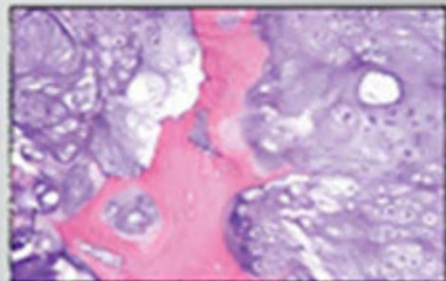
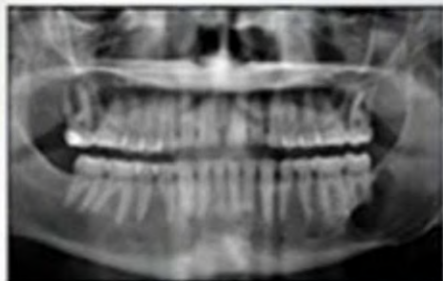
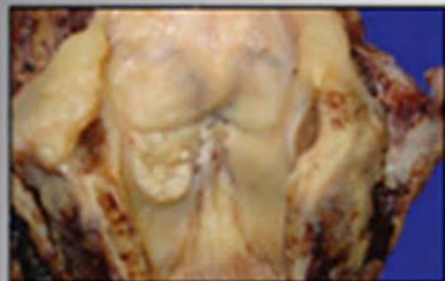


Lester D. R. Thompson  
Justin A. Bishop

# Head and Neck Pathology

THIRD EDITION



a volume in the series  
**FOUNDATIONS IN DIAGNOSTIC PATHOLOGY**

series editor  
John R. Goldblum

ELSEVIER





# Head and Neck Pathology

THIRD EDITION

A Volume in the Series Foundations in Diagnostic Pathology

## **Lester D.R. Thompson, MD**

Consultant Pathologist  
Department of Pathology  
Southern California Permanente Medical Group  
Woodland Hills, California

## **Justin A. Bishop, MD**

Associate Professor and Director of Head and Neck Pathology  
Department of Pathology  
UT Southwestern Medical Center  
Dallas, Texas

### ***Series Editor***

## **John R. Goldblum, MD, FCAP, FASCP, FACG**

Chair, Department of Anatomic Pathology  
Professor of Pathology  
Cleveland Clinic Lerner College of Medicine  
Cleveland, Ohio

ELSEVIER



## ***Other books in this series***

---



Busam: Dermatopathology, 2e  
9780323261913



Folpe and Inwards: Bone and Soft Tissue Pathology  
9780443066887



Hsi: Hematopathology, 3e  
9780323479134



Iacobuzio-Donahue and Montgomery: Gastrointestinal and Liver Pathology, 2e  
9781437709254



Marchevsky, Abdul-Karim, and Balzer: Intraoperative Consultation  
9781455748235



Nucci and Oliva: Gynecologic Pathology  
9780443069208



O'Malley, Pinder, and Mulligan: Breast Pathology, 2e  
9781437717570



Prayson: Neuropathology, 2e  
9781437709490



Procop and Pritt: Pathology of Infectious Diseases  
9781437707625



Zhou and Magi-Galluzzi: Genitourinary Pathology, 2e  
9780323188272



# ELSEVIER

1600 John F. Kennedy Blvd.  
Ste 1800  
Philadelphia, PA 19103-2899

HEAD AND NECK PATHOLOGY, THIRD EDITION  
**Copyright © 2019 by Elsevier Inc. All rights reserved.**

ISBN: 978-0-323-47916-5

No part of this publication may be reproduced or transmitted in any form or by any means, electronic or mechanical, including photocopying, recording, or any information storage and retrieval system, without permission in writing from the Publisher. Details on how to seek permission, further information about the Publisher's permissions policies and our arrangements with organizations such as the Copyright Clearance Center and the Copyright Licensing Agency, can be found at our website: [www.elsevier.com/permissions](http://www.elsevier.com/permissions).

This book and the individual contributions contained in it are protected under copyright by the Publisher (other than as may be noted herein).

## Notices

Knowledge and best practice in this field are constantly changing. As new research and experience broaden our understanding, changes in research methods, professional practices, or medical treatment may become necessary.

Practitioners and researchers must always rely on their own experience and knowledge in evaluating and using any information, methods, compounds, or experiments described herein. In using such information or methods they should be mindful of their own safety and the safety of others, including parties for whom they have a professional responsibility.

With respect to any drug or pharmaceutical products identified, readers are advised to check the most current information provided (i) on procedures featured or (ii) by the manufacturer of each product to be administered, to verify the recommended dose or formula, the method and duration of administration, and contraindications. It is the responsibility of practitioners, relying on their own experience and knowledge of their patients, to make diagnoses, to determine dosages and the best treatment for each individual patient, and to take all appropriate safety precautions.

To the fullest extent of the law, neither the Publisher nor the authors, contributors, or editors, assume any liability for any injury and/or damage to persons or property as a matter of products liability, negligence or otherwise, or from any use or operation of any methods, products, instructions, or ideas contained in the material herein.

Previous editions copyrighted in 2013, 2006.

## Library of Congress Cataloging-in-Publication Data

Names: Thompson, Lester D. R., editor. | Bishop, Justin A., editor.  
Title: Head and neck pathology / [edited by] Lester D.R. Thompson, Justin A. Bishop.  
Other titles: Head and neck pathology (Thompson) | Foundations in diagnostic pathology.  
Description: Third edition. | Philadelphia, PA : Elsevier, [2019] | Series: Foundations of diagnostic pathology | Includes bibliographical references and index.  
Identifiers: LCCN 2017051700 | ISBN 9780323479165 (hardcover : alk. paper)  
Subjects: | MESH: Head and Neck Neoplasms | Head-pathology | Neck-pathology  
Classification: LCC RC936 | NLM WE 707 | DDC 616.99/491-dc23 LC record available at <https://lccn.loc.gov/2017051700>

*Executive Content Strategist:* Michael Houston  
*Senior Content Development Manager:* Kathryn DeFrancesco  
*Publishing Services Manager:* Patricia Tannian  
*Senior Project Manager:* Sharon Corell  
*Book Designer:* Patrick Ferguson

Printed in China.

Last digit is the print number: 9 8 7 6 5 4 3 2 1



Working together  
to grow libraries in  
developing countries

[www.elsevier.com](http://www.elsevier.com) • [www.bookaid.org](http://www.bookaid.org)



**Justin A. Bishop, MD**

Associate Professor and Director of Head and Neck Pathology  
Department of Pathology  
UT Southwestern Medical Center  
Dallas, Texas, USA

**Diana Bell, MD**

Associate Professor  
Head and Neck Section  
University of Texas  
Departments of Pathology and Head and Neck Surgery  
MD Anderson Cancer Center  
Houston, Texas, USA

**Rebecca D. Chernock, MD**

Associate Professor  
Department of Pathology and Immunology  
Washington University School of Medicine  
St. Louis, Missouri, USA

**Simion I. Chiosea, MD**

Associate Professor of Pathology  
Department of Pathology  
University of Pittsburgh Medical Center  
Presbyterian Hospital  
Pittsburgh, Pennsylvania, USA

**Uta Flucke, MD, PhD**

Consultant Pathologist  
Department of Pathology  
Radboud University Medical Centre  
Nijmegen, The Netherlands

**Vickie Y. Jo, MD**

Assistant Professor  
Department of Pathology  
Brigham and Women's Hospital and Harvard Medical School  
Boston, Massachusetts, USA

**Lester D.R. Thompson, MD**

Consultant Pathologist  
Department of Pathology  
Southern California Permanente Medical Group  
Woodland Hills, California, USA

**James S. Lewis, Jr., MD**

Professor  
Department of Pathology, Microbiology, and Immunology  
Vanderbilt University Medical Center  
Nashville, Tennessee, USA

**Austin McCuiston, MD**

Resident Physician  
Department of Pathology  
The Johns Hopkins Hospital  
Baltimore, Maryland, USA

**Susan Müller, DMD, MS**

Professor Emeritus  
Emory University School of Medicine  
Atlanta, Georgia, USA

**Brenda L. Nelson, DDS, MS**

Head  
Department of Anatomic Pathology  
Naval Medical Center, San Diego  
San Diego, California, USA

**Mary S. Richardson, MD, DDS**

Professor  
Department of Pathology and Laboratory Medicine  
Medical University of South Carolina  
Charleston, South Carolina, USA



The study and practice of anatomic pathology are both exciting and somewhat overwhelming, as surgical pathology (and cytopathology) have become increasingly complex and sophisticated. It is simply not possible for any individual to master all of the skills and knowledge required to perform the daily tasks at the highest level. Simply being able to make a correct diagnosis is challenging enough, but the standard of care has far surpassed merely providing an accurate diagnosis. Pathologists are now asked to provide huge amounts of ancillary information, both diagnostic and prognostic, often on small amounts of tissue, a task that can be daunting even to the most experienced surgical pathologists.

Although large general surgical pathology textbooks remain useful resources, by necessity they cannot possibly cover many of the aspects that diagnostic pathologists need to know and include in their daily surgical pathology reports. As such, the concept behind *Foundations in Diagnostic Pathology* was born. This series is designated to cover the major areas of surgical pathology, and each volume is focused on one major topic. The goal of every book in this series is to provide the essential information that any pathologist, whether general or subspecialized, in training or in practice, would find useful in the evaluation of virtually any type of specimen encountered.

Dr. Lester Thompson and Dr. Justin Bishop, both renowned and highly prolific head and neck pathologists, have edited an outstanding state-of-the-art book on the essentials of head and neck pathology. In fact, this area is one of the most common topics encountered by any surgical pathologist, but very few pathologists actually

have formal training in this area. As such, a comprehensive reference such as this has great practical value in the day-to-day practice of any surgical pathologist. The list of contributors, as usual, includes some of the most renowned pathologists in this area, all of whom have significant expertise as practicing pathologists, researchers, and renowned educators on this topic. Each chapter is organized in an easy-to-follow manner, the writing is concise, tables are practical, and the photomicrographs are of high quality. There are thorough discussions pertaining to the handling of biopsy and resection specimens as well as frozen sections, which can be notoriously challenging in this field.

The book is organized into 29 chapters, including separate chapters that provide thorough overviews of non-neoplastic, benign, and malignant neoplasms of the larynx, hypopharynx, trachea, nasal cavity, nasopharynx, paranasal sinuses, oral cavity, oropharynx, salivary glands, ear and temporal bone, gnathic bones, and neck. Similarly, chapters describing the non-neoplastic, benign, and malignant neoplasms of the thyroid gland, parathyroid gland, and paraganglia system are included.

I am truly grateful to Dr. Thompson and Dr. Bishop as well as to all of the contributors who put forth tremendous effort to allow this book to come to fruition. It is yet another outstanding edition in the *Foundations in Diagnostic Pathology* series, and I sincerely hope you enjoy this comprehensive textbook and find it useful in your everyday practice of head and neck pathology.

**John R. Goldblum, MD**

There is an axiom in computing called Moore's law that states the computing speed of processors doubles every 2 years while the cost halves. However, if you actually read the fine print, it is the number of transistors in an average computer that would double every 2 years—a corollary if you will. Thus, the average CPU in a computer now has 904 million transistors, which clearly contributes to the overall speed, even though perhaps the “law” has slowed down.

How does this apply to pathology and medicine? Well, it seems that there is a tremendous increase in the number of discoveries, new entities being carved out of old ones, new diagnostic tools to achieve even greater precision in diagnostic terms and clinical prognostication. Even with this staggering volume of data, it must always be harnessed by a mind willing to synthesize all of the data points into a meaningful and actionable diagnosis that a clinician and patient alike can use to treat the disease and achieve the best outcome for the patient.

It is the aim of this edition to highlight several of the new diagnostic entities within the anatomic confines of the larynx, sinonasal tract, ear and temporal bone, salivary gland, oral, oropharynx, nasopharynx, gnathic, and neck regions. Clearly, the unlimited nature of the internet with countless webpages of information cannot be contained within a single book without requiring a forklift to move it around. Thus, the reader is encouraged to use this book as a starting point to make a meaningful diagnosis of the most common and frequent diagnoses that may beset a busy surgical pathologist in daily practice, while using the references and other materials to lead to greater understanding. Use the pertinent clinical, imaging, laboratory, macroscopic, microscopic, histochemical, immunohistochemical, ultrastructural, and molecular results presented herein to reach a meaningful, useful, and actionable diagnosis.

**Lester D.R. Thompson, MD, and Justin A. Bishop, MD**



## ■ ACKNOWLEDGMENTS

With the passage of time, transition and change are inevitable. As such, death seems to become more a part of life than the inherent meaning that the word suggests. And so it seems that many of those who influence you the most reach death's doorstep ahead of you, creating a vacuum and space in your heart that is never refilled. The guidance provided by a parent, especially in the early years, is an example of this type of powerful influence.

From as early as I can remember, my mother, Frances Avril Dawn Ansley Thompson (can you tell where I got all of my names!), provided love, support, and encouragement. She so wanted me to be happy, healthy, and wise. With each success or failure, triumph or rejection, I was always able to count on my mother to say the right thing—or say nothing at all, but just hold me, whether physically or emotionally. Last year as we were chatting about my projects, books, lectures, and work, she very quietly said: “It’s great that you have a written legacy, but remember to work on your spiritual, social, and emotional legacy with the same devotion and vigor.”

Those words rang loud and clear at my 25th wedding anniversary celebration the following weekend, a party she would have loved to attend, but couldn’t as she had died of complications of a ruptured thoracic aortic aneurysm. Taking her final words to heart, I find myself drawn to other pursuits, attempting to keep work in an ever shrinking box, including the time devoted to philanthropic endeavors with my wife, Pam, whose role in my life continues to grow and expand with each passing year.

Although patently obvious, the responsibility for any errors, omissions, or deviation from current orthodoxy is mine alone!

**Lester D.R. Thompson, MD**

I dedicate my work on this book to my wonderful wife, Ashley, and our beautiful children, Riley and Avery. I am very grateful for their willingness to sacrifice so much of our time together for this and other projects. I thank my parents, Debbie and Fred, my sister, Kristen, and my brother, Martin, for their unwavering support. I am also appreciative of Dr. William Westra, my mentor at The Johns Hopkins Hospital who took a chance on me and taught me much of what I know. Finally, I thank Dr. Lester Thompson for generously inviting me to co-edit the newest edition of this book. I have enjoyed working with him immensely and look forward to our many future collaborations.

**Justin A. Bishop, MD**

# Non-Neoplastic Lesions of the Nasal Cavity, Paranasal Sinuses, and Nasopharynx

■ Austin McCuiston ■ Justin A. Bishop

## ■ RHINOSINUSITIS

Rhinosinusitis is defined simply as inflammation of the nasal cavity (rhinitis), paranasal sinuses (sinusitis), or both (rhinosinusitis).

### CLINICAL FEATURES

Rhinosinusitis is a common condition that can be caused by myriad etiologies, including allergies (most common), infections, aspirin intolerance, exposures to toxins or medications, pregnancy, systemic diseases, among others. Rhinosinusitis can also be idiopathic, with no known cause. Regardless of etiology, patients share the symptoms of nasal obstruction and discharge.

Acute rhinosinusitis is typically infectious, either viral (e.g., rhinovirus, adenovirus, respiratory syncytial virus, among others) or bacterial (*Streptococcus pneumoniae*, *Haemophilus influenzae*, among others). Viral rhinosinusitis results in a watery nasal discharge, whereas bacterial disease results in a mucopurulent discharge, headache, and fever. Bacterial rhinosinusitis can occasionally be superimposed on viral disease.

Chronic rhinosinusitis (i.e., symptoms lasting longer than 12 weeks) is most often allergic in etiology as a result of an IgE-mediated reaction. Patients with allergic rhinosinusitis complain of a clear nasal discharge, sneezing, and itching after exposure to the offending allergen. Clinical examination reveals sinonasal mucosa that is edematous, pale, and sometimes bluish in color. Inflammatory polyps, as described later, are often seen in this setting.

By imaging, inflamed sinuses demonstrate opacification and mucosal thickening (Fig. 1.1A). Air-fluid levels are classically identified in acute disease (see Fig. 1.1B).

## PATHOLOGIC FEATURES

### GROSS FINDINGS

In general, the gross findings consist of fragments of soft tissue and bone with no specific changes. Inflammatory polyps (as described later) may be encountered.

### RHINOSINUSITIS—DISEASE FACT SHEET

#### Definition

- Inflammation of the nasal passages, most commonly as the result of allergies or infection

#### Incidence

- Common
- Nasal cavity and paranasal sinuses, often bilateral

#### Morbidity and Mortality

- Usually minimal, although rarely untreated bacterial sinusitis can extend to the orbit or meninges

#### Sex and Age Distribution

- Any age, no sex predilection

#### Clinical Features

- Nasal discharge, watery in allergic and viral, mucopurulent in bacterial
- Allergic disease accompanied by itching and sneezing

#### Treatment and Prognosis

- Allergic rhinosinusitis treated with antihistamines, nasal steroids, allergic desensitization
- Bacterial rhinosinusitis requires antibiotics, while viral infection is treated supportively
- Surgery is reserved for refractory, chronic disease

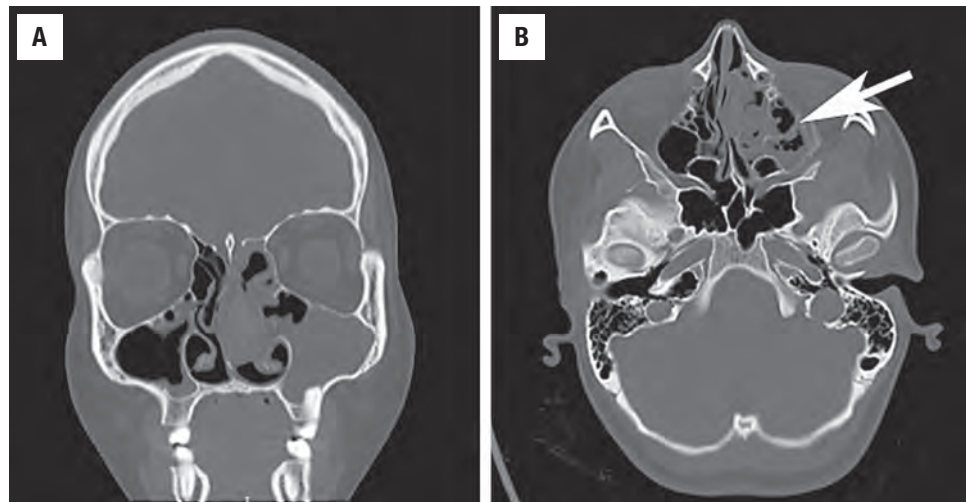


**FIGURE 1.1**

This computed tomography scan demonstrates radiographic features of both acute and chronic sinusitis. The left maxillary sinus demonstrates near complete opacification (**A**), and air-fluid levels are noted (arrow) in the left ethmoid sinus (**B**).

### MICROSCOPIC FINDINGS

Rhinosinusitis exhibits sinonasal mucosa with a submucosal inflammatory infiltrate. The inflammatory cells are generally composed of lymphocytes, plasma cells, macrophages, and eosinophils, which predominate in allergic disease (Fig. 1.2). Acute rhinosinusitis is characterized by increased neutrophils, especially when associated with a bacterial etiology. There is often a component of stromal edema, which leads to the development of inflammatory polyps (described in detail in the next topic). The surface epithelium may also demonstrate changes, including inflammation, squamous metaplasia (Fig. 1.3A), or reactive papillary hyperplasia (so-called *papillary sinusitis*) (see Fig. 1.3B).

### DIFFERENTIAL DIAGNOSIS

The diagnosis of rhinosinusitis is usually not difficult. Many of the changes overlap with sinonasal inflammatory polyps, and the distinction between the two entities is not important. In cases with squamous metaplasia and/or reactive papillary hyperplasia of the surface epithelium, sinonasal papilloma can enter the differential diagnosis. Sinonasal papillomas have squamous or squamoid epithelium that is also thickened, proliferative with endophytic and/or exophytic growth, and infiltrated by neutrophils with microabscesses. Rarely, adenocarcinoma may enter the differential diagnosis when there is a reactive proliferation of seromucinous glands.

### PROGNOSIS AND THERAPY

Acute viral rhinosinusitis is treated symptomatically, whereas bacterial disease requires antimicrobials. Chronic

### RHINOSINUSITIS—PATHOLOGIC FEATURES

#### Gross Findings

- Nonspecific

#### Microscopic Findings

- Submucosal infiltrate of lymphocytes, plasma cells, neutrophils, eosinophils, often with edema
- Surface epithelium may demonstrate squamous metaplasia, inflammation, or reactive papillary hyperplasia

#### Pathologic Differential Diagnosis

- Inflammatory polyps, sinonasal papilloma, adenocarcinoma

allergic sinusitis is treated with antihistamines, intranasal corticosteroids, and/or allergic desensitization. Patients with chronic rhinosinusitis refractory to medical therapy may require endoscopic surgery. Rhinosinusitis is generally not life-threatening, with the rare exception of untreated bacterial infection that can lead to infection of the orbit or meninges.

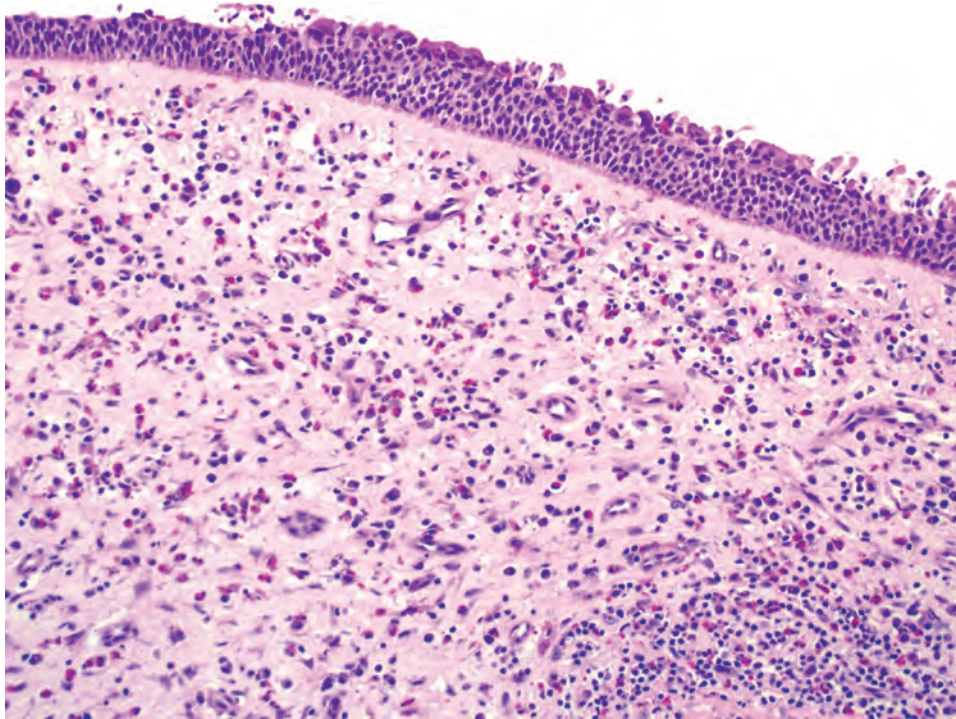
## ■ SINONASAL INFLAMMATORY POLYPS

Sinonasal inflammatory polyps are common non-neoplastic masses of sinonasal tissue that essentially result from edema within the submucosa.

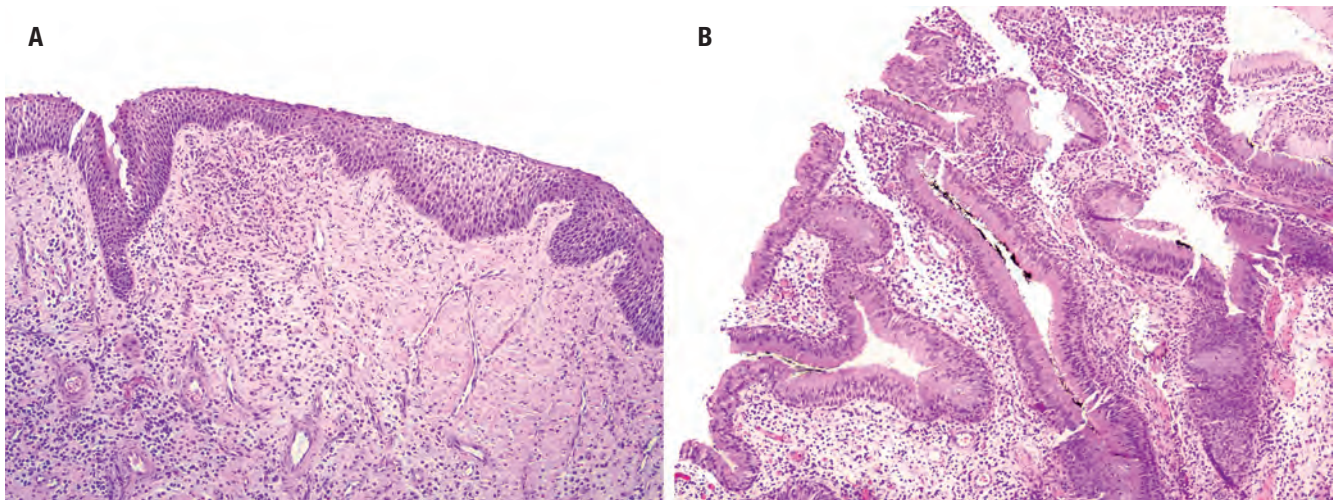
### CLINICAL FEATURES

Inflammatory polyps are associated with many conditions. They are most often seen in the setting of allergic rhinosinusitis but may also be seen in the setting of infections,



**FIGURE 1.2**

Chronic sinusitis is histologically characterized by a submucosal infiltrate of chronic inflammatory cells including lymphocytes, plasma cells, and eosinophils, which tend to predominate in allergic sinusitis.

**FIGURE 1.3**

Some cases of chronic sinusitis can demonstrate foci of surface epithelial squamous metaplasia (**A**). In addition, chronic sinusitis occasionally exhibits papillary surface epithelial hyperplasia as a reactive change. When prominent, this finding can be confused with other lesions such as respiratory epithelial adenomatoid hyperplasia or sinonasal papilloma (**B**).

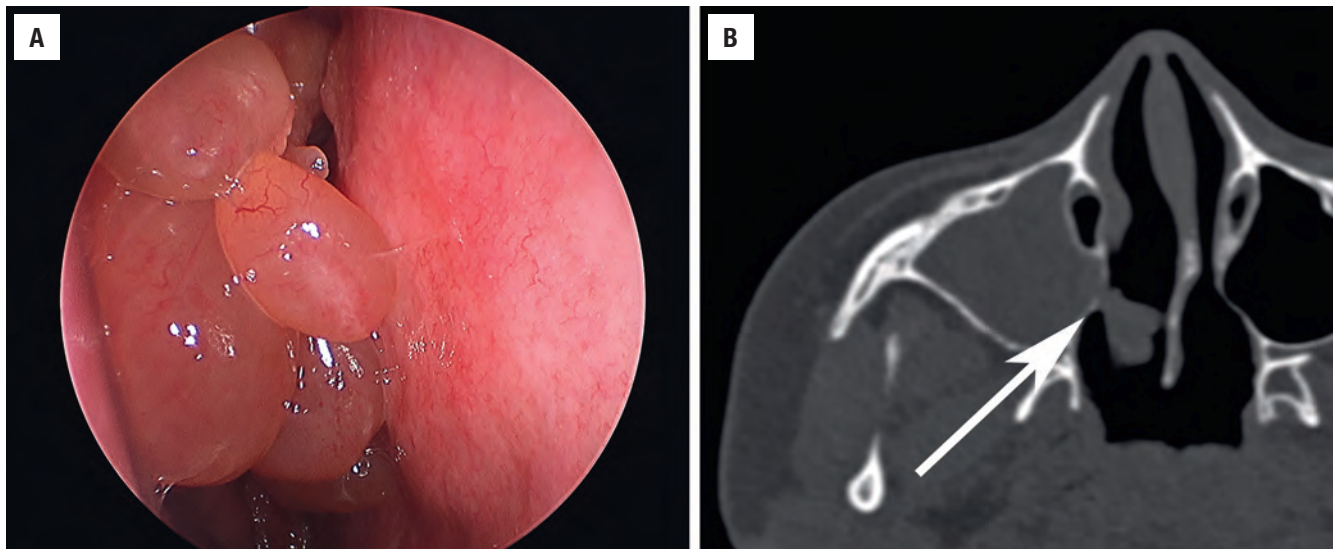
asthma, aspirin intolerance, cystic fibrosis, diabetes mellitus, and other conditions. Inflammatory polyps are typically seen in adults (except for cystic fibrosis-associated polyps), with no sex predilection. They involve the nasal cavity (especially the lateral wall) and maxillary and ethmoid sinuses and are usually bilateral (**Fig. 1.4A**). In addition to the symptoms of the underlying condition (e.g., allergies), sinonasal inflammatory polyps may cause nasal obstruction and pain. A subtype of inflammatory polyp known as antrochoanal polyp arises from the maxillary antrum and extends through the sinus ostia into the nasal cavity, nasopharynx, or oral cavity (see **Fig. 1.4B**). Antrochoanal

polyps are usually seen in younger patients (teenagers and young adults), usually males, and are typically unilateral.

## **PATHOLOGIC FEATURES**

### **GROSS FINDINGS**

Inflammatory polyps are typically translucent and mucoid in appearance (see **Fig. 1.4A**). Antrochoanal polyps tend to be elongated with a stalk and fibrotic.

**FIGURE 1.4**

The typical clinical appearance of inflammatory polyps is that of bilateral, multiple mucoid polypoid masses with a translucent appearance involving the nasal cavity (**A**). The antrochoanal polyp is a subtype of inflammatory polyp arising from the maxillary antrum and protruding into the nasal cavity through the nasal choana (**B**). (**A**, Courtesy of Dr. Douglas Reh.)

#### SINONASAL INFLAMMATORY POLYPS—DISEASE FACT SHEET

##### Definition

- Polypoid growths of sinonasal mucosa that result primarily from submucosal edema
- An allergic etiology is most common

##### Incidence

- Common
- Nasal cavity and paranasal sinuses, often bilateral
- Antrochoanal polyp is a subtype that arises from the maxillary antrum and protrudes through the sinus ostium, usually unilateral

##### Morbidity and Mortality

- Usually minimal, although rarely may lead to bone erosion or remodeling

##### Sex and Age Distribution

- Typically adults (except antrochoanal polyps in teenagers/young adults and cystic fibrosis polyps in children)

##### Clinical Features

- Symptoms of underlying disease (e.g., rhinorrhea, nasal stuffiness, headaches in allergic polyps)
- Nasal obstruction and epistaxis

##### Treatment and Prognosis

- Endoscopic removal
- Treatment of underlying disease (e.g., nasal steroids for allergic polyps)

#### SINONASAL POLYPS—PATHOLOGIC FEATURES

##### Gross Findings

- Translucent, glistening, and mucoid
- Antrochoanal polyps have a long stalk and are fibrotic

##### Microscopic Findings

- Polypoid fragments of sinonasal mucosa with abundant stromal edema
- Chronic inflammatory cell infiltrate with numerous eosinophils
- Epithelial basement membrane is usually hyalinized
- Secondary changes including infarction, hemorrhage, and fibrin deposition can be seen.
- Antrochoanal polyps are less edematous, more fibrotic, fewer eosinophils, and minimal basement membrane hyalinization.

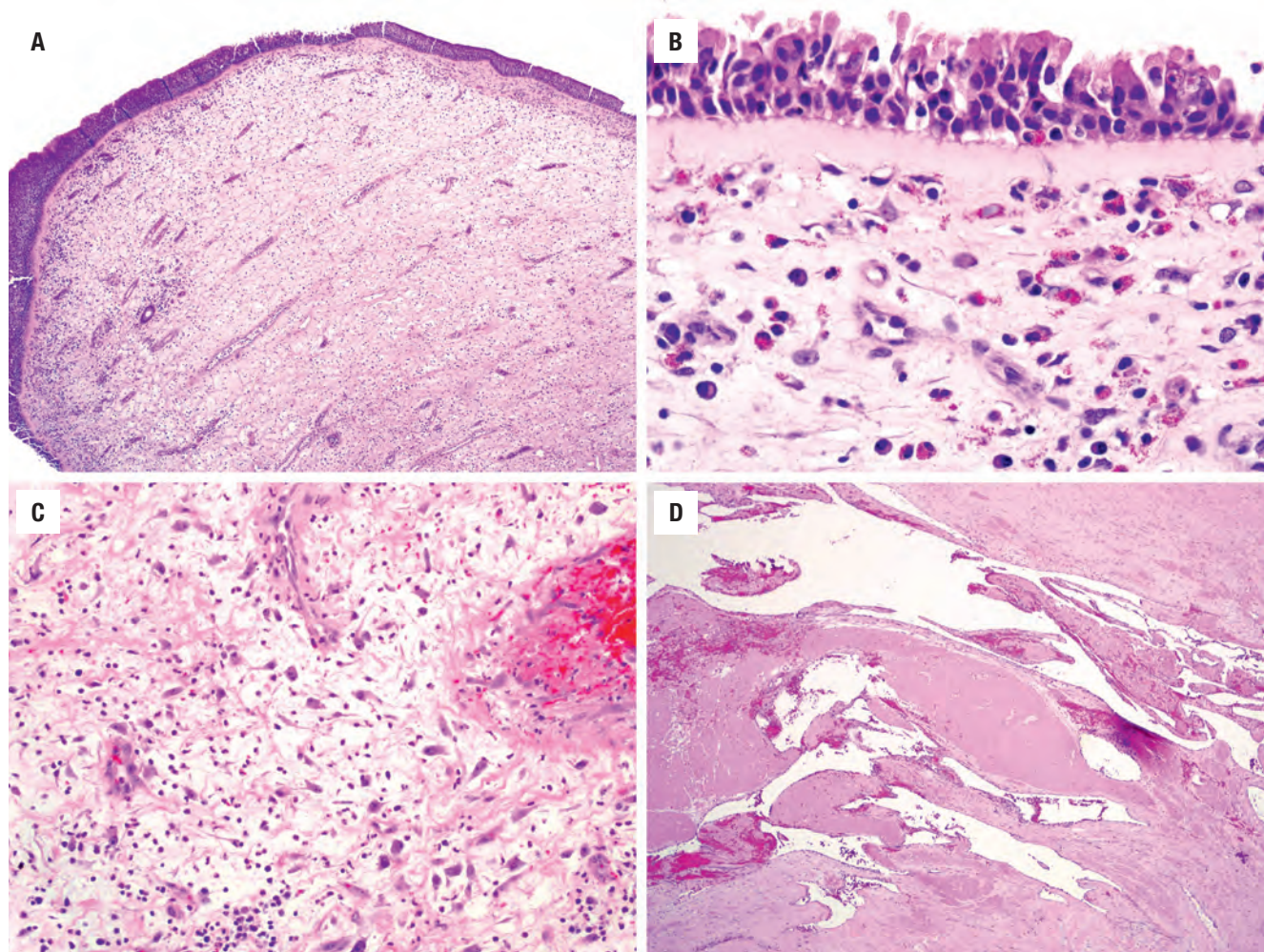
##### Pathologic Differential Diagnosis

- Amyloidosis, hemangioma, lymphangioma, infections, respiratory epithelial adenomatoid hamartoma, nasopharyngeal angiofibroma, sinonasal papilloma, embryonal rhabdomyosarcoma

#### MICROSCOPIC FINDINGS

The most prominent feature of a sinonasal inflammatory polyp is submucosal edema beneath an intact respiratory epithelium (**Fig. 1.5A**). The subepithelial basement membrane is typically hyalinized (see **Fig. 1.5B**). There is usually a mild to moderate infiltrate of chronic inflammatory cells with a predominance of eosinophils (see **Fig. 1.5B**). Scattered stellate or spindled fibroblasts are seen, some of which may exhibit enlarged, hyperchromatic nuclei (see **Fig. 1.5C**). Larger inflammatory polyps may demonstrate prominent submucosal hemorrhage with fibrin



**FIGURE 1.5**

A sinonasal inflammatory polyp consists of a rounded proliferation of sinonasal mucosa with submucosal inflammation and edema (**A**). An inflammatory polyp often has a hyalinized subepithelial basement membrane and an infiltrate of chronic inflammatory cells, especially eosinophils (**B**). Inflammatory sinonasal polyps commonly demonstrate scattered atypical stromal myofibroblasts. When prominent, a mesenchymal neoplasm is a diagnostic consideration (**C**). In the angiectatic or angiomatous variant of inflammatory polyp, there is abundant fibrin deposition (which can be mistaken for amyloid) as well as recanalizing vessels (which can be mistaken for a vascular tumor) (**D**).

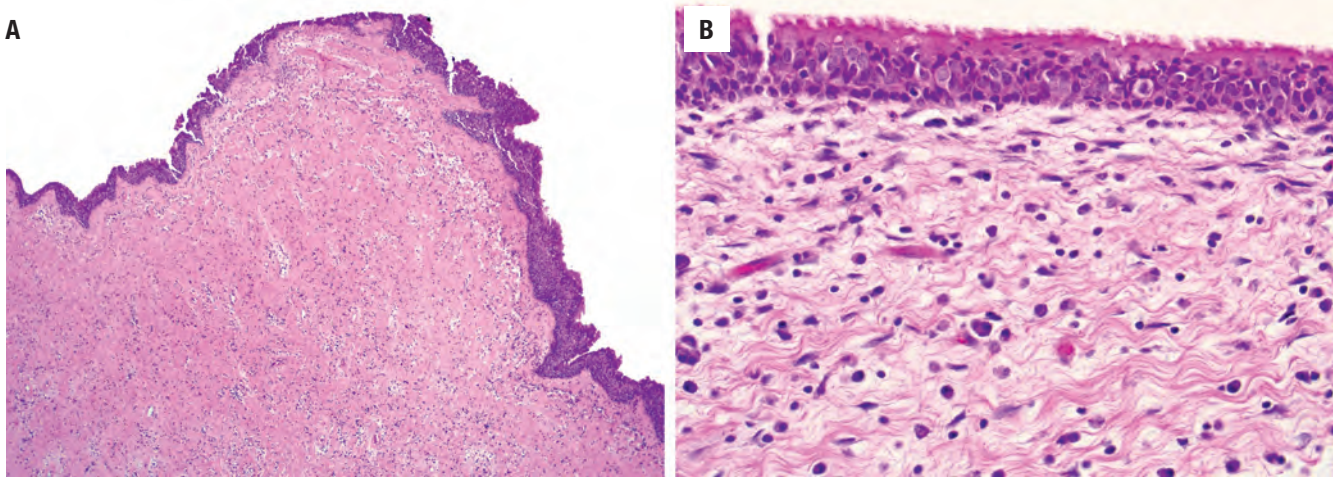
deposition or infarction, a pattern that has been referred to as “angiomatous” or “angiectatic” (see [Fig. 1.5D](#)).

Antrochoanal polyps have a similar appearance but tend to be more fibrotic and less edematous ([Fig. 1.6A](#)), have fewer eosinophils, and lack a hyalinized basement membrane (see [Fig. 1.6B](#)). Bizarre stromal cells are more common in antrochoanal polyps than in inflammatory polyps.

### DIFFERENTIAL DIAGNOSIS

The diagnosis of sinonasal inflammatory polyp is usually straightforward. When there is prominent fibrin deposition, amyloidosis is a consideration. True amyloid is positive with Congo red showing apple-green birefringence, in contrast to fibrin. In angiomatous polyps in

which recanalizing vessels are prominent, a vascular or lymphatic neoplasm could be considered. Recognizing the context of the vessels (i.e., with organizing fibrin within a sinonasal polyp) is useful in avoiding this pitfall. The fibrous stroma and occasional nasopharyngeal location of antrochoanal polyps are somewhat reminiscent of nasopharyngeal angiofibroma. In addition, both tumors, typically as unilateral masses, arise in younger men. Recognizing the dilated, “staghorn” appearance of the vessels is important for diagnosing angiofibroma; the vessels of antrochoanal polyp are typically small and inconspicuous. In difficult cases, immunohistochemistry for beta-catenin and androgen receptor may be used: the stromal cells of angiofibroma are positive for both, whereas antrochoanal polyps are negative. The atypical stromal cells of sinonasal inflammatory polyps can, in some cases, be alarming and raise the possibility of a sarcoma such as embryonal rhabdomyosarcoma.

**FIGURE 1.6**

Antrochoanal polyp is a variant of inflammatory polyp that typically exhibits more prominent subepithelial fibrosis at low power (**A**). In contrast to the usual inflammatory polyp, antrochoanal polyps have fewer eosinophils and lack a hyalinized basement membrane (**B**).

However, the atypical stromal cells of benign polyps are singly and randomly distributed, do not aggregate (e.g., no “cambium” layer characteristic of embryonal rhabdomyosarcoma), are not mitotically active, and are negative for desmin and myogenin. Respiratory epithelial adenomatoid hamartoma (REAH) tends to show widely spaced glands, surrounded by a thick, eosinophilic basement membrane, showing connections of the invaginations to the surface. Finally, one must be sure to exclude the presence of another sinonasal neoplasm such as sinonasal papilloma that are often seen in association with inflammatory polyps.

### PROGNOSIS AND THERAPY

These are benign lesions. Treatment includes endoscopic surgery in addition to treatment of the underlying medical cause (e.g., nasal steroids for allergic polyps).

## ■ PARANASAL SINUS MUCOCELE

Mucocele of the paranasal sinus result from obstruction of the sinus outflow tract with subsequent expansion of the sinus with mucin.

### CLINICAL FEATURES

Sinus mucoceles can occur in any age or sex. They result from any disease that obstructs the sinus outflow tract

### PARANASAL SINUS MUCOCELE—DISEASE FACT SHEET

#### Definition

- Expansion of the paranasal sinus by mucin resulting from obstruction of the outflow tract

#### Incidence

- Uncommon
- Frontal and ethmoid sinuses most commonly affected

#### Morbidity and Mortality

- Can result in facial deformity, brain or orbit involvement if untreated

#### Sex and Age Distribution

- Any age or sex

#### Clinical Features

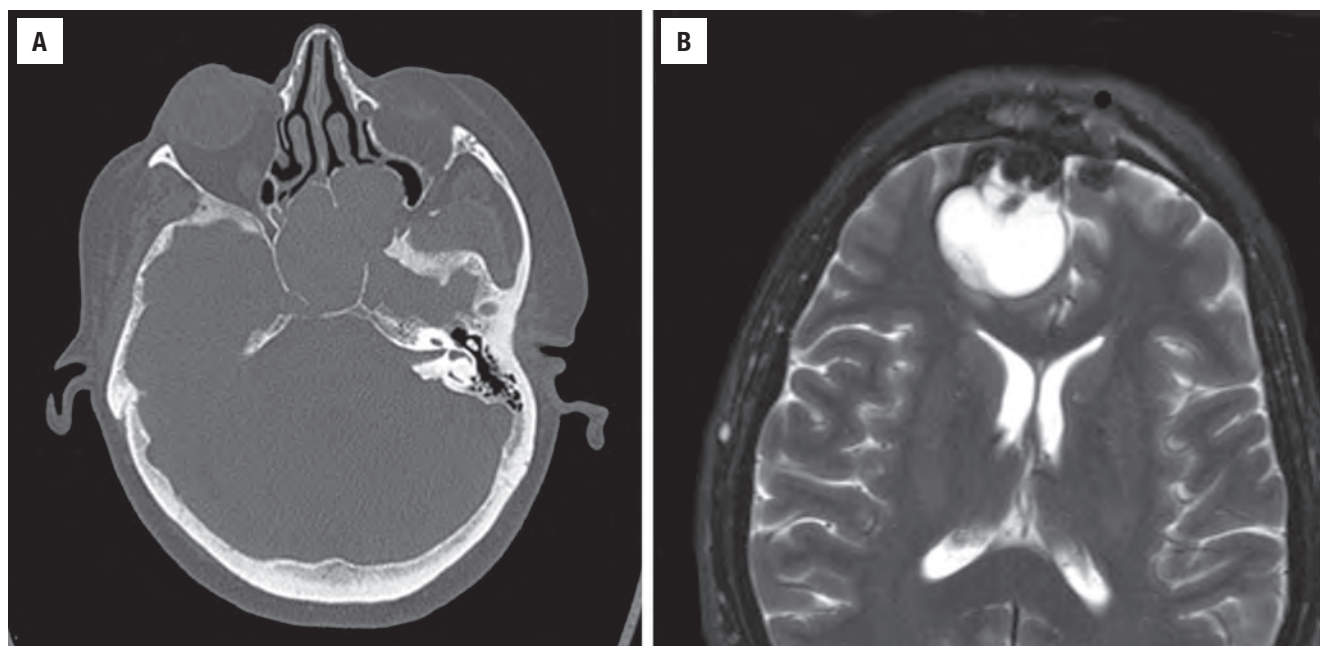
- Nasal obstruction, headaches, visual disturbances, proptosis
- Radiographs show expanded sinus with bone erosion and sclerosis and rarely invasion of the orbit or cranial cavity

#### Treatment and Prognosis

- Surgical excision
- Treatment of underlying cause (usually chronic sinusitis)

(ostium or duct), most commonly chronic sinusitis, but also occasionally trauma, neoplasms, or other causes. The obstruction leads to expansion of the involved sinus, usually frontal or ethmoid (**Fig. 1.7A**). Mucoceles can produce alarming clinical and radiographic features, including facial deformity, headaches, visual disturbances, proptosis, bone erosion and sclerosis, and rarely, invasion



**FIGURE 1.7**

This computed tomography scan demonstrates a sphenoid sinus mucocele, with expansion of the sinus with secretions and thinning and remodeling of the surrounding bones (**A**). This T2-weighted magnetic resonance imaging scan shows a fluid-filled mucocele involving the brain (**B**).

#### PARANASAL SINUS MUCOCELE—PATHOLOGIC FEATURES

##### Gross Findings

- Abundant mucin, otherwise nonspecific

##### Microscopic Findings

- Very nonspecific
- Sinonasal mucosa with inflammation, sometimes attenuation, squamous metaplasia, scarring, reactive bone, or cholesterol granulomas

##### Pathologic Differential Diagnosis

- Normal sinonasal mucosa, inflammatory polyps, unsampled neoplasm leading to obstruction

of the orbit or cranial cavity (see [Fig. 1.7B](#)). Given these dramatic symptoms and radiographic features, a neoplastic process is often suspected clinically.

#### PATHOLOGIC FEATURES

##### GROSS FINDINGS

Abundant mucin is generally apparent grossly or reported intraoperatively (if suction has removed all of the contents).

#### MICROSCOPIC FINDINGS

The microscopic features of mucoceles are typically underwhelming (particularly in the setting that is suspicious for malignancy) and closely mimic normal sinonasal tissue. The sinonasal tissue sometimes has an attenuated appearance resembling a cyst lining ([Fig. 1.8A and B](#)). Epithelial squamous metaplasia, fibrosis, a rim of reactive bone, or cholesterol granuloma formation can also be seen. Because of their nonspecific nature, a definitive diagnosis cannot be made on histologic grounds without clinical or radiographic input.

#### DIFFERENTIAL DIAGNOSIS

The main diagnostic consideration is normal sinonasal tissue. Clinical and radiographic correlation is needed to make the distinction. Sinonasal polyps or a salivary gland mucocele may also be in the differential. An unsampled neoplasm may be the cause of the obstruction leading to a mucocele.

#### PROGNOSIS AND THERAPY

Sinus mucoceles are treated by surgical excision. The underlying cause of the obstruction (e.g., chronic sinusitis) should also be addressed. The prognosis is excellent.

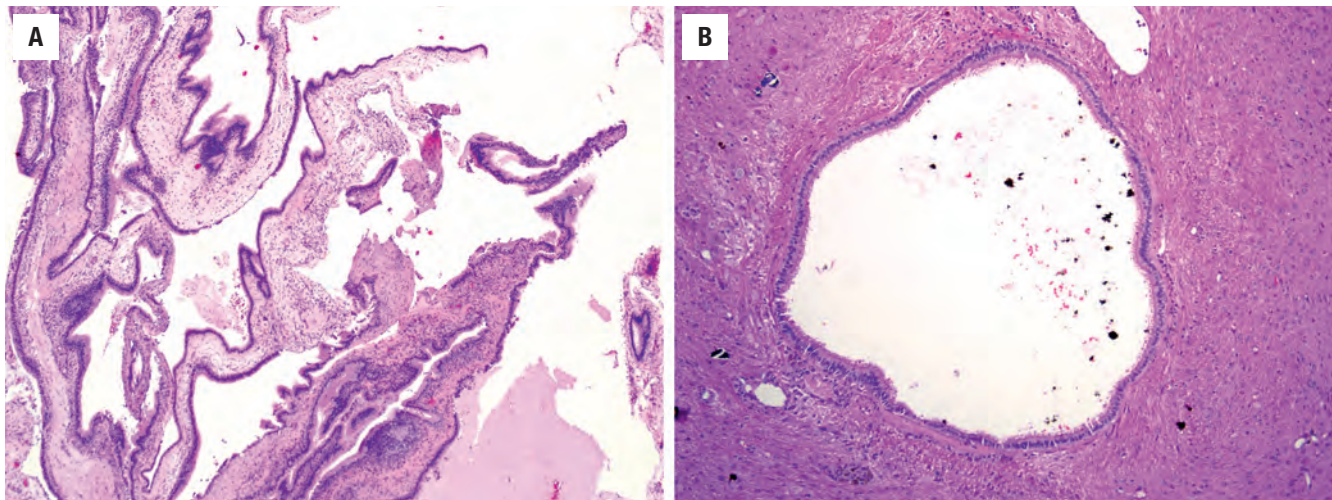


**FIGURE 1.8**

Histologically, paranasal sinus mucocoeles have a nonspecific appearance, consisting of attenuated strips of relatively normal appearing sinonasal mucosa. Radiographic correlation is needed to make the diagnosis of mucocoele (**A**). In this example of an aggressive mucocoele, normal-appearing sinonasal epithelium is seen in brain tissue (**B**).

## ■ ALLERGIC FUNGAL SINUSITIS

Allergic fungal sinusitis (AFS) is a relatively common condition believed to represent an allergic reaction to antigens from fungi (most commonly *Aspergillus* species) that have colonized the sinonasal tract.

### CLINICAL FEATURES

AFS most often affects children and young adults, with no sex predilection. Affected patients present with nasal discharge along with allergic-type symptoms such as nasal stuffiness, facial pressure, and fullness. Patients are often observed to have firm, viscous, foul-smelling mucin within their affected sinuses. In addition, patients typically exhibit peripheral eosinophilia and elevated serum IgE levels. In severe cases, patients uncommonly may exhibit facial asymmetry with bone destruction.

### PATHOLOGIC FEATURES

#### GROSS FINDINGS

Grossly, the secretions of AFS are firm, thick, and rubbery and have the quality of putty or peanut butter.

#### MICROSCOPIC FINDINGS

The microscopic hallmark of AFS is so-called *allergic mucin*: inspissated mucin that is admixed with eosinophils,

neutrophils, Charcot-Leyden crystals, fibrin, and desquamated epithelial cells (Figs. 1.9 and 1.10). The various components of allergic mucin are typically arranged in a laminated fashion, creating a striated or “tigroid” appearance (see Fig. 1.9). Fungal elements are usually not apparent on routine histology. The background

### ALLERGIC FUNGAL SINUSITIS—DISEASE FACT SHEET

#### Definition

- A noninvasive form of fungal sinusitis resulting from an allergic reaction to colonizing fungal antigens

#### Incidence and Location

- More common in warmer climates such as southern and southwestern United States

#### Morbidity and Mortality

- Typically minimal, although rarely patients may demonstrate facial asymmetry and bone destruction

#### Sex and Age Distribution

- Typically children or young adults, no sex predilection

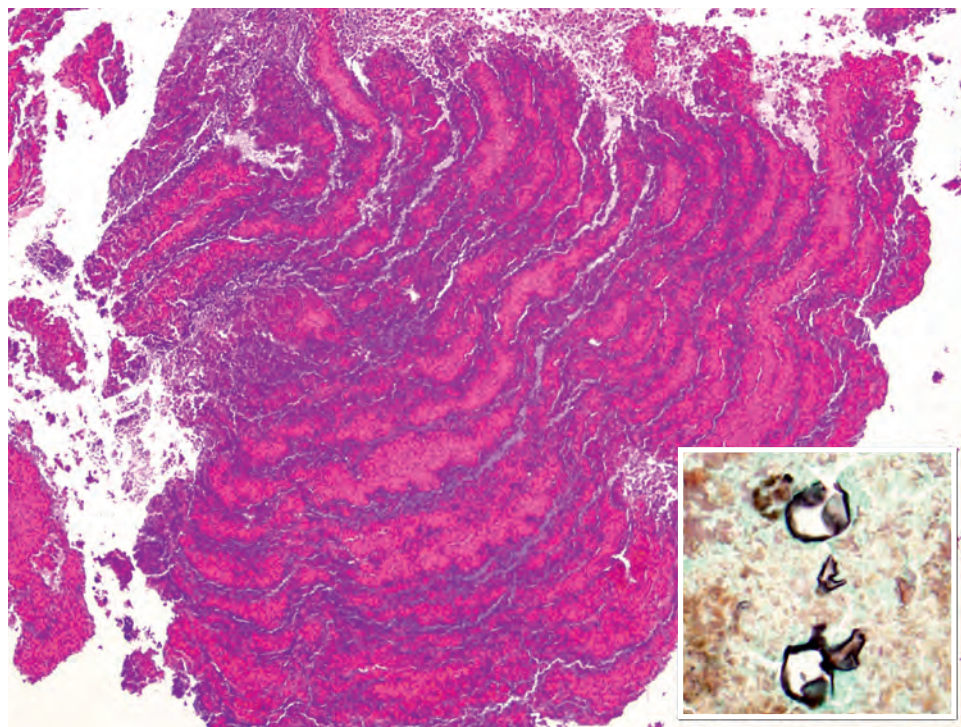
#### Clinical Features

- Nasal discharge, allergic-type symptoms
- Elevated serum IgE levels and peripheral eosinophilia
- Sinus contents with firm, rubbery, foul-smelling mucus

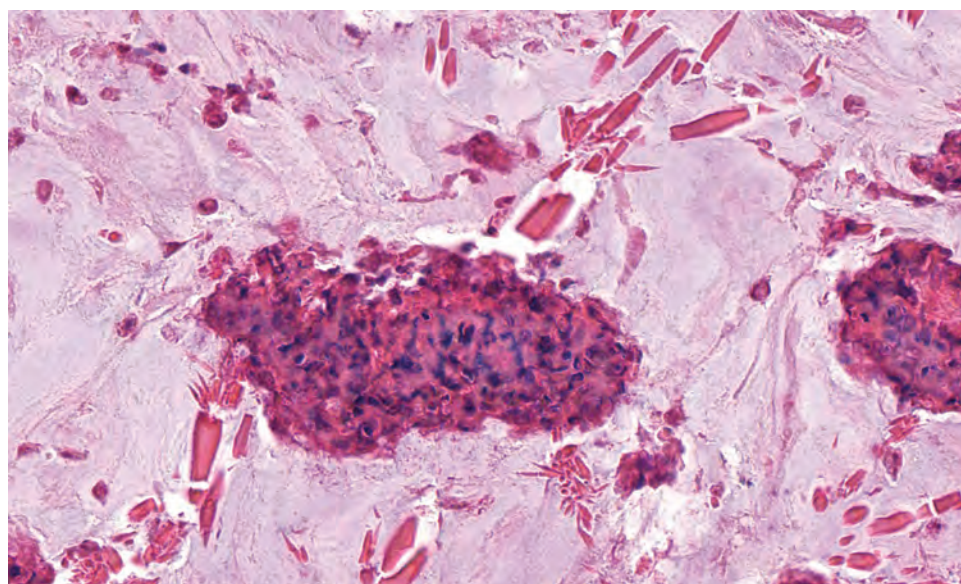
#### Treatment and Prognosis

- Evacuation of tenacious mucus
- Intranasal steroids
- Some patients benefit from fungal allergic desensitization
- Long-term therapy may be needed to control relapses



**FIGURE 1.9**

The diagnostic histologic finding is allergic mucin, which is composed of inflammatory cells (particularly eosinophils), Charcot-Leyden crystals, desquamated epithelial cells, and other debris. A lamellated ("tigroid") appearance is classic for allergic mucin. Stains for fungi (in this case, Gomori methenamine silver) highlight fungal hyphae in a subset of allergic fungal sinusitis cases. The hyphae are often degenerated and distorted, as seen here (*inset*).

**FIGURE 1.10**

Charcot-Leyden crystals are seen as long needlelike and bipyramidal-shaped crystals in this case of allergic fungal sinusitis.

sinonasal mucosa exhibits edema and chronic inflammation with frequent eosinophils.

#### ANCILLARY STUDIES

Special stains for fungi (Gomori methenamine silver [GMS] and periodic acid–Schiff [PAS]) reveal scattered fungal hyphae within the allergic mucin in about half of cases. These fungal elements are often scarce and may have an unusual, degenerated appearance (see [Fig. 1.9](#), *inset*).

#### DIFFERENTIAL DIAGNOSIS

The histologic appearance of AFS may resemble non-specific rhinosinusitis or sinonasal polyps, but the characteristic presence of allergic mucin is diagnostic for AFS. The allergic mucin of AFS may be confused with another form of noninvasive fungal sinusitis known as mycetoma or fungus ball. However, in mycetoma the debris is composed entirely of matted fungal hyphae in far greater numbers than what is seen in AFS. Mycetomas may calcify or show conidia (fungal fruiting bodies)



(Fig. 1.11A). Finally, AFS must be distinguished from acute or chronic forms of invasive fungal sinusitis, in which fungal elements invade stroma with frequent involvement of vessels (see Fig. 1.11B).

### PROGNOSIS AND THERAPY

Treatment includes removal of the mucus as a means to restore mucociliary function. Intranasal steroids are frequently used. Fungal desensitization may also be used as a treatment option. There does not appear to be a role for antifungal agents. Prognosis is good, although long-term therapy may be needed to control relapses in some patients.

#### ALLERGIC FUNGAL SINUSITIS—PATHOLOGIC FEATURES

##### Gross Findings

- Thick, viscous mucin that may resemble putty or peanut butter

##### Microscopic Findings

- Allergic mucin: a striated mixture of mucin, inflammatory cells, Charcot-Leyden crystals, and other debris
- Fungal hyphae seen in approximately half of cases with special stains
- Fungi often scarce and have a degenerated appearance

##### Pathologic Differential Diagnosis

- Nonspecific rhinosinusitis, sinonasal polyp, mycetoma (fungus ball), invasive fungal sinusitis (acute or chronic)

## NASAL GLIAL HETEROTOPIA

Nasal glial heterotopia is a benign condition resulting from the failure of the developing frontal lobe to completely retract into the cranial cavity during fetal development. Because it is not a neoplasm, the historical term “nasal glioma” should not be used.

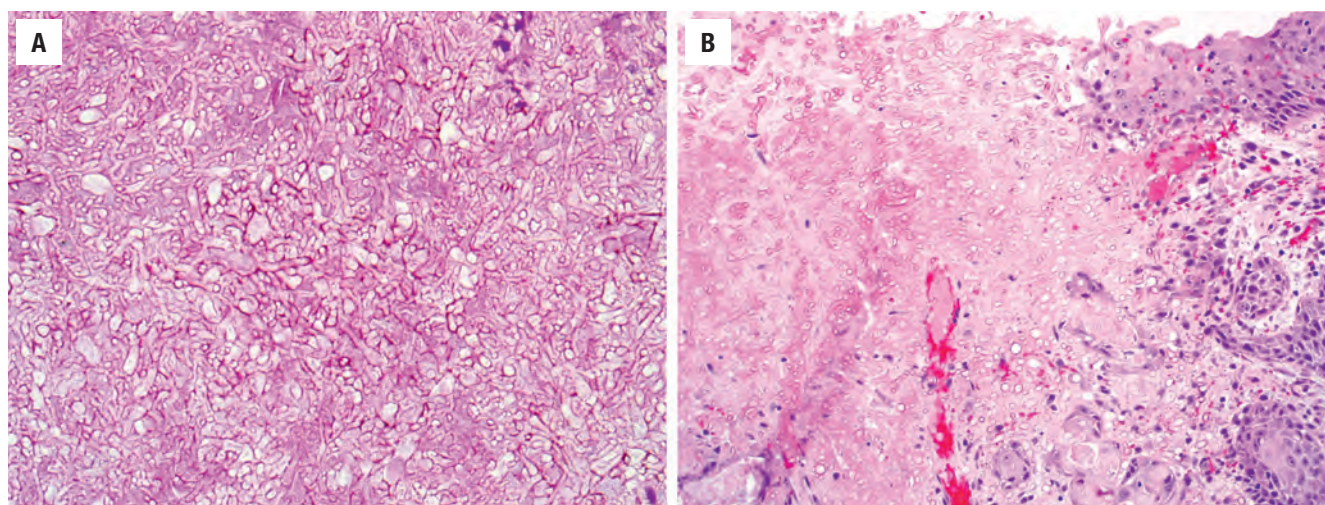
### CLINICAL FEATURES

Nasal glial heterotopia usually affects infants, although it can occasionally be encountered in older patients. There is no predilection for either sex. Glial heterotopia presents as a firm nodule that can be extranasal (60%) on the bridge or side of the nose, intranasal within the nasal cavity (30%), or both intranasal and extranasal (10%). Patients often have nasal obstruction and infants may show difficulty feeding as a result of the mass. By radiology, there is no connection to the intracranial cavity, a crucial feature that distinguishes glial heterotopia from an encephalocele (Fig. 1.12A and B).

### PATHOLOGIC FEATURES

#### GROSS FINDINGS

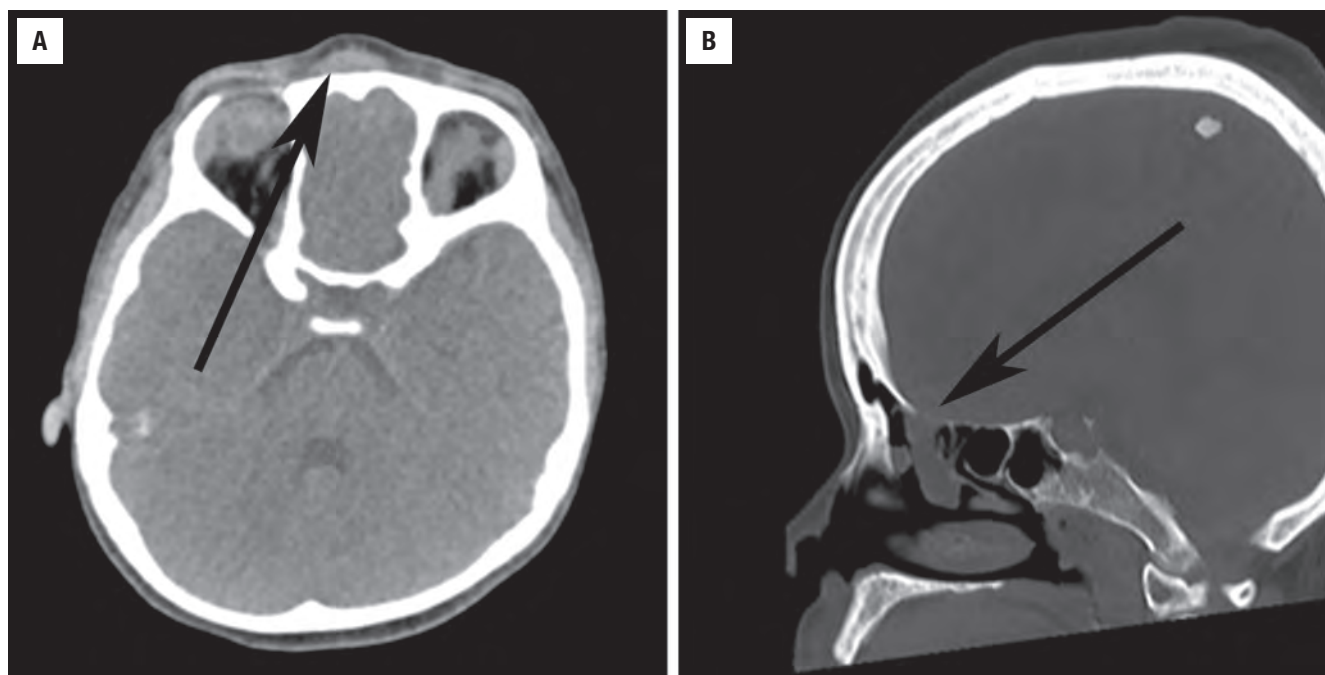
Well-circumscribed nodule of firm soft tissue, 1 to 3 cm in size, with a glistening cut surface.



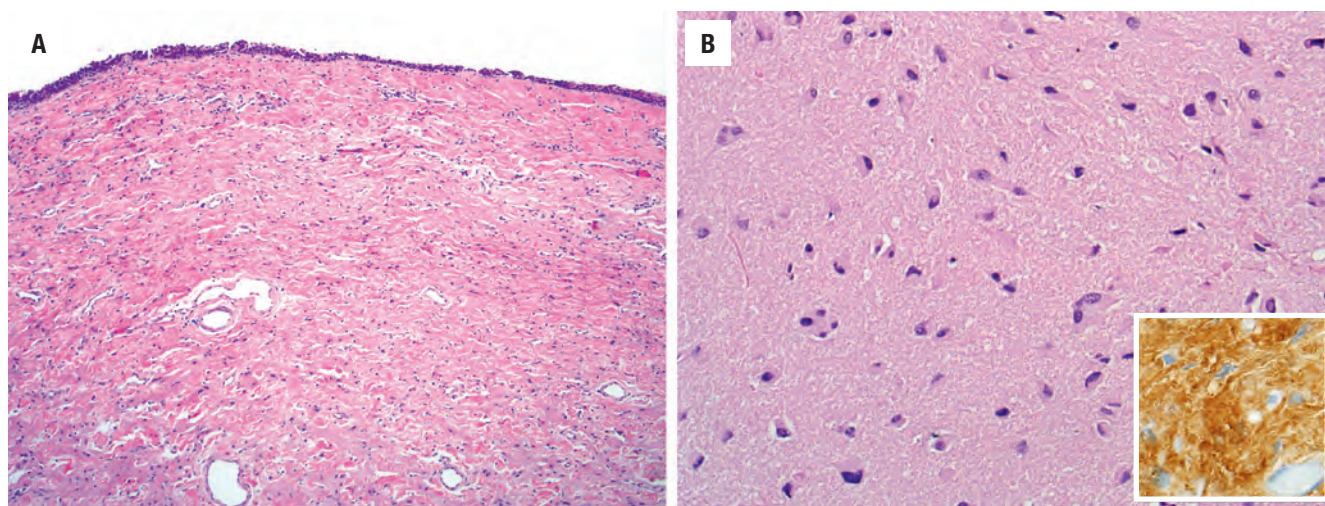
**FIGURE 1.11**

Mycetoma (fungus ball) is a form of noninvasive fungal sinusitis consisting of a matted collection of degenerating fungal hyphae growing within the sinus, with no tissue invasion (A). In contrast, fulminant invasive fungal sinusitis is characterized by invasion of tissues with necrosis and a limited inflammatory reaction (B).



**FIGURE 1.12**

Computed tomography scan of extranasal glial heterotopia (*arrow*) without a connection to the cranial cavity (**A**). In contrast, this encephalocele involving the nasal cavity has a clear connection to the cranial cavity (*arrow*) (**B**).

**FIGURE 1.13**

Nasal glial heterotopia manifests as fibrotic glial tissue in the sinonasal submucosa (**A**). At high power the glial tissue consists of scattered astrocytes in a pink, fibrillary background (**B**). Immunostaining for glial fibrillary acidic protein confirms the glial nature of the tissue (*inset*).

### MICROSCOPIC FINDINGS

Heterotopic glial tissue resembles gliotic brain tissue, with astrocytes admixed with eosinophilic fibrillary glial tissue underlying skin or sinonasal mucosa ([Fig. 1.13A and B](#)). Neurons are only rarely seen, whereas dura and meninges are not present. The glial tissue may be obscured by fibrosis, necessitating immunohistochemical confirmation.

### ANCILLARY STUDIES

Nasal glial heterotopia can be confirmed immunohistochemically by positivity for the glial markers glial fibrillary acidic protein (GFAP) (see [Fig. 1.13B](#)), S100 protein, and the newly introduced nuclear marker OLIG2.

### NASAL GLIAL HETEROTOPIA—DISEASE FACT SHEET

#### Definition

- Developmentally displaced glial tissue in the sinonasal tract *without* a connection to the cranial cavity

#### Incidence

- Uncommon
- Extranasal (bridge or side of nose) in 60%, intranasal in 30%, and mixed in 10%

#### Morbidity and Mortality

- Minimal, although can result in difficulty feeding for some infants

#### Sex and Age Distribution

- Usually infants
- No sex predilection

#### Clinical Features

- Nasal mass, often resulting in obstruction

#### Treatment and Prognosis

- Surgical excision
- Excellent prognosis after complete excision

### NASAL GLIAL HETEROTOPIA—PATHOLOGIC FEATURES

#### Gross Findings

- Small circumscribed firm nodule with a glistening cut surface

#### Microscopic Findings

- Astrocytes in a glial fibrillary matrix
- Neurons only rarely present, leptomeninges are absent
- May be fibrotic, obscuring the glial nature of the lesion

#### Ancillary Studies

- Glial tissue positive for GFAP, S100 protein, OLIG2

#### Pathologic Differential Diagnosis

- Nonspecific fibrosis in sinonasal polyp, encephalocele

### DIFFERENTIAL DIAGNOSIS

Heterotopic glial tissue can be misdiagnosed as nonspecific fibrosis in a sinonasal polyp, a distinction that can be easily addressed by immunohistochemistry for glial markers. Another diagnostic consideration is encephalocele. The distinction is not trivial, because an encephalocele, by definition, means that there is a patent connection with the cranial cavity, which puts the patient at risk for meningitis. The presence of dura/leptomeninges or well-organized glial tissue with neurons

favors an encephalocele, but these features are often lost, especially in long-standing lesions. Ultimately, the distinction requires clinical and radiographic input (see Fig. 1.12B).

### PROGNOSIS AND THERAPY

Glial heterotopia is treated with simple excision. The prognosis is excellent following complete removal of the glial tissue.

### RHINOSCLEROMA

Rhinoscleroma is a rare, chronic infectious disease caused by *Klebsiella rhinoscleromatis*, a gram-negative coccobacillus bacterium, that affects the nasal cavity and nasopharynx.

### CLINICAL FEATURES

Rhinoscleroma most often affects young adults in their second and third decades. There is a slight female predominance. It is endemic to certain parts of South America, Central America, Africa, India, and Indonesia, but is rare in North America. Rhinoscleroma affects the nasal cavity and nasopharynx, and there are three distinct clinical stages. The rhinitic or exudative stage is characterized by a foul-smelling mucopurulent nasal discharge with nasal obstruction and erythema. With progression of the disease after months or years without treatment, the florid or proliferative stage is marked by mucosal thickening by numerous small masses and subsequent nasal obstruction (Fig. 1.14). Finally, long-term rhinoscleroma is known as the fibrotic or cicatricial stage and is characterized by marked scarring and nasal stenosis. Rhinoscleroma can result in marked facial deformities, particularly in the latter stages of the disease.

### PATHOLOGIC FEATURES

#### GROSS FINDINGS

The gross pathologic appearance varies based on the clinical disease stage. The rhinitic/exudative stage has a nonspecific appearance, whereas the florid/proliferative stage produces friable nasal polyps. Finally, the fibrotic/cicatricial stage is characterized by densely fibrotic tissues.

**FIGURE 1.14**

A clinical photograph of a 42-year-old man with rhinoscleroma presenting as several years of progressive nasal ulceration, along with palatal perforation, yielding marked nasal and mid-facial distortion. (Courtesy of Dr. R. Carlos.)

### MICROSCOPIC FINDINGS

Rhinoscleroma is most often biopsied in the florid stage, where the submucosa is expanded by an inflammatory infiltrate including lymphocytes, plasma cells, neutrophils, and histiocytes. As in any disease with abundant plasma cells, Russell bodies—large cytoplasmic inclusions composed of immunoglobulin—are frequent. The diagnostic microscopic finding is the presence of “Mikulicz cells”—large histiocytes with abundant, clear, vacuolated cytoplasm (Fig. 1.15). As rhinoscleroma progresses, lesions become increasingly fibrotic and less inflammatory.

### ANCILLARY STUDIES

A Warthin-Starry stain highlights rod-shaped *Klebsiella* organisms within the Mikulicz cells (see Fig. 1.15).

### DIFFERENTIAL DIAGNOSIS

Rhinoscleroma can mimic Rosai-Dorfman disease; however, in rhinoscleroma emperipolesis is not observed

### RHINOSCLEROMA—DISEASE FACT SHEET

#### Definition

- Infectious disease caused by *Klebsiella rhinoscleromatis*, a gram-negative coccobacillus bacterium

#### Incidence and Location

- Rare
- Endemic in parts of South America, Central America, Africa, India, and Indonesia

#### Morbidity and Mortality

- Can cause marked facial deformity and nasal stenosis

#### Sex and Age Distribution

- Second and third decades
- Slight female predilection

#### Clinical Features

- Three clinical stages: rhinitic (exudative) with abundant foul-smelling mucopurulent secretions; florid (proliferative) with numerous small friable nodules causing obstruction and deformity; and fibrotic (cicatrical) with marked scarring and stenosis

#### Treatment and Prognosis

- Long-term antibiotics and possibly surgical débridement
- High relapse rates necessitate long-term follow-up

### RHINOSCLEROMA—PATHOLOGIC FEATURES

#### Gross Findings

- Nonspecific, or friable polyps, or dense sclerosis

#### Microscopic Findings

- Marked chronic inflammation with lymphocytes, plasma cells, neutrophils, and histiocytes in the sinonasal submucosa
- The diagnostic finding is the “Mikulicz cell”—large histiocytes with clear, vacuolated cytoplasm

#### Ancillary Studies

- Warthin-Starry stain highlights the rod-shaped organisms within the Mikulicz cells

#### Pathologic Differential Diagnosis

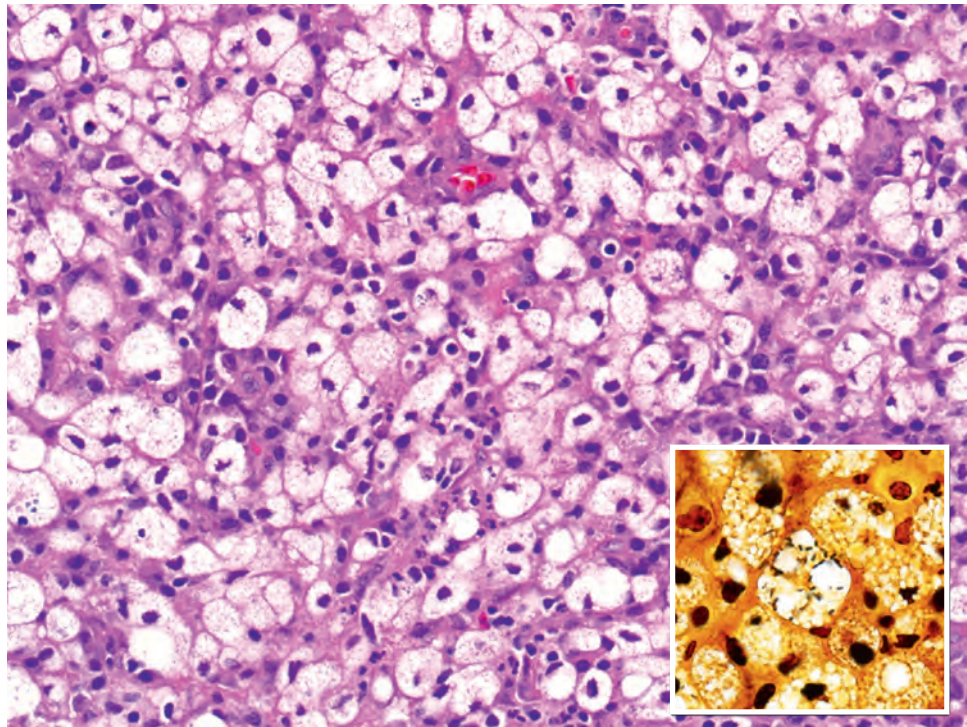
- Rosai-Dorfman disease, infections (atypical mycobacteria, leprosy, syphilis), granulomatosis with polyangiitis, clear cell epithelial neoplasms

(Fig. 1.16). Moreover, although Mikulicz cells are positive for CD68, they are negative for S100 protein. In some cases of rhinoscleroma, the Mikulicz cells can be so prominent that the lesion may be mistaken as a clear cell epithelial neoplasm such as mucoepidermoid

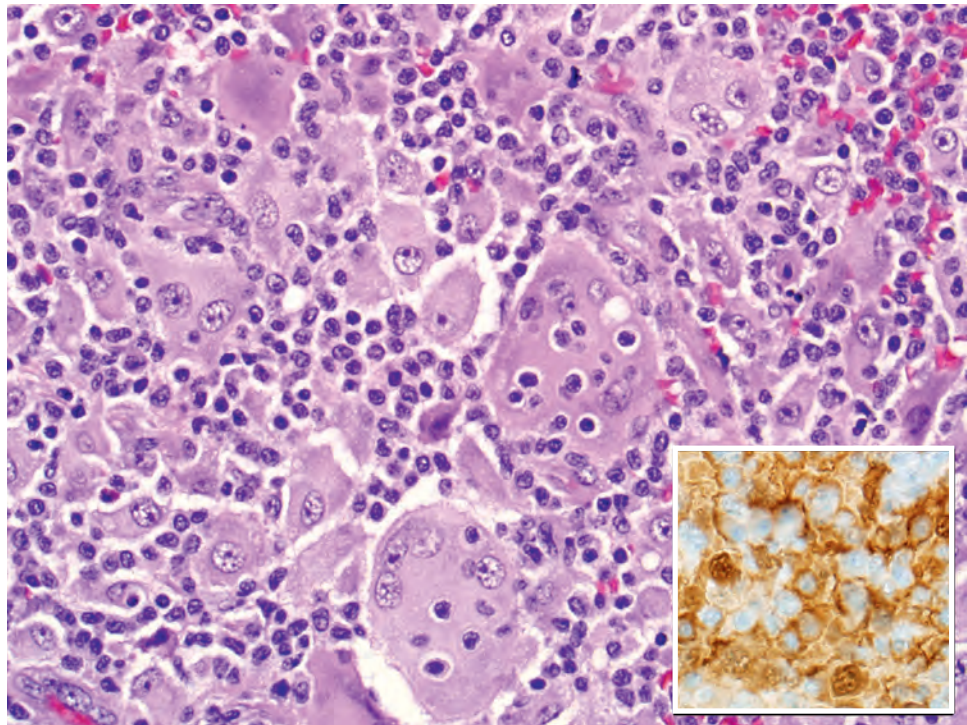


**FIGURE 1.15**

In the florid phase of rhinoscleroma, there are numerous “Mikulicz cells”—large histiocytes with abundant, clear, vacuolated cytoplasm. These cells are positive for rod-shaped bacteria on Warthin-Starry staining (*inset*).

**FIGURE 1.16**

Rosai-Dorfman disease may affect the sino-nasal tract and can mimic rhinoscleroma. The diagnostic feature of Rosai-Dorfman disease is emperipolesis—large histiocytes with intracytoplasmic lymphocytes. These histiocytes are positive for S100 protein by immunohistochemistry (*inset*).



carcinoma or myoepithelioma. This can be resolved by immunohistochemistry for CD68 (positive in rhinoscleroma) and cytokeratin (negative), as well as positive Warthin-Starry staining. Other infections (atypical mycobacteria, leprosy, and syphilis) may result in granulomata. Giant cells and granulomas may be seen in granulomatosis with polyangiitis (GPA) (Wegener), but vasculitis is not seen in rhinoscleroma.

### PROGNOSIS AND THERAPY

Long-term systemic antibiotics are indicated for rhinoscleroma. Surgical débridement may be needed to correct stenotic nasal passages. Rhinoscleroma generally shows a good response to antibiotics, but high relapse rates necessitate long-term follow-up.



## RHINOSPORIDIOSIS

Rhinosporidiosis is a chronic zoonotic infection caused by the eukaryotic organism *Rhinosporidium seeberi*.

### CLINICAL FEATURES

Rhinosporidiosis is typically localized to the sinonasal tract and conjunctiva but is rarely encountered in other anatomic sites like larynx, trachea, esophagus, genital tract, and others. It is rare in North America, but it is endemic in parts of India and Sri Lanka. Patients of any age can be affected, but it is most commonly encountered in patients in their third and fourth decades. There is a slight male predominance in patients with nasal disease. Patients with sinonasal disease complain of nasal obstruction, rhinorrhea, and nosebleeds.

### PATHOLOGIC FEATURES

#### GROSS FINDINGS

Rhinosporidiosis typically manifests as friable nasal polyps or masses, classically described as *strawberry-like* in appearance.

#### MICROSCOPIC FINDINGS

Rhinosporidiosis microscopically appears as polypoid fragments of edematous sinonasal mucosa with chronic

inflammation, similar to nonspecific inflammatory polyps. The diagnostic finding is the presence of numerous cysts (sporangia) of variable sizes (Fig. 1.17). Larger cysts (up to 300  $\mu$ m) contain numerous endospores (see Fig. 1.17). The cysts are present in the stroma but may uncommonly also involve the epithelium. On occasion, rupture of cysts can induce an acute stromal inflammatory infiltrate.

### RHINOSPORIDIOSIS—DISEASE FACT SHEET

#### Definition

- Zoonotic infection caused by the eukaryotic organism *Rhinosporidium seeberi*

#### Incidence and Location

- Rare in North America but endemic in parts of India and Sri Lanka
- Affects the mucous membranes of the sinonasal tract and less commonly conjunctiva, upper airway, genital tract, and other sites

#### Morbidity and Mortality

- Typically minimal

#### Sex and Age Distribution

- Slight male predominance
- Any age, most common in third and fourth decades

#### Clinical Features

- Nonspecific: rhinorrhea, nosebleeds, obstruction

#### Treatment and Prognosis

- Surgical
- Excellent prognosis

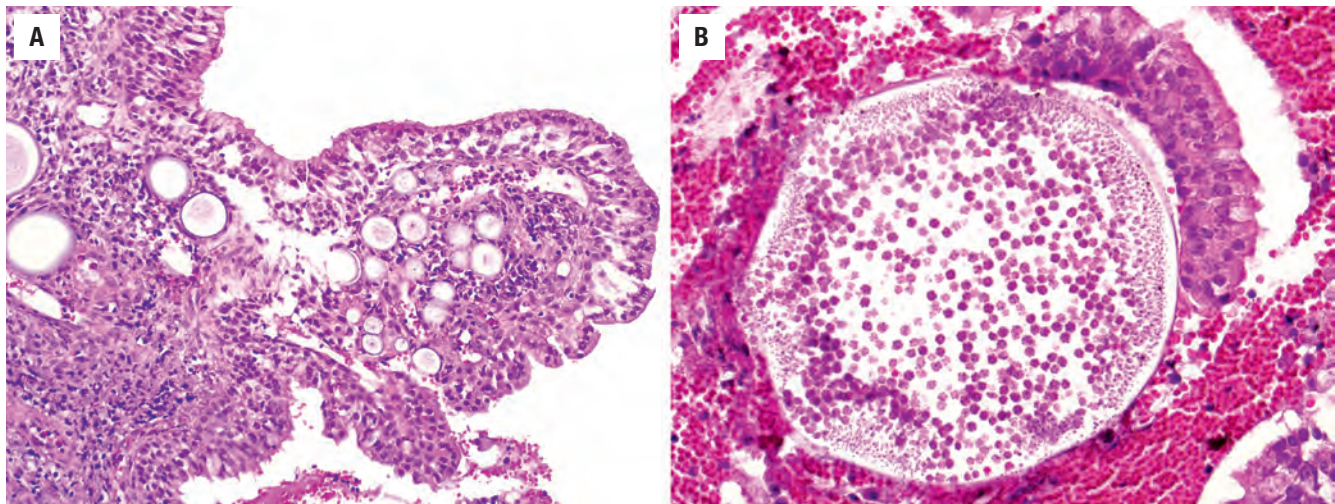


**FIGURE 1.17**

Rhinosporidiosis is an infection that exhibits presence of numerous scattered cysts (sporangia) of variable sizes (A). Larger cysts (up to 300  $\mu$ m) contain numerous endospores (B).

## RHINOSPORIDIOSIS—PATHOLOGIC FEATURES

### Gross Findings

- Friable polyps or masses

### Microscopic Findings

- Variably sized cysts up to 300  $\mu\text{m}$ , predominantly subepithelial
- The largest cysts contain small endospores
- Background nonspecific chronic inflammation and edema, acute inflammation if cysts rupture

### Ancillary Studies

- GMS and PAS highlight organisms, though usually not needed for diagnosis

### Pathologic Differential Diagnosis

- Oncocytic sinonasal papilloma, coccidiomycosis

GMS, Gomori methenamine silver; PAS, periodic acid–Schiff.

## ANCILLARY STUDIES

Special studies are not generally needed as the cysts are typically numerous and visible on routine stains, but microorganisms can be highlighted with PAS and GMS stains.

## DIFFERENTIAL DIAGNOSIS

The oncocytic type of sinonasal papilloma exhibits numerous intraepithelial microcysts that can be confused with the cysts of rhinosporidiosis. However, in oncocytic sinonasal papilloma the microcysts are confined to the epithelium. The cysts of rhinosporidiosis can be confused with the spherules of *Coccidioides immitis*, but these spherules are much smaller (up to 60  $\mu\text{m}$ ) and accompanied by a granulomatous inflammatory infiltrate.

## PROGNOSIS AND THERAPY

Rhinosporidiosis is treated by complete surgical excision. Antibiotics are not effective. The prognosis is excellent, with only occasional recurrences. The disease is not infectious to other individuals.

## ■ GRANULOMATOSIS WITH POLYANGIITIS

Granulomatosis with polyangiitis (GPA) is a systemic immune complex vasculitis of unknown etiology that often affects the sinonasal tract. Although the synonymous

term Wegener granulomatosis is still widely used, many organizations (e.g., American College of Rheumatology, the European League against Rheumatism, and the American Society of Nephrology) recommend avoiding it due to a trend against eponyms.

## CLINICAL FEATURES

GPA tends to affect middle-aged adults, with a slight male predominance. GPA classically affects the head and neck (especially sinonasal tract), lung, and kidney, but it can be localized to only one or two of these areas. Affected patients complain of nasal discharge, nasal obstruction, nosebleeds, and pain. On clinical examination, patients have a nasal septum ulcer with crusting, which can sometimes progress to perforation and collapse of the nasal cartilages (Fig. 1.18A). Respiratory disease manifests as hemoptysis, lung infiltrates, or cavitary masses, whereas renal disease results in glomerulonephritis.

## PATHOLOGIC FEATURES

### GROSS FINDINGS

The gross appearance is often a nonspecific appearing ulcer.

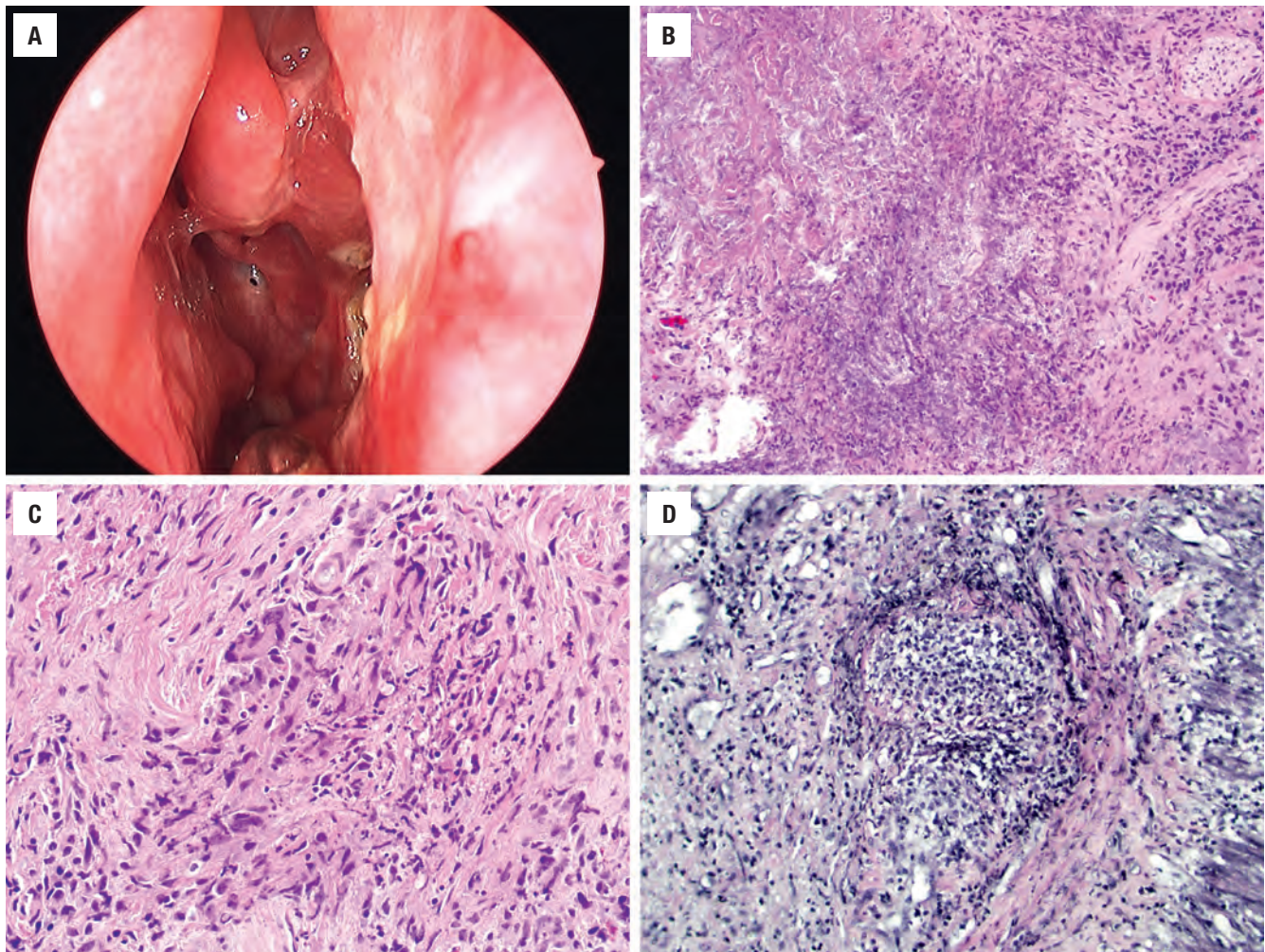
### MICROSCOPIC FEATURES

The histologic triad of GPA is biocollagenolytic (necrobiotic) necrosis, granulomatous inflammation, and vasculitis. “Biocollagenolytic” or “necrobiotic” necrosis refers to zones of geographic basophilic necrosis with granular, cellular debris (see Fig. 1.18B). The granulomatous inflammation of GPA is typically poorly formed, sometimes simply consisting of scattered giant cells (see Fig. 1.18C). Vasculitis of small to medium-sized vessels is the most specific finding but is often focal or absent. Unfortunately, most patients with GPA have biopsies that show nonspecific acute and chronic inflammation with eosinophils and sometimes neutrophilic microabscesses, and multiple biopsies may be required to establish a pathologic diagnosis.

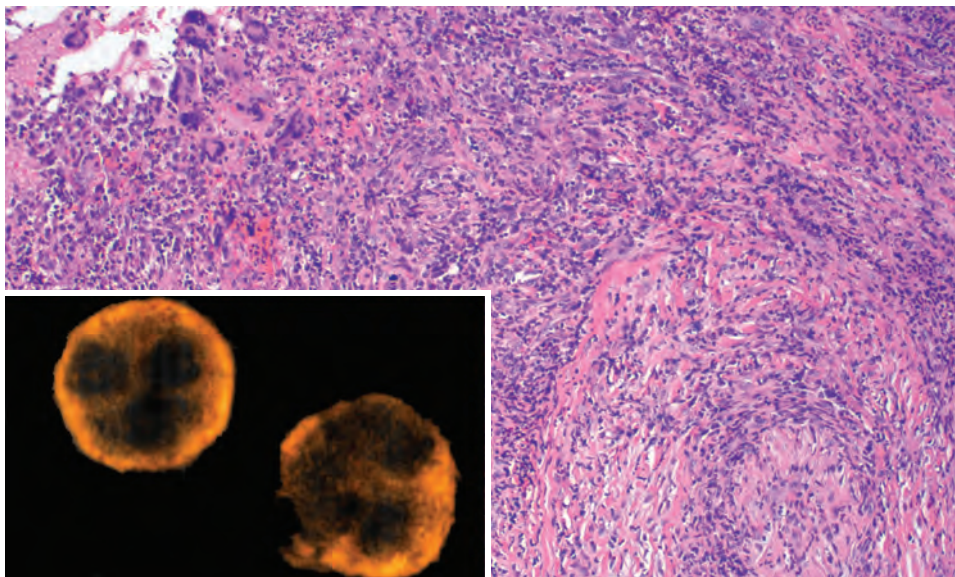
## ANCILLARY STUDIES

Elastic stains may be helpful by highlighting vessels that are involved by vasculitis (see Fig. 1.18D). Special stains for microorganisms are negative. Patients with GPA have positive serum cytoplasmic antineutrophil cytoplasmic antibodies (c-ANCA) and proteinase 3 (PR3) antibodies in approximately 80 % of cases (Fig. 1.19).



**FIGURE 1.18**

Granulomatosis with polyangiitis clinically presents as nasal erythema, crusting, ulcer, and perforation (**A**). Histologically a classic feature of granulomatosis with polyangiitis is “biocollagenolytic necrosis” (or “necrobiosis”), which is basophilic necrosis with nuclear debris (**B**). The granulomas of granulomatosis with polyangiitis are typically not well formed and may consist simply of giant cells (**C**). An elastic stain can highlight foci of vasculitis (**D**). (**A**, Courtesy of Dr. Douglas Reh.)

**FIGURE 1.19**

In granulomatosis with polyangiitis, giant cells may be present (*upper left*), but well-formed granulomas are absent. Note the vessel wall in the lower right, with destruction by the inflammatory process in an example of vasculitis. Inset: A c-ANCA shows a granular cytoplasmic pattern in a case of granulomatosis with polyangiitis.



## GRANULOMATOSIS WITH POLYANGIITIS—DISEASE FACT SHEET

### Definition

- Immune complex–mediated small vessel vasculitis of unknown etiology

### Incidence

- Uncommon
- Affects the head and neck (especially sinonasal tract), respiratory tract, and/or kidneys

### Morbidity and Mortality

- Sinonasal disease can result in significant facial deformities
- Renal and pulmonary disease can be life-threatening

### Sex and Age Distribution

- Middle-aged adults, with a slight male predominance

### Clinical Features

- Nasal disease results in nasal obstruction, pain, epistaxis, septal ulcer, and possibly perforation and deformity

### Treatment and Prognosis

- Systemic corticosteroids and/or cyclophosphamide
- Prognosis depends on extent of disease

## DIFFERENTIAL DIAGNOSIS

The differential diagnosis includes infectious granulomatous rhinosinusitis (e.g., chronic fungal sinusitis). Infectious granulomatous disease tends to produce granulomas that are better developed than those seen in GPA. Special stains for microorganisms (e.g., GMS, AFB) are helpful in addressing this possibility. Churg-Strauss disease shows granulomatosis and vasculitis and is an allergic reaction, showing asthma and tissue and peripheral eosinophilia, and may even have elevated ANCA titers. Another consideration is lymphomas in general but the NK-/T-cell lymphoma, nasal type specifically. This malignancy often exhibits vascular involvement resulting in large zones of necrosis, and the inflammatory infiltrate can be deceptively mixed and, at times, not obviously malignant. Nevertheless, on close inspection, overtly malignant lymphoma cells with marked nuclear atypia and a high mitotic rate can be found in NK-/T-cell lymphoma. In addition, NK-/T-cell lymphoma lacks granulomatous inflammation and is positive for Epstein-Barr virus (EBV) by in situ hybridization for EBV-encoded small nuclear RNA (EBER). Finally, cocaine abuse can result in nasal ulcers and perforation. The histopathologic features of cocaine abuse are typically nonspecific, but occasionally polarizable material from talc or other material used to “cut” cocaine can be identified.

## GRANULOMATOSIS WITH POLYANGIITIS—PATHOLOGIC FEATURES

### Gross Findings

- Nasal ulcer with crusting and/or perforation

### Microscopic Findings

- Classic histologic triad: biocollagenolytic necrosis (necrobiosis), vasculitis, and granulomatous inflammation
- Granulomas tend to be poorly formed and often consist simply of giant cells
- It is uncommon to see all three classic findings in a biopsy, with vasculitis being the least common

### Ancillary Studies

- Vessels with vasculitis can be highlighted by elastic stains
- Presence of serum c-ANCA and PR3 autoantibodies are quite specific

### Pathologic Differential Diagnosis

- Infectious rhinosinusitis, cocaine use, Churg-Strauss disease, NK-/T-cell lymphoma, nasal type

## PROGNOSIS AND THERAPY

GPA is treated with immunosuppressive agents such as corticosteroids or cyclophosphamide. The prognosis of GPA depends on the extent of disease. Localized disease has a good prognosis, but relapses are common. However, renal and pulmonary disease can be life-threatening.

## SINONASAL HAMARTOMAS

The sinonasal hamartomas consist of three lesions: REAH, seromucinous hamartoma (SH), and chondromesenchymal hamartoma (CMH). Despite the “hamartoma” terminology, there is evidence to suggest that each of these lesions is actually a benign neoplasm.

## CLINICAL FEATURES

All three hamartomas are rare. REAH and SH have a similar clinical profile: they tend to arise in adults with a slight male predominance and have a predilection for the posterior nasal septum (Fig. 1.20). REAH and SH present as unilateral polyps that cause nasal obstruction or epistaxis. In contrast, CMH arises most often in infants as a slow-growing, expansile lesion within the paranasal sinuses, nasal cavity, and/or orbit that can be locally aggressive. CMH has a strong association with the pleuropulmonary blastoma tumor predisposition disorder.



## PATHOLOGIC FEATURES

### GROSS FINDINGS

REAH and SH have the appearance of a nasal polyp. CMH is firm and white.

### MICROSCOPIC FINDINGS

REAH consists of downward-growing proliferations of branching glands originating from the surface epithelium (Fig. 1.21A). The glands are lined by a pseudostratified ciliated epithelium and are surrounded by a hyalinized

or edematous stroma (see Fig. 1.21B), usually showing a prominent and thickened basement membrane. SH consists of a dense proliferation of variably sized submucosal seromucinous glands lined by a single layer of cuboidal cells (Fig. 1.22A). In both REAH and SH, the

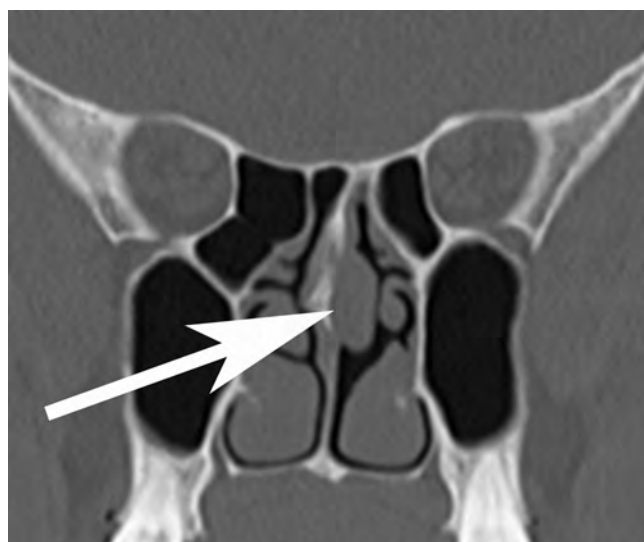


**FIGURE 1.20**

Respiratory epithelial adenomatoid hamartoma and seromucinous hamartoma have a similar radiographic appearance—a polypoid mass of the posterior nasal septum (arrow).

## SINONASAL HAMARTOMAS—DISEASE FACT SHEET

### Definition

- Benign proliferations of epithelium (REAH and SH) or stroma (CMH)

### Incidence

- All three are rare
- REAH and SH most frequently occur on the posterior nasal septum
- CMH involves the paranasal sinuses, nasal cavity, or orbit

### Morbidity and Mortality

- REAH and SH are localized lesions
- CMH may be locally aggressive

### Sex and Age Distribution

- REAH and SH involve middle-aged patients with a male predominance
- CMH usually affects infants with a male predominance

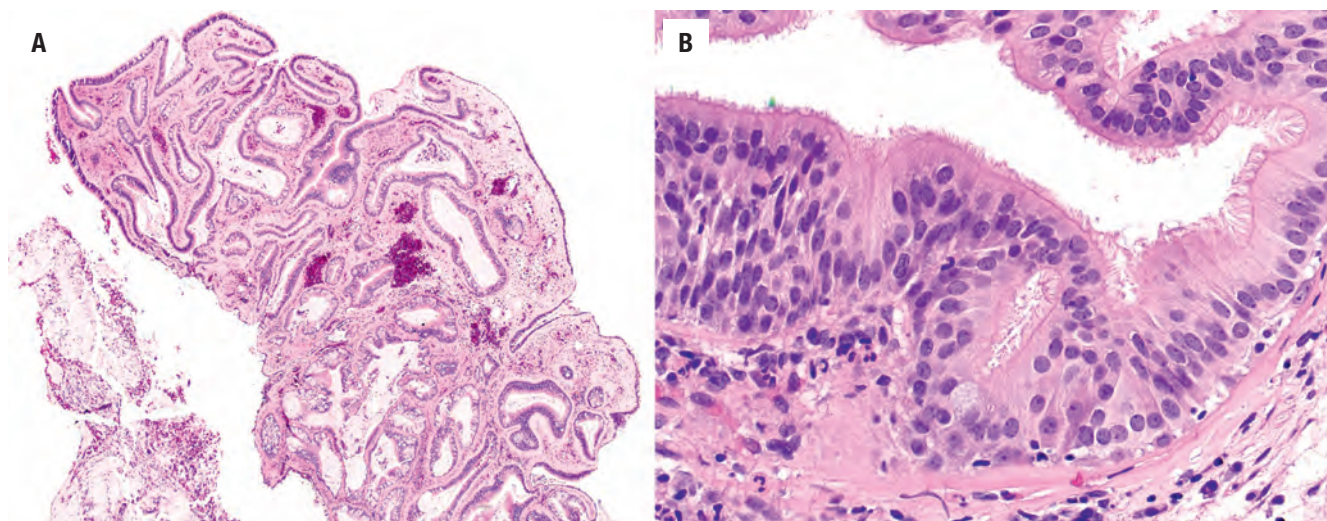
### Clinical Features

- REAH and SH present with unilateral nasal obstruction, bleeding, and polyps
- CMH presents as nasal obstruction or a mass

### Treatment and Prognosis

- Surgical excision
- Excellent prognosis

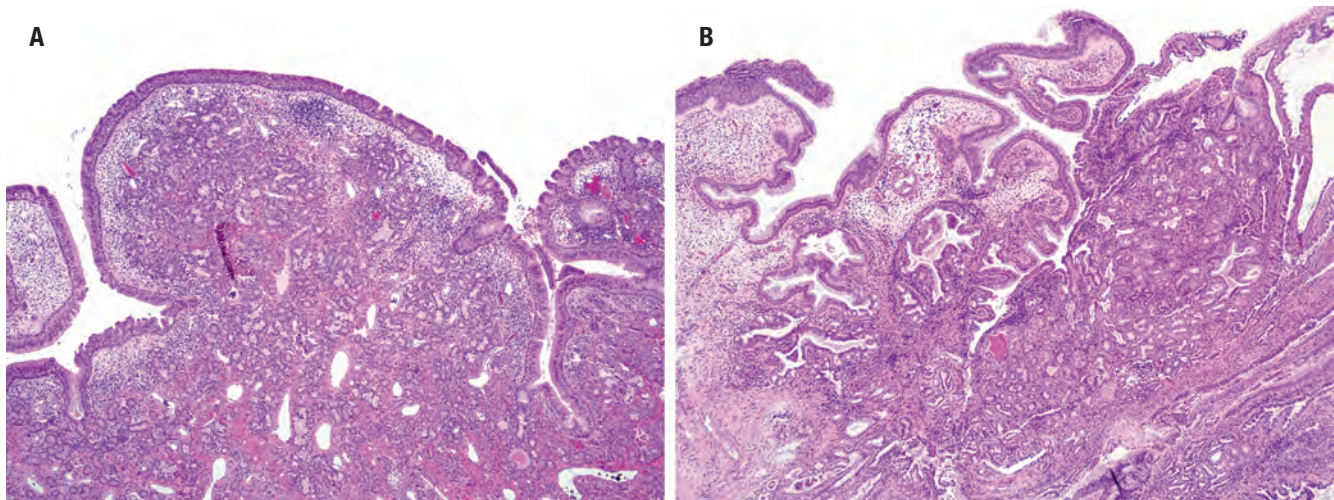
CMH, Chondromesenchymal hamartoma; REAH, respiratory epithelial adenomatoid hamartoma; SH, seromucinous hamartoma.



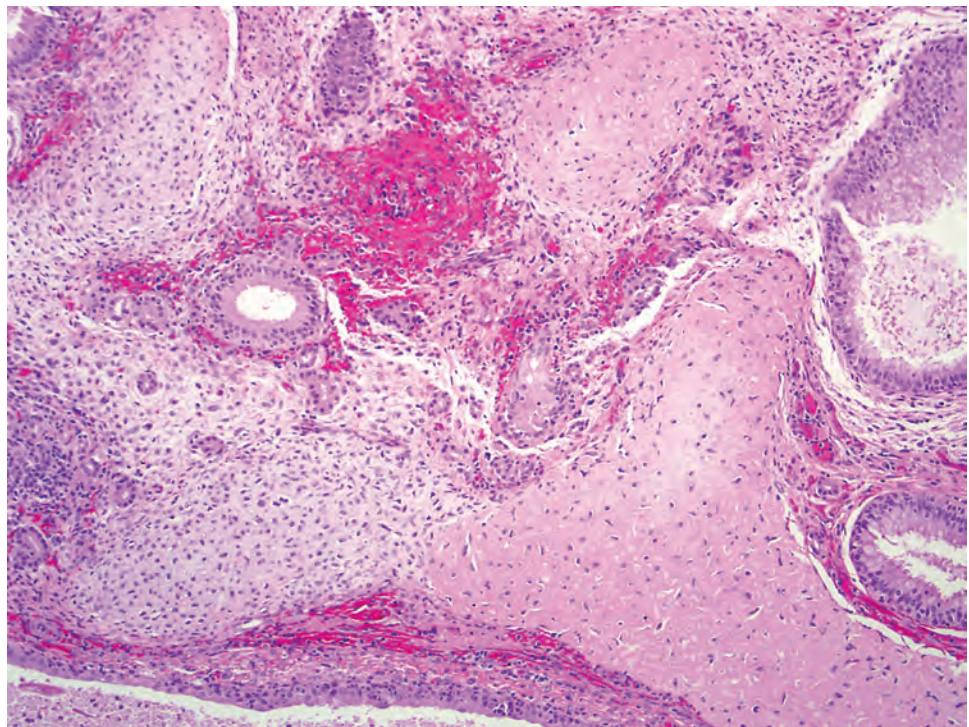
**FIGURE 1.21**

Respiratory epithelial adenomatoid hamartoma consists of a polypoid mass with a downward growth of surface epithelium (A). The glands are ciliated, pseudostratified, and often surrounded by a thick basement membrane (B).



**FIGURE 1.22**

Seromucinous hamartoma consists of an increased number of normal-appearing seromucinous glands in the submucosa (**A**). Some examples of seromucinous hamartoma have areas that closely resemble respiratory epithelial adenomatoid hamartoma (*left*), suggesting these lesions are closely related (**B**).

**FIGURE 1.23**

Chondromesenchymal hamartoma demonstrates scattered, ill-defined nodules of variably mature cartilage in the sinonasal submucosa.

glands can be dilated and lined by flattened, atrophic epithelium. REAH and SH are both frequently accompanied by chronic inflammation with edema and inflammatory polyps. It is not uncommon to see lesions with hybrid features of both REAH and SH, suggesting that the lesions exist at ends of a spectrum (see [Fig. 1.22B](#)).

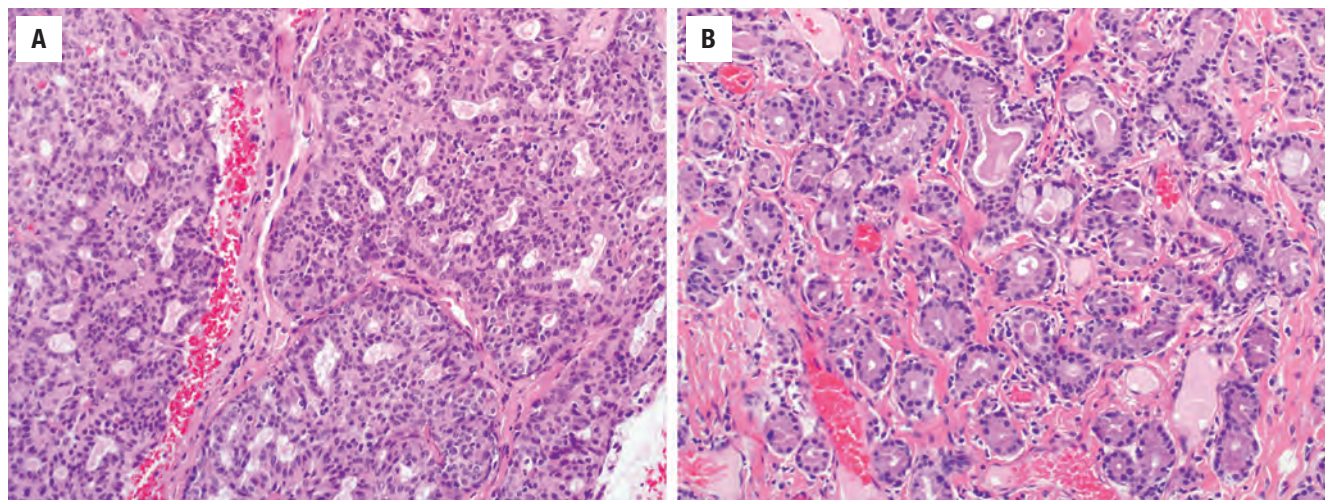
CMH consists of irregular nodules of cartilage or chondromyxoid stroma haphazardly arranged in the sinonasal submucosa ([Fig. 1.23](#)). The cartilage may be

mature or immature, and the islands are typically surrounded by a cellular fibrous stroma, often with atypical cells and even mitoses. Bony trabeculae, fat, or entrapped glands may also be seen.

#### ANCILLARY STUDIES

The role for immunohistochemistry in the diagnosis of sinonasal hamartomas is limited. The glands of REAH are



**FIGURE 1.24**

Low-grade nonintestinal sinonasal adenocarcinoma has fused, complex, back-to-back seromucinous glands without intervening stroma (**A**). In contrast, seromucinous hamartomas have stroma between the seromucinous glands (**B**).

usually surrounded by basal cells that are positive for p63, p40, and CK903, but SH typically lacks surrounding basal or myoepithelial cells. Patients with CMH usually harbor germline or somatic mutations of *DICER1* as part of the pleuropulmonary blastoma tumor predisposition disorder; CMH can be the presenting lesion of this syndrome.

### DIFFERENTIAL DIAGNOSIS

REAH may be confused with sinonasal inflammatory polyps, although glandular proliferation not commonly seen in polyps. Inverted sinonasal papilloma also exhibits downward growth of surface epithelium, but the epithelium of inverted sinonasal papilloma tends to be squamous or squamoid, thickened, and infiltrated by neutrophils with microabscesses. Biphenotypic sinonasal sarcoma shows invaginations of the surface epithelium reminiscent of REAH, but the cellular stromal spindle cell component and mixed neural and myogenic differentiation is unique. REAH and especially SH can be confused with a low-grade nonintestinal sinonasal adenocarcinoma. Although low-grade nonintestinal sinonasal adenocarcinoma is composed of similar-appearing small glands, it is architecturally more complex, with fused glands and papillary structures (Fig. 1.24A). Importantly, the glands of SH and REAH, while proliferative, are also surrounded by intervening stroma (see Fig. 1.24B). The absence of basal/myoepithelial cells is not useful in the diagnostic distinction.

CMH is more likely to be confused with a mesenchymal process such as chondromyxoid fibroma or chondroma. The young age of the patient and haphazard distribution of the cartilaginous nodules are more in keeping with CMH. Moreover, chondromyxoid fibroma typically lacks well-formed hyaline cartilage.

### SINONASAL HAMARTOMAS—PATHOLOGIC FEATURES

#### Gross Findings

- REAH and SH appear as an edematous nasal polyp
- CMH is a firm tan-white mass

#### Microscopic Findings

- REAH—downward proliferation of surface epithelial glands lined by pseudostratified ciliated epithelium
- SH—proliferation of small seromucinous submucosal glands lined by eosinophilic cuboidal epithelium
- CMH—irregular proliferation of variably mature cartilage nodules in the sinonasal submucosa with fibrotic stroma

#### Pathologic Differential Diagnosis

- REAH: sinonasal inflammatory polyp, inverted sinonasal papilloma, biphenotypic sinonasal sarcoma
- SH: low-grade nonintestinal sinonasal adenocarcinoma
- CMH: chondromyxoid fibroma, chondroma

CMH, Chondromesenchymal hamartoma; REAH, respiratory epithelial adenomatoid hamartoma; SH, seromucinous hamartoma.

### PROGNOSIS AND THERAPY

All sinonasal hamartomas are treated with surgical excision, and the prognosis for each is excellent with recurrences being uncommon.

### SUGGESTED READINGS

The complete Suggested Readings list is available online at [ExpertConsult.com](http://ExpertConsult.com).



**SUGGESTED READINGS****Rhinosinusitis**

1. Ahmad N. Allergic rhinitis and rhinosinusitis. *Otolaryngol Clin North Am.* 2008;41:267–281.
2. Ardehali MM, et al. The comparison of histopathological characteristics of polyps in asthmatic and nonasthmatic patients. *Otolaryngol Head Neck Surg.* 2009;140(5):748–751.
3. Brook I. Bacteriology of chronic sinusitis and acute exacerbation of chronic sinusitis. *Arch Otolaryngol Head Neck Surg.* 2006;132:1099–1101.
4. Ferguson BJ. Categorization of eosinophilic chronic rhinosinusitis. *Curr Opin Otolaryngol Head Neck Surg.* 2004;12:237–242.
5. Fokkens W, et al. EAACI position paper on rhinosinusitis and nasal polyps executive summary. *Allergy.* 2005;60:583–601.
6. Kennedy DW. Pathogenesis of chronic rhinosinusitis. *Ann Otol Rhinol Laryngol Suppl.* 2004;193:10–14.
7. Lee RU, et al. Aspirin-exacerbated respiratory disease: evaluation and management. *Allergy Asthma Immunol Res.* 2011;3(1):3–10.
8. Ly TH, et al. Diagnostic criteria for atrophic rhinosinusitis. *Am J Med.* 2009;122(8):747–753.
9. Mynatt RG, et al. Squamous metaplasia and chronic rhinosinusitis: a clinicopathological study. *Am J Rhinol.* 2008;22(6):602–605.
10. Naclerio RM, et al. Pathophysiology of nasal congestion. *Int J Gen Med.* 2010;3:47–57.
11. Seidman MD, et al. Guideline Otolaryngology Development Group. AAO-HNSF Clinical practice guideline: Allergic rhinitis. *Otolaryngol Head Neck Surg.* 2015;152(1Suppl):S1–S43.
12. Tammemagi CM, et al. Smoke as a potential cause of chronic rhinosinusitis. *Arch Otolaryngol Head Neck Surg.* 2010;136:327–334.

**Sinonasal Inflammatory Polyps**

1. Ardehali MM, et al. The comparison of histopathological characteristics of polyps in asthmatic and nonasthmatic patients. *Otolaryngol Head Neck Surg.* 2009;140(5):748–751.
2. Berkiten G, et al. Efficacy of systemic steroid treatment in sinonasal polyposis. *J Craniofac Surg.* 2013;24(3):e305–e308.
3. Compagno J, et al. Nasal polyposis with stromal atypia: review and follow-up of 14 cases. *Arch Pathol Lab Med.* 1976;100:224–226.
4. Gysin C, et al. Sinonasal disease in cystic fibrosis: clinical characteristics, diagnosis, and management. *Pediatr Pulmonol.* 2000;30:481–489.
5. Hellquist HB. Nasal polyps update. *Histopathology.* *Allergy Asthma Proc.* 1996;17:237–242.
6. Passali D, et al. Consensus conference on nasal polyposis. *Acta Otorhinolaryngol Ital.* 2004;24(2 suppl 77):3–61.
7. Saitoh T, et al. Role of interleukin-17A in the eosinophil accumulation and mucosal remodeling in chronic rhinosinusitis with nasal polyps associated with asthma. *Int Arch Allergy Immunol.* 2010;151(1):8–16.
8. Scadding GK. Comparison of medical and surgical treatment of nasal polyposis. *Curr Allergy Asthma Rep.* 2002;2:494–499.
9. Sheahan P, et al. Infarcted angiomatous nasal polyps. *Eur Arch Otorhinolaryngol.* 2005;262:225–230.
10. Yfantis HG, et al. Angiectatic nasal polyps that clinically simulate a malignant process: report of 2 cases and review of the literature. *Arch Pathol Lab Med.* 2000;124:406–410.
11. Zeifer B. Update on sinonasal imaging: anatomy and inflammatory disease. *Neuroimaging Clin N Am.* 1998;8:607–630.

**Paranasal Sinus Mucocoele**

1. Capra GG, et al. Paranasal sinus mucocoele. *Head Neck Pathol.* 2012;6(3):369–372.
2. Devars du Mayne M, et al. Sinus mucocoele: natural history and long-term recurrence rate. *Eur Ann Otorhinolaryngol Head Neck Dis.* 2012;129(3):125–130.
3. Kim YS, et al. Paranasal sinus mucocoeles with ophthalmologic manifestations: a 17-year review of 96 cases. *Am J Rhinol Allergy.* 2011;25(4):272–275.
4. Morita S, et al. Paranasal sinus mucocoeles with visual disturbance. *Auris Nasus Larynx.* 2010;37(6):708–712.

5. Socher JA, et al. Diagnosis and treatment of isolated sphenoid sinus disease: a review of 109 cases. *Acta Otolaryngol.* 2008;128(9):1004–1010.
6. Soon SR, et al. Sphenoid sinus mucocoele: 10 cases and literature review. *J Laryngol Otol.* 2010;124(1):44–47.

**Glial Heterotopia**

1. Capra GG, et al. Paranasal sinus mucocoele. *Head Neck Pathol.* 2012;6(3):369–372.
2. Kau T, et al. Transsphenoidal extension of heterotopic glioneuronal tissue: pathoanatomic considerations in symptomatic neonates. *Childs Nerv Syst.* 2011;27(5):771–778.
3. Meoded A, et al. Pre- and postnatal ultrasound and magnetic resonance imaging of intracranial extra-axial glioneuronal heterotopia. *Fetal Diagn Ther.* 2011;30(4):314–316.
4. Penner CR, et al. Nasal glial heterotopia: a clinicopathologic and immunophenotypic analysis of 10 cases with a review of the literature. *Ann Diagn Pathol.* 2003;7:354–359.
5. Penner CR, Thompson LD. Nasal glial heterotopia. *Ear Nose Throat J.* 2004;83(2):92–93.
6. Rahbar R, et al. Nasal glioma and encephalocele: diagnosis and management. *Laryngoscope.* 2003;113:2069–2077.
7. Theaker JM, et al. Heterotopic glial nodules: a light microscopic and immunohistochemical study. *Histopathology.* 1990;18:255–260.
8. Kardon DE. Nasal glial heterotopia. *Arch Pathol Lab Med.* 2000;124(12):1849.

**Infections**

1. Abdel Razek AA. Imaging of scleroma in the head and neck. *Br J Radiol.* 2012;85(1020):1551–1555.
2. Ahluwalia KB, et al. Rhinosporidiosis: a study that resolves etiologic controversies. *Am J Rhinol.* 1997;11:479–483.
3. Batsakis JG, et al. Rhinoscleroma and rhinosporidiosis. *Ann Otol Rhinol Laryngol.* 1992;101:879–882.
4. Chou TC, et al. Emperipolesis is not pathognomonic for Rosai-Dorfman disease: rhinoscleroma mimicking Rosai-Dorfman disease, a clinical series. *J Am Acad Dermatol.* 2013;69(6):1066–1067.
5. Cody DT 2nd, et al. Allergic fungal sinusitis: the Mayo Clinic experience. *Laryngoscope.* 1994;104:1074–1079.
6. Corey JP, et al. Allergic fungal sinusitis: allergic, infectious, or both? *Otolaryngol Head Neck Surg.* 1995;113:110–119.
7. Das S, et al. Nasal rhinosporidiosis in humans: new interpretations and a review of the literature of this enigmatic disease. *Med Mycol.* 2011;49(3):311–315.
8. Fawaz S, et al. Clinical, radiological and pathological study of 88 cases of typical and complicated scleroma. *Clin Respir J.* 2011;5(2):112–121.
9. Ferguson BJ. Eosinophilic mucin rhinosinusitis. *Laryngoscope.* 2000;110:799–813.
10. Ferreira JA, et al. Paranasal sinus fungus balls. *Head Neck.* 1997;19:481–486.
11. Gaafar HA, et al. Rhinoscleroma: an updated experience through the last 10 years. *Acta Otolaryngol.* 2011;131(4):440–446.
12. Heffner DK. Allergic fungal sinusitis is a histopathologic diagnosis; paranasal mucocoele is not. *Ann Diagn Pathol.* 2004;8:316–323.
13. Hutcheson PS, et al. Distinctions between allergic fungal rhinosinusitis and chronic rhinosinusitis. *Am J Rhinol Allergy.* 2010;24:405–408.
14. Kuhn FA, et al. Allergic fungal sinusitis: diagnosis and treatment. *Curr Opin Otolaryngol Head Neck Surg.* 2003;11:1–5.
15. Lara JF, et al. Allergic mucin with and without fungus. A comparative clinicopathologic analysis. *Arch Pathol Lab Med.* 2001;125:1442–1447.
16. Makannar JH, et al. Rhinosporidiosis: a clinicopathological study of 34 cases. *Indian J Pathol Microbiol.* 2001;44:17–21.
17. Montone KT. Pathology of fungal rhinosinusitis: a review. *Head Neck Pathol.* 2016;10(1):40–46.
18. Montone KT. The molecular genetics of inflammatory, autoimmune, and infectious diseases of the sinonasal tract: a review. *Arch Pathol Lab Med.* 2014;138(6):745–753.

19. N'gattia KV, et al. Retrospective study of the rhinoscleroma about 14 cases in ENT departments of university hospitals (Côte d'Ivoire). *Eur Ann Otorhinolaryngol Head Neck Dis.* 2011;128(1):7–10.
20. Sudarshan V, et al. Rhinosporidiosis in Raipur, Chhattisgarh: a report of 462 cases. *Indian J Pathol Microbiol.* 2007;50(4):718–721.
21. Sudasinghe T, et al. The regional sero-epidemiology of rhinosporidiosis in Sri Lankan humans and animals. *Acta Trop.* 2011;120(1–2):72–81.
22. Tan SL, et al. Rhinoscleroma: a case series. *Singapore Med J.* 2012;53(2):e24–e27.
23. Thompson LD. Rhinoscleroma. *Ear Nose Throat J.* 2002;81(8):506.
24. Zhong Q, et al. Rhinoscleroma: a retrospective study of pathologic and clinical features. *J Otolaryngol Head Neck Surg.* 2011;40(2):167–174.
16. Behery RE, et al. Translocation t(12;17)(q24.1;q21) as the sole anomaly in a nasal chondromesenchymal hamartoma arising in a patient with pleuropulmonary blastoma. *Pediatr Dev Pathol.* 2012;5(3):249–253.
17. Bullock MJ. Low-grade epithelial proliferations of the sinonasal tract. *Head Neck Pathol.* 2016;10(1):47–59.
18. Fleming KE, et al. Sinonasal seromucinous hamartoma: a review of the literature and a case report with focal myoepithelial cells. *Head Neck Pathol.* 2012;6(3):395–399.
19. Gauchotte G, et al. Respiratory epithelial adenomatoid hamartoma: a poorly recognized entity with mast cell recruitment and frequently associated with nasal polyposis. *Am J Surg Pathol.* 2013;37(11):1678–1685.
20. Jo VY, et al. Low-grade sinonasal adenocarcinomas: the association with and distinction from respiratory epithelial adenomatoid hamartomas and other glandular lesions. *Am J Surg Pathol.* 2009;33(3):401–408.
21. Mason KA, et al. Nasal Chondromesenchymal Hamartoma (NCMH): a systematic review of the literature with a new case report. *J Otolaryngol Head Neck Surg.* 2015;44:28.
22. Ozolek JA, et al. Basal/myoepithelial cells in chronic sinusitis, respiratory epithelial adenomatoid hamartoma, inverted papilloma, and intestinal-type and nonintestinal-type sinonasal adenocarcinoma: an immunohistochemical study. *Arch Pathol Lab Med.* 2007;131(4):530–537.
23. Ozolek JA, et al. Nasal chondromesenchymal hamartoma in older children and adults. Series and immunohistochemical analysis. *Arch Pathol Lab Med.* 2005;129:1444–1450.
24. Ozolek JA, Hunt JL. Tumor suppressor gene alterations in respiratory epithelial adenomatoid hamartoma (REAH). Comparison to sinonasal adenocarcinoma and inflamed sinus mucosa. *Am J Surg Pathol.* 2006;30:1576–1580.
25. Sangoi AR, et al. Respiratory epithelial adenomatoid hamartoma: diagnostic pitfalls with emphasis on differential diagnosis. *Adv Anat Pathol.* 2007;14(1):11–16.
26. Stewart DR, et al. Nasal chondromesenchymal hamartomas arise secondary to germline and somatic mutations of DICER1 in the pleuropulmonary blastoma tumor predisposition disorder. *Hum Genet.* 2014;133(11):1443–1450.
27. Toner M, et al. Chondromesenchymal hamartoma. In: El-Naggar AK, Chan JKC, Grandis JR, Takata T, Slootweg PJ, eds. *Pathology and Genetics of Head and Neck Tumours*. 4th ed. World Health Organization Classification of Tumours, Lyon, France: IARC Press; 2017:51–52. ISBN: 978-92-832-2438-9.
28. Weinreb I, et al. Seromucinous hamartomas: a clinicopathological study of a sinonasal glandular lesion lacking myoepithelial cells. *Histopathology.* 2009;54(2):205–213.
29. Weinreb I. Low grade glandular lesions of the sinonasal tract: a focused review. *Head Neck Pathol.* 2010;4(1):77–83.
30. Wenig BM, et al., eds. Respiratory epithelial lesions. In: El-Naggar AK, Chan JKC, et al. *Classification of Head and Neck Tumours*. 4th ed. World Health Organization Classification of Tumours, Lyon, France: IARC Press; 2017:31–32.
31. Wenig BM, et al. Respiratory epithelial adenomatous hamartomas of the sinonasal tract and nasopharynx: a clinicopathologic study of 31 cases. *Ann Otol Rhinol Laryngol.* 1995;104:639–645.

### Granulomatosis With Polyangiitis (Wegener Granulomatosis)

1. Chang SY, et al. IgG4-positive plasma cells in granulomatosis with polyangiitis (Wegener's): a clinicopathologic and immunohistochemical study on 43 granulomatosis with polyangiitis and 20 control cases. *Hum Pathol.* 2013;44(11):2432–2437.
2. Charles P, et al. French Vasculitis Study Group. Rituximab for induction and maintenance treatment of ANCA-associated vasculitides: a multicentre retrospective study on 80 patients. *Rheumatology (Oxford).* 2014;53(3):532–539.
3. Devaney KO, et al. Interpretation of head and neck biopsies in Wegener's granulomatosis. *Am J Surg Pathol.* 1990;14:555–564.
4. Falk RJ, et al. Granulomatosis with polyangiitis (Wegener's): an alternative name for Wegener's granulomatosis. *Ann Rheum Dis.* 2011;70:704.
5. Finkelman JD, et al. ANCA are detectable in nearly all patients with active severe Wegener's granulomatosis. *Am J Med.* 2007;120:643.e9–643.e14.
6. Heffner DK. Wegener's granulomatosis is not a granulomatous disease. *Ann Diagn Pathol.* 2002;6:329–333.
7. Jennette JC. Overview of the 2012 revised International Chapel Hill Consensus Conference nomenclature of vasculitides. *Clin Exp Nephrol.* 2013;17(5):603–606.
8. Litalo PM, et al. Diagnosis and classification of granulomatosis with polyangiitis (aka Wegener's granulomatosis). *J Autoimmun.* 2014;48–49:94–98. doi: 10.1016/j.jaut.2014.01.028.
9. Schönemarker U, et al. Treatment of ANCA-associated vasculitis. *Nat Rev Nephrol.* 2014;10(1):25–36.
10. Seo P, et al. The antineutrophil cytoplasmic antibody-associated vasculitides. *Am J Med.* 2004;117:39–50.
11. Seyer BA, et al. Aggressive destructive midfacial lesion from cocaine abuse. *Oral Surg Oral Med Oral Pathol Oral Radiol Endod.* 2002;94:465–470.
12. Takwoingi YM, et al. Wegener's granulomatosis: an analysis of 33 patients seen over a 10-year period. *Clin Otolaryngol.* 2003;28:187–194.
13. Trimarchi M, et al. Otorhinolaryngological manifestations in granulomatosis with polyangiitis (Wegener's). *Autoimmun Rev.* 2013;12(4):501–505.
14. Yi ES, et al. Wegener's granulomatosis. *Semin Diagn Pathol.* 2001;18:34–46.

### Sinonasal Hamartomas

15. Ambrosini-Spaltro A, et al. Nasal seromucinous hamartoma (microglandular adenosis of the nose): a morphological and molecular study of five cases. *Virchows Arch.* 2010;457(6):727–734.

# Benign Neoplasms of the Nasal Cavity, Paranasal Sinuses, and Nasopharynx

■ **Lester D.R. Thompson**

## ■ SINONASAL PAPILLOMAS

The mucosa of the nasal vestibule and the superior wall of the nasal cavity are lined by squamous and olfactory mucosa, respectively. The remaining nasal mucosa consists of ciliated columnar epithelium of ectodermal origin known as the schneiderian membrane. Three benign neoplastic papillomatous proliferations arise from the schneiderian membrane: inverted or endophytic papillomas (IP; most common), exophytic, fungiform, or everted papillomas (EPs; second most common), and columnar, cylindrical cell, or oncocyctic papillomas (OPs; rare). They are defined as a group of benign epithelial neoplasms arising from sinonasal (schneiderian) mucosa. Although these entities share a number of findings and are classified as “sinonasal papillomas” (SPs), there are sufficient clinical and microscopic differences to regard them as three distinctive clinicopathologic entities. The overall lack of mixed papillomas and their relation to human papillomavirus (HPV) are sufficiently different to lend further credence to this separation.

### CLINICAL FEATURES

SPs are a rare disease with an estimated annual incidence of ~2.3 cases per 100,000 population, representing < 5 % of all sinonasal tract tumors. Males are affected much more commonly than females (2 to 10:1), depending on subtype, with patients presenting over a wide age range (mean, 20 to 70 years), also type dependent. Children are rarely affected. Clinical symptoms are nonspecific and include unilateral nasal obstruction, followed by epistaxis, an asymptomatic mass, polyps, rhinorrhea, facial pressure, and headaches. Symptoms are often present for a long duration. Often, patients report previous intranasal surgery before a diagnosis of

SP is firmly established. Physical examination usually demonstrates a unilateral polypoid mass in the nasal cavity. There is well-documented evidence that exophytic papillomas have a strong HPV association (38 % to 65 %) and a weaker association with IPs but usually low-risk types 6 and 11, with only rare cases of types 16 and 57b. The association is not established for oncocyctic type. p16 at this time does not have the same surrogate expression as seen in oropharyngeal carcinoma.

SPs show a remarkable anatomic distribution according to histologic type: EPs arise almost exclusively on the nasal septum (lower anterior); IPs and OPs affect the lateral nasal wall, middle meatus, and the paranasal sinuses (maxillary, ethmoid, sphenoid, frontal sinuses). Rarely, exceptions are noted. Less than 3 % of cases are bilateral and usually reflect extension or secondary involvement of the disease from one side to the other. Rarely, cases are seen as primary lesions in nasopharyngeal, lacrimal sac, or middle ear mucosa.

### RADIOGRAPHIC FEATURES

Plain x-rays, computed tomography (CT), and magnetic resonance imaging (MRI) routinely show a unilateral polypoid mass filling the nasal cavity, although variable based on the extent of disease ([Fig. 2.1](#)). Displacement of the nasal septum and opacification of sinuses are also frequently seen. Pressure erosion of the bone is present in ~45 % of cases.

### PATHOLOGIC FEATURES

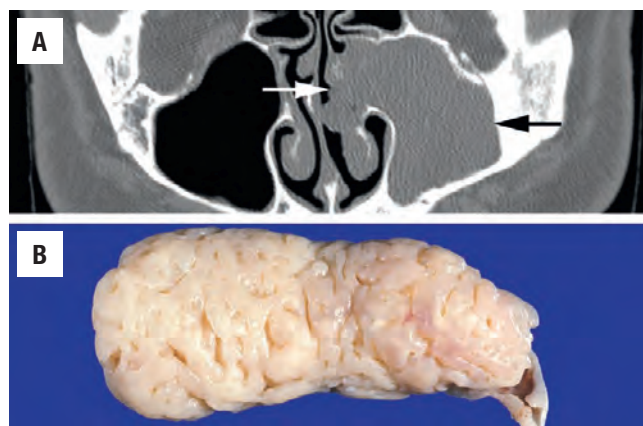
#### GROSS FINDINGS

EPs have been described as gray-tan cauliflower-like, papillary, warty, or mulberry-like verrucous papillary



**Sinonasal papilloma—disease fact sheet**

|                          | <b>Exophytic Type</b>   | <b>Inverted Type</b>   | <b>Oncocytic Type</b>  |
|--------------------------|---|--|--|
| Definition               | A papilloma derived from the schneiderian membrane composed of exophytic, papillary fronds with fibrovascular cores lined by multiple layers of well-differentiated stratified epithelial cells | A papilloma derived from the schneiderian membrane with proliferation and invagination into the underlying stroma  | A papilloma derived from the schneiderian membrane displaying exophytic fronds and endophytic invaginations lined by multilayered columnar oncocytic cells |
| Incidence and Location   | Uncommon (0.6/100,000 population)<br>Nasal septum   | Uncommon (~2.3/100,000 population)<br>Lateral nasal wall, middle meatus, paranasal sinuses<br>Rarely nasopharynx and middle ear  | Rare<br>Lateral wall of nasal cavity, paranasal sinuses  |
| Morbidity and Mortality  | Morbidity associated with nasal obstruction and epistaxis<br>No mortality   | Intracranial invasion<br>Carcinoma in 2% of cases  | Nasal obstruction, bleeding<br>Rare cases of carcinoma   |
| Sex and Age Distribution | Males > females (10:1)<br>Adults (mean, 20-50 years)  | Males > females (3:1)<br>Adults (mean, 5th-6th decade), uncommon in children   | Equal sex distribution<br>6th decade   |
| Clinical Features        | Unilateral nasal obstruction<br>Epistaxis<br>Rhinorrhea<br>Headaches  | Nasal obstruction<br>Epistaxis<br>Rhinorrhea<br>Facial pressure<br>Headaches   | Nasal obstruction<br>Epistaxis   |
| Prognosis and Treatment  | Excellent long-term prognosis, although recurrences develop (up to 50%)<br>Meticulous and complete surgical resection   | Excellent long-term prognosis (excluding cases with malignant transformation)<br>Recurrences up to 60%, depending on type of surgery<br>Carcinoma in ~2% of cases<br>Meticulous, complete surgical resection | Excellent prognosis<br>Very rare examples of carcinoma<br>Meticulous and complete surgical resection   |

**FIGURE 2.1**

(A) A computed tomography scan showing opacification and expansion of the left maxillary sinus and lateral nasal wall (arrows). (B) Surgical specimen of an inverted sinonasal papilloma with a polypoid appearance. The cerebriform surface shows numerous clefts due to exuberant endophytic epithelial proliferation.

proliferations attached to underlying mucosa by a narrow stalk, up to ~2 cm. IPs usually are large, multinodular, firm, bulky, polypoid lesions with deep clefts and intact mucosa (Fig. 2.1), creating a cerebriform appearance. Often, resections for IP include fragments of bone. Grossly,

OPs are usually small and fragmented and consist of soft pink, tan to brown papillary fragments of tissue. All of them are nontranslucent.

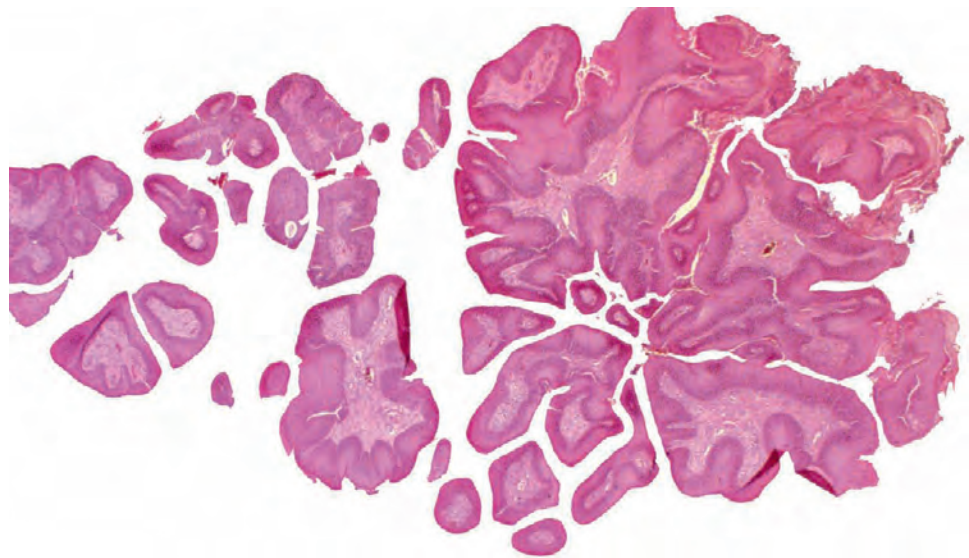
**MICROSCOPIC FINDINGS****Exophytic Papilloma**

EPs consist of branching, exophytic proliferations composed of fibrovascular cores lined by well-differentiated multilayered (up to 20 cells thick) squamous epithelium (Fig. 2.2). The epithelium ranges from basal and parabasal cells (Fig. 2.3) to well-differentiated keratinized cells with a granular cell layer and surface keratin with hyperkeratosis (Figs. 2.4 and 2.5). Koilocytic atypia may be seen. Surface keratinization is uncommon. There may be intraepithelial or luminal ciliated or goblet cells. The stroma usually contains variable numbers of seromucous glands. Mitotic figures and atypical mitoses are uncommon. Malignant change is exceptional.

**Inverted Papilloma**

IP consists of a markedly thick, inverted, or endophytic growth of multiple layers (up to 30 cells thick) of nonkeratinizing transitional cells (Fig. 2.6) associated with trans-migrating neutrophils. The inverted areas are surrounded

| Sinonasal papilloma—pathologic features |  |  |  |
|---|--|--|--|
|   | Exophytic Type   | Inverted Type  | Oncocytic Type   |
| Gross Findings                          | Gray-tan, cauliflower-like or verrucous papillary proliferation attached to mucosa by narrow stalk   | Large, multinodular, firm polypoid lesions<br>Deep clefts of inverted but intact mucosa<br>Fragments of bone in surgical specimen  | Small fragments of soft, fleshy, pink, tan, papillary tissue   |
| Microscopic Findings                    | Branching, exophytic proliferations with fibrovascular cores lined by well-differentiated stratified squamous epithelium<br>Basal and parabasal cells, well-differentiated keratinized cells, granular cell layer, surface keratin<br>Intraepithelial or luminal ciliated or goblet cells<br>Stroma with seromucous glands | Markedly thick, inverted neoplastic proliferation Transitional/squamoid epithelium<br>Transepithelial neutrophils with numerous intraepithelial microcysts containing neutrophils, mucin, and cellular debris<br>Distinct cell borders with glycogenation<br>May have ciliated columnar cells or surface keratinization<br>Foci of cytologic atypia<br>Stroma ranging from edematous, myxomatous, to fibrous<br>No seromucous glands in stroma | Both exophytic and endophytic patterns<br>Multiple layers of columnar oncocytic epithelium<br>Tumor cells have well-defined borders with eosinophilic or granular oncocytic cytoplasm<br>Round nuclei with small nucleoli<br>Cilia may be present focally on the surface<br>Intraepithelial cysts<br>Rare malignant transformation |
| Immunohistochemical Findings            |  | Coexpression of columnar and squamous epithelial keratins by the same cells  | Mitochondrial histochemical stains (phosphotungstic acid haematoxylin, PTAH)—positive<br>Cytochrome c oxidase positive   |
| Pathologic Differential Diagnosis       | Cutaneous squamous papilloma, inflammatory nasal polyp, papillary squamous cell carcinoma  | Sinonasal polyp, REAH, carcinoma   | Rhinosporeidiosis and low-grade papillary sinonasal adenocarcinoma   |

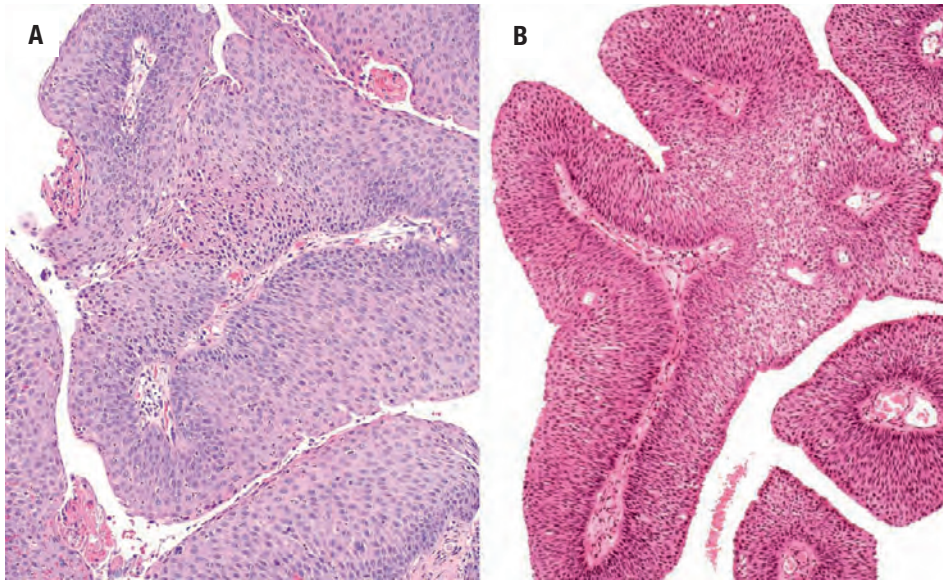


**FIGURE 2.2**  
Multiple, complex papillary projections in an exophytic sinonasal papilloma.

by a well-formed basement membrane and do not show irregular, “invasive” growth (Fig. 2.7). The epithelium in IP undergoes squamous maturation with superficial cells adopting a flattened orientation, but ciliated columnar epithelium is usually seen, whereas surface keratinization and a granular cell layer are uncommon (< 10 %). Distinct cell borders and cleared cytoplasm (due to glycogen) are frequent findings. Cellular pleomorphism may be present but is focal and not associated with dyskeratosis or increased mitotic activity. A characteristic feature is the

presence of numerous intraepithelial microcysts containing macrophages, neutrophils, mucin, and cellular debris (Fig. 2.8). These microcysts are more numerous close to the luminal surface. Mucous cells may be interspersed. Mitotic activity is variable but usually limited to basal and parabasal cells. The stroma ranges from edematous, myxomatous, to fibrous, usually showing a conspicuous absence of seromucous glands. An inflammatory infiltrate is composed of a variable mixture of neutrophils, eosinophils, and small lymphocytes (Fig. 2.8). Concurrent

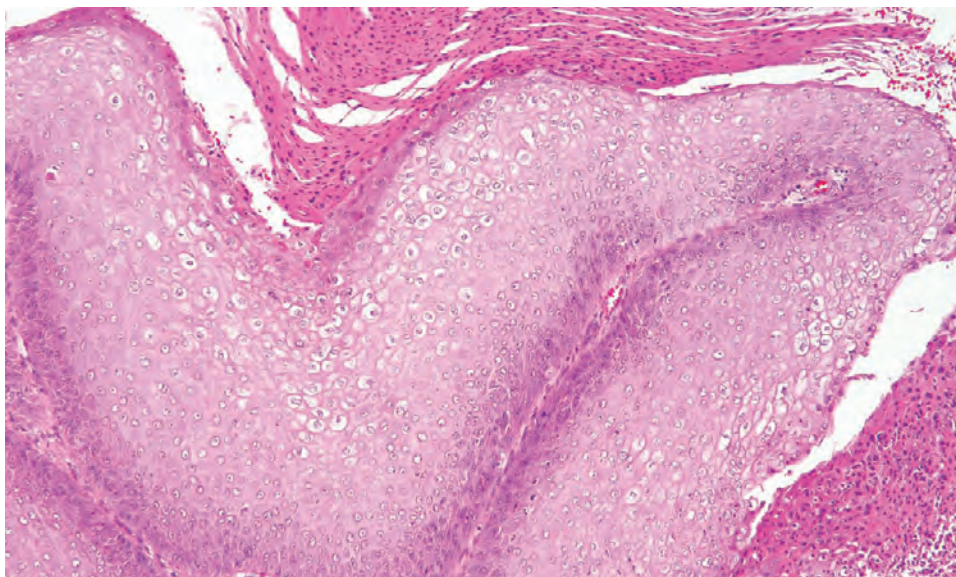


**FIGURE 2.3**

(A and B) Exophytic sinonasal papilloma lined by markedly thickened well-differentiated squamous epithelium. There are isolated inflammatory cells.

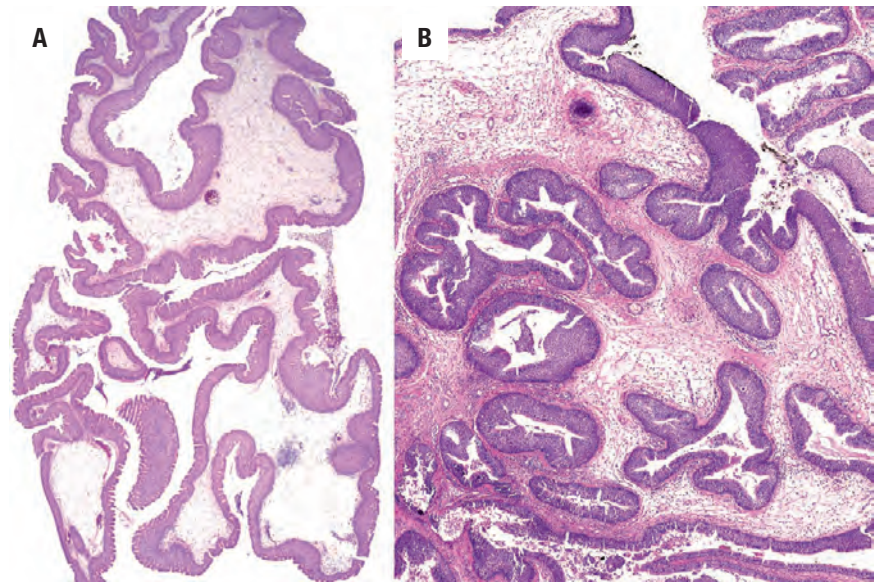
**FIGURE 2.4**

Exophytic sinonasal papilloma with papillary "finger-like" projections with a fibrovascular core lined by squamous cells.

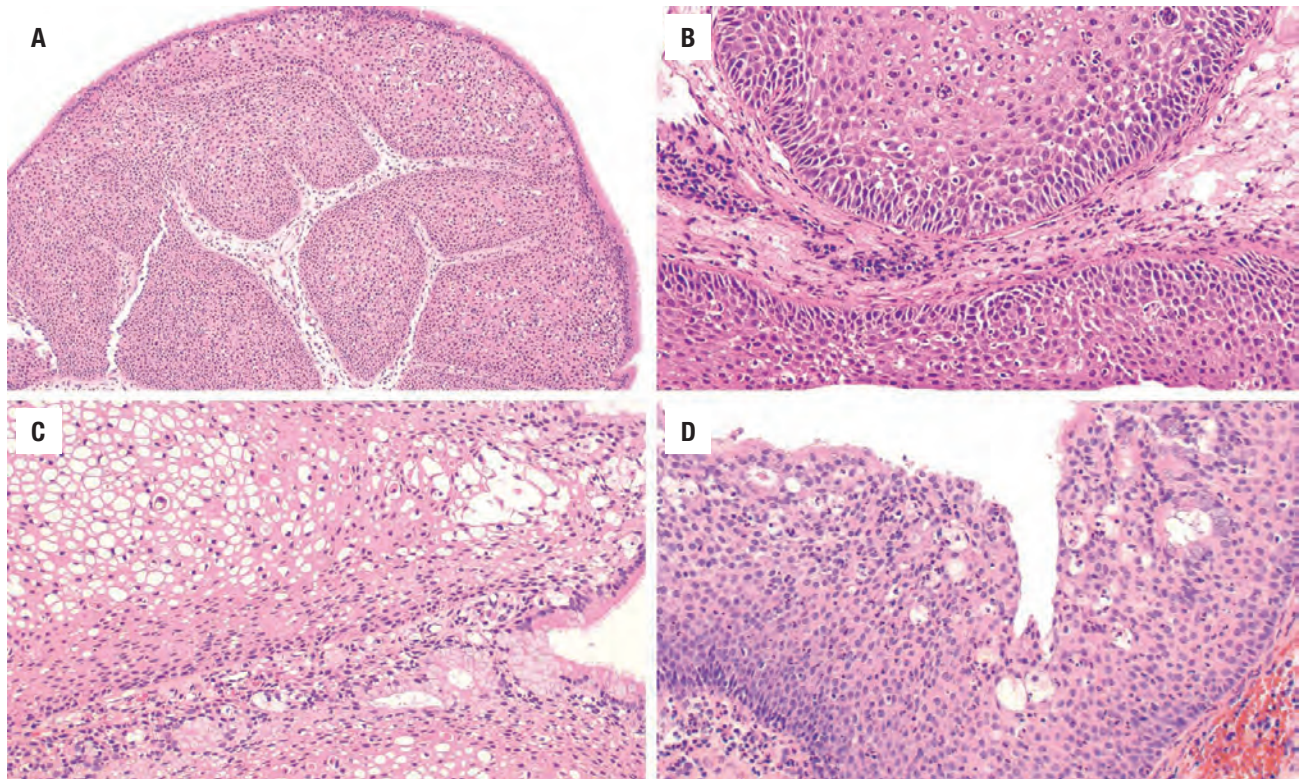
**FIGURE 2.5**

An exophytic sinonasal papilloma with koilocytic atypia, hyperkeratosis, and parakeratosis.



**FIGURE 2.6**

(**A** and **B**) Inverted sinonasal papillomas with nests of cells pushing deeply into the stroma. Note the well-developed basement membrane.

**FIGURE 2.7**

Inverted sinonasal papilloma. (**A**) An overall polypoid projection but with inverted growth. (**B**) Transitional epithelium with intraepithelial cysts with occasional macrophages. (**C**) Koilocytic atypia with areas of mucinous differentiation (*lower field*). (**D**) Small abscesses and mucinous cells.

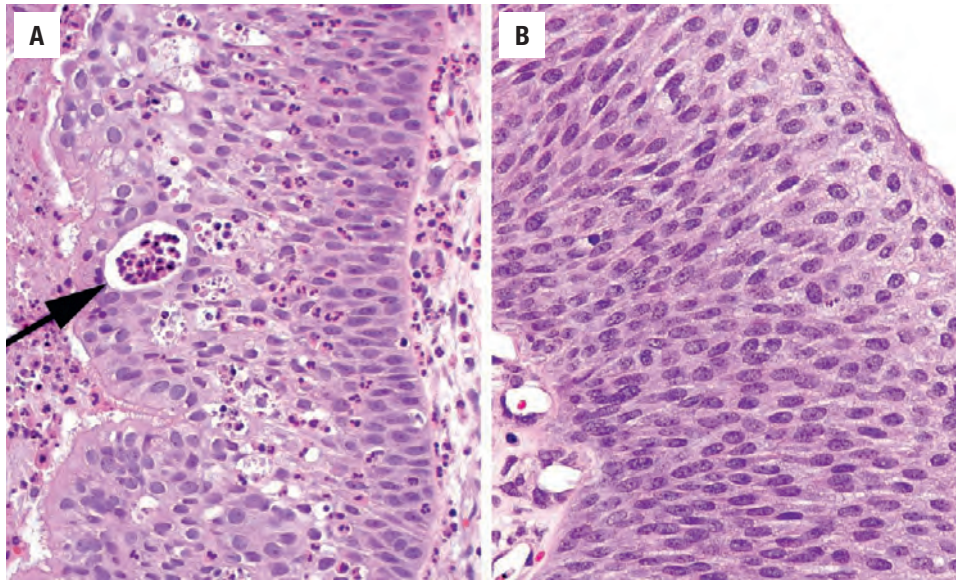
nasal inflammatory polyps may be present. Malignant transformation may be seen, identified as conventional in situ and invasive carcinomas (Fig. 2.9), developing in ~2% of patients. When carcinoma is present, it is synchronous in the majority of cases, with squamous cell carcinoma the most common tumor type, although

mucoepidermoid carcinoma, sinonasal undifferentiated carcinoma, and verrucous carcinoma may be seen.

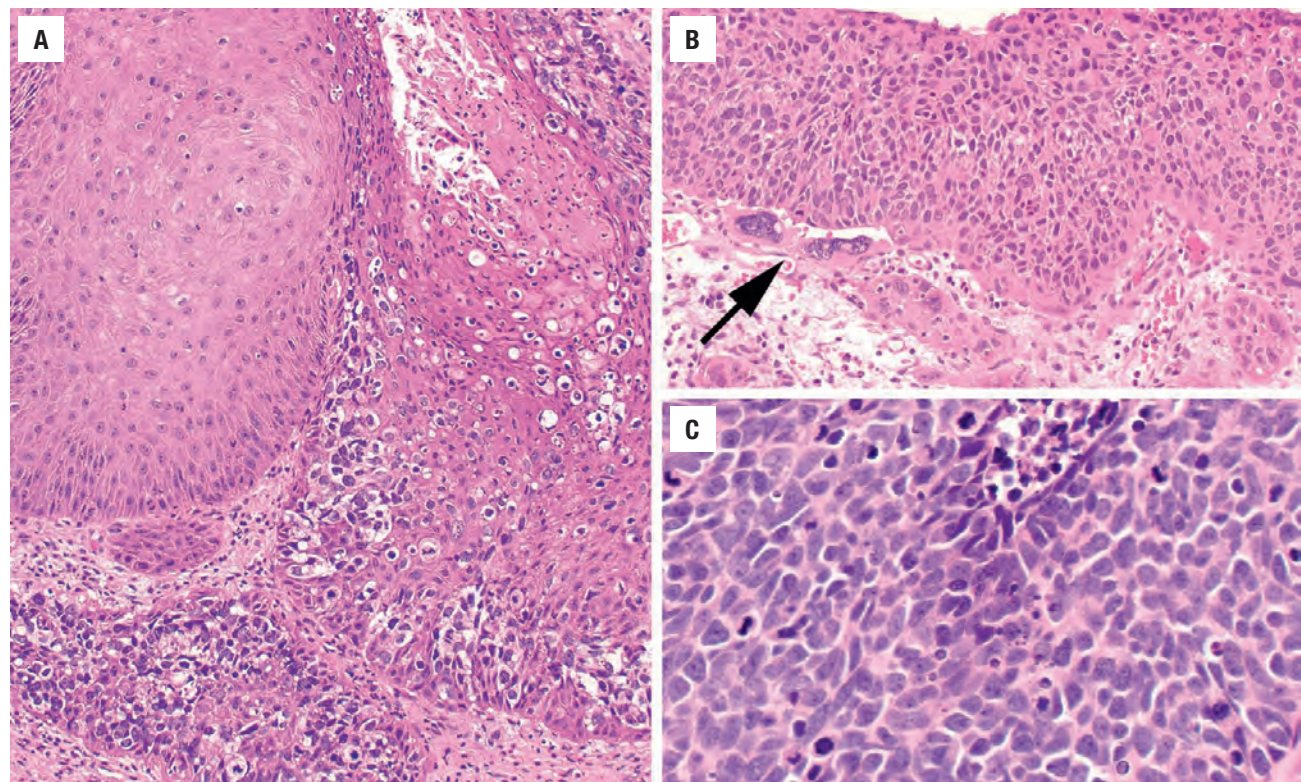
#### Oncocytic Cell Papilloma

OPs are characterized by a proliferating multilayered (two to eight cells thick) columnar or oncocytic epithelium



**FIGURE 2.8**

(A) A large number of inflammatory cells and small microabscesses (*arrow*) are noted in this inverted sinonasal papilloma. (B) There is a lack of inflammatory elements within this area of sinonasal papillomas. However, the transitional-type epithelium is easily identified.

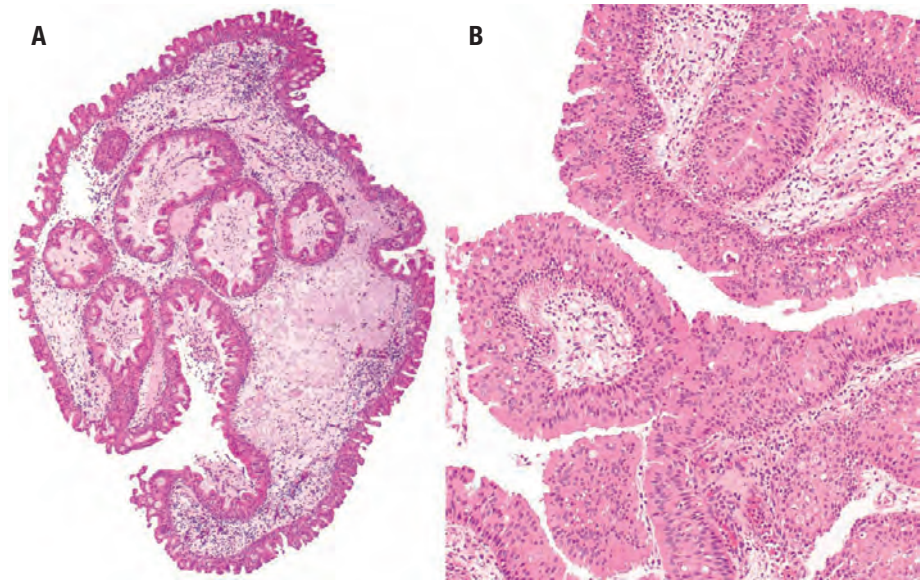
**FIGURE 2.9**

Malignant transformation of an inverted sinonasal papilloma demonstrates Pagetoid spread of neoplastic cells (A). There is profound pleomorphism with invasion into the stroma (*arrow*) (B). There is no maturation, markedly increased cellularity, and innumerable mitoses in this area of carcinoma (C).

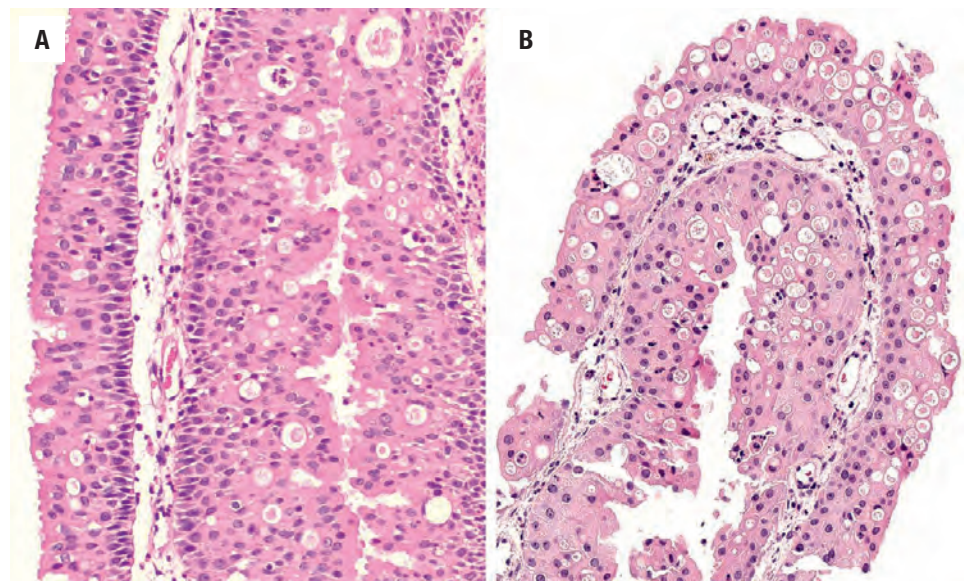
(Fig. 2.10) arranged in both exophytic and endophytic patterns, associated with intraepithelial microcysts. Most OPs have an exophytic branching papillary appearance with long delicate fibrous cores. The individual tumor cells show well-defined cell borders with eosinophilic or granular oncocytic cytoplasm. The nuclei are round,

centrally located, and uniform. Small to medium nucleoli are readily seen. The surface cells frequently show cilia (Fig. 2.11), although often with regression. Numerous small *intraepithelial* microabscesses are seen, filled with mucin and/or neutrophils. Mitotic figures are uncommon in OP. Unlike IP, seromucous glands may be seen in the



**FIGURE 2.10**

Oncocytic sinonasal papilloma. (**A** and **B**) Multilayered oncocytic epithelium arranged in a focal "tram-track" architecture. Cilia are abundant at the surface of this complex papillary growth.

**FIGURE 2.11**

(**A** and **B**) Oncocytic sinonasal papilloma with stratified columnar respiratory epithelium with oncocytic cells and small neutrophilic abscesses. These structures are present **within** the epithelium rather than in the stroma.

submucosa. Malignant transformation of OP is uncommon but may develop.

are immunoreactive with cytochrome c oxidase, as would be expected in an oncocytic cell.

## ANCILLARY STUDIES

### IMMUNOHISTOCHEMICAL FINDINGS

Immunohistochemical studies are not necessary for the diagnosis or classification of SP. Interestingly, the coexpression of keratins typical of columnar and squamous differentiation by the same cells (CK10, CK13, CK1, CK2) appears to be characteristic of sinonasal papillomas and is not seen in non-neoplastic mucosa. The cells of OP

### MOLECULAR FINDINGS

In situ hybridization and polymerase chain reaction have convincingly demonstrated an etiologic role for HPV in SP, although variation in technique and serotypes of HPV sought yield variable results. The low-risk HPV types 6 and 11 are by far the most commonly identified, but higher rates of detection in dysplastic or malignant lesions may be related to HPV integration. Although the published data are conflicting and confusing, the presence of HPV does not seem to consistently increase the risk of malignant transformation. However, activating *KRAS*

mutations are characteristically seen in oncocytic type sinonasal papilloma, as well as their associated carcinomas.

### DIFFERENTIAL DIAGNOSIS

The differential diagnosis depends on the histologic type of papilloma and includes sinonasal polyps, cutaneous squamous papilloma, verruca vulgaris, papillary squamous cell carcinoma, respiratory epithelial adenomatoid hamartoma (REAH), low-grade papillary adenocarcinoma, and rhinosporidiosis. *Sinonasal polyps* have marked stromal edema and inflammation with a nonproliferative epithelium, lacking intraepithelial microcysts, and usually show minor mucoserous glands in the subepithelial stroma. *Verruca vulgaris* has prominent keratinization with verrucoid or papillomatous growth, keratohyaline granules, and koilocytes, while lacking intraepithelial mucocytes and transepithelial neutrophils. Origin from skin rather than mucosa is also a helpful finding. *Papillary squamous cell carcinomas* are characterized by papillae with fibrovascular cores lined by clearly malignant squamous epithelium. It is important to bear in mind the possibility of a carcinoma arising in a sinonasal papilloma. *REAH* is a rare hamartoma with epithelium arranged in a glandular distribution, usually with a well-developed basement membrane. *Low-grade papillary sinonasal adenocarcinoma* has an infiltrative growth, with acinar, cystic, or trabecular growth. *Rhinosporidiosis* has characteristic sporangia and endospores within the stroma, below the epithelium rather than the microcysts within the epithelium of IPs and OPs.

### PROGNOSIS AND THERAPY

The long-term prognosis of SPs without in situ or invasive carcinoma is excellent. However, there is a considerable recurrence rate, often dependent on the extent of the tumor and initial surgical approach used. If inadequately removed, recurrences or persistence develop in up to 50 % (more common for inverted than the other types), usually developing within 5 years of initial presentation. Multiple recurrences are not uncommon. Given the anatomic confines, if neglected, significant morbidity may be experienced. There is no correlation between the number of recurrences and the development of carcinoma, if it occurs. Carcinoma is seen in ~ 2 % of cases, although exceptional in the exophytic type, and seems to be synchronous or de novo, rather than developing after many recurrences. Prognosis for carcinoma is similar to primary squamous cell carcinoma.

The treatment of choice is surgery, whether endoscopic, snare avulsion, or by a more radical excision (lateral rhinotomy and medial maxillectomy, Caldwell-Luc

procedure, craniofacial resection or midfacial degloving). Meticulous removal is imperative if recurrences are to be averted. Chemotherapy and radiation therapy are not of benefit, although radiation may be used in rare cases to treat unresectable cases.

### LOBULAR CAPILLARY HEMANGIOMA

Lobular capillary hemangiomas (LCHs) are a relatively common benign vascular neoplasm of capillary loops, representing ~ 25 % of all nonepithelial sinonasal tract neoplasms and ~ 10 % of all head and neck hemangiomas. Although the term “pyogenic granuloma” preceded “lobular capillary hemangioma,” it is a misnomer. LCHs are not “purulent,” “infectious,” or “granulomatous.” Although the pathogenesis is unknown, local trauma, hormonal factors (pregnancy or oral contraceptive use), and drugs (vemurafenib [Zelboraf]) are suggested etiologic agents (hence *epulis gravidarum* as another name). Nose picking/manipulation, nasal packing, cauterization, shaving/hair removal, and nonspecific microtrauma are all associated etiologic findings. There are isolated cases which are part of Sturge-Weber or von Hippel-Lindau syndrome.

### CLINICAL FEATURES

Approximately one-third of mucosal LCH arise in the nasal cavity (~ 60 % present in the oral cavity). When

#### LOBULAR CAPILLARY HEMANGIOMA—DISEASE FACT SHEET

##### Definition

- Benign vascular tumor with lobular architecture composed of variable size vessels with proliferating endothelial cells

##### Incidence and Location

- Common
- Anterior nasal septum (60%), nasal vestibule (20%), turbinates, and/or paranasal sinuses (20%)

##### Sex and Age Distribution

- Females in reproductive years, especially during pregnancy
- Older adults no sex differences
- Boys < 15 years

##### Clinical Features

- Intermittent, painless epistaxis
- Nasal obstruction

##### Prognosis and Treatment

- Excellent prognosis with recurrences if incompletely excised and in older patients
- Complete endoscopic resection with bleeding control



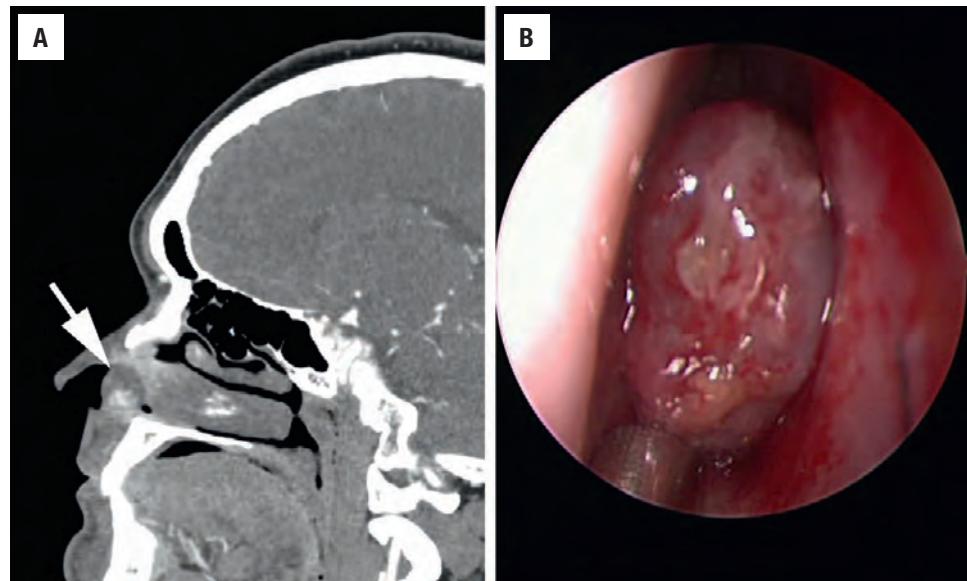


**FIGURE 2.12**

(A) A small vascular mass is noted in the anterior nasal cavity (*arrow*) on computed tomography. (B) This endoscopic view of an ulcerated polypoid mass represents a lobular capillary hemangioma.

in the oral cavity, the gingiva is most frequently affected, whereas in the nasal cavity, the anterior inferior nasal septum (Little area) accounts for ~60 % of cases (Fig. 2.12); 20 % involve the nasal vestibule and 20 % affect the turbinates and/or sinuses. These lesions usually affect boys younger than 15 years, females in their reproductive years and especially during pregnancy, and, less commonly, older adults of either sex. Patients with an inherited syndrome tend to be younger at initial presentation. Overall, females are affected more frequently than males (2:1), but in the pediatric group (up to 18 years), males are much more frequently affected than females.

Patients typically present with intermittent, painless episodes of unilateral epistaxis (in ~95 % of cases). The lesions tend to bleed easily, often with only slight trauma. Large lesions may cause nasal obstruction (in up to 35 % of cases). Tumors may present as a rapidly growing, painless, hemorrhagic mass, with patients experiencing symptoms for a relatively short duration. Rhinoscopy generally shows a well-defined, sessile or polypoid, red to purplish mass. Often, there is mucosal ulceration with a fibrinous exudate. Patients who develop tumors during pregnancy may show spontaneous involution postpartum, as hormone levels return to normal.

Radiographic studies show the anatomic site, extent, and vascular nature of the lesion (intensely enhancing) and identify feeder vessels and allow for presurgical embolization.

## **PATHOLOGIC FEATURES**

### **GROSS FINDINGS**

LCHs are polypoid (Figs. 2.12 and 2.13), nodular, or sessile masses with pink or gray-tan color. They are often

## **LOBULAR CAPILLARY HEMANGIOMA (PYOGENIC GRANULOMA)—PATHOLOGIC FEATURES**

### **Gross Findings**

- Sessile, polypoid, or nodular red to purplish mass
- Ulceration is common, with fibrinous exudate

### **Microscopic Findings**

- Lobular architecture with mixture of thin and thick blood vessels
- Central vessel surrounded by cellular lobule of closely packed capillaries
- Plump endothelial cells with bland nuclear findings and scanty to moderate eosinophilic cytoplasm
- Frequent mitotic figures
- Edematous to fibrotic stroma with mixed inflammatory infiltrate
- Ulcerated surface with fibrinous exudate simulating granulation tissue

### **Immunohistochemical Findings**

- Endothelial cells positive for CD31, CD34, FLI1, FVIIIIRAg
- Actins positive in pericytes and smooth muscle cells

### **Pathologic Differential Diagnosis**

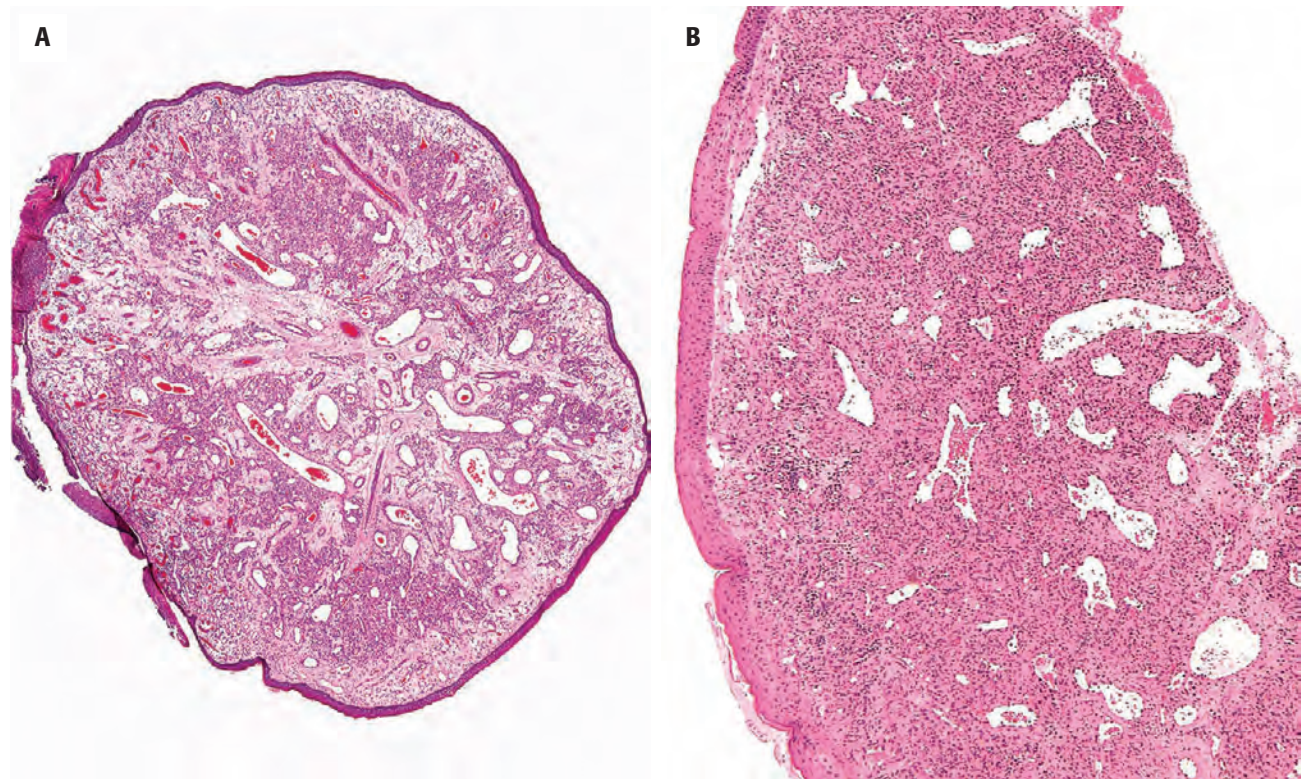
- Nasopharyngeal angiofibroma, glomangiopericytoma, angiosarcoma

soft and compressible submucosal masses. Frequently, the surgical specimen is ulcerated (~40 % of cases) and partially covered with a yellow to white fibrinous exudate. There is a wide range in size (1 to 8 cm), with a mean of ~1.5 cm.

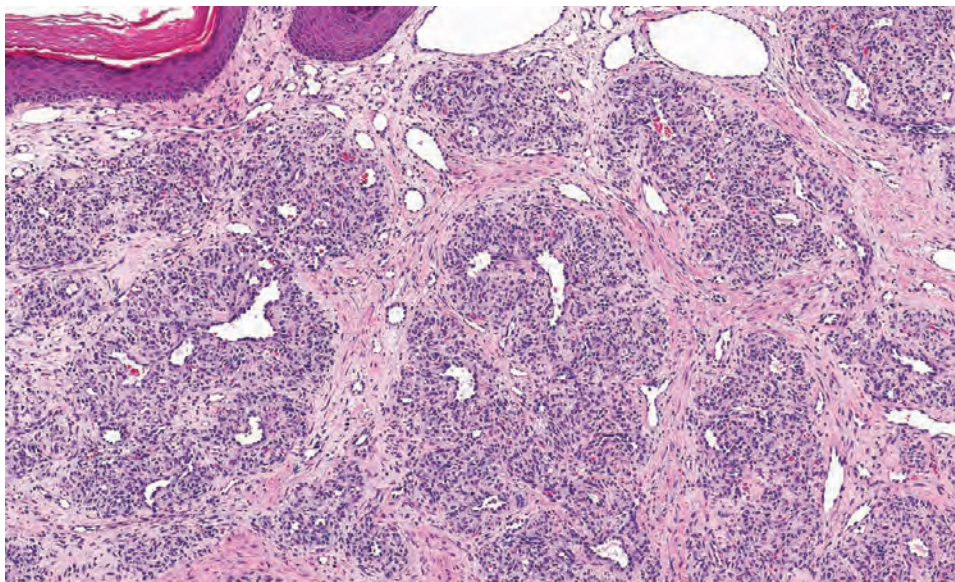
### **MICROSCOPIC FINDINGS**

The term “lobular capillary hemangioma” properly describes the microscopic appearance of this benign vascular tumor. At low power the polypoid LCH exhibits



**FIGURE 2.13**

(A) A lobular arrangement around large patulous vessels is seen in this lobular capillary hemangioma (LCH) at low power. (B) LCH with lobular architecture demonstrating cellular lobules interspersed with larger dilated blood vessels.

**FIGURE 2.14**

Lobular capillary hemangioma. The surface keratinized squamous epithelium (*upper left*) is overlying a well-developed lobular pattern of proliferating vessels. There is a "tight" architecture, with a central patulous vessel surrounded by slit-like vascular channels.

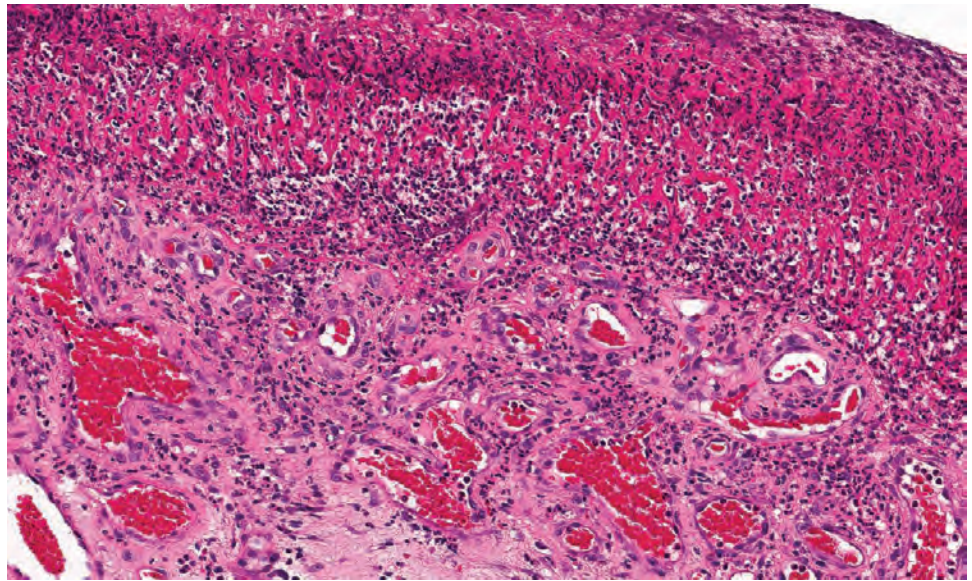
a distinct lobular architecture with a mixture of thin and thick blood vessels comprising the center of the lesion (Fig. 2.14). Surface ulceration with fibrinoid material can be seen (Fig. 2.15), sometimes with a collarette of epithelium on either side of the ulcerated area. The lobules are quite cellular and composed of small, closely packed capillaries with slit-like or indistinct lumina (Fig. 2.16). The endothelial cells are plump with bland nuclear

findings and scant to moderate eosinophilic cytoplasm (Fig. 2.17). Mitotic activity within the lobules is readily identified. The center and superficial portions of LCH show well-formed capillaries or large angulated vessels with branching lumina. These vessels may have thick walls resembling small arteries or venules. There is usually an intimate association of spindled pericytes within the perivascular spaces. The stroma ranges from edematous

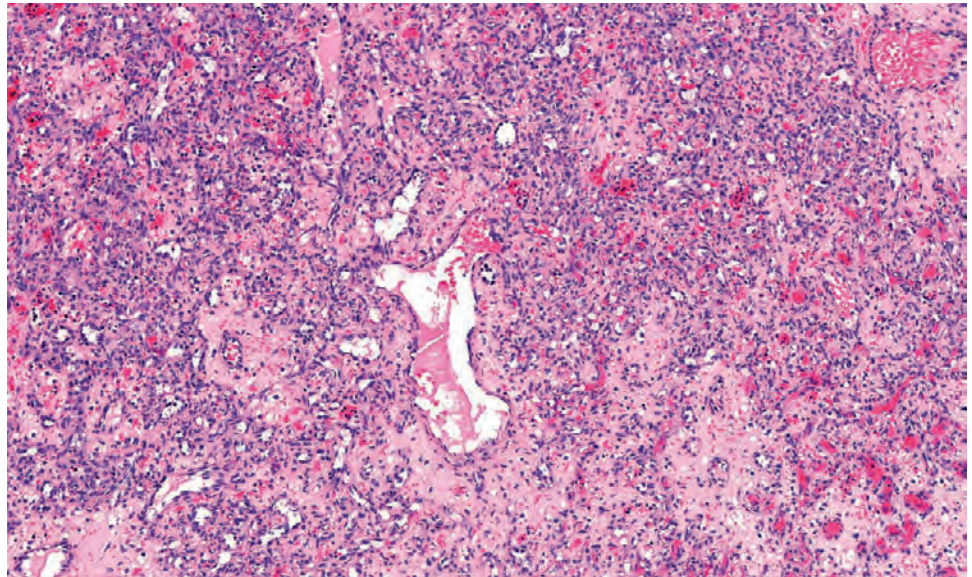


**FIGURE 2.15**

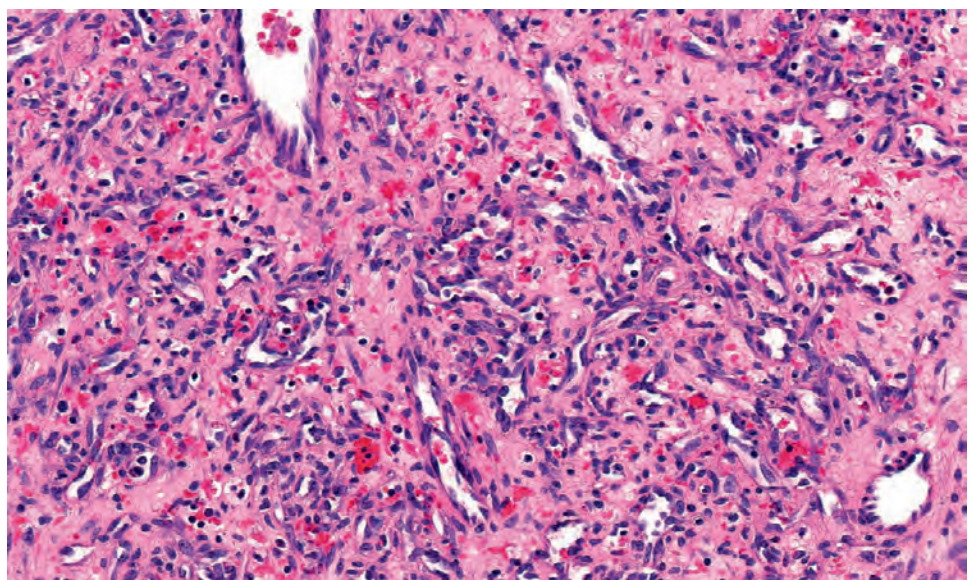
This lobular capillary hemangioma shows surface ulceration and a "granulation tissue"-like reaction. The characteristic lobular pattern was noted more deeply in this tumor.

**FIGURE 2.16**

Lobular capillary hemangioma. A patulous central vessel surrounded by lobules of endothelial-lined capillaries. Note the absence of pleomorphism and inflammatory infiltrate.

**FIGURE 2.17**

Lobular capillary hemangioma. The lobule is quite cellular and is composed of prominent endothelial cells admixed with inconspicuous pericytes. The lobule contains and is surrounded by variably sized blood vessels.





to fibrotic, the latter well-developed in older lesions. The inflammatory infiltrate is usually limited, much more prominent at the surface ulceration, where a fibrinous exudate and areas indistinguishable from conventional granulation tissue may be seen (Fig. 2.15).

### ANCILLARY STUDIES

Although unnecessary in the vast majority of cases, the endothelial cells are positive for vascular markers such as CD31, CD34, FLI1, and FVIIIIRAg, as well as variable staining with estrogen and progesterone receptors. Actin stains highlight pericytes and smooth muscle cells. Reticulin will highlight the endothelial cells, whereas elastic stains highlight fibers in the vessel walls. Although not used in diagnosis, a clonal deletion (21)(q21.2q22.12) has been identified.

### DIFFERENTIAL DIAGNOSIS

This benign tumor must be separated from nasopharyngeal angiofibroma (NPA), glomangiopericytoma (GPC), and angiosarcoma. The lobular architecture is not seen in other vascular tumors. The vascular component of *NPA*, which develops exclusively in males, is separated by thin to thick collagen fibers and spindle or stellate stromal cells. *GPC* is a cellular tumor composed of syncytia of oval to spindle cells with a characteristic perivascular hyalinization and interspersed mast cells and eosinophils. *Angiosarcoma* is widely infiltrative, composed of atypical endothelial cells lining freely anastomosing vascular channels, while showing increased mitoses. *Sinonasal polyps* have more of a haphazard vascular proliferation but are surrounded by an edematous to fibrotic stroma with mucoserous glands and eosinophils.

### PROGNOSIS AND THERAPY

LCHs are benign tumors that do not recur after complete resection, but recurrences (up to 42%) are usually seen in older patients. Biopsy should be avoided due to potential profound epistaxis. Planning of the resection should include radiographic studies to investigate the extent of the tumor and allow for possible presurgical embolization. Excision is best accomplished by wide endoscopic resection, using yttrium aluminium garnet (YAG) laser to control potential bleeding. The resection should include a rim of normal mucosa/submucosa. Aplasia of the nasal cartilages could result in potential disfigurement in young patients, so caution should be used in choosing between various surgical options.

## MENINGIOMA

Meningioma is a benign neoplasm of meningotheelial cells uncommonly identified outside the cranial cavity, occasionally involving the sinonasal tract (< 1% of sinonasal tract tumors), either as an ectopic tumor or by extra-neuraxial extension of an intracranial neoplasm.

### CLINICAL FEATURES

Meningiomas of the sinonasal tract show only a slight female predominance (female to male ratio, 1.2:1), with most patients middle aged (average, 5th decade), although women tend to be older. Symptoms include mass, obstruction, discharge, epistaxis, and sinusitis. The tumors involve the nasal cavity then paranasal sinuses.

### RADIOGRAPHIC FEATURES

The tumors are often sizeable, with imaging studies required to exclude a possible intracranial component. An en plaque tumor (extensive, collar-like or sheet-like thin involvement of the dura) can be quite subtle. Bony sclerosis and bone destruction can be seen, even though

### MENINGIOMA—DISEASE FACT SHEET

#### Definition

- A meningotheelial-derived neoplasm

#### Incidence and Location

- Rare, especially when ectopic
- Direct extension must be excluded
- Nasal cavity then paranasal sinuses, usually left sided

#### Morbidity and Mortality

- Limited, although postoperative complications are seen

#### Sex and Age Distribution

- Slight female predominance
- Mean, 5th decade (range, 13-88 years)

#### Clinical Features

- Nonspecific, with mass, polyp, or nasal obstruction
- Imaging studies performed to exclude intracranial origin

#### Prognosis and Treatment

- Usually good prognosis
- Up to 30% recurrence, usually due to incomplete excision



a benign neoplasm is present. Widening of the suture lines can hint of the diagnosis.

## **PATHOLOGIC FEATURES**

### **GROSS FINDINGS**

The generally polypoid tumors range up to 8 cm (mean, ~3.5 cm). Tumors are submitted as multiple gritty to firm grayish fragments.

### **MICROSCOPIC FINDINGS**

Histologically, they resemble their intracranial counterparts, with meningothelial the most common pattern. There are syncytial, whorled, cohesive epithelial cell clusters set within the subepithelial tissues (Fig. 2.18), but blending may be seen. The cells have a bland appearance, with a low nuclear to cytoplasmic ratio, delicate nuclear chromatin, and intranuclear cytoplasmic inclusions (Fig. 2.18). Psammoma bodies and pre-psammoma bodies may be seen (Fig. 2.18). Necrosis, pleomorphism, and atypical mitoses are uncommon. Any histologic subtype can be seen, but in this location, transitional, metaplastic, and psammomatous are most frequent.

## **MENINGIOMA PATHOLOGIC FEATURES**

### **Gross Findings**

- Polypoid masses
- Mean, 3.5 cm (up to 8 cm reported)

### **Microscopic Findings**

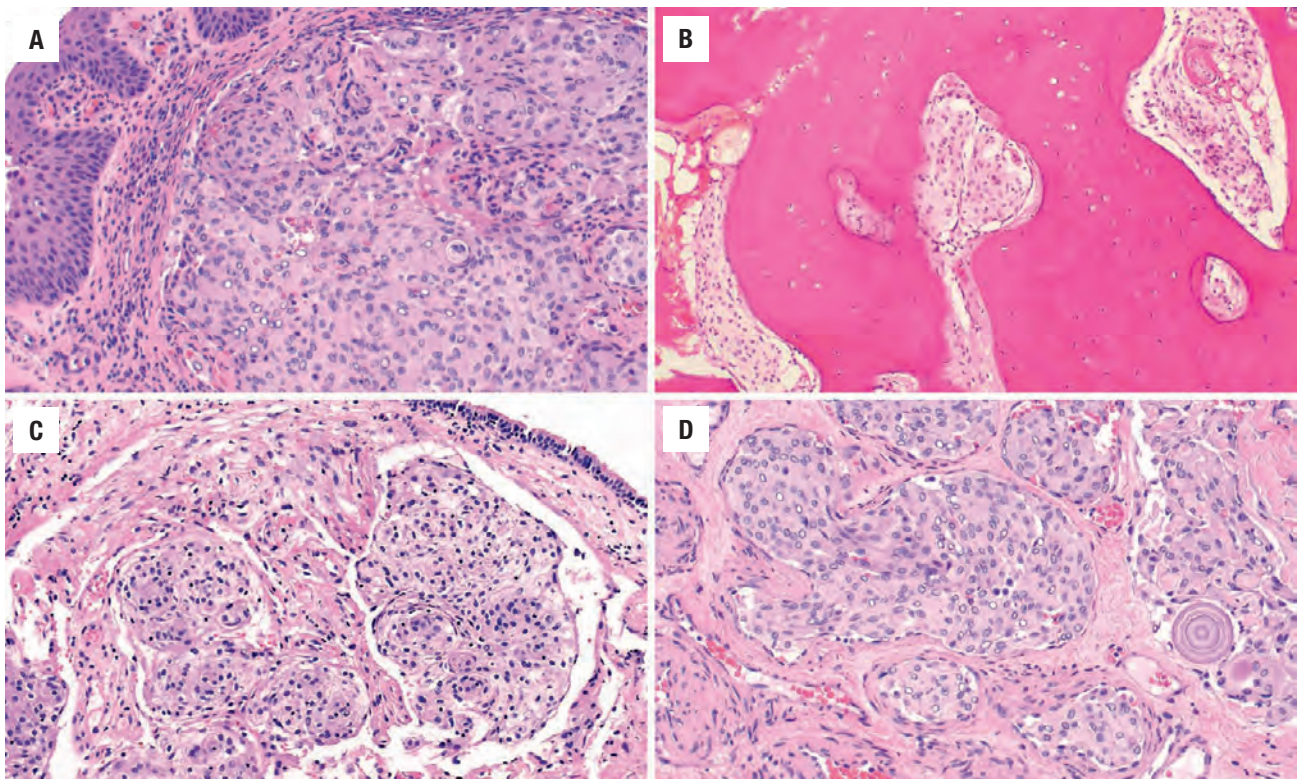
- Subepithelial unencapsulated cellular tumor
- Often blends with glands and surface invaginations
- Lobules of whorled syncytial meningothelial cells
- Bland nuclei, often with intranuclear cytoplasmic inclusions
- Psammoma bodies may be seen
- Most common types are meningothelial, transitional, psammomatous, and metaplastic (WHO grade 1 tumors)

### **Immunohistochemical Findings**

- Positive for EMA, CK7, and pancytokeratin (pre-psammomatous)
- Negative for GFAP, STAT6, and smooth muscle actin

### **Pathologic Differential Diagnosis**

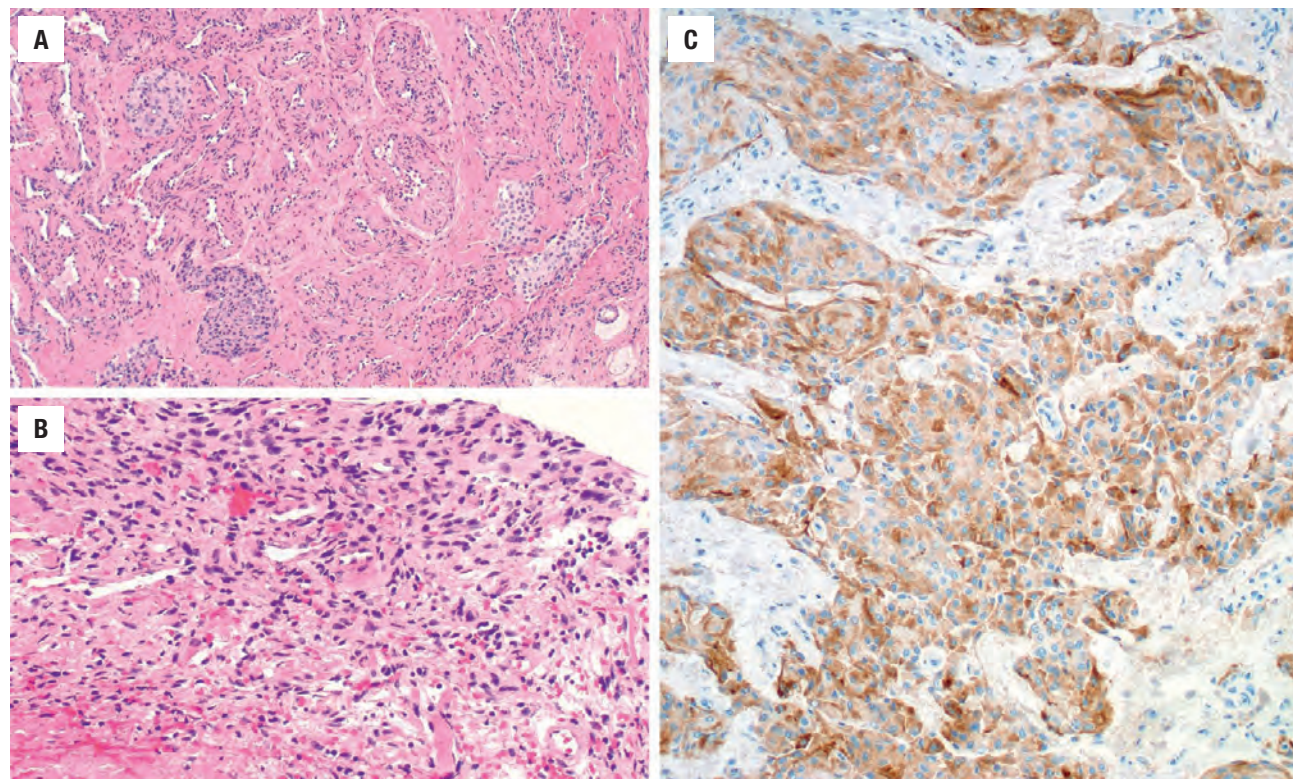
- Angiofibroma, aggressive psammomatoid ossifying fibroma, olfactory neuroblastoma, schwannoma, melanoma, paraganglioma, glomangiopericytoma, solitary fibrous tumor, meningocoele



**FIGURE 2.18**

Meningioma. The meningothelial neoplastic proliferation is noted below an intact squamous epithelium (A), interspersed within the bone (B), and within the stroma below a respiratory epithelium (C). Psammoma bodies (D) may be seen. Note the intranuclear cytoplasmic inclusions.



**FIGURE 2.19**

Meningioma is frequently noted within the stroma (A), and sometimes is quite challenging to detect on H&E-stained slides (B). The neoplastic cells show a strong, although focal EMA reaction (C).

## ANCILLARY STUDIES

### IMMUNOHISTOCHEMICAL FINDINGS

The neoplastic cells are uniformly positive with vimentin and show variable reactivity with epithelial membrane antigen (EMA) (Fig. 2.19) and progesterone receptors. The cells may show a strong CAM5.2 and CK7 reaction in a pre-psammomatous distribution.

## DIFFERENTIAL DIAGNOSIS

The differential diagnosis includes nasopharyngeal angiofibroma (NPA), aggressive psammomatoid ossifying fibroma, schwannoma, paraganglioma, olfactory neuroblastoma, melanoma, glomangiopericytoma (GPC), solitary fibrous tumor (SFT), and meningocele. Males are exclusively affected by angiofibroma, which shows a rich vascularity and collagen deposition. Psammomatoid ossifying fibroma develops in young patients, with compact to storiform stroma and innumerable calcifications. The strong S100 protein immunoreactivity in a schwannoma, along with spindled alternating cellular and hypocellular areas, and perivascular hyalinization helps make the separation. Paraganglioma will have a more nested architecture, basophilic cytoplasm, and isolated nuclear pleomorphism.

The chromaffin cells will be positive with chromogranin and synaptophysin lacking epithelial reactivity. Olfactory neuroblastoma shows much smaller cells and has a lobular pattern highlighted by S100 protein and neuroendocrine markers. GPC is highlighted by  $\beta$ -catenin and smooth muscle actin (SMA). An SFT is more collagenized and shows CD34 and STAT6 immunoreactivity. A meningocele is an acquired cystic lesion, usually associated with previous surgery, infection, or trauma, showing a similar immunohistochemistry profile as meningioma.

## PROGNOSIS AND THERAPY

Surgery or radiation is the treatment of choice, although sometimes watchful waiting is also used for the tumors. It is difficult to achieve complete extirpation, with recurrences in up to 30% of patients usually within the first 5 years. There is an ~80% 10-year survival. Metastases from sinonasal tract tumors are not reported.

## ■ GLOMANGIOPERICYTOMA (SINONASAL-TYPE HEMANGIOPERICYTOMA)

Also referred to as *sinonasal-type hemangiopericytoma*, glomangiopericytoma (GPC) is an uncommon sinonasal



tract neoplasm demonstrating perivascular myoid phenotype, showing hybrid differentiation between glomus (myoid) and hemangiopericytoma (pericyte), but it is distinctly different from soft tissue-type hemangiopericytoma.

CLINICAL FEATURES

GPC is a rare neoplasm (< 0.5% of all sinonasal neoplasms), observed slightly more frequently in females than males (1.2:1). Although any age may be affected, most patients are in the 7th decade. Most patients complain of nasal obstruction, epistaxis, and less commonly, nasal discharge, pain, sinusitis, difficulty breathing, and headaches. Symptoms are usually present for less than 1 year. Associated severe oncogenic osteomalacia is rare. Physical examination usually reveals a unilateral, polypoid mass in the nasal cavity, with rare bilateral involvement (< 5%). The paranasal sinuses are uncommonly affected.

RADIOGRAPHIC FEATURES

Radiographic studies are not distinctive, showing sinus and nasal opacification by a polypoid nasal mass. Bone

erosion and sclerosis are seen in a significant number of cases. There may be nonspecific sinusitis concurrently.

PATHOLOGIC FEATURES

GROSS FINDINGS

The generally polypoid tumors range up to 8 cm (mean, ~ 3 cm). Tumors in female patients tend to be larger than male patients. The tumors are beefy-red to grayish-pink, soft, edematous, fleshy to friable masses, often demonstrating hemorrhage.

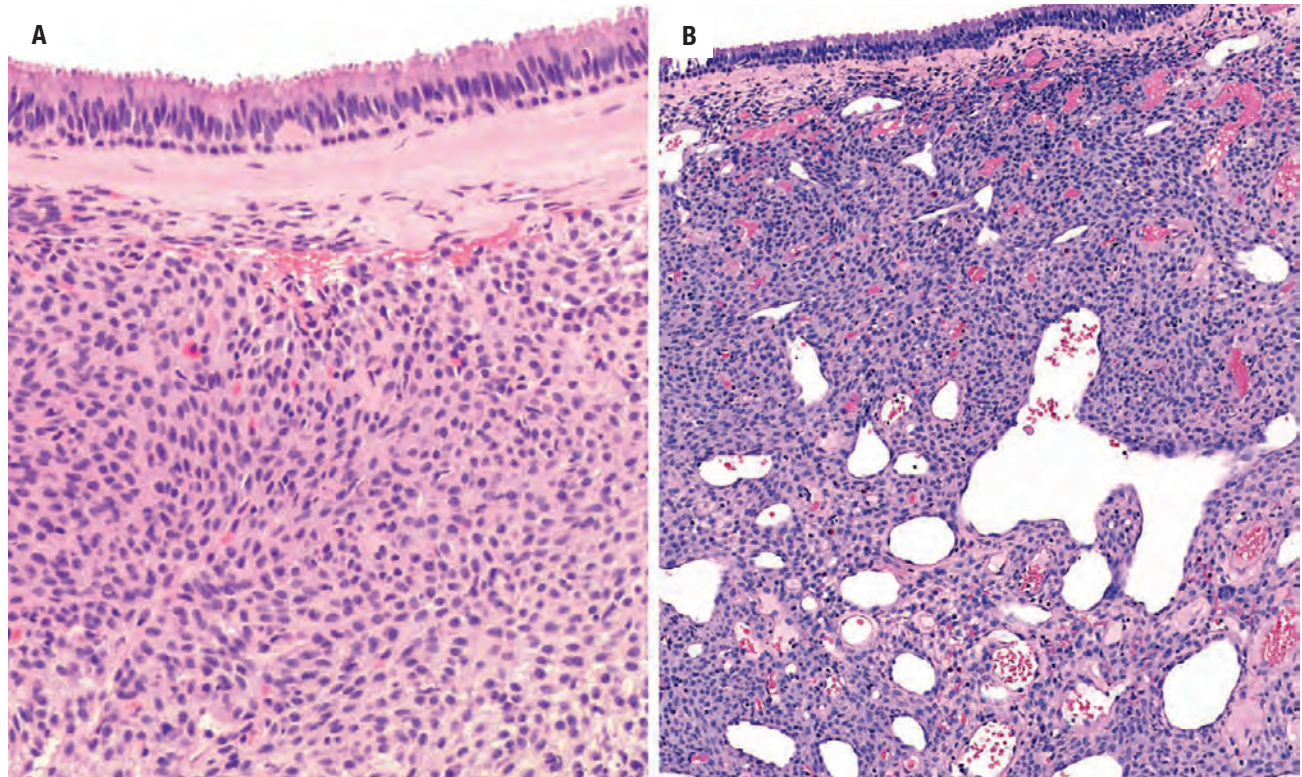
MICROSCOPIC FINDINGS

GPC is a subepithelial well-delineated but unencapsulated cellular tumor, effacing or surrounding the normal structures (Fig. 2.20). There is usually a well-developed zone of separation between the surface epithelium and the tumor. Bone remodeling can be seen but not true invasion. The tumor is composed of closely packed cells, forming short fascicles and sometimes exhibiting a storiform, whorled, or palisaded pattern, interspersed with many vascular channels (Fig. 2.21). The latter are in the form of capillary-sized to large patulous spaces that may

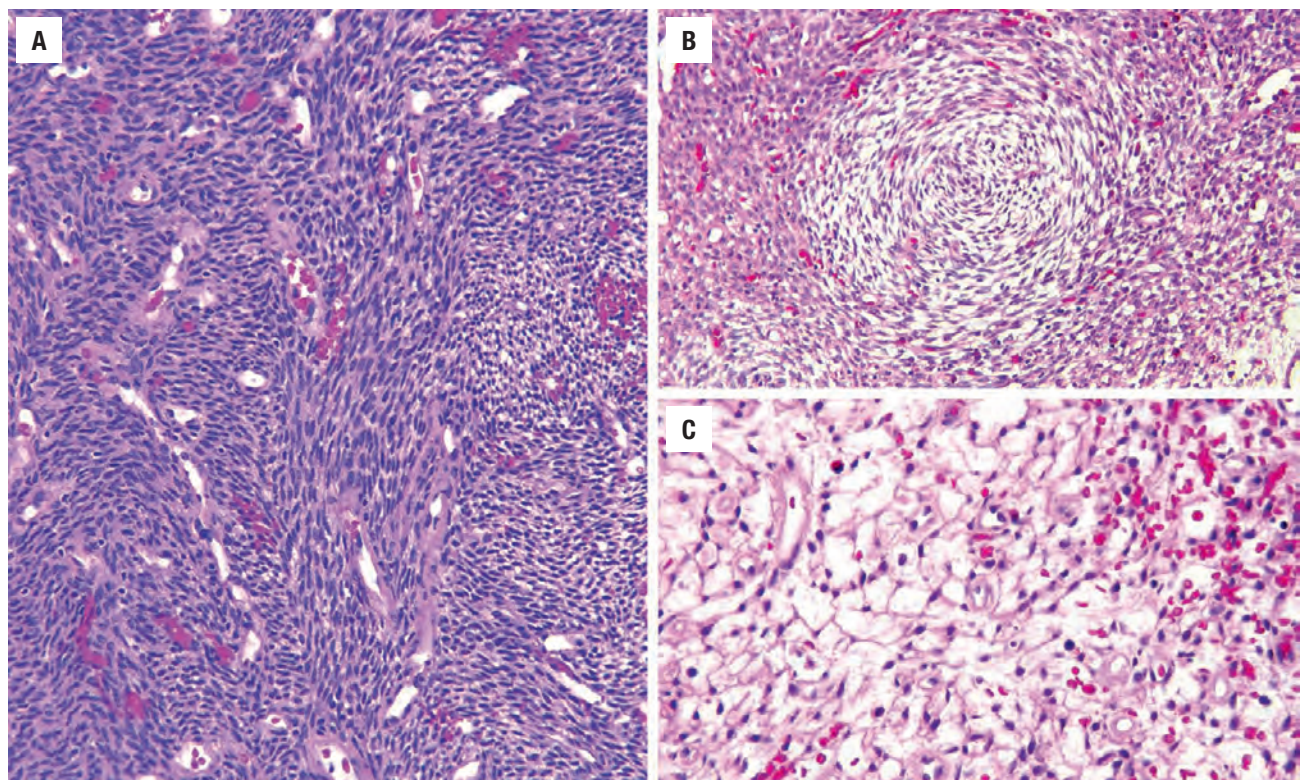
| GLOMANGIOPERICYTOMA—DISEASE FACT SHEET  |
|---|
| <b>Definition</b> <ul style="list-style-type: none"><li>■ A sinonasal tumor demonstrating perivascular myoid phenotype</li></ul>  |
| <b>Incidence and Location</b> <ul style="list-style-type: none"><li>■ Rare neoplasm (&lt; 0.5% of all sinonasal tract neoplasms)</li><li>■ Lateral nasal cavity</li><li>■ Paranasal sinuses uncommonly affected</li></ul>   |
| <b>Morbidity and Mortality</b> <ul style="list-style-type: none"><li>■ Rare malignant tumors</li></ul>  |
| <b>Sex and Age Distribution</b> <ul style="list-style-type: none"><li>■ Slight female predominance (1.2:1)</li><li>■ Mean, 7th decade (range, in utero to 90 years)</li></ul>   |
| <b>Clinical Features</b> <ul style="list-style-type: none"><li>■ Nasal obstruction</li><li>■ Epistaxis</li><li>■ Nasal discharge, pain, and headaches</li></ul>   |
| <b>Prognosis and Treatment</b> <ul style="list-style-type: none"><li>■ Indolent neoplasm with excellent prognosis (&gt; 90% 5-year survival)</li><li>■ Recurrences in up to 30%</li><li>■ Rare malignant neoplasms (2%)</li><li>■ Complete surgical resection</li></ul> |

| GLOMANGIOPERICYTOMA—PATHOLOGIC FEATURES   |
|---|
| <b>Gross Findings</b> <ul style="list-style-type: none"><li>■ Polypoid masses</li><li>■ Mean, 3 cm</li><li>■ Solid, beefy, fleshy masses with areas of hemorrhage</li></ul>   |
| <b>Microscopic Findings</b> <ul style="list-style-type: none"><li>■ Subepithelial unencapsulated cellular tumor</li><li>■ Closely packed cells, short fascicles, and storiform-whorled pattern</li><li>■ Vascular channels (staghorn) demonstrating prominent peritheliomatous hyalinization</li><li>■ Uniform, syncytial arrangement of oval to elongated cells</li><li>■ Round to spindled nuclei</li><li>■ Mast cells and eosinophils</li><li>■ Moderate to severe nuclear atypia and a mitotic rate of &gt; 4/10 HPFs associated with an increased risk of developing recurrent disease or dying with disease</li></ul> |
| <b>Immunohistochemical Findings</b> <ul style="list-style-type: none"><li>■ Positive for nuclear β-catenin, vimentin, smooth muscle actin, muscle-specific actin, cyclin-D1, factor XIIIa</li><li>■ Negative for bcl-2, keratins, CD31, FVIIIIRAg, STAT6, desmin, CD117</li></ul>   |
| <b>Pathologic Differential Diagnosis</b> <ul style="list-style-type: none"><li>■ Hemangioma, solitary fibrous tumor, glomus tumor, leiomyoma, meningioma, monophasic synovial sarcoma, fibrosarcoma, biphenotypic sinonasal sarcoma, malignant peripheral nerve sheath tumor</li></ul>  |



**FIGURE 2.20**

Glomangiopericytoma. (A and B) Characteristic diffuse growth within the submucosa with effacement. The overlying respiratory epithelium remains intact, separated by dense collagenized stroma.

**FIGURE 2.21**

Glomangiopericytoma. (A) Closely packed cells in short fascicles. The neoplastic cells may be arranged in a whorled (B) or reticulated (C) pattern.



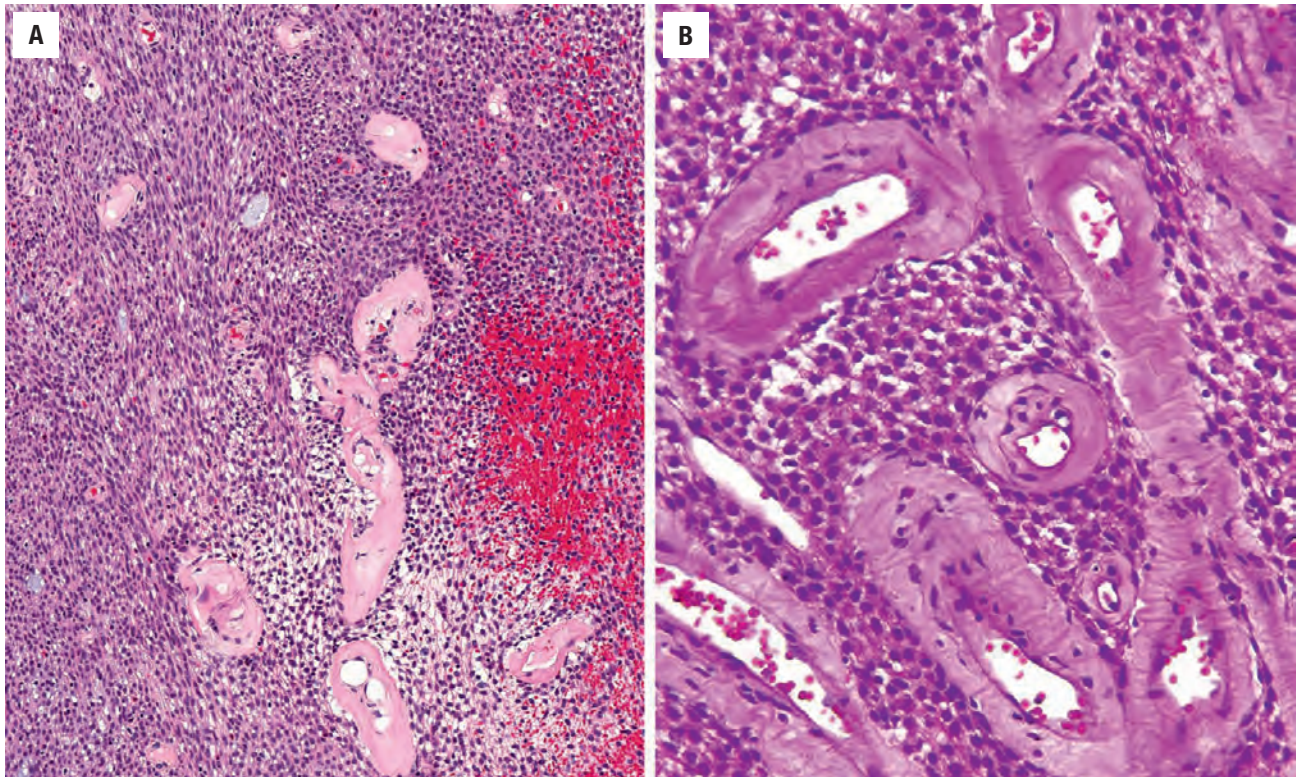


**FIGURE 2.22**

(A and B) One of the characteristic histomorphologic findings of glomangiopericytoma is the presence of prominent perivascular hyalinization.

have a “staghorn” or “antler-like” configuration. A prominent peritheliomatous hyalinization is characteristic (Fig. 2.22). The neoplastic cells are uniform, elongated to oval, and possess vesicular to hyperchromatic, round to oval to spindle-shaped nuclei, and lightly eosinophilic cytoplasm (Fig. 2.23). The cells are often syncytial in appearance. Mild nuclear pleomorphism and occasional mitotic figures may be present, but necrosis is not found. Extravasated erythrocytes, mast cells, and eosinophils are nearly ubiquitously present (Fig. 2.24). Occasionally, tumor giant cells (Fig. 2.24), fibrosis, or myxoid degeneration may be seen. Rarely, lipomatous change and hematopoiesis may be seen. Concurrently, other lesions may also be present, including SFT, fibrosarcoma, REAH, and sinonasal polyps. Moderate to severe nuclear atypia, high cellularity and a mitotic rate of  $> 4/10$  high-power fields (HPFs) has been associated with an increased risk of developing recurrent disease or dying with disease.

## ANCILLARY STUDIES

### IMMUNOHISTOCHEMICAL FINDINGS

The tumor cells are diffusely positive for vimentin, SMA, muscle-specific actin, factor XIIIa, cyclin-D1, and nuclear  $\beta$ -catenin (Fig. 2.25). Occasional focal staining for CD34 is noted in the lesional cells, but it is not as

strong as in the endothelial cells. The neoplastic cells are negative with bcl-2, keratins, CD31, FVIIIIRAg, desmin, CD99, STAT6, S100 protein, GFAP, neuron specific enolase (NSE), and CD117.

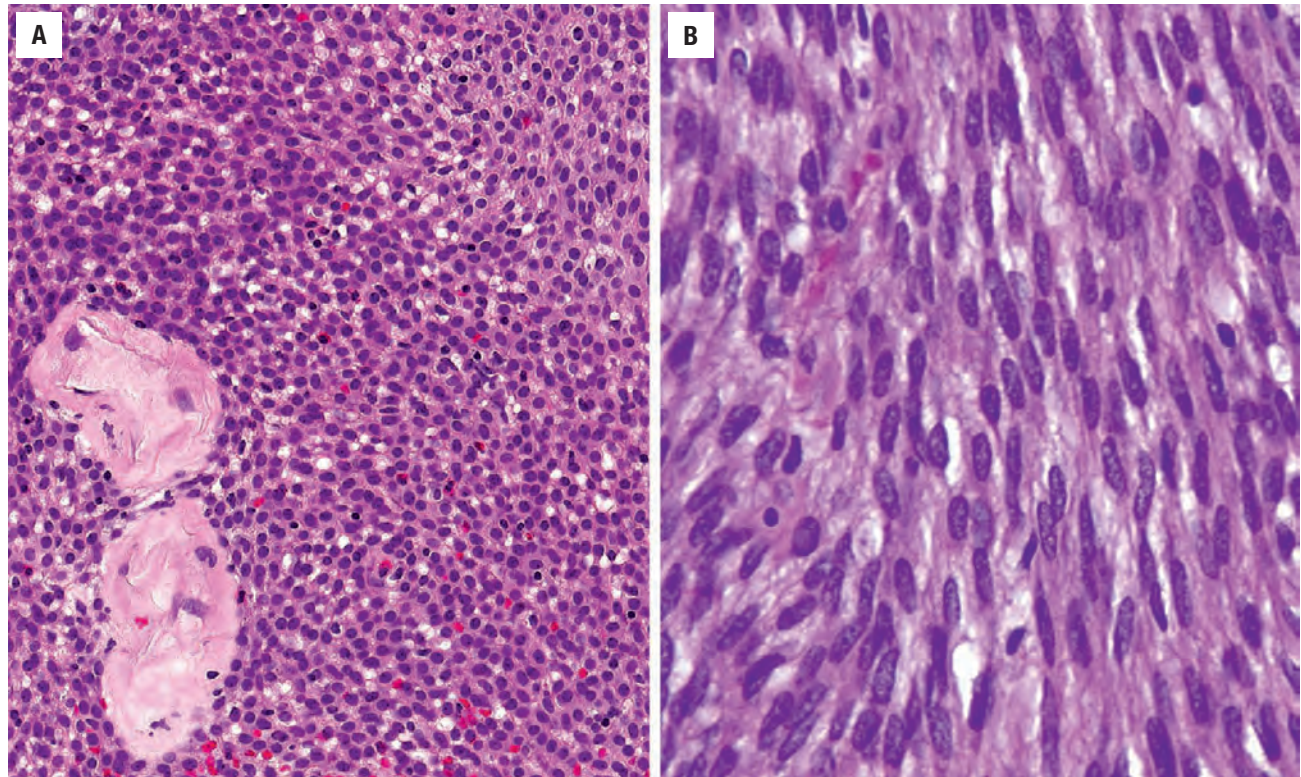
### GENETIC FINDINGS

Somatic, single nucleotide substitution heterozygous mutations in *CTNNB1* gene encoding  $\beta$ -catenin are seen, resulting in nuclear translocation and accumulation of  $\beta$ -catenin by immunohistochemistry. The upregulated cyclin-D1 leads to oncogenic activation, considered important in pathogenesis. There are not *NAB2-STAT6* or *miR143-NOTCH* fusions and no *GLI1* abnormalities, helping show GPC is a unique tumor.

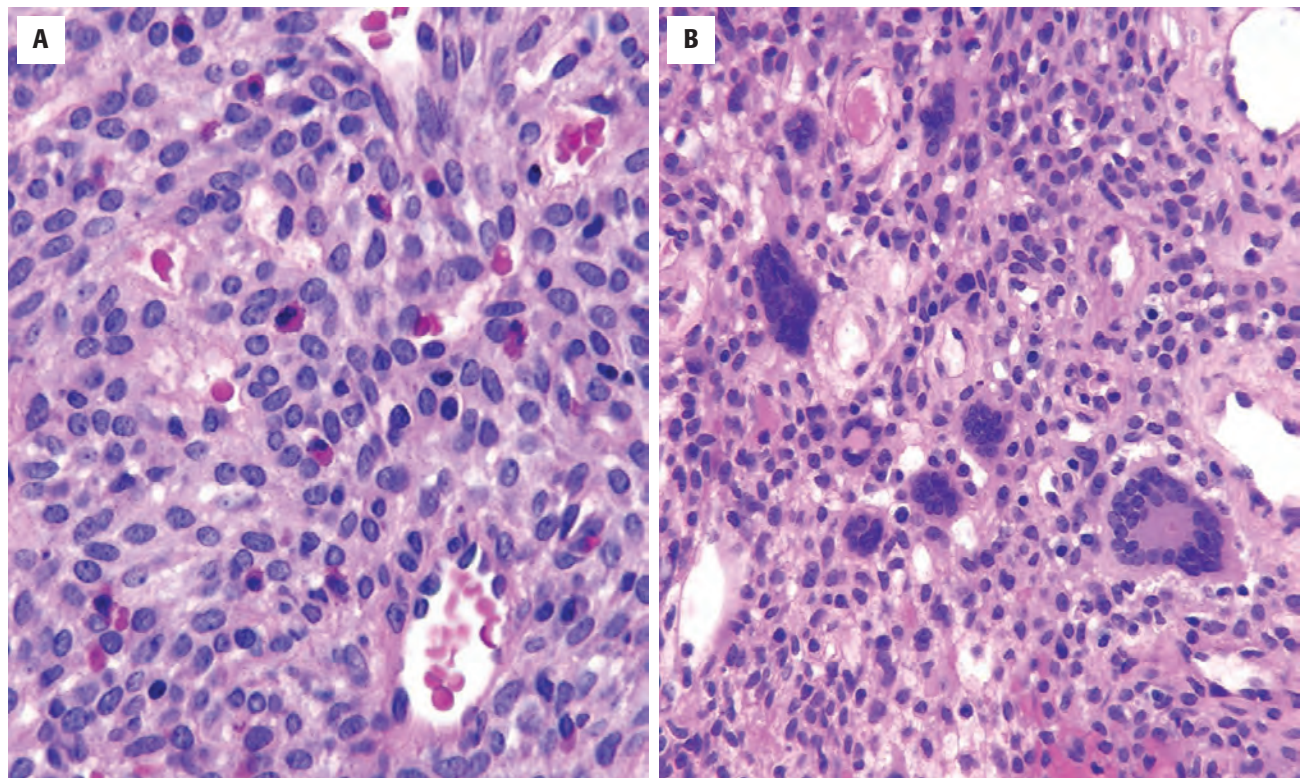
## DIFFERENTIAL DIAGNOSIS

The differential diagnosis of GPC includes a variety of benign and malignant spindle cell tumors but usually can be limited to hemangioma, SFT, glomus tumor, leiomyoma, meningioma, monophasic synovial sarcoma, fibrosarcoma, biphenotypic sinonasal sarcoma, and malignant peripheral nerve sheath tumor. *Hemangiomas* are lobular, frequently exhibit surface ulceration and do not grow in a fascicular architecture. *SFT* is often



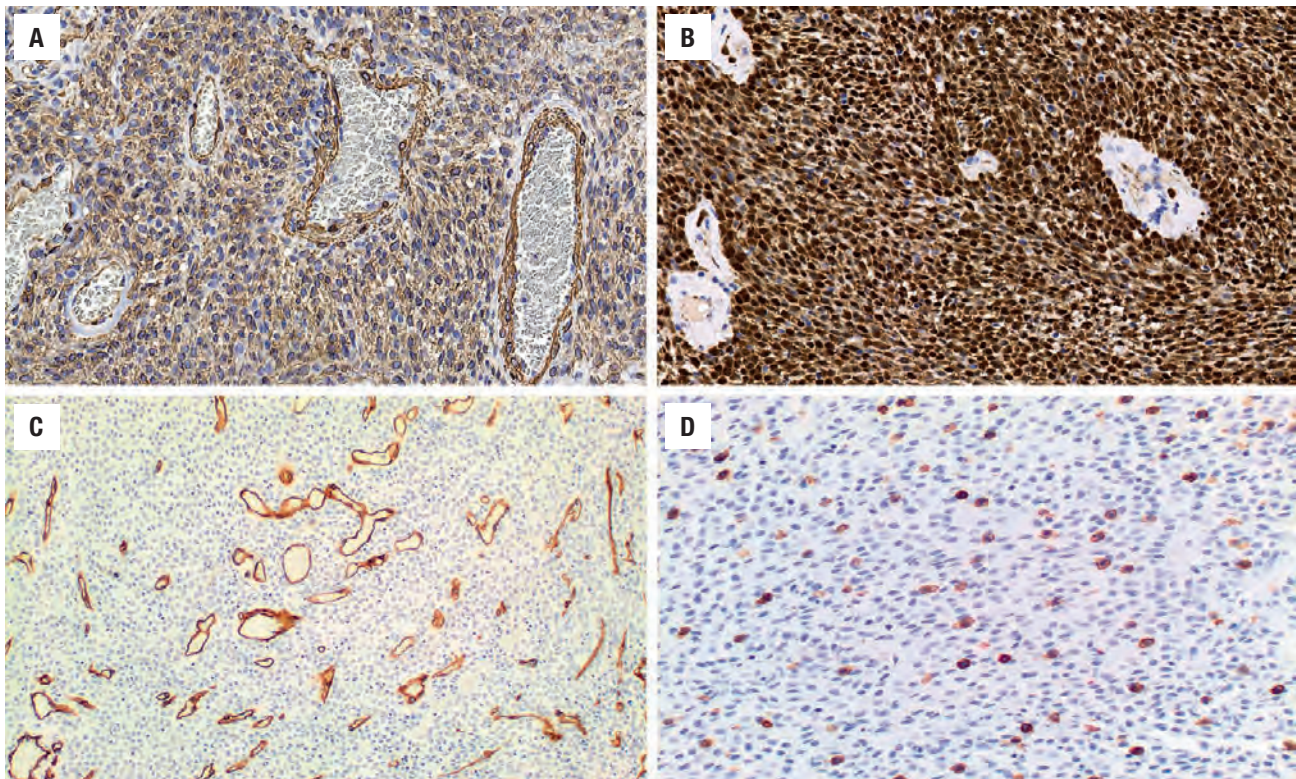
**FIGURE 2.23**

Glomangiopericytoma. A syncytial arrangement of ovoid cells with eosinophils (**A**), whereas in other areas the short spindled cells are streaming (**B**), associated with mast cells.

**FIGURE 2.24**

(**A**) Eosinophils and mast cells are common in glomangiopericytoma, along with extravasated erythrocytes. (**B**) Occasionally tumor giant cells may be seen.



**FIGURE 2.25**

Immunohistochemistry findings in glomangiopericytoma. (A) Smooth muscle actin. (B) Strong nuclear reaction with  $\beta$ -catenin. (C) No reaction in the neoplastic cells with CD31. (D) CD117 highlights the mast cells only.

hypocellular, has thick, ropy stromal collagen, lacks inflammatory cells, and is diffusely positive for CD34, STAT6, and bcl-2 (Fig. 2.26). *Glomus tumors* are composed of round, epithelioid cells forming cellular nests with organoid appearance and are exceptionally rare in the sinonasal tract. *Leiomyomas* of the sinonasal tract show a perivascular distribution with larger spindle cells. They are desmin positive in addition to the actins. All the *sarcomas* usually have significant pleomorphism, mitotic activity, and necrosis, whereas biphenotypic sinonasal sarcoma shows a characteristic blending of the spindle cells and epithelial invaginations, with both S100 protein and SMA/MSA immunoreactivity.

### PROGNOSIS AND THERAPY

GPC are indolent, with an overall excellent survival rate (> 90% 5-year survival) achieved with complete surgical excision. Recurrence, which develops in up to 40% of cases, usually develops within 1 year, a result of incomplete excision. Aggressive-behaving GPC (malignant GPC) is uncommon (2%) and usually exhibits the following findings: large size (> 5 cm), bone invasion, severe nuclear pleomorphism, increased mitotic activity (> 4/10 HPFs), atypical mitotic figures, necrosis, and proliferation index > 10%.

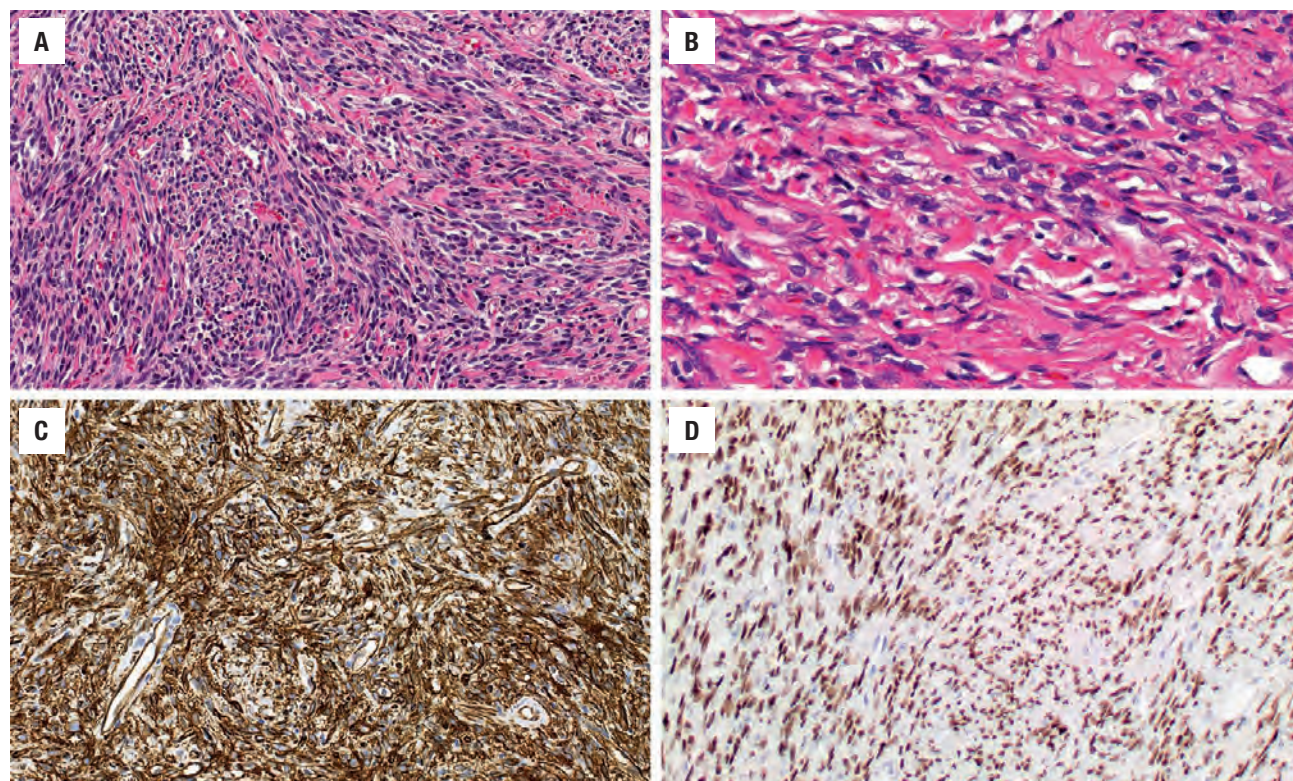
### NASOPHARYNGEAL ANGIOFIBROMA

Nasopharyngeal angiofibromas (NPAs) are benign but locally aggressive, highly cellular, and richly vascularized mesenchymal neoplasms that arise in the roof of the nose and nasopharynx in males. It is a rare tumor, accounting for < 1% of all nasopharyngeal tumors, arising in the fibrovascular stroma of the posterolateral wall of the roof of the nose. Localization studies have determined that the point of origin for most NPA is the region where the sphenoidal process of the palatine bone meets the horizontal ala of the vomer and pterygoid process. This junction forms the superior margin of the sphenopalatine foramen and the posterior margin of the middle turbinate. The tumor is thought to be testosterone dependent, with a puberty-induced growth that can be blocked with estrogen or progesterone therapy. There is a reported association with familial adenomatous polyposis.

### CLINICAL FEATURES

NPA affects almost exclusively boys and adolescent to young men, with a mean age of 17 years. NPA are uncommon tumors with an estimated incidence of 3.7 per 1,000,000 males. If a female is affected, testicular



**FIGURE 2.26**

Solitary fibrous tumor. **(A)** A solitary fibrous tumor has haphazard cellular arrangement. **(B)** Heavy collagen deposition is noted. **(C)** CD34 strongly highlights the lesional cells. **(D)** STAT6 shows a strong, nuclear reaction, unique to this tumor in the sinonasal tract.

#### NASOPHARYNGEAL ANGIOFIBROMA—DISEASE FACT SHEET

##### Definition

- A benign, highly cellular, and richly vascularized mesenchymal neoplasm that arises in the nasopharynx in males

##### Incidence and Location

- Uncommon, incidence of 3.7/1,000,000 males
- < 1% of nasopharyngeal tumors
- Posterior nasal wall, roof of nose, and nasopharynx

##### Morbidity and Mortality

- Intracranial extension in some patients
- Mortality up to 9% related to hemorrhage and intracranial extension

##### Sex and Age Distribution

- Males (exclusively)
- Peak age, 15 years (range, 6-29 years)

##### Clinical Features

- Nasal obstruction, spontaneous epistaxis, nasopharyngeal mass
- Facial deformities, proptosis, and a bulging palate
- Sinusitis, rhinolalia, otitis, tinnitus, deafness

##### Radiographic Features

- Soft tissue density with bowing of the posterior maxillary sinus
- Bony margins may be eroded
- Angiography identifies feeder vessels and permits presurgical embolization

##### Prognosis and Treatment

- Benign but locally aggressive neoplasm
- Recurrences in up to 25%, most commonly intracranial, and usually within first 2 years
- Mortality up to 9% related to hemorrhage or intracranial extension
- Complete surgical resection with preoperative embolization or hormonal therapy
- Radiotherapy for unresectable intracranial tumors

feminization has to be excluded by chromosome analysis. Although white patients tend to be fair-skinned and red-haired, this is not the case in other endemic populations (Central and South Americans, Africans, or Asians). The most common symptoms of NPA are nasal obstruction, spontaneous epistaxis, and a mass, present for 12

to 24 months in most patients. Other patients may present with facial deformities, proptosis, rhinolalia, deafness, sinusitis, otitis, and a bulging palate resulting from extension of the tumor into soft tissues of the face and orbit. Endoscopic examination usually shows a mass involving the posterior nasal wall. Various staging systems



have been proposed, with size and location determining the outcome (Table 2.1).

**RADIOGRAPHIC FEATURES**

On plain x-rays, NPA are characterized by a soft tissue mass causing bowing of the posterior wall of the maxillary

sinus and distortion and posterior displacement of the pterygoid plates (Holman-Miller or antral sign). Bony margins may be eroded but are obvious. CT and MRI show the extent of the tumor, as well as possible surgical approach (Fig. 2.27), with tumors frequently showing intracranial extension (middle cranial fossa). Angiography identifies the feeder vessel(s) and allows for presurgical embolization. A dense tumor blush is characteristic (Fig. 2.27). Due precautions are suggested before taking biopsies from these tumors because of the risk of life-threatening bleeding.

| TABLE 2.1   |  |
|---|--|
| Clinical system for staging nasopharyngeal angiofibroma |  |
| Stage   | Description  |
| Stage I   | Tumor limited to the nasopharynx with no bone destruction  |
| Stage II  | Tumor invading the nasal cavity, maxillary, ethmoid, and sphenoid sinuses with no bone destruction   |
| Stage III   | Tumor invading the pterygopalatine fossa, infratemporal fossa, orbit and parasellar region           |
| Stage IV  | Tumor with massive invasion of the cranial cavity, cavernous sinus, optic chiasm, or pituitary fossa |

**PATHOLOGIC FEATURES**

**GROSS FINDINGS**

Most NPAs are round or nodular, nonencapsulated masses with a sessile or pedunculated base. The tumors may be large (up to 22 cm), although the mean size is 4 cm. The surface of the tumors is largely covered by intact mucosa, frequently taking the shape of surrounding structures (Fig. 2.27). The cut surface is variable and shows dilated vascular channels, which give the tumors a spongy appearance. In less vascular areas the tumors appear solid and fibrotic.

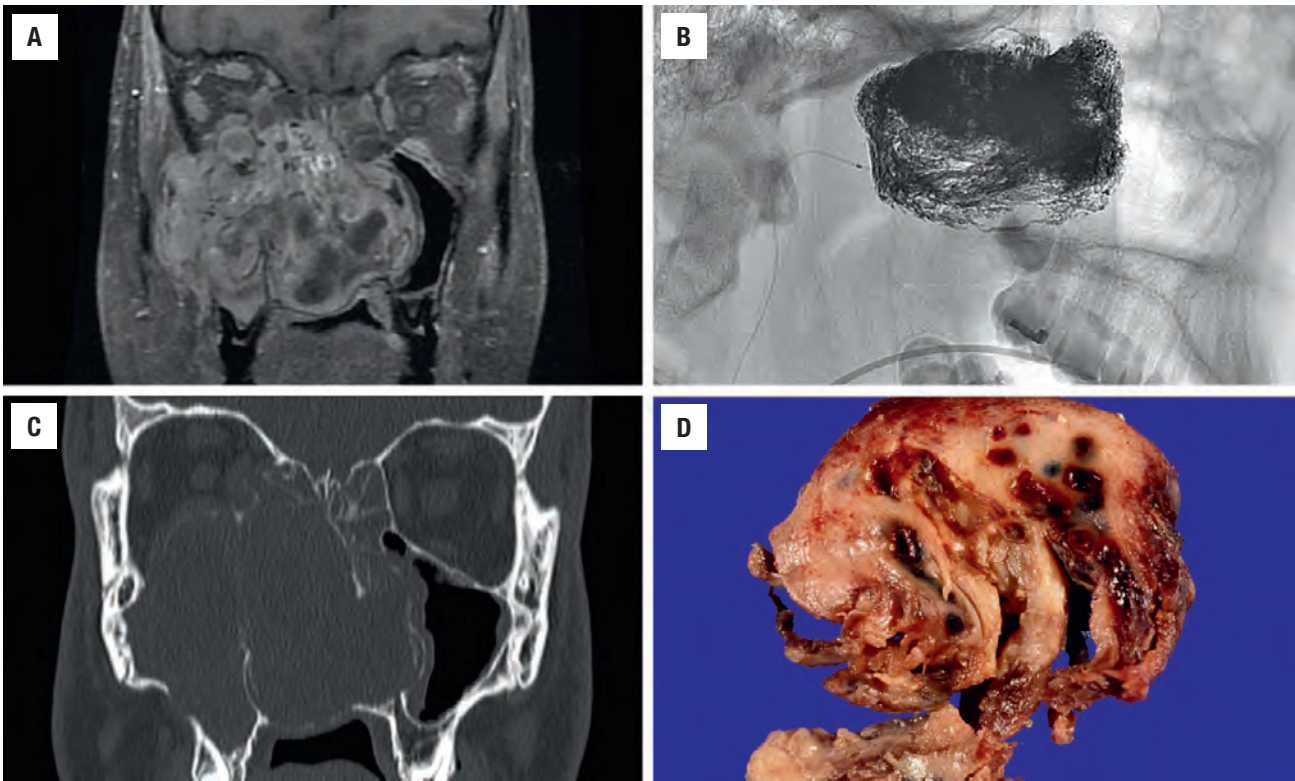


**FIGURE 2.27** Nasopharyngeal angiofibroma. (A) A magnetic resonance image shows a large mass within the nasopharynx, nasal cavity, and maxillary sinus. Note the high signal within the tumor. (B) A dense blush showing the rich vascularity of the angiofibroma and the feeder vessel by angiography. (C) A computed tomography image shows a large, destructive mass, bowing several bony structures. (D) The gross specimen cut surface shows a solid mass with large hemorrhagic areas corresponding to feeding vessels. Note how it is molded to the shape of the turinate tissue as it has filled into the nasal cavity.

### NASOPHARYNGEAL ANGIOFIBROMA—PATHOLOGIC FEATURES

#### Gross Findings

- Round or nodular, nonencapsulated masses with sessile or pedunculated base
- Intact mucosa with focal areas of ulceration and superficial hemorrhage
- Cut surface showing dilated vascular channels which give the tumors a spongy appearance or solid, fibrotic tumors
- Mean, 4 cm; but up to 22 cm

#### Microscopic Findings

- Combination of abnormal vascular network, a connective tissue stroma, and stromal cells
- Vascular network with variable sized vessels, from thin-walled, slit-like to large irregular vessels
- Muscle layer is absent, focal, pad-like, or circumferential
- Endothelium is attenuated but can be plump
- Spindle, stellate, angular stromal cells in collagenized background
- Inflammatory cells usually absent
- Increased fibrosis with treatment; embolic material may be seen

#### Immunohistochemical Findings

- Vessel walls positive with vimentin
- Endothelial cells positive for CD34; CD31; androgen, estrogen, and progesterone receptors; FVIIIIRAg
- Stromal cells positive for vimentin, nuclear  $\beta$ -catenin, androgen receptor

#### Pathologic Differential Diagnosis

- Lobular capillary hemangioma, sinonasal polyps, peripheral nerve sheath tumor, solitary fibrous tumor, desmoid tumor (desmoid-type fibromatosis)

### MICROSCOPIC FINDINGS

The microscopic appearance of NPA rests on the variable presence of three elements: an abnormal vascular network, a connective tissue stroma, and stromal cells (Fig. 2.28). The vascular network consists of mostly thin-walled, slit-like (“staghorn”) or dilated vessels, with calibers ranging from capillary to large, patulous vessels (Fig. 2.29). The muscular layer can be absent, focal, and pad-like, or circumferential (Fig. 2.30). Elastic fibers are typically absent, one of the reasons for the profuse bleeding (vessels cannot contract down). The vascular spaces and lining endothelium appear to be resting directly on the connective tissue stroma (Fig. 2.31). The endothelial cells may be plump but are usually attenuated. The fibrous connective tissue stroma consists of plump spindle, angular, or stellate-shaped cells, and a varying amount of fine and coarse collagen fibers (Fig. 2.32). Myxoid changes are seen especially in embolized specimens. The nuclei of the stromal cells are generally cytologically bland (Fig. 2.31), but they may be multinucleated or show some degree of pleomorphism in the more cellular areas, thought to represent senescent or degenerative changes. The chromatin is finely and evenly dispersed. Large stromal cells with abundant cytoplasm resembling ganglion cells can be identified. Mitotic activity and nuclear atypia are not findings of typical NPA. Mast cells may be seen, but other inflammatory elements are usually absent (except if there is surface ulceration). Long-standing lesions show increased fibrosis and diminished vasculature. Treatment with androgen receptor blockers (such as flutamide) results in increased collagenization of the stroma with fewer, but thicker-walled vessels. In specimens excised after embolization treatment, the tumor often shows areas of infarction, and embolic material can be seen in some

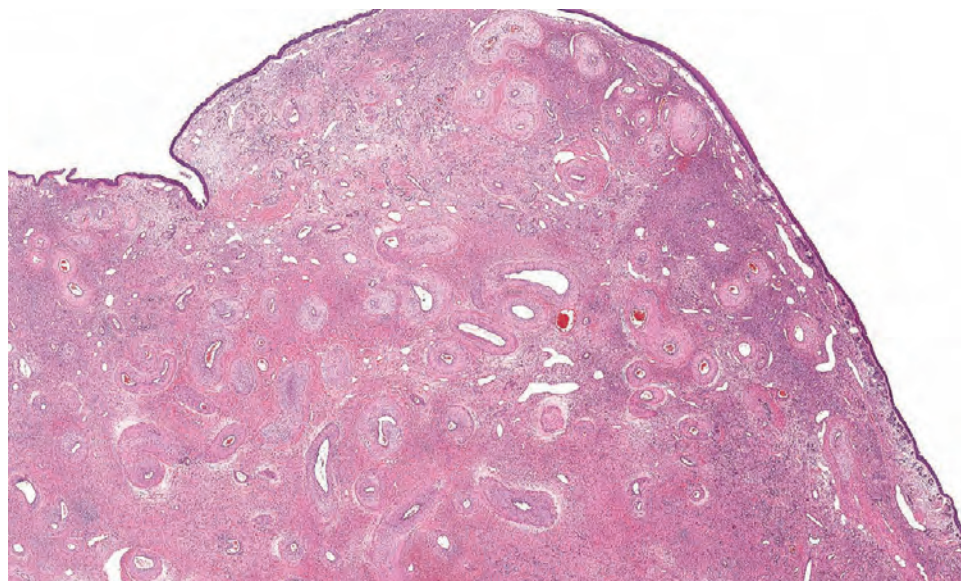


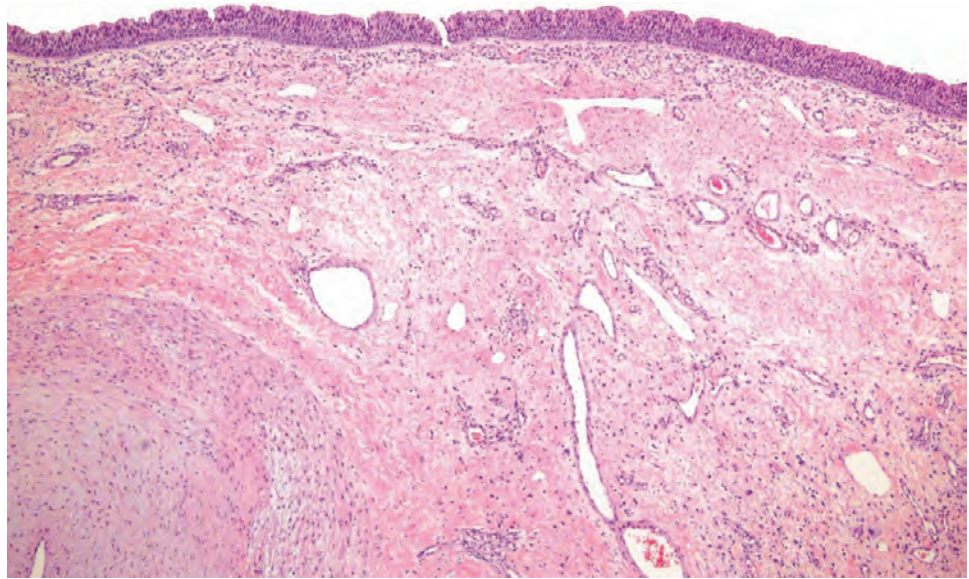
**FIGURE 2.28**

Nasopharyngeal angiofibroma. The intact respiratory epithelium (*top*) overlies a richly vascular neoplasm, which has variably sized vessels surrounded by a cellular fibroblastic stroma with collagen.

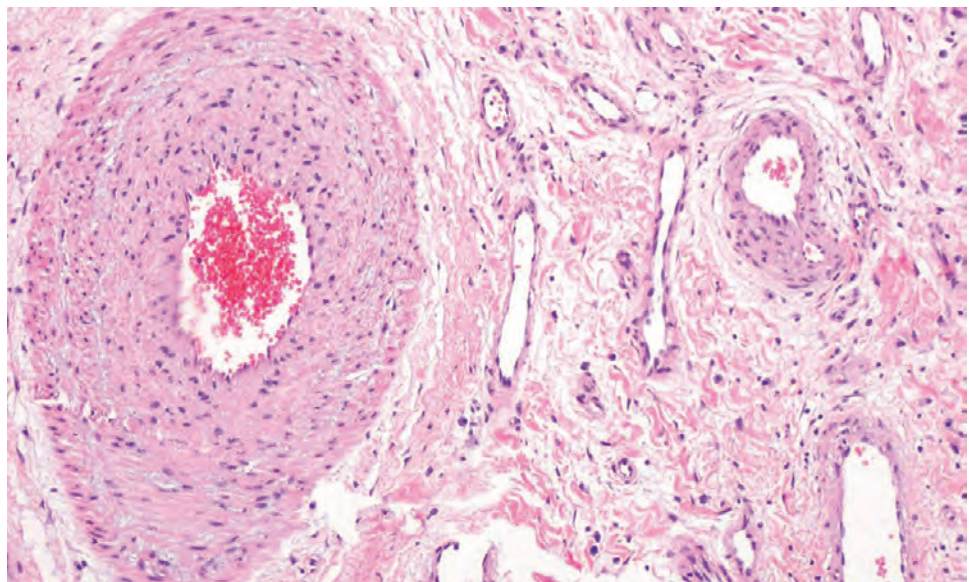


**FIGURE 2.29**

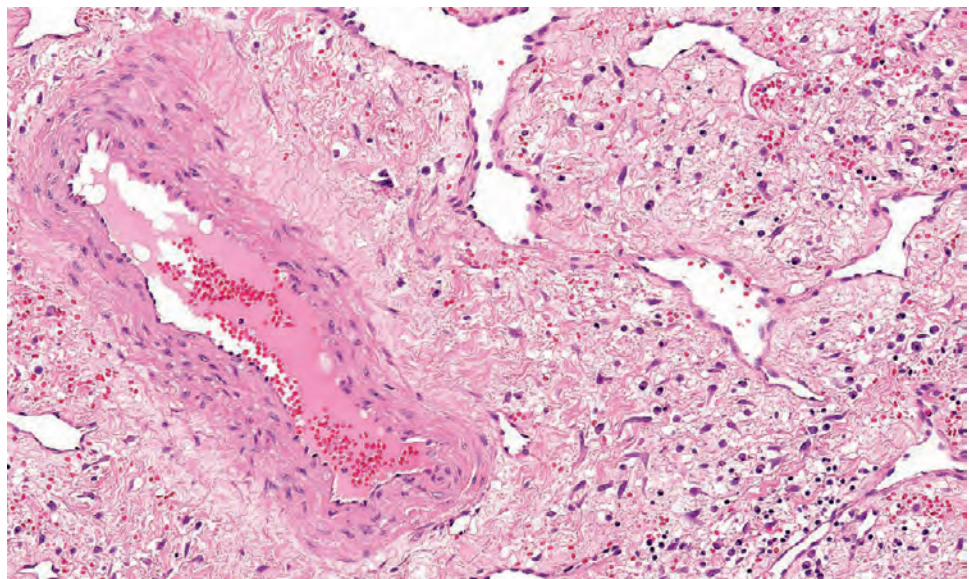
Nasopharyngeal angiofibroma. Smooth muscle walled vessels, patulous vessels, and capillaries are all surrounded by the characteristic collagenized stroma. The respiratory epithelium (*upper field*) is uninvolved.

**FIGURE 2.30**

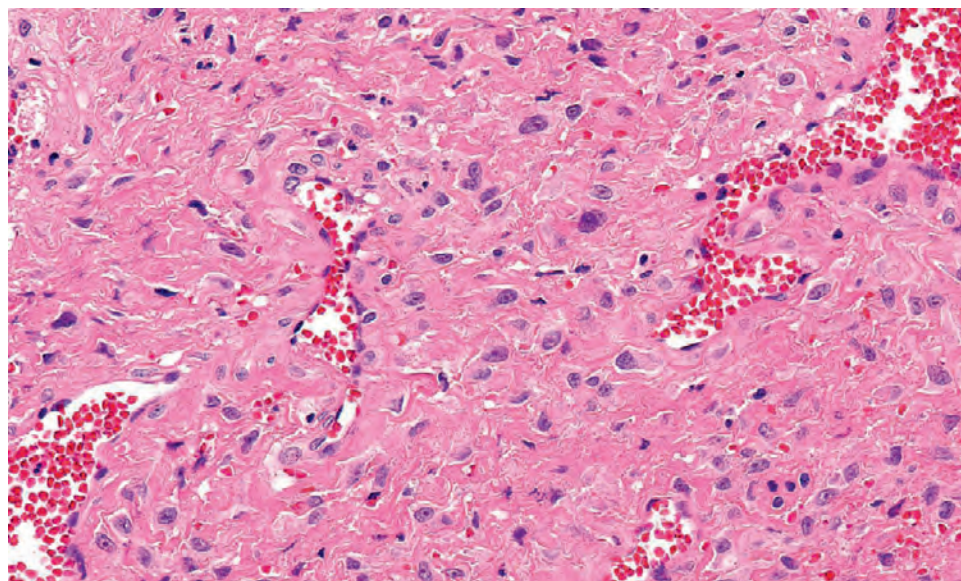
Nasopharyngeal angiofibroma. Note the remarkable variability in the nature of the vessels: muscle-walled vessels, pad-like muscle, and no muscle are all seen in the vessels of this field.

**FIGURE 2.31**

Nasopharyngeal angiofibroma. Thin-walled and thick-walled vessels surrounded by "keloid-like" collagen. Stellate fibroblasts are noted, giving a slightly "atypical" appearance.





**FIGURE 2.32**

Heavily collagenized stroma demonstrates only a few stellate fibroblastic cells in this nasopharyngeal angiofibroma.

blood vessels (Fig. 2.33). Sarcomatous transformation is an exceedingly uncommon event, usually following massive doses of radiation.

### ANCILLARY STUDIES

#### IMMUNOHISTOCHEMICAL FINDINGS

The vessel wall cells are immunoreactive with vimentin and SMA, whereas the stromal cells are immunoreactive with vimentin only, except in areas of increased fibrosis, where focal SMA may be identified. Desmin may be focally immunoreactive in larger vessels at the periphery of the tumor. FVIIIIRAg, CD34, and CD31 highlight the endothelium. Stromal and endothelial cells are usually reactive with androgen receptor (75 %; Fig. 2.33), whereas progesterone receptors are occasionally reactive. Other markers, including nuclear staining for  $\beta$ -catenin (Fig. 2.33), CD117, platelet-derived growth factor B, basic fibroblast growth factor, insulin-like growth factor type II, and nerve growth factor are also reactive. Epstein-Barr virus, S100 protein, and desmin are negative.

Somatic mutations in exon 3 of the  $\beta$ -catenin gene (*CTNNB1*) is present in most tumors, resulting in nuclear localization of  $\beta$ -catenin in > 90 % of cases. Germline mutations of *APC* and *CTNNB1* are not seen in NPA patients, but there are associations with familial adenomatous polyposis.

### DIFFERENTIAL DIAGNOSIS

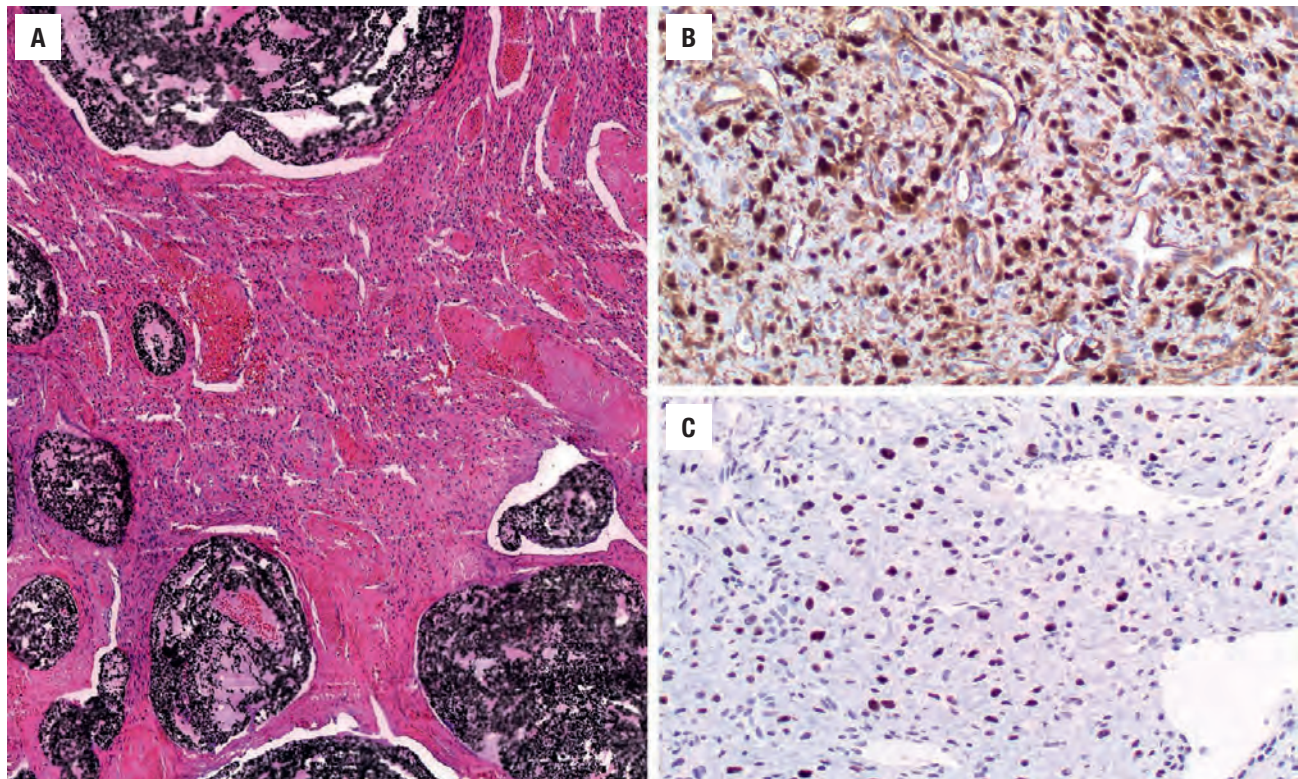
The main differential diagnoses of NPA include LCH, sinonasal polyps (including antrochoanal type), peripheral

nerve sheath tumors, SFT, and desmoid tumor. *LCHs* have a lobular architecture and lack the stromal cells and collagen of angiofibroma. *Polyps* with stromal atypia have inflammatory cells and lack the vascular pattern, most commonly arising from the maxillary antrum (antrochoanal polyps). *Peripheral nerve sheath tumors* have a fascicular architecture and are S100 protein and SOX10 positive. *SFTs* show increased cellularity, do not have the vascular pattern, and strongly express CD34 and STAT6. *Desmoid-type fibromatosis* has long sweeping fascicles and infiltrative borders without the prominent vascularity of NPA but also shows a nuclear  $\beta$ -catenin reaction, although lacking androgen receptor.

### PROGNOSIS AND THERAPY

This benign tumor is characterized by local aggressive growth, with recurrences in up to 25 % of patients, most commonly intracranial, and usually within the first 2 years after diagnosis. Mortality has ranged up to 9 % due to hemorrhage and intracranial extension, but this figure has dropped with improved radiographic and surgical techniques. Patients may be managed with selective angiographic embolization or hormonal therapy prior to definitive surgical resection (usually via a lateral rhinotomy). However, most clinicians do not wish to use hormone manipulation in pubertal males. Spontaneous regression post puberty is reported. Radiation therapy has been successfully implemented to manage large, intracranial, or recurrent tumors, but surgery is still the therapy of choice. The rare case of malignant transformation represents postradiation sarcoma.



**FIGURE 2.33**

(A) Embolic material in this nasopharyngeal angiofibroma. (B) Fibroblasts are strongly reactive with  $\beta$ -catenin, while also strongly reactive with androgen receptor (C).

## ■ ECTOPIC PITUITARY ADENOMA

A benign pituitary gland neoplasm occurring separately from and without involvement of the sella turcica (i.e., with normal anterior pituitary gland) is referred to as ectopic pituitary adenoma. Involvement of the sinonasal tract by pituitary adenomas is encountered more commonly as direct extension of an intrasellar neoplasm. It has been estimated that secondary extension into the sinonasal tract is seen in  $\sim 2\%$  of intrasellar pituitary adenomas (with pituitary adenomas accounting for  $\sim 10\%$  to  $15\%$  of all intracranial tumors). The sphenoid bone and sinus are the most frequent locations for ectopic lesions, although rarely the nasal cavity and nasopharynx may be affected. Embryologic remnants along the migration path of the Rathke pouch (intrasellar) are presumed to be the source of pituitary adenomas.

### CLINICAL FEATURES

Similarly to sellar adenomas, sinonasal pituitary adenomas are more slightly common in females than males (1.3:1), with a mean age at presentation of 54 years (range, 2 to 84 years). Patients usually have nonspecific complaints, such as nasal obstruction, chronic sinusitis, bloody nasal

discharge or epistaxis, headaches, and diplopia or other visual field defects. Approximately 50% of patients affected will have clinical evidence of hormonal hyperactivity, including Cushing syndrome, acromegaly (growth hormone [GH]), amenorrhea (prolactin, luteinizing hormone [LH] or follicle stimulating hormone [FSH]), hyperthyroidism (thyroid stimulating hormone [TSH]), and hirsutism. In endocrinologically silent tumors the diagnosis is often unsuspected before surgery, with  $\sim 10\%$  of patients asymptomatic. The vast majority of tumors involve the sphenoid sinus, although nasopharynx and nasal cavity can rarely be affected. Laboratory tests can be performed to detect hormone production with or without stimulation/suppression testing. In addition, releasing hormones can also be measured.

### RADIOGRAPHIC FEATURES

CT and MRI studies of ectopic pituitary adenomas define the extent and location of the tumor, characterized by the presence of an irregular sphenoidal or nasal mass with bone destruction in the presence of a normal pituitary gland. Thin cuts or high-resolution studies are required to show these findings. There is usually early, intense heterogeneous enhancement. With MR, T1-weighted post contrast will show strong enhancement.

**ECTOPIC PITUITARY ADENOMA—DISEASE FACT SHEET****Definition**

- A benign pituitary neoplasm occurring separately from and without involvement of the sella turcica (a normal anterior pituitary gland)

**Incidence and Location**

- Rare
- Sphenoid sinus most common location followed by nasopharynx and nasal cavity

**Morbidity and Mortality**

- Morbidity associated with hormonal manifestations and local invasion

**Sex and Age Distribution**

- Females > males (1.3:1)
- Mean age, 54 years (range, 2-84 years)

**Clinical Features**

- Nonspecific complaints including nasal obstruction, chronic sinusitis, bloody nasal discharge or epistaxis, headaches, visual field defects (diplopia)
- Approximately 50% have hormone hyperactivity

**Radiographic Features**

- Computed tomography and magnetic resonance define extent and location of tumor
- Sella may be involved by upward extension, although usually normal

**Prognosis and Treatment**

- Excellent prognosis with control of endocrine abnormalities after complete surgical resection
- Recurrence may develop in large tumors
- Surgery is curative, but only if completely removed
- Drugs (dopamine agonists, somatostatin analog) and radiation may be used postoperatively for control

Upward invasion with sellar involvement may be seen in large ectopic adenomas (Fig. 2.34). Tumor size does not seem to correlate with symptom severity.

**PATHOLOGIC FEATURES****MICROSCOPIC FINDINGS**

There is usually a polypoid, solitary mass, on average 3.4 cm in greatest dimension. The surface epithelium is usually intact and uninvolved, subtended by the unencapsulated neoplasms (Fig. 2.35). Delicate fibrovascular septa separate the tumor into solid, organoid, trabecular, festoon, ribbon, or glandular patterns (Fig. 2.36). The neoplasms are histologically identical to their intrasellar counterparts, showing a richly vascularized stroma.

**ECTOPIC PITUITARY ADENOMA—PATHOLOGIC FEATURES****Microscopic Findings**

- Submucosal location of unencapsulated tumor
- Tumors arranged in solid, organoid, and trabecular patterns separated by delicate fibrovascular septa
- Monotonous population of round or polygonal epithelial cells with eosinophilic cytoplasm
- Round or oval nuclei with “salt and pepper” chromatin and inconspicuous or small nucleoli
- Nuclear pleomorphism, mitoses, and necrosis are rare

**Immunohistochemical Findings**

- Strong keratin, chromogranin, synaptophysin, NSE reactivity
- May stain for the hormone peptides, including ACTH, prolactin, TSH, GH, FSH, and LH

**Pathologic Differential Diagnosis**

- Olfactory neuroblastoma, neuroendocrine carcinoma, Ewing/PNET, carcinoma, melanoma, lymphoma

Occasionally, the stroma may be sclerotic or heavily collagenized, obscuring the tumor cells. Most neoplasms are composed of a monotonous population of round to oval epithelial cells with eosinophilic cytoplasm, usually characterized as chromophobe adenomas. Plasmacytoid-appearing cells may be present. Gland-like spaces may be seen, but there is an absence of squamous differentiation. The nuclei are round or oval and contain clumped, neuroendocrine-type chromatin with inconspicuous or small nucleoli (Fig. 2.36). Focal profound pleomorphism may be seen, as with all endocrine-type neoplasms. Mitotic activity is inconspicuous; atypical mitoses, lymphovascular invasion, and necrosis are absent. Calcifications and/or psammoma-like concretions may be found.

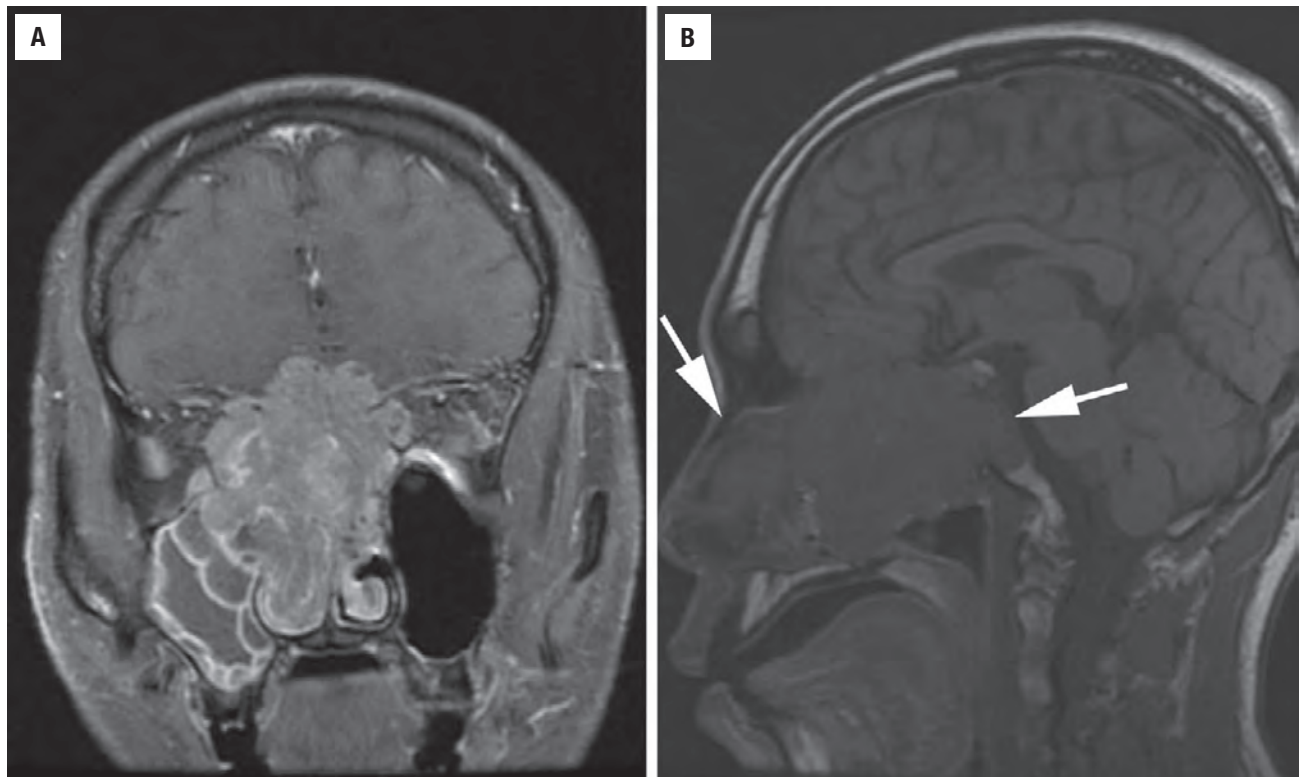
**ANCILLARY STUDIES****ULTRASTRUCTURAL FINDINGS**

The identification of intracellular neurosecretory granules confirms the neuroendocrine nature of the process, with number, variable size and shape, and type of granules specifically associated with hormone production. There is usually abundant and prominent rough endoplasmic reticulum and a large Golgi apparatus.

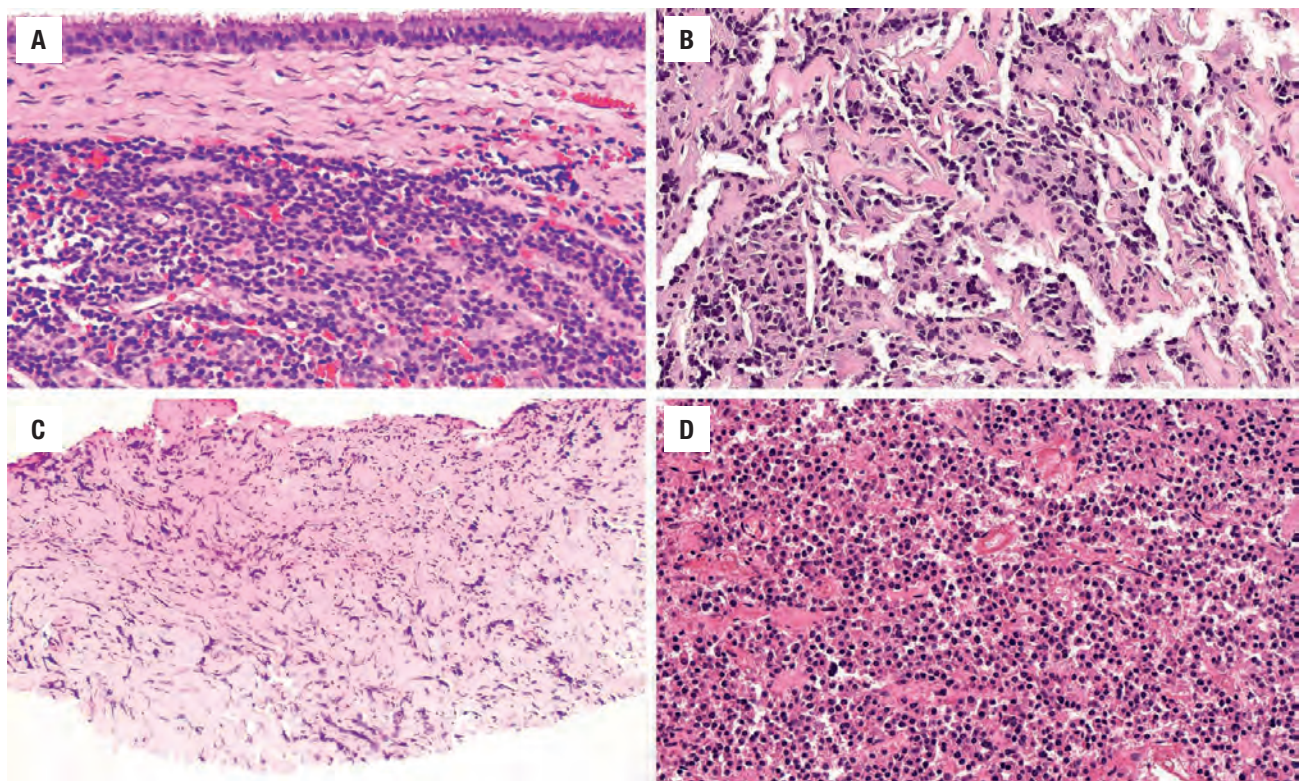
**IMMUNOHISTOCHEMICAL FINDINGS**

The tumor cells usually have strong and diffuse reactions with pan-cytokeratin (85%) and neuroendocrine markers, such as chromogranin, synaptophysin (most sensitive; Fig. 2.37), CD56, and neuron-specific enolase. A paranuclear dot-like reaction may be seen.



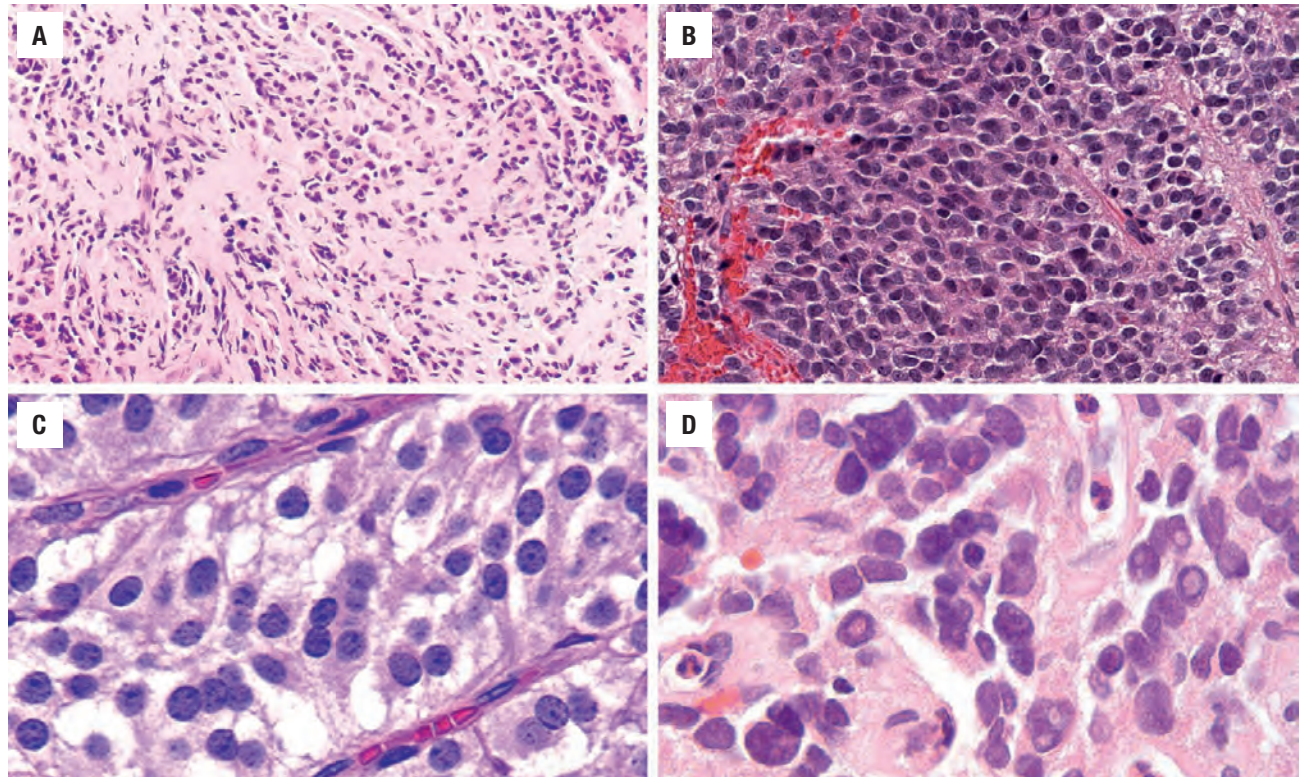
**FIGURE 2.34**

A T1-weighted magnetic resonance image of a large pituitary adenoma involving the sphenoid sinus and sella. There is strong enhancement with contrast (coronal, fat-suppressed post contrast, **A**), and the extent of the mass (*between the arrows*) can be seen on this sagittal image (no contrast, **B**).

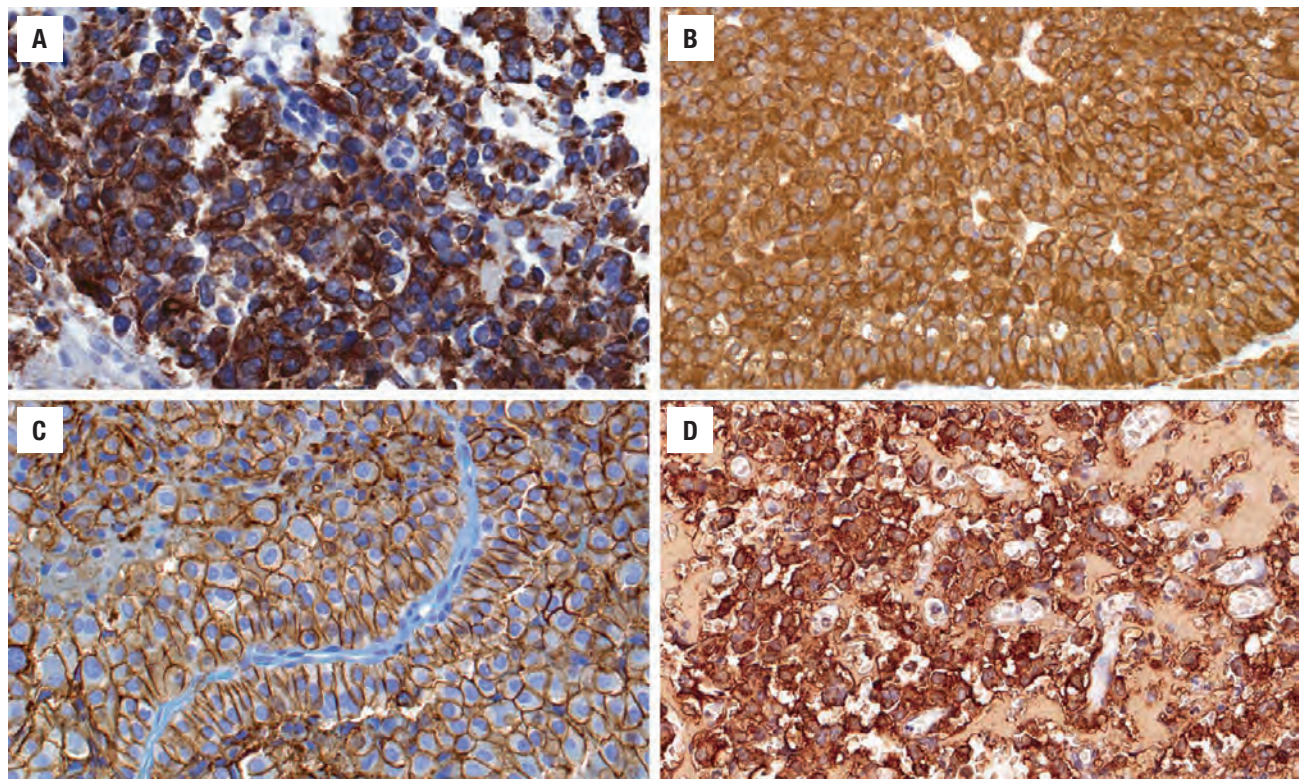
**FIGURE 2.35**

(**A**) Ectopic pituitary adenoma of the sphenoid sinus below the respiratory-ciliated mucosa. (**B**) The neoplastic cells are set within a vascularized stroma. (**C**) Heavy stromal collagen can obscure the neoplastic proliferation. (**D**) The tumor consists of lobules of monotonous epithelial cells with eosinophilic cytoplasm. Note the thin delicate fibrovascular septa.



**FIGURE 2.36**

(A) A discohesive plasmacytoid population is seen in this pituitary adenoma. (B) A greater degree of nuclear hyperchromasia is noted. (C) Delicate, salt and pepper nuclear chromatin distribution. (D) Marked pleomorphism, including intranuclear cytoplasmic inclusions may be seen in pituitary adenoma.

**FIGURE 2.37**

Ectopic pituitary adenoma. (A) Pancytokeratin. (B) Chromogranin. (C) CD56. (D) Strong prolactin reaction. The "neuroendocrine" nature of the tumor can be supported by several immunohistochemistry studies.



Specific hormones may be produced by the tumor and should be sought to confirm the diagnosis. These include adrenocorticotropin (ACTH), prolactin (Fig. 2.37), growth hormone, thyroid-stimulating hormone ( $\beta$ -TSH), pituitary-specific transcription factor (Pit-1),  $\beta$ -subunit and  $\alpha$ -subunit of glycoprotein hormones, soluble fibrin (SF-1), follicle-stimulating hormone, and luteinizing hormone. The most common immunohistochemically expressed hormones are ACTH and prolactin. Prolactin tumors tend to be chromogranin-A negative, but chromogranin-B positive. Similar to intracranial counterparts, the tumors may be monohormonal, plurihormonal, or nonhormonal.

### DIFFERENTIAL DIAGNOSIS

Keen attention to the morphologic and immunophenotypic findings is necessary if the diagnosis is to be correct. Anatomic location is a key tip-off to the diagnosis. The differential diagnosis includes olfactory neuroblastoma, neuroendocrine carcinoma (atypical carcinoid), Ewing sarcoma/primitive neuroectodermal tumor (ES/PNET), carcinoma/NOS (not otherwise specified), melanoma, rhabdomyosarcoma, and lymphoma, whereas any “small round blue cell tumor” would be included in the differential diagnosis. Neuroendocrine findings alone will not separate these first two lesions, but *olfactory neuroblastoma* involves the ethmoid sinus (cribriform plate) and has a neurofibrillary background, rosette formation, and usually S100 protein–supporting reaction and negative keratin expression. *ES/PNET* is uncommon in this location and usually has scant cytoplasm with CD99 and

FLI-1 immunoreactivity and a negative reaction with keratin and chromogranin. The separation with *carcinomas* can be extremely difficult, often resting with the identification of specific pituitary hormones or electron microscopy. *Melanoma* is confirmed by expression of melanocytic markers (HMB45, Melan-A). Rhabdomyosarcoma shows plasmacytoid findings commonly but is reactive with myogenic markers; importantly, synaptophysin and cytokeratins are frequently positive in rhabdomyosarcoma, requiring a panel of antibodies. *Lymphoma* usually has a dispersed architecture and CD45RB immunoreactivity.

### PROGNOSIS AND THERAPY

Although histologically benign, there is a potential for significant morbidity related to their local mass effects (invasion into bone and cranial cavity) and hormonal manifestations. Recurrences develop, especially if the tumors are large and incompletely excised. Most tumors are amenable to complete surgical removal, with follow-up drugs or radiation therapy if necessary to control hormone symptoms. These drugs include dopamine agonists (bromocriptine), somatostatin analogs (octreotide), corticosteroids (hydrocortisone, prednisone), and thyroxine. Stereotactic radioablation is usually used for larger or incompletely removed tumors.

### SUGGESTED READINGS

The complete Suggested Readings list is available online at [ExpertConsult.com](http://ExpertConsult.com).

## SUGGESTED READINGS

## Sinonasal Papillomas

- Altavilla G, et al. Expression of p53, p16INK4A, pRb, p21WAF1/CIP1, p27KIP1, cyclin D1, Ki-67 and HPV DNA in sinonasal endophytic Schneiderian (inverted) papilloma. *Acta Otolaryngol.* 2009;129(11):1242–1249.
- Barnes L, et al. Oncocytic Schneiderian papilloma: a reappraisal of cylindrical cell papilloma of the sinonasal tract. *Hum Pathol.* 1984;15:344–351.
- Buchwald C, et al. Sinonasal papillomas: a report of 82 cases in Copenhagen County, including a longitudinal epidemiological and clinical study. *Laryngoscope.* 1995;105:72–79.
- Carlson ML, et al. Inverting papilloma of the temporal bone: report of four new cases and systematic review of the literature. *Laryngoscope.* 2015;125(11):2576–2583.
- Christensen WN, et al. Schneiderian papillomas: a clinicopathologic study of 67 cases. *Hum Pathol.* 1986;17(4):393–400.
- Healy DY Jr, et al. Surgical risk factors for recurrence of inverted papilloma. *Laryngoscope.* 2016;126(4):796–801.
- Hunt JL, et al. Sinonasal papillomas. In: El-Naggar AK, Chan JKC, Grandis JR, Takata T, Slootweg PJ, eds. *Classification of Head and Neck Tumours*. 4th ed. World Health Organization Classification of Tumors. Lyon, France: IARC Press; 2017:28–31.
- Hyams VJ. Papillomas of the nasal cavity and paranasal sinuses. A clinicopathologic study of 315 cases. *Ann Otol Rhinol Laryngol.* 1971;80:192–206.
- Kapadia SB, et al. Carcinoma ex oncocytic Schneiderian (cylindrical cell) papilloma. *Am J Otolaryngol.* 1993;14:332–338.
- Karligkiotis A, et al. Oncocytic Schneiderian papillomas: clinical behavior and outcomes of the endoscopic endonasal approach in 33 cases. *Head Neck.* 2014;36(5):624–630.
- Lawson W, et al. The role of the human papillomavirus in the pathogenesis of Schneiderian inverted papillomas: an analytic overview of the evidence. *Head Neck Pathol.* 2008;2(2):49–59.
- Lawson W, et al. Treatment outcomes in the management of inverted papilloma: an analysis of 160 cases. *Laryngoscope.* 2003;113:1548–1556.
- Michaels L, et al. Histogenesis of papillomas of the nose and paranasal sinuses. *Arch Pathol Lab Med.* 1995;119:821–826.
- Nudell J, et al. Carcinoma ex-Schneiderian papilloma (malignant transformation): a clinicopathologic and immunophenotypic study of 20 cases combined with a comprehensive review of the literature. *Head Neck Pathol.* 2014;8(3):269–286.
- Oikawa K, et al. Clinical and pathological analysis of recurrent inverted papilloma. *Ann Otol Rhinol Laryngol.* 2007;116(4):297–303.
- Perez-Ordoñez B. Hamartomas, papillomas and adenocarcinomas of the sinonasal tract and nasopharynx. *J Clin Pathol.* 2009;62(12):1085–1095.
- Schwerer MJ, et al. Coexpression of cytokeratins typical for columnar and squamous differentiation in sinonasal inverted papillomas. *Am J Clin Pathol.* 2001;115:747–754.
- Shah AA, et al. HPV DNA is associated with a subset of Schneiderian papillomas but does not correlate with p16(INK4a) immunoreactivity. *Head Neck Pathol.* 2010;4(2):106–112.
- Stoddard DG Jr, et al. Transcriptional activity of HPV in inverted papilloma demonstrated by in situ hybridization for E6/E7 mRNA. *Otolaryngol Head Neck Surg.* 2015;152(4):752–758.
- Syrjänen K, et al. Detection of human papillomavirus in sinonasal papillomas: systematic review and meta-analysis. *Laryngoscope.* 2013;123(1):181–192.
- Thompson LD. Schneiderian papilloma of the sinonasal tract. *Ear Nose Throat J.* 2015;94(4–5):146–148.
- Udager AM, et al. Activating KRAS mutations are characteristic of oncocytic sinonasal papilloma and associated sinonasal squamous cell carcinoma. *J Pathol.* 2016;239(4):394–398.
- Vorasubin N, et al. Schneiderian papillomas: comparative review of exophytic, oncocytic, and inverted types. *Am J Rhinol Allergy.* 2013;27(4):287–292.
- Vrabec DP. The inverted Schneiderian papilloma: a 25-year study. *Laryngoscope.* 1994;104:582–605.
- Wu HH, et al. Fascin over expression is associated with dysplastic changes in sinonasal inverted papillomas: a study of 47 cases. *Head Neck Pathol.* 2009;3(3):212–216.

## Lobular Capillary Hemangioma (Pyogenic Granuloma)

- Delbrouck C, et al. Lobular capillary haemangioma of the nasal cavity during pregnancy. *J Laryngol Otol.* 2011;125(9):973–977.
- Fu YS, et al. Non-epithelial tumors of the nasal cavity, paranasal sinuses, and nasopharynx: a clinicopathologic study. I. General features and vascular tumors. *Cancer.* 1974;33:1275–1288.
- Heffner DK. Problems in pediatric otorhinolaryngic pathology. II. Vascular tumors and lesions of the sinonasal tract and nasopharynx. *Int J Pediatr Otorhinolaryngol.* 1983;5:125–138.
- Kapadia SB, et al. Pitfalls in the histopathologic diagnosis of pyogenic granuloma. *Eur Arch Otorhinolaryngol.* 1992;249(4):195–200.
- Mills SE, et al. Lobular capillary hemangioma: the underlying lesion of pyogenic granuloma. A study of 73 cases from the oral and nasal mucous membranes. *Am J Surg Pathol.* 1980;4:470–479.
- Puxeddu R, et al. Lobular capillary hemangioma of the nasal cavity: a retrospective study on 40 patients. *Am J Rhinol.* 2006;20(4):480–484.
- Smith SC, et al. Sinonasal lobular capillary hemangioma: a clinicopathologic study of 34 cases characterizing potential for local recurrence. *Head Neck Pathol.* 2013;7(2):129–134.
- Thompson LDR, et al. Haemangioma. In: El-Naggar AK, Chan JKC, Grandis JR, Takata T, Slootweg PJ, eds. *Classification of Head and Neck Tumours*. 4th ed. World Health Organization Classification of Tumors. Lyon, France: IARC Press; 2017:47–48.
- Truss L, et al. Deletion (21)(q21.2q22.12) as a sole clonal cytogenetic abnormality in a lobular capillary hemangioma of the nasal cavity. *Cancer Genet Cytogenet.* 2006;170(1):69–70.
- Yang BT, et al. Routine and dynamic MR imaging study of lobular capillary hemangioma of the nasal cavity with comparison to inverting papilloma. *AJNR Am J Neuroradiol.* 2013;34(11):2202–2207.

## Meningioma

- Bujko M, et al. EGFR, PIK3CA, KRAS and BRAF mutations in meningiomas. *Oncol Lett.* 2014;7(6):2019–2022.
- Gusella JF, et al. Merlin: the neurofibromatosis 2 tumor suppressor. *Biochim Biophys Acta.* 1999;1423(2):M29–M36.
- Iaconetta G, et al. Extracranial primary and secondary meningiomas. *Int J Oral Maxillofac Surg.* 2012;41(2):211–217.
- Mnejja M, et al. Primary sinonasal meningioma. *Eur Ann Otorhinolaryngol Head Neck Dis.* 2012;129(1):47–50.
- Perry A, et al. “Malignancy” in meningiomas: a clinicopathologic study of 116 patients, with grading implications. *Cancer.* 1999;85(9):2046–2056.
- Perry A, et al. Meningioma grading: an analysis of histologic parameters. *Am J Surg Pathol.* 1997;21(12):1455–1465.
- Perzin KH, et al. Nonepithelial tumors of the nasal cavity, paranasal sinuses, and nasopharynx. A clinicopathologic study. XIII: Meningiomas. *Cancer.* 1984;54(9):1860–1869.
- Ro JY, et al. Meningioma. In: El-Naggar AK, Chan JKC, Grandis JR, Takata T, Slootweg PJ, eds. *Classification of Head and Neck Tumours*. 4th ed. World Health Organization Classification of Tumors. Lyon, France: IARC Press; 2017:50–51.
- Rushing EJ, et al. Primary extracranial meningiomas: an analysis of 146 cases. *Head Neck Pathol.* 2009;3(2):116–130.
- Shibuya M. Pathology and molecular genetics of meningioma: recent advances. *Neurol Med Chir (Tokyo).* 2015;55(1):14–27.
- Thompson LD, et al. Extracranial sinonasal tract meningiomas: a clinicopathologic study of 30 cases with a review of the literature. *Am J Surg Pathol.* 2000;24(5):640–650.
- Torres-Martín M, et al. Whole exome sequencing in a case of sporadic multiple meningioma reveals shared NF2, FAM109B, and TPRXL mutations, together with unique SMARCB1 alterations in a subset of tumor nodules. *Cancer Genet.* 2015;208(6):327–332.

## Glomangiopericytoma (Hemangiopericytoma)

- Brandwein-Gensler M, et al. Striking pathology gold: a singular experience with daily reverberations: sinonasal hemangiopericytoma (glomangiopericytoma) and oncogenic osteomalacia. *Head Neck Pathol.* 2012;6(1):64–74.
- Compagno J, et al. Hemangiopericytoma-like intranasal tumors. A clinicopathologic study of 23 cases. *Am J Clin Pathol.* 1976;66:672–683.



3. Conrad GR, et al. FDG PET/CT findings of a glomangiopericytoma. *Clin Nucl Med*. 2011;36(6):462–464.
4. Dodwala MQ, et al. Management of sinonasal hemangiopericytomas: a systematic review. *Int Forum Allergy Rhinol*. 2013;3(7):581–587.
5. El-Naggar AK, et al. Sinonasal hemangiopericytomas. A clinicopathologic and DNA content study. *Arch Otolaryngol Head Neck Surg*. 1992;118:134–137.
6. Folpe AL, et al. Most osteomalacia-associated mesenchymal tumors are a single histopathologic entity: an analysis of 32 cases and a comprehensive review of the literature. *Am J Surg Pathol*. 2004;28(1):1–30.
7. Haller F, et al. Recurrent mutations within the amino-terminal region of  $\beta$ -catenin are probable key molecular driver events in sinonasal hemangiopericytoma. *Am J Pathol*. 2015;185(2):563–571.
8. Lasota J, et al. Nuclear expression and gain-of-function  $\beta$ -catenin mutation in glomangiopericytoma (sinonasal-type hemangiopericytoma): insight into pathogenesis and a diagnostic marker. *Mod Pathol*. 2015;28(5):715–720.
9. Morrison EJ, et al. Glomangiopericytoma: overview and role for open surgery. *ANZ J Surg*. 2012;82(9):648–650.
10. Thompson LD, et al. Sinonasal-type hemangiopericytoma: a clinicopathologic and immunophenotypic analysis of 104 cases showing perivascular myoid differentiation. *Am J Surg Pathol*. 2003;27:737–749.
11. Thompson LDR, et al. Sinonasal glomangiopericytoma. In: El-Naggar AK, Chan JKC, Grandis JR, Takata T, Slootweg PJ, eds. *Classification of Head and Neck Tumours*. 4th ed. World Health Organization Classification of Tumors. Lyon, France: IARC Press; 2017:44–45.
9. Makek MS, et al. Malignant transformation of a nasopharyngeal angiofibroma. *Laryngoscope*. 1989;99(10 Pt 1):1088–1092.
10. Maniglia MP, et al. Molecular pathogenesis of juvenile nasopharyngeal angiofibroma in Brazilian patients. *Pediatr Hematol Oncol*. 2013;30(7):616–622.
11. Neel HB, et al. Juvenile angiofibroma. Review of 120 cases. *Am J Surg*. 1973;126:547–556.
12. Pauli J, et al. Juvenile nasopharyngeal angiofibroma: an immunohistochemical characterisation of the stromal cell. *Pathology*. 2008;40(4):396–400.
13. Ponti G, et al. Wnt pathway, angiogenetic and hormonal markers in sporadic and familial adenomatous polyposis-associated juvenile nasopharyngeal angiofibromas (JNA). *Appl Immunohistochem Mol Morphol*. 2008;16(2):173–178.
14. Prasad ML, et al. Nasopharyngeal angiofibroma. In: El-Naggar AK, Chan JKC, Grandis JR, Takata T, Slootweg PJ, eds. *Classification of Head and Neck Tumours*. 4th ed. World Health Organization Classification of Tumors. Lyon, France: IARC Press; 2017:74–75.
15. Renkonen S, et al. Systems-level analysis of clinically different phenotypes of juvenile nasopharyngeal angiofibromas. *Laryngoscope*. 2012;122(12):2728–2735.
16. Sánchez-Romero C, et al. Nasopharyngeal Angiofibroma: A Clinical, Histopathological and Immunohistochemical Study of 42 Cases with Emphasis on Stromal Features. *Head Neck Pathol*. 2017 May 15 (PMID: 28508272).

### Nasopharyngeal Angiofibroma

1. Abraham SC, et al. Frequent beta-catenin mutations in juvenile nasopharyngeal angiofibromas. *Am J Pathol*. 2001;158:1073–1078.
2. Alshaikh NA, et al. Juvenile nasopharyngeal angiofibroma staging: an overview. *Ear Nose Throat J*. 2015;94(6):E12–E22.
3. Boghani Z, Husain Q, Kanumuri VV, et al. Juvenile nasopharyngeal angiofibroma: a systematic review and comparison of endoscopic, endoscopic-assisted, and open resection in 1047 cases. *Laryngoscope*. 2013;123(4):859–869.
4. Carlos R, et al. Epstein-Barr virus and human herpes virus-8 are not associated with juvenile nasopharyngeal angiofibroma. *Head Neck Pathol*. 2008;2(3):145–149.
5. Coutinho-Camillo CM, et al. Genetic alterations in juvenile nasopharyngeal angiofibromas. *Head Neck*. 2008;30(3):390–400.
6. Glad H, et al. Juvenile nasopharyngeal angiofibromas in Denmark 1981–2003: diagnosis, incidence, and treatment. *Acta Otolaryngol*. 2007;127(3):292–299.
7. Khoeir N, et al. Exclusive endoscopic resection of juvenile nasopharyngeal angiofibroma: a systematic review of the literature. *Otolaryngol Head Neck Surg*. 2014;150(3):350–358.
8. Liu Z, et al. Hormonal receptors and vascular endothelial growth factor in juvenile nasopharyngeal angiofibroma: immunohistochemical and tissue microarray analysis. *Acta Otolaryngol*. 2015;135(1):51–57.

### Pituitary Adenoma

1. Coire CI, et al. Cushing's syndrome from an ectopic pituitary adenoma with peliosis: a histological, immunohistochemical, and ultrastructural study and review of the literature. *Endocr Pathol*. 1997;8:65–74.
2. Hori A, et al. Pharyngeal pituitary: development, malformation, and tumorigenesis. *Acta Neuropathol*. 1999;98(3):262–272.
3. Hosaka N, et al. Ectopic pituitary adenoma with malignant transformation. *Am J Surg Pathol*. 2002;26:1078–1082.
4. Katabi N, et al. Ectopic pituitary adenoma. In: El-Naggar AK, Chan JKC, Grandis JR, Takata T, Slootweg PJ, eds. *Classification of Head and Neck Tumours*. 4th ed. World Health Organization Classification of Tumors. Lyon, France: IARC Press; 2017:72–73.
5. Langford L, et al. Pituitary gland involvement of the sinonasal tract. *Ann Otol Rhinol Laryngol*. 1995;104:167–169.
6. Lloyd RV, et al. Ectopic pituitary adenomas with normal anterior pituitary glands. *Am J Surg Pathol*. 1986;10:546–552.
7. Luk SC, et al. Pituitary adenoma presenting as sinonasal tumor: pitfalls in diagnosis. *Hum Pathol*. 1996;27:605–609.
8. Thompson LD, et al. Ectopic sphenoid sinus pituitary adenoma (ESSPA) with normal anterior pituitary gland: a clinicopathologic and immunophenotypic study of 32 cases with a comprehensive review of the English literature. *Head Neck Pathol*. 2012;6(1):75–100.
9. Wick MR, et al. Ectopic neural and neuroendocrine neoplasms. *Semin Diagn Pathol*. 2003;20(4):305–323.
10. Yang BT, et al. Sphenoid sinus ectopic pituitary adenomas: CT and MRI findings. *Br J Radiol*. 2010;83(987):218–224.

# Malignant Neoplasms of the Nasal Cavity, Paranasal Sinuses, and Nasopharynx

■ Justin A. Bishop ■ Lester D.R. Thompson

Malignant tumors of the sinonasal tract (SNT) are rare, comprising less than 1% of all neoplasms and about 3% of those of the upper aerodigestive tract. Squamous cell carcinoma (SCC) and adenocarcinoma are strongly associated with environmental factors, including the use of tobacco and alcohol and occupational exposures, such as heavy metal particles (nickel, chromium) and the leather, textile, furniture, and wood industries.

SNT malignancies most commonly affect the maxillary sinus (~60%), followed by the nasal cavity (~22%), ethmoid sinus (~15%), and frontal and sphenoid sinuses (~3%). SNT tumors are diverse, with the majority composed of SCC and its variants (55%), followed by nonepithelial neoplasms (20%), glandular tumors (15%), undifferentiated carcinoma (7%), and miscellaneous tumors (3%).

Carcinoma of the nasopharynx differs in many aspects from that of the nasal cavity and paranasal sinuses and is discussed as a distinct entity in this chapter.

The clinical presentations, radiologic features, and pattern of tumor spread for SCC, adenocarcinoma, and most of the other malignant neoplasms of the SNT are similar. These features are discussed in detail under the section on SCC and not repeated elsewhere. The gross appearance of SNT and nasopharyngeal malignancies has limited value in aiding diagnosis because the initial diagnosis depends on tissue obtained by endoscopy or polypectomy. With the exception of nasopharyngeal carcinoma (NPC), malignant lymphoma, and rhabdomyosarcoma (RMS), the treatment of choice for most SNT malignancies is surgical resection with clear margins. Here treatment for SCC is used as a model.

## ■ SQUAMOUS CELL CARCINOMA

SCC is a malignant epithelial neoplasm arising from surface epithelium with squamous cell differentiation. There are two major histologic subtypes: keratinizing

and nonkeratinizing (also known as transitional cell or cylindrical cell carcinoma). All SCC variants can be encountered, although less frequently in the SNT than other head and neck sites. Up to 20% to 30% of SNT SCCs harbor high-risk human papillomavirus (HPV), particularly the nonkeratinizing subtype. Sinonasal papilloma, inverted type specifically, is a precursor lesion in a subset of SCC.

## CLINICAL FEATURES

SCC represents approximately 3% of all head and neck malignancies but is the most common malignant epithelial tumor of the SNT. SCC has a male predilection (2:1), with a peak incidence in the 6th to 7th decade. The location, in order of decreasing frequency, is the maxillary sinus, nasal cavity (usually lateral wall), ethmoid sinus, frontal sinus, and sphenoid sinus. Early diagnosis is difficult because symptoms and signs are nonspecific and closely resemble those of chronic sinusitis, allergic reactions, and nasal polyposis. Initial symptoms are related to the effects of the mass causing unilateral nasal obstruction. Secondary infection is common, giving rise to a mucoid or purulent rhinorrhea. Epistaxis develops when the mucosa is ulcerated or tumor extends into the sinus wall. Tumors involving the ethmoid, maxillary, or frontal sinuses may cause proptosis, restriction of eye movements, diplopia, or loss of vision. Epiphora results from lacrimal sac or duct obstruction by the tumor. Compression of the nerve at the primary site or perineural space invasion can compromise the function of cranial nerves, resulting in numbness, paresthesia, or pain. Teeth loosening or fistula may be identified within the oral cavity. A mass or discolored lesion may be visualized endoscopically and biopsied.

Late manifestations include facial swelling and cheek paresthesia resulting from anterior maxillary extension into the soft tissue and infraorbital nerve involvement, respectively. Inferior extension into the oral cavity forms a visible mass in the palate or alveolar ridge. Posterior



### SQUAMOUS CELL CARCINOMA—DISEASE FACT SHEET

#### Definition

- Malignant neoplasm of squamous epithelial cells

#### Incidence and Location

- Most common malignant neoplasm of sinonasal tract representing ~60%-70% of sinonasal tract carcinomas
- Paranasal sinuses: maxillary sinus > ethmoid sinus
- Nasal cavity: lateral nasal wall and nasal septum

#### Morbidity and Mortality

- Mortality is 30%-40% at 5 years

#### Sex and Age Distribution

- Males > females (2:1)
- 6th to 7th decade

#### Clinical Features

- Nasal obstruction, nasal discharge, epistaxis, pain
- Orbital and eye symptoms and signs
- Cranial nerve involvement
- Mass in the nasal cavity

#### Radiographic Features

- CT and MRI complement each other
- MRI separates inflammatory from neoplastic areas and shows relationship to soft tissue
- CT is best for highlighting bony destruction and yielding extent, location, and size of tumor

#### Prognosis and Treatment

##### Nasal Cavity

- Prognosis if confined: 80% 5-year survival
- Surgery, with postoperative radiotherapy (T3 and T4)

##### Paranasal Sinuses

- Prognosis less favorable than nasal cavity, with common recurrences extending into cranial vault
- Cervical lymph node metastasis in ~20%
- Radical en bloc resection, if possible, with postoperative radiotherapy and/or chemotherapy (preoperatively or postoperatively)

extension can cause trismus from pterygoid muscle invasion. Ear symptoms suggest possible involvement of the nasopharynx, eustachian tube, and pterygoid plates. Upward extension into the skull base may lead to cranial nerve involvement and invasion of the dura. In the initial workup, it is rare to find cervical lymph node metastasis.

### RADIOGRAPHIC FEATURES

Computed tomography (CT) and magnetic resonance imaging (MRI) have largely replaced conventional radiographs in imaging SNT disease and are indispensable in evaluating the extent of disease. CT and MRI complement each other, helping to separate inflammatory disorders

### SQUAMOUS CELL CARCINOMA—PATHOLOGIC FEATURES

#### Gross Findings

- Exophytic, friable, necrotic, ulcerated mass
- Local soft tissue infiltration and bony destruction

#### Microscopic Findings

##### Nasal Cavity

- Usually keratinizing (80%-85%)
- Squamous pearls, intercellular bridges, hyperchromatic nuclei

##### Paranasal Sinus

- Usually nonkeratinizing
- Spindle cell, papillary, endophytic, verrucous types recognized

#### Immunohistochemical Findings

- Positive: p63, p40, CK5/6, CK8, CK13
- Negative: CK10

#### Pathologic Differential Diagnosis

- Pseudoepitheliomatous hyperplasia, sinonasal papilloma, squamous papilloma, nasopharyngeal carcinoma, oropharyngeal carcinoma, NUT carcinoma

and benign and malignant neoplasms and to provide pretreatment information, including location, size, extent, local invasion, and regional and distant metastasis. Of particular interest is tumor extension into the pterygopalatine and infratemporal fossae and tumor relationship to the blood vessels (especially the internal carotid artery and cavernous sinus), nerves, and cranial cavity. CT best highlights bony structures, with bony destruction and soft tissue invasion usually indicative of an aggressive lesion. MRI is superior to CT in its ability to delineate sinus tumors from inflammatory disease, and it can better delineate tumor from the adjacent soft tissues. Using MRI, inflamed mucosa, polyps, and noninspissated secretions with a high water content have high signal intensity on T2-weighted images. In contrast, cellular paranasal neoplasms have lesser amounts of water and demonstrate intermediate signal intensities on T2-weighted images. Perineural spread is best demonstrated by a gadolinium-contrasted MRI and T1-weighted images with fat suppression. CT helps detect cervical lymph node metastasis, especially when there are multiple clustered lymph nodes exceeding 1.0 cm. The status of cervical lymph nodes is best determined by positron emission tomography (PET) using <sup>18</sup>fluorodeoxyglucose (<sup>18</sup>FDG-PET) to detect tissue with increased metabolism (i.e., nodal metastasis).

### PATHOLOGIC FEATURES

#### GROSS FINDINGS

Nasal tumors are usually exophytic/fungating and prone to become friable, necrotic, and ulcerated with

increasing tumor size. Sinus tumors may be well circumscribed, filling the sinus cavity in an expansile fashion with erosion of the bone wall, while others are more destructive, inverted, necrotic, and hemorrhagic.

### MICROSCOPIC FINDINGS

In general, SCC of the nasal cavity is well differentiated and keratinizing, whereas sinus counterparts are nonkeratinizing and moderately or poorly differentiated.

As previously mentioned, SCC of the SNT is subclassified by cell type into keratinizing (80% to 85%) and nonkeratinizing (15% to 20%) subtypes. Keratinizing SCCs of the SNT are histologically indistinguishable from their counterparts of other head and neck sites, such as larynx and oral cavity. Dysplasia of the adjacent or overlying surface epithelium may be encountered. Tumor cells exhibit keratinization, intercellular bridges, dyskeratosis, and squamous “pearls” and usually have enlarged, hyperchromatic nuclei, with a variable degree of nuclear anaplasia (Fig. 3.1). Mitotic figures are usually easy to find and include atypical forms. Stromal invasion by irregular nests and cords of cells in a desmoplastic stroma is often associated with a chronic inflammatory response. However, in superficial biopsies, the only sign of stromal invasion may be in the form of single cells becoming isolated from the base of rete pegs or the tip of tongue-like protrusions. As in other sites, keratinizing SCCs of the SNT are graded as well, moderately, or poorly differentiated.

The nonkeratinizing subtype of SCC forms anastomosing ribbons and nests of variable sizes, frequently with

a smooth stromal interface and a pushing border with minimal desmoplasia (Fig. 3.2). There is a loss of polarity. Individual tumor cells reveal uniform large, round, or oval nuclei with prominent nucleoli. The cytoplasm varies from pale acidophilic to amphophilic to vacuolated. The cells may have distinct borders. Occasionally individual cell keratinization may be identified. Papillary features (malignant epithelium lining fibrovascular cores) are often encountered within the invasive or surface components (Fig. 3.2). Swirling or spindled tumor cells may be seen; when predominant, they are diagnosed as spindle cell SCC. Because of the smooth stromal interface and lack of significant desmoplasia, it is often difficult to recognize nonkeratinizing SCC as invasive, especially in superficial or small biopsies (Fig. 3.2). In these cases, correlation with radiologic evidence of local destruction confirms the invasive nature of the malignancy. Similarly, biopsies of verrucous squamous carcinoma and papillary squamous carcinoma are prone to be under diagnosed without including the base of the lesion. Variants of SCC, such as verrucous carcinoma and basaloid type, are rare in the SNT.

*HPV-related multiphenotypic sinonasal carcinoma (formerly HPV-related carcinoma with adenoid cystic-like features)* is a newly described form of SNT carcinoma that is provisionally listed in the 2017 World Health Organization (WHO) classification of head and neck tumors as a subtype of nonkeratinizing SCC. HPV-related multiphenotypic sinonasal carcinoma closely resembles salivary-type carcinomas, especially solid adenoid cystic carcinoma (ACC), with predominantly solid nests but also foci of cribriform growth and a biphasic population of ducts and basaloid myoepithelial cells. Unlike true

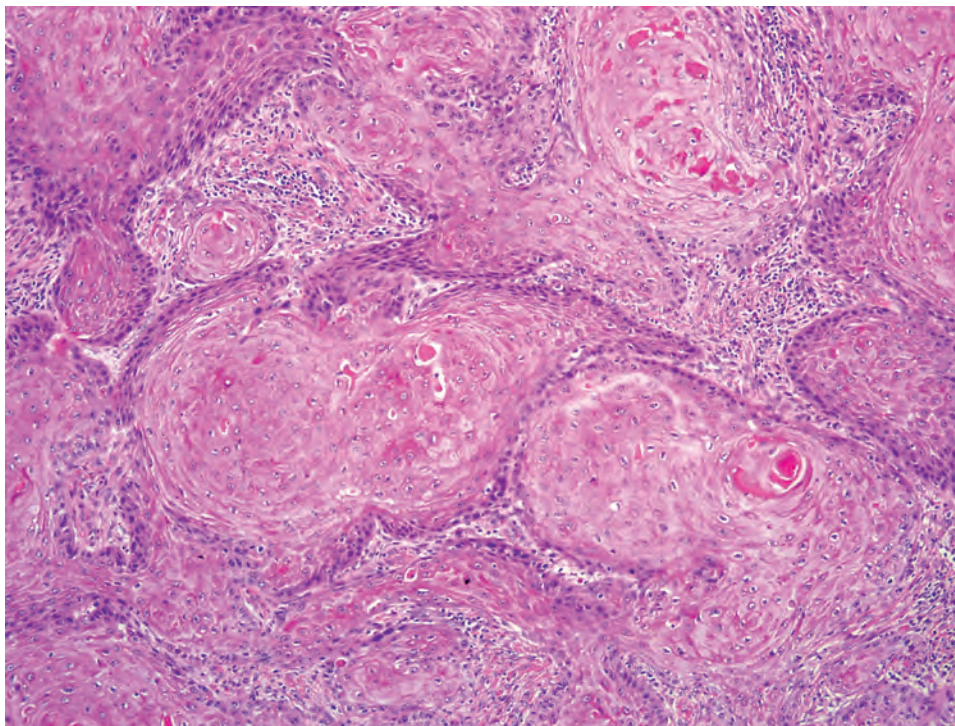


**FIGURE 3.1**

Sinonasal keratinizing squamous cell carcinomas are typically well differentiated, with angulated nests demonstrating overt keratinization and inducing a desmoplastic stromal reaction.



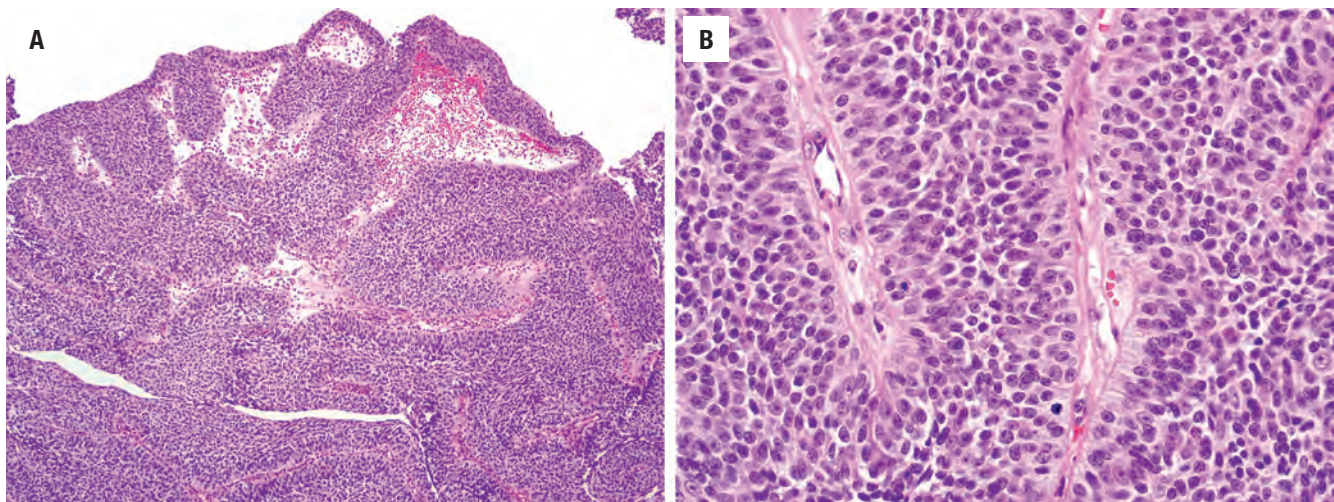


**FIGURE 3.2**

(A) Sinonasal nonkeratinizing squamous cell carcinoma consists of anastomosing ribbons of squamoid cells invading the stroma with a pushing edge. The surface demonstrates papillary features. (B) Nonkeratinizing primitive squamoid cells with nuclear atypia, numerous mitotic figures, and peripheral palisading of tumor nuclei. The stromal interface is smooth, and there is no desmoplasia.

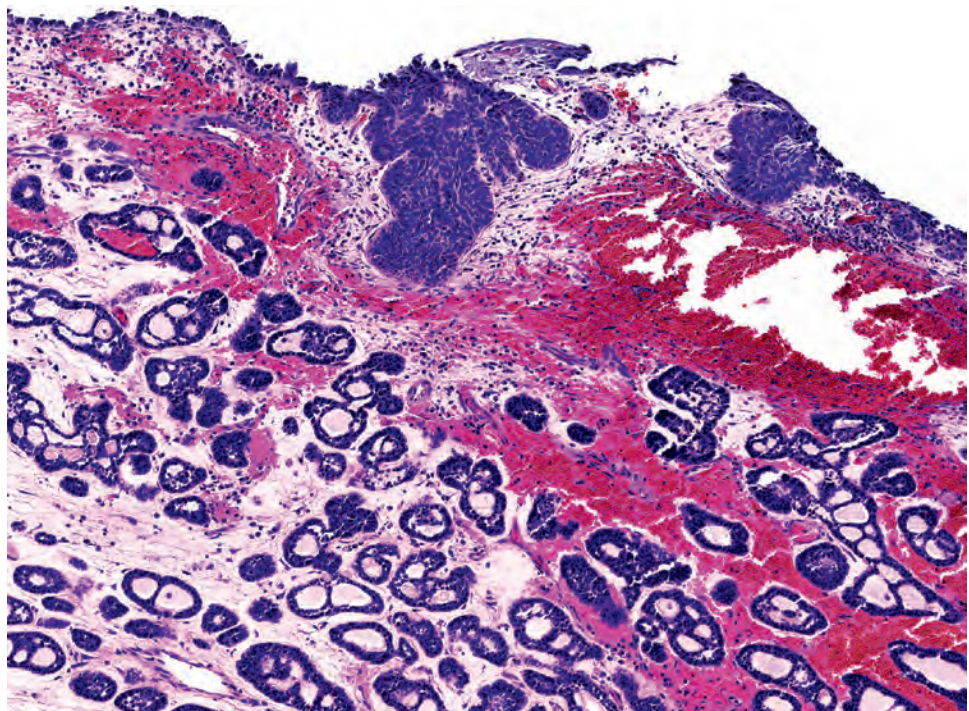


**FIGURE 3.3**

HPV-related multiphenotypic sinonasal carcinoma closely resembles adenoid cystic carcinoma as it invades as cribriform structures (*bottom*); but unlike a true adenoid cystic carcinoma, it also often shows squamous dysplasia of the surface epithelium (*top*).

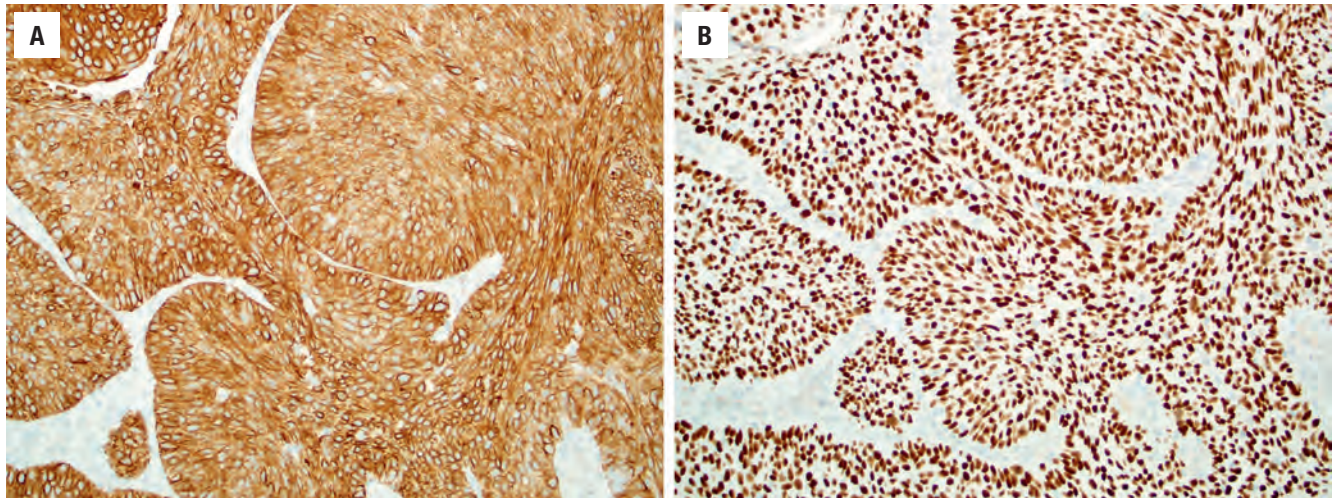
ACC, however, HPV-related multiphenotypic sinonasal carcinoma usually demonstrates foci of squamous dysplasia of the overlying surface epithelium (Fig. 3.3).

#### ANCILLARY STUDIES

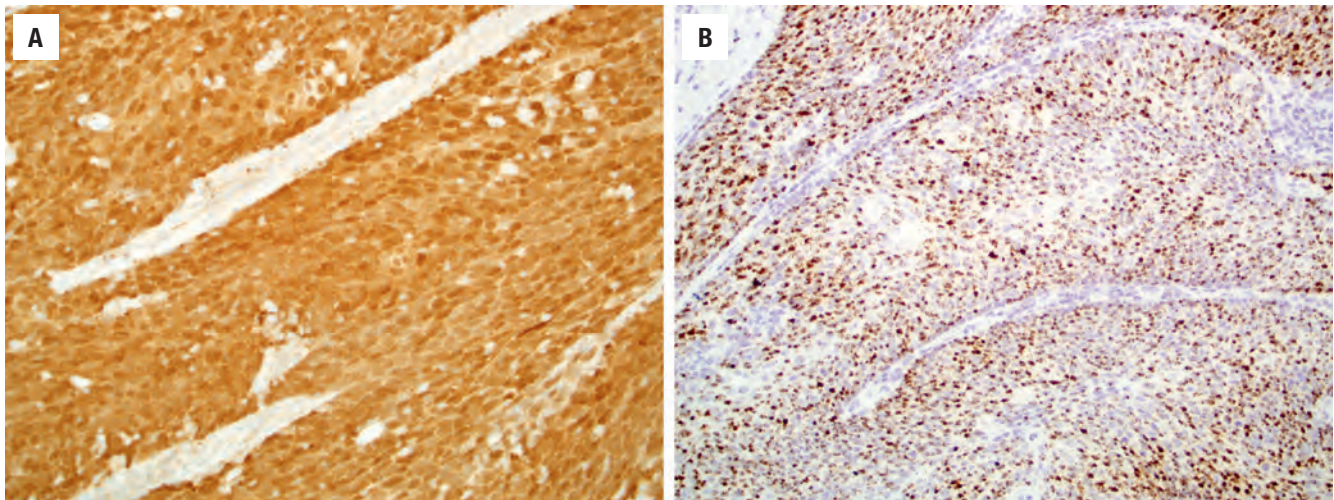
The keratinizing and nonkeratinizing subtypes have similar immunohistochemical staining patterns: cells are

diffusely immunoreactive with CK5/6 (Fig. 3.4), p63, p40 (Fig. 3.4), CK8, and CK13 but negative with CK10. Approximately 30 % to 50 % of nonkeratinizing SCCs (but only rare keratinizing SCCs) of the SNT harbor high-risk HPV (Fig. 3.5). HPV-related multiphenotypic sinonasal carcinoma has two cell populations: myoepithelial cells that are positive for p40, p63, actin, calponin, and S100 and ducts that are positive for c-kit (Fig. 3.6). HPV-related multiphenotypic sinonasal carcinoma is p16- and HPV-positive (usually the rare type 33) (Fig. 3.6).



**FIGURE 3.4**

Sinonasal squamous cell carcinomas are diffusely positive for CK5/6 (**A**) and p40 (**B**). These findings are helpful in the differential of other basaloid sinonasal neoplasms.

**FIGURE 3.5**

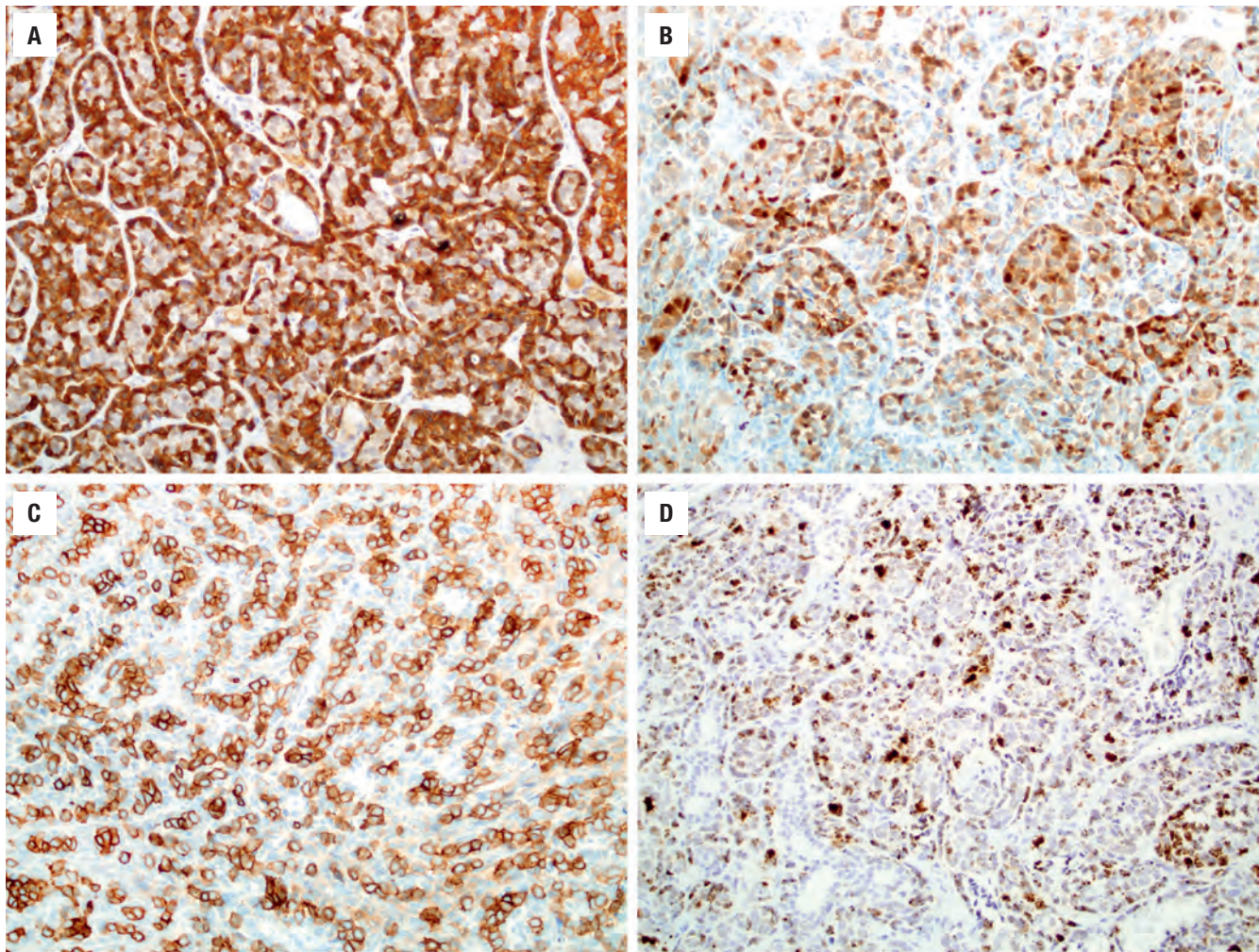
A significant portion (20% to 30%) of sinonasal squamous cell carcinomas (almost always nonkeratinizing) are HPV-related. (**A**) p16 is always positive in HPV-related squamous cell carcinomas, but it is not very specific in the sinonasal tract. (**B**) In situ hybridization for high-risk HPV RNA is much more specific.

### DIFFERENTIAL DIAGNOSIS

*Pseudoepitheliomatous hyperplasia* in the SNT region is most commonly associated with mucosal ulcer with or without prior medical intervention and may be associated with rhinoscleroma, fungal infection, and neoplastic disease (granular cell tumor, lymphoma, and fibrohistiocytic tumors). The elongated and thickened rete pegs extend into the underlying connective tissue and have smooth, sharp, and sometimes pointed borders. There is no desmoplastic stroma. The cells resemble each other and have uniform nuclei without nuclear atypia and rare mitotic figures. *Sinonasal (Schneiderian) papillomas* and *squamous papillomas* may occasionally have malignant transformation, with areas of squamous dysplasia and

carcinoma in situ. Sinonasal papillomas have inverted epithelial growth, with admixed mucocytes and intraepithelial inflammatory cysts. They lack desmoplasia, single-cell invasion, and atypical mitoses. When broad sheets of cytologically malignant squamous cells are seen in biopsies, the diagnosis of SCC should be considered even though stromal invasion is not demonstrable. Clinical and radiographic features should be requested to aid decision making. *Oropharyngeal carcinoma* is histologically indistinguishable from some forms of nonkeratinizing SCC, and both tumors are frequently p16- and HPV-positive. Fortunately spread from the oropharynx to the SNT is very rare. *Sinonasal undifferentiated carcinoma* (SNUC) shows more of a syncytial arrangement, lacks keratinization, and shows vesicular chromatin with prominent nucleoli, while it is negative or focal with



**FIGURE 3.6**

HPV-related multiphenotypic sinonasal carcinoma shows biphasic differentiation, with abluminal immunoreactivity for calponin (**A**) and S100 (**B**), while c-kit immunostaining highlights the luminal tumor component (**C**). (**D**), HPV33 RNA in situ hybridization is strongly positive in both tumor components.

p40, p63, and CK5/6. *Neuroendocrine carcinoma* should show cytologic neuroendocrine features in addition to immunohistochemistry features before the diagnosis is employed. *NUT carcinoma*, defined by the balanced chromosomal translocation t(15;19) resulting in the *BRD4-NUTM1* oncogene, tends to be a poorly differentiated carcinoma with areas of abrupt squamous differentiation; immunostaining for NUT protein or molecular studies for *NUT* rearrangement are diagnostic. *ACC* closely resembles HPV-related multiphenotypic sinonasal carcinoma; this differential is further discussed in the adenocarcinoma section of this chapter.

### PROGNOSIS AND THERAPY

If SCC is confined to the nasal cavity, the 5-year survival rate is in the range of 80 %, depending on keratinization, tumor grade, and stage. Clinical stage is most important,

while nonkeratinizing tumors have a better prognosis than keratinizing carcinomas. Involvement of the paranasal sinuses affects the prognosis adversely. Most treatment failures are related to locally advanced disease and tumor recurrence in areas inaccessible to surgical resection, such as the skull base, dura, and brain. Local recurrence is seen in up to 45 % of patients, with spread to adjacent structures. Cervical lymph node metastasis develops in up to 20 %, with uncommon distant metastases. These patients are at higher risk for the development of a second primary.

Treatment depends on the location and extent of the tumor. T1 and T2 nasal tumors are treated by surgical resection, while T3 and T4 tumors receive postoperative radiotherapy. Various surgical approaches are employed, matched to the complex anatomy of the region, with cosmetic reconstruction as permitted. Adjuvant radiotherapy is usually employed, with variable protocols based on tumor type. Chemotherapy may be used neoadjuvantly or postoperatively.

Unlike the oropharynx where high-risk HPV-related carcinomas have a good prognosis, the prognostic significance of high-risk HPV in sinonasal SCC is currently unclear and still under investigation.

## SINONASAL ADENOCARCINOMA

Malignant glandular neoplasms of the SNT can originate from the respiratory epithelium or the underlying mucoserous glands, with the majority (60%) arising from the mucoserous glands. The respiratory epithelial-derived tumors tend to develop high in the nasal cavity and ethmoid sinus, while salivary gland neoplasms develop more frequently in the lower nasal cavity and maxillary sinus. SNT adenocarcinomas are separated into salivary gland, intestinal, and nonintestinal types. By definition the intestinal-type adenocarcinomas are malignant epithelial glandular tumors of the SNT that histologically resemble intestinal adenocarcinoma.

### CLINICAL FEATURES

#### SALIVARY GLAND-TYPE ADENOCARCINOMA

The sexes are equally affected with a wide age range, although most are older patients (mean, 55 years). The majority of these tumors develop in the maxillary sinus (~60%) or a combination of sinuses and nasal cavity. Symptoms are nonspecific and include obstruction, epistaxis, and pain. Palatal swelling may be seen.

#### NON-SALIVARY GLAND-TYPE ADENOCARCINOMA

These are divided into two major categories: intestinal-type adenocarcinoma and nonintestinal-type adenocarcinoma (also nonenteric or seromucinous adenocarcinoma). The intestinal type has a strong male predominance (about 90%) and tends to affect older males (mean, 5th to 7th decade). There is a well-known occupational exposure, specifically in wood workers and leather workers. Although the carcinogenic substance is unknown, it is thought to be particulate in nature, as spouses of these workers also have an increased risk. Prolonged occupational exposure, frequently over decades, is necessary for development. These tumors tend to occur in the ethmoid sinus and nasal cavity, specifically the lower and middle turbinate in the latter. Unilateral obstruction, rhinorrhea, and epistaxis are the most common symptoms.

The nonintestinal-type adenocarcinomas are separated into low- and high-grade adenocarcinoma. Tumors tend to develop in men slightly more commonly, although high-grade tumors are much more common in men

### SINONASAL TRACT ADENOCARCINOMA—DISEASE FACT SHEET

#### Definition

- Salivary gland-type adenocarcinoma arising from mucoserous glands (60%)
- Non-salivary gland-type adenocarcinoma arising from respiratory mucosa

#### Incidence and Location

- Second most common carcinoma of sinonasal tract
- 15% of sinonasal tract carcinomas
- Paranasal sinuses > nasal cavity

#### Morbidity and Mortality

- Salivary gland-type adenocarcinomas have 40%-60% mortality
- Non-salivary gland-type adenocarcinomas have ~60% mortality, depending on grade

#### Sex and Age Distribution

##### Salivary Gland-Type Adenocarcinoma

- Equal sex distribution
- 3rd to 8th decade, mean: 55 years

##### Non-Salivary Gland-Type Adenocarcinoma

- Males > > females (specifically with industrial exposure)
- 5th to 7th decade (low grade: 6th decade; high grade: 7th decade)

#### Clinical Features

- Unilateral nasal obstruction
- Epistaxis
- Purulent or clear rhinorrhea
- Pain or visual disturbances if large
- Intestinal type has very strong association with woodworkers and leather workers (500x increased incidence)

#### Radiographic Features

- CT and MRI define extent of the tumor and identify invasion

#### Prognosis and Therapy

##### Salivary Gland-Type Adenocarcinoma

- Prognosis depends on stage and tumor type (~50% 10-year survival for adenoid cystic carcinoma)
- Recurrences common (60%)
- Complete surgical resection with optional radiation

##### Non-Salivary Gland-Type Adenocarcinoma (Intestinal Type)

- 80% 5-year survival for papillary intestinal-type adenocarcinoma, but 40% overall survival for poorly differentiated carcinoma (depending on histologic grade)
- Recurrence in 50% of patients
- Complete surgical resection with radiation

than in women. There is a wide age range, although low-grade tumors tend to occur in patients about a decade younger than those with high-grade tumors (54 years vs. 63 years, respectively). The nasal cavity and ethmoid sinus tend to be affected more commonly than other sites.



## SINONASAL TRACT ADENOCARCINOMA—PATHOLOGIC FEATURES

### Gross Findings

#### *Salivary Gland–Type Adenocarcinoma*

- Large, firm, solid, submucosal mass

#### *Non–Salivary Gland–Type Adenocarcinoma*

- Fungating, ulcerated, and friable mass, often mucoid to translucent

### Microscopic Findings

#### *Salivary Gland–Type Adenocarcinoma*

- Adenoid cystic carcinoma most common, with cribriform and cystic pattern, small basaloid cells with hyperchromatic nuclei

#### *Non–Salivary Gland–Type Adenocarcinoma*

- Intestinal and nonintestinal types
- Papillary, colonic, solid, mucinous, and mixed types
- Usually tall, nonciliated, columnar cells, mucin producing
- Tumor grade determines nuclear features
- Frequently have a background of necrosis and inflammation
- Rarely, clear cell tumor is similar to metastatic renal cell carcinoma

### Immunohistochemical Findings

- **Intestinal types** are positive for CK7, CK20, CDX-2, villin, mCEA, MUC2, MUC5, BRST-1, and B72.3
- **Nonintestinal types** are positive for CK7 and S100 but negative for CK20, CDX-2, villin, and MUCs
- Sinonasal renal cell-like carcinoma is positive for CAIX and CD10; negative for PAX8 and RCC
- p53, EGFR, c-erbB-2 expression, and RAS mutation provide prognostic value

### Pathologic Differential Diagnosis

- Sinonasal papilloma, hamartoma, metastatic colon carcinoma, metastatic renal cell carcinoma, lymphoma, olfactory neuroblastoma

## PATHOLOGIC FEATURES

### GROSS FINDINGS

Salivary gland–type adenocarcinomas tend to be large, firm, solid masses, extensively infiltrative at the time of diagnosis. Intestinal-type adenocarcinomas tend to be fungating, with an ulcerated, friable surface. Cut surface reveals gray, translucent, mucoid parenchyma.

### MICROSCOPIC FINDINGS

#### *Salivary Gland–Type Adenocarcinoma*

ACC is the most common salivary gland–type adenocarcinoma to occur in the SNT. Other salivary gland–type tumors—such as mucoepidermoid carcinoma, secretory carcinoma, and low-grade papillary adenocarcinoma—rarely involve this region. ACC is invasive, with perineural and bone invasion; it is composed of small basaloid cells with hyperchromatic nuclei and scant cytoplasm arranged

in tubules, cribriform glands, and solid sheets (Fig. 3.7). Reduplicated basement membrane material and bluish glycosaminoglycan material within the spaces is common. Predominantly solid ACC can be distinguished from undifferentiated small cell carcinomas and basaloid SCC by its lower mitotic activity and the presence of myoepithelial cell differentiation by immunohistochemistry.

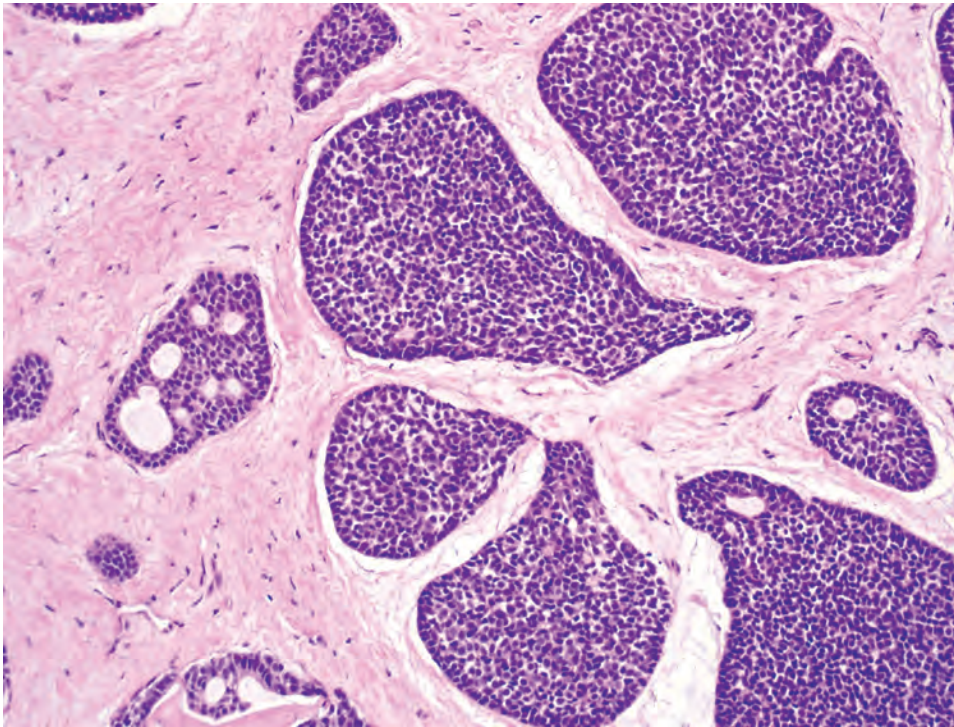
#### *Non–Salivary Gland–Type Adenocarcinoma*

This is a heterogeneous group of tumors that is divided into intestinal and nonintestinal types, with the intestinal type further separated into papillary (~25%), colonic (~45%), solid (~18%), mucinous/colloid (5%), and mixed (7%) types (Barnes classification).

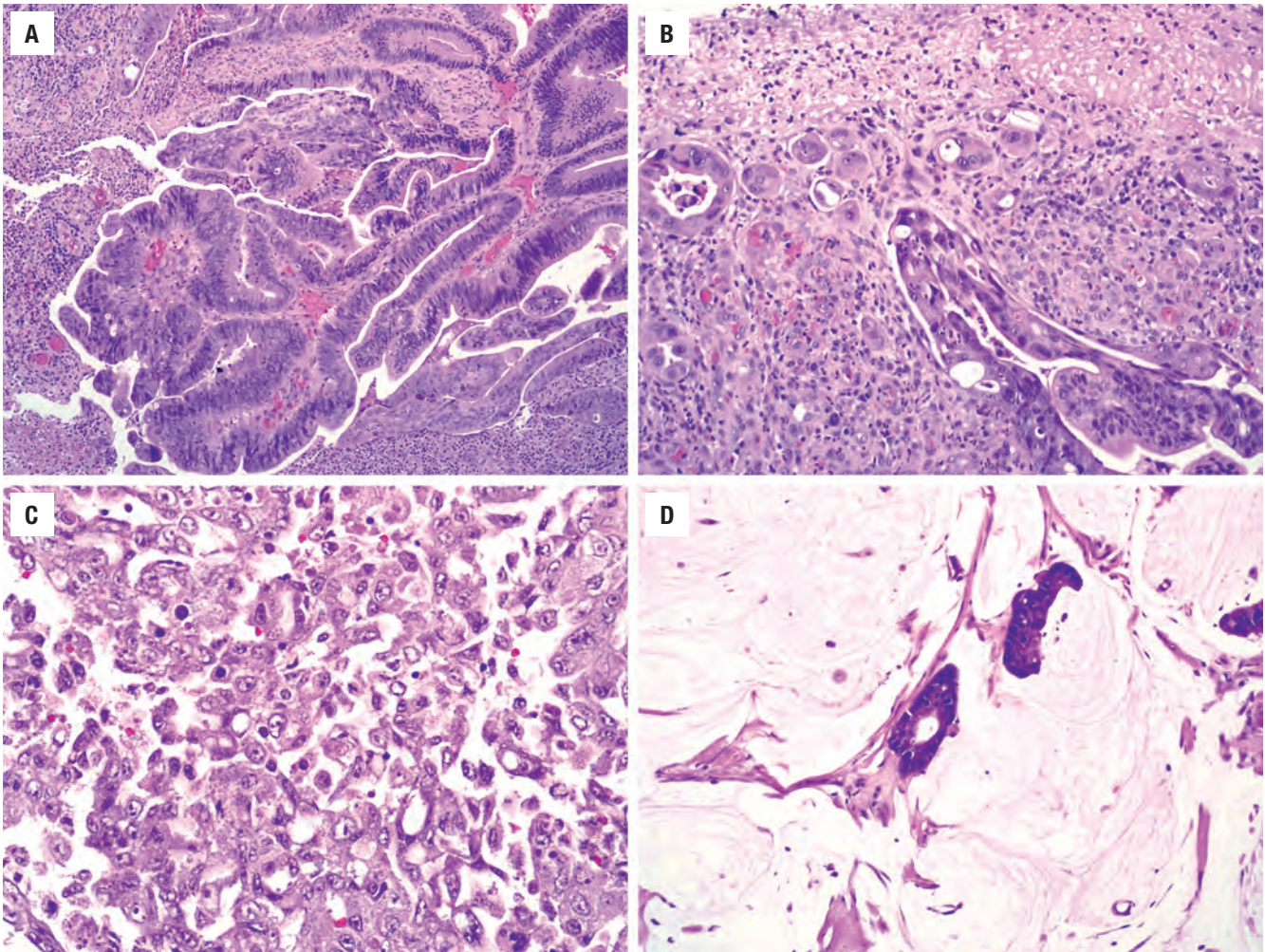
**Intestinal-Type Adenocarcinoma.** Intestinal-type adenocarcinoma is made up of absorptive cells and goblet cells forming glands, nests, and mucin. The degree of differentiation varies. Some are extremely well differentiated, having the appearance of colonic tubular and villous adenomas, with nuclear stratification and mild nuclear atypia (Fig. 3.8). Some tumors contain small intestinal-type cells, such as Paneth cells and enterochromaffin cells. Occurring at the bases of glands are a few layers of smooth muscle cells simulating muscularis mucosae. Other tumors resemble moderately differentiated colonic adenocarcinoma with confluent glands, nuclear pleomorphism, prominent nucleoli, and increased mitotic activity (Fig. 3.8). Some tumor cells produce abundant mucinous material, while others have a signet-ring formation (Fig. 3.8). Necrosis is common, while multinucleated giant cells may be seen reacting to extravasated mucin. Papillary and solid patterns are recognized. In biopsies, the presence of mucous pools and necrotic debris dissecting between the stroma, creating an alveolar pattern, should raise a suspicion of malignancy. In all cases, the patient should be examined for evidence of intestinal tumor before the neoplasm is accepted as a primary lesion of the upper respiratory tract.

**Nonintestinal-Type Adenocarcinoma.** The nonintestinal-type adenocarcinomas are also divided into low- and high-grade types on the basis of architecture, nuclear features, and mitotic activity. Low-grade adenocarcinomas are submucosal, unencapsulated proliferations of uniform cells arranged in compact acini, back-to-back confluent glands, cystic spaces, and papillae (Fig. 3.9). They maintain nonciliated tall columnar to cuboidal configurations and are arranged in a single layer with basal nuclei lacking nuclear stratification. The cytoplasm is abundant but variable in appearance, eosinophilic, basophilic, granular, or clear mucinous. The nuclear atypia is mild to moderate and nucleoli may be prominent (Fig. 3.9). The mitotic activity is generally low. High-grade adenocarcinomas are usually invasive, with angioinvasion, neurotropism, and bone destruction. They are often solid, demonstrating necrosis, nuclear pleomorphism, prominent nucleoli, and high mitotic activity. Some contain abundant signet-ring



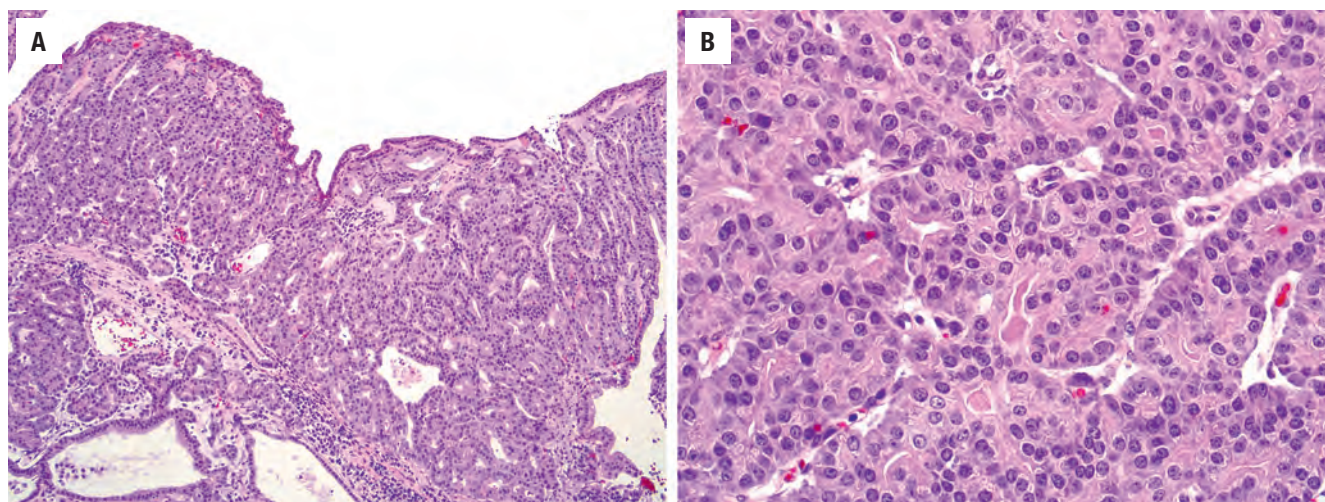
**FIGURE 3.7**

The solid variant of adenoid cystic carcinoma consists of solid nests of hyperchromatic cells with angulated nuclei (*right*) in addition to foci of more conventional-appearing, cribriform structures (*left*).

**FIGURE 3.8**

Sinonasal intestinal-type adenocarcinoma exhibits numerous architectural patterns including papillary (**A**), glandular (**B**), solid (**C**), and mucinous (**D**).



**FIGURE 3.9**

(A) This sinonasal nonintestinal-type low-grade adenocarcinoma consists of a complex proliferation of back-to-back fused glands. (B) The glands are polygonal with eosinophilic cytoplasm and uniform round nuclei demonstrating mild atypia.

cells. Special stains are helpful to identify mucus secretion. The sinonasal renal cell-like adenocarcinoma morphologically resembles metastatic renal cell carcinoma but shows more of a follicular to glandular pattern as well as peculiar intranuclear holes.

### ANCILLARY STUDIES

Mucicarmine-positive material is usually easily identified both intracytoplasmically and intraluminally. Most adenocarcinomas do not require immunohistochemical stains. ACC is positive for keratin, CK7, S100 protein, calponin, and p63. *Intestinal-type adenocarcinomas* show keratin, CK20 (up to 86 %) (Fig. 3.10), CDX-2, SATB2 (Fig. 3.10), villin, CK7, EMA, B72.3, BRST-1, mCEA, and MUC2 and MUC5 immunoreactivity. Various neuroendocrine markers may also be present (chromogranin, synaptophysin, CD56). Prognostic information may be provided by p53, epidermal growth factor receptor (EGFR), and c-erbB-2. There may be an increased proliferation rate with Ki-67. *K-* or *H-RAS* point mutations tend to be associated with a poor prognosis. The *nonintestinal-type adenocarcinomas* are positive with keratins, including CK7 and usually S100 protein (Fig. 3.10), but are negative with CK20, CDX-2, villin, and MUCs. New data suggest that a subset of nonintestinal sinonasal adenocarcinomas is positive for SOX10 (Fig. 3.10) and DOG1, suggesting a seromucinous rather than surface origin. Also recently, a subset of low-grade sinonasal nonintestinal adenocarcinomas has been shown to harbor the *ETV6-NTRK3* fusion seen in salivary secretory carcinoma and other tumors. Myoepithelial markers (p63, calponin) are negative, as are neuroendocrine markers. The renal cell-like adenocarcinoma is positive with CAIX and CD10 while negative with PAX8 and RCC.

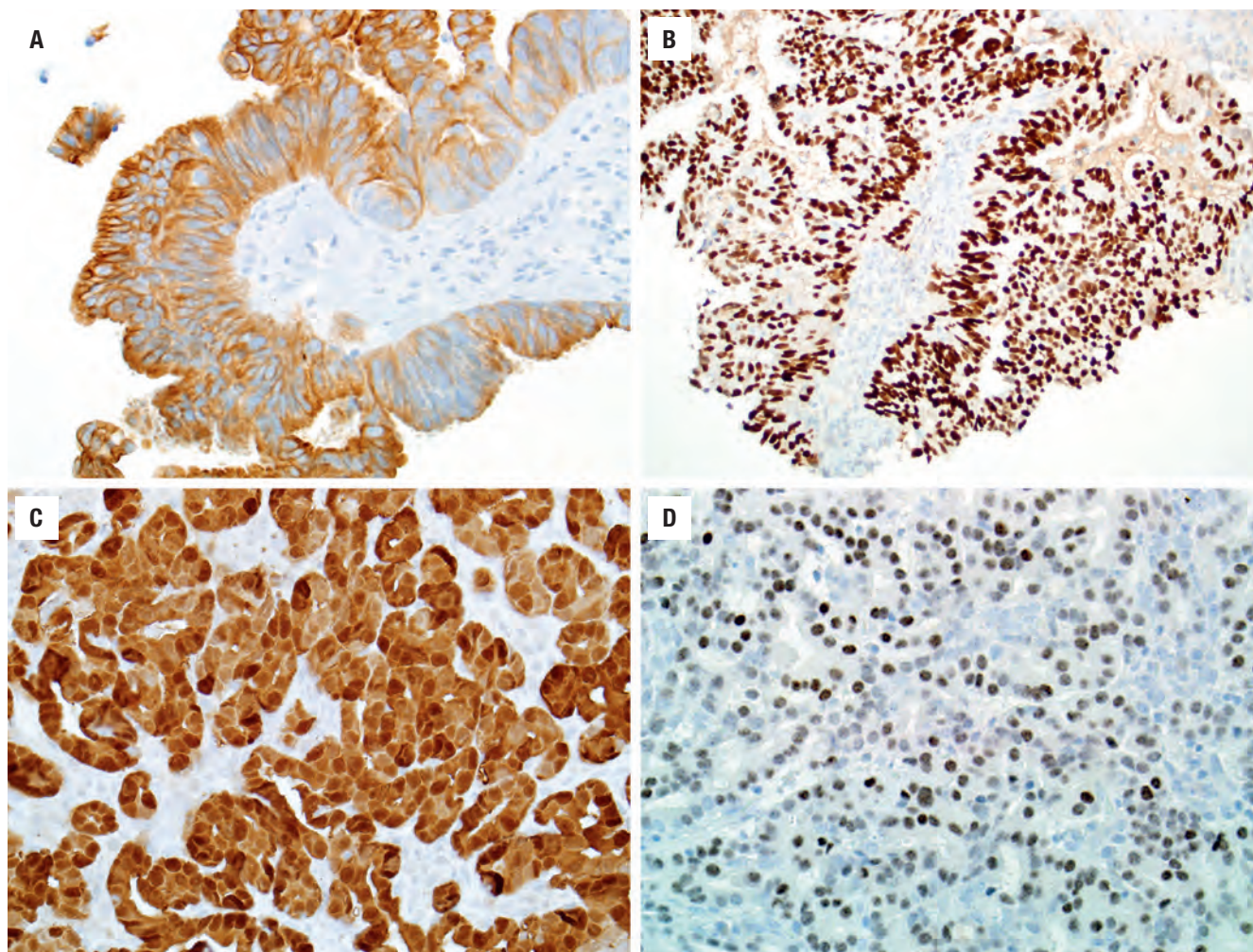
### DIFFERENTIAL DIAGNOSIS

ACC must be separated from high-grade carcinomas, lymphoma, and olfactory neuroblastoma (ONB). There is a newly reported SNT carcinoma that resembles solid ACC: *HPV-related multiphenotypic sinonasal carcinoma*. Unlike true ACC, this peculiar SNT carcinoma harbors high-risk HPV (usually type 33), often demonstrates squamous dysplasia of the overlying surface epithelium, and consistently lacks the *MYB* translocations seen in about half of ACCs. *Sinonasal papilloma* (oncocytic variant specifically) with their complex back-to-back, confluent glands and papillary architecture may be overdiagnosed as low-grade adenocarcinoma or mucoepidermoid carcinoma, but the cells are cytologically benign. *Papillary sinusitis* lacks dysplasia and infiltration. *Hamartomas* have widely separated glands with ciliated, stratified nuclei and thick basement membranes. *Metastatic adenocarcinoma* of gastrointestinal origin and clear cell tumors of any site must be excluded, especially when considering the renal cell-like adenocarcinoma category.

### PROGNOSIS AND THERAPY

The overall 10-year survival rate for ACC is 40 % to 60 %. Aggressive local therapy is warranted even in patients with distant metastases, since a significant number of patients will live for many years with their disease. Recurrences are common (up to 60 %). The treatment of choice for ACC is surgical resection with clear margins often accompanied by postoperative radiotherapy to improve local control, especially in cases with positive or close margins. The propensity for perineural spread makes it difficult to obtain clear margins.



**FIGURE 3.10**

Intestinal-type adenocarcinomas are positive for CK20 (**A**) and SATB2 (**B**) in addition to CDX2 and villin (not pictured). Nonintestinal low-grade adenocarcinoma is usually positive for S100 protein (**C**), and often SOX10 (**D**).

Among patients with non-salivary gland-type adenocarcinoma, histologic grade affects outcome. Well-differentiated tumors with predominantly papillary and tubular structures have a better prognosis (80 % 5-year survival) than their poorly differentiated counterparts (40 % 5-year survival). Patients with industrial exposure have a better outcome than the sporadic cases, perhaps because they are detected earlier owing to regular surveillance. Recurrences develop in approximately 50 % of patients, with distant metastasis in about 15 %. Overall survival is around 40 %, with death in about 3 years. Treatment is radical surgical resection with postoperative radiotherapy.

### ■ SINONASAL UNDIFFERENTIATED CARCINOMA (SNUC)

SNUC is a rare and highly aggressive undifferentiated carcinoma, showing extensive local destruction, histologic pleomorphism, and necrosis, separate from ONB. The taxonomy

is not well developed or accepted, but it is considered a distinctive carcinoma of the SNT of uncertain histogenesis lacking squamous or glandular differentiation. There is no known etiology, although isolated Epstein-Barr virus (EBV)-positive cases are reported in Asians.

### CLINICAL FEATURES

This type of undifferentiated carcinoma is a distinct clinicopathologic entity. The majority of patients present with locally advanced disease with frequent bony, cranial, or orbital involvement at diagnosis. The median age is in the 6th decade with a male predominance (2 to 3:1). Previous radiation may be an etiologic factor. Patients have nonspecific symptoms indistinguishable from those of other SNT tumors, but the symptoms are usually of short duration (rapid onset of symptoms). The nasal cavity, maxillary sinus, and ethmoid sinus are usually involved, frequently showing spread into directly contiguous sites ([Fig. 3.11](#)).



### SINONASAL UNDIFFERENTIATED CARCINOMA—DISEASE FACT SHEET

#### Definition

- High-grade aggressive undifferentiated carcinoma with extensive local disease, lacking squamous and glandular differentiation

#### Incidence and Location

- Rare
- Nasal cavity, maxillary sinus, ethmoid sinus, often combined

#### Morbidity and Mortality

- Mortality of 80% in 5 years

#### Sex and Age Distribution

- Males > females (2 to 3:1)
- Wide age range (20-76 years); mean: 6th decade

#### Clinical Features

- Nasal obstruction and/or epistaxis of short duration
- Proptosis, periorbital swelling, and facial pain
- Destructive lesion
- May have cranial nerve involvement

#### Prognosis and Therapy

- Median survival is <18 months
- About 30% have cervical lymph node metastasis
- Combination multimodality therapy (surgery, chemotherapy, radiation)

### SINONASAL UNDIFFERENTIATED CARCINOMA—PATHOLOGIC FEATURES

#### Gross Findings

- Large fungating mass (>4 cm) with bone destruction/invasion

#### Microscopic Findings

- Hypercellular tumor arranged in nests, lobules, and sheets of undifferentiated cells (no squamous or glandular differentiation)
- Polygonal cells with high nuclear/cytoplasmic ratio, with medium to large nuclei and single, variable nucleoli
- High mitotic activity
- Tumor necrosis, lymphovascular invasion, and perineural invasion are common

#### Immunohistochemical Findings

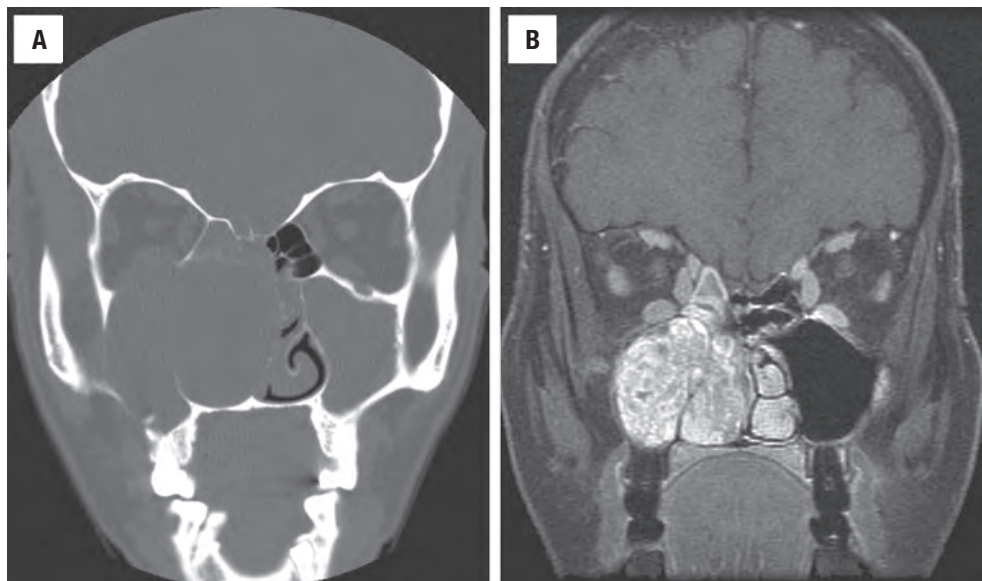
- Usually positive for pan-keratin, CK7, CK8, CK19
- Occasionally positive for EMA, NSE, p53, chromogranin/synaptophysin
- Negative or only focally positive for squamous markers p63, p40, CK5/6
- Rarely may be positive for S100 protein and CD99

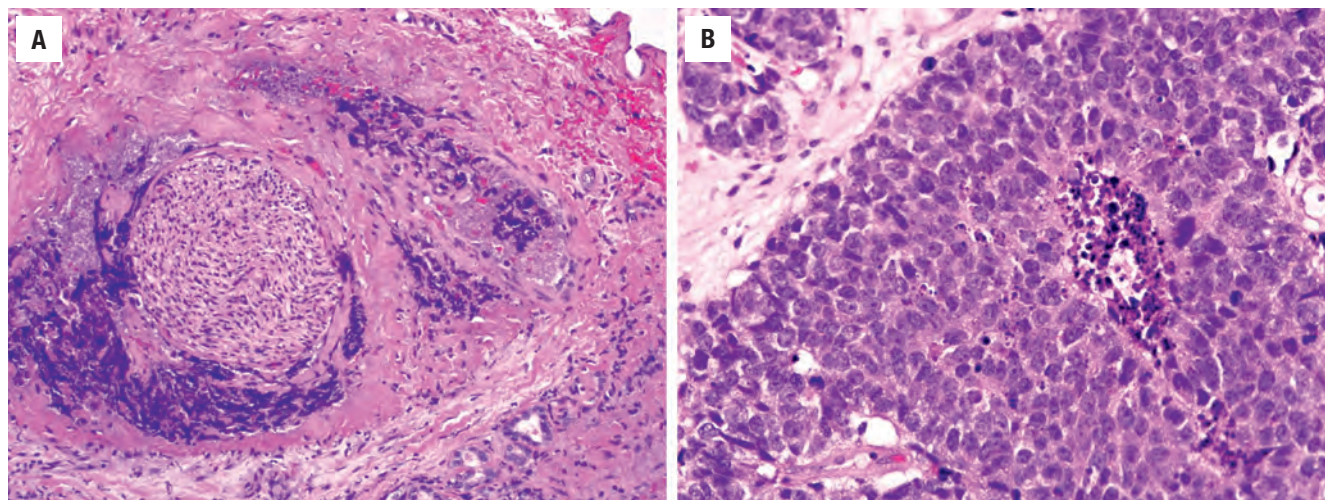
#### Pathologic Differential Diagnosis

- Olfactory neuroblastoma, neuroendocrine carcinoma, nonkeratinizing squamous cell carcinoma, nasopharyngeal carcinoma, lymphoma, melanoma, rhabdomyosarcoma, rhabdomyosarcoma, *SMARCB1*-deficient carcinoma, Ewing sarcoma/primitive neuroectodermal tumor, NUT carcinoma

**FIGURE 3.11**

Sinonasal undifferentiated carcinoma. **(A)** Computed tomography scan shows a large, destructive mass within the right maxillary sinus, filling the nasal cavity and expanding into the orbit. **(B)**, Magnetic resonance imaging of the same patient shows the significant extent of the tumor, highlighting the soft tissue component.



**FIGURE 3.12**

(A) Sinonasal undifferentiated carcinoma is typically highly invasive, here showing crushed tumor cells around a nerve (*left*) and within a vessel (*right*). (B) The carcinoma shows no squamous or glandular differentiation. The tumor cells are large, with vesicular chromatin and prominent nucleoli. Focal necrosis is seen.

## **PATHOLOGIC FEATURES**

### **GROSS FINDINGS**

Tumors are usually large (>4 cm) and fungating with poorly defined margins and bony destruction.

### **MICROSCOPIC FINDINGS**

The tumor is hypercellular; it is arranged in nests, lobules, trabeculae, and sheets without any squamous or glandular differentiation. Surface involvement is rare, but ulceration may preclude such a determination. The large polygonal cells have high nuclear/cytoplasmic ratios with medium- to large-size nuclei surrounded by scant eosinophilic cytoplasm (Fig. 3.12). The chromatin may be hyperchromatic to hypochromatic, with inconspicuous to prominent single nucleoli. Necrosis, including comedonecrosis, is common (Fig. 3.12). Mitotic figures are increased. Lymphovascular invasion and neurotropism are common findings (Fig. 3.12).

## **ANCILLARY STUDIES**

The majority of tumors react with keratins (simple keratins, especially CK7, CK8, and CK19). Epithelial membrane antigen (EMA), neuron-specific enolase (NSE), and p53 may be positive. Chromogranin and synaptophysin are occasionally focally positive. The squamous markers p63, p40, and CK5/6 are negative or, at most, focal. EBER is negative (in Western patients). p16 is commonly positive, but only rarely does SNUC harbor high-risk HPV.

## **DIFFERENTIAL DIAGNOSIS**

Separation of SNUC from high-grade ONB and neuroendocrine carcinoma remains controversial. *ONB* has a specific anatomic site of involvement, lobular architecture, and neural features and is typically keratin-negative. *Neuroendocrine carcinomas* may overlap with SNUC, a separation that at present does not have clinical implications. Nonkeratinizing SCC may resemble SNUC but is diffusely positive for squamous markers like p40. Immunohistochemical stains are valuable to diagnose NPC, lymphoma, melanoma, RMS, and Ewing sarcoma/primitive neuroectodermal tumor (ES/PNET) (Table 3.1). A *NUT carcinoma* may appear undifferentiated, showing abrupt keratinization and NUT immunoreactivity, along with t(15;19) fusion gene *BRD4-NUTM1*. A recently described undifferentiated carcinoma known as *SMARCB1-deficient sinonasal carcinoma* is characterized by loss of SMARCB1 (INI1) immunoreexpression and some degree of rhabdoid cytomorphology (Fig. 3.13). It is not yet clear whether *SMARCB1*-deficient sinonasal carcinoma is a distinct tumor entity or a group of entities.

## **PROGNOSIS AND THERAPY**

Prognosis is usually poor, with a median survival of less than 18 months, and no reported disease-free survival. There is frequent recurrence, with metastasis to lymph nodes and distant sites. A combination of chemotherapy, radiotherapy, and radical surgery provides the best chance of survival, although the exact sequence



**TABLE 3.1**  
**Differential diagnostic comparison of sinonasal tract “small round blue cell” malignant neoplasms**

| Feature                   | Squamous Cell Carcinoma                                    | Sinonasal Undifferentiated Carcinoma | Malignant Melanoma  | Olfactory Neuroblastoma                                     | Extranodal NK/T-Cell Lymphoma, Nasal                             | Rhabdomyosarcoma                                   | Ewing Sarcoma/PNET  |
|---------------------------|--|--------------------------------------|---|---|--|--|---|
| Mean age                  | 55-65 years  | 55-60 years                          | 40-70 years   | 40-45 years   | 50-60 years  | <20 years  | <30 years   |
| Site                      | Nasal cavity and/or sinuses                                | Multiple sites usually               | Anterior nasal septum > maxillary sinus                                 | Roof of nasal cavity  | Nasal cavity > paranasal sinuses > nasopharynx                   | Nasopharynx > sinonasal tract                      | Maxillary sinus > nasal cavity                            |
| Radiographic studies      | Little destruction or spread                               | Marked destruction or spread         | Central destructive mass  | “Dumbbell-shaped” cribriform plate mass                     | Early changes nonspecific; midline destruction later             | Size, extent of tumor                              | Mass lesion, with bone erosion                            |
| Prognosis                 | 60% 5-year (stage and tumor type dependent)                | <20% 5-year survival                 | 17%-47% 5-year survival   | 60%-80% 5-year survival                                     | 30%-50% 5-year survival (stage-dependent)                        | 44%-69% (age, stage- and subtype-dependent)        | 60%-70% 5-year (stage, size, <i>FLI1</i> )                |
| Cranial nerve involvement | Uncommon   | Common                               | Uncommon  | Sometimes   | Sometimes  | Uncommon   | Sometimes   |
| Pattern                   | Syncytial  | Sheets and nests                     | Protean   | Lobular   | Diffuse  | Sheets, alveolar                                   | Sheets, nests   |
| Cytology                  | Squamous differentiation, keratinization, opaque cytoplasm | Medium cells, inconspicuous nucleoli | Large, polygonal, epithelioid, rhabdoid, plasmacytoid, spindle; pigment | Salt-and-pepper chromatin, small nucleoli (grade-dependent) | Polymorphous, small to large, folded, cleaved and grooved nuclei | Round, strap, spindled, rhabdomyoblasts, primitive | Medium, round cells, vacuolated cytoplasm, fine chromatin |
| Anaplasia                 | Present  | Common                               | Common  | Occasionally and focally                                    | Common   | Common   | Minimal   |
| Mitotic figures           | Present  | High                                 | High  | Variable  | High   | Variable   | Common  |
| Necrosis                  | Limited  | Prominent                            | Limited   | Occasionally  | Prominent  | Limited  | Frequent  |
| Vascular invasion         | Rare   | Prominent                            | Rare  | Occasionally  | Prominent  | Rare   | Rare  |
| Neurofibrillary stroma    | Absent   | Absent                               | Absent  | Common  | Absent   | Absent   | Absent  |

| Feature                    | Squamous Cell Carcinoma | Sinonasal Undifferentiated Carcinoma    | Malignant Melanoma          | Olfactory Neuroblastoma   | Extranodal NK/T-Cell Lymphoma, Nasal | Rhabdomyosarcoma  | Ewing Sarcoma/PNET        |
|----------------------------|-------------------------|---|-----------------------------|---|--------------------------------------|---|---------------------------|
| Pseudorosettes             | Absent                  | Absent                                  | Rare                        | Common  | Absent                               | Absent  | Present                   |
| Keratin                    | Positive                | >90%                                    | Negative                    | Focal, weak   | Negative                             | Negative  | Rare                      |
| CK5/6                      | Present                 | Negative                                | Negative                    | Negative  | Negative                             | Negative  | n/a                       |
| EMA                        | Present                 | 50%                                     | Rare                        | Negative  | Negative                             | Negative  | n/a                       |
| NSE                        | Negative                | 50%                                     | Negative                    | >90%  | Negative                             | Negative  | Positive                  |
| S100 protein               | Negative                | <15%                                    | Positive                    | + ( sustentacular)  | Negative                             | Negative  | Rare                      |
| Chromogranin/synaptophysin | Negative                | <15%                                    | Negative                    | >90% (can be weak)  | Negative                             | Negative  | Positive                  |
| HMB45                      | Negative                | Negative                                | Positive                    | Negative  | Negative                             | Negative  | Negative                  |
| CD45RB                     | Negative                | Negative                                | Negative                    | Negative  | Positive <sup>a</sup>                | Negative  | Negative                  |
| CD56                       | Negative                | Negative                                | Negative                    | Positive  | Positive                             | Negative  | Rare                      |
| CD99                       | Negative                | <10%                                    | Negative                    | Negative  | Negative                             | Rare  | >99%                      |
| Vimentin                   | Negative                | Negative                                | Positive                    | Negative  | Positive                             | Positive  | Positive                  |
| Desmin                     | Negative                | Negative                                | Negative                    | Negative  | Negative                             | Positive <sup>b</sup>                                   | Negative                  |
| In situ EBER               | Absent                  | Absent                                  | Absent                      | Absent  | Nearly 100%                          | Negative  | Negative                  |
| Electron microscopy        | Epithelial junctions    | Junctions, rare neurosecretory granules | Premelanosomes, melanosomes | Neurite-like processes, neurofilaments, neurosecretory granules | n/a                                  | Thick and thin filaments, sarcomeres, Z-bands, glycogen | Glycogen; primitive cells |

<sup>a</sup>Lymphoma is positive with CD3e, CD2, CD56, perforin, TIA1, and granzyme B.

<sup>b</sup>Rhabdomyosarcoma is positive with desmin, actin, myoglobin, fast myosin, MYOD1, and myogenin. EMA, Epithelial membrane antigen; NSE, neuron-specific enolase; PNET, primitive neuroectodermal tumor.



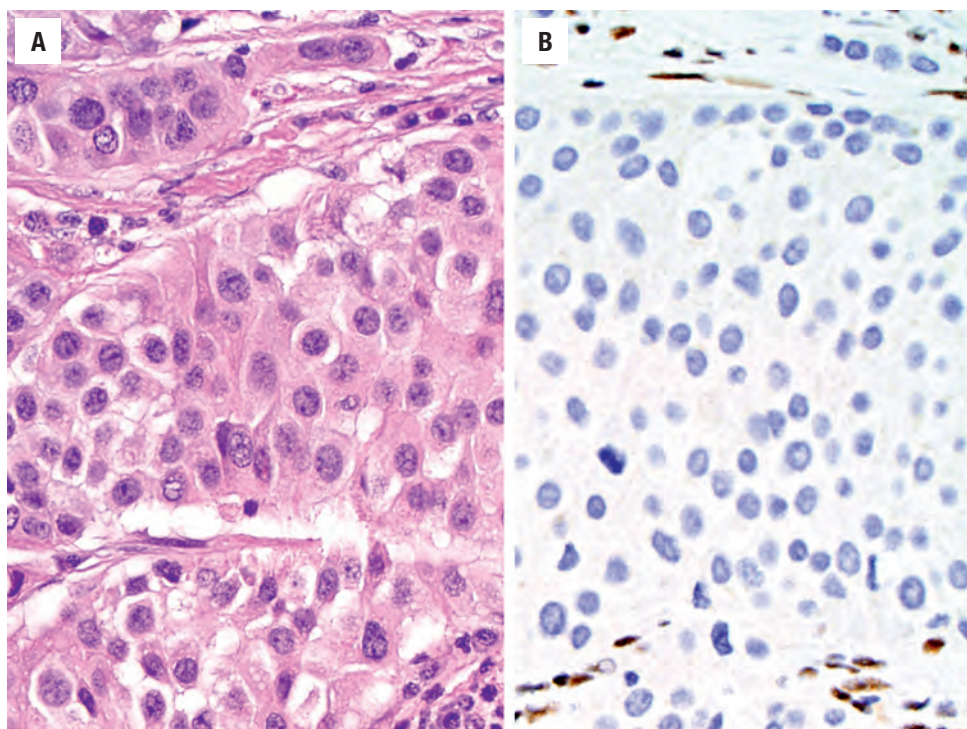


**FIGURE 3.13**

*SMARCB1* (INI-1)-deficient sinonasal carcinoma consists of nests of undifferentiated cells with variably rhabdoid features (**A**) and is defined by an absence of *SMARCB1* (INI-1) immunolabeling (**B**). Note that the normal stromal cells have retained *SMARCB1* (INI-1) expression.

of modalities and specific agents is controversial and undecided.

## ■ NUT CARCINOMA

Nuclear protein in testis (NUT) carcinoma (previously known as NUT midline carcinoma) is a poorly differentiated carcinoma defined by a genetic rearrangement of the *NUTM1* gene. NUT carcinoma can arise from virtually any anatomic site, but among head and neck sites it affects the SNT most commonly. NUT carcinoma is known for its highly aggressive clinical behavior.

### CLINICAL FEATURES

NUT carcinoma can be seen in patients of any age (0.1 to 82 years) but it occurs most often in children or young adults (median, 22 years). NUT carcinoma produces symptoms related to a rapidly growing sinonasal mass: epistaxis, nasal obstruction, nasal discharge, pain, and eye-related symptoms such as proptosis. Imaging will typically reveal an extensively invasive mass, with frequent involvement of the orbit, cribriform plate, or cranial cavity. About half of patients have regional and/or distant metastases on presentation.

### NUT CARCINOMA—DISEASE FACT SHEET

#### Definition

- Highly aggressive carcinoma, often demonstrating abrupt squamous differentiation defined by the presence of *NUTM1* gene rearrangement

#### Incidence and Location

- Rare
- Nasal cavity, maxillary sinus, ethmoid sinus, often combined

#### Morbidity and Mortality

- Mortality of >90% in 5 years

#### Sex and Age Distribution

- Females slightly > males
- Wide age range (0.1-82 years) but most often children and young adults; median 22 years

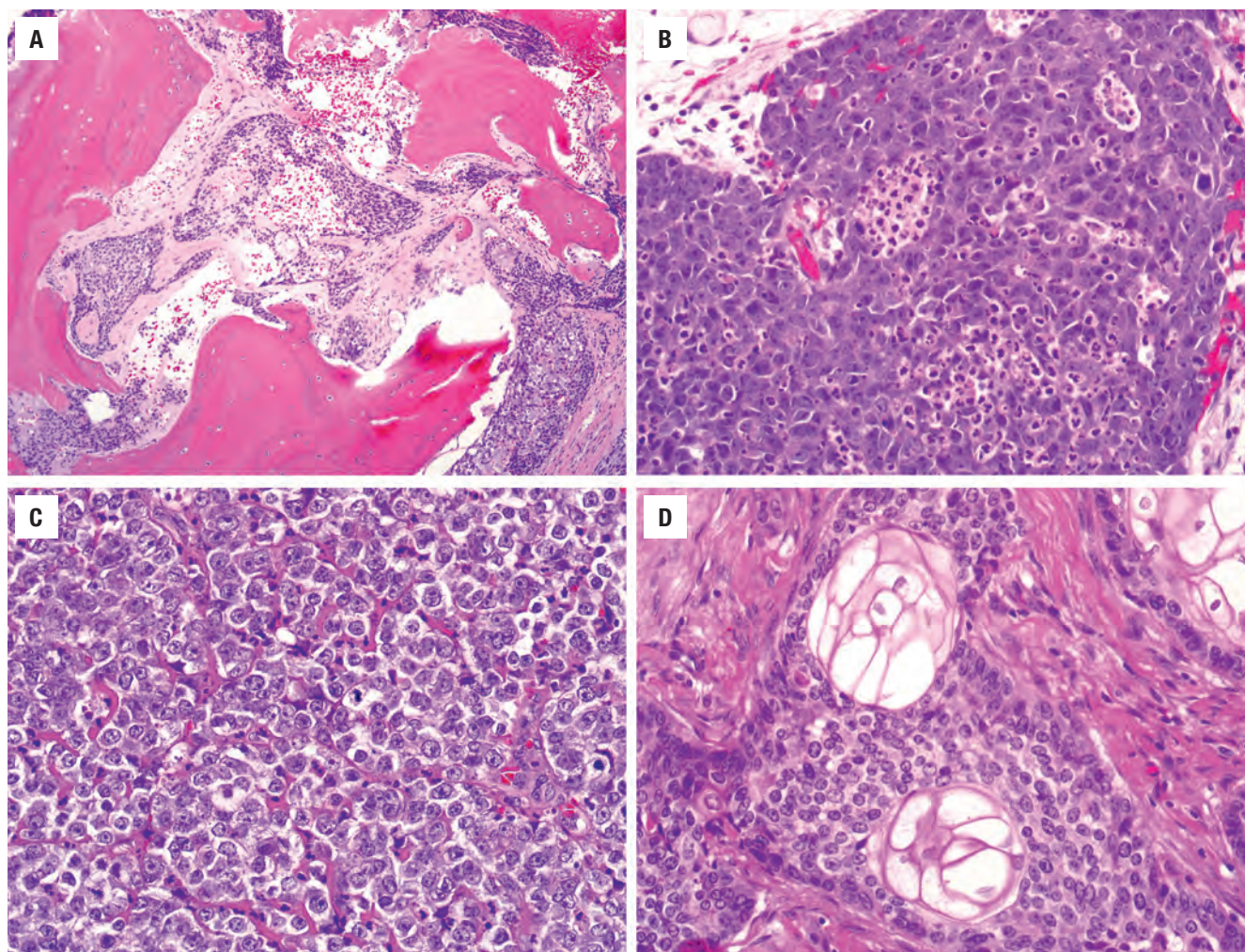
#### Clinical Features

- Nasal obstruction and/or epistaxis of short duration
- Proptosis, periorbital swelling, and facial pain
- Destructive lesion
- May have cranial nerve involvement

#### Prognosis and Therapy

- Median survival is 9.8 months
- About 50% have regional or distant metastasis at presentation
- Combination multimodality therapy (surgery, chemotherapy, radiation). Experimental targeted therapies (e.g., bromodomain inhibitors) under investigation.



**FIGURE 3.14**

NUT carcinoma is typically highly infiltrative, here with bone invasion (**A**). An infiltrate of neutrophils may be seen (**B**). NUT carcinoma comprises undifferentiated cells with monotonous round nuclei with open chromatin and prominent nucleoli (**C**). A characteristic feature of NUT carcinoma is the presence of “abrupt” keratinization (**D**).

### NUT CARCINOMA—PATHOLOGIC FEATURES

#### Gross Findings

- Not well reported because only rarely resected

#### Microscopic Findings

- Nests and sheets of undifferentiated-appearing cells
- Tumor cells are strikingly monotonous
- Squamous differentiation usually seen with an “abrupt” pattern of keratinization
- High mitotic activity
- Neutrophilic infiltrate, tumor necrosis, lymphovascular invasion, bone invasion, perineural invasion are common

#### Immunohistochemical Findings

- Positive for NUT protein in >50% of cells
- Usually positive for pan-keratin, p63, p40
- Positive for CD34 in about half of cases
- Occasionally positive for synaptophysin, p16, TTF-1, CD99

#### Pathologic Differential Diagnosis

- Sinonasal undifferentiated carcinoma, squamous cell carcinoma, neuroendocrine carcinoma, Ewing sarcoma/primitive neuroectodermal tumor, olfactory neuroblastoma

### PATHOLOGIC FEATURES

#### GROSS FINDINGS

NUT carcinoma is rarely resected, so the gross findings are not widely reported.

#### MICROSCOPIC FINDINGS

NUT carcinoma grows as nests and sheets of cells in the sinonasal submucosa. Carcinoma in situ is not seen. NUT carcinoma is highly infiltrative, with frequent invasion of nerves, vessels, and bone (**Fig. 3.14**). NUT



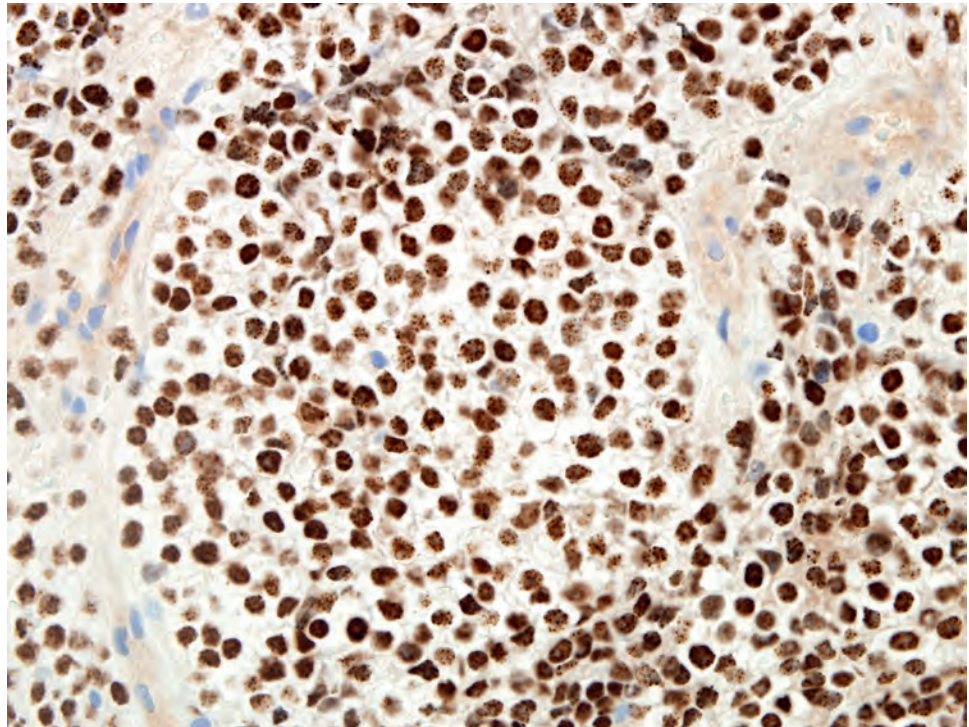


**FIGURE 3.15**

The diagnostic feature of NUT carcinoma is diffuse nuclear immunoreactivity of NUT. The staining typically demonstrates a "speckled" quality.

carcinoma demonstrates necrosis and a high mitotic rate; however, it is also characterized by a strikingly monotonous cellular population of medium-sized cells with round to oval nuclei showing minimal pleomorphism. The nuclei have open chromatin and a prominent nucleolus (Fig. 3.14). An intratumoral inflammatory infiltrate of neutrophils may be seen. Generally, NUT carcinoma demonstrates a predominantly primitive, undifferentiated appearance, but most cases exhibit foci of squamous differentiation in the form of a peculiar pattern of "abrupt" keratinization (Fig. 3.14).

#### ANCILLARY STUDIES

The diagnosis of NUT carcinoma is dependent on demonstrating a rearrangement of *NUTM1*. This can be done by molecular techniques, where the chromosomal partner is most often *BRD4*, or more simply by immunohistochemistry for NUT protein, which is highly sensitive and specific. NUT immunolabeling must be present in more than 50% cells and usually demonstrates a speckled staining pattern (Fig. 3.15). NUT carcinoma is also positive for cytokeratins and usually positive for the squamous markers p63, p40, and CK5/6. NUT carcinoma can uncommonly demonstrate neuroendocrine differentiation (synaptophysin, chromogranin) or positivity for CD99; it is rarely positive for TTF-1. NUT carcinoma is occasionally p16-positive but is not positive for high-risk HPV.

#### DIFFERENTIAL DIAGNOSIS

NUT carcinoma is commonly misdiagnosed as *SNUC*; however, *SNUC* is negative for NUT protein and does not demonstrate histologic or immunophenotypic evidence of squamous differentiation. *SCC* is another consideration, but sinonasal *SCC* typically lacks the nuclear monotony and abrupt keratinization of NUT carcinoma and is NUT-negative. The primitive cellular appearance of NUT carcinoma and occasional CD99 positivity may cause confusion with *ES/PNET*. However, *ES/PNET* typically lacks cytokeratin and p40 immunostaining and harbors a different gene fusion (most often *EWSR1-FLI1*). Finally, *ONB* and other sinonasal small round cell tumors can enter the differential diagnosis but are easily excluded by immunohistochemistry.

#### PROGNOSIS AND THERAPY

NUT carcinoma has a very poor prognosis with a median overall survival of fewer than 10 months. Complete resection with postoperative chemotherapy and radiation offers the best outcomes. There are currently trials under way that are investigating the use of bromodomain inhibitors that target the *NUTM1-BRD4* gene fusions.

## NASOPHARYNGEAL CARCINOMA

The nomenclature for carcinomas of the nasopharynx has undergone several iterations, but adenocarcinomas and salivary gland-type carcinomas are excluded from this category. NPC is an SCC originating from nasopharyngeal mucosa and encompasses nonkeratinizing carcinoma, keratinizing SCC, and basaloid SCC. In the past, synonyms included lymphoepithelial carcinoma, Schmincke-type carcinoma, Rigaud lymphoepithelioma, undifferentiated carcinoma, and anaplastic carcinoma. These terms have been abandoned in favor of the current nomenclature.

### NASOPHARYNGEAL CARCINOMA—DISEASE FACT SHEET

#### Definition

- A carcinoma arising from the nasopharynx mucosa showing evidence of squamous differentiation

#### Incidence and Location

- Incidence varies by location and population (highest in Asians)
- <0.5% of all carcinomas
- Nasopharynx

#### Morbidity and Mortality

- 5-year survival improved up to 80% in low-stage patients; usually 55%-60% overall 5-year survival

#### Sex, Race, and Age Distribution

- Males > females (3:1)
- Asians > Africans > Arctic natives
- Peak, 40-60 years

#### Clinical Features

- Neck mass, nasal obstruction, epistaxis, hearing loss, tinnitus, postnasal drip, cranial nerve involvement
- Endoscopy may show mass, fullness, or no lesion
- Migration of population from high-risk to low-risk areas does not change carcinoma risk, but subsequent generations have a reduced risk
- Strong association with Epstein-Barr virus and high levels of volatile nitrosamines in foods

#### Radiographic Features

- MRI is study of choice, showing extent of tumor
- PET is best for lymph node evaluation

#### Prognosis and Therapy

- Overall, 20%-98% 5-year survival (dependent on histology type and stage)
- Regional lymph node metastases are common
- Recurrences common, most during first 3 years postdiagnosis
- Radiotherapy is the cornerstone of management, although best for nonkeratinizing type
- Chemotherapy used for advanced disease

### CLINICAL FEATURES

NPC is both epidemic and endemic in southern parts of China, Southeast Asian countries (Thailand, Philippines, Vietnam), and North Africa and in Arctic natives, accounting for up to 18% of all cancers in these areas. The high-risk populations experience a decreased risk in subsequent generations in new places to which they migrate. There is a strong etiologic association with EBV (especially early antigen and viral capsid antigen [VCA]), diets high in volatile nitrosamines (salted fish, fermented foods), and other environmental factors (smoking, formaldehyde, chemical fumes, radiation exposure). Men are affected more commonly than women (3:1), with a wide age range at initial presentation (7 to 77 years) and a peak incidence in the 5th to 6th decade of life. Pediatric cases are increased in northern and central Africa, accounting for 10% to 20% of all cases. Owing to its anatomic location, NPC may remain clinically silent, resulting in a delay in diagnosis. The most common initial presentation is an asymptomatic cervical mass (posterior triangle or jugulodigastric) in up to 70%. When symptomatic, nasal symptoms such as nasal obstruction, discharge, postnasal drip, epistaxis, and middle ear complaints (e.g., tinnitus, earache, discharge, and hearing loss secondary to eustachian tube obstruction) are common. With disease progression, cranial nerve involvement becomes apparent, especially of cranial nerves III, V, VI, IX, and X.

### RADIOGRAPHIC FEATURES

Both CT and MRI are equally sensitive in the study of the roof and lateral wall of the nasopharynx. However, MRI provides a better separation of tumor from benign tissue. Both CT and MRI are used in assessing the local extent of the tumor for treatment planning. The status of cervical lymph nodes is best assessed by PET, which is also used in the detection of residual tumor after treatment.

### LABORATORY STUDIES

In NPC, about 90% of patients will have EBV titers, including immunoglobulin IgG or IgA against early antigens or IgA against VCAs. EBER-1 or EBNA-1 (EBV nuclear antigens) can be detected in the serum or plasma of patients by quantitative polymerase chain reaction (PCR), one of the most sensitive tests for NPC. Elevated titers may be used to screen patients or used as a marker of disease relapse.



## NASOPHARYNGEAL CARCINOMA—PATHOLOGIC FEATURES

### Gross Findings

- Superior or lateral wall mass, especially in the fossa of Rosenmüller
- Cervical metastases common

### Microscopic Findings

#### Nonkeratinizing Squamous Cell Carcinoma (85%)

- Most common type with possible surface involvement
- Solid sheets, islands, and nests with intimate lymphoid infiltrates
- Syncytial large cells with indistinct borders, vesicular nuclei with prominent, eosinophilic nucleoli, and scant cytoplasm
- Prominent mitotic figures; necrosis

#### Keratinizing Squamous Cell Carcinoma (14%)

- Invasive carcinoma with obvious squamous differentiation and keratinization
- Distinct tumor borders, intercellular bridges
- Frequent surface involvement

#### Basaloid Squamous Cell Carcinoma (<1%)

- Identical to basaloid squamous cell carcinoma in other head and neck sites (rare)

### Immunohistochemical Findings

- Positive with pan-keratin, CK5/6, 34βE12, p63, EBER in situ hybridization
- Negative: CK7, CK20, and p16

### Pathologic Differential Diagnosis

- Lymphoma, Hodgkin lymphoma, rhabdomyosarcoma, metaplasia/reactive atypia (epithelial or lymphoid), necrotizing sialometaplasia, spindle cell sarcomas, oropharyngeal nonkeratinizing carcinoma, sinonasal undifferentiated carcinoma, melanoma

## PATHOLOGIC FEATURES

### GROSS FINDINGS

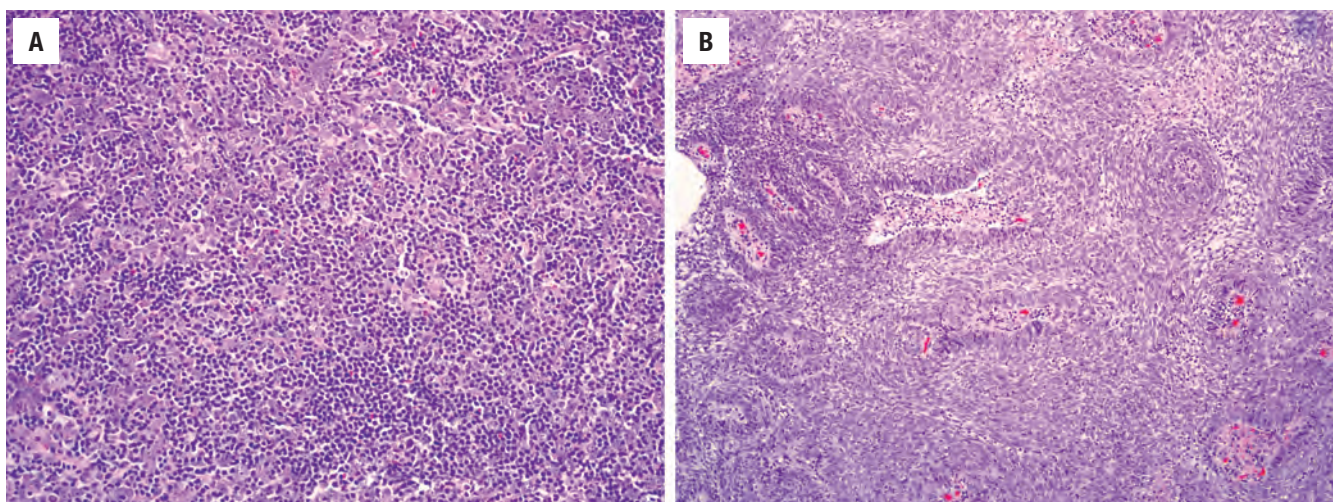
NPC arises most frequently in the lateral wall (fossa of Rosenmüller), superior wall, or vault. By endoscopy, the tumor appears as a bulging (elevated, full), infiltrative, exophytic and lobulated, or ulcerative mass. In some cases, there is no visible lesion, with the tumor identified only by random blind biopsies of the nasopharynx.

### MICROSCOPIC FINDINGS

The World Health Organization (WHO) histologic typing system for NPC includes nonkeratinizing SCC, keratinizing SCC, and basaloid SCC.

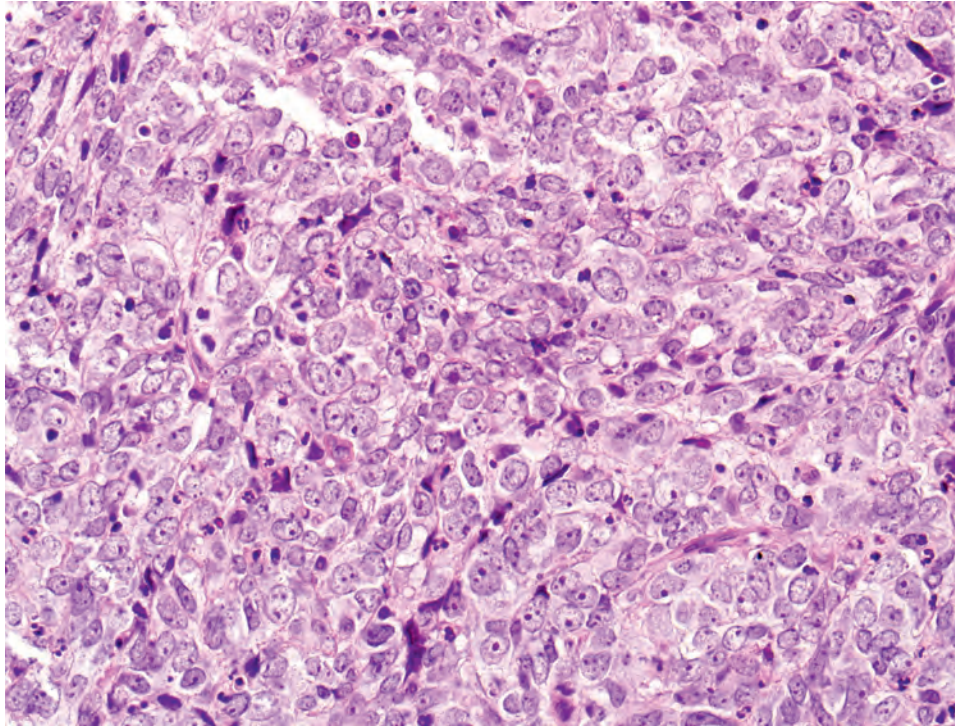
#### Nonkeratinizing Squamous Cell Carcinoma

Dysplasia or in situ surface involvement is seldom recognized, as a mass lesion is usually the dominant finding, obscuring any residual in situ component. The tumor is arranged in irregular islands, solid sheets, interconnecting cords and trabeculae, and single neoplastic cells. The neoplastic cells are intimately intermingled with lymphocytes and plasma cells, which can obscure the neoplastic cells (Fig. 3.16). Cystic change with associated necrosis is also present. The neoplastic cells are large and syncytial-appearing, lacking cell borders (Fig. 3.17). The nuclei are usually vesicular with large, central, prominent nucleoli. Sometimes a greater degree of “differentiation” is appreciated with cellular pavingmenting, cell borders, and stratification. Isolated keratinized cells may be identified (Fig. 3.16). Necrosis and mitotic figures



**FIGURE 3.16**

(A) Nonkeratinizing nasopharyngeal carcinoma with loosely cohesive tumor cells intermingling with small lymphocytes that obscure the tumor cells. (B) This example shows a more “differentiated” appearance with more defined nests and sheets of epithelioid and spindled tumor cells and few infiltrating lymphocytes.

**FIGURE 3.17**

Nonkeratinizing nasopharyngeal carcinoma comprises a syncytium of tumor cells with ill-defined cell borders, large nuclei with vesicular chromatin, and prominent nucleoli.

are easily identified. A desmoplastic stroma is uncommon. At times the lymphoid population may separate the tumor islands into individual cells, bringing the previous term *lymphoepithelial carcinoma* to mind. Eosinophils and amyloid deposits may be seen, the latter more often in indigenous populations. Tumor cells may uncommonly be spindled. More than one histologic type or pattern may be present. In metastatic deposits, the lymphoid mixture is similar to the primary, although a desmoplastic stroma and epithelioid granulomas may obscure the metastatic foci. Metastases are often cystic with central necrosis. The cells are pleomorphic showing little to absent keratinization.

#### Keratinizing Squamous Cell Carcinoma

The tumor cells have demonstrable intercellular bridges and keratin pearl formation, opaque, glassy, eosinophilic cytoplasm and well-defined cell borders. The cells grow in compact nests rather than syncytial loose cohesive aggregates. Surface epithelium is frequently affected, representing carcinoma in situ. The tumors can be graded as well, moderately and poorly differentiated. There is a desmoplastic stroma with a relatively decreased inflammatory infiltrate. This tumor tends to be a locally aggressive neoplasm, metastasizing less commonly than the nonkeratinizing type.

#### Basaloid Squamous Cell Carcinoma

This variant is morphologically identical to tumors in other head and neck sites but vanishingly rare in this location. Composed of palisaded basaloid cells with abrupt squamous differentiation (keratinization, dyskeratosis,

keratin pearl formation, dysplasia) in a variety of patterns around comedonecrosis; mucohyaline and hyaline material is frequently seen.

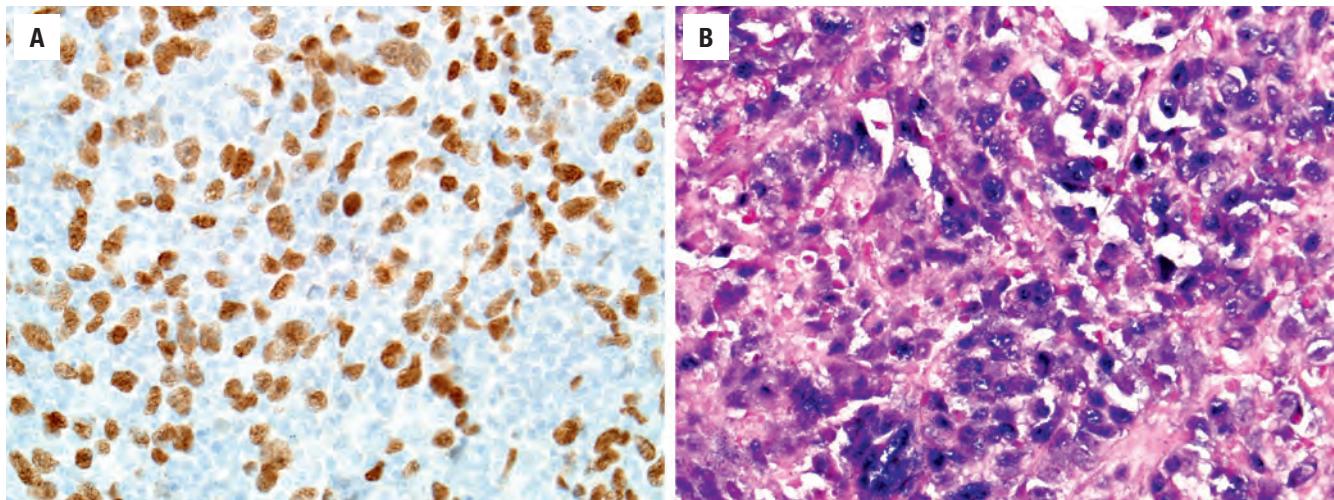
#### ANCILLARY STUDIES

NPCs as a group show strong and diffuse reactions with pan-keratin, often highlighting wisps of cytoplasm in a reticular pattern as they surround lymphocytes. High-molecular-weight keratins (CK5/6, 34 $\beta$ E12) are positive, while CK7 and CK20 are negative. p63 and p40 show a strong nuclear reaction (Fig. 3.18), while p16 is negative. EBV is found in nearly 100 % of tumors, but the technique and antigen sought influence the positivity rate: EBV latent membrane protein-1 (LMP1) is weak, patchy, and positive in only about 30 % of cases; it is thus unreliable and not recommended. The easiest and most reliable way to identify EBV is to use the in situ hybridization technique for EBER, which will show strong nuclear labeling in nearly all tumor cells (except in keratinizing type) (Fig. 3.18). The lymphoid cells react with a compartmentalized mixture of B and T cells, supporting a reactive population.

#### DIFFERENTIAL DIAGNOSIS

The histologic diagnosis of NPC can be difficult and challenging because of small biopsy size and crush artifacts.



**FIGURE 3.18**

Nasopharyngeal carcinoma is positive for the squamous marker p40 (A) and strongly positive for Epstein-Barr–encoded RNA reaction (B).

The most common differential diagnosis includes oropharyngeal nonkeratinizing carcinoma, SNUC, large cell lymphoma, Hodgkin lymphoma, melanoma, metaplastic or reactive epithelial atypia, and spindle cell sarcomas. *Oropharyngeal carcinoma* involves the base of tongue/tonsillar region and is usually p16-immunoreactive. There are occasional EBV-negative NPCs (typically in Western populations) that are HPV-positive, but often, precise staging reveals origin from the oropharynx with extension into the nasopharynx. *SNUC* involves the SNT and tends to lack an inflammatory infiltrate, and is negative for EBER. Immunohistochemical stains are essential for reaching a definitive diagnosis, as management is different for each tumor type.

### PROGNOSIS AND THERAPY

Overall, there is a relatively good prognosis of 65 % to 75 % at 5 years for nonkeratinizing type, but this is stage-dependent, with stage I showing 98 % 5-year survival and stage IV decreasing to 70 %. Prognosis is influenced by tumor stage at presentation, tumor type, young age, female sex, tumor aneuploidy, c-erb-B2, and certain human leukocyte antigen haplotypes. Recurrences are common, although the rate is lower in patients managed with induction chemotherapy before radiation. Synchronous or metachronous second primaries are seen in about 4 % of patients. Regional lymph node metastases are common, often detected at the time of initial presentation. Distant metastases (lung, bone, liver) are a late phenomenon. Keratinizing carcinomas have a 5-year survival below 20 %, probably reflecting radioresistance. Radiation (super voltage) is the cornerstone of therapy, with specific shielded ports employed. When there is advanced disease,

chemotherapy may be added (preradiation, concurrent, or postradiation).

Posttherapy biopsy samples are sometimes difficult to interpret, especially if taken within 3 months of the initiation of therapy. Radiation will induce changes in the surrounding mucosa as well as affecting the tumor cells. Maintenance of the nuclear/cytoplasmic ratio favors reactive changes. In situ EBER reaction would favor residual/recurrent tumor. In some cases, monitoring the serologic EBV DNA titer may suggest disease relapse, although it is usually a late finding.

### MUCOSAL MELANOMA

Mucosal melanoma (MM) is a neural crest–derived neoplasm originating from melanocytes and demonstrating melanocytic differentiation. There is a known formalin environmental exposure risk, but radiation and UV exposure are not associated findings. Melanocytosis is speculative.

### CLINICAL FEATURES

MM of the SNT is rare, accounting for less than 1 % of all melanomas (although between 15 % and 20 % of all skin melanomas occur in the head and neck), and less than 5 % of all SNT neoplasms. There is an equal sex distribution, with patients affected from the 5th to 8th decade of life. There appears to be an increased incidence in Japanese patients. In the SNT, the most frequently involved site is the anterior septum, followed by the

maxillary sinus. Clinically, the majority of patients have symptoms of nasal obstruction, epistaxis, nasal discharge (melanorrhoea), polyps, and pain. MRI may show high signal intensity on T1-weighted images, perhaps related to melanin content of the tumor (Fig. 3.19).

#### MUCOSAL MELANOMA—DISEASE FACT SHEET

##### Definition

- Malignant neoplasm of neural crest–derived melanocytic cells

##### Incidence and Location

- <1% of all melanomas
- <5% of all sinonasal tract neoplasms
- Anterior nasal septum > maxillary sinus

##### Morbidity and Mortality

- 17%-47% 5-year survival

##### Sex, Race, and Age Distribution

- Equal sex distribution
- Increased incidence in Japanese patients (related to melanocytosis?)
- Usually 5th to 8th decade

##### Clinical Features

- Polyp, nasal obstruction, epistaxis, or nasal discharge
- Pain uncommon

##### Prognosis and Therapy

- Generally poor prognosis (17%-47% 5-year survival)
- Recurrences common
- Poor prognosis with advanced age, tumors >3 cm, mixed anatomic sites, vascular invasion
- Radical surgery with palliative radiation

#### PATHOLOGIC FEATURES

##### GROSS FINDINGS

Nasal melanomas at the time of diagnosis have usually reached a few centimeters in size (mean, 2 to 3 cm);

#### MUCOSAL MELANOMA—PATHOLOGIC FINDINGS

##### Gross Findings

- Gray, brown, or black bulky mass with friable or gelatinous appearance

##### Microscopic Findings

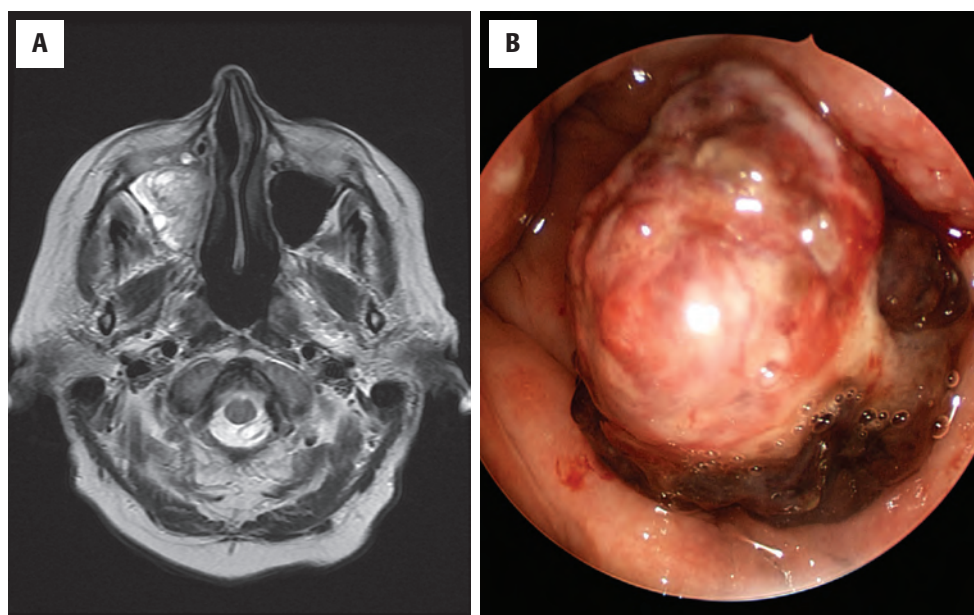
- Junctional activity and epidermal migration confirms primary site in sinonasal tract
- Epithelioid, small, spindle, and pleomorphic cell types
- Peritheliomatous growth is unique, often associated with necrotic tumors
- Usually large cells with high nuclear/cytoplasmic ratio, prominent nucleoli, intranuclear cytoplasmic inclusions
- Pigment may be present
- Mitotic figures are easily identified

##### Immunohistochemical Findings

- Positive for S100 protein, SOX10, Melan A, HMB45, tyrosinase, vimentin
- Keratin and muscle markers are negative

##### Pathologic Differential Diagnosis

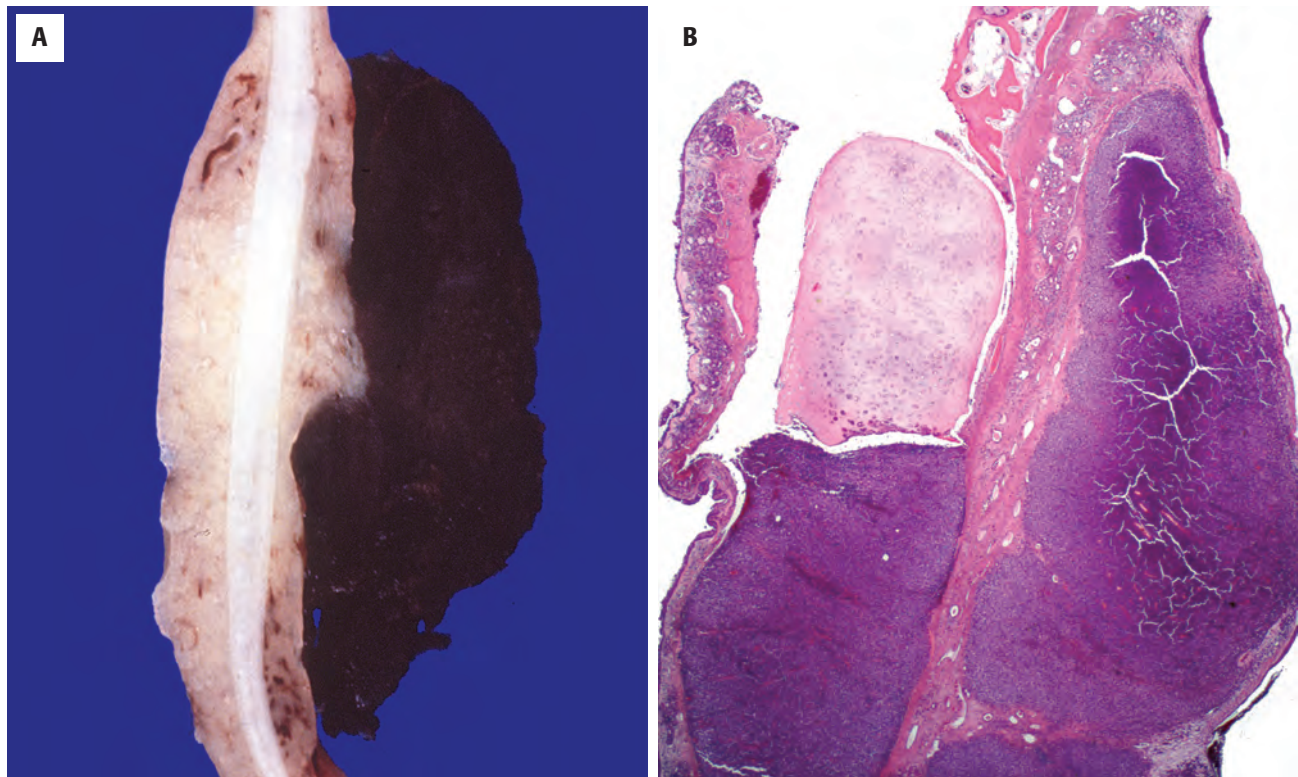
- Sinonasal undifferentiated carcinoma, lymphoma (anaplastic), plasmacytoma, angiosarcoma, sarcomas (rhabdomyosarcoma, leiomyosarcoma, fibrosarcoma), metastatic melanoma to sinonasal tract, olfactory neuroblastoma, melanotic neuroectodermal tumor of infancy, mesenchymal chondrosarcoma



**FIGURE 3.19**

Malignant mucosal melanoma. (A) Magnetic resonance imaging shows an opacifying mass within the right maxillary sinus. Note the high signal intensity on T1-weighted image. (B) An endoscopic view of the large polypoid mass. (Courtesy Dr. G. G. Calzada.)



**FIGURE 3.20**

(A) A black polypoid mass on the nasal septal cartilage was histologically a melanoma. (B) Note the destruction of the cartilage on this low-power view of a malignant mucosal melanoma. There is surface ulceration.

have a polypoid, ulcerated appearance; and vary in color from white to gray, brown, or black (Fig. 3.20).

### MICROSCOPIC FINDINGS

SNT MMs have a protean histology, mimicking that of other primary tumors. A helpful diagnostic feature is the presence of junctional activity and epithelial scatter (Fig. 3.21). Ulceration and invasion (bone, soft tissue, nerves) are common. Tumors can have many patterns of growth as well as many different cell types. Most SNT melanomas grow in sheets, nests, storiform arrangements, fascicles, and/or interlacing bundles (Fig. 3.22). A peritheliomatous distribution is unique (Fig. 3.23), showing aggregation of viable tumor cells around vessels. Large polygonal epithelioid to plasmacytoid or rhabdoid cells have vesicular nuclei, prominent nucleoli, and intranuclear cytoplasmic inclusions. Some tumor cells have small hyperchromatic nuclei and scant cytoplasm resembling anaplastic small cell carcinoma. Melanin-containing tumor cells may be found. Mitotic figures are common and necrosis and inflammation may also be seen adjacent to or within the tumor. Tumor depth of invasion (Clark) and/or thickness (Breslow) is not meaningful in the SNT and thus not measured.

### ANCILLARY STUDIES

#### ULTRASTRUCTURAL FINDINGS

The presence of premelanosomes and melanosomes confirms a melanocytic origin.

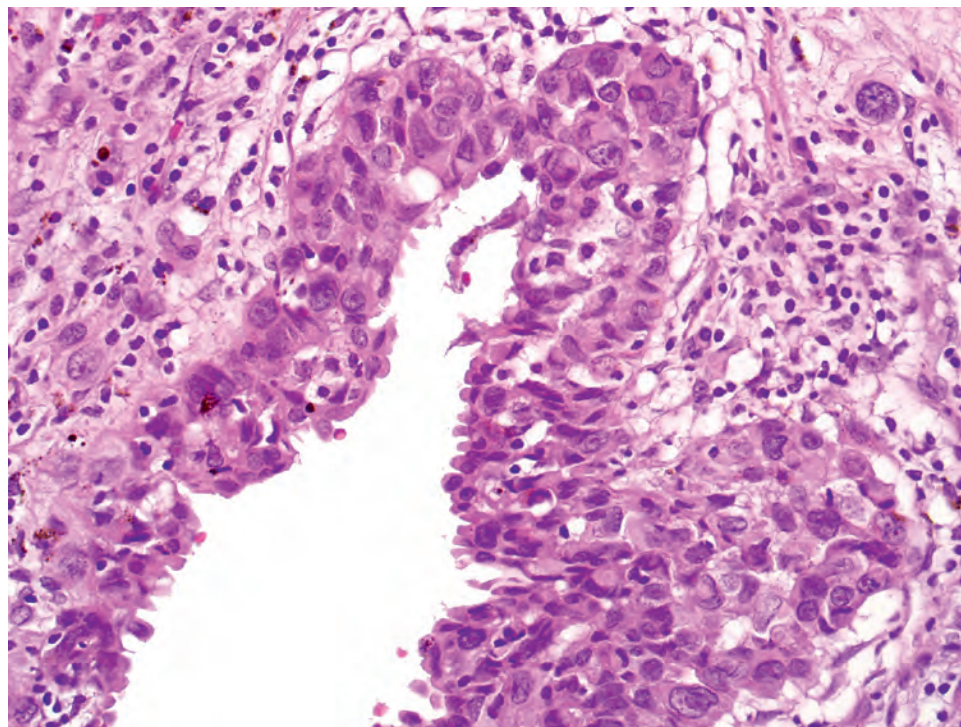
#### IMMUNOHISTOCHEMICAL FINDINGS

The neoplastic cells are immunoreactive with S100 protein (Fig. 3.24), SOX10 (Fig. 3.24), HMB45 (Fig. 3.24), Melan A (Fig. 3.24), microphthalmia transcription factor, tyrosinase, and vimentin. Unlike cutaneous melanoma, *BRAF* mutations are rare in MM; *NRAS* mutations and *KIT* mutation/amplification are more common.

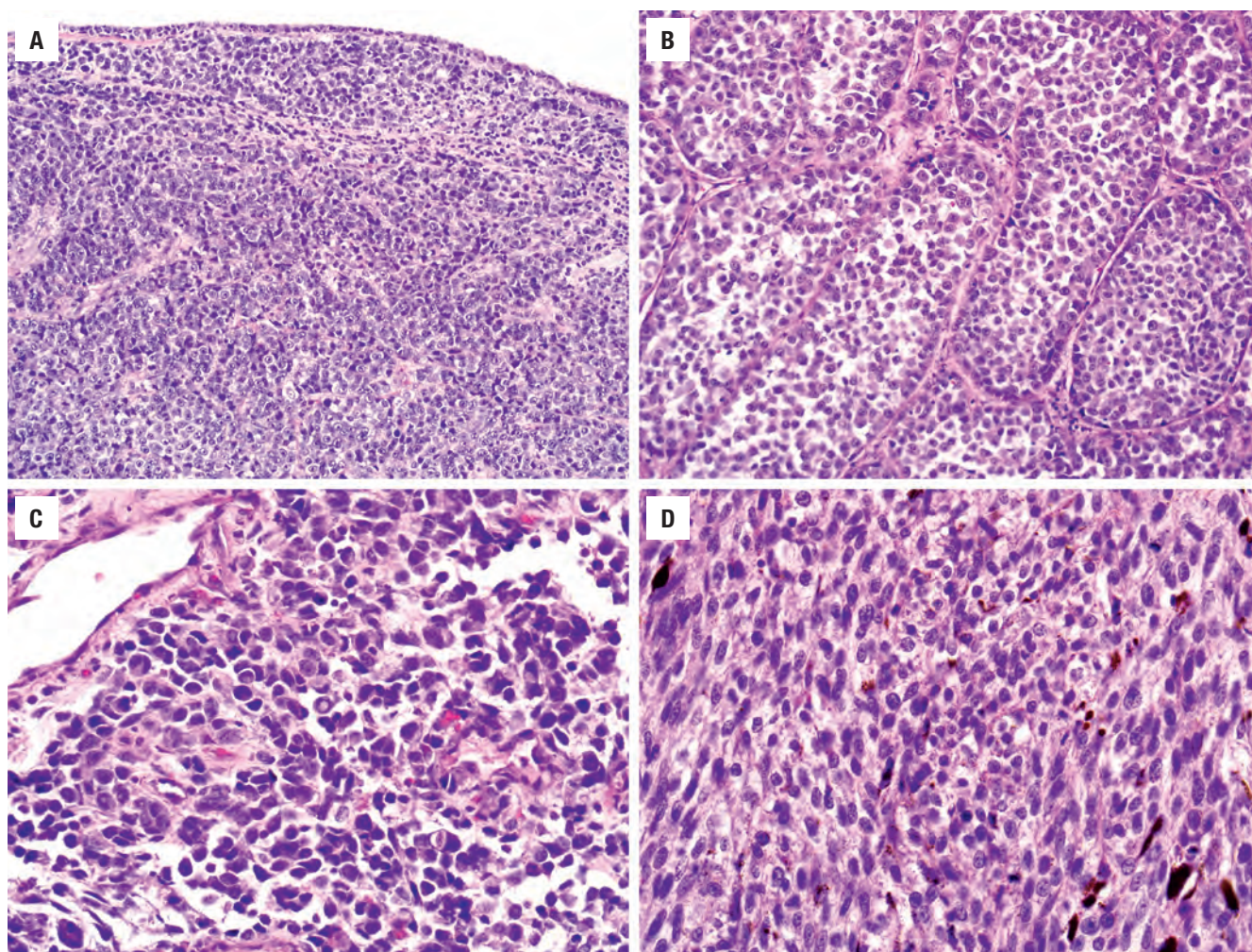
### DIFFERENTIAL DIAGNOSIS

The wide morphologic diversity includes many malignant neoplasms such as SNUC, lymphoma, ONB, melanotic neuroectodermal tumor of infancy (Fig. 3.25), RMS, LMS, fibrosarcoma, mesenchymal chondrosarcoma, plasmacytoma, angiosarcoma, and, rarely, metastatic melanoma



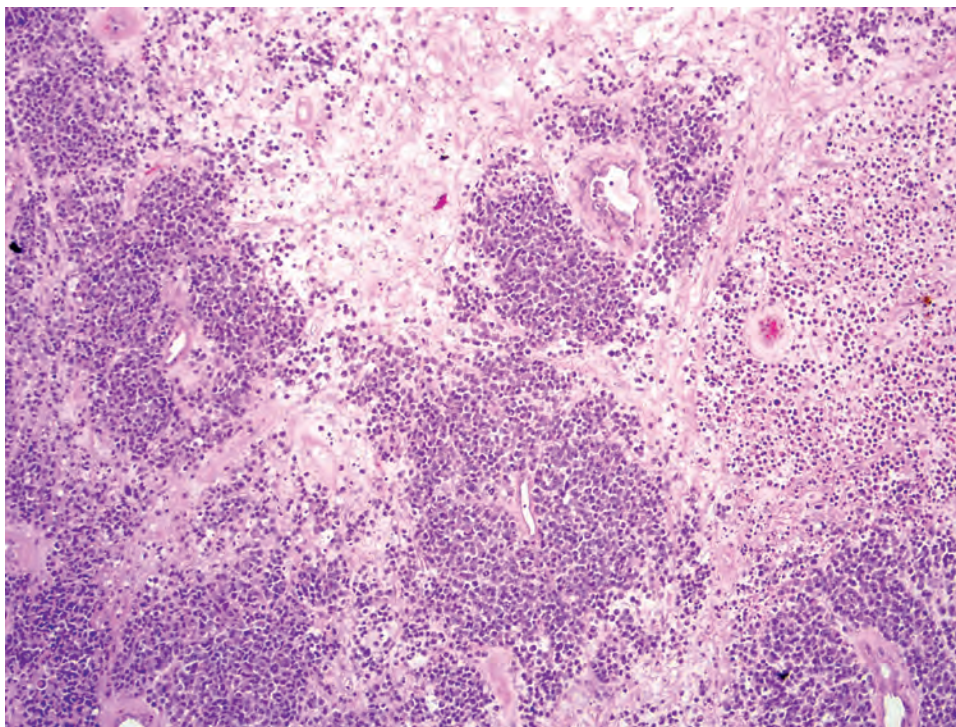
**FIGURE 3.21**

Malignant mucosal melanoma in situ with full-thickness involvement by malignant melanocytes.

**FIGURE 3.22**

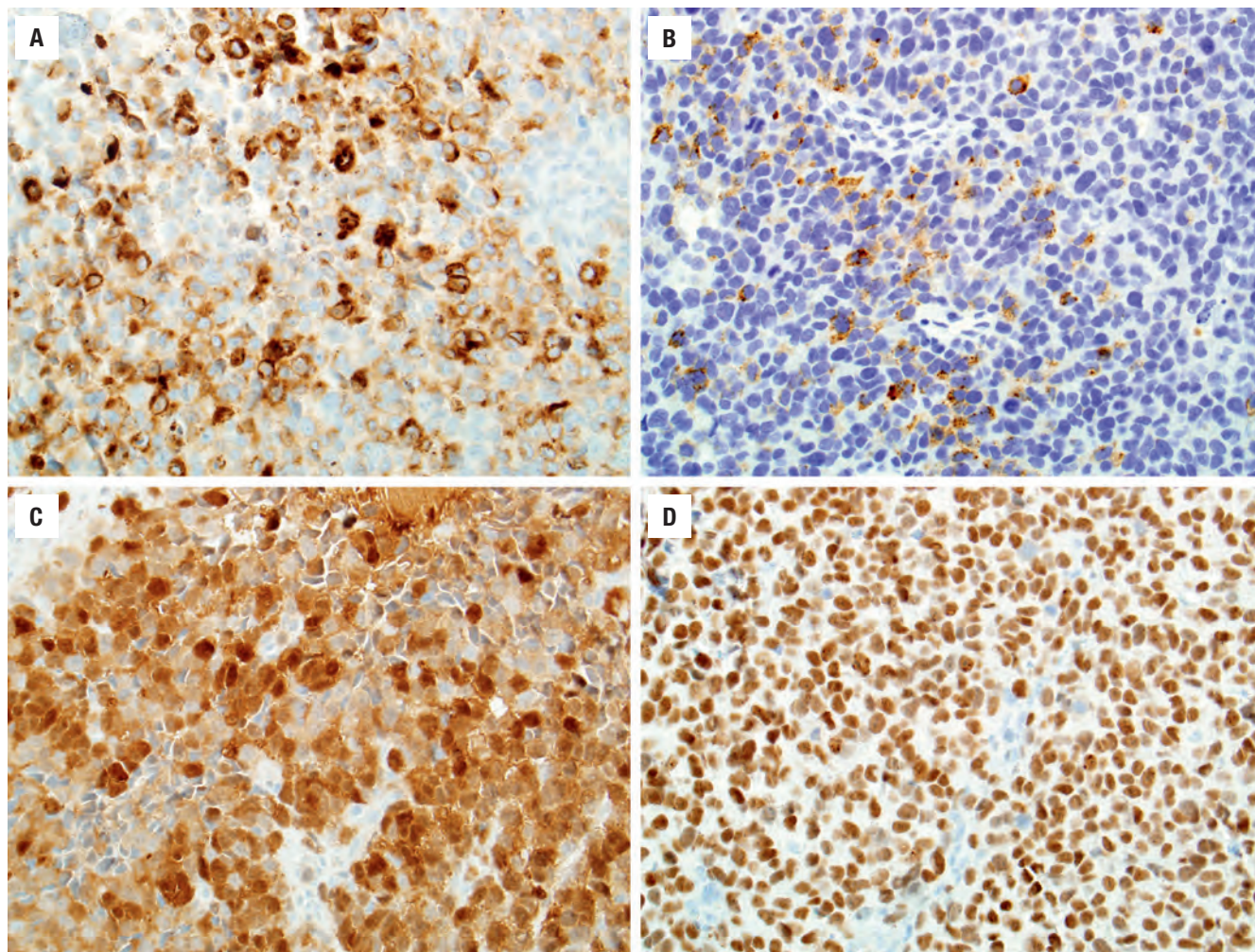
Malignant mucosal melanoma is remarkably diverse in its growth patterns, including solid (A), alveolar (B), small cell (C), and spindle cell (D). Prominent nucleoli, at least focally, are a consistent finding.





**FIGURE 3.23**

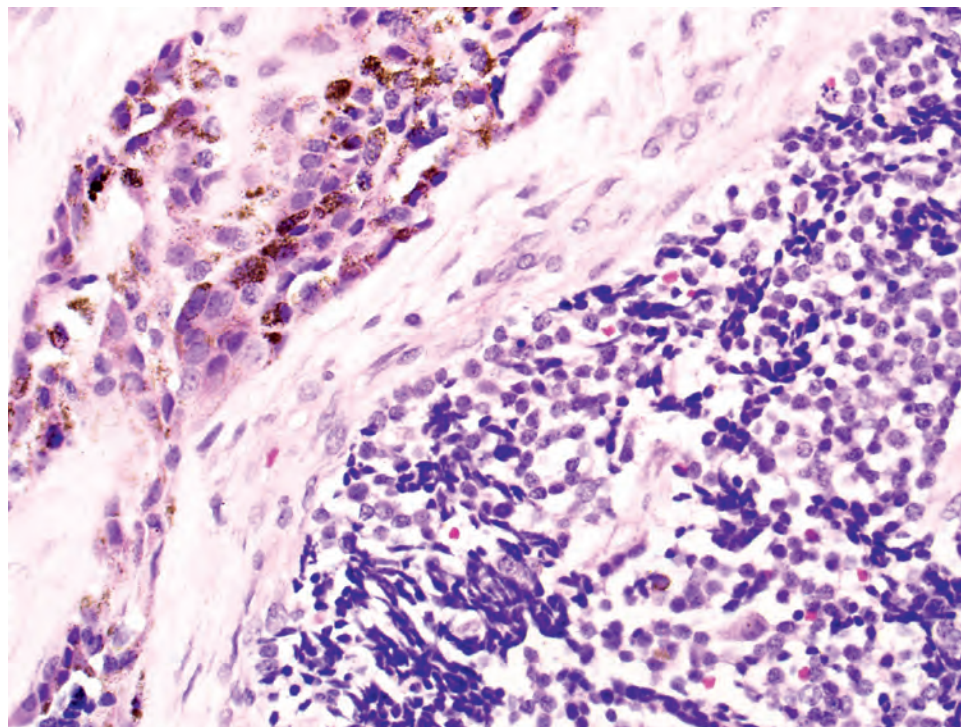
Melanomas of the sinonasal tract classically demonstrate a peritheliomatous arrangement of tumor cells, with viable tumor cells cuffing the vessels separated by abundant necrosis.



**FIGURE 3.24**

Malignant mucosal melanomas are positive (with varying degrees of intensity) for Melan A (A), HMB45 (B), S100 protein (C), and SOX10 (D).



**FIGURE 3.25**

Melanocytic neuroectodermal tumor of infancy has a dual population of large pigmented cells (*left*) and small primitive cells (*right*). The young age of the affected patient coupled with the limited cellular atypia helps to distinguish this tumor from melanoma.

to the SNT (Table 3.1). Pertinent immunohistochemical studies allow for appropriate separation. Metastatic melanoma to the SNT, if it develops, is usually a late event and part of systemic disease.

### PROGNOSIS AND THERAPY

The overall prognosis for SNT melanoma is poor, with a 5-year survival ranging from 17 % to 47 %. Recurrences are common, with a poor prognosis associated with advanced stage, obstructive symptoms, tumor greater than 3 cm in diameter, mixed anatomic sites of involvement, undifferentiated histology, high mitotic index, and vascular invasion. Matrix metalloproteinase (MMP) expression is associated with patient outcome (MMP14 expression associated with poor prognosis). Wide local excision is the treatment of choice, with radiation providing only palliation.

### ■ OLFACTORY NEUROBLASTOMA

ONB (esthesioneuroblastoma) is a malignant neoplasm thought to arise from the specialized sensory neuroepithelial (neuroectodermal) olfactory cells (bipolar neurons) normally found in the upper part of the nasal cavity, including the superior nasal concha, the upper part of the septum, the roof of the nose, and the cribriform plate

of the ethmoid sinus. Olfactory epithelium contains three cell types (basal cells, olfactory neurosensory cells, and sustentacular supporting cells), all of which are also part of the tumor.

### CLINICAL FEATURES

ONBs account for ~3 % of SNT malignancies (0.4 per 1 million population per year). There is a slight male predilection (1.2:1). The tumor may occur at any age, with a peak in the 5th to 6th decade. These slow-growing tumors most commonly cause unilateral nasal obstruction (70 %), epistaxis (50 %), headaches, pain, rhinorrhea, visual disturbances, and a mass high in the nasal cavity and ethmoid region. Anosmia is uncommon (<5 % of patients).

### RADIOGRAPHIC FEATURES

The classic presentation is with a “dumbbell-shaped” mass encompassing the cribriform plate of the ethmoid sinus (as the “waist”), with expansion into the intracranial and nasal cavity areas (Fig. 3.26). Peripheral tumor cysts in the intracranial portion are very suggestive of ONB. MRI demonstrates remarkable tumor enhancement on T1-weighted images with gadolinium contrast. Calcifications may be identified, generally best seen on CT studies.



### OLFACTORY NEUROBLASTOMA—DISEASE FACT SHEET

#### Definition

- Malignant neuroectodermal neoplasm arising from olfactory epithelium

#### Incidence and Location

- Approximately 3% of sinonasal tract malignancies
- About 0.4 per 1 million population
- Encompasses cribriform plate

#### Morbidity and Mortality

- Stage-dependent mortality, overall ~60% 5-year survival

#### Sex and Age Distribution

- Slight male predominance (1.2:1)
- Wide age range, but peak in 5th to 6th decade

#### Clinical Features

- Unilateral nasal obstruction and epistaxis most common
- Anosmia, headaches, pain, and ocular disturbances
- Often slow-growing
- Anosmia is uncommon (<5% of patients)

#### Radiographic Features

- Dumbbell-shaped mass on either side of the cribriform plate
- MRI: intense enhancement on T1-weighted imaging with gadolinium contrast

#### Prognosis and Therapy

- Prognosis is stage- and grade-dependent:
- 75%-90% 5-year survival (stage A) to 45% (stage C)
- 80% low grade vs. 25% high grade
- Approximately 30% recurrence rate, usually within 2 years
- Metastasis develops in lymph nodes (up to 35%)
- Meticulous surgical eradication with postoperative radiotherapy
- Chemotherapy and bone marrow transplantation show promise

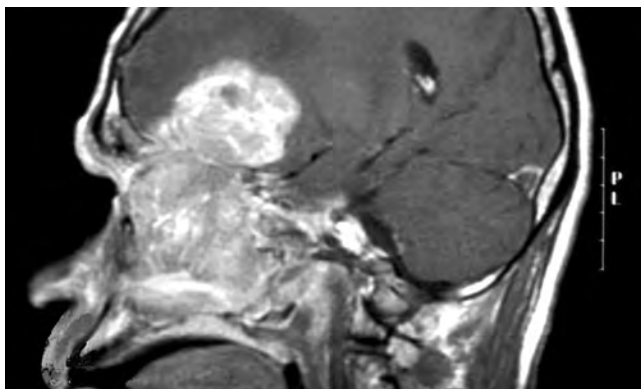


**FIGURE 3.26**

A T1-weighted gadolinium contrast-enhanced magnetic resonance image shows a dumbbell-shaped mass extending through the cribriform plate and filling the nasal vault and the intracranial cavity.

### OLFACTORY NEUROBLASTOMA—PATHOLOGIC FEATURES

#### Gross Findings

- Polypoid, glistening, soft, vascular masses high in the nasal cavity and ethmoid sinus

#### Microscopic Findings

- Circumscribed lobules separated by vascularized stroma; this pattern is maintained to some degree in all grades
- Tumor cells form solid nests, Homer Wright pseudorosettes with neurofibrillary matrix (30%), and Flexner-Wintersteiner-type true rosettes with glandular lumen (5%)
- Cells are syncytial, uniform, and small, with round nuclei and “salt-and-pepper” nuclear chromatin
- High-grade tumors have larger tumor cells, nuclear pleomorphism, and increased mitotic activity; neurofibrillary matrix is scant or absent

#### Immunohistochemical Findings

- Synaptophysin, chromogranin, CD56
- 80% of tumors are positive for neuron-specific enolase
- Calretinin is positive
- S100 protein and/or GFAP-positive cells confined to the periphery of tumor nests

#### Pathologic Differential Diagnosis

- Sinonasal undifferentiated carcinoma, lymphoma, plasmacytoma, NUT carcinoma, rhabdomyosarcoma, melanoma, neuroendocrine carcinoma, Ewing sarcoma/primitive neuroectodermal tumor, pituitary adenoma

### PATHOLOGIC FEATURES

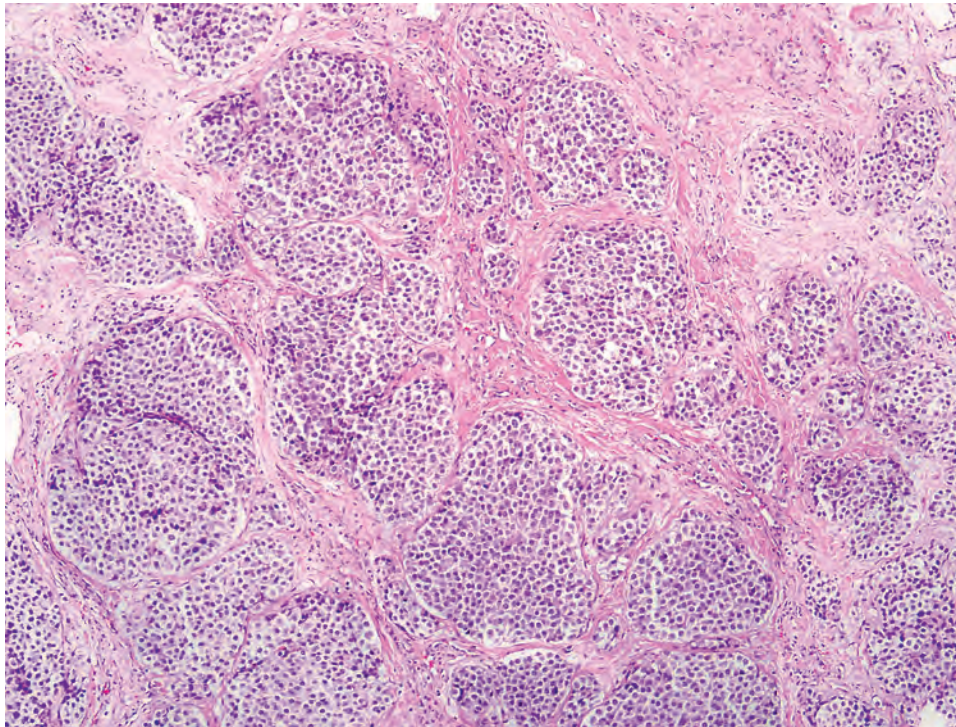
#### GROSS FINDINGS

The excised tumors vary from small polypoid nodules to large masses involving the bilateral ethmoids and nasal cavity with extension into the adjacent paranasal sinuses, superior nasal concha, turbinates, and upper septum. The cut surface appears glistening, gray-tan to pink-red, and hypervascular.

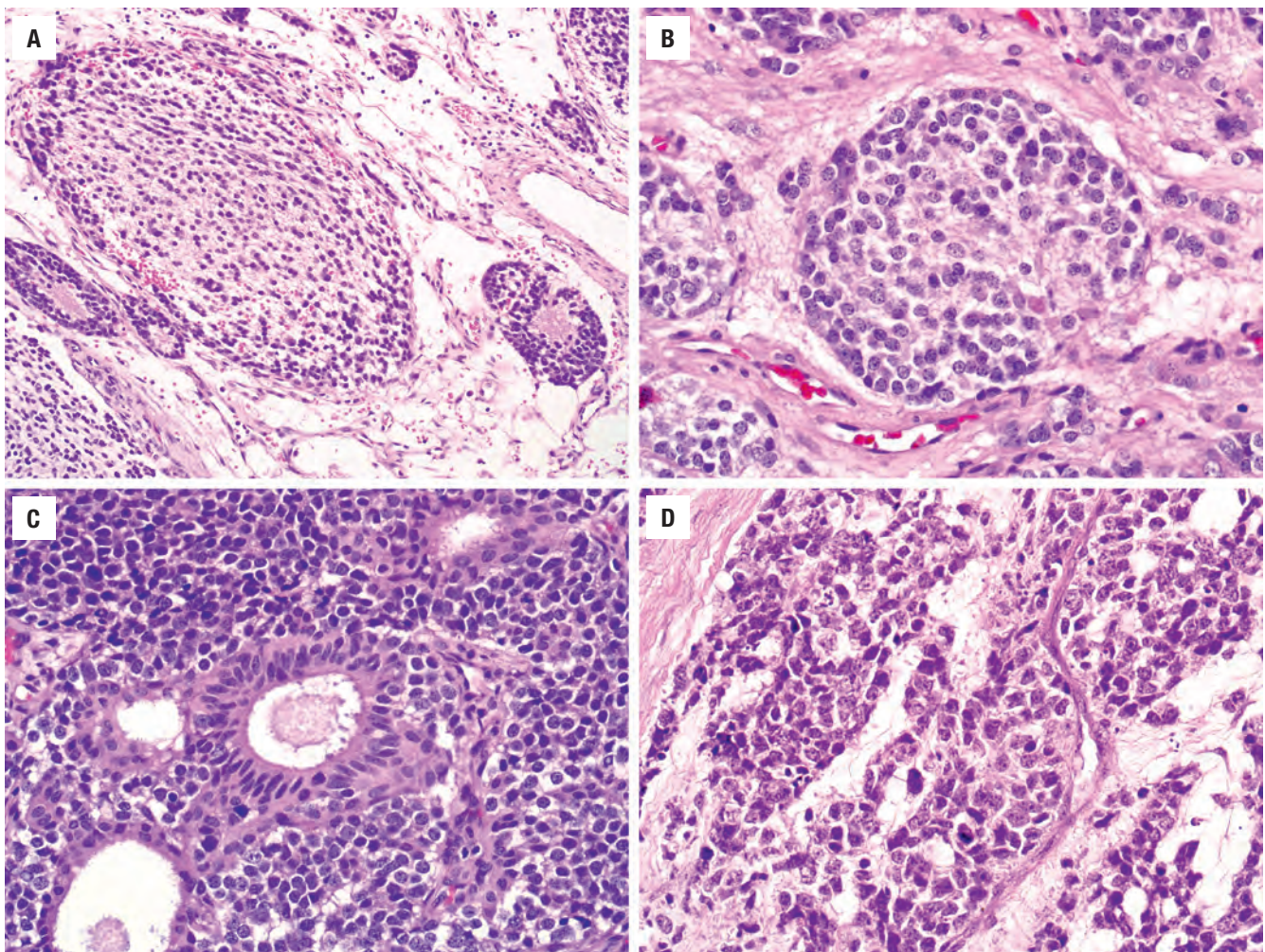
#### MICROSCOPIC FINDINGS

The histologic appearance of ONB varies by degree of differentiation, although a semblance of lobular architecture is maintained throughout (Fig. 3.27). The tumor cells are identified below an intact mucosa, often immediately subtending the olfactory epithelium. In-situ tumor is rare. Low-grade tumors contain cellular nests surrounded by fine fibrovascular septa in an organoid fashion (Fig. 3.28). Sustentacular supporting cells line these lobules or nests. The primitive neuroblastoma cells are relatively uniform, slightly larger than lymphocytes, and lie in a finely fibrillar neuronal stroma (Fig. 3.28). The syncytium of cells have a very high nuclear/cytoplasmic ratio; nuclei are small and round



**FIGURE 3.27**

Olfactory neuroblastoma with compact nests (lobules) of tumor cells separated by a vascular stroma.

**FIGURE 3.28**

Olfactory neuroblastoma. **(A)** Grade 1 olfactory neuroblastoma has a prominent fibrillary matrix, several Homer Wright pseudorosettes, and small nuclei without atypia. **(B)** Grade 2 olfactory neuroblastoma is nested with prominent fibrillary stroma but has increased nuclear atypia. **(C)** Grade 3 olfactory neuroblastoma with increased atypia, mitotic activity, and Flexner-Wintersteiner rosettes. **(D)** Grade 4 olfactory neuroblastoma with marked nuclear atypia and an elevated mitotic rate.



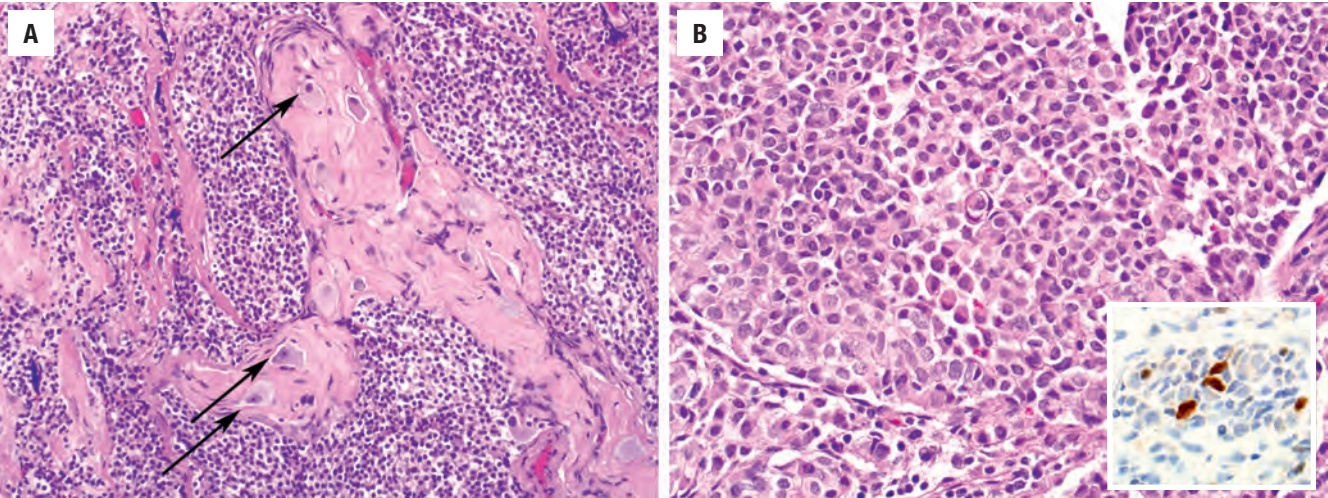


**FIGURE 3.29**  
Olfactory neuroblastoma may rarely exhibit ganglion cell (A, arrows) or rhabdomyoblastic (B) differentiation. A myogenin immunostain highlights the scattered rhabdomyoblastic tumor cells.

| TABLE 3.2<br>Hyams’ grading system for olfactory neuroblastoma |              |              |                       |                       |
|--|--------------|--------------|-----------------------|-----------------------|
| Feature  | Grade 1      | Grade 2      | Grade 3               | Grade 4               |
| Architecture   | Lobular      | Lobular      | Lobular               | Lobular               |
| Mitotic activity   | Absent       | Present      | Prominent             | Marked                |
| Nuclear pleomorphism   | Absent       | Moderate     | Prominent             | Marked                |
| Fibrillary matrix  | Prominent    | Present      | Minimal               | Absent                |
| Rosettes   | Homer Wright | Homer Wright | Flexner-Wintersteiner | Flexner-Wintersteiner |
| Necrosis   | Absent       | Absent       | Present               | Common                |

to oval with uniformly distributed fine or coarse nuclear chromatin. Homer Wright pseudorosettes (seen in up to 30 % of cases) are characterized by palisaded or cuffed neoplastic cells with finely fibrillar or granular material in the center (Fig. 3.28). True Flexner-Wintersteiner rosettes (seen in ~ 5 % of cases) form duct-like spaces lined by nonciliated columnar cells with basally placed nuclei but are identified only in higher-grade tumors (Fig. 3.28). Calcification (psammomatous or concretion) may be seen. Rarely, ganglion cells (Fig. 3.29), melanin-containing cells, and rhabdomyoblastic cells (Fig. 3.29) may be seen.

As the ONBs develop into higher grade (less differentiated) tumors, pseudorosettes and fibrillar stroma become less common. The nuclei become more pleomorphic, chromatin is coarser, mitotic figures increase, and tumor necrosis is present. Tumors are graded on the basis of the degree of differentiation, presence of neural stroma, mitotic figures, and necrosis from grades 1 to 4 (Table 3.2). The grade correlates with prognosis. Kadish staging (groups A, B, and C) is based on the clinical extent of

disease, with modifications suggested to include lymph node status.

**ANCILLARY STUDIES**

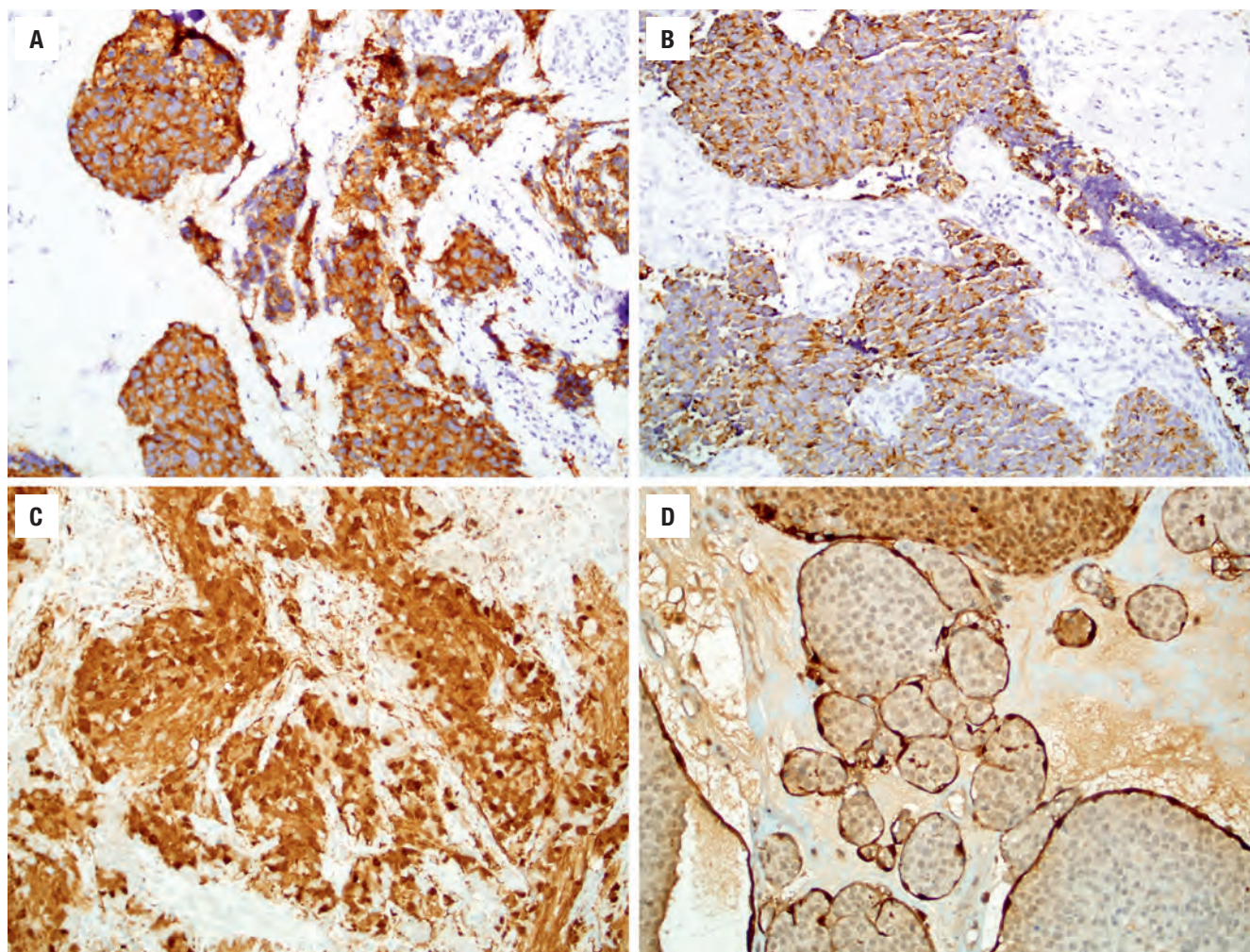
**ULTRASTRUCTURAL FINDINGS**

Membrane-bound dense core neurosecretory granules are present in the cytoplasm and in nerve processes, which additionally contain neurotubules and neurofilaments. The diameter of the granules is from 50 to 250 nm. Olfactory differentiation with olfactory vesicles and microvilli on apical borders may be seen in Flexner-Wintersteiner rosettes.

**HISTOCHEMISTRY FINDINGS**

Silver stains highlight neurosecretory granules and include Grimelius, Bodian, and Churukian–Schenk stains.



**FIGURE 3.30**

Olfactory neuroblastoma is consistently positive for synaptophysin (A), chromogranin (B), and calretinin (C). S100 protein immunohistochemistry typically demonstrates a network of sustentacular cells at the periphery of the tumor nests (D).

#### IMMUNOHISTOCHEMICAL FINDINGS

Synaptophysin (Fig. 3.30), chromogranin (Fig. 3.30), CD56, and NSE are expressed in a diffuse pattern in some 80 % of tumors. ONB is consistently positive for calretinin (Fig. 3.30). A small number of cells at the periphery of tumor nests react with the antibodies against S100 protein (Fig. 3.30) and glial fibrillary acidic protein (GFAP) to suggest Schwann cell differentiation. Keratins are occasionally positive, but usually only in isolated cells. The tumor cells are negative with CD45RB, HMB45, desmin, and CD99.

#### DIFFERENTIAL DIAGNOSIS

The small round blue cell neoplasm group of the SNT includes SNUC, NUT carcinoma, ACC, lymphoma, plasmacytoma, RMS, melanoma, neuroendocrine carcinoma, pituitary adenoma, and ES/PNET (Table 3.1).

In a small biopsy with crush artifact, misinterpretation is common, especially as edge effect and diffusion artifacts with immunohistochemistry may not resolve the differential. Carcinomas tend to have higher mitotic activity, larger nucleoli, and obvious necrosis. A targeted immunohistochemistry panel may have to be expanded to encompass the differential, especially if the lesion is high in the nasal cavity.

#### PROGNOSIS AND THERAPY

The prognosis is both stage- and grade-dependent, with stage A tumors experiencing a 75 % to 90 % 5-year survival, while stage C has a 45 % survival. Likewise, low-grade tumors have an 80 % survival, while high-grade tumors have a 25 % 5-year survival. Recurrence is common (~30 %), usually within 2 years of the initial presentation. Metastasis develops in up to 35 % of cases (lymph nodes), while distant metastasis occurs in about 10 % of patients



(lung, bone, liver, skin). En bloc resection of the tumor and cribriform plate with clear margins via a trephination and bicraniofacial approach is the treatment of choice for these tumors, although endoscopic methods are gaining popularity. Postoperative radiation is given to most patients to improve local control. Patients with advanced tumor or poorly differentiated tumor usually receive multimodality treatment, including high-dose chemotherapy and bone marrow transplantation. Poor prognostic indicators include high-grade tumor, high stage, metastases, females, below 20 or above 50 years of age at presentation, intracranial spread, high proliferation, and polyploidy/aneuploidy.

### ■ EXTRANODAL NK/T-CELL LYMPHOMA, NASAL TYPE

Lymphoma is the most common malignant nonepithelial neoplasm found in the upper respiratory tract and most often involves the nasal cavity, maxillary sinus, nasopharynx, and salivary gland. This discussion is limited to extranodal NK/T-cell lymphoma, nasal type (NK/T LNT), which is more common in the sinonasal region, although B-cell lymphomas tend to be more common in the nasopharynx, Waldeyer ring, and the sinuses (Fig. 3.31). Hodgkin lymphoma is uncommon in either location. Additionally, there are geographic differences, where Asian and South American patients have a much higher frequency of SNT lymphoma (~7% of lymphomas), with the majority NK/T LNT, while in Western countries SNT lymphomas account for less than 2% of lymphomas, with B-cell types predominating.

There are a number of differences between the types of lymphoid lesions that affect each of these locations,

most closely related to the function of tissues affected. For example, the SNT does not normally contain lymphoid tissue; therefore EBV-associated NK/T LNT tends to be more common. The nasopharynx, by contrast, has a rich lymphoid tissue, which can be affected by follicular hyperplasia or by B-cell lymphomas, most specifically mantle cell lymphoma. The distinction of NK/T LNT from other diseases that give the clinical picture of midline destructive disease cannot be overemphasized. The differences in treatment and patient outcome are diametrically opposite in many cases. Unfortunately, the diagnosis of NK/T LNT is often very challenging in the initial stages of presentation, requiring very close clinical correlation between the pathologist, otorhinolaryngologist, oncologist, and radiation therapist.

Many different names have been used for this disorder in the past: angiocentric NK/T-cell lymphoma, polymorphic reticulosis, lethal midline granuloma, Stewart granuloma, and peripheral NK/T-cell lymphoma, to name just a few. It is wisest to use the current WHO criteria since they incorporate clinical, histologic, immunophenotypic, molecular, and treatment considerations into the classification scheme.

### CLINICAL FEATURES

Peripheral T-cell lymphomas are uncommon, accounting for 10% to 15% of all non-Hodgkin lymphomas. The tumors are much more common in Asia and South and Central America than in Western countries. All ages can be affected, but patients usually present in the 5th to 6th decade, although there is a rare hydroa vacciniforme-like lymphoma in children, which is also EBV-positive. In general men are more commonly affected than women

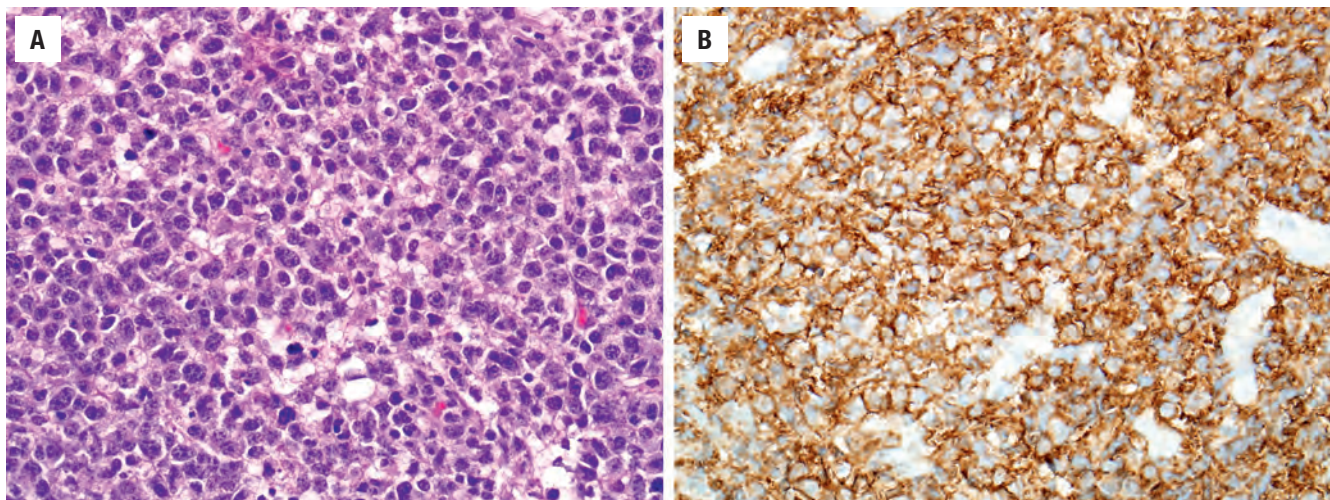


**FIGURE 3.31**

(A) A diffuse large B-cell lymphoma of the nasal tract with a sheet-like proliferation of large, atypical lymphoid cells. (B) The tumor cells are diffusely positive for the B-cell marker CD20.

**EXTRANODAL NK/T-CELL LYMPHOMA, NASAL TYPE—DISEASE FACT SHEET****Definition**

- Extranodal lymphoma with a cytotoxic phenotype universally associated with EBV, with the bulk of the disease in the sinonasal tract

**Incidence and Location**

- Most common nonepithelial malignancy of the sinonasal tract
- About 10%-15% of all non-Hodgkin lymphomas
- Nasal cavity and paranasal sinuses concurrently affected

**Morbidity and Mortality**

- Mortality in 50%-70% of patients

**Sex, Race, and Age Distribution**

- Males > females (3:1)
- Endemic in Asians and Central/Latin Americans
- Peak in 6th decade

**Clinical Features**

- Early disease difficult to detect with nonspecific symptoms
- Nasal obstruction, epistaxis, nasal discharge, and swelling
- Septal perforation and bone destruction later in course
- Uncommonly, patients have fever and weight loss
- Most patients present with low-stage disease (stage I/II)
- Very strong association with Epstein-Barr virus

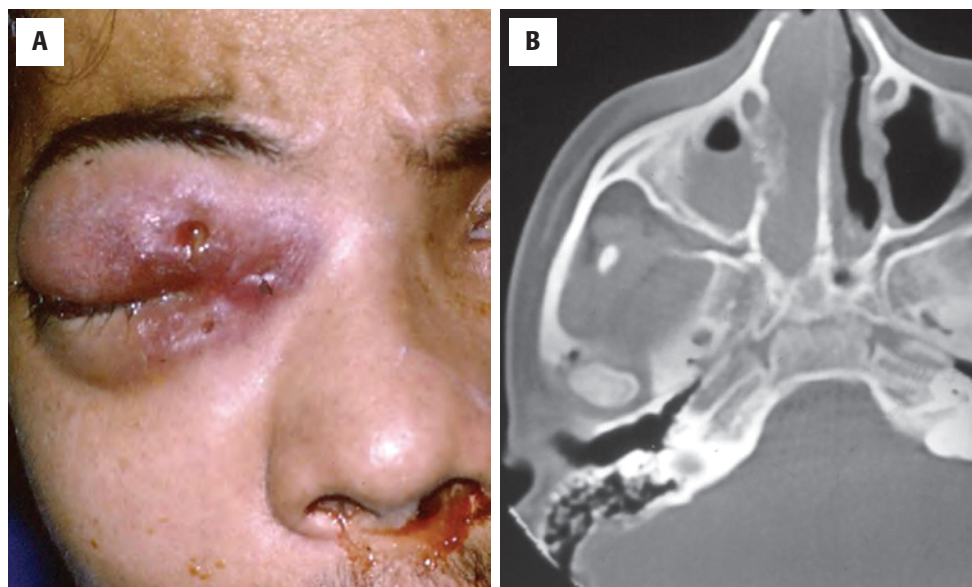
**Prognosis and Therapy**

- Overall prognosis is 30%-50%
- Relapse/recurrence develop in up to 50%
- Advanced stage, bulky disease, and systemic symptoms yield a worse prognosis
- Combined radiotherapy and chemotherapy

(3:1). The most frequent initial clinical presentation is nonspecific, with nasal discharge, sinusitis, headaches, facial and periorbital swelling, and epistaxis. As the tumor develops, the more destructive nature of the neoplasm is manifest through midline destruction (i.e., nasal cavity ulceration, paranasal sinus necrosis [frequently bilateral]), with palatal extension and fistula formation, orbital swelling, and a prominent edema (often with erythematous and “warm” skin overlying these structures) (Fig. 3.32). Pain and paresthesias develop with further destruction of the tissues. Systemic manifestations of weight loss, fever, fatigue, and profound night sweating can also be seen, especially if the stage of the lymphoma results in involvement of extra-SNT sites (skin, soft tissues, gastrointestinal tract). Most patients have stage IE or IIE disease at presentation (E meaning extranodal). Therefore, this particular type of lymphoma may be indolent or aggressive, depending on the overall morphology and the stage of lymphoma. There is a very strong association with EBV in both the endemic and nonendemic populations. Patients who are immunosuppressed (especially after organ transplantation) may develop the lymphoma more often. A few cases will have a hemato-phagocytic syndrome with pancytopenia or hyper-IgE syndrome (Job syndrome). Serum EBV-DNA copy number may be a useful tumor marker.

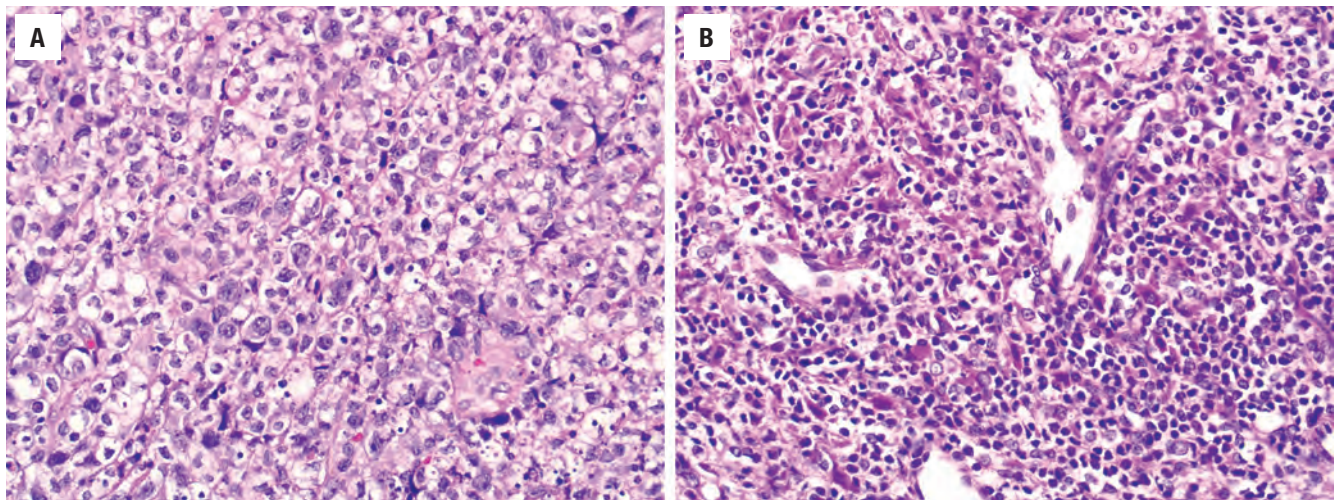
**PATHOLOGIC FEATURES****GROSS FINDINGS**

A raised polypoid unilateral lesion usually within the nasal cavity in the early stages develops progressively

**FIGURE 3.32**

Extranodal NK/T cell lymphoma, nasal type. (A) A 19-year-old presented with a large destructive lesion of the nasal cavity, maxillary sinus, and orbit, showing marked orbital edema, erythema, and crusting. (B) The medial wall of the maxillary sinus is destroyed, with a mass filling the maxillary sinus and nasal cavity in this computed tomography image. (A, Courtesy of Dr. R. Carlos.)



**FIGURE 3.33**

(A) Extranodal NK/T cell lymphoma, nasal type, consists of large pleomorphic cells with irregular tumor nuclei. (B) This tumor may be deceptively mixed in early stages, with malignant cells obscured by an infiltrate of small benign lymphocytes and/or granulocytes.

#### EXTRANODAL NK/T-CELL LYMPHOMA, NASAL TYPE— PATHOLOGIC FEATURES

##### Microscopic Findings

- Early disease difficult to detect in background reactive lymphoid infiltrate
- Diffuse infiltrate that is frequently angiocentric and angioinvasive associated with tumor necrosis
- Variable, mixed small and large lymphoid cells
- May occasionally have extensive pseudoepitheliomatous squamous hyperplasia of the epithelium

##### Immunohistochemical Findings

- Positive: CD2, cytoplasmic CD3ε, CD56, perforin, TIA1, granzyme B, EBER
- Negative: CD5, CD16, CD57

##### Pathologic Differential Diagnosis

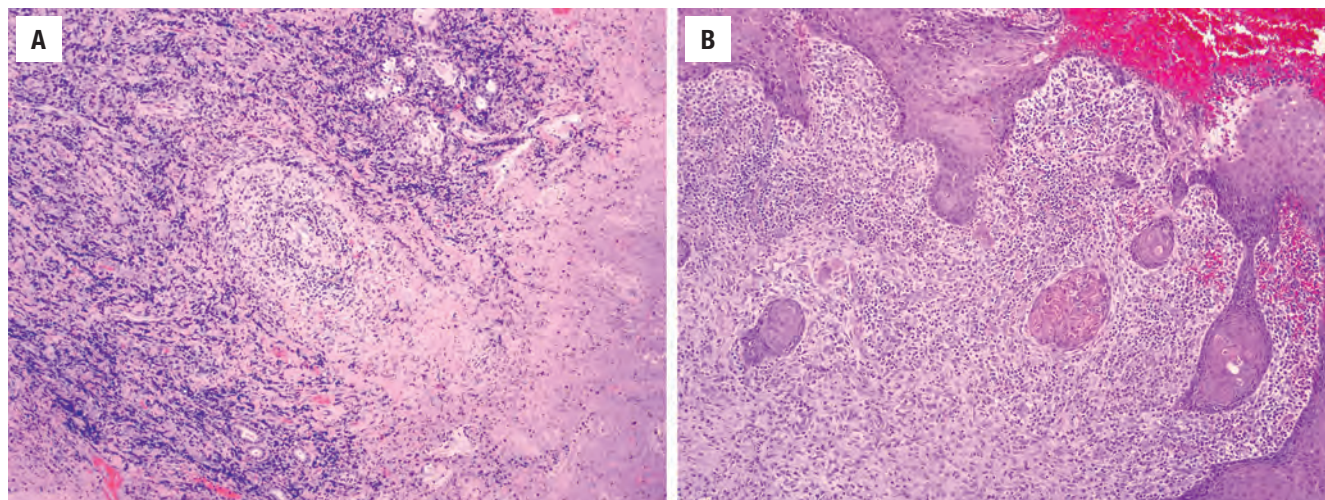
- Reactive/inflammatory infiltrate, granulomatosis with polyangiitis, lymphomatoid granulomatosis, olfactory neuroblastoma, Ewing sarcoma/primitive neuroectodermal tumor, carcinoma, melanoma

into an ulcerated and necrotic mass, which may become bilateral. The cut surface reveals gray-white, friable, homogeneous tissue.

#### MICROSCOPIC FINDINGS

NK/T LNT is a polymorphic neoplastic infiltrate with angioinvasion and/or angiodestruction with strong EBV association. In contrast to the nasopharynx and tonsils, NK/T LNT is much more common than B-cell lymphomas in the nasal cavity. There is a developmental arc associated

with disease progression. Initially, there is a subepithelial, diffuse polymorphous cellular infiltrate composed of normal appearing lymphocytes, histiocytes, immunoblasts, eosinophils, and plasma cells (Fig. 3.33). Within this milieu are a number of atypical lymphoid cells, increasing in number as the disease progresses (Fig. 3.33). These neoplastic cells have a broad cytomorphic pattern, ranging in size from small to large, the latter usually remarkably atypical. These hyperchromatic cells have irregular pleomorphic nuclei with prominent nucleoli (Fig. 3.33). Tumor cell folding, cleaving, and grooving are characteristic for an NK/T-cell lymphoma. This intermixed population of atypical NK/T cells interspersed throughout the specimen is often exceedingly difficult to identify, even with ancillary techniques. However, the presence of EBV-positive cells is strong supportive evidence of a neoplasm. The prominent background inflammatory component may completely obscure the underlying neoplasm, simulating an infectious or inflammatory condition. When the vascular walls are invaded by the neoplastic cells to the point that they occlude the lumen of the vessel, the presence of profound necrosis brings to mind the possibility of a neoplasm (Fig. 3.34). Angiocentricity and angioinvasion with necrosis are seen in some 50 % to 60 % of NK/T-LNT cases. Owing to a lack of ubiquitous angioinvasion and destruction, the WHO uses the term *extranodal NK/T-cell lymphoma, nasal type*, instead of *angiocentric NK/T-cell lymphoma*. Necrosis of the coagulative or ischemic (geographic) type may be widespread, however, further limiting interpretation, especially on small biopsies. Occasionally, pseudoepitheliomatous squamous hyperplasia (Fig. 3.34) and epitheliotropism may simulate an epithelial malignancy. Multiple and repeat biopsies are often required to render a definitive diagnosis, frequently in a patient who is deteriorating clinically!

**FIGURE 3.34**

(A) Extranodal NK/T cell lymphoma, nasal type, characteristically exhibits involvement of arteries (*center*), which leads to large zones of necrosis (*right*). (B), This tumor is sometimes accompanied by reactive pseudoepitheliomatous hyperplasia of the surface epithelium, which can lead to a misdiagnosis of squamous cell carcinoma, especially in small biopsies.

## ANCILLARY STUDIES

### HISTOCHEMICAL STUDIES

Elastic stains may be useful in identifying disruption of the elastic membrane of the vessel walls.

### IMMUNOHISTOCHEMICAL FINDINGS

By in situ hybridization, nearly 100 % of NK/T LNTs have detectable EBER, better developed in Asian patients but also present in Western patients. NK-cell lineage is seen most commonly (in up to 75 %), while T-cell lineage is seen in some 25 % to 35 % of cases. The neoplastic cells are positive with T-cell (CD3C+ [Fig. 3.35], CD2, CD5, CD8[±], CD56 [Fig. 3.35], CD94) and natural killer cell/cytotoxic-related markers (perforin, TIA1 [Fig. 3.35], granzyme B). CD43 and CD45RO may be positive. Vimentin is positive, and p63 is occasionally positive but p40 is always negative. CD16, and CD57 are usually negative. CD30 is seen in large cell morphology tumors, whereas CD5 may be seen in T-cell lineage tumors.

### MOLECULAR GENETICS

T-cell receptor (TCR) gene rearrangement will be present in T-cell tumors, but it is germline. Further, NK-cell tumors do not carry TCR gene rearrangements.

## DIFFERENTIAL DIAGNOSIS

Inflammatory (chronic rhinosinusitis), infectious lesions, and granulomatosis with polyangiitis (Wegener) are key

considerations when there is a lymphoid process. In benign conditions, nuclear atypia and mitotic activity are absent or minimal. Biocollagenolytic necrosis is usually absent in lymphoma, while antineutrophil cytoplasmic antibodies (ANCA) and proteinase 3 (PR3) will be positive in *granulomatosis with polyangiitis*. Carcinoma, melanoma, RMS, ES/PNET, and ONB have unique patterns of growth and unique immunohistochemistry profiles. Immunohistochemical stains and in situ hybridization for EBER are helpful to confirm NK/T LNT. Separation from *lymphomatoid granulomatosis* (LYG) may be nearly impossible, as the latter diagnosis significantly overlaps the clinical, morphologic, and immunophenotype features of NK/T LNT. LYG may be a T-cell-rich EBV-related B-cell lymphoproliferative disease, in which T cells are abundant and reactive in nature. In contrast, NK/T LNT is a T-cell lymphoproliferative disorder, in which EBV occurs in T and NK cells. Separation from other “small round blue cell tumors” can usually be achieved with pertinent immunohistochemistry (Table 3.1).

## PROGNOSIS AND THERAPY

The overall prognosis for NK/T LNT ranges from 30 % to 50 %, with relapses or recurrences developing in up to 50 % of patients. Prognosis is determined by stage, bulky disease, and whether systemic symptoms are present (stage IE: 70 %; stage IIE: 40 % at 5 years). Most patients present with stage I or II disease. The development of systemic disease is common. A worse prognosis is experienced by patients with bulky disease, advanced stage, multiple sites of involvement, and older age. Treatment for localized disease is radiotherapy with or without chemotherapy (specific to NK/T-cell phenotype). Early



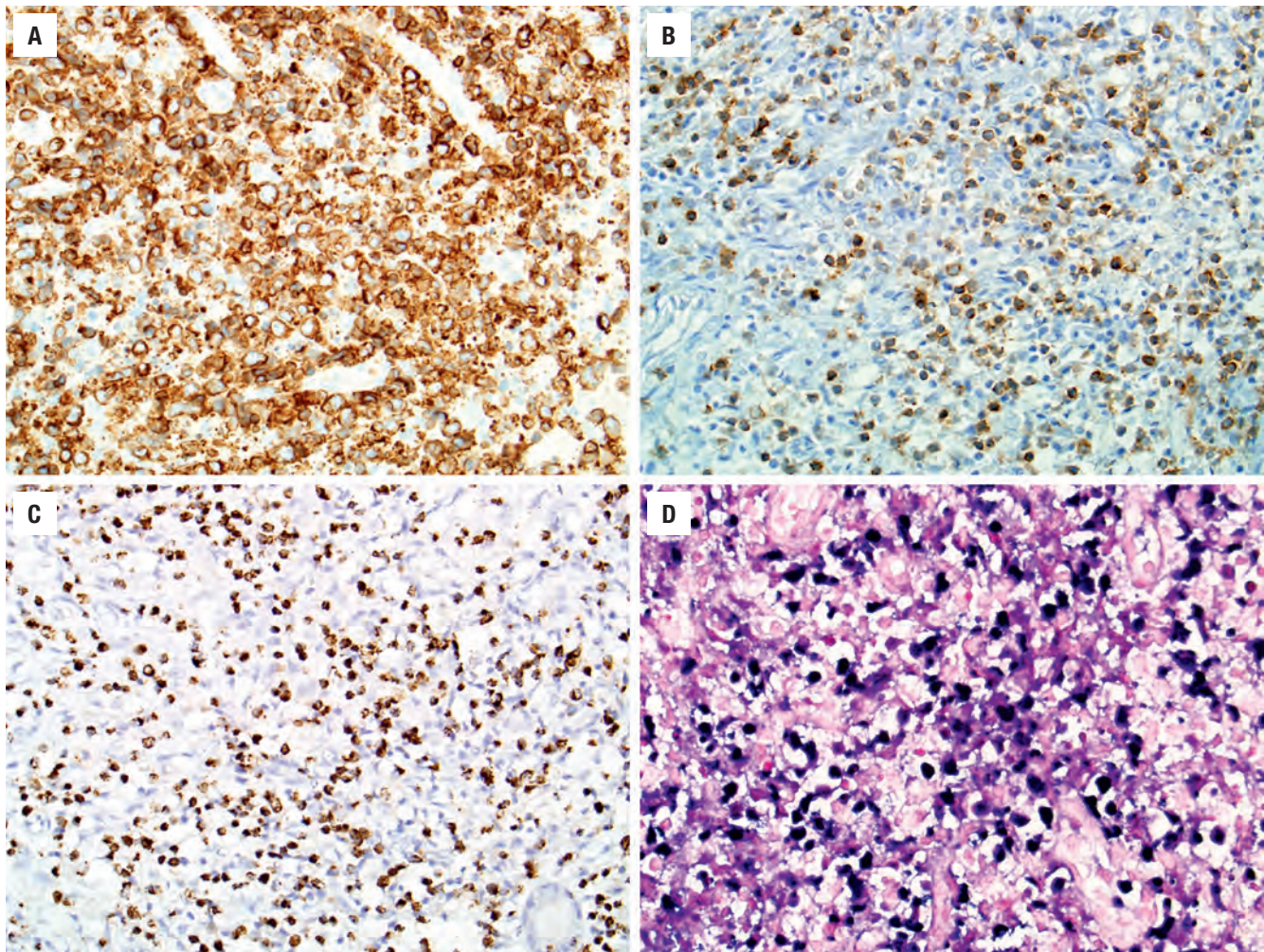


**FIGURE 3.35**

Extranodal NK/T cell lymphoma, nasal type, is positive for CD3 (cytoplasmic) (A), CD56 (B), TIA-1 (C), and Epstein-Barr–encoded RNA (D).

radiation is advocated, especially in low-stage disease. Stem cell transplantation may be beneficial. It must be stressed again that diffuse large B-cell lymphomas are managed differently, although they also show a 5-year survival of 40 % to 60 %.

## ■ MESENCHYMAL MALIGNANCIES

### RHABDOMYOSARCOMA

RMS is a primitive malignant soft tissue tumor with histologic and phenotypic features of embryonic skeletal muscle differentiation. About 40 % of all RMSs develop in the head and neck, some 20 % of which involve the SNT and nasopharynx. RMS is the most common childhood sarcoma and is subtyped, specifically in the SNT, into the following categories: embryonal (80 %) and alveolar (20 %). RMS has a peak incidence during the 1st and 2nd decade of life without a sex predilection.

The embryonal type predominates in childhood, while the alveolar type predominates in adults. Syndrome association (Li-Fraumeni, Costello, and Beckwith-Wiedemann syndromes) may be associated with childhood RMS. Patients present with difficulty breathing, epistaxis, facial swelling, visual disturbances, and sinusitis, often of a short duration. Within the head and neck, the orbit, oropharynx, ear, and temporal bone are specifically affected more often than the nasopharynx and SNT. CT and MRI delineate the size and extent of the tumor (Fig. 3.36). Tumors produce bulky, fleshy, polypoid masses simulating multiple nasal polyps (Fig. 3.36). The botryoid variant has a “grape-like” appearance, as the name implies. The surface epithelium is usually intact.

*Embryonal RMS* is made up of round to spindled cells with elongated to round hyperchromatic nuclei. The tumor has a distinct accumulation of primitive cells and rhabdomyoblasts beneath the squamous or respiratory mucosa, imparting a distinctive appearance referred to as a “cambium layer” (Fig. 3.37). In the deeper parts of the tumor, primitive cells predominate and admix with

**SARCOMA—FACT SHEET****Rhabdomyosarcoma**

- Malignant neoplasm with skeletal muscle phenotype
- About 20% of rhabdomyosarcomas involve the sinonasal tract
- Nasopharynx more commonly involved than sinonasal tract
- Age: children/young adults (embryonal subtype); adults (alveolar subtype)
- Difficulty breathing, epistaxis, facial swelling, sinusitis
- Overall mortality between 44% and 69%, depending on age, histologic subtype, and stage
- Combined multimodality therapy (chemotherapy, radiotherapy, surgery)
- Gross: large, bulky, fleshy, polypoid grape-like masses, simulating polyps
- **Embryonal type (80%):** round to spindled primitive mesenchymal cells with hyperchromatic nuclei; rhabdomyoblasts with cross-striations rare; myxoid stroma may be present, occasionally abundant
- **Alveolar type (20%):** fibrous septa separating loosely cohesive rhabdomyoblasts into alveolar spaces; multinucleated giant cells may be present; *FOXO1-PAX3* or *PAX7* fusions
- **IHC:** desmin, myoglobin, myogenin, MYOD1, and SMA positive; keratin in a small subset; CD56 in most cases
- **Differential diagnosis:** lymphoma, polyps with stromal atypia, carcinoma, Ewing sarcoma/primitive neuroectodermal tumor, olfactory neuroblastoma, melanoma

**Fibrosarcoma**

- Malignant spindle cell neoplasm with fascicular architecture and collagen deposition showing fibroblastic and/or myofibroblastic differentiation
- Uncommon, usually with a paranasal sinus location
- Equal sex distribution with a peak in 5th to 6th decade
- Nasal obstruction and epistaxis most common
- Prognosis generally good with 75% survival, although up to 60% recurrence
- Surgery is treatment of choice with adjuvant radiation
- Smooth, nodular, polypoid fleshy mass, with necrosis and hemorrhage in higher-grade tumors
- Surface epithelial invagination common
- Spindle cells arranged in short, compact fascicles at acute angles (herringbone)
- Cellularity is variable
- Fusiform cells with centrally placed hyperchromatic, needle-like nuclei and tapering cytoplasm
- Mitotic figures are variable
- Bizarre, pleomorphic cells are usually absent
- **IHC:** vimentin, and rarely, focal actin positivity
- **Differential diagnosis:** fibromatosis, glomangiopericytoma, inflammatory myofibroblastic tumor, solitary fibrous tumor, peripheral nerve sheath tumors, benign and malignant fibrous histiocytoma, synovial sarcoma, biphenotypic sinonasal sarcoma (BSNS), rhabdomyosarcoma, spindle cell melanoma, spindle cell squamous cell carcinoma

**Biphenotypic Sinonasal Sarcoma**

- Rare, recently described tumor seen only in the SNT
- Classically involves middle-aged women (mean 52 years) in the superior nasal cavity or ethmoid sinus

- Nasal obstruction and facial pressure
- Slow progressive growth with frequent local recurrences but no metastases and rare tumor-related deaths
- Infiltrative collection of spindled cells in fascicles or herringbone arrangements
- Monotonous population of bland, hypochromatic spindle cells
- Mitoses sparse, no necrosis
- Commonly entraps invaginations of surface epithelium
- **IHC:** positive (to varying degrees) for S100, actin, calponin,  $\beta$ -catenin (nuclear), occasionally focally positive for desmin, myogenin, EMA, cytokeratins, and TLE1; negative for SOX10
- **Molecular:** *PAX3* gene fusions, usually *PAX3-MAML3*
- **Differential diagnosis:** schwannoma, malignant peripheral nerve sheath tumor, solitary fibrous tumor, glomangiopericytoma, leiomyoma, fibrosarcoma, spindle cell melanoma, spindle cell squamous cell carcinoma, leiomyosarcoma, synovial sarcoma, respiratory epithelial adenomatoid hamartoma

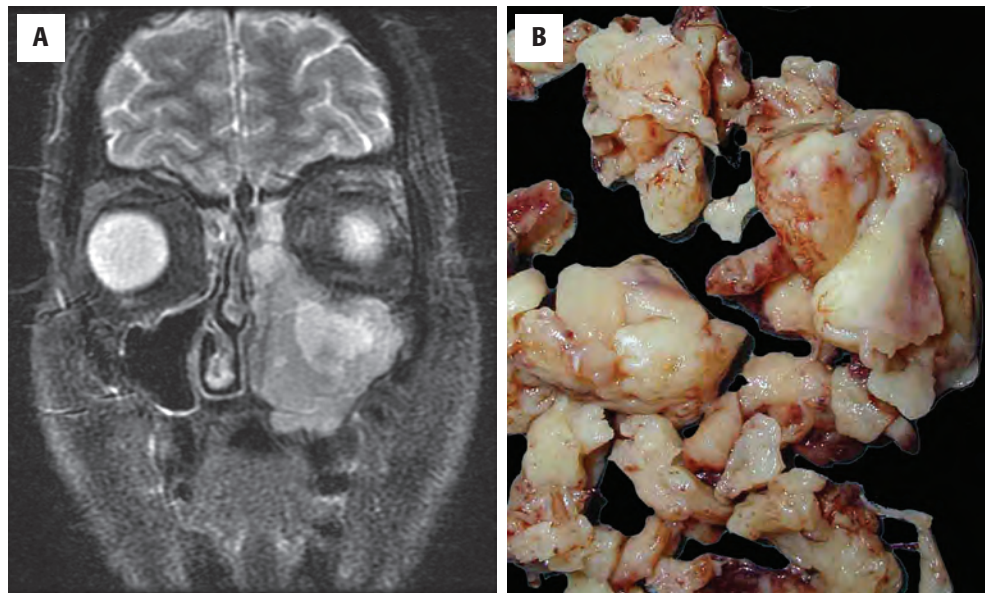
**Leiomyosarcoma**

- Malignant tumor of smooth muscle phenotype
- Arises from the vascular structures of the sinonasal tract
- All ages, although younger if Epstein-Barr virus associated
- Radical resection, with prognosis based on stage and site; recurrences are common
- Infiltrative, interlacing fascicles to storiform bundles of spindled cells
- Centrally located, blunt-ended to cigar-shaped nuclei with a perinuclear vacuole
- Increased mitoses and necrosis help confirm the diagnosis
- **IHC:** positive with vimentin, actins, and variably with desmin
- **Differential diagnosis:** leiomyoma, spindle cell squamous cell carcinoma, spindle cell melanoma, malignant peripheral nerve sheath tumor, BSNS, fibrosarcoma, rhabdomyosarcoma

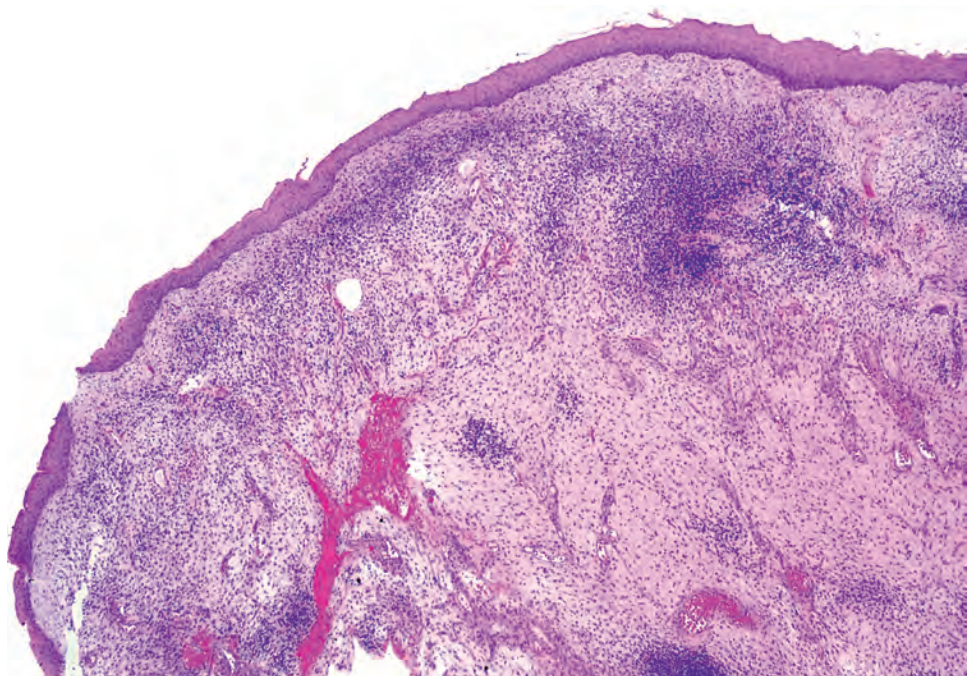
**Angiosarcoma**

- Uncommon, high-grade malignant vascular neoplasm, occasionally associated with radiation
- Patients are usually middle aged, with males > females (2:1)
- Epistaxis is the most common symptom, followed by obstruction and discharge
- Combination therapy yields best outcome, although 60% die in < 2 years
- Large, nodular, polypoid mass with soft-friable, hemorrhagic cut surfaces
- Freely anastomosing vascular channels, irregular, cleft-like with small to large spaces, lined by atypical, enlarged, spindled to epithelioid endothelial cells
- Extravasated erythrocytes and neolumen formation
- Mitoses and necrosis are common
- **IHC:** positive with CD34, CD31, ERG, factor VIII–RAG, vimentin, podoplanin
- **Differential diagnosis:** granulation tissue, lobular capillary hemangioma, angiofibroma, juvenile nasopharyngeal angiofibroma, epithelioid hemangioma, glomangiopericytoma, Kaposi sarcoma, Masson vegetant endothelial hyperplasia, intravascular papillary endothelial hyperplasia



**FIGURE 3.36**

Rhabdomyosarcoma. **(A)** Magnetic resonance imaging shows the extent of the tumor within the maxillary and ethmoid sinuses. **(B)** This macroscopic image demonstrates the gross similarity between sinonasal polyps and rhabdomyosarcoma.

**FIGURE 3.37**

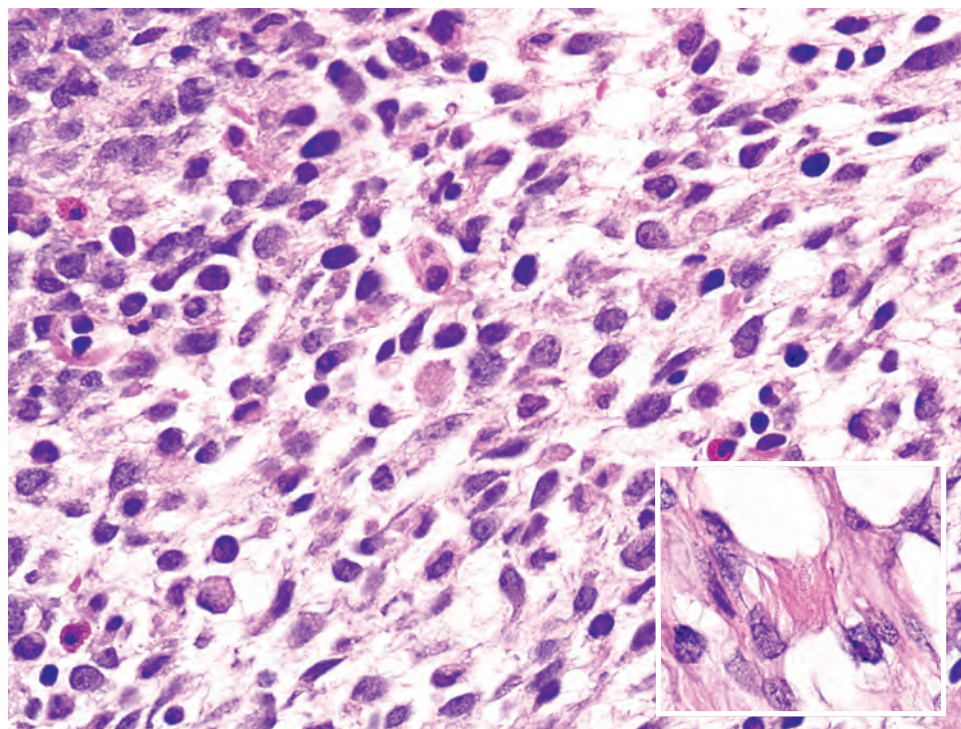
In the botryoid variant of embryonal rhabdomyosarcoma, the tumor cells often condense beneath the surface epithelium in a “cambium” layer.

a varying number of rhabdomyoblasts. Rhabdomyoblasts have many different appearances ranging from elongated strap-shaped cells to small, round “tadpole” cells, both having densely eosinophilic cytoplasm (Fig. 3.38). Cross-striations are rare (Fig. 3.38). A myxoid stroma may be present, occasionally abundant. *Spindle cell/sclerosing variant of RMS* was originally felt to represent a subtype of embryonal RMS, but in the most recent WHO classification it was regarded as a distinct tumor type. Spindle cell/sclerosing RMS is more cellular than embryonal RMS, resembling fibrosarcoma, BSNS, or LMS, and appears to

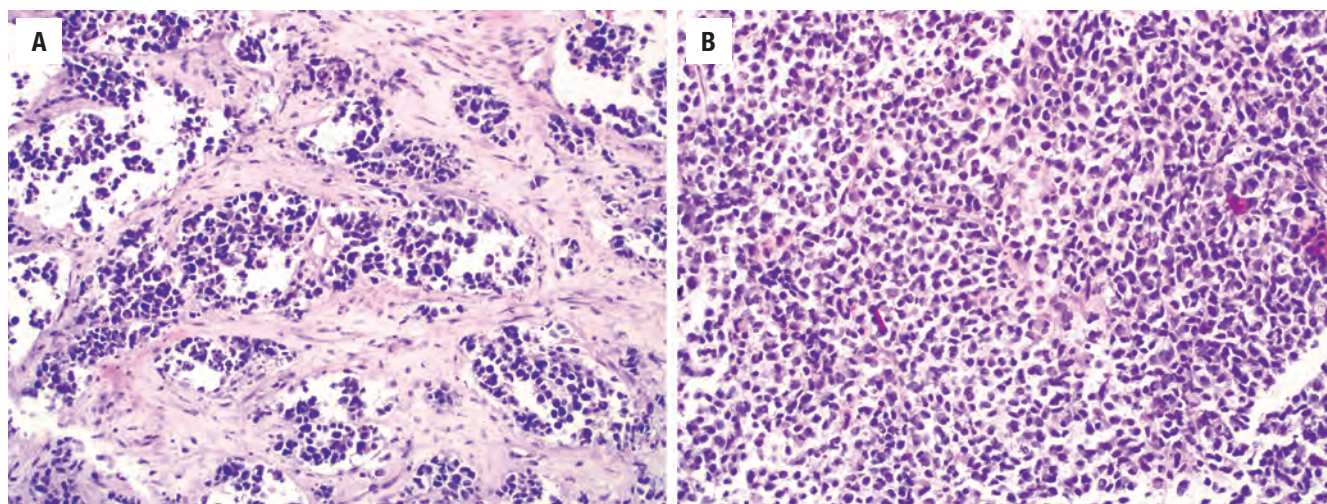
have an improved prognosis when compared to embryonal RMS. Spindle cell/sclerosing RMS has a predilection for the head and neck and extremities but is rare in the SNT.

*Alveolar RMS* shows loosely cohesive groups of small- to medium-size cells growing either in sheets (Fig. 3.39) or separated into clusters by fibrous septa, simulating a glandular neoplasm (Fig. 3.39). Rhabdomyoblasts and multinucleated giant cells may be seen (Fig. 3.40). While most rhabdomyoblasts have eosinophilic cytoplasm (often plasmacytoid or pulled to one side), some have vacuolated/cleared cytoplasm. Glycogen is easily identified.



**FIGURE 3.38**

Embryonal rhabdomyosarcoma with spindled primitive cells and rhabdomyoblasts with abundant eosinophilic cytoplasm. Rare cells demonstrate cross-striations (*inset*).

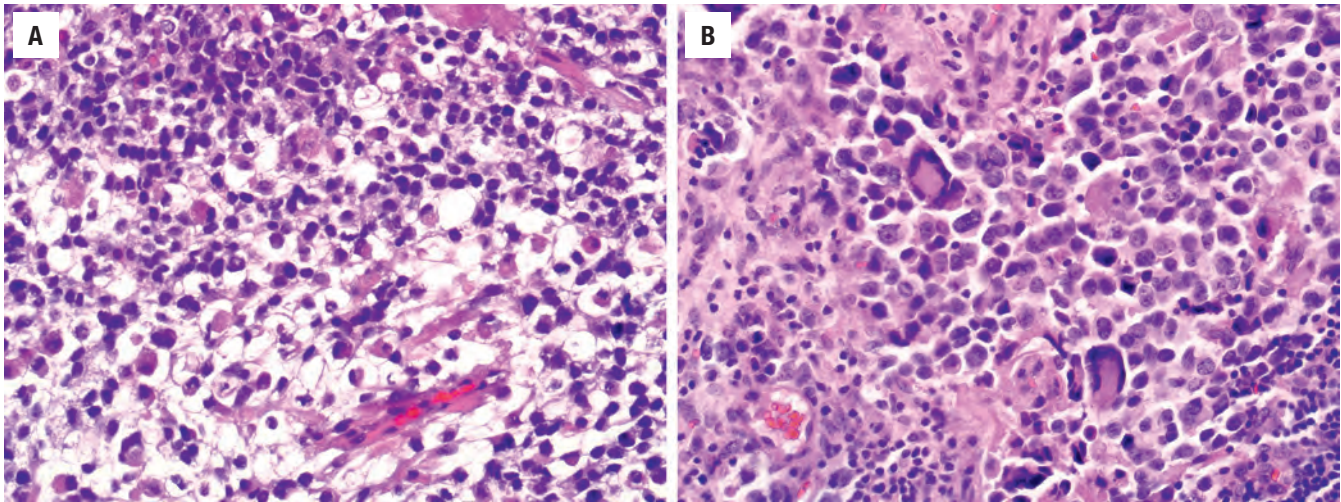
**FIGURE 3.39**

Alveolar rhabdomyosarcoma classically grows as nests of loosely cohesive small blue cells separated by fibrous septa (**A**), but it often has a more solid growth pattern (**B**).

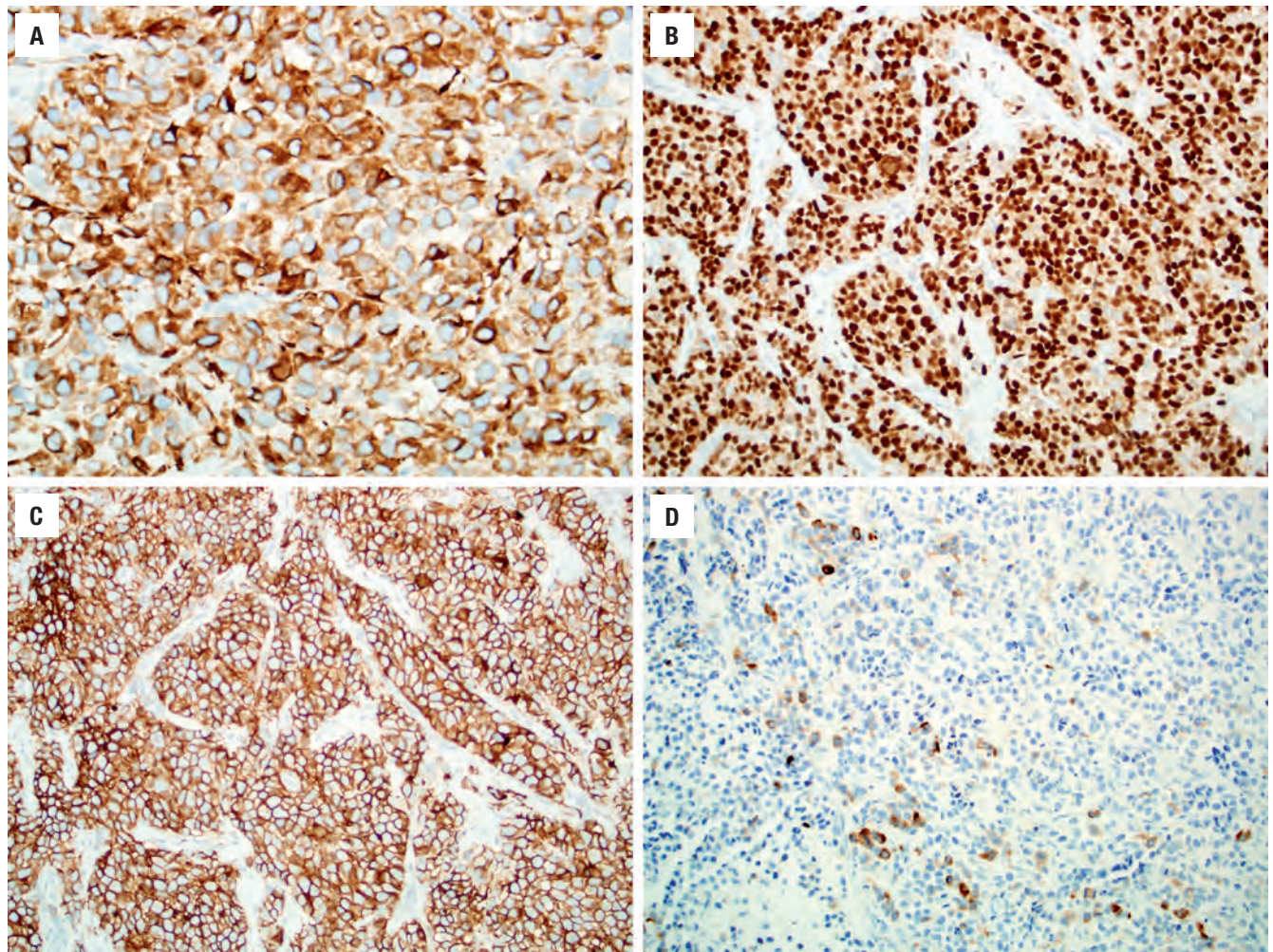
RMS expresses desmin (Fig. 3.41), myogenin (Fig. 3.41), MYOD1, muscle-specific actin, smooth muscle actin, myoglobin, fast myosin, MTF, and CD56 (Fig. 3.41). The pattern of myogenin and MYOD1 staining can be helpful: the alveolar subtype is diffusely positive, while focal staining is typical for embryonal RMS. CD99 and keratin (Fig. 3.41) may be positive (up to 50%). *FOXO1* may show gain-of-function mutations when fused with *PAX3* or *PAX7* in alveolar RMS, detected by break-apart fluorescence in situ hybridization (FISH). RMS should be separated from other small round blue cell tumors (Table 3.1). These tumors can be excluded by the use of a panel of appropriate immunohistochemical stains.

SNT polyps with stromal atypia have inflammatory cells, lack the cellularity of an RMS, and usually have different clinical findings (Fig. 3.42). The atypical spindle cells are myofibroblasts and so may have a similar immunoreactivity with actins. The overall prognosis is determined by age, histologic subtype, and the clinical stage at presentation (considered highly aggressive systemic tumors by definition). A better prognosis is seen in children and in patients with the botryoid type. Overall survival is 44% to 69% but can be as high as 90% for stage I tumors. The 5-year overall survival for children and adults is 60% and 10%, respectively, but is tumor type specific. Treatment encompasses



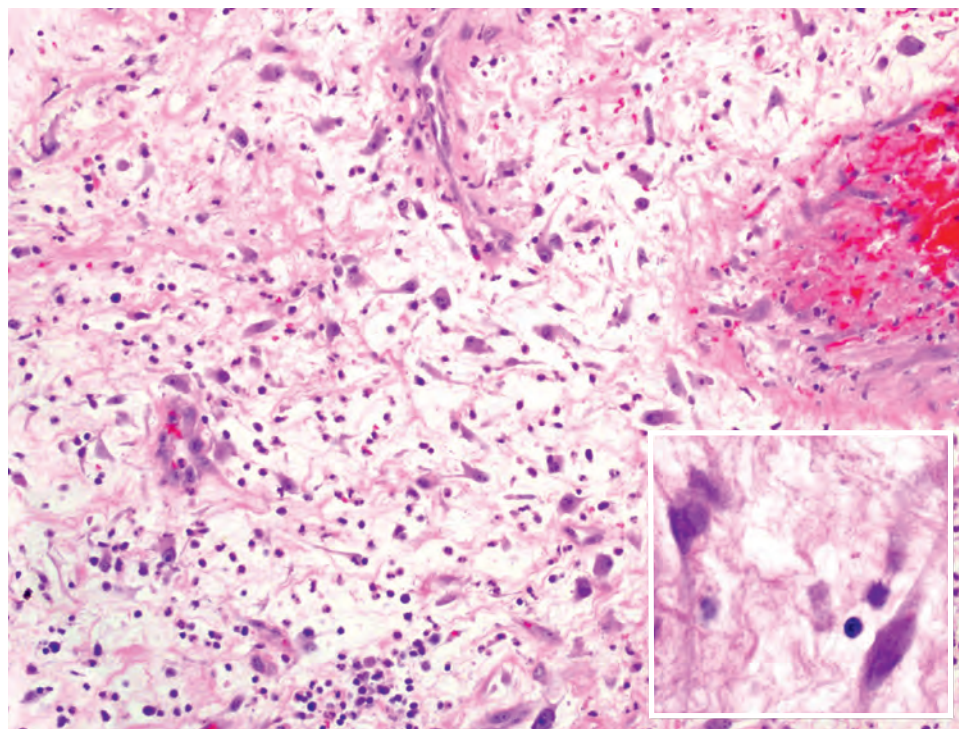
**FIGURE 3.40**

Alveolar rhabdomyosarcoma will exhibit a variable number of rhabdomyoblasts (**A**) and multinucleated giant cells (**B**).

**FIGURE 3.41**

Alveolar rhabdomyosarcoma is diffusely positive for desmin (**A**) and myogenin (**B**). In addition, alveolar RMS is almost always positive for CD56 (**C**) and is frequently focally positive for cytokeratin (**D**), findings that can cause diagnostic difficulties.



**FIGURE 3.42**

Sinonasal polyps commonly harbor atypical myofibroblasts. These cells are singly dispersed in the setting of edema and inflammation and are stellate, with low nuclear/cytoplasmic ratios (*inset*).

a multimodality approach (chemotherapy, radiation, and surgery).

## FIBROSARCOMA

Fibrosarcoma is defined as a malignant spindle cell neoplasm with fascicular architecture and collagen deposition showing fibroblastic and/or myofibroblastic differentiation. Tumors having pleomorphic, bizarre cells are excluded from fibrosarcoma and placed in the undifferentiated pleomorphic sarcoma category. This uncommon tumor (<3% of all SNT malignancies) may have prior radiation exposure as an etiologic factor. Showing an equal sex distribution, there is a peak in the 5th to 6th decade. Patients have nasal obstruction, often associated with epistaxis. Pain, sinusitis, nasal discharge, swelling, and anosmia are less common. Fibrosarcoma of the SNT occurs most frequently in the maxillary sinus, nasal cavity, and ethmoid region and is uncommonly confined to the nasal cavity alone.

In resection specimens, the tumor varies from 2 to 8 cm and has a smooth, polypoid, fleshy, white, homogeneous appearance. Necrosis and hemorrhage may be seen in higher-grade tumors. Tumors are unencapsulated, with infiltration into the bone and occasional surface ulceration. Calcification may be seen. The stroma may be vascular, with scattered capillaries mimicking hemangiopericytoma, or they may show delicate to dense bands of collagen. The cellularity is high, with the spindled cells arranged in a distinct herringbone (chevron) pattern of short, compact fascicles at acute angles (Fig. 3.43).

Occasionally a subtle fasciculation is noted, but not a storiform pattern. Although the elongated nuclei are relatively uniform in size and needle-shaped, there is evidence of nuclear atypia, altered chromatin patterns, small nucleoli, and usually increased mitotic activity in some part of the tumor (Fig. 3.43). A low mitotic activity combined with mild nuclear atypia contributes to the misdiagnosis of fibrosarcoma as fibromatosis or peripheral nerve sheath tumor. Poorly differentiated fibrosarcoma is diagnosed when there is nuclear anaplasia, high mitotic activity, scant collagenous stroma, necrosis, and hemorrhage. The majority of SNT fibrosarcomas, however, are well differentiated. By definition, the neoplastic cells are positive with vimentin only, although occasionally there may be focal, weak actin reactivity. The differential diagnosis includes a variety of spindle cell reactive and neoplastic conditions, including malignant fibrous histiocytoma, spindle cell SCC, spindle cell melanoma, malignant peripheral nerve sheath tumor, synovial sarcoma, biphenotypic sinonasal sarcoma (BSNS), RMS, glomangiopericytoma, inflammatory myofibroblastic tumor, solitary fibrous tumor, and fibromatosis (desmoid type). Before its description, many cases of BSNS were likely diagnosed as low-grade fibrosarcoma. In general, the specific architectural pattern, histologic appearance, and immunophenotype findings allow for separation. Most SNT fibrosarcomas are associated with a favorable outcome (75% 5-year survival). However, recurrences are common (up to 60%), probably because of the difficulty of obtaining clear surgical margins in the anatomic complexity of the SNT. Distant metastasis is uncommon (15%), involving the lung and bones most often. A poor



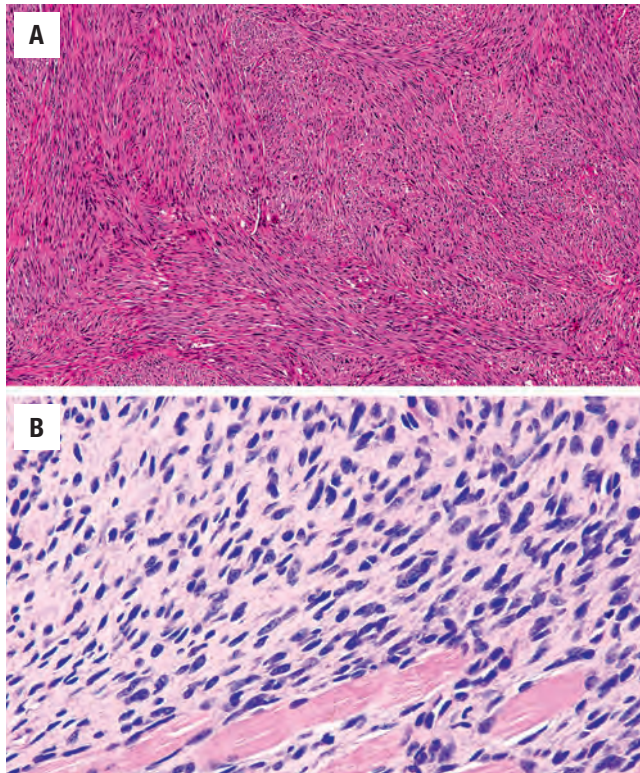


**FIGURE 3.43**

(A) Fibrosarcoma with highly cellular, compact fascicles of spindle cells arranged in short, angular intersections (herringbone or chevron), a characteristic growth pattern for this tumor type. (B) At high power, the tumor cells have elongated, "needle"-shaped nuclei that are atypical but relatively uniform. This tumor was positive for vimentin but negative for all other, more specific immunohistochemical markers (e.g., cytokeratins, desmin, S100,  $\beta$ -catenin).

prognosis is related to male patients, large tumors, advanced tumor stage (multiple sites involved), a high histologic grade, and positive surgical margins. The best prognosis is achieved with complete resection. Adjuvant radiation has been used with mixed results.

### BIPHENOTYPIC SINONASAL SARCOMA

BSNS is a recently described low-grade spindle cell sarcoma showing distinctive histologic, immunohistochemical, and molecular features. Also known as *low-grade sinonasal sarcoma with neural and myogenic differentiation*, BSNS is rare and tends to arise in middle-aged women (2:1 female-to-male ratio; mean, 52 years). BSNS can arise anywhere in the SNT but appears to have a predilection for the superior aspects of the nasal cavity and ethmoid sinuses. Patients present with nonspecific symptoms like nasal obstruction and facial pressure.

The histologic features of BSNS include an infiltrative proliferation of spindle cells arranged as fascicles or in a "herringbone" pattern (Fig. 3.44). Slit-like or staghorn vessels are common (Fig. 3.44). A characteristic feature of BSNS is its propensity to entrap benign downward invaginations of sinonasal epithelium, which in turn can

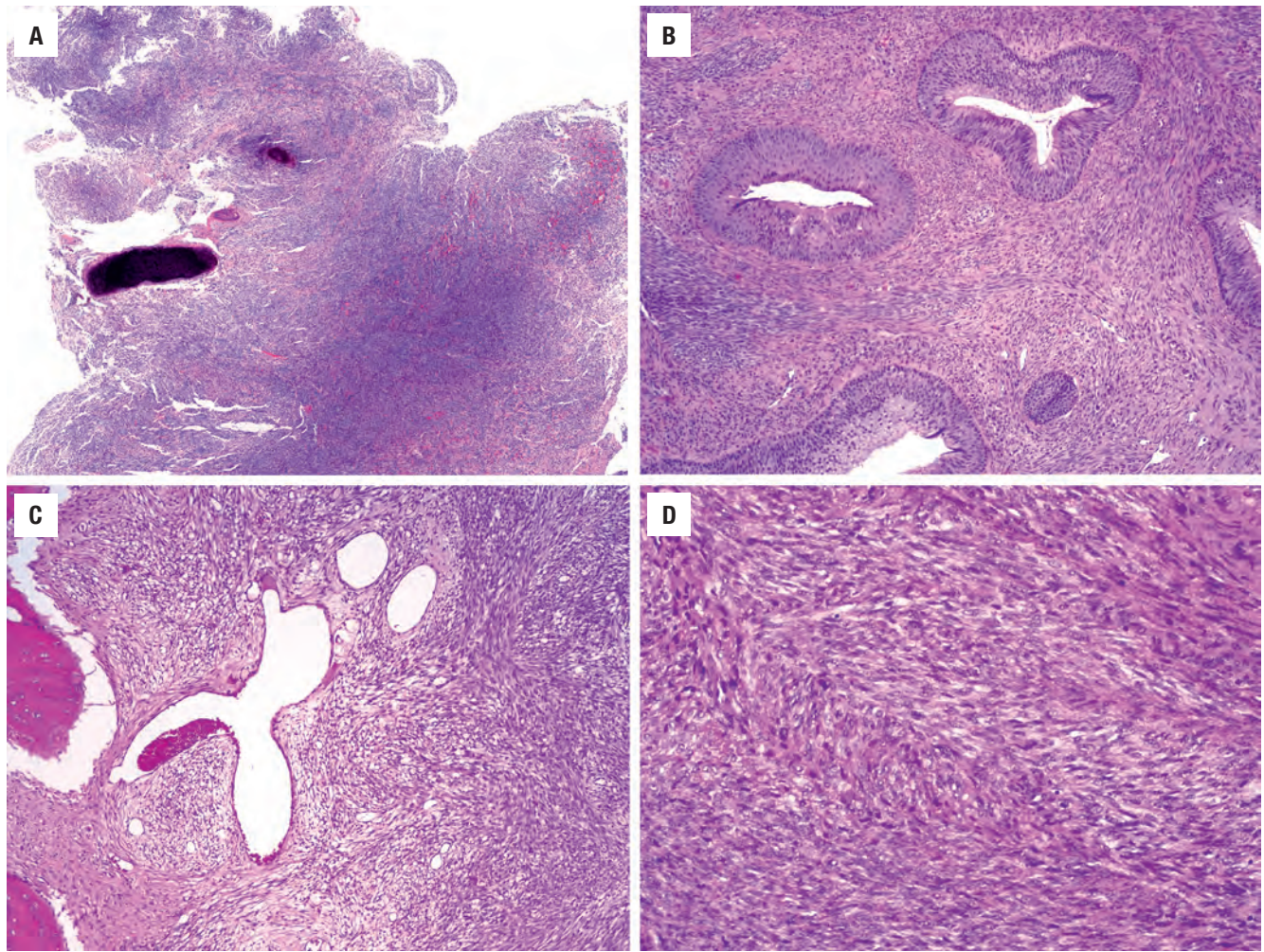
become proliferative and undergo squamous or oncocytic metaplasia (Fig. 3.44). The nuclei of BSNS are uniformly hypochromatic and slender (Fig. 3.44). Mitotic figures are uncommon and necrosis is absent. By immunohistochemistry, BSNS shows varying degrees of staining for S100 protein (Fig. 3.45), actin (Fig. 3.45), and calponin.  $\beta$ -catenin is usually positive in a nuclear distribution, ranging from focal to diffuse. BSNS may exhibit focal staining for desmin, myogenin, EMA, and cytokeratins, whereas TLE1 may be weak to patchy. Despite consistent S100 positivity, SOX10 is always negative, a helpful feature. BSNS harbors rearrangements of *PAX3*, with the most common partner being *MAML3*. Recent studies have also identified the *PAX3-NCOA1* and *PAX3-FOXO1* fusions of alveolar RMS, which appear to be associated with focal rhabdomyoblastic differentiation. BSNS is most likely to be misdiagnosed as cellular schwannoma, malignant peripheral nerve sheath tumor, fibrosarcoma, LMS, solitary fibrous tumor, glomangiopericytoma, and synovial sarcoma, whereas spindle cell melanoma and carcinoma are much less likely. BSNS is SOX10-negative, in contrast to the diffuse positivity of schwannoma and frequent focal positivity of malignant peripheral nerve sheath tumor. In addition, BSNS exhibits lower-grade histologic features than malignant peripheral nerve sheath tumors. Indeed, most tumors originally described as "low-grade" malignant peripheral nerve sheath tumor in the SNT almost certainly represent BSNS. Although the staghorn vessels of BSNS are reminiscent of solitary fibrous tumor, BSNS lacks the collagenized stroma, variability in cellularity, and CD34/STAT6 positivity of solitary fibrous tumor. Glomangiopericytoma also contains slit-like or staghorn vessels and is  $\beta$ -catenin-positive, but it has a more epithelioid appearance than BSNS and usually a much more diffuse  $\beta$ -catenin immunoreactivity. Synovial sarcoma can sometimes be difficult to differentiate from BSNS; molecular studies for the tumors' respective gene fusions may be required.

BSNS tends to demonstrate slow, progressive tumor growth. Although almost half of patients with BSNS have had local recurrences, to date none of the tumors have metastasized and only one patient to date has reportedly died of the disease.

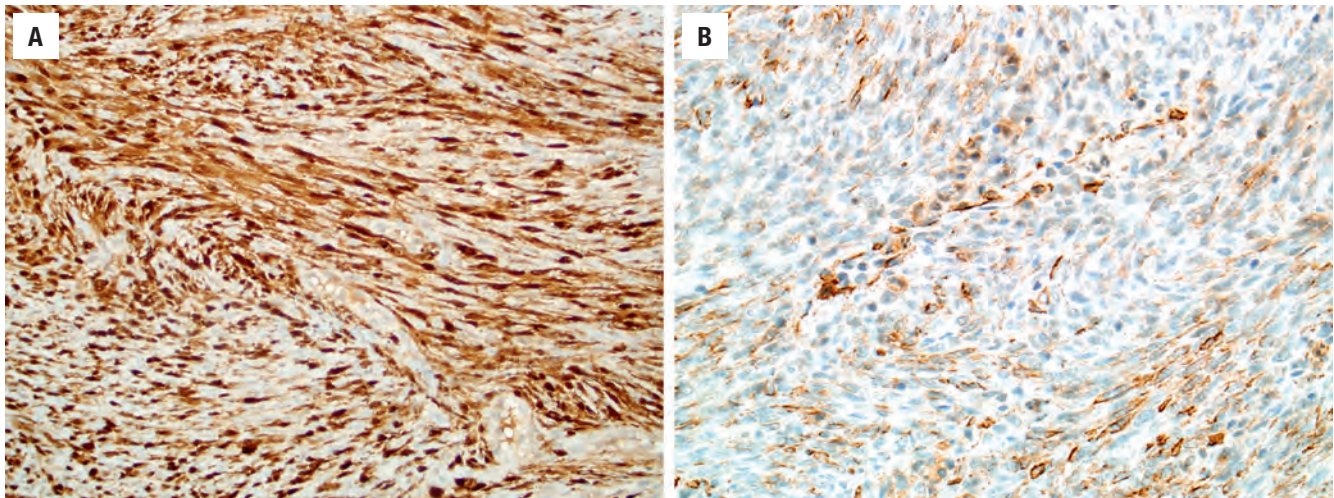
### LEIOMYOSARCOMA

LMS is a sarcoma of smooth muscle differentiation. There is a link between EBV infection in immunocompromised patients and the development of LMS. The tumor seems to arise from vascular structures in the SNT. Although patients of any age can be affected, immunocompromise-associated LMS seems to develop in children or young adults, while LMS usually develops in patients in their 6th decade or beyond. Patients have a nonspecific presentation, such as nasal obstruction, pain, and epistaxis. Radical resection is the treatment of choice, with prognosis



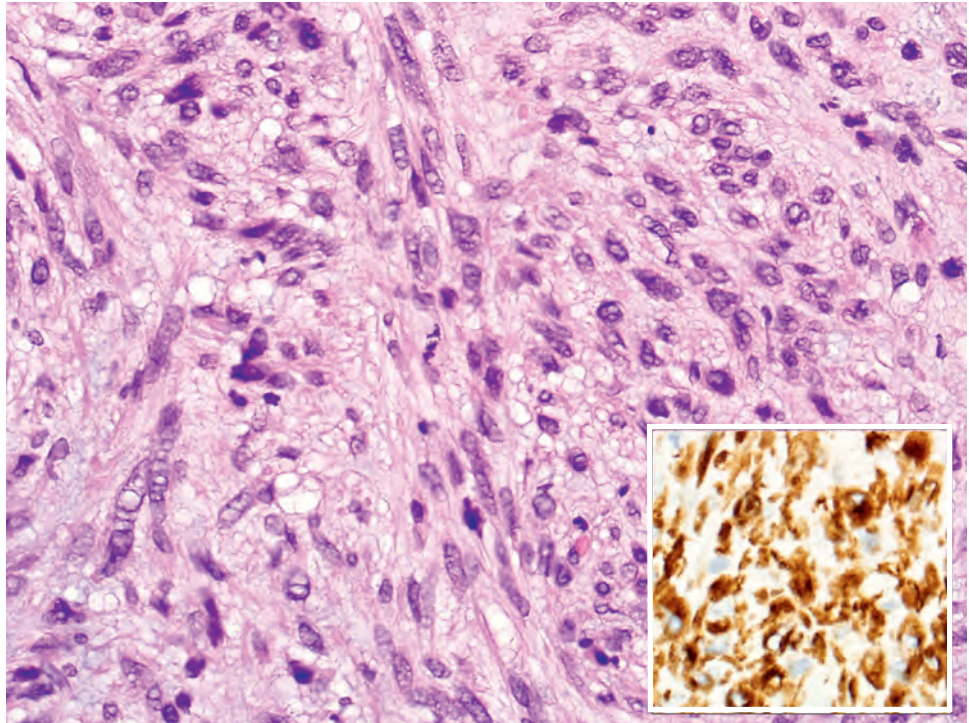
**FIGURE 3.44**

Biphenotypic sinonasal sarcoma is an infiltrative tumor, here showing bone invasion at low power (**A**). Biphenotypic sinonasal sarcoma commonly entraps invaginations of ciliated surface epithelium (**B**) and has dilated “staghorn” vessels (**C**). The tumor cells have a herringbone arrangement, with hypochromatic and elongated nuclei without significant atypia or mitotic activity (**D**).

**FIGURE 3.45**

Biphenotypic sinonasal sarcoma is positive for both S100 protein (**A**) and smooth muscle actin (**B**). The extent and strength of the immunostaining for these antibodies is variable.



**FIGURE 3.46**

Leiomyosarcoma with intersecting fascicles of elongated tumor cells with abundant pink cytoplasm and cigar-shaped nuclei with frequent perinuclear vacuoles. The tumor is diffusely desmin-positive (*inset*).

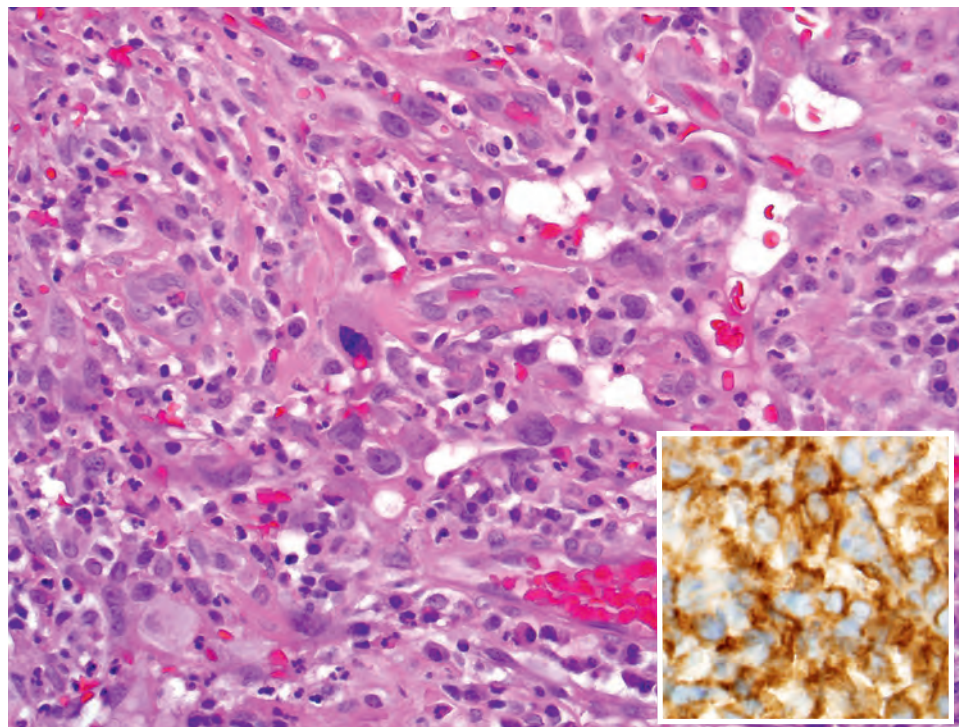
dependent on site and stage rather than histology. Recurrences are common (up to 70 %), with late distant metastasis. Tumors are large (>5 cm), nonencapsulated, tan-white, and rubbery to firm, with possible ulceration and necrosis. Histologically the tumors are infiltrative, with a richly vascularized to myxomatous stroma. The tumor cells are arranged in interlacing fascicular to storiform bundles of spindle-shaped cells, often intersecting at right angles. The tumor cells are spindle with centrally located, blunt-ended to cigar-shaped nuclei (Fig. 3.46). A perinuclear vacuole or clear halo is helpful, making the nucleus appear indented or concave (Fig. 3.46). Nuclei are variably pleomorphic, with nuclear hyperchromasia and increased mitotic activity, including atypical forms (Fig. 3.46). In general, more than mitoses per 10 high-power fields (HPFs) is worrisome for an LMS, while more than four is nearly always LMS. It is not uncommon to see multinucleated giant cells. Epithelioid cells may occasionally predominate. PAS with diastase will highlight intracellular glycogen. Tumor cells will be strongly and diffusely reactive with vimentin and actins (smooth muscle, muscle-specific) while variably positive for desmin (Fig. 3.46). Perinuclear keratin is rare. Separation must be made between LMS and leiomyoma, spindle cell SCC, malignant peripheral nerve sheath tumor, fibrosarcoma, BSNS, and RMS.

## ANGIOSARCOMA

Angiosarcoma is a very uncommon high-grade malignant vascular neoplasm that may be associated with radiation.

Nearly 50 % of all angiosarcomas develop in the head and neck, although the scalp and soft tissues are more common. Most patients are middle aged (mean, 47 years), with more males than females (2:1). Patients present with involvement of the paranasal sinuses or nasal cavity alone. Epistaxis is the most common symptom, followed by nasal discharge and obstruction. The best outcome is achieved with a combination of surgery, radiation, and chemotherapy, although in general the prognosis is poor (60 % die from disease in <2 years). Recurrences are common. A poor prognosis is associated with female sex, age above 60 years, large tumors, tumors with metastasis, and tumors with a specific etiology (radiation). Angiography identifies the extent of tumor growth and shows feeder vessel(s), allowing for presurgical angiographic embolization, if desired.

Tumors are large (mean, 4 cm), usually nodular to polypoid masses, with soft-friable cut surfaces showing hemorrhage with clots and necrosis. Tumors show ulcerated surface epithelium with associated necrosis and hemorrhage. The tumors are usually infiltrative into the adjacent soft tissues. Extravasated erythrocytes are noted throughout with freely anastomosing vascular channels. The cleft-like, irregular, small to large spaces are lined by atypical, enlarged, spindle to epithelioid endothelial cells. The atypical endothelial cells may be single, multilayered, or papillary/tufted (Fig. 3.47). The cells have intracytoplasmic vacuoles or neolumen, which frequently contain erythrocytes (Fig. 3.47). Nuclear chromatin is heavy and coarse, with irregular nuclear contours. Mitoses and necrosis are usually easily identified. Extracellular eosinophilic hyaline globules are absent. The tumor cells

**FIGURE 3.47**

Angiosarcoma consists of a richly vascularized tumor with overtly malignant pink cells forming abortive vascular structures that contain intraluminal red blood cells. The tumor cells are positive for the vascular marker CD31 (*inset*).

are positive with vimentin, CD34, CD31 (Fig. 3.47), ERG, and factor VIII–Rag. The differential includes granulation tissue, lobular capillary hemangioma, juvenile nasopharyngeal angiofibroma, epithelioid hemangioma, glomangiopericytoma, Kaposi sarcoma, and Masson vegetant endothelial hyperplasia or intravascular papillary endothelial hyperplasia.

## ■ EWING SARCOMA

ES and PNET are closely related high-grade, primitive, small round blue cell tumors with a neuroectodermal phenotype. These tumors are considered as a morphologic spectrum, with both expressing similar genetic alterations. There is a worldwide overall tumor incidence of 2 per 1 million children per year, with about 20% developing in the head and neck and 20% of these cases in the SNT. There is an association of SNT cases with retinoblastoma.

### CLINICAL FEATURES

There is a slight male predominance. The tumor is most common in children and young adults (80% of cases) who present with pain, mass, and obstruction. Elevated serum lactate dehydrogenase helps in detecting recurrence. Radiographically, there is a destructive osteolytic lesion with bony erosion and a periosteal reaction (“onion-skin”).

### EWING SARCOMA—DISEASE FACT SHEET

#### Definition

- High-grade primitive neuroectodermal neoplasm

#### Incidence and Location

- Rare (2 per 1 million children per year)
- About 20% occur in head and neck with ~20% arising in sinonasal tract
- Maxillary sinus > nasal fossa

#### Morbidity and Mortality

- Better prognosis in head and neck, with ~30% mortality

#### Sex and Age Distribution

- Slight male predominance
- Most common in children and young adults

#### Clinical Features

- Pain, mass, and obstruction

#### Prognosis and Therapy

- Size- and stage-dependent, although sinonasal tract location has better prognosis than thoracoabdominal disease
- Better prognosis when *EWSR1-FLI1* fusion is present
- Overall 60%-70% 5-year survival
- Multimodality therapy



## EWING SARCOMA—PATHOLOGIC FEATURES

### Gross Findings

- Often polypoid and multilobular, gray-white, glistening tumor with ulceration and hemorrhage
- Bone erosion/destruction is common in this large tumor (up to 6 cm)

### Microscopic Findings

- Dense, solid sheets of small- to medium-sized monotonous cells
- High nuclear to cytoplasmic ratio with round nuclei
- Fine nuclear chromatin distribution, small nucleoli
- Mitotic activity is high with coagulative tumor necrosis common
- Occasionally may have neural differentiation

### Immunohistochemical Findings

- Positive: CD99 (membranous), FLI1 (nuclear), NKX2.2 (nuclear), vimentin; rarely keratin
- May react with other neural markers (NSE, synaptophysin, S100 protein, NFP, GFAP, chromogranin)
- Rare “adamantinoma-like” variant diffusely positive for cytokeratins, p63, p40

### Molecular Findings

- t(11;22)(q24;q12) (*EWSR1-FLI1*) or t(21;22)(q22;q12) most common
- FISH (fusion or break-apart probe) or PCR detection

### Pathologic Differential Diagnosis

- Lymphoma, rhabdomyosarcoma, olfactory neuroblastoma, melanoma, sinonasal undifferentiated carcinoma, pituitary adenoma, NUT carcinoma, melanotic neuroectodermal tumor of infancy, mesenchymal chondrosarcoma, small cell osteosarcoma, small cell carcinoma

## PATHOLOGIC FEATURES

### GROSS FINDINGS

The tumors, which measure up to 6 cm, are often polypoid and multilobular, gray-white, and glistening; they are often associated with ulceration and hemorrhage. Bone erosion is common. Tumors of the head and neck are much smaller at presentation than those of other anatomic sites. Tumors are seen most commonly in the maxillary sinus, followed by the nasal cavity.

### MICROSCOPIC FINDINGS

Diffuse, densely cellular sheets and nests of uniform, small- to medium-sized round cells with scant vacuolated cytoplasm (high nuclear/cytoplasmic ratio) make up this neoplasm (Fig. 3.48). The cell borders are indistinct. The nuclei are round with fine chromatin distribution and small nucleoli (Fig. 3.48). Mitotic figures are common. Coagulative necrosis is frequently identified, while there is peritheliomatous tumor sparing. Occasionally there is

a greater degree of chromatin clumping and nuclear pleomorphism as well as the presence of true rosettes and pseudorosettes (Fig. 3.48). Atypical forms have a more lobular architecture, increased extracellular matrix, an alveolar pattern, pleomorphism, increased spindle cells, and increased mitoses.

There is a rare variant of ES/PNET known as the “adamantinoma-like” form that may arise in the head and neck, including the SNT (Fig. 3.49). Adamantinoma-like ES/PNET is characterized by prominent epithelial differentiation, particularly squamous, with some cases showing keratin pearls (Fig. 3.49). It shows other features more typical of ES/PNET and harbors the same genetic alterations.

## ANCILLARY STUDIES

### HISTOCHEMICAL STUDIES

By periodic acid–Schiff (PAS) stains, glycogen is present in the cytoplasm.

### IMMUNOHISTOCHEMICAL FINDINGS

CD99 (MIC2) represents the monoclonal antibody to *EWSR1-FLI1* fusion product and is expressed in a membranous pattern. FLI1 and NKX2.2 yield a strong nuclear stain, while vimentin is expressed in nearly all ES/PNET tumors. NSE and synaptophysin are expressed less often. Uncommonly, S100 protein, GFAP, and keratin will also be expressed.

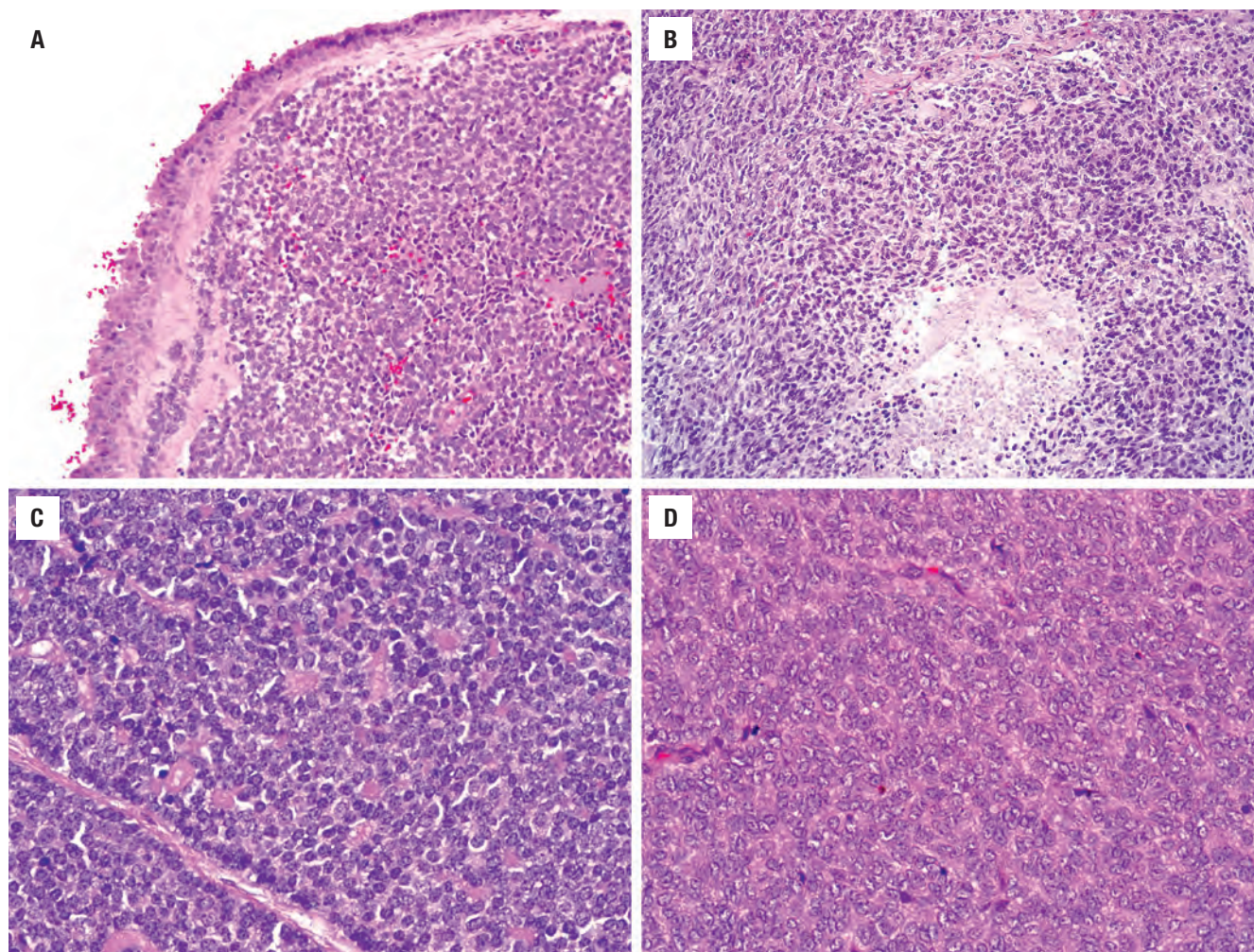
The rare adamantinoma-like variant of ES/PNET shows diffuse positivity for squamous (p63, p40, CK5/6) and epithelial markers (cytokeratins, EMA) (Fig. 3.49) but is otherwise typical of ES/PNET, with diffuse CD99 (Fig. 3.49), FLI1, and NKX2.2 immunostaining.

### MOLECULAR GENETICS

The chromosomal translocation at t(11;22)(q24;q12) or t(21;22)(q22;q12) can be identified by PCR or FISH with either a fusion method or a dual-color break-apart probe (detected in some 95 % of cases). Many chimeric *EWSR1* transcripts, representing different combinations of exons from *EWSR1* with other partner genes, are known (*ERG*, *ETV1*, *ETV4* [E1A-F], *FEV*, *ZSG*). Rare *EWSR1* fusion-negative cases have been found to harbor *CIC-DUX4* fusions; it is unclear at this time whether these tumors represent variants of ES/PNET or a distinct tumor type.

## DIFFERENTIAL DIAGNOSIS

The differential diagnosis includes all the malignant small round blue cell tumors, such as lymphoma, RMS, ONB,

**FIGURE 3.48**

(A) Ewing sarcoma/primitive neuroectodermal tumor growing as a sheet of primitive small round blue cells in the sinonasal submucosa. (B) The tumor exhibits clear cytoplasm, slight spindling, and tumor necrosis. (C) Scattered pseudorosettes are seen among the monotonous tumor cells. (D) Ewing sarcoma/primitive neuroectodermal tumor has a uniform population of cells with fine chromatin, mitotic activity, and indistinct cell borders.

mesenchymal chondrosarcoma, small cell osteosarcoma, SNUC, melanotic neuroectodermal tumor of infancy, melanoma, small cell carcinoma, NUT carcinoma, and pituitary adenoma (Table 3.1). Their distinct clinical presentations, patterns of growth, and immunohistochemical profiles allow for separation. The “adamantinoma-like” variant is particularly problematic and closely resembles NUT carcinoma; immunostaining for CD99 and NUT are necessary to distinguish the tumors.

### PROGNOSIS AND THERAPY

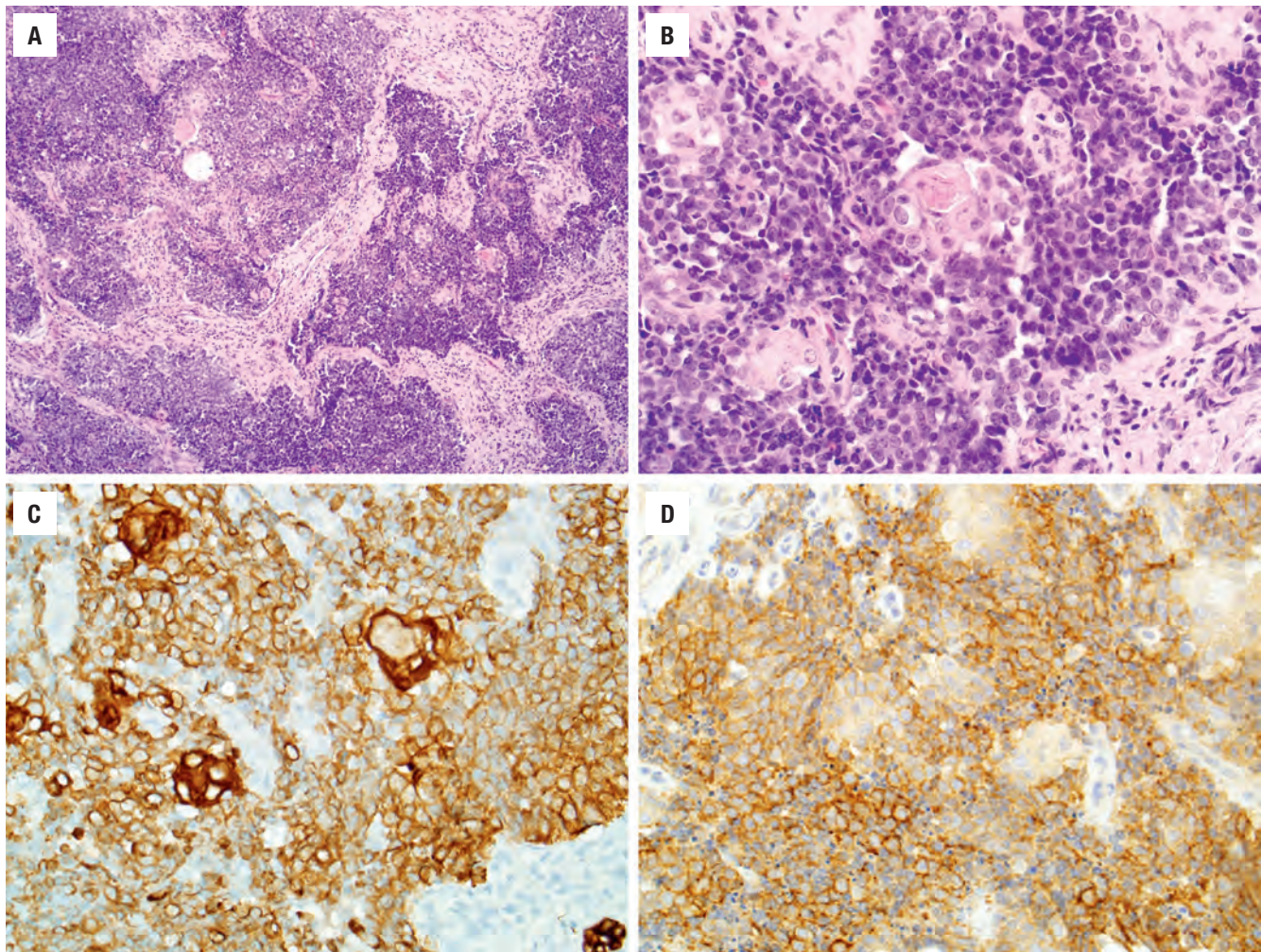
ES/PNET is considered to be a highly aggressive neoplasm, often spreading into the adjacent paranasal sinuses. Staging according to the Clinical Groups of the Intergroup RMS Study allows for a unified approach to the tumor. SNT lesions tend to have a slightly better prognosis (60 % to 70 % 5-year survival) than their thoracoabdominal

counterparts, probably owing to a smaller size at presentation (size and stage are important prognostic indicators). Patients with the *EWSR1-FLI1* fusion tend to have a better prognosis. Metastasis, seen in up to 30 % of patients, is usually to lungs, bone marrow, bone, brain, and lymph nodes. Multimodality therapy (chemotherapy, radiation, and surgery) achieves the best outcome, with autologous bone marrow or peripheral blood stem cell rescue. Poor prognostic factors include large size (tumor >8 cm), elevated white blood cell count and sedimentation rate, filigree microscopic pattern, and lack of response to chemotherapy prior to resection.

### ■ TERATOCARCINOSARCOMA

This rare, complex malignant neoplasm of SNT consists of various carcinomatous and sarcomatous elements, including immature epithelial, neuroepithelial, and



**FIGURE 3.49**

(A) Adamantinoma-like Ewing sarcoma/primitive neuroectodermal tumor growing as nests of basaloid cells separated by fibrous septae. (B) The tumor cells are not dissimilar to those seen in conventional Ewing sarcoma/primitive neuroectodermal tumor except that they demonstrate abrupt foci of keratinization (center). (C) The tumor is strongly positive for cytokeratin. (D) Like other forms of Ewing sarcoma/primitive neuroectodermal tumor, the adamantinoma-like variant is consistently positive for membranous CD99.

mesenchymal tissues resembling immature teratoma. By definition, germ cell tumors are not included (embryonal carcinoma, choriocarcinoma, seminoma). Although unproven, the tumor is thought to arise from the primitive cells in the olfactory membrane that possess the capacity to show multilineage differentiation.

#### CLINICAL FEATURES

Men are affected much more commonly than women, with a mean age of 60 years at presentation. As in the case of other malignant SNT neoplasms, nasal obstruction and epistaxis are the most common complaints, usually of short duration. The tumor occurs most commonly high in the nasal cavity, ethmoid sinus, and maxillary sinus, frequently involving more than one location. Vasopressin may be ectopically or inappropriately elevated.

#### PATHOLOGIC FEATURES

##### GROSS FINDINGS

The tumors are large (generally >4 cm), bulky, polypoid, friable to fleshy, with surface ulceration and necrosis (Fig. 3.50).

##### MICROSCOPIC FINDINGS

Teratocarcinosarcoma is a heterogeneous neoplasm containing intermingled carcinomatous and sarcomatous tissues along with teratoma-like elements (Fig. 3.51). Elements from all three germ cell layers may be present, but the components may be either benign or malignant and are topographically mixed, with transitions between the tumor elements. The carcinoma may be squamous cell or adenocarcinoma (Fig. 3.51). When present, the

**TERATOCARCINOSARCOMA—DISEASE FACT SHEET****Definition**

- A complex malignant neoplasm with immature and malignant endodermal, mesodermal, and neuroepithelial elements

**Incidence and Location**

- Extremely rare
- Ethmoid and maxillary antrum

**Morbidity and Mortality**

- 60% of patients die within 3 years

**Sex and Age Distribution**

- Males > > > females
- Mean, 60 years (adults)

**Clinical Features**

- Nasal obstruction and epistaxis of short duration

**Prognosis and Therapy**

- Poor prognosis with highly aggressive behavior
- Overall, 60% die within 3 years
- Recurrences are common usually in <3 years
- Multimodality therapy does not seem to alter prognosis

**TERATOCARCINOSARCOMA—PATHOLOGIC FEATURES****Gross Findings**

- Large (>4 cm), bulky, polypoid, friable masses, ulcerated with necrosis

**Microscopic Findings**

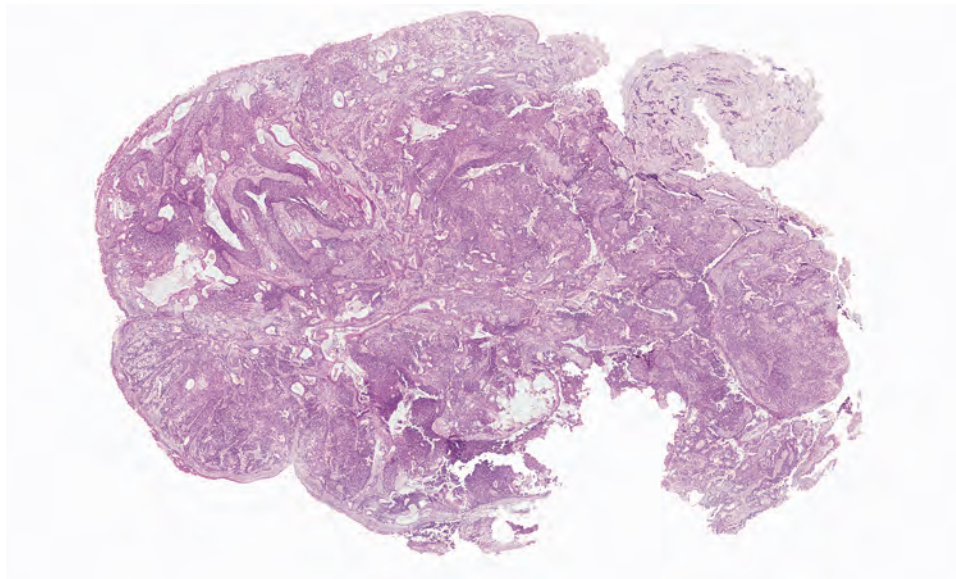
- Carcinomatous and sarcomatous component, mingled with multiple mature and immature tissues from all germ cell layers
- Carcinoma can be squamous or adenocarcinoma
- Neural elements show prominent rosettes and blastema-like cells
- Cartilage, bone, or muscle may comprise sarcoma

**Immunohistochemical Findings**

- *Neuroepithelial elements* positive: NSE, chromogranin, synaptophysin, CD56, CD99, S100 protein
- *Spindle cells* positive: vimentin, GFAP, desmin, myogenin, calponin and/or actins
- *Epithelial elements* positive: cytokeratins and EMA

**Pathologic Differential Diagnosis**

- Olfactory neuroblastoma, rhabdomyosarcoma, carcinoma (adenocarcinoma and sinonasal undifferentiated carcinoma)

**FIGURE 3.50**

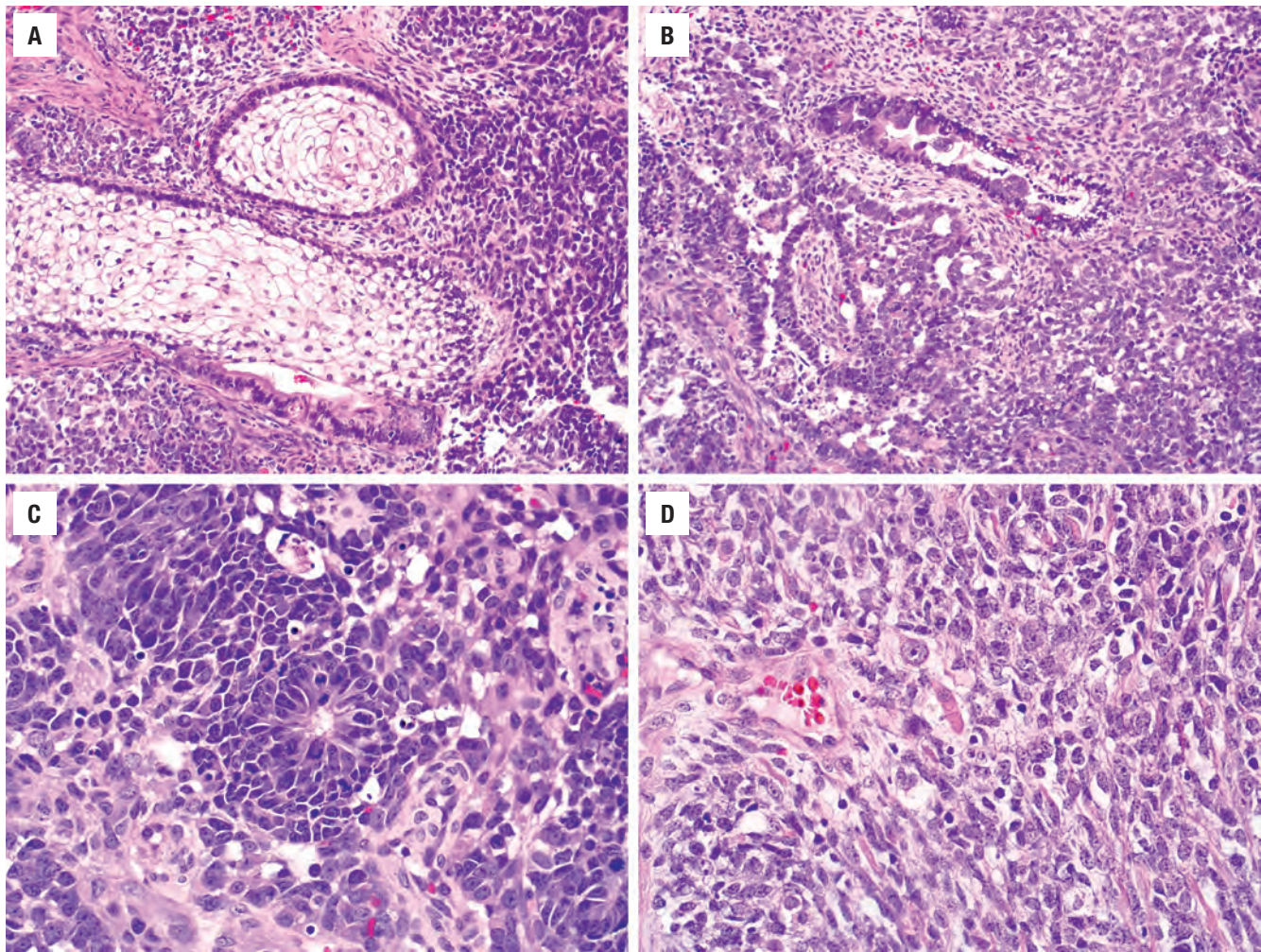
Teratocarcinosarcoma. This polypoid tumor shows a variety of different patterns of growth and different cellular compartments, including epithelial, mesenchymal, and teratomatous.

squamous epithelial component often shows a “fetal” appearance with abundant glycogenated clear cells (Fig. 3.51). The stromal elements include hypercellular immature tissue with spindle cells embedded in a myxoid matrix, whereas islands of cartilage and bone, smooth muscle, and skeletal muscle are seen in varying degrees of maturation (Fig. 3.51). Primitive neuroepithelial elements with blastomatous cells, rosettes, pseudorosettes, or neurofibrillary matrix often predominate in these tumors (Fig. 3.51).

**ANCILLARY STUDIES**

Immunohistochemistry will highlight the various constituent elements accordingly: neuroepithelial elements are usually positive with NSE, chromogranin, synaptophysin, CD56, S100 protein, and CD99; spindle cell elements express vimentin, GFAP, desmin, myogenin, calponin and/or actins; and epithelial elements are positive for cytokeratins and EMA.



**FIGURE 3.51**

Teratocarcinosarcoma is extremely heterogeneous in its cellular components. **(A)** Squamous nests with a clear cell, "fetal" appearance are seen in a background of primitive spindled cells. **(B)** Malignant tumor glands "spin off" from primitive round cells and spindle cells. **(C)** A neuroectodermal area with a true rosette. **(D)** This tumor component demonstrates rhabdomyoblastic differentiation with a strap cell (*center*).

### DIFFERENTIAL DIAGNOSIS

Depending on the cellular elements present in the biopsy, considerations include ONB, RMS, and carcinoma (SNUC and adenocarcinoma). A germ cell tumor usually has distinct embryonal, yolk sac, and seminoma features. The presence of all three elements usually confirms the diagnosis.

### PROGNOSIS AND THERAPY

This is a highly aggressive neoplasm with a poor prognosis, although ranging from 50 % to 70 % at 3 years. Most

patients (60 %) die within 3 years. Recurrences are common (up to 70 %), often with intracranial extension, which usually develops within 2 years of diagnosis. Cervical lymph node metastasis is seen in some 30 % of patients. Aggressive multimodality therapy (surgery, chemotherapy, radiation) does not seem to alter the prognosis.

### SUGGESTED READINGS

The complete Suggested Readings list is available online at [ExpertConsult.com](http://ExpertConsult.com).



## SUGGESTED READINGS

## Squamous Cell Carcinoma

- Agger A, et al. Squamous cell carcinoma of the nasal vestibule 1993-2002: a nationwide retrospective study from DAHANCA. *Head Neck*. 2009;31(12):1593-1599.
- Allen MW, et al. Long-term radiotherapy outcomes for nasal cavity and septal cancers. *Int J Radiat Oncol Biol Phys*. 2008;71(2):401-406.
- Alos L, et al. Human papillomaviruses are identified in a subgroup of sinonasal squamous cell carcinomas with favorable outcome. *Cancer*. 2009;115(12):2701-2709.
- Ansa B, et al. Paranasal sinus squamous cell carcinoma incidence and survival based on Surveillance, Epidemiology, and End Results data, 1973 to 2009. *Cancer*. 2013;119(14):2602-2610.
- Bhattacharyya N. Cancer of the nasal cavity: survival and factors influencing prognosis. *Arch Otolaryngol Head Neck Surg*. 2002;128(9):1079-1083.
- Bishop JA, et al. Human papillomavirus-related carcinoma with adenoid cystic-like features: a peculiar variant of head and neck cancer restricted to the sinonasal tract. *Am J Surg Pathol*. 2013;37(6):836-844.
- Bishop JA, et al. Human papillomavirus-related carcinomas of the sinonasal tract. *Am J Surg Pathol*. 2013;37(2):185-192.
- Bishop JA, et al. Keratinizing squamous cell carcinoma. In: el-Naggar A, et al, eds. *Classification of Head and Neck Tumours*. Bosman FT, et al, series editors. World Health Organization classification of tumours. Lyon, France: IARC Press; 2017:14-15.
- Bishop JA, et al. Non-keratinizing squamous cell carcinoma. In: El-Naggar AK, Chan JKC, Grandis JR, Takata T, Slootweg PJ, eds. *Classification of Head and Neck Tumours*. 4th ed. World Health Organization Classification of Tumors. Lyon, France: IARC Press; 2017:15-17.
- Dowley A, et al. Squamous cell carcinoma of the nasal vestibule: a 20-year case series and literature review. *J Laryngol Otol*. 2008;122(10):1019-1023.
- Dulguerov P, et al. Nasal and paranasal sinus carcinoma: are we making progress? A series of 220 patients and a systematic review. *Cancer*. 2001;92(12):3012-3029.
- El-Mofty SK, et al. Prevalence of high-risk human papillomavirus DNA in nonkeratinizing (cylindrical cell) carcinoma of the sinonasal tract: a distinct clinicopathologic and molecular disease entity. *Am J Surg Pathol*. 2005;29(10):1367-1372.
- Fasunla AJ, et al. Sinonasal malignancies: a 10-year review in a tertiary health institution. *J Natl Med Assoc*. 2007;99(12):1407-1410.
- Fu YS, et al. Pathology of the nasal cavity, paranasal sinuses, and nasopharynx. In: Fu YS, et al, eds. *Head and Neck Pathology With Clinical Correlations*. New York: Churchill Livingstone; 2001:137-230.
- Haraguchi H, et al. Malignant tumors of the nasal cavity: review of a 60-case series. *Jpn J Clin Oncol*. 1995;25(5):188-194.
- Harbo G, et al. Cancer of the nasal cavity and paranasal sinuses. A clinico-pathological study of 277 patients. *Acta Oncol*. 1997;36(1):45-50.
- Hermans R, et al. Squamous cell carcinoma of the sinonasal cavities. *Semin Ultrasound CT MR*. 1999;20(3):150-161.
- Hopkin N, et al. Cancer of the paranasal sinuses and nasal cavities. Part I. Clinical features. *J Laryngol Otol*. 1984;98:585-595.
- Hoppe BS, et al. Treatment of nasal cavity and paranasal sinus cancer with modern radiotherapy techniques in the postoperative setting—the MSKCC experience. *Int J Radiat Oncol Biol Phys*. 2007;67(3):691-702.
- Ishiyama A, et al. Papillary squamous neoplasms of the head and neck. *Laryngoscope*. 1994;104:1446-1452.
- Jackson RT, et al. Malignant neoplasms of the nasal cavities and paranasal sinuses. *Laryngoscope*. 1977;87:726-736.
- Laco J, et al. The presence of high-risk human papillomavirus (HPV) E6/E7 mRNA transcripts in a subset of sinonasal carcinomas is evidence of involvement of HPV in its etiopathogenesis. *Virchows Arch*. 2015;467(4):405-415.
- Larque AB, et al. High-risk human papillomavirus is transcriptionally active in a subset of sinonasal squamous cell carcinomas. *Mod Pathol*. 2014;27(3):343-351.
- Llorente JL, et al. Sinonasal carcinoma: clinical, pathological, genetic and therapeutic advances. *Nat Rev Clin Oncol*. 2014;11(8):460-472.
- Osborn DA. Nature and behavior of transitional tumors in the upper respiratory tract. *Cancer*. 1970;25:50-60.
- Paulino AF, et al. Epstein-Barr virus in squamous carcinoma of the anterior nasal cavity. *Ann Diagn Pathol*. 2000;4(1):7-10.
- Spiro JD, et al. Squamous carcinoma of the nasal cavity and paranasal sinuses. *Am J Surg*. 1989;158(4):328-332.
- Stelow EB, et al. Carcinomas of the upper aerodigestive tract with rearrangement of the nuclear protein of the testis (NUT) gene (NUT midline carcinomas). *Adv Anat Pathol*. 2009;16(2):92-96.
- Taxy JB. Squamous carcinoma of the nasal vestibule: an analysis of five cases and literature review. *Am J Clin Pathol*. 1997;107(6):698-703.
- Tilson MP, et al. Utility of p40 in the differential diagnosis of small round blue cell tumors of the sinonasal tract. *Head Neck Pathol*. 2014;8(2):141-145.
- Tufano RP, et al. Malignant tumors of the nose and paranasal sinuses: Hospital of the University of Pennsylvania experience 1990-1997. *Am J Rhinol*. 1999;13(2):117-123.
- Turner JH, et al. Incidence and survival in patients with sinonasal cancer: a historical analysis of population-based data. *Head Neck*. 2012;34(6):877-885.

## Sinonasal Adenocarcinoma

- Alessi DM, et al. Nonsalivary sinonasal adenocarcinoma. *Arch Otolaryngol Head Neck Surg*. 1988;114(9):996-999.
- Ariza M, et al. Comparative genomic hybridization in primary sinonasal adenocarcinomas. *Cancer*. 2004;100(2):335-341.
- Barnes L. Intestinal-type adenocarcinoma of the nasal cavity and paranasal sinuses. *Am J Surg Pathol*. 1986;10:192-202.
- Bashir AA, et al. Sinonasal adenocarcinoma: immunohistochemical marking and expression of oncoproteins. *Head Neck*. 2003;25(9):763-771.
- Bishop JA, et al. HPV-related Multiphenotypic Sinonasal Carcinoma: An Expanded Series of 49 Cases of the Tumor Formerly Known as HPV-related Carcinoma with Adenoid Cystic Carcinoma-Like Features. *Am J Surg Pathol*. In press.
- Bishop JA, et al. Human papillomavirus-related carcinoma with adenoid cystic-like features: a peculiar variant of head and neck cancer restricted to the sinonasal tract. *Am J Surg Pathol*. 2013;37(6):836-844.
- Bullock MJ. Low-grade epithelial proliferations of the sinonasal tract. *Head Neck Pathol*. 2016;10(1):47-59.
- Castillo C, et al. Signet-ring cell adenocarcinoma of sinonasal tract: an immunohistochemical study of the mucins profile. *Arch Pathol Lab Med*. 2007;131(6):961-964.
- Cathro HP, et al. Immunophenotypic differences between intestinal-type and low-grade papillary sinonasal adenocarcinomas: an immunohistochemical study of 22 cases utilizing CDX2 and MUC2. *Am J Surg Pathol*. 2004;28(8):1026-1032.
- Choi HR, et al. Sinonasal adenocarcinoma: evidence for histogenetic divergence of the enteric and nonenteric phenotypes. *Hum Pathol*. 2003;34(11):1101-1107.
- Franchi A, et al. CDX-2, cytokeratin 7 and cytokeratin 20 immunohistochemical expression in the differential diagnosis of primary adenocarcinomas of the sinonasal tract. *Virchows Arch*. 2004;445(1):63-67.
- Franchi A, et al. Clinical relevance of the histological classification of sinonasal intestinal-type adenocarcinoma. *Hum Pathol*. 1999;30:1140-1145.
- Franchi A, et al. Prognostic implications of Sialosyl-Tn antigen expression in sinonasal intestinal-type adenocarcinoma. *Eur J Cancer B Oral Oncol*. 1996;32B(2):123-127.
- Franquemont DW, et al. Histologic classification of sinonasal intestinal-type adenocarcinoma. *Am J Surg Pathol*. 1991;15:368-375.
- Gallo O, et al. Prognostic significance of c-erbB-2 oncoprotein expression in intestinal-type adenocarcinoma of the sinonasal tract. *Head Neck*. 1998;20(3):224-231.
- Hayes RB, et al. Wood-related occupations, wood dust exposure, and sinonasal cancer. *Am J Epidemiol*. 1986;124(4):569-577.
- Heffner DK, et al. Low-grade adenocarcinoma of the nasal cavity and paranasal sinuses. *Cancer*. 1982;50:312-322.
- Hermesen MA, et al. Genome-wide analysis of genetic changes in intestinal-type sinonasal adenocarcinoma. *Head Neck*. 2009;31(3):290-297.



19. Jain R, et al. Composite intestinal-type adenocarcinoma and small cell carcinoma of sinonasal tract. *J Clin Pathol.* 2009;62(7):634–637.
20. Jo VY, et al. Low-grade sinonasal adenocarcinomas: the association with and distinction from respiratory epithelial adenomatoid hamartomas and other glandular lesions. *Am J Surg Pathol.* 2009;33(3):401–408.
21. Kennedy MT, et al. Expression pattern of CK7, CK20, CDX-2, and villin in intestinal-type sinonasal adenocarcinoma. *J Clin Pathol.* 2004;57(9):932–937.
22. Kleinsasser O, et al. Adenocarcinoma of the inner nose after exposure to wood dust. Morphological findings and relationship between histopathology and clinical behavior in 79 cases. *Arch Otorhinolaryngol.* 1988;245:1–15.
23. Lee CF, et al. Sinonasal adenocarcinoma: clinical study of nine cases in Taiwan. *Acta Otolaryngol.* 2002;122(8):887–891.
24. Leivo I. Sinonasal adenocarcinoma: Update on classification, immunophenotype and molecular features. *Head Neck Pathol.* 2016;10(1):68–74.
25. Leung SY, et al. Epstein-Barr virus is present in a wide histological spectrum of sinonasal carcinomas. *Am J Surg Pathol.* 1995;19(9):994–1001.
26. Llorente JL, et al. Genetic and clinical aspects of wood dust related intestinal-type sinonasal adenocarcinoma: a review. *Eur Arch Otorhinolaryngol.* 2009;266(1):1–7.
27. López JI, et al. Intestinal-type adenocarcinoma of the nasal cavity and paranasal sinuses. A clinicopathologic study of 6 cases. *Tumori.* 1990;76(3):250–254.
28. Luna MA. Sinonasal tubulopapillary low-grade adenocarcinoma: a specific diagnosis or just another seromucous adenocarcinoma? *Adv Anat Pathol.* 2005;12(3):109–115.
29. Martínez JG, et al. Microsatellite instability analysis of sinonasal carcinomas. *Otolaryngol Head Neck Surg.* 2009;140(1):55–60.
30. Mayr SI, et al. Characterization of initial clinical symptoms and risk factors for sinonasal adenocarcinomas: results of a case-control study. *Int Arch Occup Environ Health.* 2010;83(6):631–638.
31. McKinney CD, et al. Sinonasal intestinal-type adenocarcinoma: immunohistochemical profile and comparison with colonic adenocarcinoma. *Mod Pathol.* 1995;8(4):421–426.
32. Mills SE, et al. Aggressive sinonasal lesion resembling normal intestinal mucosa. *Am J Surg Pathol.* 1982;6(8):803–809.
33. Neto AG, et al. Sinonasal tract seromucous adenocarcinomas: a report of 12 cases. *Ann Diagn Pathol.* 2003;7(3):154–159.
34. Orvidas LJ, et al. Adenocarcinoma of the nose and paranasal sinuses: a retrospective study of diagnosis, histologic characteristics, and outcomes in 24 patients. *Head Neck.* 2005;27(5):370–375.
35. Ozolek JA, et al. Basal/myoepithelial cells in chronic sinusitis, respiratory epithelial adenomatoid hamartoma, inverted papilloma, and intestinal-type and nonintestinal-type sinonasal adenocarcinoma: an immunohistochemical study. *Arch Pathol Lab Med.* 2007;131(4):530–537.
36. Perez-Ordoñez B, et al. Expression of mismatch repair proteins, beta catenin, and E cadherin in intestinal-type sinonasal adenocarcinoma. *J Clin Pathol.* 2004;57(10):1080–1083.
37. Perez-Ordoñez B. Hamartomas, papillomas and adenocarcinomas of the sinonasal tract and nasopharynx. *J Clin Pathol.* 2009;62(12):1085–1095.
38. Purgina B, et al. A subset of sinonasal non-intestinal type adenocarcinomas are truly seromucinous adenocarcinomas: A morphologic and immunophenotypic assessment and description of a novel pitfall. *Head Neck Pathol.* 2015;9(4):436–446.
39. Saber AT, et al. K-ras mutations in sinonasal adenocarcinomas in patients occupationally exposed to wood or leather dust. *Cancer Lett.* 1998;126(1):59–65.
40. Skalova A, et al. Sinonasal tubulopapillary low-grade adenocarcinoma. Histopathological, immunohistochemical and ultrastructural features of poorly recognised entity. *Virchows Arch.* 2003;443(2):152–158.
41. Skalova A, et al. The role of SATB2 as a diagnostic marker of sinonasal intestinal-type adenocarcinoma. *Appl Immunohistochem Mol Morphol.* 2016 Jun 2;[Epub ahead of print].
42. Sklar EM, et al. Sinonasal intestinal-type adenocarcinoma involvement of the paranasal sinuses. *AJNR Am J Neuroradiol.* 2003;24(6):1152–1155.
43. Stelow EB, et al. Adenocarcinoma of the upper aerodigestive tract. *Adv Anat Pathol.* 2010;17(4):262–269.
44. Stelow EB, et al. Intestinal-type adenocarcinoma. In: El-Naggar AK, Chan JKC, Grandis JR, Takata T, Slootweg PJ, eds. *Classification of Head and Neck Tumours.* 4th ed. World Health Organization Classification of Tumors. Lyon, France: IARC Press; 2017:23–24.
45. Stelow EB, et al. Non-intestinal-type adenocarcinoma. In: El-Naggar AK, Chan JKC, Grandis JR, Takata T, Slootweg PJ, eds. *Classification of Head and Neck Tumours.* 4th ed. World Health Organization Classification of Tumors. Lyon, France: IARC Press; 2017:24–26.
46. Thompson LD, et al. Sinonasal tract and nasopharyngeal adenoid cystic carcinoma: a clinicopathologic and immunophenotypic study of 86 cases. *Head Neck Pathol.* 2014;8(1):88–109.
47. Thompson LD. Intestinal-type sinonasal adenocarcinoma. *Ear Nose Throat J.* 2010;89(1):16–18.
48. Tilson MP, et al. Among sinonasal tumors, CDX-2 immunoexpression is not restricted to intestinal-type adenocarcinomas. *Head Neck Pathol.* 2014;8(1):59–65.
49. Urso C, et al. Intestinal-type adenocarcinoma of the sinonasal tract: a clinicopathologic study of 18 cases. *Tumori.* 1993;79(3):205–210.
50. Van den Oever R. Occupational exposure to dust and sinonasal cancer. An analysis of 386 cases reported to the N.C.C.S.F. Cancer Registry. *Acta Otorhinolaryngol Belg.* 1996;50(1):19–24.
51. Wenig BM, et al. Nasopharyngeal papillary adenocarcinoma. A clinicopathologic study of a low-grade carcinoma. *Am J Surg Pathol.* 1988;12:946–953.
52. Yom SS, et al. Genetic analysis of sinonasal adenocarcinoma phenotypes: distinct alterations of histogenetic significance. *Mod Pathol.* 2005;18(3):315–319.

#### Sinonasal Undifferentiated Carcinoma

1. Agaimy A, et al. SMARCB1 (INI-1)-deficient sinoansal carcinoma: a series of 39 cases expanding the morphologic and clinicopathologic spectrum of a recently described entity. *Am J Surg Pathol.* 2017;41:458–471.
2. Agaimy A, et al. SMARCB1(INI1)-deficient sinonasal basaloid carcinoma: a novel member of the expanding family of SMARCB1-deficient neoplasms. *Am J Surg Pathol.* 2014;38:1274–1281.
3. Bishop JA, et al. SMARCB1 (INI-1)-deficient carcinomas of the sinonasal tract. *Am J Surg Pathol.* 2014;38:1282–1289.
4. Cerilli LA, et al. Sinonasal undifferentiated carcinoma. Immunohistochemical profile and lack of EV association. *Am J Surg Pathol.* 2001;25:156–163.
5. Chambers KJ, et al. Incidence and survival patterns of sinonasal undifferentiated carcinoma in the United States. *J Neurol Surg B Skull Base.* 2015;76:94–100.
6. Chernock RD, et al. Receptor tyrosine kinases in sinonasal undifferentiated carcinomas—evaluation for EGFR, c-KIT, and HER2/neu expression. *Head Neck.* 2009;31:919–927.
7. Cordes B, et al. Molecular and phenotypic analysis of poorly differentiated sinonasal neoplasms: an integrated approach for early diagnosis and classification. *Hum Pathol.* 2009;40(3):283–292.
8. Ejaz A, et al. Sinonasal undifferentiated carcinoma: clinical and pathologic features and a discussion on classification, cellular differentiation, and differential diagnosis. *Adv Anat Pathol.* 2005;12(3):134–143.
9. Franchi A, et al. Sinonasal undifferentiated carcinoma, nasopharyngeal-type undifferentiated carcinoma, and keratinizing and nonkeratinizing squamous cell carcinoma express different cytokeratin patterns. *Am J Surg Pathol.* 2002;26:1597–1604.
10. Frierson HF Jr, et al. Sinonasal undifferentiated carcinoma. An aggressive neoplasm derived from schneiderian epithelium and distinct from olfactory neuroblastoma. *Am J Surg Pathol.* 1986;10:771–779.
11. Frierson HF Jr, et al. Unusual sinonasal small-cell neoplasms following radiotherapy for bilateral retinoblastomas. *Am J Surg Pathol.* 1989;13:947–954.
12. Gelbard A, et al. Molecular profiling of sinonasal undifferentiated carcinoma. *Head Neck.* 2014;36:15–21.
13. Georgiou AF, et al. Primary small cell undifferentiated (neuroendocrine) carcinoma of the maxillary sinus. *Oral Surg Oral Med Oral Pathol Oral Radiol Endod.* 2004;98:572–578.
14. Gray ST, et al. Treatment outcomes and prognostic factors, including human papillomavirus, for sinonasal undifferentiated carcinoma: a retrospective review. *Head Neck.* 2015;37:366–374.

15. Helliwell TR, et al. Anaplastic carcinoma of the nose and paranasal sinuses. Light microscopy, immunohistochemistry and clinical correlation. *Cancer*. 1986;58:2038–2045.
16. Houston GD, et al. Sinonasal undifferentiated carcinoma: a distinctive clinicopathologic entity. *Adv Anat Pathol*. 1999;6(6):317–323.
17. Iezzoni JC, et al. “Undifferentiated” small round cell tumors of the sinonasal tract: differential diagnosis update. *Am J Clin Pathol*. 2005;124(suppl):S110–S121.
18. Jeng YM, et al. Sinonasal undifferentiated carcinoma and nasopharyngeal-type undifferentiated carcinoma. Two clinically, biologically, and histopathologically distinct entities. *Am J Surg Pathol*. 2002;26:371–376.
19. Kim BS, et al. Sinonasal undifferentiated carcinoma: case series and literature review. *Am J Otolaryngol*. 2004;25(3):162–166.
20. Kramer D, et al. Sinonasal undifferentiated carcinoma: case series and systematic review of the literature. *J Otolaryngol*. 2004;33(1):32–36.
21. Levine PA, et al. Sinonasal undifferentiated carcinoma: a distinctive and highly aggressive neoplasm. *Laryngoscope*. 1987;97(8 Pt 1):905–908.
22. Lewis JS, et al. Sinonasal undifferentiated carcinoma. In: El-Naggar AK, Chan JKC, Grandis JR, Takata T, Slootweg PJ, eds. *Classification of Head and Neck Tumours*. 4th ed. World Health Organization Classification of Tumors. Lyon, France: IARC Press; 2017:18–20.
23. Mendenhall WM, et al. Sinonasal undifferentiated carcinoma. *Am J Clin Oncol*. 2006;29(1):27–31.
24. Mills SE, et al. “Undifferentiated” neoplasms of the sinonasal region: differential diagnosis based on clinical, light microscopic, immunohistochemical, and ultrastructural features. *Semin Diagn Pathol*. 1989;6(4):316–328.
25. Miyamoto RC, et al. Esthesioneuroblastoma and sinonasal undifferentiated carcinoma: impact of histological grading and clinical staging on survival and prognosis. *Laryngoscope*. 2000;110:1262–1265.
26. Musy PY, et al. Sinonasal undifferentiated carcinoma: the search for a better outcome. *Laryngoscope*. 2002;112(8 Pt 1):1450–1455.
27. Phillips CD, et al. Sinonasal undifferentiated carcinoma: CT and MR imaging of an uncommon neoplasm of the nasal cavity. *Radiology*. 1997;202(2):477–480.
28. Schmidt ER, et al. Diagnosis and treatment of sinonasal undifferentiated carcinoma: report of a case and review of the literature. *J Oral Maxillofac Surg*. 2008;66(7):1505–1510.
29. Singh L, et al. Role of p40 and cytokeratin 5/6 in the differential diagnosis of sinonasal undifferentiated carcinoma. *Ann Diagn Pathol*. 2014;18:261–265.
30. Smith SR, et al. A clinicopathological study of sinonasal neuroendocrine carcinoma and sinonasal undifferentiated carcinoma. *Laryngoscope*. 2000;110:1617–1622.
31. Stelow EB, et al. NUT rearrangement in undifferentiated carcinomas of the upper aerodigestive tract. *Am J Surg Pathol*. 2008;32(6):828–834.
32. Tilson MP, et al. Utility of p40 in the differential diagnosis of small round blue cell tumors of the sinonasal tract. *Head Neck Pathol*. 2014;8(2):141–145.
33. Wadsworth B, et al. Expression of p16 in sinonasal undifferentiated carcinoma (SNUC) without associated human papillomavirus (HPV). *Head Neck Pathol*. 2011;5:349–354.
34. Weinreb I, et al. Non-small cell neuroendocrine carcinoma of the sinonasal tract and nasopharynx. Report of 2 cases and review of the literature. *Head Neck Pathol*. 2007;1(1):21–26.
35. Wenig BM. Undifferentiated malignant neoplasms of the sinonasal tract. *Arch Pathol Lab Med*. 2009;133(5):699–712.
5. Fang W, et al. Clinicopathological significance of NUT rearrangements in poorly differentiated malignant tumors of the upper respiratory tract. *Int J Surg Pathol*. 2013;21:102–110.
6. French CA, et al. BRD4-NUT fusion oncogene: a novel mechanism in aggressive carcinoma. *Cancer Res*. 2003;63:304–307.
7. French CA, et al. Midline carcinoma of children and young adults with NUT rearrangement. *J Clin Oncol*. 2004;22:4135–4139.
8. French CA, et al. NUT carcinoma. In: El-Naggar AK, Chan JKC, Grandis JR, Takata T, Slootweg PJ, eds. *Classification of Head and Neck Tumours*. 4th ed. World Health Organization Classification of Tumors. Lyon, France: IARC Press; 2017:20–21.
9. French CA. Pathogenesis of NUT midline carcinoma. *Annu Rev Pathol*. 2012;7:247–265.
10. Haack H, et al. Diagnosis of NUT midline carcinoma using a NUT-specific monoclonal antibody. *Am J Surg Pathol*. 2009;33:984–991.
11. Solomon LW, et al. Retrospective analysis of nuclear protein in testis (NUT) midline carcinoma in the upper aerodigestive tract and mediastinum. *Oral Surg Oral Med Oral Pathol Oral Radiol*. 2015;119:213–220.
12. Stelow EB, et al. with rearrangement of the nuclear protein of the testis (NUT) gene (NUT midline carcinomas). *Adv Anat Pathol*. 2009;16:92–96.

### Nasopharyngeal Carcinoma

1. Afqir S, et al. Nasopharyngeal carcinoma in adolescents: a retrospective review of 42 patients. *Eur Arch Otorhinolaryngol*. 2009;266(11):1767–1773.
2. Armstrong RW, et al. Nasopharyngeal carcinoma in Malaysian Chinese: salted fish and other dietary exposures. *Int J Cancer*. 1998;77:228–235.
3. Dogan S, et al. Human papillomavirus and Epstein-Barr virus in nasopharyngeal carcinoma in a low-incidence population. *Head Neck*. 2014;36(4):511–516.
4. Hawkins EP, et al. Nasopharyngeal carcinoma in children—a retrospective review and demonstration of Epstein-Barr viral genomes in tumor cell cytoplasm: a report of the pediatric oncology group. *Hum Pathol*. 1990;21:805–810.
5. Hsu HC, et al. Pathology of nasopharyngeal carcinoma. Proposal of a new histologic classification correlated with prognosis. *Cancer*. 1987;59:945–951.
6. Hsu MM, et al. Nasopharyngeal carcinoma in Taiwan. Clinical manifestations and results of therapy. *Cancer*. 1983;52:362–368.
7. Kamino H, et al. Keratin and involucrin immunohistochemistry of nasopharyngeal carcinoma. *Cancer*. 1988;61:1142–1148.
8. Licitra L, et al. Cancer of the nasopharynx. *Crit Rev Oncol Hematol*. 2003;45(2):199–213.
9. Lin Z, et al. Human papillomavirus 16 detected in nasopharyngeal carcinomas in white Americans but not in endemic Southern Chinese patients. *Head Neck*. 2014;36(5):709–714.
10. Liu T, et al. FDG-PET, CT, MRI for diagnosis of local residual or recurrent nasopharyngeal carcinoma, which one is the best? A systematic review. *Radiother Oncol*. 2007;85(3):327–335.
11. Marks JE, et al. The National Cancer Data Base report on the relationship of race and national origin to the histology of nasopharyngeal carcinoma. *Cancer*. 1998;83(3):582–588.
12. Nicholls JM, et al. The association of squamous cell carcinomas of the nasopharynx with Epstein-Barr virus shows geographical variation reminiscent of Burkitt’s lymphoma. *J Pathol*. 1997;183(2):164–168.
13. Petersson BF, et al. Nasopharyngeal carcinoma. In: El-Naggar AK, Chan JKC, Grandis JR, Takata T, Slootweg PJ, eds. *Classification of Head and Neck Tumours*. 4th ed. World Health Organization Classification of Tumors. Lyon, France: IARC Press; 2017:65–70.
14. Sham JST, et al. Nasopharyngeal carcinoma in young patients. *Cancer*. 1990;65:2606–2610.
15. Shamugaratnam K, et al. Histological typing of upper respiratory tract tumor. In: *International Histological Classification of Tumors*. 2nd ed. Geneva (Switzerland): World Health Organization; 1991.
16. Singhi AD, et al. High-risk human papillomavirus in nasopharyngeal carcinoma. *Head Neck*. 2012;34(2):213–218.
17. Singhi AD, et al. Lymphoepithelial-like carcinoma of the oropharynx: a morphologic variant of HPV-related head and neck carcinoma. *Am J Surg Pathol*. 2010;34(6):800–805.
18. Tao Q, et al. Nasopharyngeal carcinoma: molecular pathogenesis and therapeutic developments. *Expert Rev Mol Med*. 2007;9(12):1–24.

### NUT Carcinoma

1. Bauer DE, et al. Clinicopathologic features and long-term outcomes of NUT midline carcinoma. *Clin Cancer Res*. 2012;18:5773–5779.
2. Bishop JA, et al. NUT midline carcinomas of the sinonasal tract. *Am J Surg Pathol*. 2012;36:1216–1221.
3. Chau NG, et al. Intensive treatment and survival outcomes in NUT midline carcinoma of the head and neck. *Cancer*. 2016 Aug 10;doi:10.1002/cncr.30242.
4. D’Souza JN, et al. Orbital involvement by NUT midline carcinoma. *Ophthal Plast Reconstr Surg*. 2015;31:e147–e150.



19. Thompson LDR. Head and Neck Cancer. In: Stewart BW, Wild CP, eds. *World Cancer Report 2014*. Lyon, France: IARC Press; 2014:422–435, [Chapter 5.8].
20. Thompson LDR. Update on nasopharyngeal carcinoma. *Head Neck Pathol*. 2007;1(1):81–86.
21. Wei WI, et al. Nasopharyngeal carcinoma. *Lancet*. 2005;365(9476):2041–2054.
22. Wenig BM. Nasopharyngeal carcinoma. *Ann Diagn Pathol*. 1999;3(6):374–385.
23. Zhang JX, et al. Epstein-Barr virus expression within keratinizing nasopharyngeal carcinoma. *J Med Virol*. 1998;55(3):227–233.

### Malignant Mucosal Melanoma

1. Akbani R, et al. Cancer Genome Atlas Network. Genomic classification of cutaneous melanoma. *Cell*. 2015;161:1681–1696.
2. Bachar G, et al. Mucosal melanomas of the head and neck: experience of the Princess Margaret Hospital. *Head Neck*. 2008;30(10):1325–1331.
3. Billings KR, et al. Clinical and pathologic distinction between primary and metastatic mucosal melanoma of the head and neck. *Arch Otolaryngol Head Neck Surg*. 1995;112:700–706.
4. Carvajal RD, et al. KIT as a therapeutic target in metastatic melanoma. *JAMA*. 2011;305:2327–2334.
5. Chan RC, et al. Mucosal melanoma of the head and neck: 32-year experience in a tertiary referral hospital. *Laryngoscope*. 2012;122:2749–2753.
6. Cheng YF, et al. Toward a better understanding of sinonasal mucosal melanoma: clinical review of 23 cases. *J Chin Med Assoc*. 2007;70(1):24–29.
7. Dauer EH, et al. Sinonasal melanoma: a clinicopathologic review of 61 cases. *Otolaryngol Head Neck Surg*. 2008;138(3):347–352.
8. Franquemont DW, Mills SE. Sinonasal malignant melanoma. A clinicopathologic and immunohistochemical study of 14 cases. *Am J Clin Pathol*. 1991;96:689–697.
9. Gal TJ, et al. Demographics and treatment trends in sinonasal mucosal melanoma. *Laryngoscope*. 2011;121:2026–2033.
10. Jethanamest D, et al. Predictors of survival in mucosal melanoma of the head and neck. *Ann Surg Oncol*. 2011;18:2748–2756.
11. Kardon DE, et al. Sinonasal mucosal malignant melanoma: report of an unusual case mimicking schwannoma. *Ann Diagn Pathol*. 2000;4(5):303–307.
12. Kim DK, et al. Ki67 antigen as a predictive factor for prognosis of sinonasal mucosal melanoma. *Clin Exp Otorhinolaryngol*. 2008;1(4):206–210.
13. Kondratiev S, et al. Expression and prognostic role of MMP2, MMP9, MMP13, and MMP14 matrix metalloproteinases in sinonasal and oral malignant melanomas. *Hum Pathol*. 2008;39(3):337–343.
14. Lazarev S, et al. Mucosal melanoma of the head and neck: a systematic review of the literature. *Int J Radiat Oncol Biol Phys*. 2014;90:1108–1118.
15. Lopez F, et al. Update on primary head and neck mucosal melanoma. *Head Neck*. 2016;38:147–155.
16. Lund VJ, et al. Sinonasal malignant melanoma: an analysis of 115 cases assessing outcomes of surgery, postoperative radiotherapy and endoscopic resection. *Rhinology*. 2012;50:203–210.
17. Martin JM, et al. Outcomes in sinonasal mucosal melanoma. *ANZ J Surg*. 2004;74(10):838–842.
18. McLean N, et al. Primary mucosal melanoma of the head and neck. Comparison of clinical presentation and histopathologic features of oral and sinonasal melanoma. *Oral Oncol*. 2008;44(11):1039–1046.
19. Moreno MA, et al. Mucosal melanoma of the nose and paranasal sinuses, a contemporary experience from the M. D. Anderson Cancer Center. *Cancer*. 2010;116:2215–2223.
20. Patel SG, et al. Primary mucosal malignant melanoma of the head and neck. *Head Neck*. 2002;24(3):247–257.
21. Prasad ML, et al. Clinicopathologic differences in malignant melanoma arising in oral squamous and sinonasal respiratory mucosa of the upper aerodigestive tract. *Arch Pathol Lab Med*. 2003;127(8):997–1002.
22. Regauer S, et al. Primary mucosal melanomas of the nasal cavity and paranasal sinuses. A clinicopathological analysis of 14 cases. *APMIS*. 1998;106(3):403–410.
23. Thompson LDR, et al. Sinonasal tract melanomas: a clinicopathologic study of 115 cases with a proposed staging system. *Am J Surg Pathol*. 2003;27:594–611.
24. Turri-Zanoni M, et al. Sinonasal mucosal melanoma: Molecular profile and therapeutic implications from a series of 32 cases. *Head Neck*. 2013;35:1066–1077.
25. van Dijk M, et al. Distinct chromosomal aberrations in sinonasal mucosal melanoma as detected by comparative genomic hybridization. *Genes Chromosomes Cancer*. 2003;36(2):151–158.
26. Williams MD, et al. Mucosal melanoma. In: El-Naggar AK, Chan JKC, Grandis JR, Takata T, Slootweg PJ, eds. *Classification of Head and Neck Tumours*. 4th ed. World Health Organization Classification of Tumors. Lyon, France: IARC Press; 2017:51–60.
27. Zebary A, et al. KIT, NRAS and BRAF mutations in sinonasal mucosal melanoma: a study of 56 cases. *Br J Cancer*. 2013;109:559–564.

### Olfactory Neuroblastoma

1. Argani P, et al. Olfactory neuroblastoma is not related to the Ewing family of tumors. Absence of EWS/FLI1 gene fusion and MIC2 expression. *Am J Surg Pathol*. 1998;22:391–398.
2. Bachar G, et al. Esthesioneuroblastoma: the Princess Margaret Hospital experience. *Head Neck*. 2008;30(12):1607–1614.
3. Bates T, et al. Ganglioneuroblastic transformation in olfactory neuroblastoma. *Head Neck Pathol*. 2012;6:150–155.
4. Bell D, et al. Olfactory neuroblastoma. In: El-Naggar AK, Chan JKC, Grandis JR, Takata T, Slootweg PJ, eds. *Classification of Head and Neck Tumours*. 4th ed. World Health Organization Classification of Tumors. Lyon, France: IARC Press; 2017:57–60.
5. Bell D, et al. Prognostic utility of Hyams histological grading and Kadish-Morita staging systems for esthesioneuroblastoma outcomes. *Head Neck Pathol*. 2015;9:51–59.
6. Bragg TM, et al. Clinicopathological review: esthesioneuroblastoma. *Neurosurgery*. 2009;64(4):764–770.
7. Devaiah AK, et al. Treatment of esthesioneuroblastoma: a 16-year meta-analysis of 361 patients. *Laryngoscope*. 2009;119(7):1412–1416.
8. Faragalla H, et al. Olfactory neuroblastoma: a review and update. *Adv Anat Pathol*. 2009;16(5):322–331.
9. Fried D, et al. Management of nonesthesioneuroblastoma sinonasal malignancies with neuroendocrine differentiation. *Laryngoscope*. 2012;122:2210–2215.
10. Gallagher KK, et al. Esthesioneuroblastoma: updating histologic grading as it relates to prognosis. *Ann Otol Rhinol Laryngol*. 2014;123:353–358.
11. Kadish S, et al. Olfactory neuroblastoma. A clinical analysis of 17 cases. *Cancer*. 1976;37:1571–1576.
12. Kauer G, et al. The prognostic implications of Hyam's subtype for patients with Kadish stage C esthesioneuroblastoma. *J Clin Neurosci*. 2013;20:281–286.
13. Miller DC, et al. Mixed olfactory neuroblastoma and carcinoma. A report of two cases. *Cancer*. 1984;54:2019–2028.
14. Mills SE, et al. Olfactory neuroblastoma. A clinicopathologic study of 21 cases. *Am J Surg Pathol*. 1985;9:317–327.
15. Ordonez NG, et al. Neuroendocrine tumors of the nasal cavity. *Pathol Annu*. 1993;28(2):77–111.
16. Ozsahin M. Outcome and prognostic factors in olfactory neuroblastoma: a rare cancer network study. *Int J Radiat Oncol Biol Phys*. 2010;78(4):992–997.
17. Platek ME, et al. Improved survival following surgery and radiation therapy for olfactory neuroblastoma: analysis of the SEER database. *Radiat Oncol*. 2011;6:41.
18. Saade RE, et al. Prognosis and biology in esthesioneuroblastoma: the emerging role of Hyams grading system. *Curr Oncol Rep*. 2015;17:423.
19. Sugita Y, et al. Olfactory neuroepithelioma: an immunohistochemical and ultrastructural study. *Neuropathology*. 2006;26(5):400–408.
20. Thompson LD. Olfactory neuroblastoma. *Head Neck Pathol*. 2009;3(3):252–259.
21. Wang SL, et al. Absence of Epstein-Barr virus in olfactory neuroblastoma. *Pathology*. 2007;39(6):565–566.
22. Wenig BM. Undifferentiated malignant neoplasms of the sinonasal tract. *Arch Pathol Lab Med*. 2009;133(5):699–712.
23. Woolf JC, et al. Calretinin staining facilitates differentiation of olfactory neuroblastoma from other small round blue cell tumors in the sinonasal tract. *Am J Surg Pathol*. 2011;35:1786–1793.

**Extranodal NK/T-Cell Lymphoma, Nasal Type**

1. Abbondanzo SL, et al. Non-Hodgkin's lymphoma of the sinonasal tract. A clinicopathologic and immunophenotypic study of 120 cases. *Cancer*. 1995;75:1281–1291.
2. Brodtkin DE, et al. Nasal-type NK/T-cell lymphoma presenting as hemophagocytic syndrome in an 11-year-old Mexican boy. *J Pediatr Hematol Oncol*. 2008;30(12):938–940.
3. Chen SW, et al. Upper aerodigestive tract lymphoma in Taiwan. *J Clin Pathol*. 2010;63(10):888–893.
4. Cheung MM, et al. Early stage nasal NK/T-cell lymphoma: clinical outcome, prognostic factors, and the effect of treatment modality. *Int J Radiat Oncol Biol Phys*. 2002;54(1):182–190.
5. Cheung MM, et al. Natural killer cell neoplasms: a distinctive group of highly aggressive lymphomas/leukemias. *Semin Hematol*. 2003;40(3):221–232.
6. Cheung MM, et al. Primary non-Hodgkin's lymphoma of the nose and nasopharynx: clinical features, tumor immunophenotype, and treatment outcome in 113 patients. *J Clin Oncol*. 1998;16(1):70–77.
7. Chuang SS, et al. Hematolymphoid tumours. In: El-Naggar AK, Chan JKC, Grandis JR, Takata T, Slootweg PJ, eds. *Classification of Head and Neck Tumours*. 4th ed. World Health Organization Classification of Tumors. Lyon, France: IARC Press; 2017:52–56.
8. Cuadra-Garcia I, et al. Sinonasal lymphoma. A clinicopathologic analysis of 58 cases from the Massachusetts General Hospital. *Am J Surg Pathol*. 1999;23:1356–1369.
9. Gaal K, et al. Sinonasal NK/T-cell lymphoma in the United States. *Am J Surg Pathol*. 2000;24:1511–1517.
10. Greer JP, et al. Natural killer-cell neoplasms. *Curr Hematol Malig Rep*. 2009;4(4):245–252.
11. Harabuchi Y, et al. Nasal natural killer (NK)/T-cell lymphoma: clinical, histological, virological, and genetic features. *Int J Clin Oncol*. 2009;14(3):181–190.
12. Heffner DK. Idiopathic midline destructive disease. *Ann Otol Rhinol Laryngol*. 1995;104(3):258.
13. Hu W, et al. Multivariate prognostic analysis of stage I(E) primary non-Hodgkin's lymphomas of the nasal cavity. *Am J Clin Oncol*. 2001;24(3):286–289.
14. Huang YH, et al. Nasopharyngeal extranodal NK/T-cell lymphoma, nasal type: retrospective study of 18 consecutive cases in Guangzhou, China. *Int J Surg Pathol*. 2011;19(1):51–61.
15. Jaffe ES, et al. Extranodal peripheral T-cell and NK-cell neoplasms. *Am J Clin Pathol*. 1999;111(1 suppl 1):S46–S55.
16. Jaffe ES, et al. Report of the workshop on nasal and related extranodal angiocentric T/NK-cell lymphomas: definition, differential diagnosis and epidemiology. *Am J Surg Pathol*. 1996;20:103–111.
17. Jaffe ES. Classification of natural killer (NK) cell and NK-like T-cell malignancies. *Blood*. 1996;87(4):1207–1210.
18. Kim K, et al. Treatment outcome of angiocentric T-cell and NK/T-cell lymphoma, nasal type: radiotherapy versus chemoradiotherapy. *Jpn J Clin Oncol*. 2005;35(1):1–5.
19. Kim TM, et al. Extranodal NK / T-cell lymphoma, nasal type: new staging system and treatment strategies. *Cancer Sci*. 2009;100(12):2242–2248.
20. Kohrt H, et al. Extranodal natural killer/T-cell lymphoma: current concepts in biology and treatment. *Leuk Lymphoma*. 2009;50(11):1773–1784.
21. Liang X, et al. Natural killer cell neoplasms. *Cancer*. 2008;112(7):1425–1436.
22. Nakashima Y, et al. Genome-wide array-based comparative genomic hybridization of natural killer cell lymphoma/leukemia: different genomic alteration patterns of aggressive NK-cell leukemia and extranodal NK/T-cell lymphoma, nasal type. *Genes Chromosomes Cancer*. 2005;44(3):247–255.
23. Nava VE, et al. The pathology of NK-cell lymphomas and leukemias. *Adv Anat Pathol*. 2005;12(1):27–34.
24. Ng SB, et al. Nasal-type extranodal natural killer/T-cell lymphomas: a clinicopathologic and genotypic study of 42 cases in Singapore. *Mod Pathol*. 2004;17(9):1097–1107.
25. Ooi GC, et al. Nasal T-cell/natural killer cell lymphoma: CT and MR imaging features of a new clinicopathologic entity. *AJR Am J Roentgenol*. 2000;174(4):1141–1145.
26. Siu LL, et al. Consistent patterns of allelic loss in natural killer cell lymphoma. *Am J Pathol*. 2000;157(6):1803–1809.
27. Strickler JG, et al. Polymorphic reticulosis: a reappraisal. *Hum Pathol*. 1994;25:659–665.
28. van Gorp J, et al. Epstein-Barr virus in nasal T-cell lymphomas (polymorphic reticulosis/midline malignant reticulosis) in western China. *J Pathol*. 1994;173:81–87.
29. Watanabe K, et al. A unique case of nasal NK/T cell lymphoma with frequent remission and relapse showing different histological features during 12 years of follow up. *J Clin Exp Hematop*. 2010;50(1):65–69.
30. Wilson WH, et al. Association of lymphomatoid granulomatosis with Epstein-Barr viral infection of B lymphocytes and response to interferon-alpha2b. *Blood*. 1996;87:4531–4537.
31. Yoon TY, et al. Nasal-type T/natural killer cell angiocentric lymphoma, Epstein-Barr virus-associated, and showing clonal T-cell receptor gamma gene rearrangement. *Br J Dermatol*. 1999;140(3):505–508.

**Rhabdomyosarcoma**

1. Bahrami A, et al. Aberrant expression of epithelial and neuroendocrine markers in alveolar rhabdomyosarcoma: a potentially serious diagnostic pitfall. *Mod Pathol*. 2008;21(7):795–806.
2. Callender TA, et al. Rhabdomyosarcoma of the nose and paranasal sinuses in adults and children. *Arch Otolaryngol Head Neck Surg*. 1995;112:252–257.
3. Coomans de Brachène A, et al. FOXO transcription factors in cancer development and therapy. *Cell Mol Life Sci*. 2016;73(6):1159–1172.
4. Franchi A, et al. Rhabdomyosarcoma. In: El-Naggar AK, Chan JKC, Grandis JR, Takata T, Slootweg PJ, eds. *Classification of Head and Neck Tumours*. 4th ed. World Health Organization Classification of Tumors. Lyon, France: IARC Press; 2017:36–38.
5. Fu YS, et al. Non-epithelial tumors of the nasal cavity, paranasal sinuses and nasopharynx: a clinicopathologic study. V. Skeletal muscle tumors (rhabdomyoma and rhabdomyosarcoma). *Cancer*. 1976;37:364–376.
6. Gerth DJ, et al. Pediatric sinonasal tumors in the United States: incidence and outcomes. *J Surg Res*. 2014;190(1):214–220.
7. Kubo T, et al. Prognostic value of PAX3/7-FOXO1 fusion status in alveolar rhabdomyosarcoma: Systematic review and meta-analysis. *Crit Rev Oncol Hematol*. 2015;96(1):46–53.
8. Parham DM, et al. Classification of rhabdomyosarcoma and its molecular basis. *Adv Anat Pathol*. 2013;20(6):387–397.
9. Sanghvi S, et al. Incidence trends and long-term survival analysis of sinonasal rhabdomyosarcoma. *Am J Otolaryngol*. 2013;34:682–689.
10. Szablewski V, et al. Adult sinonasal soft tissue sarcoma: analysis of 48 cases from the French Sarcoma Group database. *Laryngoscope*. 2015;125(3):615–623.
11. Thompson CF, et al. Sinonasal rhabdomyosarcoma: prognostic factors and treatment outcomes. *Int Forum Allergy Rhinol*. 2013;3:678–683.
12. Yasuda T, et al. Alveolar rhabdomyosarcoma of the head and neck region in older adults: genetic characterization and a review of the literature. *Hum Pathol*. 2009;40:341–348.

**Biphenotypic Sinonasal Sarcoma**

1. Huang SC, et al. Novel PAX3.NCOA1 fusions in biphenotypic sinonasal sarcoma with focal rhabdomyoblastic differentiation. *Am J Surg Pathol*. 2016;40:51–59.
2. Lewis JT, et al. Biphenotypic sinonasal sarcoma. In: El-Naggar AK, Chan JKC, Grandis JR, Takata T, Slootweg PJ, eds. *Classification of Head and Neck Tumours*. 4th ed. World Health Organization Classification of Tumors. Lyon, France: IARC Press; 2017:40–41.
3. Lewis JT, et al. Low-grade sinonasal sarcoma with neural and myogenic features: a clinicopathologic analysis of 28 cases. *Am J Surg Pathol*. 2012;36:517–525.
4. Powers KA, et al. Low-grade sinonasal sarcoma with neural and myogenic features—diagnostic challenge and pathogenic insight. *Oral Surg Oral Med Oral Pathol Oral Radiol*. 2015;119:e265–e269.
5. Rooper LM, et al. Biphenotypic sinonasal sarcoma: an expanded immunoprofile including consistent nuclear beta-catenin positivity and absence of SOX10 expression. *Hum Pathol*. 2016;55:44–50.



6. Wang X, et al. Recurrent PAX3.MAML3 fusion in biphenotypic sinonasal sarcoma. *Nat Genet.* 2014;46:666–668.
7. Wong WJ, et al. Alternate PAX3.FOXO1 oncogenic fusion in biphenotypic sinonasal sarcoma. *Genes Chromosomes Cancer.* 2016;55:25–29.

### Fibrosarcoma

1. Franchi A, et al. Fibrosarcoma. In: El-Naggar AK, Chan JKC, Grandis JR, Takata T, Slootweg PJ, eds. *Classification of Head and Neck Tumours*. 4th ed. World Health Organization Classification of Tumors. Lyon, France: IARC Press; 2017:34–35.
2. Fu YS, et al. Non-epithelial tumors of the nasal cavity, paranasal sinuses and nasopharynx: a clinicopathologic study. VI. Fibrous tissue tumors. *Cancer.* 1976;37:2912–2928.
3. Gnepp DR, et al. Desmoid fibromatosis of the sinonasal tract and nasopharynx. A clinicopathologic study of 25 cases. *Cancer.* 1996;78:2572–2579.
4. Heffner DK, et al. Sinonasal fibrosarcomas, malignant schwannomas, and “Triton” tumors. A clinicopathologic study of 67 cases. *Cancer.* 1992;70:1089–1101.
5. Patel TD, et al. Sinonasal fibrosarcoma: analysis of the Surveillance, Epidemiology, and End Results database. *Int Forum Allergy Rhinol.* 2016;6:201–205.
6. Zukerberg LR, et al. Solitary fibrous tumor of the nasal cavity and paranasal sinuses. *Am J Surg Pathol.* 1991;15:126–130.

### Leiomyosarcoma

1. Flucke U, et al. Leiomyosarcoma. In: El-Naggar AK, Chan JKC, Grandis JR, Takata T, Slootweg PJ, eds. *Classification of Head and Neck Tumours*. 4th ed. World Health Organization Classification of Tumors. Lyon, France: IARC Press; 2017:33–36.
2. Hsu JL, et al. Epstein-Barr virus-associated malignancies: epidemiologic patterns and etiologic implications. *Crit Rev Oncol Hematol.* 2000;34(1):27–53.
3. Kuruvilla A, et al. Leiomyosarcoma of the sinonasal tract. A clinicopathologic study of nine cases. *Arch Otolaryngol Head Neck Surg.* 1990;116(11):1278–1286.
4. McClain KL, et al. Association of Epstein-Barr virus with leiomyosarcomas in children with AIDS. *N Engl J Med.* 1995;332(1):12–18.
5. Szablewski V, et al. Adult sinonasal soft tissue sarcoma: analysis of 48 cases from the French Sarcoma Group database. *Laryngoscope.* 2015;125(3):615–623.
6. Ulrich CT, et al. Sinonasal leiomyosarcoma: review of literature and case report. *Laryngoscope.* 2005;115(12):2242–2248.

### Angiosarcoma

1. Bullerdiek J, et al. Angiosarcoma. In: El-Naggar AK, Chan JKC, Grandis JR, Takata T, Slootweg PJ, eds. *Classification of Head and Neck Tumours*. 4th ed. World Health Organization Classification of Tumors. Lyon, France: IARC Press; 2017:38–39.
2. Hadravsky L, et al. Angiomatoid change in polyps of the nasal and paranasal regions: an underrecognized and commonly misdiagnosed lesion—report of 45 cases. *Virchows Arch.* 2012;460(2):203–209.
3. Heffner DK. Problems in pediatric otorhinolaryngic pathology. II. Vascular tumors and lesions of the sinonasal tract and nasopharynx. *Int J Pediatr Otorhinolaryngol.* 1983;5(2):125–138.
4. Heffner DK. Sinonasal angiosarcoma? Not likely (a brief description of infarcted nasal polyps). *Ann Diagn Pathol.* 2010;14(4):233–234.
5. Nelson BL, et al. Sinonasal tract angiosarcoma: a clinicopathologic and immunophenotypic study of 10 cases with a review of the literature. *Head Neck Pathol.* 2007;1(1):1–12.
6. Smith SC, et al. Sinonasal lobular capillary hemangioma: a clinicopathologic study of 34 cases characterizing potential for local recurrence. *Head Neck Pathol.* 2013;7(2):129–134.
7. Wang ZH, et al. Sinonasal intravascular papillary endothelial hyperplasia successfully treated by endoscopic excision: a case report and review of the literature. *Auris Nasus Larynx.* 2009;36(3):363–366.
8. Yeang MS, et al. Outcomes and prognostic factors of post-irradiation and de novo sarcomas of the head and neck: a histologically matched case-control study. *Ann Surg Oncol.* 2013;20(9):3066–3075.

### Ewing Sarcoma

1. Bishop JA, et al. Adamantinoma-like Ewing family tumors of the head and neck: a pitfall in the differential diagnosis of basaloid and myoepithelial carcinomas. *Am J Surg Pathol.* 2015;39:1267–1274.
2. Cope JU, et al. Ewing sarcoma and sinonasal neuroectodermal tumors as second malignant tumors after retinoblastoma and other neoplasms. *Med Pediatr Oncol.* 2001;36(2):290–294.
3. Cordes B, et al. Molecular and phenotypic analysis of poorly differentiated sinonasal neoplasms: an integrated approach for early diagnosis and classification. *Hum Pathol.* 2009;40(3):283–292.
4. Csokonai LV, et al. Ewing’s sarcoma in the nasal cavity. *Otolaryngol Head Neck Surg.* 2001;125:665–667.
5. Dehner LP. Primitive neuroectodermal tumor and Ewing’s sarcoma. *Am J Surg Pathol.* 1993;17:1–13.
6. Huang YP, et al. Evaluation of NKX2-2 expression in round cell sarcomas and other tumors with EWSR1 rearrangement: imperfect specificity for Ewing sarcoma. *Mod Pathol.* 2016;29(4):370–380.
7. Iezzoni JC, et al. “Undifferentiated” small round cell tumors of the sinonasal tract: differential diagnosis update. *Am J Clin Pathol.* 2005;124(suppl):S110–S121.
8. Parham DM. Neuroectodermal and neuroendocrine tumors principally seen in children. *Am J Clin Pathol.* 2001;115(suppl):S113–S128.
9. Rischin D, et al. Sinonasal malignancies of neuroendocrine origin. *Hematol Oncol Clin North Am.* 2008;22(6):1297–1316, xi.
10. Toda T, et al. Primitive neuroectodermal tumor in sinonasal region. *Auris Nasus Larynx.* 1999;26:83–90.
11. Wenig BM, et al. Ewing sarcoma/primitive neuroectodermal tumors. In: El-Naggar AK, Chan JKC, Grandis JR, Takata T, Slootweg PJ, eds. *Classification of Head and Neck Tumours*. 4th ed. World Health Organization Classification of Tumors. Lyon, France: IARC Press; 2017:56–57.
12. Wenig BM. Undifferentiated malignant neoplasms of the sinonasal tract. *Arch Pathol Lab Med.* 2009;133(5):699–712.

### Teratocarcinosarcoma

1. Budrukkar A, et al. Management and clinical outcome of sinonasal teratocarcinosarcoma: single institution experience. *J Laryngol Otol.* 2010;124(7):739–743.
2. Franchi A, et al. Teratocarcinosarcoma. In: El-Naggar AK, Chan JKC, Grandis JR, Takata T, Slootweg PJ, eds. *Classification of Head and Neck Tumours*. 4th ed. World Health Organization Classification of Tumors. Lyon, France: IARC Press; 2017:26–28.
3. Heffner DK, et al. Teratocarcinosarcoma (malignant teratoma?) of the nasal cavity and paranasal sinuses. A clinicopathologic study of 20 cases. *Cancer.* 1984;53:2140–2154.
4. Kane SV, et al. Chemotherapy-induced neuronal maturation in sinonasal teratocarcinosarcoma—a unique observation. *Head Neck Pathol.* 2009;3(1):31–36.
5. Misra P, et al. Management of sinonasal teratocarcinosarcoma: a systematic review. *Am J Otolaryngol.* 2014;35:5–11.
6. Nguyen BD. Sinonasal teratocarcinosarcoma: MRI and F18- FDG-PET/CT imaging. *Ear Nose Throat J.* 2010;89(3):106–108.
7. Pai SA, et al. Teratocarcinosarcoma of the paranasal sinuses: a clinicopathologic and immunohistochemical study. *Hum Pathol.* 1998;29:718–722.
8. Salem F, et al. Teratocarcinosarcoma of the nasal cavity and paranasal sinuses: report of 3 cases with assessment for chromosome 12p status. *Hum Pathol.* 2008;39(4):605–609.
9. Shimazaki H, et al. Sinonasal teratocarcinosarcoma: ultrastructural and immunohistochemical evidence of neuroectodermal origin. *Ultrastruct Pathol.* 2000;24:115–122.
10. Smith SL, et al. Sinonasal teratocarcinosarcoma of the head and neck: a report of 10 patients treated at a single institution and comparison with reported series. *Arch Otolaryngol Head Neck Surg.* 2008;134(6):592–595.
11. Su YY, et al. Sinonasal teratocarcinosarcoma. *Am J Otolaryngol.* 2010;31(4):300–303.
12. Wei S, et al. Sinonasal teratocarcinosarcoma: report of a case with review of literature and treatment outcome. *Ann Diagn Pathol.* 2008;12(6):415–425.

# Non-Neoplastic Lesions of the Larynx, Hypopharynx, and Trachea

■ **Lester D.R. Thompson**

## ■ VOCAL CORD POLYPS AND NODULES

Vocal cord polyps and nodules represent reactive changes of laryngeal mucosa and adjacent stroma that result in a benign polypoid or nodular growth. The etiology is multifactorial, including laryngeal trauma (accidents or surgery), excessive and improper use of voice (vocal abuse), iatrogenic or functional lesions, infection, hypothyroidism, and smoking.

### CLINICAL FEATURES

A nodule and a polyp are not clinically synonymous terms, although they are frequently used interchangeably

in the pathology community. Approximately 1.5 % of the general population has hoarseness, and the presence of polyp/nodule is one of the most frequent significant causes. Nearly 2.5 % of children have nodules, with boys affected more often than girls (2:1), with attention-deficit/hyperactivity disorder (ADHD) associated with increased frequency of polyps or nodules. Among young adults, nodules are more frequent in young women. By contrast, polyps occur in any age group, with an equal sex distribution. Both lesions characteristically produce hoarseness, discomfort, vocal changes, and unstable voice. The speaking voice of singers, actors, public speakers, lecturers, and coaches is affected by excessive (overuse) and improper (abuse) use of voice. Interestingly, extroverted patients and patients who are talkative or excessively loud (vocal overdoers) are more likely to develop vocal cord polyps and nodules than quiet people who are not talkative (i.e., not me).

### VOCAL CORD POLYPS AND NODULES—DISEASE FACT SHEET

#### Definition

- Reactive changes of the laryngeal mucosa and adjacent stroma which result in a benign polypoid or nodular growth

#### Incidence and Location

- Infrequent (<1% of population)
- Approximately 2.5% of children (boys > girls; 2:1)

#### Sex and Age Distribution

- Polyps occur at any age and in both sexes equally
- Nodule is more common in young women

#### Clinical Features

- Vocal abuse or overuse, and phonation changes, hoarseness
- Other causes include infection, smoking, and hypothyroidism

#### Prognosis and Treatment

- Excellent
- Voice or speech therapy, behavior modification, vocal hygiene, and medical management before surgery

### PATHOLOGIC FEATURES

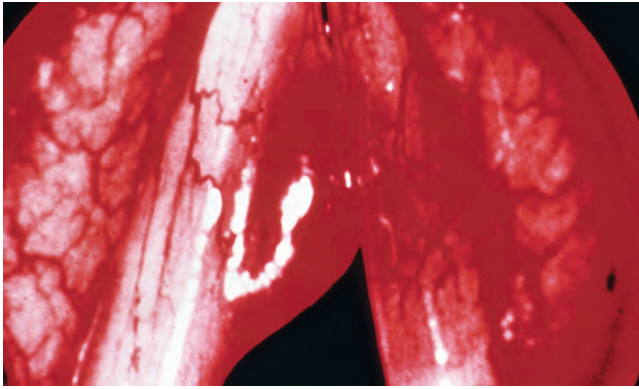
#### GROSS FINDINGS

Grossly, nodules are almost always bilateral, affecting the anterior to midportion of the true vocal cord, and presenting as an edematous, hemorrhagic, or callous-like mass, typically a few millimeters in size (Fig. 4.1). By contrast, a polyp is unilateral (>90 %), affecting the aryepiglottic fold, ventricular space, vocal fold, or Reinke space, as a sessile, raspberry-like to pedunculated soft, rubbery, translucent (edematous) to erythematous mass (Fig. 4.2) up to a few centimeters in greatest dimension.

#### MICROSCOPIC FINDINGS

There is usually no definitive histologic distinction between laryngeal nodules and polyp because they



**FIGURE 4.1**

Bilaterally edematous nodules on opposing surfaces of the vocal cords.

### VOCAL CORD POLYPS AND NODULES— PATHOLOGIC FEATURES

#### Gross Findings

- Nodules are bilateral, edematous to gelatinous, on opposing surfaces usually in the middle third of vocal cord (<0.5 cm)
- Polyps are unilateral, involve ventricular or Reinke space, and are a pedunculated soft, rubbery translucent to red mass (up to 3 cm)

#### Microscopic Findings

- Arc of development
- Edematous with proteinaceous material within interstitium
- Vascularized stroma with hemorrhage in loose myxoid stroma
- Myxoid stroma (pale blue-pink matrix material)
- Hyaline (fibrin-type material adjacent to vessels)
- Fibrous (spindle cells in dense stroma)
- Scant inflammation

#### Pathologic Differential Diagnosis

- Amyloidosis, myxoma, contact ulcer, ligneous conjunctivitis, granular cell tumor, spindle cell (sarcomatoid) squamous cell carcinoma

represent different stages within an arc of development. In the early stages, there is edema and deposition of proteinaceous material in the subepithelium and interstitium (Fig. 4.3). There is increased vascularization with subsequent hemorrhage (Fig. 4.4). Vascularity is much higher in polyps than nodules, and a thickened basement membrane is seen in nodules and not in polyps. Inflammation is scant to absent, but dilated vessels (telangiectasia) and granulation-type tissue may occasionally be seen. Myxoid stroma (pale blue-pink matrix material; Fig. 4.5) tends to be intermediate in the progression to a hyaline type, with fibrin-type material closely opposed to vascular spaces (Fig. 4.6) or a fibrous type, with spindle cells in a dense fibrous stroma (Fig. 4.7). However, any or all of these changes may be seen within the same polyp. Therefore the designations of edematous, vascular,

**FIGURE 4.2**

A polyp projects from the vocal cord on one side.

myxoid, hyaline, or fibrous types are not important, as they represent degrees of development. However, by convention, the dominant histologic pattern determines the type. The surface epithelium may become metaplastic, atrophic, keratotic, and hyperplastic. Crystals may be seen in a few polyps.

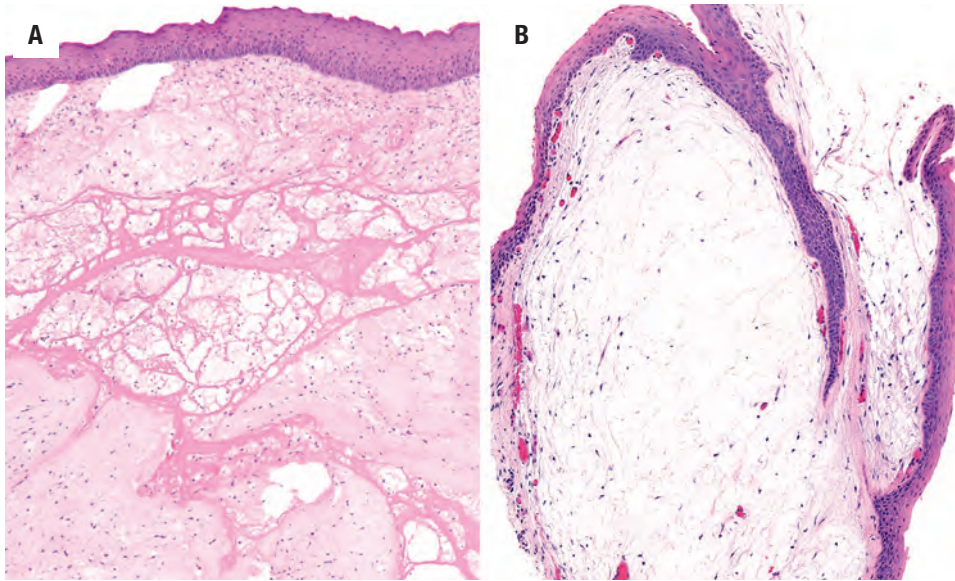
### DIFFERENTIAL DIAGNOSIS

The differential diagnosis includes amyloidosis, myxoma, contact ulcer, ligneous conjunctivitis, and, rarely, neoplasms (granular cell tumor, spindle cell [sarcomatoid] squamous cell carcinoma [SCSCC]). *Amyloidosis* shows a perivascular or periglandular accentuation of an acellular, extracellular eosinophilic matrix material. *Myxoma*, uncommon at this site, is an avascular, hypocellular lesion with occasional stellate spindle cells in an abundant basophilic, gelatinous matrix. *Contact ulcer* shows surface ulceration with fibrinoid necrosis and primarily affects opposing surfaces of the posterior true vocal cords. *Ligneous* (“woody”) *conjunctivitis*, a rare chronic condition affecting mucous membranes, results in firm, clotted fibrin-rich matrix material deposition that creates a hard, subepithelial nodule. In general, neoplasms may be easily distinguished by their unique histologic findings.

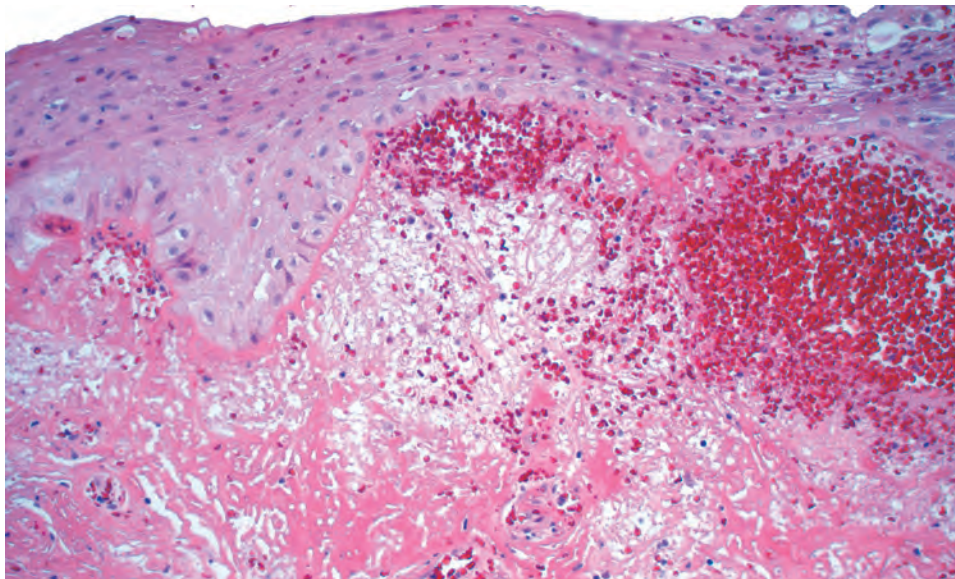
### PROGNOSIS AND THERAPY

Voice or speech therapy, behavior modification, and vocal hygiene are first line treatments for polyps and nodules. Drug therapy may also help certain underlying conditions,

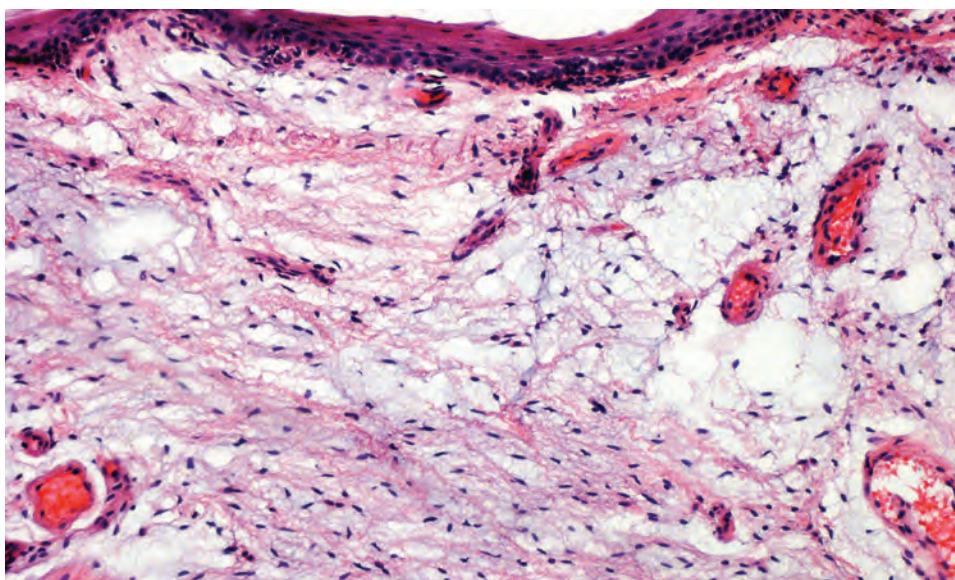


**FIGURE 4.3**

The surface epithelium of a polyp is unremarkable, covering the hypocellular, edematous stroma. The left side (**A**) is more fibrinous, whereas the right (**B**) is myxoid.

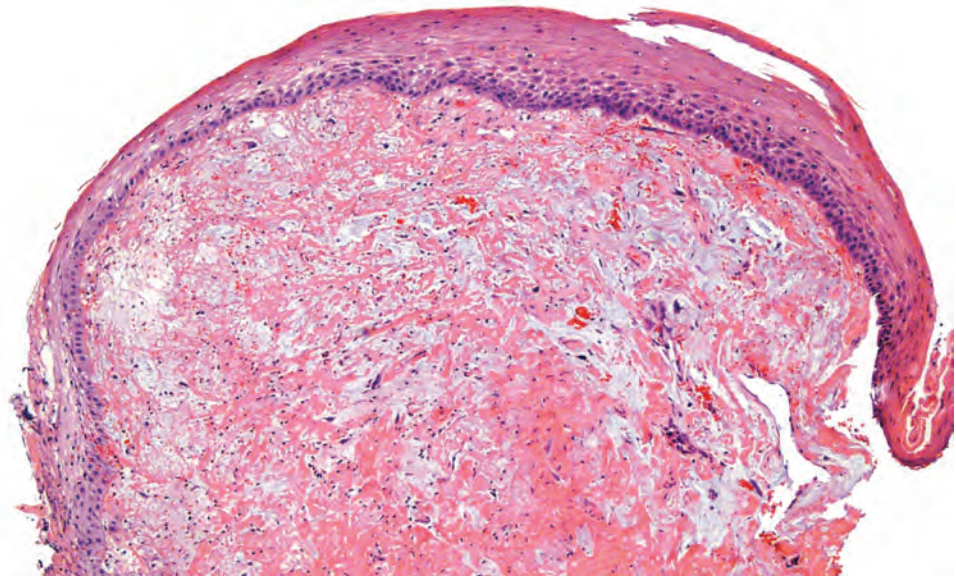
**FIGURE 4.4**

Large areas of degenerated material with edema and rich vascular investment with hemorrhage in a polyp.

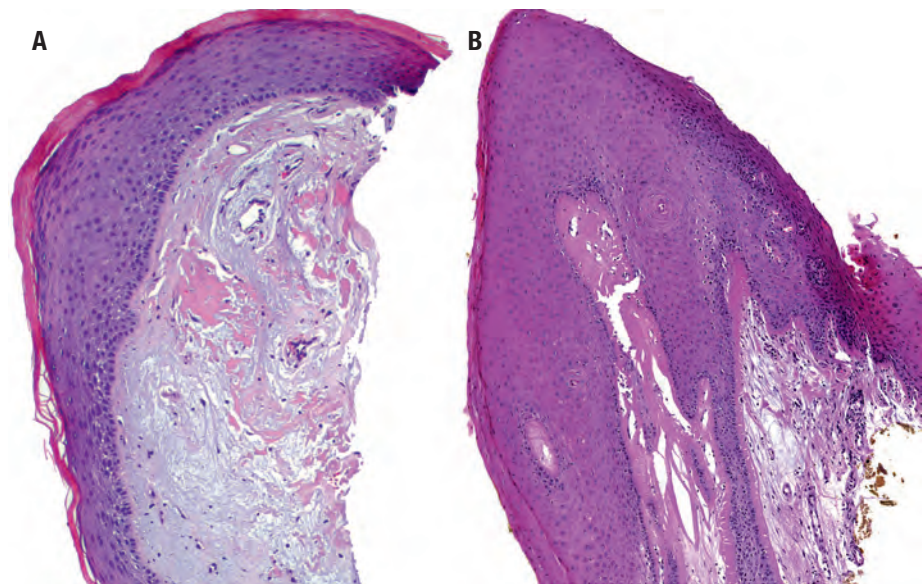
**FIGURE 4.5**

Basophilic myxoid material separates small stellate cells without cytologic atypia. The surface epithelium is intact and uninvolved.



**FIGURE 4.6**

Hyaline change in a polyp with fibrin-type material and edematous change.

**FIGURE 4.7**

Fibrous connective tissue deposition beneath a keratotic epithelium. Note a small residual area of fibrin (A), while more hyalinized material is seen in (B).

such as hypothyroidism. Surgery usually has limited value because it is the underlying cause that needs to be managed.

## ■ CONTACT ULCER

### CLINICAL FEATURES

Contact ulcer is a frequent benign reactive epithelial response to injury, generally associated with acid regurgitation, vocal abuse, and/or intubation. Gastric-laryngeal reflux or gastroesophageal reflux disease (GERD) is frequently missed because the patient is unaware of the underlying cause (hiatal hernia), although they may report heartburn and/or belching as a result of the acid reflux,

with pepsin thought to be the injurious agent rather than hydrochloric acid. When a result of intubation, females are affected more commonly, especially in the urgent setting when an inappropriately sized endotracheal tube has been selected. Otherwise, contact ulcer develops more frequently in adult men, who present with hoarseness, cough, sore throat, chronic throat clearing, habitual coughing, or pain.

### PATHOLOGIC FEATURES

#### GROSS FINDINGS

Contact ulcer usually presents as a bilateral, polypoid, or nodular mass (Fig. 4.8), up to 3 cm in size, most

**CONTACT ULCER—DISEASE FACT SHEET****Definition**

- Benign reactive epithelial response to an injury usually in the posterior larynx

**Incidence and Location**

- Frequent, especially in patients with gastroesophageal reflux disease or vocal abuse
- Posterior larynx is most common site

**Sex and Age**

- Males > females (except in postintubation distribution setting)
- Adults > children

**Clinical Features**

- Hoarseness, cough, sore throat, and pain
- Chronic throat clearing and habitual coughing
- Vocal abuse/misuse
- Gastrolaryngeal reflux disease symptoms (heartburn, belching)

**Prognosis and Treatment**

- Excellent
- Control gastroesophageal reflux disease, vocal rehabilitation, and then perhaps surgery

**CONTACT ULCER—PATHOLOGIC FEATURES****Gross Findings**

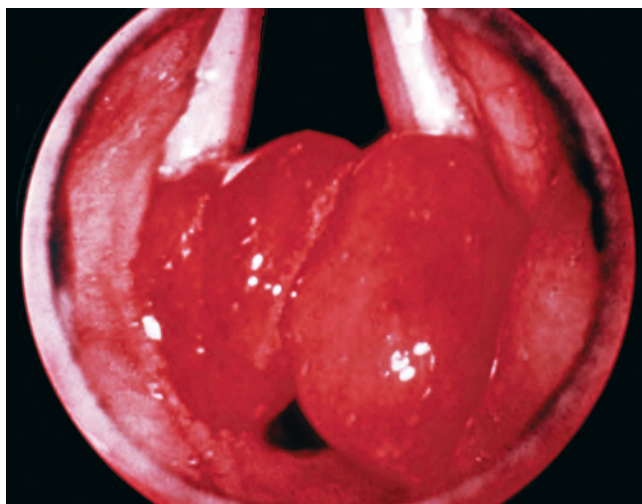
- Bilateral, ulcerated, polypoid to nodular mass
- Posterior larynx with kissing ulcer on contralateral cord
- Up to 3 cm

**Microscopic Findings**

- Surface ulceration with fibrinoid necrosis
- Exuberant granulation tissue, with vessels aligned perpendicular to surface
- Central areas may have hemosiderin-laden macrophages
- Reactive and plump endothelial cells (without atypia)
- May have surface reepithelialization with time, but fibrinoid necrosis usually remains; prominent fibrosis may develop

**Pathologic Differential Diagnosis**

- Infectious agents
- Inflammatory conditions (granulomatosis with polyangiitis)
- Vascular lesions (Kaposi sarcoma and angiosarcoma)
- Epithelial neoplasms, specifically spindle cell (sarcomatoid) squamous cell carcinoma

**FIGURE 4.8**

A laryngoscopic view of contact ulcer shows a polypoid, bilateral, beefy red mass involving the posterior vocal cords. A “kissing ulcer” is characteristic.

frequently affecting the posterior larynx. There is usually a “kissing ulcer” on the contralateral cord, with a red to beefy appearance.

**MICROSCOPIC FINDINGS**

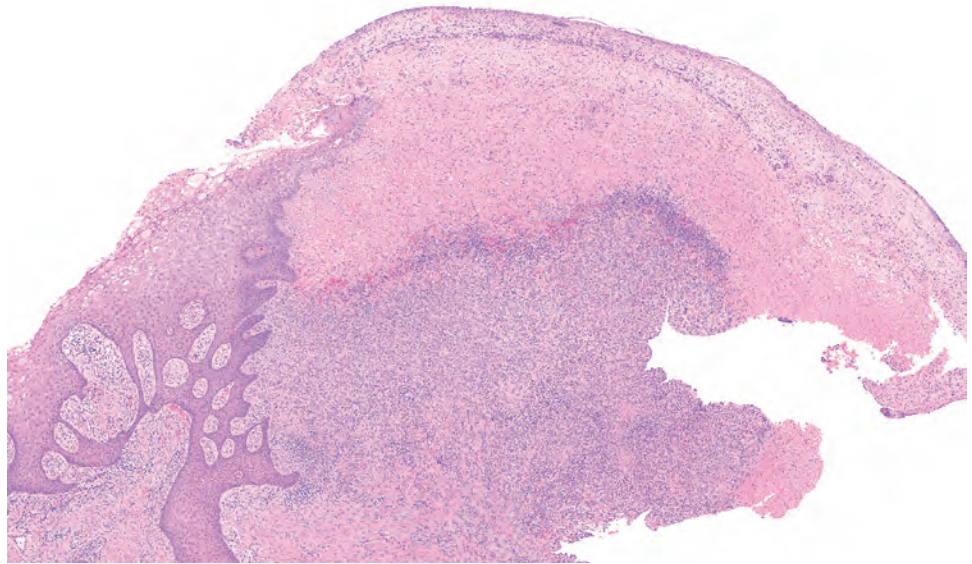
Histologic sections reveal extensive surface ulceration, covered by fibrin and/or fibrinoid necrosis, overlying exuberant granulation tissue (Figs. 4.9 and 4.10). Vessels

in the granulation tissue, often arranged perpendicular to the surface, are lined by plump reactive endothelial cells without atypia, and surrounded by marked acute and chronic inflammation, including plasma cells, histiocytes, and giant cells (Fig. 4.10). Hemosiderin-laden macrophages may be seen at the base of the polyp, especially in lesions of long clinical duration (Fig. 4.9). Surface bacterial or fungal colonization is frequently seen. In the early stages, surface ulceration without granulation tissue may be identified. Over time, the lesion may demonstrate an irregular hyperplastic epithelium secondary to regenerative surface reepithelialization, although a residuum of fibrinoid necrosis is usually identified below the new surface (Fig. 4.11). These changes characterize the chronic phase of the disease, which may also show prominent stromal fibrosis.

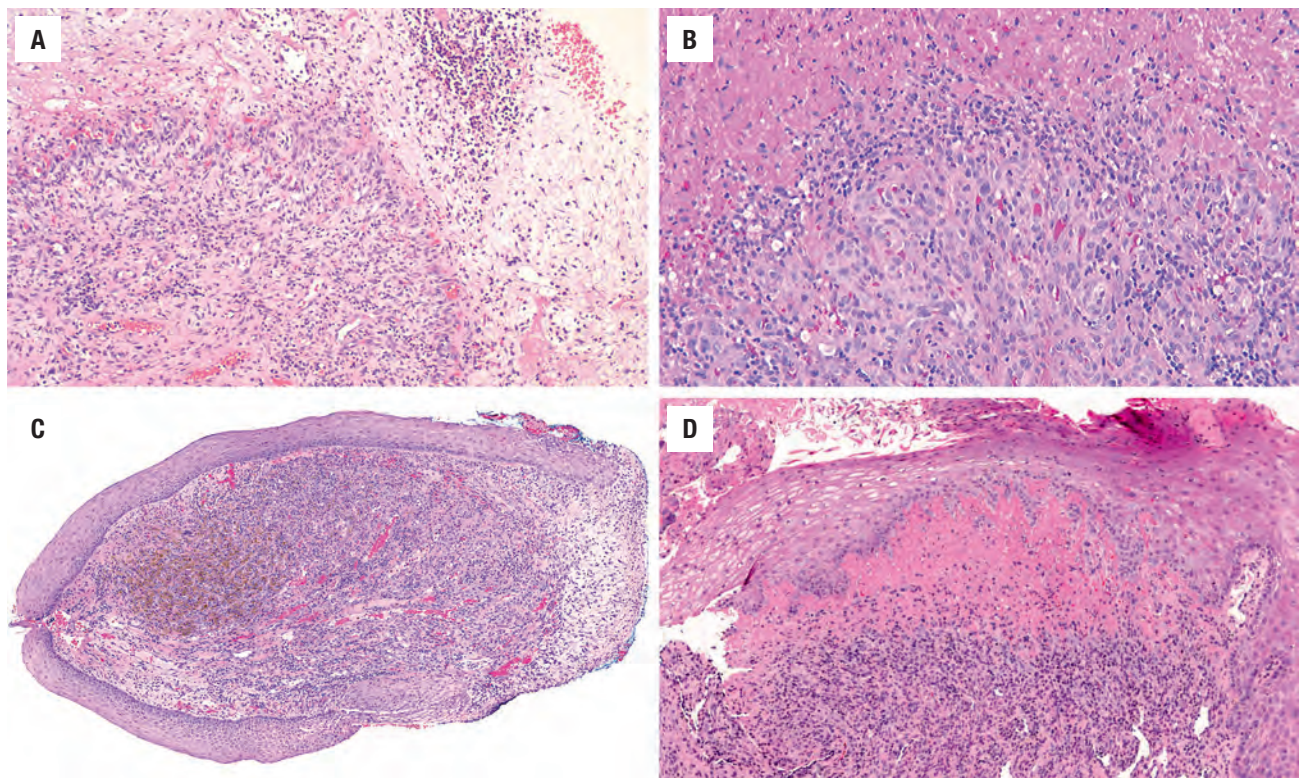
**DIFFERENTIAL DIAGNOSIS**

The diagnosis of contact ulcer is usually a clinical pathologic correlation because the histologic findings are largely nonspecific. In light of this, the morphologic differential diagnosis includes a variety of infectious agents, inflammatory conditions (granulomatosis with polyangiitis [Wegener granulomatosis], inflammatory myofibroblastic tumor), vascular lesions (Kaposi sarcoma [KS], angiosarcoma), and epithelial neoplasms (SCC, SCS). Special stains (Gomori methenamine silver [GMS], periodic acid-Schiff [PAS], Brown-Hopps [tissue Gram stain], Warthin-Starry) and culture should confirm an infectious agent. Granulomatosis with polyangiitis has geographic



**FIGURE 4.9**

A polypoid nodule has most of the surface epithelium denuded and replaced by fibrinoid necrosis overlying granulation-type tissue. Note the surface epithelium to one side.

**FIGURE 4.10**

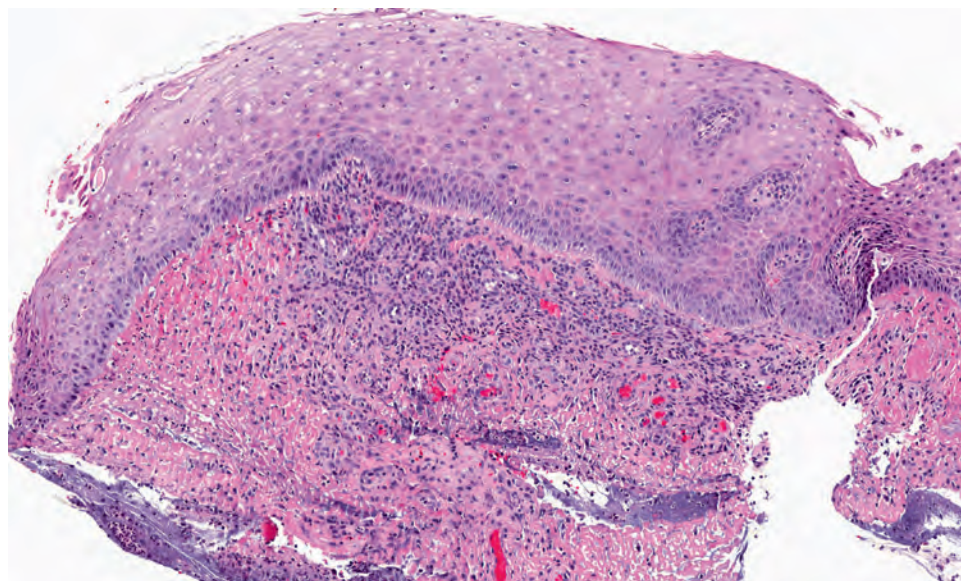
The composite shows various surface changes including fibrinoid necrosis (**A** and **B**), and hemosiderin is noted (**C**). Surface reepithelialization is present (**D**).

biocollagenolytic blue, granular necrosis, true vasculitis, and clinical findings (c-antineutrophil cytoplasmic antibodies, proteinase 3). KS and angiosarcoma are rare in the larynx but show slit-like spaces with pleomorphic cells, freely anastomosing vascular channels, spheroid hyaline globules (KS), and atypical mitotic figures.

#### PROGNOSIS AND THERAPY

After the correct diagnosis of contact ulcer is made, appropriate identification and removal of the specific inciting factor may eliminate the morbidity associated



**FIGURE 4.11**

The surface epithelium has grown over the defect, but the fibrinoid necrosis is still present to give a hint of the previous damage.

with surgery. Medical management includes aggressive acid-suppressive therapy to control GERD. In addition, vocal rehabilitation, and behavioral modifications to minimize shouting, habitual coughing, and/or throat clearing are helpful in controlling the disease.

## ■ AMYLOIDOSIS

Amyloidosis (amyloidoma) encompasses a family of different types of benign accumulations of extracellular, acellular, fibrillar, insoluble protein deposits. Laryngeal amyloidosis, both localized and primary, and is the most common site of localized disease, although rare, accounting for less than 1% of benign laryngeal tumors. Multifocal disease is present in up to 15% of patients. It may be part of mucosa-associated lymphoid tissue (MALT) or neuroendocrine tumor product. In fact, this mucosal association implies that at least a few laryngeal amyloid cases may be the result of a lymphoproliferative disorder with an origin from MALT (MALT lymphoma). Moreover, the monoclonal nature of the associated lymphoplasmacytic infiltrate in some cases, and the association with a systemic plasma cell dyscrasia, suggest a pathogenesis from an immunocyte dyscrasia.

There are a variety of classifications of amyloidosis, according to its distribution (localization), clinical type, by the presence or absence of underlying disease, its precursor protein (immunocytochemical nature), and patterns of extracellular deposition. Different sources of amyloidosis are recognized, with immunoglobulin light chains most common in the larynx.

### CLINICAL FEATURES

Almost all patients experience hoarseness or voice changes, usually caused by mechanical factors, conditioned by the size and location of the amyloid. Patients usually present as adults, although children may rarely be affected, and there is no sex predilection.

### PATHOLOGIC FEATURES

#### GROSS FINDINGS

Although there are conflicting data, the false vocal cord seems to be more frequently affected, showing a firm, “starchlike,” waxy, translucent cut surface, measuring up to 4 cm in greatest dimension. Multifocal disease elsewhere in the upper aerodigestive tract may be seen in up to 15% of patients.

#### MICROSCOPIC FINDINGS

Amyloid consists histologically (irrespective of any associated findings) of a subepithelial, extracellular, acellular, hyaline-like, homogeneous, eosinophilic matrix material dispersed throughout the stroma (Fig. 4.12), usually showing a predilection for vessels or mucoserous glands (Fig. 4.13). A sparse inflammatory infiltrate composed of lymphocytes and plasma cells (Fig. 4.14) may be seen; however, significant cytologic atypia of this lymphoplasmacytic infiltrate is not appreciated. Occasional histiocytes and giant cells may be either at the peripheral margin of, or enclosed within, the amyloid (Fig. 4.12).



**AMYLOIDOSIS—DISEASE FACT SHEET****Definition**

- Benign accumulation of extracellular, acellular, fibrillar insoluble protein deposits of amyloid

**Incidence and Location**

- <1% of all laryngeal neoplasms
- Usually in false vocal cord but may be multifocal (15%)

**Morbidity and Mortality**

- Depends on primary or systemic disease and whether single or multifocal
- May be slowly progressive

**Sex and Age Distribution**

- Equal sex distribution
- Usually adults, but rarely children are affected

**Clinical Features**

- Hoarseness and voice changes

**Prognosis and Treatment**

- Good, although dependent on localized or systemic disease and whether primary or secondary
- Surgery is the treatment of choice
- Must exclude systemic disease with clinical, radiographic, and laboratory work-up

**AMYLOIDOSIS—PATHOLOGIC FEATURES****Gross Findings**

- Firm, starchlike, waxy translucent cut surface
- Up to 4 cm

**Microscopic Findings**

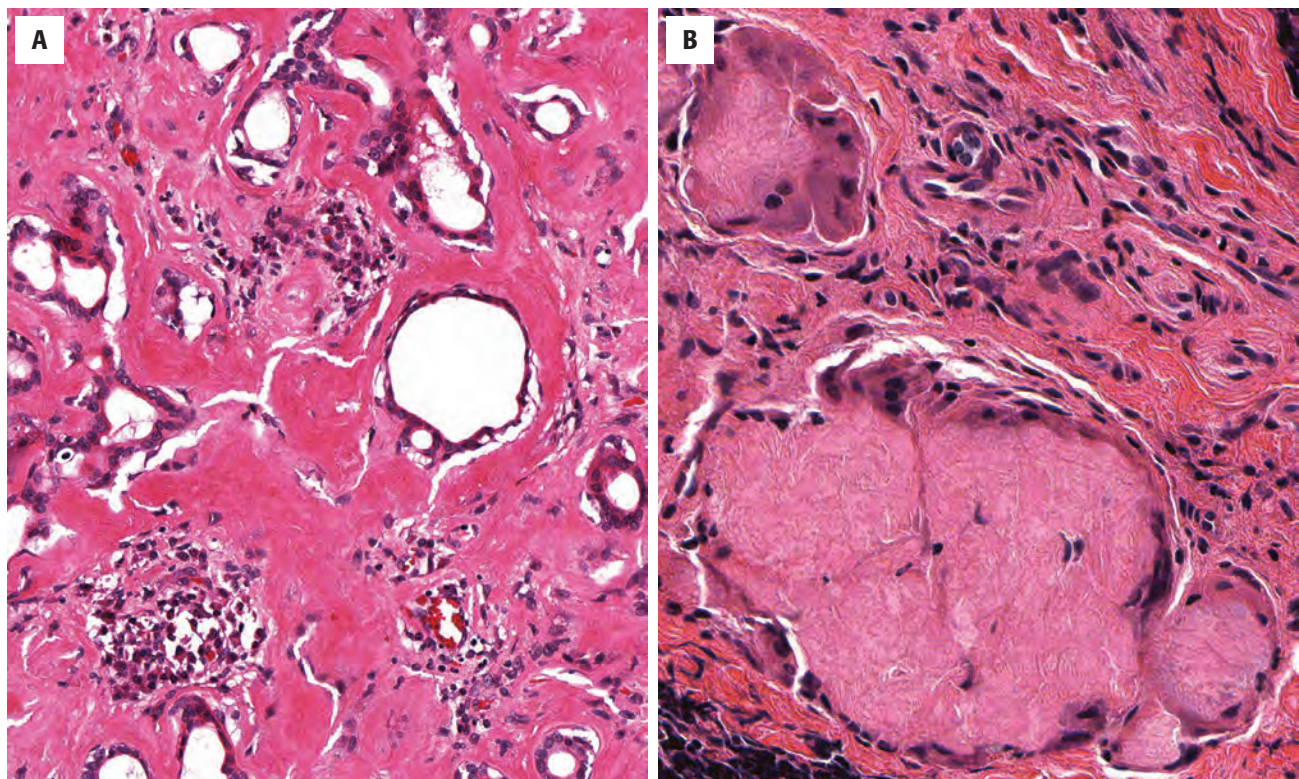
- Subepithelial deposits
- Acellular, extracellular, eosinophilic, homogeneous matrix material
- Perivascular and periglandular predilection (compression atrophy may result)
- Lymphoplasmacytic infiltrate (may be light chain restricted)
- Foreign body giant cell reaction may be seen

**Special Studies**

- "Apple-green" birefringence with polarized light using a Congo red stain
- Metachromatic with methyl violet stain
- May show kappa or lambda light chain restriction and positive amyloid P immunoreactivity

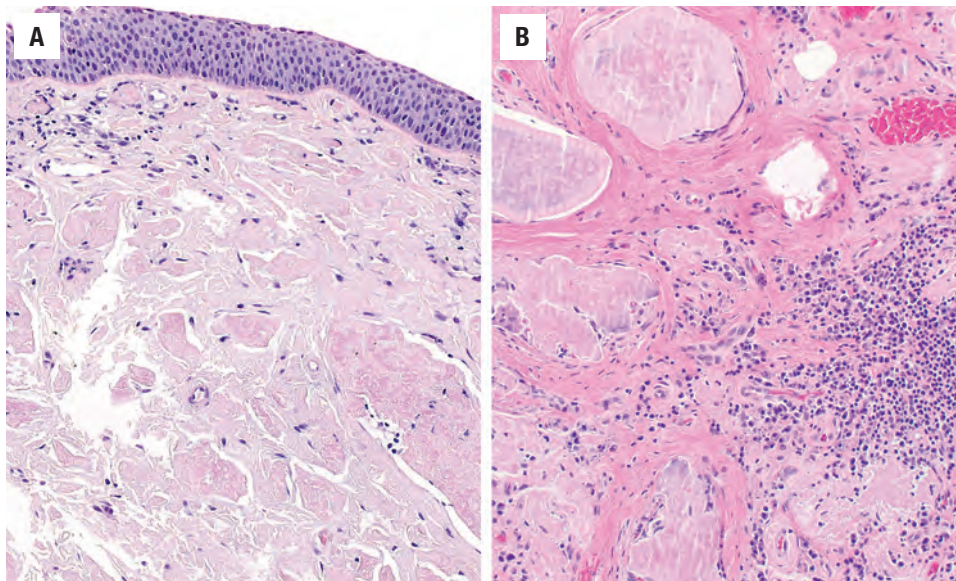
**Pathologic Differential Diagnosis**

- Mucosa-associated lymphoid tissue lymphoma, vocal cord polyps, ligneous conjunctivitis, lipid proteinosis, component of multiple myeloma, neuroendocrine carcinoma, and medullary thyroid carcinoma

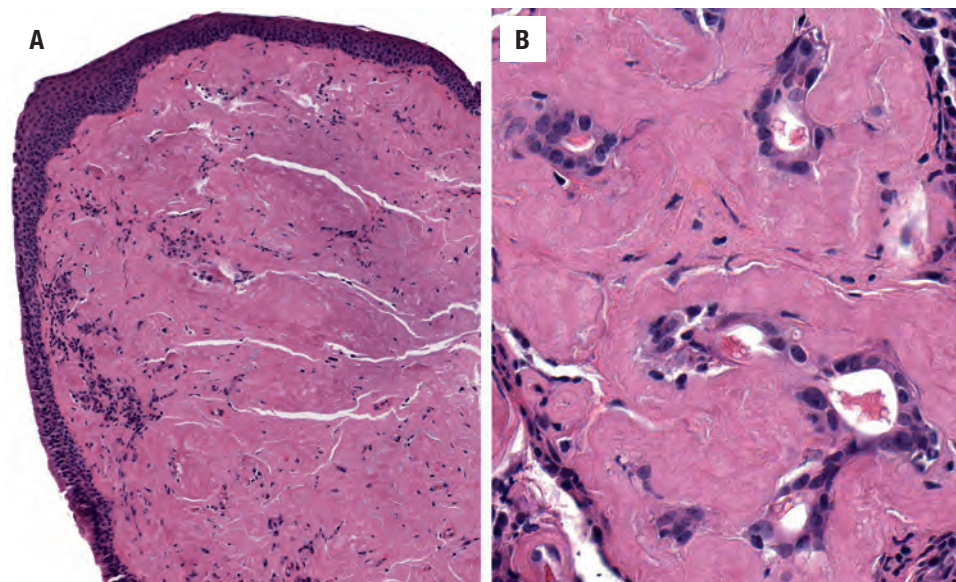
**FIGURE 4.12**

**A**, Periductal deposition with compression atrophy is characteristic for amyloid. **B**, Fragments of amorphous, acellular, eosinophilic amyloid material is found in the stroma, with a foreign body giant cell reaction.



**FIGURE 4.13**

**A**, The surface epithelium overlies a stroma filled with eosinophilic hyaline amyloid material. **B**, Note the amyloid associated with giant cell reaction but also with a rich inflammatory investment.

**FIGURE 4.14**

**A**, There is a sparse inflammatory infiltrate associated with amyloid deposition below an intact surface. **B**, Marked periductal deposition of amyloid, resulting in compression.

The amyloidosis of the larynx is composed of a protein that is immunologically identical to the variable region of the light chain fragment of immunoglobulin.

### ANCILLARY STUDIES

#### SPECIAL STAINS

Amyloid may be confirmed with histochemical techniques (Congo red, methyl violet [metachromatic pink-violet staining]), with the characteristic apple-green birefringence seen under polarized light with Congo red (Fig. 4.15) proving to be the most reliable and easy to interpret.

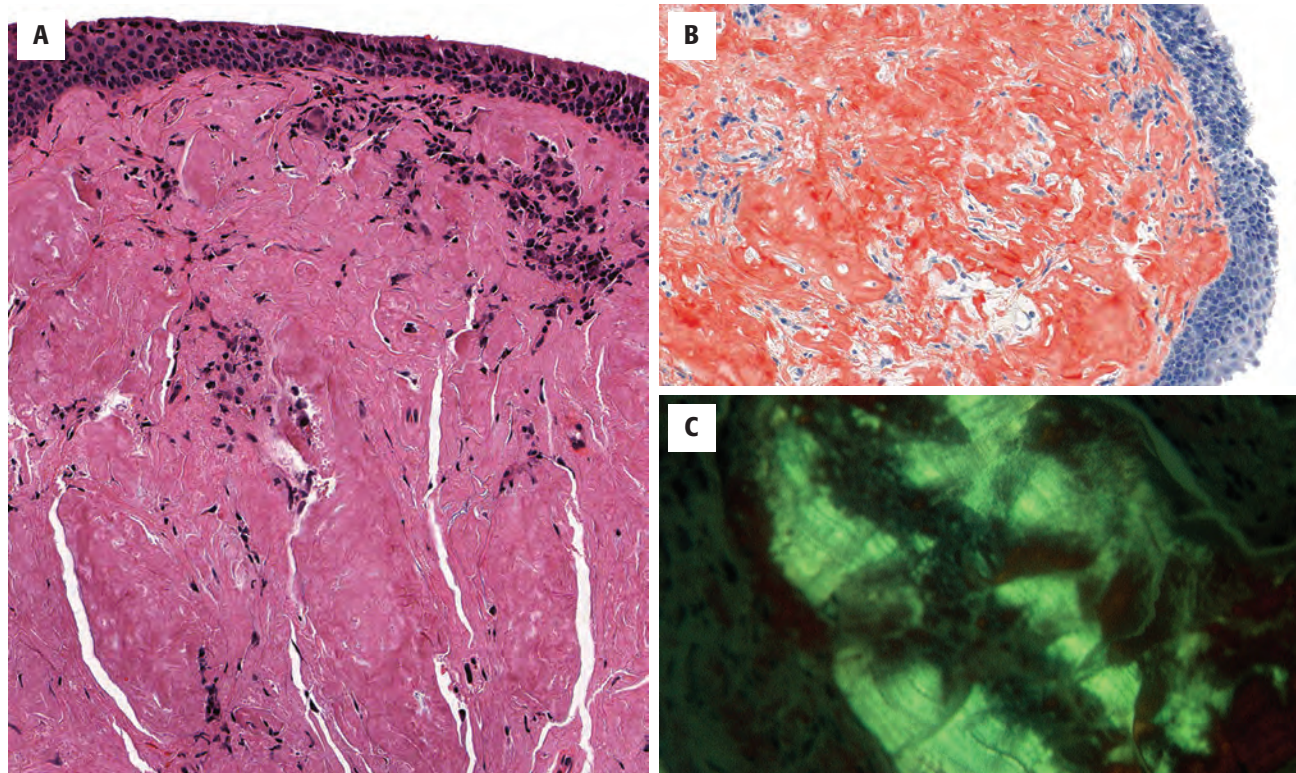
#### IMMUNOHISTOCHEMICAL FINDINGS

CD20 and CD3 highlight the admixture of B and T cells in the sparse lymphoplasmacytic infiltrate, respectively, although T cells tend to predominate, especially at the periphery of the amyloid deposits. Immunoreactivity with amyloid P and light chains ( $\kappa$  and  $\lambda$ ) is more variable, although light chain restriction of the plasma cells may be seen in some cases.

#### DIFFERENTIAL DIAGNOSIS

The differential diagnosis is limited and includes vocal cord polyps (usually lacks an associated



**FIGURE 4.15**

**A**, The acellular, eosinophilic, opaque amyloid deposition is noted below an intact surface epithelium with focal inflammation. **B**, A Congo red stain highlights the amyloid. **(C)** "Apple-green" birefringence when viewed under polarized light of a Congo red stain.

lymphoplasmacytic infiltrate), ligneous conjunctivitis (fibrin-rich nodular deposits), and lipid proteinosis (amorphous hyaline deposits), all of which are negative for amyloid studies.

It is important to note that amyloid may occur in association with multiple myeloma, laryngeal neuroendocrine tumors (atypical carcinoid, small cell carcinoma), and medullary thyroid carcinoma. In the latter scenario the determination of a serum calcitonin level may help to distinguish between a primary laryngeal neuroendocrine tumor (serum elevation absent) versus a metastatic/invasive medullary thyroid carcinoma (serum elevation present).

### PROGNOSIS AND THERAPY

Excision is usually the treatment of choice. There is a difference in the biologic behavior and clinical management between isolated laryngeal amyloidosis and other forms of amyloidosis. Multifocal or systemic disease must be ruled out by clinical, radiographic, and laboratory investigation (including quantitative immunoglobulin assay, serological test for rheumatoid arthritis and/or other chronic inflammatory conditions, urine and/or serum electrophoresis, Bence Jones protein analysis) that should be tailored to the individual patient. Prognosis depends on localized versus systemic, and primary versus secondary,

disease. The prognosis for isolated laryngeal amyloidosis is excellent because the "tumors" are slow growing, although repeated surgeries (endoscopic) may be necessary for recurrent disease. There does not appear to be any prognostic significance of amyloid deposition in association with other tumors. In these cases the prognosis is determined by the specific tumor type/morphology itself.

### ■ CYSTS OF THE LARYNX (INCLUDING LARYNGOCELE)

Cysts of the larynx may be filled with fluid or air and may be lined by different epithelia, each of which has a different name based on anatomic site as well as histologic appearance. Benign cysts (saccular, ductal, oncocytic, tonsillar) are usually distinct from laryngocele, which is usually a clinical/radiographic finding. These lesions may result from repeated increases of intralaryngeal pressure, infection, trauma, or in association with tumors.

### CLINICAL FEATURES

Outpouchings from the laryngeal ventricle and saccule of the normal laryngeal mucosa result in a laryngocele.

**CYSTS OF THE LARYNX (INCLUDING LARYNGOCELE)—  
DISEASE FACT SHEET****Definition**

- Outpouchings of the laryngeal ventricle and saccule are called laryngocele
- Saccular, ductal, oncocyctic, and tonsillar cysts are benign epithelial cysts within specific anatomic sites of the larynx

**Incidence**

- Uncommon, although more frequent in younger patients

**Sex and Age Distribution**

- Laryngocele: males > females; all ages are affected
- Cysts: equal sex distribution; usually older adults (50-60 years)

**Clinical Features**

- Divided into internal or external laryngocele
- Symptoms are variable and nonspecific, with airway obstruction, hoarseness, mass, and foreign body sensation

**Prognosis and Treatment**

- Excellent
- Marsupialization (laryngocele) or surgery for cysts

Laryngoceles are rare (1 in 2.5 million population), develop in men more often than women, across all ages, and are divided clinically into internal (expansion into the false vocal fold) and external (extension through the thyrohyoid membrane into the soft tissues of the neck). The vast majority present with an internal unilateral mass. Symptoms are variable and include airway obstruction, hoarseness, mass, or foreign body sensation; however, symptoms may spontaneously resolve when the expelled air decompresses the mass.

In general, the symptoms for patients with cysts are nonspecific and heavily overlap those of laryngocele. The most common laryngeal cysts are ductal cysts (75%), followed by saccular cysts (located between true and false cords). Tonsillar cysts show a predilection for the epiglottis, whereas ductal and oncocyctic cysts predilect to the ventricular folds and ventricle of Morgagni. Patients are usually older adults (50 to 60 years), with an equal sex distribution.

**PATHOLOGIC FEATURES****GROSS FINDINGS**

The gross appearance of laryngeal cysts is determined by the point of origin in the larynx and the type of cyst (saccular, ductal, oncocyctic, tonsillar). The cyst may be considered to be either external or internal to the larynx, based on the degree of compression by the cyst and the

**CYSTS OF THE LARYNX (INCLUDING LARYNGOCELE)—  
PATHOLOGIC FEATURES****Gross Findings**

- Point of origin and type of cyst determines the macroscopic appearance
- Internal or external to the larynx
- Cysts do not generally communicate with the lumen
- Saccular cysts (submucosal) filled with mucus affect the false cord
- Retention cysts (tonsillar) affect epiglottis
- Traumatic cysts affect the arytenoid region
- Size ranges from 0.5 to 8 cm

**Microscopic Findings**

- Cysts are surrounded by fibrous connective tissue
- Squamous or respiratory epithelium
- Vascular elements seen in vascular cysts
- Oncocyctic epithelium may line the cysts
- Inflammation within wall in tonsillar cysts

**Pathologic Differential Diagnosis**

- External jugular phlebectasia, prolapse, branchial cleft cyst, thyroglossal duct cyst, dermoid cyst, teratoma, laryngeal webs

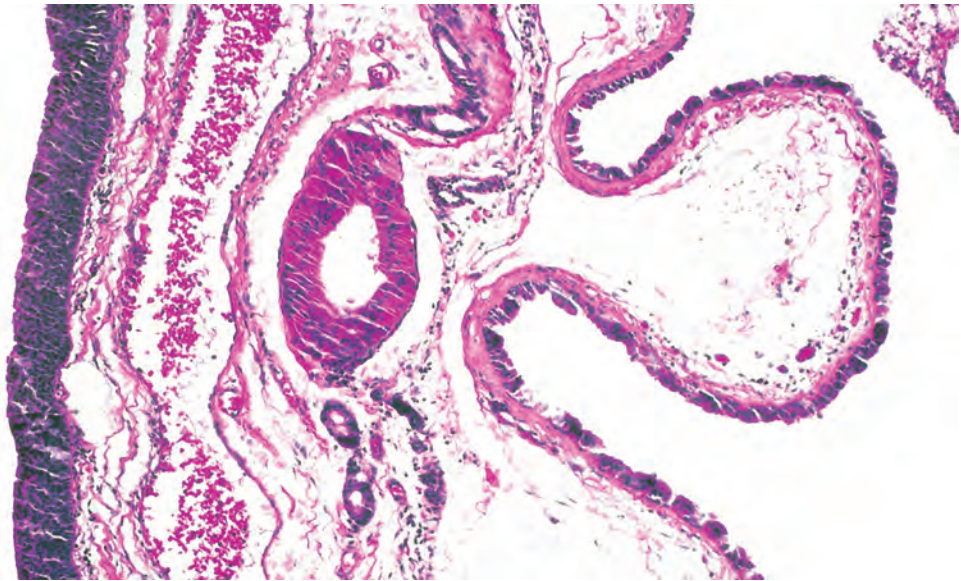
extent of disease within the larynx. Cysts generally do not communicate with the interior of the larynx, whereas a laryngocele is an air-filled herniation or dilatation of the saccule, either internal or external to the larynx, but communicating with the lumen (Fig. 4.16). Saccular cysts (anterior or lateral) are submucosal and do not communicate with the lumen but are instead filled with mucus or acute inflammatory elements. As air and fluid is forced into a laryngocele, the distinction between a laryngocele and other laryngeal cysts may be impossible. The size of these cysts ranges from 0.5 to 8 cm, depending on the location. Eversion and prolapse occur, further complicating the classification of cysts of the larynx. The cysts are variably filled with thin serous fluid to tenacious, thick, mucinous, gelatinous, or bloody fluid.

**MICROSCOPIC FINDINGS**

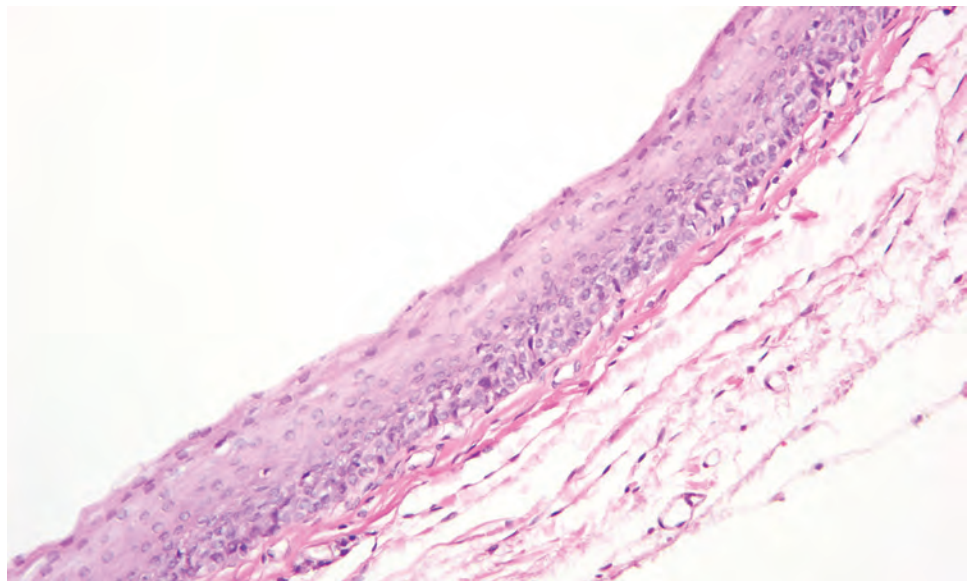
Histologic examination, although unnecessary for diagnosis of a laryngocele, will show an epithelial lined cyst containing respiratory or squamous mucosa.

Cysts have a variably thick surrounding wall of fibrous connective tissue. The lining of the cysts helps to differentiate them into a variety of subtypes. Most of the cysts are lined by squamous or respiratory epithelium (retention and saccular) (Fig. 4.17), whereas a few are lined by fibrous connective tissue. Cysts in which there is an admixture of both mesodermal and endodermal layers qualify as a *congenital* or *embryonal cyst*. This type of cyst contains squamous or respiratory epithelium, along with some other mesodermal element, intimately



**FIGURE 4.16**

An intact mucosa is seen on the left, whereas an outpouching of oncocytic epithelium on the right is part of an external laryngocele.

**FIGURE 4.17**

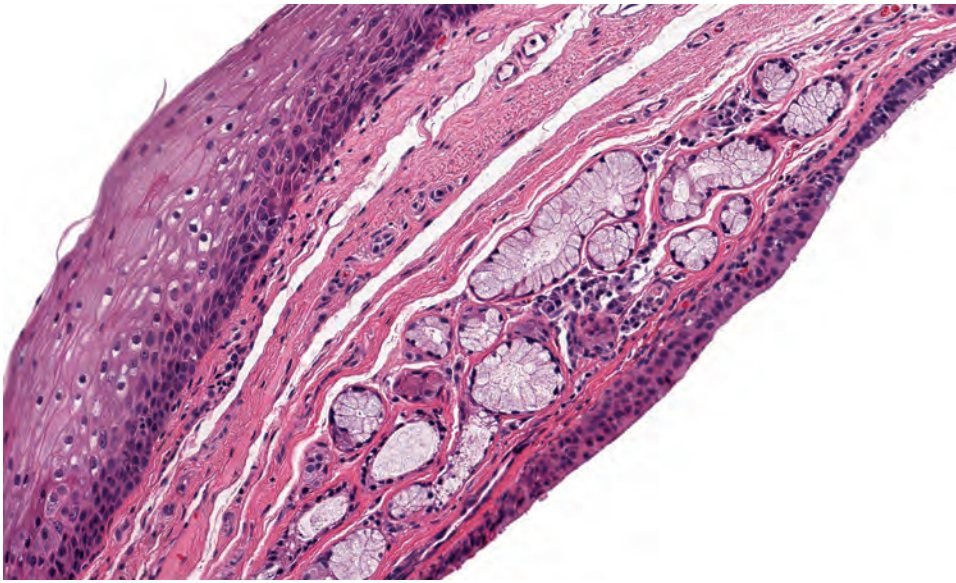
A metaplastic squamous mucosa is identified within this laryngeal cyst.

associated with the epithelial component. The *traumatic cyst* is not common but is more frequently described as surgical intervention in the larynx has increased. Small islands of tissue are implanted deep into the stroma and undergo cystic degeneration. A *saccular cyst* is lined by ciliated respiratory epithelium with increased numbers of goblet cells and a partially or completely metaplastic squamous or oncocytic epithelium (Fig. 4.18). A *ductal cyst* (which results from obstruction of intramucosal ducts of seromucinous glands) shows a double-layered cylindrical, cuboidal, or flattened ductal epithelium with squamous or oncocytic metaplasia. A *tonsillar cyst* resembles tonsillar crypt epithelium with squamous epithelium, keratin, and lymphoid tissue in the wall (Fig. 4.19). Any of the previously mentioned cysts may become infected and, when

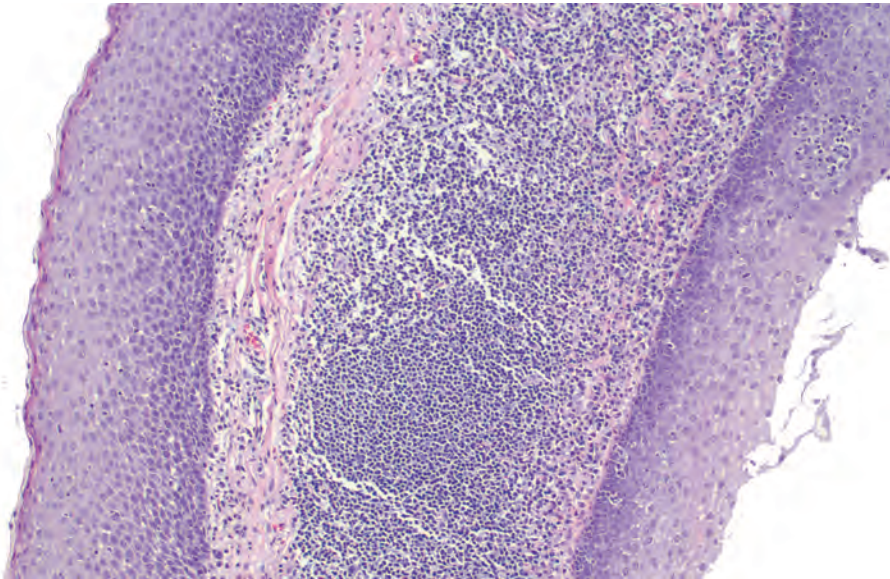
infected, are referred to as pyoceles, although still classified by the original cyst type. The larger the ventricular appendix, the more predisposed the individual is to infection or inflammation.

Oncocytes may be present within a wide variety of lesions in the larynx, including, but not limited to, oncocytic papillary cystadenoma, oncocytic cyst (Fig. 4.20), oncocytoma, oxyphilic adenoma, and oncocytic hyperplasia. Oncocytic metaplasia and/or hyperplasia are most likely aging phenomena with an aggregation of mitochondria within the cytoplasm of the lesional cells. The separation from a cyst may be difficult, although oncocytic metaplasia and/or hyperplasia should be multifocal or diffusely present within the larynx. The cells are polyhedral to round with distinct cell borders,

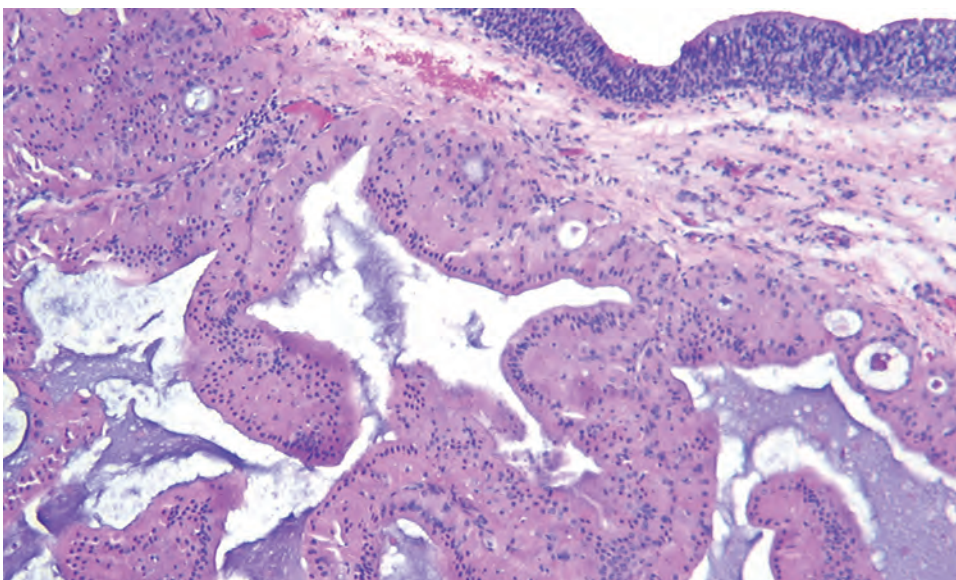


**FIGURE 4.18**

A saccular cyst shows a respiratory, oncocytic epithelium lining a space with underlying mucocytes. The squamous mucosa is the lining of the larynx.

**FIGURE 4.19**

A tonsillar cyst shows squamous epithelium associated with a lymphoid infiltrate within the wall, resembling tonsillar epithelium.

**FIGURE 4.20**

A papillary oncocytic proliferation within the larynx, composed of enlarged, polyhedral cells with abundant, opaque, oxyphilic cytoplasm. The nuclei are small and hyperchromatic.



characteristically abundant cytoplasm containing a varying number of fine to coarse, eosinophilic granules, and small, round, centrally situated, pyknotic to vesicular nuclei.

## DIFFERENTIAL DIAGNOSIS

The differential diagnosis is often limited histologically but may be quite broad clinically. For example, *external jugular phlebectasia* (a congenital dilatation of the jugular vein) frequently presents as a neck mass, particularly during straining or crying (Valsalva maneuver) similar to a laryngocele. However, it does not require surgery, although sometimes performed for cosmetic reasons. The histologic appearance is of a dilated vascular space and is different from laryngocele or other laryngeal cysts. Therefore histologic confirmation of the lesion is mandatory to help define the type of cyst. *Prolapse* of the ventricle may sometimes resemble a cyst on gross examination. However, prolapse can be “put back” to restore normal anatomy, whereas cysts cannot. *Large branchial cleft cysts* and *thyroglossal duct cysts* may push into the laryngeal spaces, thereby creating the illusion of a primary cyst of the larynx. Histologic examination, combined with the clinical site of origin should help in distinguishing these from other cysts of the region. A true *teratoma* has tissue from all three layers and is different from the developmental cysts of the larynx. Other clinical entities include laryngeal webs, vascular rings, hemangiomas, and foreign bodies. These entities can usually be excluded clinically or by biopsy. *Squamous cell carcinoma* (SCC), usually supraglottic, may be associated with laryngeal cysts, perhaps induced by the carcinoma.

## PROGNOSIS AND THERAPY

Surgical marsupialization is the treatment of choice for a laryngocele, whereas benign cysts are managed symptomatically, with aspiration or endoscopic removal only as clinically necessary to maintain a patent airway. Airway obstruction, infection (laryngopyocele), or recurrences are possible complications.

## ■ REACTIVE EPITHELIAL CHANGES

There is a lack of uniformity and an inconsistency of terminology used to describe reactive, hyperplastic, and “precancerous” epithelial lesions of the larynx, both clinically and histopathologically. This results in a lack of concordance with the term used and the biology of the lesion. Dozens of classification schemes have been proposed, but none has gained substantial support in

either the clinical or pathology communities. No matter which system is used, it is imperative that the term clearly convey to the clinician the potential biologic risk for the development of a malignant tumor.

## CLINICAL FEATURES

The spectrum of laryngeal reactive epithelial lesions is usually seen in adults, especially after age 50 years, and more frequently in men. The incidence varies, but is correlated with the same “carcinogenic” factors that result in carcinoma, including smoking, alcohol use/abuse, chronic irritation, air pollution, vocal abuse, chronic laryngitis (including infectious agents), habitual throat clearing, industrial pollution, and/or occupational exposure to specific agents (including radiation). Most of the lesions of the larynx present with nonspecific symptoms, including hoarseness, cough, airway obstruction, dysphagia, changes in phonation, and sore throat, all similar to carcinoma symptoms. Asymptomatic patients are occasionally identified. Leukoplakia, pachydermia, hyperplasia, pseudoepitheliomatous hyperplasia (PEH), metaplasia, keratosis, and contact ulcer are clinical and histologic terms that overlap with one another as well

## REACTIVE EPITHELIAL CHANGES—DISEASE FACT SHEET

### Definition

- Reactive, hyperplastic, and precancerous epithelial changes, a subset of which have a biologic potential to develop into carcinoma

### Incidence and Location

- Common and usually involve the vocal cords specifically

### Morbidity and Mortality

- True reactive lesions have no potential mortality

### Sex and Age Distribution

- Males > females
- More common > 50 years

### Clinical Features

- Associated etiologic agents include smoking and alcohol use/abuse, chronic irritation, air pollution, vocal abuse, chronic laryngitis, habitual throat clearing, industrial pollution, and/or occupation exposure to specific agents (including radiation)
- Hoarseness, cough, airway obstruction, dysphagia, changes in phonation, sore throat

### Prognosis and Treatment

- Excellent for reactive lesions
- Treat underlying etiology, although surgery is employed frequently  
(The precancerous lesions are discussed under dysplasia)

as with a number of distinctly different histologic lesions. For example, leukoplakia, used clinically, is a descriptive term designating a white patch or plaque but histopathologically may describe keratosis, PEH, dysplasia, and SCC in situ. Therefore these clinically macroscopic and microscopically morphologic diagnoses must be taken in context. Finally, there is a small but well-accepted risk of certain “reactive” lesions representing preneoplastic processes, which, if left untreated, may become carcinoma. Therefore it is imperative to recognize these various epithelial processes and to place them in a teleological arc of development when appropriate.

## PATHOLOGIC FEATURES

### GROSS FINDINGS

All of these epithelial reactions may be ulcerated, flat, polypoid, papillary, or verrucous in gross appearance, ranging from red (erythroplakic) to white (leukoplakic), and may involve a microscopic area or the entire larynx

(pachyderma laryngis), thus mimicking neoplasia clinically. Keratosis, PEH, and Teflon granuloma generally affect the true vocal cords, whereas the posterior cords and subglottis are affected by granular cell tumor and PEH; any area may be affected by radiation. However, most of these reactive lesions occur along the true vocal cords, are frequently bilateral, and rarely involve the commissures. The lesions range from a circumscribed thickening of the mucosa to an ill-defined plaque, often exhibiting a rough surface. Late radiation changes induce atrophy with glottic stenosis, whereas foreign body material is usually a firm, polypoid mass. Unfortunately, no clinical appearance has been consistently correlated to a particular underlying histology.

### MICROSCOPIC FINDINGS

It is important to remember that the overlying mucosa varies in epithelial type across the larynx, ranging from squamous epithelium on the epiglottis, transitional epithelium in the glottis, and respiratory-type epithelium in the supraglottic and infraglottic portions of the larynx. The areas of transition are normal, but in diseased states the overall histology can vary considerably.

The histologic findings may be focal or diffuse, with the overall degree or quantity influencing the diagnosis because the characteristics become more “atypical” in aggregate. The degree of each of these changes takes on importance especially because of their known association with SCC. Critical judgment, including expert consultation or multiple biopsies taken sequentially over time, is essential to an accurate diagnosis. The presence alone of any one of these reactive epithelial changes is just a morphologic diagnosis and does not necessarily equate to a specific pathologic condition. The histologic appearance is variable, with architecture and histology used simultaneously to evaluate these lesions.

Reactive lesions include hyperplasia, which is an absolute increase in the number of cells or cell layers (Fig. 4.21). This process may involve the surface or the basal (Fig. 4.22) and parabasal cell layers. There is no cytologic atypia; *atypia* is used here in the context of inflammatory and regenerative changes particularly referring to cytologic features reserving the term *pleomorphism* for precancerous lesions.

Verrucous hyperplasia and verrucous SCC are very difficult to separate, and some have suggested that they vary only in stage and size, the lesions representing a developmental spectrum. The distinction on histologic features alone, even when specialized studies have been performed (including DNA analysis), is often impossible. However, true verrucous hyperplasia shows a hyperplastic squamous epithelium with regularly spaced, verrucous projections with hyperkeratosis, and is sharply defined at the epithelial to stromal interface (Fig. 4.23). Parakeratotic crypting is not usually present. There is considerable overlap with verrucous carcinoma, which may require

## REACTIVE EPITHELIAL CHANGES—PATHOLOGIC FEATURES

### Gross Findings

- Variable and include ulcerated, flat, polypoid, papillary, verrucous, red, or white lesions
- Frequently bilateral and usually along the vocal cords

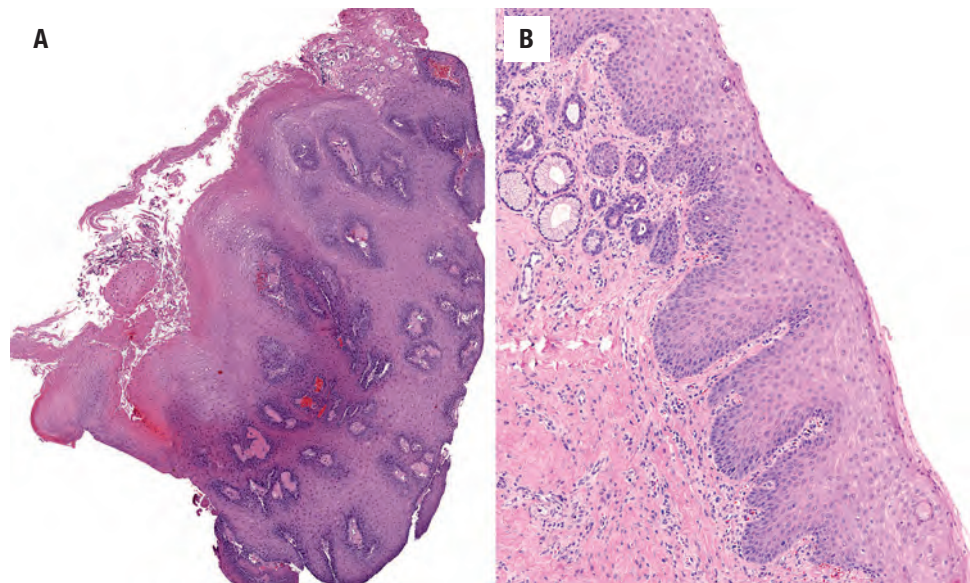
### Microscopic Findings

- Aggregate of findings is necessary before a precancerous lesion is diagnosed
- **Hyperplasia** is an increase in cell number or cell layer
- **Verrucous hyperplasia** has hyperplastic epithelium with verrucous projections, hyperkeratosis, and sharp interface with stroma, lacking parakeratotic crypting and broad bulbous rete below the adjacent epithelium
- **Pseudoepitheliomatous hyperplasia** is exuberant, large, bulbous projections of epithelium contained by an intact basement membrane without cytologic atypia
- **Metaplasia** is transformation to a simpler epithelium
- **Koilocytosis** has crenated nucleus, perinuclear halo, prominent, thick cell walls (usually in papilloma)
- **Keratosis** is an increased amount of keratin production
- **Parakeratosis** has flat nuclei with the keratosis
- **Dyskeratosis** is abnormal keratinization, usually close to the basal zone
- **Radiation changes** incorporate nuclear enlargement but in cells with a low nuclear to cytoplasmic ratio, cytoplasmic vacuolization, cellular atrophy, and vascular proliferation
- **Necrotizing sialometaplasia** is a lobular arrangement of destroyed glands with metaplastic squamous epithelium growing through the mucoserous gland structures

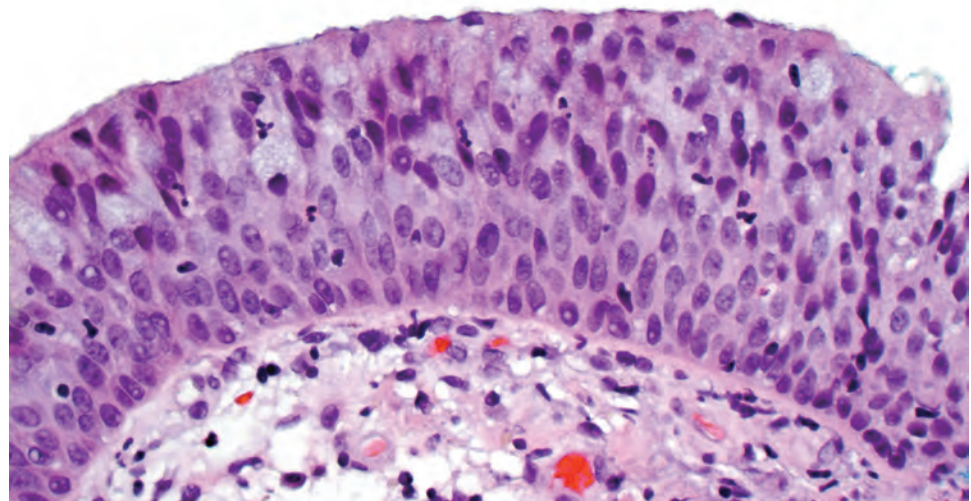
### Pathologic Differential Diagnosis

- Reactive and hyperplastic lesions, dysplasia, squamous cell carcinoma



**FIGURE 4.21**

An increase in the number of layers of squamous epithelium is called hyperplasia (**A**), with the overlying increase in keratin termed keratosis (**B**).

**FIGURE 4.22**

There is an increase of the number of cells in the basal zone, extending up to the middle one-third, where it comes to an abrupt stop. There is no cytologic atypia in this example of basal zone hyperplasia.

a larger biopsy coupled with clinical correlation and excellent communication between the pathologist and surgeon.

PEH represents an exuberant reactive overgrowth of the prickle cell layer of squamous epithelium without cytologic atypia, often with large, bulbous projections into the underlying stroma, but always respecting the basement membrane (Fig. 4.24). It is associated with fungal and mycobacterial infections (Fig. 4.25), as well as granular cell tumor (Fig. 4.24), and is frequently confused with SCC.

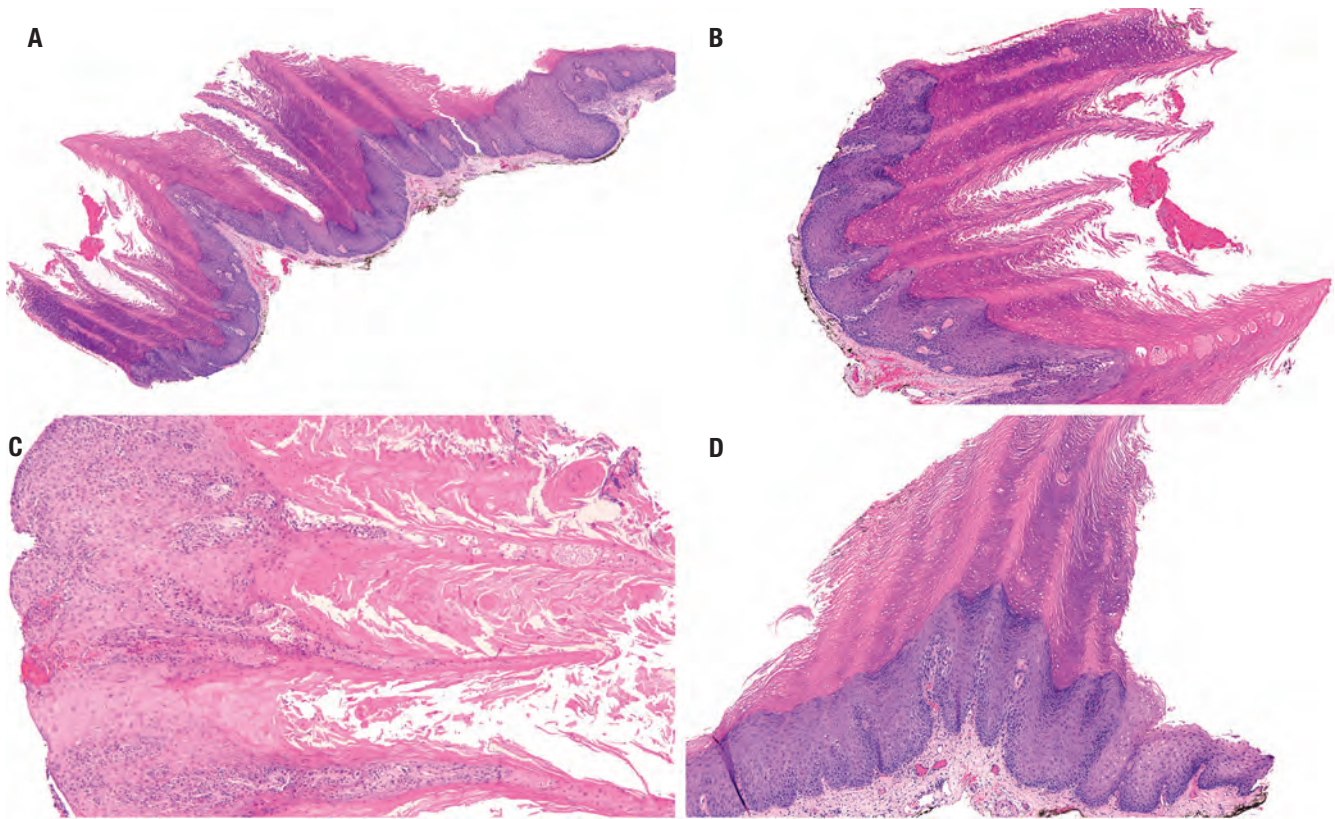
Metaplasia results when there is a change from a specialized respiratory epithelium to a simpler squamous epithelium and may occur anywhere within the larynx.

Koilocytosis is defined by a centrally placed crenated nucleus surrounded by clear cytoplasm, which forms a

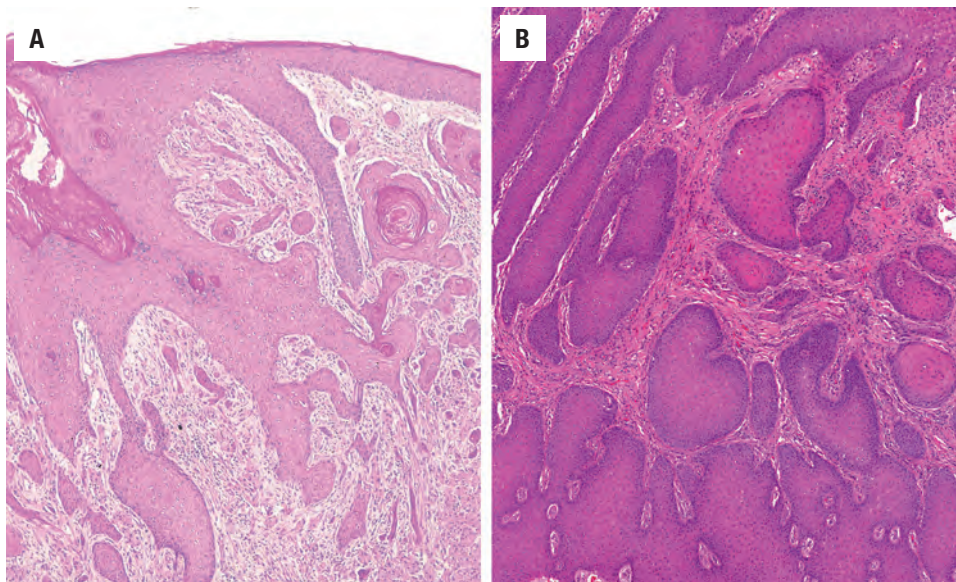
“halo,” and prominent, thick cell walls/borders (“cookie cutter” appearance). Koilocytosis is generally identified as part of a papilloma (Fig. 4.26) or carcinoma but is not identified in isolation, although glycogenation may sometimes cause diagnostic confusion.

Keratosis is separated from the other reactive and hyperplastic lesions because it may be part of all of them and so is described in a little more depth. Keratosis is an abnormal production and accumulation of keratin at the surface of the laryngeal mucosa in which the nuclei are lost and the surface epithelial cells are completely replaced by keratin (Fig. 4.27). There may be an accentuated granular layer or an irregularly hyperplastic spinous layer. The keratin is often present in an exophytic pattern. Nuclear atypia or pleomorphism is not implied by “keratosis,” although keratosis may have atypia. When the nuclei



**FIGURE 4.23**

**A-D,** Verrucous hyperplasia takes many forms, often difficult to separate from verrucous squamous cell carcinoma. There are numerous papillary fronds of squamous epithelium covered with keratin and lacking architectural and cytologic features of malignancy. The base is smooth, although an interface is lacking in one of the samples.

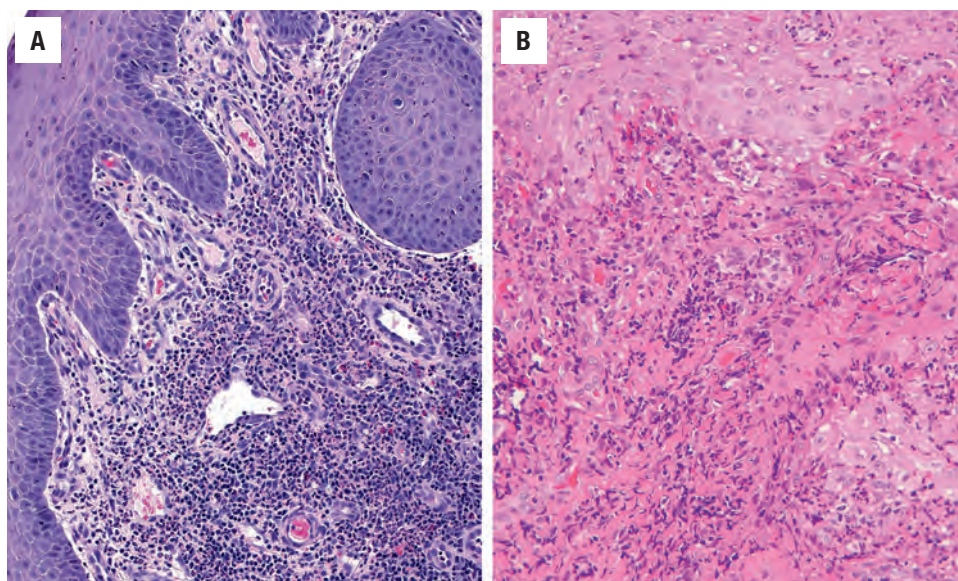
**FIGURE 4.24**

**(A and B)** Pseudoepitheliomatous hyperplasia has rounded projections into the underlying stroma, without nuclear atypia in the cells. Keratinization is frequent. Note the granular cell tumor **(A)**.

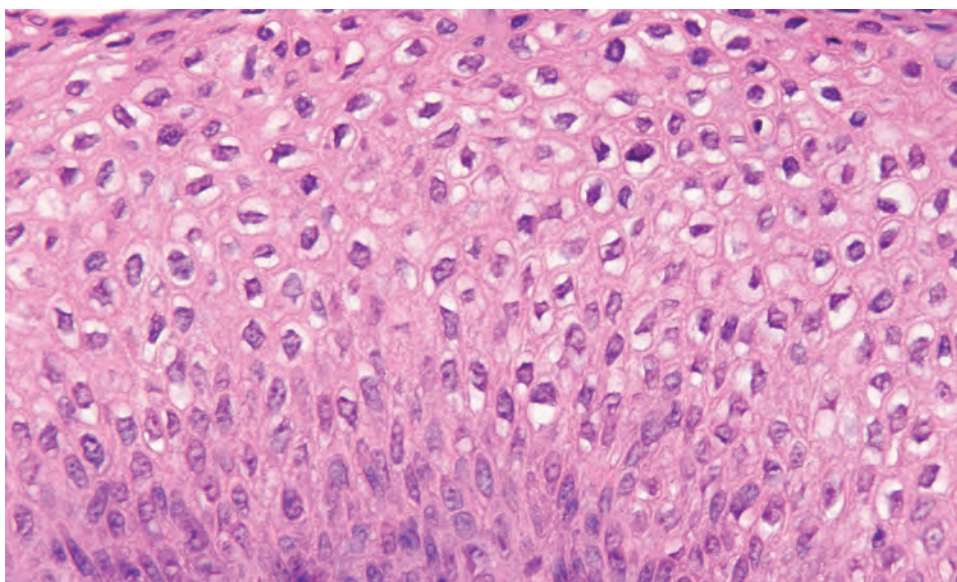
remain with incomplete keratinization, *parakeratosis* is the applied term (Fig. 4.28). Keratosis is part of the complex response seen in the larynx and does not have any prognostic significance on its own. However, keratosis has been shown to have alterations in oncogenes and tumor suppressor genes (retinoblastoma protein, p53,

p21, cyclin D1, Mcm-2, pTEN, tenascin, fibronectin) but not to the extent seen in dysplasia and carcinoma. This suggests there is an insufficient accumulation of the multiple genetic alterations known to result in the very early sequential transformation to carcinoma. There is an approximately 4% risk of subsequently identifying

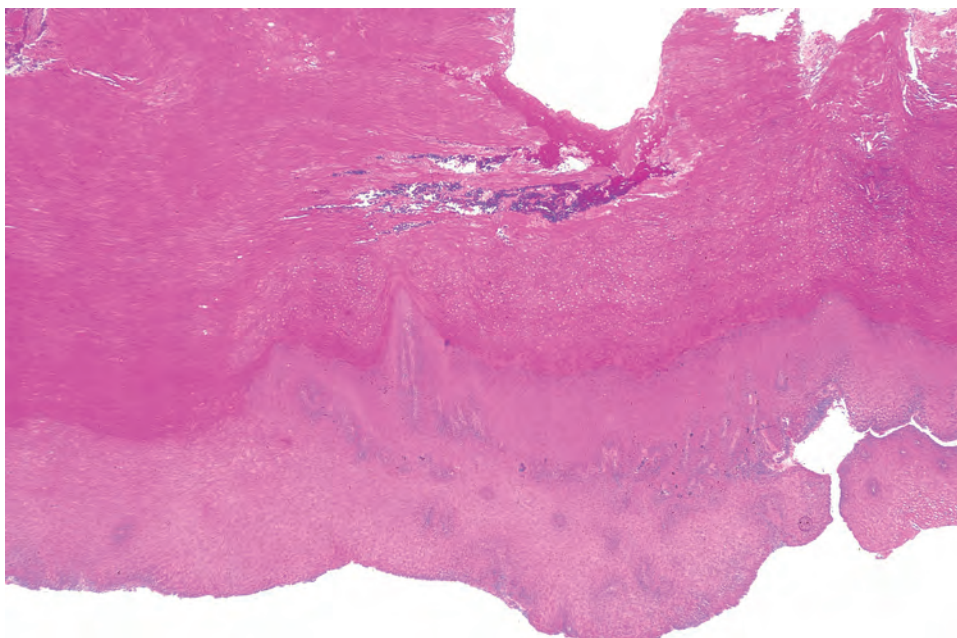


**FIGURE 4.25**

**A,** Acute inflammation is noted below a reactive squamous epithelium in this acute laryngitis. **B,** Pseudoepitheliomatous hyperplasia has an irregular proliferation of the squamous epithelium. Cryptococcus organisms were identified with special stains.

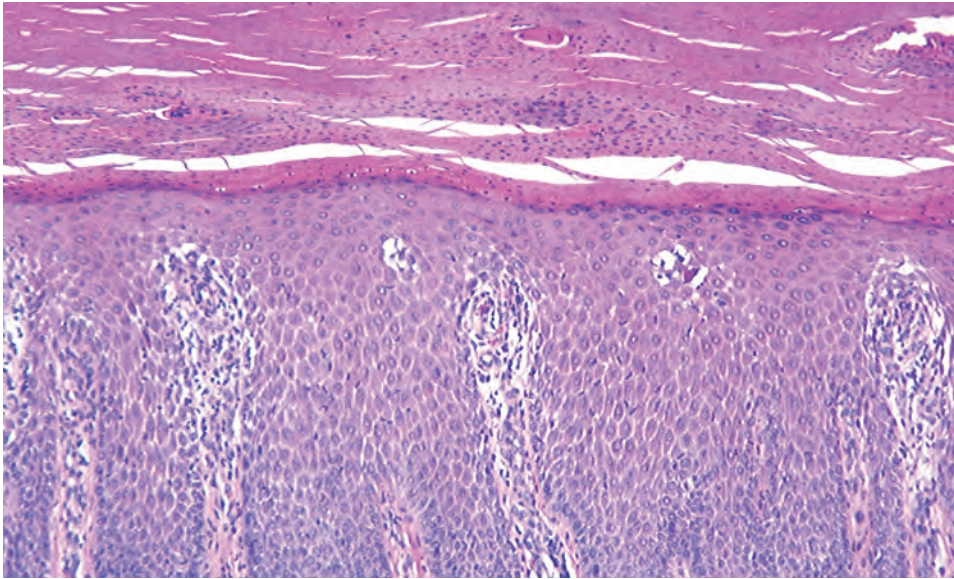
**FIGURE 4.26**

"Koilocytic" change (nuclear chromatin condensation, perinuclear halo and accentuation of the cell borders) seen in papillomas.

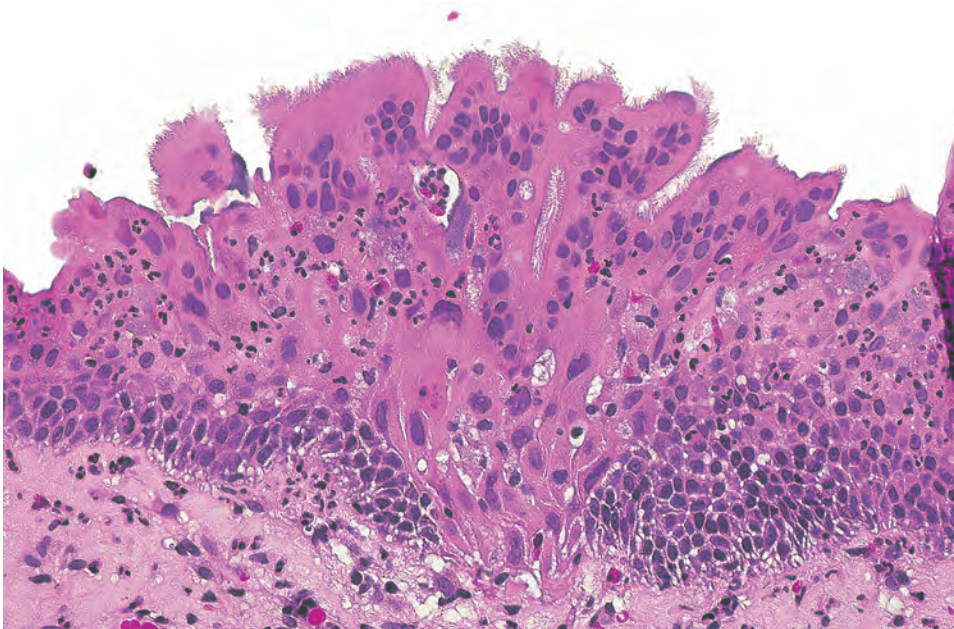
**FIGURE 4.27**

Keratosis is an accumulation of keratin at the surface.



**FIGURE 4.28**

Keratin accumulation with nuclei, referred to as parakeratosis.

**FIGURE 4.29**

An area of papillary projection is composed of remarkably enlarged cells with a low nuclear to cytoplasmic ratio and showing nuclear hyperchromasia and irregularity, with intact cilia. Acute inflammation may be seen in this example of radiation injury.

carcinoma in patients with an initial diagnosis of keratosis. Furthermore, when keratinizing dysplasia is identified, there is a strong association with abnormalities of DNA, to a much greater extent than seen in nonkeratinizing dysplasias, suggesting abnormal keratinization may be associated with a greater degree of DNA abnormalities.

Reactive epithelial changes may also be associated with radiation-induced changes. These changes are long-lasting or persistent morphologic changes affecting the surface epithelium, minor salivary glands, fibrous tissue, vessels, and cartilages. Stages of development (acute, chronic) are recognized, although the acute necrotizing inflammation of the acute stage is seldom biopsied. Features include nuclear enlargement (within epithelial, endothelial,

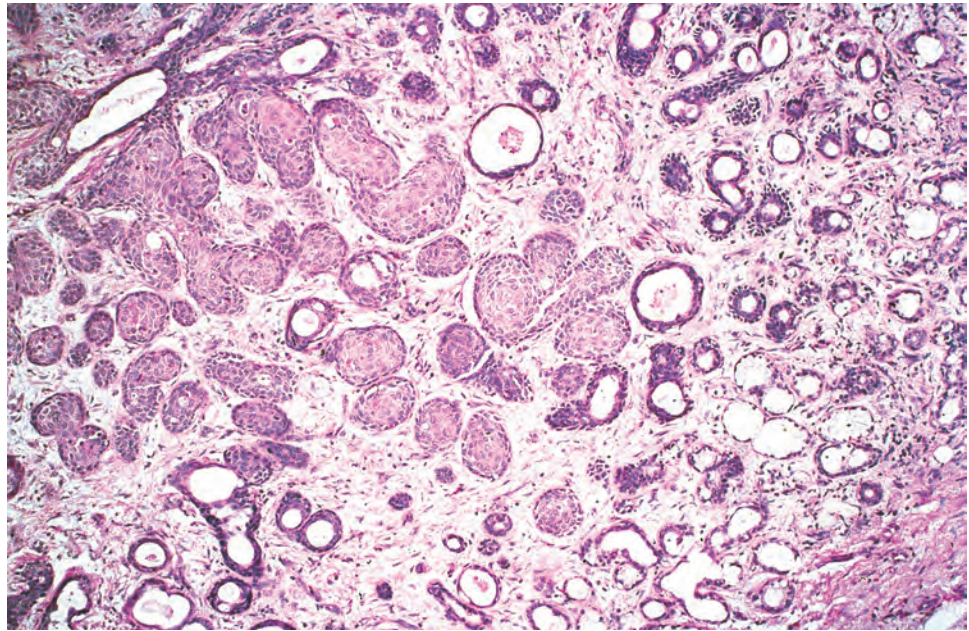
muscle, or stromal cells, which have a maintained nuclear to cytoplasmic ratio), multinucleation, cytoplasmic vacuolization, cellular atrophy, and vascular proliferation, but there are no readily identifiable changes of malignancy (recurrent or residual) (Fig. 4.29). Surface erosion and atrophy of the epithelium and minor salivary glands are common. The antecedent-inciting event (radiation) is generally known, and the difficulty generally arises in ruling out recurrent or residual disease rather than separation from a benign reactive epithelial response.

Necrotizing sialometaplasia (NS) is a benign, self-limited, reactive inflammatory process involving minor mucoserous salivary glands. The hallmark feature of this disease is the maintenance of smoothly contoured lobular architecture of the minor mucoserous glands despite

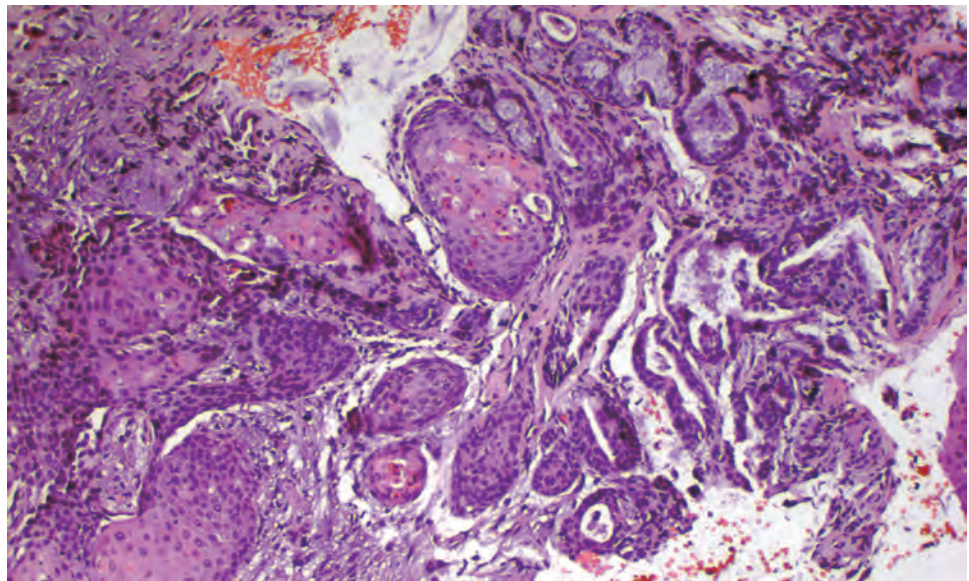


**FIGURE 4.30**

Necrotizing sialometaplasia is a lobular process, with areas of squamous metaplasia confined to the previous lobular architecture of mucoserous glands. Uninvolved mucoserous glands may be identified at the periphery.

**FIGURE 4.31**

Extensive squamous metaplasia associated within a lobular architecture, showing mucus-producing glands at the periphery (*top*).



necrosis (Fig. 4.30). In an attempt at reepithelialization, there is squamous metaplasia of the residual glands and acini (Fig. 4.31). In the immediate area, remnants of uninvolved acini and ducts may be seen along with mucin-producing cells. There is frequently an associated acute and chronic inflammation related to necrosis of the duct or acinar epithelium, in addition to mucus extravasation. Therefore the lobules of the mucoserous glands remain smooth in contour, lined by a metaplastic squamous epithelium which is bland in overall appearance. However, as with any reparative or regenerative epithelium, enlarged nuclei, prominent nucleoli, apoptosis, and mitotic figures may be seen (Fig. 4.32). The difficulty distinguishing between NS and carcinomas is especially difficult when the biopsy is small. With deeper sections

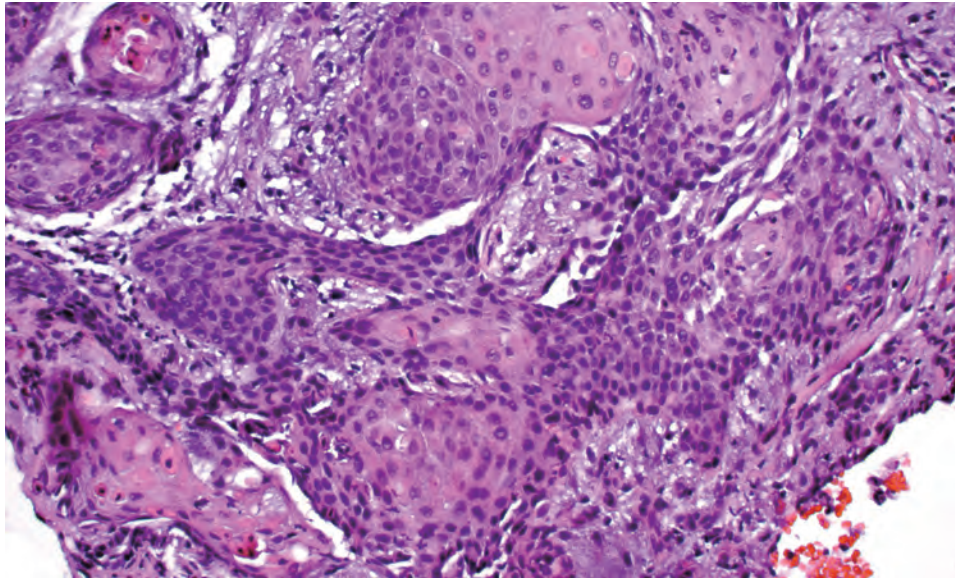
and sometimes a larger biopsy, the true nature of the lesion will become apparent.

Teflon granuloma is a foreign body granuloma caused by iatrogenic injection of Teflon paste (used to treat vocal cord paralysis). Teflon is a polarizable, birefringent foreign material with a foreign body giant cell reaction in the fibrous stroma.

#### ANCILLARY STUDIES

Immunohistochemical reactions for the subtypes of keratins have been proposed as a means for distinguishing between reactive epithelial changes and carcinoma (CK13



**FIGURE 4.32**

Although well circumscribed and surrounded by an intact basement membrane, there is atypia in the epithelial cells along with dyskeratosis and keratin pearl formation.

is expressed in normal or reactive conditions but is decreased or absent in dysplasia and carcinoma, respectively); however, from a practical standpoint, these reactions are insufficiently reliable to be used in a clinical setting. Ki-67 may be quite elevated in benign reactive conditions, and so its use in separation from preneoplastic or neoplastic lesions is exceedingly limited in practical application. p53 tends to be expressed at higher levels in premalignant lesions than in benign reactive conditions.

### DIFFERENTIAL DIAGNOSIS

The differential diagnosis encompasses different lesions within the reactive and hyperplastic category, as well as separation from dysplasia and carcinoma. It is well accepted that dysplasia (squamous intraepithelial lesion/neoplasia) is a precancerous lesion, but the issue of how much *pleomorphism* makes a lesion dysplastic is not well established and poorly reproducible between practitioners. Because there is a sequential continuum, it is nearly impossible to rigidly place a lesion into reactive versus neoplastic, as no single combination of features consistently or accurately separates reactive from dysplastic. Therefore degrees of atypia and subtle changes often portend of the impending carcinoma transformation but may at that time not represent a true “carcinoma.” Markers of dysplasia not seen in benign reactive conditions to any significant degree include dyskeratosis, a lack of maturity or irregular epithelial stratification toward the surface (“basal zone”-type cells identified above the basal zone), anisonucleosis (abnormal nuclear size), anisocytosis (abnormal cell size), pleomorphism (nuclear

shape irregularities, chromatin distribution disturbance, nuclear hyperchromasia), changes in nuclear to cytoplasmic ratio, atypical mitotic figures, premature (paradoxical) keratinization lower in the proliferating epithelium (toward the basal zone), and increased mitotic figures. It is imperative to underscore that there is a consecutive and cumulative alteration underlying the process of carcinogenesis.

### PROGNOSIS AND THERAPY

True hyperplasia and reactive epithelial lesions are self-limiting and reversible, with the majority spontaneously resolving or involuting if the etiologic agent is removed. However, after moderate to severe dysplasia develops, the persistence and/or progression to carcinoma is a well-established risk. Although diagnosis includes a biopsy, the underlying cause of the disorder should be sought and corrected. Due to the relative association of these reactive changes with malignant tumors, clinicopathologic correlation is imperative in identifying the potential risk for malignant transformation and assuring an excellent long-term prognosis. In hyperplasia, no clinical follow-up is required, but clinical follow-up is vitally important for patients with “dysplasia,” because sampling inadequacies and/or the natural progression of the lesion may result in inadequate clinical management.

### SUGGESTED READING

The complete Suggested Readings list is available online at [ExpertConsult.com](http://ExpertConsult.com).



**SUGGESTED READING****Vocal Cord Polyps and Nodules**

- Altman KW. Vocal fold masses. *Otolaryngol Clin North Am*. 2007;40(5):1091–1108.
- Bastian RW, et al. Do talkativeness and vocal loudness correlate with laryngeal pathology? A study of the vocal overdoer/underdoer continuum. *J Voice*. 2016;30(5):557–562.
- D'Alatri L, et al. Vocal fold nodules in school age children: attention deficit hyperactivity disorder as a potential risk factor. *J Voice*. 2015;29(3):287–291.
- Franco RA, et al. Common diagnoses and treatments in professional voice users. *Otolaryngol Clin North Am*. 2007;40(5):1025–1061.
- Johns MM. Update on the etiology, diagnosis, and treatment of vocal fold nodules, polyps, and cysts. *Curr Opin Otolaryngol Head Neck Surg*. 2003;11(6):456–461.
- Kambic V, et al. Vocal cord polyps: incidence, histology and pathogenesis. *J Laryngol Otol*. 1981;95:609–618.
- Marcotullio D, et al. Exudative laryngeal diseases of Reinke's space: a clinicohistopathological framing. *J Otolaryngol*. 2002;31(6):376–380.
- Nunes RB, et al. Clinical diagnosis and histological analysis of vocal nodules and polyps. *Braz J Otorhinolaryngol*. 2013;79(4):434–440.
- Stapp CE, et al. Characteristics of phonatory function in singers and nonsingers with vocal fold nodules. *J Voice*. 2011;25(6):714–724.
- Syed I, et al. Hoarse voice in adults: an evidence-based approach to the 12 minute consultation. *Clin Otolaryngol*. 2009;34(1):54–58.
- Wallis L, et al. Vocal fold nodule vs. vocal fold polyp: answer from surgical pathologist and voice pathologist point of view. *J Voice*. 2004;18(1):125–129.
- Wang CT, et al. Comprehensive outcome researches of intralesional steroid injection on benign vocal fold lesions. *J Voice*. 2015;29(5):578–587.
- Werner JA, et al. Description and clinical importance of the lymphatics of the vocal fold. *Otolaryngol Head Neck Surg*. 1990;102:13–19.
- Yamaguchi M, et al. Mucosal blood volume and oxygen saturation in the human vocal fold. *Acta Otolaryngol*. 1990;110(3–4):300–308.

**Contact Ulcer**

- Benjamin B, et al. Vocal granuloma, including sclerosis of the arytenoid cartilage: radiographic findings. *Ann Otol Rhinol Laryngol*. 1993;102(10):756–760.
- Fechner RE, et al. Pyogenic granuloma of the larynx and trachea. A causal and pathologic monomer for granulation tissue. *Arch Otolaryngol*. 1981;107:30–32.
- Koufman JA. The otolaryngologic manifestations of gastroesophageal reflux disease (GERD): a clinical investigation of 225 patients using ambulatory 24-hour pH monitoring and an experimental investigation of the role of acid and pepsin in the development of laryngeal injury. *Laryngoscope*. 1991;101:1–78.
- Powell J, et al. Mucosal changes in laryngopharyngeal reflux—prevalence, sensitivity, specificity and assessment. *Laryngoscope*. 2013;123(4):985–991.
- Qadeer MA, et al. Correlation between symptoms and laryngeal signs in laryngopharyngeal reflux. *Laryngoscope*. 2005;115(11):1947–1952.
- Shoffel-Havakuk H, et al. Lesions of the posterior glottis: clinical and pathologic considerations and treatment outcome. *J Voice*. 2014;28(2):263.e1–263.e263.
- Thompson L. Larynx contact ulcer. *Ear Nose Throat J*. 2005;84(6):340.
- Wenig BM, et al. Contact ulcers of the larynx. A reacquaintance with the pathology of an often underdiagnosed entity. *Arch Pathol Lab Med*. 1990;114:825–828.

**Amyloidosis**

- Barnes EL Jr, et al. Laryngeal amyloidosis. Clinicopathologic study of seven cases. *Ann Otol*. 1977;86:856–863.
- Bartels H, et al. Laryngeal amyloidosis: localized versus systemic disease and update on diagnosis and therapy. *Ann Otol Rhinol Laryngol*. 2004;113(9):741–748.

- Chen KTK. Amyloidosis presenting in the respiratory tract. *Pathol Ann*. 1989;24:253–273.
- Cipriani NA, et al. The clinicopathologic spectrum of benign mass lesions of the vocal fold due to vocal abuse. *Int J Surg Pathol*. 2011;19(5):583–587.
- Cohen SR. Ligneous conjunctivitis: an ophthalmic disease with potentially fatal tracheobronchial obstruction. Laryngeal and tracheobronchial features. *Ann Otol*. 1990;90:509–518.
- Eriksson M, et al. Hereditary apolipoprotein AI-associated amyloidosis in surgical pathology specimens: identification of three novel mutations in the APOA1 gene. *J Mol Diagn*. 2009;11(3):257–262.
- Lewis JE, et al. Laryngeal amyloidosis: a clinicopathologic and immunohistochemical review. *Otolaryngol Head Neck Surg*. 1992;106:372–377.
- Loyo M, et al. Plasmacytoma of the larynx. *Am J Otolaryngol*. 2013;34(2):172–175.
- Michaels L, et al. Amyloid in localized deposits and plasmacytomas of the respiratory tract. *J Pathol*. 1979;128:29–38.
- Neuner GA, et al. Complete resolution of laryngeal amyloidosis with radiation treatment. *Head Neck*. 2012;34(5):748–752.
- Penner CR, et al. Head and neck amyloidosis: a clinicopathologic study of 15 cases. *Oral Oncol*. 2006;42(4):421–429.
- Piazza C, et al. Endoscopic management of laryngo-tracheobronchial amyloidosis: a series of 32 patients. *Eur Arch Otorhinolaryngol*. 2003;260(7):349–354.
- Thompson LD, et al. Amyloidosis of the larynx: a clinicopathologic study of 11 cases. *Mod Pathol*. 2000;13:528–535.
- Wierzbicka M, et al. How to deal with laryngeal amyloidosis? Experience based on 16 cases. *Amyloid*. 2012;19(4):177–181.

**Cysts of the Larynx (Including Laryngocele)**

- Arens C, et al. Clinical and morphological aspects of laryngeal cysts. *Eur Arch Otorhinolaryngol*. 1997;254:430–436.
- Celin SE, et al. The association of laryngoceles with squamous cell carcinoma of the larynx. *Laryngoscope*. 1991;101(5):529–536.
- Civantos FJ, et al. Laryngoceles and saccular cysts in infants and children. *Arch Otolaryngol Head Neck Surg*. 1992;118:296–300.
- DeSanto LW. Laryngocele, laryngeal mucocoele, large saccules, and laryngeal saccular cysts: a developmental spectrum. *Laryngoscope*. 1974;84:1291–1296.
- Gonik N, et al. Intraoperative inflation of laryngocele with LMA. *Am J Otolaryngol*. 2013;34(6):746–748.
- Huang BY, et al. Larynx: anatomic imaging for diagnosis and management. *Otolaryngol Clin North Am*. 2012;45(6):1325–1361.
- Lundgren J, et al. Oncocytic lesions of the larynx. *Acta Otolaryngol*. 1982;94:335–344.
- Matino Soler E, et al. Laryngocele: clinical and therapeutic study of 60 cases. *Acta Otorrinolaringol Esp*. 1995;46:279–286.
- Newman BH, et al. Laryngeal cysts in adults: a clinicopathologic study of 20 cases. *Am J Clin Pathol*. 1984;81(6):715–720.
- Pennings RJ, et al. Giant laryngoceles: a cause of upper airway obstruction. *Eur Arch Otorhinolaryngol*. 2001;258(3):137–140.
- Porter PW, et al. The laryngeal saccule: clinical significance. *Clin Anat*. 2012;25(5):647–649.
- Saha D, et al. Laryngeal cysts in infants and children—a pathologist's perspective (with review of literature). *Int J Pediatr Otorhinolaryngol*. 2013;77(7):1112–1117.
- Thawley SE, et al. Oncocytic hyperplasia of the larynx. *J Laryngol Otol*. 1977;91:619–622.
- Werner RL, et al. Bilateral laryngoceles. *Head Neck Pathol*. 2014;8(1):110–113.
- Zelenik K, et al. Treatment of laryngoceles: what is the progress over the last two decades? *Biomed Res Int*. 2014;8:19453.

**Reactive Epithelial Changes**

- Blackwell KE, et al. Laryngeal dysplasia. A clinicopathologic study. *Cancer*. 1995;75:457–463.
- Calcaterra TC, et al. Dilemma of delayed radiation injury of the larynx. *Ann Otol Rhinol Laryngol*. 1972;81:501–507.
- Chatrath P, et al. Aberrant expression of minichromosome maintenance protein-2 and Ki67 in laryngeal squamous epithelial lesions. *Br J cer*. 2003;89:1048–1054.

4. Crissman JD, et al. Quantitation of DNA ploidy in squamous intraepithelial neoplasia of the laryngeal glottis. *Arch Otolaryngol Head Neck Surg.* 1991;117:182–188.
5. Crissman JD. Laryngeal keratosis and subsequent carcinoma. *Head Neck Surg.* 1979;1:386–391.
6. Cupic H, et al. Epithelial hyperplastic lesions of the larynx in biopsy specimens. *Acta Otolaryngol Suppl.* 1997;527:103–104.
7. Dedo HH, et al. Histologic evaluation of Teflon granulomas of human vocal cords. A light and electron microscopic study. *Acta Otolaryngol.* 1982;93(5–6):475–484.
8. Gale N, et al. The Ljubljana classification: a practical strategy for the diagnosis of laryngeal precancerous lesions. *Adv Anat Pathol.* 2000;7:240–251.
9. Gale N, et al. Epithelial precursor lesions: Dysplasia. In: El-Nagar AK, Chan JKC, Grandis JR, Takata T, Slootweg PJ, eds. *Classification of Head and Neck Tumours*. World Health Organization Classification of Tumours. Lyon, France: IARC Press; 2017:91–93.
10. Gillis TM, et al. Natural history and management of keratosis, atypia, carcinoma-in situ, and microinvasive cer of the larynx. *Am J Surg.* 1983;146:512–516.
11. Hamdan AL, et al. Vocal changes following radiotherapy to the head and neck for non-laryngeal tumors. *Eur Arch Otorhinolaryngol.* 2009;266(9):1435–1439.
12. Hellquist H, et al. Hyperplasia, keratosis, dysplasia and carcinoma in situ of the vocal cords—a follow-up study. *Clin Otolaryngol Allied Sci.* 1982;7(1):11–27.
13. Ioachim E, et al. Altered patterns of retinoblastoma gene product expression in benign, premalignant and malignant epithelium of the larynx: an immunohistochemical study including correlation with p53, bcl-2 and proliferating indices. *Anti cer Res.* 1999;19:541–545.
14. Koren R, et al. The spectrum of laryngeal neoplasia: the pathologist's view. *Pathol Res Pract.* 2002;198:709–715.
15. Thompson LD. Diagnostically challenging lesions in head and neck pathology. *Eur Arch Otorhinolaryngol.* 1997;254(8):357–366.
16. Vodovnik A, et al. Correlation of histomorphological criteria used in different classifications of epithelial hyperplastic lesions of the larynx. *Acta Otolaryngol Suppl.* 1997;527:116–119.
17. Wenig BM, et al. Teflonomas of the larynx and neck. *Hum Pathol.* 1990;21(6):617–623.
18. Wu M, et al. Comparative study in the expression of p53, EGFR, TGF- $\alpha$ , and cyclin D1 in verrucous carcinoma, verrucous hyperplasia, and squamous cell carcinoma of head and neck region. *Appl Immunohistochem Mol Morphol.* 2002;10:351–356.
19. Yadav UC, et al. Aldose reductase inhibition prevents metaplasia of airway epithelial cells. *PLoS ONE.* 2010;5(12):e14440.



# Benign Neoplasms of the Larynx, Hypopharynx, and Trachea

■ Justin A. Bishop

## ■ SQUAMOUS PAPILLOMAS

Squamous papillomas are the most common benign neoplasms of the larynx and trachea, characterized by an exophytic squamous epithelium lining branching fibrovascular cores, often associated with human papillomavirus (HPV) infection. They may be solitary or may present in the setting of recurrent respiratory papillomatosis (RRP), a disorder characterized by numerous, multifocal, recurrent benign squamous papillomas of the respiratory tract. Squamous papillomas have a bimodal age distribution, with a peak in children younger than 5 years (i.e., juvenile papillomas), as well as one in adults from 20 to 40 years old (i.e., adult papillomas). There is a slight male predominance (3:2) in adult papillomas, but the sex distribution is equal for the juvenile form. RRP is more common in children, with approximately 25 % of cases presenting in infancy. Squamous papillomas of the larynx are uncommon, with an estimated incidence of 4.3 cases per 100,000 children and 1.8 cases per 100,000 adults.

Squamous papillomas, especially those in the setting of RRP, are usually driven by specific types of HPV, especially types 6 and 11. These so-called low-risk types of HPV are biologically distinct from high-risk types that drive most cases of oropharyngeal carcinoma, largely due to different binding and signaling properties of their respective E6 and E7 proteins. In most pediatric cases the mode of transmission for the causative HPV is believed to be vertical (i.e., from mother to newborn via the birth canal). Indeed, an epidemiologic triad has been found to correlate with juvenile RRP cases: first-born child, vaginal delivery, and maternal age younger than 20. However, the mode of transmission in squamous papillomas that present in adults is unclear.

### CLINICAL FEATURES

Patients may present with dysphonia, hoarseness, and breathing difficulties. Symptoms are generally more severe

### SQUAMOUS PAPILLOMA—DISEASE FACT SHEET

#### Definition

- Benign neoplasm composed of papillary fronds of squamous epithelium, usually caused by infection by low-risk human papillomavirus types 6 or 11

#### Incidence and Location

- 4.3/100,000 in children, 1.8/100,000 in adults
- True or false vocal cords, ventricles, subglottis, occasionally extending beyond the larynx

#### Morbidity and Mortality

- Mortality 2%-14%, morbidity may be significant due to airway obstruction

#### Sex and Age Distribution

- Affects sexes equally in children, slight male predominance in adults
- Bimodal distribution with peaks in children <5 and adults 20-40 years

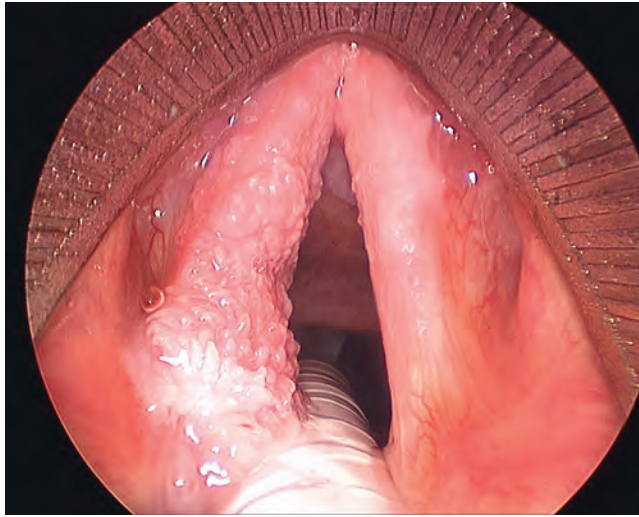
#### Clinical Features

- Hoarseness, dysphonia, stridor, more severe in children
- Exophytic masses, usually multiple, on laryngoscopic examination

#### Prognosis and Therapy

- Multiple conventional or laser surgeries, with or without antiviral agents like cidofovir
- Unpredictable course, although disease presenting in young children tends to be more progressive and more likely to transform into carcinoma

in children, possibly in part because of the smaller diameter of their airways. On clinical examination, papillomas appear as friable, exophytic masses projecting into the airway (Fig. 5.1). They tend to involve metaplastic areas where ciliated columnar transforms into squamous epithelium (squamocolumnar junction), for example, the true and false vocal cords, ventricles, and subglottis. As disease progresses, the papillomas may extend into the epiglottis and hypopharynx. Rarely (~5 % of cases)

**FIGURE 5.1**

This example of papillomatosis of the larynx shows numerous tan-pink fingerlike masses carpeting the right focal fold. (Courtesy of Dr. Simon Best.)

### SQUAMOUS PAPILLOMA—PATHOLOGIC FEATURES

#### Gross Findings

- Sessile or pedunculated, friable, exophytic tan-red mass with a lobulated surface. Often multiple

#### Microscopic Findings

- Fingerlike fronds with fibrovascular cores lined by squamous epithelium
- Epithelium often shows mild atypia in the form of basal or parabasal zone hyperplasia, increased mitoses, and “viral atypia” (koilocytes)

#### Ancillary Studies

- Majority positive: low-risk human papillomavirus (especially types 6 or 11)

#### Pathologic Differential Diagnosis

- Papillary carcinoma, dysplasia, verrucous hyperplasia, squamous cell carcinoma

papillomas can extend into the lower airway (bronchus and lung).

### PATHOLOGIC FEATURES

#### GROSS FINDINGS

Squamous papillomas are friable, exophytic tan-red masses with a lobular surface. They may be broad based or pedunculated with a stalk. They are often multiple (Fig. 5.1).

### MICROSCOPIC FINDINGS

Squamous papillomas are characterized histologically by a complex proliferation of fingerlike growths consisting of delicate fibrovascular cores lined by squamous epithelium (Fig. 5.2). There is typically little or no keratinization. Uncommonly there may also be a component of ciliated, respiratory-type epithelium. The lining epithelium is typically hyperplastic (i.e., thickened) and often exhibits mild atypia in the form of parabasal cell hyperplasia with mitotic figures elevated slightly above the basal zone (Fig. 5.3). In addition, koilocytic changes such as nuclear hyperchromasia, irregular (raisinoid) nuclear membranes, and perinuclear haloes are often identified in the superficial epithelial layers (Fig. 5.3). These types of changes should not be overinterpreted as squamous dysplasia. With that being said, in very rare instances, squamous papillomas can undergo malignant transformation into squamous cell carcinoma (Fig. 5.4).

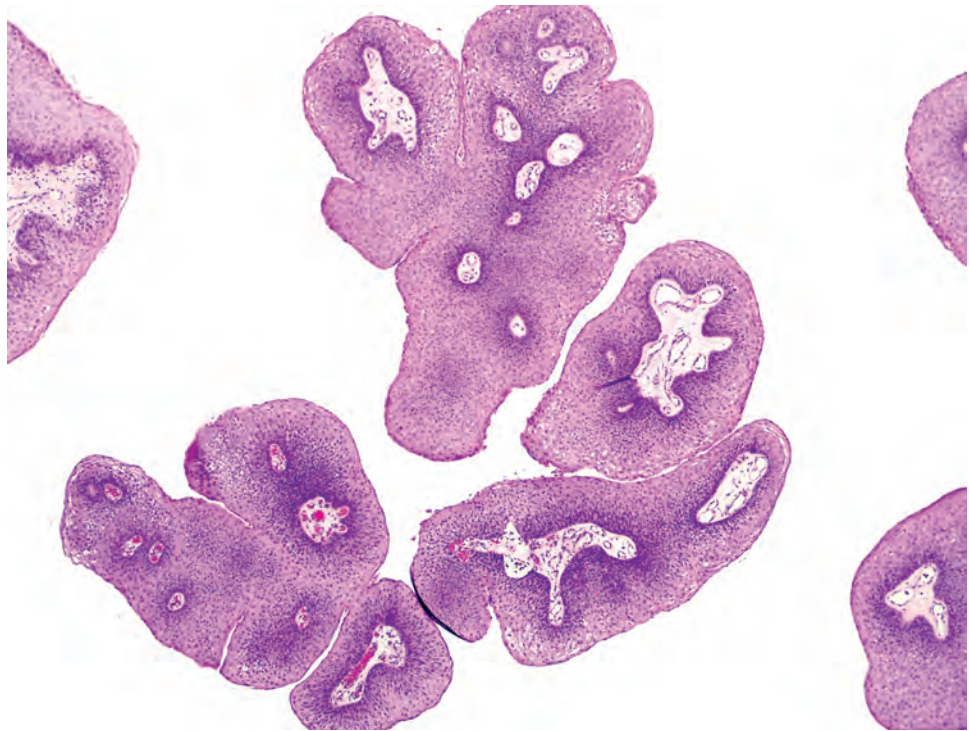
### ANCILLARY STUDIES

Squamous papillomas are usually diagnostically straightforward and ancillary studies are rarely required. Low-risk HPV types (especially 6 or 11) can be demonstrated by HPV testing techniques, most often RNA or DNA in situ hybridization in more than 90% of cases. The signals are diffuse, nuclear, and usually confined to the most superficial layers of the epithelium (Fig. 5.3). This testing is occasionally diagnostically useful (see [Differential Diagnosis](#) later) or may be requested by clinicians (e.g., for enrollment into specific clinical trials). p16 immunohistochemistry is not a useful surrogate for low-risk HPV.

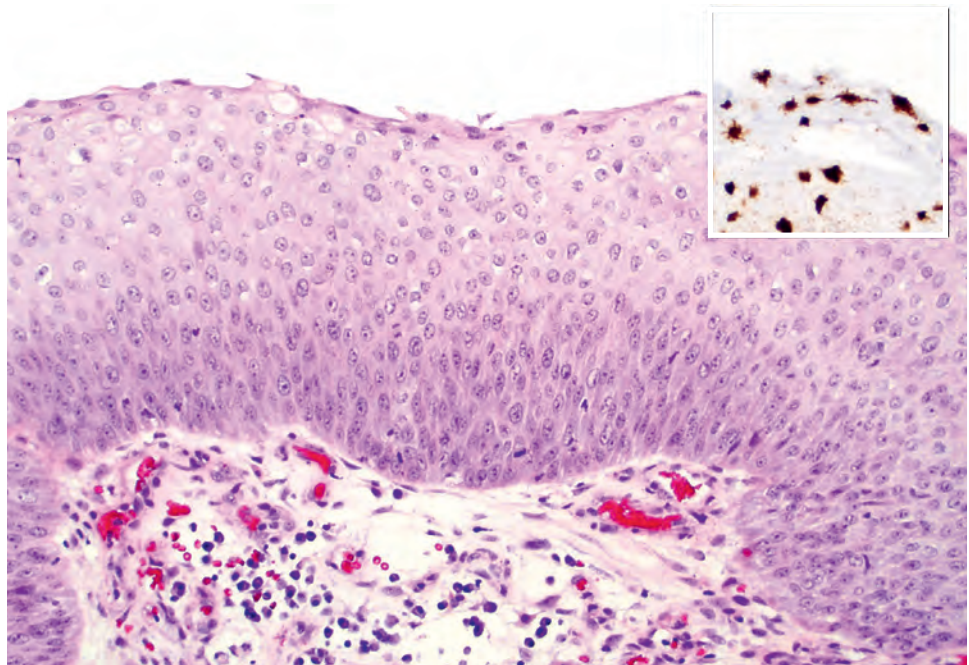
### DIFFERENTIAL DIAGNOSIS

Adult-onset squamous papillomas may be difficult to distinguish from squamous dysplasia (typically induced by smoking), which can sometimes exhibit papillary or exophytic architecture. As described previously, cellular changes that would be consistent with squamous dysplasia in some settings (e.g., parabasal hyperplasia, mitotic figures above the basal layer) are acceptable in benign squamous papillomas. In this setting, HPV 6/11 testing may be diagnostically useful, as a positive result is reassuring that the process is viral and likely not truly dysplastic. Similarly, the papillary variant of squamous cell carcinoma may be architecturally identical to squamous papilloma (Fig. 5.5A). However, this carcinoma variant exhibits overtly malignant cellular findings that are unlikely to be confused with a benign process (Fig. 5.5B). Verrucoid



**FIGURE 5.2**

Squamous papillomas at low power consist of fingerlike projections of squamous epithelium surrounding a fibrovascular core. In patients with papillomatosis, it is typical for specimens to contain numerous fragments of papillomas in the container.

**FIGURE 5.3**

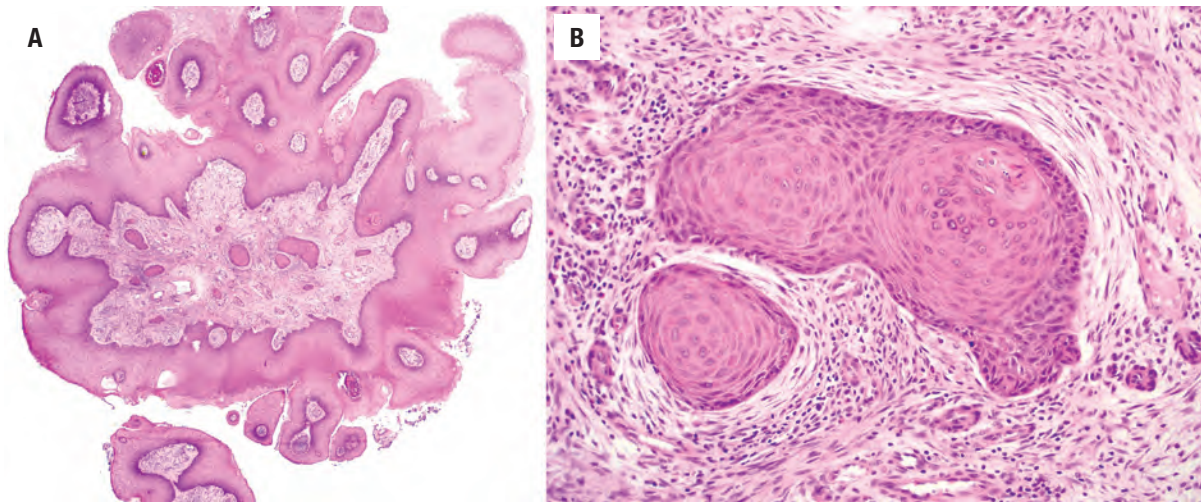
Squamous papillomas commonly exhibit mild atypia in the form of basal and parabasal layer hyperplasia and mitotic figures just above the basement membrane. In addition, cells in the superficial layers often exhibit "viral" atypia with crinkled nuclear membranes and perinuclear "haloes." These cells can usually be shown to be positive for low-risk human papillomavirus by in situ hybridization (*inset*).

lesions such as verrucous hyperplasia, verruca vulgaris, or verrucous carcinoma may be considerations because there are also exophytic squamous lesions; however, these proliferations are broad based, lack papillary fronds with fibrovascular cores, and by definition demonstrate considerable surface keratosis.

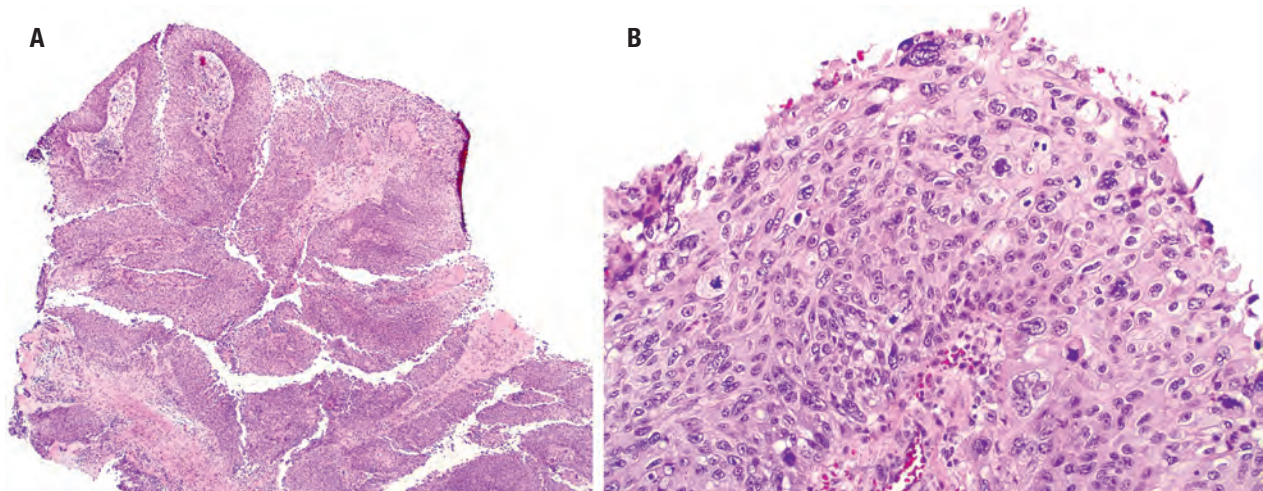
### PROGNOSIS AND THERAPY

The clinical course of patients with squamous papillomas is rather unpredictable and is often marked by alternating periods of active disease and remissions,



**FIGURE 5.4**

Very rarely, squamous cell carcinomas can arise in the setting of papillomatosis. In this case, an invasive squamous cell carcinoma is seen in the submucosa (*center*) surrounded by benign-appearing papilloma (**A**). At high power the squamous cell carcinoma is well differentiated, consisting of angulated nests of squamous epithelium eliciting a desmoplastic stromal reaction (**B**).

**FIGURE 5.5**

At low power, papillary variant of squamous cell carcinoma is virtually identical to squamous papilloma, with numerous papillary tissue fragments (**A**). However, at high power the lining epithelium of papillary variant of squamous cell carcinoma is overtly malignant at the cytologic level, with marked disorganization, nuclear pleomorphism, and atypical mitoses (**B**).

with longitudinal studies showing viral persistence in greater than 95 % (same strain at the beginning and in follow-up). Although papillomas are technically benign neoplasms, they can cause considerable morbidity due to airway obstruction and result in death in a small subset (2 % to 14 %) of patients. The aggressiveness of RRP is associated with age of onset, with disease presenting earlier in life being more progressive and more likely to undergo malignant transformation. The rare examples of malignant transformation tend to be associated with some other risk factor, such as smoking or radiation exposure, and are more often seen in RRP-induced by HPV type 11.

Patients with RRP are treated with multiple conventional or laser surgeries, often with injection of antiviral agents (e.g., cidofovir). It is hoped that widespread use of the HPV vaccine will reduce the incidence of RRP, but the vaccine effects are not yet known.

## ■ GRANULAR CELL TUMOR

Granular cell tumor is an uncommon, benign mesenchymal neoplasm of Schwann cell origin showing polygonal, large, granular cells.



### GRANULAR CELL TUMOR—DISEASE FACT SHEET

#### Definition

- Benign mesenchymal neoplasm of Schwann cell origin, composed of polygonal cells with abundant granular cytoplasm

#### Incidence and Location

- Uncommon
- Larynx is one of the more common sites of occurrence, where it usually affects the posterior vocal folds

#### Sex, Race, and Age Distribution

- No sex predilection for laryngeal tumors
- Black patients are disproportionately affected
- Third to fifth decades

#### Clinical Features

- Usually hoarseness, sometimes cough, hemoptysis, dysphagia
- Small rounded nodule on the vocal cords

#### Prognosis and Therapy

- Simple excision alone
- Excellent prognosis

### CLINICAL FEATURES

Granular cell tumor can be seen in a wide age range but most commonly affects patients in their 3rd to 5th decades. There is no predilection for either sex for laryngeal tumors, but tracheal granular cell tumors are seen more often in women. There is a predilection for black patients. In the head and neck, it is most frequently encountered in the skin, oral cavity (especially tongue), and larynx. Patients with laryngeal granular cell tumor tend to present with hoarseness, dysphagia, cough, or hemoptysis, and a small, nontender posterior vocal fold nodule is seen on laryngoscopic examination. Tracheal tumors generally occur in the cervical region of the trachea (Fig. 5.6). Approximately 10% of patients have more than one tumor.

### PATHOLOGIC FEATURES

#### GROSS FINDINGS

Grossly, granular cell tumors are small, circumscribed submucosal nodules that have a tan-white or yellowish color on cut section.

#### MICROSCOPIC FINDINGS

Granular cell tumor is poorly circumscribed and unencapsulated and typically grows as sheets or vague fascicles (Fig. 5.7A). The tumor cells of granular cell

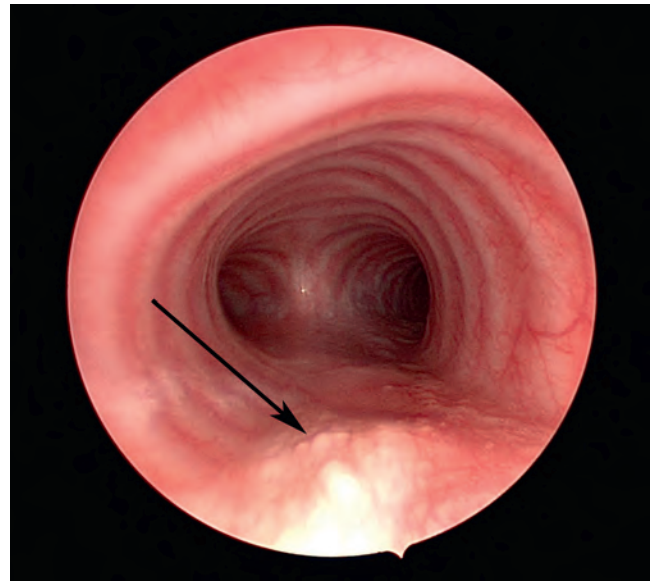


**FIGURE 5.6**

Endoscopic examination of a patient with granular cell tumor of the trachea. The nodular tumor has a whitish-yellow appearance (arrow). (Courtesy of Dr. David Tunkel.)

### GRANULAR CELL TUMOR—PATHOLOGIC FEATURES

#### Gross Findings

- Rounded submucosal nodule, nonulcerated, with tan-white or yellow appearance on cut section

#### Microscopic Findings

- Unencapsulated, poorly circumscribed proliferation of large polygonal to vaguely spindled cells with abundant pale granular cytoplasm
- Nuclei small, round, and without significant atypia
- May induce striking pseudoepitheliomatous hyperplasia of the surface epithelium
- Involvement of nerves may be seen and is not significant
- Rare malignant examples exhibit prominent spindling, elevated mitotic rates, necrosis, nuclear pleomorphism

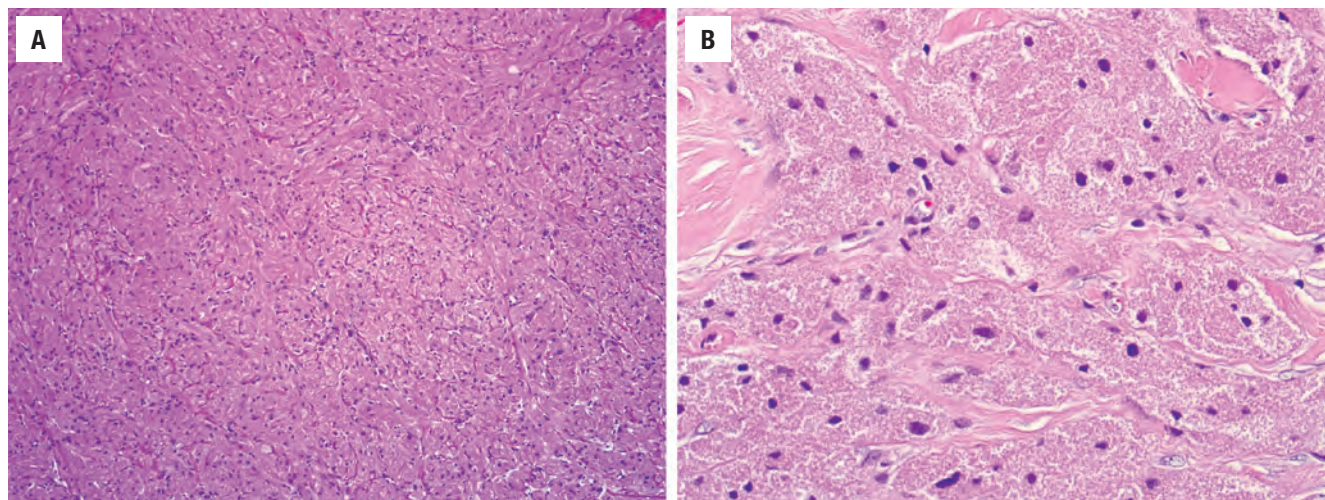
#### Ancillary Studies

- **Positive:** S100 protein, SOX10, inhibin, CD68
- **Negative:** epithelial and muscle markers

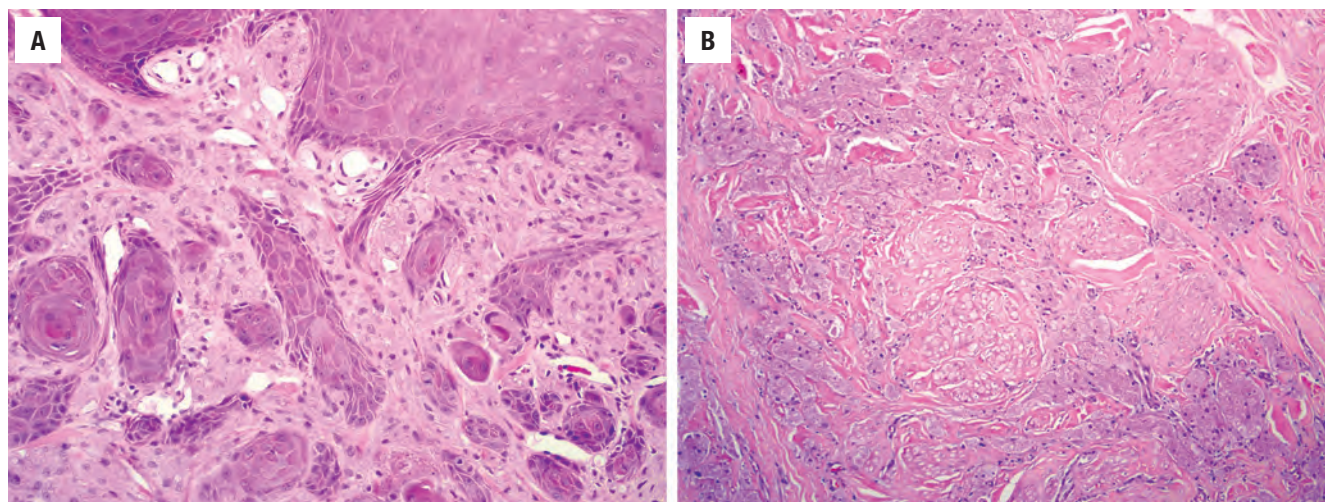
#### Pathologic Differential Diagnosis

- Adult rhabdomyoma, paraganglioma, alveolar soft parts sarcoma, PEComa, malignant granular cell tumor, squamous cell carcinoma (when pseudoepitheliomatous hyperplasia is prominent)

tumor are large polygonal cells with abundant, pale amphophilic to eosinophilic, granular cytoplasm and small round nuclei (Fig. 5.7B). Abundant cytoplasmic lysosomes are responsible for the tumor cells' granular appearance. The cells have ill-defined borders, resulting in a syncytial appearance. Nuclear atypia, cellular spindling, mitotic activity, and necrosis are typically absent, although when

**FIGURE 5.7**

Granular cell tumor at low power with sheets and vague fascicles of large, eosinophilic cells (**A**). At high power the cells of granular cell tumor are large and polygonal and have abundant, granular, eosinophilic cytoplasm with indistinct cell borders. The tumor nuclei are small and dark (**B**).

**FIGURE 5.8**

Granular cell tumor is characterized by pseudoepitheliomatous hyperplasia of the overlying squamous epithelium. When pronounced, this hyperplasia can be confused with squamous cell carcinoma if the intervening granular cells are not noticed. (**A**) It is common for granular cell tumor to involve nerves, a finding that should not be interpreted as evidence of malignancy (**B**).

these findings are present, a malignant granular cell tumor should be excluded. Granular cell tumors are sometimes accompanied by fibrosis and can also induce a very striking pseudoepitheliomatous hyperplasia of the overlying surface epithelium, which can mimic squamous cell carcinoma and obscure the granular cell tumor (Fig. 5.8A). In some cases the granular cells are closely associated with native nerve fibers, a finding that should not be interpreted as malignant behavior (Fig. 5.8B).

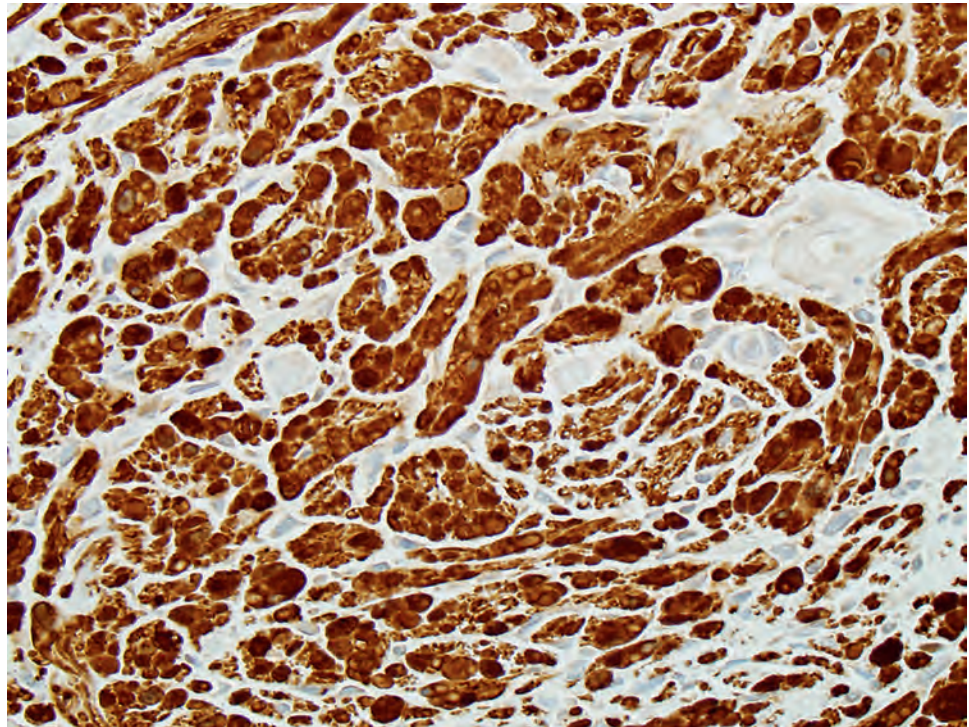
#### ANCILLARY STUDIES

Granular cell tumors are consistently positive for S100 protein (Fig. 5.9), SOX10, inhibin, and CD68, and negative for epithelial and muscle markers.

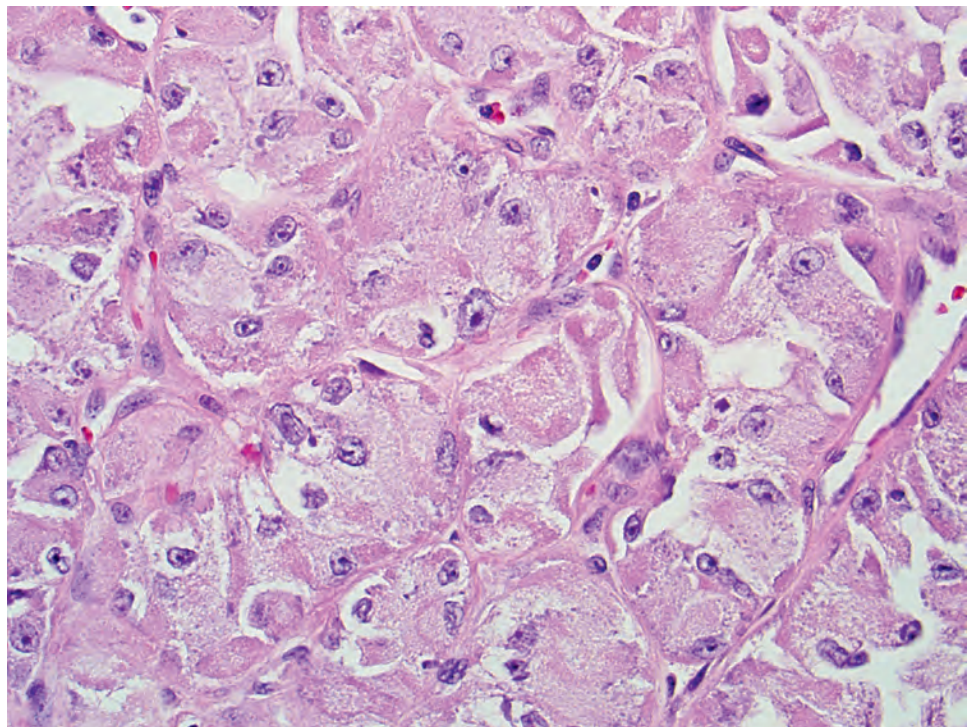
#### DIFFERENTIAL DIAGNOSIS

Granular cell tumor may mimic *adult rhabdomyoma* but lacks the fibrillary processes, cross-striations, cytoplasmic crystals, and desmin positivity that characterize rhabdomyoma. *Paraganglioma* is a tumor with nested growth, isolated pleomorphism, and is diffusely positive for synaptophysin and chromogranin, whereas S100 protein highlights a sustentacular (peripheral) population. Alveolar soft parts sarcoma also shows abundant granular cytoplasm (Fig. 5.10), but exhibits more nuclear atypia and is negative for S100 protein, SOX10, and inhibin. It should be noted that granular cell tumor is often positive for TFE3 by immunohistochemistry but consistently lacks the rearrangements of the *TFE3* gene that define alveolar soft parts sarcoma. A perivascular epithelioid cell tumor (PEComa) has large,



**FIGURE 5.9**

Granular cell tumor is characteristically positive for S100 protein in a strong, diffuse pattern.

**FIGURE 5.10**

Alveolar soft parts sarcoma resembles granular cell tumor because both neoplasms have cells with abundant granular cytoplasm. However, alveolar soft parts sarcoma usually exhibits more nuclear pleomorphism than granular cell tumor.

polygonal to epithelioid cells that often show granular cytoplasm, but the cells are positive with HMB45, Melan-A, and smooth muscle actin (SMA) and negative with S100 protein. Finally, the pseudoepitheliomatous hyperplasia induced by many granular cell tumors can be misdiagnosed as invasive squamous cell carcinoma. Distinguishing the

two rests on simply identifying the inciting neoplasm, as a diagnosis of squamous cell carcinoma should not be made in association with granular cell tumor. Helpfully, although architecturally alarming, pseudoepitheliomatous hyperplasia lacks the significant cellular atypia seen in squamous cell carcinoma (Fig. 5.8A).

## PROGNOSIS AND THERAPY

Granular cell tumors are treated with conservative but complete excision alone, which is curative. The rates of recurrence are low (<10%).

## ADULT RHABDOMYOMA

The term “rhabdomyoma” refers to a benign mesenchymal neoplasm that demonstrates skeletal muscle differentiation. However, this term may be confusing because it has historically been used for a variety of different tumor types, including cardiac neoplasms in the setting of tuberous sclerosis that are now better recognized as PEComas, as well as benign proliferations of fat and skeletal muscle in the head and neck that are probably rhabdomyomatous mesenchymal hamartomas. “True” rhabdomyomas are subclassified into adult, fetal, and genital types. The adult rhabdomyoma will be discussed here.

## CLINICAL FEATURES

Adult rhabdomyomas occur in adults, with a peak in the 6th decade and a pronounced male predilection (3-4:1). The head and neck is preferentially affected, particularly

the larynx (supraglottic or glottis), pharynx, parapharyngeal space, paratracheal soft tissue, and oral cavity (especially floor of mouth). Patients with laryngeal tumors present with hoarseness and a painless, slow-growing, circumscribed nodule.

## PATHOLOGIC FEATURES

### GROSS FINDINGS

Grossly, adult rhabdomyomas are well-circumscribed submucosal nodules ranging in size up to 8 cm (mean, 3 cm). They may be lobulated or polypoid and have a red-brown, finely granular appearance on cut section.

### MICROSCOPIC FINDINGS

Adult rhabdomyomas histologically consist of an unencapsulated, sheetlike proliferation of large polygonal cells with granular brightly eosinophilic cytoplasm (Fig. 5.11). Some tumor cells demonstrate cytoplasmic vacuolization resulting in the appearance of fibrillar processes (so-called spider cells). In addition, cross-striations or haphazardly arranged cytoplasmic rodlike or jackstrawlike crystalline structures can be seen in adult rhabdomyomas (Fig. 5.12). The nuclei of adult rhabdomyomas are small and vesicular. There is no significant nuclear atypia, mitotic activity, or necrosis.

### ADULT RHABDOMYOMA—DISEASE FACT SHEET

#### Definition

- Benign mesenchymal neoplasm of skeletal muscle differentiation

#### Incidence and Location

- Very uncommon
- Usually head and neck: larynx, pharynx, parapharyngeal space, paratracheal soft tissue, and oral cavity

#### Sex and Age Distribution

- Males > females (3 to 4:1)
- Typically adults, mean 6th decade

#### Clinical Features

- Hoarseness, slow-growing well-circumscribed submucosal nontender mass

#### Prognosis and Therapy

- Surgical excision only
- Benign, but recurrences in up to 42% of cases after incomplete excision, sometimes late

### ADULT RHABDOMYOMA—PATHOLOGIC FEATURES

#### Gross Findings

- Well-circumscribed, polypoid or lobular lesion, with red-brown cut surface

#### Microscopic Findings

- Unencapsulated sheetlike proliferation of large polygonal cells with granular brightly eosinophilic cytoplasm
- Some cells demonstrate cytoplasmic vacuolization resulting in the appearance of fibrillary processes (so-called spider cells)
- Cytoplasmic cross-striations or crystals may be seen

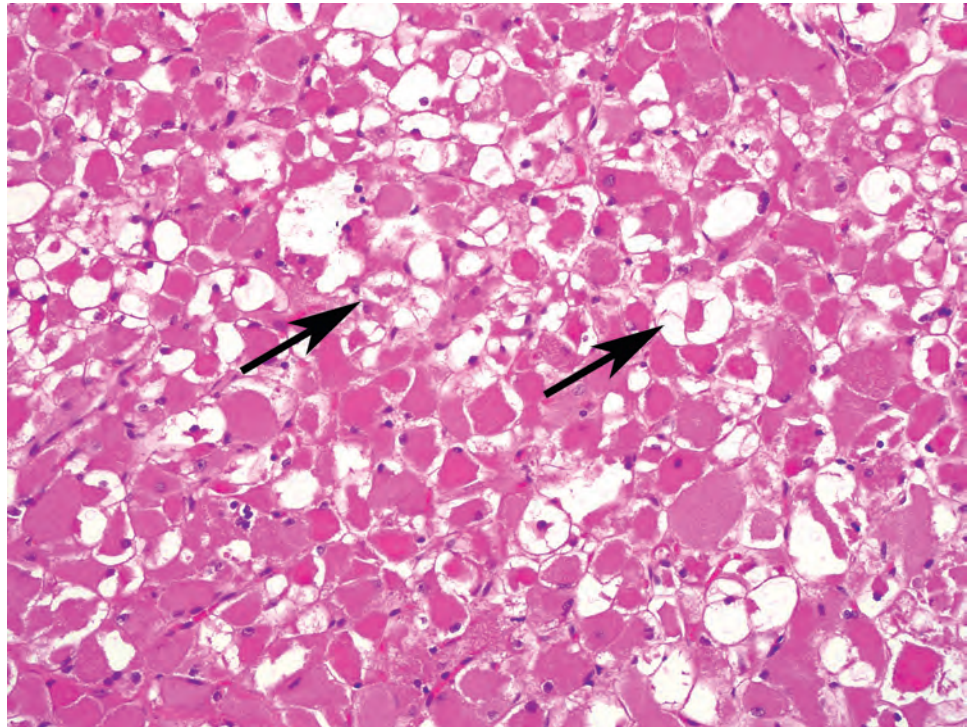
#### Special Studies

- Cytoplasmic crystals highlighted by phosphotungstic acid-hematoxylin or trichrome histochemical stains
- Positive for desmin and actin. Sometimes focally positive for S100 protein
- Negative for myogenin, epithelial markers, inhibin, SOX10, CD68

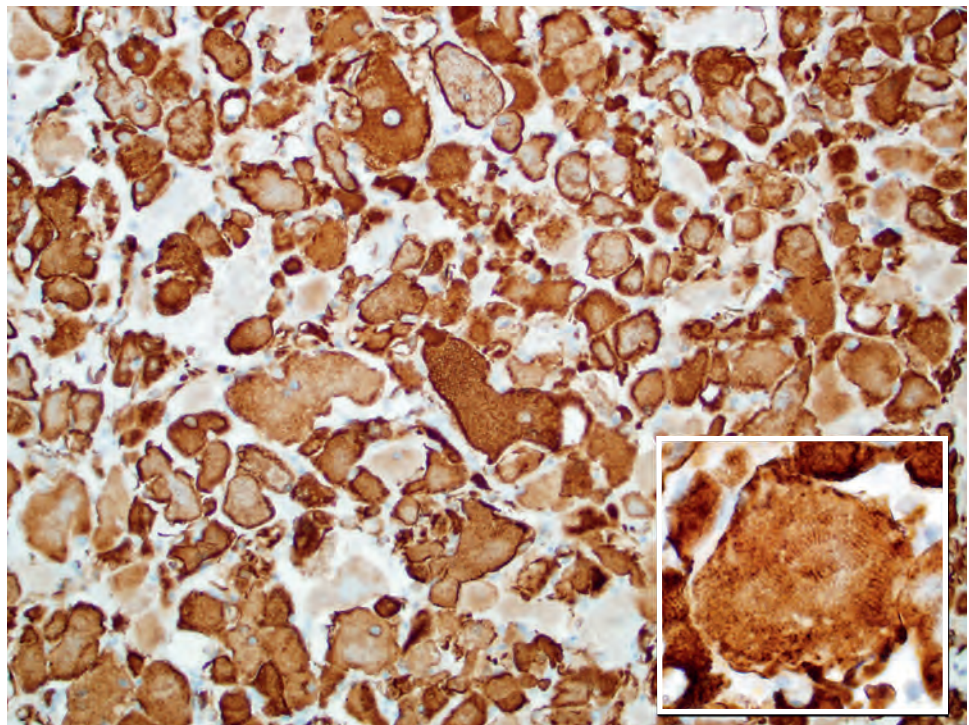
#### Pathologic Differential Diagnosis

- Granular cell tumor, paraganglioma, oncocytic epithelial tumors (e.g., oncocytoma, pleomorphic adenoma), hibernoma, myoepithelioma, crystal storing histiocytosis



**FIGURE 5.11**

The cells of adult rhabdomyoma are large with brightly eosinophilic cytoplasm. The tumor cells have cytoplasmic vacuoles that create the appearance of “spider cells” with thin, fibrillar cytoplasmic projections that resemble a spider’s web (*arrows*).

**FIGURE 5.12**

Adult rhabdomyoma is diffusely positive for desmin, consistent with its skeletal muscle origin. This immunostain is useful for highlighting cytoplasmic cross-striations (*inset*), another characteristic finding in this tumor.

### ANCILLARY STUDIES

The cytoplasmic crystals and cross-striations can be highlighted with phosphotungstic acid-hematoxylin (PTAH) or trichrome histochemical staining, and the abundant cytoplasmic glycogen is positive for periodic

acid-Schiff (PAS) (diastase sensitive). By immunohistochemistry, the tumor cells are positive for desmin (which highlights the cross-striations; [Fig. 5.12](#)) and actin. It should be remembered that, like normal mature skeletal muscle, the cells of adult rhabdomyomas are typically negative for myogenin. They are occasionally positive for S100 protein but negative for epithelial markers, inhibin, and SOX10.

## DIFFERENTIAL DIAGNOSIS

The differential diagnosis includes granular cell tumors, which lack the characteristic cytoplasmic vacuolization, cross-striations, and crystals of rhabdomyoma and are consistently desmin negative. Oncocytic epithelial tumors such as oncocytoma or myoepithelioma of the minor salivary glands may be considered, but these tumors are consistently positive for epithelial markers such as pancytokeratin. The brown fat-containing lipoma variant hibernoma may be a consideration, but it is very rare in the larynx and has distinct lipid-containing cytoplasmic vacuoles. Hibernoma is strongly positive for S100 protein and negative for desmin. Paraganglioma shows a more nested appearance and will be positive with neuroendocrine markers. Finally, crystal-storing histiocytosis, occasionally seen in the setting of lymphoplasmacytic neoplasms, can enter the differential diagnosis. These histiocytes are positive for CD68 and negative for desmin.

## PROGNOSIS AND THERAPY

Adult rhabdomyomas are treated with surgical excision only, but they may locally recur if incompletely removed. In one series, adult rhabdomyomas recurred in 42% of cases, often late (months or years after resection).

## ■ CHONDROMA

Chondroma is a benign mesenchymal neoplasm arising from the hyaline cartilage of the larynx and trachea. Chondromas are rare and much less common than its malignant counterpart, chondrosarcoma.

## CLINICAL FEATURES

Chondromas occur in men more commonly than women (2:1) over a wide age range (24 to 79; mean, 56 years). They most often arise from the cricoid cartilage (~70%), followed by the thyroid, arytenoid, and tracheal cartilages. Chondroma presents as a slow-growing endolaryngeal mass that induces hoarseness, dyspnea, dysphagia, and, rarely, a neck mass (Fig. 5.13A). Imaging studies are typically used to determine the extent of disease. Computed tomography reveals a hypodense tumor with stippled calcifications (Fig. 5.13B), and magnetic resonance imaging delineates the tumor–soft tissue border. Although radiographic evaluation is important in distinguishing chondroma from chondrosarcoma, the determination cannot be made on imaging studies alone.

## CHONDROMA—DISEASE FACT SHEET

### Definition

- Benign mesenchymal neoplasm arising from hyaline cartilage of larynx or trachea

### Incidence and Location

- Very rare
- Most common in cricoid cartilage

### Sex and Age Distribution

- Males > females (2:1)
- Wide age range (24-79), mean 56 years

### Clinical Features

- Slow-growing endolaryngeal mass inducing hoarseness, dyspnea, dysphagia

### Prognosis and Therapy

- Complete excision
- Excellent prognosis with low-risk of recurrence

## CHONDROMA—PATHOLOGIC FEATURES

### Gross Findings

- Small (usually <1 cm) submucosal mass, well circumscribed with firm, blue-white cut surface

### Microscopic Findings

- Well-circumscribed, proliferation of normal-appearing cartilage lobules
- Hypocellular, with evenly distributed chondrocytes arranged one per lacuna without atypia

### Pathologic Differential Diagnosis

- Chondrosarcoma, chondromatous metaplasia, pleomorphic adenoma, tracheopathia osteochondroplastica

## PATHOLOGIC FEATURES

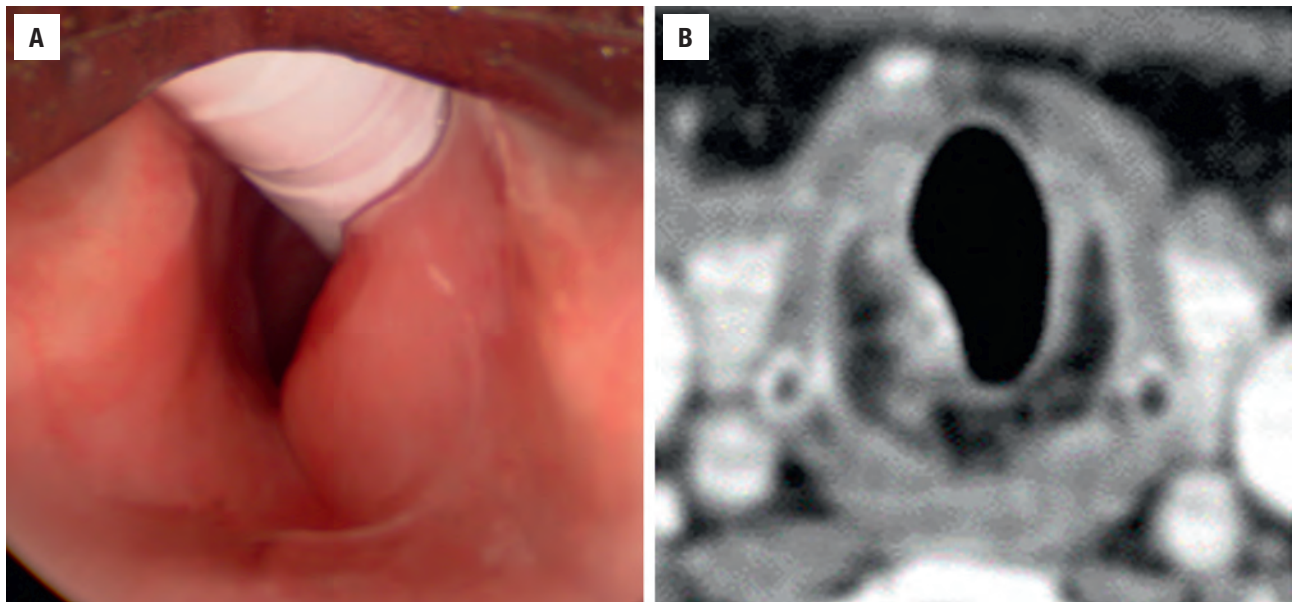
### GROSS FINDINGS

Chondroma grossly appears as a smooth, lobulated, firm submucosal mass with a blue-white cut surface. They are usually small (<1 cm).

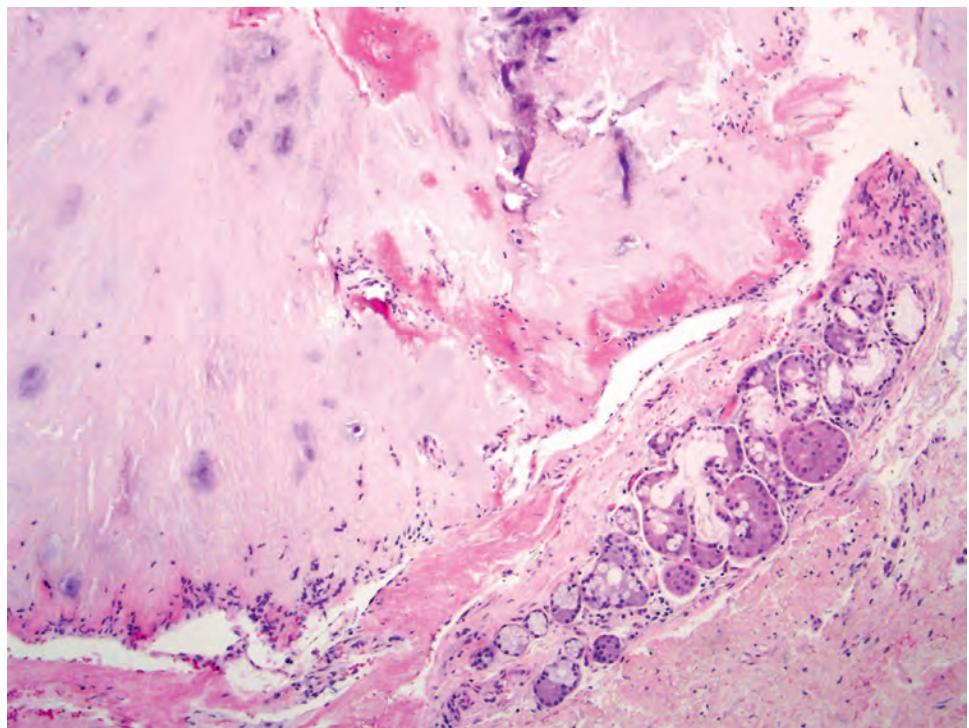
### MICROSCOPIC FINDINGS

Chondromas consist of lobules of mature, normal-appearing hyaline cartilage. They are well circumscribed and often surrounded by a thin rim of fibrous tissue resembling periosteum (Fig. 5.14). They consist of hypocellular proliferations of chondrocytes distributed evenly, one per lacuna, in the basophilic cartilaginous matrix (Fig. 5.15A). The chondrocyte nuclei are small



**FIGURE 5.13**

Chondroma of the larynx presenting as a right-sided subglottic submucosal mass bulging into the airway (**A**) and manifesting as a soft tissue density on computed tomography scanning (**B**). (Courtesy of Dr. Simon Best.)

**FIGURE 5.14**

Laryngeal chondroma with a well-circumscribed tumor border surrounded by a thin rim of connective tissue resembling periosteum.

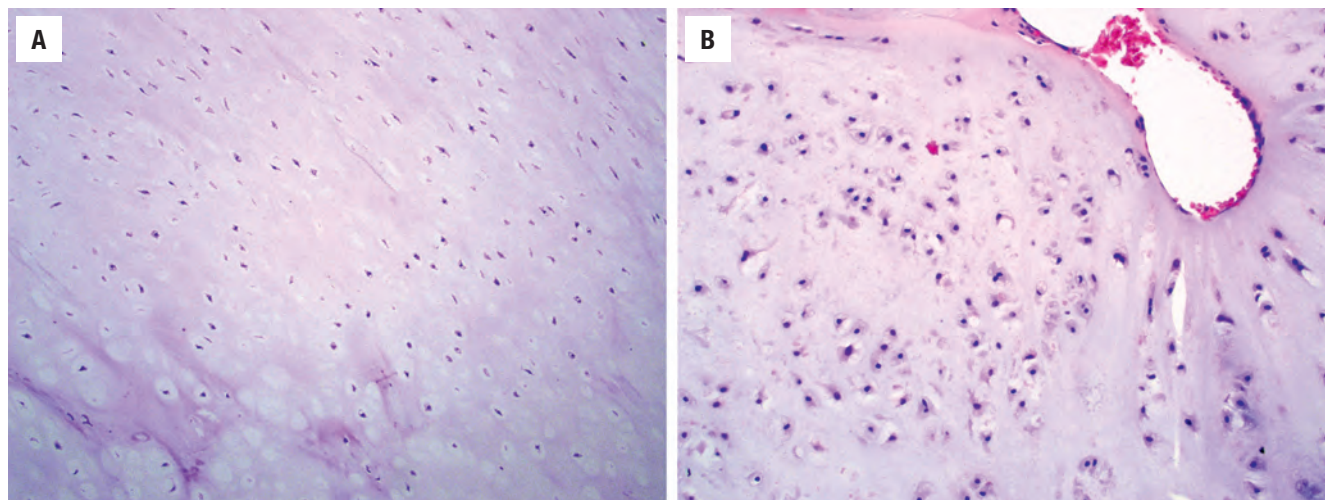
and dark, without pleomorphism, binucleation, or mitotic activity (Fig. 5.15A). Secondary calcification or ossification may be seen.

#### ANCILLARY STUDIES

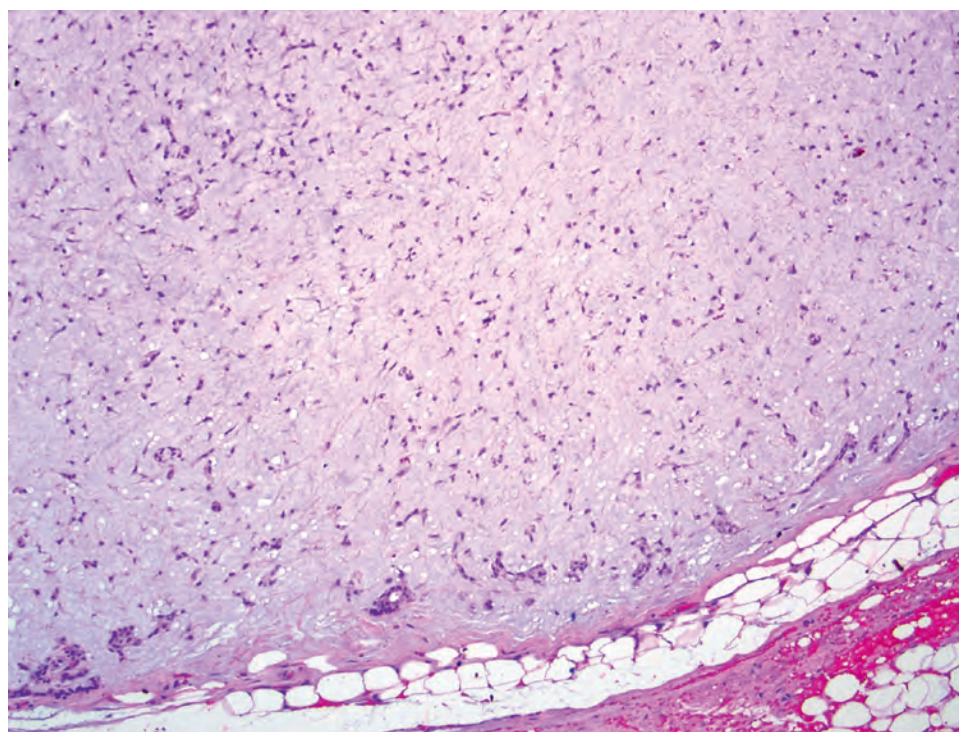
Tumor cells are positive for S100 protein and D2-40 and negative for cytokeratin.

#### DIFFERENTIAL DIAGNOSIS

Chondromas may be exceedingly difficult to distinguish from low-grade chondrosarcomas. In general, chondrosarcomas exhibit increased cellularity, binucleated cells within lacunae, and mild nuclear pleomorphism (Fig. 5.15B). However, these differences can be subtle, and there are often foci within chondrosarcomas that are indistinguishable from chondroma. As a result, a diagnosis

**FIGURE 5.15**

A benign chondroma is hypocellular with evenly spaced chondrocytes distributed singly in a bluish matrix (**A**). In comparison, a low-grade chondrosarcoma is more cellular, with chondrocytes showing slight atypia and occasional binucleation. The difference may be subtle (**B**).

**FIGURE 5.16**

A pleomorphic adenoma may have a prominent chondromyxoid stroma; however, at least focally there will be an obvious epithelial tumor component (seen here as ducts at the periphery of the tumor).

of a cartilaginous laryngeal tumor requires examination of the entire tumor and correlation with radiographic findings. Chondromatous metaplasia can be seen in various tissues of the larynx and trachea, possibly resulting from trauma. In metaplasia, the cartilage is typically more haphazardly distributed in fibrosis and does not produce a radiologic mass. Tracheopathia osteochondroplastica is an aging phenomenon, with cartilaginous protrusions from the cartilaginous or ossified trachea rings. Finally, pleomorphic adenomas with abundant chondromyxoid

stroma can be mistaken for chondromas, but pleomorphic adenomas will at least focally exhibit overt epithelial differentiation ([Fig. 5.16](#)).

#### PROGNOSIS AND THERAPY

Chondromas are benign and are treated with complete surgical excision. Recurrences are rare; in fact, tumor



recurrence suggests that the tumor is actually a low-grade chondrosarcoma. If there is ischemic change, transformation to chondrosarcoma is suggested.

■ **INFLAMMATORY MYOFIBROBLASTIC TUMOR**

Inflammatory myofibroblastic tumor (IMT) is a rare mesenchymal neoplasm characterized by a proliferation of myofibroblasts admixed with inflammatory cells. It is considered intermediate between benign and malignant tumors. In the past, terms like “inflammatory pseudotumor” and “plasma cell granuloma” were used, reflecting uncertainty about whether it was truly a neoplasm. It is now believed to be neoplastic, and these historical terms should be avoided in favor of the IMT terminology.

**CLINICAL FEATURES**

IMTs of the head and neck may affect a wide age range, including children and adolescents. They can arise in almost any head and neck site, but the larynx (especially glottis) and trachea are most common. Patients present with hoarseness, airway obstruction, or dysphonia, often having a polypoid mass protruding into the airway on laryngoscopic examination. Unlike visceral IMTs, examples of the head and neck are not associated with anemia, thrombocytopenia, or elevated sedimentation rate.

**INFLAMMATORY MYOFIBROBLASTIC TUMOR—DISEASE FACT SHEET**

**Definition**

- Benign mesenchymal neoplasm of myofibroblasts with accompanying mixed inflammatory cells

**Incidence and Location**

- Rare
- In the head and neck, larynx and trachea most common

**Sex and Age Distribution**

- Wide age range, including children and adolescents

**Clinical Features**

- Hoarseness, dysphonia, airway obstruction

**Prognosis and Therapy**

- Resection alone
- Recurrences are uncommon, and malignant behavior not reported at this site

**PATHOLOGIC FEATURES**

**GROSS FINDINGS**

IMTs grossly appear as polypoid, fleshy, or firm tan-pink masses that sometimes exhibit surface ulceration. Tumors are generally small, measuring 0.4 to 3 cm.

**MICROSCOPIC FINDINGS**

IMTs consist of an exophytic proliferation of submucosal spindled, stellate, or epithelioid cells with fibrillary cytoplasmic projections, arranged in a loose fascicular or storiform arrangement said to resemble tissue cultures (Fig. 5.17). Tumor cells have low nuclear to cytoplasmic ratios and have nuclei with open chromatin, mild pleomorphism, and prominent nucleoli (Fig. 5.18). Mitotic activity may be seen or even elevated, but atypical mitoses are not present. There is a variably intense infiltrate of chronic inflammatory cells (lymphocytes, plasma cells, eosinophils) admixed with the spindle cells (Fig. 5.18).

**ANCILLARY STUDIES**

Tumor cells are positive for actin, occasionally positive for desmin or cytokeratins, and negative for p63 and p40. ALK immunoreactivity is only seen in up to 60 %

**INFLAMMATORY MYOFIBROBLASTIC TUMOR—PATHOLOGIC FEATURES**

**Gross Findings**

- Polypoid submucosal mass, often ulcerated, fleshy, or firm on cut section

**Microscopic Findings**

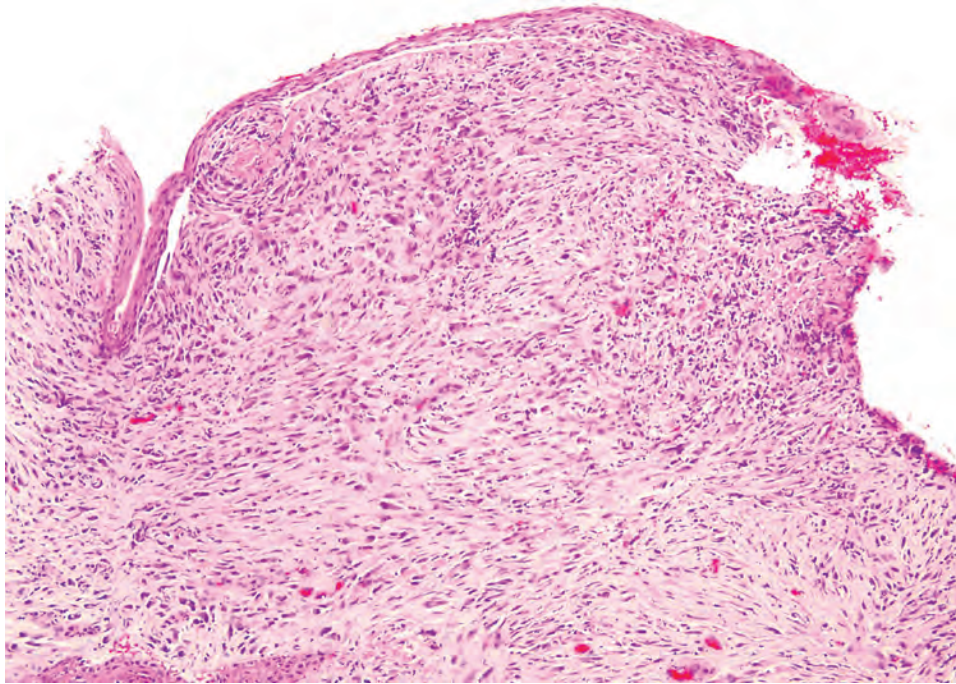
- Exophytic proliferation of spindled cells in loose fascicular or storiform arrangement
- Tumor cells have low nuclear to cytoplasmic ratios, hypochromatic nuclei with open chromatin, and prominent nucleoli
- Variably intense influx of chronic inflammatory cells
- Mitotic figures often present and may be numerous, but no atypical mitotic forms

**Ancillary Studies**

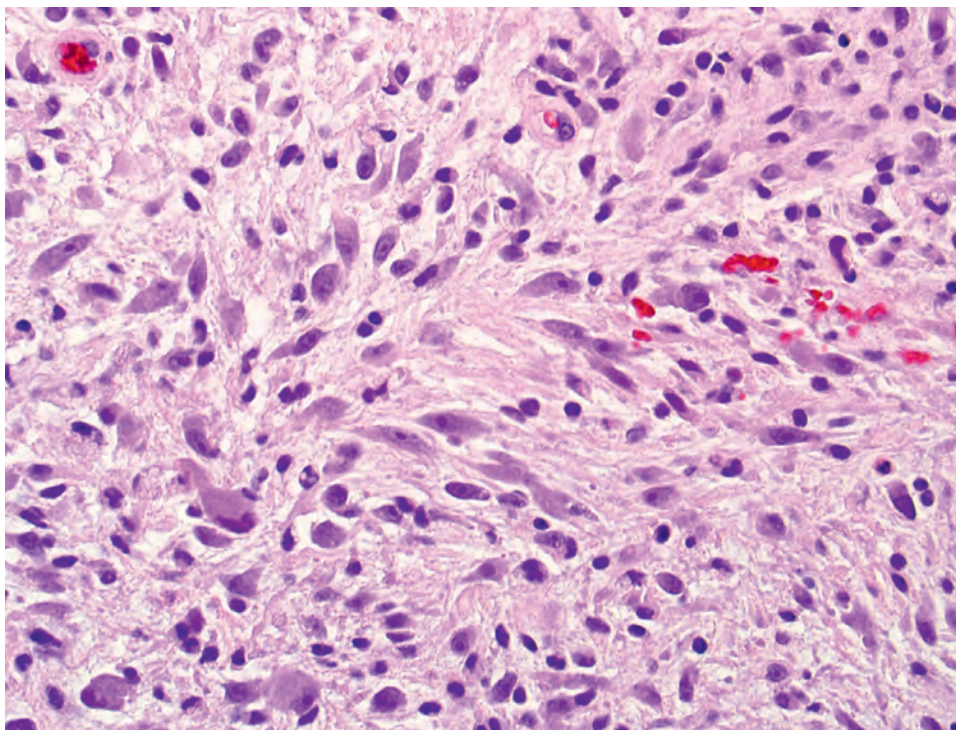
- Up to 60% positive for ALK by immunohistochemistry or gene rearrangement studies
- Often positive for actin and desmin, may be positive for cytokeratin
- Negative for p63 and p40

**Pathologic Differential Diagnosis**

- Sarcomatoid carcinoma, granulation tissue, contact ulcer, IgG<sub>4</sub>-related sclerosing disease, low-grade fibromyxoid sarcoma

**FIGURE 5.17**

Inflammatory myofibroblastic tumor, consisting of a polypoid submucosal proliferation of spindled tumor cells.

**FIGURE 5.18**

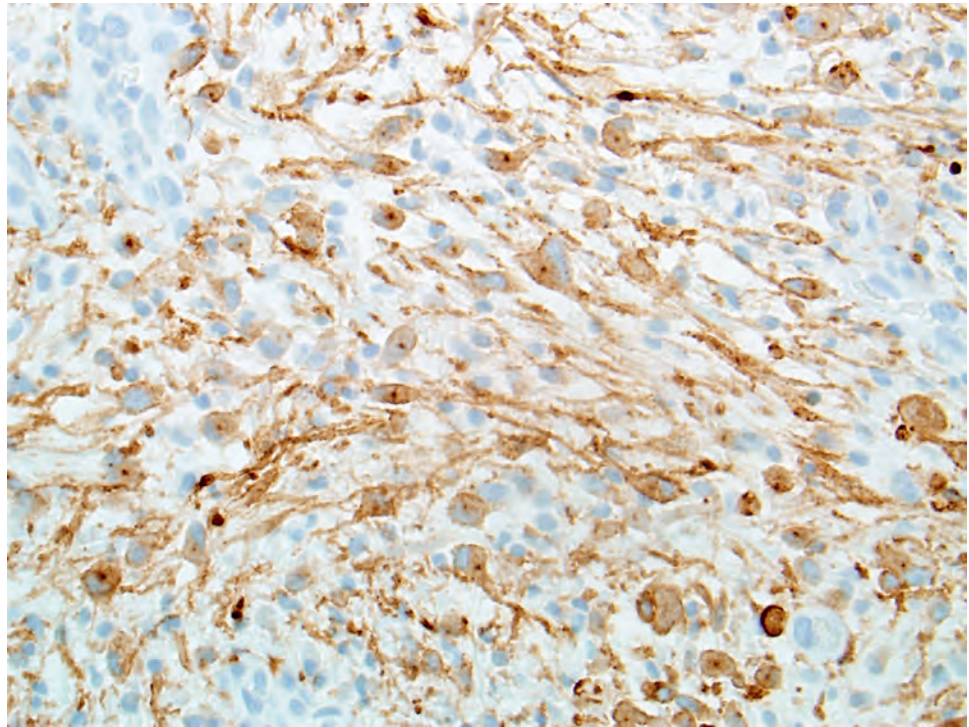
Inflammatory myofibroblastic tumor cells are often somewhat atypical, with nuclear enlargement and prominent nucleoli. However, they have low nuclear to cytoplasmic ratios and open chromatin and lack atypical mitoses. There is a sprinkling of chronic inflammatory cells associated with the tumor cells.

of cases (Fig. 5.19). The majority of IMTs (especially pediatric cases) harbor gene rearrangements of *ALK* with one of several partner genes. Interestingly, some *ALK*-negative IMTs have been reported to harbor rearrangements of *ROS1*, *ETV6*, and *NTRK3*, although these genes have not yet been well studied in IMTs of the head and neck.

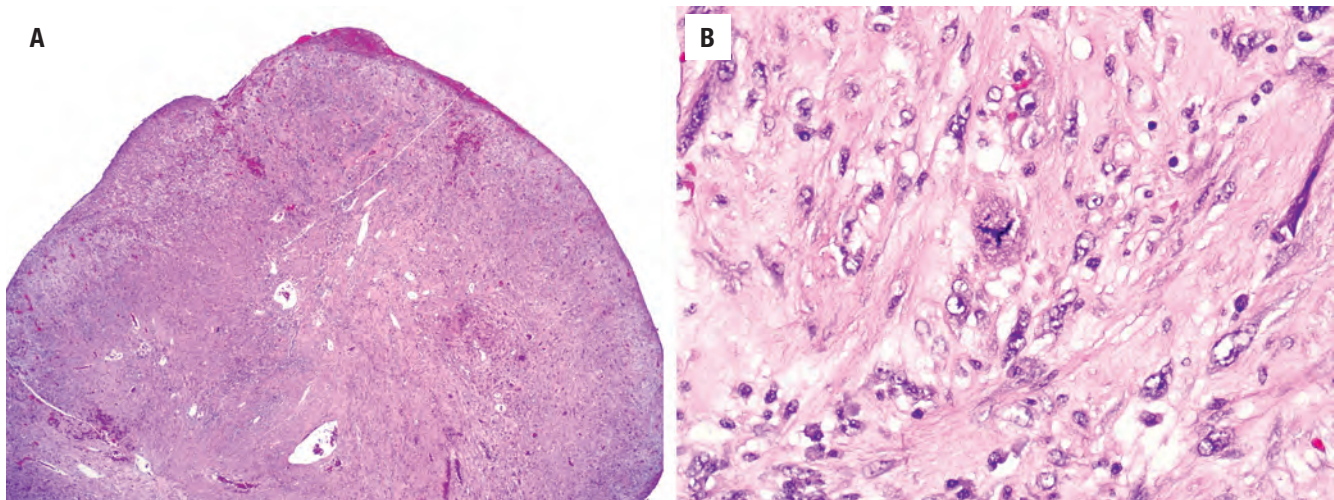
#### DIFFERENTIAL DIAGNOSIS

It is important to distinguish IMT from sarcomatoid squamous cell carcinoma, a much more common tumor in the larynx. Both tumors consist predominantly of spindled cells and may have an inflammatory infiltrate,



**FIGURE 5.19**

Inflammatory myofibroblastic tumor is often positive for ALK by immunohistochemistry. A positive result helps to distinguish inflammatory myofibroblastic tumor from some of its mimickers, such as sarcomatoid carcinoma.

**FIGURE 5.20**

Sarcomatoid carcinoma of the larynx at low power classically grows as a polypoid spindle cell proliferation beneath an ulcerated surface. This low-power appearance is very similar to that of inflammatory myofibroblastic tumor (A). However, at high power the malignant cytologic findings of sarcomatoid carcinoma are evident, with high nuclear to cytoplasmic ratios, marked pleomorphism, and an atypical mitotic figure (center) (B).

but sarcomatoid carcinoma exhibits overtly malignant cellular findings, with hypercellularity, atypical mitotic figures, and hyperchromatic nuclei showing marked nuclear pleomorphism (Fig. 5.20). In addition, many cases of sarcomatoid squamous cell carcinoma have areas of conventional squamous cell carcinoma in the invasive tumor or foci of squamous dysplasia/carcinoma in situ of the residual surface epithelium. ALK immunohistochemistry or molecular studies are helpful for confirming a diagnosis of IMT if positive, but a negative result can

be seen in either tumor. p63 and p40 are consistently negative in IMT, but positivity for cytokeratins, desmin, and actin may be seen in either tumor. The cells of IMT resemble those of a contact ulcer, but IMTs are generally much more cellular, particularly in tissue away from the ulcer bed. The histologic findings of IMT also overlap with those of IgG<sub>4</sub>-related sclerosing disease, and some cases of IMT are reported to have elevated numbers of IgG<sub>4</sub>-positive plasma cells. However, IgG<sub>4</sub>-related disease usually demonstrates obliterative phlebitis and germinal

centers and would be extremely unusual to occur in the larynx or trachea without evidence of systemic disease elsewhere (e.g., salivary glands or pancreas). Furthermore, positive ALK studies would confirm the diagnosis of IMT. Exceptional in the head and neck, a low-grade fibromyxoid sarcoma shows relatively bland spindled cells, usually associated with a myxoid matrix, with a more whorled growth pattern and a prominent vasculature. MUC4 is positive, but EMA, SMA, and p63 may also be seen, and the *FUS-CREB3L2* fusion is present in most cases.

### PROGNOSIS AND THERAPY

IMTs of the larynx and trachea are treated with surgery alone, which is usually curative. Local recurrences are

uncommon. Rare examples of visceral IMT have behaved in a malignant fashion; however, to date, malignant behavior has not been described in IMTs of the larynx or trachea.

### SUGGESTED READINGS

The complete Suggested Readings list is available online at [ExpertConsult.com](http://ExpertConsult.com).



**SUGGESTED READINGS****Squamous Papilloma/Papillomatosis**

- Bravo IG, et al. Papillomaviruses: Viral evolution, cancer and evolutionary medicine. *Evol Med Public Health*. 2015;2015(1):32–51.
- Karifi M, et al. Recurrent respiratory papillomatosis: current and future perspectives. *Ther Clin Risk Manag*. 2015;11:731–738.
- Gale N, et al. Laryngeal papillomatosis: molecular, histopathological, and clinical evaluation. *Virchows Arch*. 1994;425(3):291–295.
- Goon P, et al. Recurrent respiratory papillomatosis: an overview of current thinking and treatment. *Eur Arch Otorhinolaryngol*. 2008;265(2):147–151.
- Karatayli-Ozgursoy S, et al. Risk factors for dysplasia in recurrent respiratory papillomatosis in an adult and pediatric population. *Ann Otol Rhinol Laryngol*. 2016;125(3):235–241.
- Larson DA, et al. Epidemiology of recurrent respiratory papillomatosis. *APMIS*. 2010;118:450–454.
- Lee JH, et al. Recurrent respiratory papillomatosis: pathogenesis to treatment. *Curr Opin Otolaryngol Head Neck Surg*. 2005;13(6):354–359.
- Omland T, et al. Risk factors for aggressive recurrent respiratory papillomatosis in adults and juveniles. *PLoS ONE*. 2014;9(11):e113584.
- Richardson M, et al. Papilloma and papillomatosis. In: El-Naggar AK, Chan JKC, Grandis JR, Takata T, Slootweg PJ, eds. *Classification of Head and Neck Tumors*. 4th ed. World Health Organization Classification of Tumors. Lyon, France: IARC Press; 2017:93–95.
- Wierzbička M, et al. Effectiveness of cidofovir intralesional treatment in recurrent respiratory papillomatosis. *Eur Arch Otorhinolaryngol*. 2011;268(9):1305–1311.

**Granular Cell Tumor**

- Allen CM, et al. Granular cell tumor. In: El-Naggar AK, Chan JKC, Grandis JR, Takata T, Slootweg PJ, eds. *Classification of Head and Neck Tumors*. 4th ed. World Health Organization Classification of Tumors. Lyon, France: IARC Press; 2017:100.
- Brandwein M, et al. Atypical granular cell tumor of the larynx: an unusually aggressive tumor clinically and microscopically. *Head Neck*. 1990;12(2):154–159.
- Burton DM, et al. Granular cell tumors of the trachea. *Laryngoscope*. 1982;102:807–813.
- Chamberlain BK, et al. Alveolar soft part sarcoma and granular cell tumor: an immunohistochemical comparison study. *Hum Pathol*. 2014;45(5):1039–1044.
- Fanburg-Smith JC, et al. Malignant granular cell tumor of soft tissue: diagnostic criteria and clinicopathologic correlation. *Am J Surg Pathol*. 1998;22:779–794.
- Fine SW, et al. Expression of calretinin and the alpha-subunit of inhibin in granular cell tumors. *Am J Clin Pathol*. 2003;119(2):259–264.
- Karatayli-Ozgursoy S, et al. Non-epithelial tumors of the larynx: a single institution review. *Am J Otolaryngol*. 2016;37(3):279–285.
- Lassaletta L, et al. Immunoreactivity in granular cell tumors of the larynx. *Auris Nasus Larynx*. 1999;26(2):305–310.
- Ordonez NG, et al. Granular cell tumor: a review of pathology and histogenesis. *Ultrastruct Pathol*. 1999;23(4):207–222.
- Park JH, et al. Granular cell tumor on larynx. *Clin Exp Otorhinolaryngol*. 2010;3(1):52–55.
- Regezi JA, et al. Immunoreactivity of granular cell lesions of skin, mucosa, and jaw. *Cancer*. 1989;64:1455–1460.
- Schoolmeester JK, et al. Granular cell tumors overexpress TFE3 without corollary gene rearrangement. *Hum Pathol*. 2015;46(8):1242–1243.

**Adult Rhabdomyoma**

- Brys AK, et al. Rhabdomyoma of the larynx: case report and clinical and pathologic review. *Ear Nose Throat J*. 2005;84:437–440.
- Carta F, et al. Endoscopic management of adult-type rhabdomyoma of the glottis: case report and review of the literature. *Braz J Otorhinolaryngol*. 2016;82(2):244–247.

- Cleveland DB, et al. Adult rhabdomyoma. A light microscopic, ultrastructural, virologic, and immunologic analysis. *Oral Surg Oral Med Oral Pathol*. 1994;77(2):147–153.
- Hansen T, et al. Rhabdomyoma of the head and neck: morphology and differential diagnosis. *Virchows Arch*. 2005;447(5):849–854.
- Kapadia SB, et al. Adult rhabdomyoma of the head and neck. A clinicopathologic and immunophenotypic study. *Hum Pathol*. 1993;24(6):608–617.
- Papasprou G, et al. Adult rhabdomyoma in the parapharyngeal space: report of 2 cases and review of the literature. *Am J Otolaryngol*. 2011;32(3):240–246.

**Chondroma**

- Baatenburg de Jong RJ, et al. Chondroma and chondrosarcoma of the larynx. *Curr Opin Otolaryngol Head Neck Surg*. 2004;12(2):98–105.
- Casiraghi O, et al. Chondroid tumors of the larynx: a clinicopathologic study of 19 cases, including two dedifferentiated chondrosarcomas. *Ann Diagn Pathol*. 2004;8:189–197.
- Franco RA Jr, et al. Laryngeal chondroma. *J Voice*. 2002;16(1):92–95.
- Gale N, et al. Chondroma and chondrosarcoma. In: El-Naggar AK, Chan JKC, Grandis JR, Takata T, Slootweg PJ, eds. *Classification of Head and Neck Tumors*. 4th ed. World Health Organization Classification of Tumors. Lyon, France: IARC Press; 2017:102–104.
- Hyams VJ, et al. Cartilaginous tumors of the larynx. *Laryngoscope*. 1970;80:755–767.
- Karatayli-Ozgursoy S, et al. Non-epithelial tumors of the larynx: a single institution review. *Am J Otolaryngol*. 2016;37(3):279–285.
- Merrot O, et al. Cartilaginous tumors of the larynx: endoscopic laser management using YAG/KTP. *Head Neck*. 2009;31(2):145–152.
- Neel HB, et al. Cartilaginous tumors of the larynx: a series of 33 cases. *Otolaryngol Head Neck Surg*. 1982;90:201–207.
- Thompson LDR, et al. Chondrosarcoma of the larynx. A clinicopathologic study of 111 cases with a review of the literature. *Am J Surg Pathol*. 2002;26(7):836–851.

**Inflammatory Myofibroblastic Tumor**

- Alassiri AH, et al. ETV6-NTRK3 is expressed in a subset of ALK-negative inflammatory myofibroblastic tumors. *Am J Surg Pathol*. 2016;40(8):1051–1061.
- Alhumaid H, et al. Laryngeal myofibroblastic tumor: case series and literature review. *Int J Health Sci (Qassim)*. 2011;5(2):187–195.
- Biron VL, et al. Inflammatory pseudotumors of the larynx: three cases and a review of the literature. *J Otolaryngol Head Neck Surg*. 2008;37(2):E32–E38.
- Bishop JA, et al. Use of p40 and p63 immunohistochemistry and human papillomavirus testing as ancillary tools for the recognition of head and neck sarcomatoid carcinoma and its distinction from benign and malignant mesenchymal processes. *Am J Surg Pathol*. 2014;38(2):257–264.
- Chan JK, et al. Anaplastic lymphoma kinase expression in inflammatory pseudotumors. *Am J Surg Pathol*. 2001;25:761–768.
- Coffin CM, et al. Inflammatory myofibroblastic tumor: comparison of clinicopathologic, histologic, and immunohistochemical features including ALK expression in atypical and aggressive cases. *Am J Surg Pathol*. 2007;31(4):509–520.
- Cowan M, et al. Low-grade fibromyxoid sarcoma of the head and neck: a clinicopathologic series and review of the literature. *Head Neck Pathol*. 2016;10(2):161–166.
- Devaney KO, et al. Inflammatory myofibroblastic tumors of the head and neck: evaluation of clinicopathologic and prognostic features. *Eur Arch Otorhinolaryngol*. 2012;269(12):2461–2465.
- Idrees MT, et al. Inflammatory myofibroblastic tumor of larynx: a benign lesion with variable morphological spectrum. *Ann Diagn Pathol*. 2007;11(6):433–439.
- Völker HU, et al. Laryngeal inflammatory myofibroblastic tumors: Different clinical appearance and histomorphologic presentation of one entity. *Head Neck*. 2010;32(11):1573–1578.
- Wenig BM, et al. Inflammatory myofibroblastic tumor of the larynx. A clinicopathologic study of eight cases simulating a malignant spindle cell neoplasm. *Cancer*. 1995;76(11):2217–2229.

12. Wenig BM, et al. Inflammatory myofibroblastic tumor. In: El-Naggar AK, Chan JKC, Grandis JR, Takata T, Slootweg PJ, eds. *Classification of Head and Neck Tumours*. 4th ed. World Health Organization Classification of Tumors. Lyon, France: IARC Press; 2017: 101–102.
13. Yamamoto H, et al. ALK, ROS1 and NTRK3 gene rearrangements in inflammatory myofibroblastic tumours. *Histopathology*. 2016;69(1): 72–83.
14. Yan Q, et al. Inflammatory myofibroblastic tumor of the larynx: report of a case and review of the literature. *Int J Clin Exp Pathol*. 2015;8(10):13557–13560.



# Malignant Neoplasms of the Larynx, Hypopharynx, and Trachea

■ Lester D.R. Thompson

## ■ PRECURSOR SQUAMOUS LESIONS

Precursor lesions are difficult to define because they have an increased likelihood of progressing to squamous cell carcinoma (SCC). A constellation of architectural and cytologic features constitute dysplasia, but these features are not uniformly accepted or understood, thereby leading to differences in intra- and interobserver interpretation. It is wise to use the term *atypia* in the context of reactive, inflammatory, or regenerative changes, while reserving *dysplasia* for the premalignant group of lesions. The new World Health Organization (WHO) classification uses only two tiers, low and high grade, with carcinoma in situ (CIS) included in high-grade dysplasia. Terms like *keratosis*, *squamous intraepithelial lesion* (SIL) or *neoplasia* (SIN), *laryngeal intraepithelial neoplasia* (LIN), *basal/parabasal hyperplasia*, and *atypical hyperplasia* are preferentially replaced by the new two-tiered system for the sake of simplicity, reproducibility, and patient management. Keratinizing dysplasia is a potentially reversible alteration in epithelial cells that shows an increased likelihood of progressing to SCC. CIS is a *noninvasive* malignant alteration of the full thickness of the surface epithelium.

### CLINICAL FEATURES

Precursor lesions are mostly seen in the adult population (6th to 7th decades), with a male predilection that is especially pronounced after the 6th decade. There is a strong association with tobacco smoking and alcohol abuse, with a potentiating effect between the two; the increased risk is directly proportional to duration of use. The etiologic role of human papillomavirus (HPV) infection is very limited, detected in about 8% to 12% of cases. Symptoms depend on the location and severity of the disease and are usually present for at least a few

### PRECURSOR SQUAMOUS LESIONS—DISEASE FACT SHEET

#### Definition

- Squamous lesions with an increased risk/likelihood of progressing to squamous cell carcinoma

#### Incidence and Location

- From 2% to 40% of precursor lesions progress to carcinoma
- Supraglottic and glottic regions are most commonly affected

#### Sex and Age Distribution

- Males > females
- Peak in 6th-7th decades

#### Clinical Features

- Tobacco and alcohol abuse (with potentiating effect)
- HPV very infrequently identified as a risk factor
- Hoarseness, throat irritation, sore throat, chronic cough

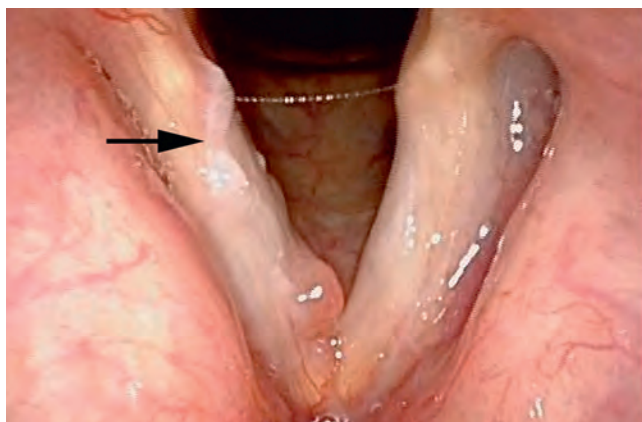
#### Prognosis and Treatment

- Progression to carcinoma is slow, but there is a well-defined risk of malignant transformation
- Surgery, laser, and radiation, dependent upon lesion

HPV, Human papillomavirus.

months before they come to clinical attention. Hoarseness, voice changes, throat irritation, sore throat, and/or chronic cough are frequently reported. Endoscopically, dysplasia has a varied appearance, ranging from discrete to diffuse, leukoplakia to erythroplakia, and a small flat patch to a large warty plaque (Fig. 6.1). Leukoplakia, in contrast to erythroplakia, tends to be well demarcated. Although inconsistent, leukoplakia alone seems to pose a lower risk of malignant transformation than pure erythroplakia.

In general it is accepted that there is an increased risk of progression to invasive SCC over time. Low-grade dysplasia is potentially reversible if the inciting factor is removed. However, as the grade of dysplasia increases,

**FIGURE 6.1**

Laryngoscopic view of true vocal cord leukoplakia (arrow), which represents a keratinizing dysplasia.

### PRECURSOR SQUAMOUS LESIONS—PATHOLOGIC FEATURES

#### Gross Findings

- Leukoplakia, erythroplakia, mixed (speckled), variegated
- Diffuse or discrete
- Flat patch or large warty plaque
- Anterior true vocal cord most often, with frequent bilateral disease

#### Microscopic Findings

- A continuum of architectural and cytologic features required, separated into low and high grade based on degree of involvement and cytologic features present
- Increased cellularity, nuclear crowding, irregular maturation, lack of polarity, dyskeratosis, irregular cell pinking, intercellular edema (prominent spinous layer), keratin pearl formation, parakeratosis, increased mitoses, atypical mitoses
- Increased nuclear-to-cytoplasmic (N:C) ratio, increased nuclear size, anisocytosis, poikilocytosis, anisonucleosis, nuclear pleomorphism, nuclear hyperchromasia, nuclear chromatin condensation, increased nucleolar size and number
- Basement membrane intact

#### Pathologic Differential Diagnosis

- Hyperplasia, regeneration, repair, inflammation, radiation changes, necrotizing sialometaplasia, SCC

SCC, Squamous cell carcinoma.

it becomes more difficult to predict which dysplasia may be reversible and which may progress to invasive carcinoma. Although quite variable, low-grade dysplasia shows a 2% risk of progression to invasive carcinoma, whereas high-grade dysplasia ranges from 23% to 40% risk of progression. The progression is usually slow, with an average latency from low-grade dysplasia to invasive SCC of just under 4 years. It is important to realize that multifocal disease is a major factor in disease development, since the entire epithelium is exposed to the same etiologic risk agents.

### PATHOLOGIC FEATURES

#### GROSS FINDINGS

There is no characteristic appearance of precursor lesions, which may be circumscribed or diffuse; smooth, granular, or irregular; flat or exophytic; and leukoplakic or erythroplakic. The anterior true vocal cords are involved most commonly (usually not the commissure), although no region of the larynx is exempt. Bilateral disease is common (30% to 60%). Invasive carcinoma may be concurrently present adjacent to or remote from the precursor lesion.

#### MICROSCOPIC FINDINGS

Dysplasia is an alteration of surface epithelium that is *more* than hyperplasia but *less* than carcinoma. Needless to say, to identify the earliest forms of dysplasia and to arbitrarily separate and rigidly divide the dysplasias into different categories is fraught with tremendous intra- and interobserver variability and an overall lack of reproducibility.

Many architectural (maturation abnormalities) and cytologic features can be seen in dysplasia, although none in isolation is pathognomonic for dysplasia. In fact, many of these same features are more fully developed in carcinoma, so a rigid segregation between lesions is nearly impossible. In general, all of the various layers begin to cytologically resemble the basal layer cells (immature or uncommitted) as the lesion progresses from low-grade dysplasia (Figs. 6.2–6.6) toward CIS. Moreover, on a continuous spectrum, there is a quantitative increase in architectural and cytologic features for the diagnosis of dysplasia (Table 6.1).

Architectural features of dysplasia include increased cellularity, nuclear crowding (Fig. 6.2), irregular maturation toward the surface, lack of polarity, dyskeratosis (Fig. 6.2), keratin pearl formation within rete, parakeratosis (Fig. 6.3), and pseudoepitheliomatous hyperplasia (PEH) or acanthosis with irregular rete extending into the submucosa. In general, dysplasia starts in the basal/parabasal zone and moves toward the surface (Fig. 6.4). Cytologic features of dysplasia include increased N:C ratio, increased nuclear size, anisocytosis, poikilocytosis, anisonucleosis, nuclear pleomorphism, nuclear hyperchromasia, nuclear chromatin condensation and contour irregularities, and increased number and size of nucleoli (Figs. 6.5 and 6.6). Mitoses are increased; they are identified above the basal zone and may include atypical mitotic figures (misalignment of chromosomes, unbalanced distribution of chromosomes, and multipolar figures). Atypical mitoses and profound pleomorphism, when present, are features of high-grade dysplasia. Obviously the basement membrane is intact. The term *carcinoma in situ* is sometimes limited to lesions that truly lack any maturation at the surface; for the most

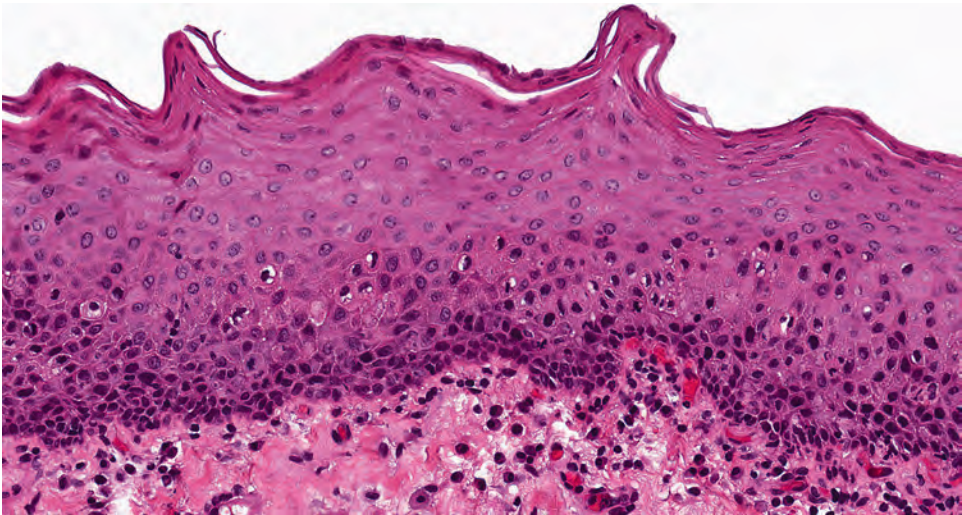


**TABLE 6.1**  
**Two-tiered system of grading laryngeal dysplasia**

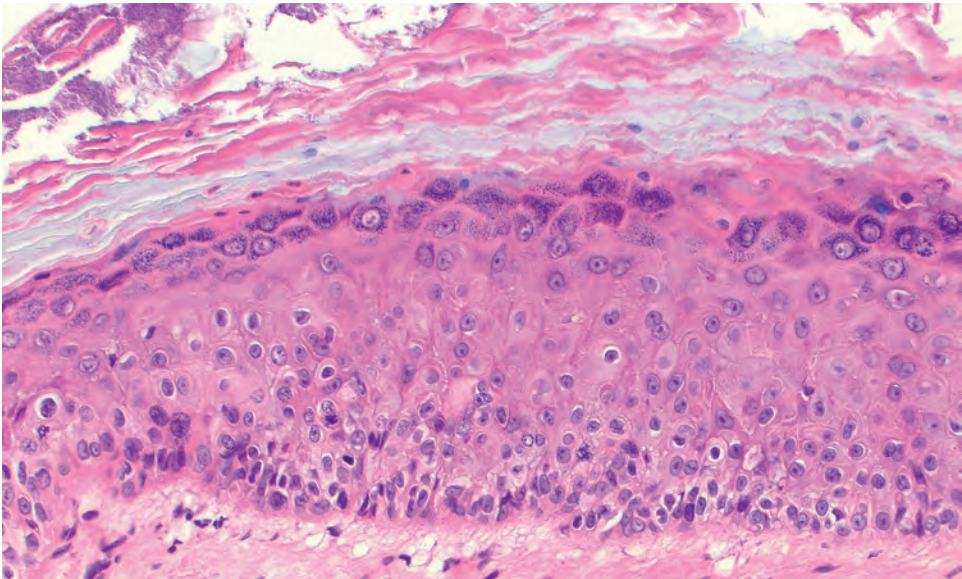
|                      |                           |   |
|----------------------|---------------------------|---|
| Low-grade dysplasia  | Architecture              | Preserved stratification, with expansion of the basal layer, often with perpendicular orientation of the nuclei, transitioning to horizontal orientation at the surface<br>Increased spinous layer, but may be confined to the upper layers of the epithelium<br>May be limited to increased basal/parabasal layers   |
|                      | Cytology                  | Limited pleomorphism at the lowest end of the spectrum<br>Parabasal cells may have slight increased cytoplasm compared with the adjacent cells, with enlarged nuclei and occasional dyskeratotic cells<br>Rare normal mitoses in and around the basal layer   |
| High-grade dysplasia | Architecture <sup>a</sup> | Abnormal maturation that extends up to the full thickness of the epithelium<br>Pleomorphic epithelium affecting at least half to full thickness of the epithelium<br>Keratinizing (spinous cell process) to nonkeratinizing (basal cell process)<br>Rete may be irregular, including bulbous or downward extension (but intact basement membrane)   |
|                      | Cytology <sup>a</sup>     | Pleomorphism is easily identified and sometimes profound, including marked variation in size, shape, and staining intensity<br>Dyskeratosis and apoptosis up to the whole epithelium<br>Increased nuclear-to-cytoplasmic ratio, irregular nuclear chromatin distribution (hyperchromasia), and prominent nucleoli<br>Increased mitoses at or above suprabasal level, with or without atypical forms |

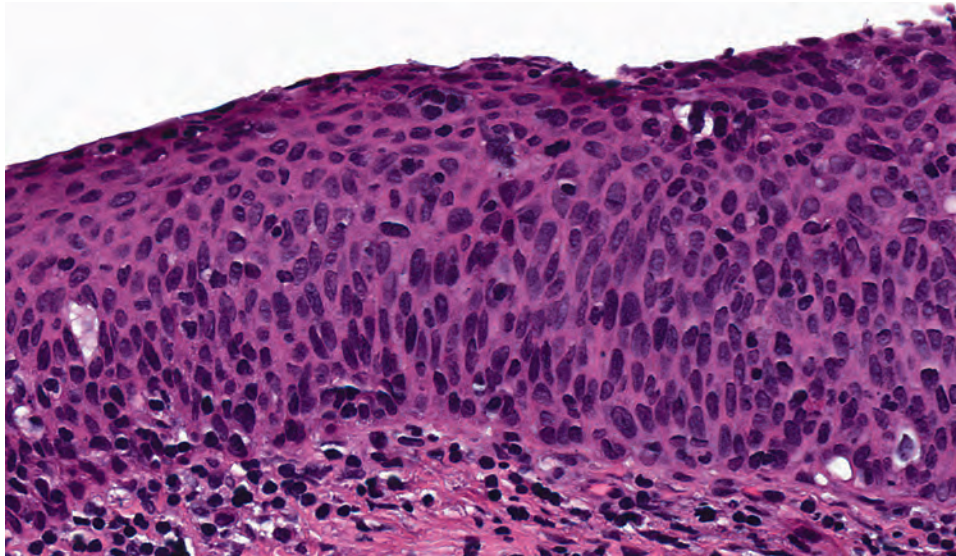
<sup>a</sup>Complete loss of polarity, profound pleomorphism and/or atypical mitoses qualifies as carcinoma in situ.

**FIGURE 6.2**  
A low-grade keratinizing dysplasia demonstrates limited disruption of the architecture and mild pleomorphism limited to the lower third of the mucosa.

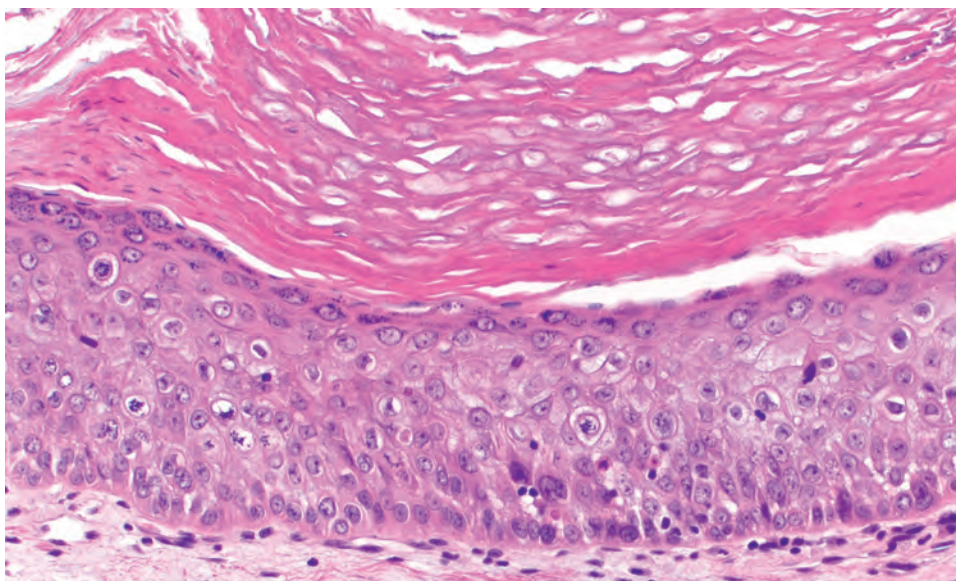


**FIGURE 6.3**  
Keratoses and a prominent granular cell layer is seen in this low-grade keratinizing dysplasia. There is loss of maturation in the lower half of the epithelium.



**FIGURE 6.4**

High-grade keratinizing dysplasia shows full-thickness replacement of the epithelium by markedly atypical cells, lacking any maturation to the surface. The basement membrane is intact.

**FIGURE 6.5**

High-grade keratinizing dysplasia with focal surface maturation. There is marked keratosis and parakeratosis as well as prominent intercellular spinous processes. Atypical mitoses are noted.

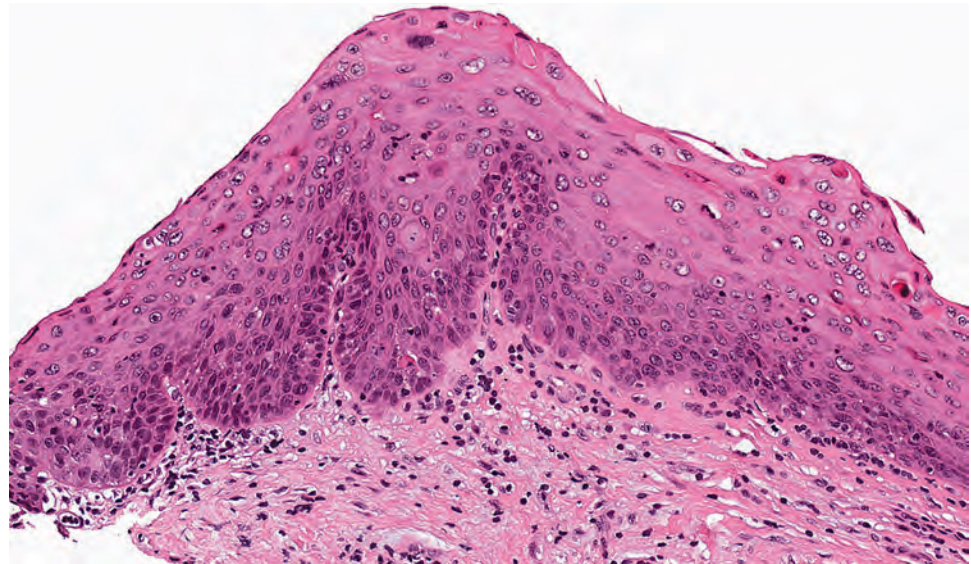
part, however, high-grade dysplasia encompasses the previous moderate and severe dysplasia and CIS. Nearly all laryngeal lesions are keratinizing dysplasia, with only isolated cases of nonkeratinizing dysplasia. An inflammatory infiltrate, occasionally intense, is common.

A commonly asked question is: How many features are necessary for the diagnosis? Here the art of pathology comes into play, with interpretation incorporating the clinical, gross, and histologic features. Other considerations include the fact that a synchronous invasive SCC is frequently present. Furthermore, invasive carcinoma may develop from a nondysplastic surface epithelium.

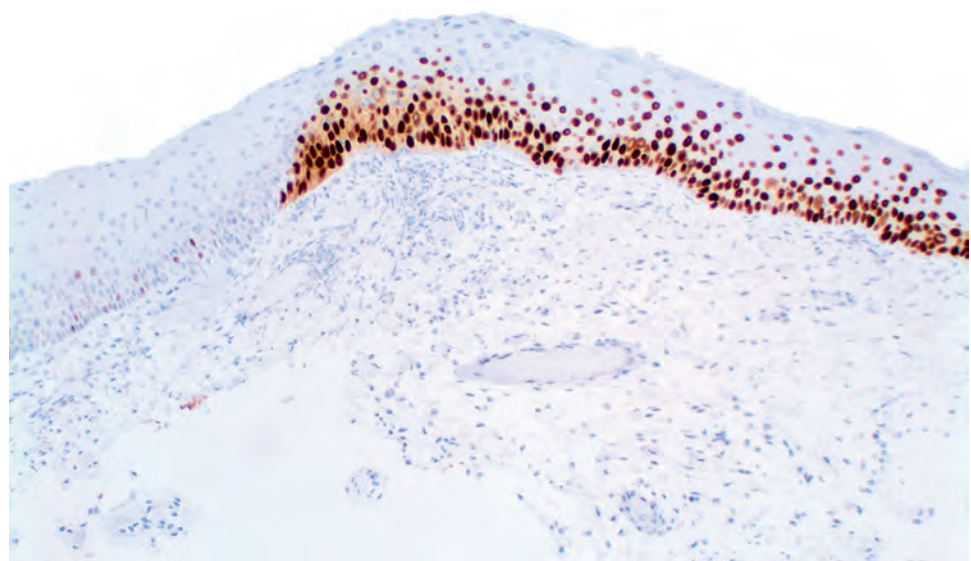
Technical factors are important to accurate diagnosis. Multiple biopsies of sufficient size from within the

diseased area are necessary to assess the full extent of the lesion. Avoiding tangential sections is paramount, which usually precludes frozen-section diagnoses. Additional deeper sections may be needed to fully demonstrate diagnostic features of dysplasia. Glandular/duct extension must not be interpreted as invasive disease. Various immunohistochemical and molecular studies have been proposed to separate hyperplasia, dysplasia, and carcinoma, including p53 (increased, [Fig. 6.7](#)), p21, p27 (decreased), cyclin D1, bcl-2, p16,  $\beta$ -catenin, EGFR, and Ki-67 (increased); but in practical application these are currently too inconsistent and have too much overlap to be clinically meaningful in an individual case.



**FIGURE 6.6**

This atypical epithelium contains dyskeratosis throughout the epithelium and pleomorphism throughout the full thickness. Previously a moderate dysplasia, this would be placed in the category of high-grade dysplasia.

**FIGURE 6.7**

A strong and nearly diffuse nuclear p53 reaction in the dysplasia epithelium may help in assessing dysplasia (note the absent staining in the normal epithelium).

## DIFFERENTIAL DIAGNOSIS

*Reactive, regenerative, reparative, or hyperplastic* squamous proliferations (e.g., in response to trauma, inflammation, irradiation, or ulceration) may manifest architectural and cytologic atypia. However, morphologic changes suggestive of the inciting event (e.g., ulceration, inflammation, hemorrhage, radiation-induced mesenchymal and/or endothelial nuclear enlargement and hyperchromasia) may be present. Infectious agents resulting in inflammatory infiltrates should be excluded with special stains or cultures. In addition, stratification and maturation is usually present and atypical mitotic figures are absent. The clinical history may also be helpful. *Transitional vocal cord epithelium* is

sometimes confused with dysplasia, but knowledge of the normal histology will help make this separation. *Basal zone hyperplasia* has a columnar arrangement to the basal cells, which maintain a vertical polarity and hyperchromatic nuclei. There is an abrupt termination of the process at the upper edge of the prickly layer with a very sharp horizontally oriented zone of transition (see laryngeal reactive lesions, Fig. 4.22). *Granular cell tumor* can cause atypical epithelial changes, most importantly PEH, which often mimics invasion but is usually limited to the extent of the granular cell tumor below. Identification of large eosinophilic cells with abundant granular cytoplasm in the stroma should confirm the diagnosis. Definitive evidence of dissociated squamous cells below the basement membrane confirms invasive SCC.

## PROGNOSIS AND THERAPY

Some precursor lesions are self-limiting and reversible, others persist, and some progress to SCC, with notable differences in incidence based on site of involvement and the presence or absence of dysplasia. Lesions that arise in the anterior commissure nearly always convert to invasive SCC, whereas other topographic sites convert only about 15 % of the time. Lesions classified as low-grade dysplasia have an approximately 2 % rate of malignant transformation, implying the need for close clinical follow-up. Patients with CIS usually require more extensive management, including close follow-up, as there is a progression rate of closer to 40 %. Treatments are not standardized but include the elimination of contributing factors, biopsy, vocal cord stripping, laser ablation, cordectomy, hemilaryngectomy and radiation, used individually or in various combinations. Recurrence or persistence may develop from gland-duct extension left behind in a stripping or ablation or as a result of persistent etiologic factors.

## ■ SQUAMOUS CELL CARCINOMA

SCC is the most common malignancy of the head and neck, accounting for more than 95 % of all laryngeal carcinomas. However, it still accounts for only about 1 % of all carcinomas, showing remarkable geographic variation between and even within countries. About 1 in 10,000 men and 1 in 100,000 women are affected. The most important risk factors are, independently and synergistically, tobacco and alcohol abuse, while susceptibility (immunologic factors and age), gastroesophageal reflux, environmental influences (including radiation), and occupational factors also play a role. Viruses (HPV, Epstein-Barr virus) are uncommonly linked to the development of laryngeal SCC. Associated genetic disorders include Lynch, Bloom, and Li-Fraumeni syndromes, among others. All of these factors interact in a multistep process.

As a malignant neoplasm characterized by squamous differentiation, SCC demonstrates infiltration into the stroma, abnormal keratinization, irregular nests of squamous epithelium, and cellular pleomorphism. Most laryngeal SCCs develop from a precursor lesion, with an arc of development, culminating in invasive SCC. But, not all dysplasias progress to invasive carcinoma.

## CLINICAL FEATURES

Men are affected much more frequently than women (M > F = 6:1), although there has been an increased incidence

## CONVENTIONAL SQUAMOUS CELL CARCINOMA—DISEASE FACT SHEET

### Definition

- A malignant epithelial neoplasm characterized by squamous differentiation

### Incidence and Location

- About 1% of all cancers, but 90% of head and neck cancers
- Marked geographic variation
- Glottic and supraglottic regions are most common

### Morbidity and Mortality

- Loss of phonation
- Up to 25% mortality (site- and stage-dependent)

### Sex and Age Distribution

- Males > females (6:1)
- 6th-7th decades; rare in children

### Clinical Features

- Tobacco and alcohol abuse
- Hoarseness, dysphagia, dysphonia, changes in phonation

### Prognosis and Treatment

- Site-, size-, and stage-specific, with ~90% 5-year survival for T1 vs. less than 50% for T4 lesions
- Glottic tumors: 80%-85%, but subglottic: 40%
- Surgery and radiation therapy

in women over recent years. All ages are affected, but patients usually present in the 6th to 7th decades of life. Patients present with symptoms referable to the anatomic site of the primary, including hoarseness, dysphagia, dysphonia, dyspnea, changes in phonation, foreign-body sensation in the throat, difficulty swallowing, and stridor.

Radiographic imaging is usually done before endoscopy, as endoscopy may decrease the sensitivity of imaging. Imaging highlights the extent of the disease, shows submucosal invasive patterns, and helps with staging (extent of disease and lymph node status). There is a high incidence of regional lymph node metastasis due to lymphovascular invasion. Endoscopy is recommended to evaluate the extent of the disease, rule out other synchronous primaries (seen in up to 10 % of patients), and obtain a biopsy.

## PATHOLOGIC FEATURES

### GROSS FINDINGS

The anatomic sites—supraglottis, glottis, and subglottis—are embryologically distinct and separately compartmentalized (Fig. 6.8), resulting in unique lymphatic drainage; consequently they have implications for



the type of surgery and oncologic management. Glottic tumors for the most part are smaller (due to early clinical presentation), whereas supraglottic tumors are often clinically silent, resulting in a much larger tumor at the time of diagnosis. Interestingly, in Europe, supraglottic tumors predominate, while glottic tumors are most common in the United States. SCCs can be ulcerative, endophytic, flat, polypoid, verrucous, or exophytic. They range from minute areas of mucosal thickened to large masses filling the luminal space, although they are usually

smaller than 2 cm. The borders are rolled, raised to irregular, and abrupt. Tumors can be erythematous to tan to white and are frequently firm.

### MICROSCOPIC FINDINGS

SCC is generally divided into two groups: superficially or deeply invasive, with additional modifiers based on histologic grade, including well differentiated (closely resembles normal squamous mucosa), moderately differentiated (distinct nuclear pleomorphism and less keratinization), or poorly differentiated (immature cells with little maturation or keratinization), along with the presence or absence of keratinization (Figs. 6.9–6.12). “Conventional” SCC is composed of a variable degree of squamous differentiation, with the neoplastic cells invading through and disrupting the basement membrane (Fig. 6.8). The overlying surface may not be atypical, yet invasion may develop from the base (Fig. 6.9). Broad infiltration may give way to small islands, irregular nests, jagged cords, or individual cells, the last correlating with a worse prognosis. SCC shows disorganized growth, a loss of polarity, dyskeratosis, keratin pearls (including paradoxical keratinization at the base), intercellular bridges, an increased N:C ratio, nuclear chromatin irregularities, prominent eosinophilic nucleoli, and increased mitoses (including atypical forms). The keratinizing type (Fig. 6.11) is seen more frequently than nonkeratinizing or poorly differentiated types, while clear cell changes may be seen. Mitoses and necrosis tend to increase as the grade of the tumor becomes more poorly differentiated (Fig. 6.12). A rich inflammatory infiltrate (usually of lymphocytes and plasma cells) is seen at the junction of tumor and stroma, along with a dense,

### CONVENTIONAL SQUAMOUS CELL CARCINOMA—PATHOLOGIC FEATURES

#### Gross Findings

- Glottic, supraglottic, subglottic, transglottic
- Flat, well defined, raised edge, polypoid, exophytic
- Surface ulceration

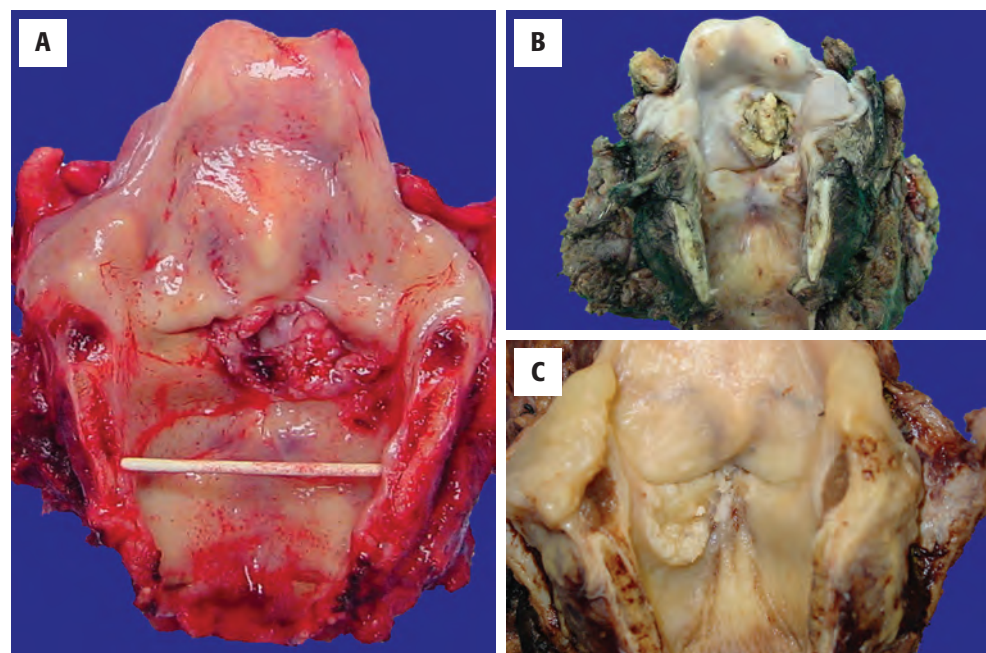
#### Microscopic Findings

- In situ, superficially or deeply invasive
- Well, moderately, or poorly differentiated
- Keratinizing or nonkeratinizing
- Disorganized growth, lack of maturation, dyskeratosis, keratin pearl formation, intercellular bridges, increased N:C ratio, irregularities in nuclear chromatin distribution, prominent nucleoli, increased mitotic figures, atypical mitotic figures
- Inflammatory infiltrate and stromal desmoplasia

#### Pathologic Differential Diagnosis

- Hyperplasia, dysplasia, radiation changes, necrotizing sialometaplasia, squamous papilloma, variants of SCC

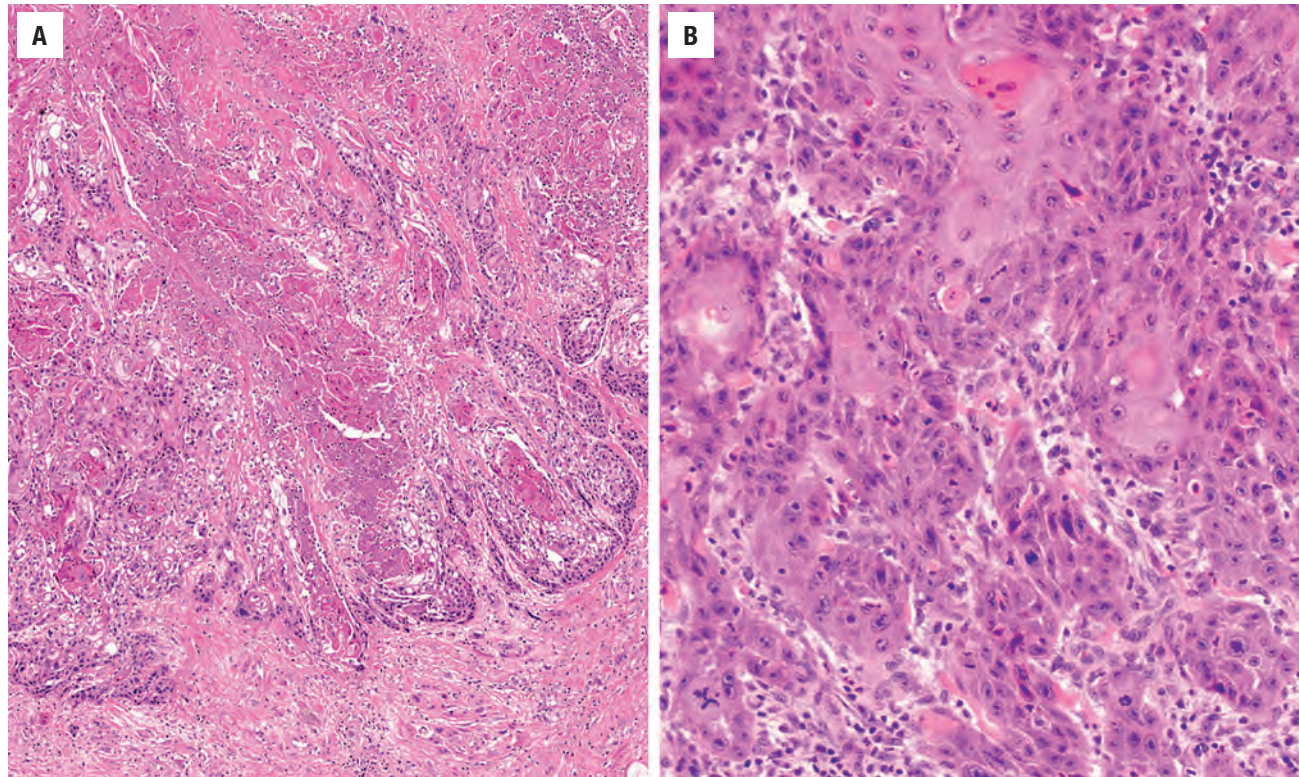
SCC, Squamous cell carcinoma.



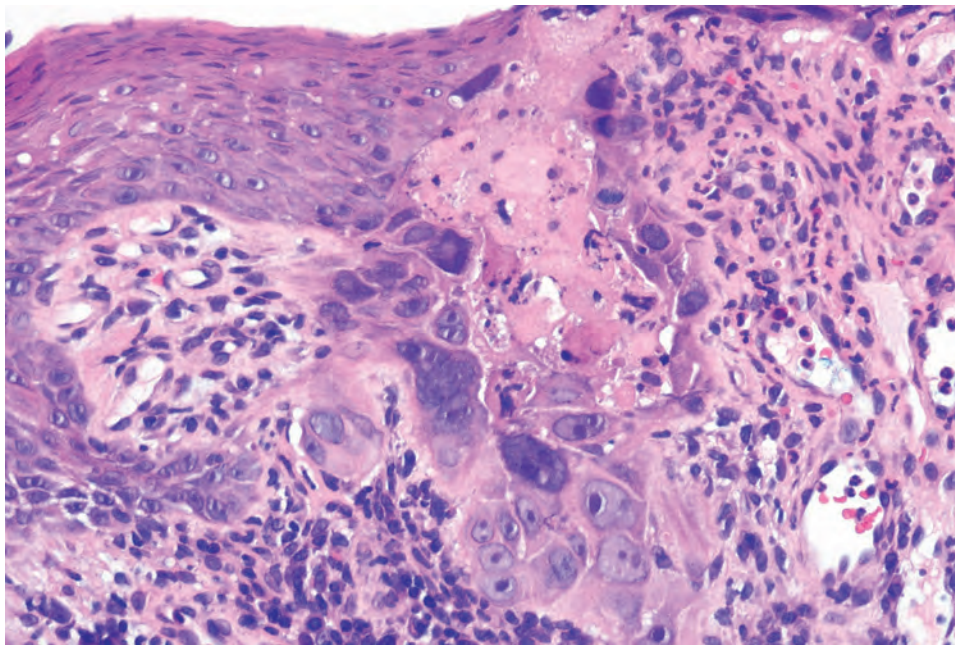
**FIGURE 6.8**

Laryngectomy specimens showing the various locations of tumor: transglottic (A), supraglottic (B), and subglottic (C). (Courtesy of J. Fowler.)



**FIGURE 6.9**

Squamous cell carcinoma (SCC) with uneven, finger-like infiltration of the SCCs into the underlying stroma. A desmoplastic stroma is noted (**A**). There is moderate nuclear pleomorphism and cellular disarray (**B**).

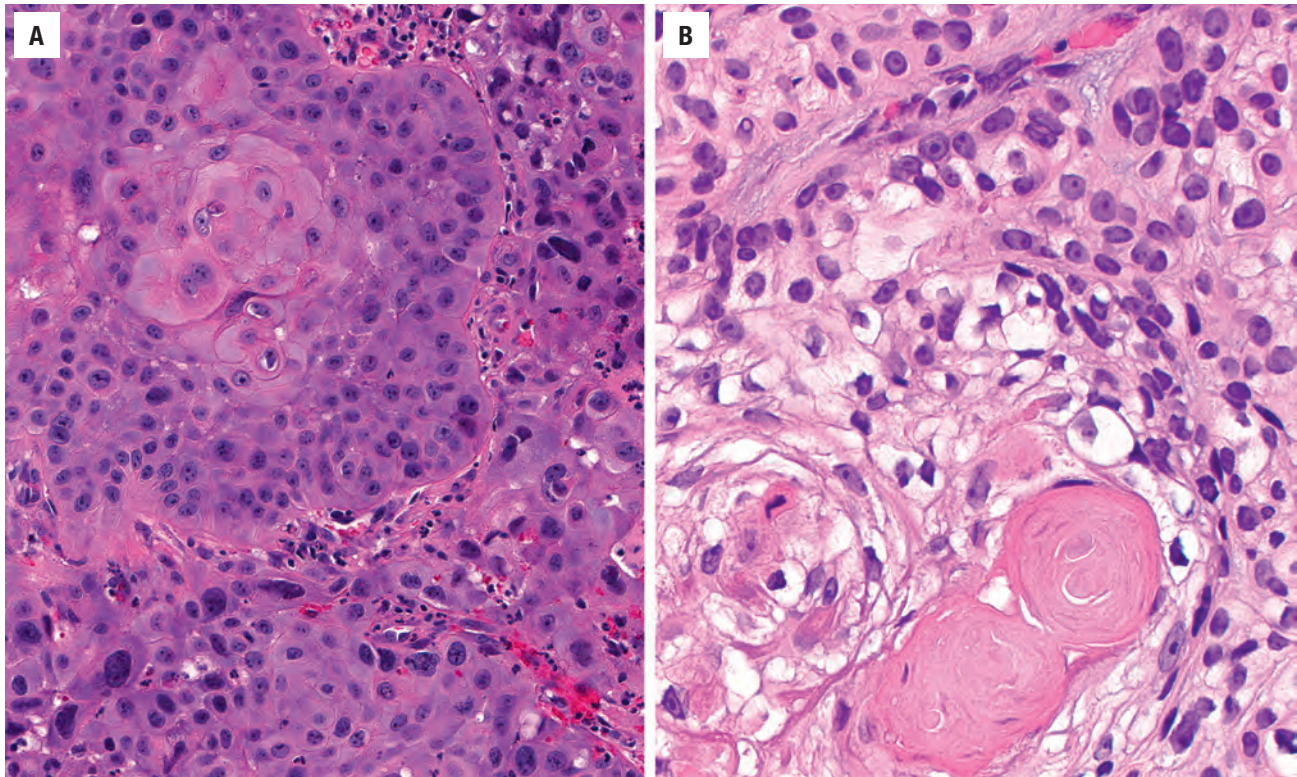
**FIGURE 6.10**

A well-differentiated squamous cell carcinoma is noted arising from an unremarkable surface epithelium, underscoring the necessity for a biopsy of adequate size and depth.

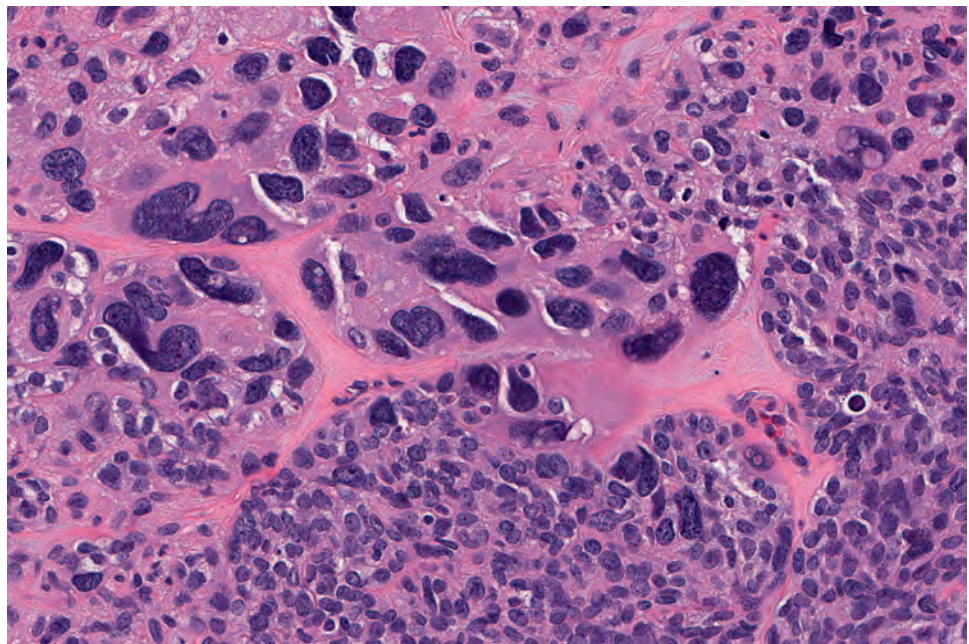
desmoplastic fibrous stroma. Perineural and lymphovascular invasion may be seen, the latter specifically correlated to metastatic potential. Tumors may directly extend into cartilage (Fig. 6.13), adjacent structures, or organs. Margins are often difficult to assess, as shrinkage

(up to 50%) may be seen after removal, and there may also be differences between frozen versus permanent sections. Special studies are rarely needed to document the epithelial nature of the tumor, although specific keratin subtypes may relate to histologic grade, degree of



**FIGURE 6.11**

(A) A moderately differentiated squamous cell carcinoma with loss of polarity, disorganization, increased nuclear-to-cytoplasmic ratio, and areas of keratinization. (B) There is clearing of the cytoplasm in many of the cells, but keratinization is still noted.

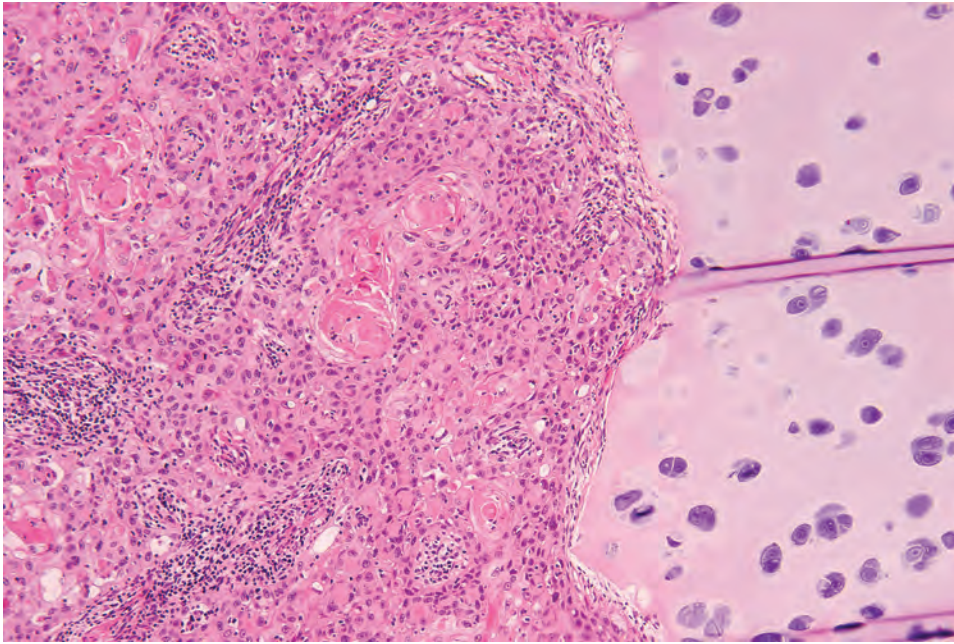
**FIGURE 6.12**

A poorly differentiated squamous cell carcinoma is arranged in a sheet-like distribution with only occasional cells showing dyskeratosis.

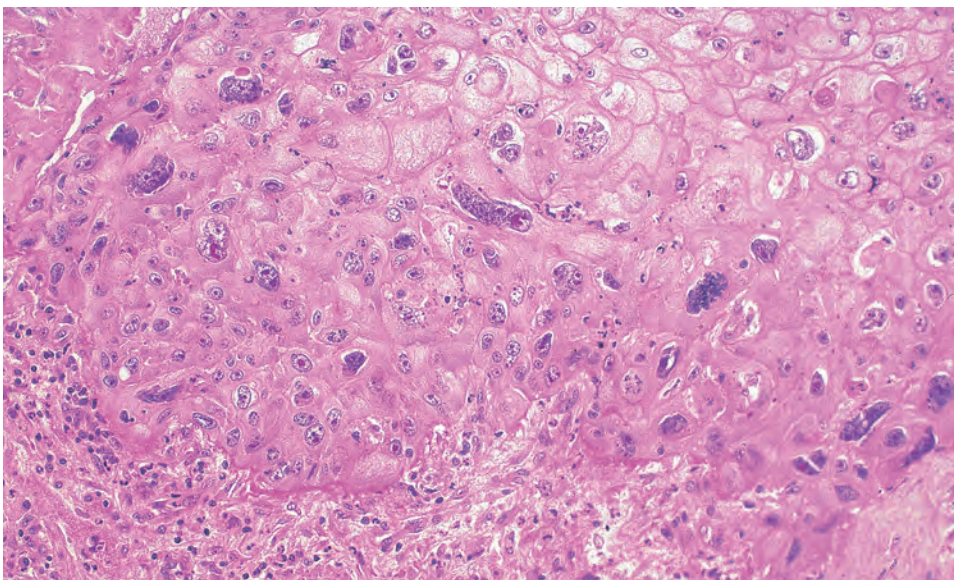
keratinization, and likelihood of metastasis. p53 mutations are an early event in carcinogenesis and may therefore help in separating benign from malignant lesions. Tumor site, size, histology (poorly differentiated), degree of invasion, positive surgical margins of resection, lymph

node metastasis (especially when there is extranodal extension), and multifocal disease all correlate with a poorer prognosis. Separation of residual carcinoma from radiation changes in the postradiation sample may be difficult. Although cellular enlargement is common,



**FIGURE 6.13**

A moderately differentiated squamous cell carcinoma approaches but does not invade the perichondrium of the laryngeal cartilage. Inflammation is noted.

**FIGURE 6.14**

Radiation can induce changes in residual carcinoma, resulting in bizarre cells and nuclei, but the cells do not appear degenerated nor do they have a low nuclear-to-cytoplasmic ratio. Nucleoli are frequently obvious in a squamous cell carcinoma after radiation therapy.

radiation usually does not change the N:C ratio, as carcinoma does (Fig. 6.14).

### DIFFERENTIAL DIAGNOSIS

The diagnosis of SCC is usually clear-cut, although occasionally other lesions—such as hyperplasia, dysplasia, radiation changes, necrotizing sialometaplasia, squamous papilloma, and the variants of SCC—are included in the differential diagnosis. Marked PEH may be mistaken for SCC. However, the reactive nature of the proliferation, lack of “finger-like” invasion, and the association with

infectious agents and granular cell tumor will help to make this distinction. Radiation changes may affect the epithelium, endothelial cells, and stroma. Glands may become atrophic. There is often profound nuclear pleomorphism; however, these cells maintain a very low N:C ratio (Fig. 6.14). Necrotizing sialometaplasia has a preserved lobular architecture despite the degree of cytologic atypia (see Nonneoplastic Larynx chapter, Figs. 4.30–4.32). A biopsy of sufficient size is necessary to secure this diagnosis. A squamous papilloma does not have disorganized growth and unequivocal morphologic features of malignancy. SCC should be separated from SCC variants (discussed further on), as there is often a difference in management and prognosis.



## PROGNOSIS AND THERAPY

Prognosis is heavily influenced by anatomic site, tumor stage, and age, while differentiation, invasive pattern, lymphovascular invasion, perineural invasion, margin status, and extranodal extension also contribute to outcome. The TNM tumor classification correlates closely with both disease-free and overall survival. Overall, 5-year survival rates approach 90 % for T1 lesions, whereas they are less than 50 % for T4 tumors. Glottic tumors have an 80 % to 85 % survival, while subglottic tumors are at about 40 %, with an intermediate 65 % to 75 % for supraglottic tumors. Regional lymph node metastases are relatively common; extracapsular extension is associated with a worse prognosis. A number of prognostic factors are available (*EGFR*, *CCND1*, *CDK4*, *CDKN2A*), although not yet commonly employed. Larynx function-preserving treatment is the goal, with negative resection margins (3 to 5 mm). Laser excision, limited resection, and radical resection along with radiation therapy are variably employed to achieve the best potentially curative voice-sparing outcome. There is a movement toward noninvasive management. Occasionally neoadjuvant chemotherapy and radiation therapy are used to maintain laryngeal function. However, if these modalities fail, delayed, salvage, partial or total laryngectomy can still achieve a good patient outcome.

## VARIANTS OF SQUAMOUS CELL CARCINOMA

Variants make up in aggregate about 4 % of all SCCs and include among others verrucous, exophytic or papillary, spindle cell, basaloid, and adenosquamous carcinomas (ASCs; Table 6.2). Rather than give an exhaustive review, only the unique features of each variant are presented here.

### VERRUCOUS SQUAMOUS CELL CARCINOMA

Verrucous SCC (VSCC; Ackerman tumor) comprises about 3 % of all SCCs, and is related to tobacco smoking, with no significant association with HPV. It is usually affects the anterior true vocal cords and measures up to 10 cm.

VSCC is a highly differentiated type of SCC that lacks cytologic features of malignancy, grows slowly, and is locally aggressive but does not usually metastasize. It is composed of an exophytic warty tumor (Fig. 6.15) with multiple filiform projections, which are thickened, club-shaped, and lined by well-differentiated squamous epithelium (Fig. 6.16). The advancing margins of the tumor are usually broad or bulbous rete ridges with a blunt, pushing rather than infiltrative appearance, occasionally showing coalescing rete (Fig. 6.17). The downward-dipping epithelium may create a “cup” or “arms” around the periphery of the

### VERRUCOUS SQUAMOUS CELL CARCINOMA

#### Definition

- Well-differentiated exophytic/verrucous growth with a pushing border of infiltration in a cytologically bland, amitotic squamous epithelium

#### Prognosis and Treatment

- 85%-95% 5-year survival (20% recurrence/persistence)
- Surgery alone; radiation employed for nonsurgical candidates

#### Gross Findings

- Broad-based, warty, exophytic, fungating mass

#### Microscopic Findings

- Broad border of pushing infiltration
- Multiple projections of well-differentiated squamous epithelium with club-shaped to filiform projections
- Maturation toward surface
- Abundant keratosis (ortho- and parakeratosis; “church spire” keratosis), parakeratotic crypting
- Limited mitotic figures, if present at all (limited to basal zone)

#### Pathologic Differential Diagnosis

- Verrucous hyperplasia, squamous papilloma, papillary/exophytic SCC, conventional SCC

SCC, Squamous cell carcinoma.

tumor, which is noted below the level of the adjacent normal basal cell layer. There is often a dense inflammatory response in the subjacent tissues, but desmoplasia is usually absent. The epithelium is extraordinarily well differentiated without any of the normally associated malignant criteria identified in SCC. The cells are arranged in an orderly maturation toward the surface, with abundant surface keratosis (parakeratosis and/or orthokeratosis; “church spire” keratosis; Fig. 6.18). Parakeratotic crypting (collections of parakeratotic cells with debris) is a common feature. Mitotic figures are not easy to identify; when found, they are not atypical (Fig. 6.19). If dysplasia is present, it is focal and limited to the basal zone. A foreign-body giant cell reaction may develop to extravasated keratin. Overexpression of p53 is seen in about 40 % of cases. A benign keratinizing hyperplasia (verrucous hyperplasia), squamous papilloma, and a very well differentiated SCC can share all of these features somewhere in the tumor, making separation of these lesions a most vexing problem. The relationship of the lesion to the stroma *must* be adequately assessed in a sample of sufficient size that has been accurately oriented (not tangential) before a definitive diagnosis can be rendered.

The major differential diagnosis rests between verrucous hyperplasia and conventional SCC. It is argued that the difference between verrucous hyperplasia and VSCC is only in stage and size, the lesions representing a developmental spectrum. The distinction on histologic

**TABLE 6.2**  
**Clinical and histologic features of squamous cell carcinoma variants**

| Feature                | Variant   |   |   |  |  |
|------------------------|---|---|---|--|--|
|                        | <i>Verrucous</i>  | <i>Papillary/Exophytic</i>  | <i>Spindle Cell (Sarcomatoid)</i>   | <i>Basaloid</i>  | <i>Adenosquamous</i>   |
| Sex                    | M > F, except oral  | M > > F   | M > > > F   | M > > F  | M slight > F   |
| Location               | Oral > larynx   | Larynx > mouth > nose   | Larynx > mouth > nose   | Base of tongue > supraglottic larynx   | Tongue > floor of mouth > nose   |
| Frequency (of all SCC) | ~ 3%  | ~ 1%  | ~ 3%  | < 1%   | < 1%   |
| Etiologic agent?       | HPV   | ? HPV   | ? Radiation   | Unknown  | Unknown  |
| Macroscopic            | Broad, based warty and fungating mass   | Polypoid, exophytic, bulky, papillary, fungiform  | Polypoid mass   | Firm to hard with central necrosis   | Indurated submucosal nodule  |
| Size (cm)              | Up to 10  | 1-1.5 (mean)  | 2 (mean)  | Up to 6  | 1 (mean)   |
| Microscopic            | Pushing border of infiltration; abrupt transition with normal; large, blunt club-shaped rete pegs; no pleomorphism; limited mitotic activity; abundant keratin, including parakeratin crypting and "church spire" keratosis | >70% exophytic or papillary architecture; "cauliflower-like" vs. "celery-like;" unequivocal cytomorphologic malignancy; surface keratinization; invasive, but difficult to demonstrate; koilocytic atypia | Biphasic: SCC present but ulcerated, blended/ transition with atypical spindle cell population; hypercellular; variable patterns of spindle cell growth; pleomorphism; opacified cytoplasm; increased mitotic figures | Biphasic: invasive, lobular, basaloid component most prominent; palisaded; high N:C ratio; abrupt squamous differentiation (metaplasia, dysplasia, CIS or invasive); ↑ mitotic figures; comedonecrosis; hyaline material | Biphasic: SCC and adenocarcinoma, undifferentiated component, separate or intermixed with areas of transition; infiltrative; ↑ mitotic figures; sparse inflammatory infiltrate |
| Special studies        | HPV identified  | None  | ~70% + with epithelial markers  | Keratin, EMA, CK7, and K903  | Mucin-positive   |
| Differential diagnosis | Verrucous hyperplasia, SCC  | In situ SCC, squamous papilloma, reactive hyperplasia   | Benign and malignant mesenchymal process, melanoma, synovial sarcoma  | Adenoid cystic carcinoma, neuroendocrine carcinoma (small cell carcinoma)  | BSCC, mucoepidermoid carcinoma, adenocarcinoma with squamous metaplasia  |
| Treatment              | Surgery   | Surgery and/or radiation  | Surgery with radiation  | Surgery, radiation, chemotherapy   | Surgery with neck dissection   |
| Prognosis              | 75% 5-year survival   | ~ 70% 5-year survival   | ~ 70% 5-year survival   | ~ 40% 2-year survival  | ~ 55% 2-year survival  |
| Pitfalls               | Inadequate biopsy, tangential sectioning, radiation is acceptable   | Orientation, adequacy of specimen   | No surface, mesenchymal markers, needs "excisional" biopsy initially  | Association with second primary, high chance of nodal metastases   | Separation on small biopsies from adenocarcinoma or SCC  |

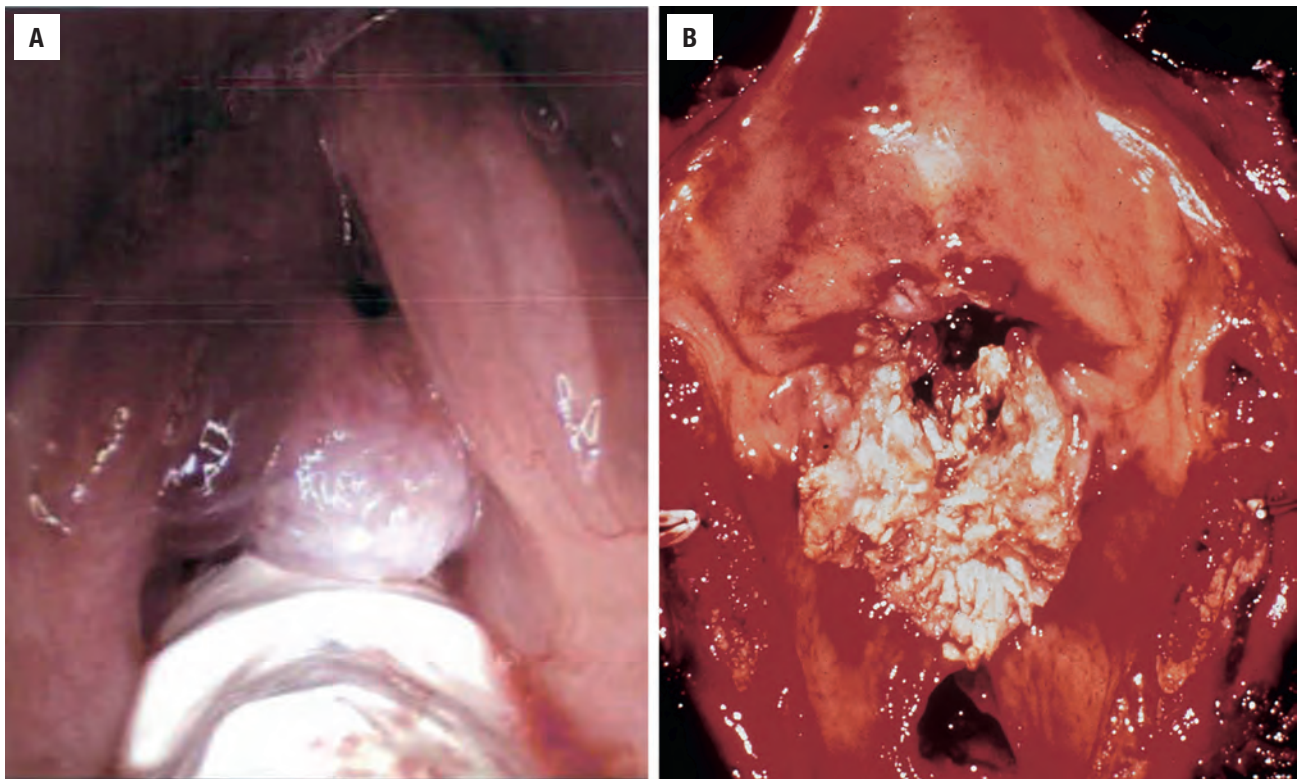
BSCC, Basaloid squamous cell carcinoma; CIS, carcinoma in situ; HPV, human papillomavirus; SCC, squamous cell carcinoma.

features alone is often impossible. True verrucous hyperplasia must be diagnosed only on a large sampling, with caution to avoid underinterpreting the extent of the lesion (Fig. 6.20). A papillary or exophytic SCC (ESCC) has pleomorphism and increased mitoses, showing lack of maturation toward the surface. VSCC can include an invasive component of "ordinary" SCC at the base or demonstrate atypical cytologic features; these are hybrid carcinomas and are managed as well-differentiated SCC.

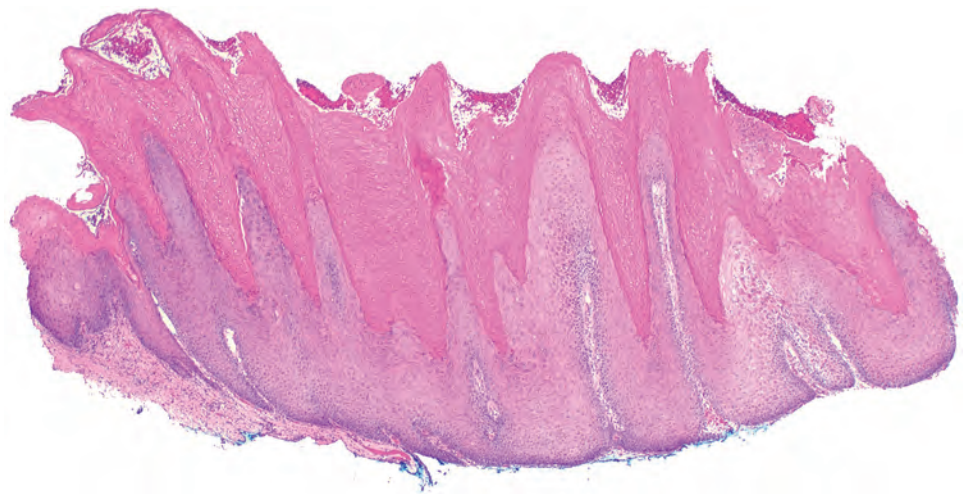
Squamous papilloma has thin, well-formed papillae, limited keratinization, and koilocytic atypia.

Biologically, VSCC behaves as an "extremely well differentiated squamous cell carcinoma," with an ~85 % to 95 % 5-year survival depending upon site and stage. Most tumors are pT1 at presentation without lymph node metastases. Persistence/recurrence is seen in up to 20 % of patients, usually as a function of the type of treatment. Voice-preservation techniques are encouraged,



**FIGURE 6.15**

(A) Laryngoscopy shows a large verruciform mass projecting into the lumen. (B) Multiple projections are seen in this macroscopic view of a large transglottic verrucous carcinoma.

**FIGURE 6.16**

The broad, pushing border of infiltration is noted below the adjacent uninvolved epithelium (far left). Keratosis and parakeratosis are noted in verrucous carcinoma.

with surgery alone the mainstay of therapy. Radiation is sometimes used for functional preservation in nonsurgical candidates.

### EXOPHYTIC AND PAPILLARY SQUAMOUS CELL CARCINOMA

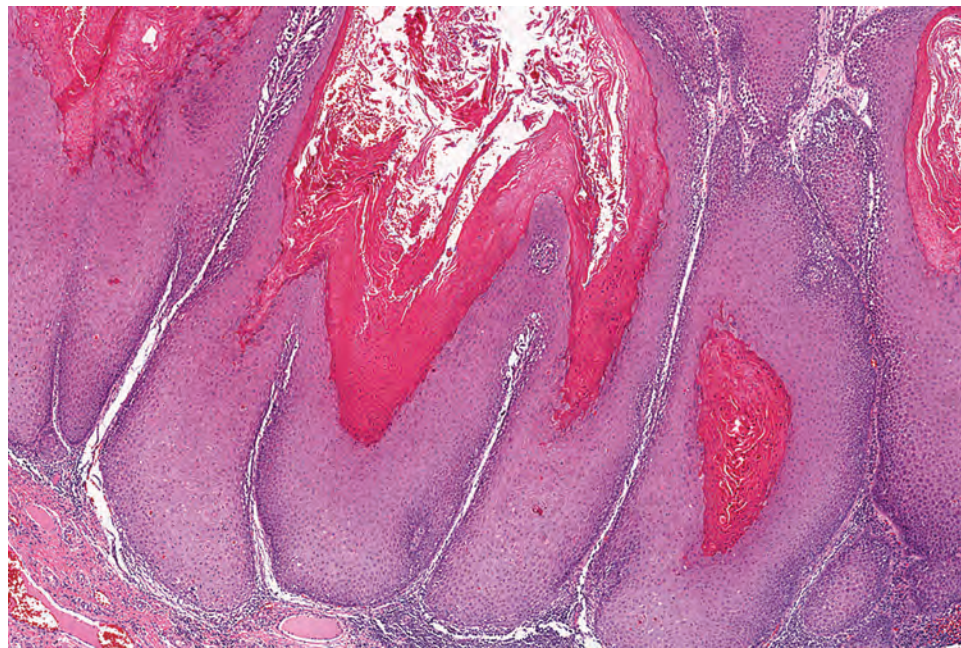
Exophytic squamous cell carcinoma (ESCC) and papillary squamous cell carcinoma (PSCC) are uncommon but distinct

variants of SCC, separable from VSCC (as outlined earlier). By definition, ESCC and PSCC are *de novo* malignancies without a pre- or coexisting benign lesion (i.e., squamous papilloma). High-risk HPV is a suggested etiology in up to 20 % of cases. The average size of exophytic and papillary tumors is between 1 and 1.5 cm. Most tumors present at a low tumor stage (T1 or T2), although multifocality is described. Tumors are seen in the supraglottis much more often than in the glottis or subglottis. Macroscopically, ESCC and PSCC are polypoid, exophytic, bulky, papillary,

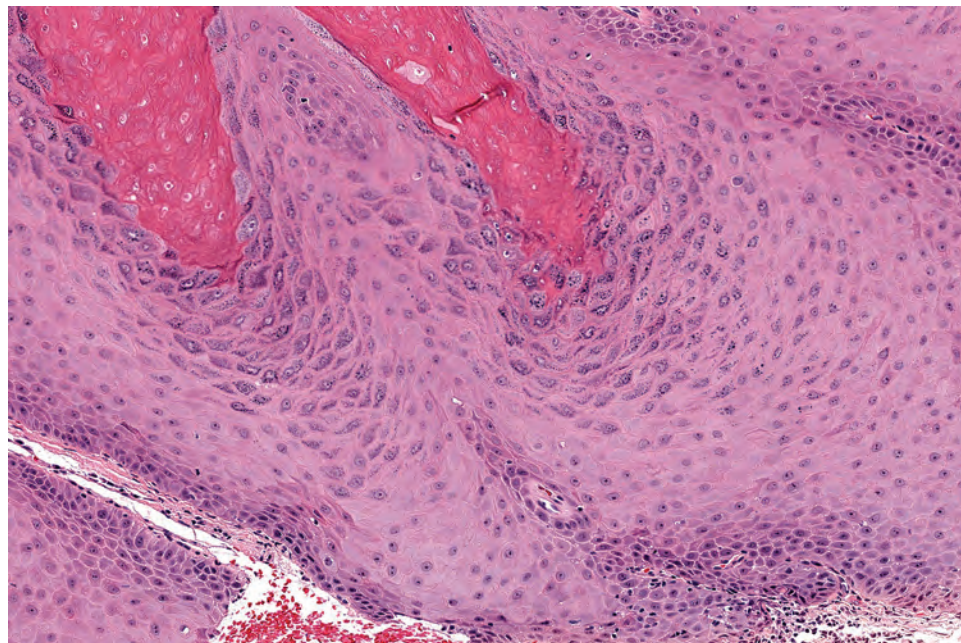


**FIGURE 6.17**

The size of the lesion is often a helpful indicator in verrucous carcinoma. Seen here is a broad, pushing border of infiltration with extensive "church spire" keratosis and parakeratotic crypting.

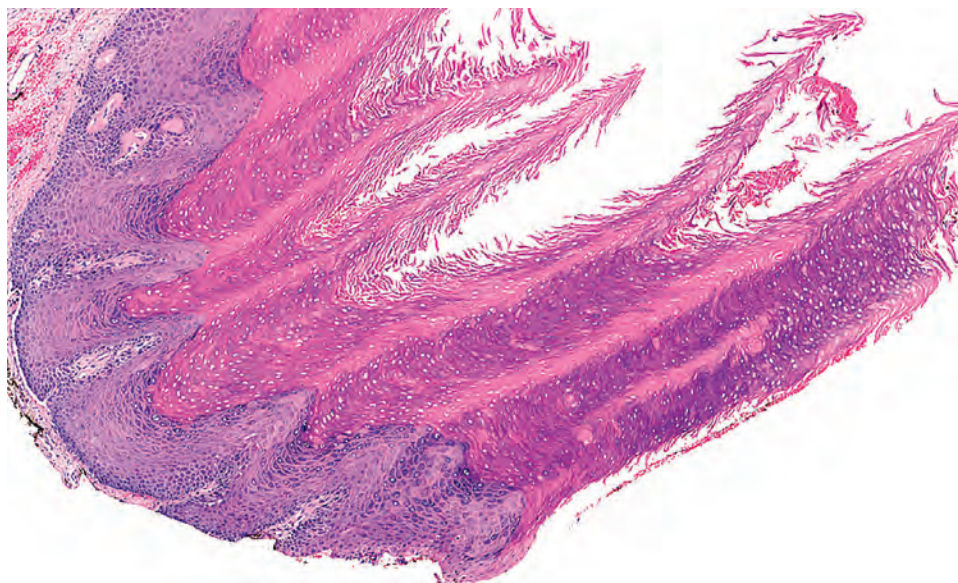
**FIGURE 6.18**

The proliferation in verrucous carcinoma is cytologically bland; it shows maturation and appropriate polarity, demonstrating a broad, bulbous type of infiltration into the stroma with associated inflammation.

**FIGURE 6.19**

The epithelium of this verrucous carcinoma lacks pleomorphism and has inconspicuous mitoses. Keratosis is noted, with a prominent granular cell layer.



**FIGURE 6.20**

Verrucous hyperplasia with fronds of squamous epithelium covered with keratin and lacking architectural and cytologic features of malignancy. The separation of verrucous hyperplasia from verrucous carcinoma is often difficult, demanding clinical correlation.

### EXOPHYTIC AND PAPILLARY SQUAMOUS CELL CARCINOMA

#### Definition

- Exophytic or papillary architecture in a SCC

#### Prognosis and Treatment

- Recurrences in about 35%
- Better prognosis than conventional SCC (site- and stage-dependent)

#### Gross Findings

- Mean of 1–1.5 cm
- Polypoid, exophytic, bulky, papillary, or fungiform

#### Microscopic Findings

- Greater than 70% exophytic or papillary architecture
- **Exophytic:** broad-based, bulbous, rounded “cauliflower-like” growth
- **Papillary:** multiple thin, delicate, filiform, finger-like projections
- Both types have malignant cytologic features
- Stromal invasion is difficult to identify

#### Pathologic Differential Diagnosis

- Squamous papilloma, SCC in situ, reactive epithelial hyperplasia, VSCC

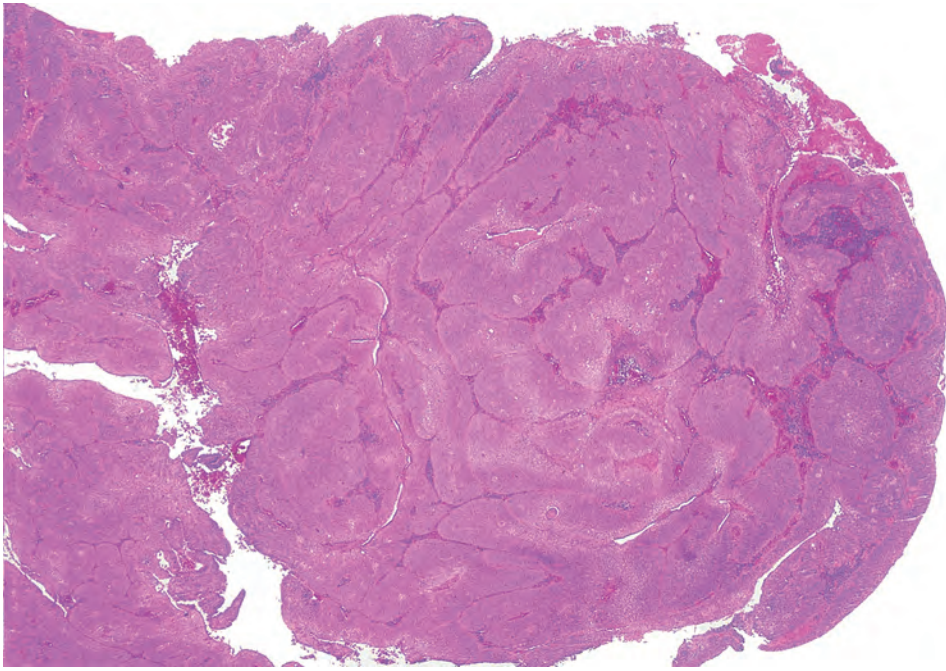
SCC, Squamous cell carcinoma; VSCC, verrucous SCC.

an immature phenotype. The exophytic pattern consists of a broad-based, bulbous to exophytic growth of the squamous epithelium (Fig. 6.21). The projections are rounded and “cauliflower-like” in growth pattern. Tangential sectioning yields a number of central fibrovascular cores, but the superficial aspect is lobular, not papillary. The papillary pattern consists of multiple, thin, delicate, filiform, finger-like papillary projections (Fig. 6.22). The papillae contain a delicate fibrovascular core surrounded by the neoplastic epithelium (Fig. 6.23). Tangential sectioning yields a number of central fibrovascular cores but appears more like a bunch of celery cut across the stalk. It is not uncommon to have extensive overlap between these patterns. When that is the case, ESCC should be the default diagnosis. Both types have the features SCC already described (Fig. 6.24). Koilocytic atypia may be noted in a few cases. Necrosis may be seen. Invasion may be difficult to define, especially in superficial biopsies. However, the significant proliferation of this carcinomatous epithelium, often forming a large clinical lesion, is rather beyond the general concept of carcinoma in situ; thus all are considered invasive by definition. When there is doubt, the significantly proliferated appearance of the lesion should be heavily weighted in the direction of carcinoma. The cytomorphologic features of malignancy would exclude the diagnosis of a papilloma as well as the consideration of a verrucous carcinoma.

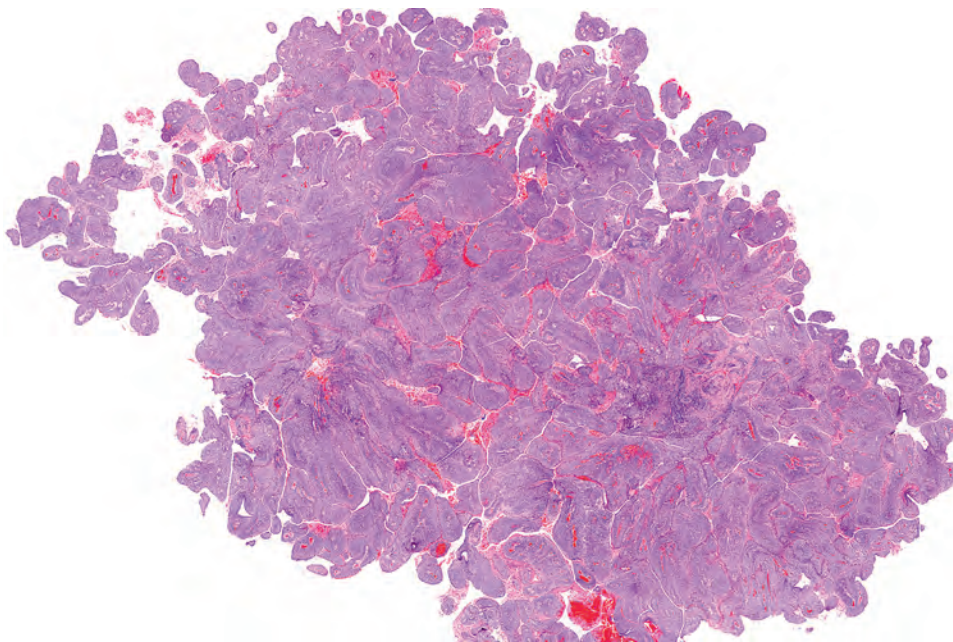
Approximately one-third of patients develop recurrence, frequently more than once. However, patients with ESCC and PSCC have a better prognosis as compared with site- and stage-matched conventional SCC patients, with PSCC behaving better than ESCC. Lymph node metastases are uncommon, and most patients present at a low stage. Radiation is used after surgery in most patients.

or fungiform tumors, soft to firm, arising from a broad base or from a narrow pedicle/stalk.

By definition, the neoplastic squamous epithelial proliferation must demonstrate a dominant (>70%) exophytic or papillary architectural growth pattern with unequivocal cytomorphologic evidence of malignancy. Cytologically, there is nuclear enlargement, pleomorphism, loss of polarity, limited surface keratosis, and

**FIGURE 6.21**

An exophytic squamous cell carcinoma with a rounded “cauliflower-like” appearance to the projections.

**FIGURE 6.22**

A papillary squamous cell carcinoma demonstrates multiple, complex papillary projections, well beyond any reactive proliferation.

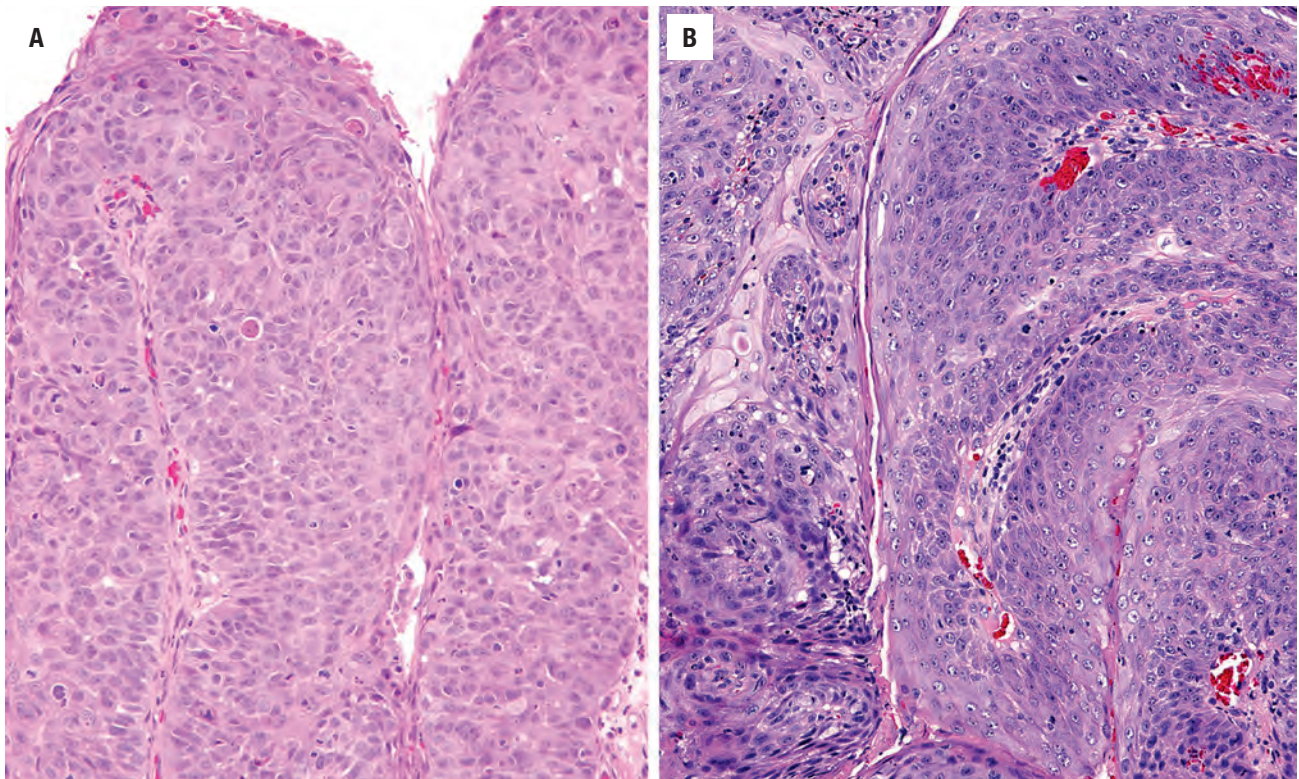
### SPINDLE CELL SQUAMOUS CELL CARCINOMA

Spindle cell SCC (SCSCC; Lane tumor) is a morphologically biphasic neoplasm containing an epithelioid and underlying spindle and/or pleomorphic proliferation. There is a profound male-to-female ratio (12:1). The majority (70%) are glottic tumors (Fig. 6.25). Nearly all cases are described as *polypoid* masses with a mean size

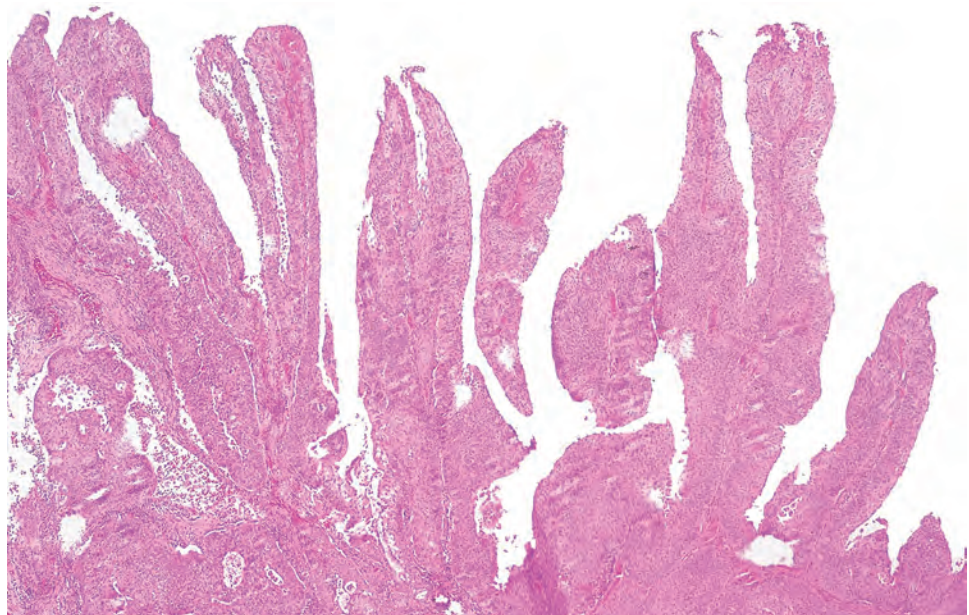
of about 2.0 cm. They are frequently ulcerated, with a covering of fibrinoid necrosis. They have a firm, fibrous cut surface.

Considering the frequency of surface ulceration with fibrinoid necrosis (Figs. 6.26 and 6.27), it may be difficult to discern the transition between the surface epithelium and the spindle cell element. In fact, the carcinomatous and sarcomatoid components will abut directly against



**FIGURE 6.24**

(A and B) Papillary squamous cell carcinoma. The papillary projections have thin fibrovascular cores and remarkably cytologically atypical epithelium lining the papillary projections. Dyskeratosis and jumbled architecture are prominent, with increased mitoses.

**FIGURE 6.23**

A papillary squamous cell carcinoma with individual, delicate finger-like projections with fibrovascular cores.



**SPINDLE CELL SQUAMOUS CELL CARCINOMA****Definition**

- Morphologically biphasic tumor with squamous cell and malignant spindle cell component with a mesenchymal appearance but an epithelial origin

**Prognosis and Treatment**

- 80% 5-year survival, with most patients having a low stage
- Surgery and radiation

**Gross Findings**

- Polypoid mass arising from true vocal cord
- Ulcerated surface and firm cut surface
- Usually <2 cm

**Microscopic Findings**

- Surface ulceration with fibrinoid necrosis
- Dysplasia, CIS, or infiltrating SCC

CIS, Carcinoma in situ; SCC, squamous cell carcinoma.

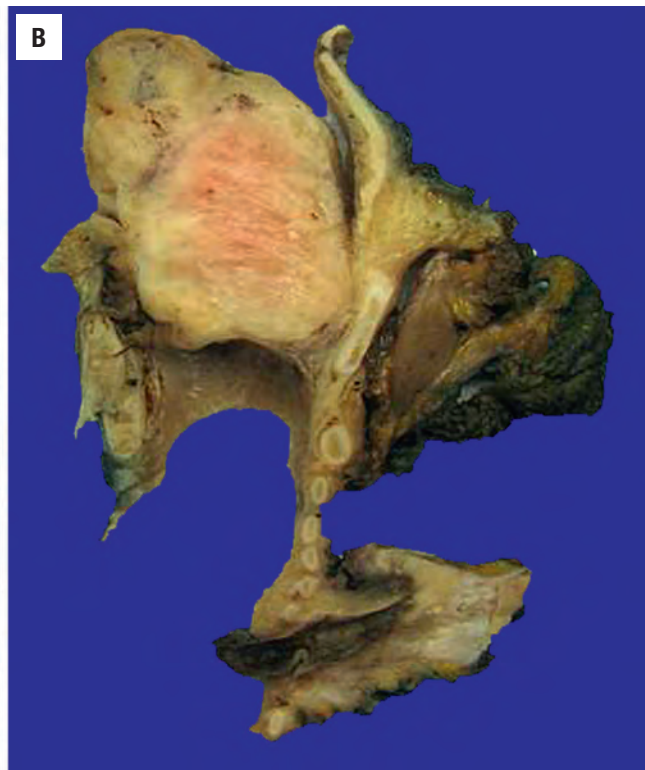
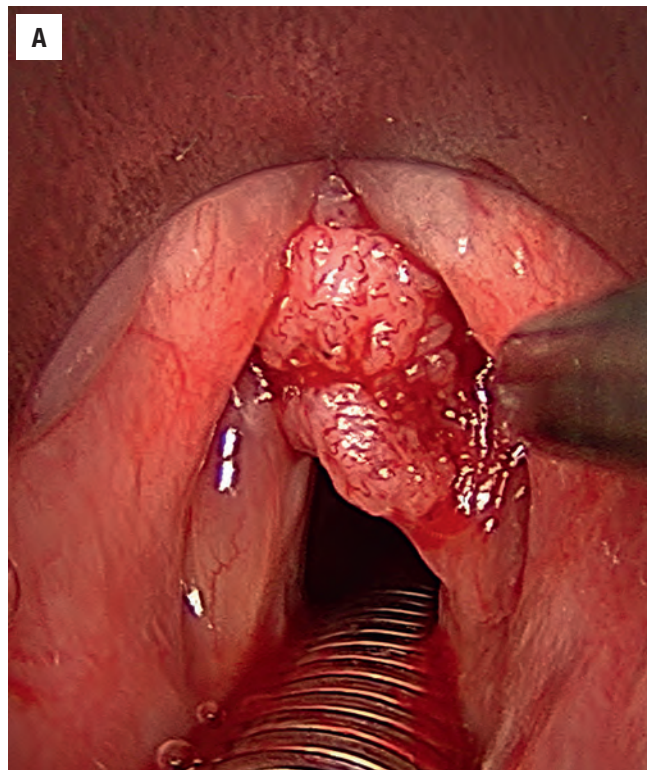
- Imperceptible blending of carcinoma with spindle cell population
- Storiform, interlacing fascicles or herringbone pattern
- Hypercellular, but also hypocellular with collagen
- Mitotic figures easily identified
- Rarely, heterologous elements may be present

**Immunohistochemical Findings**

- Pancytokeratin, EMA, CK18, p63, and p40 in epithelioid and spindle cell populations (~70% of cases)

**Pathologic Differential Diagnosis**

- Contact ulcer, inflammatory myofibroblastic tumor, synovial sarcoma, spindle cell melanoma, leiomyosarcoma

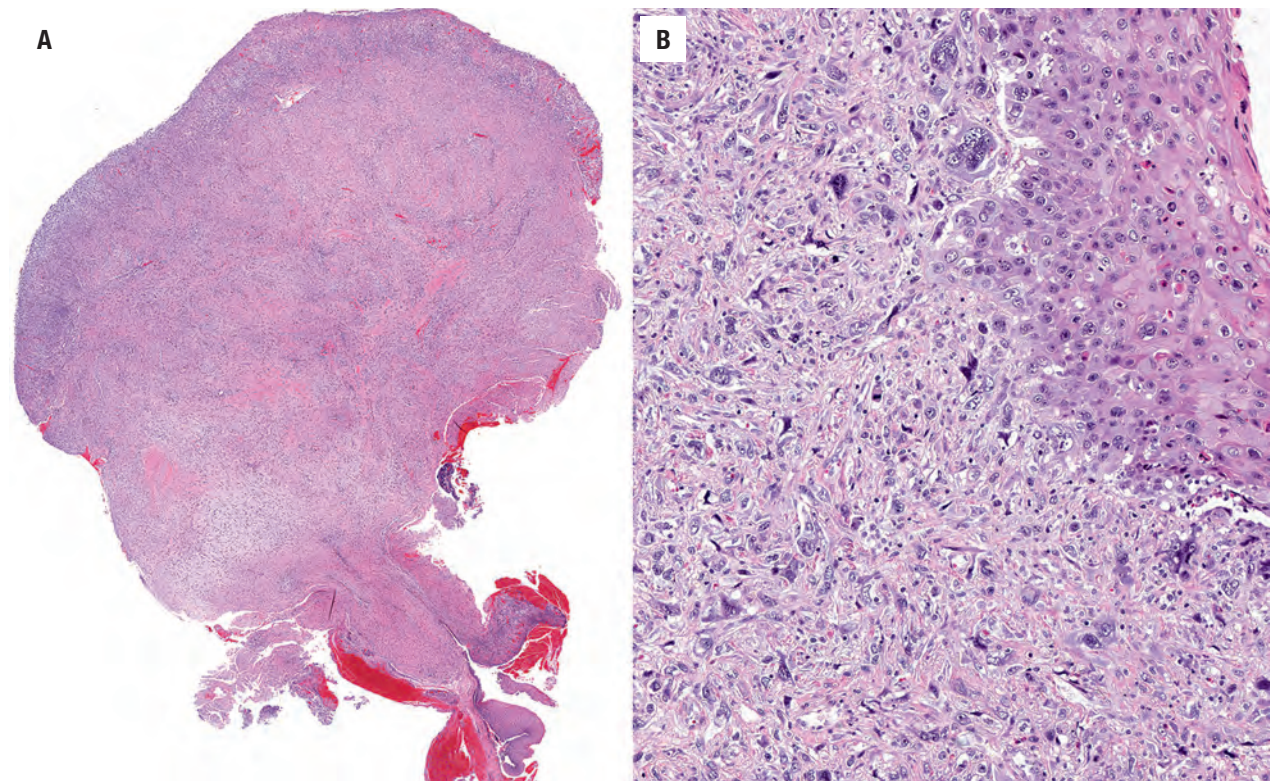
**FIGURE 6.25**

(A) A polypoid mass projects into the lumen of the larynx in this spindle cell squamous cell carcinoma. (B) This laryngectomy specimen shows a polypoid tumor with a narrow stalk of attachment.

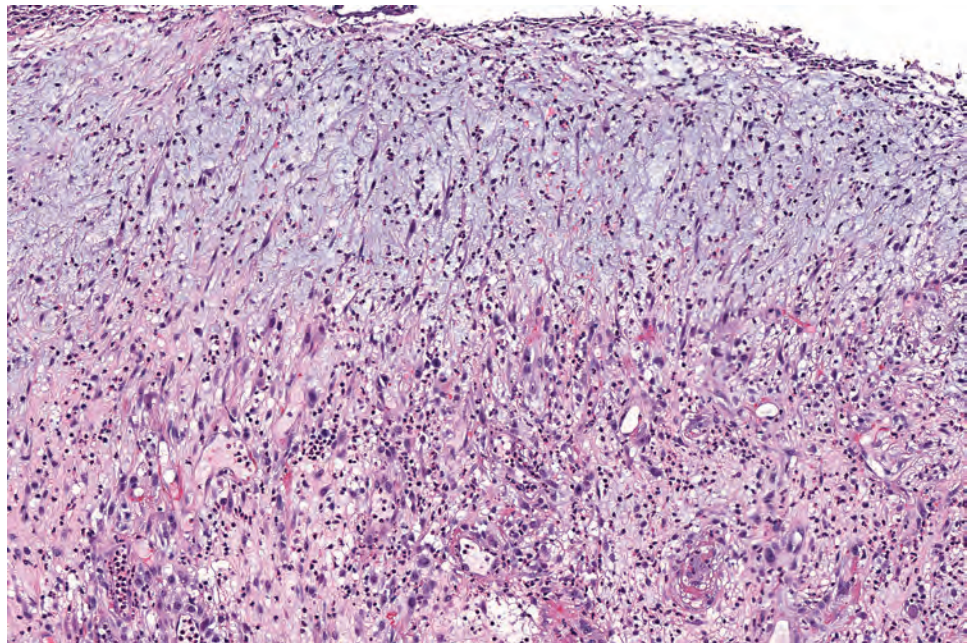
one another with imperceptible blending and continuity between them (Figs. 6.26–6.30). However, if meticulously and diligently sought, dysplasia, carcinoma in situ, or infiltrating SCC may be identified, although it is usually minor to inconspicuous, with the sarcomatoid part dominating. Frank squamous differentiation can be found at the base of the polypoid lesion, the advancing margins,

or within invaginations at the surface where the epithelium is not ulcerated or denuded (Fig. 6.29). The sarcomatoid or fusiform fraction of the tumor can be arranged in a diverse array of appearances, including storiform, interlacing bundles or fascicles, and herringbone (Fig. 6.29). Though generally hypercellular, hypocellular tumors with dense collagen deposition are also seen. A



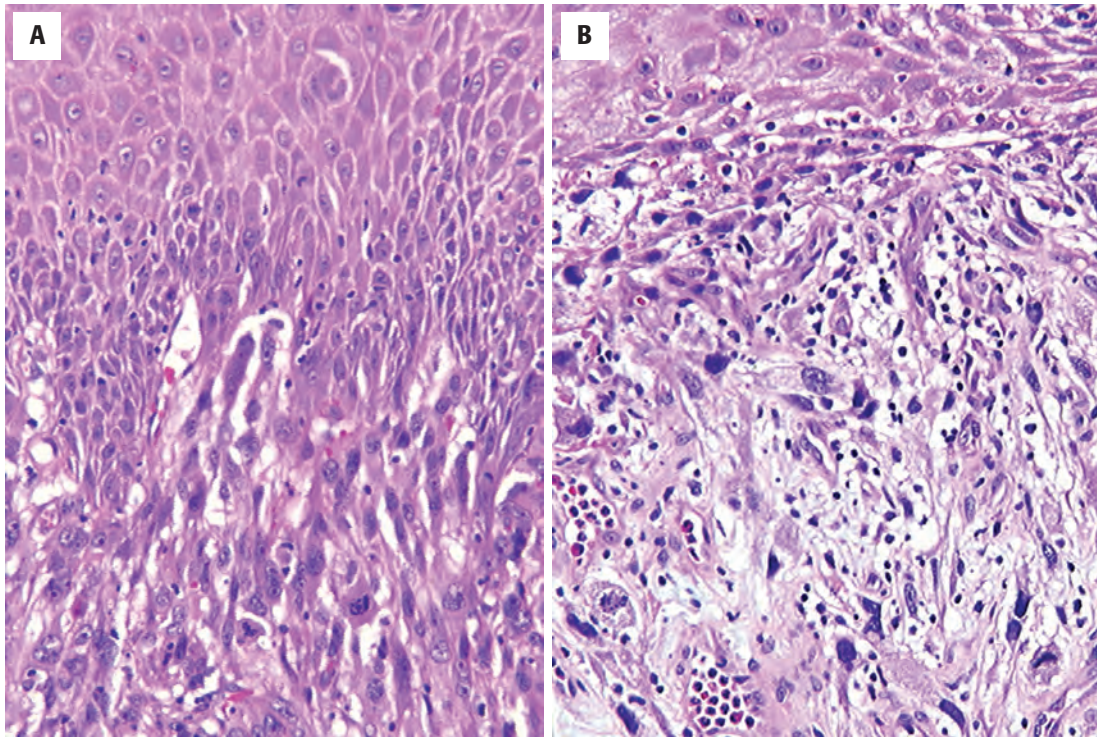
**FIGURE 6.26**

(A) A low-power view of a spindle cell squamous cell carcinoma shows the polypoid projection attached to the underlying stroma by a narrow stalk. Surface ulceration has denuded most of the epithelium, which is retained only at the base of the stalk. (B) The highly atypical surface epithelium blends imperceptibly with the equally atypical spindled to polygonal cell population in the stroma.

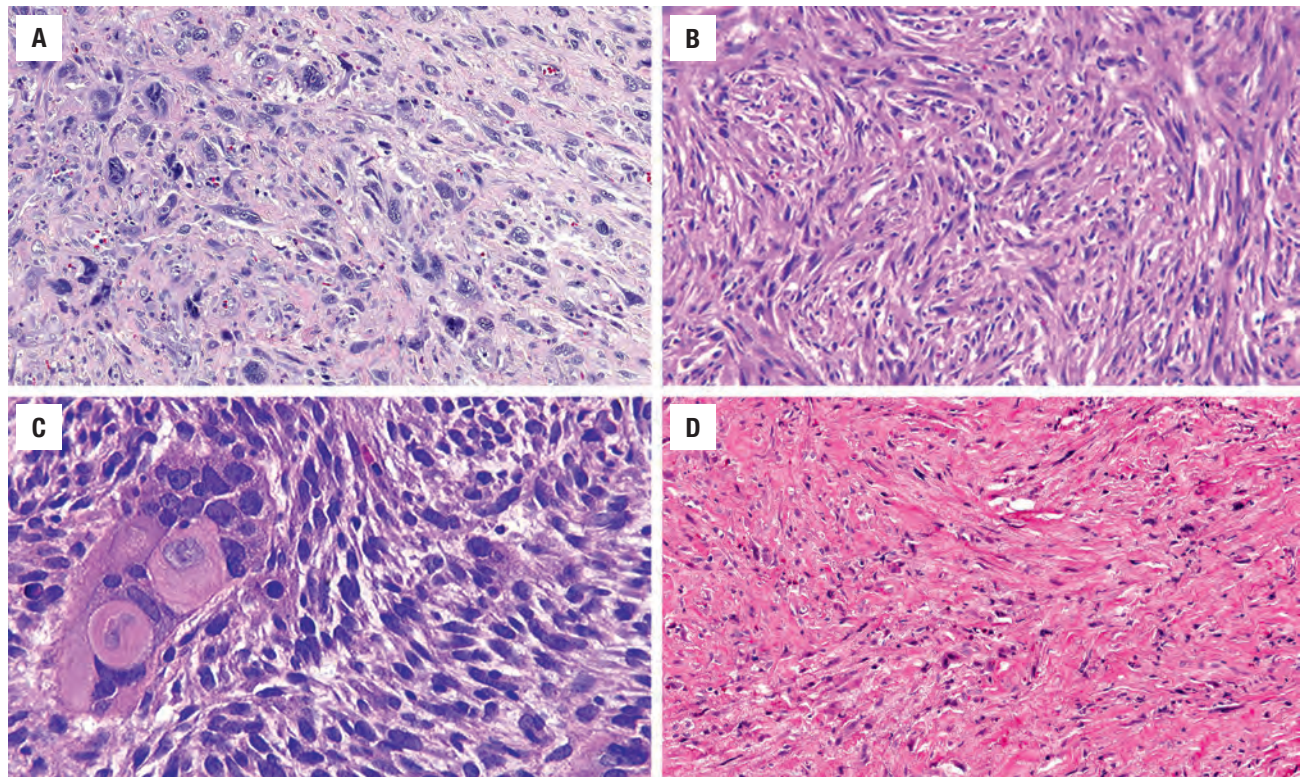
**FIGURE 6.27**

Complete loss of the surface epithelium with fibrinoid necrosis is characteristic of a spindle cell squamous cell carcinoma, with markedly atypical, hyperchromatic nuclei identified within the spindle cells of the "stroma."



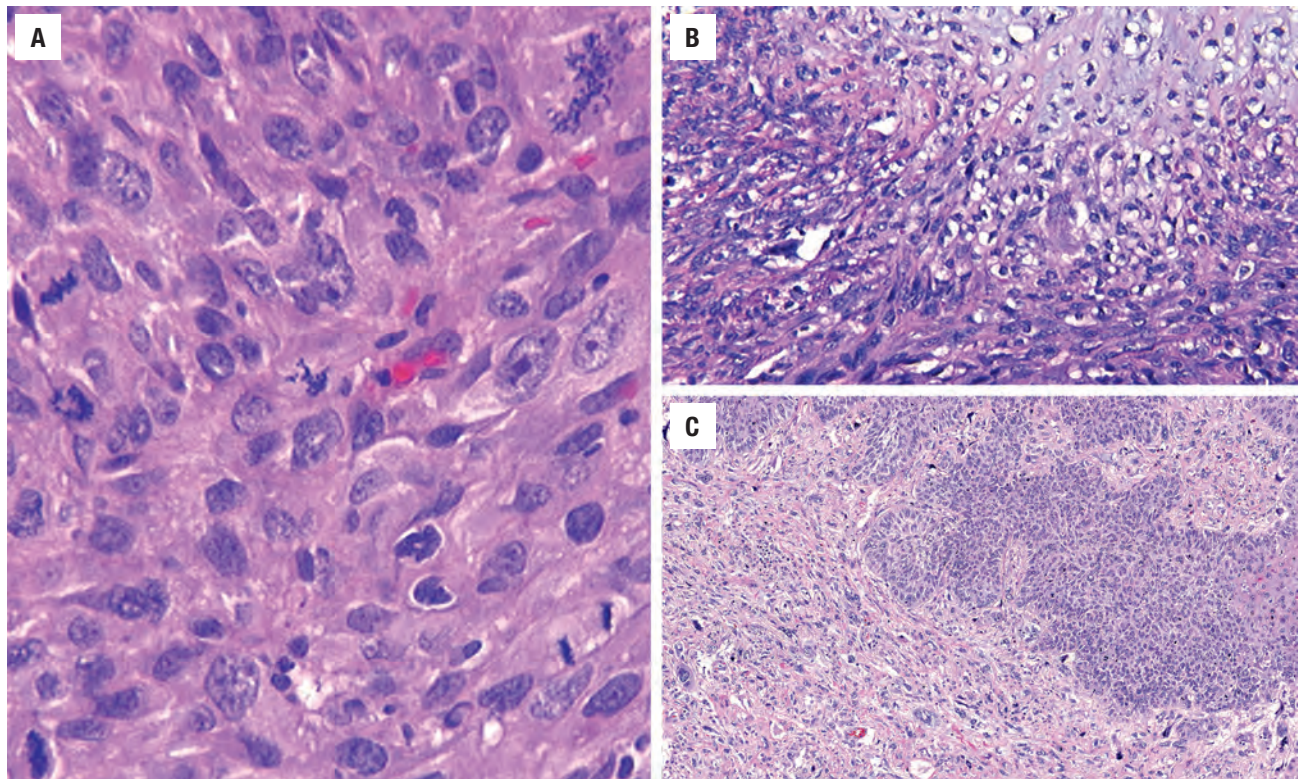
**FIGURE 6.28**

(A and B) The surface epithelium blends imperceptibly with the spindled pattern of growth. Mitotic figures, pleomorphism, and inflammation are noted.

**FIGURE 6.29**

Variable patterns of growth, including solid and compact (A), fascicular and storiform (B), a focus of abrupt squamous differentiation (C), and a hypocellular atypical spindle cell population in a heavily collagenized stroma (D).



**FIGURE 6.30**

(A) Spindle cell squamous cell carcinoma (SCSCC) composed of haphazard atypical spindle cells with increased mitoses, including atypical forms. (B) Metaplastic cartilage has undergone malignant transformation into a chondrosarcoma within this SCSCC. (C) Islands of poorly differentiated squamous cell carcinoma within the remarkably spindled cell population.

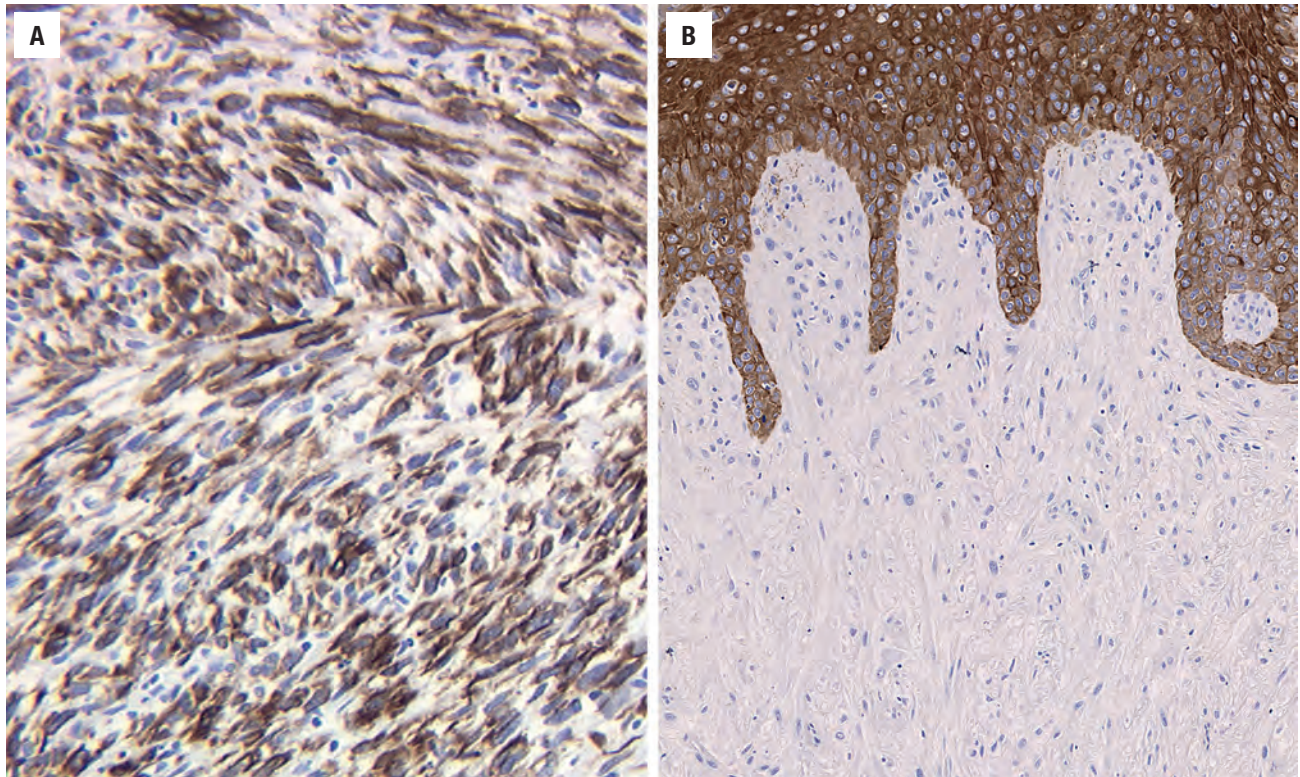
desmoplastic stroma is present in about 50 % of cases. Pleomorphism is often mild to moderate, but occasional highly pleomorphic cells may be present. The tumor cells are plump fusiform cells, although they can be rounded and epithelioid. Opacified, dense, eosinophilic cytoplasm gives a hint of squamous differentiation but is difficult to quantify or qualify accurately. Mitotic figures, including atypical forms, are easily counted in most tumors (Fig. 6.30). Necrosis is usually absent. Rarely, metaplastic or frankly neoplastic cartilage or bone may be seen (Fig. 6.30), with isolated cells showing rhabdomyoblastic differentiation.

This is the one SCC variant in which immunohistochemistry may be of value. The individual spindle neoplastic cells react variably, although most sensitively and reliably with keratin (AE1/AE3) (Fig. 6.31), EMA, and CK18, although only about 70 % of cases will yield any epithelial immunoreactivity (Fig. 6.31). In many cases, p63 and p40 are positive, while p53 is usually overexpressed. Other mesenchymal markers (SMA, MSA, S100 protein) may be identified focally, although this phenotypic plasticity or lineage infidelity supports the sarcomatoid transformation seen in SCSCC. Whereas a positive epithelial marker helps to confirm the diagnosis of SCSCC, a nonreactive or negative result should not dissuade the pathologist from the diagnosis, especially in the correct clinical setting.

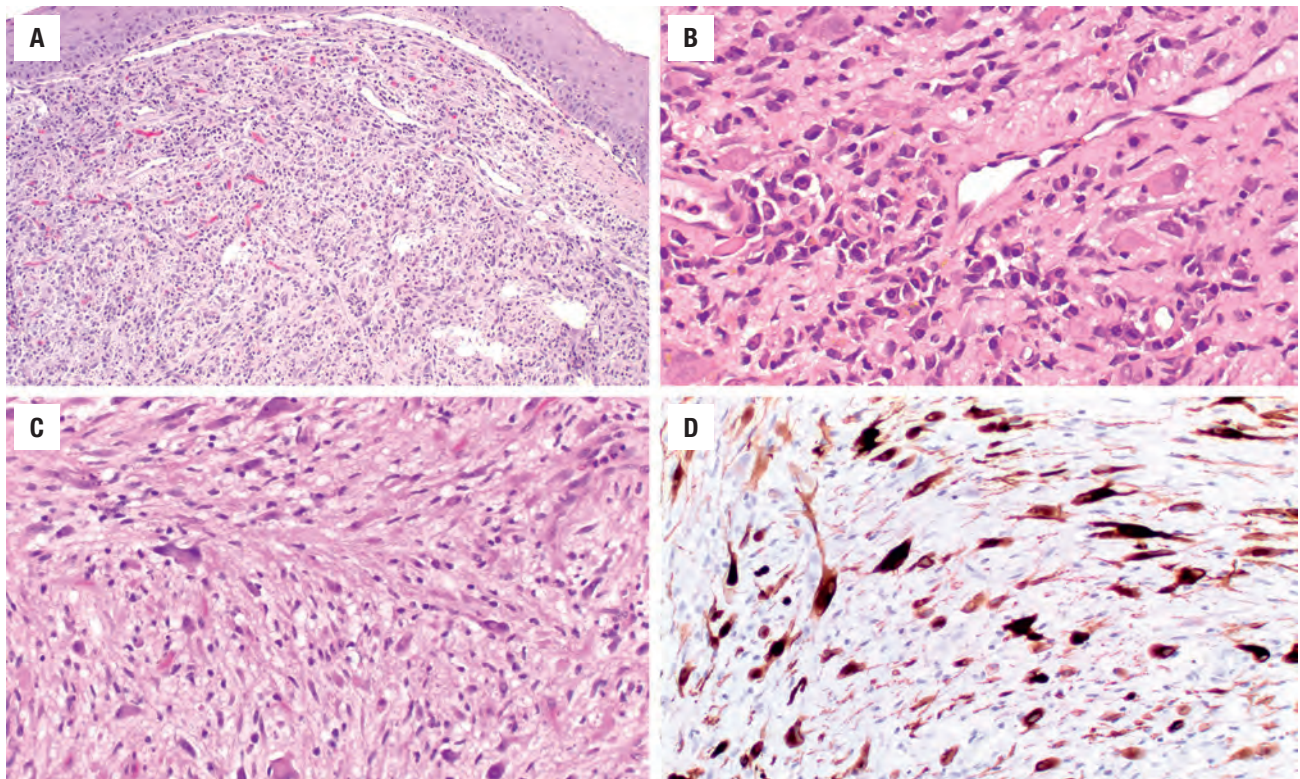
The differential diagnosis includes any spindle cell lesion, but suffice it to say that authentic primary mucosal sarcomas or benign mesenchymal tumors of the larynx are exceptional, as there is very limited stroma in the vocal cords. *Contact ulcer* has a more vascular appearance and lacks cytologic atypia. An *inflammatory myofibroblastic tumor* has a tissue culture-like growth of spindle to stellate cells with inflammatory cells throughout, often positive with anaplastic lymphoma kinase (ALK) (Fig. 6.32). *Synovial sarcoma* (especially monophasic) may cause the most diagnostic difficulty (Fig. 6.33), but the age at presentation (young people), tumor location (usually hypopharynx and soft tissue rather than mucosa), and the presence of TLE1 by immunohistochemistry along with the specific chromosomal translocation (SS18-SSX) can aid in this distinction. *Spindle cell melanoma* would react with melanocytic markers.

There is an overall 80 % 5-year survival, better than conventional SCC in age- and staged-matched controls. Most patients (85 %) present at a low stage (T1 and T2). When metastatic disease develops (about 20 %), cervical lymph nodes and pulmonary involvement is most frequent. There is a worse outcome for patients with a history of radiation, large tumors, fixed vocal cords, and the presence of epithelial markers immunohistochemically. Surgery, usually followed by radiation therapy, seems to yield the best long-term patient outcome.



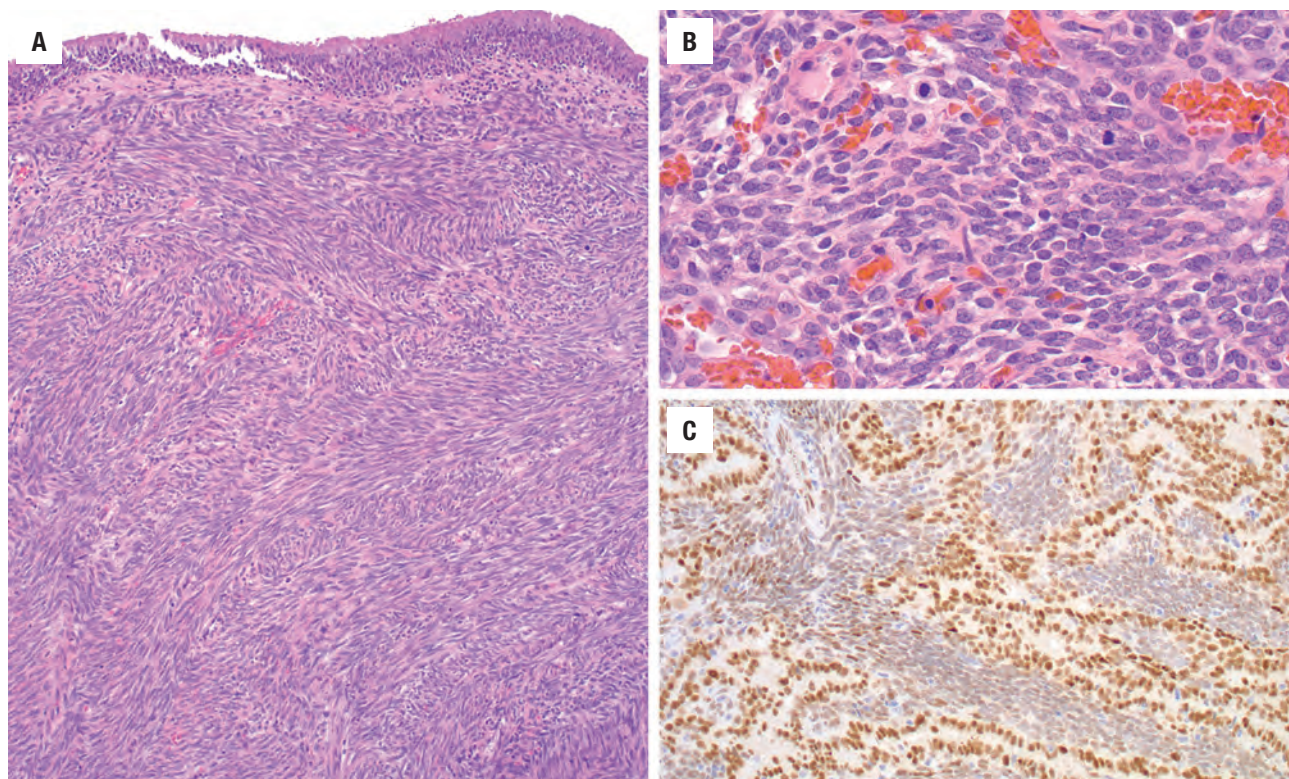
**FIGURE 6.31**

Spindle cell squamous cell carcinoma. Most tumors show a strongly immunopositive keratin reaction (**A**), while a negative stain is seen in up to 30% of cases (**B**).

**FIGURE 6.32**

(**A**) An inflammatory myofibroblastic tumor below an intact epithelium. Note the haphazard arrangement of this cellular tumor. Ganglion-like cells (**B**) are intermixed with inflammatory cells. (**C**) Eccentric cytoplasm is noted in cells with prominent nucleoli and intranuclear inclusions. (**D**) The neoplastic cells show a strong reaction with ALK1.



**FIGURE 6.33**

(A) A synovial sarcoma is usually separated from the surface epithelium and arranged in alternating bands of spindled cells. (B) There is usually limited pleomorphism but a high cellularity. (C) The neoplastic cells are strongly and diffusely immunoreactive with TLE1, a finding supportive of the diagnosis.

## BASALOID SQUAMOUS CELL CARCINOMA

Basaloid SCC (BSCC) is a high-grade SCC variant showing predominantly basaloid cells with associated squamous differentiation (keratinization, dysplasia, in situ or invasive tumor). It affects primarily men in the 7th decade. In the larynx, transcriptionally active HPV does not seem to play a significant role. As a high-grade lesion, it has a predilection for multifocal presentation and frequent cervical lymph node metastases at presentation. The piriform sinus and supraglottic areas are most frequently affected. Macroscopically, these tumors are usually firm to hard with associated central necrosis, occurring as exophytic to nodular masses measuring up to 6 cm in greatest dimension.

Many patterns are seen in this infiltrating tumor, including solid, smooth-contoured lobules; comedonecrosis (Fig. 6.34); cribriform patterns, cords, trabeculae, nests and glands, or cysts. Surface ulceration may belie the deeply invasive nature of the tumor, which has frequent lymphovascular invasion, although neurotropism is less common. The basaloid component is the most diagnostic feature, incorporating small, closely opposed, moderately pleomorphic cells with hyperchromatic to vesicular nuclei and scant cytoplasm into a lobular configuration with peripheral palisading (Fig. 6.35). These basaloid regions are in intimate association with areas of squamous differentiation, including abrupt keratinization in the form

of squamous pearls (Figs. 6.35 and 6.36), individual cell keratinization, dysplasia, or SCC (in situ or invasive). Marked mitotic activity as well as comedonecrosis in the center of the neoplastic islands is common. The tumor cells are separated by a prominently dense, pink hyaline material, often cylindrical or globular, with small cystic spaces containing mucoid material. Rosettes may be seen, with a spindle cell component in a few cases. In metastatic disease, both basaloid and squamous cell components can be seen, although the basaloid features have predominated. The neoplastic cells are reactive with pan-keratin, K903 (34 $\beta$ E12), CAM5.2, EMA, CK 7, CK5/6, p63 (Fig. 6.36), p40, and p53.

A sample of sufficient depth to show the heterogeneous nature of the tumor will usually resolve the differential consideration of a neuroendocrine carcinoma (NEC), adenoid cystic carcinoma, ASC, and SCC. A lack of neuroendocrine nuclear features and immunoreactivity eliminates *neuroendocrine carcinoma* from consideration. *Adenoid cystic carcinoma* does not have squamous differentiation, prominent pleomorphism, mitoses, or comedonecrosis; it often expresses *MYB-NFIB* gene fusion. The nuclei are angulated with no nucleoli. S100 protein is frequently positive. *Adenosquamous carcinoma* (discussed further on) shows a dual composition of true squamous carcinoma and adenocarcinoma. A poorly differentiated SCC may have a small basaloid population but without the characteristic lobular pattern with



**BASALOID SQUAMOUS CELL CARCINOMA****Definition**

- High-grade SCC variant with basaloid small cells arranged in a palisaded architecture; focal areas of squamous differentiation

**Clinical Features**

- Multifocal, older men, high cervical lymph node metastases

**Prognosis and Treatment**

- 40% survival
- Multimodality therapy (surgery, radiation, chemotherapy)

**Gross Findings**

- Firm tumors with central necrosis, up to 6 cm

**Microscopic Findings**

- Solid, lobular, comedonecrosis, cribriform, trabecular, glands, and cystic architecture

SCC, Squamous cell carcinoma.

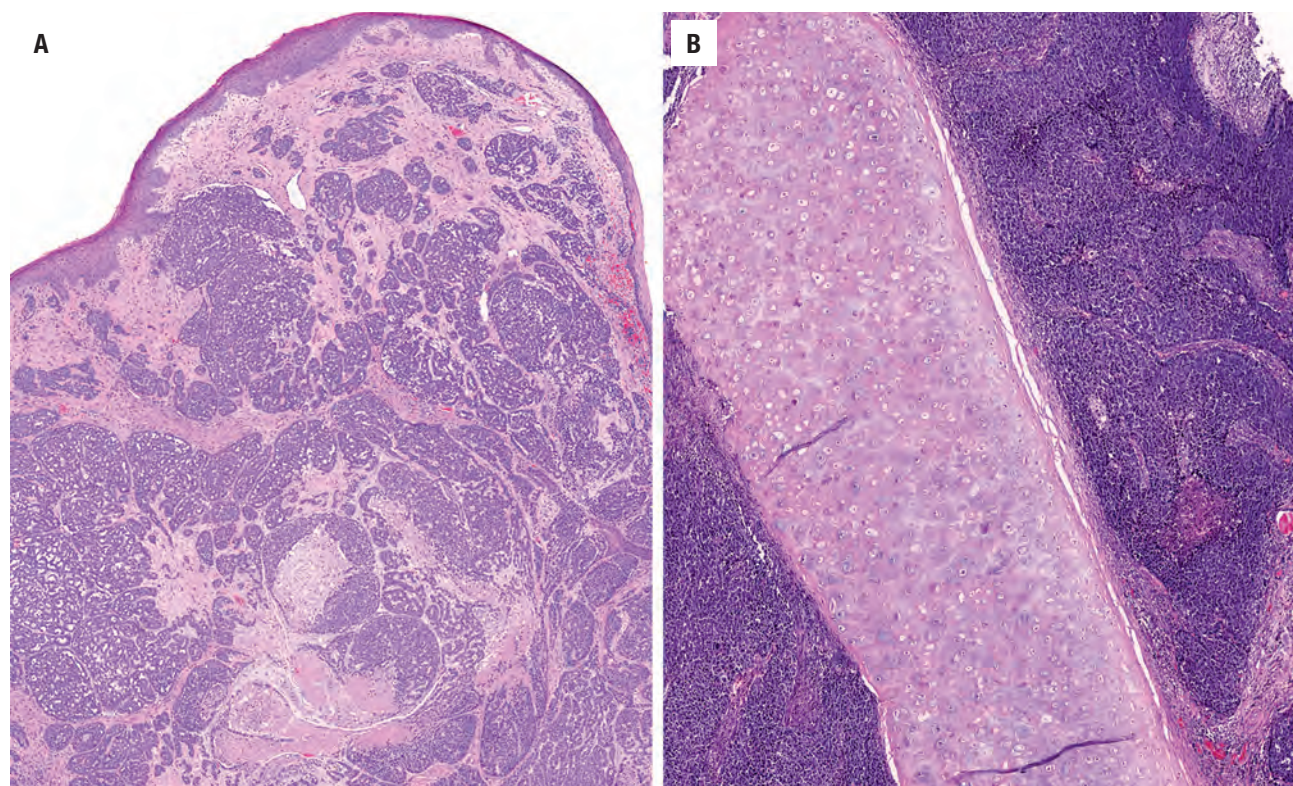
- Frequently ulcerated, easily identified lymphovascular invasion
- Basaloid cells with small, closely opposed, moderately pleomorphic cells with peripheral palisading
- Hyperchromatic to vesicular nuclei with coarse nuclear chromatin
- Abrupt keratinization, squamous pearl formation, individual cell keratinization
- High mitotic index
- Prominent eosinophilic, hyaline, cylindrical, or globular matrix material

**Immunohistochemical Findings**

- Pancytokeratin, K903 (34βE12), CAM5.2, EMA, CK7, CK5/6, p63, p40, p53

**Pathologic Differential Diagnosis**

- SCC, neuroendocrine carcinoma, adenoid cystic carcinoma, adenosquamous carcinoma, mucoepidermoid carcinoma

**FIGURE 6.34**

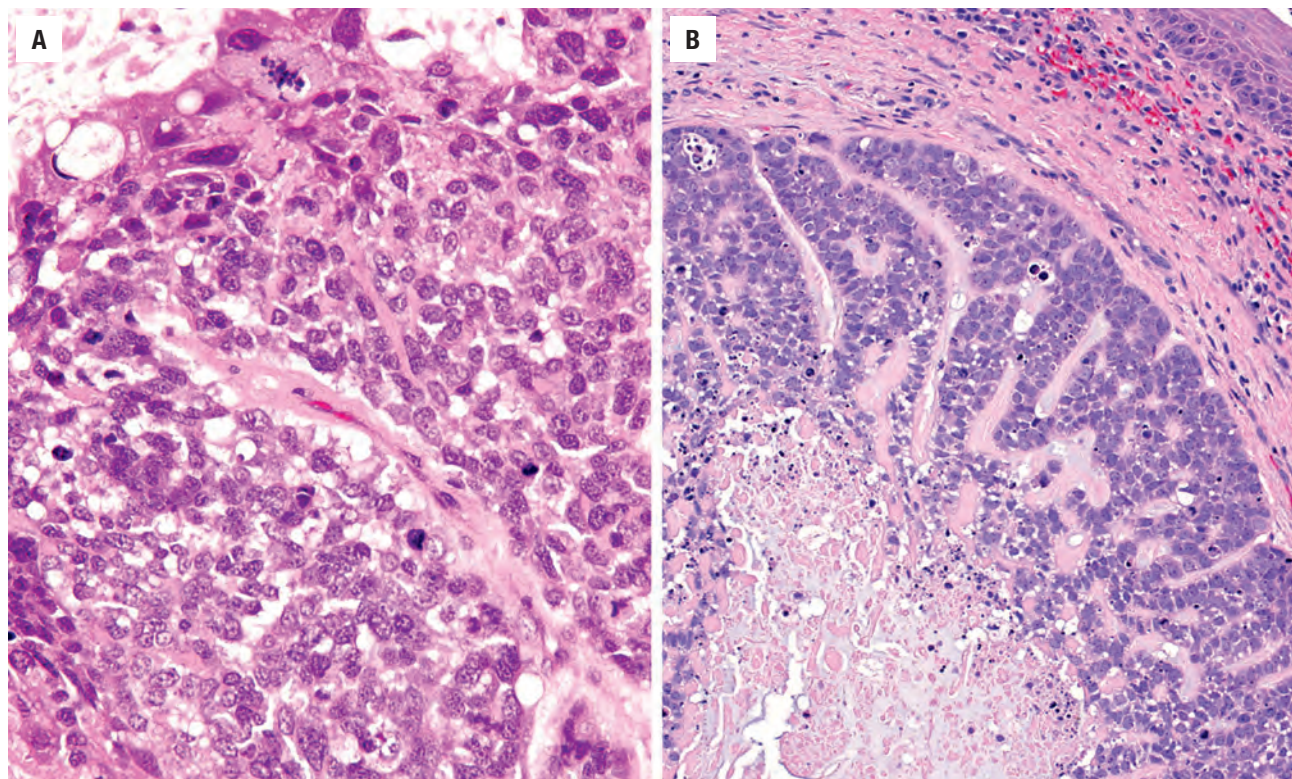
(A) The neoplastic infiltrate is dominated by a lobular arrangement of basaloid cells with areas of comedonecrosis in this basaloid squamous cell carcinoma. Note the intact surface. (B) The neoplasm surrounds the cartilage. Note the area of comedonecrosis.

comedonecrosis. When the diagnosis of a basaloid squamous carcinoma is made, there is an increased possibility of a contemporaneous primary elsewhere.

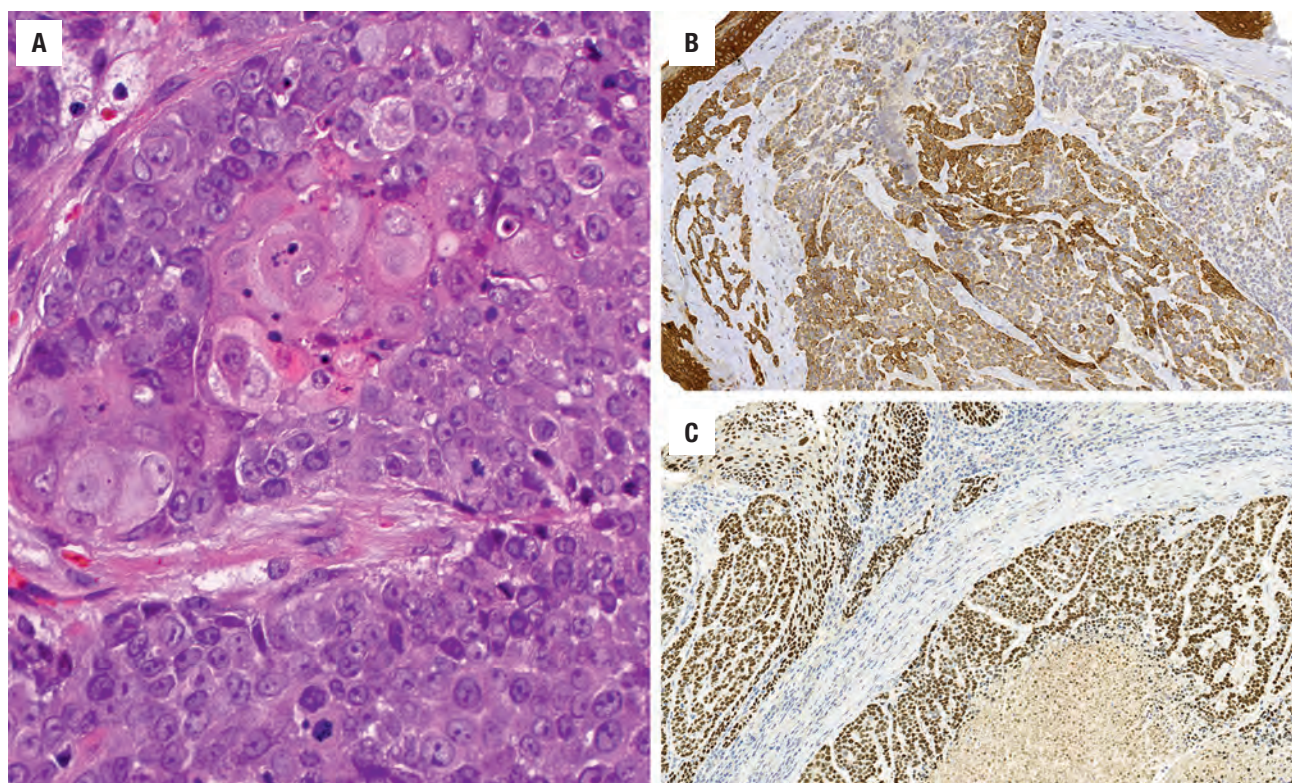
Despite aggressive therapy, the overall mortality rate is high (60% of patients die of their disease). Regional

and distant metastases are common (up to 70%). Patients present at a higher stage than those with conventional SCC. BSCC requires aggressive multimodality therapy, including radical surgery (with neck dissection), radiotherapy, and chemotherapy (especially for metastatic disease).



**FIGURE 6.35**

(A) There is focal abrupt keratinization (superior) intimately admixed with the basaloid cells of this basaloid squamous cell carcinoma. (B) There is peripheral palisading surrounding an area of necrosis. Note the reduplicated basement membrane material in a linear to globular arrangement.

**FIGURE 6.36**

(A) There is abrupt central keratinization in this otherwise more basaloid neoplasm. (B) Strong and diffuse CK5/6 immunoreactivity is seen. (C) Both the surface and deep tumor react with p63 in this basaloid squamous cell carcinoma.



## ADENOSQUAMOUS CARCINOMA

Adenosquamous carcinoma (ASC) is a high-grade variant of SCC composed of an admixture of SCC and true adenocarcinoma. Most patients (up to 75%) present with lymph node metastases. ASC occurs throughout the upper aerodigestive tract, often as an indurated, ulcerated, submucosal to exophytic nodule up to 5 cm in maximum dimension, although most are smaller than 1 cm. Any site of the larynx can be affected.

By definition the tumor demonstrates biphasic components of adenocarcinoma and SCC, with an undifferentiated cellular component in several tumors (Fig. 6.37). The SCC can be in situ or invasive, ranging from well to poorly differentiated. Squamous differentiation is confirmed by paved growth with intercellular bridges, keratin pearl formation, dyskeratosis, or individual cell keratinization. The adenocarcinoma component tends to develop away from the surface (deep), appearing tubular, alveolar, and glandular. Mucous cell differentiation is not essential for the diagnosis, but mucin production is usually easily identified. The cells in the adenocarcinoma can be basaloid, and separation from basaloid SCC can at times be arbitrary. The two carcinomas may be separate or intermixed, with areas of commingling and/or transition of the SCC to adenocarcinoma. The “undifferentiated” areas between the two distinct carcinomas

### ADENOSQUAMOUS CARCINOMA

#### Definition

- Composite of true adenocarcinoma and squamous cell carcinoma

#### Prognosis and Treatment

- Lymph node metastases in up to 75%
- Poor prognosis (20% 5-year survival)
- Surgery and radiation

#### Gross Findings

- Indurated, submucosal nodule about 1 cm (mean)

#### Microscopic Findings

- Biphasic adenocarcinoma and squamous carcinoma
- Undifferentiated or transitional components between lesions
- Separate, intermixed, commingled, transitions
- Scant inflammatory infiltrate
- Squamous component: CK7, CK5/6, p63, and p40-positive
- Glandular component: CEA and CK7-positive
- Absent *CRTC1-MAML2* translocation

#### Pathologic Differential Diagnosis

- Basaloid SCC, mucoepidermoid carcinoma, adenocarcinoma with squamous metaplasia, necrotizing sialometaplasia, adenoid SCC

SCC, Squamous cell carcinoma.

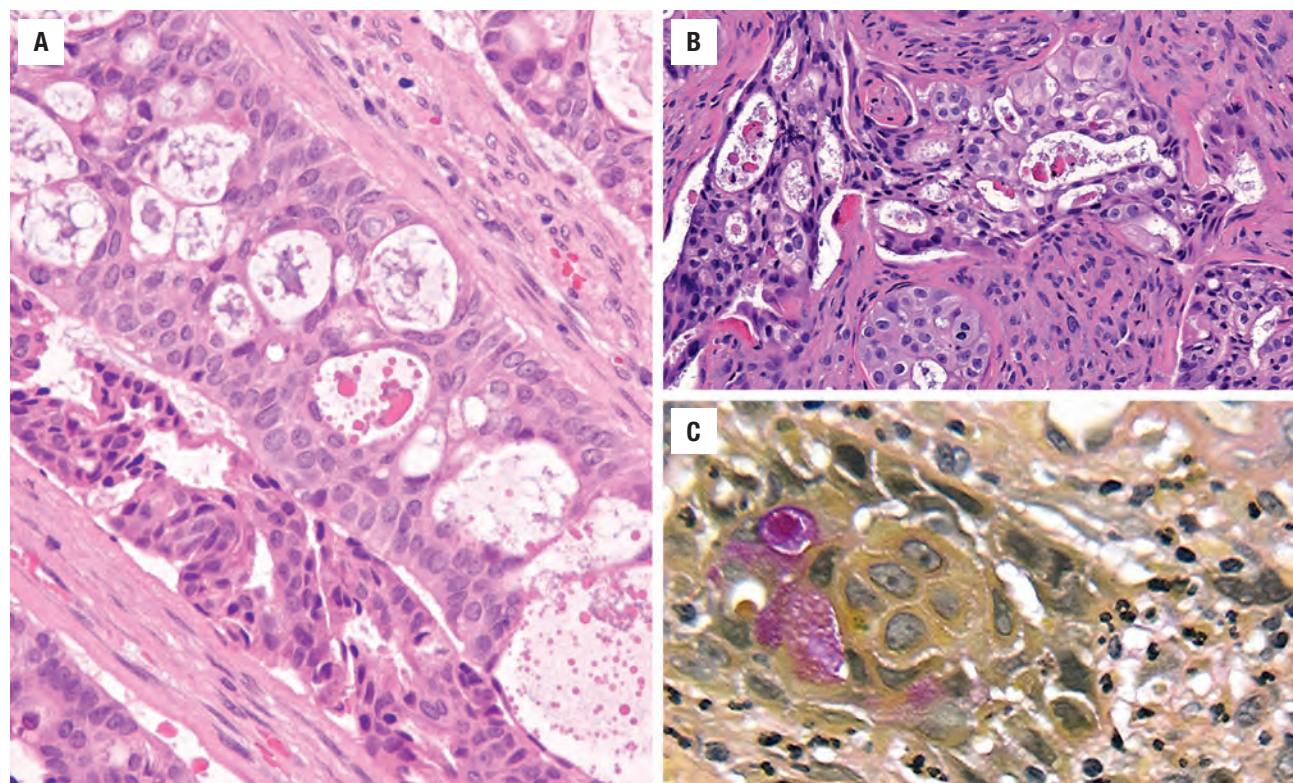


**FIGURE 6.37**

(A) This adenosquamous carcinoma demonstrates blended adenocarcinoma and squamous cell carcinoma within a single tumor mass. (B) Mucinous material is noted in the lumen of the adenocarcinoma, blended with areas of squamous differentiation. (C) A positive mucicarmine reaction is noted in the glandular component.



are often composed of clear cells. Both carcinomas may demonstrate frequent mitoses, necrosis, and infiltration into the surrounding tissue with affiliated perineural invasion. There is typically a sparse inflammatory cell infiltrate at the tumor–stromal interface with minimal to absent desmoplastic fibrosis. The squamous component is CK7, CK5/6, p63, and p40 immunoreactive, while the glandular component is CEA and CK7 positive.

In contrast to BSCC, ASC shows a prominent squamous cell component, absence of basaloid cells with peripheral nuclear palisading, and the presence of glandular differentiation. Although separation of ASC from mucoepidermoid carcinoma may be impossible in some cases, the latter demonstrates intermediate-type cells, generally does not have true squamous cell differentiation, and does not have two distinctly separate carcinomas (adenocarcinoma and SCC). *CRTC1-MAML2* translocation is not seen in ASC. An *adenocarcinoma with squamous metaplasia* generally does not demonstrate the nuclear criteria of a malignant squamous cell component. Likewise, *necrotizing sialometaplasia* shows squamous epithelium lining the scaffolding of preserved duct-gland units that have been infarcted or destroyed. A contemporaneous SCC and adenocarcinoma may affect the upper aerodigestive tract, but these lesions are usually temporally separated.

Aggressive surgery with neck dissection and follow-up radiation yields an approximately 15% to 25% 5-year survival. Along with a high lymph node metastatic rate, distant metastases are seen in about 25% of patients (lung most commonly).

## ■ NEUROENDOCRINE CARCINOMA

The terminology for this family of neoplasms is fraught with a great deal of confusion and conflict. The terms *well-differentiated* (carcinoid), *moderately differentiated* (atypical carcinoma), and *poorly differentiated* (small cell carcinoma) *neuroendocrine carcinoma*, respectively, are used by the WHO and advocated here. Paraganglioma is not considered within this group, although it is a neuroendocrine tumor also. By definition, this is a heterogeneous group of neoplasms characterized by the presence of epithelial and neuroendocrine differentiation. Systemic manifestations or paraneoplastic syndromes (Cushing, Lambert-Eaton, Schwartz-Bartter) are exceptional.

### CLINICAL FEATURES

Although there are slight differences between the various grades of neuroendocrine neoplasms, most patients are males (M > F is 3:1) between 45 and 80 years of age with a peak in the 7th decade and showing a strong tobacco association. As with all laryngeal tumors, dysphagia,

hoarseness, sore throat, hemoptysis, and the feeling of a lump are the most common presenting symptoms. Moderately differentiated NEC represents the most common nonsquamous epithelial malignancy of the larynx. Patients with poorly differentiated NEC (small cell carcinoma) frequently have lymph node metastases (50%).

### PATHOLOGIC FEATURES

#### GROSS FINDINGS

Neuroendocrine neoplasms occur most frequently in the supraglottic region, presenting as a submucosal mass in the aryepiglottic fold or arytenoid. The gross appearance ranges from polypoid (Fig. 6.38) and pedunculated to ulcerated, ranging in size up to 4 cm (1.6 cm average).

#### MICROSCOPIC FINDINGS

Neuroendocrine tumors are usually unencapsulated, although well-differentiated and moderately differentiated NECs are circumscribed and covered by an uninvolved surface mucosa. The tumors present with a variety of different histologic patterns, including an organoid or

### NEUROENDOCRINE CARCINOMA (WELL, MODERATELY, AND POORLY DIFFERENTIATED)—DISEASE FACT SHEET

#### Definition

- Malignant epithelial neoplasm with neuroendocrine differentiation by histologic and immunophenotypic findings

#### Incidence and Location

- Most common nonsquamous cell epithelial malignancy of the larynx
- Usually supraglottic

#### Morbidity and Mortality

- Variable based on histologic grade
- Metastatic disease rather than recurrence is cause of death
- Metastases usually to lymph nodes, liver, lung, and bone

#### Sex and Age Distribution

- Men > women (3:1 ratio)
- Peak in 7th decade

#### Clinical Features

- Strong tobacco association
- Dysphagia, hoarseness, sore throat, hemoptysis, lump in throat

#### Prognosis and Treatment

- Tumor-dependent:
  - Well differentiated: good long-term prognosis with surgery alone
  - Moderately differentiated: 30% metastatic disease at presentation; 50% 5-year survival with surgery and radiation
  - Poorly differentiated: rapidly fatal; 5%-20% 5-year survival

trabecular growth in well-differentiated NEC (Fig. 6.39); the addition of cords, solid, single-file, and cribriform patterns in the moderately differentiated NEC (Fig. 6.40); and all of these patterns, along with sheets, ribbons, pseudoglands, and rosette formations in small cell carcinoma. Moderately and poorly differentiated NECs may demonstrate surface ulceration. A fibrovascular stroma is generally absent in the small cell and large cell NECs, although it is seen in lower-grade NECs. Lymphovascular, perineural, and soft tissue invasion is seen in the moderate and poorly differentiated NECs. Amyloid and tumor cell spindling is occasionally noted (Fig. 6.41). Concurrent SCC may be present, creating a combined carcinoma.

The cytologic appearance of the cells is determined by the subtype of NEC. Glandular (with mucin production) or squamous differentiation can be seen in neuroendocrine neoplasms, along with occasional neural-type rosettes. The degree of cellular pleomorphism, mitotic

activity and necrosis increases as the tumor becomes more poorly differentiated (small and large cell NEC; Fig. 6.42). There is virtual absence of pleomorphism, necrosis, and mitoses in a well-differentiated NEC (Fig. 6.39), while there is prominent pleomorphism, necrosis,

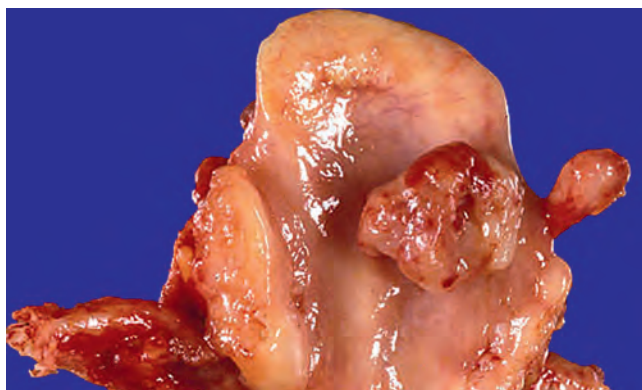


**FIGURE 6.38**

A supraglottic polypoid tumor is quite characteristic for a neuroendocrine carcinoma. (Courtesy of J. Fowler.)

#### NEUROENDOCRINE CARCINOMA (WELL, MODERATELY, AND POORLY DIFFERENTIATED)—PATHOLOGIC FEATURES

##### Gross Findings

- Supraglottic
- Submucosal mass, with ulceration in higher-grade tumors
- Polypoid, pedunculated
- Up to 4 cm (mean, 1.6 cm)

##### Microscopic Findings

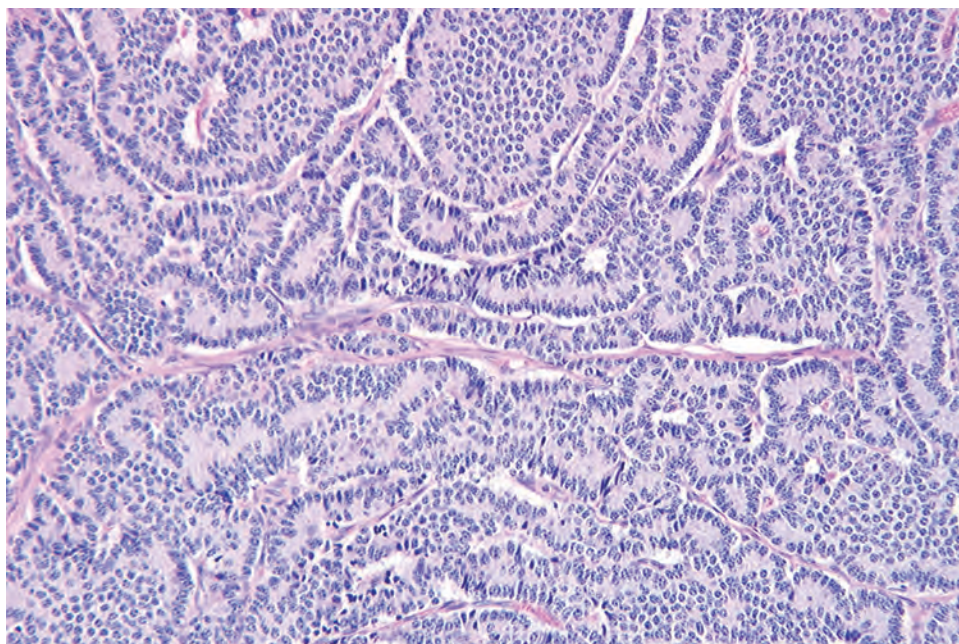
- **Well differentiated:** organoid and trabecular with monotonous cells with round nuclei and low N:C ratio and finely stippled chromatin
- **Moderately differentiated:** cords, solid and single-file infiltration, vascular invasion, vesicular to hyperchromatic nuclei with an intermediate N:C ratio, and nucleoli
- **Poorly differentiated:** sheets, ribbons, and pseudorosettes, invasive growth, pleomorphism, high N:C ratio, nuclear molding, necrosis, mitoses, crush artifact

##### Immunohistochemical Findings

- Keratin, EMA and mCEA
- Chromogranin, synaptophysin, CD56, CD57, calcitonin, and other neuroendocrine markers and hormones

##### Pathologic Differential Diagnosis

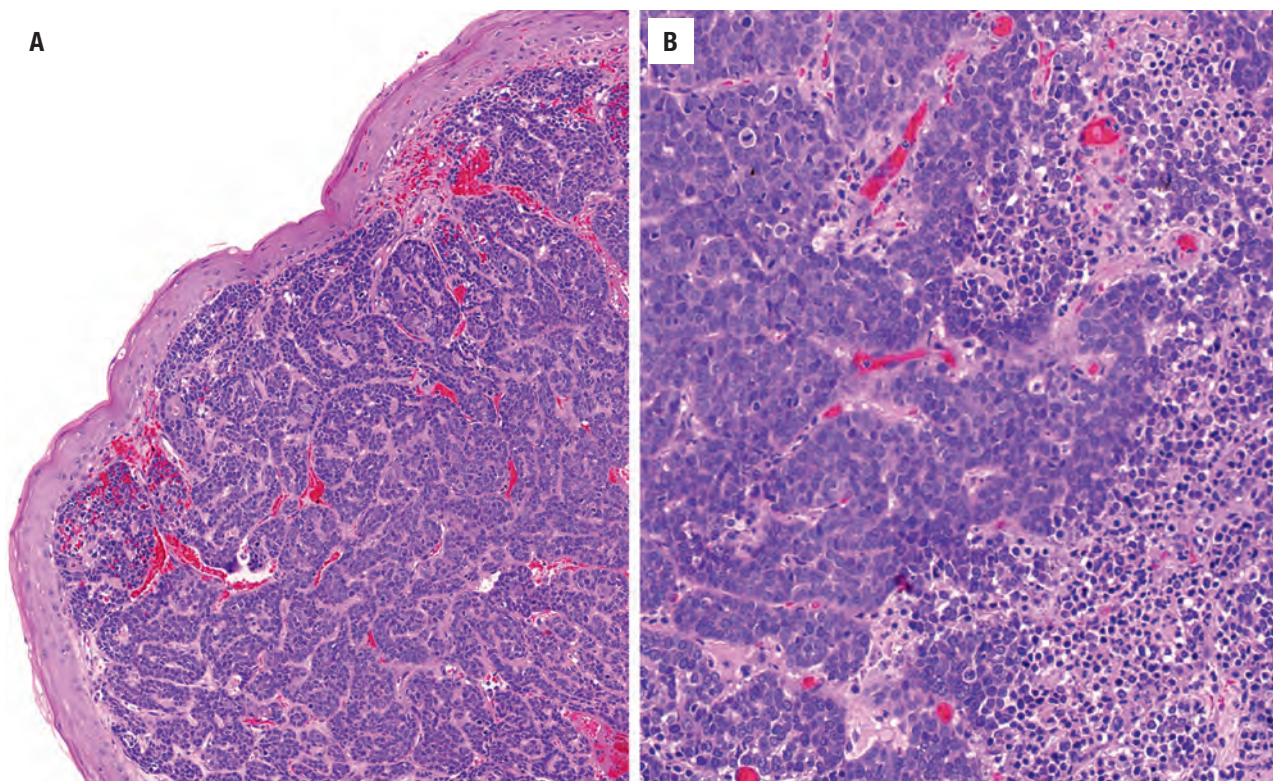
- Poorly differentiated squamous cell carcinoma, medullary thyroid carcinoma, adenoid cystic carcinoma, melanoma, lymphoma, metastatic carcinoma



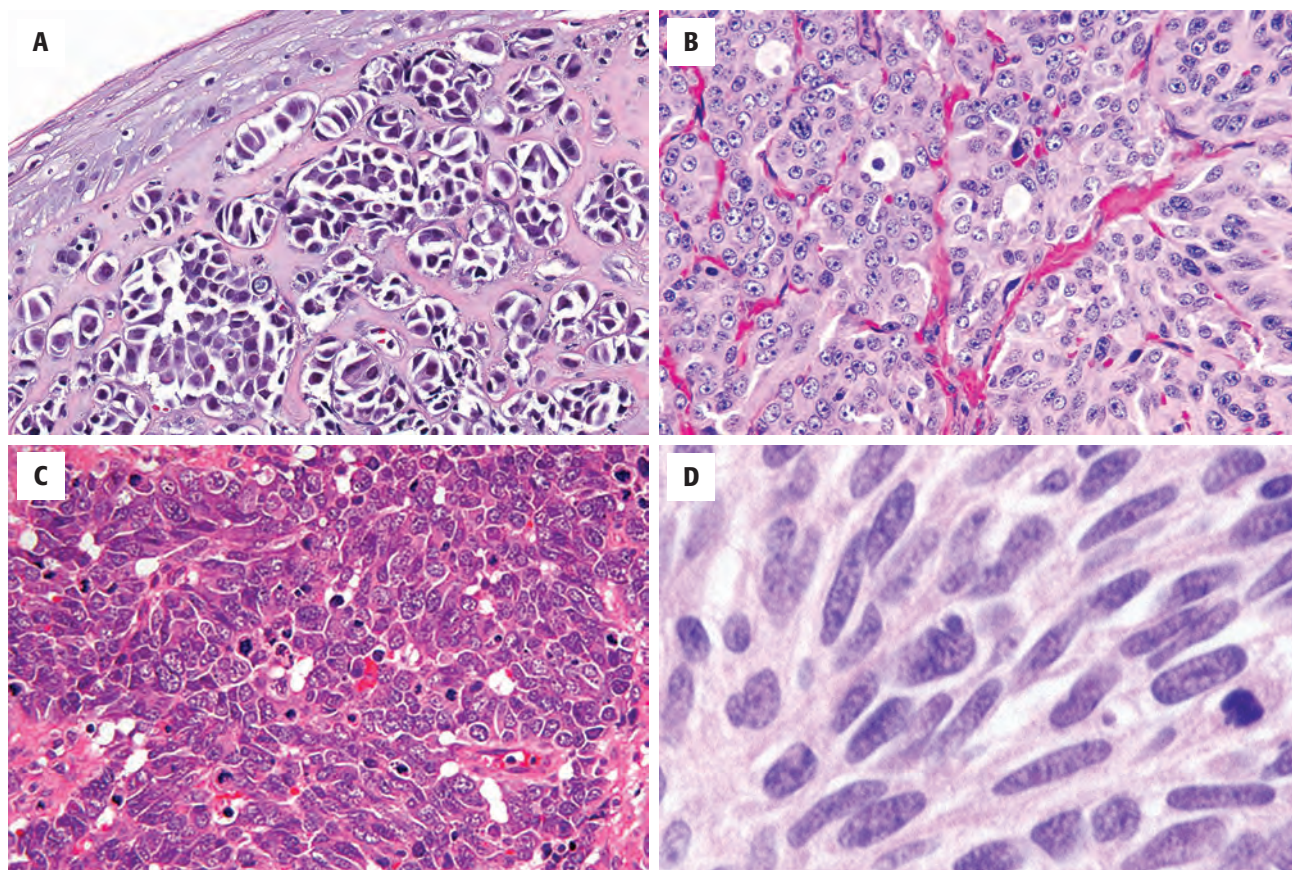
**FIGURE 6.39**

The cells are arranged in ribbons and festoons in this well-differentiated neuroendocrine carcinoma. The cells have pale cytoplasm surrounding round nuclei with salt-and-pepper chromatin distribution.



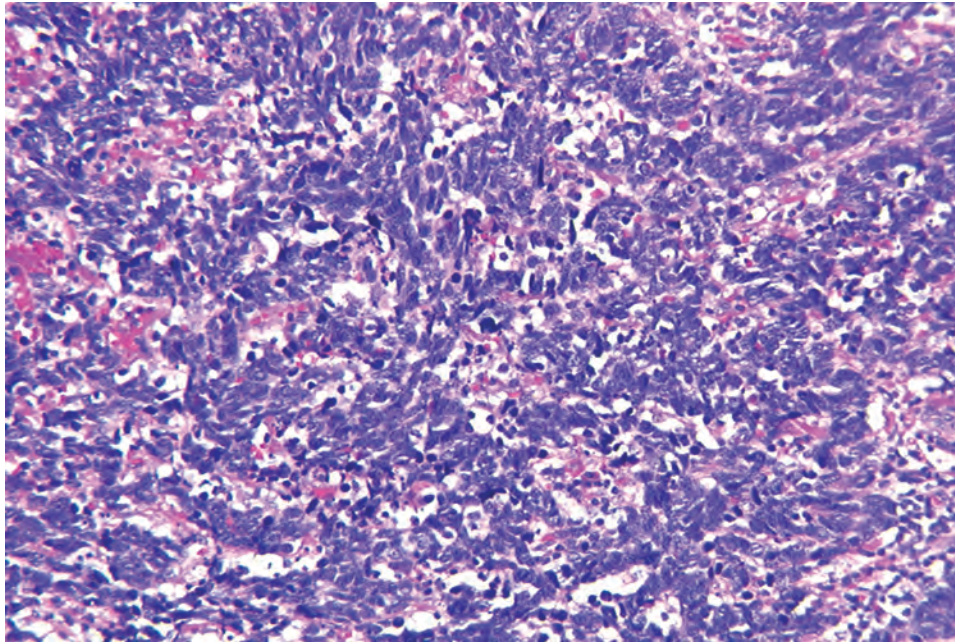
**FIGURE 6.40**

A moderately differentiated neuroendocrine carcinoma. (A) The surface epithelium is intact, with a ribbon like neoplastic proliferation below. (B) Tumor necrosis is noted, along with increased mitoses.

**FIGURE 6.41**

A moderately differentiated neuroendocrine carcinoma. The cells can be arranged in nests and balls (A), glandular profiles with round nuclei and salt-and-pepper chromatin (B), solid sheets of cells with a high nuclear-to-cytoplasmic ratio (C), or fascicles of spindle cells with stippled nuclear chromatin (D).



**FIGURE 6.42**

The “crush” artifact is characteristic of small cell neuroendocrine carcinoma, which has cells with a high nuclear-to-cytoplasmic ratio and coarse nuclear chromatin distribution.

and mitoses in a small cell carcinoma (Fig. 6.42), with moderately-differentiated NEC exhibiting intermediate features (Figs. 6.40 and 6.41). Owing to the fragility of the cells, crush artifact is frequently prominent in small cell carcinoma.

Well-differentiated NECs have small, monotonous cells with a low N:C ratio and round vesicular nuclei with finely stippled chromatin. Moderately differentiated NECs have vesicular to more hyperchromatic nuclei within polygonal cells that have an increased N:C ratio (Fig. 6.41). The location of the nucleus is variable (central, eccentric), surrounded by amphophilic to eosinophilic cytoplasm. Nucleoli are variable, from absent to prominent (Fig. 6.41). Small cell NECs and large cell NECs are hypercellular, composed of cells with a high N:C ratio, indistinct cell borders, and intensely hyperchromatic oval to spindled nuclei without nucleoli (Fig. 6.42). Nuclear molding is seen. Crush artifact, mitotic figures, necrosis, and occasional multinucleated neoplastic giant cells are present. There is usually limited stroma, which may be mucoid. Laryngeal NECs are on a morphologically continuous spectrum, with an aggregate of features distinguishing between the tumors.

## ANCILLARY STUDIES

### ULTRASTRUCTURAL FINDINGS

Electron microscopy will demonstrate membrane-bound, electron-dense neurosecretory granules, ranging from 50 to 250  $\mu\text{m}$ , decreasing in number as the tumor becomes less differentiated. Complex intercellular digitation and occasional intercellular junctions are present.

### IMMUNOHISTOCHEMICAL FINDINGS

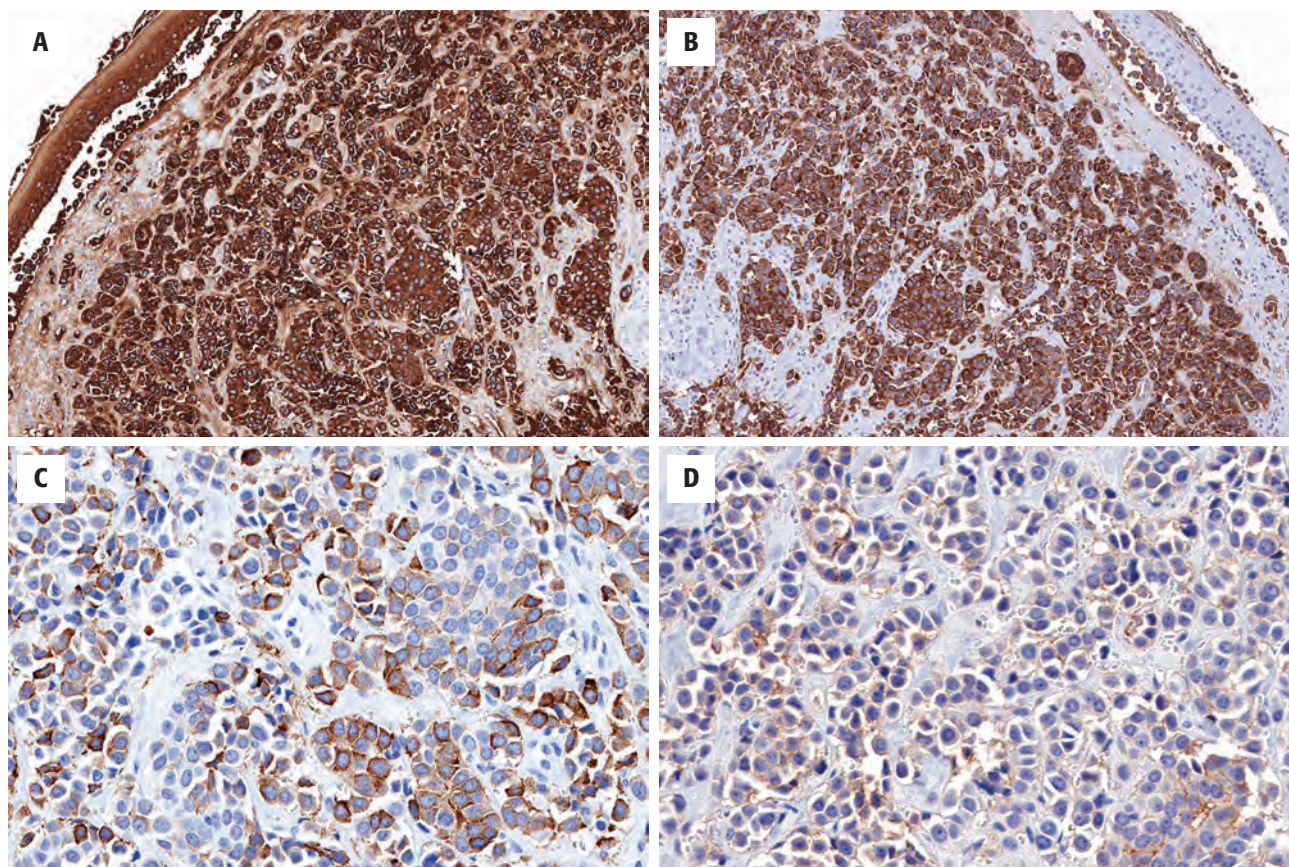
All grades of tumor variably react with pancytokeratin (Fig. 6.43), EMA, and mCEA, in addition to neuroendocrine markers (chromogranin [Fig. 6.43], synaptophysin, CD56, CD57, NSE). More than 80 % of moderately differentiated NECs are positive for calcitonin (Fig. 6.43). Almost all of these tumors are nonreactive for S100 protein, GFAP, and met-enkephalins.

## DIFFERENTIAL DIAGNOSIS

The differential diagnosis is quite broad and includes SCC, mucosal melanoma, adenoid cystic carcinoma, lymphoma, metastatic carcinoma, medullary thyroid carcinoma, and lymphoma.

Part of the reason for making a definitive diagnosis regarding neuroendocrine tumors is the difference in treatment protocols and patient outcome. A *poorly differentiated squamous cell carcinoma* (which will be negative for neuroendocrine immunohistochemistry) will respond to radiation therapy, while moderately differentiated NEC is generally insensitive to this modality. A *mucosal melanoma* more frequently involves the surface epithelium, will demonstrate greater pleomorphism, may have melanin pigment, and will show S100 protein and melanocytic marker immunoreactivity (HMB-45, SOX10, Melan-A, tyrosinase). It is imperative to exclude a *metastatic tumor* to the larynx, especially in small cell carcinoma, where a lung primary may have metastasized to the larynx and will usually be TTF1 positive. However, *medullary carcinoma of the thyroid* may metastasize to or directly invade into the larynx.



**FIGURE 6.43**

A moderately differentiated neuroendocrine carcinoma showing a variety of different immunohistochemical reactions: pancytokeratin (A), chromogranin (B), calcitonin (C), and CD56 (D).

The distinction between medullary carcinoma of the thyroid and NEC of the larynx can be nearly impossible, although amyloid and an increased serum calcitonin level are much more likely in a medullary thyroid carcinoma. *Lymphomas*, with crush artifact and a submucosal location, can be separated by the lack of neuroendocrine differentiation (either immunohistochemically or ultra-structurally) and their reaction with various lymphoid markers.

### PROGNOSIS AND THERAPY

The reason for the distinction between these tumor types relates to the differences in treatment and prognosis. Prognosis for well-differentiated NECs is excellent with excision alone, although recurrences are seen in up to 30 %, yielding a 5-year survival rate of about 80 %. Moderately differentiated NECs frequently have metastases at presentation (30 %) and are usually treated with surgery alone, as they are rather insensitive to radiation or chemotherapy. Recurrences are common (about 60 %), yielding a 50 % 5-year survival, with death usually due to metastatic disease (lungs, bone, liver). Poorly

differentiated NECs have metastasis at presentation in about 70 % of patients, with a rapidly fatal clinical course (5 % to 20 % 5-year survival). Treatment includes systemic chemotherapy and radiation. Death is usually due to metastatic disease, with the size of the tumor an important prognostic factor.

### ■ CHONDROSARCOMA

Only 2 % to 5 % of all chondrosarcomas arise in the head and neck, with laryngeal chondrosarcomas accounting for less than 1 % of all laryngeal malignancies but 75 % of laryngeal nonepithelial neoplasms. The proposed etiology for laryngeal chondrosarcomas is disordered ossification of the laryngeal cartilages, specifically the cricoid cartilage (ossification usually develops in areas of muscle insertion and is attributed to the mechanical influence of the contracting muscles). Notably, tumors do not develop in elastic cartilages (epiglottis). The ossification is found in hyaline cartilages in older adult patients, the peak age for presentation of laryngeal chondrosarcoma. It has also been suggested that ischemic change in a chondroma subjected to mechanical trauma may be a

precursor to malignant change. Interestingly, laryngeal chondromas develop on average about a decade earlier than chondrosarcomas, perhaps suggesting a developmental continuum. By definition, chondrosarcoma is a malignant neoplasm forming neoplastic hyaline cartilage.

### CLINICAL FEATURES

Men are typically affected more frequently than women (3 to 4:1) and present in the mid sixties, although there is a wide age range (25 to 91 years). As the airway is progressively narrowed or obstructed by the endolaryngeal growth, hoarseness, followed by dyspnea, dysphagia, difficulty breathing, and stridor results. Thyroid cartilage tumors are more likely to present as a mass lesion. Symptoms are frequently present for a long time (mean, >2 years), supporting the indolent tumor growth. Endoscopically, there is a subglottic swelling below an intact mucosa.

### RADIOGRAPHIC FEATURES

Either plain films or computed tomography (CT) images will show an ill-defined, destructive, hypodense mass with fine, punctate, stippled to coarse (“popcorn”) calcification (Fig. 6.44). After the tumor is identified as “cartilaginous,” the remaining features are nonspecific.

### CHONDROSARCOMA—DISEASE FACT SHEET

#### Definition

- Chondrosarcoma is a malignant tumor arising within the laryngeal cartilages and forming neoplastic hyaline cartilage

#### Incidence and Location

- Up to 1% of all laryngeal malignancies
- 75% of all laryngeal sarcomas
- Cricoid cartilage most commonly

#### Morbidity and Mortality

- Recurrences in up to 40% of patients
- Infrequently, patients die from tumor

#### Sex and Age Distribution

- Males > females (3-4:1)
- Mean, 60-65 years

#### Clinical Features

- Hoarseness, dyspnea, dysphagia, stridor
- Thyroid cartilage lesions present as a mass
- Long duration of symptoms
- Subglottic submucosal swelling on endoscopy

#### Radiographic Features

- Fine, punctate, stippled to coarse (“popcorn”) calcifications
- Ill-defined, destructive, hypodense mass

#### Prognosis and Treatment

- Greater than 90% 10-year survival
- Complete, but conservative surgery to preserve laryngeal function

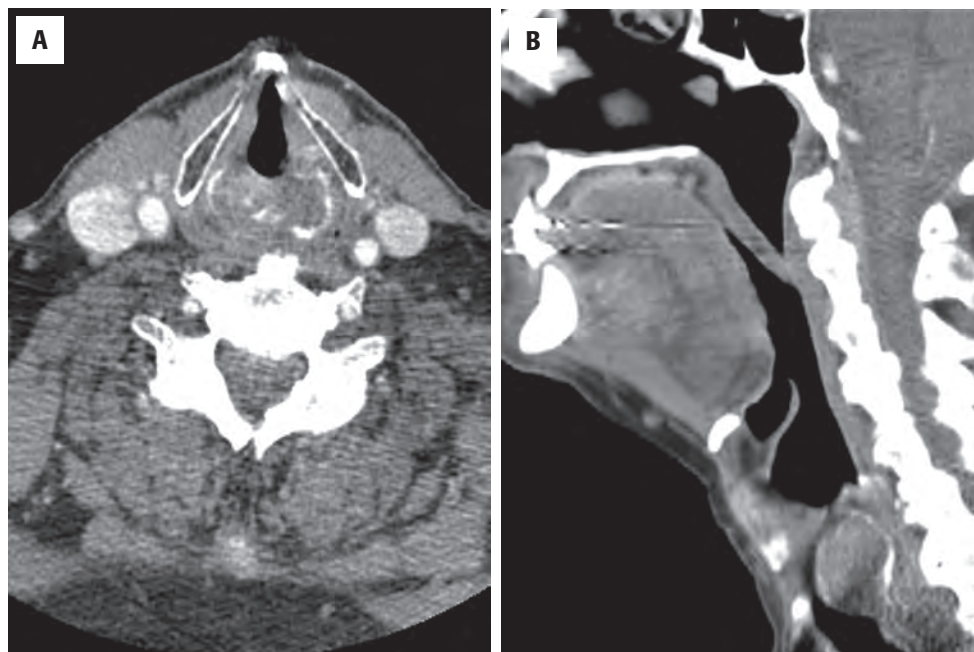


**FIGURE 6.44**

Computed tomography images of a chondrosarcoma destroying the cricoid cartilage and demonstrating stippled to coarse (“popcorn”) calcifications within the tumor (**A**, axial and **B**, sagittal).



## PATHOLOGIC FEATURES

### GROSS FINDINGS

The cricoid cartilage (specifically the inner posterior midline lamina) is affected far more frequently (in about 75 %) than other laryngeal cartilages, followed by the thyroid and arytenoid cartilages. The tumors range in size up to 12 cm, with a mean of 3.5 cm. Tumors are hard, “crunchy” or “gritty,” lobular, and glistening on the cut surface, with a blue-gray, semitranslucent, myxoid-mucinous matrix material (Fig. 6.45). Dedifferentiated chondrosarcoma has fleshy areas.

## CHONDROSARCOMA—PATHOLOGIC FEATURES

### Gross Findings

- Cricoid cartilage (posterior plate) midline mass
- Mean, 3.5 cm
- Hard, crunchy, lobular, glistening blue-gray, semitranslucent, with myxoid-mucinous matrix

### Microscopic Findings

- Bone invasion (ossification centers within cartilage)
- Increased cellularity
- Loss of normal architecture and distribution (cluster disarray)
- Nuclear atypia with bi- and multinucleation
- Increased N:C ratio
- Basophilic to metachromatic cartilaginous matrix
- Mitotic figures and necrosis only in high-grade tumors
- Separated into three grades

### Pathologic Differential Diagnosis

- Chondroma, chondrometaplasia, spindle cell squamous cell carcinoma, pleomorphic adenoma

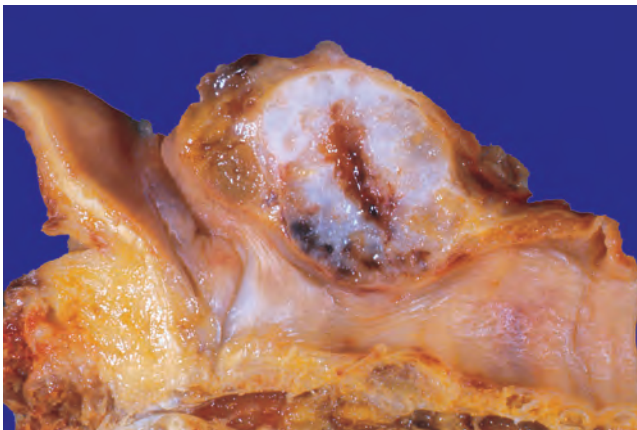


**FIGURE 6.45**

This macroscopic laryngectomy specimen shows a thin rim of bone invaded by the chondrosarcoma of the cricoid cartilage. A firm, lobular growth is noted, with central degenerative change.

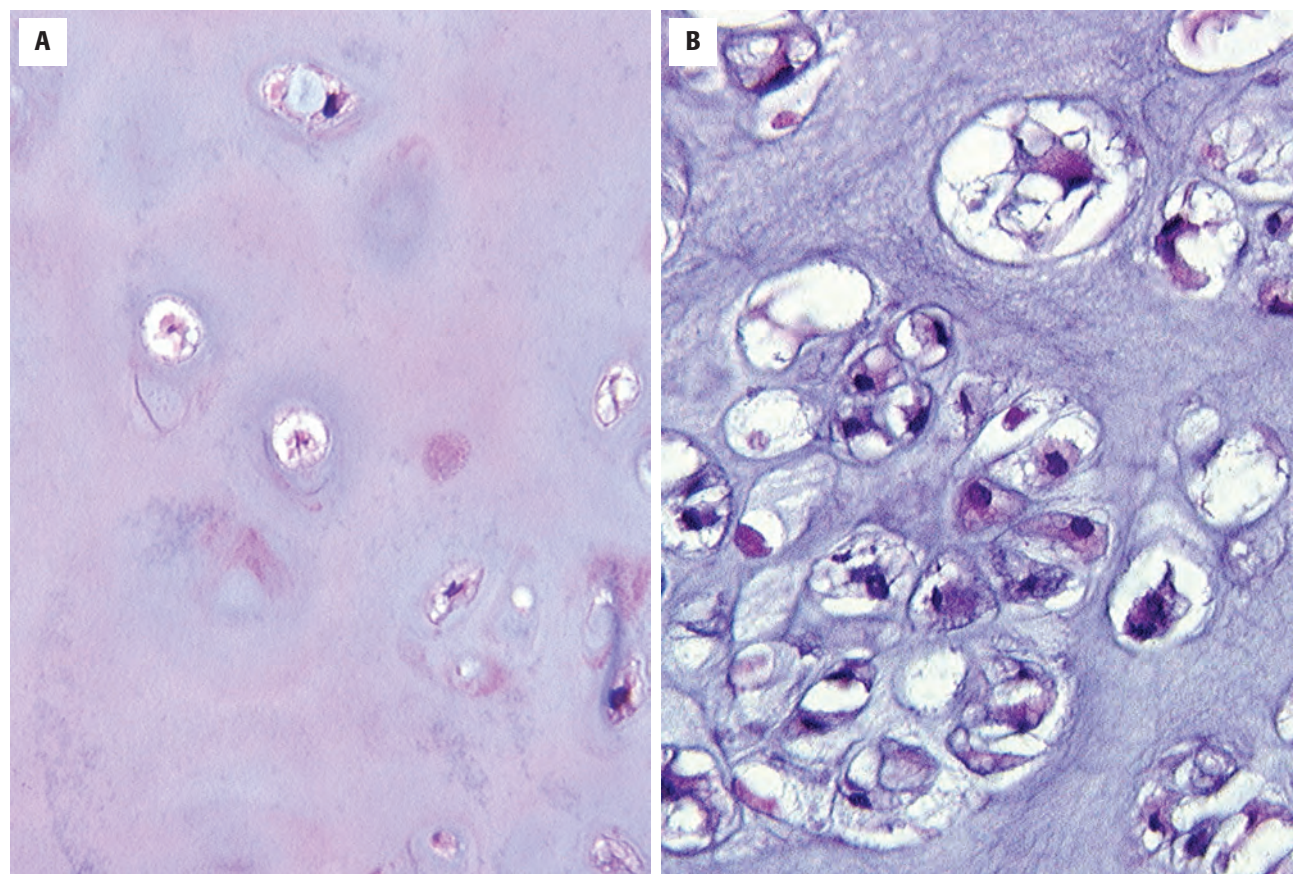
## MICROSCOPIC FINDINGS

Chondrosarcomas are recognized by their increased cellularity, nuclear pleomorphism including bi- and multinucleation (Fig. 6.46), and propensity to invade and destroy surrounding structures. Most chondrosarcomas seem to involve only a single cartilage with very little tendency to infiltrate adjacent cartilages. When the native cartilage is included in the biopsy, the cartilage is frequently ossified and will show neoplastic chondrocytes invading into the ossified regions (Fig. 6.47). The atypical, neoplastic chondrocytes are identified in a variable background of basophilic cartilaginous matrix material (Fig. 6.48) rather than the usual more pink-eosinophilic appearance of uninvolved cartilage. There is an overall loss of normal architecture and distribution of the chondrocytes (“cluster disarray”). The tumor cytomorphology varies from slightly cellular tumors composed of small, hyperchromatic nuclei surrounded by abundant cytoplasm to hypercellular neoplasms consisting of enlarged, bi- and multinucleated atypical cells with an increased N:C ratio, irregularities of nuclear chromatin distribution, and prominent nucleoli (Fig. 6.49). There is less stroma between the lacunar spaces as the grade of tumor increases. Mitotic figures, including atypical forms, are only infrequently noted and only in high-grade tumors. Tumor necrosis, usually focal and of limited geographic distribution, is usually restricted to higher-grade tumors. Ischemic change (blue, granular cytoplasm) can be seen in the background.

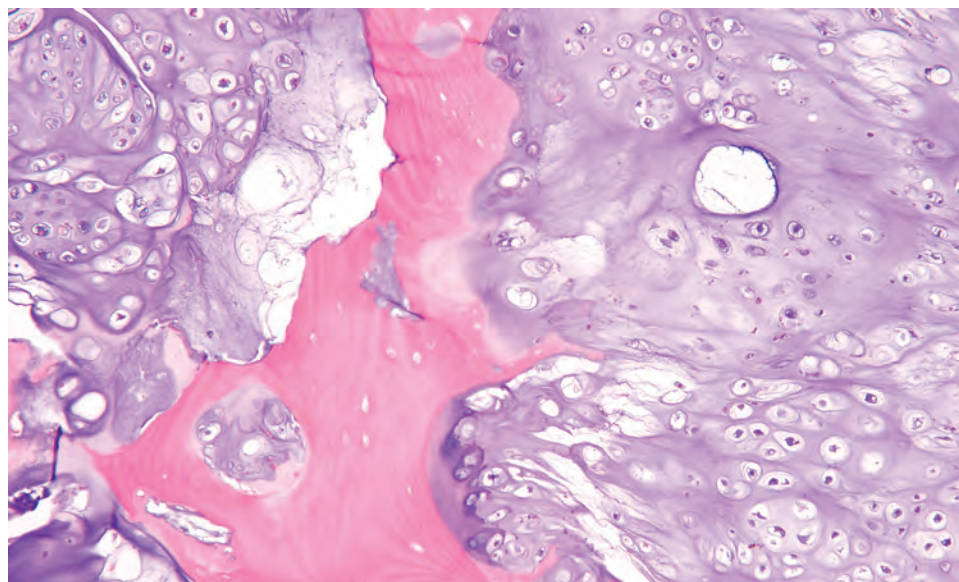
Chondrosarcomas are separated into grades based on increasing degrees of the aforementioned criteria. The vast majority (about 65 %) are well differentiated (low-grade, grade I), followed by moderately differentiated (intermediate-grade, grade II; 30 %), and poorly differentiated (high-grade, grade III; 5 %; Fig. 6.49) neoplasms. In the larynx, the grade does not seem to affect the overall patient outcome, although it does relate to recurrences. The vast majority of tumors are chondrocytic chondrosarcomas, but myxoid, mesenchymal, and dedifferentiated chondrosarcoma are described. Immunohistochemistry is unnecessary, although the tumor cells will be S100 protein, SOX9, and vimentin immunoreactive.

## DIFFERENTIAL DIAGNOSIS

The differential diagnosis is limited in practical terms to chondroma and chondrometaplasia. In general, true laryngeal *chondromas* are considered exceedingly rare; a number of authors consider all laryngeal chondromas to represent erroneous descriptions of low-grade chondrosarcomas. Given the frequent association of chondroma with chondrosarcoma, it is quite possible that “biopsy” material does not sample the malignant component. Therefore adequate tumor sampling (large biopsy) is

**FIGURE 6.46**

(A) Normal cartilage cellularity and lacunar size. (B) A chondrosarcoma has increased cellularity, pleomorphism, and increased nuclear size.

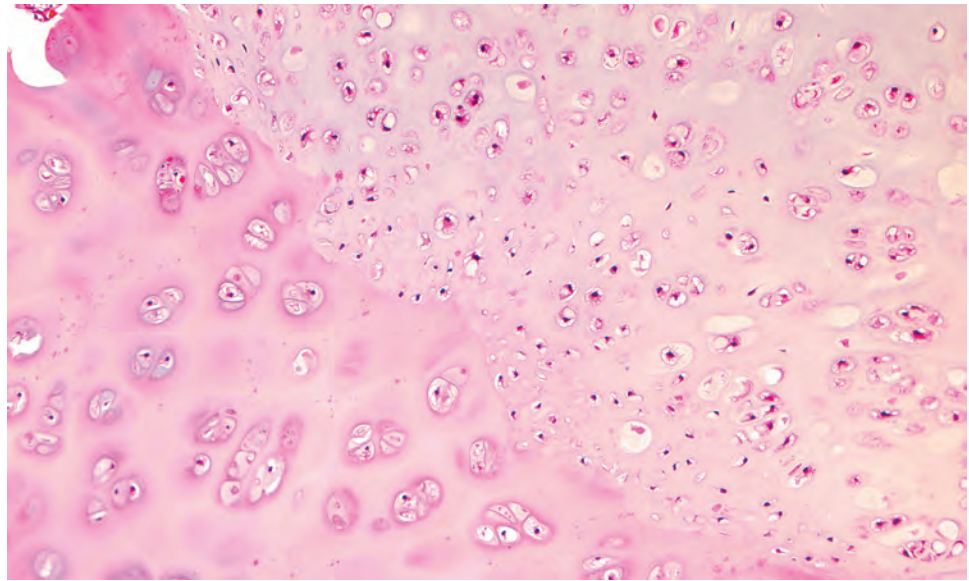
**FIGURE 6.47**

Bone is being destroyed from both sides by the low-grade (grade 1) chondrosarcoma. Note the cluster disarray.

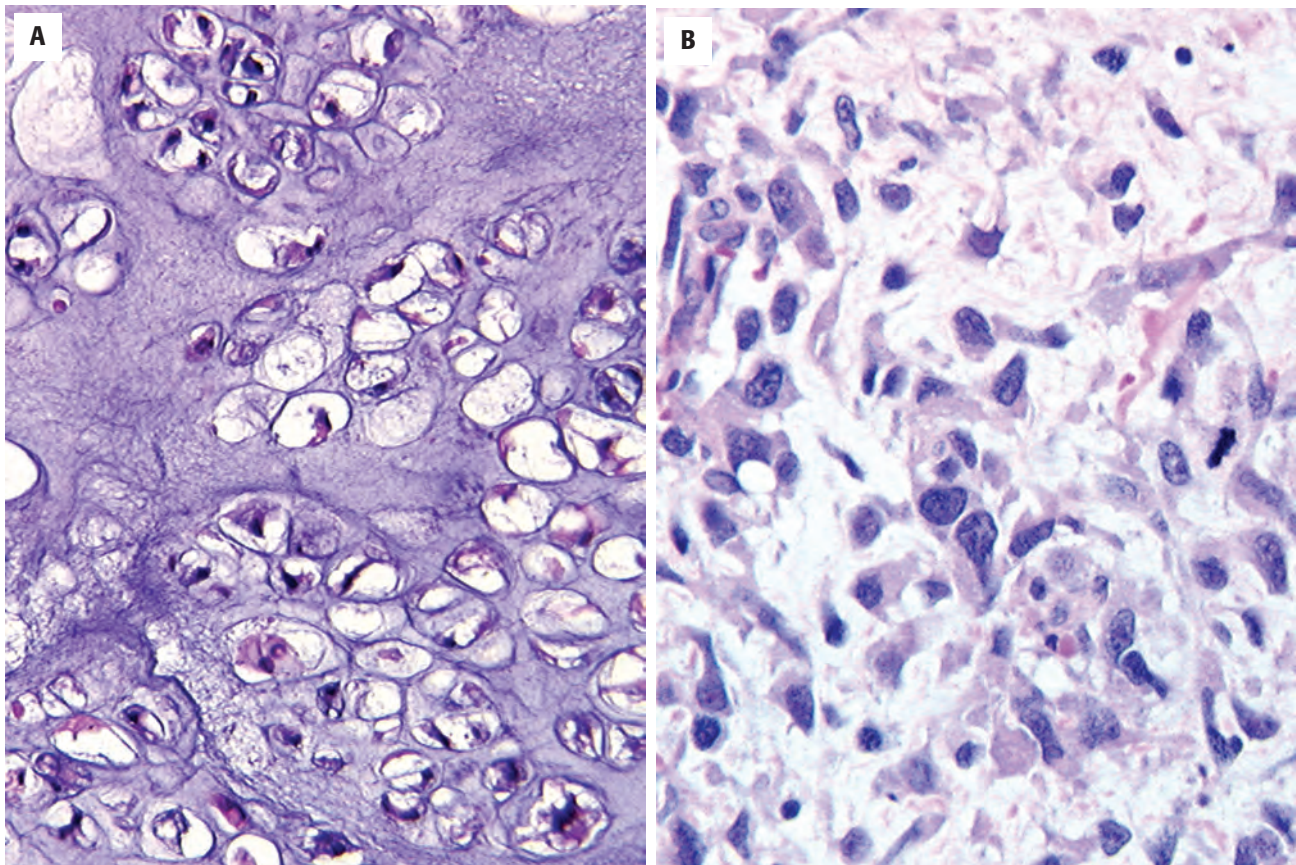
critical to the accurate identification of tumor type and grade. Although size alone is inaccurate in classification, tumors larger than 3 cm are more likely to be chondrosarcomas. The microscopic separation of chondroma from chondrosarcoma can be a very difficult one, with

chondromas containing slightly larger, albeit uniform nuclei with only slight architectural disorder. In practical terms, any *recurrent* cartilaginous tumor of the larynx should be considered a chondrosarcoma. *Spindle cell squamous cell carcinoma* may have metaplastic or



**FIGURE 6.48**

The lower left portion of the illustration demonstrates normal hyaline cartilage abutted by a grade 1 chondrosarcoma (upper and right side).

**FIGURE 6.49**

(A) A grade 2 chondrosarcoma has moderate cellularity with binucleation, nuclear atypia, and nuclear hyperchromasia. (B) A grade 3 chondrosarcoma has marked nuclear pleomorphism, multinucleation, and hyperchromatic nuclei. Mitoses are noted.

malignant cartilage as part of the tumor, but these lesions are polypoid, involve the glottis, and show keratin immunoreactivity in about 70 % of cases. *Chondrometaplasia* of the larynx consists of multiple elastic-rich cartilage nodules usually located on the vocal cords; they

are smaller than 1 cm and contain small, uniform chondrocytes without nuclear abnormalities. The margins of the lesions are indistinct, with a peripheral zone of transition between the cartilage and the surrounding tissues. A cartilaginous predominant *pleomorphic adenoma*

may also enter the differential, although identification of epithelial and/or myoepithelial components will help to resolve the matter.

### PROGNOSIS AND THERAPY

Laryngeal chondrosarcoma are considered low-grade neoplasms. Overall, there is a 90% survival with a mean follow-up of more than 10 years. Death from disease is very uncommon and is usually the result of uncontrolled local growth into vital structures of the neck. The presence of the myxoid subtype (>10% of the tumor volume) and age above 60 years at initial presentation has been reported to portend a worse patient outcome. A higher-grade tumor seems to suggest an increased chance of developing metastatic disease but not of dying from disease.

Conservative laryngeal function-preserving surgery is the treatment of choice. When recurrences develop (in up to 50% of patients), wide excision can again be employed, depending on the extent of the tumor, until functional compromise and the inability to reconstruct an adequate airway (with bone grafts or other materials) dictates the necessity for total laryngectomy. The voice-preserving surgeries allow for an improved quality of life and for a longer morbidity-free survival, which does not adversely impact the long-term patient survival.

### METASTATIC/SECONDARY TUMORS

These are defined as tumors secondarily involving the larynx or hypopharynx that originate from but are not in continuity with primary malignancies of other sites.

### CLINICAL FEATURES

Uncommon, these secondary lesions account for <0.2% of all laryngeal malignancies. Patients tend to be older men (M>F is 2:1), although sex predilection depends on tumor histology. For mucosa-based metastases, the supraglottis is most commonly affected (40%), while metastases to the cartilages tend to affect those with ossification. Up to 35% of cases have multifocal involvement. Patients present with hoarseness, voice changes, and stridor.

### PATHOLOGIC FEATURES

#### MICROSCOPIC FINDINGS

The tumors tend to be submucosal below an intact surface epithelium (Fig. 6.50). Metastases to the cartilages

tend to develop in areas of ossification and may not be identified macroscopically. The specific tumor type will dictate the histology, with melanoma and carcinoma the most common. Of the carcinomas, kidney (Fig. 6.50), breast, lung, prostate, and gastrointestinal (GI) tract account for the most common primary sites. Most tumors are adenocarcinomas. Although rare, leiomyosarcoma is the most common mesenchymal tumor to metastasize to the larynx. Pertinent, selected immunohistochemistry can be used to confirm the site of origin (Fig. 6.50).

### DIFFERENTIAL DIAGNOSIS

Primary poorly differentiated tumors may need to be separated from metastatic tumors. This is usually achieved

#### METASTATIC/SECONDARY TUMOR—DISEASE FACT SHEET

##### Definition

- Tumors secondarily involving the larynx or hypopharynx that originate from but are not in continuity with primary malignancies of other sites

##### Incidence and Location

- Rare, <0.2% of all tumors
- Supraglottis (mucosa) and cricoid cartilage

##### Morbidity and Mortality

- Usually poor owing to the systemic nature of the underlying primary

##### Sex and Age Distribution

- Males > Females (2:1)
- Older patients (owing to the nature of the underlying primary)

##### Clinical Features

- Multifocal disease
- Hoarseness, voice changes, and stridor

##### Prognosis and Treatment

- Matches underlying disease, but usually poor
- Excision for diagnosis and symptomatic relief

#### METASTATIC/SECONDARY TUMOR—PATHOLOGIC FEATURES

##### Microscopic Findings

- Submucosal mass or intracartilaginous lesion with a tumor histology based on underlying primary site

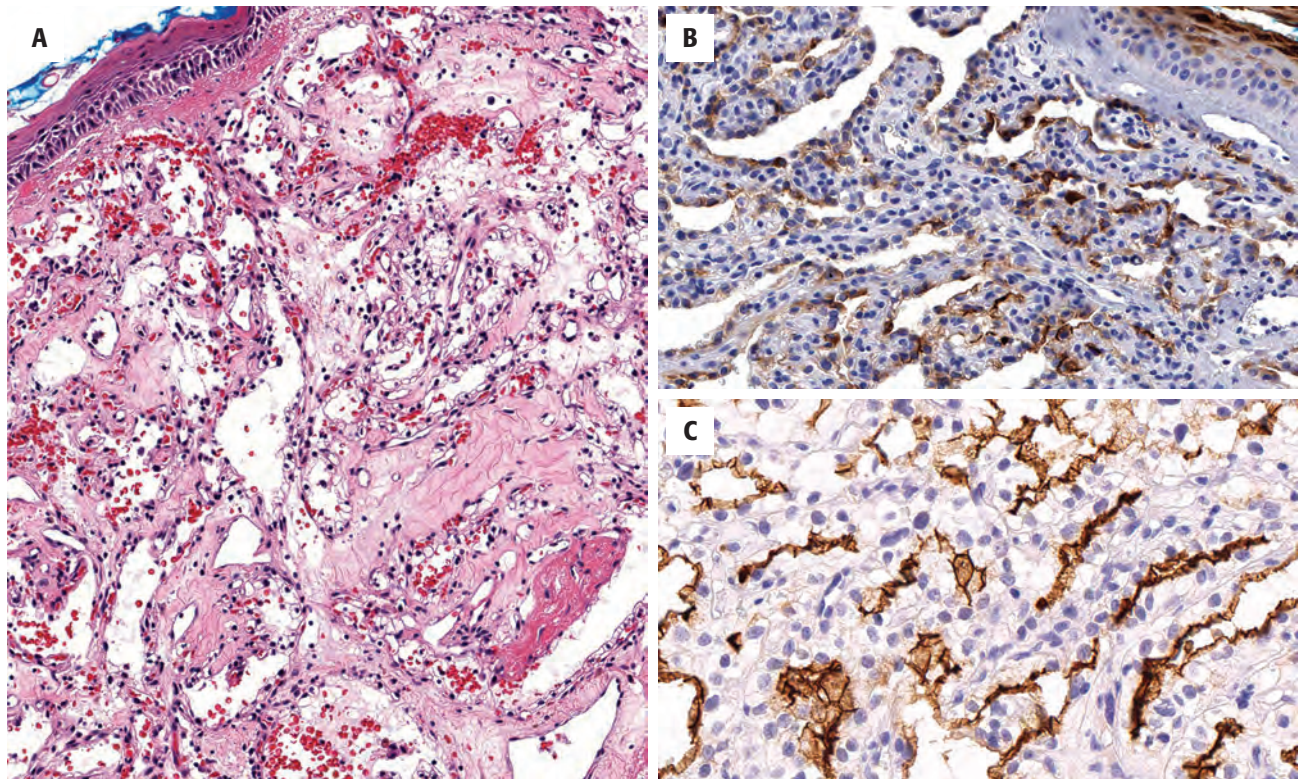
##### Immunohistochemistry Studies

- Pertinent, selected immunohistochemistry to prove origin

##### Pathologic Differential Diagnosis

- Primary tumor, direct extension from adjacent organs



**FIGURE 6.50**

(A) A metastatic renal cell carcinoma shows a pseudoalveolar pattern with extravasated erythrocytes. Note the cleared cytoplasm. The cells are immunoreactive with EMA (B) and CD10 (C), while PAX8 and CAIX would also be reactive in this tumor.

by history, radiographic studies, and immunohistochemistry. Direct extension from adjacent organs (thyroid and esophagus) and lymph nodes should also be considered.

### PROGNOSIS AND TREATMENT

The prognosis is partly based on the tumor type but largely reflects the natural course of disseminated disease, which portends a grave outcome. Renal cell carcinoma

is a possible exception, as isolated metastases, surgically removed, are associated with a good prognosis. Excision is advocated for diagnosis or symptomatic relief and not for cure, since laryngeal metastases are seldom isolated.

### SUGGESTED READINGS

The complete list of Suggested Readings is available online at [ExpertConsult.com](http://ExpertConsult.com).

## SUGGESTED READINGS

## Precursor Lesions

- Blackwell KE, et al. Laryngeal dysplasia: epidemiology and treatment outcome. *Ann Otol Rhinol Laryngol*. 1995;104(8):596–602.
- Crissman JD, et al. Preinvasive lesions of the upper aerodigestive tract: histologic definitions and clinical implications (a symposium). *Pathol Annu*. 1987;22(Pt 1):311–352.
- Crissman JD, et al. Dysplasia, in situ carcinoma, and progression to invasive squamous cell carcinoma of the upper aerodigestive tract. *Am J Surg Pathol*. 1989;13(suppl 1):5–16.
- Eversole LR. Dysplasia of the upper aerodigestive tract squamous epithelium. *Head Neck Pathol*. 2009;3(1):63–68.
- Fleskens S, et al. Grading systems in head and neck dysplasia: their prognostic value, weaknesses and utility. *Head Neck Oncol*. 2009;1:11.
- Fleskens SA, et al. Interobserver variability of laryngeal mucosal premalignant lesions—a histopathological evaluation. *Mod Pathol*. 2011;24(7):892–898.
- Gale N, et al. Evaluation of a new grading system for laryngeal squamous intraepithelial lesions—a proposed unified classification. *Histopathology*. 2014;65:456–464.
- Gale N, et al. Current review on squamous intraepithelial lesions of the larynx. *Histopathology*. 2009;54(6):639–656.
- Gale N, et al. Current views and perspectives on classification of squamous intraepithelial lesions of the head and neck. *Head Neck Pathol*. 2014;8(1):16–23.
- Gale N, et al. Tumours of the hypopharynx, larynx, trachea, and parapharyngeal space: precursor lesions: Dysplasia. In: El-Naggar AK, Chan JKC, Grandis JR, Takata T, Slootweg PJ, eds. *Classification of Head and Neck Tumours*. 4th ed. *World Health Organization Classification of Tumours*. Lyon, France: IARC Press; 2017: 91–93, in press.
- Gillis TM, et al. Natural history and management of keratosis, atypia, carcinoma-in situ, and microinvasive cancer of the larynx. *Am J Surg*. 1983;146(4):512–516.
- Halec G, et al. Biological evidence for a causal role of HPV16 in a small fraction of laryngeal squamous cell carcinoma. *Br J Cancer*. 2013;109(1):172–183.
- Hu Y, et al. Diagnostic variability of laryngeal premalignant lesions: histological evaluation and carcinoma transformation. *Otolaryngol Head Neck Surg*. 2014;150:401–406.
- Karatayli-Ozgursoy S, et al. Laryngeal dysplasia, demographics, and treatment: a single-institution, 20-year review. *JAMA Otolaryngol Head Neck Surg*. 2015;141(4):313–318.
- Lewis JS Jr, et al. Transcriptionally-active high-risk human papillomavirus is rare in oral cavity and laryngeal/hypopharyngeal squamous cell carcinomas—a tissue microarray study utilizing E6/E7 mRNA in situ hybridization. *Histopathology*. 2012;60(6): 982–991.
- López F, et al. From laryngeal epithelial precursor lesions to squamous carcinoma of the larynx: the role of cell cycle proteins and  $\beta$ -catenin. *Eur Arch Otorhinolaryngol*. 2013;270(12):3153–3162.
- Mondal D, et al. Ki67, p27 and p53 expression in squamous epithelial lesions of larynx. *Indian J Otolaryngol Head Neck Surg*. 2013;65(2):126–133.
- Mooren JJ, et al. P16(INK4A) immunostaining is a strong indicator for high-risk-HPV-associated oropharyngeal carcinomas and dysplasias, but is unreliable to predict low-risk-HPV-infection in head and neck papillomas and laryngeal dysplasias. *Int J Cancer*. 2014;134(9):2108–2117.
- Nadal A, et al. p53 expression in normal, dysplastic, and neoplastic laryngeal epithelium. Absence of a correlation with prognostic factors. *J Pathol*. 1995;175(2):181–188.
- Sarioglu S, et al. Inter-observer agreement in laryngeal pre-neoplastic lesions. *Head Neck Pathol*. 2010;4(4):276–280.
- Weller MD, et al. The risk and interval to malignancy of patients with laryngeal dysplasia; a systematic review of case series and meta-analysis. *Clin Otolaryngol*. 2010;35(5):364–372.
- Wenig BM. Squamous cell carcinoma of the upper aerodigestive tract: precursors and problematic variants. *Mod Pathol*. 2002;15(3): 229–254.
- Zhang HK, et al. Is severe dysplasia the same lesion as carcinoma in situ? 10-Year follow-up of laryngeal precancerous lesions. *Acta Otolaryngol*. 2012;132(3):325–328.

## Squamous Cell Carcinoma and Variants

- Alos L, et al. Adenosquamous carcinoma of the head and neck: criteria for diagnosis in a study of 12 cases. *Histopathology*. 2004;44(6):570–579.
- Bagnardi V, et al. Alcohol consumption and site-specific cancer risk: a comprehensive dose-response meta-analysis. *Br J Cancer*. 2015;112:580–593.
- Bahar G, et al. Basaloid squamous carcinoma of the larynx. *Am J Otolaryngol*. 2003;24(3):204–208.
- Banks ER, et al. Basaloid squamous cell carcinoma of the head and neck. A clinicopathologic and immunohistochemical study of 40 cases. *Am J Surg Pathol*. 1992;16:939–946.
- Barnes L, et al. Basaloid squamous cell carcinoma of the head and neck: clinicopathological features and differential diagnosis. *Ann Otol Rhinol Laryngol*. 1996;105:75–82.
- Batsakis JG, et al. The pathology of head and neck tumors: verrucous carcinoma, Part 15. *Head Neck Surg*. 1982;5(1):29–38.
- Batsakis JG, et al. Sarcomatoid carcinomas of the upper aerodigestive tracts. *Adv Anat Pathol*. 2000;7:282–293.
- Bice TC, et al. Disease-specific survival with spindle cell carcinoma of the head and neck. *Otolaryngol Head Neck Surg*. 2015;153:973–980.
- Bishop JA, et al. SMARCB1 (INI-1)-deficient carcinomas of the sinonasal tract. *Am J Surg Pathol*. 2014;38:1282–1289.
- Bishop JA, et al. Rhabdomyoblastic differentiation in head and neck malignancies other than rhabdomyosarcoma. *Head Neck Pathol*. 2015;9:507–518.
- Calli C, et al. Prognostic significance of p63, p53 and ki67 expression in laryngeal basaloid squamous cell carcinomas. *B-ENT*. 2011;7:37–42.
- Cattaruzza MS, et al. Epidemiology of laryngeal cancer. *Eur J Cancer B Oral Oncol*. 1996;32B:293–305.
- Chang AR, et al. Expression of epidermal growth factor receptor and cyclin D1 in pretreatment biopsies as a predictive factor of radiotherapy efficacy in early glottic cancer. *Head Neck*. 2008;30(7):852–857.
- Chernock RD, et al. Human papillomavirus-positive basaloid squamous cell carcinomas of the upper aerodigestive tract: a distinct clinicopathologic and molecular subtype of basaloid squamous cell carcinoma. *Hum Pathol*. 2010;41:1016–1023.
- Chernock RD, et al. Detection and significance of human papillomavirus, CDKN2A(p16) and CDKN1A(p21) expression in squamous cell carcinoma of the larynx. *Mod Pathol*. 2013;26:223–231.
- Choi HR, et al. Sarcomatoid carcinoma of the head and neck: molecular evidence for evolution and progression from conventional squamous cell carcinomas. *Am J Surg Pathol*. 2003;27:1216–1220.
- Chu EA, et al. Laryngeal cancer: diagnosis and preoperative work-up. *Otolaryngol Clin North Am*. 2008;41(4):673–695.
- Crissman JD, et al. Carcinoma in situ and microinvasive squamous carcinoma of the laryngeal glottis. *Arch Otolaryngol Head Neck Surg*. 1988;114:299–307.
- Damiani JM, et al. Mucoepidermoid-adenosquamous carcinoma of the larynx and hypopharynx: a report of 21 cases and a review of the literature. *Otolaryngol Head Neck Surg*. 1981;89(2):235–243.
- Dubal PM, et al. Laryngeal spindle cell carcinoma: A population-based analysis of incidence and survival. *Laryngoscope*. 2015;125:2709–2714.
- Dubal PM, et al. Laryngeal verrucous carcinoma: a population-based analysis. *Otolaryngol Head Neck Surg*. 2015;153:799–805.
- Dutta R, et al. Laryngeal papillary squamous cell carcinoma: a population-based analysis of incidence and survival. *Otolaryngol Head Neck Surg*. 2015;153:54–59.
- Ereno C, et al. Basaloid squamous cell carcinoma of the head and neck: a clinicopathological and follow-up study of 40 cases and review of the literature. *Head Neck Pathol*. 2008;2:83–91.
- Ferlito A, et al. Ackerman's tumor (verrucous carcinoma) of the larynx: a clinicopathologic study of 77 cases. *Cancer*. 1980;46(7): 1617–1630.
- Ferlito A, et al. Basaloid squamous cell carcinoma of the larynx and hypopharynx. *Ann Otol Rhinol Laryngol*. 1997;106(12):1024–1035.
- Ferlito A, et al. Mucoepidermoid carcinoma of the larynx. A clinicopathological study of 11 cases with review of the literature. *ORL J Otorhinolaryngol Relat Spec*. 1981;43(5):280–299.
- Ferlito A, et al. Mucosal adenoid squamous cell carcinoma of the head and neck. *Ann Otol Rhinol Laryngol*. 1996;105(5): 409–413.



28. Fonseca FP, et al. Molecular signature of salivary gland tumors: potential use as diagnostic and prognostic marker. *J Oral Pathol Med*. 2016;45:101–110.
29. French CA. The importance of diagnosing NUT midline carcinoma. *Head Neck Pathol*. 2013;7:11–16.
30. Fritsch VA, et al. Basaloid squamous cell carcinoma of the larynx: analysis of 145 cases with comparison to conventional squamous cell carcinoma. *Head Neck*. 2014;36:164–170.
31. Gale N, et al. Current review on squamous intraepithelial lesions of the larynx. *Histopathology*. 2009;54(6):639–656.
32. Galli J, et al. Laryngeal carcinoma and laryngo-pharyngeal reflux disease. *Acta Otorhinolaryngol Ital*. 2006;26(5):260–263.
33. Gerry D, et al. Spindle cell carcinoma of the upper aerodigestive tract: an analysis of 341 cases with comparison to conventional squamous cell carcinoma. *Ann Otol Rhinol Laryngol*. 2014;123:576–583.
34. Heffner DK. Infinitesimals, quantum mechanics, and exiguous carcinomas: how to possibly save a patient's larynx. *Ann Diagn Pathol*. 2003;7(3):187–194.
35. Hinni ML, et al. Surgical margins in head and neck cancer: a contemporary review. *Head Neck*. 2013;35:1362–1370.
36. Huang SH, et al. Truths and myths about radiotherapy for verrucous carcinoma of larynx. *Int J Radiat Oncol Biol Phys*. 2009;73(4):1110–1115.
37. Isenberg JS, et al. Institutional and comprehensive review of laryngeal leukoplakia. *Ann Otol Rhinol Laryngol*. 2008;117(1):74–79.
38. Jo VY, et al. Papillary squamous cell carcinoma of the head and neck: frequent association with human papillomavirus infection and invasive carcinoma. *Am J Surg Pathol*. 2009;33:1720–1724.
39. Kass JI, et al. Adenosquamous carcinoma of the head and neck: Molecular analysis using CRTC-MAML FISH and survival comparison with paired conventional squamous cell carcinoma. *Laryngoscope*. 2015;125:E371–E376.
40. Kau RJ, et al. Diagnostic procedures for detection of lymph node metastases in cancer of the larynx. *ORL J Otorhinolaryngol Relat Spec*. 2000;62(4):199–203.
41. Keelawat S, et al. Adenosquamous carcinoma of the upper aerodigestive tract: a clinicopathologic study of 12 cases and review of the literature. *Am J Otolaryngol*. 2002;23(3):160–168.
42. Kleist B, et al. Different risk factors in basaloid and common squamous head and neck cancer. *Laryngoscope*. 2004;114(6):1063–1068.
43. Koch BB, et al. National survey of head and neck verrucous carcinoma: patterns of presentation, care, and outcome. *Cancer*. 2001;92:110–120.
44. Kusafuka K, et al. MUC expression in adenosquamous carcinoma of the head and neck regions of Japanese patients: immunohistochemical analysis. *Pathol Int*. 2014;64:104–114.
45. Lewis JE, et al. Spindle cell carcinoma of the larynx: review of 26 cases including DNA content and immunohistochemistry. *Hum Pathol*. 1997;28(6):664–673.
46. McCaffrey TV, et al. Verrucous carcinoma of the larynx. *Ann Otol Rhinol Laryngol*. 1998;107(5 Pt 1):391–395.
47. Mehrad M, et al. Papillary squamous cell carcinoma of the head and neck: clinicopathologic and molecular features with special reference to human papillomavirus. *Am J Surg Pathol*. 2013;37:1349–1356.
48. Nakayama M, et al. Clinicopathological analyses of fifty supracricoid laryngectomized specimens: evidence base supporting minimal margins. *ORL J Otorhinolaryngol Relat Spec*. 2009;71:305–311.
49. Nappi O, et al. Sarcomatoid neoplasms of the respiratory tract. *Semin Diagn Pathol*. 1993;10:137–147.
50. Odar K, et al. Verrucous carcinoma of the head and neck - not a human papillomavirus-related tumour? *J Cell Mol Med*. 2014;18:635–645.
51. Olsen KD, et al. Spindle cell carcinoma of the larynx and hypopharynx. *Otolaryngol Head Neck Surg*. 1997;116(1):47–52.
52. Orvidas LJ, et al. Verrucous carcinoma of the larynx: a review of 53 patients. *Head Neck*. 1998;20(3):197–203.
53. Patel KR, et al. Verrucous carcinomas of the head and neck, including those with associated squamous cell carcinoma, lack transcriptionally active high-risk human papillomavirus. *Hum Pathol*. 2013;44:2385–2392.
54. Roy S, et al. Spindle cell carcinoma of the larynx with rhabdomyoblastic heterologous element: a rare form of divergent differentiation. *Head Neck Pathol*. 2013;7:263–267.
55. Russell JO, et al. Papillary squamous cell carcinoma of the head and neck: a clinicopathologic series. *Am J Otolaryngol*. 2011;32:557–563.
56. Schick U, et al. Adenosquamous carcinoma of the head and neck: report of 20 cases and review of the literature. *Oral Surg Oral Med Oral Pathol Oral Radiol*. 2013;116:313–320.
57. Sereg-Bahar M, et al. Higher levels of total pepsin and bile acids in the saliva as a possible risk factor for early laryngeal cancer. *Radiol Oncol*. 2015;49:59–64.
58. Suarez PA, et al. Papillary squamous cell carcinomas of the upper aerodigestive tract: a clinicopathologic and molecular study. *Head Neck*. 2000;22(4):360–368.
59. Thompson LD, et al. Exophytic and papillary squamous cell carcinomas of the larynx: A clinicopathologic series of 104 cases. *Otolaryngol Head Neck Surg*. 1999;120(5):718–724.
60. Thompson LD, et al. Spindle cell (sarcomatoid) carcinomas of the larynx: a clinicopathologic study of 187 cases. *Am J Surg Pathol*. 2002;26(2):153–170.
61. Thompson LDR. Squamous cell carcinoma variants of the head and neck. *Curr Diag Pathol*. 2003;9:384–396.
62. Thompson LDR. Laryngeal dysplasia, squamous cell carcinoma, and variants. *Surg Pathol Clin*. 2017;10(1):15–33.
63. Viswanathan S, et al. Sarcomatoid (spindle cell) carcinoma of the head and neck mucosal region: a clinicopathologic review of 103 cases from a tertiary referral cancer centre. *Head Neck Pathol*. 2010;4:265–275.
64. Volker HU, et al. Laryngeal inflammatory myofibroblastic tumors: Different clinical appearance and histomorphologic presentation of one entity. *Head Neck*. 2010;32:1573–1578.
65. Wagner M, et al. Occupational polycyclic aromatic hydrocarbon exposure and risk of larynx cancer: a systematic review and meta-analysis. *Occup Environ Med*. 2015;72:226–233.
66. Wenig BM. Lymphoepithelial-like carcinomas of the head and neck. *Semin Diagn Pathol*. 2015;32:74–86.
67. Wieneke JA, et al. Basaloid squamous cell carcinoma of the sinonasal tract. *Cancer*. 1999;85(4):841–854.
68. Wu M, et al. Comparative study in the expression of p53, EGFR, TGF- $\alpha$ , and cyclin D1 in verrucous carcinoma, verrucous hyperplasia, and squamous cell carcinoma of head and neck region. *Appl Immunohistochem Mol Morphol*. 2002;10:351–356.
69. Zidar N, et al. Down-regulation of microRNAs of the miR-200 family and miR-205, and an altered expression of classic and desmosomal cadherins in spindle cell carcinoma of the head and neck—hallmark of epithelial-mesenchymal transition. *Hum Pathol*. 2011;42:482–488.

## Neuroendocrine Carcinoma

1. Davies-Husband CR, et al. Primary, combined, atypical carcinoid and squamous cell carcinoma of the larynx: a new variety of composite tumour. *J Laryngol Otol*. 2010;124(2):226–229.
2. El-Naggar AK, et al. Carcinoid tumor of the larynx. A critical review of the literature. *ORL J Otorhinolaryngol Relat Spec*. 1991;53:188–193.
3. Ferlito A, et al. Paraneoplastic syndromes in patients with laryngeal neuroendocrine carcinomas: clinical manifestations and prognostic significance. *Eur Arch Otorhinolaryngol*. 2016;273(3):533–536.
4. Gillenwater A, et al. Moderately differentiated neuroendocrine carcinoma (atypical carcinoid) of the larynx: a clinically aggressive tumor. *Laryngoscope*. 2005;115(7):1191–1195.
5. Gnepp DR. Small cell neuroendocrine carcinoma of the larynx. A critical review of the literature. *ORL J Otorhinolaryngol Relat Spec*. 1991;53(4):210–219.
6. Jaiswal VR, et al. Primary combined squamous and small cell carcinoma of the larynx: a case report and review of the literature. *Arch Pathol Lab Med*. 2004;128(11):1279–1282.
7. Kao HL, et al. Head and neck large cell neuroendocrine carcinoma should be separated from atypical carcinoid on the basis of different clinical features, overall survival, and pathogenesis. *Am J Surg Pathol*. 2012;36(2):185–192.
8. Kusafuka K, et al. Mucosal large cell neuroendocrine carcinoma of the head and neck regions in Japanese patients: a distinct clinicopathological entity. *J Clin Pathol*. 2012;65(8):704–709.
9. Lewis JS Jr, et al. Large cell neuroendocrine carcinoma of the larynx: definition of an entity. *Head Neck Pathol*. 2010;4(3):198–207.
10. Mikić A, et al. Small cell neuroendocrine tumor of the larynx—a small case series. *Coll Antropol*. 2012;36(suppl 2):201–204.

11. Mills SE. Neuroectodermal neoplasms of the head and neck with emphasis on neuroendocrine carcinomas. *Mod Pathol.* 2002;15:264–278.
12. Perez-Ordóñez B, et al. Tumours of the Hypopharynx, larynx, trachea and parapharyngeal space: neuroendocrine tumours: well differentiated neuroendocrine carcinoma; moderately differentiated neuroendocrine carcinoma; poorly differentiated neuroendocrine carcinoma. In: El-Naggar AK, Chan JKC, Grandis JR, Takata T, Slootweg PJ, eds. *Classification of Head and Neck Tumours*. 4th ed. World Health Organization Classification of Tumours. Lyon, France: IARC Press;2017: 96–97.
13. Thompson ED, et al. Large cell neuroendocrine carcinoma of the head and neck: a clinicopathologic series of 10 cases with an emphasis on HPV status. *Am J Surg Pathol.* 2016;40(4):471–478.
14. van der Laan TP, et al. Clinical recommendations on the treatment of neuroendocrine carcinoma of the larynx: a meta-analysis of 436 reported cases. *Head Neck.* 2015;37(5):707–715.
15. Wenig BM, et al. Moderately differentiated neuroendocrine carcinoma of the larynx. A clinico-pathologic study of 54 cases. *Cancer.* 1988;62:2658–2676.
16. Woodruff JM, et al. Neuroendocrine carcinomas of the larynx. A study of two types, one of which mimics thyroid medullary carcinoma. *Am J Surg Pathol.* 1985;9(11):771–790.
12. Oliveira JF, et al. Laryngeal chondrosarcoma—ten years of experience. *Braz J Otorhinolaryngol.* 2014;80(4):354–358.
13. Purohit BS, et al. Dedifferentiated laryngeal chondrosarcoma: combined morphologic and functional imaging with positron-emission tomography/magnetic resonance imaging. *Laryngoscope.* 2014;124(7):E274–E277.
14. Rinaggio J, et al. Dedifferentiated chondrosarcoma of the larynx. *Oral Surg Oral Med Oral Pathol Oral Radiol Endod.* 2004;97(3):369–375.
15. Rinaldo A, et al. Laryngeal chondrosarcoma: a 24-year experience at the Royal National Throat, Nose and Ear Hospital. *Acta Otolaryngol.* 2000;120:680–688.
16. Sauter A, et al. Chondrosarcoma of the larynx and review of the literature. *Anticancer Res.* 2007;27(4C):2925–2929.
17. Thompson LDR, et al. Chondrosarcoma of the Larynx: A Clinico-pathologic Study of 111 Cases. *Am J Surg Pathol.* 2002;26:836–851.
18. Tiwari R, et al. Long-term results of organ preservation in chondrosarcoma of the cricoid. *Eur Arch Otorhinolaryngol.* 1999;256:271–276.

### Chondrosarcoma

1. Alexander J, et al. Primary laryngeal clear cell chondrosarcoma: report of a case and literature review. *Head Neck Pathol.* 2014;8(3):307–310.
2. Baatenburg de Jong RJ, et al. Chondroma and chondrosarcoma of the larynx. *Curr Opin Otolaryngol Head Neck Surg.* 2004;12(2):98–105.
3. Casiraghi O, et al. Chondroid tumors of the larynx: a clinicopathologic study of 19 cases, including two dedifferentiated chondrosarcomas. *Ann Diagn Pathol.* 2004;8(4):189–197.
4. de Vincentiis M, et al. Total cricoidectomy in the treatment of laryngeal chondrosarcomas. *Laryngoscope.* 2011;121(11):2375–2380.
5. Delaere P, et al. Organ preservation surgery for advanced unilateral glottic and subglottic cancer. *Laryngoscope.* 2007;117(10):1764–1769.
6. Devaney KO, et al. Cartilaginous tumors of the larynx. *Ann Otol Rhinol Laryngol.* 1995;104(3):251–255.
7. Dubal PM, et al. Laryngeal chondrosarcoma: a population-based analysis. *Laryngoscope.* 2014;124(8):1877–1881.
8. Garcia RE, et al. Dedifferentiated chondrosarcomas of the larynx: A report of two cases and review of the literature. *Laryngoscope.* 2002;112:1015–1018.
9. Kozelsky TF, et al. Laryngeal chondrosarcomas: the Mayo Clinic experience. *J Surg Oncol.* 1997;65(4):269–273.
10. Lewis JE, et al. Cartilaginous tumors of the larynx: clinicopathologic review of 47 cases. *Ann Otol Rhinol Laryngol.* 1997;106:94–100.
11. Merrot O, et al. Cartilaginous tumors of the larynx: endoscopic laser management using YAG/KTP. *Head Neck.* 2009;31(2):145–152.
1. Abbas A, et al. Leiomyosarcoma of the larynx: A case report. *Ear Nose Throat J.* 2005;84(7):435–436, 440.
2. Abemayor E, et al. Metastatic cancer to the larynx. Diagnosis and management. *Cancer.* 1983;52(10):1944–1948.
3. Batsakis JG, et al. Metastases to the larynx. *Head Neck Surg.* 1985;7(6):458–460.
4. Bernáldez R, et al. Pulmonary carcinoma metastatic to the larynx. *J Laryngol Otol.* 1994;108(10):898–901.
5. Coakley JF, et al. Metastasis to the larynx from a prostatic carcinoma. A case report. *J Laryngol Otol.* 1984;98(8):839–842.
6. Demir L, et al. Metastases of renal cell carcinoma to the larynx and thyroid: Two case reports on metastasis developing years after nephrectomy. *Can Urol Assoc J.* 2012;6(5):E209–E212.
7. Ferlito A, et al. Primary and secondary small cell neuroendocrine carcinoma of the larynx: a review. *Head Neck.* 2008;30(4):518–524.
8. Marioni G, et al. Laryngeal metastasis from sigmoid colon adenocarcinoma followed by peristomal recurrence. *Acta Otolaryngol.* 2006;126(6):661–663.
9. Marlowe SD, et al. Metastatic hypernephroma to the larynx: an unusual presentation. *Neuroradiology.* 1993;35(3):242–243.
10. Nicolai P, et al. Metastatic neoplasms to the larynx: report of three cases. *Laryngoscope.* 1996;106(7):851–855.
11. Prescher A, et al. Laryngeal prostatic cancer metastases: an underestimated route of metastases? *Laryngoscope.* 2002;112(8 Pt 1):1467–1473.
12. Ramanathan Y, et al. Laryngeal metastasis from a rectal carcinoma. *Ear Nose Throat J.* 2007;86(11):685–686.
13. Ritchie WW, et al. Uterine carcinoma metastatic to the larynx. *Laryngoscope.* 1985;95(1):97–98.
14. Sano D, et al. A case of metastatic colon adenocarcinoma in the larynx. *Acta Otolaryngol.* 2005;125(2):220–222.

### Metastatic – Secondary Tumors



# Non-Neoplastic Lesions of the Oral Cavity

■ Susan Müller

## ■ FORDYCE GRANULES

### CLINICAL FEATURES

Fordyce granules are considered benign ectopic sebaceous glands (not associated with hair follicles) that occur on the oral mucosa. A normal variant, they are reported in up to 80% of adults, most commonly on the upper and lower lip and the buccal mucosa. They present as multiple, uniform-sized yellow or yellow-white papules (Fig. 7.1), which may coalesce to form plaques. Usually asymptomatic, patients sometimes describe surface roughness.

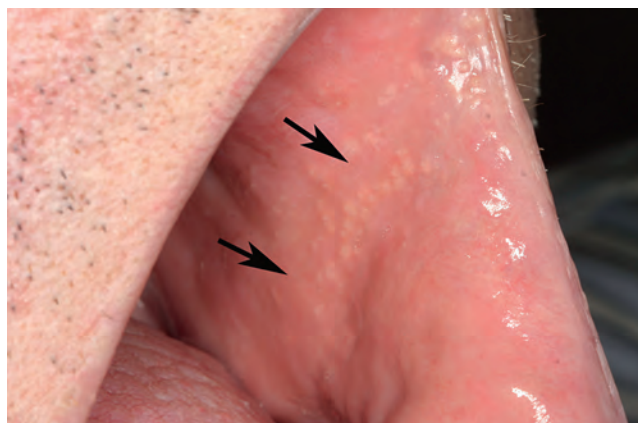


**FIGURE 7.1**

Clinical photograph of asymptomatic, multiple, small, yellow papules on the buccal mucosa (arrows) in this example of Fordyce granules.

### FORDYCE GRANULES—DISEASE FACT SHEET

#### Definition

- Benign ectopic sebaceous glands, considered to be a normal variant

#### Incidence and Location

- Reported in up to 80% of adults
- Present on the upper and lower lip and the buccal mucosa

#### Sex and Age Distribution

- Sexes equally affected
- Less clinically evident in children and adolescents

#### Clinical Features

- Asymptomatic, multiple, small yellow papules

#### Prognosis and Therapy

- Considered a normal variant

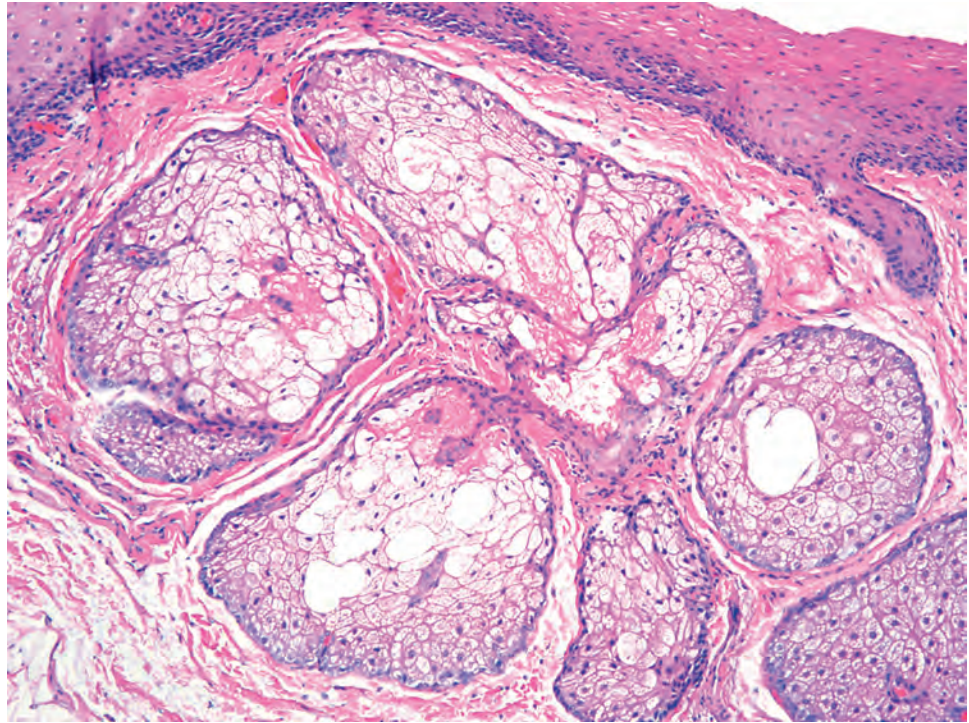
### PATHOLOGIC FEATURES

Biopsy reveals normal sebaceous glands near the surface epithelium without hair follicles (Fig. 7.2). Usually, multiple acinar lobules are present, although it may consist of one sebaceous lobule. A central duct sometimes connects the sebaceous lobules to the epithelial surface. Along the periphery, the sebaceous cells are basophilic and cuboidal, while the centrally located cells are polygonal in shape with abundant foamy cytoplasm and a centrally placed nucleus.

### FORDYCE GRANULES—PATHOLOGIC FEATURES

#### Microscopic Findings

- Normal sebaceous glands, below the surface, devoid of hair follicles

**FIGURE 7.2**

Multiple sebaceous glands in the superficial lamina propria.

### DIFFERENTIAL DIAGNOSIS

Superficial mucoceles, which can present as 1- to 3-mm papules on the lower lip, generally are blue to clear in color and spontaneously resolve.

### PROGNOSIS AND THERAPY

No treatment is indicated, although laser ablation can be offered to patients for cosmesis. Tumors arising from Fordyce granules have been reported but are extremely rare.

## ■ AMALGAM TATTOO

### CLINICAL FEATURES

Amalgam tattoo is a common localized area of blue, gray, or black pigmentation caused by amalgam that has been embedded into the oral tissues during dental procedures. Amalgam is a common material used for dental fillings and contains silver, tin, mercury, and other metals. Amalgam tattoos are most commonly located on the buccal mucosa, gingiva, and alveolar ridge (Fig. 7.3), usually

**FIGURE 7.3**

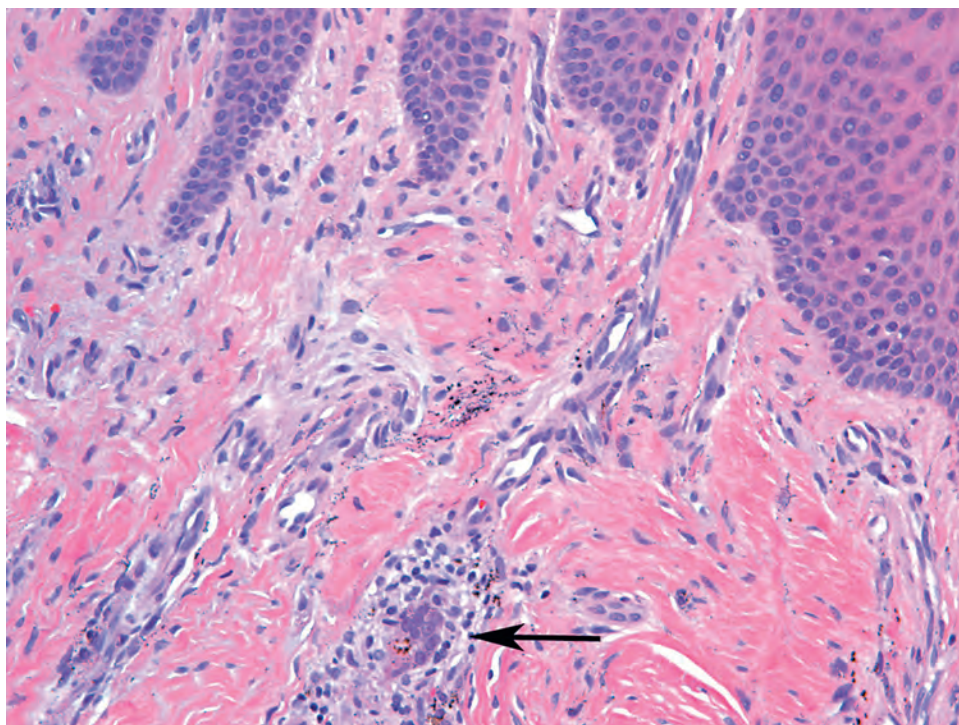
Clinical photograph of a blue-gray pigment present on the maxillary alveolar ridge. The pigmented area is flat with no ulceration or induration, and is asymptomatic.

presenting as flat macules, anywhere from a few millimeters to larger, more diffuse areas of pigmentation.

### RADIOGRAPHIC FEATURES

Generally, amalgam tattoos are not visible on dental radiographs. Larger tattoos may be visible on radiographs as densely radio-opaque lesions.



**FIGURE 7.4**

Black pigmented material is seen scattered in the lamina propria along collagen bundles and around blood vessels. The overlying epithelium is normal, and scant inflammatory cells are present. Although unusual, foreign body giant cell reactions can occur (*arrow*).

#### AMALGAM TATTOO—DISEASE FACT SHEET

##### Definition

- Localized pigmentation caused by amalgam that has been embedded in the oral tissues due to dental procedures

##### Incidence and Location

- Common
- Most common on the buccal mucosa, the gingiva, and the alveolar ridge

##### Clinical Features

- Asymptomatic flat macules ranging from a few millimeters to more diffuse areas of blue, gray, or black pigmentation

##### Prognosis and Therapy

- No treatment necessary unless for cosmetic reasons, or if the clinical diagnosis is uncertain and a melanocytic neoplasia needs to be ruled out

#### PATHOLOGIC FEATURES

An amalgam tattoo can demonstrate both discrete, fine, black granules and scattered, irregular, solid fragments (Fig. 7.4). Pigment granules are often arranged along collagen fibers and around blood vessels and nerves. Most cases elicit no tissue reaction, although a foreign body, giant cell reaction has been reported in up to 38% of cases.

#### AMALGAM TATTOO—PATHOLOGIC FEATURES

##### Microscopic Findings

- Discrete, black granules, and/or solid fragment findings of pigment arranged along collagen fibers, around blood vessels and nerves
- Foreign body reaction reported in up to 38% of cases

##### Pathologic Differential Diagnosis

- Other exogenous sources of pigmentation including pencil graphite, intentional tattoos, and coal dust

#### DIFFERENTIAL DIAGNOSIS

Other exogenous pigmentations can mimic an amalgam tattoo, including graphite, coal dust, and intentional tattooing. Melanin may be present in pigmented nevi, oral melanotic macule, oral melanoacanthoma, and melanoma. Further investigation is warranted if amalgam tattoos occur in sites distant from dental work or if the clinical diagnosis is uncertain.

#### PROGNOSIS AND THERAPY

No treatment is generally required, unless for cosmetic reasons (surgery or laser treatment) or if the clinical diagnosis is uncertain and a melanocytic neoplasm needs to be ruled out.

**FIGURE 7.5**

Clinical photograph of a lingual thyroid presenting as a midline nodular mass at the base of the tongue. The surface is smooth and hyperemic.

## ■ ECTOPIC THYROID

### CLINICAL FEATURES

Ectopic thyroid is a result of the abnormal migration of the thyroglossal duct from the foramen cecum located at the junction of the anterior two-thirds and posterior third of the tongue to its normal prelaryngeal location. While uncommon, nearly 90% of all ectopic thyroids are located on the tongue between the foramen cecum and the epiglottis. In > 70% of patients with lingual thyroid, this is the only functioning thyroid tissue. Females are affected four to seven times as frequently as males. Symptoms, including dysphagia, dyspnea, globus sensation, and dysphonia, most often coincide with puberty onset, pregnancy, or menopause corresponding to elevated thyroid-stimulating hormone (TSH). Thyroid function tests should be evaluated as part of the workup. The endoscopic appearance at the base of the tongue is of a hyperemic mass (Fig. 7.5).

### RADIOGRAPHIC FEATURES

The iodine content of the thyroid tissue results in very high signal attenuation in relation to surrounding soft tissue using computed tomography. Radioisotopic studies ( $^{131}\text{I}$  iodine and/or  $^{99\text{m}}\text{Tc}$ : technetium-99m pertechnetate) may be needed to determine size, location, and activity of thyroid tissue.

### PATHOLOGIC FEATURES

Immediately below the intact surface mucosa, unencapsulated ectopic thyroid follicles containing colloid and lined by cuboidal epithelium are identified, insinuating

### ECTOPIC THYROID—DISEASE FACT SHEET

#### Definition

- Rare developmental anomaly due to the abnormal migration of the thyroid gland from the base of the tongue

#### Incidence and Location

- Uncommon, with reported incidence of 1/100,000
- 90% of ectopic thyroids are lingual thyroids

#### Morbidity and Mortality

- Larger lesions can cause airway obstruction
- Rare reports of carcinoma development

#### Sex and Age Distribution

- Females > > > males (4-7:1)
- All ages (mean, 44 years)

#### Clinical Features

- Dysphagia, dyspnea, dysphonia, globus sensation
- One-third of patients are hypothyroid
- In > 70%, ectopic tissue is only functional thyroid tissue

#### Prognosis and Therapy

- Euthyroid and asymptomatic patients only require periodic follow-up
- Suppression therapy with thyroxine to reduce size and symptoms
- Radioactive  $^{131}\text{I}$  ablation
- Autotransplantation of lingual thyroid

### ECTOPIC THYROID—PATHOLOGIC FEATURES

#### Microscopic Findings

- Unencapsulated normal thyroid tissue insinuated through skeletal muscle
- Lymphocytic thyroiditis and adenomatoid nodules may develop

#### Pathologic Differential Diagnosis

- Metastatic thyroid carcinoma

#### Ancillary Studies

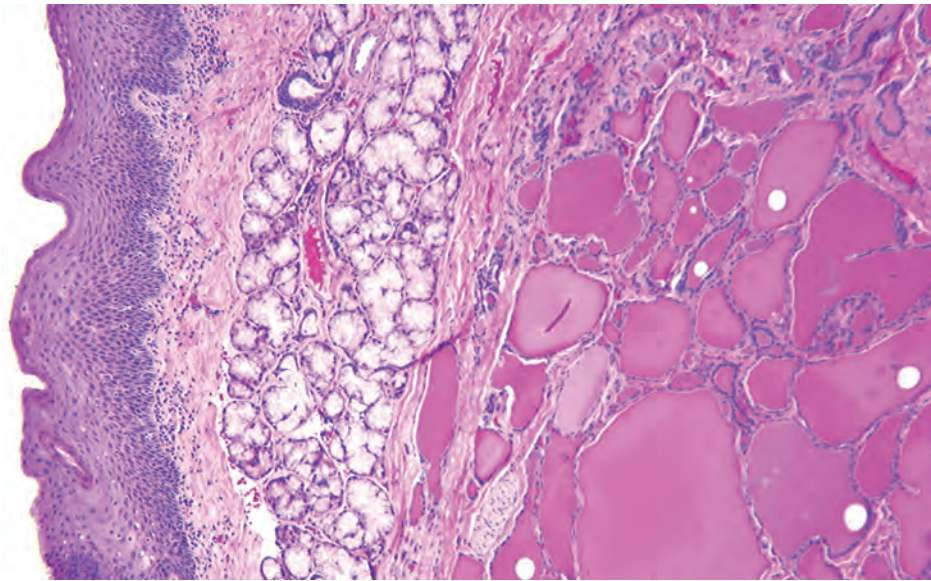
- Positive cytoplasmic staining with thyroglobulin, epithelial membrane antigen, and low-molecular weight cytokeratin
- Positive nuclear staining with TTF-1

between the tongue musculature (Fig. 7.6). Lymphocytic thyroiditis and adenomatoid nodules, as well as papillary thyroid carcinoma, have been reported.

### FINE NEEDLE ASPIRATION

Fine needle aspiration biopsy can be used to confirm the diagnosis of ectopic thyroid or to rule out neoplastic changes.



**FIGURE 7.6**

Normal stratified squamous epithelium overlying a unencapsulated collection of thyroid follicles. Note the minor mucoserous glands adjacent to the thyroid follicles.

### DIFFERENTIAL DIAGNOSIS

There are a number of clinical differential diagnostic considerations (hemangioma, lymphangioma, hypertrophic lingual tonsils, abscess, mucus retention cyst, squamous cell carcinoma), but the histologic features of ectopic thyroid are pathognomonic.

### PROGNOSIS AND THERAPY

Thyroxine suppresses TSH with a subsequent reduction in size. Surgery is used if there is uncontrollable hemorrhage, airway obstruction, or inability to eat. Radioablation may be used in nonsurgical candidates. If no “normal” thyroid is identified in the anterior neck, autotransplantation can be performed. Malignancy is a rare complication (< 1%), although it is more common in men.

## ORAL HAIRY LEUKOPLAKIA

### CLINICAL FEATURES

Oral hairy leukoplakia (OHL) is a benign epithelial disease associated with Epstein-Barr virus (EBV) and nearly always identified in human immunodeficiency virus (HIV)-infected and/or immunocompromised patients. The disease correlates with viral load and CD4 counts. OHL usually presents on the lateral border of the tongue as a white plaque, or vertical streaks, or with a corrugated surface (Fig. 7.7). The lesions can become quite extensive, and in some cases cover the entire lateral and dorsal

**FIGURE 7.7**

HIV-positive patient with a white patch on the lateral border of the tongue exhibiting a corrugated appearance in this example of oral hairy leukoplakia.

tongue. The lesion is asymptomatic and cannot be rubbed off.

### PATHOLOGIC FEATURES

OHL is characterized by marked epithelial acanthosis with elongation of the rete ridges and prominent hyperkeratosis. In the superficial spinous layer, “balloon cells,” characterized by intracellular ballooning degeneration, nuclear clearing, and margination of the chromatin indicative of a viral cytopathic effect, are present (Fig. 7.8). These nonspecific findings require documentation of EBV within the lesion.

### HISTOCHEMICAL STUDIES

Periodic acid–Schiff (PAS) highlights *Candida* organisms, identified as a secondary infection in some cases.

### ORAL HAIRY LEUKOPLAKIA—DISEASE FACT SHEET

#### Definition

- Benign, asymptomatic epithelial hyperplasia associated with Epstein-Barr virus nearly always in immunocompromised patients

#### Incidence and Location

- Less than 10% of HIV-infected patients who are on highly active antiretroviral therapy
- Non-HIV associated OHL reported in solid-organ transplant recipients and less commonly in patients with hematologic malignancies, autoimmune diseases, and other systemic inflammatory conditions
- OHL reported in immunocompetent patients on long-term inhaled, topical, and systemic corticosteroid use
- Primarily occurs on the lateral tongue, unilaterally or bilaterally

#### Sex, Race, and Age Distribution

- Identified particularly in HIV-positive men
- No racial or age predilection

#### Clinical Features

- White patches that can have a corrugated or folded surface that cannot be rubbed off
- May be quite extensive and bilateral and involve dorsal tongue

#### Prognosis and Therapy

- 10% improve spontaneously
- No specific treatment, although secondary *Candida* may need to be treated

HIV, Human immunodeficiency virus; OHL, oral hairy leukoplakia.

### IMMUNOHISTOCHEMICAL FINDINGS

Immunomarkers for EBV latent antigens (EBV nuclear antigen [EBNA], latent membrane protein [LMP]), replicative antigens (EA, VCA), or regulatory antigens (BLZF1) can be performed on both touch preps and biopsy specimens (Fig. 7.9). Depending on the immunostain used, latent versus replicative EBV infection can be determined.

### MOLECULAR STUDIES

Quantitative polymerase chain reaction (PCR) and in situ hybridization (ISH) assays (EBV-encoded small RNA

### ORAL HAIRY LEUKOPLAKIA—PATHOLOGIC FEATURES

#### Microscopic Findings

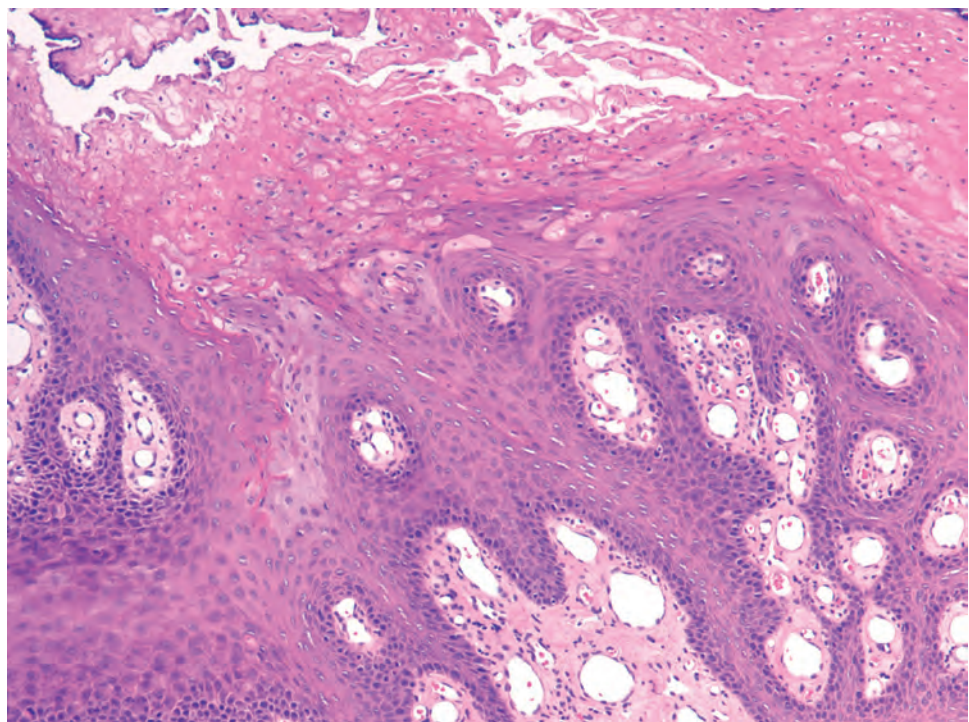
- Epithelial hyperplasia, hyperparakeratosis, and acanthosis
- Balloon cells in the upper spinous layer
- Viral cytopathic effect can sometimes be seen
- Little or no inflammation
- Secondary candidal infection may be identified

#### Ancillary Studies

- Markers for Epstein-Barr virus antigens (EBER) show punctate nuclear staining in the balloon cells

#### Pathologic Differential Diagnosis

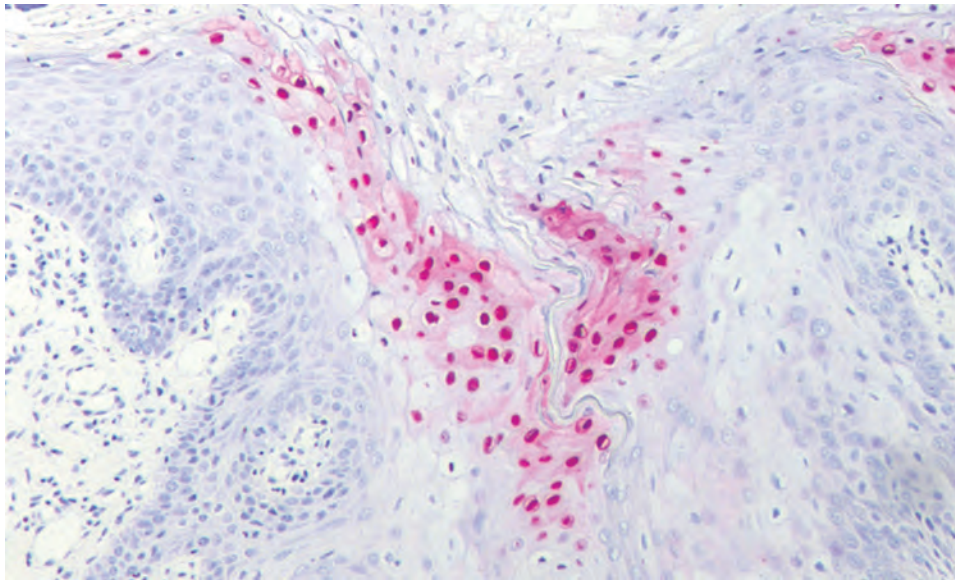
- Candidiasis, frictional keratosis, oral leukoplakia, lichen planus, and lichenoid reactions



**FIGURE 7.8**

A markedly hyperparakeratotic epithelium and a layer of balloon cells in the upper spinous layer.



**FIGURE 7.9**

In situ hybridization for Epstein-Barr virus encoded small RNA (EBER) shows strong punctate nuclear positivity in the region of the balloon cells.

[EBER]) may be useful when immunohistochemical studies fail to detect EBV, and especially when investigating EBV latent genes. EBER shows punctate nuclear staining of the spinous layer balloon cells.

### DIFFERENTIAL DIAGNOSIS

Clinically, OHL can mimic candidiasis, frictional keratosis (tongue biting), oral leukoplakia, lichen planus (LP), and lichenoid reactions. Oral candidiasis can be rubbed off the mucosa, while OHL cannot. However, OHL is frequently colonized by *Candida* sp.

### PROGNOSIS AND THERAPY

OHL does not have any malignant potential. It reportedly improves spontaneously in 10 % of cases. The incidence in HIV-infected patients has decreased to < 10 % with the use of highly active antiretroviral therapy (HAART). Treatment for concurrent *Candida* may be necessary if “burning” is described by the patient.

## ■ INFECTIONS

### CLINICAL FEATURES

There are numerous infectious conditions that can involve the oral cavity, including bacterial, fungal, viral, and protozoal infections. These infections can present as an

acute, rapidly progressive infection with constitutional symptoms, such as herpetic gingivostomatitis. Other infections can be chronic and slowly spreading, such as actinomycosis and leprosy. Sexually transmitted diseases, including syphilis and gonorrhea, can have oral manifestations. Deep fungal infections, including blastomycosis, coccidiomycosis, and histoplasmosis, can present as a nonspecific ulcer in the oral cavity. Since many infectious processes share clinical overlap, biopsy and/or culture is necessary to obtain a diagnosis. Three of the more common oral infections are caused by candidiasis, herpes simplex virus type 1 (HSV1), and actinomyces.

The most common fungal infection in the oral cavity and oropharynx is candidiasis. *Candida albicans* is the most common type, although other species have been isolated. Patients may complain of a burning sensation or a foul or salty taste, or may be entirely asymptomatic. In many infections, other factors play a role: antibiotic therapy; immunosuppression, including the use of prednisone; diabetes; pregnancy; xerostomia; and anemia.

The clinical presentations are protean, including the common acute pseudomembranous form (thrush) and erythematous (atrophic) variant (Fig. 7.10). Median rhomboid glossitis presents on the midline of the dorsal tongue as a red atrophic area (Fig. 7.11), which may become nodular over time. Angular cheilitis presents as a red scaling, fissuring area at the corners of the mouth, and is predisposed by drooling, parafunctional lip habits, and ill-fitting dentures. Hyperplastic candidiasis presents as white plaques that are *not* removable by rubbing, and occur most often on the hard palate and anterior buccal mucosa. Chronic mucocutaneous candidiasis presents as a chronic infection of the oral mucosa, nails, skin, and vagina—the familial form of which may present in early childhood and is associated with defects in cell-mediated immunity and endocrinopathies.

**FIGURE 7.10**

Clinical photograph of pseudomembranous candidiasis (thrush) presenting as creamy white plaques, which can be easily scraped off.

**FIGURE 7.11**

Clinical photograph of median rhomboid glossitis, with a red atrophic area on the midline of the dorsal tongue, corresponding to the loss of filiform papillae.

There are nearly ubiquitous antibodies (up to 90%) to the DNA of HSV1 virus, transmitted via direct contact or through saliva. Prevalence increases with age and correlates with socioeconomic status (lower status has increased prevalence). About 10% of patients when first exposed to HSV1 develop primary herpetic gingivostomatitis, while the remaining patients have subclinical

**FIGURE 7.12**

Clinical photograph of a cluster of fluid-filled vesicles of recurrent herpes simplex virus type 1 on the vermilion border.

**FIGURE 7.13**

Clinical photograph of intraoral recurrent herpes simplex virus on the mandibular attached gingiva. Intraoral vesicles rupture immediately, leaving red, eroded mucosa.

symptoms. Symptoms include fever, lymphadenopathy, malaise, mucosal erythema, vesicles, and ulcers, which resolve in 7 to 14 days. The virus remains latent within sensory and autonomic ganglion, which are reactivated in the trigeminal ganglion and result in infection of the vermilion border of the lip (herpes labialis), also called a “fever blister” or “cold sore” (Fig. 7.12). There is often a prodrome of burning, tingling, or itching at the site of the eruption, up to 24 hours before the outbreak. A cluster of fluid-filled vesicles form, rupture, crust, and heal within 7 to 10 days. Recurrent HSV1 can also occur intraorally on the hard palate and gingiva (Fig. 7.13).

*Actinomyces* are saprophytic, Gram-positive anaerobic bacteria that are part of normal oral flora. The primary pathogen is *Actinomyces israelii*, although other species can also cause infection. *Actinomyces* colonize tonsillar crypts, dental plaque, and gingival sulci. The presentation may be acute or chronic, with the bacteria entering through a site of trauma (tooth extraction



## INFECTIONS

### Definition

- **Candidiasis:** the most common oral fungal infection with a diverse clinical presentation and influenced by host immune status
- **HSV1:** a DNA virus transmitted via saliva or direct contact, with potential reactivation of latent disease
- **Actinomycosis:** acute or chronic infection by a normal saprophytic oral flora gram-positive anaerobic bacteria

### Incidence

- **Candidiasis:** *Candida* species detected in up to 50% of healthy individuals
- **HSV1:** up to 90% of adults have antibodies to HSV1
- **Actinomycosis:** uncommon, exact incidence unknown

### Morbidity and Mortality

- **Candidiasis:** usually a mild and self-limiting disease, although recurrent infections may signify an underlying disease
- **HSV1:** primary infection may be severely debilitating
- **Actinomycosis:** periostitis, osteomyelitis, and fistula formation

### Sex, Race, and Age Distribution

- **Candidiasis:** there are no sex or ethnic differences, but particularly affects the very young and elderly
- **HSV1:** prevalence increases with age and correlates with socioeconomic status (inversely proportional)
- **Actinomycosis:** no sex, ethnic, or age predilection

### Clinical Features

- **Candidiasis:** pseudomembranous, erythematous, median rhomboid glossitis, angular cheilitis, hyperplastic, and mucocutaneous types all have unique manifestations

*HSV1*, Herpes simplex virus type 1.

- **HSV1:** primary HSV1 may have fever, malaise, lymphadenopathy, multiple mucosal ulcerations, and painful erythematous gingiva; recurrent HSV1 present as fluid-filled vesicles commonly on the lip vermillion, palate, or gingiva
- **Actinomycosis:** acute form presents with painful abscesses, while chronic form may be painless, hardened, and/or result in fistula formation with trismus

### Prognosis and Therapy

- **Candidiasis:** topical and/or systemic antifungal medication
- **HSV1:** symptomatic or with topical/systemic antiviral drugs
- **Actinomycosis:** prolonged high doses of antibiotics, with abscess drainage and excision of the fistula, if present

### Microscopic Findings

- **Candidiasis:** fungal hyphae or pseudohyphae and ovoid spores (periodic acid–Schiff [PAS] positive) associated with neutrophilic microabscesses
- **HSV1:** viral cytopathic effect includes acantholysis, ballooning degeneration, chromatin margination, and multinucleation
- **Actinomycosis:** colonies of club-shaped filaments arranged in a rosette pattern surrounded by neutrophils

### Pathologic Differential Diagnosis

- **Candidiasis:** mucositis, leukoplakia, geographic tongue
- **HSV1:** erythema multiforme, herpes zoster, Epstein-Barr virus, HSV2, necrotizing ulcerative gingivitis, bacterial pharyngitis, traumatic ulcer
- **Actinomycosis:** abscess, other bacterial infections

site), infected tonsil, or soft tissue injury. In the acute suppurative phase, yellowish colonies of bacteria may be visible (“sulfur granules”), while the chronic form has extensive fibrosis, imparting a hard or “wooden” area of induration. A fistula may develop with extension to the surface, while periostitis and osteomyelitis may also develop.

## PATHOLOGIC FEATURES

### CANDIDA (INCLUDING MEDIAN RHOMBOID GLOSSITIS)

*Candida* can be seen on an exfoliative cytologic examination using either a periodic acid–Schiff (PAS; magenta-stained hyphae) or KOH stain (normal cells are lysed, but hyphae remain). The 2- $\mu$ m hyphae vary in length and can show branching along with ovoid spores or yeast forms (Fig. 7.14). In tissue sections, the organisms are seen in the parakeratin layer (Fig. 7.15 inset), highlighted with a PAS stain, while neutrophilic microabscesses may

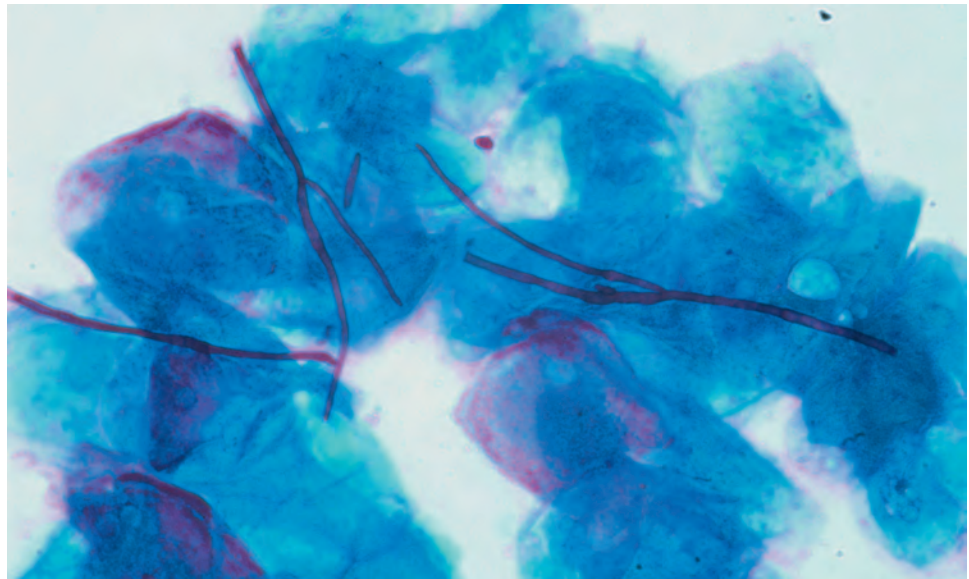
be seen along with chronic inflammatory cells in the submucosa. A PAS fungal stain is recommended whenever neutrophils are present in the parakeratin layer to help exclude a possible fungal infection.

### HERPES SIMPLEX VIRUS 1

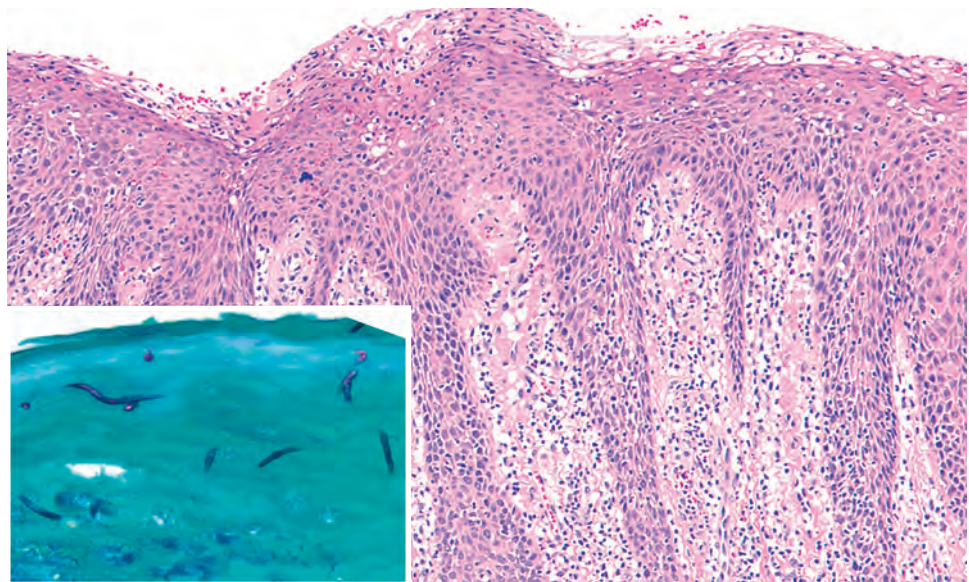
Epithelial cells infected with HSV1 show marked acantholysis (Tzanck cells), nuclear enlargement (ballooning degeneration), and condensation of the chromatin around the periphery of the nucleus (Fig. 7.16). Infected epithelial cells can fuse to form multinucleated cells. HSV1 ISH will demonstrate nuclear staining in virally infected cells (Fig. 7.16 inset). The adjacent mucosa is edematous with secondary inflammation.

### ACTINOMYCOSIS

Biopsy results show granulation tissue, with a variable number of colonies of club-shaped, basophilic, filamentous organisms arranged in a radiating rosette pattern

**FIGURE 7.14**

Exfoliative cytology with periodic acid–Schiff stain. The fungal hyphae and pseudo-hyphae appear magenta.

**FIGURE 7.15**

Marked parakeratosis and epithelial acanthosis with neutrophilic microabscesses present in hyperplastic candidiasis. *Inset:* Periodic acid–Schiff stain highlights yeast and hyphal forms noted within the parakeratin layer.

surrounded by neutrophils (so called “Splendore-Hoepli” phenomenon; [Fig. 7.17](#)). The diagnosis of *Actinomyces* can be confirmed by culture; however, due to the overgrowth of other bacteria or lack of anaerobic conditions, recovery rates are less than 30 %.

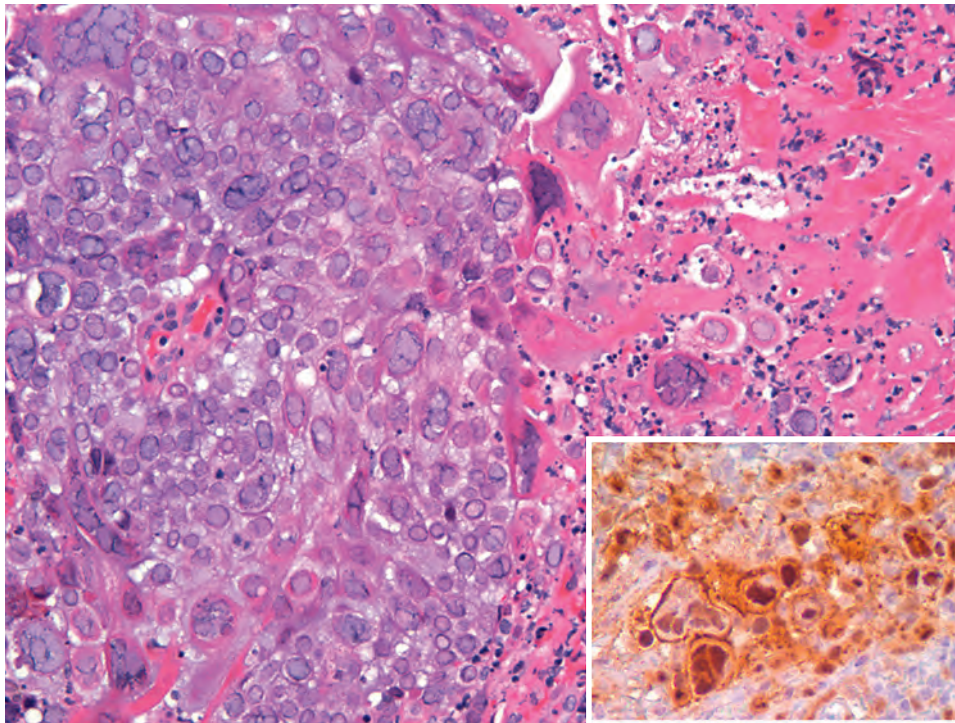
### DIFFERENTIAL DIAGNOSIS

Careful clinical history and familiarity with the clinical signs may be sufficient for arriving at a diagnosis. However, overlap in clinical presentation and lack of resolution after treatment may warrant a biopsy and/or culture. Mimics of candidiasis include severe mucositis, leukoplakia, geographic tongue, LP, and squamous cell carcinoma.

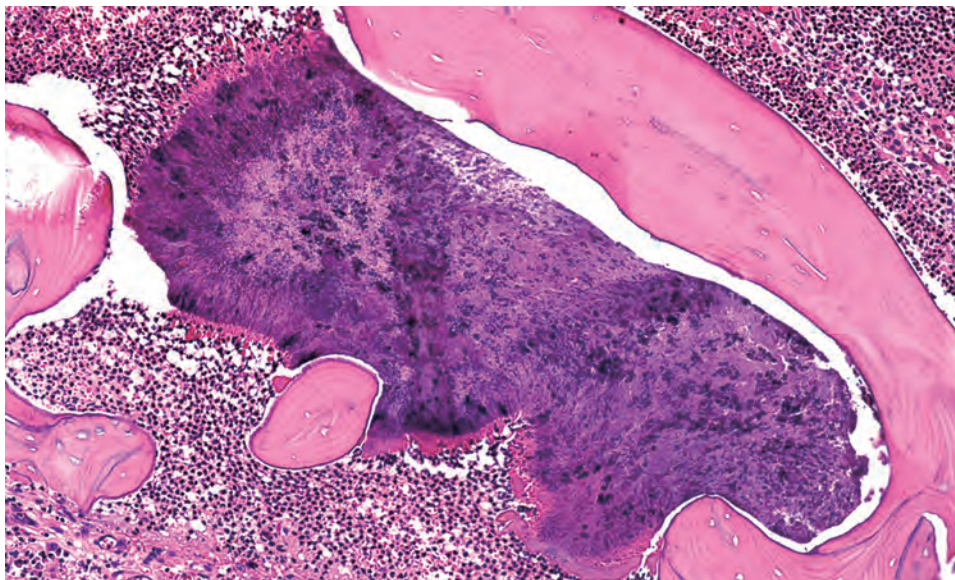
Mimics of primary HSV1, especially in adults, include erythema multiforme, necrotizing ulcerative gingivitis (NUG), pharyngotonsillitis of infectious mononucleosis, or streptococcal pharyngitis. Specific enzyme-linked immunosorbent assay (ELISA) testing of a culture from a vesicle can be performed in 24 hours and is definitive for diagnosis, while serologic tests for HSV1 antibodies document only past exposure. Changing social mores have increased the incidence of HSV2, but the infections are clinically and microscopically identical. Herpes zoster lesions can affect both keratinized and nonkeratinized mucosa, whereas HSV1 affects only keratinized mucosa.

Cervicofacial actinomycosis can masquerade as abscesses and benign or malignant neoplasms. *Nocardia* spp. are distinguished as acid-fast bacilli and stain well with a modified Ziehl-Neelsen stain, while *Actinomyces* spp. are not acid-fast.



**FIGURE 7.16**

Acantholytic epithelial cells (Tzanck cells) and cells with nuclear enlargement. Numerous multinucleated cells also show chromatin condensation at the periphery. *Inset:* In situ hybridization for herpes simplex virus type 1 shows strong nuclear staining in the virally altered acantholytic and multinucleated cells.

**FIGURE 7.17**

Colonies of club-shaped filamentous actinomycetes are arranged in a radiating rosette pattern surrounded by neutrophils and nonviable bone.

### PROGNOSIS AND THERAPY

Antimicrobial therapies represent an area of constant change and improvement, so specific drug therapies will not be included here. However, if a patient does not respond to antifungal therapy, culture is recommended to determine the definitive species of *Candida* and its drug sensitivity. If an otherwise healthy patient develops chronic oral candidiasis, then endocrine abnormalities and anemia studies should be evaluated. Any leukoplakic

lesion that exhibits dysplasia with concomitant candidiasis should be treated with appropriate antifungals and then reevaluated.

Primary HSV1, especially in pediatric patients, requires management of fever, hydration, nutritional intake, and oral pain. Topical antiviral medications are most effective when initiated during the prodrome period or within the first few hours of vesicle formation.

Chronic actinomycosis is best managed by long-term, high-dose, antibiotic therapy. Incision and drainage of any abscesses and excision of the sinus tracts are indicated.

**FIGURE 7.18**

White lace-like striae (Wickham striae) and coalescing papules affecting the buccal mucosa in a case of oral lichen planus.

**FIGURE 7.19**

Clinical photograph of erosive lichen planus of the dorsal tongue presenting with lace-like striae and plaques with erosions (arrows).

## ■ ORAL LICHEN PLANUS

### CLINICAL FEATURES

LP is a common mucocutaneous disease that can affect the skin, mucous membranes, nails, and eyes. Of patients with oral LP (OLP), only 15 % develop cutaneous disease. LP is a self-limiting disease that affects mainly middle-aged adults, with women affected more often than men (2:1). OLP is rare in the pediatric population and a slight male predilection is reported. OLP can manifest in various forms, most commonly the reticular and erosive types, without exception, showing multifocal lesions. The reticular variant is asymptomatic, presenting on the buccal mucosa with a lace-like network of fine white lines (Wickham striae; Fig. 7.18). On the dorsal tongue, it more often presents as a white plaque, rather than fine, white striae. The erosive variant causes areas of erythema and superficial ulceration, often covered by a fibrinopurulent membrane, with symptoms of pain and burning that can interfere with speech and eating. At the periphery of the erythematous or eroded area, the more typical reticular form of OLP may be observed (Fig. 7.19). Approximately 10 % of OLP is confined to the gingiva, commonly presenting with marked erythema resulting in desquamative gingivitis. The gingiva bleeds readily and can lead to gingival recession and periodontal disease.

### PATHOLOGIC FEATURES

While characteristic, the histology is not specific. OLP demonstrates hyperparakeratotic, acanthotic, and stratified squamous epithelium with either absent rete or hyperplastic rete descriptively called “saw-tooth” rete

### ORAL LICHEN PLANUS—DISEASE FACT SHEET

#### Definition

- Common chronic, self-limited inflammatory mucocutaneous disorder of unknown etiology that can affect the skin, mucous membranes, nails, and eyes

#### Incidence

- 1%-2.2% of world population

#### Sex and Age Distribution

- Females > males (2:1)
- Peak in middle-aged adults

#### Clinical Features

- Reticular variant: fine, white lace-like striae in a roughly symmetrical distribution
- Erosive variant: atrophic erythematous mucosa with ulceration

#### Prognosis and Therapy

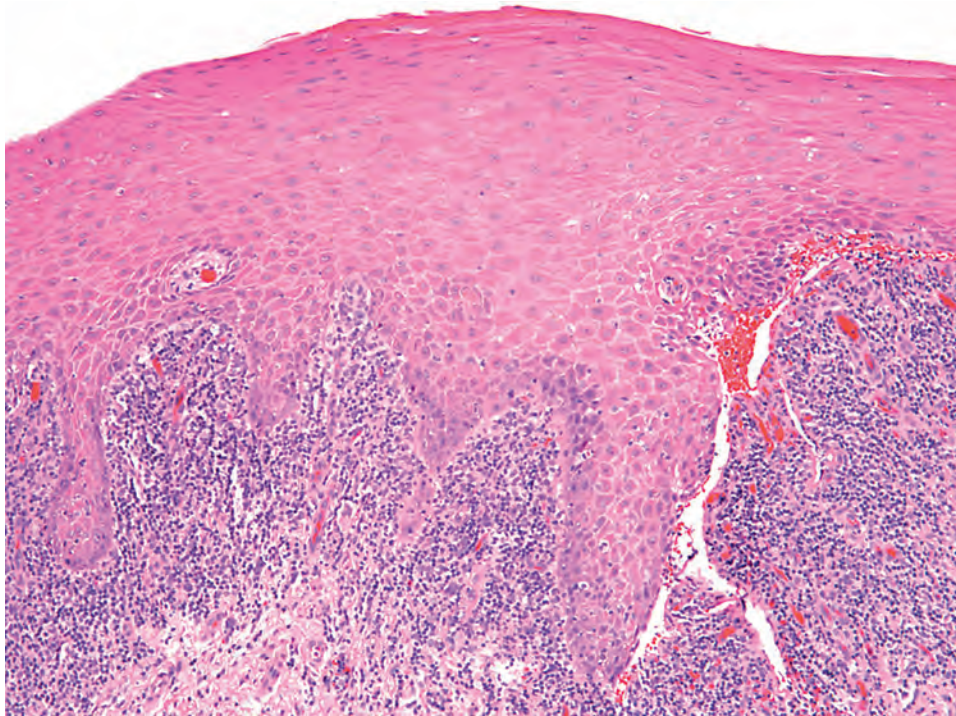
- Symptomatic lesions controlled with topical corticosteroids

(Fig. 7.20). Basal cell liquefactive degeneration with an adjacent band-like lymphocytic infiltrate and occasional degenerating keratinocytes (colloid, cytoid, or Civatte bodies) are typical features (Fig. 7.21). Biopsy samples from an erosive area may have epithelial separation or absence. Plasma cells are frequently noted in biopsies from gingival OLP. No dysplasia should be present.

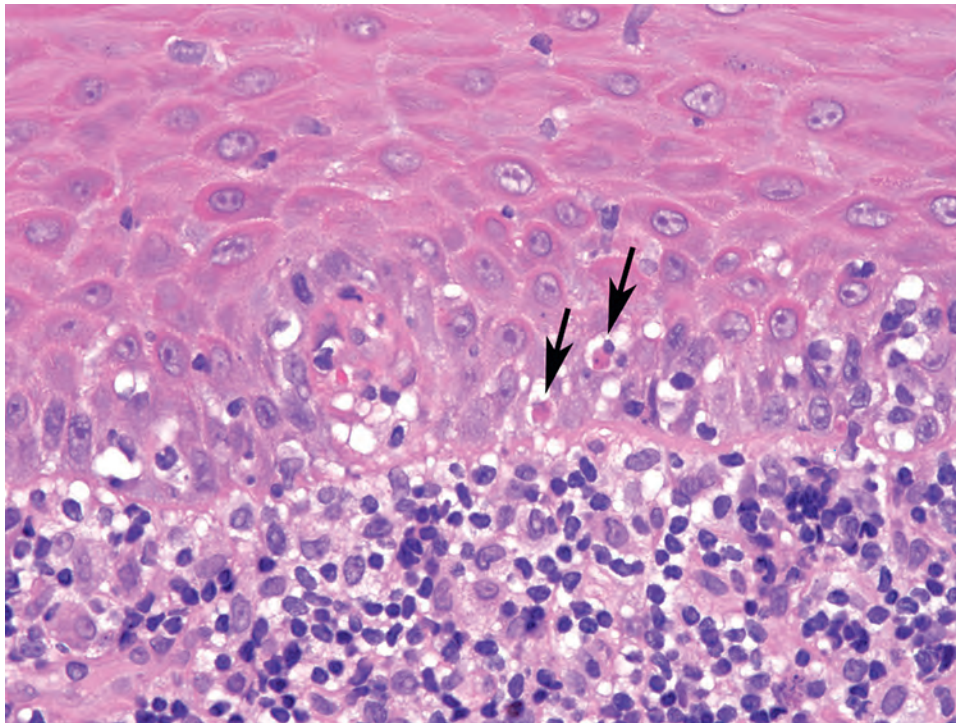
### ANCILLARY STUDIES

Direct immunofluorescence (DIF) of *perilesional* mucosa often demonstrates linear deposits of fibrin and fibrinogen



**FIGURE 7.20**

Lichen planus demonstrates parakeratotic, acanthotic stratified squamous epithelium with a band-like, lymphoplasmacytic infiltrate. The rete may be absent or "saw-tooth" as seen in this example. Subbasal separation is seen in the erosive form of lichen planus.

**FIGURE 7.21**

Interface inflammation with basal cell liquefaction and cytol bodies (*arrows*) are noted in oral lichen planus.

### ORAL LICHEN PLANUS—PATHOLOGIC FEATURES

#### Microscopic Findings

- Hyperkeratosis, acanthosis, “saw-tooth” rete
- Destruction of epithelial basal cell layer
- Band-like lymphocytic infiltrate
- Degenerating keratinocytes (cytoid, Civatte bodies)
- Erosive form may have subepithelial separation from lamina propria

#### Immunofluorescence Findings

- Direct immunofluorescence of *perilesional* tissue may show shaggy linear deposits of fibrin and fibrinogen at the basement membrane zone

#### Pathologic Differential Diagnosis

- Mucous membrane pemphigoid, lichenoid drug reaction, lichenoid reaction to amalgam, lupus, IgA disease, chronic graft-versus-host disease, chronic ulcerative stomatitis, dysplasia

at the basement membrane zone (BMZ). Although this finding is nonspecific, it is especially useful in excluding other vesiculoulcerative diseases. Indirect immunofluorescence (IDIF) is negative.

### DIFFERENTIAL DIAGNOSIS

The clinical appearance is most important, but with more complex patterns, including the erosive pattern, biopsy is often needed to rule out other vesiculoulcerative diseases. These include mucous membrane pemphigoid, lupus erythematosus, pemphigus vulgaris (PV), chronic graft-versus-host disease, linear immunoglobulin (Ig)A disease, a lichenoid reaction to dental materials (e.g., amalgam), chronic ulcerative stomatitis, and lichenoid drug reactions. Both DIF and IDIF may help in delineating these disease processes. Furthermore, OLP is never solitary and any solitary lichenoid lesion should undergo biopsy to exclude a premalignant or malignant lesion, which would have cellular enlargement, nuclear pleomorphism, and increased or abnormal mitoses.

### PROGNOSIS AND THERAPY

OLP is a chronic disease with symptoms that wax and wane over the lifetime of the patient. No treatment is necessary for asymptomatic patients, but corticosteroids are used for erosive or erythematous OLP. If extensive, a short course of systemic prednisone can reduce the symptomatic areas sufficiently so that topical corticosteroids can manage symptoms. Occasionally, topical cyclosporine and tacrolimus are employed. Extended topical corticosteroid

use places the patient at increased risk for developing oral candidiasis. While controversial, malignant transformation may rarely develop in the atrophic, erosive pattern of OLP, suggesting the need for long-term clinical follow-up of patients with symptomatic OLP.

## MUCOUS MEMBRANE PEMPHIGOID

### CLINICAL FEATURES

Mucous membrane pemphigoid (MMP) is a chronic autoimmune subepithelial blistering disease predominantly affecting the mucous membranes. The underlying pathogenesis is autoantibodies (at least 10 different types identified) that target the BMZ. Serious sequelae include subglottic stenosis, airway obstruction, conjunctival scarring, and blindness. The scarring in MMP is referred to as cicatricial pemphigoid. Middle-aged to elderly patients (50 to 70 years) are most commonly affected, with women affected more often than men (1.5 to 2:1). Almost 100 % of patients with MMP have oral involvement, with the gingiva affected in more than 60 % of oral MMP (Fig. 7.22). A positive Nikolsky sign, where clinically normal mucosa blisters on induced trauma, is seen in MMP.

### PATHOLOGIC FEATURES

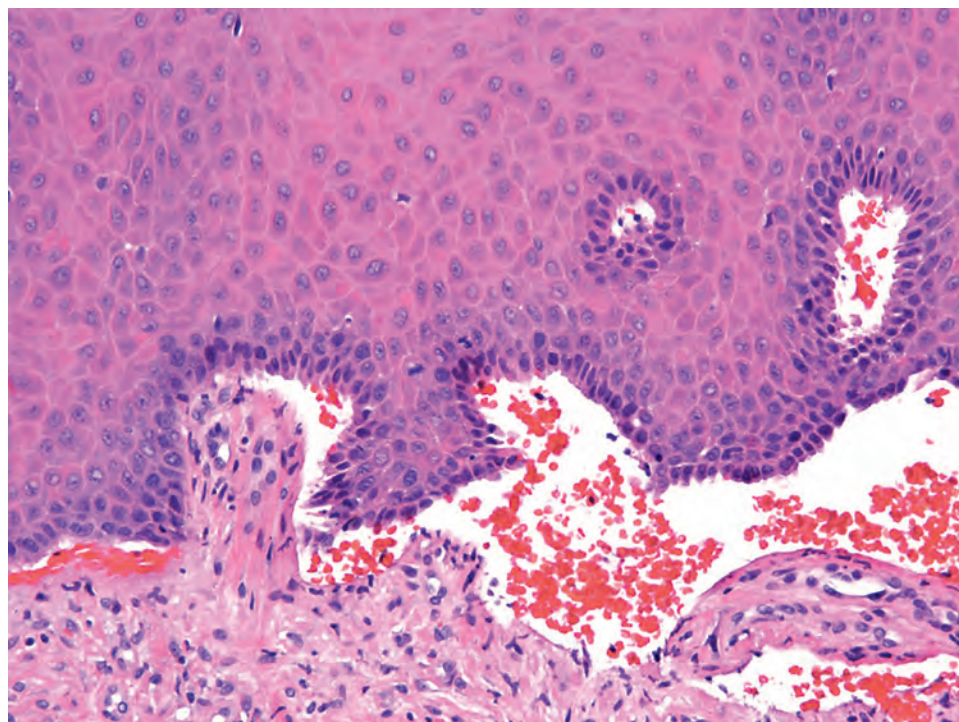
Examination of *perilesional* mucosal tissue demonstrates a subepithelial cleft, with a sparse inflammatory cell infiltrate containing lymphocytes and plasma cells in the superficial lamina propria (Fig. 7.23) with an intact basal cell layer. Occasionally, neutrophils and eosinophils are seen.



**FIGURE 7.22**

Mucous membrane pemphigoid presenting as desquamative gingivitis with large areas of red denuded mucosa resulting from sloughing of the epithelium of both the maxilla and mandible.



**FIGURE 7.23**

Perilesional tissue demonstrating subepithelial clefting and a sparse inflammatory cell infiltrate in the superficial lamina propria. There is no basal cell destruction.

### MUCOUS MEMBRANE PEMPHIGOID—DISEASE FACT SHEET

#### Definition

- An autoimmune subepithelial blistering disease predominantly affecting the mucous membranes associated with autoantibodies that target the basement membrane zone

#### Incidence

- Incidence is unknown

#### Morbidity and Mortality

- Erosions heal with scarring, which can result in blindness, airway obstruction, and epistaxis

#### Sex and Age Distribution

- Females > males (2:1)
- Mean, 50-70 years

#### Clinical Features

- Mucosal blisters, which collapse, resulting in red painful erosions
- Positive Nikolsky sign (mucosal blistering on induced trauma)

#### Prognosis and Therapy

- Waxing-waning, long-term course is usual
- Disease progression despite appropriate therapy
- Treatment includes topical and/or systemic corticosteroids, immunosuppressive therapy, and intravenous immunoglobulin

### MUCOUS MEMBRANE PEMPHIGOID—PATHOLOGIC FEATURES

#### Microscopic Findings

- Perilesional tissue shows subepithelial cleft with intact basal cells with or without stromal inflammatory cells

#### Immunofluorescence Findings

- DIF demonstrates linear deposits along the basement membrane zone of IgG and/or C3, sometimes IgA, IgM

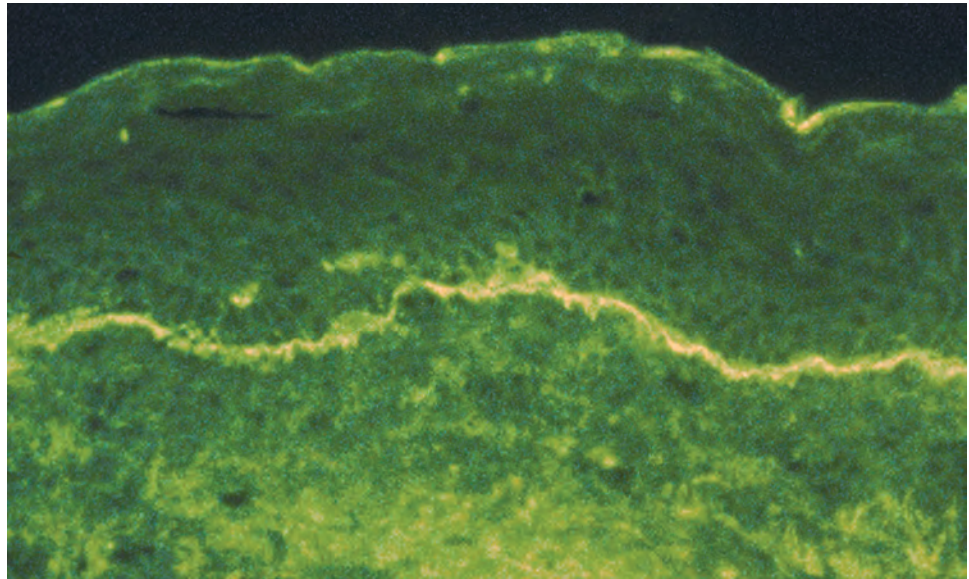
#### Pathologic Differential Diagnosis

- Lichen planus, erythema multiforme, lupus, linear IgA dermatoses, epidermolysis bullosa acquisita, pemphigoid-like drug reaction, pemphigus vulgaris, and paraneoplastic pemphigus

DIF, Direct immunofluorescence.

### ANCILLARY STUDIES

DIF of perilesional mucosa demonstrates linear deposits along the BMZ of IgG and/or C3 and sometimes IgA or IgM (Fig. 7.24) in the majority of patients (80% to 100%). These findings are not specific and require clinical correlation. Whereas IDIF of a patient's serum using salt-split skin can detect circulating antibodies to the BMZ, not all patients have detectable circulating antibodies; therefore, IDIF is not essential for the diagnosis. There is no correlation between circulating antibody titers and disease severity.

**FIGURE 7.24**

Direct immunofluorescence of perilesional mucosa from a patient with mucous membrane pemphigoid. A continuous linear band of IgG is seen at the basement membrane zone.

### DIFFERENTIAL DIAGNOSIS

MMP must be separated from other blistering diseases of the oral cavity, including erosive LP, erythema multiforme, PV, lupus erythematosus, linear IgA disease, epidermolysis bullosa acquisita, pemphigoid-like drug reactions, and paraneoplastic pemphigus (PNP). Both DIF and IDIF are essential in distinguishing MMP from these other blistering diseases.

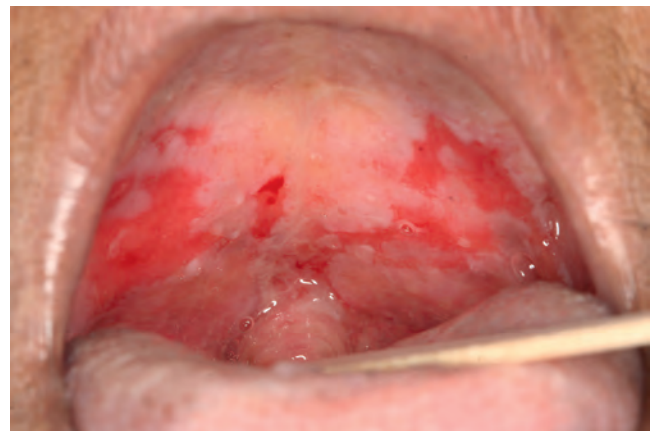
### PROGNOSIS AND THERAPY

MMP confined to the oral cavity is more amenable to treatment and is rarely associated with scarring, in contrast to involvement of the ocular, genital, laryngeal, and esophageal areas. There is often disease progression despite appropriate therapy, which includes topical corticosteroids, systemic corticosteroids, azathioprine, dapsone, and cyclophosphamide. Intravenous immunoglobulin has been used with success in patients resistant to other treatment regimens.

## ■ PEMPHIGUS VULGARIS

### CLINICAL FEATURES

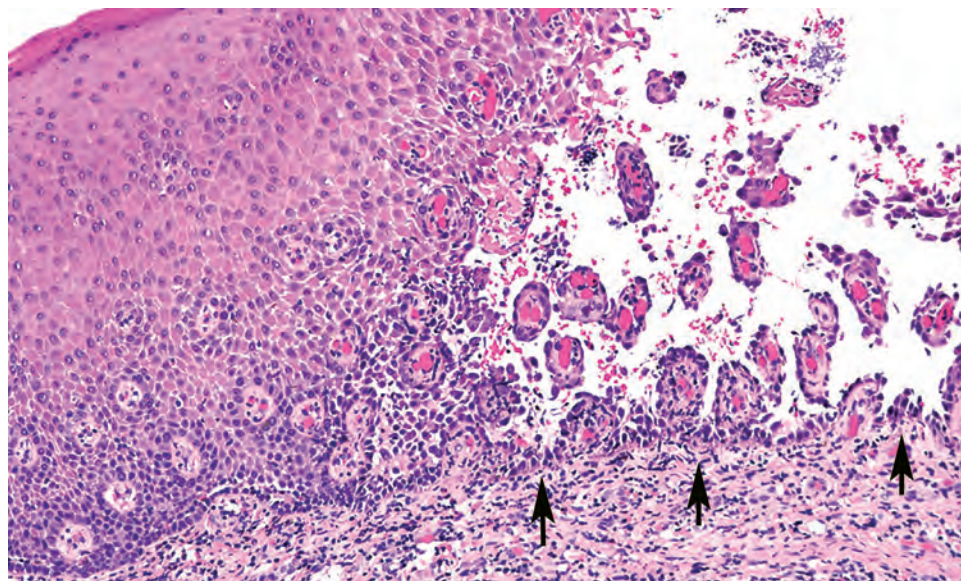
Pemphigus vulgaris (PV) is an autoimmune mucocutaneous blistering disease. Circulating IgG antibodies to desmoglein-1 and -3 (Dsg1, Dsg3) adhesion molecules of squamous epithelial cells are the underlying defects,

**FIGURE 7.25**

Large, irregularly shaped ulcers of the soft palate from a patient with oral, oropharyngeal, and esophageal pemphigus vulgaris.

causing loss of cell-to-cell adhesion. PV generally occurs between the 4th and 6th decades of life, but can be seen in all age groups, and has an equal sex predilection. Although an uncommon disease, the incidence of PV is higher in patients of Mediterranean descent and among Ashkenazi Jews. Approximately 50% to 70% of cases first present in the oral cavity with blisters that rupture, leaving painful erosions that heal without scarring (Fig. 7.25). Mucosal PV may precede cutaneous PV by an average of 5 months or may be the sole manifestation of the disease. PV can also affect other mucosal sites (esophagus, larynx, nasopharynx, conjunctiva, genitalia, anal mucosa). A flaccid blister on the upper trunk, head, neck, and/or intertriginous areas that readily ruptures is the clinical presentation. After rupture, large areas of painful, denuded epithelium remain. A positive Nikolsky sign and Asboe-Hansen sign (lateral pressure on a bulla extends it into uninvolved mucosa) are commonly seen.



**FIGURE 7.26**

Perilesional mucosa showing acantholytic epithelial cells and a suprabasilar clefting, leaving the basal cell attached to the basement membrane (“tombstoning”; arrows). A mild chronic inflammatory infiltrate is noted.

### PEMPHIGUS VULGARIS—DISEASE FACT SHEET

#### Definition

- Autoimmune mucocutaneous blistering disease associated with autoantibodies to adhesion molecules of squamous epithelium

#### Incidence and Location

- Incidence ranges from 0.08 to 3.2/100,000 population
- 50% to 70% of cases first present with oral disease

#### Morbidity and Mortality

- Morbidity related to disease severity
- Mortality rate up to 10%, due to prolonged immunosuppression

#### Sex, Race, and Age Distribution

- Peak incidence between 4th to 6th decades
- Higher incidence in Ashkenazi Jews and people of Mediterranean descent

#### Clinical Features

- Bullae/blisters readily rupture leaving irregularly shaped, painful ulcerations and erosions, which may be quite extensive
- Skin lesions are flaccid, fluid-filled blisters, which rupture and leave painful ulcers

#### Prognosis and Therapy

- Steroid and immunosuppressive therapy
- Plasmapheresis or intravenous immunoglobulins
- Long-term therapy may achieve remission, especially if the disease is mild and there is a rapid response to therapy

### PATHOLOGIC FEATURES

A biopsy sample taken from the edge of a blister will show an intraepithelial clefting above the basal layer of the epithelium (suprabasilar cleft). Round, swollen,

### PEMPHIGUS VULGARIS—PATHOLOGIC FEATURES

#### Microscopic Findings

- Intraepithelial blister above the basal cell layer (suprabasilar cleft)
- Interstitial edema, acantholysis, and loss of adhesion
- Basal cells remain attached to the basement membrane
- Mild inflammatory cell infiltrate

#### Immunofluorescence Findings

- DIF: intercellular deposits of IgG throughout the epithelium. C3 and IgA infrequent finding
- IDIF: IgG autoantibodies detected on monkey esophagus substrate

#### Pathologic Differential Diagnosis

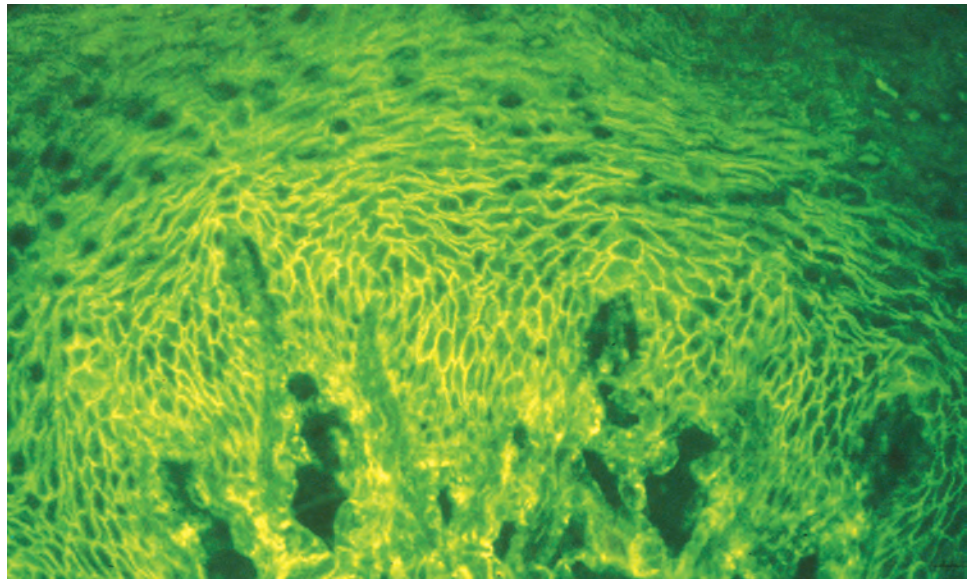
- Paraneoplastic pemphigus, pemphigus-like drug eruption, erythema multiforme, Grover disease, Hailey–Hailey disease

DIF, Direct immunofluorescence; IDIF, indirect immunofluorescence.

hyperchromatic acantholytic (Tzanck) cells are present in the cleft spaces (Fig. 7.26). The basal cells remain attached to the basement membrane, giving a “tombstone” appearance. The superficial lamina propria may contain a mild inflammatory cell infiltrate.

### ANCILLARY STUDIES

DIF of perilesional tissue demonstrates intercellular deposits of IgG throughout the epithelium (Fig. 7.27). C3 and IgA can sometimes be noted, but less frequently than IgG. IDIF, using monkey esophagus as a substrate, detects circulating IgG autoantibodies in 80% to 90% of patients with PV. The titer of circulating antibody

**FIGURE 7.27**

Perilesional mucosa showing direct immunofluorescence with deposits of IgG in the intercellular areas of the epithelium.

correlates with disease activity. ELISA can detect Dsg3 and Dsg1 autoantibodies, which correlate with disease severity.

### DIFFERENTIAL DIAGNOSIS

The clinical differential includes many desquamative-blistering disorders (see the box), including, most importantly for discussion, paraneoplastic pemphigus (PNP). PNP affects both mucosal and cutaneous sites and is associated with malignancy (lymphoma, chronic lymphocytic leukemia, carcinoma, sarcoma). There is histologic and DIF overlap between PV and PNP, but more specific tests for PNP include IDIF, using the patient's serum and a substrate (transitional epithelium of rat bladder), as well as immunoprecipitation, immunoblotting, and ELISAs for the specific antibodies targeted against proteins in the plakin family in the sera of patients with PNP.

### PROGNOSIS AND THERAPY

Mortality from PV is up to 6%, which is currently mainly due to complications from long-term immunosuppressive therapy, although mortality was much higher before the implementation of systemic corticosteroid therapy. Treatment consists of local or systemic therapy depending on the disease location and severity. Adjuvant immunosuppressants (methotrexate, azathioprine, cyclophosphamide, and cyclosporine) are used for their steroid-sparing effect. Drugs that also have an antiinflammatory effect, such as minocin, dapsone, or tetracycline, have also been used. Plasmapheresis or high-dose intravenous immunoglobulins

are used in patients resistant to other therapies. The duration of treatment is variable, with the average time to achieve complete remission ranging from 2 to 10 years. Complete remission is highest in patients who present with mild disease and have a rapid response to treatment.

## ■ RECURRENT APHTHOUS STOMATITIS

### CLINICAL FEATURES

Recurrent aphthous stomatitis (RAS), also known as canker sores, are common oral ulcers estimated to affect up to 30% to 35% of the population. These painful ulcers generally last from 10 to 30 days and range in size from a few millimeters to several centimeters. Minor aphthae, accounting for 80% of all aphthae, are characterized as small (< 1 cm) ulcers with a white, gray, or yellow fibrinopurulent membrane surrounded by an erythematous halo and present on nonkeratinized oral mucosa (buccal mucosa, labial mucosa, soft palate, floor of mouth, and lateral and ventral tongue; [Fig. 7.28](#)). These ulcers typically heal within 10 to 14 days without scarring. Major aphthae (> 1 cm) often take longer to heal and may heal with scarring. Herpetiform aphthous ulcers present as numerous pinpoint ulcers that can coalesce into a larger ulcer.

The etiology of RAS is thought to be multifactorial, including allergens, stress, anxiety, local mechanical trauma, and hormones. Reported food allergens include cinnamon, cereal products, tomatoes, nuts, citrus fruits, and chocolates. A familial association has been observed in approximately 40% of cases. No known bacterial or viral infections are associated with RAS.



## PATHOLOGIC FEATURES

The microscopic findings are of a central zone of ulceration, covered by a fibrinopurulent membrane. The underlying connective tissue exhibits increased vascularity, which contains an acute and a chronic inflammatory cell infiltrate (Fig. 7.29). The adjacent intact epithelium is spongiotic with inflammatory cell transmigration present in the lower third.



**FIGURE 7.28**

Clinical photograph of an aphthous ulcer present on the buccal mucosa. The ulcer is covered by a fibrinous membrane and surrounded by an erythematous halo.

## DIFFERENTIAL DIAGNOSIS

The clinical differential diagnosis is wide, although the microscopic differential of *nonspecific* inflammation is limited. The clinical differential includes HSV, herpangina, traumatic ulcer, pyostomatitis vegetans, and Behçet disease (ocular and orogenital ulcers). RAS typically develops

### RECURRENT APHTHOUS STOMATITIS—DISEASE FACT SHEET

#### Definition

- Common, noninfectious ulcers occurring on nonkeratinized oral mucosa of multifactorial etiology

#### Incidence

- 5%-50% with a mean of 20% of the population

#### Sex and Age Distribution

- Ulcers usually start in childhood and persist through adulthood

#### Clinical Features

- Minor or major aphthae present as ulcers with a white-gray or yellow fibrinopurulent membrane and an erythematous halo on the nonkeratinized oral mucosa (buccal and labial mucosa, floor of mouth, soft palate, lateral and ventral tongue)

#### Prognosis and Therapy

- Treatment goals include reducing pain and promoting healing with the judicious use of topical/systemic corticosteroids, and identifying specific triggers to prevent future ulcer development

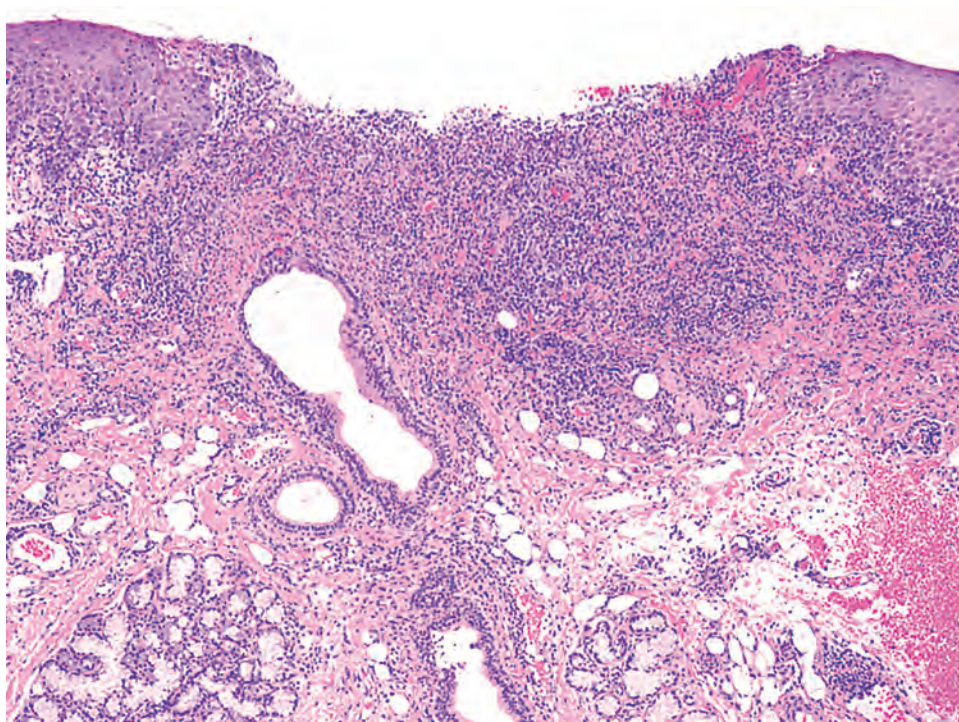


**FIGURE 7.29**

An aphthous ulcer exhibiting a fibrinopurulent membrane admixed with neutrophils. Granulation tissue beneath the ulcer bed contains inflammatory cells.

### RECURRENT APHTHOUS STOMATITIS—PATHOLOGIC FEATURES

#### Microscopic Findings

- Nonspecific ulcer with a fibrinopurulent membrane overlying edematous granulation tissue that contains a mixed inflammatory cell infiltrate

#### Pathologic Differential Diagnosis

- Traumatic ulcer, pyostomatitis vegetans, herpes simplex virus

on freely moveable mucosa, while herpes develops on “bound” or “taut” mucosa (hard palate, gingiva). Pyostomatitis vegetans is an uncommon pustular disorder that develops in patients with ulcerative colitis and is composed of microabscesses in the spinous layer. Lesions that fail to heal or respond to appropriate treatment, usually within 2 weeks, should undergo biopsy to exclude other diseases.

### PROGNOSIS AND THERAPY

The treatment of aphthous ulcer includes both over-the-counter products and prescription medications. Topical corticosteroids (triamcinolone, fluocinonide, and clobetasol) are effective in reducing the pain and decreasing healing time, while oral systemic corticosteroids can be administered to patients with severe disease. An important part of therapy is to detect and reduce local factors that trigger RAS. Elimination diets and patch testing may help in isolating the triggering agent. Patients who have more than four or five outbreaks a year should also be evaluated for systemic causes, including iron-deficiency anemia, pernicious anemia, celiac disease, and Crohn’s disease.

## ■ TRAUMATIC ULCERATIVE GRANULOMA

### CLINICAL FEATURES

Traumatic ulcerative granuloma (traumatic granuloma, traumatic ulcerative granuloma with stromal eosinophilia [TUGSE], eosinophilic granuloma) is an oral ulcer of traumatic origin with unique histopathologic features. These ulcers most often occur on the lateral border of the tongue or buccal mucosa or in sites adjacent to an identifiable source of trauma, such as a fractured or



**FIGURE 7.30**

Clinical photograph of a traumatic ulcerative granuloma on the lateral tongue. Note the zone of hyperkeratosis surrounding the ulcer.

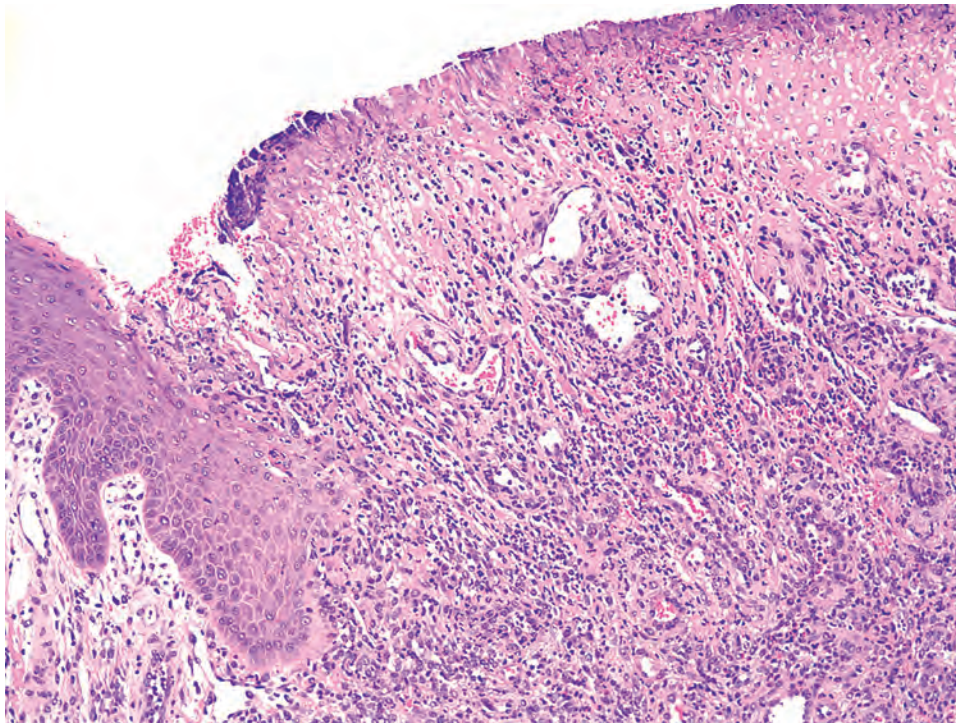
malposed tooth. The ulcers are painful and range in size from 0.1 to 1 cm. A zone of hyperkeratosis surrounding the ulcer is noted along with induration, thus mimicking squamous cell carcinoma (Fig. 7.30).

The true incidence of traumatic ulcerative granulomas is unknown but is less common than that of aphthous ulcers. These ulcers can occur in all ages. When present in an infant, it is termed Riga-Fede disease and presents as an ulceration on the ventral tongue caused by tongue thrusting against natal or neonatal teeth. Both electrical and thermal injury can induce a traumatic ulcerative granuloma as can factitious or self-induced injury, which can be observed in Lesch-Nyhan syndrome, Tourette syndrome, or obsessive-compulsive disorder.

### PATHOLOGIC FEATURES

Traumatic ulcerative granulomas have a unique histologic appearance. A thickened fibrinopurulent membrane covers the ulcer and adjacent epithelium may exhibit pseudo-epitheliomatous hyperplasia (Fig. 7.31). The ulcer bed is composed of granulation tissue with a mixed inflammatory cell infiltrate of lymphocytes, histiocytes, neutrophils, and occasionally plasma cells. The inflammation extends into the deeper tissue including skeletal muscle, and scattered eosinophils are observed (Fig. 7.32). In a subset of traumatic ulcerative granulomas, atypical CD30-positive histiocytes are noted that may exhibit pleomorphism and mitotic figures. The significance of these findings is uncertain as most cases resolve after biopsy. Necrosis may be present when the ulcer is related to thermal or electrical injury.



**FIGURE 7.31**

Traumatic ulcerative granuloma with characteristic thickened fibrinopurulent membrane with deep infiltrate of inflammatory cells. Marked epithelial hyperplasia is noted adjacent to the ulcer bed.

#### TRAUMATIC ULCERATIVE GRANULOMA—DISEASE FACT SHEET

##### Definition

- Chronic traumatic ulceration of the oral cavity with unique pathologic features

##### Incidence and Location

- Incidence unknown but most likely underreported
- Less frequent than recurrent aphthous ulcerations
- Can occur anywhere but most common on the lateral tongue

##### Sex and Age Distribution

- Males more commonly affected than females
- Can occur in all age groups including newborns (Riga-Fede disease)

##### Clinical Features

- 0.1 cm to greater than 1 cm painful ulcer
- Zone of hyperkeratosis surrounding the ulcer
- Induration mimicking squamous cell carcinoma

##### Prognosis and Therapy

- Ulcers that do not resolve may need excision
- Intralesional steroids can induce ulcer resolution
- Source of trauma must be removed if possible or recurrence is likely

#### TRAUMATIC ULCERATIVE GRANULOMA—PATHOLOGIC FEATURES

##### Microscopic Findings

- Ulcer bed composed of granulation tissue with mixed chronic inflammatory cell infiltrate
- May see pseudoepitheliomatous hyperplasia in adjacent epithelium
- Inflammation, including eosinophils, extends into skeletal muscle
- Atypical CD30+ histiocytes may be noted
- In thermal/electrical injury, necrosis may be identified

##### Differential Diagnosis

- Recurrent aphthous ulcer, cutaneous CD30+ T-cell lymphoma

#### DIFFERENTIAL DIAGNOSIS

Often, traumatic ulcerative granulomas undergo biopsy because, clinically, they mimic squamous cell carcinoma, presenting as a nonhealing ulcer with associated induration. Major aphthous ulcers may share clinical features, but on histologic examination, these ulcers are superficial and do not extend to the muscle. In the subset of traumatic ulcerative granulomas with atypical histiocytes, cutaneous CD30+ T-cell lymphoma may be considered. Despite clonal T-cell receptor rearrangements in some reported cases, no development of a T-cell lymphoproliferative disorder was noted, and results should be cautiously interpreted.

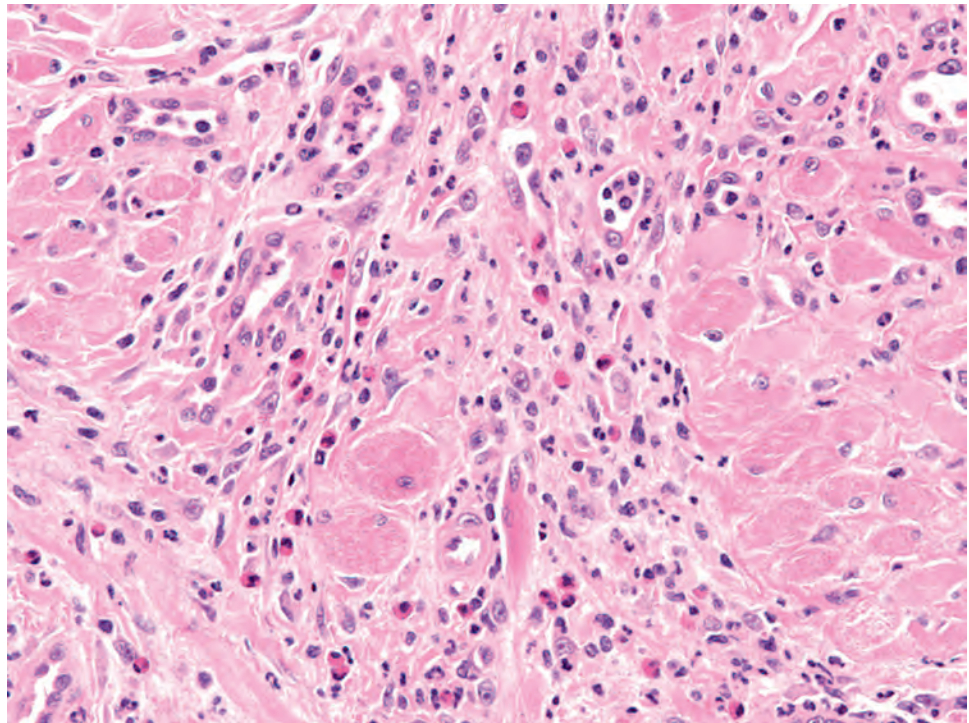


**FIGURE 7.32**

A mixed inflammatory cell infiltrate including histiocytes and numerous eosinophils are noted within the striated muscle.

#### **PROGNOSIS AND THERAPY**

Nonresolving ulcers may need total excision, although complete resolution has been reported in ulcers biopsied for diagnosis. Intralesional steroid injections are useful in resolving the ulcer. Recurrences of traumatic ulcerative

granulomas are common, particularly if the source of the trauma persists.

#### **SUGGESTED READINGS**

The complete Suggested Readings list is available online at [ExpertConsult.com](http://ExpertConsult.com).



## SUGGESTED READINGS

### Fordyce Granules

1. Alawi F, et al. Sebaceous carcinoma of the oral mucosa: case report and review of the literature. *Oral Surg Oral Med Oral Pathol Oral Radiol Endod.* 2005;99:79–84.
2. Daley TD. Intraoral sebaceous hyperplasia. Diagnostic criteria. *Oral Surg Oral Med Oral Pathol.* 1993;75:343–347.
3. Madani FM, et al. Normal variations of oral anatomy and common oral soft tissue lesions: evaluation and management. *Med Clin North Am.* 2014;98(6):1281–1298.

### Amalgam Tattoo

1. Buchner A. Amalgam tattoo (amalgam pigmentation) of the oral mucosa: clinical manifestations, diagnosis and treatment. *Refuat Hapeh Vehashinayim.* 2004;21:25–28, 92.
2. Hassona Y, et al. Prevalence and clinical features of pigmented oral lesions. *Int J Dermatol.* 2016;55(9):1005–1013.
3. Muller S. Melanin-associated pigmented lesions of the oral mucosa: presentation, differential diagnosis, and treatment. *Dermatol Ther.* 2010;23:220–229.
4. Shah G. Treatment of an amalgam tattoo with a Q-switched alexandrite (755 nm) laser. *Dermatol Surg.* 2002;28:1180–1181.

### Ectopic Thyroid

1. Adelchi C, et al. Ectopic thyroid tissue in the head and neck: a case series. *BMC Res Notes.* 2014;7:790.
2. Barnes TW, et al. Obstructive lingual thyroid causing sleep apnea: a case report and review of the literature. *Sleep Med.* 2004;5:605–607.
3. Batsakis JG, et al. Thyroid gland ectopias. *Ann Otol Rhinol Laryngol.* 1996;105:996–1000.
4. Baughman RA. Lingual thyroid and lingual thyroglossal tract remnants. A clinical and histo-pathologic study with review of the literature. *Oral Surg Oral Med Oral Pathol.* 1972;34:781–799.
5. Majumdar I, et al. Lingual thyroid as a cause of primary hypothyroidism: con-genital hypothyroidism in the neonatal period and beyond. *Clin Pediatr (Phila).* 2010;49:885–888.
6. Santangelo G, et al. Prevalence, diagnosis and management of ectopic thyroid glands. *Int J Surg.* 2016;28(suppl 1):S1–S6.
7. Turgut S, et al. Diagnosis and treatment of lingual thyroid: a review. *Rev Laryngol Otol Rhinol (Bord).* 1997;118:189–192.
8. Wei S, et al. Pathology of thyroglossal duct: an institutional experience. *Endocr Pathol.* 2015;26(1):75–79.
9. Zander DA, et al. Imaging of ectopic thyroid tissue and thyroglossal duct cysts. *Radiographics.* 2014;34(1):37–50.

### Oral Hairy Leukoplakia

1. Chambers AE, et al. Twenty-first-century oral hairy leukoplakia—a non-HIV-associated entity. *Oral Surg Oral Med Oral Pathol Oral Radiol.* 2015;119(3):326–332.
2. Greenspan JS, et al. Hairy leukoplakia; lessons learned: 30-plus years. *Oral Dis.* 2016;22(suppl 1):120–127.
3. Marcus M, et al. Oral white patches in a national sample of medical HIV patients in the era of HAART. *Community Dent Oral Epidemiol.* 2005;33:99–106.
4. Mendoza N, et al. Mucocutaneous manifestations of Epstein-Barr virus infection. *Am J Clin Dermatol.* 2008;9(5):295–305.
5. Patton LL, et al. Prevalence and classification of HIV-associated oral lesions. *Oral Dis.* 2002;8(suppl 2):98–109.
6. Prasad JL, et al. Oral hairy leukoplakia in patients without HIV: presentation of 2 new cases. *Oral Surg Oral Med Oral Pathol Oral Radiol.* 2014;118(5):e151–e160.
7. Stojanov IJ, et al. Human papillomavirus and Epstein-Barr virus associated conditions of the oral mucosa. *Semin Diagn Pathol.* 2015;32(1):3–11.
8. Walling DM, et al. Persistence and transition of Epstein-Barr virus genotypes in the pathogenesis of oral hairy leukoplakia. *J Infect Dis.* 2004;190:387–395.

## Infections

1. Arduino PG, et al. Herpes Simplex Virus Type 1 infection: overview on relevant clinico-pathological features. *J Oral Pathol Med.* 2008.
2. Boyanova L, et al. Actinomycosis: a frequently forgotten disease. *Future Microbiol.* 2015;10(4):613–628.
3. Fatahzadeh M, et al. Human herpes simplex virus infections: epidemiology, patho-genesis, symptomatology, diagnosis and management. *J Am Acad Dermatol.* 2007;57:737–763.
4. Feller L, et al. Oral candidosis in relation to oral immunity. *J Oral Pathol Med.* 2014;43(8):563–569.
5. Muzyka BC, et al. Update on oral fungal infections. *Dent Clin North Am.* 2013;57(4):561–581.
6. Pinto A, et al. Pediatric soft tissue oral lesions. *Dent Clin North Am.* 2014;58(2):437–453.
7. Reichart PA, et al. Pathology and clinical correlates in oral candidiasis and its variants: a review. *Oral Dis.* 2000;6(2):85–91.
8. Singh A, et al. Oral candidiasis: An overview. *J Oral Maxillofac Pathol.* 2014;18(suppl 1):S81–S85.
9. Stoopler ET, et al. Oral mucosal diseases: evaluation and management. *Med Clin North Am.* 2014;98(6):1323–1352.
10. Valour F, et al. Actinomycosis: etiology, clinical features, diagnosis, treatment, and management. *Infect Drug Resist.* 2014;7:183–197.
11. Woo SB, et al. Management of recurrent oral herpes simplex infections. *Oral Surg Oral Med Oral Pathol Oral Radiol Endod.* 2007;103(suppl):S12.e1–S12.e18.

### Oral Lichen Planus

1. Cheng YS, et al. Diagnosis of oral lichen planus: a position paper of the American Academy of Oral and Maxillofacial Pathology. *Oral Surg Oral Med Oral Pathol Oral Radiol.* 2016;122(3):332–354.
2. DeRossi SS, et al. Lichen planus, lichenoid drug reactions, and lichenoid mucositis. *Dent Clin North Am.* 2005;49:77–89, viii.
3. Eisen D. The clinical manifestations and treatment of oral lichen planus. *Dermatol Clin.* 2003;21:79–89.
4. Müller S. Oral manifestations of dermatologic disease: a focus on lichenoid lesions. *Head Neck Pathol.* 2011;5(1):36–40.
5. Müller S. The lichenoid tissue reactions of the oral mucosa: oral lichen planus and other lichenoid lesions. *Surg Pathol Clin.* 2011;4(4):1005–1026.
6. Schlosser BJ. Lichen planus and lichenoid reactions of the oral mucosa. *Dermatol Ther.* 2010;23:251–267.

### Mucous Membrane Pemphigoid

1. Bagan J, et al. Mucosal disease series. Number III. Mucous membrane pemphigoid. *Oral Dis.* 2005;11:197–218.
2. Chan LS, et al. The first international consensus of mucous membrane pemphigoid. *Arch Dermatol.* 2002;138:370–379.
3. Chan MH, et al. Biopsy techniques and diagnoses & treatment of mucocutaneous lesions. *Dent Clin North Am.* 2012;56(1):43–73, vii–viii.
4. Olasz EB, et al. Bullous pemphigoid and related subepidermal autoimmune blistering diseases. *Curr Dir Autoimmun.* 2008;10:141–166.
5. Sollecito TP, et al. Mucous membrane pemphigoid. *Dent Clin North Am.* 2005;49:91–106, viii.
6. Stoopler ET, et al. Oral mucosal diseases: evaluation and management. *Med Clin North Am.* 2014;98(6):1323–1352.
7. Taylor J, et al. World workshop on oral medicine VI: a systematic review of the treatment of mucous membrane pemphigoid. *Oral Surg Oral Med Oral Pathol Oral Radiol.* 2015;120(2):161–171.e20.
8. Xu HH, et al. Mucous membrane pemphigoid. *Dent Clin North Am.* 2013;57(4):611–630.

### Pemphigus Vulgaris

1. Kelly S, et al. Comparative study of five serological assays for the diagnosis of paraneoplastic pemphigus. *Pathology.* 2015;47(1):58–61.
2. McMillan R, et al. World Workshop on Oral Medicine VI: a systematic review of the treatment of mucocutaneous pemphigus vulgaris. *Oral Surg Oral Med Oral Pathol Oral Radiol.* 2015;120(2):132–142.e61.

3. Patricio P, et al. Autoimmune bullous dermatoses: a review. *Ann NY Acad Sci.* 2009;1173:203–210.
4. Santoro FA, et al. Pemphigus. *Dent Clin North Am.* 2013;57(4): 597–610.
5. Stoopler ET, et al. Oral mucosal diseases: evaluation and management. *Med Clin North Am.* 2014;98(6):1323–1352.
6. Zhou T, et al. Comparative study of indirect immunofluorescence, enzyme-linked immunosorbent assay, and the Tzanck smear test for the diagnosis of pemphigus. *J Oral Pathol Med.* 2016.

### Recurrent Aphthous Stomatitis

1. Cui RZ, et al. Recurrent aphthous stomatitis. *Clin Dermatol.* 2016;34(4):475–481.
2. Gürkan A, et al. Recurrent aphthous stomatitis in childhood and adolescence: a single-center experience. *Pediatr Dermatol.* 2015;32(4):476–480.
3. Stoopler ET, et al. Oral mucosal diseases: evaluation and management. *Med Clin North Am.* 2014;98(6):1323–1352.
4. Stoopler ET, et al. Recurrent oral ulcers. *JAMA.* 2015;313(23): 2373–2374.

### Traumatic Ulcerative Granuloma

1. Gagari E, et al. Traumatic ulcerative granuloma with stromal eosinophilia: a lesion with alarming histopathologic presentation and benign clinical course. *Am J Dermatopathol.* 2011;33(2):192–194.
2. Hirshberg A, et al. Traumatic ulcerative granuloma with stromal eosinophilia: a reactive lesion of the oral mucosa. *Am J Clin Pathol.* 2006;126:522–529.
4. Salisbury CL, et al. T-cell receptor gene rearrangement and CD30 immunoreactivity in traumatic ulcerative granuloma with stromal eosinophilia of the oral cavity. *Am J Clin Pathol.* 2009;132:722–727.
4. Sarantopoulos GP, et al. Mimics of cutaneous lymphoma: report of the 2011 Society for Hematopathology/European Association for Hematopathology workshop. *Am J Clin Pathol.* 2013;139(4):536–551.
5. Sciallis AP, et al. Mucosal CD30-positive T-cell lymphoproliferations of the head and neck show a clinicopathologic spectrum similar to cutaneous CD30-positive T-cell lymphoproliferative disorders. *Mod Pathol.* 2012;25(7):983–992.
6. Yacovone L, et al. Riga-Fede disease: a rare sublingual traumatic ulcerative lesion in a child. *Otolaryngol Head Neck Surg.* 2012;146(2):333–334.



# Benign Neoplasms of the Oral Cavity

■ Brenda L. Nelson

## ■ FIBROMA

The term *fibroma*, unless further qualified (e.g., ossifying fibroma, ameloblastic fibroma), refers to a localized proliferation of fibrous connective tissue in response to tissue irritation. As such, oral fibromas are reactive in nature, with some advocating the use of alternative designations, such as “traumatic fibroma” or “irritation fibroma.” It is believed that these terms more accurately reflect the true reactive nature of this lesion, whereas the term “fibroma” may imply a neoplastic process.

### CLINICAL FEATURES

Fibroma is the most common “tumor” encountered in the oral cavity. It occurs more often in women than in men by a 2:1 ratio. It usually presents during the fourth to sixth decades of life but may be found across a wide age range that includes children and the elderly. There is no racial predilection. Distribution within the oral cavity, not surprisingly, reflects those sites most prone to trauma. Consequently, fibromas favor the buccal mucosa, specifically along the bite (occlusal) line, and the lateral border of the tongue. They may, however, arise on the lips and gingiva as well. The classic clinical appearance is that of an elevated sessile nodule surfaced by smooth mucosa (Fig. 8.1). Although fibromas are painless, patients tend to report them as a nuisance.

### PATHOLOGIC FEATURES

#### GROSS FINDINGS

Oral fibromas are generally seen as a round nodule with a smooth mucosal surface. The cut surface is solid and gray with a consistency that ranges from soft to firm.

### FIBROMA—DISEASE FACT SHEET

#### Definition

- A localized proliferation of fibrous connective tissue in response to tissue irritation

#### Incidence and Location

- Most common “tumor” encountered in the oral cavity
- Most common in oral sites prone to irritation/injury (e.g., buccal mucosa along the occlusal line, lateral tongue)

#### Sex and Age Distribution

- Females > males (2:1)
- Most common between 30 and 50 years

#### Clinical Features

- Painless and asymptomatic
- Submucosal nodules with limited growth potential (usually a few millimeters in diameter)

#### Prognosis and Therapy

- Conservative surgical resection is curative
- Potential for recurrence if inciting trauma persists

Most are only a few millimeters, and only the rare lesion reaches a diameter of 1 to 2 cm.

### MICROSCOPIC FINDINGS

The histologic picture is dominated by the nodular deposition of submucosal collagen (Fig. 8.2). Spindled fibroblasts and small blood vessels are dispersed among the pink, dense collagen bundles (Fig. 8.3). The periphery of the nodule may be rounded and sharply demarcated or it may blend imperceptibly with the surrounding fibrous connective tissues. The overlying squamous epithelium may be attenuated with flattening of its rete ridges as if it were being tightly stretched over the nodular mass. Trauma to the nodule may incite secondary changes ranging from friction-induced hyperkeratosis to ulceration.

The fibroblasts of irritation fibromas are spindled and inconspicuous. The presence of larger stellate fibroblasts

with large and multiple nuclei is characteristic of the *giant cell fibroma* (Fig. 8.4). In contrast to the more common irritation fibroma, the giant cell fibroma is not associated with trauma, tends to occur in a younger age group, and favors the tongue and gingiva.

### DIFFERENTIAL DIAGNOSIS

Although fibromas are common and clinically inconsequential, surgical removal with microscopic examination is prudent to rule out various benign and malignant neoplasms that may simulate the clinical appearance of fibromas, such as schwannomas, neurofibromas, granular cell tumors, and

salivary gland neoplasms. This broad clinical differential diagnosis, however, is easily resolved by microscopic examination, carefully observing any keloid-like collagen seen in a scar; vascular proliferation, which may be a sign of an organizing lobular capillary hemangioma; or large, polygonal cells with eosinophilic granules seen in granular cell tumor.

### PROGNOSIS AND THERAPY

As a reactive non-neoplastic process, fibromas have no malignant potential. Simple surgical resection is curative. If the source of inciting trauma has not been adequately addressed, the lesion may rarely recur.



**FIGURE 8.1**

This fibroma arose along the occlusal line of the oral mucosa, seen as a raised sessile nodule with a smooth surface.

### FIBROMA—PATHOLOGIC FEATURES

#### Gross Findings

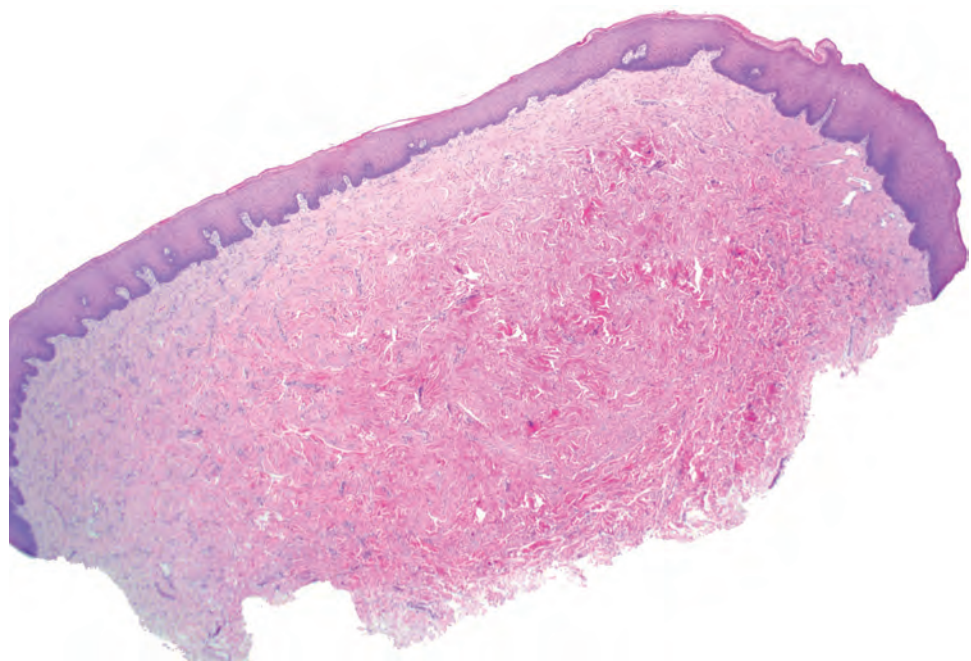
- Dome-shaped nodule ranging from a few millimeters to 2 cm
- Smooth surface unless secondarily ulcerated

#### Microscopic Findings

- Histologic picture dominated by submucosal collagen
- Inconspicuous spindled fibroblasts sparsely dispersed among collagen bundles
- Squamous epithelium is usually unremarkable, but may demonstrate varying degrees of rete atrophy, hyperkeratosis, and/or superficial ulceration

#### Pathologic Differential Diagnosis

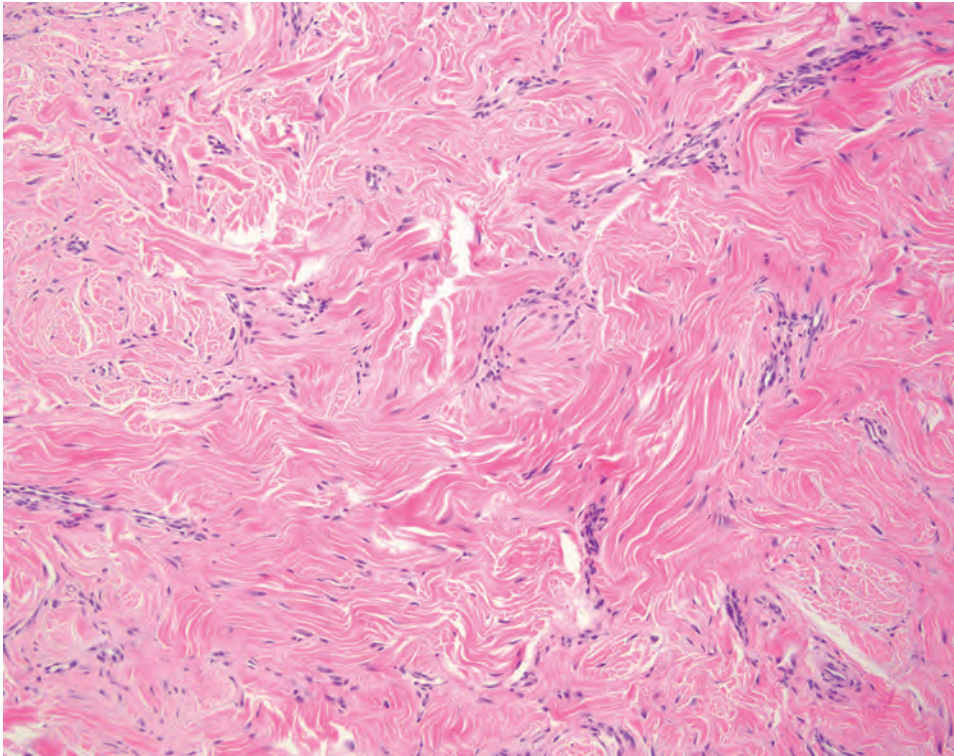
- Generally obvious, but granular cell tumor, scar, and lobular capillary hemangioma may be considered



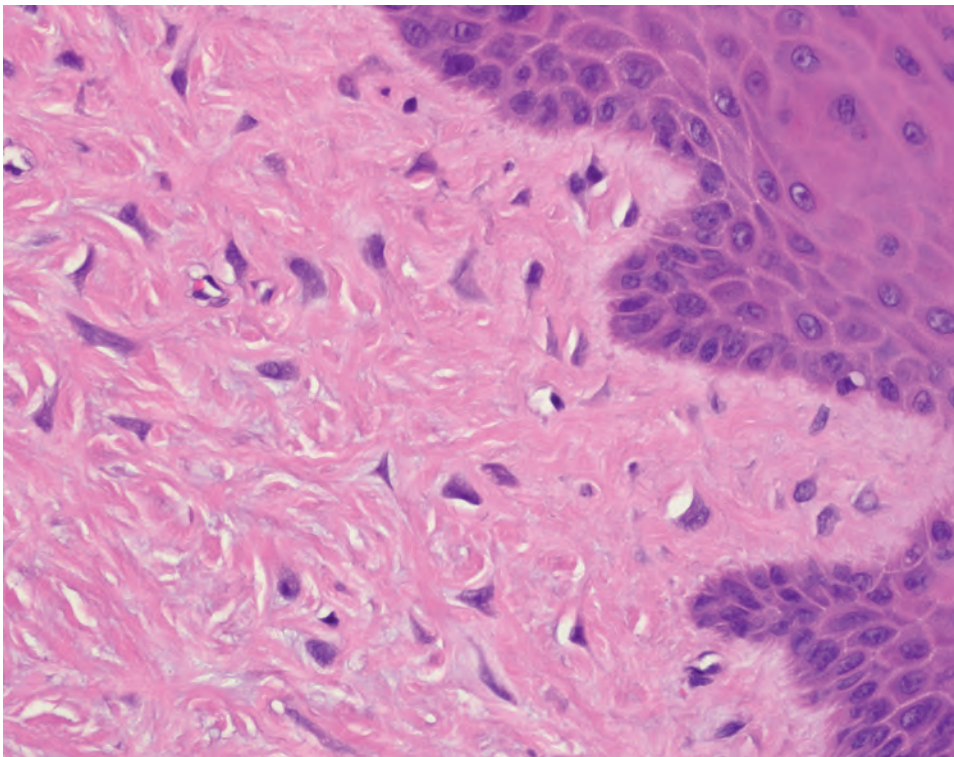
**FIGURE 8.2**

At low power, the deposition of connective tissue forms a discrete submucosal nodule.



**FIGURE 8.3**

At higher power, the nodule is composed of inconspicuous fibroblasts in a collagen-rich stroma. Note the skeletal muscle.

**FIGURE 8.4**

A giant cell fibroma findings stellate fibroblasts with large hyperchromatic nuclei.

## ■ SQUAMOUS PAPILLOMA (INCLUDING VERRUCA AND CONDYLOMA)

Squamous papilloma (SP) of the oral cavity is a localized benign exophytic proliferation of the squamous epithelium. Its classic microscopic presentation is that of a proliferation of keratinizing stratified squamous epithelium supported by fibrovascular connective tissue cores. It is one of several lesions of the oral cavity that has been associated with the human papillomavirus (HPV). Other HPV-associated lesions of the oral mucosa include verruca vulgaris (common wart) and condyloma acuminatum (venereal wart, sexually transmitted). The HPV serotypes 6 and 11 are most consistently detected in oral SPs and condyloma, whereas HPV serotypes 2 and 4 are associated with verruca vulgaris.

### CLINICAL FEATURES

SPs represent the most common benign neoplasm originating from the oral mucosa. They occur across a broad age range, affecting both children and adults. Most lesions, however, are diagnosed in individuals 30 to 50 years of age. Some large studies indicate that males are affected more commonly than females and white more than black patients. They may arise from any intraoral mucosal location, but they show a definite predilection for the hard and soft palate and uvula.

SPs are clinically observed as soft, white pedunculated nodules that usually measure less than 1 cm (Fig. 8.5). Their hallmark frond-like projections give rise to surface irregularities that range from granular, to spiny, to convoluted (i.e., “cauliflower-like”). Most SPs of the oral cavity are solitary and may have a history of being present for years, reflecting the low virulence and infectivity of this lesion. In contrast, verruca vulgaris and condyloma acuminatum frequently present as multiple or clustered lesions reflecting their more infectious nature.

### PATHOLOGIC FEATURES

#### GROSS FINDINGS

The SP tends to be exophytic, warty, friable, and white to gray. The degree of its surface irregularities reflects the length and complexity of the papillae.

#### MICROSCOPIC FINDINGS

The trademark feature of SP, namely its papillary extensions, is histologically characterized by



**FIGURE 8.5**

This squamous papilloma is seen as an exophytic cauliflower-like mass having a convoluted surface.

### SQUAMOUS PAPILLOMA (INCLUDING VERRUCA AND CONDYLOMA)—DISEASE FACT SHEET

#### Definition

- A localized benign exophytic warty proliferation of the squamous epithelium driven in part by human papillomavirus, particularly by the nononcogenic serotypes 6 and 11

#### Incidence and Location

- Most common benign neoplasm originating from the surface epithelium
- May originate from any intraoral mucosal site, but with a preference for the hard and soft palate and uvula

#### Morbidity and Mortality

- Benign proliferations with little potential to undergo malignant transformation

#### Sex, Race, and Age Distribution

- Males slightly more often than females
- White patients slightly more often than black patients
- Broad age range, but peak between 30 and 50 years; verruca vulgaris, on average, in younger individuals

#### Clinical Features

- Painless and asymptomatic
- Warty exophytic growth
- Usually solitary and small (<1 cm); condyloma and verruca vulgaris are frequently multiple

#### Prognosis and Therapy

- Conservative surgical resection or laser ablation is curative



multilayered squamous epithelium supported by a central fibrovascular core (Fig. 8.6). The squamous layer is often thickened, but it demonstrates normal maturation. Hyperplasia of the basal cell layer with increased mitotic figures is not uncommon and should not be interpreted as a precursor (i.e., dysplastic) lesion. HPV-induced cytopathic changes may sometimes be appreciated in cells within the prickly cell layer. These altered cells are referred to as koilocytes, and they are characterized by dark condensed and crenated nuclei surrounded by cleared cytoplasm and prominent cell borders (Fig. 8.7, *inset*).

Verruca vulgaris demonstrates hyperkeratotic squamous epithelium (church spire appearance) supported by underlying fibrovascular connective cores. Distinguishing findings are a prominent granular cell layer with occasional keratohyaline granules and rete ridges that converge at the base of the lesion (Fig. 8.8). Oral condyloma is characterized by acanthosis with wide rete ridges. The epithelium often displays impressive koilocytic change.

#### ANCILLARY STUDIES

In situ hybridization using type-specific HPV probes is a fairly reliable method of documenting the presence of HPV 6 or 11 in oral SPs, but this technique plays no

#### SQUAMOUS PAPILLOMA—PATHOLOGIC FEATURES

##### Gross Findings

- Exophytic, warty, friable, and white to gray
- Surface irregularities ranging from granular, to spiny, to convoluted

##### Microscopic Findings

- Fibrovascular cores lined by mature, stratified squamous epithelium
- The cells of the prickly layer may show koilocytic change: crenated, hyperchromatic nuclei surrounded by clear cytoplasm ("halos") and prominent cell borders
- Hyperplasia of the basal cell layer is common and should not be mistaken as a precursor (i.e., dysplastic) lesion

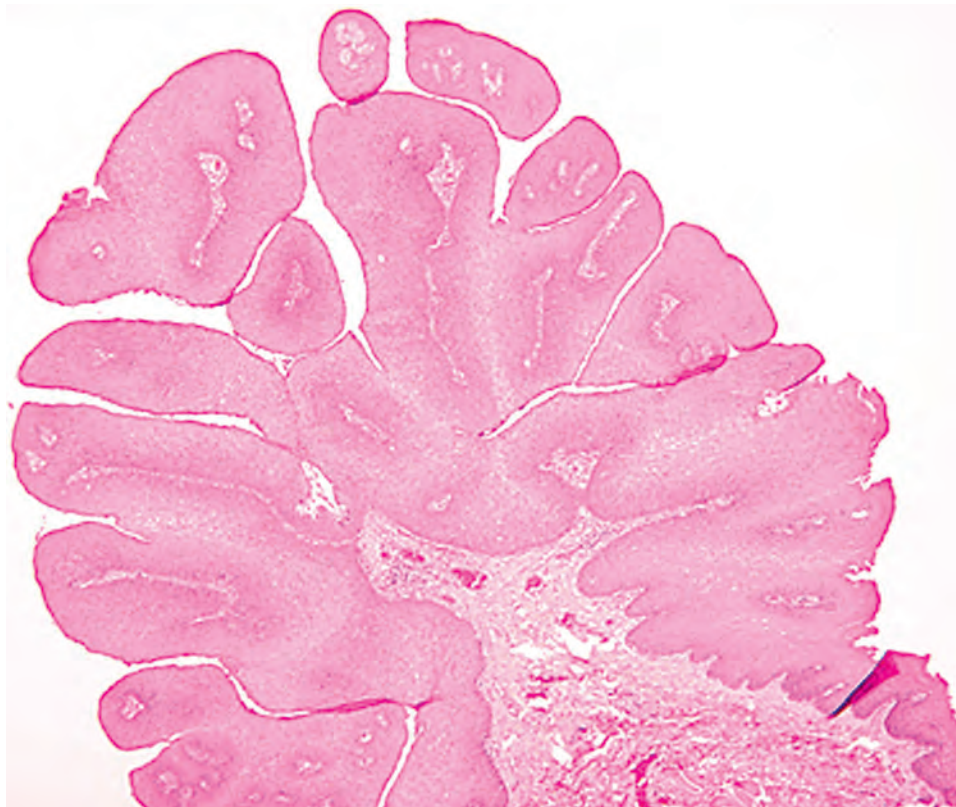
##### Pathologic Differential Diagnosis

- Verruca vulgaris, condyloma acuminatum, multifocal epithelial hyperplasia, reactive papillary hyperplasia, proliferative verrucous leukoplakia, papillary squamous cell carcinoma

practical role in diagnosing SP, determining treatment, or predicting clinical behavior.

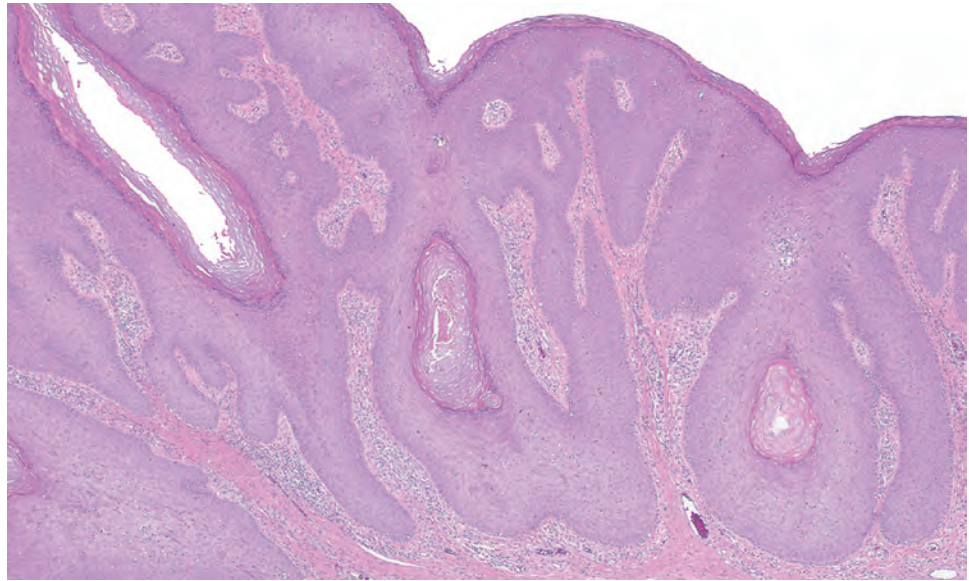
#### DIFFERENTIAL DIAGNOSIS

SPs can be distinguished from other HPV-associated lesions of the oral cavity based on clinical and

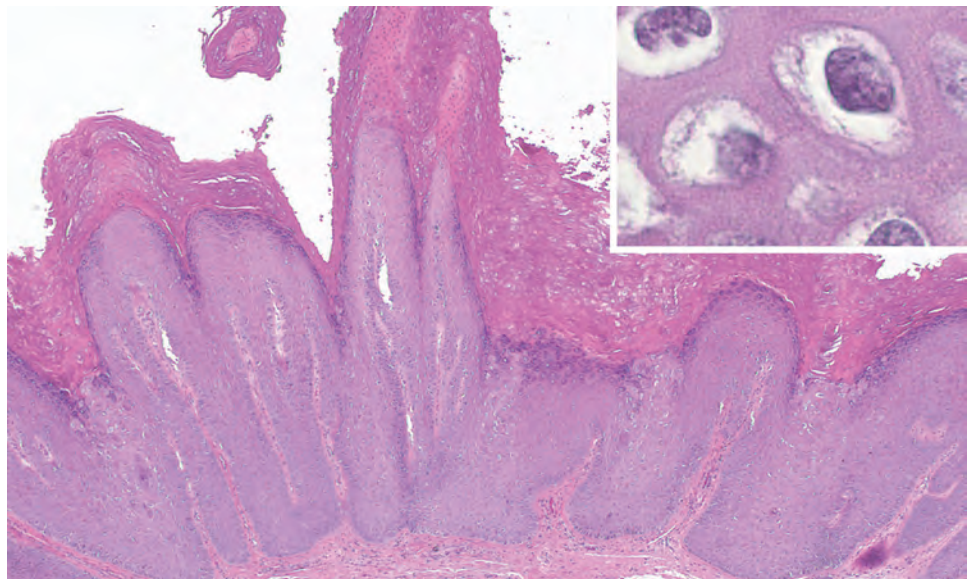


**FIGURE 8.6**

A low-power view demonstrates the complex branching papillary structures of a squamous papilloma.

**FIGURE 8.7**

Oral condyloma exhibits papillary fronds that are broader and more blunted than the papillary projections of squamous papilloma.

**FIGURE 8.8**

Low-power view of verruca vulgaris. In contrast to the squamous papilloma, verruca has a broad flat base, a prominent granular layer, and extensive hyperkeratosis. The inset demonstrates cells with dark condensed nuclei surrounded by a zone of cytoplasmic clearing. These koilocytic changes are viral-induced and are characteristic of human papillomavirus-related lesions of the oral cavity.

histopathologic characteristics. *Verruca vulgaris* usually occurs as warty excrescences located along the vermilion border, labial mucosa, and/or the anterior tongue of children. Histologically, verruca vulgaris will have projections of epithelium that appear to converge at the base. The epithelium demonstrates a prominent granular layer with spires of hyperkeratosis (see Fig. 8.8). *Oral condyloma*, a sexually transmitted disease, is seen most commonly in young adults at sites of sexual contact (e.g., labial mucosa, soft palate), as clusters of pink nodules that coalesce into broad-based exophytic masses. Microscopically, its papillary fronds are broader and more blunted than the papillary projections of SP. Koilocytes are usually more prominent (see Fig. 8.7). Multifocal epithelial hyperplasia shows multiple lesions,

with acanthosis, and expanded and often fused rete and mitosoid cells.

Other oral lesions that may be considered in the differential diagnosis include reactive *papillary hyperplasia*, *proliferative verrucous leukoplakia (PVL)*, and *papillary squamous cell carcinoma*. The distinction between SP and papillary hyperplasia is usually determined clinically. Papillary hyperplasia is a reactive process that is generally seen in association with ill-fitting prostheses, usually dentures. PVL is characterized by multifocal lesions that may appear histologically similar to SPs. This condition represents a varied process that relentlessly spreads and progresses to malignancy. Papillary squamous cell carcinoma may share some of the architectural findings of SP but will have malignant cytology.



## PROGNOSIS AND THERAPY

As a benign neoplasm with a limited growth potential, the oral SP is cured by local excision or laser ablation. Local recurrence is uncommon and malignant transformation is exceedingly rare. Importantly, they do not share with juvenile laryngeal papillomas the penchant for multifocality, widespread growth, and rapid recurrence.

## MULTIFOCAL EPITHELIAL HYPERPLASIA

Multifocal epithelial hyperplasia (MFEH), also referred to as “Heck disease,” is a virus-induced benign proliferation of the oral squamous epithelium that arises primarily in children and adolescents. The original indigenous North America ethnic predilection is no longer supported, with populations from around the world affected. HPV is the responsible agent, with HPV serotypes 13 and 32 being the most consistently identified.

## CLINICAL FEATURES

MFEH is not common, and incidence rates vary widely depending on age and ethnicity. The ethnic incidence of MFEH is broader than initially reported and it has been reported in populations from North, South, and Central America, Africa, and the Middle East, among other groups. Most initial diagnoses involve children and adolescents, and in certain ethnic groups, nearly 40% of children are affected. However, lesions can be seen throughout life. In some ethnic populations, females are affected more frequently than males by a 2:1 ratio. MFEH has also been reported among those who are HIV positive and, interestingly, its frequency increases with the introduction of highly active antiretroviral therapy (HAART). This has also been seen with SPs and other HPV-associated lesions of the oral cavity.

MFEH has a distinct clinical appearance. It is seen as multiple clustered flat-topped papules and rounded nodules that have a predilection for the labial, lingual, and buccal mucosae (Fig. 8.9). Individual papules are discrete and small (a few millimeters to 1 cm), but tightly clustered papules may coalesce to form large confluent lesions. Papules tend to be soft and painless.

## PATHOLOGIC FEATURES

### GROSS FINDINGS

MFEH is grossly seen as tan, soft nodules with a sessile base and a smooth surface.



**FIGURE 8.9**

Multifocal epithelial hyperplasia involving the labial mucosa. Small, tightly packed papules merge to form larger confluent lesions.

## MULTIFOCAL EPITHELIAL HYPERPLASIA—DISEASE FACT SHEET

### Definition

- A localized benign simple hyperplasia of the squamous epithelium driven in part by human papillomavirus, particularly by the nononcogenic serotypes 13 and 32

### Incidence and Location

- Very uncommon overall, but disproportionately affects certain ethnic groups
- Predilection for the labial, lingual, and buccal mucosa

### Morbidity and Mortality

- Benign squamous proliferation with no potential for malignant progression
- Spontaneous regression is common

### Sex, Race, and Age Distribution

- Females > males (2:1) in some ethnic groups
- First reported in American Indians and Inuits, but recognized in a broad range of ethnic groups
- Generally considered to present in childhood, but can be seen throughout life
- Sometimes involves HIV-positive adults (HAART-associated)

### Clinical Features

- Painless and asymptomatic
- Multifocal slightly raised flat papules and rounded nodules
- Individual lesions are small (<1 cm) but may coalesce to form large patches of mucosal involvement

### Prognosis and Therapy

- Harmless lesions that often spontaneously regress
- Treatment is not necessary, but conservative surgical resection or laser ablation for cosmetic purposes is optional when lesions are few in number

HAART, Highly active antiretroviral therapy; HIV, human immunodeficiency virus.

### MICROSCOPIC FINDINGS

The hallmark histologic feature is acanthosis of the squamous epithelium (Fig. 8.10). The rete ridges are expanded and often fused. The keratinocytes show orderly maturation without atypia. Parakeratosis is a common finding. Virus-induced cellular alterations are sometimes present in the superficial keratinocytes. These alterations include koilocytic changes typical of HPV infection, and a more unique type of alteration characterized by fragmentation of the nuclei in a way that resembles a mitotic figure (the “mitosoid cell”) (Fig. 8.11).

### MULTIFOCAL EPITHELIAL HYPERPLASIA— PATHOLOGIC FEATURES

#### Gross Findings

- Tan, soft nodules with a sessile base and smooth surface

#### Microscopic Findings

- Abrupt acanthosis (simple squamous hyperplasia) with orderly maturation
- Expansion, clubbing, and fusion of the rete ridges
- Virus-induced alterations include koilocytes and a peculiar form of nuclear fragmentation resembling a mitotic figure (“mitosoid cell”)

#### Differential Diagnosis

- Condyloma acuminatum, squamous papilloma

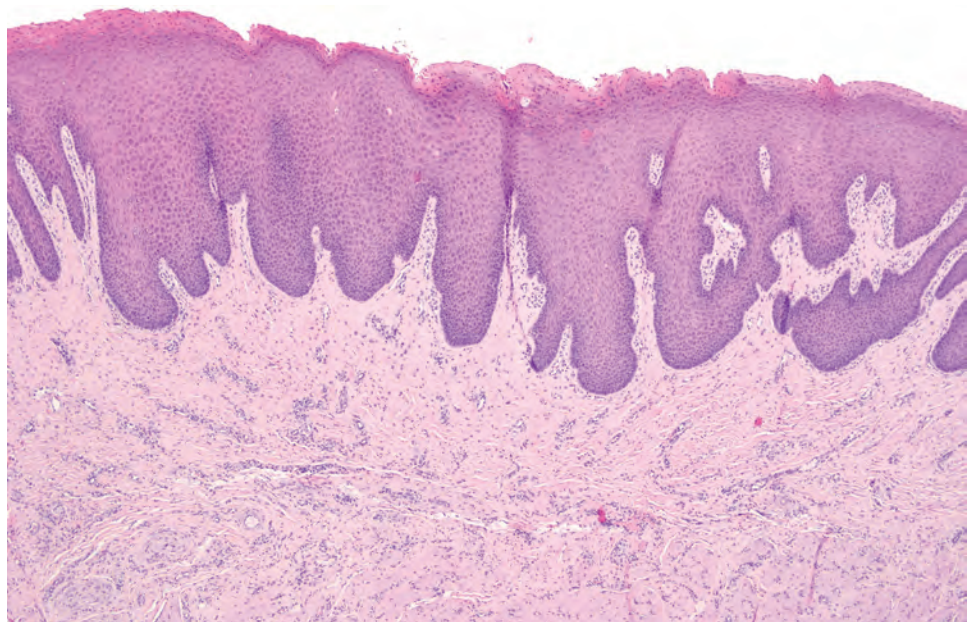


**FIGURE 8.10**

Low-power view of multifocal epithelial hyperplasia showing acanthosis of the squamous epithelium with expansion and clubbing of rete ridges.

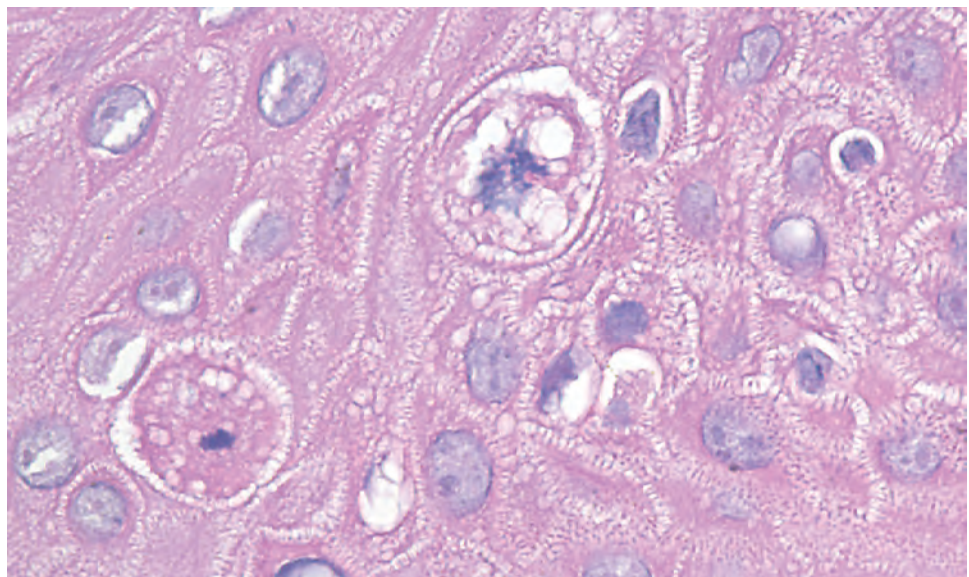


**FIGURE 8.11**

High-power view of “mitosoid cells”: The pattern of nuclear fragmentation in this keratinocyte has the appearance of a mitotic figure.



## ANCILLARY STUDIES

The presence of HPV can be documented using a variety of detection methods ranging from electron microscopy to type-specific DNA in situ hybridization. Viral detection, however, is a matter more of academic interest than of diagnostic relevance and methods of detection are generally not commercially available. Additionally, these techniques do not play any significant role in diagnosing MFEH or predicting its clinical behavior.

## DIFFERENTIAL DIAGNOSIS

Careful correlation of the clinical and pathologic findings should allow ready distinction of MFEH from other papular eruptions of the oral cavity. *Condyloma acuminatum*, for example, may clinically present as multifocal coalescent nodules of the oral mucosa. At the microscopic level, however, condyloma acuminatum and its family of HPV-related oral warts are characterized by a papillary growth as opposed to the simple squamous hyperplasia of MFEH. The distinction is important as lesions submitted from children may raise a question of sexual abuse.

## PROGNOSIS AND THERAPY

MFEH is a benign epithelial proliferation that often undergoes spontaneous regression. Removal of individual lesions by surgical excision or laser ablation for cosmetic purposes is feasible when a few lesions are present but impractical when lesions are more numerous and widespread.

## LOBULAR CAPILLARY HEMANGIOMA

Lobular capillary hemangioma (LCH), also referred to as “pyogenic granuloma,” is a reactive soft tissue growth with a predilection for the oral cavity that is histologically characterized by a lobular arrangement of proliferating small blood vessels. The term “pyogenic granuloma,” while entrenched in the culture and literature, is misleading because the lesion is neither infectious (related to pyogenic organisms) nor granulomatous. The designation LCH better reflects its true nature.

## CLINICAL FEATURES

LCH occurs in all age groups. Although it occurs equally in both sexes overall, some have noted an

## LOBULAR CAPILLARY HEMANGIOMA—DISEASE FACT SHEET

### Definition

- An acquired polypoid form of capillary hemangioma that is histologically characterized by a lobular arrangement of proliferating vessels

### Incidence and Location

- Common
- In the oral cavity, the most frequently involved sites are the lips, gingiva, cheek, and tongue

### Morbidity and Mortality

- Benign with no potential for invasive growth or malignant progression

### Sex and Age Distribution

- Equal sex distribution
- A hormonally driven form affects a small percentage (1%) of pregnant women
- Occurs in all ages

### Clinical Features

- Nonpainful, purple-red, polypoid mass that is friable and bleeds easily

### Prognosis and Therapy

- Conservative local excision is usually curative, but a small percentage may locally recur if incompletely excised.
- Pregnancy-associated lesions usually regress following parturition.

unequal sex distribution across different age groups: Patients younger than 18 years are predominantly male, patients between 18 and 39 years are predominantly female, and patients older than 39 years are more evenly distributed. The proportional increase in females during reproductive years reflects the contribution of hormonally driven lesions that occur during early stages of pregnancy.

The most frequently involved oral sites are the lips, gingiva, cheek, and tongue. Those lesions that arise during pregnancy almost exclusively involve the gingiva and are sometimes referred to as a *pregnancy tumor*. About one-third develop following minor trauma, whereas others are the result of a reaction to local irritation. Lesions of the oral cavity are almost always solitary. The clinical presentation is that of a nonpainful, purple-red polypoid mass that is friable and bleeds easily; not surprisingly, bleeding is the most common clinical complaint (Fig. 8.12). The surface is often ulcerated and sometimes covered with an exudate. Most lesions range in size from a few millimeters to a few centimeters.

## **PATHOLOGIC FEATURES**

### **GROSS FINDINGS**

LCH is grossly seen as a polypoid, often pedunculated, gray-tan mass. The surface is usually ulcerated, and the presence of an underlying exuberant granulation tissue often forms a prominent cap on a narrower stalk (Fig. 8.13).

### **MICROSCOPIC FINDINGS**

At low magnification, LCH is an exophytic growth connected to the oral mucosa by a broad stalk that is often collared by hyperplastic squamous epithelium (see Fig. 8.13). The fundamental microscopic makeup is that of a lobulated capillary hemangioma. Each lobule

consists of a compact proliferation of capillaries around a central larger feeding vessel (see Fig. 8.13). In the presence of ulceration, the stroma becomes inflamed and edematous, particularly in the superficial aspect of the lesion (Fig. 8.14). When these secondary stromal changes are pronounced, the lobular pattern is lost and the distinction between an LCH and an exuberant granulation tissue is obscured. The endothelial cells lining the capillaries are often plump with an epithelioid appearance. Mitotic activity is variable and may be robust.



**FIGURE 8.12**

This pyogenic granuloma of the lip is seen as a purple polypoid nodule.

## **LOBULAR CAPILLARY HEMANGIOMA— PATHOLOGIC FEATURES**

### **Gross Findings**

- Smooth, polypoid, pedunculated gray-tan mass

### **Microscopic Findings**

- Lobular arrangement of compact capillaries around a central larger feeding vessel
- Surface ulceration with varying degrees of stromal edema, inflammation, and fibrosis

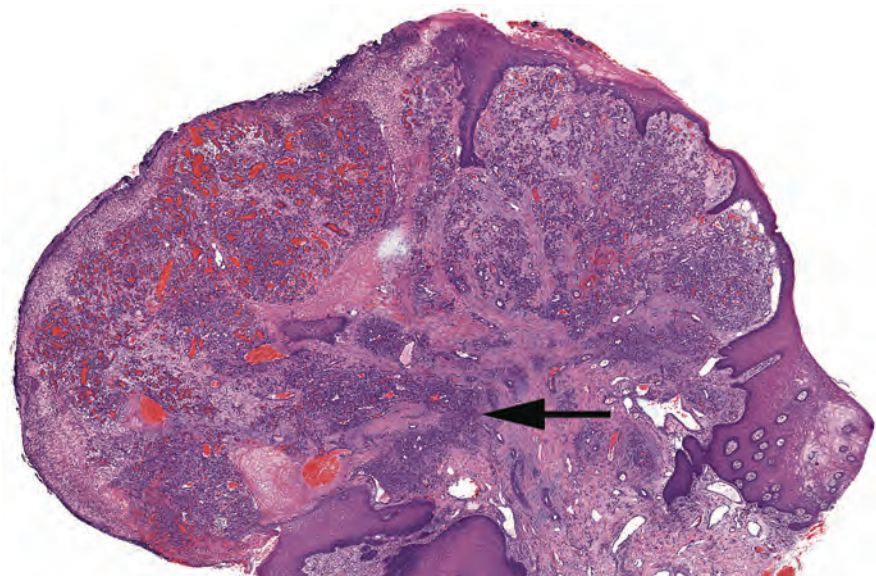
### **Immunohistochemical Findings**

- Positive: FVIII-Rag, CD34, CD31, ERG, FLI1

### **Pathologic Differential Diagnosis**

- Granulation tissue, nasopharyngeal angiofibroma, aggressive vascular neoplasms (e.g., Kaposi sarcoma, angiosarcoma, hemangiopericytoma)

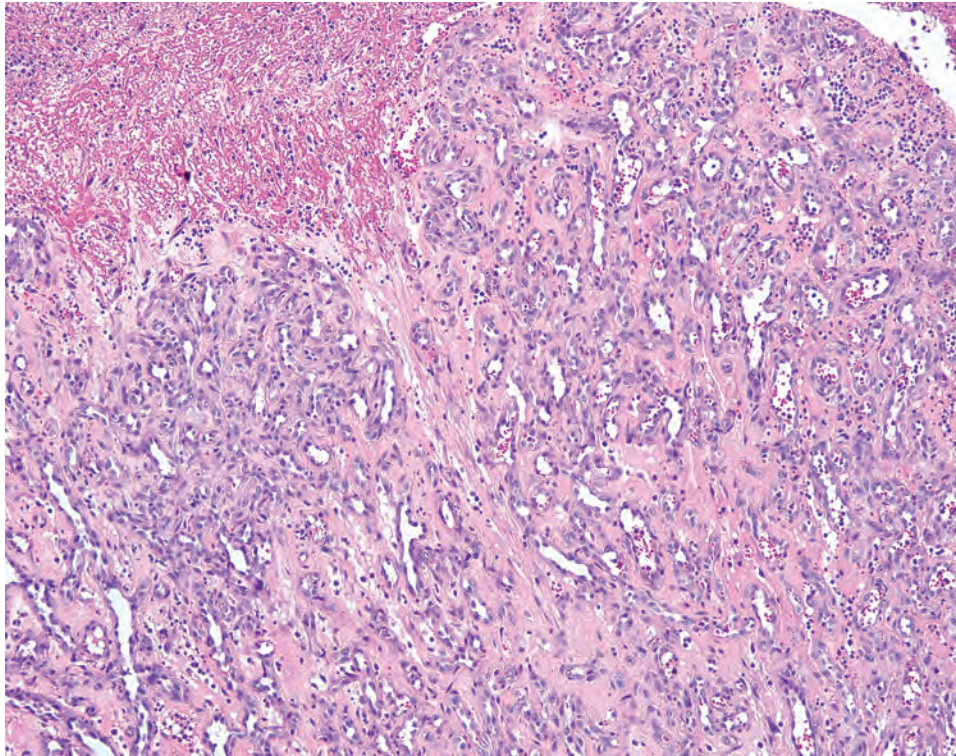
*FLI1*, Friend leukemia integration 1; *FVIII-Rag*, factor VIII-related antigen.



**FIGURE 8.13**

Low-power view showing the characteristic zonal pattern. The superficial aspect of this pyogenic granuloma is ulcerated, edematous, and inflamed. The lobular proliferation of small blood vessels is best appreciated in the deeper portion of the lesion (arrow).



**FIGURE 8.14**

High-power view of a lobule shows the compact proliferation of capillaries around a central larger feeding vessel.

### ANCILLARY STUDIES

The vascular component of LCH is immunoreactive with endothelial markers, including factor VIII-related antigen (FVIII-RAg), CD34, CD31, ERG, and Friend leukemia integration 1 (FLI1); it is not immunoreactive for epithelial markers (e.g., cytokeratin) or melanocytic markers (e.g., S100 protein, HMB45, Melan-A/Mart-1). Immunohistochemical documentation of its vascular nature has diagnostic utility when the epithelioid appearance of some cellular LCH causes confusion with an epithelial or melanocytic neoplasm.

### DIFFERENTIAL DIAGNOSIS

The differential diagnosis for an LCH is broad. Lesions with classic histology are not a diagnostic dilemma; however, lesions with prominent stromal edema may be dismissed as exuberant granulation tissue or as revolving mucocles. In turn, LCHs that are in the process of resolving may share histologic findings with fibroma. Malignancy must be excluded because LCH with a predominant solid growth pattern and brisk mitotic activity may be mistaken for more aggressive vascular lesions, such as *angiosarcoma*, *Kaposi sarcoma*, and *hemangiopericytoma*. When the endothelial cells in these solid areas take on a more epithelioid appearance, the lesion can mimic *epithelioid hemangioma*, *angiolymphoid*

*hyperplasia with eosinophilia*, and even carcinoma or melanoma. Brisk mitotic activity may lead to increased concerns of a possible malignancy. Unlike malignant vascular, epithelial, and melanocytic tumors, LCH is exophytic and circumscribed without infiltration of surrounding structures.

### PROGNOSIS AND THERAPY

LCH is a benign vascular neoplasm with no potential for locally invasive tumor growth or metastatic spread. Conservative local excision is usually curative, but a small percentage may locally recur if incompletely excised. Gingival lesions should be excised down to periosteum and any local irritants must be managed to prevent recurrence/persistence. Pregnancy-associated lesions usually regress following parturition.

## ■ PERIPHERAL OSSIFYING FIBROMA

Peripheral ossifying fibroma (POF) is a reactive non-neoplastic proliferation of fibrous tissue with focal mineralization forming a gingival mass (*peripheral* implies soft tissue involvement, whereas *central* implies within bone). The central ossifying fibroma is not, however, considered to be an intraosseous counterpart to the POF, as the former is a true neoplasm.

## CLINICAL FEATURES

POF is a common lesion that occurs exclusively on the gingiva or alveolar ridge. It more commonly affects the maxilla than the mandible, and favors the interdental papilla of the incisor/canine region. In some cases, a source of chronic irritation (e.g., ill-fitting dentures, orthodontics) or trauma is identified. It occurs over a broad age range with a peak among teenagers and young adults. Females are affected more commonly than males (1.7:1). POF appears clinically as a sessile or pedunculated nodule that ranges in size from a few millimeters to 2 cm (Fig. 8.15). The surface is often ulcerated.

### PERIPHERAL OSSIFYING FIBROMA—DISEASE FACT SHEET

#### Definition

- A reactive, non-neoplastic proliferation of fibrous tissue with mineralized material forming a gingival mass

#### Incidence and Location

- Common
- Almost exclusively involves the gingiva, usually arising from the interdental papilla

#### Morbidity and Mortality

- Reactive process with no malignant potential

#### Sex and Age Distribution

- More common in females
- Peak incidence in the second decade

#### Clinical Features

- Sessile or pedunculated nodule that ranges in size from a few millimeters to 2 cm
- Surface ulceration is common

#### Prognosis and Therapy

- Local surgical excision down to periosteum
- May recur locally



**FIGURE 8.15**

This peripheral ossifying fibroma arises from the interdental papilla as a lobulated smooth, sessile nodule.

## PATHOLOGIC FEATURES

### GROSS FINDINGS

POF is grossly seen as a polypoid, sometimes pedunculated, nodule. The surface may be intact or ulcerated.

### MICROSCOPIC FINDINGS

The fundamental makeup of the POF is fibroblastic tissue with randomly distributed deposits of mineralized material (Fig. 8.16). However, there is some inconstancy in its histologic appearance due to variations in the cellularity and the extent and type of mineralization, as a result of lesion maturation. The fibroblastic proliferation is covered by a stratified squamous epithelium, but this epithelium is often ulcerated and replaced by an inflammatory exudate. The overall cellularity of the fibroblastic component varies according to the relative proportion of plump fibroblasts and stromal collagen. The nature of the mineralized material varies from dystrophic calcification to cementum-like material to well-formed bone (Fig. 8.17). Mineralization may be scant, requiring review of multiple sections and levels. Multinucleated giant cells may be present, but not numerous.

## DIFFERENTIAL DIAGNOSIS

POFs can be confused with other fibrous lesions of the gingiva. Ulcerated lesions without conspicuous mineralization may be confused with *LCH*. A thorough microscopic examination, however, is usually sufficient to establish a diagnosis of POF by demonstrating the presence of focal mineralized deposits and the absence of a lobular proliferation of capillaries. Although individual or clustered multinucleated giant cells are present in a subset of POFs, they are not nearly as numerous as in *peripheral giant cell granuloma*. The stroma is histologically similar

### PERIPHERAL OSSIFYING FIBROMA—PATHOLOGIC FEATURES

#### Gross Findings

- Polypoid sometimes pedunculated gray-tan mass

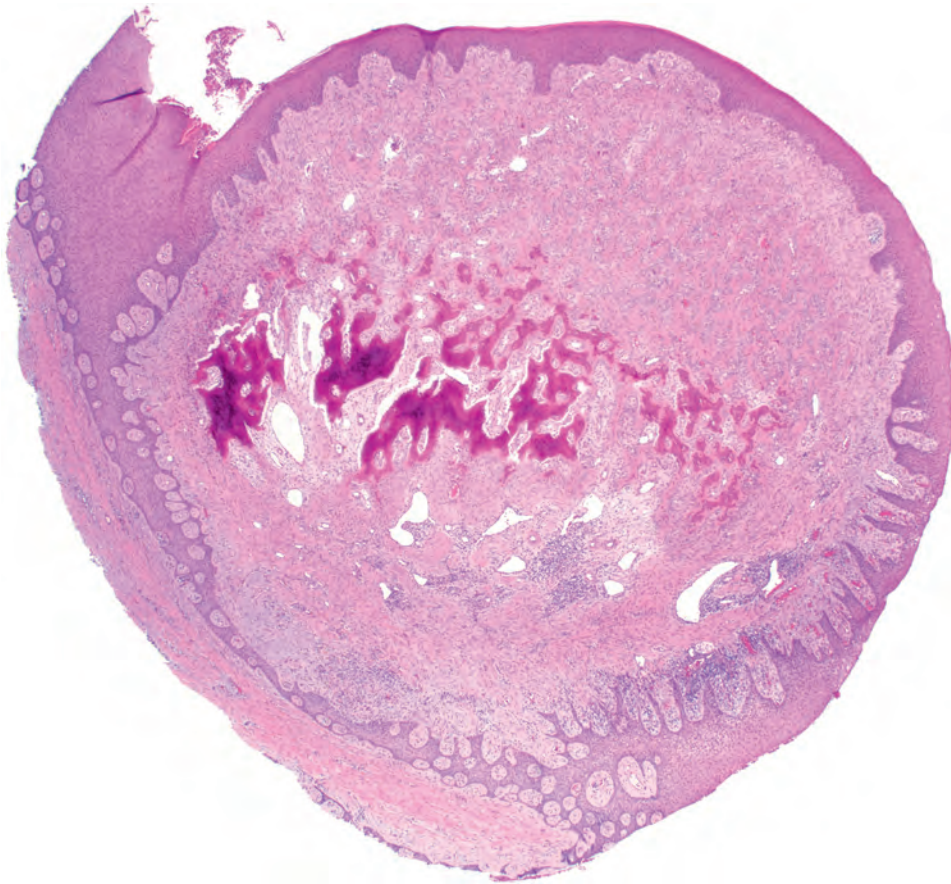
#### Microscopic Findings

- Fibroblast proliferation with randomly distributed deposits of mineralized material (e.g., dystrophic calcifications, cementum, bone)

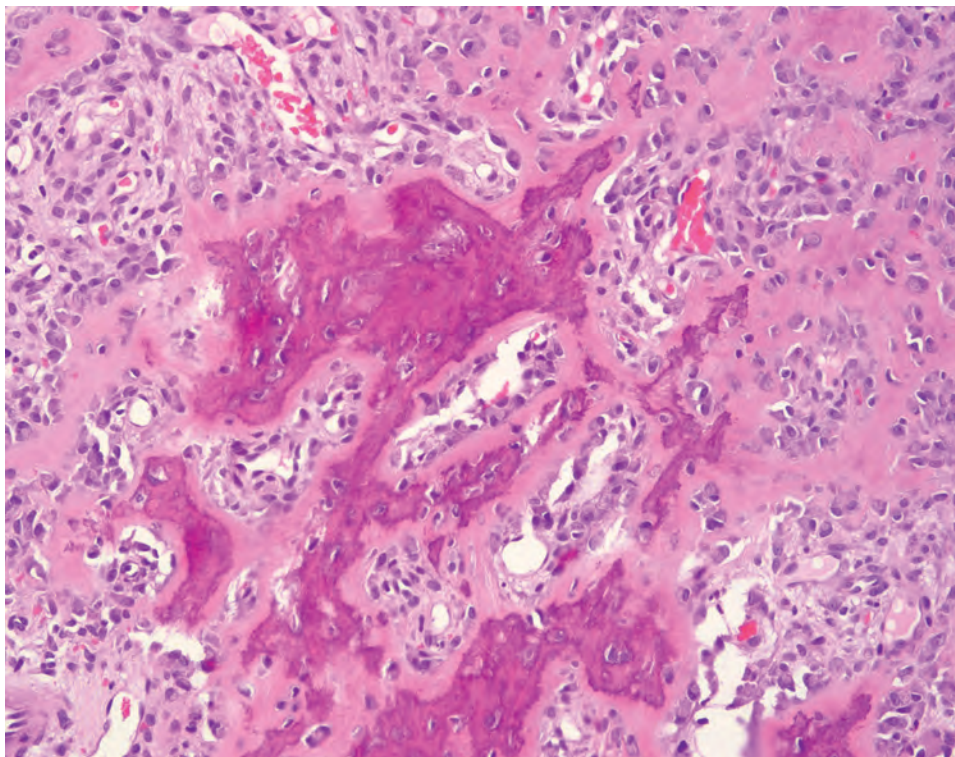
#### Pathologic Differential Diagnosis

- Pyogenic granuloma, peripheral giant cell granuloma, fibroma



**FIGURE 8.16**

Low-power view demonstrates an exophytic mass of exuberant fibroconnective tissue emanating from a central nidus of mineralization.

**FIGURE 8.17**

High power view shows the mineralized component to be composed of reactive, newly formed bone.

between fibroma and POF, with the mineralized material helping make the separation.

### PROGNOSIS AND THERAPY

Even though a reactive, non-neoplastic process, approximately 16% of POFs recur following local surgical excision. Therefore, aggressive excision, down to the periosteum, along with the removal of the underlying inciting irritant, is recommended as a means of minimizing the long-term risk of local recurrence.

## PERIPHERAL GIANT CELL GRANULOMA

Peripheral giant cell granuloma (PGCG) is a reactive proliferation caused by chronic irritation of the gingival mucosa. It is microscopically seen as an exuberant proliferation of multinucleated giant cells. The traditional term *peripheral giant cell reparative granuloma* is inaccurate, because the multinucleated giant cells have little if any capacity for local tissue repair. *Peripheral* implies soft tissue involvement, whereas *central* implies an intraosseous location.

### CLINICAL FEATURES

PGCG is a relatively common exophytic lesion of the oral cavity. It occurs over a broad age range, but most patients are between 40 and 60 years of age. Females are affected slightly more often than males. The PGCG presumably arises from the periodontal ligament and thus occurs exclusively on the gingiva, usually between the permanent molars and incisors. The mandible and maxilla are involved at an almost equal frequency. PGCG classically presents as a solitary broad-based reddish-blue polypoid nodule (Fig. 8.18). The surface epithelium is frequently ulcerated.



**FIGURE 8.18**

This peripheral giant cell granuloma arises from the gingiva as a broad-based reddish-blue polypoid nodule.

### PERIPHERAL GIANT CELL GRANULOMA—DISEASE FACT SHEET

#### Definition

- An exuberant reactive proliferation of multinucleated giant cells forming a gingival mass

#### Incidence and Location

- Relatively common
- Almost exclusively involves the gingiva

#### Morbidity and Mortality

- Reactive process with no malignant potential

#### Sex and Age Distribution

- More common in females
- Most patients 40-60 years old

#### Clinical Features

- Reddish-blue rubbery nodules that range in size from a few millimeters to 3 cm
- Surface ulceration is common

#### Prognosis and Therapy

- Local surgical excision down to bone
- May recur locally

### RADIOGRAPHIC FEATURES

Unlike central giant cell granuloma, the PGCG does not arise within the craniofacial bones. Nonetheless, it may occasionally induce focal resorption of underlying alveolar bone, thus giving rise to a superficial cup-shaped radiolucency on imaging.

### PATHOLOGIC FEATURES

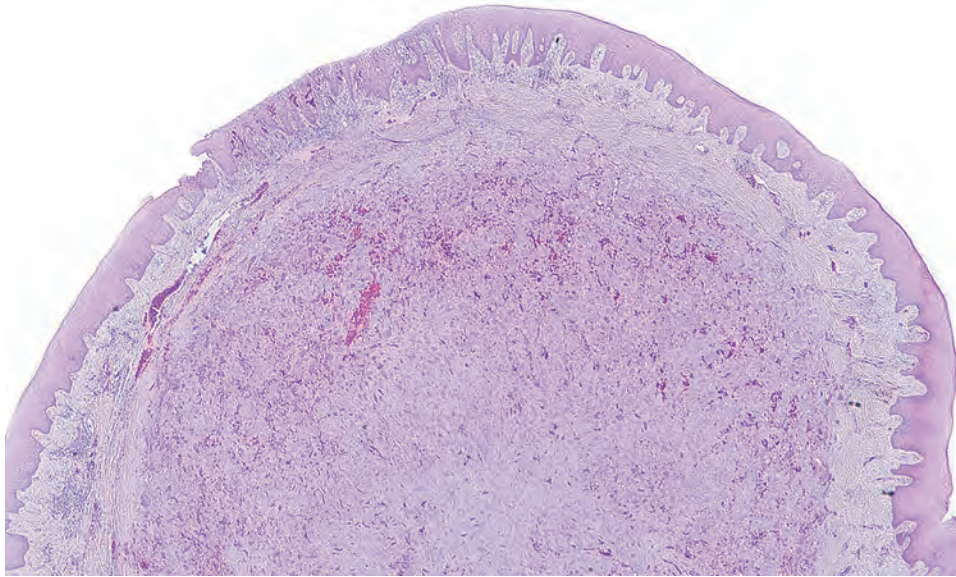
#### GROSS FINDINGS

PGCG grossly appears as a soft to rubbery, broad-based polypoid nodule that measures a few millimeters up to 3 cm. Its surface tends to be smooth.

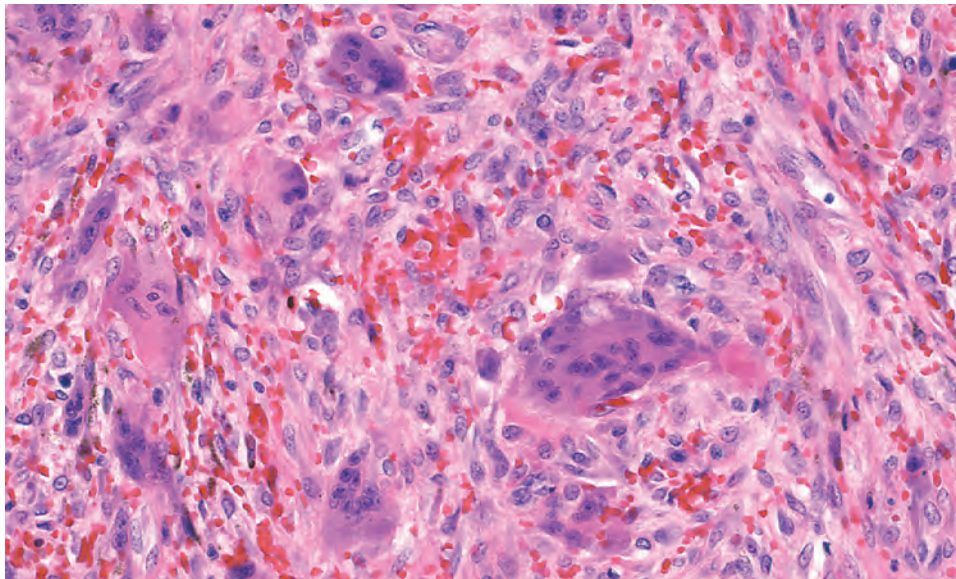
#### MICROSCOPIC FINDINGS

The microscopic appearance is characterized by an exuberance of multinucleated giant cells (Figs. 8.19 and 8.20). They are abundantly present and dominate the microscopic picture. The relationship of these cells to true osteoclasts is unclear, but they are certainly osteoclast-like in their appearance having abundant cytoplasm containing up to 100 nuclei (Fig. 8.21). These multinucleated giant cells are interspersed among spindled to oval

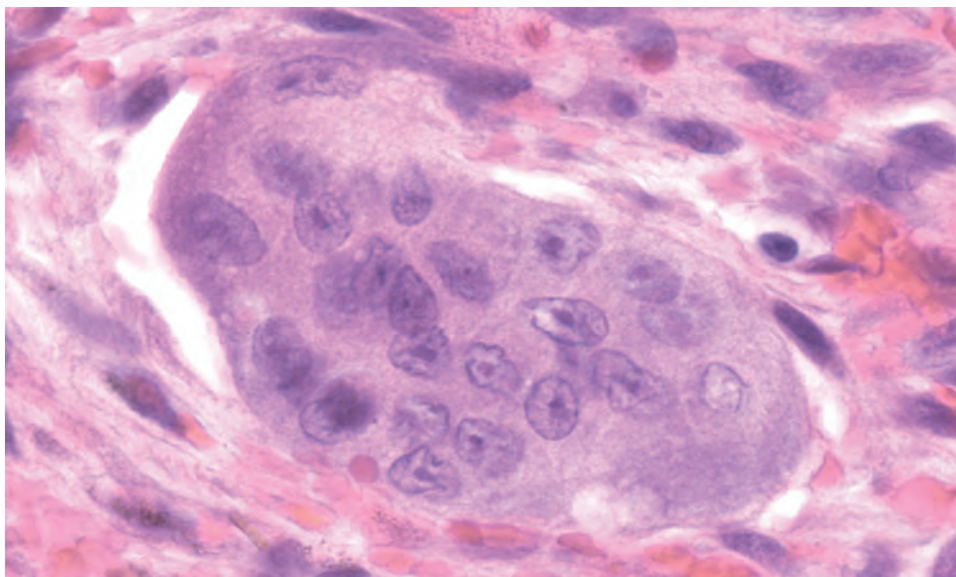


**FIGURE 8.19**

Proliferation of giant cells forms a sub-mucosal nodule.

**FIGURE 8.20**

Giant cells are interspersed among stromal mononuclear cells in a hemorrhagic background.

**FIGURE 8.21**

Giant cells have an abundant cytoplasm that contains numerous nuclei, usually many dozen.

### PERIPHERAL GIANT CELL GRANULOMA— PATHOLOGIC FEATURES

#### Gross Findings

- Broad-based rubbery polypoid nodule with smooth surface

#### Microscopic Findings

- Histologic picture dominated by multinucleated giant cells admixed with mononuclear stromal cells
- Background findings include hemorrhage, hemosiderin deposition, chronic inflammation, and islands of metaplastic bone

#### Pathologic Differential Diagnosis

- Other giant cell-rich tumors include central giant cell tumor, brown tumor of hyperparathyroidism, and cherubism

mononuclear cells. Secondary background findings include hemorrhage, hemosiderin deposition, chronic inflammation, and islands of metaplastic bone.

### DIFFERENTIAL DIAGNOSIS

There are a handful of lesions that closely resemble the PGCG in their histologic appearance. These include central *giant cell granuloma*, *brown tumor of hyperparathyroidism*, and *cherubism*. However, all of these occur within the craniofacial bones, in contrast to PGCG. Thus, the clinical findings and radiographic findings are essential when it comes to distinguishing between the various giant cell-rich lesions of the oral cavity. Additionally, such correlation may assist in ruling out a central lesion that has perforated the bone, resulting in a gingival mass. Of course, giant cells may be found in other lesions, so the defining findings of those entities must be considered before the diagnosis of PGCG is rendered.

### PROGNOSIS AND THERAPY

The standard treatment of PGCG is surgical excision down to the bone. Failure to include the periosteum or periodontal ligament may result in an increased risk of local recurrence, which occurs in approximately 10 % of lesions. In addition, efforts should be taken to identify and remove any inciting source(s) of chronic irritation.

### ■ GRANULAR CELL TUMOR

Granular cell tumor is an uncommon benign soft tissue neoplasm that has a predilection for the oral cavity, skin,



**FIGURE 8.22**

Clinical image demonstrates a granular cell tumor appearing as a sessile submucosal mass of the anterior tongue.

and subcutaneous tissues. Previously thought to arise from skeletal muscle tissues, it is currently thought to be of Schwann cell-derivation.

### CLINICAL FEATURES

Granular cell tumors favor the head and neck with tumors of the tongue, usually the dorsal surface, accounting for well over half of all reported cases. Other intraoral locations include the buccal mucosa, the floor of the mouth, and the palate. Although occasionally reported in children, tumors are most frequently found in adults in the fourth to sixth decades. Women are affected by intraoral tumors with a frequency three times that of men. Tumors generally present as solitary sessile masses; however, multiple lesions are reported in up to 25 % of individuals. The tumors generally are surfaced by normal appearing mucosa, and a slight yellow color is sometimes reported (Fig. 8.22).

### PATHOLOGIC FEATURES

#### GROSS FINDINGS

Granular cell tumors are generally pink-yellow masses with a smooth nonulcerated surface. The cut surface is homogeneous, firm, and tan to yellow.

#### MICROSCOPIC FINDINGS

The granular cell tumor is a nonencapsulated collection of distinctive plump, polygonal to elongated eosinophilic granular cells. The nuclei are centrally located, small, and round or oval. Cells grow in sheets and cords, blending with surrounding tissues, often skeletal muscle and



**GRANULAR CELL TUMOR—DISEASE FACT SHEET****Definition**

- A benign tumor arising from Schwann cells

**Incidence and Location**

- Uncommon
- Over half of tumors affect the dorsal surface of the tongue.
- Buccal mucosa, floor of the tongue, and the palate are other intraoral site

**Morbidity and Mortality**

- Rarely, large tumors may affect function
- Rare reports of malignant granular cell tumors

**Sex and Age Distribution**

- Females > males (3:1)
- Fourth to sixth decade, rare in children

**Clinical Features**

- Smooth sessile masses
- Surfaced by normal pink mucosa or may have a slight yellow appearance

**Prognosis and Therapy**

- Local conservative resection is curative
- Recurrence is uncommon

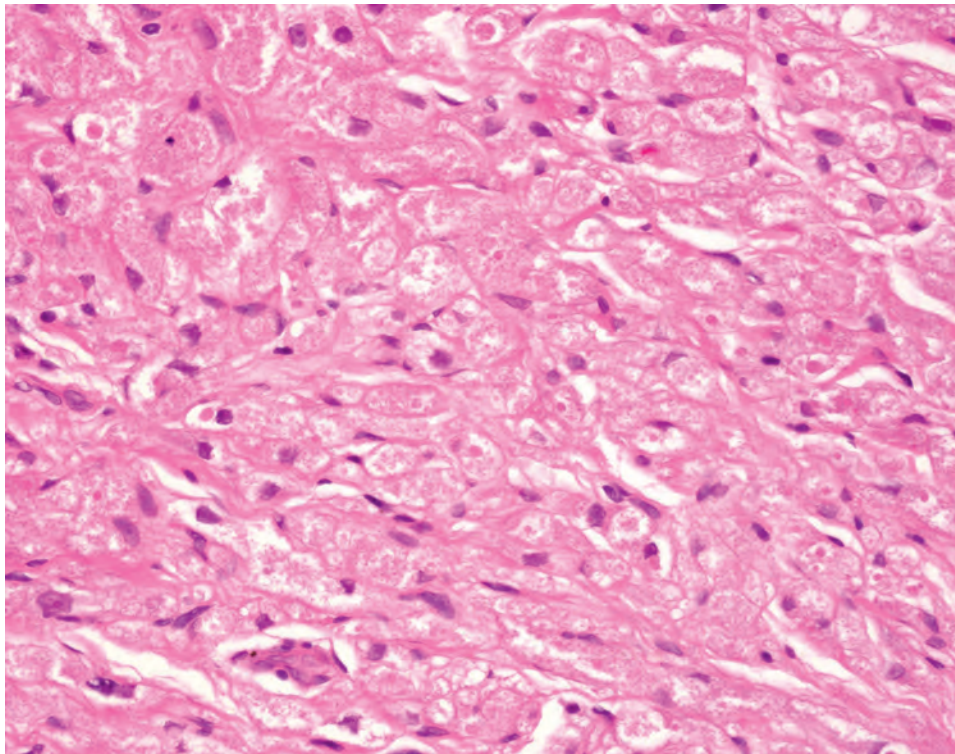
around nerves. A syncytial appearance is created by the indistinct cell membranes of tumor cells (Fig. 8.23). The overlying surface may demonstrate pseudoepitheliomatous hyperplasia (PEH), reported in 30 % to 50 % of cases (Fig. 8.24).

**ANCILLARY STUDIES**

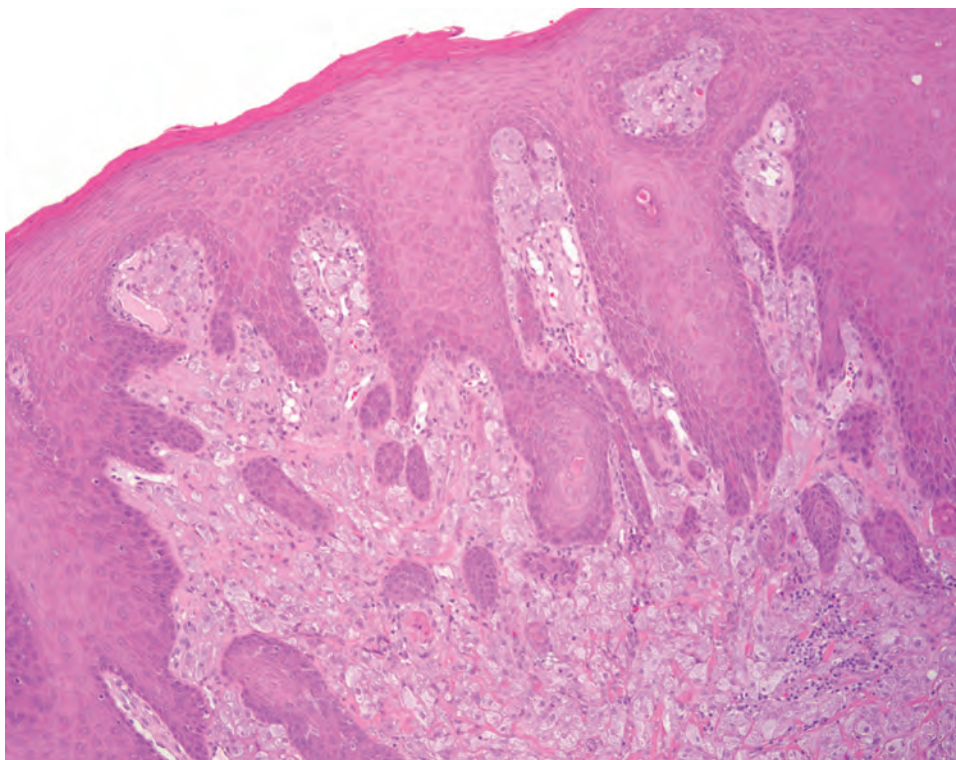
Immunohistochemical studies may be of assistance because granular cell tumors are strongly and uniformly reactive, both nuclear and cytoplasmic, for S100 protein, while showing a nuclear reaction with SOX10. CD68 yields nonspecific reactivity. Additionally, the granules of the cells are periodic acid–Schiff (PAS) positive and diastase resistant.

**DIFFERENTIAL DIAGNOSIS**

Granular cell tumor and congenital granular cell epulis (CGCE) are microscopically similar. Close examination of the clinical presentation and patient demographics is helpful in narrowing the differential diagnosis. CGCE, discussed in the next section, is found primarily in

**FIGURE 8.23**

High-power image shows the granular cells with abundant pale eosinophilic cytoplasm.

**FIGURE 8.24**

Low-power image shows the surface pseudoepitheliomatous hyperplasia overlying a granular cell tumor of the tongue.

#### GRANULAR CELL TUMOR—PATHOLOGIC FEATURES

##### Gross Findings

- Smooth-surfaced nodule
- Cut surface is of a firm texture, pale tan-yellow

##### Microscopic Findings

- Nonencapsulated collection of cells that blend with the surrounding tissue
- Submucosal proliferation of cells with abundant eosinophilic granular cytoplasm
- Syncytial appearance
- Central small, dark nuclei
- Overlying PEH in up to 50% of cases

##### Immunohistochemical Findings

- Positive: S100 protein, SOX10, CD68

##### Pathologic Differential Diagnosis

- Congenital granular cell epulis, alveolar soft part sarcoma, rhabdomyoma
- Squamous cell carcinoma may be considered when PEH is a feature

PEH, Pseudoepitheliomatous hyperplasia.

epithelium is usually intact and atrophic in a CGCE, whereas the epithelium of a granular cell tumor may demonstrate impressive PEH. Other pink cell tumors that can involve the oral cavity include *alveolar soft part sarcoma* and *rhabdomyoma*. Both of these entities are relatively rare in the oral cavity and have different immunohistochemical profiles. Both also lack PEH. The PEH of a granular cell tumor, however, may bring into consideration a squamous cell carcinoma. Small and superficial biopsies are at particular risk for this potential pitfall. Review of multiple step sections should assist in ruling out a malignancy. A squamous cell carcinoma should show considerable atypia, whereas the islands of PEH should be bland.

#### PROGNOSIS AND THERAPY

Complete excision is the treatment of choice with recurrence reported at less than 10%. Those with multiple tumors may require closer clinical follow-up.

#### ■ CONGENITAL GRANULAR CELL EPULIS

newborns and young children and tends to favor the alveolar ridge. Although histologically the granular cells for both entities are identical, the cells of the granular cell tumor are strongly immunoreactive for S100 protein, whereas CGCE is nonreactive. The overlying surface

CGCE is a rare benign mesenchymal tumor composed of large cells with coarse granular cytoplasm. It is also known as *congenital epulis*, or as *congenital epulis of the newborn*, although the latter is redundant. It classically arises from the anterior alveolar ridge of the newborn.



Its cell of origin remains elusive, and it is not to be regarded as the congenital counterpart of the Schwann cell–derived adult granular cell tumor.

### CLINICAL FEATURES

CGCE is a rare tumor that occurs almost exclusively in newborns. Females are affected much more commonly than males at a ratio of approximately 9:1. CGCE is a lesion of the alveolar ridge with a particular predilection for the gingiva overlying the future canine and lateral incisor teeth. The maxilla is involved more commonly than the mandible. They tend to be seen as smooth nonulcerated polypoid masses with a broad-based attachment to the alveolar ridge. The bone and teeth are uninvolved. Most lesions measure about 1 cm, but they may achieve sizes of greater than 5 cm. Affected newborns often present with a mass protruding from the oral cavity (Fig. 8.25). Mechanical obstruction may cause problems with feeding and respiration.

### PATHOLOGIC FEATURES

#### GROSS FINDINGS

CGCE typically presents as a tan-pink, polypoid mass with a smooth nonulcerated surface (Fig. 8.26). The cut surface is homogeneous, firm, and tan to yellow.

#### MICROSCOPIC FINDINGS

The CGCE is composed of large, polygonal granular cells, characterized by an abundance of eosinophilic granular cytoplasm and round or oval basophilic nuclei.



**FIGURE 8.25**

This congenital granular cell epulis arises from the alveolar ridge of the maxilla and emanates from the oral cavity as a large polypoid mass.

These distinctive cells grow in a sheet-like pattern supported by delicate fibrovascular septa (Fig. 8.27). Incorporation of odontogenic epithelium is occasionally seen. The overlying surface epithelium is usually intact and atrophic.

### CONGENITAL GRANULAR CELL EPULIS—DISEASE FACT SHEET

#### Definition

- A benign mesenchymal tumor arising from the anterior alveolar ridge of the newborn and composed of large cells with coarse granular cytoplasm

#### Incidence and Location

- Rare
- Almost exclusively involves the alveolar ridge with a distinct preference for gingiva overlying the future canine and lateral incisor teeth
- The maxilla is involved more commonly than the mandible

#### Morbidity and Mortality

- Obstructive masses may cause difficulty with respiration and feeding

#### Sex and Age Distribution

- Females > > > males (9:1)
- Newborns

#### Clinical Features

- Smooth nonulcerated polypoid masses with a broad-based attachment to the alveolar ridge

#### Prognosis and Therapy

- Stops growing at birth and often regresses over time
- Local conservative resection is curative
- Does not recur (even after incomplete excision).

### CONGENITAL GRANULAR CELL EPULIS—PATHOLOGIC FEATURES

#### Gross Findings

- Tan-pink polypoid mass with a smooth nonulcerated surface

#### Microscopic Findings

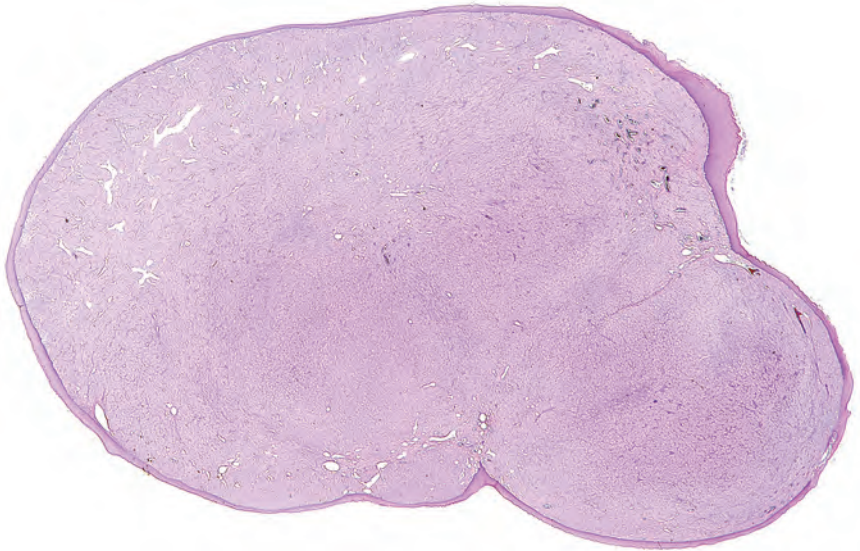
- Submucosal proliferation of cells with abundant eosinophilic granular cytoplasm

#### Immunohistochemical Findings

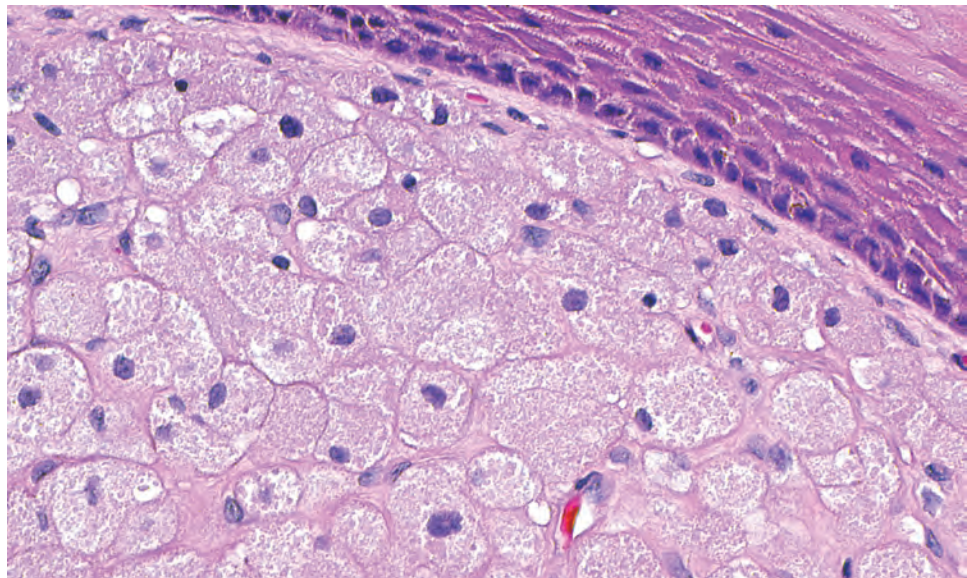
- Absence of S100 protein and SOX10 staining, in contrast to adult granular cell tumors

#### Pathologic Differential Diagnosis

- Adult granular cell tumor, alveolar soft part sarcoma, rhabdomyoma

**FIGURE 8.26**

Low-power view showing sheets of granular cells filling the submucosa.

**FIGURE 8.27**

Higher-power view demonstrating the abundant pink granular cytoplasm of the granular cells.

### ANCILLARY STUDIES

Immunohistochemical studies have focused on questions related to histogenesis, because the cell of origin remains elusive. The absence of staining for muscle markers, epithelial markers, and neural markers suggests an origin from an uncommitted mesenchymal cell. Notably, the lack of S100 protein, SOX10, pancytokeratin, actin, and desmin support the contention that, histologic similarities aside, the CGCE and the Schwann cell-derived granular cell tumor are distinct, unrelated lesions. Moreover, electron microscopy fails to reveal any evidence of Schwannian differentiation.

### DIFFERENTIAL DIAGNOSIS

The granular cells in CGCE and *granular cell tumors* are microscopically identical, but they should not be regarded as equivalent tumors. In contrast to CGCE, granular cell tumors usually affect adults, have a site predilection for the tongue, are immunoreactive for S100 protein and SOX10, and are associated with hyperplasia of the overlying epithelium (i.e., PEH). As with the differential diagnosis of granular cell tumors, *alveolar soft part sarcoma* and *rhabdomyoma* should at least be considered, but these rarely cause diagnostic confusion when the histologic picture is considered together with the age of the patient and location of the mass.



## PROGNOSIS AND THERAPY

The tumor stops growing at birth and regresses over time. In fact, complete regression without therapy has been reported. Most tumors are surgically excised. As they do not recur, even following incomplete removal, surgical excision should be conservative, to ensure the preservation of underlying developing teeth.

## ■ ECTOMESENCHYMAL CHONDROMYXOID TUMOR

Ectomesenchymal chondromyxoid tumor (EMCMT) is a benign mesenchymal neoplasm showing a mixed lineage of both myoepithelial and neural crest origin. Originally described in the anterior tongue only, it is known to develop rarely in other intraoral sites.

## CLINICAL FEATURES

EMCMT is a rare tumor occurring over a wide age range, with a peak in the fourth decade, without any sex predilection. Affecting the oral cavity exclusively, the vast majority of tumors affect the dorsal tongue. Patients present with

a submucosal, painless mass often present for a long duration.

## PATHOLOGIC FEATURES

### GROSS FINDINGS

Small tumors that are relatively circumscribed, showing a gelatinous appearance.

### MICROSCOPIC FINDINGS

EMCMT is not encapsulated, although often well circumscribed, but showing an intimate relationship with the surrounding tongue musculature, which may simulate a malignancy. The tumor grows in a lobular pattern separated by bands of fibrosis that frequently cleft away from the tumor (Fig. 8.28). The neoplastic cells are round to spindled, showing cords or reticulated cells within a myxoid or chondromyxoid stroma. The cells have ample amphophilic to eosinophilic cytoplasm, arranged in a syncytial appearance (see Fig. 8.28). The nuclei may show indentations or irregular periphery, with hyperchromasia and intranuclear cytoplasmic inclusions.

### ECTOMESENCHYMAL CHONDROMYXOID TUMOR—DISEASE FACT SHEET

#### Definition

- A benign mesenchymal neoplasm showing myoepithelial and primitive neural crest differentiation

#### Incidence and Location

- Rare
- Almost exclusively affects the anterior dorsal tongue

#### Morbidity and Mortality

- None

#### Sex and Age Distribution

- Equal sex distribution
- Wide age range; mean in fourth decade

#### Clinical Features

- Painless, submucosal dorsal tongue mass present for a long duration

#### Prognosis and Therapy

- Local conservative resection is curative
- Rare recurrence if incompletely removed

### ECTOMESENCHYMAL CHONDROMYXOID TUMOR—PATHOLOGIC FINDINGS

#### Gross Findings

- Nonulcerated, submucosal, unencapsulated gelatinous mass

#### Microscopic Findings

- Irregular periphery of tumor lobules, frequently entrapping skeletal muscle
- Bands of fibrosis dissect the round to spindled neoplastic cells, often showing a cleft
- Cords or reticulated pattern of cells within a myxoid or chondromyxoid stroma
- Syncytium of cells with ample cytoplasm, often showing nuclei with indentations or inclusions
- Mitoses are inconspicuous

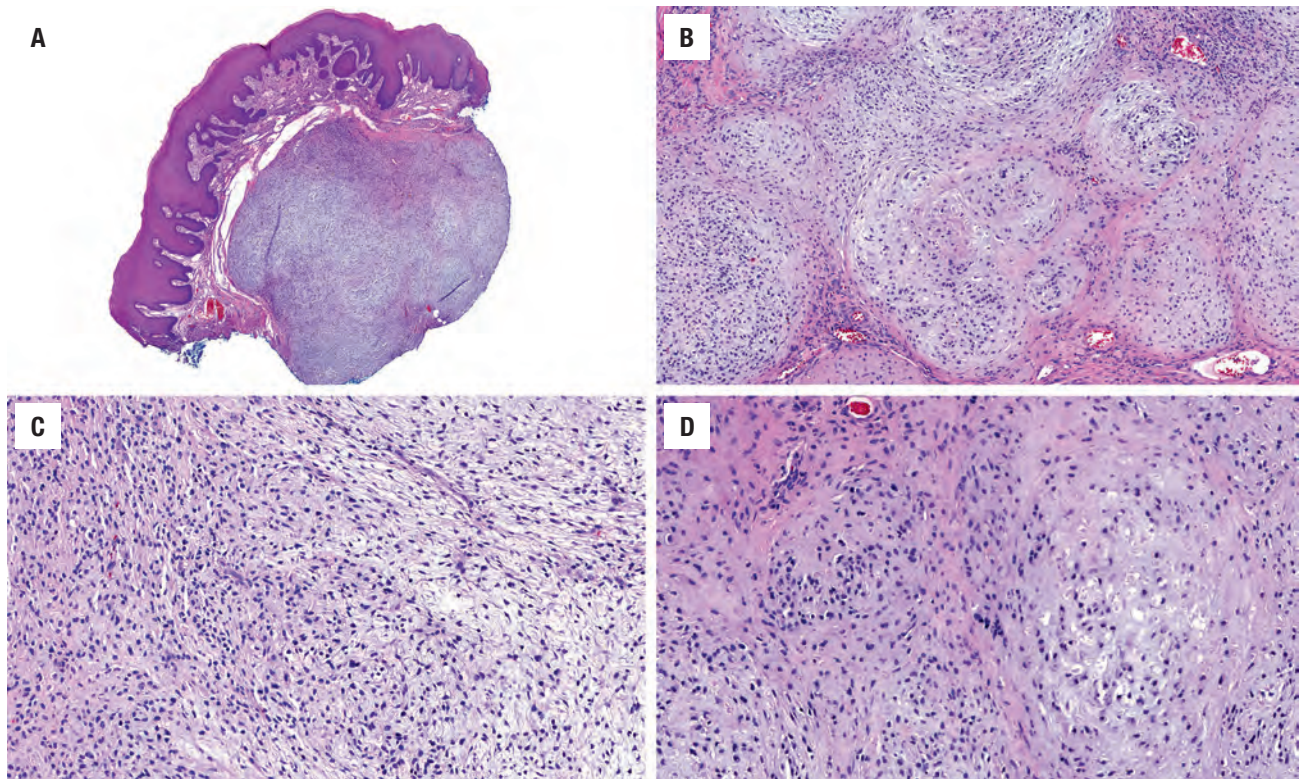
#### Immunohistochemical Findings

- Positive: GFAP, S100 protein, actin, pancytokeratin
- Negative: EMA, desmin, p63, calponin (usually)

#### Pathologic Differential Diagnosis

- Pleomorphic adenoma, myoepithelioma, myxoid neurofibroma, nerve sheath myxoma (classic neurothekeoma), extraskelatal myxoid chondrosarcoma, chondroid choristoma, focal oral mucinosis, fetal rhabdomyoma, mucous retention phenomenon (mucocele)

EMA, Epithelial membrane antigen; GFAP, glial fibrillary acidic protein.

**FIGURE 8.28**

Several images of an ectomesenchymal chondromyxoid tumor. **(A)** The tumor is identified below an intact squamous mucosa, lacking a capsule. **(B)** The tumor is often arranged in nodules that are separated by fibrous bands. **(C)** The cells are arranged in a myxoid background. **(D)** There is a vaguely chondroid appearance, with bland cells showing eosinophilic cytoplasm surrounding round to regular nuclei.

Mitoses are inconspicuous. Plasmacytoid cells and ductal or glandular differentiation is absent.

#### ANCILLARY STUDIES

Alcian blue and mucicarmine will highlight the stromal matrix, but PAS is nonreactive. The neoplastic cells are nearly always reactive with glial fibrillary acidic protein (GFAP), whereas pancytokeratin, S100 protein, and smooth muscle actin are variably reactive. Epithelial membrane antigen (EMA), desmin, p63, and calponin are usually negative. Recent evidence has shown that a subset of EMCMTs harbor *EWSR1* gene fusions. This finding, coupled with overlapping morphologic and immunophenotypic findings, suggests that EMCMT may be analogous to soft tissue myoepithelioma.

#### DIFFERENTIAL DIAGNOSIS

The differential diagnosis is usually quite broad, including pleomorphic adenoma, myoepithelioma, myxoid

neurofibroma, nerve sheath myxoma, extraskeletal myxoid chondrosarcoma, chondroid choristoma, focal oral mucinous, fetal rhabdomyoma, and mucous retention. However, careful review of the histologic findings coupled with pertinent reactions with selected immunohistochemistry studies helps to make the distinction between these entities.

#### PROGNOSIS AND THERAPY

After complete, but conservative excision, there is an excellent long-term outcome, with rare recurrences reported after incomplete excision.

#### SUGGESTED READINGS

The complete Suggested Readings list is available online at [ExpertConsult.com](http://ExpertConsult.com).



**SUGGESTED READINGS****Fibroma**

1. Buchner A, et al. Relative frequency of localized reactive hyperplastic lesions of the gingiva: a retrospective study of 1675 cases from Israel. *J Oral Pathol Med*. 2010;39:631–638.
2. de Santana Santos T, et al. Focal fibrous hyperplasia: A review of 193 cases. *J Oral Maxillofac Pathol*. 2014;18(suppl 1):S86–S89.
3. Esmeli T, et al. Common benign oral soft tissue masses. *Dent Clin North Am*. 2005;49(1):223–240.
4. Neville BW, et al. Soft tissue tumors. In: Neville BW, Damm DD, Allen CM, Chi AC, eds. *Oral and Maxillofacial Pathology*. 4th ed. New York: WB Saunders; 2015.
5. Regezi JA, et al. Connective tissue lesions. In: Regezi JA, Sciubba JJ, Jordan RCK, eds. *Oral Pathology: Clinical Pathologic Correlations*. 7th ed. St. Louis: Saunders; 2016.

**Squamous Papilloma (Including Verruca and Condyloma)**

1. Abbey LM, et al. The clinical and histopathologic features of a series of 464 oral squamous cell papillomas. *Oral Surg Oral Med Oral Pathol*. 1980;49:419–428.
2. Carneiro TE, et al. Squamous papilloma: clinical, histologic and immunohistochemical analyses. *J Oral Sci*. 2009;51(3):367–372.
3. Dalla Torre D, et al. Comparison of the prevalence of human papilloma virus infection in histopathologically confirmed premalignant oral lesions and healthy oral mucosa by brush smear detection. *Oral Surg Oral Med Oral Pathol Oral Radiol*. 2015;119(3):333–339.
4. Frigerio M, et al. Clinical, histopathological and immunohistochemical study of oral squamous papillomas. *Acta Odontol Scand*. 2015;73(7):508–515.
5. Garlick JA, et al. Human papillomavirus of the oral mucosa. *Am J Dermatopathol*. 1991;13:386–395.
6. Jaiswal R, et al. Condyloma acuminatum of the buccal mucosa. *Ear Nose Throat J*. 2014;93(6):219–223.
7. Müller S, et al. Squamous cell papilloma. In: El-Naggar AK, Chan JKC, Grandis JR, Takata T, Slootweg PJ, eds. *Classification of Head and Neck Tumors*. 4th ed. World Health Organization Classification of Tumours. Lyon, France: IARC Press; 2017:115–116.
8. Nguyen HP, et al. Human papillomavirus infections of the oral mucosa and upper respiratory tract. *Curr Probl Dermatol*. 2014;45:132–153.

**Multifocal Epithelial Hyperplasia**

1. Archard HO, et al. Focal epithelial hyperplasia: an unusual oral mucosal lesion found in Indian children. *Oral Surg Oral Med Oral Pathol*. 1965;20:201–212.
2. Carlos RB, et al. Multifocal papilloma virus epithelial hyperplasia. *Oral Surg Oral Med Oral Pathol*. 1994;77:631–635.
3. Feller L, et al. Focal epithelial hyperplasia (Heck disease) related to highly active antiretroviral therapy in an HIV-seropositive child. A report of a case, and a review of the literature. *SADJ*. 2010;65(4):172–175.
4. Moerman M, et al. Recurrent focal epithelial hyperplasia due to HPV13 in an HIV-positive patient. *Dermatology*. 2001;203:339–341.
5. Said AK, et al. Focal epithelial hyperplasia – an update. *J Oral Pathol Med*. 2013;42(6):435–442.
6. Vigneswaran N, et al. Multifocal epithelial hyperplasia. In: El-Naggar AK, Chan JKC, Grandis JR, Takata T, Slootweg PJ, eds. *Classification of Head and Neck Tumors*. 4th ed. World Health Organization Classification of Tumours. Lyon, France: IARC Press; 2017:117–118.
7. Padayachee A, et al. Human papillomavirus (HPV) DNA in focal epithelial hyperplasia by in situ hybridization. *J Oral Pathol Med*. 1991;20:210–214.

**Lobular Capillary Hemangioma**

1. Bhaskar SN, et al. Pyogenic granuloma: clinical features, incidence, histology and result of treatment—report of 242 cases. *J Oral Surg*. 1966;24:391–398.
2. Bullerdiek J, et al. Haemangioma. In: El-Naggar AK, Chan JKC, Grandis JR, Takata T, Slootweg PJ, eds. *Classification of Head and*

*Neck Tumors*. 4th ed. World Health Organization Classification of Tumours. Lyon, France: IARC Press; 2017.

3. Gordón-Núñez MA, et al. Oral pyogenic granuloma: a retrospective analysis of 293 cases in a Brazilian population. *J Oral Maxillofac Surg*. 2010;68:2185–2188.
4. Kapadia SB, et al. Pitfalls in the histopathologic diagnosis of pyogenic granuloma. *Eur Arch Otorhinolaryngol*. 1992;249:195–200.
5. Marla V, et al. The histopathological spectrum of pyogenic granuloma: a case series. *Case Rep Dent*. 2016;2016:1323798.
6. Mills SE, et al. Lobular capillary hemangioma: the underlying lesion of pyogenic granuloma: a study of 73 cases from the oral and nasal membranes. *Am J Surg Pathol*. 1980;4:471–479.

**Peripheral Ossifying Fibroma**

1. Buchner A, et al. The histomorphologic spectrum of peripheral ossifying fibroma. *Oral Surg Oral Med Oral Pathol*. 1987;63:452–461.
2. Gardner DG. The peripheral odontogenic fibroma: an attempt at clarification. *Oral Surg Oral Med Oral Pathol*. 1982;54:40–48.
3. Kendrick F, et al. Managing a peripheral ossifying fibroma. *ASDC J Dent Child*. 1996;63:135–138.
4. Franco-Barrera MJ, et al. An update on peripheral ossifying fibroma: case report and literature review. *Oral Maxillofac Surg*. 2016;20(1):1–7.
5. Zain RB, et al. Fibrous lesions of the gingiva: a histopathologic analysis of 204 cases. *Oral Surg Oral Med Oral Pathol*. 1990;70:466–470.

**Peripheral Giant Cell Granuloma**

1. Katsikeris N, et al. Peripheral giant cell granuloma. Clinicopathologic study of 224 cases and review of 956 reported cases. *Int J Oral Maxillofac Surg*. 1988;17:94–99.
2. Lester SR, et al. Peripheral giant cell granulomas: a series of 279 cases. *Oral Surg Oral Med Oral Pathol Oral Radiol*. 2014;118(4):475–482.
3. Neville BW, et al. Soft tissue tumors. In: Neville BW, Damm DD, Allen CM, Chi AC, eds. *Oral and Maxillofacial Pathology*. 4th ed. New York: WB Saunders; 2015.
4. Vidyantath S, et al. Reactive hyperplastic lesions of the oral cavity: A survey of 295 cases at a Tertiary Health Institution in Kerala. *J Oral Maxillofac Pathol*. 2015;19(3):330–334.

**Granular Cell Tumor**

1. Allen CM, et al. Granular cell tumour. In: El-Naggar AK, Chan JKC, Grandis JR, Takata T, Slootweg PJ, eds. *Classification of Head and Neck Tumors*. 4th ed. World Health Organization Classification of Tumours. Lyon, France: IARC Press; 2017:121–122.
2. Andrade ES, et al. Isolated intra-oral granular cell tumor: report of two cases and review of the literature. *Acta Odontol Latinoam*. 2010;23(2):99–104.
3. Bomfin LE, et al. Multiple granular cell tumors of the tongue and parotid gland. *Oral Surg Oral Med Oral Pathol Oral Radiol Endod*. 2009;107(5):e10–e13.
4. Brannon RB, et al. Oral granular cell tumors: an analysis of 10 new pediatric and adolescent cases and a review of the literature. *J Clin Pediatr Dent*. 2004;29(1):69–74.
5. Collins BM, et al. Multiple granular cell tumors of the oral cavity: report of a case and review of the literature. *J Oral Maxillofac Surg*. 1995;53(6):707–711.

**Congenital Epulis**

1. Allen CM, et al. Congenital granular cell epulis. In: El-Naggar AK, Chan JKC, Grandis JR, Takata T, Slootweg PJ, eds. *Classification of Head and Neck Tumors*. 4th ed. World Health Organization Classification of Tumours. Lyon, France: IARC Press; 2017:1119.
2. Conrad R, et al. Congenital granular cell epulis. *Arch Pathol Lab Med*. 2014;138(1):128–131.
3. Filie AC, et al. Immunoreactivity of S100 protein, alpha-1-antitrypsin, and CD68 in adult and congenital granular cell tumors. *Mod Pathol*. 1996;9:888–892.

4. Kumar RM, et al. Congenital epulis of the newborn. *J Oral Maxillofac Pathol.* 2015;19(3):407.
5. Lack EE, et al. Gingival granular cell tumors of the newborn (congenital "epulis"): a clinical and pathologic study of 21 patients. *Am J Surg Pathol.* 1981;5:37–46.
6. Lapid O, et al. Congenital epulis. *Pediatrics.* 2001;107:E22.
7. Ritwik P, et al. Spontaneous regression of congenital epulis: a case report and review of the literature. *J Med Case Rep.* 2010;4:331.
8. Zuker RM, et al. Congenital epulis: review of the literature and case report. *J Oral Maxillofac Surg.* 1993;51:1040–1043.
- eds. *Classification of Head and Neck Tumors.* 4th ed. World Health Organization Classification of Tumours. Lyon, France: IARC Press; 2017:119–121.
3. Goveas N, et al. Ectomesenchymal chondromyxoid tumour of the tongue: Unlikely to originate from myoepithelial cells. *Oral Oncol.* 2006;42(10):1026–1028.
4. Laco J, et al. Cyclin D1 Expression in ectomesenchymal chondromyxoid tumor of the anterior tongue. *Int J Surg Pathol.* 2016;24(7):586–594.
5. Smith BC, et al. Ectomesenchymal chondromyxoid tumor of the anterior tongue. Nineteen cases of a new clinicopathologic entity. *Am J Surg Pathol.* 1995;19(5):519–530.
6. Argyris PP, et al. A subset of ectomesenchymal chondromyxoid tumors of the tongue show EWSR1 rearrangements and are genetically linked to soft tissue myoepithelial neoplasms: a study of 11 cases. *Histopathol.* 2016;69(4):607–613.

### Ectomesenchymal Chondromyxoid Tumor

1. Aldojain A, et al. Ectomesenchymal chondromyxoid tumor: a series of seven cases and review of the literature. *Head Neck Pathol.* 2015;9(3):315–322.
2. Bishop JA, et al. Ectomesenchymal chondromyxoid tumour. In: El-Naggar AK, Chan JKC, Grandis JR, Takata T, Slootweg PJ,



# Malignant Neoplasms of the Oral Cavity

■ Susan Müller

## ■ SQUAMOUS CELL CARCINOMA

### CLINICAL FEATURES

Squamous cell carcinoma (SCC) is the most common cancer of the oral cavity, accounting for greater than 90% of oral cancers. Although lip, oral cavity, and oropharyngeal SCC (OSCC) have different etiologies, most

cancer statistics currently include both lip and/or oropharynx when calculating the estimated number of new oral cavity cases. In 2016 it is estimated that 48,330 new cases of OSCC will occur in these three anatomic sites, accounting for 2.9% of all new cancer cases. However, the overall number of oral cavity cancers is decreasing and the increased number of reported cases is related to oropharyngeal SCC. The only site in the oral cavity that shows an increased incidence is the lateral border of the tongue and this is true for both sexes and all races. In the United States, the rate of OSCC incidence is similar in black and white men (~12/100,000).

Carcinogen exposure, diet, and preexisting medical conditions may all play a role in tumor development. Tobacco is the most important risk factor for oral cavity SCC. Depending on the number of cigarettes smoked ("pack years"), the risk of oral cavity is 5 to 17 times higher. Betel quid chewing, commonly used in Southeast Asia, South Asia, and other parts of the world, increases the risk of oral cancer whether or not tobacco is added. Although less substantial, other risk factors include snuff and chewing tobacco. Alcohol consumption has a synergistic association with smoking. Another risk factor is chronic sun exposure, which is a major cause of carcinoma of the vermilion border of the lip. Some inherited genetic mutations are associated with a higher risk of oral cancer development including Fanconi anemia, Li-Fraumeni syndrome, and dyskeratosis congenita. Although human papillomavirus (HPV), in particular, type 16, is a well-recognized etiology in OSCC, less than 3% of oral SCCs are HPV related. Proliferative verrucous leukoplakia (PVL) is a distinct form of oral precancer of unknown etiology with a multifocal presentation and a progressive course, with high recurrence rates and malignant transformation in as many as 70% of cases.

Oral cavity carcinomas most commonly arise in the lateral border and ventral tongue followed by floor of mouth, gingiva, and other parts of the mouth. The remaining cancers are found in the lip and minor salivary glands. SCCs of the oral cavity are generally preceded by clinically visible, premalignant mucosal lesions that appear

### SQUAMOUS CELL CARCINOMA—DISEASE FACT SHEET

#### Definition

- A malignant neoplasm arising from the mucosal epithelium of the oral cavity
- Related to incidence and location
- Most common malignancy of the oral cavity (> 90%)
- More than 48,000 cases diagnosed in the United States each year (includes oropharynx)
- Most commonly arises from the tongue (lateral border and ventral), gingiva, floor of mouth, and other oral sites followed by lip

#### Sex, Race, and Age Distribution

- Males > Females (~3:1)
- Equally occurs in blacks and whites
- Most patients > 50 years old, average age is 62

#### Clinical Features

- Premalignant changes present as white (leukoplakia) or red (erythroplakia) mucosal patches
- Invasive carcinomas range from small cancers that mimic benign disease to depressed ulcerated lesions to fungating masses
- Many patients have cervical lymph node metastases at presentation

#### Prognosis and Treatment

- Tumor stage has a dramatic impact on outcome and therapy
- Surgery with or without radiation and chemotherapy standard treatment for all oral cavity carcinomas; relative survival ~64% at 5 years; although ranges from 38% to 83% depending on stage

as leukoplakia, mixed (speckled) leukoplakia, and erythroplakia. Leukoplakia is a clinical term that refers to a white patch in the oral cavity (Fig. 9.1) and corresponds to the presence of surface keratin. Leukoplakia varies in thickness, and its surface ranges from granular to nodular to fissured. Leukoplakia has a 2 % prevalence in Western countries and less than 25 % of biopsies from oral leukoplakia show dysplasia. Erythroplakia is a clinical term that refers to a thin, red patch of the oral mucosa and is less common than leukoplakia. Erythroleukoplakia or speckled leukoplakia has both erythroplasia and leukoplakic components (Fig. 9.2). Unlike leukoplakia, erythroplasia is much more likely to be associated with dysplasia or carcinoma (> 90 %). During cancer progression, these lesions may evolve into expanding, nonhealing

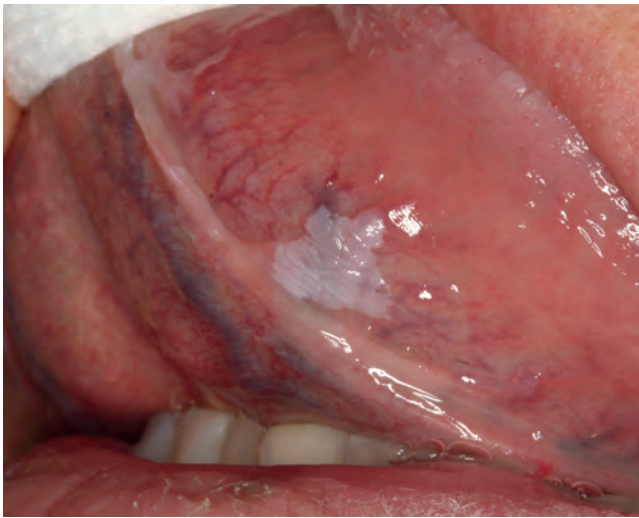


**FIGURE 9.1**

Leukoplakia presenting as a white thickened patch of the ventral tongue. Biopsy showed low-grade dysplasia.

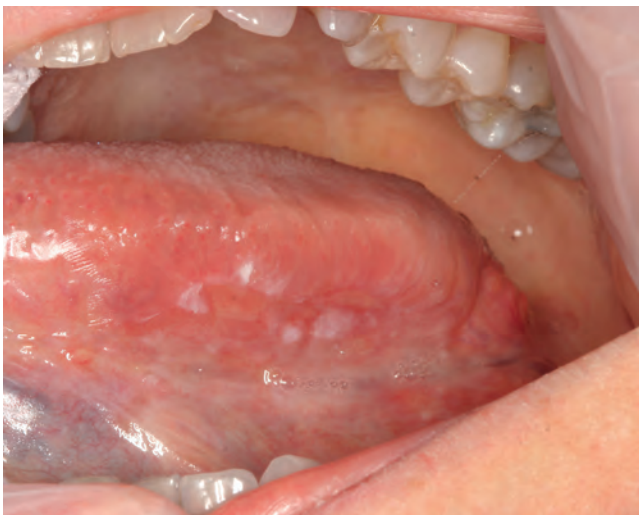


**FIGURE 9.2**

Erythroleukoplakia of the lateral tongue was positive for carcinoma-in-situ on biopsy.

ulcers. Tumor invasion is heralded by bleeding, loosening of teeth, dysphagia, dysarthria, odynophagia, or a palpable neck mass.

The clinical appearance of invasive carcinomas is highly variable, ranging from small asymptomatic cancers that mimic other noncancerous oral lesions, to depressed, ulcerated lesions, to fungating masses (Fig. 9.3). Approximately 40 % of patients with oral SCC present with spread to regional/cervical lymph nodes. Distant metastases are uncommon in oral SCC at presentation.

### RADIOGRAPHIC FEATURES

Radiographic evaluation including computed tomography, magnetic resonance imaging, and occasionally positron emission tomography is primarily used for staging purposes to evaluate primary disease extent and presence of metastatic spread to regional lymph nodes or distantly (Fig. 9.4).

### PATHOLOGIC FEATURES

#### MICROSCOPIC FINDINGS

Dysplastic changes include abnormal cellular organization, increased mitotic activity, and nuclear enlargement with pleomorphism. Although terminology varies, dysplasia limited to the lower one-third of the epithelium is generally referred to as mild dysplasia (Fig. 9.5A), dysplasia limited to the lower two-thirds as moderate dysplasia (Fig. 9.5B), and dysplasia involving the full thickness as severe dysplasia/carcinoma in situ (Fig. 9.5C and D). However,



**FIGURE 9.3**

Squamous cell carcinoma of the lateral tongue with surface ulceration and an adjacent area of leukoplakia in a 43-year-old male.



**FIGURE 9.4**

Magnetic resonance imaging findings in a T4 oral tongue squamous cell carcinoma showing the primary lesion with numerous positive cervical lymph node metastases.

forms of severe dysplasia can certainly have less than full-thickness atypia. A recently described subset of oral dysplasia is positive for high-risk HPV. The epithelium exhibits full-thickness dysplastic changes with karyorrhexis and apoptosis and the cells are strongly positive for p16 by immunohistochemistry (Fig. 9.6). The malignant transformation rate of this subset of dysplasia is unknown.

Most OSCCs are well-to-moderately differentiated (Grade 1 and 2). Well-differentiated SCC shows islands and nests of epithelium with squamous differentiation with interconnecting nests of cells with pink cytoplasm, intercellular bridges, and keratin pearl formation, often associated with inflammation (Fig. 9.7). The tumor can extend into the underlying connective tissue in a cohesive or noncohesive pattern and with advanced tumor growth, tumor nests invade skeletal muscle and craniofacial bones and frequently develop perineural and lymphovascular invasion. There are several recognized subtypes of OSCC including basaloid SCC (BSCC), spindle cell carcinoma (SpCC), adenosquamous carcinoma, carcinoma cuniculatum, verrucous carcinoma, papillary SCC (PSCC), acantholytic SCC, and lymphoepithelial SCC.

Certain variants of SCC depart from the typical appearance of conventional SCC and are most commonly seen in the oral cavity.

1. *Verrucous squamous cell carcinoma* (VSCC) is common in the oral cavity, accounting for more than 75 % of reported cases. VSCC presents as a well-demarcated carpet of epithelium with a warty or papillary

## SQUAMOUS CELL CARCINOMA—PATHOLOGIC FEATURES

### Gross Findings

- Leukoplakia and erythroplakia cannot be distinguished clinically from hyperkeratosis
- Exophytic and endophytic growth patterns that may show ulceration, induration, friable or firm tumor mass, and necrosis

### Microscopic Findings

- Premalignant (noninvasive) stage (dysplasia):
  - Dysplastic cells limited to the surface squamous epithelium that have abnormal cellular organization and maturation, increased mitotic activity, and nuclear enlargement with pleomorphism
- Malignant (invasive) stage:
  - Infiltrating nests and cords of cells showing varying degrees of squamous differentiation (pink cytoplasm, intercellular bridges, and keratin pearl formation)
  - Desmoplastic stromal reaction including stromal fibrosis and chronic inflammation
  - Specific variants include VSCC, PSCC, SpCC, BSCC, acantholytic SCC, carcinoma cuniculatum, or lymphoepithelial SCC

### Fine Needle Aspiration

- Atypical squamous cells in a background of keratinous and necrotic cystic debris

### Immunohistochemical Findings

- Immunoreactivity for epithelial markers (e.g., p63, p40 and cytokeratins 5/6, and 34βE12)

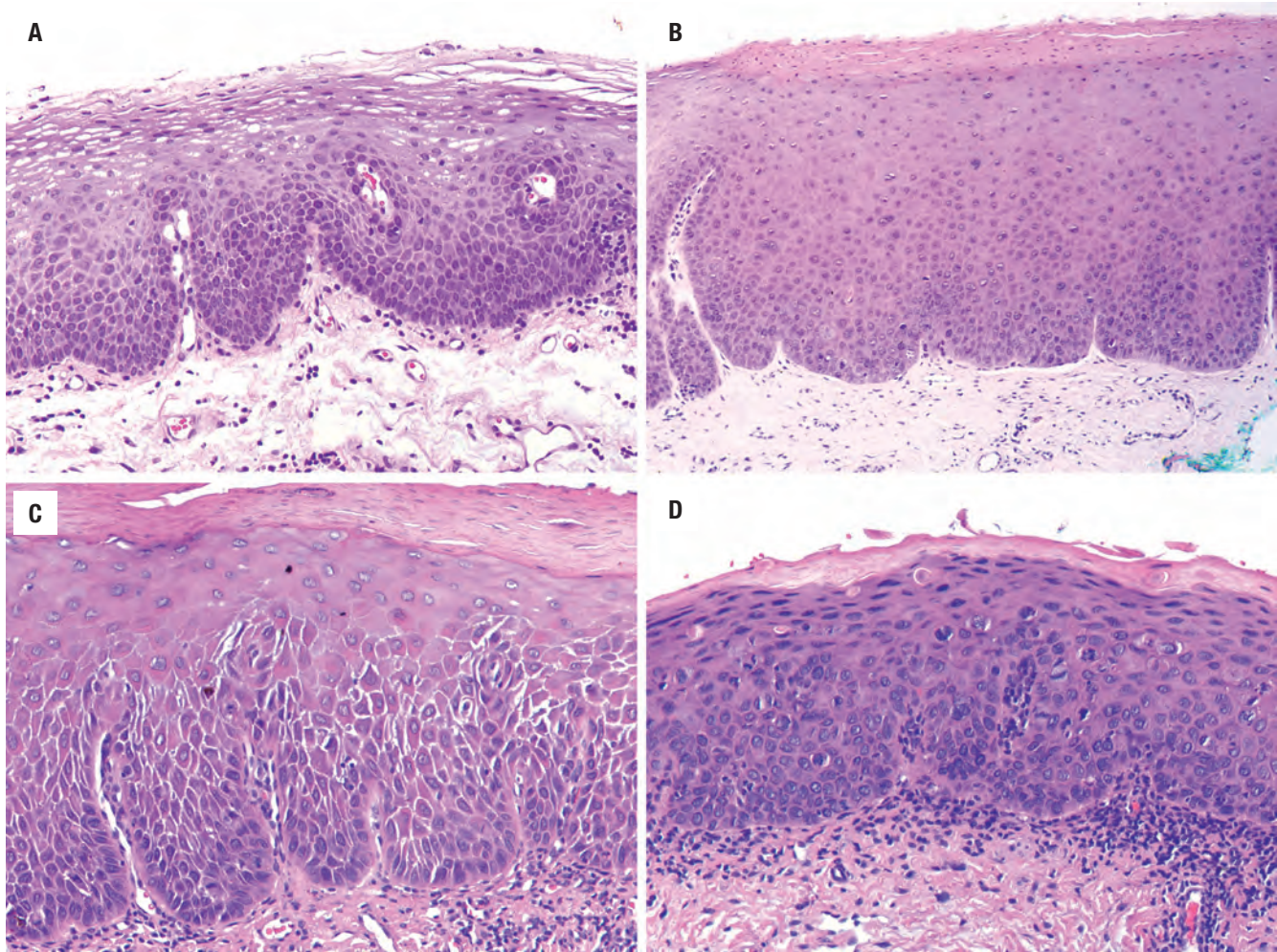
### Pathologic Differential Diagnosis

- Pseudoepitheliomatous hyperplasia, verrucous hyperplasia, necrotizing sialometaplasia, squamous papilloma, sarcoma, malignant melanoma, solid variant of adenoid cystic carcinoma, high-grade neuroendocrine carcinoma

BSCC, Basaloid squamous cell carcinoma; PSCC, papillary squamous cell carcinoma; SCC, squamous cell carcinoma; SpCC, spindle cell carcinoma; VSCC, verrucous squamous cell carcinoma.

hyperkeratotic surface. Surface ulceration is unusual and may indicate a hybrid lesion of SCC and VSCC. Histologically, VSCC is a broad-based epithelial proliferation with marked parakeratosis with keratin plugging (parakeratotic crypting). The bulbous rete ridges are usually associated with inflammation but the basement membrane is intact (Fig. 9.8). There is lack of cytologic atypia, normal maturation, and no metastatic potential.

2. *Spindle cell squamous cell carcinoma* (SpCC) is a subtype of SCC found chiefly in the upper aerodigestive tract with a predilection for males who have a positive tobacco history. After the larynx, the oral cavity is a common site for SpCC and the gross appearance is typically of an exophytic, bosselated mass often with surface ulceration (Fig. 9.9). SpCC presents as a biphasic tumor characterized by sheets of spindled and/or pleomorphic cells, usually admixed with a component of typical invasive

**FIGURE 9.5**

(A) Mild dysplasia of the oral cavity with budding of the rete and increased nuclear-to-cytoplasmic ratio but an otherwise normal maturation sequence. (B) Moderate dysplasia with nuclear pleomorphism present in the lower half of the epithelium. (C and D) Severe dysplasia/carcinoma in situ with the atypical cells involving the full thickness of the epithelium.

squamous carcinoma (Fig. 9.10). At times, only the spindle cell component is evident and can be diagnostically challenging because it mimics other malignant tumors. Cytokeratin markers including CK-pan, p63, p40, AE1/AE3, and CK5/6 may highlight the epithelial cells in the stroma, although absent immunoreactivity is reported in up to 30 % of cases (Fig. 9.10).

## ANCILLARY STUDIES

### FINE NEEDLE ASPIRATION

Although fine needle aspiration (FNA) is not usually performed on primary OSCC, many patients present with cervical metastases, some without an obvious primary lesion. FNA is effective in establishing a diagnosis of metastatic SCC. Cytologic smears are often cellular with

both syncytial fragments of large pleomorphic cells as well as singly dispersed cells. These cells characteristically have large nuclei, prominent nucleoli, and dense, pink (“squamoid” appearing) cytoplasm on Papanicolaou staining.

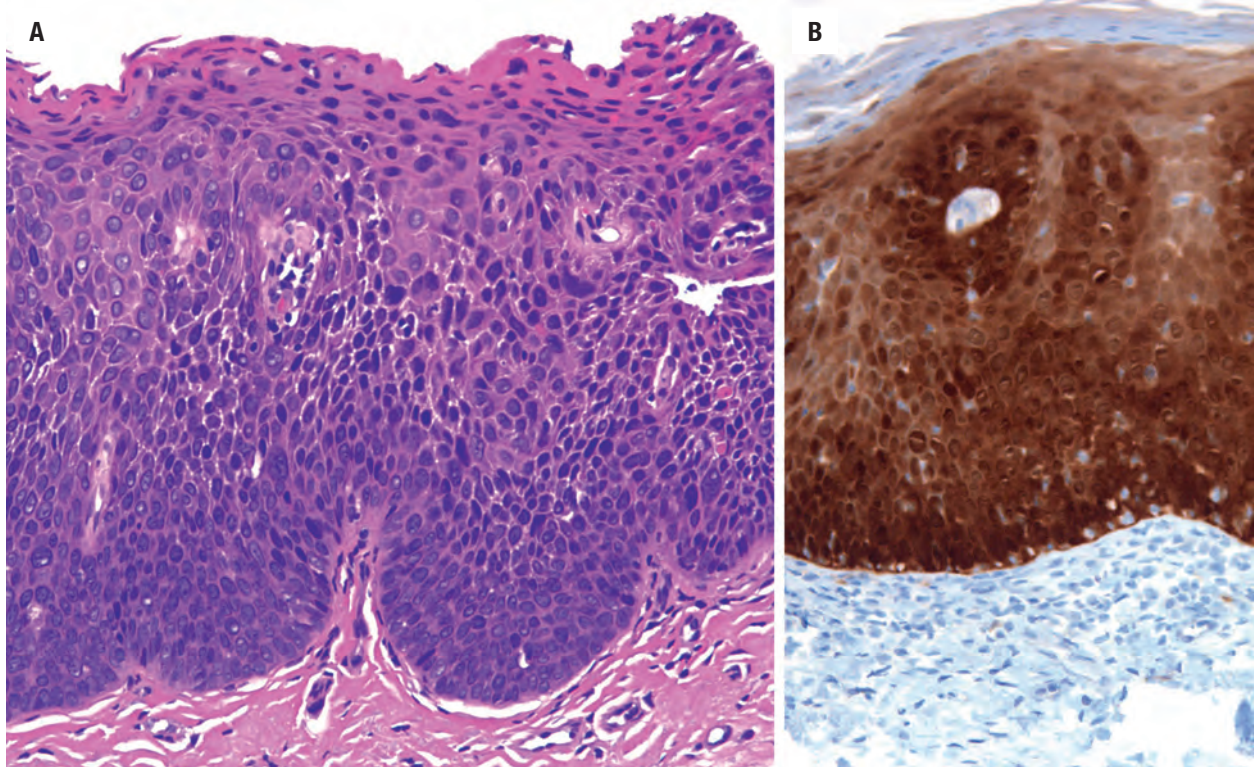
### IMMUNOHISTOCHEMICAL FINDINGS

Immunohistochemistry is only rarely necessary in diagnosing OSCC and usually only needed for poorly differentiated SCC and SpCC. Most SCCs express a wide spectrum of cytokeratins and p63, and lack expression of lymphoid, melanocytic, and mesenchymal markers.

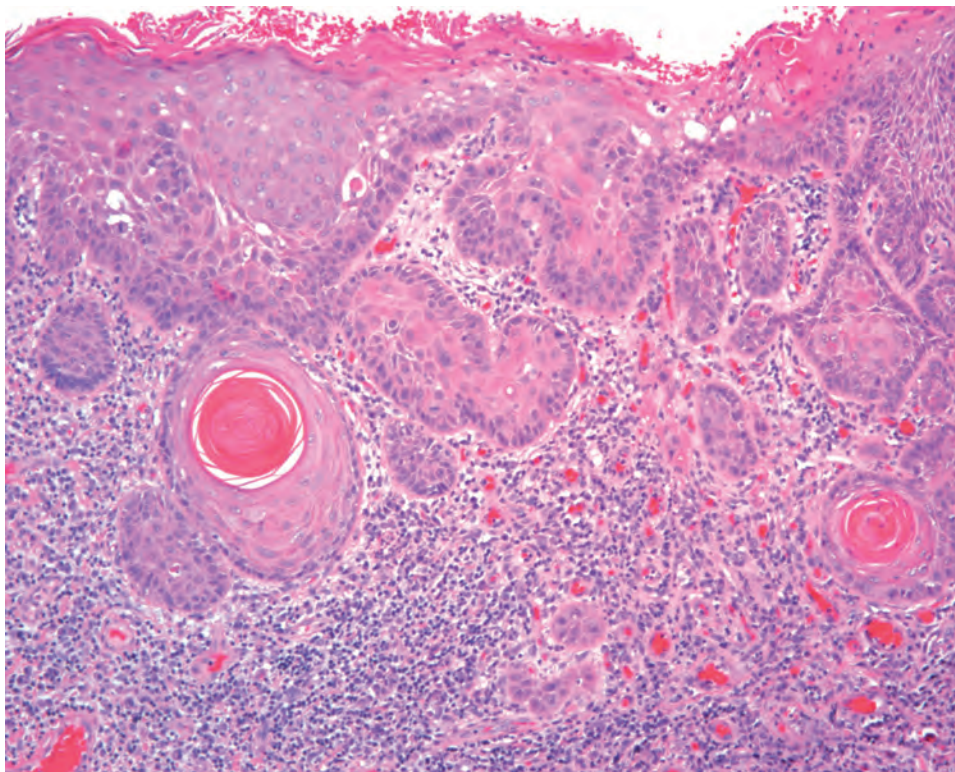
## DIFFERENTIAL DIAGNOSIS

SCC can be mistaken for reactive non-neoplastic squamous proliferations of the oral cavity such as



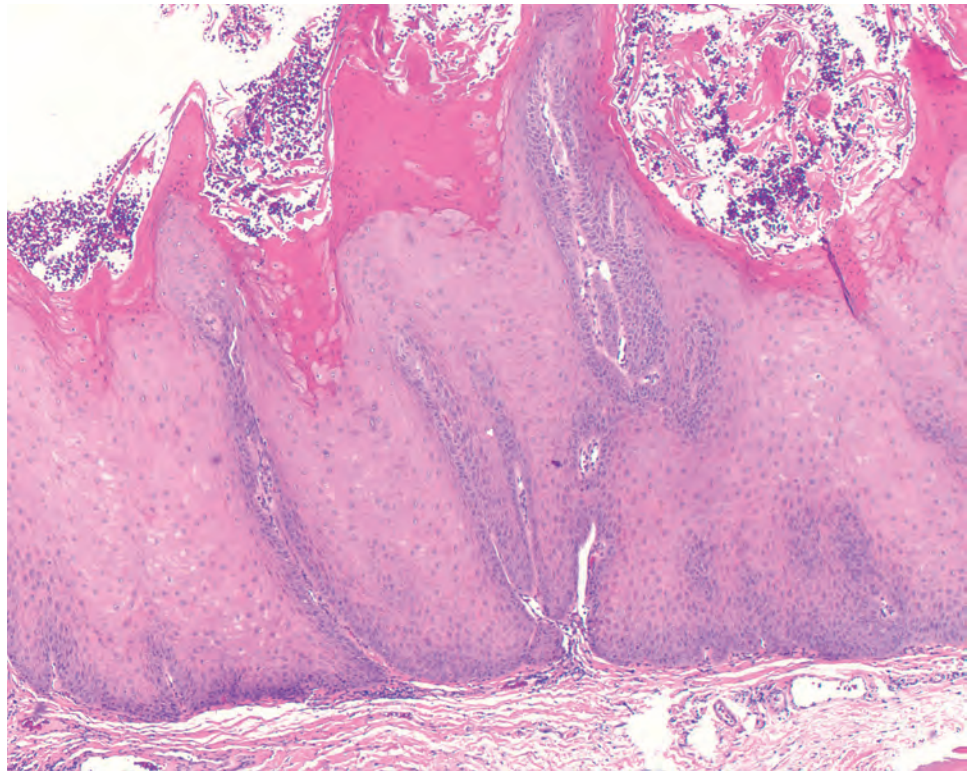
**FIGURE 9.6**

Human papillomavirus-associated oral dysplasia. **(A)** The epithelium has a marked basophilic appearance and undulating contour with full-thickness dysplastic changes, karyorrhexis, and apoptosis. **(B)** The cells are strongly positive for p16 by immunohistochemistry.

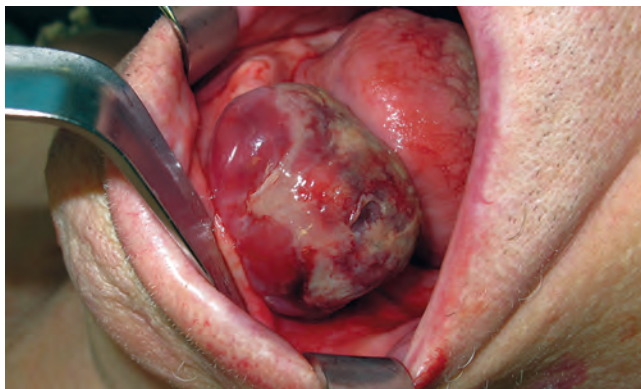
**FIGURE 9.7**

Histologic findings of well-differentiated keratinizing squamous cell carcinoma, showing a tumor with irregular nests of cells that have abundant eosinophilic cytoplasm arising from the dysplastic surface epithelium. There is a prominent inflammatory response to the malignant islands of epithelium.



**FIGURE 9.8**

Verrucous carcinoma consists of a broad-based epithelial proliferation with marked parakeratosis with keratin plugging and thick, eosinophilic (“glassy”) epithelium without atypia.

**FIGURE 9.9**

In spindle cell squamous cell carcinoma, the gross appearance is usually of an exophytic, smooth and partially ulcerated, polypoid mass. (Courtesy of Dr. B. Nussenbaum.)

pseudoepitheliomatous hyperplasia, radiation-induced atypia, and necrotizing sialometaplasia—a proliferation of metaplastic squamous cells within the ducts and acini of minor salivary glands. These reactive processes are generally preceded by an inciting event (e.g., ulceration, radiation), and in contrast to SCC, do not display infiltrative growth, stromal desmoplasia, or overtly malignant cytology. At the other extreme, poorly differentiated and nonkeratinizing SCCs can be confused with various nonepithelial malignancies such as melanoma, sarcoma, or lymphoma. In this setting, immunohistochemistry may play a useful role in establishing the diagnosis of

carcinoma by demonstrating positive staining for keratins and p63, and no staining for melanocytic, mesenchymal, or lymphoid markers. In addition, occasional tumors may resemble the solid variant of adenoid cystic carcinoma or a high-grade neuroendocrine tumor.

### PROGNOSIS AND THERAPY

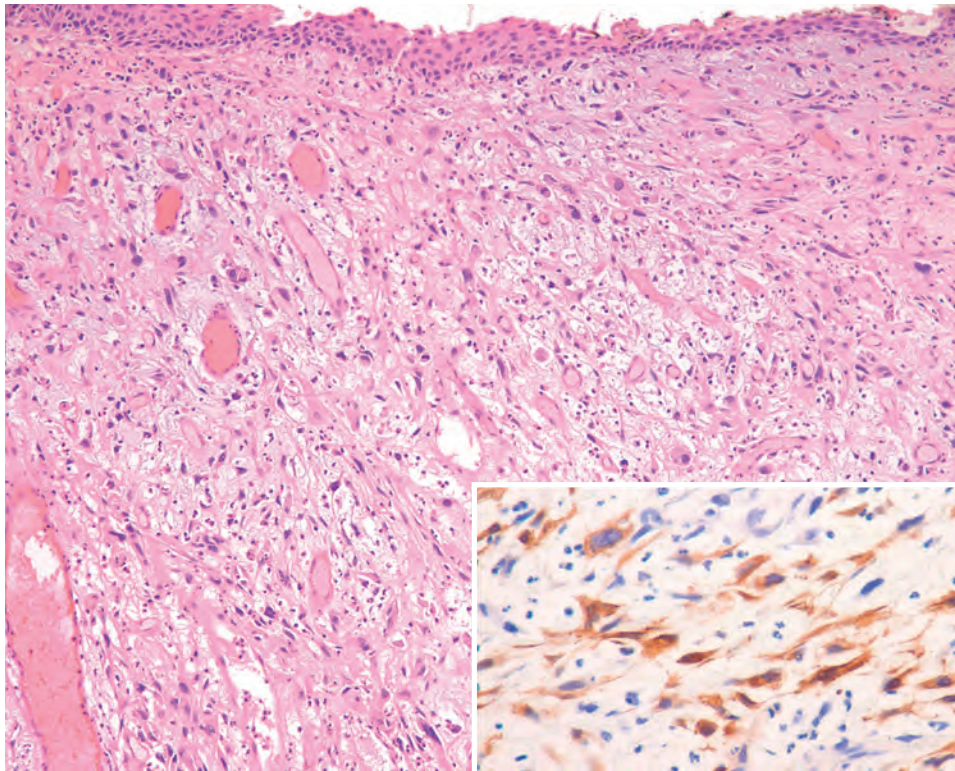
The overall 5-year survival rate for oral cavity SCC is ~64%. However, the tumor stage greatly determines outcome: stage I SCC of the oral cavity is associated with survival rates of 83%, but this drops to 38% for locally or regionally advanced disease (stage III or IV).

Treatment options are highly variable and depend on many factors, including size and location of the primary tumor, spread to regional lymph nodes or distant sites, and the patient's ability to tolerate treatment. Primary surgery is the standard treatment with adjuvant radiation and chemotherapy used for more advanced stage disease.

### ■ KAPOSI SARCOMA

Kaposi sarcoma (KS) is a locally aggressive vascular neoplasm of intermediate grade uniformly associated with human herpes virus 8 (HHV8). KS is an acquired immune deficiency syndrome (AIDS)-defining illness.



**FIGURE 9.10**

In spindle cell squamous cell carcinoma, the spindled cells can be mistaken for a sarcoma as in this example where the overlying epithelium shows minimal atypia. The stroma consists of sheets of malignant pleomorphic and spindled cells. Immunohistochemistry for pan-cytokeratin (CK-PAN) shows strong immunoreactivity of the spindled cells (*inset*).

### CLINICAL FEATURES

Four distinct clinical subtypes of KS are recognized: (1) the *classic* form occurs primarily in older men of Eastern European (especially Ashkenazi Jews) or Mediterranean descent; (2) the *endemic* form is common to regions of Africa and particularly prevalent among young Bantu children of South Africa; (3) the *transplant-associated* form occurs after high doses of immunosuppressive therapy; and (4) the *AIDS-associated* form is particularly prevalent among human immunodeficiency virus (HIV)-infected homosexual and bisexual males. In fact, KS develops in as many as 20% of patients with AIDS and is considered an AIDS-defining illness. Regardless of the form, all KS lesions are infected with HHV8. Immunosuppression is a critical cofactor in the pathogenesis and clinical expression of the disease.

The AIDS-associated form is the most likely subtype to be encountered in the oral cavity. KS represents the most frequent HIV-associated oral cancer (followed by non-Hodgkin lymphoma). In the HIV-infected population, oral KS is most common in homosexual and bisexual men with a peak incidence in the 4th to 5th decade. The palate is the most common subsite, often showing multiple lesions; moreover, concurrent cutaneous and visceral organ lesions are frequently present. The clinical appearance changes with lesion progression. Early lesions are flat, red, and asymptomatic, and later lesions become

larger, darker, and raised (Fig. 9.11). With continued growth, these large nodular lesions may become ulcerated and painful.

### PATHOLOGIC FEATURES

#### GROSS FINDINGS

Early lesions are small, flat, and red. Advanced lesions are larger, deep-red to purple, and nodular.

#### MICROSCOPIC FINDINGS

KS is a nonencapsulated, infiltrative lesion. The histomorphology varies with stage of progression. The patch stage shows an ill-defined proliferation of dilated, irregular, angulated blood vessels dissecting collagen bundles, often parallel to the epithelium, with associated chronic inflammatory cells. As the lesions progress (plaque stage), the dilated vascular channels become surrounded by aggregates of spindle cells with intra- and extracellular hyaline globules, extravasated erythrocytes, and hemosiderin (Fig. 9.12). In the nodular stage, the histology is dominated by an infiltrative, highly cellular proliferation of spindle cells with increased atypia and mitoses. A lymphangiomatic variant is characterized by large dilated anastomosing vessels with papillary tufting.

### KAPOSI SARCOMA—DISEASE FACT SHEET

#### Definition

- A vascular neoplasm unique to certain patient populations, most notably in individuals with AIDS
- Related to incidence and location
- Non-AIDS related forms of KS are rare and mostly confined to older men of Eastern European or Mediterranean ancestry, individuals in certain regions of Africa, and transplant recipients
- KS is common in patients with AIDS (~15% to 20%)
- Hard palate, followed by the gingiva and dorsal tongue are the most common oral sites

#### Sex and Age Distribution

- In the HIV-infected population, oral KS is most commonly encountered in homo- and bisexual men with peak incidence in the 4th to 5th decade

#### Clinical Features

- Oral lesions commonly multifocal
- Early lesions: flat, red, and asymptomatic
- Older lesions: larger, darker, nodular, and ulcerated

#### Prognosis and Treatment

- Mortality is dependent on the patient's immunologic status, presence of opportunistic infections, disease stage, and other factors
- General treatment: active antiretroviral therapy, radiation, chemotherapy
- Local treatment of problematic oral lesions: surgery, cryotherapy, laser ablation, intralesional injections of chemotherapeutic or sclerosing agents

*AIDS*, Acquired immune deficiency syndrome; *HIV*, human immunodeficiency virus; *KS*, Kaposi sarcoma.



**FIGURE 9.11**

HIV-associated Kaposi sarcoma presenting as a dusky red flat macule in the maxillary alveolus of a 37-year-old male.

### KAPOSI SARCOMA—PATHOLOGIC FEATURES

#### Gross Findings

- Early lesions: small, red, and flat
- Advanced lesions: large, deep-red to purple, and nodular

#### Microscopic Findings

- Early lesions (patch stage): proliferation of dilated, irregular blood vessels
- Maturing lesions (plaque stage): dilated vascular channels surrounded by aggregates of spindle cells
- Advanced lesions (nodular stage): cellular proliferation of spindle cells, slit-like vascular spaces, extravasated blood cells, hemosiderin deposits, and hyaline globules

#### Immunohistochemical Findings

- HHV8 and variable expression for endothelial markers (D2-40, CD31, CD34, LYVE1, VEGFR3, PROX1)

#### Pathologic Differential Diagnosis

- Reactive vascular ectasia, bacillary angiomatosis, lobular capillary hemangioma, well-differentiated angiosarcoma

*HHV8*, Human herpes virus 8.

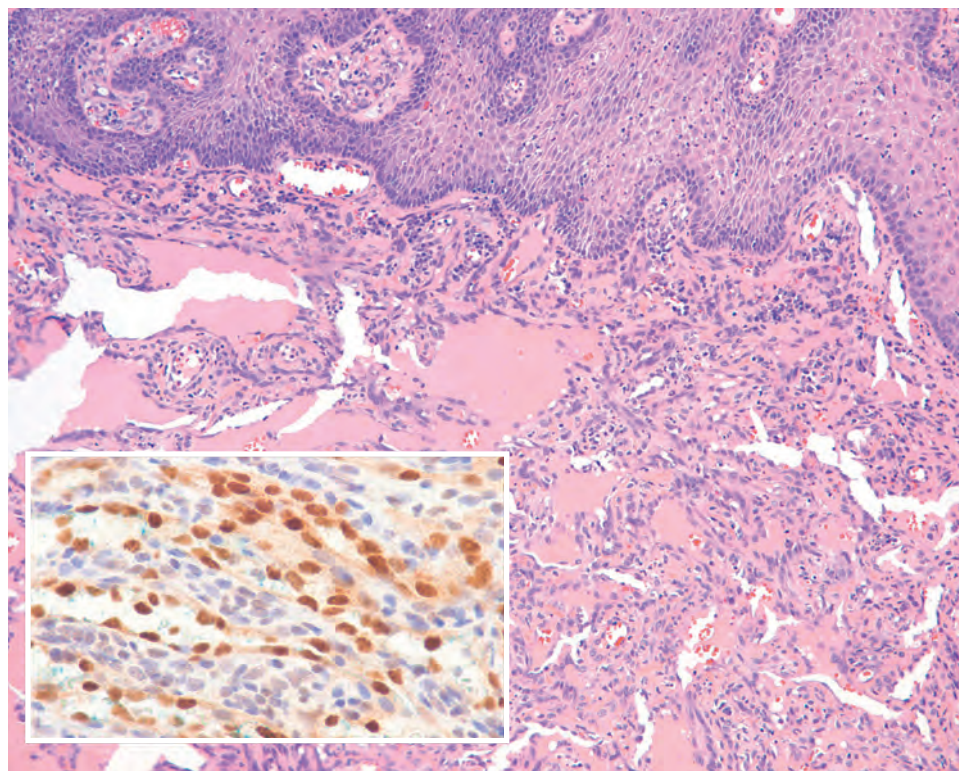
### ANCILLARY STUDIES

KS tumor cells are immunoreactive for podoplanin (D2-40), LYVE1, VEGFR3, PROX1, CD34, CD31, and other endothelial markers. However, as the differential diagnosis is virtually limited to other vascular proliferations, immunohistochemical confirmation of endothelial differentiation is not helpful. In contrast, the HHV8-specific immunohistochemical stain is often helpful in separating KS from other vascular lesions (Fig. 9.12).

### DIFFERENTIAL DIAGNOSIS

The differential diagnosis is largely contingent on the histologic stage. Early lesions, due to their subtle changes, may be dismissed as reactive vascular ectasia. As the lesion progresses, the proliferation of vessels becomes more apparent, and may cause confusion with lobular capillary hemangioma, bacillary angiomatosis, kaposiform hemangioendothelioma, and angiosarcoma. Lobular capillary hemangioma has a lobular growth pattern lacking hyaline globules and is negative for HV8. In bacillary angiomatosis, a Warthin starry stain will reveal the slender bacilli of *Bartonella henselae* among the granular material in the interstitium. Kaposiform hemangioendothelioma is rare and usually occurs in the 1st decade of life with no association with HIV or HHV8 infection. Angiosarcoma, with its classic endothelial “hobnailing,” may show greater pleomorphism, mitoses, and necrosis, and is not HHV8-associated.



**FIGURE 9.12**

Kaposi sarcoma shows numerous vascular spaces of varying sizes in the submucosa composed of spindle endothelial cells. Erythrocytes are noted both within and between the vessels. Tumor cells show strong diffuse nuclear immunoreactivity for HHV8 (*inset*).

### PROGNOSIS AND THERAPY

The improved management and survival in HIV due to antiretroviral therapy, especially highly active antiretroviral therapy (HAART), has dramatically decreased the incidence of oral KS. Moreover, without correction of the underlying immunodeficiency, survival is poor, hence the institution (or reinstitution) of HAART in combination with radiation and/or chemotherapy, which are the more general standard treatments of KS. Local symptoms can be controlled by intralesional injection of chemotherapeutic or sclerosing agents, or by removal via surgery, cryotherapy, or laser therapy. Nonetheless, the disease course and overall behavior depends greatly on the clinical subtype, amount of dissemination, disease stage, and the presence of systemic symptoms and related comorbidities.

### ■ ORAL MUCOSAL MELANOMA

Oral mucosal melanoma (OMM) is a malignant neoplasm of neural crest origin demonstrating melanocytic differentiation.

#### CLINICAL FEATURES

OMM is a rare entity and an accurate assessment of the incidence is difficult. It is estimated that less than

#### ORAL MUCOSAL MELANOMA—DISEASE FACT SHEET

##### Definition

- Malignant neural crest-derived neoplasm with melanocytic differentiation

##### Incidence and Location

- Rare, accounting for <3% of all melanomas
- Palate and maxillary alveolus account for ~80% of cases
- Other sites include mandibular gingivae, buccal mucosa, floor of mouth, and tongue

##### Sex, Race, and Age Distribution

- No sex predilection
- More common in Asians, Africans, Hispanics, and Asian Indians
- Mean age is 6th to 7th decade, rare in pediatric population

##### Clinical Features

- Asymmetric pigmented lesion (black, red, gray) with irregular borders (15% are amelanotic)
- Early lesions are macular and later lesions become nodular with ulceration
- Positive cervical lymph nodes in 30% of cases at presentation
- Distant metastases in 50% of cases at presentation

##### Prognosis and Treatment

- Poor prognosis with median survival of 2 years; 5-year survival 5%-10%; high rates of distant metastases to liver, brain, and lung
- General treatment: radical surgical excision ± adjuvant therapy
- Chemotherapy is not used as a single modality agent; radiation used for palliation

**FIGURE 9.13**

Primary mucosal melanoma of the hard palate presenting as a diffuse black pigmented lesion with irregular borders. The palate is the most common site for oral mucosal melanoma accounting for ~80% of cases.

3% of mucosal melanomas arise in the head and neck area and most of these occur in the sinonasal tract. Based on reported cases there is no sex predilection and median age of diagnosis is 55 to 68 years, although OMM may occur in any age group. There is a reported higher incidence of OMM in Asians, Africans, Hispanics, and Asian Indians; however Caucasians predominate in studies from North America. The pathogenesis of OMM is unknown and no risk factors have been identified. Melanocytes are present in oral mucosa from 20 weeks of gestation but their exact role is unclear. OMM is often incidentally discovered. More than 80% of OMM occur on the hard palate and alveolus (Fig. 9.13). Most OMMs arise *de novo*, although some cases are preceded by a pigmented lesion or melanosis. Patients present typically with a painless asymmetric brown, black, purple, or gray pigmented macule that may, over time, become nodular with ulceration and bleeding. A small percentage of OMMs are amelanotic. Satellite lesions adjacent to the tumor can be noted. Other symptoms may include ill-fitting dentures or neck mass from a metastatic lymph node, because cervical lymph node metastases are reported in up to 30% of cases at presentation.

## **PATHOLOGIC FEATURES**

### **GROSS FINDINGS**

Early lesions are flat macules with brown to black pigment and irregular borders ranging in size from 1.5 to 4 cm (radial growth phase). Advanced lesions are nodular and satellite lesions may be present (nodular growth phase).

## **ORAL MUCOSAL MELANOMA—PATHOLOGIC FEATURES**

### **Gross Findings**

- Brown to black pigmented lesion with irregular borders
- Early lesions: flat macular extending lateral (radial growth phase)
- Advanced lesions: large, nodular, often with ulceration (vertical growth phase)
- Satellite lesions are common

### **Microscopic Findings**

- Radial growth phase is like acral lentiginous melanoma—pagetoid spread within epithelium and atypical melanocytes in basal layer spreading laterally. Invasion of melanoma cells into connective tissue
- Nodular growth phase: epithelioid or spindle-shaped morphology containing melanin (15% are amelanotic); bone and/or cartilage invasion, surface ulceration

### **Immunohistochemical Findings**

- S100 protein, SOX10, HMB-45, MITF positive in most cases. Variable positivity with tyrosinase, Melan-A, CD117

### **Pathologic Differential Diagnosis**

- Spindle cell squamous cell carcinoma, pleomorphic sarcoma, metastatic melanoma

## **MICROSCOPIC FINDINGS**

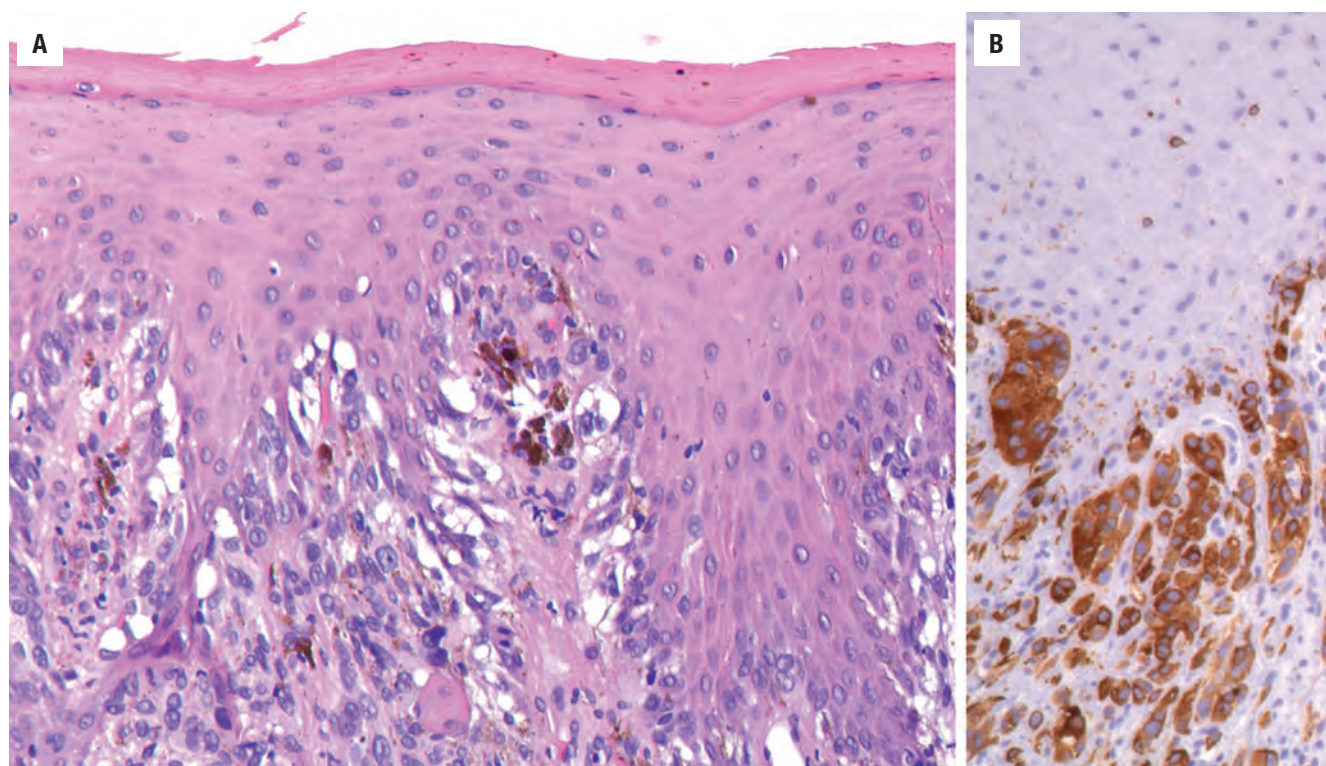
The radial growth phase is similar to acral lentiginous melanoma with pagetoid spread of atypical melanocytes in the basal cell epithelium spreading laterally (Fig. 9.14A). Individual melanocytes can be seen invading the upper level of the epithelium. Invasion into the superficial lamina propria of melanoma cells, usually containing fine melanin granules, is present. An inflammatory infiltrate, sometimes quite dense, can be present and may partially obscure the melanoma cells.

The nodular growth phase shows a polymorphic cell population consisting of spindle cells, epithelioid cells, “round blue cells,” or clear cells, often with melanin. An organoid or nesting, and rarely a pseudo-alveolar growth pattern, may be seen. Bone and/or cartilage invasion is present in up to one-third of cases. Overlying squamous ulceration or atrophy is frequently present. Vascular and perineural invasion is usually not identified. Depth of invasion is difficult to assess for OMM and is not used for staging purposes.

## **ANCILLARY STUDIES**

When melanin is present, the diagnosis of OMM is straightforward; however, immunohistochemistry is necessary for confirmation. OMMs express S100 protein, SOX10, HMB-45, vimentin, and MITF in most cases (Fig. 19.14B). Variable positivity with tyrosinase, Melan-A,



**FIGURE 9.14**

(A) Radial growth phase of oral mucosal melanoma with histologic features similar to acral lentiginous melanoma. Atypical melanocytes, some pigmented, are seen in the basal layer spreading laterally and invading the submucosa. (B) HMB-45 highlights the melanocytes in the basal layer and in the submucosa.

and CD117 has been reported. With all immunohistochemical stains, the reactivity can be patchy or focal. OMMs show a much higher prevalence of *KIT* and *RAS* mutations, while *BRAF* plays only a minor role, distinctly different from cutaneous melanoma.

### DIFFERENTIAL DIAGNOSIS

When melanin pigment is not apparent, immunohistochemistry is essential because other entities may present with similar histology. SpCC is a high-grade tumor that often presents with surface ulceration obscuring its surface origin. The tumor typically is highly pleomorphic with increased mitoses. The tumor cells are immunoreactive for epithelial markers, p63 and p40 and lack melanoma markers. Undifferentiated pleomorphic sarcomas are high-grade tumors that are negative for both epithelial and melanoma markers. Although rare, metastatic melanoma to the oral cavity has been reported. The most common location is tongue, buccal mucosa, and lip. Clinical history is essential and further diagnostic tests are required for this diagnosis, including molecular testing.

There are benign pigmented lesions that occur with some frequency in the oral cavity, which may cause alarm to the clinician and patient. These include oral nevi, melanoacanthoma, physiologic pigmentation, smoker's

melanosis, medication-related melanosis, melanin related to systemic diseases (Addison disease, Peutz-Jeghers syndrome, and Laugier-Hunziker syndrome), and foreign body tattoo. However, histologic examination would readily rule out OMM.

### PROGNOSIS AND THERAPY

OMM is an aggressive disease with an overall poor prognosis. Surgical resection with or without lymph node dissection is the primary treatment modality. Due to the anatomic location and associated vital structures, clear margins are not always possible. Surgery is also advocated for local recurrence. Some institutions recommend neck dissection in a clinically negative neck due to the frequent cervical lymph node metastases in OMM. Postoperative radiotherapy is often used; however, its benefit for overall survival is unclear.

Systemic treatments including immunotherapy and chemotherapy have been developed for mucosal melanoma although overall survival benefits are not known.

### SUGGESTED READINGS

The complete Suggested Readings list is available online at [ExpertConsult.com](http://ExpertConsult.com).

**SUGGESTED READINGS****Squamous Cell Carcinoma**

1. Akrish S, et al. Oral squamous cell carcinoma associated with proliferative verrucous leukoplakia compared with conventional squamous cell carcinoma—a clinical, histologic and immunohistochemical study. *Oral Surg Oral Med Oral Pathol Oral Radiol.* 2015;119(3):318–325.
2. Arnaoutakis D, et al. Recurrence patterns and management of oral cavity premalignant lesions. *Oral Oncol.* 2013;49(8):814–817.
3. Bice TC, et al. Disease-specific survival with spindle cell carcinoma of the head and neck. *Otolaryngol Head Neck Surg.* 2015;153(6):973–980.
4. Fitzpatrick SG, et al. Histologic lichenoid features in oral dysplasia and squamous cell carcinoma. *Oral Surg Oral Med Oral Pathol Oral Radiol.* 2014;117(4):511–520.
5. Gerry D, et al. Spindle cell carcinoma of the upper aerodigestive tract: an analysis of 341 cases with comparison to conventional squamous cell carcinoma. *Ann Otol Rhinol Laryngol.* 2014;123(8):576–583.
6. Gillenwater AM, et al. Proliferative verrucous leukoplakia (PVL): a review of an elusive pathologic entity! *Adv Anat Pathol.* 2013;20(6):416–423.
7. Ohba S, et al. Spindle cell carcinoma arising at the buccal mucosa: a case report and review of the literature. *Cranio.* 2015;33(1):42–45.
8. Patel KR, et al. Verrucous carcinoma with dysplasia or minimal invasion: a variant of verrucous carcinoma with extremely favorable prognosis. *Head Neck Pathol.* 2015;9(1):65–73.
9. Rosko AJ, et al. Tumor biomarkers in spindle cell variant squamous cell carcinoma of the head and neck. *Otolaryngol Head Neck Surg.* 2016;155(1):106–112.
10. Sloan P, et al. Squamous cell carcinoma. In: El-Naggar AK, Chan JKC, Grandis JR, Takata T, Slootweg PJ, eds. *Classification of Head and Neck Tumors*. 4th ed. World Health Organization Classification of Tumors. Lyon, France: IARC Press; 2017:109–111.
11. Speight PM, et al. Interobserver agreement in dysplasia grading: toward an enhanced gold standard for clinical pathology trials. *Oral Surg Oral Med Oral Pathol Oral Radiol.* 2015;120(4):474–482, e2.
12. Stojanov IJ, et al. Human papillomavirus and Epstein-Barr virus associated conditions of the oral mucosa. *Semin Diagn Pathol.* 2015;32(1):3–11.
13. Syrjänen S, et al. Human papillomaviruses in oral carcinoma and oral potentially malignant disorders: a systematic review. *Oral Dis.* 2011;17(suppl 1):58–72.
14. Viswanathan S, et al. Sarcomatoid (spindle cell) carcinoma of the head and neck mucosal region: a clinicopathologic review of 103 cases from a tertiary referral cancer centre. *Head Neck Pathol.* 2010;4(4):265–275.
15. Watson RF, et al. Spindle cell carcinomas of the head and neck rarely harbor transcriptionally-active human papillomavirus. *Head Neck Pathol.* 2013;7(3):250–257.
16. Woolgar JA, et al. Squamous cell carcinoma and precursor lesions: clinical pathology. *Periodontol 2000.* 2011;57(1):51–72.
2. Goncalves PH, et al. Cancer prevention in HIV-infected populations. *Semin Oncol.* 2016;43(1):173–188.
3. Goncalves PH, et al. Kaposi sarcoma herpesvirus-associated cancers and related diseases. *Curr Opin HIV AIDS.* 2017;12(1):47–56.
4. Hu D, et al. Induction of Kaposi's sarcoma-associated herpesvirus-encoded viral interleukin-6 by X-box binding protein 1. *J Virol.* 2015;90(1):368–378.
5. Polizzotto MN, et al. 18F-fluorodeoxyglucose positron emission tomography in kaposi sarcoma herpesvirus-associated multicentric castlemann disease: correlation with activity, severity, inflammatory and virologic parameters. *J Infect Dis.* 2015;212(8):1250–1260.
6. Polizzotto MN, et al. Clinical features and outcomes of patients with symptomatic kaposi sarcoma herpesvirus (KSHV)-associated Inflammation: prospective Characterization of KSHV inflammatory cytokine syndrome (KICS). *Clin Infect Dis.* 2016;62(6):730–738.
7. Thompson LDR, et al. Kaposi sarcoma. In: El-Naggar AK, Chan JKC, Grandis JR, Takata T, Slootweg PJ, eds. *Classification of Head and Neck Tumors*. 4th ed. World Health Organization Classification of Tumors. Lyon, France: IARC Press; 2017:124–126.

**Oral Mucosal Melanoma**

1. Breik O, et al. Survival outcomes of mucosal melanoma in the head and neck: case series and review of current treatment guidelines. *J Oral Maxillofac Surg.* 2016;74(9):1859–1871.
2. Chatzistefanou I, et al. Primary mucosal melanoma of the oral cavity: current therapy and future directions. *Oral Surg Oral Med Oral Pathol Oral Radiol.* 2016;122(1):17–27.
3. Francisco AL, et al. Head and neck mucosal melanoma: clinicopathological analysis of 51 cases treated in a single cancer centre and review of the literature. *Int J Oral Maxillofac Surg.* 2016;45(2):135–140.
4. López F, et al. Update on primary head and neck mucosal melanoma. *Head Neck.* 2016;38(1):147–155.
5. Lourenço SV, et al. Head and neck mucosal melanoma: a review. *Am J Dermatopathol.* 2014;36(7):578–587.
6. Mikkelsen LH, et al. Mucosal malignant melanoma—a clinical, oncological, pathological and genetic survey. *APMIS.* 2016;124(6):475–486.
7. Smith MH, et al. Melanoma of the oral cavity: an analysis of 46 new cases with emphasis on clinical and histopathologic characteristics. *Head Neck Pathol.* 2016;10(3):298–305.
8. Song H, et al. Prognostic factors of oral mucosal melanoma: histopathological analysis in a retrospective cohort of 82 cases. *Histopathology.* 2015;67(4):548–556.
9. Thlholoe MM, et al. Oral mucosal melanoma: some pathobiological considerations and an illustrative report of a case. *Head Neck Pathol.* 2015;9(1):127–134.
10. Williams MD, et al. Oral mucosal melanoma. In: El-Naggar AK, Chan JKC, Grandis JR, Takata T, Slootweg PJ, eds. *Classification of Head and Neck Tumors*. 4th ed. World Health Organization Classification of Tumors. Lyon, France: IARC Press; 2017:126–127.
11. Wushou A, et al. The management and site-specific prognostic factors of primary oral mucosal malignant melanoma. *J Craniofac Surg.* 2015;26(2):430–434.

**Kaposi's Sarcoma**

1. Bhutani M, et al. Kaposi sarcoma-associated herpesvirus-associated malignancies: epidemiology, pathogenesis, and advances in treatment. *Semin Oncol.* 2015;42(2):223–246.



# Malignant Neoplasms of the Oropharynx

■ James S. Lewis, Jr.

## ■ SQUAMOUS CELL CARCINOMA

Squamous cell carcinoma (SCC) arises not only from the surface epithelium of the oropharynx but also from the tonsillar crypts. It is steadily increasing in incidence due to high-risk human papillomavirus (HPV), and HPV-positive oropharyngeal SCC is a biologically and clinically distinct type of head and neck cancer.

### CLINICAL FEATURES

SCC constitutes the majority of oropharyngeal malignancies (> 90%). Most develop in white men (male to female, 3:1) between the ages of 55 and 60 years. Unlike for most other types of head and neck carcinoma, which are declining, the rate of oropharyngeal SCC is increasing dramatically (as much as 5% per year) due to HPV, particularly type 16. It is a global problem but is most important in the United States, Canada, and parts of Northern Europe, where as many as 80% of oropharyngeal SCCs are HPV-positive. The virus is sexually transmitted. Patients have histories of more sex partners and more oral sex exposure than HPV-negative patients. HPV-positive SCC patients are approximately 5 years younger, on average. Carcinogen exposure, diet, and preexisting medical conditions all also play a role in tumor development. Smoking (tobacco) exposure is less important in oropharyngeal than in oral and laryngeal SCC. More than 95% of patients with HPV-negative oropharyngeal SCC are smokers, whereas 60% to 75% of HPV-positive oropharyngeal SCC are current or former smokers, with less exposure overall.

Oropharyngeal carcinomas classically present as small primary tumors usually arising from the palatine tonsils followed by the base of the tongue. These sites harbor a large amount of lymphoid tissue associated with invaginated “crypt” epithelium, for which HPV is tropic. For HPV-positive oropharyngeal SCCs, no obvious precursor

### SQUAMOUS CELL CARCINOMA—DISEASE FACT SHEET

#### Definition

- A malignant neoplasm arising from the squamous epithelium of the oropharyngeal surface or tonsillar crypts

#### Incidence and Location

- Most common malignancy of the oropharynx
- More than 25,000 cases diagnosed in the United States each year
- Most common in the palatine tonsils followed by the tongue base

#### Sex, Race, and Age Distribution

- Males > females (~3:1)
- Higher incidence among whites than blacks
- Most patients 50-60 years of age

#### Clinical Features

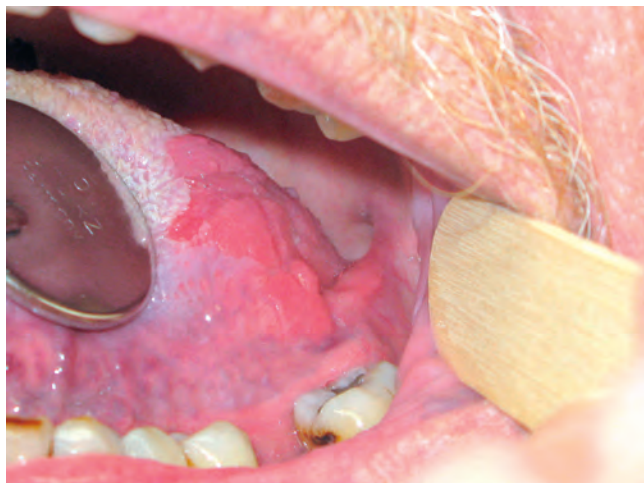
- Surface mucosa preinvasive lesions can either be leukoplakic (white patch) or erythroplakic (red patch) with varying degrees of dysplasia. HPV-positive examples do not have preinvasive lesions.
- Invasive carcinomas range from depressed ulcerated lesions to fungating masses; many are small and soft, hidden deep in the tonsillar parenchyma
- Most patients have cervical lymph node metastases at presentation

#### Prognosis and Treatment

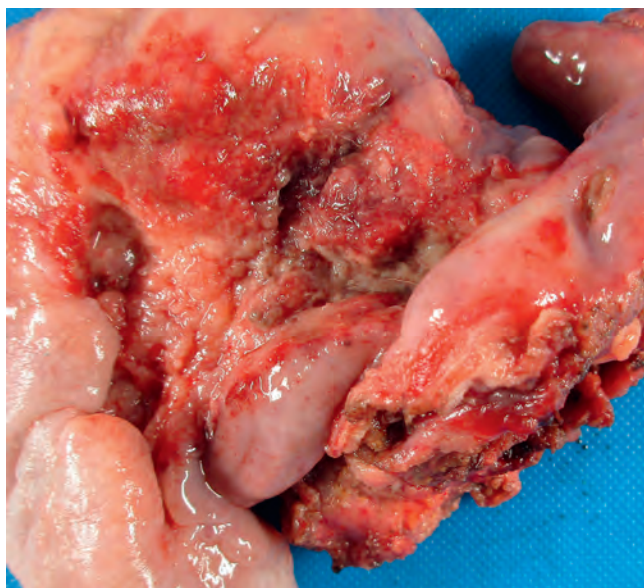
- Tumor stage has a significant impact on outcome and therapy
- Primary chemoradiation is the most common treatment approach, with transoral surgical resection used at many centers, particularly for early stage disease. Both are effective treatment types; survival at 5 years is approximately 50% for HPV negative and approximately 80% for HPV positive

HPV, Human papillomavirus.

lesions have been identified, probably because the crypt epithelium has a discontinuous basement membrane and may be permissive to early metastasis. HPV-negative SCCs are clinically much more like other head and neck SCC, with fungating or ulcerated masses that may be associated

**FIGURE 10.1**

Extensive erythroplakia of the tongue base and posterior oral tongue. (Courtesy of Dr. J. Netterville.)

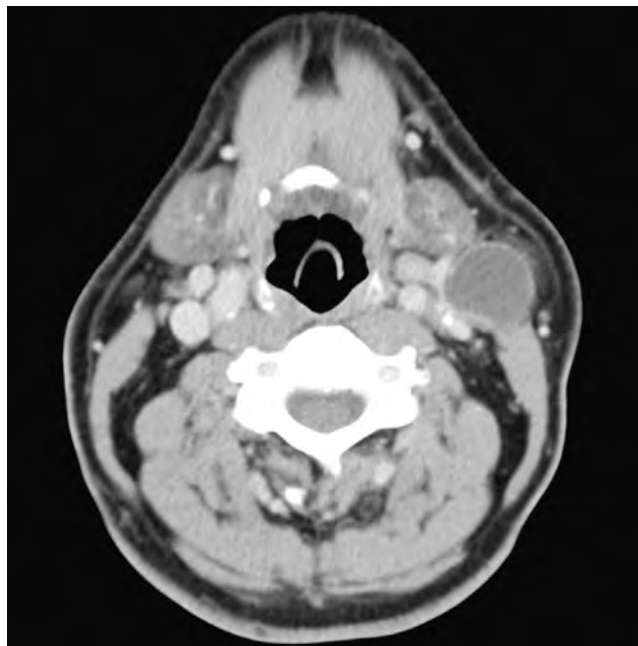
**FIGURE 10.2**

An ulcerated, granular, and friable keratinizing-type squamous cell carcinoma of the base of tongue and extending onto the floor of mouth and lateral tongue.

with leukoplakia or erythroplakia (Figs. 10.1 and 10.2). Approximately 80 % to 90 % of patients present with spread to regional/cervical lymph nodes. In fact, oropharyngeal SCC not infrequently presents as a clinically undetectable tumor or, after thorough work-up, truly is of “unknown primary.”

#### RADIOGRAPHIC FEATURES

Radiographic evaluation is primarily used for staging purposes. Computed tomography, magnetic resonance

**FIGURE 10.3**

Computed tomography scan findings in a patient with metastatic HPV-positive oropharyngeal squamous cell carcinoma. The nodal metastasis is exquisitely cystic with a thin wall. (Courtesy of Dr. A. Langerman.)

imaging, and occasionally positron emission tomography are used to determine the extent of local invasion and presence of metastatic spread to regional lymph nodes or distantly. There are no distinct radiographic findings of primary oropharyngeal SCC, but nodal metastases are often (and characteristically) cystic with thin walls and central necrotic material or fluid (Fig. 10.3). More than 90 % of patients have metastases to level II nodes.

#### PATHOLOGIC FEATURES

##### GROSS FINDINGS

The gross appearance of squamous lesions varies from subtle grayish-white thickening of the mucosa (specifically with keratinizing-type SCC) to large ulcerated, flat, or fungating masses with invasion of local structures. Depending on the degree of desmoplasia and tumor necrosis, the cut surface of invasive tumors ranges from relatively soft and inconspicuous to solid and firm to cystic and friable.

##### MICROSCOPIC FINDINGS

Dysplasia refers to neoplastic alterations of the surface epithelium prior to invasion of the submucosa. These changes include abnormal cellular organization, increased mitotic activity, and nuclear enlargement



## SQUAMOUS CELL CARCINOMA—PATHOLOGIC FEATURES

### Gross Findings

- Can be ulcerated, flat, or fungating masses but more frequently presents as small, relatively soft, ill-defined submucosal lesions

### Microscopic Findings

#### *Premalignant (Noninvasive) Stage (Dysplasia)*

- For HPV-negative neoplasia, dysplastic cells can be limited to the surface squamous epithelium with abnormal cellular organization and maturation, increased mitotic activity, and nuclear enlargement with pleomorphism

#### *Malignant (Invasive) Stage*

- **Keratinizing-type SCC:** infiltrating nests and cords of cells showing varying degrees of squamous differentiation (pink cytoplasm, intercellular bridges, and keratin pearl formation)
  - Desmoplastic stromal reaction including stromal fibrosis and chronic inflammation
- **Nonkeratinizing-type SCC:** large, rounded nests of blue cells with little cytoplasm and hyperchromatic, ovoid nuclei; brisk mitotic activity and little keratinizing maturation which may be haphazardly present and may be at the periphery of the nests
- Specific variants can be seen, including basaloid, papillary, lymphoepithelial-like (“undifferentiated”), spindle cell, and adenosquamous

### Fine Needle Aspiration

- Ranges from atypical squamous cells in a background of keratinous and necrotic cystic debris to clusters of cells with high nuclear to cytoplasmic ratios, inconspicuous nucleoli, and background cyst contents and/or necrotic debris

### Immunohistochemical Findings

- Immunoreactivity for epithelial markers (e.g., p40 p63, and cytokeratins 5/6 and 34βE12)
- p16 positivity (prognostic marker and surrogate marker of HPV-positive SCC): strong and diffuse nuclear and cytoplasmic expression (although patchy staining common when used on fine needle aspiration cytology cell block preparations)

### Pathologic Differential Diagnosis

- **Keratinizing type SCC:** pseudoepitheliomatous hyperplasia, verrucous hyperplasia, necrotizing sialometaplasia
- **Nonkeratinizing type SCC:** solid pattern of adenoid cystic carcinoma, high-grade neuroendocrine carcinoma, true basaloid SCC, lymphoma

HPV, Human papillomavirus; SCC, squamous cell carcinoma.

with pleomorphism. It is seen in the oropharynx but is applicable only for surface mucosal lesions and is most commonly associated with keratinizing-type (or conventional, usually HPV-negative) SCC. Although terminology varies, pleomorphism limited to the lower third of the epithelium is generally referred to as mild dysplasia, pleomorphism limited to the lower two-thirds as moderate dysplasia, and pleomorphism involving the full thickness as severe dysplasia/carcinoma in situ. However, forms of severe dysplasia certainly can have less than full-thickness atypia, but they usually show very undulating rete with “teardrop”-type arrangement

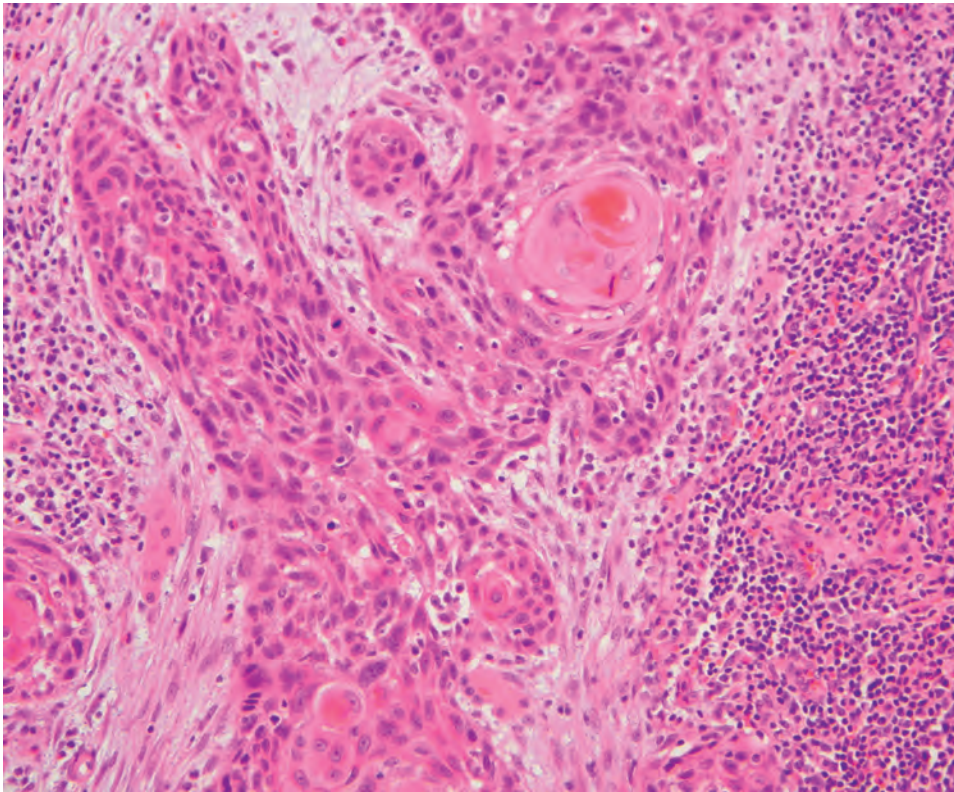
with the downward pushing rete filled with dysplastic cells with nuclear atypia, hyperchromasia, and increased mitotic activity.

With progression, cells invade through the basement membrane. With advanced tumor growth, tumor nests invade skeletal muscle and craniofacial bones and may develop perineural and lymphovascular space invasion. Tumor grade in keratinizing-type SCC varies from well to poorly differentiated, from large, maturing nests, to infiltrative small nests and single cells, although histologic grading is minimally predictive of clinical behavior. Regardless of tumor grade, nests of infiltrating keratinizing type SCC tend to elicit a prominent host fibrotic stromal reaction (desmoplasia) (Fig. 10.4).

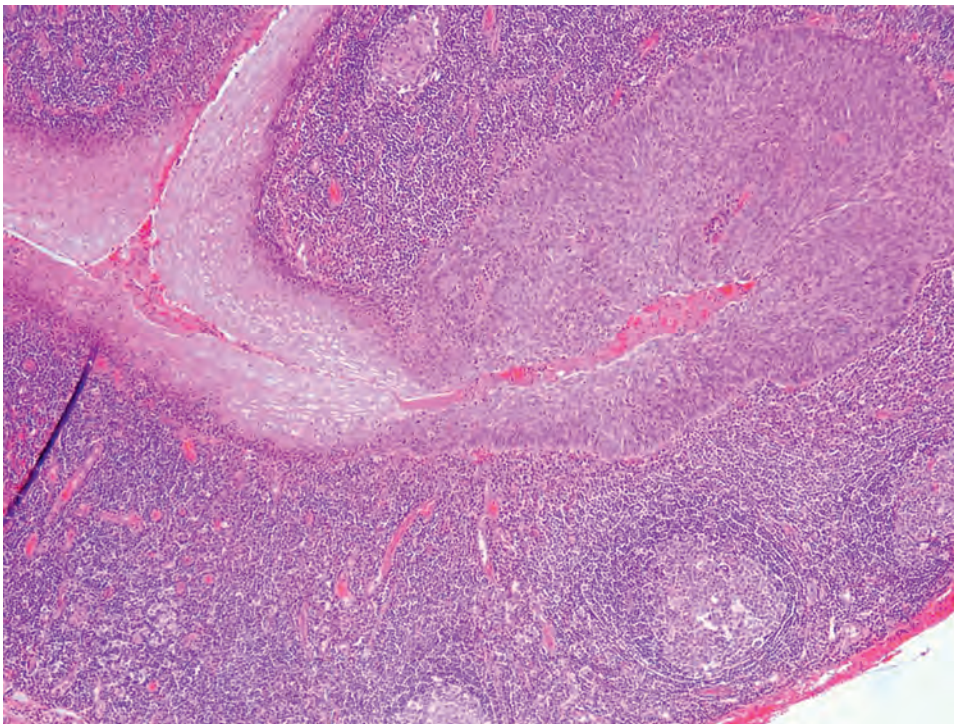
In contrast, HPV-positive oropharyngeal SCC usually does not involve the surface mucosa at all; instead, early lesions arise from, and appear to line, the crypt epithelium (Fig. 10.5). It adopts a “blue cell” morphology in 65 % to 80 % of patients, characterized by scant cytoplasm and hyperchromatic nuclei, referred to as “nonkeratinizing” SCC. This type usually lacks surface involvement and has large nests with smooth edges, little or no stromal reaction, and no (or limited) squamous maturation (Figs. 10.6 and 10.7) that, when present, is often at the periphery of the nests. Mitotic activity is brisk. Hybrid types having both keratinizing and nonkeratinizing findings are also occasionally seen (sometimes called “nonkeratinizing with maturation”). Although some early lesions may appear to be “in situ” along the tonsillar crypt epithelium, it has a discontinuous basement membrane so is a poor barrier to spread. As such, there is no morphologically definable in situ carcinoma—the term should be avoided at this anatomic subsite (see Fig. 10.5).

Certain variants of SCC depart from the typical appearance of conventional SCC. All of these can occur in the oropharynx as the result of HPV.

1. *Papillary SCC* is common in the oropharynx and is characterized by prominent exophytic papillae with delicate fibrovascular cores (Fig. 10.8). In contrast to benign squamous papillomas, these papillary fronds are diffusely lined by overtly malignant squamous cells. There is usually a frankly invasive component, and approximately 80 % are HPV positive.
2. *Basaloid SCC* is also relatively common in the oropharynx. It is characterized by expanding lobules of hyperchromatic, round, basaloid cells that have a “jigsaw puzzle” pattern, hyalinized, nodular stroma, and only focal areas of mature squamous differentiation (Fig. 10.9). Approximately 75 % to 80 % are HPV positive and, when so, they have a very good prognosis. HPV-negative basaloid SCC, in the oropharynx and from other sites, by contrast, is extremely aggressive with high rates of metastasis.
3. *Spindle cell (or sarcomatoid) carcinoma* is quite uncommon in the oropharynx. It classically presents

**FIGURE 10.4**

Invasive keratinizing-type squamous cell carcinoma of the oropharynx showing angulated nests of tumor cells with abundant, eosinophilic cytoplasm, scattered keratin pearls, and prominent stromal desmoplasia.

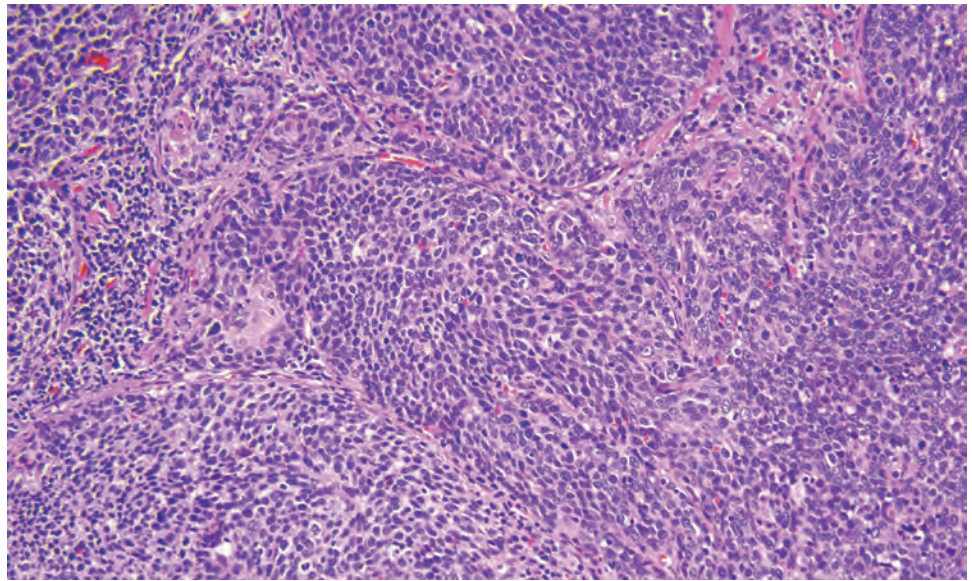
**FIGURE 10.5**

Nonkeratinizing squamous cell carcinoma along crypts can mimic in situ carcinoma but should not be diagnosed as such because the crypt epithelium is an ineffective barrier to tumor spread.

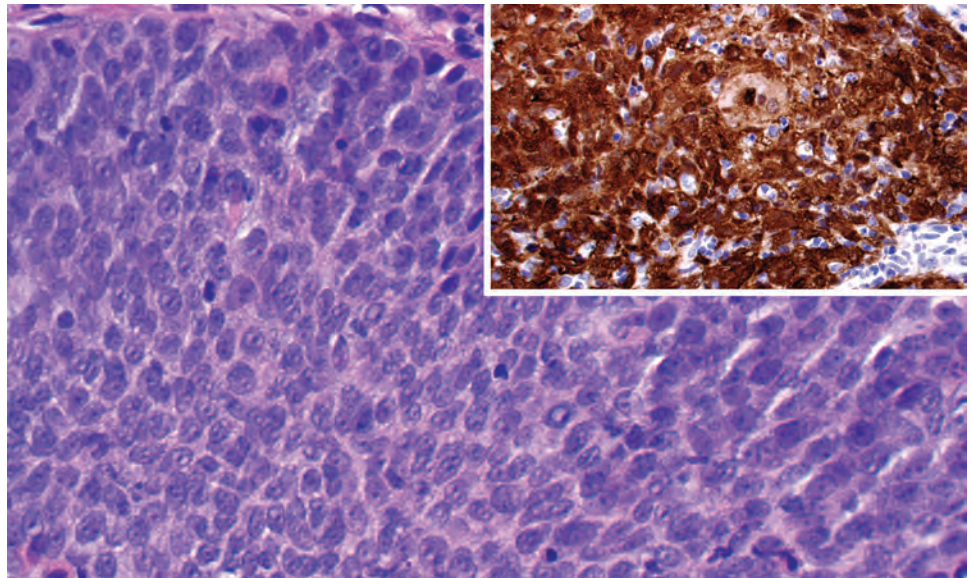


**FIGURE 10.6**

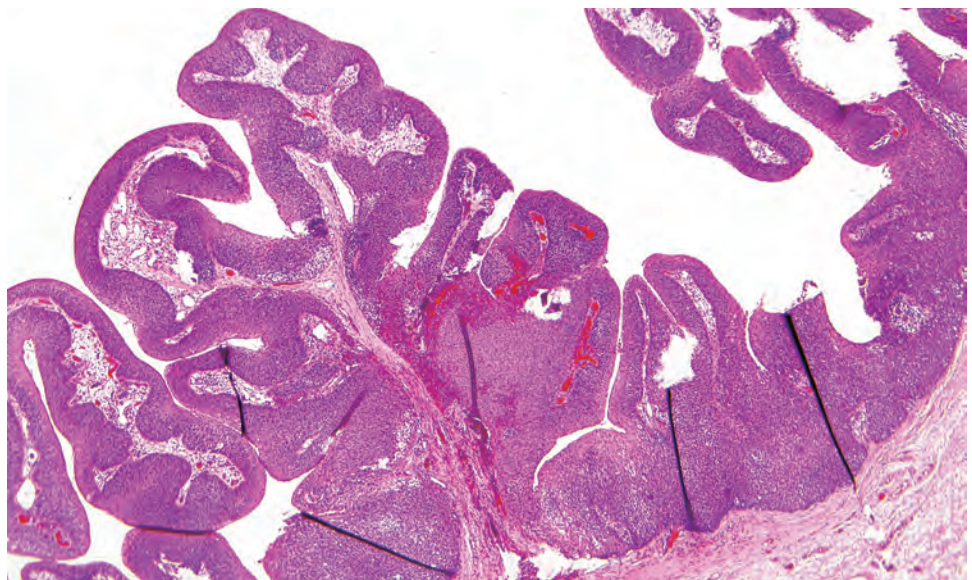
Nonkeratinizing squamous cell carcinoma of the oropharynx consisting of large sheets of tumor cells with oval nuclei, little cytoplasm, and no obvious maturing squamous differentiation. These findings are typical of human papillomavirus-related oropharyngeal carcinomas.

**FIGURE 10.7**

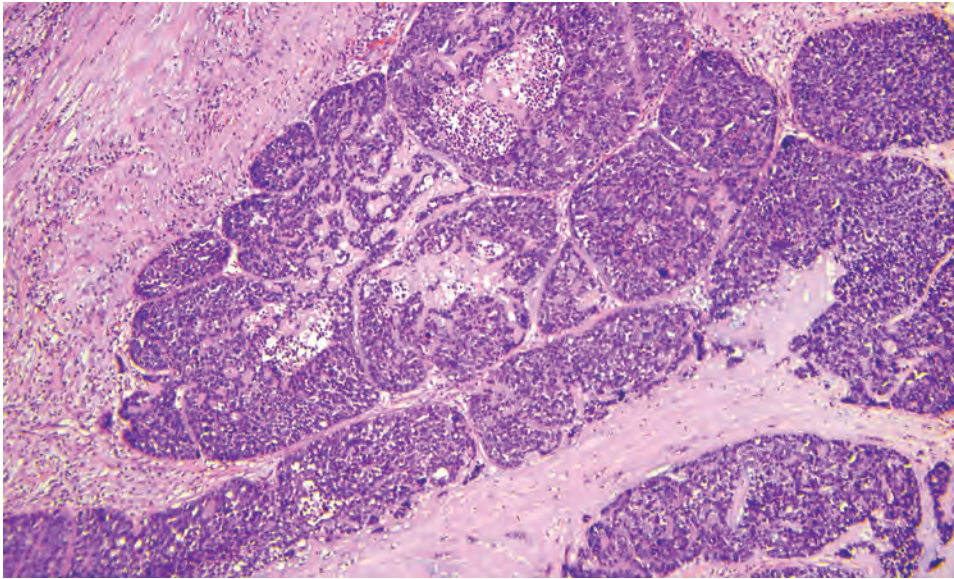
A nonkeratinizing squamous cell carcinoma with a sheet-like collection of tumor cells with spindling. *Inset:* Strong, diffuse, nuclear, and cytoplasmic reactivity with p16 immunohistochemistry.

**FIGURE 10.8**

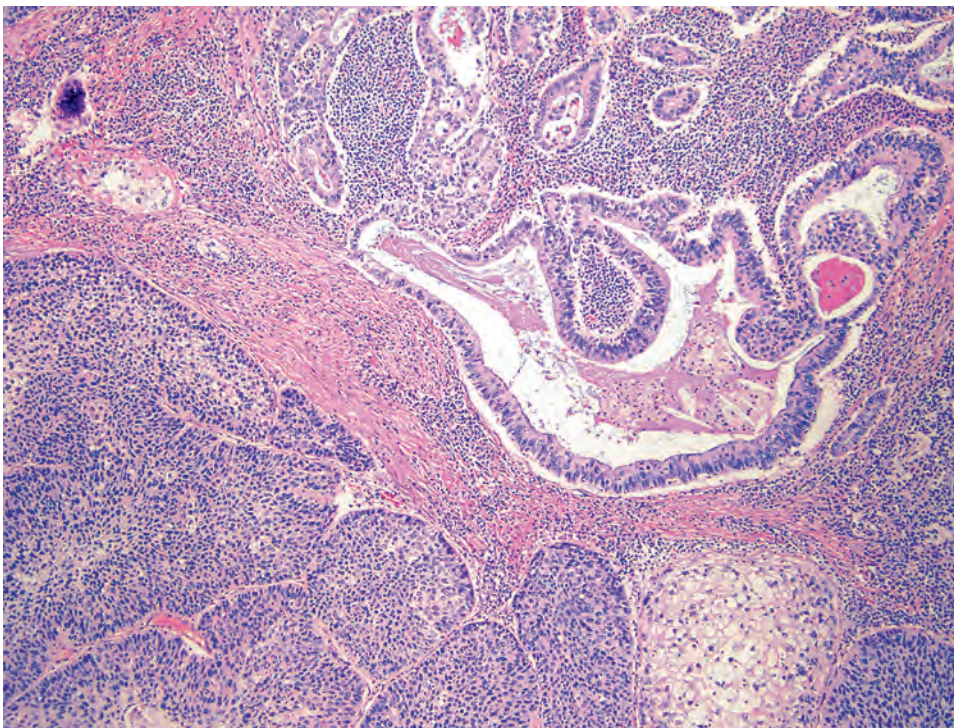
Papillary squamous cell carcinoma is defined by the delicate, papillary fronds lined diffusely by full-thickness squamous cell carcinoma, with or without an obviously invasive component.





**FIGURE 10.9**

Basaloid squamous cell carcinoma infiltrates as rounded lobules of tumor cells having high nuclear to cytoplasmic ratios. The nests of tumor cells characteristically mold to one another, leaving only thin lines of intervening stroma.

**FIGURE 10.10**

Adenosquamous carcinoma shows a mixture of squamous cell carcinoma with areas where tumor cells form true glands with punched out spaces, smooth cell edges, and frequent intraluminal mucin.

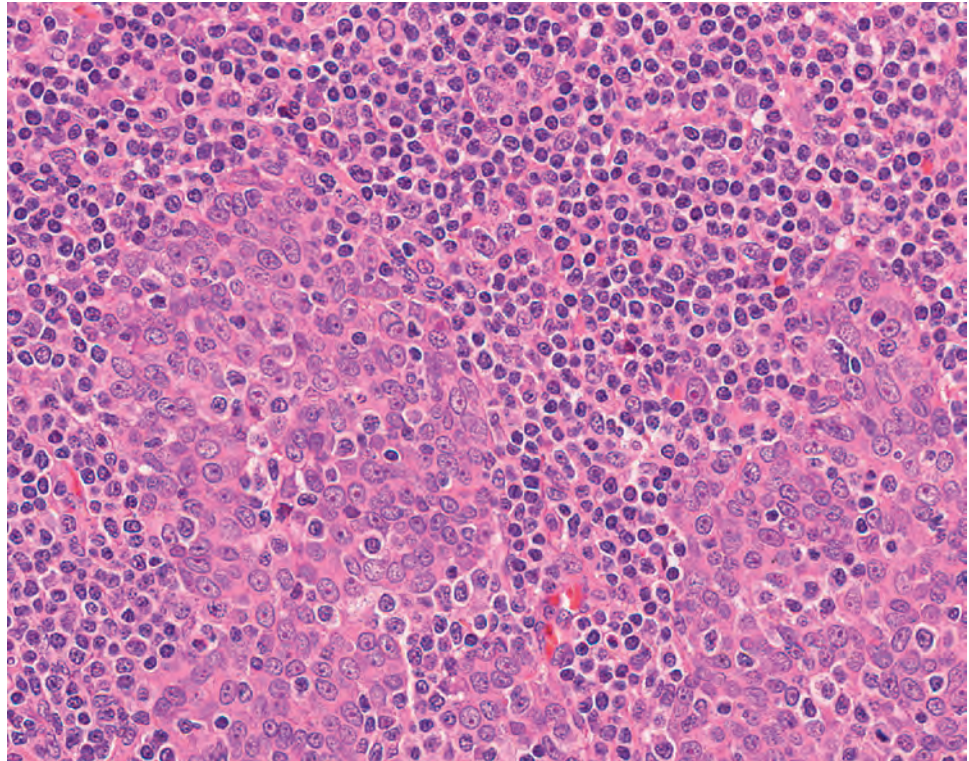
as an exophytic, bosselated mass and is characterized by sheets of spindled and/or pleomorphic cells, usually admixed with a component of typical invasive squamous carcinoma. Rare oropharyngeal cases are HPV-positive, but the prognostic significance of this variant is unknown.

4. *Adenosquamous carcinoma* is uncommon in the oropharynx and is defined by the presence of an SCC component admixed with true, rounded glands that are usually, but not always, associated with

mucin production (Fig. 10.10). Many HPV-positive adenosquamous carcinomas have been reported. HPV-positive examples sometimes can have tumor cells with apical cilia, mimicking a benign process. In general, it has a worse prognosis than keratinizing SCC, but when HPV-positive, it is probably favorable, just as with other HPV-positive SCC.

5. *Lymphoepithelial-like (or “undifferentiated”) carcinoma* is seen in approximately 3% of oropharyngeal carcinomas and morphologically is indistinguishable



**FIGURE 10.11**

Lymphoepithelial-like carcinoma consists of sheets and ill-defined nests of cells with moderate cytoplasm, poorly defined cell borders, round nuclei with vesicular chromatin and prominent nucleoli, and a brisk lymphoplasmacytic inflammatory infiltrate.

from the same tumor of the nasopharynx. Histologically, it has poorly defined collections of tumor cells with ill-defined cell borders, round nuclei with prominent nucleoli, and a dense lymphoplasmacytic inflammatory infiltrate (Fig. 10.11). It is almost always HPV-positive in the oropharynx and has a very good prognosis.

## ANCILLARY STUDIES

### FINE NEEDLE ASPIRATION

More than 50% of patients present with cervical metastases, and some do not have an obvious primary lesion. Fine-needle aspiration is effective in establishing a diagnosis of metastatic SCC. Cytologic smears from keratinizing-type SCC are often cellular with both syncytial fragments of large pleomorphic cells as well as singly dispersed cells. These cells characteristically have large nuclei, prominent nucleoli, and dense, pink or orangeophilic (“squamoid”-appearing) cytoplasm on Papanicolaou staining. However, most oropharyngeal SCC are nonkeratinizing. These tumors show sheets and clusters of cells with high nuclear to cytoplasmic ratios, inconspicuous nucleoli, very few single cells, hyperchromatic, overlapping nuclei, and background cyst contents and/or necrotic debris. If the node is cystic, it is recommended to obtain cyst contents but to attempt to sample

the more solid portions of the wall. Material for a cell block preparation is recommended to use for HPV testing, which is prognostic and may help to suggest an oropharyngeal primary site. Liquid-based HPV DNA testing can also be performed.

### IMMUNOHISTOCHEMICAL FINDINGS

Immunohistochemistry is only rarely necessary for the diagnosis of oropharyngeal SCC and most often arises out of the need to exclude small cell carcinoma or lymphoma, which can also have the “blue cell” appearance. Almost all SCCs express a wide spectrum of cytokeratins (pan-keratin, cytokeratins 5/6, 34 $\beta$ E12) and p63 and/or p40 (diffuse pattern) and lack expression of lymphoid, melanocytic, and neuroendocrine markers. In the oropharynx, p16, a tumor suppressor protein that is aberrantly overexpressed in HPV-related carcinoma cells, is strongly and diffusely expressed in the nuclei and cytoplasm in HPV-related SCC (Figs. 10.12 to 10.14). Given the prognostic significance of HPV in this site, routine p16 immunostaining is recommended for all oropharyngeal SCCs.

## DIFFERENTIAL DIAGNOSIS

Keratinizing-type oropharyngeal SCCs, just like those at other sites such as the oral cavity and larynx, can

be mistaken for reactive non-neoplastic squamous proliferations such as pseudoepitheliomatous hyperplasia, radiation-induced atypia, and necrotizing sialometaplasia—a proliferation of metaplastic squamous cells within the ducts and acini of minor salivary glands. These reactive processes are generally preceded by an inciting event (e.g., ulceration, radiation) and, in contrast to SCC, do not display infiltrative growth, stromal desmoplasia, or overtly malignant cytology. At the other extreme, nonkeratinizing SCCs can be confused with other “blue cell” neoplasms such as small cell carcinoma, solid adenoid cystic carcinoma, or lymphoma. In this setting, immunohistochemistry may play a useful role in establishing the diagnosis of carcinoma by demonstrating positive staining for high-molecular-weight cytokeratins and p40 (in a diffuse pattern) and no staining for neuroendocrine or lymphoid markers.

### PROGNOSIS AND THERAPY

Oropharyngeal SCC has two distinct prognostic types—those related to high-risk HPV and those that are not. Marked overexpression of p16 is an effective surrogate marker for HPV status and is a very strong prognostic marker as an individual test. It should be performed on all new oropharyngeal SCC specimens. Overall 5-year survival for p16-positive cases is approximately 80% compared with 40% to 50% for negative ones. Given the marked differences in behavior, staging systems unique to HPV-positive (p16-positive) oropharyngeal SCC are now recommended.

Treatment options are highly variable and depend on many factors, including size and location of the primary tumor, spread to regional lymph nodes or distant sites, and the patient's ability to tolerate treatment. Primary chemotherapy and radiation is extremely effective because the HPV-positive tumors are very sensitive. However, there is an emerging role for primary surgery due to the development of transoral approaches such as laser or robotic surgery, particularly for early stage SCC and for those with small primary tumors, with decisions on adjuvant radiation (and sometimes chemotherapy) depending on the pathology findings.

### ■ SMALL CELL CARCINOMA

Small cell carcinoma is a malignant neoplasm in which the cells show neuroendocrine differentiation histologically and immunohistochemically. It is also known as high-grade neuroendocrine carcinoma and, although rare in the oropharynx with approximately 30 cases reported in the literature, may be on the rise due to HPV.

### CLINICAL FEATURES

Small cell carcinomas occur in patients between 50 and 70 years old and are slightly more common in men than women. Patients are almost always smokers, usually current and with heavy use. They present similarly to oropharyngeal SCC, with nodal metastases, many complaining of a neck mass as their primary symptom, but some patients present with throat pain or odynophagia. Paraneoplastic syndromes, such as can be seen in lung small cell carcinomas, are exceedingly rare in tumors from the head and neck. Approximately 10 patients have been described with HPV-positive oropharyngeal small cell carcinoma. Despite otherwise having similar demographics to typical patients, a few of these HPV-positive patients have been nonsmokers of slightly younger age.

### PATHOLOGIC FEATURES

#### GROSS FINDINGS

There are no distinct gross findings of oropharyngeal small cell carcinomas. They present similarly to SCC, as

#### SMALL CELL CARCINOMA—DISEASE FACT SHEET

##### Definition

- A high-grade carcinoma that has neuroendocrine differentiation and aggressive clinical behavior

##### Incidence and Location

- Oropharyngeal small cell carcinoma is very rare, being more common in the larynx

##### Sex and Age Distribution

- Common in men
- Patients between 50 and 70 years old

##### Clinical Features

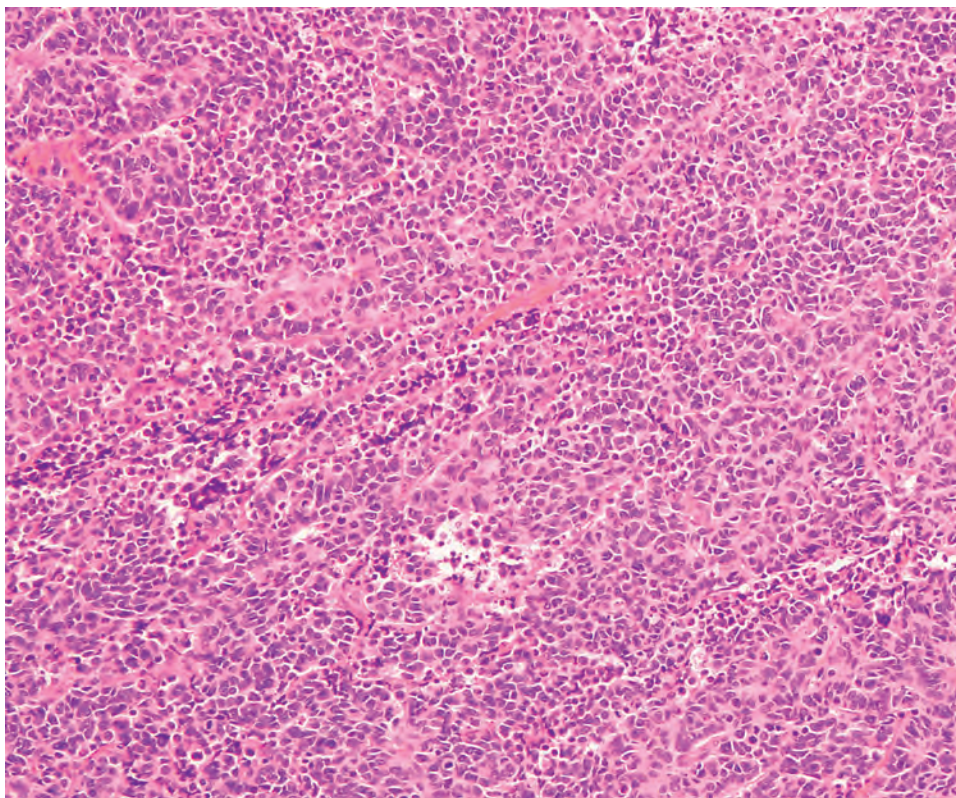
- Neck symptoms are present in most patients and are usually the presenting symptom
- Some patients present with throat pain, odynophagia, or hemoptysis
- Most patients are smokers, often with heavy exposure

##### Prognosis and Treatment

- The optimal treatment is with primary chemotherapy and radiation, with surgery reserved for rare, very early stage tumors
- More than 80% of patients die of widely disseminated disease, generally within 2 years
- Occasional patients with HPV-related carcinomas have been cured of their disease by primary chemotherapy and radiation

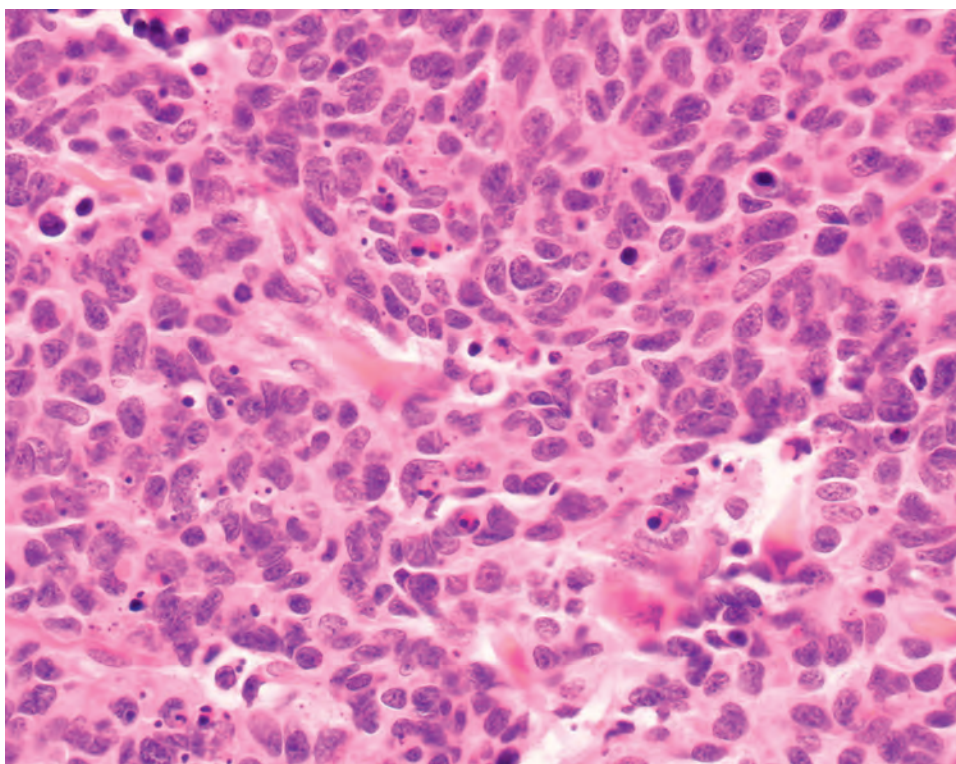
HPV, Human papillomavirus.





**FIGURE 10.12**

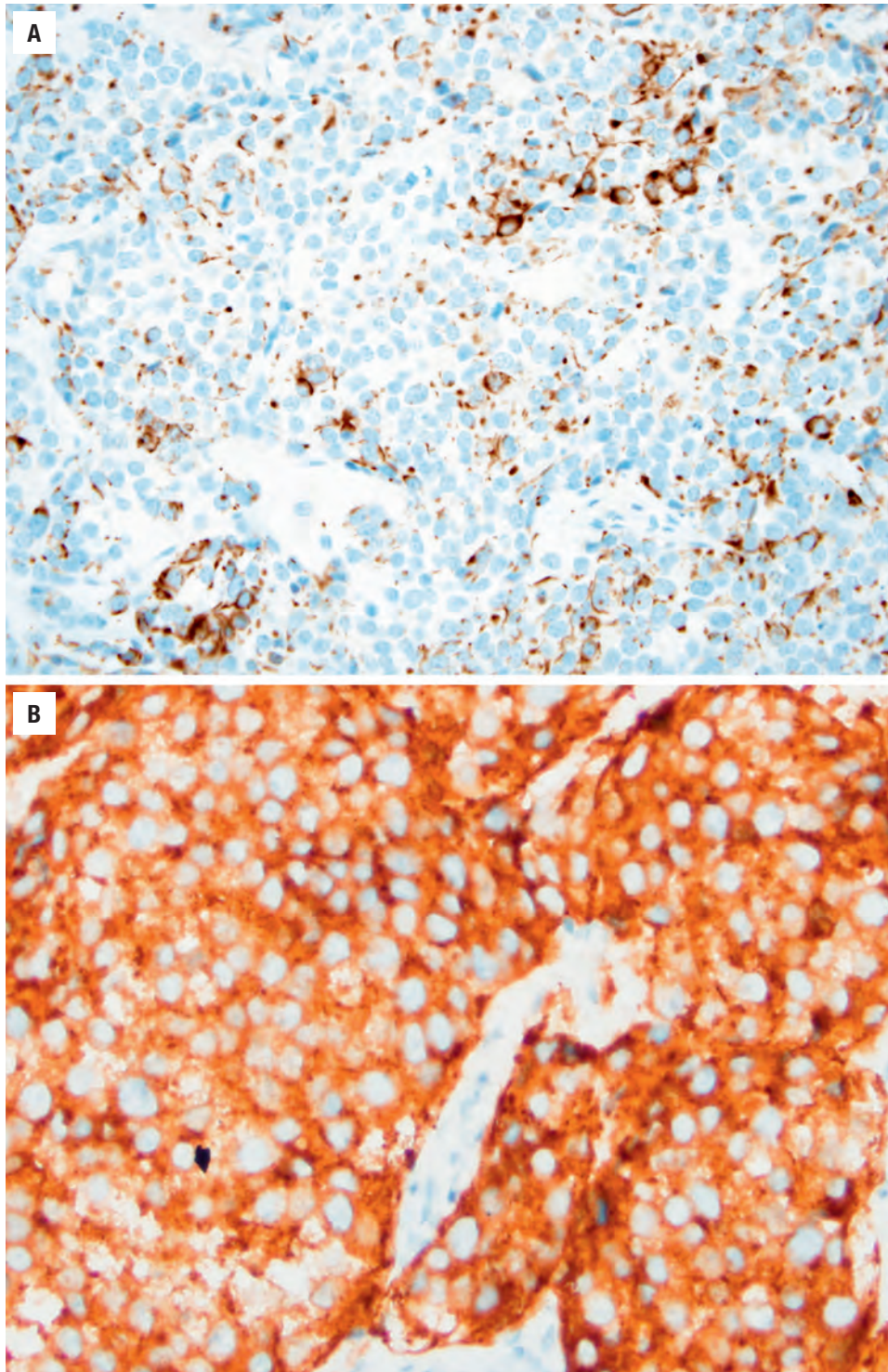
Small cell carcinoma with sheets of markedly basophilic tumor with abundant apoptosis.



**FIGURE 10.13**

Small cell carcinoma tumor cells have nuclei that are angulated, with tapered or "teardrop" shapes, hyperchromasia, apoptosis, and mitosis.



**FIGURE 10.14**

Immunohistochemistry for pancytokeratin (**A**) shows dot-like reactivity in small cell carcinoma and chromogranin and synaptophysin (**B**) are usually expressed.

firm, tan masses involving the surface and underlying tonsillar parenchyma.

#### MICROSCOPIC FINDINGS

The key low-power feature of small cell carcinoma is its “blue cell” appearance. It is arranged in variably sized, and poorly defined, nests. There is frequent necrosis. On

mid and higher power, tumor cells have very high nuclear to cytoplasmic ratios and nuclei are hyperchromatic and angulated. They frequently are drawn out into tapered or “teardrop” shapes, have speckled chromatin, and mold to each other. Apoptosis and mitosis are frequent. Rosettes, which are rounded foci with central areas lacking nuclei, are sometimes seen; in some cases crush artifact may also be seen. Approximately 30% will be combined



### SMALL CELL CARCINOMA—PATHOLOGIC FEATURES

#### Gross Findings

- No distinct gross findings; firm, tan masses

#### Microscopic Findings

- Haphazardly arranged, poorly defined nests of very blue appearing tumor cells
- Very high nuclear to cytoplasmic ratios with speckled chromatin, nuclear molding and teardrop shapes, abundant apoptosis and mitosis
- Approximately 30% are mixed with SCC, which can either be keratinizing or nonkeratinizing but is more frequently the latter, especially in HPV-related tumors

#### Immunohistochemical Findings

- Positive for cytokeratins with dot-like, perinuclear pattern
- Positive, although variably, for neuroendocrine markers synaptophysin, chromogranin, and CD56
- A minority of tumors are positive for TTF-1, which is not specific for lung small cell carcinoma

#### Pathologic Differential Diagnosis

- Nonkeratinizing SCC
- Lymphoma
- Metastatic small cell carcinoma from other sites, such as the lung

HPV, Human papillomavirus; SCC, squamous cell carcinoma.

with SCC, which can either be nonkeratinizing or keratinizing type.

### ANCILLARY STUDIES

Immunohistochemistry for cytokeratins is positive, classically with a dot-like, perinuclear staining pattern. The neuroendocrine markers synaptophysin, chromogranin-A, and CD56 are variably positive, although almost all express at least one of these markers. Immunohistochemistry can be positive for p63, although it is usually weak and/or focal. However, small cell carcinomas are negative for p40. Some tumors are positive for TTF-1, which is not specific for lung small cell carcinoma. Because of their

aggressive nature, prognostic HPV testing is not clearly indicated in routine clinical practice, and caution should be observed with p16, which is positive in almost all small cell carcinomas, including in lung and other head and neck anatomic subsites, regardless of HPV status.

### DIFFERENTIAL DIAGNOSIS

The key to the diagnosis is to recognize the subtle neuroendocrine histologic features. This is critical because the main differential diagnosis is nonkeratinizing SCC. Both have the blue tumor appearance and have abundant apoptosis and mitosis. However, nonkeratinizing SCC is a little less haphazardly arranged, and the nuclei are more round to oval without speckled chromatin and without nuclear molding. Small cell carcinoma has angulated, densely hyperchromatic cells, and, although both nonkeratinizing SCC and small cell carcinoma have high nuclear to cytoplasmic ratios, it is even higher in small cell carcinoma. Prominent crush artifact favors small cell carcinoma. Lymphoma is easily excluded by morphology and immunohistochemistry for keratins and lymphoid markers.

### PROGNOSIS AND THERAPY

The prognosis for oropharyngeal small cell carcinoma is poor. The vast majority of patients present with high-stage disease. Patients are treated with radiation and chemotherapy. Although small cell carcinomas, just like their lung counterparts, tend to respond initially to chemotherapy, the disease is rapidly progressive and more than 80 % of patients die of distant metastases. Patients with HPV-related tumors do not appear to have a better prognosis, most dying with distant metastases. However, a few of the reported HPV-positive patients have been cured, so there may be a slightly better biology compared to HPV-negative small cell carcinoma patients.

### SUGGESTED READINGS

The complete suggested readings list is available online at [ExpertConsult.com](http://ExpertConsult.com).

**SUGGESTED READINGS****Squamous Cell Carcinoma**

1. Ang KK, et al. Human papillomavirus and survival of patients with oropharyngeal cancer. *N Engl J Med*. 2010;363:24–35.
2. Bishop JA, et al. Use of p40 and p63 immunohistochemistry and human papillomavirus testing as ancillary tools for the recognition of head and neck sarcomatoid carcinoma and its distinction from benign and malignant mesenchymal processes. *Am J Surg Pathol*. 2014;38:257–264.
3. Bishop JA. Non-squamous variants of human papillomavirus-related head and neck carcinoma. *Diagn Histopathol*. 2014;20:301–307.
4. Bishop JA, et al. Ciliated HPV-related carcinoma: a well-differentiated form of head and neck carcinoma that can be mistaken for a benign cyst. *Am J Surg Pathol*. 2015;39:1591–1595.
5. Chaturvedi AK, et al. Human papillomavirus and rising oropharyngeal cancer incidence in the United States. *J Clin Oncol*. 2011;29:4294–4301.
6. D'Souza G, et al. Case-control study of human papillomavirus and oropharyngeal cancer. *N Engl J Med*. 2007;356:1944–1956.
7. Gondim DD, et al. Histologic typing in oropharyngeal squamous cell carcinoma—a 4-year prospective practice study with p16 and high risk HPV mRNA testing correlation. *Am J Surg Pathol*. 2016;40:1117–1124.
8. Lewis JS Jr. P16 immunohistochemistry as a standalone test for risk stratification in oropharyngeal squamous cell carcinoma. *Head Neck Pathol*. 2012;6:S75–S82.
9. Masand RP, et al. Adenosquamous carcinoma of the head and neck: relationship to human papillomavirus and review of the literature. *Head Neck Pathol*. 2011;5:108–116.
10. Mehrad M, et al. Papillary squamous cell carcinoma of the head and neck: clinicopathologic and molecular features with special reference to human papillomavirus. *Am J Surg Pathol*. 2013;37:1349–1356.
11. O'Sullivan B, et al. HPV-mediated (p16 +) oropharyngeal cancer. In: Amin MB, ed. *AJCC Cancer Staging Manual*. 8th ed. Switzerland: Springer Nature; 2016.
12. Radkay-Gonzalez L, et al. Ciliated adenosquamous carcinoma: expanding the phenotypic diversity of human papillomavirus-associated tumors. *Head Neck Pathol*. 2016;10:167–175.
13. Singhi A, et al. Comparison of human papillomavirus in situ hybridization and p16 immunohistochemistry in the detection of human papillomavirus-associated head and neck cancer based on a prospective clinical experience. *Cancer*. 2010;116:2166–2173.
14. Singhi AD, et al. Lymphoepithelial-like carcinoma of the oropharynx: a morphologic variant of HPV-related head and neck carcinoma. *Am J Surg Pathol*. 2010;34:800–805.
15. Westra WH. The changing face of head and neck cancer in the 21st century: the impact of HPV on the epidemiology and pathology of oral cancer. *Head Neck Pathol*. 2009;3:78–81.
16. Westra WH, et al. Squamous cell carcinoma, HPV-positive. In: El-Naggar A, Chan JKC, et al, eds. *Classification of Head and Neck Tumors*. 4th ed. World Health Organization Classification of Tumors. Lyon, France: IARC Press; 2017:136–138.

**Small Cell Carcinoma**

1. Bates T, et al. Small cell neuroendocrine carcinoma of the oropharynx harbouring oncogenic HPV-infection. *Head Neck Pathol*. 2014;8:127–131.
2. Bishop JA, et al. Human papillomavirus-related small cell carcinoma of the oropharynx. *Am J Surg Pathol*. 2011;35:1679–1684.
3. Kraft S, et al. HPV-associated neuroendocrine carcinoma of the oropharynx: a rare new entity with potentially aggressive clinical behavior. *Am J Surg Pathol*. 2012;36:321–330.
4. Lewis JS Jr., et al. Squamous and neuroendocrine specific immunohistochemical markers in head and neck squamous cell carcinoma: a tissue microarray study. *Head Neck Pathol*. 2017; in press.
5. Perez-Ordóñez B, et al. Poorly differentiated neuroendocrine carcinoma. In: El-Naggar A, Chan JKC, et al, eds. *Classification of Head and Neck Tumors*. 4th ed. World Health Organization Classification of Tumors. Lyon, France: IARC Press; 2017:97–98.
6. Westra WH, et al. Squamous cell carcinoma, HPV-positive. In: El-Naggar A, Chan JKC, et al, eds. *Classification of Head and Neck Tumors*. 4th ed. World Health Organization Classification of Tumors. Lyon, France: IARC Press; 2017:136–138.



# Non-Neoplastic Lesions of the Salivary Glands

■ **Mary S. Richardson**

## ■ DEVELOPMENTAL LESIONS, INCLUDING HETEROTOPIA AND ONCOCYTOSIS

Salivary glands are composed of three paired major glands—the parotid, submandibular, and sublingual—and approximately 1000 minor seromucous glands that are distributed throughout the sinonasal tract, oral cavity, pharynx, larynx, and lower respiratory tract. The minor salivary glands secrete continuously, whereas the major glands secrete mainly in response to parasympathetic activity induced by stimuli. All the glands develop from ingrowths of surface epithelium and have a common architecture with varying acinar compositions of serous and mucous cell types. The parotid glands are almost entirely serous, the sublingual glands are predominantly mucous, and the submandibular glands contain both serous and mucous cells. These secretory units empty into excretory ducts lined by cuboidal to columnar epithelium. All salivary glands are vulnerable to the same disorders.

Not only are lesions of salivary glands uncommon, but they encompass a heterogeneous group of disorders. Enlargement of salivary glands is most often due to non-neoplastic or inflammatory conditions, including developmental abnormalities, hyperplasia, metaplasia, cysts, and inflammatory diseases. Of these, heterotopia and oncocytosis will be discussed.

### CLINICAL FEATURES

Heterotopia of salivary gland is the existence of salivary gland tissue in locations external to the major and minor salivary glands. In contrast, accessory salivary glands are defined as isolated lobules of glands situated along a major salivary duct. Heterotopic or ectopic salivary gland tissue has been reported in a myriad of anatomic locations (Table 11.1) and is usually found incidentally, although it may be discovered due to signs and symptoms associated with inflammation or neoplasia. The more common sites

for heterotopic salivary gland are the middle ear, neck, mandible, and pituitary gland. Sites outside the head and neck include the mediastinum, stomach, prostate gland, rectum, and vulva. Removal of these salivary gland tissue deposits may occur for cosmetic reasons, as intervention for a congenital abnormality (oncocytosis), or due to neoplasia. In the case of malignancy, confusion may arise, particularly if the remaining normal gland architecture has been destroyed, as to whether the tumor is primary in heterotopic salivary gland tissue versus a metastatic deposit from a nearby salivary gland.

### DEVELOPMENTAL LESIONS, INCLUDING HETEROTOPIA AND ONCOCYTOSIS—DISEASE FACT SHEET

#### Definition

- Heterotopia: salivary gland tissue in a location external to the major and minor salivary glands
- Oncocytes are transformed acinar or ductal cells with finely granular eosinophilic cytoplasm, categorized as oncocytic metaplasia, oncocytosis (nodular or diffuse), and oncocytoma

#### Incidence and Location

- Heterotopia most commonly involves the parotid and cervical lymph nodes
- Oncocytic tumors of salivary gland are rare (<1%)

#### Sex and Age Distribution

- Salivary gland heterotopia has no known age or sex predilection
- Oncocytic lesions are uncommon in patients <50 years, with a peak incidence in the 7th to 9th decade

#### Clinical Features

- Heterotopia is usually found incidentally or as a mass secondary to an inflammatory or neoplastic process
- Oncocytic lesions (oncocytosis/oncocytoma) may be multifocal within the gland, unilateral, or bilateral

#### Prognosis and Therapy

- Simple excision if clinically indicated for heterotopia
- Oncocytic lesions are usually not recurrent; however, oncocytoma has a 0%-30% recurrence rate

**TABLE 11.1**  
**Reported sites of heterotopic salivary tissues**

|  |                        |
|--|------------------------|
| Middle ear                               | Mediastinum            |
| External auditory canal                  | Pituitary gland        |
| Neck                                     | Cerebellopontine angle |
| Thyroglossal duct cyst and thyroid gland | Stomach                |
| Mandible (intraosseous)                  | Rectum                 |
| Cervical and paraparotid lymph nodes     | Prostate gland         |

Oncocytes are characterized by the presence of abundant finely granular, bright eosinophilic cytoplasm surrounding a round nucleus that contains a single nucleolus. The granular cytoplasm is due to an overabundance of mitochondria. The number and distribution of oncocytic cells in salivary gland vary, as does the growth pattern. The occurrence of oncocytic cells in salivary gland can be categorized as oncocytic metaplasia within a duct or isolated aggregate, focal and diffuse oncocytosis, multifocal oncocytic hyperplasia, and oncocytoma. *Oncocytic metaplasia* involves the abnormal change or transformation (metaplasia) of acinar cells (serous, mucous, and sero-mucous) and/or striated ducts to oncocytes. Oncocytic metaplasia is uncommon before the age of 50 and increases with advancing age. The metaplasia is usually seen focally within a duct and may be found in conjunction with salivary gland neoplasms (pleomorphic adenoma, muco-epidermoid carcinoma). *Oncocytosis* is an unencapsulated (mass-forming) collection of oncocytes, which may occur in minor or major salivary glands. This alteration may involve either ducts, predominantly, or acini and may be associated with fatty infiltration and acinar atrophy. The rare condition *nodular oncocytic hyperplasia (NOH)* is characterized by multiple nodules of oncocytic cells in a lobular distribution within one or both parotid glands (bilateral in 40 % of cases) (Fig. 11.1). NOH has been reported associated with oncocytoma and benign or malignant salivary gland neoplasms. These nodules or islands may be large, but they lack the encapsulation of an oncocytoma. The oncocytic islands of NOH may involve the intraparotid lymph nodes, which often contain salivary gland ducts, or the hilum of the lymph node. It is worth highlighting that these oncocytic islands within the lymph nodes can be incorrectly confused with meta-static deposits.

**PATHOLOGIC FEATURES**

**GROSS FINDINGS**

On gross examination, the heterotopic salivary gland tissue has the characteristic findings of normal salivary

**DEVELOPMENTAL LESIONS, INCLUDING HETEROTOPIA AND ONCOCYTOSIS—PATHOLOGIC FEATURES**

**Gross Findings**

- Oncocytic nodules may measure up to 7 cm, with small, cystic areas

**Microscopic Findings**

- Oncocytic cells are characterized by finely granular, eosinophilic cytoplasm
- There is a single round nucleus with conspicuous nucleolus
- Architectural growth patterns are usually organoid with variable areas showing cording and prominent capillaries
- Oncocytes may undergo “clear cell” change

**Ancillary Studies**

- PTAH stain accentuates granules

**Pathologic Differential Diagnosis**

- When clear cell oncocytes are present, differential includes metastasis from clear cell mucoepidermoid carcinoma, clear cell acinic cell, and renal cell carcinoma

*PTAH*, Phosphotungstic acid–hematoxylin stain.

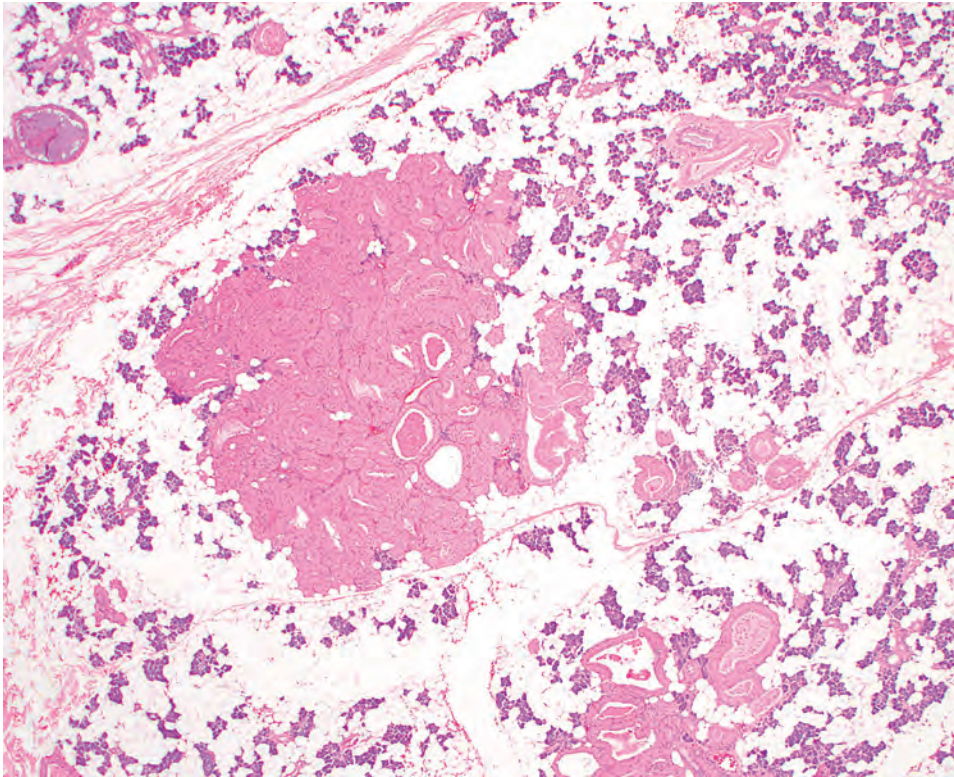
gland tissue, which usually has a yellow-tan firm and lobulated appearance. There is no definitive gross appearance for oncocytosis, but larger lesions (which may measure up to 7 cm) may reveal tan to light brown nodules.

**MICROSCOPIC FINDINGS**

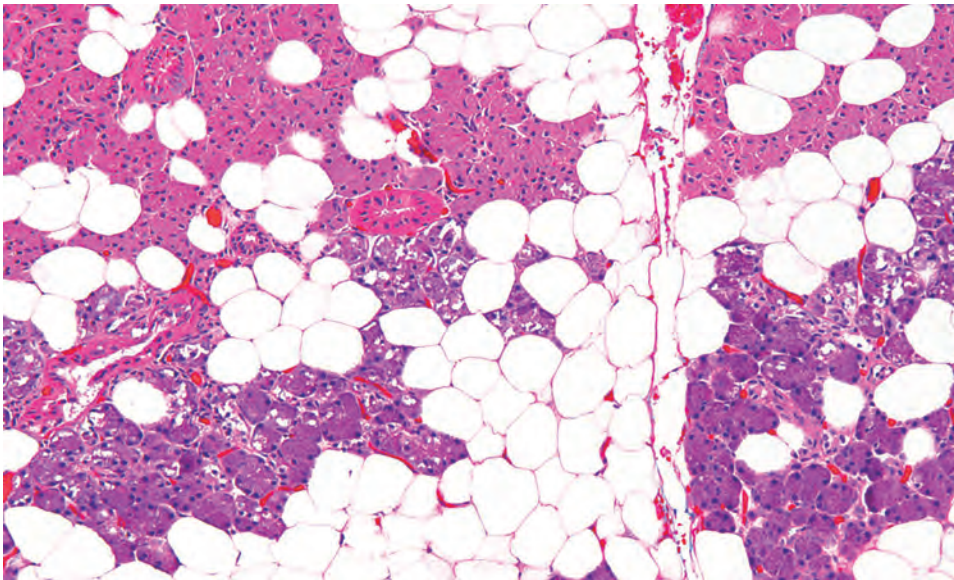
Like any salivary gland, histologic sections of heterotopia reveal a variably mixed population of large pale mucous cells with poorly staining mucigen granules and condensed peripheral nuclei and the more basophilic serous cells with strongly staining zymogen granules and central nuclei. Intermixed are the intercalated ducts with a lining of cuboidal secretory cells.

Histologic examination of an oncocytic lesion shows the characteristic polygonal cells with abundant finely granular eosinophilic cytoplasm. This oncocytic transformation can involve acinar and ductal cells, and the cytologic distinction can be striking (Fig. 11.2). The nuclei are usually uniformly round with granular chromatin and contain a single nucleolus. Mitotic figures are absent or rare. The presence of a complete or partial fibrous capsule surrounding an oncocytoma will aid in the distinction between an oncocytoma and NOH. Oncocytes may grow as a solid nodule of cells or within ducts. There may be unencapsulated focal cystic areas with papillary proliferations within ducts or as an isolated parenchymal aggregate. The architectural growth pattern of the cells within a solid nodule is often organoid or



**FIGURE 11.1**

At medium power, notice the distribution of nodular oncocytic hyperplasia within the salivary gland tissue. The nodular proliferations are seen diffusely throughout the parotid gland tissue.

**FIGURE 11.2**

At medium power, the tinctorial difference between the basophilic acinar cells and the eosinophilic oncocytes is easily noted. Oncocytic metaplasia may be seen in acinar and ductal cells.

forming cords in a hepatoid pattern. The individual cells show a variable eosinophilic staining quality (Fig. 11.3) and, on a rare occasion, may contain focal or diffuse clear cells.

#### ANCILLARY STUDIES

Although not necessary for the diagnosis, the following may be useful in demonstrating the presence of mitochondria within oncocytic lesions.

#### ULTRASTRUCTURAL FINDINGS

On ultrastructural evaluation, abundant mitochondria may completely fill the cytoplasmic compartment. The mitochondria show some variability in their shape, ranging from round to irregular and elongate. Desmosomal cell attachments are identified.

#### HISTOCHEMICAL FINDINGS

A phosphotungstic acid–hematoxylin stain (PTAH) will stain mitochondria varying intensities of blue.

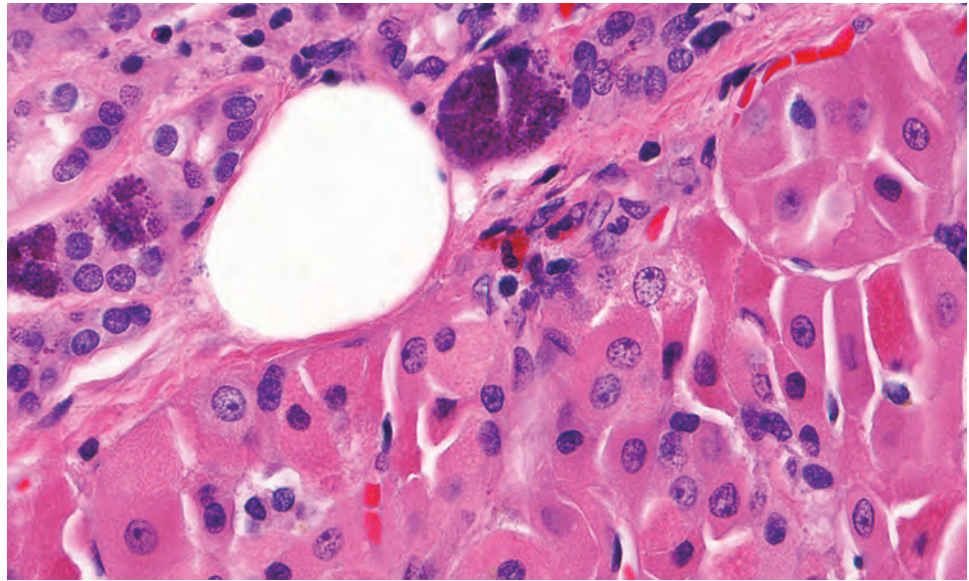


**FIGURE 11.3**

At high power, the finely granular eosinophilic cytoplasm and round nuclei with a single nucleolus are seen. Note the variability in eosinophilic staining of the oncocytic cytoplasm.

However, the results of this stain are not always consistent.

#### FINE NEEDLE ASPIRATION

On fine needle aspiration, oncocytes are easily identified with abundant, well-defined, finely granular cytoplasm and large round nuclei with prominent nucleoli. However, distinguishing oncocytic metaplasia from oncocytomas is done on excised lesions.

#### DIFFERENTIAL DIAGNOSIS

Distinguishing between nodular hyperplasia, nodular oncocytosis, and oncocytoma may be problematic and sometimes impossible. Some authorities define an oncocytoma as a *single* nodule, whereas others require the presence of at least a partial *capsule*. The distinction between oncocytic hyperplasia and neoplasia is still not well defined. Oncocytic metaplasia and a variety of clear cell neoplasms are included in the differential diagnosis with oncocytoma. Areas of oncocytic metaplasia have been reported in pleomorphic adenomas and within mucoepidermoid carcinomas; however, these areas are usually isolated. Furthermore, oncocytomas lack the architectural patterns of these two neoplasms: Focal mucus cell differentiation and squamous metaplasia are exceedingly rare within oncocytomas and help to distinguish oncocytoma from mucoepidermoid carcinoma; and oncocytomas do not have myoepithelial cell proliferation with ductal structures, or myxoid or chondroid differentiation, which is characteristic of pleomorphic adenoma.

Acinic cell carcinoma may be difficult to distinguish from a multi NOH. However, the presence of zymogen

granules combined with the microcystic and papillary follicular growth patterns of acinic cell carcinoma is not seen in oncocytic hyperplasia.

#### PROGNOSIS AND THERAPY

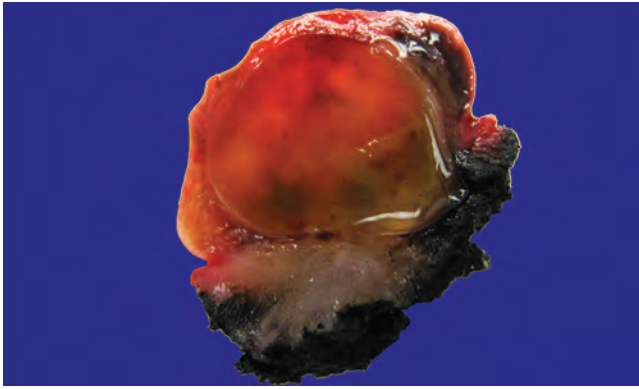
Oncocytic metaplasia and oncocytosis are usually identified in a gland removed for another reason. No therapy is necessary for these benign reactions. Heterotopias are excised for symptomatic relief in some cases, with an excellent prognosis.

#### ■ MUCUS RETENTION CYST, MUCOCELE, AND SIALOLITHIASIS

##### CLINICAL FEATURES

The most common non-neoplastic lesion of salivary gland tissue is the mucocele. The mucocele is defined as the pooling of mucin in a cystic cavity. Two types of mucoceles are described: (1) the retention type (Fig. 11.4), characterized by mucin pooling confined within a dilated excretory duct (Figs. 11.5 and 11.6), and (2) the extravasation type (Fig. 11.7), showing escape of salivary-secreted mucin from the duct system into connective tissue (Figs. 11.8 and 11.9). The mucus retention cyst is more common in the parotid and submandibular glands, and the peak incidence is in the 7th to 8th decade. The extravasated type is the most common mucocele, and its peak incidence is in the 3rd decade. The lower lip is the most common site, followed by the tongue, floor of mouth, palate, and

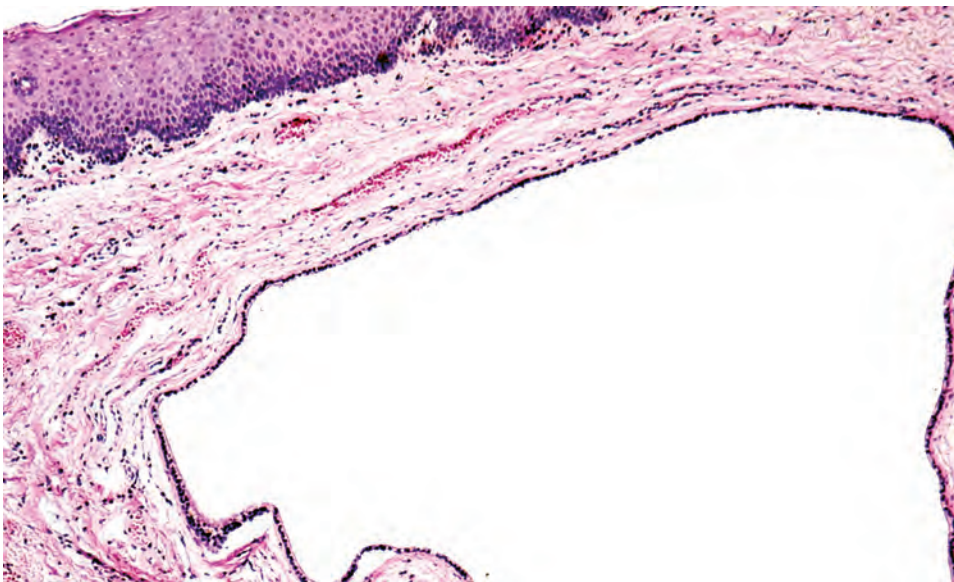


**FIGURE 11.4**

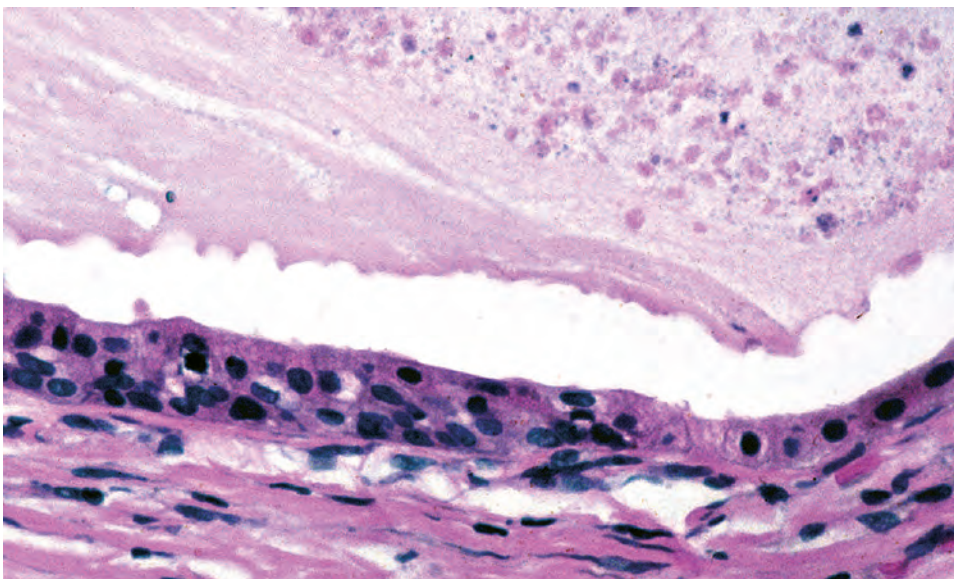
Macroscopic view of a mucocoele showing a well-defined border filled with mucin.

buccal mucosa. The extravasated type most commonly occurs in the lower lip, often appearing as blue-tinged, dome-shaped swellings. A large mucocoele that may arise in the floor of the mouth from the sublingual or minor salivary gland and descend into the soft tissues of the floor of the mouth is called a *ranula*.

A sialolith is a collection of often laminated concretions that form a stone within the salivary gland excretory duct system. Sialolithiasis most frequently involves the submandibular gland and may cause a chronic sclerosing sialadenitis distal to the stone (Fig. 11.10). The stone will cause distention of the duct system and retention of secreted fluids, resulting in glandular swelling and pain.

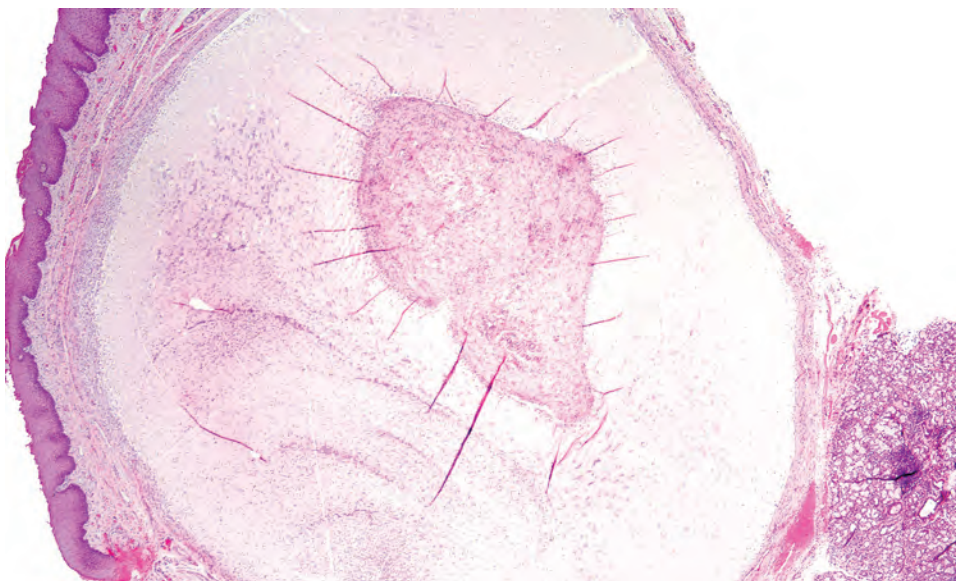
**FIGURE 11.5**

At low power, the dilated, epithelial lined cavity of a mucus cyst is apparent. The mucus has not extravasated into the tissues.

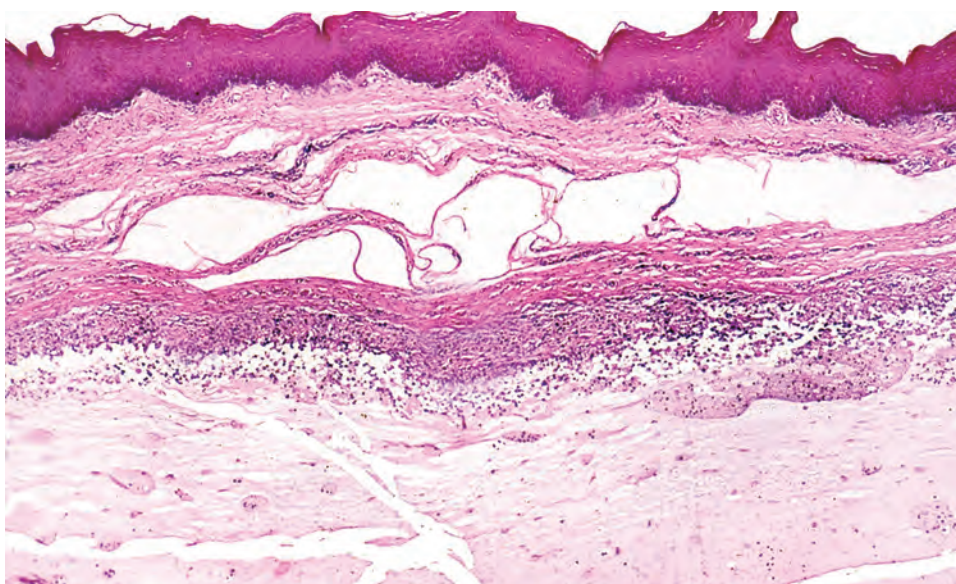
**FIGURE 11.6**

At high power, the low cuboidal lining of the cyst is seen. There is very little inflammatory response in the subjacent connective tissue.

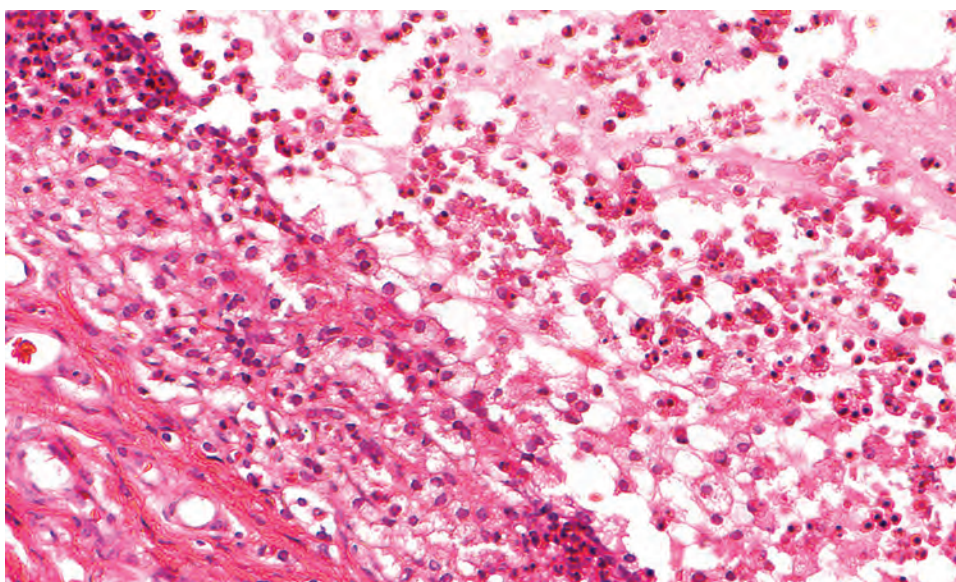


**FIGURE 11.7**

At low power, the circumscribed extravasated mucus is identified.

**FIGURE 11.8**

At medium power, the absence of an epithelial lining and mixed inflammatory infiltrate is noted at the mucus and connective tissue interface.

**FIGURE 11.9**

At high power, a prominent inflammatory infiltrate and foamy, mucin-laden macrophages are noted within the connective tissue and within the mucin. No epithelium is identified.



## RADIOGRAPHIC FEATURES

Sialoliths are always visible on radiographic examination. The Wharton duct of the submandibular gland is the most common site for a sialolith, which can be visualized easily on a radiograph (Fig. 11.10).

### MUCUS RETENTION CYST AND MUCOCELE—DISEASE FACT SHEET

#### Definition

- The pooling of salivary mucus within a cystic cavity resulting from blockage/rupture of a salivary gland duct

#### Incidence and Location

- Most common non-neoplastic lesion of salivary glands
- Lower lip is the most common site, followed by tongue, floor of mouth, palate, and buccal mucosa
- Mucocèles in the floor of mouth are called “ranula”

#### Sex and Age Distribution

- Equal sex distribution
- Peak incidence in 3rd decade
- Most common intraoral lesion in the first two decades of life

#### Clinical Features

- Soft, fluctuant, semitranslucent, painless swelling that may be noted to occur after a traumatic event
- The lesion may fluctuate with meals or when ruptured secondary to trauma
- Lesion may be recurrent to the same site

#### Prognosis and Therapy

- Complete excision, including minor salivary gland, usually is adequate
- Recurrence is usually seen with inadequate excision

## PATHOLOGIC FEATURES

Histologically, the retention cyst captures the mucus within an epithelium-lined lumen. The cyst shows an attenuated epithelium. There is usually minimal inflammatory infiltrate within the wall (Fig. 11.5) unless there is adjacent rupture. In contrast, the lesions of extravasated mucin (mucocele) show compression of the adjacent connective tissue with a brisk inflammatory reaction circumscribing the mucin pool (Fig. 11.8). Often within the infiltrate of the mucocele wall, there are numerous foamy macrophages containing phagocytized mucin (Fig. 11.9). As the lesion progresses, granulation tissue from the wall becomes more prominent and organizes to obliterate the lumen of the mucocele. In a primarily granulation tissue-laden lesion, a mucicarmine

### MUCUS RETENTION CYST AND MUCOCELE—PATHOLOGIC FEATURES

#### Gross Findings

- Cystic cavity within connective tissue containing glistening fluid

#### Microscopic Findings

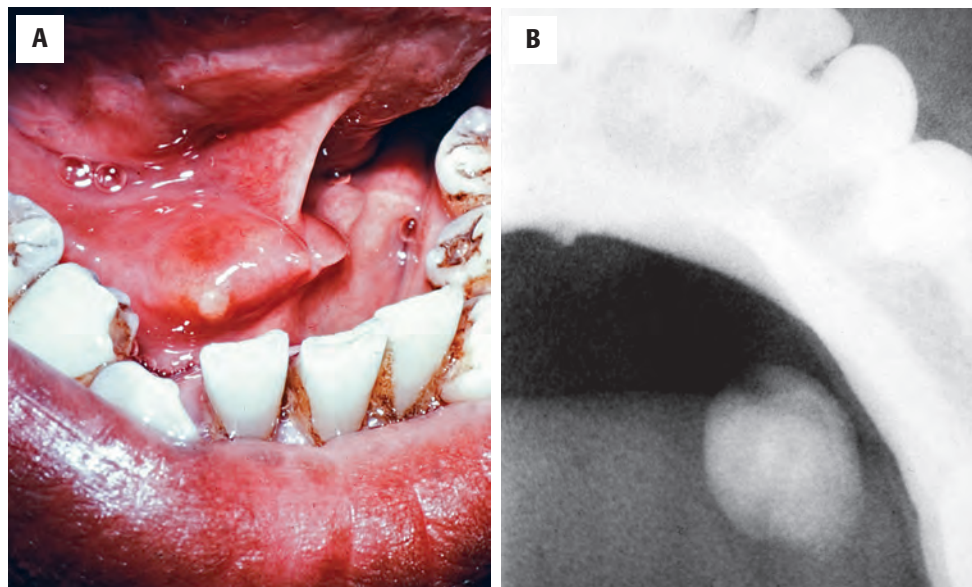
- Circumscribed mucin with inflammation within the wall
- Retention cyst has epithelial lining of the lumen

#### Ancillary Studies

- Periodic acid Schiff (PAS) and mucicarmine stain mucin

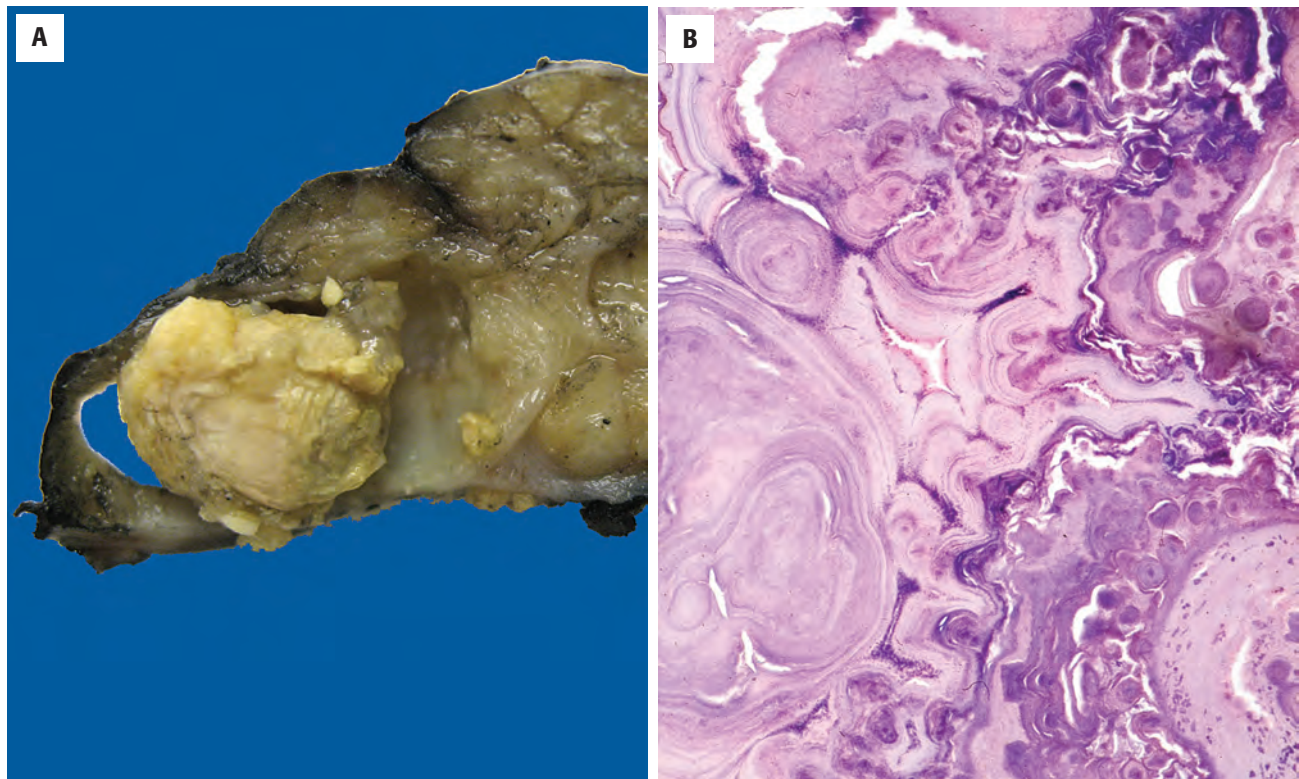
#### Pathologic Differential Diagnosis

- Organizing hematoma



**FIGURE 11.10**

(A) A sialolith (stone) present at the orifice of Wharton duct is just beginning to protrude from the lumen of the duct. (B) Sialoliths are common in Wharton duct of the submandibular gland. The lamination of the sialolith can be appreciated on this radiograph.

**FIGURE 11.11**

(A) Macroscopically, there is a sialolith within the duct of the submandibular gland. (B) At low power, the laminated concretions around nidi of cellular debris are seen in this section of a sialolith.

stain will highlight the residual mucin-containing macrophages.

A sialolith will frequently demonstrate a nidus of cellular debris found in the center of the concentric laminated calcium deposits (Fig. 11.11).

### DIFFERENTIAL DIAGNOSIS

Few entities enter into the differential diagnosis of an extravasated-type mucocele. Certainly, a resolving extravasated mucocele with only remaining granulation tissue may be misinterpreted as a small hematoma or a thrombus. However, the use of mucicarmine would illustrate the presence of mucin-laden macrophages and aid in this distinction. The mucus retention cyst is lined by a thin layer of cuboidal epithelium with little to no inflammatory cell infiltrate. Mucoepidermoid carcinoma could enter the differential diagnosis of a mucus retention cyst. However, mucoepidermoid carcinoma contains three cell types: mucus goblet cells, intermediate cells, and squamous cells. Moreover, within mucus retention cysts, the epithelium is attenuated and it lacks papillary projections that often protrude into the lumen of a mucoepidermoid carcinoma.

### PROGNOSIS AND THERAPY

Surgical excision to include the minor mucoserous gland is suggested, as clinically indicated by the patient's condition. Alginate has been used by some with varying results. Recurrence is seen in patients with inadequate excision. Lithotripsy, sialoendoscopy, and other supportive measures are used for symptomatic sialoliths.

## ■ NECROTIZING SIALOMETAPLASIA

### CLINICAL FEATURES

Necrotizing sialometaplasia is an uncommon destructive reactive inflammatory process of the salivary gland. The clinical and histologic characteristics resemble those of malignant neoplasms and can lead to misdiagnosis and inappropriate therapy. The age range of reported patients with necrotizing sialometaplasia is from 1.5 to 83 years, with the average age of ~46 years. The lesion has a 2:1 predominance in men. Its etiology is somewhat speculative, although strong evidence suggests the cause may be



vascular compromise leading to ischemic necrosis. The vast majority of these lesions affect the minor salivary glands in the hard palate or at the junction of the hard and soft palate (Fig. 11.12). Lesions are most commonly unilateral; however, occasional bilateral or midline lesions develop. Other common sites for this lesion are oral cavity, lower lip, retromolar trigone, tongue, and buccal mucosa, although the entire upper aerodigestive tract can be affected. Occurrence of this lesion in major salivary glands, primarily the parotid gland, is uncommon, representing 8.5% of necrotizing sialometaplasia cases.

Clinically, the lesion appears in the palate as a deep, sharply defined, up to 3 cm crater-like ulcer that develops rapidly over a few days and fails to heal for an extended

period of time. Duration of healing of this lesion can range up to 6 months, although most heal within 1 month. All such lesions that fail to resolve usually undergo a biopsy. Other symptoms associated with this lesion (pain or numbness) may simulate malignancy.

## **PATHOLOGIC FEATURES**

### **GROSS FINDINGS**

On gross examination, there is only a slight suggestion of softening of these submucosal tissues with a glistening cut surface. Usually there is no distinguishing mass.

### **MICROSCOPIC FINDINGS**

Microscopically, the characteristic feature of necrotizing sialometaplasia is ischemic necrosis or infarction, which

## **NECROTIZING SIALOMETAPLASIA—DISEASE FACT SHEET**

### **Definition**

- Ischemic necrosis of salivary gland tissue that maintains a lobular distribution

### **Incidence and Location**

- Palate is most frequent site of involvement

### **Sex and Age Distribution**

- Male predominance
- All ages affected

### **Clinical Features**

- Rapid swelling of the mucosa with ulceration in a few days
- Lesion slowly heals over several weeks
- Patients complain of pain or numbness which simulates malignancy

### **Prognosis and Therapy**

- No therapy is necessary for this self-healing process

## **NECROTIZING SIALOMETAPLASIA—PATHOLOGIC FEATURES**

### **Gross Findings**

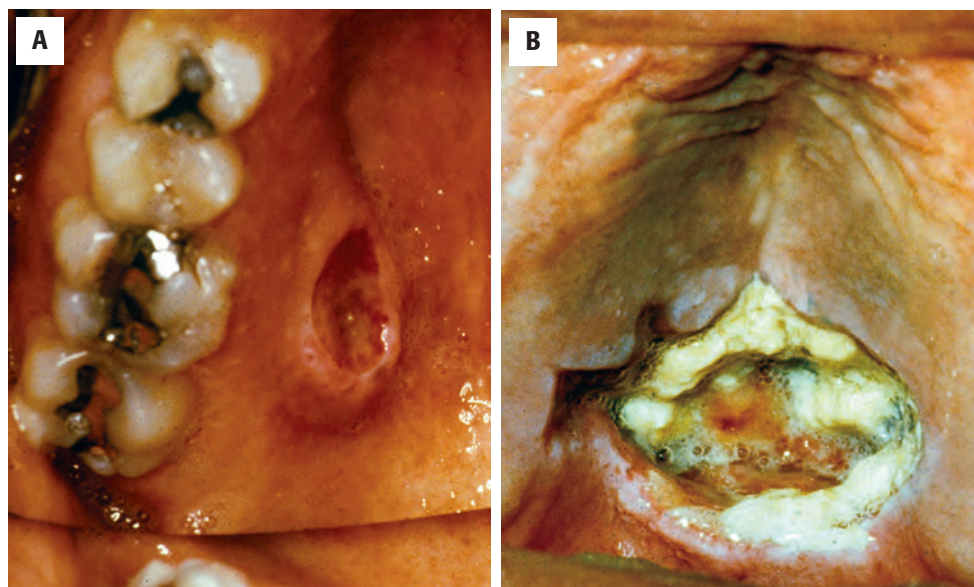
- Usually the overlying mucosa shows ulceration
- Ulcer may be up to 3 cm

### **Microscopic Findings**

- Lobular coagulative necrosis of glandular acini
- Prominent squamous metaplasia of salivary gland ducts
- Inflammation is present
- Pseudoepitheliomatous hyperplasia of the overlying mucosal epithelium may be seen

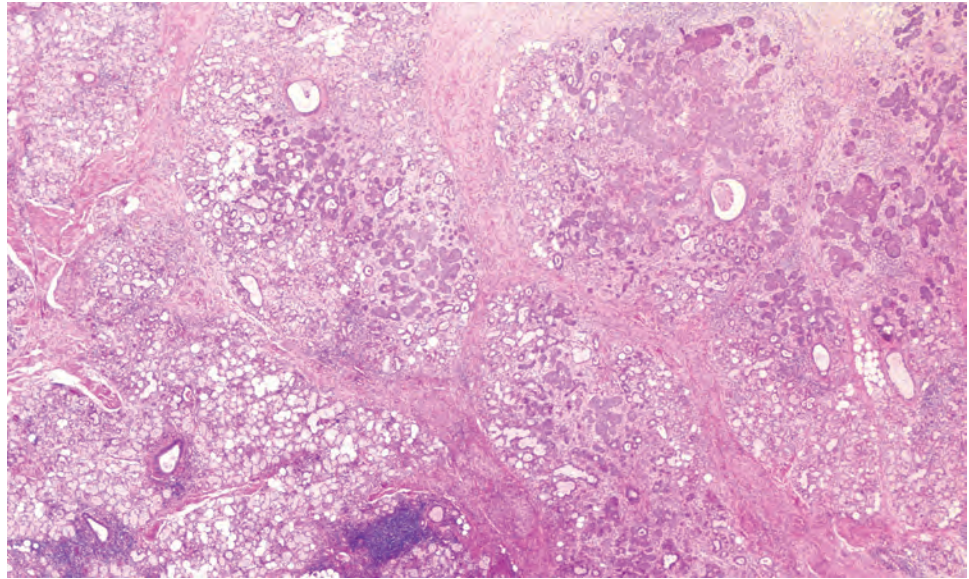
### **Pathologic Differential Diagnosis**

- Squamous cell carcinoma, mucoepidermoid carcinoma



**FIGURE 11.12**

Two cases of necrotizing sialometaplasia as seen in the palate. (A) A unilateral ulcer, showing a raised border and center crater. (B) A large, crater-like ulceration in the midline. It is sharply defined, filled with exudate.

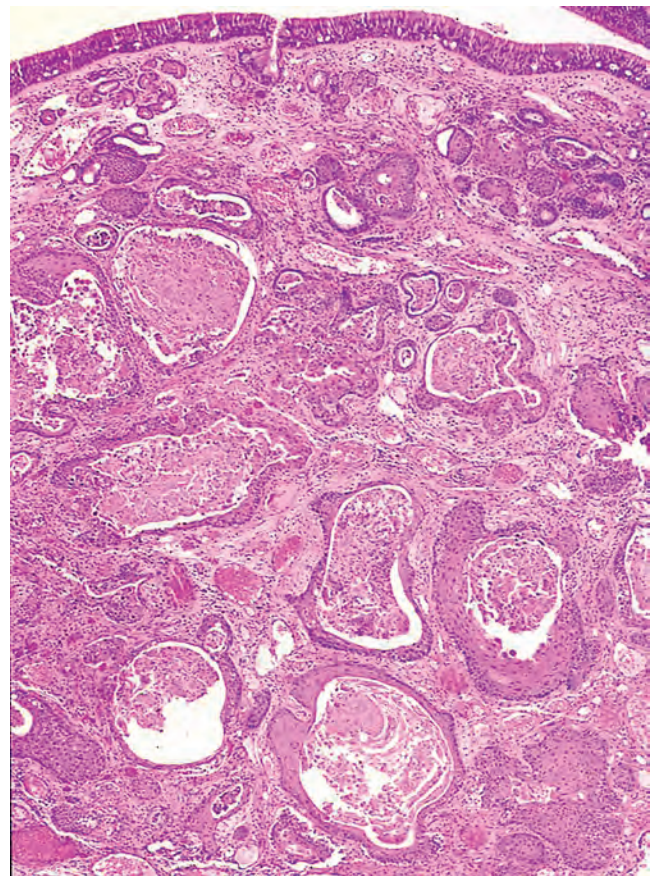
**FIGURE 11.13**

Lobules of salivary gland show multiple areas of squamous metaplasia as it replaces the areas of coagulative necrosis. Fibrosis is noted between the lobules.

is thought to be the primary pathogenic mechanism of this lesion, with preservation of the lobular architecture. The key histologic findings in identifying this lesion are (1) lobular coagulative necrosis of the salivary gland acini (Fig. 11.13), (2) prominent and proliferative squamous metaplasia of the excretory ducts (Fig. 11.14), (3) pseudoepitheliomatous hyperplasia of the overlying mucosa, and (4) prominent inflammatory infiltrate. The most prominent and useful findings histologically are the coagulative necrosis and ductal metaplasia (Fig. 11.15). In addition, the overall acinar architecture is preserved, despite necrotic mucinous acini showing the “ghosted” outline of coagulative necrosis, and with associated salivary ducts showing metaplastic squamous mucosa (Fig. 11.16).

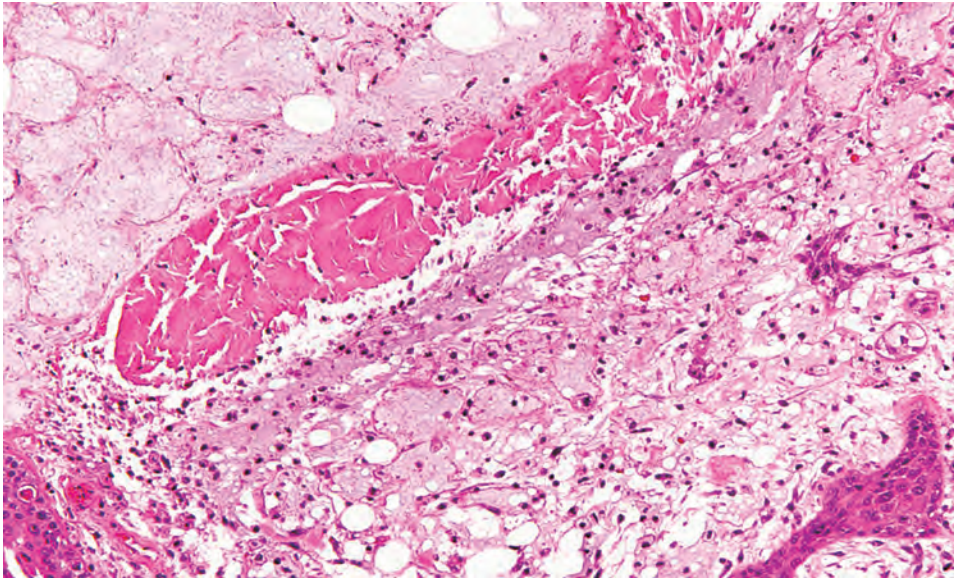
### DIFFERENTIAL DIAGNOSIS

The diagnosis of necrotizing sialometaplasia can be problematic if the biopsy is not adequate or oriented properly. The chief differential diagnoses for this lesion are mucosal squamous cell carcinoma and mucoepidermoid carcinoma. In an adequately oriented biopsy, it is easy to distinguish these lesions based on the maintenance of the salivary gland lobular architecture. The cytologic findings of necrotizing sialometaplasia are bland. In addition, the inflammatory infiltrate characterizing necrotizing sialometaplasia is more prominent than that frequently associated with squamous cell carcinoma and mucoepidermoid carcinoma. Moreover, these two malignancies infiltrate the salivary gland parenchyma.

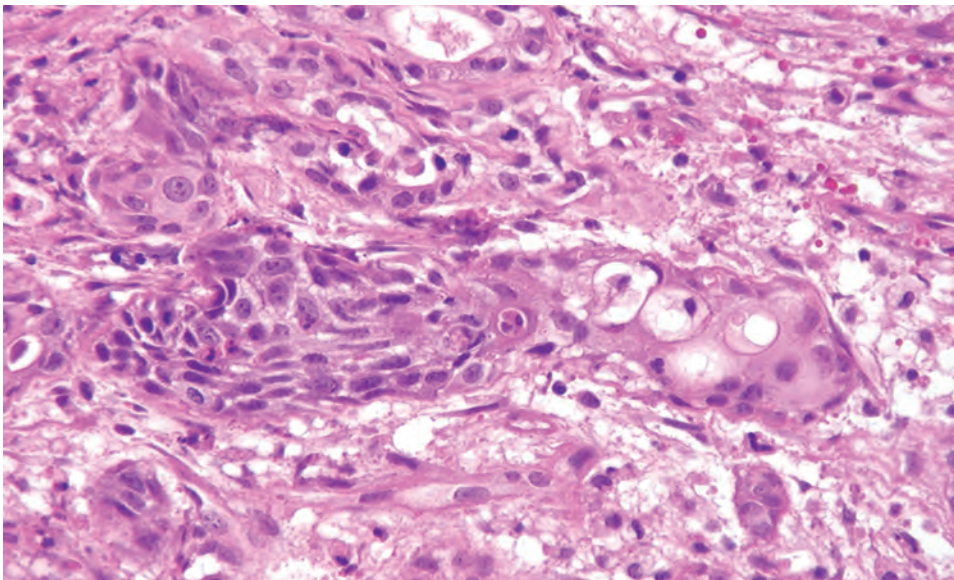
**FIGURE 11.14**

At low power, prominent cystic degeneration of squamous metaplasia within the sinonasal seromucous gland units may mimic squamous cell carcinoma.



**FIGURE 11.15**

At medium power, there is extensive degeneration and necrosis with islands of squamous metaplasia (*lower*).

**FIGURE 11.16**

At high power, islands of squamous metaplasia are cytologically bland, not to be confused with malignancy. There is inflammation surrounding the outlines of the acini and ducts.

### PROGNOSIS AND THERAPY

No specific therapy is required for necrotizing sialometaplasia. These lesions are self-healing.

### ■ LYMPHOEPITHELIAL SIALADENITIS

Lymphoepithelial sialadenitis (LESA), also known as benign lymphoepithelial lesion and myoepithelial sialadenitis, is used to describe a characteristic effacement of salivary parenchyma by a dense lymphocytic infiltrate.

The term does not commit to an etiologic cause but refers to histologic findings.

### CLINICAL FEATURES

Clinically, the lesions present as unilateral, bilateral, or diffuse enlargement of salivary glands (usually parotid) or lacrimal glands. This lesion may occur in children and adults of either sex; however, most cases present in women in the 4th and 5th decade. LESA is associated with, or a precursor to, Sjögren syndrome, a systemic autoimmune disease characterized by chronic inflammation in exocrine

**LYMPHOEPITHELIAL SIALADENITIS—DISEASE FACT SHEET****Definition**

- Salivary gland tissue with an intense lymphocytic infiltrate with associated epimyoepithelial islands

**Incidence**

- Uncommon lesion

**Morbidity and Mortality**

- Increased risk of lymphoma

**Sex and Age Distribution**

- Female predominance
- Mean age, 50 years

**Clinical Features**

- 85% of cases occur in the parotid gland
- Diffuse swelling of the affected gland

**Prognosis and Therapy**

- Prognosis relates to development of lymphoma, which is usually a low-grade extranodal marginal zone B-cell lymphoma (MALT lymphoma)
- Surgery

MALT, Mucosa-associated lymphoid tissue.

organs. In some cases, it is a precursor lesion to salivary mucosa-associated lymphoid tissue (MALT) lymphoma. Patients experience facial swelling with or without pain, dry mouth, and keratoconjunctivitis.

**PATHOLOGIC FEATURES****GROSS FINDINGS**

On gross examination, LESA may be seen as diffuse enlargement of the gland or present as discrete tan micronodules. The gross appearance can be mistaken for a neoplastic process due to the multinodularity; however, the capsule in major salivary glands is intact.

**MICROSCOPIC FINDINGS**

LESA is characterized histologically by irregular, multifocal islands of epithelial proliferations surrounded by a dense lymphocytic infiltrate, known as “epimyoepithelial islands” (Fig. 11.17). The extent of the lymphocytic infiltrate can vary within a lobule and ultimately progresses to total acinar atrophy with only remaining ducts (Fig. 11.18). The remaining excretory ducts are usually infiltrated by intermediate-sized lymphocytes. Similar changes to those seen in the major salivary glands in LESA can occur in the minor salivary glands of patients

**BENIGN LYMPHOEPITHELIAL LESION—PATHOLOGIC FEATURES****Gross Findings**

- Small tan nodules to diffuse replacement of gland by creamy tan tissue

**Microscopic Findings**

- Heavy lymphocytic infiltrate associated with destruction of salivary acini
- Proliferating epimyoepithelial islands

**Pathologic Differential Diagnosis**

- Lymphoma

with Sjögren syndrome. The changes in minor glands include a chronic lymphocytic sialadenitis usually without epithelial hyperplasia. The changes seen in a labial minor salivary gland biopsy are supportive but not pathognomonic evidence for the diagnosis of Sjögren syndrome (Fig. 11.19). Numeric grading systems are used based on the number of lymphocytic aggregates present in salivary gland lobules, but clinical and serologic confirmation is required for a definitive diagnosis. An aggregate (50 lymphocytes) is referred to as a “focus,” resulting in a “focus score.” It is important that the sample be obtained from normal tissue (i.e., not infected, inflamed, ulcerated, etc.) and that lymphocytes must be within the parenchyma, not in a periductal (sialodochitis) location or in association with heavy fibrosis (chronic sialadenitis).

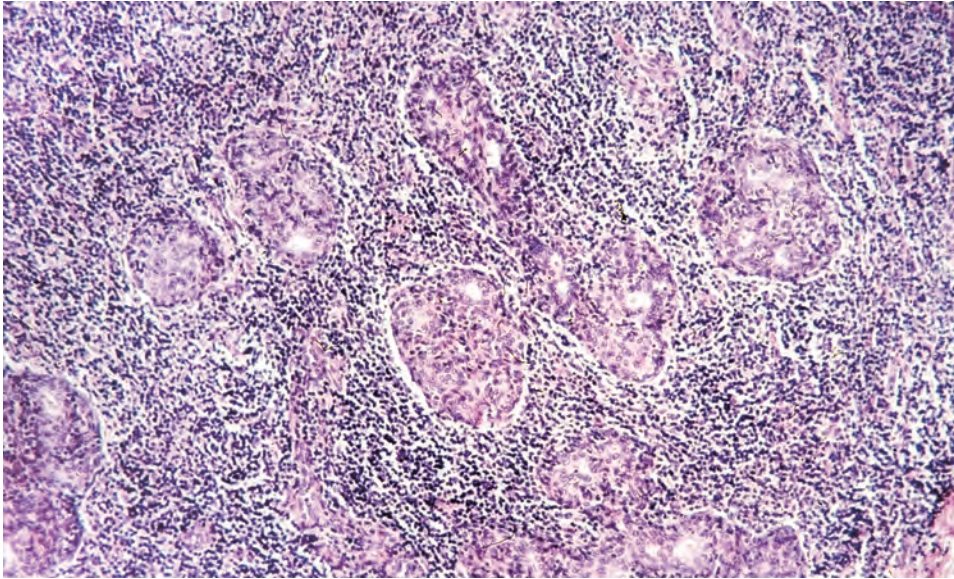
**ANCILLARY STUDIES**

The lymphoid infiltrate that is present in these lesions is a mixture of T and B lymphocytes similar to those seen in hyperplastic lymph nodes. Plasma cells, eosinophils, and polymorphonuclear leukocytes are not usually present. Use of immunohistochemistry for CD3 (T-cell marker) or CD20 (B-cell marker) can reveal a mixed population of T and B lymphocytes. Fresh tissue at the time of biopsy may be submitted for flow cytometry analysis and gene rearrangement studies to exclude a lymphoma.

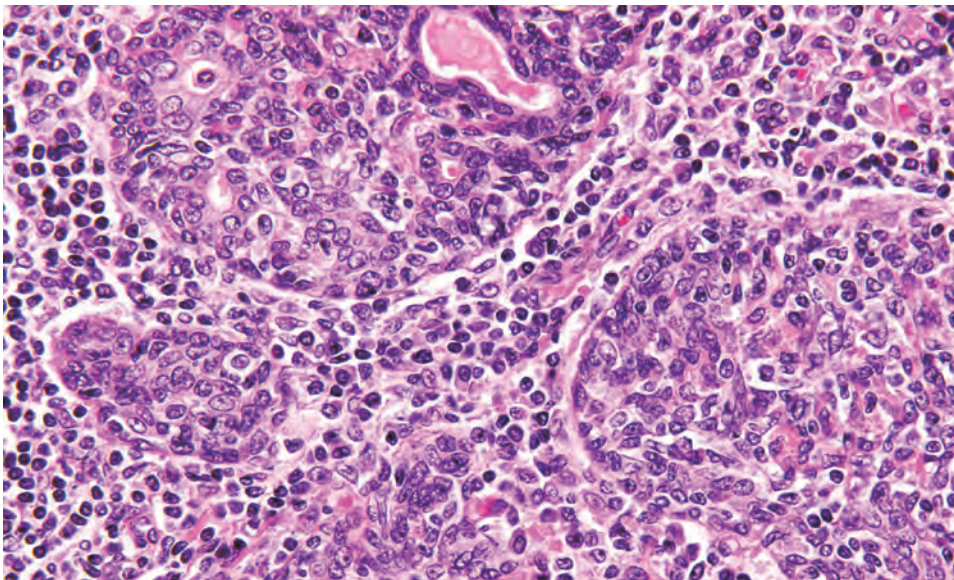
**DIFFERENTIAL DIAGNOSIS**

The differential diagnosis includes malignant lymphoma, metastatic carcinoma, chronic sialadenitis, and sarcoidosis. The following are helpful in distinguishing lymphoma from a LESA: the infiltrate remaining within the normal lobular architecture of the gland, lack of invasion of capsule and

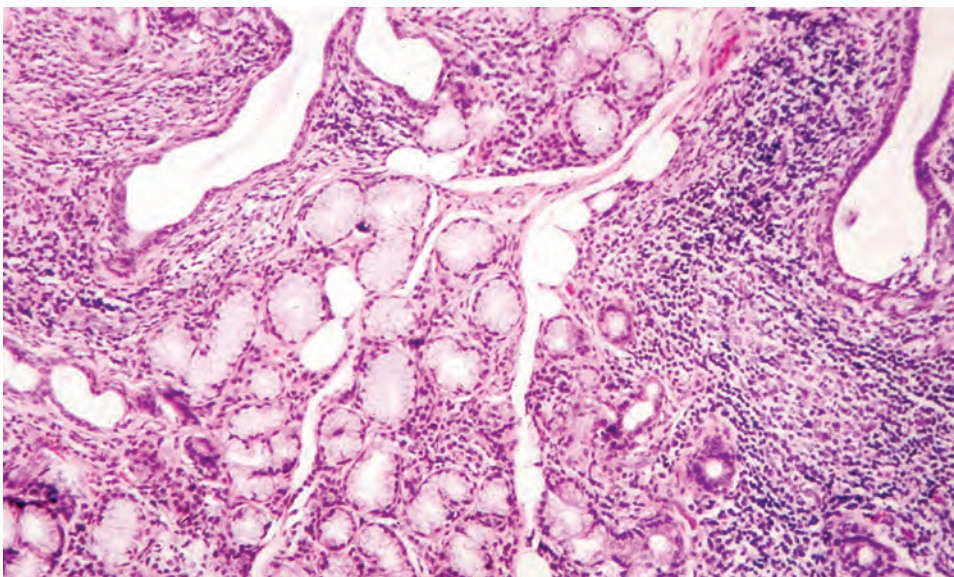


**FIGURE 11.17**

At intermediate power, the proliferative ductal epithelium is evident. The epimyoepithelial islands show infiltration by the lymphocytic infiltrate.

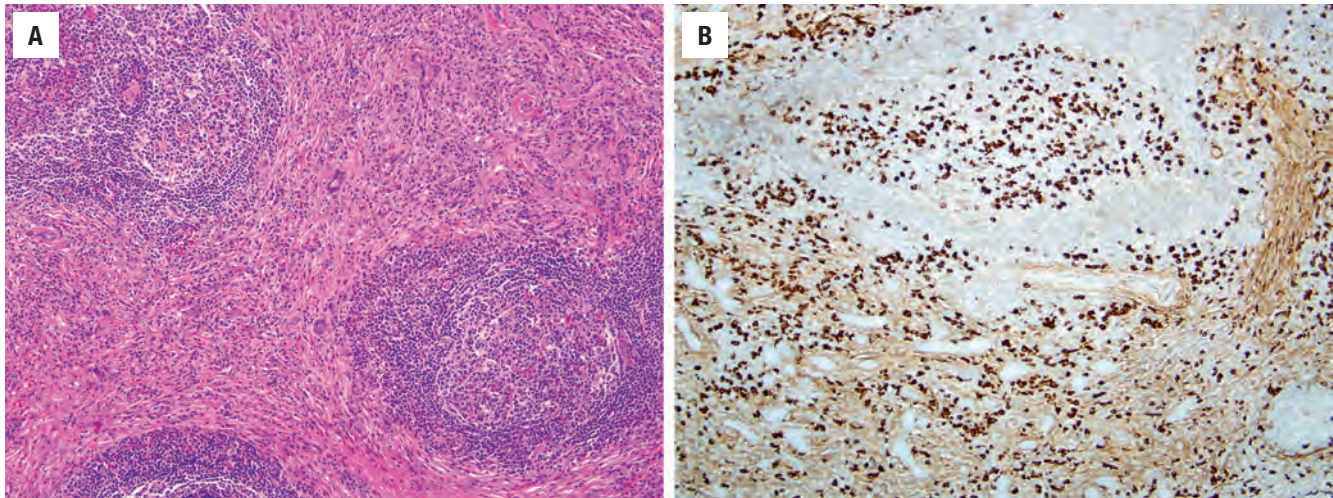
**FIGURE 11.18**

A well-developed example of lymphoepithelial sialadenitis shows an epimyoepithelial cell proliferation. There are many infiltrating lymphocytes.

**FIGURE 11.19**

Focal lymphocytic sialadenitis is adjacent to normal-appearing acini. Germinal center formation in the lymphocytic infiltrate is noted. This biopsy specimen is from a patient with Sjögren syndrome.



**FIGURE 11.20**

(A) IgG<sup>4</sup>-related sialadenitis demonstrates chronic inflammation with lymphoid follicles in addition to cellular fibrosis in a storiform pattern. (B) IgG<sup>4</sup> immunostain highlights numerous positive plasma cells.

periglandular tissue, lack of infiltrated epithelial islands, and lack of the atypical nuclear findings of malignant lymphocytes. Metastatic carcinoma can be excluded by the benign appearance of the cells within the myoepithelial islands. The distinction between chronic sialadenitis and sarcoidosis is often not quite as clear. Chronic sialadenitis is composed of a mixed chronic inflammatory infiltrate containing plasma cells and neutrophils with prominent fibrosis. If the infiltrate has a prominent plasma cell component, tumefactive fibrosis and obliterative phlebitis, then *IgG<sup>4</sup>-related sialadenitis* should enter the differential diagnosis (Fig. 11.20). Sarcoidosis is characterized by noncaseating granulomas.

### PROGNOSIS AND THERAPY

Lymphomas arising in LESA are most frequently characterized as low-grade B-cell lymphomas similar to lymphomas of other MALT. Any salivary gland undergoing biopsy for Sjögren syndrome or for a persistent mass should have material submitted for flow cytometry analysis, immunohistochemical techniques, and gene arrangements to exclude the possibility of lymphoma. Lymphoepithelial carcinomas, although rare, may arise in a setting of LESA. These lesions have only been reported in major salivary glands, usually the parotid gland, and women seem to be affected more often than men. However, there are two subgroups who are particularly affected: Inuits (Eskimos) and Chinese. These carcinomas may present with regional lymph node metastasis. Within Inuits this lesion has more commonly been reported in parotid, whereas within the Chinese, it is more common in the submandibular gland with less frequent regional lymph node disease.

## ■ LYMPHOEPITHELIAL CYST

### CLINICAL FEATURES

The benign cystic salivary gland lesions known as lymphoepithelial cysts occur most commonly in the parotid glands and oral cavity. The name reflects the two histologic components that constitute the lesions: lymphoid tissue and epithelium-lined cysts. The male-to-female ratio is 3:1, with a peak incidence in the 4th decade. These lesions are seen in a small minority of HIV-positive individuals, among whom it is more common in children. Although they may be present at birth, they may not become clinically obvious until later in adult life (Fig. 11.21). They frequently present as a unilateral painful swelling. However, pain may occur due to secondary infection or nerve compression.

### PATHOLOGIC FEATURES

#### GROSS FINDINGS

On gross examination, the cysts measure 0.1 to 8 cm. The cyst contents are usually a straw-colored serous fluid.

#### MICROSCOPIC FINDINGS

Microscopically, the cyst lining is composed of squamous, columnar, or cuboidal epithelium (Fig. 11.22). Occasionally, there may be goblet cells or oncocytic metaplasia identified within the cyst lining. The cyst wall is composed of lymphoid tissue that will contain germinal centers. Depending on the location of the cyst,



**LYMPHOEPITHELIAL CYST—DISEASE FACT SHEET****Definition**

- A cyst lined by epithelium that is surrounded by a dense lymphoid infiltrate

**Incidence and Location**

- Uncommon lesion
- Parotid gland most commonly affected

**Morbidity and Mortality**

- There may be facial nerve dysfunction with compression when involving the parotid gland

**Sex and Age Distribution**

- Males > females (3:1)
- Peak incidence in 4th decade
- HIV-associated lymphoepithelial cysts are more common in children

**Clinical Features**

- Lesions are usually asymptomatic with occasional associated pain or tenderness and rarely facial nerve dysfunction
- Unilateral or bilateral (HIV-related) parotid enlargement
- Small nodules may be located in minor salivary glands (floor of mouth, lateral tongue) or tonsillar tissues

**Prognosis and Therapy**

- Usually treated by surgical excision and is not known to recur

**LYMPHOEPITHELIAL CYST—PATHOLOGIC FEATURES****Gross Findings**

- Well-demarcated nodule or mass that varies in size by location from 0.1 cm (intraoral sites) to 8 cm (parotid)

**Microscopic Findings**

- Epithelium-lined cysts composed of stratified squamous, cuboidal, columnar, or pseudostratified-ciliated type
- Lymphoid tissue within the cyst wall, which may show follicular hyperplasia
- The lumen may be filled with desquamated cells
- In HIV-associated cysts, associated proliferating epimyoeplithelial islands may be seen

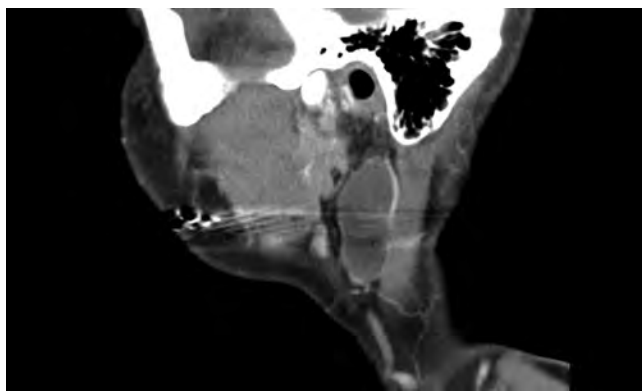
**Fine Needle Aspiration**

- Composed of lymphocytes and desquamated squamous cells

**Pathologic Differential Diagnosis**

- Warthin tumor, cystic metastatic squamous carcinoma, metastatic nasopharyngeal carcinoma

findings on aspiration are fairly nonspecific. There can be a predominance of lymphoid cells with interspersed squamous cells. The differential diagnosis of an aspirate from these lesions may include cystadenoma and Warthin tumor.

**FIGURE 11.21**

A sagittal computed tomography scan showing a large cyst within the parotid gland. This was part of a bilateral presentation in this HIV-positive patient.

it may be within an intraparotid lymph node or cervical lymph node.

**ANCILLARY STUDIES**

Due to the accessibility of lymphoepithelial cysts, they frequently undergo fine needle aspiration. However,

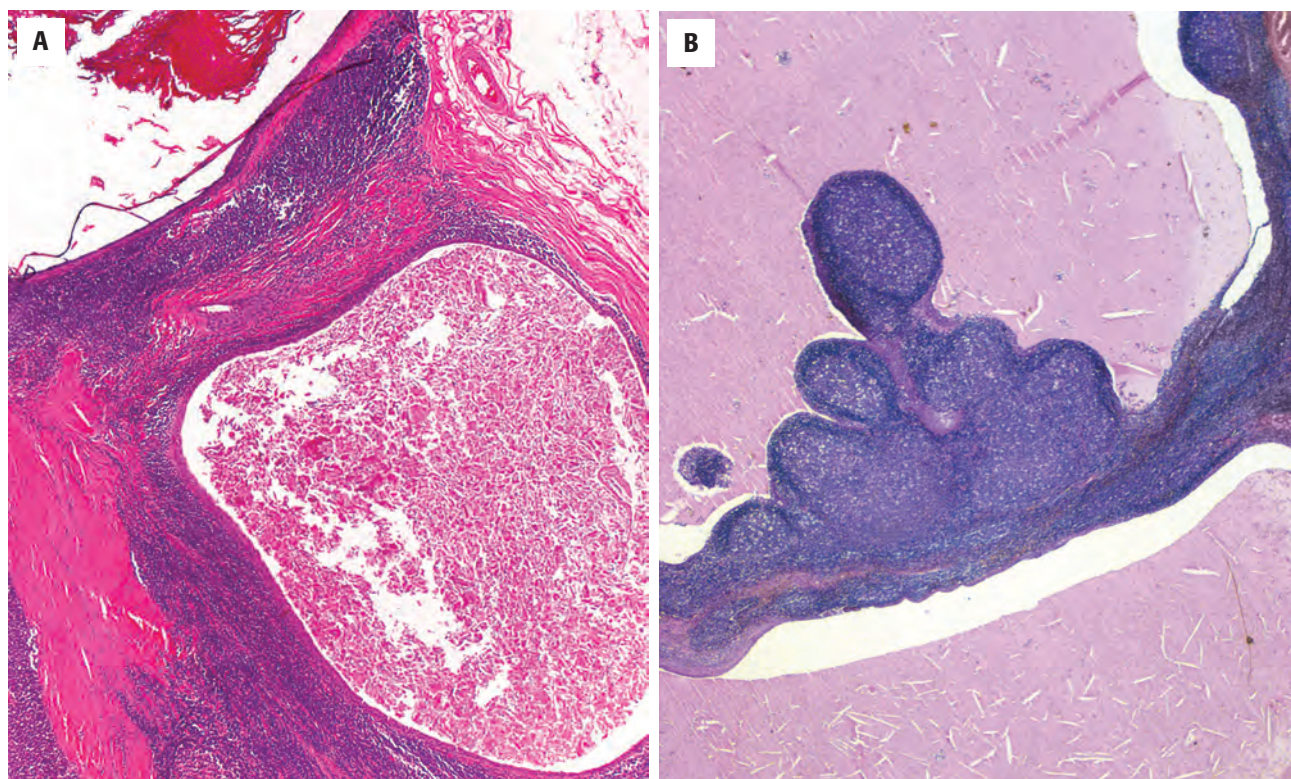
**DIFFERENTIAL DIAGNOSIS**

These cysts are frequently misdiagnosed as neoplasms. They may be mistaken histologically for cystic low-grade mucoepidermoid carcinomas or metastatic cystic squamous cell carcinoma. However, the lining of the lymphoepithelial cyst is a benign squamous lining with no pleomorphism (Fig. 11.23). The lining epithelium will be immunoreactive with keratin but negative for p16. p16 may show focal reactivity in areas where inflammatory cells are within the epithelium. In addition, lymphoepithelial cysts generally lack mucin cells with microcystic and macrocystic structures, contain no papillary projections, and have no intermediate cells.

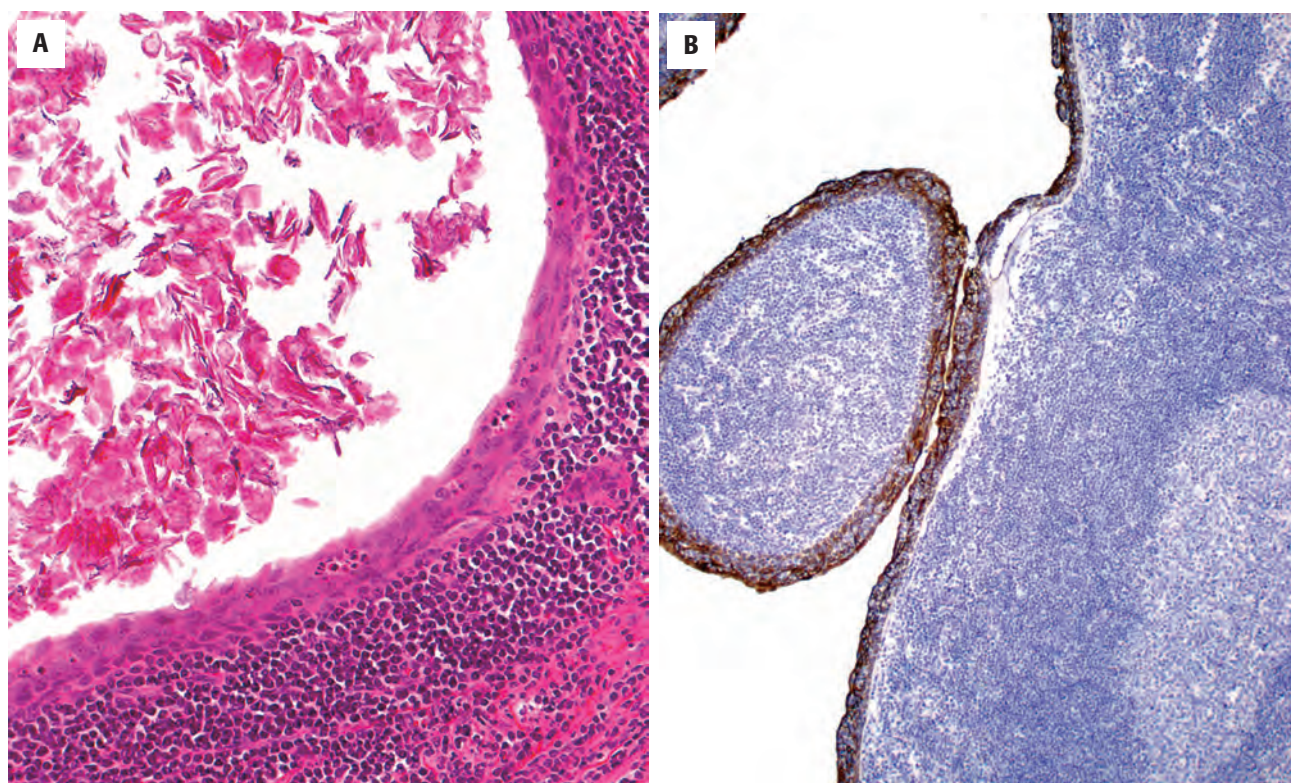
**PROGNOSIS AND THERAPY**

Surgical excision is curative. If a fistulous tract is present, then it is necessary to remove the sinus tract or fistula to prevent recurrence. There are alternative treatments to surgery for HIV-positive patients. Frequently, the only purpose for removing the cyst is for cosmetic reasons.



**FIGURE 11.22**

(A and B) Two lymphoepithelial cysts. The dilated squamous-lined cysts are surrounded by a lymphocytic infiltrate within the parotid. Fine-needle aspirate findings of squamous cells and lymphocytes are easily explained by the above tissue architecture.

**FIGURE 11.23**

(A) High power shows the attenuated benign squamous lining of a lymphoepithelial cyst. (B) Although not required, the epithelium will be positive with keratin immunohistochemistry.



## ■ SCLEROSING POLYCYSTIC ADENOSIS

Sclerosing polycystic adenosis (SPA) is a peculiar proliferation first described in 1996 that resembles proliferative fibrocystic changes of the breast. SPA is presumed to be non-neoplastic; however, it frequently gives rise to intraductal neoplasia. Interestingly, a single study using polymorphism of the human androgen receptor suggested that some cases are monoclonal, indicating that SPA could actually be neoplastic.

### CLINICAL FEATURES

SPA usually involves the parotid gland, where it manifests as a painless, slow-growing mass. SPA is rare, with only ~ 60 cases reported. There appears to be a slight female predominance (3:1), and virtually any ages can be affected (7 to 84 years), with a peak in the 5th decade.

### PATHOLOGIC FEATURES

#### GROSS FINDINGS

On gross examination, SPA is a firm and well-circumscribed mass. On cut section, multiple cystic spaces are often seen.

### SCLEROSING POLYCYSTIC ADENOSIS—DISEASE FACT SHEET

#### Definition

- A rare, benign epithelial salivary gland proliferation that resembles proliferative fibrocystic changes of the breast

#### Incidence and Location

- Rare lesion
- Parotid gland in >70%. Less commonly submandibular gland, oral cavity, and nasal cavity

#### Morbidity and Mortality

- Benign tumor with a low risk of recurrence
- Even cases with intraductal carcinoma within them behave in a benign manner

#### Sex and Age Distribution

- Females > males
- 7-84 years, mean 40 years

#### Clinical Features

- Painless, slow-growing mass

#### Prognosis and Therapy

- Surgical excision only
- Excellent prognosis

### MICROSCOPIC FINDINGS

Microscopically, SPA consists of a well-circumscribed mass composed of irregular lobules of ducts, acini, and myoepithelial cells separated by bands of fibrosis (Figs. 11.24 and 11.25). The ducts exhibit varying degrees of dilatation with intraluminal secretory material, and also frequently exhibit apocrine metaplasia. This appearance resembles, to some degree, fibrocystic changes and sclerosing adenosis of the breast. SPA frequently exhibits varying degrees of intraluminal ductal proliferation with some examples reminiscent of atypical ductal hyperplasia of the breast and others with marked atypia and necrosis similar to high-grade ductal carcinoma in situ. However, there is only one report of an invasive carcinoma arising in this setting.

### ANCILLARY STUDIES

Very few studies have published the fine needle aspiration findings of SPA. They have described syncytial tissue fragments of apocrine ductal cells associated with foamy histiocytes and secretory cystic material. Immunostains for myoepithelial cells (e.g., S100, p40, calponin) will demonstrate that any intraductal proliferation is confined by an intact myoepithelial cell layer.

### DIFFERENTIAL DIAGNOSIS

The differential diagnosis of SPA is broad, ranging from other non-neoplastic conditions to malignant neoplasms. The dilated ducts and fibrosis may raise the possibility

### SCLEROSING POLYCYSTIC ADENOSIS—PATHOLOGIC FEATURES

#### Gross Findings

- Firm, well-delineated mass

#### Microscopic Findings

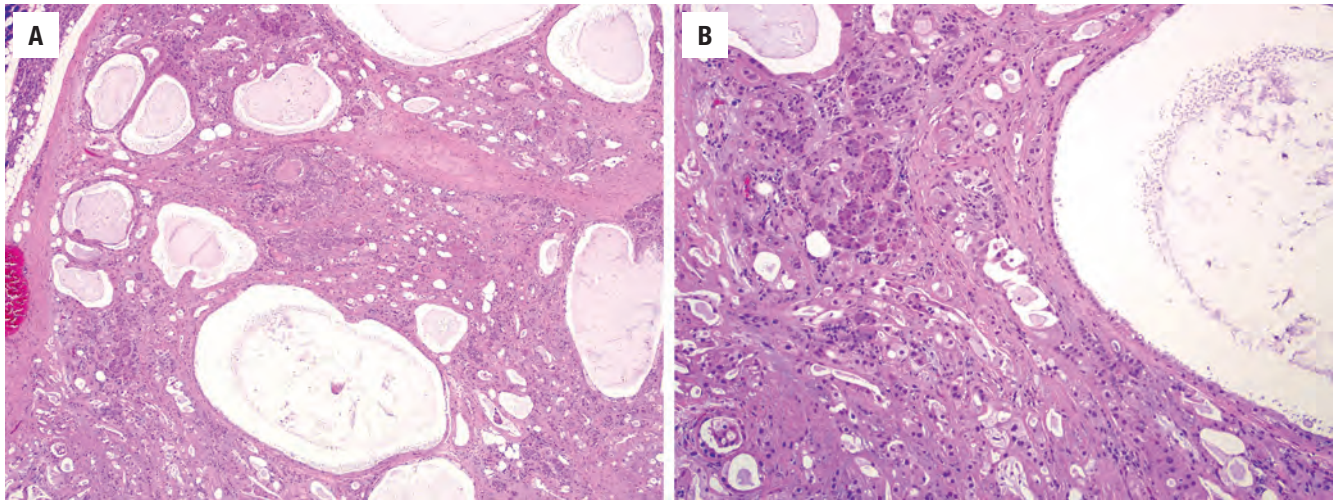
- Well-circumscribed proliferation of irregular lobules separated by fibrosis
- Lobules contain variably cystic ducts with frequent apocrine changes, admixed with acini and myoepithelial cells

#### Fine Needle Aspiration

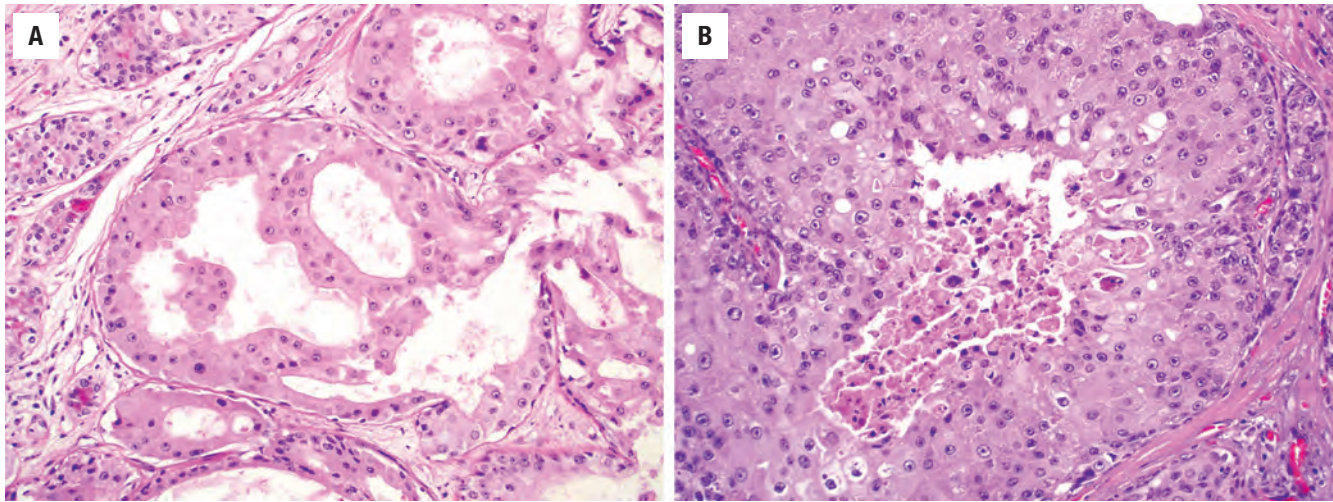
- Foamy histiocytes, apocrine ductal cells

#### Pathologic Differential Diagnosis

- Acinic cell carcinoma, sialadenitis/sialofibrosis, benign mixed tumor, salivary duct carcinoma

**FIGURE 11.24**

(A) Sclerosing polycystic adenosis consists of a well-circumscribed nodule of epithelial elements with varying degrees of fibrosis. (B) The lesion is composed of a mixture of acini, myoepithelial cells, and ducts that are often cystic.

**FIGURE 11.25**

(A) Sclerosing polycystic adenosis commonly shows areas of apocrine ductal proliferation. In this case the ductal lesion resembles atypical ductal hyperplasia of the breast with rigid "Roman bridges" of cells. (B) This case has an intraductal carcinoma component, with solid nests of malignant apocrine cells with necrosis.

of duct dilatation with sialofibrosis, possibly the result of sialoliths. However, SPA is much more proliferative than what is encountered in the setting of simple obstructive changes. Pleomorphic adenoma may be considered as the most common benign tumor of the salivary glands, but SPA lacks the chondromyxoid stroma of this neoplasm. The presence of acinic cells within the tumor may cause confusion for acinic cell carcinoma. Recognizing the admixture of other salivary elements along with the acinic cells, along with the lobular nature of SPA, will differentiate the two. Finally, intraductal carcinomas within SPA can appear identical to an intraductal, noninvasive salivary duct carcinoma. In this case recognizing the background changes of SPA in addition to the intraductal carcinoma is key.

### PROGNOSIS AND THERAPY

SPA is treated with surgery alone. SPA recurs in 11% of cases but does not metastasize, even in cases with intraductal dysplasia or carcinoma.

### ■ INTERCALATED DUCT HYPERPLASIA

Intercalated duct hyperplasia (IDH) is a benign proliferation of intercalated ducts and myoepithelial cells that may represent a precursor lesion to salivary gland neoplasms.



**CLINICAL FEATURES**

IDH is rare, with fewer than 100 reported cases. There is a male-to-female ratio of 3:2. A wide age range is affected, with a peak in the 6th decade. Most (~85%) have been identified in the parotid gland, with rare cases of the submandibular gland and oral cavity. Most cases of IDH are found incidentally.

**INTERCALATED DUCT HYPERPLASIA—DISEASE FACT SHEET****Definition**

- A benign, non-neoplastic proliferation of ducts and myoepithelial cells that could represent a neoplastic precursor

**Incidence and Location**

- Rare lesion
- Parotid gland most often (85%), rarely oral cavity or submandibular gland

**Morbidity and Mortality**

- Benign lesion

**Sex and Age Distribution**

- Males > females (3:2)
- Wide age range, mean 52 years

**Clinical Features**

- Incidentally found next to other tumors (e.g., basal cell adenoma)

**Prognosis and Therapy**

- Benign, non-neoplastic lesion with excellent prognosis

**PATHOLOGIC FEATURES****GROSS FINDINGS**

Often not evident grossly. If identified, they consist of well-circumscribed, tan nodules.

**MICROSCOPIC FINDINGS**

Microscopically, IDH consists of a nodule of proliferating ducts. The intercalated ductal cells are surrounded by a layer of attenuated myoepithelial cells (Fig. 11.26). All cellular components are cytologically bland. Although

**INTERCALATED DUCT HYPERPLASIA—PATHOLOGIC FEATURES****Gross Findings**

- Usually not seen grossly. When it is, it consists of a well-circumscribed tan nodule

**Microscopic Findings**

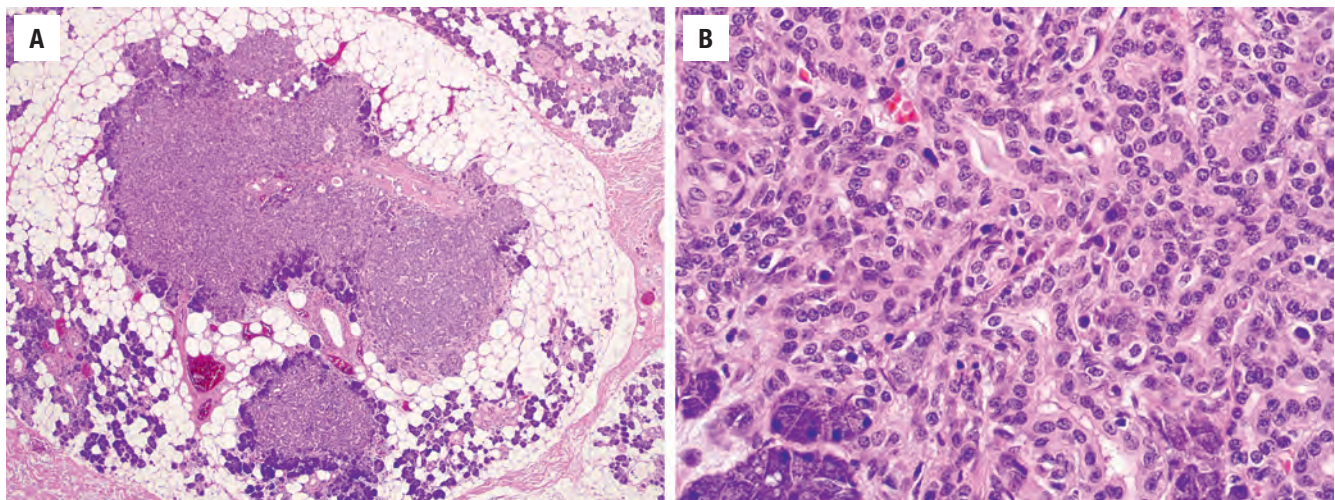
- Nodule of bland ducts and myoepithelial cells, often with an irregular edge
- Often seen adjacent to another salivary gland neoplasm like basal cell adenoma

**Fine Needle Aspiration**

- Not well described

**Pathologic Differential Diagnosis**

- Basal cell adenoma, striated duct adenoma

**FIGURE 11.26**

(A) Intercalated duct hyperplasia consists of an unencapsulated nodule, often adjacent to a salivary gland neoplasm (not depicted here). (B) Lesion is made up of intercalated ducts and surrounding myoepithelial cells. There is no cellular atypia.

well circumscribed at low power, unlike an adenoma, IDH lacks a capsule and typically has an irregular border, with lesional ducts intermingling with normal acini or fat. IDH is most often found incidentally next to a salivary gland neoplasm, usually basal cell adenoma or epithelial-myoepithelial carcinoma. Given its frequent proximity to neoplasms and histologic similarities, it has been suggested that IDH represents a non-neoplastic precursor lesion.

#### ANCILLARY STUDIES

IDH is usually diffusely positive for S100 protein. The myoepithelial cell component is positive for S100 protein, actin, p63, and other myoepithelial markers. Fine needle aspiration findings are not well described.

#### DIFFERENTIAL DIAGNOSIS

The differential diagnosis includes basal cell adenoma and striated duct adenoma, which are larger, have a smooth tumor edge, and are often encapsulated.

#### PROGNOSIS AND THERAPY

IDH is benign, hyperplastic, and usually found incidentally upon surgical resection. No additional therapy is needed.

#### SUGGESTED READINGS

The complete Suggested Readings list is available online at [ExpertConsult.com](http://ExpertConsult.com).



**SUGGESTED READINGS****Developmental Lesions, Including Heterotopia and Oncocytosis**

1. Azevedo LR, et al. Age-related changes in human sublingual glands: a post mortem study. *Arch Oral Biol*. 2005;50:565–574.
2. Bouquot JE, et al. Intraosseous salivary tissue: jawbone examples of choristomas, hamartomas, embryonic rests, and inflammatory entrapment. *Oral Surg Oral Med Oral Pathol Oral Radiol Endod*. 2000;90:205–217.
3. Brandwein MS, et al. Oncocytic tumors of major salivary glands. A study of 68 cases with follow-up of 44 patients. *Am J Surg Pathol*. 1991;15:514–528.
4. Chang A, et al. Oncocytes, oncocytosis, and oncocytic tumors. *Pathol Annu*. 1992;27(Pt 1):263–304.
5. Lassaletta-Atienza L, et al. Salivary gland heterotopia in the lower neck: a report of five cases. *Int J Pediatr Otorhinolaryngol*. 1998;43:153–161.
6. Loreti A, et al. Diffuse hyperplastic oncocytosis of the parotid gland. *Br J Plast Surg*. 2002;55:151–152.
7. Scott J, et al. Histological analysis of parotid and submandibular glands in chronic alcohol abuse: a necropsy study. *J Clin Pathol*. 1988;41:837–840.
8. Toh H, et al. Incidence and histology of human accessory parotid glands. *Anat Rec*. 1993;236:589–590.
9. Zajtcuk JT, et al. Cervical heterotopic salivary gland neoplasms: a diagnostic dilemma. *Otolaryngol Head Neck Surg*. 1982;90:178–181.
6. Rice DH. Noninflammatory, non-neoplastic disorders of the salivary glands. *Otolaryngol Clin North Am*. 1999;32:835–843.
7. Suresh L, et al. Subacute necrotizing sialadenitis: a clinicopathological study. *Oral Surg Oral Med Oral Pathol Oral Radiol Endod*. 2007;104:385–390.

**Lymphoepithelial Sialadenitis**

1. Bloemena E, et al. Lymphoepithelial sialadenitis. In: el-Naggar AK, Chan JKC, Grandis JR, Takata T, Slootweg PJ, eds. *WHO Classification of Head and Neck Tumours*. IARC Press; 2017:196–197.
2. Cleary KR, et al. Undifferentiated carcinoma with lymphoid stroma of the major salivary gland. *Ann Otol Rhinol Laryngol*. 1990;99:236–238.
3. DiGiuseppe JA, et al. Lymphoid infiltrates of the salivary glands: pathology, biology, and clinical significance. *Curr Opin Oncol*. 1996;8:232–237.
4. Falzon M, et al. The natural history of benign lymphoepithelial lesion of the salivary gland in which there is a monoclonal population of B cells. *Am J Surg Pathol*. 1991;15:59–65.
5. Godwin JT. Benign lymphoepithelial lesion of the parotid gland (adenolymphoma, chronic inflammation, lymphoepithelioma, lymphocytic tumor, Mikulicz disease): report of eleven cases. *Cancer*. 1952;5:1089–1093.
6. Saw D, et al. Malignant lymphoepithelial lesion of the salivary gland. *Hum Pathol*. 1986;17:914–923.
7. Wallace AC, et al. Salivary gland tumors in Canadian Eskimos. *Cancer*. 1963;16:1338–1353.

**Mucus Retention Cyst, Mucocele, and Sialolithiasis**

1. Arduino PG, et al. Non-neoplastic salivary gland diseases. *Minerva Stomatol*. 2006;55:249–270.
2. Ben Lagha N, et al. Lithiasis of minor salivary glands: current data. *Oral Surg Oral Med Oral Pathol Oral Radiol Endod*. 2005;100:345–348.
3. Chi A, et al. Oral mucoceles: a clinicopathologic review of 1,824 cases, including unusual variants. *J Oral Maxillofac Surg*. 2011;69:1086–1093.
4. Deshpande V. IgG4 related disease of the head and neck. *Head Neck Pathol*. 2015;9:24–31.
5. Eveson JW. Superficial mucoceles: pitfall in clinical and microscopic diagnosis. *Oral Surg Oral Med Oral Pathol*. 1988;66:318–322.
6. Gnepp DR, et al. Salivary and lacrimal glands. In: Gnepp DR, ed. *Diagnostic Surgical Pathology of the Head and Neck*. Philadelphia: WB Saunders; 2001:332–334.
7. Guerre A, et al. Extracorporeal shockwave lithotripsy (ESWL) for salivary gland stones: a retrospective study of 1571 patients. *Rev Stomatol Chir Maxillofac*. 2011;112:75–79, [in French].
8. Harrison JD. Causes, natural history, and incidence of salivary stones and obstructions. *Otolaryngol Clin North Am*. 2009;42:927–947.
9. Hayashida AM, et al. Mucus extravasation and retention phenomena: a 24-year study. *BMC Oral Health*. 2010;10:15.
10. Layfield LJ, et al. Cystic lesions of the salivary glands: cytologic features in fine-needle aspiration biopsies. *Diagn Cytopathol*. 2002;27:197–204.
11. Peel RL. Diseases of the salivary glands. In: Barnes L, ed. *Surgical Pathology of the Head and Neck*. 2nd ed. New York: Marcel Dekker; 2001:642–644.
12. Raymond AK, et al. Angiothiasis and sialolithiasis in the head and neck. *Ann Otol Rhinol Laryngol*. 1992;101:455–457.

**Lymphoepithelial Cyst**

1. Cleary KR, et al. Lymphoepithelial cysts of the parotid region: a “new face” on an old lesion. *Ann Otol Rhinol Laryngol*. 1990;99:162–164.
2. d’Agay MF, et al. Cystic benign lymphoepithelial lesion of the salivary glands in HIV-positive patients. *Virchows Arch A Pathol Anat*. 1990;417:353–356.
3. Huang RD, et al. Benign cystic vs. solid lesions of the parotid gland in HIV patients. *Head Neck*. 1991;13:522–527.
4. Layfield LJ, et al. Cystic lesions of the salivary glands: cytologic features in fine needle aspiration biopsies. *Diagn Cytopathol*. 2002;27:197–204.
5. Mandel L, et al. HIV-associated parotid lymphoepithelial cysts. *J Am Dent Assoc*. 1999;130:528–532.

**Sclerosing Polycystic Adenosis**

1. Canas Marques R, et al. Invasive carcinoma arising from sclerosing polycystic adenosis of the salivary gland. *Virchows Arch*. 2014;464(5):621–625.
2. Etit D, et al. Fine-needle aspiration biopsy findings in sclerosing polycystic adenosis of the parotid gland. *Diagn Cytopathol*. 2007;35:444–447.
3. Gnepp DR, et al. Sclerosing polycystic adenosis of the salivary gland. *Am J Surg Pathol*. 2006;30:154–164.
4. Petersson F. Sclerosing polycystic adenosis of salivary glands: a review with some emphasis on intraductal epithelial proliferations. *Head Neck Pathol*. 2013;7(suppl 1):S97–S106.
5. Seethala RR, et al. Sclerosing polycystic adenosis. In: el-Naggar AK, Chan JKC, Grandis JR, Takata T, Slootweg PJ, eds. *WHO Classification of Head and Neck Tumours*. IARC Press; 2017:195.
6. Smith BC, et al. Sclerosing polycystic adenosis of major salivary glands: a clinicopathologic analysis of nine cases. *Am J Surg Pathol*. 1996;20:161–170.
7. Skalova A, et al. Sclerosing polycystic adenosis of parotid gland with dysplasia and ductal carcinoma in situ. Report of three cases with immunohistochemical and ultrastructural examination. *Virchows Arch*. 2002;440:29–35.
8. Skálová A, et al. Clonal nature of sclerosing polycystic adenosis of salivary glands demonstrated by using the polymorphism of the human androgen receptor (HUMARA) locus as a marker. *Am J Surg Pathol*. 2006;30:939–944.

**Necrotizing Sialometaplasia**

1. Abrams AM, et al. Necrotizing sialometaplasia. A disease of simulating malignancy. *Cancer*. 1973;32:130–135.
2. Brannon RB, et al. Necrotizing sialometaplasia. *Oral Surg Oral Med Oral Pathol*. 1991;72:317–325.
3. Carlson DL. Necrotizing sialometaplasia: a practical approach to the diagnosis. *Arch Pathol Lab Med*. 2009;133:692–698.
4. Flint SR. Necrotizing sialometaplasia: an important diagnosis—review of the literature and spectrum of clinical presentation. *J Ir Dent Assoc*. 2005;51:26–28.
5. Gnepp DR, et al. Salivary and lacrimal glands. In: Gnepp DR, ed. *Diagnostic Surgical Pathology of the Head and Neck*. Philadelphia: WB Saunders; 2001:336–349.

**Intercalated Duct Hyperplasia**

1. Chetty R. Intercalated duct hyperplasia: possible relationship to epithelial-myoepithelial carcinoma and hybrid tumours of salivary gland. *Histopathology*. 2000;37(3):260–263.
2. Chiosea S, et al. Intercalated duct hyperplasia. In: el-Naggar AK, Chan JKC, Grandis JR, Takata T, Slootweg PJ, eds. *WHO Classification of Head and Neck Tumours*. IARC Press; 2017:197.
3. Di Palma S. Epithelial-myoepithelial carcinoma with co-existing multifocal intercalated duct hyperplasia of the parotid gland. *Histopathology*. 1994;25(5):494–496.
4. Montalli VA, et al. Tubular variant of basal cell adenoma shares immunophenotypical features with normal intercalated ducts and is closely related to intercalated duct lesions of salivary gland. *Histopathology*. 2014;64(6):880–889.
5. Weinreb I, et al. Intercalated duct lesions of salivary gland: a morphologic spectrum from hyperplasia to adenoma. *Am J Surg Pathol*. 2009;33(9):1322–1329.



# Benign Neoplasms of the Salivary Glands

■ **Mary S. Richardson**

## ■ PLEOMORPHIC ADENOMA

Pleomorphic adenoma (PA), also called benign mixed tumor or mixed tumor, is a benign salivary gland neoplasm composed of ductal epithelial and myoepithelial cell proliferations set within a mesenchymal stroma. This tumor displays remarkable histomorphologic diversity, including varying cellularity, cell morphology, matrix type, and encapsulation.

### CLINICAL FEATURES

PA is the most common neoplasm within the salivary glands, accounting for 54 % to 76 % of all neoplasia. The vast majority of PAs are diagnosed in the parotid gland, followed by the minor salivary glands (especially the palate) and the submandibular gland. In adults, females are affected more often than males, with a wide age range peaking in the 4th to 5th decades. In children and adolescents, the incidence peaks between 5 and 15 years of age, and males are affected more frequently.

Presentation usually consists of a painless, slowly growing, firm mass. Mucosal ulceration or paresthesia (due to nerve compression) is a rare finding. Nodules tend to be singular and mobile and may become very large if neglected.

### PATHOLOGIC FEATURES

#### GROSS FINDINGS

The surgical specimen of a PA is typically a well-circumscribed, smooth to slightly lobular, round to oval mass. Encapsulation is highly variable, ranging from thick to nonexistent. The cut surface is white to tan and often shiny to translucent (Fig. 12.1). Recurrent tumors are

commonly multifocal, ranging in size from about 1 mm to several centimeters.

#### MICROSCOPIC FINDINGS

The histologic range of appearances of PAs is enormously varied; however, all mixed tumors display epithelial ductal structures, myoepithelial cells, and a mesenchymal stroma (Fig. 12.2). Three main groups of tumors may be found: myxoid (“stroma-rich”; ~80 % stroma), cellular (“cell-rich,” “myoepithelial predominant”; ~80 % cellular), and mixed (classic), with the stroma-rich variant being more prone to recurrence.

### PLEOMORPHIC ADENOMA—DISEASE FACT SHEET

#### Definition

- A benign neoplasm composed of ductal epithelial cells and myoepithelial cells set within a mesenchymal stroma

#### Incidence and Location

- Most common salivary gland neoplasm
- Comprises approximately 60% of parotid, submandibular, and minor salivary gland tumors

#### Sex and Age Distribution

- Females > males
- Males > females, in children and adolescents (peak 5-15 years)
- Peak incidence in 4th to 5th decades

#### Clinical Features

- Asymptomatic, slowly growing mass
- May become very large if neglected

#### Prognosis and Therapy

- 20%-45% recurrence rate with enucleation
- Multinodular recurrences with potential for malignant transformation in up to 7% of patients
- Superficial or total parotidectomy, submandibular gland resection, or wide excision

### PLEOMORPHIC ADENOMA—PATHOLOGIC FEATURES

#### Gross Findings

- Well-circumscribed, round to oval, variably encapsulated mass
- White-tan, possibly shiny or translucent cut surface

#### Microscopic Findings

- Epithelial glandular/ductal structures
- Myoepithelial cells in spindle, plasmacytoid, epithelioid, stellate, or basaloid morphologies
- Mesenchymal stroma either myxoid, mucochondroid, hyalinized, osseous, and/or fatty

#### Immunohistochemical Findings

- Reactive with cytokeratin cocktail, S100 protein, SOX10, SMA, p63, p40, calponin, MSA, GFAP, and CD10

#### Pathologic Differential Diagnosis

- *Benign*: myoepithelioma, basal cell adenoma
- *Malignant*: adenoid cystic carcinoma, polymorphous adenocarcinoma

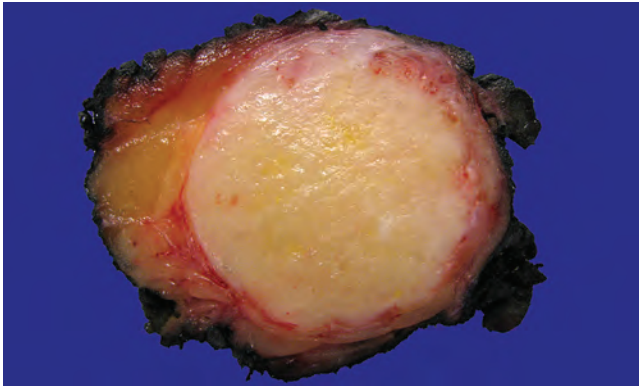


**FIGURE 12.1**

A very well circumscribed and encapsulated neoplasm within the parotid gland. Note the shiny translucent cut surface of this pleomorphic adenoma.

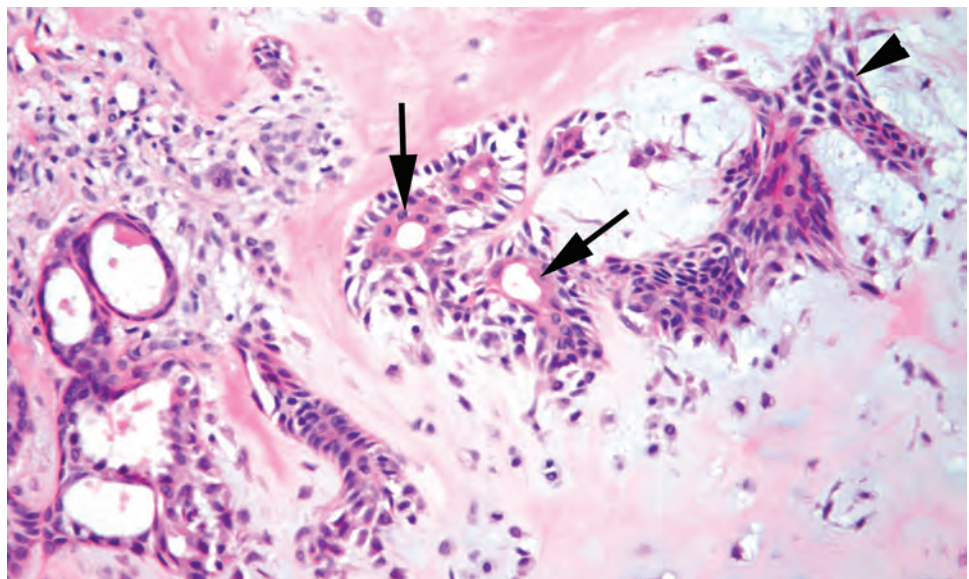
Encapsulation is inconsistent in PAs, ranging from significant and well developed to nonexistent. Lack of encapsulation is particularly evident in tumors of the minor salivary glands (especially the palate) or those that are stroma-rich, with a direct interface between the tumor and the surrounding gland or connective tissues (Fig. 12.3).

Ductal epithelial cells constitute the minority of the cell population, forming variably sized ductal or cystic structures. The remainder of the cellularity is myoepithelial, with a wide range of cytomorphology, including spindled, plasmacytoid, squamoid, stellate, and basaloid cells. Neoplastic myoepithelial cells may be abluminal, individual and scattered, or in nests, solid sheets, or trabeculae (Fig. 12.4). Oncocytic and sebaceous cells as well as adipocytes may be present to a variable degree.

Myxochondroid stromal changes are most frequent. However, the amount of collagenation is variable, with stroma appearing from loose and myxoid to dense and hyalinized (Fig. 12.4). Chondroid, osteoid, and adipose-like tissues may also occur.

Multinodular growth, although rare in primary mixed tumors, is common in recurrent disease. The nodules tend to be stroma-rich, widely scattered in the prior surgical area, and can number in excess of 100 (Fig. 12.5).

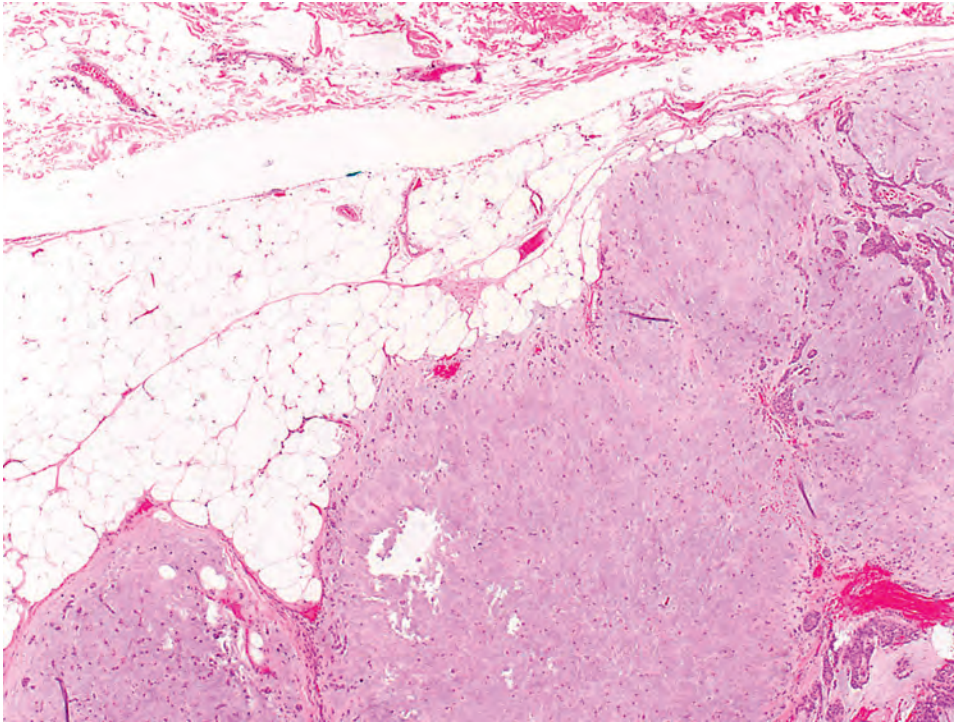
PAs that display mild-to-moderate pleomorphism, prominent nucleoli, or numerous mitotic figures may be termed *atypical*. If malignant features such as tumor necrosis, atypical mitoses, and profound nuclear pleomorphism are present but limited to the interior of the neoplasm (i.e., without capsular invasion), the diagnosis *carcinoma ex mixed tumor, noninvasive type (or in situ)* is appropriate. Other than indicating a stronger need for close clinical follow-up, these features do not appreciably alter the prognosis.



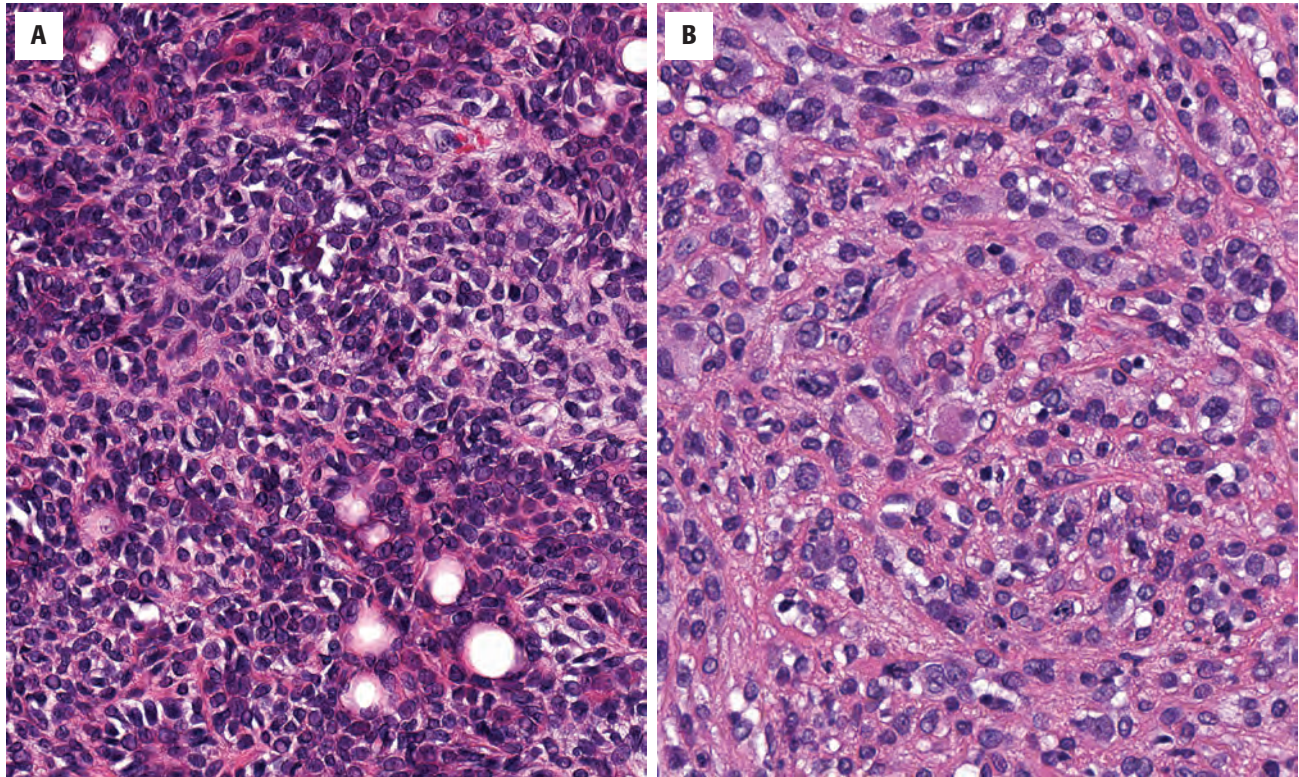
**FIGURE 12.2**

Pleomorphic adenoma with ductal structures (arrows) surrounded by abluminal myoepithelial cells, which are also present in sheets (arrowhead) and singly scattered. Hyalinized, myxoid, and chondromyxoid stroma types are evident.



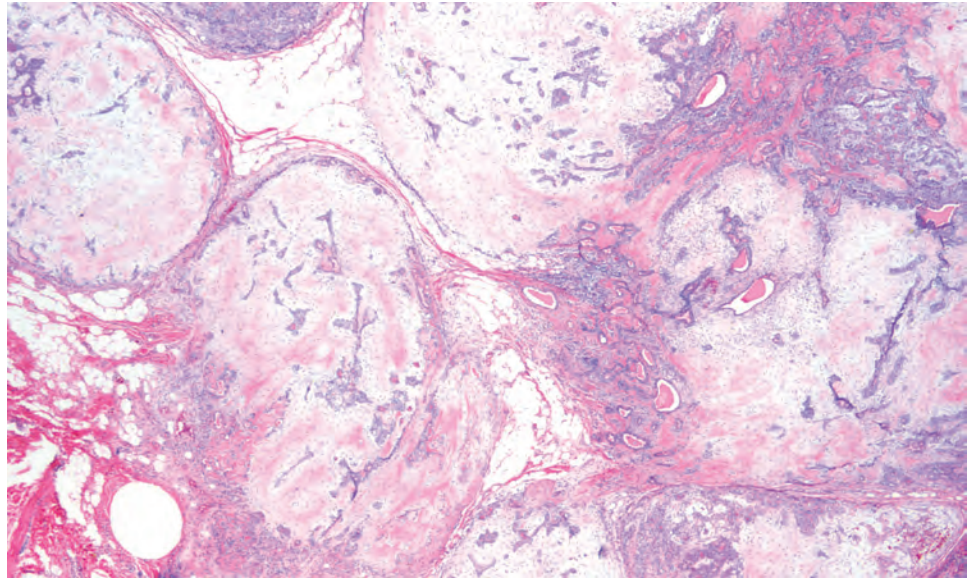
**FIGURE 12.3**

Unencapsulated, myxoid variant pleomorphic adenoma (stroma-rich) showing direct apposition with the adjacent adipose tissue. Note the small tumor extensions into the fat.

**FIGURE 12.4**

Pleomorphic adenoma may be quite cellular, with a focal small ductal lumen (**A**). Stromal hyalinization instead of a myxoid stroma may also be present (**B**), a feature that is seen more frequently in cases with malignant transformation.



**FIGURE 12.5**

Recurrent pleomorphic adenoma with numerous variably sized nodules characterizing recurrent disease.

## ANCILLARY STUDIES

### IMMUNOHISTOCHEMICAL FINDINGS

Cytokeratin cocktail is strongly reactive in ductal epithelial and squamoid myoepithelial cells and variably reactive in other myoepithelial forms. Vimentin, S100 protein, SOX10, p63, glial fibrillary acidic protein (GFAP), smooth muscle actin (SMA), calponin, smooth muscle myosin heavy chain, and CD10 decorate the myoepithelial component. CK7 highlights plasmacytoid cells. However, the staining patterns are irregular, with strongest reactivity for GFAP in the myxoid areas and SMA in the spindle cells.

### FINE NEEDLE ASPIRATION

Aspirates are variably cellular, with a biphasic appearance of luminal (ductal) epithelial cells and abluminal myoepithelial cells. The ductal cells display ample cytoplasm with round to oval nuclei and small nucleoli. Myoepithelial cells may be single or clustered and plasmacytoid, spindle-shaped, or stellate (Fig. 12.6). Mucoid to myxoid background material may also be present, taking on a bright, fibrillar, magenta quality with Wright- or Diff-Quik-stained material.

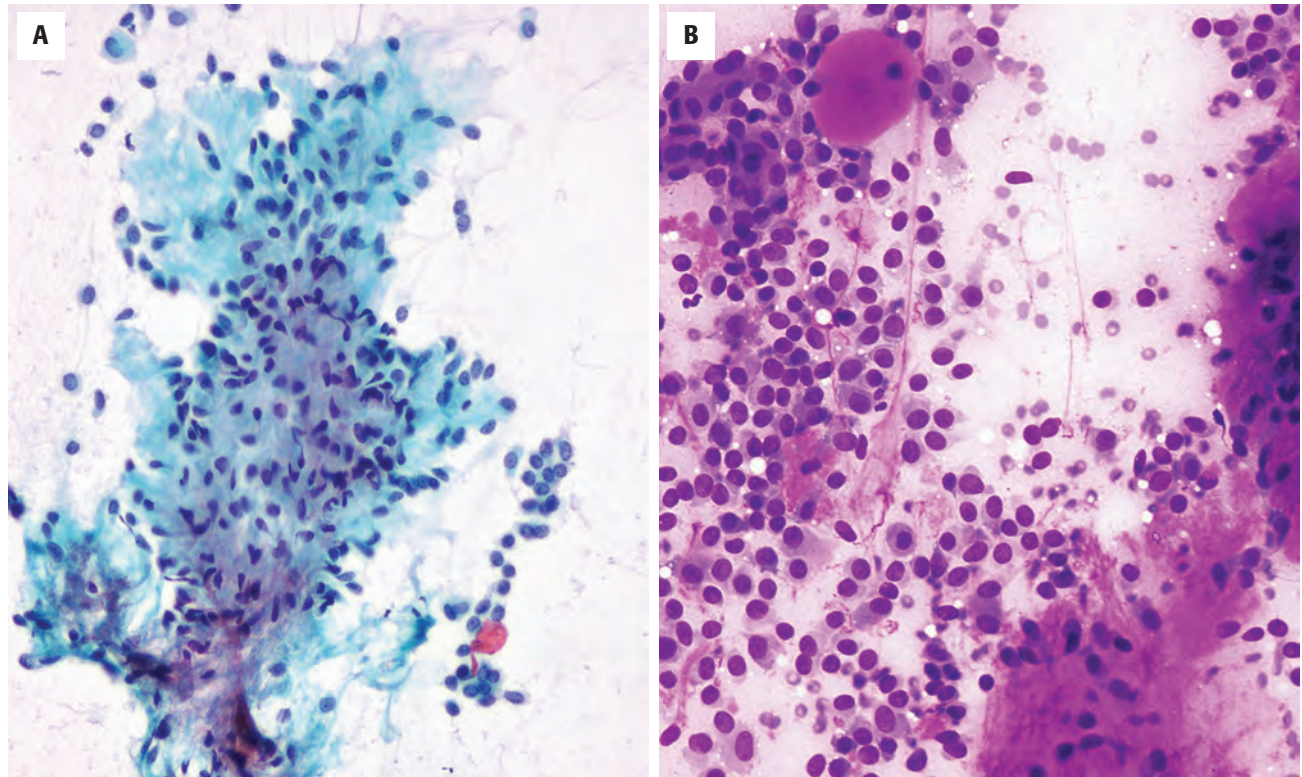
## DIFFERENTIAL DIAGNOSIS

The differential includes myoepithelioma, a benign epithelial salivary gland neoplasm composed entirely of myoepithelial cells. This neoplasm may represent one end of the spectrum of mixed tumor, in which ductal structures and myxoid matrix are absent. Plasmacytoid (Fig. 12.7) or spindled (Fig. 12.8) myoepithelial cells predominate, although any myoepithelial form may be present. Basal cell adenoma is also included in the differential. Unencapsulated tumors, especially those of the palate, may appear infiltrative, mimicking malignancies such as polymorphous adenocarcinoma or adenoid cystic carcinoma.

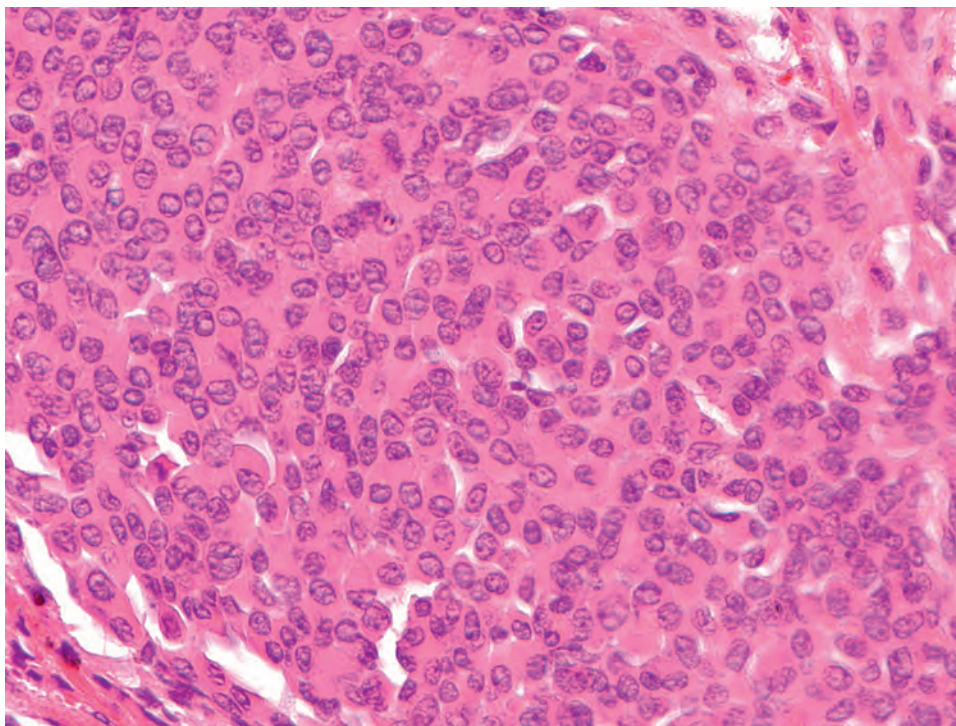
## PROGNOSIS AND THERAPY

The recurrence rate after simple tumor enucleation approaches 45%. This is because of the lack of encapsulation, which potentiates incomplete removal or tumor rupture with spillage. Therefore, superficial or total parotidectomy, resection, or excision with a rim of uninvolved tissue is the treatment of choice for parotid, submandibular, or minor salivary gland tumors, respectively.

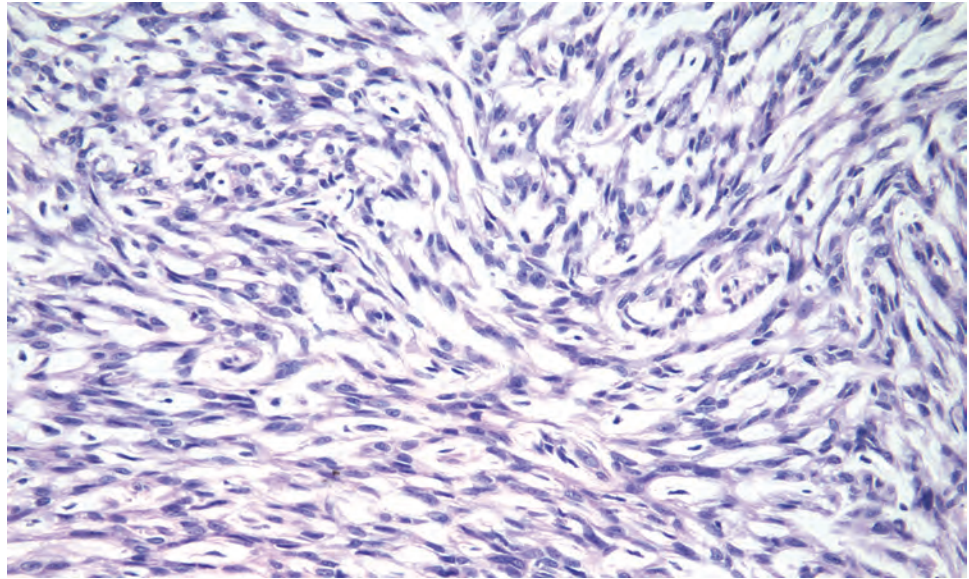


**FIGURE 12.6**

(A) Papanicolaou-stained fine needle aspiration (FNA) specimen shows small glands with a fibrillar matrix material intermixed with the epithelial component. (B) May-Grünwald-Giemsa preparation stains the mucochondroid material bright magenta in this FNA specimen. The matrix material is intimately blended with the epithelial component.

**FIGURE 12.7**

Myoepithelioma, plasmacytoid variant, lacking any well developed ductal structures and/or myxoid matrix material.

**FIGURE 12.8**

Myoepithelioma, spindle cell variant, demonstrates interlacing cords without a myxochondroid matrix.

Recurrence rate with such treatment is up to 2.5%, with most occurring in less than 10 years. Recurrent disease tends to include multiple nodules, with a resultant higher degree of surgical difficulty and risk of further recurrences. Malignant change develops in 2% to 7%. Influencing factors include multiple recurrences, age above 40 years, male sex, a nodule larger than 2 cm in diameter, and deep lobe tumors.

## ■ BASAL CELL ADENOMA

Basal cell adenoma is a benign salivary gland epithelial neoplasm composed of a proliferation of small basaloid cells in solid, tubular, trabecular, or membranous patterns. Histogenesis is most likely from intercalated ducts or the basal cells of striated ducts.

### CLINICAL FEATURES

Basal cell adenoma represents about 2% of salivary gland neoplasms, with a peak incidence in the 6th decade. The usual presentation is of an asymptomatic, solitary, slowly growing mass, with almost 75% arising within the parotid gland. Females are affected slightly more commonly than males.

The membranous pattern of basal cell adenoma, however, has a different presentation. Males are affected more frequently and the tumor has a propensity for multicentricity. In addition, the membranous type (also known as *dermal analogue tumor*) may be part of the “skin/salivary gland tumor diathesis,” a rare complex that includes concomitant skin neoplasms such as dermal cylindroma, trichoepithelioma, and eccrine spiradenoma.

### BASAL CELL ADENOMA—DISEASE FACT SHEET

#### Definition

- Benign epithelial salivary gland neoplasm composed of small basaloid cells in solid, trabecular, tubular, or membranous growth patterns

#### Incidence and Location

- Represents 2% of salivary gland neoplasms
- 75% within the parotid gland, the remainder in submandibular and minor salivary glands

#### Sex and Age Distribution

- Females > males in solid and tubulotrabeular forms
- Males > females in membranous variant
- Peak incidence in the 6th decade

#### Clinical Features

- Asymptomatic slow-growing mass
- Membranous variant is associated with multifocality and skin adnexal tumors

#### Prognosis and Therapy

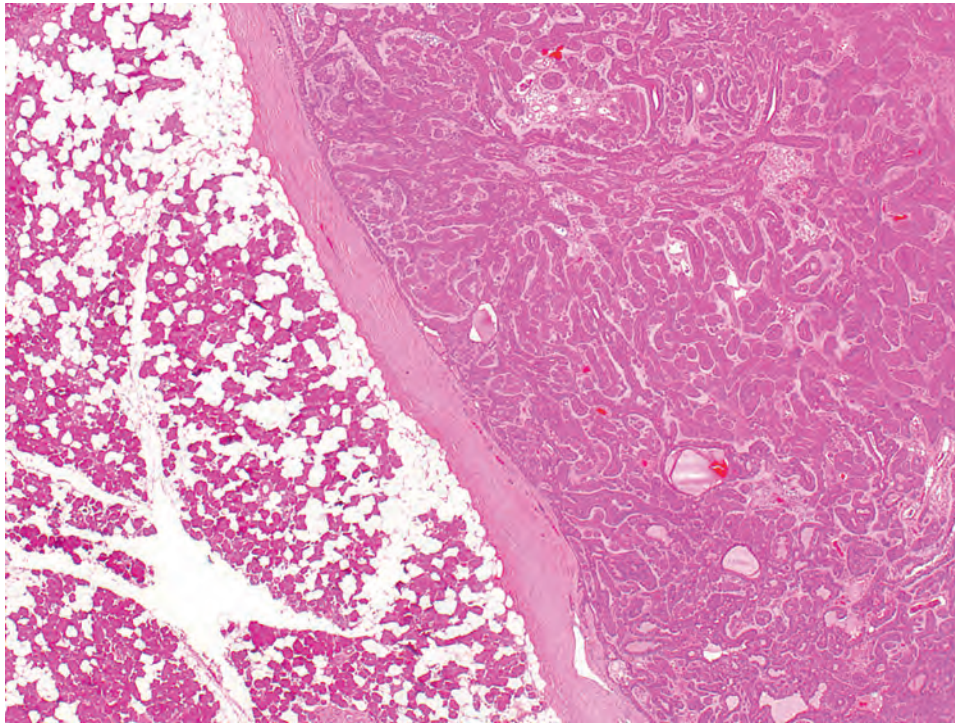
- 25% recurrence rate and small chance of malignant transformation for membranous type
- Low recurrence rate for other forms
- Surgical excision with possible parotidectomy

### PATHOLOGIC FEATURES

#### GROSS FINDINGS

Grossly, the tumor is well circumscribed, pink-brown, and smooth in texture, simulating an enlarged lymph node. It may be large but is generally less than 3 cm in diameter.



**FIGURE 12.9**

Basal cell adenoma, solid type, showing an encapsulated tumor comprised of nests of basaloid cells with peripheral palisading.

### BASAL CELL ADENOMA—PATHOLOGIC FEATURES

#### Gross Findings

- Well-circumscribed, encapsulated, pink-brown mass

#### Microscopic Findings

- Solid, trabecular, tubular, and membranous patterns
- Small basaloid cells with peripheral palisading around sheets and islands
- Focal squamous metaplasia with keratinization

#### Immunohistochemical Findings

- *Inner luminal cells:* cytokeratin cocktail, CK7, and CD117
- *Peripheral basaloid cells:* S100 protein, SOX10, p63, SMA, MSA,  $\beta$ -catenin (nuclear)

#### Pathologic Differential Diagnosis

- *Benign:* canaliculal adenoma
- *Malignant:* basal cell adenocarcinoma, adenoid cystic carcinoma

### MICROSCOPIC FINDINGS

Basal cell adenoma is a well-circumscribed, usually encapsulated epithelial tumor that classically displays two cell morphologies. Peripheral cells line the outer surface of tumor nodules, often in a palisade-like fashion. These basaloid cells are small, with scant cytoplasm and dense basophilic nuclei. Central cells form the bulk of

the nodules and solid sheets. Polygonal or angular in shape, these cells are larger with more abundant cytoplasm and pale round nuclei (Fig. 12.9). Small ductal structures or squamous metaplasia, including keratinization, may be observed.

Four basic architectural patterns are seen: solid, trabecular (Fig. 12.10), and membranous (Fig. 12.11). A solitary tumor may display all patterns, but a specific configuration generally predominates. The membranous type is characterized by a “jigsaw” puzzle pattern, with nodules surrounded and separated by a dense, periodic acid–Schiff–positive hyaline band (Fig. 12.12). The hyaline material may also form small round globules within the cellular islands. The membranous type may be multifocal or unencapsulated, with limited infiltration into the surrounding parenchyma.

### ANCILLARY STUDIES

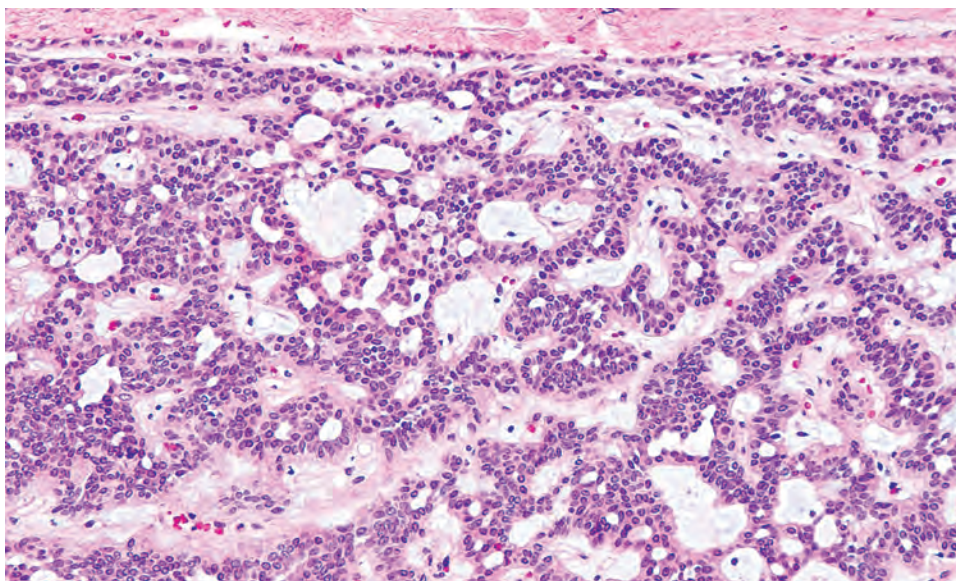
#### IMMUNOHISTOCHEMICAL FINDINGS

Cytokeratin cocktail is reactive in all tumors, albeit with variable distribution and density. S100 protein, SOX10, p63, SMA, and muscle-specific actin may display variable reactivity in the basal aspect of the peripheral epithelial cells (Fig. 12.13), while CK7 and CD117 highlight the luminal cells. Recent studies have shown that the basaloid cells of basal cell adenomas are usually positive for  $\beta$ -catenin in a nuclear distribution, related to the underlying consistent *CTNNB1* mutations.

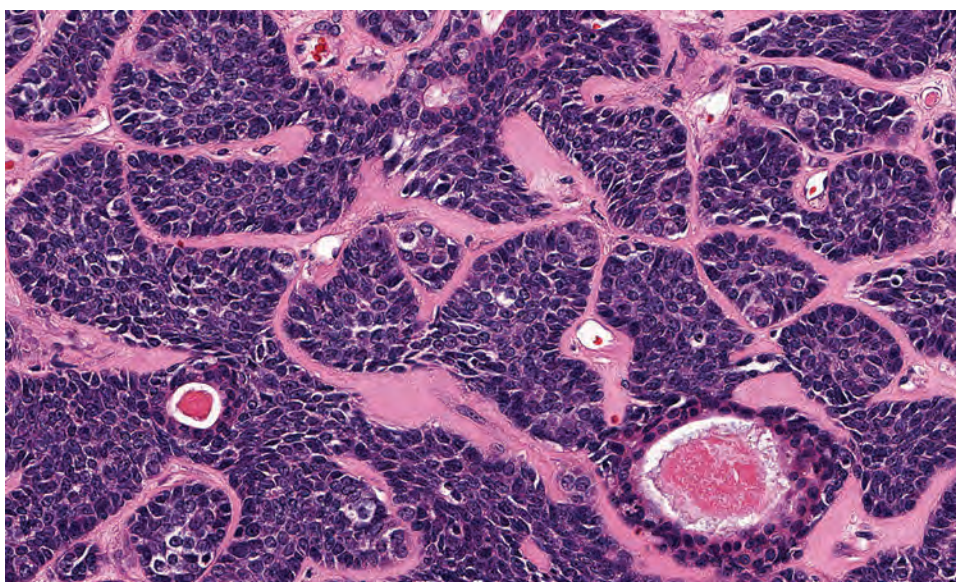


**FIGURE 12.10**

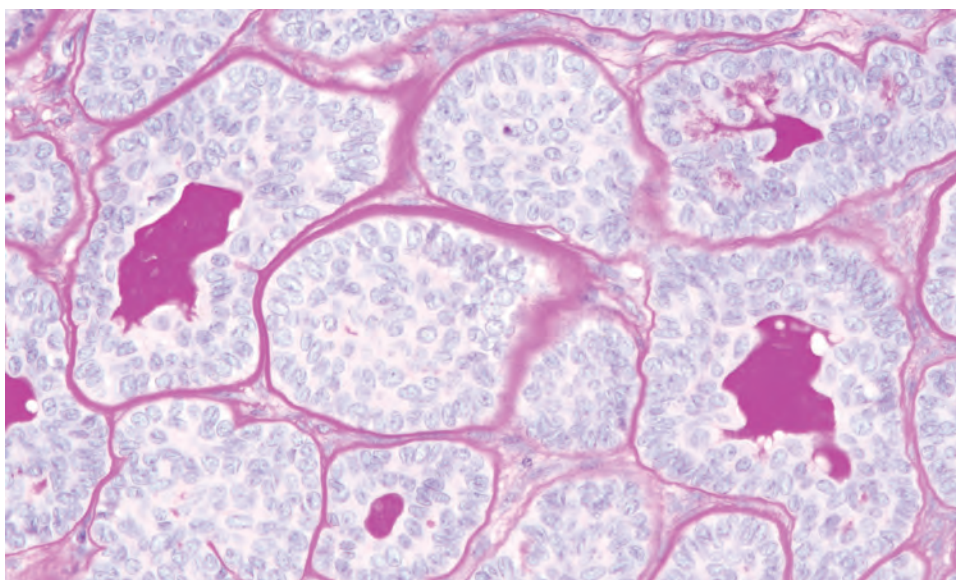
Basal cell adenoma, trabecular type, demonstrates an encapsulated neoplasm composed of variably thick chains of basaloid cells in a loose fibrous stroma.

**FIGURE 12.11**

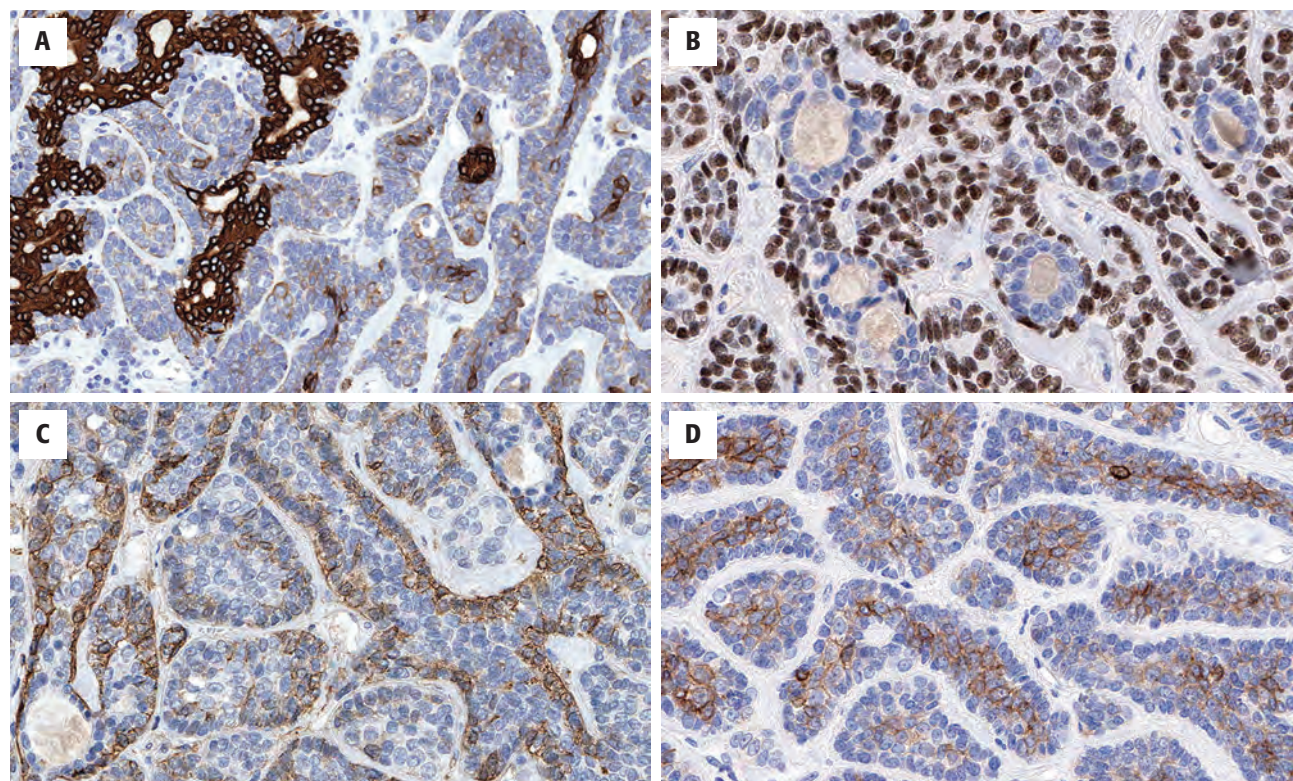
Basal cell adenoma, membranous type, showing nests of basaloid cells surrounded by a distinct hyaline band.

**FIGURE 12.12**

Basal cell adenoma, membranous type. The periodic acid–Schiff special stain accentuates the hyaline bands surrounding the basaloid cell nests.





**FIGURE 12.13**

A variety of immunohistochemistry studies can be used to highlight the biphasic appearance of the neoplastic cells. **(A)** Keratin highlights the inner luminal cells. **(B)** p63 highlights the basal cells. **(C)** Smooth muscle actin highlights the basal-myoepithelial zone. **(D)** CD117 preferentially highlights the luminal cells.

### FINE NEEDLE ASPIRATION

Aspirates consist of sheets or syncytial fragments of bland oval cells with scanty cytoplasm and round-to-oval nuclei. Nests or groups may be surrounded by a bright green (Papanicolaou) or pale magenta (Diff-Quik) hyaline band.

### DIFFERENTIAL DIAGNOSIS

The differential diagnosis may include malignancies such as basal cell adenocarcinoma or adenoid cystic carcinoma. However, features of malignancy—such as cytologic pleomorphism, tumor necrosis, significant glandular infiltration, or perineural invasion—are seen in carcinoma but not in adenoma. Benign entities such as canaliculal adenoma, PA, or myoeptelioma may also be considered, but they usually have different patterns of growth.

### PROGNOSIS AND THERAPY

Surgical excision, to possibly include parotidectomy, is the treatment of choice. Although very low for most

forms, the recurrence rate for membranous type is up to 25 %, possibly owing to capsular infiltration or multifocality. In addition, malignant degeneration or concomitant skin lesions are possible with this variant.

## CANALICULAR ADENOMA

Canaliculal adenoma is a benign epithelial salivary gland neoplasm characterized by chains of columnar cells and reported exclusive involvement of the minor salivary glands. An excretory duct origin is likely.

### CLINICAL FEATURES

Canaliculal adenoma is almost invariably associated with minor salivary glands, especially those of the upper lip, with occasional cases in the buccal mucosa or palate. Indeed, it is the second most common salivary gland neoplasm of the upper lip, just behind PA. It typically presents as an asymptomatic, firm to fluctuant, slow-growing, 1- to 2-cm submucosal nodule in the 7th decade of life. Although normally solitary, multifocal tumors may occur. Females are more commonly affected, as are blacks.



## PATHOLOGIC FEATURES

### GROSS FINDINGS

Canalicular adenomas are well circumscribed yet unencapsulated. The cut surface is pinkish-brown to tan, with a solid or cystic consistency.

### CANALICULAR ADENOMA—DISEASE FACT SHEET

#### Definition

- Benign epithelial salivary gland neoplasm characterized by chains of columnar cells and a loose connective tissue stroma

#### Incidence and Location

- 1% of all salivary gland neoplasms; 4% of all minor salivary gland neoplasms
- Minor salivary glands: especially of the upper lip

#### Sex, Race, and Age Distribution

- Females > males
- Black > white
- Peak incidence in the 7th decade

#### Clinical Features

- Asymptomatic, potentially multinodular mass

#### Prognosis and Therapy

- Recurrence rare
- Simple excision with clear margins

### MICROSCOPIC FINDINGS

Canalicular adenoma is commonly composed of long, single-layered strands or tubules of cuboidal to short columnar epithelial cells within a loose, lightly collagenized stroma (Fig. 12.14). The strands may run parallel to one another with a thin “canal-like” space in between and then attach to one another and separate again, creating a “beaded” appearance (Fig. 12.15). Cystic degeneration is common. The tumor may be multifocal, with

### CANALICULAR ADENOMA—PATHOLOGIC FEATURES

#### Gross Findings

- Well-circumscribed, unencapsulated, solid or cystic, pink-tan up to 2-cm mass

#### Microscopic Findings

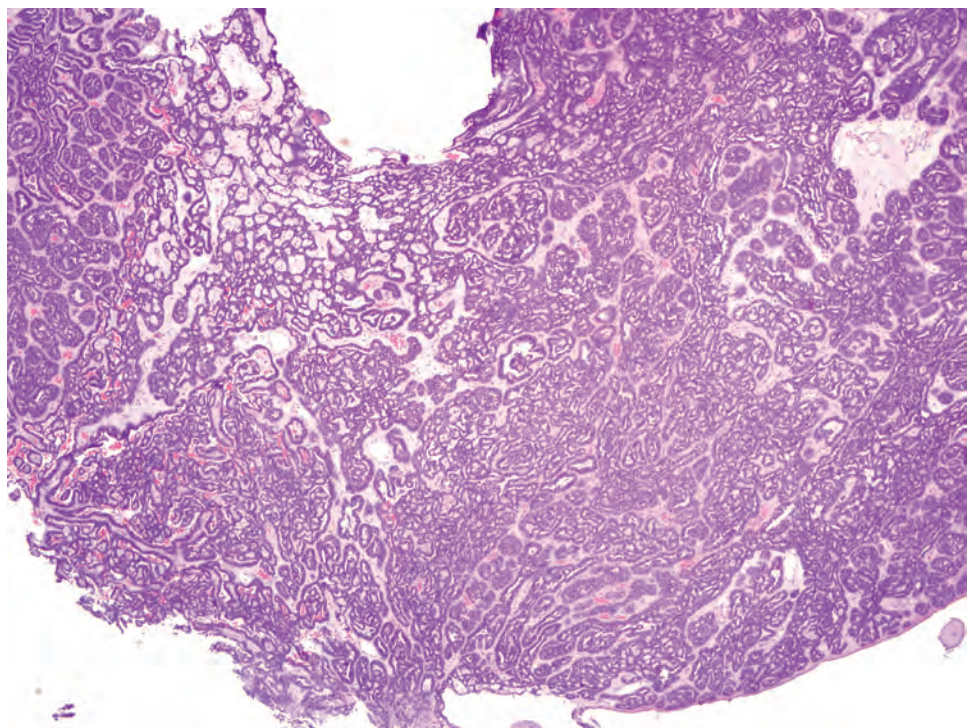
- Long chains of columnar cells that may join and then separate
- Tubules, duct-like forms, and rare solid groups
- Loose, lightly collagenous stroma

#### Immunohistochemical Findings

- Reactive with cytokeratin and S100 protein
- Reactive with GFAP at tumor/connective tissue interface

#### Pathologic Differential Diagnosis

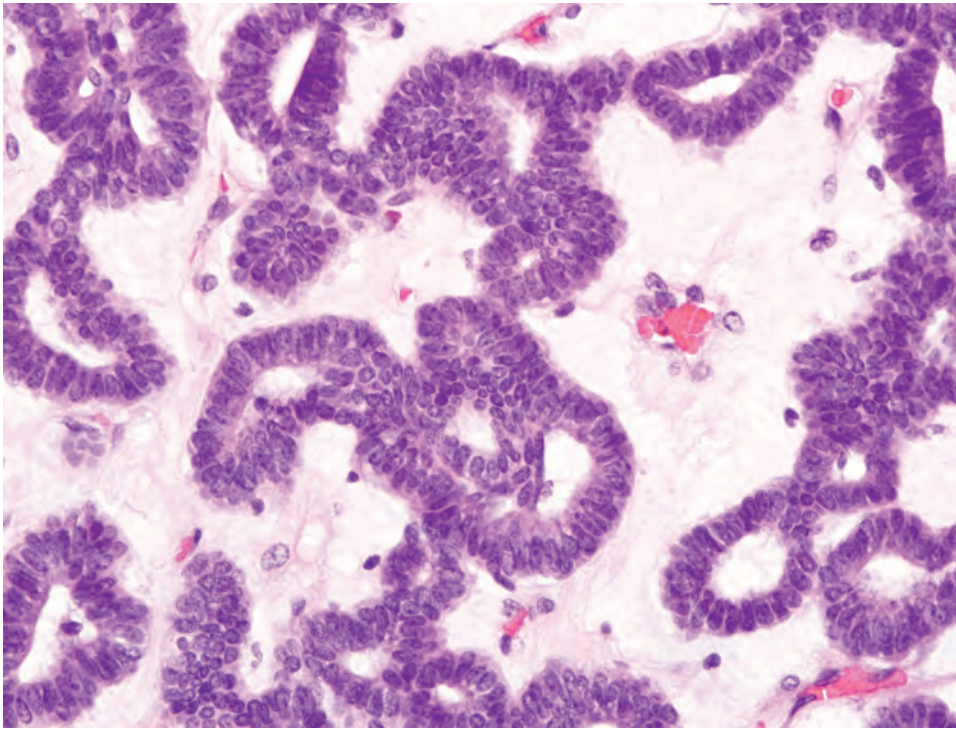
- *Benign*: pleomorphic adenoma, basal cell adenoma
- *Malignant*: adenoid cystic carcinoma, polymorphous adenocarcinoma



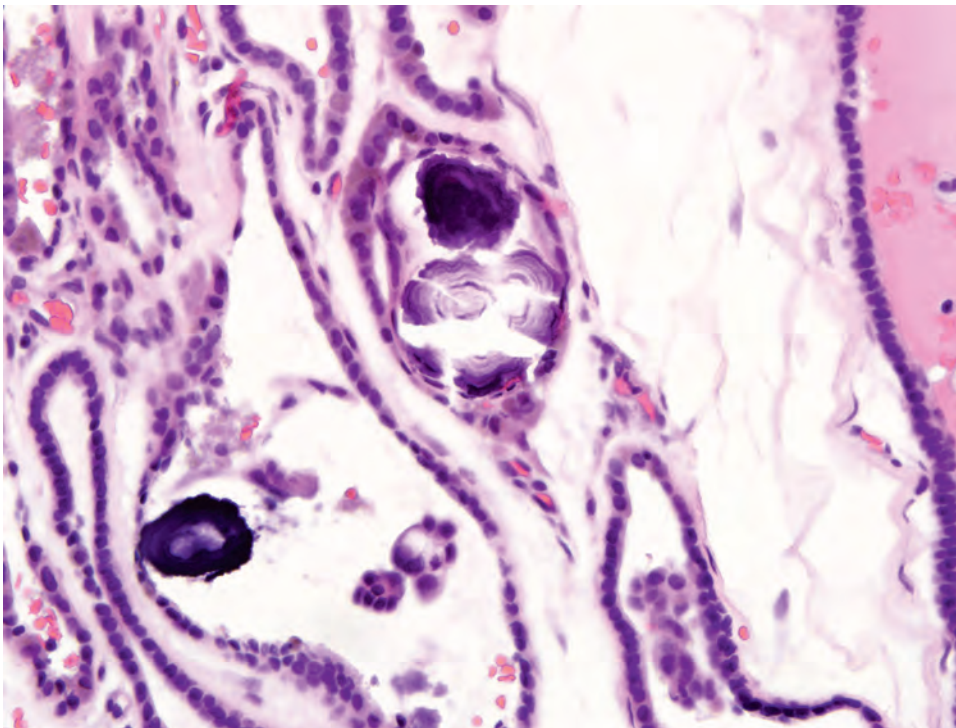
**FIGURE 12.14**

A canalicular adenoma shows a well-circumscribed neoplasm displaying chains of cells in a loose fibrous stroma. Note the numerous cystically dilated spaces.



**FIGURE 12.15**

Canalicular adenoma, high power. Short columnar to basaloid cells are arranged in a palisaded architecture with intervening loose stroma. "Beading" is noted where the cells come together and then separate again.

**FIGURE 12.16**

Canalicular adenoma showing single-file chains of columnar cells with oval nuclei set in a loose stroma characterize this entity. Psammomatous calcifications are seen.

possible small, unencapsulated, “incipient” tumors evident within surrounding minor salivary glands. Calcifications (psammomatous bodies) may be seen.

The cuboidal or columnar cells have eosinophilic cytoplasm and basophilic, oval nuclei (Fig. 12.16). Pleomorphism is minimal and mitotic figures are rare. Solid nests or sheets of smaller squamoid (morular appearing) cells may also be evident, with the larger cuboidal to columnar cells present at the periphery.

### ANCILLARY STUDIES

The cells are diffusely reactive for cytokeratin cocktail, S100 protein, and SOX10 while nonreactive for actins, p63, p40, and calponin. GFAP reactivity is focal, often at the tumor–connective tissue interface.

### DIFFERENTIAL DIAGNOSIS

The differential comprises benign neoplasms, including PA and basal cell adenoma. Malignancies commonly affecting the minor salivary glands, primarily adenoid cystic carcinoma and polymorphous adenocarcinoma, may also be considered.

### PROGNOSIS AND THERAPY

Simple local excision to include a rim of normal surrounding tissue is the treatment of choice. Although true recurrence is rare, the presence of multiple lesions may set the stage for possible clinical persistence or recurrence.

## ■ ONCOCYTOMA

Oncocytoma (oncocyctic adenoma) is a putative neoplastic proliferation of oncocytically altered cells. Histogenesis may be associated with therapeutic radiation exposure.

### CLINICAL FEATURES

Oncocytoma typically presents as an asymptomatic, slowly growing mass in the 7th to 8th decades of life. It affects the parotid gland in 80% to 90% of cases and represents about 1% of all parotid gland neoplasms. A slight female predominance is noted. Approximately 7% of tumors have a bilateral presentation. Whites are affected much more commonly than other races.

### ONCOCYTOMA—DISEASE FACT SHEET

#### Definition

- Neoplasm composed of large polygonal cells containing abundant abnormal mitochondria

#### Incidence and Location

- Approximately 1% of all parotid gland neoplasms
- Parotid > submandibular gland

#### Sex, Race, and Age Distribution

- Females > males
- Predominantly affects whites
- Peak incidence in the 7th to 8th decades

#### Clinical Features

- Asymptomatic slow-growing mass

#### Prognosis and Therapy

- Minimal recurrence with adequate excision
- Parotidectomy

### PATHOLOGIC FEATURES

#### GROSS FINDINGS

Oncocytoma presents as a soft, well-circumscribed, tan-brown nodule. It is usually solitary, ranging from 1 to 7 cm in size.

#### MICROSCOPIC FINDINGS

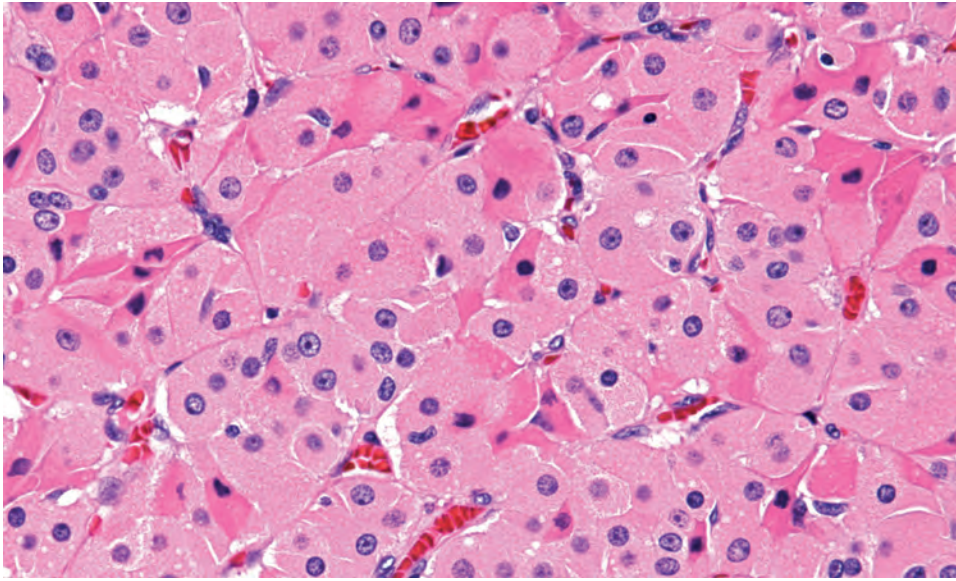
*Oncocytes* are polygonal cells with abundant eosinophilic, finely granular cytoplasm and uniform round, centrally placed nuclei with or without nucleoli (Fig. 12.17). Oncocytes may accumulate copious amounts of intracytoplasmic glycogen and, because of processing artifacts, appear “clear” and devoid of cytoplasmic staining (Fig. 12.18).

*Oncocytic metaplasia* is identified as solitary or small groups of acinar cells (mucous or serous) that have undergone cellular changes to become oncocytes, a process that increases with advancing age and becomes practically universal in individuals over 70 years of age. A distinct and immediate transformation of one cell type to another occurs without alteration of the glandular architecture.

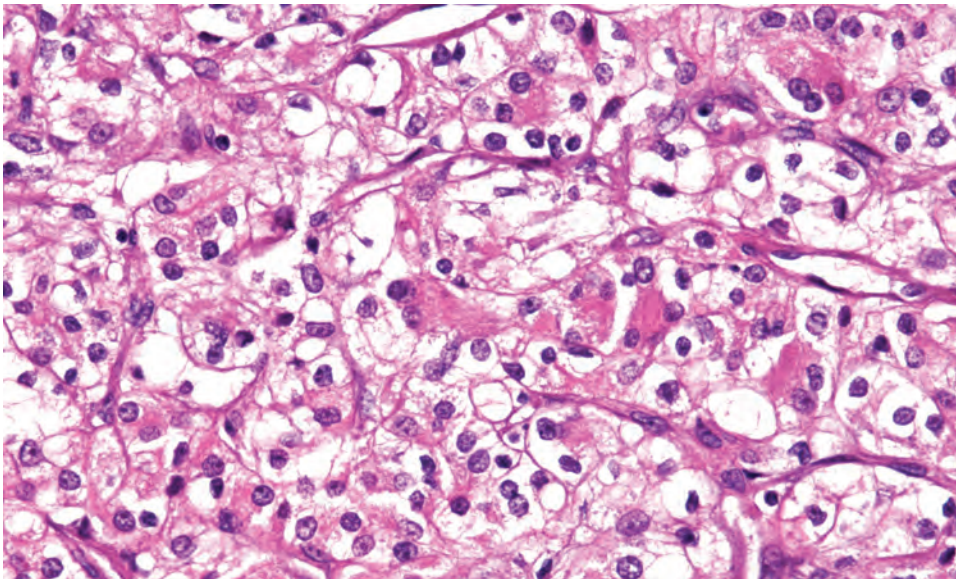
*Oncocytosis (oncocyctic hyperplasia)* includes multiple areas of oncocytic change, ranging from isolated variably sized cellular groupings (*nodular form*) to a diffuse process affecting a majority of the gland (*diffuse form*). An intimate, unencapsulated relationship between the glandular parenchyma and the oncocytic nodule is present and may include normal acini intermixed with oncocytes (Fig. 12.19).

*Oncocytoma* is well circumscribed with variably thick encapsulation (Fig. 12.20). Architectural patterns include

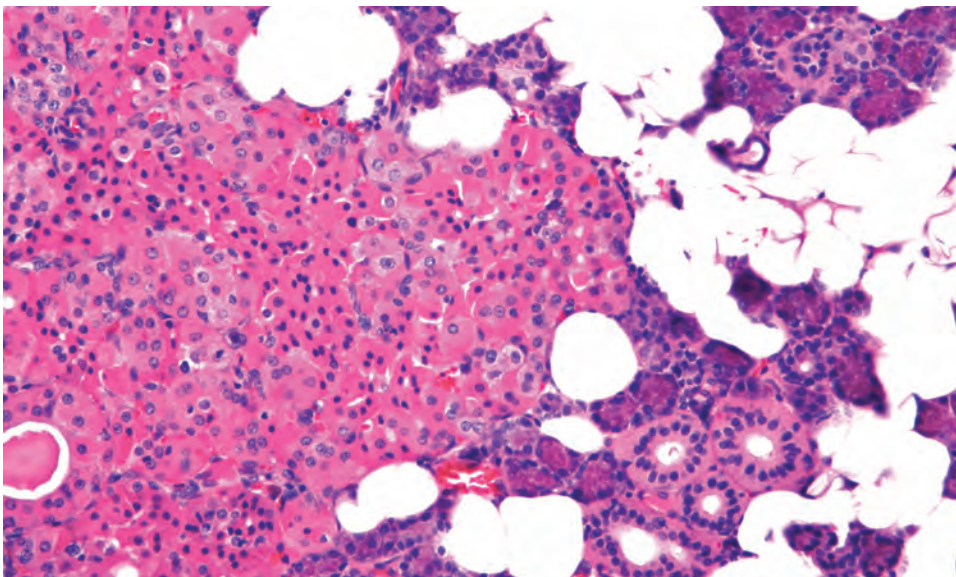


**FIGURE 12.17**

Oncocytes are polygonal cells with abundant granular eosinophilic cytoplasm and round, centrally placed nuclei, with or without nucleoli.

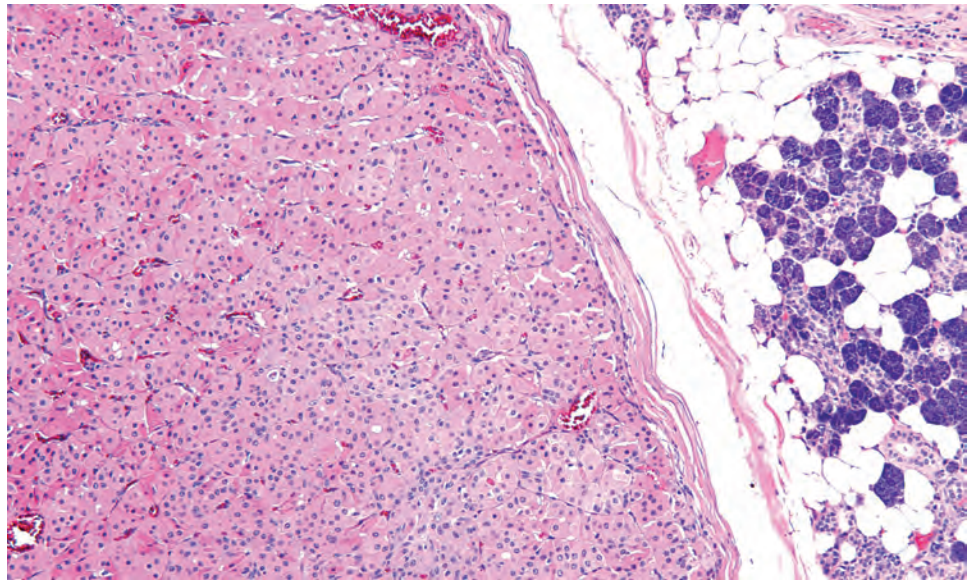
**FIGURE 12.18**

Oncocytoma, clear cell variant. Note scattered cells still possessing eosinophilic granular cytoplasm.

**FIGURE 12.19**

Oncocytosis with sheets of oncocytes (*left*) showing an intimate association with the salivary gland parenchyma.



**FIGURE 12.20**

Oncocytoma shows a well-encapsulated neoplasm composed of sheets of oncocytically altered cells.

### ONCOCYTOMA—PATHOLOGIC FEATURES

#### Gross Findings

- Single, soft, well-circumscribed tan-brown nodule

#### Microscopic Findings

- Large polygonal cells with abundant eosinophilic granular cytoplasm
- Solid, acinar, trabecular, or follicular patterns
- Clear cell change can be seen

#### Ancillary Studies

- Reactive with cytokeratin, p63, and phosphotungstic acid–hematoxylin

#### Pathologic Differential Diagnosis

- *Benign*: Warthin tumor, nodular oncocytic hyperplasia
- *Malignant*: acinic cell adenocarcinoma, metastatic renal cell carcinoma, oncocytic carcinoma

monotonous solid sheets, acinar, trabecular, papillary-cystic, or follicular arrangements. Slight nuclear pleomorphism may be identified, including prominent nucleoli. Significant stromal hyalinization or vascularity is possible. It is common to appreciate focal areas of oncocytosis in conjunction with an oncocytoma. The term *clear cell oncocytosis/oncocytoma* may be applied if the majority of the oncocytes display cleared cytoplasm. Some examples have fatty elements interspersed between oncocytes; this tumor that has been referred to as *oncocytic lipoadenoma* (Fig. 12.21).

### ANCILLARY STUDIES

#### HISTOCHEMICAL FINDINGS

Phosphotungstic acid–hematoxylin (PTAH) highlights the abundant mitochondria, seen as deep blue cytoplasmic

granularity and ranging from focal or patchy to diffuse. Striated duct epithelial cells, with their basally oriented interdigitating cytoplasmic processes and associated columns of mitochondria, may act as a positive internal control.

#### ULTRASTRUCTURAL FINDINGS

The organelles are shifted within the cytoplasm by an overwhelming number of surrounding mitochondria, many of which will show abnormal cristae (Fig. 12.22).

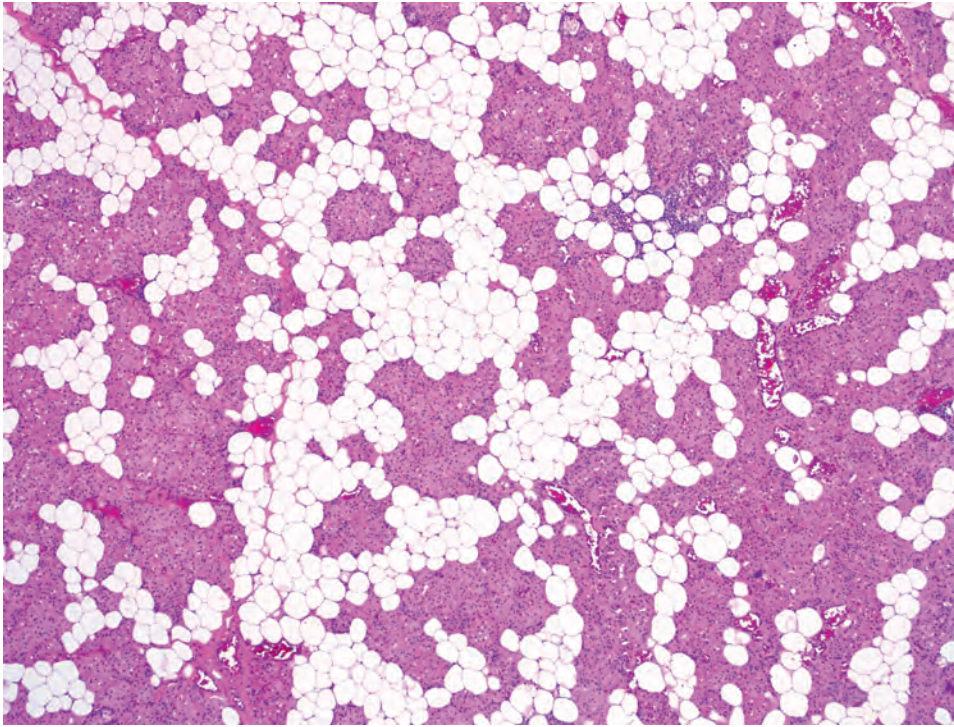
#### FINE NEEDLE ASPIRATION

Aspirates contain polygonal epithelial cells in papillary fragments, sheets, acinar-like structures, or singly (Fig. 12.23). Prominent nucleoli may be noted, but mitoses are rare to nonexistent. There is no background lymphoid component.

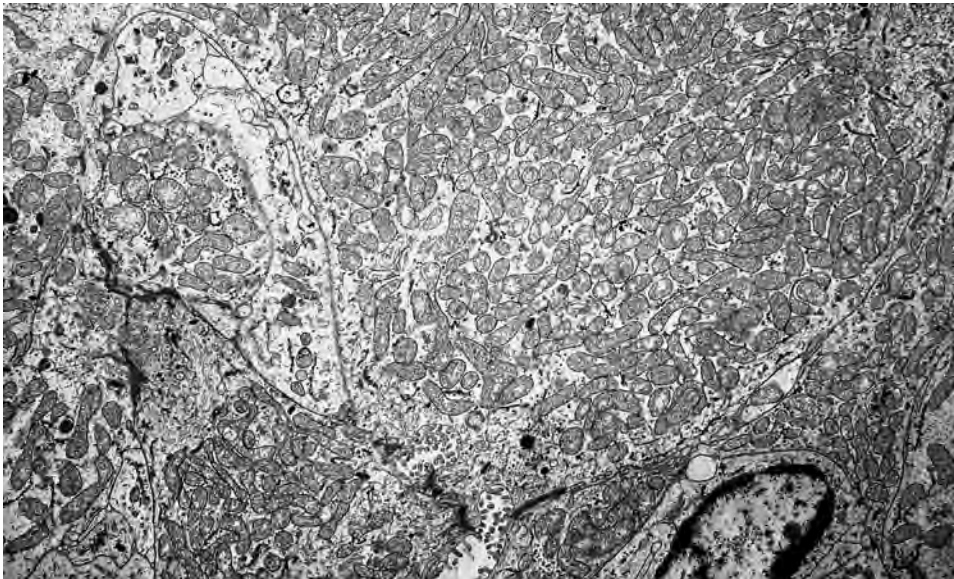
### DIFFERENTIAL DIAGNOSIS

The benign differential includes Warthin tumor and a dominant nodule within oncocytic hyperplasia. Warthin tumor has prominent lymphoid elements and the oncocytic hyperplasia often blends with the surrounding parenchyma. Malignancies may include acinic cell carcinoma or metastatic renal cell carcinoma, especially if clear cells predominate. Special studies usually help to resolve this differential. Oncocytic carcinoma is invasive, with profound pleomorphism and necrosis. Oncocytoma and oncocytic carcinoma are reactive for p63 in a basal cell distribution, while metastatic renal cell carcinoma is nonreactive for this marker.



**FIGURE 12.21**

This oncocytic lipoadenoma consists of nodules of oncocytic epithelium separated by fat lobules.

**FIGURE 12.22**

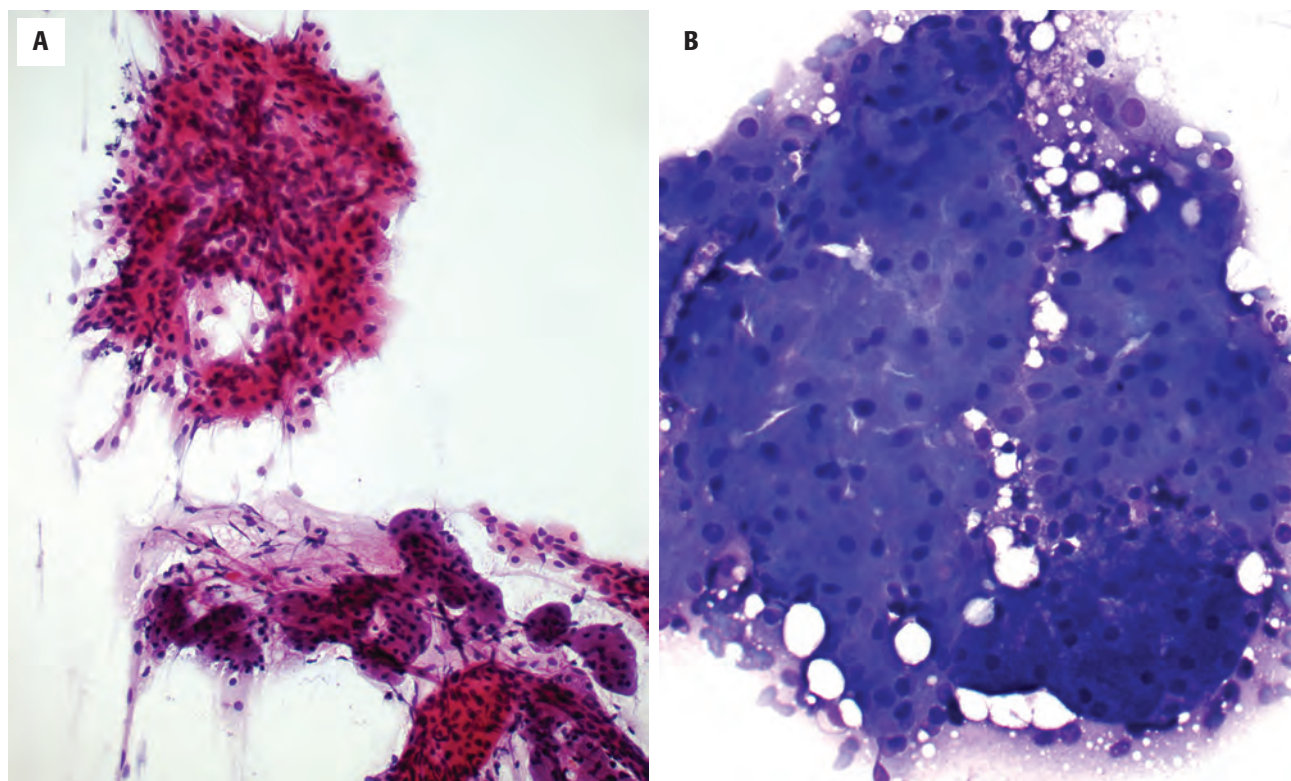
Cytoplasm of this oncocytoma is laden with mitochondria, as identified by electron microscopy. A small lumen is noted, along with tight junctions and short microvilli. (Courtesy of Dr. I. Dardick.)

### PROGNOSIS AND THERAPY

Superficial parotidectomy for lateral tumors or total parotidectomy for deep lobe tumors is the treatment of choice. Recurrence is minimal but may happen owing to multifocality or incomplete removal. The rare tumors of the minor salivary glands require complete excision with a small margin of uninvolved tissue.

### ■ WARTHIN TUMOR

Warthin tumor (papillary cystadenoma lymphomatosum) is a relatively common lesion composed of a double layer of oncocytic epithelium; this has a papillary and cystic architectural pattern and a dense lymphoid stroma. It is thought likely to arise from entrapped salivary tissue in intraparotid or periparotid lymph nodes.

**FIGURE 12.23**

Fine needle aspiration shows sheets and nests of large cells with abundant granular-eosinophilic cytoplasm. (A) Unremarkable acini are present in the lower field (Papanicolaou stain). (B) Seen here are large polygonal cells with small nuclei and abundant cytoplasm (Diff-Quik stained).

### CLINICAL FEATURES

Warthin tumor is the second most common benign salivary gland tumor and characteristically presents in the lower portion of the lateral lobe of the parotid gland. With a slight white male predominance, presentation normally occurs in the 6th to 7th decades as an asymptomatic, slow-growing 1- to 4-cm mass. Bilaterality or multifocality occurs more frequently than with any other salivary gland tumor. Warthin tumor may also be synchronously identified with other salivary gland neoplasms. Cigarette smoking is a likely etiologic factor.

### PATHOLOGIC FEATURES

#### GROSS FINDINGS

Macroscopically, Warthin tumor is circumscribed, solid, papillary, or cystic, and brown, yellow, or red. Cysts may contain yellow-brown fluid.

#### MICROSCOPIC FINDINGS

The synonym *papillary cystadenoma lymphomatosum*, though cumbersome, correctly describes the overall

### WARTHIN TUMOR—DISEASE FACT SHEET

#### Definition

- Biphasic tumor composed of bilayered oncocytic cells forming cysts and papillary fronds set within a dense lymph node–like stroma

#### Incidence and Location

- Second most common salivary gland tumor
- Parotid gland

#### Sex, Race, and Age Distribution

- Males > females
- White > black
- Peak incidence in the 6th to 7th decades

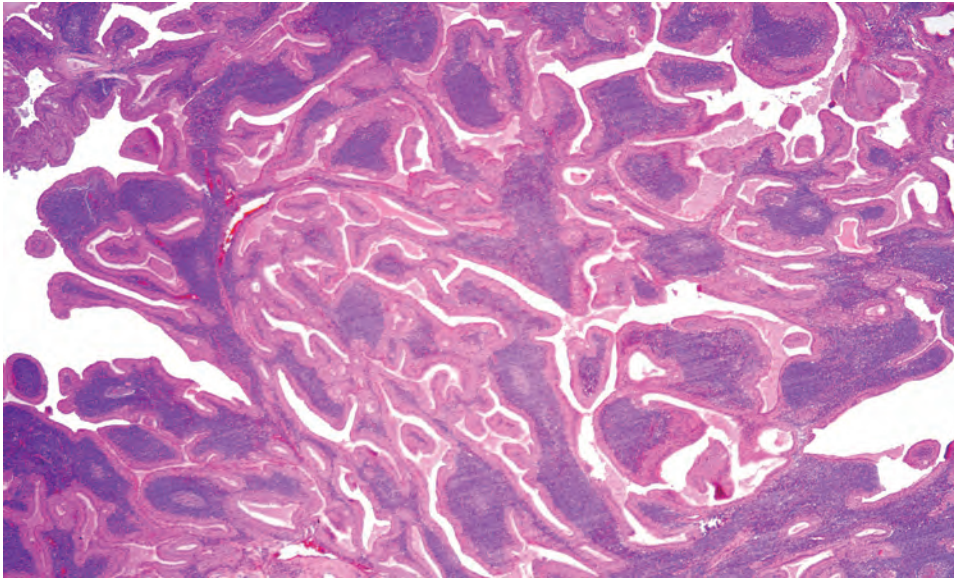
#### Clinical Features

- Asymptomatic slow-growing mass
- Most common bilateral and “second” (synchronous) tumor

#### Prognosis and Therapy

- Recurrence rate 4%-25%
- Lumpectomy to parotidectomy



**FIGURE 12.24**

Warthin tumor, low power. This papillary-cystic tumor is associated with a dense lymphoid stroma.

### WARTHIN TUMOR—PATHOLOGIC FEATURES

#### Gross Findings

- Circumscribed, firm to cystic, brown, yellow, or red mass

#### Microscopic Findings

- Double layer of oncocytic epithelium with cuboidal basal cells and overlying columnar luminal cells
- Numerous cysts with papillary infoldings
- Dense lymph node–like stroma with possible reactive germinal centers

#### Immunohistochemical Findings

- Epithelial component is keratin-reactive
- Lymphoid component is reactive with B- and T-cell markers

#### Pathologic Differential Diagnosis

- Lymph node metastases, sebaceous lymphadenoma, cystadenoma

microscopic appearance of Warthin tumor (Fig. 12.24). Papillary fronds and cystic spaces are lined with oncocytic epithelium, consisting of cuboidal basal cells supporting tall columnar cells with palisaded nuclei (Fig. 12.25), often creating a “tram tracking” nuclear appearance. The cystic spaces may be filled with fluid, desquamated epithelial cells, or lymphoid cells. Intimately associated with the epithelial component is a dense lymph node–like stroma, including reactive germinal centers. The proportion of the three elements is variable. Isolated mucocytes can be seen.

Trauma may lead to cyst rupture and a subsequent foreign-body giant cell reaction, fibrosis, squamous metaplasia, or necrosis. Such findings may occur spontaneously or after fine needle aspiration (FNA).

### ANCILLARY STUDIES

#### IMMUNOHISTOCHEMICAL FINDINGS

The epithelial component is reactive for a cytokeratin cocktail. The lymphoid portion is similar to a reactive lymph node, including  $\kappa$  and  $\lambda$  light-chain polyclonality.

#### FINE NEEDLE ASPIRATION

Aspirates display small collections of epithelial cells surrounded by lymphocytes. These epithelial islands demonstrate a “honeycomb” pattern, with well-defined cell borders and relatively large, centrally placed nuclei (Fig. 12.26). Squamoid cells may also be evident. Background lymphoid elements are easily identified. The cytoplasm appears opacified and “blue” with Romanovsky (Diff-Quik, MGG) preparations (Fig. 12.26).

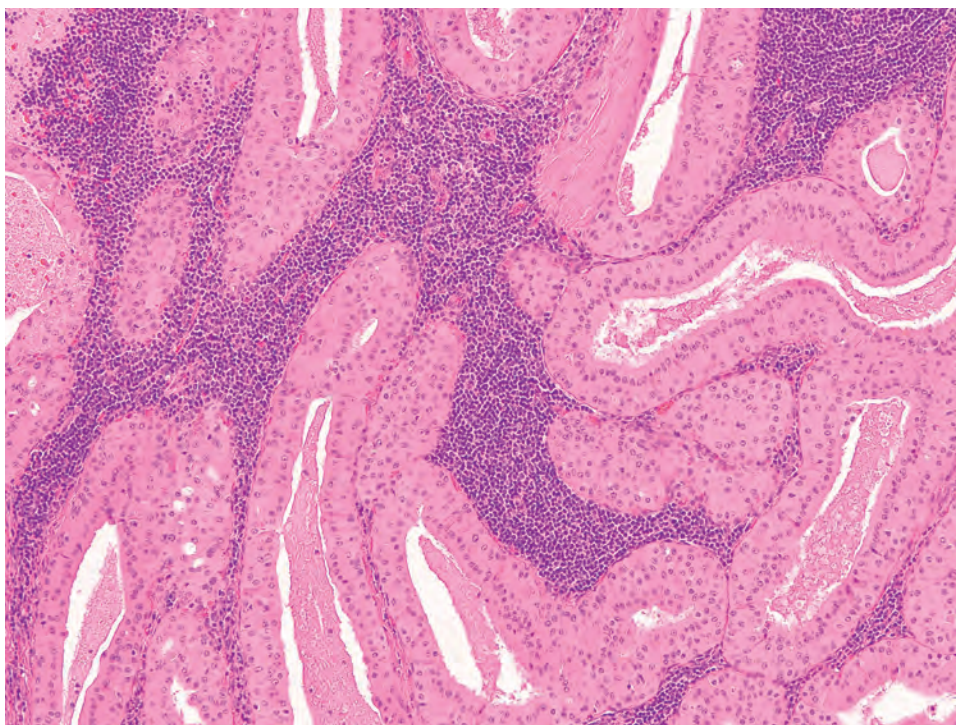
### DIFFERENTIAL DIAGNOSIS

The differential diagnosis includes lymph node metastasis and sebaceous lymphadenoma. However, the cytologically bland, bilayered, oncocytic epithelial element militates against both. Cystadenomas may be oncocytic but do not have the lymphoid stroma and usually have small, multilocular cystic spaces.

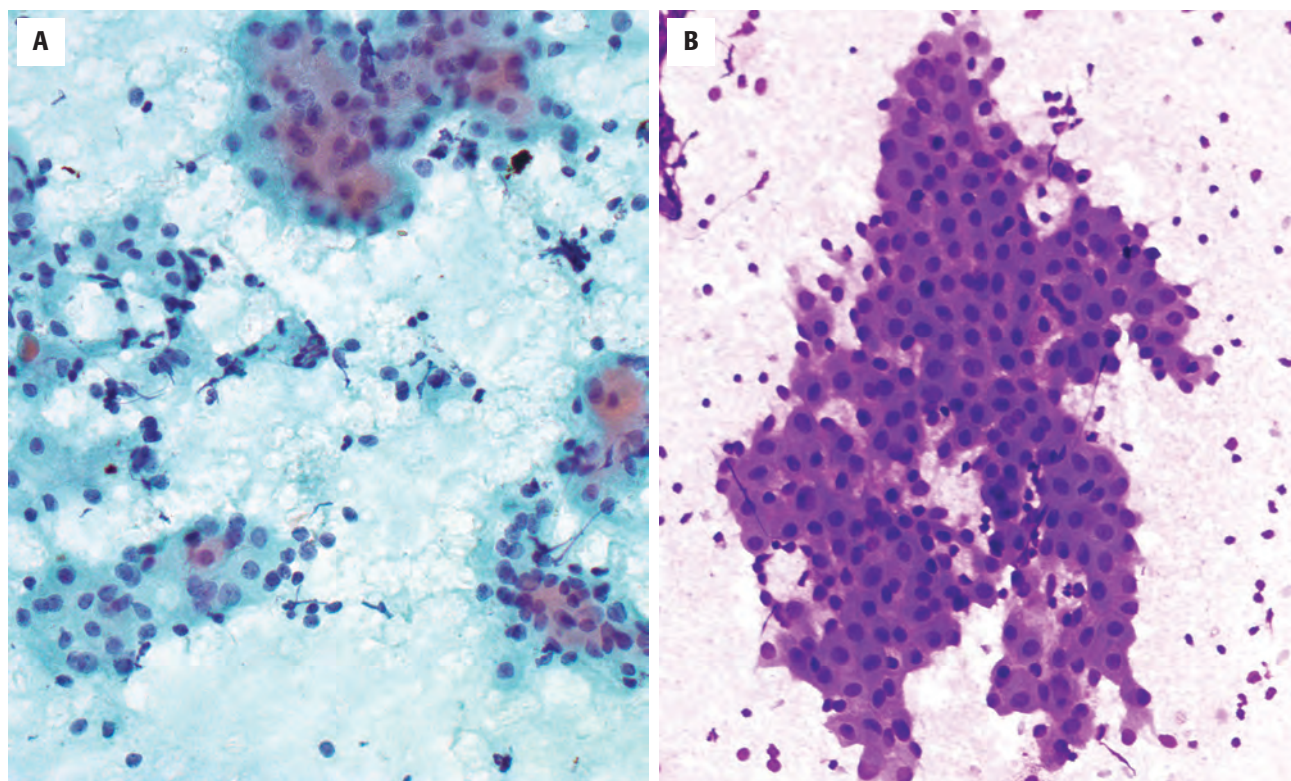
### PROGNOSIS AND THERAPY

The recurrence rate after excision is 4 % to 25 %, likely associated with multifocality or incomplete excision.



**FIGURE 12.25**

A Warthin tumor demonstrates papillary fronds and cystic spaces lined by a double cell layer of oncocytes.

**FIGURE 12.26**

(A) Papanicolaou-stained smear demonstrating cohesive clusters of oncocytic epithelial cells in a honeycomb pattern with well-defined cell borders and background lymphocytes. (B) Diff-Quik preparation has stained this papillary frond of epithelium a light blue. Lymphocytes and histiocytes are noted in the bloody background.



Treatment may range from lumpectomy to total parotidectomy, depending on size and location. A low malignant transformation rate of 1% is recognized, interestingly giving rise to various carcinomas (from epithelial component) or a low-grade B-cell lymphoma (from the lymphoid component).

## ■ SEBACEOUS ADENOMA/LYMPHADENOMA

Sebaceous adenoma is a benign epithelial neoplasm composed of proliferating, incompletely differentiated sebaceous glands. Sebaceous lymphadenoma is a rare variant in which the epithelial proliferation is supported by a dense lymphoid stroma; it possibly arises from entrapped salivary gland tissue within intraparotid or periparotid lymph nodes.

### CLINICAL FEATURES

The clinical presentations of both neoplasms are similar; they are therefore discussed together. Both represent less than 1% of all salivary gland neoplasms and are rarely reported outside of the parotid gland. Males and females are affected equally, with most lesions presenting in the 6th to 7th decades of life as an asymptomatic slow-growing mass.

#### SEBACEOUS ADENOMA/LYMPHADENOMA—DISEASE FACT SHEET

##### Definition

- Benign epithelial neoplasms composed of proliferating, incompletely differentiated sebaceous glands set within a fibrous (sebaceous adenoma) or dense lymphoid (sebaceous lymphadenoma) stroma

##### Incidence and Location

- Approximately 0.1% of all salivary gland neoplasms
- Parotid gland

##### Sex and Age Distribution

- Equal sex distribution
- Peak incidence in the 6th to 7th decades

##### Clinical Features

- Slow-growing asymptomatic mass

##### Prognosis and Therapy

- Minimal recurrence rate
- Surgical excision with rim of normal tissue

### PATHOLOGIC FEATURES

#### GROSS FINDINGS

Both sebaceous adenoma and lymphadenoma are firm, well-circumscribed masses. Cut section is pinkish-gray to white or yellow and may be solid or cystic (Fig. 12.27).

#### MICROSCOPIC FINDINGS

Sebaceous adenoma is a well-circumscribed neoplasm composed of solid and cystic epithelial structures surrounded by a dense fibrous stroma (Fig. 12.28). Epithelial nests are squamoid, displaying peripheral basaloid cells maturing inwardly into sebaceous cells (Fig. 12.29).

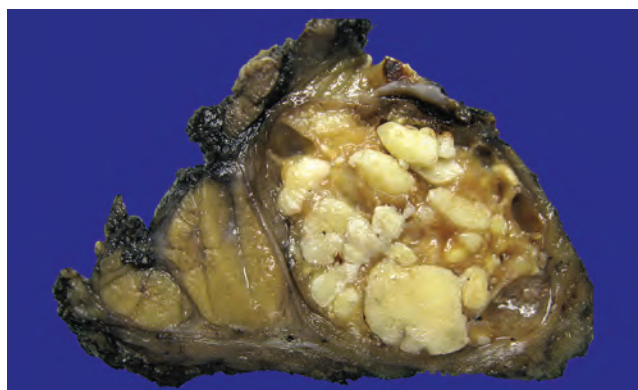


**FIGURE 12.27**

Sebaceous lymphadenoma showing a greasy cut surface, with multiple cystic spaces filled with sebaceous material.

#### SEBACEOUS ADENOMA/LYMPHADENOMA—PATHOLOGIC FEATURES

##### Gross Findings

- Well-circumscribed, solid or cystic, pink-gray mass

##### Microscopic Findings

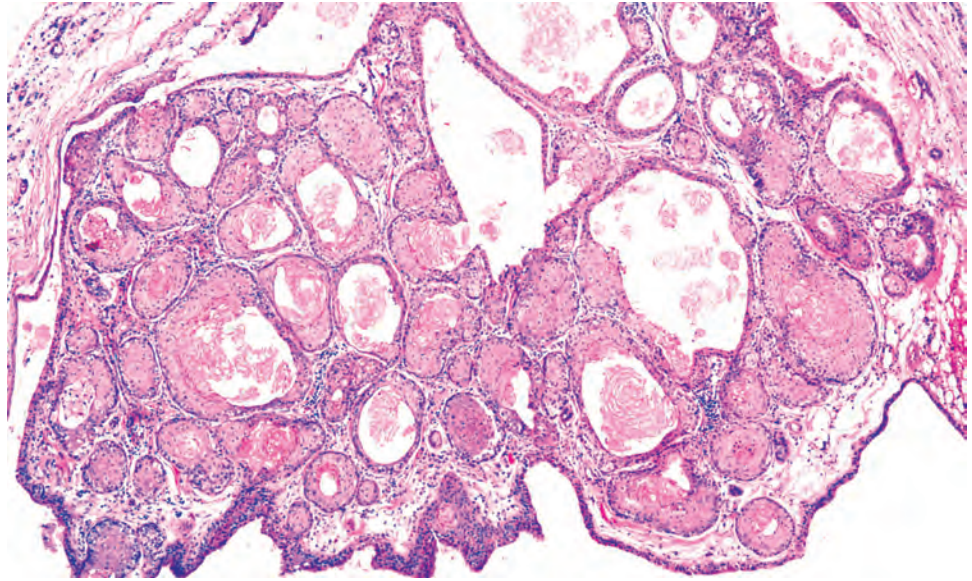
- Solid nests or cystic structures
- Mature sebaceous differentiation in center of nodules or wall of cysts
- Fibrous stroma (*sebaceous adenoma*) or dense lymph node–like stroma (*sebaceous lymphadenoma*)

##### Immunohistochemical Findings

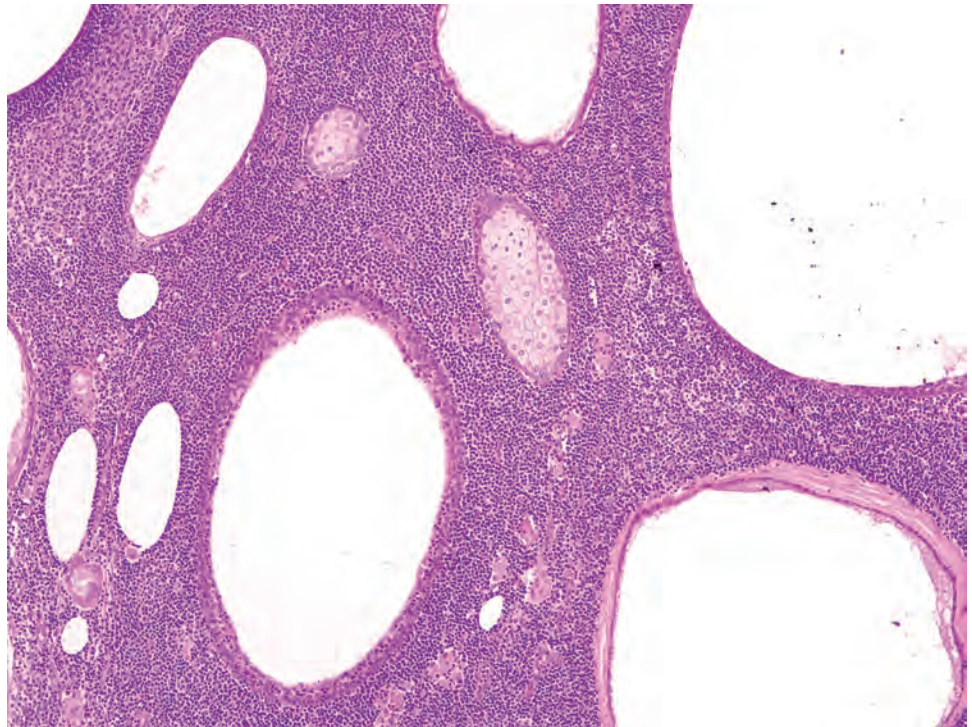
- Epithelial component is reactive with cytokeratin and EMA

##### Pathologic Differential Diagnosis

- *Sebaceous adenoma*: mucoepidermoid carcinoma and sebaceous adenocarcinoma
- *Sebaceous lymphadenoma*: Warthin tumor and metastatic carcinoma

**FIGURE 12.28**

Sebaceous adenoma with numerous solid and cystically dilated nests of squamoid cells.

**FIGURE 12.29**

Sebaceous adenoma with nests of squamoid cells displaying central sebaceous cell differentiation.

Sebaceous cells, either singly or in groups, may also be found within cyst walls.

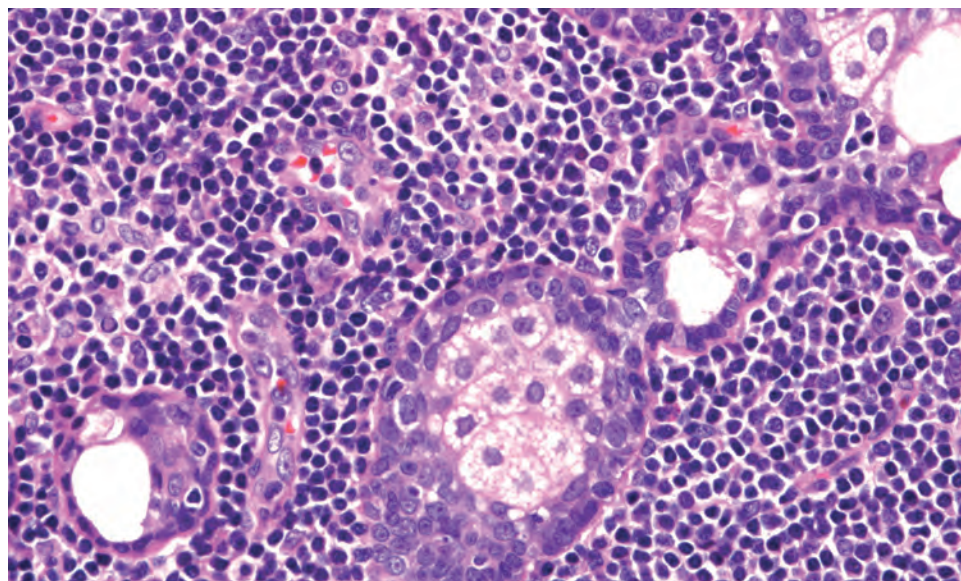
Sebaceous lymphadenoma is composed of a similar epithelial component that is evenly distributed throughout the tumor. However, instead of a fibrous background, the stroma consists of a dense population of lymphocytes perhaps including reactive germinal centers (Fig. 12.30). A histologically similar tumor devoid of sebaceous differentiation is termed *lymphadenoma*.

## ANCILLARY STUDIES

### IMMUNOHISTOCHEMICAL FINDINGS

Cytokeratin cocktail and epithelial membrane antigen are reactive in the epithelial proliferation. Androgen receptor highlights the sebocytes. S100 protein and SMA are nonreactive. As with Warthin tumor, the lymphoid component in sebaceous lymphadenoma is similar to a reactive lymph node.



**FIGURE 12.30**

Sebaceous lymphadenoma with solid and cystic nests of squamoid cells with sebaceous differentiation amid a dense lymphoid stroma.

### FINE NEEDLE ASPIRATION

Aspirates of sebaceous adenoma demonstrate aggregates of large cells with foamy cytoplasm and central crenated nuclei, consistent with sebaceous cells. Less mature squamoid forms with dense cytoplasm and round to oval nuclei are also present. Sebaceous lymphadenoma is similar but also displays a background of small mature lymphocytes.

### DIFFERENTIAL DIAGNOSIS

The sebaceous adenoma differential includes mucoepidermoid carcinoma and sebaceous adenocarcinoma. Sebaceous lymphadenoma may be confused with Warthin tumor and metastatic squamous cell carcinoma.

### PROGNOSIS AND THERAPY

Treatment includes surgical excision with a rim of normal surrounding tissue. The recurrence rate is minimal following complete removal.

## ■ HEMANGIOMA

Hemangioma is a soft tissue tumor composed of variably mature blood vessels and endothelial cells. All histologic variants of hemangioma occur in the salivary glands. However, this discussion is limited to the most common form, *juvenile (capillary) hemangioma* (JH).

### CLINICAL FEATURES

JH affects the very young, arising at birth or shortly thereafter; it is the most common salivary gland neoplasm to arise in this time frame. Females predominate, and the parotid gland is the affected site in the vast majority of cases. Bilaterality is found in about 25%. A rapid growth phase is followed by a very slow involutional phase. The tumor may become large, affecting more than half of the face, and can extend into the ear, lip, subglottis, or nose. Although it is usually asymptomatic, complications such as cutaneous ulceration, bleeding, airway compression, or, rarely, congestive heart failure may arise.

### HEMANGIOMA (JUVENILE)—DISEASE FACT SHEET

#### Definition

- Soft tissue tumor composed of variably mature blood vessels and endothelial cells

#### Incidence and Location

- Rare
- Parotid gland

#### Sex and Age Distribution

- Females > males
- Perinatal or neonatal

#### Clinical Features

- Rapid growth followed by slow involution
- Usually asymptomatic

#### Prognosis and Therapy

- Most resolve spontaneously over time
- Pharmacologic therapy if required

## **PATHOLOGIC FEATURES**

### **GROSS FINDINGS**

Macroscopically, parotid JH is hemorrhagic, lobular, and red to brown. As opposed to a discrete mass, the lesion diffusely affects the lobes of the gland.

### **MICROSCOPIC FINDINGS**

JH appears as a diffuse replacement of the salivary gland parenchyma. The lobular architectural pattern and anatomic boundaries of the salivary gland are maintained, with replacement of the serous acini by sheets of small endothelial cells and immature capillaries (Fig. 12.31). Striated ducts and peripheral nerves, however, seem unaffected.

The endothelial cells are small, with indistinct cell borders. Nuclei are oval or irregular, with possible grooves and occasional inconspicuous nucleoli. Mitotic figures, normal in morphology, may be numerous. Dense cellularity may mask the vascular differentiation (Fig. 12.32). Erythrocytes are noted within the lumens.

## **ANCILLARY STUDIES**

### **IMMUNOHISTOCHEMICAL FINDINGS**

The endothelial cells are reactive with the endothelial cell markers CD31, CD34, ERG, and factor VIII-related antigen (FVIII-RAG). GLUT1 is relatively specific for juvenile hemangiomas. Reticulin accentuates the vascularity. Cytokeratin cocktail highlights the residual ductal structures.

### **FINE NEEDLE ASPIRATION**

Aspirates consist of a spindle cell proliferation, including cohesive groups of bland cells in a bloody background or hypercellular groups arranged in compact, three-dimensional coils. The cells have scant to moderate cytoplasm and oval nuclei (Fig. 12.33). Needless to say, FNA is not recommended if the clinical differential includes a vascular neoplasm.

## **DIFFERENTIAL DIAGNOSIS**

Angiosarcoma is very rare in this age group, yet it is at the top of the differential. Bland cytomorphology and maintenance of glandular architecture favor JH.

### **HEMANGIOMA (JUVENILE)—PATHOLOGIC FEATURES**

#### **Gross Findings**

- Hemorrhagic, lobular, red-brown

#### **Microscopic Findings**

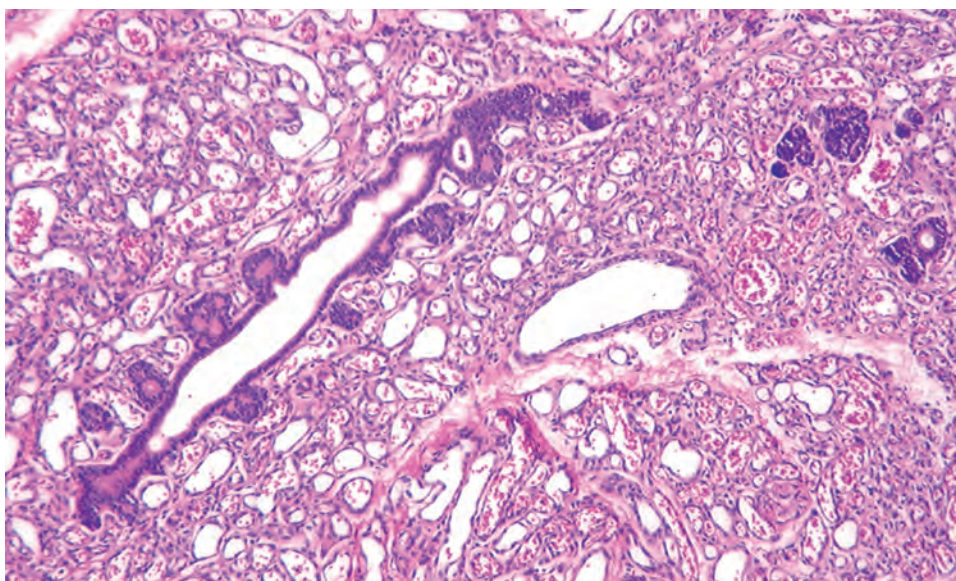
- Interdigitation between salivary acini and intercalated ducts by immature endothelial cells and small capillaries
- Lobular architecture of salivary gland remains intact

#### **Immunohistochemical Findings**

- Endothelial cells are reactive with CD31, CD34, ERG, FVIII-RAG, and GLUT1

#### **Pathologic Differential Diagnosis**

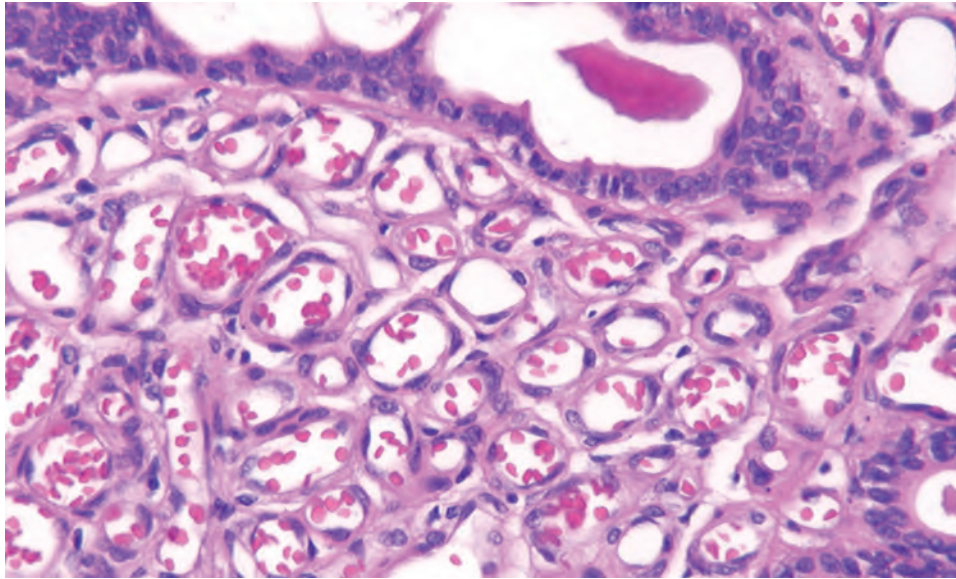
- Angiosarcoma



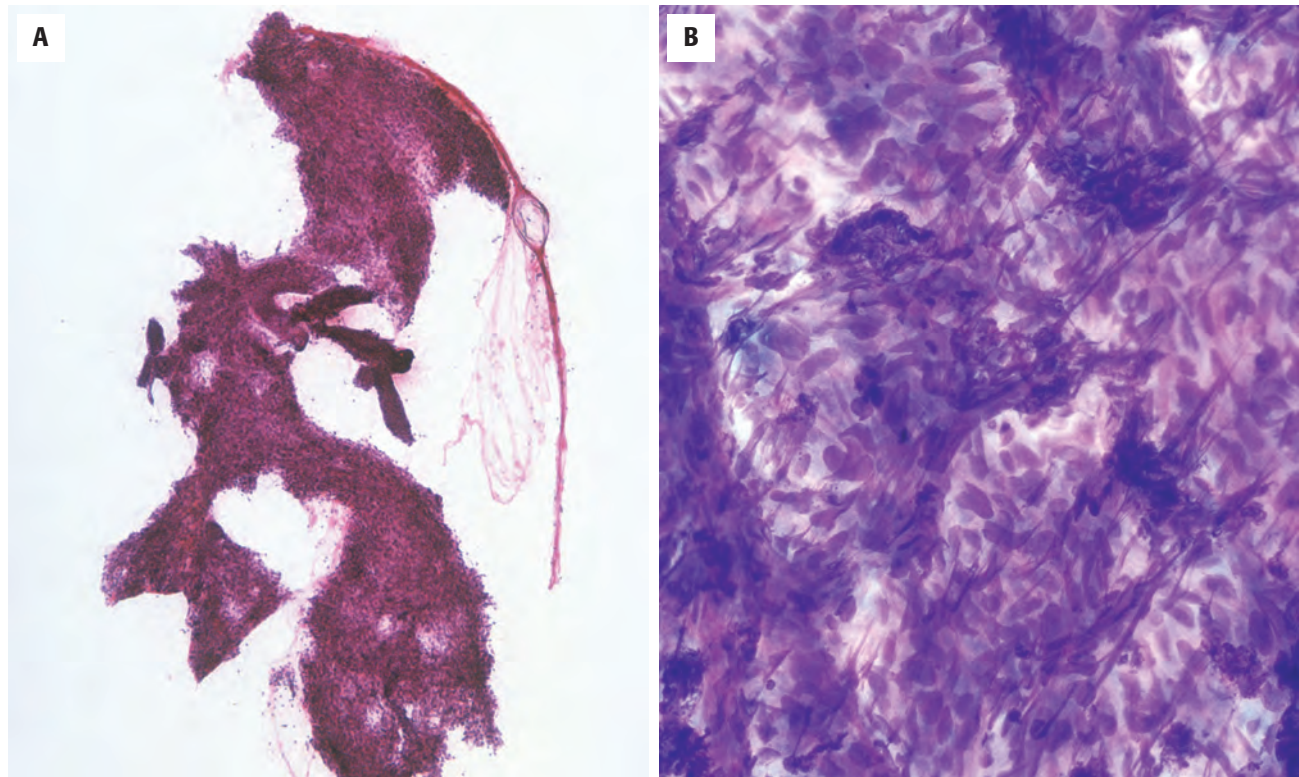
**FIGURE 12.31**

Juvenile capillary hemangioma showing salivary gland lobules replaced by endothelial cells and small blood vessels. Note that the glandular architecture and excretory ducts are still intact.



**FIGURE 12.32**

Juvenile capillary hemangioma showing small uniform endothelial cells and small capillaries pushing aside the glandular acini. Note the residual excretory ducts.

**FIGURE 12.33**

(A) This Papanicolaou-stained smear shows a hypercellular, compact, three-dimensional cluster or coil. There is a relative lack of blood. (B) Diff-Quik-stained material shows cohesive clusters of spindled cells without significant pleomorphism. This is a cellular smear of a hemangioma.

### PROGNOSIS AND THERAPY

Most JHs involute over time, with 75 % to 95 % displaying spontaneous regression by 7 years. However, pharmacologic therapy, including corticosteroids and/or interferon ( $\alpha$ -2a or  $\alpha$ -2b), may be required if complications develop.

Resection is not advised because of blood loss or possible injury to the facial nerve.

### SUGGESTED READINGS

The complete Suggested Readings list is available online at [ExpertConsult.com](http://ExpertConsult.com).

**SUGGESTED READINGS****Pleomorphic Adenoma**

- Alves FA, et al. Pleomorphic adenoma of the submandibular gland: clinicopathologic and immunohistochemical features of 60 cases in Brazil. *Arch Otolaryngol Head Neck Surg*. 2002;128:1400–1403.
- Bell D, et al. Tumours of salivary glands: Pleomorphic adenoma. In: el-Naggar AK, Chang JKC, Grandis JR, Takata T, Slootweg PJ, eds. *Classification of Head and Neck Tumors*. 4th ed. World Health Organization Classification of Tumours. Lyon, France: IARC Press; 2017:185–186.
- Buening JE, et al. Giant pleomorphic adenoma of the parotid gland: case report and review of the literature. *Ear Nose Throat J*. 1998;77:634–640.
- Colella G, et al. Meta-analysis of surgical approaches to the treatment of parotid pleomorphic adenomas and recurrence rates. *J Craniomaxillofac Surg*. 2015;43:738–745.
- Dardick I. Myoepithelioma: definitions and diagnostic criteria. *Ultrastruct Pathol*. 1995;19:335–345.
- Fonseca I, et al. Tumours of salivary glands: Myoepithelioma. In: el-Naggar AK, Chang JKC, Grandis JR, Takata T, Slootweg PJ, eds. *Classification of Head and Neck Tumours*. 4th ed. World Health Organization Classification of Tumours. Lyon, France: IARC Press; 2017:186–187.
- Glas AS, et al. Surgical treatment of recurrent pleomorphic adenoma of the parotid gland: a clinical analysis of 52 patients. *Head Neck*. 2001;23:311–316.
- Guntinas-Lichius O, et al. Pleomorphic adenoma of the parotid gland: a 13-year experience of consequent management by lateral or total parotidectomy. *Eur Arch Otorhinolaryngol*. 2004;261:143–146.
- Kawahara A, et al. Characterization of the epithelial components in pleomorphic adenoma of the salivary gland. *Acta Cytol*. 2002;46:1095–1100.
- Marioni G, et al. Benign metastasizing pleomorphic adenoma of the parotid gland: a clinicopathologic puzzle. *Head Neck*. 2003;25:1071–1076.
- Mendenhall WM, et al. Salivary gland pleomorphic adenoma. *Am J Clin Oncol*. 2008;31:95–99.
- Nishimura T, et al. Differential diagnosis of pleomorphic adenoma by immunohistochemical means. *J Laryngol Otol*. 1991;105:1057–1060.
- Simpson RHW, et al. Benign myoepithelioma of the salivary glands: a true entity? *Histopathology*. 1995;27:1–9.
- Stennert E, et al. Histopathology of pleomorphic adenoma in the parotid gland: a prospective unselected series of 100 cases. *Laryngoscope*. 2001;111:2195–2200.
- Stennert E, et al. Recurrent pleomorphic adenoma of the parotid gland: a prospective histopathological and immunohistochemical study. *Laryngoscope*. 2004;114:158–163.
- Stenman G. Fusion oncogenes and tumor type specificity-insights from salivary gland tumors. *Semin Cancer Biol*. 2005;15:224–235.
- Stenman G. Fusion oncogenes in salivary gland tumors: molecular and clinical consequences. *Head and Neck Pathol*. 2013;7(suppl 1):S12–S19.
- Stenman G, et al. Diagnostic and therapeutic implications of new molecular biomarkers in salivary gland cancers. *Oral Oncol*. 2014;50:683–690.
- Valentini V, et al. Surgical techniques in the treatment of pleomorphic adenoma of the parotid gland: our experience and review of the literature. *J Craniofac Surg*. 2001;12:565–568.
- Jo VY, et al. Distinctive patterns of CTNNB1 ( $\beta$ -Catenin) alterations in salivary gland basal cell adenoma and basal cell adenocarcinoma. *Am J Surg Pathol*. 2016;40(8):1143–1150.
- Jungehulsing M, et al. Turban tumor with involvement of the parotid gland. *J Laryngol Otol*. 1999;113:779–783.
- Kawahara A, et al. Fine-needle aspiration cytology of basal cell adenoma of the parotid gland: characteristic cytologic features and diagnostic pitfalls. *Diagn Cytopathol*. 2007;35:85–90.
- Kawahara A, et al. Nuclear  $\beta$ -catenin expression in basal cell adenomas of salivary gland. *J Oral Pathol Med*. 2011;40(6):460–466.
- Kawata R, et al. Basal cell adenoma of the parotid gland: a clinicopathologic study of nine cases—basal cell adenoma versus pleomorphic adenoma and Warthin tumor. *Eur Arch Otorhinolaryngol*. 2010;267:779–783.
- Li J, et al. Tumours of salivary glands: Basal cell adenoma. In: el-Naggar AK, Chang JKC, Grandis JR, Takata T, Slootweg PJ, eds. *Classification of Head and Neck Tumours*. 4th ed. World Health Organization Classification of Tumours. Lyon, France: IARC Press; 2017:187–188.
- Sahu K, et al. Basal cell adenoma, solid variant, diagnosed by fine needle aspiration cytology. *Acta Cytol*. 1999;43:1198–1200.
- Scott AR, et al. Parotid mass in a woman with multiple cutaneous cylindromas. *Head Neck*. 2010;32:684–687.
- Yu GY, et al. Histogenesis and development of membranous basal cell adenoma. *Oral Surg Oral Med Oral Pathol*. 1998;86:446–451.
- Yu GY, et al. Membranous basal cell adenoma of the salivary gland: a clinicopathologic study of 12 cases. *Acta Otolaryngol*. 1998;118:588–593.
- Zarbo RJ, et al. Salivary gland basal cell and canalicular adenomas: immunohistochemical demonstration of myoepithelial participation and morphogenetic considerations. *Arch Pathol Lab Med*. 2000;124:401–405.

**Canalicular Adenoma**

- Bloemena E, et al. Tumours of salivary glands: Canalicular adenoma and other ductal adenomas. In: el-Naggar AK, Chang JKC, Grandis JR, Takata T, Slootweg PJ, eds. *Classification of Head and Neck Tumours*. 4th ed. World Health Organization Classification of Tumours. Lyon, France: IARC Press; 2017:194.
- Curran AE, et al. Distinctive pattern of glial fibrillary acidic protein reactivity useful in distinguishing fragmented pleomorphic adenoma, canalicular adenoma and polymorphous low-grade adenocarcinoma of minor salivary glands. *Head Neck Pathol*. 2007;1:27–32.
- Furuse C, et al. Comparative immunoprofile of polymorphous low-grade adenocarcinoma and canalicular adenoma. *Ann Diagn Pathol*. 2003;7:278–280.
- Harmse JL, et al. Recurrent canalicular adenoma of the minor salivary glands in the upper lip. *J Laryngol Otol*. 1997;111:985–987.
- Neville BW, et al. Labial salivary gland tumors. *Cancer*. 1988;61:2113–2116.
- Rousseau A, et al. Multiple canalicular adenomas: a case report and review of the literature. *Oral Surg Oral Med Oral Pathol*. 1999;87:346–350.
- Suarez P, et al. Palatal canalicular adenoma: report of 12 cases and review of the literature. *Ann Diagn Pathol*. 1998;2:224–228.
- Thompson LDR, et al. Canalicular adenoma: a clinicopathologic and immunohistochemical analysis of 67 cases with a review of the literature. *Head and Neck Pathol*. 2015;9(2):181–195.
- Waldron CA, et al. Tumors of the intraoral minor salivary glands: a demographic and histologic study of 426 cases. *Oral Surg Oral Med Oral Pathol*. 1988;66:323–333.

**Basal Cell Adenoma**

- Batsakis JG, et al. Basaloid monomorphic adenomas. *Ann Otol Rhinol Laryngol*. 1991;100:687–690.
- Dardick I, et al. Trabecular and solid-cribriform types of basal cell adenoma: a morphologic study of two cases of an unusual variant of monomorphic adenoma. *Oral Surg Oral Med Oral Pathol*. 1992;73:75–83.
- Ferreiro JA. Immunohistochemistry of basal cell adenoma of the major salivary glands. *Histopathol*. 1994;24:539–542.
- Galed-Placed I, et al. Synchronous, double parotid tumor: fine needle aspiration cytology diagnosis of the membranous basal cell adenoma component. *Acta Cytol*. 2000;44:1120–1122.

**Oncocytoma**

- Brandwein MS, et al. Oncocytic tumors of major salivary glands: a study of 68 cases with follow-up of 44 patients. *Am J Surg Pathol*. 1991;15:514–528.
- Capone RB, et al. Oncocytic neoplasms of the parotid gland: a 16-year institutional review. *Oto Head Neck Surg*. 2002;126:657–662.
- Dardick I, et al. Differentiation and the cytomorphology of salivary gland tumors with specific reference to oncocytic metaplasia. *Oral Surg Oral Med Oral Pathol*. 1999;88:691–701.



4. Davy CL, et al. Relationship of clear cell oncocytoma to mitochondrial-rich (typical) oncocytomas of parotid salivary gland. *Oral Surg Oral Med Oral Pathol*. 1994;77:469–478.
5. Ellis GL. “Clear cell” oncocytoma of salivary gland. *Hum Pathol*. 1988;19:862–867.
6. Kanazawa H, et al. Oncocytoma of an intraoral minor salivary gland: report of a case and review of the literature. *J Oral Maxillofac Surg*. 2000;58:894–897.
7. Katabi N, et al. Tumours of salivary glands: Oncocytoma. In: el-Naggar AK, Chang JKC, Grandis JR, Takata T, Slootweg PJ, eds. *Classification of Head and Neck Tumours*. 4th ed. World Health Organization Classification of Tumours. Lyon, France: IARC Press; 2017: 189–190.
8. Lau SK, et al. Oncocytic lipoadenoma of the salivary gland: a clinicopathologic analysis of 7 cases and review of the literature. *Head and Neck Pathol*. 2015;9:39–46.
9. McHugh JB, et al. p63 immunohistochemistry differentiates salivary gland oncocytoma and oncocytic carcinoma from metastatic renal cell carcinoma. *Head Neck Pathol*. 2007;1(2):123–131.
10. McLoughlin PM, et al. Oncocytoma of the submandibular gland. *Int J Oral Maxillofac Surg*. 1994;23:294–295.
11. Palmer TJ, et al. Oncocytic adenomas and oncocytic hyperplasia of salivary glands: a clinicopathological study of 26 cases. *Histopathology*. 1990;16:487–493.
12. Verma K, et al. Salivary gland tumors with a prominent oncocytic component: cytologic findings and differential diagnosis of oncocytomas and Warthin tumor on fine needle aspirates. *Acta Cytol*. 2003;47:221–226.
2. Batsakis JG, et al. Sebaceous lesions of salivary glands and oral cavity. *Ann Otol Rhinol Laryngol*. 1999;99:416–418.
3. Dardick I, et al. Lymphadenoma of parotid gland: two additional cases and a literature review. *Oral Surg Oral Med Oral Pathol Oral Radiol Endod*. 2008;105(4):491–494.
4. Firat P, et al. Sebaceous lymphadenoma of the parotid gland. *J Otol*. 2000;29:114–116.
5. Gnepp DR, et al. Sebaceous neoplasms of salivary gland origin: report of 21 cases. *Cancer*. 1984;53:2155–2170.
6. Gnepp DR, et al. Tumours of salivary glands: Sebaceous adenoma. In: el-Naggar AK, Chang JKC, Grandis JR, Takata T, Slootweg PJ, eds. *Classification of Head and Neck Tumours*. 4th ed. World Health Organization Classification of Tumours. Lyon, France: IARC Press; 2017:193–194.
7. Iezzi G, et al. Sebaceous adenoma of the cheek. *Oral Oncol*. 2002;38:111–113.
8. Izutsu T, et al. Sebaceous adenoma in the retromolar region: report of a case with a review of the English literature. *Int J Oral Maxillofac Surg*. 2003;32:423–426.
9. Maffini F, et al. Sebaceous lymphadenoma of salivary gland: a case report and a review of the literature. *Acta Otorhinolaryngol Ital*. 2007;27(3):147–150.
10. Prasad ML, et al. Tumours of salivary glands: Lymphadenoma. In: el-Naggar AK, Chang JKC, Grandis JR, Takata T, Slootweg PJ, eds. *Classification of Head and Neck Tumours*. 4th ed. World Health Organization Classification of Tumours. Lyon, France: IARC Press; 2017:190–191.
11. Seethala RR, et al. Lymphadenoma of the salivary gland: clinicopathological and immunohistochemical analysis of 33 tumors. *Mod Pathol*. 2012;25(1):26–35.

#### Warthin Tumor

1. Batsakis JG, et al. Warthin tumor. *Ann Otol Rhinol Laryngol*. 1990;99:588–591.
2. Gallo O. New insights into the pathogenesis of Warthin tumor. *Oral Oncol Eur J Cancer*. 1995;31B:211–215.
3. Nagao T, et al. Tumours of salivary glands: Warthin tumour. In: el-Naggar AK, Chang JKC, Grandis JR, Takata T, Slootweg PJ, eds. *Classification of Head and Neck Tumours*. 4th ed. World Health Organization Classification of Tumours. Lyon, France: IARC Press; 2017:188–189.
4. Sadetzki S, et al. Smoking and risk of parotid gland tumors: a nationwide case-control study. *Cancer*. 2008;112(9):1974–1982.
5. Seven H, et al. Multifocal synchronous Warthin tumor: a case report. *Am J Otolaryngol*. 1999;20:346–349.
6. Shikhani AH, et al. Warthin tumor-associated neoplasms: report of two cases and review of the literature. *Ear Nose Throat J*. 1993;72:264–273.
7. To EWH, et al. Warthin tumor with multiple sarcoid-like granulomas: a case report. *J Oral Maxillofac Surg*. 2002;60:585–588.
8. Vories AA, et al. Warthin tumor and cigarette smoking. *South Med J*. 1997;90:416–418.
9. Yoo GH, et al. Warthin tumor: a 40-year experience at the Johns Hopkins hospital. *Laryngoscope*. 1994;104:799–803.

#### Sebaceous Adenoma/Lymphadenoma

1. Apple SK, et al. Sebaceous adenoma of the parotid gland: a case report with fine needle aspiration findings and histologic correlation. *Acta Cytol*. 2009;53(4):419–422.

#### Hemangioma

1. Bruder E, et al. Vascular and perivascular lesions of skin and soft tissues in children and adolescents. *Pediatr Dev Pathol*. 2012;15(suppl):26–61.
2. Childers ELB, et al. Hemangioma of the salivary glands: a study of ten cases of a rarely biopsied/excised lesion. *Ann Diag Pathol*. 2002;6:339–344.
3. Damiani S, et al. Primary angiosarcoma of the parotid gland arising from benign congenital hemangioma. *Oral Surg Oral Med Oral Pathol Oral Radiol Endod*. 2003;96:66–69.
4. Flucke U, et al. Tumours of salivary glands: Haemangioma. In: el-Naggar AK, Chang JKC, Grandis JR, Takata T, Slootweg PJ, eds. *Classification of Head and Neck Tumours*. 4th ed. World Health Organization Classification of Tumours. Lyon, France: IARC Press; 2017:198.
5. Greene AR, et al. Management of parotid hemangioma in 100 children. *Plast Recon Surg*. 2004;113:53–60.
6. Khurana KK, et al. The role of fine-needle aspiration biopsy in the diagnosis and management of juvenile hemangioma of parotid gland and cheek. *Arch Pathol Lab Med*. 2001;125:1340–1343.
7. North PE, et al. GLUT1: a newly discovered immunohistochemical marker for juvenile hemangiomas. *Hum Pathol*. 2000;31(1): 11–22.

# Malignant Neoplasms of the Salivary Glands

■ Simion I. Chiosea ■ Lester D.R. Thompson

## ■ MUCOEPIDERMOID CARCINOMA

### CLINICAL FEATURES

Mucoepidermoid carcinoma (MEC) is the most common malignant salivary gland tumor (12% to 29%). Over half of all cases involve major glands, particularly the parotid (Fig. 13.1). Other sites include the mouth, particularly the palate (Fig. 13.1), buccal mucosa, lips, retromolar trigone, and the upper and lower respiratory tracts. Rarely, intrabony tumors form in the mandible and maxilla.

Women are more commonly affected than men (3:2), with a mean age in the 5th decade. MEC is the most common salivary gland malignancy in children. The tumor usually forms a painless, fixed, slowly growing swelling of widely varying duration; sometimes it shows a recent accelerated growth phase. Symptoms include tenderness, pain, evidence of nerve involvement, otorrhea, dysphagia, and trismus. Intraoral tumors are often bluish-red and fluctuant and may resemble mucoceles or vascular lesions. The tumor occasionally invades the underlying bone.

### PATHOLOGIC FEATURES

#### GROSS FINDINGS

MEC may be circumscribed and variably encapsulated or infiltrative and fixed, particularly in the higher-grade tumors. Most tumors are less than 4 cm in diameter. Areas of scarring are relatively common. Cysts of variable sizes are often present and usually contain brownish, glairy fluid (Fig. 13.2). Occasionally, tumors appear to be unicystic.

#### MICROSCOPIC FINDINGS

The cells of MEC form sheets, islands, duct-like structures, and cysts of varying sizes (Fig. 13.3). Cysts

### MUCOEPIDERMOID CARCINOMA—DISEASE FACT SHEET

#### Definition

- A malignant glandular epithelial neoplasm characterized by mucous, intermediate, and epidermoid cells

#### Incidence and Location

- Most common malignant salivary gland tumor (12%-29%)
- Nearly 60% in major salivary glands (usually parotid)
- Others develop in the mouth and upper and lower respiratory tracts

#### Morbidity and Mortality

- About 40% of cases recur locally
- Spread to regional lymph nodes and distant sites occurs in some 15% of cases
- Overall 5-year survival is 80%

#### Sex and Age Distribution

- Females > males (3:2)
- Mean, 47 years (range, 8-92 years)
- Most common salivary malignancy in children

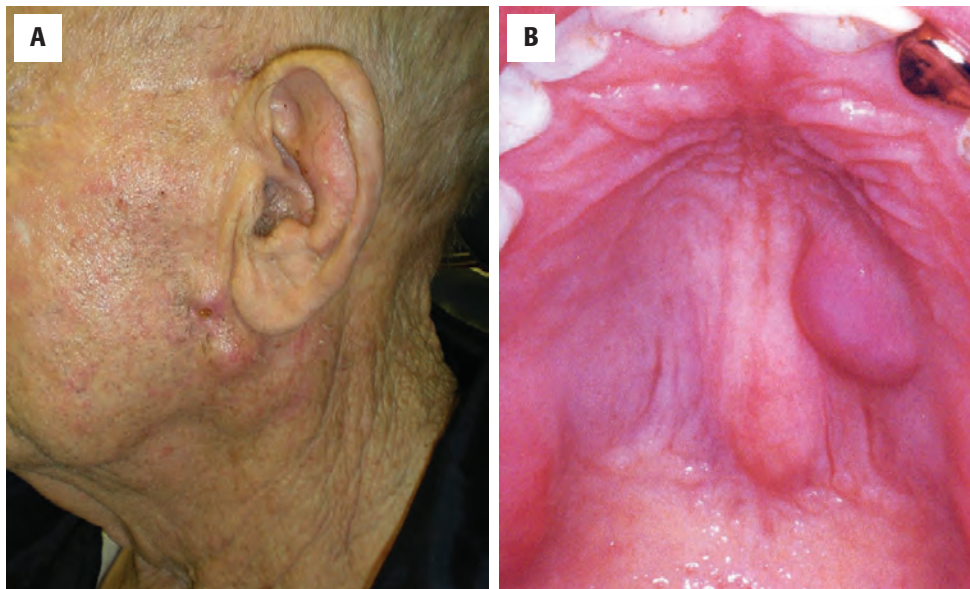
#### Clinical Features

- Usually forms a painless, fixed, slow-growing swelling
- Intraoral tumors, often bluish red, may mimic mucoceles or vascular tumors
- Symptoms include pain, evidence of nerve involvement, otorrhea, dysphagia, and trismus

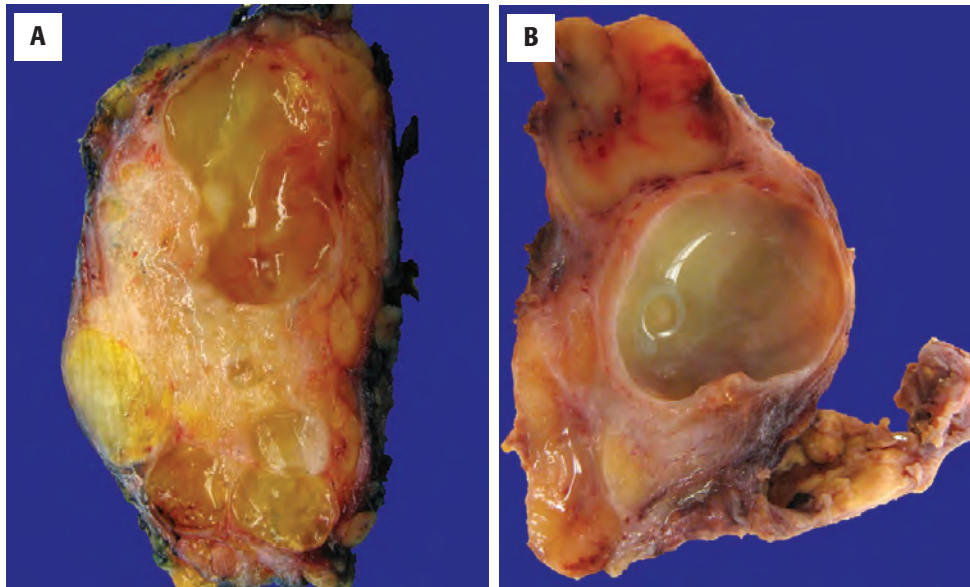
#### Prognosis and Therapy

- Prognosis depends on clinical stage, site, grading, and adequacy of surgical excision
- Most tumors are of low grade with an excellent prognosis
- Tumors of the submandibular gland have a poorer prognosis
- Tumors, particularly those of high grade, can show spread to regional lymph nodes and distant sites, including the lungs, bone, and brain
- Surgery, with or without neck dissection, is the treatment of choice; palliative radiotherapy may be used in some cases



**FIGURE 13.1**

(**A**) A multinodular mass is noted in the left parotid gland. There is erythema and focal ulceration. (**B**) A mucosa-covered slightly bluish mass in the left palate represents a mucoepidermoid carcinoma, although this finding is not specific.

**FIGURE 13.2**

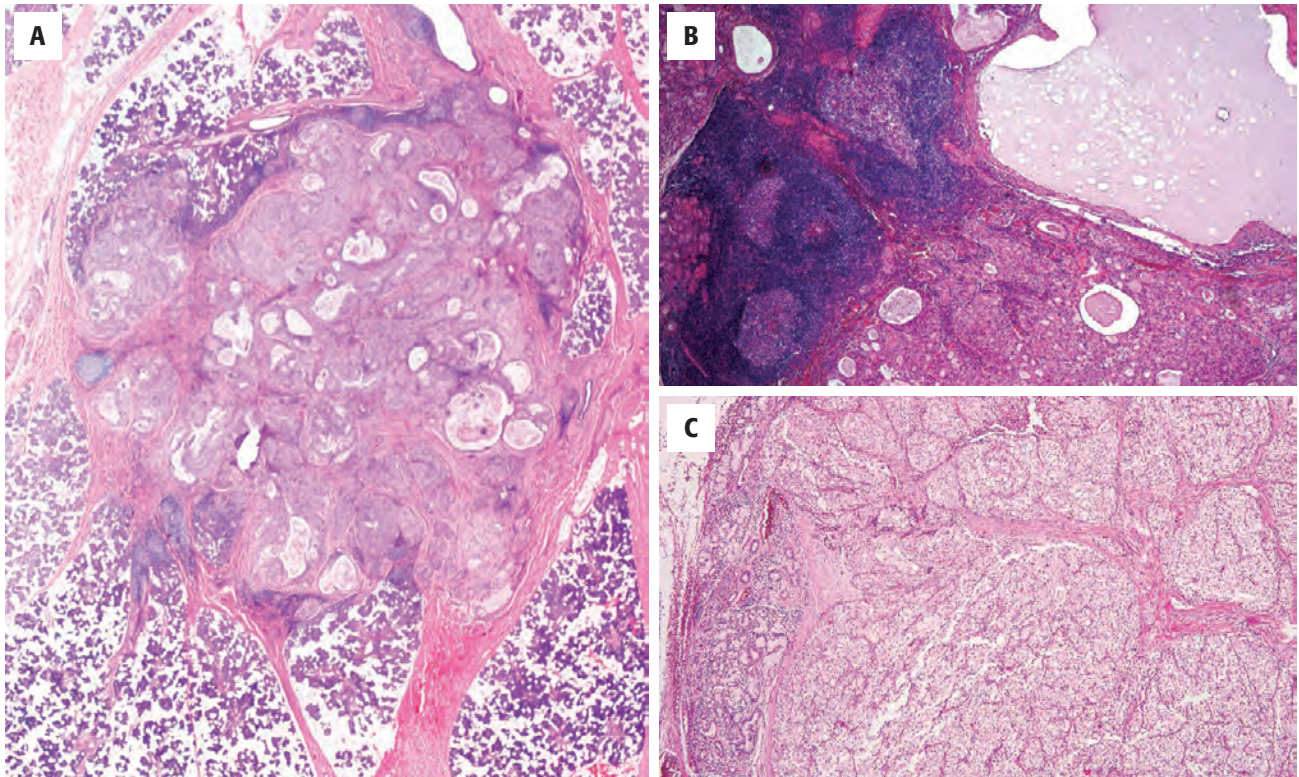
(**A**) Gross photograph shows a tumor with a tan-yellow cut surface. Mucoïd material glistens within the multiple cystic spaces. (**B**) This gross photograph demonstrates a predominantly unilocular cyst of a mucoepidermoid carcinoma. The fluid is thick, mucoid, and tenacious. Note the lymph node (*upper*).

may be lined by intermediate, mucous, or epidermoid cells and are filled with mucus (Fig. 13.4). Larger cysts often rupture, spreading tumor cells into the adjacent tissue and evoking an inflammatory reaction, with hemorrhage, hemosiderin deposition, cholesterol cleft formation, and fibrosis. Some tumors show extensive mucinous lakes (mucin-rich variant). Papillary processes may extend into the cyst lumen, and occasionally, this is conspicuous.

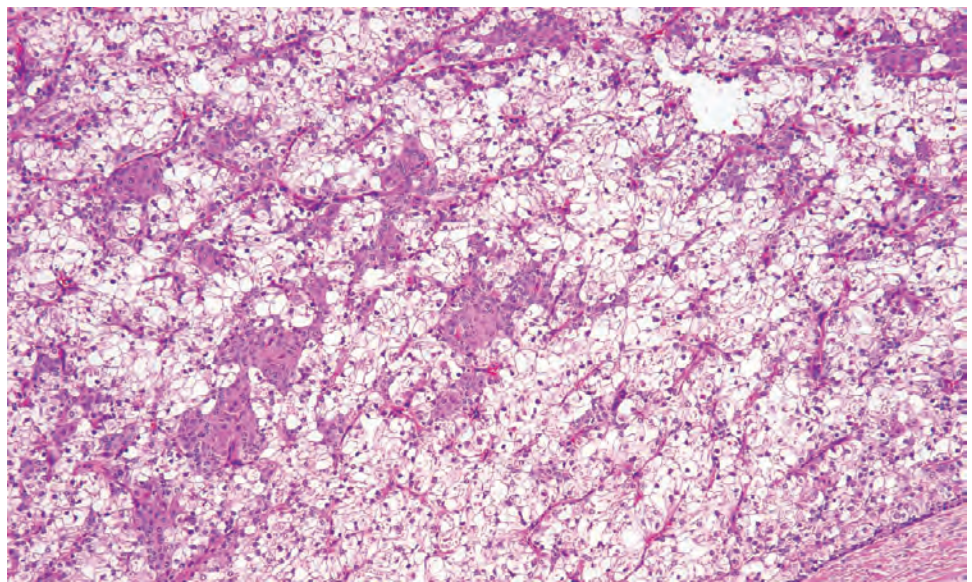
MEC consists predominantly of three cell types in widely varying proportions: epidermoid, mucous, and intermediate (Fig. 13.5). Less common cell types seen include clear cells, columnar cells, and oncocytes. Intermediate cells frequently predominate and range in size from small basal cells with scanty basophilic cytoplasm (“maternal” cells) to larger and more oval cells with more

abundant pale, eosinophilic cytoplasm that appears to merge into epidermoid or mucous cells (Fig. 13.6). The intermediate cells form islands or sheets and may be the basally located cells of intratumoral cysts. Mucous cells (mucocytes) can occur singly or in clusters and have pale and sometimes foamy cytoplasm, a distinct cell boundary, and peripherally placed, small, compressed nuclei. They often form the lining of cysts or duct-like structures (Fig. 13.7). Occasionally, mucocytes are so scanty that they can be identified with confidence only by using stains such as mucicarmine (Fig. 13.7) or Alcian blue. Epidermoid cells may be uncommon and focally distributed. They have abundant eosinophilic cytoplasm but rarely show extracellular keratin pearl formation or dyskeratosis unless there has been a biopsy or fine needle aspiration (FNA).



**FIGURE 13.3**

(**A**) Mucoepidermoid carcinoma (MEC) often shows a variable growth pattern with cystic spaces and fibrosis. (**B**) Tumor-associated lymphoid proliferation (TALP) is noted adjacent to the tumor. (**C**) Predominantly mucinous epithelium is seen in this field of a MEC.

**FIGURE 13.4**

Sheet-like distribution of intermediate and mucous cells in this mucoepidermoid carcinoma.

Focal areas of clear cells are common but occasionally form the bulk of the tumor. The cells have distinct outlines, water-clear cytoplasm, and small, centrally located nuclei (Fig. 13.8). They contain minimal sialomucin but usually have plentiful glycogen content, as demonstrated with periodic acid-Schiff diastase (PAS/D) staining. Columnar cells are uncommon and typically

form the lining of cysts. Focal or generalized oncocytic metaplasia (known as the oncocytic variant) is seen occasionally.

Higher-grade tumors may show cytologic atypia, a high mitotic frequency, areas of necrosis, and neural invasion (Fig. 13.9). Rarely, low-grade MECs undergo high-grade transformation (HGT; “dedifferentiation”).



**MUCOEPIDERMOID CARCINOMA—PATHOLOGIC FEATURES****Gross Findings**

- May be circumscribed and variably encapsulated or infiltrative
- Cysts often present and contain brownish, viscid fluid

**Microscopic Findings**

- Consists of mucous, intermediate, and epidermoid cells
- Other cells include clear cells, columnar cells, and oncocytes
- Tumors show cystic and solid areas in varying proportions along with other patterns
- Inflammation and fibrosis are common
- Tumors are separated into low, intermediate, and high grades

**Immunohistochemical Findings**

- Intermediate and epidermoid cells are immunoreactive for cytokeratin, p63, p40, and frequently EMA

**Molecular Findings**

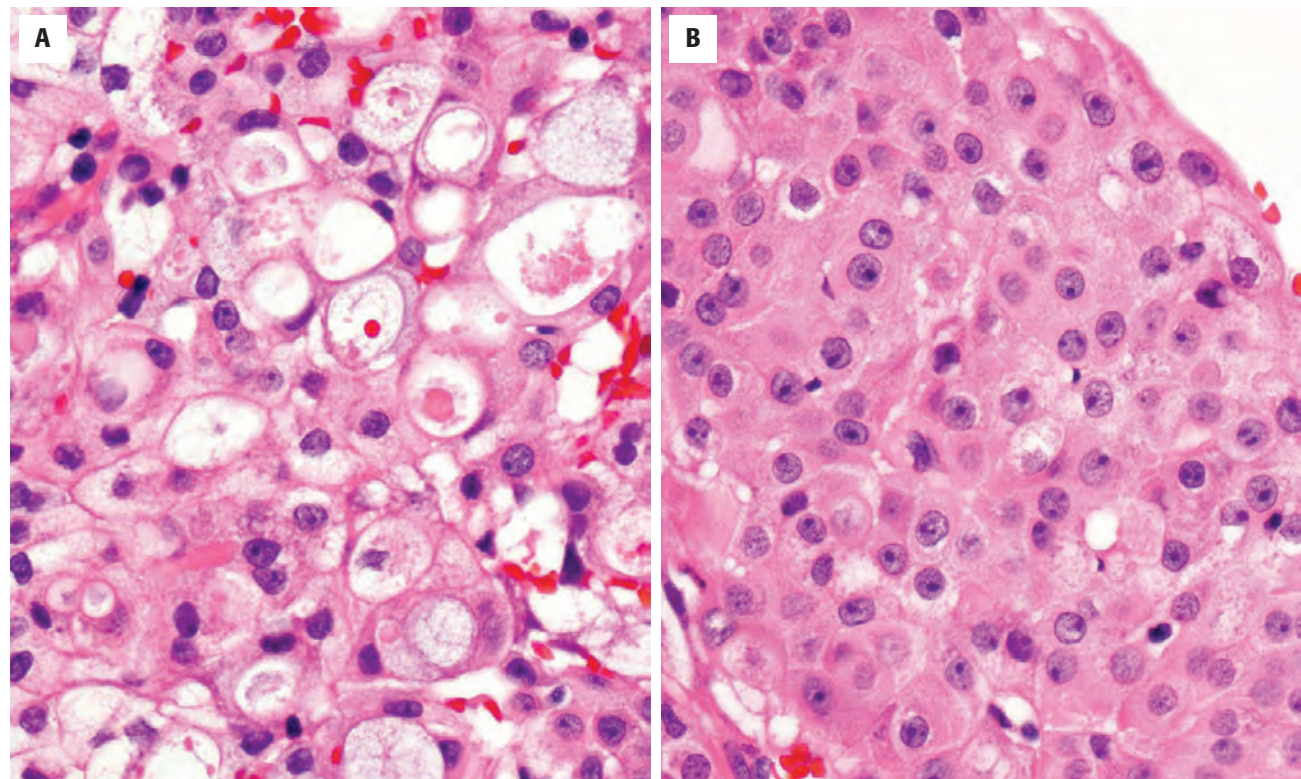
- *MAML2* rearrangement is identified in 78%-85% of cases, independent of grade

**Fine Needle Aspiration**

- Cellular smears with background of mucinous material
- Cohesive epithelial clusters with sheets of cells and cells streaming in the mucus
- Mucocytes help to confirm diagnosis in presence of intermediate and epidermoid cells

**Pathologic Differential Diagnosis**

- Necrotizing sialometaplasia, mucocele, cystadenoma, cystadenocarcinoma, squamous cell carcinoma (of mucosal or cutaneous origin), adenosquamous carcinoma, clear cell neoplasms, metastasis, secretory carcinoma, and salivary duct carcinoma

**FIGURE 13.5**

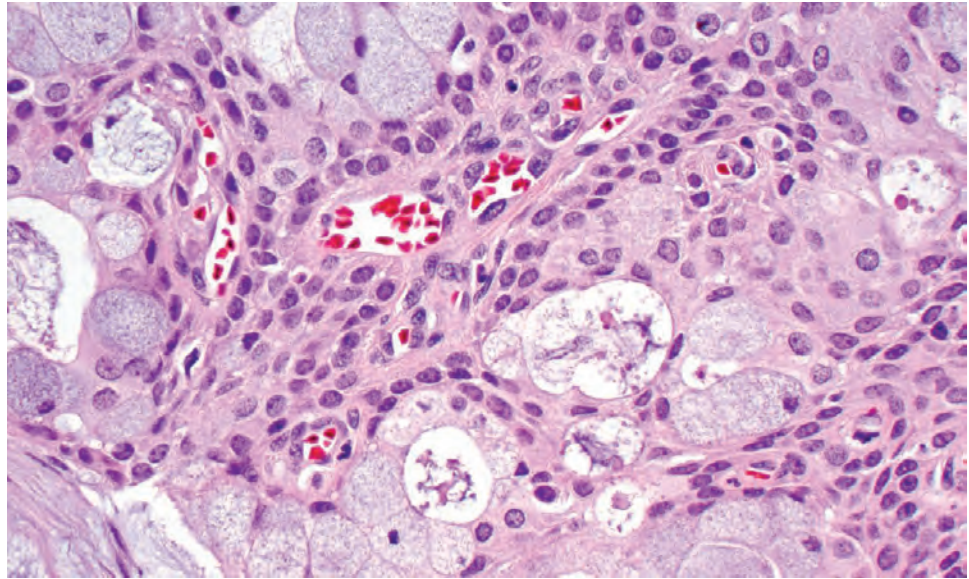
(**A**) Intermediate cells are blending imperceptibly with the mucocytes in this mucoepidermoid carcinoma. (**B**) A field of epidermoid cells. Note the lack of intercellular bridges and “hard” keratinization.

**TUMOR GRADING**

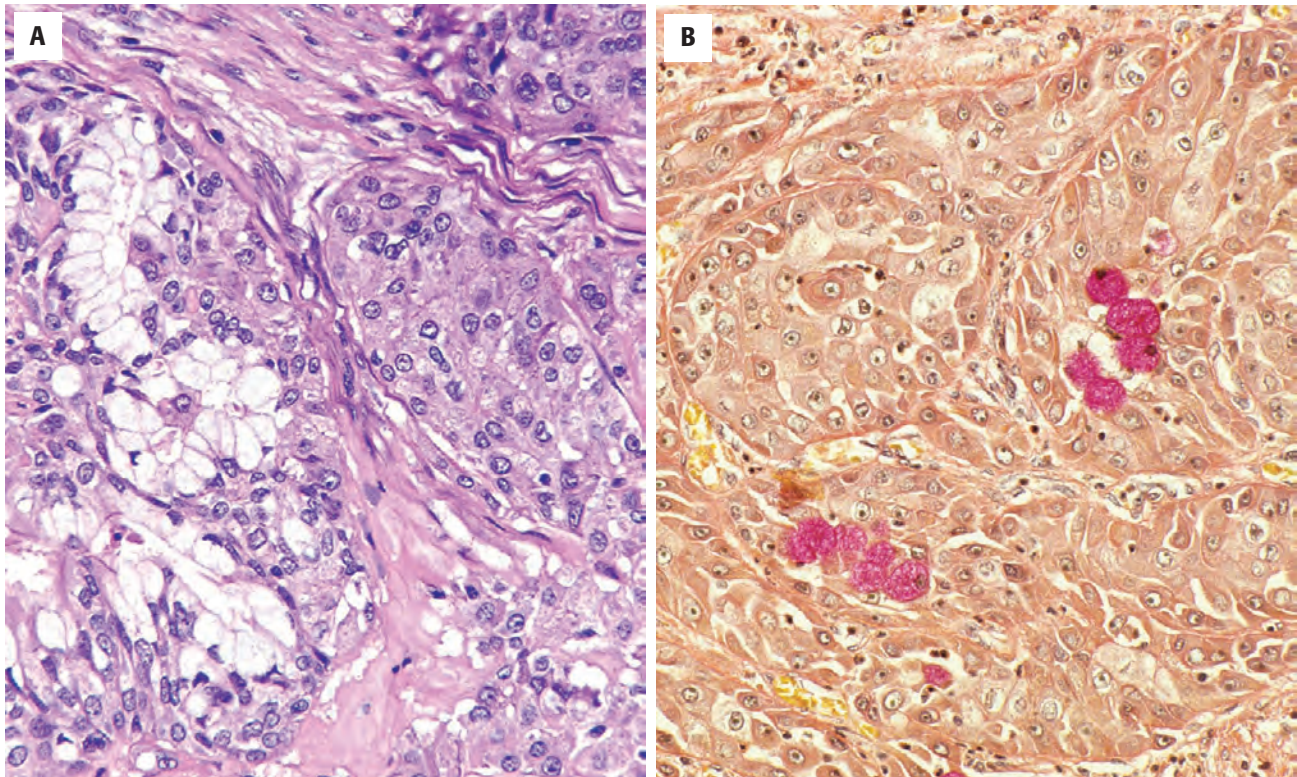
MEC shows variability in clinical behavior, and several microscopic grading systems have been advocated to predict outcome. Many rely on subjective evaluation of

the relative proportions of the various cell types as well as (1) the cystic component, (2) neural invasion ([Fig. 13.10](#)), (3) necrosis, (4) increased mitoses, and (5) cellular pleomorphism (anaplasia). Low-grade tumors tend to be cystic, have abundant mucocytes, and show minimal atypia or mitotic activity. However, they usually show



**FIGURE 13.6**

Intermediate cells are noted in small islands and form the “basal zone” below the cystic spaces lined by mucocytes. Mucocytes have fluffy cytoplasm.

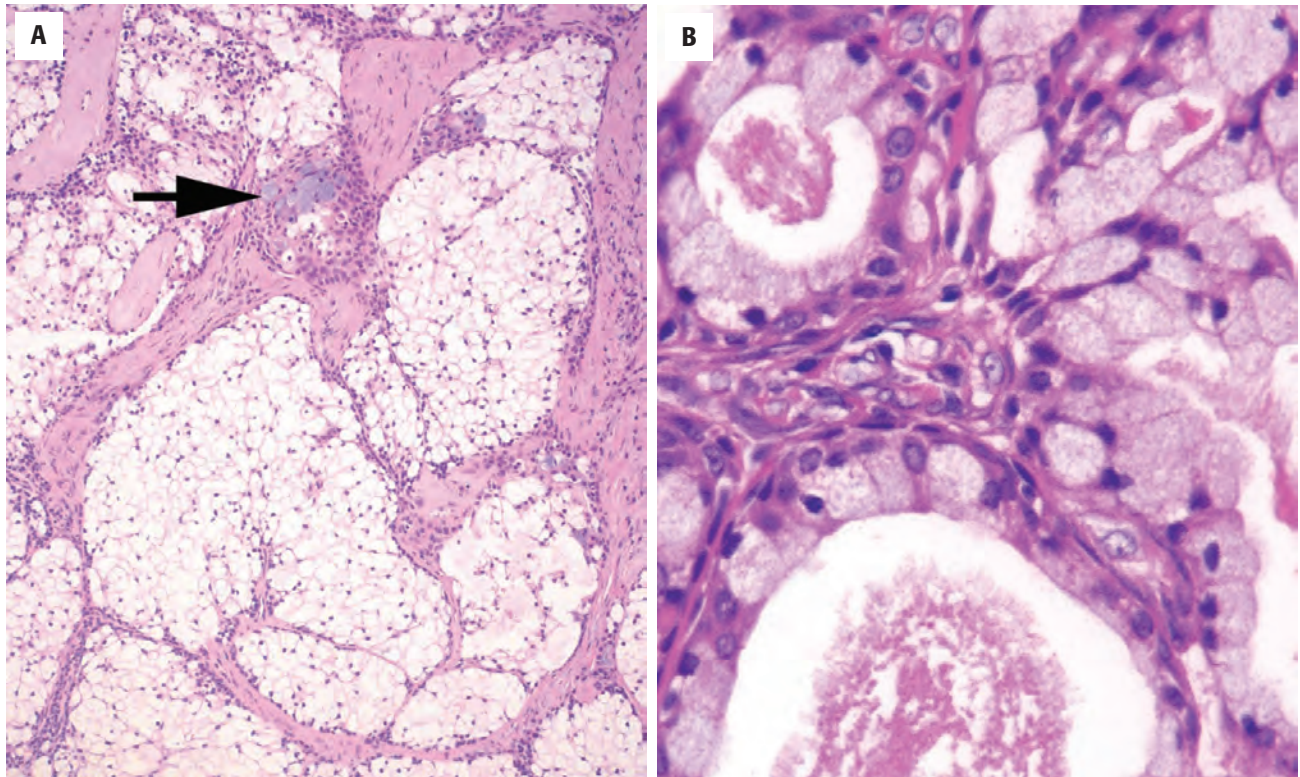
**FIGURE 13.7**

(A) Mucocytes are identified in a cyst with intermediate cells at the base. (B) Mucicarmine highlights intracytoplasmic mucin, especially in cells with eccentric, squashed nuclei.

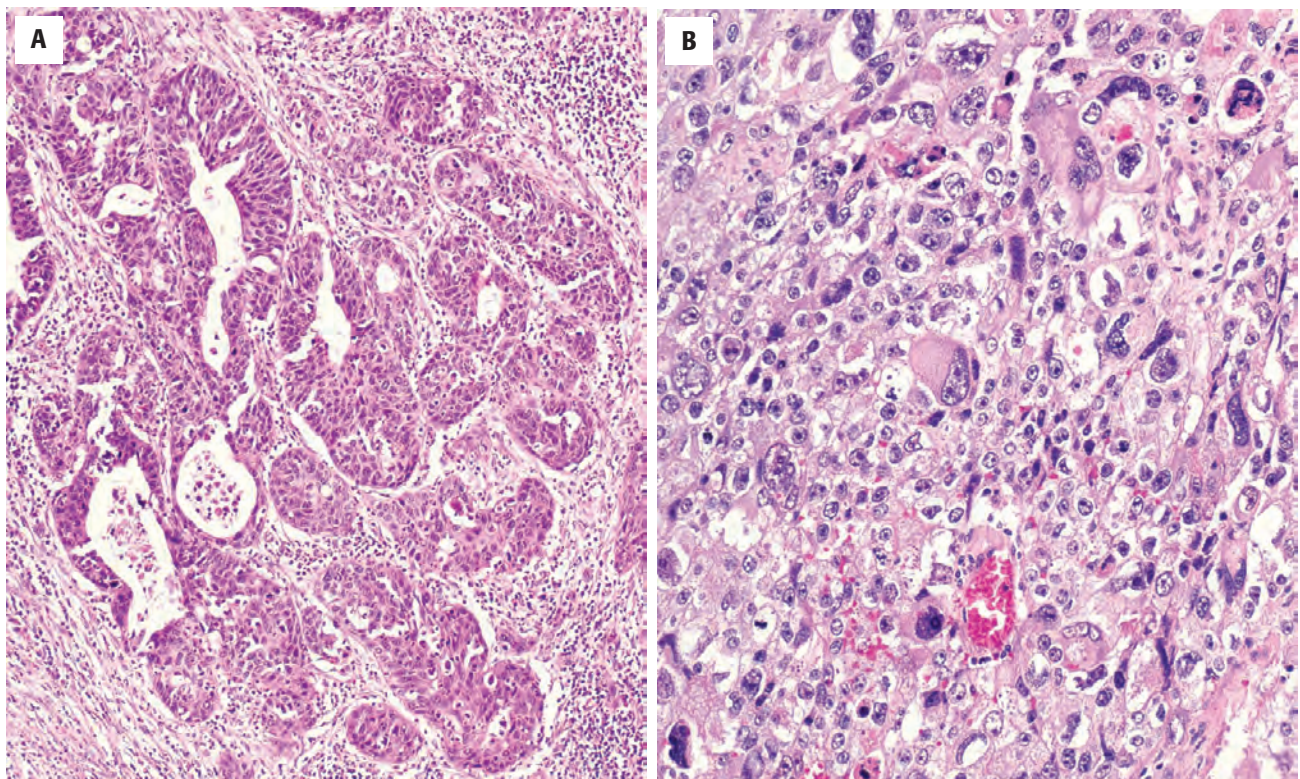
evidence of invasion. Higher-grade tumors are more cellular, with minimal cyst formation (Fig. 13.11). They have few mucocytes, consist mainly of cells similar to squamous cell carcinoma, and may show necrosis and neural or vascular invasion. A numerical grading system using point scoring of five parameters appears to be useful in defining the tumors as low, intermediate, or high grade

and predicting their behavior (Table 13.1). However, the grading of MEC of the submandibular gland using this system has been less reliable. A seven-point grading system, including the additional parameters of the nature of the invasive front and bone invasion, has been proposed but requires additional validation. Lymphovascular invasion has not been included in grading schemes to date.



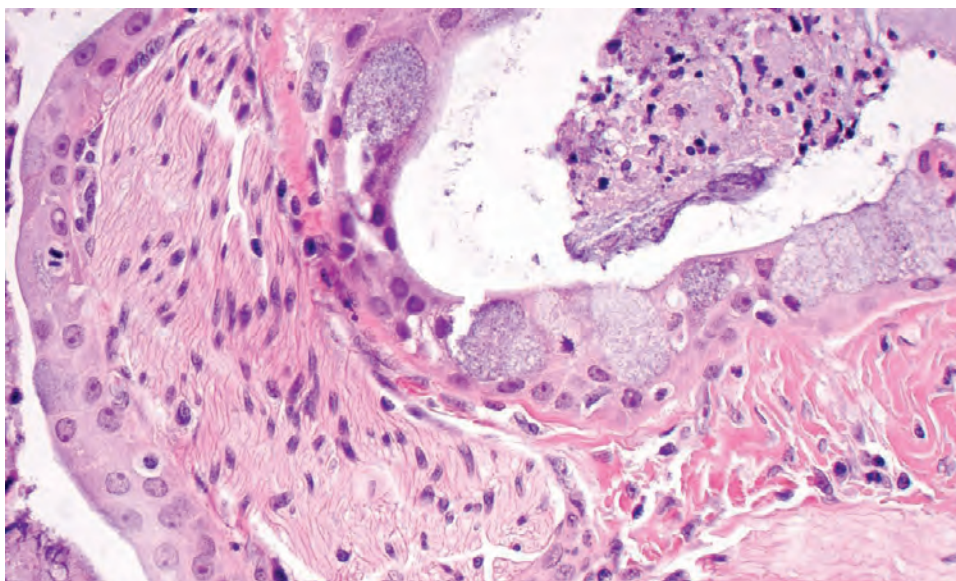
**FIGURE 13.8**

(A) This mucoepidermoid carcinoma shows a predominantly clear cell pattern, although isolated mucocytes are noted (*arrow*). (B) The mucocytes have fluffy cytoplasm and may surround secretions within the duct spaces.

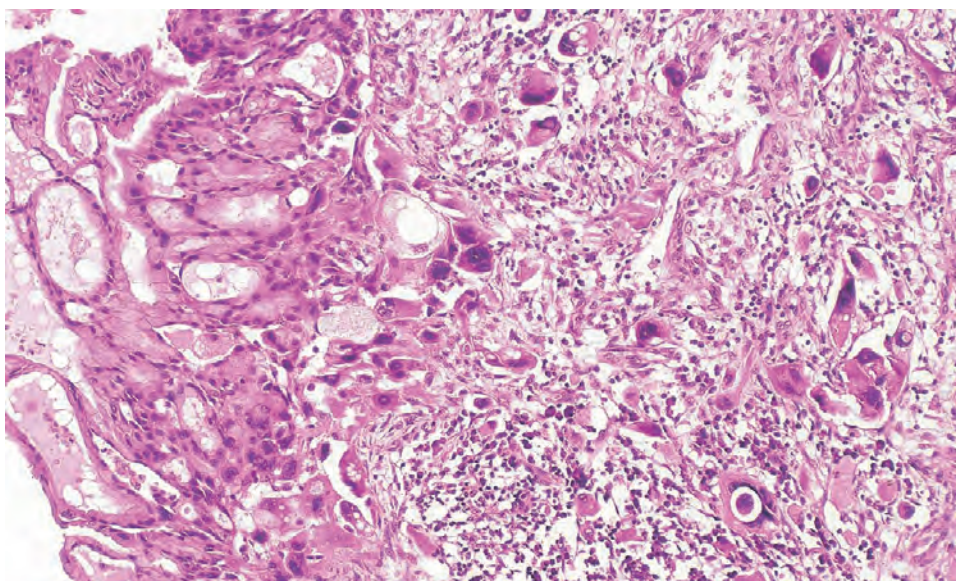
**FIGURE 13.9**

(A) Intermediate-grade mucoepidermoid carcinoma showing limited cyst formation and nearly absent mucocytes. (B) A high-grade tumor with increased mitoses and profound pleomorphism.



**FIGURE 13.10**

The degree of cytologic atypia is not profound, but there is well-developed perineural invasion in this tumor.

**FIGURE 13.11**

A low-grade tumor is noted to undergo dedifferentiation into a sarcomatoid carcinoma appearance (*right-sided*). This abrupt transition is usually the tip-off to sarcomatous transformation.

## ANCILLARY STUDIES

### IMMUNOHISTOCHEMICAL FINDINGS

Intermediate, epidermoid, and columnar cells are usually positive for cytokeratin, but clear cells show inconsistent reactivity and mucocytes are negative. Epithelial membrane antigen (EMA) is positive in most tumor cells, but staining with this and other immunohistochemical markers (such as CK5/6 and p63) does not correlate with histologic grading (Fig. 13.12).

### MOLECULAR FINDINGS

*MAML2* rearrangement is identified in 78 % to 85 % of cases regardless of grade. The presence of *MAML2*

rearrangement is of pure diagnostic value without any prognostic significance.

### FINE NEEDLE ASPIRATION

Smears of an MEC may be difficult to separate from a mucocoele or other benign cyst. However, MEC usually has cellular smears with abundant mucinous material and debris in the background (Fig. 13.13). There are cohesive groups of epithelial cells arranged in sheets or streaming within the mucin (Fig. 13.13). Cells are separated into mucocytes, intermediate cells, and epidermoid cells in variable proportions. Most of the cells have ample cytoplasm surrounding nuclei that are only mildly pleomorphic. Higher-grade tumors have less mucin and greater nuclear pleomorphism, which may be difficult to diagnose accurately on FNA. Occasionally, a diagnosis



**TABLE 13.1****Grading and outcome for mucoepidermoid carcinomas**

| Parameter                           | Point Value |                 |
|-------------------------------------|-------------|-----------------|
| Intracystic component<br>< 20%      | 2           |                 |
| Neural invasion                     | 2           |                 |
| Necrosis                            | 3           |                 |
| Mitotic figures $\geq 4/10$<br>HPFs | 3           |                 |
| Anaplasia                           | 4           |                 |
| Grade                               | Total Score | Dead of Disease |
| Low                                 | 0–4         | 3.3%            |
| Intermediate                        | 5–6         | 9.7%            |
| High                                | $\geq 7$    | 46.3%           |

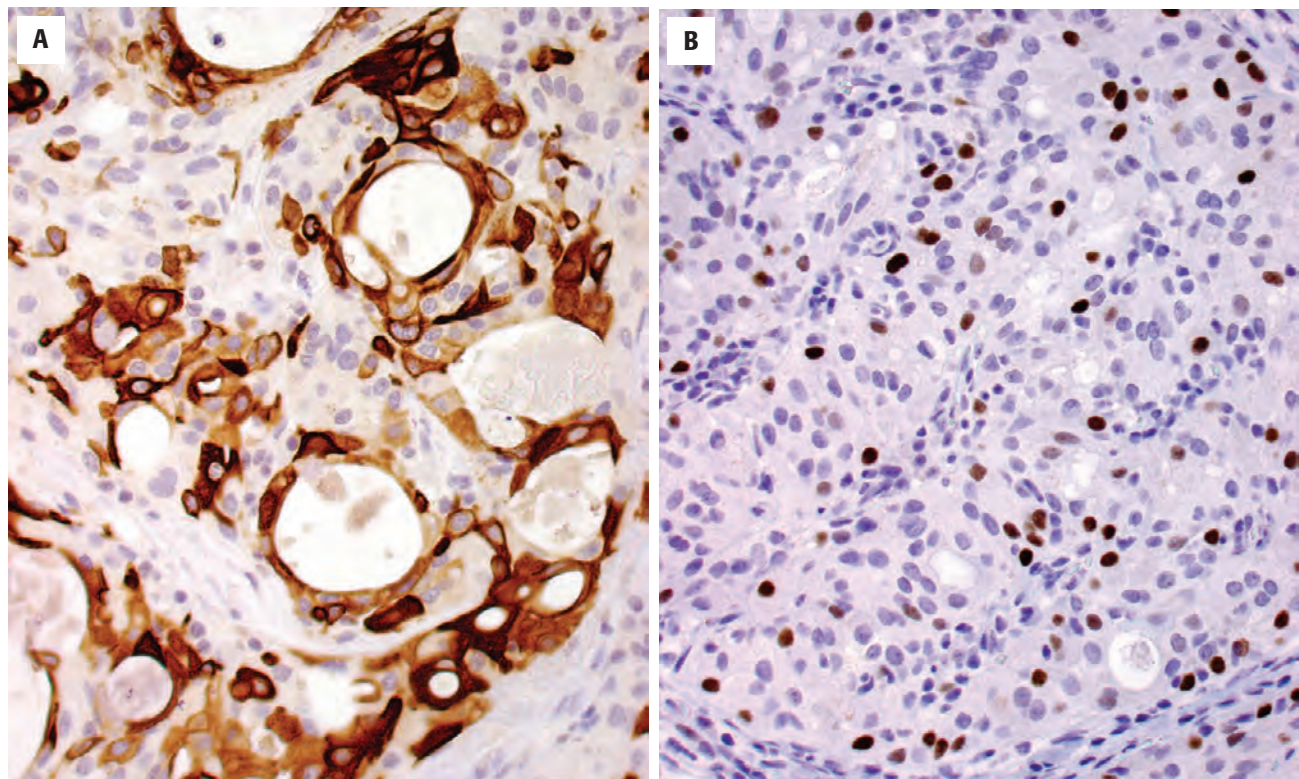
HPFs, High-power fields.

of “mucus-producing lesion” may be the only diagnosis that can be rendered with accuracy.

**DIFFERENTIAL DIAGNOSIS**

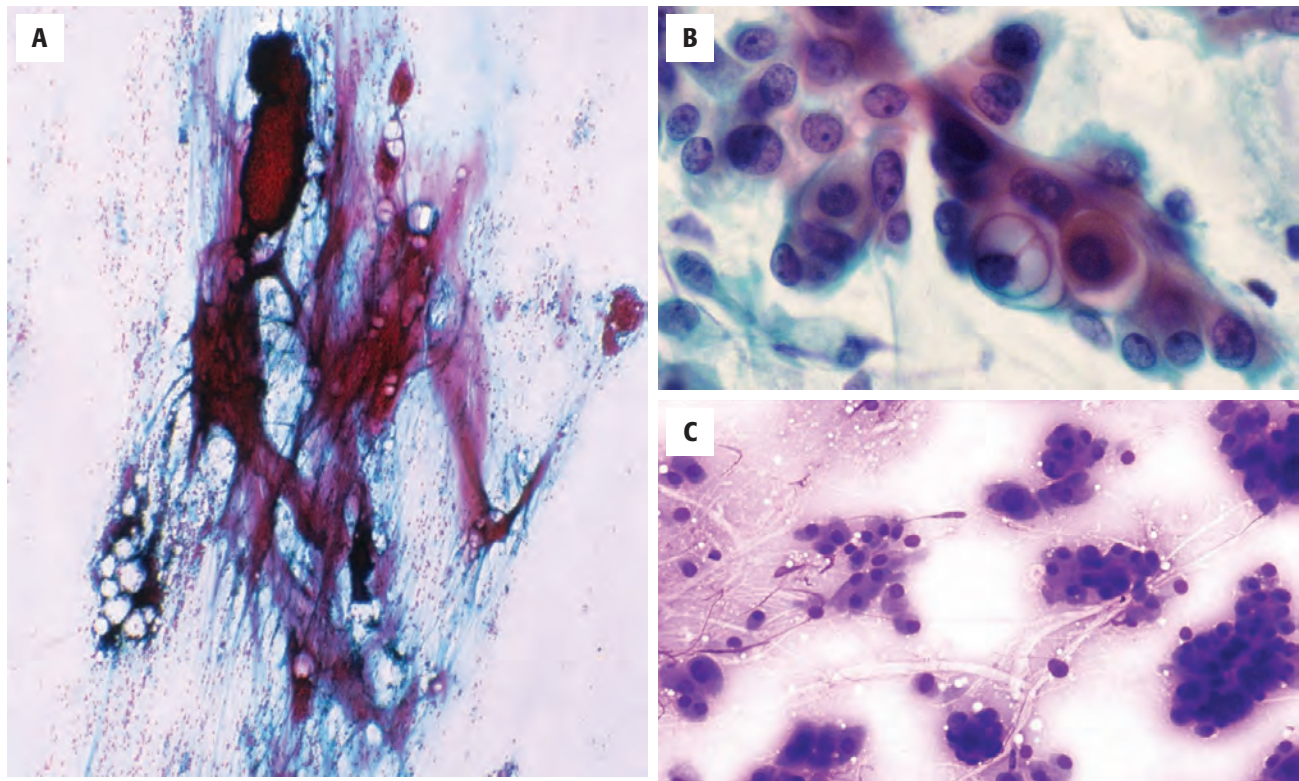
Both MEC and necrotizing sialometaplasia (NSM) can show squamous proliferation with foci of mucocytic differentiation in an inflamed, fibrous stroma. NSM, however, has a lobular distribution and usually shows areas of transition from the ducts to the solid islands of squamous cells formed by intraductal regenerative hyperplasia (Fig. 13.14). There are no intermediate cells, and cyst formation is not a feature.

High-grade tumors may resemble nonkeratinizing squamous cell carcinoma, but appropriate stains can demonstrate the presence of scattered mucocytes. In addition, it is rare for MECs to show keratinization. Other mimics of high-grade MEC include adenosquamous carcinoma and salivary duct carcinoma (SDC). The sclerosing variant of MEC may be confused with chronic sialadenitis. Predominantly clear cell MEC must be distinguished from tumors such as epithelial-myoepithelial carcinoma (EMC), clear cell carcinoma, and metastatic tumors. The pattern of p63 or p40 positivity may be of

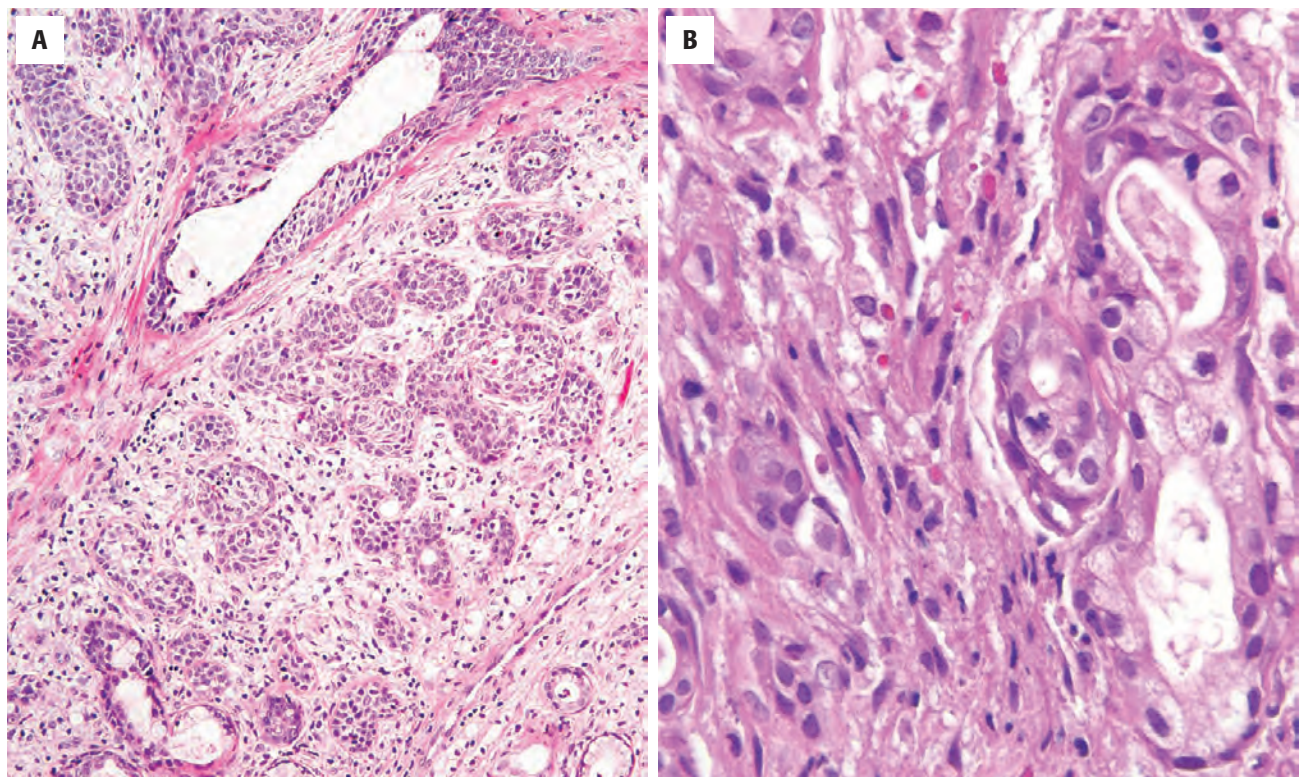
**FIGURE 13.12**

Immunohistochemistry can help to confirm the epithelial nature of the process and perhaps highlight the epidermoid cells (CK5/6, **A**), although basal markers (p63, **B**) are also positive.



**FIGURE 13.13**

(A) Epithelial cells are set in a sea of mucinous material. This type of mucinous material is the clue to the diagnosis. (B) A cellular smear with intermediate-epidermoid cells arranged in sheets and streaming groups. Note the mucocyte in the center with mucin vacuoles (alcohol-fixed, Papanicolaou stain). (C) A cellular smear with a background of mucinous material. Groups of epithelial cells with opaque cytoplasm constitute the intermediate component (air-dried, Diff-Quik stain).

**FIGURE 13.14**

(A) Necrotizing sialometaplasia has a lobular architecture with squamous metaplasia of the duct/lobular units. (B) Residual mucocytes are replaced by metaplastic squamous epithelium. Inflammatory cells are noted in the background.



help. Specifically, p63 and p40 will highlight the dual cell population of EMC. Almost all cells in clear cell carcinoma are p63- and p40-positive. In MEC, p63 and p40 will highlight epidermoid cells and a subset of intermediate cells.

### PROGNOSIS AND THERAPY

The prognosis is dependent on clinical stage, site, grading, and adequacy of surgery. Most MECs are low grade and the prognosis for these tumors is generally good (> 95 % survival with only rare regional metastases). The mortality rate, however, increases to about 45 % in the much less common group of high-grade tumors. In addition, incompletely excised tumors have a very high recurrence rate, particularly high-grade tumors. Also, MEC in the submandibular gland, floor of mouth, tongue, and maxillary antrum has a poorer prognosis. Death is usually due to uncontrolled locoregional disease and/or metastases to lung, bone, and brain. Treatment is by surgical excision with or without neck dissection. Radiotherapy is generally palliative in advanced tumors but has little impact on outcome.

## ■ ACINIC CELL CARCINOMA

### CLINICAL FEATURES

Acinic cell carcinoma (AcCC) accounts for about 6 % of all salivary gland tumors and up to 17.5 % of all salivary malignancies. About 95 % form in the parotid gland. The possibility of secretory carcinoma (SC) should be considered before the diagnosis of AcCC is rendered for a tumor outside of major salivary glands (Fig. 13.15). About 4 % arise in the submandibular gland and 1 % in the sublingual. There is a female predominance (3:2). Most patients with conventional AcCC are diagnosed in the 4th to 5th decades (mean, 48 years), while patients with AcCC with HGT are diagnosed in the 7th decade. AcCC is the second most common malignant salivary gland tumor in children.

AcCC usually presents as a slow-growing mass with a duration ranging from a few weeks to 40 years. Pain or tenderness is present in up to half of patients. The tumor may be freely mobile or fixed to the skin or underlying tissues. Facial nerve involvement is seen in up to 10 % of cases.

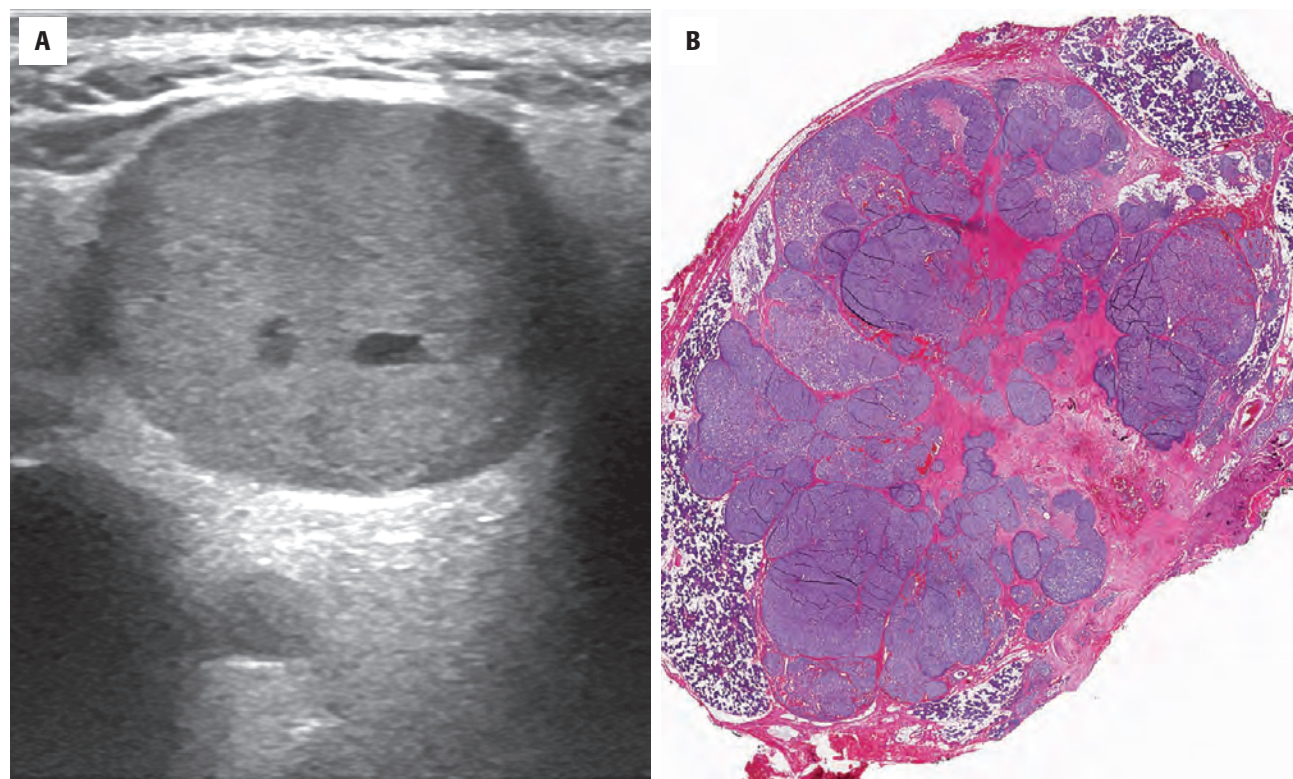


**FIGURE 13.15**

(A) Ultrasound shows a well-circumscribed mass with focal cystic change. (B) There is an irregular, invasive periphery to this multinodular tumor. A capsule is not well developed, although internal tumor fibrosis is present.

**ACINIC CELL CARCINOMA—DISEASE FACT SHEET****Definition**

- A malignant epithelial neoplasm demonstrating serous acinar cell differentiation with cytoplasmic zymogen secretory granules

**Incidence and Location**

- About 6% of salivary gland tumors
- 95% involve the major salivary glands

**Morbidity and Mortality**

- 5-year and 10-year survival rates are 82% and 68%, respectively

**Sex and Age Distribution**

- Females > males (3:2)
- 2nd-7th decades (mean, 44 years)
- Second most common malignant salivary gland tumor in children

**Clinical Features**

- Slow-growing mobile or fixed mass
- Duration varies from weeks to several decades
- Pain or tenderness in up to half of patients
- Facial nerve involvement in 5%-10% of cases

**Prognosis and Therapy**

- About 35% develop recurrences
- Behavior does not correlate with patterns of growth
- Regional and distant metastases and worse overall survival are associated with high-grade transformation (cellular pleomorphism, increased mitotic frequency, presence of necrosis, and loss of serous acinar differentiation)
- Complete surgical excision is the treatment of choice

**PATHOLOGIC FEATURES****GROSS FINDINGS**

Most tumors are less than 3 cm in diameter and usually form a rubbery or firm, circumscribed, oval, or round mass (Fig. 13.15). Some have poorly defined margins or multifocal nodules and areas of hemorrhage or cystic change.

**MICROSCOPIC FINDINGS**

AcCC is defined by serous acinar cells, but several other cell types may be present as well, including vacuolated and clear cells. Individual tumors may show several cell types or one type may predominate. *Serous acinar* cells are the most common (Fig. 13.16). They resemble serous cells of the normal salivary gland and have abundant basophilic cytoplasm containing dense, grayish, or blue zymogen granules. The granules may be fine or coarse (Fig. 13.17) and are variably PAS/D-positive. Nuclei are round and basophilic or occasionally more vesicular and are usually located peripherally. Cells with *clear*

**ACINIC CELL CARCINOMA—PATHOLOGIC FEATURES****Gross Findings**

- Rubbery or firm tumors usually < 3 cm
- Usually circumscribed (occasionally irregular)
- May show hemorrhage or cystic change

**Microscopic Findings**

- Characteristic cell is serous acinar type with basophilic zymogen granules in the cytoplasm (usually accentuated at the lumen)
- Other cell types include vacuolated and clear cells
- Solid and follicular growth patterns
- May have tumor associated lymphoid proliferation (TALP)/infiltrate, occasionally prominent

**Ancillary Studies**

- PAS-positive, diastase-resistant zymogen granules
- Acinic cells may stain positively for amylase, transferrin, lactoferrin, DOG1, and SOX10
- About 10% show some positivity for S100 protein (usually weaker than adjacent nerves)

**Fine Needle Aspiration**

- Cellular smears with clean background
- Cohesive, small, tight clusters
- Ample granular to vacuolated cytoplasm surrounding round and regular nuclei with coarse chromatin (lymphocyte-like nuclei)

**Pathologic Differential Diagnosis**

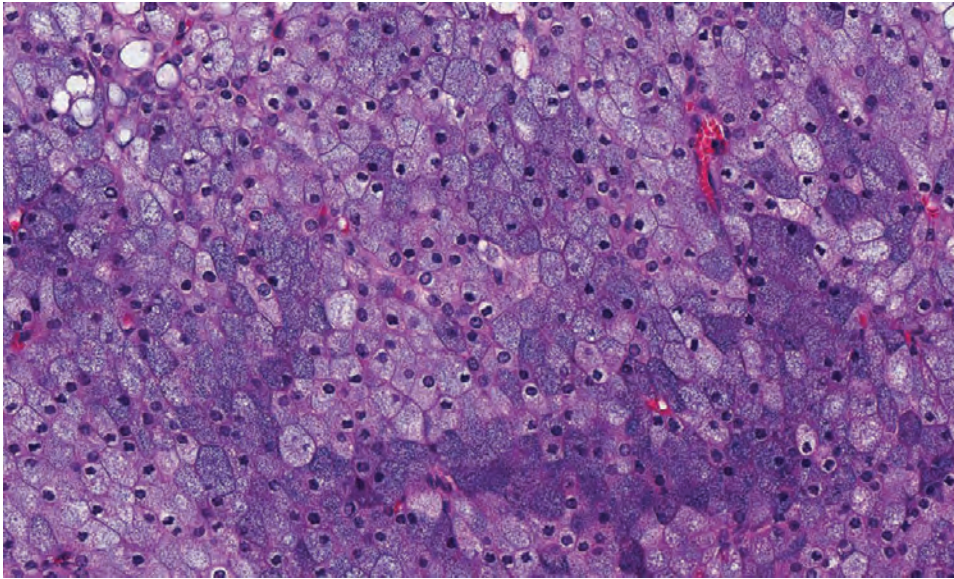
- For conventional AcCC: Normal salivary gland, sialadenitis, cystadenocarcinoma (especially papillary variants), mucoepidermoid carcinoma, secretory carcinoma, clear cell tumors
- For AcCC with high-grade transformation: high-grade carcinomas, such as salivary duct carcinoma, and other salivary-type carcinomas with high-grade transformation

AcCC, Acinic cell carcinoma; PAS, periodic acid–Schiff.

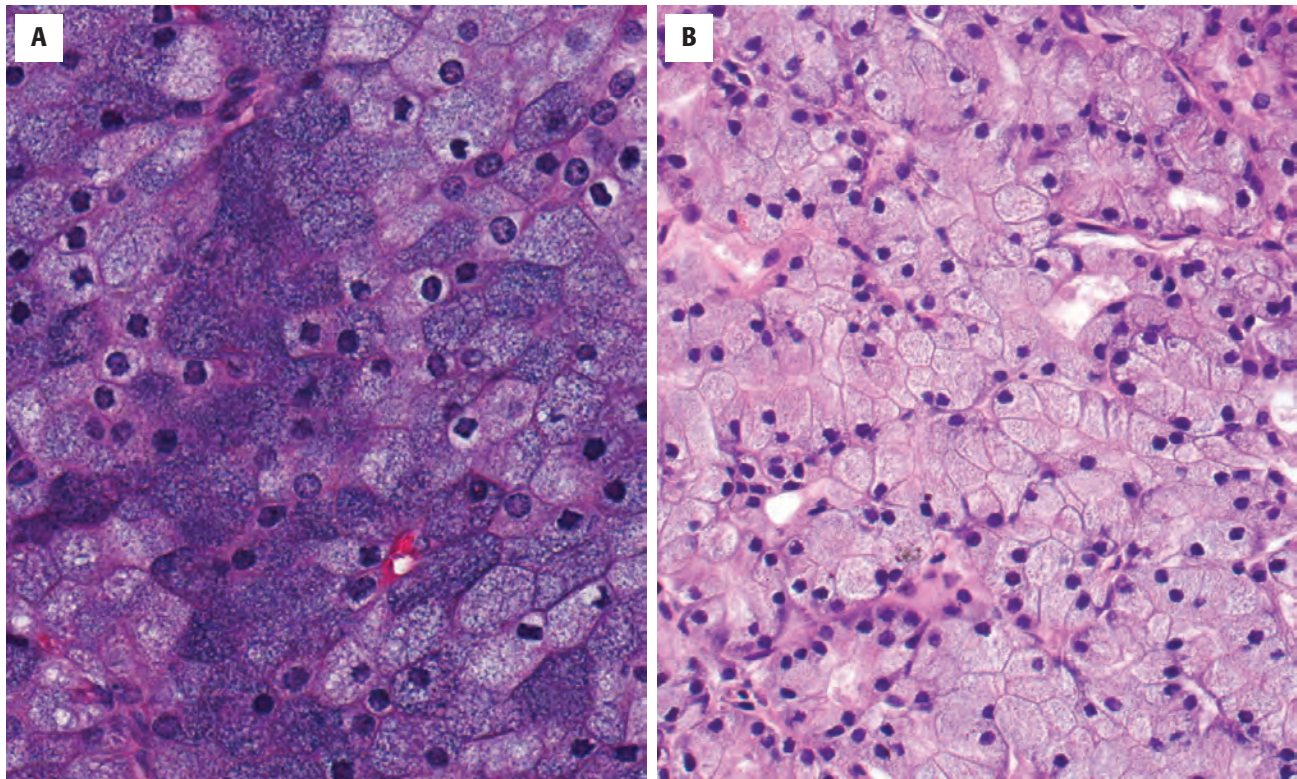
cytoplasm and conspicuous cell boundaries are usually seen only focally. They do not contain glycogen and may represent fixation or processing artifacts. *Vacuolated* cells may be a conspicuous feature. They have clear PAS/D-negative cytoplasmic vacuoles, and some cells also contain zymogen granules. *Intercalated duct-type* cells are smaller because they contain less cytoplasm, which is usually eosinophilic, and the nuclei tend to be central. These cells surround luminal spaces of varying size. *Nonspecific glandular* cells are polygonal or round and are usually smaller than acinar cells. The cytoplasm is eosinophilic or amphophilic, PAS/D-negative, and lacks granules. The nonspecific glandular cells often form sheets of cells with indistinct borders. The predominance of nonspecific glandular or intercalated duct-type cells should raise the possibility of SC.

Growth patterns of AcCC include solid (Fig. 13.17) and follicular/microcystic (Fig. 13.18) types; individual tumors may show several configurations. In the *solid* type, the cells are closely aggregated in sheets or nodules



**FIGURE 13.16**

Serous acinar cells have abundant pale to basophilic, heavily granular cytoplasm in this low-grade acinar cell carcinoma.

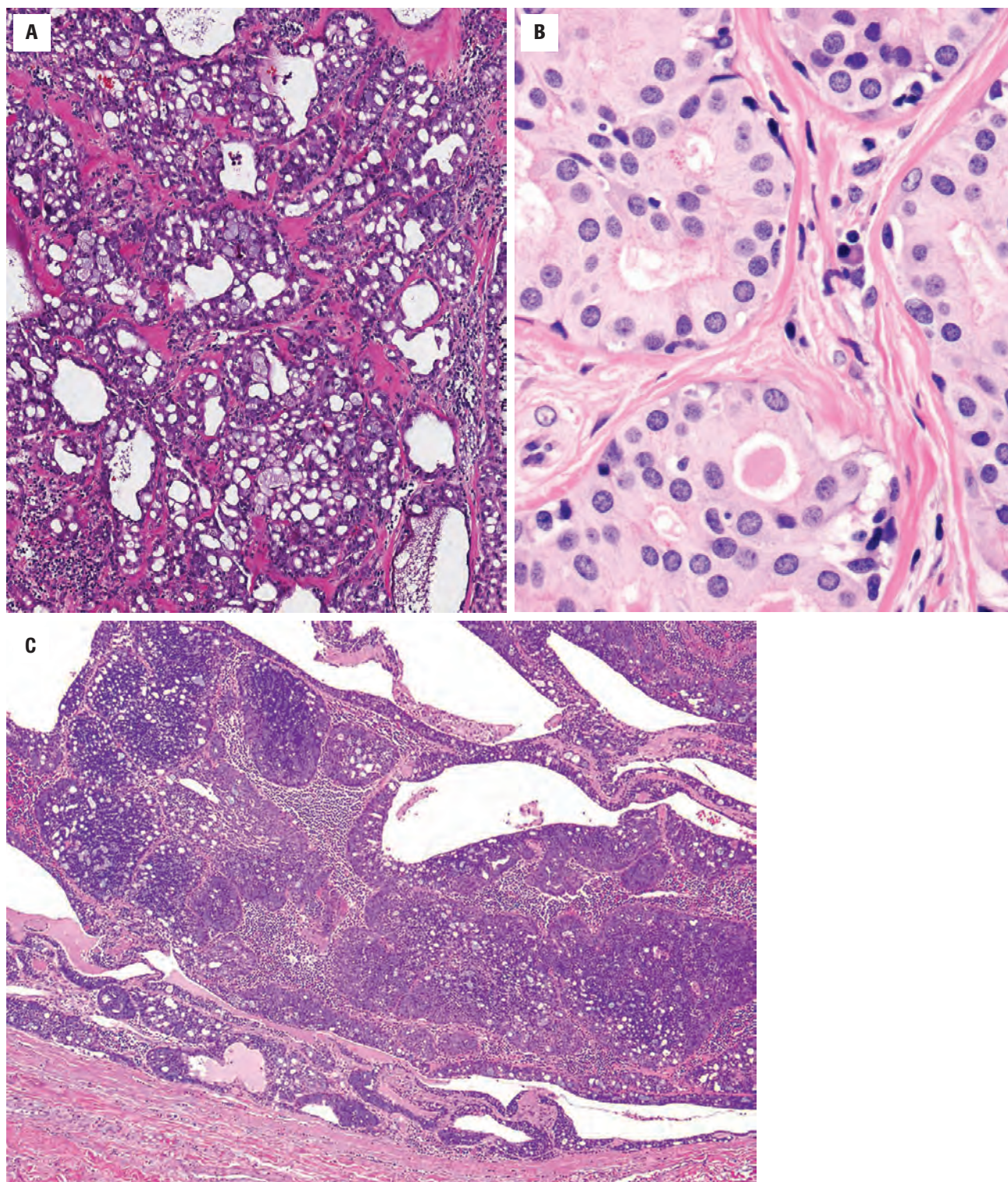
**FIGURE 13.17**

(A) The granules, representing zymogen granules, are variable in size and often accentuated along the luminal border in acinar cell carcinoma. (B) Sometimes the granules are less well developed, although the cell borders are usually quite prominent.

without the intervening ducts characteristic of normal salivary tissue. Since the recognition of SC, the *papillary-cystic growth* has been shown to be much less frequent in AcCC. In addition to the acinar cells, vacuolated and intercalated types of cells are common. The *follicular variant* consists of multiple variably sized cystic spaces. Psammoma bodies are sometimes seen in a variety of AcCC types and may be a conspicuous feature.

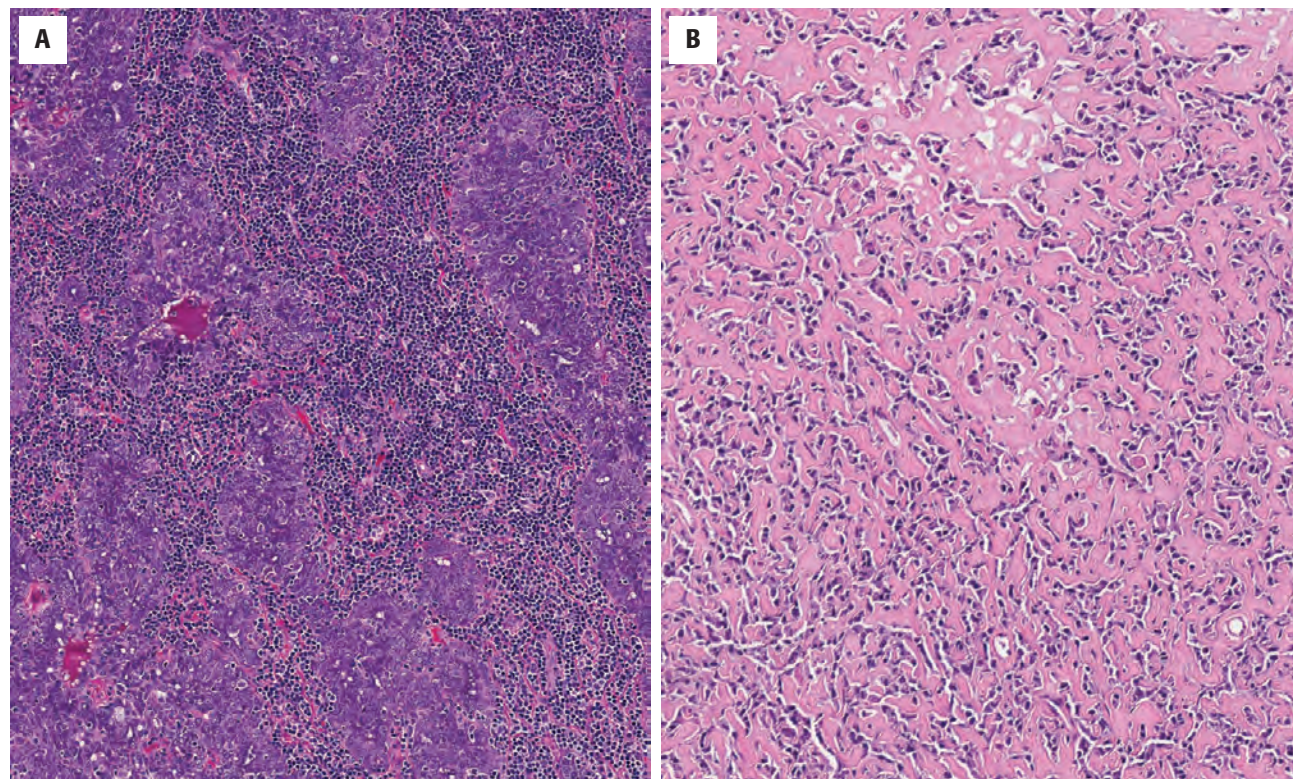
Many tumors show focal areas of stromal infiltration by lymphocytes, but some have a very striking lymphocytic stroma in which germinal centers develop (Fig. 13.19). These tumors are well circumscribed or encapsulated and are usually of the solid or microcystic type. They may have a better prognosis than conventional types. A prominent tumor-associated lymphoid proliferation (TALP) should not be confused with lymph node



**FIGURE 13.18**

(A) Lattice-like appearance is dominant in this case, with fibrous bands noted. Secretions are frequently present. (B) This tumor shows a follicular pattern with glandular-like spaces and concretions. Note the fine granules surrounding the lumen at the center of the image. (C) An acinic cell carcinoma with cystic pattern.



**FIGURE 13.19**

(A) Stroma is infiltrated by lymphocytes (tumor-associated lymphoid proliferation) in this acinic cell carcinoma. (B) Dense stromal fibrosis compressed the tumor cells into cords, making them difficult to classify accurately.

involvement: even the most exuberant TALP lacks the structures of a lymph node (i.e., lymph node capsule, sinuses). Stromal fibrosis or sclerosis may be associated with a slightly worse prognosis (Fig. 13.19). HGT of conventional AcCC is defined by diminished serous acinar differentiation, increased mitotic activity, and necrosis (Fig. 13.20).

### ANCILLARY STUDIES

#### ULTRASTRUCTURAL FINDINGS

Although uncommonly used to identify tumors in modern practice, identification of secretory zymogen granules in the cytoplasm can help to confirm the diagnosis (Fig. 13.21).

#### IMMUNOHISTOCHEMICAL FINDINGS

AcCC shows reactivity with a variety of immunoagents, but staining with amylase, transferrin, and lactoferrin tends to be unpredictable and of little value in diagnosis. For instance, staining for amylase is frequently weak or absent in routinely processed tissue. Acinic cells stain positively for DOG1 (Fig. 13.22) and SOX10. p63 and

p40 are negative and help to highlight the absence of normal salivary ducts, especially in small biopsies. About 10 % of tumors show weak positivity for S100 protein.

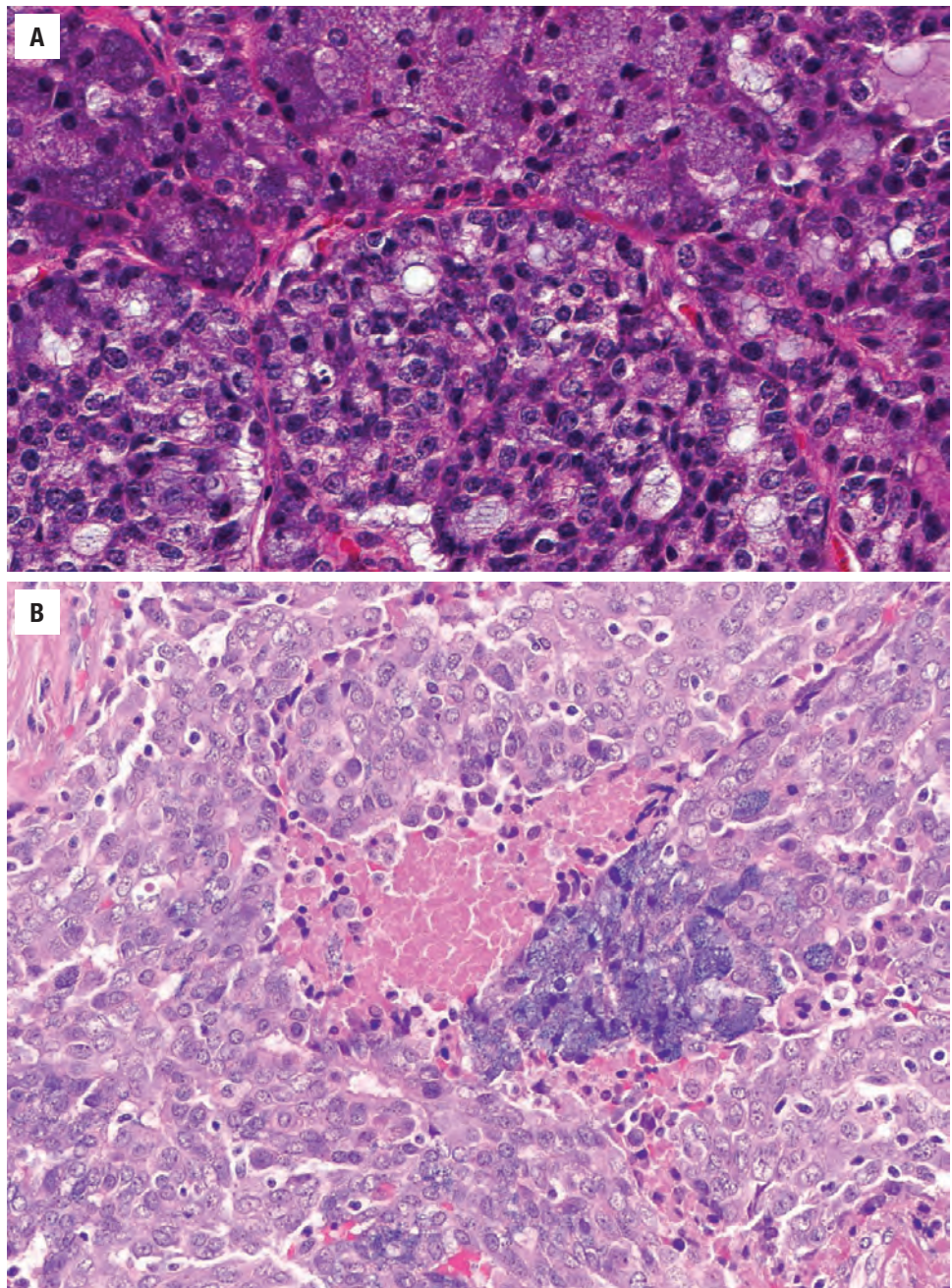
#### FINE NEEDLE ASPIRATION

AcCC tends to yield cellular smears with a clean background. Tumor cells are cohesive and arranged in small tight clusters, occasionally demonstrating a small central fibrovascular core (Figs. 13.23 and 13.24). The nuclei are usually round and regular with little pleomorphism; they are surrounded by abundant eosinophilic, finely granular to vacuolated cytoplasm (Fig. 13.24). Separating other tumors from an acinic cell tumor on FNA preparations may be difficult.

### DIFFERENTIAL DIAGNOSIS

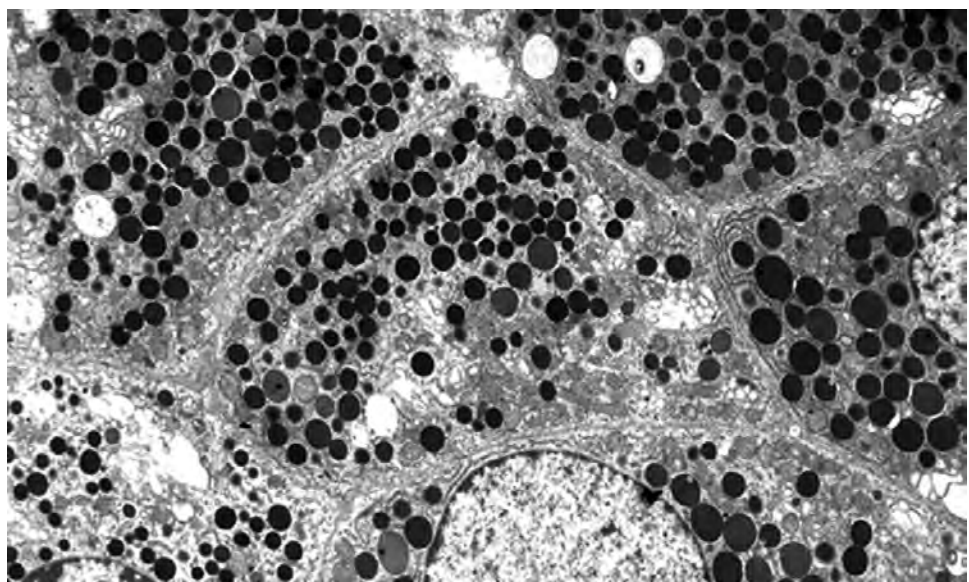
The lack of salivary ducts and adipose tissue, or *sialadenitis*, helps to distinguish AcCC from normal salivary tissue, especially if there is limited material. Microcystic and papillary-cystic variants with predominant intercalated ductal cells must be differentiated from SC. Zymogen granules and vacuolated cells would support the diagnosis





**FIGURE 13.20**

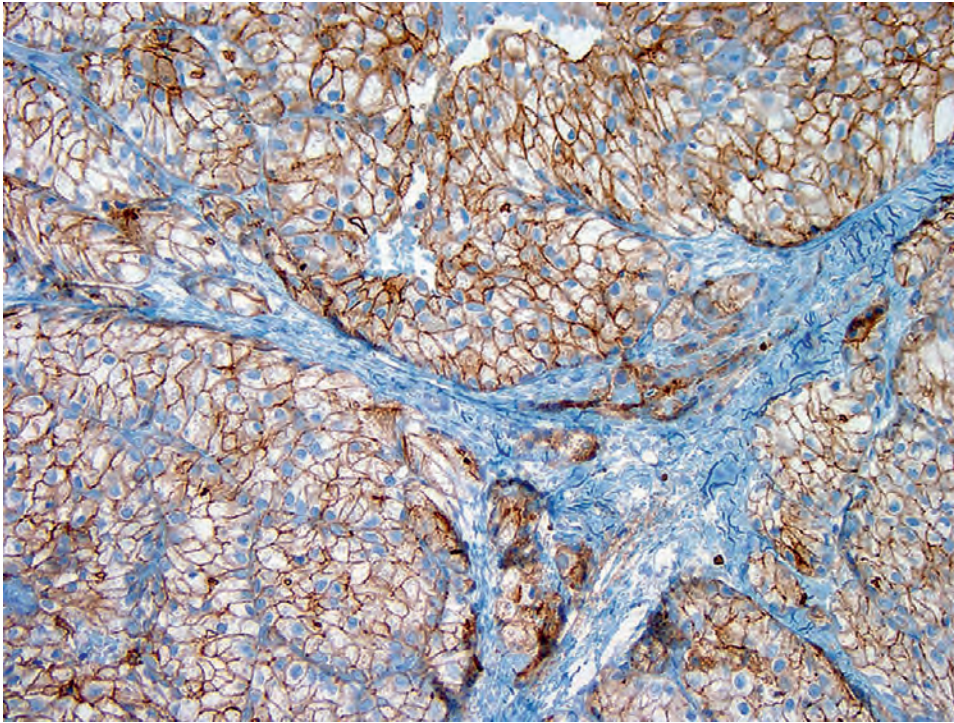
(**A** and **B**) High-grade transformation can be seen in acinic cell carcinoma. In the center (**B**), there is a comedo-type necrosis. The majority of the neoplastic cells lost basophilic zymogen granules and acquired a more eosinophilic appearance. Some cells still show a basophilic cytoplasmic tinge, indicative of preserved zymogen granules.



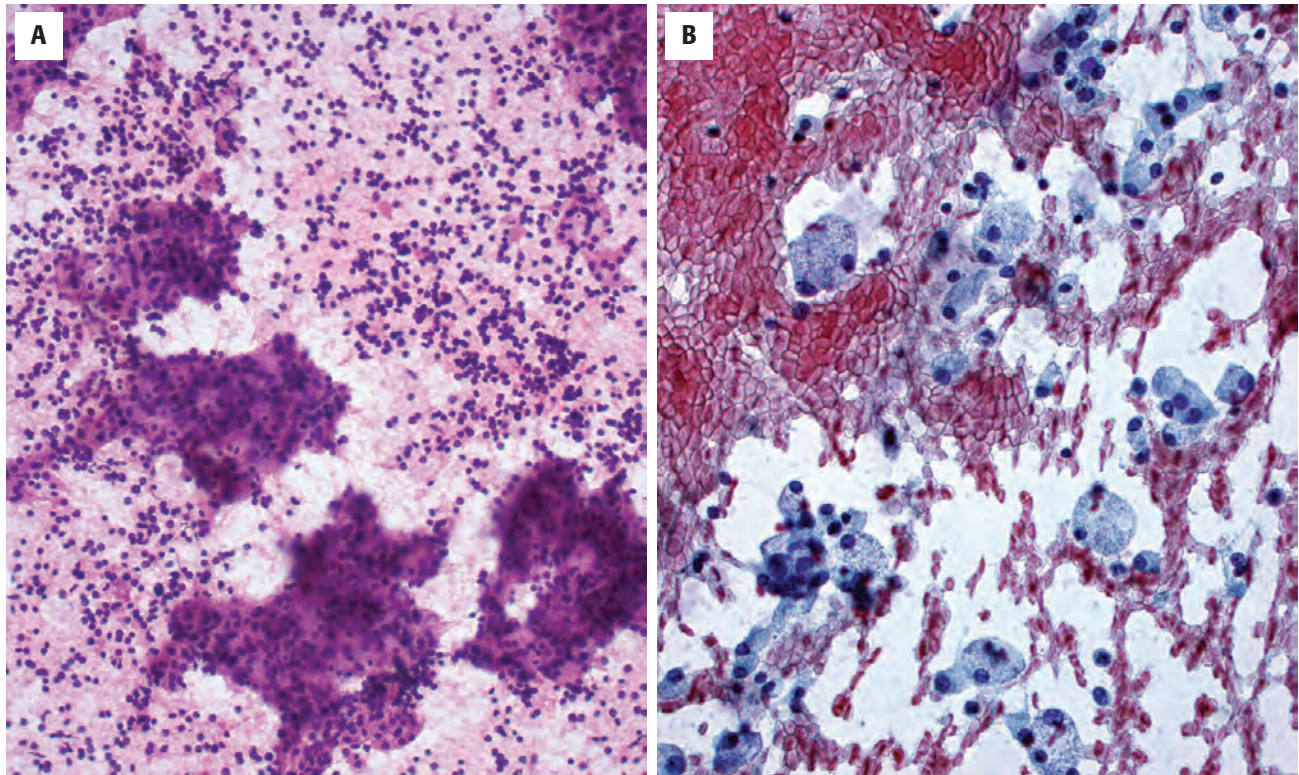
**FIGURE 13.21**

This ultrastructural examination demonstrates secretory zymogen granules. (Courtesy of Dr. I. Dardick.)



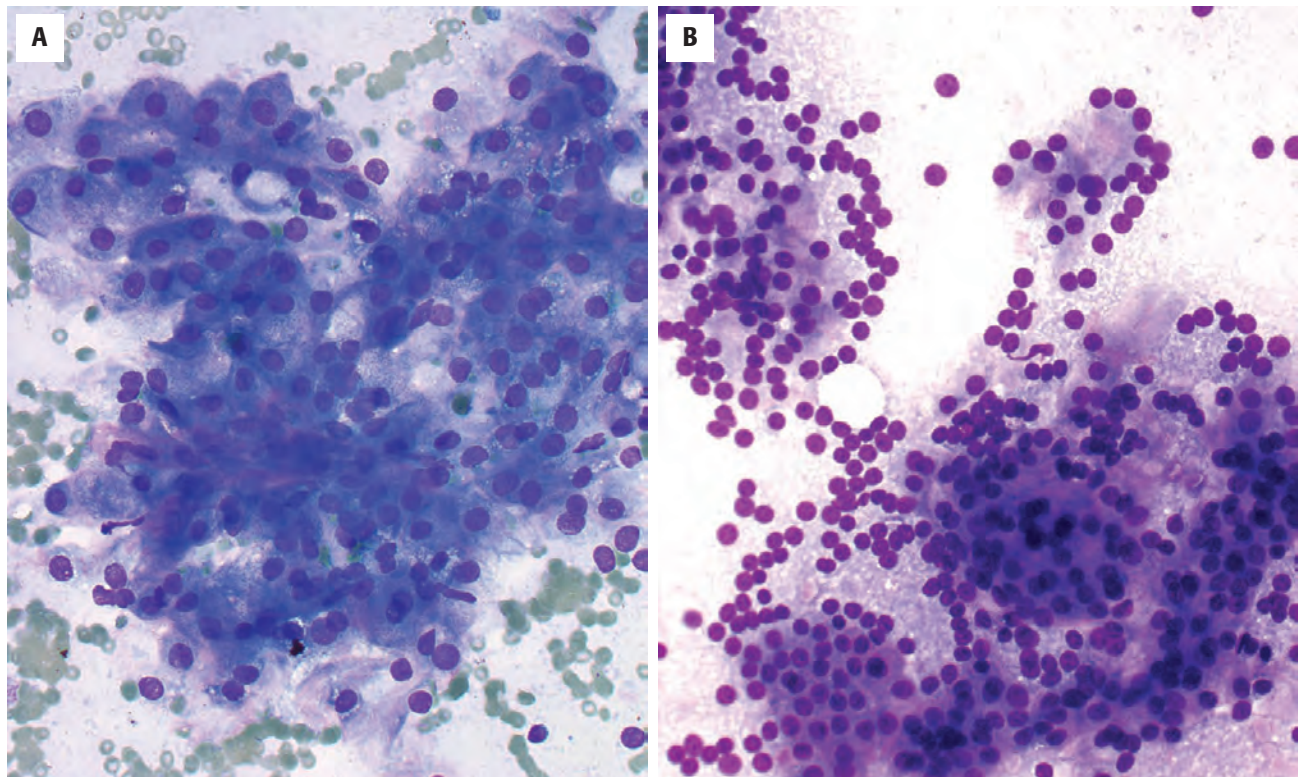
**FIGURE 13.22**

Acinic cell carcinoma DOG1 immunohistochemistry shows intense complete membranous staining.

**FIGURE 13.23**

Acinic cell carcinoma. (A) An acinar arrangement of cells with round, regular nuclei and granular cytoplasm along with numerous naked nuclei in the background (alcohol-fixed, hematoxylin and eosin stain). (B) Isolated tumor cells with bubbly cytoplasm can suggest macrophages rather than epithelial cells (alcohol-fixed, Papanicolaou stain).



**FIGURE 13.24**

(A and B) A cohesive cluster of cells is noted in a background of blood. There is only slight nuclear variability. Note the finely granular to vacuolated cytoplasm in these acinic cell carcinomas (air-dried, Diff-Quik stain).

of AcCC. Microcystic variants may be misdiagnosed as *MECs* owing to the strong mucicarmine positivity of the cystic spaces and the presence of small spaces that are interpreted as mucocytes. AcCC with HGT should be distinguished from SDC (which are SOX10- and DOG1-negative and are almost uniformly positive for androgen receptor).

#### PROGNOSIS AND THERAPY

Recurrences develop in about 35 % of patients, usually in AcCC with HGT. There are overall 5- and 10-year survival rates of 82 % and 68 %, respectively. The tumor may involve regional lymph nodes, and the most common sites for distant spread are lung and bones. Further grading (beyond distinguishing conventional and high-grade transformed cases) is not reliable. There is no correlation between prognosis and the main histomorphologic patterns. Histologic features thought to be associated with poor prognosis include HGT (defined by cellular pleomorphism, increased mitotic frequency, areas of necrosis, perineural invasion, and decreased serous differentiation). Large size, involvement of the deep lobe of the parotid, multiple recurrences, multinodularity, and regional and

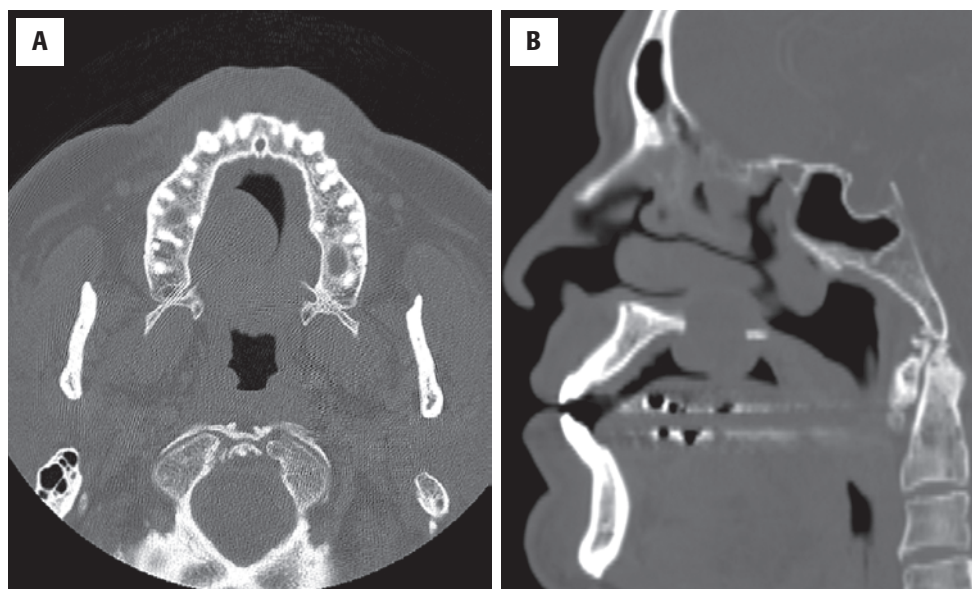
distant metastases are indicators of poor prognosis. Complete surgical excision is the treatment of choice, and failure to clear the tumor is associated with a poor outcome.

### ■ ADENOID CYSTIC CARCINOMA

#### CLINICAL FEATURES

Adenoid cystic carcinoma (AdCC) accounts for 10 % of all malignant salivary gland tumors. It affects a wide age range with a peak incidence in 40- to 60-year-olds. There is a slight female predominance. Minor glands of the mouth, particularly the palate, and of the upper aerodigestive tract account for about half of all cases (Fig. 13.25). Other common sites include the parotid (21 %), submandibular gland (5 %), and sinonasal tract (11 %). The tumor usually presents as a slow-growing mass of long duration. It may be tender or painful, and cranial nerve lesions, particularly facial nerve palsy, may be the presenting findings. Tumors of minor glands often show ulceration of the overlying mucosa.



**FIGURE 13.25**

A tumor within the palate shows a projection into the oral cavity (**A**), while destroying the bony floor of the nasal cavity (**B**), in these computed tomography scans of adenoid cystic carcinoma.

### ADENOID CYSTIC CARCINOMA—DISEASE FACT SHEET

#### Definition

- Adenoid cystic carcinoma is a basophilic tumor with a dual cell population (epithelial and basal/myoepithelial) in variable morphologic configurations, including cribriform, tubular, and solid patterns

#### Incidence and Location

- Accounts for about 10% of salivary gland neoplasms
- About 75% arise in minor glands, particularly in palate, with 25% in major glands, mainly the parotid gland

#### Morbidity and Mortality

- 5- and 10-year survival rates are 62% and 40%, respectively
- Most patients die of or with the tumor

#### Sex and Age Distribution

- Females > males (3:2)
- Peak in 5th-7th decades (wide age range)
- Rare in children

#### Clinical Features

- Usually forms a slow-growing mass that may be painful
- Cranial nerve involvement is common, especially in causing facial nerve palsy
- Submucosal tumors may ulcerate

#### Prognosis and Therapy

- Main prognostic factors are site, tumor size, clinical stage, histologic pattern (solid has a worse prognosis), and high-grade transformation
- Frequent recurrence, especially in the first 5 postoperative years
- Submandibular gland tumors have a worse prognosis
- Metastasis to lung, bone, brain, and liver seen in up to 60%
- Treated with wide local excision and adjuvant radiotherapy

### PATHOLOGIC FEATURES

#### GROSS FINDINGS

The tumor is usually firm and may be well circumscribed, particularly when it is small. Most are unencapsulated. The gross appearance belies the true extent of the tumor, as neural infiltration is not discernible on macroscopic examination.

#### MICROSCOPIC FINDINGS

AdCC has three main morphologic patterns: cribriform or cylindromatous, tubular, and solid, in decreasing order of frequency. A mixture of these patterns may be seen, but the hallmark of AdCC is a dual cell population with inner ductal, usually more eosinophilic cells forming true lumina filled with pink secretions and abluminal basal/myoepithelial cells surrounding pseudolumina with basement membrane-like material ([Fig. 13.26](#)). The *cribriform* pattern consists of islands of modified myoepithelial cells containing rounded pseudolumina filled with basement membrane-like material ([Figs. 13.27](#) and [13.28](#)). They are composed of glycosaminoglycans and reduplicated basement membrane material. True glands comprising ductal cells are present within the myoepithelial areas but may be inconspicuous. The *tubular* variant is also double-layered and has more obvious ductal differentiation ([Fig. 13.26](#)). There is an inner layer of eosinophilic duct-lining cells and the abluminal basal/myoepithelial cells with irregular, angular nuclei ([Fig. 13.26](#)). The uncommon *solid* variant consists of islands or sheets of basaloid cells with larger and less angular nuclei ([Fig. 13.29](#)). There is diagnostic and prognostic value in distinguishing AdCC with solid growth and AdCC

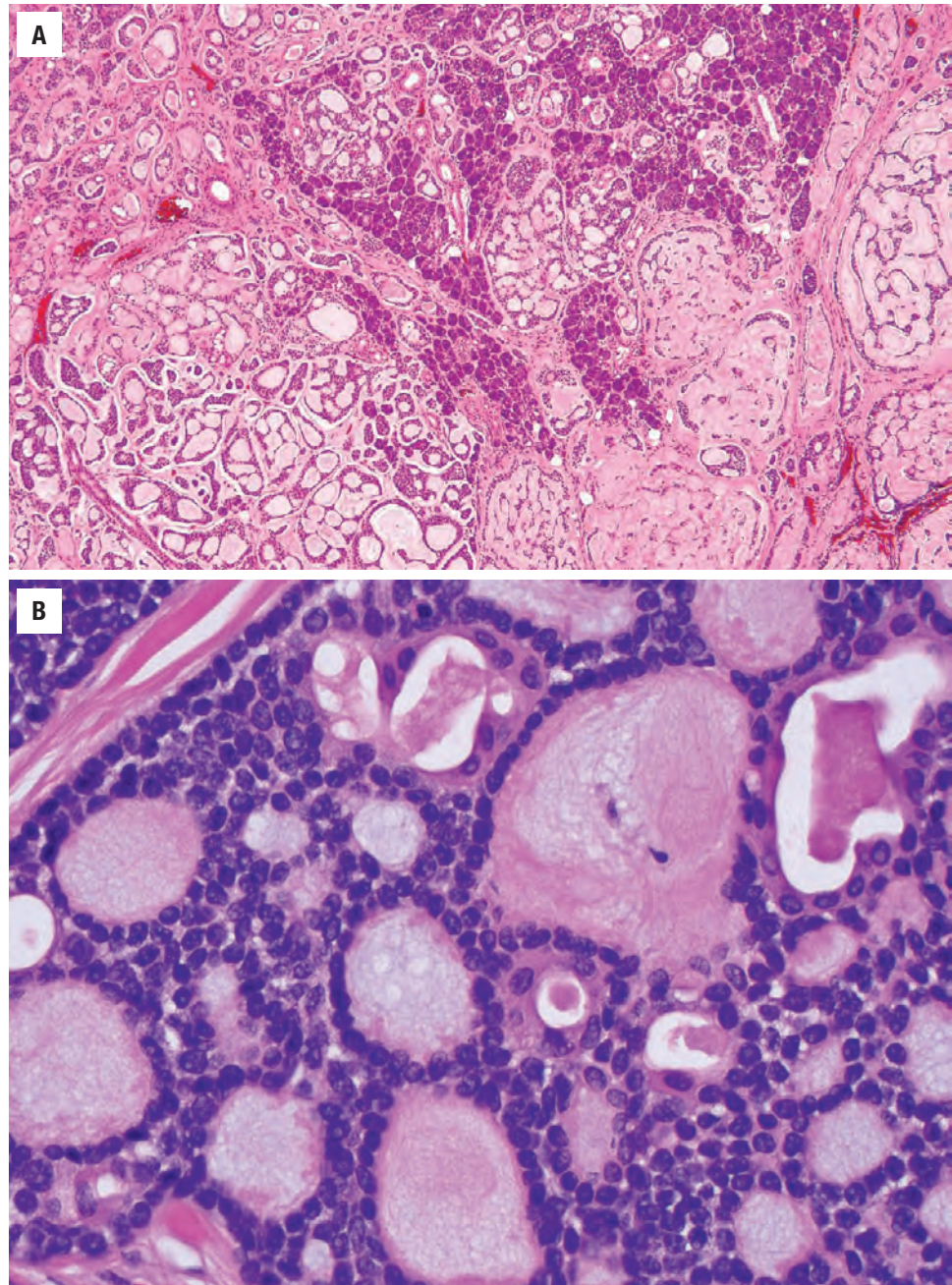


**FIGURE 13.26**

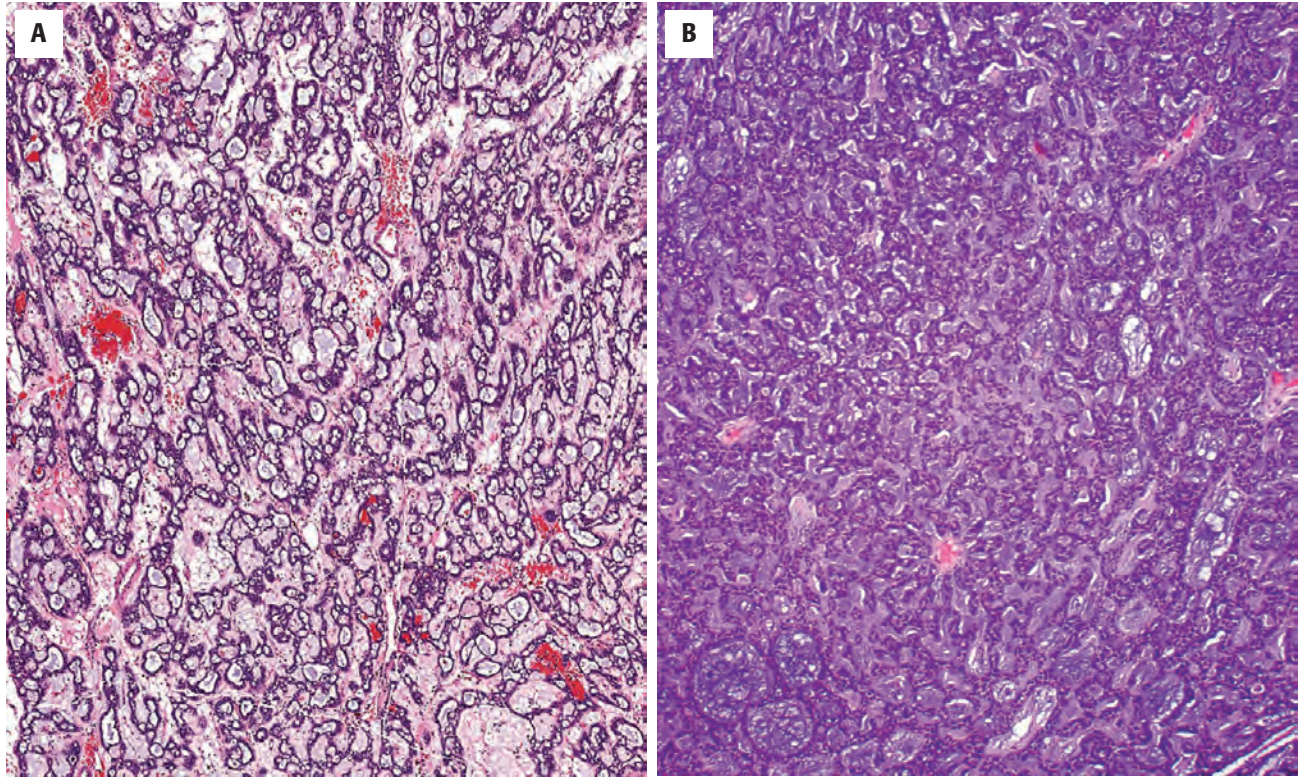
(A) An adenoid cystic carcinoma showing multiple patterns of growth, although the cribriform and tubular areas predominate. Notice how the tumor is infiltrating between and around the parenchyma. (B) The dual cell population of adenoid cystic carcinoma. In the center, true ducts lined by cuboidal eosinophilic cells and with pink secretions are more prominent. Abluminal basal cells surround larger and easily identifiable pseudolumina filled with basement membrane–like material.

with HGT (Fig. 13.30). The conventional solid component may coexist with areas of high-grade transformed AdCC. The solid conventional component is usually represented by smaller, rounded nests of neoplastic cells, while areas of HGT are usually more irregular and confluent. The stroma of the solid component tends to be hyaline or myxoid, while the stroma of the HGT component is desmoplastic. The comedonecrosis is usually punctate in solid areas and more confluent in HGT areas. The layer of p63- or p40-positive basal/myoepithelial cells is preserved in solid areas and absent or incomplete in HGT cases of AdCC (Fig. 13.30). Mitoses are sparse in

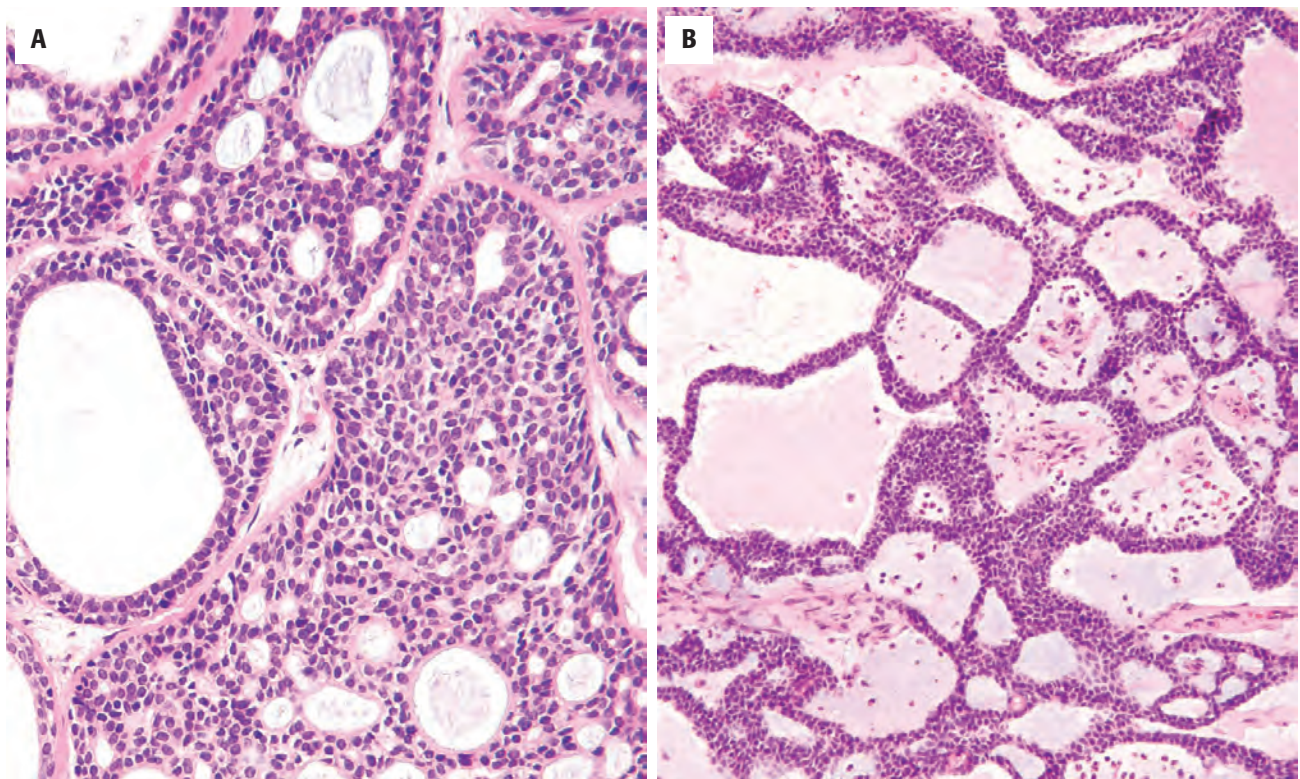
the cribriform and tubular patterns but may be frequent in the solid type.

AdCC is composed of luminal ductal cells and abluminal, modified myoepithelial cells. The latter predominate and have indistinct cell borders and frequently sparse amphophilic cytoplasm. The nuclei are uniform in size, with dense chromatin; they may be round or angular (peg-shaped). Ductal cells surround small and sometimes indistinct true lumina (Fig. 13.31). The ductal cells are cuboidal and have more abundant eosinophilic cytoplasm and round, uniform nuclei that may contain small nucleoli.



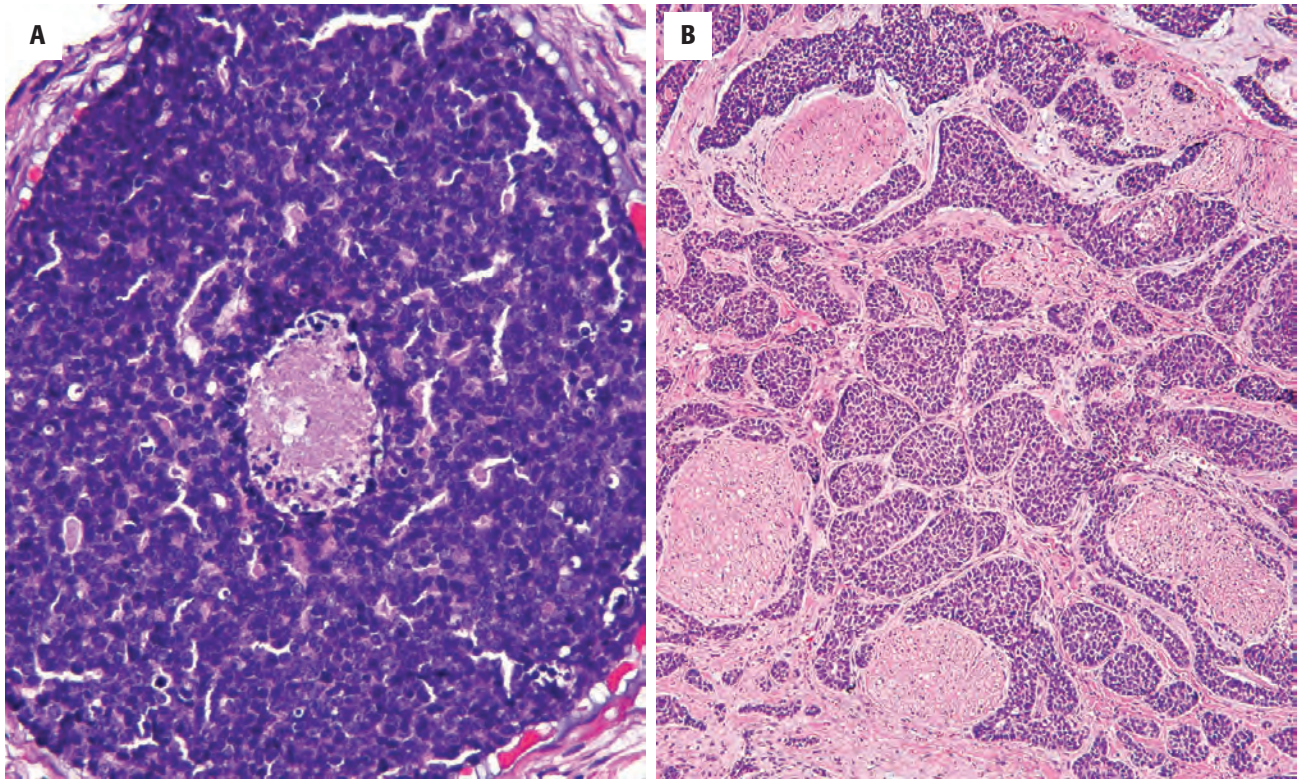
**FIGURE 13.27**

(A) The characteristic cribriform or cylindromatous pattern is seen in this adenoid cystic carcinoma. (B) Note a more trabecular appearance, although the glycosaminoglycan material is very prominent in this adenoid cystic carcinoma.

**FIGURE 13.28**

(A) There is a mixture of patterns, but the peg-shaped nuclei are seen along with small duct-like spaces within the proliferation. (B) This pattern suggests a canalicular adenoma pattern, although the matrix material is not similar.



**FIGURE 13.29**

(A) The solid variant of adenoid cystic carcinoma has large nests of cells with a high nuclear-to-cytoplasmic ratio. Central comedonecrosis is noted. (B) There is extensive perineural invasion in this tumor.

### ADENOID CYSTIC CARCINOMA—PATHOLOGIC FEATURES

#### Gross Findings

- Usually firm, often well circumscribed, but unencapsulated

#### Microscopic Findings

- Composed of duct-lining cells and abluminal modified myoepithelial cells
- Main patterns are cribriform, tubular, and solid in decreasing order of frequency; mixed patterns are common
- Pseudocysts filled with basophilic mucoid (“blue goo”) or hyaline, eosinophilic material (reduplicated basement membrane material)
- Perineural invasion common and frequently extensive
- Cells are small with a high nuclear-to-cytoplasmic ratio
- Nuclei are peg-shaped (“carrot”-shaped) to columnar with dense nuclear chromatin distribution
- Stroma is hyalinized in conventional AdCC and desmoplastic in AdCC with high-grade transformation

#### Ancillary Studies

- Pseudocysts positive for PAS, Alcian blue, laminin, and type IV collagen
- Epithelial cells positive for low-molecular-weight keratins, EMA, and CD117
- Myoepithelial cells positive with calponin, SMA, S100 protein, and p63 or p40

#### Fine Needle Aspiration

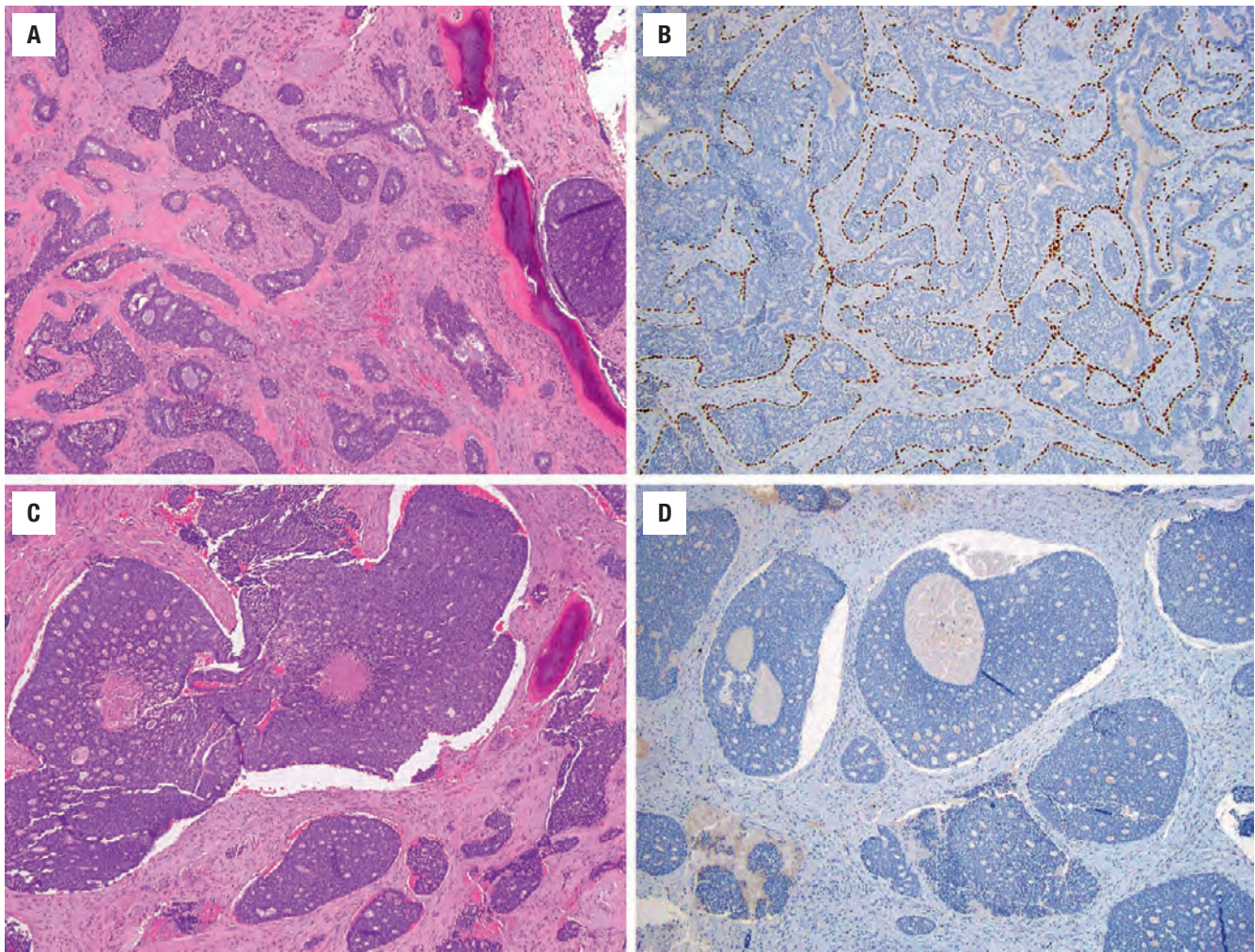
- Usually cellular smears with cohesive sheets of monotonous, only mildly atypical epithelial cells
- Cells surround spherical hyaline globules (reduplicated basement membrane material resembling pink “gum balls”), best seen on air-dried preparations (bright magenta on Romanowsky stains)
- Nuclei are hyperchromatic and peg shaped/cuboidal within cells that have high nuclear-to-cytoplasmic ratios

#### Pathologic Differential Diagnosis

- Other salivary tumors with dual cell populations, such as: epithelial-myoepithelial carcinoma, pleomorphic adenoma (on FNA and limited samples), basal cell adenoma, and basal cell adenocarcinoma
- AdCC with high-grade transformation should be distinguished from other high-grade carcinomas, such as basaloid squamous cell carcinoma, salivary duct carcinoma
- Polymorphous adenocarcinoma comprises one cell type—ductal; this feature can be highlighted by immunostaining (p40-negative) and used to distinguish it from AdCC
- HPV-related multiphenotypic sinonasal carcinoma:—sinonasal tract only, HPV-positive, negative for *MYB* translocations, surface squamous dysplasia often present

AdCC, adenoid cystic carcinoma; EMA, epithelial membrane antigen; FNA, fine needle aspiration; PAS, periodic acid–Schiff; SMA, smooth muscle actin.



**FIGURE 13.30**

(**A** and **B**) Solid variant of adenoid cystic carcinoma with smaller nests, individual cell necrosis, and preserved layer of p63-positive basal/myoepithelial cells. (**C** and **D**) In areas of adenoid cystic carcinoma with high-grade transformation, tumor nests are larger, confluent, with easily identifiable comedo-type necrosis. The layer of p63-positive basal cells is incomplete to absent.

The stroma of AdCC is usually hyalinized; in some cases it is so abundant that tumor cells are attenuated into strands (Fig. 13.32). It is continuous, though appearing separated in histologic sections. Perineural or intraneural invasion is common and frequently conspicuous, and the tumor can extend along nerves over a wide area (Fig. 13.29). It may invade bone extensively before there is any radiographic evidence of bone destruction. Lymph node involvement is often due to contiguous spread rather than lymphatic permeation or embolization.

## ANCILLARY STUDIES

### HISTOCHEMICAL AND IMMUNOHISTOCHEMICAL FINDINGS

The pseudocysts/pseudolumina are positive for PAS and Alcian blue (Fig. 13.31) and react with antibodies

to basement membrane components such as laminin and type IV collagen. The epithelial cells are positive for low-molecular-weight keratins (including CK5/6), EMA, and CD117; the myoepithelial cells are positive for markers such as calponin, smooth muscle actin (SMA), p63, p40, and S100 protein (Figs. 13.33 and 13.34).

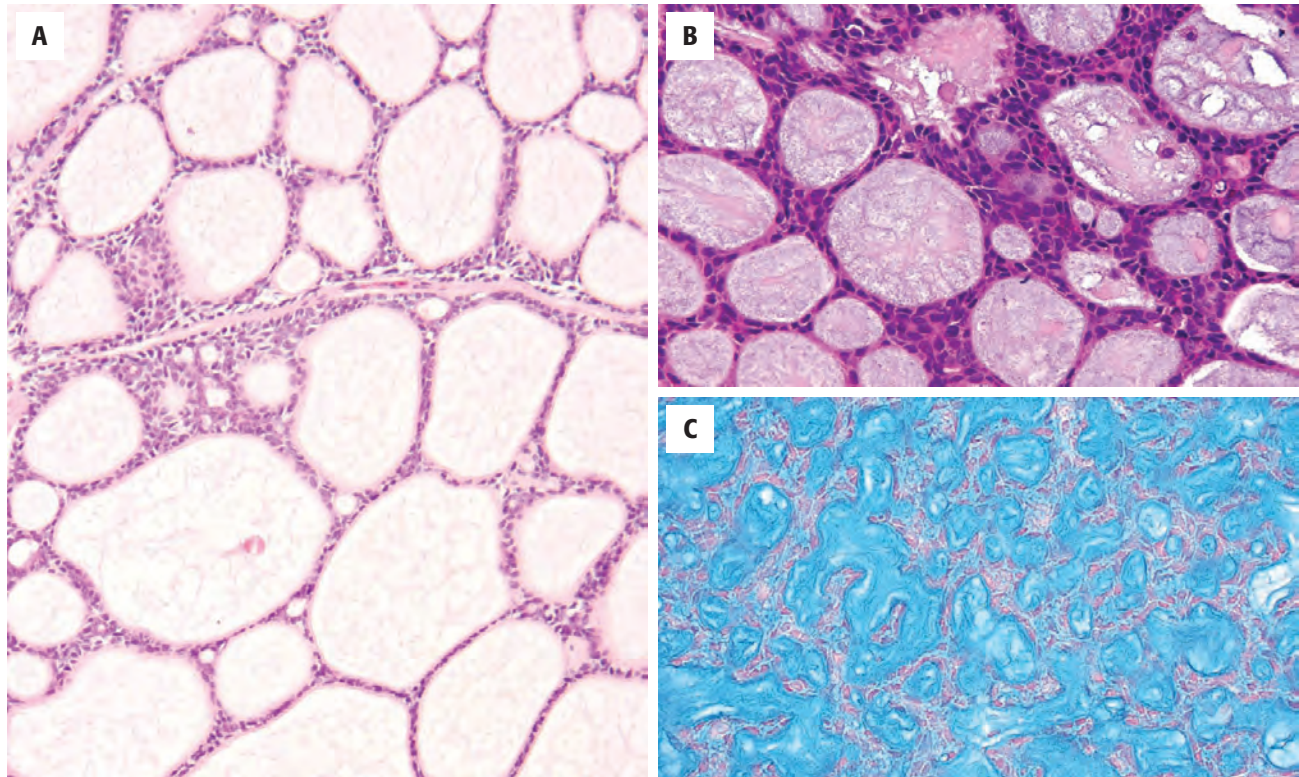
### MOLECULAR FINDINGS

AdCC shows *MYB* activation, commonly by *MYB-NFIB* fusion in 40 % to 60 % of cases.

### FINE NEEDLE ASPIRATION

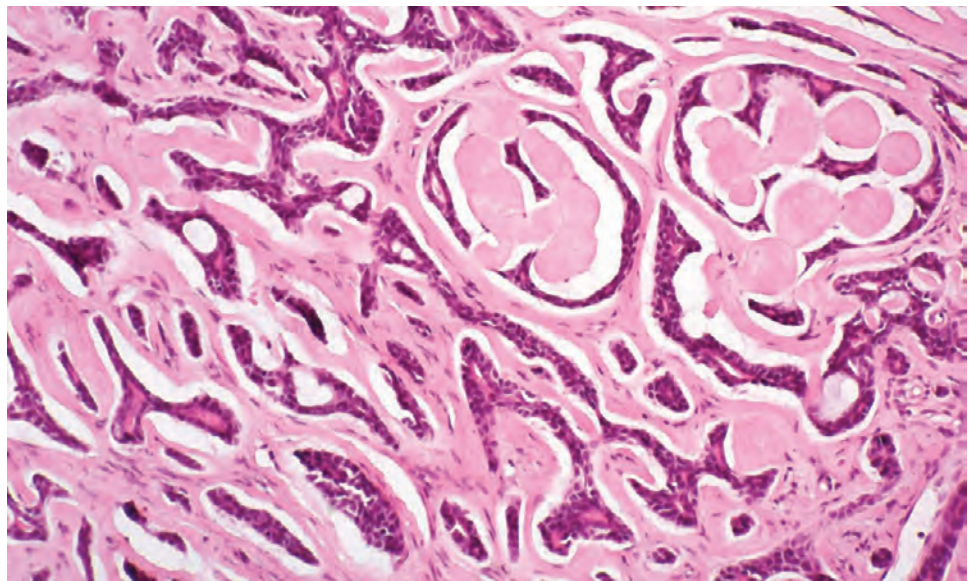
AdCC contains intensely metachromatic spherical hyaline globules (resembling pink “gum balls”), which represent the reduplicated basement membrane material intimately surrounded by the neoplastic cells (Fig. 13.35). This is best seen on air-dried preparations (they





**FIGURE 13.31**

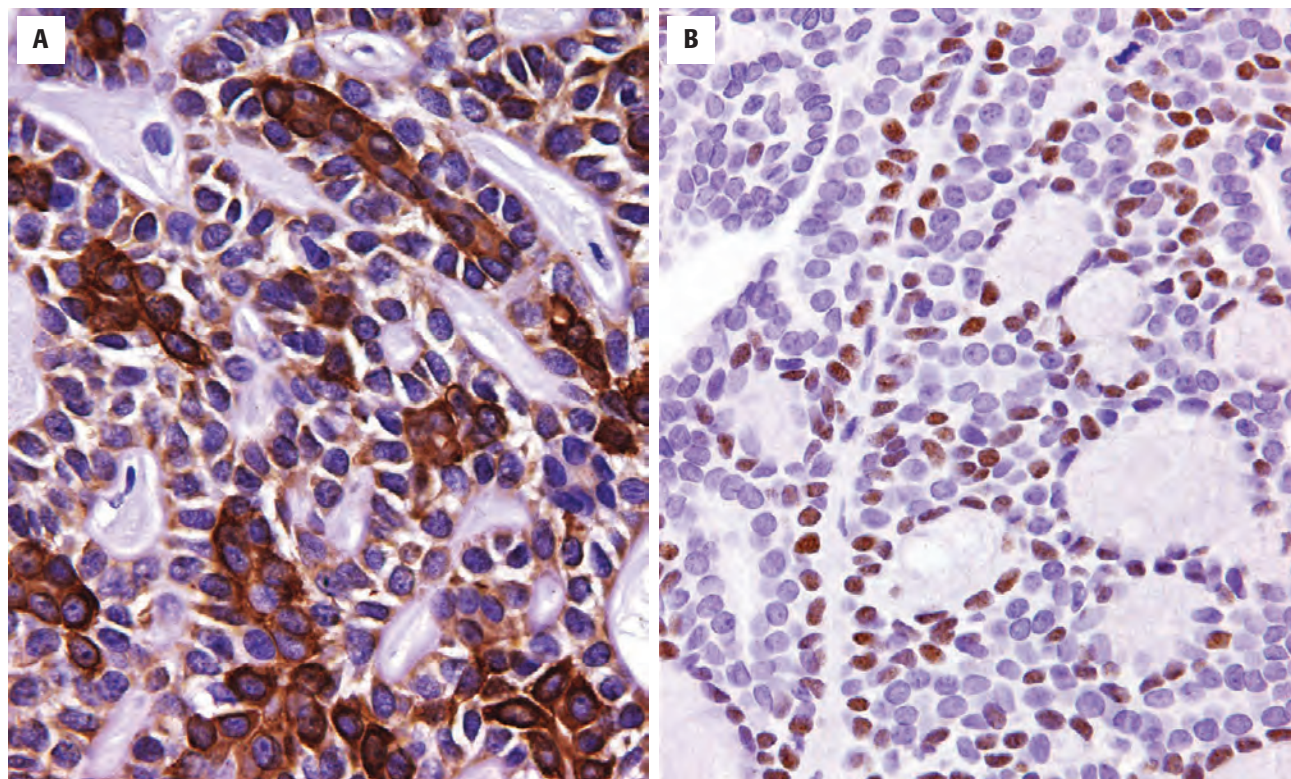
(A) Pseudocystic spaces with mucoïd and eosinophilic material. Note the peg-shaped nuclei, especially at the periphery of the cell groups, as well as small duct-like spaces. (B) A cylindrical appearance with mucoïd basophilic material in the center. (C) Alcian blue highlights the pseudocystic glycosaminoglycan material.



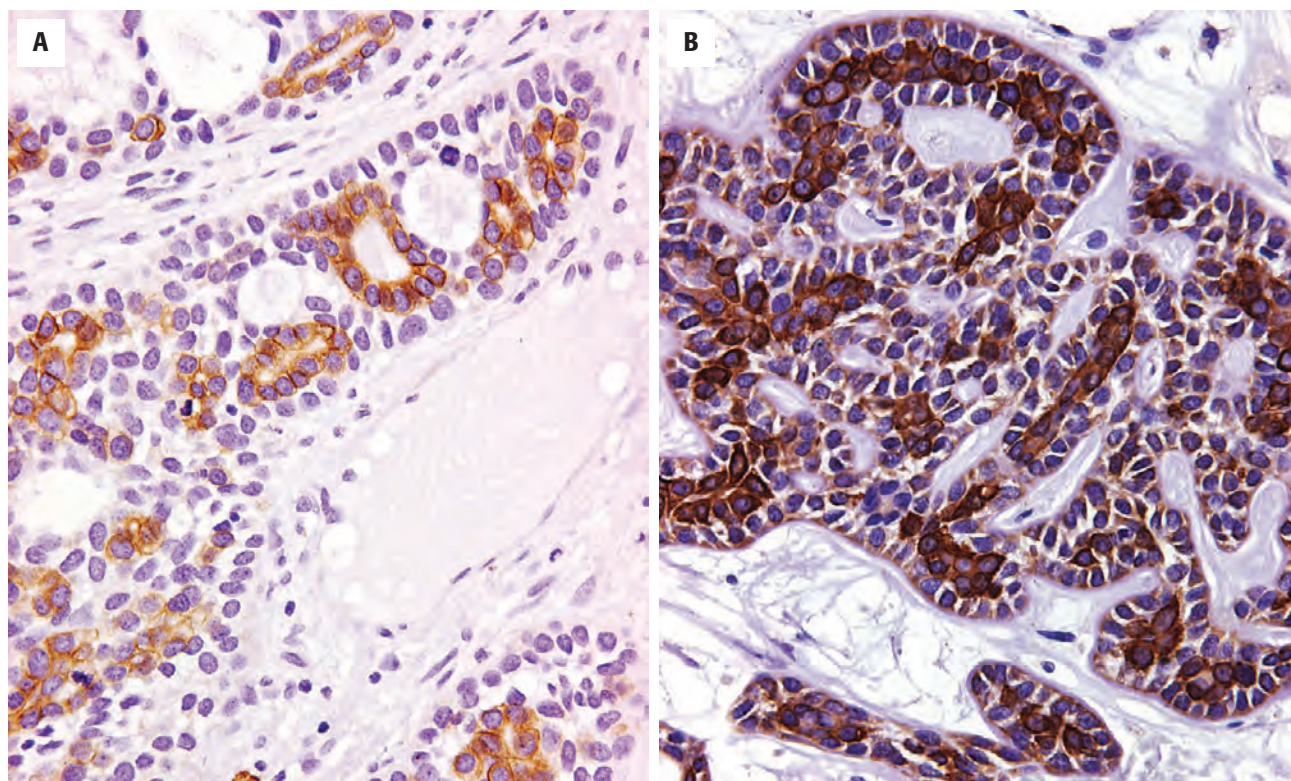
**FIGURE 13.32**

A heavily hyalinized stroma has compressed the neoplastic cells in this adenoid cystic carcinoma. The retraction artifact is most prominent between the cellular component and stroma (in epithelial myoepithelial carcinomas, retraction is between the two cell types [ductal and myoepithelial]).



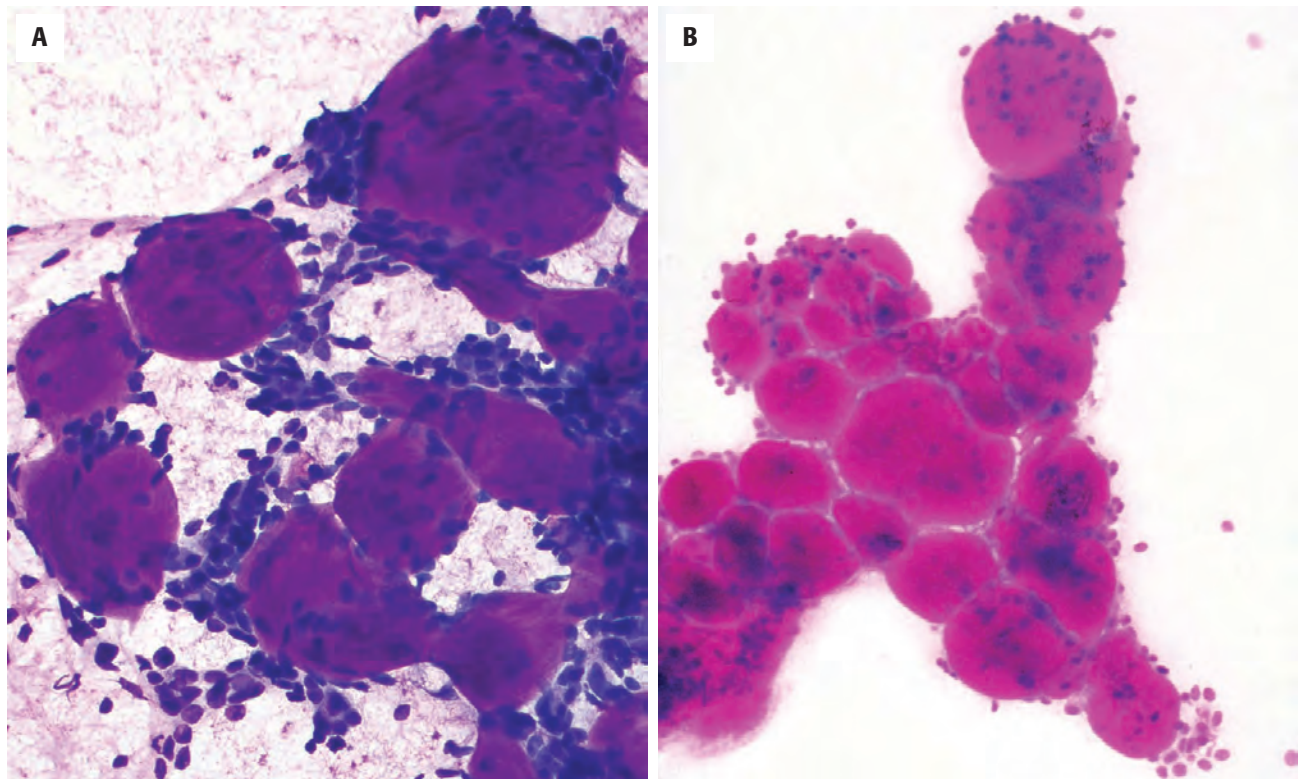
**FIGURE 13.33**

(A) Keratin immunohistochemistry highlights the luminal epithelial cells. (B) p63 immunohistochemistry highlights the basal-myoepithelial cells.

**FIGURE 13.34**

(A) CD117 tends to highlight the luminal cells preferentially. (B) Many times the luminal cells are highlighted with CK5/6.



**FIGURE 13.35**

(A and B) Air-dried Romanowsky-stained fine needle aspiration material highlights the spherical hyaline globules; the intimately associated cells have small hyperchromatic nuclei. Note the arrangement of the nuclei, which appear peripherally rather than within the matrix.

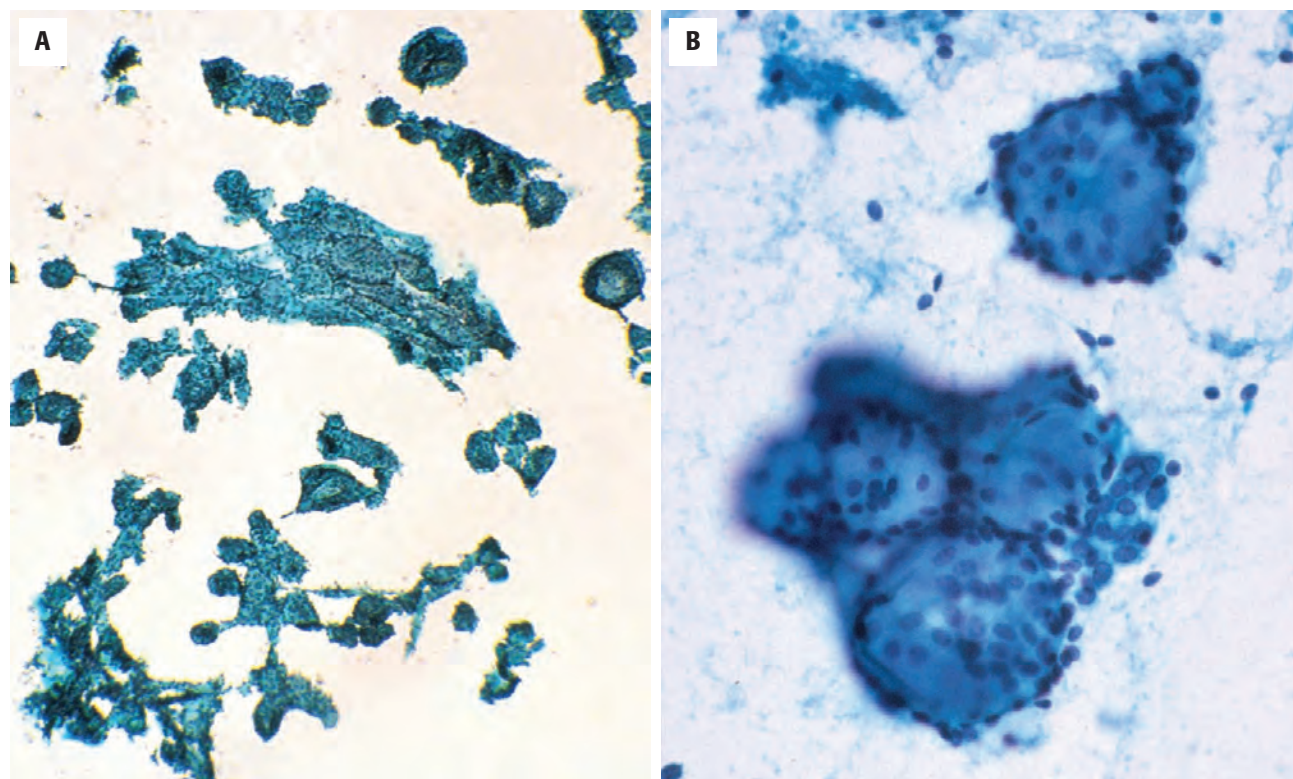
stain pale blue or pink on Papanicolaou [Pap] stain). The globules do not have a fibrillar or feathery edge, as seen in pleomorphic adenoma (PA). There are often rounded stromal structures between the nests of tumor cells. The tumor cells are cohesive, often showing high cellularity and cellular overlap of cells that have little pleomorphism (Fig. 13.36). The nuclei are often peg-shaped, identified in cells with a high nuclear-to-cytoplasmic ratio. The chromatin is heavy and coarse in distribution. On FNA, it may be difficult to separate an AdCC from a PA.

### DIFFERENTIAL DIAGNOSIS

It is important to distinguish AdCC from *polymorphous adenocarcinoma* (PAC), previously known as polymorphous *low-grade* adenocarcinoma. Although both neoplasms have similar patterns of growth, PAC consists of a uniform ductal cell population with cytologically bland round or oval vesicular nuclei and pale eosinophilic cytoplasm. PAC has infiltrating single cords of cells and also a striking targetoid arrangement, often centered on a nerve. The nuclei of PAC resemble those of papillary thyroid carcinoma, a feature that is not seen in conventional AdCC. Unlike AdCC, PAC is S100 protein- and

p63-positive but p40-negative. *Basaloid squamous cell carcinoma* can resemble the solid variant of AdCC but typically involves the hypopharynx and glottic region, shows squamous differentiation, is diffusely p63- and p40-positive, and may show squamous dysplasia in the overlying mucosa. Both EMC and the tubular variant of AdCC can show double-layered duct-like structures with an abluminal layer of clear cells. However, the retraction artifact (the “split”) in AdCC tends to be between the cellular component and the stroma, while the split in EMC is usually most prominent between the two cell types (i.e., between the ductal and myoepithelial cells). The presence of a preexisting PA component is more commonly seen in the setting of EMC. Both AdCC and EMC may undergo HGT. In AdCC with HGT, the HGT component is represented exclusively by the ductal-type p63-negative cells, while in EMC the HGT component is most commonly represented by myoepithelial p63-positive cells. Finally, in the sinonasal tract, AdCC should be distinguished from the newly described HPV-related multiphenotypic sinonasal carcinoma (described in detail in Chapter 3). Briefly, HPV-related multiphenotypic sinonasal carcinoma at times closely resembles true AdCC at the histologic and immunophenotypic levels but is encountered only in the sinonasal tract, is HPV-positive (usually type 33), and often exhibits foci of surface squamous dysplasia overlying the carcinoma. Moreover,



**FIGURE 13.36**

(A and B) The epithelial cells form cohesive sheets that show rounded void areas, corresponding to the hyaline globules. These globules do not stain with Papanicolaou preparations but appear as voids.

unlike many cases of AdCC, HPV-related multiphenotypic sinonasal carcinoma is always negative for *MYB* rearrangements.

### PROGNOSIS AND THERAPY

The 5- and 10-year survival rates are 62% and 40%, respectively, although most patients usually die of or with the tumor. Local recurrence is very common, especially in the first 5 years after surgery. The main prognostic factors are site, tumor size, clinical stage, and histologic pattern. Bone involvement and failure of primary surgery are associated with poor prognosis. Correlations between tumor morphology and outcome have yielded conflicting results owing to the overall poor long-term prognosis. However, it appears that the tubular and cribriform variants have a better outcome than tumors with a solid component, especially if the solid component exceeds 30% of the tumor volume. Tumors in the submandibular gland have a poorer prognosis than those in the parotid. The relationship between nerve involvement and survival is a subject of contention, but invasion of larger nerves appears to correlate with more aggressive behavior. Lymph node involvement is relatively uncommon, but distant metastases to lung, bone, brain, and

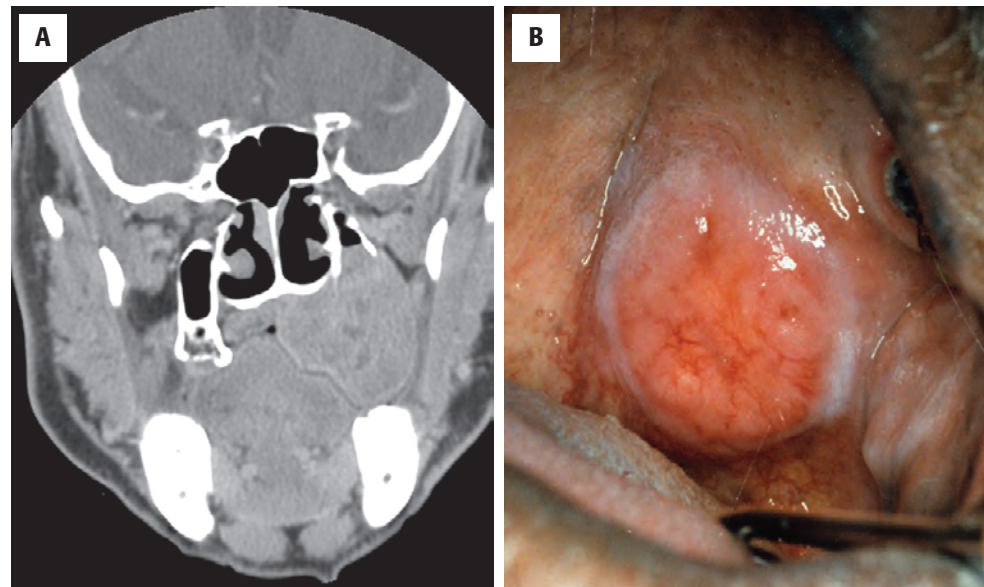
liver are seen in up to 60% of cases. Wide local excision together with adjuvant radiotherapy offers the best hope of local control.

## POLYMORPHOUS ADENOCARCINOMA

### CLINICAL FEATURES

Polymorphous adenocarcinoma (PAC) was previously known as polymorphous *low-grade* adenocarcinoma. Since high-grade PACs have been reported, the descriptor “low grade” was dropped. Cribriform adenocarcinoma of minor salivary glands (CAMSG) is considered to be a variant of PAC in the World Health Organization classification of salivary gland tumors.

PAC is found almost exclusively in minor glands and accounts for about a quarter of the malignant tumors in these sites. Most present in patients aged 50 to 70 years, with a female predominance (2:1). The most common site is the palate (60%), especially at the junction of the hard and soft palates (Fig. 13.37). Other intraoral sites include the lip (particularly the upper), buccal mucosa, retromolar areas, and posterior third of the tongue. Rarely, tumors arise in the lacrimal gland,

**FIGURE 13.37**

(A) There is a large tumor growing from the palate into the base of the nasal cavity, resulting in bone destruction (computed tomography scan). (B) An intact mucosa overlies a mass at the junction of the hard and soft palates. Note the vascular pattern. No surface ulceration is present.

sinonasal tract, nasopharynx, and upper and lower respiratory tracts. Tumors usually form a slow-growing mass that may have been present for many years. Ulceration, bleeding, and pain are uncommon presenting features.

## **PATHOLOGIC FEATURES**

### **GROSS FINDINGS**

The tumor usually forms a circumscribed, nonencapsulated, pale yellow or tan colored mass. Most measure up to 3 cm.

### **MICROSCOPIC FINDINGS**

PAC is an invasive tumor that is often circumscribed but not encapsulated; it is frequently identified immediately below an intact surface epithelium (Fig. 13.38). There is typically a wide variety of morphologic patterns within individual tumors. The most common configurations include lobular arrangements, solid nests or thèques, cribriform areas, and duct-like structures of varying sizes (Figs. 13.39 and 13.40). Concentric targeting or whorling, usually by cells in a single-file arrangement and producing an “eye of the storm” appearance, can often be seen around nerves and, less commonly, blood vessels and small ducts (Figs. 13.41 and 13.42). The perineural infiltration is usually present within or close to the body of the tumor (Fig. 13.42). Foci of oncocytic, mucous, and squamous metaplasia are occasionally present. Normal salivary gland acini are frequently incarcerated within the tumor (Fig. 13.41). A characteristic stromal

## **POLYMORPHOUS ADENOCARCINOMA—DISEASE FACT SHEET**

### **Definition**

- A malignant epithelial tumor characterized by an infiltrative growth of cytologically uniform ductal-type cells arranged in architecturally diverse patterns (“polymorphous”)

### **Incidence and Location**

- Accounts for about 25% of intraoral malignant salivary gland tumors
- 60% of cases involve the palate; other sites include lip, buccal mucosa, retromolar areas, and tongue

### **Morbidity and Mortality**

- Spread to regional lymph nodes in 9%-15% of cases
- Death due to disease is uncommon

### **Sex and Age Distribution**

- Females > males (2:1)
- Peak in 6th-8th decades (wide age range)
- Rare in children

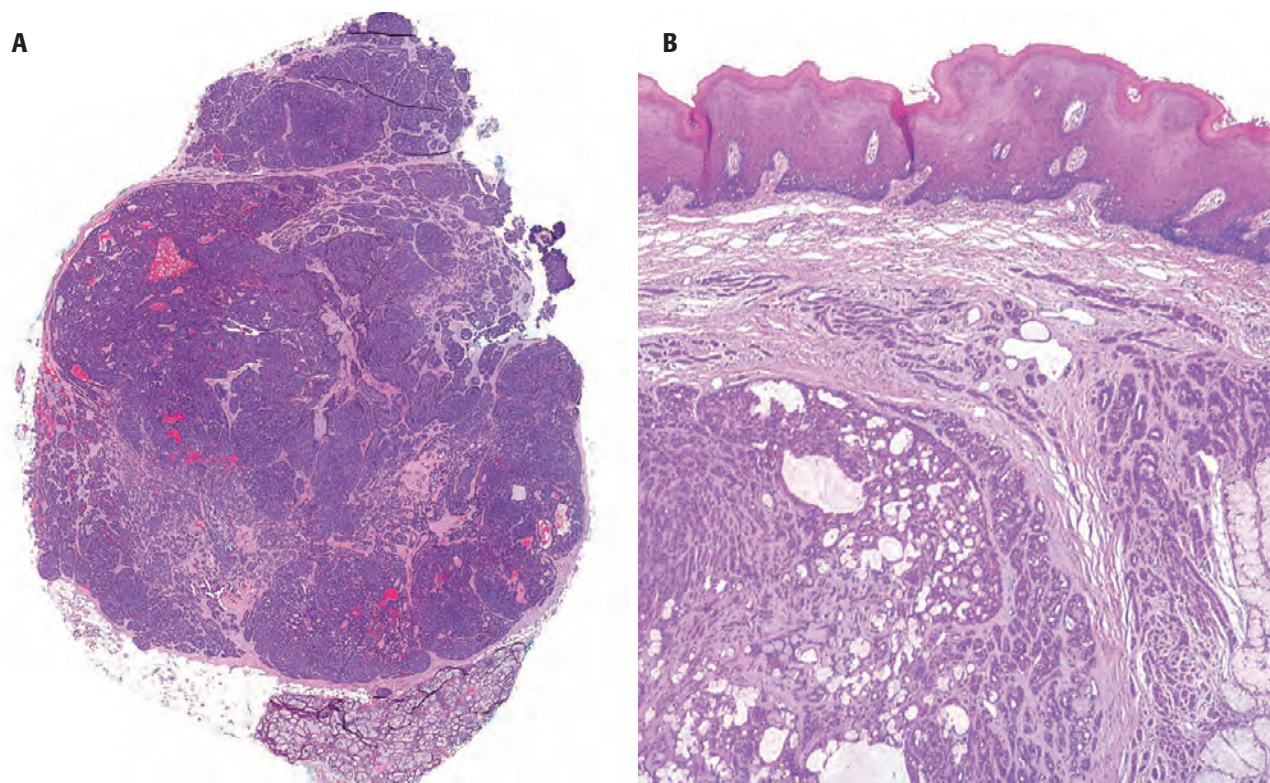
### **Clinical Features**

- Usually forms a painless, slow-growing mass
- Tumors are often present for many years
- Tumors may be mobile or fixed
- Ulceration, pain, and bleeding are uncommon

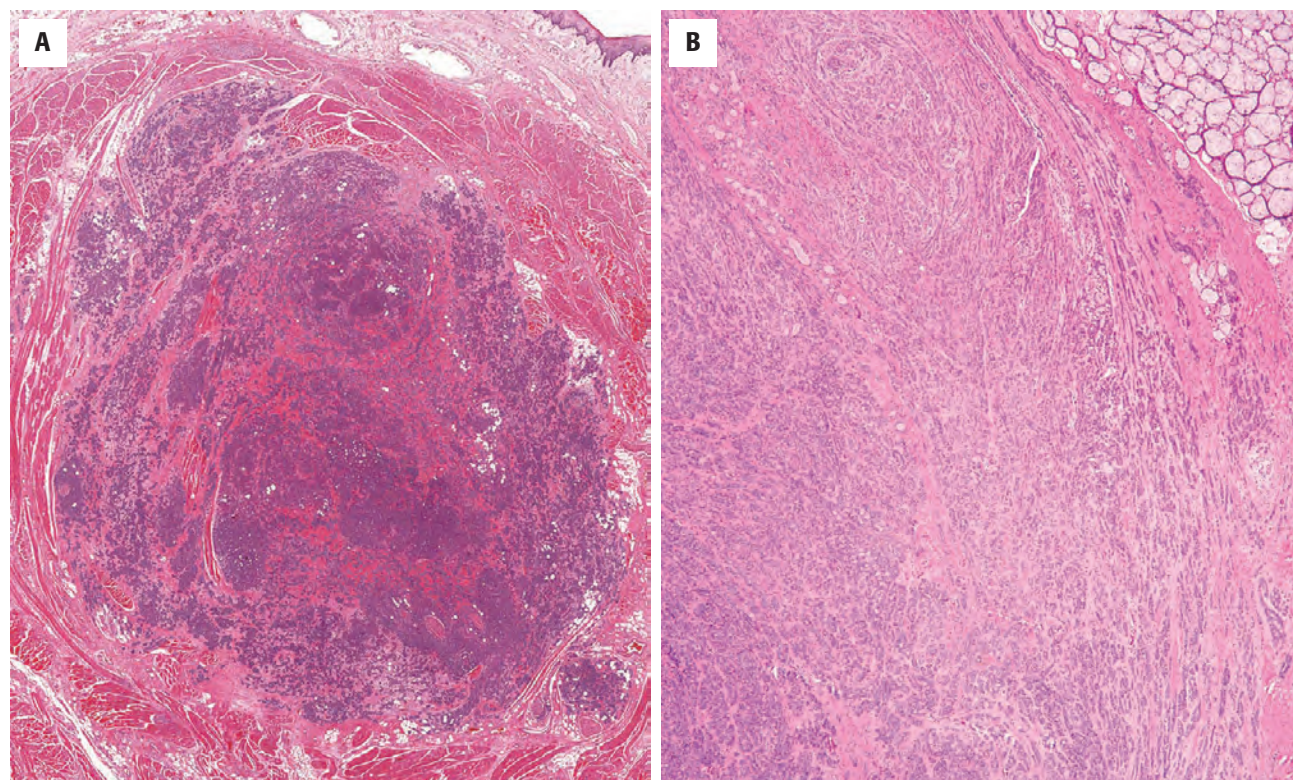
### **Prognosis and Therapy**

- Prognosis usually excellent
- Local recurrences in 9%-17% of cases
- Questionable aggressive behavior in younger patients
- Conservative surgery is the treatment of choice



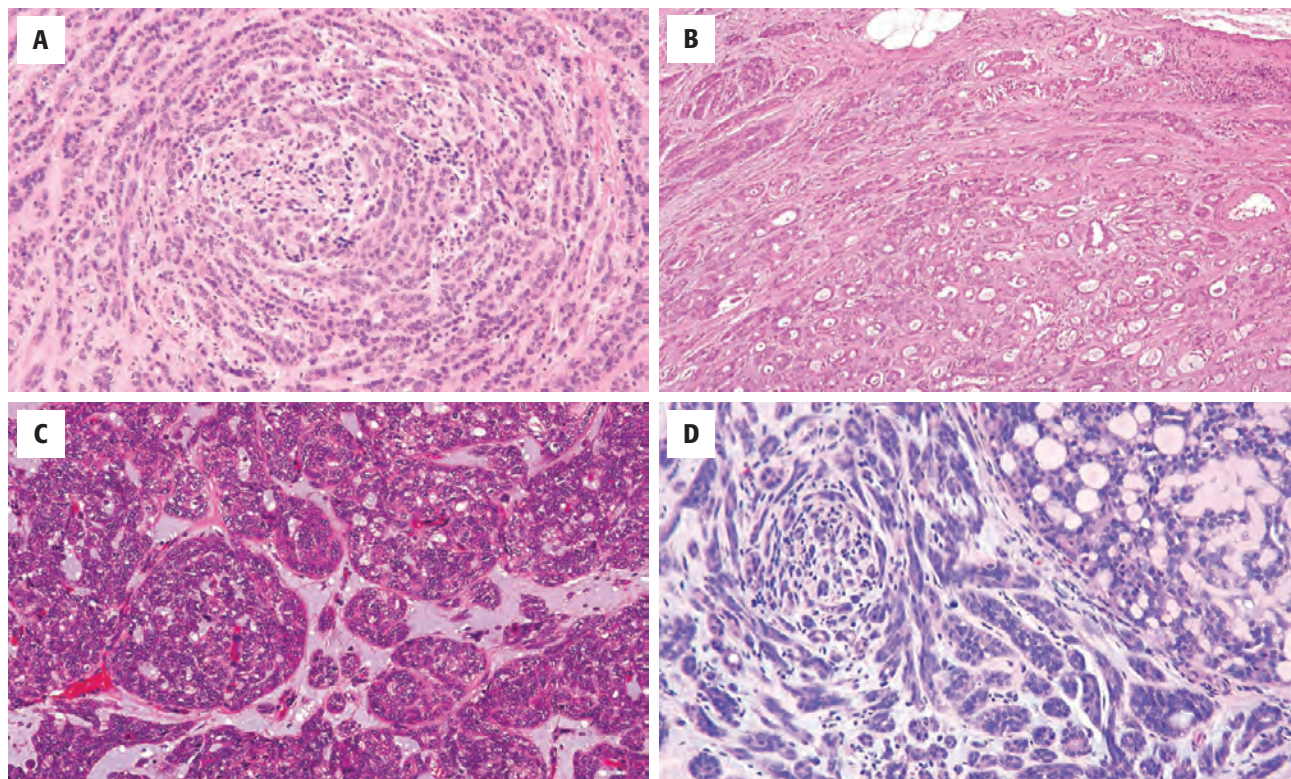
**FIGURE 13.38**

(A) Low power shows an invasive tumor arranged in several patterns. (B) A low-power magnification of polymorphous adenocarcinoma showing a well-circumscribed though unencapsulated mass with a variety of different growth patterns. The surface is intact and uninvolved. Note the encasement of the mucous glands (*far right*).

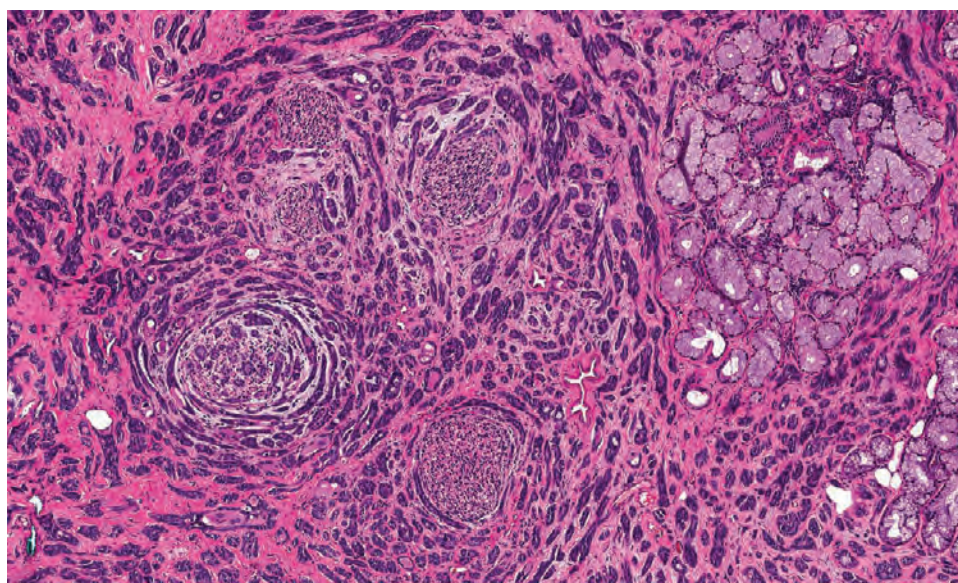
**FIGURE 13.39**

(A) Low power shows a number of different patterns in this unencapsulated tumor. (B) Note the single-file infiltration at the periphery of this variably patterned tumor.



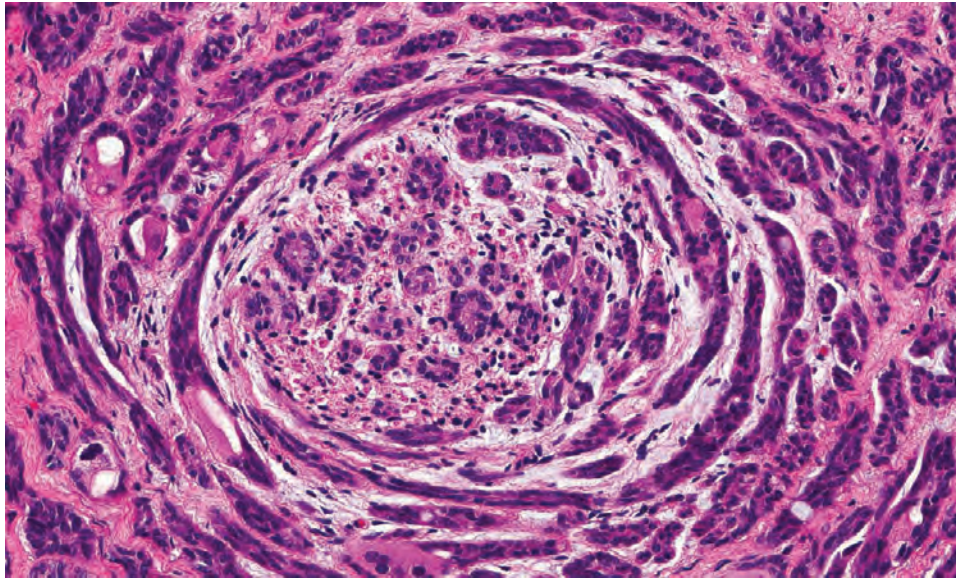
**FIGURE 13.40**

(A–D) Variable architectures are seen within a single tumor, including cribriform, tubular, and trabecular. Note the stroma in the background, which can be mucinous, myxoid, and slate gray–blue to eosinophilic and hyalinized.

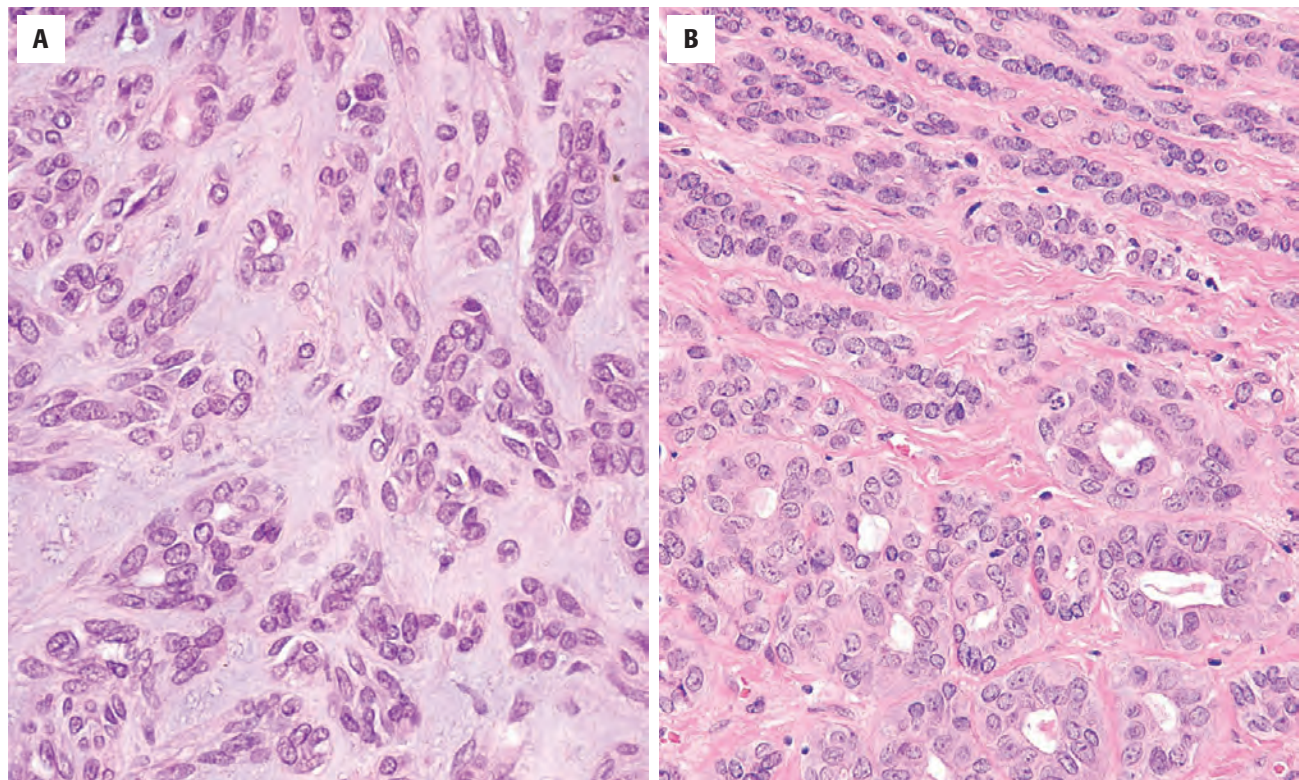
**FIGURE 13.41**

A targetoid pattern with a single-file, concentric arrangement of the cells. Nerves are usually in the center of these targets. Note the entombed minor mucoserous glands (surrounded but not destroyed).



**FIGURE 13.42**

A targetoid arrangement around a nerve, with intraneural and perineural invasion easily identified in this polymorphous adenocarcinoma.

**FIGURE 13.43**

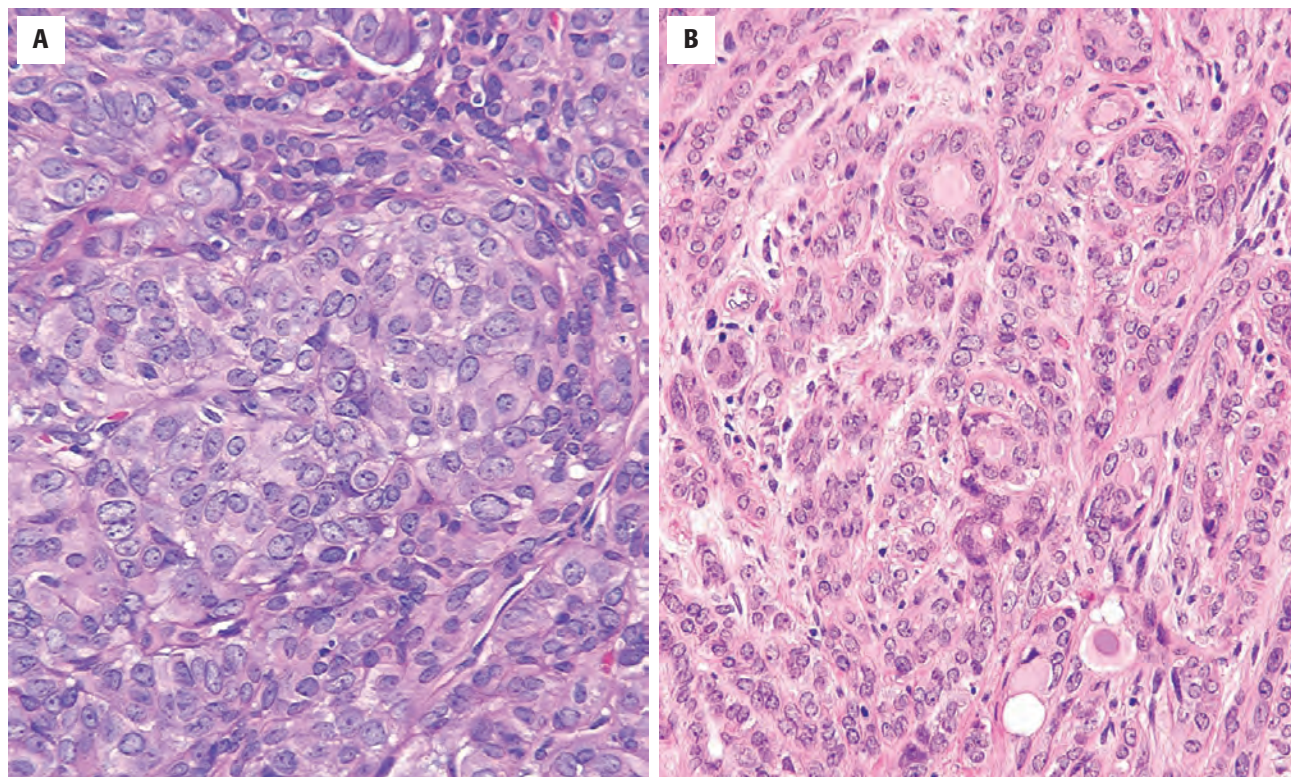
(A and B) Stromal hyalinization and a slate-gray-blue mucinous material in the background is quite characteristic of a polymorphous adenocarcinoma. Note the open vesicular nuclear chromatin and delicate small nucleoli.

hyalinization with a slate-gray appearance is common (Fig. 13.43), but chondroid or myxochondroid areas are not seen. One of the defining features of PAC is uniform nuclear changes that resemble those of papillary thyroid carcinoma (chromatin clearing, nuclear enlargement, and irregularities of nuclear membrane).

PAC is characterized by cytologic uniformity and architectural diversity (“polymorphous”). The cells

are isomorphic, small to medium in size, with pale eosinophilic cytoplasm. They have cytologically bland, pale-staining (vesicular) round or oval nuclei (Figs. 13.43 and 13.44). Mitotic figures or areas of necrosis are seen in high-grade PAC (Figs. 13.45 and 13.46). CAMSG tend to have nests with more prominent solid growth and slit-like spaces and a component of papillary growth (Fig. 13.47).



**FIGURE 13.44**

(A and B) The nuclei are round to oval, with vesicular pale nuclear chromatin, and small nucleoli. Mitotic figures are inconspicuous.

### POLYMORPHOUS ADENOCARCINOMA—PATHOLOGIC FEATURES

#### Gross Findings

- Circumscribed but usually unencapsulated mass
- Usually 1-3 cm

#### Microscopic Findings

- Cytologically uniform and architecturally diverse
- Wide variety of morphologic patterns in individual tumors
- Concentric targeting around nerves and blood vessels
- Encasement of benign residual salivary gland tissue
- Stromal hyalinization or myxoid/mucinous change (slate-gray in color)
- Isomorphic, small to medium-sized cells with eosinophilic cytoplasm
- Cytologically bland, pale-staining (vesicular), round or oval nuclei resembling those of papillary thyroid carcinoma

PAC, Polymorphous adenocarcinoma.

- Mitoses and necrosis uncommonly seen and define high-grade PAC

#### Immunohistochemical Findings

- Positive for cytokeratin, vimentin, S100 protein, and SOX10
- p63-positive cells are randomly distributed; p40 negative

#### Molecular Findings

- *PRKD* family genes; mutations or rearrangements

#### Pathologic Differential Diagnosis

- Limited biopsy specimens make diagnosis difficult; pleomorphic adenoma, adenoid cystic carcinoma, cystadenocarcinoma

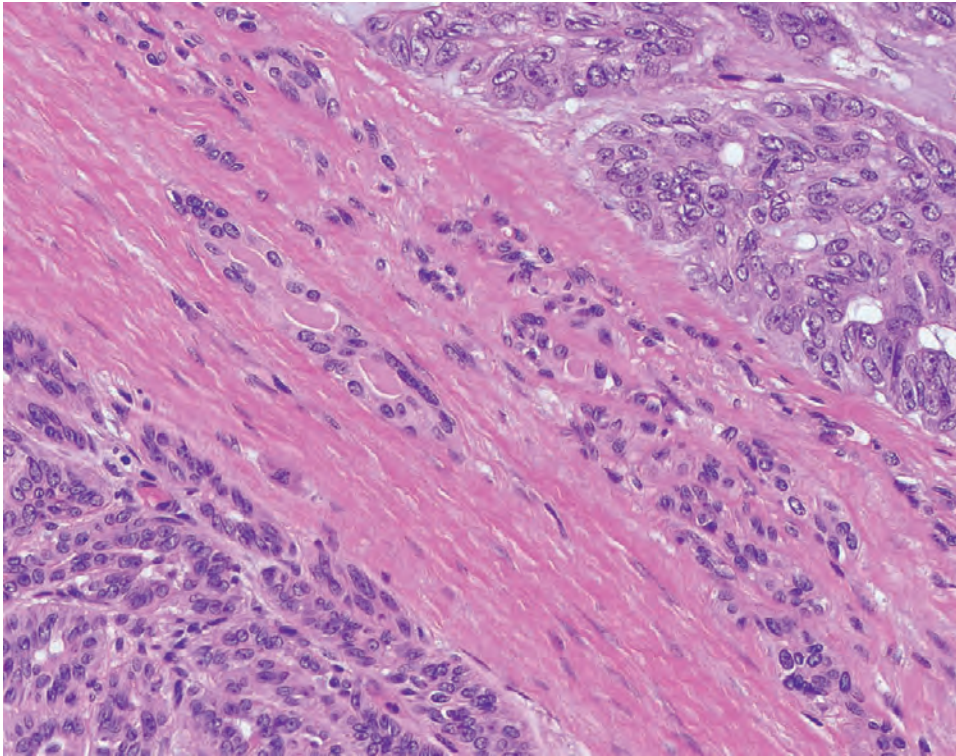
### ANCILLARY STUDIES

Most cases of PAC express p63 (randomly distributed cells without evidence of a dual cell population) (Fig. 13.48) but not p40. S100 protein (Fig. 13.49) and SOX10 are the most consistent markers and will decorate most of the cells with strong intensity.

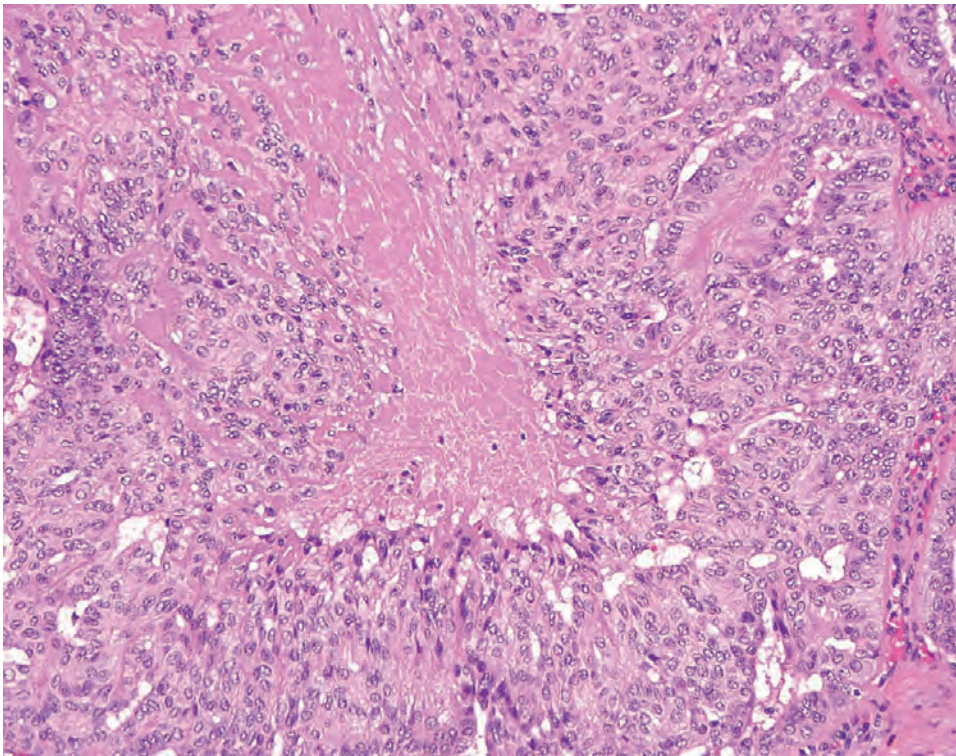
### DIFFERENTIAL DIAGNOSIS

The differential diagnosis includes PA, AdCC, and papillary variants of cystadenocarcinoma. This separation is hampered if the biopsy is small. Typically PA is circumscribed and often shows plasmacytoid differentiation in minor glands. Although both tumors can show stromal



**FIGURE 13.45**

Polymorphous adenocarcinoma interface between a conventional low-grade area (*left lower corner*) and a high-grade area (*right upper corner*).

**FIGURE 13.46**

High-grade polymorphous adenocarcinoma. Note comedo-type necrosis and enlarged vesicular nuclei.



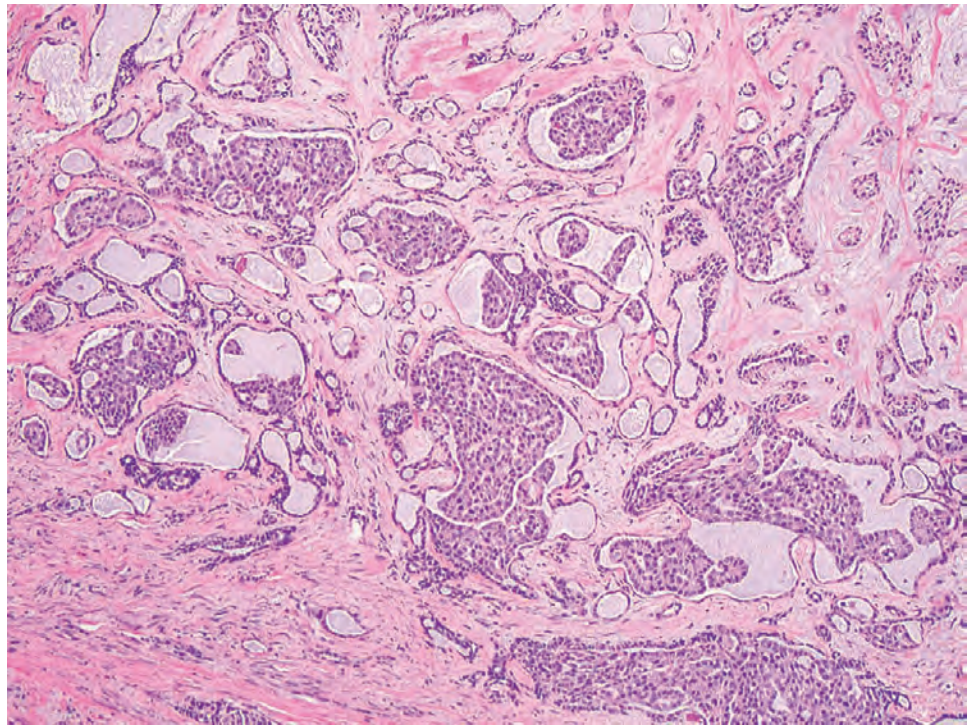


**FIGURE 13.47**

An example of cribriform adenocarcinoma of the salivary gland (with known *PRKD1* rearrangement), a variant of polymorphous adenocarcinoma.

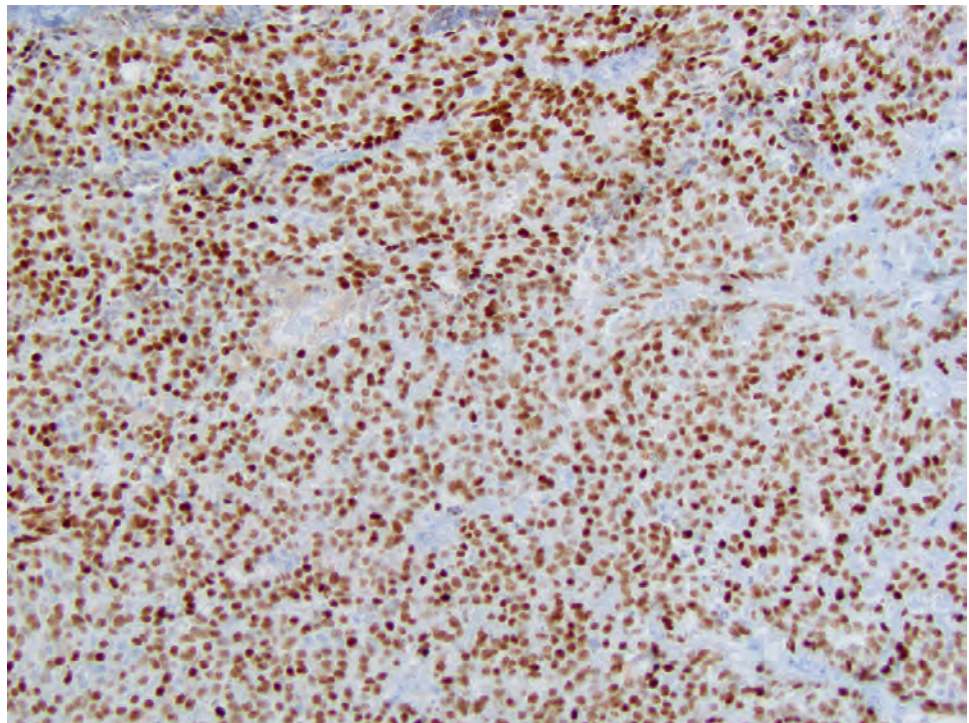


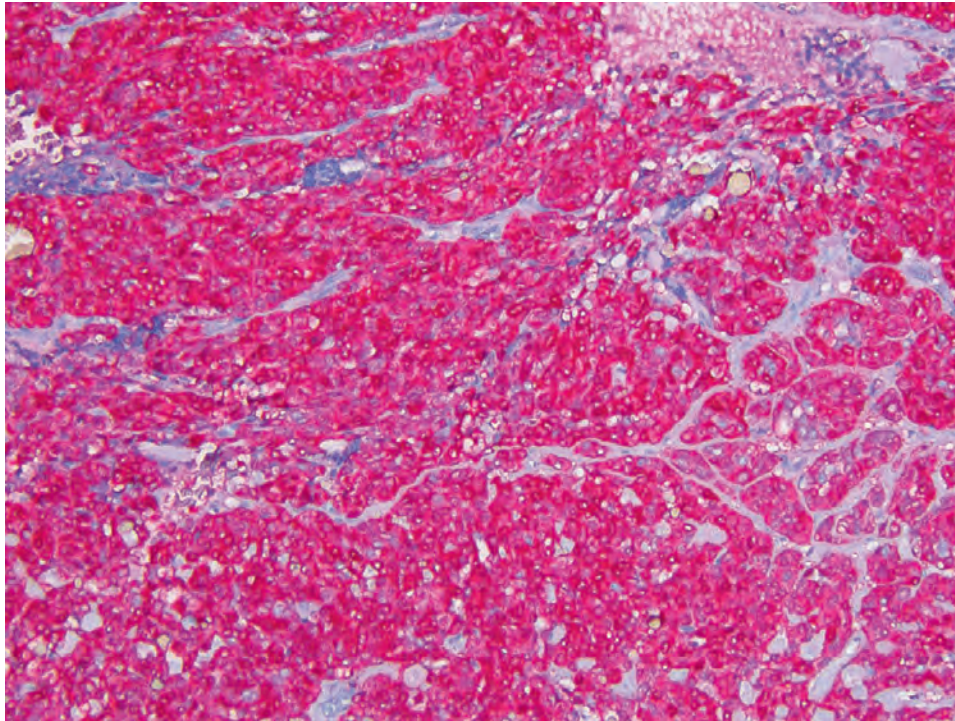
**FIGURE 13.48**

Polymorphous adenocarcinoma p63 immunohistochemistry highlights most of the cells and shows no evidence of a dual cell population.

mucinosi and elastosis, myxochondroid or chondroid matrix is not seen in PAC. It has been reported that staining for GFAP is very strong in PAs but weak or absent in PAC. AdCC has a dual cell population (luminal ductal cells and abluminal basal-myoeptithelial cells) with

hyperchromatic nuclei and a much higher nuclear-to-cytoplasmic ratio; it tends to be more extensively infiltrative. *Cystadenocarcinoma* usually has a conspicuous papillary architecture and nuclear pleomorphism with mitotic figures.



**FIGURE 13.49**

Polymorphous adenocarcinoma S100 protein immunohistochemistry strongly highlights most of the cells and shows no evidence of a dual cell population.

### PROGNOSIS AND THERAPY

The long-term prognosis is usually excellent. There is local recurrence in 9% to 17% of cases and spread to regional lymph nodes is seen in 9% to 15% of cases. Distant metastases are very rare and death due to disease is uncommon. PAC with prominent papillary growth has a more aggressive behavior. Complete but conservative surgery is the treatment of choice, together with neck dissection in cases with proven regional metastases.

## ■ EPITHELIAL-MYOEPITHELIAL CARCINOMA

### CLINICAL FEATURES

Epithelial-myoepithelial carcinoma (EMC) is a malignant neoplasm demonstrating a characteristic biphasic pattern of inner ductal cells and an outer layer of myoepithelial cells. EMC accounts for about 1% of salivary gland tumors. It is usually seen in older age groups (50–60 years) and is rare in children. Women are affected twice as often as men. Most cases arise in the parotid gland, where the tumor typically forms as a slowly growing, painless mass, often of long duration. It can also arise from minor glands of the mouth and the upper and lower respiratory tracts, where it has a tendency to ulcerate. Tumors with HGT may undergo rapid growth and cause pain or facial nerve palsy.

### PATHOLOGIC FEATURES

#### GROSS FINDINGS

The tumor typically forms a well-defined but usually nonencapsulated mass 2 to 8 cm in diameter. The tumors are often lobulated and cystic areas are common (Fig. 13.50). Tumors in minor glands tend to be less well demarcated.

#### MICROSCOPIC FINDINGS

The characteristic feature of EMC is the formation of double-layered duct-like structures (Fig. 13.51), occasionally with a prominent split between the two cell layers (Fig. 13.52). The luminal cells form a single cuboidal or columnar layer and have finely granular, eosinophilic cytoplasm and a central round or oval nucleus. The outer cells may form single or multiple layers and have abundant clear cytoplasm that is usually rich in glycogen; they typically have eccentric and vesicular nuclei. However, in about 20% of cases, there is little evidence of clear cells (Fig. 13.53). The proportion of each cell type and their architectural arrangement is extremely variable. The duct-like structures may be surrounded and separated by hyaline material or fibrous tissue (Fig. 13.53). They can also form more cohesive sheets, and the ductal configuration may not be immediately apparent. Tumors may consist predominantly of clear cells with only scattered duct-lining cells, which may form solid islands without canalization. Cystic or papillary areas are seen

**EPITHELIAL-MYOEPITHELIAL CARCINOMA—DISEASE FACT SHEET****Definition**

- A malignant neoplasm with biphasic duct-like structures composed of an inner layer of ductal cells and an outer layer of clear myoepithelial cells

**Incidence and Location**

- About 1% of salivary gland tumors
- 60% of cases involve the parotid gland
- Also seen in the mouth and the upper and lower respiratory tracts

**Morbidity and Mortality**

- Spread to regional lymph nodes and distant sites (about 15%)
- 5-year survival rate of 80%

**Sex and Age Distribution**

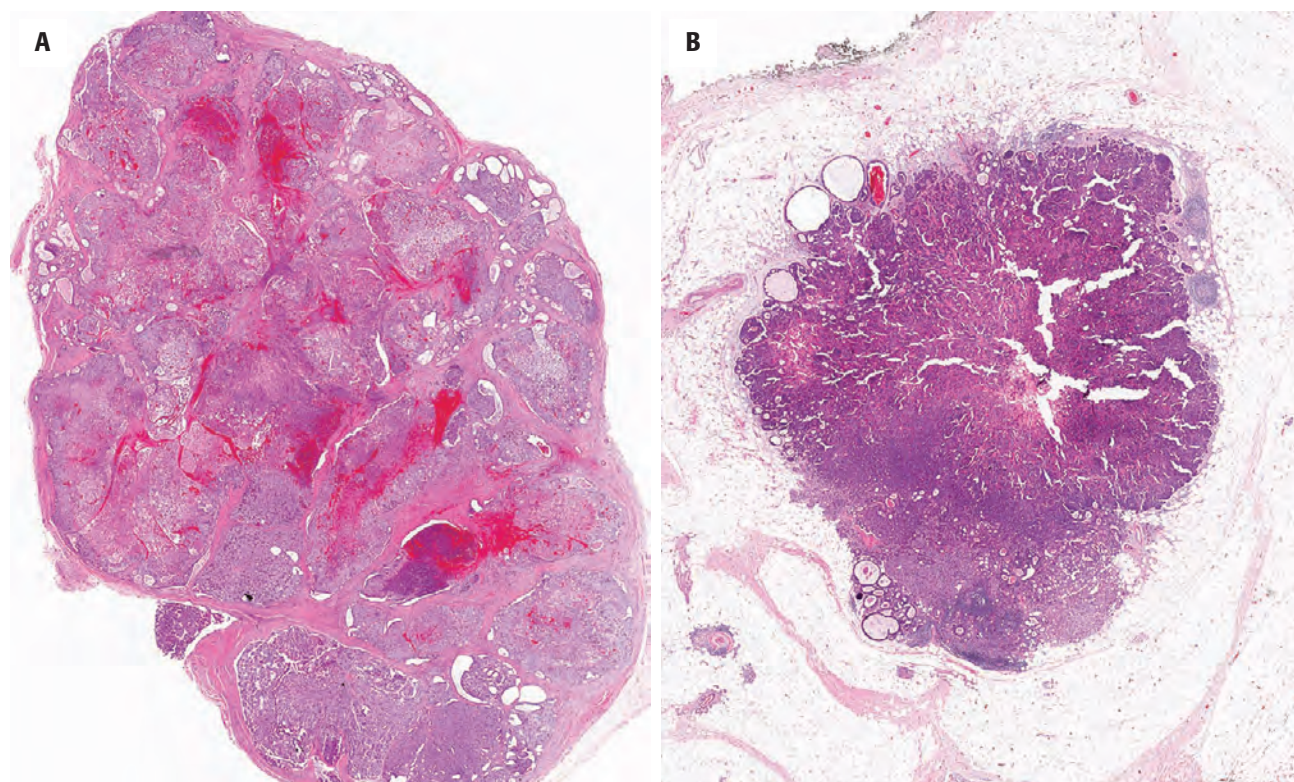
- Females > males (2:1)
- Peak incidence in 6th-7th decades
- Rare in children

**Clinical Features**

- Painless slow-growing mass
- Tumors are often present for long periods
- Tumors involving mucosal sites often ulcerate
- Occasionally, tumors are rapidly growing and painful and may cause nerve palsies

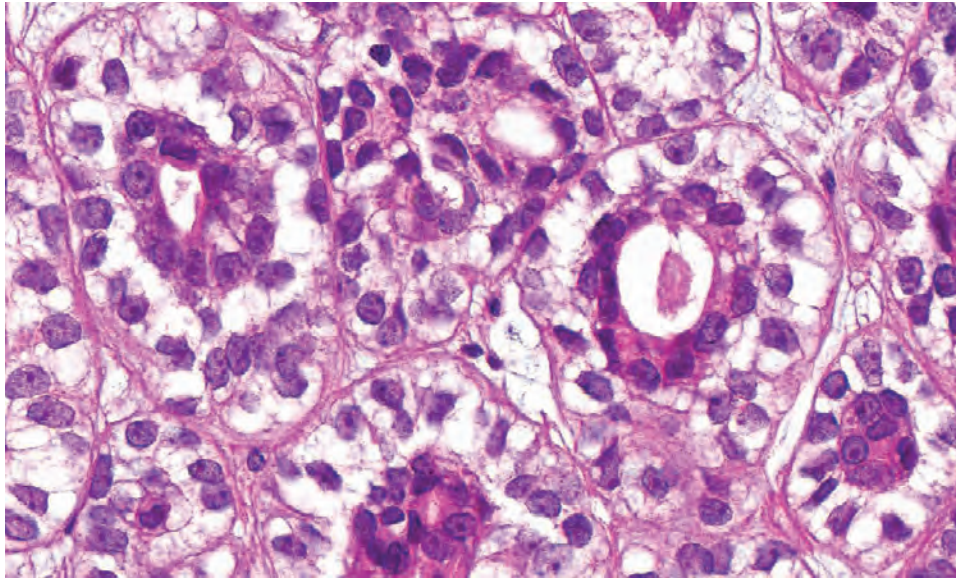
**Prognosis and Therapy**

- Prognosis is usually good (5-year survival of 80%), although recurrences are common (40%)
- Clinical indicators of poor prognosis include incomplete surgical excision, large size, rapid growth, and involvement of minor salivary glands
- Microscopic features associated with a poor outcome include cellular atypia, high mitotic count, and necrosis
- Surgery is the treatment of choice, supplemented by radiotherapy in advanced or recurrent cases

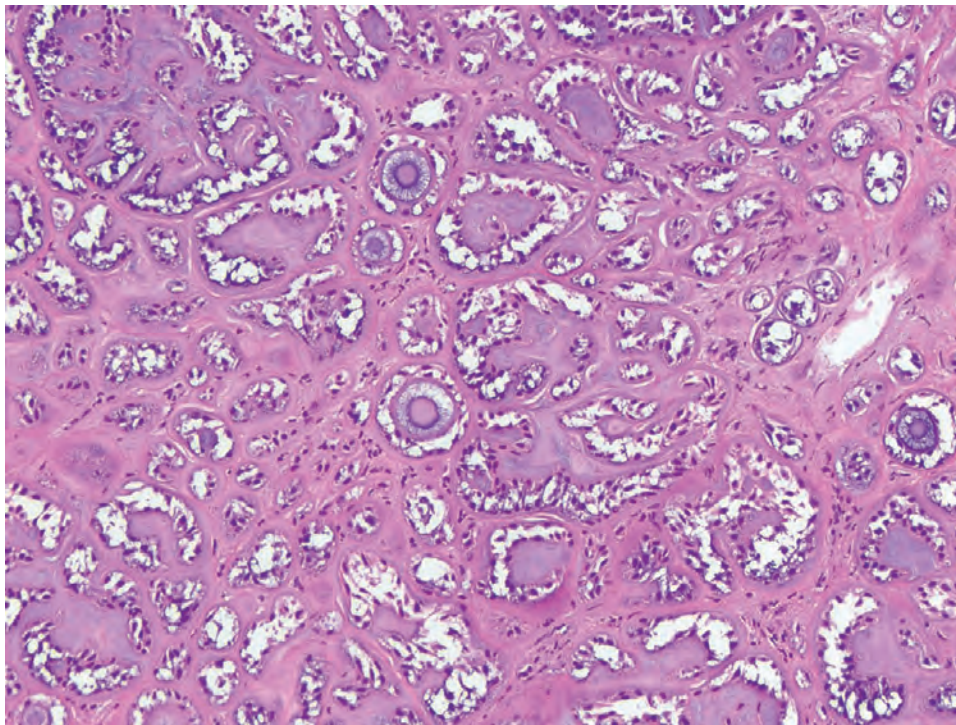
**FIGURE 13.50**

(A) There is a well-defined but unencapsulated tumor showing invasion and irregular borders in this epithelial-myoepithelial carcinoma. (B) An ill-defined tumor is noted in this minor salivary gland location.



**FIGURE 13.51**

High power shows eosinophilic cytoplasm of the inner luminal duct-like cells. The myoepithelial cells have cleared cytoplasm with more vesicular nuclear chromatin.

**FIGURE 13.52**

Epithelial-myoepithelial carcinoma with prominent artifactual retraction ("split") between the two cell layers.

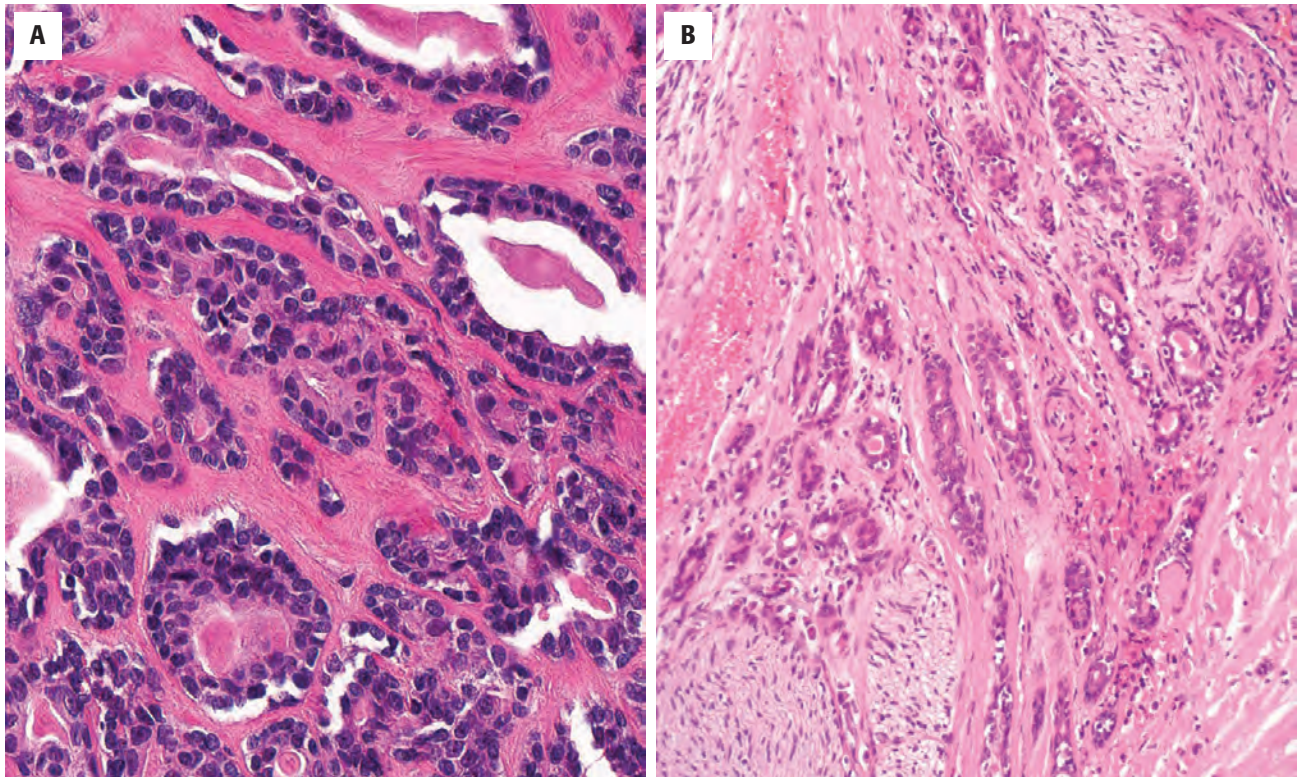
in about 20 % of cases. Less commonly, areas show spindle cell or squamous differentiation, or oncocytic metaplasia, typically of the luminal cells ([Fig. 13.54](#)). Mitoses are usually sparse and rarely exceed 2 per 10 high-power fields (HPFs). Perineural and vascular involvement is relatively common and bone invasion is occasionally seen ([Fig. 13.53](#)). EMC may arise from a PA and a few cases of hybrid tumors with components of EMC and another tumor type (e.g., AdCC) have been described. Cases of EMC showing HGT have been reported ([Fig. 13.55](#)).

Recently described but rare variants include oncocytic-sebaceous EMC and apocrine EMC.

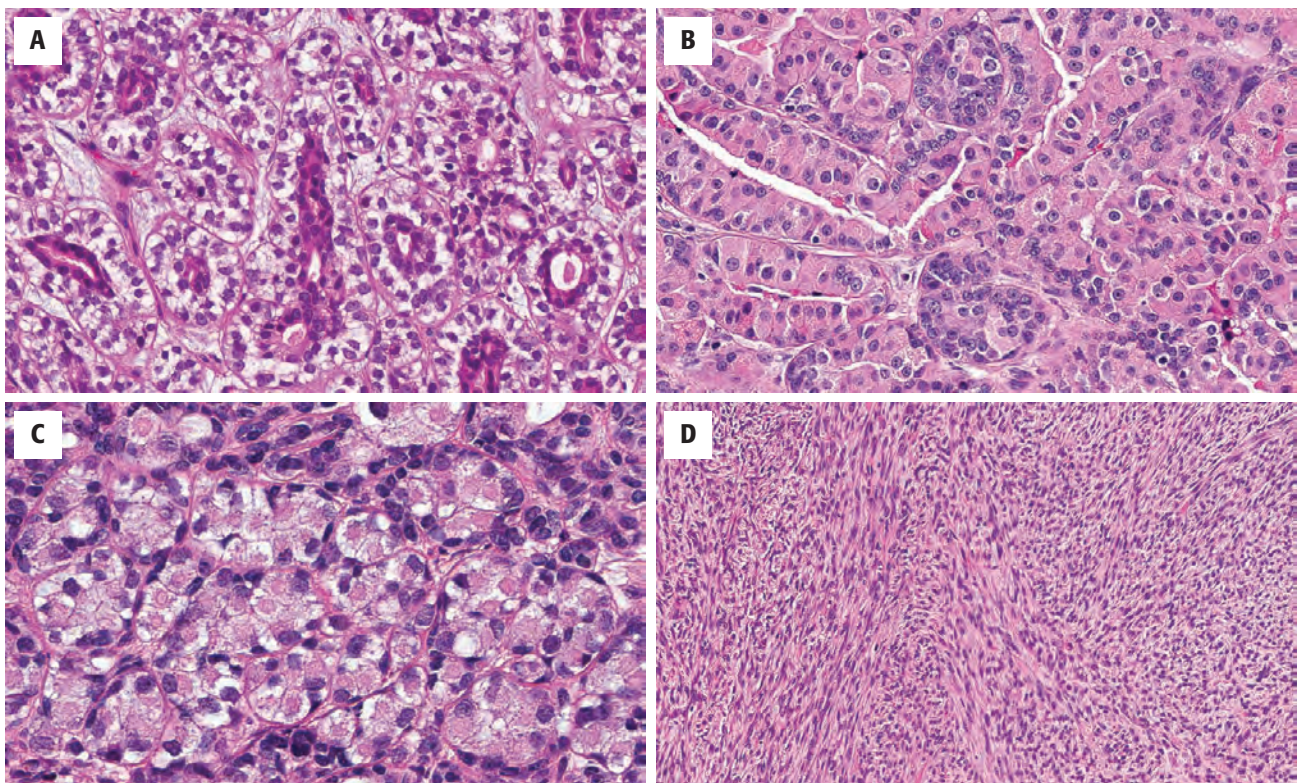
#### ANCILLARY STUDIES

The inner duct-lining cells stain with low-molecular-weight cytokeratins, CAM5.2, and EMA ([Fig. 13.56](#)). The outer clear cells stain with myoepithelial markers



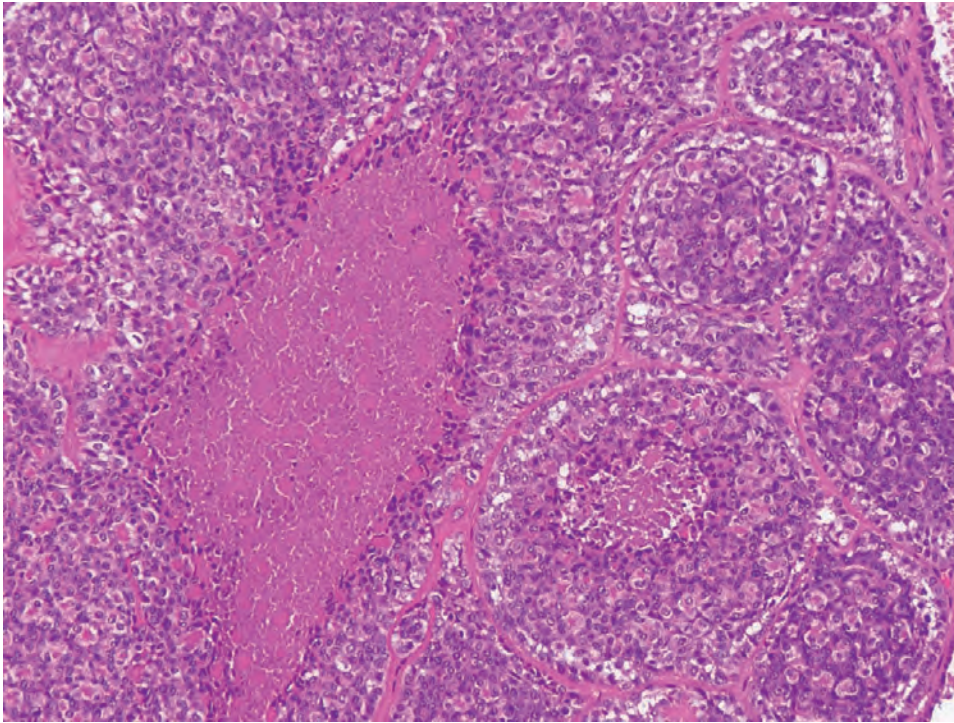
**FIGURE 13.53**

(A) Duct-like structures separated by fibrous connective tissue. Note the double layer of inner cuboidal cells surrounded by myoepithelial cells. (B) Perineural invasion is prominent.

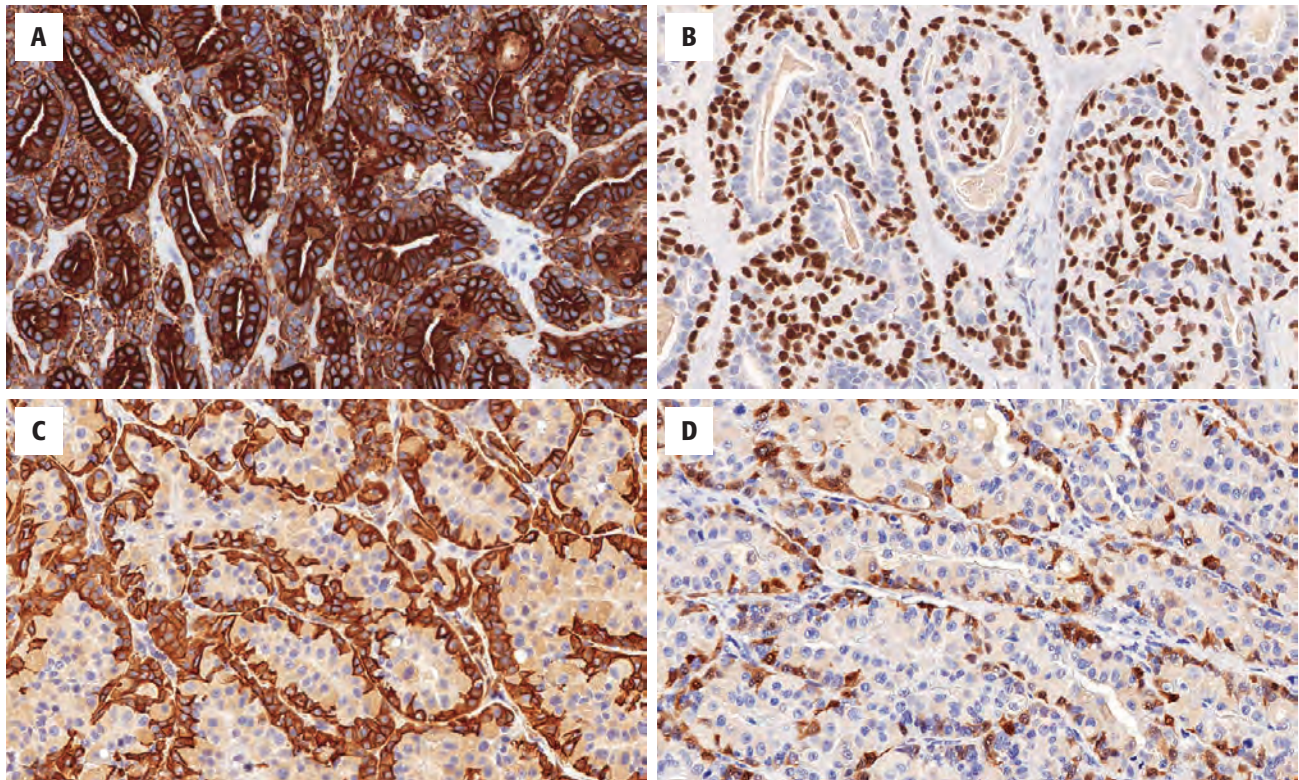
**FIGURE 13.54**

A variety of different cell types can be seen in an epithelial-myoepithelial carcinoma. (A) The classic central duct-like structures surrounded by syncytial myoepithelial cells with cleared cytoplasm. (B) The cells have an oncocytic appearance, although the biphasic appearance is still noted with the darker myoepithelial cells. (C) A more solid area shows granular cytoplasm in the ductal cells and darker basaloid cells. (D) The tumor cells are arranged in a spindled pattern without any easily identified epithelial component. Immunohistochemistry would be valuable in this setting.



**FIGURE 13.55**

Epithelial-myoepithelial carcinoma with high-grade transformation (note extensive necrosis).

**FIGURE 13.56**

(A) Keratin highlights the inner ductal-type cells. (B) p63 highlights the basal myoepithelial cells. (C) A smooth muscle actin strongly stains the basal-myoepithelial cells. (D) An S100 protein stain accentuates the outer myoepithelial cells.



### EPITHELIAL-MYOEPITHELIAL CARCINOMA—PATHOLOGIC FEATURES

#### Gross Findings

- Well-defined but usually nonencapsulated mass, 2–8 cm in diameter
- Often lobulated, cystic areas common
- Tumors in minor glands less well demarcated

#### Microscopic Findings

- Double-layered duct-like structures
- Inner cuboidal duct-lining cells and outer, single or multiple layers of myoepithelial cells with clear cytoplasm and eccentric vesicular nuclei
- Wide variation in proportions of each cell type
- Duct-like structures may be widely separated by fibrous tissue or merge into cohesive sheets
- Papillary and cystic areas are present in 20% of cases
- Spindle cell areas and squamous metaplasia occasionally present
- Mitoses uncommon (2 per 10 HPFs)
- Perineural and vascular invasion commonly seen

#### Immunohistochemical Findings

- Inner cells positive with keratins
- Outer myoepithelial cells positive with calponin, SMA, p63, and, less reliably, S100 protein; CD117 and bcl-2 frequently positive

#### Molecular Findings

- EMC arising ex pleomorphic adenoma frequently shows *PLAG1* or *HMG2* rearrangements, and about one-third of EMCs harbor *HRAS* mutations

#### Pathologic Differential Diagnosis

- Pleomorphic adenoma, adenoid cystic carcinoma (tubular variant), myoepithelioma, clear cell oncocytoma, mucoepidermoid carcinoma, clear cell carcinoma, and metastases from the kidney and thyroid gland

EMCs, Epithelial-myoepithelial carcinomas; HPFs, high-power fields; SMA, smooth muscle actin.

such as calponin, SMA, p63, p40, and, less reliably, S100 protein (Fig. 13.56).

### DIFFERENTIAL DIAGNOSIS

The differential diagnosis of EMC includes tumors showing double-layered duct-like structures and those consisting predominantly of clear cells. Double-layered duct-like structures can be seen in PA, basal cell adenoma or adenocarcinoma, and the tubular variant of AdCC. The clear cells in these tumors tend to be focal, have less abundant cytoplasm, and have hyperchromatic angular nuclei. Nuclear palisading allows the identification of basal cell adenoma and basal cell adenocarcinoma. In addition, the clear cells of EMC are typically rich in glycogen. Tumors showing focal or extensive areas of

predominantly clear cells include clear cell variants of PA, myoepithelioma, oncocytoma, and MEC, as well as clear cell carcinoma. *Metastases* from the kidney and thyroid glands may have to be excluded by staining for p63, calponin, renal cell carcinoma (RCC) marker, PAX8, PAX2, thyroglobulin, and TTF1.

### PROGNOSIS AND THERAPY

EMC is a moderately aggressive salivary gland tumor with a high recurrence rate (40%) and metastases to regional lymph nodes and distant sites—such as the lung, liver, and kidney—seen in nearly 15% of cases. The 5-year survival rate is 80% and the 10-year survival is 72%. Clinical findings indicating a poorer prognosis include incomplete surgical excision, large size, rapid growth, and involvement of minor salivary glands. Microscopic features associated with a poor outcome include cellular atypia, high mitotic count, and necrosis. Surgery is the treatment of choice, and neck dissection should be included in patients with evidence of regional lymph node spread. This can be supplemented by radiotherapy in advanced or recurrent cases.

### ■ SECRETORY CARCINOMA (MAMMARY ANALOGUE SECRETORY CARCINOMA)

#### CLINICAL FEATURES

Secretory carcinoma (SC), also known *mammary analogue secretory carcinoma*, is a recently described malignant salivary gland tumor. SC predominantly involves major glands, particularly the parotid, but is also frequently reported at other sites including buccal mucosa, lip, and base of tongue. Whereas most cases develop in the breast and salivary glands, rare cases arising in unusual sites like skin and thyroid gland have been reported.

Men are more commonly affected than women (1.2:1), with a mean age of patients with conventional SC in the 5th decade. Patients with SC with HGT (SC-HGT) usually present later in the 6th decade. The tumor usually forms a painless mass that is discovered incidentally. SC-HGT may present with facial nerve paralysis or distant metastases.

#### PATHOLOGIC FEATURES

##### GROSS FINDINGS

SC may be well defined, infiltrative, and fixed or, rarely, (< 10%) encapsulated. Most tumors are less than 4 cm in largest dimension. About one-third of tumors are cystic.



**SECRETORY CARCINOMA—DISEASE FACT SHEET****Definition**

- A malignant glandular epithelial neoplasm comprising intercalated duct-type cells arranged in follicular, solid, and microcystic patterns

**Incidence and Location**

- Recently described entity with uncertain incidence
- Major and minor salivary glands throughout the upper and lower aerodigestive tract

**Morbidity and Mortality**

- Up to 20% of cases recur locally
- Spread to regional lymph nodes in up to 25% of cases
- Distant metastases are known to occur
- Instances of death from disease are known

*SC-HGT*, SC with high-grade transformation.

**Sex and Age Distribution**

- Males > females (1.2:1)
- Mean, 47 years (for patients with SC-HGT, 56 years)

**Clinical Features**

- Usually forms a painless mass, often discovered incidentally

**Prognosis and Therapy**

- SCs with high-grade transformation have a higher incidence of regional lymph node involvement and greater chance of local recurrence
- Most tumors are conventional (formal grading scheme not yet developed)
- Surgery with or without neck dissection is the treatment of choice

**SECRETORY CARCINOMA—PATHOLOGIC FEATURES****Gross Findings**

- May be circumscribed or infiltrative

**Microscopic Findings**

- Consists of intercalated duct-type cells, flattened or cuboidal, with central nucleolus and eosinophilic cytoplasm
- Tumors show cystic, papillary, microfollicular, and solid growth
- Predominance of solid growth, loss of secretory activity, enlarged vesicular nuclei, and necrosis are features of SC with high-grade transformation

**Immunohistochemical Findings**

- S100 protein and mammaglobin are positive in over 95% of cases
- GCDFP-15 is positive in about 80% of SC
- SOX10 is positive in about 70% of cases
- In up to one-third of SCs, p63 outlines short stretches of preserved basal cells

SC, Secretory carcinoma

**Molecular Findings**

- *ETV6* rearrangement is a hallmark of SC

**Fine Needle Aspiration**

- Round nuclei with nucleoli, reduced cellular cohesion, and transgressing vessels
- Cytoplasmic microvacuoles

**Pathologic Differential Diagnosis**

- Conventional SCs are most commonly confused with low-grade cribriform cystadenocarcinoma (also known as intraductal carcinoma)
- SCs with high-grade transformation mimic salivary duct carcinomas
- At unusual sites (outside of the oral cavity and major salivary glands—for example, lymph nodes, thyroid gland), SC may be confused with papillary thyroid carcinoma, especially on small biopsies and fine needle aspirates

**MICROSCOPIC FINDINGS**

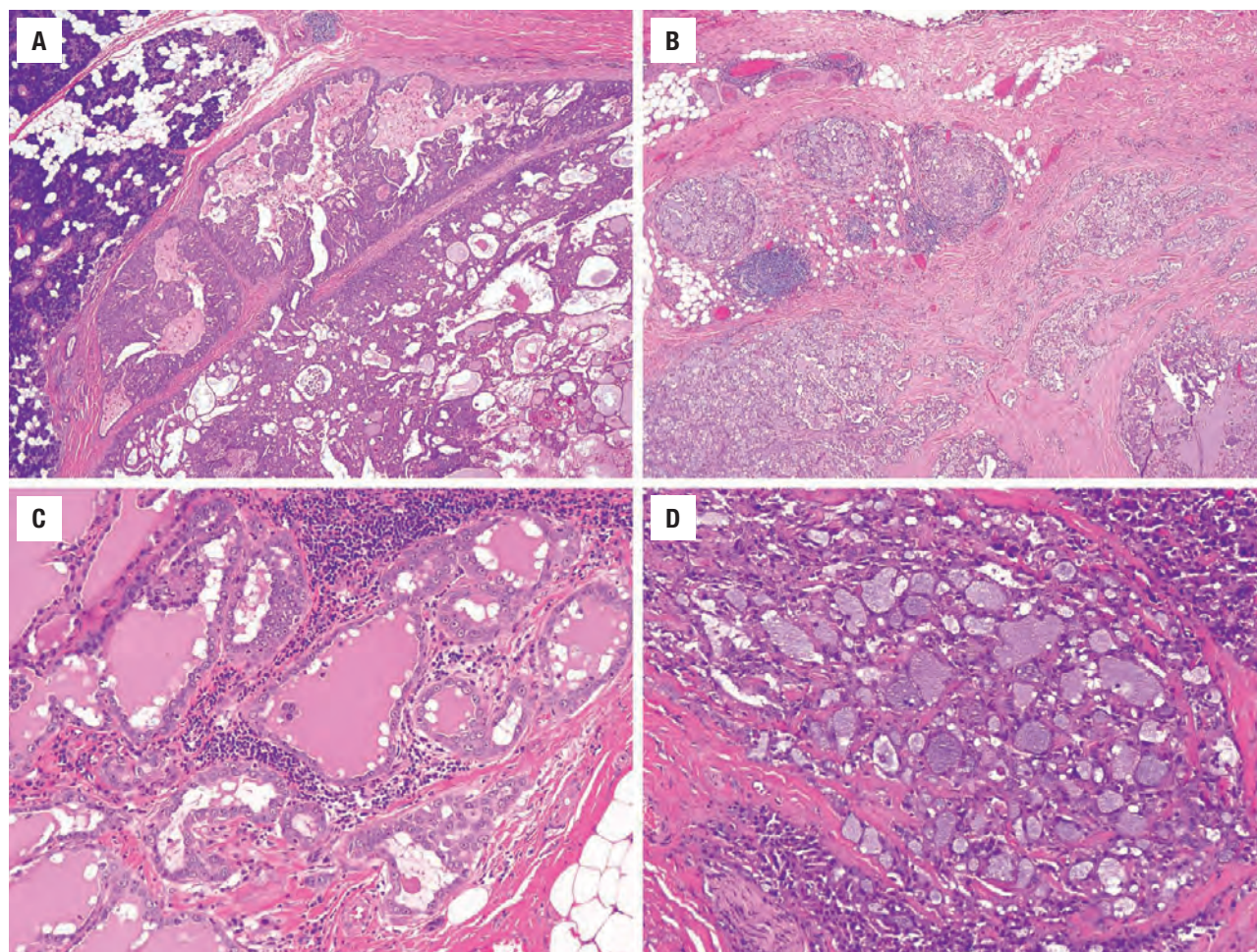
About one-third of conventional SCs show pushing and lobulated growth, while one-third have invasive growth (Fig. 13.57). About 20% of SCs show perineural invasion (Fig. 13.58). The neoplastic cells of conventional SCs are flattened or cuboidal with a central nucleolus and eosinophilic cytoplasm. The cells of SCs are of the intercalated duct type and form follicles filled usually with eosinophilic colloid-like secretions (Fig. 13.57). Occasionally, secretions are more basophilic rather than eosinophilic (Fig. 13.57D). Some cases show cysts filled with eosinophilic colloid-like material and

with papillae (Fig. 13.59). Larger cysts may rupture, leading to an inflammatory reaction with hemorrhage, hemosiderin deposition, and cholesterol cleft formation (Fig. 13.60). Tumors arising in the palate or lip may undergo infarction due to trauma or FNA (Fig. 13.60).

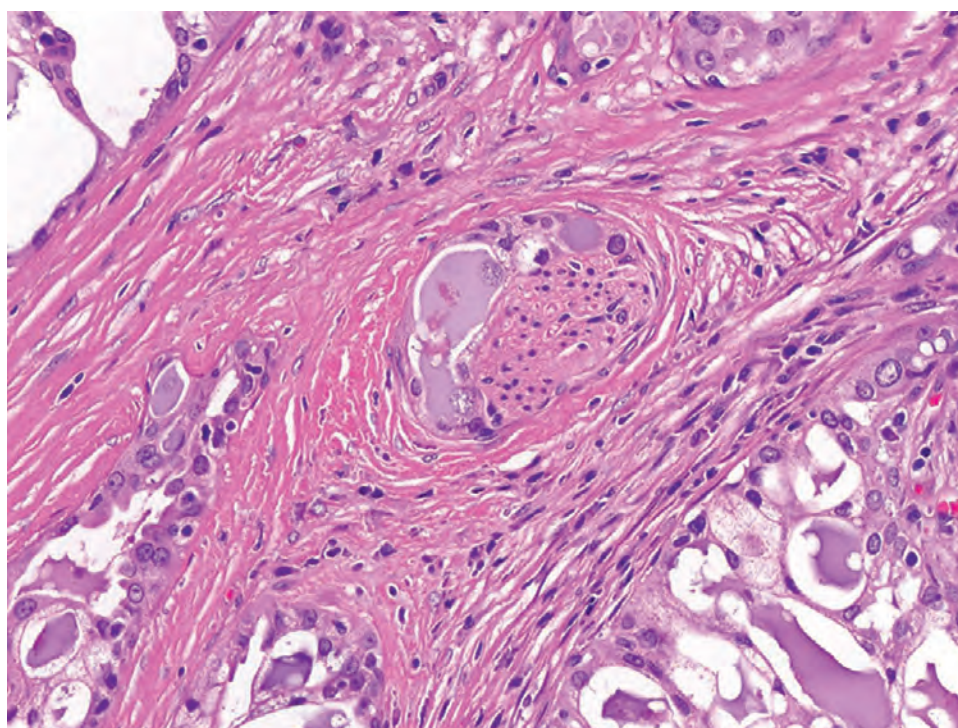
**TUMOR GRADING**

There is no formal SC grading scheme. However, loss of secretory activity, enlarged vesicular nuclei, increased



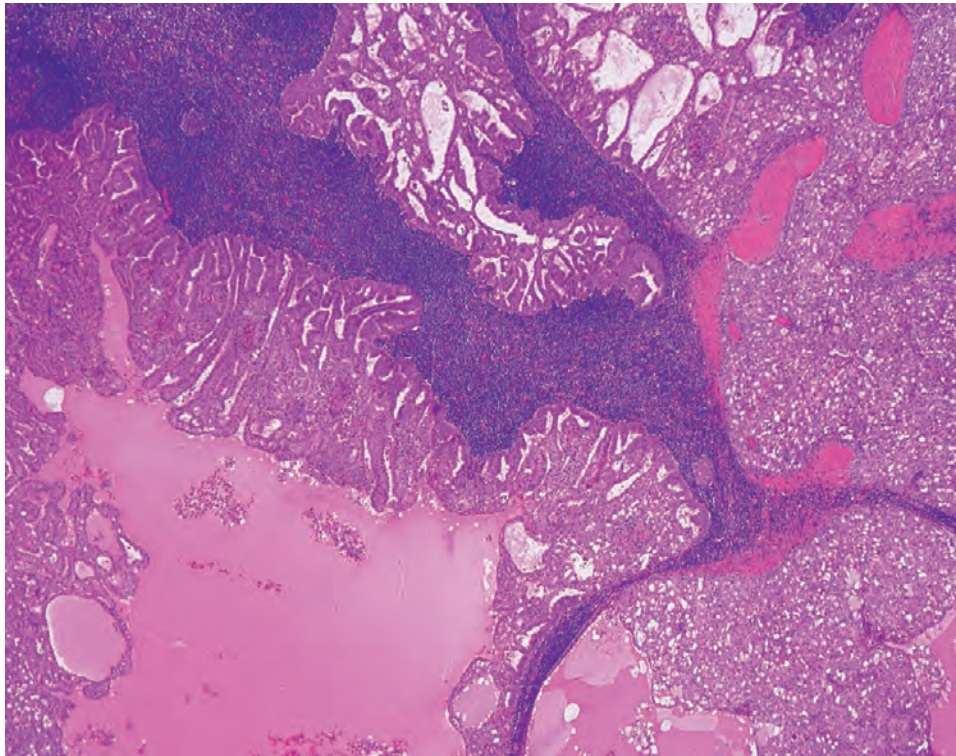
**FIGURE 13.57**

Secretory carcinoma, conventional. (A) Well-circumscribed lobulated growth pattern. (B) Infiltrative growth and fibrosis. (C) Tumor follicles lined by intercalated duct-type cells and filled with eosinophilic colloid-like fluid, mimicking well-differentiated thyroid carcinoma. (D) Occasionally, secretions are more basophilic.

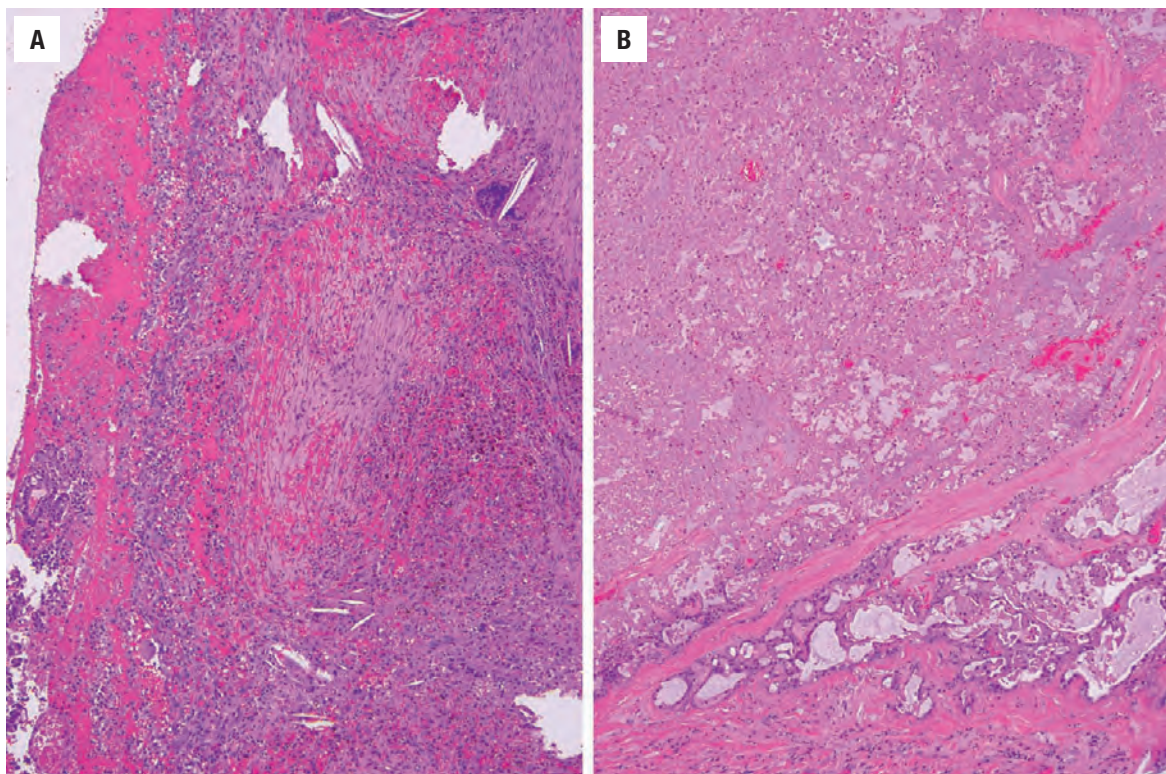
**FIGURE 13.58**

About 20% of cases of secretory carcinoma show perineural invasion.





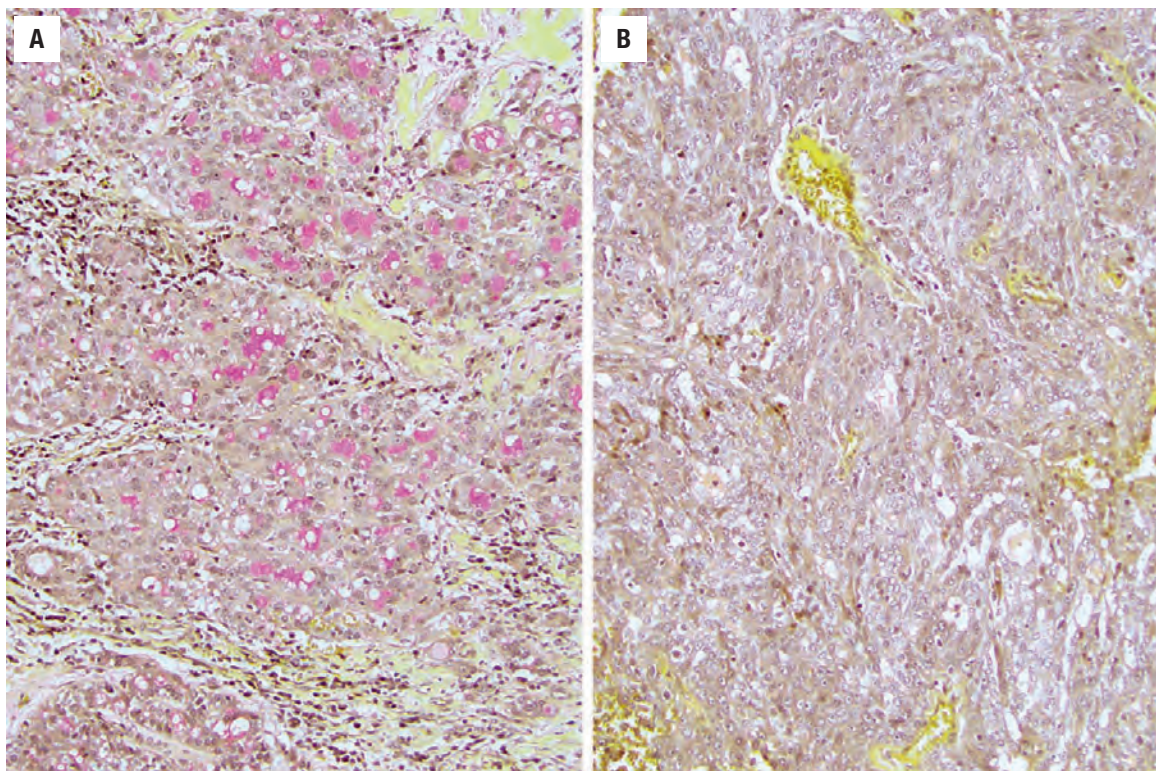
**FIGURE 13.59**  
Lymph node metastasis of a secretory carcinoma with papillary cystic growth.



**FIGURE 13.60**

Secretory carcinoma secondary changes. **(A)** Reaction to escaped cystic content with cholesterol granuloma, granulation tissue, and hemosiderin. Small areas of viable carcinoma are seen in the left quarter of the image. **(B)** Extensive post-fine needle aspiration infarct. Viable carcinoma is seen in the lower third of the image.



**FIGURE 13.61**

Secretory carcinoma. **(A)** Mucicarmine highlights secretions and preserved secretory activity in conventional areas. **(B)** Mucicarmine is negative in solid areas. Such areas may show increased mitotic activity and necrosis, consistent with high-grade transformation.

mitotic activity ( $> 3$  per 40x HPF), and necrosis are findings of SC with HGT (Figs. 13.61 and 13.62).

## ANCILLARY STUDIES

### IMMUNOHISTOCHEMICAL FINDINGS

S100 protein and mammaglobin are positive in over 95 % of SCs. At least one of these markers is positive in the great majority of SCs. The breast markers GCDPF-15 and GATA3 are positive in most cases as well. SOX10 is positive in over two-thirds of cases. In about 10 % of SCs, DOG-1 may show predominantly apical staining. In up to one-third of SCs, p63 or p40 outlines short stretches of preserved basal cells.

### MOLECULAR FINDINGS

*ETV6* rearrangement defines SC and, in the context of salivary tumors, is specific to SC.

### FINE NEEDLE ASPIRATION

Cytologically, SC is characterized by round nuclei with nucleoli, reduced cellular cohesion, and transgressing vessels. The cytoplasm shows microvacuoles that are more clearly appreciated on Papanicolaou stain (Fig. 13.63).

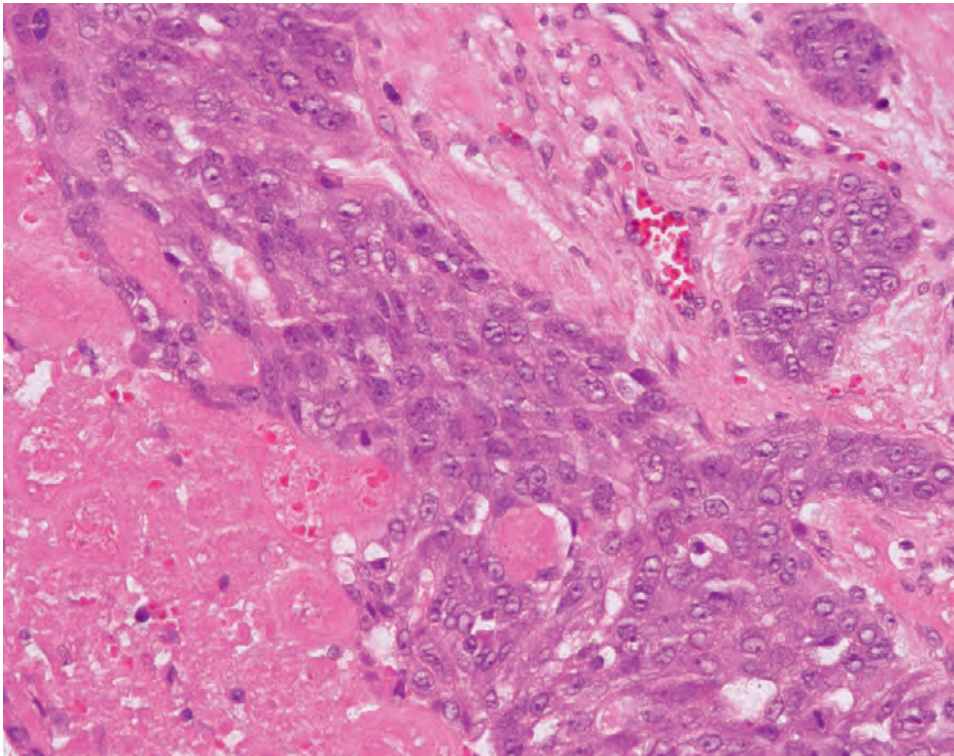
## DIFFERENTIAL DIAGNOSIS

The differential diagnosis for SC depends on tumor site and grade. At unusual sites (outside of oral cavity and major salivary glands—for example, lymph nodes, thyroid gland), SC may be confused with papillary thyroid carcinoma, especially on small biopsies and FNAs. Importantly, SCs are TTF1 negative, while even papillary thyroid carcinomas with *ETV6* rearrangement are TTF1-positive. SC with HGT mimics SDCs. Of note, SCs lack apocrine differentiation and are androgen receptor negative, while SDCs are S100 protein-negative. Conventional SCs are most commonly confused with low-grade cribriform cystadenocarcinoma (LGCCA, also known as intraductal carcinoma). If *ETV6* status is unknown, the pattern of p63 expression is most helpful in distinguishing SC from LGCCA. LGCCAs are usually almost entirely intraductal and surrounded by a layer of basal/myoepithelial cells (Fig. 13.64).

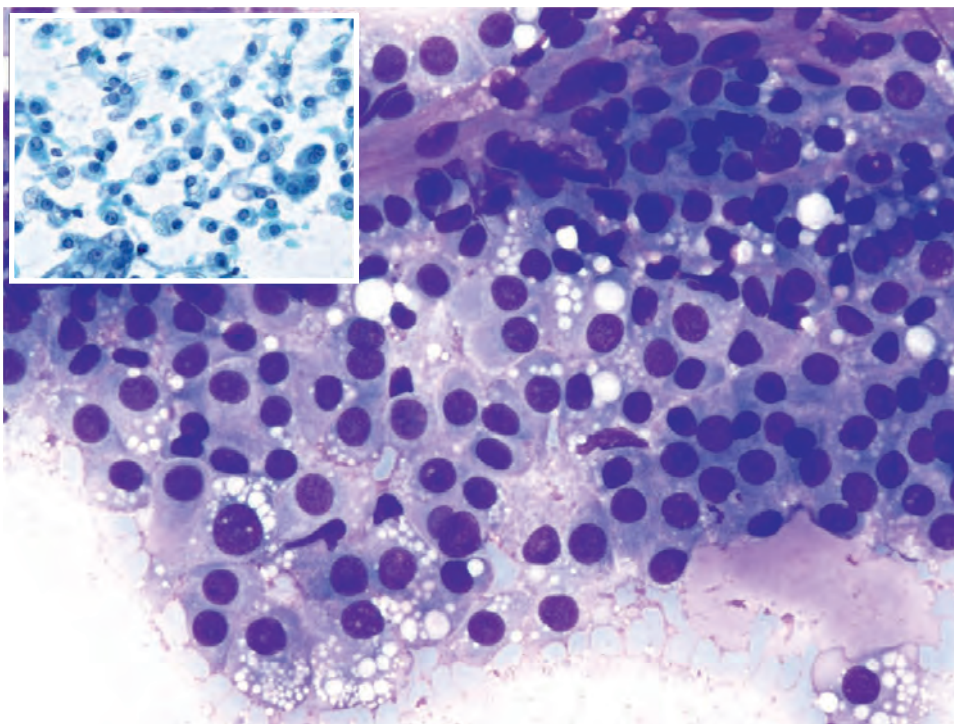
## PROGNOSIS AND THERAPY

The prognostic factors are not yet well established. It appears that prognosis and therapeutic approaches are similar to those for AcCC.



**FIGURE 13.62**

Secretory carcinoma with solid growth, enlarged vesicular nuclei and necrosis, consistent with high-grade transformation.

**FIGURE 13.63**

Secretory carcinoma Diff-Quick–stained fine-needle aspirate reveals round nuclei with nucleoli, transgressing vessels, and cytoplasm with microvacuoles (best appreciated on Papanicolaou stain, inset). (Image courtesy of Dr. R. Seethala.)



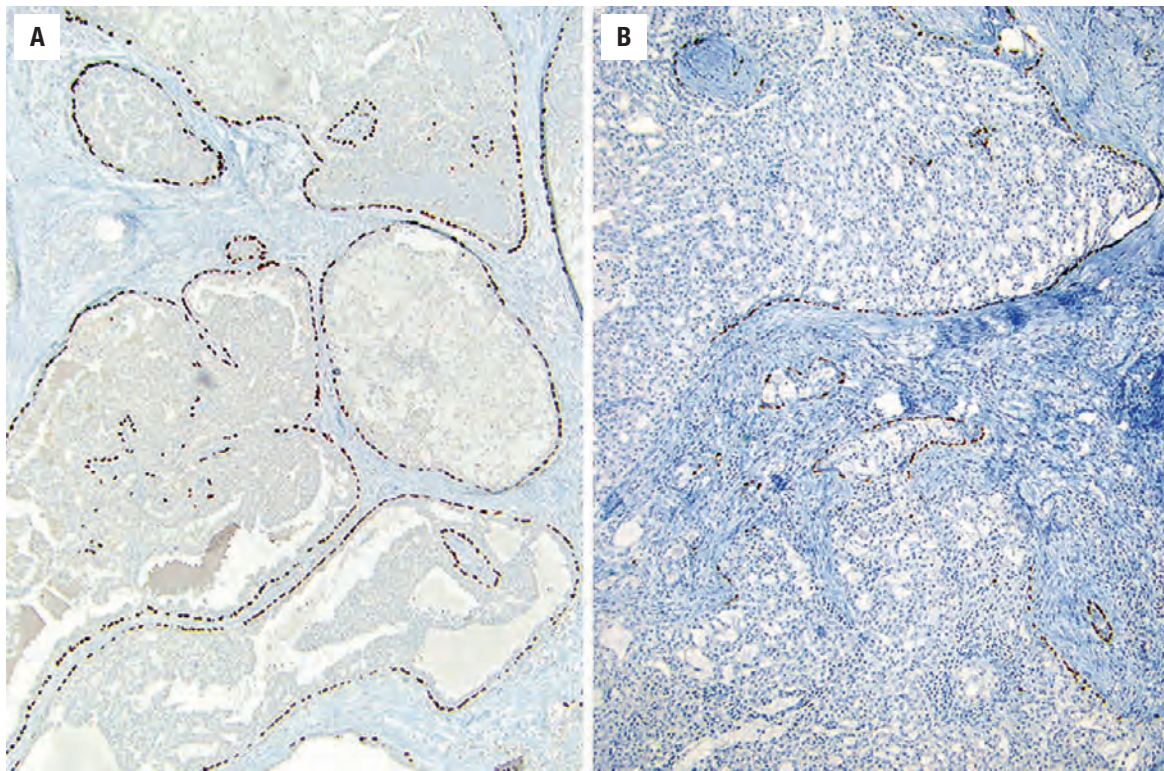


**FIGURE 13.64**

P63 immunohistochemistry patterns in low-grade cribriform cystadenocarcinoma/intraductal carcinoma (A) and secretory carcinoma (B).

## ■ SALIVARY DUCT CARCINOMA

### CLINICAL FEATURES

Salivary duct carcinoma (SDC) can arise *de novo* or, in up to 70 % of cases, develop ex PA (SDC ex PA). SDC accounts for about 9 % of malignant salivary gland tumors. The age at presentation ranges from 22 to 91 years, but most patients are older than 50 years. There is a striking male predominance (8:1). The vast majority of cases arise in the major glands (96 %), predominantly the parotid (Fig. 13.65) and rarely in the sinonasal tract and lacrimal gland. The tumor usually presents as a rapidly growing mass, with ulceration and facial nerve palsy relatively common. In carcinomas arising ex PA, there may be a history of a long-standing mass with recent enlargement.

### PATHOLOGIC FEATURES

#### GROSS FINDINGS

The cut surface is predominantly solid; white, gray, or tan; with cysts, necrosis, and hemorrhage commonly seen. The tumor usually shows invasion into surrounding tissues but occasionally, cases appear to be relatively well

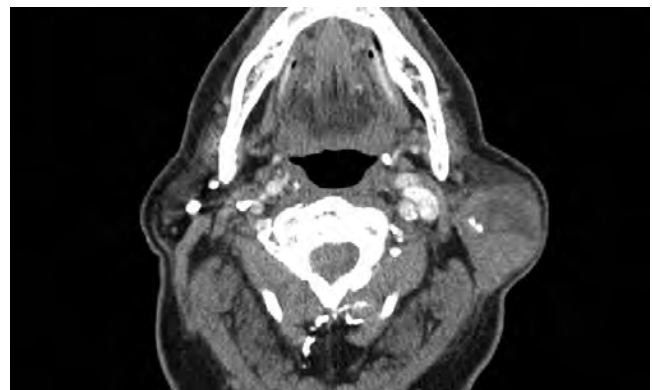


**FIGURE 13.65**

Computed tomography scan showing a right parotid gland tumor with cystic degeneration and small calcifications. The latter finding suggests a previous pleomorphic adenoma.

circumscribed (Fig. 13.66). Macroscopic findings typical of a preexisting PA may be present.

#### MICROSCOPIC FINDINGS

SDC resembles *in situ* (intraductal) and infiltrative ductal adenocarcinoma of the breast, specifically the “luminal androgen receptor positive/molecular apocrine” type. The most characteristic feature is the formation of multiple large ducts with cribriform configurations,



**SALIVARY DUCT CARCINOMA—DISEASE FACT SHEET****Definition**

- Salivary duct carcinoma is a high-grade adenocarcinoma with apocrine differentiation, resembling a subset of breast ductal adenocarcinoma—"luminal androgen receptor positive/molecular apocrine"

**Incidence and Location**

- Represents about 9% of malignant salivary gland tumors
- One of the most common types of malignancy arising ex pleomorphic adenoma
- Overwhelming majority affect major glands (usually parotid)

**Morbidity and Mortality**

- About one-third of cases recur locally
- 65% of patients die from disease within 5 years of diagnosis

**Sex and Age Distribution**

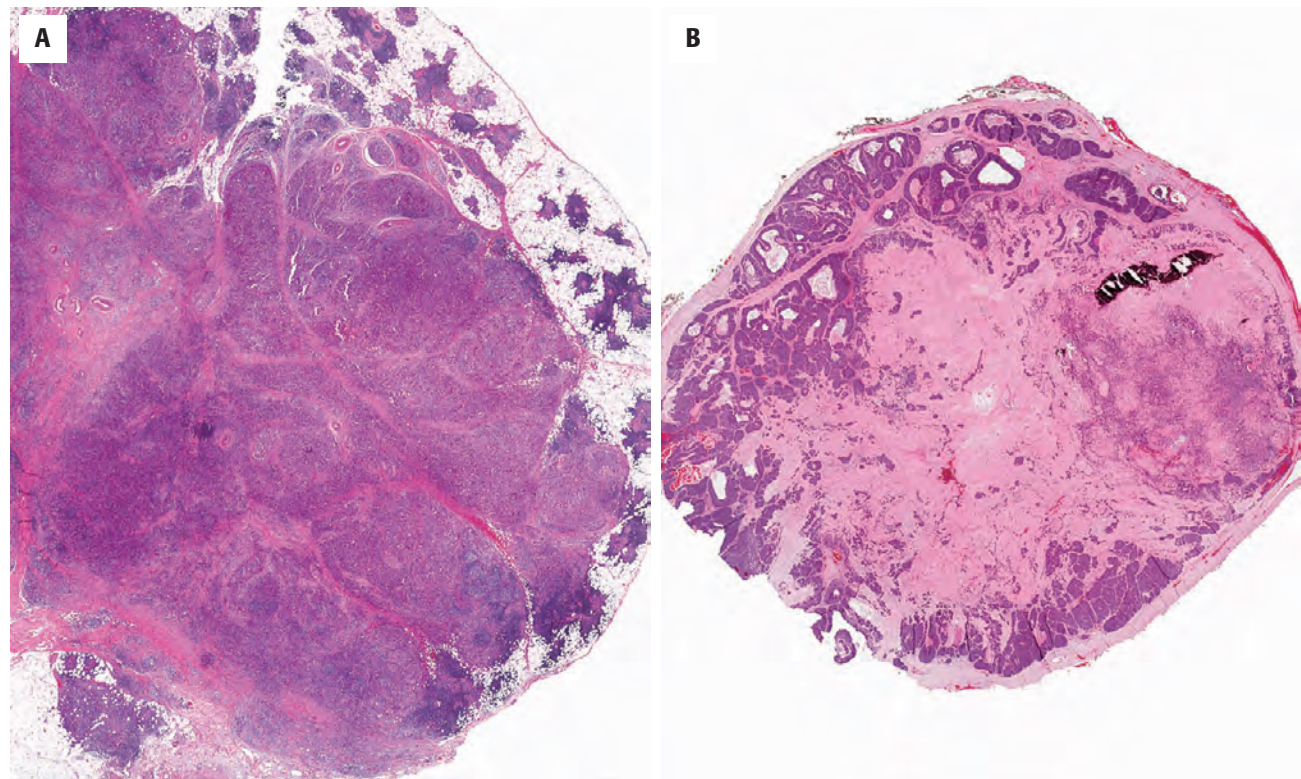
- Males > > > females (8:1)
- Peak incidence in 6th-7th decades

**Clinical Features**

- Presents as rapidly growing mass
- Ulceration and facial nerve palsy common
- If arising in a pleomorphic adenoma, there is rapid enlargement of a long-standing mass

**Prognosis and Therapy**

- Most aggressive salivary gland tumor with regional metastasis in about 60% and distant spread in about 50% of cases
- Features associated with a poor outcome include large tumor size and distant metastases
- Radical surgery with adjuvant radiotherapy and chemotherapy (antiandrogen and trastuzumab)

**FIGURE 13.66**

(A and B) Low-power view of two tumors showing an infiltrating pattern in both. The right-sided tumor shows extensive hyalinization and calcification with associated pleomorphic adenoma. The "carcinoma" of a carcinoma ex pleomorphic adenoma is frequently a salivary duct carcinoma.

"Roman-bridging," and comedonecrosis (Fig. 13.67). Hypocellular hyalinized stroma, fibrosis, or infarction and inflammatory infiltration are often conspicuous features (Fig. 13.68). Vascular and neural invasion is common and frequently extensive (Fig. 13.69). The tumor typically consists of cytologically pleomorphic cells with abundant pink cytoplasm and apical snouts indicative of apocrine-type secretion (Figs. 13.70 and 13.71). The

nuclei are large and hyperchromatic with prominent nucleoli, and there is usually a high mitotic index. Tumors occasionally show a malignant spindle cell component and sarcomatoid stroma (Fig. 13.72). Several other variants have been described and are practically always accompanied by areas of conventional apocrine morphology. The mucin-rich variant shows lakes of epithelial mucin containing malignant cells, in addition to more



## SALIVARY DUCT CARCINOMA—PATHOLOGIC FEATURES

### Gross Findings

- Predominantly solid white, gray, or tan
- Cysts, necrosis, and hemorrhage common
- Usually shows invasion into surrounding tissues
- Macroscopic features typical of a preexisting pleomorphic adenoma may be present

### Microscopic Findings

- Resembles “luminal androgen receptor positive/molecular apocrine” ductal adenocarcinoma of breast
- Vascular and neural invasion
- Large ducts with cribriform configurations, Roman-bridging, and comedonecrosis
- Solid and papillary areas may be present
- Cytologically pleomorphic cells with apocrine-type secretion (apical snout-like projections)
- Large, hyperchromatic nuclei with prominent nucleoli and high mitotic frequency

### Immunohistochemical Findings

- Positive for a wide range of cytokeratins, Carcinoembryonic Antigen (CEA), and EMA
- ~98% are positive for androgen receptor (negative for estrogen and progesterone receptors)
- About one-third show overexpression of HER-2–neu protein

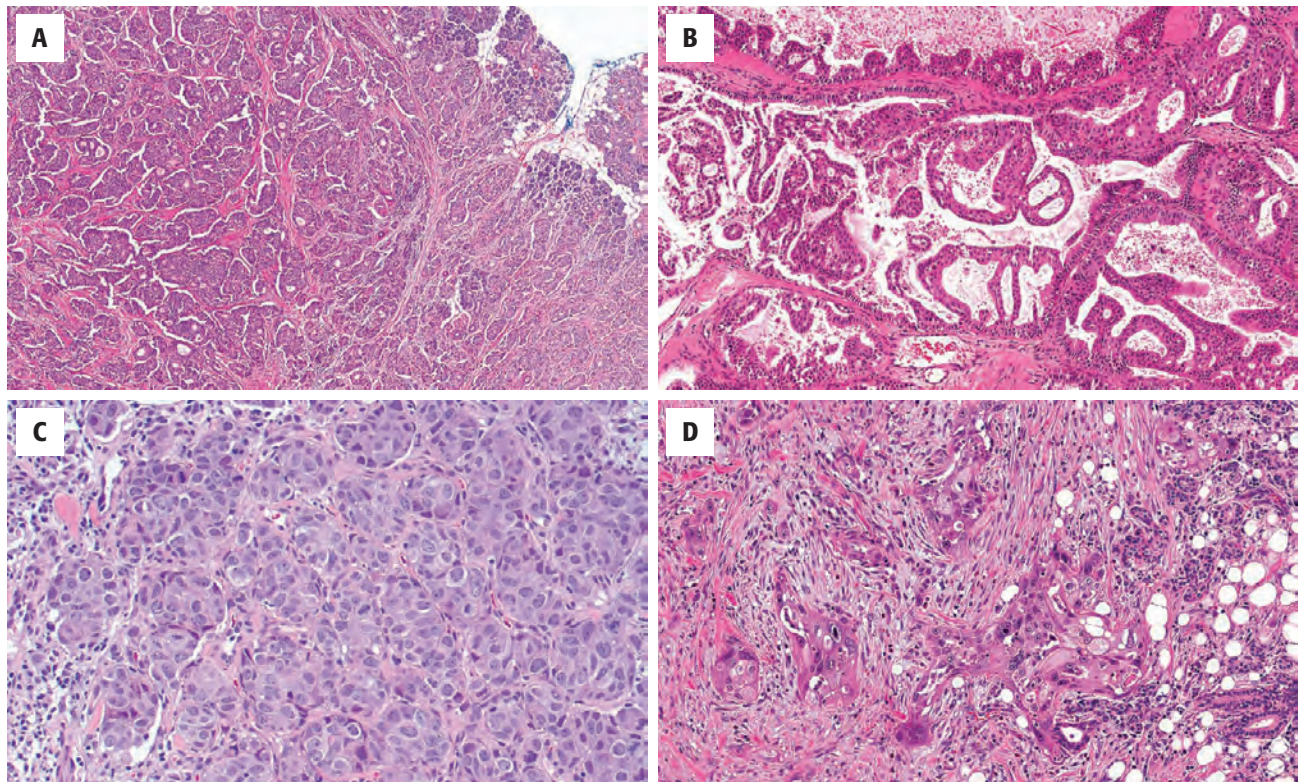
### Molecular Findings

- About one-third of cases harbor *PLAG1* rearrangement, while one-eighth have *HMGA2* rearrangement
- Most de novo SDCs harbor combined *HRAS*–*PIK3CA* mutations
- Many SDC ex PA have *HER-2–neu* amplification, *TP53* abnormalities, and *HRAS* or *PIK3CA* mutations

### Pathologic Differential Diagnosis

- Metastatic breast or prostate carcinoma, squamous cell carcinoma (i.e., metastatic to parotid area), oncocytic carcinoma, cystadenocarcinoma, other salivary-type carcinomas with high-grade transformation

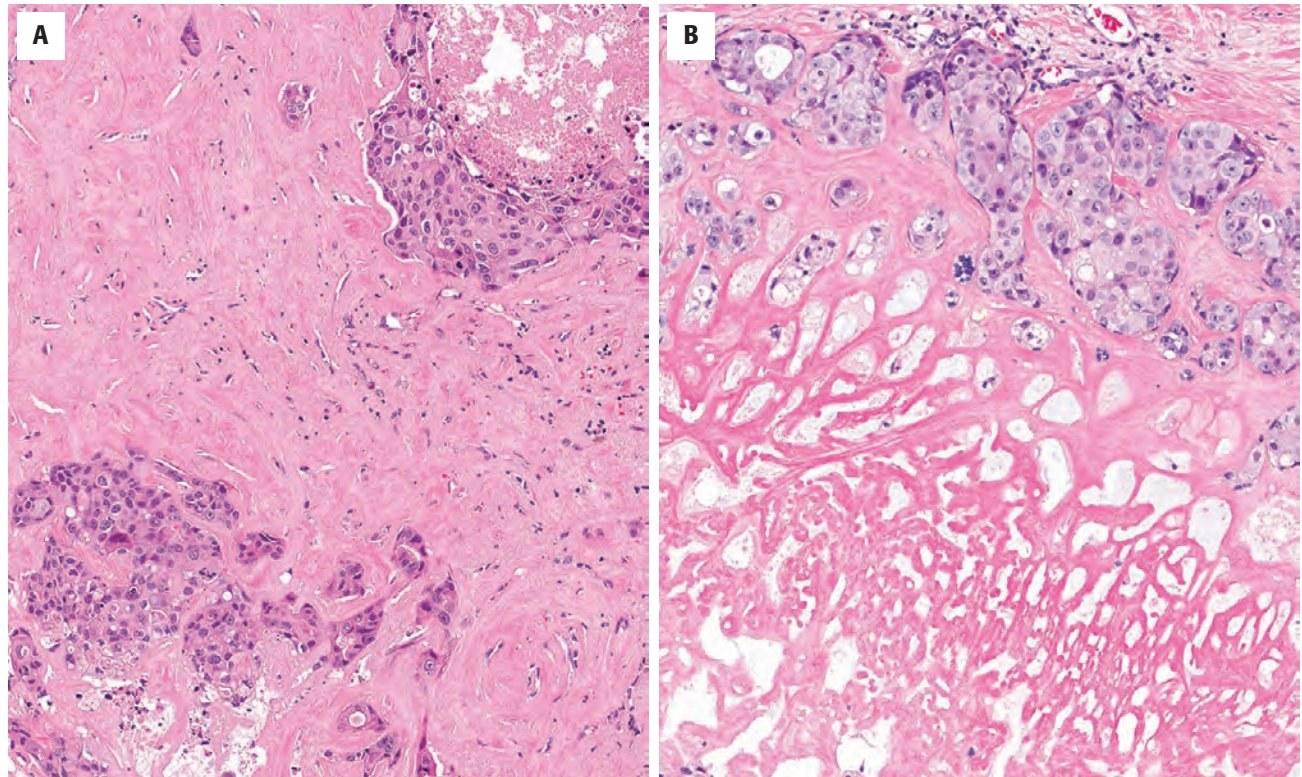
EMA, Epithelial membrane antigen; SDC, salivary duct carcinoma.



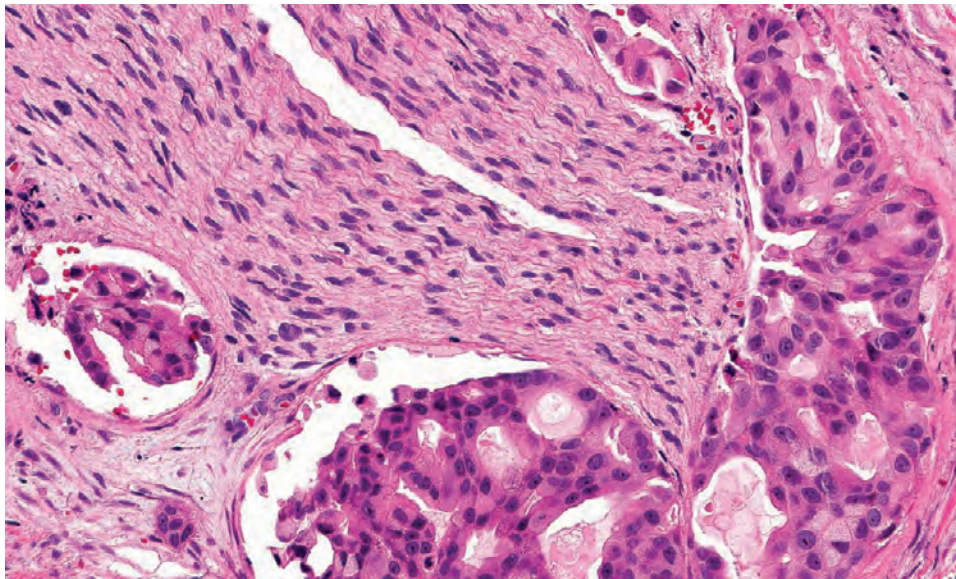
**FIGURE 13.67**

A number of different patterns of growth can be seen. **(A)** A micropapillary architecture is noted in this tumor, which infiltrates into the surrounding parenchyma. **(B)** There is a well-developed papillary and “Roman bridge” pattern in this tumor. **(C)** A more solid pattern of growth is noted, composed of large polygonal tumor cells. **(D)** This area shows a sarcomatoid pattern to the cells, which are infiltrating into the adjacent fat and parenchyma.



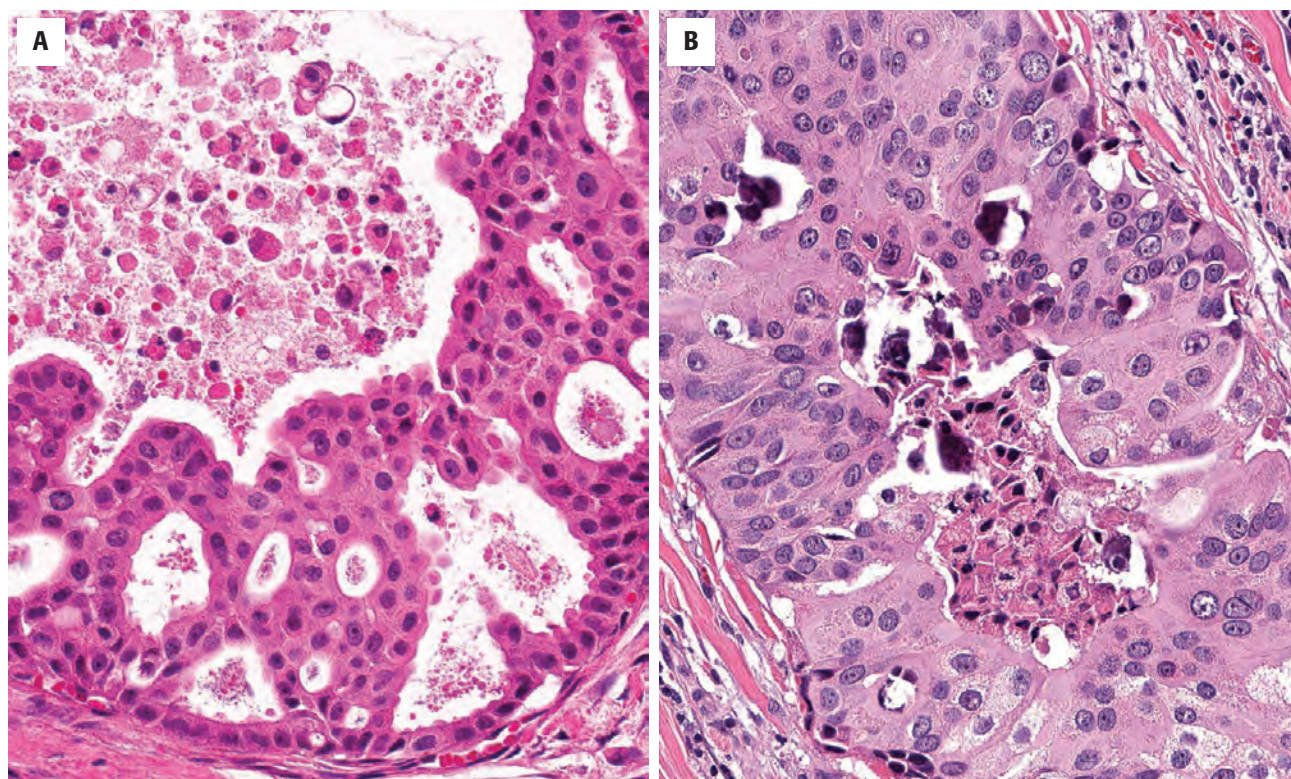
**FIGURE 13.68**

(A) Pleomorphic cells are arranged as tumor nests, set in a heavy stromal fibrosis and showing infarction (B).

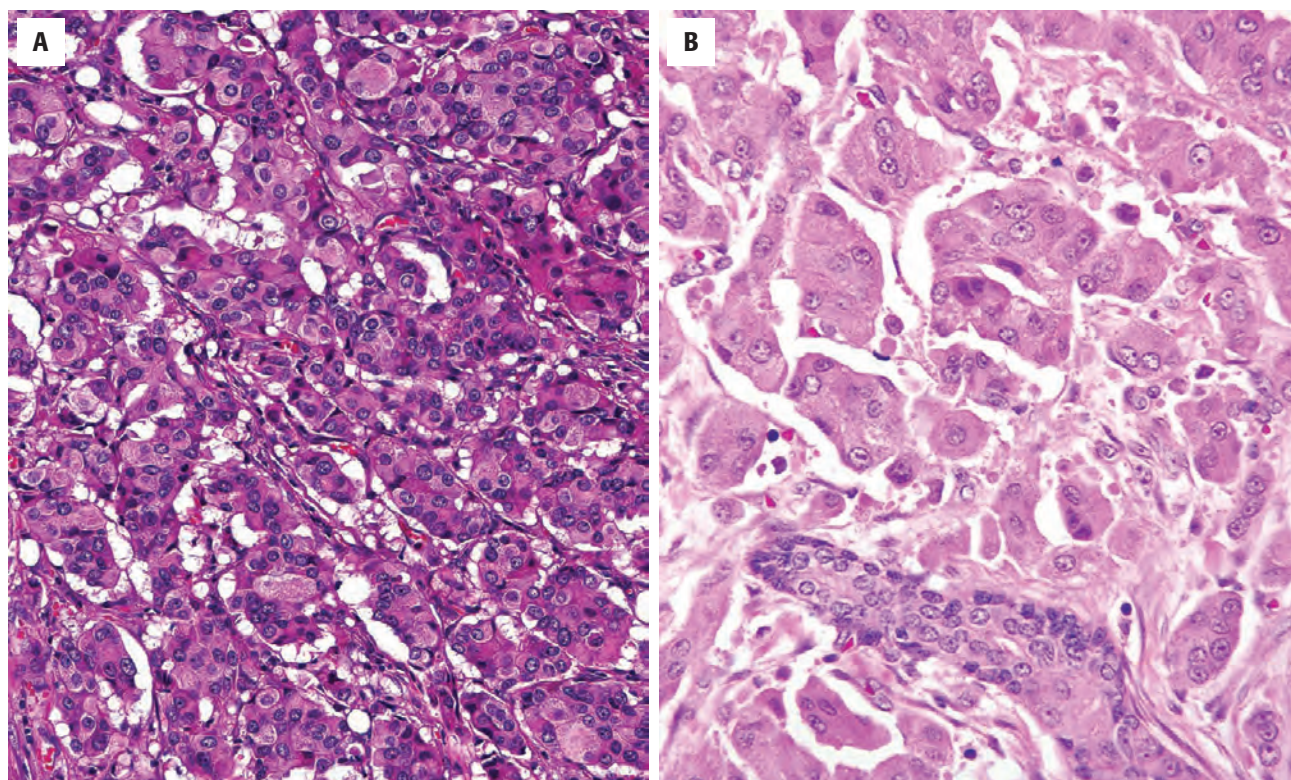
**FIGURE 13.69**

Characteristic cribriform pattern of tumor growth is identified within and adjacent to nerves.



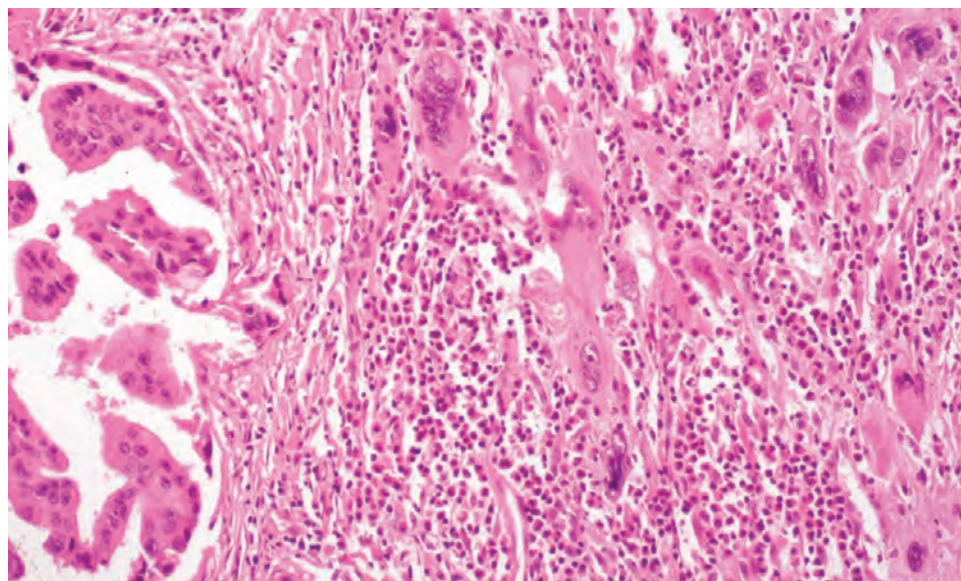
**FIGURE 13.70**

(A) Cribriform areas with a "Roman bridge" formation and comedonecrosis are seen in this salivary duct carcinoma. Note the pleomorphism and mitotic figures. (B) An area of comedonecrosis is noted.

**FIGURE 13.71**

(A) There are small packets of neoplastic cells showing a pseudoalveolar pattern with ample granular-eosinophilic cytoplasm. (B) These cytologically pleomorphic cells have abundant granular eosinophilic cytoplasm (normal duct in lower field).



**FIGURE 13.72**

Papillary architecture blends into an area of spindle cell or “sarcomatoid” transformation in this salivary duct carcinoma.

typical areas. Some tumors have an invasive micropapillary component and a strong propensity for lymphovascular and neural spread; these have a particularly poor prognosis.

### ANCILLARY STUDIES

#### IMMUNOHISTOCHEMICAL FINDINGS

SDC is usually positive for a wide range of cytokeratins, including cytokeratin 7 and EMA. It shows strong nuclear positivity for androgen receptor (Fig. 13.73) and is usually negative for myoepithelial, estrogen, and progesterone markers. SDC is characteristically positive for the breast markers GCDFP and GATA3. p63 or p40 are negative in neoplastic cells and highlight residual basal and myoepithelial cells, helping to identify in situ/intraductal components. Up to 5 % of SDCs are positive for prostate-specific antigen and prostatic acid phosphatase. About one-third of SDCs shows overexpression of HER-2/neu protein with strong membrane staining (Fig. 13.73).

#### FINE NEEDLE ASPIRATION

The smears are usually very cellular, with abundant background debris and necrotic material. The cells are arranged in cohesive three-dimensional papillary clusters. A cribriform pattern can be seen. The cells range from round to polygonal; they are occasionally spindled, with abundant finely granular to vacuolated cytoplasm. Nuclei are large, pleomorphic, and often hyperchromatic. Nucleoli are frequently prominent. Mitotic figures can easily be identified. The background will frequently contain isolated highly atypical epithelial cells, frequently clustered at the periphery of the cell groups (Fig. 13.74).

### DIFFERENTIAL DIAGNOSIS

Squamous cell carcinomas (SCCs) of cutaneous or mucosal origin must be considered, especially when the bulk of the tumor is extraparotid or almost exclusively involves intraparotid lymph nodes. SCCs are diffusely p63-positive and androgen receptor-negative.

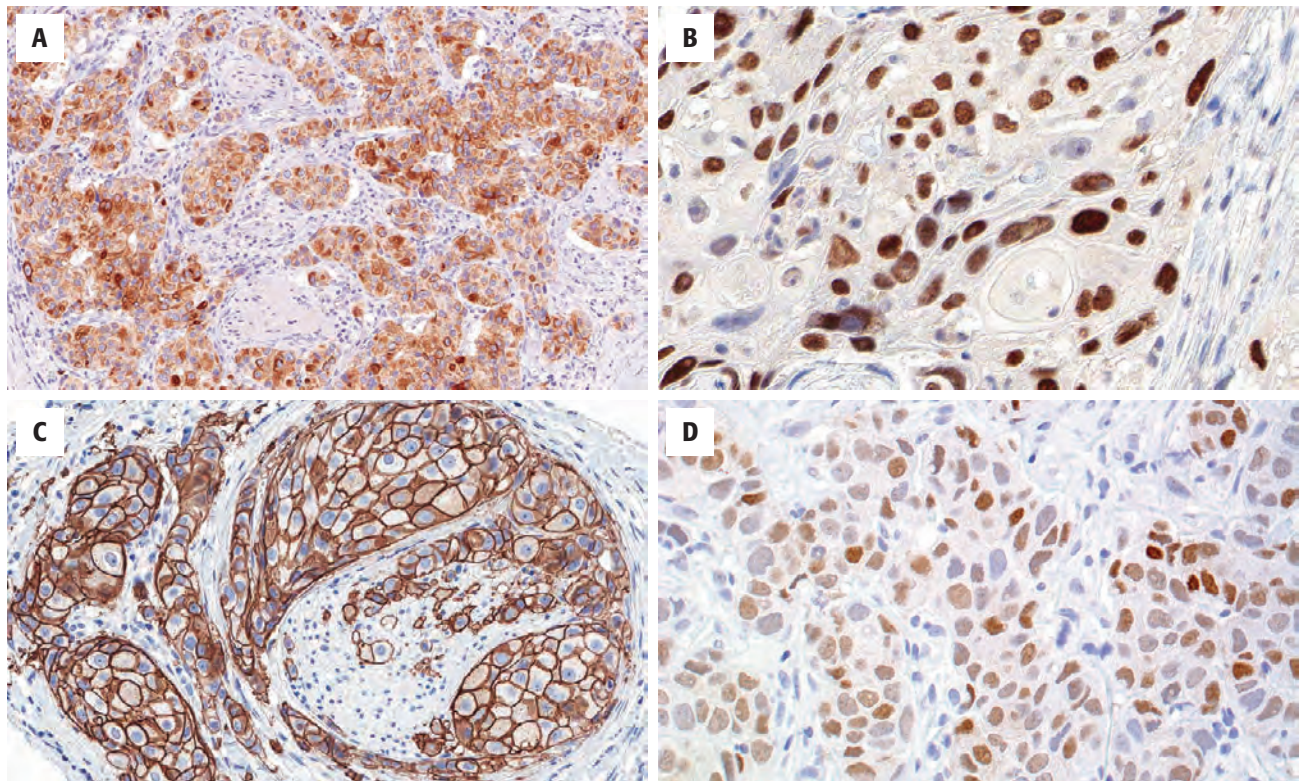
Other salivary-type carcinomas with HGT (e.g., comedo-type necrosis) may be confused with SDC. Up to 98 % of SDCs are androgen receptor-positive and p63- (or p40-) negative; in the absence of such an immunoprofile, a search for more conventional lower-grade areas typical of other salivary tumors is most helpful in avoiding confusion with SDC.

Papillary areas can resemble cystadenocarcinoma, but these are usually focal and show more cellular pleomorphism in SDC. SDC must be distinguished from metastatic breast or prostate carcinoma.

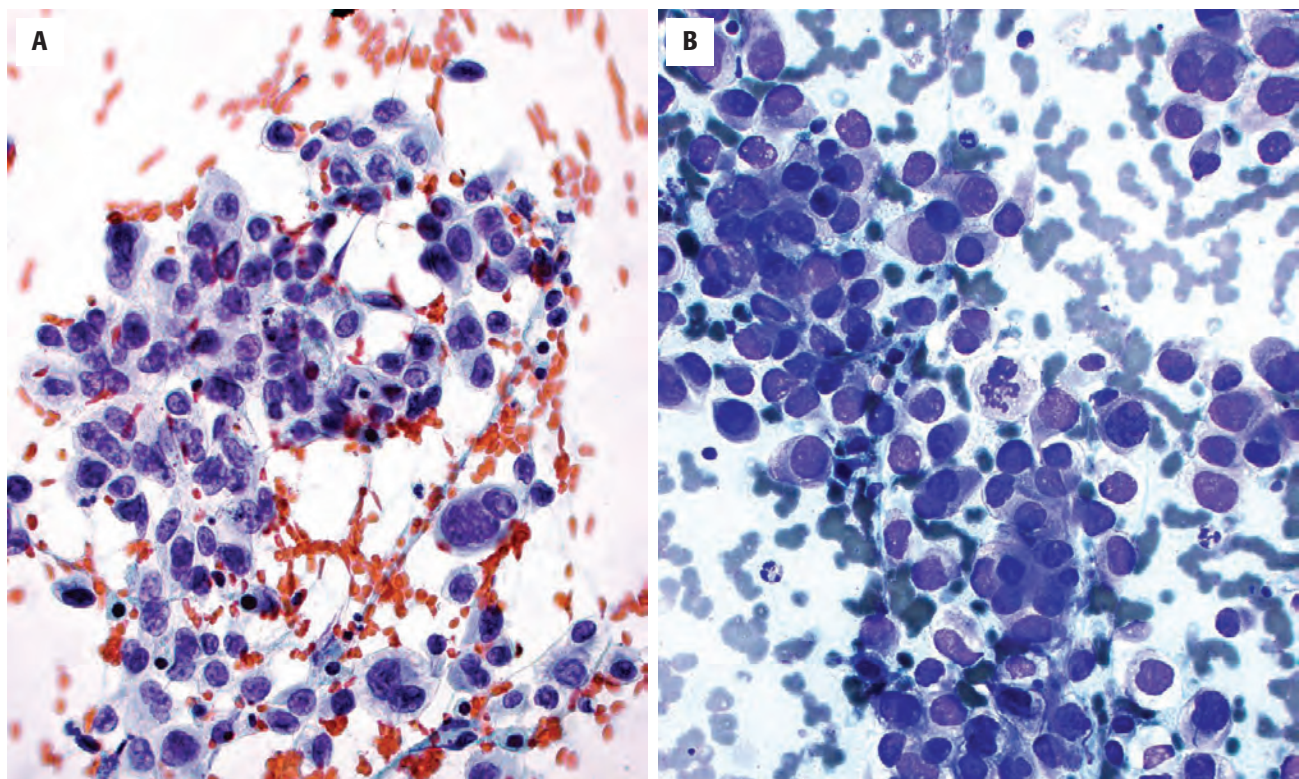
### PROGNOSIS AND THERAPY

SDC is the most aggressive salivary gland tumor, with an overall survival rate of about 35 %; most patients die within 4 years. About one-third of cases show local recurrence and about 60 % develop metastasis to regional lymph nodes. Systemic metastases to lung and bone are seen in up to 50 % of cases. A large primary tumor and evidence of metastases appear to be indicators of poorer prognosis. The presence of preexisting PA, proliferation rate, and TP53 mutational status show no correlation with outcome. The treatment usually includes a total parotidectomy with a neck dissection and adjuvant radiotherapy. Antiandrogen, trastuzumab (Herceptin),



**FIGURE 13.73**

Immunohistochemistry highlights several different features. **(A)** Epithelial membrane antigen highlights many of the neoplastic cells (nerve is negative). **(B)** Up to 50% of SDC show *TP53* abnormalities. Strong nuclear staining is usually indicative of a point missense mutation. **(C)** HER-2/neu usually gives a strong, diffuse, circumferential membrane reaction of more than 30% of the tumor cells. **(D)** Androgen receptor gives a strong diffuse reaction in most of the tumor cell nuclei.

**FIGURE 13.74**

**(A)** Cellular smears with loose clusters of atypical epithelial cells. The chromatin is coarse to open (alcohol-fixed Papanicolaou stain). **(B)** Slightly cohesive cells with a high nuclear-to-cytoplasmic ratio. Note the mitotic figure in the center (air-dried Diff-Quik stain).



anti-*BRAF*, and anti-*PIK3CA* drugs have been used for systemic therapy in patients with advanced disease.

## CARCINOMA EX PLEOMORPHIC ADENOMA

### CLINICAL FEATURES

Carcinoma ex pleomorphic adenoma (Ca ex PA) accounts for about 4% of all salivary tumors and about 12% of salivary malignancies. The sites of origin are usually the parotid (67%), minor glands (18%), and submandibular (15%) and sublingual glands (< 1%). Most cases are seen in 6th and 7th decades; Ca ex PA is rare in children. There is an equal sex distribution. The typical history is that of a long-standing mass with recent rapid enlargement or previous surgery for a PA (Fig. 13.75). These tumors are often painless but some are painful, and about 40% of patients have nerve palsies.

### PATHOLOGIC FEATURES

#### GROSS FINDINGS

Tumors range up to 25 cm in largest dimension. An area of circumscribed PA may be apparent, associated with an extensively infiltrative component often showing areas of hemorrhage and necrosis. The preexisting PA may be represented by an area of rounded hypocellular hyalinized scar.

### CARCINOMA EX PLEOMORPHIC ADENOMA—DISEASE FACT SHEET

#### Definition

- A carcinoma arising in association with a PA; a specific histologic type of Ca ex PA must be specified

#### Incidence and Location

- 4% of all salivary tumors; 12% of salivary malignancies
- Parotid (67%), submandibular (15%), minor glands (18%)

#### Morbidity and Mortality

- Dependent on tumor size, type, grade, and extent of invasion
- 25%-65% at 5 years; 24%-50% at 10 years; 10%-35% at 15 years for tumors with more than 4-6 mm of invasion

#### Sex and Age Distribution

- Equal sex distribution
- Usually seen in 6th and 7th decades
- Rare in children

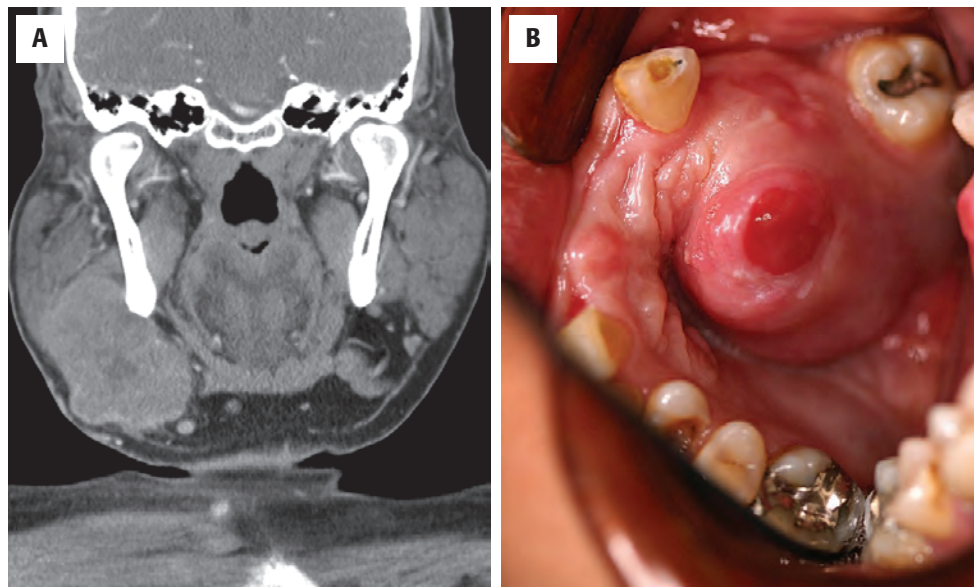
#### Clinical Features

- Typical history of long-standing mass with recent rapid enlargement
- Previous surgery for PA often reported
- Often painless but some are painful and nearly 40% experience nerve palsies

#### Prognosis and Therapy

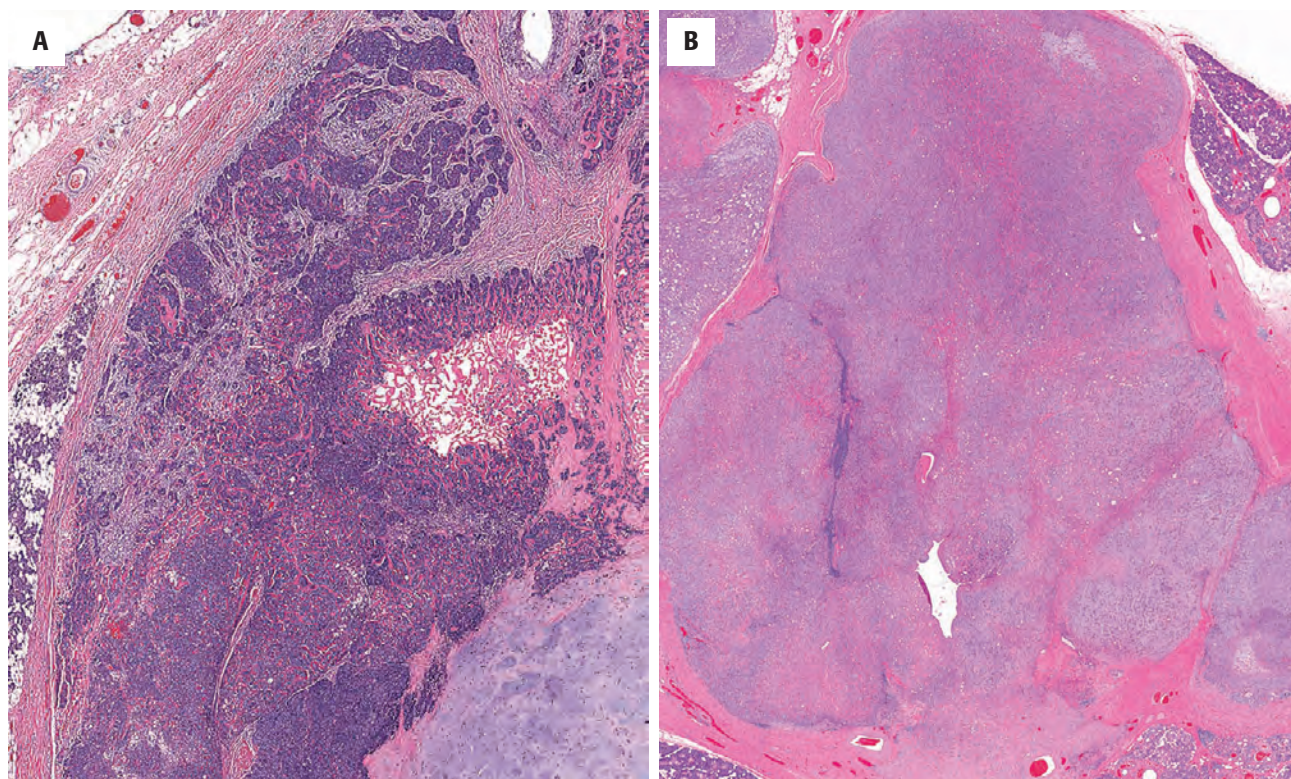
- Noninvasive carcinomas have same prognosis as PA
- About 25%-50% have local recurrence, usually within 5 years
- Minimally invasive tumors; low grade Ca ex PA ( $\leq$  4-6 mm); relatively good prognosis
- Invasive tumors ( $>$  4-6 mm) have a poor prognosis
- Large and histologically high-grade tumors have a poor prognosis
- Wide resection is the treatment of choice

PA, Pleomorphic adenoma.



**FIGURE 13.75**

(A) There is a mass in the parotid gland showing extensive necrosis and multinodularity. (B) Tumor in the palate, showing ulceration and erythema. Neither of these images is specific for a carcinoma ex pleomorphic adenoma.

**FIGURE 13.76**

Two examples of carcinoma ex pleomorphic adenoma. **(A)** The pleomorphic adenoma is noted in the lower right, with a malignant tumor expanding outward. **(B)** There is extensive hyalinization in this tumor, which has a multinodular-bosselated appearance.

### MICROSCOPIC FINDINGS

The relative proportions of preexisting PA and Ca ex PA vary widely. Some tumors show a carcinoma in direct juxtaposition to a typical PA (Fig. 13.76); sometimes the benign remnant may be difficult to find, particularly in scarred tumors. The malignant component may overgrow the benign element, but the diagnosis can be implied on the basis of clinical history. The tumor frequently shows invasion, which may involve soft tissue, nerve, or vasculature (Figs. 13.77 and 13.78). Ca ex PA has been subclassified into noninvasive, minimally invasive ( $\leq 4$ -6 mm), and invasive ( $> 4$ -6 mm) (Figs. 13.79 and 13.80). Noninvasive carcinomas have also been referred to as intracapsular carcinomas, in situ Ca ex PA, or severely dysplastic PA. They show a PA with focal or diffuse areas of cytologically malignant cells but without evidence of invasion into the surrounding tissues. These areas are commonly associated with increased mitotic activity. The malignant component is frequently a SDC (Fig. 13.81). However, many other types of salivary gland carcinomas have been described in Ca ex PA, and some cases show diverse differentiation with several distinct types within the tumor mass (Fig. 13.82).

### CARCINOMA EX PLEOMORPHIC ADENOMA—PATHOLOGIC FEATURES

#### Gross Findings

- Range from small to massive (25 cm)
- Area of circumscribed PA associated with infiltrative component

#### Microscopic Findings

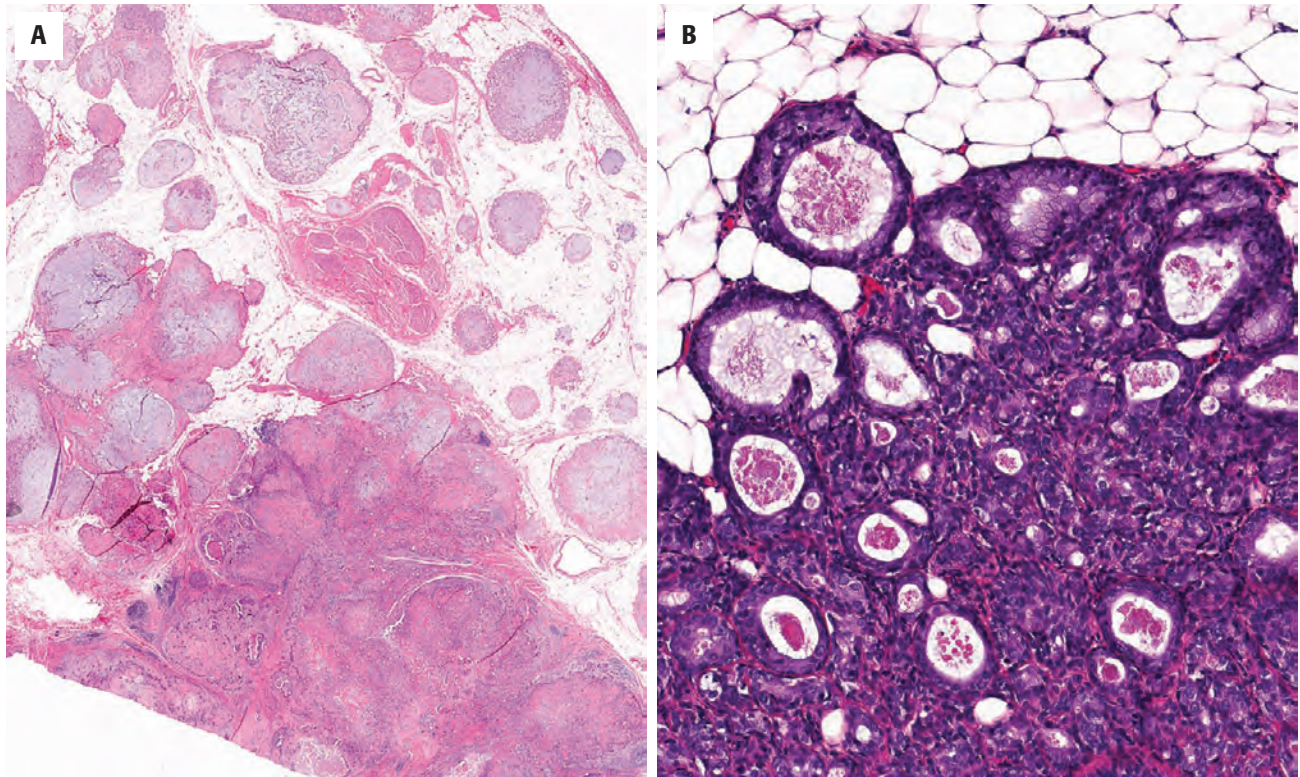
- Proportions of preexisting PA and Ca ex PA widely variable
- Original PA may scar or be overgrown by malignant component
- Malignant element is frequently a salivary duct carcinoma
- There may be several distinct carcinomatous components
- Sarcoma, carcinoma, and PA combinations are rare

#### Pathologic Differential Diagnosis

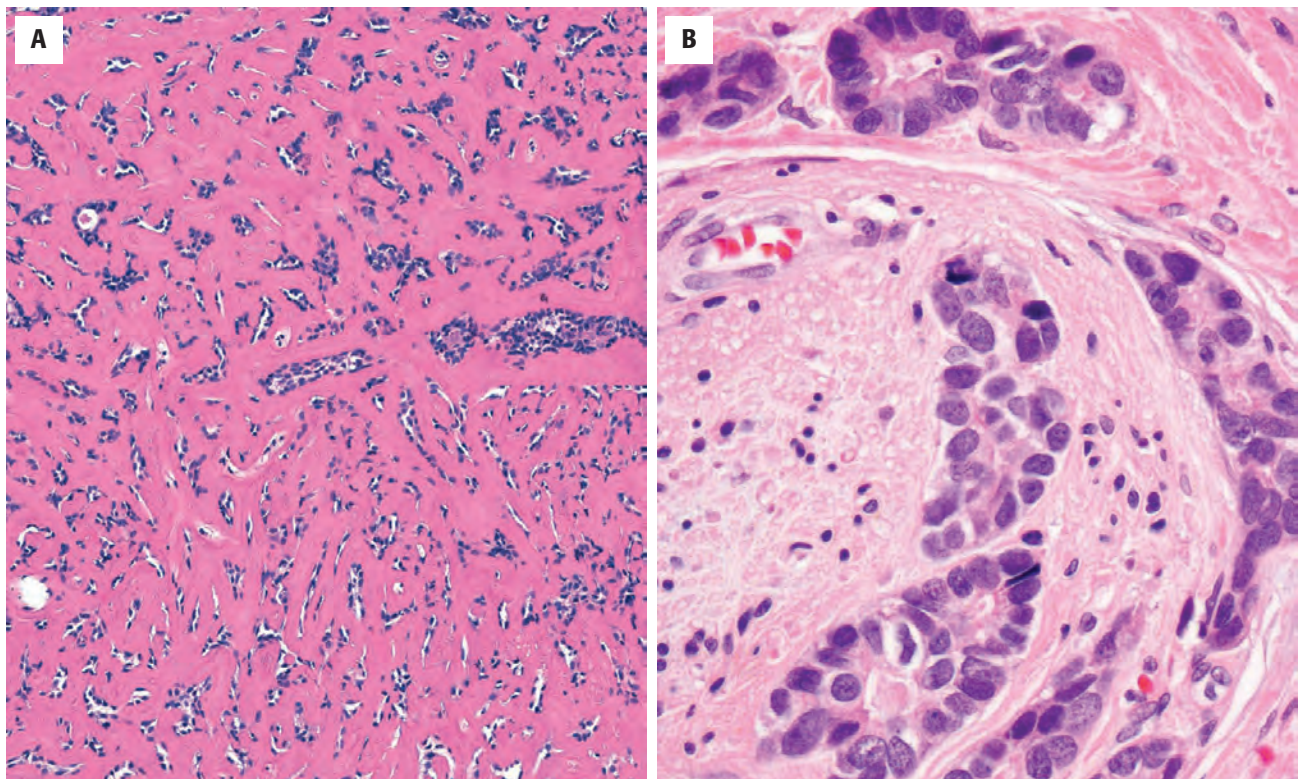
- FNA or infarction of PA, separation of noninvasive and invasive tumor, foci of carcinoma in hyalinized PA easily missed

PA, Pleomorphic adenoma.



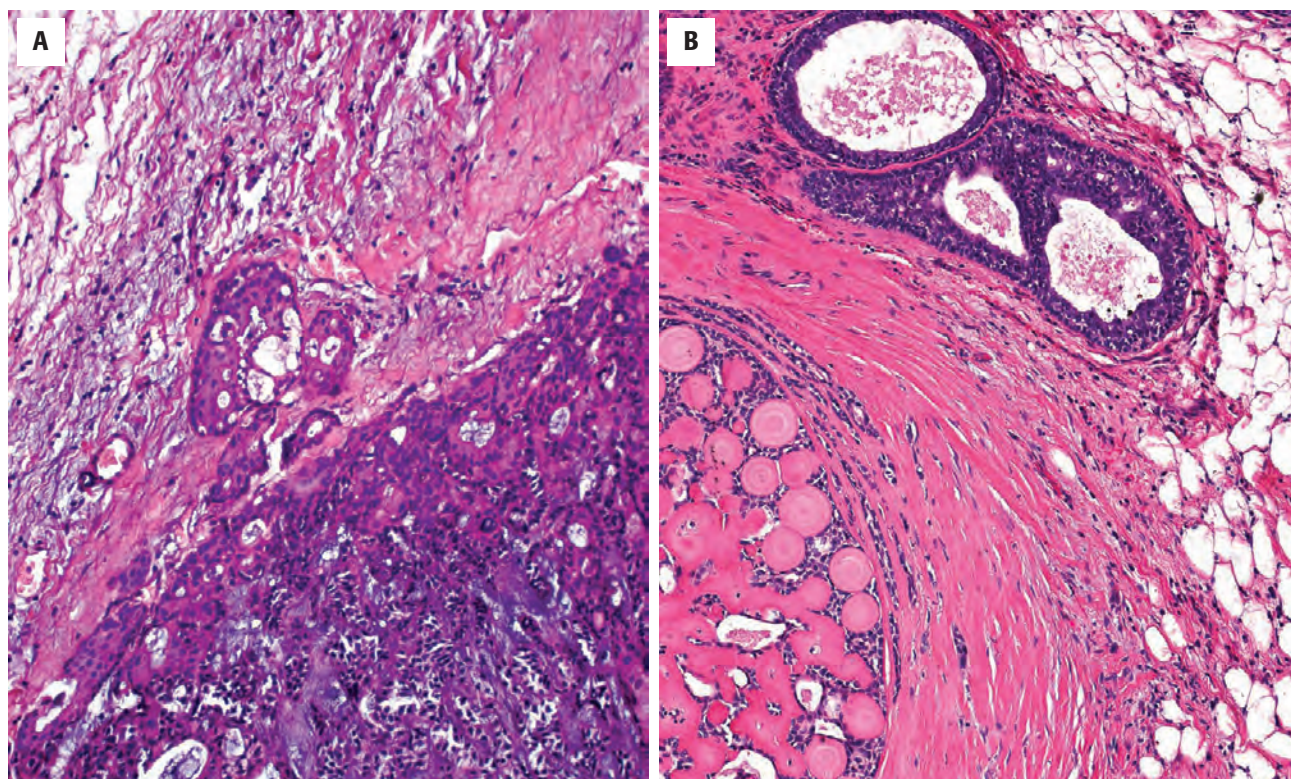
**FIGURE 13.77**

(A) There are multiple nodules of tumor within the adipose tissue. These represent the recurrent pleomorphic adenoma. However, the area of carcinoma is noted in the lower part of the field. (B) Note the infiltration of this carcinoma into the adjacent adipose tissue.

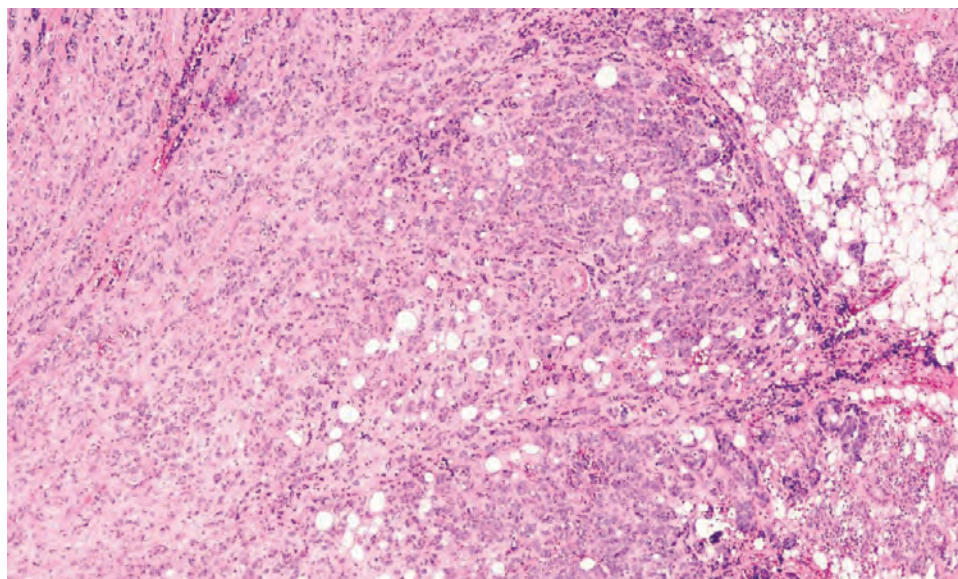
**FIGURE 13.78**

(A) This tumor shows extremely heavy sclerosing or scarring, nearly completely obscuring the underlying tumor. (B) Perineural invasion by the malignant epithelial cells.



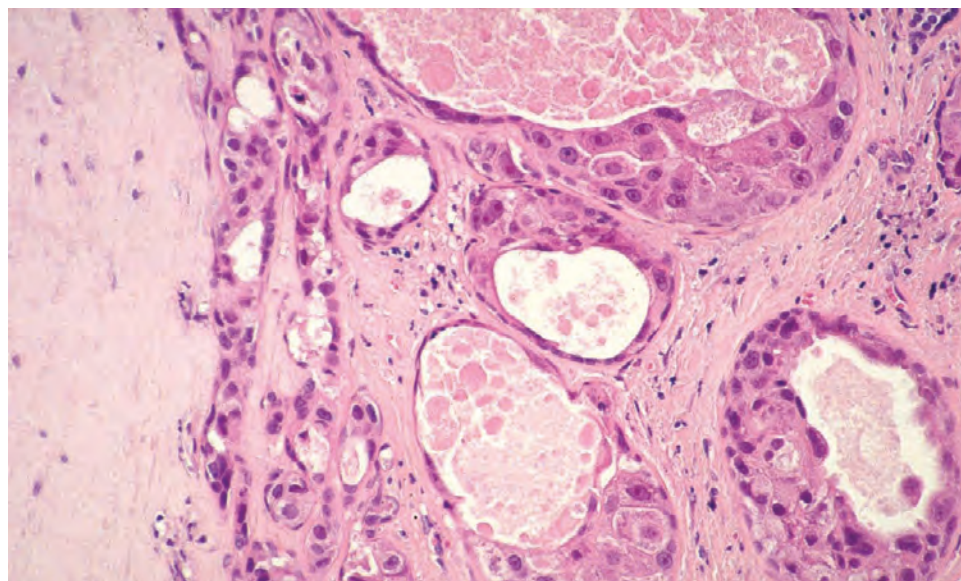
**FIGURE 13.79**

(A) A small nest of malignant epithelium extending beyond the contour of the tumor would be classified as minimally invasive. (B) This tumor showed multiple areas of greater than 4-6 mm of invasion, qualifying it as an invasive type.

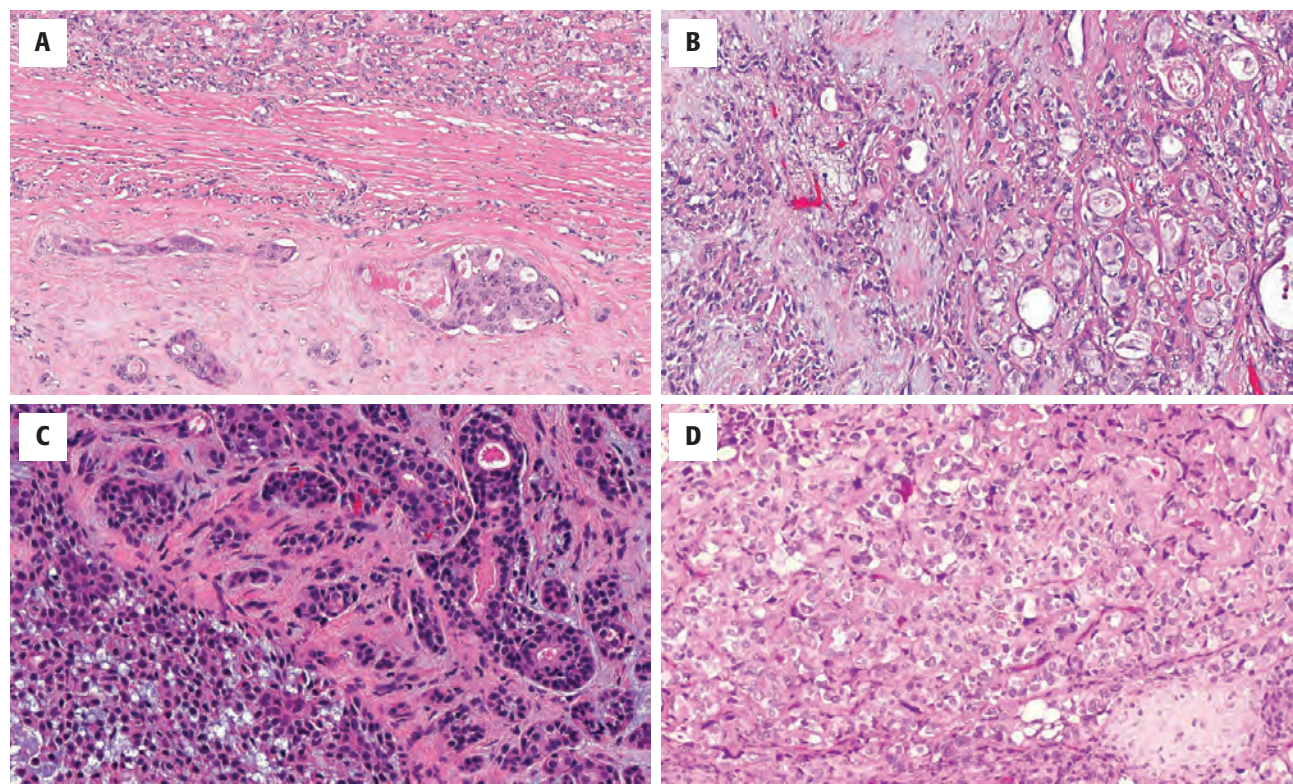
**FIGURE 13.80**

Benign pleomorphic adenoma (*upper left*) associated with areas of invasion into the adjacent parenchyma and adipose tissue by the carcinomatous elements.



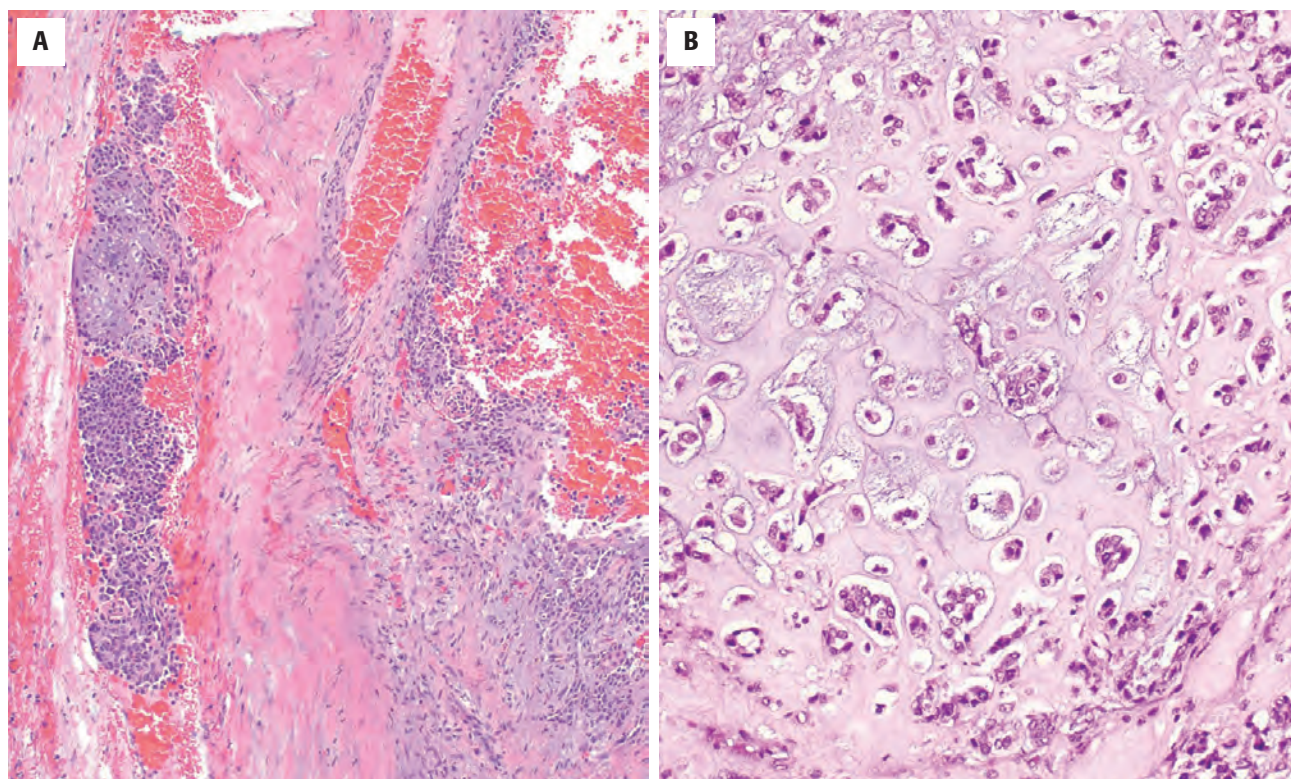
**FIGURE 13.81**

Benign pleomorphic adenoma (*left*) blends with a high-grade carcinoma with features of a salivary duct carcinoma in this carcinoma ex pleomorphic adenoma.

**FIGURE 13.82**

Multiple different patterns of growth and tumor types can be seen in carcinoma ex pleomorphic adenoma. (A) Vascular invasion and areas of sclerosis. (B) Adenocarcinoma, not otherwise specified. (C) Adenoid cystic carcinoma pattern. (D) Oncocytic carcinoma with small area of chondroid matrix (*lower field*).



**FIGURE 13.83**

(A) Benign metastasizing pleomorphic adenoma shows benign epithelium within vascular spaces, not malignant epithelium. (B) Chondrosarcoma present within a true malignant mixed tumor or carcinosarcoma.

### DIFFERENTIAL DIAGNOSIS

FNA or spontaneous infarction of PA can cause secondary degenerative changes that may be confused with Ca ex PA. These include hemorrhage, necrosis, inflammation, reactive cellular atypia, and squamous or mucous metaplasia. It is important to distinguish between noninvasive, minimally invasive, and invasive tumors, as there are clear prognostic implications. Foci of carcinoma may develop in a hyalinized PA and be easily missed, particularly in large tumors. A *metastasizing PA* may be caused by surgical manipulation of a previous PA, with benign-appearing epithelial elements in the sites of metastasis (Fig. 13.83).

### PROGNOSIS AND THERAPY

Noninvasive carcinomas have the same prognosis as conventional PA. Invasive carcinomas are usually aggressive but show a range of behavior. About 25 % to 50 % of cases recur locally, usually within 5 years. Up to 70 % show regional or distant metastases, usually to lung, bone, liver, brain, and elsewhere. Tumors with invasion of more than 4-6 mm have a poor prognosis, ranging from 25 % to 65 % at 5 years to 0 % to 35 % at 20 years.

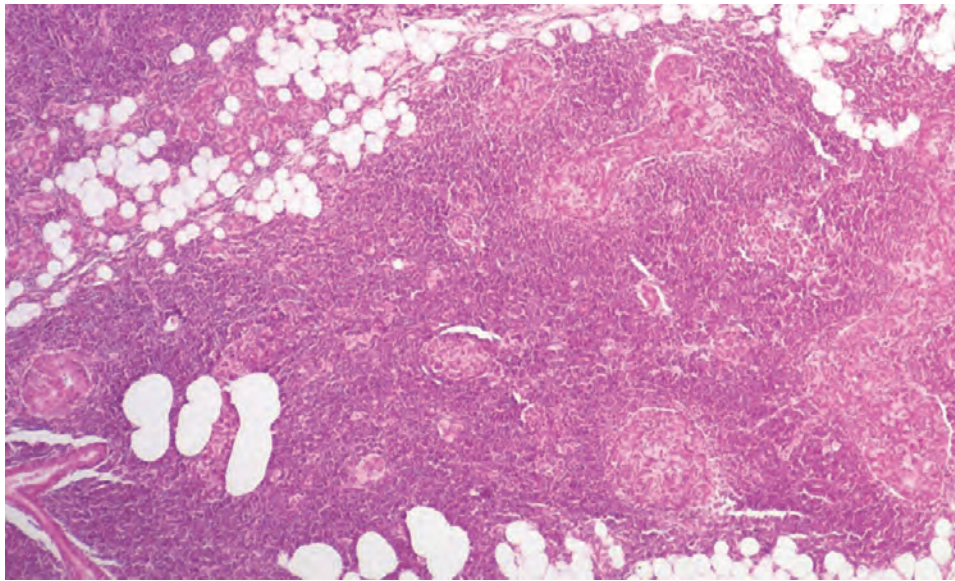
Minimally invasive low-grade tumors (< 4-6 mm) appear to have a relatively good prognosis. Large and histologically high-grade tumors have a poor prognosis, as do carcinomas with a myoepithelial phenotype. Wide resection is the treatment of choice.

### ■ EXTRANODAL MARGINAL ZONE B-CELL LYMPHOMA OF SALIVARY GLANDS

#### CLINICAL FEATURES

Extranodal marginal zone B-cell lymphoma (EMZBCL) of mucosa-associated lymphoid tissue is an uncommon low-grade B-cell salivary neoplasm. It is usually seen in the context of lymphoepithelial sialadenitis (LESA), previously referred to as either benign lymphoepithelial lesion or myoepithelial sialadenitis (MESA), associated with either primary or secondary Sjögren syndrome. Most patients are in the range of 55 to 65 years old, with a striking female predilection (9:1). Over 80 % of cases involve the parotid glands (unilaterally or bilaterally), and the tumors usually cause painless swelling. Despite their neoplastic nature, these swellings may be remarkably episodic and, in some cases, enlargement can be exacerbated by secondary ascending bacterial infection, when pain may also be a feature.



**FIGURE 13.84**

Lymphoepithelial sialadenitis shows a multifocal inflammatory infiltrate with “epimyoeplithelial” islands and reactive germinal centers in a major salivary gland.

#### EXTRANODAL MARGINAL ZONE B-CELL LYMPHOMA OF SALIVARY GLANDS—DISEASE FACT SHEET

##### Definition

- An extranodal low-grade B-cell lymphoma arising in mucosa-associated lymphoid tissue

##### Incidence and Location

- Predominantly seen in patients with Sjögren syndrome
- 80% of cases involve the parotid gland
- May be bilateral

##### Morbidity and Mortality

- Typically indolent, without significant morbidity or mortality
- Spontaneous regression reported

##### Sex and Age Distribution

- Females > > > males (9:1)
- Age range 55-65 years

##### Clinical Features

- Patients may have xerostomia and xerophthalmia associated with Sjögren syndrome
- Chronic and sometimes episodic parotid enlargement
- Occasionally painful owing to superimposed ascending infection

##### Prognosis and Therapy

- Most patients can be followed without active treatment
- Infrequent transformation into higher-grade lymphomas may require additional therapy

#### PATHOLOGIC FEATURES

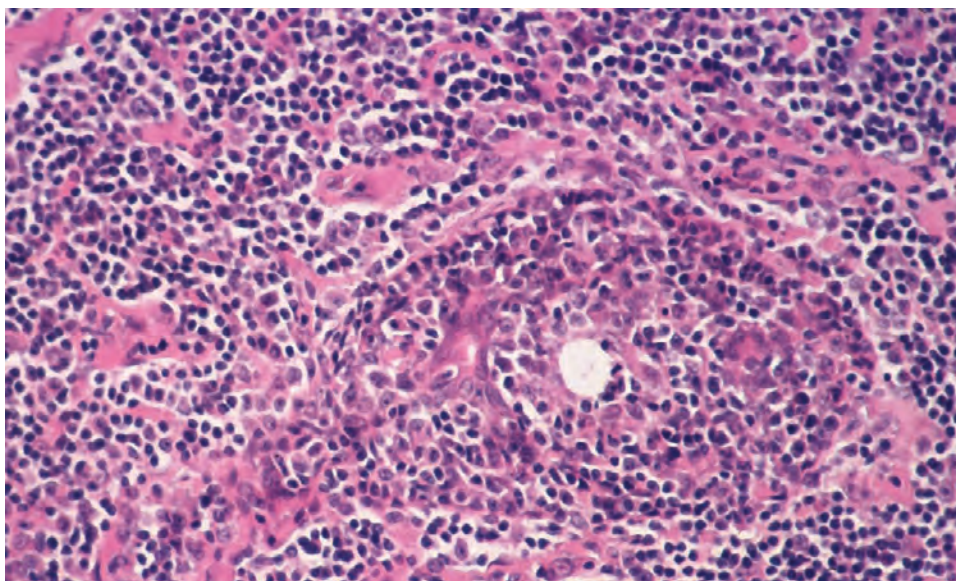
##### GROSS FINDINGS

The tumor forms a firm mass with a yellowish, tan to pale, “fish-flesh” cut surface. The tumor is usually homogeneous, but small cysts are occasionally present.

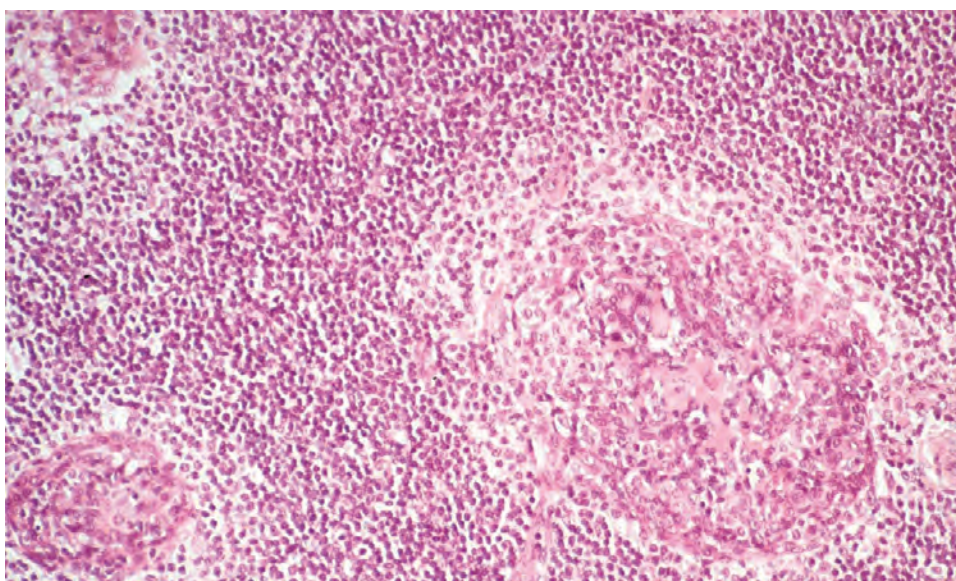
##### MICROSCOPIC FINDINGS

EMZBCL is usually seen in salivary glands involved with LESA. The two components of LESA are lymphoid infiltration and epimyoeplithelial islands. The lymphoid infiltrate is initially multifocal and periductal and spreads centrifugally, progressively destroying the adjacent acinar tissue (Fig. 13.84). Reactive follicles are frequent and consist of polytypic B cells. The interfollicular lymphoid tissue consists predominantly of T cells. The “epimyoeplithelial islands” consist of ducts that have undergone hyperplasia and frequently show luminal obliteration (Fig. 13.85). The role, if any, of myoeplithelial cells in this process is a subject of contention. The islands frequently contain hyaline material derived from basement membrane. In addition, the islands are infiltrated by B and T cells. When EMZBCL develops in LESA, halos of monocytoid and centrocyte-like B cells surround and progressively invade and destroy the epimyoeplithelial islands or “lymphoepithelial islands” (Fig. 13.86). In addition, immunoblasts and lymphoplasmacytic cells are present and plasma cell differentiation may be a striking feature. Colonization of reactive germinal follicles by neoplastic B cells is frequent. A few large cells are commonly present; sometimes they are more numerous and form focal aggregates (Fig. 13.87). Occasionally, diffuse large B-cell lymphoma develops within this setting. The

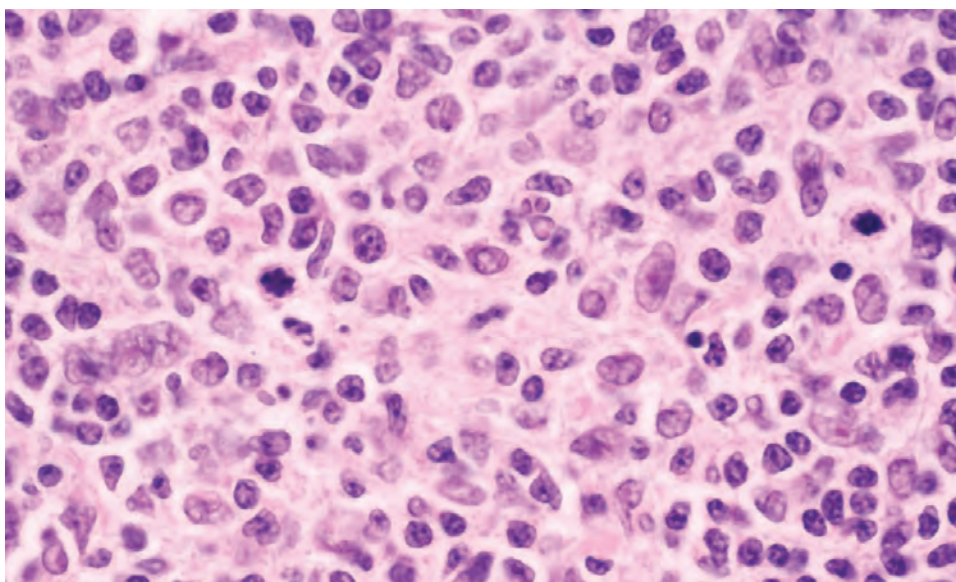


**FIGURE 13.85**

An "epimyoeipithelial" island has small hyperplastic ducts associated with a mixed inflammatory infiltrate.

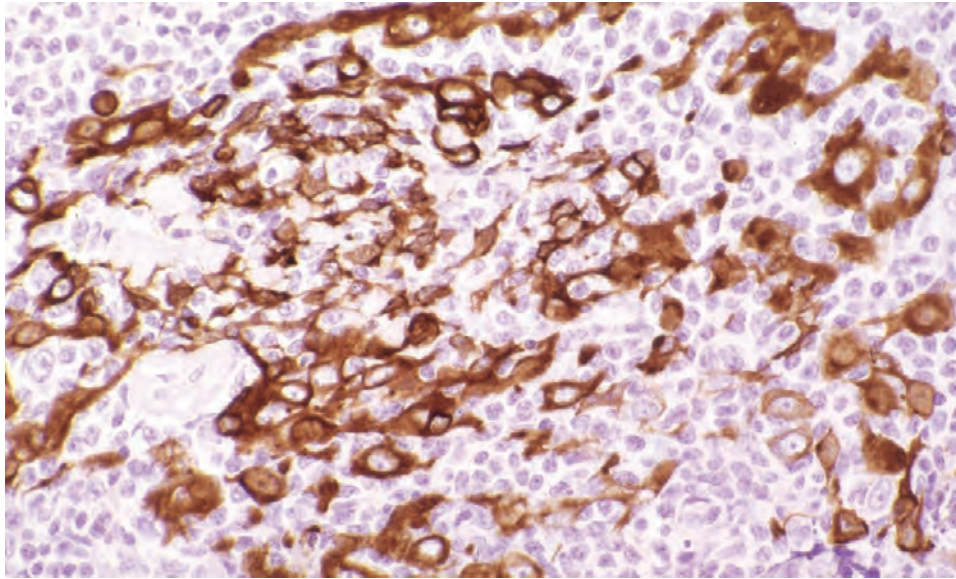
**FIGURE 13.86**

Halos of monocytoid cells around "epimyoeipithelial" islands, a few containing hyaline material, in this extranodal marginal-zone B-cell lymphoma.

**FIGURE 13.87**

Immunoblasts or lymphoplasmacytic cells are associated with increased mitotic figures in this area of extranodal marginal zone B-cell lymphoma.



**FIGURE 13.88**

Keratin immunohistochemistry highlights the epithelial component in a lymphoepithelial lesion, which develops in extranodal marginal zone B-cell lymphoma.

### EXTRANODAL MARGINAL ZONE B-CELL LYMPHOMA OF SALIVARY GLANDS—PATHOLOGIC FEATURES

#### Gross Findings

- Firm, with yellowish-tan, “fish-flesh” cut surface
- Usually homogeneous or may show microcysts

#### Microscopic Findings

- Background of LESA
- Epimyoepithelial islands, frequently infiltrated by lymphocytes
- Nodules of diffuse heterogeneous B-cell infiltrate
- Halos of monocytoid B cells around follicles
- Infiltrate consists of atypical small lymphocytes, centrocyte-like cells, monocytoid B cells, immunoblasts, and plasma cells
- Reactive germinal centers common and may be colonized by neoplastic B cells

#### Immunohistochemical Findings

- B-cell phenotype of CD20 and/or CD79a
- B cells colonizing reactive follicles are often reactive with bcl-2
- Monoclonality demonstrated by light-chain restriction
- Remnants of epimyoepithelial islands highlighted by cytokeratin staining

#### Pathologic Differential Diagnosis

- LESA, follicular lymphoma, rarely diffuse large B-cell lymphoma

LESA, lymphoepithelial sialadenitis.

lymphoid cells infiltrate the interlobular septa and gland capsule and extend into the periglandular tissues.

### ANCILLARY STUDIES

The predominance of B cells can be confirmed by immunostaining for CD20 or CD79a. The neoplastic

nature of the infiltrate can be demonstrated by light-chain restriction ( $\kappa$  or  $\lambda$ ). The significance of clonal rearrangements of immunoglobulin genes in diagnosing malignant transformation of LESA is less clear. Neoplastic B cells colonizing reactive follicles often show bcl-2 positivity. Remnants of the epithelial islands can be readily highlighted with keratin immunohistochemistry (Fig. 13.88).

### DIFFERENTIAL DIAGNOSIS

In some cases, it may not be possible to distinguish between EMZBCL and LESA using conventional microscopy. Effacement of the interlobular septa and infiltration of lymphocytes into periglandular tissue suggest lymphomatous transformation. Both may contain reactive follicles, but, in EMZBCL, colonizing B cells are usually bcl-2–positive. Demonstration of light-chain restriction is typical of a B-cell lymphoma. Nodular tumors may be confused with *follicular lymphoma* but, in addition to more extensive immunoreactivity for bcl-2, the latter is typically also positive for CD10 and bcl-6, although follicular lymphoma is very unusual in salivary glands. Rarely, there is development of a *diffuse large B-cell lymphoma*.

### PROGNOSIS AND THERAPY

EMZBCL usually has an excellent prognosis, and most patients can be followed without active treatment. Some cases appear to show spontaneous regression. Occasionally, there is transformation into higher-grade tumors and development of extrasalivary gland lymphoma. Treatment is usually limited to regular follow-up.



**FIGURE 13.89**

There is a large mass occupying the salivary gland of this boy, less than 1 year of age. It expands into the adjacent cervical and preauricular regions. The tumor had grown rapidly in the past several weeks.

## ■ SIALOBLASTOMA

### CLINICAL FEATURES

Sialoblastoma is a very rare and potentially aggressive tumor seen predominantly in major salivary glands. It is usually present at birth and recapitulates the primitive salivary anlage. Synonyms include embryoma, congenital basal cell adenoma, basaloid AC, and congenital hybrid basal cell adenoma–AdCC. About 50 cases have been reported. Most tumors are seen in the perinatal or neonatal period and some cases are detected in utero. Isolated cases in adults have recently been reported. There is no sex predilection. Most cases have involved the parotid or submandibular gland. The tumor usually presents as a firm, painless swelling, but some cases are large and rapidly growing (Fig. 13.89). There may also be facial nerve involvement and ulceration.

### PATHOLOGIC FEATURES

#### GROSS FINDINGS

Tumors range from 1.5 cm to 15 cm in diameter and usually form a multilobulated and variably circumscribed

### SIALOBLASTOMA—DISEASE FACT SHEET

#### Definition

- Sialoblastoma is a rare and potentially aggressive tumor that recapitulates primitive salivary development

#### Incidence and Location

- Very rare
- Large majority of cases involve major glands, mainly the parotid

#### Morbidity and Mortality

- Local recurrence in about 20% of cases

#### Sex and Age Distribution

- Equal sex incidence
- Mainly perinatal or neonatal

#### Clinical Features

- Usually forms a slow-growing mass but can show rapid expansion
- Pain or facial nerve involvement seen in a minority of cases
- Tumors may ulcerate and involve underlying bone

#### Prognosis and Therapy

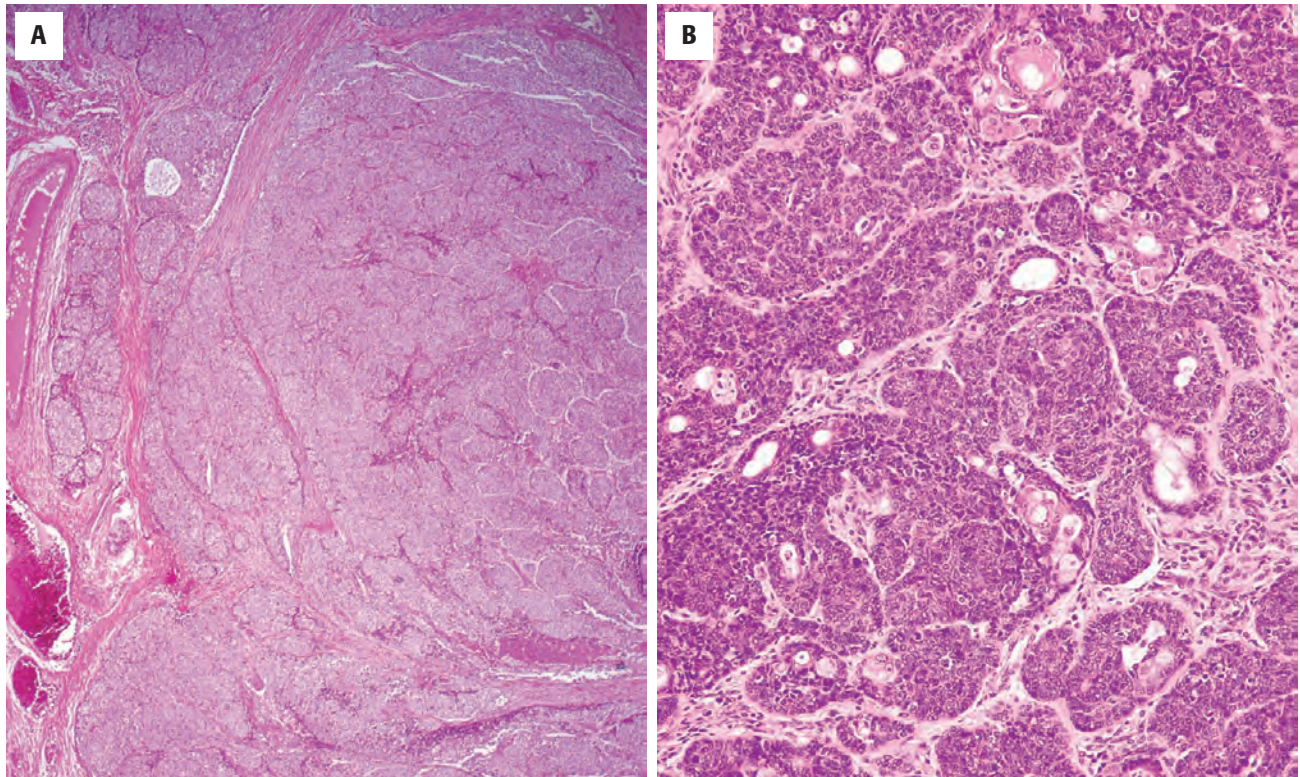
- Locoregional and distant metastasis uncommon
- Surgery is the treatment of choice

mass that may show local infiltration (Fig. 13.90). The cut surface is usually tan or yellow and there may be foci of hemorrhage or necrosis.

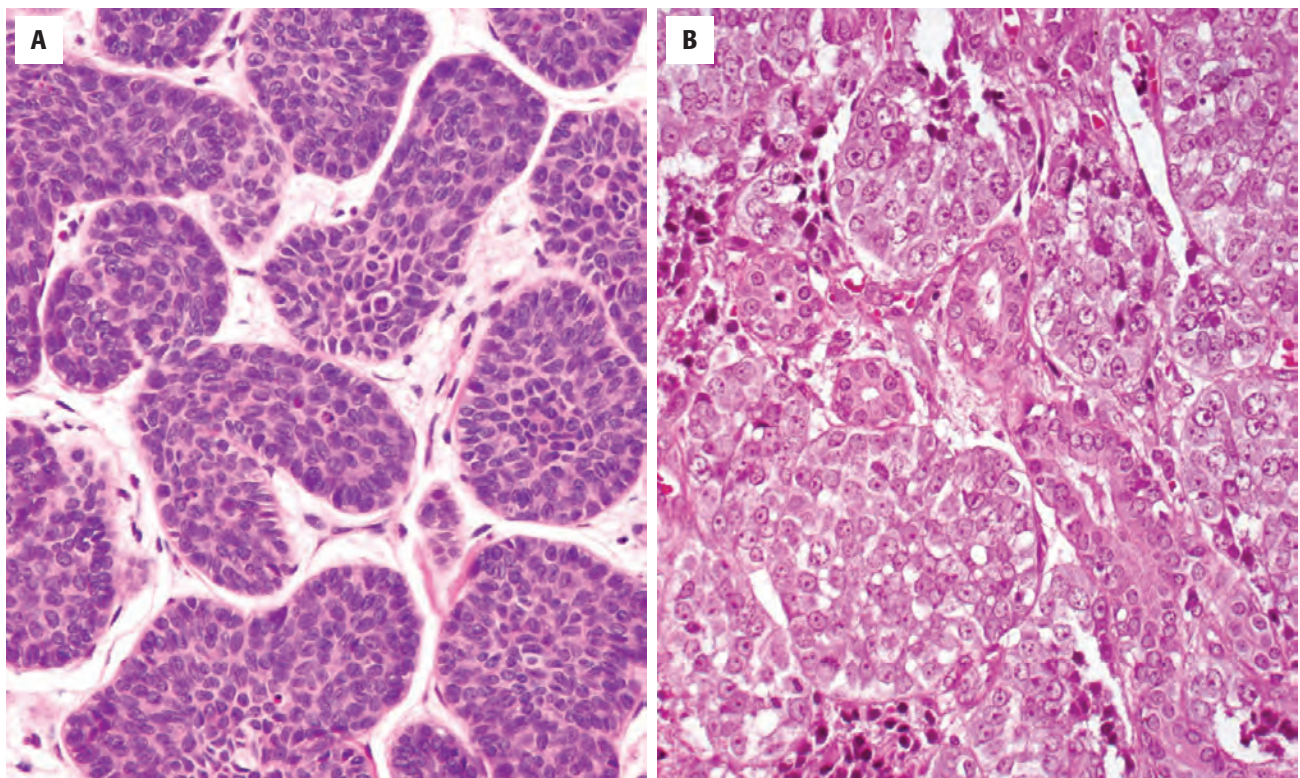
### MICROSCOPIC FINDINGS

The tumor consists predominantly of primitive basaloid cells with round or oval vesicular nuclei. The eosinophilic cytoplasm may be scanty or abundant, and cell borders tend to be indistinct (Fig. 13.91). Some tumors are cytologically bland, whereas others show variable degrees of pleomorphism with hyperchromatic nuclei, a high nuclear-to-cytoplasmic ratio, and a high frequency of usually normal mitotic figures (Figs. 13.91 and 13.92). There may be foci of apoptosis and frank necrosis. The cells are usually arranged in solid nests, which may show nuclear palisading peripherally (Fig. 13.91). Cribriform areas may be present focally. In addition, there may be small, duct-like structures lined by cuboidal or columnar cells; some show small terminal nests of cells resembling the anlage of the developing salivary gland (Fig. 13.91). In addition, there may be evidence of myoepithelial, squamous, or sebaceous differentiation (Fig. 13.90). The stroma ranges from thin, sparsely cellular fibrous septa to abundant, cellular, and fibroblastic areas.



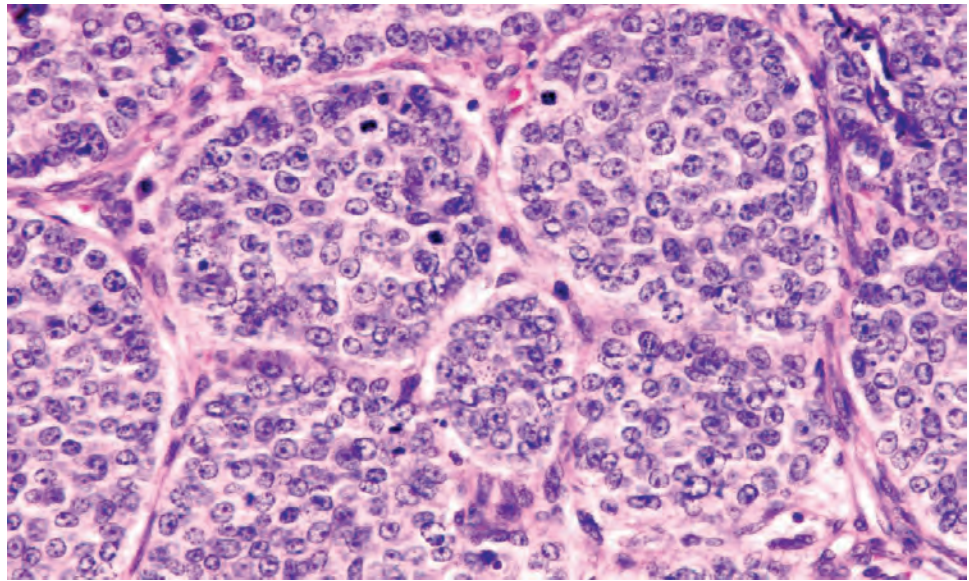
**FIGURE 13.90**

(A) A multinodular and lobulated periphery shows an extensive infiltration into the adjacent tissues. There is necrosis (*lower field*). (B) A well-differentiated tumor shows cytologically bland cells arranged in solid nests and duct-like structures. There are scattered foci of sebaceous differentiation in this sialoblastoma.

**FIGURE 13.91**

(A) Basaloid nests of tumor arranged in a multinodular appearance, separated by fibrous connective tissue stroma. (B) High power of a less-differentiated tumor showing nests of basaloid cells with numerous scattered mitotic figures. Note the more mature cuboidal cells arranged in ductules.



**FIGURE 13.92**

A vaguely nodular to sheet-like distribution of cells with a high nuclear-to-cytoplasmic ratio, vesicular nuclear chromatin, and a single prominent nucleolus. Mitotic figures are frequent.

### SIALOBLASTOMA—PATHOLOGIC FEATURES

#### Gross Findings

- Usually multilobulated and at least partly circumscribed
- May show local invasion
- Foci of hemorrhage and necrosis in higher-grade tumors

#### Microscopic Findings

- Primitive basaloid cells
- Solid nests with peripheral palisading
- Variable pleomorphism and sometimes high mitotic rate

#### Immunohistochemical Findings

- Keratin markers including pan-cytokeratin, EMA, CK5/6, CK7, and CK14
- “Myoepithelial” markers including S100 protein and p63

#### Pathologic Differential Diagnosis

- Basal cell adenoma, basal cell adenocarcinoma, adenoid cystic carcinoma

### ANCILLARY STUDIES

Sialoblastoma is variably positive for a number of keratin markers including pan-cytokeratin, EMA, CK5/6, CK7, and CK14 but is negative for CK20. The abluminal cells stain with a variety of “myoepithelial” markers including S100 protein and p63. The Ki-67 proliferation index varies widely (3% to 80%).

### DIFFERENTIAL DIAGNOSIS

The differential diagnosis of sialoblastoma includes other predominantly basaloid tumors such as *basal cell adenoma*,

*basal cell adenocarcinoma*, and *AdCC*. In contrast to basal cell adenoma, sialoblastoma shows more primitive cellular features, a higher mitotic rate, and a tendency to local infiltration. In addition, all of these tumors are exceptionally rare in children, and the distinction is usually straightforward.

### PROGNOSIS AND THERAPY

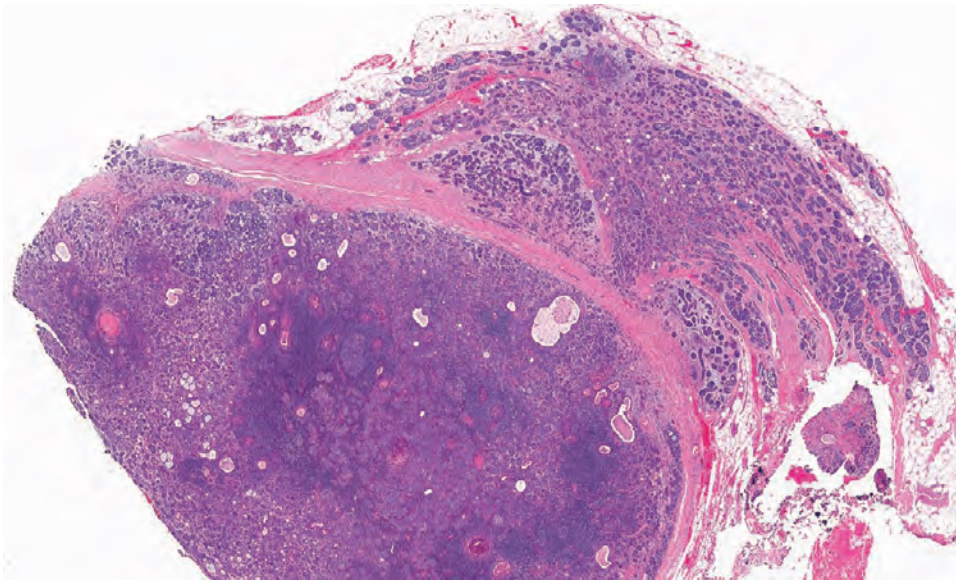
The behavior of sialoblastoma is variable, and the paucity of reported cases makes it difficult to assess prognosis accurately. About 20% of cases recur, and a small number have undergone regional or distant metastases. It has been suggested that cases could be divided into favorable and unfavorable subtypes. Favorable tumors are at least partially encapsulated, are cytologically bland, and show abundant stroma. Unfavorable subtypes show variable degrees of anaplasia, limited stroma, and evidence of neural or vascular invasion. They may additionally show alpha fetoprotein reactivity and have a high Ki-67 proliferative index. The treatment of choice is complete surgical excision. The value of radiotherapy and chemotherapy has not been established, but a recent report suggests that neoadjuvant chemotherapy may be an alternative to mutilating surgery in locally invasive tumors.

## ■ UNCOMMON CARCINOMAS

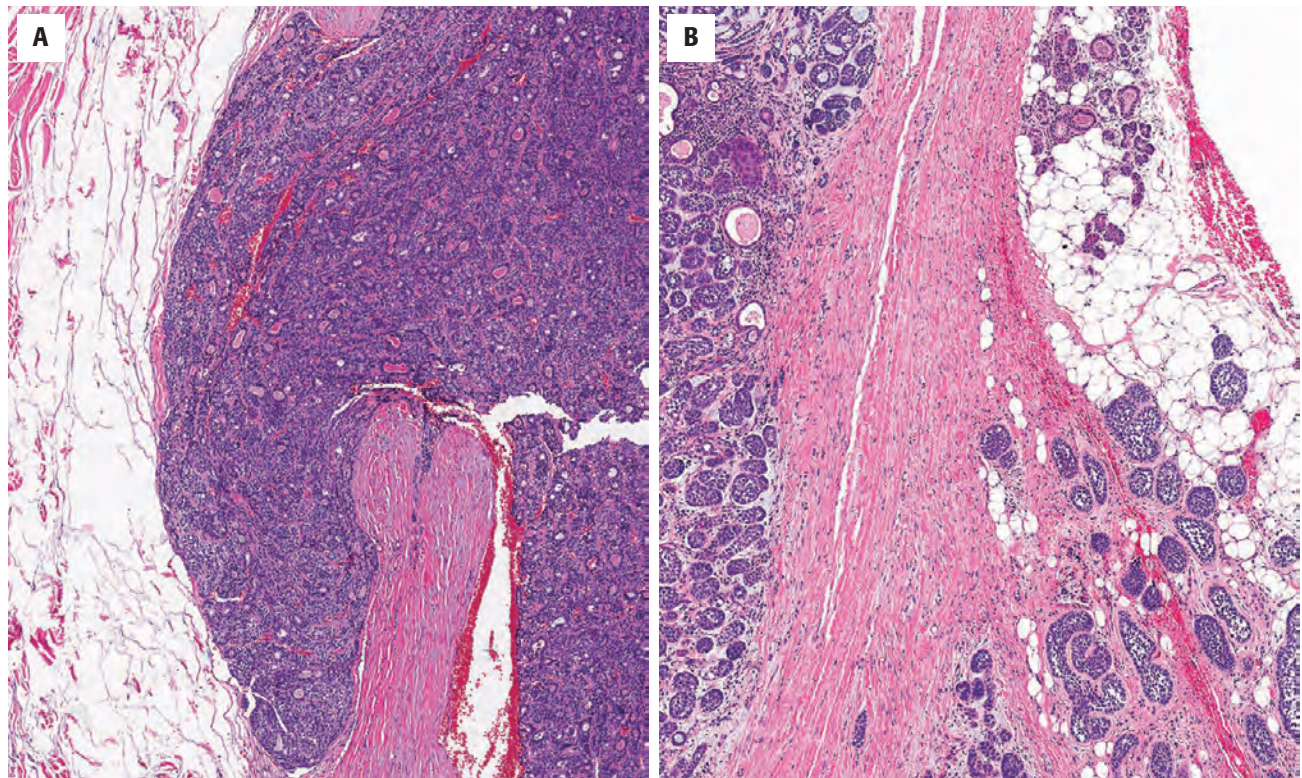
### BASAL CELL ADENOCARCINOMA

Basal cell adenocarcinoma (AC) consists of basaloid epithelial cells cytologically and histomorphologically similar to those of basal cell adenoma but in an infiltrative epithelial neoplasm (Figs. 13.93 and 13.94) with a



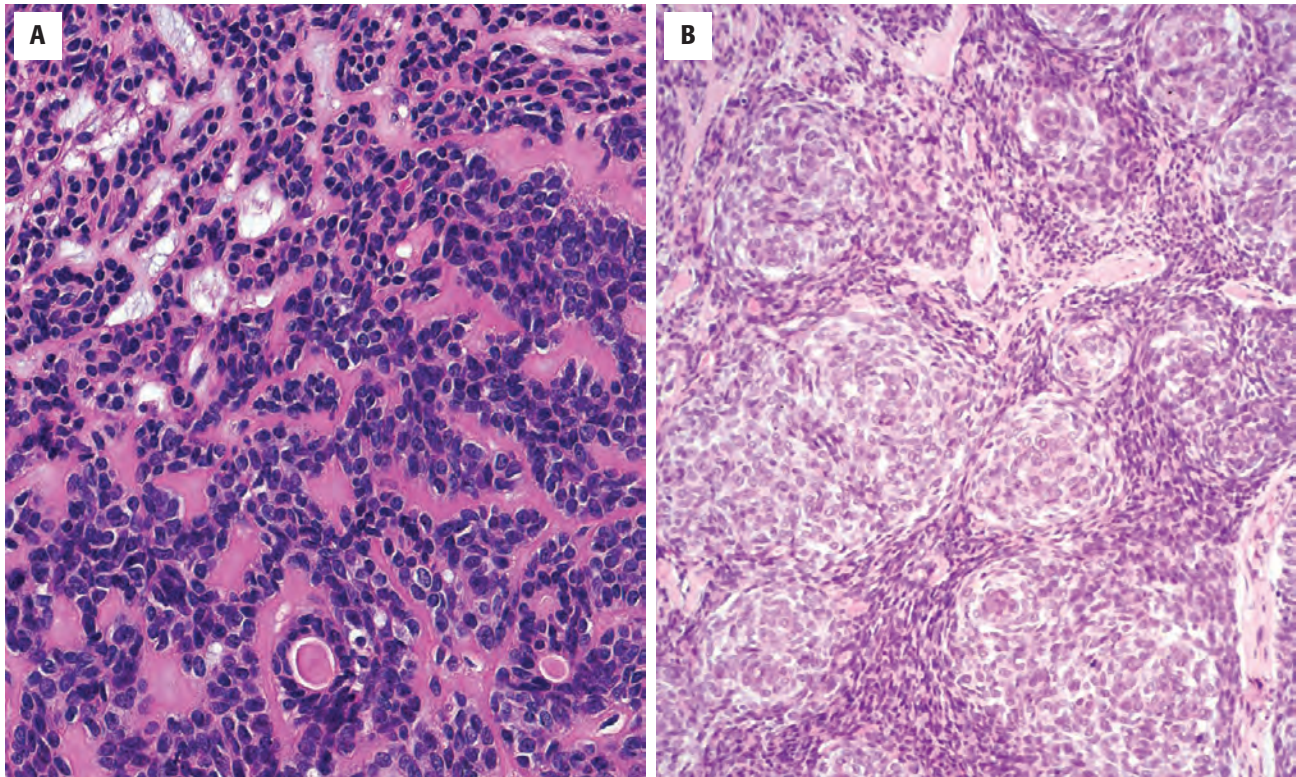
**FIGURE 13.93**

Tumor is surrounded by a very well-formed capsule but shows extensive infiltration into the adjacent soft tissue and fat in this basal cell adenocarcinoma.

**FIGURE 13.94**

(**A** and **B**) The basaloid cells of this basal cell adenocarcinoma are seen invading adjacent soft tissue and fat.



**FIGURE 13.95**

(A) Small dark cells with scant cytoplasm are noted surrounding larger polygonal cells with eosinophilic cytoplasm separated by basement membrane material in this basal cell adenocarcinoma. (B) Areas of squamous differentiation are quite prominent in this basal cell adenocarcinoma.

potential for metastasis. Rare cases have arisen from a preexisting basal cell adenoma. Basal cell AC accounts for less than 2 % of all salivary gland tumors. It has been reported in only adults, with an average age of 60 years at presentation. Over 90 % of cases involve the parotid gland, and tumors in the oral cavity are rare. Most present as painless swellings, sometimes of many years' duration.

The tumor consists of basaloid epithelial cells, which may be small and dark with scanty cytoplasm or larger and polygonal, with eosinophilic or amphophilic cytoplasm (Fig. 13.95). As in basal cell adenoma, there are three main histomorphologic patterns: solid, membranous, and tubulotrabeular. In the *solid* variant, the tumor islands are separated by collagenous septa of variable thickness. The basement membrane zone of the *membranous* variant is thick and densely hyalinized, and frequently, there are hyaline droplets within the tumor islands. Peripheral palisading and cellular whorling, sometimes with squamous differentiation, may be seen in both of these variants (Fig. 13.95). The *tubulotrabeular* pattern consists of interconnecting cords of basaloid cells with varying degrees of luminal differentiation (highlighted with immunohistochemistry) (Fig. 13.96). Cellular and nuclear pleomorphism is rarely conspicuous, and mitotic activity is often minimal. A Ki-67 proliferation index is low. However, these tumors are infiltrative and frequently

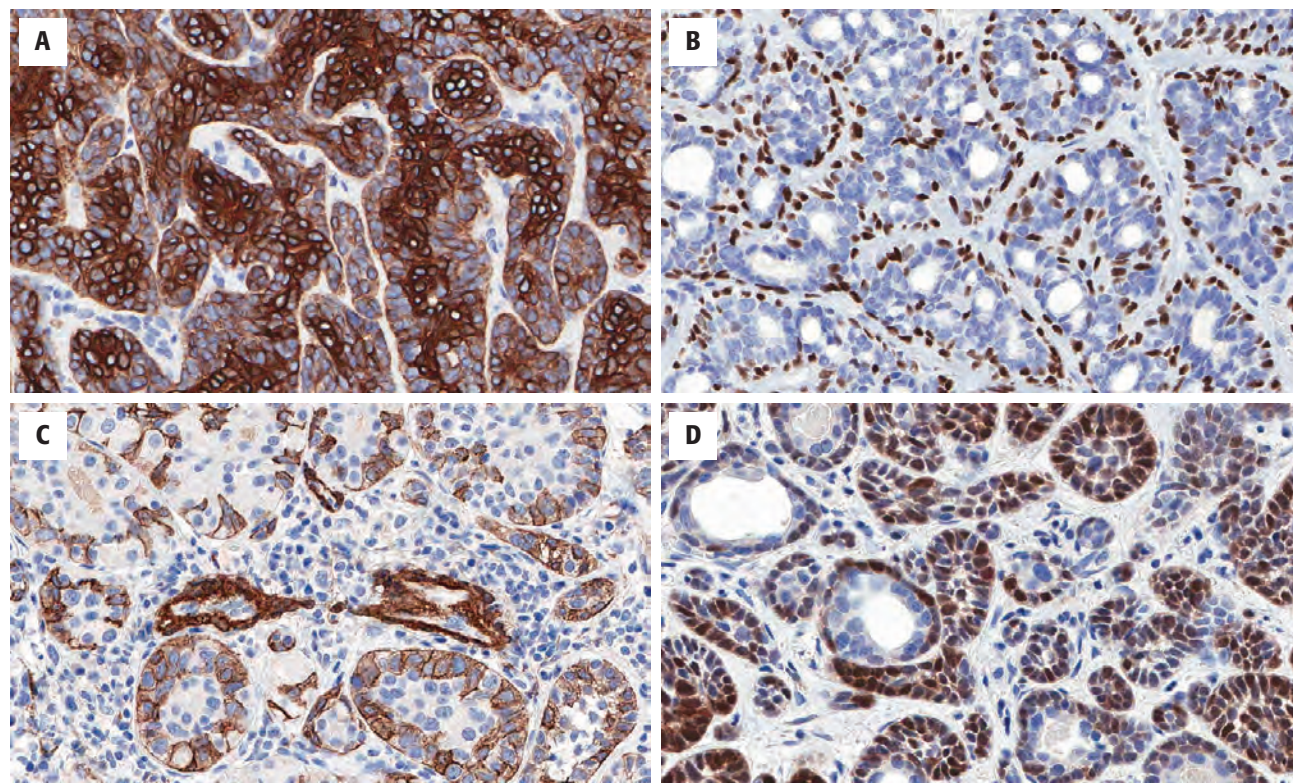
extend widely into the surrounding tissues. Perineural and lymphovascular invasion is present in about a quarter of cases, but regional and distant metastases are uncommon. Although basal cell AC is locally destructive, the long-term prognosis is good and the tumor is regarded as low grade. High-grade basal cell AC shows necrosis (Fig. 13.97). A subset of basal cell AC harbors beta-catenin mutations, leading to nuclear beta-catenin and nuclear LEF-1 immunoreexpression (Fig. 13.98).

### CLEAR CELL CARCINOMA

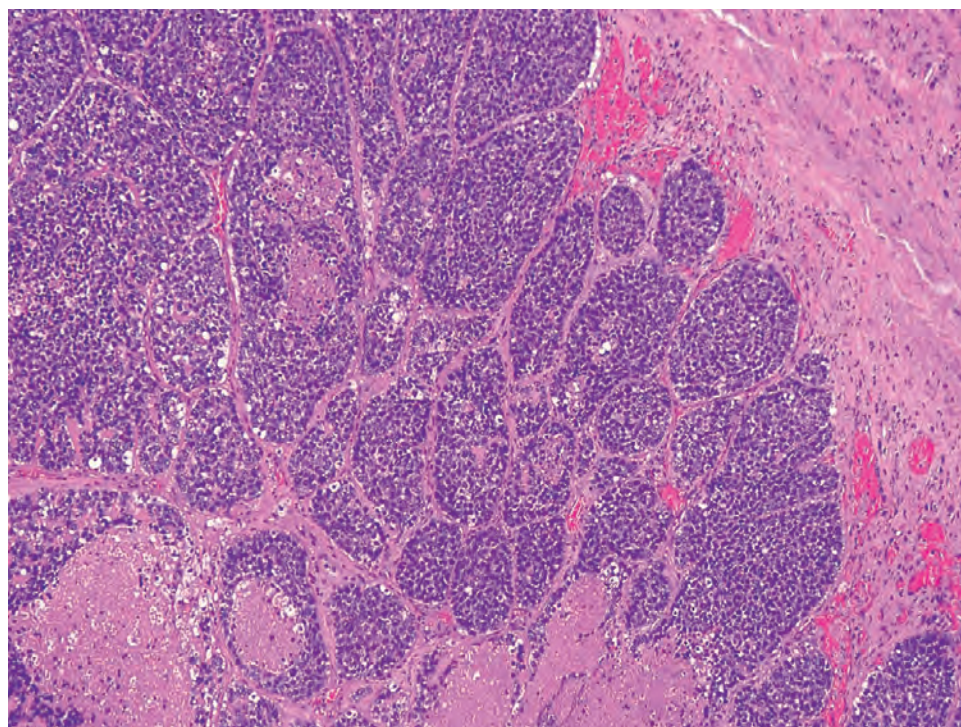
Clear cell carcinoma (CCC), also known as *hyalinizing* clear cell carcinoma, is a malignant epithelial neoplasm composed of a monomorphous population of cells that have optically clear cytoplasm (Fig. 13.99). It is distinguished from other salivary gland tumors containing clear cells by the absence of their characteristic features and its monomorphous population of cells. The peak incidence is in the age range of 40 to 70 years, and about 60 % involve intraoral minor glands, particularly the palate. Most present as a painless swelling without ulceration, with a history ranging from a few weeks to many years.

CCC is unencapsulated and infiltrates the surrounding tissues. Microscopy shows a uniform population of



**FIGURE 13.96**

The biphasic appearance of basal cell adenocarcinoma is highlighted with keratin (A), p63 (B), smooth muscle actin (C), and S100 protein (D).

**FIGURE 13.97**

High-grade basal cell adenocarcinoma; note necrosis in the lower left corner.



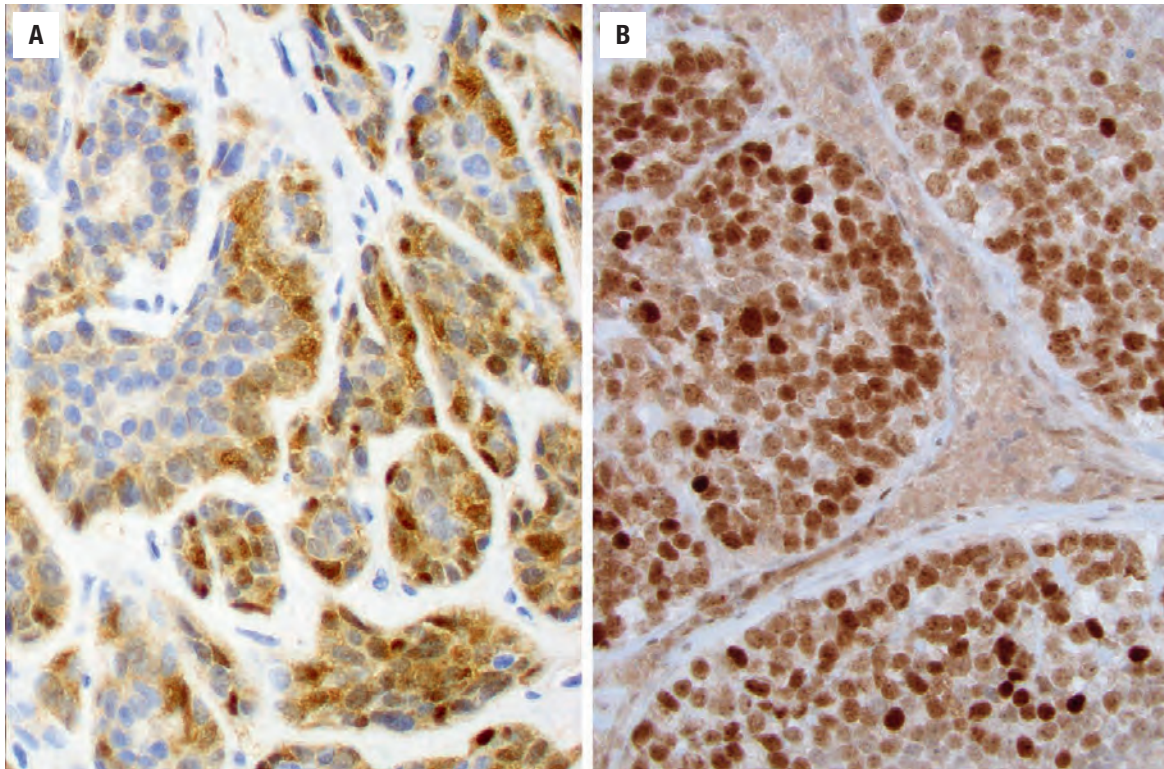


**FIGURE 13.98**

Basal cell adenocarcinoma showing a lack of nuclear  $\beta$ -catenin staining (**A**) while showing a strong nuclear LEF-1 reaction (**B**).

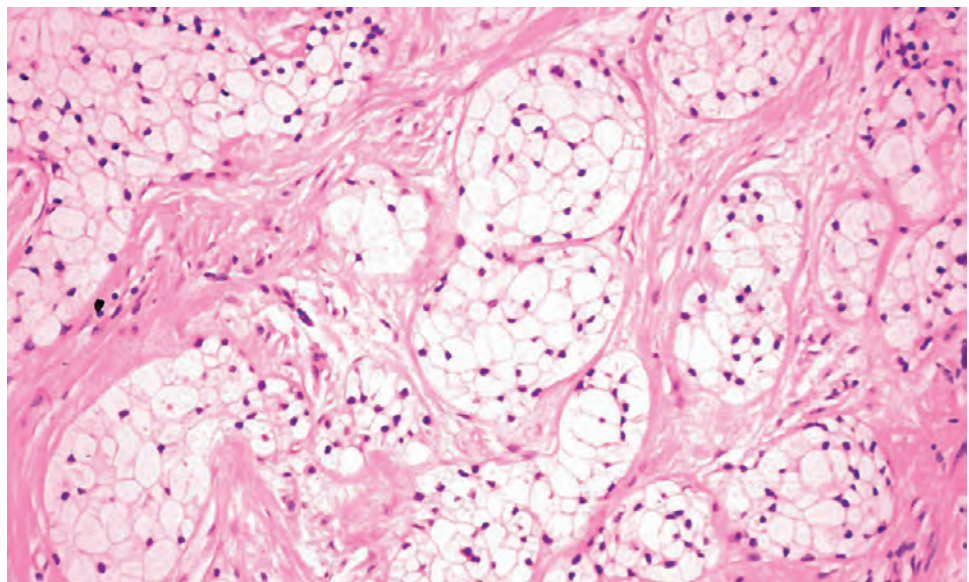


**FIGURE 13.99**

Clear cell carcinoma. A monotonous population of cells with clear cytoplasm containing small hyperchromatic nuclei. There are prominent cell borders. Fibrous bands separate the nodules of tumor. There is no ductal differentiation.

polygonal or round cells with distinct cell borders (Figs. 13.99 and 13.100). Cells with optically clear cytoplasm usually predominate, although occasional CCCs have more eosinophilic cells with a minor population of clear cells. The cytoplasm contains variable amounts of glycogen

(Fig. 13.100) but has no significant mucin content. Nuclei are round and eccentric and, though there may occasionally be moderate pleomorphism, mitoses are few. The cells are arranged in nests, sheets, and cords with no evidence of ductal differentiation. There is a fibrous



**UNCOMMON CARCINOMAS—FACT SHEET****Basal Cell Adenocarcinoma***Clinical*

- Basaloid cell neoplasm with invasive growth
- Represents less than 2% of salivary gland tumors
- Adults, mean 60 years
- More than 90% occur in the parotid gland
- Locally destructive, but good long-term prognosis

*Pathology*

- Infiltrative border
- Basaloid cells, which may be small and dark with scant cytoplasm or larger, polygonal cells with eosinophilic/amphophilic cytoplasm
- Solid, membranous, and tubulotrabecular patterns
- Separated by variable hyalinizing material
- Mitotic figures scant
- Perineural and vascular invasion can be seen

**Clear Cell Carcinoma***Clinical*

- Malignant epithelial tumor of monotonous optically clear cytoplasm (no other tumor features present)
- Represents less than 2% of salivary gland tumors
- Adults, peak in the 40- to 70-year age range
- About 60% occur in minor salivary glands (palate)
- Locally infiltrative but low grade, cured by surgery

*Pathology*

- Unencapsulated with infiltrative growth
- Uniform population of polygonal/round cells with distinct borders, clear cytoplasm, small nuclei, and fibrosis separating the tumor groups
- Must be separated from metastatic renal cell carcinoma and other clear cell variants of salivary gland neoplasms
- Clear cell carcinomas show *EWSR1* rearrangement

**Sebaceous Adenocarcinoma***Clinical*

- Malignant tumor with sebaceous cells of variable maturity with pleomorphism and invasive growth

- Represents less than 1% of salivary gland tumors
- Adults, peaks in 3rd and 7th decades
- More than 90% occur in the parotid gland
- May be very painful, with facial nerve palsy
- Wide excision yields a 5-year survival of about 70%

*Pathology*

- Sheets, islands, and trabeculae with ductal structures that may become cystic
- Sebaceous differentiation is variable, with occasional tumors showing only rare sebaceous cells
- Cytologic atypia and mitotic figures usually in basaloid and squamous cells
- Necrosis is common, with perineural invasion seen in about 20%

**Oncocytic Carcinoma***Clinical*

- Cytomorphologically malignant oncocytes arranged in an adenocarcinoma pattern with invasion
- Represents less than 1% of salivary gland tumors
- Adults, mean age 65 years
- Males > females
- 80% occur in the parotid gland
- A mass lesion, which may be associated with pain or facial palsy
- A high-grade tumor with frequent recurrences and metastasis

*Pathology*

- Unencapsulated tumors composed of large, round, polygonal cells with abundant, granular, eosinophilic cytoplasm
- Large nuclei with prominent nucleoli
- Variable pleomorphism
- Neural and vascular invasion is common
- Must be separated from oncocytic variants of other salivary gland tumors (e.g., mucoepidermoid carcinoma)

stroma of variable thickness and cellularity (Figs. 13.99 and 13.100). CCC is diffusely p63- and p40-positive, and about 80% of cases harbor *EWSR1* rearrangement. CCC is locally infiltrative and may invade nerves. This tumor must be separated from clear cell variants of other salivary gland neoplasms and from metastatic RCC. The tumor is usually low grade and is cured by conservative surgery.

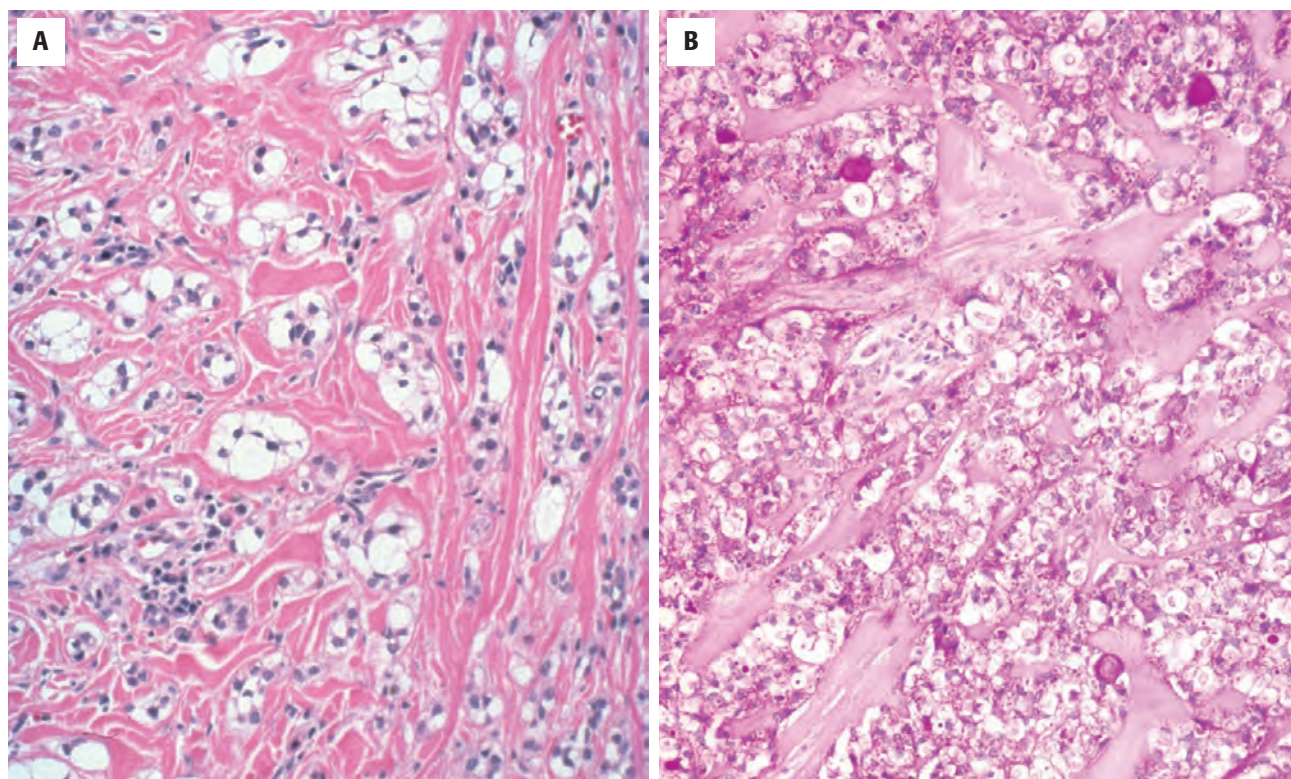
**SEBACEOUS ADENOCARCINOMA**

Sebaceous adenocarcinoma is a malignant tumor composed of sebaceous cells of varying maturity that are arranged in sheets and/or nests with different degrees of pleomorphism, nuclear atypia, and invasiveness. It is a rare tumor with bimodal peaks appearing in the 3rd and 7th decades.

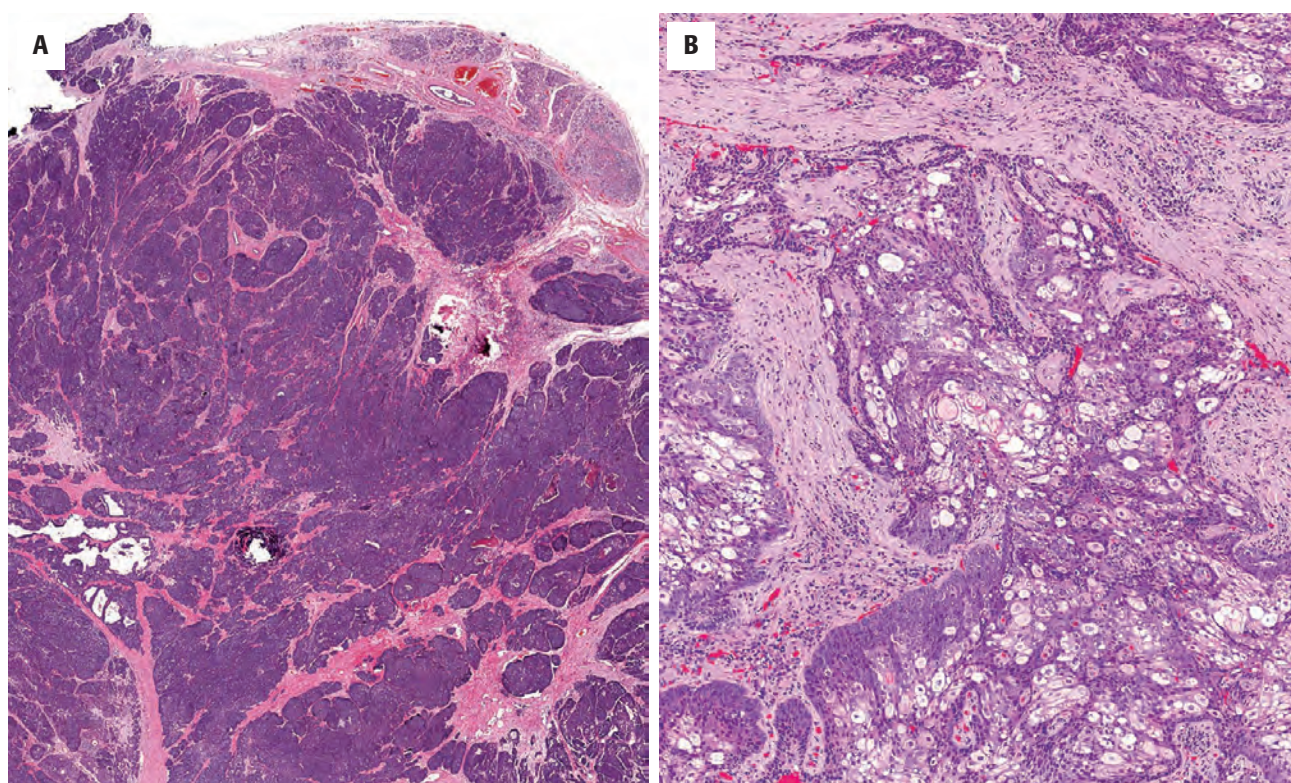
Over 90% arise in the parotid gland, and the tumor usually presents as a variably painful mass, sometimes with facial nerve palsy.

The tumor can form sheets, islands, and trabeculae (Fig. 13.101). Ductal structures are common and may become cystic. The degree of sebaceous differentiation is quite variable; in some tumors, basaloid or squamous cell types predominate, and sebaceous cells may be difficult to find (Figs. 13.101 and 13.102). Cytologic atypia and mitotic activity are usually seen in the basaloid and squamous cells. Areas of necrosis are common, and neural invasion is present in about one-fifth of cases. Immunohistochemistry can be used to confirm the sebaceous differentiation (i.e., CD15, androgen receptor, adipophilin, or EMA) (Fig. 13.103). The 5-year survival rate in the small number of reported cases was about 70%, and wide surgical excision is the treatment of choice.



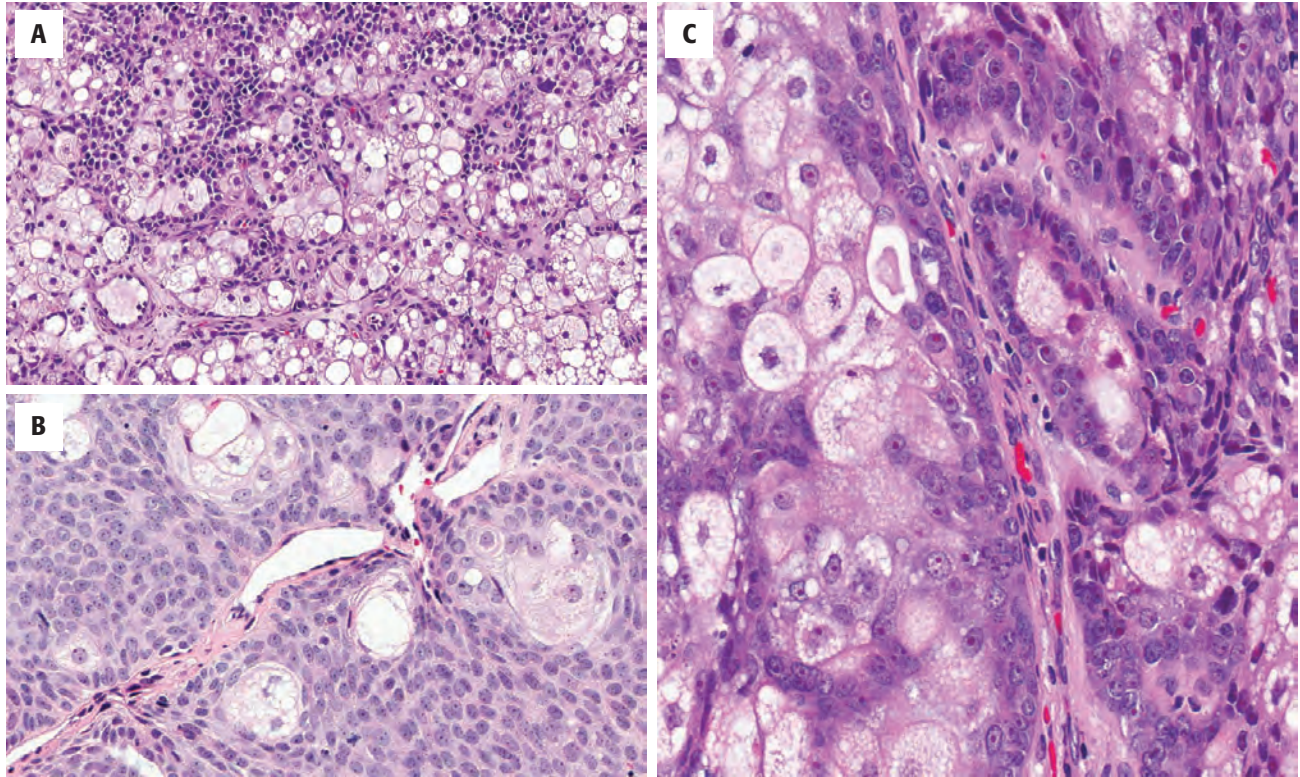
**FIGURE 13.100**

(A) Bands of heavy fibrosis dissect the tumor into multiple small nests of tumor cells. There is abundant clear cytoplasm. (B) A strong periodic acid–Schiff without diastase reaction highlights the glycogen in the cytoplasm.

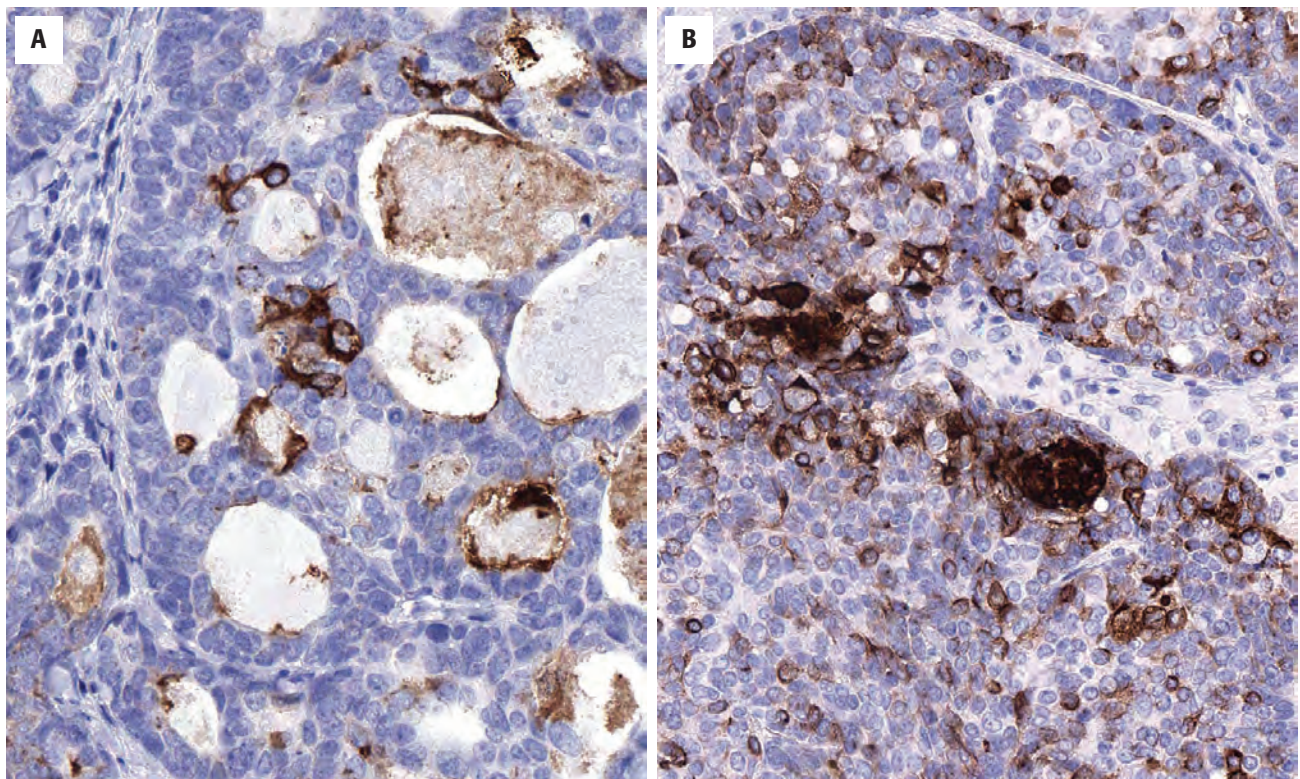
**FIGURE 13.101**

(A) Nests of neoplastic cells with a "dark" appearance are shown infiltrating into the adjacent tissue. (B) Basaloid cells arranged in trabeculae in this sebaceous carcinoma. Note the areas of sebaceous differentiation throughout.



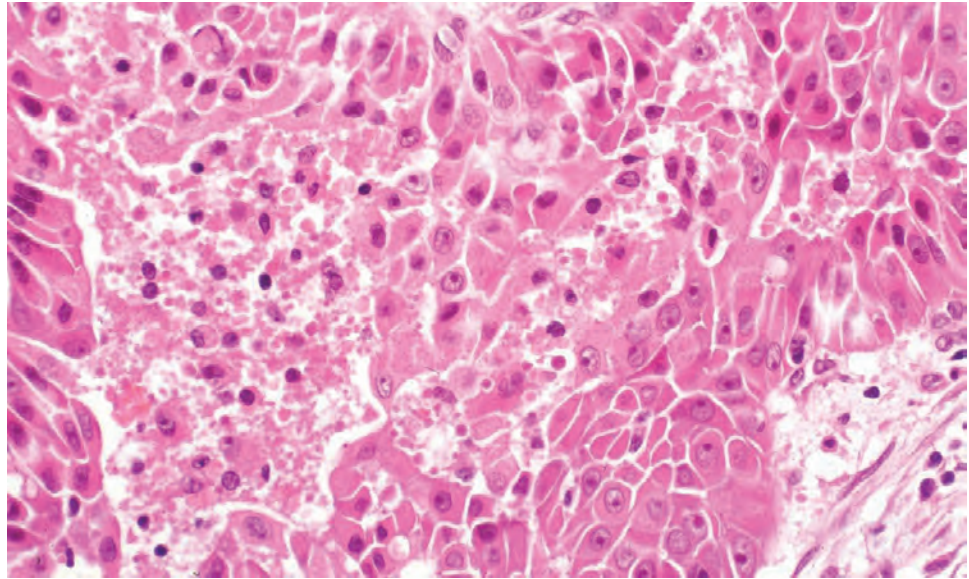
**FIGURE 13.102**

(A–C) The variable degree of sebaceous differentiation is shown. It is important to note that the cells should show true microvesiculation and not degenerative change. Nucleoli are frequently quite prominent.

**FIGURE 13.103**

(A) CD15 highlights the sebaceous cells in this sebaceous carcinoma. (B) Epithelial membrane antigen preferentially highlights the sebocytes, although other cells are also positive.



**FIGURE 13.104**

Large polygonal cells with ample oncocyctic-oxophilic cytoplasm surround nuclei with prominent nucleoli. Note the necrosis.

### ONCOCYTIC CARCINOMA

Oncocytic carcinoma is a proliferation of cytomorphologically malignant oncocytes with an adenocarcinomatous architectural phenotype, including infiltrative qualities. It is rare, accounting for less than 1% of all salivary gland tumors. About 80% involve the parotid gland, with the remainder arising in the submandibular and minor glands. The age range is from 29 to 91 years (mean, 65 years), and there is a male predominance. Parotid tumors usually form a nondescript mass that is often associated with pain or facial palsy.

The tumor is unencapsulated and consists of large round or polyhedral cells with abundant granular and eosinophilic cytoplasm and large, centrally placed nuclei with prominent nucleoli (Fig. 13.104). The mitochondria-rich cytoplasm usually shows intensely blue, granular positivity with PTAH stain. There is variable pleomorphism and some tumors have cytologically bland areas, suggesting that they have arisen from a preexisting oncocytoma. Ki-67 staining may be of value in differentiating between benign and malignant oncocytic tumors. The cells are arranged in sheets, thèques, and cords, and sometimes duct-like structures are present. The tumor shows infiltration into surrounding tissue, and neural and lymphovascular invasion is common (Fig. 13.105). The diagnosis is usually made after oncocytic variants of other salivary gland malignancies have been excluded. Oncocytic carcinoma is often high grade, showing frequent local recurrence and both regional and distant metastases.

### ■ UNDIFFERENTIATED CARCINOMAS

Undifferentiated carcinomas are rare, high-grade malignant salivary tumors. They are too poorly differentiated

to be placed in any other specific category of carcinoma but are now divided into three independent groups: small and large cell carcinomas and lymphoepithelial carcinoma (LEC).

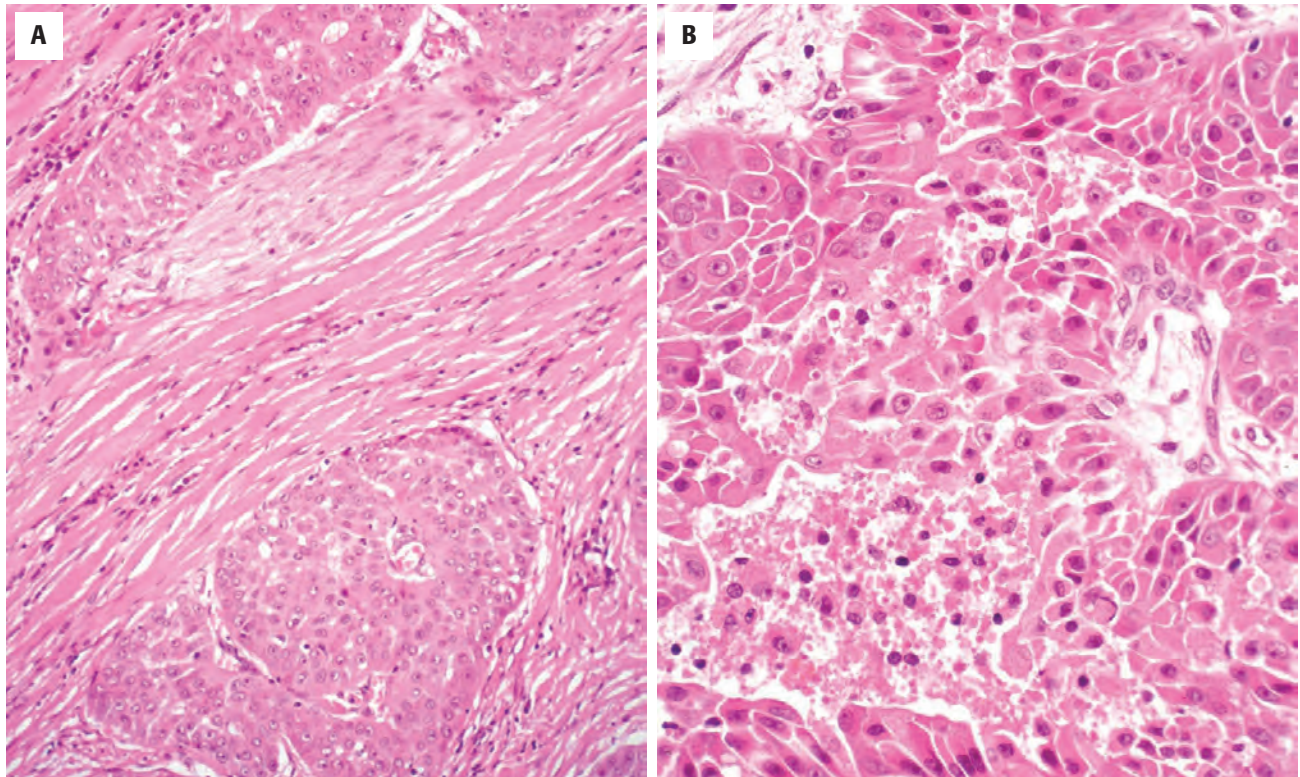
### SMALL CELL CARCINOMA

Small cell carcinoma is a type of undifferentiated carcinoma characterized by a proliferation of small anaplastic cells with scanty cytoplasm, fine nuclear chromatin, and inconspicuous nucleoli. Most show evidence of neuroendocrine differentiation. Small cell carcinoma is very rare in the salivary glands and most cases involve the parotid gland. There is a slight male predominance and the peak incidence is in the 5th to 7th decades. The tumor usually presents as a painless but rapidly growing mass, and facial nerve and regional lymph node involvement is common.

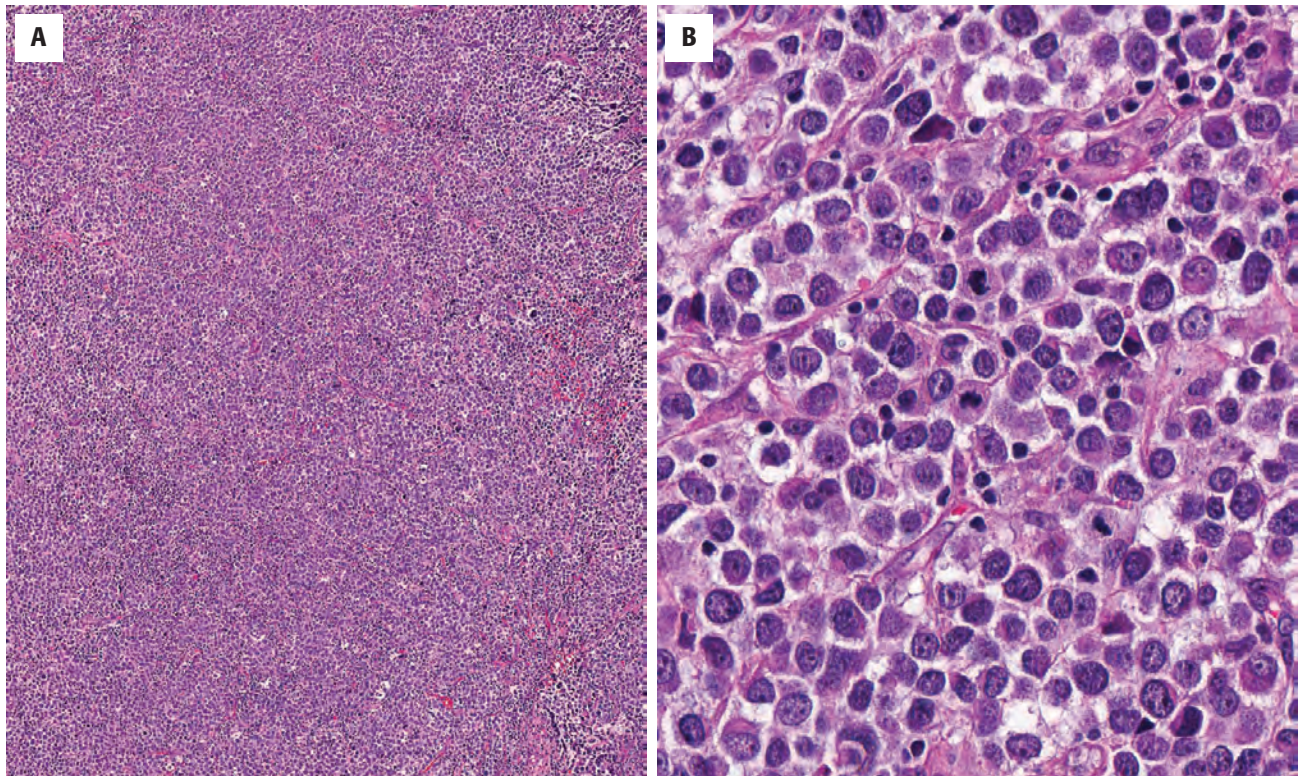
Small cell carcinoma typically forms a poorly circumscribed, infiltrative mass. It consists of sheets, cords, or nests of uniform anaplastic cells that are usually less than 30 µm in largest diameter (Fig. 13.106). Occasional larger or fusiform cells are present, often displaying cellular or nuclear molding. The nuclear chromatin is finely granular and there are no nucleoli. The cytoplasm is scanty and cell borders are ill defined (Fig. 13.107). Crush artifacts with nuclear smearing are usually present. Cells at the periphery of nests may show a suggestion of palisading, and occasionally, cells are arranged in organoid or rosette-like patterns. Occasionally too, there are small foci of ductal or squamous differentiation. There can be extensive areas of necrosis. There is a high mitotic frequency, and vascular and neural invasion is common.

Small cell carcinomas usually show focal pan-cytokeratin expression, which may have a characteristic



**FIGURE 13.105**

(A and B) Oncocytic carcinoma cells are arranged in gland- or duct-like structures seen surrounding a nerve in this infiltrative neoplasm. The cells have prominent nucleoli.

**FIGURE 13.106**

(A and B) Small cell carcinoma showing sheets of small cells with densely hyperchromatic nuclei. Note the high nuclear-to-cytoplasmic ratio.



## UNDIFFERENTIATED CARCINOMAS—FACT SHEET

### Small Cell Carcinoma

#### Clinical

- A type of undifferentiated carcinoma characterized by a proliferation of small anaplastic cells, most showing evidence of neuroendocrine differentiation
- Represent less than 1% of salivary gland tumors
- Peak incidence in 5th-7th decades
- Usually painless but rapidly growing mass with frequent facial nerve and cervical lymph node involvement
- Highly aggressive, with 5-year survival of less than 50%

#### Pathology

- Poorly circumscribed infiltrative mass often with areas of hemorrhage and necrosis
- Sheets, cords, trabeculae of anaplastic small cells
- May show focal palisading or organoid patterns
- Numerous mitoses; crush artifacts, necrosis, neural and vascular invasion
- Focal pan-cytokeratin paranuclear dot-like staining
- Must be separated from solid variant of adenoid cystic carcinoma, lymphoma, melanoma, Merkel cell carcinoma, metastases

### Large Cell Carcinoma

#### Clinical

- A rare high-grade, undifferentiated, malignant salivary tumor composed of pleomorphic, large cells with abundant cytoplasm
- Represents less than 1% of salivary gland tumors
- Most cases involve major glands, particularly the parotid gland
- Peak incidence at 60-70 years
- Rapidly growing, firm, fixed mass, which is often tender or painful
- Facial nerve and regional lymph node involvement common
- Very aggressive, with frequent local recurrence and distant metastases

#### Pathology

- Poorly circumscribed infiltrative mass, often with areas of necrosis
- Characterized by lack of differentiation, with occasional foci of ductal or squamous differentiation

- Sheets, cords, or trabeculae of loosely cohesive cells in fibrous stroma
- Cells more than 30  $\mu$ m in diameter with abundant pale eosinophilic or clear cytoplasm
- Nuclei round or polygonal and vesicular with prominent nucleoli and frequent mitoses
- Lymphovascular and neural invasion frequent
- Must be separated from metastases, carcinoma, component of carcinoma ex pleomorphic adenoma, melanoma, anaplastic large cell lymphoma

### Lymphoepithelial Carcinoma

#### Clinical

- A large cell undifferentiated carcinoma with prominent non-neoplastic lymphoplasmacytic infiltrate
- Represents less than 0.4% of salivary gland tumors
- 80% parotid, 20% submandibular
- Mean age, 40 years; range, 2nd-9th decades
- Much higher incidence in Inuit and southern Chinese populations; strong association with Epstein-Barr virus
- Often presents as a long-standing mass with recent rapid growth as well as pain or nerve involvement
- 5-year survival rate of 60%-80%

#### Pathology

- Solid, firm mass that may be circumscribed and lobulated or extensively infiltrative
- Sheets, cords, nests of tumor cells in dense lymphoid stroma
- Carcinoma cells large and polyhedral with faintly eosinophilic, abundant cytoplasm and indistinct cell borders
- Nuclei round or oval with vesicular chromatin, conspicuous nucleoli, and frequent mitoses
- Must be separated from metastatic nasopharyngeal carcinoma, lymphoepithelial sialadenitis, large cell undifferentiated carcinoma, lymphoma

parinuclear dot-like reactivity. Some tumors show a similar staining pattern for CK20 (Fig. 13.108), referred to as Merkel cell type. Many are positive for EMA and occasional tumors are reactive with TTF1. Most tumors show immunoreactivity with neuroendocrine markers, including neuron-specific enolase (NSE), leu-7 (CD57), CD56, chromogranin A, and synaptophysin (Fig. 13.108), among others. Smears show a dispersed to loose clustering of small to intermediate cells with mild to moderate pleomorphism. There is smudging of the nuclei along with nuclear molding. Rosettes or multinucleated giant cells may be seen (Fig. 13.109).

The differential diagnosis of small cell carcinoma includes the solid variant of *AdCC*, *lymphoma*, and *melanoma*, and particularly *metastases* from the lung or cutaneous *Merkel cell carcinoma*.

Small cell carcinoma is highly aggressive, with over half of patients developing recurrence and regional or

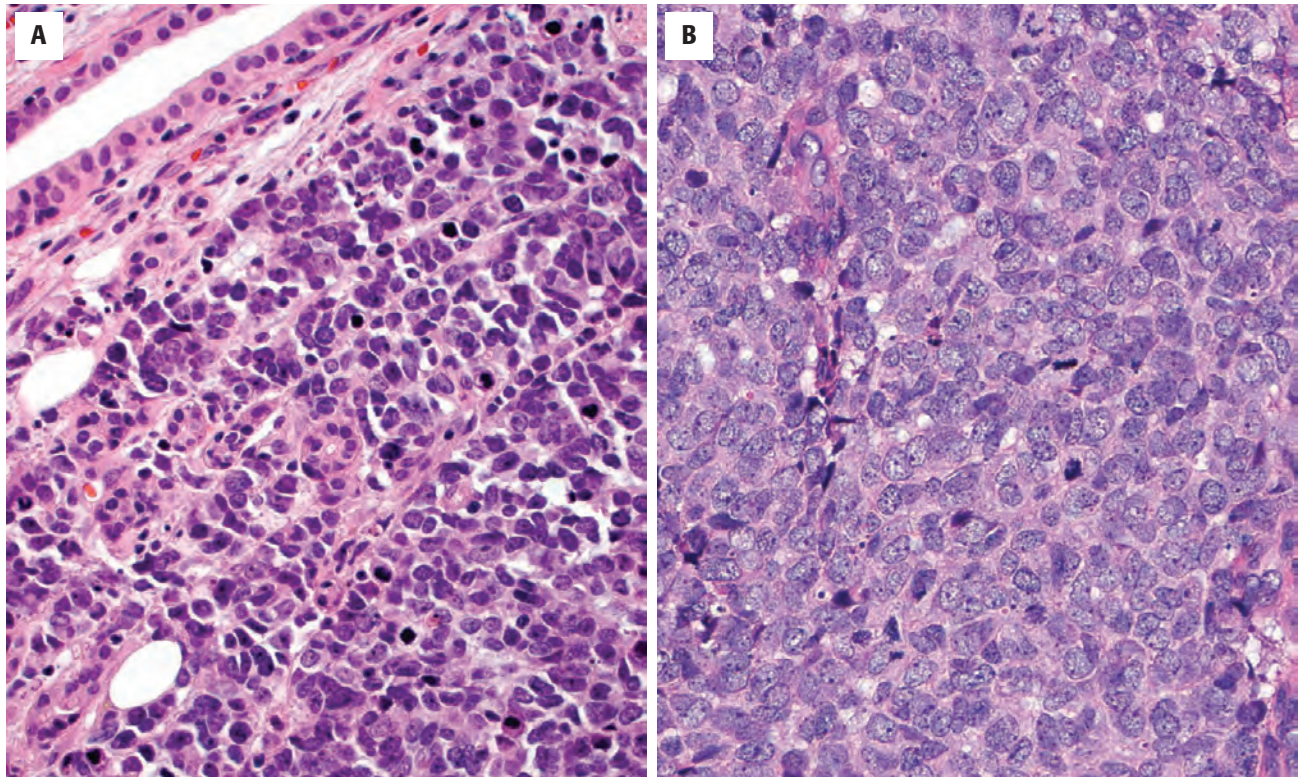
distant metastases. Treatment is usually wide surgical excision and regional lymph node dissection for patients with no evidence of distant metastases. This is often supplemented by radiotherapy and chemotherapy.

## LARGE CELL CARCINOMA

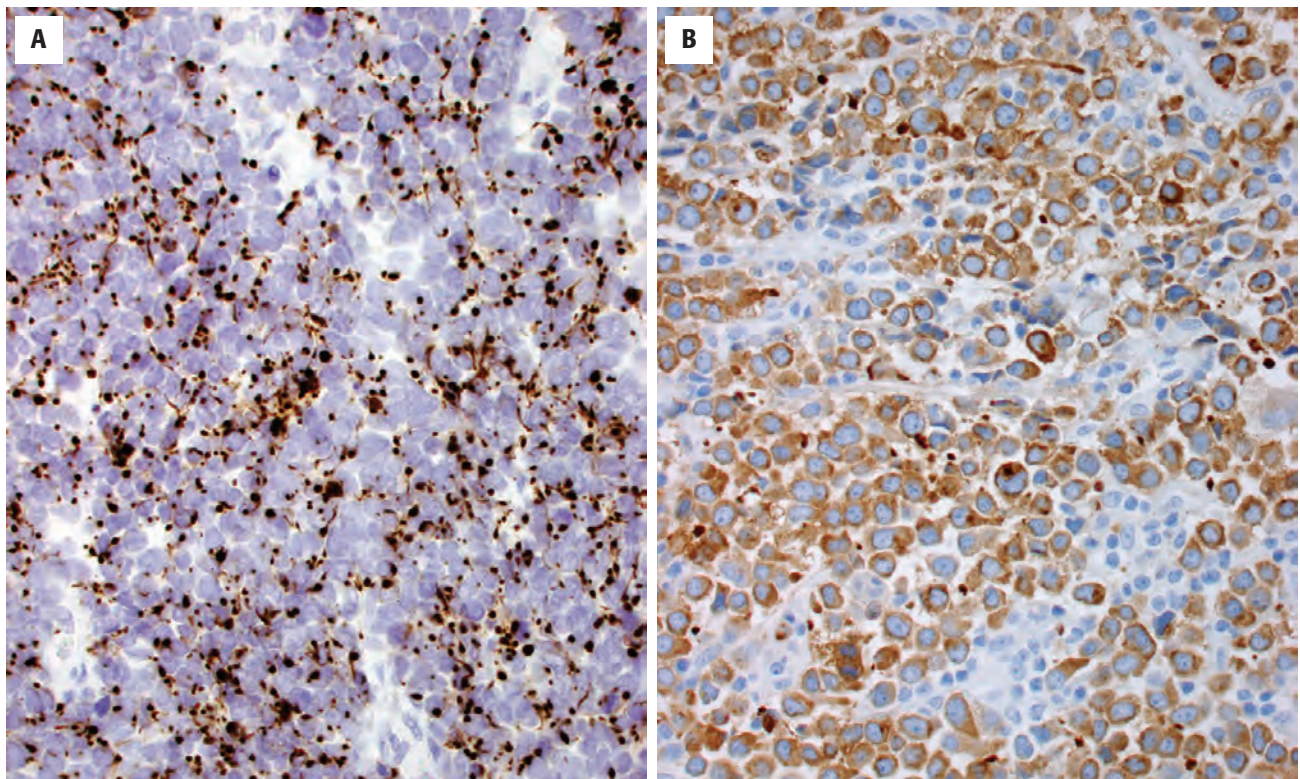
Large cell carcinoma (LCC) is a rare, high-grade malignant salivary gland tumor composed of pleomorphic, large cells with abundant cytoplasm. It lacks the specific features of other salivary gland carcinomas. It is difficult to characterize precisely due to the paucity of reported cases. In addition, some LCCs show neuroendocrine differentiation and are termed *large cell neuroendocrine carcinomas*.

LCCs are very rare (< 1% of salivary neoplasms). Most involve major glands, particularly the parotid gland. They are seen mainly in elderly patients with a peak



**FIGURE 13.107**

(A) A streaming architecture of small cells with a high nuclear-to-cytoplasmic ratio. There is a normal duct in the upper left. (B) A slightly larger cell appearance, with vesicular open nuclear chromatin and a small but easily identified nucleolus. Note the numerous mitoses.

**FIGURE 13.108**

(A) A dot-like, paranuclear CK20 immunoreaction in a small cell carcinoma of Merkel type. (B) The neoplastic cells show a strong cytoplasmic reaction with synaptophysin.



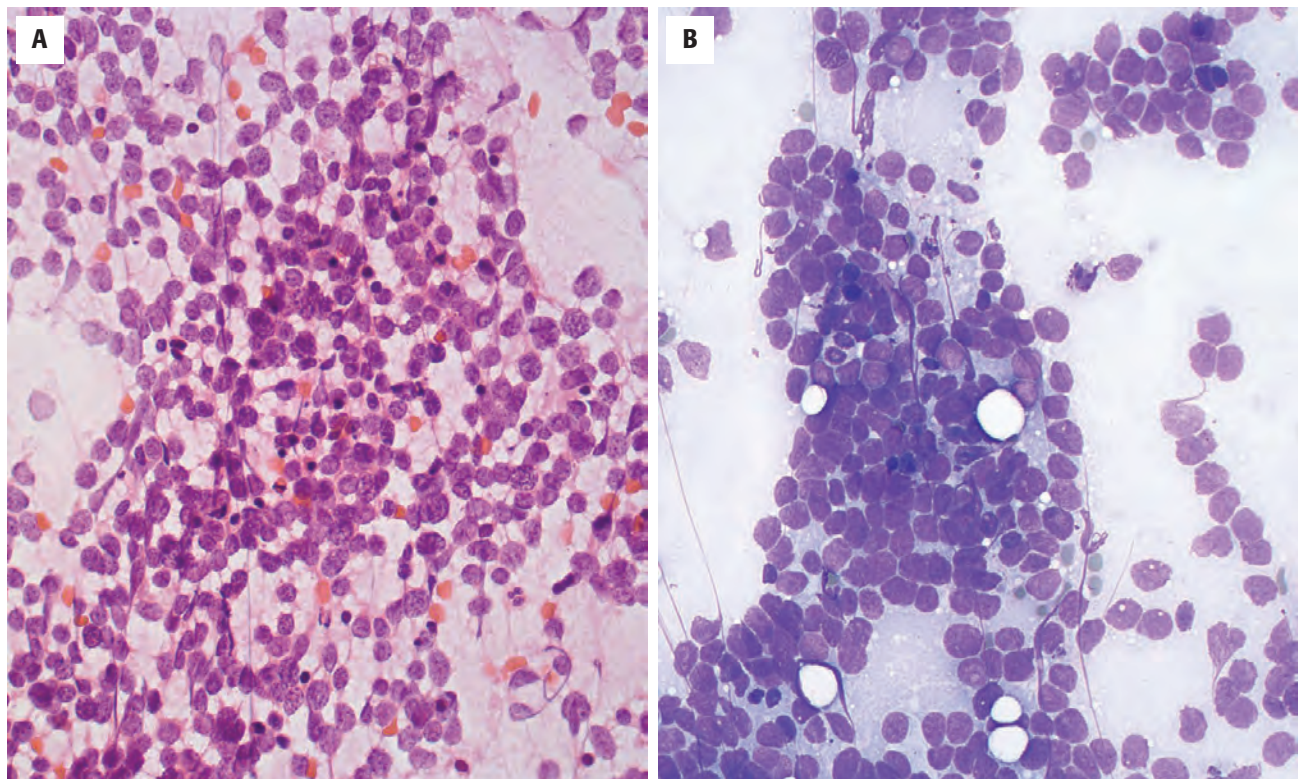


**FIGURE 13.109**

(A) A cellular smear with dispersed small to intermediate-sized cells with mild pleomorphism. Almost no cytoplasm is visible. There are no lymphoglandular bodies (alcohol-fixed, Papanicolaou stain). (B) Small cells with nuclear molding and a high nuclear-to-cytoplasmic ratio. Mitotic figures are present (air-dried, Diff-Quik stain).

incidence in the 7th and 8th decades. There is no significant sex predilection. The tumor usually forms as a rapidly growing firm and fixed mass. This is often tender or painful, and both facial nerve and regional lymph node involvement are common.

LCC is characterized by its lack of differentiation and features that would allow it to be allocated to a more specific designation. Despite this, occasional and small foci of ductal or squamous differentiation can be accepted. The tumor consists of sheets, cords, or trabeculae of loosely cohesive cells in a fibrous stroma. Necrosis is common. The cells are typically larger than 30  $\mu\text{m}$  and have abundant pale eosinophilic or clear cytoplasm. Nuclei are round or polygonal or, less commonly, fusiform. They are vesicular and often contain prominent nucleoli. Occasionally, there are bizarre anaplastic cells and osteoclast-like multinucleated giant cells. Intracytoplasmic glycogen is sometimes present, but there is no evidence of mucocytic differentiation. Mitotic figures are usually numerous and many are abnormal. A minority show a conspicuous mixed inflammatory infiltrate, and necrosis is common. Lymphovascular and neural invasion is frequent.

LCC is typically positive for pan-cytokeratin and EMA. Additionally, rare large cell neuroendocrine carcinomas are also positive for at least one neuroendocrine marker other

than NSE. There is a high (> 50%) Ki-67 proliferative index, and diffuse p53 nuclear staining is frequent.

It is essential to exclude the possibility of metastatic disease. Therefore, additional clinical and imaging studies, particularly of the nasopharynx, may be necessary to establish the diagnosis. Undifferentiated carcinoma can form a significant component of Ca ex PA. Melanoma and anaplastic large cell lymphoma can be distinguished from LCC by using appropriate immunohistochemical markers.

LCC is very aggressive, with frequent local recurrence together with cervical lymph node and distant metastases. The usual treatment is wide local surgical excision and adjuvant radiotherapy.

### LYMPHOEPITHELIAL CARCINOMA

LEC is a large cell undifferentiated carcinoma with a prominent non-neoplastic lymphoplasmacytic infiltrate. Most LECs arise de novo, but some can be preceded by LESA.

LEC is rare, accounting for only 0.4% of salivary tumors. However, there is a much higher incidence in some ethnic groups, including Inuits and southern Chinese populations. It affects a wide age range (2nd to 9th



decades) with a median age of 40 years. There is no significant sex predilection. About 80 % of cases involve the parotid gland and most of the remainder are in the submandibular gland. Intraoral minor glands are rarely affected. The tumor usually presents as a long-standing, firm mass with a history of recent more rapid growth. There may be pain or facial nerve palsy, and nearly half of cases have regional lymphadenopathy. In Mongolian populations and in Inuits, there is a consistent association with Epstein-Barr virus (EBV), but this is rarely seen in Caucasian patients.

The tumor forms a solid, firm mass that ranges from 1 to 10 cm. It can be circumscribed and lobulated but often extensively infiltrates the surrounding soft tissues. LEC forms sheets, cords, and nests of tumor cells in a dense lymphoid stroma. The carcinoma cells are usually large and polygonal with faintly eosinophilic, abundant cytoplasm and indistinct cell borders (Fig. 13.110). This often produces a syncytial appearance. Occasionally, plumper or spindle-shaped cells are present. The nuclei are round or oval and have vesicular chromatin and conspicuous nucleoli. Extreme nuclear pleomorphism is rarely conspicuous. There is usually a high mitotic rate, and focal necrosis is common. Foci of squamous differentiation are infrequent. Some tumors show evidence of neural and lymphovascular invasion. The stroma consists

of a dense lymphoid infiltrate with smaller numbers of plasma cells. This infiltrate may be so dense that it can initially mask the underlying malignant component. Lymphocytes surround and permeate the tumor islands. Germinal centers are an inconsistent feature. Many tumors show pale, reactive histiocytes imparting a “starry sky” appearance. In some cases, the surrounding salivary parenchyma can show evidence of LESA. LEC cells are positive for pan-cytokeratin and EMA. There is increased expression of p53 and a high Ki-67 proliferative index. The lymphoid component is polyclonal and consists of B and T cells, with the latter predominating. CD4<sup>+</sup> T cells are prominent in the stroma and CD8<sup>+</sup> T cells predominate in the epithelial islands. EBV-encoded small RNA (EBER) can usually be detected by in situ hybridization in the carcinoma cells of endemic cases.

The differential diagnosis includes metastatic *nasopharyngeal carcinoma*, *LESA*, *large cell undifferentiated carcinoma*, and *lymphoma*. In endemic populations, it may not be possible to exclude metastatic nasopharyngeal carcinoma of the lymphoepithelial type on the basis of morphology, immunocytochemistry, or virology.

Locoregional lymph node metastasis is common (40 %), and about 20 % of cases show distant metastases. Despite this, the 5-year survival rate is about 60 % to 80 %. Most cases are treated with a combination of local radical

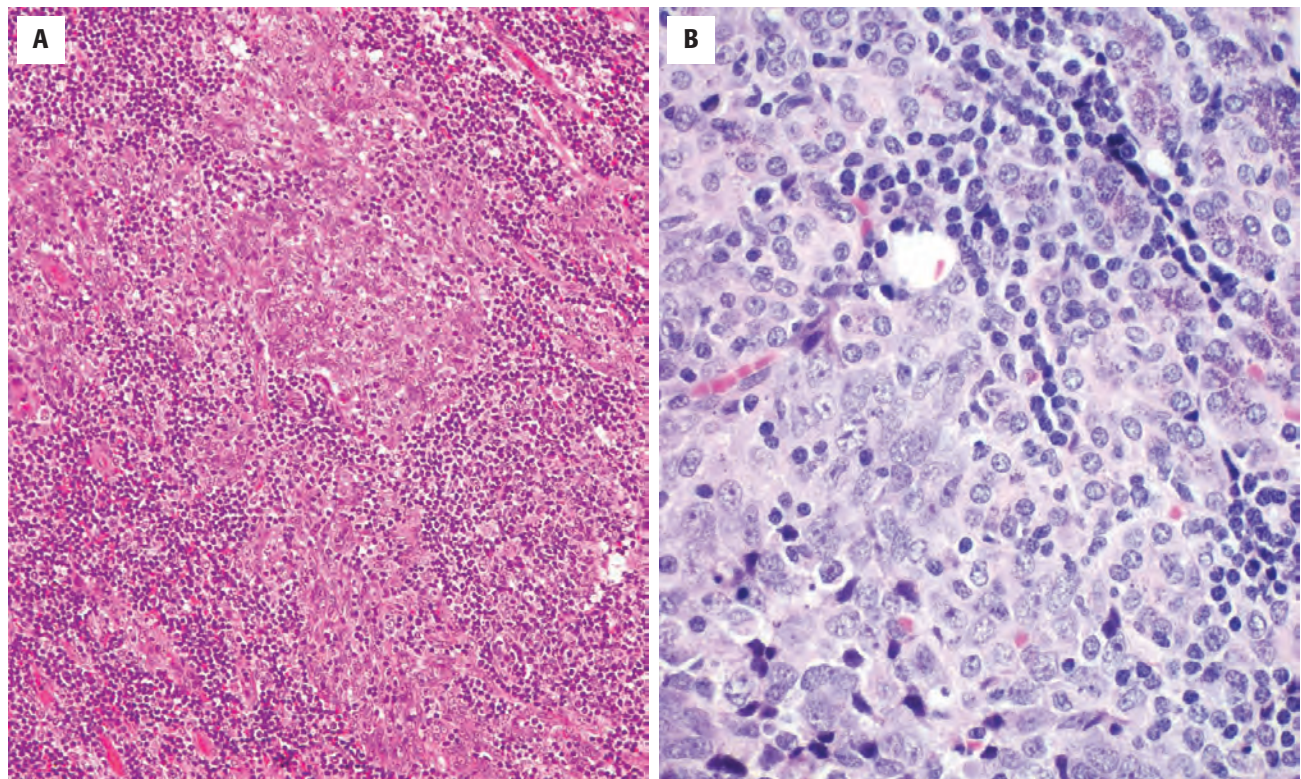


**FIGURE 13.110**

(A) Lymphoepithelial carcinoma showing islands of epithelial cells surrounded and infiltrated by lymphocytes. (B) The cells have a syncytial arrangement with prominent nucleoli identified in nuclei with vesicular nuclear chromatin. Note the heavy inflammatory infiltrate.

surgical excision and adjuvant radiotherapy to the surgical site and ipsilateral neck. Elective neck dissection is usually limited to patients with proven cervical metastases.

## ■ ADENOCARCINOMA, NOT OTHERWISE SPECIFIED

### CLINICAL FEATURES

Adenocarcinoma not otherwise specified (AC [NOS]) is a diagnosis of exclusion; the variable reporting of these tumors makes the interpretation of published data difficult. There is a slight female preponderance, and the peak age incidence is in the 6th decade. It is rare in children. About 60% arise in the major glands, predominantly the parotid. Common intraoral sites are the junction of the hard and soft palates, buccal mucosa, and lips. The tumor usually presents as a slow-growing, painless mass of 1- to 10-year duration. Tumors involving minor glands may ulcerate and extend into underlying bone.

#### ADENOCARCINOMA, NOT OTHERWISE SPECIFIED—DISEASE FACT SHEET

##### Definition

- Adenocarcinoma not otherwise specified is a malignant salivary gland tumor that shows ductal differentiation but lacks the histomorphologic features that characterize other specific types of salivary gland carcinoma

##### Incidence and Location

- Uncertain
- May involve major and minor glands

##### Morbidity and Mortality

- 15-year survival rate of 54%-3%, depending on grade (low grade to high grade)

##### Sex and Age Distribution

- Slight female predominance
- Peak incidence in the 6th decade
- Very rare in children

##### Clinical Features

- Usually forms a slow-growing mass
- Pain or facial nerve involvement in 20% of cases
- Tumors of minor glands may ulcerate and involve underlying bone

##### Prognosis and Therapy

- Prognostic factors include tumor grading, stage, and location
- Tumors in minor glands have a better prognosis than those in major glands
- Surgery is treatment of choice, with radiotherapy and neck dissection in advanced or recurrent cases

### PATHOLOGIC FEATURES

#### GROSS FINDINGS

The tumor is well defined or has an irregular, infiltrative margin. There may be areas of intratumoral hemorrhage and necrosis.

#### MICROSCOPIC FINDINGS

AC (NOS) shows duct-like structures with evidence of an infiltrative growth pattern (Fig. 13.111). By definition, it lacks the characteristic features of more specific tumor types. There is wide variability in growth patterns, which can include ductal configurations, thèques, sheets, and trabeculae (Fig. 13.111).

Cytologic variability can be used to grade these tumors into low-, intermediate-, and high-grade types. In most tumors, the cells are cuboidal or oval; in low-grade AC (NOS), there is minimal cytologic atypia and infrequent mitotic figures. Ductal differentiation is typically a conspicuous feature of these tumors. Intermediate- and high-grade tumors show increasing cellular pleomorphism with hyperchromatism, a high nuclear-to-cytoplasmic ratio, frequent and abnormal mitoses, and foci of hemorrhage and necrosis (Figs. 13.112 and 13.113). The stroma is often fibrous and cellular in low-grade tumors but more scanty in higher-grade tumors, which often have a solid growth pattern with minimal ductal differentiation. There may be evidence of lymphovascular and nerve involvement.

#### ADENOCARCINOMA NOT OTHERWISE SPECIFIED—PATHOLOGIC FEATURES

##### Gross Findings

- Well defined or shows irregular outline
- Hemorrhage and necrosis common in high-grade tumors

##### Microscopic Findings

- Duct-like structures with infiltrative growth
- Patterns include ducts, thèques, sheets, and trabeculae
- Cytologic variability used to grade the tumors into low-, intermediate-, and high-grade types
- Perineural and lymphovascular invasion may be seen

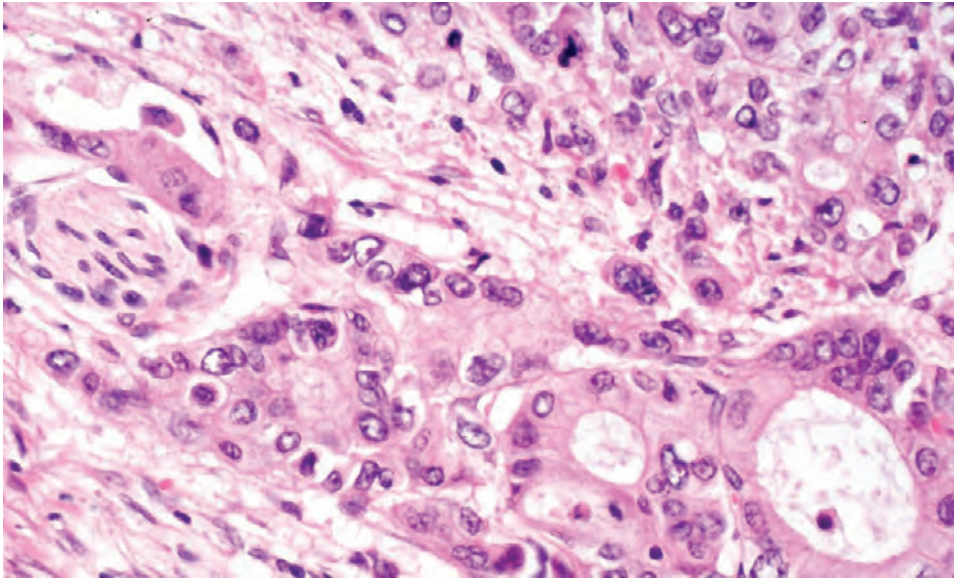
##### Fine Needle Aspiration

- Cellular smears with loose cohesion
- Features of malignancy include cytologic variability, nuclear pleomorphism, and occasional mucous cells

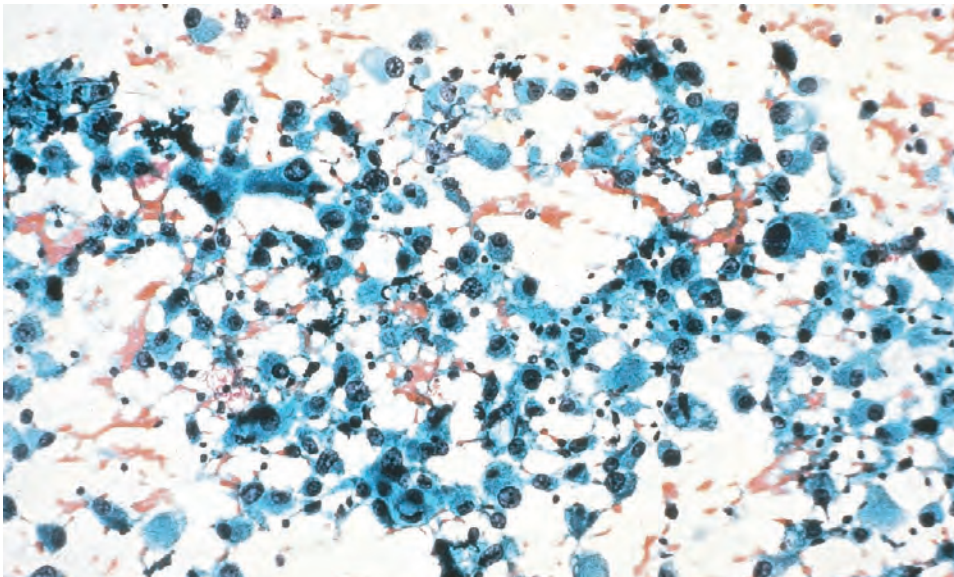
##### Pathologic Differential Diagnosis

- Diagnosis of exclusion, metastatic adenocarcinoma, undifferentiated carcinoma

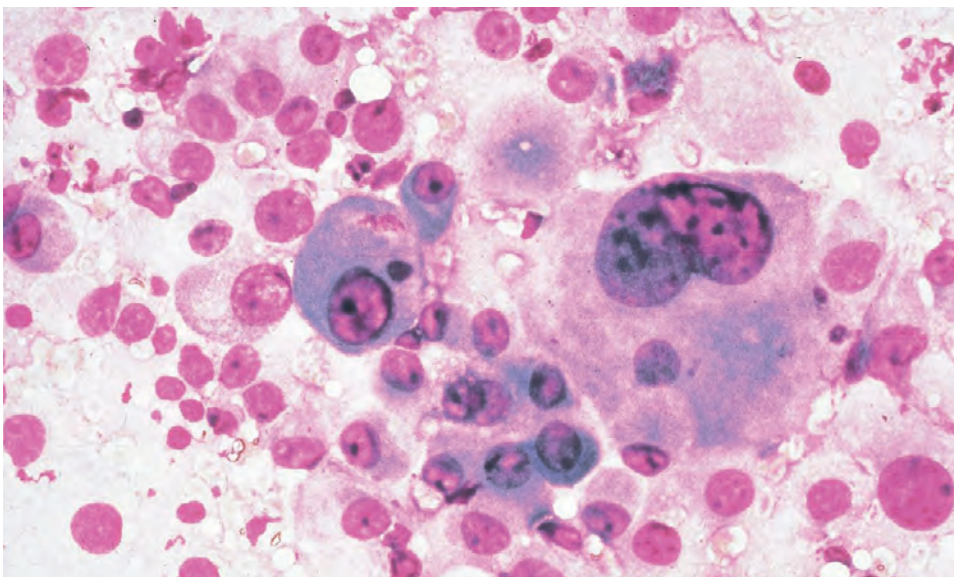


**FIGURE 13.111**

A high-grade adenocarcinoma, NOS shows glandular profiles with perineural invasion (*far left*). Mitotic figures are easily identified.

**FIGURE 13.112**

Highly cellular smear with slight dyscohesion of cells with a high nuclear-to-cytoplasmic ratio and focal mucin production (alcohol-fixed, Papanicolaou stain).

**FIGURE 13.113**

High power shows profound nuclear pleomorphism, confirming a high-grade malignancy but no specific tumor type in this fine needle aspiration smear (air-dried, Diff-Quik stain).

## ANCILLARY STUDIES

### IMMUNOHISTOCHEMICAL FINDINGS

There are no characteristic immunohistochemical findings.

### FINE NEEDLE ASPIRATION

The aspirates of AC (NOS) are often diagnosed as “salivary gland neoplasm,” covering a wide variety of tumors. Salivary gland tumors often have variable patterns within the same tumor, making FNA smears difficult to interpret. However, separation into benign and malignant tumors can usually be accomplished, with a low- versus high-grade designation. Cellular features of malignancy, remarkable cytologic variability, vague glandular differentiation, and rare mucin production may help in establishing a high-grade neoplasm, with definitive classification reserved for the surgical specimen (Figs. 13.112 and 13.113).

## DIFFERENTIAL DIAGNOSIS

The diagnosis of AC (NOS) is based on the exclusion of other specific tumor types. Metastatic disease must always

be considered. Evidence of ductal differentiation aids in the distinction from undifferentiated carcinoma.

## PROGNOSIS AND THERAPY

Variability in the criteria used to define these tumors makes the determination of prognostic factors and assessment of outcome problematic. Prognostic factors include tumor grading, clinical stage, and location. Tumors in minor glands have a better prognosis than those in major glands. In the largest survey of this tumor, the 15-year survival rates for low-, intermediate-, and high-grade tumors were 54 %, 31 %, and 3 %, respectively. Tumors of low grade and stage are treated with complete surgical excision; in higher-grade tumors, neck dissection and adjuvant radiotherapy must be considered.

## SUGGESTED READINGS

The complete Suggested Readings list is available online at [ExpertConsult.com](http://ExpertConsult.com).



**SUGGESTED READINGS****Mucoepidermoid Carcinoma**

1. Auclair PL, et al. Mucoepidermoid carcinoma of intraoral salivary glands. Evaluation and application of grading criteria in 143 cases. *Cancer*. 1992;69:2021–2030.
2. Boahene DK, et al. Mucoepidermoid carcinoma of the parotid gland: the Mayo Clinic experience. *Arch Otolaryngol Head Neck Surg*. 2004;130:849–856.
3. Brandwein MS, et al. Mucoepidermoid carcinoma: a clinicopathologic study of 80 patients with special reference to histological grading. *Am J Surg Pathol*. 2001;25:835–845.
4. Brandwein-Gensler M, et al. Mucoepidermoid carcinoma. In: El-Naggar AK, Chan JKC, Grandis JR, Takata T, Slootweg PJ, eds. *Classification of Head and Neck Tumours*. 4th ed. World Health Organization Classification of Tumours. Lyon, France: IARC Press; 2017:163–164.
5. Chenvert J, et al. Mucoepidermoid carcinoma: a five-decade journey. *Virchows Arch*. 2011;458:133–140.
6. Ellis GL. Clear cell neoplasms in salivary glands: clearly a diagnostic challenge. *Ann Diagn Pathol*. 1998;2:61–78.
7. Fadare O, et al. Sclerosing mucoepidermoid carcinoma of the parotid gland. *Arch Pathol Lab Med*. 2004;128:1046–1049.
8. Fujimaki M, et al. Oncocytic mucoepidermoid carcinoma of the parotid gland with CRTC-MAML2 fusion transcript: report of a case and review of literature. *Hum Pathol*. 2011;42:2052–2055.
9. Goode RK, et al. Mucoepidermoid carcinoma of the major salivary glands: clinical and histopathologic analysis of 234 cases with evaluation of grading criteria. *Cancer*. 1998;82:1217–1224.
10. Guzzo M, et al. Mucoepidermoid carcinoma of the salivary glands: clinicopathologic review of 108 patients treated at the National Cancer Institute of Milan. *Ann Surg Oncol*. 2002;9:688–695.
11. Luna MA. Salivary mucoepidermoid carcinoma: revisited. *Adv Anat Pathol*. 2006;13:293–307.
12. Mendelson AA, et al. Sclerosing mucoepidermoid of the salivary gland: case report and literature review. *Ear Nose Throat J*. 2010;89:600–603.
13. Nagao T, et al. Dedifferentiation in low-grade mucoepidermoid carcinoma of the parotid gland. *Hum Pathol*. 2003;34:1068–1072.
14. Saade RE, et al. Role of CRTC1/MAML2 translocation in the prognosis and clinical outcomes of mucoepidermoid carcinoma. *JAMA Otolaryngol Head Neck Surg*. 2016;142(3):234–240.
15. Seethala RR. Histologic grading and prognostic biomarkers in salivary gland carcinomas. *Adv Anat Pathol*. 2011;18:29–49.
16. Seethala RR, et al. A reappraisal of the MECT1/MAML2 translocation in salivary mucoepidermoid carcinoma. *Am J Surg Pathol*. 2010;34:1106–1121.
17. Urano M, et al. Sclerosing mucoepidermoid carcinoma with eosinophilia of the salivary glands. *Pathol Res Pract*. 2002;198:305–310.

**Acinic Cell Carcinoma**

1. Bishop JA, et al. Most nonparotid "acinic cell carcinomas" represent mammary analog secretory carcinomas. *Am J Surg Pathol*. 2013;37(7):1053–1057.
2. Chênevert J, et al. DOG1: a novel marker of salivary acinar and intercalated duct differentiation. *Mod Pathol*. 2012;25(7):919–929.
3. Chiosea SI, et al. The profile of acinic cell carcinoma after recognition of mammary analog secretory carcinoma. *Am J Surg Pathol*. 2012;36(3):343–350.
4. Colmenero C, et al. Acinic cell carcinoma of the salivary glands. A review of 20 new cases. *J Craniomaxillofac Surg*. 1991;19:260–266.
5. Ellis GL, et al. Acinic cell adenocarcinoma. A clinicopathologic analysis of 294 cases.
6. Hellquist HB, et al. Tumour growth fraction and apoptosis in salivary gland acinic cell carcinomas. Prognostic implications of Ki-67 and bcl-2 expression and of in situ end labelling (TUNEL). *J Pathol*. 1997;181:323–329.
7. Ihrler S, et al. Differential diagnosis of salivary acinic cell carcinoma and adenocarcinoma (NOS). A comparison of (immuno-) histochemical markers. *Pathol Res Pract*. 2002;198:777–783.
8. Michal M, et al. Well-differentiated acinic cell carcinoma of salivary glands associated with lymphoid stroma. *Hum Pathol*. 1997;28:595–600.

9. Omlie JE, et al. Acinic cell carcinoma of minor glands: a clinicopathologic study of 21 cases. *J Oral Maxillofac Surg*. 2010;68:2053–2057.
10. Simpson RHW, et al. Acinic cell carcinoma. In: El-Naggar AK, Chan JKC, Grandis JR, Takata T, Slootweg PJ, eds. *Classification of Head and Neck Tumours*. 4th ed. World Health Organization Classification of Tumours. Lyon, France: IARC Press; 2017:166–167.
11. Thompson LD. Salivary gland acinic cell carcinoma. *Ear Nose Throat J*. 2010;89:530–532.
12. Thompson LD, et al. Clinicopathologic and immunophenotypic characterization of 25 cases of acinic cell carcinoma with high-grade transformation. *Head Neck Pathol*. 2016;10(2):152–160.
13. Vander Poorten V, et al. Salivary acinic cell carcinoma: reappraisal and update. *Eur Arch Otorhinolaryngol*. 2016;273(11):3511–3531.

**Adenoid Cystic Carcinoma**

1. Barrett AW, et al. Perineural invasion in adenoid cystic carcinoma of the salivary glands: a valid prognostic indicator? *Oral Oncol*. 2009;45:936–940.
2. Bishop JA, et al. Human papillomavirus-related carcinoma with adenoid cystic-like features: a peculiar variant of head and neck cancer restricted to the sinonasal tract. *Am J Surg Pathol*. 2013;37(6):836–844.
3. Bradley PJ. Adenoid cystic carcinoma of the head and neck: a review. *Curr Opin Otolaryngol Head Neck Surg*. 2004;12:127–132.
4. Edwards PC, et al. C-kit expression in the salivary gland neoplasms adenoid cystic carcinoma, polymorphous low-grade adenocarcinoma, and monomorphic adenoma. *Oral Surg Oral Med Oral Pathol Oral Radiol Endod*. 2003;95:586–593.
5. Garden AS, et al. The influence of positive margins and nerve invasion in adenoid cystic carcinoma of the head and neck treated with surgery and radiation. *Int J Radiat Oncol Biol Phys*. 1995;32:619–626.
6. Gondivkar SM, et al. Adenoid cystic carcinoma: a rare clinical entity and literature review. *Oral Oncol*. 2011;47:231–236.
7. Hamper K, et al. Prognostic factors for adenoid cystic carcinoma of the head and neck: a retrospective evaluation of 96 cases. *J Oral Pathol Med*. 1990;19:101–107.
8. Ho AS, et al. The mutational landscape of adenoid cystic carcinoma. *Nat Genet*. 2013;45(7):791–798.
9. Martins C, et al. Cytogenetic similarities between two types of salivary gland carcinomas: adenoid cystic carcinoma and polymorphous low-grade adenocarcinoma. *Cancer Genet Cytogenet*. 2001;128:130–136.
10. Rettig EM, et al. MYB rearrangement and clinicopathologic characteristics in head and neck adenoid cystic carcinoma. *Laryngoscope*. 2015;125(9):E292–E299.
11. Rettig EM, et al. Whole-Genome Sequencing of Salivary Gland Adenoid Cystic Carcinoma. *Cancer Prev Res (Phila)*. 2016;9(4):265–274.
12. Seethala RR, et al. Adenoid cystic carcinoma with high-grade transformation: a report of 11 cases and review of the literature. *Am J Surg Pathol*. 2007;31:1683–1694.
13. Seethala RR, et al. Progressive genetic alterations of adenoid cystic carcinoma with high-grade transformation. *Arch Pathol Lab Med*. 2011;135:123–130.
14. Spiro RH. Distant metastasis in adenoid cystic carcinoma of salivary origin. *Am J Surg*. 1997;174:495–498.
15. Spiro RH, et al. Stage means more than grade in adenoid cystic carcinoma. *Am J Surg*. 1992;164:623–628.
16. Stenman G, et al. Adenoid cystic carcinoma. In: El-Naggar AK, et al, eds. *Classification of Head and Neck Tumours*. 4th ed. World Health Organization Classification of Tumours. Lyon, France: IARC Press; 2017:164–165.

**Polymorphous Adenocarcinoma**

1. Castle JT, et al. Polymorphous low grade adenocarcinoma: a clinicopathologic study of 164 cases. *Cancer*. 1999;86:207–219.
2. Clarke BA, et al. Novel PRKD gene rearrangements and variant fusions in cribriform adenocarcinoma of salivary gland origin. *Genes Chromosomes Cancer*. 2014;53(10):845–856.

3. Curran AE, et al. Polymorphous low-grade adenocarcinoma versus pleomorphic adenoma of minor salivary glands: resolution of a diagnostic dilemma by immunohistochemical analysis with glial fibrillary acidic protein. *Oral Surg Oral Med Oral Pathol Oral Radiol Endod.* 2001;91:194–199.
4. Darling MR, et al. Polymorphous low-grade adenocarcinoma and adenoid cystic carcinoma: a review and comparison of immunohistochemical markers. *Oral Oncol.* 2002;38:641–645.
5. El-Naaj IA, et al. Polymorphous low grade adenocarcinoma: case series and review of surgical management. *J Oral Maxillofac Surg.* 2011;69:1967–1972.
6. Evans HL, et al. Polymorphous low-grade adenocarcinoma: a study of 40 cases with long-term follow up and an evaluation of the importance of papillary areas. *Am J Surg Pathol.* 2000;24:1319–1328.
7. Fonseca I, et al. Polymorphous adenocarcinoma. In: El-Naggar AK, Chan JKC, Grandis JR, Takata T, Slootweg PJ, eds. *Classification of Head and Neck Tumours*. 4th ed. World Health Organization Classification of Tumours. Lyon, France: IARC Press; 2017:167–168.
8. Kumar M, et al. Polymorphous low-grade adenocarcinoma—a rare and aggressive entity in adolescence. *Br J Oral Maxillofac Surg.* 2004;42:195–199.
9. Nagao T, et al. Polymorphous low-grade adenocarcinoma of the major salivary glands: report of three cases in an unusual location. *Histopathology.* 2004;44:164–171.
10. Penner CR, et al. C-kit expression distinguishes salivary gland adenoid cystic carcinoma from polymorphous low-grade adenocarcinoma. *Mod Pathol.* 2002;15:687–691.
11. Rooper LM, et al. Polymorphous low grade adenocarcinoma has a consistent p63+/p40- immunophenotype that helps distinguish it from adenoid cystic carcinoma and cellular pleomorphic adenoma. *Head Neck Pathol.* 2015;9(1):79–84.
12. Seethala RR, et al. Polymorphous low-grade adenocarcinoma: the University of Pittsburgh experience. *Arch Otolaryngol Head Neck Surg.* 2010;136:385–392.
13. Skalova A, et al. Cribriform adenocarcinoma of minor salivary gland origin principally affecting the tongue: characterization of new entity. *Am J Surg Pathol.* 2011;35:1168–1176.
14. Weinreb I, et al. Hotspot activating PRKD1 somatic mutations in polymorphous low-grade adenocarcinomas of the salivary glands. *Nat Genet.* 2014;46(11):1166–1169.

### Epithelial-Myoepithelial Carcinoma

1. Chiosea SI, et al. HRAS mutations in epithelial-myoepithelial carcinoma. *Head Neck Pathol.* 2014;8(2):146–150.
2. Cho KJ, et al. Epithelial-myoepithelial carcinoma of salivary glands. A clinicopathologic, DNA flow cytometric, and immunohistochemical study of Ki-67 and HER-2/neu oncogene. *Am J Clin Pathol.* 1995;103:432–437.
3. Fonseca I, et al. Epithelial-myoepithelial carcinoma of the salivary glands. A study of 22 cases. *Virchows Arch A Pathol Anat Histopathol.* 1993;422:389–396.
4. Fonseca I, et al. Dedifferentiation in salivary gland carcinomas. *Am J Surg Pathol.* 2000;24:469–471.
5. Nagao T, et al. Hybrid carcinomas of the salivary glands: report of nine cases with a clinicopathologic, immunohistochemical, and p53 gene alteration analysis. *Mod Pathol.* 2002;15:724–733.
6. Roy P, et al. Epithelial-myoepithelial carcinoma with high grade transformation. *Am J Surg Pathol.* 2010;34:1258–1265.
7. Seethala RR, et al. Epithelial-myoepithelial carcinoma: a review of the clinicopathologic spectrum and immunophenotypic characteristics in 61 tumors of the salivary glands and upper aerodigestive tract. *Am J Surg Pathol.* 2007;31:44–57.
8. Seethala RR, et al. New variants of epithelial-myoepithelial carcinoma: oncocytic-sebaceous and apocrine. *Arch Pathol Lab Med.* 2009;133:950–959.
9. Seethala RR, et al. Epithelial-myoepithelial carcinoma. In: El-Naggar AK, Chan JKC, Grandis JR, Takata T, Slootweg PJ, eds. *Classification of Head and Neck Tumours*. 4th ed. World Health Organization Classification of Tumours. Lyon, France: IARC Press; 2017:175–176.
10. Tralongo V, et al. Epithelial-myoepithelial carcinoma of the salivary glands: a review of literature. *Anticancer Res.* 1998;18:603–608.
11. Wang B, et al. Primary salivary clear cell tumors—a diagnostic approach: a clinicopathologic and immunohistochemical study of 20 patients with clear cell carcinoma, clear cell myoepithelial carcinoma, and epithelial-myoepithelial carcinoma. *Arch Pathol Lab Med.* 2002;126:676–685.

### Secretory Carcinoma

1. Bishop JA. Unmasking MASC: bringing to light the unique morphologic, immunohistochemical and genetic features of the newly recognized mammary analogue secretory carcinoma of salivary glands. *Head Neck Pathol.* 2013;7(1):35–39.
2. Bishop JA, et al. Most nonparotid "acinic cell carcinomas" represent mammary analog secretory carcinomas. *Am J Surg Pathol.* 2013;37(7):1053–1057.
3. Bishop JA, et al. Cytopathologic features of mammary analogue secretory carcinoma. *Cancer Cytopathol.* 2013;121(5):228–233.
4. Bishop JA, et al. Utility of mammaglobin immunohistochemistry as a proxy marker for the ETV6-NTRK3 translocation in the diagnosis of salivary mammary analogue secretory carcinoma. *Hum Pathol.* 2013;44(10):1982–1988.
5. Bishop JA, et al. Secretory carcinoma of the skin harboring ETV6 gene fusions: a cutaneous analogue to secretory carcinomas of the breast and salivary glands. *Am J Surg Pathol.* 2017;41(1):62–66.
6. Chiosea SI, et al. Clinicopathological characterization of mammary analogue secretory carcinoma of salivary glands. *Histopathology.* 2012;61(3):387–394.
7. Dettloff J, et al. Mammary analog secretory carcinoma (MASC) involving the thyroid gland: a report of the first 3 cases. *Head Neck Pathol.* 2017;11(2):124–130.
8. Dogan S, et al. Mammary analog secretory carcinoma of the thyroid gland: a primary thyroid adenocarcinoma harboring ETV6-NTRK3 fusion. *Mod Pathol.* 2016;29(9):985–995.
9. Griffith CC, et al. The cytological features of mammary analogue secretory carcinoma: a series of 6 molecularly confirmed cases. *Cancer Cytopathol.* 2013;121(5):234–241.
10. Schwartz LE, et al. GATA3 immunohistochemical expression in salivary gland neoplasms. *Head Neck Pathol.* 2013;7(4):311–315.
11. Skalova A. Mammary analogue secretory carcinoma of salivary gland origin: an update and expanded morphologic and immunohistochemical spectrum of recently described entity. *Head Neck Pathol.* 2013;7(suppl 1):S30–S36.
12. Skálová A, et al. Mammary analogue secretory carcinoma of salivary glands, containing the ETV6-NTRK3 fusion gene: a hitherto undescribed salivary gland tumor entity. *Am J Surg Pathol.* 2010;34(5):599–608.
13. Skálová A, et al. Mammary analogue secretory carcinoma of salivary glands with high-grade transformation: report of 3 cases with the ETV6-NTRK3 gene fusion and analysis of TP53,  $\beta$ -catenin, EGFR, and CCND1 genes. *Am J Surg Pathol.* 2014;38(1):23–33.
14. Skalova A, et al. Secretory carcinoma. In: El-Naggar AK, Chan JKC, Grandis JR, Takata T, Slootweg PJ, eds. *Classification of Head and Neck Tumours*. 4th ed. World Health Organization Classification of Tumours. Lyon, France: IARC Press; 2017:177–178.

### Salivary Duct Carcinoma

1. Barnes L, et al. Salivary duct carcinoma. Part I. A clinicopathologic evaluation and DNA image analysis of 13 cases with review of the literature. *Oral Surg Oral Med Oral Pathol.* 1994;78:64–73.
2. Cheuk W, et al. Advances in salivary gland pathology. *Histopathology.* 2007;51:1–20.
3. Chiosea SI, et al. Subsets of salivary duct carcinoma defined by morphologic evidence of pleomorphic adenoma, PLAG1 or HMGA2 rearrangements, and common genetic alterations. *Cancer.* 2016;122(20):3136–3144.
4. Etges A, et al. Salivary duct carcinoma: immunohistochemical profile of an aggressive salivary gland tumour. *J Clin Pathol.* 2003;56:914–918.
5. Fan CY, et al. Expression of androgen receptor and prostatic specific markers in salivary duct carcinoma: an immunohistochemical analysis of 13 cases and review of the literature. *Am J Surg Pathol.* 2000;24:579–586.



6. Griffith CC, et al. Salivary duct carcinoma and the concept of early carcinoma ex pleomorphic adenoma. *Histopathology*. 2014;65(6):854–860.
7. Hungermann D, et al. Salivary duct carcinomas comprise phenotypically and genotypically diverse high-grade neoplasms. *Histopathology*. 2007;50:956–958.
8. Johnson CJ, et al. Her-2/neu expression in salivary duct carcinoma: an immunohistochemical and chromogenic in situ hybridization study. *Appl Immunohistochem Mol Morphol*. 2008;16:54–58.
9. Nabili V, et al. Salivary duct carcinoma: a clinical and histologic review with implications for trastuzumab therapy. *Head Neck*. 2007;29:907–912.
10. Nagao T, et al. Invasive micropapillary salivary duct carcinoma: a distinct histologic variant with biologic significance. *Am J Surg Pathol*. 2004;28:319–326.
11. Nagao T, et al. Sarcomatoid variant of salivary duct carcinoma: clinicopathologic and immunohistochemical study of eight cases with review of the literature. *Am J Clin Pathol*. 2004;122:222–231.
12. Nagao T, et al. Salivary duct carcinoma. In: El-Naggar AK, Chan JKC, Grandis JR, Takata T, Slootweg PJ, eds. *Classification of Head and Neck Tumours*. 4th ed. World Health Organization Classification of Tumours. Lyon, France: IARC Press; 2017:173–174.
13. Schwartz LE, et al. GATA3 immunohistochemical expression in salivary gland neoplasms. *Head Neck Pathol*. 2013;7(4):311–315.
14. Simpson RH, et al. Mucin-rich variant of salivary duct carcinoma: a clinicopathologic and immunohistochemical study of four cases. *Am J Surg Pathol*. 2003;27:1070–1079.
15. Simpson RH, et al. Salivary duct carcinoma in situ of parotid gland. *Histopathology*. 2008;53:416–425.
16. Skalova A, et al. Expression of HER-2/neu gene and protein in salivary duct carcinomas of parotid gland as revealed by fluorescence in-situ hybridization and immunohistochemistry. *Histopathology*. 2003;42:348–356.
17. Williams MD, et al. Differential expression of hormonal and growth factor receptors in salivary duct carcinomas: biologic significance and potential role in therapeutic stratification of patients. *Am J Surg Pathol*. 2007;31:1645–1652.
18. Williams MD, et al. Genetic and expression analysis of HER-2 and EGFR genes in salivary duct carcinoma: empirical and therapeutic significance. *Clin Cancer Res*. 2010;16:2266–2274.
19. Williams L, et al. Salivary duct carcinoma: the predominance of apocrine morphology, prevalence of histologic variants, and androgen receptor expression. *Am J Surg Pathol*. 2015;39(5):705–713.
20. Tortoledo ME, et al. Carcinomas ex pleomorphic adenoma and malignant mixed tumors. Histomorphologic indexes. *Arch Otolaryngol*. 1984;110:172–176.
21. Williams MD, et al. Carcinoma ex pleomorphic adenoma. In: El-Naggar AK, Chan JKC, Grandis JR, Takata T, Slootweg PJ, eds. *Classification of Head and Neck Tumours*. 4th ed. World Health Organization Classification of Tumours. Lyon, France: IARC Press; 2017:176–177.

### Extranodal Marginal Zone B-Cell Lymphoma of Salivary Glands

1. Anaya JM, et al. Clinicopathological factors relating to malignant lymphoma in Sjögren's syndrome. *Semin Arthritis Rheum*. 1996;25:337–346.
2. Cheuk W, et al. Extranodal marginal zone lymphoma of mucosa associated lymphoid tissue (MALT lymphoma). In: El-Naggar AK, Chan JKC, Grandis JR, Takata T, Slootweg PJ, eds. *Classification of Head and Neck Tumours*. 4th ed. World Health Organization Classification of Tumours. Lyon, France: IARC Press; 2017:201–202.
3. Ellis GL. Lymphoid lesions of salivary glands: malignant and benign. *Med Oral Patol Oral Cir Bucal*. 2007;12:E479–E485.
4. Isaacson PG, et al. Malignant lymphoma of the salivary gland. In: Isaacson PG, Norton AJ, eds. *Extranodal Lymphomas*. New York: Churchill Livingstone; 1994.
5. Jaffe ES, et al. *Pathology and Genetics of Tumors of Haemopoietic and Lymphoid Tissues*. Lyon (France): IARC Press; 2001.
6. Masaki Y, et al. Lymphoproliferative disorders in Sjögren's syndrome. *Autoimmun Rev*. 2004;3:175–182.
7. Quintana PG, et al. Salivary gland lymphoid infiltrates associated with lymphoepithelial lesions: a clinicopathologic, immunophenotypic, and genotypic study. *Hum Pathol*. 1997;28:850–861.
8. Royer B, et al. Lymphomas in patients with Sjögren's syndrome are marginal zone B-cell neoplasms, arise in diverse extranodal sites, and are not associated with viruses. *Blood*. 1997;90:766–777.
9. Voulgarelis M, et al. Mucosa associated lymphoid tissue lymphoma in Sjögren's syndrome: risks, management, and prognosis. *Rheum Dis Clin North Am*. 2008;34:291–293.

### Sialoblastoma

1. Adkins GF. Low grade basaloid adenocarcinoma of salivary gland in childhood—the so-called hybrid basal cell adenoma—adenoid cystic carcinoma. *Pathology*. 1990;22:187–190.
2. Alvarez-Mendoza A, et al. Diagnostic and therapeutic approach to sialoblastoma: report of a case. *J Pediatr Surg*. 1999;34:1875–1877.
3. Batsakis JG, et al. Embryoma (sialoblastoma) of salivary glands. *Ann Otol Rhinol Laryngol*. 1992;101:958–960.
4. Brandwein M, et al. Sialoblastoma: clinicopathological/immunohistochemical study. *Am J Surg Pathol*. 1999;23:342–348.
5. Brandwein-Gensler M, et al. Sialoblastoma. In: El-Naggar AK, Chan JKC, Grandis JR, Takata T, Slootweg PJ, eds. *Classification of Head and Neck Tumours*. 4th ed. World Health Organization Classification of Tumours. Lyon, France: IARC Press; 2017:183–184.
6. Dardick I, et al. Sialoblastoma in adults: distinction from adenoid cystic carcinoma. *Oral Surg Oral Med Oral Pathol Oral Radiol Endod*. 2010;109:109–116.
7. Luna MA. Sialoblastoma and epithelial tumors in children: their morphologic spectrum and distribution by age. *Adv Anat Pathol*. 1999;6:287–292.
8. Ozdemir I, et al. Congenital sialoblastoma (embryoma) associated with premature centromere division and high level of alpha-fetoprotein. *Prenat Diagn*. 2005;25:687–689.
9. Patil DT, et al. Sialoblastoma: utility of Ki-67 and p53 as a prognostic tool and review of literature. *Pediatr Dev Pathol*. 2010;13:32–38.
10. Prigent M, et al. Sialoblastoma of salivary glands in children: chemotherapy should be discussed as an alternative to mutilating surgery. *Int J Pediatr Otorhinolaryngol*. 2010;74:942–945.
11. Seifert G, et al. The congenital basal cell adenoma of salivary glands. Contribution to the differential diagnosis of congenital salivary gland tumours. *Virchows Arch*. 1997;430:311–319.
12. Simpson PR, et al. Congenital hybrid basal cell adenoma—adenoid cystic carcinoma of the salivary gland. *Pediatr Pathol*. 1986;6:199–208.

### Carcinoma ex Pleomorphic Adenoma

1. Brandwein M, et al. Noninvasive and minimally invasive carcinoma ex mixed tumor: a clinicopathologic and ploidy study of 12 patients with major salivary tumors of low (or no?) malignant potential. *Oral Surg Oral Med Oral Pathol Oral Radiol Endod*. 1996;81:655–664.
2. Chiosea SI, et al. Subsets of salivary duct carcinoma defined by morphologic evidence of pleomorphic adenoma, PLAG1 or HMGA2 rearrangements, and common genetic alterations. *Cancer*. 2016;122(20):3136–3144.
3. Gnepp DR. Malignant mixed tumors of the salivary glands: a review. *Pathol Annu*. 1993;28(Pt 1):279–328.
4. Katabi N, et al. Prognostic factors of recurrence in carcinoma ex pleomorphic adenoma, with emphasis on the carcinoma histologic subtype: a clinicopathologic study of 43 cases. *Hum Pathol*. 2010;41:927–934.
5. Li S, et al. Worrisome histologic alterations following fine-needle aspiration of benign parotid lesions. *Arch Pathol Lab Med*. 2000;124:87–91.
6. LiVolsi VA, et al. Malignant mixed tumors arising in salivary glands. I. Carcinomas arising in benign mixed tumors: a clinicopathologic study. *Cancer*. 1977;39:2209–2230.
7. McHugh JB, et al. Update on selected salivary gland neoplasms. *Arch Pathol Lab Med*. 2009;113:1763–1764.
8. Olsen KD, et al. Carcinoma ex pleomorphic adenoma: a clinicopathologic review. *Head Neck*. 2001;23:705–712.
9. Rito M, et al. Carcinoma ex-pleomorphic adenoma of the salivary glands has a high risk of progression when the tumor invades more than 2.5 mm beyond the capsule of the residual pleomorphic adenoma. *Virchows Arch*. 2016;468(3):297–303.

13. Taylor GP. Congenital epithelial tumor of the parotid-sialoblastoma. *Pediatr Pathol.* 1988;8:447–452.
14. Verret DJ, et al. Sialoblastoma: a rare submandibular gland neoplasm. *Ear Nose Throat J.* 2006;85:440–442.
15. Williams SB, et al. Sialoblastoma: a clinicopathologic and immunohistochemical study of 7 cases. *Ann Diagn Pathol.* 2006;10:320–326.

### Uncommon Carcinomas

1. Antonescu CR, et al. EWSR1-ATF1 fusion is a novel and consistent finding in hyalinizing clear-cell carcinoma of salivary gland. *Genes Chromosomes Cancer.* 2011;50(7):559–570.
2. Brandwein MS, et al. Oncocytic tumors of salivary glands. A study of 68 cases with follow-up of 48 cases. *Am J Surg Pathol.* 1991;15:514–528.
3. Casani AP, et al. Clear cell adenocarcinoma of the base of the tongue: a case report and review of the literature. *Ear Nose Throat J.* 2011;90:E9–E16.
4. Dardick I, et al. Clear cell carcinoma: review of its histomorphogenesis and classification as a squamous cell lesion. *Oral Surg Oral Med Oral Pathol Oral Radiol Endod.* 2009;108:399–405.
5. Ellis GL, et al. Basal cell adenocarcinomas of the major salivary glands. *Oral Surg Oral Med Oral Pathol.* 1990;69:461–469.
6. Ellis GL, et al. Other malignant epithelial neoplasms. In: Ellis GL, Auclair PL, et al, eds. *Surgical Pathology of Salivary Glands.* Philadelphia: WB Saunders; 1991:455–488.
7. Fonseca I, et al. Basal cell adenocarcinoma. In: El-Naggar AK, Chan JKC, Grandis JR, Takata T, Slootweg PJ, eds. *Classification of Head and Neck Tumours.* 4th ed. World Health Organization Classification of Tumours. Lyon, France: IARC Press; 2017:169–170.
8. Gnepp DR. Sebaceous neoplasms of salivary gland origin: a review. *Pathol Annu.* 1983;18(Pt 1):71–102.
9. Gnepp DR, et al. Sebaceous adenocarcinoma. In: El-Naggar AK, Chan JKC, Grandis JR, Takata T, Slootweg PJ, eds. *Classification of Head and Neck Tumours.* 4th ed. World Health Organization Classification of Tumours. Lyon, France: IARC Press; 2017:178–179.
10. Ito K, et al. Benign and malignant oncocytoma of the salivary glands with an immunohistochemical evaluation of Ki-67. *ORL J Otorhinolaryngol Relat Spec.* 2000;62:338–341.
11. Nagao T, et al. Oncocytic carcinoma. In: El-Naggar AK, Chan JKC, Grandis JR, Takata T, Slootweg PJ, eds. *Classification of Head and Neck Tumours.* 4th ed. World Health Organization Classification of Tumours. Lyon, France: IARC Press; 2017:182–183.
12. O'Sullivan-Mejia ED, et al. Hyalinizing clear cell carcinoma: report of eight cases and review of literature. *Head Neck Pathol.* 2009;3:179–185.
13. Qudus MR, et al. Basal cell adenocarcinoma of the salivary gland: an ultrastructural and immunohistochemical study. *Oral Surg Oral Med Oral Pathol Oral Radiol Endod.* 1999;87:485–492.
14. Simpson RH, et al. Clear cell carcinoma of minor salivary glands. *Histopathology.* 1990;17:433–438.
15. Wang H, et al. Sebaceous carcinoma of the oral cavity: a case report and review of the literature. *Oral Surg Oral Med Oral Pathol Oral Radiol Endod.* 2010;110:e37–e40.
16. Weinreb I. Hyalinizing clear cell carcinoma of salivary gland: a review and update. *Head Neck Pathol.* 2013;7 Suppl 1:S20–S29.
17. Wenig BM, et al. Clear cell carcinoma. In: El-Naggar AK, Chan JKC, Grandis JR, Takata T, Slootweg PJ, eds. *Classification of Head and Neck Tumours.* 4th ed. World Health Organization Classification of Tumours. Lyon, France: IARC Press; 2017:168–169.
18. Zhou CX, et al. Primary oncocytic carcinoma of the salivary glands: a clinicopathologic and immunohistochemical study of 12 cases. *Oral Oncol.* 2010;46:773–778.
4. Chan JKC, et al. Specific association of Epstein-Barr virus with lymphoepithelial carcinoma among tumors and tumorlike lesions of the salivary gland. *Arch Pathol Lab Med.* 1994;118:994–997.
5. Chan JK, et al. Cytokeratin 20 immunoreactivity distinguishes Merkel cell (primary cutaneous neuroendocrine) carcinomas and salivary gland small cell carcinomas from small cell carcinomas of various sites. *Am J Surg Pathol.* 1997;21:226–234.
6. Cheuk W, et al. Immunostaining for thyroid transcription factor 1 and cytokeratin 20 aids the distinction of small cell carcinoma from Merkel cell carcinoma, but not pulmonary from extrapulmonary small cell carcinomas. *Arch Pathol Lab Med.* 2001;125:228–231.
7. Chiosea S, et al. Poorly differentiated carcinoma. In: El-Naggar AK, Chan JKC, Grandis JR, Takata T, Slootweg PJ, eds. *Classification of Head and Neck Tumours.* 4th ed. World Health Organization Classification of Tumours. Lyon, France: IARC Press; 2017:180–181.
8. de Vicente Rodríguez JC, et al. Small cell undifferentiated carcinoma of the submandibular gland with neuroendocrine features. *Ann Otol Rhinol Laryngol.* 2004;113:55–59.
9. Gnepp DR, et al. Small cell carcinoma of the major salivary glands: an immunohistochemical study. *Cancer.* 1990;66:185–192.
10. Gnepp DR, et al. Small cell carcinoma of the major salivary glands. *Cancer.* 1986;58:705–714.
11. Hamilton-Dutoit SJ, et al. Undifferentiated carcinoma of the salivary gland in Greenlandic Eskimos: demonstration of Epstein-Barr virus DNA by in situ nucleic acid hybridization. *Hum Pathol.* 1991;22:811–815.
12. Hayashi Y, et al. Undifferentiated carcinoma of the parotid gland with bizarre giant cells: clinicopathologic report with ultrastructural study. *Acta Pathol Jpn.* 1983;33:169–176.
13. Hui KK, et al. Undifferentiated carcinoma of the major salivary glands. *Oral Surg Oral Med Oral Pathol.* 1990;69:76–83.
14. Jen KY, et al. Mutational events in LMP1 gene of Epstein-Barr virus in salivary gland lymphoepithelial carcinomas. *Int J Cancer.* 2003;105:654–660.
15. Kotsianti A, et al. Undifferentiated carcinoma of the parotid gland in a white patient: detection of Epstein-Barr virus by in situ hybridization. *Hum Pathol.* 1996;27:87–90.
16. Kraemer BB, et al. Small cell carcinomas of the parotid gland: a clinicopathologic study of three cases. *Cancer.* 1983;52:2115–2121.
17. Kuo T, et al. Lymphoepithelioma-like salivary gland carcinoma in Taiwan: a clinicopathological study of nine cases demonstrating a strong association with Epstein-Barr virus. *Histopathology.* 1997;31:75–82.
18. Larsson LG, et al. Large cell neuroendocrine carcinoma of the parotid gland: fine needle aspiration, and light microscopic and ultrastructural study. *Acta Cytol.* 1999;43:534–536.
19. Leung SY, et al. Lymphoepithelial carcinoma of the salivary gland: in situ detection of Epstein-Barr virus. *J Clin Pathol.* 1995;48:1022–1027.
20. Lewis JS, et al. Lymphoepithelial carcinoma. In: El-Naggar AK, et al, eds. *Classification of Head and Neck Tumours.* 4th ed. World Health Organization Classification of Tumours. Lyon, France: IARC Press; 2017:181–182.
21. Mair S, et al. Small cell undifferentiated carcinoma of the parotid gland: cytologic, histologic, immunohistochemical and ultrastructural features of a neuroendocrine variant. *Acta Cytol.* 1989;33:164–168.
22. Merrick Y, et al. Familial clustering of salivary gland carcinoma in Greenland. *Cancer.* 1986;57:2097–2102.
23. Mineta H, et al. Immunohistochemical analysis of small cell carcinoma of the head and neck: a report of four patients and a review of sixteen patients in the literature with ectopic hormone production. *Ann Otol Rhinol Laryngol.* 2001;110:76–82.
24. Mutoh H, et al. Analysis of the p53 gene in parotid gland cancers: a relatively high frequency of mutations in low-grade mucoepidermoid carcinomas. *Int J Oncol.* 2001;18:781–786.
25. Nagao K, et al. Histopathologic studies of undifferentiated carcinoma of the parotid gland. *Cancer.* 1982;50:1572–1579.
26. Nagao T, et al. Epstein-Barr virus-associated undifferentiated carcinoma with lymphoid stroma of the salivary gland in Japanese patients: comparison with benign lymphoepithelial lesion. *Cancer.* 1996;78:695–703.
27. Nagao T, et al. Primary large-cell neuroendocrine carcinoma of the parotid gland: immunohistochemical and molecular analysis of two cases. *Mod Pathol.* 2000;13:554–561.
28. Nagao T, et al. Dedifferentiation in low-grade mucoepidermoid carcinoma of the parotid gland. *Hum Pathol.* 2003;34:1068–1072.

### Undifferentiated Carcinomas

1. Autio-Harmainen H, et al. Familial occurrence of malignant lymphoepithelial lesion of the parotid in a Finnish family with dominantly inherited trichoepithelioma. *Cancer.* 1988;61:161–166.
2. Batsakis JG, et al. Undifferentiated carcinomas of salivary glands. *Ann Otol Rhinol Laryngol.* 1991;100:82–84.
3. Casas P, et al. Large cell neuroendocrine carcinoma of the parotid gland: case report and literature review. *Auris Nasus Larynx.* 2005;32: 89–93.



29. Nagao T, et al. Small cell carcinoma of the major salivary gland: clinicopathologic study with emphasis on cytokeratin 20 immunoreactivity and clinical outcome. *Am J Surg Pathol*. 2004;28:762–770.
30. Nielsen NH, et al. Incidence of salivary gland neoplasms in Greenland with special reference to an anaplastic carcinoma. *Acta Path Microbiol Scand A*. 1978;86:185–193.
31. Pierce ST, et al. Bone marrow metastases from small cell cancer of the head and neck. *Head Neck*. 1994;16:266–271.
32. Saemundsen AK, et al. Epstein-Barr virus in nasopharyngeal and salivary carcinomas of Greenland Eskimos. *Br J Cancer*. 1982;46:721–728.
33. Schneider M, et al. Lymphoepithelial carcinoma of the parotid gland and its relationship with benign lymphoepithelial lesion. *Arch Pathol Lab Med*. 2008;132:278–282.
34. Siciliano S, et al. Primary neuroendocrine carcinoma of the parotid gland: a case report. *J Oral Maxillofac Surg*. 2001;59:1359–1362.
35. Soini Y, et al. Low p53 protein expression in salivary gland tumours compared with lung carcinomas. *Virchows Arch A Pathol Anat Histopathol*. 1992;421:415–420.
36. Takata T, et al. Undifferentiated tumors of salivary glands: immunocytochemical investigations and differential diagnosis of 22 cases. *Pathol Res Pract*. 1987;182:161–168.
37. Toyosawa S, et al. Small cell undifferentiated carcinoma of the submandibular gland: immunohistochemical evidence of myoepithelial, basal and luminal cell features. *Pathol Int*. 1999;49:887–892.
38. Wang CP, et al. Lymphoepithelial carcinoma versus large cell undifferentiated carcinoma of the major salivary glands. *Cancer*. 2004;101:2020–2027.
39. Yaku Y, et al. Undifferentiated carcinoma of the parotid gland: case report with electron microscopic findings. *Virchows Arch A Pathol Anat Histopathol*. 1983;401:89–97.
40. Yazdi HM, et al. Malignant lymphoepithelial lesion of the submandibular gland. *Am J Clin Pathol*. 1984;82:344–348.

#### Adenocarcinoma Not Otherwise Specified

1. Leivo I, et al. Adenocarcinoma, NOS. In: El-Naggar AK, Chan JKC, et al, eds. *Classification of Head and Neck Tumours*. 4th ed. World Health Organization Classification of Tumours. Lyon, France: IARC Press; 2017:171–172.
2. Matsuba HM, et al. Adenocarcinomas of major and minor salivary gland origin: a histopathologic review of treatment failure patterns. *Laryngoscope*. 1988;98:784–788.
3. Nagao K, et al. Histopathologic studies on adenocarcinoma of the parotid gland. *Acta Pathol Jpn*. 1986;36:337–347.
4. Sheahan P, et al. Neck dissection findings in primary head and neck high-grade adenocarcinoma. *J Laryngol Otol*. 2004;118:532–536.
5. Spiro RH, et al. Adenocarcinoma of salivary origin. Clinicopathologic study of 204 patients. *Am J Surg*. 1982;44:423–431.
6. Wahlberg P, et al. Carcinoma of the parotid and submandibular glands—a study of survival in 2,465 patients. *Oral Oncol*. 2002;38:706–713.

# Non-Neoplastic Lesions of the Gnathic Bones

■ Uta Flucke ■ Lester D.R. Thompson

## ■ OSTEOMYELITIS

Osteomyelitis (osteitis) is an inflammatory or infectious process in the marrow cavities of the bone. It may be either acute or chronic. There are many classification schemes, including composition of the infiltrate (acute, subacute, chronic, granulomatous), infectious agent (bacteria, fungi, virus), method of acquisition (hematogenous, direct extension, or contamination), and site of involvement. It originates as inflammation of the bone marrow connective tissue or organic bone matrix, with avascular and ischemic necrosis associated with lowered oxygen tension. Injury, teeth cleaning, dental work, surgery, nonsterile needles, diabetes, sickle cell disease, and hypertension are risk factors associated with disease development.

### CLINICAL FEATURES

Osteomyelitis is uncommon in the head and neck, but poor oral hygiene, tobacco use, alcoholism, malnutrition, and immunosuppression are associated findings. Patients with acute osteomyelitis show all signs and symptoms of an acute inflammatory disease, such as fever, malaise, and regional lymphadenopathy. Often a dental infection, extraction, or surgery may incite the initial infection, whereas fractures may introduce oral flora into the bony interstices. In chronic osteomyelitis, signs and symptoms usually are less prominent and may fluctuate in severity; they include swelling, pain, sinus formation, sequestration, and, in case of bone loss, pathologic fractures. The disease may occur at any age, but jaw disease seems to be more common in the sixth to seventh decades, with males affected more often than females. The mandible is more commonly involved (usually posterior body), but the maxilla is more often affected in children and infants due to a greater surface area and more rich blood supply. Many different organisms are etiologically related, but

### OSTEOMYELITIS—DISEASE FACT SHEET

#### Definition

- Inflammatory or infectious changes in the jaw bones causing both loss and increase of bone.

#### Sex and Age Distribution

- Males > females
- Usually sixth to seventh decades

#### Clinical Features

- Fever, chills, regional lymphadenopathy in case of acute osteomyelitis
- Swelling, pain, and draining fistulae both in acute and chronic osteomyelitis
- Mandible most often involved in adults, maxilla in children
- Localized bony swelling in case of proliferative periostitis
- Neck pain or dysphagia seen in chronic osteomyelitis
- Many organisms may cause osteomyelitis

#### Radiographic Features

- MRI is the best study to show extent of disease, including soft tissue involvement
- Bone scan is the most sensitive, but not very specific
- Plain films show mixed radiodense and radiolucent lesions but are very difficult to interpret due to anatomic structures of the jaws

#### Prognosis and Treatment

- Depends on eradication of the causative organisms and removal of necrotic bone
- Cultures must be obtained, with appropriate drug treatment (often for > 4 weeks to avoid relapse)
- Removal of foreign objects as potential nidus of infections
- Complications of osteonecrosis, septic arthritis, altered growth and fistula formation may be seen
- Bone grafts for bone stability

pneumococcus and *Haemophilus influenzae* are most common.

Sclerosing osteomyelitis and proliferative periostitis are specific subtypes. Sclerosing osteomyelitis causes recurrent pain, swelling of the cheek, and restricted jaw



movement and may be either diffuse or focal. Proliferative periostitis is a periosteal reaction to inflammatory changes in the underlying jaw bone causing facial swelling and bony enlargement.

### RADIOGRAPHIC FEATURES

Radiographs show an irregular pattern of bone loss and increased density of bone, but generally only after 3 weeks of disease. Plain films are difficult to interpret, whereas MRI is much better at identifying extent of disease and showing bone marrow and soft tissue involvement, highlighting sequestration. Bone scan, considered to be the most sensitive study, is able to see hyperperfused tissues 2 to 3 days after an infection. However, there is a low specificity. Cortical duplicating or “onion-skinning” is the radiographic hallmark of proliferative periostitis.

### PATHOLOGIC FEATURES

#### GROSS FINDINGS

Gross findings are nonspecific, usually identified as curettings. Lesions may be up to 5 cm, the larger lesions usually associated with soft tissue extension and abscess formation.

#### MICROSCOPIC FINDINGS

Marrow fibrosis or edema is the hallmark of osteomyelitis, with bone necrosis identified by marrow fibrosis and inflammation. It is important not to overinterpret

lack of osteocytes as necrosis, especially if there is over-decalcification. Acute osteomyelitis shows necrotic bone fragments with neutrophilic granulocytes and thick layers of microorganisms (Fig. 14.1). Bone death is present, with bone resorption identified by osteoclastic activity and release of neutrophil neutral proteases. Subacute disease shows both neutrophils and chronic inflammatory cells, coupled with marrow fibrosis, bone death, and resorption. In chronic osteomyelitis, sclerotic bone masses combine with chronic inflammation and dense fibrosis (Fig. 14.2). New bone formation is often seen. Squamous lined fistulae/sinuses may extend from the oral mucosa.

In case of proliferative periostitis, one sees bony trabeculae that lie in a linear parallel pattern (Fig. 14.3).

### DIFFERENTIAL DIAGNOSIS

Acute osteomyelitis generally does not pose any differential diagnostic problems, although fracture repair is sometimes considered. There is generally a lack of acute inflammation and dead bone. Chronic osteomyelitis may be confused with fibrous dysplasia, osseous dysplasia, Paget disease, or osteonecrosis. Paget disease shows highly vascular bone marrow with abundant osteoclasts. A mosaic pattern of reversal lines in the bone is not a reliable diagnostic tool as this can occur in osteomyelitis as well. Fibrous dysplasia is distinguished from chronic osteomyelitis by its slender trabeculae of woven bone that differ from the sclerotic lamellar bone masses in osteomyelitis. Osteonecrosis usually shows bone death and necrosis with very active remodeling and chronic inflammation. A radiation or drug therapy (such as bisphosphonates) history can generally be elicited. The main differential diagnostic problem occurs with osseous dysplasia, which sometimes also consists of large masses of sclerotic lamellar bone. Criteria that may be useful in this context are discussed under that specific heading. Sinuses or fistulae lined by squamous epithelium should not be confused with squamous cell carcinoma infiltrating the bone. Absence of cellular atypia rules out this possibility. Rarely, lymphoma may be seen within a setting that can mimic osteomyelitis.

### PROGNOSIS AND THERAPY

Treatment of acute osteomyelitis consists of antibiotics and removal of dead bone. It is imperative to obtain cultures and use appropriate drug therapy, often for a prolonged period and sometimes as intravenous therapy (for base of skull disease). Chronic osteomyelitis is more difficult to manage, unless all necrotic bone and organisms are removed. Foreign objects should be

### OSTEOMYELITIS—PATHOLOGIC FEATURES

#### Gross Findings

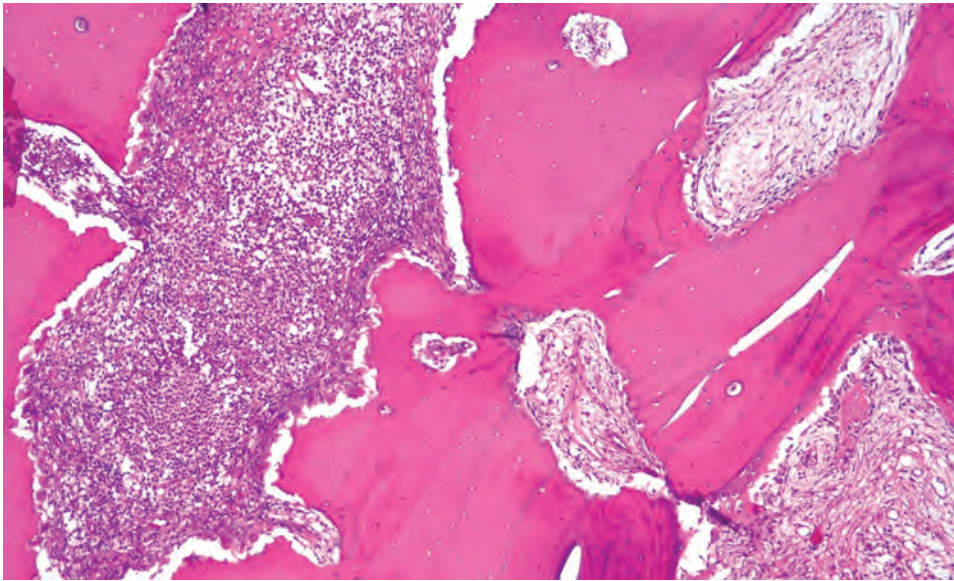
- Nonspecific, usually curettings, ranging up to 5 cm
- Abscesses may be seen along with soft tissue extension

#### Microscopic Findings

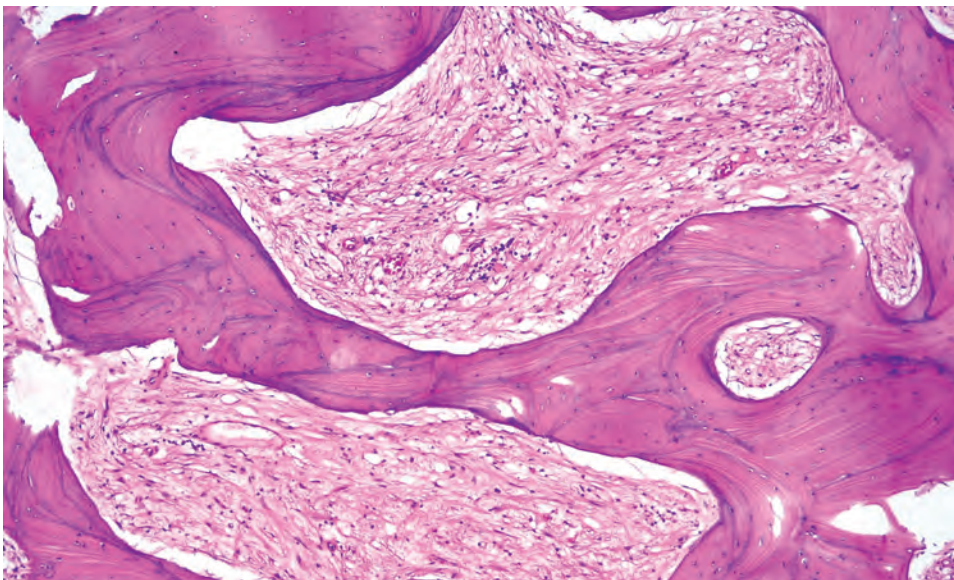
- Marrow fibrosis or edema, with necrotic bone identified by marrow fibrosis and inflammation
- Necrotic bone may be invested with microorganisms
- Sclerotic bone
- Infiltrate of neutrophils
- Granulation tissue
- Squamous lined fistulae/sinuses may be seen

#### Pathologic Differential Diagnosis

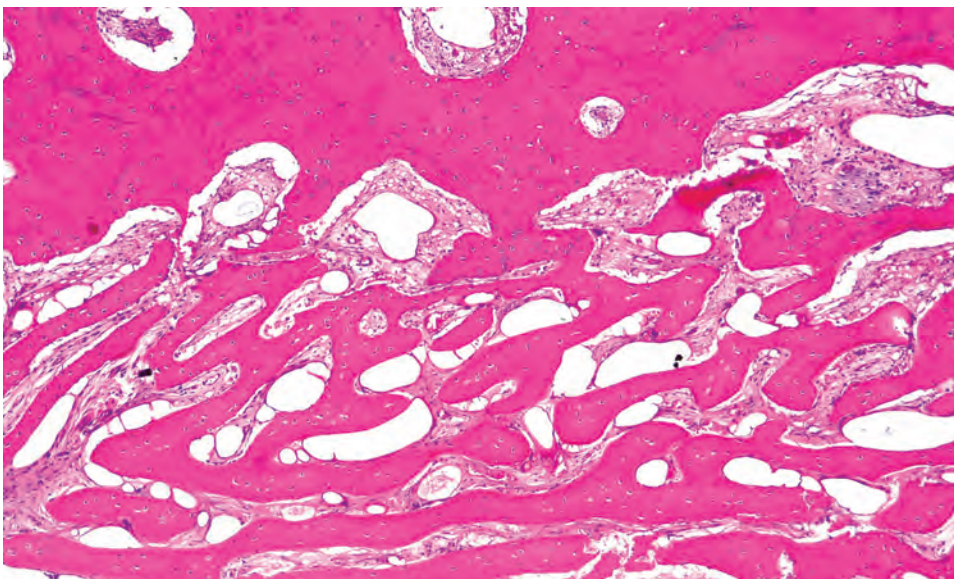
- Fracture repair, lymphoma, osteonecrosis, Paget disease, fibrous dysplasia, osseous dysplasia

**FIGURE 14.1**

Osteomyelitis; bone recognizable as dead due to empty osteocyte lacunae. The marrow cavities are partly filled with an infiltrate of polymorphonuclear granulocytes, partly with fibrous tissue. The surface of the bone is irregular and multinuclear osteoclasts form a covering rim in an attempt to resorb the dead bony tissue.

**FIGURE 14.2**

Chronic sclerosing osteomyelitis is characterized by coarse trabeculae composed of lamellar bone. The intervening marrow cavities contain fibrous tissue with sparse lymphocytes.

**FIGURE 14.3**

In case of chronic periostitis, reactive bone formation occurs parallel to the outer surface of the adjacent cortical bone.



removed to prevent a nidus of recurrent infection. In some cases, bone grafts are used for bone stability and reconstruction.

## ■ DENTIGEROUS CYST

A dentigerous cyst (sometimes called follicular cyst) is a developmental fluid-filled “bag” that surrounds the crown of an unerupted tooth at the cemento-enamel junction, mostly the maxillary canine or the mandibular third molar.

### CLINICAL FEATURES

The most common developmental cyst, dentigerous cysts account for approximately 25 % of all jaw cysts. They occur twice as often in males as in females and have the highest incidence between 10 and 40 years of age (mean, 33 years), although seen over a wide age range. The mandible is affected twice as often as the maxilla, where the mandibular third molars are most commonly affected, followed by maxillary canines, maxillary third molars, and then mandibular second premolars. Usually identified in asymptomatic patients during routine radiographs, it is only when they are large that they

result in pain, resorption of adjacent teeth, and possible infections.

### RADIOGRAPHIC FEATURES

Dentigerous cysts present as unilocular radiolucent lesions with a well-defined sclerotic border, into which the crown of an unerupted tooth protrudes (Fig. 14.4). However, there may be a central, lateral, or circumferential relationship to the crown of the tooth. The cyst may be multilocular when large, associated with tooth displacement.

### PATHOLOGIC FEATURES

#### GROSS FINDINGS

Gross pathology shows a fluid-filled “bag” or cyst that is attached to the tooth at the cemento-enamel junction, forming a collar (Fig. 14.4). However, this relationship is lost in most extraction procedures.

#### MICROSCOPIC FINDINGS

The cyst wall is lined by a thin layer (usually 2-3 cells thick) of cuboidal to squamoid epithelium (Fig. 14.5). The epithelium may be significantly thickened if associated with inflammation, resulting in hyperplastic rete ridges. Cholesterol clefts and Rushton bodies (degenerated, hypereosinophilic keratin flakes) may be seen. Mucous cells, sebocytes, and ciliated cells may be observed (Fig. 14.5). The cyst wall, composed of fibrous or fibromyxoid connective tissue, may contain varying amounts of odontogenic epithelial nests (up to 20 % of cases) and occasional dystrophic calcifications.

### DENTIGEROUS CYST—DISEASE FACT SHEET

#### Definition

- A cyst that arises from fluid accumulation between enamel organ and enamel surface in an unerupted tooth

#### Incidence and Location

- One of the more common odontogenic cysts, mostly associated with lower third molar or upper canine tooth

#### Sex, Race, and Age Distribution

- Males > females (2:1)
- Blacks > whites (5:1)
- Highest incidence in second, third, and fourth decades

#### Clinical Features

- Mostly none
- Slight swelling when large and pain in case of concomitant infection with inflammation

#### Radiographic Features

- Circumscribed radiolucency surrounding the crown of the involved tooth

#### Prognosis and Treatment

- Cured by simple enucleation

### DENTIGEROUS CYST—PATHOLOGIC FEATURES

#### Gross Findings

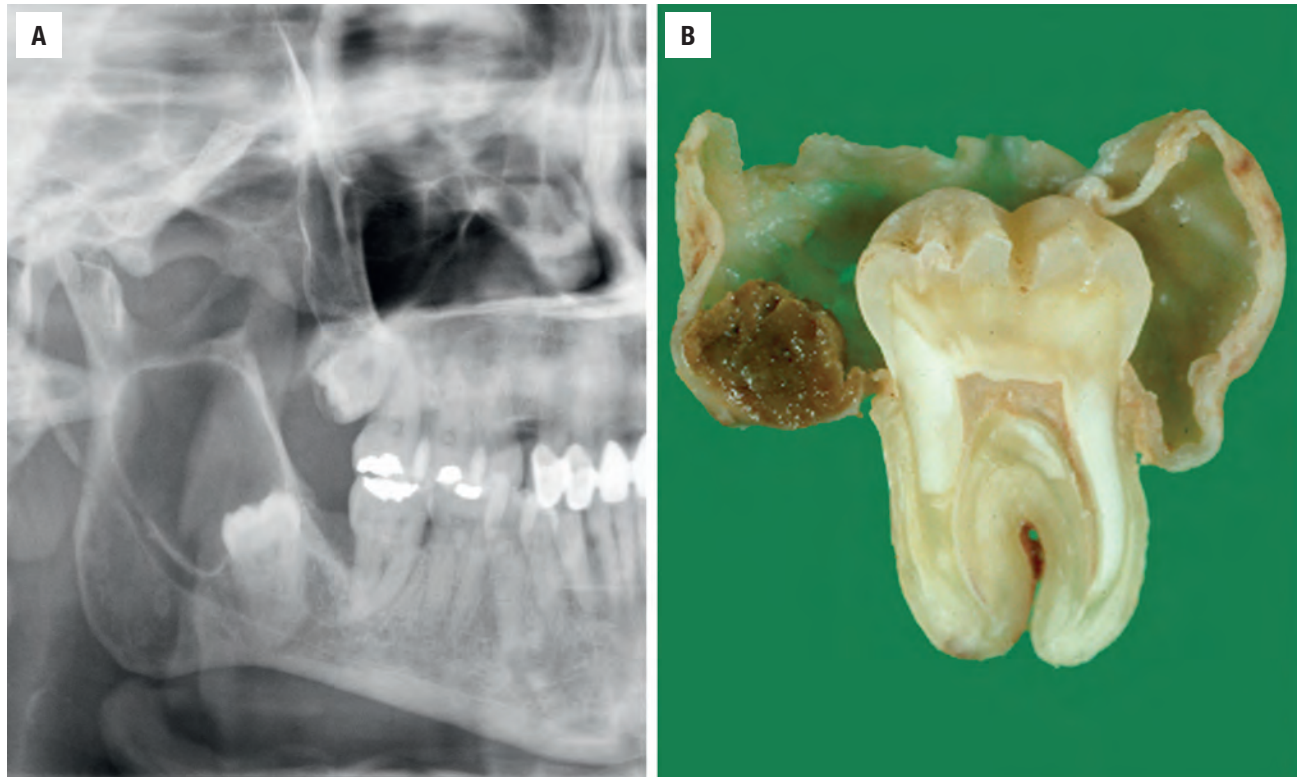
- A tooth partly covered by a soft tissue bag/sac

#### Microscopic Findings

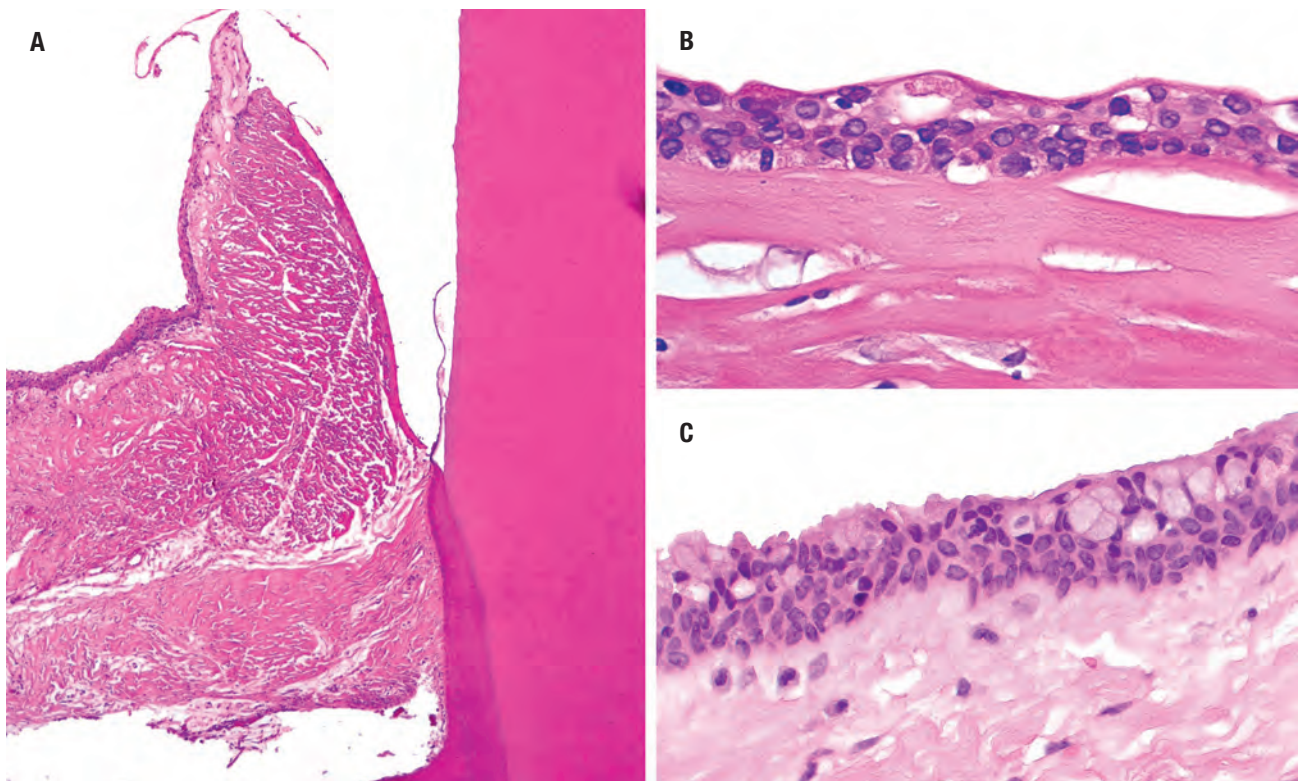
- Epithelial lining mostly consisting of bilayered cuboidal cells; sometimes mucoid cells, ciliated columnar cells
- Spongiotic squamous epithelium in case of inflammation
- Fibrous wall sometimes showing focal mucoid transformation and contains nests and strands of odontogenic epithelium

#### Pathologic Differential Diagnosis

- Eruption cyst (dental follicle), unicystic ameloblastoma, odontogenic keratocyst, odontogenic myxoma, glandular odontogenic cyst

**FIGURE 14.4**

(A) An orthopantomograph of a dentigerous cyst showing the crown of tooth #32 surrounded by a well-defined radiolucency with a sclerotic border. (B) Gross specimen of a dentigerous cyst. The cyst wall surrounds the tooth crown and is attached at the neck of the tooth at the cemento-enamel junction.

**FIGURE 14.5**

(A) Junction of the enamel (*right*) with the cyst epithelial lining may be preserved histologically. (B) In classical appearance, the epithelial lining of a dentigerous cyst consists of two to three cell layers of cuboidal epithelial cells. (C) Mucocytes may be seen in the epithelium of a dentigerous cyst.



## DIFFERENTIAL DIAGNOSIS

An *eruption cyst* (dental follicle) is a specific type of dentigerous cyst located in the gingival soft tissues overlying the crown of an erupting tooth. It generally lacks a cystic epithelium and is usually less than 3 to 4 mm in size. Although there is radiographic overlap, histologic examination will separate odontogenic keratocyst and unicystic ameloblastoma from dentigerous cyst. Odontogenic keratocysts are lined by a basal palisade of epithelial cells with a characteristic superficial corrugated parakeratosis. Unicystic ameloblastoma shows a basal layer of cylindrical cells with hyperchromatic nuclei, occasional reverse polarity, and an overlying layer of spindle-shaped cells with intervening edema resembling stellate reticulum. Fibromyxomatous areas in the connective tissue wall of the dentigerous cyst may be confused with an odontogenic myxoma. However, myxomas are not cystic and lack an epithelial lining. Glandular odontogenic cyst develops in the fifth decade, usually associated with cortical perforation of the anterior mandible. There is a squamous epithelium that shows plaque-like thickenings or whorls; hobnail cells and duct-like structures may be seen.

## PROGNOSIS AND THERAPY

Removal of the cyst wall and extraction of the involved tooth will yield a permanent cure, although sometimes marsupialization is used for large cysts. There is a very low rate of recurrence.

## ■ PERIAPICAL CYST/GRANULOMA

Periapical cyst and granuloma, sometimes covered by the term radicular cyst, is a lesion defined by an arc of development, starting out as an epithelial lined cyst that undergoes involution, resulting in inflammation and fibrosis only. It is an inflammatory odontogenic cyst identified at the root tips of nonvital teeth, mostly due to dental caries.

## CLINICAL FEATURES

Periapical cyst is the most common jaw cyst and accounts for approximately 75 % of periapical lesions. There is a wide age range and equal sex distribution. Most patients are asymptomatic, with lesions identified by routine dental imaging. When there is inflammation, then pain, sensitivity to temperature changes, and swelling may be seen. In general, caries result in tooth cavitation, resulting in

## PERIAPICAL CYST/GRANULOMA—DISEASE FACT SHEET

### Definition

- An inflammatory odontogenic cyst located at the root tip of a nonvital tooth

### Incidence and Location

- Most common jaw cyst, approximately 75% of all periapical lesions
- Root tip of any nonvital tooth

### Sex and Age Distribution

- Equal sex distribution
- Wide age range

### Clinical Features

- Asymptomatic, identified by routine dental imaging
- Swelling, temperature sensitivity, and pain in case of inflammation

### Radiographic Features

- Circumscribed radiolucency located at the root tip or lateral root surface of a nonvital tooth

### Prognosis and Treatment

- Tooth extraction or apical resection with curettage of the periapex
- Antibiotic therapy for infection and endodontic treatment if necessary

bacterial invasion of the tooth pulp, which results in tooth devitalization.

## RADIOGRAPHIC FEATURES

In general, there is a radiolucent lesion located at the root tip of a nonvital tooth, often associated with root resorption (Fig. 14.6). The radiolucency must be associated with the tooth root or lateral root surface. There may be caries, fracture, restoration, or other endodontic apparatus in place.

## PATHOLOGIC FEATURES

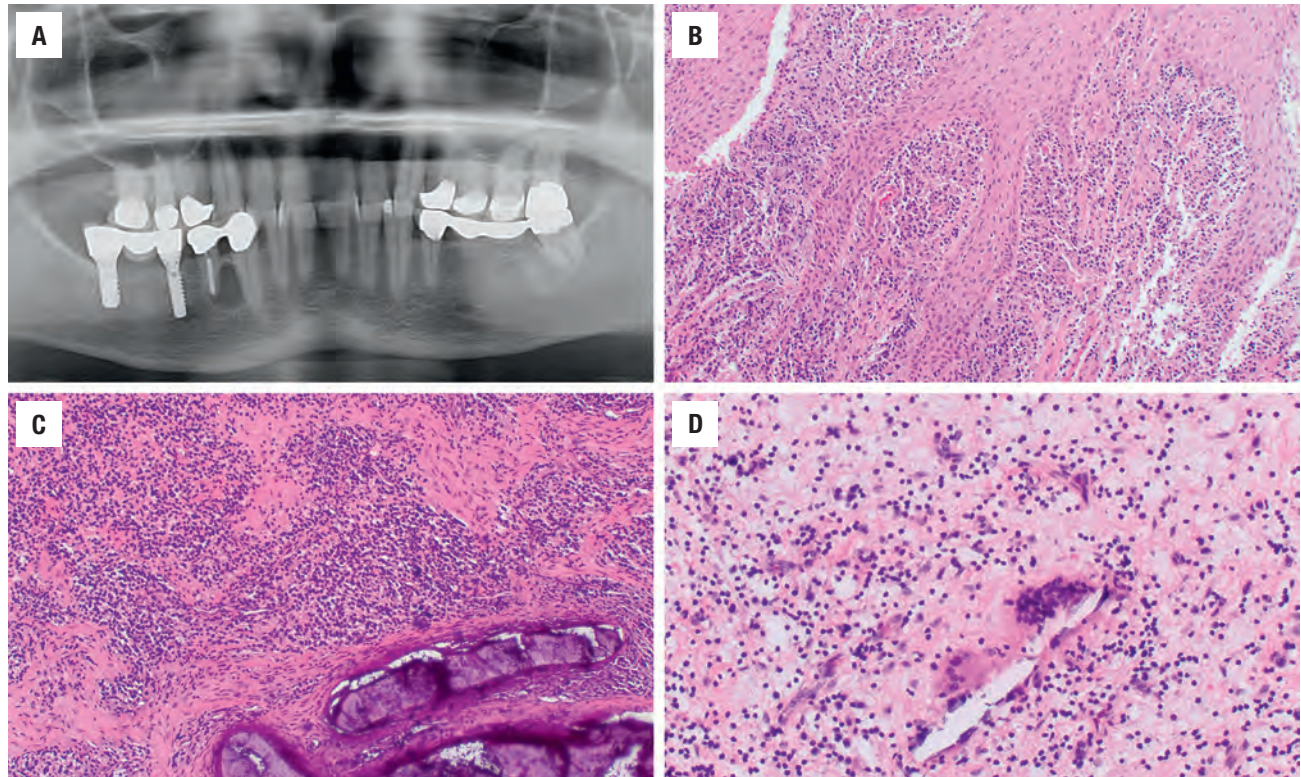
### GROSS FINDINGS

There is usually a thick-walled cyst related to the tooth apex.

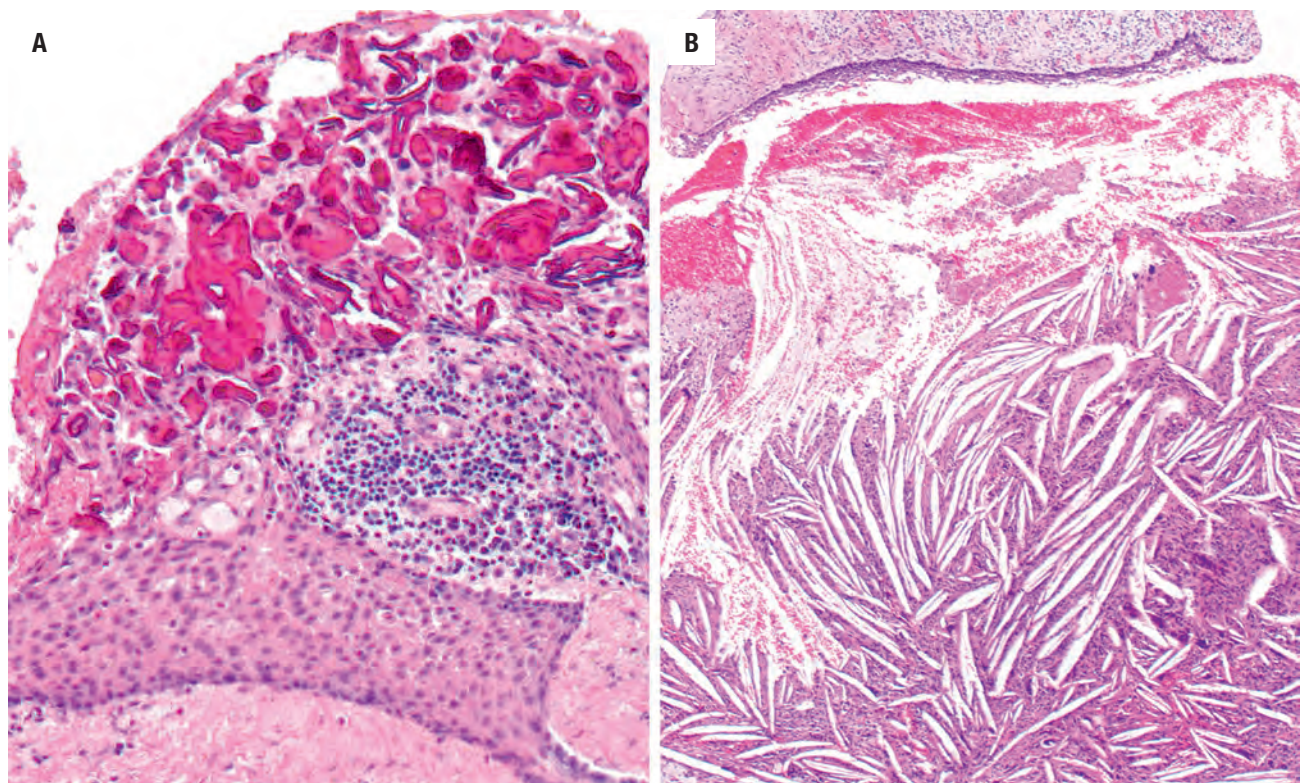
### MICROSCOPIC FINDINGS

The cysts are lined by nonkeratinizing squamous epithelium that may show elongated rete processes (Fig. 14.6). Cholesterol clefts with foreign body giant cells are frequently present (Fig. 14.7). Chronic inflammation is prominent and stromal calcifications may be seen. Intraepithelial hyaline



**FIGURE 14.6**

Periapical cyst and granuloma. (A) There is a nonvital tooth with a radiolucency at the lateral and periapical border of the right mandible. (B) There is an inflamed squamous epithelium in this periapical cyst. (C) The inflammatory infiltrate can be quite pronounced, shown here with fragments of bone. (D) Cholesterol cleft with giant cell reaction and a background of inflammation.

**FIGURE 14.7**

(A) Periapical cyst lined by nonkeratinizing squamous epithelium. An inflammatory infiltrate is present, associated with Rushton bodies. (B) The epithelium is thin and attenuated (*upper field*), while the dominant finding is cholesterol clefts and inflammation in this periapical cyst.



### PERIAPICAL CYST/GRANULOMA—PATHOLOGIC FEATURES

#### Gross Findings

- Thick-walled cyst related to the tooth apex

#### Microscopic Findings

- Nonkeratinizing squamous epithelium sometimes admixed with mucous or ciliated cells
- Marked mixed inflammation, although predominantly lymphoplasmacytic
- Cholesterol clefts with adjacent giant cells
- Intraepithelial hyaline bodies (Rushton bodies)

#### Pathologic Differential Diagnosis

- Other (inflamed) jaw cysts, odontogenic and nonodontogenic; nasopalatine duct cyst

bodies, so-called Rushton bodies, may be present, but these are not a specific finding (Fig. 14.7).

### DIFFERENTIAL DIAGNOSIS

Given the fact that the histology is nonspecific, other jaw cysts, both odontogenic and nonodontogenic, can give an identical appearance, especially in cases with extensive inflammation. Therefore, it should be noted that a periapical cyst is strongly associated with the root of a decayed and nonvital tooth. A nasopalatine duct cyst may be confused with central maxilla lesions, but the histologic features are characteristic.

### PROGNOSIS AND THERAPY

Tooth extraction or apical resection with curettage of the periapex usually is an adequate treatment. Endodontic treatment with a root canal may be used with tooth restoration. Antibiotic therapy is often used for infections. When a cyst is left behind after extraction of the corresponding tooth, it is called a residual cyst.

## ■ FIBROUS DYSPLASIA

Fibrous dysplasia is a sporadic skeletal overgrowth disorder that occurs in three clinical subtypes: monostotic (one bone), polyostotic (multiple bones), and more rarely, McCune-Albright syndrome, in which polyostotic disease is accompanied by skin hyperpigmentation and

endocrine disturbances leading to precocious puberty, hyperthyroidism, growth hormone excess, and Cushing syndrome. Activating missense mutations in the *GNAS1* gene coding for the  $\alpha$ -subunit of the stimulatory G protein are a consistent finding in the various forms of fibrous dysplasia but are considered acquired rather than inherited. Mutations occur somatically and result in mosaicism, explaining the extreme heterogeneity of the condition. Thus it should probably be considered as a benign neoplasm rather than a reactive condition.

### CLINICAL FEATURES

Fibrous dysplasia occurs predominantly in children and adolescents. The maxilla is more often involved than the mandible. Polyostotic disease is more common in females and shows craniofacial involvement in virtually all cases. Bone pain, fractures, and deformity are the most common presenting features. Skull base involvement may lead to cranial nerve compression with corresponding neurologic symptoms. When part of McCune-Albright, nearly all cases are diagnosed before 15 years of age.

### RADIOGRAPHIC FEATURES

The classical appearance is described as “orange-skin” or “ground-glass” radio-opacity without defined borders, blending with the surrounding bone. In less typical cases, the afflicted bone may be mainly radiolucent or predominantly sclerotic or show a cotton-wool appearance. In the maxilla, fibrous dysplasia may extend by continuity across suture lines to involve adjacent bones (Fig. 14.8). Calcifications may be seen.

### PATHOLOGIC FEATURES

#### GROSS FINDINGS

Resected specimens consist of gritty fragments of bony tissue.

#### MICROSCOPIC FINDINGS

Fibrous dysplasia shows replacement of the normal bone by moderately cellular fibrous tissue containing irregularly shaped (“alphabet soup”) trabeculae consisting of woven bone *without* osteoblastic rimming (Fig. 14.9).

**FIBROUS DYSPLASIA—DISEASE FACT SHEET****Definition**

- A sporadic skeletal overgrowth disorder of fibrous tissue with woven bone causing bone expansion, associated with activating mutations of *GNAS1*

**Incidence and Location**

- Rare lesion
- Maxilla more often involved than mandible

**Sex and Age Distribution**

- Polyostotic form is more common in females
- Young adults and adolescents
- When part of McCune-Albright syndrome, nearly always identified < 15 years

**Clinical Features**

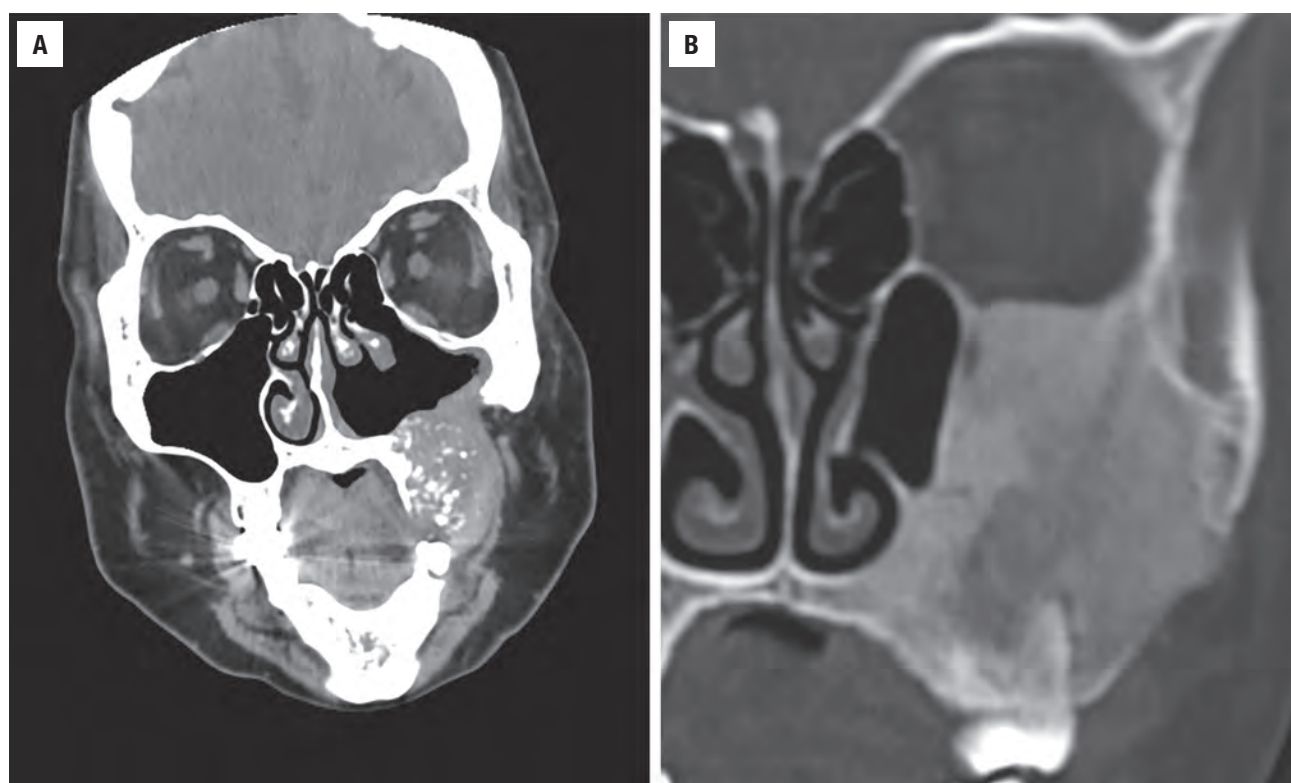
- Bone pain, fractures, and deformity
- Cranial nerve dysfunction with skull base disease
- Pigmented skin spots and endocrine dysfunction in polyostotic cases

**Radiographic Features**

- Ground-glass appearance blending with adjacent bone (across suture lines)
- Less specific: radiolucencies, radio-opacities, and multiple coalescing radio-opacities causing a cotton-wool appearance

**Prognosis and Treatment**

- Self-limiting disease sometimes requiring surgical intervention for cosmetic reasons or to decompress cranial nerves

**FIGURE 14.8**

Two computed tomography scans show fibrous dysplasia, one involving the maxilla with calcifications (**A**), while the right image (**B**) shows near complete obliteration and opacification of the maxillary sinus.

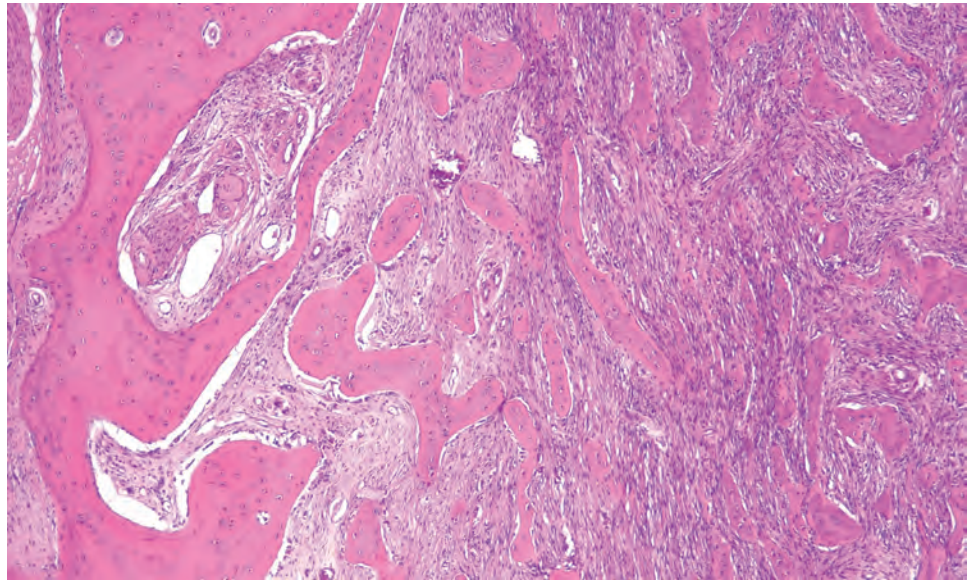
Jaw lesions may also show lamellar bone (**Fig. 14.10**). Sometimes, tiny calcified spherules may be present.

**DIFFERENTIAL DIAGNOSIS**

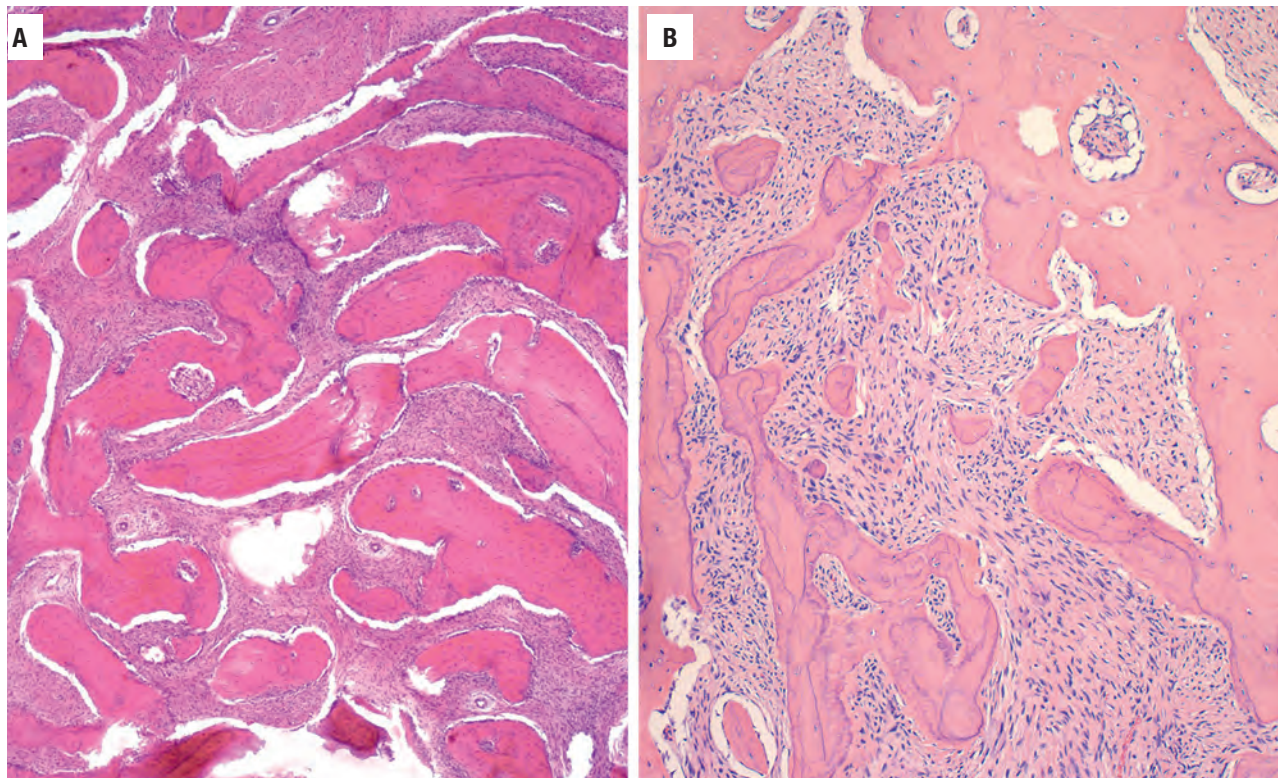
Fibrous dysplasia must be distinguished from ossifying fibroma, osseous dysplasia, low-grade osteosarcoma,

and sclerosing osteomyelitis. None of these is composed of woven bone trabeculae fusing with adjacent uninvolved bone. Ossifying fibroma and osseous dysplasia have a variety of appearances of mineralized material and stromal cellularity. Low-grade osteosarcoma invades through the cortical bone into soft tissues and exhibits slight atypia. Sclerosing osteomyelitis shows coarse lamellar bone and edematous intervening stroma containing lymphocytes.



**FIGURE 14.9**

Continuity between the lesional bone (*right*) and the adjacent cortical bone (*left*) is clearly visible in this example of fibrous dysplasia.

**FIGURE 14.10**

Bony trabeculae in fibrous dysplasia may show a parallel arrangement (**A**) or a more characteristic “alphabet soup” appearance (**B**). There is a near complete absence of osteoblastic rimming of the bony trabeculae.

### FIBROUS DYSPLASIA—PATHOLOGIC FEATURES

#### Gross Findings

- Gritty fragments of bony tissue

#### Microscopic Findings

- Moderately cellular fibrous tissue intermingled with immature woven bone and occasionally lamellar bone
- Lesional bone fusing with adjacent cancellous or cortical bone

- Irregular shaped (alphabet soup) trabecular *without* osteoblastic rimming

#### Pathologic Differential Diagnosis

- Ossifying fibroma, osseous dysplasia, low-grade osteosarcoma, chronic sclerosing osteomyelitis

## PROGNOSIS AND THERAPY

Usually, fibrous dysplasia is a self-limiting disease. Therefore, treatment is required only in case of problems due to local increase in size. Development of osteosarcoma is a rare complicating event.

## ■ OSTEONECROSIS

Osteoradionecrosis (ORN) is a complication of irradiation resulting in avascular bone necrosis, whereas medication-related osteonecrosis (MRON) is identical but caused by antiresorptive medications (such as bisphosphonates). Thus, the term osteonecrosis is favored.

In the head and neck, osteonecrosis occurs as a complication from radiotherapy for primary tumors, most commonly squamous cell carcinoma. However, medications, such as bisphosphonates used to treat diseases like osteoporosis and Paget disease, result in osteoclastic activity blockade, which lowers bone turnover. Whether due to medication or a compromised microvasculature, death of osteoblasts, and resultant dead bone, there is an overall unregulated fibroblastic activity, causing a failure of bone to heal. Infection may ensue but is not necessarily present.

## CLINICAL FEATURES

MRON is recognized in up to 7% of patients receiving bisphosphonates, although it is dose and duration dependent, as well as being more common in certain tumor types (multiple myeloma > breast cancer). ORN is detected in approximately 5% of patients treated by radiation, more commonly seen when brachytherapy is used and with greater than 60 Gy of radiation exposure, usually seen between 4 and 24 months after radiation. Generally identified in older patients, there are sex differences: women more often with MRON due to a higher incidence of osteoporosis and treatments associated with breast cancer; men more often for ORN. Patients present with pain and teeth loosening, with the mandible affected more often than the maxilla. Tooth extraction is often a precipitating event. Sinuses may develop, as well as mucosal ulceration exposing dead bone. Pathologic fractures may develop.

## RADIOGRAPHIC FEATURES

Ill-defined areas of radiolucency alternate with areas of increased radiopacity. In general, the findings are non-specific, with either localized or diffuse osteosclerosis,

## OSTEONECROSIS—DISEASE FACT SHEET

### Definition

- Avascular bone necrosis due to irradiation or antiresorptive medications (such as bisphosphonates)

### Incidence and Location

- 7% of patients after medical therapy
- 5% of patients after radiation
- Mandible > maxilla

### Sex and Age Distribution

- MRON for osteoporosis or breast carcinoma: females > males
- ORN: males > females
- Older patients in general

### Clinical Features

- Pain, teeth loosening; fistulae late in disease

### Radiographic Features

- Ill-defined radiolucencies and opacities

### Prognosis and Treatment

- Difficult to cure
- Hyperbaric oxygen and removal of dead bone
- Infections aggressively treated
- Avoid extraction, with endodontic procedures preferred

MRON, Medication-related osteonecrosis; ORN, osteoradionecrosis.

with osteolysis often seen. In general, computed tomography is more sensitive than plain films or dental imaging.

## PATHOLOGIC FEATURES

### GROSS FINDINGS

There are no specific gross findings, although the bone is often soft due to nonviability.

### MICROSCOPIC FINDINGS

Histologically, there is a large overlap with osteomyelitis. In fact, cases with only minor inflammatory changes mimic chronic sclerosing osteomyelitis (Fig. 14.11). Cases in which concomitant infection develops more closely resemble acute osteomyelitis, with acute inflammation and necrosis (Fig. 14.12). In this setting, clinical history is required for the distinction. In general, the nonvital bone shows a lack of osteocytes with a scalloped resorption pattern. Osteoclasts may be seen away from the bone interface. Neutrophils are often seen in the soft tissue, whereas bacterial colonization may be seen adjacent to bone. There is an arc of development, with changes in the endothelium first, followed by an increased fibroblastic



### OSTEONECROSIS—PATHOLOGIC FEATURES

#### Gross Findings

- Softening of bone due to nonviability

#### Microscopic Findings

- Arc of development results in variable features
- Nonvital bone lacking osteocytes
- Fibrosis
- Neutrophils in soft tissues

#### Pathologic Differential Diagnosis

- Osteomyelitis, recurrent squamous cell carcinoma (when fistula present)

activity, and finally tissue remodeling is noted. Fistula formation is often present.

### DIFFERENTIAL DIAGNOSIS

Infection and concomitant inflammation may form fistulae showing “invading” strands of squamous epithelium, quite often in contact with necrotic bone. This ominous appearance is readily mistaken for (recurrent) squamous cell cancer. The epithelium, however, shows reactive alterations, such as pronounced intraepithelial edema and absence of cytologic atypia indicating malignancy. It is imperative to use medication and treatment history in reaching a diagnosis.

**FIGURE 14.11**

Prominent reversal lines indicate active bone remodeling in a case of osteoradionecrosis. The adjacent stroma contains lymphocytes. The features are virtually identical to chronic sclerosing osteomyelitis.

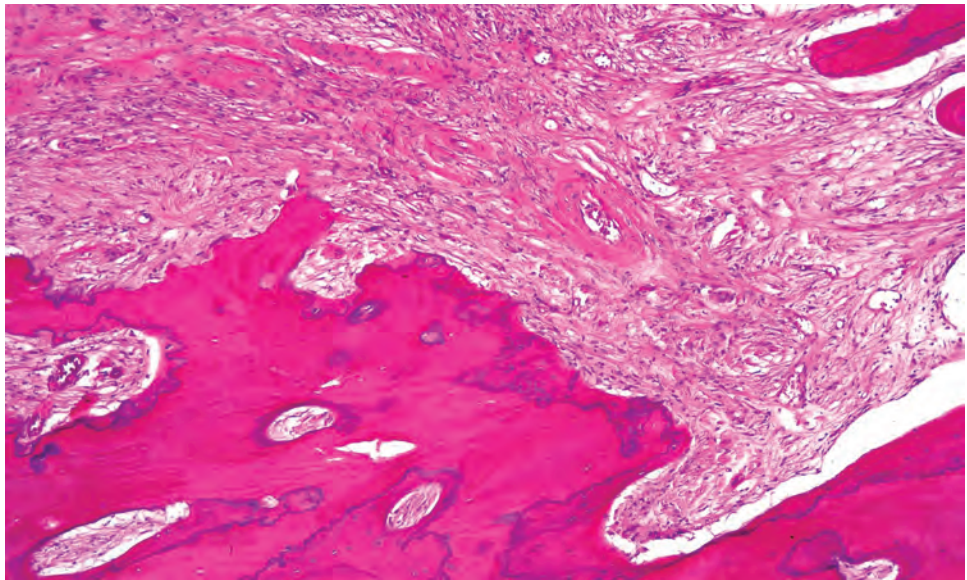
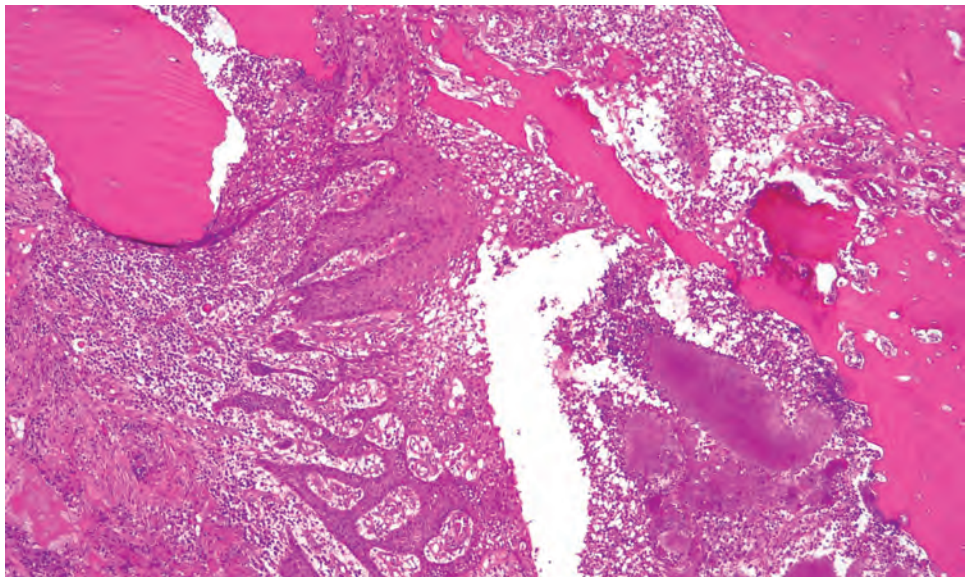


**FIGURE 14.12**

In case of infection, osteoradionecrosis shows abundant acute inflammatory cells with squamous epithelium lining a fistula tract. Colonies of microorganisms are apparent.



## PROGNOSIS AND THERAPY

In some cases, treatment with hyperbaric oxygen may ameliorate the symptoms. Ideally, conservative surgery is best, but quite often, treatment requires the removal of large areas of diseased bone due to intractable and severe pain. Infections must be treated aggressively. Tooth extraction should be avoided, with endodontic treatments preferred. Overall, there is a risk of ORN for life, even though it is lower as time passes. Pathologic fracture may be seen in progressive disease.

## SIMPLE (SOLITARY) BONE CYST

The solitary or simple bone cyst is a lesion with a poorly understood pathogenesis, although a remnant of intraosseous hemorrhage is the favored hypothesis.

## CLINICAL FEATURES

There are seldom clinical features because they are usually discovered incidentally on oral radiographs taken for a different reason. Patients are usually young (second decade), with males affected slightly more often than females. The mandible is affected much more commonly than the maxilla (9:1), with lesions usually identified in the molar region.

### SIMPLE (SOLITARY) BONE CYST—DISEASE FACT SHEET

#### Definition

- Fluid-filled bone cavity lacking a definable wall

#### Incidence and Location

- Rare
- Mandible > > > maxilla (9:1)

#### Sex, Race, and Age Distribution

- Slight male predominance
- No racial predilection
- Most common in second decade of life

#### Clinical Features

- Usually an incidental finding on dental imaging

#### Radiographic Features

- Well-circumscribed radiolucency

#### Prognosis and Treatment

- Excellent, no specific treatment required

## RADIOGRAPHIC FEATURES

Radiographs show a well-circumscribed radiolucent cavity of variable size (Fig. 14.13). Mandibular cases may occupy the entire body and ramus.

## PATHOLOGIC FEATURES

### GROSS FINDINGS

At surgical exploration, one encounters a fluid-filled cavity. Material for histologic examination may be difficult to obtain as a soft tissue lining of the bony cavity may be entirely absent or very thin.

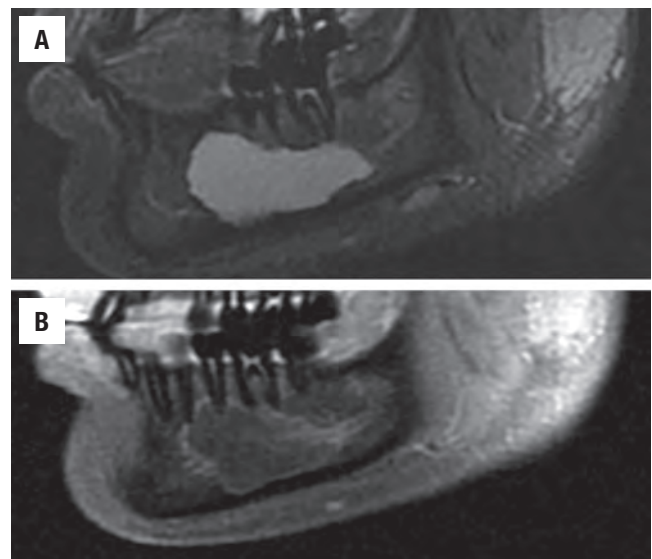


FIGURE 14.13

A mandible simple bone cyst identified by magnetic resonance imaging. The sagittal T2 image shows a very bright and high signal intensity, highlighting the fluid-filled cavity (A), whereas the T1 postcontrast image shows no central enhancement, although there is a rim of enhancement (B).

### SIMPLE (SOLITARY) BONE CYST—PATHOLOGIC FEATURES

#### Gross Findings

- Fluid-filled cavity at surgery, but contents may be lost during processing

#### Microscopic Findings

- Loose fibrovascular tissue, granulation tissue, fibrin, or hemorrhage with cholesterol clefts

#### Pathologic Differential Diagnosis

- Inadequate sampling of another odontogenic cyst



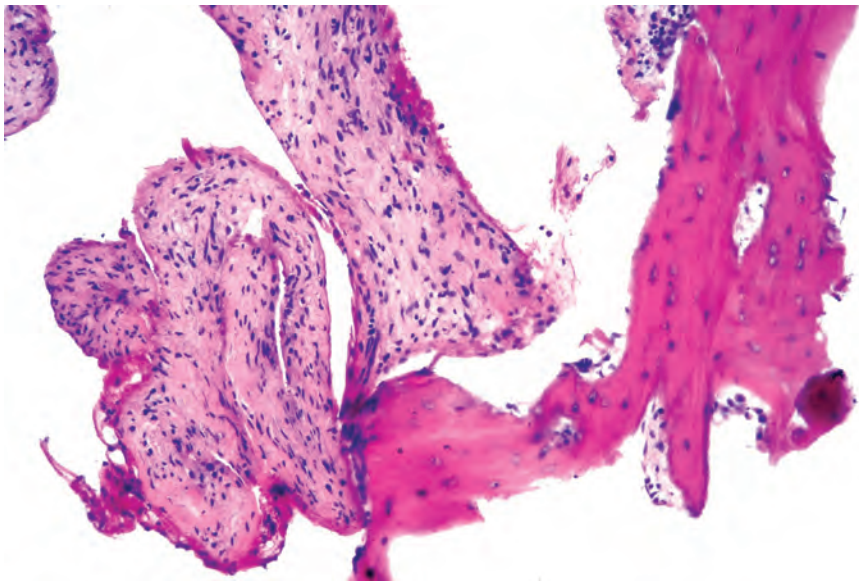


**FIGURE 14.14**  
Biopsies of simple bone cyst contain thin pieces of lamellar bone and some fibrous tissue.

**MICROSCOPIC FINDINGS**

The cyst wall usually consists of loose fibrovascular tissue (Fig. 14.14); it may also contain granulation tissue with signs of previous hemorrhage, such as cholesterol clefts and hemosiderin-laden macrophages. Dystrophic calcification may also occur. Sometimes, the cyst is associated with osseous dysplasia.

**DIFFERENTIAL DIAGNOSIS**

There is not usually a difficulty in diagnosis, although it is important to realize that insufficiently sampled gnathic cysts may have histologic overlap with a solitary bone cyst.

**PROGNOSIS AND THERAPY**

No therapy is required after the diagnosis has been made.

**NASOPALATINE DUCT CYST**

Nasopalatine duct cysts arise within the nasopalatine canal, connecting the nasal and oral cavity, from epithelial remnants of the nasopalatine duct.

**CLINICAL FEATURES**

Nasopalatine duct cysts are seen most commonly in the fourth to sixth decades of life, with a male predilection.

**NASOPALATINE DUCT CYST—DISEASE FACT SHEET**

|  |
|--|
| <b>Definition</b>  |
| ■ A cyst in the nasopalatine canal and derived from the nasopalatine duct remnants |
| <b>Incidence and Location</b>  |
| ■ One of the more common jaw cysts, confined to the anterior maxilla               |
| <b>Sex and Age Distribution</b>  |
| ■ More often in males  |
| ■ Fourth to sixth decades  |
| <b>Clinical Features</b>   |
| ■ Swelling of the anterior palate  |
| ■ Pain in case of concomitant inflammation   |
| <b>Radiographic Features</b>   |
| ■ Pear-shaped radiolucency between roots of left and right central incisor teeth   |
| ■ Roots diverging to give way to the expanding cyst                                |
| <b>Prognosis and Treatment</b>   |
| ■ Excision is curative   |

Occurrence in children is rarely seen. They manifest as a swelling in the anterior part of the palate. In case of concomitant inflammation, pain may also be present.

**RADIOGRAPHIC FEATURES**

They present as midline, pear-shaped radiolucent lesions situated between the roots of the maxillary central incisor

teeth. Thus the roots are noted to diverge around the expanded cyst.

### **PATHOLOGIC FEATURES**

The cyst lining may be pseudostratified columnar ciliated epithelium, stratified squamous epithelium, columnar or cuboidal epithelium, or combinations of these. As surgical treatment comprises emptying the nasopalatine canal, the specimen includes the artery and nerve that run through it (Fig. 14.15). As a matter of fact, the artery and the nerve may be the most diagnostic feature as the epithelial histomorphology is nonspecific and may be obscured by inflammatory changes.

### **DIFFERENTIAL DIAGNOSIS**

Nasopalatine duct cyst may be mimicked by a periapical cyst associated with one or both nonvital central incisor

#### **NASOPALATINE DUCT CYST—PATHOLOGIC FEATURES**

##### **Microscopic Findings**

- A fibrous cyst wall lined by columnar, ciliated, and/or mucous cells
- Large vessels and nerve bundles most helpful

##### **Pathologic Differential Diagnosis**

- Periapical cyst or granuloma

teeth. Distinction between both cyst types may be impossible when one of these teeth is nonvital and the cyst wall shows inflammatory alterations with reactive squamous metaplasia of the epithelial lining. However, when teeth are vital, a periapical cyst can be effectively ruled out.

### **PROGNOSIS AND THERAPY**

Excision of the cyst is the appropriate treatment. Recurrences may develop in up to 11 % of patients.

### **TORI**

Tori are common reactive irregular bony outgrowths (exostoses), seen in the palate (torus palatinus: midline) or mandible (torus mandibularis), the latter defined by bony growths along the lingual mandible above the mylohyoid bone usually in the molar-premolar region.

### **CLINICAL FEATURES**

These lesions can present at any age but are usually noted in early adult life. They are common, detected in 25 % to 40 % of the United States population (higher incidence in torus palatinus). There is a female predominance for torus palatinus and a slight male predilection for torus mandibularis. There is a higher incidence seen in Asians and Inuit patients.

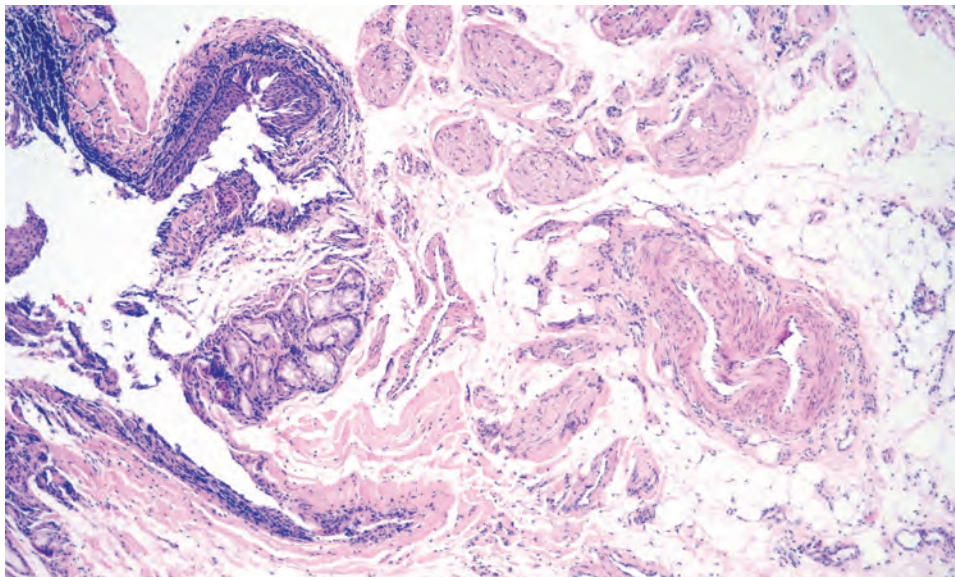


**FIGURE 14.15**

Note the nerve bundles and vessels in the nasopalatine duct cyst wall. The epithelium may be either squamous or columnar.



**TORI—DISEASE FACT SHEET****Definition**

- Irregular bony outgrowths (exostoses)

**Incidence and Location**

- Common
- Palate or mandible

**Sex, Race, and Age Distribution**

- Females more often for torus palatinus; males for torus mandibularis
- Higher incidence in Asians and Inuits
- Any age but peak detection in early adulthood

**Clinical Features**

- Bony swellings covered with intact mucosa

**Radiographic Features**

- Cloudy radiopacities superimposed on the teeth contour

**Prognosis and Treatment**

- Only corrective jaw contouring needed for mechanical difficulties with mastication or denture fitting

**RADIOGRAPHIC FEATURES**

Tori present as ill-defined cloudy radiopacities, although torus palatinus is generally not detected with routine dental films.

**PATHOLOGIC FEATURES****GROSS FINDINGS**

Multilobular bony fragments, frequently asymmetric, most less than 2 cm.

**MICROSCOPIC FINDINGS**

Tori consist of dense, mature lamellar bone (Fig. 14.16), with minimal osteoblastic activity and a limited marrow space.

**DIFFERENTIAL DIAGNOSIS**

Characteristic clinical appearance precludes any differential diagnostic problems. However, bony growths along the facial aspect of the maxilla or mandible are called buccal exostosis, and an osteoma can look histologically similar, although usually showing more osteoblastic

**TORI—PATHOLOGIC FEATURES****Gross Findings**

- Bony fragments, usually < 2 cm

**Microscopic Findings**

- Dense, lamellar bone with minimal osteoblastic activity
- Limited marrow space

**Pathologic Differential Diagnosis**

- Buccal exostosis, osteoma

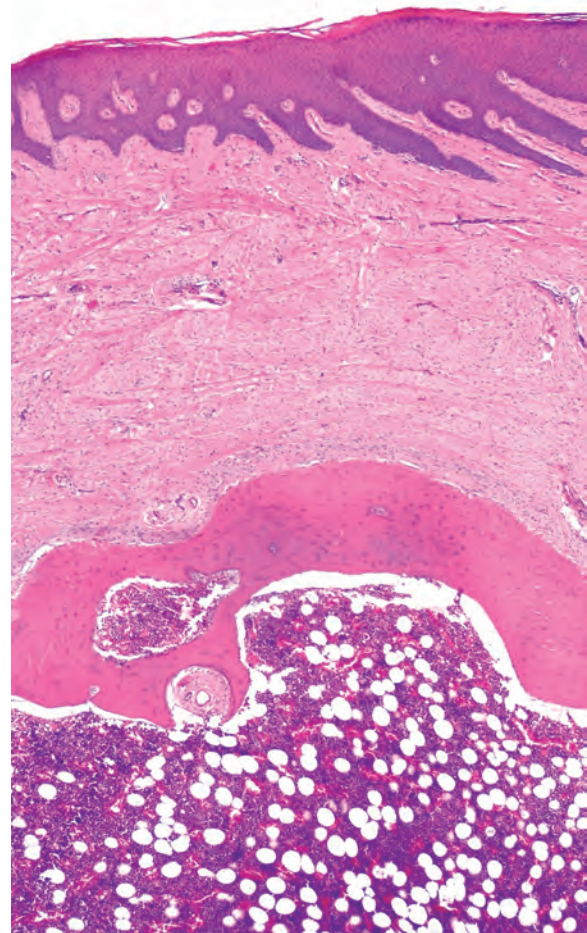


**FIGURE 14.16**

Tori consists of lamellar bone, with hematopoietic marrow in this case. Periosteum and mucosa do not show any abnormalities.

activity and usually showing more of a pedicle or point of attachment to the underlying bone.

**PROGNOSIS AND THERAPY**

Treatment is not necessary except in cases of mechanical problems, such as denture use or difficulties with

mastication. The lesions may slowly increase in size over decades or spontaneously resorb.

## ■ CHERUBISM

Cherubism is a rare, inherited disease characterized by progressive, painless, and symmetrical expansion of the jaws, resulting in the clinical appearance of a cherub (putti): a rounded face with an upward gaze toward heaven. It is usually an autosomal dominant inherited disease of childhood that is usually self-limited. The disorder is caused by mutations in *SH3BP2* (4p16.3).

### CLINICAL FEATURES

Very rare, patients nearly always present before 5 years of age, with males affected more commonly than females (2:1). Interestingly, there is a 100% penetrance of the disease in males and 50% to 70% in females. The mandible is affected most often, particularly the ascending rami, followed by the posterior maxilla. The symptoms depend on the severity of the disease, occasionally resulting in extremely grotesque physical deformity but in

patients of normal mental ability. Usually, there is a symmetrical, hard, and painless swelling of the jaws, giving an angelic appearance. When the infraorbital maxilla is involved, the inferior sclera is more prominent, resulting in the “eyes toward heaven” appearance (Fig. 14.17). Dental complications with malalignment of the teeth and impacted teeth may be seen.

### RADIOGRAPHIC FEATURES

Bilateral, symmetrical involvement of the mandible and maxilla is usually seen, although the extent of involvement can range from minor to massive. There are bilateral, multilocular radiolucencies, showing cortical expansion and thinning. Teeth may be displaced or appear to float in cyst-like spaces.

### PATHOLOGIC FEATURES

#### GROSS FINDINGS

The submitted material mostly consists of brown hard to soft tissue fragments. Teeth or tooth germs may also be recognized if removed. Periosteum is not usually seen.

### CHERUBISM—DISEASE FACT SHEET

#### Definition

- Bilateral progressive, painless and symmetrical jaw expansion due to an autosomal dominant inherited mutation in *SH3BP2*

#### Incidence and Location

- Rare
- Bilateral jaw deformity (maxilla and/or mandible)

#### Sex and Age Distribution

- Males > females (2:1)
- Usually present before 5 years of age

#### Clinical Features

- Bony expansion of the jaws leading to symmetrical, hard, painless facial swelling
- Symptoms depend on disease severity
- Angelic facies with prominent inferior sclera (heavenly gaze)

#### Radiographic Features

- Bilateral, symmetrical, multilocular soap bubble-like radiolucencies with displaced teeth

#### Prognosis and Treatment

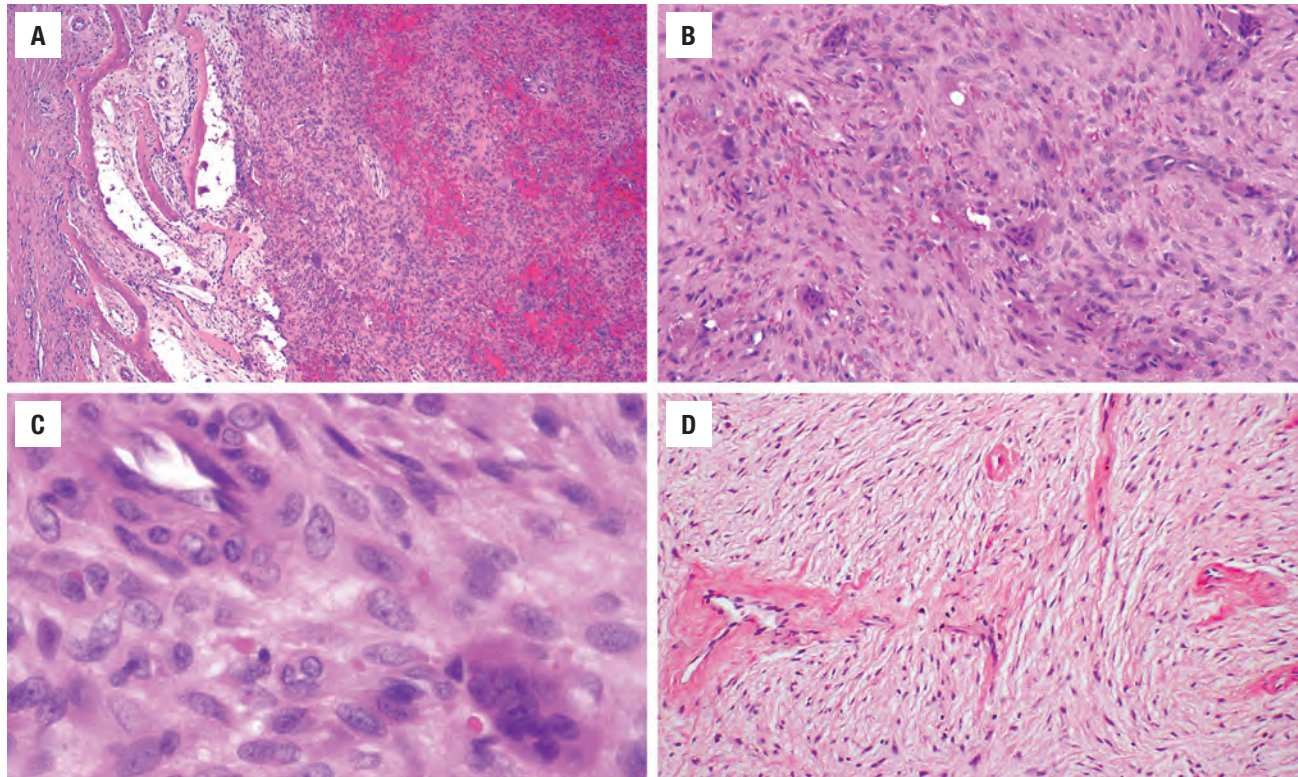
- Watchful waiting, as disease burns out with onset of puberty
- Cosmetic surgery for facial deformity but late in disease to avoid recurrence or progression
- Radiation is contraindicated



**FIGURE 14.17**

Young boy showing the maxillary swelling typical for cherubism (shown with permission).



**FIGURE 14.18**

(A) Cherubism does not show bone formation, but instead, reactive remodeled bone is seen at the border or periphery of the lesion. (B) Fibrous connective tissue with osteoclastic giant cells. (C) The nuclei of the giant cells are different from the surrounding stroma. (D) Perivascular hyalinization is quite characteristic. (D, courtesy Dr. J. Wright.)

### CHERUBISM—PATHOLOGIC FEATURES

#### Gross Findings

- Brown soft tissue fragments, sometimes including teeth or tooth germs

#### Microscopic Findings

- Clinical-radiographic-pathologic correlation mandatory
- Fibrocellular tissue with osteoclast-like giant cells, mostly clustering in areas of hemorrhage
- Perivascular eosinophilic collagen cuffing is unique
- Bone formation usually reactive on lesion periphery

#### Pathologic Differential Diagnosis

- Fibrous dysplasia, hyperparathyroidism, odontogenic lesions, central giant cell lesion

### MICROSCOPIC FINDINGS

A diagnosis cannot be rendered without clinical and radiographic correlation because the histologic findings are often nonspecific. There is a vascularized fibrous stroma, often showing a whorled pattern. A perivascular eosinophilic collagen cuffing (Fig. 14.18) is quite helpful in yielding the diagnosis. Osteoclast-like giant cells are usually numerous, seen preferentially near hemorrhage or degenerated material. Mitoses are present but are not

increased nor atypical. Bone formation is usually confined to the periphery of the lesion as a reactive remodeling or woven bone (Fig. 14.18). There may also be immature odontogenic tissue due to developing tooth germs lying within the lesional tissue.

### DIFFERENTIAL DIAGNOSIS

Cherubism needs to be distinguished from fibrous dysplasia, hyperparathyroidism, odontogenic lesions, and central giant cell lesion. All of these lesions may show histologic overlap but do not show the symmetric involvement of multiple jaw quadrants seen in cherubism, and children are rarely affected by these other disorders. Hyperparathyroidism/brown tumor should be clinically excluded. Concomitant presence of immature odontogenic tissues should not be interpreted as evidence for an odontogenic tumor such as an ameloblastic fibroma or immature odontoma.

### PROGNOSIS AND THERAPY

With the onset of puberty, the lesions lose their activity and may mature to fibrous tissue and bone. Thus a

watchful waiting approach for natural involution in adulthood is advocated. However, surgery for cosmesis should be avoided early in the disorder because it seems to result in recurrences or progression. Radiation is absolutely contraindicated. Ultimately, there is an excellent prognosis but often delayed up to 20 to 30 years later.

## ■ CEMENTO-OSSEOUS DYSPLASIA

Also called osseous dysplasia, cemento-osseous dysplasia is a pathologic process of unknown etiology affecting the tooth-bearing areas of the jaw in the vicinity of vital teeth. The lesion is considered a reactive process with origins from the periodontal ligament, with fibroblasts that may deposit bone and/or cementum.

### CLINICAL FEATURES

Cemento-osseous dysplasia occurs in various histologically identical but clinically and radiographically different types. Therefore radiographic studies are imperative before rendering a diagnosis. *Periapical osseous dysplasia* occurs in the anterior mandible and involves only a few adjacent teeth. A similar limited lesion in a posterior jaw quadrant is known as *focal osseous dysplasia*. *Florid osseous dysplasia* is also nonexpansile but involves more than one jaw quadrant and is typically seen in middle-aged black females. *Familial gigantiform cementoma* is expansile, involves multiple quadrants, and occurs at a young age.

### RADIOGRAPHIC FEATURES

Lesions are either predominantly radiolucent, predominantly radiodense, or mixed, depending on the ratio of hard to soft tissue. They are characteristically located in the tooth-bearing part of the jaw from which they may spread to adjacent areas. However, there is often a well-defined, thin peripheral radiolucent rim, with a separation of the periodontal ligament from the teeth.

### PATHOLOGIC FEATURES

#### GROSS FINDINGS

Generally, there are gritty fragments of bony tissue.

#### MICROSCOPIC FINDINGS

Cemento-osseous dysplasia consists of cellular fibrous tissue, trabeculae of woven and/or lamellar bone, and

### CEMENTO-OSSEOUS DYSPLASIA—DISEASE FACT SHEET

#### Definition

- Tooth-associated lesions consisting of fibrous tissue and bone occurring in several clinical subtypes

#### Incidence and Location

- 2.6 cases per 1,000 patients for periapical osseous dysplasia
- Periapical osseous dysplasia in the anterior mandible
- Focal osseous dysplasia in the posterior mandible
- Florid osseous dysplasia in several jaw quadrants simultaneously
- Familial gigantiform cementoma in all jaw quadrants simultaneously

#### Sex, Race, and Age Distribution

- Periapical osseous dysplasia more common in black women, usually > 25 years
- Focal osseous dysplasia mostly in white females and occurring in the fourth to fifth decades
- Florid osseous dysplasia mainly in middle-aged black females
- Familial gigantiform cementoma in young children

#### Clinical Features

- No clinical features in case of periapical and focal osseous dysplasia
- Pain and swelling in case of florid osseous dysplasia due to frequent concomitant infection
- Swelling in case of familial gigantiform cementoma

#### Radiographic Features

- Mixed radiodense radiolucent lesions adjacent to the roots of the teeth
- Anterior mandible in case of periapical osseous dysplasia
- Posterior mandible in case of focal osseous dysplasia
- Extensive jaw involvement with gigantiform cementoma

#### Prognosis and Treatment

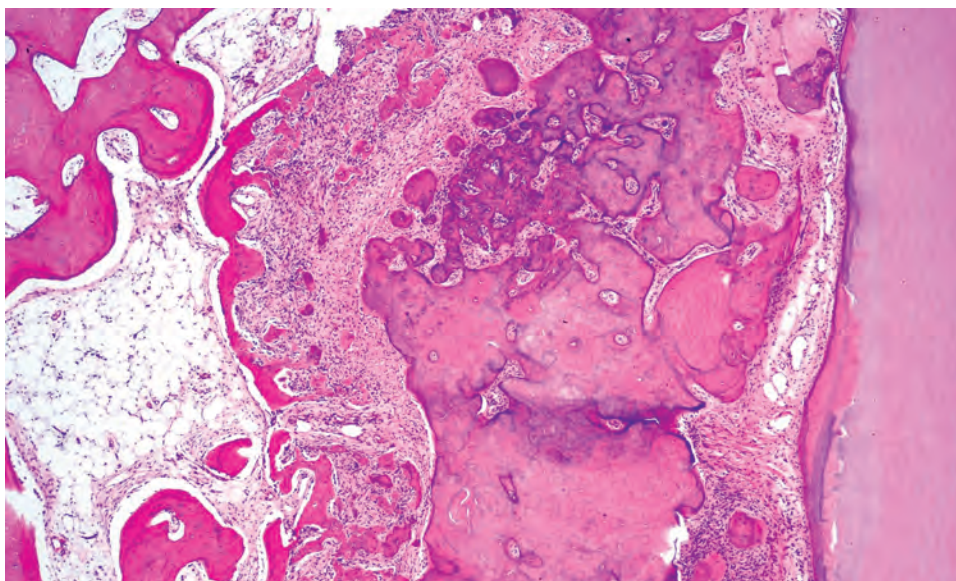
- Only treated for infection or cosmetic deformity

spherules of cementum-like material. Moreover, deeply basophilic amorphous particles may be present. Osteoblastic rimming is uncommon. Cemento-osseous dysplasia lacks demarcation and will merge with the adjacent cortical or medullary bone, but the mineralized tissue does not connect with the root surface (Fig. 14.19). Inflammatory changes are absent, although sometimes a rich vascularity can be seen, resulting in hemorrhagic foci.

### DIFFERENTIAL DIAGNOSIS

The differential diagnosis includes ossifying fibroma, fibrous dysplasia, and sclerosing osteomyelitis. Ossifying fibroma is a single, expansive, predominantly radiolucent lesion. Separation by histology alone may be impossible, requiring radiographic and clinical features. Sclerosing lamellar bone and well-vascularized fibrous tissue with lymphocytes and plasma cells define sclerosing



**FIGURE 14.19**

Osseous dysplasia is interposed between bone (*left side*) and tooth surface (*right side*). The lesional tissue may fuse with surrounding bone, but the tooth surface is not touched. The variation in size, outline, and tinctural qualities of bone in osseous dysplasia is also illustrated in this case.

#### CEMENTO-OSSEOUS DYSPLASIA—PATHOLOGIC FEATURES

##### Gross Findings

- Gritty fragments of bone

##### Microscopic Findings

- Fibrous tissue of varying cellularity with woven as well as lamellar bone, lacking demarcation (merges with adjacent bone)
- Amorphous basophilic calcifications
- Smoothly contoured acellular particles resembling cementum
- Osteoblastic rimming is uncommon

##### Pathologic Differential Diagnosis

- Ossifying fibroma, fibrous dysplasia, chronic sclerosing osteomyelitis

osteomyelitis. Fibrous dysplasia is composed of irregular woven bone without osteoblastic rimming, whereas cemento-osseous dysplasia shows woven and lamellar bone and mineralized particles resembling cementum.

#### PROGNOSIS AND THERAPY

Treatment for all forms of cemento-osseous dysplasia is needed only when there is infection or sclerotic bone masses that result in cosmetic deformities.

#### SUGGESTED READINGS

The complete Suggested Readings list is available online at [ExpertConsult.com](http://ExpertConsult.com).

**SUGGESTED READINGS****Osteomyelitis**

1. Aitasalo K, et al. A modified protocol for early treatment of osteomyelitis and osteoradionecrosis of the mandible. *Head Neck*. 1998;20(5):411–417.
2. Dudkiewicz M, et al. Acute mastoiditis and osteomyelitis of the temporal bone. *Int J Pediatr Otorhinolaryngol*. 2005;69(10):1399–1405.
3. Krakowiak PA. Alveolar osteitis and osteomyelitis of the jaws. *Oral Maxillofac Surg Clin North Am*. 2011;23(3):401–413.
4. Marshall AH, et al. Osteomyelitis of the frontal bone secondary to frontal sinusitis. *J Laryngol Otol*. 2000;114(12):944–946.
5. Perloff JR, et al. Bone involvement in sinusitis: an apparent pathway for the spread of disease. *Laryngoscope*. 2000;110(12):2095–2099.
6. Prasad KC, et al. Osteomyelitis in the head and neck. *Acta Otolaryngol*. 2007;127(2):194–205.
7. Schneider LC, et al. Differences between florid osseous dysplasia and chronic diffuse sclerosing osteomyelitis. *Oral Surg Oral Med Oral Pathol*. 1990;70:308–312.
8. Sethi A, et al. Tubercular and chronic pyogenic osteomyelitis of cranio-facial bones: a retrospective analysis. *J Laryngol Otol*. 2008;122(8):799–804.
9. Sharkawy AA. Cervicofacial actinomycosis and mandibular osteomyelitis. *Infect Dis Clin North Am*. 2007;21(2):543–556, viii.
10. Swei Y, et al. Chronic recurrent multifocal osteomyelitis involving the mandible. *Oral Surg Oral Med Oral Pathol*. 1994;78:156–162.

**Dentigerous Cyst**

1. Al-Otaibi O, et al. Syndecan-1 (CD 138) surface expression marks cell type and differentiation in ameloblastoma, keratocystic odontogenic tumor, and dentigerous cyst. *J Oral Pathol Med*. 2013;42(2):186–193.
2. Dunsche A, et al. Dentigerous cyst versus unicystic ameloblastoma—differential diagnosis in routine histology. *J Oral Pathol Med*. 2003;32:486–491.
3. Farah CS, et al. Pericoronal radiolucencies and the significance of early detection. *Aust Dent J*. 2002;47(3):262–265.
4. Grossmann SM, et al. Demographic profile of odontogenic and selected nonodontogenic cysts in a Brazilian population. *Oral Surg Oral Med Oral Pathol Oral Radiol Endod*. 2007;104(6):e35–e41.
5. Lin HP, et al. A clinicopathological study of 338 dentigerous cysts. *J Oral Pathol Med*. 2013;42(6):462–467.
6. Malčić A, et al. Alterations of FHIT and P53 genes in keratocystic odontogenic tumor, dentigerous and radicular cyst. *J Oral Pathol Med*. 2008;37(5):294–301.
7. Mosqueda-Taylor A, et al. Odontogenic cysts. Analysis of 856 cases. *Med Oral*. 2002;7(2):89–96.
8. Yeo JF, et al. Clinicopathological study of dentigerous cysts in Singapore and Malaysia. *Malays J Pathol*. 2007;29(1):41–47.

**Periapical Cyst/Granuloma**

1. Dammaschke T, et al. Long-term survival of root-canal-treated teeth: a retrospective study over 10 years. *J Endod*. 2003;29(10):638–643.
2. Das SN, et al. A survey of 4478 biopsy specimens of oral lesions. *J Pierre Fauchard Acad*. 1994;8(4):143–147.
3. Kirkevang LL, et al. Frequency and distribution of endodontically treated teeth and apical periodontitis in an urban Danish population. *Int Endod J*. 2001;34(3):198–205.
4. Lustmann J, et al. Radicular cysts arising from deciduous teeth. Review of the literature and report of 23 cases. *Int J Oral Surg*. 1985;14(2):153–161.
5. Mass E, et al. A clinical and histopathological study of radicular cysts associated with pri-mary molars. *J Oral Pathol Med*. 1995;24(10):458–461.
6. Nair PN. New perspectives on radicular cysts: do they heal? *Int Endod J*. 1998;31(3):155–160.
7. Philipsen HP, et al. The inflammatory paradental cyst: a critical review of 342 cases from a literature survey, including 17 new cases from the author's files. *J Oral Pathol Med*. 2004;33(3):147–155.

8. Silva TA, et al. Paradental cyst mimicking a radicular cyst on the adjacent tooth: case report and review of terminology. *J Endod*. 2003;29(1):73–76.
9. Siqueira JF Jr, et al. Bacteria in the apical root canal of teeth with primary apical periodontitis. *Oral Surg Oral Med Oral Pathol Oral Radiol Endod*. 2009;107(5):721–726.
10. Slootweg PJ. Lesions of the jaws. *Histopathology*. 2009;54:401–418.
11. Wood RE, et al. Radicular cysts of primary teeth mimicking premolar dentigerous cysts: report of three cases. *ASDC J Dent Child*. 1988;55(4):288–290.

**Fibrous Dysplasia**

1. Berlucchi M, et al. Endoscopic surgery for fibrous dysplasia of the sinonasal tract in pediatric patients. *Int J Pediatr Otorhinolaryngol*. 2005;69(1):43–48.
2. Brannon RB, et al. Benign fibro-osseous lesions: a review of current concepts. *Adv Anat Pathol*. 2001;8:126–143.
3. Chan EK. Ethmoid fibrous dysplasia with anterior skull base and intraorbital extension. *Ear Nose Throat J*. 2005;84(10):627–628.
4. Conejero JA, et al. Management of incidental fibrous dysplasia of the maxilla in a patient with facial fractures. *J Craniofac Surg*. 2007;18(6):1463–1464.
5. Ebata K, et al. Chondrosarcoma and osteosarcoma arising in polyostotic fibrous dysplasia. *J Oral Maxillofac Surg*. 1992;50:761–764.
6. Edmundson AC, et al. Overgrowth syndromes. *J Pediatr Genet*. 2015;4:136–143.
7. Galvan O, et al. Fibro-osseous lesion of the middle turbinate: ossifying fibroma or fibrous dysplasia? *J Laryngol Otol*. 2007;121(12):1201–1203.
8. Gerceker M, et al. Fibrous dysplasia in the retropharyngeal area. *Ear Nose Throat J*. 2006;85(7):446–447.
9. Hempel JM, et al. Fibrous dysplasia of the frontal bone. *Ear Nose Throat J*. 2006;85(10):654, 656–657.
10. Hullar TE, et al. Paget's disease and fibrous dysplasia. *Otolaryngol Clin North Am*. 2003;36(4):707–732.
11. Kim YH, et al. Role of surgical management in temporal bone fibrous dysplasia. *Acta Otolaryngol*. 2009;129(12):1374–1379.
12. Mäkitie AA, et al. Bisphosphonate treatment in craniofacial fibrous dysplasia—a case report and review of the literature. *Clin Rheumatol*. 2008;27(6):809–812.
13. Mendonça Caridad JJ, et al. Fibrous dysplasia of the mandible: surgical treatment with platelet-rich plasma and a corticocancellous iliac crest graft—report of a case. *Oral Surg Oral Med Oral Pathol Oral Radiol Endod*. 2008;105(4):e12–e18.
14. Mendonça-Caridad JJ, et al. Frontal sinus obliteration and craniofacial reconstruction with platelet rich plasma in a patient with fibrous dysplasia. *Int J Oral Maxillofac Surg*. 2006;35(1):88–91.
15. Menezes AH. Craniovertebral junction neoplasms in the pediatric population. *Childs Nerv Syst*. 2008;24(10):1173–1186.
16. Nelson BL, et al. Fibrous dysplasia of bone. *Ear Nose Throat J*. 2003;82(4):259.
17. Ozbek C, et al. Fibrous dysplasia of the temporal bone. *Ann Otol Rhinol Laryngol*. 2003;112(7):654–656.
18. Panda NK, et al. A clinicoradiologic analysis of symptomatic craniofacial fibro-osseous lesions. *Otolaryngol Head Neck Surg*. 2007;136(6):928–933.
19. Post G, et al. Endoscopic resection of large sinonasal ossifying fibroma. *Am J Otolaryngol*. 2005;26(1):54–56.
20. Riminucci M, et al. The histopathology of fibrous dysplasia of bone in patients with activating mutations of the Gsα gene: site-specific patterns and recurrent histological hallmarks. *J Pathol*. 1999;187:249–258.
21. Slootweg PJ. Maxillofacial fibro-osseous lesions: classification and differential diagnosis. *Semin Diagn Pathol*. 1996;13:104–112.
22. Song JJ, et al. Monostotic fibrous dysplasia of temporal bone: report of two cases and re-view of its characteristics. *Acta Otolaryngol*. 2005;125(10):1126–1129.
23. Wenig BM, et al. Fibro-osseous, osseous, and cartilaginous lesions of the orbit and paraorbi-tal region. Correlative clinicopathologic and radiographic findings, including the diagnostic role of CT and MR imaging. *Radiol Clin North Am*. 1998;36(6):1241–1259, xii.
24. Yu Hon Wan A, et al. Fibrous dysplasia of the temporal bone presenting with facial nerve palsy and conductive hearing loss. *Otol Neurotol*. 2008;29(7):1039–1040.



### Osteonecrosis

- Barasch A, et al. Risk factors for osteonecrosis of the jaws: a case-control study from the CONDOR dental PBRN. *J Dent Res*. 2011;90(4):439–444.
- Benlier E, et al. Massive osteoradionecrosis of facial bones and soft tissues. *J BUON*. 2009;14(3):523–527.
- Cohen EE, et al. Efficacy and safety of treating T4 oral cavity tumors with primary chemoradiotherapy. *Head Neck*. 2009;31(8):1013–1021.
- Ferguson HW, et al. Advances in head and neck radiotherapy to the mandible. *Oral Maxillofac Surg Clin North Am*. 2007;19(4):553–563, vii.
- Freiberger JJ, et al. Multimodality surgical and hyperbaric management of mandibular osteoradionecrosis. *Int J Radiat Oncol Biol Phys*. 2009;75(3):717–724.
- Hamadeh IS, et al. Drug induced osteonecrosis of the jaw. *Cancer Treat Rev*. 2015;41(5):455–464.
- Hansen T, et al. Osteonecrosis of the jaws in patients treated with bisphosphonates—histomorphologic analysis in comparison with infected osteoradionecrosis. *J Oral Pathol Med*. 2006;35:155–160.
- Hellstein J. Osteochemonecrosis: an overview. *Head Neck Pathol*. 2014;8(4):482–490.
- McLeod NM, et al. Management of patients at risk of osteoradionecrosis: results of survey of dentists and oral & maxillofacial surgery units in the United Kingdom, and suggestions for best practice. *Br J Oral Maxillofac Surg*. 2010;48(4):301–304.
- Otmani N. Oral and maxillofacial side effects of radiation therapy on children. *J Can Dent Assoc*. 2007;73(3):257–261.
- Peterson DE, et al. Osteoradionecrosis in cancer patients: the evidence base for treatment-dependent frequency, current management strategies, and future studies. *Support Care Cancer*. 2010;18(8):1089–1098.
- Reuther T, et al. Osteoradionecrosis of the jaws as a side effect of radiotherapy of head and neck tumour patients—a report of a thirty year retrospective review. *Int J Oral Maxillofac Surg*. 2003;32:289–295.
- Yazdi PM, et al. Dentoalveolar trauma and minor trauma as precipitating factors for medication-related osteonecrosis of the jaw (ONJ): a retrospective study of 149 consecutive patients from the Copenhagen ONJ Cohort. *Oral Surg Oral Med Oral Pathol Oral Radiol*. 2015;119(4):416–422.
- Harnet JC, et al. Solitary bone cyst of the jaws: a review of the etiopathogenic hypotheses. *J Oral Maxillofac Surg*. 2008;66(11):2345–2348.
- Saito Y, et al. Simple bone cyst. A clinical and histopathologic study of fifteen cases. *Oral Surg Oral Med Oral Pathol*. 1992;74:487–491.
- Shimoyama T, et al. So-called simple bone cyst of the jaw: a family of pseudocysts of diverse nature and etiology. *J Oral Sci*. 1999;41(2):93–98.
- Slootweg PJ. Lesions of the jaws. *Histopathology*. 2009;54(4):401–418.
- Suei Y, et al. A comparative study of simple bone cysts of the jaw and extracranial bones. *Dentomaxillofac Radiol*. 2007;36(3):125–129.
- Suei Y, et al. Simple bone cyst of the jaws: evaluation of treatment outcome by review of 132 cases. *J Oral Maxillofac Surg*. 2007;65(5):918–923.
- Tong AC, et al. Variations in clinical presentations of the simple bone cyst: report of cases. *J Oral Maxillofac Surg*. 2003;61:1487–1491.

### Tori

- Antoniades DZ, et al. Concurrence of torus palatinus with palatal and buccal exostoses: case report and review of the literature. *Oral Surg Oral Med Oral Pathol Oral Radiol Endod*. 1998;85:552–557.
- Chohayeb AA, et al. Occurrence of torus palatinus and mandibularis among women of different ethnic groups. *Am J Dent*. 2001;14(5):278–280.
- Jainkittivong A, et al. Prevalence and clinical characteristics of oral tori in 1,520 Chulalongkorn University Dental School patients. *Surg Radiol Anat*. 2007;29(2):125–131.
- Jainkittivong A, et al. Buccal and palatal exostoses: prevalence and concurrence with tori. *Oral Surg Oral Med Oral Pathol Oral Radiol Endod*. 2000;90:48–53.

### Cherubism

- Beaman FD, et al. Imaging characteristics of cherubism. *AJR Am J Roentgenol*. 2004;182(4):1051–1054.
- Carvalho Silva E, et al. Cherubism: clinicoradiographic findings, treatment, and long-term follow-up of 8 cases. *J Oral Maxillofac Surg*. 2007;65(3):517–522.
- Carvalho VM, et al. Novel mutations in the SH3BP2 gene associated with sporadic central giant cell lesions and cherubism. *Oral Dis*. 2009;15(1):106–110.
- Hatani T, et al. Adaptor protein 3BP2 and cherubism. *Curr Med Chem*. 2008;15(6):549–554.
- Jing X, et al. Fine-needle aspiration cytological findings of cherubism. *Diagn Cytopathol*. 2008;36(3):188–189.
- Kadlub N, et al. Defining a new aggressiveness classification and using NFATc1 localization as a prognostic factor in cherubism. *Hum Pathol*. 2016;58:62–71.
- Kozakiewicz M, et al. Cherubism—clinical picture and treatment. *Oral Dis*. 2001;7(2):123–130.
- Mortellaro C, et al. Diagnosis and treatment of familial cherubism characterized by early onset and rapid development. *J Craniofac Surg*. 2009;20(1):116–120.
- Ozkan Y, et al. Clinical and radiological evaluation of cherubism: a sporadic case report and review of the literature. *Int J Pediatr Otorhinolaryngol*. 2003;67:1005–1012.
- Peñarocha M, et al. Cherubism: a clinical, radiographic, and histopathologic comparison of 7 cases. *J Oral Maxillofac Surg*. 2006;64(6):924–930.
- Reichenberger EJ, et al. The role of SH3BP2 in the pathophysiology of cherubism. *Orphanet J Rare Dis*. 2012;7(suppl 1):S5.
- Tiziani V, et al. The gene for cherubism maps to chromosome 4p16. *Am J Hum Genet*. 1999;65:158–166.
- Von Wöern N. Cherubism: a 36-year long-term follow-up of 2 generations in different families and review of the literature. *Oral Surg Oral Med Oral Pathol Oral Radiol Endod*. 2000;90:765–772.
- Yamaguchi T, et al. Cherubism: clinicopathologic findings. *Skeletal Radiol*. 1999;28(6):350–353.
- Allard RH, et al. Nasopalatine duct cyst. Review of the literature and report of 22 cases. *Int J Oral Surg*. 1981;10(6):447–461.
- Elliott KA, et al. Diagnosis and surgical management of nasopalatine duct cysts. *Laryngoscope*. 2004;114:1336–1340.
- Escoda Francolí J, et al. Nasopalatine duct cyst: report of 22 cases and review of the literature. *Med Oral Patol Oral Cir Bucal*. 2008;13(7):E438–E443.
- Hertzanu Y, et al. Nasopalatine duct cyst. *Clin Radiol*. 1985;36(2):153–158.
- Jones RS, et al. Nonodontogenic cysts of the jaws and treatment in the pediatric population. *Oral Maxillofac Surg Clin North Am*. 2016;28:31–44.
- Spinelli HM, et al. Nasopalatine duct cysts and the role of magnetic resonance imaging. *J Craniofac Surg*. 1994;5(1):57–60.
- Suter VG, et al. The nasopalatine duct cyst—epidemiology, diagnosis and therapy. *Schweiz Monatsschr Zahnmed*. 2007;117(8):824–839 [in French, German].
- Swanson KS, et al. Nasopalatine duct cyst: an analysis of 334 cases. *J Oral Maxillofac Surg*. 1991;49:268–271.
- Vasconcelos R, et al. Retrospective analysis of 31 cases of nasopalatine duct cyst. *Oral Dis*. 1999;5:325–328.

### Simple Bone Cyst

- Copete MA, et al. Solitary bone cyst of the jaws: radiographic review of 44 cases. *Oral Surg Oral Med Oral Pathol Oral Radiol Endod*. 1998;85(2):221–225.
- Cortell-Ballester I, et al. Traumatic bone cyst: a retrospective study of 21 cases. *Med Oral Patol Oral Cir Bucal*. 2009;14(5):E239–E243.

**Osseous Dysplasia**

1. Brannon RB, et al. Benign fibro-osseous lesions: a review of current concepts. *Adv Anat Pathol*. 2001;8:126–143.
2. Schneider LC, et al. Differences between florid osseous dysplasia and chronic diffuse sclerosing osteomyelitis. *Oral Surg Oral Med Oral Pathol*. 1990;70:308–312.
3. Slootweg PJ. Maxillofacial fibro-osseous lesions: classification and differential diagnosis. *Semin Diagn Pathol*. 1996;13:104–112.
4. Su L, et al. Distinguishing findings of focal cemento-osseous dysplasias and cemento-ossifying fibromas. II. A clinical and radiologic spectrum of 316 cases. *Oral Surg Oral Med Oral Pathol Oral Radiol Endod*. 1997;84:540–549.
5. Summerlin DJ, et al. Focal cemento-osseous dysplasia: a clinico-pathologic study of 221 cases. *Oral Surg Oral Med Oral Pathol*. 1994;78:611–620.



# Benign Neoplasms of the Gnathic Bones

■ Brenda L. Nelson

## ■ OSSIFYING FIBROMA

Ossifying fibroma is a benign neoplasm that falls in to the broader category of benign fibro-osseous lesions (BFOLs). All BFOLs are characterized by the replacement of native bone by fibrous and mineralized tissues and are grouped together due to their histologic similarities despite having different clinical features and treatments. The other BFOLs, fibrous dysplasia and the cemento-osseous dysplasias, can be difficult to differentiate microscopically, and therefore all BFOLs require radiographic and clinical correlation to make an accurate diagnosis. Bone and/or cementum may be present in an ossifying fibroma, and so *cemento-ossifying fibroma (COF)* may also be used interchangeably. By convention the term ossifying fibroma generally refers to the cemento-ossifying type, which is associated with tooth-bearing areas, whereas juvenile ossifying fibroma (discussed separately) is denoted by the term “juvenile.” Distinguishing these entities is important due to their differing biologic behavior, treatment, and prognosis.

### CLINICAL FEATURES

Ossifying fibromas are relatively rare and are found more commonly in the mandible (90%) than the maxilla, specifically affecting the molar-premolar area. Patients in the third to fourth decades are most affected, with a high female-to-male ratio (5:1). Small lesions are usually asymptomatic, often incidental findings on routine dental radiographs. Larger lesions may result in significant cosmetic and functional morbidity.

### RADIOGRAPHIC FEATURES

Radiographic images are essential to the diagnosis, and a diagnosis should not be rendered without radiographs

or their reliable interpretation. Ossifying fibromas are characteristically well-demarcated unilocular or multilocular radiolucent lesions with varying degrees of radiopacity (Fig. 15.1). The radiopacities correlate with the mineralized component of the tumor. Large lesions may cause displacement of teeth, root divergence, or alterations of adjacent structures. Furthermore, a characteristic downward bowing of the mandible may be helpful in developing a radiographic differential diagnosis.

### OSSIFYING FIBROMA—DISEASE FACT SHEET

#### Definition

- A well-demarcated neoplasm of gnathic bones composed of fibrocellular tissue and mineralized material of varying appearances

#### Incidence and Location

- Mandible > > maxilla (90%), premolar-molar area specifically

#### Morbidity and Mortality

- Aggressive behavior is reported with functional morbidity and cosmetic disruption

#### Sex and Age Distribution

- Females > > males (5:1)
- Wide age range with a predilection for third to fourth decade

#### Clinical Features

- Small lesions are asymptomatic, incidentally discovered
- Larger lesions may cause facial deformity, malocclusion, and pain

#### Prognosis and Treatment

- Clinical follow-up for recurrences
- Surgical curettage or enucleation

**FIGURE 15.1**

(**A**, axial and **B**, coronal view) Computed tomography studies. The lesion is a well-defined, unilocular, radiolucent defect in the anterior right mandible. There is variable radiopacity and a sclerotic border.

## **PATHOLOGIC FEATURES**

### **GROSS FINDINGS**

Lesions are well demarcated, frequently described as “shelling out” of the bone. The intact tumor is a smooth, glistening, white, firm-elastic mass.

### **MICROSCOPIC FINDINGS**

Microscopically, lesions are composed of varying amounts of stellate fibrous stroma with diverse types and degrees of mineralized material. The fibrous tissue may be dense (Fig. 15.2) to nearly acellular. The mineralized tissue may appear as cementum-like basophilic deposits, trabeculae of lamellar bone, or trabeculae of woven bone (Fig. 15.3). Characteristically, plump osteoblasts are seen to rim the bony trabeculae. Rare mitotic figures may be seen, in addition to areas of pseudocystic degeneration and hemorrhage.

## **DIFFERENTIAL DIAGNOSIS**

Quality radiographs and a complete clinical history are *required* because other BFOLs may be virtually

## **OSSIFYING FIBROMA—PATHOLOGIC FEATURES**

### **Gross Findings**

- Lesions are well circumscribed, usually with a smooth surface
- Easily separated from bone (“shelling out”)

### **Microscopic Findings**

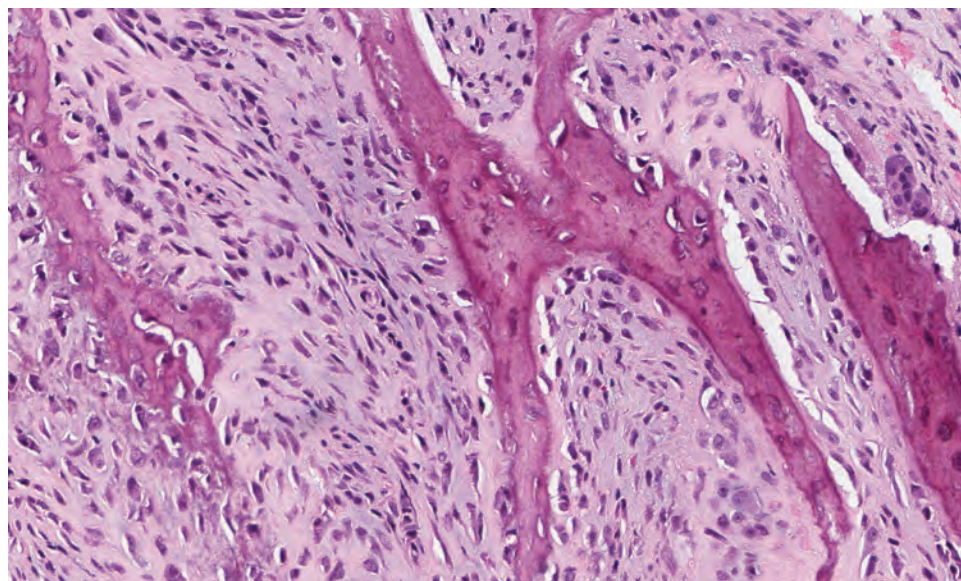
- Variably cellular fibrous stroma with calcified tissue
- Mineralized material may be cementum-like basophilic deposits or trabeculae of lamellar or woven bone
- Osteoblastic rimming is noted along with mitotic figures

### **Pathologic Differential Diagnosis**

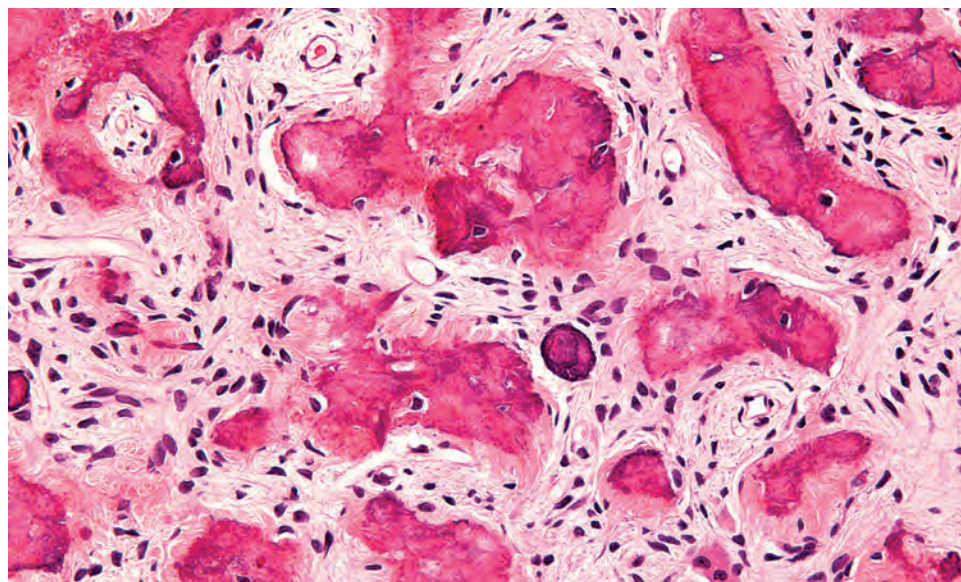
- Fibrous dysplasia, cemento-osseous dysplasia, active ossifying fibroma

indistinguishable histologically. Radiographically, *fibrous dysplasia* classically appears with a radiodense “orange-peel or ground-glass” texture that blends imperceptibly into normal bone. *Cemento-osseous dysplasia* has a varied presentation, with immature lesions appearing primarily radiolucent and more mature lesions becoming more sclerotic and radiodense. The cemento-osseous dysplasias (periapical, focal, and florid variants) are always intimately associated with the tooth-bearing areas of the jaws. An ossifying fibroma is usually a well-defined radiolucent



**FIGURE 15.2**

A cellular fibroblastic stroma with osteoid formation. Note the presence of osteoblastic rimming.

**FIGURE 15.3**

Osteoid and cementum-like material in a cellular stroma.

lesion with variable radiodensities. The BFOLS also present very differently macroscopically and intraoperatively. Grossly, *cemento-osseous dysplasia* is usually submitted as small mineralized, gritty fragments, the result of curetting. *Fibrous dysplasia* is frequently submitted in a small block or core, the consequence of sampling a lesion that is difficult to distinguish from surrounding normal bone. Finally, ossifying fibroma is generally an intact tumor mass or submitted as large fragments. It is worth noting that osteoblastic rimming is seen less frequently in the other benign fibrous osseous lesions than it is in ossifying fibroma. If no radiographic or clinical information is available, a preliminary diagnosis of BFOL may be rendered until more information can be obtained. However, definitive diagnosis is important because the treatment and prognosis of these lesions are different.

### PROGNOSIS AND THERAPY

Small lesions may be treated with enucleation and curettage, whereas larger lesions may require more extensive surgery with reconstruction. Close clinical follow-up is indicated to monitor the patient for recurrences.

### ■ JUVENILE OSSIFYING FIBROMA

Juvenile ossifying fibroma (JOF) is an ossifying fibroma variant characterized by rapid and destructive growth. These neoplasms have been further categorized into juvenile trabecular ossifying fibroma (JTOF) and juvenile



**FIGURE 15.4**

A young man from a developing nation with a large and distorting juvenile ossifying fibroma of the anterior maxilla. (Courtesy of Dr. S. R. Clarke.)

psammomatoid ossifying fibroma (JPOF) by the World Health Organization (WHO). Historically the term *active ossifying fibroma* instead of juvenile ossifying fibroma has been used because these tumors do not occur exclusively in young patients.

#### CLINICAL FEATURES

The juvenile ossifying fibromas are uncommon and are seen with considerably less frequency than their conventional counterpart. Although the trabecular variant is found most commonly in children less than 15 years old and favors the maxilla, the psammomatoid variant is generally seen in those 20 years and older and is most common to the paranasal sinuses. However, both subtypes may occasionally affect older patients. Small lesions may be detected on routine examination or patients may present with rapid, disfiguring growth (Fig. 15.4).

#### RADIOGRAPHIC FEATURES

Radiographically, the lesion presents as a well-delineated, expansile radiolucent lesion with variable focal calcifications. Lesions may demonstrate invasive growth and affect adjacent structures.

#### PATHOLOGIC FEATURES

##### GROSS FINDINGS

The juvenile ossifying fibromas are generally well circumscribed and usually demonstrate a smooth surface. Like their conventional ossifying fibroma counterpart,

#### JUVENILE OSSIFYING FIBROMA—DISEASE FACT SHEET

##### Definition

- Ossifying fibroma variant characterized by rapid and destructive growth and an increased cellularity

##### Incidence and Location

- Uncommon
- Maxilla and paranasal sinuses more common than mandible

##### Morbidity and Mortality

- Radical surgery may be associated with an increased morbidity

##### Sex and Age Distribution

- Equal sex distribution
- Trabecular variant: usually seen in patients < 15 years
- Psammomatoid variant: 20 years or older

##### Clinical Features

- Rapid, disfiguring growth

##### Radiographic Features

- Well-delineated, expansile radiolucent lesion with variable, focal calcifications

##### Prognosis and Treatment

- Recurrences reported in up to 58% of cases, requiring potentially disfiguring surgery
- Complete (radical) surgery

#### JUVENILE OSSIFYING FIBROMA—PATHOLOGIC FEATURES

##### Gross Findings

- Lesions are well circumscribed, usually with a smooth surface

##### Microscopic Findings

- Cellular proliferation of spindle cells
- Trabecular variant: immature osteoid, and trabeculae of immature bone with distinct osteoblastic rimming
- Psammomatoid variant: cementum-like psammomatous structures are variably present
- Thick, irregular collagenous rim
- Osteoclastic giant cells are commonly found
- Mitotic figures are noted

##### Pathologic Differential Diagnosis

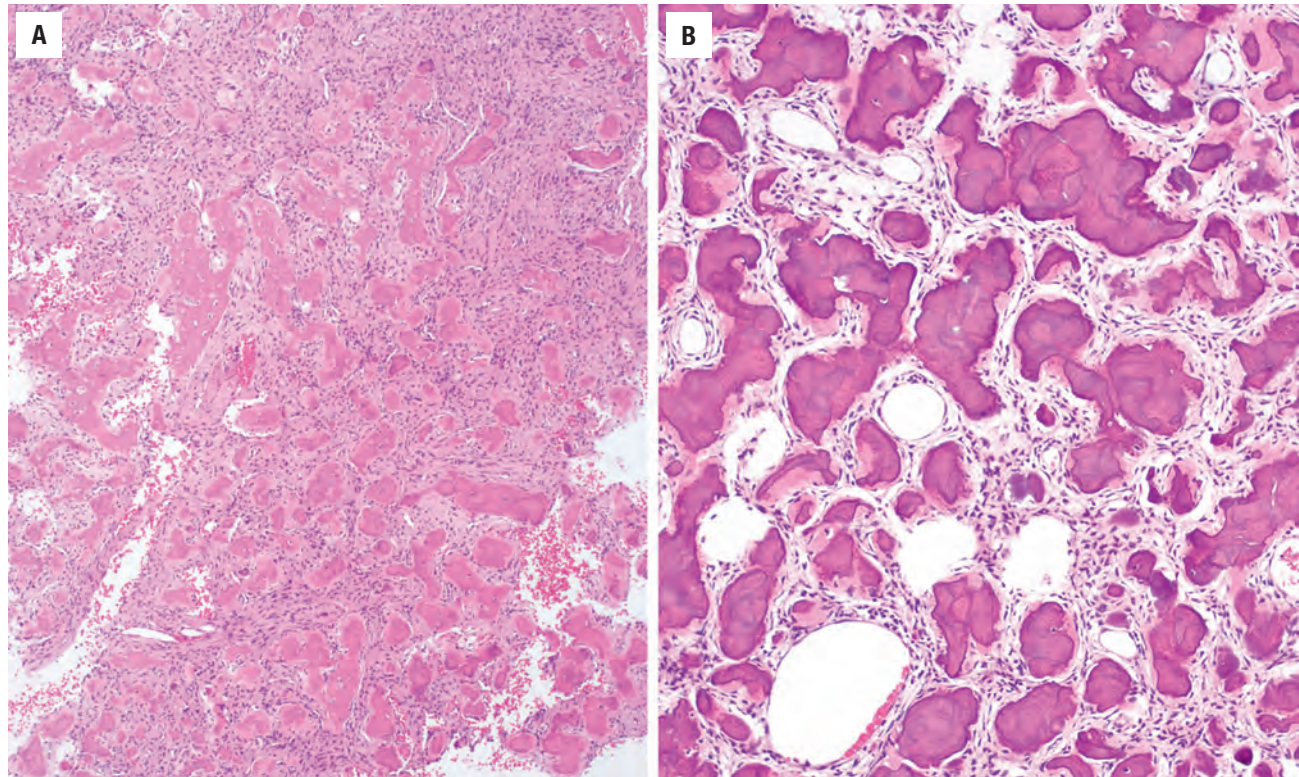
- Ossifying fibroma, extracranial meningioma

intraoperative findings may include the tumor “shelling out.” However, some lesions will grossly have a more infiltrative relationship to the surrounding bone.

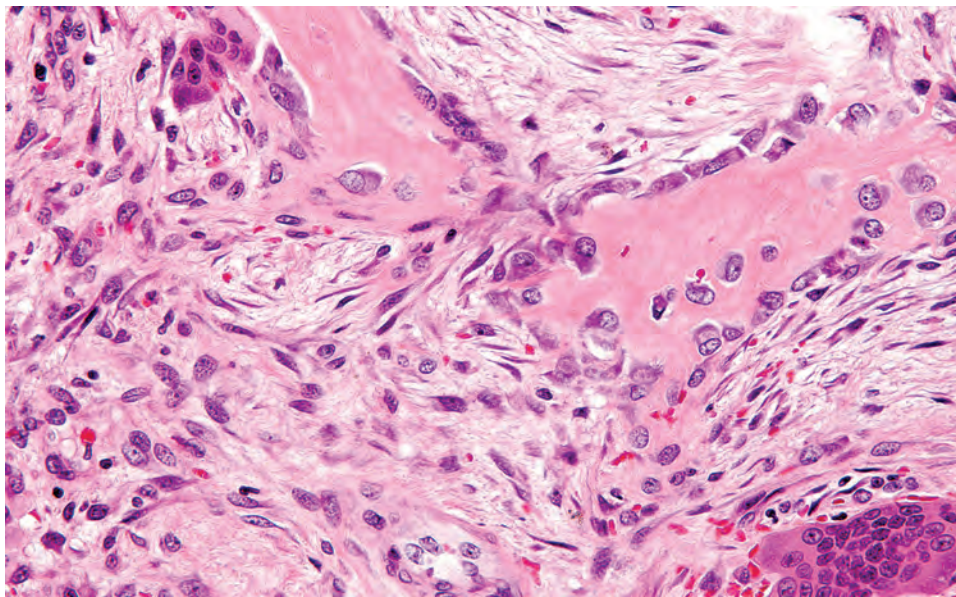
##### MICROSCOPIC FINDINGS

The JTOF is characterized by a cellular fibrous background containing trabeculae of immature bone. This



**FIGURE 15.5**

(A and B) Two separate cases showing immature trabeculae of bone with marked calcification, spheroid ossicles, and a collagenous rim. Note the high cellularity of the stroma in these juvenile ossifying fibromas.

**FIGURE 15.6**

Plump active osteoblasts lining the osteoid. Multinucleated giant cells are present in this juvenile ossifying fibroma.

bone is varied in shape, often with a thick, irregular collagenous rim (Fig. 15.5). Osteoblastic rimming is a feature of the immature bone. The JPOF has a variably cellular background with small spherical ossicles with distinct osteoblastic rimming (Fig. 15.6). Psammomatous structures are a classic feature of this lesion (Fig. 15.5B), although sometimes scant. Concentrically laminated particles may occasionally simulate a genuine psammoma body. In addition, multinucleated giant cells and

scattered mitotic figures are commonly seen in either variant.

#### DIFFERENTIAL DIAGNOSIS

The differential diagnosis includes the other BFOLs to include conventional ossifying fibroma. Differentiation

**CENTRAL ODONTOGENIC FIBROMA—DISEASE FACT SHEET****Definition**

- A benign mesenchymal neoplasm of odontogenic origin

**Incidence and Location**

- Rare
- Predilection for the anterior maxilla

**Sex and Age Distribution**

- Females > males (3:1)
- Peak incidence in second to fourth decades

**Clinical Features**

- Usually asymptomatic
- Larger lesions may cause painless jaw expansion
- Anterior maxillary lesions result in a distinctive palatal cleft

**Radiographic Features**

- Most present as well-defined unilocular radiolucencies
- Well-defined sclerotic border
- Rarely, they may be a mixed radiolucent-radiopaque multilocular lesion
- Occasionally associated with crown of unerupted tooth

**Prognosis and Treatment**

- Recurrence is rare
- Enucleation and curettage

of these lesions may require clinical, radiographic, and intraoperative data. *Extracranial meningioma*, especially with lesions of the maxilla, should be a consideration. The clinical and radiographic histories are helpful. The true psammoma bodies of a meningioma are different, as is the pattern of growth (whorled, meningothelial architecture).

**PROGNOSIS AND THERAPY**

Tumors continue to enlarge if left untreated, thereby necessitating complete surgical excision. Recurrences are common (up to 58%), resulting in potentially disfiguring surgery requiring reconstruction.

**■ CENTRAL ODONTOGENIC FIBROMA**

Central odontogenic fibroma is a rare benign mesenchymal neoplasm of dental origin. Previous publications established the practice of separating the central lesion into two histologic subtypes; however, this distinction has little clinical significance and is unnecessarily confusing.

Finally, it is helpful to note the peripheral ossifying fibroma is generally thought to be a reactive lesion and unrelated to the central ossifying fibroma.

**CLINICAL FEATURES**

Central odontogenic fibromas show a predilection for women (3:1) and an increased incidence in the second to fourth decades. Lesions may be asymptomatic, although larger lesions may cause jaw expansion and occasional perforation of the cortical plate. The tumor is generally described as a painless mass. Central odontogenic fibromas occur more frequently in the anterior maxilla and may result in a distinctive palatal cleft or depression, considered characteristic of this tumor.

**RADIOGRAPHIC FEATURES**

Radiographically, most central odontogenic fibromas are unilocular radiolucencies (Fig. 15.7), although multilocular lesions are seen. Lesions frequently present with a well-defined sclerotic border and may be associated with the crown of an unerupted tooth. Rarely, central odontogenic fibromas may appear as mixed radiolucent-radiopaque lesions. In addition, large lesions may affect adjacent structures, move teeth, or even cause root resorption.

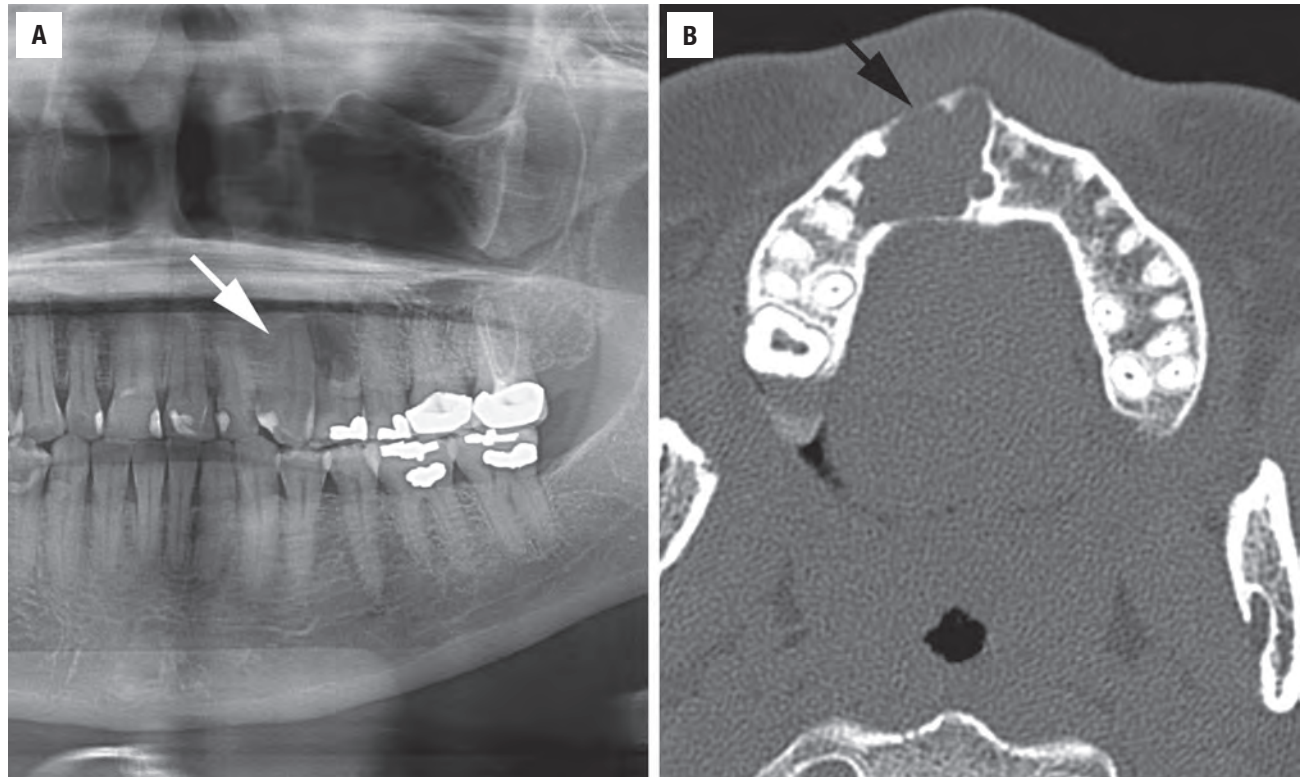
**PATHOLOGIC FEATURES****GROSS FINDINGS**

Specimens are usually encapsulated, firm smooth masses. Surgeons may state the lesion “shells out.”

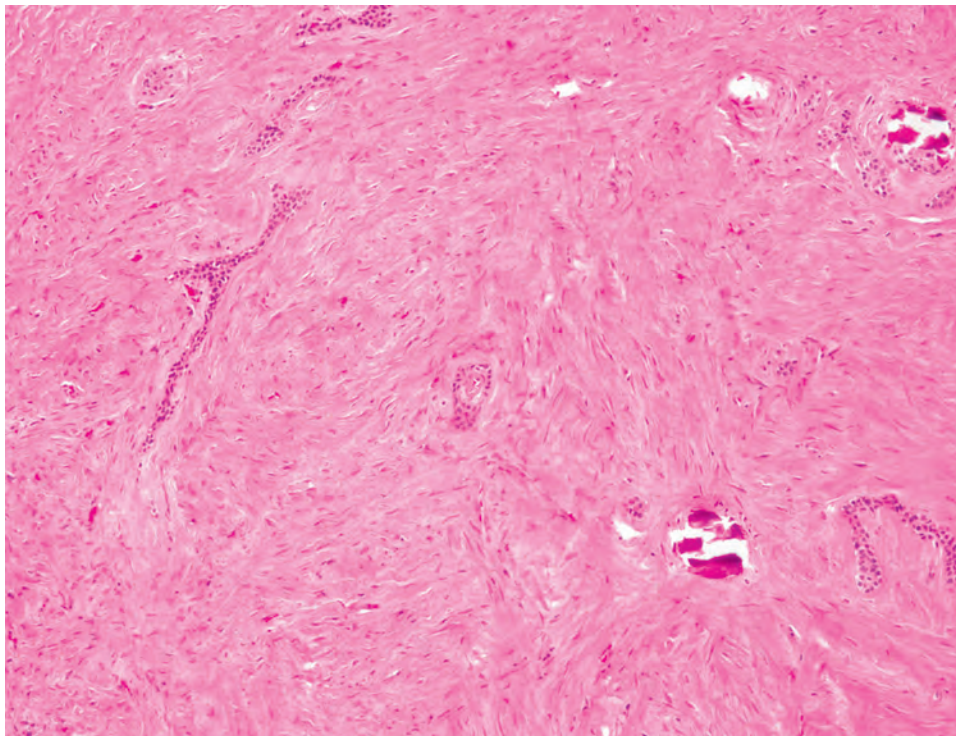
**MICROSCOPIC FINDINGS**

There is a wide variation of histologic appearances, ranging from densely hyalinized and cellular, to loose and myxomatous, to nearly acellular (Fig. 15.8). Delicate collagen fibers are occasionally identified along with fibromyxoid stroma. It is this variation that has resulted in the historical separation into two types: *epithelium-poor type* (formally referred to as the simple type) or *epithelium-rich type* (formally referred to as the WHO type). Features of odontogenic fibromas include inactive-looking odontogenic epithelium that, when present, may appear proliferative (Fig. 15.9) or form irregular islands and cords. In addition, calcifications may or may not be present, simulating cementum, osteoid, or dentin. A rare granular cell odontogenic fibroma variant also exists.

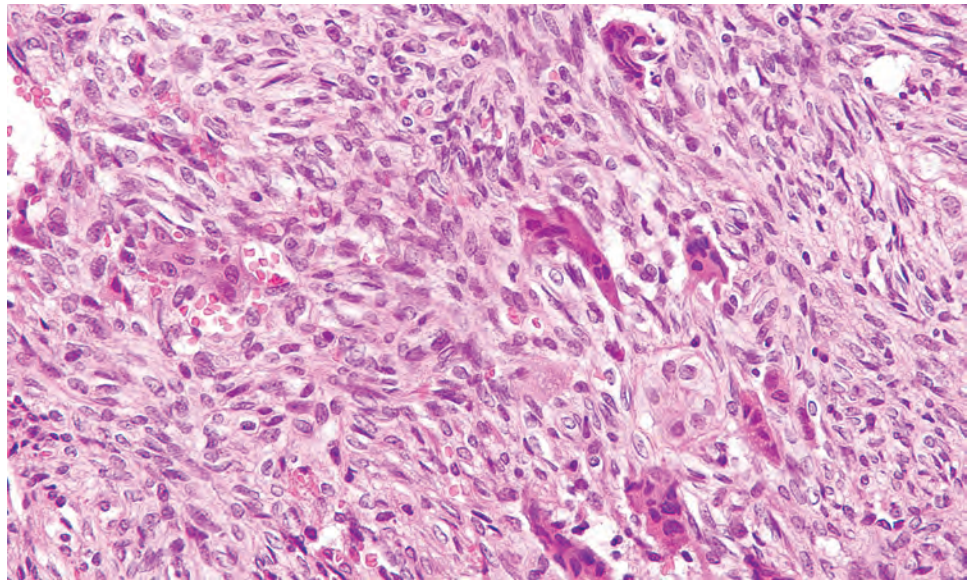


**FIGURE 15.7**

(A) A panoramic radiograph shows a radiolucent lesion adjacent to tooth roots #11 and 12 (*arrow*). (B) The corresponding computed tomography scan shows a radiolucent cyst (*arrow*) of the maxilla.

**FIGURE 15.8**

Loosely arranged fibroblasts and collagen fibrils with a deposit of cementum-like material. Note the small nest of odontogenic epithelium.

**FIGURE 15.9**

This more cellular fibrous lesion with focal nest of odontogenic epithelium is characteristic of the epithelium-rich type of central odontogenic fibroma.

#### CENTRAL ODONTOGENIC FIBROMA— PATHOLOGIC FEATURES

##### Gross Findings

- Encapsulated, firm, smooth yellow-white mass

##### Microscopic Findings

- Wide variation of histologic appearances, ranging from loose myxomatous to densely hyalinized stroma
- Odontogenic epithelium usually inactive, although proliferative type may be present
- Calcifications may or may not be present

##### Pathologic Differential Diagnosis

- Hyperplastic dental follicle, desmoplastic fibroma

#### DIFFERENTIAL DIAGNOSIS

For lesions that are epithelium poor, the microscopic appearance is similar to a *dental follicle*. Excluding a dental follicle is based on the radiographic and clinical appearance including size and location. Usually this is not a difficult distinction, and one should remember that a hyperplastic dental follicle is a very common entity, whereas the central odontogenic fibroma is exceedingly rare. A cellular central odontogenic fibroma, epithelium-rich variant, may appear similar to a *desmoplastic fibroma*. However, a desmoplastic fibroma does not have an odontogenic epithelial component nor is it found in association with teeth. In addition, desmoplastic fibromas generally demonstrate a locally infiltrative quality.

#### PROGNOSIS AND THERAPY

Surgical enucleation and curettage is usually the treatment of choice. Recurrences are rare.

#### ■ OSTEOLASTOMA

An osteoblastoma is a benign bone-forming tumor that arises from osteoblasts. It is histologically similar to osteoid osteoma but is larger than 2 cm.

#### CLINICAL FEATURES

Osteoblastoma, as a group, is a relatively rare bone lesion with approximately 10% occurring in the craniofacial bones. The mandible is affected more frequently than the maxilla, particularly the ramus, coronoid process, and condyle. The majority of cases present before 30 years of age, and there is a definite male predilection. Pain, particularly nocturnal, is a common symptom and may mimic a toothache but not relieved by aspirin.

#### RADIOGRAPHIC FEATURES

Osteoblastomas are typically well-circumscribed, round to oval lesions that are radiolucent to radiopaque. Patchy



**OSTEOBLASTOMA/OSTEOID OSTEOMA—DISEASE FACT SHEET****Definition**

- A benign bone-forming tumor of bone composed of anastomosing trabeculae of osteoid

**Incidence and Location**

- Uncommon, osteoblastomas are more common than osteoid osteoma in the gnathic bones
- 15% arise in the jaws, involving mandible > maxilla

**Morbidity and Mortality**

- May cause functional problems with increased size

**Sex and Age Distribution**

- Males > females (2:1)
- Peak incidence in second decade; most present less than 30 years

**Clinical Features**

- Bone expansion may cause pain
- Pain not relieved by aspirin in osteoblastomas but is in osteoid osteoma

**Radiographic Features**

- Osteoblastomas may be well defined or ill defined, lacking surrounding sclerosis
- Osteoid osteomas may have an identifiable radiopaque nidus and typically have a distinct rim of sclerosis

**Prognosis and Treatment**

- Recurrence is rare, especially for jaw lesions
- Conservative surgery

scattered calcifications may be seen. Osteoblastomas near teeth may rarely cause resorption or displacement.

**PATHOLOGIC FEATURES****GROSS FINDINGS**

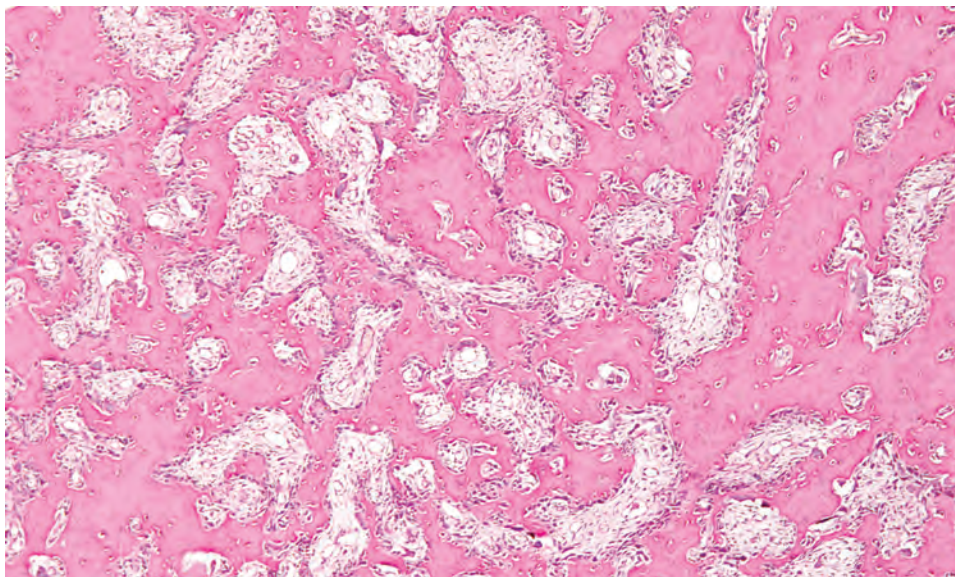
Osteoblastomas are larger than 2 cm and are usually sharply circumscribed. Specimens submitted usually consist of fragments of red to brown gritty bone.

**MICROSCOPIC FINDINGS**

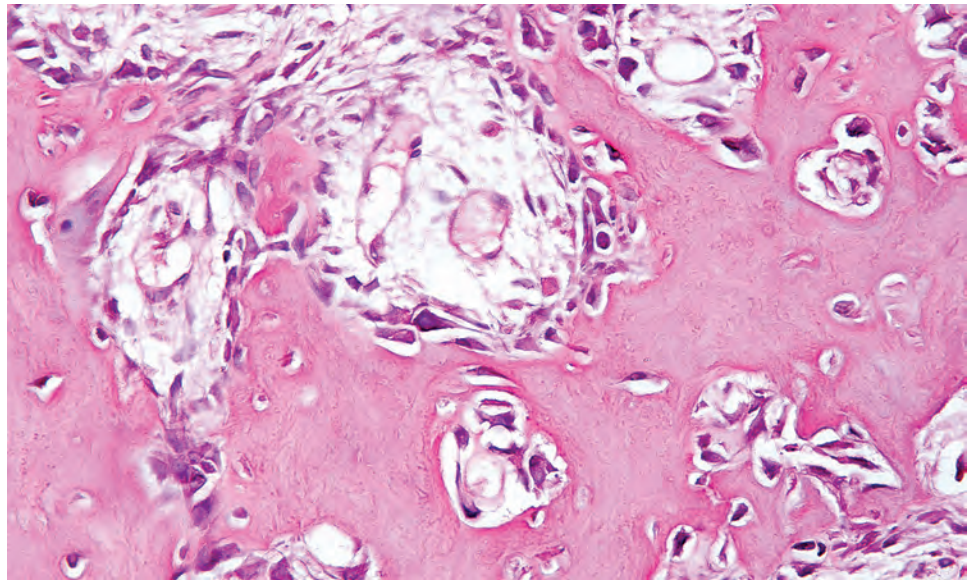
Although there may be subtle histologic differences between osteoblastoma and osteoid osteoma, they are essentially identical. They consist of anastomosing trabeculae of osteoid in a loose fibrovascular stroma (Fig. 15.10). The mineralized component usually shows noticeable osteoblastic rimming along with a characteristic basophilic appearance (Fig. 15.11). Osteoclastic giant cells are usually present and may even be a predominant feature. Extravasated erythrocytes are common.

**DIFFERENTIAL DIAGNOSIS**

The most obvious differential diagnosis is determining whether the lesion in question is an osteoblastoma or an osteoid osteoma, determined primarily based on the size of the lesion. However, differentiating between an osteoblastoma and a *low-grade osteosarcoma* is most

**FIGURE 15.10**

Anastomosing trabeculae of osteoid with prominent osteoblastic rimming in this osteoblastoma.

**FIGURE 15.11**

High-power view showing characteristic osteoblastic rimming in an osteoblastoma.

#### OSTEOBLASTOMA/OSTEOID OSTEOMA—PATHOLOGIC FEATURES

##### Gross Findings

- Conventional osteoblastomas larger than 2 cm, osteoid osteoma usually less than 2 cm
- Removed as fragments of red-brown gritty bone

##### Microscopic Findings

- Anastomosing trabeculae of osteoid in a loose fibrovascular stroma
- The basophilic mineralized component shows prominent osteoblastic rimming
- Osteoclasts are often present
- Extravasated erythrocytes common

##### Pathologic Differential Diagnosis

- Osteosarcoma, cementoblastoma, ossifying fibroma

important. Osteosarcoma has atypical features which include pleomorphism, infiltrative growth, and atypical mitosis. The clinical presentation of an osteosarcoma includes pain, loosening of the teeth, and paresthesia. BFOLs are also a consideration, although these lesions generally have a distinct clinical and radiographic appearance. *Cementoblastoma*, which histologically may be identical to osteoblastoma, is distinguished by direct and intimate association with the tooth root.

#### PROGNOSIS AND THERAPY

Usually conservative excision is adequate. Some large lesions may require larger resections resulting in the need

for subsequent reconstruction. On rare occasions, lesions have been reported to be locally aggressive.

#### ■ OSTEOID OSTEOMA

Osteoid osteoma is a benign bone-forming tumor within bone, which shares histologic features with osteoblastoma, previously discussed. An osteoid osteoma has limited growth potential and is, by definition, less than 2 cm.

#### CLINICAL FEATURES

Osteoid osteoma is even more rare than osteoblastoma in the craniofacial bones. Pain, especially at night, is frequently reported and often described as disproportionate to the size of the lesion. In contrast to osteoblastoma the pain is generally described as being relieved by aspirin.

#### RADIOGRAPHIC FEATURES

Osteoid osteomas typically are well-circumscribed lesions with a distinct rim of sclerosis. An identifiable radiopaque nidus is a distinctive feature.

#### PATHOLOGIC FEATURES

##### GROSS FINDINGS

Osteoid osteomas are less than 2 cm. Specimens submitted usually consist of fragments of red to brown gritty bone.



### MICROSCOPIC FINDINGS

As previously stated, osteoblastoma and osteoid osteoma are essentially identical microscopically. They consist of anastomosing trabeculae of osteoid in a loose fibrovascular stroma (Fig. 15.10). The mineralized component usually shows noticeable osteoblastic rimming along with a characteristic basophilic appearance (Fig. 15.11). Osteoclastic giant cells may be a predominant feature. Extravasated red blood cells are common.

### DIFFERENTIAL DIAGNOSIS

An osteoblastoma should be excluded; this can be done based on the tumor size. The remaining differential diagnosis remains the same as reported for osteoblastoma. Just as with osteoblastoma the possibility of a *low-grade osteosarcoma* must be considered. The atypical features of osteosarcoma should not be present in an osteoid osteoma. A BFOL and *cementoblastoma* are also part of the differential diagnosis; radiographic and clinical correlation will assist in ruling these entities in or out.

### PROGNOSIS AND THERAPY

Conservative excision is the treatment of choice. Recurrence is very rare.

## ■ CEMENTOBLASTOMA

Cementoblastoma is a rare benign neoplasm that forms cementum-like material attached to the tooth root.

### CLINICAL FEATURES

Cementoblastomas are rare, accounting for only approximately 4% of cementum-containing lesions. There is no significant sex predilection, and lesions are generally discovered in the second to third decades. Lesions present with varied levels of pain and a swelling of the buccal or lingual aspect of the alveolar ridges as a result of bone expansion. Smaller lesions may be asymptomatic and detected on routine dental radiographs. The involved tooth usually remains vital. There is a predilection for the mandible, particularly the mandibular permanent first molar.

### RADIOGRAPHIC FEATURES

The tumors are a well-defined, radiopaque or mixed-density, rounded mass, intimately associated with the tooth root (Fig. 15.12). In addition, a thin radiolucent rim surrounds the tumor, representing the periodontal ligament. Root resorption is common but may be obscured by the neoplasm.

### PATHOLOGIC FEATURES

#### GROSS FINDINGS

The lesion appears as a mass of yellow-white cementum fused to the roots of a tooth. Surgical extraction may result in the fragmentation of the specimen.

#### MICROSCOPIC FINDINGS

A cementoblastoma is composed of a dense mass of cementum in a loose fibrovascular stroma. Lesions usually show prominent cementoblastic rimming and may demonstrate a characteristic basophilic appearance and reversal lines of the cementum (Fig. 15.13). Multinucleated osteoclastic

### CEMENTOBLASTOMA—DISEASE FACT SHEET

#### Definition

- A benign neoplasm of cementum-like material connected with the tooth root

#### Incidence and Location

- Approximately 4% of cementum-containing lesions
- Predilection for the posterior mandible, first molar specifically

#### Sex and Age Distribution

- Equal sex distribution
- Peak in the second to third decades

#### Clinical Features

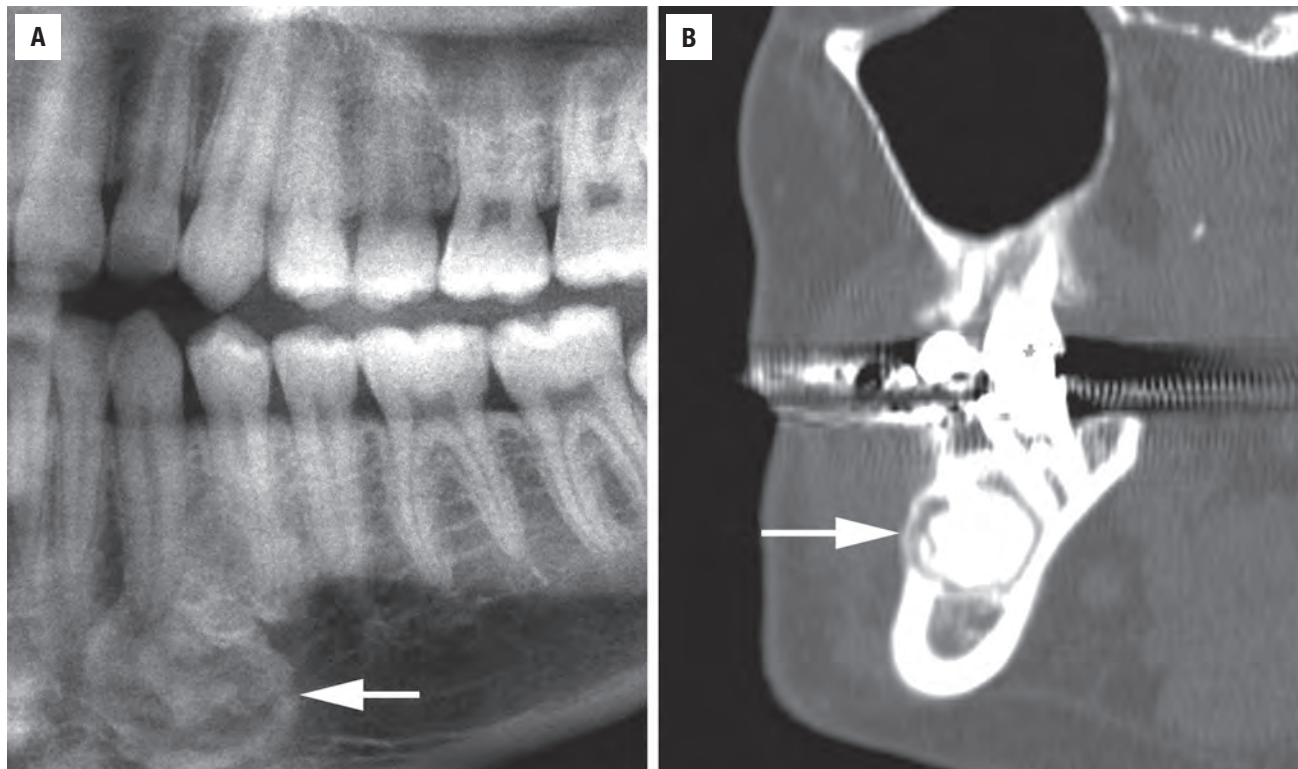
- Local expansion of bone causes buccal swelling of the alveolar ridges
- Variable pain

#### Radiographic Features

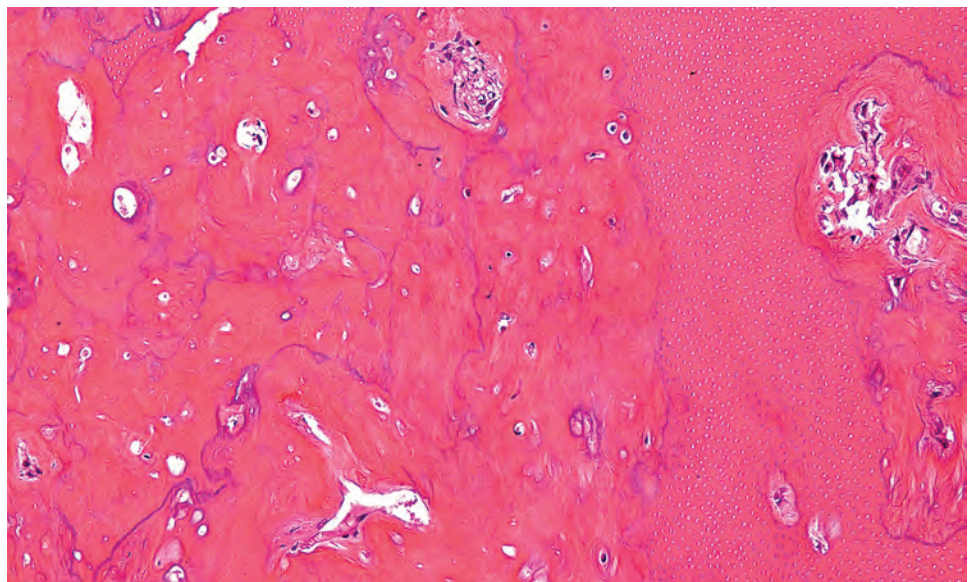
- Well-defined, radiopaque or mixed density, rounded mass
- Intimately associated with the tooth root
- A narrow radiolucent rim surrounds the tumor, representing the periodontal ligament

#### Prognosis and Treatment

- Recurrences only occur if incompletely excised
- Excision of mass and associated tooth

**FIGURE 15.12**

(A) A radiographic image of a radiodense calcified mass attached to a tooth root (*arrow*) is characteristic for a cementoblastoma. Note the thin radiolucent rim surrounding the tumor. Root resorption is present. (B) A computed tomography shows a very dense mass intimately in continuity with the tooth root (*arrow*), also showing a radiolucent rim.

**FIGURE 15.13**

The relationship between the tooth root (*right*) and the cemental mass (*left*) is demonstrated in this cementoblastoma.

#### CEMENTOBLASTOMA—PATHOLOGIC FEATURES

##### Gross Findings

- A mass of yellow-white cementum fused to the tooth root

##### Microscopic Findings

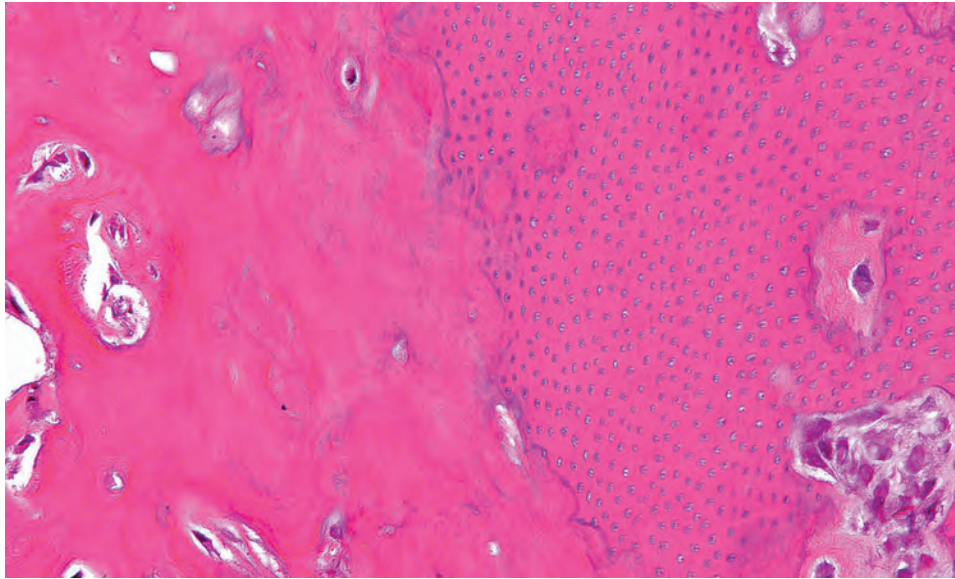
- A dense mass of cementum-like tissue with prominent basophilic reversal lines

- Variably cellular fibrovascular background stroma
- Cementoblasts, cementoclasts, and multinucleated giant cells are found

##### Pathologic Differential Diagnosis

- Osteoblastoma, osteosarcoma



**FIGURE 15.14**

The dentin tubules are seen in the root structure adjacent to the nodular mass of cementum, which is lined by plump cementoblasts.

giant cells are usually present. The periphery may have radiating columns of unmineralized tissue (Fig. 15.14).

### DIFFERENTIAL DIAGNOSIS

Cementoblastomas are essentially identical to *osteoblastoma* or *osteoid osteoma* microscopically, although cementoblastoma has an intimate association with the tooth root. *Osteosarcoma* must also be excluded. Both lesions require radiographic and clinical correlation.

### PROGNOSIS AND THERAPY

Treatment requires removal of the mass and associated tooth, usually a surgical extraction. Occasionally a molar tooth may have only one root affected. In these cases the individual root may be removed while the remaining tooth is treated with endodontic therapy, preserving function. Recurrences do not occur, unless the lesion is incompletely removed.

## ■ AMELOBLASTOMA

Ameloblastoma is the most common clinically significant odontogenic tumor of the gnathic bones. It is characterized as a benign but persistent, locally aggressive neoplasm. The majority of ameloblastomas occur in the posterior mandible, with a wide variety of radiographic and clinical presentations, each carrying treatment and prognostic

implications. The tumor arises from the enamel organ or its progenitor cell lines, resulting in the development of the soft tissue components of the odontogenic tumor without production of any calcified products. Mutations of genes that belong to the mitogen-activated protein kinase (MAPK) pathway have been detected in 90 % of ameloblastomas, primarily *BRAF* V600E, while *KRAS*, *NRAS*, *HRAS*, and *FGFR2* mutations are also noted.

### CLINICAL FEATURES

Ameloblastomas manifest in three major clinical-radiographic forms: conventional (either solid or multicystic), unicystic, or peripheral (gingiva). Conventional ameloblastomas are invasive by definition and require aggressive therapy. Conventional ameloblastomas occur within a wide age range, with most presenting in the fourth to fifth decades and represent more than 85 % of all ameloblastomas. Sinonasal tumors are unique because they have a propensity to occur in males, develop in much older patients (sixth to seventh decades), and present with sinusitis and epistaxis. Approximately 80 % occur in the posterior mandible, many associated with unerupted teeth. Bony expansion is seen, usually at a later stage of development, with untreated tumors having the potential to become very large. Large lesions are often disfiguring and may threaten vital structures. Unicystic ameloblastomas occur in a younger population, approximately two decades earlier than conventional tumors, and require less aggressive treatment. Unicystic ameloblastomas have neoplastic tissue that is confined to the lumen of the cyst and represent approximately 10 % to 15 % of ameloblastomas.

## AMELOBLASTOMA—DISEASE FACT SHEET

### Definition

- Most common significant benign epithelial odontogenic tumor, which is slow growing, but locally aggressive, persistent, and frequently recurrent

### Incidence and Location

- Most common odontogenic tumor
- 80% in mandible and 20% in maxilla
- Two-thirds located in the posterior mandible (ramus area)

### Sex, Race, and Age Distribution

- Equal sex and race distribution
- Wide age range, second to sixth decades
- Mean age: conventional (44 years); unicystic (22 years)

### Clinical Features

- Most small tumors are asymptomatic
- Variably sized jaw swellings, peripheral tumors appear as gingiva nodules
- Pain or paresthesia are rare

### Radiographic Features

- Unilocular or multilocular radiolucencies, resembling cysts with scalloped borders
- An unerupted/impacted tooth is frequently associated
- Resorption of the roots of adjacent teeth is common
- Cortical bony expansion in long-standing tumors

### Prognosis and Treatment

- Prognosis and treatment varies with clinical type of tumor
- Unicystic tumors: enucleation with 5% recurrence
- Conventional tumors: en bloc resection with 25%-55% recurrence
- Peripheral tumors: excise down to periosteum with rare recurrence

Finally, peripheral ameloblastomas represent only 1% of ameloblastomas and are limited exclusively to the soft tissue. These tumors present as elevated smooth-surfaced nodules on the gingiva resembling an irritation fibroma. The superficial nature of peripheral ameloblastomas, lacking bone involvement, translates into simple excision.

## RADIOGRAPHIC FEATURES

Multicystic lesions may form large radiolucent loculations within the cortex of the bone with numerous distinct bony septa forming the walls of the compartments (Fig. 15.15). Conventional tumors progress anteriorly and posteriorly through the central medullary bone through the path of least resistance. An involved impacted tooth

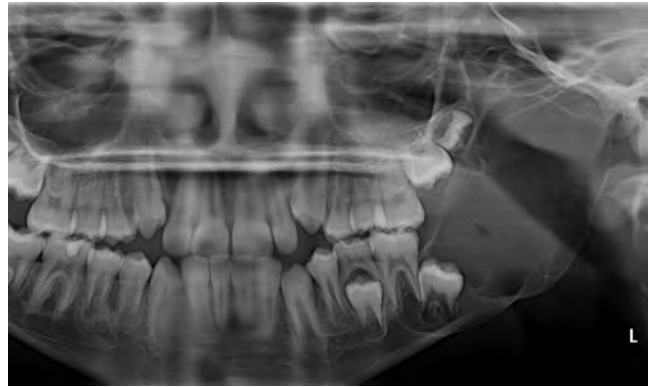


**FIGURE 15.15**

Orthopantomograph shows an expansive, multiloculated cystic ameloblastoma of the left posterior mandible, inferiorly displacing the molar tooth and forming fine bony septa in the ramus.

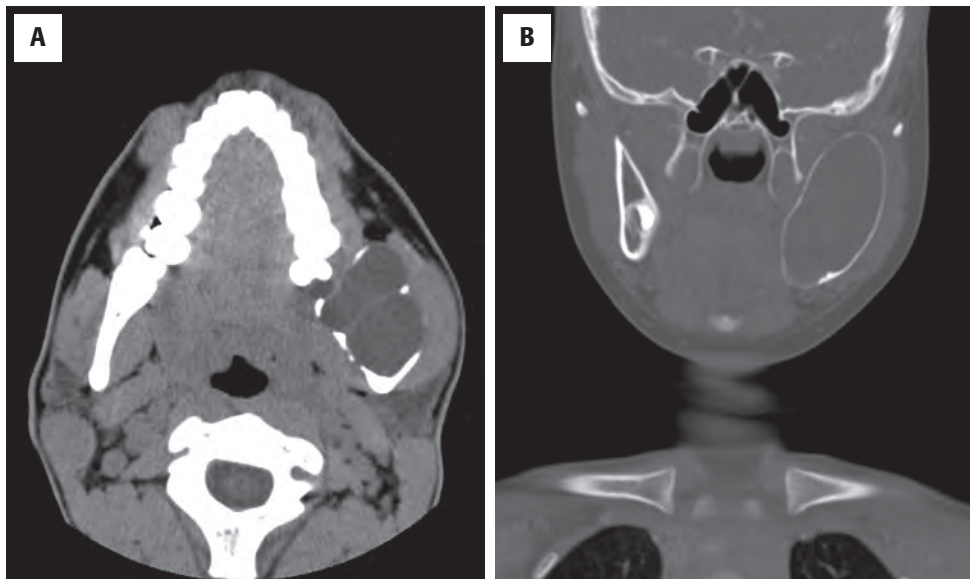
may be significantly displaced, with tooth resorption seen only in later stages of development. Large, long-standing lesions may perforate cortical bone; however, more frequently, thinning and expansion of the cortical plate are seen (Fig. 15.16). Some conventional ameloblastomas may become very large. Unicystic lesions are solitary radiolucent cysts, generally associated with an impacted tooth. The cortical plate may be expanded and a dense sclerotic border is seen at the leading edge of the slowly expanding tumor. The unicystic appearance radiographically is part of the criteria for the diagnosis of unicystic ameloblastoma, so radiographic correlation is required. Maxillary tumors may show less distinct radiographic borders, often filling the maxillary sinus and appearing as a diffuse solid semiradiopaque mass within the sinus. Desmoplastic ameloblastoma, a histologic variant of conventional ameloblastoma, usually presents as a mixed radiolucency/radiopacity. These lesions are often thought to represent a BFOL radiographically and are more common in the maxilla.

## PATHOLOGIC FEATURES

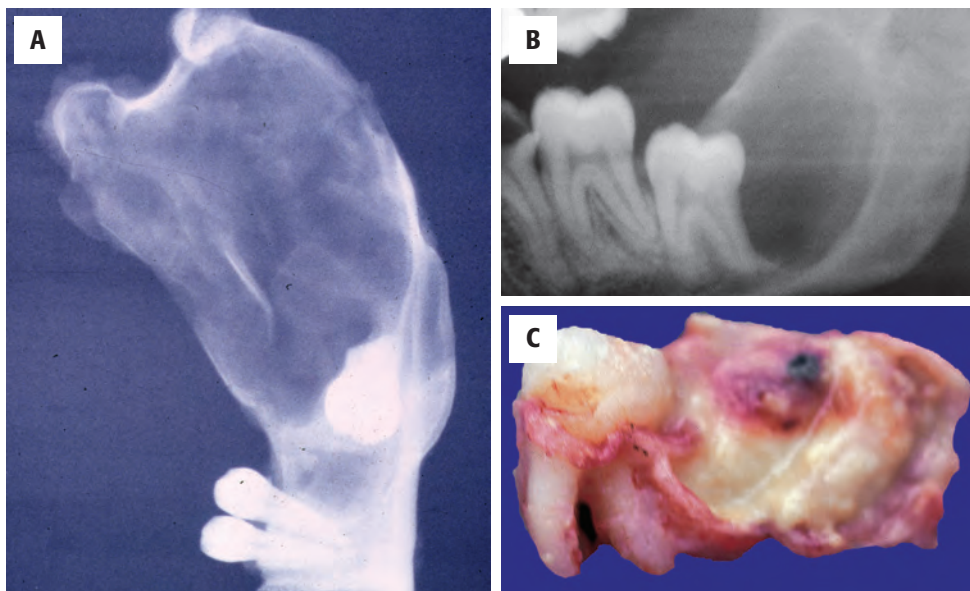
### GROSS FINDINGS

Early conventional and unicystic ameloblastomas are typically cysts that have thick walls with rough luminal surface elevations. The cyst wall in early unicystic tumors is thin, uniform, and often filled by gray-brown gelatinous material representing tumor (Fig. 15.17). Some conventional tumors may initially appear unicystic but thickening of the wall with corresponding variegated coloration of the luminal surface likely indicates the infiltrating tumor of a conventional ameloblastoma. These areas should be thoroughly sampled. Late-stage conventional tumors are removed as en bloc resections of bone with tumor filling



**FIGURE 15.16**

Computed tomography demonstrates an intraosseous ameloblastoma. **(A)** Multilocular cyst with bone remodeling and tooth displacement. **(B)** A unilocular ameloblastoma of the left mandible, showing a rim of bone around the periphery.

**FIGURE 15.17**

**(A)** Specimen radiograph showing the remarkable extent of the tumor in this en bloc resection. **(B)** Radiographic features of a solitary, unilocular radiolucent cystic ameloblastoma of right mandible with distinct sclerotic peripheral margin. **(C)** Gross specimen with attached bisected cyst, showing intact cyst wall with hemorrhagic-appearing area representing a plexiform unicystic ameloblastoma.

### AMELOBLASTOMA—PATHOLOGIC FEATURES

#### Gross Findings

- **Unicystic:** simple cyst with irregular wall filled with gray-brown-yellow gelatinous material; a simple cyst appearance is a required criterion for this diagnosis
- **Conventional:** compartmentalized bone filled with fibrous stroma containing gray cystic or necrotic foci
- **Peripheral:** nodule of soft tissue surfaced by mucosa or ulcer

#### Microscopic Findings

- **Unicystic:** cyst with lining forming reticulated plexiform, stranded, meshwork of cuboidal cells lacking characteristic ameloblastic features; the lack of infiltration into the surrounding tissue is a criterion for this diagnosis
- **Conventional:** may show one or more of the histologic variants
  - **Follicular pattern:** most common; epithelial islands with a center composed of loosely arranged stellate cells, surrounded by ameloblastic cells with reverse polarity

- **Plexiform pattern:** sheets and cords of odontogenic epithelium surrounded by ameloblastic cells with reverse polarity
- **Acanthomatous pattern:** areas with squamous metaplasia and keratin formation within odontogenic epithelial islands
- **Granular cell pattern:** center of the odontogenic islands shows a proliferation of granular cells
- **Desmoplastic:** dense fibrous proliferation with widely placed odontogenic cords, lacking the conspicuous ameloblastic findings

#### Pathologic Differential Diagnosis

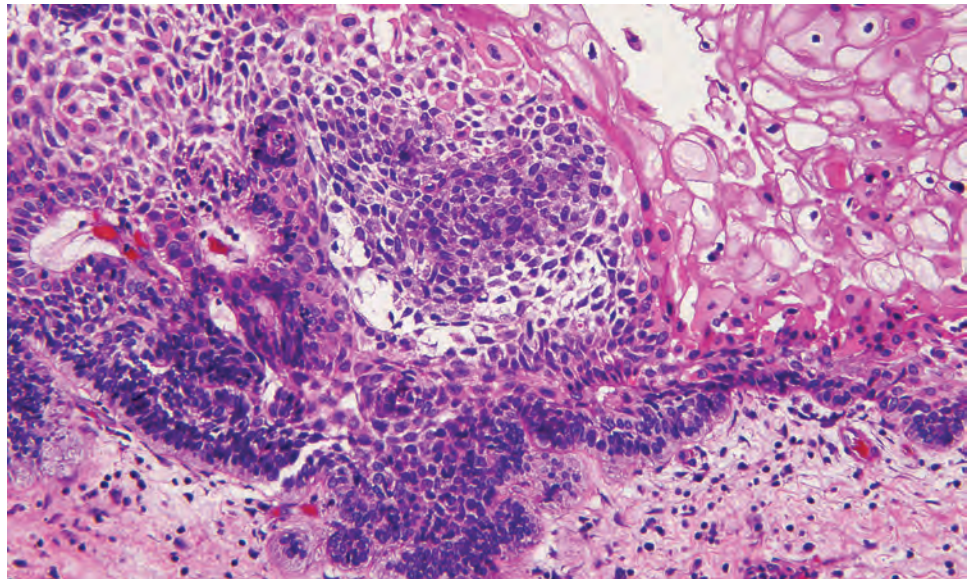
- Dentigerous cyst, odontogenic keratocyst, ameloblastic fibroma, ameloblastic fibro-odontoma, adenomatoid odontogenic tumor, odontogenic myxoma, benign fibro-osseous lesion, ameloblastic carcinoma

medullary spaces and appearing as dense fibrous tissue with cystic spaces.

#### MICROSCOPIC FINDINGS

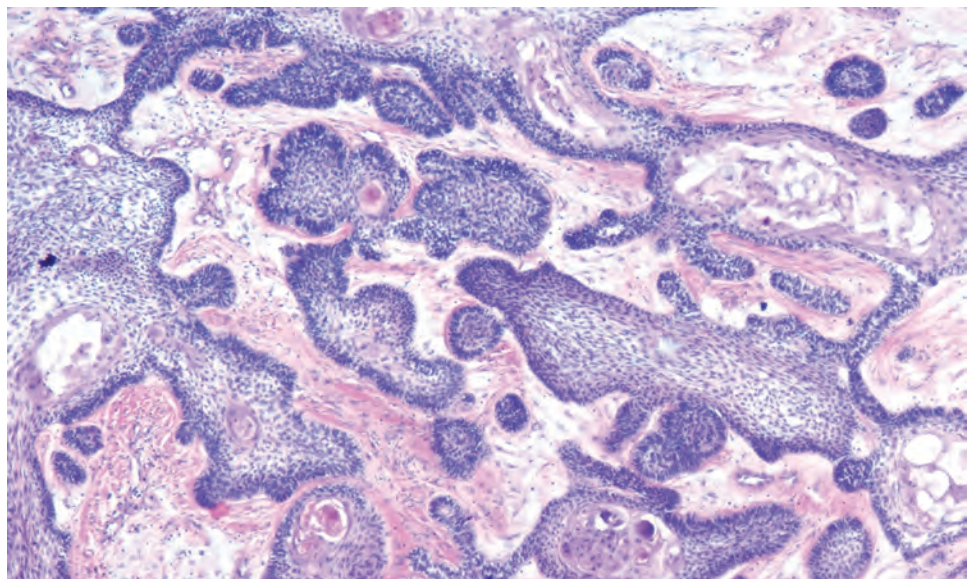
The classic histologic (follicular) features as described by Vickers and Gorlin, are seen in conventional tumors and characterized by islands of proliferating odontogenic epithelium reminiscent of the enamel organ (Fig. 15.18). Epithelial tumor islands are enmeshed in hyperplastic fibrous connective tissue, displaying pale hyalinized areas at the epithelial connective tissue interface (Fig. 15.19).

The odontogenic elements are composed of basophilic columnar cells at the periphery, exhibiting reverse polarization of nuclei away from the connective tissue with vacuolization. The central portions of the epithelial islands are less cellular, are edematous, and mimic the stellate reticulum of the enamel organ (Fig. 15.20). Follicular histologic features are seen in most ameloblastomas; however, other patterns are also seen: acanthomatous (Fig. 15.21), basaloid, granular cell (Fig. 15.22), and plexiform variations. Cyst formation is common, varying in size from microscopic to several centimeters (Figs. 15.23 and 15.24). The desmoplastic variant shows little to no evidence of



**FIGURE 15.18**

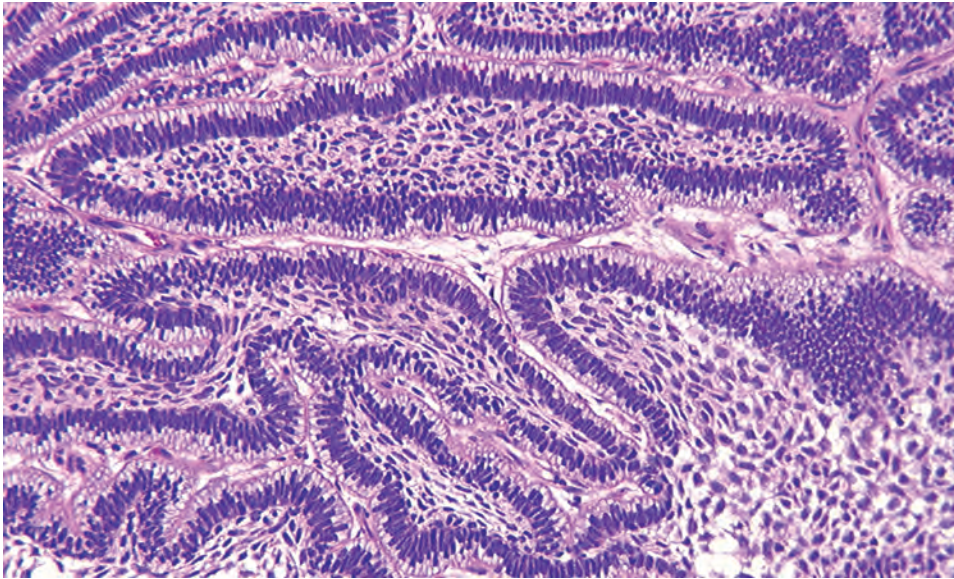
The characteristic columnar ameloblasts with reverse polarized nuclei, a stellate reticulum, and squamoid epithelial cells.



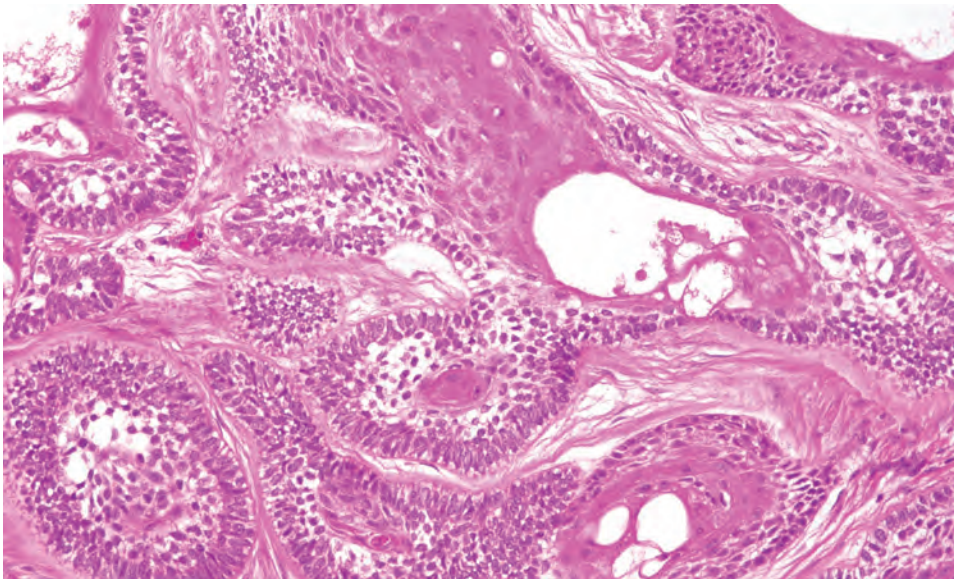
**FIGURE 15.19**

Low-power view of a follicular pattern ameloblastoma with anastomosing islands of basophilic epithelium set in a loose connective tissue stroma with eosinophilic inductive hyalinized change at the connective tissue/epithelial interface.



**FIGURE 15.20**

Hyperchromatic nuclei within columnar basal cells are seen showing vacuolization, reverse polarization, and less cellular central areas reminiscent of stellate reticulum of the enamel organ.

**FIGURE 15.21**

Medium-power view of ameloblastoma with follicular and acanthomatous patterns showing cystic acanthomatous central areas with dyskeratotic cells.

the classic ameloblastic features but rather widely scattered small islands and cords of bland odontogenic epithelium set in a dense collagenous stroma (Fig. 15.25).

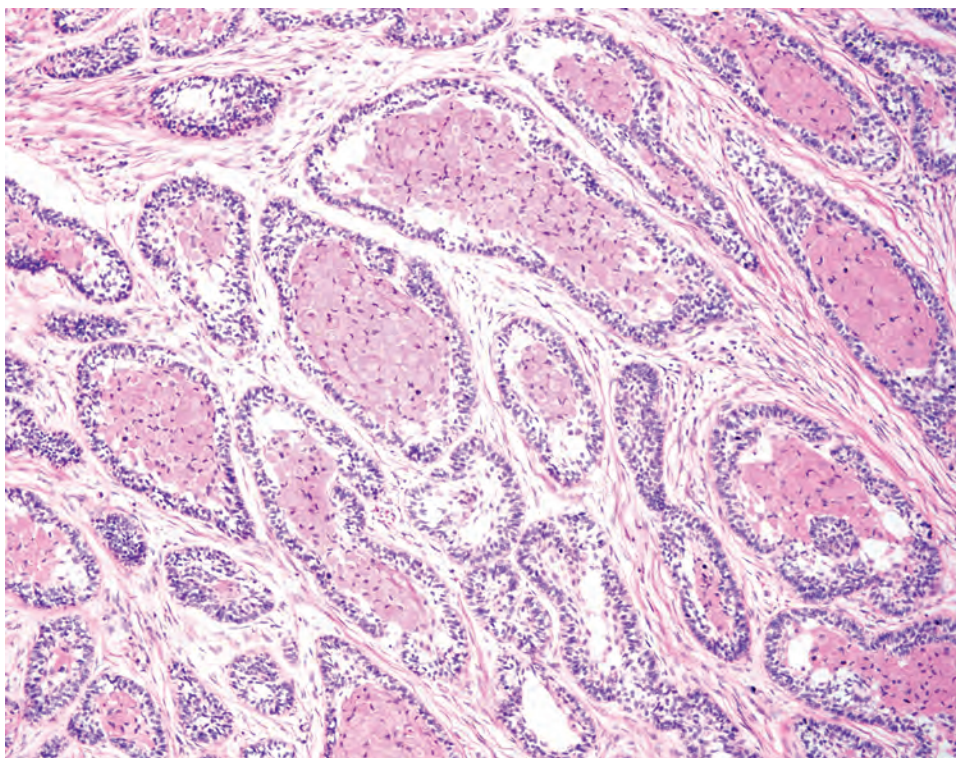
Unicystic tumors and sinonasal tumors seldom show the classic Vickers and Gorlin features but rather a loose “basketweave” luminal lining with intraluminal proliferation of plexiform tumor (Fig. 15.26). Unicystic tumors are filled with interlacing strands and cords, forming a reticulated plexiform pattern of cells with little evidence of a follicular character and reverse polarization. Peripheral ameloblastomas typically have a follicular histologic pattern and are circumscribed by dense fibrous connective

tissue. All histologic variants of ameloblastomas are cytologically bland with little pleomorphism or mitotic activity. When pleomorphism, hypercellularity, or mitotic activity is encountered, ameloblastic carcinoma should be considered.

#### DIFFERENTIAL DIAGNOSIS

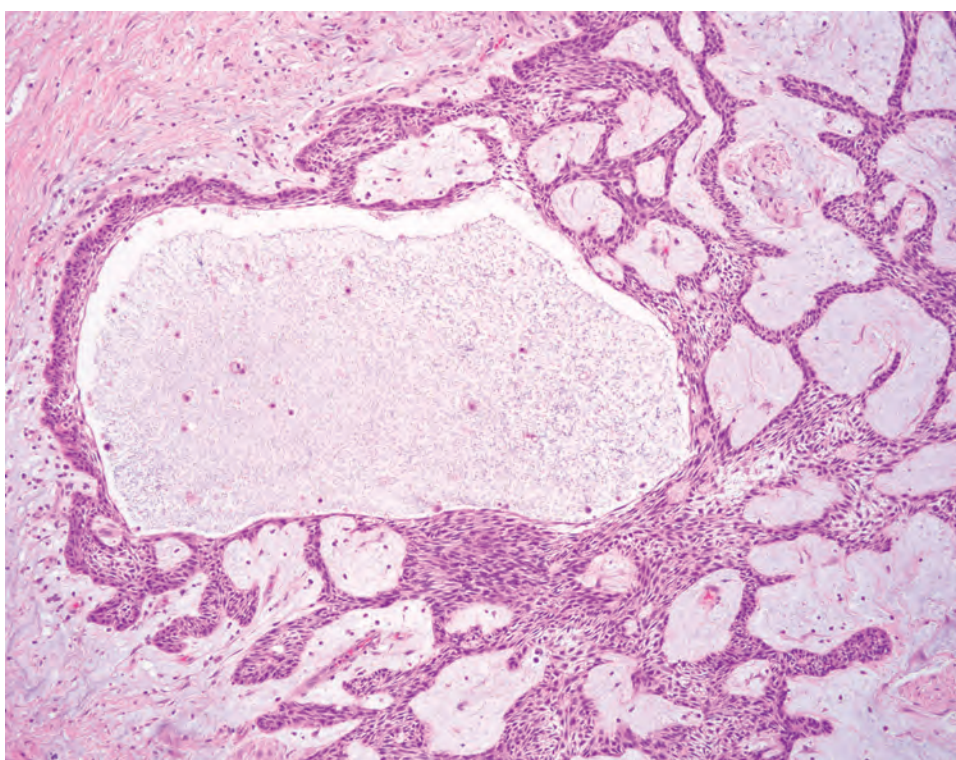
The clinical differential diagnostic consideration for unicystic lesions includes benign odontogenic cysts and





**FIGURE 15.22**

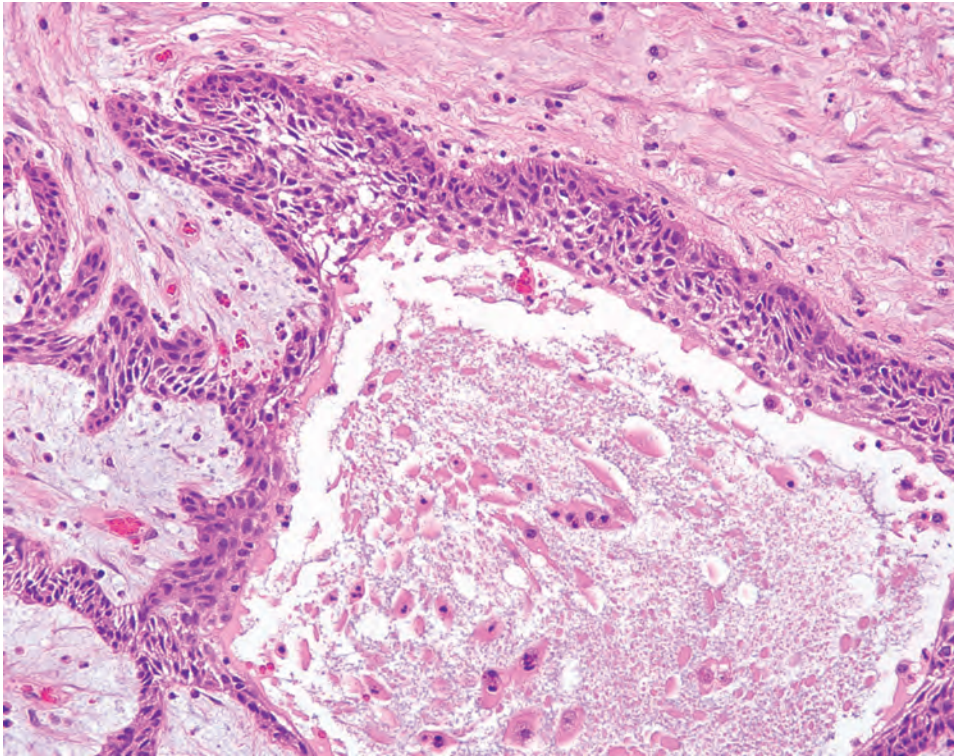
A granular cell variant shows numerous granular cells replacing the central stellate reticulum area.



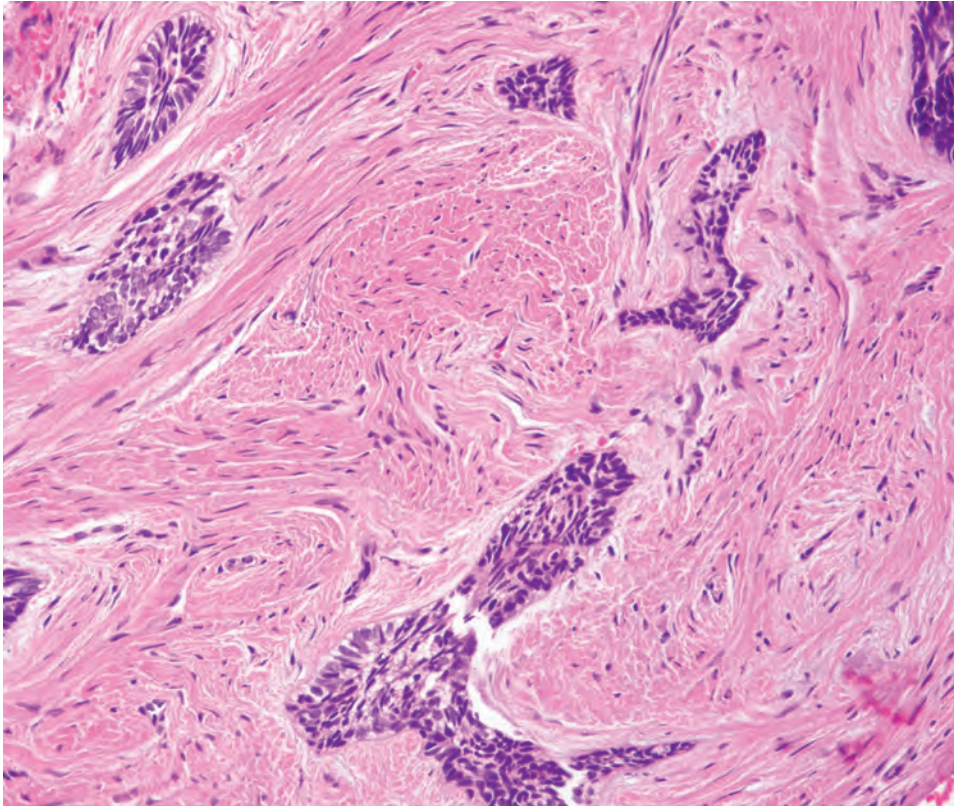
**FIGURE 15.23**

Low-power view of plexiform ameloblastoma with reticulated strands of epithelium proliferating into the cystic lumen and focal extension of a follicular pattern ameloblastoma into the fibrous wall.



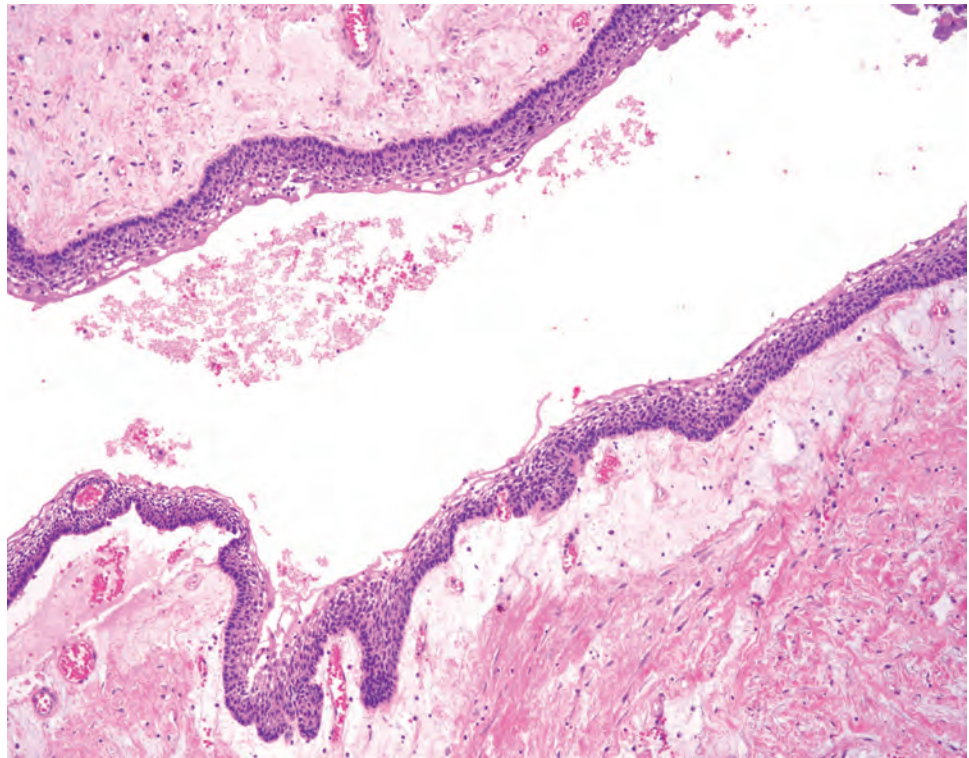
**FIGURE 15.24**

High-power view shows strands of plexiform ameloblastoma free floating in a cyst with little reverse polarization and a "basketweave" surface.

**FIGURE 15.25**

Medium-power view of desmoplastic ameloblastoma showing no evidence of Vickers and Gorlin changes, presenting as irregular islands of squamous epithelium circumscribed by edematous halos consistent with inductive effect.



**FIGURE 15.26**

A unicystic ameloblastoma showing a loose basketweave central portion, subtended by the basaloid cells with a peripheral palisade.

neoplasms. The histologic differential considerations are limited due to the distinctive histology of ameloblastomas. Other histologic considerations include ameloblastic fibroma, ameloblastic fibro-odontoma, and ameloblastic odontoma. *Ameloblastic fibroma* and *ameloblastic fibro-odontoma* have a unique appearance showing the characteristic “ameloblastic” islands, which are smaller, fail to open into a large follicular island, and are set in a background of primitive mesenchyme containing widely scattered stellate fibroblasts in a myxoid matrix. *Ameloblastic odontomas* display similar histology in the epithelial elements but are associated with hard tissue forming an odontoma. Adenomatoid odontogenic tumor (AOT) demonstrates reverse polarity away from a central lumen, whereas an ameloblastoma shows reverse polarity surrounding an island of odontogenic cells with a stellate-like appearance. Adenomatoid odontogenic tumors generally have a very distinct gland-like appearance with a very thick capsule.

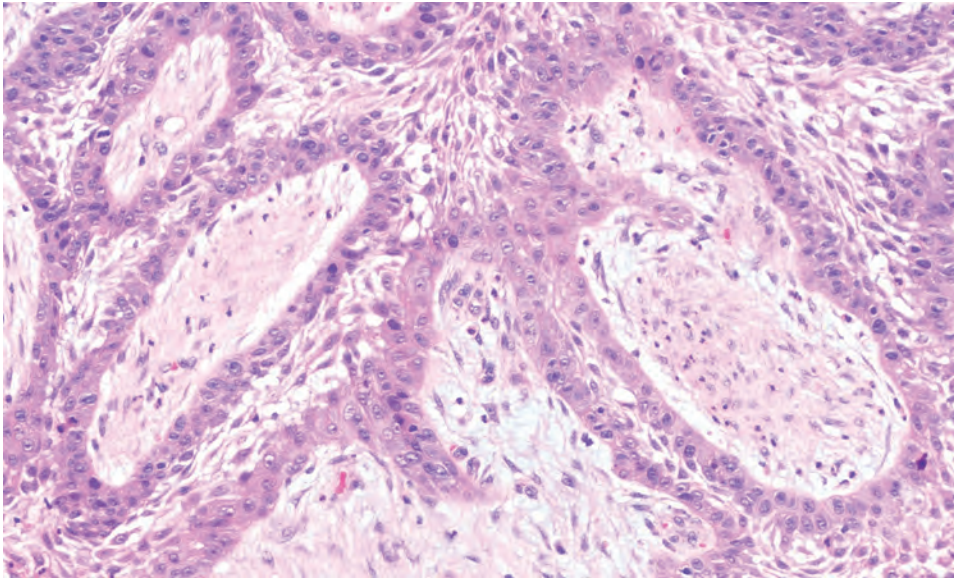
### PROGNOSIS AND THERAPY

Historically, ameloblastomas have been treated with wide (1 cm) local surgical resection. Surgical resection continues to be the favored treatment for conventional

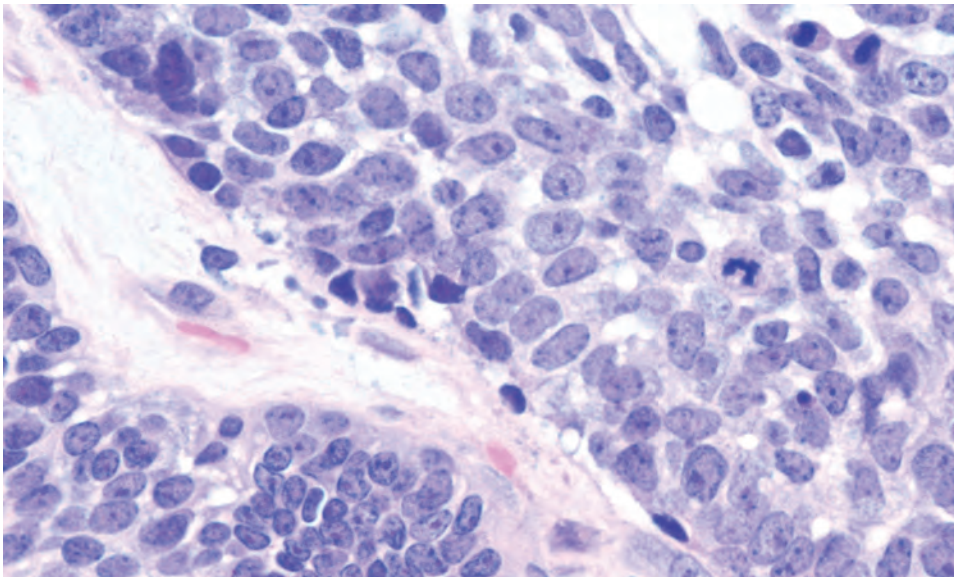
tumors. Conventional tumors treated with a 1-cm surgical margin have recurrence rates of between 25 % and 55 %. Patients should be placed on long-term periodic follow-up because tumors frequently recur many years after the initial surgical procedure. Unicystic ameloblastomas require less aggressive therapy, necessitating only enucleation of the cystic tumor with curettage and possible “bone burring” deemed adequate. Unicystic lesions treated less aggressively have recurrence rates of approximately 5 %. Peripheral tumors are excised down to periosteum when they present on the gingiva and seldom recur.

On rare occasions, an ameloblastoma will metastasize as a solitary lesion, which has been termed “metastasizing ameloblastoma or malignant ameloblastoma,” despite its cytologic benignity. However, the “true malignant” counterpart of the ameloblastoma is an ameloblastic carcinoma. It is a high-grade tumor and may be widely metastatic, with a 50 % mortality rate in some series. The character of ameloblastic carcinomas is reminiscent of the benign counterpart; however, they show less polarization at the connective tissue interface, a more solid cellular central area, considerable cytologic pleomorphism, and significant mitotic activity (Fig. 15.27). Ameloblastic carcinomas are often solid basaloid tumors (Fig. 15.28) that are locally aggressive (not slowly progressive), eroding bony margins early, as well as potentially metastatic.



**FIGURE 15.27**

Medium-power view of ameloblastic carcinoma shows a condensed layer of atypical peripheral basal cells lacking columnar cells, vacuolar changes, and reverse polarization.

**FIGURE 15.28**

At high power, ameloblastic carcinoma displays a distinct connective tissue epithelial interface with unorganized basal cell layer, marked pleomorphism, and numerous mitoses.

## ■ ODONTOGENIC KERATOCYST

The odontogenic keratocyst (OKC) is a distinctive odontogenic cyst, believed to arise from the dental lamina. Although also referred to as keratocystic odontogenic tumor (KCOT or KOT), the current WHO has reclassified this entity as OKC. The previous name change, keratocystic odontogenic tumor, was intended to stress the neoplastic-like growth potential, supported by biologic potential and molecular studies.

## CLINICAL FEATURES

Representing between 10% and 12% of all odontogenic cysts, the OKC is a distinctive cystic neoplasm of the mandible and maxilla, arising most commonly in the posterior mandible in the region of the third molar. OKCs may develop at any age, although they are found most commonly in the second to third decades, with a slight predilection for males. Many lesions are discovered incidentally during routine dental radiographs. However, some patients present with pain, swelling, and drainage, frequently related to a

### ODONTOGENIC KERATOCYST—DISEASE FACT SHEET

#### Definition

- A developmental odontogenic cyst of the jaw that may exhibit aggressive clinical behavior, characterized by a unicystic or multicystic intraosseous tumor with a distinct lining of parakeratinized stratified squamous epithelium

#### Incidence

- Represents 10%-12% of odontogenic cysts

#### Morbidity and Mortality

- Morbidity is low, although high recurrence may require disfiguring surgery

#### Sex, Race, and Age Distribution

- Males > females (approximately 1.2:1)
- Incidence is higher among whites
- Any age, with peak in second to third decades

#### Clinical Features

- Most lesions are incidental and asymptomatic
- If symptomatic, pain, swelling, and drainage are most common
- Lesions of children, as well as multiple lesions, may be associated with nevoid basal cell carcinoma syndrome (NBCCS)

#### Radiographic Features

- Well-defined, radiolucent, unilocular lesion
- Larger lesions may become multilocular
- Smooth corticated borders
- Unerupted tooth present (40%)

#### Prognosis and Treatment

- Frequent recurrences require close follow-up
- Association with the NBCCS
- Surgery

secondary infection of the cyst. Of clinical significance is the presence of OKCs as one of the most consistent features of nevoid basal cell carcinoma syndrome (NBCCS), or Gorlin syndrome. NBCCS is an autosomal dominant disorder, associated with loss of function of the *PTCH1* gene (chromosome 9q22.3–q31). The syndrome has many signs and symptoms including, but not limited to, numerous basal cell carcinomas of the skin (usually at a young age and in non-sun-exposed areas), skeletal abnormalities (rib and vertebra), palmar and plantar pits, calcification of the falx cerebri, an increased frequency of certain neoplasms (cardiac and ovarian fibromas, medulloblastoma), along with multiple OKCs.

### RADIOGRAPHIC FEATURES

An OKC usually presents as a radiolucent, unilocular, well-defined lesion (Fig. 15.29). However, as lesions increase in size they may become multilocular and may



**FIGURE 15.29**

A panoramic radiograph shows a well-defined, large unilocular left mandibular radiolucency, with smooth corticated border.

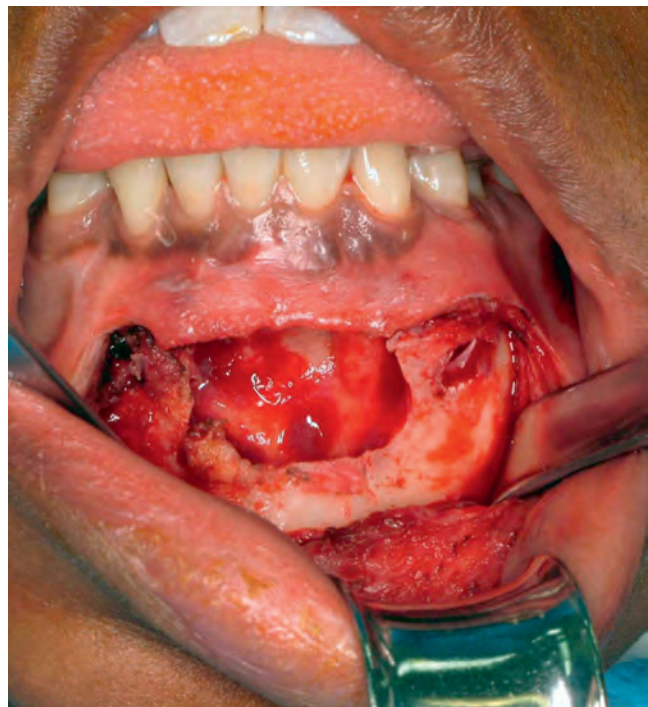


**FIGURE 15.30**

This intraoperative view demonstrates a large mandibular swelling, expanding the bone significantly, and showing a cystic space.

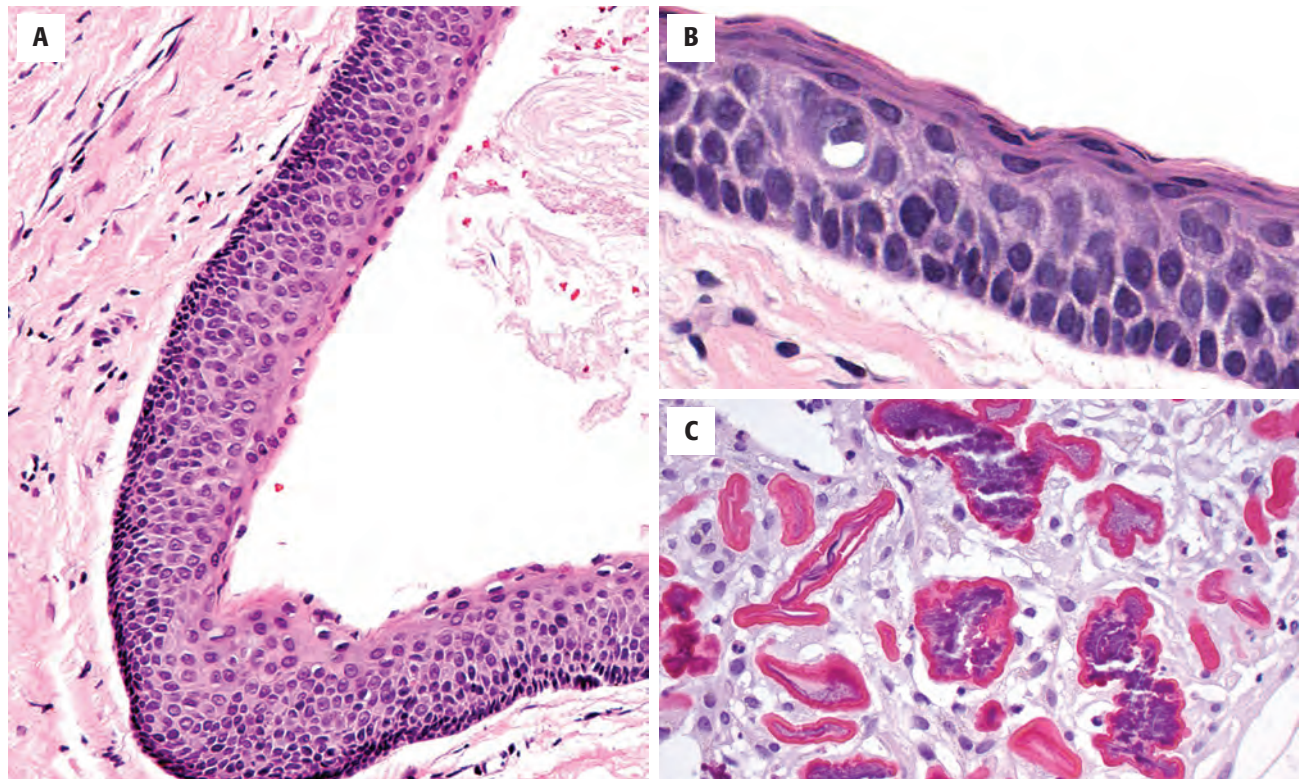
perforate the cortex (Fig. 15.30). Lesions usually have a smooth margin, without bone expansion or generally limited expansion. OKCs are often associated with unerupted teeth (40%).

### PATHOLOGIC FEATURES

#### GROSS FINDINGS

OKCs have a fibrous cyst wall with a lumen that may be filled with either clear fluid or yellow-white keratin (Fig. 15.30). However, specimens may be fragmented due to



**FIGURE 15.31**

(A) Note the thin parakeratotic epithelial lining with a focal area of keratinaceous debris in an odontogenic keratocyst. The epithelial layer is six to eight cells thick and demonstrates darkly stained cuboidal cells making up a distinct basal layer artifactually cleaved from the stroma. (B) There is a parakeratinized refractile surface keratin layer. (C) Rushton bodies are composed of refractile keratin material.

#### ODONTOGENIC KERATOCYST—PATHOLOGIC FEATURES

##### Gross Findings

- A thin friable cyst wall filled with either clear fluid or yellow-white keratin
- Unerrupted tooth may be seen

##### Microscopic Findings

- Uniformly thin epithelium, usually six to eight cells thick, with minimal rete ridges
- Artifacts cleaving below epithelium
- Luminal epithelial cells show corrugated refractile parakeratotic surface
- Palisaded cuboidal or columnar basal cell layer
- Lumen contains keratinaceous debris
- Inflammation may alter the histologic features

##### Pathologic Differential Diagnosis

- Dentigerous cyst, orthokeratinized odontogenic cyst, calcifying odontogenic cyst, ameloblastoma

curettage. In addition, an unerupted tooth may be submitted with the cyst.

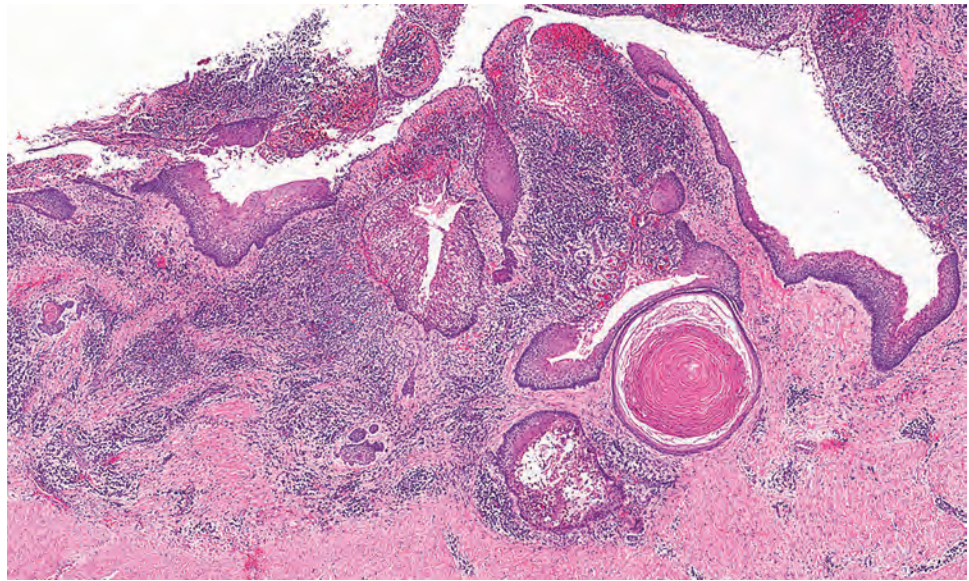
#### MICROSCOPIC FINDINGS

The histopathologic features of OKCs are distinctive. The epithelial lining is uniformly thin, usually six to eight cells

thick (Fig. 15.31). The cystic neoplasm shows a distinct lack of rete ridges, resulting in a characteristic, although artifactual, separation of the epithelial lining from the underlying fibrous connective tissue. The luminal surface shows corrugated parakeratotic epithelial cells, with an underlying basal cell layer composed of palisaded and hyperchromatic cuboidal or columnar epithelial cells. The keratinization on the surface is refractile, a feature highlighted by dropping the substage condenser (Fig. 15.31). The lumen may contain varying amounts of keratinaceous material. Epithelial hyaline bodies (Rushton bodies) may be seen, representing refractile brightly eosinophilic curvilinear bodies of keratin (Fig. 15.31). OKCs may also show satellite cysts and islands of odontogenic epithelium; the latter features are more common, although still rare, in those patients who have NBCCS (Fig. 15.32). It is important to note that inflammation or previous biopsy may alter the features making definitive diagnosis more difficult.

#### DIFFERENTIAL DIAGNOSIS

Other odontogenic cysts must be considered in the differential diagnosis. A *dentigerous cyst*, the most common odontogenic cyst, lacks the basal palisading and corrugated parakeratinized surface. Of note, a dentigerous cyst is, by definition, always associated with an unerupted tooth.

**FIGURE 15.32**

Multiple daughter cysts are seen in this OKC, a tumor associated with nevoid basal cell carcinoma syndrome. There is concurrent inflammation in this case, distorting some of the classic histologic features.

The *orthokeratinized odontogenic cyst* may share some histologic features with OKC but is orthokeratinized (not parakeratinized) and lacks the palisaded basal cell layer. A *calcified odontogenic cyst* has basal palisading but has very distinctive ghost cells. An *ameloblastoma*, although in the differential diagnosis radiographically, shows a loosely arranged stellate reticulum, a feature which recapitulates the developing tooth.

### PROGNOSIS AND THERAPY

Close patient follow-up is required to monitor for recurrences. Young patients and patients with multiple lesions should be evaluated for NBCCS. Complete removal is essential if recurrences are to be avoided. Controversy exists about how to achieve complete removal, with treatments including peripheral osseous curettage, ostectomy, en bloc resection, and marsupialization followed by surgery.

## ■ CALCIFYING EPITHELIAL ODONTOGENIC TUMOR

The calcifying epithelial odontogenic tumor (CEOT), also referred to as Pindborg tumor, is a rare, distinctive locally invasive jaw tumor characterized by amyloid-like material that may become calcified.

### CLINICAL FEATURES

Accounting for less than 1% of odontogenic tumors, CEOT occurs without a sex predilection in patients 20

### CALCIFYING EPITHELIAL ODONTOGENIC TUMOR—DISEASE FACT SHEET

#### Definition

- A rare, locally invasive, epithelial odontogenic neoplasm characterized by the presence of amyloid material that may become calcified (aka Pindborg tumor)

#### Incidence and Location

- < 1% of odontogenic tumors
- Mandible > maxilla (2:1), specifically premolar/molar region

#### Sex and Age Distribution

- Equal sex distribution
- Usually between 20 and 60 years

#### Clinical Features

- Slowly enlarging painless mass of the jaw
- Peripheral (extraosseous) type appears as nondescript gum bumps (6% of cases)

#### Radiographic Features

- Well-circumscribed unilocular or multilocular radiolucencies with variable opaque flecks
- Calcifications described as “driven snow” or “plowed snow”
- Up to 60% associated with crown of unerupted tooth

#### Prognosis and Treatment

- Long-term follow-up for recurrences (especially if incompletely excised or in clear cell variant)
- Conservative surgery

to 60 years old. Tumors present as slowly enlarging painless masses of the jaw. Rarely, the gingiva may be affected. The mandible is affected twice as often as the maxilla, with a distinct predilection for the premolar/molar region.



## RADIOGRAPHIC FEATURES

Tumors are well-circumscribed unilocular or multilocular, mixed radiolucent-radiopaque lesions with variable opaque flecks (Fig. 15.33). The calcifications are characteristically described as “driven snow.” Up to 60% of lesions are associated with the crown of an unerupted tooth.



**FIGURE 15.33**

Panoraphic radiograph of a calcifying epithelial odontogenic tumor represented by a multilocular left posterior mandible radiolucent lesion containing larger calcifications.

## PATHOLOGIC FEATURES

### GROSS FINDINGS

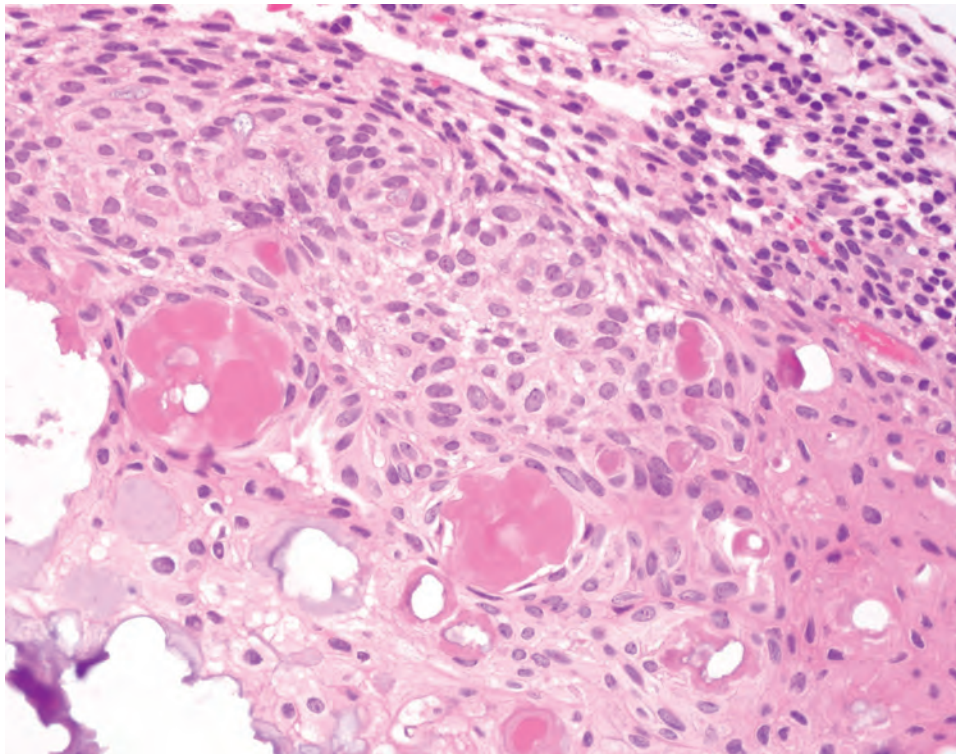
Grossly, lesions appear solid and well circumscribed, with varying amounts of calcification.

### MICROSCOPIC FINDINGS

The tumor is composed of sheets and islands of polyhedral epithelial cells with abundant eosinophilic cytoplasm and distinct intercellular bridges. Nuclei may show considerable pleomorphism (Fig. 15.34). However, mitotic figures are rare. Characteristically, there is abundant, eosinophilic, homogeneous, hyaline matrix material, proved to be amyloid (Fig. 15.35). Concentric, basophilic ring calcification of this material results in the classic finding of Liesegang rings. Clear cell and noncalcifying variants are described (Fig. 15.36).

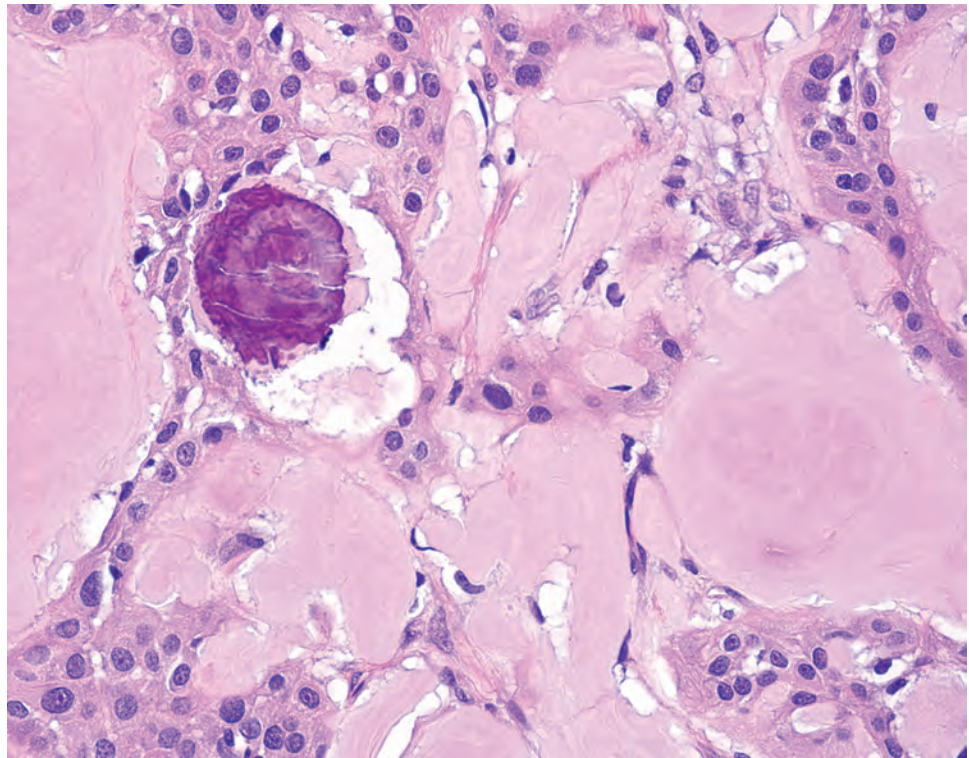
### ANCILLARY STUDIES

The amyloid-like material, when stained with Congo red, demonstrates the classic apple-green birefringence when viewed with polarized light. The tumor cells react with cytokeratins and epithelial membrane antigen.

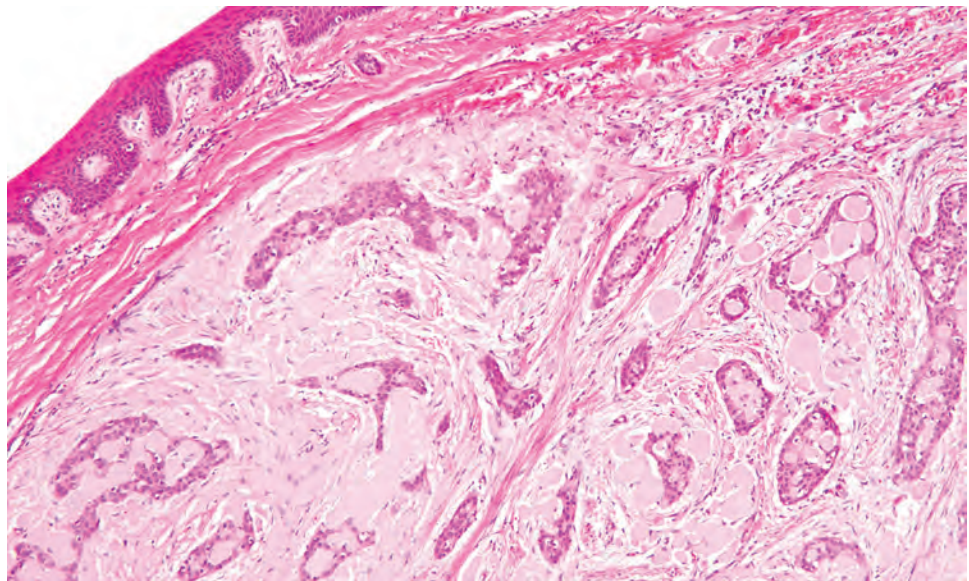


**FIGURE 15.34**

Sheets of polyhedral epithelial cells with abundant cytoplasm and distinct intercellular bridges. Extracellular, acellular matrix material (pink amyloid-like material) is readily identified in a calcifying epithelial odontogenic tumor.

**FIGURE 15.35**

This calcifying epithelial odontogenic tumor shows islands and cords of epithelial cells surrounding acellular, extracellular eosinophilic amyloid-type material.

**FIGURE 15.36**

Rare peripheral variant of calcifying epithelial odontogenic tumor shows cords and nests of epithelial cells separated by fibrous connective tissue and associated acellular eosinophilic matrix (amyloid) material. The surface epithelium is intact.

## DIFFERENTIAL DIAGNOSIS

*Squamous cell carcinoma (SCC)*, either primary or metastatic, is sometimes raised in the differential diagnosis. However, SCC is generally more pleomorphic and lacks amyloid and calcifications. A *clear cell odontogenic carcinoma* and *metastatic renal cell carcinoma* may also need to be considered when the clear cell variant of CEOT is

in the differential diagnosis, but typically show a distinct immunohistochemistry profile.

## PROGNOSIS AND THERAPY

Long-term follow-up is suggested because there is a known recurrence risk, especially if incompletely excised and/



**CALCIFYING EPITHELIAL ODONTOGENIC TUMOR—PATHOLOGIC FEATURES****Gross Findings**

- Solid, well-circumscribed mass with calcifications

**Microscopic Findings**

- Sheets and strands of polyhedral epithelial cells with abundant eosinophilic cytoplasm with distinct intercellular bridges
- Nuclear pleomorphism may be remarkable
- Mitotic figures are rare
- Abundant, eosinophilic, homogeneous, hyaline matrix material (amyloid)
- Concentric, basophilic ring calcification (Liesegang rings)
- “Clear cell” and “noncalcifying” variants described

**Ancillary Studies**

- Amyloid material has Congo red, apple-green birefringence with polarized light (crystal violet and thioflavin T may be used)
- Reactivity with cytokeratins and EMA

**Pathologic Differential Diagnosis**

- Squamous cell carcinoma, clear cell odontogenic carcinoma, metastatic renal cell carcinoma

or in the clear cell variant. Treatment is usually conservative surgery (enucleation or local resection).

**ADENOMATOID ODONTOGENIC TUMOR**

The adenomatoid odontogenic tumor (AOT) is a rare benign tumor of odontogenic epithelium with distinctive duct-like areas embedded in a mature connective tissue stroma.

**CLINICAL FEATURES**

AOT accounts for approximately 5% of odontogenic tumors. Females are affected twice as frequently as males, with greater than 90% of patients diagnosed before age 30 years (nearly 50% as teenagers). Asian and black patients are more commonly affected than are white patients. The maxilla is affected twice as often as the mandible; an unerupted canine is often involved. The “two-thirds rule” has been popularized by clinicians for this lesion: two-thirds less than 20 years of age; two-thirds female; two-thirds in the maxilla; and two-thirds involving the canine. Peripheral types appear as a nondescript mass of the gingival tissue and are bone-hard, palpable masses with or without pain. Tooth displacement may be an additional finding.

**ADENOMATOID ODONTOGENIC TUMOR—DISEASE FACT SHEET****Definition**

- A benign tumor of odontogenic duct-like epithelium embedded in a mature connective tissue stroma

**Incidence and Location**

- Approximately 5% of odontogenic tumors
- Predilection for the anterior maxilla

**Sex, Race, and Age Distribution**

- Females > males (2:1)
- Asian and black patients more commonly affected than white patients
- > 90% present before 30 years (peak, second decade)

**Clinical Features**

- Usually asymptomatic
- May be bone-hard, palpable mass with or without pain
- Associated with unerupted tooth, most commonly canines
- Tooth displacement is reported
- Rare peripheral type is a nondescript gingival mass

**Radiographic Features**

- Intraosseous, well-circumscribed, unilocular radiolucent mass
- Associated with crown or part of the root of an unerupted permanent tooth
- Occasionally, opaque flecks representing calcifications noted
- May cause divergence of adjacent roots

**Prognosis and Treatment**

- Recurrence is extremely rare
- Conservative, local excision

**RADIOGRAPHIC FEATURES**

Most AOTs present as intraosseous, well-circumscribed, unilocular radiolucent lesions, often around the crown and part of the root of an unerupted permanent tooth (Fig. 15.37). Some tumors may have opaque flecks that represent small calcifications. Larger lesions may cause divergence of adjacent roots. Saucerization (erosion) of the alveolar bone is an occasional feature of peripheral tumors.

**PATHOLOGIC FEATURES****GROSS FINDINGS**

Lesions are well circumscribed, often with a distinct fibrous capsule. The submitted tissue may be accompanied by an associated tooth. Tumors are usually less than 3.0 cm. Focal cystic areas and calcifications may be seen on serial sectioning.

### MICROSCOPIC FINDINGS

Histologically, nodules of odontogenic epithelium are separated by minimal stromal connective tissue. The tumor comprises two cell types. The duct-like, tubular, or cord-like areas are lined by cuboidal to columnar epithelial cells (Fig. 15.38), with nuclei polarized away from the central duct-like space, imparting an appearance reminiscent of ameloblastoma. The duct-like spaces are pseudolumina containing secretions of the columnar cells. The second component is a spindled to polyhedral eosinophilic cell component, which creates a nodular, nested, and swirling pattern, often containing collections



**FIGURE 15.37**

Occlusal radiograph. Radiolucent lesion of the anterior mandible between the incisor and canine, showing a well-circumscribed unilocular lesion.

of eosinophilic, amorphous amyloid-like material (Fig. 15.39). These globular masses may show varying degrees of mineralization, and in their most advanced form may show distinct laminations (Fig. 15.40). Minimal, loose stroma with thin-walled vessels is present, usually accentuated at the periphery.

### ADENOMATOID ODONTOGENIC TUMOR— PATHOLOGIC FEATURES

#### Gross Findings

- Well-circumscribed by a fibrous capsule
- Often associated with the crown of an extracted tooth
- Focal cystic areas and calcification may be seen

#### Microscopic Findings

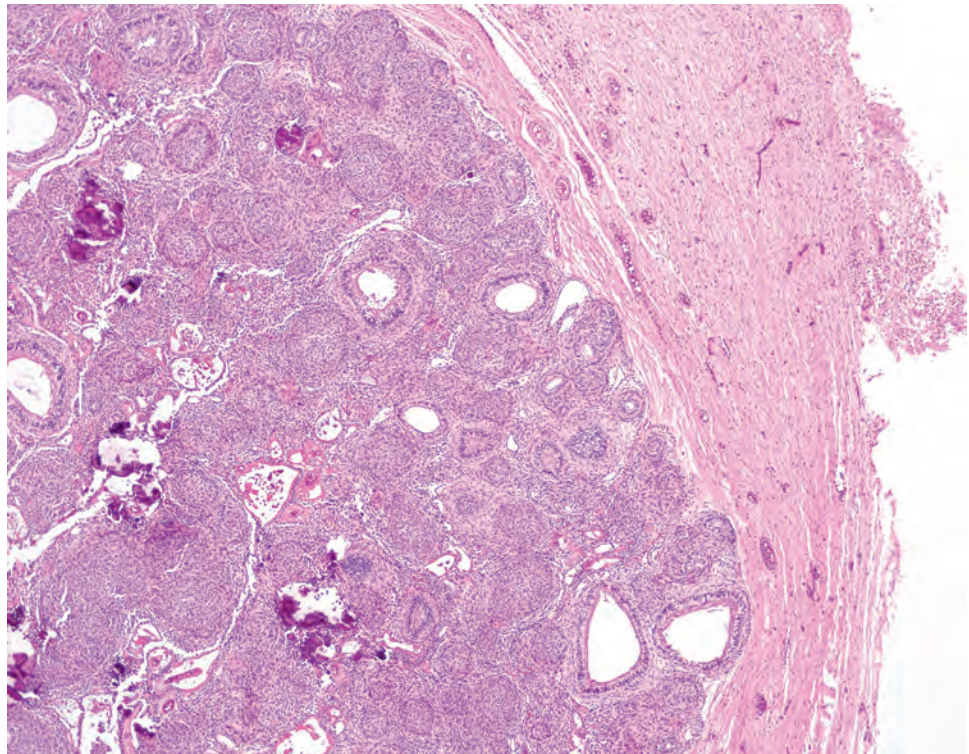
- A distinctive fibrous capsule is usually noted
- Nodules of odontogenic epithelium
- Duct-like, tubular, or cord-like areas lined by cuboidal to columnar cells with reverse polarized nuclei
- Spindled to polyhedral eosinophilic cells in nodular, nested swirling patterns
- Collections of eosinophilic, amorphous amyloid-like material
- Areas of calcification with lamination may be seen

#### Ancillary Studies

- Ultrastructurally appears like enamel matrix
- Histochemical stains support amyloid

#### Pathologic Differential Diagnosis

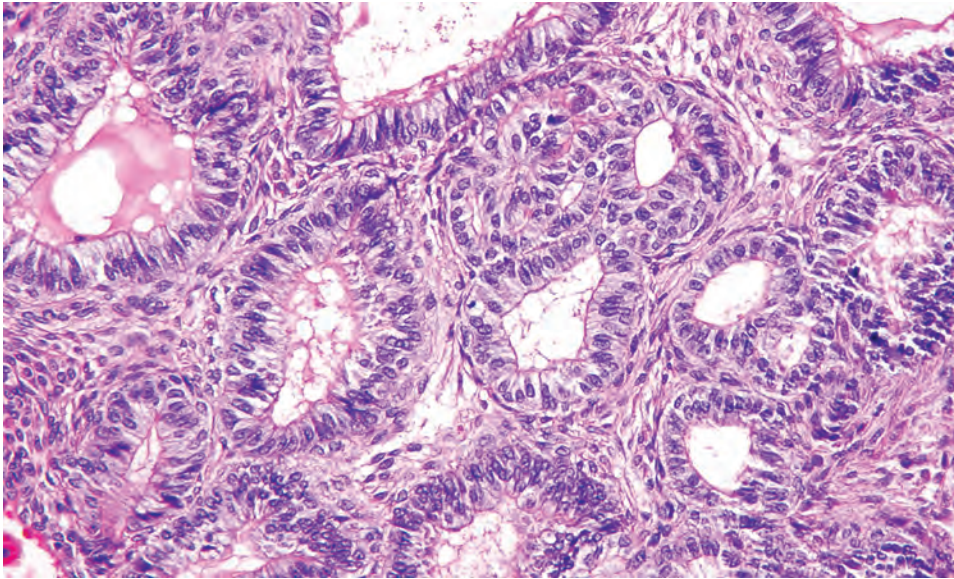
- Ameloblastoma, salivary gland tumors



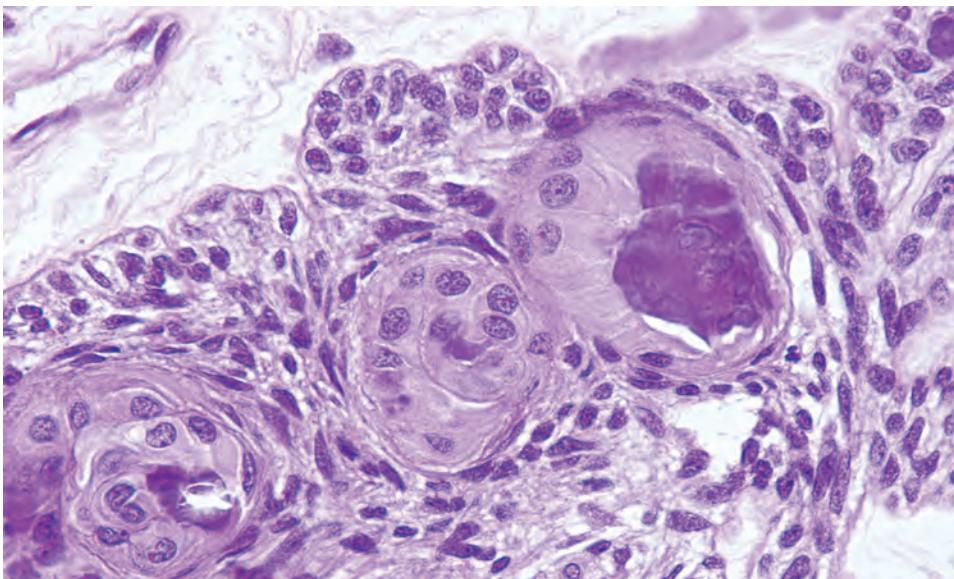
**FIGURE 15.38**

This low-power view of an adenomatoid odontogenic tumor shows a well-defined border with duct-like structures set in a spindle cell background. Intralesional microcalcifications are noted.



**FIGURE 15.39**

Nuclei of the duct-like spaces are polarized away from the duct lumen, reminiscent of ameloblastoma.

**FIGURE 15.40**

Calcifications adjacent to the spindle and columnar epithelial cells. Note the area of lamination, a feature helpful in confirming a diagnosis of adenomatoid odontogenic tumor.

### ANCILLARY STUDIES

Ultrastructural findings reveal a fibrillar to granular quality to the eosinophilic deposits, suggesting they may represent enamel matrix or perhaps amyloid.

### DIFFERENTIAL DIAGNOSIS

Although AOT histology is characteristic, an *ameloblastoma* must be ruled out, and occasionally salivary gland tumors may enter the differential diagnosis.

### PROGNOSIS AND THERAPY

Recurrences are extremely rare. Conservative, local excision is curative and made easier by a thick capsule.

### ■ CENTRAL GIANT CELL LESION

The central giant cell lesion is a localized lytic lesion of the jawbones associated with fibrosis, hemorrhage, hemosiderin-laden macrophages, reactive bone, and osteoclastic giant cells. In the past the terms *reparative*

*giant cell granuloma* and *central giant cell granuloma* have been used as synonyms but are to be discouraged.

### CLINICAL FEATURES

Central giant cell lesions are found in a wide age range, although the average is 20 years. Females are affected more often than males (1.5 to 2:1), and there is a definitive predilection for the mandible. Lesions show a range of biologic potential with some cases acting in a nonaggressive manner: usually asymptomatic, incidental findings, although aggressive lesions may present with pain, paresthesias, and resorption of teeth.

### RADIOGRAPHIC FEATURES

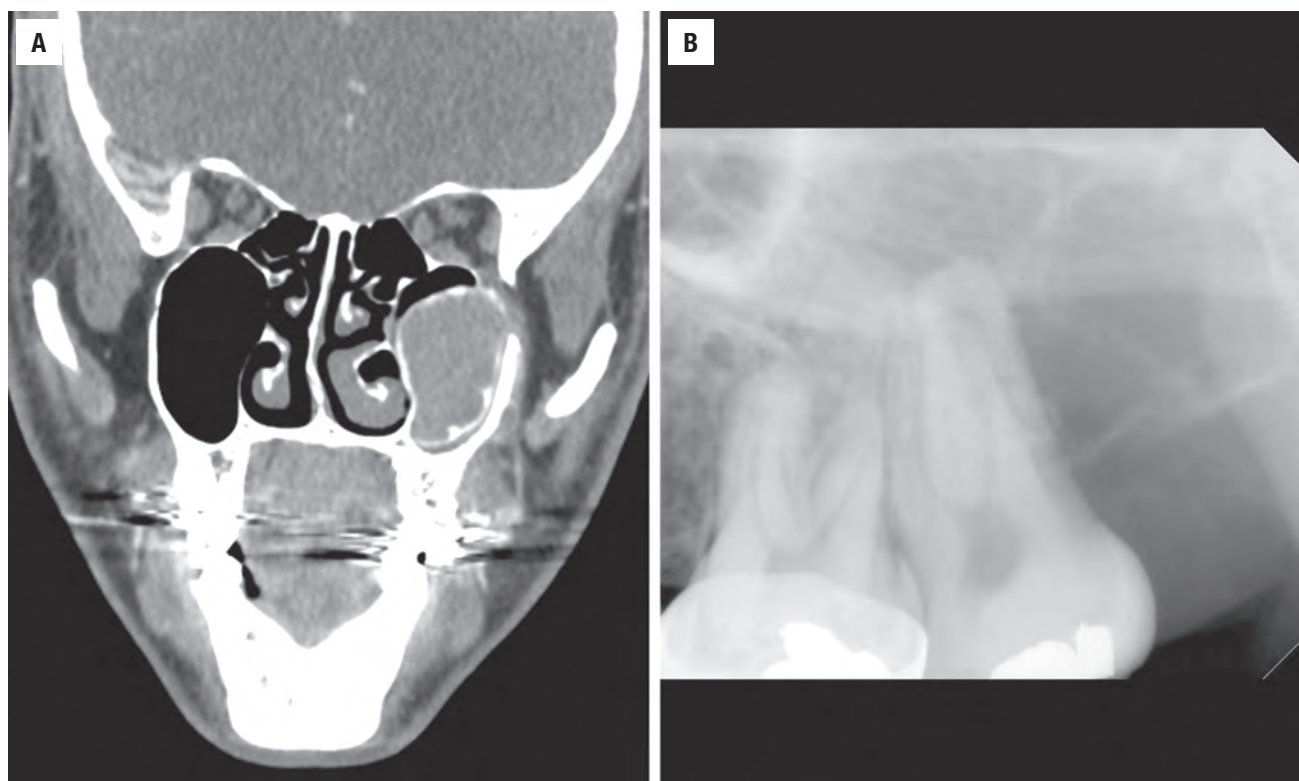
Central giant cell lesions present as expansile unilocular or multilocular radiolucent defects with scalloped and usually well-defined borders (Fig. 15.41). Tooth displacement may be seen. Intralesional bony septa are helpful, although radiographic features are not diagnostic.

### PATHOLOGIC FEATURES

The lesion consists of oval to spindle-shaped fibroblastic cells; some lesions are highly cellular, while others are loose and myxoid. A richly vascularized stroma is associated with extravasated erythrocytes (hemorrhage), hemosiderin-laden macrophages, and giant cells (Fig. 15.42). The osteoclastic giant cell population is variable, without an absolute number required for the diagnosis. Although multinucleated, the number of nuclei is quite variable (Fig. 15.43). Lobules of collagen and metaplastic bone traverse the lesion, although accentuated at the periphery. Mitoses are not uncommon but are not atypical. Aggressiveness is clinically and radiographically determined.

### DIFFERENTIAL DIAGNOSIS

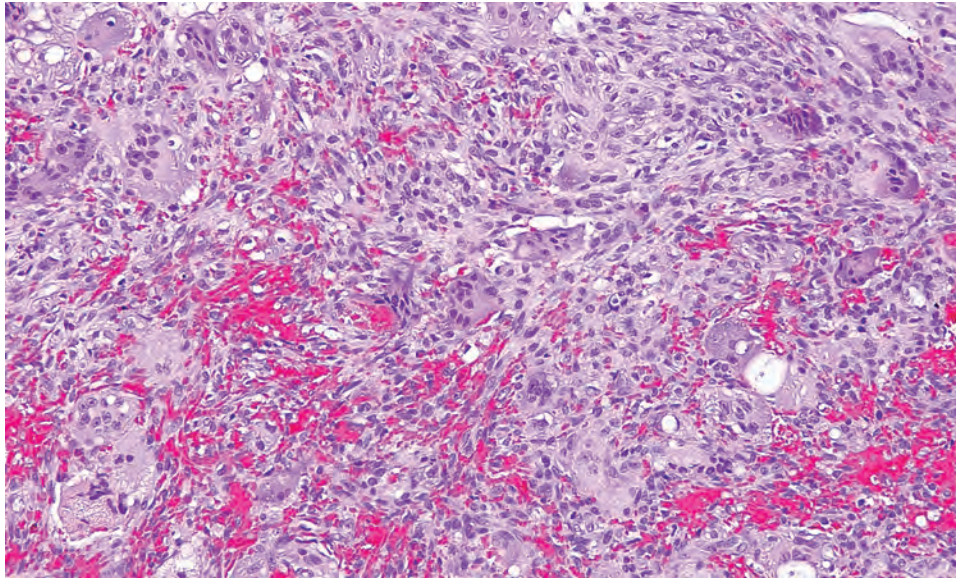
The central giant cell lesion is histologically identical to a *brown tumor of hyperparathyroidism*. Therefore the diagnosis of this entity as *central giant cell lesion*, rule out *hyperparathyroidism* may be most prudent, and patient's serum calcium and parathyroid hormone levels should be evaluated. Histologic separation from *cherubism* may



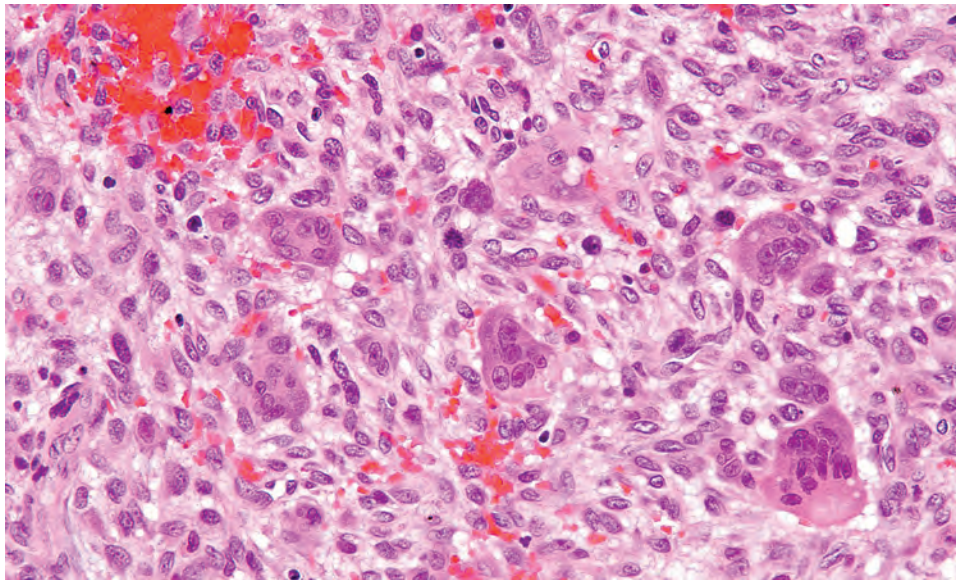
**FIGURE 15.41**

(A) Computed tomography image showing a large expanding radiolucent lesion of the posterior maxilla. (B) Periapical dental radiograph shows a multilocular radiolucency with intralesional septae, a helpful feature in the diagnosis of a central giant cell lesion.



**FIGURE 15.42**

Many multinucleated giant cells are set within a cellular mesenchymal tissue within the bone in a central giant cell lesion. Note the extravasated erythrocytes.

**FIGURE 15.43**

Multinucleated foreign body giant cells in a stroma of ovoid to spindle-shaped cells. Note the erythrocyte extravasation in this central giant cell lesion. A mitotic figure is present.

### CENTRAL GIANT CELL LESION—DISEASE FACT SHEET

#### Definition

- A localized osteolytic lesion of the jaw bones associated with fibrosis, hemorrhage, hemosiderin-laden macrophages, reactive bone, and osteoclastic giant cells

#### Incidence and Location

- Uncommon
- Mandible > maxilla (2:1)

#### Sex and Age Distribution

- Females > males (1.5-2:1)
- Average 20 years (> 90% before 30 years)

#### Clinical Features

- Separated by radiographic and clinical features into nonaggressive and aggressive

- Usually asymptomatic
- Painless expansion of the jaw, paresthesias, and tooth resorption

#### Radiographic Features

- Range from unilocular, well-circumscribed radiolucent lesions to large, expansile multilocular lytic lesions
- Root resorption and displacement of teeth may be seen
- Intralesional bony ("wavy") septa may be seen

#### Prognosis and Treatment

- Long-term prognosis is good, although histology does not predict behavior
- Complete enucleation, although steroid injection, alpha-interferon injections, and calcitonin treatments are effective

**CENTRAL GIANT CELL LESION—PATHOLOGIC FEATURES****Gross Findings**

- Red to brown hemorrhagic tissue with associated bone

**Microscopic Findings**

- Multinucleated, osteoclastic giant cells in a background of ovoid to spindle-shaped fibroblastic cells
- Richly vascularized; associated with extravasated erythrocytes and hemosiderin-laden macrophages
- Metaplastic bone and osteoid traverse the lesion
- Mitotic figures are common (although not atypical)

**Pathologic Differential Diagnosis**

- Brown tumor of hyperparathyroidism, cherubism

be difficult; however, the finding of eosinophilic ring-like deposits surrounding vessels plus the clinical (especially a patient's age) and radiographic information, most importantly, will allow for proper separation.

**PROGNOSIS AND THERAPY**

Histology does not predict behavior. Recurrences are rare if there is unaffected bone at the margins of the resection. Complete enucleation has traditionally been the treatment of choice, but steroid injection, alpha-interferon injections, and calcitonin treatments have proved effective. The nonsurgical techniques require months before regression is seen.

**■ ODONTOMA (COMPLEX AND COMPOUND)**

Odontoma is the most common odontogenic tumor, although it may best be classified as a hamartoma, composed of enamel, dentin, pulpal tissue, and cementum. Academically, odontomas are subclassified into two types; however, management is identical: *compound* when composed of rudimentary teeth-like structures and *complex* when composed of haphazardly arranged products of odontogenesis.

**CLINICAL FEATURES**

Odontomas occur more frequently than all other odontogenic tumors combined. There is no sex predilection and they develop most commonly in the first two decades (the same time that normal teeth are developing and erupting). Most odontomas are asymptomatic,

**ODONTOMA (COMPLEX AND COMPOUND)—DISEASE FACT SHEET****Definition**

- A tumor-like malformation (hamartoma) composed of enamel, dentin, pulpal tissue, and cementum separated into compound and complex types

**Incidence and Location**

- Most common odontogenic tumor
- Compound odontomas predilect to anterior maxilla
- Complex odontomas predilect to posterior mandible

**Sex and Age Distribution**

- Equal sex distribution
- Prevalence in the first two decades

**Clinical Features**

- Usually asymptomatic
- Unusually large lesions may expand the jaws, preventing normal tooth eruption

**Radiographic Features**

- Radiodense calcified mass surrounded by thin radiolucent rim
- Appearance of small, malformed teeth

**Prognosis and Treatment**

- Prognosis is good
- Conservative enucleation of odontoma and associated dental follicle or cyst

found incidentally on routine dental radiographs, whereas larger lesions may interfere with eruption of normal adjacent teeth, prompting radiographic investigation. Rarely, an odontoma may erupt into the oral cavity.

**RADIOGRAPHIC FEATURES**

Odontomas present as a radiodense calcified mass surrounded by a thin radiolucent rim (Fig. 15.44). Compound odontomas will appear like small, malformed teeth, whereas complex odontomas present as radiodense masses of calcified tooth material.

**PATHOLOGIC FEATURES****GROSS FINDINGS**

Compound odontomas have a predilection for the anterior maxilla, whereas complex odontomas favor the posterior



mandible. Compound odontomas appear as a collection of small malformed teeth (Fig. 15.44). Complex odontomas may appear as a collection of mineralized material, usually yellow-white in color. Both subtypes may be associated with soft fibrous connective tissue. They are frequently described as “shelling out” of the bone.

#### MICROSCOPIC FINDINGS

Microscopically, odontomas are composed of the normal elements of tooth structure: dentin, enamel, cementum, and pulpal tissue (Figs. 15.45 and 15.46). These tissues are histologically characteristic and are usually readily identified. In compound odontomas the normal organized relationship of enamel matrix, dentin, and pulpal elements is intact (Fig. 15.45). By contrast, complex odontoma

has a haphazardly arranged enamel matrix, tubular dentin, and pulpal tissue (Fig. 15.46). Note that mature enamel, being so highly mineralized, is lost during tissue decalcification. Immature enamel, or enamel matrix, is usually readily identified, however. Dental follicular tissue, a dentigerous cyst, or, rarely, an odontogenic tumor may be seen in association with an odontoma.

#### DIFFERENTIAL DIAGNOSIS

The only real differential diagnosis is normal teeth, which are removed from consideration by clinical and radiographic correlation. A supernumerary tooth may be considered. Supernumerary teeth are generally defined

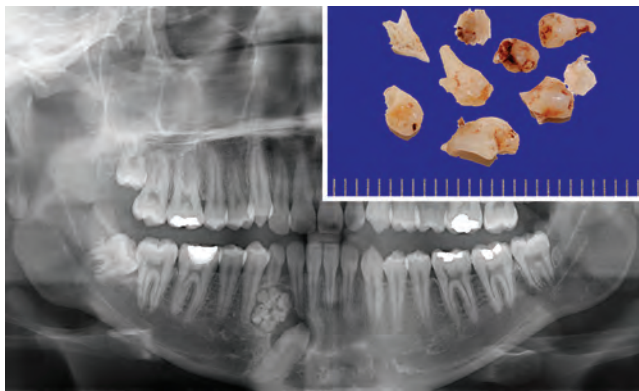


**FIGURE 15.44**

Panoraphic radiograph showing a radiopaque mass in the anterior mandible resulting in impaction of the canine. The appearance is of multiple malformed teeth (compound odontoma). *Inset:* Nine malformed teeth measuring a few millimeters each are seen.

#### ODONTOMA (COMPLEX AND COMPOUND)— PATHOLOGIC FEATURES

##### Gross Findings

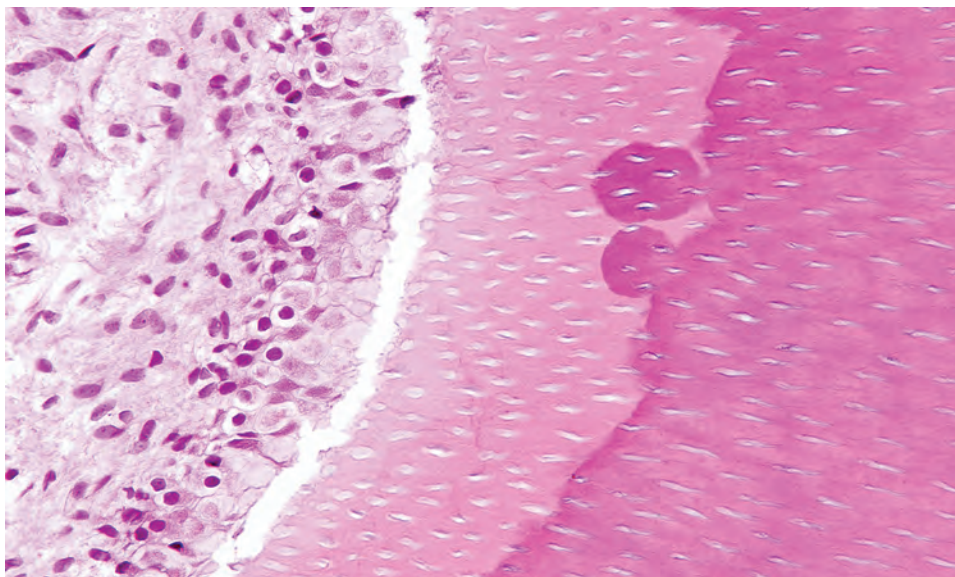
- Compound odontomas may appear as a collection of small, malformed teeth
- Complex odontomas may appear as a collection of mineralized material, usually yellow-white

##### Microscopic Findings

- Compound odontomas have enamel, dentin, cementum, and pulpal tissue recapitulating normal teeth (odontoids)
- Complex odontomas have enamel, dentin, cementum, and pulpal tissue arranged in a disorganized, haphazard manner

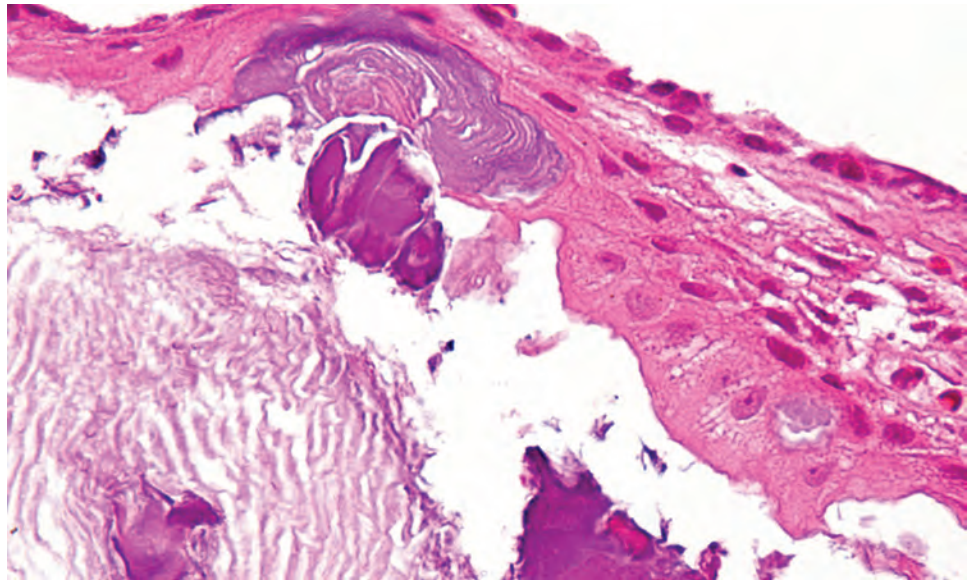
##### Pathologic Differential Diagnosis

- Normal teeth or supernumerary teeth



**FIGURE 15.45**

Distinctive pulpal tissue adjacent to predentin and mature dentin helps to confirm the diagnosis of compound odontoma.

**FIGURE 15.46**

Enamel matrix, with a distinctive fish scale appearance, and odontogenic epithelium in a complex odontoma.

as additional teeth to the normal component of teeth, with the latter more fully formed. The treatment of a supernumerary tooth and an odontoma are essentially the same, and in well-formed (compound) odontomas the terms may be used interchangeably.

#### **PROGNOSIS AND THERAPY**

Treatment is conservative enucleation, including the associated dental follicle or cyst. There is no recurrence

and prognosis is excellent. If the eruption of normal teeth was affected, orthodontic procedures may be necessary to correct the resulting malocclusion.

#### **SUGGESTED READINGS**

The complete Suggested Readings list is available online at [ExpertConsult.com](http://ExpertConsult.com).



**SUGGESTED READINGS****Ossifying Fibroma**

- Childers EL, et al. Giant peripheral ossifying fibroma: a case report and clinicopathologic review of 10 cases from the literature. *Head Neck Pathol.* 2013;7(4):356–360.
- El-Mofty SK. Fibro-osseous lesions of the craniofacial skeleton: an update. *Head Neck Pathol.* 2014;8(4):432–444.
- Eversole LR, et al. Ossifying fibroma: a clinicopathologic study of sixty-four cases. *Oral Surg Oral Med Oral Pathol.* 1985;60:505–511.
- McCarthy EF. Fibro-osseous lesions of the maxillofacial bones. *Head Neck Pathol.* 2013;7(1):5–10.
- Mohanty S, et al. Retrospective analysis of ossifying fibroma of jaw bones over a period of 10 years with literature review. *J Maxillofac Oral Surg.* 2014;13(4):560–567.
- Mohapatra M, et al. Cemento-ossifying fibroma of mandible: An unusual case report and review of literature. *J Oral Maxillofac Pathol.* 2015;19(3):405.
- Prabhu S, et al. Fibro-osseous lesions of the oral and maxillo-facial region: Retrospective analysis for 20 years. *J Oral Maxillofac Pathol.* 2013;17(1):36–40.
- Su L, et al. Distinguishing features of focal cemento-osseous dysplasia and cemento-ossifying fibromas, I. A pathologic spectrum of 316 cases. *Oral Surg Oral Med Oral Pathol.* 1997;84:301–309.
- Su L, et al. Distinguishing features of focal cemento-osseous dysplasia and cemento-ossifying fibromas, II. A clinical and radiologic spectrum of 316 cases. *Oral Surg Oral Med Oral Pathol.* 1997;84:540–549.
- Titinchi F, et al. Ossifying fibroma: analysis of treatment methods and recurrence patterns. *J Oral Maxillofac Surg.* 2016.

**Juvenile/Active Ossifying Fibroma**

- El-Mofty SK. Fibro-osseous lesions of the craniofacial skeleton: an update. *Head Neck Pathol.* 2014;8(4):432–444.
- Han J, et al. Juvenile ossifying fibroma of the jaw: a retrospective study of 15 cases. *Int J Oral Maxillofac Surg.* 2016;45(3):368–376.
- Mohapatra M, et al. Cemento-ossifying fibroma of mandible: An unusual case report and review of literature. *J Oral Maxillofac Pathol.* 2015;19(3):405.
- Owosho AA, et al. Psammomatoid and trabecular juvenile ossifying fibroma: two distinct radiologic entities. *Oral Surg Oral Med Oral Pathol Oral Radiol.* 2014;118(6):732–738.
- Prabhu S, et al. Fibro-osseous lesions of the oral and maxillo-facial region: Retrospective analysis for 20 years. *J Oral Maxillofac Pathol.* 2013;17(1):36–40.
- Peterson BR, et al. Juvenile active ossifying fibroma. *Head Neck Pathol.* 2015;9(3):384–386.
- Ranganath K, et al. Juvenile psammomatoid ossifying fibroma of maxillary sinus: case report with review of literature. *J Maxillofac Oral Surg.* 2014;13(2):109–114.
- Rogozhin DV, et al. Benign fibro-osseous lesions of the cranio-facial area in children and adolescents: a review. *Arkh Patol.* 2015;77(4):63–70.
- Williams HK, et al. Juvenile ossifying fibroma. An analysis of eight cases and a comparison with other fibro-osseous lesions. *J Oral Pathol Med* 2000;29(1):13–18.

**Osteoblastoma**

- Barlow E, et al. Osteoid osteoma and osteoblastoma: novel histological and immunohistochemical observations as evidence for a single entity. *J Clin Pathol.* 2013;66(9):768–774.
- Jones AC, et al. Osteoblastoma of the maxilla and mandible: a report of 24 cases, review of the literature, and discussion of its relationship to osteoid osteoma of the jaws. *Oral Surg Oral Med Oral Pathol Oral Radiol Endod.* 2006;102(5):639–650.
- Lucas DR, et al. Osteoblastoma: clinicopathologic study of 306 cases. *Hum Pathol.* 1994;25:117–134.
- Mahajan A, et al. Osteoblastoma in the retromolar region - Report of an unusual case and review of literature. *J Maxillofac Oral Surg.* 2013;12(3):338–340.

- Pandiar D, et al. Benign osteoblastoma of maxilla: a case report emphasizing the histopathological differential diagnosis. *J Clin Diagn Res.* 2014;8(10):ZD21–ZD23.
- Panigrahi RG, et al. Non aggressive mandibular osteoblastoma - a rare maxillofacial entity. *J Clin Diagn Res.* 2016;10(4):ZD6–ZD8.

**Cementoblastoma**

- Damm DD. Apical lesion of mandibular bicuspid. Apical lesion of maxillary molar. Cemento-osseous dysplasia. Cementoblastoma. *Gen Dent.* 2015;63(3):78–79.
- Gulses A, et al. A case of a benign cementoblastoma treated by enucleation and apicoectomy. *Gen Dent.* 2012;60(6):e380–e382.
- Slootweg PJ. Cementoblastoma and osteoblastoma: a comparison of histologic features. *J Oral Pathol Med.* 1996;13:104–112.

**Ameloblastoma**

- da Silva AD, et al. Ameloblastic neoplasia spectrum: a cross-sectional study of MMPS expression and proliferative activity. *Oral Surg Oral Med Oral Pathol Oral Radiol.* 2016;121(4):396–401.e1.
- Kar IB, et al. Ameloblastic carcinoma: A clinicopathologic dilemma - Report of two cases with total review of literature from 1984 to 2012. *Ann Maxillofac Surg.* 2014;4(1):70–77.
- Milman T, et al. Ameloblastoma: 25 year experience at a single institution. *Head Neck Pathol.* 2016.
- Schafer DR, et al. Primary ameloblastoma of the sinonasal tract: a clinicopathologic study of 24 cases. *Cancer.* 1998;82:667–674.
- Seintou A, et al. Unicystic ameloblastoma in children: systematic review of clinicopathological features and treatment outcomes. *Int J Oral Maxillofac Surg.* 2014;43(4):405–412.
- Vickers RA, et al. Ameloblastoma: delineation of early histopathologic features of neoplasia. *Cancer.* 1970;26:699–710.

**Odontogenic Keratocyst**

- Antonoglou GN, et al. Non-syndromic and syndromic keratocystic odontogenic tumors: systematic review and meta-analysis of recurrences. *J Craniomaxillofac Surg.* 2014;42(7):e364–e371.
- Avelar RL, et al. Odontogenic cysts: a clinicopathological study of 507 cases. *J Oral Sci.* 2009;51(4):581–586.
- Brannon RB. The odontogenic keratocyst—a clinicopathologic study of 312 cases. Part I: clinical features. *Oral Surg Oral Med Oral Pathol.* 1976;42:54–72.
- Brannon RB. The odontogenic keratocyst—a clinicopathologic study of 312 cases. Part II: histologic features. *Oral Surg Oral Med Oral Pathol.* 1977;43:233–255.
- Carlson ER, et al. Nevroid basal cell carcinoma syndrome and the keratocystic odontogenic tumor. *J Oral Maxillofac Surg.* 2015;73(12 suppl):S77–S86.
- Castro-Núñez J. Decompression of odontogenic cystic lesions: past, present, and future. *J Oral Maxillofac Surg.* 2016;74(1):104.e1–104.e9.
- Cheng YS, et al. Multiple orthokeratinized odontogenic cysts: a case report. *Head Neck Pathol.* 2015;9(1):153–157.
- Cunha JF, et al. Clinicopathologic features associated with recurrence of the odontogenic keratocyst: a cohort retrospective analysis. *Oral Surg Oral Med Oral Pathol Oral Radiol.* 2016;121(6):629–635.
- Gorlin RJ, et al. Multiple nevoid basal-cell epithelioma, jaw and bifid rib syndrome. *N Engl J Med.* 1960;262:908–914.
- Nayak MT, et al. Odontogenic keratocyst: what is in the name? *J Nat Sci Biol Med.* 2013;4(2):282–285.
- Ramesh M, et al. Gorlin-Goltz syndrome: case report and literature review. *J Oral Maxillofac Pathol.* 2015;19(2):267.
- Sansare K. Response to the critique of “Keratocystic odontogenic tumor: systematic review with analysis of 72 additional cases from Mumbai, India”. *Oral Surg Oral Med Oral Pathol Oral Radiol.* 2014;117(5):649–653.
- Warburton G, et al. Keratocystic odontogenic tumor (KCOT/OKC)-clinical guidelines for resection. *J Maxillofac Oral Surg.* 2015;14(3):558–564.

### Calcifying Epithelial Odontogenic Tumor

1. Azevedo RS, et al. Calcifying epithelial odontogenic tumor (CEOT): a clinicopathologic and immunohistochemical study and comparison with dental follicles containing CEOT-like areas. *Oral Surg Oral Med Oral Pathol Oral Radiol.* 2013;116(6):759–768.
2. Park CM, et al. Clinicopathologic correlation: a mixed radio-opaque and radiolucent lesion of the posterior maxilla. *Oral Surg Oral Med Oral Pathol Oral Radiol.* 2014;118(4):387–391.
3. Philipsen HP, et al. Calcifying epithelial odontogenic tumour: biological profile based on 181 cases from the literature. *Oral Oncol.* 2000;36:17–26.
4. Pindborg JJ, et al. The calcifying epithelial odontogenic tumor. A review of recent literature and report of a case. *APMIS.* 1991;23(suppl):152–157.
5. Shetty SJ, et al. Peripheral clear cell variant of calcifying epithelial odontogenic tumor: case report and review of the literature. *Head Neck Pathol.* 2016.
6. Urias Barreras CM, et al. Clear cell cystic variant of calcifying epithelial odontogenic tumor. *Head Neck Pathol.* 2014;8(2):229–233.

### Adenomatoid Odontogenic Tumor

1. de Matos FR, et al. Adenomatoid odontogenic tumor: retrospective study of 15 cases with emphasis on histopathologic features. *Head Neck Pathol.* 2012;6(4):430–437.
2. Gomez RS, et al. Adenomatoid odontogenic tumor associated with odontoma: a case report and critical review of the literature. *Head Face Med.* 2013;9:20.
3. Naidu A, et al. Adenomatoid odontogenic tumor with peripheral cemento-osseous reactive proliferation: report of 2 cases and review of the literature. *Oral Surg Oral Med Oral Pathol Oral Radiol.* 2015.
4. Philipsen HP, et al. Adenomatoid odontogenic tumor: biologic profile based on 499 cases. *J Oral Pathol Med.* 1991;20:149–158.

### Central Giant Cell Lesion

1. Aghbali A, et al. Correlation of histopathologic features with demographic, gross and radiographic findings in giant cell granulomas of the jaws. *J Dent Res Dent Clin Dent Prospects.* 2013;7(4):225–229.
2. Ficcarra G, et al. Giant cell lesions of the jaw: a clinicopathologic and cytometric study. *Oral Surg Oral Med Oral Pathol.* 1987;64:44–49.
3. Gomes CC, et al. The highly prevalent H3F3A mutation in giant cell tumours of bone is not shared by sporadic central giant cell lesion of the jaws. *Oral Surg Oral Med Oral Pathol Oral Radiol.* 2014;118(5):583–585.
4. Waldrom CA, et al. The central giant cell reparative granuloma of the jaw. An analysis of 38 cases. *Am J Clin Pathol.* 1966;45:437–447.

### Odontoma

1. Astekar M, et al. Histopathological insight of complex odontoma associated with a dentigerous cyst. *BMJ Case Rep.* 2014;2014.
2. Bereket C, et al. Complex and compound odontomas: Analysis of 69 cases and a rare case of erupted compound odontoma. *Niger J Clin Pract.* 2015;18(6):726–730.
3. Budnick SD. Compound and complex odontomas. *Oral Surg.* 1976;42:501–506.
4. Sekerci AE, et al. Odontogenic tumors: a collaborative study of 218 cases diagnosed over 12 years and comprehensive review of the literature. *Med Oral Patol Oral Cir Bucal.* 2015;20(1):e34–e44.
5. Sun L, et al. Multiple complex odontoma of the maxilla and the mandible. *Oral Surg Oral Med Oral Pathol Oral Radiol.* 2015;120(1):e11–e16.



# Malignant Neoplasms of the Gnathic Bones

■ Uta Flucke

## ■ OSTEOSARCOMA

Osteosarcoma (OS) is defined as a group of malignant tumors whose neoplastic cells produce bone. It is the most common primary malignant bone tumor. Aggressive behavior is usually associated with high-grade morphology of the atypical osteoid-producing osteoblasts. Tumors of the jaw are the fourth most common site of OSs, accounting for approximately 6% of all OSs. Other sites are paranasal sinuses and skull base.

### CLINICAL FEATURES

Affected patients are one to two decades older than patients with peripheral OS, with an average age of 33 to 36 years, without a sex predilection. Most patients present with swelling and pain; tooth displacement and overlying ulceration are possible. Previous radiation or Paget disease of bone are predisposing factors to tumor development in a small subset of patients. There are more tumors in the mandible than maxilla.

Low-grade OSs (central and parosteal, [Table 16.1](#)) are genetically characterized by *MDM2* amplification, whereas high-grade OSs show complex genetic changes.

### RADIOGRAPHIC FEATURES

Radiographs show a poorly defined mixed radiodense and radiolucent lesion, usually with soft tissue extension ([Fig. 16.1](#)). Symmetrical widening of the periodontal ligament space in tooth bearing areas and sunburst periosteal reaction are radiologic hallmarks.

### OSTEOSARCOMA—DISEASE FACT SHEET

#### Definition

- Bone-producing sarcoma, frequently high grade

#### Incidence and Location

- Most common primary malignant bone tumor
- 6% develop in the jaws
- Mandible > maxilla

#### Sex, Race, and Age Distribution

- Equal sex distribution
- Tend to be younger than appendicular skeleton, mean 35 years

#### Clinical Features

- Swelling and pain
- Possibly tooth displacement and overlying ulceration
- Radiation and Paget disease of bone may predispose

#### Radiographic Features

- Poorly defined, mixed radiodense and radiolucent
- Symmetrical widening of the periodontal ligament space in tooth bearing areas
- Sunburst periosteal reaction

#### Prognosis and Treatment

- Mortality is usually due to local disease, with distant metastases, usually in high-grade tumors
- Oncologic resection

### PATHOLOGIC FEATURES

#### GROSS FINDINGS

OSs are (multi)nodular, tan-gray-white, gritty masses. Some tumors are very hard due to heavy mineralization. There is destruction of preexisting bone and often extension into soft tissue. Cartilaginous differentiation shows

**TABLE 16.1**  
**Osteosarcoma classification scheme**

| Type                        | Variants             | Grade        |
|-----------------------------|----------------------|--------------|
| Central<br>(intramedullary) | Conventional:        | High         |
|                             | Osteoblastic         |              |
|                             | Chondroblastic       |              |
|                             | Fibroblastic         |              |
|                             | Rare variants:       |              |
| Surface<br>(juxtacortical)  | Teleangiectatic      | Low          |
|                             | Small cell           |              |
|                             | Epithelioid          |              |
|                             | Giant cell-rich      |              |
|                             | Osteoblastoma-like   |              |
|                             | Chondroblastoma-like |              |
|                             | Low-grade central    |              |
|                             | Parosteal            | Low          |
|                             | Periosteal           | Intermediate |
|                             | High-grade surface   | High         |

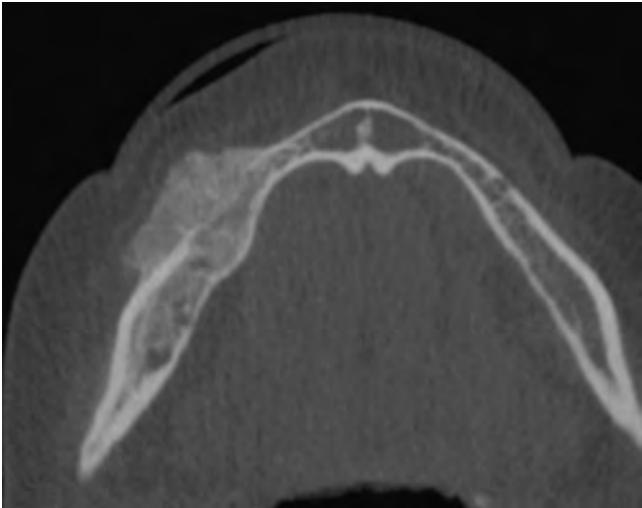


**FIGURE 16.1**  
Poorly defined, mixed radiodense and radiolucent lesion with expansion into soft tissue.

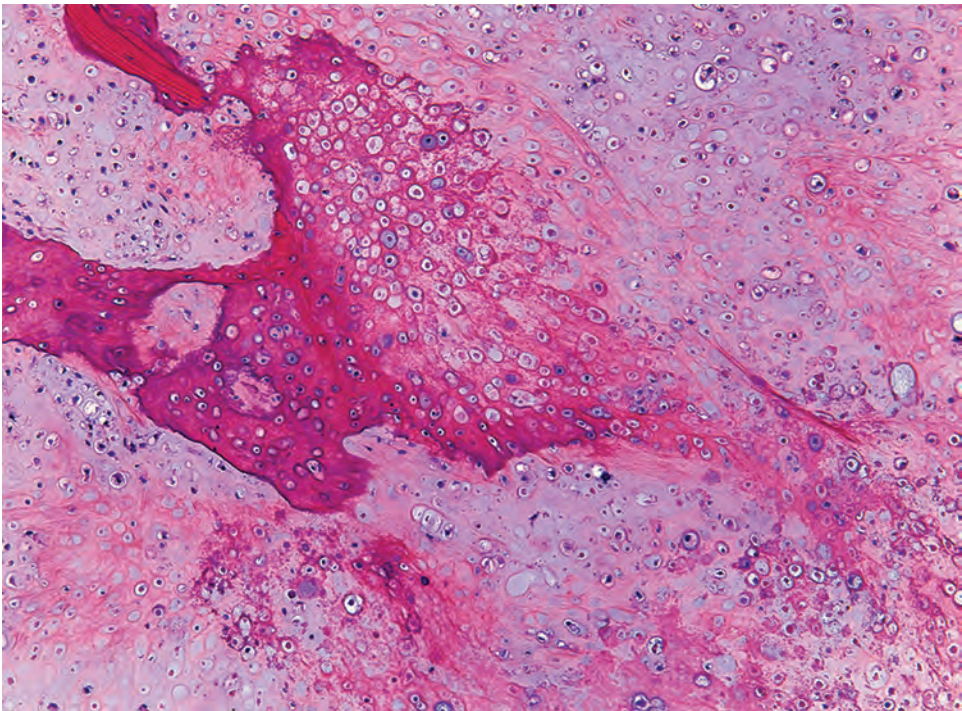


**FIGURE 16.2**  
Chondroblastic osteosarcoma showing pleomorphic cells, which produce osteoid and a chondroid matrix.

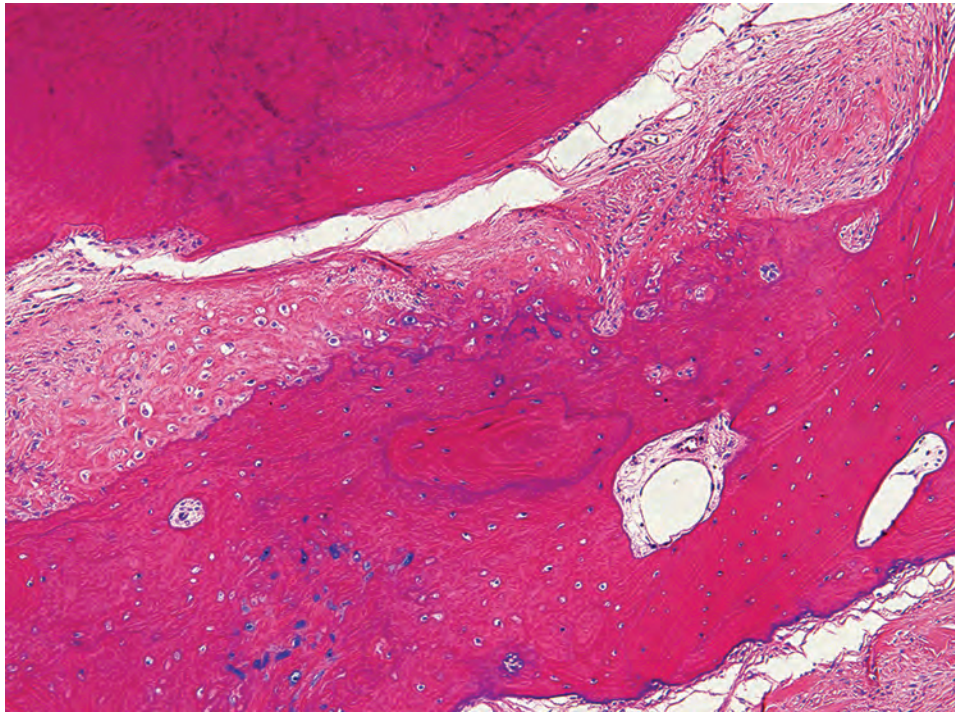
a gray, glistening cut surface like chondroid tumors. Sometimes there is a mucoid matrix, cystic degeneration, or hemorrhage.

**MICROSCOPIC FINDINGS**

The histologic pattern can vary. Essential is the identification of neoplastic bone, which may be focal,

immature to lace-like, and in other cases very sclerotic and heavily mineralized. Tumor cells in high-grade lesions are pleomorphic showing hyperchromatic nuclei (Fig. 16.2). Low-grade lesions are well differentiated with slight pleomorphism and often obvious osteoblastic differentiation (Fig. 16.3). Mitoses are often scarce, especially in low-grade tumors. Subtypes are listed in Table 16.1, but in general the dominant matrix defines the variant:



**FIGURE 16.3**

Low-grade osteosarcoma shows slight pleomorphism of the osteoblastic cells. The matrix shows maturation in comparison to high-grade tumors.

### OSTEOSARCOMA—PATHOLOGIC FEATURES

#### Gross Findings

- (Multi)nodular tan-gray-white gritty and hard mass showing destruction of bone and infiltration into soft tissue

#### Microscopic Findings

- Histology is variable
- By definition, neoplastic bone must be identified
- Bone may be focal, immature, lace-like, sclerotic, or heavily mineralized
- Many subtypes are recognized, but in the jaws chondroblastic is most common
- Extension into soft tissue helps to diagnose low-grade tumors

#### Pathologic Differential Diagnosis

- Chondrosarcoma, benign fibro-osseous lesions (ossifying fibroma)

chondroblastic, osteoblastic, and fibroblastic subtypes. Chondroblastic OS is more common in the jaw bones and must be separated from chondrosarcoma (CS), which is quite rare in this site.

### DIFFERENTIAL DIAGNOSIS

When osteoid production is low in the chondroblastic subtype, a CS must be considered. However, the presence of neoplastic bone, in any volume, defines OS. Low-grade OS should be distinguished from benign fibro-osseous

lesions, such as ossifying fibroma, by cellular atypia and infiltration of the surrounding soft tissue.

### PROGNOSIS AND THERAPY

High mortality is due to local disease. Hematogenous spread in high-grade OS seems to be much more infrequent (up to 21 % of patients) and seems to occur later in the course of disease compared with peripheral OS. The vast majority of patients are managed by complete resection. Multimodality treatment should be critically evaluated because the benefit in jaw tumors is not well documented.

### ■ CHONDROSARCOMA

CS is a bone tumor that produces cartilage. Tumors of craniofacial bones are rare, accounting for only approximately 4 % of all CS. The maxilla is more commonly affected than the mandible, but any site can be involved. In the mandible, the symphysis, coronoid process, and condyle are more often affected, sites corresponding to regions of endochondral ossification.

### CLINICAL FEATURES

CS is a tumor of adulthood; however, the child/adolescent population may rarely be affected. The

**CHONDROSARCOMA—DISEASE FACT SHEET****Definition**

- A bone tumor that produces cartilage

**Incidence and Location**

- Rare, with jaw tumors representing 4% of chondrosarcoma
- Maxilla > mandible

**Sex and Age Distribution**

- Males slightly more than females
- The peak age at presentation is the 4th decade

**Clinical Features**

- Pain, swelling, and nasal obstruction
- Rare association with syndromes (Ollier disease, Maffucci syndrome)

**Radiographic Features**

- Radiolucent lesions with more or less evenly distributed punctuate or ring-like opacities

**Prognosis and Treatment**

- Recurrence and uncontrolled local extension is associated with a poor prognosis
- Oncologic resection is the treatment of choice

peak age at presentation is the 4th decade, with men affected slightly more often than women. Swelling and nasal obstruction are common complaints. Syndrome (Maffucci syndrome or Ollier disease) association is rare.

**RADIOGRAPHIC FEATURES**

Cartilage neoplasms are radiolucent lesions with more or less evenly distributed punctuate or ring-like opacities. These discrete calcified opacities are the radiologic hallmark. There is variation from predominant lytic to heavily calcified with consolidated areas of opacity, difficult to distinguish from bone-forming lesions.

**PATHOLOGIC FEATURES****GROSS FINDINGS**

Lesions have a lobulated architecture composed of translucent hyaline nodules resembling more or less normal cartilage. Mineralized areas are chalk-like. Myxoid change, hemorrhage, and necrosis may be found, the latter usually a sign of a high-grade tumor.

**CHONDROSARCOMA—PATHOLOGIC FEATURES****Gross Findings**

- Lobulated architecture composed of translucent hyaline nodules

**Microscopic Findings**

- Uniformly cartilaginous and lobulated with a partially calcified or myxoid matrix
- Cluster disarray and increased cellularity
- Grading (I–III) depends on cellularity, atypia, and mitoses

**Ancillary Studies**

- Positive: S100 protein, SOX9, podoplanin
- *IDH1/2* hot spot mutations

**Pathologic Differential Diagnosis**

- Chondroblastic osteosarcoma, chondrometaplasia, pleomorphic adenoma

**MICROSCOPIC FINDINGS**

Tumors should be uniformly cartilaginous and lobulated with a partially calcified or myxoid matrix. Low-grade tumors (grade 1) show cluster disarray, slightly increased cellularity, and occasional nuclei with pleomorphism or binucleation, only slightly different from enchondroma. Grade II CS is characterized by a definite increased cellularity (Fig. 16.4). The atypical chondrocytes are more or less evenly distributed with occurrence of loose clusters. Nuclei are enlarged with open chromatin and often distinct nucleoli. Binucleated cells are frequent and atypical multinucleated cells may be seen. Myxoid changes are frequently present. Myxoid CSs are classified as grade II, even when the cellularity is relatively low (Fig. 16.5). High-grade CSs (grade III) are rare and characterized by high cellularity, prominent nuclear atypia, and the presence of mitotic figures. Importantly, chondroblastic OS is much more common in the jaws than primary CS.

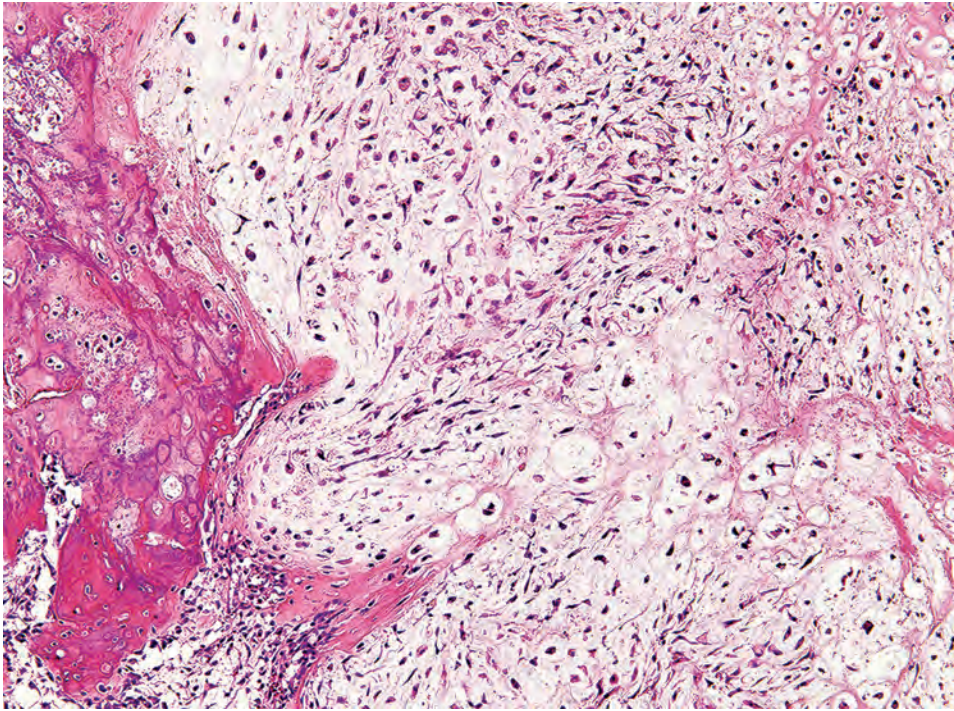
**ANCILLARY STUDIES**

Seldom used, but CS are immunoreactive with S100 protein, SOX9, and podoplanin. Hot spot mutations in *IDH1/2* are a genetic feature of CS in general.

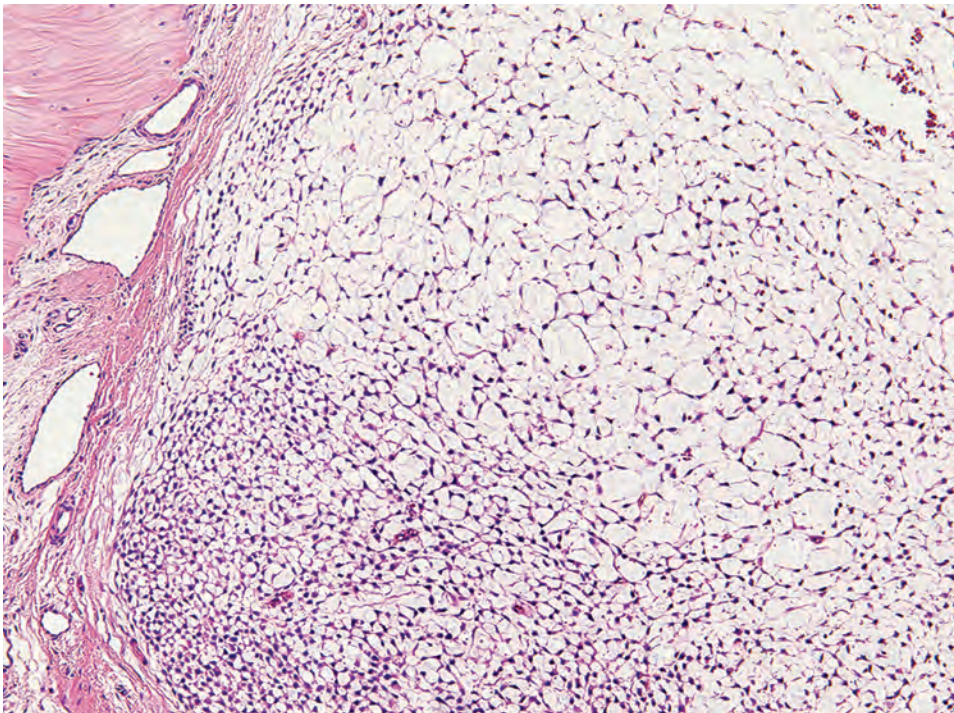
**DIFFERENTIAL DIAGNOSIS**

Chondroblastic OS shows bone-forming areas. Reactive nodular proliferation of cartilage in the nasal septum may be misinterpreted as CS, while cartilaginous differentiation may be seen in pleomorphic adenoma.



**FIGURE 16.4**

Grade II chondrosarcoma depicting increased cellularity, pleomorphism, and isolated mitoses. Destructive invasion into native bone is noted (left side).

**FIGURE 16.5**

Grade II chondrosarcoma with a myxoid matrix yielding a "string of pearls" appearance.

### PROGNOSIS AND THERAPY

Resection is the treatment of choice. Wide oncologic margins are associated with a low recurrence rate. Recurrence and uncontrolled local extension is associated with a poor prognosis. Distant metastases are rare.

### ■ MESENCHYMAL CHONDROSARCOMA

Mesenchymal chondrosarcoma (MCS) is a distinct and translocation-associated malignancy defined by a biphasic appearance of small blue round cells with focal cartilaginous differentiation. MCS is an extremely rare sarcoma

and has a predilection for the facial skeleton, particularly the jaws, which are involved in approximately 25 % of the cases.

### CLINICAL FEATURES

MCS tends to affect children and young adults, although the age range is broad, without a sex predilection. Blacks and Latinas are more commonly affected. Swelling or mass and pain are the main symptoms. Additional site-dependent symptoms include loosening teeth, sinusitis, nasal obstruction, visual change, headaches, epistaxis, or signs of nerve dysfunction.

### RADIOGRAPHIC FEATURES

Radiographic features nearly always suggest malignancy with a destructive growth pattern. It appears as a radiolucent lesion with varying degrees of stippled calcification.

### MESENCHYMAL CHONDROSARCOMA—DISEASE FACT SHEET

#### Definition

- Distinct and translocation-associated, small, blue round cell tumor with focal cartilaginous differentiation

#### Incidence and Location

- Extremely rare
- Predilection for the facial skeleton

#### Sex, Race, and Age Distribution

- Equal sex distribution
- Blacks and Latinos more commonly affected
- Age range is broad but mainly children and young adults

#### Clinical Features

- Swelling, mass, pain
- Site-dependent symptoms may be seen

#### Radiographic Features

- Destructive growth pattern
- Radiolucent lesion with varying degrees of stippled calcification

#### Prognosis and Treatment

- Aggressive behavior with early and very late metastases
- Surgery is treatment of choice
- Protracted and relentless clinical course, requiring long-term follow-up

### PATHOLOGIC FEATURES

#### GROSS FINDINGS

The tumor is usually well-demarcated from the surrounding bone and soft tissue, when involved, and may have a lobulated architecture. The tissue is gray to pink with foci of cartilage with or without calcification.

#### MICROSCOPIC FINDINGS

MCS is a small blue round cell tumor with a distinct biphasic appearance, characterized by undifferentiated round to spindled cells and a hyaline cartilaginous component, which is the hallmark (Fig. 16.6). However, the amount of cartilage may be very limited, frequently requiring many tumor sections and/or levels/deepers to reveal the cartilaginous foci. A staghorn-like vasculature is often present and prominent. The chondroid matrix may calcify and/or ossify.

### ANCILLARY STUDIES

Immunohistochemically, CD99 and SOX9 are expressed in the small cells, whereas S100 protein highlights the cartilaginous component. The *HEY1-NCOA2* fusion appears to be a helpful genetic marker. However, there is some genetic heterogeneity with alternate fusion partners. *IDH1/2* mutations are absent.

### MESENCHYMAL CHONDROSARCOMA—PATHOLOGIC FEATURES

#### Gross Findings

- Well-demarcated, lobulated, gray to pink tumor with foci of cartilage with or without calcification

#### Microscopic Findings

- Biphasic tumor with undifferentiated small blue round cells and a hyaline cartilaginous component
- Cartilage is often extremely limited requiring many tumor sections and/or deepers/levels
- Prominent staghorn-like vasculature

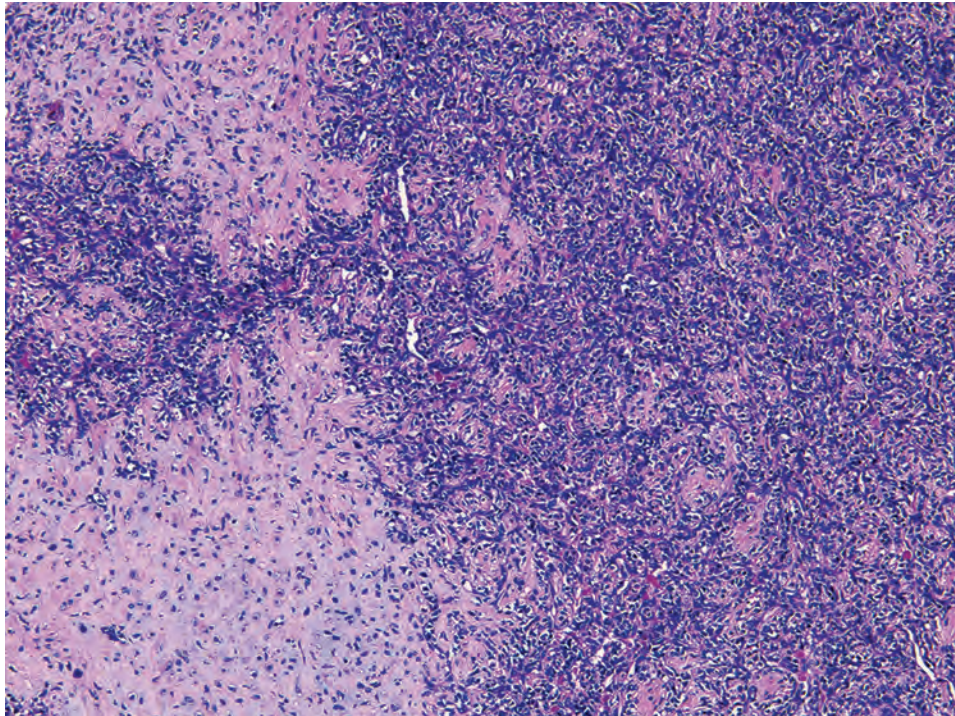
#### Ancillary Studies

- Positive: CD99, SOX9 in small cells; S100 protein in cartilaginous component
- Consistent fusion gene *HEY1-NCOA2*

#### Pathologic Differential Diagnosis

- Ewing sarcoma/primitive neuroectodermal tumor, synovial sarcoma, alveolar rhabdomyosarcoma, lymphoma, melanoma, undifferentiated carcinoma



**FIGURE 16.6**

Mesenchymal chondrosarcoma consisting of a small blue round cell component and a cartilaginous component. Note the hemangiopericytoma-like vessels.

### DIFFERENTIAL DIAGNOSIS

Other small blue round cell tumors, such as Ewing sarcoma, synovial sarcoma, alveolar rhabdomyosarcoma, undifferentiated carcinoma, melanoma, and lymphoma lack the chondroid component.

### PROGNOSIS AND THERAPY

MSCs are generally aggressive with early and very late metastases. Metastases can occur everywhere in the body. Surgery is the mainstay of treatment. The role of chemotherapy and radiation is uncertain. The clinical course is frequently protracted and relentless, making long-term follow-up mandatory. Some studies suggest the prognosis is more favorable for lesions arising in the jaws compared with other sites.

## ■ AMELOBLASTIC CARCINOMA

Ameloblastic carcinoma (AC) is a very rare odontogenic malignancy that combines the histologic features of ameloblastoma and cellular pleomorphism, considered the malignant counterpart of ameloblastoma. They arise de novo or rarely from a preexisting ameloblastoma.

### CLINICAL FEATURES

Adults are affected with a mean age of approximately 50 years, with males at slightly greater frequency than females. Most lesions arise in the mandible, posterior more often than anterior, although any location may be affected. Patients complain of diffuse and slow-growing swelling. Other symptoms are pain, bleeding, tooth mobility, and dysphasia.

### RADIOGRAPHIC FEATURES

ACs are irregular radiolucent lesions showing destructive growth with cortical expansion. Perforation with extension into adjacent soft tissue is not uncommon.

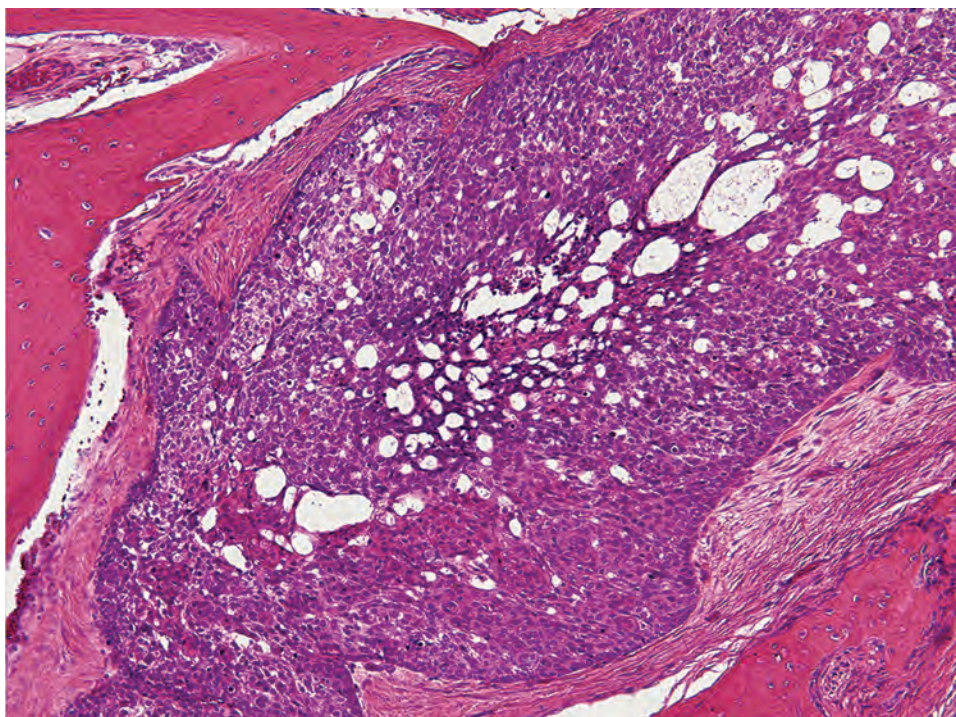
### PATHOLOGIC FEATURES

#### GROSS FINDINGS

Irregular and ill-defined white-gray mass, often with necrotic areas and hemorrhage.

#### MICROSCOPIC FINDINGS

AC is characterized by the histologic pattern of ameloblastoma and anaplasia. The latter consists of

**FIGURE 16.7**

Ameloblastic carcinoma shows the pattern of ameloblastoma and cytological atypia.

#### AMELOBLASTIC CARCINOMA—DISEASE FACT SHEET

##### Definition

- Odontogenic malignancy combining the histologic features of ameloblastoma and cytologic pleomorphism

##### Incidence and Location

- Extremely rare
- Mandible (posterior > anterior) most commonly

##### Sex and Age Distribution

- Males slightly more frequently affected than females
- Mean: 50 years

##### Clinical Features

- Diffuse and slow-growing swelling
- Other symptoms are pain, bleeding, tooth mobility, and dysphasia

##### Radiographic Features

- Irregular radiolucent lesions with destructive bone growth, showing perforation and soft tissue extension

##### Prognosis and Treatment

- Wide local excision with clear margins
- Aggressive clinical course
- Multiple local recurrences, with frequent lung metastases
- Overall 5-, 10- and 15-year survival rates: 90%, 45%, and 20%, respectively

#### AMELOBLASTIC CARCINOMA—PATHOLOGIC FEATURES

##### Gross Findings

- Irregular and ill-defined white-gray mass with necrosis

##### Microscopic Findings

- Combination of ameloblastoma with pleomorphism
- Hypercellularity, basaloid, and/or pseudosarcomatous differentiation of the stellate reticulum, loss of ameloblastic differentiation, follicular budding, presence of clear cells, nuclear pleomorphism, hyperchromasia, increased nuclear to cytoplasmic (N:C) ratio
- High mitotic rate
- Infiltrative growth pattern, neural and vascular invasion, and necrosis

##### Ancillary Studies

- CK18 and CK19 are highly expressed
- SOX2 shows diffuse nuclear staining
- *BRAF* mutations in a subset of cases

##### Pathologic Differential Diagnosis

- Ameloblastoma, squamous cell carcinoma, clear cell odontogenic carcinoma, metastatic carcinomas

hypercellularity, basaloid and/or pseudosarcomatous differentiation of the stellate reticulum, loss of ameloblastic differentiation, follicular budding, presence of clear cells, nuclear pleomorphism, hyperchromasia, increased nuclear to cytoplasmic ratio, and a high mitotic count (Fig. 16.7). Infiltrative growth pattern, perineural and lymphovascular invasion and necrosis are also present. However, as many of these features are not observed in the same tumor, no single characteristic can be used, with diagnosis requiring a combination of them.



### ANCILLARY STUDIES

As in ameloblastomas, CK18 and CK19 are highly expressed, whereas SOX2 shows a strong nuclear reaction. The Ki-67 proliferation index is higher in AC than in ameloblastoma. The *BRAF* mutations in AC are identical to ameloblastoma.

### DIFFERENTIAL DIAGNOSIS

Ameloblastoma lacks atypia and mitotic activity. Intraosseous squamous cell carcinoma, clear cell odontogenic carcinomas (CCOCs), and metastatic carcinomas are usually distinct.

### PROGNOSIS AND THERAPY

Because of its aggressive clinical course, AC is usually treated with wide local excision with clear margins. Radiotherapy remains a questionable adjuvant approach for incompletely resected tumors. Multiple local recurrences are common (30%). Metastases are seen in approximately 30% of patients to the lung, whereas cervical lymph node metastases are uncommon. Overall 5-, 10-, and 15-year survival rates are 90%, 45%, and 20%, respectively.

## ■ PRIMARY INTRAOSSEOUS CARCINOMA

Primary intraosseous carcinoma (PIOC) is a rare malignant odontogenic tumor that originates from odontogenic epithelial remnants and arises in the jaw bones. It also may derive from odontogenic keratocyst and benign odontogenic cysts, thus squamous differentiation is most common.

### CLINICAL FEATURES

PIOCs are rare, representing < 2% of all odontogenic tumors. Mean age is 55 years, with a male to female ratio of 2:1. However, cases have been encountered during infancy. The mandible to maxilla ratio is 4:1, with posterior mandibular and anterior maxillary tumors most common. Swelling and pain are the most commonly

### PRIMARY INTRAOSSEOUS CARCINOMA—DISEASE FACT SHEET

#### Definition

- Malignant odontogenic tumor that originates from odontogenic epithelial remnants and arises in the jaws
- May derive from odontogenic keratocyst and benign odontogenic cysts

#### Incidence and Location

- Less than 2% of all odontogenic tumors
- Mandible > > maxilla (4:1)

#### Sex and Age Distribution

- Males > females (2:1)
- Mean age 55 years

#### Clinical Features

- Swelling and pain are the most common symptoms

#### Radiographic Features

- Osteolytic, radiolucent, irregular lesions with possible cortical expansion and destruction

#### Prognosis and Treatment

- Resection and adjuvant radiation (multimodality therapy)
- Poor prognosis because of local failure and frequent metastases (regional lymph nodes, lung)

associated symptoms. Strict diagnostic criteria are difficult to apply because odontogenic origin may be obscured or benign precursor remnants difficult to identify. Interestingly, PIOCs are usually seen above the inferior dental canal, whereas metastases are more frequently below the canal.

### RADIOGRAPHIC FEATURES

PIOCs are osteolytic. The margins of the radiolucency are often irregular and noncorticated. Cortical expansion and destruction are obvious in larger lesions, with root resorption and perforation.

### PATHOLOGIC FEATURES

#### GROSS FINDINGS

Irregular and ill-defined white-gray mass, often with necrotic areas and hemorrhage. Extension into adjacent

### PRIMARY INTRAOSSEOUS CARCINOMA—PATHOLOGIC FEATURES

#### Gross Findings

- Irregular and ill-defined white-gray mass with extension into adjacent soft tissue through the periodontal ligament

#### Microscopic Findings

- Diagnosis of exclusion
- Atypical squamous cells (well to poorly differentiated)
- Keratinizing is uncommon and necrosis limited to absent
- Rarely, associated with odontogenic keratocyst and benign odontogenic cysts, showing transition to malignancy

#### Pathologic Differential Diagnosis

- Squamous cell carcinoma from adjacent sites or metastatic tumors

soft tissue through the periodontal ligament are possible.

#### MICROSCOPIC FINDINGS

Histologically, the tumor is composed of atypical squamous cells ranging from well to poorly differentiated, like squamous cell carcinoma (SCC) at other sites. Rarely, there is a connection with odontogenic keratocysts and benign odontogenic cysts. Keratinization is uncommon. Necrosis is limited to absent. It is important to remember that PIOC is a diagnosis of exclusion. If benign remnants are seen with dysplasia and then transition to carcinoma, a primary lesion can be confirmed.

### DIFFERENTIAL DIAGNOSIS

Alveolar mucosal squamous cell carcinoma, SCC originating from the maxillary sinus, or metastatic SCC can morphologically not be distinguished, and must be ruled out clinically or radiologically.

### PROGNOSIS AND THERAPY

Resection and adjuvant radiation seem to provide the best treatment results. However, the prognosis is poor because of local failure within the first 2 years and frequent metastases to regional lymph nodes and the lungs. Multimodality therapy yields the best outcome.

### SCLEROSING ODONTOGENIC CARCINOMA—DISEASE FACT SHEET

#### Definition

- Odontogenic carcinoma characterized by infiltrative strands of bland cuboidal or polygonal cells set in a prominent sclerotic stroma

#### Incidence and Location

- Rare
- Mandible > maxilla

#### Sex and Age Distribution

- Adults with equal sex distribution

#### Clinical Features

- Expansile intragnathic mass

#### Radiographic Features

- Ill-defined expansile radiolucencies with possible extension into soft tissue; radiopaque areas may be present

#### Prognosis and Treatment

- Prognosis is excellent after complete resection

## ■ SCLEROSING ODONTOGENIC CARCINOMA

Sclerosing odontogenic carcinoma is a recently defined odontogenic carcinoma, showing a highly infiltrative growth by carcinoma cells with very bland cytology set in a prominent sclerotic stroma.

### CLINICAL FEATURES

Patients are adults with equal sex distribution presenting with an expansile intragnathic mass, either in mandible (more often) or maxilla.

### RADIOGRAPHIC FEATURES

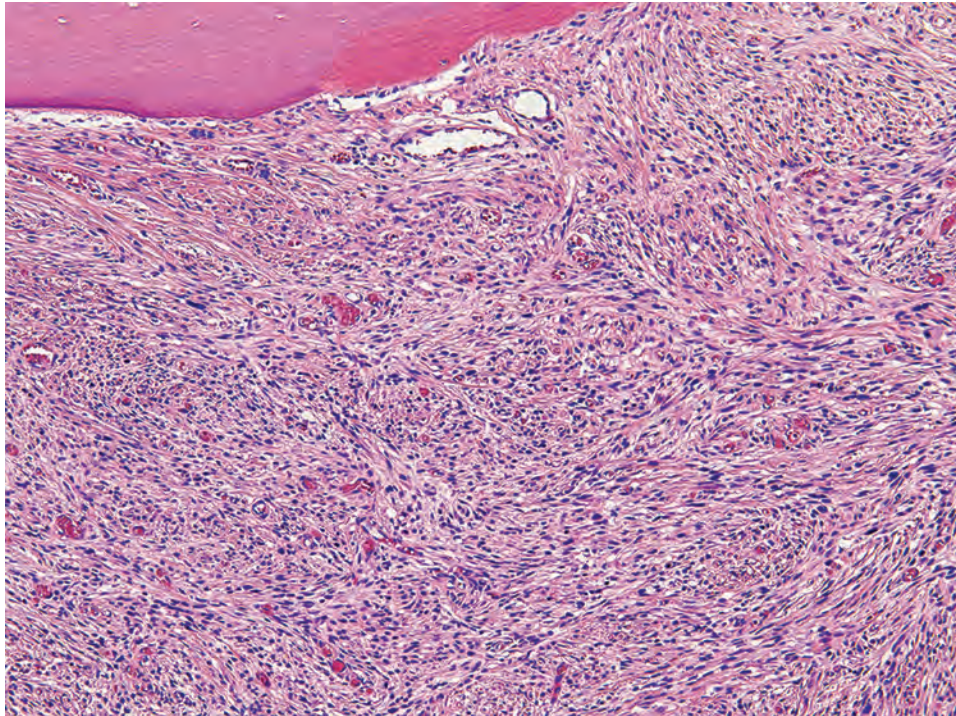
Radiographs show ill-defined, expansile radiolucencies with possible extension into soft tissue. Radiopaque areas may be present.

### PATHOLOGIC FEATURES

#### GROSS FINDINGS

Solid, white-gray, irregular mass with destruction of the bone.



**FIGURE 16.8**

Sclerosing odontogenic carcinoma show thin strands and nests of epithelial cells in a prominent sclerotic stroma. The cells are cuboidal or polygonal with hyperchromatic and slightly pleomorphic nuclei.

### SCLEROSING ODONTOGENIC CARCINOMA— PATHOLOGIC FEATURES

#### Gross Findings

- Solid white-gray irregular destructive mass

#### Microscopic Findings

- Single-file strands and nests of bland cuboidal or polygonal epithelial cells in a prominent sclerotic stroma
- Distinct cytoplasmic borders with eosinophilic or rarely clear cytoplasm
- Low to absent mitotic activity

#### Immunohistochemical Findings

- Positive: CK5/6, p63, CK19
- Negative: CAM5.2, CK20
- Variable expression with CK7

#### Pathologic Differential Diagnosis

- Metastatic carcinoma, desmoplastic ameloblastoma, squamous odontogenic tumor, epithelium-rich variant of central odontogenic fibroma, calcifying epithelial odontogenic tumor, clear cell odontogenic carcinoma, normal odontogenic rests

### MICROSCOPIC FINDINGS

The tumor is defined by thin, single-file strands, cords, and nests of bland epithelial cells in a prominent sclerotic stroma. The strands or cords are linear, tadpole-like, club-shaped, or helix-like and reminiscent of odontogenic rests found in normal gingival tissues or of the epithelial component of odontogenic fibroma. The cells are cuboidal

or polygonal with distinct cytoplasmic borders. The cytoplasm is eosinophilic or rarely clear with signet ring appearance, but there is no mucus. Mitotic activity is very low to absent (Fig. 16.8). Acellular stromal calcifications may be present. Other striking features are extraosseous expansion with invasion of skeletal muscle and perineurium. Inflammatory reactions can camouflage epithelial nests and strands.

### ANCILLARY STUDIES

Tumor cells are positive for CK5/6, p63, and CK19, whereas CAM5.2 and CK20 are negative. CK7 is variably positive. Although unnecessary for the diagnosis, immunohistochemistry may serve to highlight the epithelial cells within the sclerotic stroma.

### DIFFERENTIAL DIAGNOSIS

The possibility of metastatic disease should be ruled out. Other differential diagnostic considerations are desmoplastic ameloblastoma (thin cords and small nests are absent in contrast to stellate-shaped neoplastic islands), squamous odontogenic tumor (larger epithelial islands occasionally with cystic degeneration), epithelium-rich variant of central odontogenic fibroma (fibroblastic and no sclerotic stroma), calcifying epithelial odontogenic tumor (hyalinized material that stains positive for amyloid), CCOC (sheets or large islands of vacuolated

cells), and normal odontogenic rests (localized phenomenon without atypia).

### PROGNOSIS AND THERAPY

Complete resection is curative, whereas curettage may be associated with recurrence. Metastatic disease is not reported.

## CLEAR CELL ODONTOGENIC CARCINOMA

Clear cell odontogenic carcinoma (CCOC) is a malignant neoplasm showing sheets and islands of vacuolated and clear cells, harboring *EWSR1* rearrangements, with *ATF1* the most common fusion partner.

### CLINICAL FEATURES

CCOC affects patients of a wide age range but is most often seen in the 6th decade. There is a preponderance of females, with most cases reported in the mandible

(mandible to maxilla ratio, 7:1). Signs include swelling and loosening of teeth.

### RADIOGRAPHIC FEATURES

CCOC presents as an ill-defined radiolucency with possible root resorption (Fig. 16.9).

### PATHOLOGIC FEATURES

#### GROSS FINDINGS

Irregular, infiltrative, white-gray mass.



**FIGURE 16.9**

Clear cell odontogenic carcinoma present as an ill-defined radiolucency, as other malignant odontogenic tumors.

### CLEAR CELL ODONTOGENIC CARCINOMA—DISEASE FACT SHEET

#### Definition

- A malignant odontogenic carcinoma showing sheets and island of clear to vacuolated cells associated with a consistent fusion (*EWSR1-ATF1*)

#### Incidence and Location

- Rare
- Mandible > > > maxilla (7:1)

#### Sex and Age Distribution

- Females > males (1.6:1)
- Wide age range, mean in the 6th decade

#### Clinical Features

- Swelling and teeth loosening

#### Radiographic Features

- Ill-defined radiolucency with possible root resorption

#### Prognosis and Treatment

- Indolent to recurrent
- Approximately 10% develop metastases (lymph nodes, lung), with death reported in ~15%
- Resection with tumor-free margins is the treatment of choice

### CLEAR CELL ODONTOGENIC CARCINOMA—PATHOLOGIC FEATURES

#### Gross Findings

- Irregular infiltrative white-gray mass

#### Microscopic Findings

- Three patterns: biphasic, monomorphic, and ameloblastomatous
- **Biphasic:** clear cells arranged in a linear architecture with peripheral palisading of hyperchromatic polygonal cells with eosinophilic cytoplasm
- **Ameloblastomatous:** clear cells arranged in islands with peripheral palisaded columnar cells
- Hyalinized to fibrocellular stroma in all cases

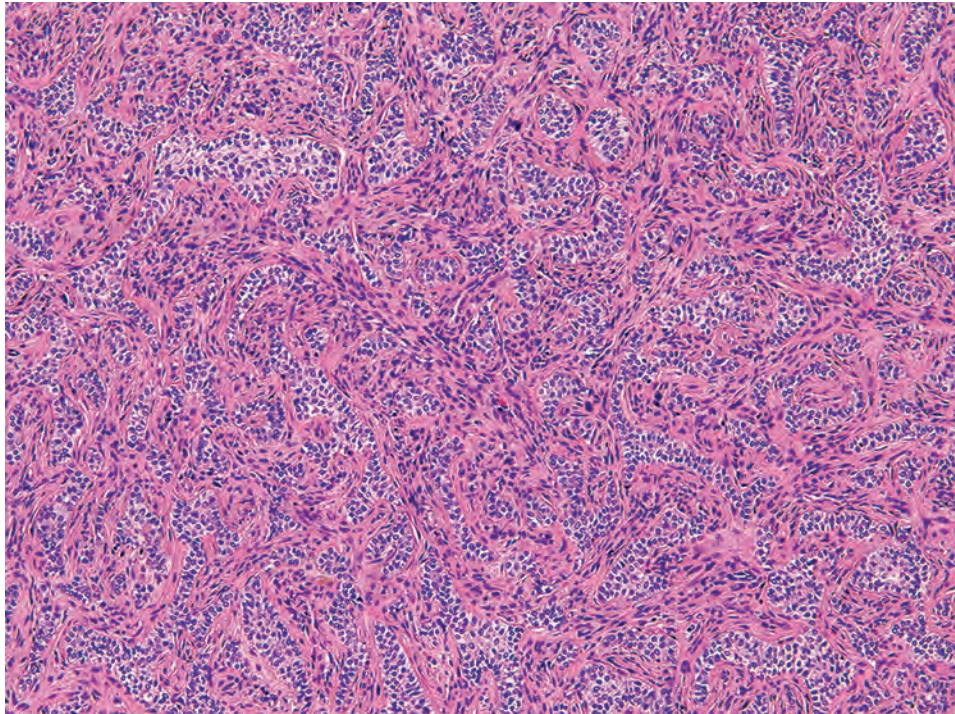
#### Ancillary Studies

- Positive: pancytokeratin, CK5/6, p63, CK19, EMA
- Negative: vimentin, S100 protein, desmin, HMB45, CD10
- *EWSR1* rearrangements by FISH

#### Pathologic Differential Diagnosis

- Salivary gland tumors with clear cell features, melanoma, renal cell carcinoma, clear cell variant of calcifying epithelial odontogenic tumor



**FIGURE 16.10**

The monomorphic pattern of a clear cell odontogenic carcinoma is entirely composed of clear cells. Note the fibrocellular stroma.

### MICROSCOPIC FINDINGS

Three histomorphologic patterns are described: biphasic, monomorphic, and ameloblastomatous. In general, the epithelial cells show clear cytoplasm, well-demarcated membranes, and dark-staining nuclei. The cells are arranged in sheets, trabeculae, or strands, showing basaloid cells at the periphery. The monomorphic pattern is entirely composed of clear cells (Fig. 16.10). The ameloblastomatous pattern is rare and shows clear cells organized in islands with peripheral palisading columnar cells. All cases harbor a hyalinized to fibrocellular stroma without amyloid. The latter is in contrast to calcifying epithelial odontogenic tumor. High-grade tumors may show necrosis, pleomorphism, and perineural invasion.

### ANCILLARY STUDIES

CCOC is positive for pancytokeratin (AE1/AE3), CK5/6, CK19, p63, and EMA, whereas CK7, S100 protein, SMA, calponin, desmin HMB45, GFAP, and vimentin are negative. *EWSR1* gene rearrangements can be detected by fluorescence in situ hybridization (FISH).

### DIFFERENTIAL DIAGNOSIS

Salivary gland tumors with clear cell features, especially hyalinizing clear cell carcinoma, are included in the

differential diagnosis. However, there is morphologic, immunohistochemical, and molecular genetic overlap showing *EWSR1-ATF1* fusion genes in both tumor types. Thus, clinical and imaging findings may help with separation. Melanotic tumors and metastatic renal cell carcinoma have a specific immunophenotype. The clear cell variant of calcifying epithelial odontogenic tumor has an amyloid-rich stroma.

### PROGNOSIS AND THERAPY

CCOC varies from indolent to more aggressive, with recurrences. Metastases are uncommon (12 % of cases), usually to lung and lymph nodes, followed by bone. Recurrences may be seen years after the primary. Resection with tumor-free margins is the treatment of choice.

### ■ GHOST CELL ODONTOGENIC CARCINOMA

Ghost cell odontogenic carcinoma (GCOC) is a malignant epithelial odontogenic neoplasm with ghost-cell keratinization and dentinoid deposition. This tumor represents a heterogeneous group with variable clinical, radiologic, and histopathologic features. They may arise de novo or from calcifying cystic odontogenic tumor (CCOT) and/or dentinogenic ghost cell tumor (DGCT).

**GHOST CELL ODONTOGENIC CARCINOMA—DISEASE FACT SHEET****Definition**

- Malignant epithelial odontogenic neoplasm with aberrant ghost cell keratinization and dentinoid deposition
- May develop in association with calcifying cystic odontogenic tumor and/or dentinogenic ghost cell tumor

**Incidence and Location**

- Rare
- Maxilla > mandible (2:1)

**Sex, Race, and Age Distribution**

- Males >> females (4:1)
- More common in Asians
- Wide age range with a peak in the 4th decade

**Clinical Features**

- Main symptoms: swelling, loosening teeth, and paresthesia

**Radiographic Features**

- Ill-defined mixed radiolucent and radiopaque lesions

**Prognosis and Treatment**

- Unpredictable, ranging from indolent to highly aggressive
- Extensive surgical treatment with clear margins
- Five-year survival rate 73%
- Local, regional, and distant metastases are rare

**CLINICAL FEATURES**

This is a rare neoplasm, primarily affecting patients in the 4th decade, with males more frequently affected than females (4:1), with an increased incidence in Asian patients. The maxilla is twice as commonly affected as the mandible. The tumor may be most common within Asians. Swelling, loosening teeth, and paresthesia are the main symptoms.

**RADIOGRAPHIC FEATURES**

GCOCs present as ill-defined, mixed radiolucent and radiopaque lesions.

**PATHOLOGIC FEATURES****GROSS FINDINGS**

Irregular infiltrative white-gray mass is present.

**MICROSCOPIC FINDINGS**

The histologic spectrum is diverse, showing various tumor components. Tumors may be cystic or solid and consist of malignant rounded epithelial cells showing infiltrative growth, necrosis, pleomorphism, increased mitoses, and aberrant (ghost cell) keratinization. Precursor lesions (DGCT or CCOT) may be seen. Ghost cells vary in portion and show faint outlines of the nucleus with aberrant keratinization (Fig. 16.11). Dentin may be present. There is destruction of bone with expansion into adjacent soft tissue. Most cases show p53

**GHOST CELL ODONTOGENIC CARCINOMA—PATHOLOGIC FEATURES****Gross Findings**

- Irregular infiltrative white-gray mass

**Microscopic Findings**

- Wide spectrum
- Lesions are cystic or solid
- Malignant rounded epithelial with a high mitotic index
- Ghost cells vary in portion and show a faint outline of the nucleus and aberrant keratinization
- Dentin and necrosis may be present
- Destruction of bone with expansion into adjacent soft tissue

**Pathologic Differential Diagnosis**

- Benign calcifying odontogenic cyst

immunoreactivity, along with an increased Ki-67 proliferation index.

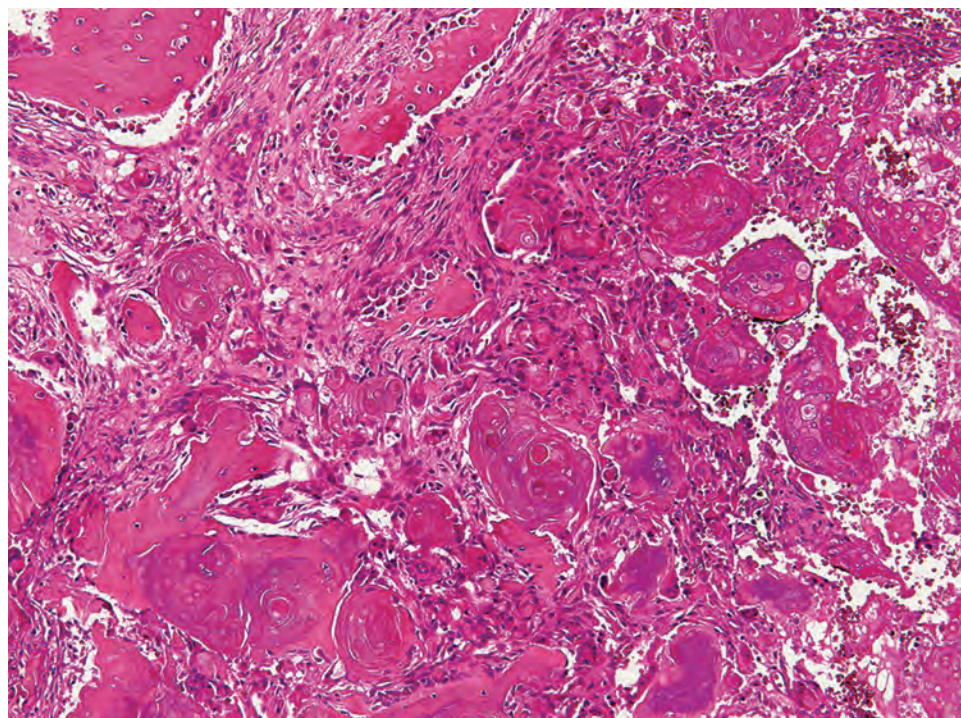
**DIFFERENTIAL DIAGNOSIS**

Discrimination from benign calcifying odontogenic cyst may be challenging, with cytologic atypia and necrosis being the most helpful.

**PROGNOSIS AND THERAPY**

Lesions can be indolent or highly aggressive. Extensive surgical treatment with clear margins is mandatory. The 5-year survival rate is 73%. Local, regional, and distant metastases are rare.



**FIGURE 16.11**

Ghost cell odontogenic carcinoma show ghost cells in varying portions with a faint outline of the nucleus and aberrant keratinization.

## ■ ODONTOGENIC SARCOMA

Odontogenic sarcomas are rare malignant tumors characterized by a benign epithelial and a malignant mesenchymal component. They comprise ameloblastic fibrosarcoma (malignant counterpart of ameloblastic fibroma), ameloblastic fibrodentinosa (including dentin), or fibro-odontosarcoma (including dentin and enamel). This subclassification has no prognostic value. Tumors may arise *de novo* or from preexistent ameloblastic fibroma or ameloblastic fibro-odontoma.

### CLINICAL FEATURES

The incidence is highest in the 2nd and 3rd decades of life and the mandible is the most common site (mandible to maxilla, 4:1). Males are affected slightly more often than females (1.5:1). Malignant transformation of a preexistent benign lesion (ameloblastic fibroma or ameloblastic fibro-odontoma) is possible. Swelling and pain are the most common features.

### RADIOGRAPHIC FEATURES

Lesions exhibit a varied radiographic appearance, with the majority of reported cases showing extensive areas of bone destruction with irregular and indistinct margins.

### ODONTOGENIC SARCOMA—DISEASE FACT SHEET

#### Definition

- A mixed odontogenic tumor with benign epithelial component and malignant mesenchymal component

#### Incidence and Location

- Very rare
- Mandible > > maxilla (4:1)

#### Sex and Age Distribution

- Males > females (1.5:1)
- 2nd and 3rd decades of life

#### Clinical Features

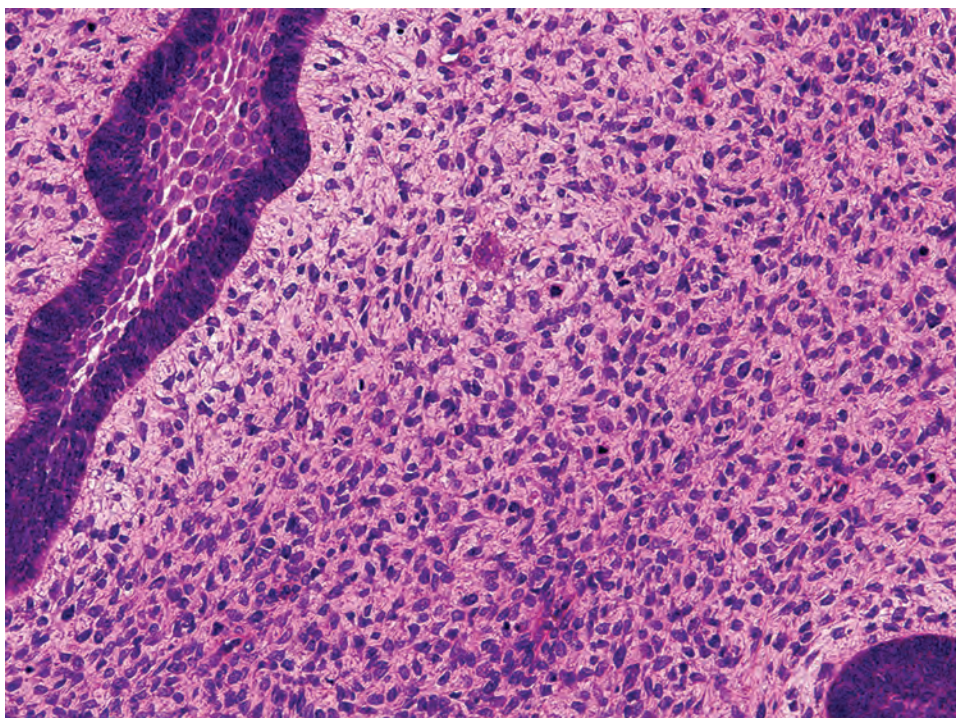
- Swelling and pain are the most common findings
- Malignant transformation of a preexistent benign lesion (ameloblastic fibroma or ameloblastic fibro-odontoma) is possible

#### Radiographic Features

- Varied appearance, with irregular margins and bone destruction

#### Prognosis and Treatment

- Locally aggressive with low incidence of metastases
- Radical resection with clear margins
- Neck dissection is not indicated
- Adjuvant radiotherapy may decrease recurrences

**FIGURE 16.12**

Ameloblastic fibrosarcoma show a benign epithelial component similar to ameloblastic fibroma and a malignant mesenchymal component with marked cellularity, nuclear pleomorphism, and mitotic figures.

### ODONTOGENIC SARCOMA—PATHOLOGIC FEATURES

#### Gross Findings

- Irregular infiltrative white-gray mass, like other malignancies
- Cysts can be present

#### Microscopic Findings

- Biphasic pattern with an epithelial component similar to ameloblastic fibroma
- Sarcoma component shows marked cellularity, nuclear pleomorphism, and a moderate to high number of mitotic figures
- Dentinoid and enamel lead to the diagnosis of ameloblastic fibrodentinosa sarcoma (dentin) or fibro-odontosarcoma (dentin and enamel)

#### Pathologic Differential Diagnosis

- Ameloblastic fibroma, ameloblastic fibro-odontoma

features. Unlike ameloblastic fibroma, the mesenchymal component typically shows marked cellularity, nuclear pleomorphism, and a moderate to high number of mitoses (Fig. 16.12). Deposition of dentinoid and enamel leads to the diagnosis of ameloblastic fibrodentinosa sarcoma (includes dentin) or fibro-odontosarcoma (includes dentin and enamel).

### DIFFERENTIAL DIAGNOSIS

Ameloblastic fibroma and ameloblastic fibro-odontoma show a mesenchymal component without atypia or increased mitotic figures.

### PROGNOSIS AND THERAPY

Prognosis for the odontogenic sarcomas is apparently better than for other jaw fibrosarcomas. It is considered a locally aggressive neoplasm with a low incidence of metastases. Treatment is radical resection with clear margins. Neck dissection is not indicated in view of the usual absence of lymph node metastases. Sarcomas generally show hematogenous spread. Adjuvant radiotherapy decreases recurrence in some cases.

### PATHOLOGIC FEATURES

#### GROSS FINDINGS

Irregular, infiltrative, white-gray mass, like other malignancies, is found. Cysts may be present.

#### MICROSCOPIC FINDINGS

Tumors show a biphasic pattern with an epithelial component similar to ameloblastic fibroma showing benign

### SUGGESTED READINGS

The complete Suggested Readings list is available online at [ExpertConsult.com](http://ExpertConsult.com).



**SUGGESTED READINGS****Osteosarcoma**

1. Baumhoer D, et al. Osteosarcomas of the jaws differ from their peripheral counterparts and require a distinct treatment approach. Experiences from the DOESAK Registry. *Oral Oncol.* 2014;50:147–153.
2. Baumhoer D, et al. Odontogenic and maxillofacial bone tumours: Osteosarcoma. In: El-Naggar AK, Chan JKC, Grandis JR, Takata T, Slootweg PJ, eds. *Classification of Head and Neck Tumors*. 4th ed. World Health Organization Classification of Tumours. Lyon, France: IARC Press; 2017:244.
3. Boon E, et al. Impact of chemotherapy on the outcome of osteosarcoma of the head and neck in adults. *Head Neck.* 2017;39:140–146.
4. Demicco EG, et al. Well differentiated osteosarcoma of the jaw bones: a clinicopathologic study of 15 cases. *Am J Surg Pathol.* 2010;34:1647–1655.
5. Fernandes R, et al. Osteogenic sarcoma of the jaw: a 10-year experience. *J Oral Maxillofac Surg.* 2007;65(7):1286–1291.
6. Gadwal SR, et al. Primary osteosarcoma of the head and neck in pediatric patients: a clinico-pathologic study of 22 cases with a review of the literature. *Cancer.* 2001;91:598–605.
7. Garrington GE, et al. Osteosarcoma of the jaws. Analysis of 56 cases. *Cancer.* 1967;20:377–391.
8. Sarkar R. Pathological and clinical features of primary osseous tumors of the jaw. *J Bone Oncol.* 2014;3:90–95.
9. Shao Z, et al. Computed tomography findings in radiation induced osteosarcoma of the jaws. *Oral Surg Oral Med Oral Pathol Oral Radiol Endod.* 2010;109(3):e88–e94.
10. Smeele LE, et al. Osteosarcoma of the head and neck: meta-analysis of the nonrandomized studies. *Laryngoscope.* 1998;108(6):946.
11. Stewart BD, et al. Bone- and cartilage-forming tumors and Ewing sarcoma: an update with a gnathic emphasis. *Head Neck Pathol.* 2014;8:454–462.

**Chondrosarcoma**

1. Baumhoer D, et al. Odontogenic and maxillofacial bone tumours: Chondrosarcoma. In: El-Naggar AK, Chan JKC, Grandis JR, Takata T, Slootweg PJ, eds. *Classification of Head and Neck Tumors*. 4th ed. World Health Organization Classification of Tumours. Lyon, France: IARC Press; 2017:243.
2. Gadwal SR, et al. Primary chondrosarcoma of the head and neck in pediatric patients: a clinicopathologic study of 14 cases with a review of the literature. *Cancer.* 2000;88:2181–2188.
3. Hong P, et al. Chondrosarcoma of the head and neck: report of 11 cases and literature review. *J Otolaryngol Head Neck Surg.* 2009;38(2):279–285.
4. Inwards CY. Update on cartilage forming tumors of the head and neck. *Head Neck Pathol.* 2007;1:67–74.
5. Soderstrom M, et al. Molecular profiling of human chondrosarcomas for matrix production and cancer markers. *Int J Cancer.* 2002;10:144–151.
6. Stewart BD, et al. Bone- and cartilage-forming tumors and Ewing sarcoma: an update with a gnathic emphasis. *Head Neck Pathol.* 2014;8:454–462.

**Mesenchymal Chondrosarcoma**

1. Baumhoer D, et al. Odontogenic and maxillofacial bone tumours: Mesenchymal chondrosarcoma. In: El-Naggar AK, Chan JKC, Grandis JR, Takata T, Slootweg PJ, eds. *Classification of Head and Neck Tumors*. 4th ed. World Health Organization Classification of Tumours. Lyon, France: IARC Press; 2017:244.
2. Inwards CY. Update on cartilage forming tumors of the head and neck. *Head Neck Pathol.* 2007;1:67–74.
3. Knott PD, et al. Mesenchymal chondrosarcoma of the sinonasal tract: a clinicopathological study of 13 cases with a review of the literature. *Laryngoscope.* 2003;113(5):783–790.

4. Lockhart R, et al. Mesenchymal chondrosarcoma of the jaws. Report of four cases. *Int J Oral Maxillofac Surg.* 1998;27(5):358–362.
5. Stewart BD, et al. Bone- and cartilage-forming tumors and Ewing sarcoma: an update with a gnathic emphasis. *Head Neck Pathol.* 2014;8:454–462.
6. Takahashi K, et al. Mesenchymal chondrosarcoma of the jaw—report of a case and review of 41 cases in the literature. *Head Neck.* 1993;15(5):459–464.
7. Tien N, et al. Mesenchymal chondrosarcoma of the maxilla: case report and literature review. *J Oral Maxillofac Surg.* 2007;65(6):1260–1266.
8. Wang L, et al. Identification of a novel, recurrent HEY1-NCOA2 fusion in mesenchymal chondrosarcoma based on a genome-wide screen of exon-level expression data. *Genes Chromosomes Cancer.* 2012;51:127–139.

**Ameloblastic Carcinoma**

1. Brunner P, et al. BRAF p.V600E mutations are not unique to ameloblastoma and are shared by other odontogenic tumors with ameloblastic morphology. *Oral Oncol.* 2015;51:e77–e78.
2. Dutta M, et al. Ameloblastic carcinoma of mandible: facts and dilemmas. *Tumori.* 2014;100(5):e189–e196.
3. Lei Y, et al. Evaluation of SOX2 as a potential marker for ameloblastic carcinoma. *Oral Surg Oral Med Oral Pathol Oral Radiol.* 2014;117(5):608–616.
4. Li J, et al. Ameloblastic carcinoma: An analysis of 12 cases with a review of the literature. *Oncol Lett.* 2014;8(2):914–920.
5. Loyola AM, et al. Ameloblastic carcinoma: a Brazilian collaborative study of 17 cases. *Histopathology.* 2016;69:687–701.
6. Matsushita Y, et al. Spindle cell variant of ameloblastic carcinoma: a case report and literature review. *Oral Surg Oral Med Oral Pathol Oral Radiol.* 2016;121(3):e54–e61.
7. Odell EW, et al. Odontogenic and maxillofacial bone tumours: Ameloblastic carcinoma. In: El-Naggar AK, Chan JKC, Grandis JR, Takata T, Slootweg PJ, eds. *Classification of Head and Neck Tumors*. 4th ed. World Health Organization Classification of Tumours. Lyon, France: IARC Press; 2017:206.
8. Safadi RA, et al. Immunohistochemical expression of K6, K8, K16, K17, K19, maspin, syndecan-1 (CD138),  $\alpha$ -SMA, and Ki-67 in ameloblastoma and ameloblastic carcinoma: diagnostic and prognostic correlations. *Oral Surg Oral Med Oral Pathol Oral Radiol.* 2016;121(4):402–411.
9. Sánchez-Romero C, et al. Immunohistochemical expression of podoplanin (D2-40), lymphangiogenesis, and neoangiogenesis in tooth germ, ameloblastomas, and ameloblastic carcinomas. *J Oral Pathol Med.* 2016 Nov 10.
10. Sánchez-Romero C, et al. Immunohistochemical expression of GLUT-1 and HIF-1 $\alpha$  in tooth germ, ameloblastoma, and ameloblastic carcinoma. *Int J Surg Pathol.* 2016;24(5):410–418.
11. Yoon HJ, et al. Comparative immunohistochemical study of ameloblastoma and ameloblastic carcinoma. *Oral Surg Oral Med Oral Pathol Oral Radiol Endod.* 2011;112(6):767–776.

**Primary Intraosseous Carcinoma**

1. Naruse T, et al. Clinicopathological study of primary intraosseous squamous cell carcinoma of the jaw and a review of the literature. *J Oral Maxillofac Surg.* 2016;74:2420–2427.
2. Nomura T, et al. Primary intraosseous squamous cell carcinoma of the jaw: two new cases and review of the literature. *Eur Arch Otorhinolaryngol.* 2013;270(1):375–379.
3. Odell EW, et al. Odontogenic and maxillofacial bone tumours: Primary intraosseous carcinoma, NOS. In: El-Naggar AK, Chan JKC, Grandis JR, Takata T, Slootweg PJ, eds. *Classification of Head and Neck Tumors*. 4th ed. World Health Organization Classification of Tumours. Lyon, France: IARC Press; 2017:207.
4. Slootweg P. *Pathology of the Maxillofacial Bones. A Guide to Diagnosis*. Switzerland: Springer International Publishing; 2015.
5. Woolgar JA, et al. Intraosseous carcinoma of the jaws: a clinicopathologic review. Part III: Primary intraosseous squamous cell carcinoma. *Head Neck.* 2013;35(6):906–909.

### Sclerosing Odontogenic Carcinoma

1. Hussain O, et al. Sclerosing odontogenic carcinoma in the maxilla: a rare primary intraosseous carcinoma. *Oral Surg Oral Med Oral Pathol Oral Radiol.* 2013;116(4):e283–e286.
1. Koutlas IG, et al. Sclerosing odontogenic carcinoma. A previously unreported variant of a locally aggressive odontogenic neoplasm without apparent metastatic potential. *Am J Surg Pathol.* 2008;32:1613–1619.
2. Odell EW, et al. Odontogenic and maxillofacial bone tumours: Sclerosing odontogenic carcinoma. In: El-Naggar AK, Chan JKC, Grandis JR, Takata T, Slootweg PJ, eds. *Classification of Head and Neck Tumors*. 4th ed. World Health Organization Classification of Tumours. Lyon, France: IARC Press; 2017:209.
3. Richardson MS, et al. Malignant odontogenic tumors: an update on selected tumors. *Head Neck Pathol.* 2014;8:411–420.
4. Saxena S, et al. Sclerosing odontogenic carcinoma—an enigma. *Oral Surg Oral Med Oral Pathol Oral Radiol.* 2013;115(6):840.

### Clear Cell Odontogenic Carcinoma

1. Bilodeau EA, et al. Clear cell carcinoma and clear cell odontogenic carcinoma: a comparative clinicopathologic and immunohistochemical study. *Head Neck Pathol.* 2011;5(2):101–107.
2. Bilodeau EA, et al. Clear cell odontogenic carcinomas show EWSR1 rearrangements: a novel finding and a biological link to salivary clear cell carcinomas. *Am J Surg Pathol.* 2013;37(7):1001–1005.
3. Harbhajanka A, et al. Cytomorphology and immunohistochemistry of a recurrent clear cell odontogenic carcinoma with molecular analysis: A case report with review of literature. *Diagn Cytopathol.* 2015;43(9):743–746.
4. Loyola AM, et al. Clear cell odontogenic carcinoma: report of 7 new cases and systematic review of the current knowledge. *Oral Surg Oral Med Oral Pathol Oral Radiol.* 2015;120(4):483–496.
5. Odell EW, et al. Odontogenic and maxillofacial bone tumours: Clear cell odontogenic carcinoma. In: El-Naggar AK, Chan JKC, Grandis JR, Takata T, Slootweg PJ, eds. *Classification of Head and Neck Tumors*. 4th ed. World Health Organization Classification of Tumours. Lyon, France: IARC Press; 2017:210.

6. Richardson MS, et al. Malignant odontogenic tumors: an update on selected tumors. *Head Neck Pathol.* 2014;8:411–420.
7. Tanguay J, et al. What the EWSR1-ATF1 fusion has taught us about hyalinizing clear cell carcinoma. *Head Neck Pathol.* 2013;7(1):28–34.
8. Yancoskie AE, et al. EWSR1 and ATF1 rearrangements in clear cell odontogenic carcinoma: presentation of a case. *Oral Surg Oral Med Oral Pathol Oral Radiol.* 2014;118(4):e115–e118.
9. Zhang J, et al. Clear cell odontogenic carcinoma: report of 6 cases and review of the literature. *Med Oncol.* 2011;28(suppl 1):S626–S633.

### Ghost Cell Odontogenic Carcinoma

1. Ledesma-Montes C, et al. International collaborative study on ghost cell odontogenic tumours: calcifying cystic odontogenic tumour, dentinogenic ghost cell tumour and ghost cell odontogenic carcinoma. *J Oral Pathol Med.* 2008;37:302–308.
2. Odell EW, et al. Odontogenic and maxillofacial bone tumours: Ghost cell odontogenic carcinoma. In: El-Naggar AK, Chan JKC, Grandis JR, Takata T, Slootweg PJ, eds. *Classification of Head and Neck Tumors*. 4th ed. World Health Organization Classification of Tumours. Lyon, France: IARC Press; 2017:211.
3. Richardson MS, et al. Malignant odontogenic tumors: an update on selected tumors. *Head Neck Pathol.* 2014;8:411–420.

### Odontogenic Carcinosarcoma

1. Chen SJ, et al. Ameloblastic fibro-odontosarcoma of the mandible in a pediatric patient. *Eur Ann Otorhinolaryngol Head Neck Dis.* 2016;133:419–421.
2. El-Mofty SK. Odontogenic and maxillofacial bone tumours: Odontogenic carcinosarcoma. In: El-Naggar AK, Chan JKC, Grandis JR, Takata T, Slootweg PJ, eds. *Classification of Head and Neck Tumors*. 4th ed. World Health Organization Classification of Tumours. Lyon, France: IARC Press; 2017:213.
3. Richardson MS, et al. Malignant odontogenic tumors: an update on selected tumors. *Head Neck Pathol.* 2014;8:411–420.
4. Slootweg PJ. Lesions of the jaw. *Histopathology.* 2009;54:401–418.



# Non-Neoplastic Lesions of the Ear and Temporal Bone

■ **Lester D.R. Thompson**

## ■ FIRST BRANCHIAL CLEFT ANOMALIES

First branchial cleft anomalies include a spectrum of benign congenital fistulas, sinuses, and cysts and result from incomplete fusion of the first and second branchial arches, with persistence of the ventral component of the first branchial cleft. The first branchial cleft gives rise to the external auditory canal, whereas the first branchial arch gives rise to the mandible, muscles of mastication, incus, and head of malleus; and the first branchial pouch gives rise to the eustachian tube, middle ear, and mastoid air cells. The most commonly used classification for first branchial cleft anomalies is the Work and Proctor 2-type system. Type I lesions are ectodermal in origin with close proximity to the external auditory canal. Type II lesions contain ectodermal components of the first branchial cleft and mesodermal components of the first and second branchial arches and are more medially and inferiorly located. First branchial cleft anomalies comprise approximately 10% of all branchial cleft anomalies.

### CLINICAL FEATURES

Work type I branchial cleft anomalies usually manifest as periauricular cysts, rather than sinuses or fistulas. They are usually located anterior, inferior, or posterior to the conchal cartilage and pinna; if a sinus tract is present, it parallels the external auditory canal. Although most are discovered in childhood, some are not diagnosed until adulthood, when they are often misdiagnosed as epidermal inclusion cysts or as abscesses, in cases of secondary infection. Incision and drainage by itself results in persistence or recurrence over years.

Work type II branchial cleft anomalies, more common than type I, usually come to medical attention in the first year of life as a result of a draining sinus tract with otorrhea or periauricular drainage rather than as a cyst; the lesions are frequently infected at the time of diagnosis.

### FIRST BRANCHIAL CLEFT ANOMALIES—DISEASE FACT SHEET

#### Definition

- A spectrum of benign congenital cysts, fistulas, and sinuses resulting from incomplete fusion of the first and second branchial arches

#### Incidence and Location

- Uncommon (< 10% of all branchial cleft anomalies)
- Periauricular with sinuses/fistulas in anterolateral neck or external auditory canal

#### Morbidity and Mortality

- Secondary infection common with potential facial nerve injury

#### Sex and Age Distribution

- Females > males (2:1)
- Most discovered in early childhood, but type I anomalies may present in adults (range: 13–81 years)

#### Clinical Features

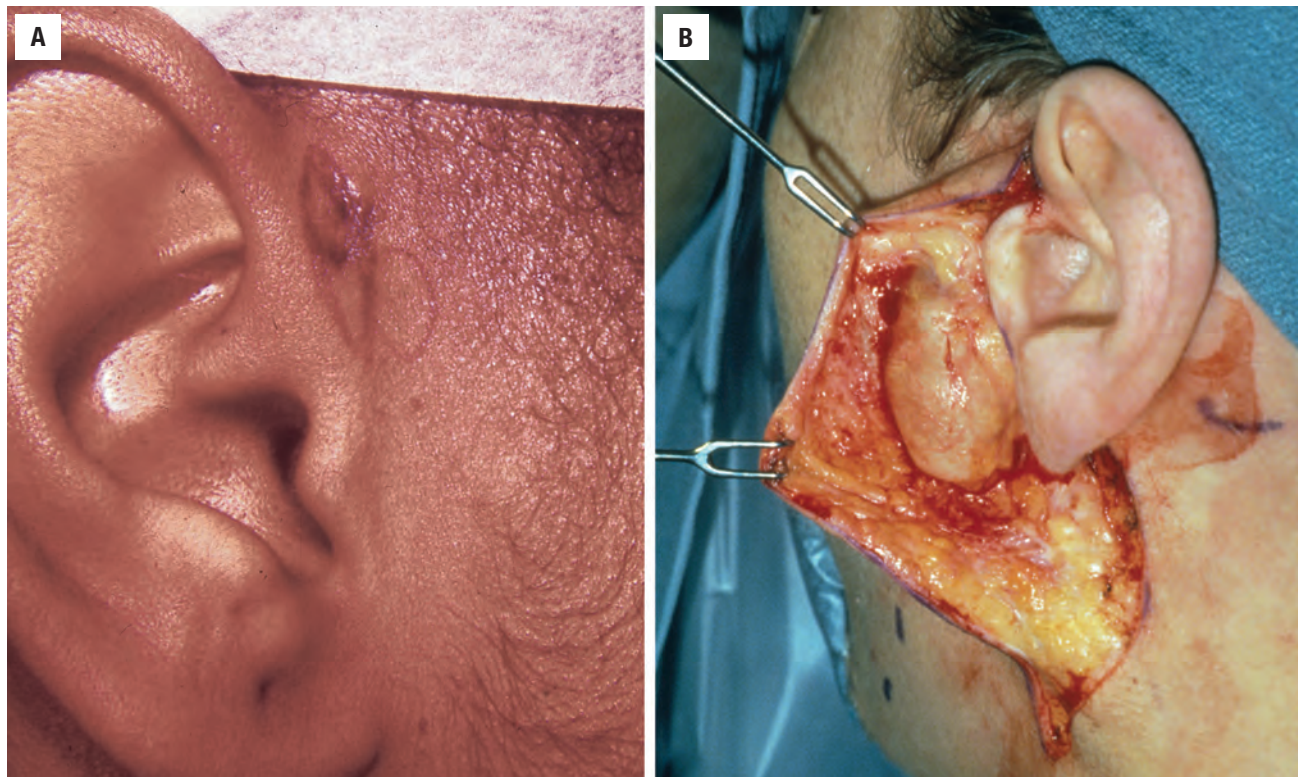
- Painless cyst, draining sinus tract on skin of neck, otorrhea, or purulent drainage from ear canal

#### Prognosis and Treatment

- Benign
- Complete excision of cyst, sinus, and/or fistula, with antibiotic treatment prior to surgery, if infected

They may present as a mass with a sinus or a fistulous tract between the neck and the ear canal (Fig. 17.1). A sinus may open from a fistulous track, usually anterior to the sternocleidomastoid muscle and superior to the hyoid bone, or in the external auditory canal. The spatial relationship to the facial nerve is variable, requiring a cautious surgical approach (see Fig. 17.1).

Females are affected twice as often as males. A careful physical examination with particular attention to the periauricular region and lateral neck is essential, including otologic examination to exclude a tract which

**FIGURE 17.1**

**A.** A preauricular fistula is present in a patient with a first branchial cleft anomaly. The lesion was secondarily infected and produced purulent drainage. **B.** Resection photograph of a first branchial cleft cyst. Note the close relationship to the ear.

communicates with the external auditory canal or rarely, the middle ear space. High-resolution, contrast-enhanced computed tomography (CT) is the preferred radiographic study for accurate delineation of the extent and course of the anomaly prior to surgery, where they are classified based on “anatomic site” (Arnot classification system).

### **PATHOLOGIC FEATURES**

#### **GROSS FINDINGS**

Discrete cysts (up to 4 cm), sinuses, or fistulas, or a combination of structures may be seen, with the cysts frequently containing viscous cloudy fluid, or, if infected, purulent material and necrotic debris. Cartilaginous components may be noticed on sectioning.

#### **MICROSCOPIC FINDINGS**

The cysts, sinuses, and fistulas may be lined by either stratified squamous epithelium or ciliated respiratory epithelium (Fig. 17.2). The cyst wall may contain lymphoid aggregates, sometimes with germinal centers (Fig. 17.3), as commonly seen in second branchial cleft anomalies. If the lesion is infected, the epithelium

### **FIRST BRANCHIAL CLEFT ANOMALIES—PATHOLOGIC FEATURES**

#### **Gross Findings**

- Cyst with viscous cloudy fluid
- Sinus tracts/fistulas extending from neck skin or from external auditory canal
- Abscess with purulent contents if secondarily infected

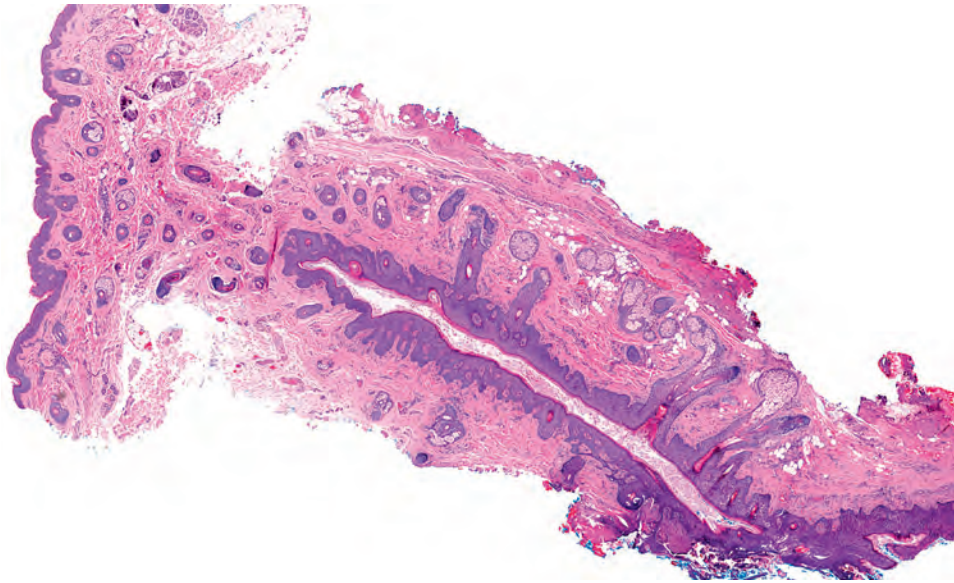
#### **Microscopic Findings**

- Cyst, sinus, or fistula lined by stratified squamous or ciliated respiratory epithelium
- Lymphoid aggregates may be present in cyst wall
- Granulation tissue or purulent material if infected, with denuded epithelium
- Work type I: epithelial component (ectodermal)
- Work type II: epithelial lining and cutaneous adnexal structures and/or cartilage (ectodermal and mesodermal)

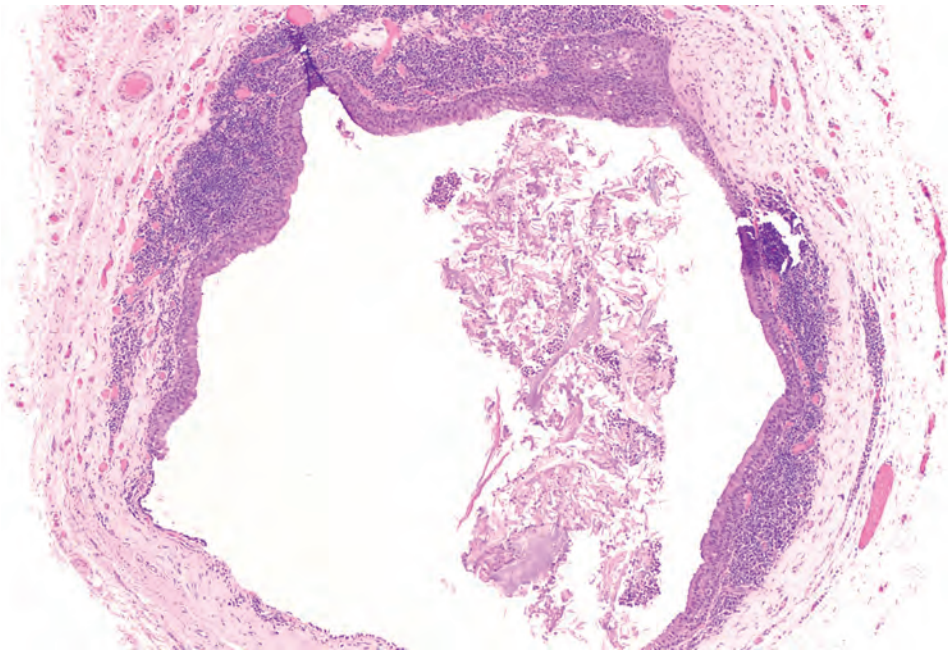
#### **Pathologic Differential Diagnosis**

- Epidermal inclusion cyst, cholesteatoma, lymphoepithelial cyst, folliculitis, accessory tragus, chondrocutaneous vestige, cystic squamous cell carcinoma



**FIGURE 17.2**

A Work type II anomaly of the first branchial cleft. There is a well-developed tract, lined by keratinizing squamous epithelium with cutaneous adnexal structures.

**FIGURE 17.3**

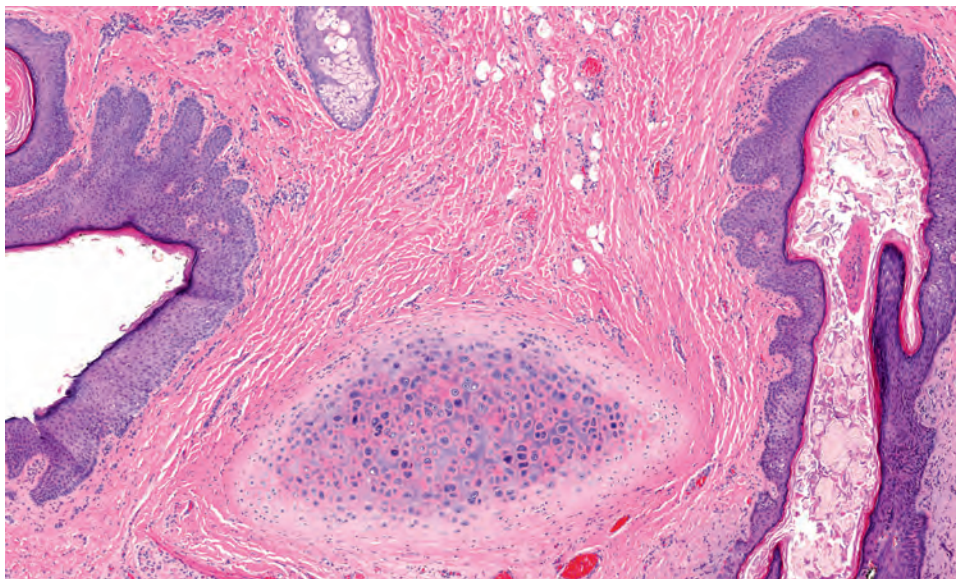
The lining of the tract shows ciliated respiratory epithelium, surrounded by lymphoid tissue.

may be largely denuded, replaced by heavily inflamed granulation tissue. Type II anomalies are distinguished by the presence of cutaneous adnexal structures and cartilage (Fig. 17.4), the result of a mesodermal component in their development. These lesions are p16 negative.

#### DIFFERENTIAL DIAGNOSIS

The pathologic differential diagnosis includes epidermal inclusion cyst, cholesteatoma, benign lymphoepithelial cyst, folliculitis/abscess, accessory tragus, chondrocutaneous vestige, and, in adults, cystic metastatic squamous cell

carcinoma. *Epidermal inclusion cysts* and *cholesteatomas* contain intracystic keratinous debris. However, without clinical or imaging information, an epidermal inclusion cyst in this anatomic site may be histologically identical. A lymphoepithelial cyst lacks a sinus/fistula. Folliculitis is centered on a follicle and dermis based. An accessory tragus recapitulates the external auricle, showing a central core of cartilage without a cyst. A chondrocutaneous vestige develops at the anterior border of the sternocleidomastoid muscle, usually in lower third of the neck, and has a cartilaginous core without a cyst. The benign cytologic features of branchial cleft anomalies contrasts with the atypia and loss of polarity encountered in *cystic metastatic squamous cell carcinoma*. These metastases usually develop in the jugulodigastric region and not within the area of a

**FIGURE 17.4**

Cartilage is noted adjacent to the squamous epithelial lined sinus tract of this Work type II anomaly. Note the sebaceous glands.

first branchial cleft anomaly. Performing p16 immunohistochemistry can help to confirm an oropharyngeal primary, but patchy strong reactivity may be seen in the epithelial cells immediately adjacent to lymphocytes within the epithelium.

### PROGNOSIS AND THERAPY

First branchial cleft anomalies are benign congenital lesions, commonly given to secondary infection. Treatment consists of complete surgical excision of the malformation, including cysts, and any associated sinus or fistula. In some cases, superficial parotidectomy may be required for complete removal. Complications of surgery may be seen.

## ■ CYSTIC CHONDROMALACIA

Idiopathic cystic chondromalacia, also known as pseudocyst of the auricle, is an uncommon degenerative cystic lesion of the auricular cartilaginous plate. There is no well-established etiology, but some possibilities include ischemic necrosis (related to repetitive minor trauma), abnormal release of lysosomal enzymes by chondrocytes, and an embryologic fusion defect.

### CLINICAL FEATURES

Cystic chondromalacia tends to be more common in young males (mean, 35 years), with a 9:1 male to female

### CYSTIC CHONDROMALACIA—DISEASE FACT SHEET

#### Definition

- A non-neoplastic degenerative lesion of the auricular cartilage resulting in a cleft-like pseudocyst within the cartilaginous plate

#### Incidence and Location

- Rare
- Usually involves helix or antihelix, with 80% in the scaphoid fossa

#### Sex, Race, and Age Distribution

- Males > females (9:1)
- Higher incidence in Chinese and Malay population
- Any age but commonly young adults (mean 35 years)

#### Clinical Features

- Usually unilateral, painless, fusiform swelling of helix or antihelix with normal overlying skin
- Often fluctuant; viscous clear fluid may be aspirated

#### Prognosis and Treatment

- Benign
- Usually treated for cosmetic reasons with aspiration followed by compression sutures; unroofing of anterior wall of pseudocyst followed by application of sclerosing agent

ratio, although either sex and all ages may be affected. An increased incidence has been noted in Chinese and Malay males, although cystic chondromalacia has been reported in patients of all racial backgrounds. The typical presentation is a unilateral, fusiform, slightly fluctuant swelling of the helix or antihelix (scaphoid fossa) (Fig. 17.5). The lesion is painless, and there are no changes in the overlying skin.



## PATHOLOGIC FEATURES

### GROSS FINDINGS

If the full thickness of the cartilaginous plate has been excised, a central, slit-like cleft can be seen in the cartilage (Fig. 17.6). When incised, the cyst exudes viscous, clear to olive oil-colored fluid, usually less than 2 mL in volume. The cystic area, especially in long-standing lesions, may be lined by a thin brown-tinged layer, representing old hemorrhage and granulation tissue, or may be completely replaced by fibrosis (there is no epithelial lining). Often the specimen is fragmented, especially if the cyst is “unroofed” (Fig. 17.7), making prior knowledge of the clinical appearance helpful for diagnosis.



**FIGURE 17.5**

A young adult has a fusiform fluctuant mass on the antihelix which was histologically idiopathic cystic chondromalacia

### MICROSCOPIC FINDINGS

The cartilaginous plate contains a central cleft with no epithelial lining, hence the term “pseudocyst.” The contour of the cleft may be slightly irregular, and a thin inner rim of fibrous tissue or granulation tissue with plump fibroblasts may be seen (Figs. 17.6–17.8). Hemosiderin deposits may be present. In long-standing cases the fibrous tissue may obliterate the cystic space.

### DIFFERENTIAL DIAGNOSIS

Cystic chondromalacia is easily distinguished from *relapsing polychondritis* by its lack of an inflammatory component, and from *chondrodermatitis nodularis helices* by the normal skin overlying it. Both of these lesions are associated with pain. Traumatic perichondritis usually shows acute inflammation without a cyst.

### CYSTIC CHONDROMALACIA—PATHOLOGIC FEATURES

#### Gross Findings

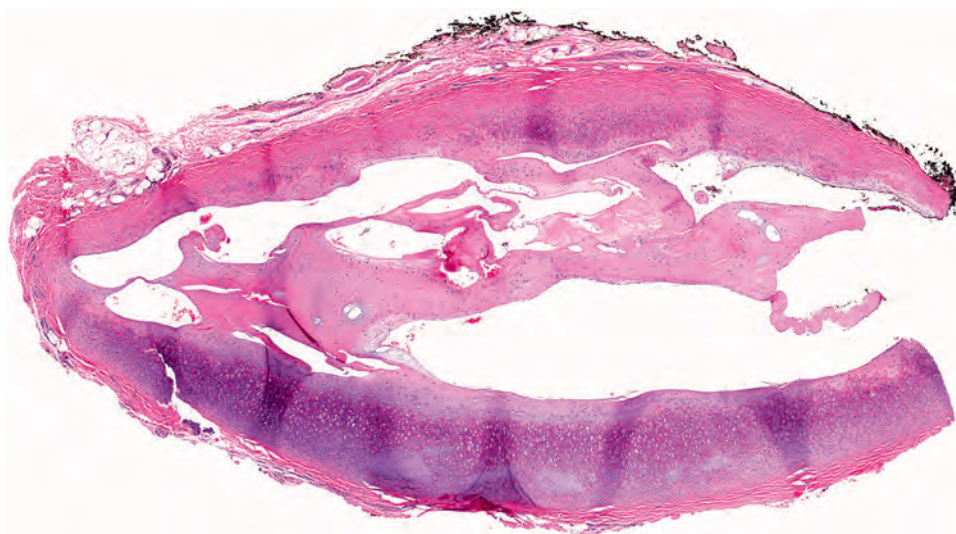
- Cleft-like space centrally located within cartilaginous plate
- Cleft filled with viscous clear to olive oil-colored fluid
- Obliterated by fibrous tissue or granulation tissue in long-standing lesions

#### Microscopic Findings

- Central slit-like cleft in cartilage without an epithelial lining
- Cleft may contain fibrous tissue and/or granulation tissue with hemosiderin

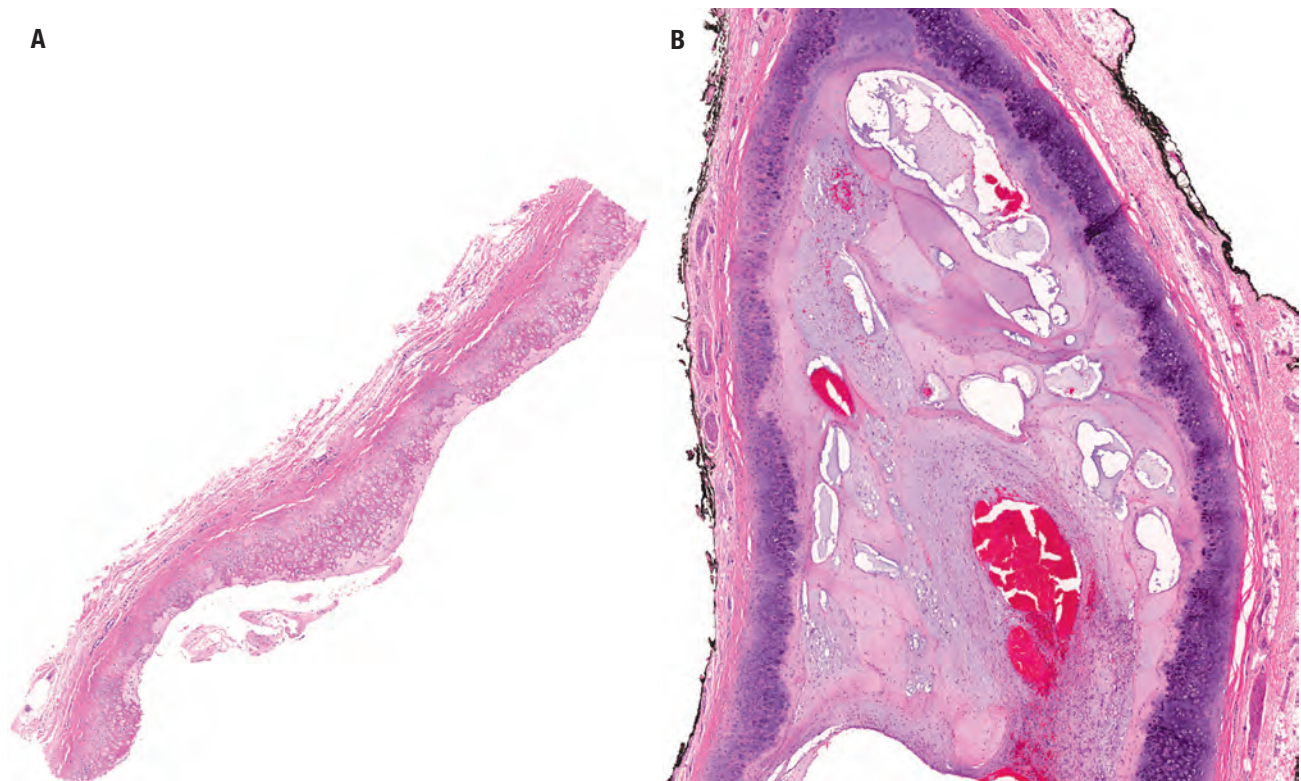
#### Pathologic Differential Diagnosis

- Relapsing polychondritis, chondrodermatitis nodularis helices, traumatic perichondritis

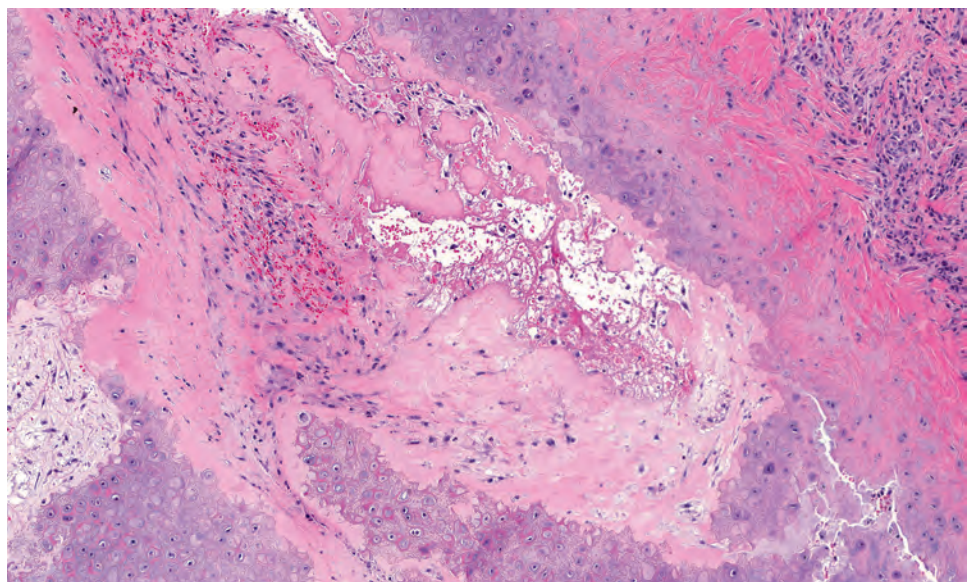


**FIGURE 17.6**

The cartilaginous plate contains an elongated cleft and has lost some of its normal basophilic staining in this idiopathic cystic chondromalacia.

**FIGURE 17.7**

**A**, A “de-roofed” lesion shows only the cartilage and some area of degeneration, but the plates are not present on both sides of the cyst. **(B)** A blood-filled cyst is associated with granulation-type tissue. The cartilage plate is separated, with fluid in part of the spaces.

**FIGURE 17.8**

Granulation tissue forms the pseudo cyst lining, seen adjacent to the degenerating cartilaginous plate. A cystic space with debris is present.

### PROGNOSIS AND THERAPY

Cosmetic concerns for this benign lesion often prompt therapeutic intervention. Treatment is usually directed at extirpation of the pseudocyst while preserving the underlying architecture of the cartilaginous plate. Incision

and drainage with curettage has had variable success. Needle aspiration alone has limited value but is quite effective when combined with compression suture therapy using “button” bolsters. Unroofing of the pseudocyst by removal of its anterior wall followed by application of a sclerosing agent, or by suture compression, has the lowest incidence of recurrence.



## ■ CHONDRODERMATITIS NODULAR HELICIS

Chondrodermatitis nodularis helicis (CDNH) is a non-neoplastic, inflammatory, and degenerative process of the external ear characterized by necrobiotic changes in the dermis which extend down to the perichondrium, with associated alterations in the cartilaginous plate. The dermal injury is thought to be caused by a combination of factors: local trauma, actinic damage, and the relatively tenuous vascularity of the auricle. The necrobiotic dermal collagen and sometimes cartilaginous matrix are extruded through a crater-like defect in the epidermis; thus CDNH is considered to be one of the transepidermal elimination disorders. Distal narrowing of the arterioles in the perichondrium may play a role in the ischemic injury of the cartilage. Systemic diseases associated with microangiopathy may predispose individuals to CDNH; these include cardiovascular disease, diabetes mellitus, lupus erythematosus, rheumatoid arthritis, and autoimmune and connective tissue disorders.

### CLINICAL FEATURES

CDNH presents as an exquisitely painful nodule, usually on the helix or antihelix; however, it may develop on any portion of the auricle. Lesions of the helix are twice as common as those of the antihelix. CDNH begins as a reddish, round, indurated nodule, measuring several millimeters in diameter; over a period of days to a few weeks, the nodule develops a central crater, which contains crust-like material (Fig. 17.9). CDNH is more common in males; however, lesions of the antihelix are more common in females. Most patients are in the sixth decade. Cell phone–induced injury seems to be an etiologic factor.

### PATHOLOGIC FEATURES

#### GROSS FINDINGS

CDNH is usually removed by shave biopsy. The nodule is firm, round, circumscribed, and nodular, with a central crater containing yellow to brown necrotic material. Most examples measure between 5 and 15 mm in diameter. Sectioning may demonstrate cartilage at the deep aspect of the biopsy, but the sharp interface between the cartilaginous plate and dermis is obscured.

#### MICROSCOPIC FINDINGS

There is a central crater filled with acellular necrotic debris, fibrin, and a variable number of inflammatory cells. The epidermis surrounding the crater is acanthotic

### CHONDRODERMATITIS NODULAR HELICIS—DISEASE FACT SHEET

#### Definition

- Inflammatory transepidermal elimination disorder characterized by necrobiosis of dermal collagen and degenerative changes in the cartilaginous plate

#### Incidence and Location

- Relatively common
- Helix most often, followed by antihelix (more common in females)

#### Sex and Age Distribution

- Males > females
- Usually sixth decade

#### Clinical Features

- Unilateral, painful, circumscribed indurated nodule with central crater filled with brown debris

#### Prognosis and Treatment

- Benign disorder, often removed to alleviate pain
- Intralesional steroid injection successful in 50% of cases
- Persistent or recurrent lesions adequately treated by conservative excision or deep shave biopsy

### CHONDRODERMATITIS NODULAR HELICIS—PATHOLOGIC FEATURES

#### Gross Findings

- Rounded, circumscribed nodule with central crater filled with necrotic debris
- 5–15 mm diameter
- Cartilage may be seen at deep aspect of biopsy

#### Microscopic Findings

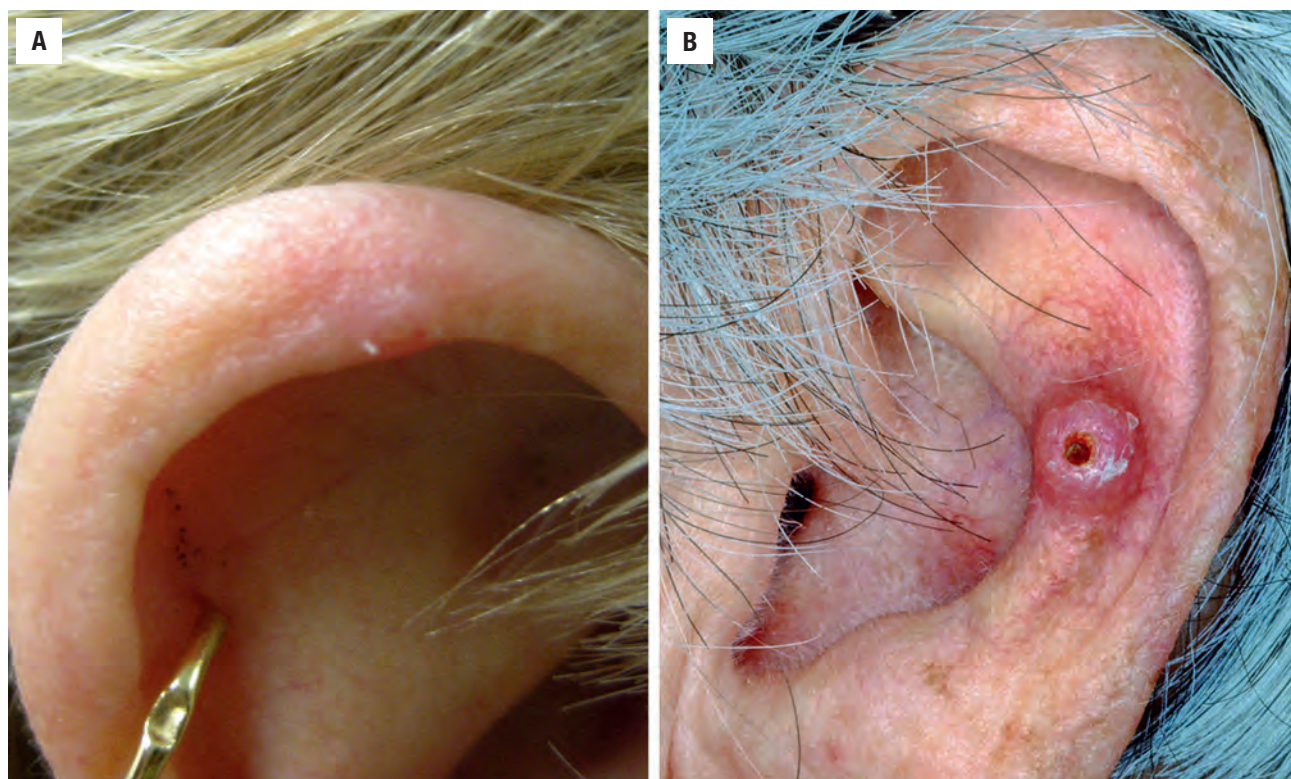
- Squamous epithelial hyperplasia surrounding central crater
- Crater filled with acellular necrotic debris, fibrin, and inflammatory cells
- Homogenous, eosinophilic dermal collagen may extrude through the crater
- Underlying cartilage loses normal basophilia
- Interface between cartilaginous plate and dermis is blurred

#### Pathologic Differential Diagnosis

- Relapsing polychondritis, cystic chondromalacia, squamous cell carcinoma, actinic keratosis

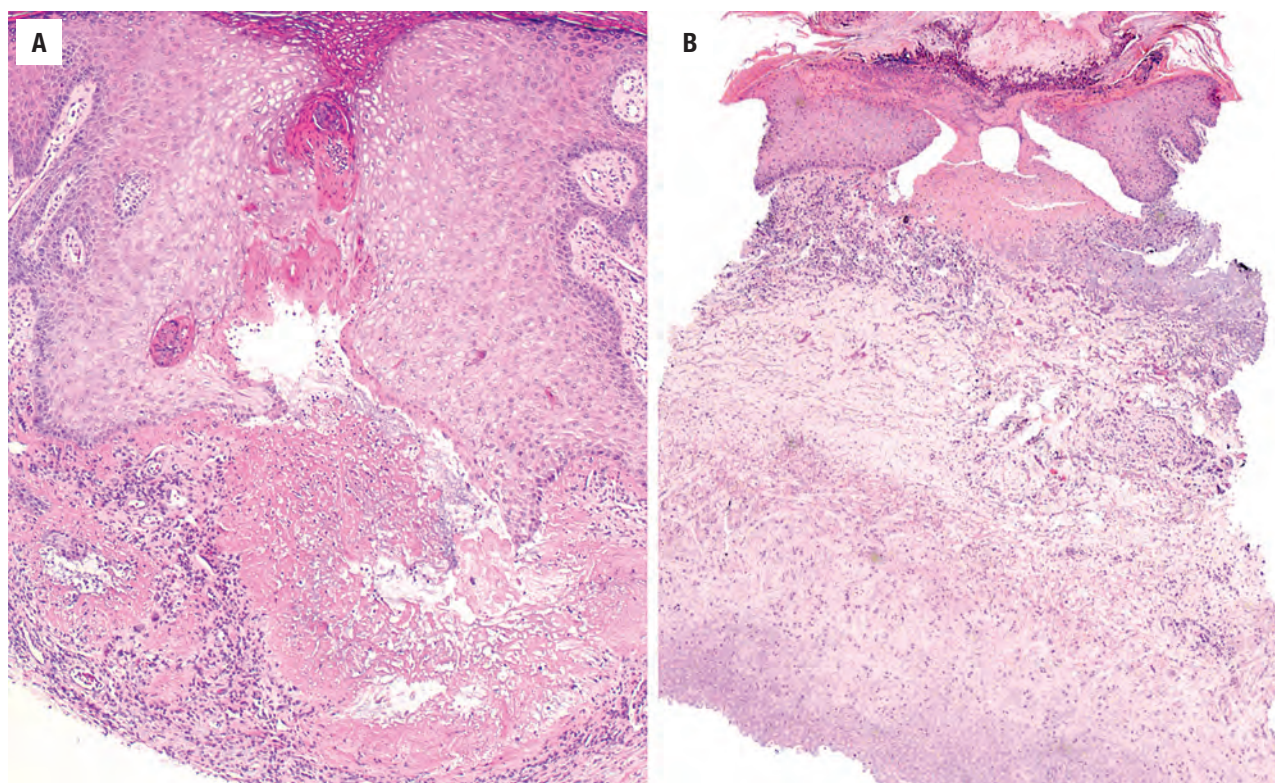
with hyperkeratosis (Fig. 17.10). The dermal collagen underlying the crater is homogeneous and eosinophilic, admixed with fibrin (Fig. 17.11), with edema in the surrounding viable dermis. The degenerative changes extend to the level of the perichondrium and are associated with loss of the normal basophilia of the underlying





**FIGURE 17.9**

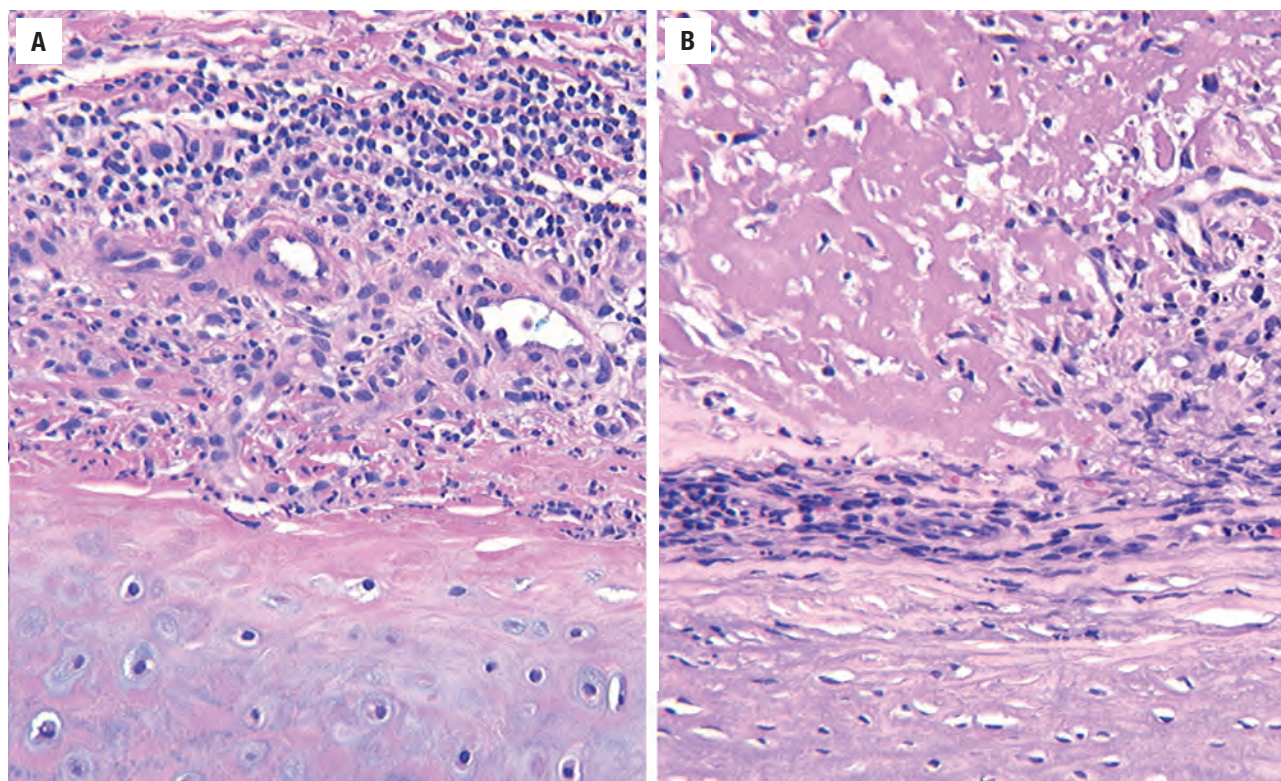
**A.** There is a nodule with a small center crater on the helix of this patient. **B.** This firm nodule with a central crater is seen on the antihelix of an elderly female with chondrodermatitis nodularis helices; antihelical lesions are more common in women. ([**A**] Courtesy of Dr. C. Chia. [**B**] Courtesy of Dr. S. A. Norton.)



**FIGURE 17.10**

Eosinophilic degenerative dermal collagen appears ready to extrude from a central crater in chondrodermatitis nodularis helices (**A**). The underlying interface between the cartilaginous plate and the dermis is blurred, and the cartilage has lost its normal basophilia (**B**).



**FIGURE 17.11**

Deep biopsies of chondrodermatitis nodularis helcis may show extensive inflammation (**A**) or degenerated collagen and fibrinoid necrosis (**B**), both immediately adjacent to the cartilage.

cartilage, focal fibrosis with increased cellularity, and dropout of chondrocytes. The necrobiotic material and fibrin spew from the crater through a disrupted epidermis. In some cases, portions of the cartilage are also extruded through the crater. Nerve twigs are frequently “captured” by this destructive inflammatory process, perhaps accounting for the exquisite pain clinically.

#### DIFFERENTIAL DIAGNOSIS

CDNH is very commonly confused clinically with *squamous cell carcinoma*, occasionally leading to overtreatment. The histologic findings may be mistaken for relapsing polychondritis, cystic chondromalacia, squamous cell carcinoma, or actinic keratosis because of the prominent squamous epithelial hyperplasia and underlying solar elastosis typically encountered in CDNH. However, the central crater and cartilage involvement (often identified with levels) usually confirm the diagnosis.

#### PROGNOSIS AND THERAPY

CDNH is a benign disorder, treated by surgery, pressure relief, and/or topical nitroglycerin therapies, although

many unconventional therapies are used. Surgery has the highest cure rate and should be the first line treatment. Removal of the lesion often alleviates the associated pain.

#### ■ ANGIOLYMPHOID HYPERPLASIA WITH EOSINOPHILIA

Angiolymploid hyperplasia with eosinophilia (ALHE; also known as epithelioid hemangioma) is an uncommon, benign, subcutaneous, vascular proliferation associated with a peculiar inflammatory infiltrate. There are some histologic similarities to Kimura disease, but the clinical features are different. It is thought to be a reaction to trauma and/or arteriovenous shunting.

#### CLINICAL FEATURES

The lesions most often occur in the auricle, in and around the external auditory canal, but may also be seen on the scalp and face. In all lesions, there is no sex difference, with a mean age in the fourth decade. Some cases have been associated with pregnancy. They are characterized by intensely pruritic, red-tan papules, which may bleed

## ANGIOLYMPHOID HYPERPLASIA WITH EOSINOPHILIA— DISEASE FACT SHEET

### Definition

- An idiopathic non-neoplastic vascular proliferation with chronic inflammatory cell infiltrate, characterized by epithelioid endothelial cells

### Incidence and Location

- Rare
- Usually involves the auricle or periauricular area, and sometimes the scalp or face

### Sex, Race, and Age Distribution

- Equal sex distribution
- No racial predominance
- Any age but commonly middle-aged adults (fourth decade)

### Clinical Features

- Usually unilateral, multiple red-tan papules on or around the auricle; papules may coalesce into plaque
- Typically present with intense pruritis with secondary bleeding; some associated with pregnancy

### Prognosis and Treatment

- Benign
- Usually treated because of pruritis, with cryotherapy and pulsed dye laser

secondary to scratching. A minority of cases are associated with peripheral blood eosinophilia. Lymphadenopathy is rarely present.

## PATHOLOGIC FEATURES

### GROSS FINDINGS

ALHE generally presents with clusters of red-tan, firm papules or subcutaneous, nodular lesions, usually a few millimeters in diameter. With time the papules may transform into a larger plaque.

### MICROSCOPIC FINDINGS

The lesion of ALHE is a circumscribed, nodular proliferation of variably sized blood vessels, capillaries to small arteries and veins with a distinctive prominent “epithelioid” endothelial lining (Fig. 17.12). The endothelial cells are plump, enlarged, with abundant eosinophilic cytoplasm, and large, somewhat pleomorphic nuclei. The prominent endothelial cells protrude into the vessel lumina, with a “bumpy” hobnail-like appearance. The vessels may be arranged in a lobular pattern or may be irregularly distributed within the lesion (Fig. 17.12).

## ANGIOLYMPHOID HYPERPLASIA WITH EOSINOPHILIA— PATHOLOGIC FEATURES

### Gross Findings

- Red-tan, firm papules in clusters, to plaques
- 5–15 mm

### Microscopic Findings

- Vascular proliferation, usually somewhat lobular
- Enlarged, plump, “epithelioid” endothelial cells with abundant eosinophilic cytoplasm and enlarged nuclei
- Hobnail pattern of endothelium protruding into vessel lumen
- Mixed lymphoid infiltrate with variable eosinophils
- Lacks lymph node architecture

### Pathologic Differential Diagnosis

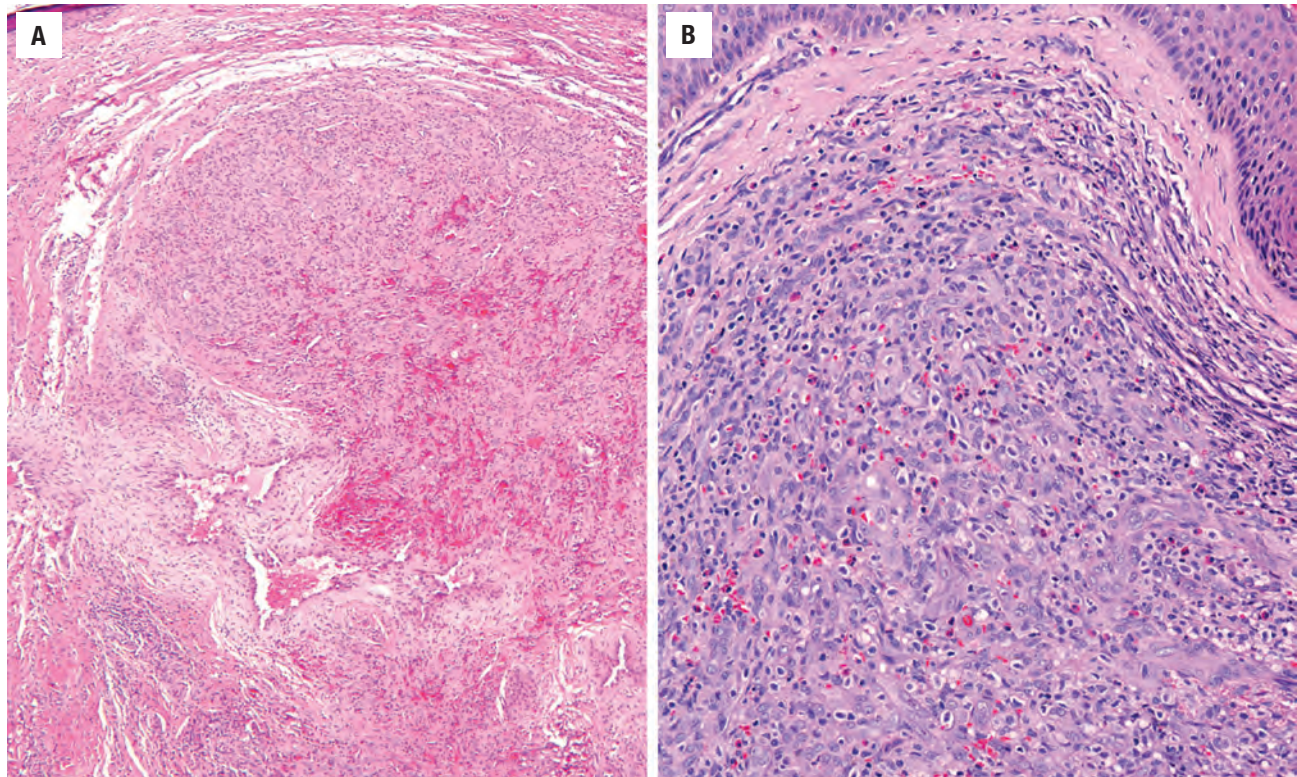
- Kimura disease, lobular capillary hemangioma, angiosarcoma, Kaposi sarcoma, metastatic papillary thyroid carcinoma

They may be ectatic or they may have thickened walls (Fig. 17.13). The background inflammatory infiltrate is often so dense that the lesion may resemble a lymph node at first glance. However, closer inspection fails to reveal the nodal architectural elements, such as sinuoids and a subcapsular sinus, even though lymphoid follicles are common. The inflammatory cells include lymphocytes and histiocytes, with a variable component of eosinophils. The eosinophils are usually prominent, suggesting the diagnosis, but occasionally they are inconspicuous.

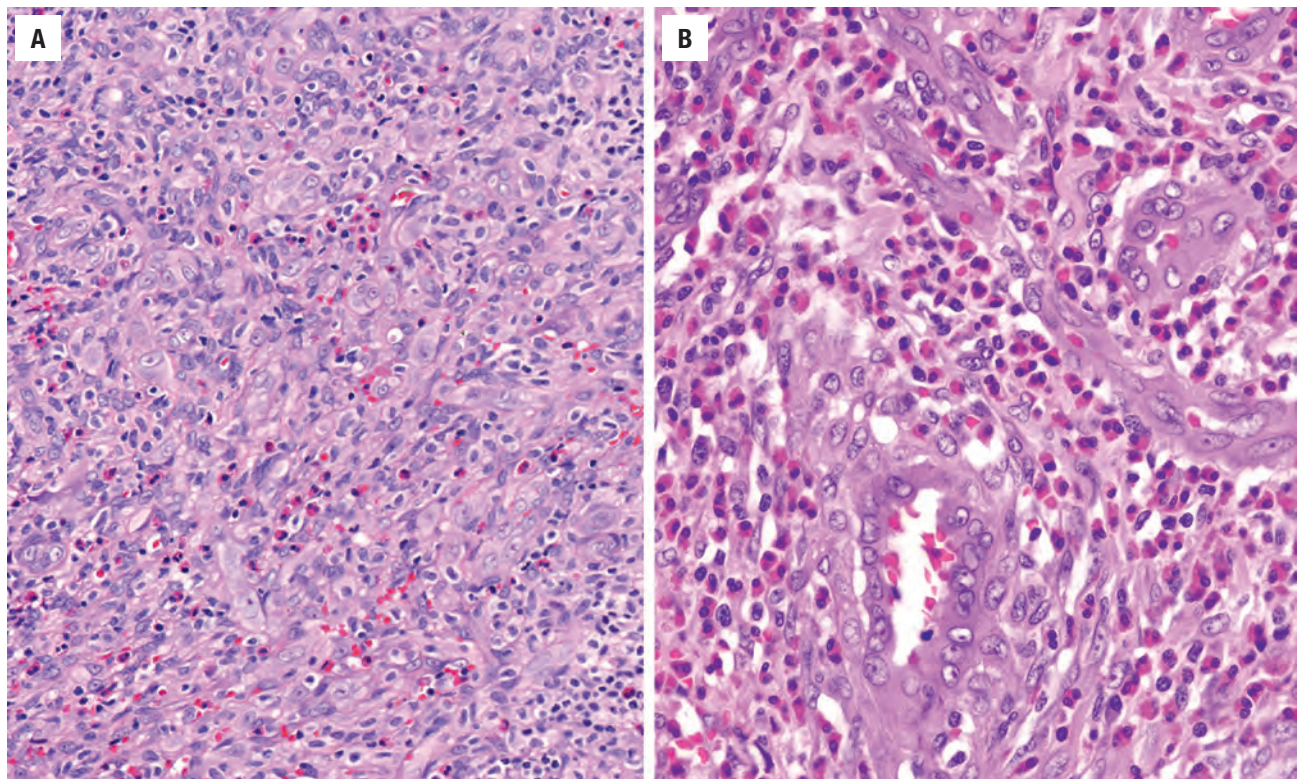
## DIFFERENTIAL DIAGNOSIS

The chief differential diagnostic consideration is *Kimura disease*, which unlike ALHE, is more commonly seen in Asian males. It is frequently associated with lymphadenopathy and with peripheral blood eosinophilia. The lesions of Kimura disease are usually larger and deeper in the subcutis or underlying soft tissue. Follicle lysis with eosinophilic abscesses and a prominent immunoglobulin E (IgE) immunohistochemistry are seen. *Lobular capillary hemangioma* is distinguished from ALHE by its characteristic lobular growth pattern, absent prominent epithelioid endothelial cells, and usually a lack of a heavy inflammatory infiltrate. *Angiosarcoma*, unlike ALHE, is defined by an infiltrative pattern, anastomosing and poorly formed vascular spaces, striking nuclear atypia with increased mitotic activity, and a usually absent inflammatory infiltrate. Rarely, *metastatic papillary thyroid carcinoma* may yield a similar histologic appearance. Thyroglobulin and TTF1 stains would help to make the separation.



**FIGURE 17.12**

(**A** and **B**) Low-power appearance of angiolymphoid hyperplasia with eosinophilia demonstrates a mixed lymphoid infiltrate associated with a vascular proliferation. There is an intact squamous epithelium (top of **B**).

**FIGURE 17.13**

(**A** and **B**) Vascular proliferation in angiolymphoid hyperplasia with eosinophilia is characterized by enlarged, plump, high "epithelioid" endothelial cells with abundant eosinophilic cytoplasm and large nuclei with prominent nucleoli. Note the numerous eosinophils in both images.



## PROGNOSIS AND THERAPY

ALHE is adequately treated by local excision in most cases, although spontaneous resolution has been documented. Cryotherapy and pulsed dye laser have reported success. Occasionally, the lesions recur after treatment, especially in young patients, patients with a long disease duration, and in patients with bilateral and/or multiple lesions.

## ■ RELAPSING POLYCHONDritis

Relapsing polychondritis is a rare autoimmune connective tissue inflammatory disorder with antibodies that target type II collagen and matrilin-1. The disease is usually seen in cartilage of the ear, nose, larynx, joints, tracheobronchial tree, and cardiovascular system, often resulting in structural damage and deformity. Humoral and cell-mediated immunity seem to play a role in the destructive inflammatory process, with various chemokines (such as interferon- $\gamma$ , interleukin-12 and -2) matching changes in disease activity. A genetic association between relapsing polychondritis and different human leukocyte antigen (HLA) types, particularly HLA-DR4, is well developed. There is an increased incidence (up to 35%) of other autoimmune disorders, such as rheumatoid arthritis, Hashimoto thyroiditis, systemic lupus erythematosus, Sjögren syndrome, systemic vasculitides, inflammatory bowel disease, diabetes mellitus, and primary biliary cirrhosis. It is also associated with myelodysplastic syndromes and leukemia. Relapsing polychondritis has also been reported in human immunodeficiency virus (HIV)-infected patients without associated autoimmune connective tissue disorders.

## CLINICAL FEATURES

Relapsing polychondritis has an estimated incidence of 3.5 cases per million population per year in the United States. Occurring over a wide age range, the disease is most often seen in the fourth to fifth decades, with an equal sex predilection. Nearly 40% of patients are initially affected in the ear (auricle specifically), although eventually approximately 90% will have ear involvement. The ears become red to purple, swollen, and painful, except for the noncartilaginous lobule, which is spared. Inflammatory episodes may last a few days or several weeks. After repeated attacks or a prolonged episode, the cartilaginous framework is damaged, becoming “flabby” and resulting in a “cauliflower ear” deformity (Fig. 17.14). When the external auditory canal and eustachian tube are involved, they may become narrowed, leading to

## RELAPSING POLYCHONDritis—DISEASE FACT SHEET

### Definition

- Rare, autoimmune connective tissue inflammatory disorder with antibodies to type II collagen and/or matrilin-1 which lead to destruction of cartilaginous tissues of the ear, nose, larynx, tracheobronchial tree, eye, heart, and blood vessels

### Incidence and Location

- 3.5/1,000,000 population/year in United States
- Auricle most common site, affected in up to 85%

### Morbidity and Mortality

- Leading cause of death is airway compromise due to tracheobronchial damage
- 10-year survival of 55%–94%
- Associated with myelodysplasia or leukemia

### Sex and Age Distribution

- Equal sex distribution
- Fourth to fifth decades

### Clinical Features

- In acute phase the ears become red, edematous, and tender, although noncartilaginous lobule is spared
- After repeated bouts, floppy ear and/or saddle nose deformity develops
- Other symptoms relate to other anatomic sites, including laryngotracheal disease, nonerosive arthritis, ophthalmologic disease, and cardiovascular disease
- HLA-DR4 association
- Associated autoimmune disorder in 25%–35%; some in human immunodeficiency virus infection

### Prognosis and Treatment

- Depends on severity of disease and number of anatomic sites affected, with airway compromise, secondary infections, and cardiovascular disease the most common causes of death
- Corticosteroids, nonsteroidal anti-inflammatory drugs, and immunomodulators have variable success
- Advanced age, anemia, and tracheobronchial stricture are poor prognostic factors

decreased auditory acuity (conductive type) and otitis media. Other anatomic sites may also be affected, with nasal chondritis (25%–50%) producing a saddle nose deformity; laryngotracheopulmonary disease (50%) causing obstruction, collapse, and a predisposition to pulmonary infections; arthritis/arthropathy (60%) causing nonerosive changes of the knees and small joints of the hand; ophthalmologic changes (up to 60%); cardiovascular disease (up to 50%) presenting with vasculitis and valvular dysfunction.

Biopsy is unnecessary as the diagnosis can be made clinically based on: (1) the presence of chondritis in two of three sites (auricle, nose, laryngotracheal tree); or (2) in one of those sites along with two other features (ocular inflammation, audiovestibular damage, or seronegative arthritis).



## PATHOLOGIC FEATURES

### GROSS FINDINGS

After long-standing or repeated episodes of active inflammation, the auricular cartilage becomes physically “floppy,” owing to loss of structural integrity of the pinna.

### MICROSCOPIC FINDINGS

The initial histologic finding in relapsing polychondritis is loss of the normal basophilia of the cartilage accompanied by an infiltration of the perichondrium by neutrophils, lymphocytes, plasma cells, and eosinophils, blurring the usually sharp interface between the cartilaginous

plate and the surrounding soft tissue (Figs. 17.15 and 17.16). The damaged cartilage (initially vacuolated) is gradually replaced by granulation tissue and fibrous tissue, with any residual cartilage demonstrating an irregular moth-eaten border (see Fig. 17.16). Immunofluorescence studies may show deposition of immunoglobulins and C3 at the periphery of the cartilage and within the walls of perichondral vessels.

## DIFFERENTIAL DIAGNOSIS

The differential diagnosis includes *necrotizing (malignant) external otitis* (an infection due to *Pseudomonas aeruginosa*), *granulomatosis with polyangitis (Wegener granulomatosis)*, *extranodal natural killer (NK)/T-cell lymphoma*,

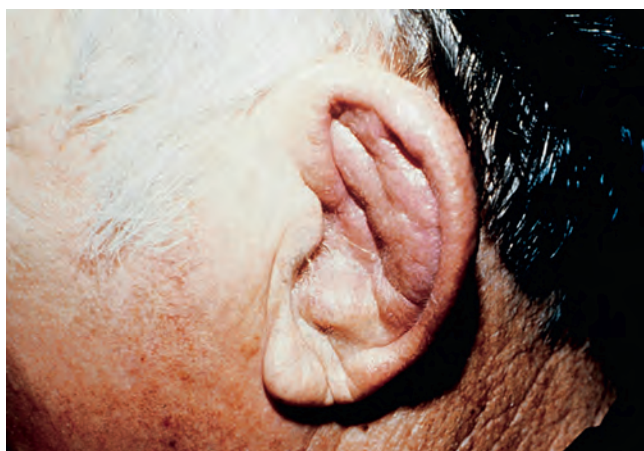


**FIGURE 17.14**

After multiple acute episodes of auricular chondritis, this patient's auricle is deformed and floppy as a result of destruction of the cartilaginous plate in this relapsing polychondritis. (Courtesy of Dr. V. J. Hyams.)

## RELAPSING POLYCHONDritis—PATHOLOGIC FEATURES

### Gross Findings

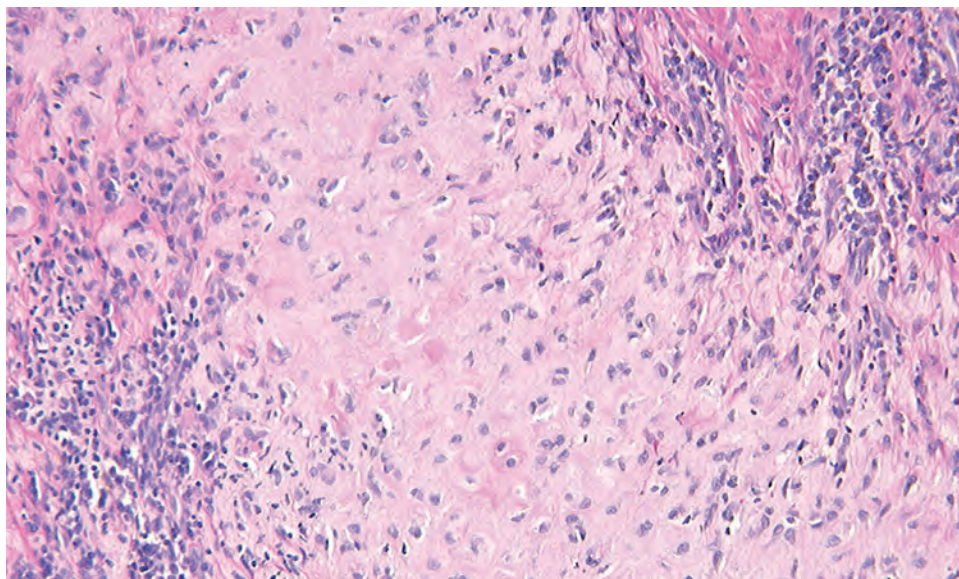
- Acute phase: erythematous, edematous pinna, with sparing of lobule
- After multiple episodes: floppy, deformed pinna with loss of cartilaginous structure

### Microscopic Findings

- Loss of basophilia in cartilaginous plate (earliest change)
- Perichondrium infiltrated by mixed inflammation
- Damaged cartilage has moth-eaten appearance and areas are replaced by granulation tissue

### Pathologic Differential Diagnosis

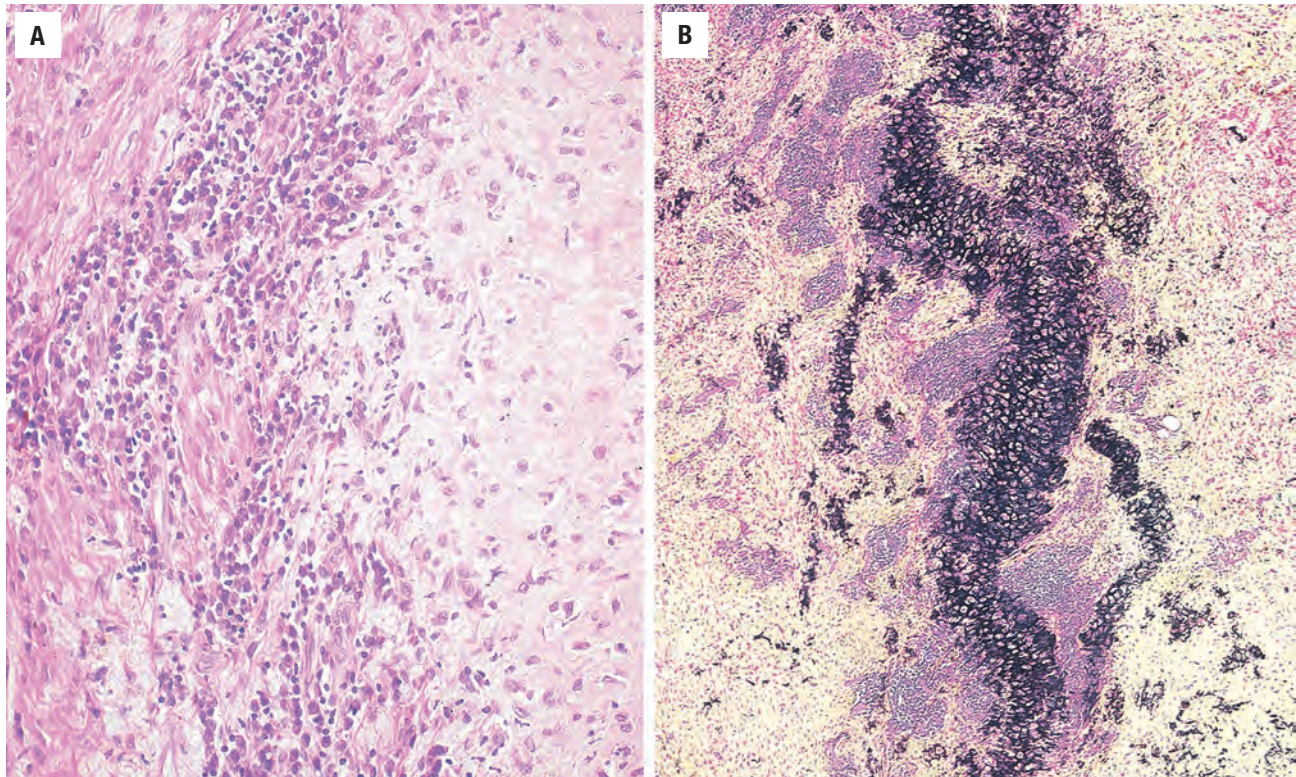
- Malignant external otitis, granulomatosis with polyangitis, extranodal NK/T-cell lymphoma, nasal type, cystic chondromalacia



**FIGURE 17.15**

Interface between the cartilage and perichondrium is blurred by a mixed inflammatory infiltrate in relapsing polychondritis.



**FIGURE 17.16**

**A**, Inflammatory cells are predominantly small lymphocytes and plasma cells. The normal basophilia of the cartilage has been lost. **B**, A Movat stain highlights the extensive damage to the cartilaginous plate, which appears black. Moth-eaten appearance is typical of relapsing polychondritis.

*nasal type*, in upper aerodigestive tract locations, and cystic chondromalacia. The ears are not usually affected by polyangitis or lymphoma.

### PROGNOSIS AND THERAPY

Due to the rarity of the disorder, optimal therapy is yet to be defined. Various medical therapies, including corticosteroids (methyl-prednisone), nonsteroidal anti-inflammatory drugs, immunomodulators (e.g., methotrexate, azathioprine, and cyclosporine A), and tumor necrosis factor alpha antagonists (rituximab, tocilizumab, abatacept) have all had some degree of success depending on the severity of disease. Autologous stem cell transplantation has induced complete remission of disease in some patients who have failed other treatments. Ear treatments are usually not critical, but surgery may be needed for patients with severe airway compromise, as well as aortic grafting and valve replacement for cardiovascular disease. The leading causes of death in patients with relapsing polychondritis are airway compromise, secondary infections, and cardiovascular disease. Factors which have a negative impact on survival include advanced age at diagnosis, anemia, and tracheobronchial stricture. The 10-year survival rate varies from 55 % to 94 %, depending on the study.

## ■ CHOLESTEATOMA

Cholesteatoma is a misnomer because it contains no “cholesterol” and it is not a true “neoplasm.” It simulates a neoplasm clinically by the propensity to destroy surrounding tissues (including bone) and to recur after excision. With negative pressure and eustachian tube dysfunction, accumulation of desquamated keratin results in obstruction. Trapped bacteria cause infection, resulting in increased inflammatory cells, with release of cytokines, causing epithelial proliferation. Collagenase production by the squamous epithelium (“matrix”) is thought to result in the bone destruction. The cystic lesion, filled with keratinous debris and lined by keratinizing squamous epithelium, is found within the middle ear or mastoid region. The presence of squamous epithelium in the middle ear, which is normally lined by cuboidal or columnar glandular epithelium, is abnormal, no matter by which mechanism it arrives there. Acquired and congenital forms of cholesteatoma are recognized.

### CLINICAL FEATURES

Cholesteatomas are common and usually unilateral. Older children and young adults (third to fourth decades) will



**CHOLESTEATOMA—DISEASE FACT SHEET****Definition**

- Destructive squamous epithelial cyst of middle ear or mastoid region, usually secondary to chronic otitis media but occasionally congenital

**Incidence and Location**

- Common
- Origin in superior posterior middle ear and/or petrous apex but may demonstrate locally aggressive growth into adjacent structures

**Morbidity and Mortality**

- Chronic middle ear disease and progressive conductive hearing loss
- Intracranial extension may lead to lethal complications such as meningitis, epidural abscess, brain parenchymal abscess, or lateral sinus thrombosis

**Sex and Age Distribution**

- Equal sex distribution
- Any age, including congenital examples; highest incidence in third to fourth decades

**Clinical Features**

- Long history of unilateral, severe, chronic otitis media
- Progressive conductive hearing loss, foul-smelling discharge, otalgia, otorrhea (in part due to underlying chronic ear disease); tinnitus and vertigo less common
- Facial nerve palsy, vomiting, severe vertigo, severe headache suggests advanced destructive disease or suppurative infection
- Otoscopic appearance: white-gray to yellow irregular mass associated with chronic otitis media or perforated tympanic membrane

**Radiographic Features**

- Bone destruction with medial displacement of the ossicles
- Computed tomography and magnetic resonance imaging are complimentary

**Prognosis and Treatment**

- Surgical extirpation of the squamous epithelial lining essential
- Recurrence if incompletely excised (20%)
- Increased incidence of recurrence includes: < 20 years of age, marked ossicular erosion, polypoid mucosal inflammatory disease, extensive disease
- Serious complications include labyrinthine fistula, sigmoid sinus or facial nerve canal erosion, cranial nerve dysfunction, meningitis, epidural or brain parenchymal abscess

present with a foul-smelling aural discharge and conductive hearing loss. The tympanic membrane is perforated (usually at the superior margin) in the acquired form, and intact in the congenital form. Both are usually associated with a long history of severe chronic otitis media, giving an otoscopic appearance of a white-gray to yellow irregular mass associated with chronic otitis media (Fig. 17.17). Facial nerve dysfunction, vomiting, severe vertigo, and very severe headaches may indicate advanced

**CHOLESTEATOMA—PATHOLOGIC FEATURES****Gross Findings**

- Specimen fragmented, but may contain flecks of white to yellow keratinous (grumous) material
- All tissue should be processed

**Microscopic Findings**

- Cystic, sac-like mass
- Acellular, keratinous material
- Thin, stratified squamous epithelium with prominent granular layer
- Inflamed granulation or fibrous tissue
- Giant cell granulomatous reaction to keratinous debris and cholesteatoma may coexist

**Immunohistochemical Findings**

- Strong Ki67 immunoreactivity confirms proliferation

**Pathologic Differential Diagnosis**

- Squamous cell carcinoma, otitis media, cholesterol granuloma

destructive disease or a suppurative infection, either one requiring immediate intervention.

**RADIOGRAPHIC FEATURES**

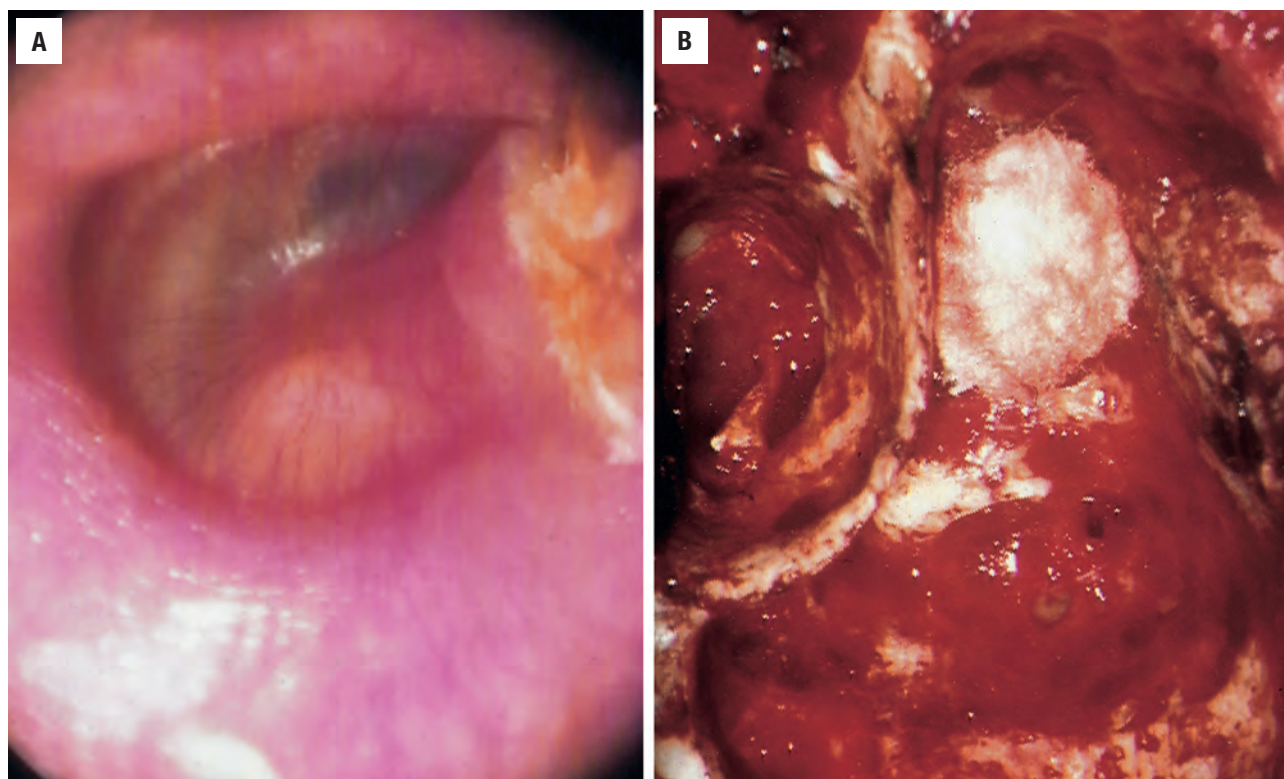
CT and magnetic resonance imaging (MRI; non-echo planar diffusion-weighted imaging) are essential and complimentary, showing a soft tissue mass displacing the ossicles medially, with a variable degree of bone destruction (Fig. 17.18). Associated changes of chronic middle ear infection are common. There is usually prolongation of the signal in both T1 and T2 MRI signals, with T1-weighted signal intensity being low, while T2-weighted signal intensity is high. There may be peripheral enhancement, if degenerated.

**PATHOLOGIC FEATURES****GROSS FINDINGS**

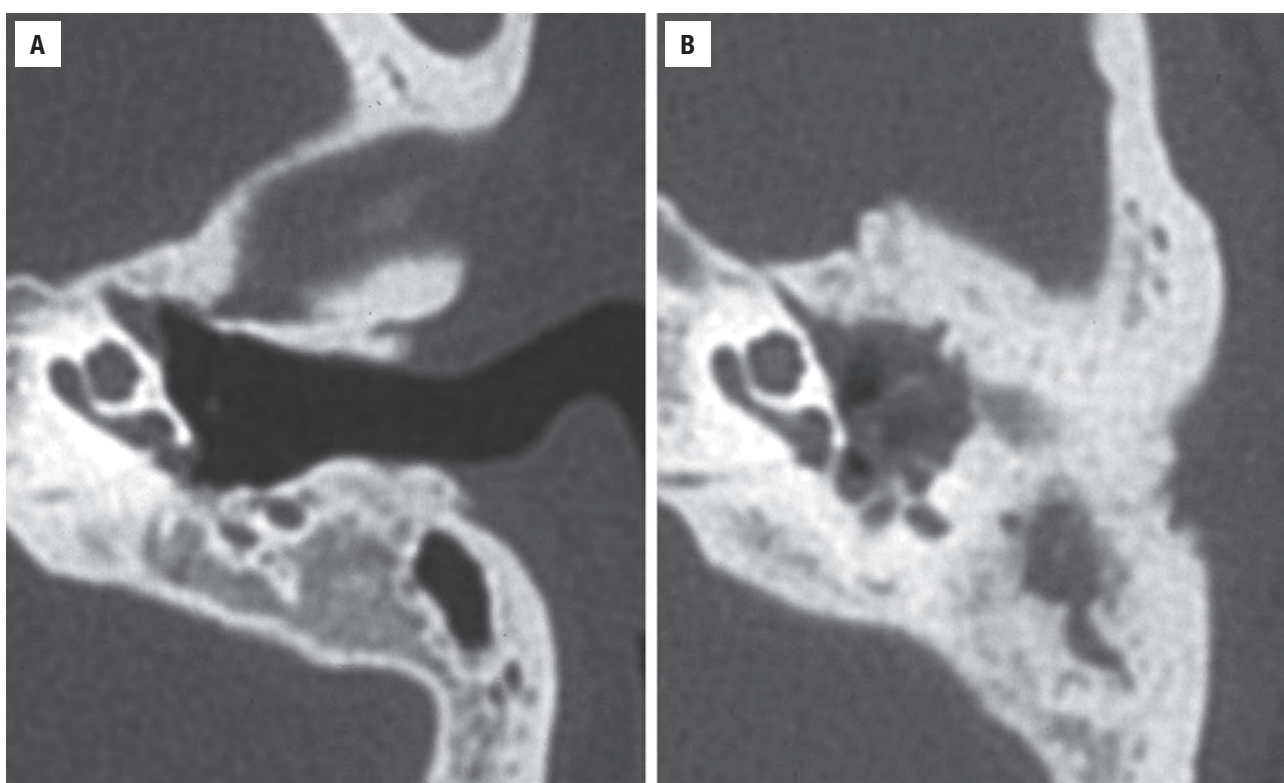
Rarely is a cholesteatoma received intact for pathologic examination. The specimen usually consists of multiple fragments of flakey, white keratinous debris, accompanied by soft tissue fragments. A foul aroma and associated chronic otitis media with bone destruction may be noted at surgery, with bone fragments submitted to pathology.

**MICROSCOPIC FINDINGS**

Three components are essential for the diagnosis of cholesteatoma: (1) keratinous material; (2) stratified

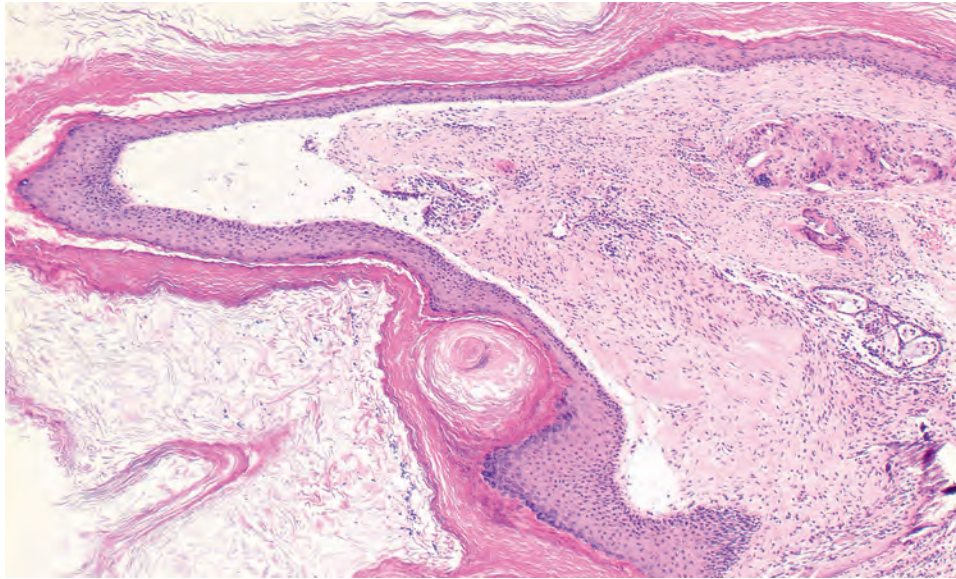
**FIGURE 17.17**

**A**, Otoscopic view demonstrates an irregular yellow to white mass behind the perforated tympanic membrane in this cholesteatoma. **B**, Surgical exposure reveals a yellow white mass that represents a cholesteatoma. Specimens received in pathology are typically fragmented.

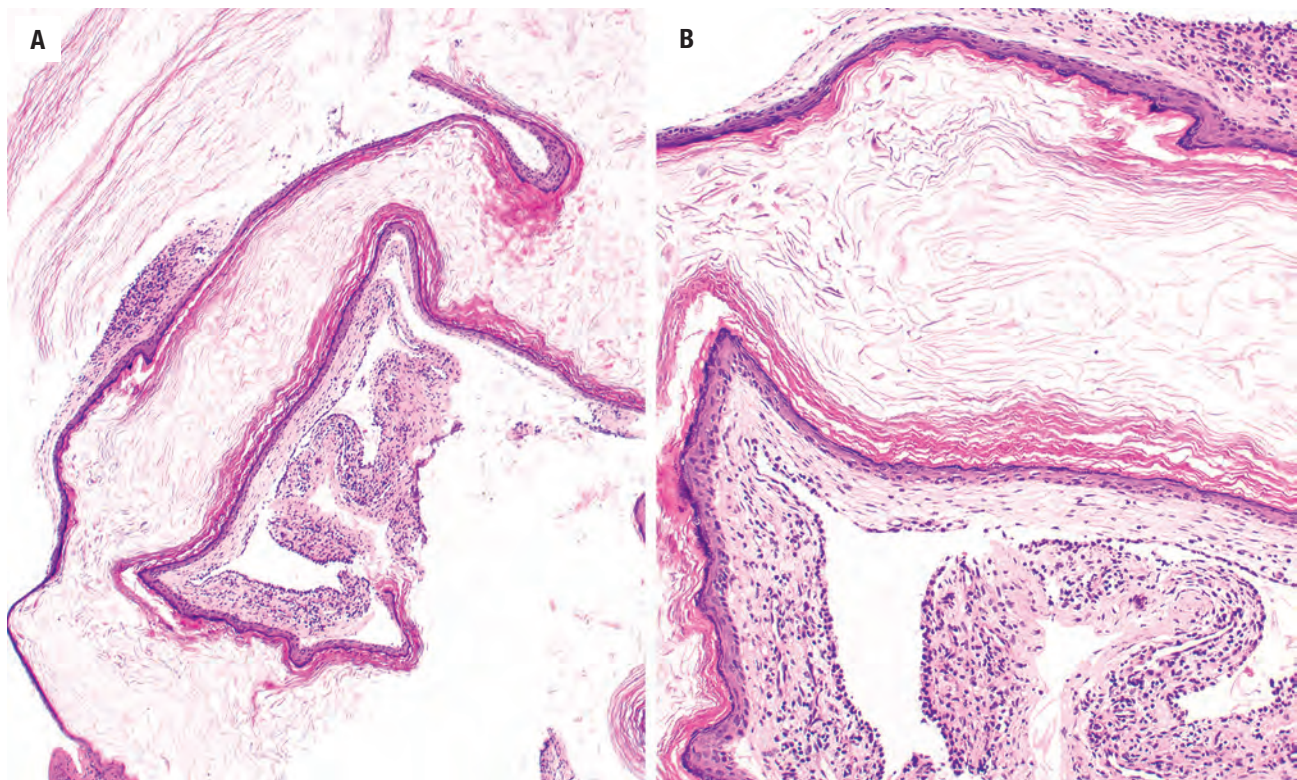
**FIGURE 17.18**

**A**, Computed tomography (CT) image of a *normal* ear. **B**, In comparison, the CT shows a soft tissue mass in the middle ear space. The stapes is present in both views.



**FIGURE 17.19**

Essential elements of a cholesteatoma include inflamed granulation or fibrous tissue, keratinizing squamous epithelium, and acellular keratinous material.

**FIGURE 17.20**

(A and B) Squamous epithelium, or “matrix,” has a granular layer in a cholesteatoma, associated with flakes of keratin and debris.

squamous epithelium with a prominent granular layer; and (3) inflamed granulation or fibrous tissue (Figs. 17.19 and 17.20). The squamous epithelium is usually bland and atrophic, lacking rete pegs and without reactive changes expected in an inflammatory process. A giant cell granulomatous reaction to the keratinous material may be seen.

The thin epithelium lines a sac filled with exfoliated anucleate squames (see Fig. 17.20). Occasionally, other disorders accompany the cholesteatoma and include cholesterol granuloma, aural polyps, tympanosclerosis, acquired encephalocele (herniation of normal brain tissue through a bony defect), and tumors (such as middle ear adenoma).

## ANCILLARY STUDIES

Fluorescence in situ hybridization studies have demonstrated extra copies of chromosome 7 in over half of cholesteatomas, which correlates with proliferative activity. Additionally, this abnormality may be useful in identifying those cases that will exhibit more aggressive behavior.

## DIFFERENTIAL DIAGNOSIS

The pathologic differential diagnosis is relatively limited to *squamous cell carcinoma*, *otitis media*, and *cholesterol granuloma*. Carcinoma contains pleomorphic epithelium, not seen in cholesteatoma. Cholesterol granuloma, discussed later, may be a concurrent lesion, just like otitis media.

## PROGNOSIS AND THERAPY

Excision, exteriorization with reconstruction, of a cholesteatoma can be achieved by a modified radical (all ossicles left) or radical mastoidectomy (stapes left). The goals of therapy are a nondischarging, but hearing ear. Recurrence can occur if incompletely excised, with a failure rate of about 20%. Other factors associated with increased incidence of recurrence include age less than 20 years, marked ossicular erosion, polypoid mucosal inflammatory disease, and extensive disease. Serious complications include labyrinthitis, labyrinthine fistula, sigmoid sinus or facial nerve canal erosion, cranial nerve dysfunction, meningitis, and epidural or brain parenchymal abscess.

## ■ CHOLESTEROL GRANULOMA

Cholesterol granuloma of the mastoid or middle ear is a stromal reaction to hemorrhage and cholesterol crystals associated with breakdown of red blood cells and other necrotic tissues. When there is exposed marrow tissue, cholesterol granuloma is thought to develop.

## CLINICAL FEATURES

Cholesterol granuloma is seen at any age, with no sex preference, usually in patients with a history of chronic ear disease, such as serous otitis media or acute suppurative otitis media. Trauma or surgical procedures that

## CHOLESTEROL GRANULOMA—DISEASE FACT SHEET

### Definition

- Stromal reaction to hemorrhage and cholesterol crystals from cell breakdown of erythrocytes

### Incidence and Location

- Incidence unknown due to coexistence with other diseases
- Middle ear and petrous apex, but occur in any location

### Morbidity and Mortality

- Conductive hearing loss and chronic middle ear disease
- Petrous apex lesions may be more aggressive, with sensorineural hearing loss, cranial nerve deficits, or intracranial extension

### Sex and Age Distribution

- Equal sex distribution
- Any age

### Clinical Features

- History of chronic middle ear disease
- Trauma or surgical procedure predispose in some cases
- Otoscopic appearance: blue to black tympanic membrane if associated with bloody middle ear effusion, or submucosal brown mass
- Unilateral conductive hearing loss, tinnitus, balance disturbances, bloody otorrhea

### Radiographic Features

- Well-defined intraosseous cystic lesion with bone remodeling
- No gadolinium enhancement by computed tomography
- Magnetic resonance imaging T1- and T2-weighted high-intensity signal

### Prognosis and Treatment

- Drainage and aeration of middle ear–mastoid compartment
- Aggressive petrous apex lesions may require more aggressive surgery

produce obstruction may also predispose to these lesions. Patients present with unilateral conductive hearing loss, tinnitus, disturbances of balance, or episodes of bloody otorrhea. Otoscopic examination often demonstrates a blue to black tympanic membrane secondary to a middle ear bloody effusion. When cholesterol granulomas occur in the petrous apex, the clinical course may be more aggressive, with sensorineural hearing loss, deficits of other cranial nerves (V, VI, VII), and, in advanced cases, extension into the middle or posterior cranial fossa.

## RADIOGRAPHIC FEATURES

Cholesterol granuloma is readily identified by CT or MRI, where it is characterized by a well-defined intraosseous cystic lesion with associated bone remodeling. Gadolinium



enhancement is not present; cholesterol granuloma demonstrates high-intensity signal with both T1- and T2-weighted images by MRI.

## PATHOLOGIC FEATURES

### GROSS FINDINGS

The specimen is usually fragmented, consisting of yellow-brown or red friable tissue, sometimes with overlying mucosa. The entire specimen should be processed to exclude an associated cholesteatoma or neoplasm.

### MICROSCOPIC FINDINGS

The cholesterol granuloma consists of granulation tissue or fibrous tissue, with recent hemorrhage and elongated clefts (left by cholesterol crystals dissolved by processing) surrounded by multinucleated giant cells, foamy and hemosiderin-laden histiocytes, and extracellular accumulations of hemosiderin pigment (Fig. 17.21). The overlying mucosa may demonstrate reactive changes, but a pure cholesterol granuloma will not include a proliferation of keratinizing squamous epithelium, which would indicate a coexisting cholesteatoma.

## DIFFERENTIAL DIAGNOSIS

The cholesterol granuloma is frequently simultaneously present with other lesions, such as cholesteatoma, middle ear adenoma, and endolymphatic sac tumor. Therefore

## CHOLESTEROL GRANULOMA—PATHOLOGIC FEATURES

### Gross Findings

- Fragmented, friable, yellow-brown to red friable tissue
- Processing of all material required to exclude associated cholesteatoma or neoplasm

### Microscopic Findings

- Granulation or fibrous tissue with recent hemorrhage
- Elongated clefts (left by cholesterol crystals) surrounded by multinucleated giant cells, foamy and hemosiderin-laden macrophages
- Extracellular aggregates of hemosiderin pigment
- Reactive epithelium, but no keratinizing squamous epithelium in pure cholesterol granuloma

### Pathologic Differential Diagnosis

- Look for associated lesions: cholesteatoma, middle ear adenoma, endolymphatic sac tumor

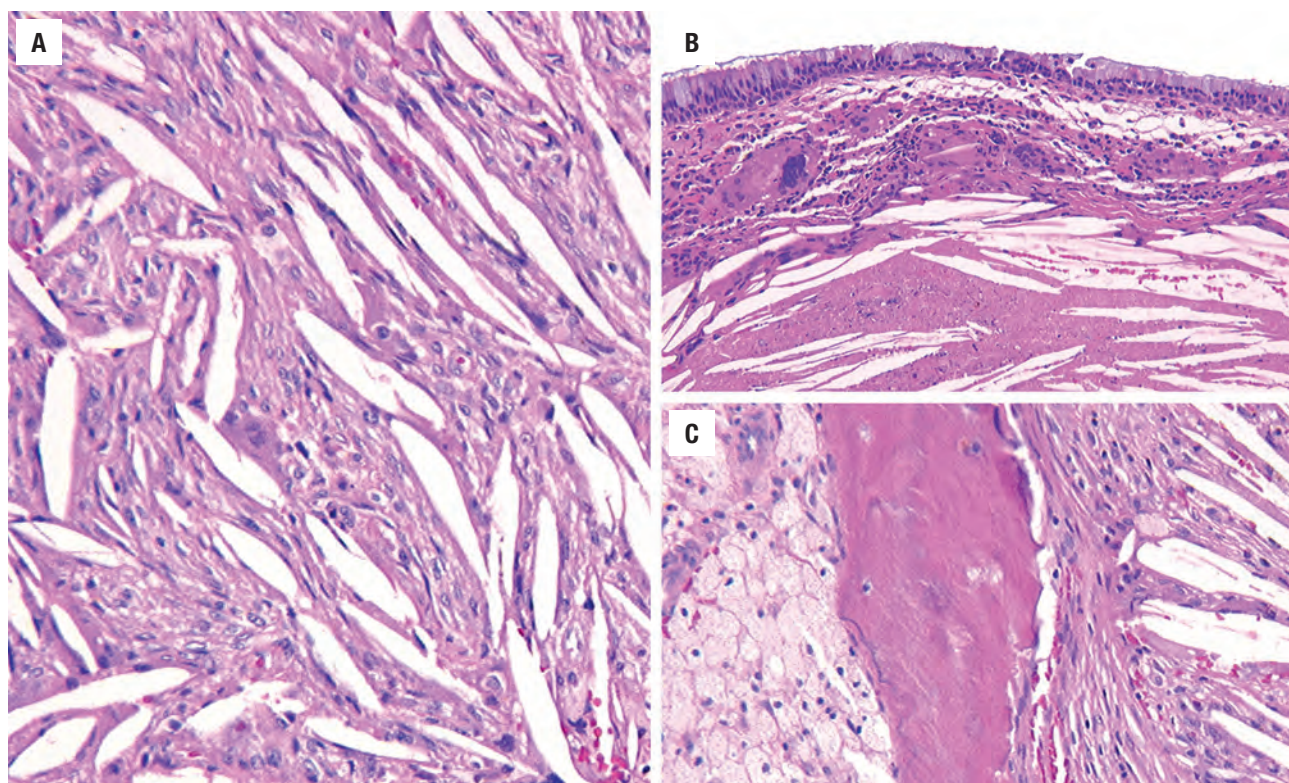


**FIGURE 17.21**

**A**, Submucosal stroma demonstrates fusiform clefts left by cholesterol crystals which have been dissolved during processing. **B**, Many of the cholesterol crystals are engulfed by multinucleated giant cells below an intact respiratory-type epithelium. **C**, Bone with histiocytes (*left side*) and cholesterol clefts (*right side*).

it is imperative to search for these other possible lesions.

### PROGNOSIS AND THERAPY

Treatment of a cholesterol granuloma requires drainage and aeration of the middle ear–mastoid compartment, removing the predisposing factors for development of

these lesions. Petrous apex lesions may require drainage (through a variety of techniques), depending on the presence or absence of residual hearing. Nonaggressive petrous apex lesions, often incidental, may be followed clinically and radiographically.

### SUGGESTED READINGS

The complete Suggested Readings list is available online at [ExpertConsult.com](http://ExpertConsult.com).



**SUGGESTED READINGS****First Branchial Cleft Anomalies**

1. Al-Khateeb TH, et al. Congenital neck masses: a descriptive retrospective study of 252 cases. *J Oral Maxillofac Surg.* 2007;65:2242–2247.
2. Begovic N, et al. Cervical chondrocutaneous branchial remnants—report of 17 cases. *Int J Pediatr Otorhinolaryngol.* 2014;78(11):1961–1964.
3. Hickey SA, et al. Defects of the first branchial cleft. *J Laryngol Otol.* 1994;108:240–243.
4. Krishnamurthy A, et al. A Type I first branchial cleft cyst masquerading as a parotid tumor. *Natl J Maxillofac Surg.* 2014;5(1):84–85.
5. Magdy EA, et al. First branchial cleft anomalies: presentation, variability and safe surgical management. *Eur Arch Otorhinolaryngol.* 2013;270(6):1917–1925.
6. Schroeder JW, et al. Branchial anomalies in the pediatric population. *Otolaryngol Head Neck Surg.* 2007;137:289–295.
7. Shinn JR, et al. First branchial cleft anomalies: otologic manifestations and treatment outcomes. *Otolaryngol Head Neck Surg.* 2015;152(3):506–512.
8. Spinelli C, et al. Branchial cleft and pouch anomalies in childhood: a report of 50 surgical cases. *J Endocrinol Invest.* 2016;39(5):529–535.
9. Thompson LDR, et al. The clinical importance of cystic metastatic squamous cell carcinomas in the neck: a study of 136 cases. *Cancer.* 1998;82:944–956.
10. Triglia J-M, et al. First branchial cleft anomalies. A study of 39 cases and a review of the literature. *Arch Otolaryngol Head Neck Surg.* 1998;124:291–295.

**Cystic Chondromalacia**

1. Grigoryan KV, et al. Surgical derofing procedure for the treatment of an auricular pseudocyst. *Dermatol Surg.* 2015;41(10):1198–1200.
2. Heffner DK, et al. Cystic chondromalacia (endochondral pseudocyst) of the auricle. *Arch Pathol Lab Med.* 1986;110:740–743.
3. Liu Y, et al. The treatment of 176 cases of auricular pseudocyst by the probe microwave burning. *Lin Chung Er Bi Yan Hou Tou Jing Wai Ke Za Zhi.* 2014;29(8):763–764.
4. Nemade SV, et al. Treatment of auricular seroma: a conservative, innovative, and effective approach. *Ann Otol Rhinol Laryngol.* 2014;123(11):749–753.
5. Shan Y, et al. Novel modified surgical treatment of auricular pseudocyst using plastic sheet compression. *Otolaryngol Head Neck Surg.* 2014;151(6):934–938.
6. Sheaffer A, et al. Pseudocyst of the auricle: an uncommon entity of the ear. *Skinmed.* 2012;10(2):104–106.
7. Zhu L, et al. Histological examination of the auricular cartilage and pseudocysts of the auricle. *J Laryngol Otol.* 1992;106:103–104.

**Chondrodermatitis Nodular Helicis**

1. Bruns NM, et al. Surgical treatment of chondrodermatitis nodularis helicis via a retroauricular incision. *J Dtsch Dermatol Ges.* 2015;13(10):1049–1051.
2. Elgart ML. Cell phone chondrodermatitis. *Arch Dermatol.* 2000;136:1568.
3. Kechichian E, et al. Management of chondrodermatitis nodularis helicis: a systematic review and treatment algorithm. *Dermatol Surg.* 2016;42(10):1125–1134.
4. Kulendra K, et al. Long-term recurrence rates following excision and cartilage rim shave of chondrodermatitis nodularis chronica helicis and antihelicis. *Clin Otolaryngol.* 2014;39(2):121–126.
5. Magro CM, et al. Chondrodermatitis nodularis helicis as a marker of internal syndromes associated with microvascular injury. *J Cutan Pathol.* 2005;32:329–333.
6. Moncrief M, et al. Effective treatment of chondrodermatitis nodularis chronica helicis using a conservative approach. *Br J Dermatol.* 2004;150:892–894.
7. Santa Cruz DJ. Chondrodermatitis nodularis helicis: a transepidermal perforating disorder. *J Cutan Pathol.* 1980;7:70–76.
8. Shah S, et al. Chondrodermatitis nodularis helicis: A review of current therapies. *Dermatol Ther.* 2016;PMID: 27723195.

9. Upile T, et al. Advances in the understanding of chondrodermatitis nodularis chronica helicis: the perichondral vasculitis theory. *Clin Otolaryngol.* 2009;34:147–150.

**Angiolymphoid Hyperplasia With Eosinophilia**

1. Adler BL, et al. Epidemiology and treatment of angiolymphoid hyperplasia with eosinophilia (ALHE): A systematic review. *J Am Acad Dermatol.* 2016;74(3):506–512.e11.
2. Bhattacharjee P, et al. Human herpesvirus-8 is not associated with angiolymphoid hyperplasia with eosinophilia. *J Cutan Pathol.* 2004;31:612–615.
3. Buder K, et al. Angiolymphoid hyperplasia with eosinophilia and Kimura's disease - a clinical and histopathological comparison. *J Dtsch Dermatol Ges.* 2014;12(3):224–228.
4. Chen H, et al. Kimura disease: a clinicopathologic study of 21 cases. *Am J Surg Pathol.* 2004;28:505–513.
5. Guo R, et al. Angiolymphoid hyperplasia with eosinophilia. *Arch Pathol Lab Med.* 2015;139(5):683–686.
6. Hamaguchi Y, et al. IgG4-related skin disease, a mimic of angiolymphoid hyperplasia with eosinophilia. *Dermatology.* 2011;223(4):301–305.
7. Olsen TG, et al. Angiolymphoid hyperplasia with eosinophilia: a clinicopathologic study of 116 patients. *J Am Acad Dermatol.* 1985;12:781–796.
8. San Nicolás M, et al. Angiolymphoid hyperplasia with eosinophilia of the external ear: case report and review of the literature. *Eur Arch Otorhinolaryngol.* 2013;270(10):2775–2777.

**Relapsing Polychondritis**

1. Arnaud L, et al. Pathogenesis of relapsing polychondritis: a 2013 update. *Autoimmun Rev.* 2014;13(2):90–95.
2. Cantarini L, et al. Diagnosis and classification of relapsing polychondritis. *J Autoimmun.* 2014;48:49:53–59.
3. Frances C, et al. Dermatologic manifestations of relapsing polychondritis. A study of 200 cases at a single center. *Medicine (Baltimore).* 2001;80:173–179.
4. Lahmer T, et al. Relapsing polychondritis: an autoimmune disease with many faces. *Autoimmun Rev.* 2010;9:540–546.
5. Longo L, et al. Relapsing polychondritis: A clinical update. *Autoimmun Rev.* 2016;15(6):539–543.
6. Mathew SD, et al. Relapsing polychondritis in the Department of Defense population and review of the literature. *Semin Arthritis Rheum.* 2012;42(1):70–83.
7. O'Connor Reina C, et al. When is a biopsy justified in a case of relapsing polychondritis? *J Laryngol Otol.* 1999;113:663–665.
8. Yang H, et al. Clinical analysis of 15 patients with relapsing auricular polychondritis. *Eur Arch Otorhinolaryngol.* 2014;271(3):473–476.

**Cholesteatoma**

1. Chawla A, et al. Computed tomography features of external auditory canal cholesteatoma: a pictorial review. *Curr Probl Diagn Radiol.* 2015;44(6):511–516.
2. Goycoolea MV, et al. The theory of the trigger, the bridge, and the transmigration in the pathogenesis of acquired cholesteatoma. *Acta Otolaryngol.* 1999;119:244–248.
3. Harris AT, et al. Pooled analysis of the evidence for open cavity, combined approach and reconstruction of the mastoid cavity in primary cholesteatoma surgery. *J Laryngol Otol.* 2016;130(3):235–241.
4. Huisman MA, et al. Cholesteatoma epithelium is characterized by increased expression of Ki-67, p53, and p21, with minimal apoptosis. *Acta Otolaryngol.* 2003;123:377–382.
5. Louw L. Acquired cholesteatoma: summary of the cascade of molecular events. *J Laryngol Otol.* 2013;127(6):542–549.
6. Luers JC, et al. Surgical anatomy and pathology of the middle ear. *J Anat.* 2016;228(2):338–353.
7. Kuo CL, et al. Updates and knowledge gaps in cholesteatoma research. *Biomed Res Int.* 2015;2015:854024.
8. Kuo CL. Etiopathogenesis of acquired cholesteatoma: prominent theories and recent advances in biomolecular research. *Laryngoscope.* 2015;125(1):234–240.

9. Maniu A, et al. Molecular biology of cholesteatoma. *Rom J Morphol Embryol*. 2014;55(1):7–13.
10. Mor N, et al. Middle ear cholesteatoma treated with a mastoidectomy: a systematic review of the measures used. *Otolaryngol Head Neck Surg*. 2014;151(6):923–929.
11. Presutti L, et al. Results of endoscopic middle ear surgery for cholesteatoma treatment: a systematic review. *Acta Otorhinolaryngol Ital*. 2014;34(3):153–157.
12. Soldati D, et al. Knowledge about cholesteatoma, from the first description to modern histopathology. *Otol Neurotol*. 2001;22:723–730.
13. van Egmond SL, et al. A systematic review of non-echo planar diffusion-weighted magnetic resonance imaging for detection of primary and postoperative cholesteatoma. *Otolaryngol Head Neck Surg*. 2016;154(2):233–240.
2. DeGuine C, et al. Blue ear drum and cholesterol granuloma. *Ear Nose Throat J*. 2000;79:542.
3. Ferlito A, et al. Clinicopathological consultation. Ear cholesteatoma versus cholesterol granuloma. *Ann Otol Rhinol Laryngol*. 1997;106:79–85.
4. Hoa M, et al. Petrous apex cholesterol granuloma: maintenance of drainage pathway, the histopathology of surgical management and histopathologic evidence for the exposed marrow theory. *Otol Neurotol*. 2012;33(6):1059–1065.
5. Iannella G, et al. Tympanomastoid cholesterol granuloma: radiological and intraoperative findings of blood source connection. *Eur Arch Otorhinolaryngol*. 2016;273(9):2395–2401.
6. Mosnier I, et al. Management of cholesterol granulomas of the petrous apex based on clinical and radiologic evaluation. *Otol Neurotol*. 2002;23:522–528.

### Cholesterol Granuloma

1. Brackmann DE, et al. Surgical management of petrous apex cholesterol granulomas. *Otol Neurotol*. 2002;230:529–533.



# Benign Neoplasms of the Ear and Temporal Bone

■ **Lester D.R. Thompson**

## ■ CERUMINOUS ADENOMA

Ceruminous adenoma is a benign glandular neoplasm of ceruminous glands (modified apocrine sweat glands) that arises solely from the external auditory canal (EAC).

### CLINICAL FEATURES

Ceruminous adenoma accounts for less than 1% of all external ear tumors, usually affecting middle-aged (mean, 55 years) patients, without a sex difference. Patients usually present with a mass in the posterior wall of the outer one-third to one-half of the EAC. There may be associated pain, hearing loss (sensorineural and conductive), tinnitus, or even paralysis of the nerves.

### CERUMINOUS ADENOMA—DISEASE FACT SHEET

#### Definition

- Benign ceruminous gland neoplasm

#### Incidence and Location

- Rare
- Outer half of the external auditory canal

#### Morbidity and Mortality

- None

#### Sex and Age Distribution

- Equal sex distribution
- Wide age range but usually 6th decade

#### Clinical Features

- Mass with hearing changes, pain, tinnitus

#### Prognosis and Treatment

- Excellent; surgery alone, although recurrences may develop

## PATHOLOGIC FEATURES

### GROSS FINDINGS

Most tumors are small (mean, 1.2 cm), nonulcerating, superficial masses found in the outer one-third to one-half of the EAC, covered by intact skin. Grossly polypoid, these masses are usually fragmented during removal. As benign tumors, extension into the mastoid bone, middle ear, and base of the skull is not identified.

### MICROSCOPIC FINDINGS

Ceruminous adenomas are well circumscribed but unencapsulated (Fig. 18.1). Surface involvement (not *origin*) may be seen, whereas ulceration is absent. Tumors are divided into three subtypes based on specific histologic

### CERUMINOUS ADENOMA—PATHOLOGIC FEATURES

#### Gross Findings

- Nonulcerated, superficial mass in outer half of EAC
- Size: 1.2 cm

#### Microscopic Findings

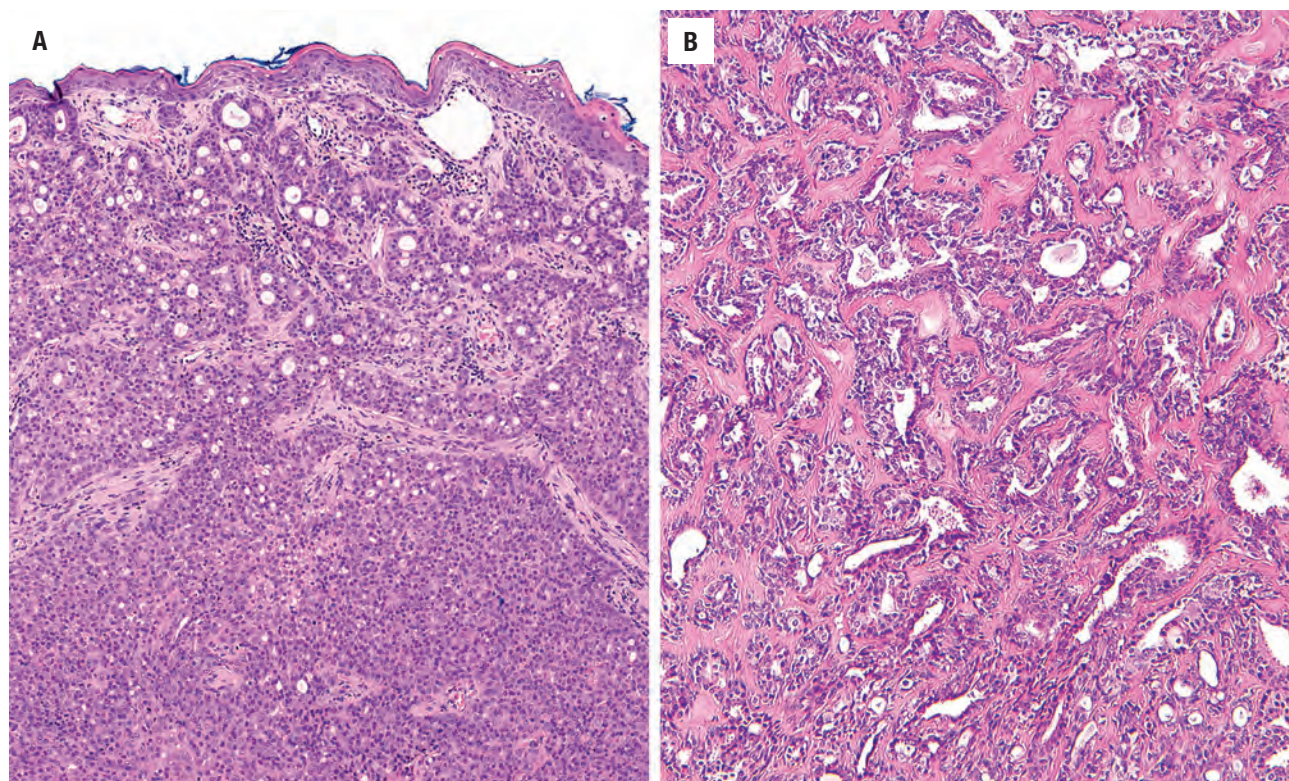
- Circumscribed but unencapsulated mass with glandular and cystic pattern
- Dual cell population, with inner apocrine cells showing decapitation secretion surrounded by outer basal-myoeepithelial cells
- Luminal cells with cytoplasmic yellow-brown, cerumen pigment granules
- Dense, sclerotic fibrosis

#### Immunohistochemical Findings

- Positive: CK7, CD117 (luminal) secretory cells
- Positive: CK5/6, p63, S100 protein basal-myoeepithelial cells

#### Pathologic Differential Diagnosis

- Ceruminous gland adenocarcinoma, middle ear adenoma, paraganglioma, parotid gland primary

**FIGURE 18.1**

Ceruminous adenoma. There is an unencapsulated neoplastic proliferation of ceruminous glands. The surface epithelium is uninvolved (**A**), with easily identified glandular and cystic profiles, separated by heavy fibrosis (**B**).

findings: ceruminous adenoma, ceruminous pleomorphic adenoma (chondroid syringoma), and ceruminous syringocystadenoma papilliferum. There is frequently a background of dense, sclerotic fibrosis that may simulate invasion. The tumors are moderately cellular, arranged in a mixture of glandular and cystic patterns each composed of a dual cell population ([Fig. 18.2](#)). The inner luminal secretory cells have apocrine decapitation secretions or blebs and abundant granular, eosinophilic cytoplasm. Specifically, there are yellow-brown, ceroid, lipofuscin-like (cerumen, wax; acid-fast fluorescent) pigment granules within the cytoplasm of these luminal cells ([Fig. 18.3](#)). These cells are surrounded by basal, myoepithelial cells lined up along the basement membrane ([Fig. 18.2](#)). There is usually very limited pleomorphism, occasional nucleoli, rare mitoses, and a lack of necrosis.

A *ceruminous pleomorphic adenoma* is identical to a salivary gland pleomorphic adenoma, thus showing chondromyxoid matrix material (not native cartilage) juxtaposed to, and blended with, epithelium, with the added feature of ceruminous differentiation among the epithelial and “duct-like” cells ([Fig. 18.4](#)). It is important to separate a primary EAC tumor from a parotid salivary gland tumor with local extension into the EAC. The *ceruminous papillary cystadenoma papilliferum* has papillary projections lined by cuboidal to columnar cells, a

dense plasmacytic infiltrate, and cells with ceruminous differentiation ([Fig. 18.4](#)).

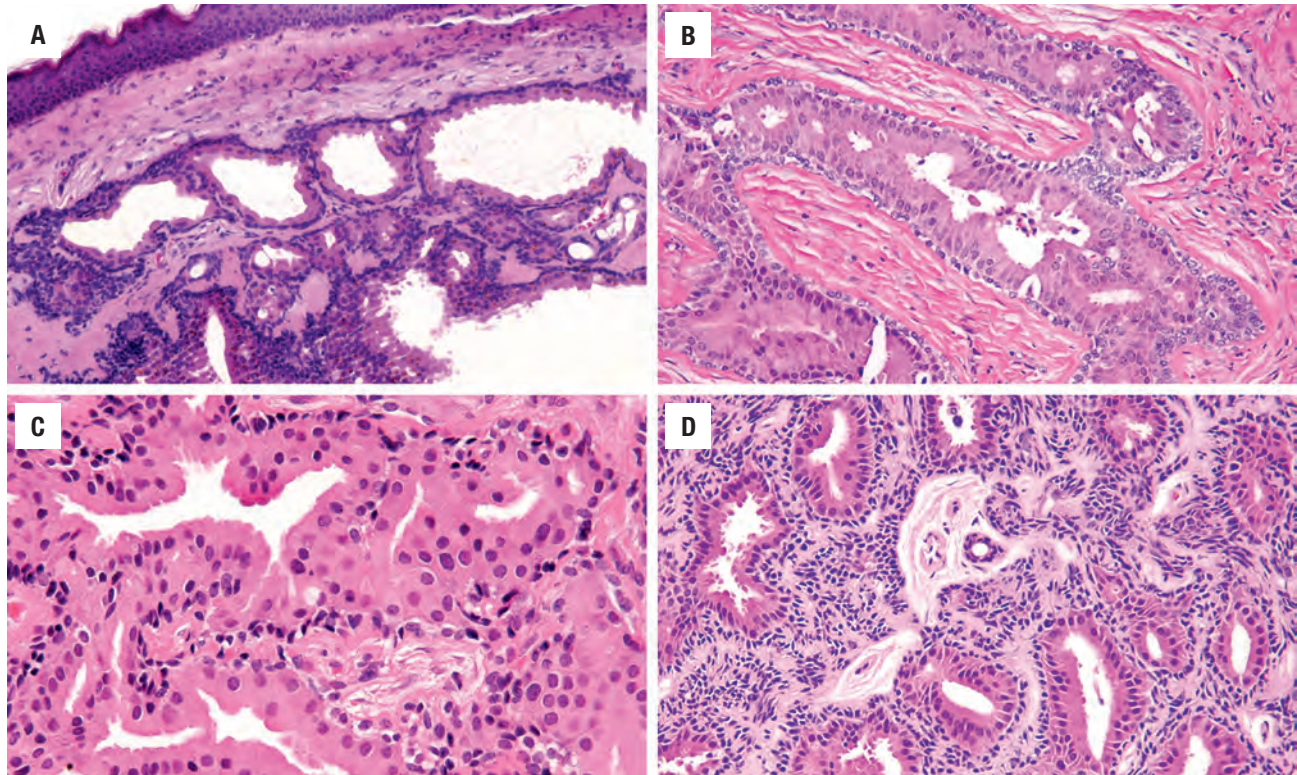
#### ANCILLARY STUDIES

Immunohistochemistry is not necessary for the diagnosis, but stains can be used to highlight the biphasic nature of the tumor cells. Both cell types stain for epithelial membrane antigen (EMA) and pancytokeratin; the luminal cells uniquely stain for CK7 and preferentially stain for CD117, whereas the basal-luminal cells will stain with CK5/6, p63, and S100 protein ([Fig. 18.5](#)). The cells lack a reaction with neuroendocrine markers and CK20.

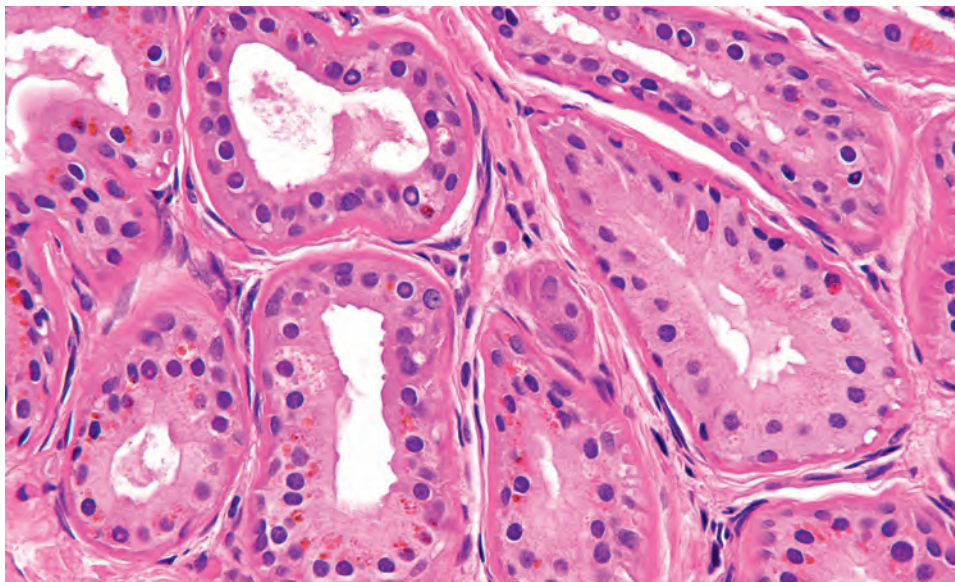
#### DIFFERENTIAL DIAGNOSIS

This tumor type is unique to the EAC, with infrequent confusion with other tumors. *Ceruminous adenocarcinoma* has an infiltrative and destructive growth pattern, greater cellularity, cribriform growth, and pronounced nuclear pleomorphism with prominent nucleoli. Mitoses and necrosis may be seen. Ceroid pigmentation, seen in the luminal cells of benign adenoma, is notably absent. A



**FIGURE 18.2**

A variety of different patterns and histologic appearances of a ceruminous adenoma. (A) Inner luminal secretory cells with cerumen granules subtended by basal myoepithelial cells demonstrate the dual cell population. (B) Abundant eosinophilic cytoplasm is seen in the luminal cells which show decapitation secretion. (C) Glandular profiles with a delicate basal layer. (D) The inner cells are surrounded by a proliferation of basal myoepithelial cells.

**FIGURE 18.3**

Yellow-brown "ceroid" lipofuscin-like material is seen in the cytoplasm of the ceruminous cells in a ceruminous adenoma.

*middle ear adenoma* may expand from the middle ear into the medial aspect of the EAC. This tumor also has a biphasic appearance, but the cells are plasmacytoid to cuboidal, have salt and pepper nuclear chromatin distribution, lack decapitation secretions, and have no ceroid granules in the cytoplasm. Furthermore, they are positive for neuroendocrine and peptide markers. A *paraganglioma*

shows a classic zellballen (nested) architecture, cells with basophilic, slightly granular cytoplasm, and isolated pleomorphism. The paraganglia cells are immunoreactive with chromogranin, synaptophysin, and/or CD56, consistent with their neuroendocrine origin, whereas the sustentacular (supporting) cells will stain with S100 protein.



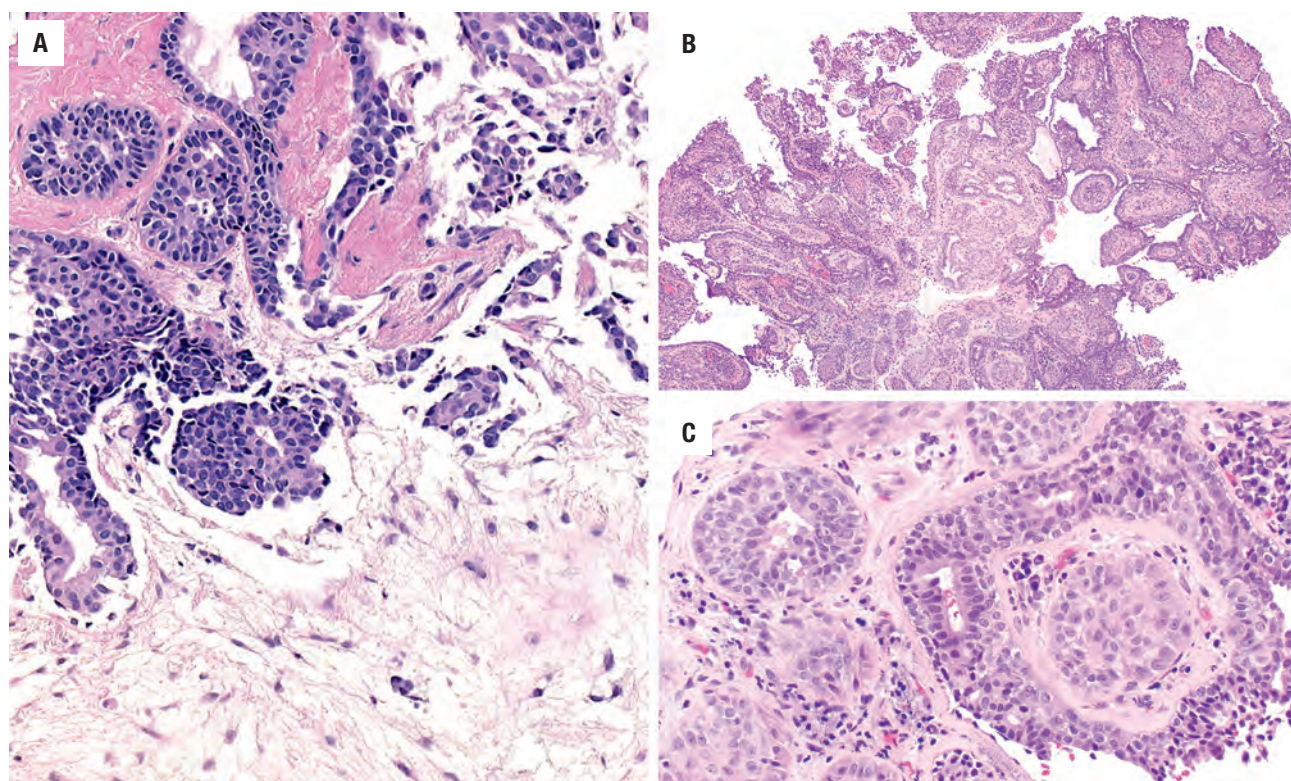


**FIGURE 18.4**

(A) Ceruminous pleomorphic adenoma, showing the characteristic chondromyxoid stroma with the epithelial elements. (B) Low-power showing the papillary architecture of a ceruminous syringo cystadenoma papilliferum, and C shows collections of plasma cells adjacent to bilayered epithelium.

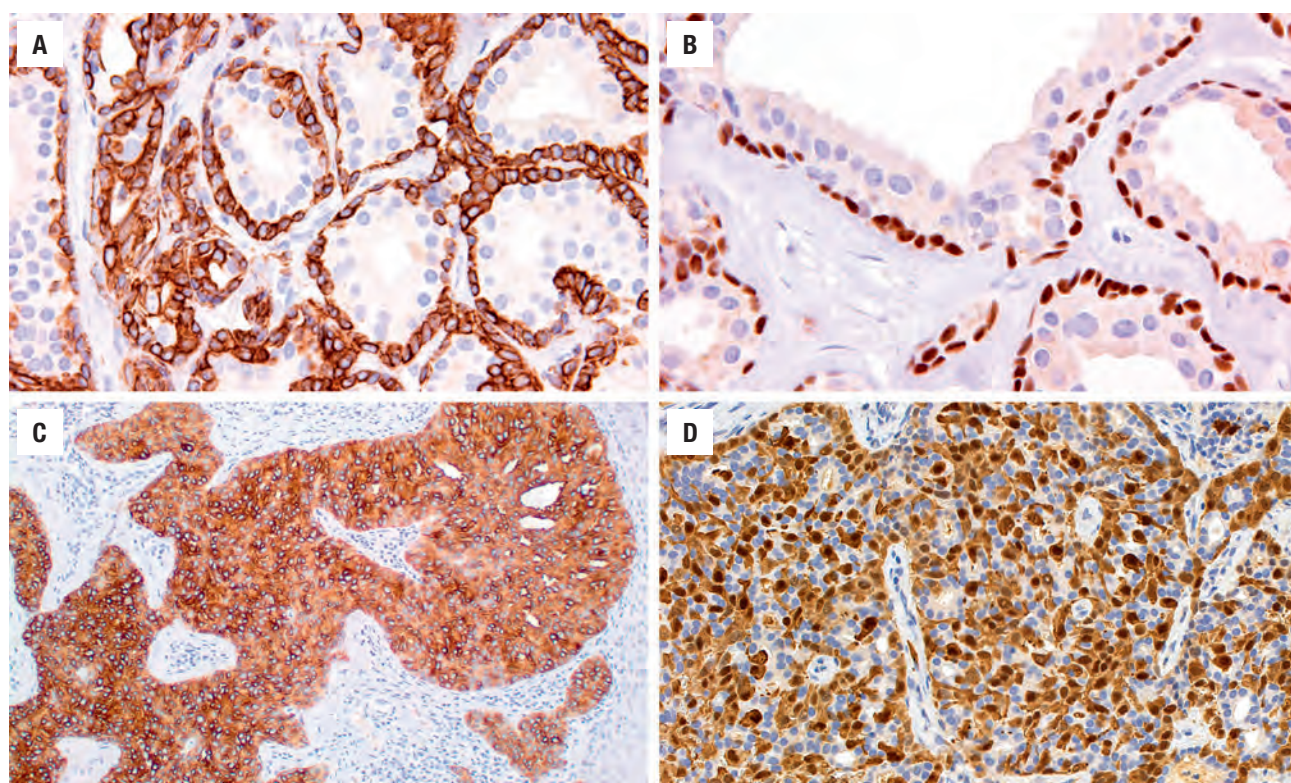


**FIGURE 18.5**

Differential immunohistochemical staining highlights the luminal cells from the basal, myoepithelial cells of a ceruminous adenoma: CK5/6 (A), p63 (B), CK7 (C), and S100 protein (D).



## PROGNOSIS AND THERAPY

Complete excision will be curative, although difficult to achieve due to the complex anatomy of the EAC. Therefore incomplete excision is not uncommon and is associated with an increased risk of recurrence.

## ■ LANGERHANS CELL HISTIOCYTOSIS

Langerhans cell histiocytosis (LCH) is a neoplastic clonal proliferation of Langerhans cells, a dendritic antigen-presenting cell type found most commonly in the epithelium of the skin and various mucosal sites. The Langerhans cells participate in specific immune reactions by capturing foreign antigens and presenting them to the T lymphocytes. LCH includes isolated lesions of Langerhans cell origin as well as multifocal and systemic disease. It was previously known as histiocytosis X, a general term that included eosinophilic granuloma, Hand-Schüller Christian-disease, and Letterer-Siwe disease. “Eosinophilic granuloma” referred to the disease in general, or to an individual lesion, usually of bone. Hand-Schüller-Christian disease referred to multifocal lytic bone lesions (usually of the skull) with exophthalmos and diabetes insipidus due to pituitary involvement. Letterer-Siwe disease is a severe systemic form of the disease seen in young children, with skin, mucosal, and solid organ involvement.

## CLINICAL FEATURES

LCH is rare (~5/1,000,000 population), more common in males, with a peak incidence in the 20s and 30s. Nearly 60% to 80% of cases develop in the head and neck, with ~25% part of multisystem disease. The bone, particularly the skull, is most frequently affected, whereas only ~4% of patients have ear/temporal bone involvement. Lesions of the middle ear and temporal bone may present with otorrhea, hearing loss, expansion of the temporal bone with a mass effect, pain, vertigo, otitis media, or skin ulceration. Bilateral temporal bone involvement is frequent.

## RADIOGRAPHIC FEATURES

LCH may demonstrate single or multiple lesions, usually readily detected by imaging studies as sharply circumscribed lytic lesions. Lesions of the skull characteristically have a “beveled” margin. If multiple lesions are present, the appearance may vary; some may have a poorly defined

## LANGERHANS CELL HISTIOCYTOSIS—DISEASE FACT SHEET

### Definition

- Neoplastic clonal proliferation of a unique histiocyte: the Langerhans cell; may be localized or systemic

### Incidence and Location

- Prevalence in children: 5/1,000,000 population annually
- Up to 80% show head and neck disease, although only 4% affect ear/temporal bone region

### Morbidity and Mortality

- Isolated bone lesions readily treated by curettage; multiple bone lesions may be difficult to control locally
- Systemic disease with solid organ and skin involvement have poor prognosis

### Sex and Age Distribution

- Slightly more common in males
- Peak in the 20s and 30s for localized, solitary lesion

### Clinical Features

- Lytic lesions of skull and jaws
- Otorrhea, hearing loss, and mass effect with pain and vertigo; otitis media and/or destructive temporal bone involvement if localized

### Prognosis and Treatment

- Dependent on extent of local involvement or systemic disease
- Localized bone lesions usually cured by surgical curettage
- Systemic disease has poor prognosis even with chemotherapy

sclerotic border, which may reflect regression of the LCH and replacement by reactive bone. LCH tends to involve cortical bone, whereas rhabdomyosarcoma tends not to involve bone.

## PATHOLOGIC FEATURES

### GROSS FINDINGS

Because the specimens are generally either biopsies or curettings, the gross appearance is not distinctive. The fragments may be hemorrhagic and red-brown or firm and yellow, depending on the age of the lesion.

### MICROSCOPIC FINDINGS

The characteristic feature of LCH is the Langerhans cell, with its irregular, convoluted nucleus. The nuclei are somewhat bean shaped, with grooves and indentations that give them a cerebriform appearance (Figs. 18.6 and 18.7). The chromatin pattern is fine and dispersed, with slight condensation along the nuclear membrane. Nucleoli are not prominent. Mitotic activity is variable but rarely

exceeds 5/10 high-power fields. The cytoplasm is scant to moderate in volume and may be pale or eosinophilic and may contain hemosiderin or lipid droplets. In addition to the Langerhans cells, the lesions contain an admixture of usual histiocytes, eosinophils, plasma cells, and neutrophils. The number of eosinophils is variable; they may

be scattered individually throughout the lesion or may form large sheets with central necrotic patches. Charcot-Leyden crystals are sometimes seen if eosinophils are numerous. Bone, if present, is usually seen as a reactive rim at the margin of the lesion. Regressing lesions are more fibrotic and may be more difficult to identify as LCH due to the paucity of the diagnostic cells.

#### LANGERHANS CELL HISTIOCYTOSIS—PATHOLOGIC FEATURES

##### Gross Findings

- Yellowish softened bone fragments in curettings

##### Microscopic Findings

- Prominent Langerhans cells, mononuclear, with enlarged nuclei with irregular, grooved, and convoluted contours; cytoplasm is pale to eosinophilic
- Multinucleated cells with irregular nuclei
- Eosinophils increased, often prominent (eosinophilic abscesses)

##### Ultrastructural Findings

- Langerhans cells have irregular, cerebriform nuclear contours
- Cell membranes have Birbeck granules: invaginated pentalaminar structures with fusiform distal expansion, giving “tennis racquet” appearance

##### Immunohistochemistry Findings

- Positive: S100 protein, CD1a, CD207 (Langerin), CD68

##### Molecular Findings

- *BRAF*<sup>V600E</sup> mutations are detected in ~50% of cases

##### Pathologic Differential Diagnosis

- Rosai-Dorfman disease, Hodgkin lymphoma, simple reactive histiocytosis, infectious granulomatous processes

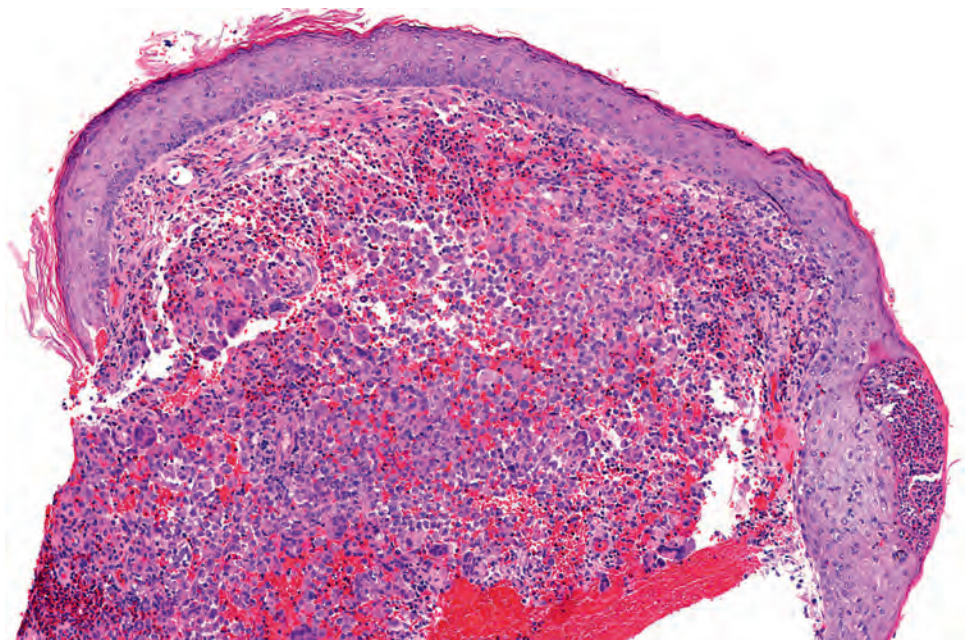
#### ANCILLARY STUDIES

##### ULTRASTRUCTURAL FINDINGS

Electron microscopy is rarely used in the diagnosis of LCH because the combination of histologic features and immunohistochemistry for S100 protein and CD1a is considered confirmatory. The identification of the Birbeck granule, an elongated pentalaminar structure with a “zipper-like” pattern of cross-striations, emanating from the cell membrane, is diagnostic. Some Birbeck granules have bulbous expansions which lend them a “tennis racquet” appearance.

##### IMMUNOHISTOCHEMISTRY

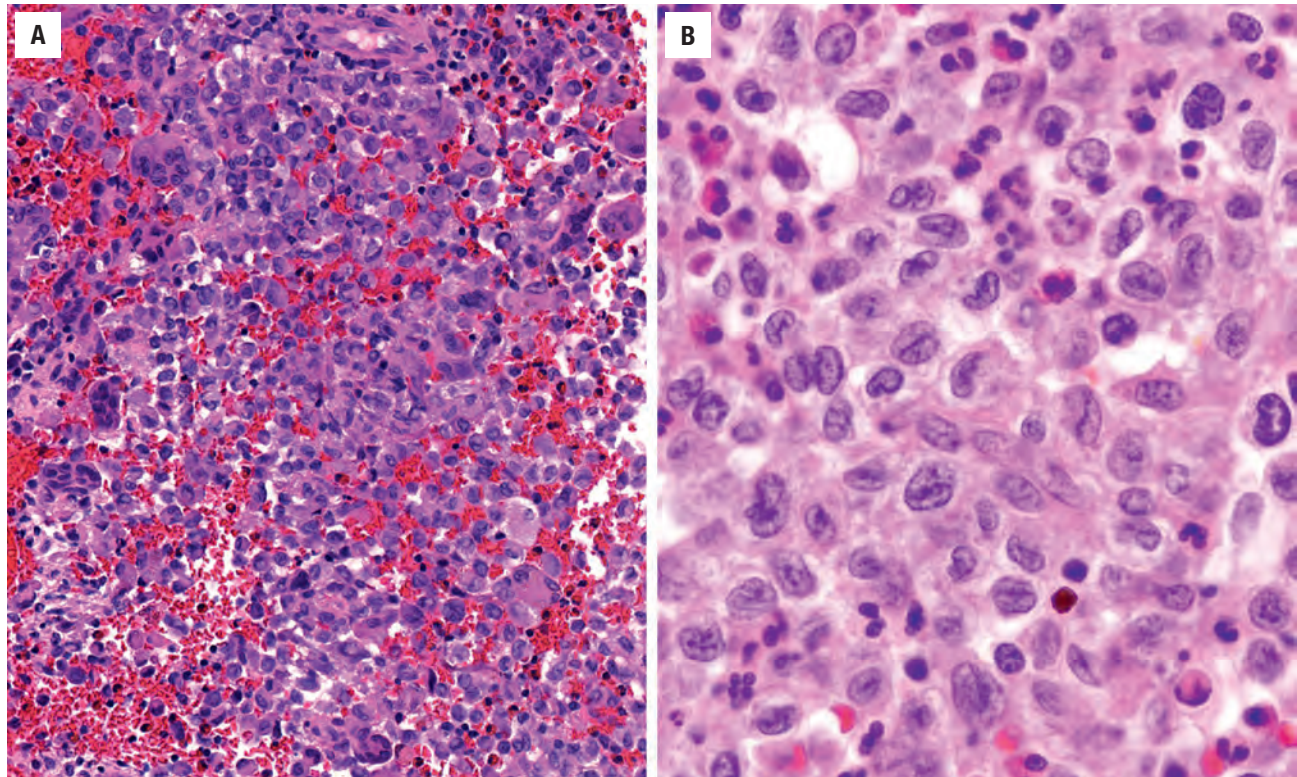
The Langerhans cells are identified by their positive immunoreactivity for S100 protein, CD1a (Figs. 18.8 and 18.9), and CD207 (Langerin). Reactivity for CD1a, a relatively specific finding, is helpful in excluding the many other entities that are S100 protein positive, such as melanocytic lesions, Rosai-Dorfman disease, and xanthogranulomas. CD68 is also positive in the lesional cells (Fig. 18.9). Langerin, a transmembrane protein which mediates the formation of Birbeck granules, is also sensitive and relatively specific for LCH.



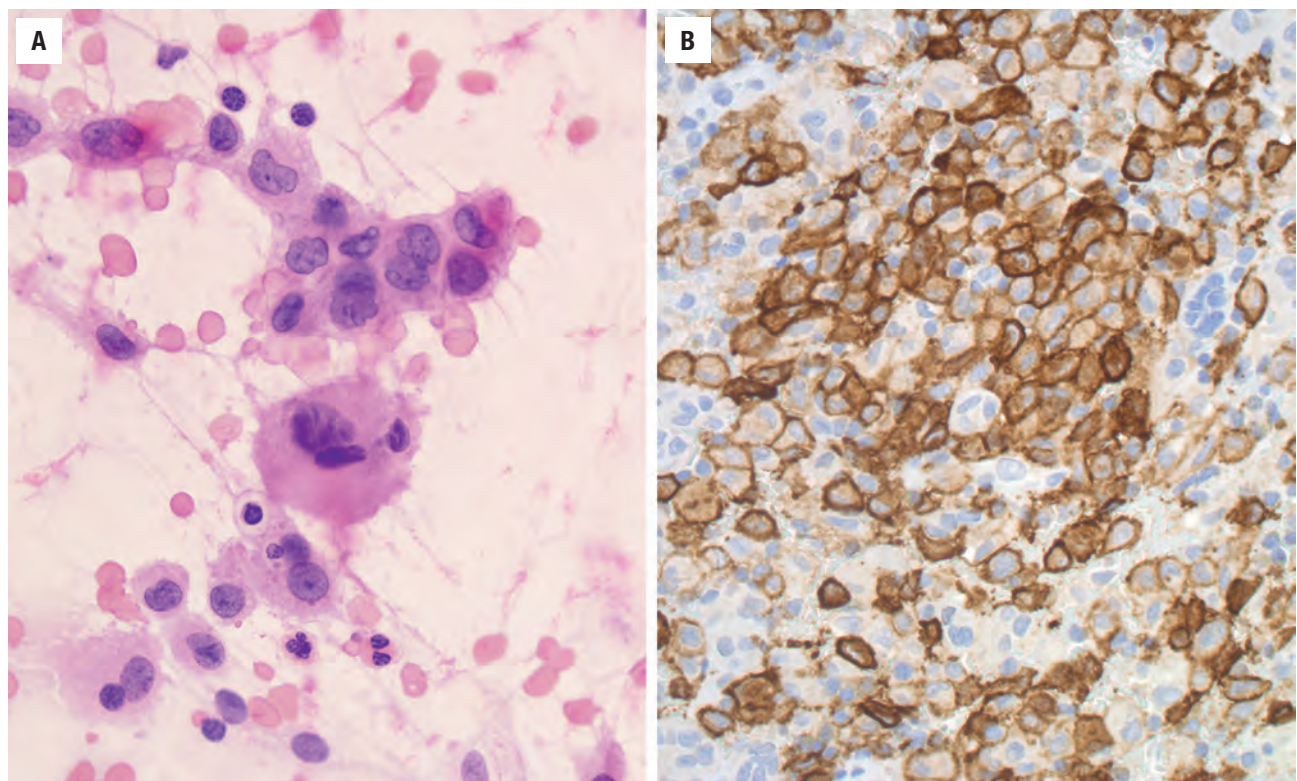
**FIGURE 18.6**

Surface epithelium is intact, overlying a rich inflammatory infiltrate with blood. Close inspection is required to correctly identify the lesional cells.



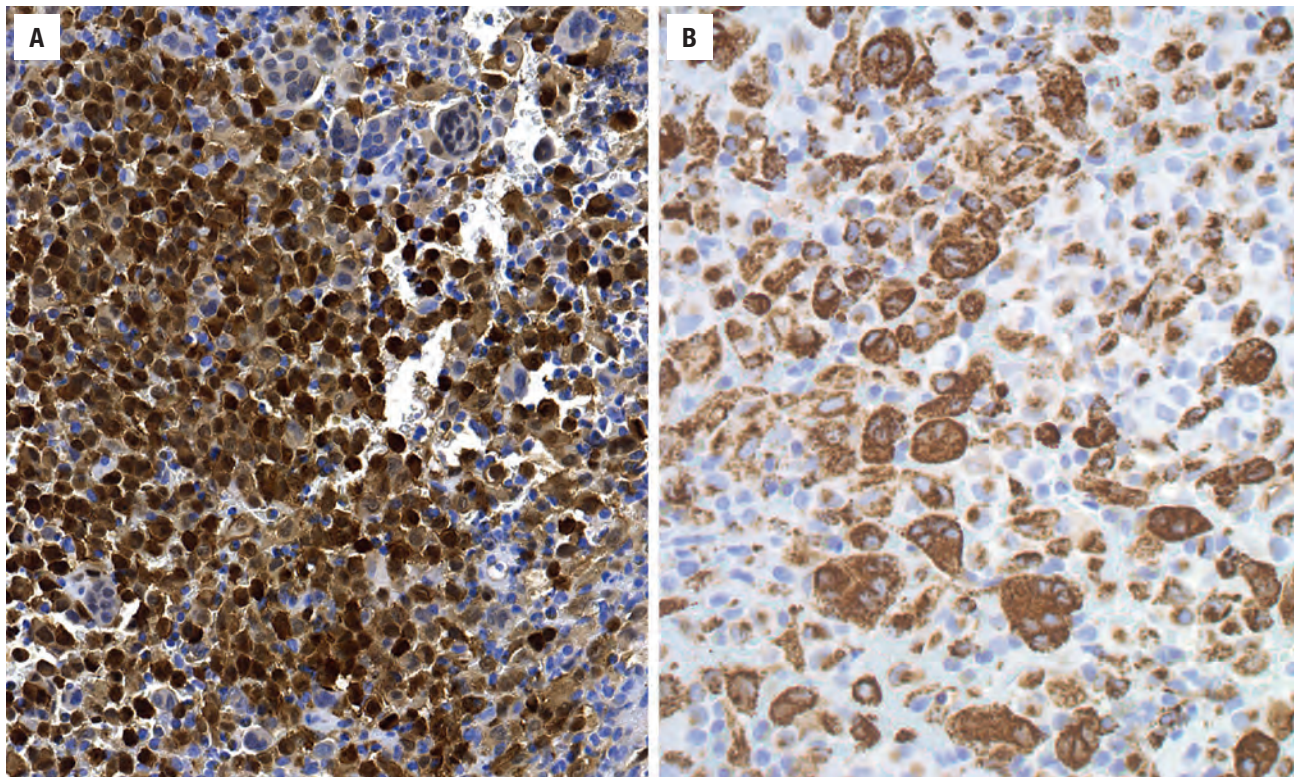
**FIGURE 18.7**

(A) Characteristic Langerhans cell with a number of giant cells and eosinophils in the background. The Langerhans cells are admixed with a variable infiltrate of lymphocytes, plasma cells, and eosinophils. (B) Nuclei are convoluted, folded, or grooved, yielding a coffee bean shape. In some cases, such as this one, the eosinophils are conspicuous, but in other cases their presence is subtle.

**FIGURE 18.8**

(A) Fine needle aspirate (H&E smear) demonstrates the distinctive nucleus of the Langerhans histiocyte with a very irregular, grooved contour, lending it a cerebriform appearance. (B) The lesional cells show a strong and diffuse cytoplasmic reaction with CD1a.



**FIGURE 18.9**

(A) Strong and diffuse nuclear and cytoplasmic S100 protein reaction in the Langerhans cells, whereas the giant cells are negative. (B) Strong and diffuse CD68 reaction in the cytoplasm of the lesional cells and in the giant cells.

### MOLECULAR FINDINGS

Immunoglobulin heavy chain and/or T-cell receptor gamma gene clonal rearrangements may be detected in up to 30 % of cases, whereas *BRAF*<sup>V600E</sup> mutations are detected in ~50 % of cases.

### DIFFERENTIAL DIAGNOSIS

Differential diagnostic considerations based on clinical presentation include *infectious granulomatous processes*, *osteomyelitis*, *Rosai-Dorfman disease*, and *Hodgkin lymphoma*. However, the suggestive radiographic appearance of punched-out lytic lesions of the craniofacial skeleton and identification of the Langerhans cell component by immunohistochemistry readily excludes these other lesions from further consideration.

### PROGNOSIS AND THERAPY

As noted previously, some lesions spontaneously regress or “heal.” Most isolated lesions of the skull are amenable to curettage or intralesional steroid injection. Such lesions

have a very good prognosis. Low-dose radiation therapy is also useful, particularly in lesions not readily accessible surgically, whereas chemotherapy is also frequently used for multisystem disease. Extensive disease in younger patients portends a less favorable prognosis, particularly in the setting of visceral involvement. Long-term organ damage (hearing loss) may develop. Long-term follow-up is required due to high relapse, especially in multisystem disease.

### ■ PERIPHERAL NERVE SHEATH TUMOR (SCHWANNOMA)

Schwannoma (acoustic neuroma or neurilemmoma) is a benign peripheral nerve sheath tumor (PNST) arising within the internal auditory canal (IAC) or intralabyrinthine, and is the most common neoplasm of the temporal bone. The tumor arises from the myelin-forming Schwann cells, usually from the vestibular portion of the vestibulocochlear (eighth) cranial nerve, and accounts for 80 % to 90 % of all cerebropontine angle (CPA) tumors. Approximately 95 % of tumors are unilateral and sporadic, but if bilateral or presenting in a young patient, association with neurofibromatosis type 2 (NF2) is high.



**PERIPHERAL NERVE SHEATH TUMOR—DISEASE FACT SHEET****Definition**

- Benign Schwann cell–derived neoplasm arising within the internal auditory canal or intralabyrinthine

**Incidence and Location**

- Most common cerebellopontine angle tumor (80%–90%)
- 95% unilateral and sporadic
- If bilateral or young age, neurofibromatosis type 2 (NF2) association is high

**Morbidity and Mortality**

- Loss of hearing, especially in NF2 associated tumors
- No mortality

**Sex and Age Distribution**

- Equal sex distribution
- 5th to 6th decade; younger for NF2 patients

**Clinical Features**

- Progressive sensorineural hearing loss
- Tinnitus (high-pitched, steam kettle-type hissing)
- Extended (~20 years) occupational exposure to extremely loud noise

**Radiographic Features**

- Cerebropontine angle mass with funnel-shaped widening of the internal auditory canal
- Magnetic resonance imaging (MRI): hyperintense mass on T2-weighted images

**Prognosis and Treatment**

- Excellent prognosis, with recurrences in up to 15%
- Surgery or serial MRI scans to follow slow growing lesions

**CLINICAL FEATURES**

Patients usually present in the 5th to 6th decades of life but tend to be younger (< 21 years) when NF2 associated. Progressive, unilateral sensorineural (not *conductive*) hearing loss and tinnitus (steam kettle–type hissing) occur in > 90% of patients, occasionally accompanied by headache, vertigo, altered balance and gait, facial pain, facial weakness, and changes in taste (the latter three symptoms due to brainstem compression by the tumor). Although the etiology is unknown, extended (~20 years) occupational exposure to extremely loud noise, may be a risk factor in tumor development.

**RADIOGRAPHIC FEATURES**

The best radiographic diagnostic clue is a CPA mass, with a funnel-shaped widening of the IAC or small

**PERIPHERAL NERVE SHEATH TUMOR—PATHOLOGIC FEATURES****Gross Findings**

- Attached to the vestibular or cochlear division of cranial nerve VIII
- Globular to mushroom shaped, usually < 2 cm, rubbery yellow mass, myxoid, and cystic

**Microscopic Findings**

- Cellular Antoni A areas with closely backed bundles of spindled cells and Verocay bodies
- Hypocellular Antoni B areas with microcystic degeneration
- Fusiform cells with fibrillar cytoplasm
- Spindled, wavy/buckled, pointy nuclei (often palisaded)
- Medium-sized dilated vessels with hyalinization

**Immunohistochemical Findings**

- Diffuse, strong S100 protein, SOX10, and vimentin reactions
- Glial fibrillary acidic protein and neuron-specific enolase occasionally positive
- CD34 fibroblasts within degenerated areas

**Genetic Studies**

- 90% of mutations in neurofibromatosis type 2 coded by *merlin* at 22q12

**Pathologic Differential Diagnosis**

- Meningioma, neurofibroma, solitary fibrous tumor, paraganglioma, malignant peripheral nerve sheath tumor

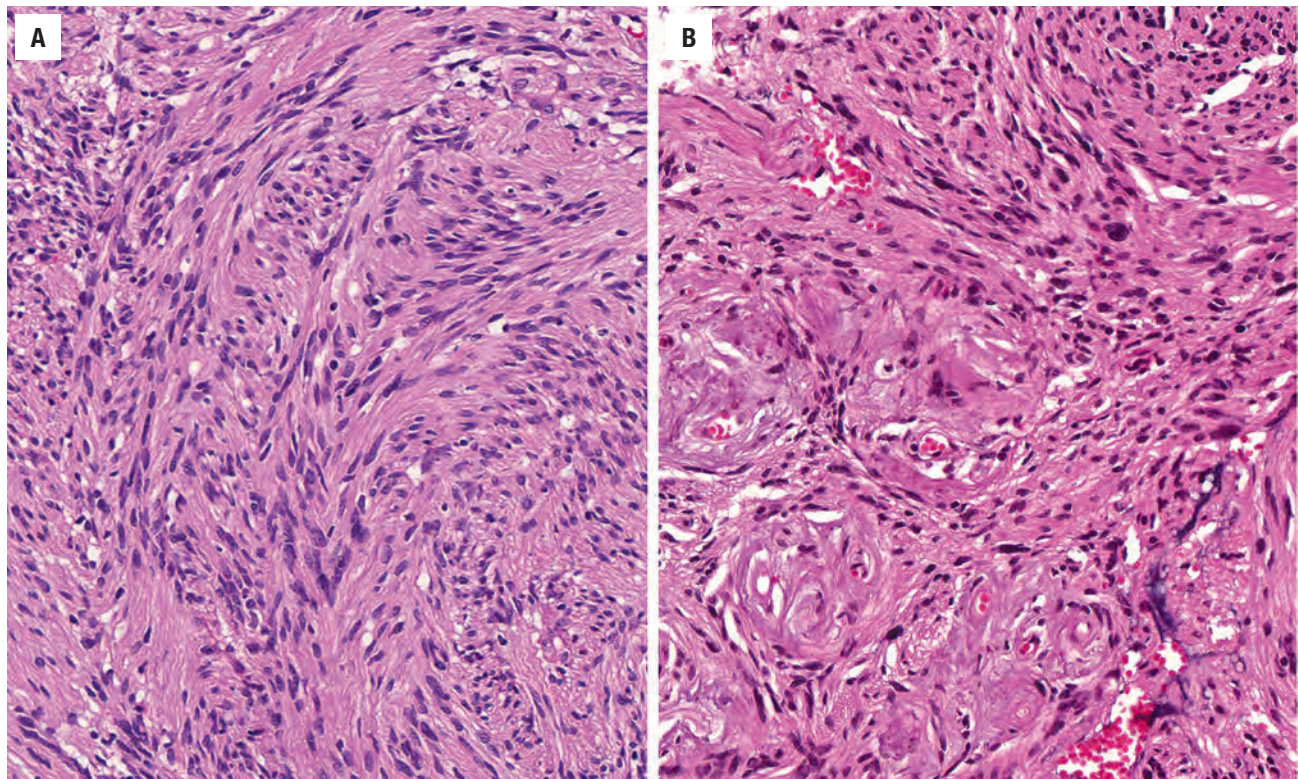
indentation of bone. Magnetic resonance imaging (MRI) shows a hyperintense mass on T2-weighted images (with gadolinium contrast) with intense enhancement into the porus acusticus. Tumors are radiographically staged based on size, extent, and exact tumor location.

**PATHOLOGIC FEATURES****GROSS FINDINGS**

The tumors are usually small (< 2 cm), globular to mushroom-shaped masses frequently eccentrically attached to the vestibular division of the eighth (vestibulocochlear) cranial nerve (CN), growing centrally along the CPA (“mushroom”) and peripherally along the IAC (“stalk”). When the cochlear division is involved, the nerve is stretched rather than attached. Cross-sections are smooth, gray-tan to yellow, rubbery to firm, and solid to myxoid and cystic. Intratumoral hemorrhage is common.

**MICROSCOPIC FINDINGS**

Histologically, the tumor cells are arranged in cellular (Antoni A) closely packed bundles of spindle cells

**FIGURE 18.10**

(A) Hypercellular Antoni A area with fascicular arrangement of cells with fibrillar cytoplasm. (B) Small vessels showing perivascular hyalinization.

(Fig. 18.10) adjacent to microcystic or loosely reticular (Antoni B) areas (Fig. 18.11). When these spindled cells have their nuclei lined up in a palisaded architecture, they are called Verocay bodies. The spindled or fusiform cells have fibrillar cytoplasm surrounding buckled to wavy, elongated, and pointy nuclei. Small- to medium-sized vessels are characteristically ectatic with distinctive perivascular hyalinization (Fig. 18.10). Mitoses are uncommon, and necrosis is usually absent. However, extensive degenerative changes (“ancient schwannoma”) can occur (including xanthoma-type histiocytes) and may result in only a thin rim of recognizable tumor. Calcification is rare. Extensive pleomorphism, necrosis, and mitoses suggest malignancy.

of slender cells in the loose, Antoni B areas. Neurofilament is absent. Interestingly, the proliferation index (using Ki-67 antibody) is higher in schwannomas of NF2 patients than in sporadic, solitary lesions.

#### GENETIC STUDIES

NF2 (distinct from NF1 or von Recklinghausen disease) is an autosomal dominant disease, with more than 200 identified mutations involving *NF2*, a tumor suppressor gene at 22q12 that encodes the protein *merlin* or *schwannomin*. Approximately 90% of mutations result in a truncated protein that cannot carry out its normal tumor suppressor function.

#### ANCILLARY STUDIES

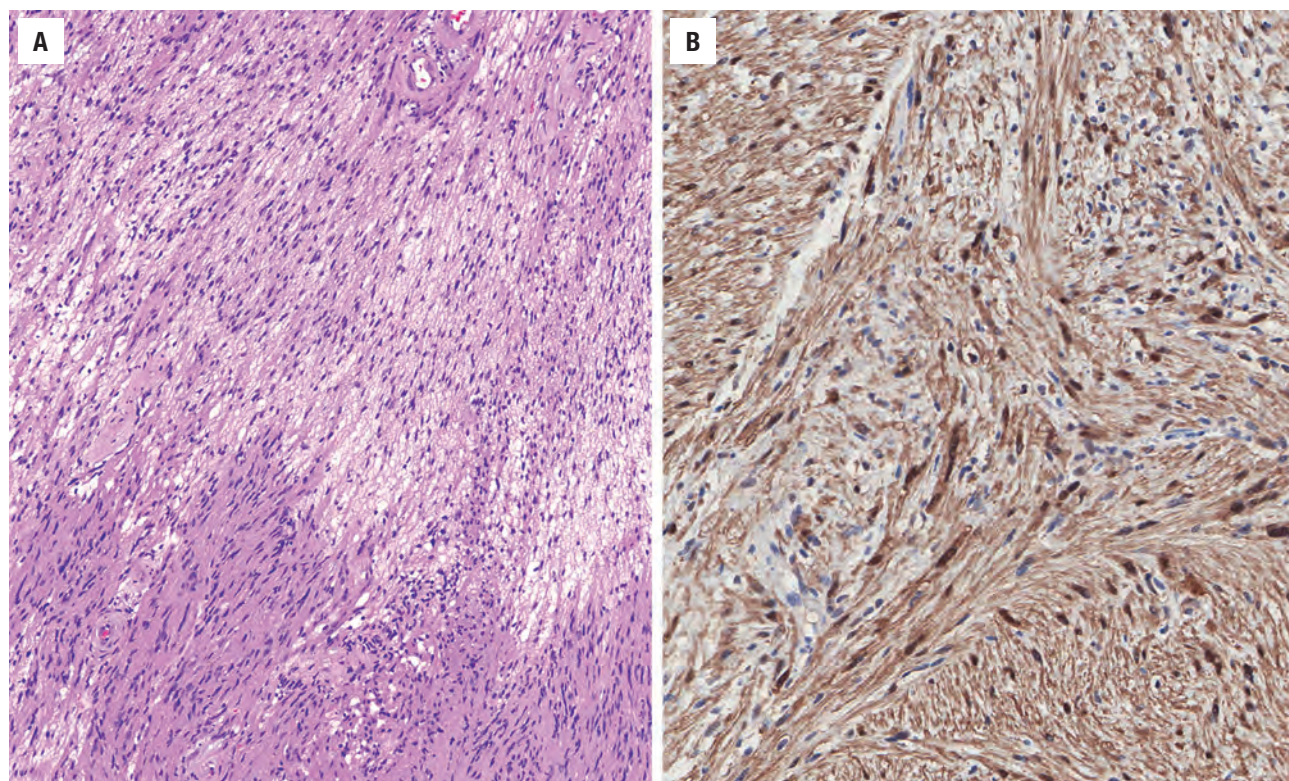
##### IMMUNOHISTOCHEMICAL FINDINGS

The neoplastic cells of schwannoma show a strong and diffuse nuclear and cytoplasmic immunoreactivity for S100 protein (Fig. 18.11) and nuclear SOX10, along with vimentin (the latter is nonspecific). Glial fibrillary acidic protein (GFAP) and neuron-specific enolase (NSE) may occasionally be positive. CD34 stains a subpopulation

#### DIFFERENTIAL DIAGNOSIS

The uniqueness of this anatomic site (CPA) raises a limited differential that includes only meningioma, neurofibroma, solitary fibrous tumor, paraganglioma, and malignant PNST (MPNST). Meningioma is characterized by a whorled epithelioid proliferation with psammoma bodies, intranuclear cytoplasmic inclusions, and EMA immunoreactivity. Neurofibromas are exceptionally rare in the ear and temporal bone and lack the classic



**FIGURE 18.11**

(A) Hypocellular areas show a myxoid degeneration between the spindle cells. (B) S100 protein reaction in the nucleus and cytoplasm of the lesional cells.

alternating Antoni A and B areas, Verocay bodies, and perivascular hyalinization. Solitary fibrous tumor is more collagenized, lacking a palisade of nuclei, and showing strong CD34, STAT6, and bcl-2 reactivity. Paraganglioma is arranged in nests, showing focal pleomorphism, and generally positive with neuroendocrine markers, whereas S100 protein highlights the sustentacular cells.

### PROGNOSIS AND THERAPY

Schwannoma is a benign tumor with a very low recurrence potential. Surgical removal by any one of various approaches (translabyrinthine, suboccipital, middle cranial fossa, or by stereotactic gamma knife surgery) is standard therapy, with the goal of preserving hearing and vestibular function. It is more difficult to preserve hearing and facial nerve function in schwannomas of NF2 patients because they tend to infiltrate the nerves to a greater extent and also grow more rapidly. However, in small tumors (generally < 18 mm) or elderly patients (> 70 years), management can include watchful waiting using serial MRI scans to monitor growth (up to 4 mm per year). Radiotherapy can be used but may fail in up to 15% of patients.

### ■ PARAGANGLIOMA

Paraganglioma is a neuroendocrine neoplasm arising from paraganglia (chemoreceptors derived from neural crest responding to changes in blood oxygen and carbon dioxide levels) situated in the vicinity of the jugular bulb (glomus jugulare) or the medial cochlea promontory of the middle ear (glomus tympanicum), together representing nearly 80% of all head and neck paragangliomas. Paraganglioma is the preferred term for this most common neoplasm of the middle ear, but chemodectoma and glomus tumor are frequently used clinically. It is important to note that “glomus” used here is not synonymous with *glomus tumor*, which is a specific pericytic smooth muscle vascular tumor. The tumors arise from the adventitia of the jugular bulb or paraganglion associated with Jacobson nerve.

### CLINICAL FEATURES

Familial and solitary paragangliomas are recognized. Sporadic tumors show a strong female predilection (female to male ratio, 5:1), whereas inherited or familial tumors are more common in males. There is a wide age range at initial presentation, with a mean in the 6th decade,

## PARAGANGLIOMA—DISEASE FACT SHEET

### Definition

- A benign neoplasm arising from the paraganglia (chemoreceptors) of the jugular bulb or medial cochlea promontory of the middle ear

### Incidence and Location

- Uncommon (represent 80% of all head and neck paragangliomas)
- Jugular bulb, middle ear
- Rule of 10%: (multifocal, bilateral, familial, pediatric, and malignant) is probably outdated due to higher familial association

### Morbidity and Mortality

- Approximately 15% mortality

### Sex and Age Distribution

- 90% are solitary tumors, more common in women
- 10% are familial tumors, more common in men
- Wide age range; mean in 6th decade

### Clinical Features

- Pulsatile tinnitus (90%) and conductive hearing loss (50%)

### Radiographic Features

- Angiography shows blood supply and feeder vessels
- Computed tomography: well-defined hypervascular, heterogeneous mass with bony changes
- Magnetic resonance imaging: serpentine signal voids on T1 and hyperintense areas on T2
- Octreotide or <sup>131</sup>I-meta-iodobenzylguanidine scintigraphy may find clinically occult tumors

### Prognosis and Treatment

- Slow growing but invasive, with 15% mortality rate
- Watchful waiting, embolization, surgery, and radiation therapy

although there are bimodal peaks (30s and 60s). The previous “rule of 10”: 10 % multicentric, 10 % bilateral, 10 % pediatric, 10 % malignant, and 10 % familial, is perhaps outdated because nearly 30 % are thought to have a syndrome or familial association. Patients report pulsatile tinnitus (~90 % of patients), hearing loss (~50 % of patients; conductive rather than sensorineural), otalgia and/or facial nerve paralysis, whereas examination reveals a vascular retrotympenic mass. Biopsy is contraindicated because it can result in profound bleeding. Rarely, catecholamine hypersecretion may be found.

## RADIOGRAPHIC FEATURES

Radiographs will accurately define the location, size, and extent of the tumor. Angiography highlights feeder vessels and blood supply while also permitting presurgical embolization. MR and computed tomography (CT) show

## PARAGANGLIOMA—PATHOLOGIC FEATURES

### Gross Findings

- Fragmented, irregular, reddish firm up to 6-cm mass with hemorrhage

### Microscopic Findings

- Poorly encapsulated, infiltrative tumors
- Cellular tumors with clusters, alveolar or *zellballen* architecture
- Small, uniform cells with granular basophilic cytoplasm
- Richly vascularized stroma

### Immunohistochemical Findings

- Paraganglia: chromogranin, synaptophysin, CD56, neuron-specific enolase positive
- Sustentacular cells: S100 protein and glial fibrillary acidic protein positive

### Genetic Studies

- Inactivating mutations in subunits of the succinate-ubiquinone oxidoreductase gene (*SDH*): *PGL1* (11q23), *PGL2* (11q13.1), *PGL3* (1q21-q23)

### Pathologic Differential Diagnosis

- Schwannoma, meningioma, middle ear adenoma

complimentary features with the former showing an enhancing, vascular mass, and the latter highlighting bony changes, including expansion and erosion of the jugular foramen or ossicular chain (Fig. 18.12). More recently, nuclear imaging, including a positron emission tomography (PET) scan with F18-FDG and octreotide and/or <sup>131</sup>I-meta-iodobenzylguanidine (MIBG) scintigraphy helps to confirm the “neuroendocrine” nature of the neoplasm, as well as identify occult or familial tumors.

## PATHOLOGIC FEATURES

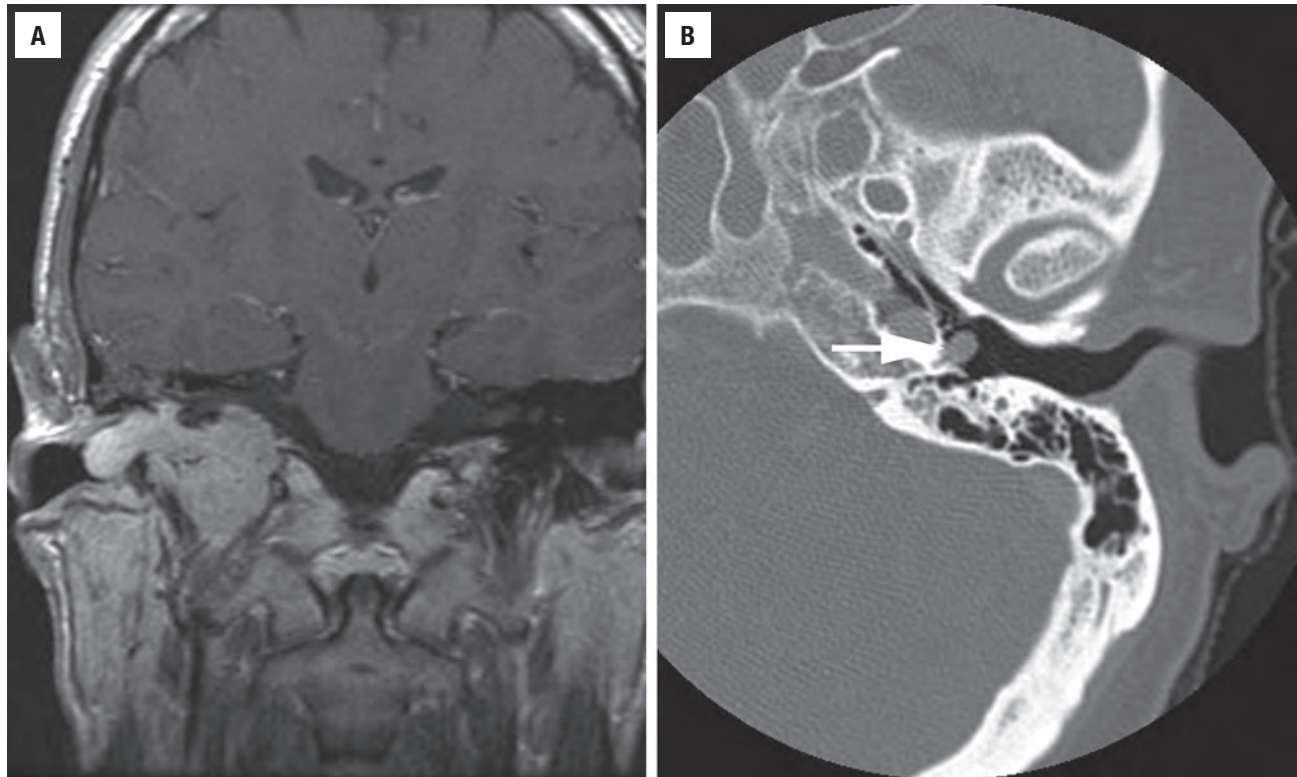
### GROSS FINDINGS

The tumors are irregular, firm, reddish masses, ranging from 0.3 cm up to 6 cm, and are usually fragmented upon removal. The cut surface is often variegated with cystic degeneration and hemorrhage. The tympanic membrane is usually intact. The appearance is modified by preoperative embolization or other treatments.

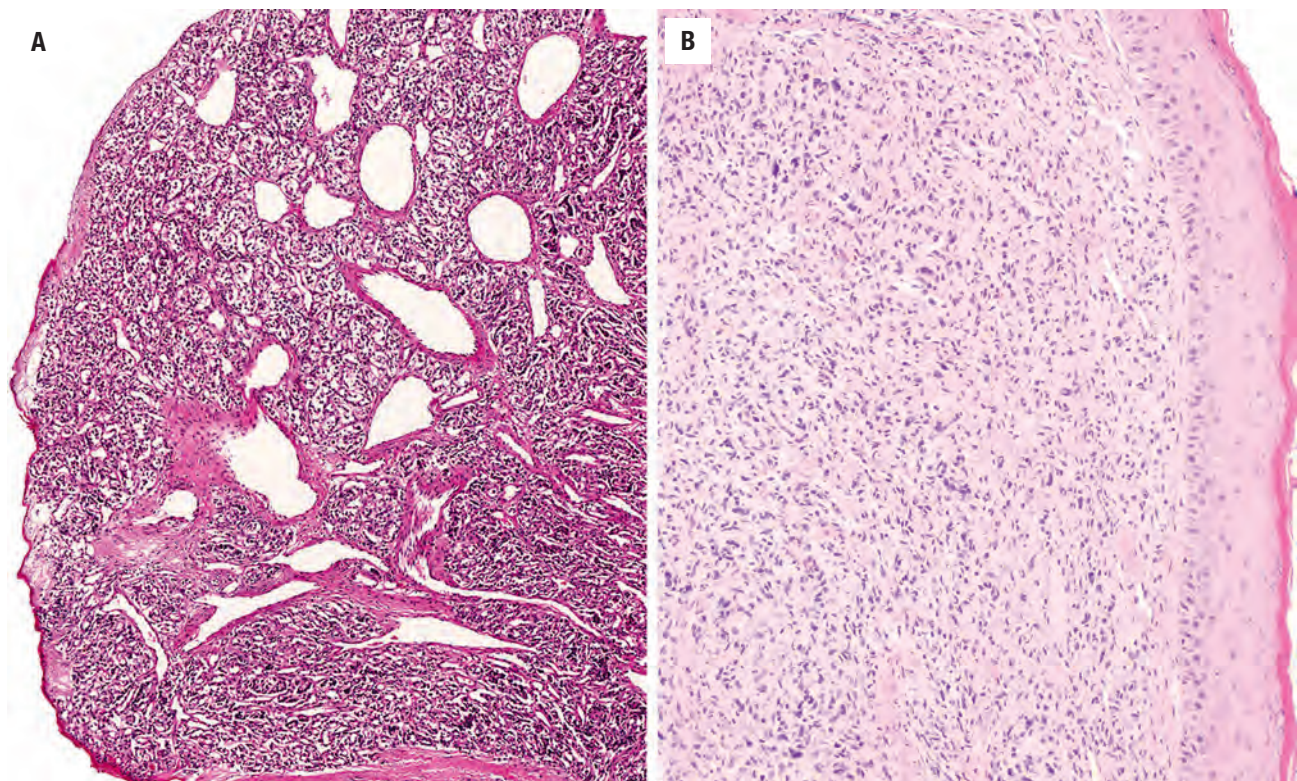
### MICROSCOPIC FINDINGS

Histologically, these tumors are usually infiltrative (usually into bone), lacking encapsulation or circumscription and are arranged in a characteristic clustered or *zellballen* architecture (Figs. 18.13 and 18.14). The balls or nests of paraganglia are surrounded by a layer of supporting or sustentacular cells (not readily appreciable



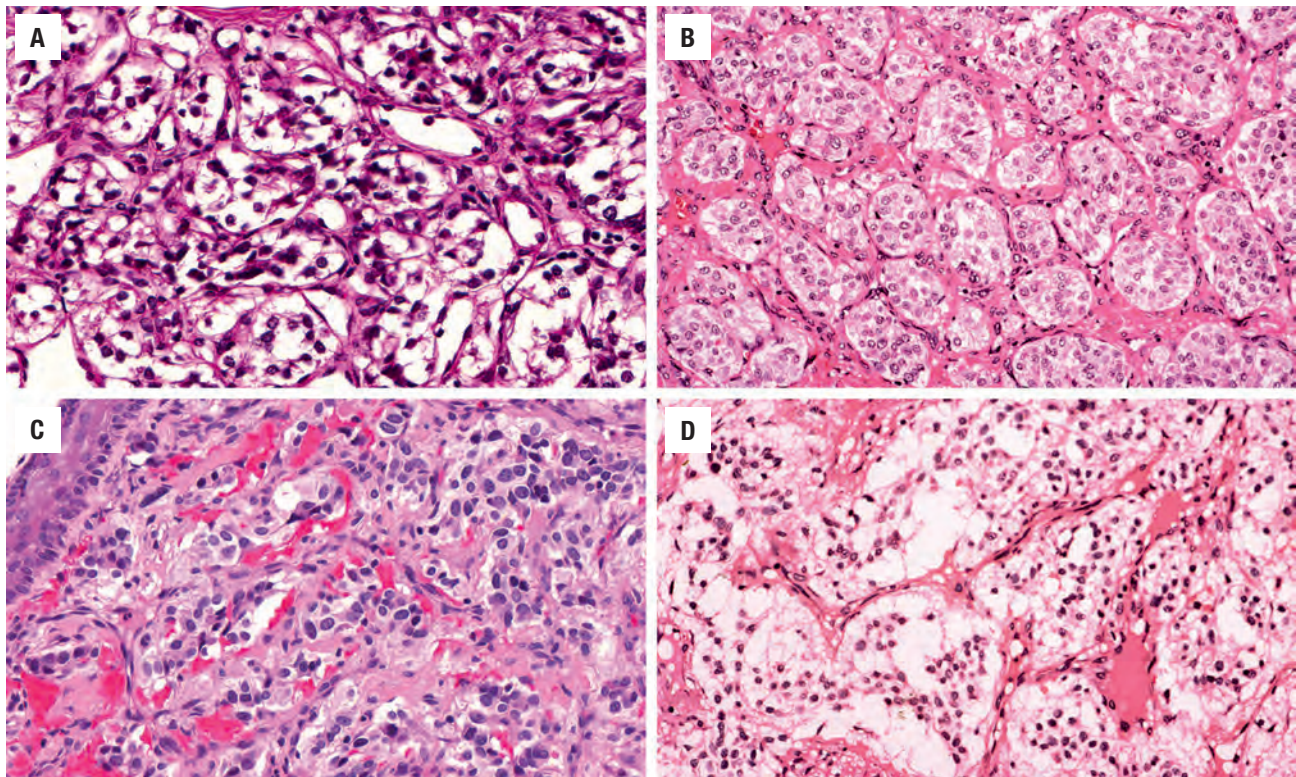
**FIGURE 18.12**

Imaging studies help to define the extent of paraganglioma. **(A)** This coronal magnetic resonance imaging T1-weighted postcontrast image demonstrates an enhancing large right jugular paraganglioma. **(B)** A computed tomography image shows a 3-mm left-sided tumor next to the promontory behind the tympanic membrane.

**FIGURE 18.13**

**(A)** Polypoid tumor with a rich vascularity and a nested, alveolar (*zellballen*) pattern. **(B)** Intact squamous epithelium with a vaguely nested tumor in the stroma.



**FIGURE 18.14**

A variety of different patterns and size of Zellballen can be seen, along with variability in cytoplasmic quality (**A**, cleared; **B**, granular; **C**, basophilic; **D**, fibrillar).

by H&E alone) and invested by a richly vascularized stroma (Fig. 18.14). In isolated cases, intravascular invasion may be seen. Tumors are moderately cellular, composed of small to intermediate cells containing ample granular to basophilic cytoplasm (Fig. 18.14). The nuclei are rather monotonous, although isolated marked pleomorphism may be seen. Nuclear chromatin is usually delicate to coarse. Mitoses are uncommon to rare. Multinucleated cells are occasionally present. Degenerative changes, especially after embolization, will result in cyst formation and hemorrhage, with hemosiderin-laden macrophages and fibrosis.

## ANCILLARY STUDIES

### IMMUNOHISTOCHEMICAL FINDINGS

The paraganglia cells will be immunoreactive with chromogranin, synaptophysin (Fig. 18.15), NSE, and/or CD56 (membrane staining), confirming the neuroendocrine differentiation of the cells. The supporting sustentacular framework cells will react with S100 protein or with GFAP. There is no pancytokeratin, p63, CEA, or human pancreatic polypeptide (HPP) immunoreactivity. Loss of immunoreactivity for succinate dehydrogenase B (SDHB) protein is significantly correlated with germline mutation within the SDH complex of genes and may help to guide genetic screening.

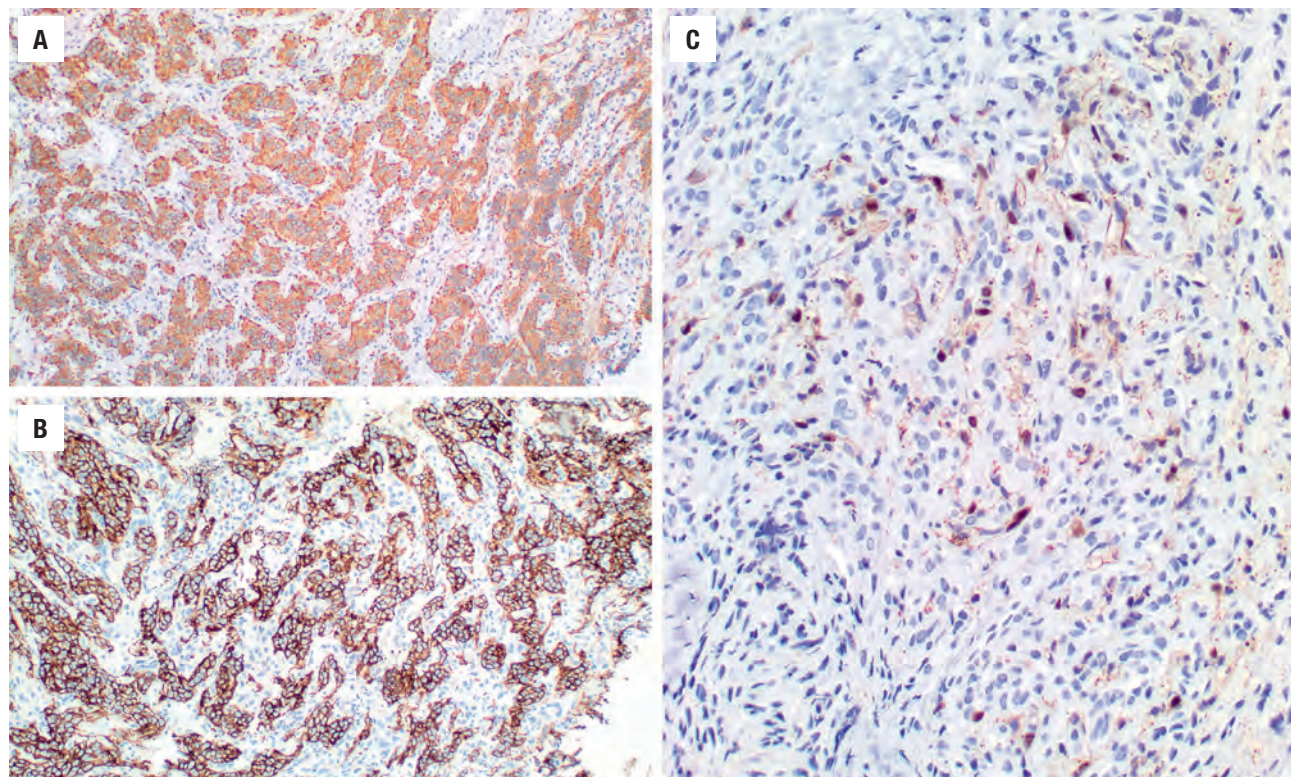
### GENETIC STUDIES

Up to 30 % of head and neck paragangliomas are familial and inherited as an autosomal dominant trait with genomic imprinting. The most common genetic loci associated with paragangliomas are within several genes encoding various subunits of the succinate dehydrogenase gene (*SDH*): paraganglioma 1 (*PGL1*) at 11q23, *PGL2* at 11q13.1, and *PGL3* at 1q21–q23, which are inactivating mutations in *SDHB*, *SDHC*, and *SDHD*, respectively. Hereditary syndromes such as neurofibromatosis and pheochromocytoma-paraganglioma syndrome may be seen.

### DIFFERENTIAL DIAGNOSIS

The differential is limited when considering anatomic site alone because nearly 90 % of masses in the jugular foramen are paraganglioma, with schwannoma, meningioma, and middle ear adenoma accounting for the remaining lesions. Nonetheless, the small size of biopsies from the middle ear is the principal reason for diagnostic difficulties. For example, a minute specimen may cause confusion with middle ear adenoma, but keratin immunoreactivity should make the distinction obvious. Moreover, necrosis due to embolization may suggest an underlying malignancy. However, the presence of embolic material



**FIGURE 18.15**

Paraganglia cells are strongly and diffusely immunoreactive with synaptophysin (**A**) and CD56 (**B**), whereas the supporting, sustentacular cells are highlighted by S100 protein (**C**).

in certain cases will assist in confirming the correct diagnosis.

### PROGNOSIS AND THERAPY

Jugulotympanic paragangliomas are slow growing but can be locally invasive. Due to the vital structures in the region, mortality rates of 15 % can be expected even though it is a benign neoplasm in 90 % of cases. Watchful waiting can be used, although surgery is the standard therapy, with or without presurgical embolization. Radiation therapy plays a role in poor surgical candidates. Distant metastases are very rare. Lack of immunostaining for SDHB is associated with an increased risk of metastasis.

## MENINGIOMA

Meningioma is a common, benign neoplasm of meningotheelial cells within the ear and temporal bone. This tumor arises from the arachnoid cells (arachnoid granulations, pacchionian bodies), which normally line the inner aspect of the arachnoid membrane, and fill the cores of the arachnoid villi that project into the lumens of dural veins and venous sinuses. Extranaxial (extracranial, ectopic,

extracalvarial) meningiomas are usually divided into four groups based on suggested etiologies: (1) direct extension of a primary intracranial meningioma through pressure necrosis/absorption of the bone, or through an iatrogenic or natural opening; (2) extracranial metastasis from an intracranial meningioma; (3) extracranial meningioma originating from pia-arachnoid cell clusters in the sheaths of the cranial nerves (or vessels) as they exit through the foramina or suture lines of the skull; (4) extracranial meningioma without any apparent demonstrable connection with foramina, cranial nerves, or intracranial primaries. Most of the reported cases involving the ear and temporal bone fall into the first group, representing secondary extension from an intracranial lesion, a phenomenon seen in up to 20 % of intracranial meningiomas. A true primary meningioma of the ear and temporal bone should be diagnosed only when there is clinical and radiographic support (i.e., a lack of any detectable intracranial mass or “dural enhancement”).

### CLINICAL FEATURES

Meningioma comprises ~10 % of ear and temporal bone tumors, affecting predominantly middle-aged patients (mean, 50 years). There is a 2:1 female to male ratio, and women tend to be older than men at presentation.

## MENINGIOMA—DISEASE FACT SHEET

### Definition

- A benign neoplasm of meningotheial cells

### Incidence and Location

- Up to 10% of ear and temporal bone tumors
- Internal auditory meatus, jugular foramen, middle ear (cleft)

### Morbidity and Mortality

- Mastoiditis

### Sex and Age Distribution

- Females > males (2:1) (women are usually older at presentation)
- Broad age range, mean: 50 years

### Clinical Features

- Hearing loss, tinnitus, otitis, pain, headaches, dizziness, vertigo

### Radiographic Features

- Direct CNS extension should be sought or excluded (en plaque)
- Magnetic resonance: T1: isointense; T2: hyperintense
- Computed tomography: focal bone erosion, sclerosis, or hyperostosis

### Prognosis and Treatment

- Good outcome (85% 5-year survival)
- 20% recurrence rate
- Wide surgical excision with clear margins

Patients present with hearing loss, tinnitus, otitis, pain, headaches, dizziness, and/or vertigo. The most common locations are the internal auditory meatus, jugular foramen, middle ear, and the eustachian tube roof. Meningioma may be seen in NF2.

## RADIOGRAPHIC FEATURES

Radiographic studies are performed with an eye to excluding direct CNS extension. MR tends to be more yielding than CT. The tumor is usually isointense to gray matter on T1-weighted MR images, and isointense to hyperintense on T2-weighted images. A direct extension or central nervous system association should be sought and/or excluded. Specifically, en plaque lesions (flat, “carpet-like” growth along the dura) must also be actively sought and excluded.

## PATHOLOGIC FEATURES

### GROSS FINDINGS

Most tumors of the ear and temporal bone are relatively small (< 1.5 cm), unless an intracranial component is

## MENINGIOMA—PATHOLOGIC FEATURES

### Gross Findings

- Infiltrative into bone (suture lines), sparing mucosa/skin
- Usually < 1.5 cm
- Granular mass with gritty consistency and calcifications

### Microscopic Findings

- Meningothelial and whorled architecture
- Syncytial and epithelioid cells with indistinct borders
- Bland, round nuclei with delicate chromatin and intranuclear cytoplasmic inclusions
- Psammoma bodies or pre-psammoma bodies

### Immunohistochemical Findings

- EMA focal and weak
- Keratin (CAM5.2, CK7) in pre-psammoma body pattern

### Pathologic Differential Diagnosis

- Middle ear adenoma, schwannoma, paraganglioma, and meningocele

identified. Macroscopically, the tumors are usually infiltrative into the bone through crevices and suture lines, while sparing the mucosal surface (or skin if it involves the EAC). The cut surface is gray-white and granular, with a gritty consistency due to calcifications and bony fragments that are frequently grossly visible.

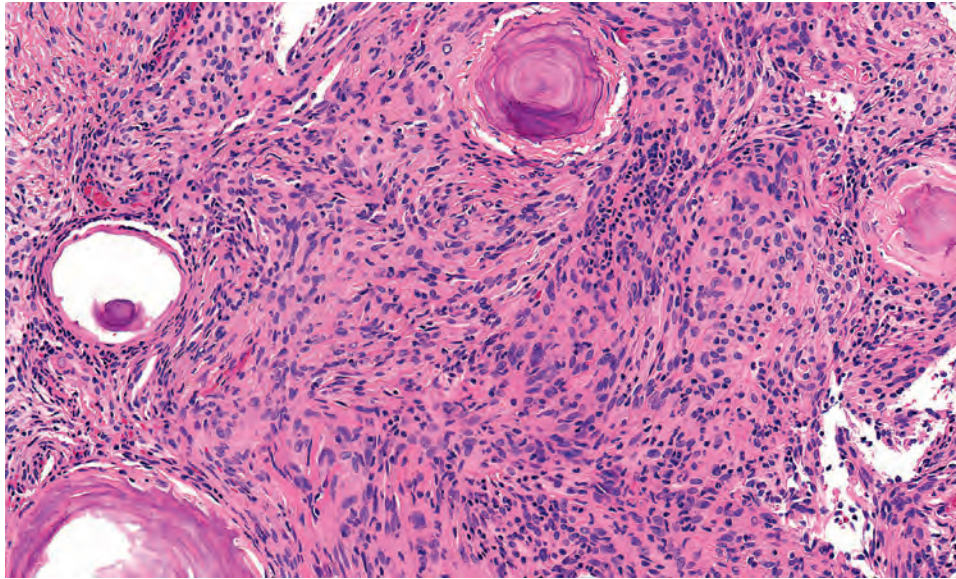
## MICROSCOPIC FINDINGS

The tumor cells have a syncytial, epithelioid appearance and are arranged in lobules or nests with a meningotheial and whorled architecture (Fig. 18.16). In general, the cells are bland with round to oval nuclei, delicate nuclear chromatin, and intranuclear cytoplasmic inclusions (Fig. 18.17). True psammoma bodies or “pre-psammoma” bodies are often present (Figs. 18.16 and 18.17). Pleomorphism and necrosis are usually absent and mitoses are uncommon. Multiple patterns of growth may be seen. An infiltrative growth pattern is defined by bone and soft tissue invasion (assessed by imaging or histology) and is identified in many cases. Notably, it does not appear to have a bearing on overall patient outcome. Nearly all tumors are World Health Organization grade I, with the meningotheial (syncytial) and psammomatous variants, respectively, the most frequently occurring.

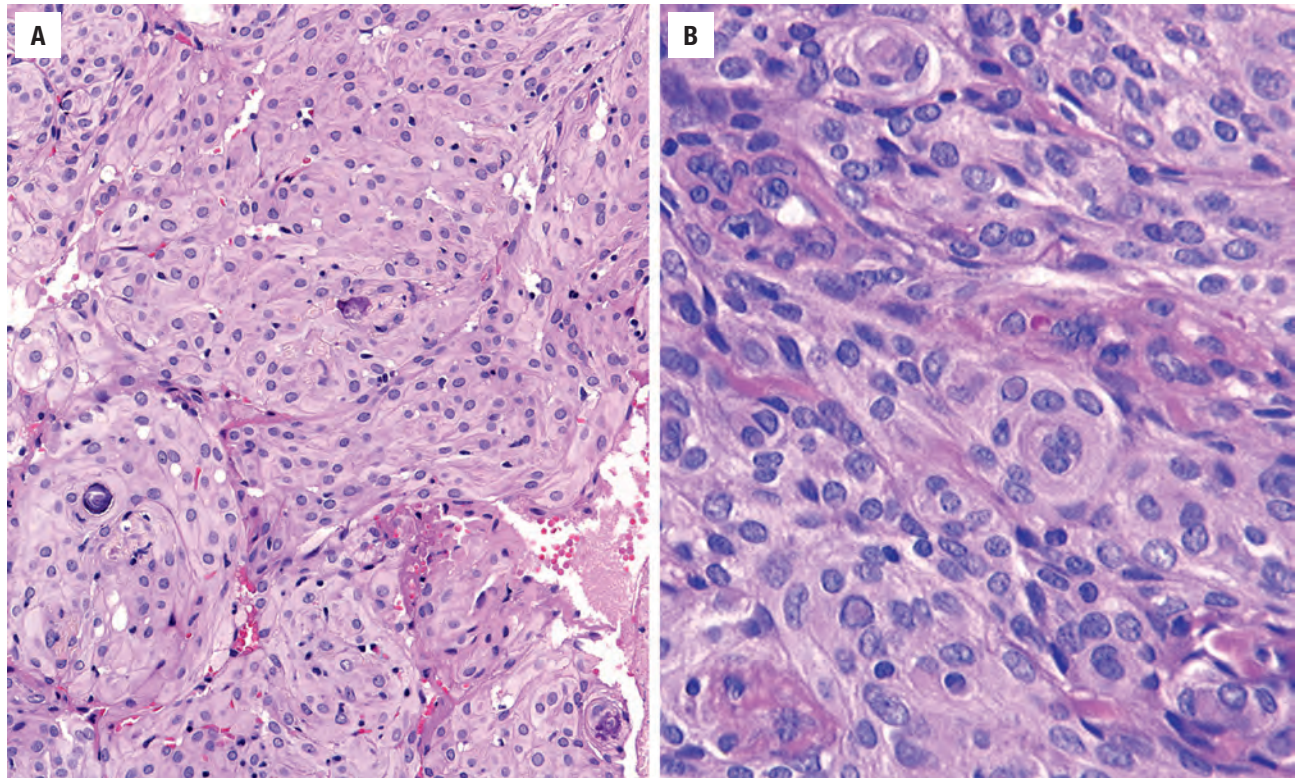
## ANCILLARY STUDIES

Nearly all meningiomas react with vimentin and have a weak, focal, but genuine reactivity for EMA (Fig. 18.18),



**FIGURE 18.16**

Typical meningotheliomatous meningioma with a whorled syncytial architecture with several psammoma bodies.

**FIGURE 18.17**

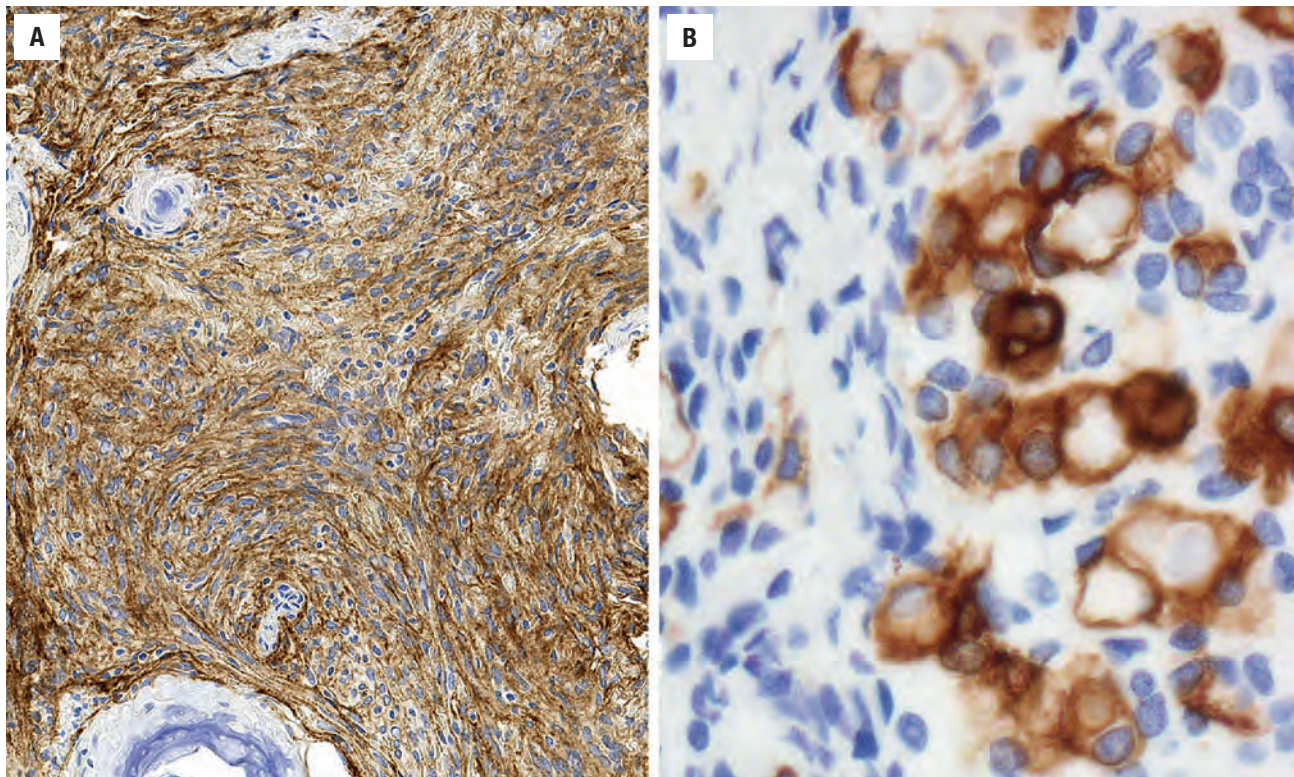
(A) Small psammoma bodies are seen within a whorled, meningothelial meningioma. (B) A variety of different growth patterns can be seen, but the meningothelial nature of the neoplasm is maintained. Note the intranuclear-cytoplasmic inclusions.

which is often helpful in making the diagnosis. It is not uncommon to also exhibit focal immunoreactivity with S100 protein. Keratin stains (CK7, CAM5.2) in a pre-psammoma body pattern only (Fig. 18.18). There is a strong reaction with claudin-1 and progesterone receptors. The proliferation index is usually less than 5%.

#### DIFFERENTIAL DIAGNOSIS

The differential diagnosis for meningiomas includes middle ear adenoma, schwannoma, paraganglioma, and meningocele. The general histologic features and immunohistochemical findings can usually distinguish between



**FIGURE 18.18**

(A) Neoplastic cells are reactive with EMA in a diffuse fashion in this tumor. (B) Note the numerous “pre-psammoma bodies” that are highlighted by CK7 immunohistochemistry.

these tumors. A middle ear adenoma has a more organoid growth with neuroendocrine nuclear features and strong keratin and neuroendocrine immunoreactivity. A spindle cell tumor with alternating cellular (Antoni A) and hypocellular (Antoni B) areas, perivascular hyalinization, and strong and diffuse nuclear and cytoplasmic S100 protein and/or SOX10 immunoreactivity confirms a diagnosis of schwannoma. Paraganglioma shows a zellballen (nested) architecture with basophilic cells and a distinctive immunoprofile: chromogranin-positive paraganglia cells and S100 protein-positive supporting sustentacular cells. A meningocele, or protrusion of the meninges through a bony defect, can occur in the middle ear and temporal bone, but these are histologically cystic lesions with a connection to the central nervous system. They can be congenital or “acquired” after surgery, infection, or trauma.

### PROGNOSIS AND THERAPY

Wide excision with clear margins is required. In the case of skull base involvement, surgical approaches are complex and challenging (transpetrosal, subtemporal, transtentorial). Adjuvant radiation therapy is used in poor surgical candidates or in cases of incomplete surgical resection. Overall, there is a good 5-year survival of 80%. However,

recurrences are frequent (20% of patients), although some of these cases may actually represent persistent or residual disease instead of true recurrence. In spite of additional surgery, occasionally patients will die with disease (although “from” disease is difficult to determine). Cerebral spinal fluid (CSF) leak and hearing loss are the most common complications, whereas others such as mastoiditis, meningitis, and sepsis may result in patient death.

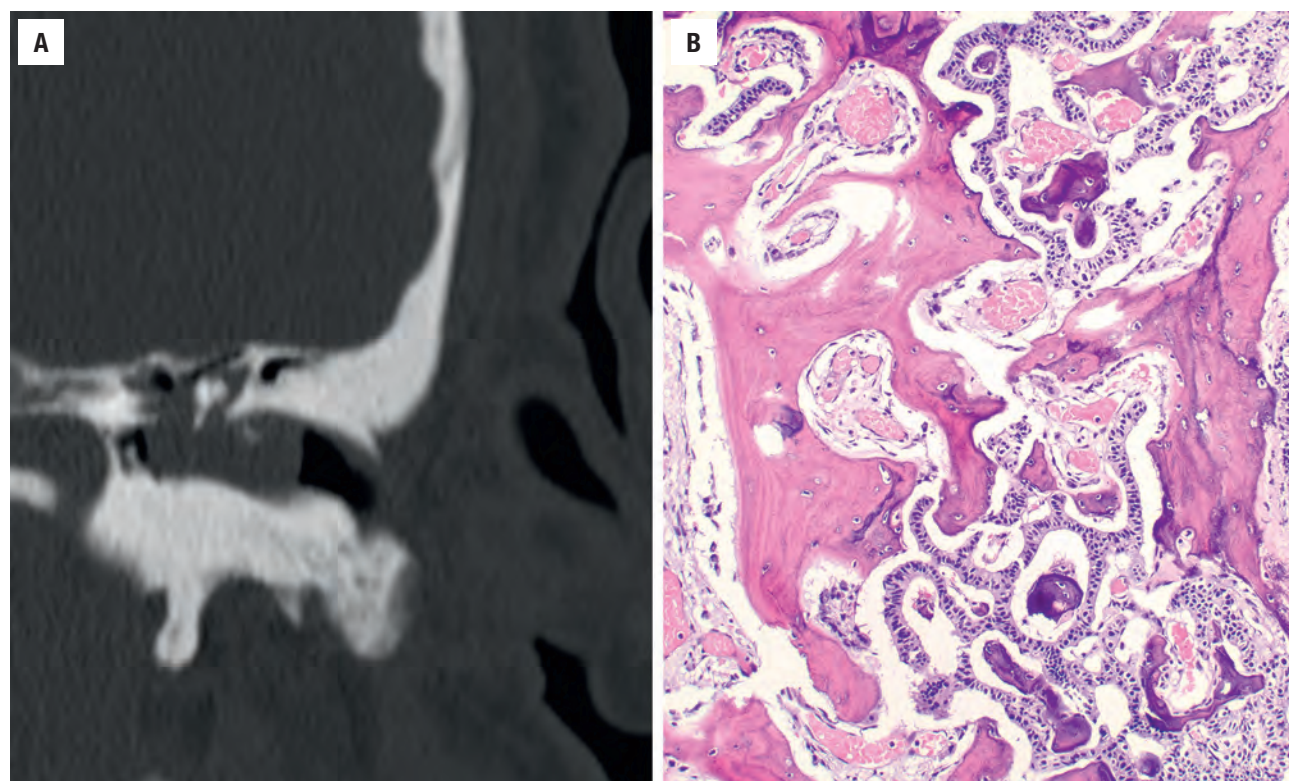
### MIDDLE EAR ADENOMA (NEUROENDOCRINE ADENOMA OF THE MIDDLE EAR)

Middle ear adenoma, carcinoid, or neuroendocrine adenoma of the middle ear (NAME) is a benign glandular neoplasm of the middle ear showing both cytomorphic and immunohistochemical evidence of mixed mucinous and neuroendocrine differentiation.

### CLINICAL FEATURES

This is an uncommon tumor (< 2% of ear tumors) usually presenting in the 5th decade, with an equal sex



**FIGURE 18.19**

(A) High resolution computed tomography study shows a left middle ear adenoma completely encasing the ossicles. (B) Expansion into the ossicular bones is seen histologically.

#### MIDDLE EAR ADENOMA—DISEASE FACT SHEET

##### Definition

- Benign glandular and neuroendocrine neoplasm arising in the middle ear

##### Incidence and Location

- Uncommon (< 2% of ear tumors)
- Middle ear

##### Morbidity and Mortality

- Mastoiditis
- No mortality

##### Sex and Age Distribution

- Equal sex distribution
- Mean, 5th decade

##### Clinical Features

- Unilateral conductive hearing loss, pressure, and tinnitus

##### Prognosis and Treatment

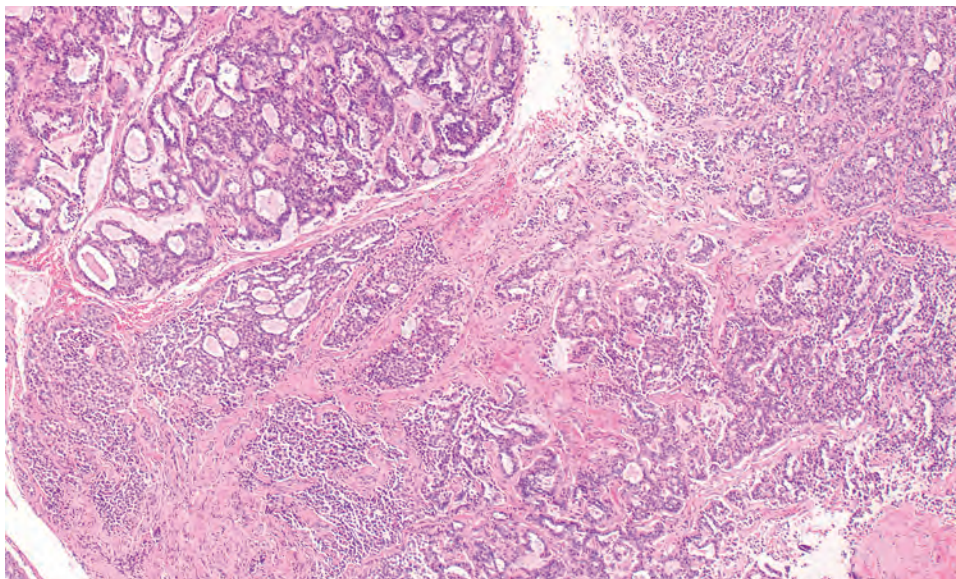
- Excellent, although recurrence/persistence in ~15%
- Complete surgical excision, including ossicular chain

distribution. Patients present with unilateral disease and associated tinnitus, fullness or pressure, otitis media, and conductive hearing loss, especially if the ossicular chain is involved. In early stages, otoscopy shows an intact tympanic membrane with a dark brownish-red mass behind it. The tumor may later expand to and involve the ossicular chain, thus causing conductive hearing loss, and may even penetrate the tympanic membrane. Occasionally, it may extend into the EAC or into the mastoid bone and eustachian tube. Despite its neuroendocrine origin, there is no serologic evidence of peptide hyperproduction. Imaging studies show the extent of involvement, highlighting ossicular encasement (Fig. 18.19).

#### PATHOLOGIC FEATURES

##### GROSS FINDINGS

Most tumors are quite small, less than < 1 cm in greatest dimension. Because they tend to encase the ossicular chain, the tumor is usually peeled away from the bone upon resection. Therefore, surgical specimens are highly fragmented and consist of whitish-yellow to gray, soft to rubbery tissue. Tumors are unencapsulated and abut the overlying intact surface epithelium.

**FIGURE 18.20**

Middle ear adenoma shows a wide variety of different patterns of growth, including solid, glandular, trabecular, and single cell. Fibrosis separates the neoplastic cells.

### MIDDLE EAR ADENOMA—PATHOLOGIC FEATURES

#### Gross Findings

- < 1 cm fragmented mass within the middle ear
- Avascular, rubbery, unencapsulated gray-yellow mass

#### Microscopic Findings

- Many patterns: glandular, ribbon, festoon, solid, single cell architecture
- “Infiltrative” growth is common
- Dual cell population: inner luminal cells with eosinophilic cytoplasm and outer, cuboidal/columnar cells with indistinct cytoplasm
- Ovoid, eccentrically placed nuclei with “salt and pepper” nuclear chromatin distribution and no nucleoli

#### Ultrastructural Findings

- Two distinct cell types:
  - Apical cells with elongated microvilli and secretory granules (type A cells)
  - Basal cells with neurosecretory granules (type B cells)

#### Immunohistochemical Findings

- Pancytokeratin, CAM5.2, CK7 (the latter in luminal cells) positive
- Chromogranin, synaptophysin, CD56, islet-1, human pancreatic polypeptide preferentially outer cells

#### Pathologic Differential Diagnosis

- Ceruminous adenoma, paraganglioma, meningioma, metastatic adenocarcinoma

ossicular chain is not uncommon (Fig. 18.19). The glandular pattern consists of duct-like structures with focal “back-to-back” gland configuration and luminal secretions (Fig. 18.21). The ducts are lined by a dual cell population composed of an inner (luminal), flattened, slightly more intensely eosinophilic mucinous cell, surrounded by an outer (basal), cuboidal to short columnar neuroendocrine cell with eosinophilic and homogeneous to finely granular cytoplasm and indistinct cytoplasmic borders (Fig. 18.22). There is no myoepithelial cell population. The nuclei tend to be round to oval, eccentrically placed (“plasmacytoid”), with minimal pleomorphism and “salt and pepper” chromatin distribution. Nucleoli are inconspicuous and mitoses are essentially absent.

An “infiltrative” pattern is characterized by small irregular groups and strands of cells in a moderately desmoplastic stroma. This pattern gives the illusion of tumor cells dissecting the collagen bundles in an uncontrolled and aggressive fashion (Fig. 18.21). The cells tend to be smaller than those within the other patterns and have a higher nuclear to cytoplasmic ratio. However, findings of malignancy such as mitotic activity, pleomorphism, necrosis, and invasion into bone, nerves, or lymphovascular spaces are not noted. Additional features may include a concurrent cholesteatoma and/or cholesterol granuloma.

### ANCILLARY STUDIES

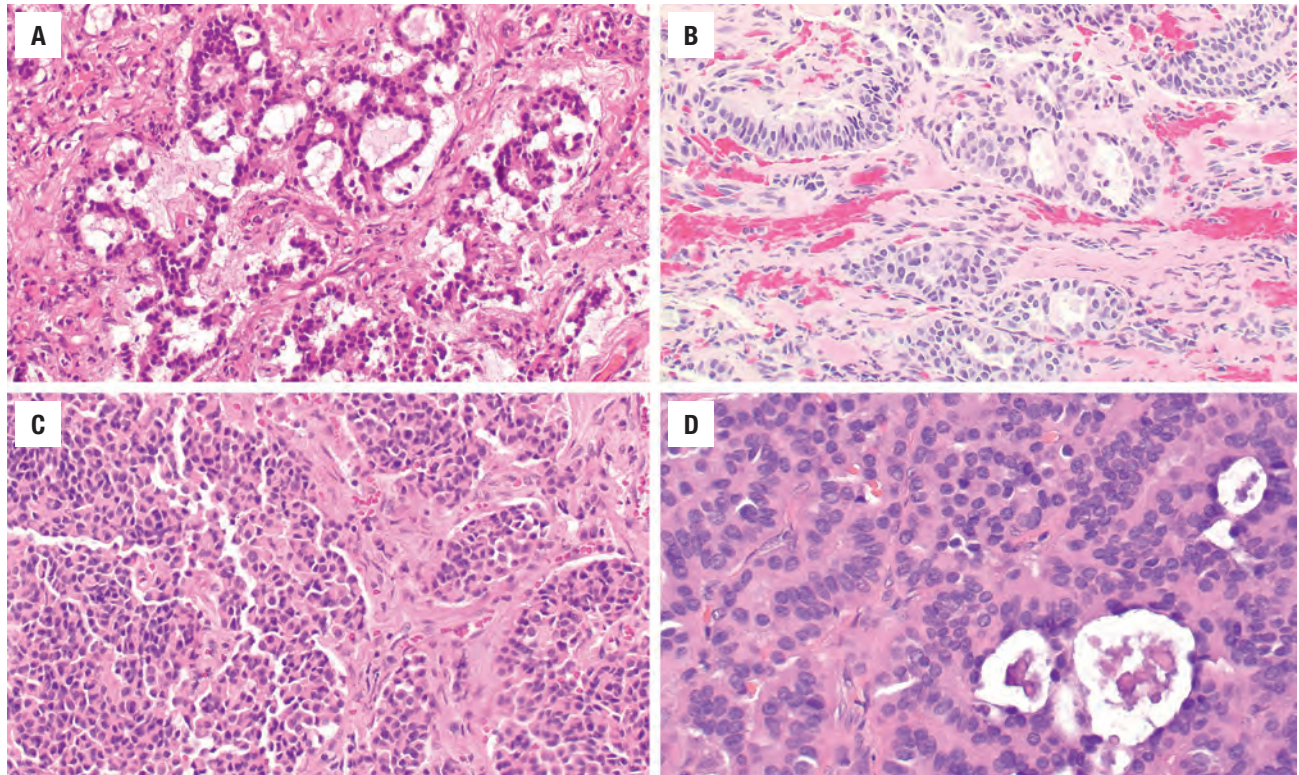
#### ULTRASTRUCTURAL FINDINGS

Electron microscopy demonstrates two distinct cell types: (1) apical cells with elongated microvilli and secretory mucus granules (type A cells) and (2) basal cells with neurosecretory granules (type B cells).

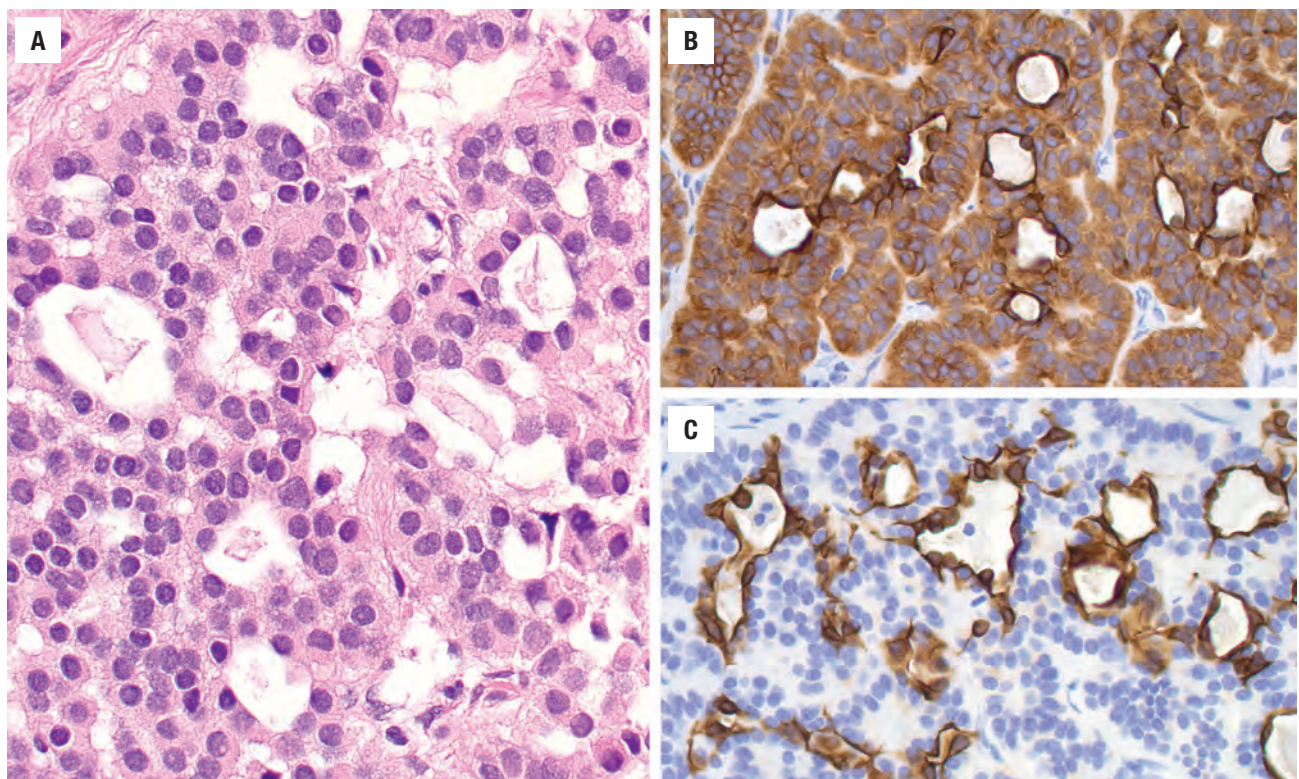
#### MICROSCOPIC FINDINGS

These tumors are moderately cellular, with an infiltrative growth arranged in a variety of different patterns: glandular, trabecular, cord-like, festoon-like, solid, and single cell, although the glandular pattern predominates (Fig. 18.20). Involvement of the bony interstices of the



**FIGURE 18.21**

Middle ear adenoma displaying multiple growth patterns, to include glandular (A), infiltrative (B), organoid (C), solid, trabecular, and glandular with secretions (D).

**FIGURE 18.22**

(A) Cuboidal to columnar cells with oval nuclei demonstrating "salt and pepper" nuclear chromatin, with an easily identifiable inner, flattened cellular layer. All neoplastic cells react with pancytokeratin (B) with a heavier reaction seen with the inner lining cells, further highlighted by the CK7 (C).



Transitional forms with features of both cell types have been described.

#### HISTOCHEMICAL FINDINGS

Mucin content can be confirmed in the gland lumen, and rarely within the cytoplasm, by periodic acid–Schiff (PAS) and alcian blue histochemical stains. A Grimelius stain may demonstrate granular cytoplasmic positivity at the base of the cells (periphery of the glands), corresponding to the location of the neurosecretory granules by electron microscopy.

#### IMMUNOHISTOCHEMICAL FINDINGS

The neoplastic cells have both epithelial and neuroendocrine marker immunoreactivity. These cells stain with a variety of keratin antibodies, including pancytkeratin, CK7, and CAM5.2, although CK7 preferentially highlights the inner (luminal) layer of the glandular cells (Fig. 18.22). Neuroendocrine marker immunoreactivity includes chromogranin, NSE, synaptophysin, and CD56, along with various hormone polypeptides (serotonin, glucagon, leu-7, HPP) and transcription factors (such as islet-1 [ISL1]), preferentially expressed in the outer basal cells (Fig. 18.23). The cells are negative with S100 protein, p63, PAX8, EMA, GFAP, and TTF1.

#### DIFFERENTIAL DIAGNOSIS

Histologically, ceruminous adenoma, paraganglioma, and metastatic adenocarcinoma can be included in the differential diagnosis. However, the anatomic site of origin makes this a unique tumor, distinctly separable from the other lesions by histology and immunohistochemistry. Because glandular (mucosal) metaplasia of the middle ear epithelium is common in chronic inflammation, such as otitis media, adenoma would seem to be the benign neoplastic counterpart of this reactive process.

#### PROGNOSIS AND THERAPY

Complete surgical excision is generally curative and must include the ossicular chain to prevent recurrence. Recurrence (persistence) is likely to develop in ~15% of patients, especially when the ossicular chain is involved but not removed. Facial nerve paralysis or paresthesia is usually mass-related compression rather than invasion, whereas parotid gland involvement usually represents direct extension rather than metastatic disease. Although controversial, there appears to be an extremely low risk of metastatic disease.

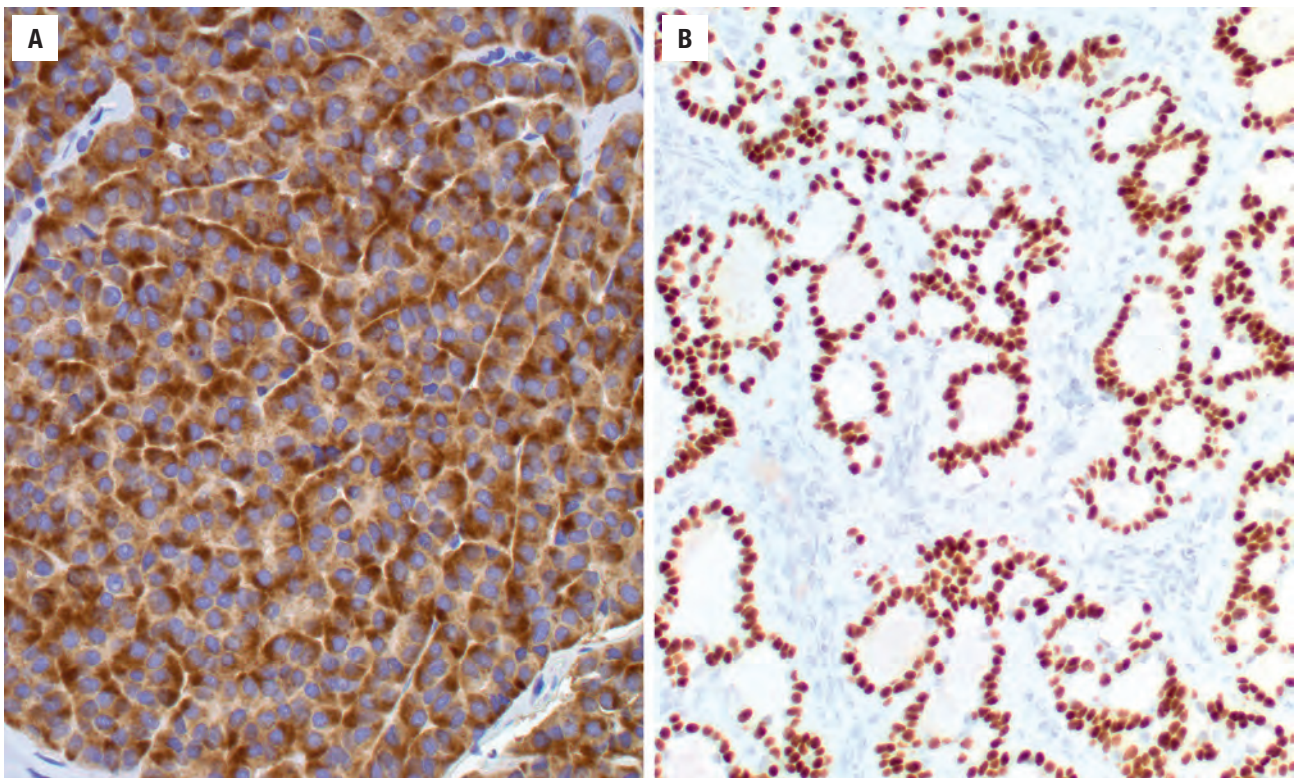


**FIGURE 18.23**

(A) Synaptophysin and (B) islet-1 react with the neoplastic cells, highlighting the neuroendocrine findings of the tumor.



## ■ ENDOLYMPHATIC SAC TUMOR

Endolymphatic sac tumor (ELST) is a low-grade papillary epithelial neoplasm arising within the endolymphatic sac/duct, showing a high association (up to one-third) with von Hippel-Lindau (VHL) syndrome. Growth into the middle ear is common. This tumor shows an intermediate behavior, more than a benign tumor but not quite malignant, because there is no metastatic potential.

### CLINICAL FEATURES

Approximately 1 in 35,000 to 40,000 people have VHL, of which ~10% to 15% develop ELSTs, with ~30% of these bilateral. There is a wide age range at presentation, although most patients are between 30 and 40 years. There is no sex difference. The most common symptoms include ipsilateral hearing loss (sensorineural > conductive, although can be mixed), tinnitus, facial nerve palsy, and vestibular dysfunction (vertigo, ataxia) resembling Ménière disease. Many patients report a long history of

symptoms, which suggests that these are slow growing tumors.

Given the strong association with VHL, it is appropriate to assess patients who present with an ELST for the corresponding gene mutation at 3p25–26 involving *VHL*, a tumor suppressor gene. Importantly, patients may show signs of VHL at other anatomic sites (such as kidney, pancreas, cerebellum). When tumors are bilateral, they are nearly always associated with VHL.

### RADIOGRAPHIC FEATURES

The best radiographic studies are a combination of MR and CT. MR shows a hyperintense (hypervascular) heterogeneous mass with T1-weighted images, whereas CT will show a lytic lesion with bone destruction, often with a multilocular appearance centered on the endolymphatic sac (between the IAC and sigmoid sinus). Tumor expansion into neighboring structures (especially middle and posterior cranial fossae and cerebellopontine angle) may also be seen.

### ENDOLYMPHATIC SAC TUMOR—DISEASE FACT SHEET

#### Definition

- Low-grade papillary epithelial neoplasm arising within or near the endolymphatic sac

#### Incidence and Location

- Rare
- Temporal bone and occasionally middle ear

#### Morbidity and Mortality

- Locally destructive with cranial nerve damage
- Death may result due to large, destructive lesion in vital areas

#### Sex and Age Distribution

- Equal sex distribution
- Wide age range, mean between 30 and 40 years

#### Clinical Features

- Ipsilateral hearing loss, tinnitus, vestibular dysfunction and facial nerve palsy
- Strong association with von Hippel-Lindau (VHL) syndrome

#### Radiographic Features

- MR: hyperintense heterogeneous mass on T1-weighted images
- Computed tomography: lytic, multilocular lesion with bone destruction centered on endolymphatic sac

#### Prognosis and Treatment

- Good prognosis, although dependent on extent of tumor
- Recurrent if not completely excised (difficult due to site)
- Surgery; all patients with VHL should be screened for endolymphatic sac tumor

### PATHOLOGIC FEATURES

#### GROSS FINDINGS

The tumors will frequently expand into the posterior cranial fossa, ranging up to 10 cm in greatest dimension. Older patients tend to have larger tumors.

### ENDOLYMPHATIC SAC TUMOR—PATHOLOGIC FEATURES

#### Gross Findings

- Large (10 cm) tumor centered on the endolymphatic sac region

#### Microscopic Findings

- Unencapsulated with bone invasion
- Coarse, papillary projections into cystic, fluid filled spaces
- Bland, cuboidal cells with little pleomorphism
- Glands with colloid-like material in lumens

#### Immunohistochemical Findings

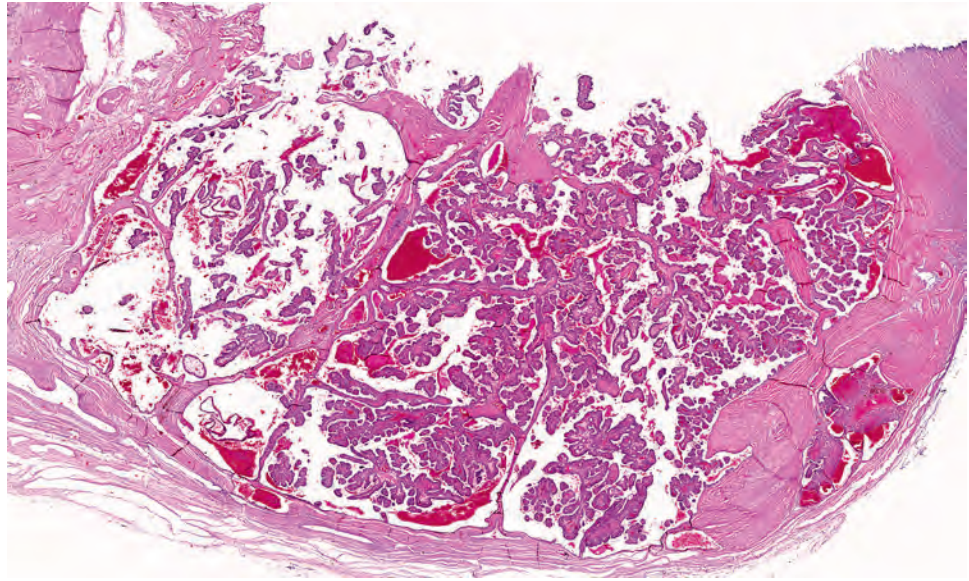
- Positive: keratin, CK7, CAM5.2, EMA, S100 protein, CAIX, PAX8
- Negative: thyroglobulin, TTF1, PSA, CD10 RCC

#### Genetic Studies

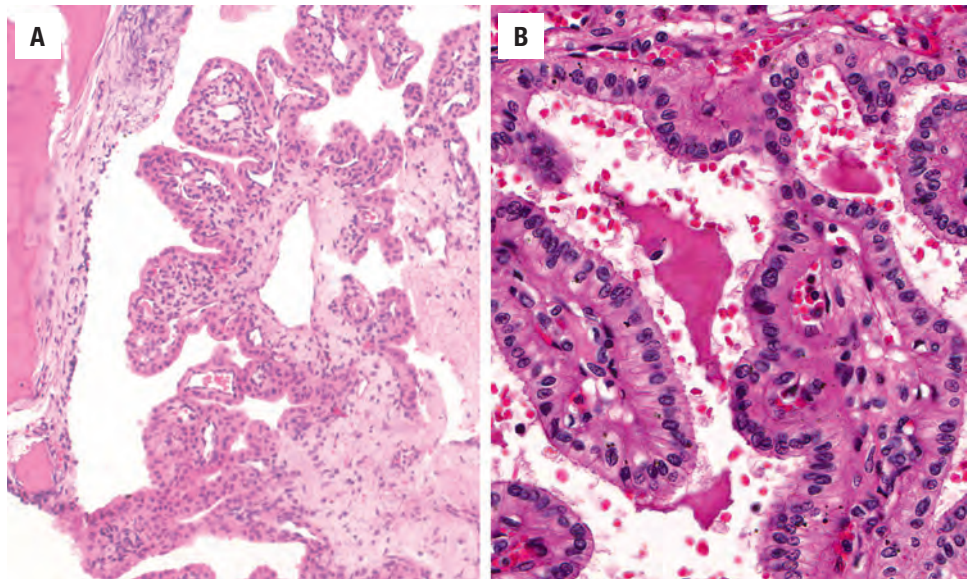
- Germline mutations of the *VHL* tumor suppressor gene (3p25–26)

#### Pathologic Differential Diagnosis

- Choroid plexus papilloma, middle ear adenoma, metastatic papillary thyroid carcinoma, metastatic adenocarcinoma (lung, kidney, colon, prostate)

**FIGURE 18.24**

There is a very complex papillary architecture to this endolymphatic sac tumor.

**FIGURE 18.25**

(A) Complex, although broad papillae within a cystic cavity adjacent to bone. (B) Single layer of cuboidal cells with small, hyperchromatic nuclei, line the papillary projections.

### MICROSCOPIC FINDINGS

The tumors are unencapsulated, locally destructive lesions with “bone invasion” commonly identified. The classic histologic appearance consists of a cystically dilated cavity with coarse, interdigitating, papillary projections (Fig. 18.24). Fibrovascular cores are seen within these papillae, which are lined by a single layer of low cuboidal to columnar epithelial cells (Fig. 18.25), similar to the normal endolymphatic sac lining. These cells contain uniformly round to oval nuclei with coarse nuclear chromatin deposition and eosinophilic, granular cytoplasm with indistinct cell membranes. A histologic similarity to thyroid follicles is common (Fig. 18.26), with dilated glands containing secretions. Pleomorphism, mitotic

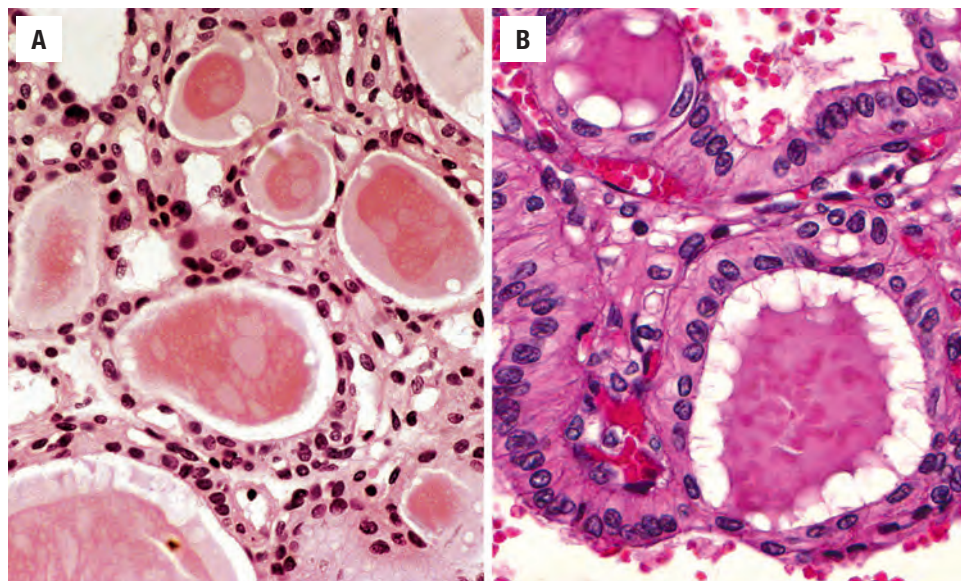
figures, and necrosis are absent. Granulation tissue, hemosiderin, chronic inflammation, and cholesterol clefts may be associated.

### ANCILLARY STUDIES

#### IMMUNOHISTOCHEMICAL FINDINGS

Cytokeratin, CK7, CAM5.2, PAX8, CAIX, EMA, and S100 protein are immunoreactive, although the latter two are often focal and weak. GFAP may occasionally be weakly positive, whereas thyroglobulin, TTF1, PSA, RCC, and CD10 are always negative.



**FIGURE 18.26**

(A and B) There are acini with eosinophilic secretions resembling thyroid gland follicles with colloid. However, TTF1 and thyroglobulin are negative.

### GENETIC STUDIES

Germline mutations of the *VHL* tumor suppressor gene (3p25–26) are usually detected in these patients, although sporadic cases may lack such abnormalities. *VHL* has multiple functions, including the upregulation of the hypoxic response (via hypoxia-inducible factor [*HIF*]-1  $\alpha$ ). Mutations prevent production of any functional *VHL* protein or result in a change of structure of *VHL* protein. Because individuals who have inherited one mutated copy have such a high probability of developing a second mutation in the other allele (the “two-hit” hypothesis), the inheritance pattern is autosomal dominant.

### DIFFERENTIAL DIAGNOSIS

A choroid plexus papilloma is generally confined to the midline and is not associated with destruction of the temporal bone. Metastatic carcinomas (lung, kidney, colon, prostate) can be distinguished with the help of immunohistochemistry. For example, reactivity with thyroglobulin and/or TTF1 confirms a metastatic papillary thyroid carcinoma. Metastatic renal cell carcinoma (clear cell type) is usually not papillary, shows a greater degree

of pleomorphism, and has extravasated erythrocytes in a pseudoalveolar pattern, with most cases immunoreactive with CD10, PAX8, CAIX, and renal cell carcinoma (RCC). Thus, the RCC and CD10 reactions are unique to metastatic renal cell carcinoma. Middle ear adenoma is a biphasic tumor with neuroendocrine immunophenotype and does not have a papillary architecture.

### PROGNOSIS AND THERAPY

Surgery, often radical, is the treatment of choice, often associated with morbidity. Nonetheless, surgery is performed with the goal of preserving hearing. Radiotherapy is used for advanced tumors. All patients with VHL should be radiographically screened for ELSTs because the incidence can be high (up to 30%). The prognosis is dependent on the extent of the disease, with death occasionally reported due to destruction of vital structures, as a result of the indolent but progressive course.

### SUGGESTED READINGS

The complete Suggested Readings list is available online at [ExpertConsult.com](http://ExpertConsult.com).

**SUGGESTED READINGS****Ceruminous Adenoma**

1. Lott Limbach AA, et al. Middle ear adenomas stain for two cell populations and lack myoepithelial cell differentiation. *Head Neck Pathol.* 2012;6(3):345–353.
2. Magliulo G, et al. Adenoma of the ceruminous gland. *Otolaryngol Head Neck Surg.* 2010;143(3):459–460.
3. Mansour P, et al. Ceruminous gland tumours: a reappraisal. *J Laryngol Otol.* 1992;106:727–732.
4. Markou K, et al. Primary pleomorphic adenoma of the external ear canal. Report of a case and literature review. *Am J Otolaryngol.* 2008;29(2):142–146.
5. Maruyama A, et al. Pleomorphic adenoma presenting with conductive hearing loss in the ear canal: a case report and review of the literature. *J Med Case Rep.* 2014;8:178.
6. Mills RG, et al. “Ceruminoma”—a defunct diagnosis. *J Laryngol Otol.* 1995;109:180–188.
7. Oda T, et al. Polygonal cells with ceroid granules and myoepithelial cells in fine needle aspiration cytology of ceruminous adenoma. *Cytopathology.* 2014;25(1):67–68.
8. Orendorz-Fraczkowska K, et al. Middle-ear ceruminous adenoma as a rare cause of hearing loss and vertigo: case reports. *Auris Nasus Larynx.* 2005;32(4):393–397.
9. Shen WQ, et al. Expression of Glut-1, HIF-1 $\alpha$ , PI3K and p-Akt in a case of ceruminous adenoma. *Head Neck Oncol.* 2012;4:18.
10. Thompson LDR, et al. Ceruminous adenomas: a clinicopathologic study of 41 cases with a review of the literature. *Am J Surg Pathol.* 2004;28:308–318.

**Langerhans Cell Histiocytosis**

1. Al-Ammar AY, et al. Langerhans' cell histiocytosis: paediatric head and neck study. *J Otolaryngol.* 1999;28:266–272.
2. Chen W, et al. Detection of clonally lymphoid receptor gene rearrangements in Langerhans cell histiocytosis. *Am J Surg Pathol.* 2010;34:1049–1057.
3. Chevallier KM, et al. Differentiating pediatric rhabdomyosarcoma and Langerhans cell histiocytosis of the temporal bone by imaging appearance. *AJNR Am J Neuroradiol.* 2016;37(6):1185–1189.
4. Cochrane LA, et al. Langerhans cell histiocytosis in the paediatric population: presentation and treatment of head and neck manifestations. *J Otolaryngol.* 2003;32:33–37.
5. Lau SK, et al. Immunohistochemical expression of langerin in Langerhans cell histiocytosis and non-Langerhans cell histiocytic disorders. *Am J Surg Pathol.* 2008;32:615–619.
6. Lieberman PH, et al. Langerhans' cell (eosinophilic) granulomatosis: a clinicopathologic study encompassing 50 years. *Am J Surg Pathol.* 1997;20:519–552.
7. Modest MC, et al. Langerhans cell histiocytosis of the temporal bone: A review of 29 cases at a single center. *Laryngoscope.* 2016;126(8):1899–1904.
8. Mueller RJ, et al. Langerhans cell histiocytosis of the auditory canal detected by 18F-FDG PET/CT. *Clin Nucl Med.* 2012;37(9):908–909.

**Peripheral Nerve Sheath Tumor (Schwannoma)**

1. Abram S, et al. Stereotactic radiation techniques in the treatment of acoustic schwannomas. *Otolaryngol Clin North Am.* 2007;40(3):571–588, ix.
2. Bennett M, et al. Surgical approaches and complications in the removal of vestibular schwannomas. *Otolaryngol Clin North Am.* 2007;40(3):589–609, ix-x.
3. Edwards CG, et al. Exposure to loud noise and risk of acoustic neuroma. *Am J Epidemiol.* 2006;163:327–333.
4. Huang MY, et al. Clinical perspectives regarding patients with internal auditory canal or cerebellopontine angle lesions: surgical and radiation oncology perspectives. *Semin Ultrasound CT MR.* 2003;24(3):124–132.
5. Irving RM, et al. A molecular, clinical, and immunohistochemical study of vestibular schwannoma. *Otolaryngol Head Neck Surg.* 1997;116:426–430.

6. Kasantikul V, et al. Acoustic neurilemmoma: clinico-anatomical study of 103 patients. *J Neurosurg.* 1980;52:28–35.
7. Liu W, et al. How to address small- and medium-sized acoustic neuromas with hearing: a systematic review and decision analysis. *World Neurosurg.* 2015;84(2):283–291.e1.
8. Maniakas A, et al. Conservative management versus stereotactic radiation for vestibular schwannomas: a meta-analysis of patients with more than 5 years' follow-up. *Otol Neurotol.* 2012;33(2):230–238.
9. Merkus P, et al. Less than 1% cerebrospinal fluid leakage in 1,803 translabyrinthine vestibular schwannoma surgery cases. *Otol Neurotol.* 2010;31:276–283.
10. Mirzayan MJ, et al. Management of vestibular schwannomas in young patients-comparison of clinical features and outcome with adult patients. *Childs Nerv Syst.* 2007;23(8):891–895.
11. Mornet E, et al. Vestibular schwannoma and cell-phones. Results, limits and perspectives of clinical studies. *Eur Ann Otorhinolaryngol Head Neck Dis.* 2013;130(5):275–282.
12. Nikolopoulos TP, et al. Acoustic neuroma growth: a systematic review of the evidence. *Otol Neurotol.* 2010;31(3):478–485.
13. Rosenberg SI. Natural history of acoustic neuromas. *Laryngoscope.* 2000;110(4):497–508.
14. Samii M, et al. Management of 1000 vestibular schwannomas (acoustic neuromas): surgical management and results with an emphasis on complications and how to avoid them. *Neurosurgery.* 1997;40:11–23.
15. Sanna M, et al. Surgical management of jugular foramen schwannomas with hearing and facial nerve function preservation: a series of 23 cases and review of the literature. *Laryngoscope.* 2006;116(12):2191–2204.
16. Schroeder RD, et al. NF2/merlin in hereditary neurofibromatosis 2 versus cancer: biologic mechanisms and clinical associations. *Oncotarget.* 2014;5(1):67–77.
17. Sekiya T, et al. A comprehensive classification system of vestibular schwannomas. *J Clin Neurosci.* 2000;7:129–133.
18. Slattery WH. Neurofibromatosis type 2. *Otolaryngol Clin North Am.* 2015;48(3):443–460.
19. Stangerup SE, et al. Epidemiology and natural history of vestibular schwannomas. *Otolaryngol Clin North Am.* 2012;45(2):257–268, vii.
20. Tan M, et al. Trends in the management of vestibular schwannomas at Johns Hopkins 1997-2007. *Laryngoscope.* 2010;120:144–149.
21. Torres-Martín M, et al. Genome-wide methylation analysis in vestibular schwannomas shows putative mechanisms of gene expression modulation and global hypomethylation at the HOX gene cluster. *Genes Chromosomes Cancer.* 2015;54(4):197–209.
22. Tos M, et al. Incidence of vestibular schwannomas. *Laryngoscope.* 1999;109:736–740.

**Paraganglioma**

1. Al-Mefty O, et al. Complex tumors of the glomus jugulare: criteria, treatment, and outcome. *J Neurosurg.* 2002;97(6):1356–1366.
2. Álvarez-Morujó RJ, et al. Management of multicentric paragangliomas: Review of 24 patients with 60 tumors. *Head Neck.* 2016;38(2):267–276.
3. Borba LA, et al. Surgical management of glomus jugulare tumors: a proposal for approach selection based on tumor relationships with the facial nerve. *J Neurosurg.* 2010;112:88–98.
4. Carlson ML, et al. Glomus tympanicum: a review of 115 cases over 4 decades. *Otolaryngol Head Neck Surg.* 2015;152(1):136–142.
5. Carlson ML, et al. Natural history of glomus jugulare: a review of 16 tumors managed with primary observation. *Otolaryngol Head Neck Surg.* 2015;152(1):98–105.
6. Fayad JN, et al. Jugular foramen tumors: clinical characteristics and treatment outcomes. *Otol Neurotol.* 2010;31:299–305.
7. Fishbein L, et al. Inherited mutations in pheochromocytoma and paraganglioma: why all patients should be offered genetic testing. *Ann Surg Oncol.* 2013;20(5):1444–1450.
8. Kaygusuz I, et al. Carotid body tumor: clinical features. *J Craniofac Surg.* 2015;26(7):e586–e589.
9. Pellitteri PK, et al. Paragangliomas of the head and neck. *Oral Oncol.* 2004;40:563–575.



10. Rao AB, et al. From the archives of the AFIP. Paragangliomas of the head and neck: radiologic-pathologic correlation. *Radiographics*. 1999;19:1605–1632.
11. Schiavi F, et al. Paraganglioma syndrome: SDHB, SDHC, and SDHD mutations in head and neck paragangliomas. *Ann N Y Acad Sci*. 2006;1073:190–197.
12. Tasar M, et al. Glomus tumors: therapeutic role of selective embolization. *J Craniofac Surg*. 2004;15(3):497–505.
13. Wang Z, et al. Surgical management of extensive jugular paragangliomas: 10-year experience with a large cohort of patients in China. *Int J Surg*. 2013;11(9):853–857.

## Meningioma

1. Bacciu A, et al. Intracranial meningioma: clinical features, radiologic findings, and surgical management. *Otol Neurotol*. 2007;28:391–399.
2. Bakar B. Jugular foramen meningiomas: review of the major surgical series. *Neurol Med Chir (Tokyo)*. 2010;50:89–96.
3. Chang CY, et al. Meningiomas presenting in the temporal bone: the pathways of spread from an intracranial site of origin. *Otolaryngol Head Neck Surg*. 1998;119:658–664.
4. Deveze A, et al. Transpetrosal approaches for meningiomas of the posterior aspect of the petrous bone Results in 43 consecutive patients. *Clin Neurol Neurosurg*. 2007;109:578–588.
5. Gyure KA, et al. A clinicopathological study of 15 patients with neuroglial heterotopias and encephalocoeles of the middle ear and mastoid region. *Laryngoscope*. 2001;110:1731–1735.
6. Hamilton BE, et al. Imaging and clinical characteristics of temporal bone meningioma. *AJNR Am J Neuroradiol*. 2006;27:2204–2209.
7. O'Reilly RC, et al. Primary extracranial meningioma of the temporal bone. *Otolaryngol Head Neck Surg*. 1998;118:690–694.
8. Nakamura M, et al. Meningiomas of the internal auditory canal. *Neurosurgery*. 2004;55(1):119–128.
9. Nam SI, et al. Temporal bone histopathology in neurofibromatosis type 2. *Laryngoscope*. 2011;121(7):1548–1554.
10. Prayson RA. Middle ear meningiomas. *Ann Diagn Pathol*. 2000;4:149–153.
11. Rushing EJ, et al. Primary extracranial meningiomas: an analysis of 146 cases. *Head Neck Pathol*. 2009;3:116–130.
12. Shihada R, et al. Skull base meningiomas mimicking otitis media. *J Laryngol Otol*. 2012;126(6):619–624.
13. Stevens KL, et al. Middle ear meningiomas: a case series reviewing the clinical presentation, radiologic features, and contemporary management of a rare temporal bone pathology. *Am J Otolaryngol*. 2014;35(3):384–389.
14. Thompson LDR, et al. Primary ear and temporal bone meningiomas: a clinicopathologic study of 36 cases with a review of the literature. *Mod Pathol*. 2003;16:236–245.
15. Wu ZB, et al. Posterior petrous meningiomas: 82 cases. *J Neurosurg*. 2005;102:284–289.

## Middle Ear Adenoma

1. Agaimy A, et al. 'Neuroendocrine' middle ear adenomas: consistent expression of the transcription factor ISL1 further supports their neuroendocrine derivation. *Histopathology*. 2015;66(2):182–191.
2. Batsakis JG. Adenomatous tumors of the middle ear. *Ann Otol Rhinol Laryngol*. 1989;98:749–752.
3. Bittencourt AG, et al. Middle ear adenoma with neuroendocrine differentiation: relate of two cases and literature review. *Int Arch Otorhinolaryngol*. 2013;17(3):340–343.
4. Bold EL, et al. Adenomatous lesions of the temporal bone immunohistochemical analysis and theories of histogenesis. *Am J Otol*. 1995;16:146–152.
5. Cruz Toro P, et al. Neuroendocrine adenoma of the middle ear. *Otol Neurotol*. 2012;33(1):e7–e8.
6. Davies JE, et al. Middle ear neoplasms showing adenomatous and neuroendocrine components. *J Laryngol Otol*. 1989;103:404–407.
7. Devaney KO, et al. Epithelial tumors of the middle ear—are middle ear carcinoids really distinct from middle ear adenomas? *Acta Otolaryngol*. 2003;123:678–682.
8. Duderstadt M, et al. Adenomatous tumors of the middle ear and temporal bone: clinical, morphological and tumor biological

- characteristics of challenging neoplastic lesions. *Eur Arch Otorhinolaryngol*. 2012;269(3):823–831.
9. Gobel Y, et al. Recurrent neuroendocrine adenoma of the middle ear: a case report. *Eur Ann Otorhinolaryngol Head Neck Dis*. 2014;131(4):267–268.
10. Hale RJ, et al. Middle ear adenoma: tumour of mixed mucinous and neuroendocrine differentiation. *J Clin Pathol*. 1991;44:652–654.
11. Hyams VJ, et al. Benign adenomatous neoplasm (adenoma) of the middle ear. *Clin Otolaryngol Allied Sci*. 1976;1:17–26.
12. Lott Limbach AA, et al. Middle ear adenomas stain for two cell populations and lack myoepithelial cell differentiation. *Head Neck Pathol*. 2012;6(3):345–353.
13. Mills SE, et al. Middle ear adenoma. A cytologically uniform neoplasm displaying a variety of architectural patterns. *Am J Surg Pathol*. 1984;8:677–685.
14. Mooney EE, et al. Middle ear carcinoid: an indolent tumor with metastatic potential. *Head Neck*. 1999;21(1):72–77.
15. Pelosi S, et al. Adenomatous tumors of the middle ear. *Otolaryngol Clin North Am*. 2015;48(2):305–315.
16. Ramsey MJ, et al. Carcinoid tumor of the middle ear: clinical features, recurrences, and metastases. *Laryngoscope*. 2005;115:1660–1666.
17. Stanley MW, et al. Carcinoid tumors of the middle ear. *Am J Clin Pathol*. 1987;87(5):592–600.
18. Thompson LD. Neuroendocrine adenoma of the middle ear. *Ear Nose Throat J*. 2005;84:560–561.
19. Torske KR, et al. Adenoma vs. carcinoid tumor of the middle ear: A study of 48 cases and review of the literature. *Mod Pathol*. 2002;15:543–555.
20. Wassef M, et al. Middle ear adenoma. A tumor displaying mucinous and neuroendocrine differentiation. *Am J Surg Pathol*. 1989;13:838–847.

## Endolymphatic Sac Tumor

1. Bell D, et al. Endolymphatic sac tumor (aggressive papillary tumor of middle ear and temporal bone): sine qua non radiology-pathology and the University of Texas MD Anderson Cancer Center experience. *Ann Diagn Pathol*. 2011;15(2):117–123.
2. Bisceglia M, et al. Endolymphatic sac papillary tumor (Heffner tumor). *Adv Anat Pathol*. 2006;13:131–138.
3. Carlson ML, et al. Management of primary and recurrent endolymphatic sac tumors. *Otol Neurotol*. 2013;34(5):939–943.
4. Choo D, et al. Endolymphatic sac tumors in von Hippel-Lindau disease. *J Neurosurg*. 2004;100:480–487.
5. Devaney KO, et al. Endolymphatic sac tumor (low-grade papillary adenocarcinoma) of the temporal bone. *Acta Otolaryngol*. 2003;123:1022–1026.
6. El-Naggar AK, et al. Tumors of the middle ear and endolymphatic sac. *Pathol Annu*. 1994;29(Pt 2):199–231.
7. Heffner DK. Low-grade adenocarcinoma of probable endolymphatic sac origin: a clinicopathologic study of 20 cases. *Cancer*. 1989;64:2292–2302.
8. Horiguchi H, et al. Endolymphatic sac tumor associated with a von Hippel-Lindau disease patient: an immunohistochemical study. *Mod Pathol*. 2001;14(7):727–732.
9. Kim HJ, et al. Surgical resection of endolymphatic sac tumors in von Hippel-Lindau disease: findings, results, and indications. *Laryngoscope*. 2013;123(2):477–483.
10. Lonser RR, et al. Tumors of the endolymphatic sac in von Hippel-Lindau disease. *N Engl J Med*. 2004;350:2481–2486.
11. Manski TJ, et al. Endolymphatic sac tumors. A source of morbid hearing loss in von Hippel-Lindau disease. *JAMA*. 1997;277:1461–1466.
12. Megerian CA, et al. Evaluation and management of endolymphatic sac and duct tumors. *Otolaryngol Clin North Am*. 2007;40(3):463–478, viii.
13. Michaels L. Origin of endolymphatic sac tumor. *Head Neck Pathol*. 2007;1:104–111.
14. Patel NP, et al. The radiologic diagnosis of endolymphatic sac tumors. *Laryngoscope*. 2006;116(1):40–46.
15. Skalova A, et al. Endolymphatic sac tumor (aggressive papillary tumor of middle ear and temporal bone): report of two cases with analysis of the VHL gene. *Pathol Res Pract*. 2008;204:599–606.
16. Thompson LD. Endolymphatic sac tumor. *Ear Nose Throat J*. 2013;92(4–5):184–188.

# Malignant Neoplasms of the Ear and Temporal Bone

■ **Lester D.R. Thompson**

## ■ **SQUAMOUS CELL CARCINOMA (EXTERNAL AUDITORY CANAL AND MIDDLE EAR)**

Squamous cell carcinoma (SCC) is a malignant tumor of squamous keratinocytes. Ultraviolet (UV) radiation is considered etiologic for external ear lesions, whereas chronic inflammation (otitis media) may be associated with middle ear tumors.

### CLINICAL FEATURES

#### SQUAMOUS CELL CARCINOMA (EXTERNAL & MIDDLE EAR)—DISEASE FACT SHEET

##### Definition

- An invasive epithelial tumor with squamous differentiation (keratinocytes)

##### Incidence and Location

- Common tumor (similar frequency to basal cell carcinoma)
- Pinna, external canal, and middle ear

##### Sex and Age Distribution

- Males > females (3:1) for external ear tumors
- Females > males for external auditory canal tumors
- Elderly patients

##### Clinical Features

- Mass lesion, often with ulceration
- Pain, hearing loss, and drainage of blood or pus (middle ear/external auditory canal [EAC])
- Tumor plaque, polypoid mass, or ulcer with everted edges
- Obstructed external canal

##### Prognosis and Treatment

- Dependent on stage of disease but usually good for external ear lesions, although less so for EAC tumors
- Recurrences are common
- Death is usually due to intracranial extension
- Surgical excision and/or irradiation

SCCs of the external auditory canal (EAC) are uncommon (1/million population), quite different from pinna SCC. Patients are usually older (mean, 55 to 65 years), but women are affected more often than men for EAC carcinomas, opposite of pinna carcinomas. A serious problem with EAC and middle ear tumors is the delay in diagnosis because of the nonspecific symptoms that may be present ([Fig. 19.1](#)), different from much earlier detection of pinna lesions due to their prominent position. Chronic otitis media and radiation exposure are etiologies considered, quite different from ultraviolet exposure or frostbite for pinna tumors. Transformation of squamous papilloma is rare. Patients present with a mass, otitis media, otitis externa, pain, hearing loss, discharge, and/or bleeding. In the later stages, there may be dissolution of the tympanic membrane with invasion into the middle ear, bone, and internal auditory meatus. Tumor may also enter the middle ear by posterior canal entry into the mastoid air spaces ([Fig. 19.2](#)). Isolated cases (usually younger patients) may show middle ear confined tumors. Interestingly, concomitant cholesteatoma is usually not found.

### PATHOLOGIC FEATURES

#### GROSS FINDINGS

The gross appearance ranges from papules to nodules to plaque-like lesions, which may be exophytic, ulcerated, or hemorrhagic, frequently occluding the EAC and/or destroying the tympanum.

#### MICROSCOPIC FINDINGS

SCC of the EAC and middle ear is similar to other sites, separated into well, moderately, and poorly differentiated; keratinizing and nonkeratinizing; and in situ versus invasive ([Fig. 19.2](#)). There are nests, sheets, and infiltrative cords, keratin pearl formation, atypical



**FIGURE 19.1**

This squamous cell carcinoma presented as an ulcerated mass filling the external auditory canal. (Courtesy Dr. Carsten Palme.)

### SQUAMOUS CELL CARCINOMA (EXTERNAL AND MIDDLE EAR)—PATHOLOGIC FEATURES

#### Gross Findings

- Nodular or plaque-like mass arising from skin
- Invasion of elastic cartilage

#### Microscopic Findings

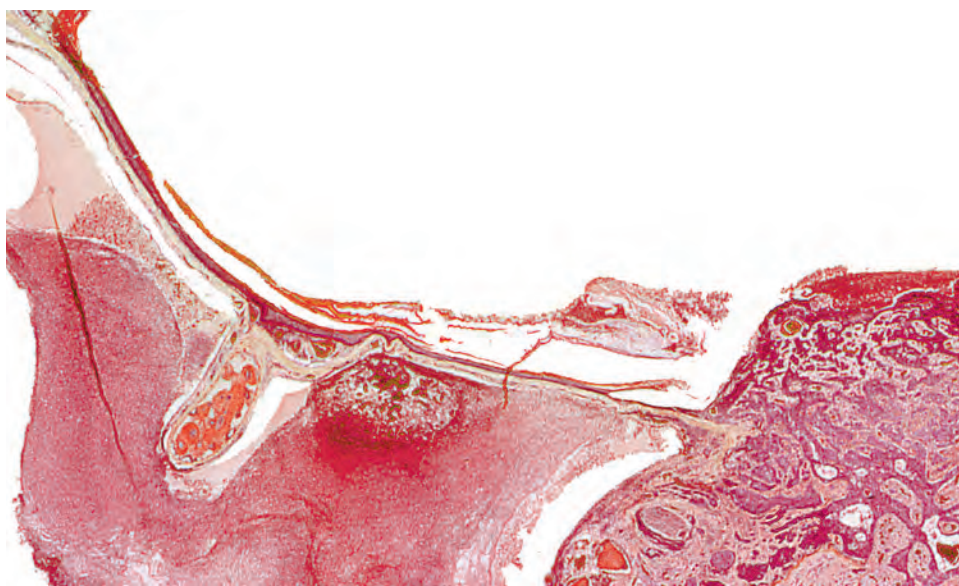
- Squamous cell carcinoma with invasion of atypical cells
- Well, moderately, or poorly differentiated
- Keratinizing or nonkeratinizing
- Multiple patterns of growth, perhaps with perineural invasion
- Stromal response with desmoplasia and inflammation
- Variant patterns may have higher risk of recurrence/death

#### Immunohistochemical Findings

- CK5/6, CK903 (34βE12), p63, and p40
- Ber-Ep4 negative (positive in basal cell carcinoma)

#### Pathologic Differential Diagnosis

- Basal cell carcinoma, normal middle ear corpuscles, reactive conditions, metastatic carcinoma, atypical fibroxanthoma

**FIGURE 19.2**

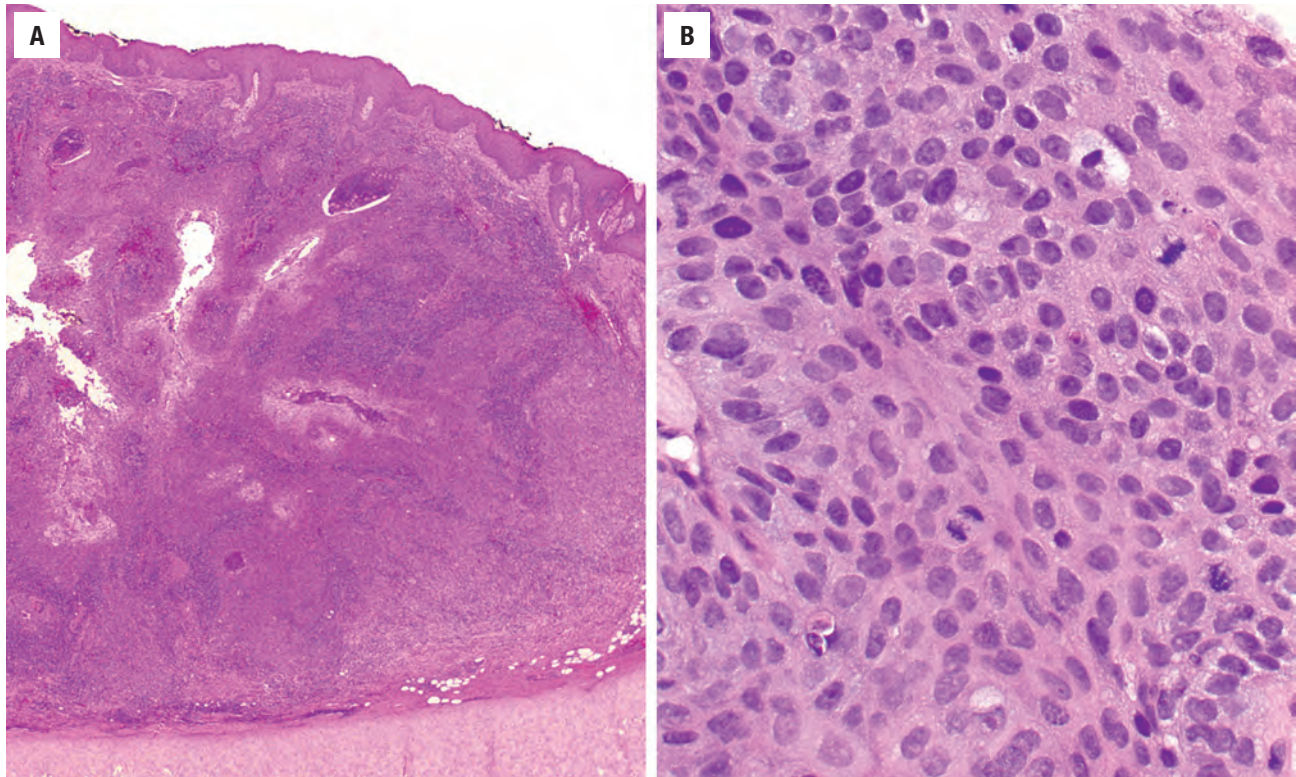
Low-power temporal bone section shows an intact tympanic membrane with fibrinoid and necrotic material resulting from acute inflammation in association with a squamous cell carcinoma at the deep end of the external canal near the eardrum annulus but not penetrating it.

keratinization, polarity loss, intercellular bridges, opacified cytoplasm, nuclear chromatin condensation, and increased mitotic figures, including atypical forms (Fig. 19.3). Perineural invasion is associated with a high rate of local recurrence and increased risk of metastasis. Middle ear tumors may show chronic inflammation and often marked desmoplastic stroma. In cases arising deeply within the ear canal, there is often dissolution of the tympanic membrane and a concomitant origin from the middle ear epidermis (squamous metaplasia arising from the simple cuboidal epithelium), although passage into the middle ear is possible without damage to the eardrum

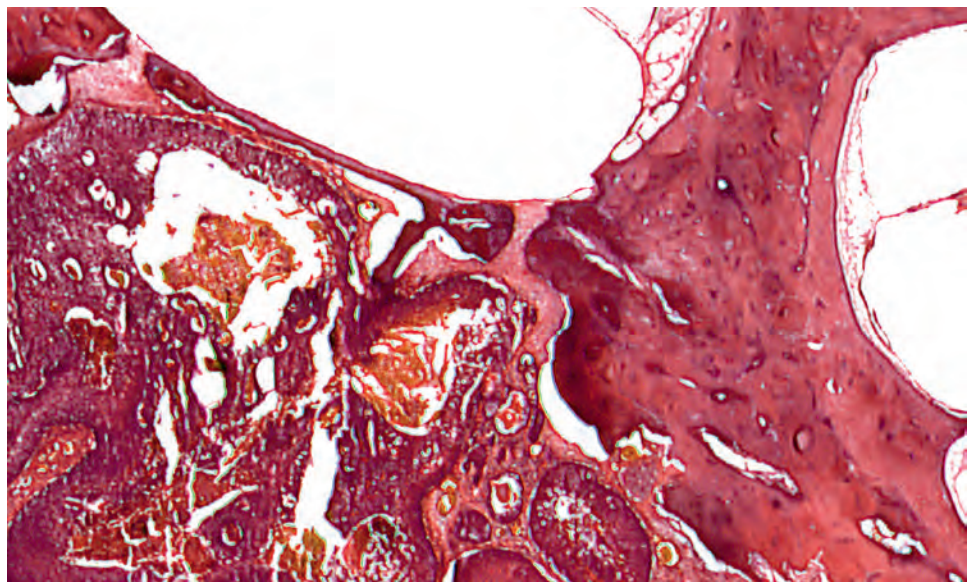
(Fig. 19.4). An origin directly from middle ear epithelium may also be seen. Other variants include verrucous, spindle cell, and adenoid squamous cell carcinoma. High-risk patterns include spindle cell/sarcomatoid (Fig. 19.5), basaloid, adenosquamous, and desmoplastic SCCs.

Although cholesteatoma may be concurrently identified with SCC, SCC does *not* develop from cholesteatoma. Spread of SCC within the middle ear is extremely rare due to the peculiar resistance of the bone of the otic capsule to direct spread of the tumor. Nonetheless, this spread begins with early erosion through the thin bony plate (up to 1 mm thick) that separates the medial wall



**FIGURE 19.3**

**A**, Invasive squamous cell carcinoma associated with inflammation and extension to the cartilage (*lower field*). **B**, A well-differentiated invasive tumor with large number of mitoses.

**FIGURE 19.4**

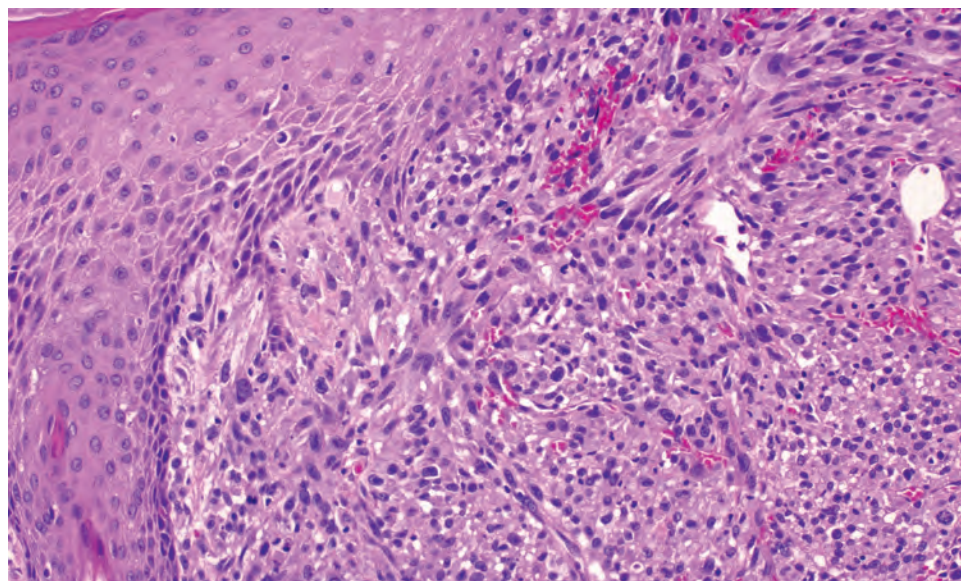
Low-power view of squamous carcinoma in middle ear showing sparing of otic capsule bone. The vestibule with saccule and utricle lies above. The footplate of the stapes is seen bordering the vestibule below. This thin bony plate is not invaded by the neoplasm. To the right is seen the cochlea, surrounded also by otic capsule bone. There is a little erosion of this bone by adjacent tumor.

of the middle ear at its junction with the eustachian tube from the carotid canal. Further extension along the carotid canal eventually allows for easy extension to the sympathetic nerves, making the tumor impossible to eradicate surgically. In addition, tumor spreads through the bony walls of the posterior mastoid air cells to the dura of the posterior surface of the temporal bone.

#### ANCILLARY STUDIES

Immunostains are used primarily for poorly differentiated and spindle cell tumors. High-molecular-weight (HMW) cytokeratins 5/6 and CK903 (34 $\beta$ E12) are the most sensitive markers for squamous differentiation and, along



**FIGURE 19.5**

Spindle-cell squamous cell carcinoma shows association with the overlying surface and a spindled cell morphology.

with p63 or p40, help to confirm the diagnosis in these more difficult cases.

### DIFFERENTIAL DIAGNOSIS

Middle ear corpuscles, concentrically laminated balls of collagen formed on bone-free mastoid air cell partitions, are more common in the elderly and may be difficult to separate from SCC, particularly in frozen sections. However, there is an absence of cells in the laminated corpuscles. Cholesteatoma does not show pleomorphism, desmoplastic stroma, or atypical mitoses. Otic polyp shows chronic inflammation without well-developed epithelial atypia or atypical mitoses.

### PROGNOSIS AND THERAPY

Squamous carcinoma of the external canal and middle ear is an aggressive disease with a high propensity for local recurrence. Poor prognostic features include high clinical stage, > 8 mm tumor depth, perineural, and/or lymphovascular invasion. Death is usually due to direct intracranial extension. Lymph node metastasis is unusual (< 10%) and hematogenous spread even more rare. Optimal therapy is complete surgical excision, with radiation therapy.

If the middle ear is involved, the neoplasm is surgically incurable if either or both (1) the thin plate of bone between the internal carotid artery and the tympanic end of the eustachian tube and (2) the bone in the posterior wall of the mastoid, bordering the posterior cranial fossa, are breached by tumor. In the absence of these features middle

ear squamous carcinoma is often treated by “petrousectomy,” which is by no means a resection of the whole petrous bone but a subtotal resection or extirpation of the middle ear components involved by tumor.

### CERUMINOUS ADENOCARCINOMA

Malignant neoplasms derived from the apocrine (ceruminous glands) of the EAC are rare. These neoplasms take the form of adenoid cystic carcinoma, mucoepidermoid carcinoma, and adenocarcinoma, not otherwise specified (NOS).

### CLINICAL FEATURES

These rare tumors (< 3% of ear tumors), arising from the ceruminous glands of the outer one-third to one-half of the EAC, occur more frequently in females than males (1.5:1). Patients tend to be middle aged at presentation (mean, 49 years). Patients present with pain, a mass, hearing changes (conductive hearing loss), drainage, and/or neurologic deficits. Symptoms are frequently present for 8 to 12 months on average.

### RADIOGRAPHIC FEATURES

Imaging studies are usually recommended to help exclude direct extension from the parotid gland (Fig. 19.6) or nasopharynx and to define the extent of the tumor for surgical planning.

**CERUMINOUS ADENOCARCINOMA—DISEASE FACT SHEET****Definition**

- Malignant tumor derived from apocrine glands in the cartilaginous part of the external auditory canal

**Incidence**

- Rare neoplasm

**Morbidity and Mortality**

- Hearing loss
- Mortality is variable but ~50% dead of disease

**Sex and Age Distribution**

- Females > males (~1.5:1)
- Usually 5th-6th decades

**Clinical Features**

- Pain, mass, hearing changes (conductive hearing loss), drainage, and/or neurologic deficits

**Radiographic Features**

- Imaging used to exclude direct extension from parotid gland or nasopharynx

**Prognosis and Treatment**

- Overall, 50% at 5 years
- Frequent recurrences, direct invasion of the brain, and metastasis (lung) will often result in death
- Wide, radical resection and/or radiation

**CERUMINOUS ADENOCARCINOMA—PATHOLOGIC FEATURES****Microscopic Findings**

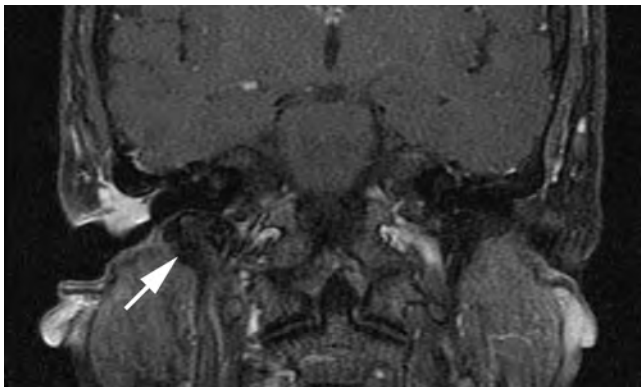
- Tumors are often polypoid (mean, 1.4 cm)
- Tumors are infiltrative with epithelial ulceration
- Range from solid to cystic, glandular or cribriform
- Increased cellularity, nuclear pleomorphism, prominent nucleoli, mitotic figures
- Cerumen granules (pigment) not present in carcinoma
- Necrosis and perineural invasion uncommon but diagnostic of carcinoma
- Adenoid cystic type usually displays the characteristic cribriform pattern with a tendency to perineural infiltration

**Immunohistochemical Findings**

- Keratin, CK7, and CD117 highlight luminal cells
- p63, CK5/6, and S100 protein highlight basal cells if present

**Pathologic Differential Diagnosis**

- Metastatic adenocarcinoma, direct extension from salivary gland carcinoma, benign ceruminous adenomas

**FIGURE 19.6**

An invasive ceruminous adenocarcinoma is seen in this magnetic resonance imaging T1-weighted fat-suppressed coronal view (arrow).

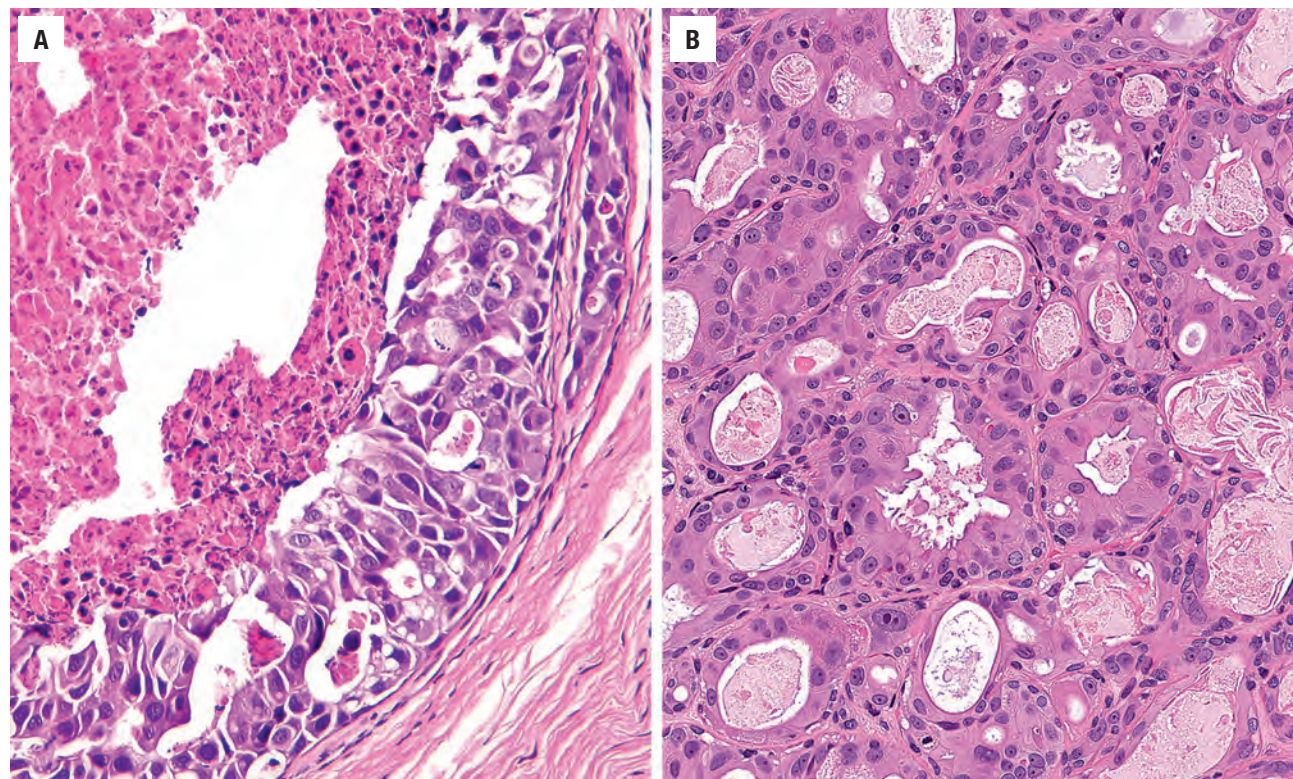
**PATHOLOGIC FEATURES**

Ranging up to 3 cm (mean, 1.4 cm) in greatest dimension, these tumors are often polypoid, tend to involve the posterior canal, and are highly invasive. Although not arising from the surface epithelium, there is frequent

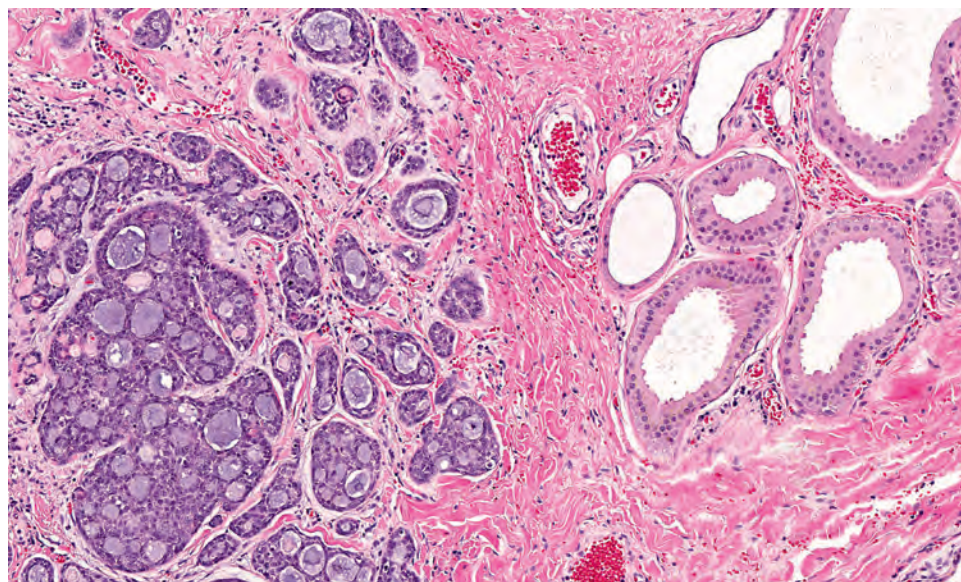
surface epithelial involvement. Histologically, these tumors are cellular and may be arranged in a variety of different patterns: solid, cystic, cribriform, glandular, and even single cell. Uncommonly, a dual cell population is noted but is not the dominant histology. There is usually cellular pleomorphism, with nuclear variability and prominent nucleoli. Regardless of subtype, these tumors infiltrate into the surrounding soft tissue, benign ceruminous glands, and even cartilage or bone. Perineural invasion and central comedonecrosis (Fig. 19.7), features only identified in carcinoma, may be seen.

As previously mentioned, these tumors are separated into three main subtypes: (1) ceruminous adenocarcinoma, NOS; (2) ceruminous adenoid cystic carcinoma; and (3) ceruminous mucoepidermoid carcinoma. *Ceruminous adenocarcinoma, NOS* may be recognized by the eosinophilic character of the tumor cells and increased mitotic figures, including atypical forms. Notably, the apocrine-type secretion and myoepithelial layer characteristic of benign ceruminous adenomas are not usually present in the malignant form. The ceroid (cerumen, wax) pigment granules normally found in the cytoplasm of benign ceruminous glands are absent (Fig. 19.7). The *ceruminous adenoid cystic carcinoma* subtype shows identical features to the same lesion growing from major and minor salivary glands, composed of masses of small cells with hyperchromatic, carrot-shaped nuclei, surrounding punched-out round spaces containing a basophilic secretion and reduplicated basement membrane (Figs. 19.8 and 19.9) and clefting from the surrounding stroma. Mucoepidermoid carcinoma shows similar features to salivary gland primaries (Fig. 19.9).



**FIGURE 19.7**

**A**, High-grade ceruminous adenocarcinoma with central comedo-type necrosis. Severe nuclear pleomorphism is noted. **B**, Back-to-back glandular pattern with cells that show apocrine-type snouting.

**FIGURE 19.8**

Benign apocrine ceruminous glands are seen to the right of an adenoid cystic carcinoma, which is composed of small cells arranged in a cribriform pattern.

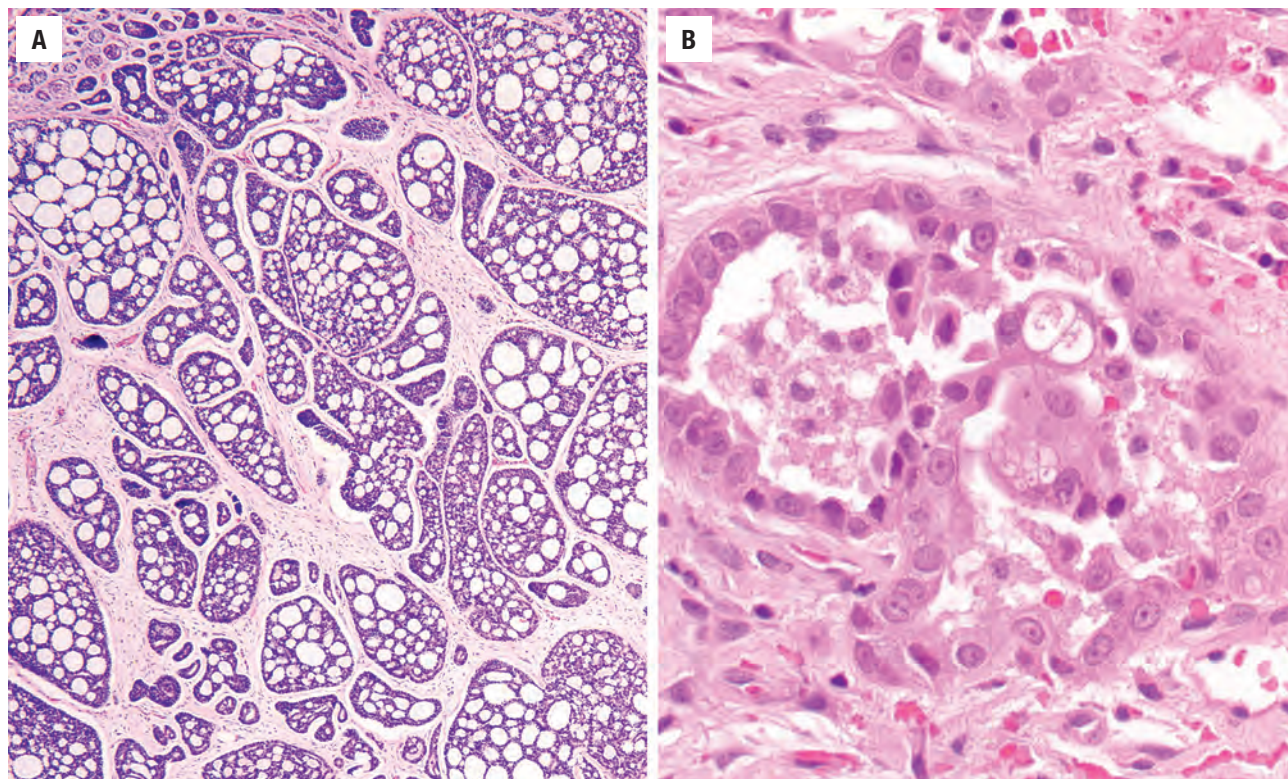
#### ANCILLARY STUDIES

Immunohistochemistry may highlight the basal cells (p63, p40, CK5/6, S100 protein) if they are present, whereas the luminal tumor cells are uniquely CK7 and preferentially CD117 positive. Ki-67 highlights an increased proliferation index.

#### DIFFERENTIAL DIAGNOSIS

The most important aspect of the differential diagnosis is to exclude direct invasion from a parotid gland primary, best achieved through careful imaging. Metastatic adenocarcinomas (discussed later) may also be raised in the differential diagnosis, but a clinical history and unique



**FIGURE 19.9**

**A.** Multiple patterns are seen in adenoid cystic carcinoma, including the cribriform pattern composed of punched out spaces filled with blue-pink amorphous material. **B.** This mucoepidermoid ceruminous carcinoma shows mucinous differentiation with a transitional-type epithelium.

histology should make the distinction. Separation from ceruminous adenoma is difficult on small biopsy. However, carcinomas are invasive, have pleomorphism and mitotic figures, and lack ceroid.

### PROGNOSIS AND THERAPY

A wide, radical (complete) resection is required, especially for ceruminous adenoid cystic carcinoma. Radiation is only used for palliation and usually for cases of ceruminous adenocarcinoma, NOS and mucoepidermoid carcinoma. Multiple recurrences (especially if the margins are positive) and metastasis (lung rather than lymph nodes) may be seen. The overall prognosis is approximately 50 % at 5 years.

### ■ METASTATIC NEOPLASMS

Excluding neoplasms that directly invade from a contiguous site into the ear, metastatic tumors spread by blood or lymphatic channels from a noncontiguous site. Lymphomas and leukemias, as systemic diseases, are excluded by definition. Metastases to the ear and temporal bone generally occur late in the course of the cancer

producing the metastases. Although unusual in surgical pathology material during life, autopsy studies show temporal bone involvement in approximately 20 % of cancer patients, virtually all of whom also had disseminated malignant disease.

### CLINICAL FEATURES

Patients tend to be older, and females are more frequently affected than males, although this is dependent on tumor type. Most lesions that metastasize to the ear and temporal bone are carcinomas and melanomas, with few sarcomas identified. Presentation is often late in the underlying disease course. Most patients are asymptomatic but may present with hearing loss, dizziness, tinnitus, facial palsy, otalgia, and/or otorrhea. Tumors are usually bilateral and multifocal. The petrous apex is the most common site (~80 %), although the mastoid bone, internal auditory canal, and middle ear can also be affected.

### PATHOLOGIC FEATURES

Tumors that develop as a consequence of hematogenous spread (lymphovascular invasion) include breast (~25 %;



**METASTATIC NEOPLASMS—DISEASE FACT SHEET****Definition**

- Metastatic tumors spread by blood or lymphatic channels from noncontiguous sites (not direct invasion from adjacent neoplasms)

**Incidence and Location**

- Approximately 20% of patients with disseminated malignant tumors will have ear/temporal bone metastasis
- Petrous apex most common (80%)

**Sex and Age Distribution**

- Sex differences based on primary site
- Usually older patients with widely disseminated disease

**Clinical Features**

- Usually asymptomatic
- Hearing loss, tinnitus, vertigo, facial palsy, otalgia, otorrhea
- Tumors usually bilateral and multifocal

**Prognosis and Treatment**

- Generally poor outcome reflecting underlying stage of primary tumor
- Surgery for symptomatic relief, with adjuvant therapy for palliation

(Fig. 19.10), lung (~10%), kidney, gastrointestinal tract (Fig. 19.11), prostate (~10%), and melanoma (~6%). Virtually any tumor, including mesenchymal tumors, can metastasize to this location. In general, metastatic deposits maintain the phenotype of the primary. Rarely are the ear and temporal bone metastases the initial presentation of the disease, and consequently an extensive clinical or histologic work-up is seldom necessary. Direct extension from the parotid gland region (Fig. 19.12), eustachian tube, posterior fossa (skull), and external ear is seen.

**METASTATIC NEOPLASMS—PATHOLOGIC FEATURES****Microscopic**

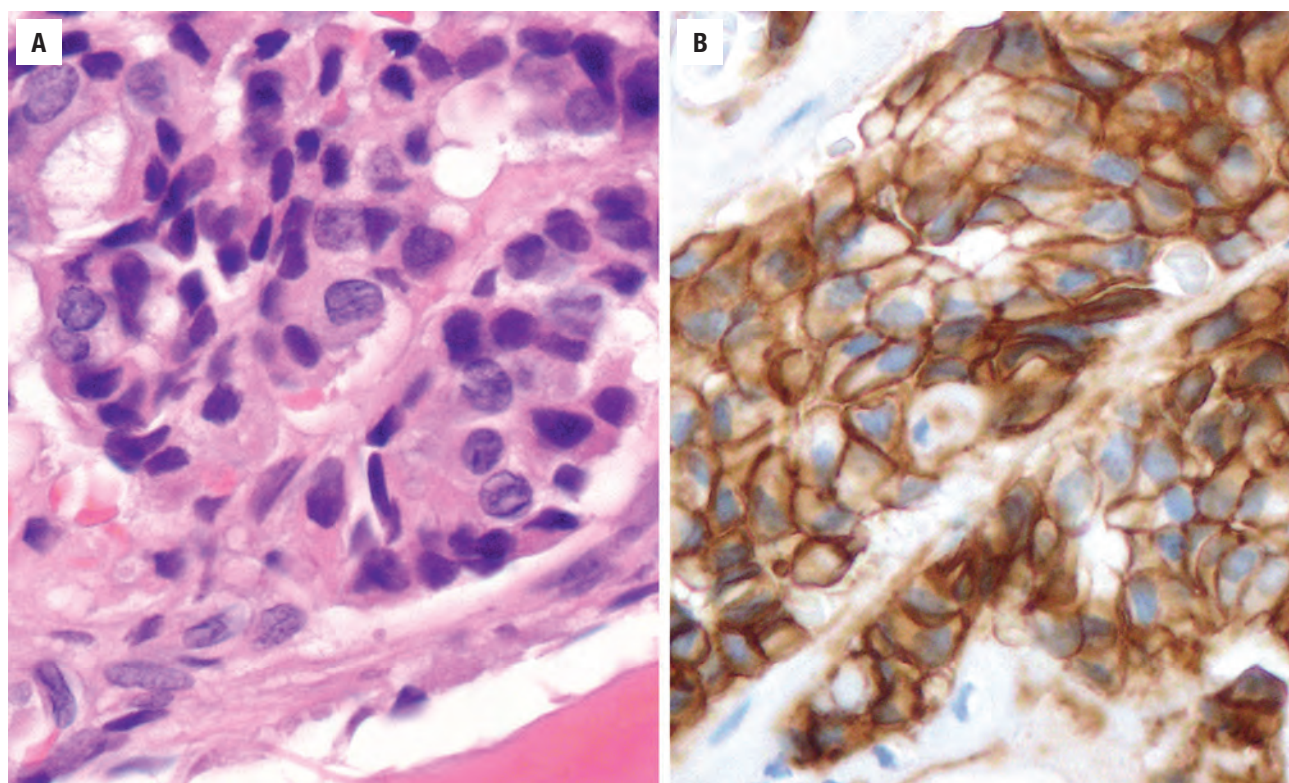
- Primary adenocarcinoma is vanishingly rare, so metastasis should be excluded first
- Main sources are carcinomas of breast, lung, kidney, gastrointestinal tract, prostate, thyroid, larynx
- Melanoma and mesenchymal tumors also seen
- Histology mimics primary tumor

**Immunohistochemical Findings**

- Selected and pertinent to primary site

**Pathologic Differential Diagnosis**

- Ceruminous adenocarcinoma, direct invasion from adjacent sites/organs, primary ear adenocarcinoma

**FIGURE 19.10**

**A**, Metastatic breast carcinoma within the temporal bone. Gland formation is prominent. **B**, HER-2/neu immunoreactivity may help to support a diagnosis of breast carcinoma.



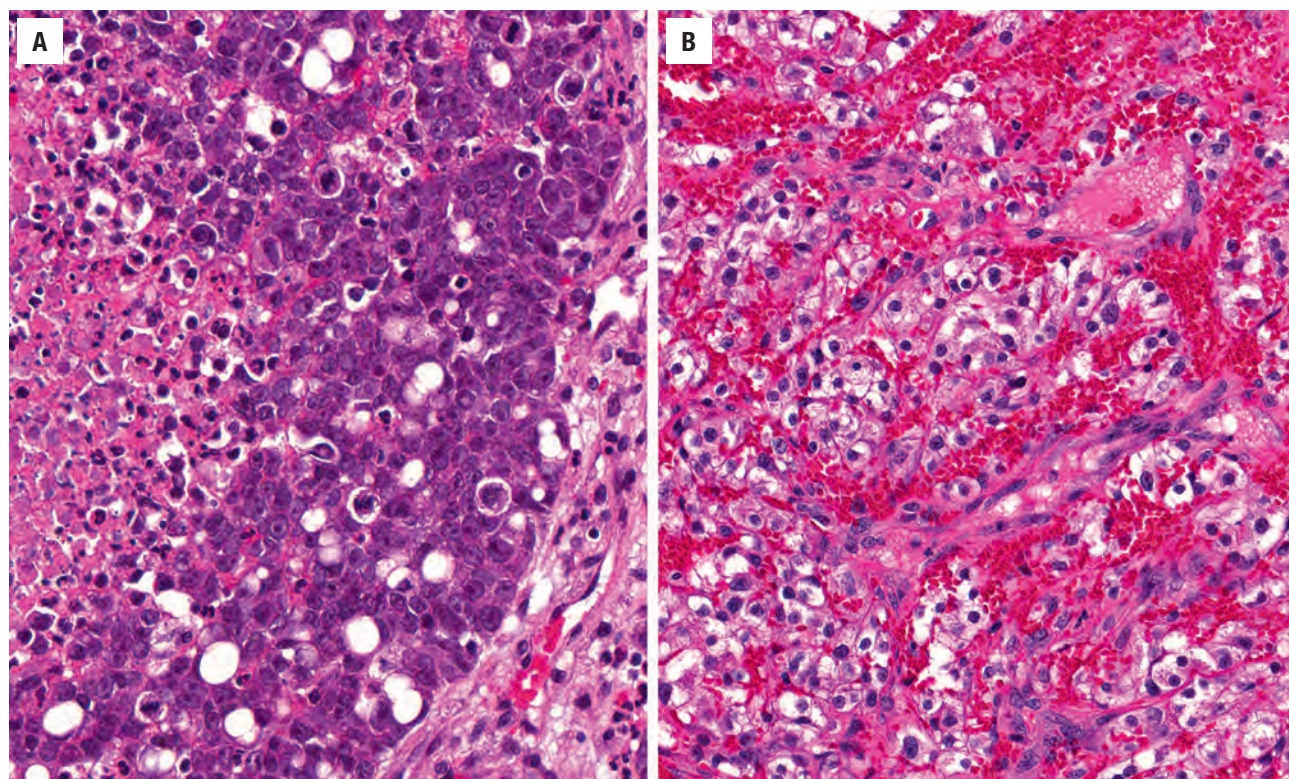


**FIGURE 19.11**

**A**, Metastatic colon adenocarcinoma usually has a different histologic appearance than primary ear/temporal bone tumors. **B**, Metastatic renal cell carcinoma, clear cell type, shows a pseudoalveolar architecture with extravasated erythrocytes.

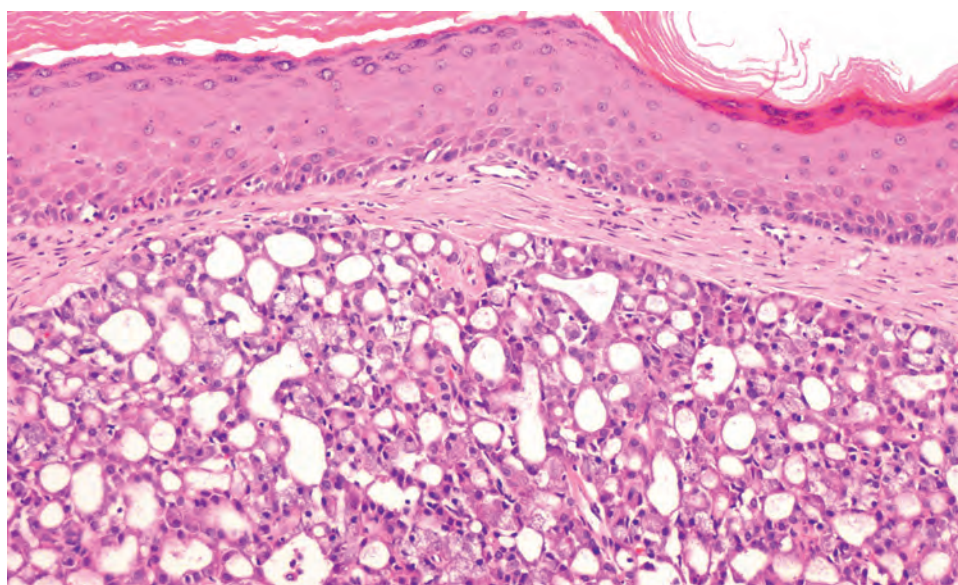


**FIGURE 19.12**

Direct infiltration into the ear canal from an acinic cell carcinoma of the parotid gland. Note the intact surface epithelium.



**ANCILLARY STUDIES**

Because primary adenocarcinoma of the ear and temporal bone is vanishingly rare, adenocarcinomas should be presumed to be metastatic. Selective use of immunostains helps to confirm the metastasis and reveal the tissue of origin. In general, it is important to consider how primary ear lesions may react and use this as a point of comparison or exclusion.

**DIFFERENTIAL DIAGNOSIS**

A poorly differentiated ear primary may mimic a metastatic tumor. Separation is often achieved by careful examination of architectural and histologic features

judicious use of immunohistochemistry, and correlation with clinical history and radiographic studies.

**PROGNOSIS AND THERAPY**

The overall prognosis matches the underlying disease; however, ear metastasis generally occurs in the setting of disseminated disease and thus portends a relatively poor prognosis. Surgery may be of value in selected cases for symptomatic relief, whereas adjuvant therapy can occasionally have a palliative effect.

**SUGGESTED READINGS**

The complete Suggested Readings list is available online at [ExpertConsult.com](http://ExpertConsult.com).

## SUGGESTED READINGS

**Squamous Cell Carcinoma (External Auditory Canal and Middle Ear)**

1. Bibas AG, et al. Squamous cell carcinoma of the temporal bone. *J Laryngol Otol*. 2008;122:1156–1161.
2. Fleiner F, et al. Cancer of the external auditory canal—diagnostic and treatment. *Indian J Otolaryngol Head Neck Surg*. 2009;61(4):270–274.
3. Hosokawa S, et al. Carcinoma of the external auditory canal: histological and treatment groups. *B-ENT*. 2014;10(4):259–264.
4. Johns ME, et al. Squamous cell carcinoma of the external auditory canal. A clinicopathologic study of 20 cases. *Arch Otolaryngol*. 1974;100(1):45–49.
5. Liang J, et al. Immunohistochemical characterization of the epidermoid formation in the middle ear. *Laryngoscope*. 2003;113:1007–1014.
6. Mazzoni A, et al. Primary squamous cell carcinoma of the external auditory canal: surgical treatment and long-term outcomes. *Acta Otorhinolaryngol Ital*. 2014;34(2):129–137.
7. Michaels L, et al. Squamous cell carcinoma of the middle ear. *Clin Otolaryngol*. 1980;5:235–248.
8. Moody SA, et al. Squamous cell carcinoma of the external auditory canal: an evaluation of a staging system. *Am J Otol*. 2000;21:582–588.
9. Nyrop M. Cancer of the external auditory canal. *Arch Otolaryngol Head Neck Surg*. 2002;128:834–837.
10. Ouaz K, et al. Cancer of the external auditory canal. *Eur Ann Otorhinolaryngol Head Neck Dis*. 2013;130(4):175–182.
11. Repanos C, et al. Great auricular nerve perineural spread of squamous cell carcinoma. *ANZ J Surg*. 2012;82(3):179–180.
12. Shockley WW, et al. Squamous cell carcinoma of the external ear: a review of 75 cases. *Otolaryngol Head Neck Surg*. 1987;97:308–312.
13. Shu MT, et al. Radiation-induced squamous cell carcinoma of the external auditory canal. *Otol Neurotol*. 2011;32(3):e24–e25.
14. Stafford ND, et al. Verrucous carcinoma in the external auditory canal. *Am J Otol*. 1986;7:443–445.
15. Tay G, et al. Squamous cell carcinoma of the ear arising in patients after radiotherapy for nasopharyngeal carcinoma. *Eur Arch Otorhinolaryngol*. 2014;271(1):149–156.
16. Wermker K, et al. Prediction score for lymph node metastasis from cutaneous squamous cell carcinoma of the external ear. *Eur J Surg Oncol*. 2015;41(1):128–135.
17. Zhang T, et al. The misdiagnosis of external auditory canal carcinoma. *Eur Arch Otorhinolaryngol*. 2013;270(5):1607–1613.
8. Jan JC, et al. Ceruminous adenocarcinoma with extensive parotid, cervical, and distant metastases: case report and review of literature. *Arch Otolaryngol Head Neck Surg*. 2008;134(6):663–666.
9. Lynde CW, et al. Tumors of ceruminous glands. *J Am Acad Dermatol*. 1984;11:841–847.
10. Mansour P, et al. Ceruminous gland tumours: a reappraisal. *J Laryngol Otol*. 1992;106:727–732.
11. Michel RG, et al. Ceruminous gland adenocarcinoma: a light and electron microscopic study. *Cancer*. 1978;41:545–553.
12. Mills RG, et al. Ceruminoma—a defunct diagnosis. *J Laryngol Otol*. 1995;109:180–188.
13. Mourad WF, et al. Trimodality approach for ceruminous muco-epidermoid carcinoma of the external auditory canal. *J Laryngol Otol*. 2013;127(2):203–206.
14. Nádasdy T, et al. Adenocarcinoma of ceruminous glands. Ultrastructural, immunohistochemical and lectin histochemical studies. *Acta Morphol Hung*. 1991;39(2):157–165.
15. Perzin KH, et al. Adenoid cystic carcinoma involving the external auditory canal. A clinicopathologic study of 16 cases. *Cancer*. 1982;50:2873–2883.
16. Pulec JL. Glandular tumors of the external auditory canal. *Laryngoscope*. 1977;87:1601–1612.
17. Wetli CV, et al. Tumors of ceruminous glands. *Cancer*. 1972;29(5):1169–1178.

**Metastatic Neoplasms**

1. Bakhos D, et al. Two cases of temporal bone metastases as presenting sign of lung cancer. *Eur Ann Otorhinolaryngol Head Neck Dis*. 2012;129(1):54–57.
2. Carson HJ, et al. Metastasis of colonic adenocarcinoma to the external ear canal: an unusual case with a complex pattern of disease progression. *Ear Nose Throat J*. 2005;84(1):36–38.
3. Cumberworth VL, et al. Late metastasis of breast carcinoma to the external auditory canal. *J Laryngol Otol*. 1994;108:808–810.
4. Della Puppa A, et al. Internal auditory canal metastasis. *J Neurosurg Sci*. 2010;54(4):159–162.
5. Gloria-Cruz TI, et al. Metastases to temporal bones from primary nonsystemic malignant neoplasms. *Arch Otolaryngol Head Neck Surg*. 2000;126:209–214.
6. Imauchi Y, et al. Metastasis of cervical esophageal carcinoma to the temporal bone—a study of the temporal bone histology. *Auris Nasus Larynx*. 2001;28(2):169–172.
7. Michaelson PG, et al. Metastatic renal cell carcinoma presenting in the external auditory canal. *Otolaryngol Head Neck Surg*. 2005;133(6):979–980.
8. Sahin AA, et al. Temporal bone involvement by prostatic adenocarcinoma: report of two cases and review of the literature. *Head Neck*. 1991;13:349–354.
9. Saldanha CB, et al. Metastasis to the temporal bone, secondary to carcinoma of the bladder. *J Laryngol Otol*. 1989;103(6):599–601.
10. Shrivastava V, et al. Prostate cancer metastatic to the external auditory canals. *Clin Genitourin Cancer*. 2007;5(5):341–343.
11. Suzuki T, et al. Sudden hearing loss due to meningeal carcinomatosis from rectal carcinoma. *Auris Nasus Larynx*. 2006;33(3):315–319.
12. Thirunavukarasu V, et al. Post-aural ache: an unusual presentation of a metastatic temporal bone lesion from a primary adenocarcinoma of the lung. *J Laryngol Otol*. 2013;127(10):1017–1019.
13. Vasileiadis I, et al. External auditory canal mass as the first manifestation of a bronchogenic carcinoma: report of a rare case. *Ann Otol Rhinol Laryngol*. 2013;122(6):378–381.
14. Yasumatsu R, et al. Metastatic hepatocellular carcinoma of the external auditory canal. *World J Gastroenterol*. 2007;13(47):6436–6438.
15. Yildirim-Baylan M, et al. Bladder cancer metastases to the temporal bone. *Otol Neurotol*. 2011;32(5):e40–e41.
1. Aikawa H, et al. Adenoid cystic carcinoma of the external auditory canal: correlation between histological features and MRI appearances. *Br J Radiol*. 1997;70:530–532.
2. Crain N, et al. Ceruminous gland carcinomas: a clinicopathologic and immunophenotypic study of 17 cases. *Head Neck Pathol*. 2009;3:1–17.
3. Dehner LP, et al. Primary tumors of the external and middle ear. Benign and malignant glandular neoplasms. *Arch Otolaryngol*. 1980;106:13–19.
4. Dong F, et al. Adenoid cystic carcinoma of the external auditory canal. *Laryngoscope*. 2008;118(9):1591–1596.
5. Hicks GW. Tumors arising from the glandular structures of the external auditory canal. *Laryngoscope*. 1983;93(3):326–340.
6. Ito K, et al. An immunohistochemical study of adenoid cystic carcinoma of the external auditory canal. *Eur Arch Otorhinolaryngol*. 1993;250:240–244.
7. Iqbal A, et al. Ceruminous gland neoplasia. *Br J Plast Surg*. 1998;51(4):317–320.

**Ceruminous Adenocarcinoma**



# Non-Neoplastic Lesions of the Neck (Soft Tissue, Bone, and Lymph Node)

■ Diana Bell

Non-neoplastic lesions of the neck can be broadly classified into developmental cystic anomalies; infections and related diseases/lesions; and reactive, inflammatory, and tumor-like lesions.

## ■ BRANCHIAL CLEFT ANOMALIES

Branchial cleft anomalies are divided according to the branchial apparatus involved and are further divided into cysts, sinuses, or fistulas. When the name *branchial cyst* is used without further qualifications, it generally refers to a cyst of second branchial cleft origin, which accounts for 80% to 90% of all branchial cleft anomalies. Branchial cleft cysts constitute 17% of all congenital cervical cysts in children and encompass branchial cysts, sinuses, and/or fistulas.

### CLINICAL FEATURES

Patients usually present with a painless mass measuring up to 6 cm. The location is dependent on the cleft origin, and second-cleft anomalies are characteristically located along the anterior border of the sternocleidomastoid muscle, from the hyoid bone to the suprasternal notch. There is no sex difference and 75% of patients are between 20 and 40 years of age at the time of diagnosis. The cysts are usually nontender masses unless they become secondarily inflamed or infected. They may be bilateral, especially when they are associated with congenital syndromes.

### RADIOGRAPHIC FEATURES

The radiology will characteristically show a well-circumscribed cystic mass with a smooth cavity and a dense wall.

## PATHOLOGIC FEATURES

### GROSS FINDINGS

Grossly, the cysts are unilocular and between 2 and 6 cm in diameter; they usually contain clear to grumous material (Fig. 20.1).

### MICROSCOPIC FINDINGS

A branchial cleft cyst is usually lined by stratified squamous epithelium (90%), occasionally by respiratory epithelium (8%), or, rarely, by both (2%) (Fig. 20.2). Lymphoid aggregates with or without reactive germinal

## BRANCHIAL CLEFT ANOMALIES—DISEASE FACT SHEET

### Definition

- A lateral cervical cyst that results from congenital/developmental defects arising from the primitive second branchial apparatus

### Incidence and Location

- 17% of all congenital cervical cysts
- Lateral neck, with most near the mandibular angle

### Sex and Age Distribution

- Equal sex distribution
- 75% of patients are 20–40 years of age
- Less than 3% occur in patients > 50 years

### Clinical Features

- Mass along the anterior border of the sternocleidomastoid muscle
- Painless mass of long duration
- May become secondarily infected, which will bring it to clinical attention

### Prognosis and Therapy

- Complete excision
- Recurrence rate about 3%

**FIGURE 20.1**

There is a thick, fibrous wall of connective tissue surrounding this cyst, which is filled with tan-yellow material.

centers are found beneath the epithelial lining in some 70% to 85% of cysts (Figs. 20.2 and 20.3). However, as no true lymph node architecture is present, there are no sinuses, medullary regions, or interfollicular zones. Keratinaceous debris may be present within the cavity. Acute and chronic inflammation, foreign-body giant cell reaction, and fibrosis are secondary changes often seen in the wall of the cyst.

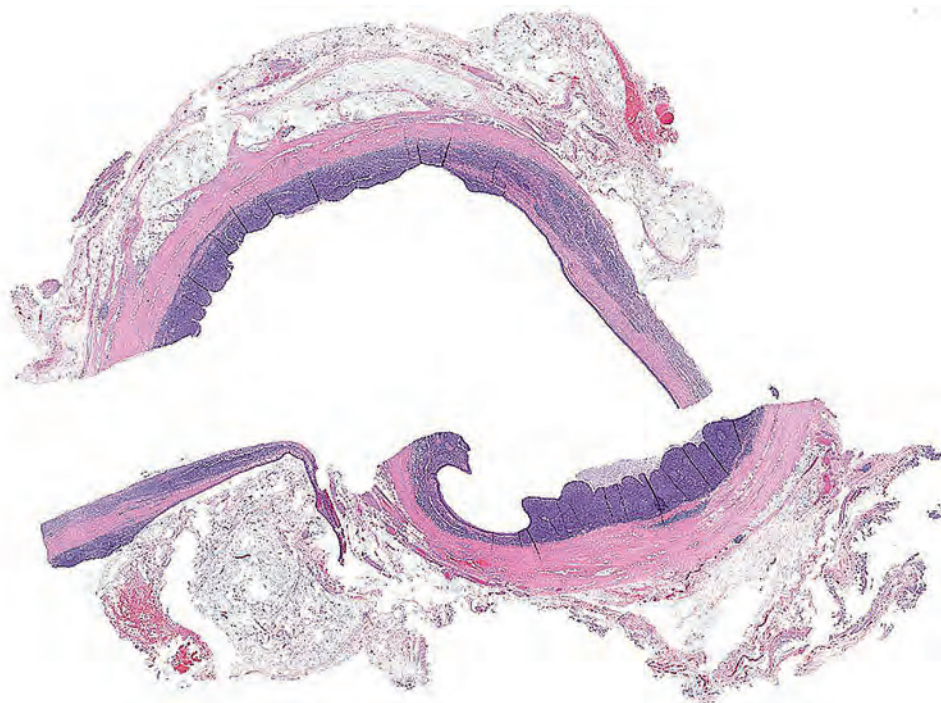
### ANCILLARY STUDIES

#### IMMUNOHISTOCHEMICAL FINDINGS

The epithelial lining expresses cytokeratins of different types, depending on the type of lining—pseudostratified respiratory, transitional, stratified keratinizing, or non-keratinizing. However, these cysts are negative for high-risk human papillomavirus (HPV), a useful feature for distinguishing them from metastatic cystic squamous cell carcinoma. It is important to realize that up to 50% of benign branchial cleft cysts may show p16 immunopositivity, necessitating the use of a more specific HPV testing method (e.g., in situ hybridization).

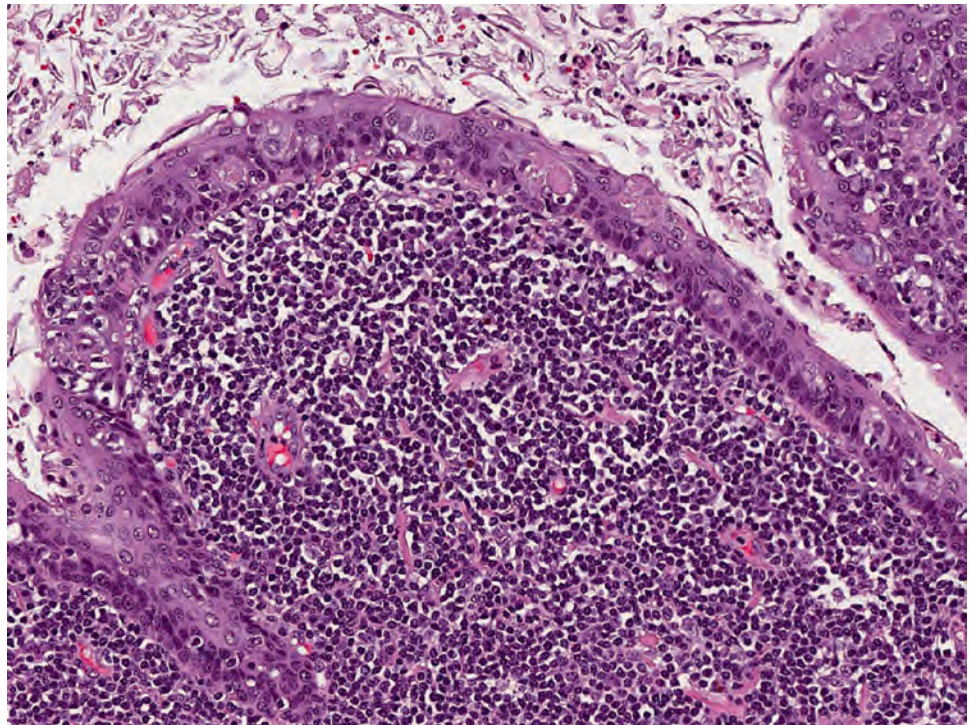
#### FINE NEEDLE ASPIRATION

Fine needle aspiration (FNA) of a branchial cleft cyst will yield a thick, yellow, pus-like material, which microscopically is composed of anucleate squames, amorphous debris and macrophages, and variable lymphoid cells (Fig. 20.4). Viable mature squamous epithelial cells and occasionally columnar respiratory epithelial

**FIGURE 20.2**

This unilocular branchial cleft cyst has a very thin, well-defined squamous lining subtended by a rich inflammatory infiltrate with the formation of lymphoid germinal centers.



**FIGURE 20.3**

Keratinaceous debris is frequently present; the cyst may be stratified ciliated columnar epithelium or squamous epithelium.

### BRANCHIAL CLEFT ANOMALIES—PATHOLOGIC FEATURES

#### Gross Findings

- Cystic mass up to 6 cm, containing fluid

#### Microscopic Findings

- Cysts lined by squamous epithelium (90%), respiratory epithelium (8%), or both (2%)
- Keratinaceous debris
- Lymphoid tissue, nodular or diffuse (70%–85%)
- Fibrosis and secondary changes in the cyst wall

#### Fine Needle Aspiration

- Mature squamous epithelium
- Anucleate squames
- Debris, including macrophages
- Lymphoid infiltrate

#### Immunohistochemical Findings

- Cytokeratins-positive (type dependent on lining)
- Negative for ISH high-risk HPV, though p16 may be positive

#### Pathologic Differential Diagnosis

- Metastatic cystic squamous cell carcinoma, thymic cyst, bronchial cyst, thyroglossal duct cyst

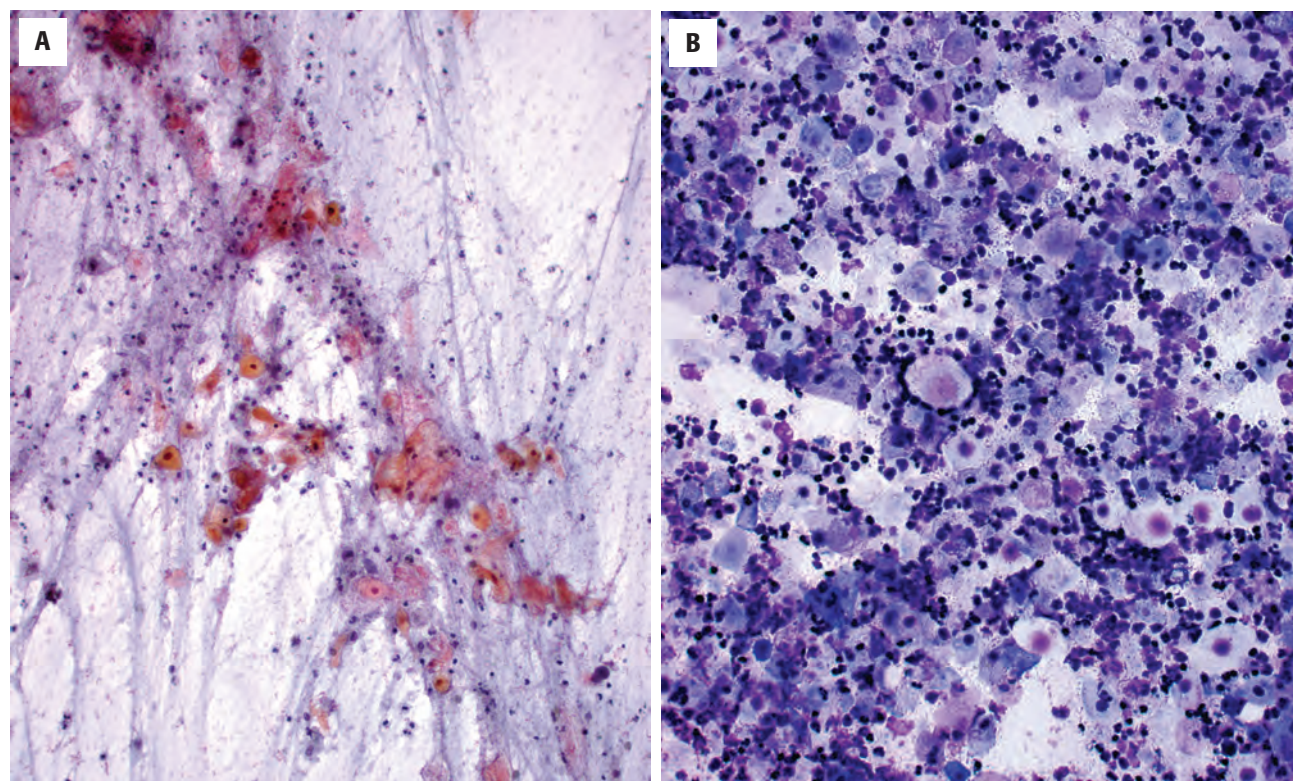
HPV, Human papillomavirus.

cells are often noted. Significant epithelial atypia should not be present, and, in the right clinical setting, atypia would suggest potential malignancy.

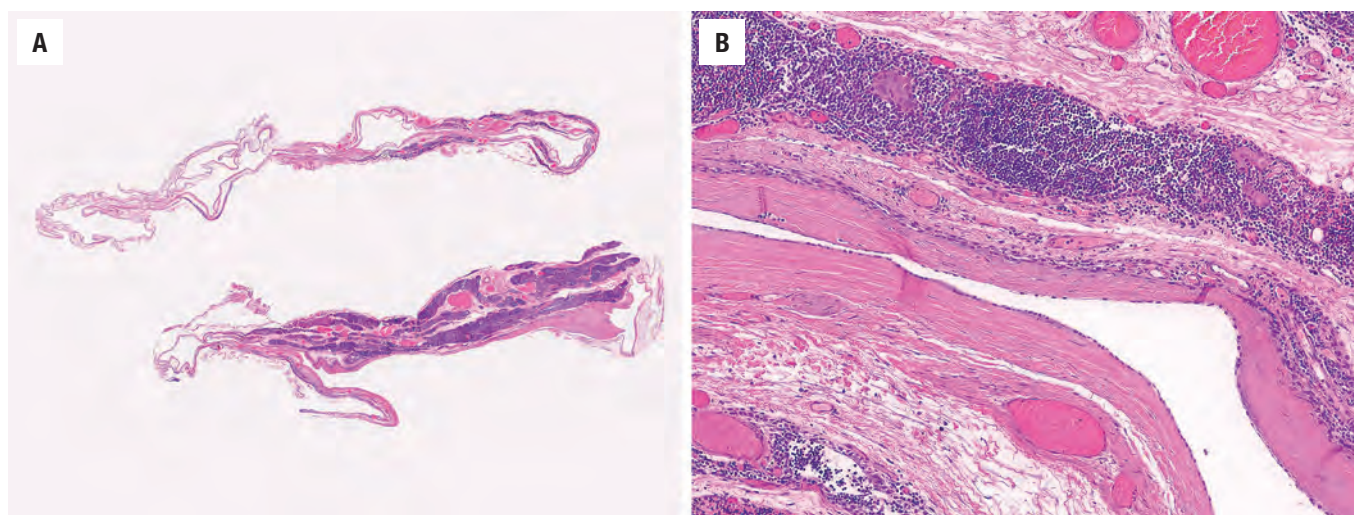
### DIFFERENTIAL DIAGNOSIS

*Thymic cysts* contain thymic tissue within the wall, including Hassall corpuscles (concentric island of squamous cells with central keratinization; Fig. 20.5). A *thyroglossal duct cyst* occurs in the midline and is often associated with thyroid tissue. *Bronchial cysts* are more common in the subcutaneous tissue of the supraclavicular region and are lined by respiratory mucosa with smooth muscle and bronchial glands in the wall. *Dermoid cysts* can also be in the differential, although these will present in a midline location and, histologically, will show adnexal structures within the wall. The most important differential diagnostic consideration, however, particularly if the lesion is in an adult, is *metastatic cystic squamous cell carcinoma*. These lesions usually have a malignant epithelial lining and may be positive for p16 and HPV (by immunohistochemistry and in situ hybridization, respectively), especially when the primary tumor is from the oropharynx. Metastatic HPV-related oropharyngeal carcinomas may even rarely retain cilia, further mimicking a benign cyst. Confusion and controversy exists between the diagnosis of metastatic squamous cell carcinoma and that of a carcinoma arising in a branchiogenic cyst. Evidence suggests that cases of purported *branchiogenic carcinoma* almost always represent



**FIGURE 20.4**

Keratinaceous debris with inflammatory cells is diagnostic of a branchial cleft cyst in fine needle aspiration smears as long as there are no atypia in the epithelial component. **(A)** Alcohol-fixed, Papanicolaou-stained smear. **(B)** Air-dried, Diff-Quik-stained smear.

**FIGURE 20.5**

**(A, B)** The wall of this thymic cyst contains lymphoid aggregates, fat, and Hassall corpuscles; this appearance may sometimes mimic that of a branchial cleft cyst.



metastatic HPV-related squamous cell carcinomas from the oropharynx that are clinically occult.

PROGNOSIS AND THERAPY

The recurrence rate is about 3 % for cases with no history of infection or prior surgery. However, recurrence is more common in second operations or when the lesion is infected at the time of operation (14 % and 21 %, respectively). A complete excision of the cyst is indicated.

CAT SCRATCH DISEASE (GRANULOMATOUS INFLAMMATION)

Many infectious agents can affect the skin, soft tissues, and lymph nodes of the neck. Cat scratch disease (CSD; cat scratch fever, cat scratch adenitis, Debre syndrome, Foshay-Mollaret syndrome) will be highlighted as a single example. CSD is a zoonotic infection caused by any one of a group of rickettsial microorganisms of the alpha-2 subgroup of alpha-protobacteria, specifically *Bartonella henselae*, with some taxonomic overlap with *Afipia felis* and *B. quintana*. *B. henselae* is a gram-negative pleomorphic rod-shaped bacillus. CSD occurs worldwide and is more common in autumn and winter, especially in dwellings where cats are kept as pets.

CLINICAL FEATURES

The characteristic clinical syndrome consists of an initial lesion that develops at the site of inoculation followed by enlargement of regional lymph nodes. The primary lesion, a cat scratch or bite, will cause skin erythema within 3 to 5 days and may be slightly painful (in some cases, this initial injury goes unnoticed). Within 3 weeks of inoculation, acute regional lymphadenopathy develops proximal to the inoculation site. The affected lymph nodes are those that drain the primary lesion; they become enlarged and tender. Occasionally they drain to the surface, forming a fistula. Lymphadenopathy involves only one nodal region in about 85 % of patients, while matted, suppurative lymph nodes are seen in some 15 % of patients. Constitutional symptoms may be present; these include a low-grade fever, headaches, and malaise. Most infections occur in children and young adults, usually less than 21 years of age. In general, most cases are self-limited and resolve within 3 to 4 months, although lymphadenitis may persist for years. Atypical presentations include ocular, neurologic, or visceral organ involvement. Erythema nodosum, an erythematous nodular panniculitis associated with a variety of conditions, is

CAT SCRATCH DISEASE (GRANULOMATOUS INFLAMMATION)—FACT SHEET

Definition

- A zoonotic infection caused by a group of gram-negative rickettsial bacilli, specifically *Bartonella henselae*, *Afipia felis*, and *B. quintana*

Incidence

- Worldwide; most common in autumn and winter
- Found especially in dwellings where cats are kept as pets

Morbidity and Mortality

- No mortality unless patients are immunosuppressed

Sex and Age Distribution

- Equal sex distribution
- Children and young adults between 3 and 21 years (majority < 8 years)

Clinical Features

- Usually associated with a cat scratch or bite
- Solitary, tender lymphadenopathy
- Constitutional symptoms including low-grade fever, malaise, and headaches

Prognosis and Therapy

- Excellent prognosis
- Supportive therapy is adequate, although ciprofloxacin has been advocated by a few
- Excision and drainage plus antibiotics may yield best overall results

seen in only 2 % of patients. Serology for *B. henselae* antibodies does not work well, and culture, using brain-heart infusion agar with incubation at 32°C, is difficult to perform owing to the organism’s fastidious and slow growth.

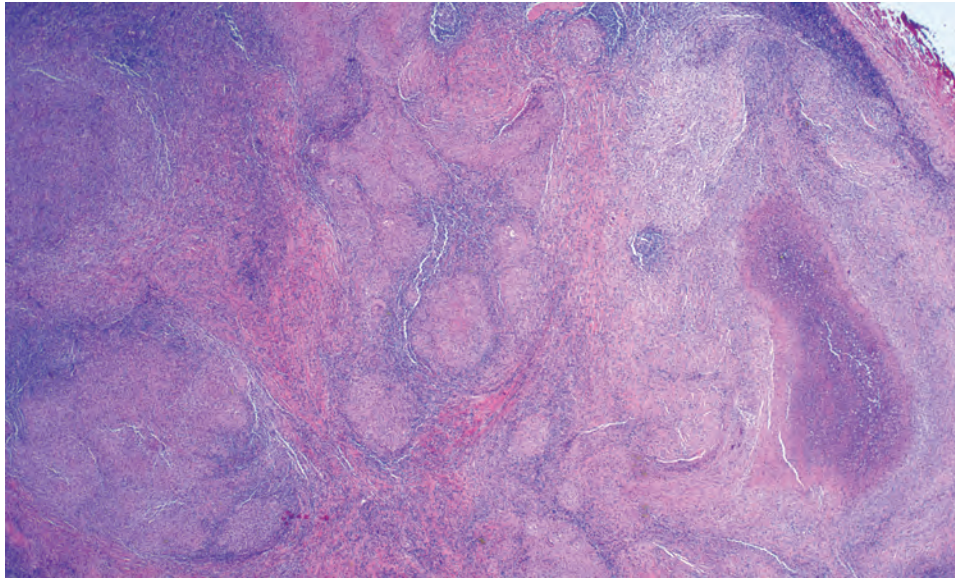
PATHOLOGIC FEATURES

GROSS FINDINGS

The lymph nodes are soft and swollen and have foci of necrosis on the cut surface. They measure up to 10 cm.

MICROSCOPIC FINDINGS

The histology can be divided into three stages of progression. Histologically, early lesions show foci of swollen capillaries, which have a pink hyaline appearance and are associated with lymphoid follicular hyperplasia. As the foci of suppuration grow, they coalesce to form stellate abscesses (Fig. 20.6), which become surrounded by histiocytes, epithelioid cells, and occasionally giant cells. Eventually a granulomatous perimeter surrounding a central area of caseation remains. The caseous center,

**FIGURE 20.6**

This characteristic stellate abscess has central area of necrosis surrounded by a granulomatous reaction and inflammatory cells, in this case indicative of cat scratch disease.

### CAT SCRATCH DISEASE (GRANULOMATOUS INFLAMMATION)—PATHOLOGIC FEATURES

#### Gross Findings

- Enlarged, swollen lymph nodes with areas of necrosis

#### Microscopic Findings

- Three stages of progression are generally identified:
  - Early stage shows follicular hyperplasia
  - Stellate abscess surrounded by histiocytes, epithelioid cells, and occasionally giant cells
  - Late stage shows granulomas with central caseation

#### Fine Needle Aspiration

- Granulomatous inflammation with epithelioid histiocytes and occasional giant cells
- Lymphoid infiltrate
- Necrotic debris, depending on stage

#### Special Techniques

- Warthin-Starry stain for rod-shaped organisms
- Immunoperoxidase stain
- DNA primer for use with polymerase chain reaction
- Culture using brain-heart agar at 32°C

#### Pathologic Differential Diagnosis

- Primarily infectious agents (brucellosis, tuberculosis, lymphogranuloma venereum)
- May also resemble other reactive nodal conditions, including Kikuchi-Fujimoto disease and Kimura disease
- Lymphoma

unlike the centers of tuberculosis lesions, is rarely calcified. Obviously these changes are nonspecific, requiring additional studies to document the causative agent.

### ANCILLARY STUDIES

#### HISTOCHEMICAL FINDINGS

Tissue Gram stain will demonstrate the bacillus, but a Warthin-Starry silver impregnation technique stains the 1- to 3- $\mu$ m pleomorphic bacteria black, highlighting the organisms in the wall of the vessels in the early stages and in the suppurative areas in the later stages. Stains are often difficult to interpret because of high background staining in the necrotic debris.

#### FINE NEEDLE ASPIRATION

The features on FNA are those of a granulomatous inflammation and are nonspecific. Epithelioid histiocytes, Langhans-type giant cells, inflammatory cells, and debris are present to a variable degree depending on stage. However, additional studies, including culture and/or special studies, are necessary to confirm the diagnosis.

#### IMMUNOHISTOCHEMICAL FINDINGS

An indirect immunoperoxidase stain has been developed to demonstrate the organisms. However, it is capricious, requiring a specific volume of cases to achieve quality, reproducible results, so it is not of much practical value.



ADDITIONAL STUDIES

DNA primers have been developed for use with a polymerase chain reaction (PCR) for the evaluation of CSD.

DIFFERENTIAL DIAGNOSIS

Stellate abscesses, characteristic of CSD, are also seen in a broad range of *infectious etiologies*, including mycobacterial infections, fungal infections, toxoplasmosis, tularemia, brucellosis, leishmaniasis, chancroid, granuloma inguinale, and lymphogranuloma. However, many of these are exceedingly rare or nonexistent in the head and neck region or have very specific culture findings. *Metastatic disease* will show neoplastic cells with areas of necrosis, while *lymphoma* will show specific atypical lymphoid elements, with ancillary studies supporting monoclonality. *Sarcoidosis* shows tight, well-formed, small granulomas without necrosis, while a *branchial cleft cyst* usually lacks granulomatous or suppurative inflammation. *Kikuchi-Fujimoto disease* is a histiocytic necrotizing lymphadenitis characterized by crescentic histiocytes and marked karyorrhectic debris without neutrophils. Most helpful in diagnosing CSD is a high index of suspicion based on the clinical history, leading to the demonstration of bacilli by silver impregnation or by culture. *Kimura disease* is a rare benign chronic inflammatory disease that usually involves deep subcutaneous tissue and lymph nodes of the head and neck with regional lymphadenopathy and salivary gland enlargement. The disease is more common in middle-aged Asian populations; elevated serum immunoglobulin E (IgE) levels and peripheral blood eosinophilia are common. The histologic features of Kimura disease include preserved nodal architecture; follicular hyperplasia with reactive germinal centers; well-formed mantle zones; eosinophilic infiltrates involving the interfollicular areas, sinusoidal areas, perinodal soft tissue, and subcutaneous tissue; and proliferation of postcapillary venules.

PROGNOSIS AND THERAPY

The prognosis is excellent with supportive treatment alone. Antibiotics are generally not required to relieve symptoms, but ciprofloxacin has been advocated by a few. Excision with drainage and antibiotics yields the best overall outcome.

■ BACILLARY ANGIOMATOSIS

Bacillary angiomatosis is a vascular, proliferative form of *Bartonella* (*B. henselae* or *B. quintana*) infection that occurs primarily in immunocompromised persons.

CLINICAL FEATURES

Bacillary angiomatosis almost always occurs in immunocompromised patients and is characterized by reddish, berry-like lesions on the skin surrounded by a collar of scale, which may bleed significantly if traumatized. Lesions can also occur on the oral mucosa, tongue, oropharynx, and nose. Infection with *B. henselae* is spread by fleas from cats, while *B. quintana* is spread by lice. Disease may spread throughout the reticuloendothelial system, causing bacillary peliosis, mainly in patients carrying human immunodeficiency virus (HIV). Patients with bacillary angiomatosis commonly have a history of HIV infection, organ transplantation, leukemia, or chemotherapy. Inoculation bartonellosis may be evident in immunocompetent individuals as a pyogenic granuloma-like nodule at the site of a cat scratch.

PATHOLOGIC FEATURES

MICROSCOPIC FINDINGS

Some bacillary angiomatosis lesions have two distinct regions of vascular proliferation, a superficial one resembling a pyogenic granuloma or popular angiokeratoma and a deeper one similar to hemangioma, with a proliferation of small blood vessels lined by protuberant endothelial cells closely adherent to one another in an epithelioid pattern (Fig. 20.7A and B). The presence of neutrophils adjacent to blood vessels is noteworthy and may be an important diagnostic clue. Granular material resembling fibrin may adjoin neutrophils. This bacterium is observed

BACILLARY ANGIOMATOSIS—DISEASE FACT SHEET

Definition

- A vascular, proliferative form of *Bartonella* (*B. henselae* or *B. quintana*) infection

Risk Factors

- HIV infections, CLL/SLL, chemotherapy, organ transplantation, cat contact, low socioeconomic status

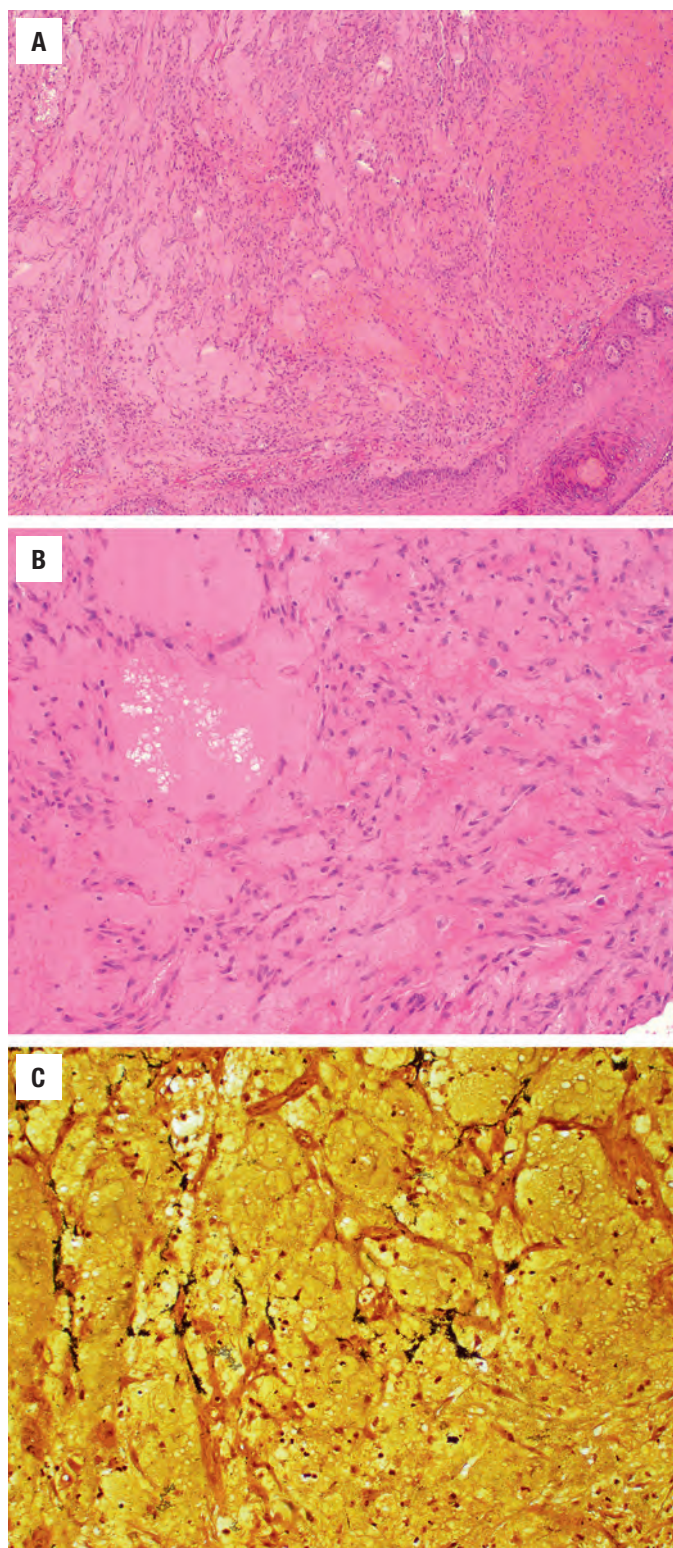
Sex Distribution

- Approximately 90% of the patients are male, probably as disproportionate number of HIV patients are also men

Prognosis and Therapy

- Prognosis is excellent; antibiotics are mostly curative with lesions resolving completely after treatment with erythromycin or doxycycline

CLL/SLL, Chronic lymphocytic leukemia/small lymphocytic lymphoma.

**FIGURE 20.7**

Bacillary angiomatosis. (A) Lesion showing masses of blood vessels of varying dimensions lined by swollen endothelial cells. (B) Blood vessels of variable dimensions lined by swollen endothelial cells that contain bacilli. (C) Black, rod-shaped organisms accentuated with the Warthin–Starry silver stain.

best with either Warthin–Starry (Fig. 20.7C) or Steiner stain.

### ANCILLARY STUDIES

As in the case of cat scratch disease, Gram stain will demonstrate the bacillus; both Warthin–Starry and Steiner silver impregnation stains will highlight the organisms. An immunohistochemical stain for anti-HHV8 antibody is negative, excluding a Kaposi sarcoma.

### DIFFERENTIAL DIAGNOSIS

On histologic grounds, hemangiomas/epithelioid hemangiomas show lobulated architectural growth, with the absence of granular material or neutrophilic debris. Angiosarcoma and Kaposi sarcoma display interconnecting vascular channels, a slit-like appearance, extravasated red blood cells, endothelial cytologic atypia, and piled-up, hyaline globular inclusions. Neutrophilic infiltrates, debris, and granular deposits are absent. Immunoreactivity with anti-HHV8 is helpful for a Kaposi sarcoma. Verruca peruana is endemic to Peru.

### PROGNOSIS AND THERAPY

The prognosis is excellent, with most lesions resolving after treatment with erythromycin or doxycycline. Persistent disease may require longer management.

### BACILLARY ANGIOMATOSIS—PATHOLOGIC FEATURES

#### Gross Findings

- Cutaneous reddish lesions that may have crusting or scaling, or mucosal pyogenic granulomas

#### Microscopic Findings

- Well-circumscribed lobular capillary proliferation similar to lobular capillary hemangioma
- Small capillaries arranged around ectatic vessels lined by prominent endothelial cells
- Absence of cytological atypia, itosis, and necrosis
- Presence of neutrophils and debris adjacent to capillary proliferations, and associated granular bacterial clumps

#### Special Techniques

- Warthin–Starry stain, polymerase chain reaction, cultures

#### Pathologic Differential Diagnosis

- Lobular capillary hemangioma, angiosarcoma, Kaposi sarcoma, verruca peruana, verruca, angiokeratoma



## ■ CERVICOFACIAL ACTINOMYCOSIS

Cervical actinomycosis is a subacute-to-chronic disease characterized by abscess formation, draining sinus tracts, fistulas, and tissue fibrosis.

### CLINICAL FEATURES

Actinomycosis can mimic malignancy and granulomatous disease; therefore it is included in the differential of any head and neck soft tissue swelling. Cervicofacial involvement accounts for half of the cases of actinomycosis. Cervicofacial actinomycosis (lumpy jaw) is caused by branching gram-positive bacteria of Actinomycetales order, family Actinomycetaceae, genus *Actinomyces*. *Mycobacterium mycobacterium* and *Nocardia* species also belong to the same order, and infections caused by these are difficult to distinguish from *Actinomyces*. Organisms of the

*Actinomyces* species are non-spore-forming anaerobes with morphologic variability that colonize the normal oral flora within tonsillar crypts, periodontal pockets, dental plaques, and carious teeth. Actinomycosis is rare. Improved dental hygiene and antibiotics have contributed to the declining incidence of this disease.

Patients with cervical actinomycosis present with nodular lesions at the jaw angle (Fig. 20.8A). These progress in size and number, with multiple abscesses, and ultimately, form sinuses with cheek or submandibular openings. Sulfur granules may be noted in the exudates. Lymphadenopathy is not typical. When masticator muscles are involved, trismus is usually present.

### RADIOGRAPHIC FEATURES

Computed tomography (CT) scanning reveals an infiltrative mass into surrounding tissues, with areas of attenuation that enhance with contrast.

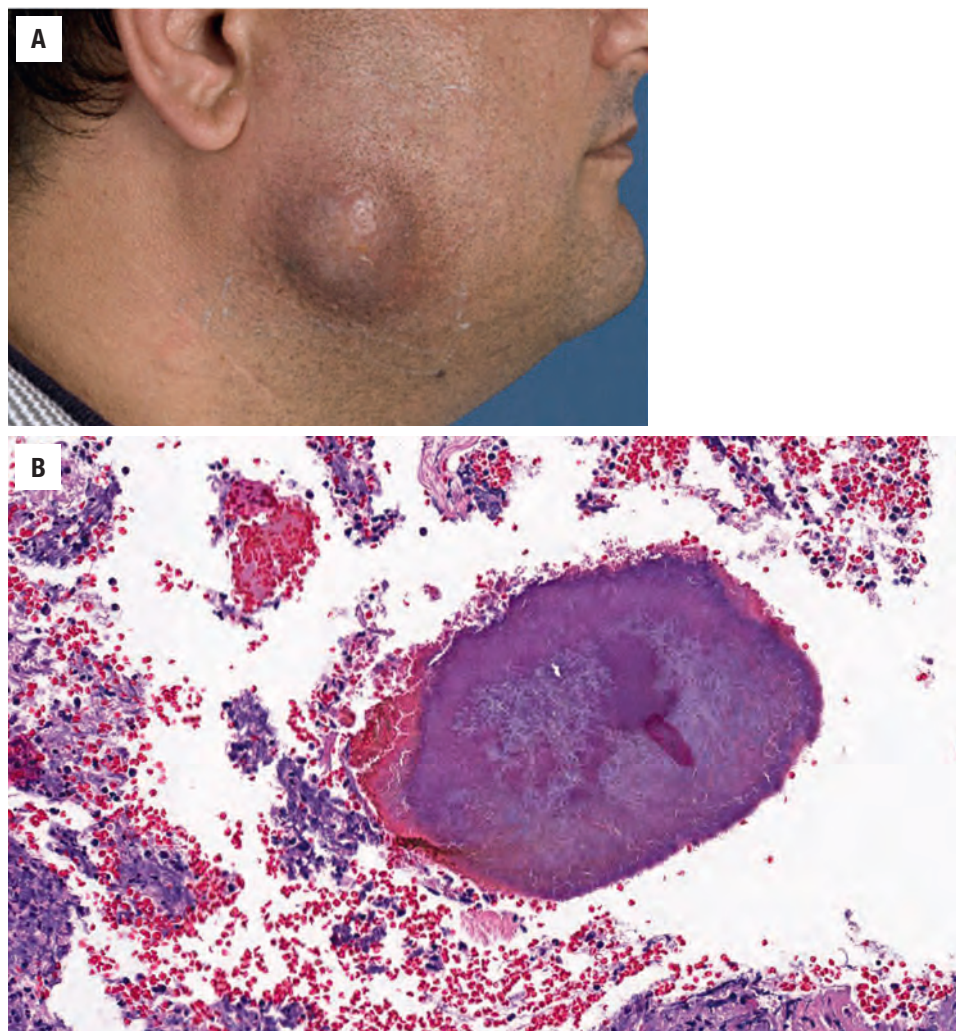


**FIGURE 20.8**

(A) Swelling of the cheek in a patient with actinomycosis. Note the possible beginning of a sinus tract. (Reproduced with permission from PMID: PMC3731091.)  
(B) Abundant inflammatory cells surrounding basophilic sulfur granules, which are composed of a large number of filaments arranged in a radiating pattern.

**CERVICOFACIAL ACTINOMYCOSIS—DISEASE FACT SHEET****Definition**

- Actinomycosis is a suppurative and granulomatous anaerobic infectious disease, caused by *Actinomyces israelii*, that spreads into adjacent soft tissue without regard for tissue planes or lymphatic drainage; it may also be associated with a draining sinus tract

**Risk Factors**

- Dental caries, dental manipulations, and oromaxillofacial trauma are the most common triggering effects, including osteonecrosis of the jaw or maxilla with radiation therapy or bisphosphonates use

**Sex and Age Distribution**

- More common in men (males > females (3:1))
- Affects all ages, with most cases reported in young to middle-aged adults (age 20–50 years)

**Prognosis and Therapy**

- With early diagnosis and appropriate treatment with penicillin G, prognosis is excellent
- Drain abscess and excise fistula

**PATHOLOGIC FEATURES****MICROSCOPIC FINDINGS**

Actinomycosis is characterized by mixed suppurative and granulomatous inflammatory reactions, connective tissue proliferation, and the pathognomonic sulfur granules (Fig. 20.8B). The sulfur granules are yellow particles up to 1 mm in diameter and are visible to the naked eye. Gram stain shows gram-positive microcolonies and intertwined branching filaments with radially arranged peripheral hyphae; associated companion gram-positive and gram-negative cocci and rods are present.

**SPECIAL TECHNIQUES**

Direct identification and/or isolation of the infectious organism from a clinical specimen or from sulfur granules is necessary for definitive diagnosis.

A preliminary diagnosis alternatively, can be made by examining the sulfur granules crushed between two slides, stained with methylene blue, and microscopically examined for the characteristic features of actinomycetes.

**PROGNOSIS AND THERAPY**

A high dose of penicillin G over a prolonged period is the cornerstone of therapy for actinomycosis. Surgical options may include incision and drainage of abscesses or excision of the sinus tract.

**CERVICOFACIAL ACTINOMYCOSIS—PATHOLOGIC FEATURES****Gross Findings**

- Multiple small, communicating abscesses with sinus tracts that produce a purulent discharge

**Microscopic Findings**

- Distinctive yellowish sulfur granules (rounded or spherical particles, < 1 mm) or tangled masses or branched and unbranched wavy bacterial filaments

**■ NODULAR FASCIITIS**

Nodular fasciitis is a mass-forming myofibroblastic proliferation that usually occurs in the subcutaneous tissues and typically displays a tissue culture-like growth pattern. Cranial fasciitis and intravascular fasciitis are histologically related lesions. Nearly 30% of nodular fasciitis develops in the head and neck.

**CLINICAL FEATURES**

Most patients give a history of a rapidly growing mass present for only a short duration (up to 3 weeks). It usually measures less than 3 cm and almost always less than 5 cm. Nodular fasciitis is almost always subcutaneous, although occasional cases are intramuscular. The upper extremities and head and neck are the most frequently affected regions. It has been reported in the neck, face, orbit, oral cavity, and ear. Nodular fasciitis is more common in children and young adults up to 35 years of age. It is rare in adults above age 60. There is no sex predilection. Trauma is considered an etiologic factor, although the trauma may be slight or of a limited degree (e.g., seat belt pushing against the neck).

**RADIOGRAPHIC FEATURES**

The presence of an infiltrative growth pattern and significant edema on imaging studies, coupled with a rapidly growing mass, are worrying imaging features.

**PATHOLOGIC FEATURES****GROSS FINDINGS**

The lesion consists of a round to oval, nodular, non-encapsulated mass usually measuring less than 3 cm in



greatest dimension (Fig. 20.9). There is often attachment to the fascia. The cut surfaces may be firm and gray-white or soft and gelatinous. Areas of cystic change are frequently noted.

#### MICROSCOPIC FINDINGS

Nodular fasciitis is a reactive soft tissue lesion, poorly circumscribed and irregularly stellate in appearance. It is composed of bundles of loosely arranged fibroblasts and myofibroblasts resembling the cells found in tissue culture or granulation tissue, with areas of central degeneration and extravasated erythrocytes (Fig. 20.10). Of note,

small, thin-walled vessels with an arborizing pattern and pools of stromal mucin can be seen. The fibroblasts have oval, pale-staining nuclei with prominent nucleoli and are arranged in short, irregular bundles and storiform fascicles (Fig. 20.11). Mitotic figures are common, but atypical mitoses are never seen (Fig. 20.12). Chronic

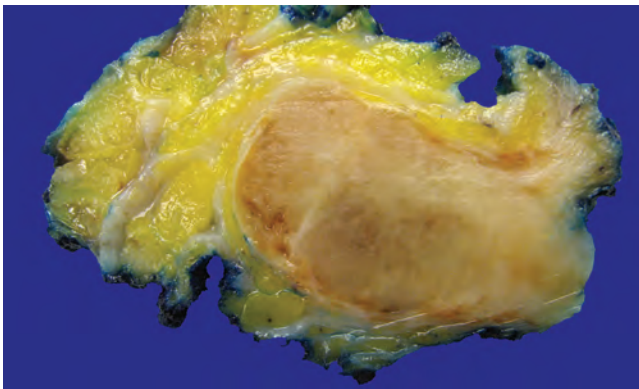


**FIGURE 20.9**

This focus of nodular fasciitis shows an oval, well-circumscribed but unencapsulated mass with a distinct appearance compared with the adjacent fat.

#### NODULAR FASCIITIS—DISEASE FACT SHEET

##### Definition

- A mass-forming myofibroblastic proliferation, usually within subcutaneous tissues

##### Incidence and Location

- Uncommon lesion
- Most common in upper extremities and head and neck

##### Sex and Age Distribution

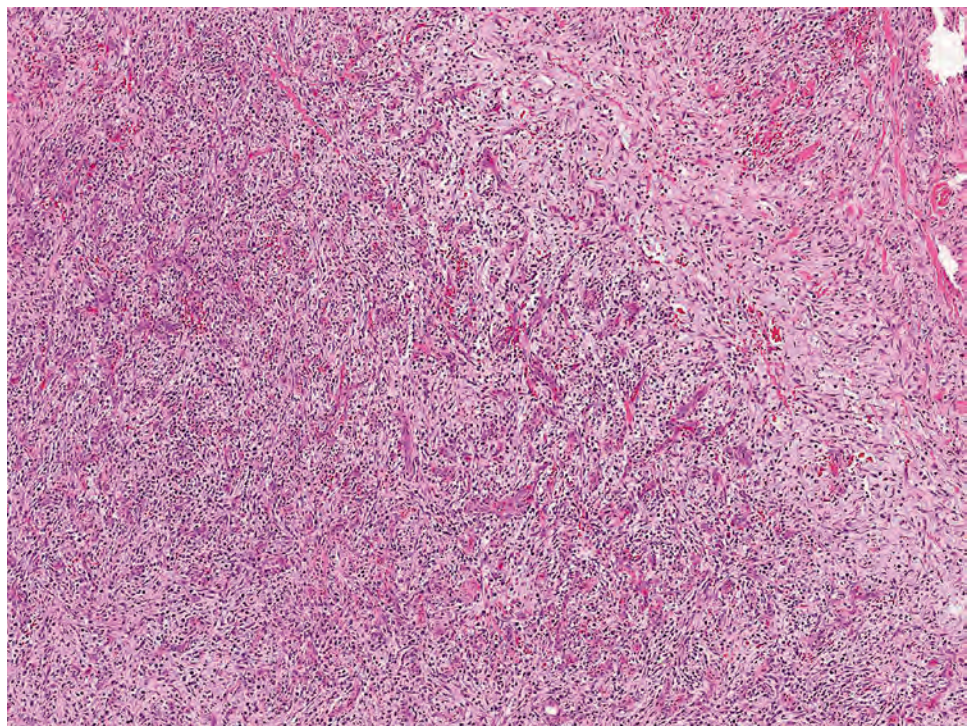
- Equal sex distribution
- Up to 35 years most commonly (rare after 60 years)

##### Clinical Features

- Rapidly growing mass of up to 3 weeks' duration
- Usually less than 3 cm mass
- Neck, orbit, and ear
- Trauma may play an etiologic role

##### Prognosis and Therapy

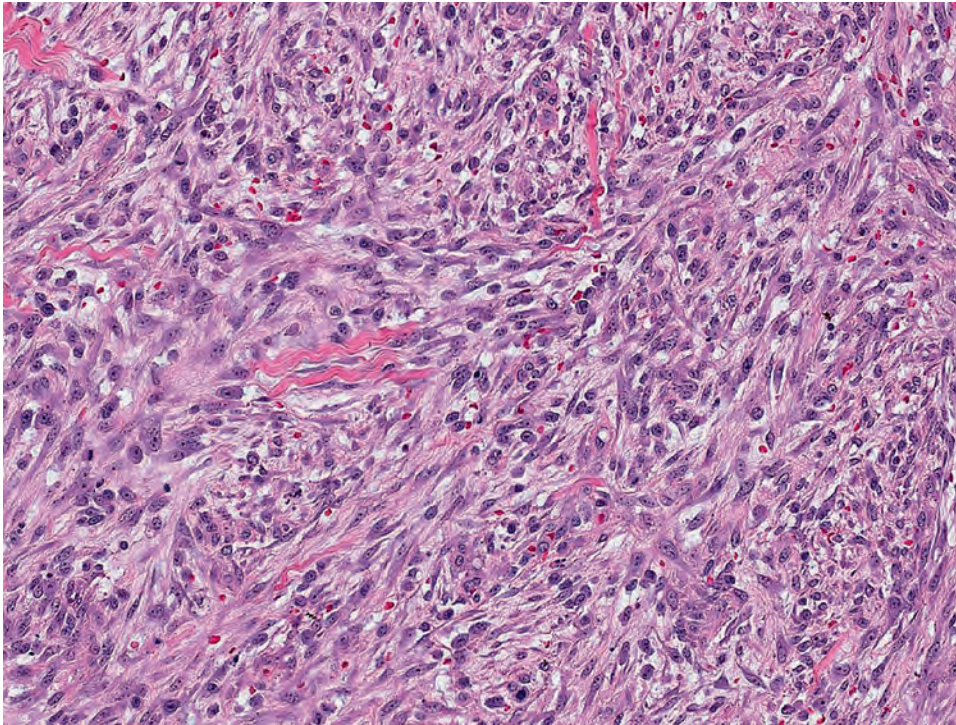
- Excellent prognosis with less than 2% recurrence rate
- Complete surgical excision



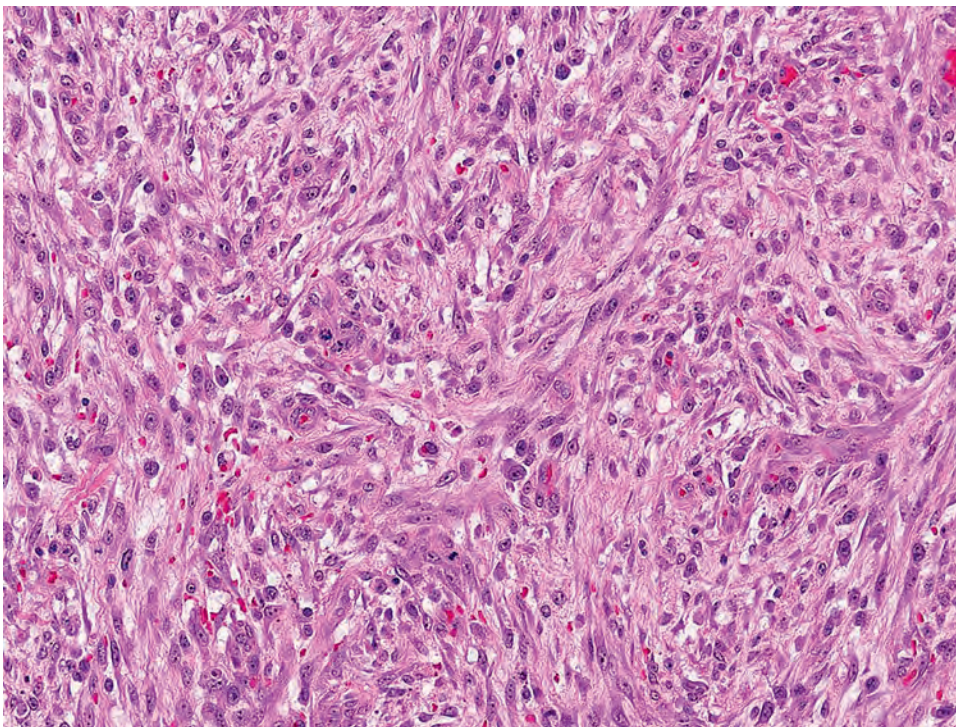
**FIGURE 20.10**

Nodular fasciitis with a tissue culture-like growth and myxoid degeneration.



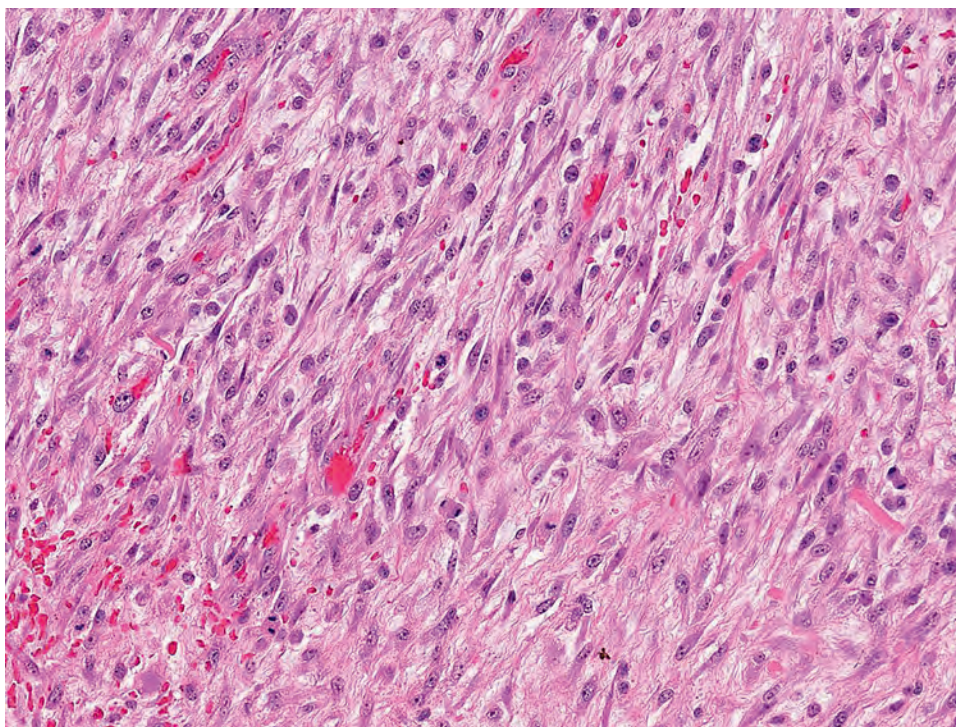
**FIGURE 20.11**

Tissue culture-like growth with collagen deposition and extravasated erythrocytes. A storiform growth pattern is typical for nodular fasciitis.

**FIGURE 20.12**

Short irregular bundles of fibroblasts arranged in a storiform pattern.



**FIGURE 20.13**

Collagen and fibroblasts with extravasated erythrocytes in nodular fasciitis.

### NODULAR FASCIITIS—PATHOLOGIC FEATURES

#### Gross Findings

- Solid to cystic nonencapsulated mass
- Usually less than 3 cm

#### Microscopic Findings

- Plump, immature fibroblasts resembling tissue culture
- Cystic spaces or areas of degeneration common
- Mitoses are abundant but not atypical
- Extravasated erythrocytes, inflammatory cells, keloid-like collagen, and giant cells often present

#### Fine Needle Aspiration

- Cellular smears
- Plump, spindled fibroblasts with wispy cytoplasmic extensions
- Binucleated forms may be seen
- Finely dispersed chromatin without atypia
- Blood, giant cells, and bundles of collagen occasionally present

#### Immunohistochemical Findings

- Not necessary for diagnosis, but actins are positive
- CD68-positive histiocytes
- Negative for keratin and S100 protein

#### Pathologic Differential Diagnosis

- Fibrosarcoma, rhabdomyosarcoma, fibromatosis, fibrous histiocytoma, fetal rhabdomyoma

inflammatory cells and giant cells are variably present. The deposition of keloid-like collagen increases with time, from small amounts in early lesions to extensive amounts at later stages (Fig. 20.13). Variants are defined by location: cranial fasciitis (involves skull and soft tissue of the scalp, may involve dura and meninges); intramuscular fasciitis (involves skeletal muscle); intravascular fasciitis (involves small to large veins and arteries); parosteal fasciitis (also known as ossifying fasciitis or fasciitis ossificans, involving periosteum).

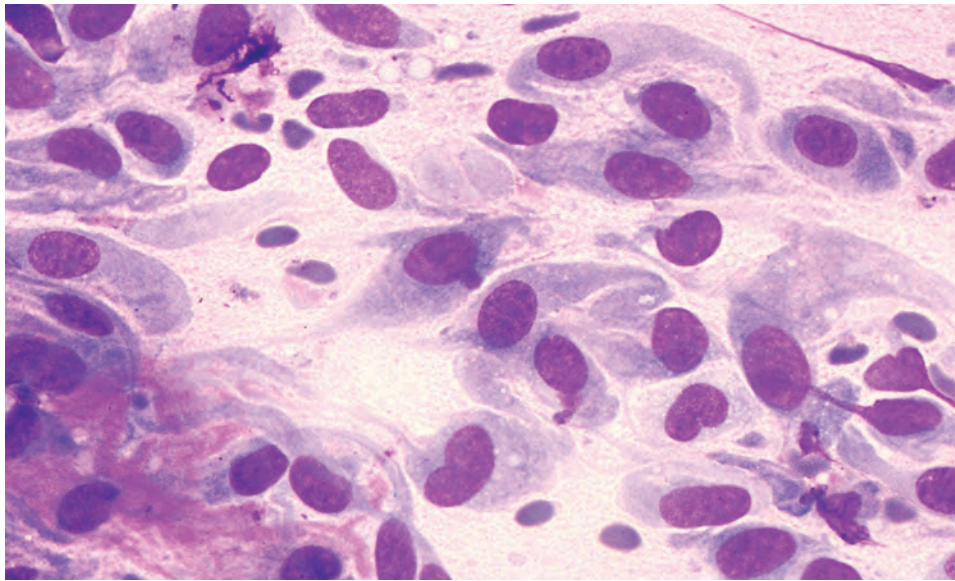
### ANCILLARY STUDIES

#### ULTRASTRUCTURAL FINDINGS

The elongated, bipolar fibroblastic cells have abundant rough endoplasmic reticulum and cisternae with granular, electron-dense material. Intracytoplasmic bundles of microfilaments are also seen. There is a fine distribution of the nuclear chromatin. Collagen fibers are seen in the background.

#### IMMUNOHISTOCHEMICAL FINDINGS

Immunohistochemistry is not usually necessary for the diagnosis. The fibroblasts are positive with actins, while the histiocytes will be reactive with CD68. Desmin

**FIGURE 20.14**

Fine needle aspiration of nodular fasciitis. The cellular smear is composed of single, spindle, bipolar cells in a background of myxoid material. The slightly vacuolated cytoplasm appears wispy and “tadpole”-like, while the nuclear chromatin is delicate and evenly distributed. Nucleoli are prominent. (Air-dried May–Grünwald–Giemsa stain)

may rarely be positive, but keratin and S100 protein are typically negative.

#### MOLECULAR FINDINGS

Rearrangement of the ubiquitin-specific protease 6 (*USP6*) gene has been reported as a recurrent and specific finding in nodular fasciitis. Fluorescence in situ hybridization (FISH) analysis for *USP6* rearrangement is valuable in challenging cases, particularly small biopsies, in which the morphologic features of nodular fasciitis are not entirely represented.

#### FINE NEEDLE ASPIRATION

FNA will typically demonstrate a cellular smear composed of short, plump, spindled fibroblasts in a slightly myxoid background (Fig. 20.14). The cells may be binucleated, with eccentric nuclear placement. Mitotic figures are common, but there is no evidence of atypia. Blood and giant cells are seen in the background, and occasionally collagen may be present.

#### DIFFERENTIAL DIAGNOSIS

Nodular fasciitis is often clinically worrisome because of the presentation of a rapidly enlarging mass. The clinical differential diagnosis will include a variety of neoplastic conditions. Indeed, the histologic appearance can also be worrisome, and these lesions can be misdiagnosed as sarcoma (fibrosarcoma, rhabdomyosarcoma) or a variety of benign lesions. The cells in *fibrosarcoma* are

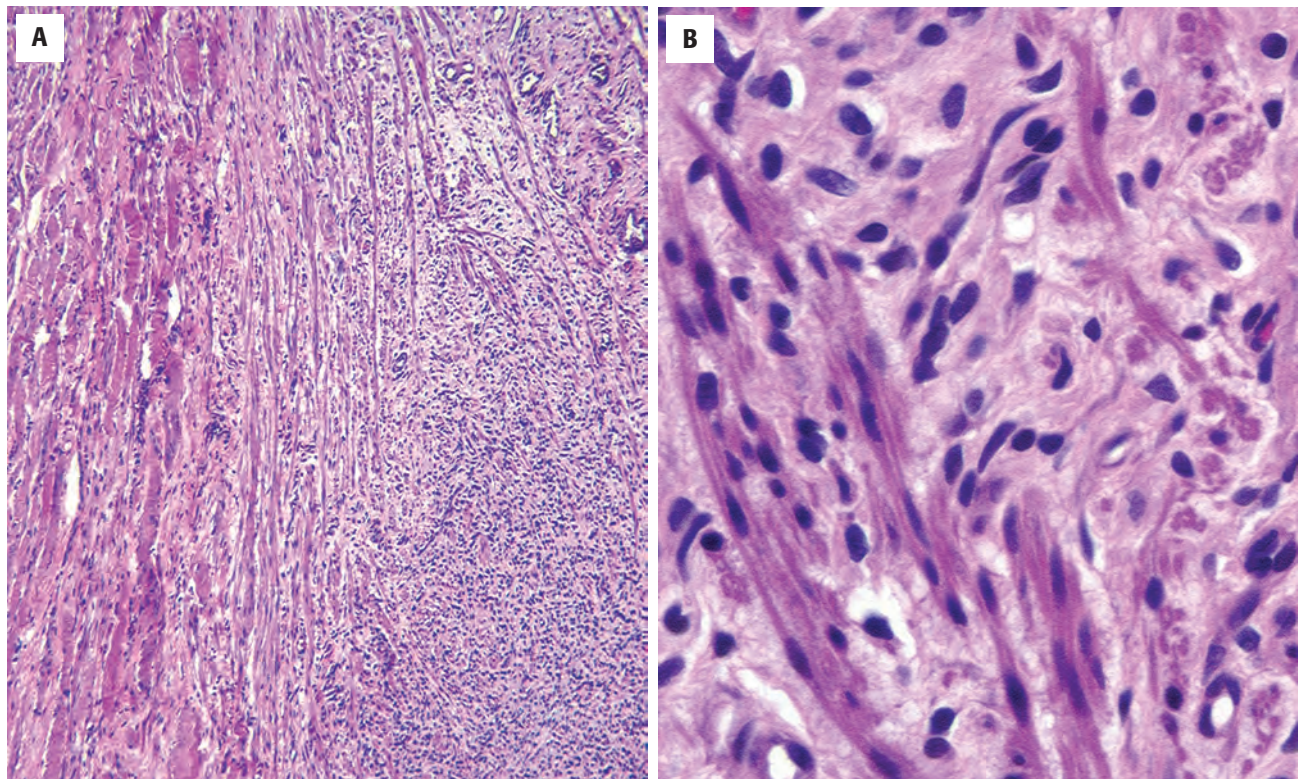
densely packed without stroma and are arranged in short, tight “herringbone” or “chevron” bundles. The individual cells differ much more in size and shape than those seen in nodular fasciitis and will often have numerous atypical mitoses. *Rhabdomyosarcoma* may occasionally have spindle-shaped cells, but it also tends to have pleomorphic cells with increased mitotic figures. Its unique immunohistochemical (muscle marker reactivity) and molecular profile (e.g., *FOXO1* gene fusions for alveolar type) will be quite useful in this differentiation.

The benign entities in the differential diagnosis of nodular fasciitis include fibromatosis, fibrous histiocytoma, and fetal rhabdomyoma. *Fibromatosis* is less circumscribed and usually larger; it often has an “invasive” growth pattern. It is characterized by slender spindle-shaped fibroblasts that are arranged in long sweeping fascicles separated by abundant, dense collagen. Although usually not necessary, immunohistochemistry will show strong nuclear reactivity for  $\beta$ -catenin. *Fibrous histiocytoma* is made up of more rounded cells that are arranged in a storiform pattern. *Fetal rhabdomyoma* has a gradient of cellularity, with large cells showing cross striations (strap cells) set in a bland but cellular stromal background (Fig. 20.15).

#### PROGNOSIS AND THERAPY

Complete excision is the treatment of choice. Recurrences are seen in some 2% of cases and usually develop shortly after surgery; this may represent a “reaction” to the trauma of surgery.



**FIGURE 20.15**

(A) Fetal rhabdomyoma with a gradient of cellularity and elongated strap-like cells. There is unremarkable skeletal muscle on the far left. (B) Large strap-like cells with cross striations are set in a cellular stroma of benign-appearing cells.

### ■ SINUS HISTIOCYTOSIS WITH MASSIVE LYMPHADENOPATHY (ROSAI-DORFMAN DISEASE)

Rosai-Dorfman disease (sinus histiocytosis with massive lymphadenopathy [SHML]) is a rare, idiopathic, histiocytic proliferation usually involving lymph nodes and following an indolent disease course. However, extranodal manifestations are frequent, especially in the upper aerodigestive tract. The histiocytes are considered to be part of the mononuclear phagocyte and immunoregulatory effector (M-PIRE) system belonging to the macrophage/histiocyte family. There is no known etiology, although immunodeficiency, autoimmune disease, or even a neoplastic process may be involved.

#### CLINICAL FEATURES

SHML is an uncommon condition that predominantly affects young black women (African and Caribbean origin), who present with massive lymphadenopathy, most commonly involving the cervical lymph nodes. However, nearly half of the affected patients will develop extranodal involvement, the majority of which (75%) occurs within the head and neck, such as the eyes, ocular

adnexae, paranasal sinuses, and nasal cavity. Extranodal disease may be part of generalized disease or separate from nodal disease. Typically, these patients with head and neck involvement present with local mass-effect symptoms related to the location, such as nasal obstruction, proptosis, ptosis, stridor, pain, and/or cranial nerve deficits. Patients with SHML may also present with fever, an elevated white blood cell count, and an elevated erythrocyte sedimentation rate, but the antineutrophil cytoplasmic antibody (ANCA) and proteinase 3 are negative.

#### RADIOGRAPHIC FEATURES

The radiographic features will depend on the location of the disease. In the sinonasal tract, for example, paranasal sinus disease can appear as a bulky, homogeneous mass, mimicking lymphoma.

#### PATHOLOGIC FEATURES

##### GROSS FINDINGS

Lymph nodes show remarkable enlargement but generally lack necrosis or cystic change. Sinonasal tract

**SINUS HISTIOCYTOSIS WITH MASSIVE LYMPHADENOPATHY (ROSAI-DORFMAN)—DISEASE FACT SHEET****Definition**

- Rosai-Dorfman disease is an idiopathic histiocytic proliferation

**Incidence and Location**

- Rare
- Majority have head and neck involvement, with about 50% demonstrating extranodal disease (ocular, paranasal sinuses)

**Morbidity**

- Direct mass effect into the cranial cavity

**Sex, Race, and Age Distribution**

- Females > males
- Predisposition in black patients
- Usually young

**Clinical Features**

- Cervical lymphadenopathy common
- Nasal obstruction, proptosis, cranial nerve deficits, and mass lesion
- Fever, elevated white blood cells, and erythrocyte sedimentation rate

**Prognosis and Therapy**

- Prognosis determined by extent and stage
- Spontaneous remission or death from complications both occur uncommonly
- Steroids conservatively manage localized disease, with surgery and/or radiation for more extensive disease

involvement results in polypoid to nodular masses, which may be fibrotic, with a gray to yellow cut surface.

**MICROSCOPIC FINDINGS**

In SHML, there is a characteristic pronounced dilation of the lymphoid sinuses, with an abundant lymphoplasmacytic infiltrate in the background (Fig. 20.16). The low-power appearance of these cellular compartments imparts a mottled appearance. Fibrosis may be associated with the dilated spaces. These sinuses are filled with abundant pale, histiocytic cells that demonstrate the nearly pathognomonic lymphophagocytosis or *emperipolesis* (Fig. 20.17A and B). There is often a clear halo around the phagocytized cells, a feature highlighted with S100 protein staining. The histiocytes tend to form clusters or nests. There is an overall lack of pleomorphism, and the nuclei do not have longitudinal grooves or folds. Of note, extranodal SHML tends to be more fibrotic and may demonstrate less *emperipolesis* than the nodal form. Furthermore, the plasma cell population, which may include Russell bodies, may be so heavy as to obscure the histiocytes. Although axiomatic, special stains for organisms will be negative.

**SINUS HISTIOCYTOSIS WITH MASSIVE LYMPHADENOPATHY (ROSAI-DORFMAN)—PATHOLOGIC FEATURES****Gross Findings**

- Greatly enlarged lymph nodes
- Polypoid masses in the sinonasal tract, which may be fibrotic

**Microscopic Findings**

- Marked dilation of the lymphoid sinuses
- Abundant lymphoplasmacytic infiltrate in the background
- Pale histiocytic cells in the sinuses demonstrating lymphophagocytosis or *emperipolesis*

**Immunohistochemical Findings**

- Positive with S100 protein, CD68, CD163,  $\alpha$ -1-chymotrypsin, Leu M3, lysozyme
- Negative with CD1a and CD207 (Langerin)

**Pathologic Differential Diagnosis**

- Rhinoscleroma, lepromatous leprosy, histiocytic lymphomas

**ANCILLARY STUDIES****ULTRASTRUCTURAL FINDINGS**

The histiocytes contain fat vacuoles and lack Birbeck granules.

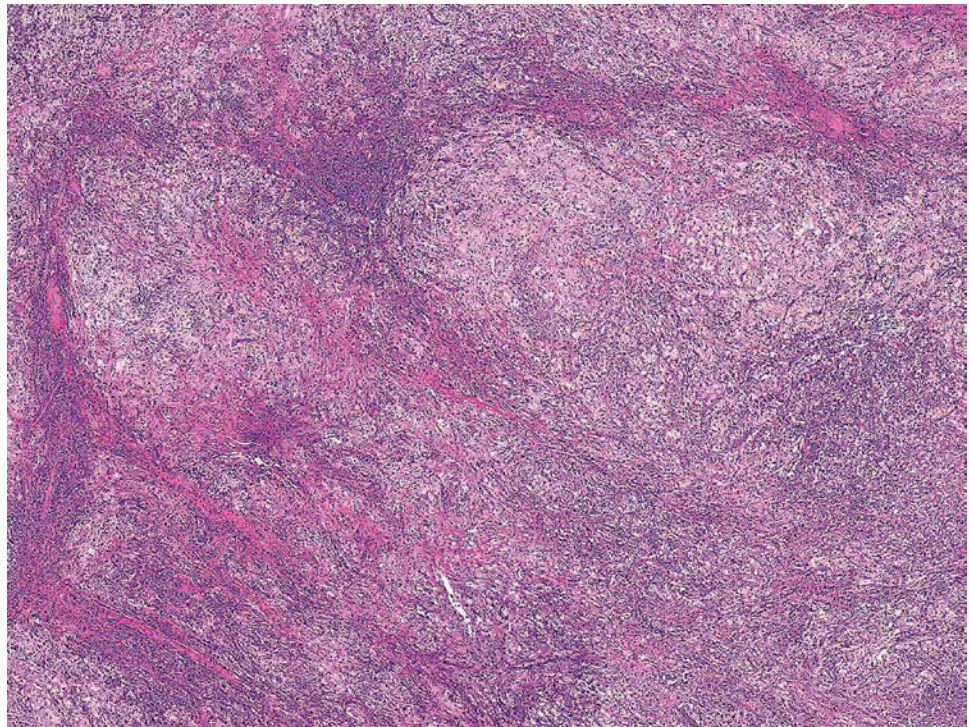
**IMMUNOHISTOCHEMICAL FINDINGS**

The histiocytes of SHML are diffusely and strongly positive for S100 protein while variably positive with macrophage antigens such as CD68, CD163, MAC387, Leu M3, lysozyme, and  $\alpha$ -1-chymotrypsin. However, they are negative for CD1a and CD207 (Langerin), allowing for an important distinction to be made. Interestingly, these histiocytic cells are thought to be recently recruited blood monocytes.

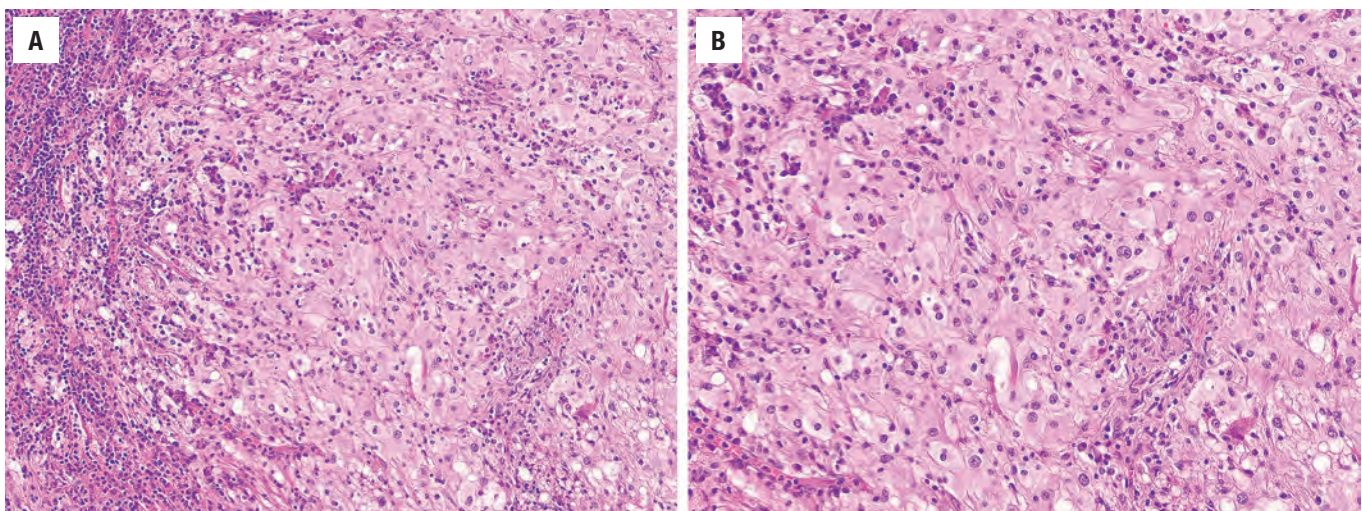
**DIFFERENTIAL DIAGNOSIS**

The differential diagnosis includes other processes rich in histiocytes, such as rhinoscleroma, lepromatous leprosy, Langerhans cell histiocytosis (LCH), granulomatosis with polyangiitis (Wegener granulomatosis), and, rarely, histiocytic lymphomas. The histiocytes of the infectious diseases are smaller and not arranged within sinuses, and they lack S100 protein immunoreactivity. Special stains will also help to highlight respective microorganisms. B-cell lymphomas may rarely exhibit *emperipolesis*, but they will also be S100 protein-negative. Granulomatosis with polyangiitis is a complex, largely autoimmune



**FIGURE 20.16**

These lymphocytes are separated by lakes of histiocytes within expanded sinuses in a case of sinus histiocytosis with massive lymphadenopathy.

**FIGURE 20.17**

(A) Sinus histiocytosis composed of histiocytes with phagocytosis. (B) Histiocyte with emperipolesis: Numerous plasma cell and lymphocyte nuclei are seen within the cytoplasm of the histiocyte in this example of sinus histiocytosis with massive lymphadenopathy.

disease with a characteristic clinical presentation and laboratory studies.

Steroids may conservatively manage localized disease, but surgery (often extensive) and radiation may be necessary owing to involvement of adjacent structures.

### PROGNOSIS AND THERAPY

The prognosis is determined by the extent of the disorder and “stage” of the disease. Patients may experience spontaneous remission, but occasionally some patients may die of complications of the disorder, including infectious disease and amyloid-related organ dysfunction.

### ■ LANGERHANS CELL HISTIOCYTOSIS

Langerhans cell histiocytosis (LCH), formerly histiocytosis X, represents a rare interrelated group of diseases including eosinophilic granuloma (EG), Hand-Schüller-Christian syndrome, and Letterer-Siwe disease. All of these lesions



contain an unusual clonal histiocyte, which contains Birbeck granules on electron microscopy. Although requiring additional evaluation, new evidence suggests that mutations in *BRAF* may support a neoplastic etiology.

### CLINICAL FEATURES

The disease has an estimated prevalence of 1 per 200,000 children per year. It can be localized or can present with systemic findings, including multiorgan involvement. The head and neck are frequently involved in LCH, often affecting the flat bones of the skull or the jaws, the ear, and the sinonasal tract. Although it is common for patients to present initially in the first two decades of life, the disease can affect a broad age range, from a few months to the 6th decade. Males are affected more frequently than females. Clinical symptoms can be very nonspecific, such as otitis media, hearing loss, bone pain, vertigo, or a destructive bone lesion.

### RADIOGRAPHIC FEATURES

Radiographically, osseous involvement by LCH produces sharply punched-out single or multiple radiolucencies. Extensive involvement of the gnathic alveolus causes the teeth to appear as if they were “floating in air.”

### PATHOLOGIC FEATURES

The Langerhans histiocytes are characterized as enlarged cells, containing delicate-appearing pale or eosinophilic cytoplasm, often finely vacuolated, and occasionally showing phagocytized cellular debris. The most characteristic cytologic feature, however, is the vesicular nucleus with an indented, notched, lobated, folded, grooved, reniform, vesicular, or “coffee bean”-shaped appearance, and one or two nucleoli (Fig. 20.18). An increased number of eosinophils may be seen intermingled with the Langerhans cells, which may be concentrated in collections, usually around areas of necrosis. Other inflammatory cells are also seen, such as lymphocytes, plasma cells, and neutrophils. Multinucleated giant cells and hemorrhage may be present (Fig. 20.19).

### ANCILLARY STUDIES

#### ULTRASTRUCTURAL FINDINGS

On electron microscopy, the characteristic folded, convoluted, and lobulated nuclei of Langerhans cells are

### LANGERHANS CELL HISTIOCYTOSIS—DISEASE FACT SHEET

#### Definition

- A interrelated group of diseases that are manifestations of a unique histiocyte containing Birbeck granules on electron microscopy

#### Incidence

- Estimated prevalence in children is 1 per 200,000 per year

#### Morbidity and Mortality

- Morbidity can result from multifocal involvement of the skull
- Multiorgan involvement unresponsive to chemotherapy has a dismal prognosis

#### Sex and Age Distribution

- Males affected more often than females
- Usually young (< 20 years), but a broad age range

#### Clinical Features

- Head and neck involvement occurs in flat bones of the skull or jaws
- Presents with otitis media and/or destructive temporal bone lesions (if the disease is localized)

#### Prognosis and Therapy

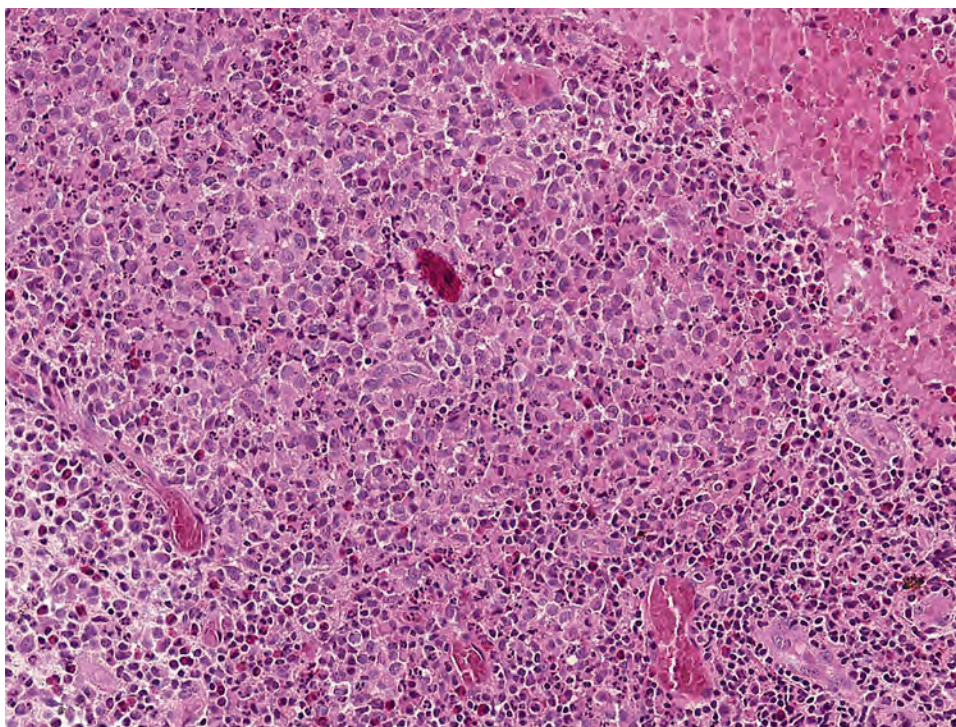
- Prognosis depends on stage and whether disease is localized or systemic
- Disease progression is common if there is multiorgan involvement
- Surgery for localized disease has an excellent prognosis
- Combination chemotherapy and radiation for systemic disease

readily appreciated. Cytoplasmic filipodial extensions create an uneven cell contour. Most important, the cell contains a variable number of invaginations of the cell membrane called Birbeck or Langerhans granules. The granules are disk-shaped, but when cross-sectioned they appear rod-shaped. The granules are pentalaminar, showing cross striations, often with the characteristic vesicular expansions imparting the unique “tennis racquet” appearance classically associated with the Langerhans cell.

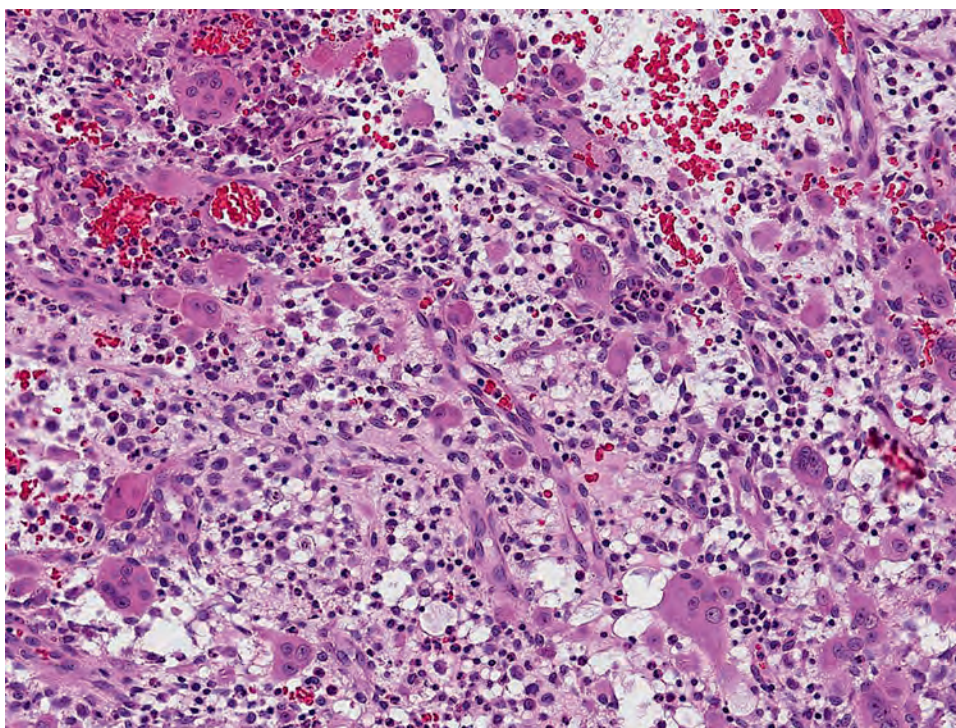
#### IMMUNOHISTOCHEMICAL FINDINGS

The immunohistochemical antigenic profile of Langerhans cells is remarkably wide, but in practical terms S100 protein, CD1a, and CD68 will all yield a positive reaction (Fig. 20.20). A relatively new marker, CD207, also referred to as “langerin” (Fig. 20.20D), appears to have excellent sensitivity and specificity for the Langerhans cell histiocyte. Langerin is a type II transmembrane cell-surface receptor localized in the Birbeck granules. Occasionally, sialated Leu M1, peanut agglutinin, ATPase, or T-6 antigenic determinants and HLA-DR (CD74) may be used to confirm the diagnosis. The macrophage antigens



**FIGURE 20.18**

Langerhans cell histiocytosis demonstrates cleaved, "coffee bean"-shaped nuclei within a rich inflammatory background filled with eosinophils.

**FIGURE 20.19**

Langerhans histiocytes are seen within a heavy inflammatory background including multiple giant cells and blood.



### LANGERHANS CELL HISTIOCYTOSIS— PATHOLOGIC FEATURES

#### Microscopic Findings

- Langerhans cells are enlarged cells with delicate, pale cytoplasm surrounding vesicular nuclei with indented, notched, lobated, folded, grooved, or “coffee-bean” nuclei
- Increased eosinophils are often present, occasionally forming microscopic abscesses

#### Ultrastructural Findings

- Langerhans cells have folded, convoluted, and lobulated nuclei
- Cell membrane invaginations forming Birbeck or Langerhans granules: disk shaped, pentilaminar, giving a “tennis racquet” appearance

#### Immunohistochemical Findings

- Broadly reactive with many histiocytic markers
- The diagnosis is usually confirmed with S100 protein, CD68, CD1a, and CD207 (langerin)

#### Pathologic Differential Diagnosis

- Hodgkin lymphoma, extranodal NK/T-cell lymphoma, Rosai-Dorfman disease, Erdheim-Chester disease

generally demonstrate a concentration in the perinuclear space and Golgi region.

#### MOLECULAR FINDINGS

About half of LCH cases tested, show an oncogenic *BRAF* V600E mutation, raising the possibility of pharmacogenomic inhibitor therapy. There is some recent evidence of a high level of PD-L1 expression in histiocytoses, along with frequent *BRAF* and other *ERK* pathway gene mutations; this provides additional support for testing combination therapeutic approaches for patients with multisystem and/or refractory forms of histiocytoses.

#### DIFFERENTIAL DIAGNOSIS

The differential in the head and neck is usually limited to Hodgkin lymphoma, extranodal SHML (Rosai-Dorfman disease), extranodal NK/T-cell lymphoma, and perhaps Erdheim-Chester disease. *Rosai-Dorfman disease* shows a different pattern of growth, has emperipolesis, and is reactive with S100 protein, while the lesional cells are negative with CD1a and CD207. *Hodgkin lymphoma* may have a pronounced eosinophilic infiltrate but has Reed–Sternberg cells, with immunoreactivity for CD15

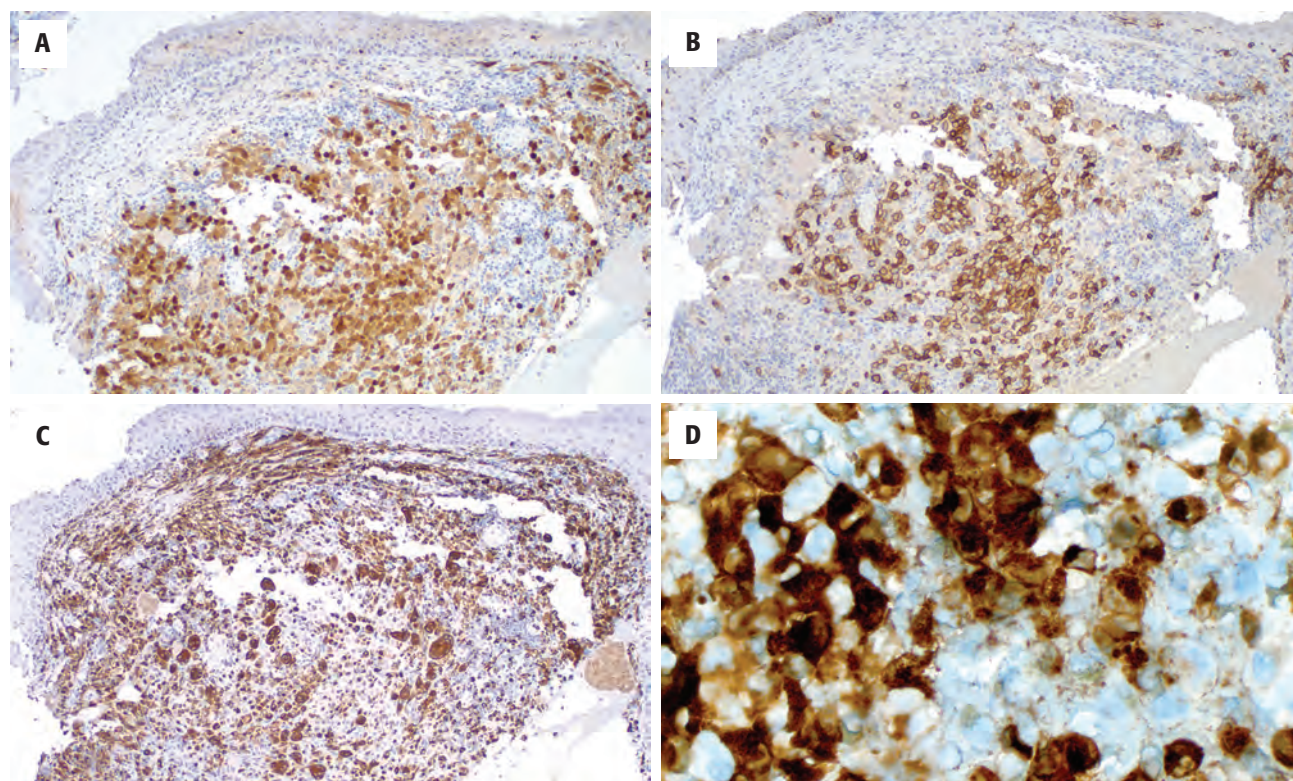


**FIGURE 20.20**

Immunohistochemistry of Langerhans cell histiocytosis. (A) S100 protein. (B) CD1a. (C) CD68. (D) Langerin (CD207).



and CD30 but not CD1a. *NK/T-cell lymphoma* may have irregular and grooved nuclei as well as eosinophils in the background, but it will show angiocentricity and an NK- or T-cell lineage. *Erdheim-Chester disease* is an idiopathic true histiocytic disorder whose cells are S100 protein-positive but CD1a-negative, without the presence of Birbeck granules.

### PROGNOSIS AND THERAPY

LCH may be a localized or systemic disease, and a complex staging system is applied. Localized disease, frequently

the case in the head and neck, requires conservative surgery to achieve an excellent prognosis. If no new lesions develop within 1 year, the patient is considered cured. If systemic disease is identified, combination chemotherapy is used along with radiation as necessary. Adverse prognostic findings include a young age at onset, extensive bone and/or visceral involvement, and multiple recurrences (usually within 6 months of diagnosis).

### SUGGESTED READINGS

The complete Suggested Readings list is available online at [ExpertConsult.com](http://ExpertConsult.com).

**SUGGESTED READINGS****Branchial Cleft Anomalies**

- Adams A, et al. Branchial cleft anomalies: a pictorial review of embryological development and spectrum of imaging findings. *Insights Imaging*. 2016;7(1):69–76.
- Bishop JA, et al. Ciliated HPV-related carcinoma: a well-differentiated form of head and neck carcinoma that can be mistaken for a benign cyst. *Am J Surg Pathol*. 2015;39(11):1591–1595.
- Cao D, et al. Expression of p16 in benign and malignant cystic squamous lesions of the neck. *Hum Pathol*. 2010;41(4):535–539.
- Doshi J, et al. Branchial cyst side predilection: fact or fiction? *Ann Otol Rhinol Laryngol*. 2007;116(2):112–114.
- Glosser JW, et al. Branchial cleft or cervical lymphoepithelial cysts: etiology and management. *J Am Dent Assoc*. 2003;134(1):81–86.
- Goins MR, et al. Pediatric neck masses. *Oral Maxillofac Surg Clin North Am*. 2012;24(30):457–468.
- Kadhim AL, et al. Pearls and pitfalls in the management of branchial cyst. *J Laryngol Otol*. 2004;118(12):946–950.
- Kajosaari L, et al. Second branchial cleft fistulae: patient characteristics and surgical outcome. *Int J Pediatr Otorhinolaryngol*. 2014;78(9):1503–1507.
- Mandell DL. Head and neck anomalies related to the branchial apparatus. *Otolaryngol Clin North Am*. 2000;33:1309–1332.
- Nicoucar K, et al. Management of congenital fourth branchial arch anomalies: a review and analysis of published cases. *J Pediatr Surg*. 2009;44(7):1432–1439.
- Ozolek JA. Selective pathologies of the head and neck in children: a developmental perspective. *Adv Anat Pathol*. 2009;16(5):332–358.
- Pai RK, et al. p16 (INK4A) immunohistochemical staining may be helpful in distinguishing branchial cleft cysts from cystic squamous cell carcinoma originating in the oropharynx. *Cancer*. 2009;117(2):108–119.
- Prosser JD, et al. Branchial cleft anomalies and thymic cysts. *Otolaryngol Clin North Am*. 2015;48(1):1–14.
- Radkay-Gonzalez L, et al. Ciliated adenosquamous carcinoma: expanding the phenotypic diversity of human papillomavirus-associated tumors. *Head Neck Pathol*. 2016;10(2):167–175.
- Rea PA, et al. Third and fourth branchial pouch anomalies. *J Laryngol Otol*. 2004;118:19–24.
- Strassen U, et al. Bronchogenic cancer: it still exists. *Laryngoscope*. 2016;126(3):638–642.
- Thompson LD. Branchial cleft cyst. *Ear Nose Throat J*. 2004;83(11):740.
- Todd NW. Common congenital anomalies of the neck. Embryology and surgical anatomy. *Surg Clin North Am*. 1993;73(4):599–610.

**Cat Scratch Disease (Granulomatous Inflammation)**

- Adal KA, et al. Cat scratch disease, bacillary angiomatosis, and other infections due to *Rochalimaea*. *N Engl J Med*. 1994;330:1509–1515.
- Caponetti G, et al. Cat-scratch disease lymphadenitis. *Ear Nose Throat J*. 2007;86(8):449–450.
- Caponetti GC, et al. Evaluation of immunohistochemistry in identifying Bartonella henselae in cat-scratch disease. *Am J Clin Pathol*. 2009;131(2):250–256.
- Cheuk W, et al. Confirmation of diagnosis of cat scratch disease by immunohistochemistry. *Am J Surg Pathol*. 2006;30(2):274–275.
- Chomel BB. Cat-scratch disease. *Rev - Off Int Epizoot*. 2000;19(1):136–150.
- Lamps LW, et al. Cat scratch disease: historic, clinical and pathologic perspectives. *Am J Clin Pathol*. 2004;121:S71–S80.
- Nelson CA, et al. Cat-scratch disease in the United States, 2005–2013. *Emerg Infect Dis*. 2016;22(10):1741–1746.

**Bacillary Angiomatosis**

- Amsbaugh S, et al. Bacillary angiomatosis associated with pseudoepitheliomatous hyperplasia. *Am J Dermatopathol*. 2006;28(1):32–35.
- Batsakis JG, et al. Bacillary angiomatosis. *Ann Otol Rhinol Laryngol*. 1995;104(8):668–672.
- Hnatuk LA, et al. Bacillary angiomatosis: a new entity in acquired immunodeficiency syndrome. *J Otolaryngol*. 1994;23(3):216–220.

- Radu O, et al. Kaposi sarcoma. *Arch Pathol Lab Med*. 2013;137(2):289–294.
- Wick MR, et al. Selected pseudoneoplastic lesions of the skin. *Arch Pathol Lab Med*. 2010;134(3):369–377.

**Cervical Actinomycosis**

- Lancella A, et al. Two unusual presentations of cervicofacial actinomycosis and review of the literature. *Acta Otorhinolaryngol Ital*. 2008;28(2):89–93.
- Moghimi M, et al. Treatment of cervicofacial actinomycosis: a report of 19 cases and review of the literature. *Med Oral Patol Oral Cir Bucal*. 2013;18(1):e627–e632.
- Oostman O, et al. Cervicofacial actinomycosis: diagnosis and management. *Curr Infect Dis Rep*. 2005;7(3):170–174.
- Sharkawy AA. Cervicofacial actinomycosis and mandibular osteomyelitis. *Infect Dis Clin North Am*. 2007;21(2):543–556.

**Nodular Fasciitis**

- Allison DB, et al. Nodular fasciitis: a frequent diagnostic pitfall on fine-needle aspiration. *Cancer*. 2014;125(1):20–29.
- Forcucci JA, et al. Benign soft tissue lesions that may mimic malignancy. *Semin Diagn Pathol*. 2016;33(1):50–59.
- Gibson TC, et al. Parotid gland nodular fasciitis: a clinicopathologic series of 12 cases with a review of 18 cases from the literature. *Head Neck Pathol*. 2015;9(3):334–344.
- Hourani R, et al. Fibroblastic and myofibroblastic tumors of the head and neck: comprehensive imaging-based review with pathologic correlation. *Eur J Radiol*. 2015;84(2):250–260.
- Ng E, et al. Characterising benign fibrous-soft tissue tumor in adult: why is it so difficult and what do we need to know? *Clin Radiol*. 2015;70(7):684–697.
- Nishio J. Updates on the cytogenetics and molecular cytogenetics of benign and intermediate soft tissue tumors. *Oncol Lett*. 2013;5(1):12–18.
- Oliveira AM, et al. USP6-induced neoplasms: the biologic spectrum of aneurysmal bone cyst and nodular fasciitis. *Hum Pathol*. 2014;45(1):1–11.
- Shin C, et al. USP6 gene rearrangement in nodular fasciitis and histological mimics. *Histopathology*. 2016;69(5):784–791.

**Sinus Histiocytosis With Massive Lymphadenopathy (Rosai-Dorfman Disease)**

- Ahsan SF, et al. Otolaryngologic manifestations of Rosai-Dorfman disease. *Int J Pediatr Otorhinolaryngol*. 2001;59(3):2210227.
- Carbone A, et al. Review of sinus histiocytosis with massive lymphadenopathy (Rosai-Dorfman disease) of head and neck. *Ann Otol Rhinol Laryngol*. 1999;108:1095–1104.
- Eisen RN, et al. Immunophenotypic characterization of sinus histiocytosis with massive lymphadenopathy (Rosai-Dorfman disease). *Semin Diagn Pathol*. 1990;7(1):74–82.
- Foucar E, et al. Sinus histiocytosis with massive lymphadenopathy (Rosai-Dorfman disease): review of the entity. *Semin Diagn Pathol*. 1990;7(1):19–73.
- Goodnight JW, et al. Extranodal Rosai-Dorfman disease of the head and neck. *Laryngoscope*. 1996;106(3 Pt 1):253–256.
- Hagemann M, et al. Nasal and paranasal sinus manifestation of Rosai-Dorfman disease. *Rhinology*. 2005;43(3):229–232.
- La Barge DV 3rd, et al. Sinus histiocytosis with massive lymphadenopathy (Rosai-Dorfman disease): imaging manifestations in the head and neck. *AJR Am J Roentgenol*. 2008;19(6):W299–W306.
- Lai KL, et al. Rosai-Dorfman disease: presentation, diagnosis and treatment. *Head Neck*. 2013;35(3):E85–E88.
- Maeda Y, et al. Rosai-Dorfman disease revealed in the upper airway: a case report and review of the literature. *Auris Nasus Larynx*. 2004;31(3):279–282.
- Montgomery EA, et al. Rosai-Dorfman disease of soft tissue. *Am J Surg Pathol*. 1992;16(2):122–129.
- Paulli M, et al. Immunophenotypic characterization of the cell infiltrate in five cases of sinus histiocytosis with massive



- lymphadenopathy (Rosai-Dorfman disease). *Hum Pathol.* 1992;23(6):647–654.
12. Rosai J, et al. Sinus histiocytosis with massive lymphadenopathy. A newly recognized benign clinicopathological entity. *Arch Pathol.* 1969;87(1):63–70.
  13. Rosai J, et al. Sinus histiocytosis with massive lymphadenopathy: a pseudolymphomatous benign disorder. Analysis of 34 cases. *Cancer.* 1972;30(5):1174–1188.
  14. Wenig BM, et al. Extranodal sinus histiocytosis with massive lymphadenopathy (Rosai-Dorfman disease) of the head and neck. *Hum Pathol.* 1993;24(5):483–492.
  6. Imashuku S, et al. Langerhans cell histiocytosis with multifocal bone lesions: comparative clinical features between single and multi-systems. *Int J Hematol.* 2009;90(4):506–512.
  7. Lau SK, et al. Immunohistochemical expression of Langerin in Langerhans cell histiocytosis and non-Langerhans cell histiocytic disorders. *Am J Surg Pathol.* 2008;32(4):615–619.
  8. Lieberman PH, et al. Langerhans cell (eosinophilic) granulomatosis. A clinicopathologic study encompassing 50 years. *Am J Surg Pathol.* 1996;20(5):519–552.
  9. Nicollas R, et al. Head and neck manifestation and prognosis of Langerhans' cell histiocytosis in children. *Int J Pediatr Otorhinolaryngol.* 2010;74(6):669–673.
  10. Sachdev R, et al. CD163 expression is present in cutaneous histiocytomas but not in atypical fibroxanthomas. *Am J Clin Pathol.* 2010;133(6):915–921.
  11. Wang J, et al. Langerhans cell histiocytosis of bone in children: a clinicopathologic study of 108 cases. *World J Pediatr.* 2010;6(3):255–259.
  12. Willman CL. Detection of clonal histiocytes in Langerhans cell histiocytosis: biology and clinical significance. *Br J Cancer Suppl.* 1994;23:S29–S33.
  13. Willman CL, et al. Langerhans'-cell histiocytosis (histiocytosis X)—a clonal proliferative disease. *N Engl J Med.* 1994;331(3):154–160.

### Langerhans Cell Histiocytosis

1. Abba O, et al. Langerhans cell histiocytosis: current concepts and treatments. *Cancer Treat Rev.* 2010;36(4):354–359.
2. Badalian-Very G, et al. Recurrent BRAF mutations in Langerhans cell histiocytosis. *Blood.* 2010;116(11):1919–1923.
3. Davis SE, et al. Langerhans' cell histiocytosis: current trends and the role of the head and neck surgeon. *Ear Nose Throat J.* 2004;83:340–344.
4. Devaney KO, et al. Head and neck Langerhans cell histiocytosis. *Ann Otol Rhinol Laryngol.* 1997;106:526–532.
5. Gatalica Z, et al. Disseminated histiocytoses biomarkers beyond BRAFV600E: frequent expression of PD-L1. *Oncotarget.* 2015;6(23):19819–19825.

# Benign Neoplasms of the Neck (Soft Tissue, Bone, and Lymph Node)

■ **Diana Bell**

## ■ LYMPHANGIOMA (CYSTIC HYGROMA)

Lymphangiomas are rare congenital lymphatic malformations, with up to 70% reported in the head and neck. They are separated into three types: capillary, cavernous, and cystic (cystic hygroma). Lymphangiomas comprise approximately 25% of all vascular neoplasms in children and adolescents; approximately 25% of cervical cysts are lymphangiomas.

### CLINICAL FEATURES

Approximately two-thirds of lymphangiomas are noted shortly after birth, and 95% are present by the end of the second year of life. Cystic hygroma may also be detected in utero with ultrasonography. Cystic hygroma may be associated with fetal hydrops and several genetic abnormalities, most notably Turner syndrome (Fig. 21.1) but also Noonan syndrome and trisomies 13, 18, and 21. In general, symptoms are related to pressure caused by the slowly enlarging mass or extension of the mass into the posterior neck or, less commonly, into the anterior compartment, cheek, mediastinum, or axilla. When the hygroma is located superior to the hyoid bone, it may cause dysphagia or airway compression. Ultrasound will show a cystic lesion, frequently identified prenatally, while computed tomography (CT) studies will show a nonenhancing multilocular cystic mass.

Cavernous lymphangioma forms an ill-defined, spongy, compressible mass and is found most commonly in the tongue, cheek, floor of mouth, and lips; it is uncommon in the soft tissues. In contrast, capillary lymphangioma is usually confined to the skin and is clinically the least significant of the three types.

### LYMPHANGIOMA (CYSTIC HYGROMA)—DISEASE FACT SHEET

#### Definition

- A benign cystic neoplasm composed of dilated lymph vessels

#### Incidence and Location

- Represents 25% of congenital cervical cysts
- Up to 70% of lymphangiomas occur in the head and neck

#### Morbidity and Mortality

- Mortality 3%-7% (via pressure destruction of adjacent vital structures)

#### Sex and Age Distribution

- No significant sex difference
- Most present shortly after birth and 95% by the second year

#### Clinical Features

- Slowly enlarging painless mass
- May produce pressure symptoms owing to its size
- Associated with fetal hydrops and Turner syndrome

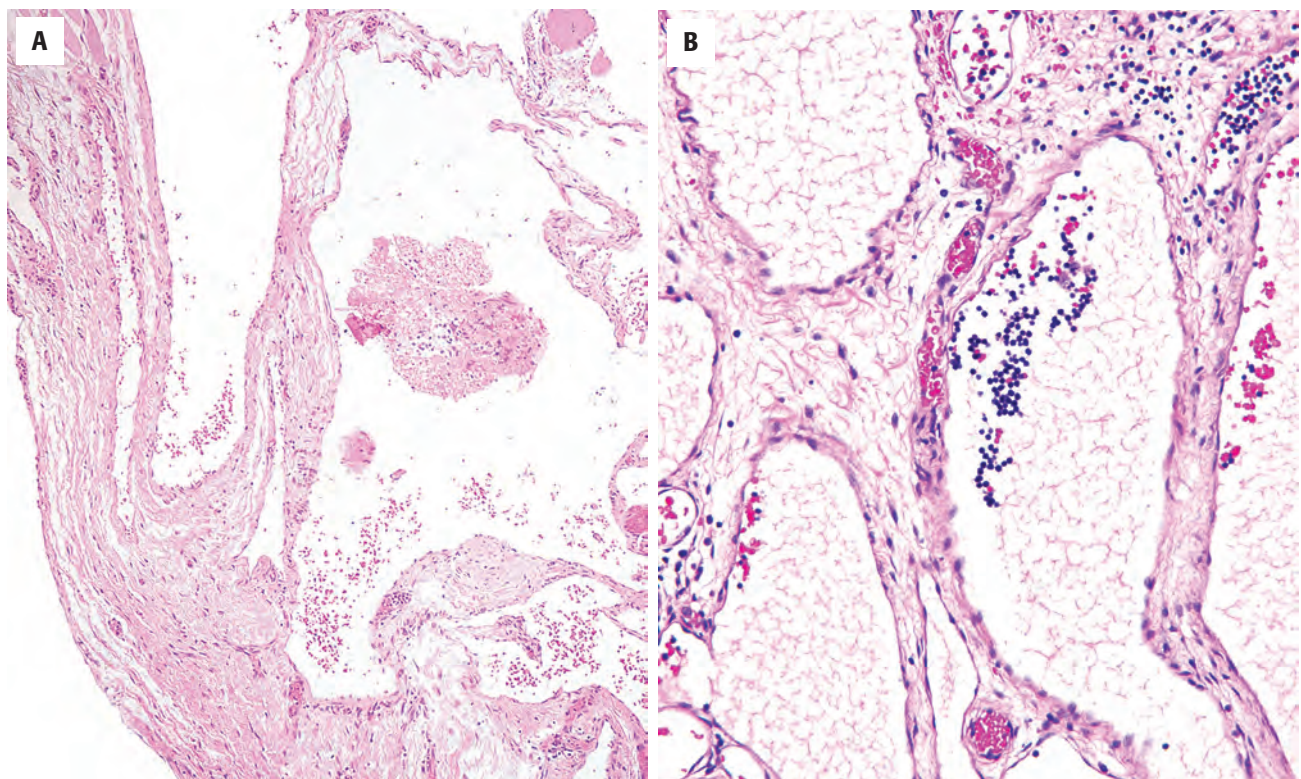
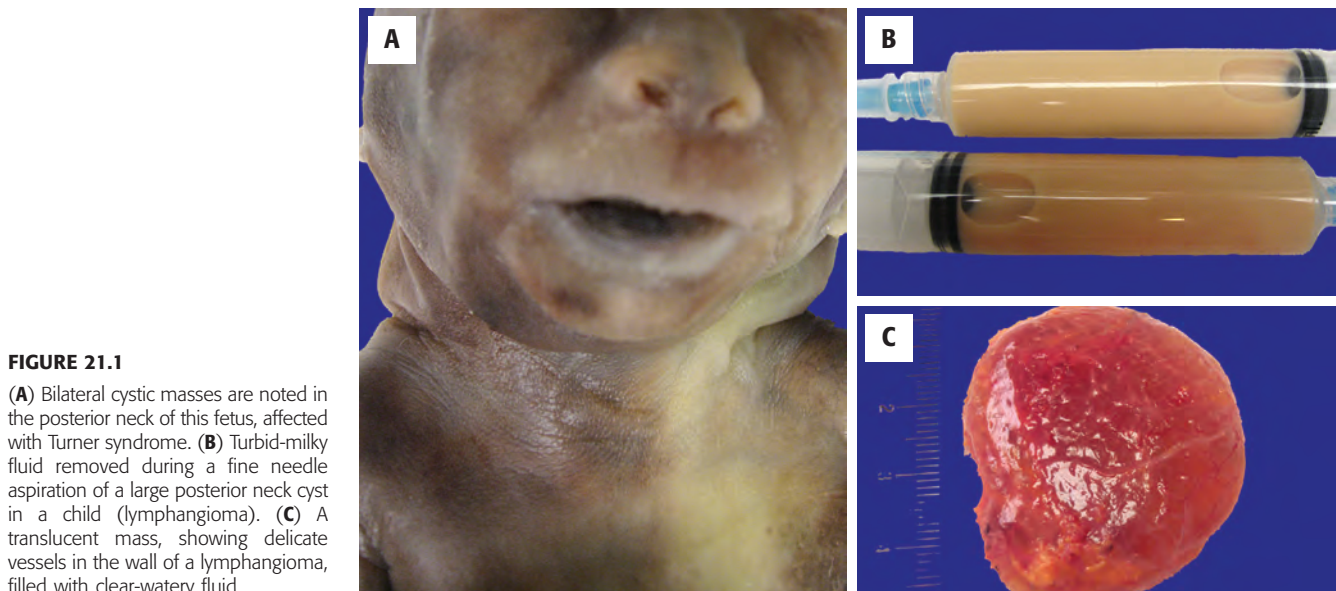
#### Prognosis and Treatment

- May become secondarily infected
- Surgery is the treatment of choice; sclerosing agents and laser can be used
- Up to 50% recurrence depending on size and site of lesion (due to incomplete excision)

### PATHOLOGIC FEATURES

Cystic lymphangiomas (hygromas) vary from a single soft mass with a pseudocontour to lobulated multicystic masses (Fig. 21.1). They contain clear to white-turbid fluid, described as milk-like (Fig. 21.1). Histologically,



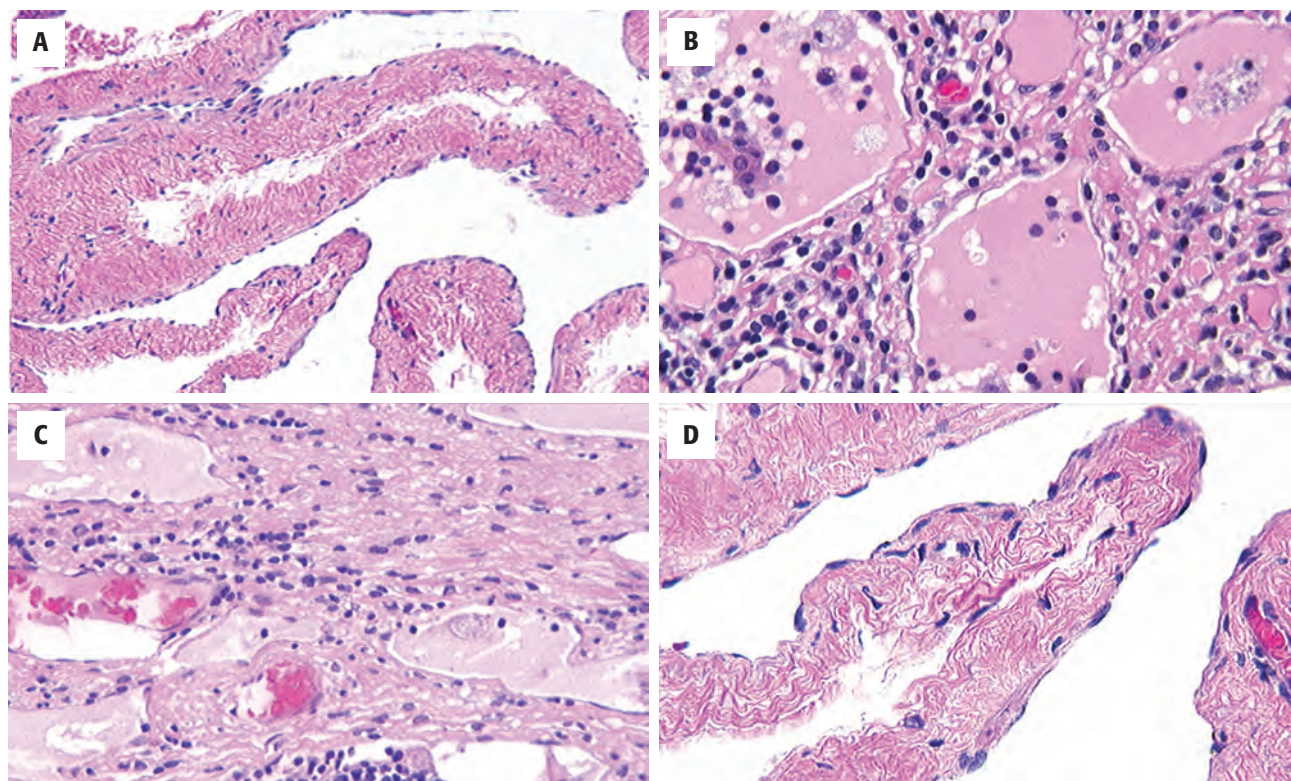


they consist of dilated, thin-walled spaces filled with eosinophilic, proteinaceous fluid and lined by flat endothelial cells (Fig. 21.2). The intervening stroma contains scattered lymphoid aggregates and wisps of smooth muscle fibers (Fig. 21.3). Fibrosis may be increased in lesions that have been present for a long time.

#### ANCILLARY STUDIES

Endothelial markers (factor VIII–related antigen [FVIII-RAG], CD31, CD34, and *Ulex europaeus*) can be expressed by endothelial cells in both hemangiomas and



**FIGURE 21.3**

(A) Lymphatic spaces subtended by smooth muscle. (B) Lymphoid cells and proteinaceous fluid. (C) Lymphoid elements with fibrosis surrounding fluid-filled spaces. (D) Flat, attenuated endothelial cells line the cavity.

lymphangiomas. D2-40 (podoplanin) may be a lymphatic-specific marker, along with CD9 and lymphatic vessel endothelial receptor 1 (LYVE-1), although podoplanin may be easier to interpret.

### DIFFERENTIAL DIAGNOSIS

The most common differential diagnosis is with cavernous hemangioma. Lymphangioma contains proteinaceous fluid and the surrounding tissues are usually infiltrated by lymphocytes, whereas *cavernous hemangiomas* are filled with red blood cells and lack valve structures. *Metastatic papillary thyroid carcinoma* may have flattened cells along the spaces, but TTF1 and/or thyroglobulin will be positive. Furthermore, a lymph node architecture should be recognizable, often at the periphery.

### PROGNOSIS AND THERAPY

Mortality rates are between 3% and 7%, specifically related to pressure destruction of vital structures of the neck. Lymphangiomas may occasionally become infected and may cause difficulty swallowing or respiratory distress. Surgery is the treatment of choice, while laser

### LYMPHANGIOMA (CYSTIC HYGROMA)— PATHOLOGIC FEATURES

#### Gross Findings

- Sponge-like cystic mass

#### Microscopic Findings

- Dilated, thin-walled spaces filled with proteinaceous fluid
- Lined by flat endothelial cells
- Lymphoid aggregates in stroma
- Wisps of smooth muscle in the wall

#### Immunohistochemical Findings

- Positive with factor VIII–related antigen, CD31, CD34, Ulex europaeus
- D2-40 (podoplanin) may be specific lymphatic marker (also CD9 and LYVE-1, although less common)

#### Pathologic Differential Diagnosis

- Cavernous hemangioma, metastatic papillary thyroid carcinoma

treatment or injected sclerosing agents (such as bleomycin) are alternative therapies. Recurrence rates range from 15% to 50% and are highest when the lymphangioma is incompletely removed. Malignant transformation is not documented.



## ■ TERATOMA

Teratomas are neoplasms composed of elements from each of the three germ cell layers (ectoderm, endoderm, and mesoderm). About 1 in 4000 live births have a teratoma, with approximately 2% involving the head and neck, most commonly the neck, oropharynx, nasopharynx, and orbit. Specifically, cervical teratomas represent less than 3% of all teratomas and less than 1% of all neck masses in children. Teratomas are separated, histologically, into mature or immature, solid or cystic, and are classified as benign or malignant depending on the degree of tissue maturation. In general, teratomas of the neck in neonates or infants are clinically benign, although they may be histologically mature or immature. By comparison, teratomas in adults are more likely to be clinically malignant and histologically immature.

### CLINICAL FEATURES

More than 90% of cervical teratomas occur in neonates or infants and are rare in patients older than 1 year. They occur with similar frequency in boys and girls. In addition to a neck mass, severe respiratory distress is notable in neonates, frequently leading to airway compromise and requiring immediate surgery. Polyhydramnios and other malformations may be seen in approximately 20% of patients, many of whom will show an elevated  $\alpha$ -fetoprotein concentration in amniotic fluid. Failure of midline structure development may result in fetal demise, even though the lesion is histologically benign. If detected prenatally by ultrasonographic examination, surgical

planning may yield a better outcome. CT or magnetic resonance imaging (MRI) usually shows a multilocular mass (Fig. 21.4). Cervical teratomas in adults are extremely rare, with patients reporting a rapidly enlarging neck mass.

### TERATOMA—DISEASE FACT SHEET

#### Definition

- Neoplasm composed of mature or immature elements from ectoderm, endoderm, and mesoderm

#### Incidence and Location

- Cervical teratomas represent 3% of all teratomas
- Less than 1% of pediatric neck masses

#### Morbidity and Mortality

- High morbidity but low mortality in neonates and infants
- High mortality in older children and adults

#### Sex and Age Distribution

- Equal sex distribution
- More than 90% occur in neonates or infants

#### Clinical Features

- Neck mass
- Respiratory distress
- Frequent association with congenital malformations
- Polyhydramnios seen in 20% of neonatal lesions

#### Prognosis and Treatment

- Prognosis is very good in neonates and infants but guarded in older children and adults
- Surgery

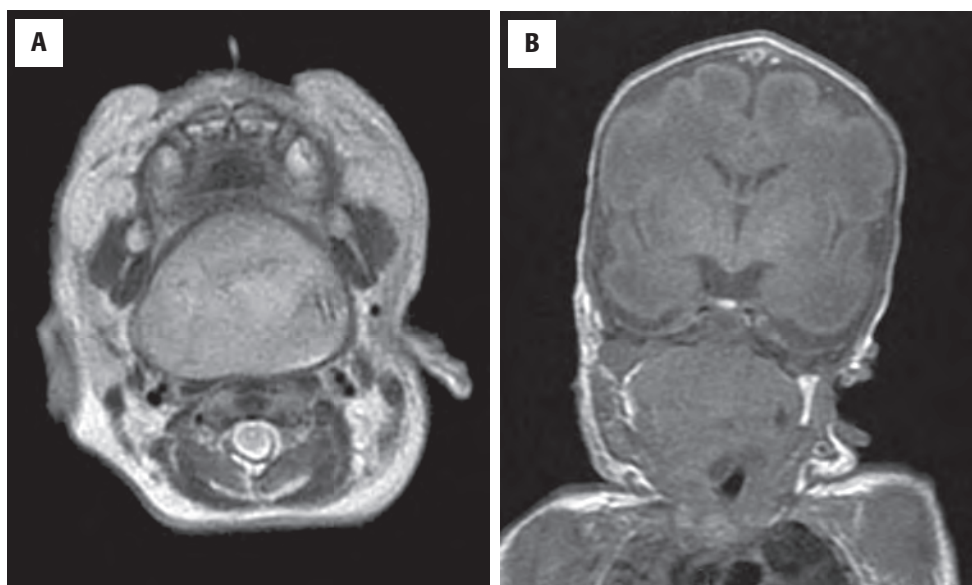


**FIGURE 21.4**

Magnetic resonance imaging demonstrates a large mass involving the oropharynx, nasopharynx, and neck. (A) Axial T2-weighted image. (B) Coronal T1-weighted image.

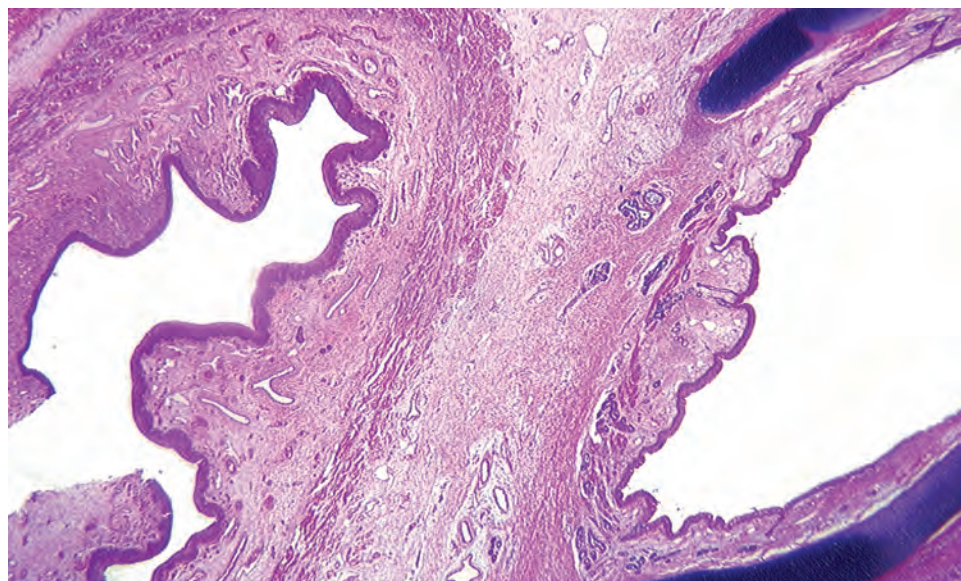
**PATHOLOGIC FEATURES****GROSS FINDINGS**

Grossly, the tumors are encapsulated, lobulated, and usually cystic, but they can be solid or multiloculated. They measure up to 12 cm in greatest diameter.

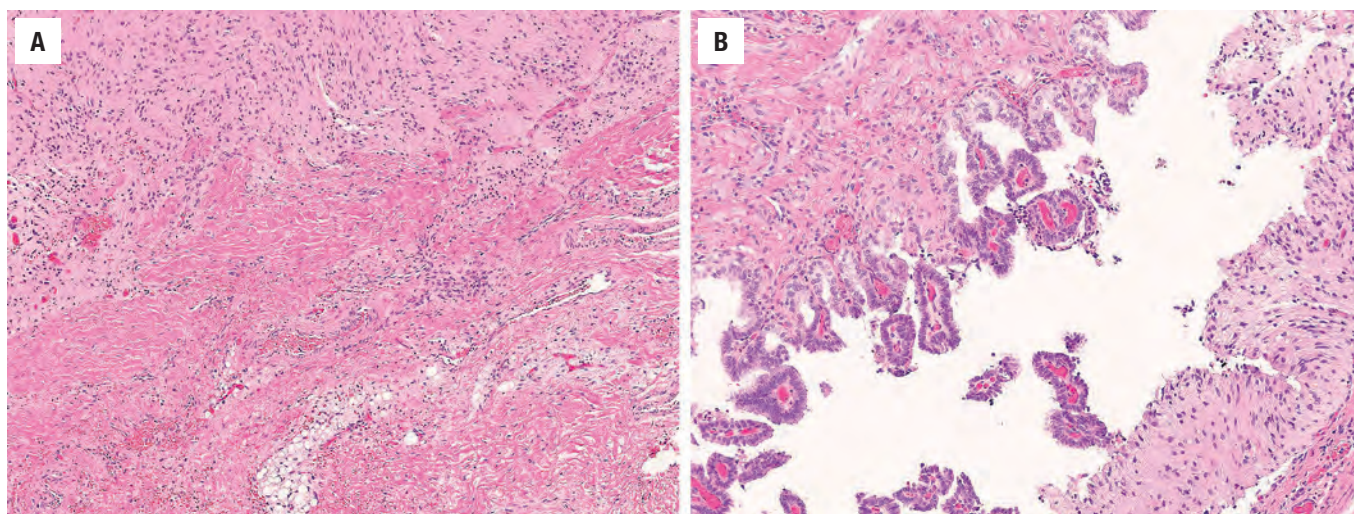
**MICROSCOPIC FINDINGS**

Histologically, the tumors are composed of an assemblage of mature or immature tissues from the three embryonic germ cell layers: ectoderm, endoderm,

mesoderm (Fig. 21.5). The most common finding is neural tissue arranged in islands, tubules, and rosette-like formations of immature neuroepithelium or mature glial tissue (Fig. 21.6), including retinal anlage epithelium (Fig. 21.7). A variety of epithelia are seen, including squamous, respiratory, and enteric-type mucosa, with solid organ tissues occasionally noted (pancreas, liver, thyroid; Fig. 21.7). The epithelium may line a cyst, with sebaceous units and hair frequently identified. Nodules of cartilage, fat, and muscle blend with the surrounding epithelial or glial tissues. The tissue may be mature or immature (embryonic), with the volume of immature tissues determining the overall grade of the tumor. The designation *benign mature* is used for tumors containing only

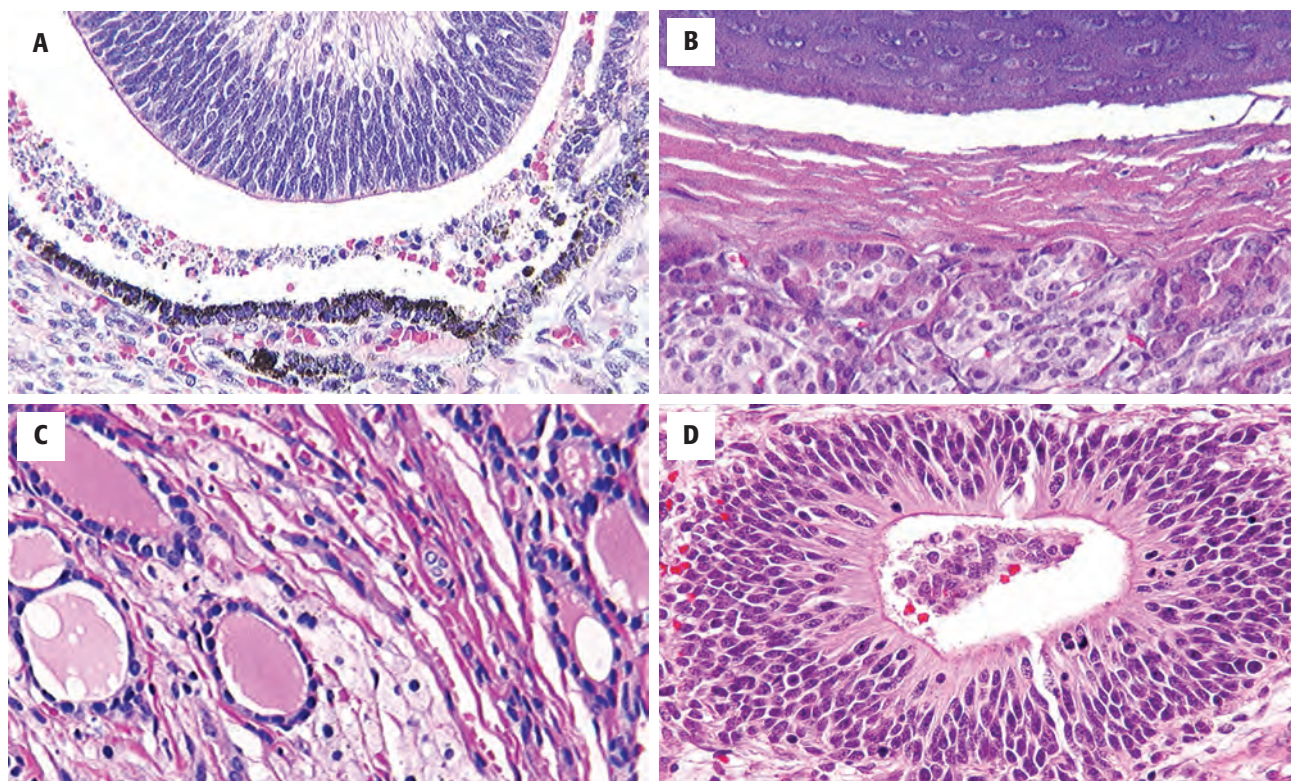
**FIGURE 21.5**

This benign, mature teratoma contains a primitive esophagus adjacent to a primitive trachea. Elements from other germ cell layers were noted elsewhere.

**FIGURE 21.6**

(A) Teratoma containing neuroglial tissue with focal fibrosis. (B) Adjacent focus showing ependymal and choroid plexus elements.



**FIGURE 21.7**

(A) Retinal anlage epithelium. (B) Mature cartilage adjacent to pancreatic tissue. (C) Thyroid parenchyma with immature fat. (D) A rosette of immature glial tissue.

### TERATOMA—PATHOLOGIC FEATURES

#### Gross Findings

- Cystic, solid, or multilocular lobulated mass

#### Microscopic Findings

- Mature or immature tissues from all germ cell layers
- Squamous, respiratory, glandular, and cuboidal epithelium
- Organ differentiation may be seen
- Neural tissues, including glial elements, choroid plexus, immature neuroblastoma, and pigmented retinal anlage
- Bone, cartilage, muscle, and fat

#### Immunohistochemical Findings

- $\alpha$ -fetoprotein and human chorionic gonadotropin if yolk sac tumor or choriocarcinoma are present (respectively)

#### Pathologic Differential Diagnosis

- Hamartoma, neuroblastoma, malignant germ cell tumors, metastatic testicular teratoma

mature elements; *benign immature* is used if there are foci of immature elements within a tumor that has a majority of mature elements; and *malignant* is used if the majority of the tumor is composed of immature elements. Foci of malignant germ cell tumor (such as

yolk sac tumor, embryonal carcinoma, or choriocarcinoma), while uncommon, automatically place the tumor in the malignant category.

### ANCILLARY STUDIES

Immunohistochemical stains with  $\alpha$ -fetoprotein and human chorionic gonadotropin may be of help in finding islands of yolk sac tumor or choriocarcinoma, respectively, in malignant teratomas. However, immunohistochemistry is generally not necessary for diagnosis.

### DIFFERENTIAL DIAGNOSIS

A broad differential diagnosis exists with these heterogeneous tumors when initially evaluated on small biopsy samples, offering limited sampling. Hamartoma, choristoma, ectopia, encephalocele, neuroblastoma, rhabdomyosarcoma, and malignant germ cell tumors may all be considered in the differential. However, attention to the nondescript mesenchymal background and heterogeneity

of elements, including embryonic forms, provides a clue to the diagnosis. A hamartoma is readily ruled out by the presence of tissues that are not indigenous to the location and/or that have an immature appearance. Depending on the patient's age, cervical metastasis from a gonadal teratoma should also be considered in the differential diagnosis.

### PROGNOSIS AND THERAPY

The prognosis of cervical teratoma in newborns and infants is excellent, although teratomas of the neck, despite their favorable histology, may cause significant morbidity owing to their important location. Tracheotomy or oral intubation may be required, along with a nasogastric tube for feeding. Death does occur as a result of associated developmental malformations of the vital structures of the neck. Therefore, surgery should be instituted without delay because the preoperative mortality is significant. Many advocate delivering a fetus by an ex utero intra-partum treatment (EXIT) procedure to yield the best possible outcome. In adults, in whom a malignant histology is more common, the biologic behavior of the tumors is more aggressive, with a poorer clinical outcome, as expected. Metastasis to lymph nodes and lung is common. Surgery with adjuvant chemotherapy and radiation is advocated, although often with mixed results.

## ECTOPIC HAMARTOMATOUS THYMOMA

Ectopic hamartomatous thymoma (EHT) is a rare benign neoplasm characteristically composed of a mixture of spindle cells, epithelial cells, mature adipose tissue, and lymphocytes. It is thought to arise from misplaced derivatives of the branchial pouch (remnant of cervical sinus of His). There is no evidence that the tumor is related to the thymus; some studies suggest that it originates from the salivary gland. Alternate terminology includes *branchial anlage mixed tumor* and *biphenotypic branchioma*.

### CLINICAL FEATURES

EHT occurs in the soft tissue of lower neck/supraclavicular, suprasternal, and presternal regions, and most patients are men, who present at a mean age of 46 years. It is usually seen as a slow-growing, well-circumscribed mass. It does not affect the thyroid gland, the larger vessels of the neck, or the mediastinum.

### ECTOPIC HAMARTOMATOUS THYMOMA—DISEASE FACT SHEET

#### Definition

- Subcutaneous tumor composed of bland spindle cells, nests of epithelioid cells, and adipocytes

#### Incidence and Location

- Rare neoplasm
- Low neck and supraclavicular/suprasternal notch region

#### Sex and Age Distribution

- Male predominance (M:F 3.4:1)
- Peak incidence in the 5th decade

#### Clinical Features

- Slow-growing, well-circumscribed swelling/mass in the lower neck or supraclavicular region

#### Prognosis and Treatment

- Benign clinical course
- No recurrence after local excision
- Rare malignant transformation



**FIGURE 21.8**

The cut surface of the mass shows gray-white, solid tumor with scattered, small cystic spaces and yellow foci of adipose tissue. (From Seok SH, Lee DH, Kang SH, Bae YK. Ectopic hamartomatous thymoma- a case report along with a review of the literature concerning the histogenesis and new nomenclature. Korean J Pathol. 2006;40:292–296.)

### PATHOLOGICAL FEATURES

#### GROSS FINDINGS

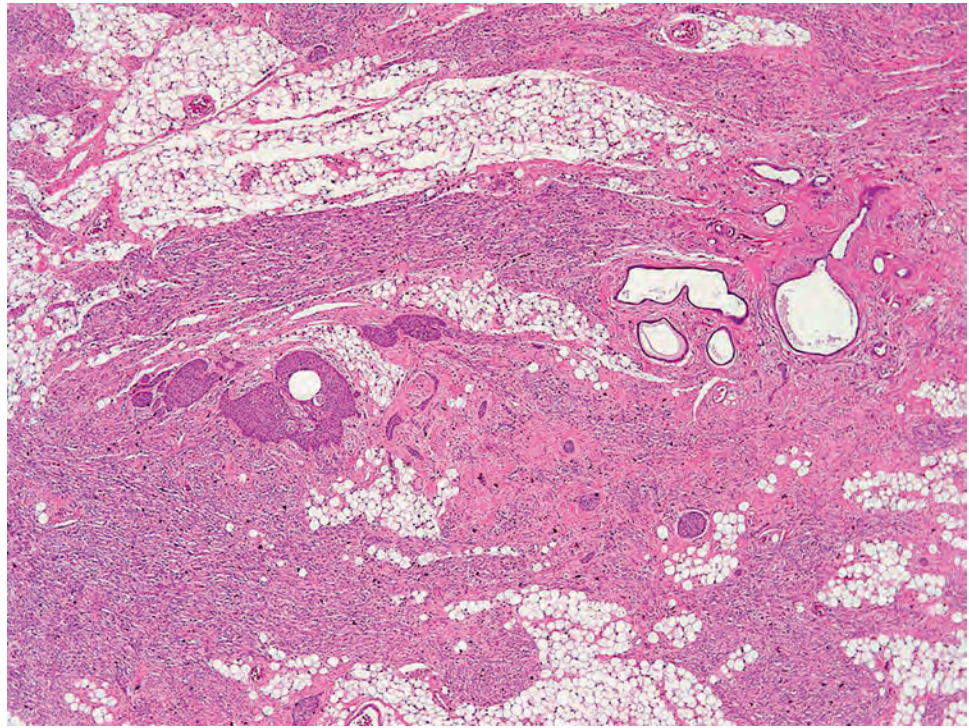
EHT is usually a well-circumscribed mass, measuring up to 5 cm. These tumors have a rubbery consistency and a gray-white to tan cut surface. Cyst formation can be seen (Fig. 21.8).



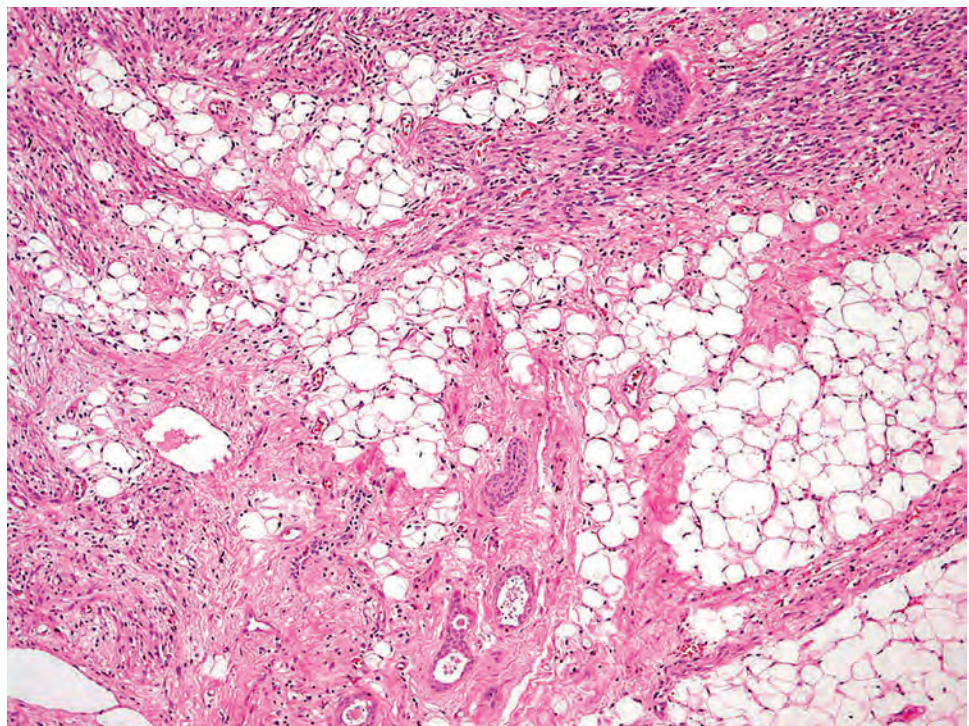
**MICROSCOPIC FINDINGS**

EHTs are composed of a mix of spindle and epithelial cells, with islands of mature adipose tissue (Fig. 21.9). The spindle cells are an admixture of plump and delicate cells; the epithelial component may show squamous, glandular,

or clear cell differentiation (Figs. 21.10 and 21.11; see also Fig. 21.9). Occasionally, focal smooth muscle and psammoma bodies have been reported. There is no cytologic atypia, mitotic activity is very low, and necrosis is absent. Rare cases with malignant transformation are documented.

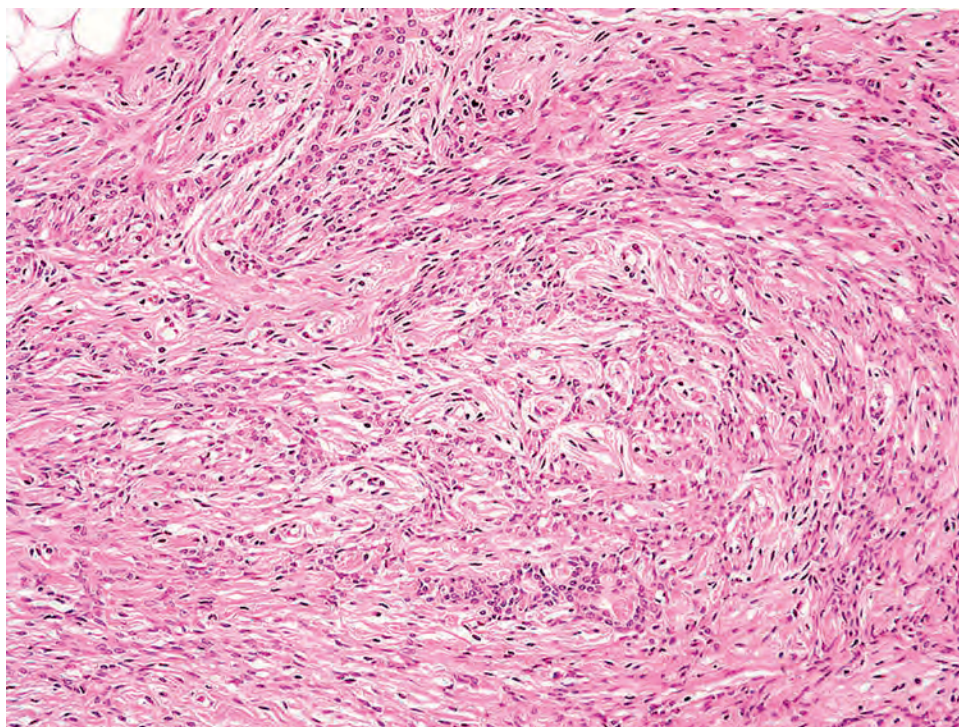
**FIGURE 21.9**

Tumor is composed of spindle cells entrapping epithelial and mature adipose tissue components.

**FIGURE 21.10**

Spindle cell component with fascicular arrangement; epithelial component with glands and cystic structures.



**FIGURE 21.11**

Epithelial component showing interanastomotic strands of squamous cells.

#### ECTOPIC HAMARTOMATOUS THYMOMA— PATHOLOGIC FEATURES

##### Gross Findings

- Well-circumscribed mass, nonencapsulated

##### Microscopic Findings

- Triphasic histology: spindle cells (predominant, bland, plump to thin); epithelioid nests and cords haphazardously arranged (squamous, glandular, clear cells); mature adipocytes
- No immature T cells
- No evidence of thymic differentiation

##### Ancillary Studies

- Smooth muscle actin-, keratin-, p63-positive
- Occasional CD34 positivity

##### Pathologic Differential Diagnosis

- Mixed tumors of skin adnexal or salivary gland origin, spindle cell/pleomorphic lipoma, sarcomatoid carcinoma, synovial sarcoma, cystic teratoma

tumor is negative for S100 protein and glial fibrillary acidic protein, while rarely showing focal reactivity with CD34.

#### DIFFERENTIAL DIAGNOSIS

The differential diagnosis includes mixed tumors of skin adnexal or salivary gland origin (EHT lacks chondroid/cartilaginous foci), spindle cell/pleomorphic lipoma (CD34-positive), sarcomatoid carcinoma (cytologically malignant), synovial sarcoma, cystic teratoma (the origin is deep-seated), and glandular malignant peripheral nerve sheath tumor (patchy S100 protein and strong SOX10 positivity).

#### PROGNOSIS AND THERAPY

The tumor usually does not recur after local excision.

#### ANCILLARY STUDIES

##### IMMUNOHISTOCHEMICAL FINDINGS

The spindled areas display strong and diffuse positivity for cytokeratin and epithelial membrane antigen. Myo-epithelial phenotype with the coexpression of keratins and smooth muscle actin has been also reported. The

#### ■ SPINDLE CELL LIPOMA/ PLEOMORPHIC LIPOMA

Spindle cell and pleomorphic lipomas are distinctive types of lipoma histologically on a continuum and characterized by replacement of mature fat cells by bland spindle cells, hyperchromatic round cells, and multinucleated giant



cells, including the characteristic “floret cell,” in association with ropy collagen. These tumors account for approximately 1.5 % of all adipose tissue neoplasms, with a lipoma:spindle cell lipoma ratio of 60:1.

### CLINICAL FEATURES

More than 90 % of spindle cell/pleomorphic lipomas occur in men (men outnumbering women 10:1), with a peak incidence in the 6th decade. Almost all of the tumors are located in the subcutaneous tissue of the posterior neck, upper back, and shoulder girdle. Rarely, the salivary gland, lip, tongue, and maxillofacial region will be affected. Patients are usually asymptomatic but may present with a painless, mobile, subcutaneous mass that has often been present for many years. Characteristically, the tumors are solitary, although rarely they may be familial and multiple.

### PATHOLOGIC FEATURES

#### GROSS FINDINGS

Spindle cell/pleomorphic lipomas range in size from 1 to 13 cm (mean, 5 cm). Grossly, they resemble an ordinary lipoma (Fig. 21.12), although some are gray-white or pale-pink, and deeper tumors may be myxoid.

### MICROSCOPIC FINDINGS

Microscopically, at one end of the histologic spectrum, spindle cell lipoma is composed of varying proportions of mature adipocytes and fibroblast-like

### SPINDLE CELL LIPOMA/PLEOMORPHIC LIPOMA—DISEASE FACT SHEET

#### Definition

- A distinct group of lipomas composed of spindle cells, adipocytes, and multinucleated giant cells associated with ropy collagen

#### Incidence and Location

- About 1.5% of all adipose tissue tumors
- Subcutaneous tissues of posterior neck and upper back most frequently

#### Sex and Age Distribution

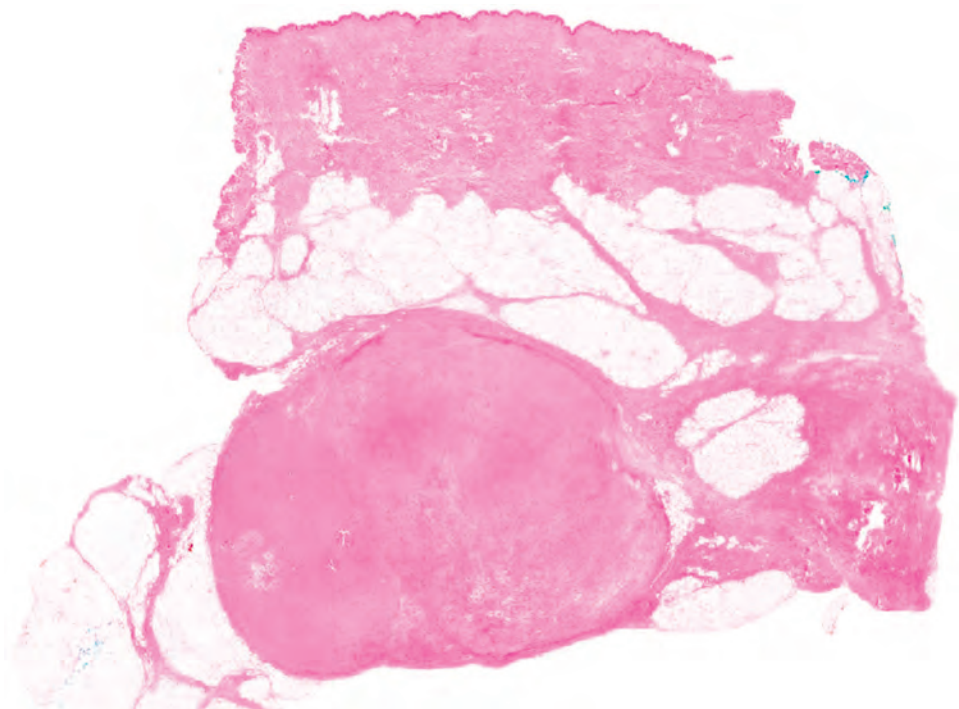
- Males > > > females (10:1)
- Mean age: 55 years

#### Clinical Features

- Painless, subcutaneous, mobile mass
- Posterior neck, upper back, shoulders
- Seldom multiple

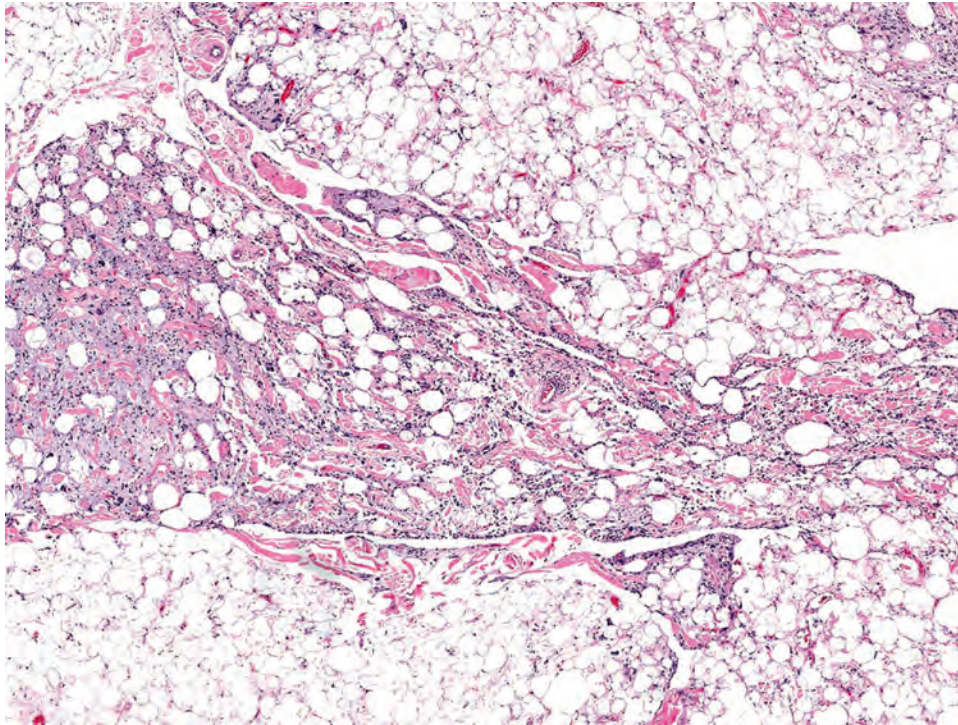
#### Prognosis and Treatment

- Excellent, although there are isolated reports of recurrence
- Surgery

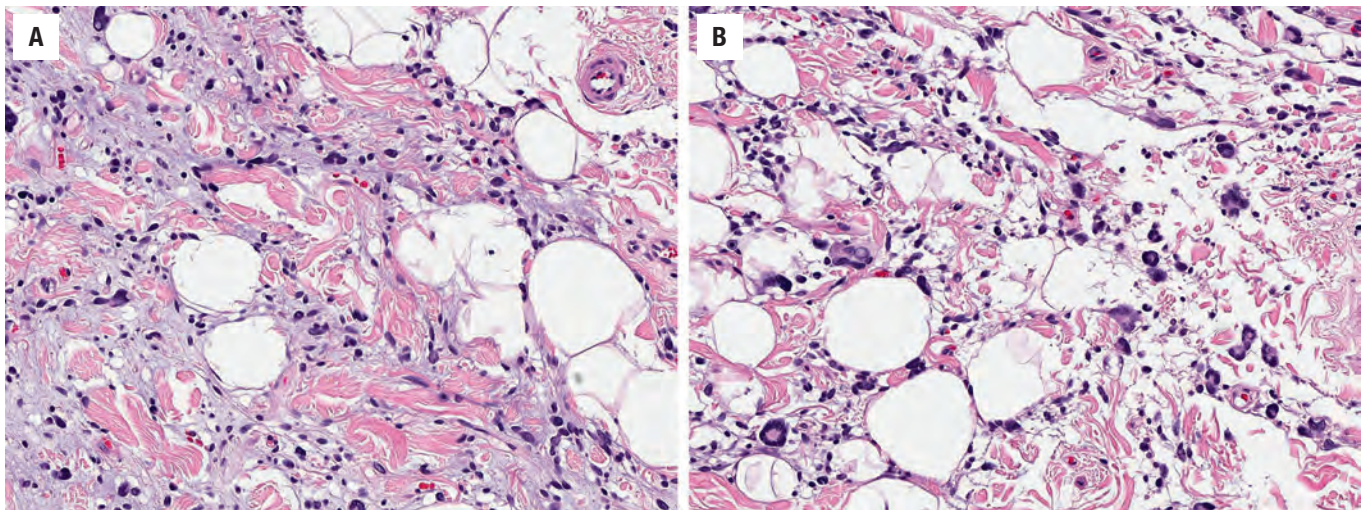


**FIGURE 21.12**

Well-circumscribed and encapsulated, intramuscular spindle cell lipoma. Note the myxoid appearance from low power as well as areas of increased cellularity.

**FIGURE 21.13**

Spindle cell lipoma with bland spindle cells in a background of adipocytes. Note the areas of thick, ropy collagen fibers.

**FIGURE 21.14**

(A) Marked myxoid stroma with delicate collagen fibers and fibroblasts in a spindle cell lipoma. (B) Pleomorphic lipoma: Hyperchromatic nuclei are seen in cells separated by dense collagen. There are a few floret-like (“petal”) multinucleated giant cells associated with mast cells and collagenized stroma.

spindle cells admixed with wire- or rope-like collagen fibers (“ropy collagen”) and myxoid stroma (Figs. 21.13 and 21.14). The fibroblast-like cells may be arranged in a parallel fashion. Mast cells are frequently numerous. It is important to note that fat may be sparse and difficult to find in selected tumors. The myxoid stroma may be a dominant finding. Profound but focal nuclear pleomorphism can be seen and is considered “degenerative” or “ancient change.” Mitoses are usually absent.

At the opposite end of the spectrum lies pleomorphic lipoma, which is characterized by small, round hyperchromatic cells and multinucleated giant cells with radially arranged “floret-like” nuclei—so named for their resemblance to the petals of a flower (Fig. 21.14). Cases with mixed features of spindle cell and pleomorphic lipoma occur quite often, making any distinction impossible and arbitrary. Secondary changes of fat necrosis or hyalinization can be seen and may also be associated with “aging” or “ancient” change. By definition, lipoblasts are absent.



### SPINDLE CELL LIPOMA/PLEOMORPHIC LIPOMA—PATHOLOGIC FEATURES

#### Gross Findings

- Yellow to gray-white to pale-pink circumscribed mass
- Mean, 5 cm (range, 1–13 cm)

#### Microscopic Findings

- Mixture of bland spindle cells arranged in parallel, adipocytes, and multinucleated giant cells (“floret-like”)
- Bands of mature rope-like collagen fibers
- Mast cells may be numerous

#### Ancillary Studies

- Spindle cells of both types of lipoma express CD34
- Negative for S100 protein
- Loss of 13q and/or 16q

#### Pathologic Differential Diagnosis

- Atypical lipomatous tumor/well-differentiated liposarcoma, neurofibroma, schwannoma, myxoma, nuchal fibroma

### ANCILLARY STUDIES

#### ULTRASTRUCTURAL FINDINGS

Electron microscopic studies have revealed spindle cells thought to represent fibroblasts or fibroblast-like cells analogous to the stellate mesenchymal cells seen in primitive fat lobules.

#### IMMUNOHISTOCHEMICAL FINDINGS

Immunohistochemically, the spindle cells in spindle/pleomorphic lipomas express CD34 and vimentin. Rare isolated cells may be positive for S100 protein, but this is quite different from the strong reaction usually seen in ordinary lipocytes. MDM2 immunostaining is negative.

#### FINE NEEDLE ASPIRATION

Smears will contain large, atypical, floret-type cells within a background of mature adipocytes. Needless to say the cells are frequently interpreted to be malignant.

#### MOLECULAR STUDIES

Loss of chromosomes 13q (13q12 and 13q14-q22) and/or 16q (16q13-qter) is characteristic of this family of

lipomas (seen in about 70% of cases). These genetic findings support distinction from both conventional lipoma and atypical lipomatous tumor/well-differentiated liposarcoma (ALT/WDLPS). The same alteration is seen in mammary-type myofibroblastoma, as well as in cellular angiofibroma.

### DIFFERENTIAL DIAGNOSIS

The differential diagnosis includes ALT/WDLPS (owing to the adipocytic component) and the common neural neoplasms, neurofibroma and schwannoma (owing to the spindle cell component); myxoma, nuchal fibroma, and fibrous hamartoma of infancy are occasionally considerations. The uniformity of the spindle cells, association with mature collagen fibers, and absence of lipoblasts—combined with the characteristic location, patient age, and overall circumscription of the lesion—support the diagnosis of spindle cell lipoma over ALT/WDLPS. Spindle cell/pleomorphic lipoma lacks the *MDM2* amplification characteristic of ALT/WDLPS. *Neurofibroma*, which tends to be infiltrative, contains spindle cells that are more randomly arranged and may contain characteristic Wagner-Meissner bodies (eosinophilic-appearing touch corpuscles). *Schwannoma* has buckled-wavy nuclei, cellular Antoni A areas, and perivascular hyalinization. S100 protein and SOX10 are usually strongly and diffusely immunoreactive. *Myxoma* is very hypocellular, lacks fat, and does not have thick bundles of collagen. A *nuchal-type fibroma* has fat but has a much heavier collagen deposition and entrapped nerves. *Fibrous hamartoma of infancy* most commonly involves soft tissue of shoulder, axilla, and upper arm in infants (within the first 2 years of life). It is composed of three distinctive tissue types: (1) well-differentiated fibroblastic/myofibroblastic cells, (2) mature adipose tissue, and (3) whorls of primitive mesenchymal areas.

### PROGNOSIS AND THERAPY

Complete local excision is curative for both types of lipomas.

### SUGGESTED READINGS

The complete Suggested Readings list is available online at [ExpertConsult.com](http://ExpertConsult.com).

**SUGGESTED READINGS****Lymphangioma (Cystic Hygroma)**

- Chervenak FA, et al. Fetal cystic hygroma. Cause and history. *N Engl J Med*. 1983;309:822–825.
- Coffin CM, et al. Vascular tumors in children and adolescents: a clinicopathologic study of 228 tumors in 222 patients. *Pathol Annu*. 1993;28:97–120.
- Erovic BM, et al. CD9 expression in lymphatic vessels in head and neck mucosa. *Mod Pathol*. 2003;16:1028–1034.
- Gedikbasi A, et al. Cystic hygroma and lymphangioma: associated findings, perinatal outcome and prognostic factors in live-born infants. *Arch Gynecol Obstet*. 2007;276(5):491–498.
- Hsieh YY, et al. Pathologic analysis of congenital cervical cysts in children: 20 years of experience at Chang Gung Memorial Hospital. *Chang Gung Med J*. 2003;26:107–113.
- Kraus J, et al. Cystic lymphangioma of the neck in adults: a report of three cases. *Wien Klin Wochenschr*. 2008;120(7–8):242–245.
- Mosca RC, et al. Cystic hygroma: characterization by computerized tomography. *Oral Surg Oral Med Oral Pathol Oral Radiol Endod*. 2008;105(5):e65–e69.
- Okazaki T, et al. Treatment of lymphangioma in children: our experience of 128 cases. *J Pediatr Surg*. 2007;42(2):386–389.
- Weiss SW, et al. Tumors of lymph vessels. In: Weiss SW, Goldblum JR, eds. *Enzinger and Weiss's soft tissue tumors*. 6th ed. St. Louis: Mosby; 2014:735.
- Fetsch JF, et al. Ectopic hamartomatous thymoma: clinicopathologic, immunohistochemical, and histogenetic considerations in four new cases. *Hum Pathol*. 1990;17(6):572–574.
- Henderson CJ, et al. Ectopic hamartomatous thymoma: a case study and review of the literature. *Pathology*. 2000;32(2):142–146.
- Kazakov DV, et al. Ectopic hamartomatous thymoma. *Histopathology*. 2004;45(2):202–204.
- Rosai J, et al. Ectopic hamartomatous thymoma: a distinctive benign lesion of lower neck. *Am J Surg Pathol*. 1984;8(7):501–513.
- Sato K, et al. Ectopic Hamartomatous Thymoma: A Review Of The Literature With Report Of New Cases And Proposal Of A New Name: Biphenotypic Branchioma. *Head Neck Pathol*. 2017;doi:10.1007/s12105-017-0854-6.
- Seok SH, et al. Ectopic hamartomatous thymoma- a case report along with a review of the literature concerning the histogenesis and new nomenclature. *Korean J Pathol*. 2006;40:292–296.
- Weissferdt A, et al. Ectopic hamartomatous thymoma- new insights into a challenging entity: a clinicopathologic and immunohistochemical study of 9 cases. *Am J Surg Pathol*. 2016;40(11):1571–1576.

**Teratoma**

- Alexander VR, et al. Head and neck teratomas in children- a series of 23 cases at Great Ormond Street Hospital. *Int J Pediatr Otorhinolaryngol*. 2015;79(12):2008–2014.
- Azizkhan RG, et al. Diagnosis, management, and outcome of cervicofacial teratomas in neonates: a Children's Cancer Group study. *J Pediatr Surg*. 1995;30:312–316.
- Batsakis JG, et al. Teratomas of the head and neck with emphasis on malignancy. *Ann Otol Rhinol Laryngol*. 1995;104:456–500.
- Berge SJ, et al. Diagnosis and management of cervical teratoma. *Br J Oral Maxillofac Surg*. 2004;42:41–45.
- Celik M, et al. Congenital teratoma of the tongue: a case report and review of the literature. *J Pediatr Surg*. 2006;41(11):e25–e28.
- Freitas Rda S, et al. Epignathus: two cases. *Br J Oral Maxillofac Surg*. 2008;46(4):317–319.
- Hassan S, et al. Massive lingual teratoma in a neonate. *Singapore Med J*. 2007;48(8):e212–e214.
- Jordan RB, et al. Cervical teratomas: an analysis, literature review and proposed classification. *J Pediatr Surg*. 1988;23:583–591.
- Torsigliori AJ Jr, et al. Pediatric neck masses guidelines for evaluation. *Int J Pediatr Otorhinolaryngol*. 1988;16:199–210.

**Ectopic Hamartomatous Thymoma**

- Fetsch JF, et al. Ectopic hamartomatous thymoma: a clinicopathological and immunohistochemical analysis of 21 cases with data supporting reclassification as branchial anlage mixed tumor. *Am J Surg Pathol*. 2004;28(10):1360–1380.
- Fetsch JF, et al. Ectopic hamartomatous thymoma: clinicopathologic, immunohistochemical, and histogenetic considerations in four new cases. *Hum Pathol*. 1990;17(6):572–574.
- Henderson CJ, et al. Ectopic hamartomatous thymoma: a case study and review of the literature. *Pathology*. 2000;32(2):142–146.
- Kazakov DV, et al. Ectopic hamartomatous thymoma. *Histopathology*. 2004;45(2):202–204.
- Rosai J, et al. Ectopic hamartomatous thymoma: a distinctive benign lesion of lower neck. *Am J Surg Pathol*. 1984;8(7):501–513.
- Sato K, et al. Ectopic Hamartomatous Thymoma: A Review Of The Literature With Report Of New Cases And Proposal Of A New Name: Biphenotypic Branchioma. *Head Neck Pathol*. 2017;doi:10.1007/s12105-017-0854-6.
- Seok SH, et al. Ectopic hamartomatous thymoma- a case report along with a review of the literature concerning the histogenesis and new nomenclature. *Korean J Pathol*. 2006;40:292–296.
- Weissferdt A, et al. Ectopic hamartomatous thymoma- new insights into a challenging entity: a clinicopathologic and immunohistochemical study of 9 cases. *Am J Surg Pathol*. 2016;40(11):1571–1576.

**Spindle Cell Lipoma/Pleomorphic Lipoma**

- Billings SD, et al. Diagnostically challenging spindle cell lipomas: a report of 34 “low-fat” and “fat-free” variants. *Am J Dermatopathol*. 2007;29(5):437–442.
- Bolen JW, et al. Spindle-cell lipoma. A clinical, light- and electron-microscopical study. *Am J Surg Pathol*. 1981;5(5):435–441.
- Cheah A, et al. Spindle cell/pleomorphic lipomas of the face: an under-recognized diagnosis. *Histopathology*. 2015;66(3):430–437.
- Choi JW, et al. Spindle cell lipoma of the head and neck: CT and MRI imaging findings. *Neuroradiology*. 2013;55(1):101–106.
- del Cin P, et al. Lesions of 13q may occur independently of deletions of 16q in spindle cell/pleomorphic lipomas. *Histopathology*. 1997;31:222–225.
- Domaniski HH, et al. Distinct cytologic features of spindle cell lipoma. A cytologic-histologic study with clinical, radiologic, electron microscopic and cytogenetic correlation. *Cancer*. 2001;93:381–389.
- Enzinger FM, et al. Spindle cell lipoma. *Cancer*. 1975;36:1852–1859.
- Fanburg-Smith JC, et al. Multiple spindle cell lipomas: a report of 7 familial and 11 nonfamilial cases. *Am J Surg Pathol*. 1998;22(1):40–48.
- Fletcher CD, et al. Spindle cell lipoma: a clinicopathological study with some original observations. *Histopathology*. 1987;11(8):803–817.
- Mentzel T, et al. Well-differentiated spindle cell liposarcoma (“atypical spindle cell lipomatous tumor”) does not belong to the spectrum of atypical lipomatous tumor but has a close relationship to spindle cell lipoma: clinicopathologic, immunohistochemical, and molecular analysis of six cases. *Mod Pathol*. 2010;23(5):729–736.
- Mentzel T. Cutaneous lipomatous neoplasms. *Semin Diagn Pathol*. 2001;18(4):250–257.
- Sachdeva MP, et al. Low-fat and fat-free pleomorphic lipomas: a diagnostic challenge. *Am J Dermatopathol*. 2009;31(5):423–426.



# Malignant Neoplasms of the Neck (Soft Tissue and Lymph Node)

■ Vickie Y. Jo

## ■ METASTATIC SQUAMOUS CELL CARCINOMA

Metastatic squamous cell carcinoma (SCC) in the neck often presents without a clinically apparent primary. The majority of cases of metastatic SCC to cervical lymph nodes are associated with high-risk human papillomavirus (HPV) from the oropharynx (base of tongue and tonsil), although conventional SCC from the upper aerodigestive tract is also common. The rich lymphatic plexus in the oropharynx can lead to early metastatic disease via the jugulodigastric lymph node chain, even for small and clinically inapparent primary tumors. Furthermore, tumors that involve the tonsils and tongue base will frequently localize to deep crypt locations, with little evidence for surface mucosal alterations. Metastatic SCC is often cystic, which may pose certain diagnostic difficulties, especially in younger patients.

Rarely, specific variants of SCC must be considered in the neck, such as nasopharyngeal carcinoma (which is associated with Epstein-Barr virus [EBV]) and NUT carcinoma (characterized by *NUTM1* gene rearrangement), the latter representing an extremely aggressive subtype.

### CLINICAL FEATURES

Patients most frequently present with a short history (< 6 months) of a painless mass in the upper neck involving the jugulodigastric lymph nodes. Patients may have bilateral disease (10%). There may be a history of smoking and/or alcohol abuse, especially in the context of conventional SCC. Most patients present during the 6th decade of life, with a strong male predilection (4:1). After the diagnosis of metastatic SCC is established, a primary tumor is discovered in at least 80% of patients, with the majority located in the oropharynx. Other primary sites can include the nasopharynx, oral cavity, esophagus, and laryngotracheal region. In up to 10% of patients a primary is never found, despite an extensive workup.

### METASTATIC SQUAMOUS CELL CARCINOMA—DISEASE FACT SHEET

#### Definition

- SCC that has metastasized to cervical lymph nodes

#### Incidence and Location

- Approximately one-third of cervical metastatic SCCs are cystic
- Many are from an oropharyngeal primary and are associated with high-risk HPV
- Primary oropharyngeal HPV-associated SCC may be occult and small

#### Morbidity and Mortality

- Mucositis and xerostomia (secondary to radiotherapy and/or chemotherapy)
- Approximately 30% mortality at 5 years

#### Sex and Age Distribution

- Males > > females (4:1)
- Mean presentation in 6th decade

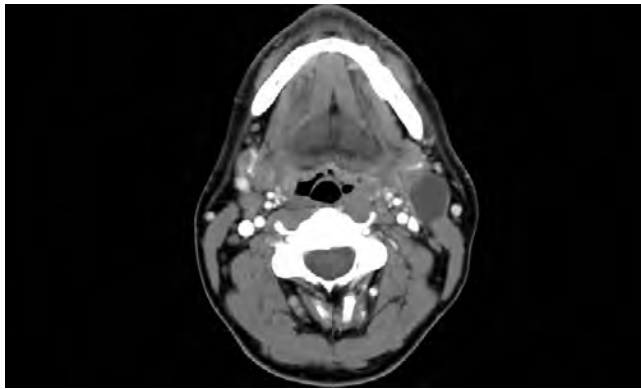
#### Clinical Features

- Painless mass involving jugulodigastric lymph nodes
- Usually short duration (<6 months)
- May have bilateral disease (10%)
- Often have smoking and alcohol abuse history
- Once metastatic disease is diagnosed, nearly 70% will have an oropharyngeal primary

#### Prognosis and Treatment

- 70%-80% 5-year survival
- Identification of the primary may require extensive examination under anesthesia, pan-endoscopy, high-resolution radiographic studies, and/or ipsilateral tonsillectomy
- Selected lymphadenectomy (used to make diagnosis) followed by focused radiation therapy (targeted to primary or Waldeyer ring if no primary is identified)

HPV, Human papillomavirus; SCC, squamous cell carcinoma.

**FIGURE 22.1**

A computed tomography scan demonstrates typical findings for metastatic squamous cell carcinoma to neck. There is a well-defined mass deep to the sternocleidomastoid muscle in the left neck, with a thick capsule. In addition, the primary mass in the oropharynx is present, which creates asymmetry.

### RADIOGRAPHIC FEATURES

Computed tomography (CT) or magnetic resonance imaging (MRI) shows a cystic or multilocular mass with a thick capsule in the region of the jugulodigastric lymph nodes (Fig. 22.1).

### PATHOLOGIC FEATURES

#### GROSS FINDINGS

The metastatic lesions can range in size from 1.5 to 12 cm (average size of approximately 4 cm). There is often a thick, fibrotic capsule defining the well-circumscribed lymph node border. Tumors with extracapsular extension have irregular borders and infiltration into adjacent fibroadipose tissue or skeletal muscle. Matted lymph nodes of confluent metastases may be seen. The cut surface is unilocular or multilocular, with cyst(s) filled with granular, thick, tenacious, and purulent yellow-brown to hemorrhagic fluid.

#### MICROSCOPIC FINDINGS

On microscopic examination, a dense, fibrous connective tissue capsule will often surround the lymph node that contains metastatic tumor (Fig. 22.2). The cystic spaces are lined by a ribbon-like growth of squamous epithelium, which has a generally uniform thickness (Fig. 22.3). Metastatic SCC can vary in appearance, ranging from transitional, basaloid, and nonkeratinizing morphology to a more conventional keratinizing squamous appearance. In some areas, metastatic tumor has an endophytic growth pattern, budding into the lymphoid stroma, whereas in other areas it is exophytic or papillary,

### METASTATIC SQUAMOUS CELL CARCINOMA—PATHOLOGIC FEATURES

#### Gross Findings

- Typically well-circumscribed, thickly encapsulated cystic mass
- Thick, tenacious, purulent, yellow-brown to hemorrhagic fluid
- Mean size of 4 cm (but may be large, up to 12 cm)

#### Microscopic Findings

- Thick, desmoplastic fibrous capsule
- Metastases are often cystic, with cyst spaces lined by ribbon-like growth of malignant squamous cells
- Conventional SCC may be well, moderately, or poorly differentiated with varying degrees of keratinization and atypia
- HPV-SCC appears nonkeratinizing, with trabecular and ribbon-like growth of uniform squamous cells lacking maturation that demonstrate loss of polarity, high nuclear to cytoplasmic ratio, and mitotic figures; profound pleomorphism is typically absent
- Extranodal extension should be noted

#### Immunohistochemical Findings

- Keratins and p63/p40 are positive, but usually not necessary for diagnosis
- Diffuse p16 nuclear positivity is an excellent surrogate marker of high-risk HPV
- High-risk HPV can be detected by ISH or sequencing
- Nasopharyngeal carcinoma is positive for EBV (best detected by ISH)
- NUT carcinoma shows punctate nuclear staining for NUT immunohistochemistry

#### Fine Needle Aspiration

- Cellular smears
- Anucleate squames and debris
- Atypical squamous cells with dyskeratosis, irregular nuclear contours, nuclear hyperchromasia, and increased nuclear to cytoplasmic ratio

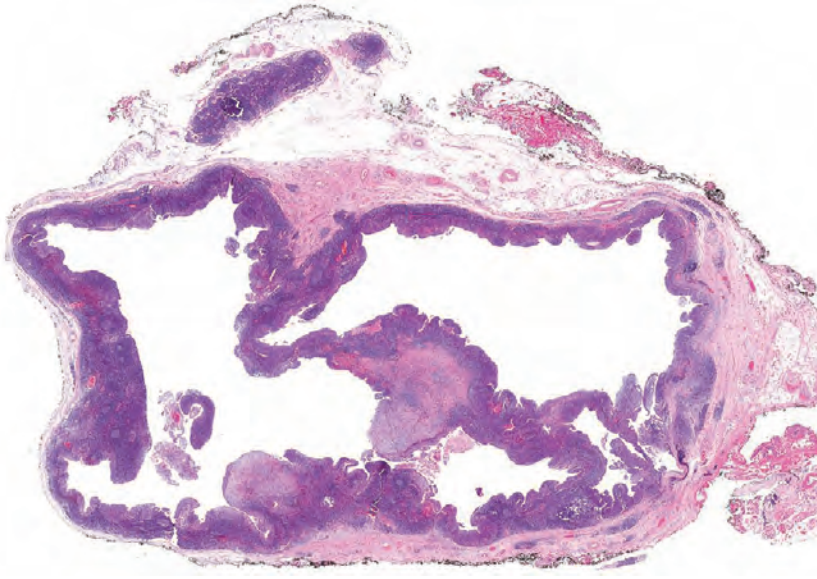
#### Pathologic Differential Diagnosis

- Branchial cleft cyst, thymopharyngeal cyst, thymic cyst, bronchial cyst
- Pilomatricoma
- High-grade mucoepidermoid carcinoma

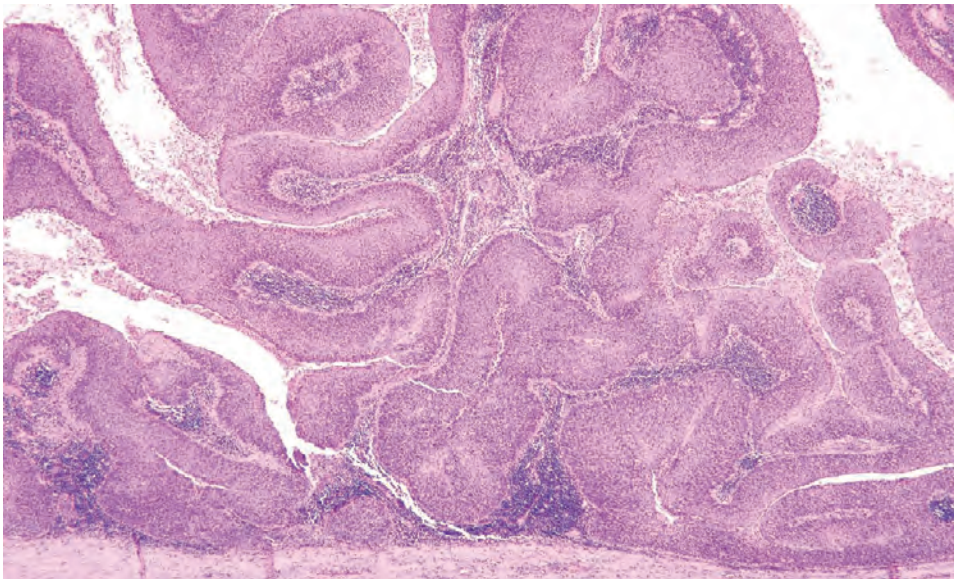
EBV, Epstein-Barr virus; HPV, human papillomavirus; ISH, in situ hybridization; SCC, squamous cell carcinoma.

with projections into the cyst spaces. The cyst contents are often washed away during fixation and histologic processing, leaving these variably sized spaces largely empty. For metastatic oropharyngeal HPV-related squamous cell carcinoma (HPV-SCC) in particular, the overall histologic appearance may be somewhat bland, recapitulating the normal squamous or transitional-type epithelium that is present in a normal deep tonsillar crypt (Fig. 22.4). In exceptional cases of metastatic HPV-SCC, the tumor cells even retain cilia, an extremely rare finding in malignant neoplasms (Fig. 22.5). Nonetheless, the cells are enlarged with a high nuclear to cytoplasmic ratio, no appreciable degree of surface maturation, and limited

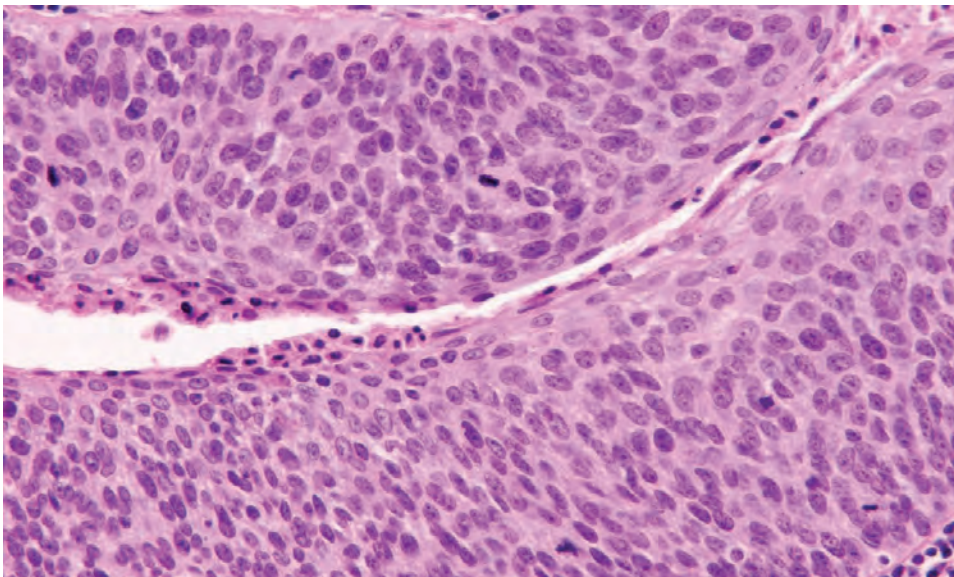


**FIGURE 22.2**

There is a thickened capsule at the periphery of this lymph node that is replaced by metastatic squamous cell carcinoma. The cystic metastasis shows a thin ribbon of malignant epithelial cells around the periphery. Note a smaller uninvolved lymph node at the top of the field.

**FIGURE 22.3**

Ribbon-like growth pattern of the metastatic squamous cell carcinoma can form papillary infoldings into the cystic spaces of the replaced lymph node.

**FIGURE 22.4**

Atypia of human papillomavirus-associated squamous cell carcinoma can be subtle. Note the loss of polarity and disorganization, increased mitotic figures, and overall mild nuclear pleomorphism.



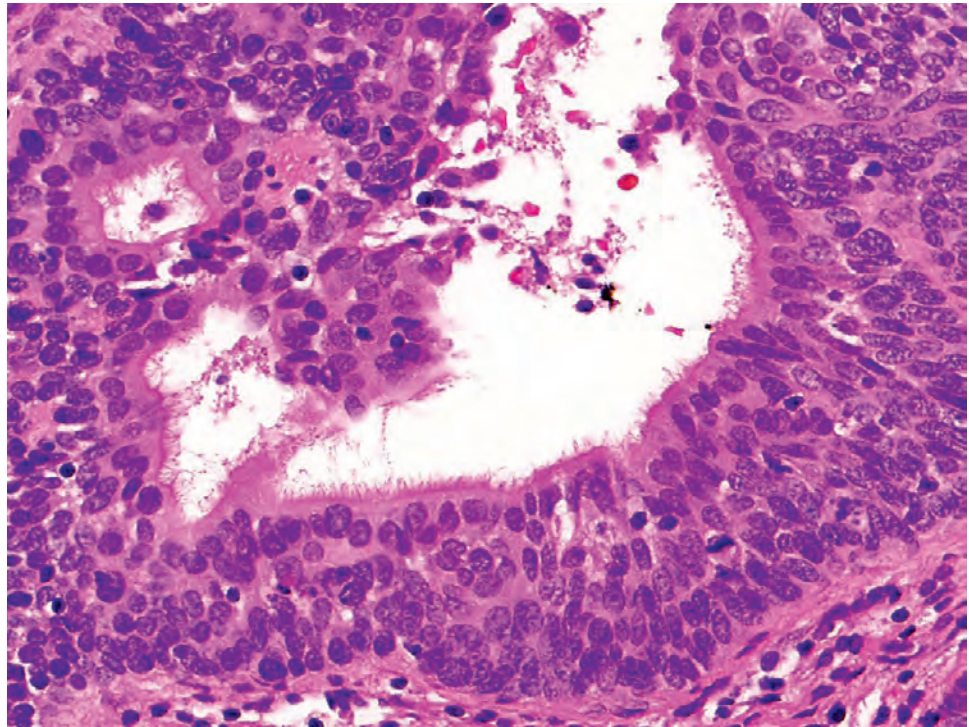


**FIGURE 22.5**

Rare examples of human papillomavirus–related squamous cell carcinomas are ciliated. Although this feature may cause confusion for a benign cyst, the carcinoma still exhibits significant cellular atypia.

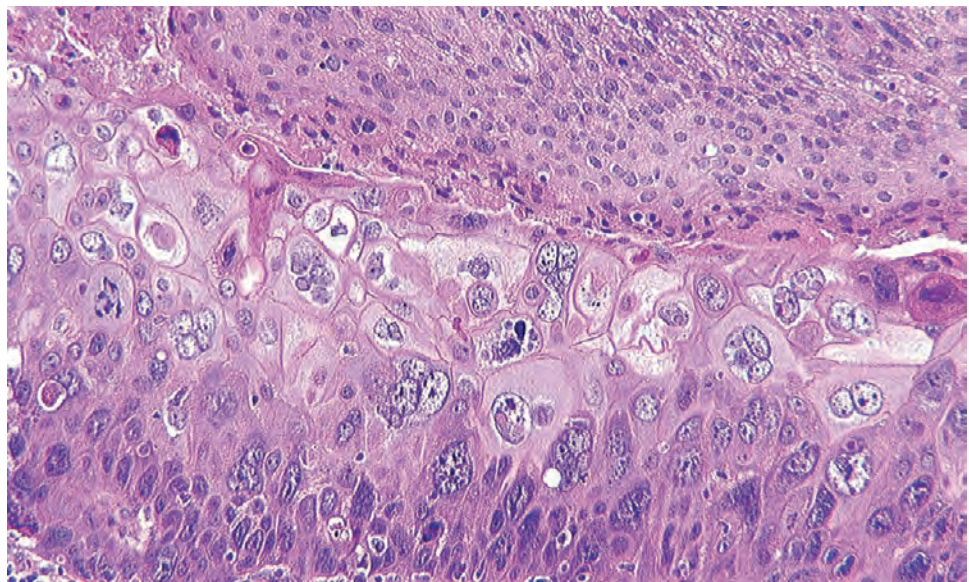


**FIGURE 22.6**

Metastatic squamous cell carcinoma can show focally severe pleomorphism.

keratinization. Occasionally, an abrupt transition to remarkably atypical epithelium can be seen, facilitating the diagnosis (Fig. 22.6). Because of the often bland histologic appearance on initial low-power examination, these lesions may require careful inspection to make the correct diagnosis. Notably, extranodular extension should be noted although for oropharyngeal HPV-associated primaries, it may not be associated with prognosis.

Specific rare variants of SCC that are nonkeratinizing or primitive appearing may need to be considered in the absence of HPV. Nasopharyngeal carcinoma is associated with a dense lymphocytic infiltrate (but may appear indistinct from normal lymph node), and tumor cells

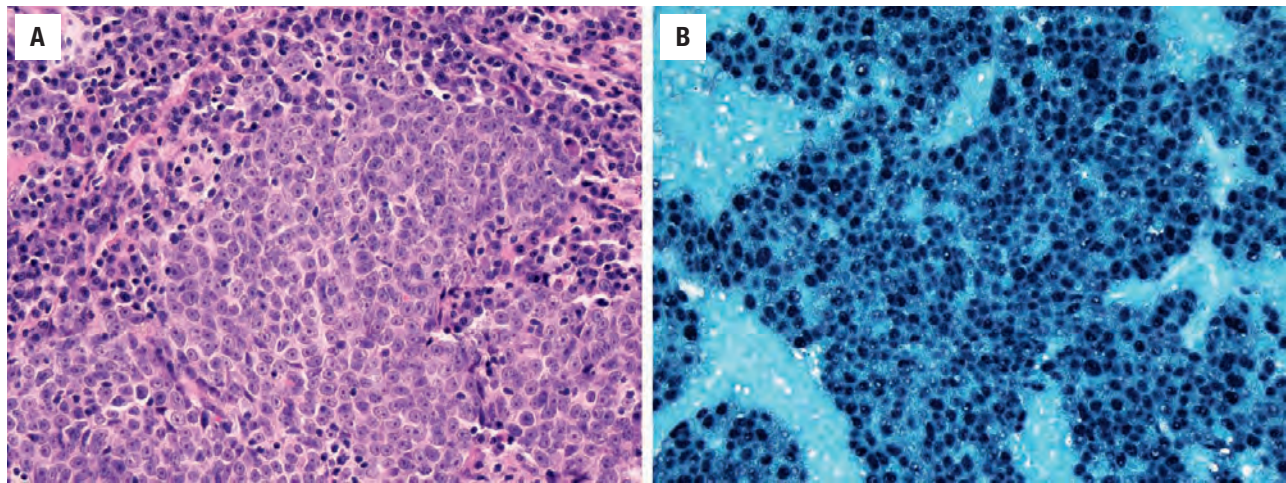
often have large vesicular nuclei and prominent nucleoli (Fig. 22.7). NUT carcinoma is composed predominantly of a uniform undifferentiated epithelioid morphology, but careful histologic examination will usually identify abrupt small foci of keratinization (Fig. 22.8).

## ANCILLARY STUDIES

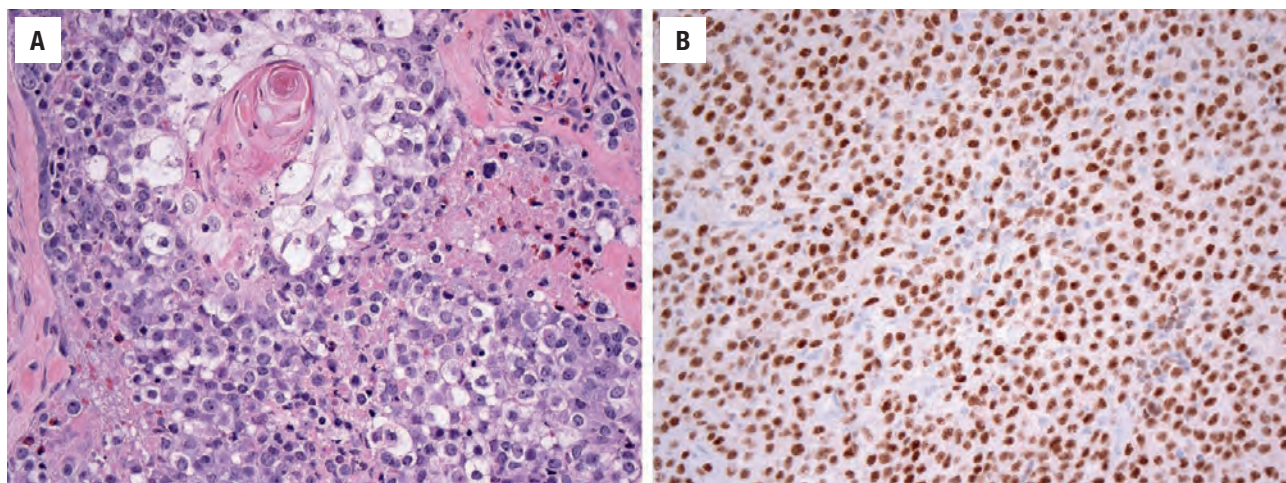
### IMMUNOHISTOCHEMICAL AND MOLECULAR FINDINGS

Immunohistochemistry is often not necessary for the recognition of SCC. However, tumor cells are positive



**FIGURE 22.7**

(A) Nasopharyngeal carcinoma can appear as an undifferentiated carcinoma. Diagnosis can be confirmed by in situ hybridization for Epstein-Barr virus (B).

**FIGURE 22.8**

(A) NUT carcinoma shows foci of abrupt keratinization within an otherwise monotonous population of undifferentiated-appearing epithelioid cells. (B) NUT immunohistochemistry shows a positive punctate nuclear staining pattern.

with a variety of keratins (AE1/AE3, CK5, CK8, CK14, and CK19), although CK7 is usually negative. Squamous differentiation can be identified by p63 and its more squamous-specific isoform, p40, which is helpful for poorly differentiated tumors.

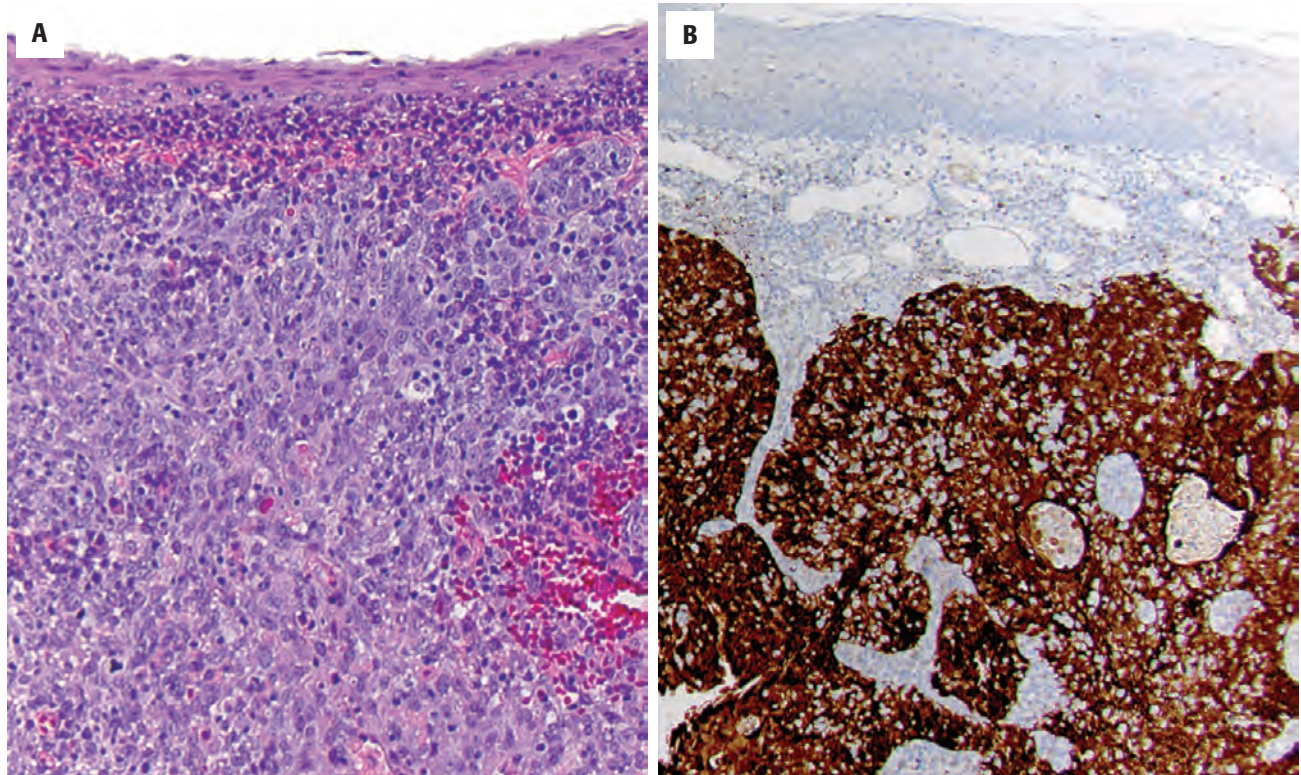
Given the high frequency (70%) of patients with HPV-SCC who present with cervical lymph node metastases, all cases of metastatic SCC in the neck should undergo testing for high-risk HPV. p16 is an excellent immunohistochemical surrogate marker for high-risk HPV; to be regarded as positive, nuclear and cytoplasmic staining should be present in at least 70% of tumor cells (Fig. 22.9). The detection of HPV is helpful in localizing the primary oropharyngeal site but also has clinical implications given that HPV-SCC is associated with better outcomes in comparison to conventional SCC.

In most cases, p16 positivity is sufficient for identifying HPV-SCC if the histologic features (i.e., nonkeratinizing

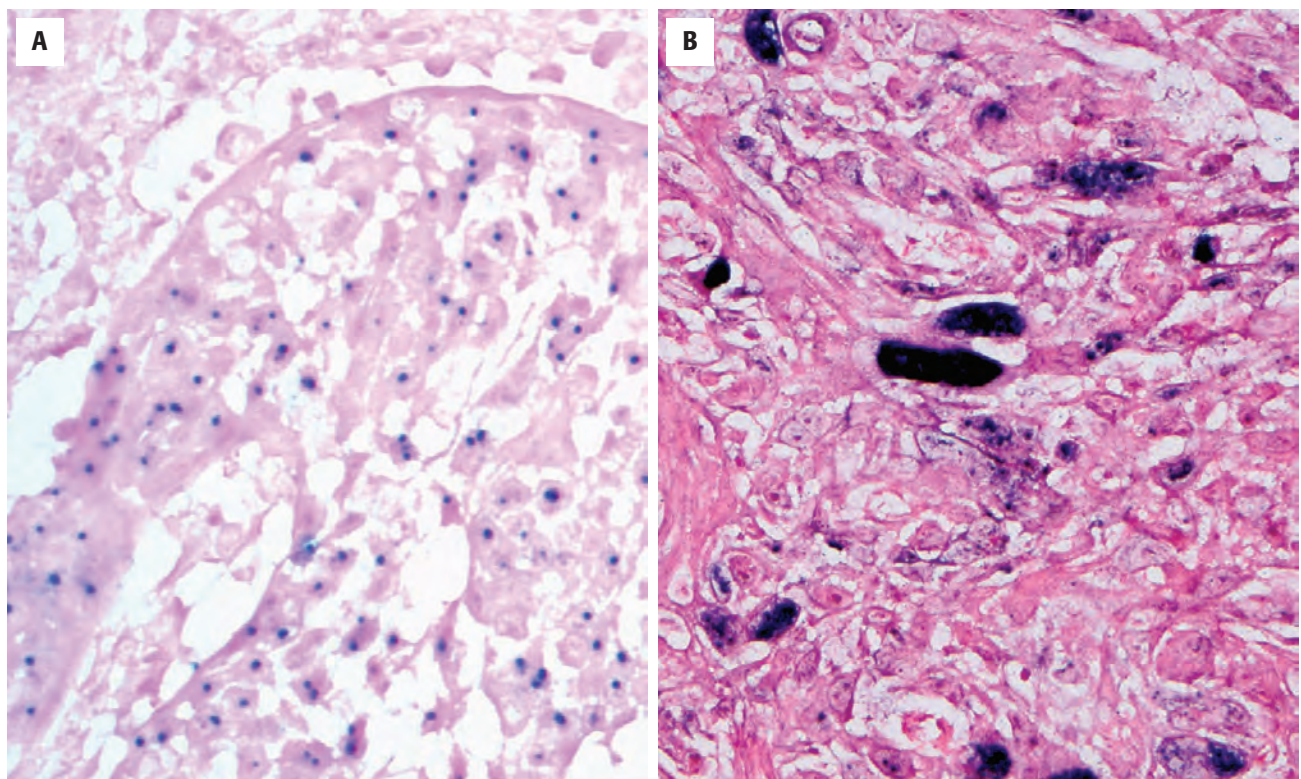
morphology) and clinical context (i.e., level 2 or 3 lymph node, oropharyngeal or unknown primary) are typical. However, there are more pitfalls in the interpretation of p16 in the neck than in the oropharynx because metastatic lung and skin carcinomas and even benign cysts can be p16 positive. For that reason, many laboratories follow positive p16 staining with confirmatory HPV detection by a more specific technique. High-risk HPV can be detected via *in situ* hybridization (ISH) or through amplification detection via sequencing. ISH has the advantage of assessing cellular location, which distinguishes between episomal and integrated virus by two distinct staining patterns: punctate (dot-like) staining with integrated virus and diffuse nuclear staining with episomal virus (Fig. 22.10).

EBV can be detected in nasopharyngeal carcinoma by ISH (Fig. 22.7). NUT carcinoma will show punctate nuclear immunoreactivity for NUT (Fig. 22.8); *NUTM1*



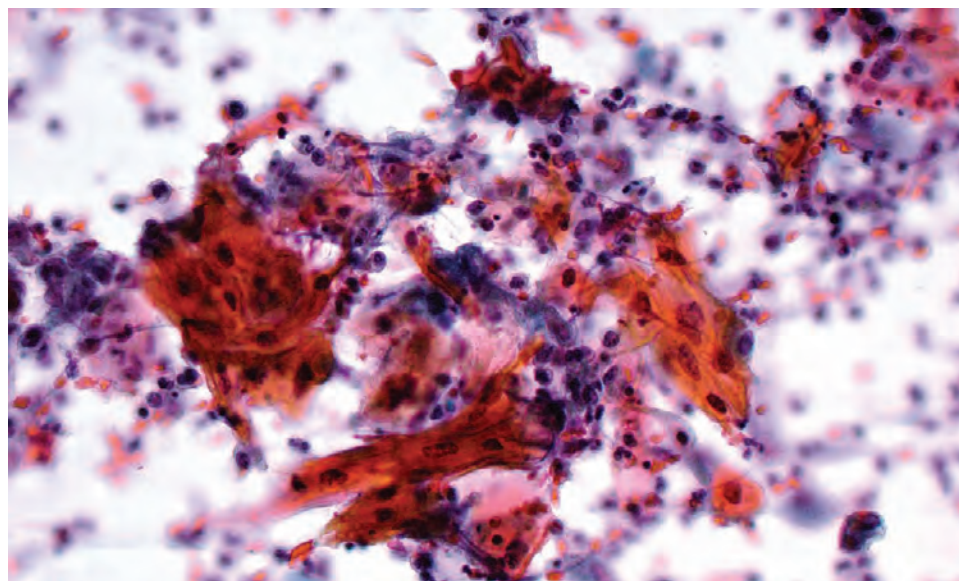
**FIGURE 22.9**

(A) Human papillomavirus (HPV)-associated squamous cell carcinoma from a tonsillar primary shows a typical nonkeratinizing morphology. (B) Strong, diffuse, nuclear and cytoplasmic p16 immunoreactivity is a surrogate marker for high-risk HPV.

**FIGURE 22.10**

In situ hybridization for high-risk human papillomavirus in a metastatic oropharyngeal squamous cell carcinoma. (A) Integrated virus showing a punctate staining pattern. (B) Episomal virus showing diffuse nuclear staining.



**FIGURE 22.11**

Aspirate smear of squamous cell carcinoma is composed of atypical squamous cells with "tadpole"-like cytoplasmic extensions, nuclear hyperchromasia, and nuclear membrane contour irregularity; a tumor diathesis in the background is commonly seen (alcohol fixed, Papanicolaou stained).

rearrangements can be detected using fluorescence in situ hybridization (FISH) break-apart probe for the *NUT* locus on 15q14 or by sequencing the *NUT-BRD4* fusion gene.

#### FINE NEEDLE ASPIRATION

Aspirate smears of metastatic SCC are often quite cellular and, in many cases, dominated by anucleate squamous and debris from the cyst contents. Fragments of atypical squamous epithelium are often present, as well as individual atypical keratinocytes (Fig. 22.11). Nuclear atypia, pleomorphism, increased nuclear to cytoplasmic ratio, and mitotic figures all help to confirm the diagnosis. All cytologic specimens, especially with cell block material of metastatic SCC should be assessed for high-risk HPV, and if initially negative, studies should be repeated on any subsequent surgical specimens. Notably, p16 immunostaining is less consistently strong and diffuse in cytology material than it is in tissue specimens.

#### DIFFERENTIAL DIAGNOSIS

Especially in younger patients, cystic, metastatic SCC must be distinguished from a branchial cleft cyst. *Branchial cleft cysts* will usually not have a thickened or desmoplastic capsule and will often contain clear fluid. The epithelium in branchial cleft cyst may be variable, with areas of respiratory epithelium and squamous epithelium, which can show keratinization; however, frank atypia is absent. Immunoreactivity for p16 may be seen in the epithelium of branchial cleft cysts but is usually limited to areas infiltrated by inflammatory cells. Ciliated HPV-related carcinomas are particularly treacherous as the presence

of cilia in a lateral neck cyst is sometimes presumed to be diagnostic of a branchial cleft cyst. Using an HPV-specific testing such as ISH will resolve this diagnostic dilemma. Other benign developmental cystic lesions that may enter the differential include thymopharyngeal cyst, thymic cyst, and bronchial cyst, which can be identified by the presence of thymic or respiratory components.

Pilomatricomas are another diagnostic pitfall, especially for HPV-SCC. Pilomatricoma is characterized by a monomorphous basaloid cell population and abundant "ghost" cells (anucleate squames with pale central zone) admixed with keratin. An adjacent inflammatory infiltrate and giant cell reaction and large dystrophic calcifications are common in pilomatricoma, but these features may also be seen as reactive changes to metastatic SCC. Pilomatricomas are more likely in younger patients and show a female predominance. The absence of cytologic atypia favors pilomatricoma; SCC should be considered if there is significant pleomorphism, hyperchromatic nuclei with prominent nucleoli, and significant mitotic activity with atypical forms.

Metastatic salivary gland neoplasms may need to be considered, namely high-grade mucoepidermoid carcinoma, as well as salivary duct carcinoma and carcinoma ex pleomorphic adenoma. High-grade mucoepidermoid carcinoma shows a predominance of the squamoid cells and limited cyst formation and absence or paucity of mucocytes. Careful histologic examination is necessary to find focal glandular differentiation, which may be visualized by mucicarmine special stain. Genetic testing may be helpful because mucoepidermoid carcinoma harbors recurrent *MECT1-MAML2* fusion gene (or rarely alternate *CRCT3-MAML2*). Salivary duct carcinoma has foci resembling high-grade in situ ductal carcinoma of breast. Most salivary duct carcinomas are positive for

androgen receptor, and a subset show membranous expression of Her2/neu (30%). Carcinoma ex pleomorphic adenoma (including salivary duct carcinoma ex pleomorphic adenoma) often shows cytologic and architectural heterogeneity and a myoepithelial immunophenotype, and the subsets arising from a precursor harboring either *PLAG1* or *HMGA2* rearrangement will show overexpression of the corresponding protein.

### PROGNOSIS AND THERAPY

After the diagnosis of metastatic SCC is accurately classified, efforts toward identifying the primary tumor are typically undertaken and include extensive physical examination under anesthesia, pan-endoscopy (nasopharynx, larynx, esophagus, nasal cavity), and detailed, high-resolution CT or MRI studies of the oropharynx and Waldeyer ring area. Again, this search is informed by initial assessment of the metastatic lesion for the presence of high-risk HPV. If these studies do not identify the primary, then prophylactic lingual and palatine tonsillectomy, specifically on the ipsilateral side, should be performed, with complete embedding of the tonsils and thorough sectioning. Still, attempts at identifying the primary tumor will be defied in an appreciable proportion of patients (up to 10%). Radiation therapy in the region of Waldeyer ring, after selected lymph node dissection, will yield a good long-term clinical outcome of 70% to 80% survival at 5 years. Patients with HPV-SCC may be managed with intensity-modulated or brachy-radiation treatment. Concurrent radiation and multiagent chemotherapy may be used. A common complication of radiotherapy or chemotherapy is mucositis and xerostomia. Overall, HPV-SCC are associated with a better outcome (up to 80% 5-year survival, stage dependent) in comparison to conventional SCC of the upper aerodigestive tract (survival rates of <35% at 5 years).

## ■ METASTATIC NEOPLASM OF UNKNOWN PRIMARY

The term “occult primary tumor” refers to a primary neoplasm that has not been found in a patient with lymph node, organ, or soft tissue metastasis, even after thorough clinical evaluation. Evaluation includes pan-endoscopy, radiographic studies, and serologic markers. A fine needle aspiration (FNA) or core needle biopsy is frequently the initial procedure. Neck metastasis may represent disease from a regional or distant primary neoplasm. Despite aggressive assessment, in up to 10% of patients, a primary tumor will not be identified. Axiomatic, lymphomas must always be excluded because their management is unique from that of metastatic carcinoma.

## CLINICAL FEATURES

The most common symptom is a painless mass in the neck. The most frequent sites of adenopathy are upper jugulodigastric (70%), midjugular (22%), supraclavicular (18%), and posterior cervical lymph nodes (12%), frequently with more than one site affected. The mass may be present for quite some time and is often slowly enlarging. The mean age at presentation is in the 6th decade, although this depends on the primary tumor type. When the primaries are from the upper aerodigestive system or salivary gland, men are affected more commonly than women (4:1), with many patients reporting a history of heavy smoking and drinking. Non-head and non-neck carcinoma primary sites include melanoma, lung, gastrointestinal tract, breast, pancreas, ovary, kidney, prostate, and less rarely sarcomas.

### METASTATIC NEOPLASM OF UNKNOWN PRIMARY—DISEASE FACT SHEET

#### Definition

- An unidentified primary neoplasm with cervical metastasis

#### Incidence and Location

- Neck lymph node metastasis is frequent
- Upper jugular lymph nodes account for site of most metastatic tumors (70%)

#### Morbidity and Mortality

- Mortality depends on primary tumor

#### Sex and Age Distribution

- For upper aerodigestive tract and salivary primaries, males > females (4:1)
- Usually adults, with a mean presentation in the 6th decade
- Other primaries are sex and age specific

#### Clinical Features

- Painless cervical mass
- Slow growing over several months
- Primary sites include oropharynx, nasopharynx, larynx, and esophagus; and lung, gastrointestinal tract, breast, pancreas, and prostate account for carcinomas outside of the head and neck region
- Melanoma and sarcoma also present as metastatic tumors
- For a subset of patients (up to 10%), no known primary is identified after thorough work-up

#### Prognosis and Treatment

- Prognosis is determined by the underlying primary but is usually poor as metastatic disease is already present
- Initial FNA evaluation guides clinical management, which includes lymph node dissection and radiation



## **PATHOLOGIC FEATURES**

### **GROSS FINDINGS**

Involved lymph nodes may be solid, unicystic or multicystic, white, gray to dark, and hemorrhagic. The size may reach 10 cm in greatest dimension (mean, 3 cm). The primary tumor type will frequently dictate the gross appearance of the metastasis.

### **MICROSCOPIC FINDINGS**

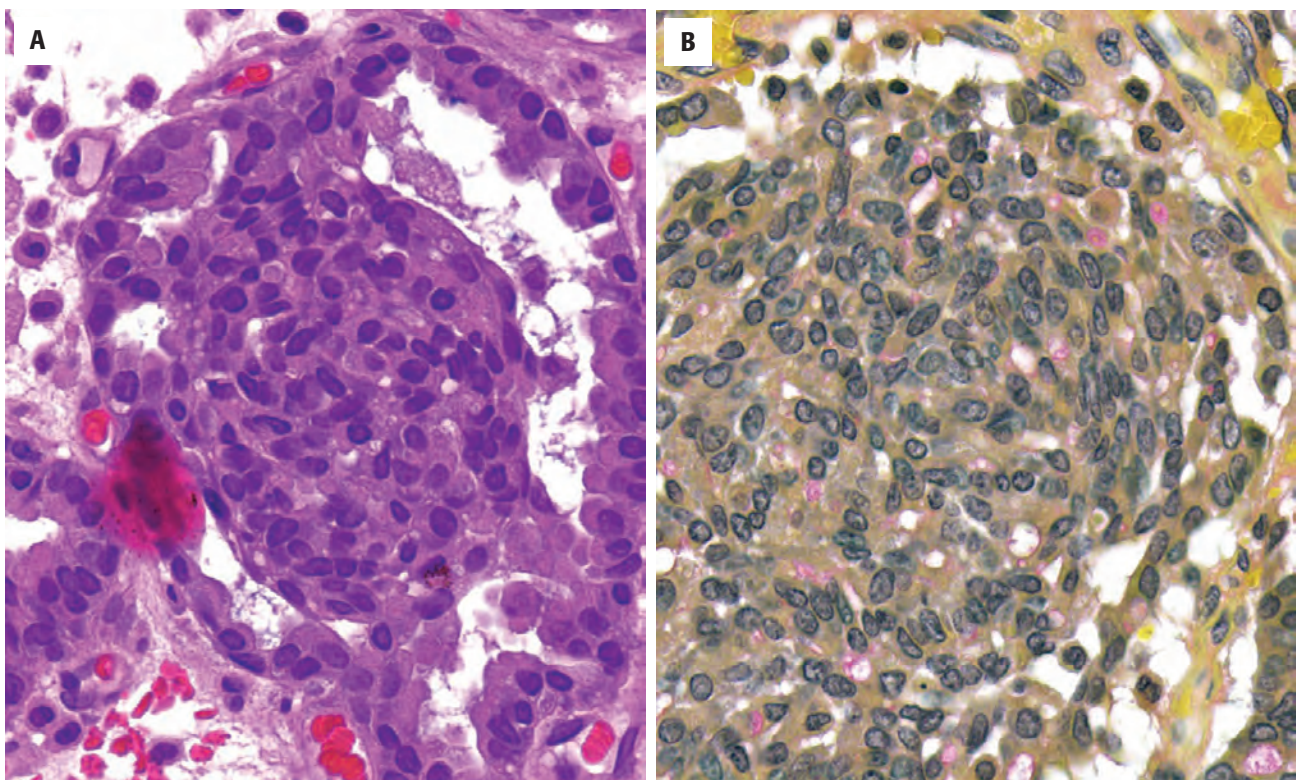
Nearly every known malignancy may result in metastatic deposits in cervical lymph nodes, and the histologic features are highly variable based on the tumor of origin. However, the most common metastatic primary sites in the cervical lymph nodes are conventional and HPV-associated SCC (60%), adenocarcinoma (20%; Fig. 22.12), undifferentiated carcinoma (12%), and melanoma (5%; Fig. 22.13); other, miscellaneous tumor types comprise the remainder (3%). Adenocarcinomas, undifferentiated carcinoma, and thyroid carcinomas are more common in the supraclavicular and scalene lymph nodes. Melanoma may also present initially as a lymph node metastasis and notoriously shows a wide morphologic spectrum and can show epithelioid, spindled, pleomorphic, or small

cell appearances. Typical cases will show nested growth of ovoid cells having large hyperchromatic nuclei with macronucleoli and amphophilic cytoplasm; some cases may have melanin pigmentation facilitating diagnosis, but a significant proportion of metastatic malignant melanoma are amelanotic.

## **ANCILLARY STUDIES**

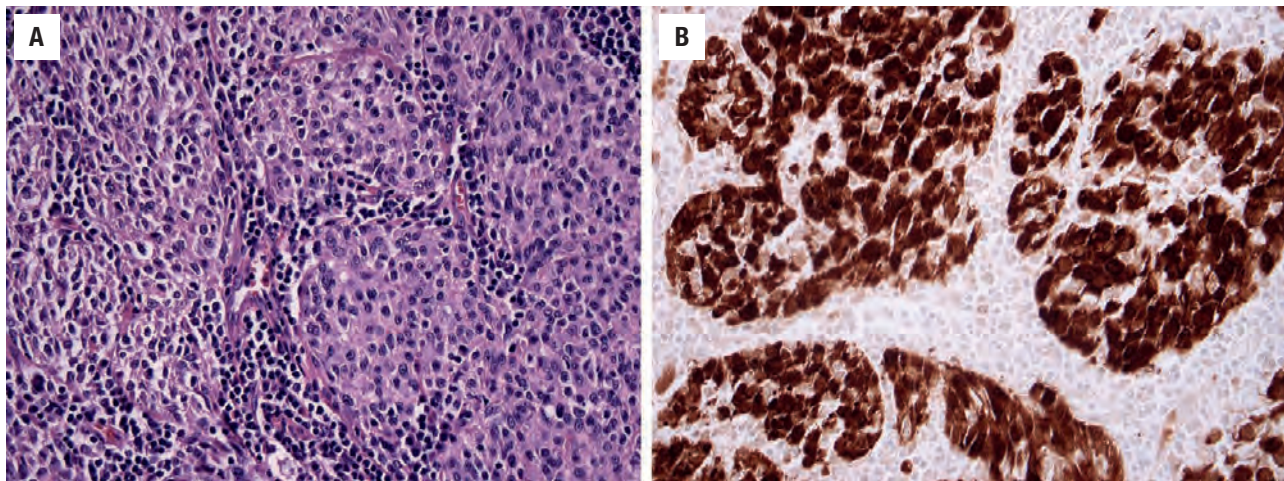
### **HISTOCHEMICAL AND IMMUNOHISTOCHEMICAL FINDINGS**

The clinical history, including the patient's sex, age, physical examination, and laboratory studies should direct the immunohistochemical work-up. Mucicarmine remains a useful histochemical stain that can highlight intracytoplasmic mucin to identify glandular differentiation in adenocarcinoma or high-grade mucoepidermoid carcinoma (Fig. 21.12). For metastatic SCC, detection of HPV helps to distinguish metastatic oropharyngeal from cutaneous or lung primaries. In many cases a targeted immunohistochemical panel will help to suggest a primary site. Keratin, p63, S100 protein, and desmin are often used as initial screening studies, to help narrow the selection of additional antibodies. For many metastatic adenocarcinomas, CK7 and CK20 will help to localize the primary



**FIGURE 22.12**

(A) Metastatic adenocarcinoma from the breast demonstrates lumina and a suggestion of intracytoplasmic vacuoles of mucin. (B) Mucicarmine stain highlights the intracytoplasmic mucin vacuoles.

**FIGURE 22.13**

(**A**) Metastatic melanoma is frequently amelanotic, and typically shows nested growth of spindled and epithelioid cells. (**B**) The diagnosis is supported by S100 protein immunoreactivity, among other immunomarkers.

#### METASTATIC NEOPLASM OF UNKNOWN PRIMARY— PATHOLOGIC FEATURES

##### Gross Findings

- Solid or cystic mass
- Up to 10 cm in size (mean, approximately 3 cm)

##### Microscopic Findings

- SCC, papillary thyroid carcinoma, adenocarcinoma, undifferentiated carcinoma, melanoma, sarcoma, and lymphoma are all considerations, with carcinomas most common
- Malignant melanoma may show a wide morphologic spectrum and can be amelanotic

##### Ancillary Studies

- Variable depending on the histologic type
- Screening panel should include keratin, p63, S100 protein, LCA, and desmin
- Mucicarmine is helpful in identifying glandular differentiation (i.e., adenocarcinoma)
- For adenocarcinomas, CK7 and CK20 should be performed, followed by relevant site-specific markers
- HPV testing such as in situ hybridization can distinguish metastatic oropharyngeal HPV-SCC from lung and cutaneous primaries

##### Pathologic Differential Diagnosis

- Developmental cysts, lymphoma, ectopic nests in the lymph node

HPV, Human papillomavirus; SCC, squamous cell carcinoma.

#### FINE NEEDLE ASPIRATION

FNA is an excellent screening study; it is a rapid, inexpensive, and safe procedure. For carcinomas, separation can usually be made between SCC and adenocarcinoma, with additional histochemical or immunohistochemical studies performed directly on smears or cell block sections. More generally, a diagnosis of lymphoma, carcinoma, melanoma, or sarcoma as major categories is also helpful for directing the search in a specific direction, eliminating the need for more invasive and costly procedures while also directing treatment planning.

#### DIFFERENTIAL DIAGNOSIS

The differential diagnosis usually encompasses benign and reactive versus neoplastic lesions; however, given the lymph node location, any identified epithelial neoplasm is reasonably assumed to be malignant. Benign entities are also in the differential and include branchial cleft cysts, developmental cysts, ectopia, infections, and reactive inflammatory lymphoid hyperplasia, most of which can usually be easily separated.

#### PROGNOSIS AND THERAPY

The prognosis is determined largely by the underlying primary, although the presence of metastases at the time of diagnosis already portends a poorer prognosis. Rare exceptions do exist, however. Lymph node dissection and radiation can often palliate tumor progression.

(Table 22.1). Table 22.1 summarizes useful site-specific immunohistochemical antibodies in the work-up of carcinoma of unknown primary. In the absence of keratin positivity, CD45 should be performed to rule out a lymphoproliferative disorder.



**TABLE 22.1****Site-specific immunohistochemical markers of common occult metastatic carcinomas (non-H&N) to cervical lymph nodes**

|                    | CK7 | CK20 | TTF1 | ER  | CDX2 | SATB2 | SMAD4* | Pax8 | WT1 | NKX3.1 |
|--------------------|-----|------|------|-----|------|-------|--------|------|-----|--------|
| Lung               | +   | –    | +    | –   | –    | –     | +      | –    | –   | –      |
| Breast             | +   | –    | –    | +/- | –    | –     | +      | –    | –   | –      |
| Upper GI           | +   | -/+  | –    | –   | -/+  | -/+   | +      | –    | –   | –      |
| Lower GI           | –   | +    | –    | –   | +    | +     | +      | –    | –   | –      |
| Pancreaticobiliary | +   | -/+  | –    | –   | -/+  | -/+   | –      | –    | –   | –      |
| Ovary              | +   | –    | –    | +   | –    | –     | +      | +    | +   | –      |
| Kidney             | +   | –    | –    | –   | –    | –     | +      | +    | –   | –      |
| Prostate           | -/+ | -/+  | –    | –   | –    | –     | +      | –    | –   | +      |

\*Loss of expression is considered diagnostic.

## ■ SYNOVIAL SARCOMA

Synovial sarcoma (SS) is a spindle cell sarcoma that may show epithelial differentiation and a specific chromosomal translocation t(X;18)(p11;q11), resulting in *SS18* fusion with *SSX1*, *SSX2*, or *SSX4*. SS accounts for approximately 10% of all soft tissue sarcomas. Although there is a predilection for the extremities, approximately 10% occur in the head and neck, usually in the neck, oropharynx, or hypopharynx. The World Health Organization (WHO) designates SS as a tumor of uncertain histogenesis.

### CLINICAL FEATURES

Although all age groups may be affected, there is a bimodal presentation, with most affected patients young adults (mean, 25 years) and a second peak in the 50s. Males are affected more commonly than females (3:1). Many patients report a long history of a slowly growing tumor mass. Typically, the symptoms are nonspecific, manifesting as a solitary, painless mass. Occasionally, hoarseness, upper respiratory distress, and dysphagia may be present.

### RADIOGRAPHIC FEATURES

A soft tissue mass is appreciable on radiographic studies in most cases, with CT often informative about the site and extent of the tumor. Irregular calcifications may be present (20% of cases).

### SYNOVIAL SARCOMA—DISEASE FACT SHEET

#### Definition

- Spindle cell sarcoma characterized by translocation t(X;18)(p11;q11); a subset show epithelial differentiation

#### Incidence and Location

- Represents approximately 10% of all soft tissue sarcomas
- Approximately 10% occur in the head and neck

#### Morbidity and Mortality

- 5-year and 10-year survival in children and adolescents is 83% and 75%, respectively
- 5-year and 10-year survival in adults is 62% and 52%, respectively
- Approximately 30% die of disease

#### Sex and Age Distribution

- Males > females (3:1)
- Median age, 25 years
- Bimodal distribution during 2nd-to-3rd and 6th decades

#### Clinical Features

- Painless, solitary mass in neck or hypopharynx
- May be slowly growing over a long time period (multiple years)
- Hoarseness, upper respiratory distress, or dysphagia may occur

#### Radiographic Features

- Soft tissue mass on computed tomography
- Calcifications within the tumor may help with diagnosis

#### Prognosis and Treatment

- Approximately 25% develop recurrence
- Approximately 50% of patients develop distant metastases
- Tumor size <5.0 cm, age <20 years, and negative surgical margins portend a better prognosis
- Wide surgical excision with adjuvant multimodality therapy

## **PATHOLOGIC FEATURES**

### **GROSS FINDINGS**

Head and neck SS ranges in size from 1 to 12 cm. Tumors are partially encapsulated and variably circumscribed, solid to cystic. The cut surface is yellow to gray-white with a firm, gritty, and friable to soft, boggy, and rubbery consistency (Fig. 22.14). It usually has a whorled appearance, with areas of cyst formation, and mucoid or hemorrhagic degeneration.

### **MICROSCOPIC FINDINGS**

SS is a spindle cell sarcoma and tumors composed solely of spindle cell morphology are referred to as monophasic SS (Fig. 22.15). Tumors with additional epithelial differentiation are referred to as biphasic SS

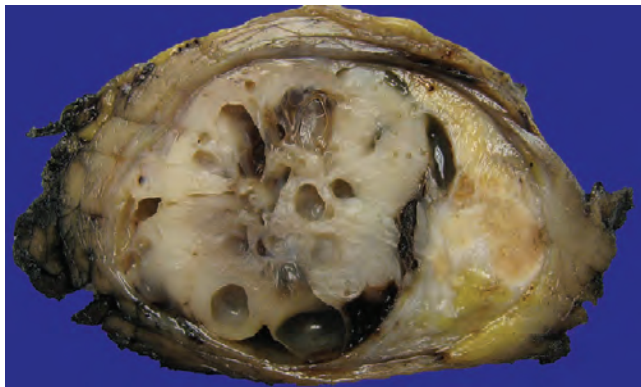


**FIGURE 22.14**

Synovial sarcoma appears grossly well circumscribed and has a variably nodular, fibrous, and cystic cut surface.

## **SYNOVIAL SARCOMA—PATHOLOGIC FEATURES**

### **Gross Findings**

- Solid or multicystic mass with calcifications
- Partially encapsulated with variable circumscription
- Cut surface is yellow, gray-white
- Firm, gritty to soft and boggy
- Mucoid and hemorrhagic degeneration may be present

### **Microscopic Findings**

- Fascicles and sheets of spindle cells with overlapping ovoid nuclei and indistinct cell borders
- Wiry stromal collagen and thin-walled HPC-like vessels are present
- Biphasic SS has an epithelial component admixed with the spindle cell component
- Epithelial component comprised of cuboidal to columnar cells with more abundant pale eosinophilic cytoplasm, arranged in cords, nests, and pseudoglandular spaces
- Calcifications may be present
- Poorly differentiated SS commonly shows round cell morphology

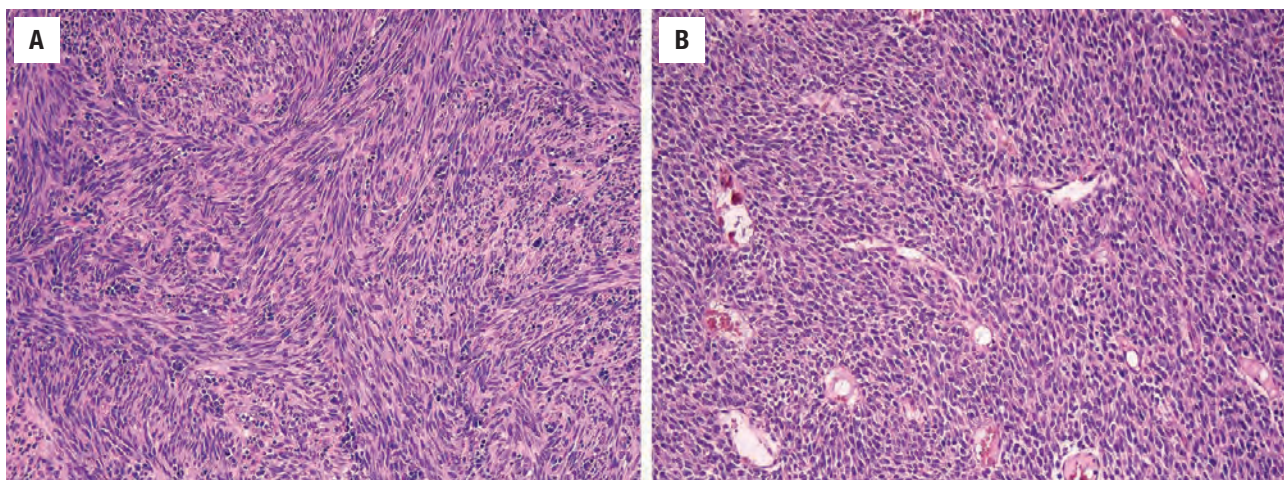
### **Ancillary Studies**

- Keratin and EMA are positive in both epithelial and spindle cell components
- TLE1 shows diffuse and strong nuclear staining
- Translocation t(X;18)(p11.2;q11.2) resulting in *SS18-SSX* fusion gene

### **Pathologic Differential Diagnosis**

- Malignant peripheral nerve sheath tumor, leiomyosarcoma, spindle cell RMS, spindle cell carcinoma, metastatic adenocarcinoma

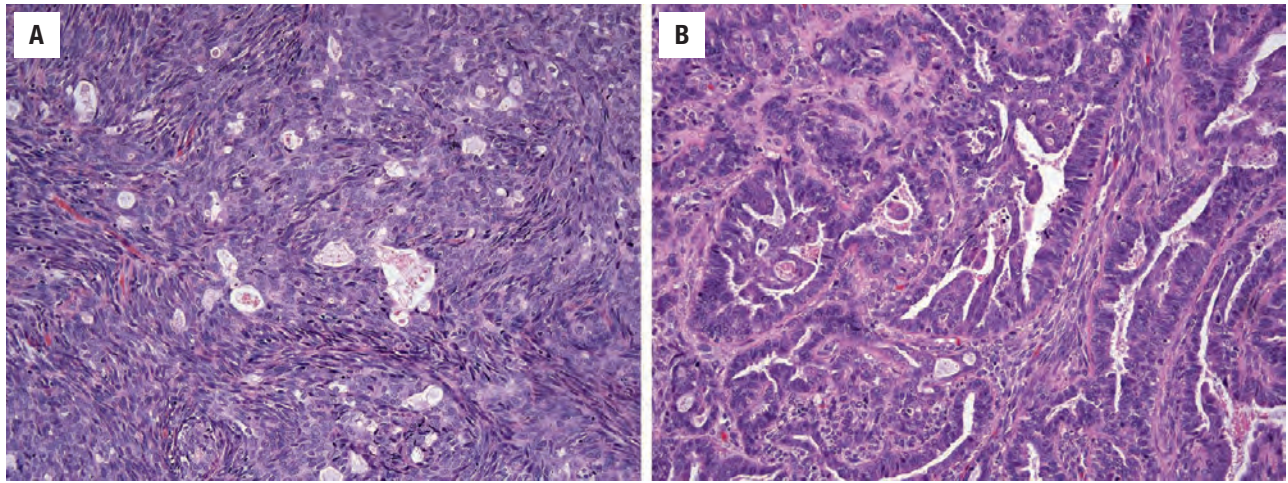
*HPC*, Hemangiopericytoma; *RMS*, rhabdomyosarcoma.



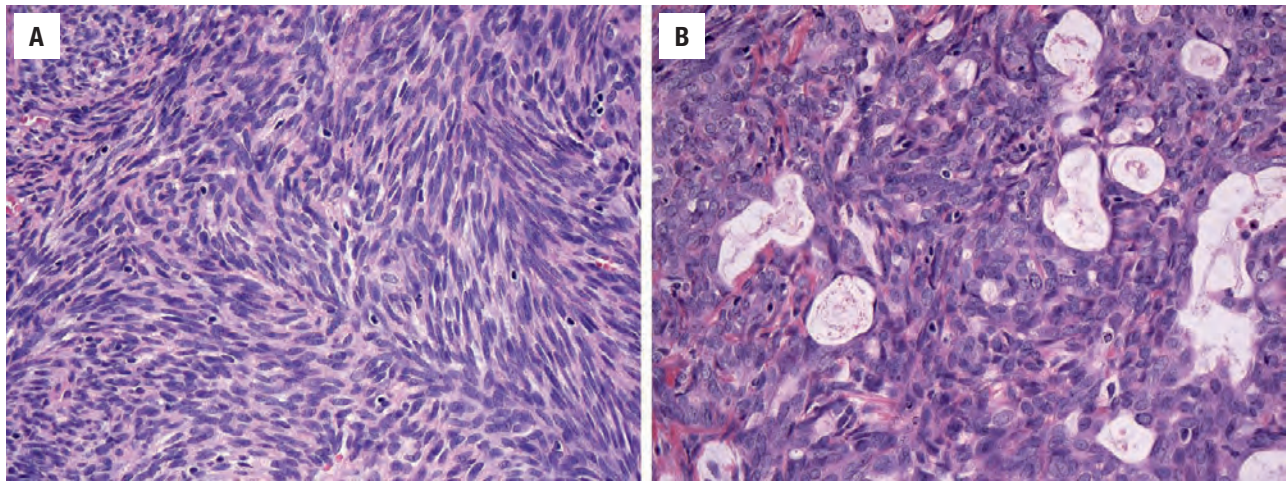
**FIGURE 22.15**

Synovial sarcoma. (A) Spindle cell component (which predominates in monophasic synovial sarcoma) is arranged in fascicles and sheets; fascicles are densely cellular with overlapping tumor cell nuclei. (B) Thin-walled hemangiopericytoma-like vessels are a feature of synovial sarcoma.



**FIGURE 22.16**

(A) In biphasic synovial sarcoma, there is an epithelial component that is often gland forming, admixed with the spindled cells. (B) Some examples may have prominent glandular differentiation that mimics adenocarcinoma.

**FIGURE 22.17**

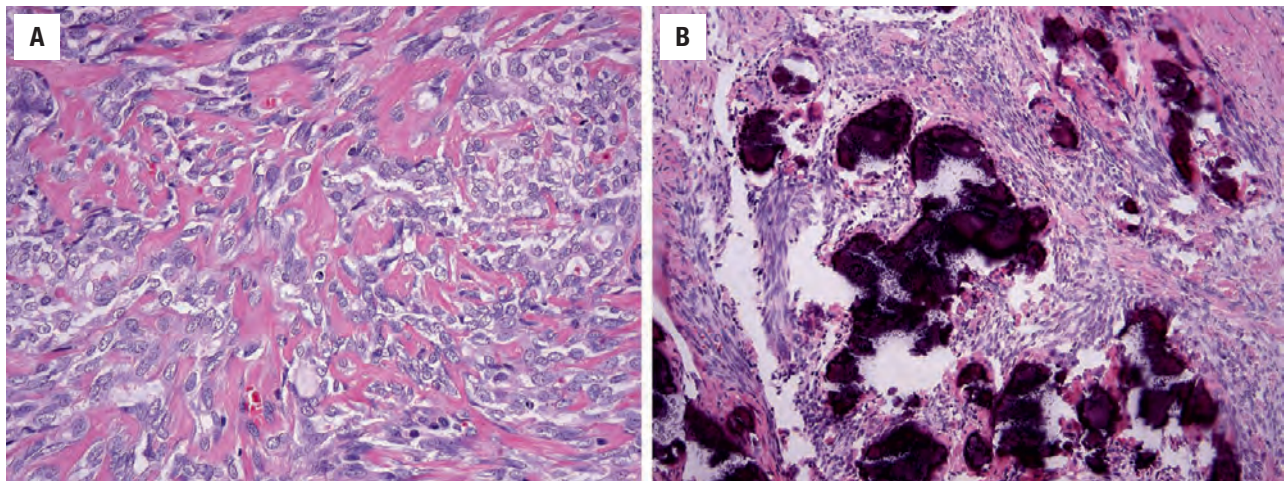
Synovial sarcoma. (A) The spindle cell nuclei are variably ovoid and spindle shaped and are vesicular or hyperchromatic; cytoplasm is scant and with indistinct cellular boundaries. (B) The epithelial component shows cuboidal to columnar cells with more abundant pale eosinophilic cytoplasm.

(Fig. 22.16). There is no clinical difference between monophasic and biphasic tumors. At low power, tumors may show variable “marbling” with alternating hypercellular (dark) and hypocellular (light) areas. The spindle cells are arranged in densely packed, interlacing fascicles and sheets of spindle cells with overlapping nuclei. The nuclei are variably ovoid and spindled and are vesicular or hyperchromatic; cytoplasm is scant and cell borders are indistinct (Fig. 22.17). When present, the epithelial component is composed of cuboidal or columnar cells arranged in cords, nests, whorls, or pseudoglandular spaces, having round to oval vesicular nuclei encompassed by abundant, pale eosinophilic or clear cytoplasm (Fig. 22.17). Occasional examples have an extensive epithelial

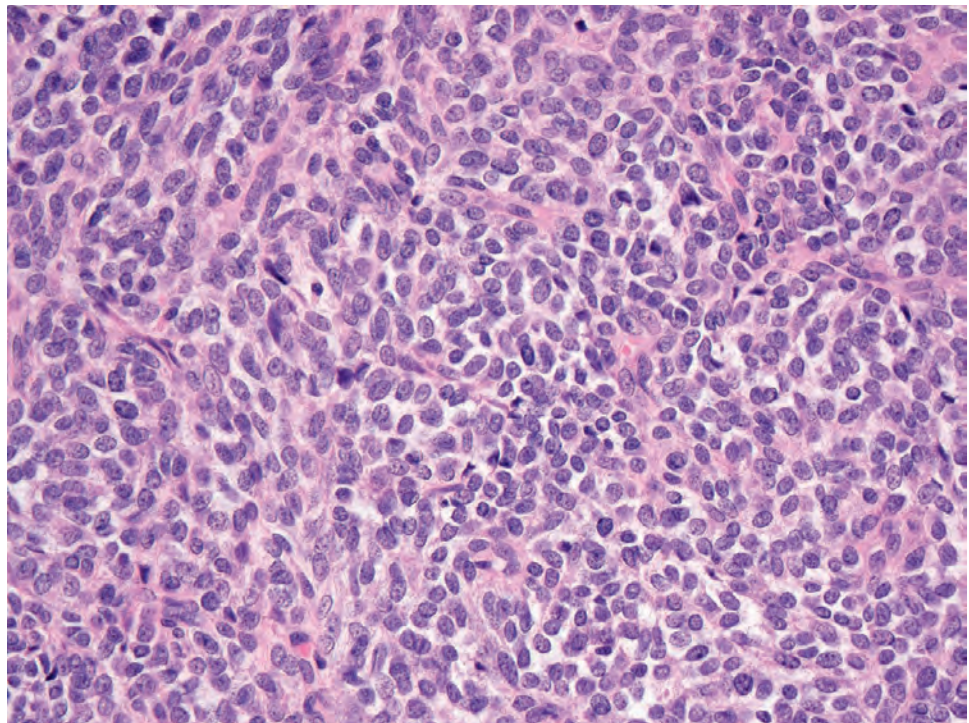
component that may mimic adenocarcinoma (Fig. 22.16B). SS shows frequent mitotic activity. Large stromal calcifications can be seen, as well as areas of myxoid change or necrosis. Tumors have a rich vascular component of slit-like, thin-walled vessels, many times creating a hemangiopericytoma (HPC)-like pattern. Stromal collagen varies from scant, delicate and wiry, or thickly hyalinized (Fig. 22.18). SS typically imparts a uniform cytologic appearance, although pleomorphism is seen in occasional examples.

Poorly differentiated SS is hypercellular with nuclear irregularity, prominent nucleoli, or irregular chromatin, and often characterized by round cell morphology (Fig. 22.19).



**FIGURE 22.18**

(A) Some examples of synovial sarcoma have prominent thick hyalinized stromal collagen. (B) Large stromal calcifications are common.

**FIGURE 22.19**

Poorly differentiated synovial sarcoma showing predominantly small round cell morphology and hypercellularity, reminiscent of Ewing sarcoma.

## ANCILLARY STUDIES

### IMMUNOHISTOCHEMICAL FINDINGS

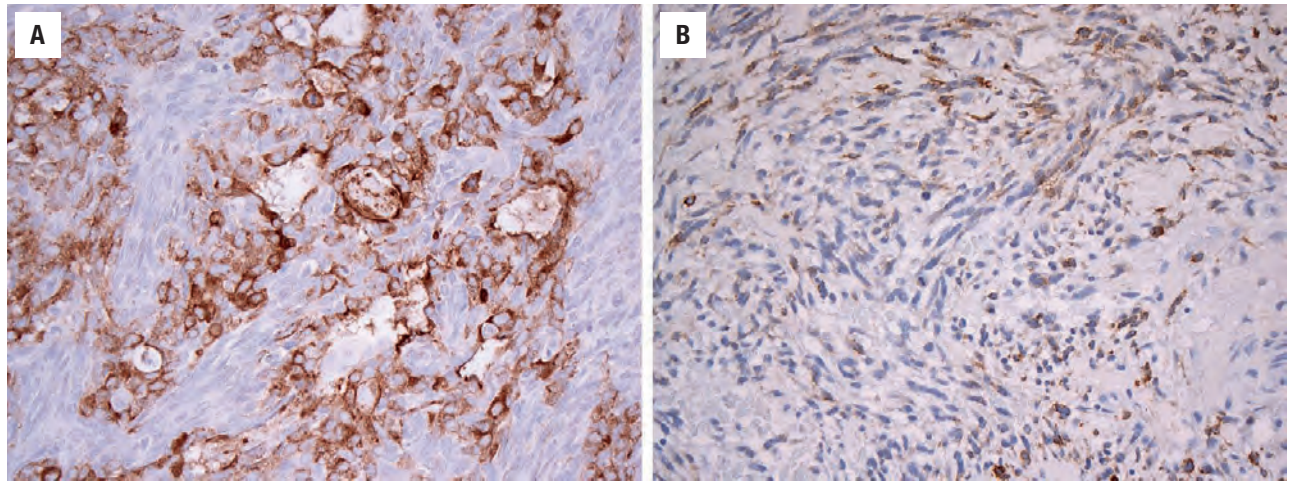
SS expresses low- and high-molecular-weight keratins, CK7, CK19, and epithelial membrane antigen (EMA) in the epithelial component; the spindle cells often show variably weak or focal staining for epithelial markers (80%; Fig. 22.20). CD99 is positive in approximately 60% of cases but is a nonspecific marker. TLE1 shows strong and diffuse nuclear reactivity in spindle cell and epithelial components (Fig. 22.21); however, nonspecific

weak staining may be seen in mimics, such as malignant peripheral nerve sheath tumor (MPNST).

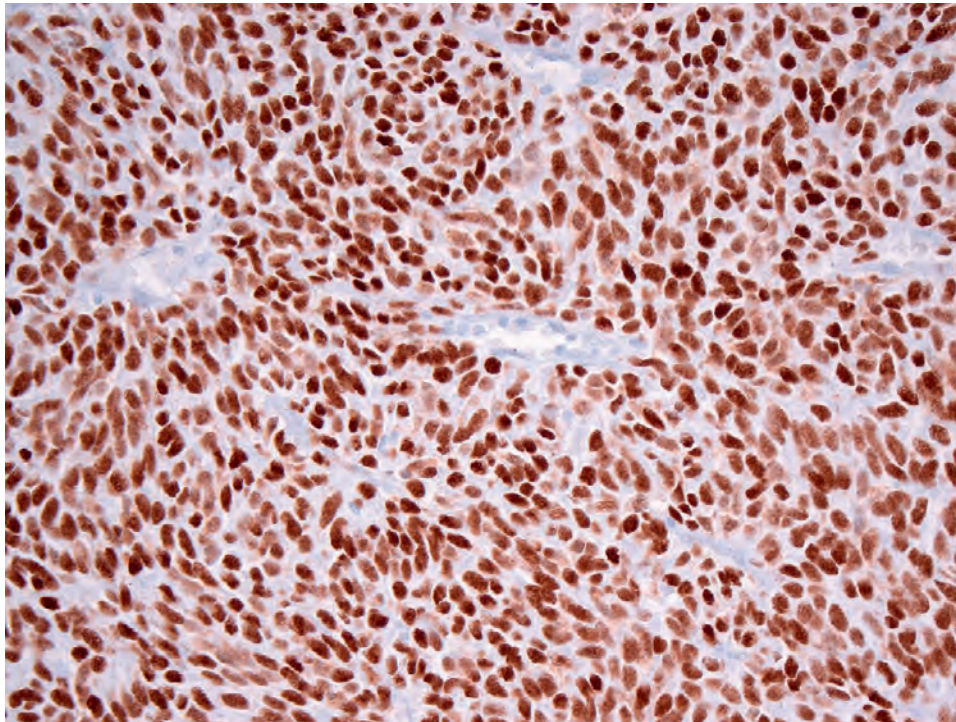
### FINE NEEDLE ASPIRATION

Smears from SS are densely cellular, composed of three-dimensional tissue fragments with irregular borders and numerous singly dispersed ovoid and spindle tumor cells (including bare nuclei; Fig. 22.22). There is an accentuation of the proliferation around a capillary vascular plexus or network. Nuclei are ovoid to spindled, with delicate, even chromatin distribution. In biphasic SS, small gland-like or duct-like structures may be seen.



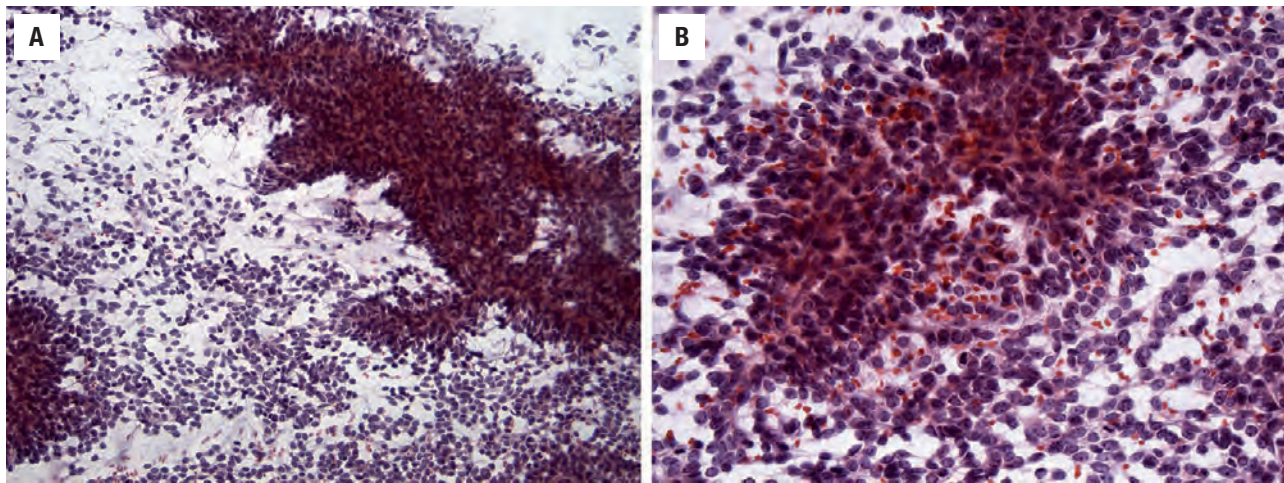
**FIGURE 22.20**

Epithelial markers (EMA shown here) are positive in the epithelial component of biphasic synovial sarcoma (**A**) and may also show focal reactivity in spindle cells, even in monophasic synovial sarcoma (**B**).

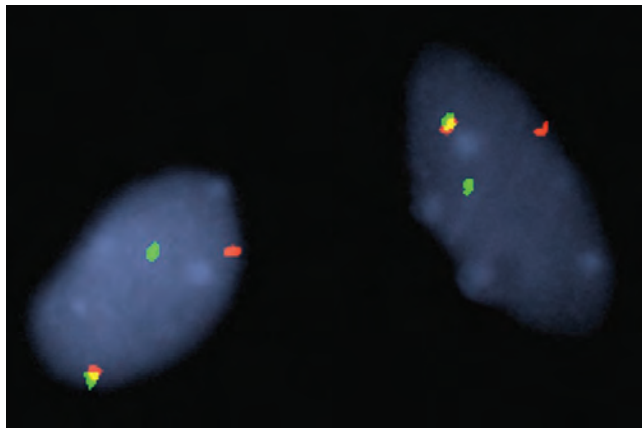
**FIGURE 22.21**

TLE1 shows a strong and diffuse nuclear reactivity in synovial sarcoma.



**FIGURE 22.22**

(A) Aspirate smears of synovial sarcoma are hypercellular, with large tissue fragments and singly dispersed tumor cells (alcohol fixed, Papanicolaou stained). (B) The uniform population of spindled and ovoid tumor cells have hyperchromatic nuclei, indistinct nucleoli, and scant cytoplasm; naked nuclei are common (alcohol fixed, Papanicolaou stained).

**FIGURE 22.23**

Fluorescence in situ hybridization (FISH) confirms *SS18* gene rearrangement in synovial sarcoma. This FISH break-apart probe shows single red and green signals in each cell, confirming the separation of the two probes that normally flank the breakpoint region. (A normal result shows a yellow signal (red and green fluorescing together) indicating that the locus is intact.) (Courtesy of Anhthu Nguyen.)

### MOLECULAR FINDINGS

By use of FISH or sequencing, the characteristic balanced, reciprocal translocation  $t(X;18)(p11.2;q11.2)$  can be confirmed (Fig. 22.23). The translocation results in rearrangement of *SS18* (on chromosome 18) with partners *SSX1*, *SSX2*, or *SSX4* from the X chromosome.

### DIFFERENTIAL DIAGNOSIS

The differential diagnosis can be broad. For monophasic SS, the differential includes MPNST, leiomyosarcoma, spindle cell rhabdomyosarcoma (RMS), and spindle cell

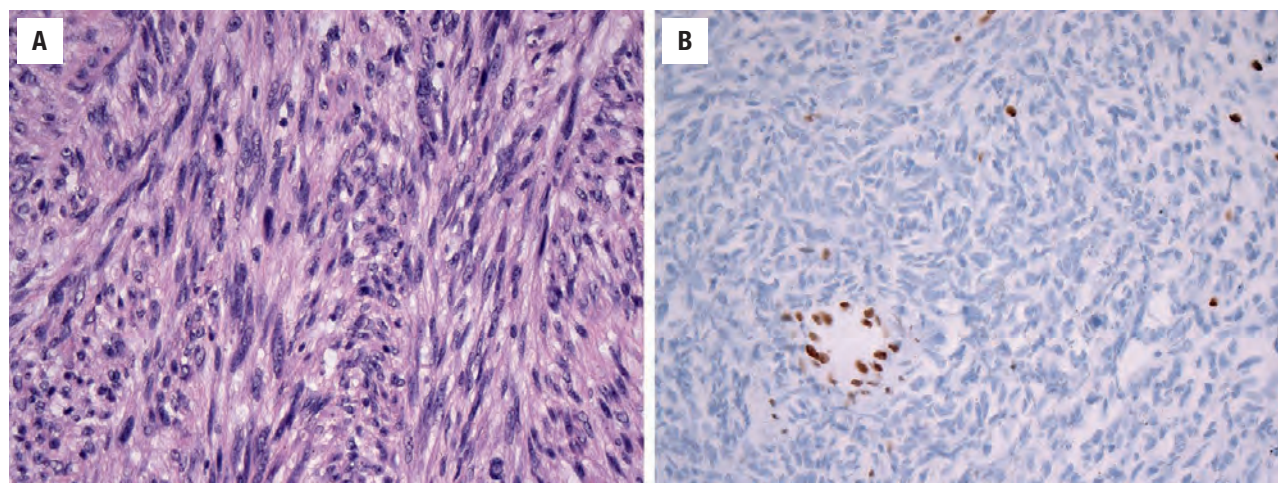
SCC. A broad immunohistochemical panel in the work-up of a spindle cell sarcoma should include keratin, EMA, S100 protein, desmin, and smooth muscle actin (SMA). MPNST is often indistinguishable from SS, showing similar features of fascicular growth, alternating hypercellular and hypocellular areas, and HPC-like vessels (Fig. 22.24); rarely MPNST can also show glandular differentiation. Furthermore, MPNST can show weak multifocal positivity for TLE1, and only up to 30% are positive for S100 and SOX10. Loss of expression of H3K27me3 is a useful marker for MPNST (Fig. 22.24). H3K27me3 loss occurs secondary to inactivation of *PRC2*, which results from inactivating mutations of its constituents *SUZ12* or *EED1*. A history of neurofibromatosis type 1, or association with a nerve, favors MPNST. Metastatic adenocarcinoma may also be considered in cases with prominent epithelial differentiation. Leiomyosarcoma is positive for SMA, desmin, and caldesmon; spindle cell RMS is positive for desmin, myogenin, and MyoD1 and is associated with *MyoD1* or *NCOA2* mutations.

The differential diagnosis for poorly differentiated SS includes other round cell neoplasms, such as alveolar RMS and Ewing sarcoma. Immunohistochemistry will resolve most cases: alveolar RMS shows diffuse desmin and myogenin staining, and Ewing sarcoma shows a diffuse membranous CD99 staining and strong nuclear FLI-1 and NKX2.2 positivity.

### PROGNOSIS AND THERAPY

Most patients are treated by surgery combined with multimodality therapy (radiation and chemotherapy). Local recurrence develops in approximately 25% of patients, with approximately 25% also demonstrating distant metastases (usually to lung). Approximately



**FIGURE 22.24**

(A) Malignant peripheral nerve sheath tumor (MPNST) shows fascicles of atypical spindle cells. (B) At least 50% of MPNST show immunohistochemical loss of expression of H3K27me3, which indicates loss of tri-methylation of lysine 27 of histone H3 secondary to *PRC2* inactivation.

one-third of patients die from disease. In children and adolescences, the 5- and 10-year survivals in children and adolescents are 83 % and 75 %, respectively; in adults, the 5- and 10-year survivals in adults are 62 % and 52 %, respectively. There is better prognosis associated with small tumors, young age at presentation, and low mitotic indexes. Poorly differentiated SS shows more aggressive behavior.

## ■ CHORDOMA

Chordomas are malignant tumors that recapitulate the notochord. Sites of involvement are: sacrococcygeal (60 %), speno-occipital (25 %), and vertebral (15 %). Approximately 10 % of all tumors are cervical. Most cases are sporadic. Isolated cases show an autosomal dominant inheritance pattern, associated with duplication of the brachyury (*T*) gene.

### CLINICAL FEATURES

Chordomas account for approximately 4 % of malignant bone tumors, with incidence of 0.08 per 100,000 population. Tumors arise most commonly during the 5th to 7th decade. Overall, males are more commonly affected than females. The most common symptoms in the neck include neurologic symptoms (nerve impingement) and progressive pain, and headaches may develop if the lesion encroaches on the skull base. Rarely, a parapharyngeal mass may occur in cervical lesions, as the mass protrudes forward. Tumors are slow growing and locally destructive.

### CHORDOMA—DISEASE FACT SHEET

#### Definition

- A malignant tumor of notochord differentiation

#### Incidence and Location

- Represents approximately 4% of malignant bone tumors
- Cervical tumors account for approximately 10%

#### Morbidity and Mortality

- For cervical lesions, approximately 60% ultimately die of disease
- Recurrence rates up to 60%
- 40% develop distant metastases

#### Sex and Age Distribution

- Males > females (2:1)
- Mean age, 56 years

#### Clinical Features

- Neurologic symptoms referable to nerve roots
- Progressive pain
- Parapharyngeal mass if mass protrudes forward

#### Prognosis and Treatment

- Overall median survival of 7 years, and depends on tumor site and size (i.e., resectability)
- Radical, complete surgical removal yields best outcome
- Radiotherapy may be used if unresectable
- Dedifferentiated chordoma have worse prognosis with frequent distant metastases

### RADIOGRAPHIC FEATURES

Chordomas are typically solitary, central, lytic, expansile, and destructive lesions. CT and MRI are complementary imaging modalities, with MRI showing soft tissue changes and CT highlighting bony changes. An adjacent

extraosseous soft tissue component is frequent. Matrix calcification is radiographically evident in the majority (70%) of cases.

## **PATHOLOGIC FEATURES**

### **GROSS FINDINGS**

Chordomas are expansive, lobulated tumors with a myxoid or gelatinous, and occasionally chondroid, gross appearance. Tumors of the neck involve the vertebral column, almost always destroying the vertebral disc space, with extension into the surrounding tissues. These tumors range in size from 1 to 20 cm (mean, 5 cm).

### **MICROSCOPIC FINDINGS**

The classic microscopic appearance of chordoma is a lobulated growth of cords and clusters of tumor cells separated by fibrous septa. Tumor cells are embedded within an abundant myxoid stroma (Fig. 22.25). The two constituent populations are epithelioid cells having clear or pale eosinophilic cytoplasm and large “physaliphorous” cells having abundant vacuolated cytoplasm (Fig. 22.26); these components may be variably present within a given tumor. Tumor cells may have round nuclei that may appear uniform with mild atypia or exhibit higher-grade features. Approximately 5% of chordomas contain islands of hyaline-type chondroid or cartilaginous matrix and are designated “chondroid chordomas” (Fig. 22.27); contrary to earlier studies, there is no evidence that chondroid chordomas behave differently.

A subset of chordomas, especially in younger patients, show increased cellularity, cytologic atypia, increased mitotic activity, and solid growth and are designated “poorly differentiated chordomas” (Fig. 22.28). Less than

## **CHORDOMA—PATHOLOGIC FEATURES**

### **Gross Findings**

- Expansive, lobulated, glistening mass with a variably gelatinous or chondroid appearance

### **Microscopic Findings**

- Lobular architecture with fibrous septa
- Cords and island of epithelioid cells with clear and eosinophilic cytoplasm embedded in an extracellular chondromyxoid matrix
- Physaliphorous cells with abundant “bubbly” vacuolated cytoplasm
- Chondroid chordoma has islands of hyaline chondroid matrix
- Poorly differentiated tumors show hypercellularity, cytologic atypia, increased mitotic activity, and solid growth

### **Immunohistochemical Findings**

- Express keratin, EMA, and S100 protein
- Brachyury expression is highly sensitive and specific for chordoma
- Poorly differentiated chordomas show loss of expression of SMARCB1 (INI1)

### **Pathologic Differential Diagnosis**

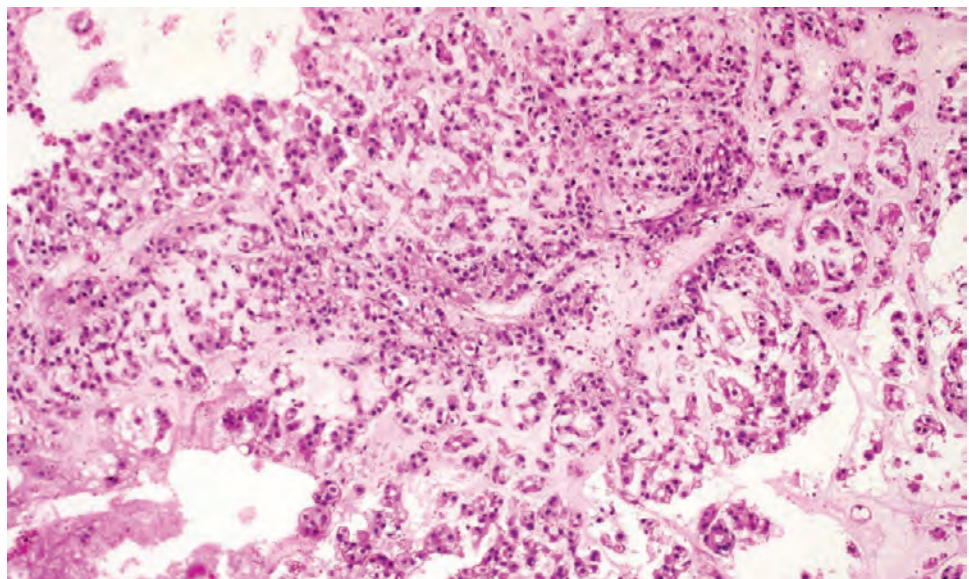
- Chondrosarcoma, pleomorphic adenoma, carcinoma ex pleomorphic adenoma, metastatic carcinoma

5% of chordomas show “dedifferentiation” with juxtaposed high-grade undifferentiated spindle cell tumor or osteosarcoma.

## **ANCILLARY STUDIES**

### **IMMUNOHISTOCHEMICAL FINDINGS**

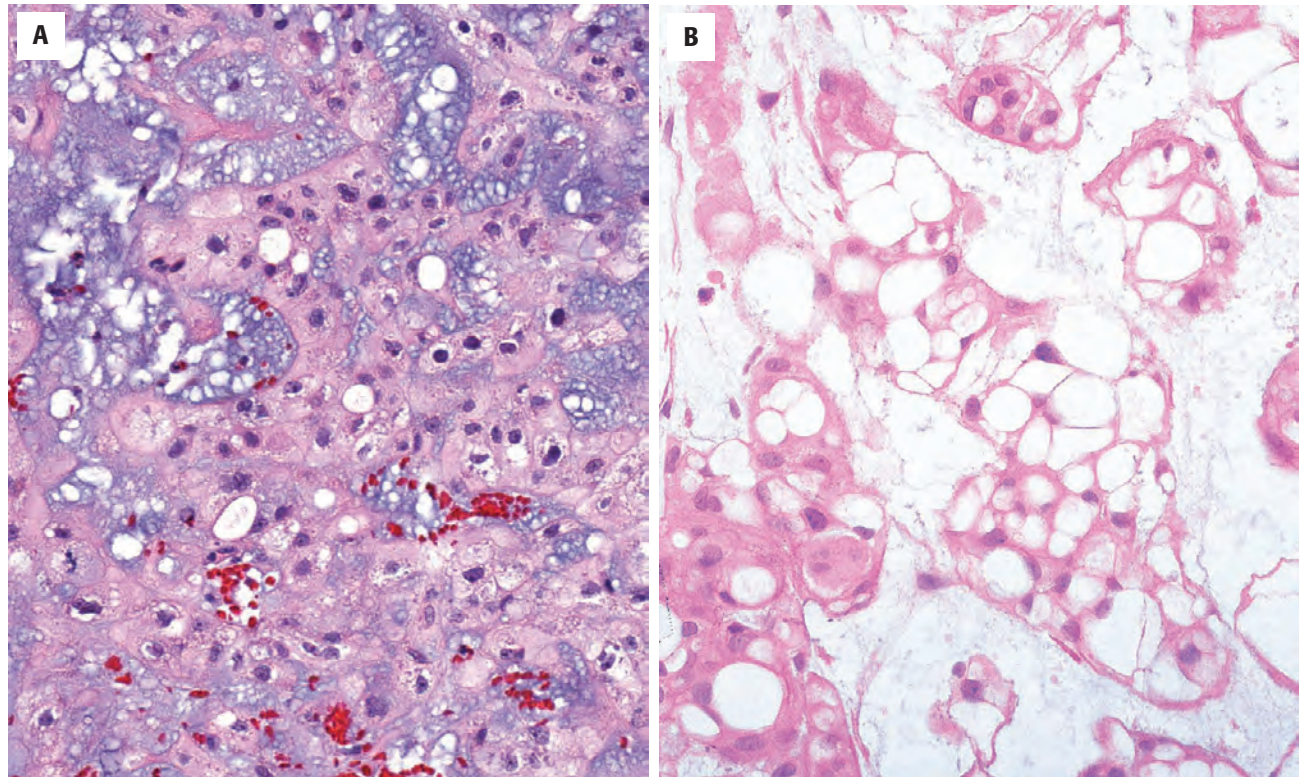
Chordomas are immunoreactive with keratin, EMA, and S100 protein (Fig. 22.29). Staining for these



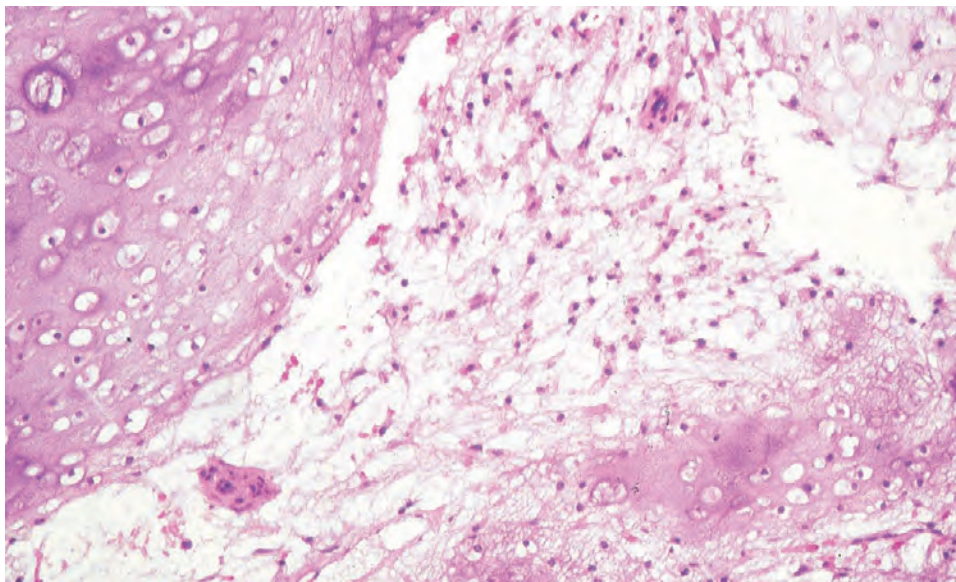
**FIGURE 22.25**

Chordoma shows lobulated architecture of cords and islands of epithelioid cells within an abundant myxoid stroma.



**FIGURE 22.26**

Chordoma is composed of a dual cell population embedded in an abundant myxoid background. **(A)** Epithelioid polygonal cells with clear or palely eosinophilic cytoplasm arranged singly and in clusters and cords. **(B)** Physaliphorous cells show abundant vacuolated cytoplasm.

**FIGURE 22.27**

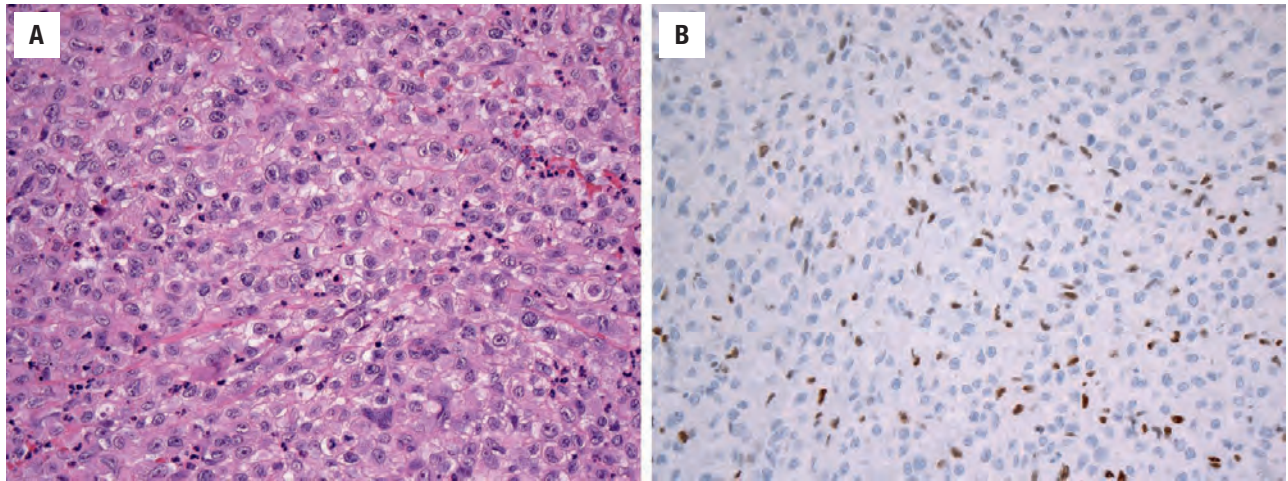
Chondroid chordoma has shown areas of hyaline chondroid matrix.

conventional markers can be variable and may range from strong and diffuse to weak and focal. Nuclear staining for brachyury is a sensitive and specific marker for chordoma (Fig. 22.29). Tumor cells are negative with glial fibrillary acidic protein (GFAP). Poorly differentiated chordomas show loss of SMARCB1 (INI1) expression (Fig. 22.28).

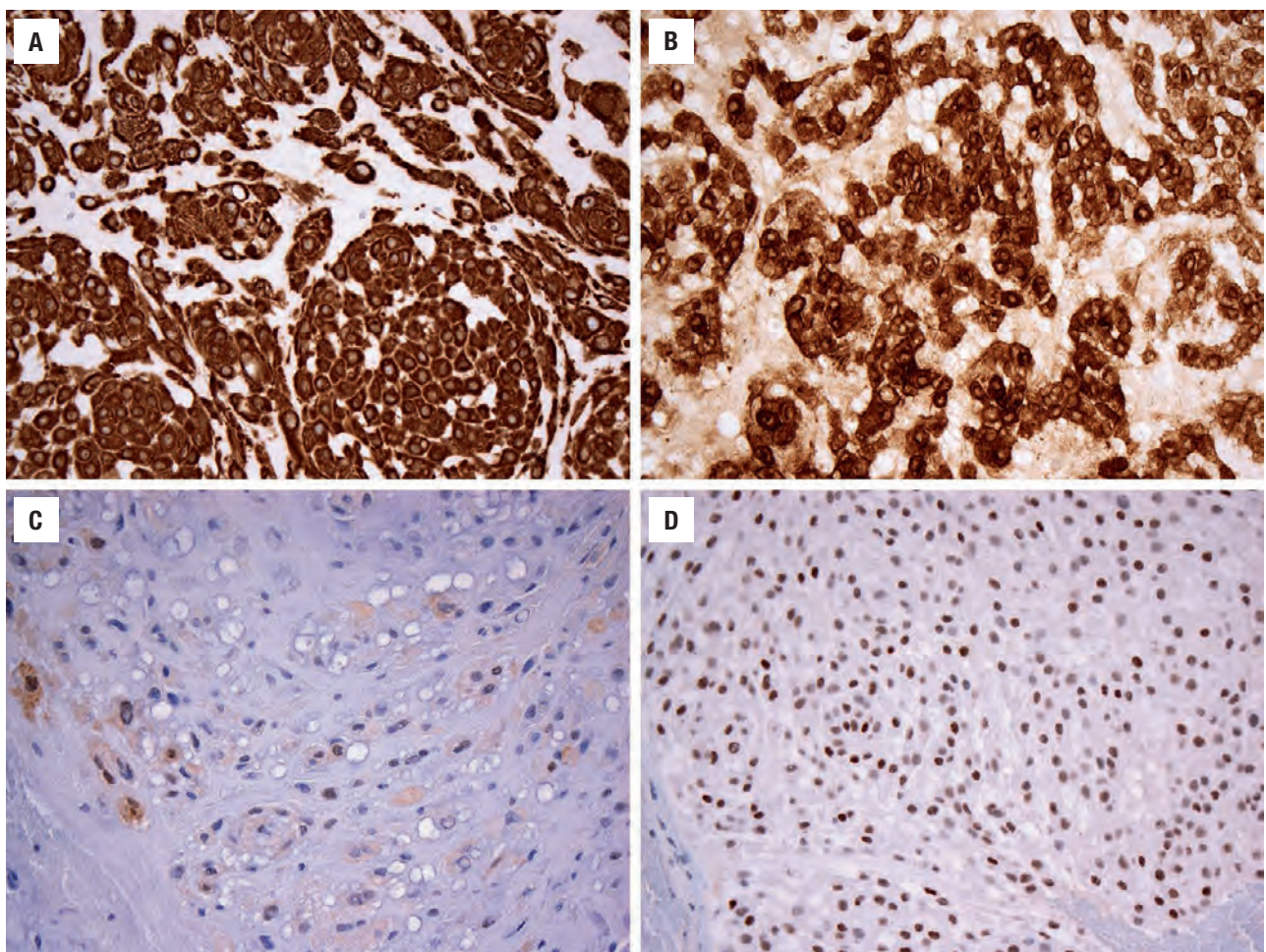
#### FINE NEEDLE ASPIRATION

Smears of chordoma are usually cellular with abundant, chondromyxoid background matrix (Fig. 22.30). The epithelioid cells are embedded within the chondromyxoid matrix, may be seen singly or in small groups, and show varying degrees of nuclear atypia.



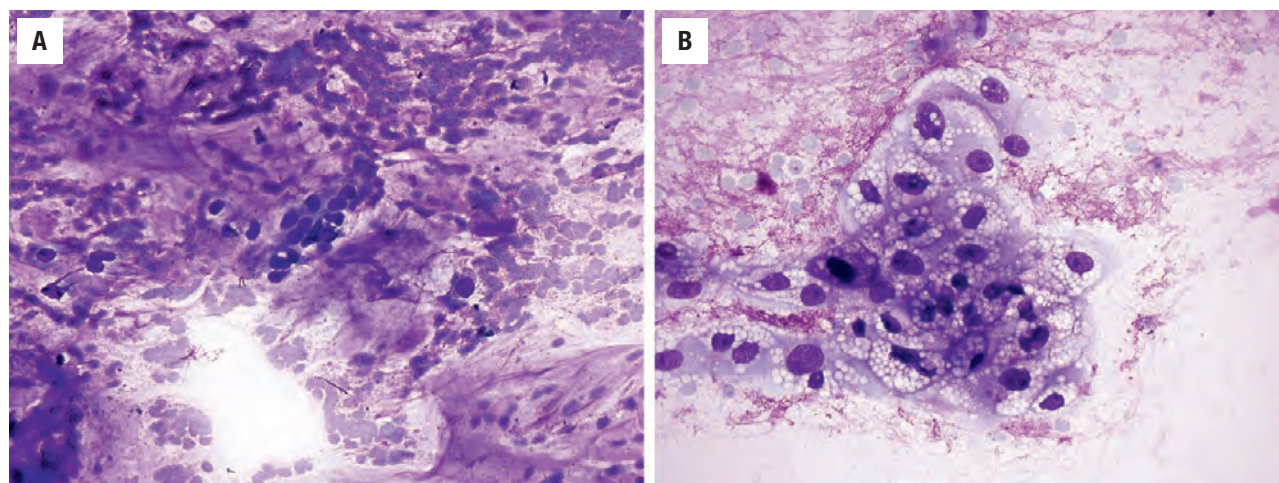
**FIGURE 22.28**

(A) Poorly differentiated chordoma is rare and shows increased cellularity, cytologic atypia, increased mitotic activity, and solid growth. (B) These tumors show loss of SMARCB1 (INI1) expression.

**FIGURE 22.29**

Most chordomas show expression of pan-keratin (A) and EMA (B). S100 protein is frequently positive (C) but has lower sensitivity than epithelial markers (D). Nuclear staining for brachyury is highly sensitive and specific for chordoma.



**FIGURE 22.30**

(A) Aspirate smears show abundant extracellular myxoid matrix with scattered epithelioid cells, which may be sparsely present (air dried, Diff-Quik–stained).  
 (B) The characteristic physaliphorous cells are larger with more abundant vacuolated cytoplasm (air dried, Diff-Quik–stained).

The larger physaliphorous cells, with abundant bubbly cytoplasm, are distributed throughout but may be sparsely represented.

#### MOLECULAR FINDINGS

Cytogenetic studies have shown several numerical and structural rearrangements, most commonly monosomy of chromosome 1 and chromosome 7 gains. In addition, comparative genomic hybridization studies have shown that 70 % of chordomas harbor either homozygous or heterozygous loss of *CDKN2A* and *CDKN2B*. Other common events include copy number gains of *T (brachyury)* (encoded on 7q33) and *EGFR7* (encoded on 7p12). Duplication of *T (brachyury)* is associated with autosomal dominant familial cases. Both heterozygous and homozygous deletions of the *SMARCB1 (INI1)* gene (encoded on 22q11) are present in poorly differentiated chordomas.

#### DIFFERENTIAL DIAGNOSIS

In the neck the main differential diagnoses are epithelial neoplasms (e.g., mucinous or poorly differentiated adenocarcinoma, salivary gland neoplasms) and chondrosarcoma, along with benign notochord tumors. The lobulation, physaliphorous cells, and S100 protein and brachyury immunoreactivity distinguish chordoma from

*carcinoma*; clinical correlation for a previous malignancy is also helpful. The presence of ductal structures and the immunoreactivity for GFAP, PLAG1, or HMGA2 distinguish *pleomorphic adenoma* and *carcinoma ex pleomorphic adenomas* from chordoma. *Chondrosarcoma* may show S100 positivity but is negative for cytokeratin and brachyury. *Benign notochord tumors* lack intercellular myxoid matrix and do not show bone destruction.

#### PROGNOSIS AND THERAPY

The overall median survival is 7 years and depends on the site and size of the tumor. Radical, complete surgical removal of the chordoma is associated with longer survival and delayed recurrences but is often difficult to achieve in the anatomic confines of the neck. Up to 40 % of patients develop distant metastases and nearly 60 % ultimately die from disease. Worse prognosis, including metastases to lung, bone, and lymph node, is associated with dedifferentiated chordoma. For unresectable tumors, adjuvant radiotherapy is used. Complications (cerebrospinal fluid leak, meningitis, paralysis, fistula formation) are frequently seen after surgery.

#### SUGGESTED READINGS

The complete list of Suggested Readings is available online at [ExpertConsult.com](http://ExpertConsult.com).

**SUGGESTED READINGS****Metastatic Squamous Cell Carcinoma**

1. Ang KK, et al. Human papillomavirus and survival of patients with oropharyngeal cancer. *N Engl J Med*. 2010;363(1):24–35.
2. Begum S, et al. Detection of human papillomavirus-16 in fine-needle aspirates to determine tumor origin in patients with metastatic squamous cell carcinoma of the head and neck. *Clin Cancer Res*. 2007;13(4):1186–1191.
3. Bishop JA, et al. Ciliated HPV-related carcinoma: a well-differentiated form of head and neck carcinoma that can be mistaken for a benign cyst. *Am J Surg Pathol*. 2015;39(11):1591–1595.
4. Cao D, et al. Expression of p16 in benign and malignant cystic squamous lesions of the neck. *Hum Pathol*. 2010;41(4):535–539.
5. El-Mofty SK, et al. Histologic identification of human papillomavirus (HPV)-related squamous cell carcinoma in cervical lymph nodes: a reliable predictor of the site of an occult head and neck primary carcinoma. *Head Neck Pathol*. 2008;2(3):163–168.
6. Goldenberg D, et al. Cystic lymph node metastasis in patients with head and neck cancer: An HPV-associated phenomenon. *Head Neck*. 2008;30(7):898–903.
7. Haack H, et al. Diagnosis of NUT midline carcinoma using a NUT-specific monoclonal antibody. *Am J Surg Pathol*. 2009;33(7):984–991.
8. Iganej S, et al. Metastatic squamous cell carcinoma of the neck from an unknown primary: management options and patterns of relapse. *Head Neck*. 2002;24(3):236–246.
9. Marur S, et al. HPV-associated head and neck cancer: a virus-related cancer epidemic. *Lancet Oncol*. 2010;11(8):781–789.
10. Maxwell JH, et al. Extracapsular spread in head and neck carcinoma: impact of site and human papillomavirus status. *Cancer*. 2013;119(18):3302–3308.
11. Pai RK, et al. p16(INK4A) immunohistochemical staining may be helpful in distinguishing branchial cleft cysts from cystic squamous cell carcinomas originating in the oropharynx. *Cancer*. 2009;117(2):108–119.
12. Singhi AD, et al. Comparison of human papillomavirus in situ hybridization and p16 immunohistochemistry in the detection of human papillomavirus-associated head and neck cancer based on a prospective clinical experience. *Cancer*. 2010;116(9):2166–2173.
13. Thompson LD, et al. The clinical importance of cystic squamous cell carcinomas in the neck: a study of 136 cases. *Cancer*. 1998;82(5):944–956.

**Metastatic Neoplasm of Unknown Primary**

1. Ansari-Lari MA, et al. . The prevalence and significance of clinically unsuspected neoplasms in cervical lymph nodes. *Head Neck*. 2003;25(10):841–847.
2. Bishop JA, et al. HPV analysis in distinguishing second primary tumors from lung metastases in patients with head and neck squamous cell carcinoma. *Am J Surg Pathol*. 2012;36(1):142–148.
3. Califano J, et al. Unknown primary head and neck squamous cell carcinoma: molecular identification of the site of origin. *J Natl Cancer Inst*. 1999;91(7):599–604.
4. Conner JR, et al. . Metastatic carcinoma of unknown primary: diagnostic approach using immunohistochemistry. *Adv Anat Pathol*. 2015;22(3):149–167.
5. Koivunen P, et al. Cervical metastasis of unknown origin: a series of 72 patients. *Acta Otolaryngol*. 2002;122(5):569–574.
6. McDowell LJ, et al. p16-positive lymph node metastases from cutaneous head and neck squamous cell carcinoma: No association with high-risk human papillomavirus or prognosis and implications for the workup of the unknown primary. *Cancer*. 2016;122(8):1201–1208.
7. Talmi YP, et al. Patterns of metastases to the upper jugular lymph nodes (the “submuscular recess”). *Head Neck*. 1998;20(8):682–686.
8. Tong CC, et al. Cervical nodal metastases from occult primary: undifferentiated carcinoma versus squamous cell carcinoma. *Head Neck*. 2002;24(4):361–369.

9. Werner JA, et al. Functional anatomy of the lymphatic drainage system of the upper aerodigestive tract and its role in metastasis of squamous cell carcinoma. *Head Neck*. 2003;25(4):322–332.

**Synovial Sarcoma**

1. Bergh P, et al. Synovial sarcoma: identification of low and high risk groups. *Cancer*. 1999;85(12):2596–2607.
2. Bixby SD, et al. Synovial sarcoma in children: imaging features and common benign mimics. *AJR Am J Roentgenol*. 2010;195(4):1026–1032.
3. Foo WC, et al. Immunohistochemical staining for TLE1 distinguishes synovial sarcoma from histologic mimics. *Am J Clin Pathol*. 2011;135(6):839–844.
4. Kosemehmetoglu K, et al. TLE1 expression is not specific for synovial sarcoma: a whole section study of 163 soft tissue and bone neoplasms. *Mod Pathol*. 2009;22(7):872–878.
5. Krieg AH, et al. Synovial sarcomas usually metastasize after >5 years: a multicenter retrospective analysis with minimum follow-up of 10 years for survivors. *Ann Oncol*. 2011;22(2):458–467.
6. Ladanyi M, et al. Impact of SYT-SSX fusion type on the clinical behavior of synovial sarcoma: a multi-institutional retrospective study of 243 patients. *Cancer Res*. 2002;62(1):135–140.
7. Murphey MD, et al. From the archives of the AFIP: Imaging of synovial sarcoma with radiologic-pathologic correlation. *Radiographics*. 2006;26(5):1543–1565.
8. Pai S, et al. Head and neck synovial sarcomas. *J Surg Oncol*. 1993;54(2):82–86.
9. Srinivasan R, et al. Synovial sarcoma: diagnosis on fine-needle aspiration by morphology and molecular analysis. *Cancer*. 2009;117(2):128–136.
10. Sultan I, et al. Comparing children and adults with synovial sarcoma in the Surveillance, Epidemiology, and End Results program, 1983 to 2005: an analysis of 1268 patients. *Cancer*. 2009;115(15):3537–3547.

**Chordoma**

1. Antonelli M, et al. SMARCB1/INI1 involvement in pediatric chordoma: a mutational and immunohistochemical analysis. *Am J Surg Pathol*. 2017;41(1):56–61.
2. Jeffrey PB, et al. Chondroid chordoma. A hyalinized chordoma without cartilaginous differentiation. *Am J Clin Pathol*. 1995;103(3):271–279.
3. Jambhekar NA, et al. Revisiting chordoma with brachyury, a “new age” marker: analysis of a validation study on 51 cases. *Arch Pathol Lab Med*. 2010;134(8):1181–1187.
4. Kay PA, et al. Chordoma. Cytomorphologic findings in 14 cases diagnosed by fine needle aspiration. *Acta Cytol*. 2003;47(2):202–208.
5. Kelley MJ, et al. Characterization of T gene sequence variants and germline duplications in familial and sporadic chordoma. *Hum Genet*. 2014;133(10):1289–1297.
6. Mobley BC, et al. Loss of SMARCB1/INI1 expression in poorly differentiated chordomas. *Acta Neuropathol*. 2010;120(6):745–753.
7. Oakley GJ, et al. Brachyury, SOX-9, and podoplanin, new markers in the skull base chordoma vs chondrosarcoma differential: a tissue microarray-based comparative analysis. *Mod Pathol*. 2008;21(12):1461–1469.
8. Vujovic S, et al. Brachyury, a crucial regulator of notochordal development, is a novel biomarker for chordomas. *J Pathol*. 2006;209(2):157–165.
9. Wang L, et al. Clinical features and surgical outcomes of patients with skull base chordoma: a retrospective analysis of 238 patients. *J Neurosurg*. 2017;6:1–11.
10. Wasserman JK, et al. Chordoma of the Head and Neck: A Review. *Head Neck Pathol*. 2017; doi:10.1007/s12105-017-0860-8. PMID: 28980142.
11. Yamaguchi T, et al. Benign notochordal cell tumors: A comparative histological study of benign notochordal cell tumors, classic chordomas, and notochordal vestiges of fetal intervertebral discs. *Am J Surg Pathol*. 2004;28(6):756–761.
12. Yang XR, et al. T (brachyury) gene duplication confers major susceptibility to familial chordoma. *Nat Genet*. 2009;41(11):1176–1178.



# Non-Neoplastic Lesions of the Thyroid Gland

■ Rebecca D. Chernock ■ Lester D.R. Thompson

## ■ THYROGLOSSAL DUCT CYST

The thyroglossal duct represents the tract in the midline neck through which the thyroid anlage descends during embryonic development. It begins at the foramen cecum at the base of the tongue, continues around the hyoid bone, and ends at the normal position of the thyroid gland in the pretracheal lower neck. Persistence of the thyroglossal duct postnatally can give rise to cysts (thyroglossal duct cysts), fistula tracts, and sinuses anywhere along the tract.

### CLINICAL FEATURES

Thyroglossal duct cysts represent the most common midline mass in children but may also be found in adults and in the elderly. At least one-third occur after the age of 30 years. There is no sex predilection. The classic presentation is of a midline, mobile neck mass located either at or immediately below the hyoid bone (75%) (Fig. 23.1). Less commonly, such cysts may be suprahyoid, submental, intrathyroidal, and rarely intralingual. Slightly off-midline examples may be seen; in such cases, the presence of a fibrous tract or cord emanating from the hyoid bone is a helpful finding. Cysts can be linked to the skin or foramen cecum by a sinus tract.

In most cases, the patient is asymptomatic but may have pain, a draining sinus, a fistula (10% to 20%), dysphagia, or rarely airway obstruction. Infection occurs in one-third of cysts. The cysts may fluctuate in size, especially if infected. Thyroglossal duct cysts move vertically with swallowing or protrusion of the tongue.

### RADIOGRAPHIC FEATURES

Radiographic studies usually show a cystic mass, often with bright signal on magnetic resonance imaging (MRI)

### THYROGLOSSAL DUCT CYST—DISEASE FACT SHEET

#### Definition

- Cystic change of a persistent tract representing the embryologic migratory path of the thyroid anlage in the midline anterior neck

#### Incidence and Location

- Most common pediatric midline neck mass; at least one-third occur after the age of 30 years
- 75% in anterior midline of neck at or immediately below the hyoid bone; the remainder are found in intralingual, suprahyoid (submental), and intrathyroidal loci

#### Morbidity and Mortality

- May become secondarily infected
- Thyroid carcinoma, usually papillary type, develops in up to 3% of cases; this is associated with a favorable prognosis

#### Sex and Age Distribution

- Equal sex distribution
- Most common in children or young adults

#### Clinical Features

- Asymptomatic midline neck mass
- Draining sinus or fistula and pain, if infected

#### Prognosis and Therapy

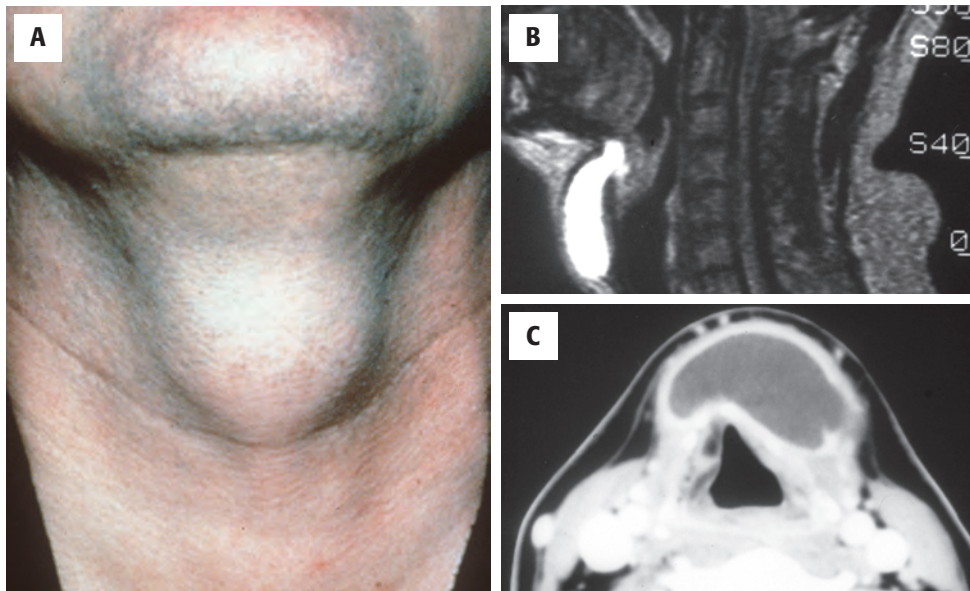
- Preferred treatment is the Sistrunk procedure
- 4%–6% recurrence rate with Sistrunk procedure

studies. These cysts are usually found at midline, with the point of origin frequently identified.

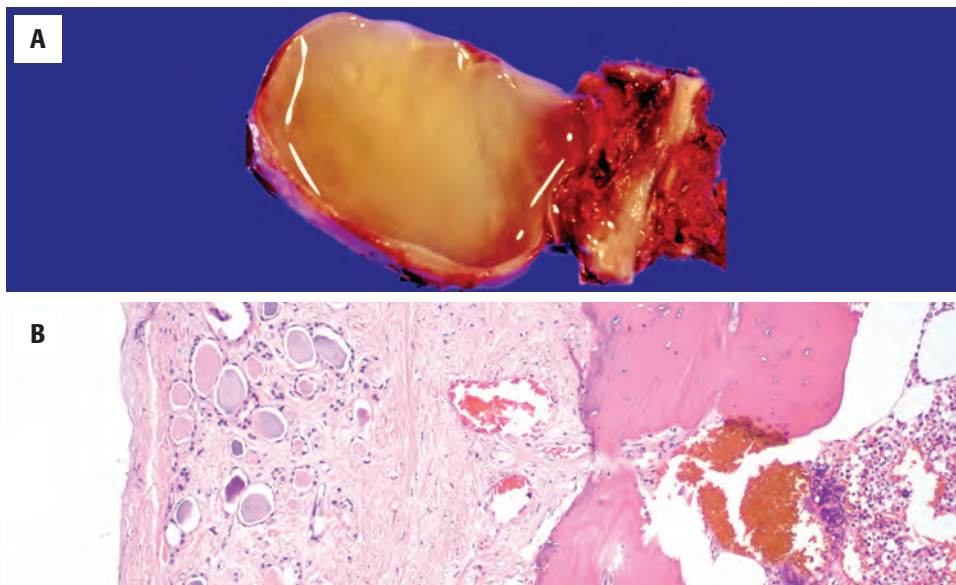
### PATHOLOGIC FEATURES

#### GROSS FINDINGS

The surgical specimen usually consists of the thyroglossal duct cyst as well as the fibrous tract/duct extending to the foramen cecum and the central 1 to 2 cm of the hyoid bone (Fig. 23.2). The mean cyst size is around

**FIGURE 23.1**

**A**, Neck mass in the midline, encompassing the hyoid bone, which moves with swallowing. **B**, Magnetic resonance image showing a bright signal of the fluid-filled thyroglossal duct cyst as it extends from the foramen cecum. **C**, Computed tomography scan showing a large fluid-filled cyst anterior to the larynx. Note a slight “shift” to the left of midline.

**FIGURE 23.2**

**A**, This thyroglossal duct cyst is from a Sistrunk procedure and includes the cyst, the tract of the thyroglossal duct, and the midsection of the hyoid bone. **B**, Thyroid parenchyma is noted at the left side, while a portion of bone and marrow is noted immediately adjacent.

2.5 cm, although cysts up to 8.5 cm have been reported. The cyst may contain clear mucoid fluid or, if infected, purulent material. Solid or firm areas should be carefully sampled to exclude an associated neoplasm.

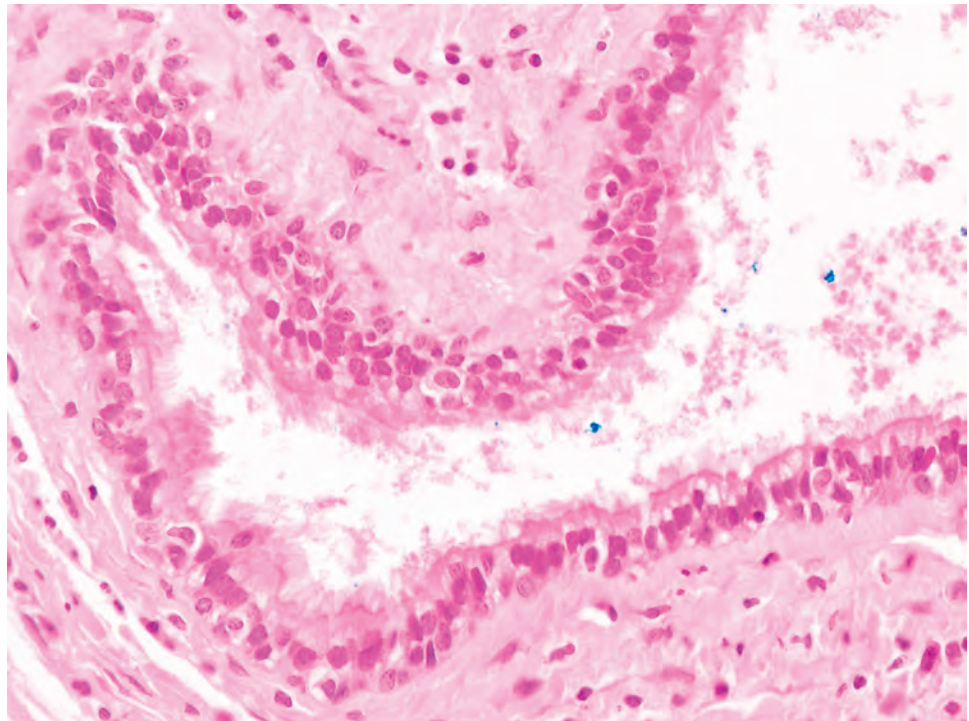
#### MICROSCOPIC FINDINGS

The thyroglossal duct cyst is normally lined by respiratory epithelium, but squamous metaplasia is quite common and most cysts contain a mixture of squamous and respiratory epithelium (Figs. 23.3 and 23.4). About 10% are purely squamous-lined. If the cyst has been infected, the lining epithelium may be replaced by granulation tissue, sometimes with granulomatous elements such as foamy histiocytes and multinucleated giant cells (Fig. 23.4). Fibrosis and chronic inflammation

are often found in the cyst wall. Thyroid tissue is not invariably present but is quite common, found in up to 71% of cases with careful examination (Fig. 23.5). Seromucinous glands and cartilage may also be found in the wall.

The associated thyroid tissue may harbor any inflammatory, hyperplastic, or neoplastic alteration that can be seen in the normal follicular epithelial component of the thyroid gland. Up to 3% of thyroglossal duct cysts will have an associated carcinoma, with papillary thyroid carcinoma (PTC) representing at least 90% of cases. Thyroglossal duct cysts in elderly patients are much more likely to harbor malignancies. No examples of medullary carcinoma have been documented, presumably due to the different embryologic origin of the C cells from the ultimobranchial body.



**FIGURE 23.3**

Thyroglossal duct cyst. The cyst is lined in this case by respiratory epithelium and is surrounded by fibrous tissue.

#### THYROGLOSSAL DUCT CYST—PATHOLOGIC FEATURES

##### Gross Findings

- Cyst filled with mucoid or purulent material
- Fibrous tract from area of foramen cecum to hyoid bone
- One-third present as fistulas, usually due to infection
- Solid areas sampled to exclude neoplasm

##### Microscopic Findings

- Cyst lined by respiratory and/or squamous epithelium
- If the cyst is infected, granulation tissue may replace epithelium
- Fibrosis and chronic inflammation in cyst wall
- Thyroid tissue identified in at least two-thirds of cases
- If carcinoma is present, at least 90% are of the papillary type

##### Fine Needle Aspiration

- Thick mucoid or purulent material, sparsely cellular and with inflammatory material

##### Pathologic Differential Diagnosis

- Epidermoid and dermoid cysts, plunging ranula, degenerated adenomatoid nodules

confirm a clinically suspected malignancy in a thyroglossal duct cyst. Aspirates consist of thick mucoid or purulent material and are sparsely cellular; inflammatory cells tend to outnumber the benign squamous or respiratory epithelial cells.

#### DIFFERENTIAL DIAGNOSIS

*Epidermoid cysts* of the thyroid, *plunging ranula* of salivary origin, or degenerated cystic *adenomatoid nodules* may be considered in the differential diagnosis; but the midline location and respiratory and/or squamous epithelial lining are key elements in making the diagnosis of thyroglossal duct cyst. When a thyroid carcinoma arising in a thyroglossal duct cyst is under consideration, the possibility of a metastatic tumor from the thyroid proper should be excluded.

#### PROGNOSIS AND THERAPY

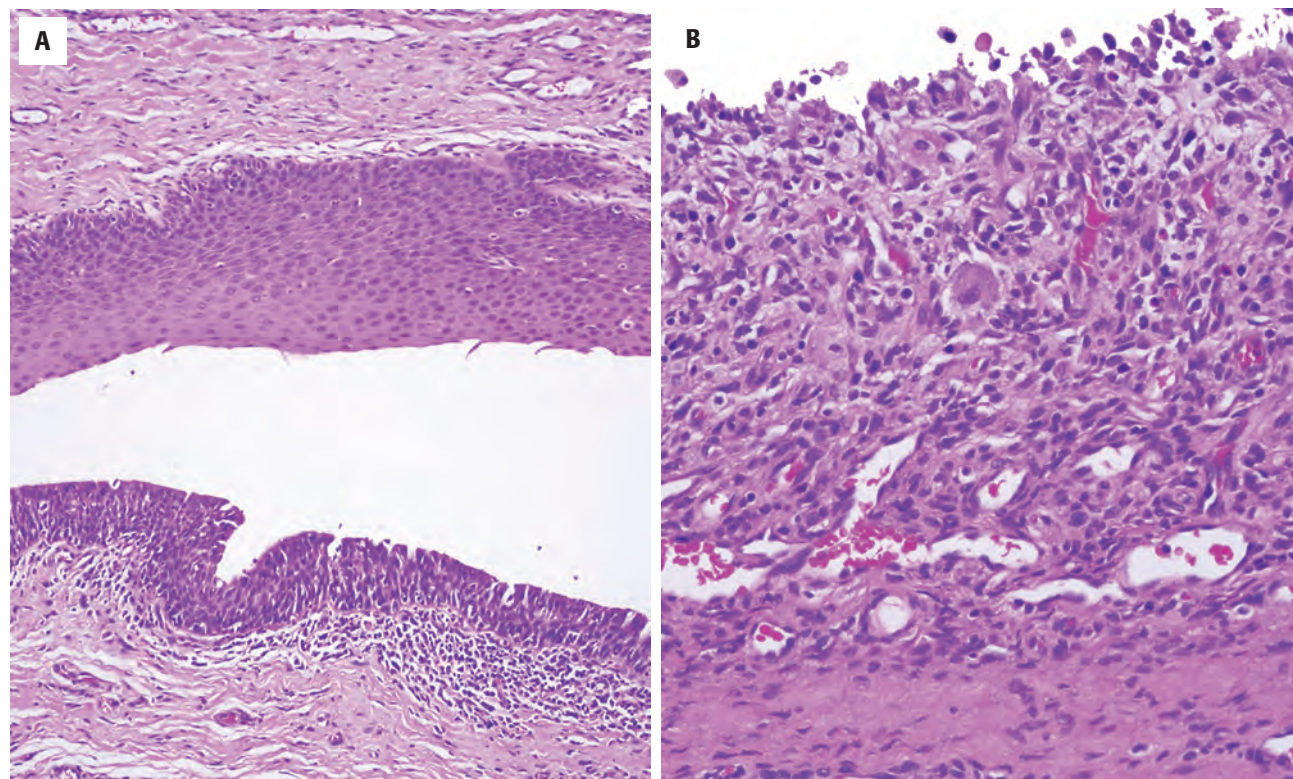
The preferred treatment for a thyroglossal duct cyst is the Sistrunk procedure, which requires resection of the entire tract of the thyroglossal duct along with the cyst or fistula and the central 1 to 2 cm of the hyoid bone. The recurrence rate after this procedure is 4% to 6%; if the hyoid bone segment is not removed, the recurrence rate increases to above 25%. Well-differentiated thyroid carcinoma arising in a thyroglossal duct cyst has an

#### ANCILLARY STUDIES

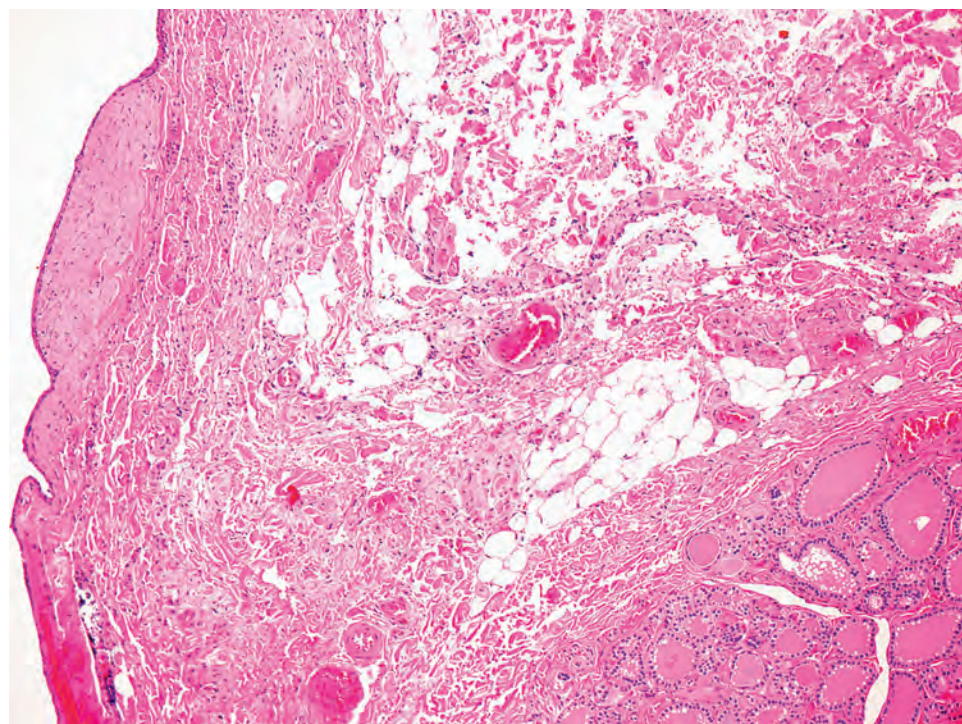
##### FINE NEEDLE ASPIRATION

Fine needle aspiration (FNA) is not widely used in the diagnosis of thyroglossal duct cysts because of the limited cytologic findings, but it is useful in documenting other lesions that may form midline neck masses or to



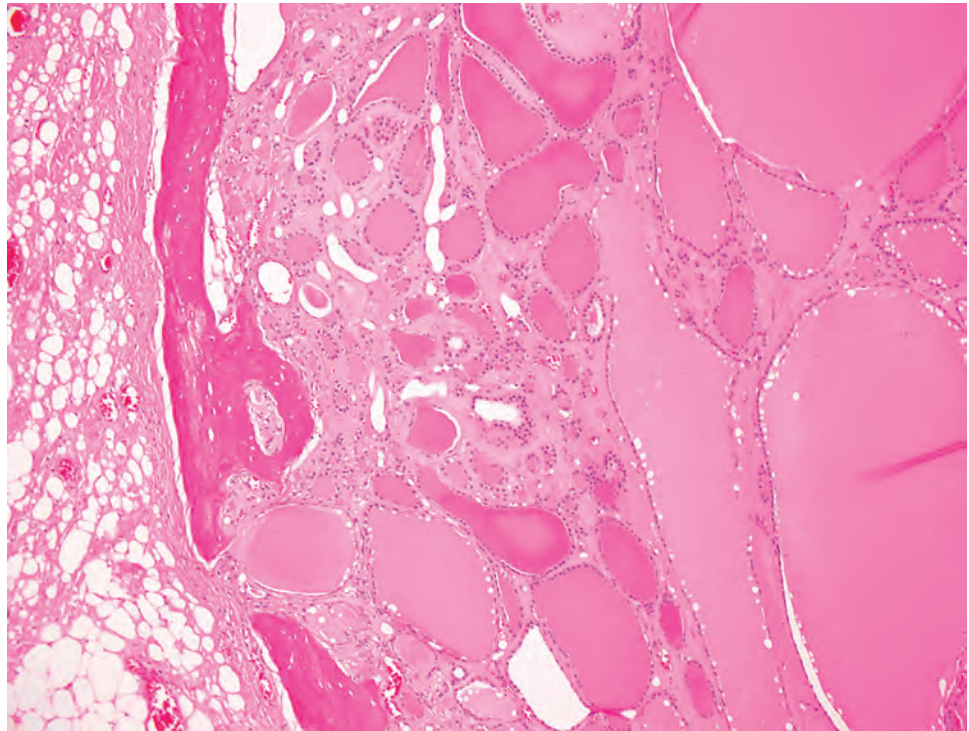
**FIGURE 23.4**

**A**, Cyst lining is both squamous epithelium (*upper*) and respiratory type (*lower*) in this thyroglossal duct cyst. **B**, Infection may cause denudation of the epithelial lining, which is replaced by granulation tissue.

**FIGURE 23.5**

Thyroid parenchyma is seen in the cyst wall (*lower right*) of this thyroglossal duct cyst (*left*).



**FIGURE 23.6**

Ectopic thyroid tissue is present within the hyoid bone and should not be mistaken for metastatic carcinoma.

excellent prognosis with the Sistrunk procedure. Total thyroidectomy is not usually required for benign cysts except in high-risk patients or in the instance of carcinoma arising in the thyroglossal duct cyst.

## ■ THYROID ECTOPIA AND LINGUAL THYROID

As the embryonic thyroid descends down the anterior neck, remnants of thyroid tissue, usually microscopic, can be distributed along the tract in the neck soft tissue or even in the hyoid bone (ectopic thyroid tissue) (Fig. 23.6). Less commonly, ectopic thyroid tissue has been reported at other sites in the neck and exceptionally in the mediastinum, abdomen, or other sites. Its existence in the lateral neck is controversial. If thyroid tissue is encountered lateral to the jugular vein, especially if intranodal, it most likely represents a metastasis from a well-differentiated PTC. Rarely, the thyroid gland fails to migrate down the thyroglossal duct and remains at the foramen cecum, forming a submucosal mass at the base of tongue known as lingual thyroid, a type of thyroid ectopia.

### CLINICAL FEATURES

Most thyroid ectopia is clinically occult and discovered incidentally in patients undergoing surgery for another

indication. Lingual thyroid is the most common type of clinically detected thyroid ectopia (90% of cases). In addition, most patients have no other thyroid tissue in the neck (complete thyroid ectopia). It can present at any age and is more common in women. The male-to-female ratio is 1:5.

Patients with lingual thyroid may present with symptoms including cough, hoarseness, and sleep apnea, but most are asymptomatic. Airway obstruction is rare. Over half of patients are hypothyroid. Clinically visible lingual thyroids appear as a submucosal, smooth mass at the base of the tongue.

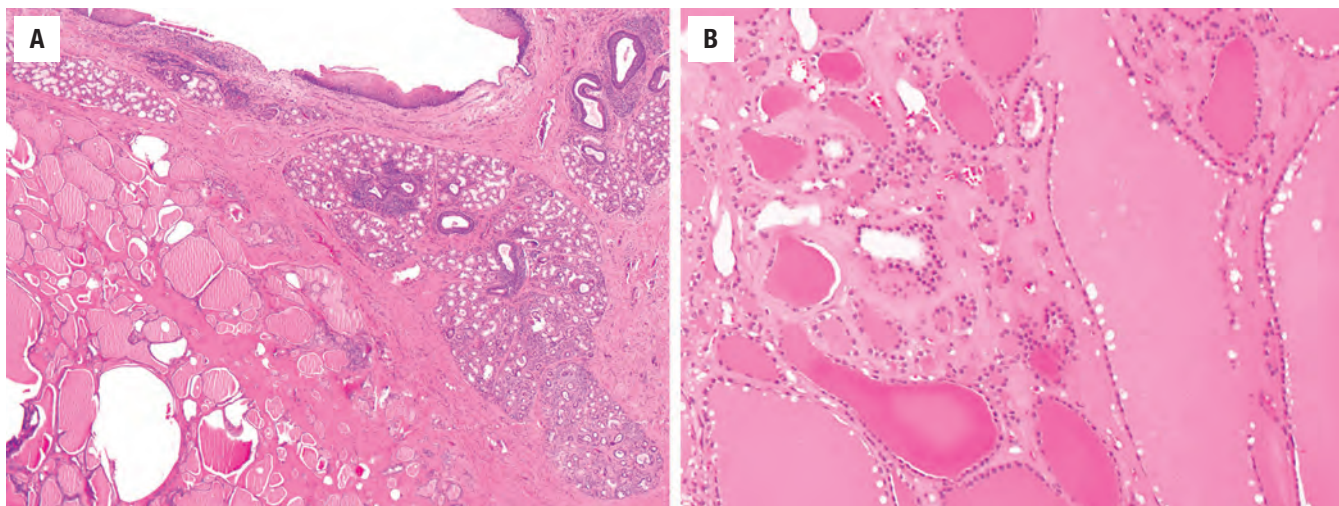
### RADIOGRAPHIC FEATURES

Radionuclide scanning either with  $^{99m}\text{Tc}$  pertechnetate,  $^{123}\text{I}$ , or  $^{131}\text{I}$  is virtually diagnostic of thyroid ectopia.

### PATHOLOGIC FEATURES

#### GROSS FINDINGS

Although most thyroid ectopias are not grossly visible but rather encountered incidentally under the microscope, those that form a mass appear similar to normal thyroid tissue. They are well circumscribed with a glistening brown cut surface. Nodular hyperplasia (adenomatoid nodules) may be present.

**FIGURE 23.7**

**A**, Ectopic thyroid tissue is present beneath the surface mucosa (*top*) of the base of tongue in lingual thyroid. **B**, The thyroid parenchyma is histologically identical to the normal thyroid gland.

#### THYROID ECTOPIA AND LINGUAL THYROID—DISEASE FACT SHEET

##### Definition

- Thyroid tissue located outside the normal pretracheal location of the thyroid gland; lingual thyroid is a type of thyroid ectopia located at the base of tongue

##### Incidence and Location

- Usually an incidental finding in the central neck
- Approximately 90% of clinically detected cases are located at the base of the tongue (lingual thyroid)

##### Morbidity and Mortality

- Lingual thyroid is associated with hypothyroidism
- Patients may have cough, hoarseness, and sleep apnea

##### Sex and Age Distribution

- Lingual thyroid is more common in females than males (5:1)
- Can occur at any age

##### Clinical Features

- Lingual thyroids appear as smooth domed, submucosal masses at the base of tongue

##### Prognosis and Therapy

- No treatment is necessary unless the patient is symptomatic
- Hypothyroidism is treated with hormone replacement

#### THYROID ECTOPIA AND LINGUAL THYROID—PATHOLOGIC FEATURES

##### Gross Findings

- Well-circumscribed brown glistening mass
- Often not grossly visible

##### Microscopic Findings

- Similar to normal thyroid tissue

##### Fine Needle Aspiration

- Not usually indicated unless the diagnosis is clinically unsuspected
- Clusters of thyroid follicular epithelium in a background of watery colloid

##### Pathologic Differential Diagnosis

- Metastatic well-differentiated thyroid carcinoma

#### ANCILLARY STUDIES

##### FINE NEEDLE ASPIRATION

FNA is rarely necessary to establish the diagnosis of thyroid ectopia but may be used when the diagnosis is not suspected. Aspirates usually consist of watery colloid and clusters of follicular epithelial cells.

#### DIFFERENTIAL DIAGNOSIS

*Metastatic well-differentiated PTC* is the main consideration in the differential diagnosis of thyroid ectopia. Thyroid ectopia lacks nuclear features of PTC, but metastases of papillary thyroid carcinoma can be

#### MICROSCOPIC FINDINGS

Thyroid ectopia is histologically identical to normal thyroid (*Fig. 23.7*). Lingual thyroids often have intervening skeletal muscle. Changes typical of nodular hyperplasia, variability in follicle size, cyst formation, fibrosis, and calcification may be present. Thyroid carcinoma is rare (1%).



deceptively bland; therefore, careful examination is important. In the lateral neck, thyroid tissue usually represents metastatic disease rather than ectopia, especially in a lymph node.

### PROGNOSIS AND THERAPY

No treatment is required for asymptomatic thyroid ectopia/lingual thyroid. If symptomatic, thyroid hormone replacement may be used to shrink the thyroid tissue. Surgery or radioactive iodine ablation can be used to treat more severe symptoms in patients who are not surgical candidates. Associated hypothyroidism is treated by hormone replacement. Death from airway obstruction is very rare.

## ■ ULTIMOBRANCHIAL BODY REMNANTS (SOLID CELL NESTS) AND OTHER INTRATHYROIDAL INCLUSIONS

Small remnants of the ultimobranchial apparatus, or “solid cell nests,” are associated with the embryologic development of the C-cell (calcitonin-producing) population of the thyroid. They are encountered as an incidental finding, usually in the posteromedial and posterolateral lobes but never in the isthmus.

### CLINICAL FEATURES

Solid cell nests, which are fairly common, are of no clinical significance. They are identified in some 25 % of thyroid resection specimens; their discovery is largely related to the generosity of sampling of “normal” thyroid tissue.

### PATHOLOGIC FEATURES

Ultimobranchial remnants (solid cell nests) are quite small, most measuring no more than 0.1 mm. They are represented by a cluster of small, round, or lobulated epithelial nests and may be solid or partially cystic (Fig. 23.8). Occasionally, several foci may be found in a gland. The epithelial cells are small and ovoid to polygonal, with slightly elongated nuclei; they are called “main cells.” The chromatin is finely granular and evenly dispersed. A longitudinal nuclear groove is often present (Fig. 23.9). The overall histologic pattern is very similar to that of immature squamous metaplasia, but keratinization and intercellular bridges are not visible. A minor population of cells with clear cytoplasm comprises C-cells. Degenerative changes are thought to account for

### ULTIMOBRANCHIAL BODY REMNANTS—DISEASE FACT SHEET

#### Definition

- Small remnant of the ultimobranchial apparatus that delivers C-cells to the thyroid gland

#### Incidence and Location

- Incidental finding in some 25% of thyroid specimens
- Posteromedial and posterolateral areas of lobes; *never* in the isthmus

#### Clinical Features

- None (incidental microscopic finding)

#### Prognosis and Therapy

- No clinical significance

### ULTIMOBRANCHIAL BODY REMNANTS—PATHOLOGIC FEATURES

#### Microscopic Findings

- Small, round, or lobulated nests of polygonal epithelial cells resembling immature squamous metaplasia, usually  $\leq 0.1$  mm
- Some examples are partially cystic
- No keratinization or intercellular bridges
- Nuclei ovoid, with evenly distributed chromatin and frequent longitudinal nuclear grooves
- Occasional clear cells and mucoid material may be seen

#### Immunohistochemical Findings

- Main cells p63-positive but negative for thyroglobulin, thyroid transcription factor-1, and calcitonin
- Scattered C-cells positive for neuroendocrine markers, calcitonin, and carcinoembryonic antigen (CEA)

#### Pathologic Differential Diagnosis

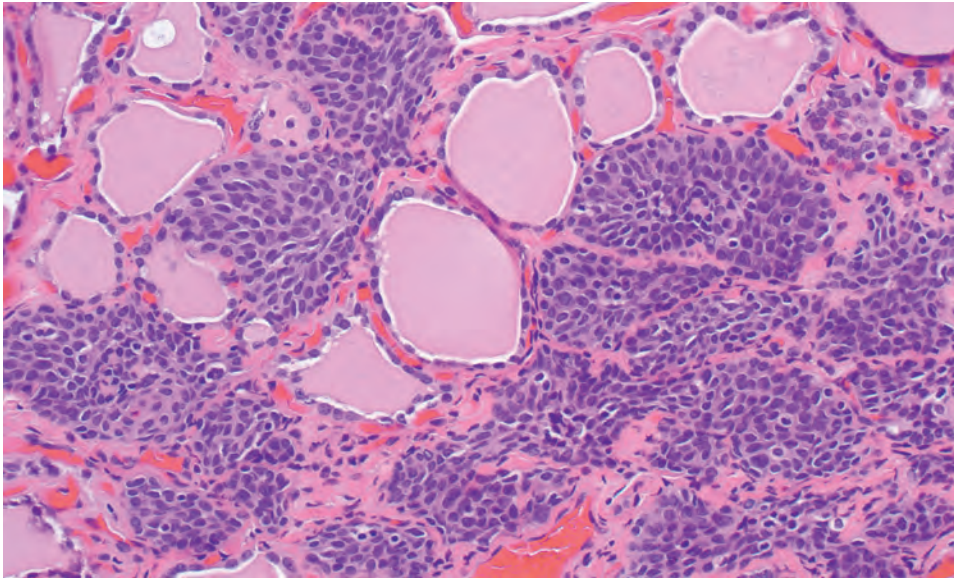
- Incidental papillary thyroid carcinoma, C-cell hyperplasia/small medullary carcinoma, and squamous metaplasia

the occasional presence of mucicarmine-positive material in ultimobranchial remnants.

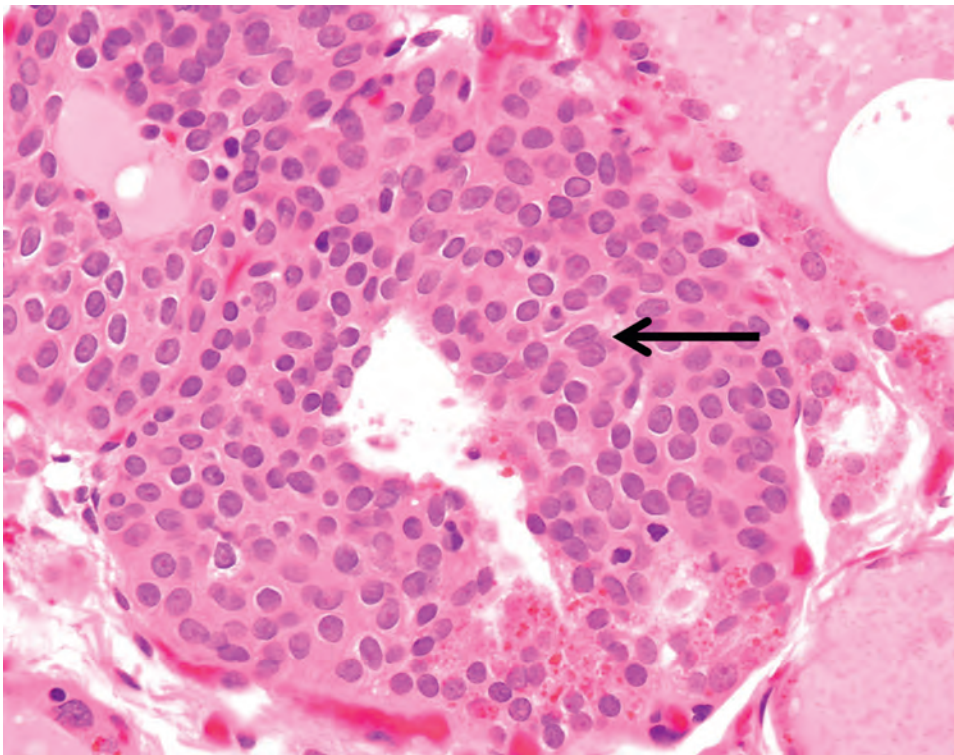
### ANCILLARY STUDIES

#### IMMUNOHISTOCHEMICAL FINDINGS

Although immunohistochemical studies are certainly not necessary for making a diagnosis, the staining pattern of ultimobranchial remnants is fairly distinctive. Main cells are positive for p63, bcl-2, CK19, and galectin-3 but negative for thyroglobulin, thyroid transcription factor-1 (TTF1), and calcitonin. The scattered C-cells are positive for neuroendocrine markers, calcitonin, carcinoembryonic antigen (CEA), and galectin-3.

**FIGURE 23.8**

The ultimobranchial body remnant is a solid cell nest, adjacent to normal thyroid parenchyma, and is an incidental finding. It often consists of multiple solid, round nests of cells that appear to encase and replace thyroid follicles.

**FIGURE 23.9**

The ultimobranchial body epithelium is reminiscent of immature squamous metaplasia. Note the lack of keratinization and intercellular bridges. The nuclei are ovoid, often with a longitudinal groove (arrow).

### DIFFERENTIAL DIAGNOSIS

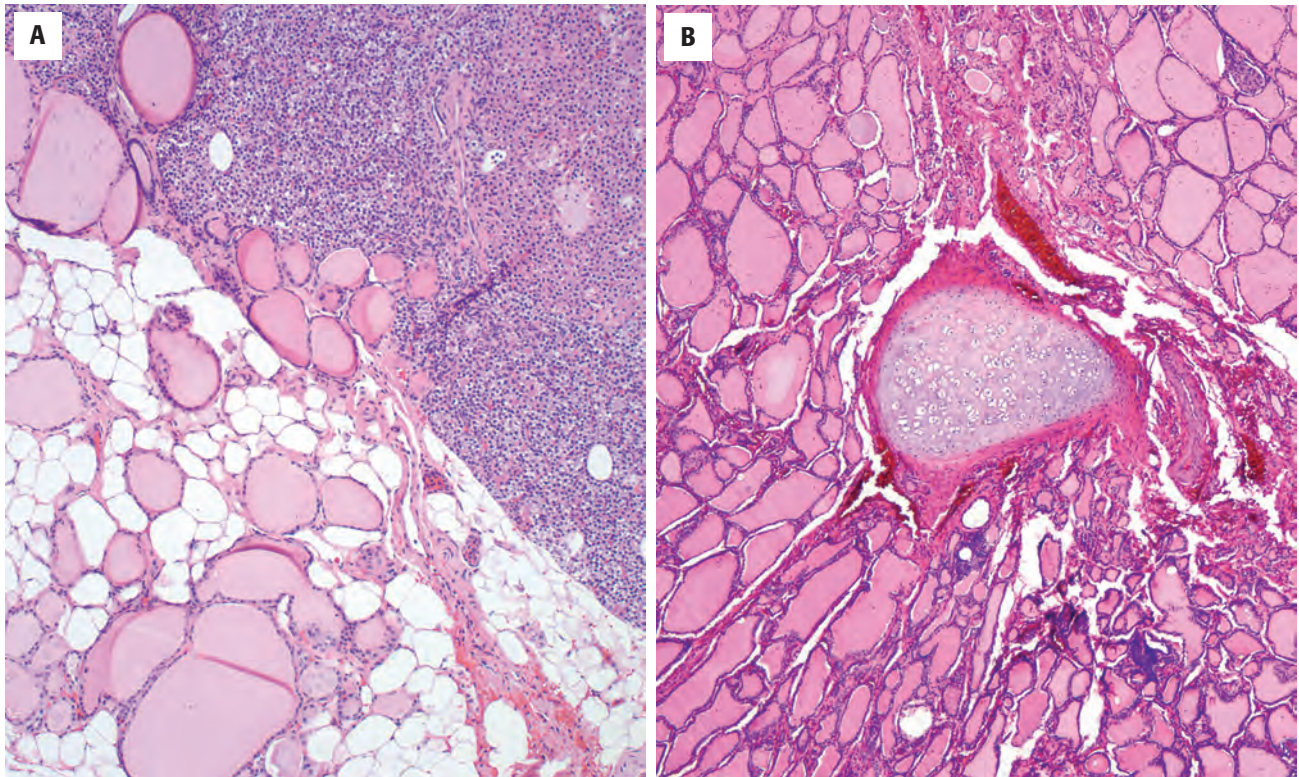
Ultimobranchial remnants are sometimes mistaken for squamous metaplasia, incidental microscopic *PTC*, or a *small medullary carcinoma/C-cell hyperplasia*. Although nuclear grooves are frequent in ultimobranchial remnants, these lesions lack the other nuclear features of *PTC* (overlapping nuclei, ground-glass chromatin pattern, intranuclear inclusions) as well as an adjacent stromal desmoplastic reaction.

C-cell hyperplasia or a small medullary carcinoma may have similar nodular growth. However, C-cells (which

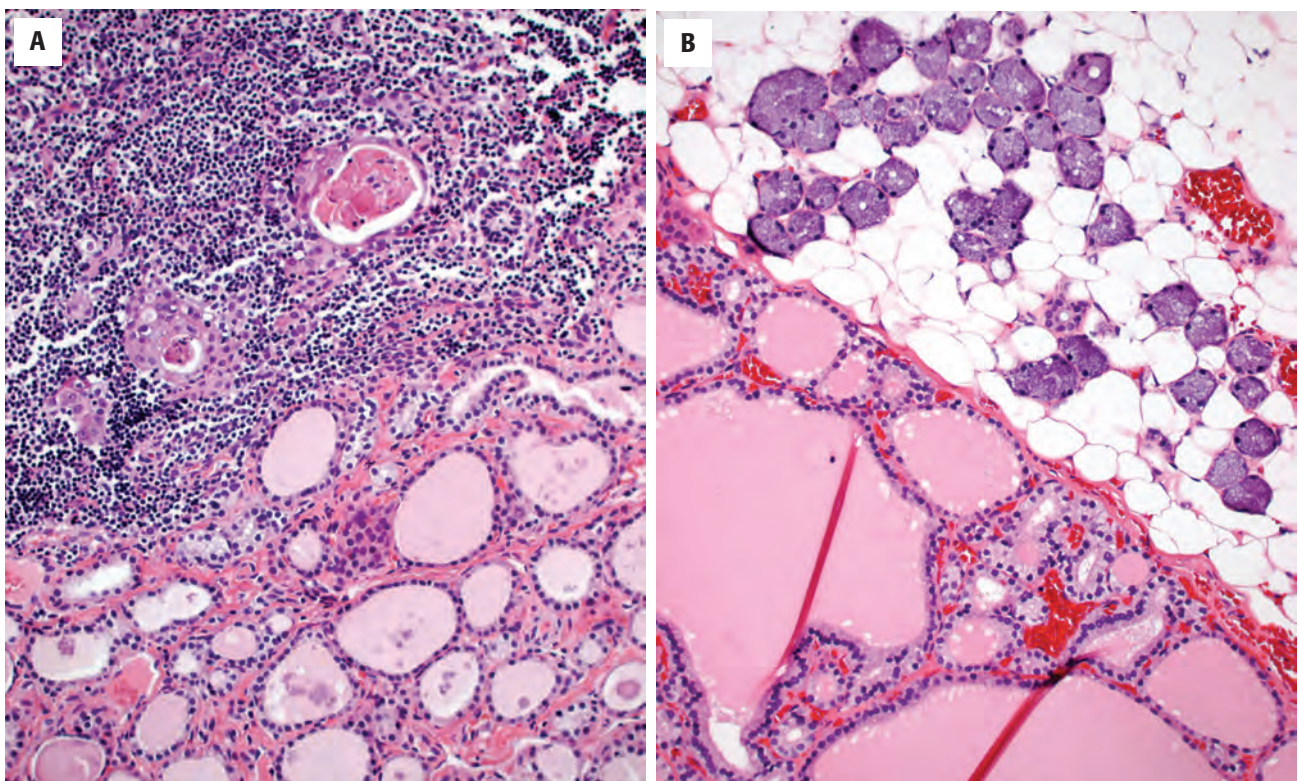
give rise to both hyperplasia and medullary carcinoma) are plasmacytoid; they have granular chromatin and more abundant pale pink to clear cytoplasm than solid cell nests. Small medullary carcinomas show expansile growth, stromal fibrosis, and/or amyloid deposition as well. Scattered calcitonin or neuroendocrine marker staining should not be mistaken for C-cell neoplasia, as C-cells are normally present in solid cell nests.

While not necessarily within the differential diagnosis, *endodermally derived tissues* may be encountered in the thyroid gland, including cartilage, parathyroid gland (Fig. 23.10), thymic tissue, and salivary gland tissue (Fig. 23.11). These “inclusions” are usually of no clinical



**FIGURE 23.10**

There may be inclusions of other tissue types identified within the thyroid gland. Here is an intrathyroidal parathyroid (**A**) and a small fragment of cartilage (**B**).

**FIGURE 23.11**

Thymic tissue (**A**) is noted in direct continuity with the thyroid gland. Salivary gland tissue **B**, is noted adjacent to unremarkable thyroid parenchyma. These are normal tissue elements without any tissue reaction.



significance, typically representing incidental findings in surgical resection specimens. *Thymic tissue* retains its lobulated appearance, has small cystic islands of squamous epithelium (Hassall corpuscles) with an abundant lymphoid component that may be mistaken for lymphocytic thyroiditis or a lymph node (Fig. 23.11). *Parathyroid tissue*, particularly if it is hyperplastic or neoplastic, can be difficult to distinguish from a cellular adenomatoid nodule or follicular thyroid neoplasm. *Oxyphilic change* makes separation a challenge. Parathyroid cells often have perinuclear clearing and the nuclei are very small, round, and hyperchromatic, with rather coarse chromatin that suggests a neuroendocrine cell type.

### PROGNOSIS AND THERAPY

No therapy is necessary as this is an incidental finding.

## ■ ACUTE THYROIDITIS

Acute inflammation with a neutrophilic inflammatory infiltrate in the thyroid parenchyma is rare and accounts for less than 1 % of all thyroid disease. A wide spectrum of bacterial, fungal, and rarely parasitic pathogens are responsible. Routes of infection include congenital piriform sinus fistula (usually presenting in the 1st decade of life), direct extension from a neck or retropharyngeal abscess, penetrating trauma (including fine needle aspiration), hematogenous spread from a systemic infection, and esophageal perforation. The immunosuppressed population and patients with underlying thyroid abnormalities (e.g., malignancies, chronic lymphocytic thyroiditis, or goiter) are at increased risk.

### CLINICAL FEATURES

Patients are usually febrile and complain of chills, malaise, and pain and swelling of the anterior neck. Dysphagia or hoarseness may also be noted. While most patients are euthyroid, occasional patients demonstrate clinical and laboratory evidence of hyperthyroidism or hypothyroidism.

### PATHOLOGIC FEATURES

#### GROSS FINDINGS

The thyroid is seldom removed for acute thyroiditis. A specimen is usually submitted as part of an incision

### ACUTE THYROIDITIS—DISEASE FACT SHEET

#### Definition

- Acute inflammation of the thyroid parenchyma associated with a local or systemic bacterial or fungal infection

#### Incidence and Location

- Rare (< 1% of all thyroid disease)
- Most cases are associated with congenital piriform sinus fistulae, generalized sepsis, immunosuppression, or trauma

#### Clinical Features

- Fever, chills, malaise, pain, swelling of anterior neck
- Occasionally dysphagia or hoarseness
- Most patients are euthyroid; occasionally hypothyroid or hyperthyroid

#### Prognosis and Therapy

- Prognosis related to underlying condition (sepsis, trauma, etc.)
- Cultures to determine causative agent
- Aggressive antibiotic or antifungal therapy, with surgery reserved for abscess drainage, injury debridement, or excision of piriform sinus fistula tract to prevent recurrence in such cases

and drainage of an abscess or debridement following neck trauma. The gland is erythematous and soft and may contain pockets of purulent exudate or areas of necrosis.

### MICROSCOPIC FINDINGS

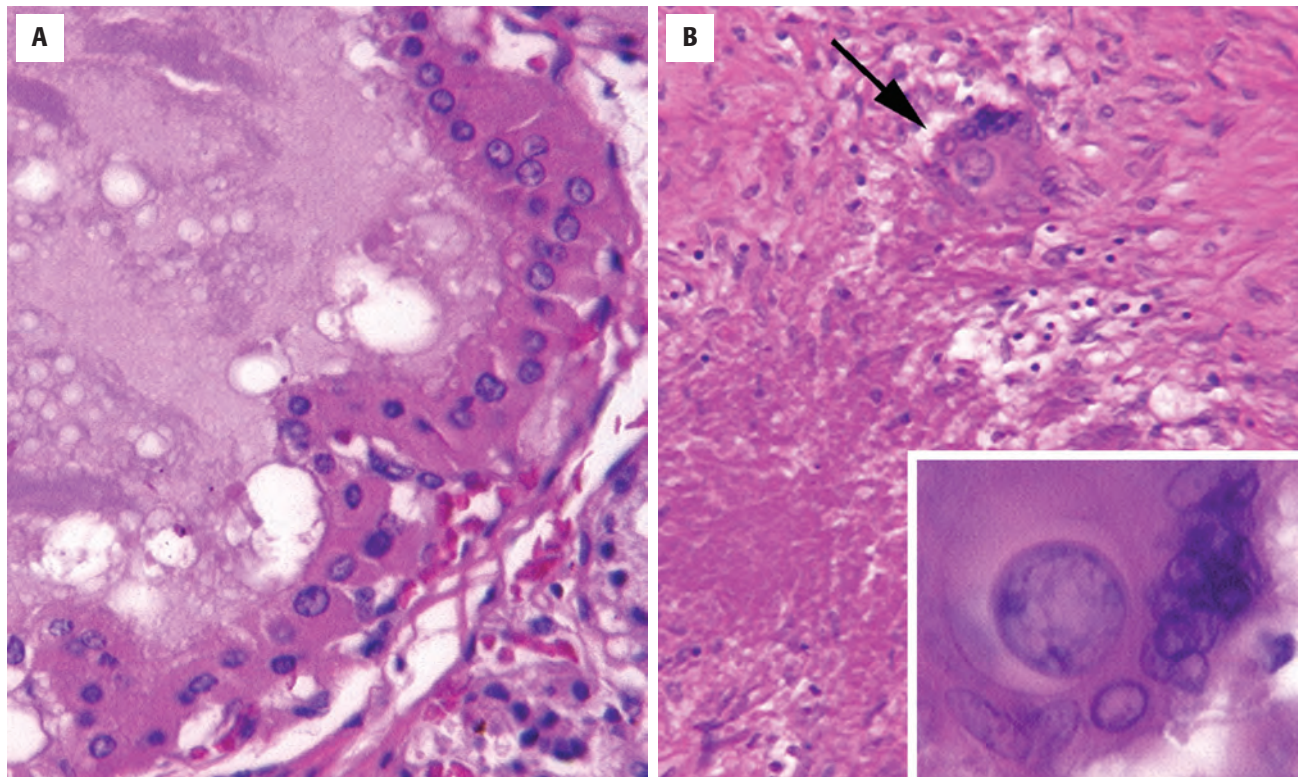
The key finding is the presence of polymorphonuclear leukocytes infiltrating the thyroid parenchyma. Microabscesses, foci of necrosis (Fig. 23.12), and vasculitis may be seen. Identification of a causative organism may be possible with histochemical stains, such as tissue Gram stains, Gomori methenamine silver, or periodic acid–Schiff (PAS) stains for fungi or mycobacterial stains (Ziehl–Neelsen). Immunosuppressed patients may develop an acute infectious thyroiditis rather than the typical granulomatous type in response to fungal or mycobacterial organisms. Tissue cultures are invaluable in identifying the organism and in determining its sensitivity to antibiotic therapy.

### ANCILLARY STUDIES

#### FINE NEEDLE ASPIRATION

FNA is useful to obtain material for culture and for therapeutic drainage of fluid collections. Aspirates typically show neutrophils and cellular debris.



**FIGURE 23.12**

**A.** Thyroid follicular epithelium is oncocytic with organisms identified within the colloid. **B.** Coccidioidomycosis organisms (arrow and inset) are identified in a background of necrosis in this case of acute thyroiditis.

### ACUTE THYROIDITIS—PATHOLOGIC FEATURES

#### Gross Findings

- Thyroid erythematous and soft, with pockets of purulent exudate or necrosis

#### Microscopic Findings

- Infiltration of parenchyma by neutrophils
- Microabscesses, foci of necrosis, vasculitis common
- Organisms may be identified on histology in some cases, highlighted with special studies

#### Pathologic Differential Diagnosis

- Subacute (granulomatous) thyroiditis, acute inflammation associated with malignancy

### DIFFERENTIAL DIAGNOSIS

*Subacute (granulomatous) thyroiditis* also involves a neutrophilic infiltrate in its early phase, but it is folliculocentric with accompanying histiocytes, lymphocytes, and multinucleated giant cells. No infectious agent is identified. Secondary infection and acute inflammation can also accompany an underlying malignancy.

### PROGNOSIS AND THERAPY

The prognosis is favorable with treatment and in the absence of underlying predisposing factors such as immunosuppressive states or extensive neck trauma, which may carry their own risk of poor outcome. Appropriate treatment requires identification of the infectious agent, preferably by culture, and initiation of effective antibiotic therapy. If abscesses or areas of infarction are present, surgical incision and drainage or debridement may be necessary.

### ■ SUBACUTE GRANULOMATOUS THYROIDITIS (DE QUERVAIN THYROIDITIS)

Also known as de Quervain thyroiditis (named after Fritz de Quervain, 1868–1940), subacute granulomatous thyroiditis is a self-limited inflammatory disorder widely suspected to be related to a systemic viral infection. Association with viral epidemics such as mumps, influenza, coxsackievirus, and measles has been reported. Some cases have also been associated with Epstein–Barr virus and with immunosuppressive therapy. Although

seasonal variation corresponding to peak enteroviral incidence has been noted in the past, some recent studies show only a modest increase in cases during the spring and summer. An autoimmune component is also postulated due to the presence of thyroidal autoantibodies in some patients.

### CLINICAL FEATURES

The annual incidence in the United States is estimated at 5 per 100,000 population. Women are more commonly affected than men, with a female-to-male ratio of 3.5:1. The mean age of onset is in the 5th decade (range, 14 to 87 years). The most common presenting symptom is pain in the thyroid region, sometimes radiating to the jaw. Other complaints include dysphagia, sore throat, low-grade fever, arthralgia, myalgia, tremor, excessive sweating, and weight loss. Physical examination is notable for pain on palpation of the thyroid. The entire gland is usually involved; however, the changes may be localized to one lobe or to a distinct nodule. Thyroid function often varies with disease activity. In the early phase, patients may be hyperthyroid owing to destruction of follicles and release of thyroglobulin. Rarely, a life-threatening thyrotoxicosis or “thyroid storm” occurs early in the disease. With disease progression, thyroid epithelium is destroyed, resulting in hypothyroidism. However, most patients regain normal thyroid function after resolution of the disease.

### RADIOGRAPHIC FEATURES

Radioactive iodine (RAI) uptake is decreased.

### LABORATORY STUDIES

Serum thyroid-stimulating hormone (TSH) is suppressed and total and free T3 and T4 are elevated early in the course of disease. In the subsequent hypothyroid phase, TSH is elevated and total and free T3 and T4 are low.

### PATHOLOGIC FEATURES

#### GROSS FINDINGS

Surgery is unnecessary, but the rare resection specimen shows asymmetric enlargement of the thyroid, vague nodularity, and a somewhat firm consistency.

### SUBACUTE GRANULOMATOUS THYROIDITIS—DISEASE FACT SHEET

#### Definition

- Self-limited inflammatory disorder thought to be related to systemic viral illness and possible autoimmune factors
- Also called de Quervain thyroiditis

#### Incidence

- About 5 per 100,000 population per year
- Seasonal increase in spring and summer may occur

#### Sex and Age Distribution

- Females > males (3.5:1)
- Peak in 5th decade (range, 14–87 years)

#### Clinical Features

- Pain in the thyroid region, tender to palpation
- Other symptoms include dysphagia, “sore throat,” fever, arthralgia, myalgia, tremor, excessive sweating, weight loss
- Entire gland usually involved, but inflammation may be localized
- Thyroid function varies: hyperthyroidism may occur early; hypothyroidism may develop in midphase
- Most patients are euthyroid after resolution

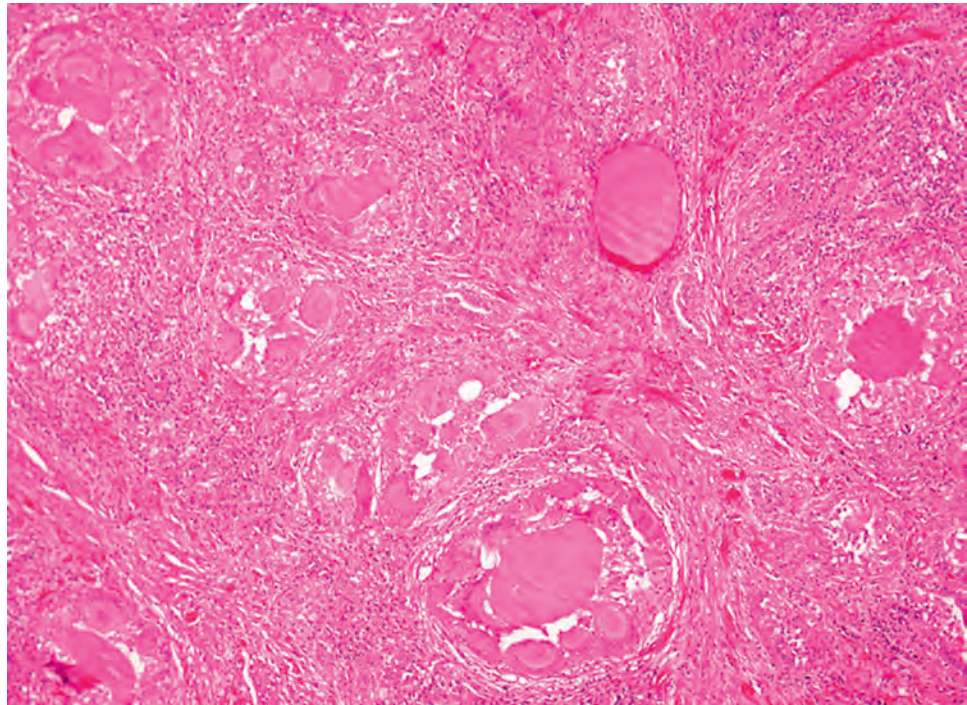
#### Prognosis and Therapy

- Usually self-limiting disease that resolves in months, although it may recur (years after initial disease)
- 5% remain hypothyroid
- Treatment includes aspirin, nonsteroidal anti-inflammatory drugs, steroids, and beta-blocking agents if hyperthyroidism present

### MICROSCOPIC FINDINGS

Histologic features are usually seen throughout the gland. The inflammatory infiltrate is distributed in a relatively nodular fashion and includes lymphocytes, plasma cells, foamy histiocytes, epithelioid histiocytes, multinucleated giant cells, and neutrophils (Fig. 23.13). A variable background of fibrosis is also present. In the hyperthyroid phase of the disease, the inflammatory process is centered on the follicle. A group of follicles is surrounded and disrupted by a lymphohistiocytic infiltrate; aggregates of neutrophils within the follicular lumens are very characteristic of this phase (Fig. 23.14). Multinucleated giant cells, often containing engulfed colloid, become more prominent in the hypothyroid phase. The inflammatory infiltrate is largely composed of lymphocytes, plasma cells, and histiocytes during this phase (Fig. 23.15). Much of the follicular epithelium has been destroyed by this stage, making it less obvious that the process was centered on the thyroid follicle. With time, the gland recovers, with regeneration of the follicles and, in most cases, resolution of the fibrosis and inflammatory infiltrate.



**FIGURE 23.13**

In subacute granulomatous thyroiditis, the thyroid is affected by nodules of a follicle-centered inflammatory infiltrate including lymphocytes, plasma cells, histiocytes, giant cells, and neutrophils. The follicles are destroyed by the process.

### SUBACUTE GRANULOMATOUS THYROIDITIS—PATHOLOGIC FEATURES

#### Gross Findings

- Rarely removed, but shows asymmetrically enlarged, firm, vaguely nodular gland

#### Microscopic Findings

- Whole gland affected
- *Early stage*: follicle-centered with groups of follicles disrupted by lymphohistiocytic infiltrate and neutrophils aggregated in follicle lumens
- *Late stage*: multinucleated giant cells more prominent and neutrophils absent, with extensive destruction of follicular epithelium, obscuring follicle-centered disease
- *Resolution*: follicular regeneration, little fibrosis remains

#### Fine Needle Aspiration

- Aggregates of lymphocytes, histiocytes, plasma cells, multinucleated giant cells
- Neutrophils may be prominent in early phase
- Giant cells may contain colloid fragments
- Colloid and follicular epithelial cells usually scant

#### Pathologic Differential Diagnosis

- Sarcoidosis, mycobacterial or fungal granulomatous infection, palpation thyroiditis, postoperative granuloma

### ANCILLARY STUDIES

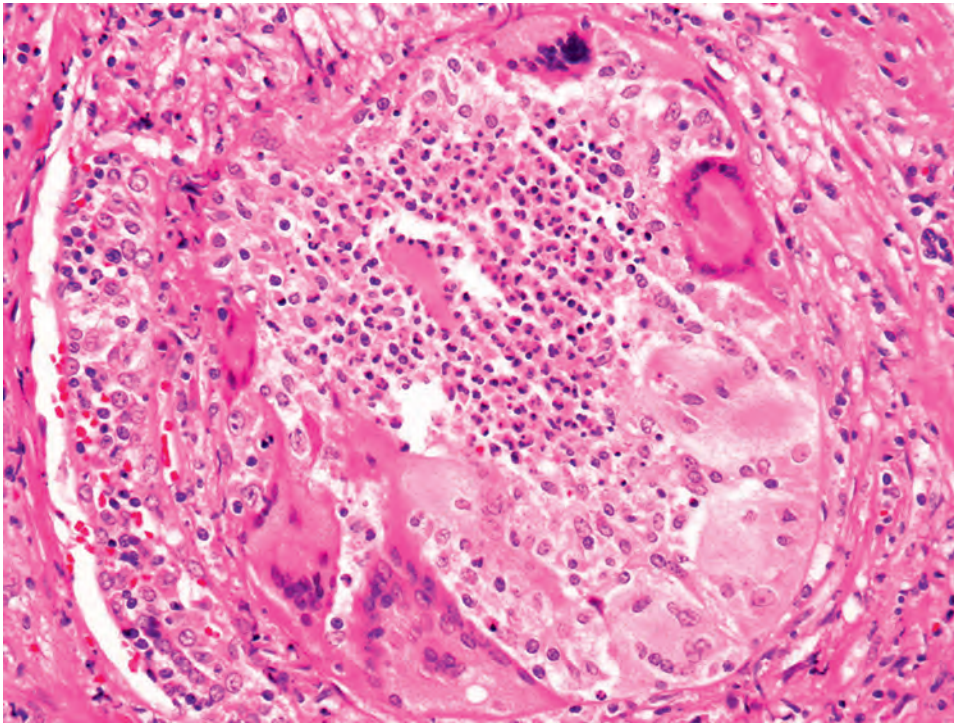
#### FINE NEEDLE ASPIRATION

In most patients, the diagnosis of granulomatous thyroiditis can be made on clinical evidence alone. Occasionally, FNA may be requested, particularly in the minority of patients without thyroid pain. The aspirate contains a mixed inflammatory infiltrate, including lymphocytes, plasma cells, foamy and epithelioid histiocytes, and multinucleated giant cells (Figs. 23.16 and 23.17); neutrophils are seen in the early phase of the disease. Follicular cells vary in number with the phase of disease: early-phase aspirates often contain small sheets of follicular cells or isolated cells (Fig. 23.16). Colloid may be present within small acinar groups or as isolated fragments. Abundant thin colloid, as seen in normal glands or in adenomatoid nodules, is not present.

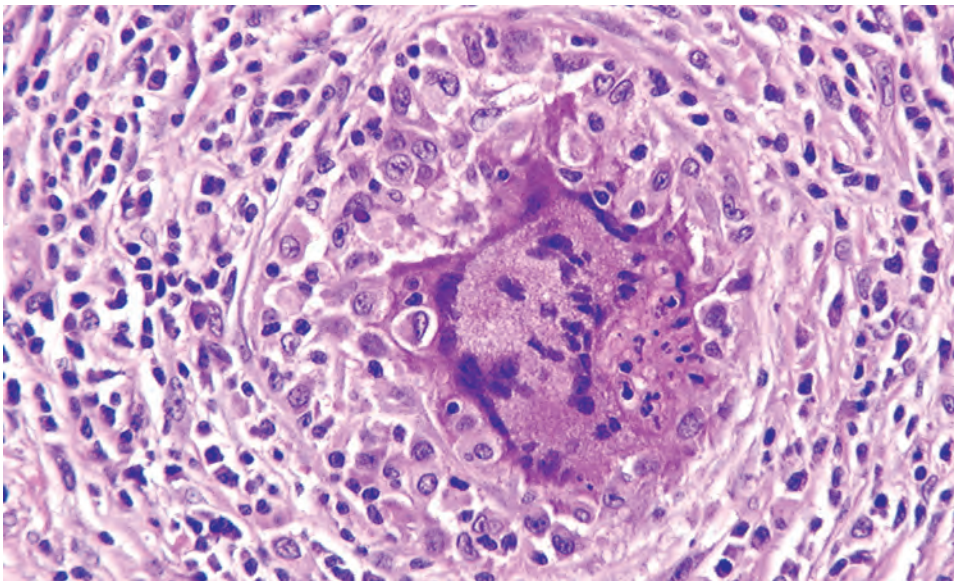
### DIFFERENTIAL DIAGNOSIS

The pathologic differential diagnosis of granulomatous thyroiditis includes other granulomatous processes that may involve the thyroid, including infectious processes, sarcoidosis, palpation thyroiditis, and postoperative granulomas. *Tuberculosis* or *fungal thyroiditis* is usually characterized by necrotizing granulomas (Fig. 23.18), in



**FIGURE 23.14**

Aggregates of neutrophils within the destroyed follicles, or “follicle abscesses,” are very common in the early phase of subacute granulomatous thyroiditis. Giant cells also surround the follicles.

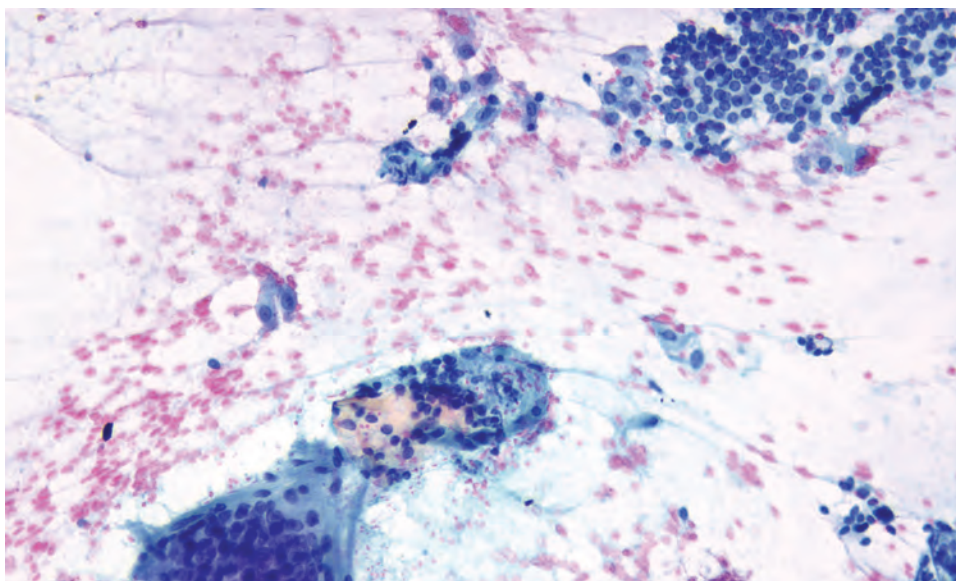
**FIGURE 23.15**

Follicular epithelium is replaced by a layer of histiocytes with a large giant cell, more prominent in the later phases of subacute granulomatous thyroiditis.

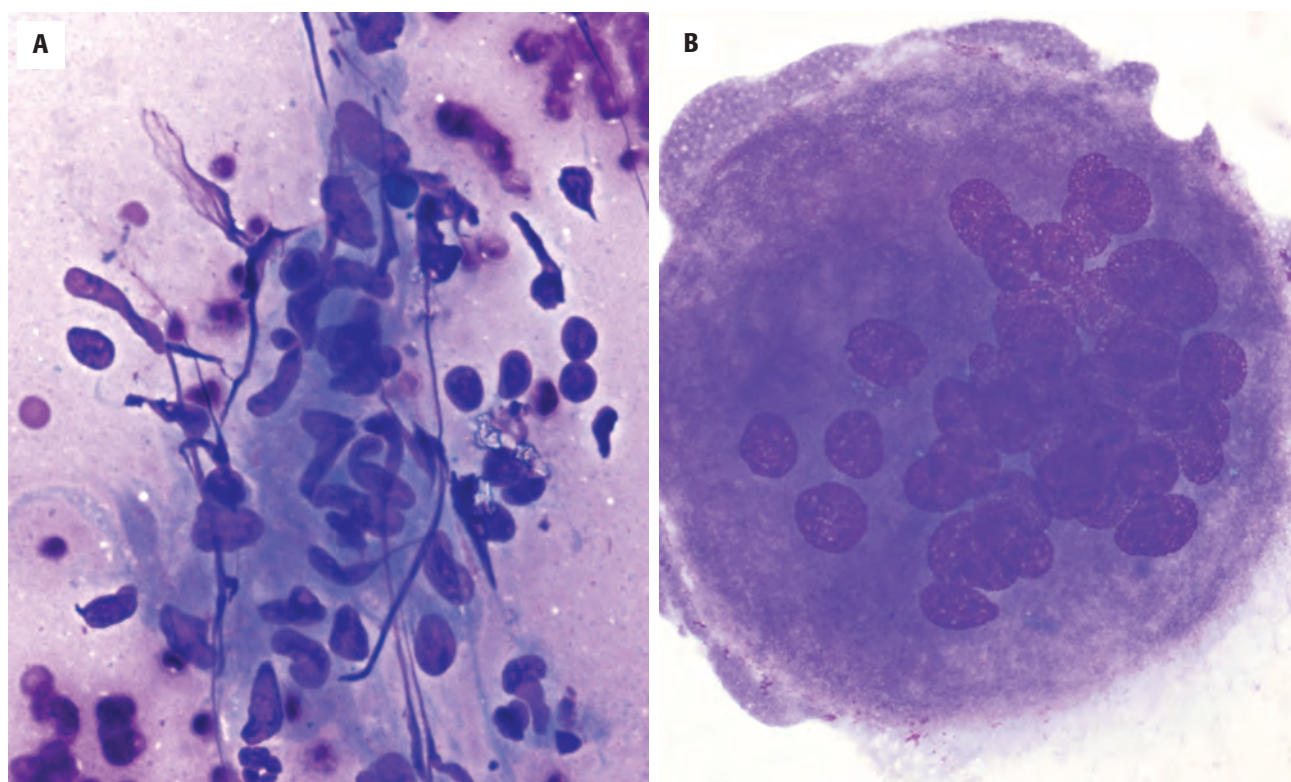
contrast to granulomatous thyroiditis. *Sarcoidal granulomas* are small and compact; they are usually located in the interstitium rather than centered on the thyroid follicles (Fig. 23.19). *Palpation thyroiditis*, an incidental finding of no clinical consequence, shares some histologic features with subacute granulomatous thyroiditis in that it is follicle-centric and granulomatous. Follicles contain aggregates of foamy histiocytes, a few lymphocytes, and

occasional multinucleated giant cells (Fig. 23.20). However, palpation thyroiditis lacks neutrophils and is focal/very patchy in its distribution. It is thought to be secondary to trauma-related rupture of individual thyroid follicles (commonly caused by palpation of thyroid nodules during physical examination). *Postoperative granulomas* are a recognized procedural phenomenon supported by the clinical history.



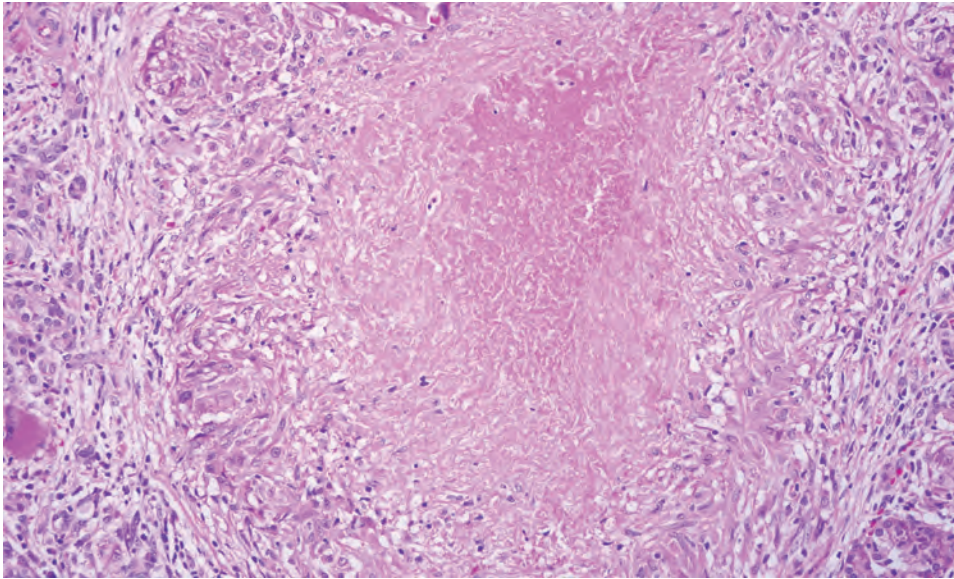
**FIGURE 23.16**

Fine needle aspiration from a patient with subacute granulomatous thyroiditis demonstrates a sheet of benign follicular epithelium with a mixed inflammatory infiltrate, which includes lymphocytes, histiocytes, and multinucleated giant cells (alcohol-fixed, Papanicolaou stain).

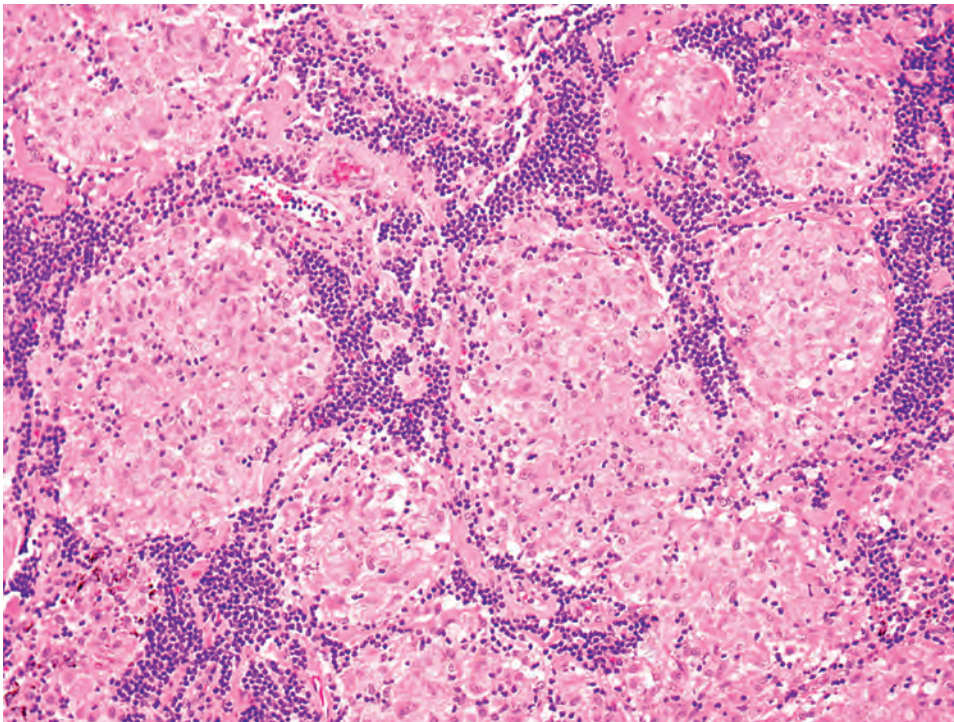
**FIGURE 23.17**

**A**, Aggregates of epithelioid histiocytes suggest the granulomatous nature of this process. **B**, A multinucleated giant cell. While typical of this type of subacute granulomatous thyroiditis, giant cells are not specific as they may be seen in adenomatoid nodules, lymphocytic thyroiditis, and papillary thyroid carcinoma (air-dried, Diff-Quik stain).



**FIGURE 23.18**

Patient has disseminated tuberculosis with extensive granulomatous inflammation in the thyroid. The central necrosis distinguishes these granulomas from those seen in subacute thyroiditis, palpation thyroiditis, and sarcoidosis.

**FIGURE 23.19**

Sarcoid granulomas are small, compact, and interstitial rather than centered on the follicles.

### PROGNOSIS AND THERAPY

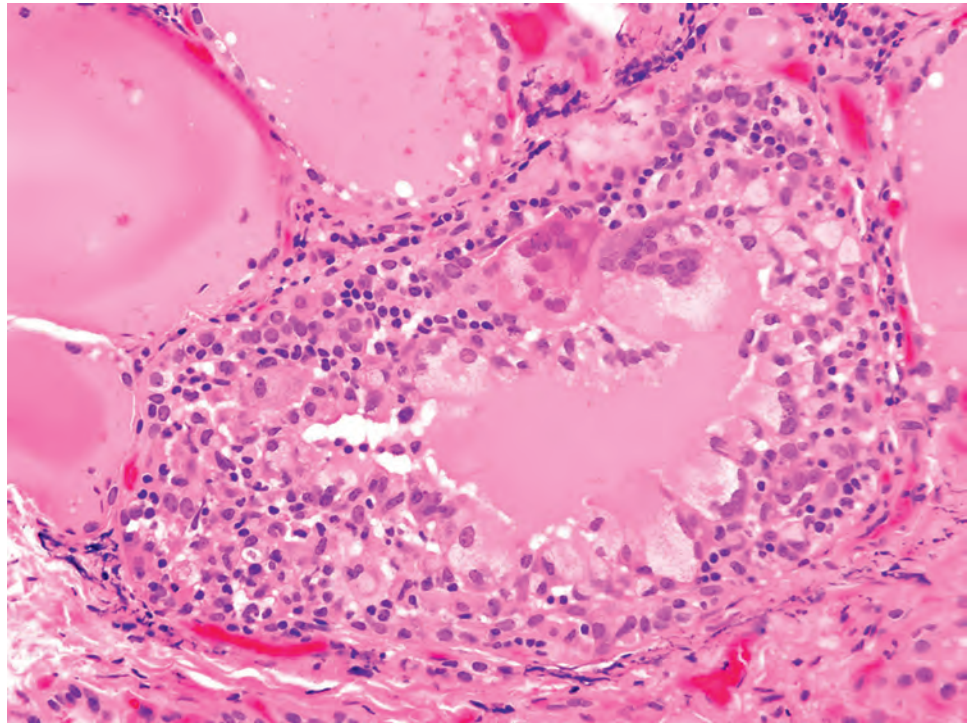
Most patients with granulomatous thyroiditis experience a self-limiting disease that resolves within several months. Treatment modalities include aspirin, nonsteroidal anti-inflammatory drugs, prednisone (for more severe symptoms), and, if thyrotoxicosis is present, beta-adrenergic blocking agents such as propranolol. A small number of patients experience recurrence of disease years after the initial episode. Permanent hypothyroidism

occurs in some 5% of patients with granulomatous thyroiditis.

### ■ INVASIVE FIBROUS THYROIDITIS (IgG<sub>4</sub>-RELATED THYROIDITIS; RIEDEL THYROIDITIS)

Invasive fibrous thyroiditis, also known as Riedel thyroiditis (named after Bernhard Moritz Carl Ludwig Riedel,



**FIGURE 23.20**

Palpation thyroiditis with foamy histiocytes, lymphocytes, and occasional multinucleated giant cells colonizing occasional follicles. The inflammatory process is focal and not diffuse, as it is in subacute granulomatous thyroiditis.

1846–1916), is a rare, fibrosing form of chronic thyroiditis that is now considered to be part of the IgG<sub>4</sub>-related disease spectrum (IgG<sub>4</sub>-related thyroiditis). IgG<sub>4</sub>-related diseases are fibrosclerosing disorders of unknown etiology characterized by increased density of IgG<sub>4</sub>-positive plasma cells in tissue sections, often with elevated serum IgG<sub>4</sub> titers. Various organ systems may be involved, including the retroperitoneum, mediastinum, eyes, hepatobiliary tree, lung, and especially the pancreas. When the thyroid gland is affected, it is replaced by dense fibrous tissue, often extending beyond the thyroid gland to involve the soft tissues of the neck.

### CLINICAL FEATURES

Invasive fibrous thyroiditis is noted in less than 0.3% of thyroidectomy specimens. The disease is much more common in women (female-to-male ratio is 5:1). There is a peak in the 5th decade, although identified over a wide range of 23 to 77 years. An enigmatic association with smoking has been noted. Nearly one-third of patients develop IgG<sub>4</sub>-related disease in another organ within a 10-year period, supporting the common pathogenesis and systemic nature of this disease.

In thyroid disease, patients have a subacute to chronic presentation with a firm goiter (thyroid enlargement) often associated with pressure symptoms, such as discomfort in the anterior neck, dysphagia, dyspnea, or stridor. The infiltrative nature of the disease may cause damage to the recurrent laryngeal nerve (vocal cord

paralysis and hoarseness) or to the sympathetic trunk (Horner syndrome). In addition, adherence to surrounding structures can be mistaken clinically for an invasive malignancy. Advanced fibrosis in the neck may produce vascular compromise, such as superior vena cava syndrome or hypoparathyroidism secondary to parathyroid gland destruction. In fact, while most patients are euthyroid at the time of diagnosis, up to 40% develop hypothyroidism over a period of 10 years. Although variable, thyroglobulin and thyroid peroxidase antibodies are slightly elevated in up to two-thirds of patients.

### RADIOGRAPHIC FEATURES

CT scans shows low attenuation of the thyroid gland with poor enhancement. MRI demonstrates homogeneous hypointensity on both T1- and T2-weighted images, findings distinct from all the other forms of thyroiditis and thyroid neoplasia.

### LABORATORY STUDIES

Serum IgG<sub>4</sub> levels are unfortunately not very sensitive or specific. Serum elevations are seen in only about 50% of cases and are not restricted to IgG<sub>4</sub>-related disease. Elevated IgG<sub>4</sub> levels may also be seen in other entities, such as malignancy and allergic disease of the upper airways.

**INVASIVE FIBROUS THYROIDITIS—DISEASE FACT SHEET****Definition**

- Rare IgG<sub>4</sub>-related disease characterized by extensive replacement of thyroid parenchyma by dense fibrosis

**Incidence and Location**

- < 0.3% of thyroidectomy specimens
- May also affect other organs, particularly the retroperitoneum, lung, mediastinum, biliary tree, pancreas, kidney, subcutis

**Morbidity and Mortality**

- Vascular compromise, recurrent laryngeal nerve damage, hypoparathyroidism

**Sex and Age Distribution**

- Females > > males (5:1)
- Peak in 5th decade (range, 23–77 years)

**Clinical Features**

- Most present with a very firm goiter
- Symptoms include dysphagia, hoarseness, stridor, Horner syndrome, fever, neck pain
- Mass may be mistaken for malignant neoplasm
- Most euthyroid at diagnosis but up to 40% develop hypothyroidism

**Prognosis and Therapy**

- Benign disease
- About one-third develop another fibrosing disorder within 10 years
- 40% develop hypothyroidism over 10 years
- Poor outcome is associated with fibrosis in other organs
- Corticosteroid useful in control or reversal of disease
- Surgery may be necessary for symptoms of compression

**PATHOLOGIC FEATURES****GROSS FINDINGS**

The thyroid is usually diffusely abnormal without normal tissue; rarely will only one lobe be affected. The gland is pale tan to white, with a woody consistency. The surgical margins of the specimen are typically ragged due to extension of the fibrosing process into perithyroidal soft tissue (Fig. 23.21). Remnants of strap muscle may be adherent to the gland's surface.

**MICROSCOPIC FINDINGS**

There is a distinctive fibroinflammatory process extensively involving the gland, extending into the perithyroidal soft tissue and strap muscles (Fig. 23.22). The interface between thyroid gland and soft tissue of the neck is lost. The fibrosis typically predominates over the inflammatory infiltrate, with broad zones of acellular

**INVASIVE FIBROUS THYROIDITIS—PATHOLOGIC FEATURES****Gross Findings**

- Diffuse enlargement of thyroid with adherence to strap muscle and perithyroidal soft tissue
- Surgical margins "ragged" because of difficult dissection
- Cut surface white, with a woody texture

**Microscopic Findings**

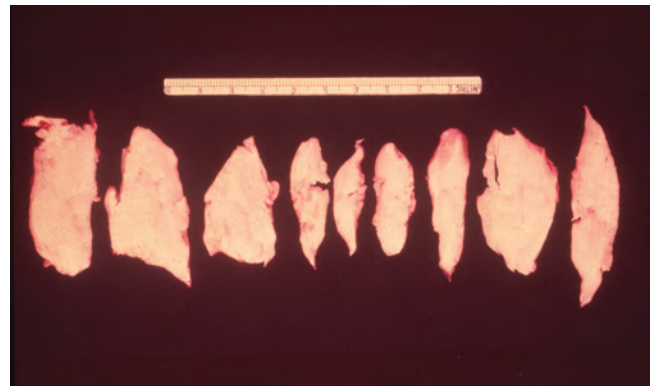
- Extensive fibrosis predominates over inflammatory infiltrate with extension into soft tissue
- Patchy infiltrate of lymphocytes, plasma cells, monocytes, neutrophils, and occasional eosinophils
- Rare peripheral entrapped thyroid follicles
- *Occlusive phlebitis* with small to medium-sized veins infiltrated by inflammatory cells with thickened walls and myxoid change
- Increased numbers of IgG<sub>4</sub> plasma cells

**Fine Needle Aspiration**

- Paucicellular to acellular aspirates
- Scant material with atypical spindle cells is misleading

**Pathologic Differential Diagnosis**

- Undifferentiated thyroid carcinoma, diffuse sclerosing variant of papillary carcinoma, fibrous variant of Hashimoto thyroiditis, Hodgkin lymphoma, sarcoma

**FIGURE 23.21**

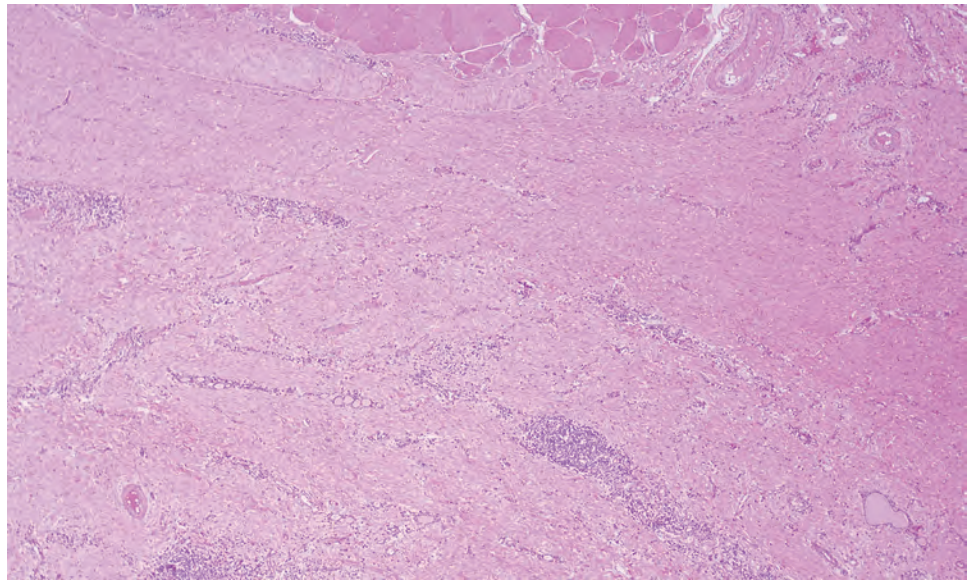
The thyroid gland in invasive fibrous thyroiditis (IgG<sub>4</sub>-related or Riedel thyroiditis) is pale and woody. The surgical border of the gland is quite ragged following a difficult dissection resulting from extrathyroidal extension of the fibrosing process.

fibrosis. The inflammatory infiltrate consists of patchy aggregates of lymphocytes, plasma cells, monocytes, neutrophils, and eosinophils (Fig. 23.23). A vascular alteration characteristic of IgG<sub>4</sub>-related disease, *occlusive phlebitis* (Fig. 23.24), is pathognomonic. Small and medium-sized veins are marked by a sparse infiltrate of lymphocytes and plasma cells. The vessel walls are thickened, often with myxoid change. If residual thyroid tissue is present, rare entrapped follicles, often with atrophic epithelium, may be identified in the sclerotic periphery (Fig. 23.25). Oxyphilic/oncocytic follicular

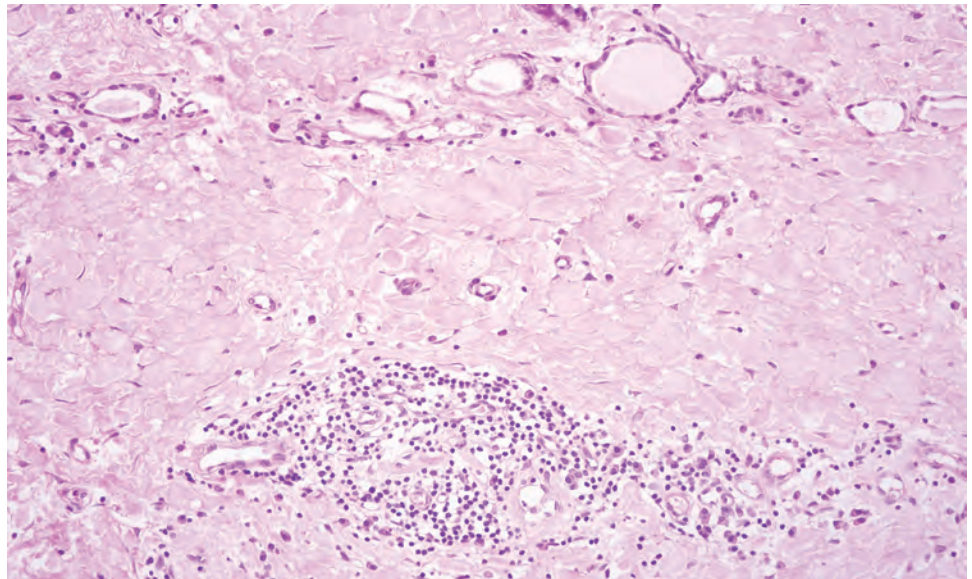


**FIGURE 23.22**

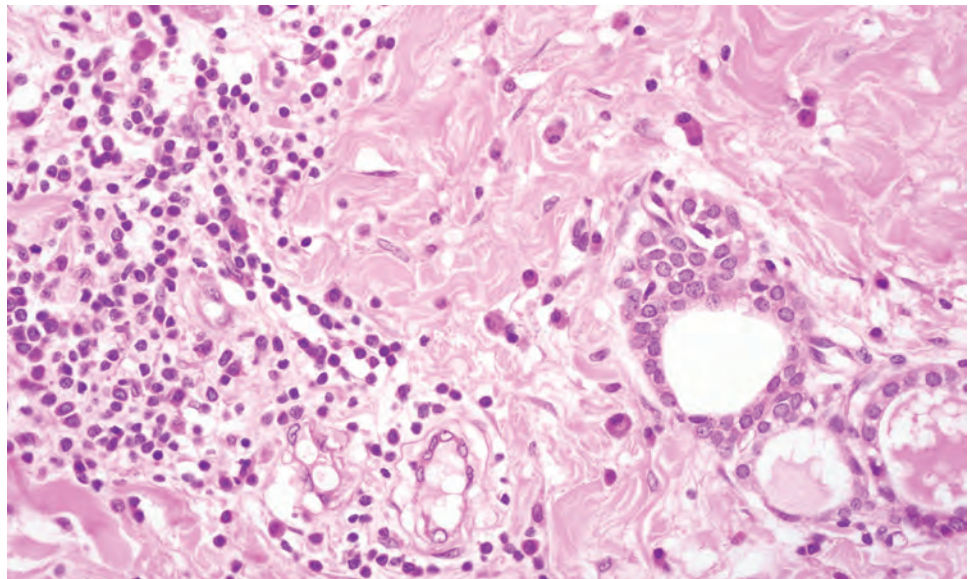
Low-power view of invasive fibrous thyroiditis demonstrates the dense fibrosis obscuring the architecture of the thyroid and extending into the perithyroidal soft tissue. Note the skeletal muscle at the upper edge.

**FIGURE 23.23**

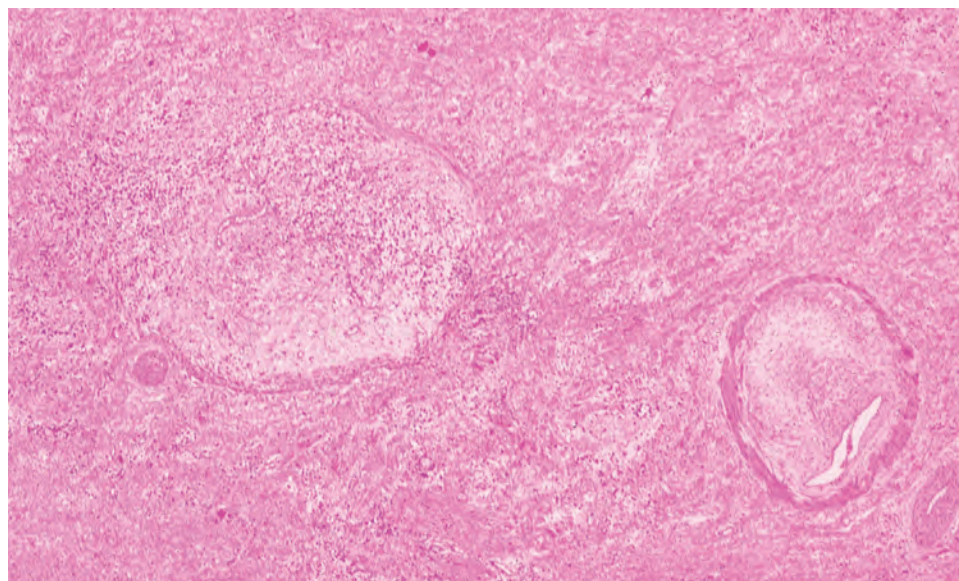
Lobular pattern of the thyroid has been destroyed by the fibroinflammatory process in invasive fibrous thyroiditis. Only scattered residual follicles remain in this gland.

**FIGURE 23.24**

Inflammatory infiltrate in invasive fibrous thyroiditis includes lymphocytes, plasma cells, and occasional eosinophils. Note the atrophic appearance of the follicular epithelium.





**FIGURE 23.25**

Occlusive phlebitis is characteristic of invasive fibrous thyroiditis. Several small and medium-sized veins demonstrate thickening of the vessel walls with myxoid degeneration and a chronic inflammatory infiltrate.

epithelial metaplasia (characteristic of Hashimoto thyroiditis) is absent.

### ANCILLARY STUDIES

#### IMMUNOHISTOCHEMICAL FINDINGS

IgG<sub>4</sub>/IgG immunohistochemistry is helpful to confirm the diagnosis. Increased numbers of IgG<sub>4</sub> plasma cells with a ratio of IgG<sub>4</sub> to IgG of greater than 40 % should be present.

#### FINE NEEDLE ASPIRATION

FNA is typically unsuccessful, with paucicellular to acellular aspirates due to the densely fibrotic gland. The scant material may, in fact, be misleading. Rare atypical spindle cells, sometimes with intranuclear cytoplasmic intrusions (pseudoinclusions), should not be over interpreted as undifferentiated (anaplastic) carcinoma.

### DIFFERENTIAL DIAGNOSIS

Invasive fibrous thyroiditis must be separated from undifferentiated carcinoma, solitary fibrous tumor, fibrous variant of Hashimoto thyroiditis, diffuse sclerosing variant of papillary carcinoma, Hodgkin lymphoma, and sarcoma. The paucicellular variant of *undifferentiated thyroid carcinoma* includes areas of infarction or necrosis, highly atypical spindle or epithelioid cells with a high mitotic rate, and at least focal positive staining for cytokeratin or follicular epithelial markers such as PAX8. *Solitary*

*fibrous tumor* is circumscribed and lacks the inflammatory infiltrate of thyroiditis. Immunohistochemical studies for STAT6, CD34, and bcl-2 are positive. The *fibrous variant of Hashimoto thyroiditis* has significant deposition of dense fibrous tissue with effacement of the thyroid architecture and follicular atrophy. Whether a subset of these cases is also IgG<sub>4</sub>-related is controversial. However, unlike invasive fibrous thyroiditis, the process is limited to the thyroid gland, and oncocytic metaplasia is characteristically present. The *diffuse sclerosing variant of papillary carcinoma* demonstrates numerous psammoma bodies, lymphocytic thyroiditis, and areas of tumor with the diagnostic nuclear features of papillary carcinoma. *Hodgkin lymphoma* (nodular sclerosis type) should have Reed–Sternberg cells and lacunar cells positive for CD15 and/or CD30 and an appropriate background of inflammatory elements. *Sarcomas* will have cytologic atypia, necrosis, and mitotic figures.

### PROGNOSIS AND THERAPY

Invasive fibrous thyroiditis is a benign and often self-limiting, disease. The chief morbidity is related to hypothyroidism, since the local effects of the goiter can be addressed surgically, if necessary. Other potential complications include hypoparathyroidism and nerve injury related either to the disease or to the difficulty of surgery in these patients. In those individuals with multifocal systemic fibrosclerosis, other organ systems may be affected by life-threatening disease. Corticosteroid therapy has been successful in the majority of patients in controlling disease progression or in complete or partial reversal of symptoms.



## ■ CHRONIC LYMPHOCYTIC THYROIDITIS (HASHIMOTO THYROIDITIS)

Widely known by its eponym, Hashimoto thyroiditis (named after Hakaru Hashimoto, 1881–1934), chronic lymphocytic thyroiditis is an autoimmune chronic inflammatory disorder of the thyroid associated with diffuse enlargement of the gland and several thyroid autoantibodies. A fibrous variant is associated with marked fibrosclerosis and atrophy of the thyroid epithelium. The mechanism of autoimmunity is not clearly understood. A combination of genetic and environmental factors (the latter including high iodine intake, infections, medications, pregnancy, and smoking) likely play a role and ultimately lead to a breakdown of immune tolerance. Major histocompatibility complex class II proteins, HLA-DR, HLA-DP, and HLA-DQ are expressed by the follicular epithelial cells in patients with chronic lymphocytic thyroiditis; these proteins are necessary for presentation of antigen to CD4+ T-cells. The activated helper T-cells, in turn, stimulate autoreactive B-cells to be recruited into the thyroid, where they secrete autoantibodies. The key target antigens for this autoimmune reaction are thyroglobulin, thyroid peroxidase, and the thyrotropin (TSH) receptor. TSH receptor antibodies may contribute to hypothyroidism by blocking the binding capacity for TSH. The activated helper T-cells also recruit cytotoxic CD8+ T-cells, which may be responsible for the destruction of follicular epithelial cells, ultimately leading to hypothyroidism in many patients.

### CLINICAL FEATURES

Chronic lymphocytic thyroiditis is common, affecting about 1% of the general population, but a subset of cases are subclinical. It can be found over a wide age range, although it shows a peak in middle age. Women are much more frequently affected; the female-to-male ratio is 5 to 10:1. An exception to this is the fibrous variant of Hashimoto thyroiditis, which is more common in older men. The risk of the disease seems highest in countries with the highest iodine intake (United States and Japan).

A familial association is seen, while there is also an increased incidence in individuals with Down syndrome, Turner syndrome, and familial Alzheimer disease. HLA-DR3, HLA-DR4, and HLA-DR5 have been linked to the disease. Other autoimmune diseases may coexist, including pernicious anemia, type 1 diabetes mellitus, multiple sclerosis, rheumatoid arthritis, Addison disease, Graves disease, and Sjögren syndrome.

Patients with chronic lymphocytic thyroiditis have a gradual, diffuse enlargement of a firm, nontender thyroid gland, usually 2 to 3 times the normal weight. Occasionally patients with the fibrous variant of Hashimoto thyroiditis

have rapid enlargement of the gland; however, this finding should raise the suspicion of thyroid lymphoma in a patient with a history of autoimmune thyroiditis. Hypothyroidism is common but not invariably present at the time of presentation. Symptoms of hypothyroidism include constipation, skin changes, bradycardia, menstrual cycle abnormalities, depression, and myxedema. Severe hypothyroidism is commonly associated with the fibrous variant of the disease. Rare patients present with hyper- rather than hypothyroidism, known as hashitoxicosis.

Juvenile Hashimoto thyroiditis, usually seen in adolescents and young adults, may present with hypothyroidism or hyperthyroidism; the patients often have a strong family history of thyroid disease. Some patients also have hypoadrenalism (Schmidt syndrome), hypoparathyroidism, diabetes mellitus, or hypogonadism.

### RADIOGRAPHIC FEATURES

Radiographic imaging is not necessary in the diagnosis of autoimmune thyroiditis unless there are coexisting

### CHRONIC LYMPHOCYTIC THYROIDITIS (HASHIMOTO)—DISEASE FACT SHEET

#### Definition

- Autoimmune chronic inflammatory disorder of the thyroid associated with diffuse enlargement, thyroid autoantibodies, and hypothyroidism

#### Incidence

- Affects some 1% of the general population but a subset of cases is subclinical
- Familial cases well documented

#### Sex, Race, and Age Distribution

- Females > > > males (5–10:1) except for fibrous variant
- Highest incidence in the United States and Japan related to high iodine intake
- Peak in middle age (mean, 59 years), but wide age range

#### Clinical Features

- Diffusely enlarged, nontender gland
- Enlargement usually gradual
- Hypothyroidism common, but rarely hyperthyroidism (hashitoxicosis)
- Other associated autoimmune disorders

#### Laboratory Studies

- Serum thyroid antibodies are elevated (various types)

#### Prognosis and Treatment

- Increased incidence of thyroid lymphoma (up to 80-fold increase)
- Synthetic levothyroxine for hypothyroidism and antithyroid drugs for hashitoxicosis
- Surgery if symptomatic or for suspicious nodules

nodules and may, in fact, be misleading. Ultrasound characteristically shows heterogeneous parenchyma with innumerable small hypoechoic nodules separated by echogenic septae. Radioactive iodine uptake is usually normal or increased in Hashimoto thyroiditis, suggesting Graves disease, even in patients with hypothyroidism.

### LABORATORY STUDIES

Laboratory assessment requires testing for serum thyroid antibodies (antithyroglobulin and antithyroperoxidase [TPO] antibodies). Anti-TPO antibodies are the most sensitive and specific marker, found in 95 % of patients while very rare in healthy controls. Antithyroglobulin antibodies are less sensitive and are not specific to patients with thyroiditis. Serum TSH and free thyroxine (T4) measurement is important to monitor thyroid function.

### PATHOLOGIC FEATURES

#### GROSS FINDINGS

Thyroidectomy is often performed because of a coexisting thyroid nodule. The gland is diffusely enlarged and pale gray to white, with a consistency of lymphoid tissue (Fig. 23.26). If the disease is of long standing, it may contain distinct nodules and bands of fibrous tissue. The fibrous variant is very firm and fibrotic, with a multinodular cut surface resembling cirrhosis of the liver. The thyroid gland may be quite small (< 5 g) in the late stage (“fibrous atrophy variant”). While the gross appearance of the thyroid in the fibrous variant may resemble invasive

fibrous thyroiditis, the periphery of the thyroid gland is smooth in chronic lymphocytic thyroiditis rather than ragged.

#### MICROSCOPIC FINDINGS

The histologic features of classic Hashimoto thyroiditis include diffuse and rather dense infiltration of the gland by

### CHRONIC LYMPHOCYTIC THYROIDITIS (HASHIMOTO)–PATHOLOGIC FEATURES

#### Gross Findings

- Diffusely enlarged gland, may be lobulated or nodular
- Pale white cut surface resembles lymphoid tissue
- Smooth periphery

#### Microscopic Findings

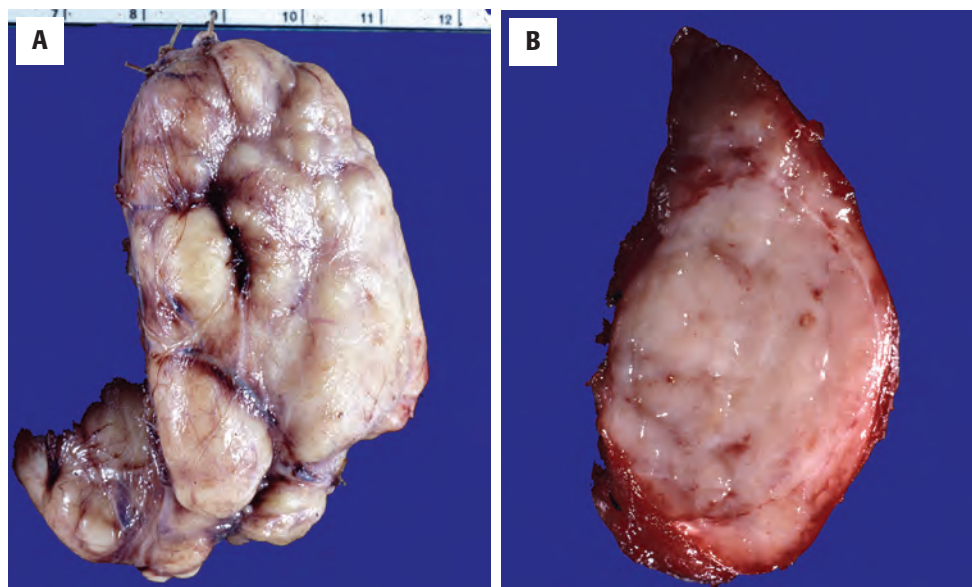
- Diffuse, dense lymphoplasmacytic infiltrate, often with well-developed germinal centers
- Follicular atrophy with decrease in colloid
- Oxyphilic/oncocyctic (Hürthle) cell metaplasia
- Squamous metaplasia is common
- Fibrous variant shows dense lymphoid infiltrate, extensive fibrosis, and minimal residual follicular epithelium

#### Fine Needle Aspiration

- Mixed polymorphic lymphoplasmacytic infiltrate
- Occasional multinucleated giant cells and histiocytes
- Oxyphilic epithelial cells in small clusters and sheets, may have nuclear atypia
- Scant colloid in most cases

#### Pathologic Differential Diagnosis

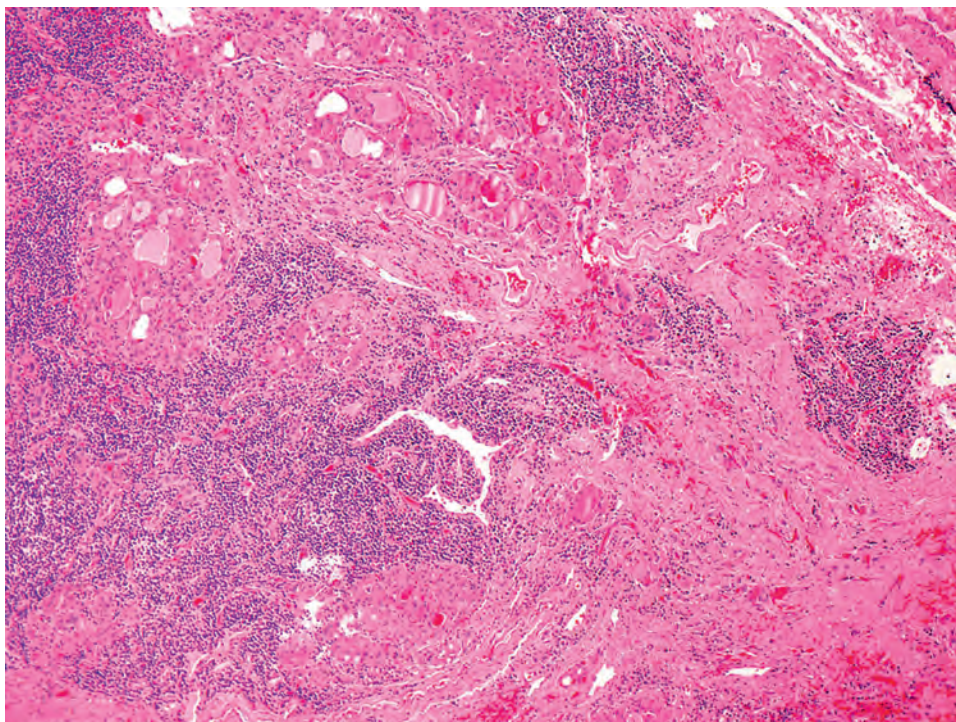
- Papillary thyroid carcinoma, extranodal marginal zone B-cell lymphoma, invasive fibrous thyroiditis, nonspecific lymphocytic thyroiditis, painless or silent thyroiditis



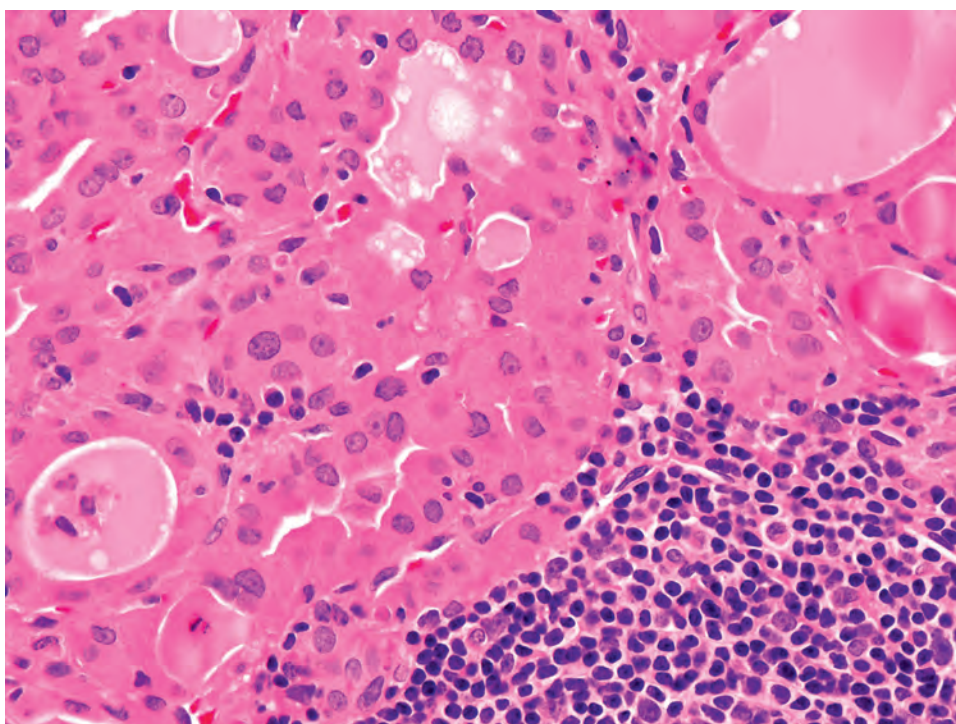
**FIGURE 23.26**

**A**, The thyroid is often enlarged, with a lobulated appearance in chronic lymphocytic thyroiditis (Hashimoto thyroiditis). The pale white tan color reflects the dense lymphoid infiltrate. **B**, The cut surface of lymphocytic thyroiditis bears a striking resemblance to lymph node tissue.



**FIGURE 23.27**

There is a dense, diffuse chronic inflammatory infiltrate with germinal centers in chronic lymphocytic thyroiditis. Note the atrophy of the thyroid follicles.

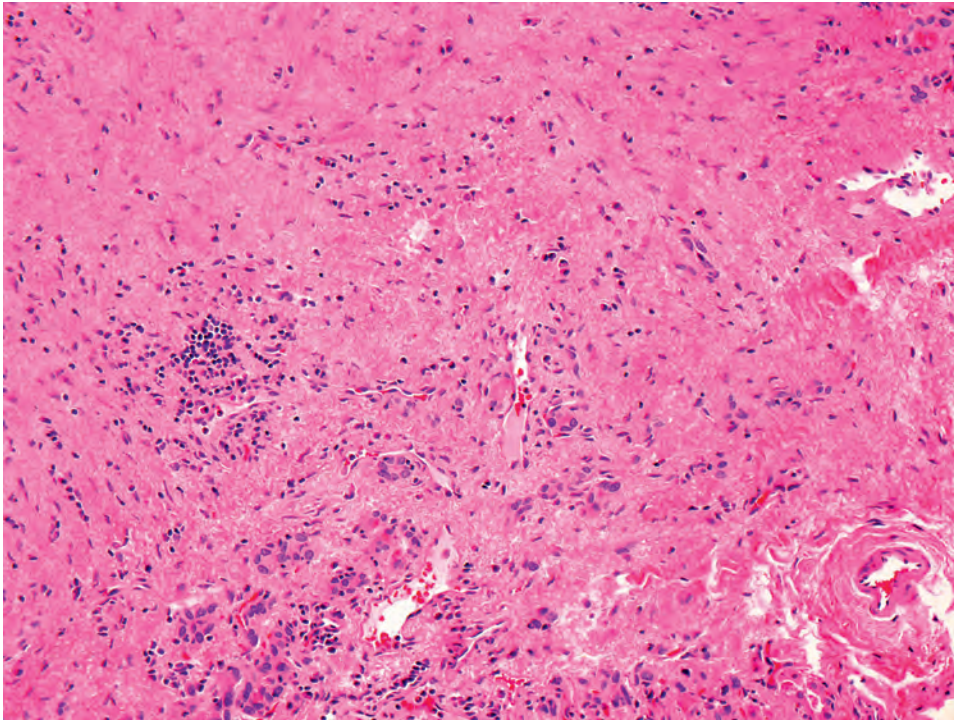
**FIGURE 23.28**

Key histologic features of chronic lymphocytic thyroiditis include a dense lymphocytic infiltration of the gland, atrophy of the follicular epithelial component, and oxyphilic/oncocyte change in the follicular epithelial cells, as shown here.

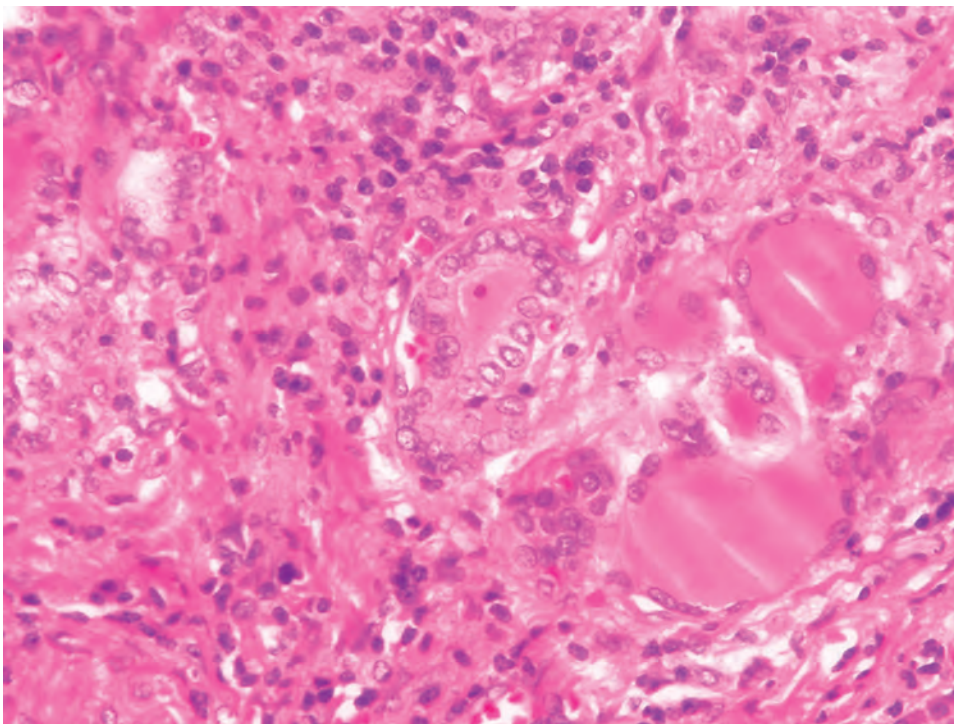
predominantly small lymphocytes but often with germinal centers as well; plasma cells, histiocytes, and, sometimes, giant cells may be present. At low power, the lobular pattern of the thyroid is preserved (Fig. 23.27). The lymphocytic infiltrate is usually confined to the thyroid but rarely extends into the adjacent soft tissue. The appearance of the follicular epithelium may vary from area to area, with some follicles remaining intact. The hallmark

of Hashimoto thyroiditis, however, is follicular atrophy accompanied by oncocyte (Hürthle cell) metaplasia of the follicular epithelial cells (Figs. 23.28 and 23.29). The follicles may be small, with scant colloid, or they may be destroyed, leaving small islands of oxyphilic epithelium surrounded by an intense lymphoid infiltrate or areas of fibrosis (Fig. 23.29). The oncocyte (Hürthle) cells are strikingly different from normal follicular epithelial cells. The



**FIGURE 23.29**

Areas of fibrosis with parenchymal extinction may be prominent in some cases of chronic lymphocytic thyroiditis.

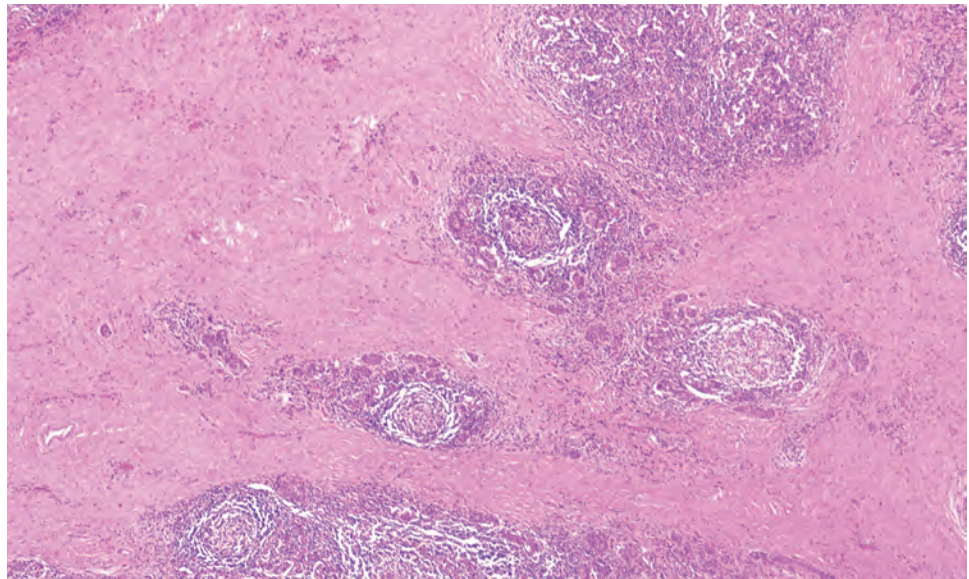
**FIGURE 23.30**

Oxyphilic cells may have rather striking nuclear atypia, with features that overlap with papillary thyroid carcinoma. Note that the nuclei are optically clear, but they are immediately associated with lymphocytes, lacking any “mass” or tumor formation.

nuclei are enlarged, often with irregular nuclear contours, vesicular chromatin, and grooving, which may be confused with those of PTC (Fig. 23.30). Prominent nucleoli are frequently observed. The cytoplasm of the oxyphilic cells is abundant, eosinophilic, and very granular. Squamous metaplasia is common in the atrophic follicular epithelium, particularly in more advanced cases and in the fibrous variant. Squamous or respiratory epithelium-lined cysts

are occasionally present; if they are unusually large, they may suggest a branchial cleft anomaly (“lymphoepithelial cysts”). Long-standing Hashimoto thyroiditis tends to become nodular. The nodules have a pushing border, as seen in adenomatoid nodules; however, they are frequently quite cellular. The juvenile form has the lymphocytic infiltrate but tends to include minimal follicular atrophy and oncocyctic metaplasia.



**FIGURE 23.31**

In the fibrosing variant of Hashimoto thyroiditis, little remains of the thyroid parenchyma; small islands of epithelium are found among the patches of chronic inflammation.

The fibrous variant of Hashimoto thyroiditis, also known as “advanced lymphocytic thyroiditis,” represents ~10% of cases. Fibrosis dominates the histologic picture; it has a dense keloidal appearance (Fig. 23.31). A lobular pattern is still evident from the distribution of the lymphoid infiltrate around the severely atrophic follicles. The atrophic variant (“fibrous atrophy”) has more extreme follicular atrophy and likely represents end-stage disease.

## ANCILLARY STUDIES

### IMMUNOHISTOCHEMICAL FINDINGS

Immunohistochemical studies are rarely necessary for making the diagnosis of Hashimoto thyroiditis; however, if extranodal lymphoma is a diagnostic concern, particularly in the patient with rapid enlargement of the thyroid, they may be helpful in excluding malignancy. If lymphoma is suspected, it may be prudent to reserve fresh tissue in transportation media for flow cytometric immunophenotyping.

The infiltrate in Hashimoto thyroiditis demonstrates a mixed B- and T-cell population, which includes CD20-, CD4-, and CD8-positive cells. The plasma cells in the background are polyclonal for immunoglobulin heavy and light chains. Increased numbers of IgG<sub>4</sub> plasma cells may be present in a subset of cases. Whether or not these cases fall within the spectrum of IgG<sub>4</sub>-related disease is controversial.

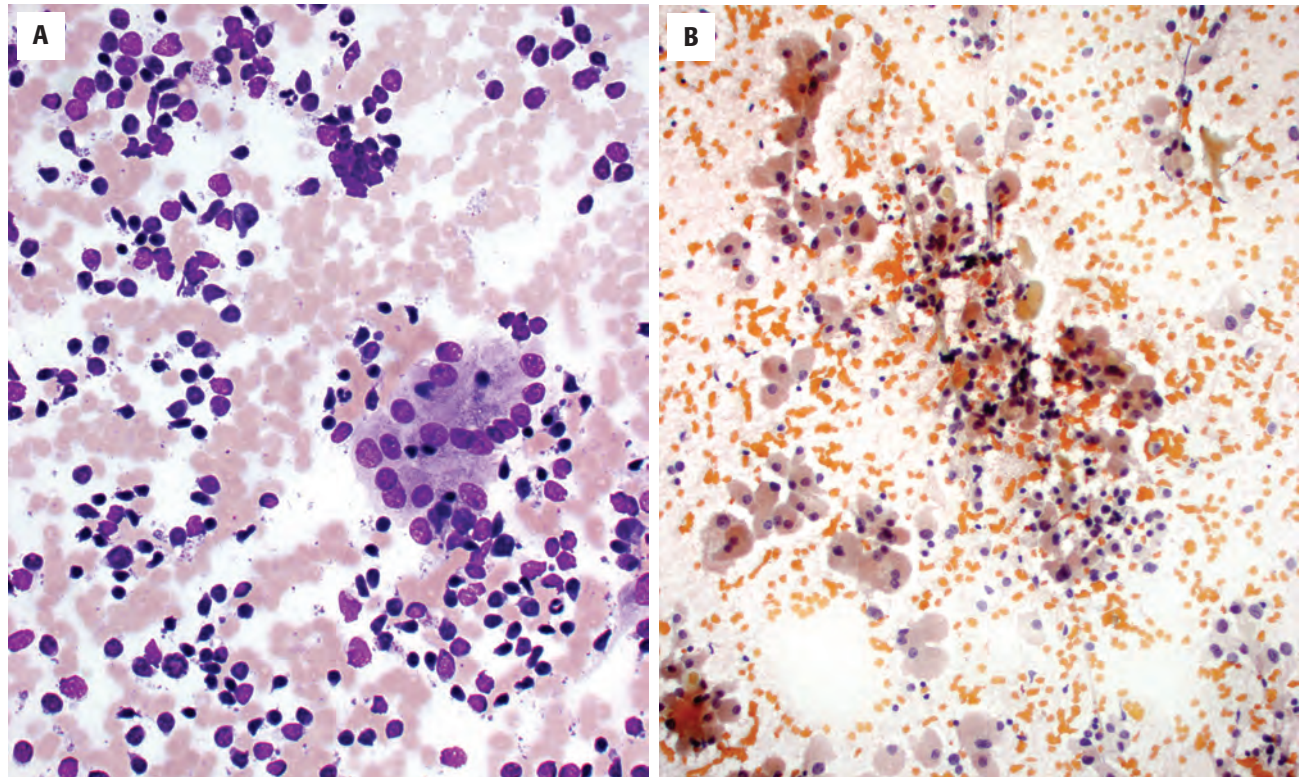
### FINE NEEDLE ASPIRATION

The cytologic features of Hashimoto thyroiditis include a mixed polymorphic lymphoplasmacytic infiltrate with

a spectrum of lymphoid cells ranging from small round lymphocytes to the activated cells found in germinal centers (Fig. 23.32). Histiocytes and the occasional multinucleated giant cell may be seen. Colloid is usually sparse in well-developed Hashimoto thyroiditis. The follicular epithelium is usually scant, found in small flat sheets or as single cells. The cytoplasm is very granular and oxyphilic. The nuclei of the epithelial cells may be enlarged; they may include vesicular or “pale” chromatin and irregular nuclear contours. Oncocytic cells are probably the most significant pitfall in thyroid aspiration cytology, but a sheet-like architecture, lack of syncytial cell groups, the intense oxyphilia of the follicular cell cytoplasm, and the background lymphoid cells should be helpful in distinguishing thyroiditis from PTC. Cellular adenomatoid nodules may be indistinguishable from a follicular neoplasm by cytology alone; examination of the periphery of the nodule histologically is necessary to make that distinction.

## DIFFERENTIAL DIAGNOSIS

Extranodal marginal zone B-cell lymphoma (“MALT” lymphoma), PTC, invasive fibrous thyroiditis, painless or silent thyroiditis, and nonspecific inflammation are differential considerations. There is an increased risk of *MALT lymphoma* in patients with lymphocytic thyroiditis (up to 80-fold). Rapid enlargement of the gland, a diffuse, sheet-like effacement of the thyroid parenchyma, lymphoepithelial lesions, and supporting immunohistochemistry and/or flow cytometry will help to make the diagnosis of lymphoma. Nuclear irregularities can be pronounced in the follicular epithelial cells near lymphocytic thyroiditis, thus mimicking a PTC. However, the oxyphilia in

**FIGURE 23.32**

**A.** In cytologic preparations of chronic lymphocytic thyroiditis, the oxyphilic follicular cells may be scant in number. They are usually seen as small sheets of polygonal cells with abundant granular blue cytoplasm. Numerous lymphocytes and plasma cells are noted (air-dried, Diff-Quik stain). **B.** A fine needle aspiration yields a dense infiltrate with a polymorphous lymphoplasmacytic population with oncocyctic follicular epithelium appearing orangeophilic (alcohol-fixed, Papanicolaou stain).

multiple foci and the lack of architectural features and infiltrative pattern should make the separation possible. *Invasive fibrous thyroiditis* has a diffuse pattern of effacement by fibrosis that infiltrates beyond the thyroid gland and is accompanied by vasculitis. *Focal/mild nonspecific lymphocytic thyroiditis* (Fig. 23.33), which is typically patchy in its distribution within the gland, lacks the clinical and laboratory features of an autoimmune thyroid disorder. It is frequently encountered as an incidental finding in thyroids resected for other reasons and not accompanied by oncocyctic metaplasia. *Painless or silent thyroiditis* (sporadic or postpartum) is considered by some to be a variant of chronic lymphocytic thyroiditis. It is characterized by transient hyperthyroidism followed by hypothyroidism that eventually resolves in most cases. Postpartum cases occur following pregnancy. The histopathology is not well characterized. However, thyroid glands typically contain a lymphoplasmacytic infiltrate without significant oncocyctic metaplasia.

#### PROGNOSIS AND THERAPY

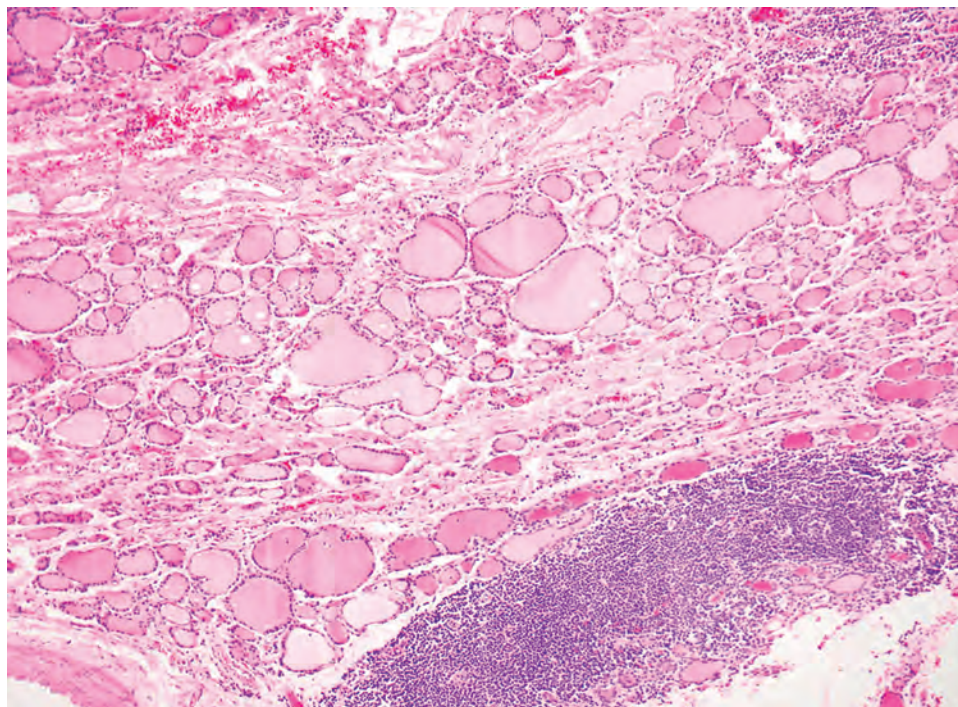
Treatment depends on the clinical manifestations in a given patient. Those with hypothyroidism require thyroid hormone replacement (synthetic levo-thyroxine), usually

lifelong, while those presenting with hyperthyroidism are treated accordingly. Surgery may be recommended if the thyroid enlargement is symptomatic or if suspicious nodules develop. The increased incidence of lymphoma, usually an extranodal marginal zone B-cell lymphoma (although transformation to a diffuse large B-cell lymphoma also occurs) suggests lifelong monitoring to exclude this development.

#### ■ DIFFUSE HYPERPLASIA (GRAVES DISEASE)

Widely known by its eponym (named after Robert James Graves, 1796–1853), Graves disease is an autoimmune condition of the thyroid that results in diffuse hyperplasia with excess thyroid hormone production that is unchecked by the normal feedback loop between the pituitary gland and the thyroid. The immune abnormality is mediated by antibodies to the thyrotropin receptor found on follicular epithelial cells. The most specific antibody, known as thyroid-stimulating immunoglobulin (TSI), when bound to the TSH receptor, mimics the action of pituitary TSH, stimulating the follicular epithelium to produce hormone. Other antibodies are often present in Graves disease, including thyroid growth-stimulating immunoglobulin, which is associated with thyrocyte proliferation, and



**FIGURE 23.33**

Focal/mild nonspecific thyroiditis is characterized by much more sparse and scattered lymphoid aggregates in an otherwise normal thyroid gland. Diffuse oxyphilic/oncocyctic metaplasia, follicular atrophy, and fibrosis are not observed.

TSH-binding antibodies, which may either inhibit or stimulate TSH activity. The clinical effect of this autoimmune process is thyrotoxicosis (hyperthyroidism), accompanied by diffuse thyroid enlargement, an infiltrative ophthalmopathy in about 25 % of patients, and a spectrum of systemic effects of thyroid hormone excess.

### CLINICAL FEATURES

Graves disease is the most common cause of spontaneous hyperthyroidism, representing up to 80 % of all cases. The incidence is approximately 1 % to 2 % of the population, with a slightly higher incidence in areas of particularly high iodine intake (United States and Japan). It is 5 to 10 times more common in women than in men. Graves disease is most common in the 3rd to 4th decades. Men, however, tend to develop Graves disease at an older age, often with a more severe form of thyrotoxicosis.

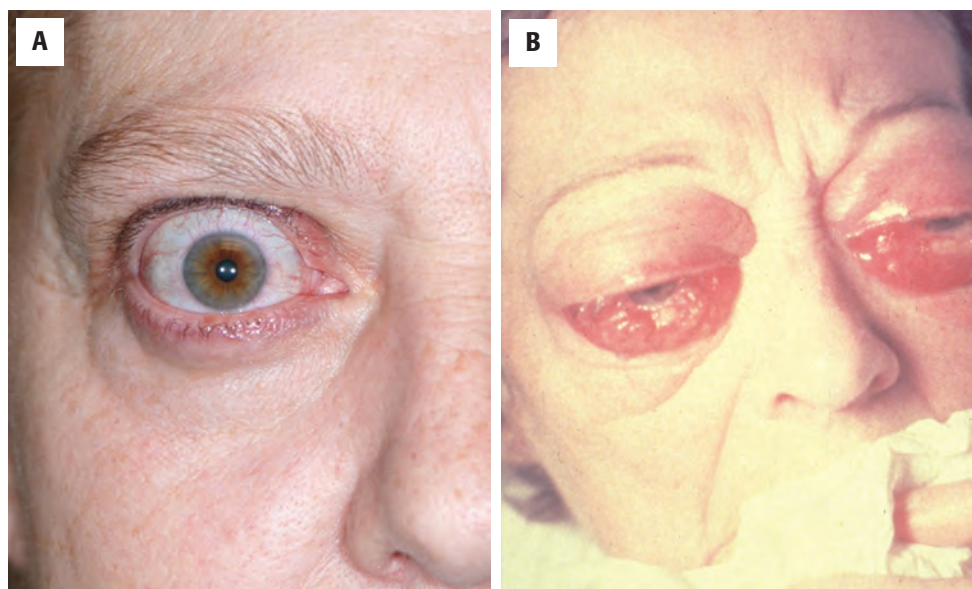
Genetic factors play a role, with familial clustering common. However, although susceptibility has been associated with polymorphisms within the HLA region (particularly DR3) and in the *CTLA-4* gene (cytotoxic T-lymphocyte-associated gene), environmental factors—such as infections, stress, smoking, and gonadal steroid hormones—are also involved in the etiology of this disease.

The symptoms of Graves disease reflect the effect of thyrotoxicosis and of the autoimmune process on multiple organ systems. The spectrum of signs and symptoms includes weight loss, heat intolerance, fatigue, weakness, palpitations, dyspnea on exertion, stridor due to tracheal compression, hoarseness, chest pain, dysphagia,

oligomenorrhea, hair loss or change in hair texture, a “gritty” sensation in the eyes, proptosis, conjunctivitis, memory loss, poor attention span, emotional lability, muscle weakness, and irritability or agitation. Physical examination findings include localized myxedema (particularly pretibial and most often in females); hair loss; a wide-eyed stare or proptotic appearance (Fig. 23.34); irritative keratoconjunctivitis; lid lag; diplopia; tachycardia; smooth, warm, and velvety skin; and hyperactive reflexes. In addition, the thyroid is diffusely enlarged and a bruit may be appreciated over the thyroid area. Also, long-standing or treated Graves disease is often characterized by the development of nodules. It is important to note that elderly patients may show few of the classic signs and symptoms mentioned (“apathetic hyperthyroidism”). The diagnosis should be considered in patients with new-onset atrial fibrillation, unexplained weight loss, worsening cardiovascular disease, and new onset of tremor. A life-threatening exacerbation of thyrotoxicosis, “thyroid storm,” is usually precipitated by surgery, infection, or trauma and is characterized by central nervous system agitation or depression and high fever.

### RADIOGRAPHIC FEATURES

RAI scans demonstrate a diffuse increase in uptake within the thyroid; however, this is not a specific finding and is not usually necessary for establishing the diagnosis of Graves disease. Ultrasound shows bilateral increased thyroid gland volume with hypervascularity, occasionally with nodules (Fig. 23.35).

**FIGURE 23.34**

One of the most striking features of diffuse hyperplasia (Graves disease) is a proptotic wide-eyed stare, keratoconjunctivitis, and limited movement of the extraocular muscles. **A**, Note the remarkable lid lag and proptosis. **B**, In this very advanced case of Graves disease, the enlarged extraocular muscles are visible. (**A**, Courtesy Dr. K.B. Krantz. **B**, Courtesy Dr. C.S. Heffess.)

### DIFFUSE HYPERPLASIA (GRAVES DISEASE)—DISEASE FACT SHEET

#### Definition

- Autoimmune process that results in clinical hyperthyroidism and histologic diffuse hyperplasia of the follicular epithelium

#### Incidence and Location

- Incidence 1%–2% worldwide
- Somewhat higher incidence in areas with highest iodine intake
- Responsible for 80% of cases of hyperthyroidism

#### Sex and Age Distribution

- Females > > > males (5–10:1)
- Peak in 3rd to 4th decades

#### Clinical Features

- Greatest risk factor is positive family history
- Common symptoms of thyrotoxicosis include weight loss, heat intolerance, fatigue, weakness, palpitations, dyspnea on exertion, stridor due to compression, hoarseness, chest pain, tremor, oligomenorrhea, amenorrhea, hair loss, change in hair texture, conjunctival irritation, proptosis, poor attention span, emotional lability, agitation
- Physical findings including localized myxedema (especially pretibial), hair loss, wide-eyed stare or proptosis,

keratoconjunctivitis, lid lag, diplopia, tachycardia, hyperactive reflexes

- “Apathetic hyperthyroidism” in elderly shows atrial fibrillation, weight loss, worsening cardiac disease, tremor
- Thyroid usually diffusely enlarged although sometimes nodular

#### Radiographic Features

- RAI uptake is homogeneously increased

#### Laboratory Studies

- T3 and free T4 elevated; thyroid-stimulating hormone markedly suppressed
- Thyroid antibodies (especially thyroid-stimulating immunoglobulin) present

#### Prognosis and Treatment

- Overall prognosis is excellent, although thyroid storm is a life-threatening exacerbation requiring rapid antithyroid drug therapy
- Therapy includes antithyroid drugs, RAI, and surgery
- Drug failure (up to 40%) requires RAI or surgery
- Permanent hypothyroidism can be a complication

RAI, Radioactive iodine.

### LABORATORY STUDIES

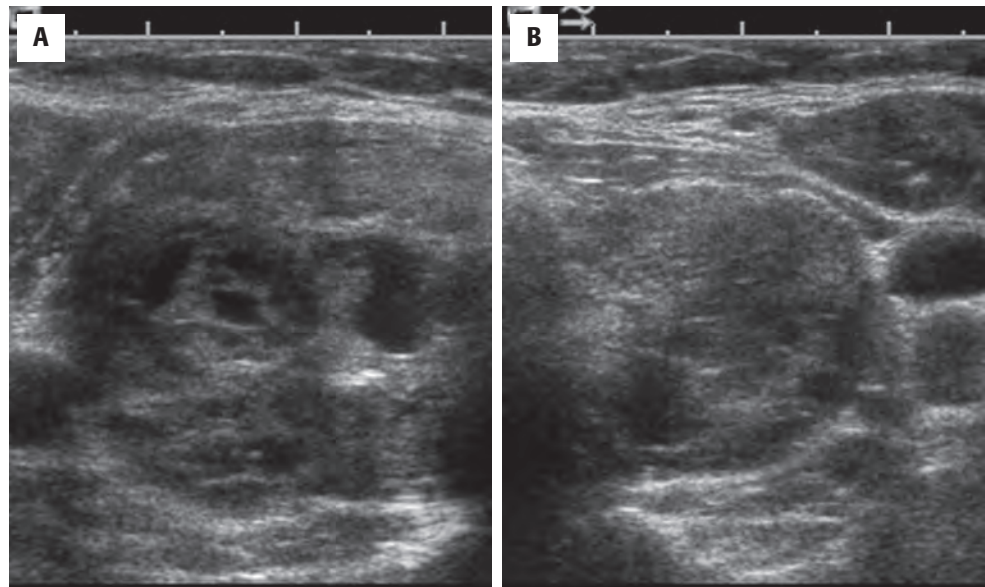
Elevated levels of free thyroxine (T4) and triiodothyronine (T3) and low TSH support the diagnosis of Graves disease in the appropriate clinical setting. If the diagnosis is uncertain, TSH-receptor antibodies can be measured.

### PATHOLOGIC FEATURES

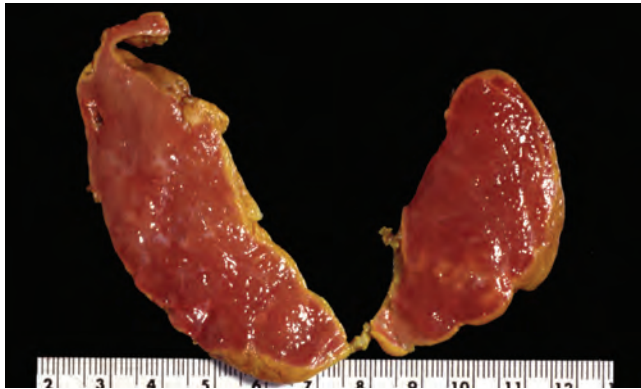
#### GROSS FINDINGS

The thyroid gland is diffusely and symmetrically enlarged and characteristically beefy red owing to increased vascularity (Fig. 23.36). Vague nodularity may



**FIGURE 23.35**

**A** and **B**, Right and left lobes of the thyroid gland showed increased size with multiple nodules on ultrasound, which are nonspecific findings in this patient with Graves disease.

**FIGURE 23.36**

This thyroidectomy specimen from a child with hyperthyroidism is enlarged and hyperemic, with a “beefy red” appearance due to increased vascularity. (With permission from Wenig BM, Heffess CS, Adair CF. *Atlas of Endocrine Pathology*. Philadelphia: WB Saunders; 1997.)

be present. Average weights range from 50 to 150 g. If the patient has been treated, if the Graves disease is of long standing, or if it is “burnt out,” the gland may contain multiple nodules or patches of fibrosis.

#### MICROSCOPIC FINDINGS

The low-power appearance of the gland is remarkable for accentuation of its normal lobular pattern. This is due to increased fibrous tissue in the interlobular septa (Fig. 23.37). A patchy lymphocytic infiltrate is present in the perifollicular stroma (Fig. 23.38); the density varies from case to case. It is sparse in some patients, but conspicuous, with germinal centers in others, related to the autoimmune nature of the underlying process.

An important microscopic finding of Graves disease is the diffuse nature of the pathologic features (Fig. 23.37): *the entire gland is affected*. The thyroid follicles are lined

#### DIFFUSE HYPERPLASIA (GRAVES DISEASE)— PATHOLOGIC FEATURES

##### Gross Findings

- Beefy red, diffusely enlarged thyroid gland
- Average weights range from 50 to 150 g
- Treatment may result in nodules and prominent fibrosis

##### Microscopic Findings

- Highly cellular gland with little colloid
- Hyperplastic, redundant follicular epithelium with papillary infoldings
- Enlarged, columnar follicular cells with eosinophilic granular cytoplasm
- If colloid is present, scalloping is seen (small vacuoles along the apical border of epithelial cells)
- Patchy lymphocytic infiltrate
- After medical treatment, follicles regain colloid; mild hyperplastic changes persist
- Following radioactive iodine, gland may become nodular, with increased fibrosis and cytologic atypia of follicular epithelial cells

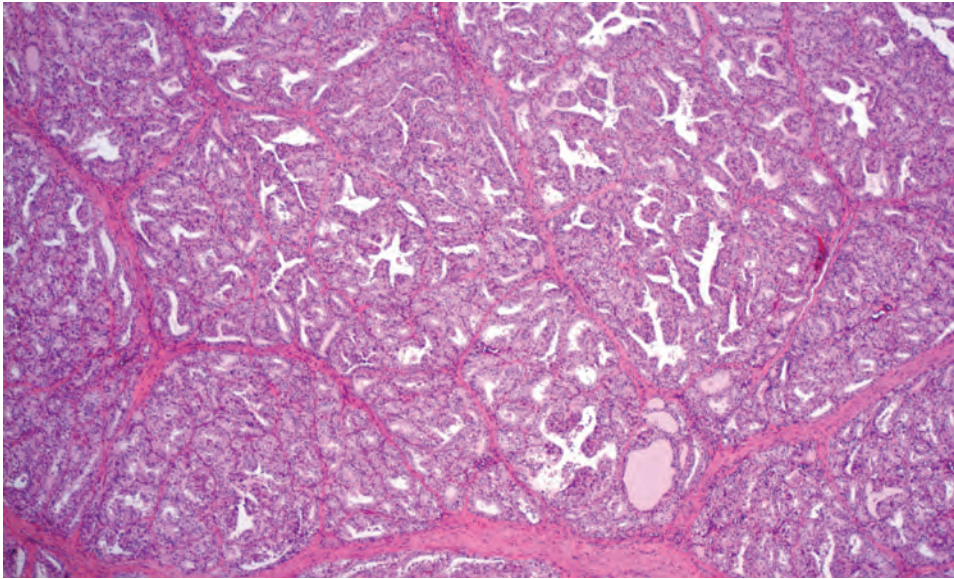
##### Fine Needle Aspiration

- Highly cellular smears; minimal or no colloid
- Sheets of follicular epithelial cells
- Follicular cells have abundant granular cytoplasm (“flame cells”), nuclei with compact chromatin

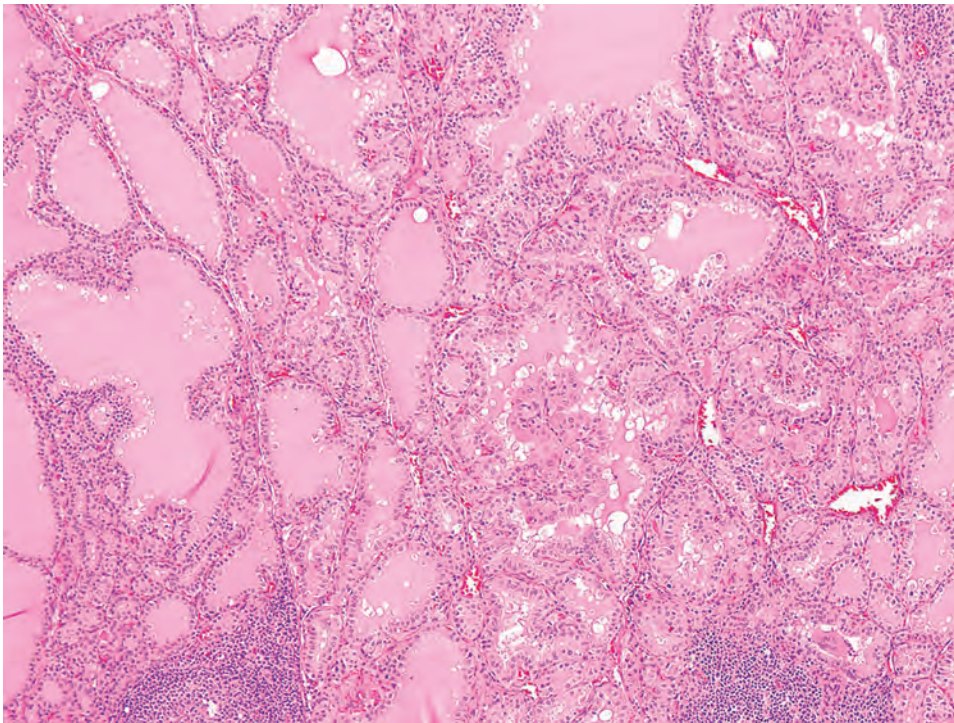
##### Pathologic Differential Diagnosis

- Papillary thyroid carcinoma, toxic nodular goiter (Plummer disease), Hashimoto thyroiditis, follicular carcinoma (posttreatment)

by columnar epithelial cells with basally located, enlarged, round nuclei with relatively dense chromatin; the cytoplasm is abundant, granular, and eosinophilic (Fig. 23.39). The hyperplastic follicular epithelium forms papillary infoldings into the lumen of the follicle (Fig. 23.40). These papillary

**FIGURE 23.37**

Gland with diffuse hyperplasia is intensely cellular, with little colloid. Note the prominence of the somewhat fibrotic interlobular septae, which are usually inapparent in a normal thyroid gland.

**FIGURE 23.38**

Patches of lymphoid cells are noted in this hyperplastic gland (*bottom*). Because Graves is an autoimmune disorder, inflammation is not uncommon but is usually much less than that seen in Hashimoto thyroiditis.

infoldings must not be mistaken for evidence of PTC (Figs. 23.39 and 23.40). Colloid is reduced, often with vacuoles along the apical aspect of the follicular cells, giving the colloid a scalloped appearance (Fig. 23.41).

In cases of *treated* Graves disease, the histologic appearance depends on the type and duration of treatment. Potassium iodide causes involution, with follicular cells reverting to their normal cuboidal or flattened appearance, alternating with areas retaining some of the features of hyperplasia (Fig. 23.42). RAI therapy may produce a nodular gland, with nodules that are often quite cellular and may exhibit striking nuclear atypia (Fig. 23.42). The

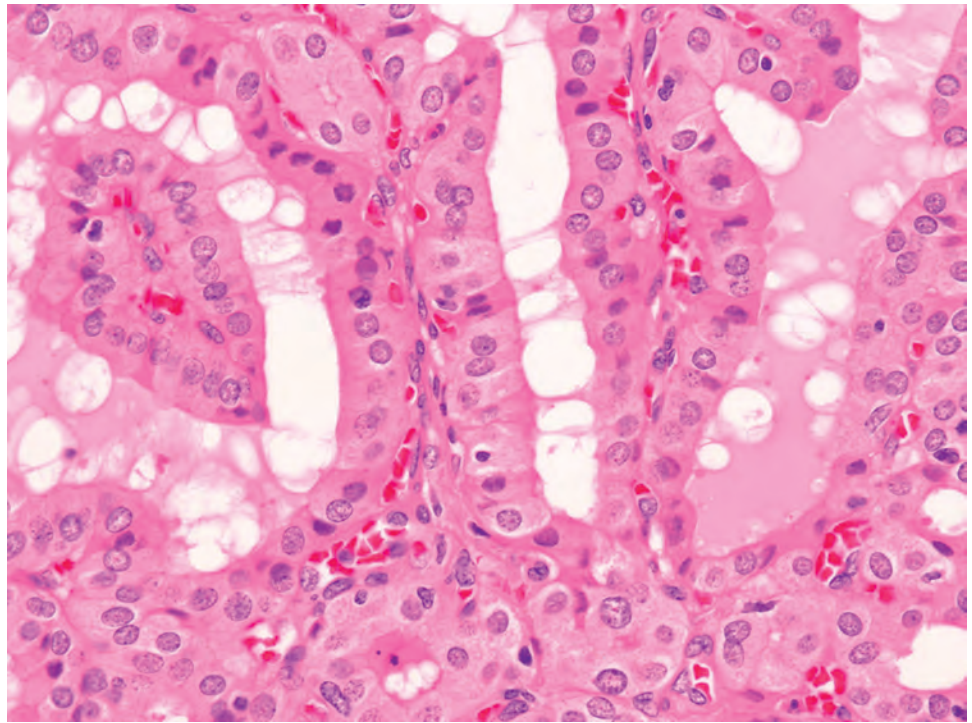
periphery of such nodules should be scrutinized for evidence of capsular or vascular invasion that would identify them as follicular carcinomas. Fibrosis and areas of follicular atrophy are frequently present.

### ANCILLARY STUDIES

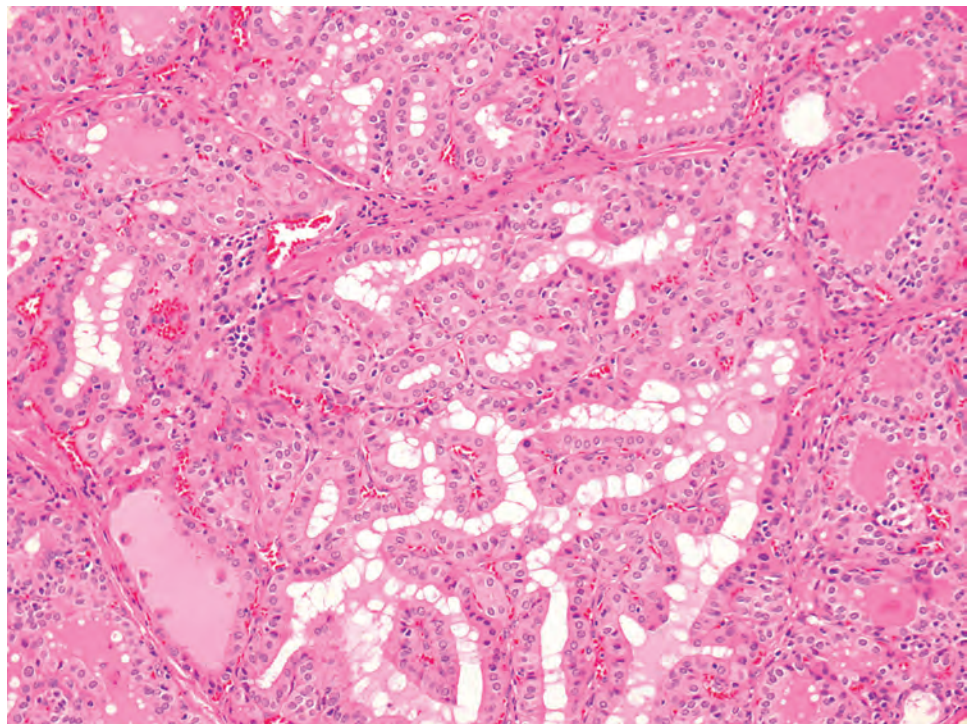
#### FINE NEEDLE ASPIRATION

Cytologic examination of diffuse hyperplasia is treacherous and seldom attempted in patients with active clinical



**FIGURE 23.39**

Follicular epithelial cells are hyperplastic and columnar in shape with abundant granular, eosinophilic cytoplasm. Nuclei are basally located, round, and enlarged with relatively dense chromatin.

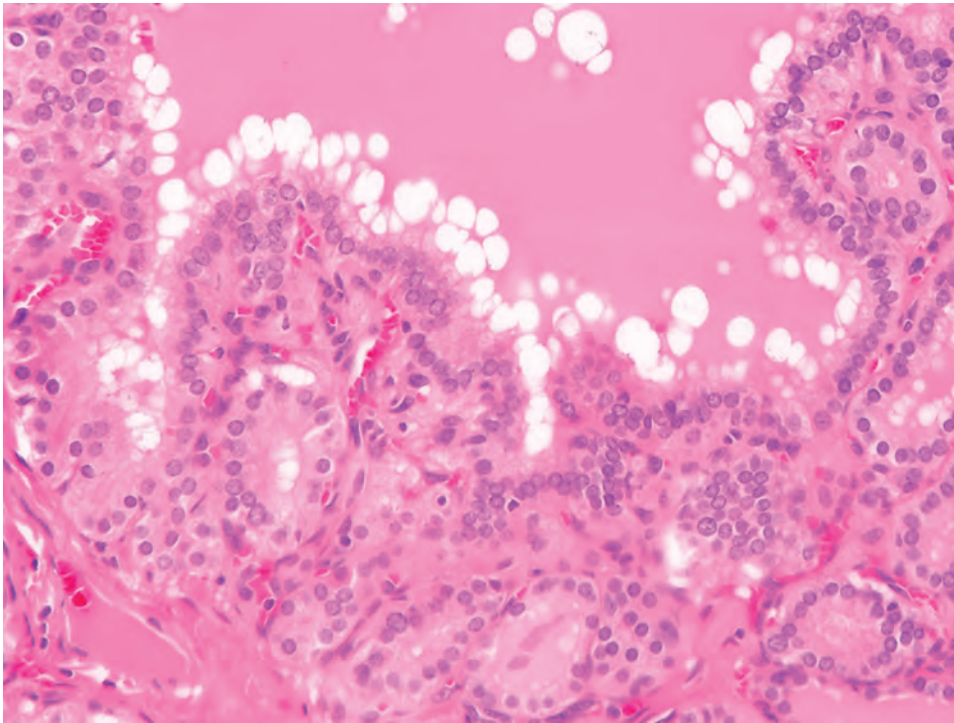
**FIGURE 23.40**

In diffuse hyperplasia, papillary infoldings are present in many of the follicles and the amount of colloid in the follicles is reduced.

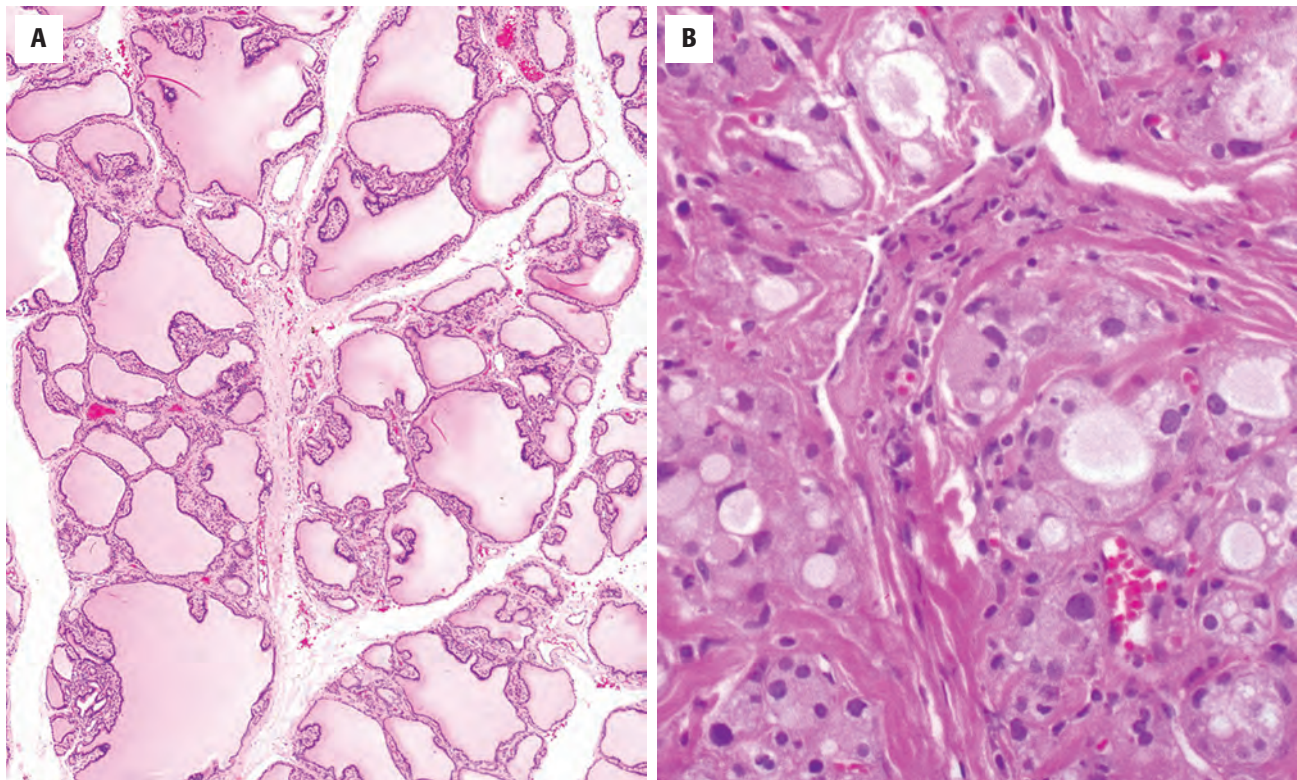
disease. However, FNA may be requested in two settings: (1) a patient with a nodule, in order to exclude malignancy, and (2) a patient with treated Graves disease who has developed a nodule, or nodules, months to years after treatment. In the patient with active disease, the aspirate is typically extremely cellular, consisting of columnar cells with round nuclei and dense chromatin. The cytoplasm

is usually intensely granular (“flame cells”), suggesting oxyphilia on both Romanowsky- and Papanicolaou-stained smears (Fig. 23.43). If the clinical information regarding Graves disease is not provided, a follicular neoplasm is almost invariably favored. Because of the degree of cellularity inherent in this setting, FNA is useful in excluding only PTC and not a follicular neoplasm.



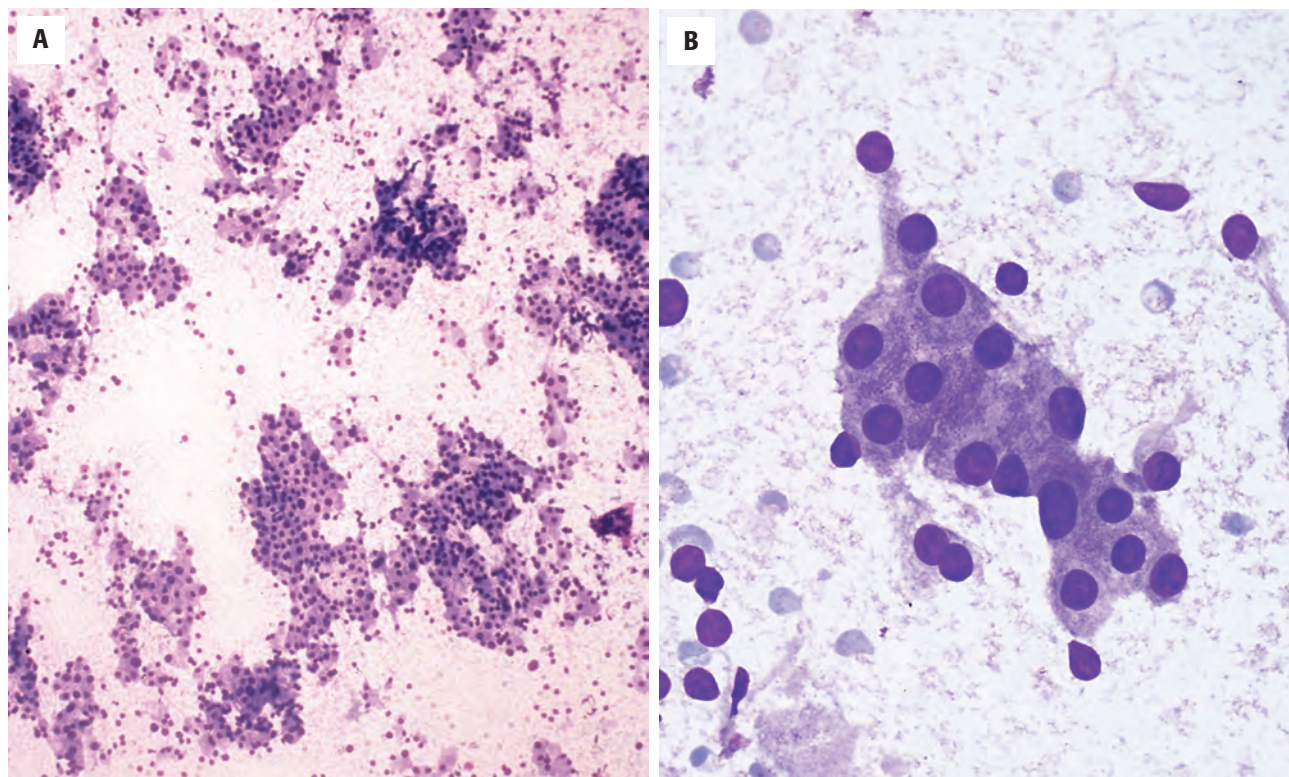
**FIGURE 23.41**

Reduction of colloid in diffuse hyperplasia often causes the formation of vacuoles along the periphery of the follicles, giving the colloid a ruffled or scalloped edge. This is referred to as “scallop” of the colloid.

**FIGURE 23.42**

**A**, In previously treated Graves disease, there is significant involution with increased colloid but still showing focal hyperplastic changes including papillary infoldings throughout the gland. **B**, The gland still demonstrates some degree of hyperplastic change, with nuclear atypia prominent in this example of radiation treatment effect.



**FIGURE 23.43**

**A**, Fine needle aspiration yields a very cellular sample, with minimal colloid in a patient with active Graves disease and a somewhat nodular gland (air-dried, Diff-Quik stain). **B**, Epithelial cells have abundant granular (oxyphilic) cytoplasm (air-dried, Diff-Quik stain).

The patient with Graves disease treated remotely with radioactive iodine or medical therapy who presents with a nodular gland is similarly problematic. Cellular adenomatoid nodules are common in these patients; they cannot be distinguished cytologically from follicular neoplasms. The presence of nuclear atypia, which may be bizarre in some instances, should not prompt a diagnosis of malignancy. FNA is useful, again, in excluding PTC in this setting.

### DIFFERENTIAL DIAGNOSIS

Sometimes Graves disease is mistaken for *PTC*. Findings that may suggest the diagnosis include papillary infoldings of the hyperplastic follicular epithelium, sometimes with small fibrovascular cores, and the rare occurrence of true psammoma bodies in Graves disease. Much more commonly, dystrophic calcifications and inspissated colloid aggregates should be distinguished from psammoma bodies. The small, round, basally oriented nuclei with preserved nuclear polarity and dense chromatin pattern seen in Graves disease are quite different from the nuclei of *PTC*, which are enlarged and overlapping, with irregular contours and fine, evenly distributed “powdery” chromatin (Fig. 23.39).

Other causes of hyperthyroidism may be clinically confused with Graves disease, but they are usually readily distinguished by gross and histologic examination. *Hashimoto thyroiditis* may present with thyrotoxicosis. It is distinguished from Graves disease by the density of the lymphoid infiltrate (often with germinal centers), striking epithelial oxyphilia, and areas of follicular atrophy. *Toxic nodular goiters* (Plummer disease) contain multiple nodules, some of which display hyperplastic changes similar to the diffuse changes that are characteristic of Graves disease. In treated Graves disease, cellular nodules may be difficult to separate from follicular neoplasms. Capsular and/or vascular invasion is required to diagnose a *follicular carcinoma*.

### PROGNOSIS AND THERAPY

The overall prognosis is excellent. Thyroid storm is a life-threatening exacerbation of thyrotoxicosis with severe central nervous system and cardiac manifestations; it requires rapid treatment, usually with antithyroid drugs for initial control. Incidental *PTCs* may be identified.

The three chief treatment options for Graves disease are antithyroid drugs, RAI, and surgery. Medical therapy includes antithyroid drug therapy (methimazole and

propylthiouracil). A failure rate of about 50 % forces these patients to consider RAI or surgery. RAI therapy is the most popular treatment modality among endocrinologists in North America. It is very effective in controlling Graves disease, but at the cost of permanent hypothyroidism in over 80 % of patients, requiring lifelong medical replacement therapy. Surgery is preferred in patients with a suspicious or malignant nodule, in those with severe ophthalmopathy, and in children. It is also indicated for those who are intolerant of medical therapy and for whom RAI is not desired or is contraindicated. Beta-blockers are also often part of the initial treatment until thyroid hormone levels can be normalized.

## ■ NODULAR HYPERPLASIA (ADENOMATOID NODULES, MULTINODULAR GOITER)

The multinodular goiter represents diffuse enlargement of the thyroid with varying degrees of nodularity. The histologic descriptor is *nodular hyperplasia* and individual nodules are often referred to as *adenomatoid* nodules. Most patients are euthyroid (“nontoxic goiter”), but a minority may have or subsequently develop hyperthyroidism (clinically referred to as *toxic multinodular goiter* or Plummer disease) due to a hyperfunctioning nodule or nodules. Nodular hyperplasia may be sporadic or endemic (the latter attributable to iodine deficiency). In either case, the histopathologic features are similar. Nodular hyperplasia is very common and therefore may coexist with other thyroid diseases, both benign (Graves disease, Hashimoto thyroiditis) and malignant.

A variety of factors are involved in the development of multinodular goiters; most are associated with some impairment of thyroid hormone production. The response is increased secretion of TSH, which stimulates proliferation of the follicular epithelium and increased thyroglobulin production in a compensatory process, with increased thyroid mass and hormone-producing capacity. In iodine-deficient areas of the world, multinodular goiters at one time affected over half of adolescent girls; this was essentially reversed by iodine supplementation. Excess iodine intake, including iodine-containing medications or other goitrogens, can also induce multinodular goiter by interfering with efficient organification of iodine in the production of thyroid hormone. A genetic component may also play a role in the development of multinodular goiter.

### CLINICAL FEATURES

Nodular hyperplasia is found in ~ 10 % of autopsies (up to 50 % if microscopic nodules are included), but clinically detectable nodules are found in less than 5 % of individuals. Nodules are more common in women than in men

### NODULAR HYPERPLASIA—DISEASE FACT SHEET

#### Definition

- Diffuse enlargement of the thyroid with varying degrees of nodularity, usually associated with some impairment of thyroid hormone production and increased thyroid-stimulating hormone secretion

#### Incidence and Location

- Clinically detectable nodules found in < 5% of the general population
- Highest incidence in areas with iodine-deficient diets (endemic); may also occur with excess iodine intake

#### Sex and Age Distribution

- Females > > > males (8:1)
- Wide age range, although patients are usually adults

#### Clinical Features

- One or more thyroid nodules usually discovered by patient or health care provider
- Most patients are euthyroid but some may have hyperthyroidism (“toxic multinodular goiter”)
- A dominant nodule is difficult to distinguish from a thyroid neoplasm clinically
- Tracheal compression or dysphagia may develop with large nodules

#### Prognosis and Treatment

- Treatment is usually initiated for cosmetic or comfort reasons
- Thyroxine therapy is often used to suppress nodules
- Surgery is typically chosen for cosmetic reasons or for a dominant nodule that may be suspicious for neoplasm
- RAI ablation for poor surgical candidates or toxic nodules
- Hypothyroidism may develop, especially after surgical or RAI therapy

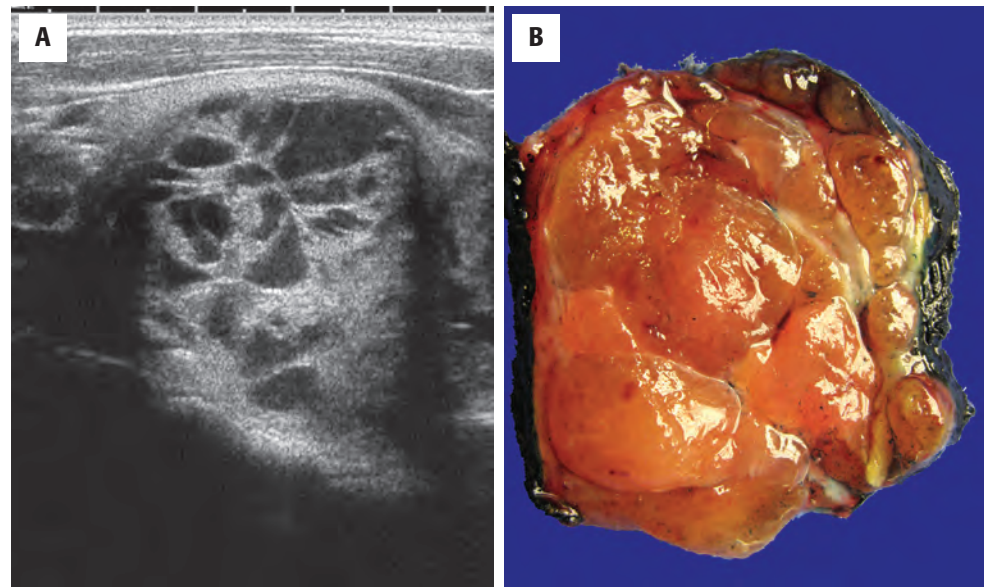
RAI, Radioactive iodine.

(8:1); they occur over a very wide age range but tend to come to attention in adulthood. Nodules often become noticeable during pregnancy. The nodules are usually multiple, but one may be dominant and suggest a solitary nodule. Nodules that attain a large size may produce symptoms due to compression of adjacent structures (dysphagia, hoarseness, stridor) or cause cosmetic disfigurement.

### RADIOGRAPHIC FEATURES

Ultrasound (the preferred imaging modality) often demonstrates the multiplicity and heterogeneous appearance of nodules (Fig. 23.44). However, the nodules can be difficult to distinguish from benign and malignant neoplasms on imaging. As a result, there are published guidelines recommending which nodules should be biopsied to exclude malignancy.



**FIGURE 23.44**

**A**, Ultrasound shows multiple nodules, with fibrous bands dissecting between them in this patient with nodular hyperplasia. **B**, Many gelatinous fleshy nodules bulge from the cut surface macroscopically.

### LABORATORY STUDIES

Thyroid function studies may be performed periodically to exclude the development of toxic multinodular goiter.

### PATHOLOGIC FEATURES

#### GROSS FINDINGS

The thyroid is diffusely enlarged and nodular (Figs. 23.44 to 23.46). The weight of the gland is quite variable, up to several hundred grams or more. Sectioning may reveal nodules that are similar in texture, with a fleshy gelatinous surface; colloid may exude from the cut surface on scraping with a scalpel blade (Fig. 23.45), while other nodules are characterized by their heterogeneity (Fig. 23.45). Nodules may demonstrate hemorrhage in the form of central hematomas or areas of organization, with brown patches representing hemosiderin deposits. Cystic degeneration is common, particularly in larger nodules or following FNA, and may go on to develop into thick fibrous pseudocapsules. Fibrous scars may be seen in some nodules; degenerated nodules are often calcified and may require decalcification prior to histologic processing. Necrosis, if present, is usually central and confluent due to vascular insufficiency. Sections from the periphery of nodules are more useful than those from the center of the lesion (Fig. 23.46). It is always prudent to remember that a multinodular goiter can easily harbor a thyroid neoplasm among its nodules. Therefore tan-white nodules or those with “capsules” should be generously sampled, concentrating on the periphery or “capsule of the lesion” to exclude carcinoma.

### NODULAR HYPERPLASIA—PATHOLOGIC FEATURES

#### Gross Findings

- Enlarged gland with multiple nodules of variable size
- May be gelatinous, with colloid exuding from cut surface
- Degenerative changes include hemorrhage, central scars, fibrous pseudocapsules, cystic change, and calcification
- Histologic sections taken from the periphery to exclude malignancy

#### Microscopic Findings

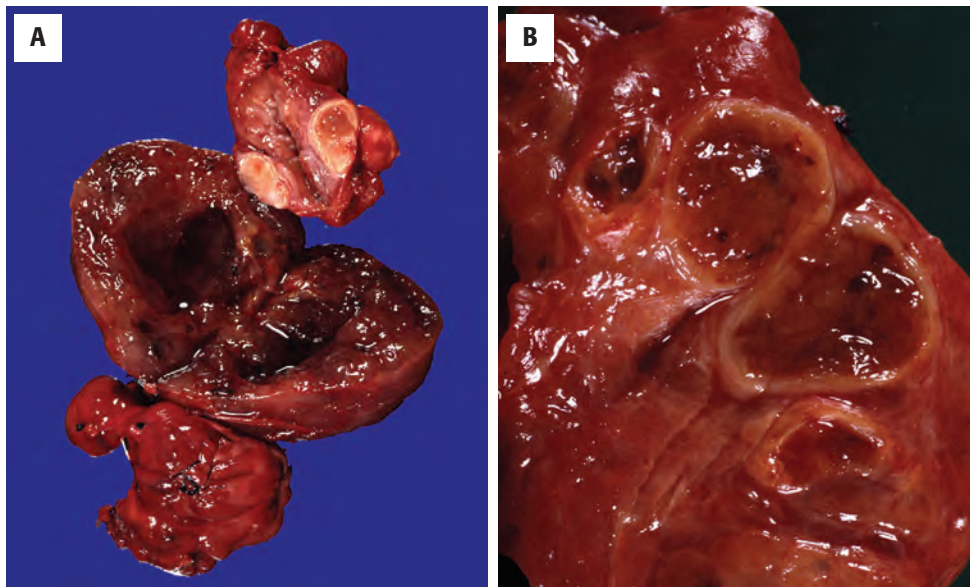
- Nodules have a pushing border that merges with the surrounding follicles or may have a pseudocapsule
- Hemorrhage is common, with hemosiderin-laden macrophages and cystic change
- Most nodules contain large follicles distended with colloid; the lining epithelium is low, cuboidal, and inconspicuous
- Cellular nodules (solid, microfollicular) have little colloid
- Papillary fronds may be dominant, but with round, basally oriented nuclei
- Epithelial cells may demonstrate prominent oxyphilia and mild nuclear atypia

#### Fine Needle Aspiration

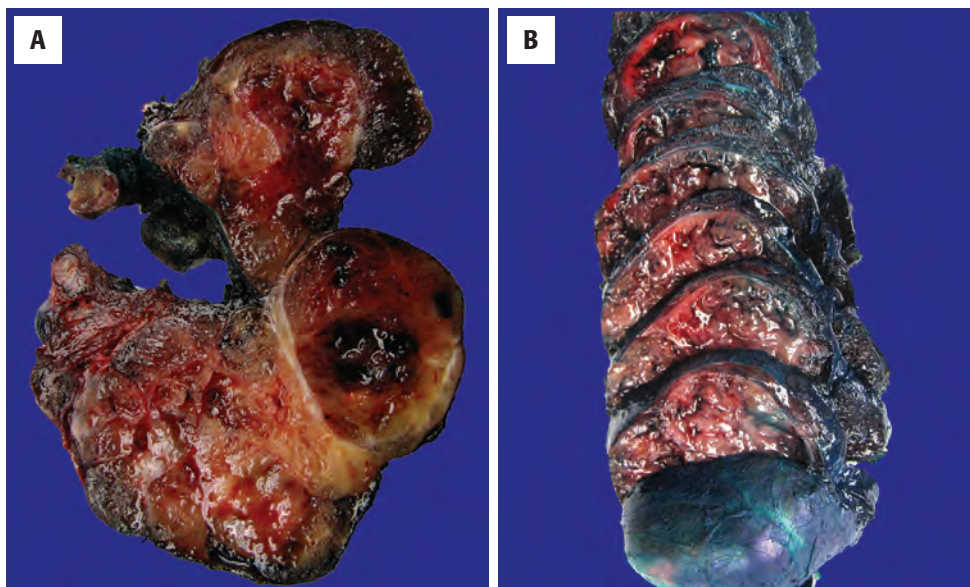
- Usually low cellularity and abundant thin colloid, often with scratches, waves, or cracks
- Sheets of follicular epithelium with small, round, dense nuclei arranged in a “honeycomb pattern”
- Hemosiderin-laden macrophages if degeneration is present
- Cellular nodules have high cellularity and scant colloid, difficult to distinguish from follicular neoplasm

#### Pathologic Differential Diagnosis

- Papillary thyroid carcinoma, follicular neoplasm, hyperfunctioning (“toxic”) nodule versus Graves disease

**FIGURE 23.45**

**A**, This gland illustrates a spectrum of adenomatoid nodules, including one with cystic degeneration and another with fibrosis. Nodules with a “capsule” should be carefully examined histologically to exclude a carcinoma. **B**, Multiple adenomatoid nodules showing heterogeneity.

**FIGURE 23.46**

**A**, Multiple variably sized nodules are seen in this thyroid lobe. Note the “pseudocapsule” and hemorrhage. Colloid is honey-colored and shiny. **B**, Serial sections through the gland demonstrate multiple nodules. Sections submitted from the periphery rather than from the center of the nodule are more helpful in yielding a diagnosis.

### MICROSCOPIC FINDINGS

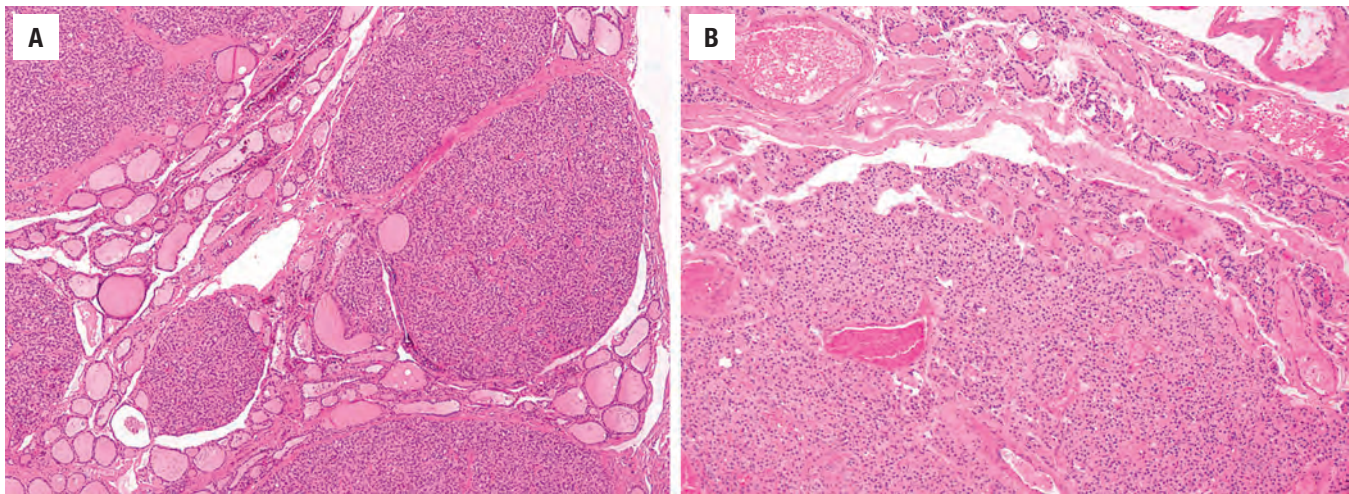
The histologic features are as heterogeneous as the gross findings. Nodules are circumscribed and generally unencapsulated but may have a partial capsule (Fig. 23.47). Most nodules are composed of variably sized follicles including some that are enlarged and distended with colloid, lined by low cuboidal follicular epithelial cells (Fig. 23.48). Cellular-appearing solid areas with minimal colloid and microfollicles may be present and in some cases predominate (Fig. 23.47). Some nodules, usually those with cystic change, develop papillary

structures that can be mistaken for PTC (Figs. 23.49 and 23.50).

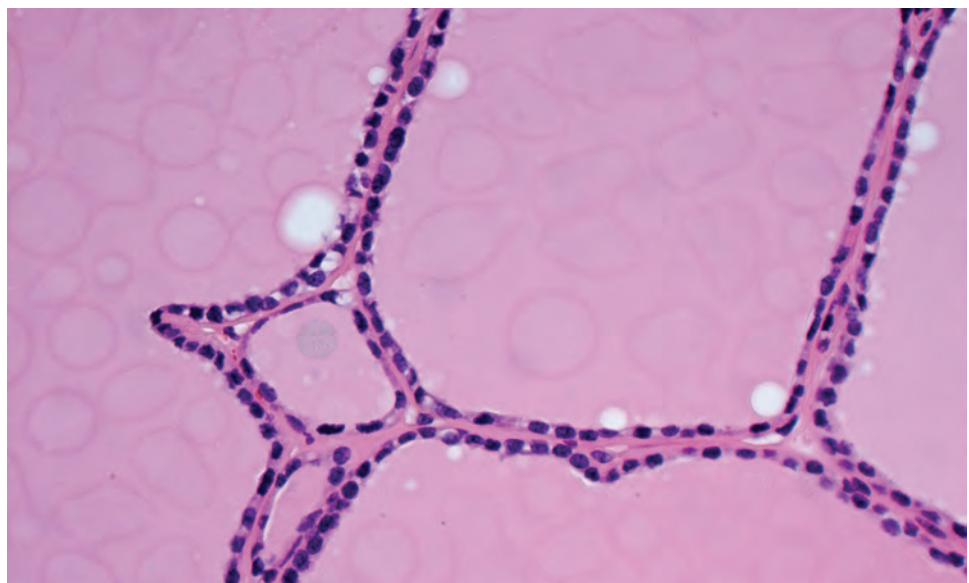
The cytologic appearance varies, but the nuclei are typically round and hyperchromatic. Oxyphilic cells (common) (Fig. 23.50) and clear cells (occasional) may be present within the nodules (Fig. 23.50). It is important to realize that oxyphilic cells may exhibit mild nuclear atypia, including nuclear enlargement, vesicular chromatin, and irregular nuclear contours (Fig. 23.51). These changes should not be overdiagnosed as PTC.

Hemorrhage and cystic degeneration often go hand in hand (Fig. 23.52). Hemosiderin may be seen deposited



**FIGURE 23.47**

**A**, This lobe contains multiple cellular adenomatoid nodules. **B**, The periphery of the nodule is demarcated from the surrounding thyroid but there is no capsule in this case. Partial encapsulation may be present in some cases.

**FIGURE 23.48**

Classic adenomatoid nodule is composed of large follicles distended with colloid and lined by flattened follicular epithelium.

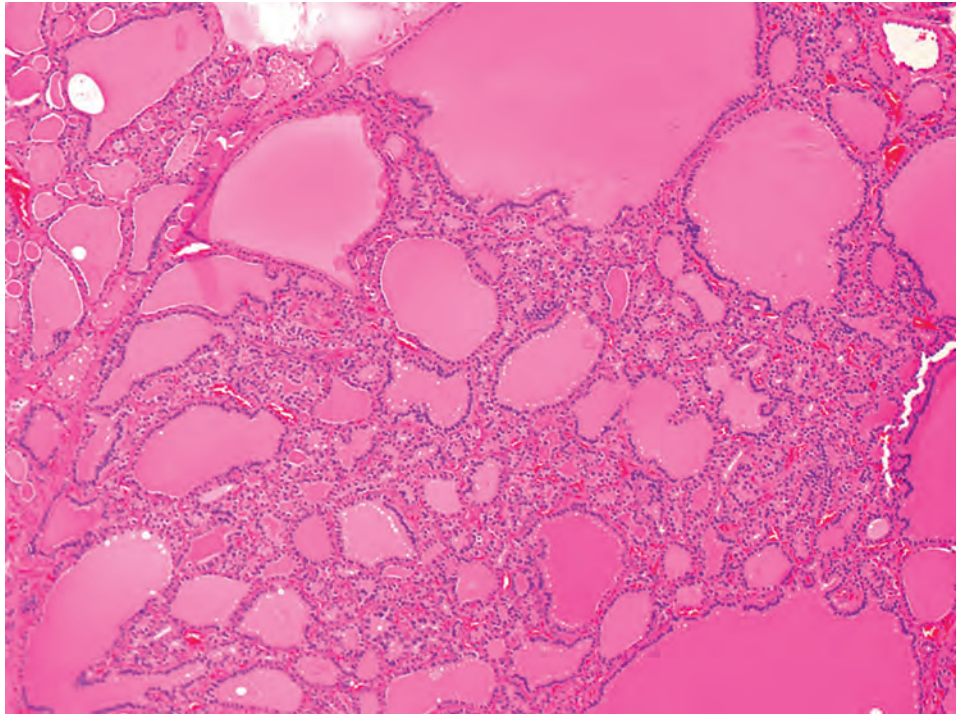
in granulation tissue or fibrous scar tissue in areas of degeneration. Hemosiderin-laden macrophages are often seen in the cystic areas and in adjacent parenchyma. In areas of marked hemorrhage, small granules of hemosiderin may be present in the cytoplasm of follicular cells, giving them a red-brown appearance (Fig. 23.53). A chronic inflammatory infiltrate may be present. A variety of metaplastic changes may be seen, including fatty, squamous, cartilaginous, and osseous metaplasia.

In addition to the large macroscopic nodules, one usually finds small areas of incipient nodularity scattered through the grossly unremarkable portions of the thyroid (Fig. 23.54). They are seen as nodular groupings of

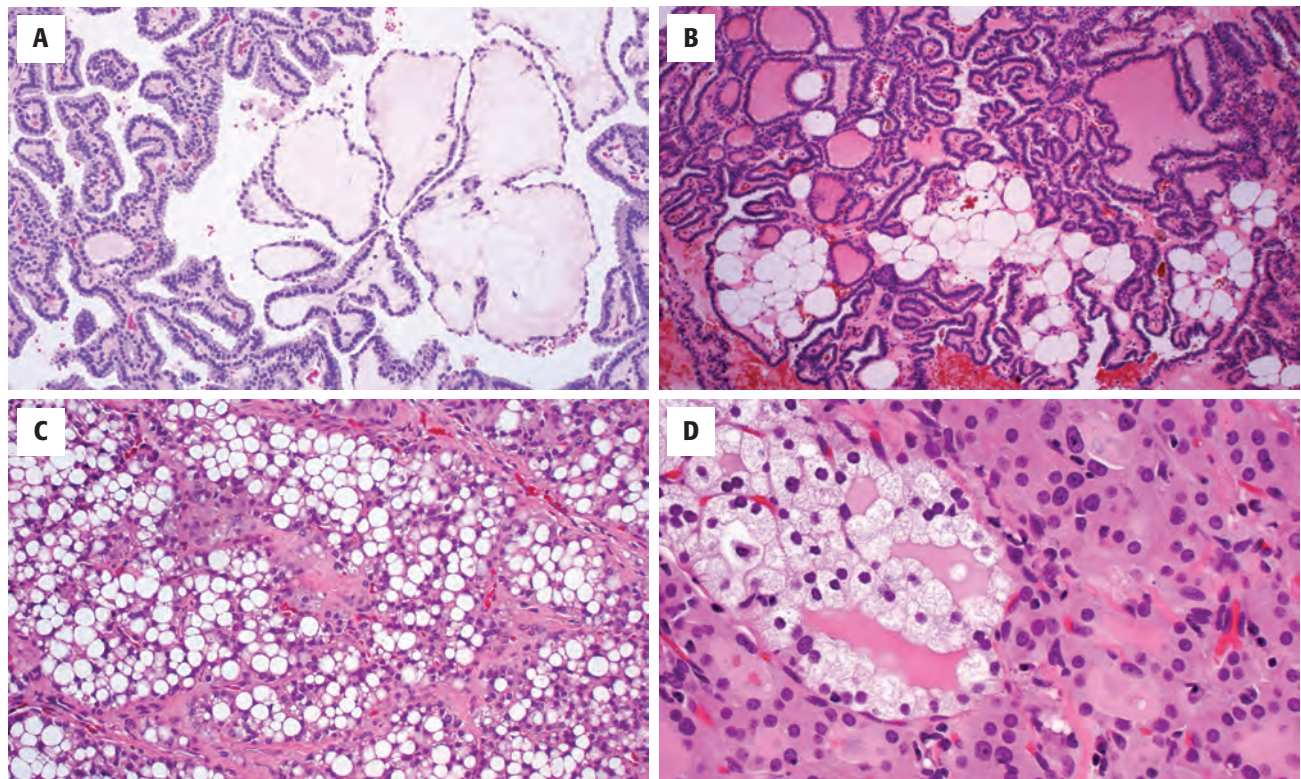
variably sized follicles, which stand out among the normal background follicles.

A phenomenon that occasionally causes confusion, particularly during frozen section examination, is the parasitic nodule (Fig. 23.55). This represents a nodule of thyroid tissue which has become separated from the thyroid gland, often demonstrating either nodular hyperplasia or nodular chronic lymphocytic thyroiditis. The attachment to the thyroid is by an inconspicuous cord of fibrous tissue, often overlooked intraoperatively. The histologic appearance is usually that of an adenomatoid nodule; however, in cases associated with a dense lymphocytic infiltrate, such a nodule may resemble lymph



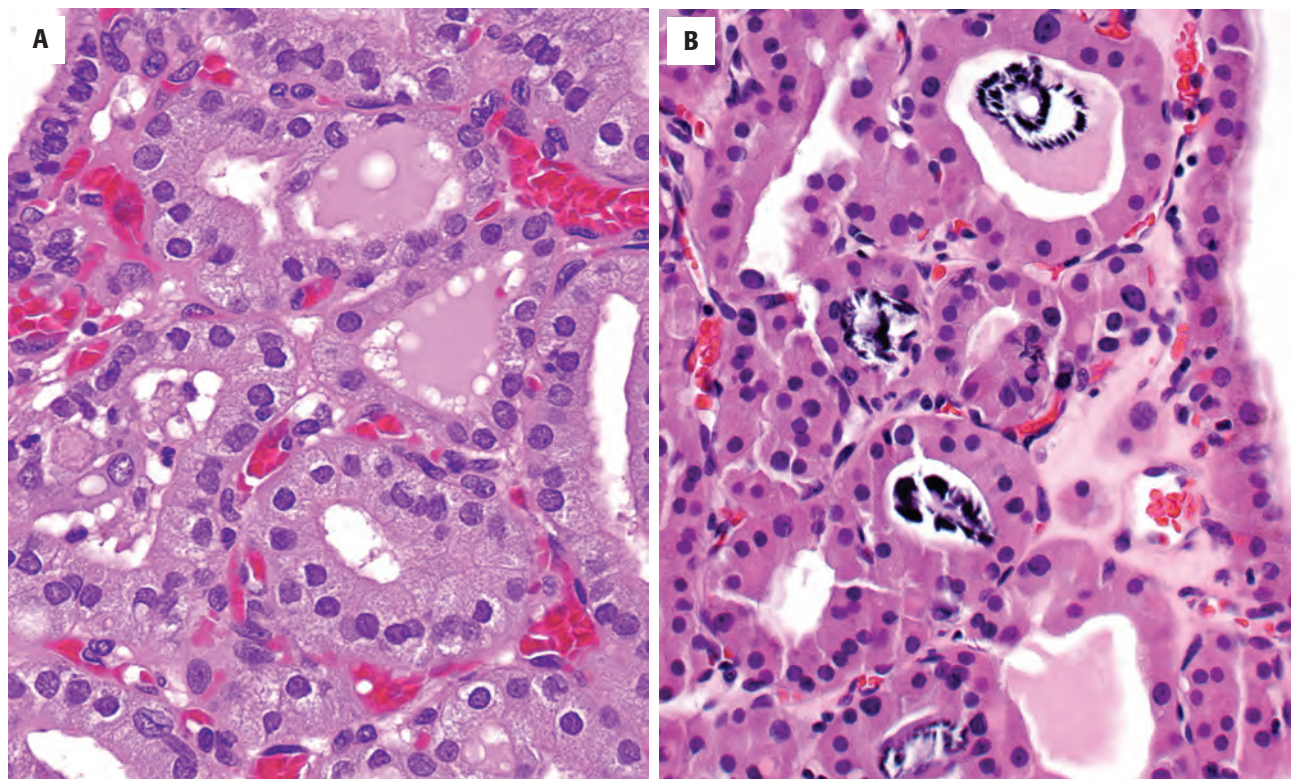
**FIGURE 23.49**

Some nodules may have cystic change with papillary infoldings. In this example the papillae are broad-based.

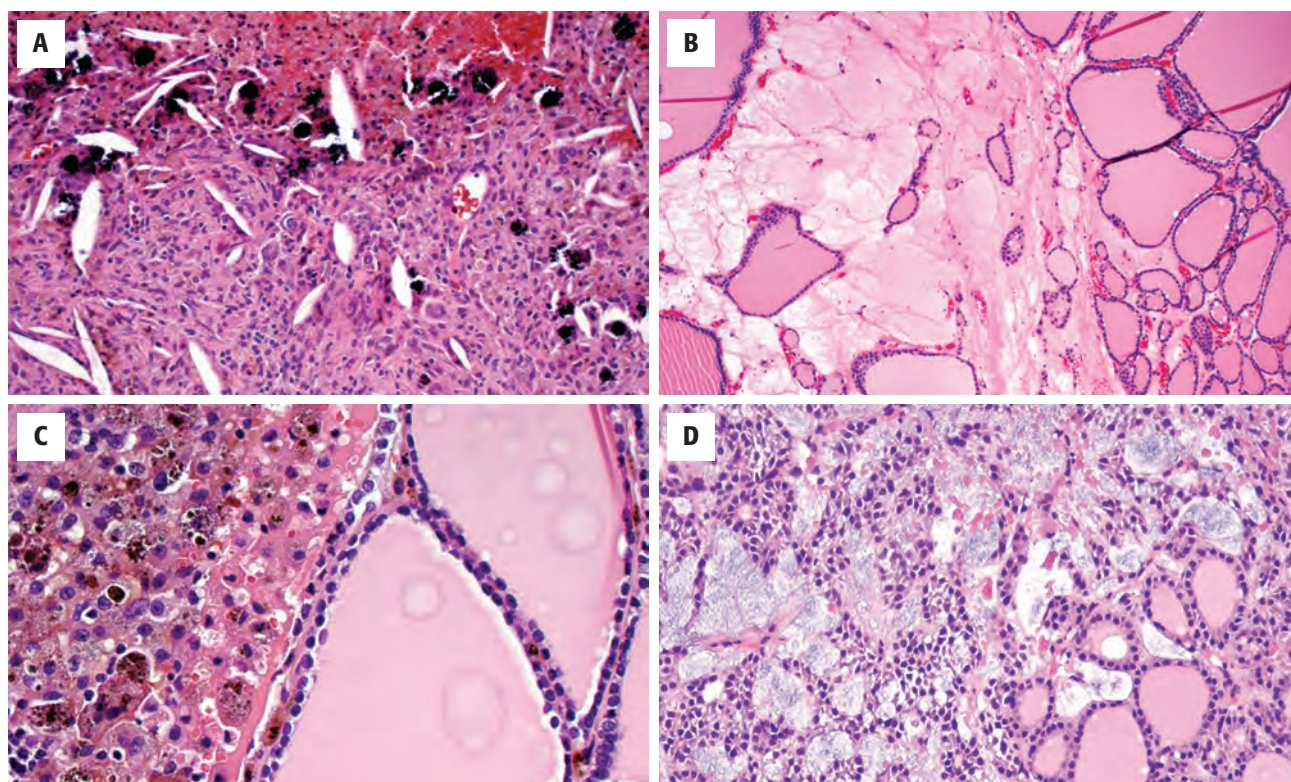
**FIGURE 23.50**

A variety of histologic changes may be seen in adenomatoid nodules. Examples are shown here. **A**, Papillary structures in adenomatoid nodules may be quite prominent and edematous/ bulbous or fine and arborizing. **B**, Papillary structures with fat and colloid. **C**, Clear cell change within the cytoplasm of the follicular epithelium. **D**, Oncocytic cells, focally showing early clear cell change.



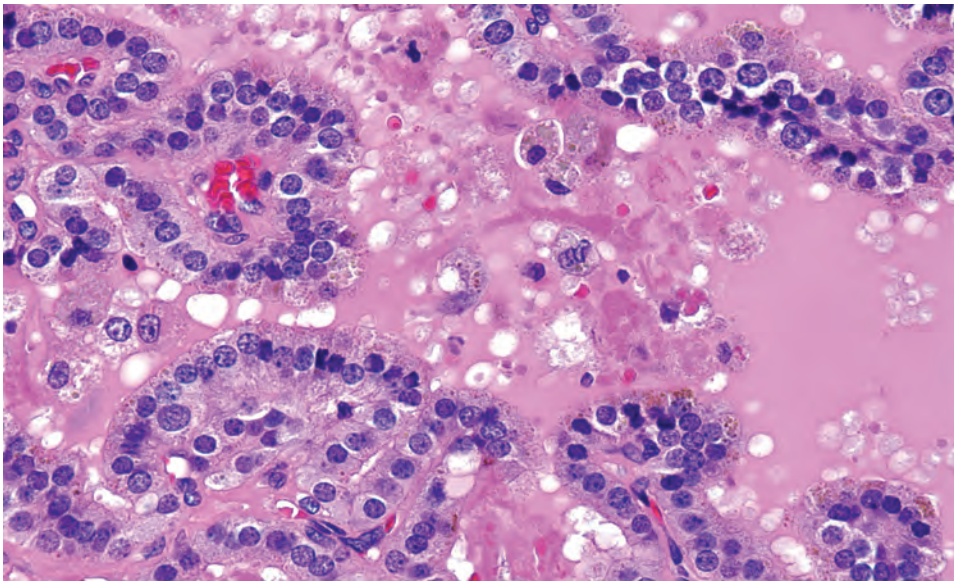
**FIGURE 23.51**

Oxyphilic/oncocyctic change is common in adenomatoid nodules. Oncocytic cytoplasm is well developed in these cases. **A**, Granular cytoplasm surrounds nuclei that are focally irregular. The nuclear chromatin is coarse and heavy. **B**, Note the calcifications within the colloid. These calcifications are not psammoma bodies.

**FIGURE 23.52**

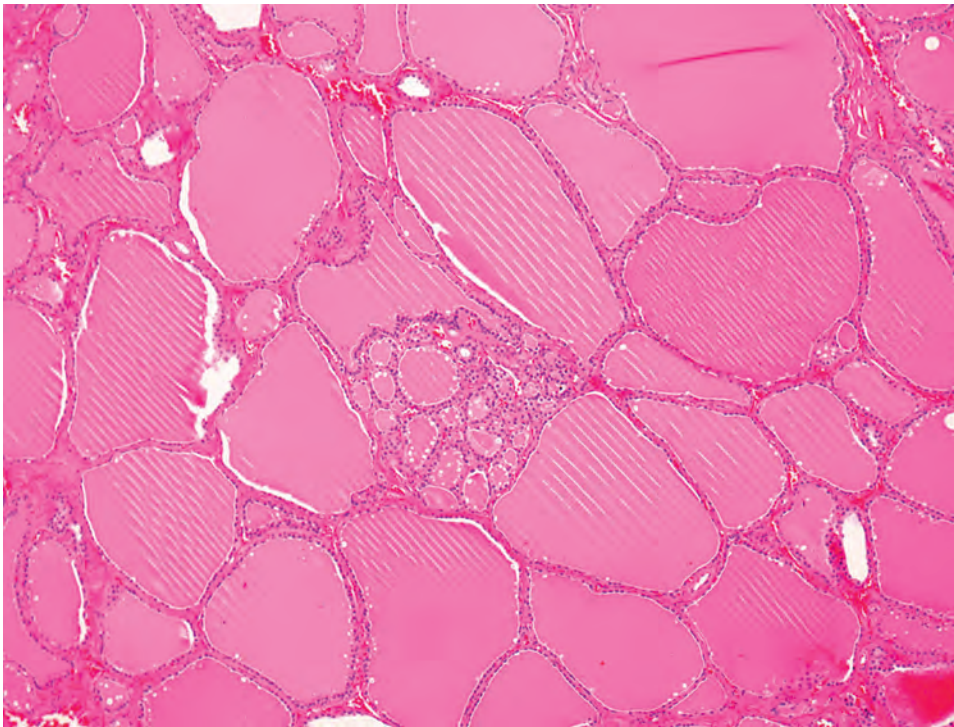
**A**, Hemorrhage, hemosiderin-laden macrophages, cholesterol clefts, and a reactive fibrosis in a degenerated adenomatoid nodule. **B**, Edematous change is frequent in nodules. **C**, Hemosiderin-laden macrophages nearly completely replace the colloid in part of this nodule. **D**, Myxoid degeneration can sometimes be seen in adenomatoid nodules.





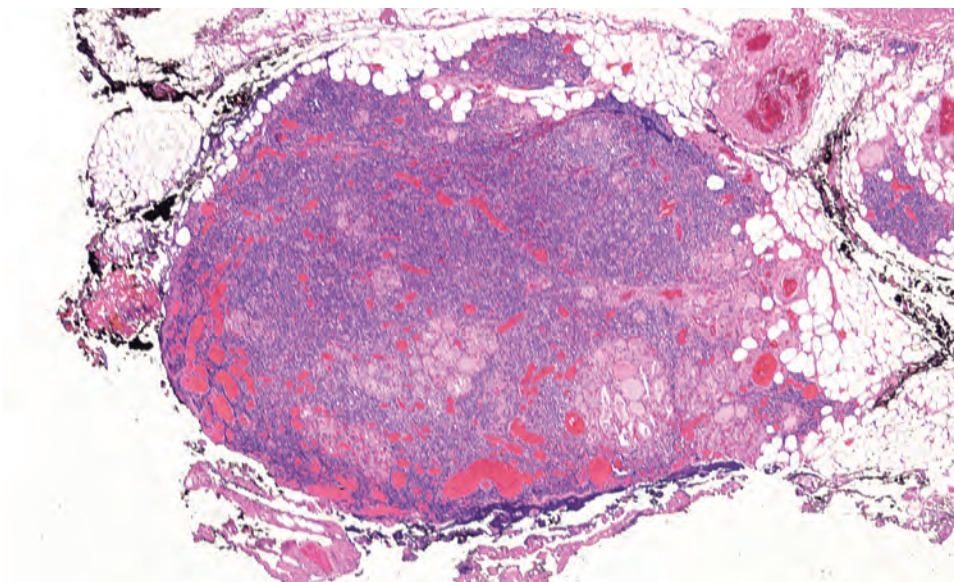
**FIGURE 23.53**

Hemosiderin is noted within the histiocytes but is also present within the cytoplasm of the follicular epithelial cells. This is a common occurrence in adenomatoid nodules but very rare in papillary carcinoma.



**FIGURE 23.54**

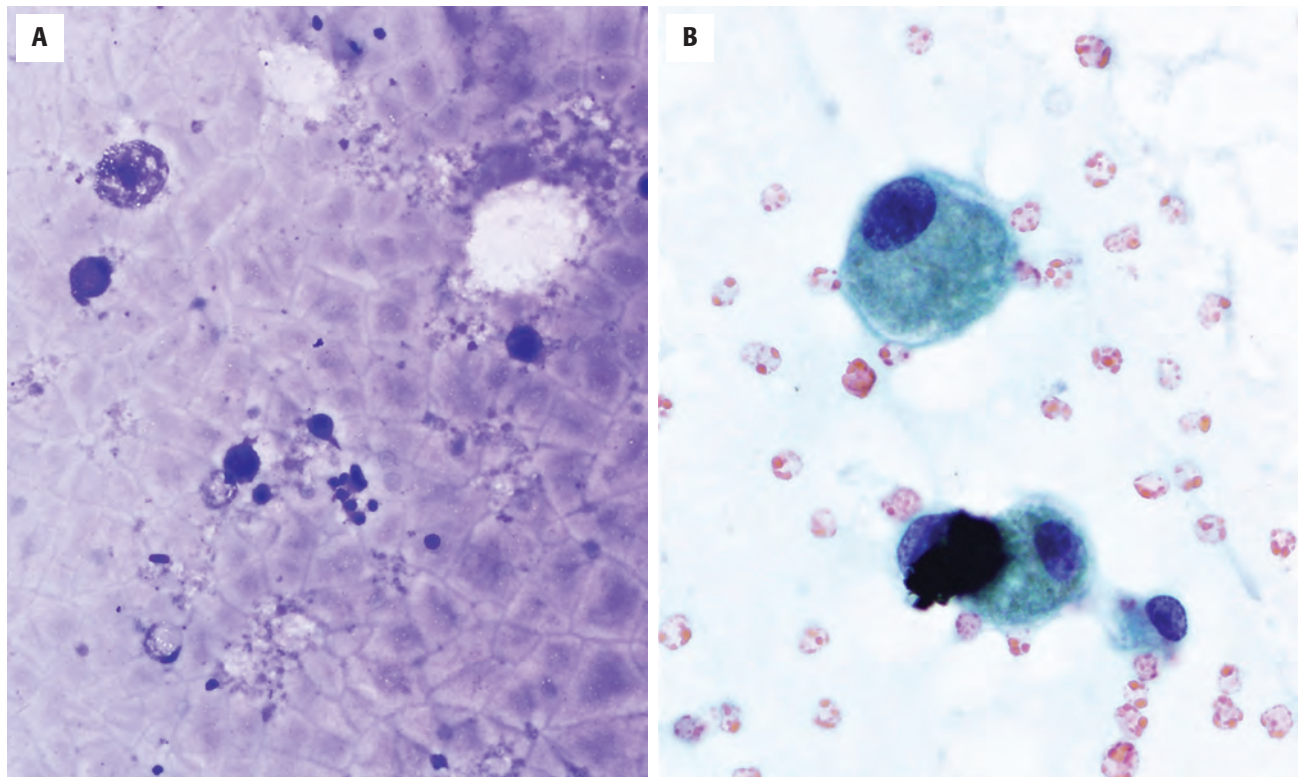
Incipient nodularity may be seen scattered throughout grossly unremarkable portions of the thyroid gland.



**FIGURE 23.55**

This patient had a multinodular goiter with a background of lymphocytic thyroiditis. Small fragments of inflamed thyroid epithelium, detached from the gland, may resemble lymph nodes intraoperatively and histologically.



**FIGURE 23.56**

**A**, Colloid is abundant in fine needle aspiration samples of typical adenomatoid nodules. The colloid often has a wavy or cracked appearance (air-dried, Diff-Quik stain). **B**, Cystic degeneration or hemorrhage results in the presence of hemosiderin-laden macrophages in many cases (alcohol-fixed, Papanicolaou stain).

node, especially when submitted as such during intra-operative assessment. Because parasitic nodules lack the structures of a lymph node (subcapsular sinus, sinusoids, etc.), the misdiagnosis of metastatic PTC in a lymph node can be averted.

## ANCILLARY STUDIES

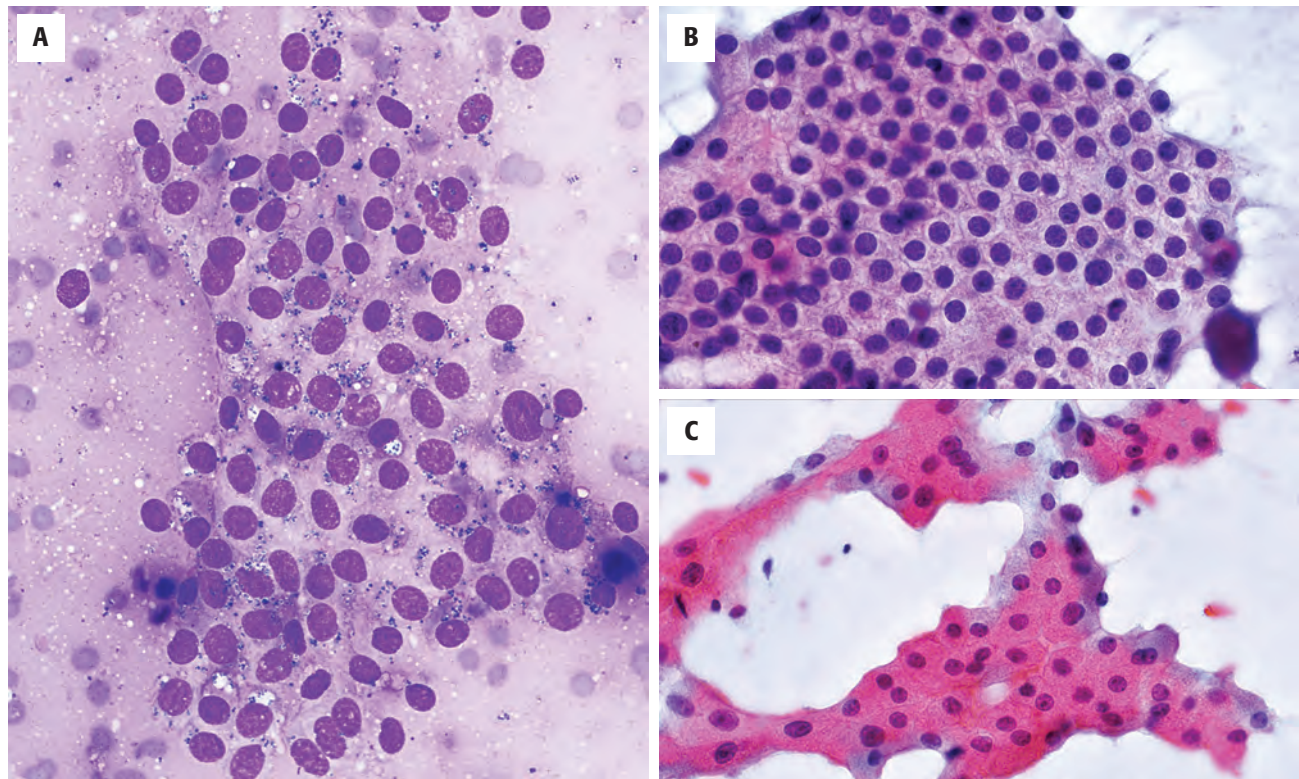
### FINE NEEDLE ASPIRATION

The cytologic features include abundant, usually thin, colloid and relatively low cellularity with hemosiderin-laden macrophages (Fig. 23.56). The follicular epithelial cells from the large follicles ruptured by the aspiration process are usually found as large flat sheets, with evenly spaced round nuclei in a honeycomb pattern. The nuclei of the follicular cells have dense chromatin and are not crowded or overlapping (Fig. 23.57). In lesions with degenerative changes, the follicular cells may be somewhat oxyphilic. Reactive or reparative follicular cells may be present; they are elongated and may demonstrate nuclear enlargement and prominent nucleoli. Occasionally, based on cytologic examination alone, aspirates of cellular nodules that have little colloid are indistinguishable

from those of follicular neoplasms. These are considered to be indeterminate or “suggestive of neoplasm”; surgical removal of the nodule is usually required in such cases.

## DIFFERENTIAL DIAGNOSIS

The chief differential diagnostic problems arise when nodules are cellular or when papillary hyperplasia is present, requiring separation from follicular neoplasms and PTC. Cellular nodules may have a pseudocapsule associated with degenerative changes; prominent cystic degeneration is more often found in adenomatoid nodules than in follicular neoplasms, although FNA may induce such changes in neoplasms. Examination of the nodule’s periphery for capsular or lymphovascular invasion is necessary to exclude a minimally invasive *follicular carcinoma* in such cases. Once invasion is excluded, the distinction between nodular hyperplasia and a follicular adenoma is of no clinical significance and may, in fact, be impossible. A true neoplasm usually has smooth muscle-walled vessels in the fibrous capsule, but this is not always identifiable. Adenomatoid nodules with extensive papillae lack the nuclear features of PTC and

**FIGURE 23.57**

**A.** Follicular epithelium appears as flat sheets, in this case with hemosiderin present within the cytoplasm (air-dried, Diff-Quik stain). **B.** Sheets of follicular epithelium usually have a “honeycomb” appearance due to their polarity and distinct cell borders (alcohol-fixed, Papanicolaou-stained). **C.** This cellular adenomatoid nodule has scant colloid, high cellularity, and oxyphilic change; separation from a neoplasm is often impossible by fine needle aspiration smears alone (alcohol-fixed, Papanicolaou stain).

have an orderly, polarized arrangement of their cells. The differential diagnosis of a parasitic nodule and thyroid carcinoma is described in the preceding text.

Graves disease is also in the differential diagnosis when a nodule is hyperfunctioning (“toxic”). Hyperfunctioning nodules may show prominent papillary infoldings and scalloping similar to that seen in Graves disease. However, in Graves disease these features are present diffusely throughout the thyroid gland, whereas in nodular hyperplasia they are limited to the nodule or nodules.

### PROGNOSIS AND THERAPY

Multinodular goiters are not life-threatening, and treatment is usually for cosmetic or comfort issues or to exclude a neoplasm in radiographically and cytologically indeterminate nodules. There is no increased incidence of thyroid carcinoma. The therapeutic approach to multinodular goiter includes medical therapy (thyroxin administration for suppression of the gland), RAI ablation, and thyroidectomy. RAI ablation is not widely used in the United States for treatment of multinodular goiter

but may be useful in patients who are not surgical candidates or for those with toxic multinodular goiter. Hypothyroidism is a risk in any patient treated surgically for multinodular goiter.

### ■ DYSHORMONOGENETIC GOITER

Dyshormonogenesis is due to a genetic defect in thyroid hormone synthesis leading to insufficient production of thyroid hormone. It has an autosomal recessive inheritance pattern and accounts for 15 % to 20 % of cases of congenital hypothyroidism. A wide variety of mutations have been reported in various genes including those involved in thyroglobulin synthesis, iodine transport (sodium-iodide symporter, pendrin), iodide oxidation, and organification (TPO), coupling of MIT (mono-iodotyrosine) and DIT (di-iodotyrosine), and iodide recycling. TPO mutations are the most common. The resulting effect is hypothyroidism with a lack of negative feedback on pituitary secretion of TSH. Over time, patients develop goiters (dyshormonogenetic goiter) from continuous TSH stimulation of the thyroid gland.



## CLINICAL FEATURES

Dyshormonogenetic goiter is rare, with a prevalence estimated to be 1 in 30,000 to 50,000. It is the second most frequent cause of permanent congenital hypothyroidism after dysgenesis (abnormal thyroid gland development and/or migration). However, only patients with the most severe impairment in thyroid hormone production present clinically in infancy with cretinism. The average age at presentation is 16 years, but patients from neonates to adults may be affected. Approximately two-thirds of patients are known to have hypothyroidism prior to recognition of the goiter, which tends to develop later in life. There is a slight female predominance. A family history of hypothyroidism and/or goiter is elicited in 20% of patients. Pendred syndrome is an association of dyshormonogenetic goiter with familial deaf-mutism due to sensorineural deafness; it is very rare, involving *SLC26A4* at 7q31.

## LABORATORY STUDIES

Laboratory studies show a low to absent T4 and/or T3 and high TSH.

### DYSHORMONOGENETIC GOITER—DISEASE FACT SHEET

#### Definition

- Thyroid hyperplasia secondary to hypothyroidism resulting from a number of inherited genetic defects in thyroid hormone production

#### Incidence

- Rare (estimated 1 in 30,000 to 50,000)
- Family history of hypothyroidism in 20%

#### Sex and Age Distribution

- Females slightly > males
- Mean, 16 years (wide age range)
- Severe impairment presents in infancy; may be associated with cretinism; partial defects in hormone synthesis may present later in life

#### Clinical Features

- Permanent congenital hypothyroidism
- Hypothyroidism recognized prior to goiter in two-thirds
- Diffuse thyroid enlargement, often nodular with time
- Rarely Pendred syndrome (familial deaf-mutism and dyshormonogenetic goiter)

#### Prognosis and Treatment

- No increased risk of thyroid carcinoma
- Lifelong hormone replacement therapy necessary
- Symptomatic goiter treated with total thyroidectomy

## PATHOLOGIC FEATURES

### GROSS FINDINGS

The thyroid gland can be massively enlarged, with weights up to 600 grams; it may also be nodular. The nodules resemble nodular hyperplasia, but colloid does not exude from the cut surfaces and they have a more opaque rather than a translucent appearance (Fig. 23.58).

### MICROSCOPIC FINDINGS

All of the thyroid tissue has an abnormal histologic appearance (Fig. 23.59), different from the relatively normal thyroid seen between adenomatoid nodules of nodular hyperplasia. The nodules of dyshormonogenetic goiter vary in their appearance, probably as a result of the different enzyme defects and the duration of the disease (age of patient) at the time of diagnosis. The most common finding is the presence of hypercellular nodules with solid or microfollicular patterns. Papillary and insular patterns may also be observed. Colloid is usually scant if it is present at all (Fig. 23.60). Fibrosis is often a prominent finding and may be so extensive that it distorts the contours of the nodules, suggesting an invasive pattern, as seen in follicular carcinoma.

### DYSHORMONOGENETIC GOITER—PATHOLOGIC FEATURES

#### Gross Findings

- Thyroid can be massively enlarged, asymmetric, nodular
- Weighs up to 600 grams
- Nodules have a more opaque appearance

#### Microscopic Findings

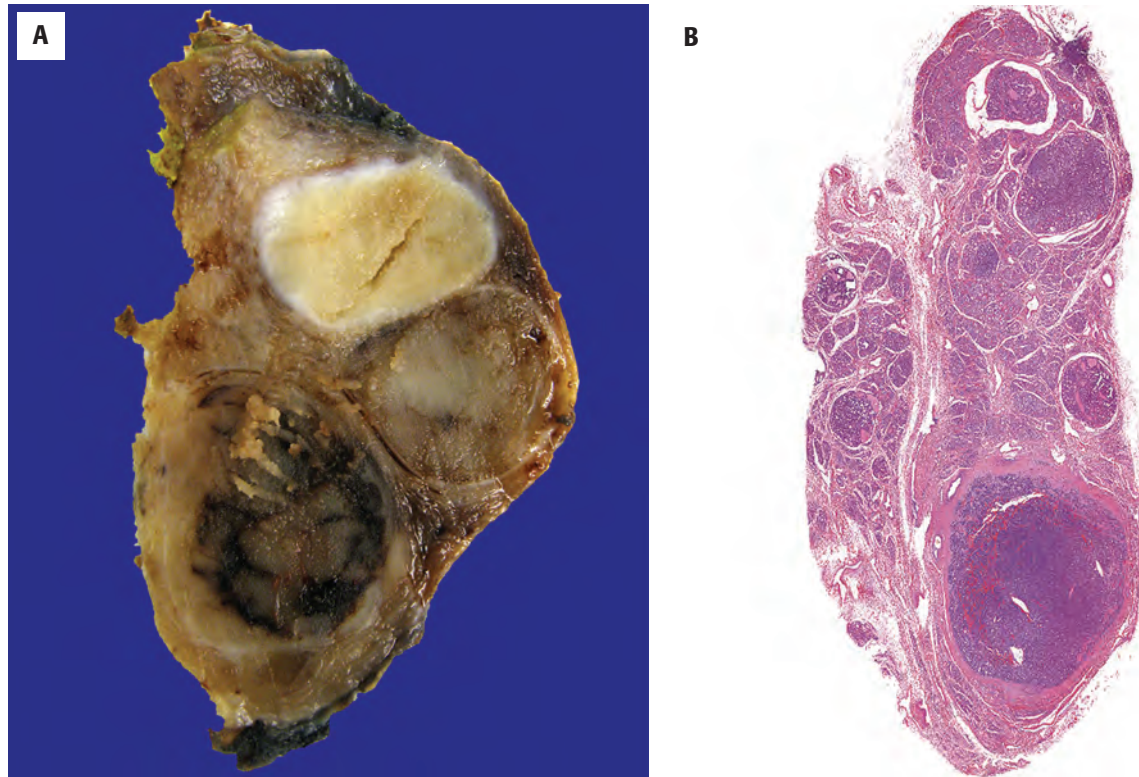
- Most often nodules are hypercellular, with microfollicular or solid patterns and little if any colloid
- Some glands may have a hyperplastic appearance similar to that seen in Graves disease, with empty follicles
- Fibrosis is often prominent and may distort the borders of the nodules
- Cytologic atypia may be striking, especially in parenchyma between nodules

#### Fine Needle Aspiration

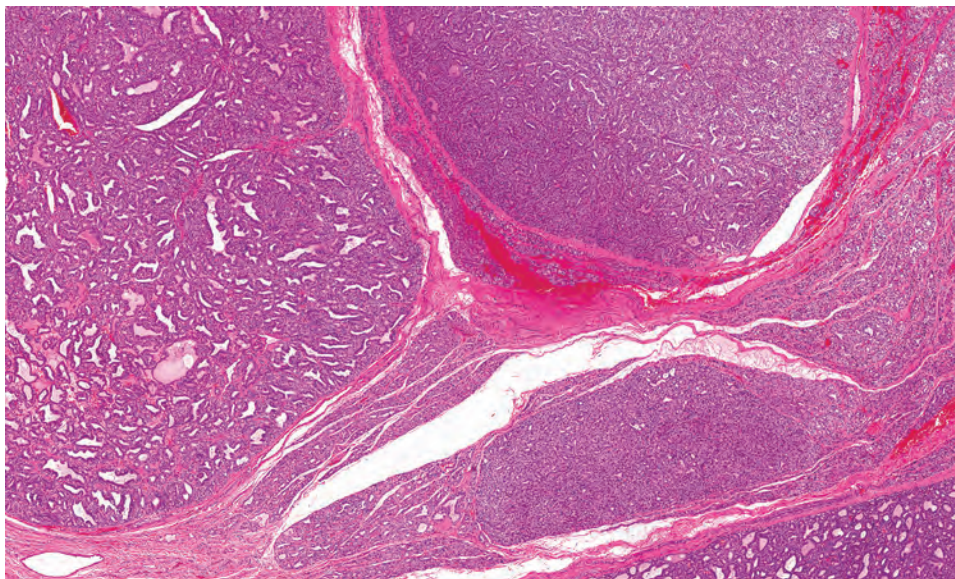
- Highly cellular aspirate, with small sheets and clusters of follicular epithelial cells
- Little or no colloid
- Follicular cells often have cytoplasmic oxyphilia and marked nuclear atypia, with enlarged, hyperchromatic, and irregularly shaped nuclei
- Impossible to exclude a follicular neoplasm based on cytology alone

#### Pathologic Differential Diagnosis

- Follicular neoplasm, diffuse hyperplasia (Graves disease), radiation thyroiditis

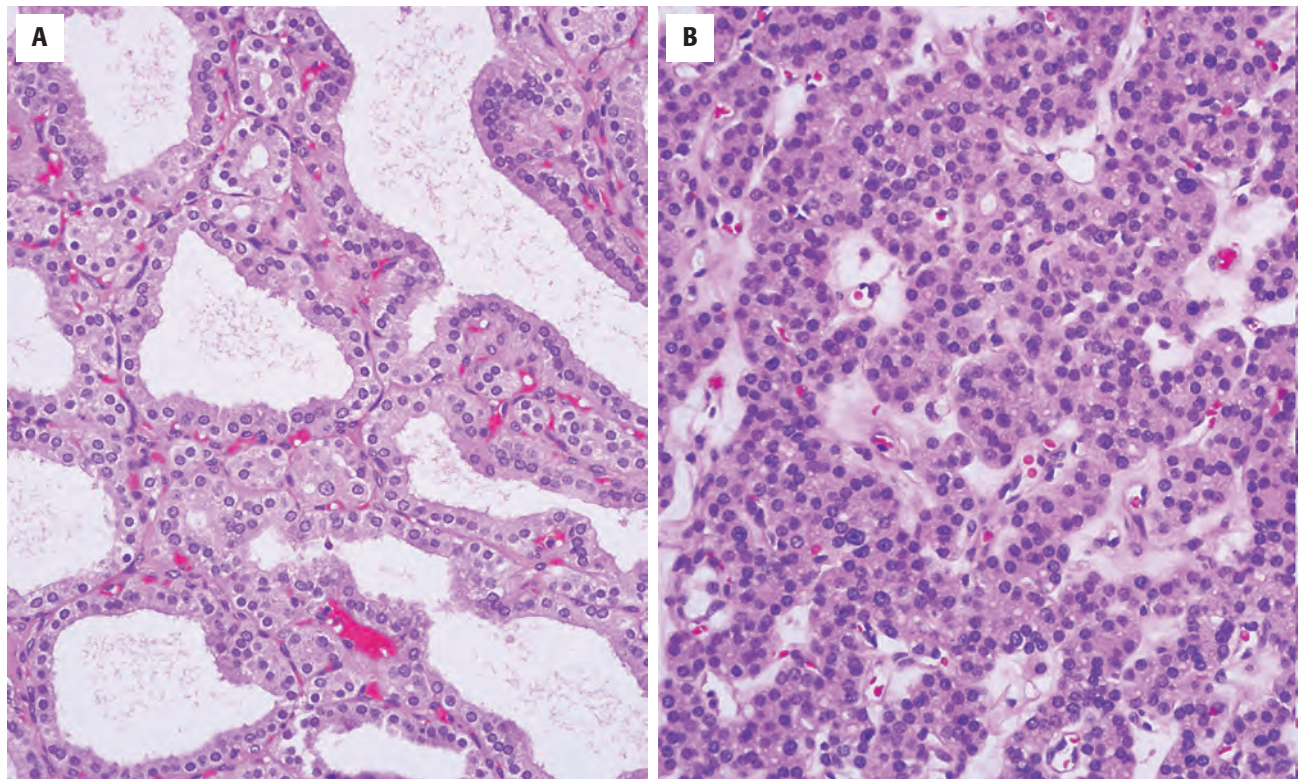
**FIGURE 23.58**

**A**, Thyroid gland in dysmorphogenetic goiter shows a multinodular appearance. Each nodule is different, lacking easily identified colloid. **B**, There is almost no colloid in this low-power view of the thyroid gland, showing multiple nodules.

**FIGURE 23.59**

This example of dysmorphogenetic goiter bears a resemblance to Graves disease, with diffuse hyperplastic changes throughout the gland, creating multiple asymmetric nodules. The tissue between the nodules is also abnormal.



**FIGURE 23.60**

**A**, There is a complete lack of normal colloid. **B**, The nodules may be quite cellular in dys hormonogenetic goiter, so as to suggest a follicular neoplasm.

Cytologic atypia is present in many cases and may be quite striking, similar to that seen in radiation thyroiditis (Fig. 23.61), with an accentuation of this finding in the cells between the nodules.

### ANCILLARY STUDIES

#### FINE NEEDLE ASPIRATION

The aspirates are remarkably cellular, with little or no colloid and often with prominent nuclear atypia. These findings make exclusion of a follicular neoplasm impossible, even if the history of dys hormonogenetic goiter is known. Aspiration cytology in these cases is useful primarily for ruling out PTC.

### DIFFERENTIAL DIAGNOSIS

The differential diagnosis includes follicular carcinoma, diffuse hyperplasia (Graves disease), and radiation thyroiditis. The cellularity, fibrosis, and cellular atypia make a diagnosis of follicular carcinoma extremely challenging in the setting of dys hormonogenetic goiter. However, a *follicular carcinoma* has the presence of

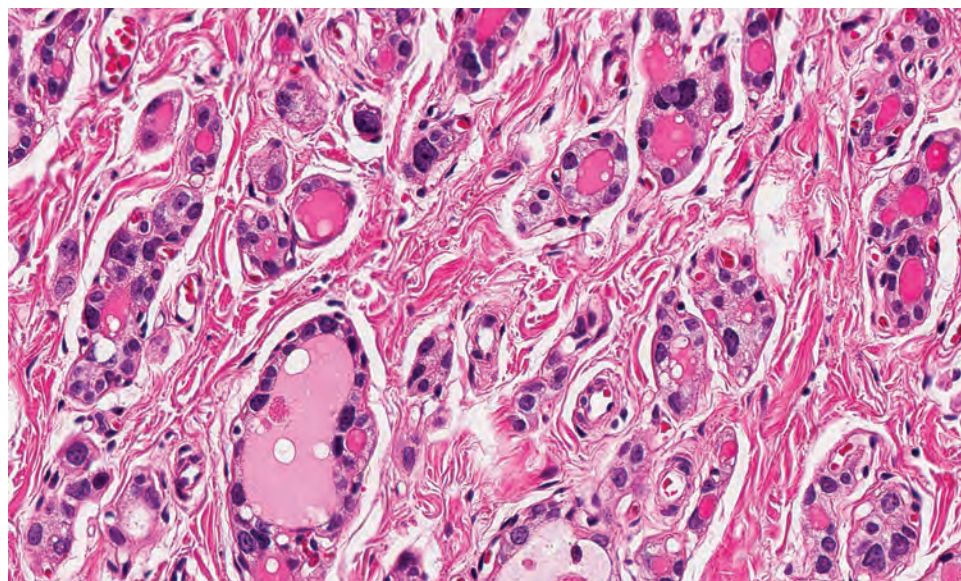
*definitive capsular or lymphovascular invasion. Diffuse hyperplasia* involves clinical hyperthyroidism, often with lymphoid aggregates and usually has some colloid present. *Radiation thyroiditis* may demonstrate cellular nodules with cytologic atypia and increased fibrosis within the gland. An accurate clinical history should readily enable the distinction from dys hormonogenetic goiter.

### PROGNOSIS AND THERAPY

Treatment of the hypothyroidism associated with dys hormonogenetic goiter is the primary goal. Patients have a favorable outcome with thyroid hormone replacement therapy. There is no increased risk of thyroid carcinoma. For symptomatic goiter, total thyroidectomy is the procedure of choice.

### ■ AMYLOID GOITER

Amyloid goiter represents a symptomatic mass or clinically detectable thyroid enlargement due to extracellular deposition of amyloid. While amyloid deposition may be quite common in the thyroid in the setting of systemic amyloidosis, clinical enlargement of the gland (amyloid

**FIGURE 23.61**

Cytologic atypia is common in dysplastic goiter. It should not be overinterpreted as malignancy. All of this area is between nodules.

goiter) is rare. There are several settings in which amyloid deposition occurs including monoclonal Ig light chain disease/hematolymphoid malignancy (primary systemic disease), chronic inflammatory disease (such as rheumatoid arthritis, Crohn disease, familial Mediterranean fever), hereditary amyloidosis, and dialysis-related illness. Chronic inflammatory conditions are the most common cause of amyloid goiter.

### CLINICAL FEATURES

Amyloid goiter is very rare and occurs over a wide age range, from adolescents (especially with juvenile rheumatoid arthritis or familial Mediterranean fever) to the elderly (with hematolymphoid neoplasia); there is no sex predilection. Patients usually detect a palpable mass, which, if symptomatic, may have caused dysphagia, dyspnea, and hoarseness. Rapid enlargement may mimic malignancy. Patients are usually euthyroid.

### PATHOLOGIC FEATURES

#### GROSS FINDINGS

The thyroid is variably enlarged and firm, with a pale tan “waxy” cut surface; nodules may be present.

#### MICROSCOPIC FINDINGS

The amyloid deposition is usually diffuse, but nodular deposits may occur. Amyloid appears as extracellular,

### AMYLOID GOITER—DISEASE FACT SHEET

#### Definition

- Amyloid goiter represents thyroid enlargement due to the intercellular deposition of amyloid

#### Incidence

- Extremely rare

#### Sex and Age Distribution

- Equal sex distribution
- Wide age range

#### Clinical Features

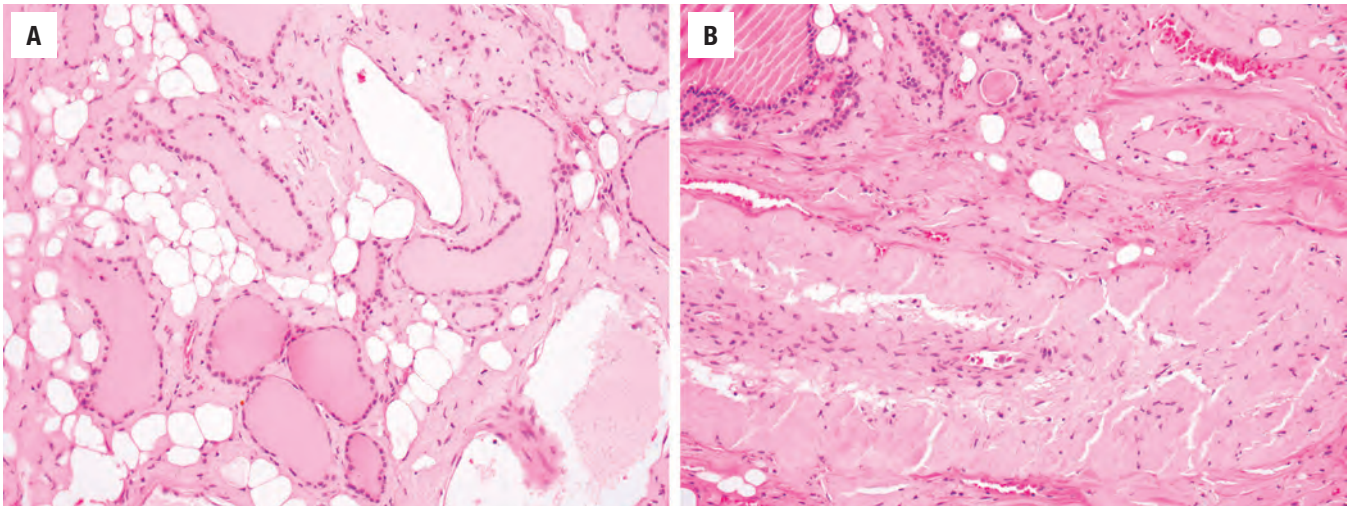
- Most cases associated with systemic inflammatory disease
- Palpable mass
- Patients may have dysphagia, dyspnea, and hoarseness
- Patients are usually euthyroid
- Associated disease: juvenile rheumatoid arthritis and other rheumatologic disease, familial Mediterranean fever, hematolymphoid neoplasms

#### Prognosis and Treatment

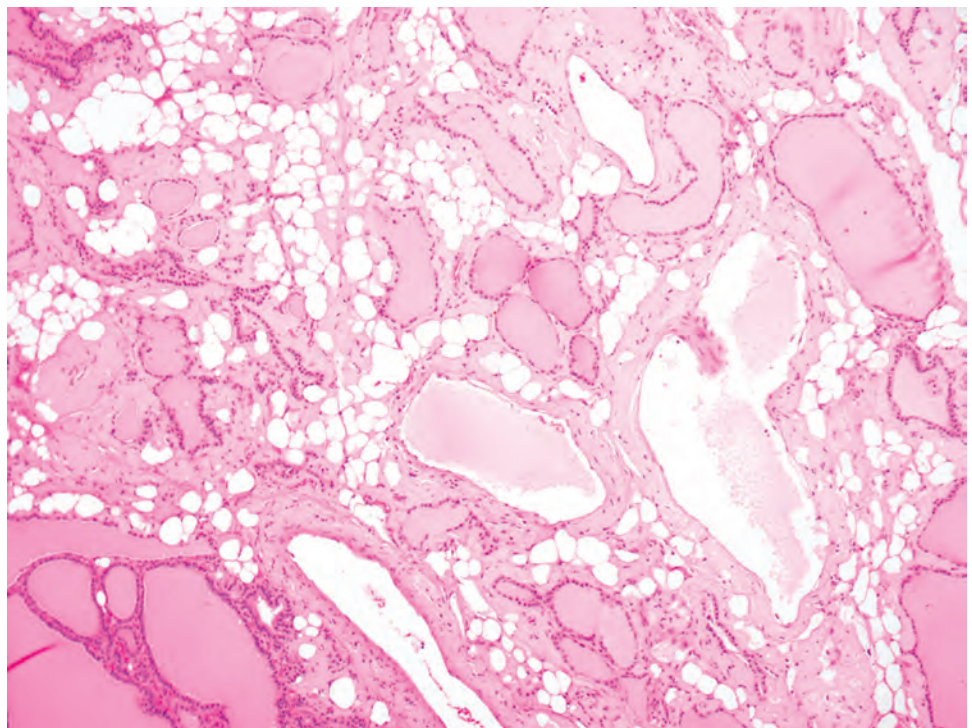
- Prognosis largely related to underlying disorder (especially hematolymphoid malignancy)
- Compressive symptoms may be relieved by thyroidectomy

acellular, homogeneous pale eosinophilic material, classically accentuated in and around vessels (Fig. 23.62). Adipose tissue is often prominent throughout the thyroid gland (Fig. 23.63). Follicles are often remarkably elongated. Not uncommonly, a chronic inflammatory cell infiltrate and sometimes multinucleated giant cells may be present. Squamous metaplasia may be present.



**FIGURE 23.62**

**A**, Thyroid is diffusely infiltrated by intercellular deposits of amorphous eosinophilic amyloid, crowding out the thyroid follicles. Intervening adipose tissue is frequently observed in amyloid goiter. **B**, Perivascular amyloid deposition is also present.

**FIGURE 23.63**

Prominent adipose tissue separating the thyroid follicles throughout the gland may be the initial diagnostic clue on low power of amyloid goiter.

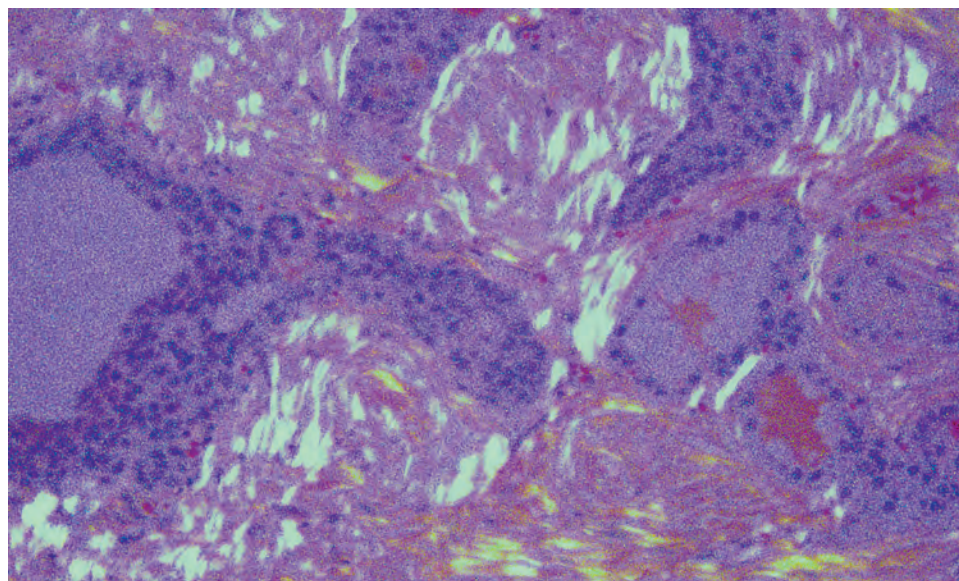
## ANCILLARY STUDIES

### ULTRASTRUCTURAL FINDINGS

Electron microscopy is rarely necessary for the diagnosis but shows masses of nonbranching filaments ranging in size from 50 to 150 Å.

### HISTOCHEMICAL FINDINGS

Amyloid can be demonstrated with crystal violet (metachromatic amorphous material), thioflavin-T, and Congo red. The Congo red stain is most commonly used and exhibits apple-green birefringence when polarized (Fig. 23.64).

**FIGURE 23.64**

Congo red stain highlights the amyloid deposits with “apple-green” birefringence when polarized.

### AMYLOID GOITER—PATHOLOGIC FEATURES

#### Gross Findings

- Thyroid diffusely enlarged with a firm, pale, tan, waxy cut surface
- Nodules may be present

#### Microscopic Findings

- Amyloid deposits usually diffuse but occasionally nodular
- Extracellular accumulation of acellular homogeneous, pale, eosinophilic material
- Angiocentric deposits and amyloid in walls of blood vessels
- Atrophy of follicular component of thyroid, with scattered follicles entrapped in amyloid deposits
- Groups of fat cells scattered through gland
- Squamous metaplasia is common
- Chronic inflammatory infiltrate, sometimes with multinucleated giant cells

#### Histochemical Findings

- Crystal violet: amyloid metachromatic
- Thioflavin T positive
- Congo red positive deposits are rose-colored, with apple-green birefringence with polarization

#### Pathologic Differential Diagnosis

- Fibrous variant of Hashimoto thyroiditis, invasive fibrous thyroiditis, nodular hyperplasia, lymphoplasmacytic neoplasm, medullary thyroid carcinoma

### DIFFERENTIAL DIAGNOSIS

Amyloid is usually distinctive, with the adipose tissue an initial clue to the diagnosis. Collagenous tissue seen in the *fibrous variant of Hashimoto thyroiditis* or *invasive fibrous thyroiditis* is darker and will stain differently with histochemical stains. *Nodular hyperplasia* may have fatty infiltration but does not have amyloid present. A *neoplastic plasma cell* or *lymphoplasmacytic neoplasm* may not be obvious in the setting of amyloid goiter; immunohistochemical stains for assessing immunophenotype and clonality ( $\kappa$  and  $\lambda$ ) are useful in this regard. Lastly, it is important to recognize that the most common cause of amyloid deposition in the thyroid is *medullary thyroid carcinoma*. Malignant cells should not be associated with the amyloid deposition in amyloid goiter.

### PROGNOSIS AND THERAPY

Both prognosis and therapy are dependent on the underlying cause of amyloid goiter: primary systemic amyloidosis, secondary to chronic inflammatory disease, hereditary or dialysis-related. If there are compressive symptoms, thyroidectomy may be necessary. The more ominous findings are involvement of other organs, such as the heart, kidneys, or liver.

### MASS SPECTROMETRY

Mass spectrometry is the most sensitive and specific method for amyloid typing (over 25 different proteins can cause amyloid deposition) and is preferred over immunohistochemistry. It may be clinically useful in cases where the underlying cause of amyloid deposition is not known.

### ■ AMIODARONE-INDUCED THYROID DISEASE

A wide variety of drugs may alter thyroid function and in some cases cause overt hypo- or hyperthyroidism.



These include lithium, interferon- $\alpha$ , tyrosine kinase inhibitors, and amiodarone, among others. However, with the exception of amiodarone, the histopathologic features are poorly characterized.

Amiodarone, a drug used to treat cardiac arrhythmias, has a wide variety of adverse effects. It has a high iodine content and is structurally similar to T3 and T4 hormones. Not surprisingly, amiodarone therapy has a complex effect on thyroid function. Preexisting thyroid disease (Hashimoto thyroiditis, Graves disease, and nodular hyperplasia) can be exacerbated, resulting in either clinical hypo- or hyperthyroidism. Amiodarone can also cause thyrotoxicosis in patients without underlying thyroid disease.

## CLINICAL FEATURES

Amiodarone-associated hypothyroidism or thyrotoxicosis is seen in about 10% to 20% of patients taking the drug. The clinical features are no different from hypo- or hyperthyroidism in other disease. Drug history is helpful.

### AMIODARONE-INDUCED THYROID DISEASE—DISEASE FACT SHEET

#### Definition

- Either hypo- or hyperthyroidism as a result of amiodarone therapy

#### Incidence

- Some 10%–20% of patients taking amiodarone
- Hypo- or hyperthyroidism may be caused by exacerbation of underlying thyroid disease
- A subset of patients with amiodarone-induced thyrotoxicosis have no preexisting thyroid disease

#### Clinical Features

- No different from other causes of either hypo- or hyperthyroidism (thyrotoxicosis)

#### Laboratory Studies

- Serum levels of TSH, T3, and T4 may be altered with initiation of amiodarone therapy but eventually return to normal in euthyroid patients (rT3 may remain elevated)
- Thyroid function tests show the expected abnormalities in hypo- and hyperthyroid patients

#### Prognosis and Treatment

- Most patients return to a euthyroid state with amiodarone cessation unless underlying thyroid disease is present
- Underlying thyroid disease should be treated
- Cessation of amiodarone may not be possible in all cases
- Glucocorticosteroids are first-line treatment for thyrotoxicosis unrelated to preexisting thyroid disease

## LABORATORY STUDIES

The laboratory diagnosis of hypo- or hyperthyroidism is no different in this setting. However, it is important to be aware of changes in thyroid function studies at the initiation of amiodarone therapy; these generally resolve over time. Serum T4 is initially increased and T3 is decreased in patients taking amiodarone but levels return to normal after the first few weeks. rT3 may remain elevated. TSH rises at the start of therapy but returns to normal after 2 to 3 months in euthyroid patients.

## PATHOLOGIC FEATURES

### GROSS FINDINGS

Little is known about the pathologic features of amiodarone-induced hypothyroidism. The pathologic features of amiodarone-induced thyrotoxicosis are better described. The gross appearance of the thyroid is not particularly remarkable. The cut surface is dark brown and glistening due to the abundance of colloid.

### MICROSCOPIC FEATURES

The most prominent finding microscopically is the diffuse marked atrophy and flattening of the follicular epithelium in patients with thyrotoxicosis (Fig. 23.65). Granular or vacuolated cytoplasm may be seen. Colloid is abundant. Inflammation is sparse but scattered foamy macrophages are often present in the colloid, evidence of follicular destruction (Fig. 23.65). Small foci of fibrosis may be present between the follicles.

### AMIODARONE-INDUCED THYROID DISEASE—PATHOLOGIC FEATURES

#### Gross Findings

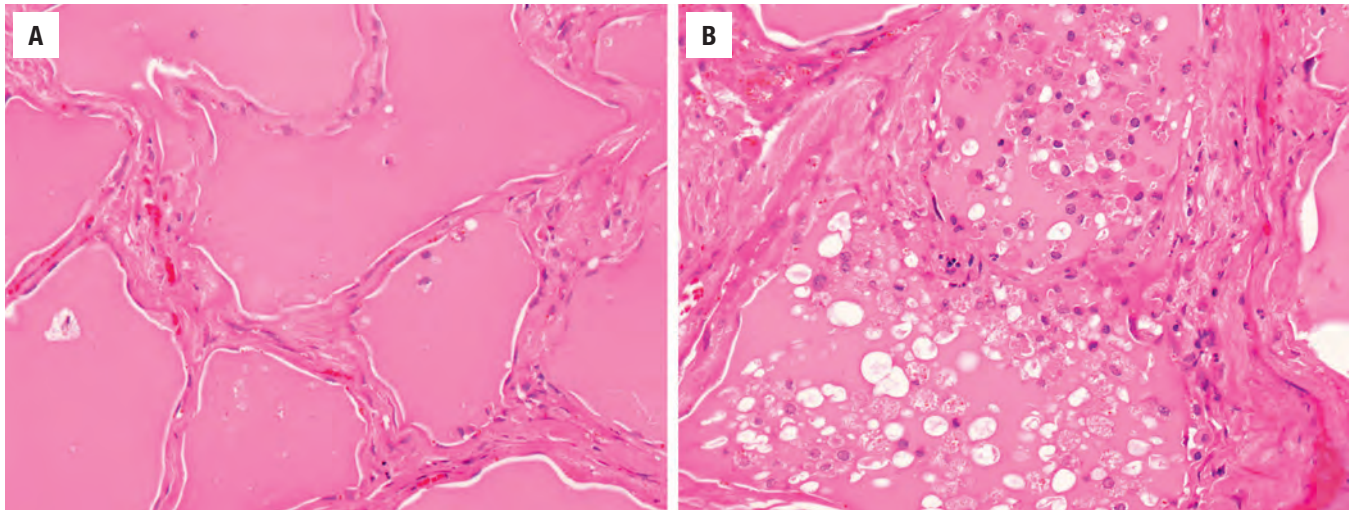
- Gross findings are related to underlying thyroid disease if present

#### Microscopic Findings

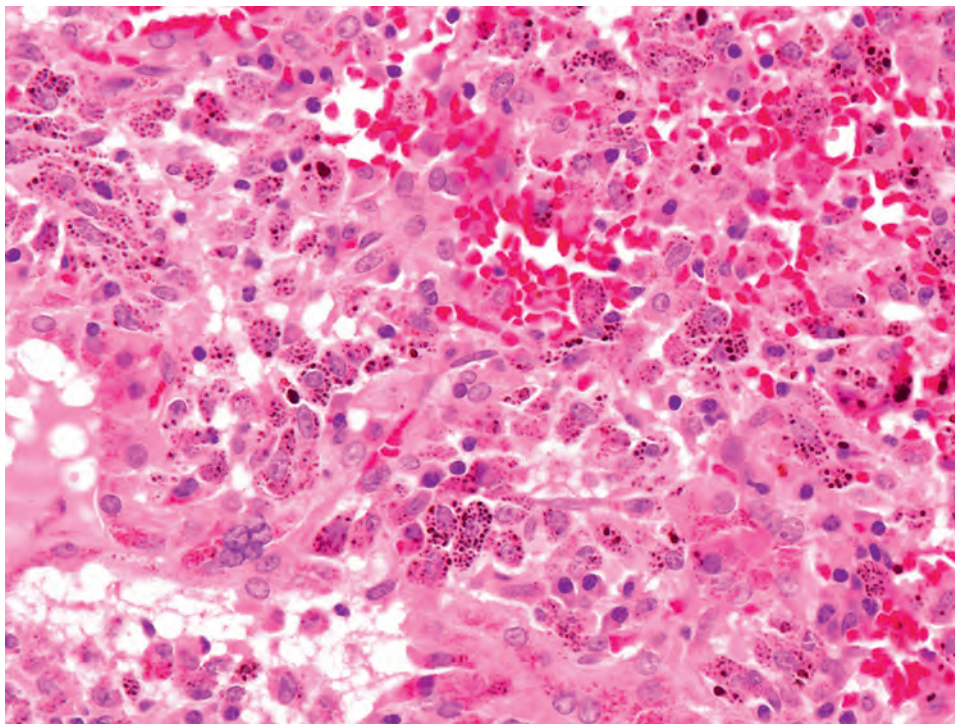
- Thyrotoxicosis associated with diffuse atrophy and flattening of the follicular epithelium with preserved colloid
- Scattered intrafollicular foamy macrophages
- Small foci of fibrosis

#### Pathologic Differential Diagnosis

- Palpation thyroiditis, subacute granulomatous thyroiditis
- Minocycline and indocyanine green cause pigment deposition in the thyroid distinct from the histopathology of amiodarone

**FIGURE 23.65**

**A**, Diffuse atrophy and flattening of the follicular epithelium is seen in amiodarone-induced thyrotoxicosis. **B**, Scattered foamy macrophages are often present within the colloid.

**FIGURE 23.66**

Minocycline is associated with granular dark-brown pigment deposition in the follicular epithelial cells and colloid.

### DIFFERENTIAL DIAGNOSIS

The differential diagnosis is limited in the clinical setting of amiodarone treatment. Foci of foamy macrophages may resemble *palpation thyroiditis* or *subacute granulomatous thyroiditis*, but the accompanying diffuse follicular atrophy is a helpful diagnostic finding.

Although not diagnostic considerations in this setting, other drugs may cause characteristic histopathologic

changes in the thyroid gland. *Minocycline* is the best known and is associated with a “black thyroid” due to pigment deposition. This is usually an incidental finding in a thyroid removed for another indication and clinical thyroid dysfunction is rare. The thyroid is characteristically brown-black on gross examination. Histologically, granular dark-brown pigment can be seen within the cytoplasm of follicular epithelial cells (Fig. 23.66). Macrophages and colloid often contain pigment as well. Anecdotally, *indocyanine green*, an iodine-containing drug



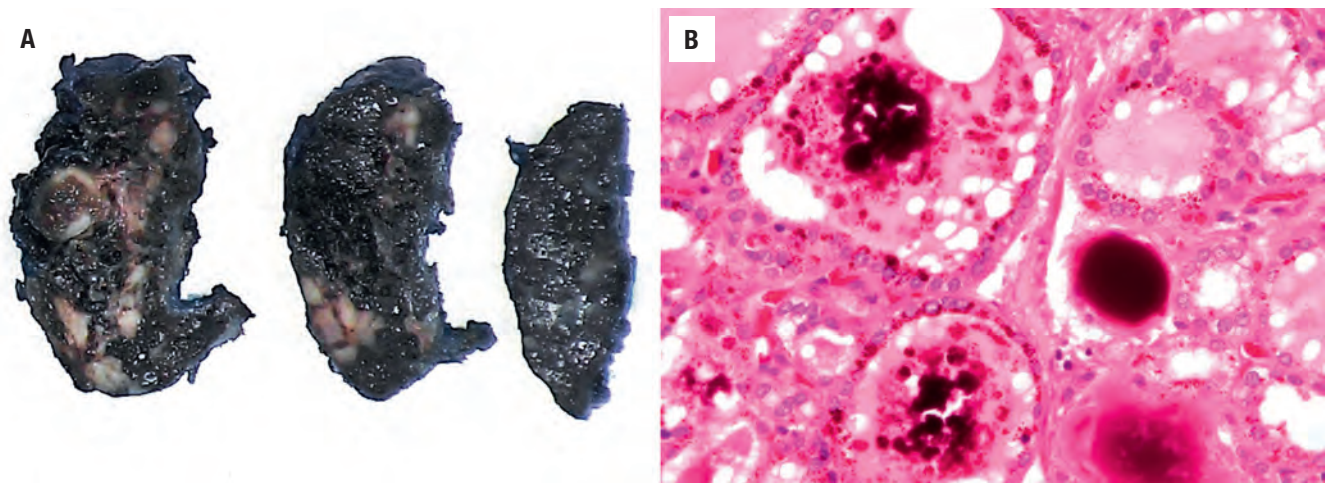


**FIGURE 23.67**

Indocyanine green, an iodine-containing drug used for fluorescent imaging, can cause brown-black discoloration of the thyroid gland. **A**, Dark discoloration of the thyroid gland is seen in a patient who received indocyanine green intraoperatively, similar in appearance to minocycline-induced “black thyroid.” **B**, Histologically, brown granular pigment is seen in the follicular epithelial cells and colloid.

used for fluorescent imaging, can cause similar gross and histologic pigment deposition (Fig. 23.67).

#### PROGNOSIS AND THERAPY

If amiodarone is discontinued, most patients will return to a euthyroid state. However, discontinuation is not always an option clinically. For patients with underlying

thyroid disease, the treatment is similar as for patients not taking amiodarone. Glucocorticosteroids are the first line of treatment for patients with thyrotoxicosis unrelated to preexisting thyroid disease. Surgery and RAI are also options for refractory cases.

#### SUGGESTED READINGS

The complete list of Suggested Readings is available online at [ExpertConsult.com](http://ExpertConsult.com).

**SUGGESTED READINGS****Thyroglossal Duct Cyst**

1. Arabi A, et al. Papillary carcinoma arising in a thyroglossal duct cyst; two case reports and a review of the literature. *Int Surg.* 2007;29:187–190.
2. Brousseau VJ, et al. Thyroglossal duct cysts: presentation and management in children versus adults. *Int J Pediatric Otorhinolaryngol.* 2003;67:1285–1290.
3. Dedivitis RA, et al. Thyroglossal duct: a review of 55 cases. *J Am Coll Surg.* 2002;194:274–277.
4. Gioacchini FM, et al. Clinical presentation and treatment outcomes of thyroglossal duct cysts: a systematic review. *Int J Oral Maxillofac Surg.* 2015;44:119–126.
5. Pradeep PV, et al. Thyroglossal cysts in a pediatric population: apparent differences from adult thyroglossal cysts. *Ann Saudi Med.* 2013;33(1):45–48.
6. Shaffer MM, et al. Thyroglossal duct cysts: diagnostic criteria by fine-needle aspiration. *Arch Pathol Lab Med.* 1996;120:1039–1043.
7. Thompson LDR, et al. A clinicopathologic series of 685 thyroglossal duct remnant cysts. *Head and Neck Pathol.* 2016;10(4):465–474.
8. Thompson LDR, et al. Thyroglossal duct cyst carcinomas: a clinicopathologic series of 22 cases with staging recommendations. *Head Neck Pathol.* 2017 Jun;11(2):175–185.
9. Wei S, et al. Pathology of thyroglossal duct: an institutional experience. *Endocr Pathol.* 2015;26(1):75–79.

**Thyroid Ectopia and Lingual Thyroid**

1. Block MA, et al. Does benign thyroid tissue occur in the lateral part of the neck? *Am J Surg.* 1966;112:476–481.
2. Gandhi A, et al. Lingual thyroid ectopia: diagnostic SPECT/CT imaging and radioactive iodine treatment. *Thyroid.* 2016;26(4):573–579.
3. Leon BGC, et al. Lingual thyroid: 35-year experience at a tertiary care referral center. *Endocr Pract.* 2016;22:343–349.
4. Massine RE, et al. Lingual thyroid carcinoma: a case report and review of the literature. *Thyroid.* 2001;11:1191–1196.
5. Triantafyllou A, et al. Incidental findings of thyroid tissue in cervical lymph nodes: old controversy not yet resolved? *Eur Arch Otorhinolaryngol.* 2016;273(10):2867–2875.

**Ultimobranchial Body Remnants (Solid Cell Nests) and Other Intrathyroidal Inclusions**

1. Abscher KJ, et al. Parathyroid cytology: avoiding diagnostic pitfalls. *Head Neck.* 2002;24:157–164.
2. Beckner ME, et al. Solid and cystic ultimobranchial body remnants in the thyroid. *Arch Pathol Lab Med.* 1992;116:461.
3. Buyukyavuz I, et al. Ectopic thymic tissue as a rare and confusing entity. *Eur J Pediatr Surg.* 2002;12:327–329.
4. Cameselle-Teijeiro J, et al. Solid cell nests of the thyroid: light microscopy and immunohistochemical profile. *Hum Pathol.* 1994;25:684–693.
5. Cameselle-Teijeiro J, et al. Intrathyroidal salivary gland-type tissue in multinodular goiter. *Virchow's Arch.* 1994;425:331–334.
6. de la Cruz Vigo F, et al. Pathologic intrathyroidal parathyroid glands. *Int Surg.* 1997;82:87–90.
7. Harach HR. Solid cell nests of the thyroid. *J Pathol.* 1988;155:191–200.
8. McIntyre RC, et al. Intrathyroidal parathyroid glands can be a cause of failed cervical exploration for hyperparathyroidism. *Am J Surg.* 1997;174:750–753.
9. Sawady J, et al. The intrathyroidal hyperfunctioning parathyroid gland. *Mod Pathol.* 1989;2:652–657.

**Acute Thyroiditis**

1. Berger SA, et al. Infectious diseases of the thyroid gland. *Rev Infect Dis.* 1983;5:108–122.
2. Cabizuca CA, et al. Acute thyroiditis due to septic emboli derived from infective endocarditis. *Postgrad Med J.* 2008;84:445–446.
3. Jeng LBB, et al. Acute suppurative thyroiditis: a ten-year review in a Taiwanese hospital. *Scand J Infect Dis.* 1994;26:297–300.

4. Paes JE, et al. Acute bacterial suppurative thyroiditis: a clinical review and expert opinion. *Thyroid.* 2010;20(3):247–255.
5. Singer PA. Thyroiditis. Acute, subacute, and chronic. *Med Clin North Am.* 1991;75:61–77.

**Subacute Granulomatous Thyroiditis (de Quervain Thyroiditis)**

1. Bartalena L, et al. Graves' disease occurring after subacute thyroiditis: report of a case and review of the literature. *Thyroid.* 1996;6:345–348.
2. deBruin TW, et al. An outbreak of thyrotoxicosis due to atypical subacute thyroiditis. *J Clin Endocrinol Metab.* 1990;70:396–402.
3. Desailoud R, et al. Viruses and thyroiditis: an update. *Virol J.* 2009;6:5.
4. Fatourechi V, et al. Clinical features and outcome of subacute thyroiditis in an incidence cohort: Olmstead County, Minnesota study. *J Clin Endocrinol Metab.* 2003;88:2100–2105.
5. Manson CM, et al. Postoperative necrotizing granulomas of the thyroid. *Histopathology.* 1992;21:392–393.
6. Mizukami V, et al. Sarcoidosis of the thyroid gland manifested initially as thyroid tumor. *Pathol Res Pract.* 1994;190:1201–1205.
7. Obuobie K, et al. Subacute thyroiditis in an immunosuppressed patient. *J Endocrinol Invest.* 2002;25:169–171.
8. Oksa H, et al. No seasonal distribution in subacute deQuervain's thyroiditis in Finland. *J Endocrinol Invest.* 1989;12:495.
9. Sherman SI, et al. Subacute thyroiditis causing thyroid storm. *Thyroid.* 2007;17:283.
10. Singer PA. Thyroiditis. Acute, subacute and chronic. *Med Clin North Am.* 1991;75:61–77.
11. Swinburne JL, et al. A rare case of subacute thyroiditis causing thyroid storm. *Thyroid.* 2007;17:73–76.
12. Volpe R. The management of subacute (deQuervain's) thyroiditis. *Thyroid.* 1993;3:253–255.
13. Volta C, et al. Atypical subacute thyroiditis caused by Epstein-Barr virus infection in a three-year-old girl. *Thyroid.* 2005;15:1189–1191.
14. Walfish PG. Syndromes of thyrotoxicosis with low radioactive iodine uptake. *Endocrinol Metab Clin North Am.* 1998;27:169–185.

**Invasive Fibrous Thyroiditis (IgG<sub>4</sub>-Related Thyroiditis; Riedel Thyroiditis)**

1. Blumenfeld W. Correlation of cytologic and histologic findings in fibrosing thyroiditis. *Acta Cytol.* 1997;41:1337–1340.
2. Caraway NP, et al. Diagnostic pitfalls in thyroid fine-needle aspiration: a review of 394 cases. *Diagn Cytopathol.* 1993;9:345–350.
3. Dahlgren M, et al. Riedel's thyroiditis and multifocal fibrosclerosis are part of the IgG<sub>4</sub>-related systemic disease spectrum. *Arthritis Care Res.* 2010;62:1312–1318.
4. Dehner LP, et al. Idiopathic fibrosclerotic disorders and other inflammatory pseudotumors. *Semin Diagn Pathol.* 1998;15:161–173.
5. Deshpande V. IgG<sub>4</sub> related disease of the head and neck. *Head and Neck Pathol.* 2015;9:24–31.
6. Deshpande V, et al. Consensus statement on the pathology of IgG<sub>4</sub>-related disease. *Mod Pathol.* 2012;25:1181–1192.
7. Fatourechi MM, et al. Invasive fibrous thyroiditis (Riedel thyroiditis): the Mayo Clinic experience, 1976–2008. *Thyroid.* 2011;21:765–772.
8. Heufelder AE, et al. Evidence of autoimmune mechanisms in the evolution of invasive fibrous thyroiditis (Riedel's struma). *Clin Invest.* 1994;72:788–793.
9. Papi G, et al. Riedel thyroiditis: clinical, pathological, and imaging features. *Int J Clin Pract.* 2002;56:65–67.
10. Papi G, et al. Riedel's thyroiditis and fibrous variant of Hashimoto's thyroiditis: a clinicopathologic and immunohistochemical study. *J Endocrinol Invest.* 2003;26:444–449.
11. Papi G, et al. Current concepts on Riedel thyroiditis. *Am J Clin Pathol.* 2004;121(suppl 1):S50–S63.
12. Tutuncu NB, et al. Multifocal idiopathic fibrosclerosis manifesting with Riedel's thyroiditis. *Endocr Pract.* 2000;6:447–449.
13. Wan S, et al. Paucicellular variant of anaplastic thyroid carcinoma: a mimic of Riedel's thyroiditis. *Am J Clin Pathol.* 1996;105:388–393.



### Chronic Lymphocytic Thyroiditis (Hashimoto Thyroiditis)

- Ahmed R, et al. Hashimoto thyroiditis: a century later. *Adv Anat Pathol*. 2012;19:181–186.
- Caturegli P, et al. Hashimoto thyroiditis: clinical and diagnostic criteria. *Autoimmun Rev*. 2014;13:391–397.
- Dayan CM, et al. Chronic autoimmune thyroiditis. *N Engl J Med*. 1996;335:99–107.
- LiVolsi VA. The pathology of autoimmune thyroid disease: a review. *Thyroid*. 1994;4:333–339.
- Louis DN, et al. Multiple branchial cleft-like cysts in Hashimoto's thyroiditis. *Am J Surg Pathol*. 1989;13:45–49.
- Raess PW, et al. Overlapping morphologic and immunohistochemical features of Hashimoto thyroiditis and IgG4-related disease. *Endocr Pathol*. 2015;26:170–177.
- Roman SH, et al. Genetics of autoimmune thyroid disease: lack of evidence for linkage to HLA within families. *J Clin Endocrinol Metab*. 1992;74:496–503.
- Samuels MH. Subacute, silent and postpartum thyroiditis. *Med Clin North Amer*. 2012;96(2):223–233.
- Tamai H, et al. Resistance to autoimmune thyroid disease is associated with HLA-DQ. *J Clin Endocrinol Metab*. 1994;78:94–97.
- Vanderpump MP, et al. The incidence of thyroid disorders in the community: a twenty-year follow-up of the Whickham survey. *Clin Endocrinol*. 1995;43:55–68.
- Volpe R. A perspective on human autoimmune thyroid disease: is there an abnormality of the target cell which predisposes to the disorder? *Autoimmunity*. 1992;13:3–9.
- Weetman AP, et al. Autoimmune thyroiditis: further developments in our understanding. *Endocr Rev*. 1994;15:788–830.
- Day TA, et al. Multinodular goiter. *Otolaryngol Clin North Am*. 2003;26:35–54.
- Derwahl M, et al. Nodular goiter and goiter nodules: where iodine deficiency falls short of explaining the facts. *Exp Clin Endocrinol Diabetes*. 2001;109:250–260.
- Glinoe D. Radioiodine therapy of non-toxic multinodular goiter. *Clin Endocrinol*. 1994;41:713–714.
- Glinoe D, et al. Goiter and pregnancy: a new insight into an old problem. *Thyroid*. 1992;2:65–70.
- Krohn K, et al. Molecular pathogenesis of euthyroid and toxic multinodular goiter. *Endocr Rev*. 2005;26:504–524.
- Siegel RD, et al. Toxic nodular goiter. *Endocrinol Metab Clin North Am*. 1998;27:151–168.
- Studer H, et al. Natural heterogeneity of thyroid cells: the basis for understanding thyroid function and nodular goiter growth. *Endocr Rev*. 1989;10:125–135.
- Tollin SR, et al. The use of fine-needle aspiration under ultrasound guidance to assess the risk of malignancy in patients with a multinodular goiter. *Thyroid*. 2000;10:235–241.

### Dyshormonogenetic Goiter

- Ghossein RA, et al. Dyshormonogenetic goiter: a clinicopathologic study of 56 cases. *Endocr Pathol*. 1997;8:283–292.
- Matos PS, et al. Dyshormonogenetic goiter. A morphological and immunohistochemical study. *Endocr Pathol*. 1994;5:49–58.
- Medeiros-Neto GA, et al. Defective organification of iodide causing hereditary goitrous hypothyroidism. *Thyroid*. 1993;3:143–159.
- Ramesh BG, et al. Genotype-phenotype correlations of dyshormonogenetic goiter in children and adolescents from South India. *Indian J Endocrinol Metab*. 2016;20(6):816–824.
- Shacham EC, et al. Minimally invasive follicular thyroid carcinoma developed in dyshormonogenetic multinodular goiter due to thyroid peroxidase gene mutation. *Thyroid*. 2012;22(5):542.

### Diffuse Hyperplasia (Graves Disease)

- Alsaanea O, et al. Treatment of Graves' disease: the advantage of surgery. *Endocrinol Metab Clin North Am*. 2000;29:321–337.
- Bahn RS. Understanding the immunology of Graves' ophthalmopathy. Is it an autoimmune disease? *Endocrinol Metab Clin North Am*. 2000;29:287–296.
- Brown RS. Immunoglobulins affecting thyroid growth: a continuing controversy. *J Clin Endocrinol Metab*. 1995;80:1506–1508.
- Burch HB, et al. Management of Graves disease: a review. *JAMA*. 2015;314(23):2544–2554.
- Carnell NE, et al. Thyroid nodules in Graves' disease: classification, characterization, and response to treatment. *Thyroid*. 1998;8:647–652.
- Cooper DS. Antithyroid drugs for the treatment of hyperthyroidism caused by Graves' disease. *Endocrinol Clin North Am*. 1998;27:225–246.
- Dabon-Almirante CLM, et al. Clinical and laboratory diagnosis of thyrotoxicosis. *Endocrinol Metab Clin North Am*. 1998;27:25–35.
- Gough SCL. The genetics of Graves' disease. *Endocrinol Metab Clin North Am*. 2000;29:255–266.
- Graves PN, et al. New insights into the thyroid-stimulating hormone receptor. *Endocrinol Clin North Am*. 2000;29:267–286.
- Kaplan MM, et al. Treatment of hyperthyroidism with radioactive iodine. *Endocrinol Metab Clin North Am*. 1998;27:205–223.
- McIver B, et al. The pathogenesis of Graves' disease. *Endocrinol Metab Clin North Am*. 1998;27:73–89.
- Motomura K, et al. Mechanisms of thyroid hormone action. *Endocrinol Clin North Am*. 1998;27:1–23.

### Amyloid Goiter

- Alvarez-Sala R, et al. Amyloid goiter and hypothyroidism secondary to cystic fibrosis. *Postgrad Med J*. 1995;7:307–308.
- García Villanueva A, et al. Surgical considerations about amyloid goiter. *Endocrinol Nutr*. 2013;60(5):254–259.
- Hamed G, et al. Amyloid goiter. A clinicopathologic study of 14 cases and review of the literature. *Am J Clin Pathol*. 1995;104:306–312.
- Law JH, et al. Symptomatic amyloid goiters: report of five cases. *Thyroid*. 2013;23(11):1490–1495.
- Ojha SS, et al. Amyloid goiter: cytomorphological features and differential diagnosis on fine needle aspiration cytology: a case report. *Anal Quant Cytopathol Histopathol*. 2014;36(4):241–244.
- Ozemir IA, et al. Amyloid goiter related with Crohn's disease: a rare association: amyloid goiter secondary to Crohn's disease. *Int J Surg Case Rep*. 2014;5(8):480–483.
- Yaeger KA, et al. Amyloid goiter. *Diagn Cytopathol*. 2010;38(10):742–743.

### Amiodarone-Induced Thyroid Disease

- Bogazzi F, et al. Amiodarone and the thyroid: a 2012 update. *J Endocrinol Invest*. 2012;35(3):340–348.
- Czarnywojtek A, et al. Dysfunction of the thyroid gland during amiodarone therapy: a study of 297 cases. *Ther Clin Risk Manag*. 2016;12:505–513.
- Nakazawa T, et al. Histopathology of the thyroid in amiodarone-induced hypothyroidism. *Pathol Internat*. 2008;58:55–58.
- Smyrk TC, et al. Pathology of the thyroid in amiodarone-associated thyrotoxicosis. *Am J Surg Pathol*. 1987;11(3):197–204.
- Surks MI, et al. Drugs and thyroid function. *N Engl J Med*. 1995;333(25):1688–1694.
- Taurog A, et al. Minocycline and the thyroid: antithyroid effects of the drug, and the role of thyroid peroxidase in minocycline-induced black pigmentation of the gland. *Thyroid*. 1996;6(3):211–219.

### Adenomatoid Nodules (Multinodular Goiter)

- Aeschmann S, et al. Morphological and functional polymorphism within clonal thyroid nodules. *J Clin Endocrinol Metab*. 1993;77:846–851.
- Apel RL, et al. Clonality of thyroid nodules in sporadic goiter. *Diagn Mol Pathol*. 1995;4:113–121.
- Berghout A, et al. Interrelationships between age, thyroid volume, thyroid nodularity, and thyroid function in patients with sporadic non-toxic goiter. *Am J Med*. 1990;89:602–608.

# Benign Neoplasms of the Thyroid Gland

■ **Lester D.R. Thompson** ■ **Rebecca D. Chernock**

## ■ FOLLICULAR ADENOMA

Follicular adenoma (FA) is a benign encapsulated neoplasm of follicular epithelial origin and is the most common neoplasm of the thyroid gland. Autopsy studies show that 3% to 5% of adult thyroid glands harbor an FA. A subset may represent a precursor lesion to follicular carcinoma.

### CLINICAL FEATURES

The most common tumor of the thyroid gland, FA is often discovered incidentally during routine physical exam as a solitary, painless, mobile mass or during radiographic studies for other reasons; sometimes patients present with a history of a slow-growing nodule present for months to years. Iodine deficiency, radiation, and inherited syndromes (PTEN–hamartoma tumor syndrome [Cowden, Proteus syndrome]; Carney complex; Werner, McCune–Albright, and Li–Fraumeni syndromes) may have an etiologic relationship to FA development, which is thought to be a monoclonal proliferation. Multiple FAs should raise clinical suspicion for an inherited syndrome. Women are affected more frequently than men (4 to 5:1). Patients present over a wide age range, but there is a peak in the 5th to 6th decade. Patients are typically euthyroid and only rarely develop hyperfunction (“toxic adenoma”) or hypofunction. Neck pain or pressure may be reported if bleeding into the tumor has occurred or due to compressive symptoms in large tumors. Initial management includes a fine needle aspiration (FNA) with or without ultrasonographic guidance.

### RADIOGRAPHIC FEATURES

Imaging studies cannot reliably separate benign from malignant neoplasms, but ultrasound (US) is the best

### FOLLICULAR ADENOMA—DISEASE FACT SHEET

#### Definition

- Benign encapsulated tumor with evidence of follicular cell differentiation

#### Incidence

- About 3%-5% of the population

#### Morbidity and Mortality

- None (although hypoparathyroidism or recurrent laryngeal nerve damage may occur during surgery)

#### Sex and Age Distribution

- Females > > males (4-5:1)
- Wide age range, but usually 5th to 6th decade

#### Clinical Features

- Painless neck mass, often present for years
- Solitary nodule involving only one lobe

#### Radiographic Features

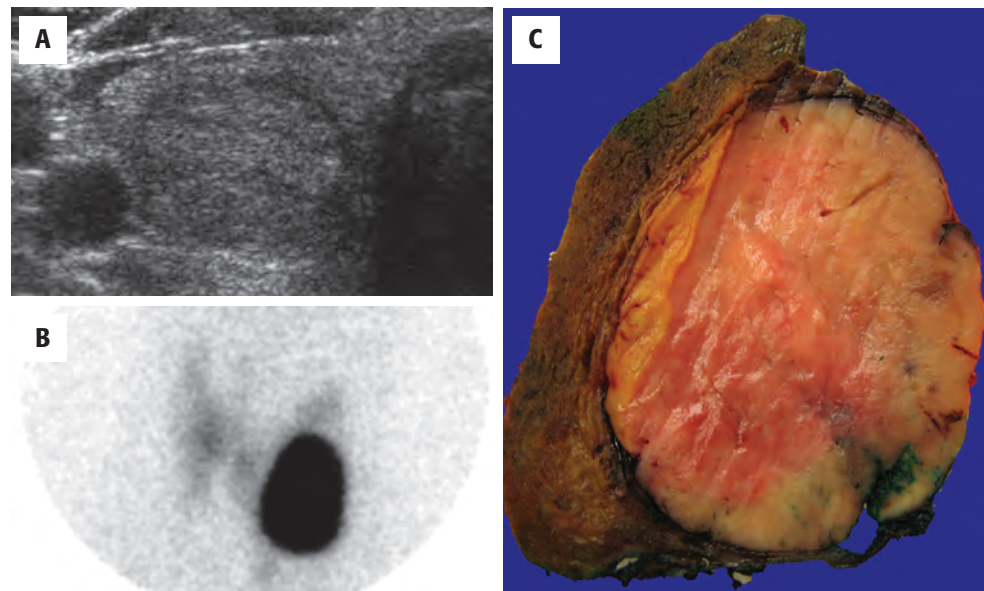
- Ultrasound typically shows hypoechoic halo at the periphery of a solid mass
- Imaging guides fine needle aspiration biopsy

#### Prognosis and Therapy

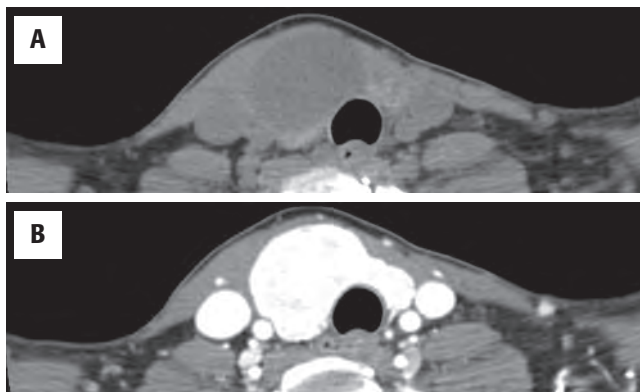
- Excellent
- Surgery (lobectomy)

study, helping to identify the size, location, and character of the nodule (Fig. 24.1). US may aid in guiding a FNA for deep-seated or nonpalpable masses. Since adenomas are encapsulated, they are easily identified by a well-defined hypoechoic halo at the periphery of an otherwise solid, homogeneous mass. Color Doppler gives a “spoke and wheel” appearance of peripheral blood vessels extending toward the center of the lesion. Nuclear imaging studies are “cold,” although a functional or “hot” nodule can rarely be seen (Fig. 24.1). Computed tomography



**FIGURE 24.1**

(A) Ultrasound shows an echo-poor halo at the periphery of a solid nodule. (B) A "hot" nodule in the left lobe of the thyroid gland demonstrates increased uptake of the radiolabeled  $^{125}\text{I}$ . (C) A single encapsulated follicular adenoma with a different cut appearance than the surrounding thyroid parenchyma.

**FIGURE 24.2**

(A) Computed tomography scan showing a well-defined nodule in the right thyroid gland, brightly enhancing with contrast (B).

tends to be nonspecific, showing a hypodense intrathyroid mass and enhancement with contrast (Fig. 24.2).

## **PATHOLOGIC FEATURES**

### **GROSS FINDINGS**

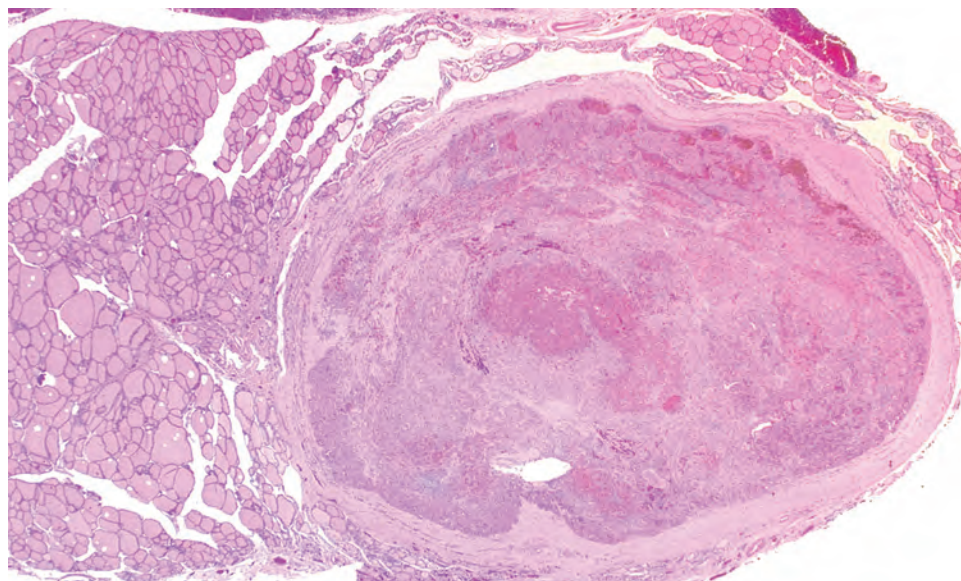
FAs are usually solitary, well demarcated, and encapsulated masses identified in one lobe or in the isthmus (Fig. 24.1). The capsule is usually thin but distinct (Fig. 24.3); a thick capsule should raise suspicion for a follicular carcinoma. Adenomas are usually round to spherical, measuring about 1 to 3 cm on average, although this may be quite variable depending on clinical presentation (palpable versus incidental radiographic feature). The cut surface is rubbery to firm with a homogeneous solid appearance. Gray-white lesions are usually more cellular,

while brown-tan lesions tend to have more colloid. Cystic change, degeneration, calcification, and infarction are common and may alter the physical appearance. The *oncocytic adenoma* (10% to 15% of FAs) tends to have a mahogany-brown cut surface with central scarring.

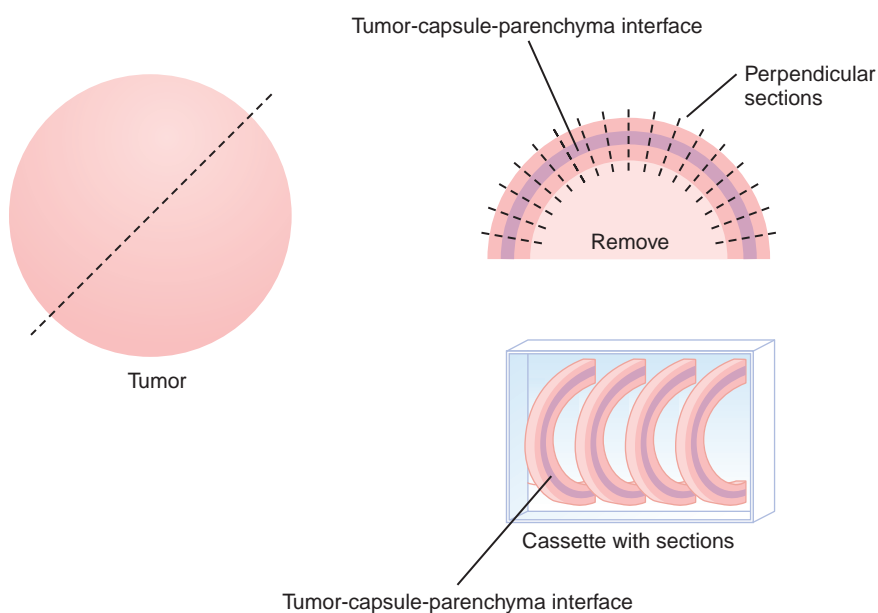
Thoroughly sampling the capsule for invasion (capsular or lymphovascular) is critical, as invasion leads to a diagnosis of follicular carcinoma rather than FA. It is our practice to submit the whole periphery. If this is not feasible, a minimum of three sections per 1 cm of tumor diameter should be submitted. If the tumor looks macroscopically homogeneous after being bivalved, then the center of the tumor is of less interest and should be sampled only representatively. The tumor is serially sectioned perpendicular to the capsule, making 2- to 3-mm thick sections. Then the very periphery of the tumor to capsule to parenchymal interface is embedded. As many as five sections, 3 mm thick and 2.5 cm long, can be placed side by side in the cassette. With this technique, most tumors can be placed in fewer than 10 blocks, allowing for complete evaluation of the capsule (Fig. 24.4).

### **MICROSCOPIC FINDINGS**

A well-defined, variably thick fibrous connective tissue capsule encloses the neoplastic cells, separating them from the compressed or atrophic thyroid parenchyma (Figs. 24.5 and 24.6). If the capsule is very thick, additional sections should be evaluated to exclude a carcinoma. Small to medium-sized smooth muscle-walled vessels can usually be seen within the fibrous connective tissue (Fig. 24.7). A reticulin or elastic stain can highlight fibers in a true capsule. Invasion is absent by definition, although entrapped epithelium can be seen. FNA may result in iatrogenic defects in the capsule, but these

**FIGURE 24.3**

A variably thick fibrous connective tissue capsule surrounds a follicular adenoma showing oncocytic change. Central degeneration is a result of previous fine needle aspiration.

**FIGURE 24.4**

Prosection of an encapsulated thyroid tumor. The tumor is cross-sectioned. The central portion is removed and representatively sampled. Serial sections are cut perpendicular to the tumor-capsule-parenchymal interface. Sections are submitted to ensure that the interface is sufficiently examined.

### FOLLICULAR ADENOMA—PATHOLOGIC FEATURES

#### Gross Findings

- Solitary, well-demarcated encapsulated spherical mass; mean size 3 cm
- Interior of tumor distinct from remaining thyroid parenchyma

#### Microscopic Findings

- Surrounded by intact, easily identified capsule (no invasion)
- Smooth muscle-walled vessels present in the fibrous tissue help confirm a true capsule
- Appearance of tumor cells is distinct and separate from parenchyma
- Colloid is usually present, although sometimes limited in oncocytic tumors
- Cells are slightly enlarged with low nuclear:cytoplasmic ratio
- Variants include oncocytic, trabecular, fetal, papillary, clear cell, signet-ring cell, spindle, among others

#### Immunohistochemical Findings

- TTF1, thyroglobulin, pancytokeratin, PAX8

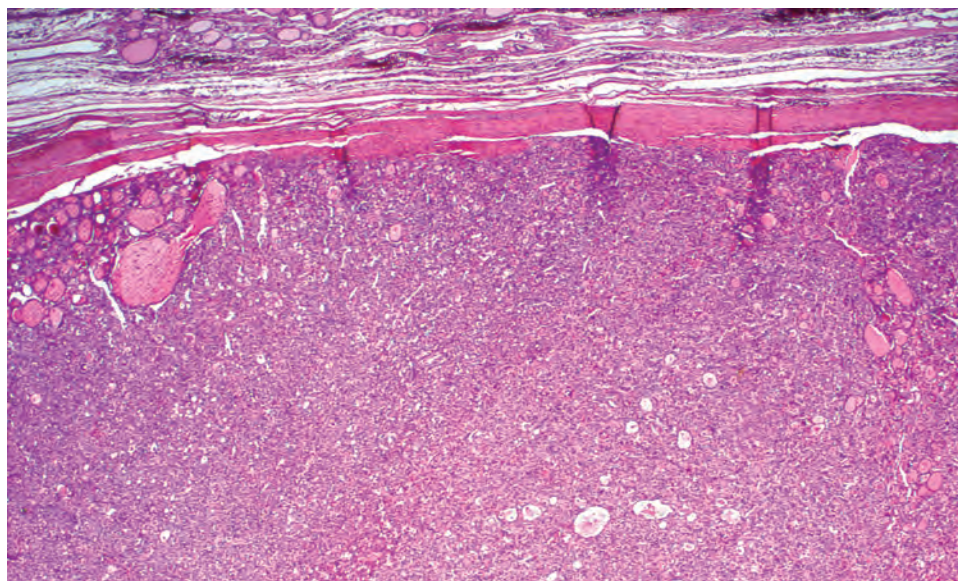
#### Fine Needle Aspiration

- Cellular smears with ample colloid (usually)
- Follicular groups without nuclear features of papillary carcinoma
- Cannot reliably separate between adenomatoid nodule, follicular adenoma, and follicular carcinoma

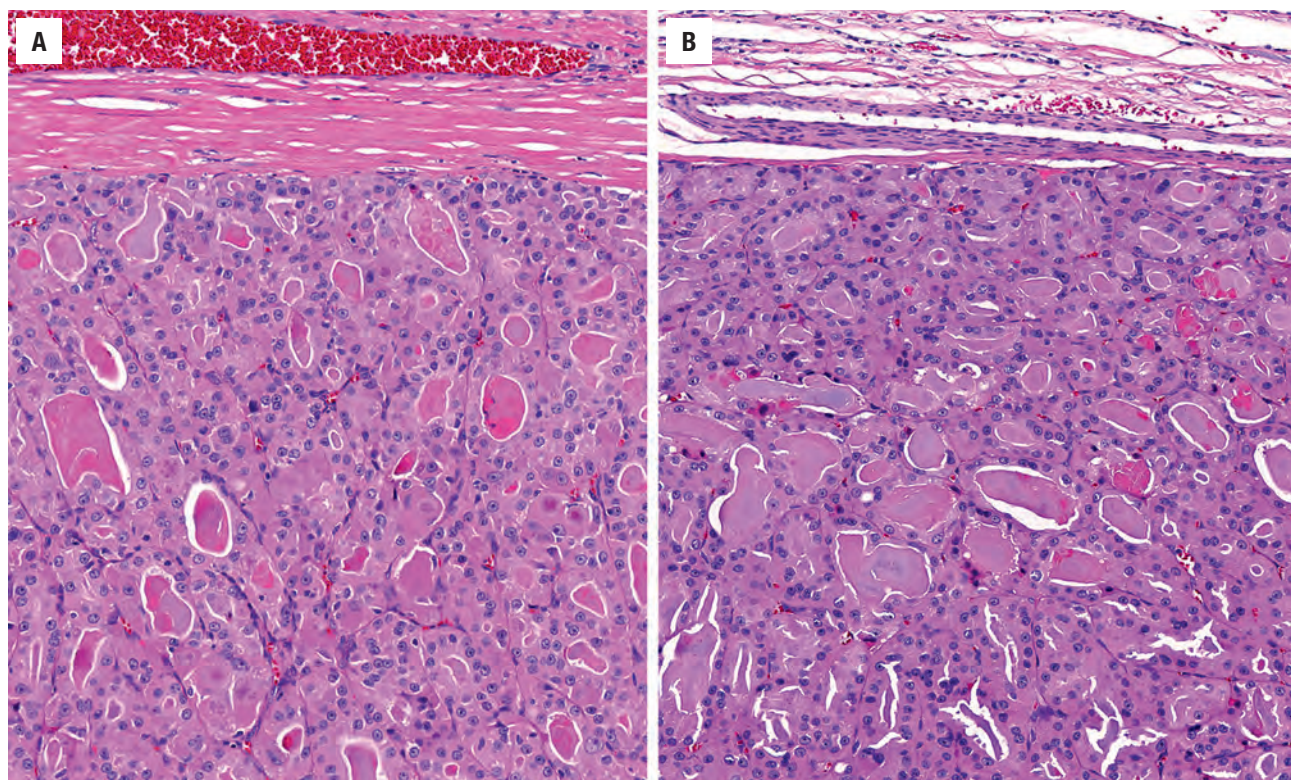
#### Pathologic Differential Diagnosis

- Cellular/dominant adenomatoid nodule, follicular carcinoma, papillary thyroid carcinoma, noninvasive follicular thyroid neoplasm with papillary-like nuclear features (NIFTP), hyalinizing trabecular tumor, metastatic carcinoma



**FIGURE 24.5**

A cellular follicular adenoma is surrounded by a thin but well-formed capsule. Compressed parenchyma is noted at the periphery.

**FIGURE 24.6**

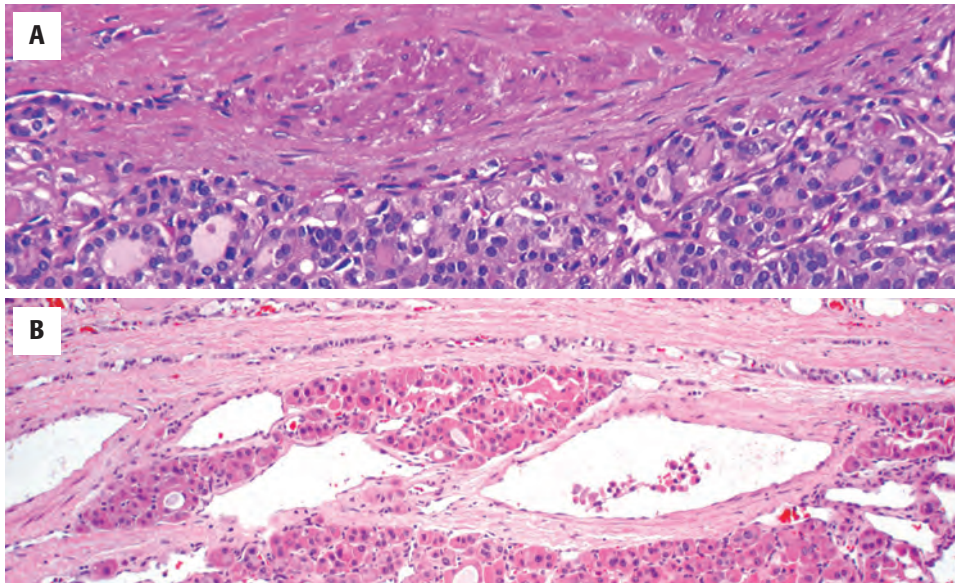
(A) A well-formed, thick capsule surrounds this oncocytic tumor. (B) There is a very thin capsule, exhibiting an elongated vessel.

are usually associated with a linear tract, extravasated erythrocytes, hemosiderin-laden macrophages, “reactive” fibrosis, and endothelial hyperplasia (Fig. 24.8). The site of puncture often has a “sharp edge” of transgression, suggesting a mechanical device rather than biologic aggression.

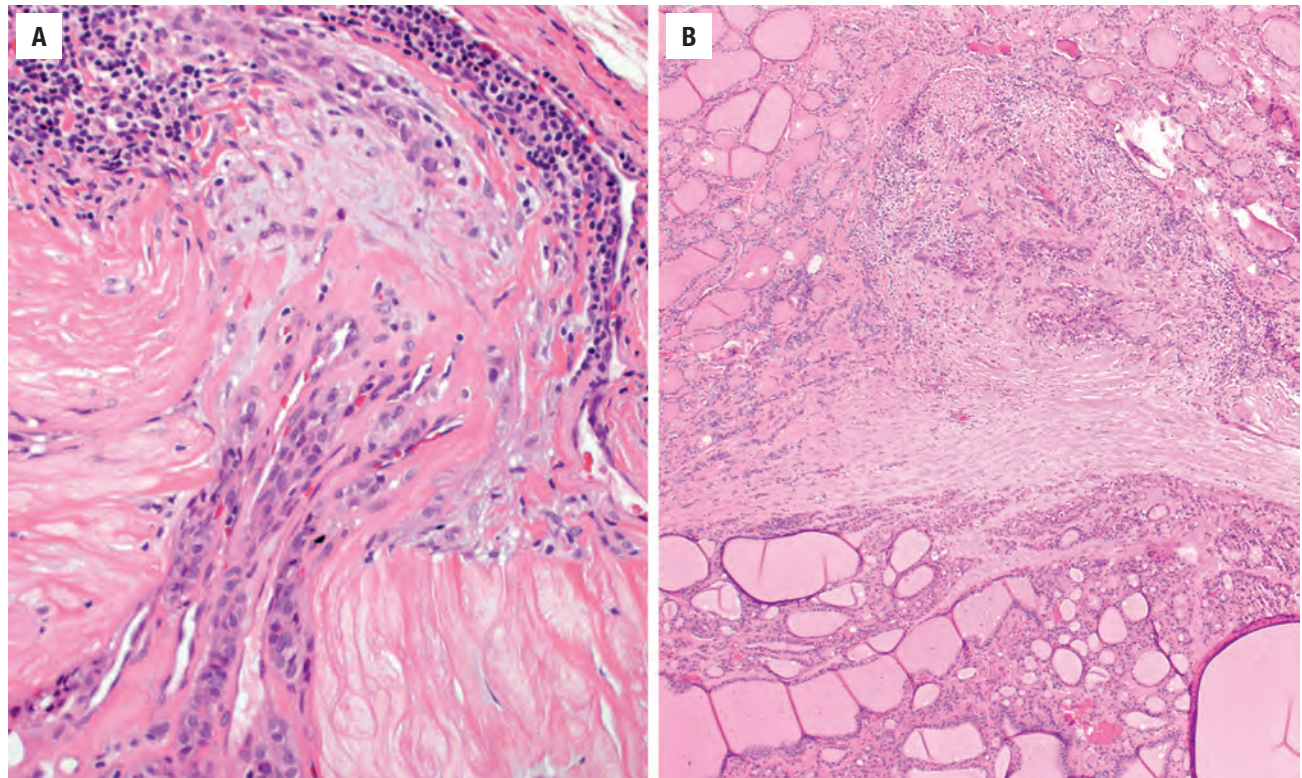
The cells are arranged in a variety of patterns with a variable amount of colloid, usually distinctive from the surrounding parenchyma. While the patterns of growth

have been given “type” or “variant” designations (normofollicular [Fig. 24.9], macrofollicular, microfollicular, fetal, embryonal, solid, trabecular [Fig. 24.10], spindled [Fig. 24.11], insular, organoid, papillary), these terms are of no clinical consequence. The follicles are usually uniform with a single architectural pattern predominating. Colloid may be highlighted by a periodic acid–Schiff (PAS) stain if it is limited. Delicate capillaries are easily identified, but intratumoral fibrosis is uncommon. The cells



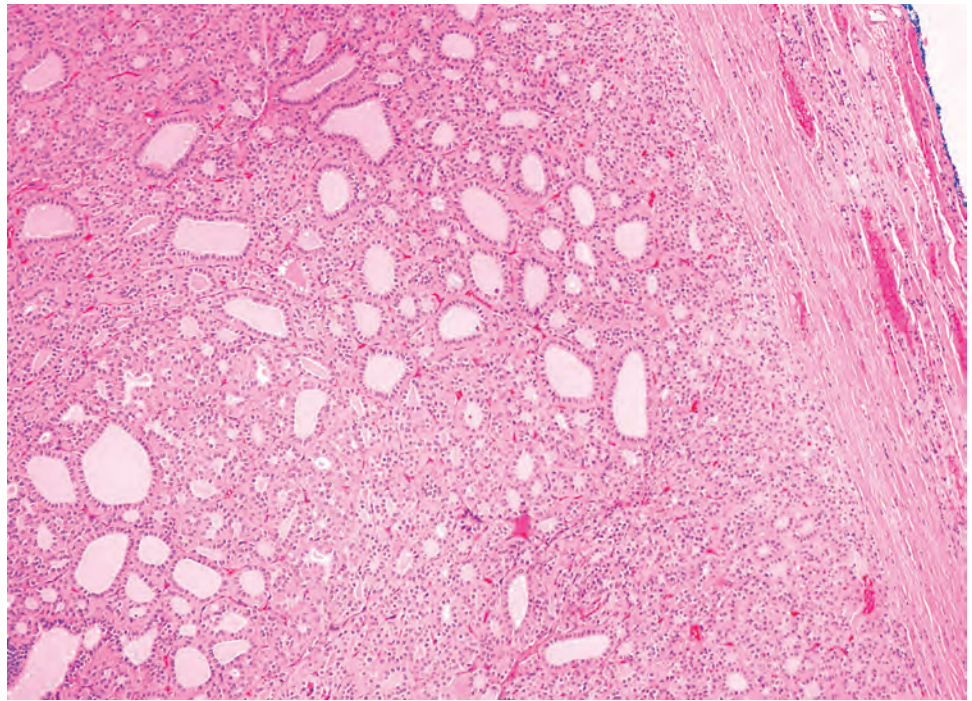
**FIGURE 24.7**

(A) A smooth muscle-walled vessel is identified within the capsule of a follicular adenoma. (B) Multiple vessels within the capsule have entrapped follicles between them. This finding does not represent invasion in this follicular adenoma.

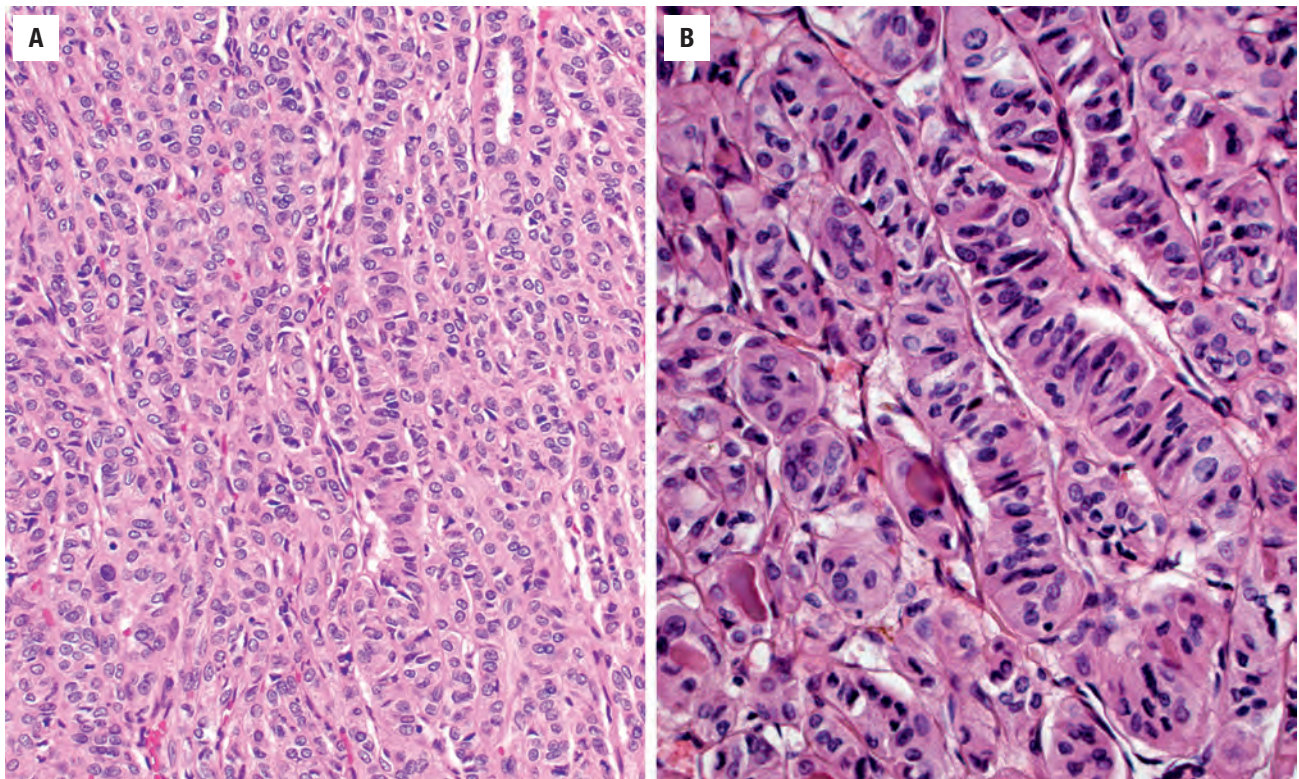
**FIGURE 24.8**

(A) Note the sharp edge of transgression, with follicular cells associated with lymphocytes and histiocytes in this post-fine needle aspiration site. (B) A reactive vascular proliferation at the edge of the capsule, associated with blood is characteristic for a fine needle aspiration site. These changes do not represent capsular invasion.



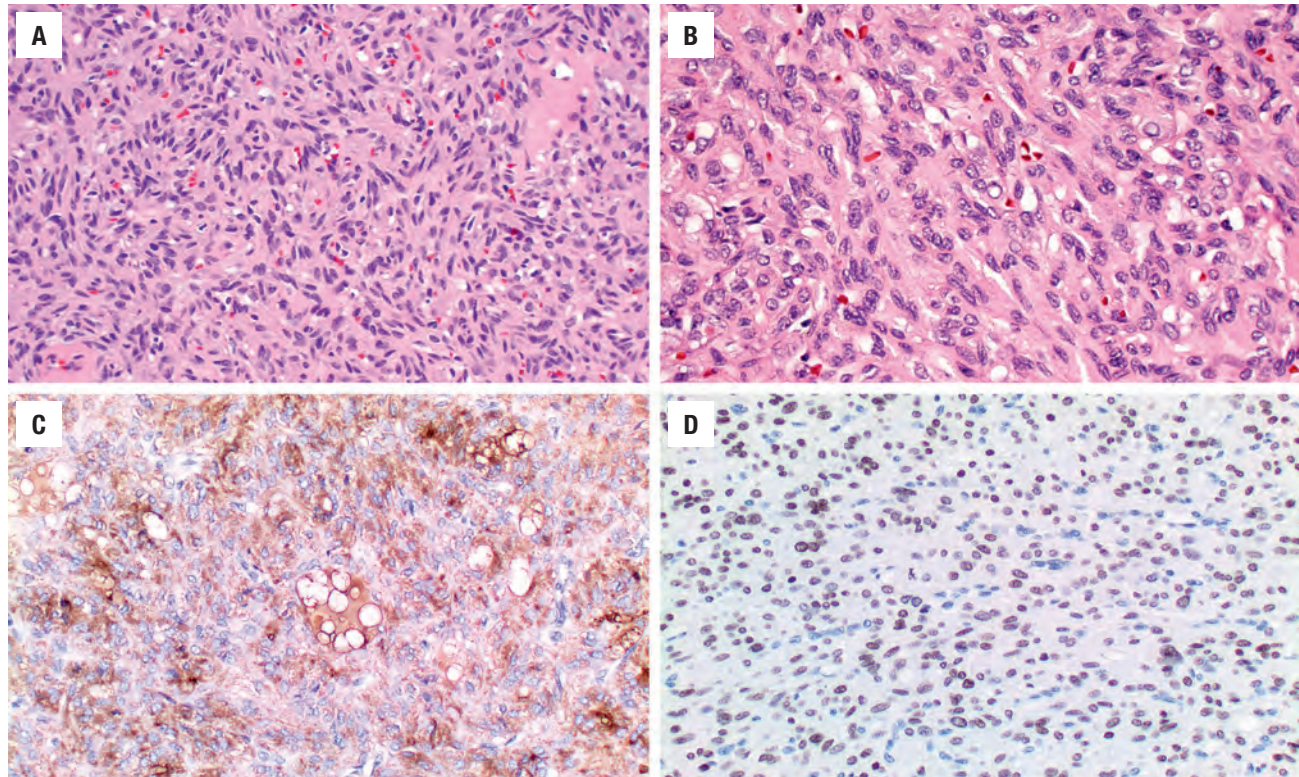
**FIGURE 24.9**

A follicular adenoma with normofollicular architecture showing easily identified colloid. The tumor is distinctly different from the surrounding parenchyma.

**FIGURE 24.10**

(A) A trabecular-to-insular architecture is noted in this adenoma with scant colloid. (B) There is no intratumoral fibrosis, although vascular channels are noted surrounding the trabeculae.



**FIGURE 24.11**

(A) Lesional cells show a spindled architecture. (B) Nuclei are elongated with grooves but set within a spindled cell population. (C) Spindled cells are strongly positive with thyroglobulin. (D) They are also reactive with TTF1 in this example of a spindle cell adenoma.

are monotonous and only slightly enlarged. There is a low nuclear:cytoplasmic ratio with well-defined cell borders in the cuboidal to columnar cells. The nuclei are usually aligned in an orderly arrangement along the basal aspect of the cell. Ample cytoplasm, ranging from eosinophilic, oncocytic (Fig. 24.12), amphophilic, granular to clear, or signet-ring (Fig. 24.13), surrounds round and regular nuclei with a coarse to heavy nuclear chromatin distribution. Nucleoli are inconspicuous, although they may be prominent and centrally placed in an oncocytic FA (Fig. 24.12). Profound nuclear pleomorphism may be seen but is usually focal (Fig. 24.12). Mitotic figures are generally inconspicuous but may be increased, particularly in the post-FNA setting. Degenerative and cystic changes include edema, fibrosis, hemorrhage, cyst formation, and calcification, but tumor necrosis is not identified. Infarction, especially in oncocytic tumors, may be associated with prior FNA or decreased blood supply. Viable tumor cells may be limited to the periphery. Fat is rarely noted (lipid-rich adenoma) within the tumor cells and presents as intracytoplasmic, oil red O–positive vesicles (Fig. 24.14). This is distinct from lipoadenoma, in which mature fat is interspersed between the follicular epithelial cells (Fig. 24.15). Squamous metaplasia may be seen but is more common in papillary carcinoma.

*Oncocytic* (oxyphilic, Hürthle cell, Ashkenazi cell) *adenoma* typically has less colloid production, frequently resulting in inspissated colloid that can mimic psammoma

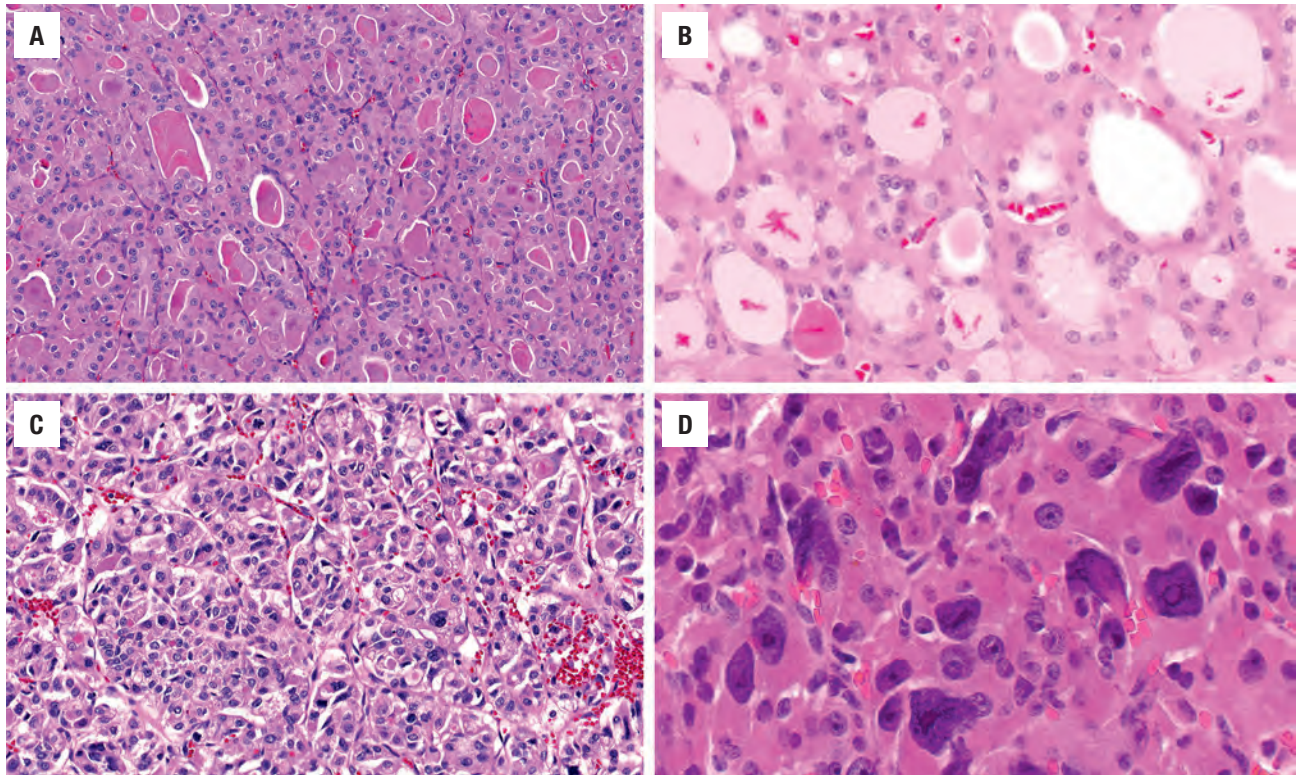
bodies (Figs. 24.12 and 24.16, left). Tumor cells tend to have a greater degree of nuclear atypia (Fig. 24.12), with vesicular nuclear chromatin, nuclear contour irregularity, and prominent nucleoli. The cytoplasm is eosinophilic and granular. However, oncocytic adenoma is a histologic description only and *does not* imply a different biologic potential. To be qualified as a *clear cell variant*, the tumor should be predominantly or exclusively composed of cells with clear cytoplasm (Fig. 24.13). The nuclei are usually centrally situated and are hyperchromatic. *Signet-ring cell adenoma* is extremely rare but has cells with large intracytoplasmic vacuoles, which compress the nucleus to the side (Fig. 24.13). These vacuoles contain diastase-resistant PAS-positive material, which is strongly thyroglobulin-immunoreactive, suggesting an abnormal thyroglobulin accumulation. Metastatic adenocarcinoma may rarely give a similar histologic appearance.

## ANCILLARY STUDIES

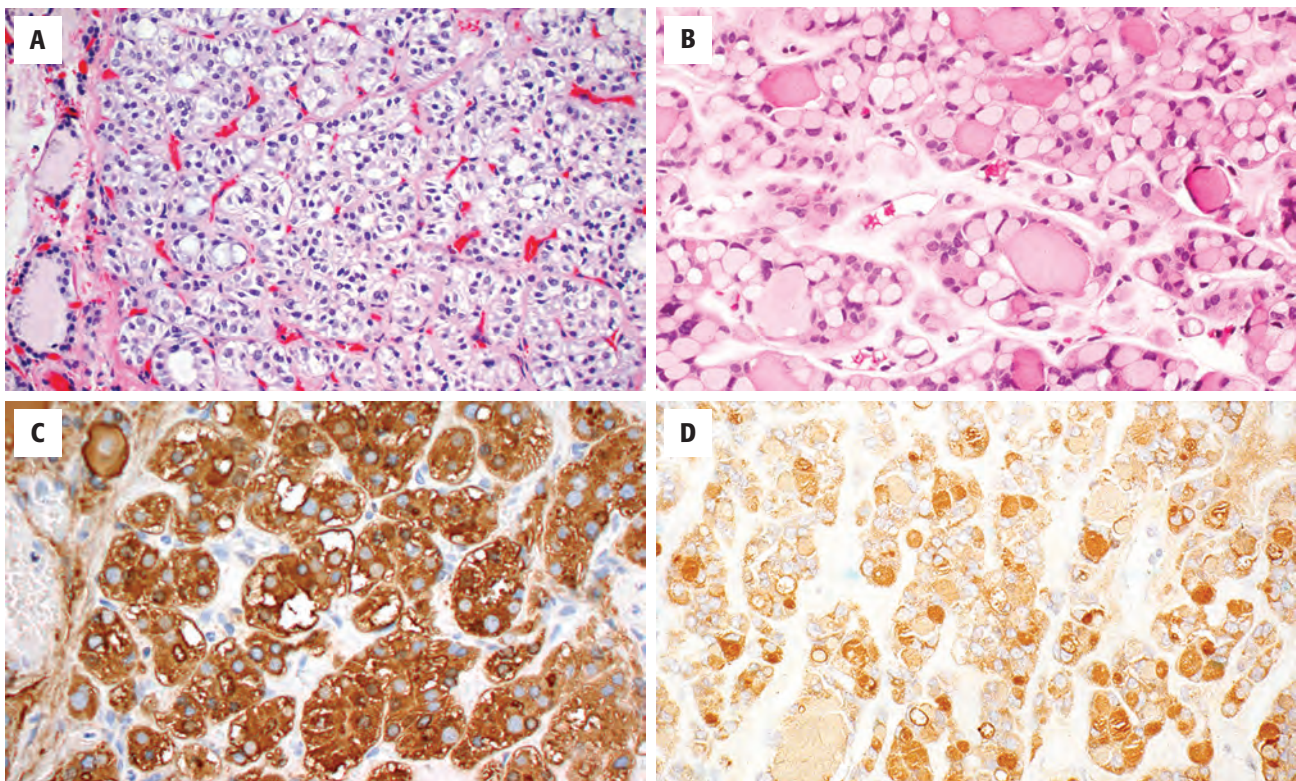
### IMMUNOHISTOCHEMICAL FINDINGS

Immunohistochemistry is seldom necessary for the diagnosis, but in cases where the diagnosis is in question, the neoplastic cells will be immunoreactive to thyroglobulin (Figs. 24.11, 24.13, and 24.16), TTF1 (Figs. 24.11



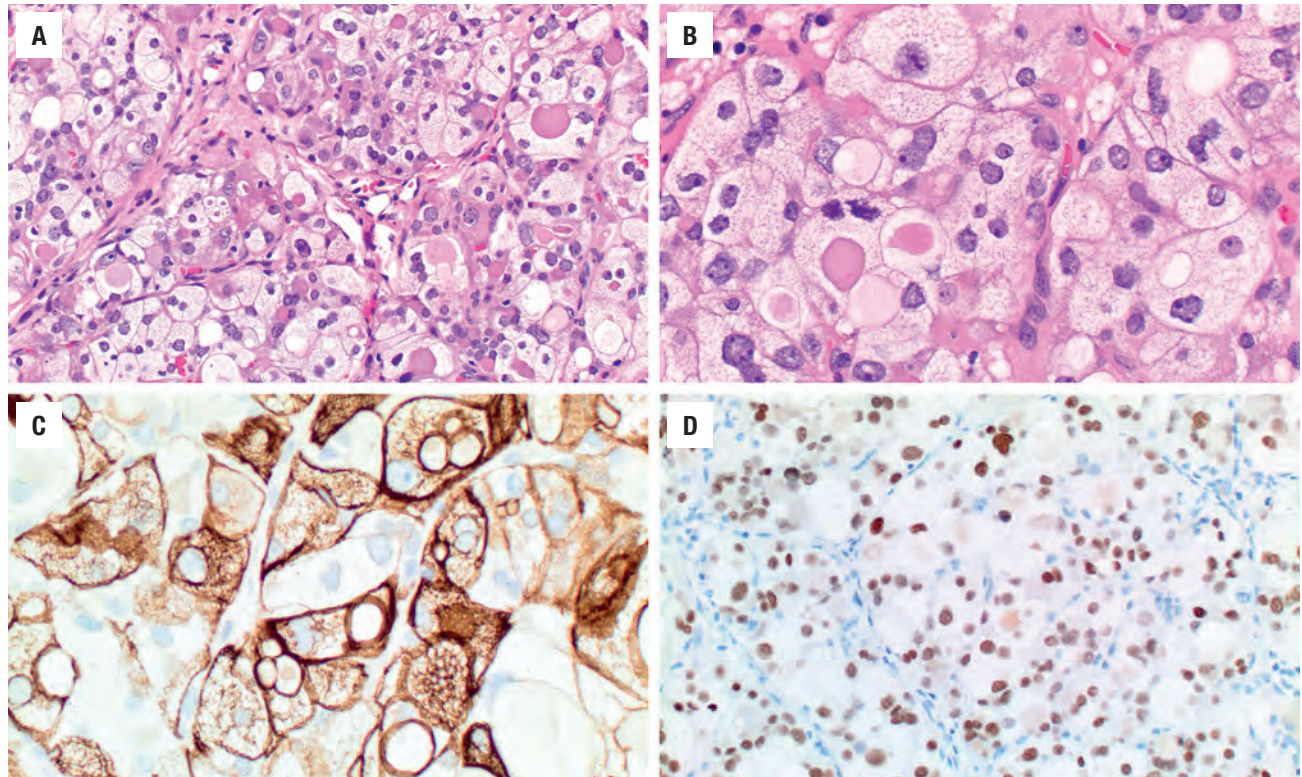
**FIGURE 24.12**

A series of follicular adenomas with oncocytic cells, showing the diversity that may be seen (A-D). There is abundant eosinophilic, granular cytoplasm surrounding nuclei that are generally round and regular, sometimes with prominent nucleoli. (D) Profound but focal nuclear pleomorphism may be seen in endocrine organ neoplasms—a finding that does not confer malignancy.

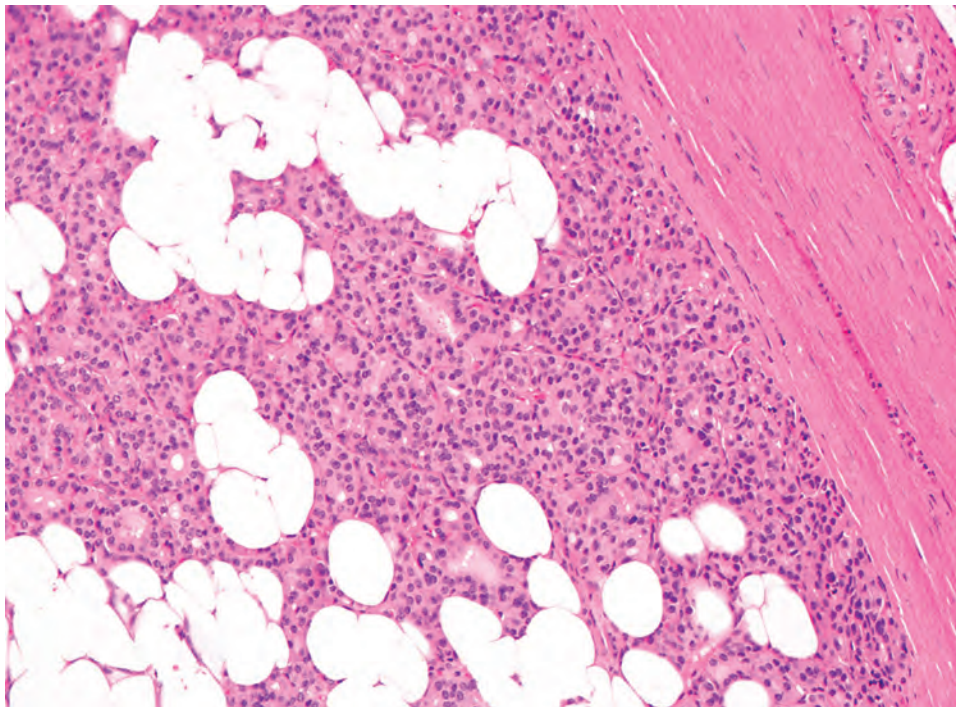
**FIGURE 24.13**

A follicular adenoma is composed exclusively of clear cells in this case (A), although colloid production can still be highlighted with a thyroglobulin (C). (B) A signet-ring adenoma is composed of cells with a large cytoplasmic vacuole that compresses the nucleus. (D) Thyroglobulin highlights the vacuoles in a signet-ring adenoma.



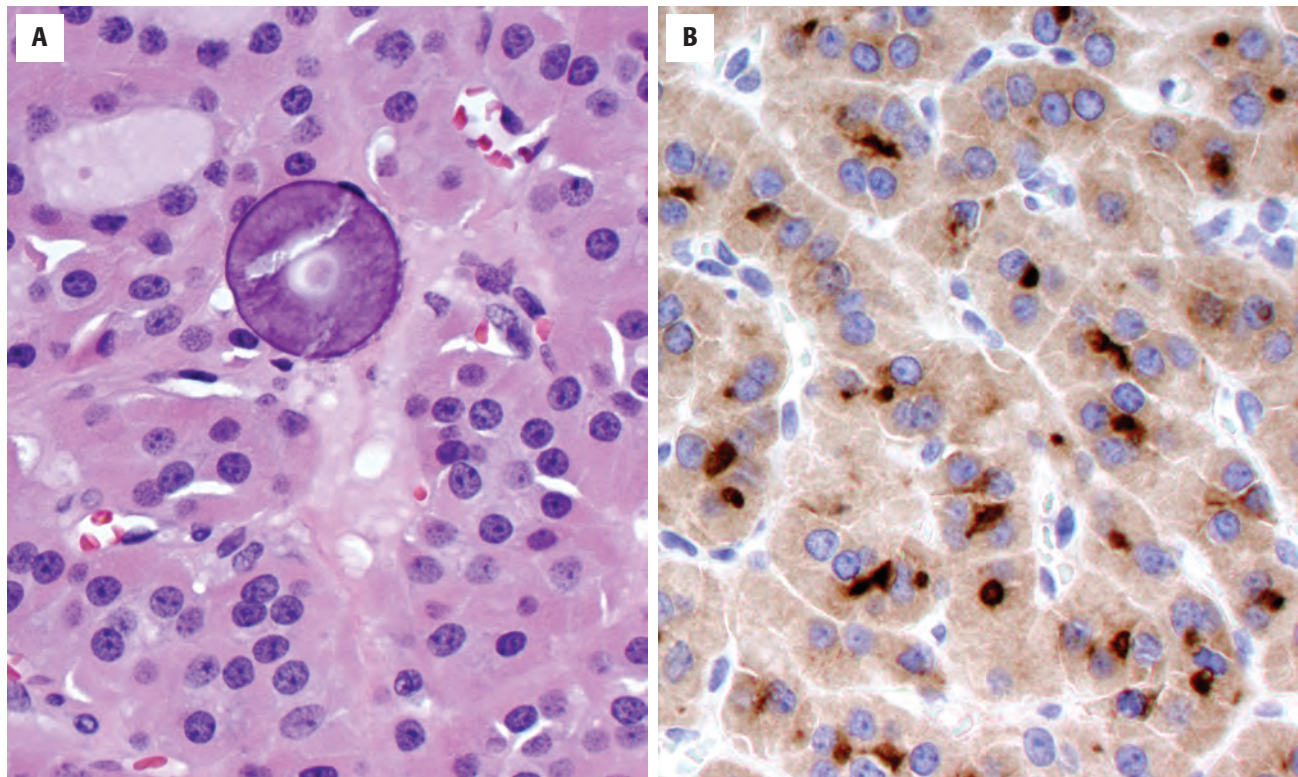
**FIGURE 24.14**

A lipid-rich follicular adenoma shows a follicular architecture (A), with higher magnification showing the microvesicular cytoplasmic quality (B). Neoplastic cells are positive with CK19 (C), which highlights the vacuoles, while the nuclei react strongly with TTF1 (D).

**FIGURE 24.15**

A lipoadenoma contains fat cells interspersed between the follicles.



**FIGURE 24.16**

(A) Colloid has become inspissated and calcified, but the nuclei are round and regular in this oncocytic follicular adenoma. (B) Thyroglobulin may help to confirm the follicular derivation of tumors with limited to absent colloid production.

and 24.14), PAX8, and keratin (CAM5.2, AE1/AE3, CK7). Oncocytic tumors must be interpreted with caution owing to high background and nonspecific staining.

#### FINE NEEDLE ASPIRATION

FNA is the first-line evaluation technique. Unfortunately FNA does not reliably distinguish between a cellular and a dominant adenomatoid nodule, FA, or follicular carcinoma with any degree of certainty or reproducibility. After adequacy is assessed (five or six follicular epithelial groups of at least 10 epithelial cells per group), a follicular neoplasm may be favored over an adenomatoid nodule (colloid goiter). Features that favor a neoplasm are syncytial groups with a microfollicular arrangement in a cellular smear in which there is increased cellularity compared with the amount of colloid and uniform, monotonous cells that vary little from one another (Fig. 24.17). The epithelial groups are arranged as small spherical aggregates surrounding a colloid droplet. Oncocytic adenomas have large polygonal cells with granular cytoplasm. The nucleoli tend to be more prominent. Adenomatoid nodules tend to have cellular variability and often show extensive degenerative changes. The diagnosis of “follicular neoplasm” or “suspicious for a follicular neoplasm” will result in appropriate surgery for a solitary thyroid mass (equivalent to Bethesda System for Reporting Thyroid Cytopathology category IV).

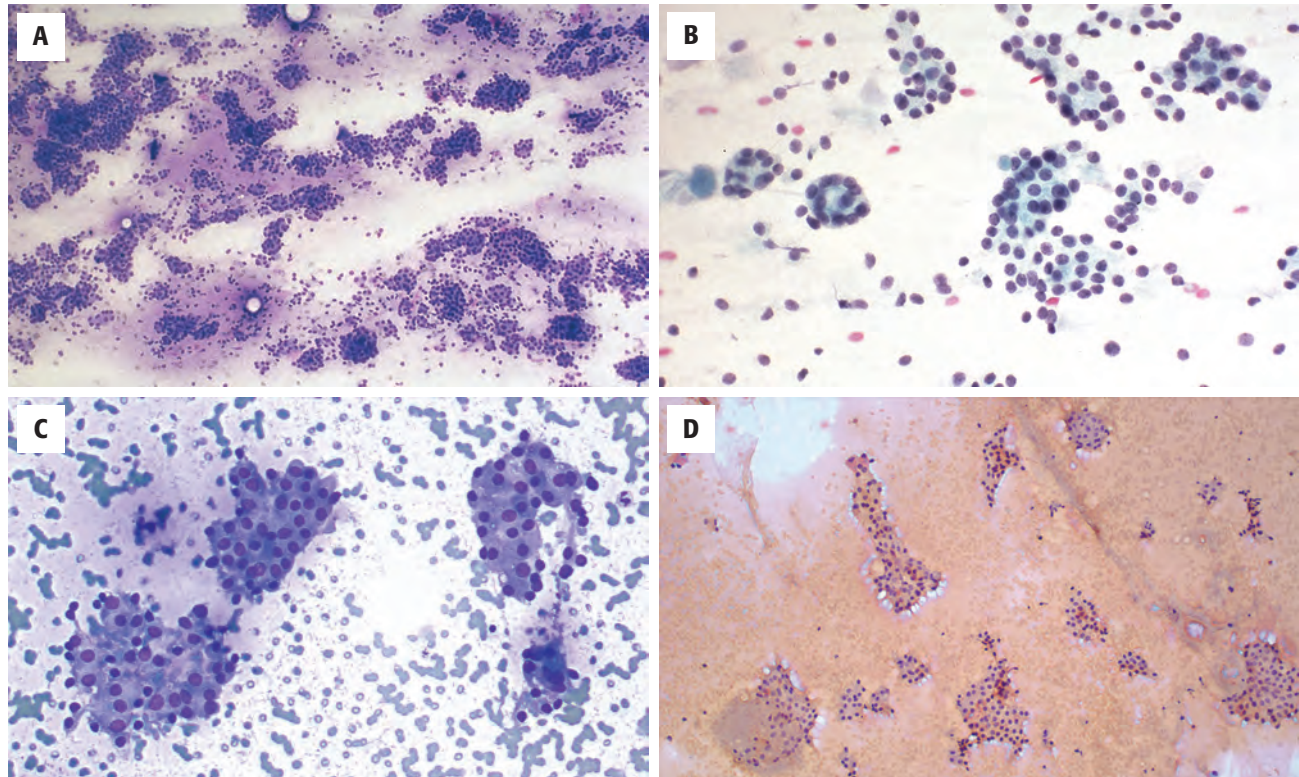
#### INTRAOPERATIVE FROZEN SECTION

Intraoperative consultation cannot reliably separate FA from follicular carcinoma because extensive sampling is needed to exclude invasion; therefore it is not helpful, and should be deferred.

#### GENETICS

Numerical chromosome changes can be seen, with trisomy 7 seen in some 15 % of FAs, while tetrasomy is seen in about 45 % of oncocytic adenomas. Translocations involving 2p21 (*THADA*) and 19q13 (*ZNF331-RITA*) are seen in approximately 10 % and 20 %, respectively, of FAs. The *PAX8-PRAR* $\gamma$  rearrangement, characteristic of follicular carcinoma, is also found in less than 10 % of FAs. *PAX8-PRAR* $\gamma$ -rearranged tumors often have thickened capsules, a feature worrisome for malignancy. Infrequent *TERT* promoter mutations have been associated with atypia and aggressive behavior. Thus, *PAX8-PRAR* $\gamma$ -rearranged and *TERT*-mutated FAs may represent follicular carcinoma precursors or, in some cases, undersampled follicular carcinomas. In these cases, more extensive sampling to identify invasion is advocated.

Activating point mutations of *RAS* genes (specifically *NRAS* and *HRAS*) are most prevalent and detected in about 20 % to 30 % of cases overall, but they are less common in oncocytic adenomas. *RAS* mutations are not

**FIGURE 24.17**

Fine needle aspiration of follicular adenomas usually generates a Bethesda category IV: “follicular neoplasm” or “suspicious for follicular neoplasm.” Cellular smears with syncytial groups of uniform and monotonous cells are seen. Scant colloid is present (**A** and **C**, air-dried, Diff-Quik stain; **B** and **D**, alcohol-fixed, Papanicolaou stain). Note the oncocyctic appearance of the cells in **C** and **D**.

restricted to FA and occur in all types of thyroid neoplasms, including follicular, papillary, and medullary carcinomas and even occasionally in nodular hyperplasia. Somatic mutations in mitochondrial DNA (mtDNA) are found in oncocyctic tumors. Thyroid-stimulating hormone (TSH) receptor gene mutations have been described in hyperfunctioning “toxic” adenomas.

### DIFFERENTIAL DIAGNOSIS

The differential diagnosis includes cellular or dominant adenomatoid nodules, follicular or papillary thyroid carcinoma (PTC), noninvasive follicular thyroid neoplasm with papillary-like nuclear features (NIFTP), medullary carcinoma, hyalinizing trabecular tumor, and metastatic carcinomas. Definitive separation between FA and *adenomatoid nodule* is arbitrary and sometimes semantic, as both are benign lesions calling for no difference in management. With that said, adenomatoid nodules are usually multiple, lack a capsule with smooth muscle-walled vessels, and usually have much more abundant colloid and degenerative changes than an adenoma. Oncocyctic cells can be seen in either.

Without definitive capsular or vascular invasion, a diagnosis of *carcinoma* cannot be rendered in the case

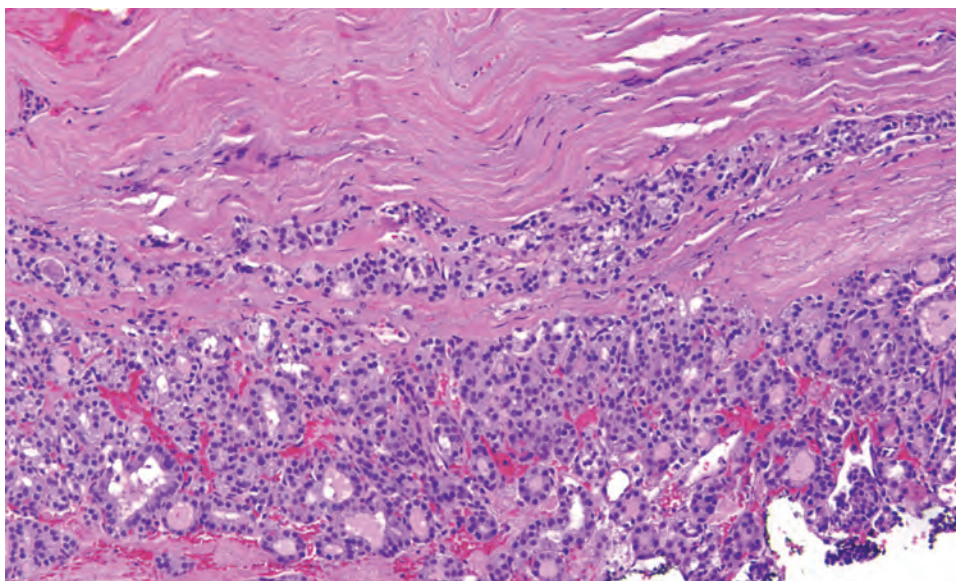
of a follicular neoplasm. However, features that raise the suspicion of carcinoma include a remarkably thickened fibrous capsule, increased cellularity (especially at the periphery of the tumor), increased mitotic activity, atypical mitotic figures, and tumor necrosis. Still, invasion must be present to call the tumor a follicular carcinoma. The designation *atypical adenoma* may be used in circumstances where a definitive separation is impossible (Fig. 24.18). To date, cytogenetic and molecular studies cannot reliably separate follicular tumors.

Oxyphilia often results in nuclear contour irregularities and intranuclear cytoplasmic inclusions (any cell with abundant cytoplasm is prone to intranuclear cytoplasmic invaginations), both features seen in PTC. However, additional architectural and cytomorphologic features of papillary carcinoma must be present before making the diagnosis: invasive growth, intratumoral fibrosis, thick eosinophilic colloid, and the characteristic nuclear features of enlargement, crowding, irregular placement around the follicle, grooves, folds, and contour irregularities, with chromatin clearing and margination. Nuclear features of papillary carcinoma alone in a follicular neoplasm are no longer sufficient to render a diagnosis of papillary carcinoma; architecture, pattern of growth, cytoplasmic qualities, and invasion must be taken into consideration. Otherwise, a diagnosis of *NIFTP* must be considered (see next section for discussion of NIFTP). The most



**FIGURE 24.18**

A very thick fibrous connective tissue capsule with irregularities in the contour, focal areas of “entrapment,” and an increased cellularity at the periphery are worrisome for a follicular carcinoma but not quite definitive for invasion. “Atypical adenoma” may be employed as the diagnosis.



significant distinguishing feature between FA and NIFTP is the presence of nuclear features of PTC in the latter, as both are noninvasive.

*Medullary thyroid carcinoma* should be considered in any FA that lacks well-developed colloid, especially if spindled or clear cells are present; it should be assessed with immunohistochemistry (calcitonin, synaptophysin, chromogranin). Other *clear cell tumors*, such as some parathyroid neoplasms or metastatic renal cell carcinoma (CAIX, CD10, RCC), can usually be separated on immunohistochemical grounds as well. *Hyalinizing trabecular tumor* shows a trabecular growth pattern with a perpendicular arrangement of nuclei, grooves, and pseudoinclusions; it demonstrates a distinctive membranous staining pattern with Dako Ki-67 antibody (MIB-1).

### PROGNOSIS AND THERAPY

There is an excellent long-term clinical prognosis without recurrences or metastasis when the lesion is removed by conservative surgery (lobectomy alone). Hypoparathyroidism and recurrent laryngeal nerve damage may result from surgery, but they are uncommon complications.

### ■ NONINVASIVE FOLLICULAR THYROID NEOPLASM WITH PAPILLARY-LIKE NUCLEAR FEATURES

The diagnostic term *NIFTP* represents a reclassification of the entity previously known as noninvasive encapsulated follicular variant of PTC. It is a noninvasive, follicular-patterned tumor with nuclei resembling those

seen in papillary carcinoma. The terminology change reflects growing evidence that these tumors have extremely low malignant potential when completely excised and therefore should not be classified as malignant. NIFTP, like FA, is a noninvasive tumor, so it is equally important to exclude invasive growth with extensive sampling of the periphery of the tumor (i.e., complete submission of periphery). The absence of invasion in NIFTP distinguishes it from papillary carcinoma. A set of inclusion and exclusion criteria must be applied to diagnose NIFTP (Fig. 24.19), described in the following paragraphs.

### CLINICAL FEATURES

Similar to FA, NIFTP typically presents as a painless, mobile thyroid nodule. The nodule may be palpable or incidentally discovered on imaging performed for another indication. Large tumors may cause compressive symptoms. Patients are euthyroid. Although NIFTP is a new diagnostic category, the incidence of NIFTP can be estimated from that of encapsulated follicular variant of PTC, which was about 10% to 20% of all PTCs. Thus, the incidence in the general population is estimated to be roughly 1 in 100,000. NIFTP is more common in women (female-to-male ratio of 3 to 4:1), who most often present in the 5th decade of life.

### RADIOGRAPHIC FEATURES

Ultrasound features are nonspecific, although a hypoechoic rim may be present. NIFTP is often solid and well defined on imaging.

## ALGORITHM FOR DIAGNOSIS OF NIFTP

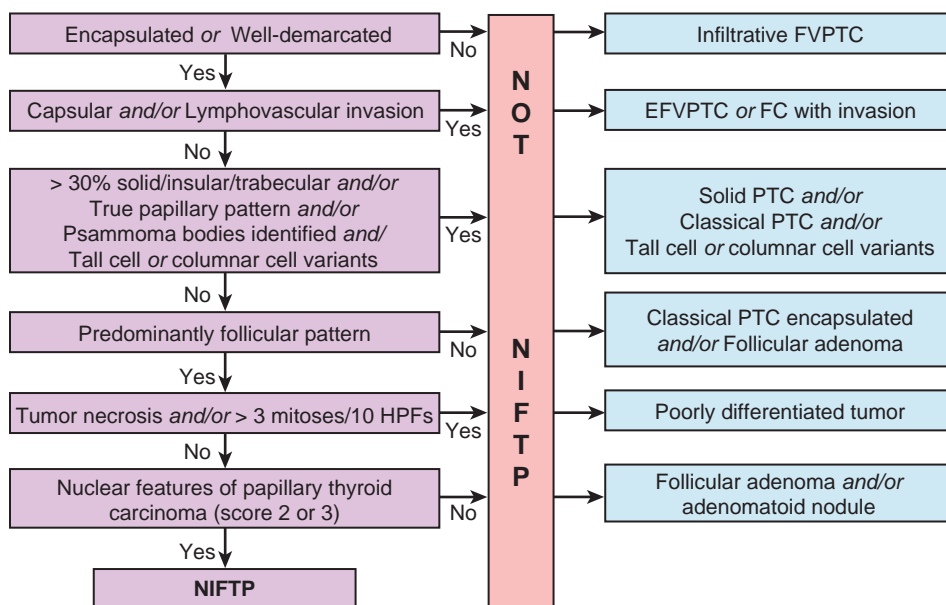


FIGURE 24.19

Algorithm for the diagnosis of NIFTP. EFV, Encapsulated follicular variant; FC, follicular carcinoma; FV, follicular variant; HPF, high power fields; NIFTP, noninvasive follicular thyroid neoplasm with papillary-like nuclear findings; PTC, papillary thyroid carcinoma.

## NONINVASIVE FOLLICULAR THYROID NEOPLASM WITH PAPILLARY-LIKE NUCLEAR FEATURES—DISEASE FACT SHEET

## Definition

- Noninvasive follicular neoplasm with nuclear features resembling PTC with an extremely low malignant potential

## Incidence

- Incidence of ~1 per 100,000

## Morbidity and Mortality

- Recurrence is possible with incomplete excision

## Sex and Age Distribution

- Females > males (3-4:1)
- Wide age range (20-80); mean, 46 years

## Clinical Features

- Painless neck mass
- Palpable or discovered on imaging

## Prognosis and Therapy

- Excellent with conservative surgery alone

PTC, Papillary thyroid carcinoma.

## PATHOLOGIC FEATURES

## GROSS FINDINGS

The gross appearance is similar to that of FA. Tumors are circumscribed or grossly encapsulated and usually 2 to 4 cm in diameter, but they may be much larger. The

cut surface is tan-white or brown, the latter resembling normal thyroid. NIFTP should be grossed in an identical manner to FA with thorough sampling of the periphery (i.e., complete submission or at the very least three sections per centimeter of tumor diameter) to exclude invasive growth, which, if present, would be diagnostic of PTC.

## MICROSCOPIC FINDINGS

As the name implies, NIFTP is a follicular-patterned thyroid neoplasm that shows a noninvasive growth (encapsulated or well demarcated) and nuclei resembling those seen in PTC (Figs. 24.20 and 24.21). NIFTP is diagnosed based on the presence of four histologic criteria and the absence of any exclusionary criteria. A diagnostic algorithm may be helpful in reaching a diagnosis (Fig. 24.19).

The *inclusion criteria* are as follows: (1) clear demarcation/circumscription and/or a complete capsule (Fig. 24.20), (2) noninvasive growth (no capsular or lymphovascular invasion), (3) follicular architecture, and (4) nuclear features of PTC (Fig. 24.21). The nuclear features frequently show a patchy (sprinkled) distribution or are not as well developed as in classical PTC. Intranuclear pseudoinclusions are rarely identified. Use of a 3-point scoring system to evaluate the nuclei may be helpful: 1 point is given for nuclear enlargement, crowding, and overlap; 1 point for nuclear contour irregularity including grooves, folds, and pseudoinclusions; and 1 point for nuclear clearing, margination, or glassy nuclei. A total of 2 or more points is sufficient for the diagnostic category.

The *exclusion criteria* are as follows: (1) the presence of true papillae with fibrovascular cores (abortive papillae



### NONINVASIVE FOLLICULAR THYROID NEOPLASM WITH PAPILLARY-LIKE NUCLEAR FEATURES—PATHOLOGIC FEATURES

#### Gross Findings

- Solitary, well-demarcated/encapsulated spherical mass
- Extensive sampling of the periphery necessary to exclude malignancy

#### Microscopic Findings

- Encapsulated or well-demarcated predominantly follicular-patterned neoplasm
- Noninvasive growth (no capsular or lymphovascular invasion)
- Papillary nuclear features present
- No true papillae; no psammoma bodies
- Solid, trabecular or insular growth in < 30% of the tumor
- No necrosis or increased mitotic activity
- No morphologic features of other variants of papillary carcinoma (i.e., tall cell, columnar cell, cribriform morular, oncocytic, etc.)

PTC, Papillary thyroid carcinoma.

#### Immunohistochemical Findings

- Positive for thyroglobulin, TTF1, PAX8, CK7, and keratin

#### Fine Needle Aspiration

- Cellular aspirate with scant colloid
- Lack of three-dimensional papillary structures; no psammoma bodies
- Nuclear enlargement and grooves may lead to an atypia of undetermined significance or suspicious for PTC diagnosis
- PTC is a pitfall, but noninvasive follicular thyroid neoplasm with papillary-like nuclear features is rarely diagnosed as such

#### Pathologic Differential Diagnosis

- Follicular variant papillary carcinoma, follicular adenoma, follicular carcinoma

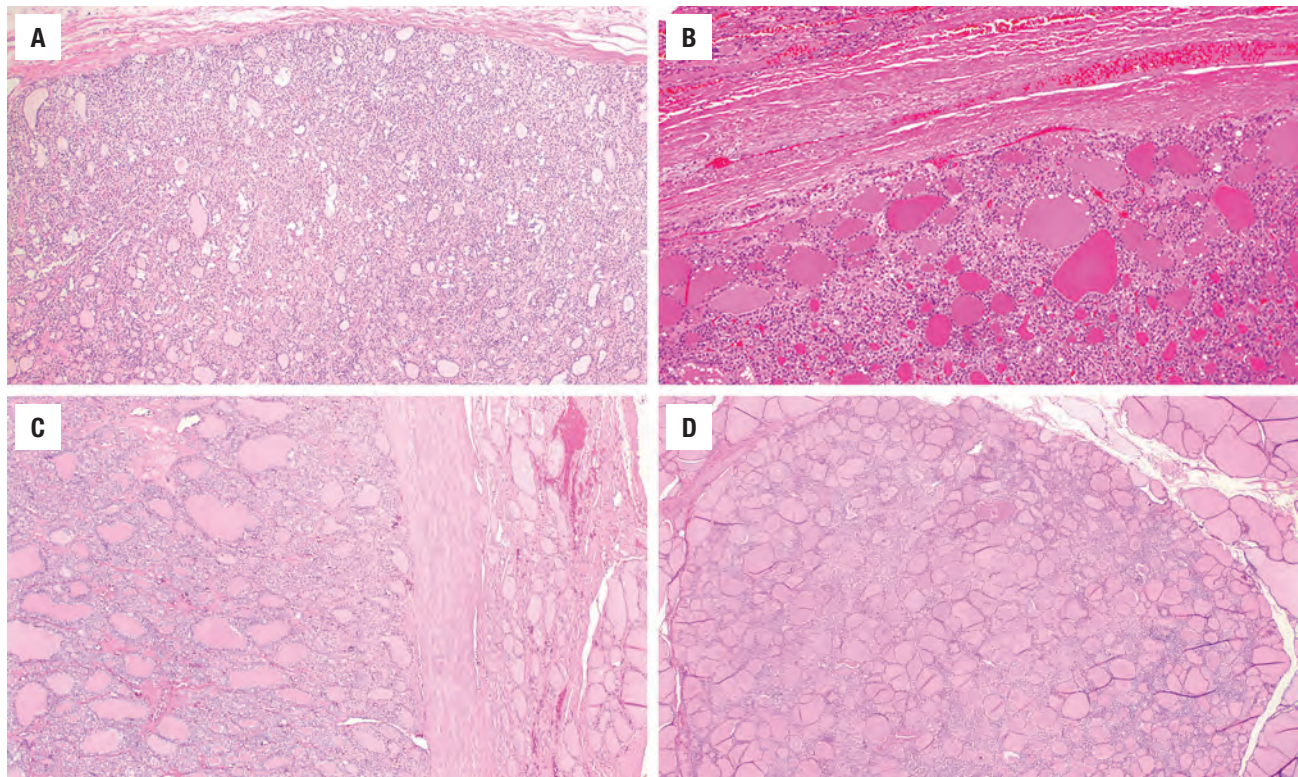


**FIGURE 24.20**

NIPTP shows a distinct neoplasm in comparison to the surrounding tissue. A capsule (**A** to **C**) is usually present, showing variable thickness. (**D**) A well-demarcated but unencapsulated tumor is distinct from the surrounding thyroid parenchyma.

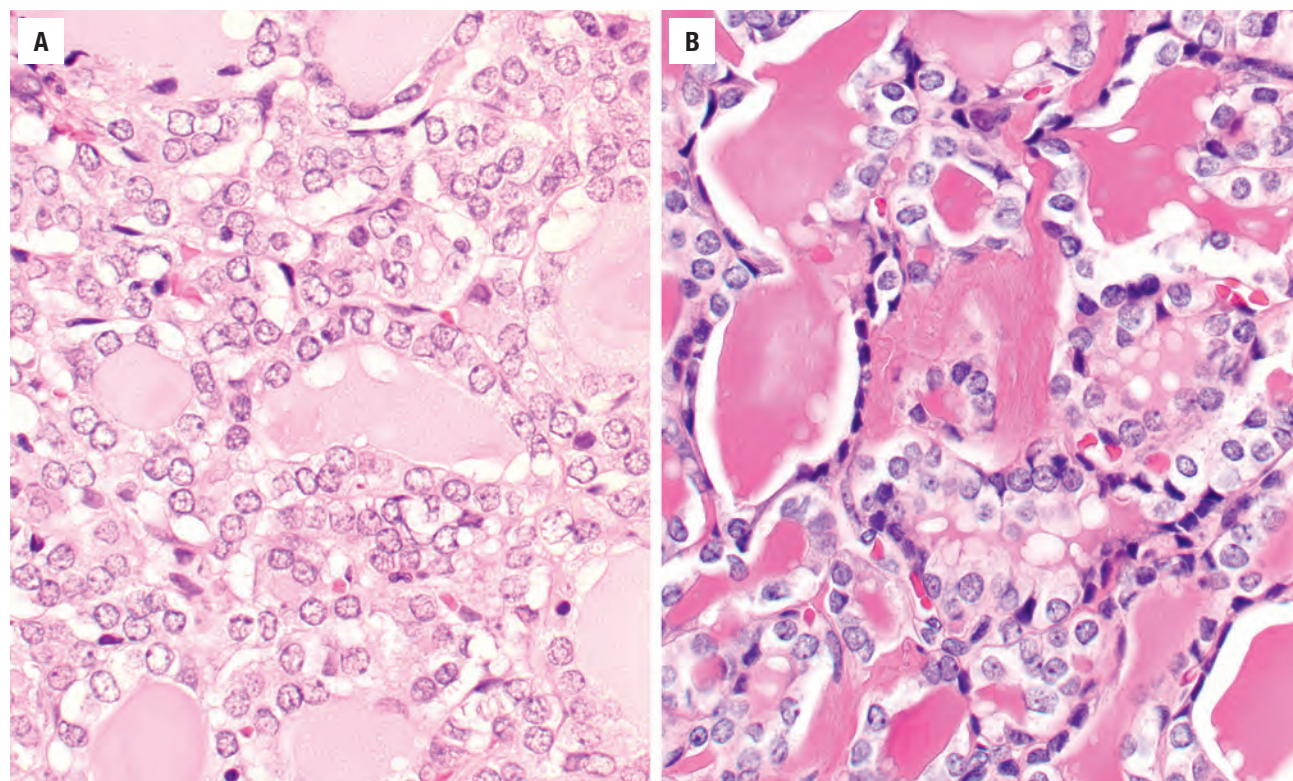
are acceptable); (2) psammoma bodies (evidence of true papillae); (3) more than 30% solid/trabecular/insular growth; (4) tumor necrosis; (5) mitotic activity equal to or greater than three mitoses per 10 high power fields; (6) morphology characteristic of other variants of papillary carcinoma (tall cell, columnar cell, cribriform-morular, etc.).

### ANCILLARY STUDIES

#### IMMUNOHISTOCHEMICAL FINDINGS

The neoplastic cells are positive for thyroglobulin, TTF1, PAX8, CK7, and keratins. HBME-1, CITED1,



**FIGURE 24.21**

(A and B) Nuclear features of papillary thyroid carcinoma are present in NIFTP, including nuclear enlargement, overlapping, and crowding; nuclear contour irregularities (grooves, folds); and nuclear chromatin clearing or margination. Intratumoral fibrosis is noted (B).

galectin-3, CK19, and other markers have been suggested but show significant individual variability of staining both within and between tumors.

#### FINE NEEDLE ASPIRATION

FNAs usually show cellular groups of follicular epithelial cells with scant colloid. Microfollicles may be present. Nuclear features are often inconspicuous and, as a result, the majority are diagnosed as follicular lesion of undetermined significance (FLUS), atypia of undetermined significance (AUS [Fig. 24.22]), or suspicious for follicular neoplasm (SFN) (Bethesda System for Reporting Thyroid Cytopathology categories III and IV) on FNA. The remaining cases are usually classified as suspicious for malignancy (Bethesda category V). A diagnosis of PTC may rarely be made. This is a known pitfall of NIFTP on cytology. However, if three-dimensional papillary structures or psammoma bodies are present, a NIFTP diagnosis is excluded.

#### GENETICS

The molecular alterations overlap with other benign and malignant thyroid neoplasms. *RAS* mutations are common, while other reported alterations include *PPAR $\gamma$*  and *THADA* fusions and *BRAF*-K601E (but not V600E) mutations.

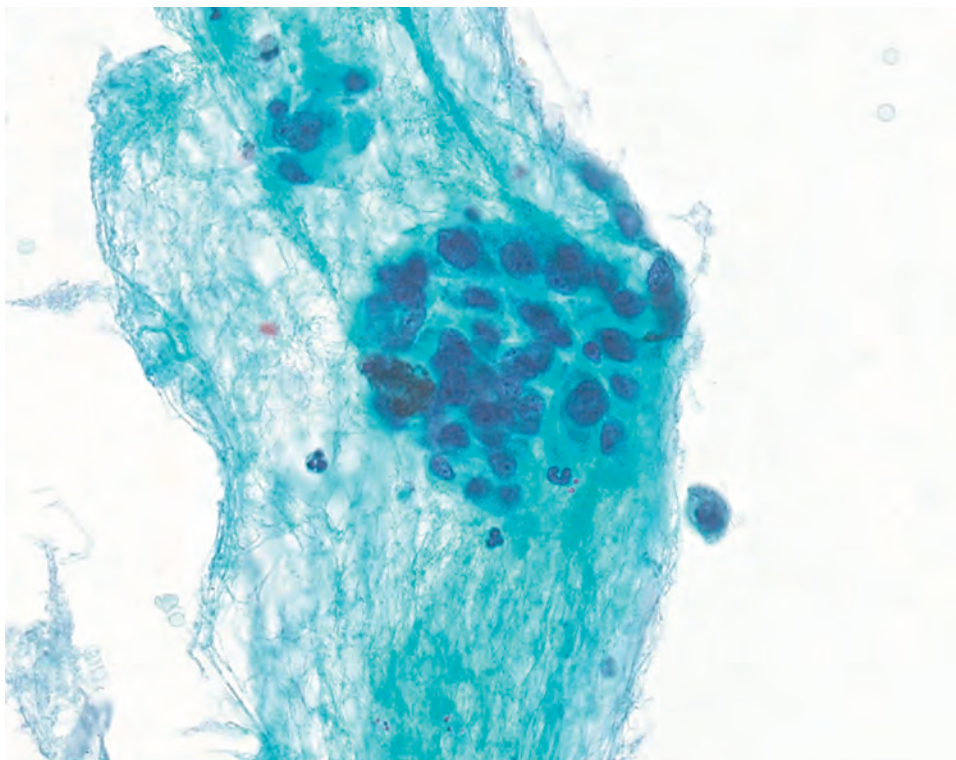
#### DIFFERENTIAL DIAGNOSIS

The differential diagnosis includes adenomatoid nodule, FA, PTC, and follicular carcinoma. The distinction from FA and adenomatoid nodule rests on identification of nuclear features of PTC, which are present in NIFTP and absent in both FA and adenomatoid nodule. However, the nuclear features can be subtle and/or patchy in NIFTP. Use of the previously described 3-point system for scoring nuclear features (with a score of 2 or 3 considered positive) may be helpful. The distinction between NIFTP and carcinoma (either papillary or follicular) is made based on the presence of capsular or lymphovascular invasion in carcinoma. A diagnosis of carcinoma may be rendered in the absence of invasion if NIFTP exclusion criteria are present (as discussed).

#### PROGNOSIS AND THERAPY

As long as the tumor is completely excised, the risk of recurrence is significantly less than 1%. Completion thyroidectomy and radioablative iodine are not necessary.



**FIGURE 24.22**

This is a fine needle aspiration biopsy of a noninvasive follicular thyroid neoplasm with papillary-like nuclear findings that was interpreted as atypia of undetermined significance. Nuclear crowding and overlap with irregular nuclear contours are present.

## ■ HYALINIZING TRABECULAR TUMOR

Hyalinizing trabecular tumors (HTTs) are very rare follicular neoplasms with trabecular growth and intratrabecular hyalinization; they seem to have a molecular link to papillary thyroid carcinoma (*RET-PTCH1* rearrangements but not *BRAF*). A few cases have occurred following radiation exposure. The overwhelming majority have noninvasive growth and behave in a benign manner. Some refer to these as *hyalinizing trabecular adenoma*. Extremely rare examples with invasive growth and metastasis have been described (*hyalinizing trabecular carcinoma*).

### CLINICAL FEATURES

Women are affected much more commonly than men (female-to-male ratio, 6:1) with a wide age range at initial presentation, although the mean age is 50 years. Patients usually have an asymptomatic neck mass that is discovered incidentally during routine physical examination or found in multinodular glands removed for a different reason. Patients are usually euthyroid. Ultrasonography shows a solid nodule with hypoechoic or heterogeneous echogenicity. Most but not all nodules are “cold” on scintigraphy.

### HYALINIZING TRABECULAR TUMOR—DISEASE FACT SHEET

#### Definition

- Hyalinizing trabecular tumor is a follicular cell neoplasm with a trabecular growth pattern and heavy intratrabecular hyalinization

#### Incidence

- Rare

#### Morbidity and Mortality

- None without invasive growth

#### Sex and Age Distribution

- Females > > males (6:1)
- Usually presents in 5th to 6th decade

#### Clinical Features

- Solitary, usually asymptomatic mass
- Palpable or incidentally found
- Rare association with radiation

#### Prognosis and Therapy

- By definition, excellent
- Rare metastases associated with invasive growth (hyalinizing trabecular carcinoma)

## PATHOLOGIC FEATURES

### GROSS FINDINGS

Most commonly, a solitary encapsulated to well-circumscribed thyroid tumor that is usually small, with a mean size of 2.5 cm, is found, but tumors up to 7.5 cm have been reported. The cut surface is usually solid with a slight yellow tinge; it is delicately lobulated and occasionally shows patulous vessels. Grossly evident calcifications are uncommon.

### MICROSCOPIC FINDINGS

The cellular and solid tumors are well demarcated and surrounded by a well-formed but thin fibrous connective tissue capsule in a subset of cases. Vascular and/or capsular invasion is almost always absent; when present, it indicates a hyalinizing trabecular carcinoma. The cells are arranged in trabecular and insular patterns (Fig. 24.23), resulting in straight to curvilinear bands of tumor cells two to four cells thick. The nests are formed by a dense, heavily hyalinized eosinophilic fibrovascular stroma. The basement membrane material may resemble amyloid but is Congo red negative. Colloid is limited to absent. The nuclei are arranged perpendicular to the long axis of the trabeculae and fibrovascular stroma (Fig. 24.24). The cells are medium to large, polygonal to fusiform, with variable cytoplasm surrounding the oval to elongated nuclei. Intranuclear cytoplasmic inclusions are common, with easily identified nuclear grooves (Fig. 24.25). Perinucleolar halos are often present.

## HYALINIZING TRABECULAR TUMOR— PATHOLOGIC FEATURES

### Gross Findings

- Solitary, solid, circumscribed/encapsulated neoplasm
- Usually small, mean diameter: 2.5 cm

### Microscopic Findings

- Well-demarcated or thin fibrous connective tissue capsule
- Trabecular to insular growth pattern
- Hyalinized stroma separating neoplastic cells into trabeculae
- Scant to absent colloid
- Calcific bodies
- Medium-sized to large polygonal to fusiform cells, arranged perpendicularly to the long axis of the trabeculae
- Variable cytoplasm, sometimes containing yellow paranuclear bodies
- Prominent nuclear grooves and perinucleolar halos
- Prominent intranuclear cytoplasmic inclusions

### Immunohistochemical Findings

- Positive: thyroglobulin, TTF1, CK7
- Membrane MIB-1 (Ki-67) immunoreactivity (Dako only)

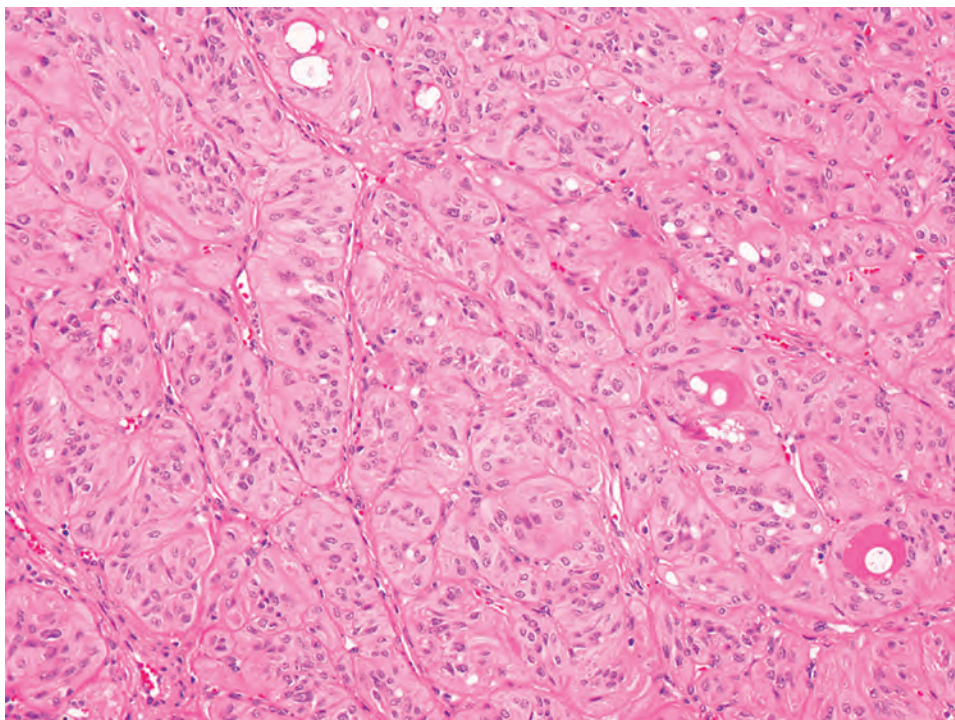
### Fine Needle Aspiration

- Cellular aspirates
- Elongated nuclei with grooves and pseudoinclusions may be misinterpreted as PTC
- Lumpy basement membrane material

### Pathologic Differential Diagnosis

- Paraganglioma, medullary thyroid carcinoma, PTC, FA, follicular carcinoma

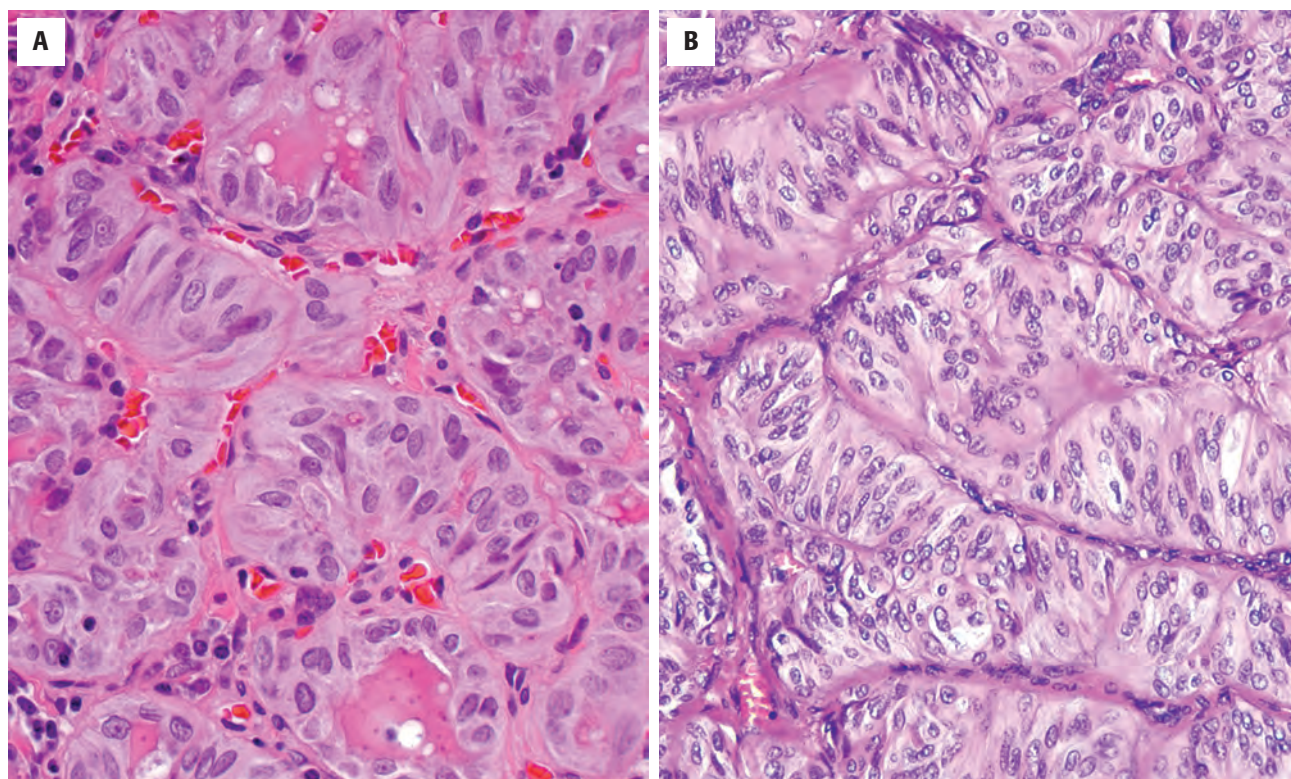
FA, Follicular adenoma; PTC, papillary thyroid carcinoma.



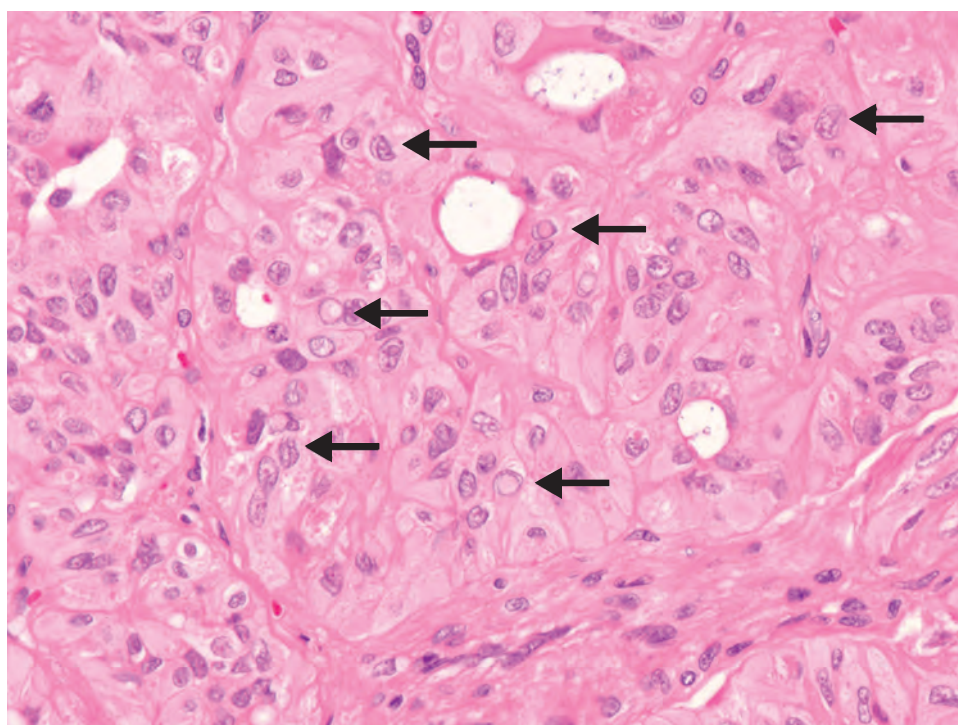
**FIGURE 24.23**

A hyalinizing trabecular tumor with cells arranged in trabeculae separated by fibrous connective tissue, often showing basement membrane material within the groups.



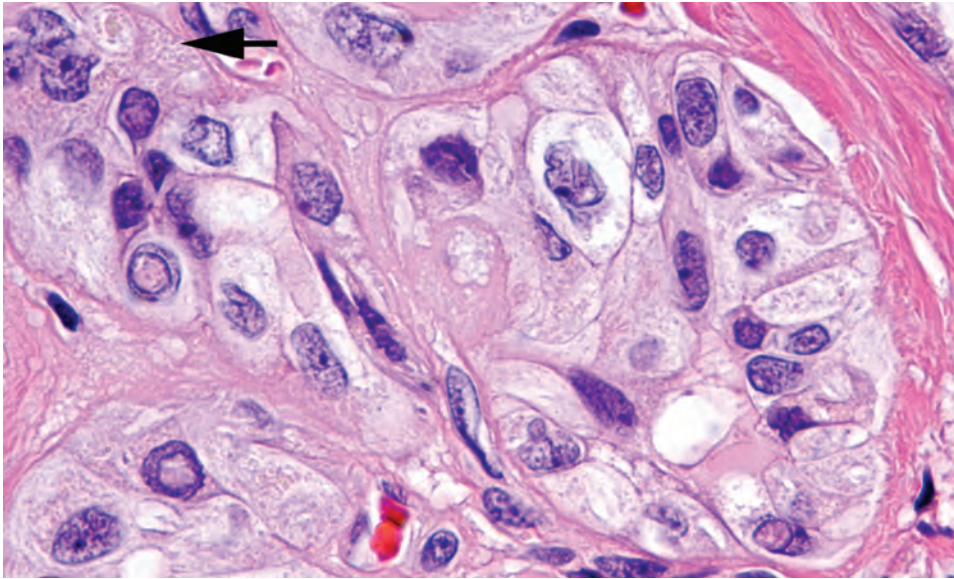
**FIGURE 24.24**

(A and B) Fusiform cells are arranged perpendicular to the fibrovascular stroma in these hyalinizing trabecular tumors.

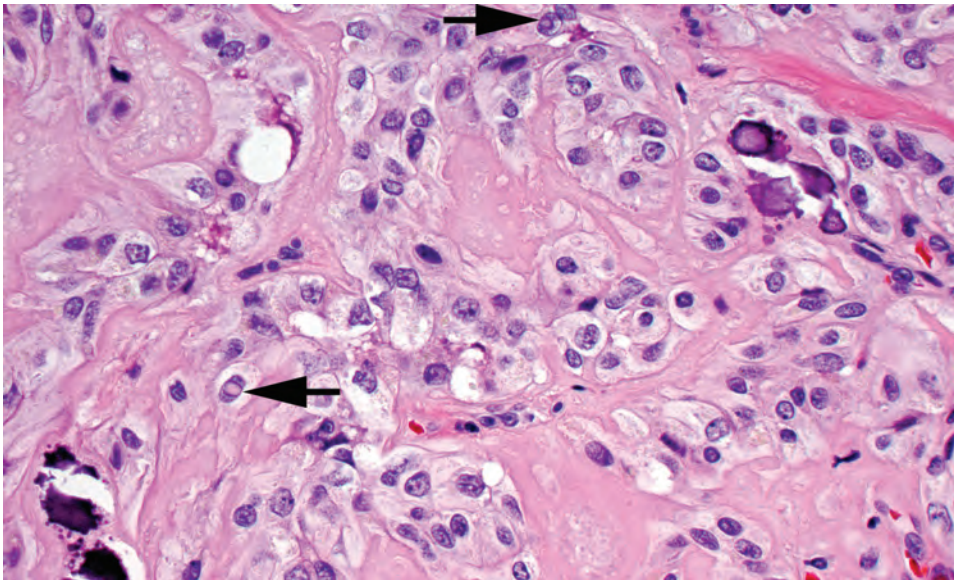
**FIGURE 24.25**

Intranuclear pseudoinclusions and nuclear grooves are very common (*arrows*). Perinuclear halos may also be seen.



**FIGURE 24.26**

There are slightly yellow paranuclear cytoplasmic bodies (*arrow*), a unique feature in hyalinizing trabecular tumors.

**FIGURE 24.27**

Calcifications may be present in hyalinizing trabecular tumors. Multiple intranuclear cytoplasmic inclusions (*arrows*) and perinucleolar halos are present.

Distinctive small, round, refractile, slightly yellow intracytoplasmic bodies may be seen in a paranuclear distribution (Fig. 24.26). Lymphocytic thyroiditis may be present in the background thyroid parenchyma. Occasional calcospherites (psammoma bodies) may be seen within the tumor (Fig. 24.27).

## ANCILLARY STUDIES

### IMMUNOHISTOCHEMICAL FINDINGS

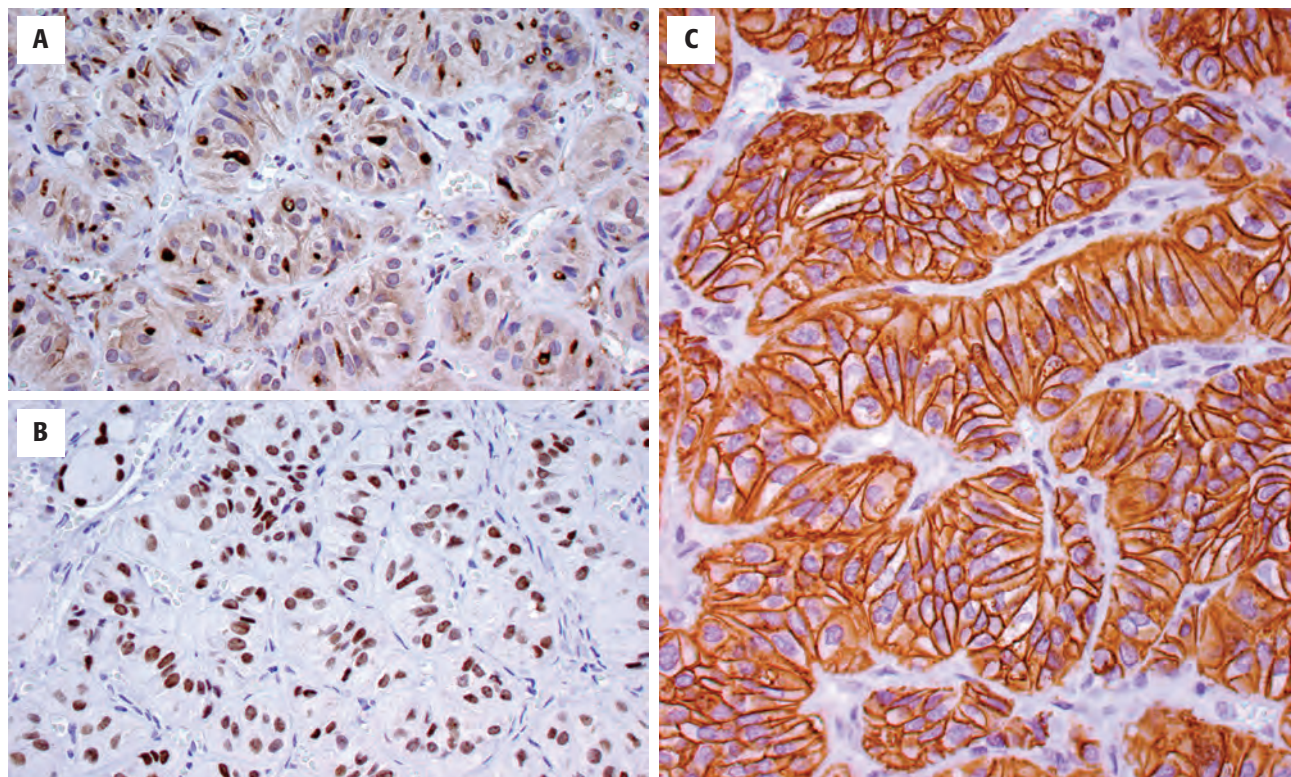
The neoplastic cells are reactive with thyroglobulin (Fig. 24.28), TTF1, CK7, keratin, and vimentin; they are nonreactive with neuroendocrine markers, calcitonin, and S100 protein. Strong membranous Ki-67 (with the

MIB-1, Dako antibody only) staining is distinctive (Fig. 24.28).

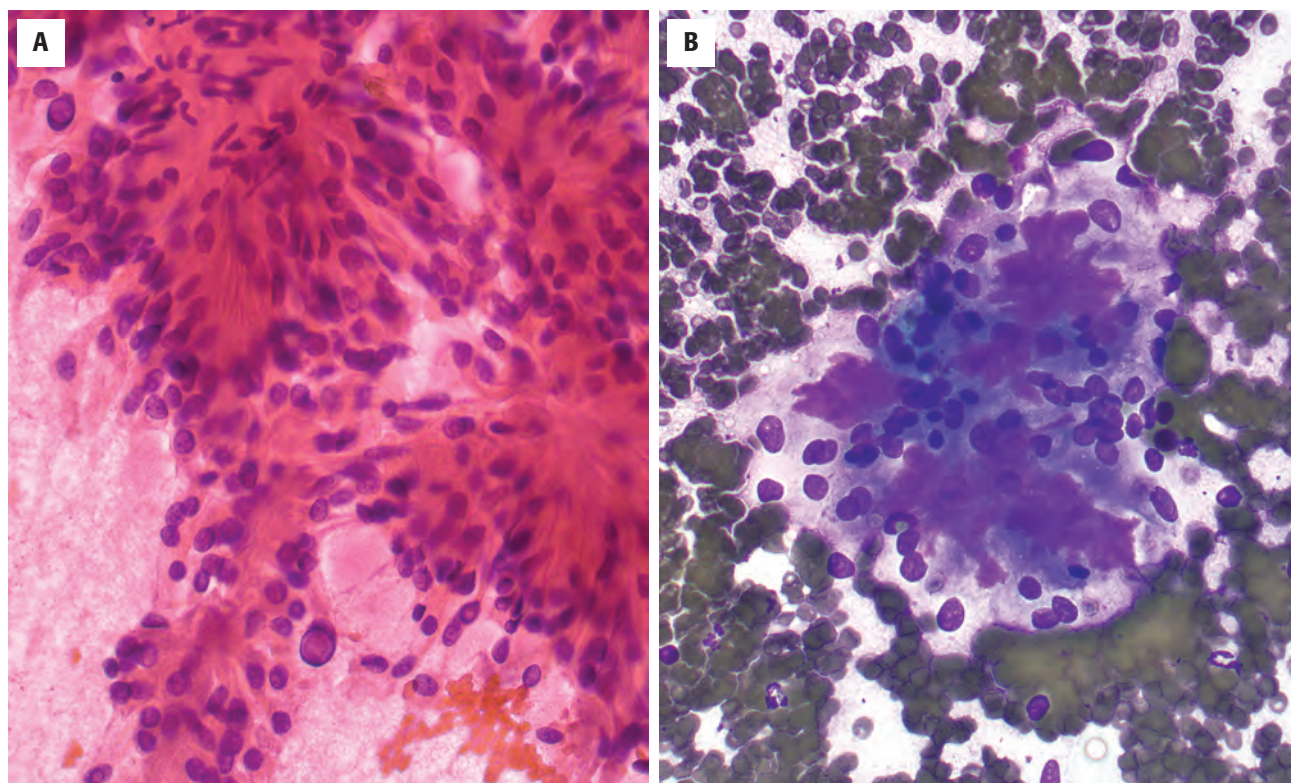
### FINE NEEDLE ASPIRATION

Aspirates are cellular, with cohesive clusters of cells and abundant cytoplasm. Nuclei are elongated with evenly dispersed chromatin, intranuclear cytoplasmic inclusions, and nuclear grooves. Most cases are diagnosed as PTC or suspicious for PTC on FNA, given the overlapping nuclear features (grooves and pseudoinclusions). The dense, lumpy basement membrane material between cells may help with the diagnosis but may be difficult to appreciate (Fig. 24.29). When present, this material is often radially oriented around cells, accounting for the hyalinized nature of this tumor. A known diagnostic pitfall in thyroid cytology, HTT is fortunately quite rare.



**FIGURE 24.28**

(A) There is cytoplasmic immunoreactivity with thyroglobulin along with highlighting the colloid. (B) Strong, diffuse nuclear TTF1 reactivity. (C) The MIB-1 (Dako antibody) gives a unique membranous reaction for Ki-67 in hyalinizing trabecular tumors.

**FIGURE 24.29**

(A) Fine needle aspiration of a hyalinizing trabecular tumor shows a cellular smear with intranuclear cytoplasmic inclusions in the round to regular nuclei (alcohol-fixed, Papanicolaou stain). The dense, basement membrane material can be seen in both images, although highlighted in magenta-purple with the Diff-Quik preparation (B).



## DIFFERENTIAL DIAGNOSIS

The differential diagnosis includes paraganglioma, medullary thyroid carcinoma, PTC, FA, and follicular carcinoma. *Paraganglioma*, rare in the thyroid, can be readily ruled out by its characteristic immunophenotype (neuroendocrine markers positive, with S100 protein staining the sustentacular cells; cytokeratin negative). *Medullary thyroid carcinoma* lacks colloid and contains amyloid, which may resemble the stromal hyalinization in HTT but is much less evenly dispersed. The immunophenotype is diagnostic (positive: calcitonin, neuroendocrine markers, carcinoembryonic antigen [CEA]). A trabecular pattern of growth can be seen in papillary, medullary, and follicular neoplasms. *Follicular carcinoma* with trabecular architecture, by definition, will have invasion. The nuclei are not usually arranged perpendicular to the trabecula axis. Both follicular carcinoma and FA lack the frequent nuclear grooves and pseudoinclusions present in HTT. Molecular *RET-PTCH1* studies of HTT have shown a possible link with PTC, but other mutations are not detected. A trabecular growth, lack of colloid, extensive intratrabecular stromal hyalinization, and cytoplasmic yellowish bodies/vacuoles favor HTT. NIFTP is not a diagnostic consideration because trabecular growth is an exclusion criterion.

## PROGNOSIS AND THERAPY

Complete but conservative surgery yields an excellent prognosis. Although data are limited, in the few well-documented cases, metastases occur in tumors that show invasive growth (capsular and lymphovascular invasion). Such cases can be termed *hyalinizing trabecular carcinoma*.

## ■ TERATOMA

Tumors of the cervical region are regarded as thyroid teratomas if:

- The tumor occupies a portion of the thyroid gland,
- There is direct continuity or close anatomic relationship between the tumor and the thyroid gland, or
- A cervical teratoma is accompanied by total absence of the thyroid gland

In a given case, it can be difficult to rule out the possibility that the thyroid tissue found adjacent to the teratoma may represent either normal thyroid gland secondarily replaced by a primary teratoma or just a component of the teratoma. The tumors histologically display mature or immature tissues from all three embryonic germ cell layers: ectoderm, endoderm, and mesoderm.

They are further separated into mature, immature, and malignant types.

## CLINICAL FEATURES

Teratoma is a rare tumor comprising less than 0.1 % of all primary thyroid neoplasms. Patients range from newborn to 85 years of age at initial presentation, although the peak and median fall within the newborn period. The average age, however, is skewed by *older* patients who usually have *malignant* teratomas. In fact, more than 90 % of the tumors in the neonatal group will be benign teratomas, whereas 50 % or more of the child/adult group will have malignant teratomas. There is no sex predilection. All patients present with an anterior neck mass, often reaching a significant size. Patients may also experience dyspnea, difficulty breathing, and/or stridor. Benign teratomas, whether mature or immature, may result in the patient's death due to tracheal compression or maldevelopment of the neck organs.

### TERATOMA—DISEASE FACT SHEET

#### Definition

- Neoplasm within the thyroid displaying mature or immature tissues from ectoderm, endoderm, and mesoderm

#### Incidence and Location

- Less than 0.1% of all thyroid primary neoplasms

#### Morbidity and Mortality

- Significant respiratory distress and associated malformations of neck vital structures due to mass effect
- Malignant teratomas have a high mortality rate

#### Sex and Age Distribution

- Equal sex distribution
- Biphasic age distribution
  - Benign in neonates and infants; malignant in older children and adults

#### Clinical Features

- Mass lesion, often of significant size
- Dyspnea, difficulty breathing, and stridor
- Maldevelopment of neck organs and/or tracheal compression

#### Radiographic Features

- In utero ultrasound may define extent of disease
- Multicystic mass lesions
- Inhomogeneous mass arising within the thyroid/anterior neck

#### Prognosis and Therapy

- Proportion of immaturity determines prognosis and correlates with tumor size and age
- Death may occur due to tracheal compression or lack of development of neck organs
- 30% of malignant teratomas have recurrence and dissemination



## RADIOGRAPHIC FEATURES

Radiographic images can be obtained in utero, at the time of birth, or in the adult patient. Ultrasonographic techniques provide the best information and are easiest to perform in utero or in the neonatal period. A multicystic mass lesion of the thyroid gland is most frequently identified. Computed tomography images show an inhomogeneous mass arising in the thyroid gland and compressing the upper airway in either the benign or malignant teratomas (Fig. 24.30). The presence of enlarged, peripherally enhancing lymph nodes in the neck suggests a malignant teratoma.

## PATHOLOGIC FEATURES

### GROSS FINDINGS

The tumors average 6 to 7 cm in diameter but can be quite large. The outer tumor surface is lobulated and smooth with a variable consistency, from firm to soft and cystic (Fig. 24.30). It may be well circumscribed to widely infiltrative. A gray-tan to translucent cut surface is common. Small multiloculated cysts may contain

white-tan creamy material, mucoid glairy material, or dark-brown hemorrhagic fluid with necrotic debris. “Brain” tissue is frequent, while black pigmentation (retinal anlage) is less common. Bone and cartilage can be recognized macroscopically.

### MICROSCOPIC FINDINGS

Teratoma, choristoma, hamartoma, heterotopia, epignathus, and dermoid are all unique lesions. Although these separations are semantic, they are well accepted. The term *teratoma* should be applied only to a tumor with *trilineage* differentiation. Thyroid parenchyma should be identified somewhere within the mass for it to qualify as a thyroid teratoma (Fig. 24.31), although in malignant teratomas residual thyroid follicles are frequently scarce or absent. There may be a wide array of tissue types and growth patterns within a single lesion (Fig. 24.32). A host of small cystic spaces are lined by a variety of different epithelia (Fig. 24.33): squamous, pseudostratified ciliated columnar (respiratory), cuboidal (with and without goblet cells), glandular, and transitional. Pilosebaceous and other adnexal structures are seen in association with squamous epithelium. True “organ” differentiation (pancreas, liver, lung) is uncommonly noted. Nearly all cases contain neural tissue, which consists of mature glial elements, choroid plexus,

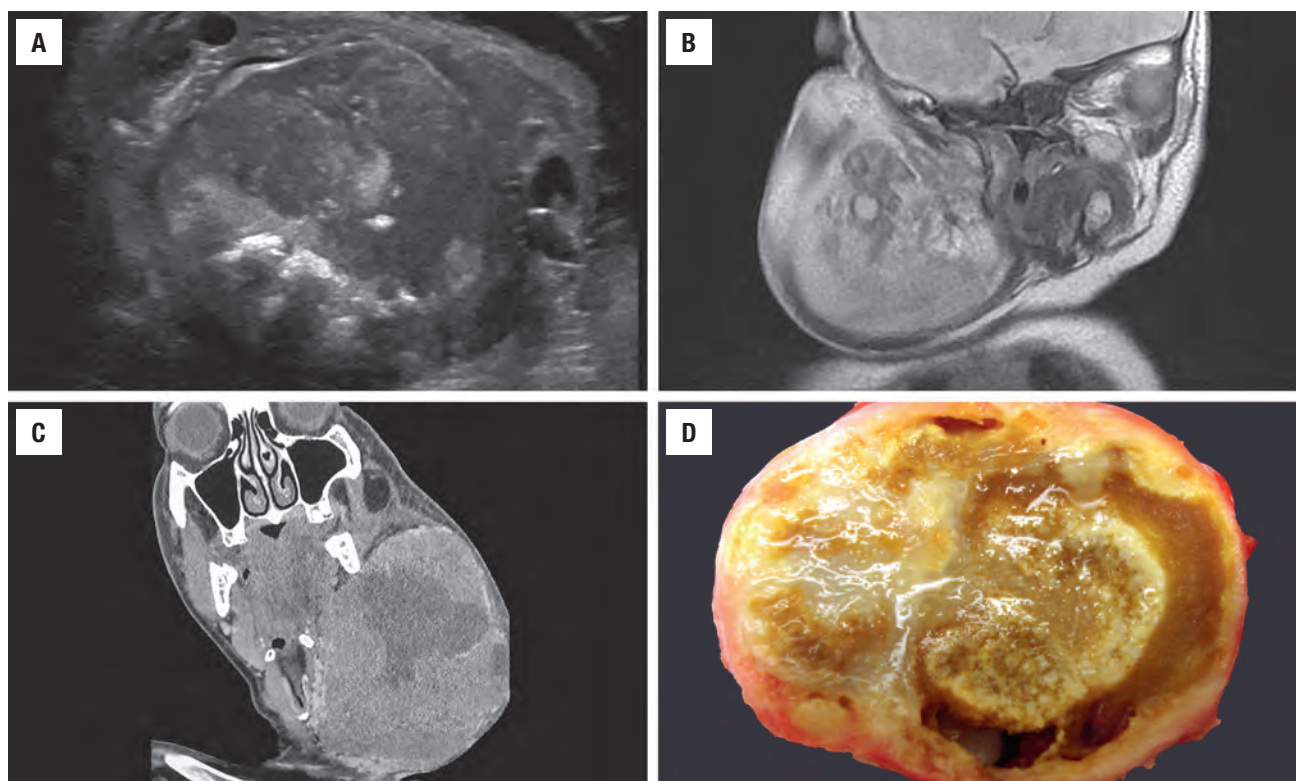


**FIGURE 24.30**

(A) This computed tomography scan demonstrates a large multicystic thyroid teratoma in the anterior neck that completely replaces the thyroid gland. (B and C) The teratoma has a multinodular and variable appearance. (D) Cystic and calcified areas are noted with myxoid-mucinous areas.

**TERATOMA—PATHOLOGIC FEATURES****Gross Findings**

- Mean diameter: 6–7 cm
- Lobulated, smooth with variable consistency
- Multiloculated cysts with white-tan creamy material, mucoid glairy material, or dark hemorrhagic fluid with necrotic debris
- “Brain” tissue is usually present
- Gritty material represents bone or cartilage

**Microscopic Findings**

- Thyroid parenchyma should be identified
- Mature or immature tissues from all germ cell layers
- Squamous, respiratory, glandular, and cuboidal epithelium
- Organ differentiation may be seen
- Neural tissues, including glial elements, choroid plexus, immature neuroblastoma, and pigmented retinal anlage
- Bone, cartilage, muscle, and fat
- Separated into benign, immature, and malignant based on degree and extent of immature neuroectodermal elements

**Immunohistochemical Findings**

- Variable for each specific element within teratoma
- Immature glial elements can be highlighted with S100 protein, GFAP, NSE, and NFP

**Fine Needle Aspiration**

- Cellular smears with various elements often misdiagnosed as “contamination” or “missed lesion”
- Immature/malignant neural elements are called “malignant” but not specific for teratoma

**Pathologic Differential Diagnosis**

- Benign: epignathus, choristoma, hamartoma, heterotopia, dermoid cyst

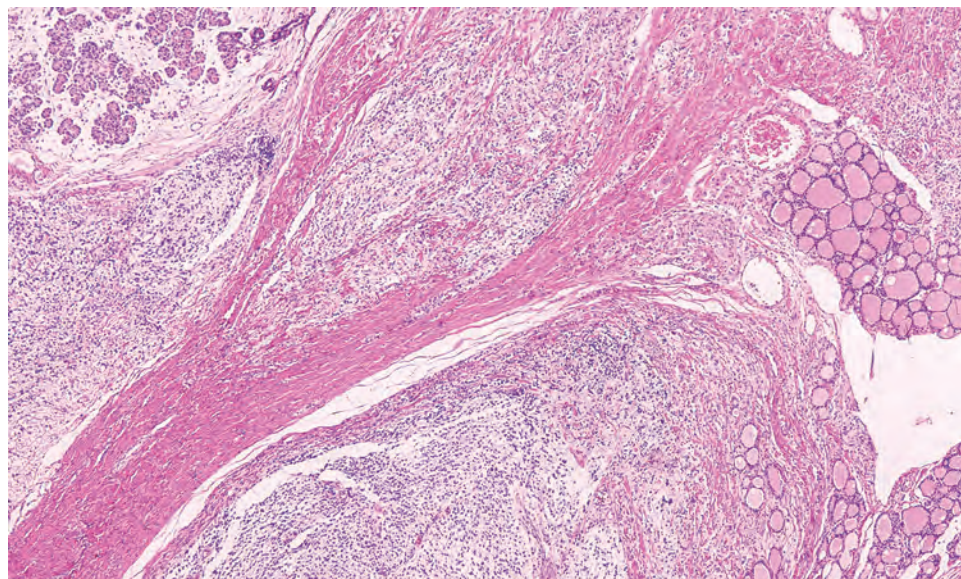
GFAP, Glial fibrillary acidic protein; NFP, neural filament protein; NSE, neuron-specific enolase.

pigmented retinal anlage, or immature neuroblastomal elements resembling embryonic tissue. Neuroblastic elements often arranged in sheets or rosette-like structures (Homer Wright or Flexner–Wintersteiner) are characterized by small to medium-sized cells with dense hyperchromatic nuclei and mitoses (Fig. 24.34). Mitotic figures are common in these immature areas. Cartilage, bone, striated skeletal muscle (Fig. 24.35), smooth muscle, adipose tissue, and loose myxoid to fibrous embryonic mesenchymal connective tissue are seen intermixed with the neural and epithelial elements.

The maturation of the neural-type tissue determines the grade. Benign mature teratomas contain only mature elements (grade 0). The term *benign immature teratoma* encompasses tumors with a limited degree of immaturity: (1) embryonal-type tissue in only one low-power (x4 objective, x10 ocular) field (grade 1) and (2) tumors with more than one but less than four low-power fields of immature foci (grade 2). “Malignant teratomas” contain more than four low-power fields of immature tissue (Fig. 24.36), along with mitoses and cellular atypia (grade 3). The presence of embryonal carcinoma or yolk sac tumor would place a teratoma into the malignant category by definition.

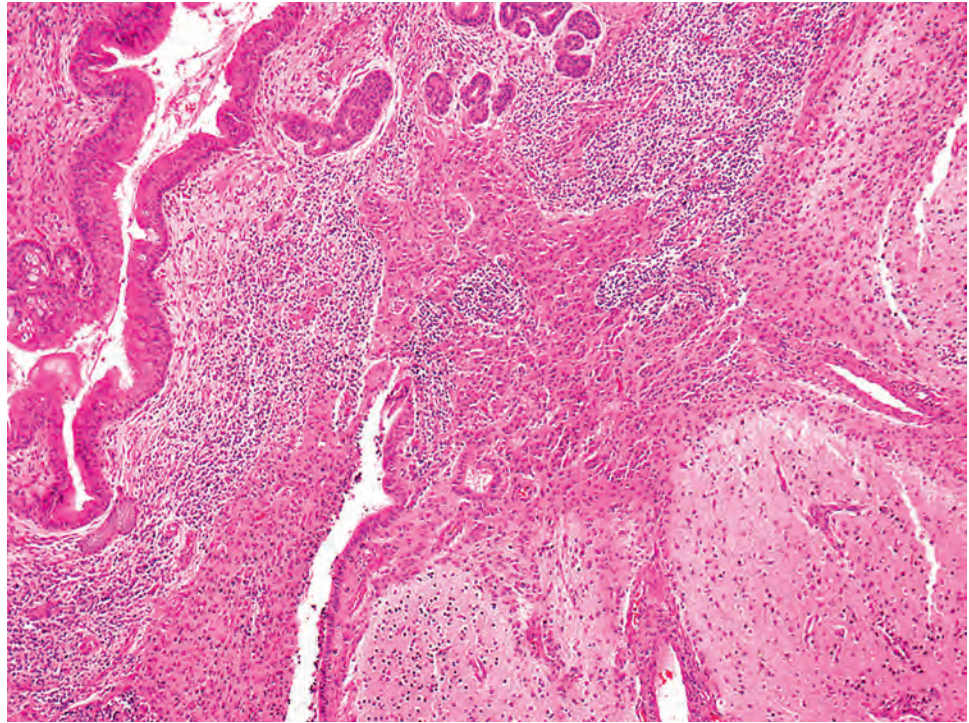
**ANCILLARY STUDIES****IMMUNOHISTOCHEMICAL FINDINGS**

Immunohistochemistry for S100 protein, glial fibrillary acidic protein, neuron-specific enolase, neural filament protein, desmin, myogenin, or MYOD1 may be of value for the characterization of the various immature elements.

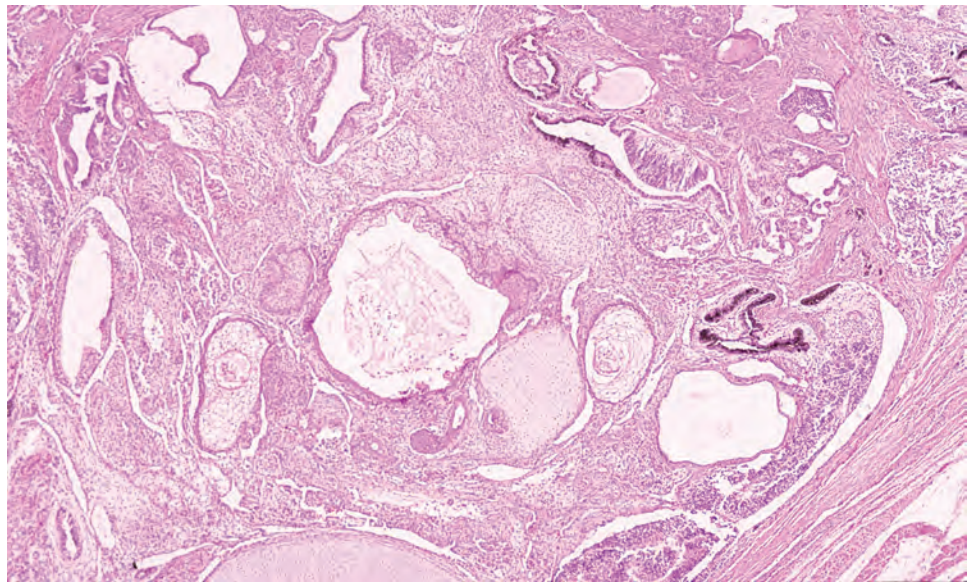
**FIGURE 24.31**

Benign mature teratoma. Mature thyroid follicular epithelium is compressed to the periphery by mature glial and salivary gland tissue.



**FIGURE 24.32**

Respiratory epithelium and mucoserous glands are adjacent to mature glial tissue in this benign mature teratoma.

**FIGURE 24.33**

Multiple cystic spaces are lined by squamous, cuboidal, and respiratory-type epithelium in this benign mature teratoma. Neural tissue and pigmented retinal anlage are also noted.

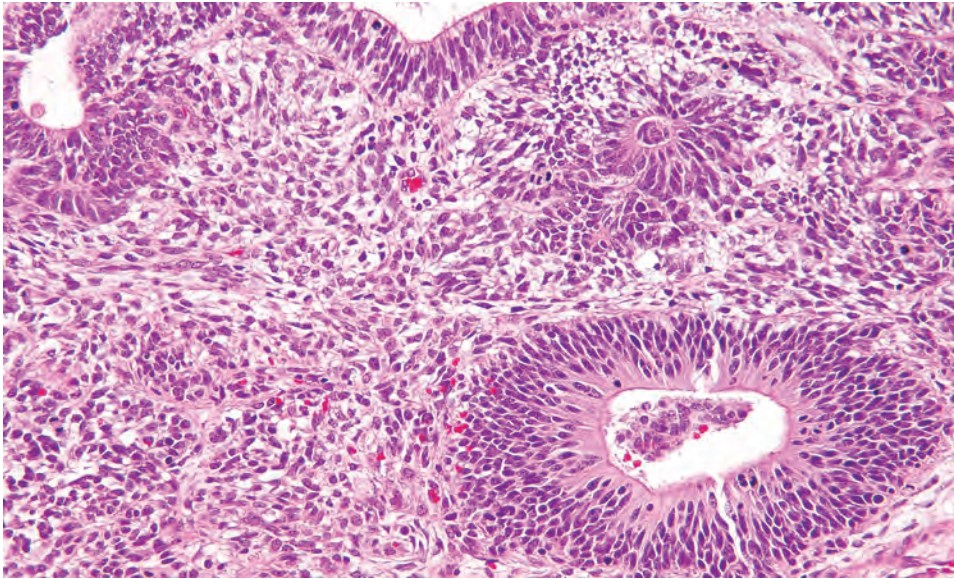
#### FINE NEEDLE ASPIRATION

Smears will demonstrate various cellular components, often misinterpreted as representing a contamination or a “missed” lesion. In malignant teratomas, the FNA smears will show a “neuroepithelial” small round blue cell appearance when taken from the immature/malignant neural elements. These cells are frequently interpreted as “malignant cells” rather than giving a specific diagnosis of malignant teratoma.

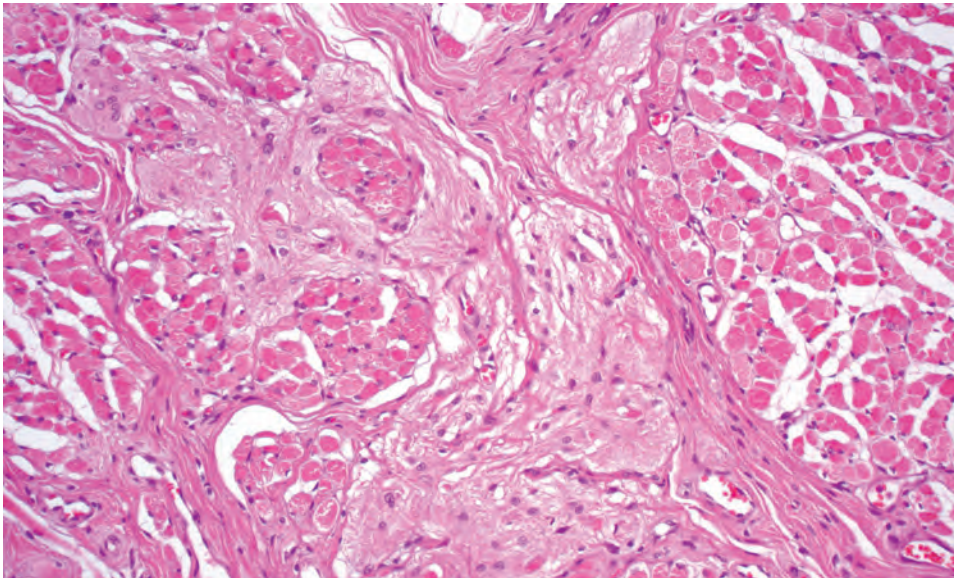
#### DIFFERENTIAL DIAGNOSIS

The term *choristoma* is used to designate histologically normal tissues in a location other than the site at which it is normally detected. *Hamartoma* refers to a disorganized collection of normal mature tissues for the anatomic area. *Heterotopias* are normal tissue in an abnormal location (misplaced or displaced). *Epignathus* designates a tumor of the palate; it is sometimes considered to be

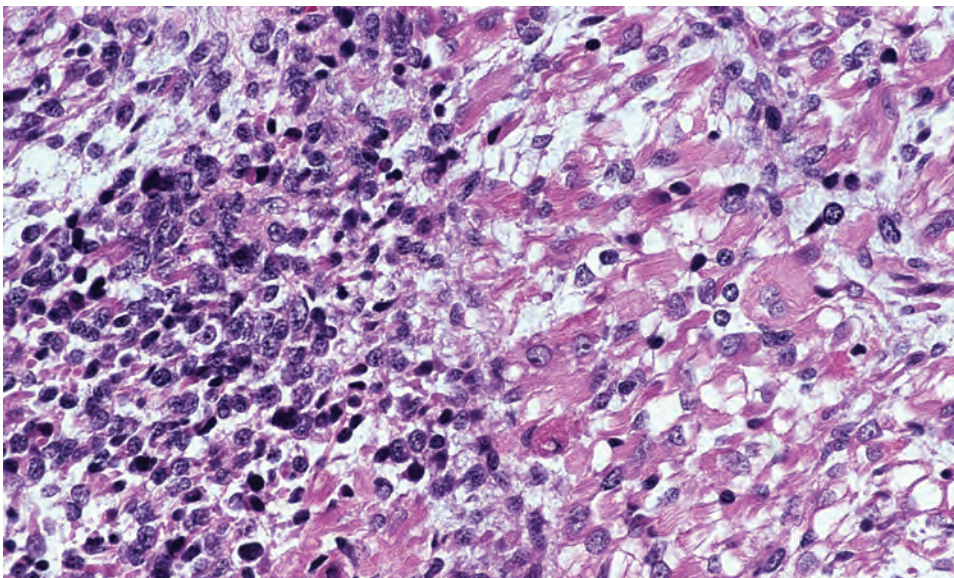


**FIGURE 24.34**

Benign immature teratoma. Immature neuroectodermal tissue arranged in Flexner-Wintersteiner rosettes.

**FIGURE 24.35**

This benign mature teratoma has a haphazard arrangement of skeletal muscle with mature glial tissue.

**FIGURE 24.36**

Malignant teratoma. This tumor has immature neuroectodermal and rhabdomyosarcomatous differentiation.



a parasitic fetus containing nearly all of the tissues seen in a complete fetus. *Dermoid cyst* (“resembling skin”) generally contains only ectodermal and mesodermal elements, specifically skin and hair.

The majority of thyroid teratomas are easily recognizable as such on clinical, radiographic, and pathologic grounds. However, when immature elements predominate, extraskeletal Ewing sarcoma, small cell carcinoma, lymphoma, and rhabdomyosarcoma enter the differential diagnosis. The diagnosis of teratoma under these circumstances is largely dependent on the identification of other tissue elements, the immature/malignant neural tissues, and a confirmatory immunohistochemical panel.

### PROGNOSIS AND THERAPY

The outcome for thyroid teratomas is dependent largely on the age of the patient, the size of the tumor at initial presentation, and the presence and proportion of immaturity. Even though histologically benign teratomas (whether mature or immature) do not invade or metastasize, they

can still result in the patient’s death from tracheal compression or lack of development of vital neck structures during fetal growth. Prompt surgical intervention, including in utero procedures (ex utero intrapartum treatment [EXIT] procedure), may be necessary to yield a good patient outcome. Age at presentation and tumor histology are strongly correlated: neonates nearly always have benign or immature teratomas; they do not die from disease (but may die with disease); children and adults tend to have malignant teratomas and may die from disease. Recurrence and dissemination are known to occur in about one-third of patients with malignant teratomas, nearly all of whom are adults. Lymph node metastasis is usually followed by lung disease. These patients are managed with radiation and chemotherapy, although this is generally considered palliative with an almost uniformly fatal outcome. Staging is not usually applied since the local effect is more prognostically significant than other features.

### SUGGESTED READINGS

The complete Suggested Readings list is available online at [Expertconsult.com](http://Expertconsult.com).

**SUGGESTED READINGS****Follicular Adenoma**

- Baloch ZW, et al. Fine-needle aspiration of the thyroid: today and tomorrow. *Best Pract Res Clin Endocrinol Metab.* 2008;22(6):929–939.
- Baloch ZW, et al. Follicular-patterned afflictions of the thyroid gland: reappraisal of the most discussed entity in endocrine pathology. *Endocr Pathol.* 2014;25:12–20.
- Bisi H, et al. The prevalence of unsuspected thyroid pathology in 300 sequential autopsies, with special reference to the incidental carcinoma. *Cancer.* 1989;64(9):1888–1893.
- Bocker W, et al. Immunohistochemical and electron microscope analysis of adenomas of the thyroid gland. II. Adenomas with specific cytological differentiation. *Virchows Arch A Pathol Anat Histol.* 1978;380:205–220.
- Cameselle Teijeiro J, et al. Thyroid pathology findings in cowden syndrome: a clue for the diagnosis of the PTEN hamartoma tumor syndrome. *Am J Clin Pathol.* 2015;144(2):322–328.
- Carcangiu ML, et al. Clear cell change in primary thyroid tumors: a study of 38 cases. *Am J Surg Pathol.* 1985;9:705–722.
- Carcangiu ML, et al. Follicular Hürthle cell tumors of the thyroid gland. *Cancer.* 1991;68:1944–1953.
- Chetty R. Thyroid follicular adenoma composed of lipid-rich cells. *Endocr Pathol.* 2011;22(1):31–34.
- Faquin WC. The thyroid gland: recurring problems in histologic and cytologic evaluation. *Arch Pathol Lab Med.* 2008;132(4):622–632.
- Feng X, et al. Characteristics of benign and malignant thyroid disease in familial adenomatous polyposis patients and recommendations for disease surveillance. *Thyroid.* 2015;25(3):325–332.
- Fischer S, et al. Application of immunohistochemistry to thyroid neoplasms. *Arch Pathol Lab Med.* 2008;132(3):359–372.
- Flint A, et al. Hürthle-cell neoplasms of the thyroid gland. *Pathol Annu.* 1990;25:37–52.
- Freitas BCG, et al. Genetic markers differentiating follicular thyroid carcinoma from benign lesions. *Mol Cell Endocrinol.* 2010;77–85.
- Gherardi G. Signet ring cell ‘mucinous’ thyroid adenoma: a follicle cell tumour with ab-normal accumulation of thyroglobulin and a peculiar histochemical profile. *Histopathology.* 1987;11:317–326.
- Gnepp DR, et al. Fat-containing lesions of the thyroid gland. *Am J Surg Pathol.* 1989;13:605–612.
- Hunt JL. Molecular alterations in hereditary and sporadic thyroid and parathyroid diseases. *Adv Anat Pathol.* 2009;16(1):23–32.
- Ko HM, et al. Clinicopathologic analysis of fine needle aspiration cytology of the thyroid. A review of 1,613 cases and correlation with histopathologic diagnoses. *Acta Cytol.* 2003;47:727–732.
- Koren R, et al. Black thyroid adenoma. Clinical, histochemical, and ultrastructural features. *Appl Immunohistochem Mol Morphol.* 2000;8(1):80–84.
- Krohn K, et al. Clonal origin of toxic thyroid nodules with constitutively activating thyrotropin receptor mutations. *J Clin Endocrinol Metab.* 1998;83(1):130–134.
- Layfield LJ, et al. Thyroid aspiration cytology: current status. *CA Cancer J Clin.* 2009;59(2):99–110.
- Mai KT, et al. Follicular adenoma with papillary architecture: a lesion mimicking papillary thyroid carcinoma. *Histopathology.* 2001;39(1):25–32.
- Namba H, et al. Point mutations of ras oncogenes are an early event in thyroid tumorigenesis. *Mol Endocrinol.* 1990;4(10):1474–1479.
- Osamura RY, et al. Current practices in performing frozen sections for thyroid and parathyroid pathology. *Virchows Arch.* 2008;453(5):433–440.
- Radkay LA, et al. Thyroid nodules with KRAS mutations are different from nodules with NRAS and HRAS mutations with regard to cytopathologic and histopathologic outcome characteristics. *Cancer Cytopathol.* 2014;122:873–882.
- Rigaud C, et al. Mucin producing microfollicular adenoma of the thyroid. *J Clin Pathol.* 1985;38:277–280.
- Rosai J, et al. Pitfalls in thyroid tumour pathology. *Histopathology.* 2006;49(2):107–120.
- Schröder S, et al. Signet-ring-cell thyroid tumors: follicle cell tumors with arrest of folliculogenesis. *Am J Surg Pathol.* 1985;9:619–629.
- Scognamiglio T, et al. Diagnostic usefulness of HBME1, galectin-3, CK19, and CITED1 and evaluation of their expression in encapsulated lesions with questionable features of papillary thyroid carcinoma. *Am J Clin Pathol.* 2006;126(5):700–708.
- Serra S, et al. Controversies in thyroid pathology: the diagnosis of follicular neoplasms. *Endocr Pathol.* 2008;19(3):156–165.
- Tóth K, et al. Lipid-rich cell thyroid adenoma: histopathology with comparative lipid analysis. *Virchows Arch.* 1990;417(3):27–36.
- Wang N, et al. TERT promoter mutation as an early genetic event activating telomerase in follicular thyroid adenoma (FTA) and atypical FTA. *Cancer.* 2014;120:2965–2979.
- Wang TS, et al. Management of follicular tumors of the thyroid. *Minerva Chir.* 2007;62(5):373–382.
- Yamashina M. Follicular neoplasms of the thyroid. Total circumferential evaluation of the fibrous capsule. *Am J Surg Pathol.* 1992;16:392–400.
- Yeung MJ, et al. Management of the solitary thyroid nodule. *Oncologist.* 2008;13(2):105–112.

**Noninvasive Follicular Thyroid Neoplasm With Papillary-Like Nuclear Findings (NIFTP)**

- Baloch ZW, et al. Noninvasive follicular thyroid neoplasm with papillary-like nuclear features (NIFTP): a changing paradigm in thyroid surgical pathology and implications for thyroid cytopathology. *Cancer Cytopathol.* 2016;124(9):616–620.
- Chetty R. Follicular patterned lesions of the thyroid gland: a practical algorithmic approach. *J Clin Pathol.* 2011;64:737–741.
- Ganly I, et al. Invasion rather than nuclear features correlates with outcome in encapsulated follicular tumors: further evidence for the reclassification of the encapsulated papillary thyroid carcinoma follicular variant. *Hum Pathol.* 2015;46:657–664.
- Nikiforov YE, et al. Nomenclature revision for encapsulated follicular variant of papillary thyroid carcinoma: a paradigm shift to reduce overtreatment of indolent tumors. *JAMA Oncol.* 2016;2(8):1023–1029.
- Thompson LDR. Ninety-four cases of encapsulated follicular variant of papillary thyroid carcinoma: a name change to noninvasive follicular thyroid neoplasm with papillary-like nuclear features would help prevent overtreatment. *Mod Pathol.* 2016;29(7):698–707.

**Hyalinizing Trabecular Tumor**

- Bakuła Zalewska E, et al. Hyaline matrix in hyalinizing trabecular tumor: Findings in fine needle aspiration smears. *Diagn Cytopathol.* 2015;43(9):710–713.
- Carney JA, et al. Hyalinizing trabecular adenoma of the thyroid gland. *Am J Surg Pathol.* 1987;11:583–591.
- Carney JA, et al. Hyalinizing trabecular tumors of the thyroid gland are almost all benign. *Am J Surg Pathol.* 2008;32(12):1877–1889.
- Casey MB, et al. Hyalinizing trabecular adenoma of the thyroid gland: cytologic features in 29 cases. *Am J Surg Pathol.* 2004;28(7):859–867.
- Evenson A, et al. Hyalinizing trabecular adenoma—an uncommon thyroid tumor frequently misdiagnosed as papillary or medullary thyroid carcinoma. *Am J Surg.* 2007;193(6):707–712.
- Gaffney RL, et al. Galectin-3 expression in hyalinizing trabecular tumors of the thyroid gland. *Am J Surg Pathol.* 2003;27(4):494–498.
- Hirokawa M, et al. Cell membrane and cytoplasmic staining for MIB-1 in hyalinizing trabecular adenoma of the thyroid gland. *Am J Surg Pathol.* 2000;24:575–578.
- Leonardo E, et al. Cell membrane reactivity of MIB1 antibody to Ki67 in human tumors: fact or artifact? *Appl Immunohisto Mol Morphol.* 2007;15(2):220–223.
- Li M, et al. Abnormal intracellular and extracellular distribution of basement membrane material in papillary carcinoma and hyalinizing trabecular tumors of the thyroid: implication for deregulation of secretory pathways. *Human Pathol.* 1997;28(12):1366–1372.
- LiVolsi VA. Hyalinizing trabecular tumor of the thyroid: adenoma, carcinoma, or neoplasm of uncertain malignant potential? *Am J Surg Pathol.* 2000;24(12):1683–1684.
- Nosé V, et al. Hyalinizing trabecular tumor of the thyroid: an update. *Endocr Pathol.* 2008;19(1):1–8.
- Rothenberg HJ, et al. Hyalinizing trabecular adenoma of the thyroid gland: recognition and characterization of its cytoplasmic yellow body. *Am J Surg Pathol.* 1999;23(1):118–125.



13. Rothenberg HJ, et al. Prevalence and incidence of cytoplasmic yellow bodies in thyroid neoplasms. *Arch Pathol Lab Med*. 2003;127(6):715–717.
14. Salvatore G, et al. Molecular profile of hyalinizing trabecular tumours of the thyroid: high prevalence of RET/PTC rearrangements and absence of B-raf and N-ras point mutations. *Eur J Cancer*. 2005;41(5):816–821.
15. Volante M, et al. A practical diagnostic approach to solid/trabecular nodules in the thyroid. *Endocr Pathol*. 2008;19(2):75–81.
5. Furtado LV, et al. Yolk sac tumor of the thyroid gland: a case report. *Pediatr Dev Pathol*. 2011;14(6):47–59.
6. Furtado LV, et al. Thyroid: Germ cell tumour. In: Lloyd RV, Klöppel G, et al, eds. *World Health Organization Classification of Tumours of Endocrine Organ*. 4th ed. Lyon, France: IARC Press; 2017:139–141.
7. Jordan RB, et al. Cervical teratomas: an analysis, literature review and pro-proposed classification. *J Pediatr Surg*. 1988;23:583–591.
8. Lack EE. Extragonadal germ cell tumors of the head and neck region: review of 16 cases. *Hum Pathol*. 1985;16:56–64.
9. Riedlinger WF, et al. Primary thyroid teratomas in children: a report of 11 cases with a proposal of criteria for their diagnosis. *Am J Surg Pathol*. 2005;29(5):700–706.
10. Thompson LD, et al. Primary thyroid teratomas: a clinicopathologic study of 30 cases. *Cancer*. 2000;88(5):1149–1158.
11. Tsang RW, et al. Malignant teratoma of the thyroid: aggressive chemoradiation therapy is required after surgery. *Thyroid*. 2003;13(4):401–404.
12. Vujančić GM, et al. Thyroid/cervical teratomas in children: immunohistochemical studies for specific thyroid epithelial cell markers. *Pediatr Pathol*. 1994;14(2):369–375.
13. Wolvos TA, et al. An unusual thyroid tumor: a comparison to a literature review of thyroid teratomas. *Surgery*. 1985;97(5):613–617.
14. Zerella JT, et al. Obstruction of the neonatal airway from teratomas. *Surg Gynecol Obstet*. 1990;170(2):126–131.

### Teratoma

1. Alexander VR, et al. Head and neck teratomas in children A series of 23 cases at Great Ormond Street Hospital. *Int J Pediatr Otorhinolaryngol*. 2015;79(12):2008–2014.
2. Arezzo A, et al. Immature malignant teratoma of the thyroid gland. *J Exp Clin Cancer Res*. 1998;17(1):109–112.
3. Azizkhan RG, et al. Diagnosis, management, and outcome of cervicofacial teratomas in ne-onates: a Children's Cancer Group study. *J Pediatr Surg*. 1995;30(2):312–316.
4. Craver RD, et al. Malignant teratoma of the thyroid with primitive neuroepithelial and mesenchymal sarcomatous components. *Ann Diagn Pathol*. 2001;5:285–292.

# Malignant Neoplasms of the Thyroid Gland

■ **Lester D.R. Thompson**

Thyroid gland malignancies account for about 3 % of all cancers (13.5/100,000 population), while representing the most common malignancy of the endocrine system. In general, thyroid cancer afflicts young to middle-aged adults with environmental, genetic, and hormonal factors often playing an etiologic role. Iodine is essential for normal thyroid function and consequently, radioactive iodine can be used in treatment. Women are affected by thyroid diseases nearly four times as frequently as men. Fine needle aspiration (FNA) has contributed significantly to the assessment of thyroid nodules, especially ultrasound-detected masses, with a corresponding decline in use of nuclear scintigraphy. FNA is satisfactory or unsatisfactory, making certain to meet the adequacy criteria as established by the Bethesda system. Satisfactory lesions are then separated into benign, follicular lesion of undetermined significance, neoplasms, suspicious for malignancy, and malignant. There is a sensitivity for cancer of 65 % to 98 %, specificity of 72 % to 100 %, and a positive predictive value of 90 % to 96 %. The false negative rate is from 1 % to 11 %, while the false positive rate is less than 1 %. Most of the tumors are of thyroid follicular cell derivation and, for the most part, carry an excellent long-term prognosis.

Adequacy of tumor sampling is frequently a question. It is my practice to submit at least one section per centimeter of tumor diameter, but with an attempt to submit the whole periphery of the tumor. If the tumor looks macroscopically homogeneous after being bivalved, then the center of the tumor is not as critical to examine. The tumor is serially sectioned at 2 to 3 mm. Then, only the very periphery of the tumor to capsule to parenchymal interface is embedded. As many as five sections, 3 mm thick and up to 2.5 cm long, can be placed side by side in the 2.5 cm wide cassette. With this technique, the periphery of most tumors can be entirely embedded in 4 to 8 blocks, allowing for complete evaluation of the capsule.

## ■ **PAPILLARY THYROID CARCINOMA**

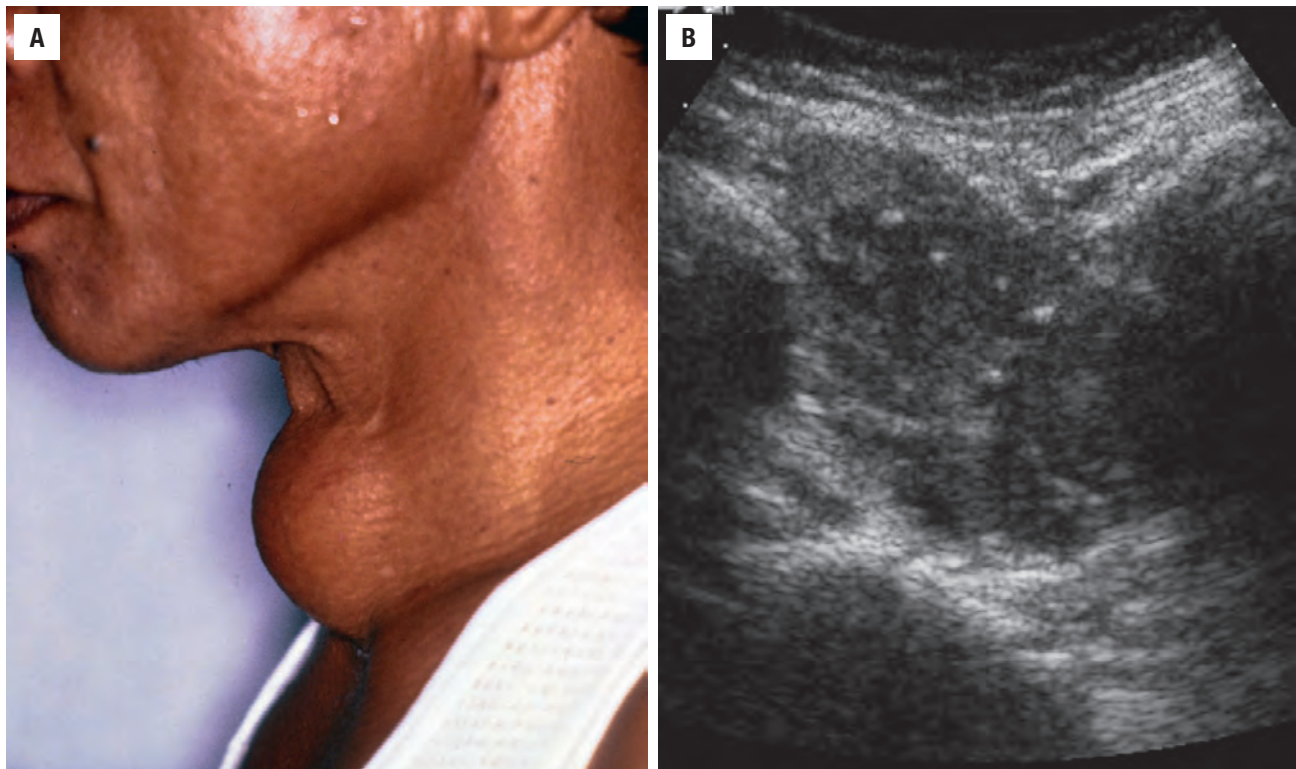
“A malignant epithelial tumor showing evidence of follicular cell differentiation and a set of distinctive nuclear

features. Either papillae or invasion are required” is a somewhat vague World Health Organization (WHO) definition of papillary thyroid carcinoma (PTC). However, with a constellation of architectural and cytomorphologic features, accurate diagnosis of papillary carcinoma is achievable.

### **CLINICAL FEATURES**

Papillary carcinoma represents about 80 % to 85 % of all malignant thyroid neoplasms and occurs largely in middle-aged adults with a 3:1 female-to-male ratio, and a median age at presentation of 50 years. Even though rare in children, papillary carcinoma is still the most common pediatric thyroid malignancy. Whites are affected more commonly than blacks. Curiously, there is about a 20 % prevalence of PTC (autopsy studies), supporting the overall excellent long-term prognosis and highlighting the difficulty in deciding appropriate patient management. There is a close link with radiation exposure, an association much more highly developed in children (especially for the solid variant of PTC). There is also a higher incidence of carcinoma in regions with high dietary iodine intake, in patients who have preexisting benign thyroid disease, and in some inherited disorders (Carney complex; familial adenomatous polyposis [FAP]). Patients present with a solitary, painless otherwise asymptomatic thyroid gland mass (Fig. 25.1) or with cervical lymphadenopathy (metastatic disease in about 30 %). Dysphagia, stridor, and cough are usually seen in patients with large tumors due to compression. There are many “incidental” papillary carcinomas (discussed later), which are frequently discovered during routine radiographic studies for unrelated reasons or in patients with other thyroid diseases. FNA is the initial study of choice for a thyroid nodule, with excellent positive predictive value. Thyroid function studies are not useful in the initial evaluation of patients as there is rarely functional compromise. However, serum thyroglobulin levels can be used to monitor disease status (if elevated).



**FIGURE 25.1**

(A) A clinical photograph shows a large, protuberant mass at the level of the thyroid gland. (B) An irregular mass within the thyroid with mixed echogenicity by ultrasound, showing punctate calcifications, characteristic for a papillary carcinoma.

### PAPILLARY THYROID CARCINOMA—DISEASE FACT SHEET

#### Definition

- A malignant epithelial tumor showing evidence of follicular cell differentiation and a set of distinctive nuclear features

#### Incidence and Location

- Thyroid malignancies represent about 3% of all carcinomas
- 80%-85% of thyroid malignancies are papillary thyroid carcinoma

#### Morbidity and Mortality

- Recurrent laryngeal nerve damage and hypoparathyroidism
- Excellent long term outcome (> 90% 20-year survival)

#### Sex and Age Distribution

- Females > > Males (3 : 1)
- Age: 20-60 years; median: 50 years

#### Clinical Features

- Associated with radiation exposure
- Usually a palpable painless (asymptomatic) mass lesion, often with neck lymph nodes
- Uncommonly, dysphagia or hoarseness

#### Radiographic Features

- Ultrasound shows a solid or cystic mass and guides FNA
- Computed tomography is useful to determine extent of the mass and lymph node disease
- Nuclear scintigraphy seldom used

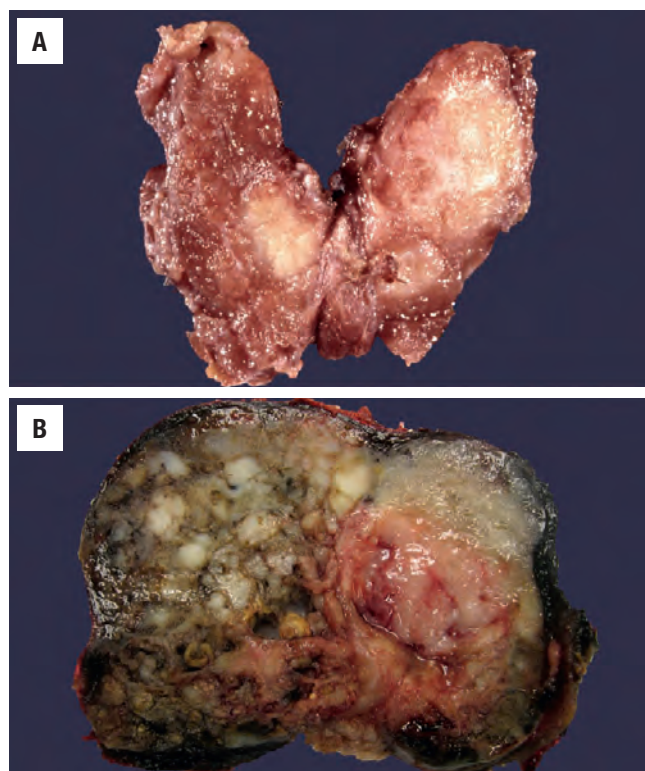
#### Prognosis and Therapy

- Excellent long term prognosis (> 90 % 20-year survival)
- Surgery (lobectomy or thyroidectomy) with follow-up radioactive iodine (in total thyroidectomy patients)

### RADIOGRAPHIC FEATURES

Ultrasound will usually establish the size and whether the lesion is solid or cystic, while also being a valuable adjunct for guiding FNA. Punctate microcalcifications are

frequently present (Fig. 25.1), with high central blood flow on color Doppler. While nuclear scintigraphy was widely used to demonstrate functionality (“cold” without uptake; “hot” increased uptake) in comparison to the uninvolved thyroid parenchyma, it has been almost completely replaced by ultrasound and FNA as the techniques of

**FIGURE 25.2**

(A) Three separate primaries are noted, with the largest lesion in the left upper lobe. There is an infiltrative border to these sclerotic tumors. (B) A large, irregular, multilobular mass nearly completely replaces the thyroid lobe. Note the areas of more fleshy tumor compared to cystic areas of degeneration. This tumor fit within the columnar variant of papillary carcinoma. (A, Courtesy of Dr. J. A. Ohara.)

choice in initial evaluation of a thyroid nodule. CT or MRI scans are valuable in highlighting enlarged, cystic lymph nodes, which may suggest metastatic disease, showing increased signal intensity on T1-weighted images, and may reveal punctate calcifications.

## **PATHOLOGIC FEATURES**

### **GROSS FINDINGS**

Most clinical tumors are discrete, ill-defined but circumscribed, often with an irregular and infiltrative border (Fig. 25.2). Ranging from microscopic to 20 cm, infiltration into the surrounding thyroid parenchyma is frequently noted, along with extension beyond the thyroid gland periphery. Gritty, dystrophic calcification is common, while cystic change and hemorrhage may also be present. Multifocality is occasionally identified macroscopically. The cut surface can be shaggy to papillary, with irregular areas of fibrosis. The best sections to submit capture the “tumor-to-capsule-to-parenchyma” interface.

## **PAPILLARY THYROID CARCINOMA—PATHOLOGIC FEATURES**

### **Gross Findings**

- Discrete, grey-white, firm mass with irregular borders, although often circumscribed
- Calcifications give a “gritty” cut surface
- Extrathyroidal extension may be seen
- Up to 20 cm; average about 3 cm

### **Microscopic Findings**

- **Architecture:** Variable growth patterns, complex papillae, elongated and twisted follicles, invasive growth, psammoma bodies, “bright eosinophilic” colloid, crystals, and giant cells in colloid
- **Cytology:** Enlarged cells, increased nuclear to cytoplasmic ratio; nuclear enlargement, nuclear overlapping and crowding, loss of polarity; nuclear contour irregularities, grooves, folds or “crescent moons,” nuclear chromatin is cleared, pale, fine delicate to even, with intranuclear cytoplasmic inclusions
- Intratumoral fibrosis, psammoma bodies, colloid scalloping

### **Immunohistochemical Results**

- TTF1, thyroglobulin, PAX8, CK7, CK19
- Panel: HBME-1, galectin-3, CITED1 positive

### **Fine Needle Aspiration**

- Cellular aspirate with papillary and monolayered sheets, cuboidal cells with enlarged and overlapped nuclei, powdery nuclear chromatin with nuclear grooves and intranuclear cytoplasmic inclusions, andropy, “bubble-gum” colloid

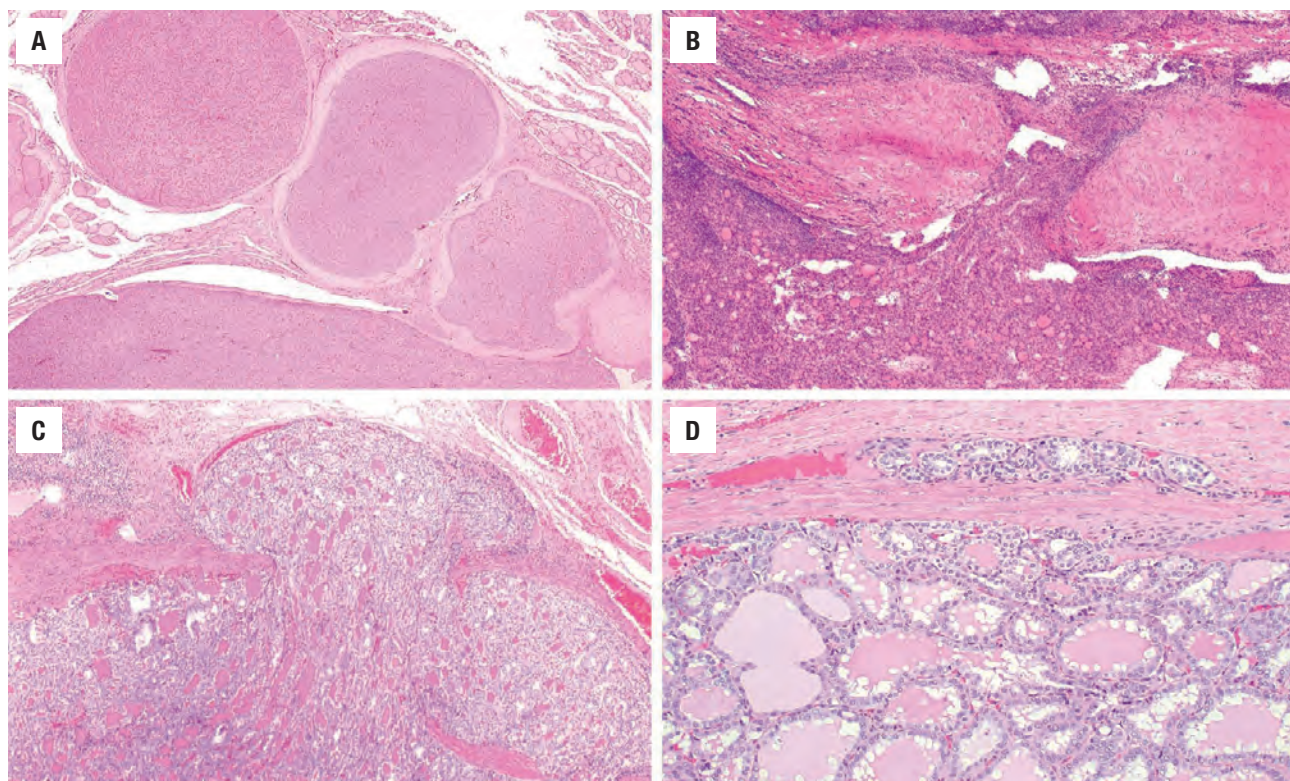
### **Pathologic Differential Diagnosis**

- Adenomatoid nodules, diffuse hyperplasia (Graves’ disease), dysmorphogenetic goiter, follicular adenoma, papillary carcinoma variants, follicular carcinoma, medullary carcinoma, metastatic tumors

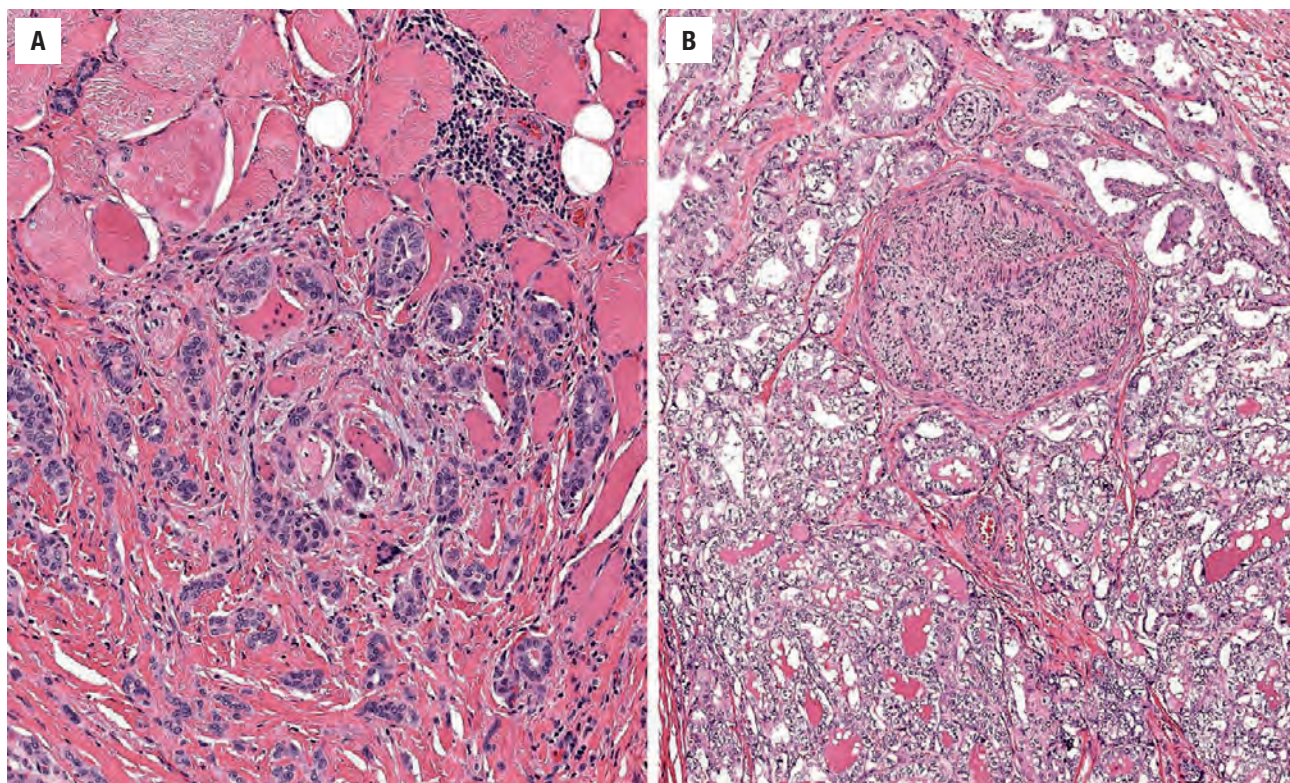
## **MICROSCOPIC FINDINGS**

The diagnosis of papillary carcinoma is made by using an aggregate of architectural and cytologic features, with no one single feature being diagnostic. The exact number of features necessary for the diagnosis is undefined, but the nuclear features must be present to be diagnostic. Multinodular and multifocal tumors are common (Fig. 25.3), seen in about 50 % of cases. An irregular and invasive border is common, with both capsular and lymphovascular invasion (Fig. 25.3). Extrathyroidal extension involves expansion of tumor into skeletal muscle (Fig. 25.4), adipose tissue, around nerves, and adjacent to large perithyroidal vessels. Only macroscopic evidence of extrathyroidal extension, however, is evaluated in staging. The architectural features in PTC include variable growth patterns (papillary, solid, trabecular, micro- or macrofollicular, cystic); elongated and/or twisted follicles; complex, arborizing, delicate, narrow papillae; intratumoral dense acellular fibrosis; “bright,” hypereosinophilic, intense colloid (distinct from surrounding thyroid



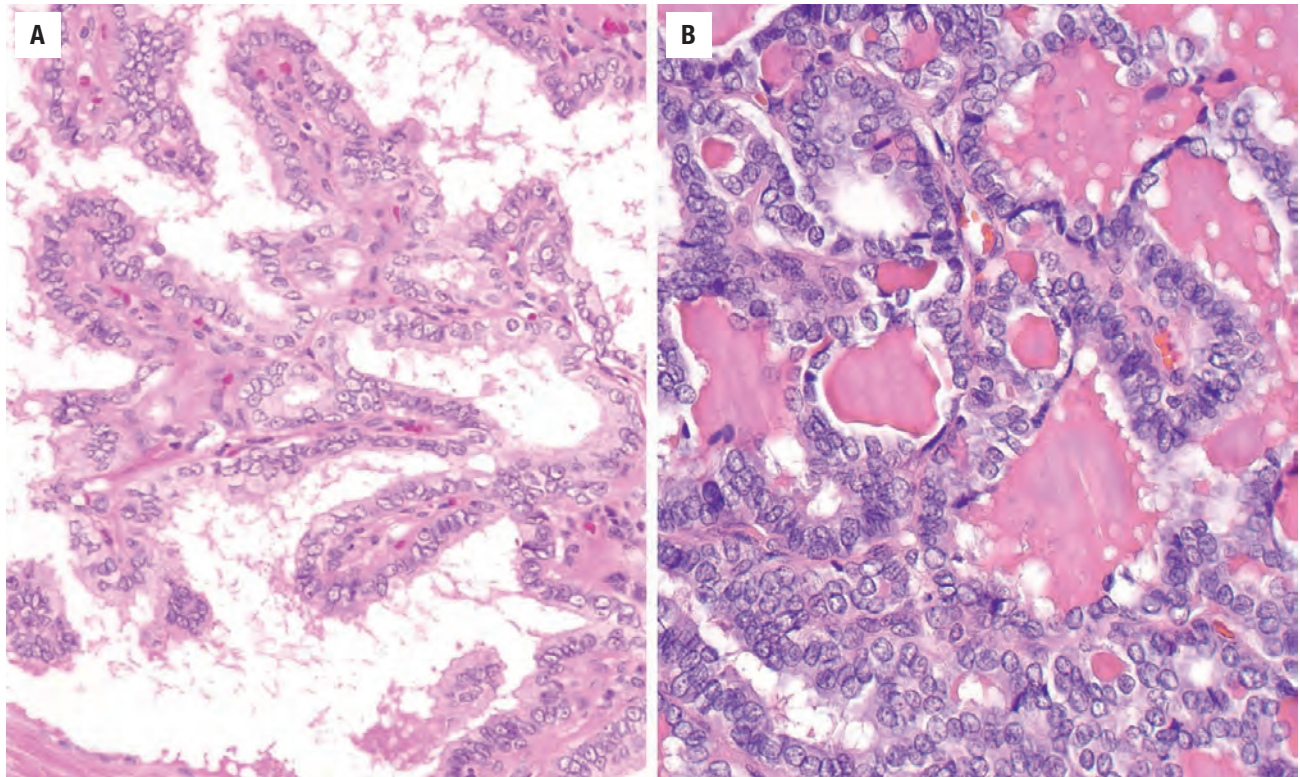
**FIGURE 25.3**

(A) Multiple nodules of papillary carcinoma are surrounded by dense fibrosis. (B) A frozen section sample just happens to have caught an area of invasion. (C) A mushroom of invasion through the capsule. (D) An area of vascular invasion, filling the lymphatic space.

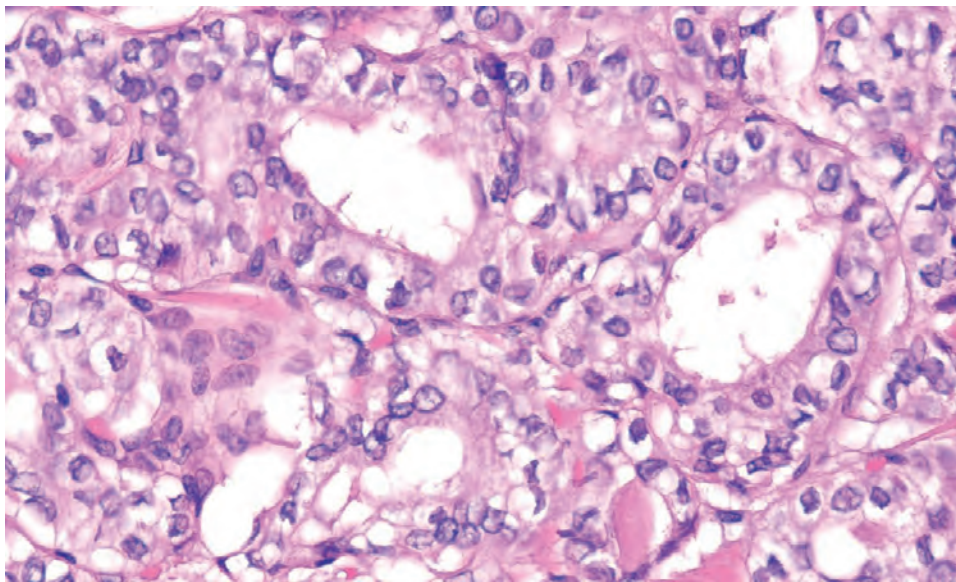
**FIGURE 25.4**

(A) A PTC shows infiltration into the adjacent skeletal muscle, while growth around a large perithyroidal nerve (B) is also seen in these examples of microscopic extrathyroidal extension.



**FIGURE 25.5**

(A) Delicate and complex papillary fronds lined by cells with an increased nuclear-to-cytoplasmic ratio, disorganized placement of the nuclei within the cell, and nuclear crowding and overlap. (B) Nuclear overlapping and crowding with isolated papillae are seen.

**FIGURE 25.6**

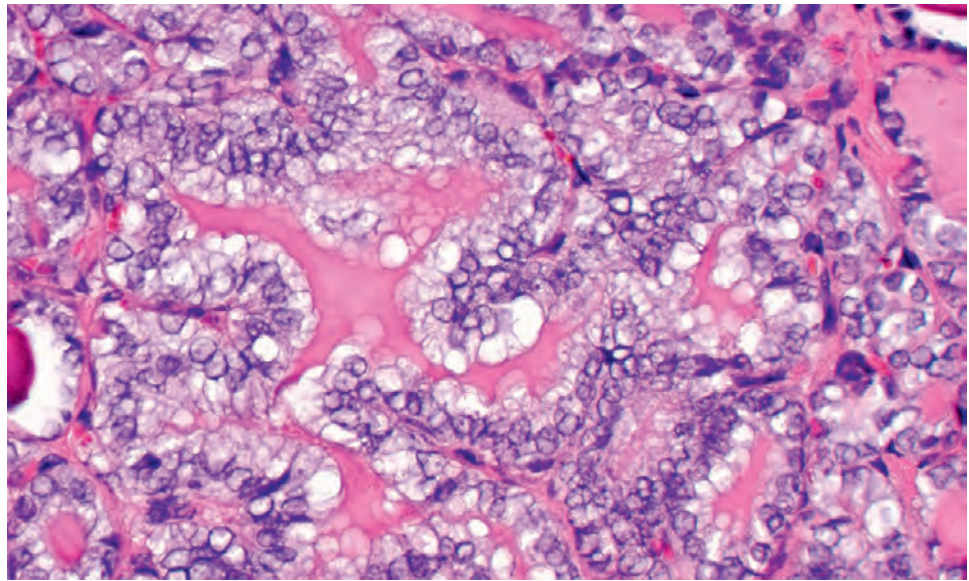
The classic features seen in PTC: irregular placement of the nuclei around the follicle, nuclear crowding, nuclear contour irregularities, nuclear "crescent-moon" formation, nuclear grooves, nuclear folds, and nuclear chromatin clearing.

parenchyma); and psammoma bodies (concentrically laminated calcific bodies; [Figs. 25.5–25.10](#)). If a single tumor has many different growth patterns, suspicion for papillary carcinoma should be raised.

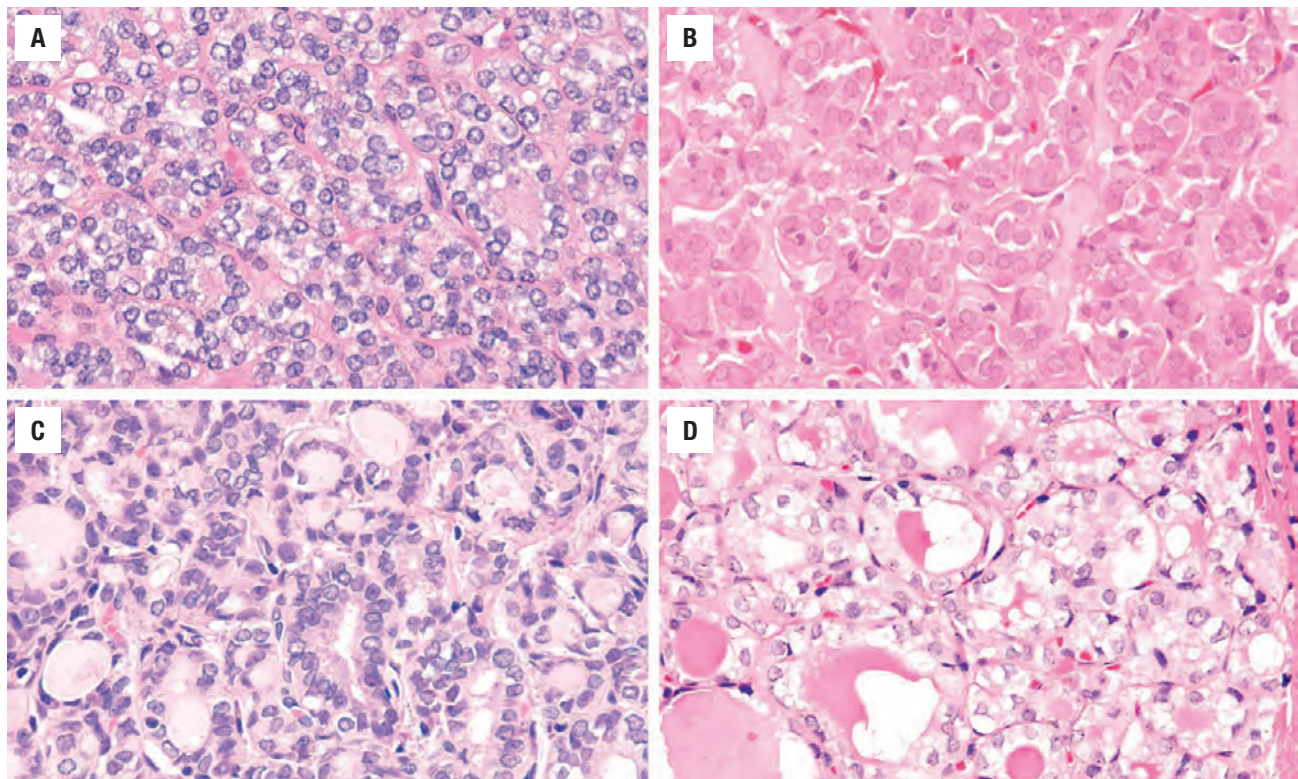
The cytomorphic and nuclear features are vital in the diagnosis of papillary carcinoma and are usually constant even between the variants. These features are

best assessed at the periphery of the tumor, where comparison can be made to the adjacent, uninvolved normal thyroid tissue. These features include enlarged cells with a high nuclear-to-cytoplasmic ratio; nuclear enlargement of oval to elongated nuclei; variability in size and shape, with nuclear overlapping and crowding; and loss of polarity and disorganized nuclear placement within the cell



**FIGURE 25.7**

There is nuclear crowding and overlapping within hypereosinophilic colloid that shows peripheral scalloping. There is well-developed nuclear chromatin clearing (optical clearing: Orphan Annie nuclei).

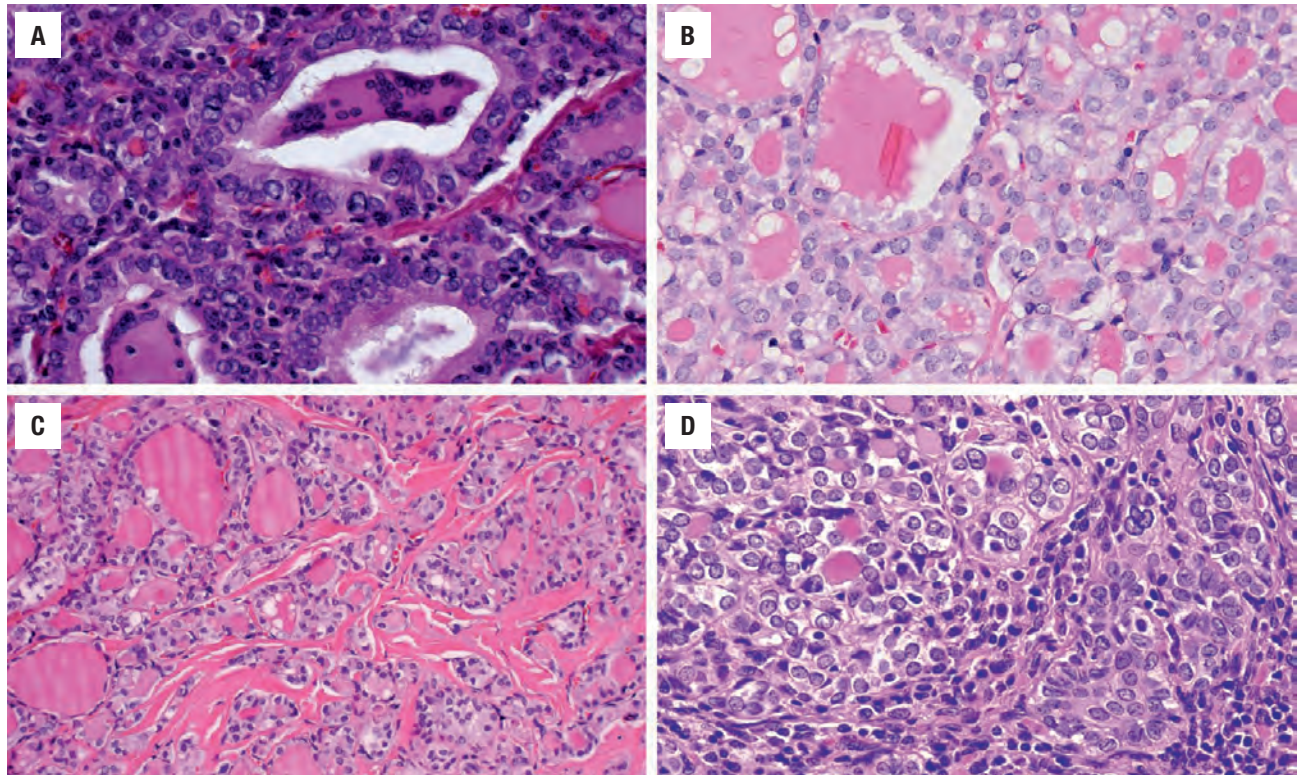
**FIGURE 25.8**

Cytomorphologic features in PTC. (A) Nuclear crowding and chromatin clearing. (B) Fine, ground glass nuclear chromatin. (C) Nuclear overlapping, chromatin irregularities, and loss of nuclear polarity. (D) Pale nuclear chromatin in irregular nuclei surrounding follicles with scalloped, dense colloid.

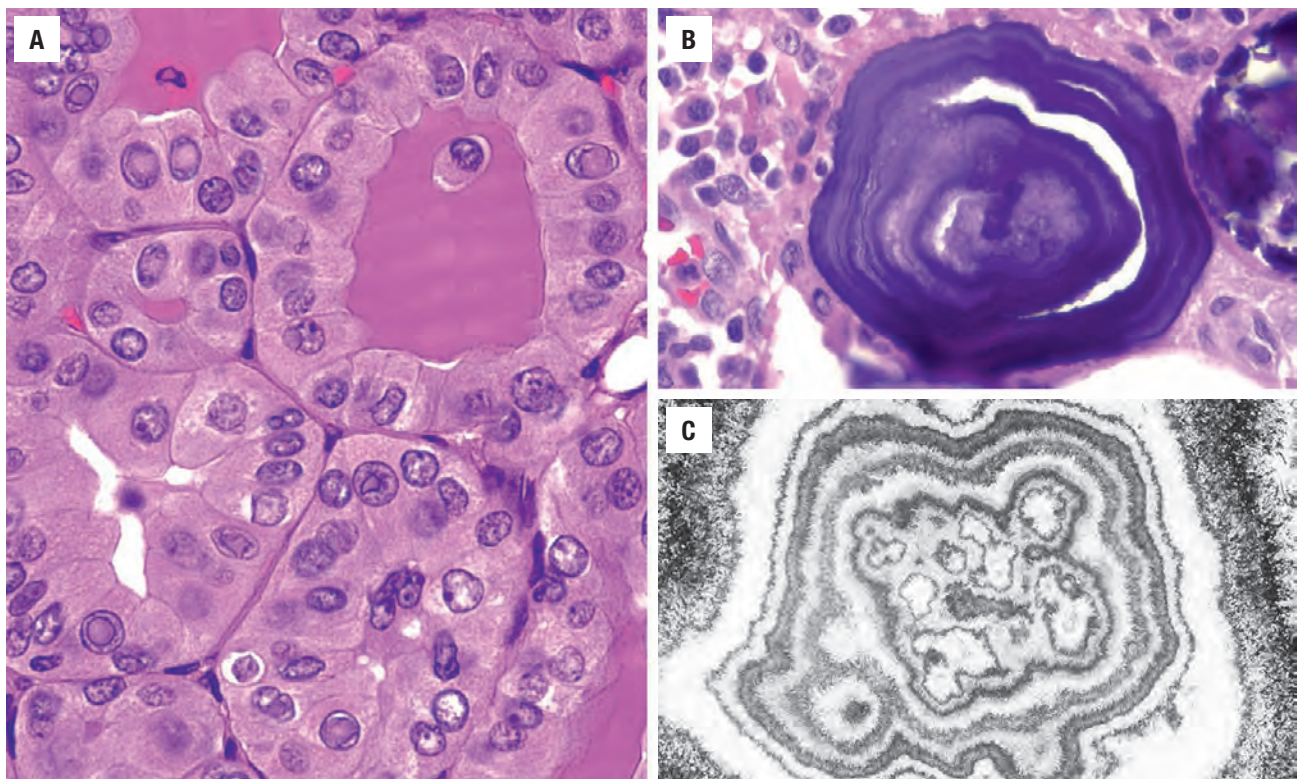
(Figs. 25.5–25.9). The nuclear crowding creates a “herd,” “lake,” or “egg-basket” appearance (Figs. 25.5 and 25.7). The nuclear chromatin is fine, delicate, even, and pale (“ground glass”) with chromatin margination or condensation (thick membranes) and clearing (“Orphan Annie” nuclei; Figs. 25.7 and 25.8). If slides are left on the heating block for too long or in an aqueous solution during processing, “false” intranuclear bubbles are created.

Formalin fixation creates the clearing, since it is not seen in frozen section material nor in alcohol fixatives (SafeFix, HistoChoice). Nuclear grooves and longitudinal folds creating a “crescent moon,” triangular, angulated, or convoluted shape (“coffee bean,” “popcorn”) are characteristic (Figs. 25.6 and 25.9). Nuclear envelope irregularities are more difficult to assess on frozen section material. Intranuclear cytoplasmic inclusions (pseudoinclusions) are recognized



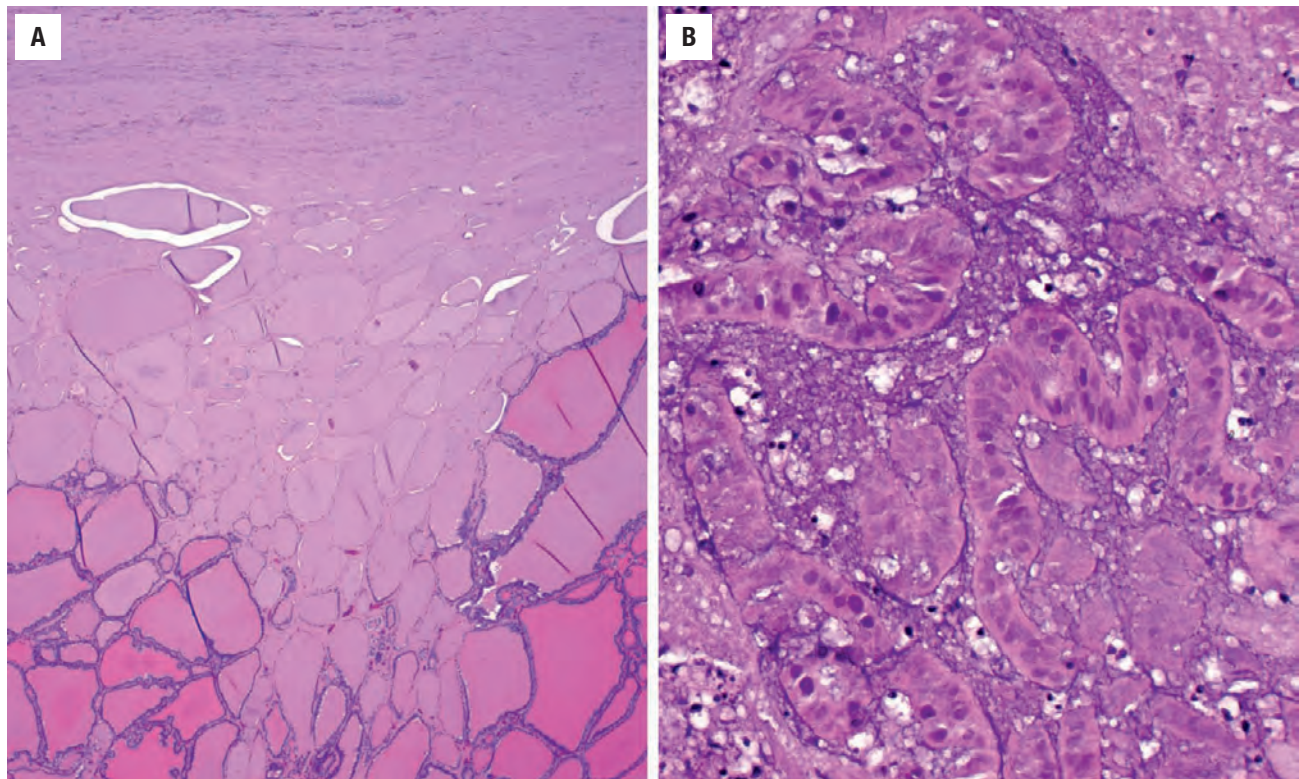
**FIGURE 25.9**

Associated findings in PTC. (A) Giant cells within the colloid. (B) Crystals within the colloid. Nucleoli are noted along the nuclear membrane. (C) Dense fibrosis separating the tumor cells. (D) Squamous metaplasia (*lower right corner*) within a PTC.

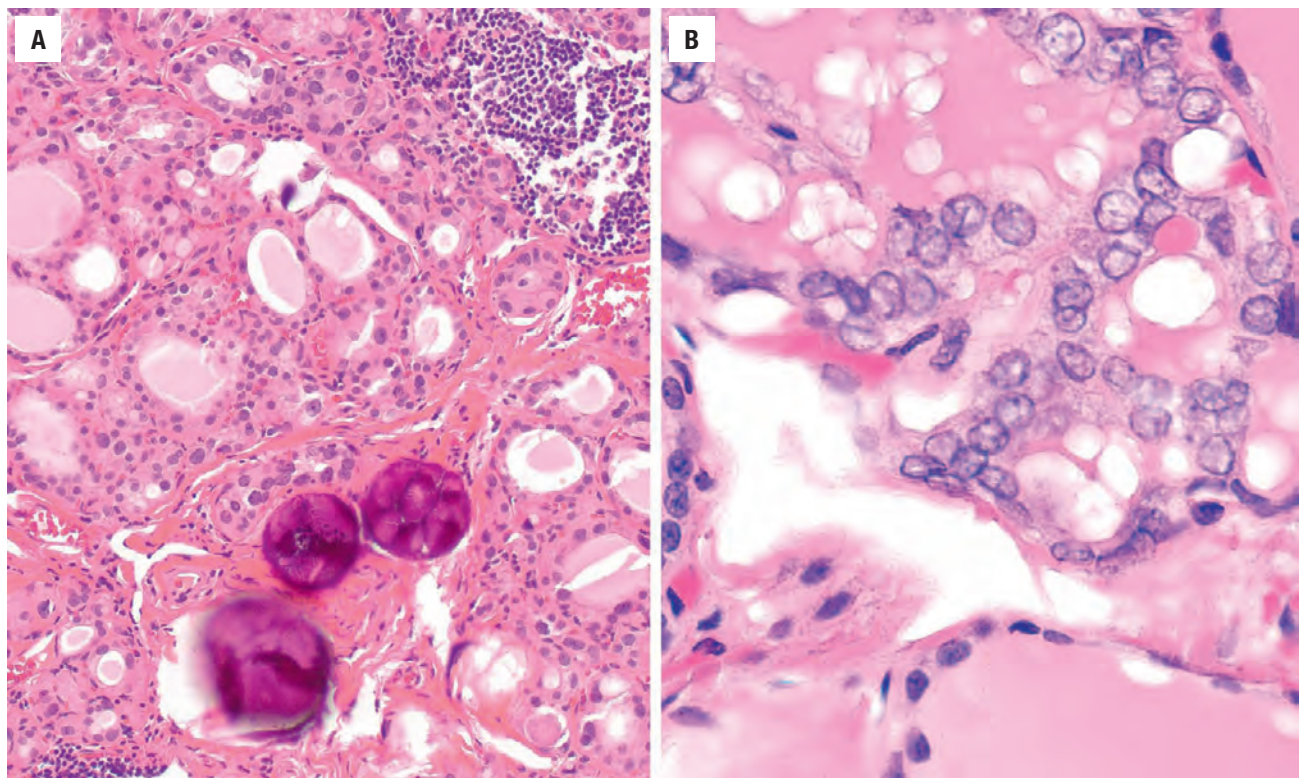
**FIGURE 25.10**

(A) Multiple intranuclear cytoplasmic inclusions contain material the same color as the cytoplasm. (B) Light microscopic appearance of a psammoma body with concentric laminations. (C) Electron micrograph of a psammoma body showing concentric lamination and crenated nuclei in the center. (Courtesy of Dr. C. S. Heffess.)



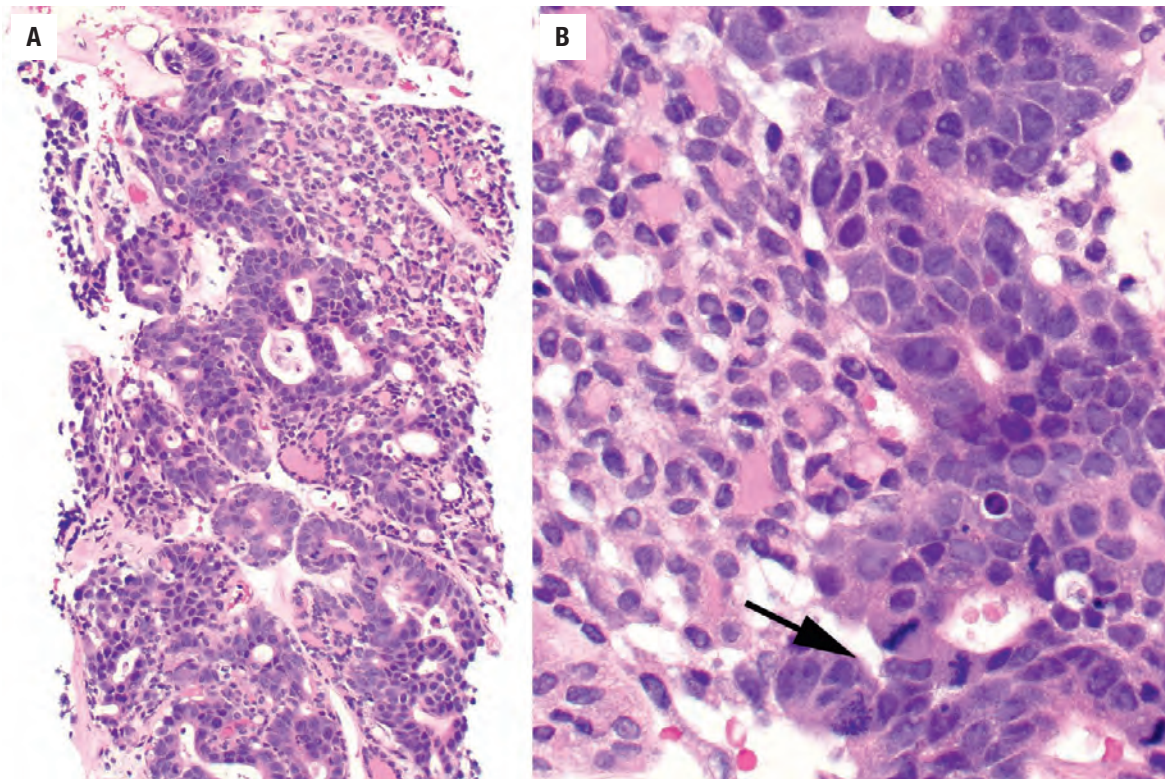
**FIGURE 25.11**

(A) "Mummification" of the cells, at the periphery of the tumor, creating a wedge shape is an uncommon, but unique feature of papillary carcinoma. (B) Tumor infarction results in ghost cell outlines, still showing papillae, but no longer viable tumor cells.

**FIGURE 25.12**

(A) Psammoma bodies are noted in this case of diffuse hyperplasia, with a microscopic papillary thyroid carcinoma noted elsewhere in the lobe. (B) Papillary carcinoma within a lymphatic unassociated with any fibrosis. Benign thyroid parenchyma is noted in the lower portion of the figure.



**FIGURE 25.13**

(A) Poorly differentiated carcinoma is considered in the presence of increased mitoses, necrosis, and high cellularity. (B) Note there are three mitoses in just this one high power field (arrow).

by the contents of the inclusion having an appearance similar to the cytoplasm—and not an artifactual “vacuole” formed secondary to fixation (Fig. 25.10). Nucleoli, if present, are usually small and inconspicuous and seem to touch the nuclear membrane rather than being centrally located (Fig. 25.9). The cytoplasm is variable and usually not helpful in the diagnosis, although variants are named according to the cytoplasm (clear, oncocytic, hobnail, columnar). Giant cells in the colloid and the presence of crystals are “soft” criteria, also seen in other lesions (Fig. 25.9). Squamous metaplasia, cyst formation, and degeneration are not uncommon, with infarction induced by FNA (Figs. 25.9 and 25.11). Psammoma bodies are *not* the same as dystrophic calcification of colloid in the center of a follicle. Psammoma bodies (Greek for “salt-like”) represent apoptotic cells that form the nidus for concentric lamellation of calcium (Fig. 25.10). Present in up to 50% of cases, they are often identified within lymphovascular channels, diagnostic of intraglandular spread. Likewise, their presence in lymph nodes is pathognomonic for metastatic disease (any papillary pattern tumor may cause psammoma bodies), although potentially excluded in staging systems.

Mummification (peripheral cell death) is infrequently seen, but quite characteristic for papillary carcinoma (Fig. 25.11). Separation of multifocal versus intraglandular spread of PTC can be difficult. Intraglandular spread is suggested when there are psammoma bodies

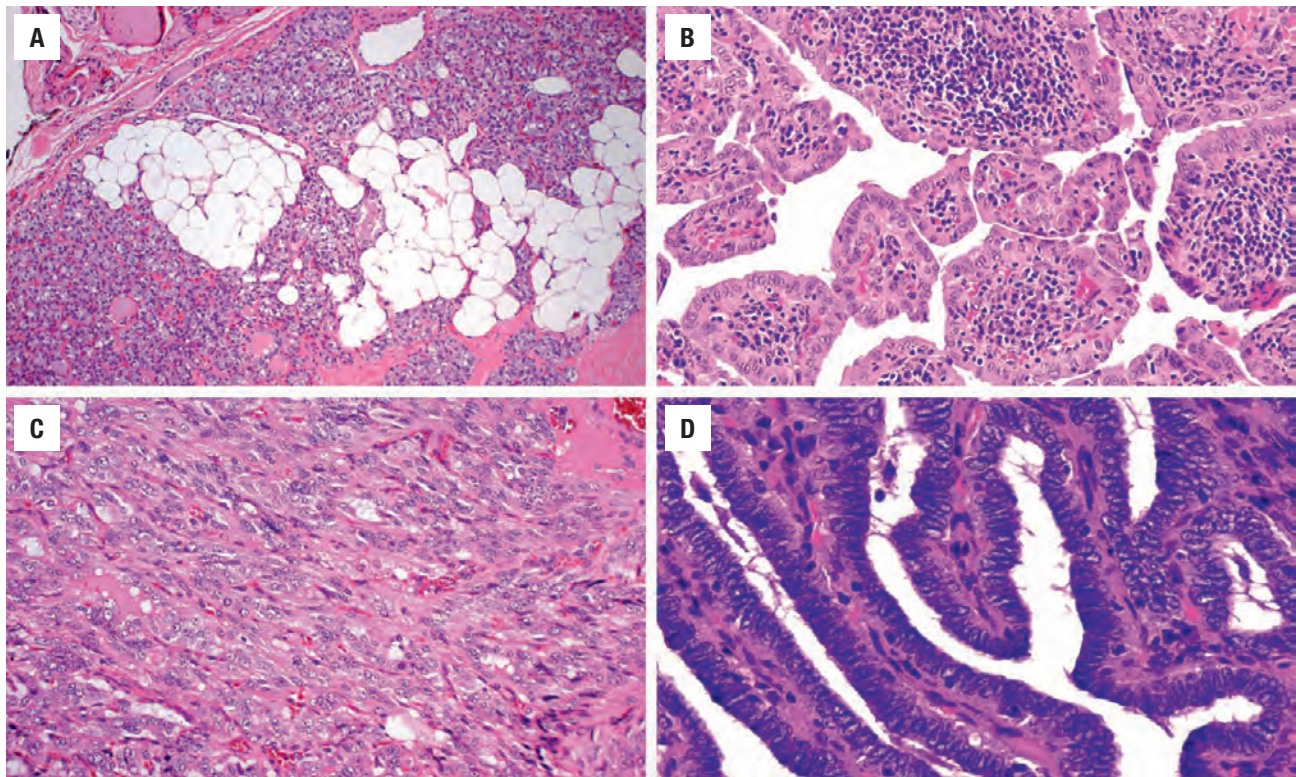
within the septa or when there is viable tumor within a lymphovascular channel and has no stellate fibrosis at the periphery (Fig. 25.12). Intratumoral fibrosis is an acellular, sclerotic, dense, eosinophilic fibrosis found in up to 90% of cases. The fibrosis is often irregular to stellate, a feature that is useful during gross examination to select areas for microscopic examination. Papillary carcinoma is not routinely graded, as nearly all are considered well differentiated. However, when there are increased mitoses ( $> 3/10$  high power fields; Fig. 25.13) and tumor necrosis, then the tumor would be considered a poorly differentiated carcinoma. Tumor necrosis is uncommon in PTC, with its detection away from an FNA tract suggesting a more aggressive (poorly differentiated or undifferentiated) component within the tumor. A heavy lymphocytic response is frequently seen both adjacent to and within the tumor (Fig. 25.14). Fatty metaplasia, spindled tumor cells and limited colloid may be seen (Fig. 25.14). Variants are described in the next section.

## ANCILLARY STUDIES

### IMMUNOHISTOCHEMICAL FINDINGS

Immunohistochemistry is seldom of value in diagnosing PTC, although it may play a role in metastatic disease.



**FIGURE 25.14**

Uncommon features in PTC. (A) Fatty metaplasia. (B) Lymphocytes and plasma cells, sometimes referred to as “Warthin” variant of papillary carcinoma. (C) Tumor cell spindling. (D) No colloid is seen in this tumor with marked nuclear overlapping and stratification.

The neoplastic cells are strongly and diffusely immunoreactive with keratin, CK7, thyroglobulin, TTF1, and PAX8, while other markers (HBME-1 [Fig. 25.15], galectin-3, S100 protein, CITED1, CK19 [Fig. 25.15]) yield variable results. In challenging cases, there is good sensitivity and specificity when using a panel approach: HBME-1 (membranous), galectin-3 (nuclear and cytoplasmic), and CITED1. However, for more than 98 % of cases, immunohistochemistry is unnecessary. p27 (lost) and cyclin D1 (up regulation) shows differential staining in tumors that are more likely to metastasize.

#### FINE NEEDLE ASPIRATION

FNA is considered the test of choice for the diagnosis and management of thyroid nodules, having an excellent sensitivity, specificity, and positive predictive value. An initial pass using a 25-gauge needle—without suction—yields excellent material uncontaminated by blood. In general practice, about 70 % of thyroid FNAs are benign, 10 % are indeterminate, 15 % are unsatisfactory, and 5 % are malignant.

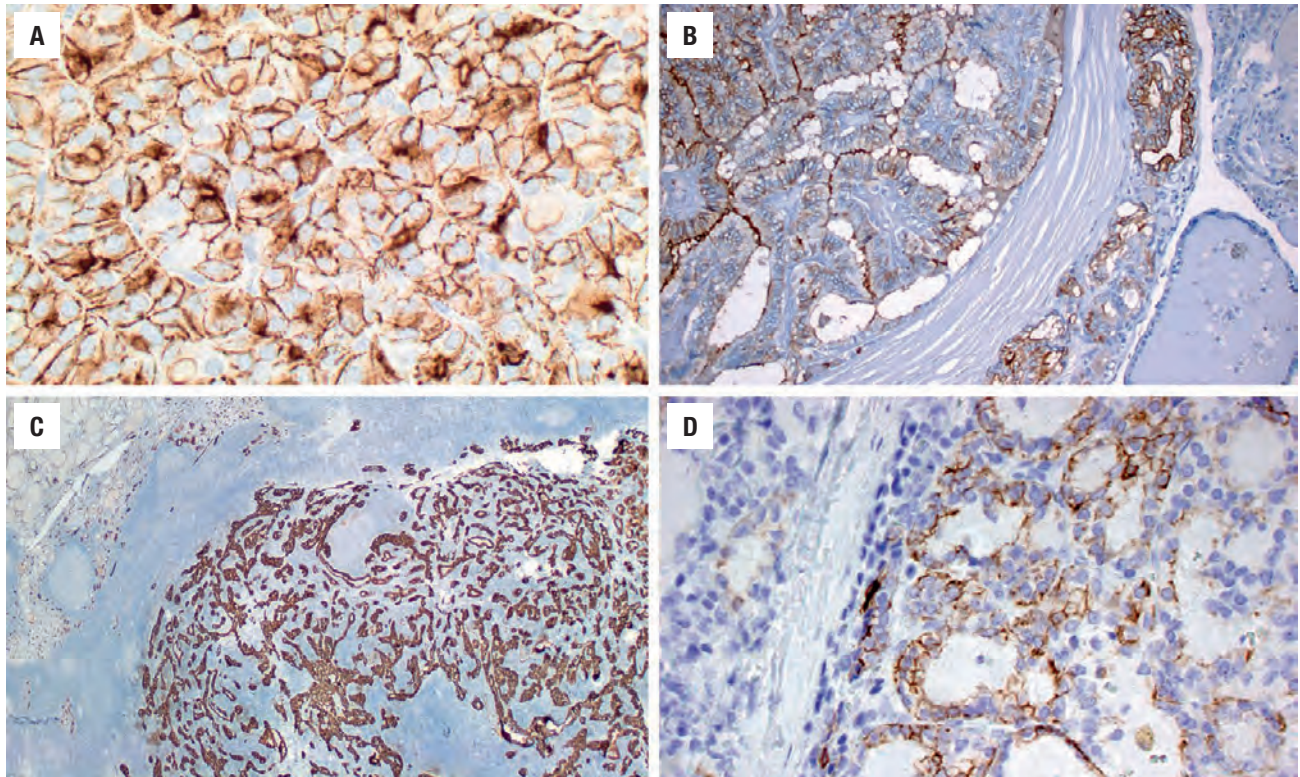
Aspirates from papillary carcinomas are usually diagnostic, meeting the adequacy criteria (at least 6 follicular groups with greater than 10 follicular cells per group) and are characteristically cellular, with monolayered sheets (syncytium) and three-dimensional clusters of enlarged cells (Fig. 25.16). The nuclei are enlarged

and overlapped with irregular borders, but with a powdery/dusty, delicate nuclear chromatin on alcohol fixed preparations. Nuclear folds or grooves and intranuclear cytoplasmic inclusions are also common. The cytoplasm is often pale or foamy, but not distinctive on FNA. Colloid is often scant and thickened (“chewing gum” or ropy), with occasional multinucleate giant cells and, rarely, psammoma bodies. The features of papillary carcinoma are best appreciated with alcohol-preserved Papanicolaou preparations rather than with air-dried material. With noninvasive follicular pattern tumors now recognized separately, they may show the nuclear features of papillary carcinoma. Thus, the definitive diagnosis of PTC on FNA material should be limited to those smears that show three-dimensional papillary structures and/or psammoma bodies.

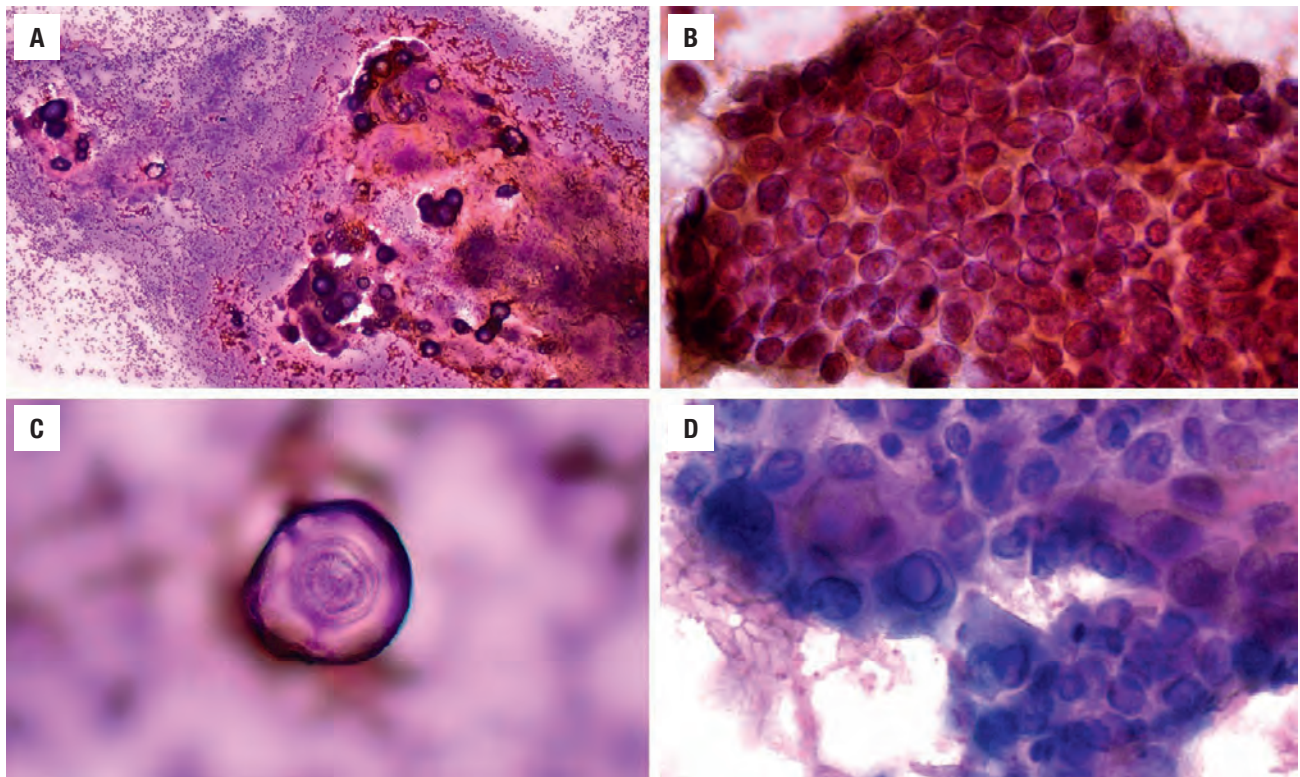
#### MOLECULAR FINDINGS

Results are quite dependent on technique and the specific histologic variant. Most genetic alterations are mutually exclusive, with a majority of cases activating the mitogen-activated protein kinase (MAPK) pathway. In general, point mutations (such as *BRAF* V600E, *NRAS*), gene fusions, or gene copy number variations account for the usual molecular findings. Point mutations in the *BRAF* gene are identified in up to 60 % of papillary carcinomas (valine-to-glutamate substitution at residue



**FIGURE 25.15**

HMBE-1. Note the variable membrane and cytoplasmic expression in the tumor cells (heavy in **A**), including an area of invasion (**B**). CK19. There is strong cytoplasmic reactivity (**C**), while in other areas it is only delicate, partial membranous staining (**D**).

**FIGURE 25.16**

(**A**) Three-dimensional clusters in a cellular smear with psammoma bodies noted (Diff-Quik). (**B**) A syncytium of cells with enlarged nuclei and nuclear grooves (alcohol fixed, Papanicolaou stain). (**C**) A psammoma body is characteristic of papillary carcinoma (Diff-Quik). (**D**) Three-dimensional papillae around a central fibrovascular core showing nuclei with intranuclear cytoplasmic inclusions (air dried, Diff-Quik stain).



600: V600E), while other *BRAF* mutations (K601E) account for a minority of lesions. *RAS* gene (*NRAS*, *HRAS*, *KRAS*) mutations are seen in up to 15 % of tumors, but almost exclusively in follicular patterned tumors. *EIF1AX* is also seen in follicular patterned tumors. Fusion genes often involve *RET* gene, while *NTRK3*, *NTRK1*, *ALK*, and others are also recognized. *TERT* mutations seem to be associated with higher risk of recurrence, distant metastases, and tumor-related mortality. Each mutation/fusion/rearrangement has distinct phenotypic and biologic properties. While not necessary for diagnosis, there may be value in inherited papillary carcinoma syndromes, such as FAP coli or Cowden syndrome, for genetic studies to help in patient management.

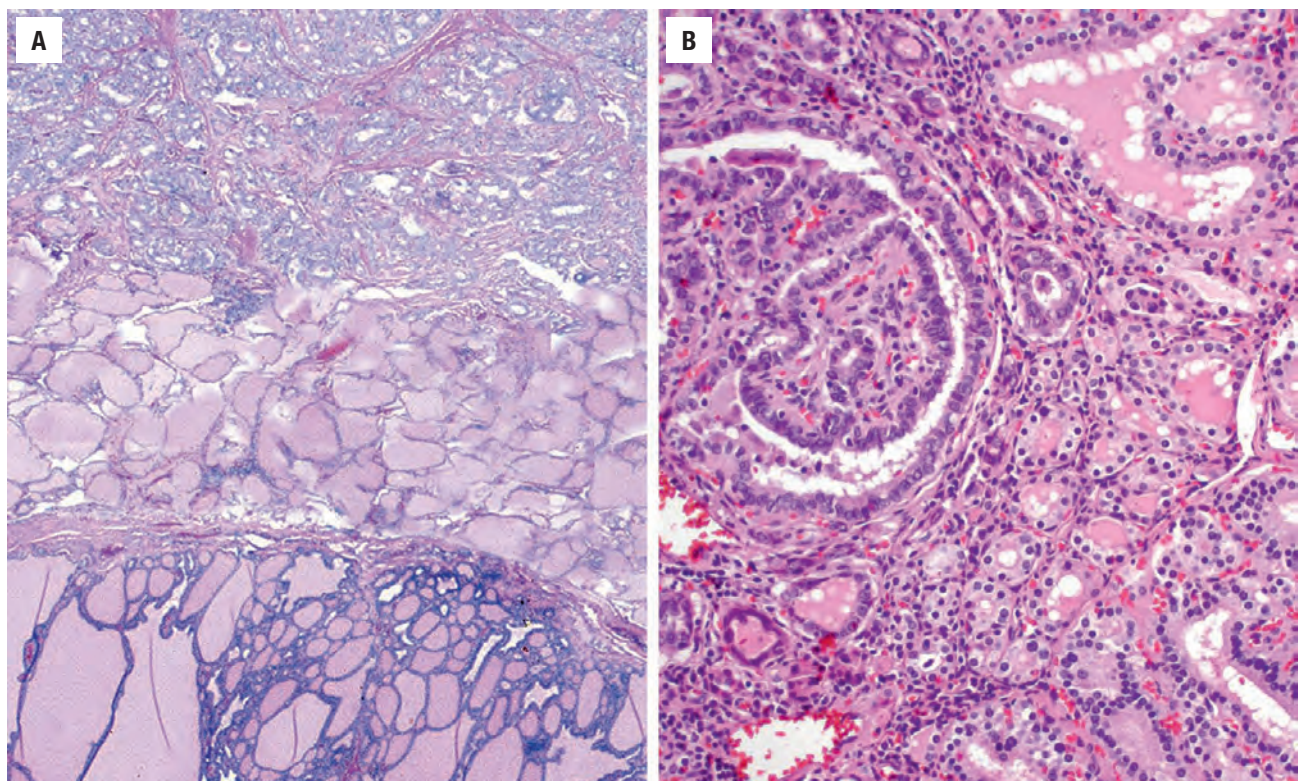
### DIFFERENTIAL DIAGNOSIS

The principal differential diagnosis includes a number of disorders with papillae, including adenomatoid nodules (Figs. 25.17 and 25.18), diffuse hyperplasia (Graves disease, Fig. 25.17), and dyshormonogenetic goiter, while follicular adenoma (FA), follicular thyroid carcinoma (FTC), medullary thyroid carcinoma (MTC), and metastatic tumors are also considered. In general, the papillae

of all of these other lesions are short, simple, nonbranching, and often “thick.” The nuclei are round, regular, basally located, and hyperchromatic. Intracytoplasmic hemosiderin pigment is nearly always lacking in PTC. Although a nuclear feature or two may be present in these other lesions, there is both a qualitative and quantitative difference in their appearance. Many lesions that have oncocyctic cytoplasm may induce nuclear enlargement, but other features of PTC are lacking. It is worth noting that noninvasive follicular thyroid neoplasm with papillary-like nuclear features is included in the differential diagnosis of follicular patterned tumors, and will be further discussed in the chapter on benign neoplasms.

### PROGNOSIS AND THERAPY

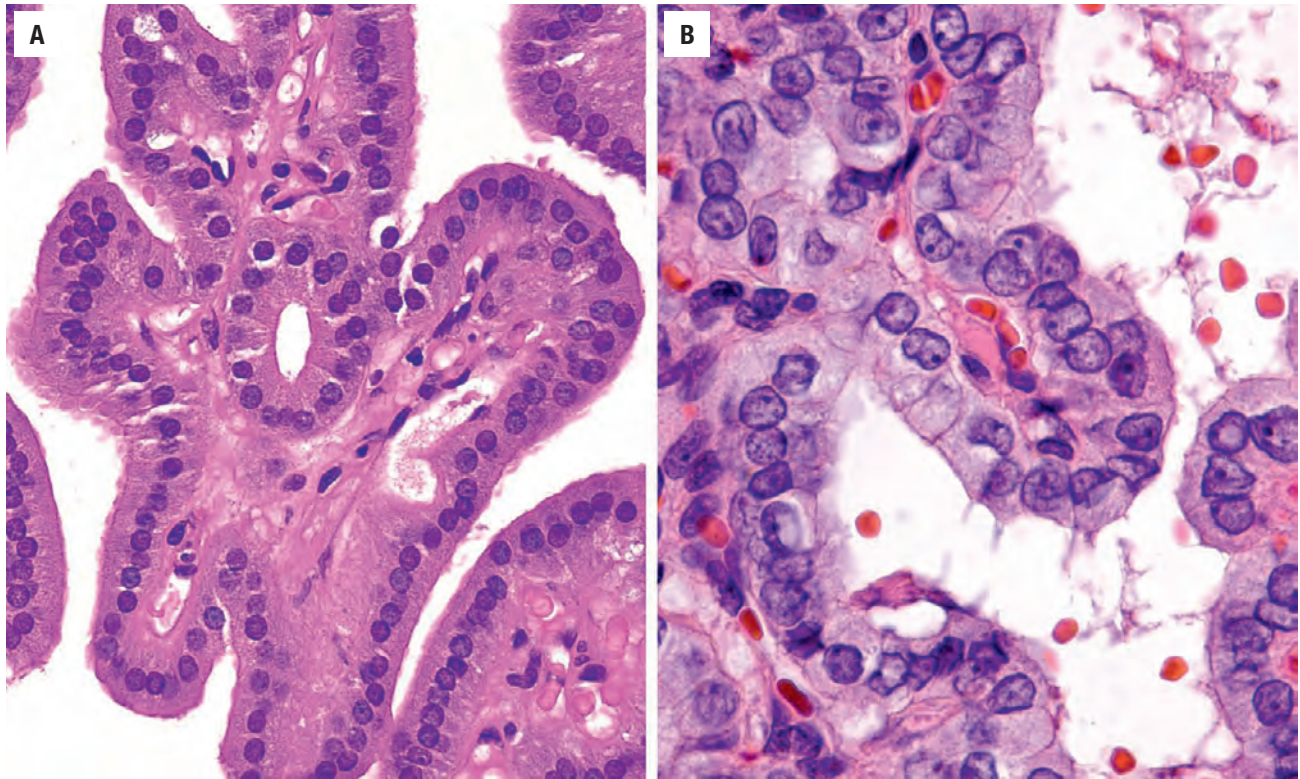
Papillary carcinoma spreads preferentially by lymphatic channels, with the regional lymph nodes affected most commonly, and in a significant proportion of cases (Fig. 25.19). Intraglandular spread, including the contralateral lobe, is common. However, the prognosis is excellent, with greater than 90 % 20-year survival rate and a less than 0.2 % mortality rate. Macroscopic extrathyroidal extension into the adjacent fat or skeletal muscle places



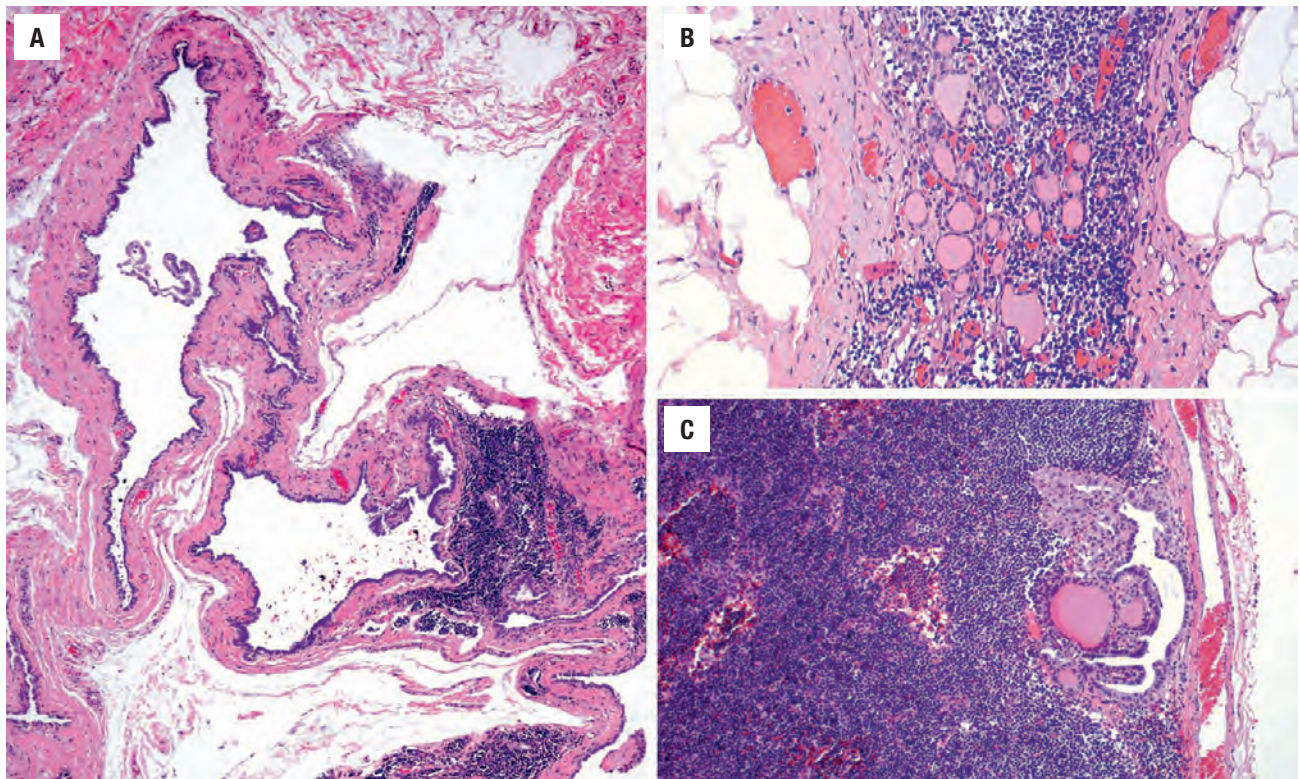
**FIGURE 25.17**

(A) Adenomatoid nodule (lower half) and papillary carcinoma (upper half) frequently co-exist. There are differences in architecture and cytology, even at this low magnification. (B) A papillary carcinoma (right upper) has a completely different appearance than the background of diffuse hyperplasia.



**FIGURE 25.18**

(A) An adenomatoid nodule has small cells in an orderly arrangement around the follicles with coarse/heavy nuclear chromatin distribution. (B) Papillary carcinoma has large cells with an increased nuclear-to-cytoplasmic ratio, irregular placement of the nuclei, nuclear contour irregularities, nuclear grooves and folds, and delicate to fine nuclear chromatin distribution (same magnification).

**FIGURE 25.19**

(A) A predominantly cystic metastasis can sometimes simulate a lymphangioma or branchial cyst. (B) Almost "normal" appearing follicles within a lymph node. However, this represented metastatic disease from an ipsilateral primary papillary carcinoma. (C) Papillary projections and colloid of metastatic papillary carcinoma in a lymph node.



## HISTOLOGIC VARIANTS OF PAPILLARY THYROID CARCINOMA

### Encapsulated Variant

- Classical histologic and architecture features of papillary carcinoma but in an entirely encapsulated tumor with only limited invasion

### Follicular Variant

- Most are encapsulated or very well circumscribed
- Almost exclusively small follicles with scant, bright colloid
- Classic nuclear features of papillary carcinoma
- No tumor necrosis, increased mitoses, or dominant solid or other pattern
- Invasion used to separate from noninvasive follicular thyroid neoplasm with papillary-like nuclei

### Macrofollicular Variant

- Enlarged follicles with remaining features similar to follicular variant although nuclei are often flattened
- Abortive, rigid papillae may be seen
- Separation from adenomatoid nodule is imperative

### Oncocytic Variant

- 30%–70% papillary architecture (criteria vary by study)
- Enlarged cells with abundant oncocytic, glassy cytoplasm, apically-oriented enlarged nuclei with papillary features, increased number of intranuclear cytoplasmic inclusions
- Degenerative changes common

### Clear Cell Variant

- Clear cytoplasm, although occasionally oncocytic and clear cells are combined
- Must be separated from medullary and metastatic renal cell carcinoma

### Spindle Cell Variant

- Focal to diffuse tumor cells spindling of proven epithelial cells (keratin and/or TTF1) that lack pleomorphism increased mitoses and necrosis
- Follicular adenoma, follicular carcinoma, papillary carcinoma, paraganglioma, hyalinizing trabecular tumor, amyloid goiter, undifferentiated carcinoma, metastatic tumor, lymphoma

### Diffuse Sclerosing Variant

- Diffuse, bilateral involvement, extensive fibrosis, innumerable psammoma bodies, extensive intravascular growth and extrathyroidal extension, florid squamous metaplasia, dense lymphocytic thyroiditis, solid or papillary growth of papillary carcinoma cells

- Nearly all have extensive lymph node metastases

### Tall Cell Variant

- 30%–70% of tumor area composed of cells that are at least three times as tall as they are wide, usually oncocytic cytoplasm, sharply defined cellular borders, increased intranuclear cytoplasmic inclusions, centrally placed nuclei within the cell
- Papillary structures and parallel elongated follicles with limited colloid

### Columnar Cell Variant

- Prominent papillary growth, parallel follicles (“railroad tracks”), scant colloid, syncytial architecture with prominent nuclear stratification, coarse nuclear chromatin, subnuclear cytoplasmic vacuolization, squamous metaplasia as “morules,” and increased mitotic figures
- CDX2 and TTF1 reactive

### Solid/Insular Variant

- Solid or insular pattern with nuclear features of papillary carcinoma
- More common in children
- Must lack features of another variant
- Lacks increased mitoses and necrosis

### Cribriform-Morular Variant

- Almost exclusively in female patients with FAP
- Multiple encapsulated tumors, mixed patterns, cribriform dominant
- Morules or whorls of squamous cells without keratinization, showing optical clearing
- Columnar cells often have grooves and folds
- Nuclear  $\beta$ -catenin strong and diffuse; TTF1 and thyroglobulin: weak, focal and patchy

### Hobnail Variant

- At least 30% of cells must have hobnail appearance, with protrusion into the colloid, apically placed nuclei with prominent nucleoli
- Higher association with extrathyroidal extension, lymphovascular invasion, necrosis, and increased mitoses

### Size Variation

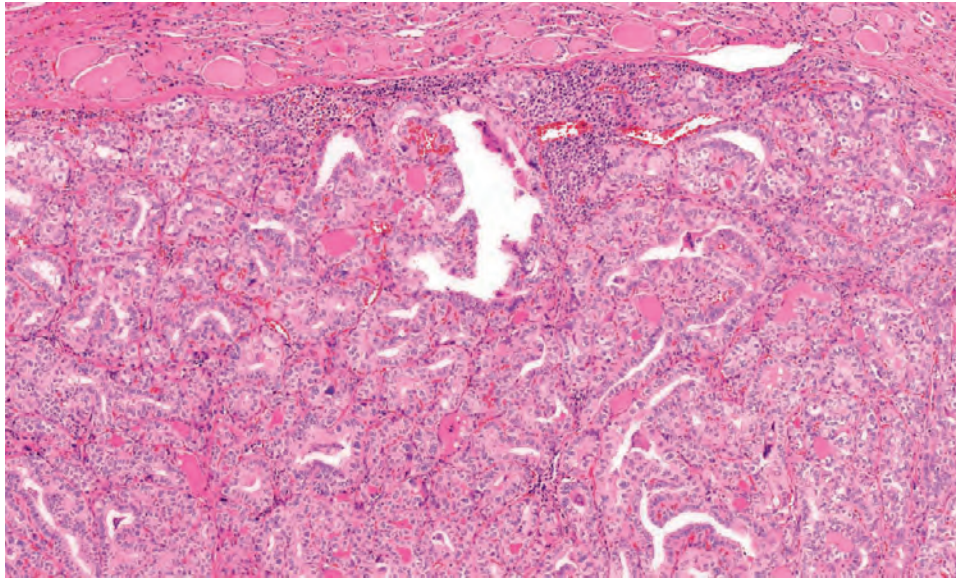
- Incidentally found,  $\leq 1$  cm papillary carcinoma with a proclivity for thyroid subcapsular location—designated “microcarcinoma” when not the reason for the surgery

the tumor in the American Joint Committee on Cancer (AJCC) stage pT3b (2017 criteria), but microscopic extension does not change stage. Age ( $<55$  years) and sex (female) are the most important prognostic factors, although tumor size ( $> 4$  cm), gross extrathyroidal extension, and metastasis are significant for patients  $\geq 55$  years. Surgery is the treatment of choice, although the extent of surgery (lobectomy, subtotal, or total thyroidectomy) remains controversial. Recurrent laryngeal nerve damage and hypoparathyroidism are known surgical complications. Radioablative iodine therapy is incorporated after a total thyroidectomy. However, the tumor needs to show

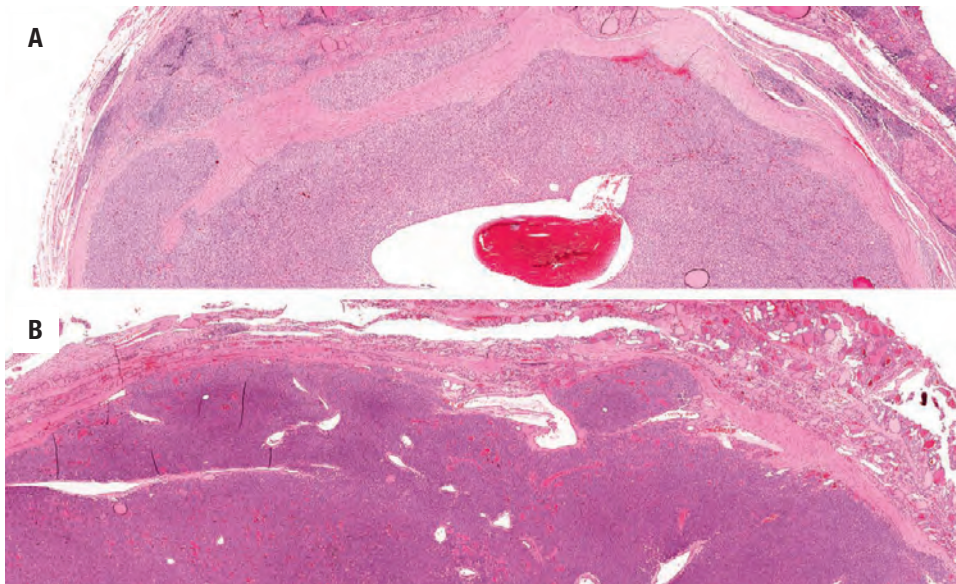
uptake of the radiolabeled iodine to be therapeutically sensitive. Lymph node sampling is advocated only if there is clinical or radiographic enlargement.

## ■ HISTOLOGICAL VARIANTS OF PAPILLARY CARCINOMA

Variants of papillary carcinoma have specific features that may be associated with a different patient outcome or cause difficulty with the differential diagnosis. In

**FIGURE 25.20**

There is a very thin and delicate fibrous connective tissue capsule completely surrounding this classical papillary carcinoma without invasion.

**FIGURE 25.21**

**(A and B)** A very thick capsule surrounds a tumor that shows a monotonous follicular tumor with hyper eosinophilic colloid. Note the areas of invasion in both tumors.

general, the changes should be the dominant finding to qualify as a histologic variant.

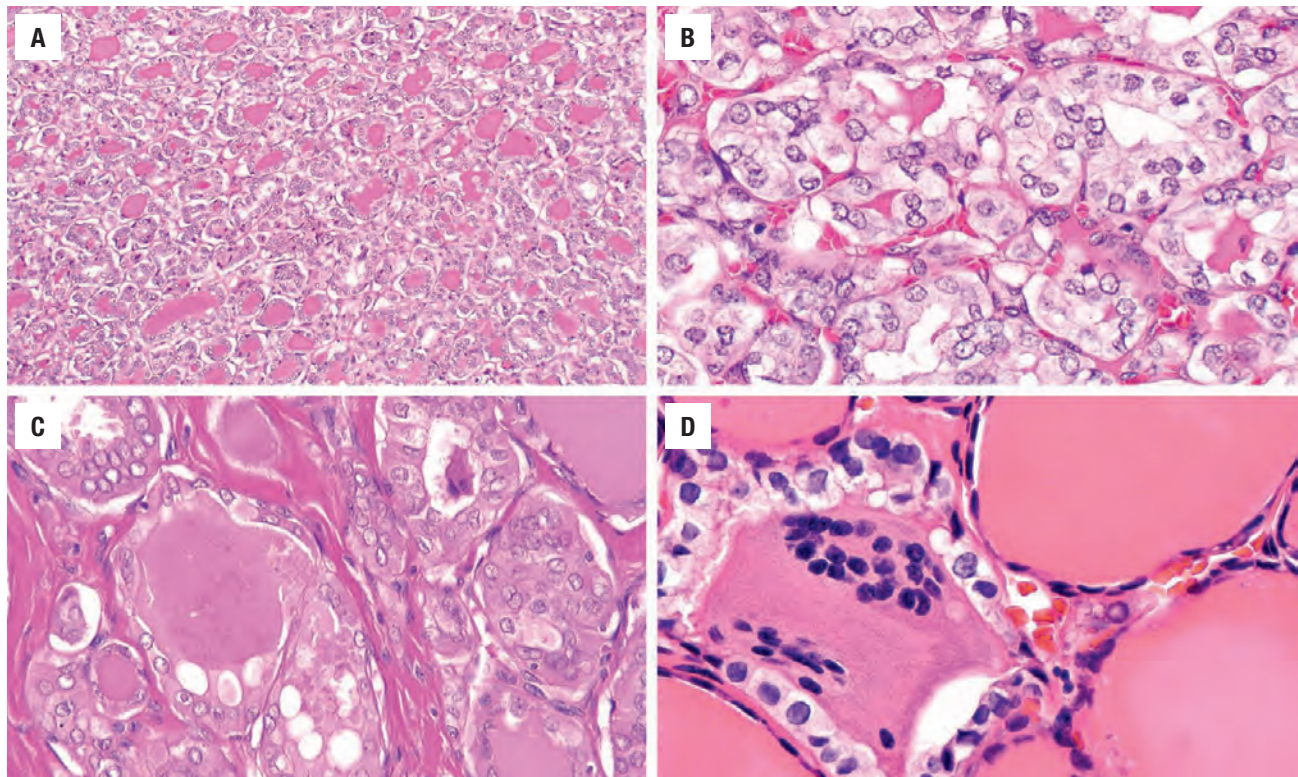
### ENCAPSULATED VARIANT

Classical architecture and nuclear features of papillary carcinoma in a tumor that is totally encapsulated (Fig. 25.20) with only limited evidence of invasion. In these cases, “encapsulated variant with invasion” is used to qualify the type of invasion. This tumor is separated from FA with papillary hyperplasia by the presence of classical papillary nuclear features. The papillary structures exclude a noninvasive follicular thyroid neoplasm with papillary-like nuclear features (NIFTP).

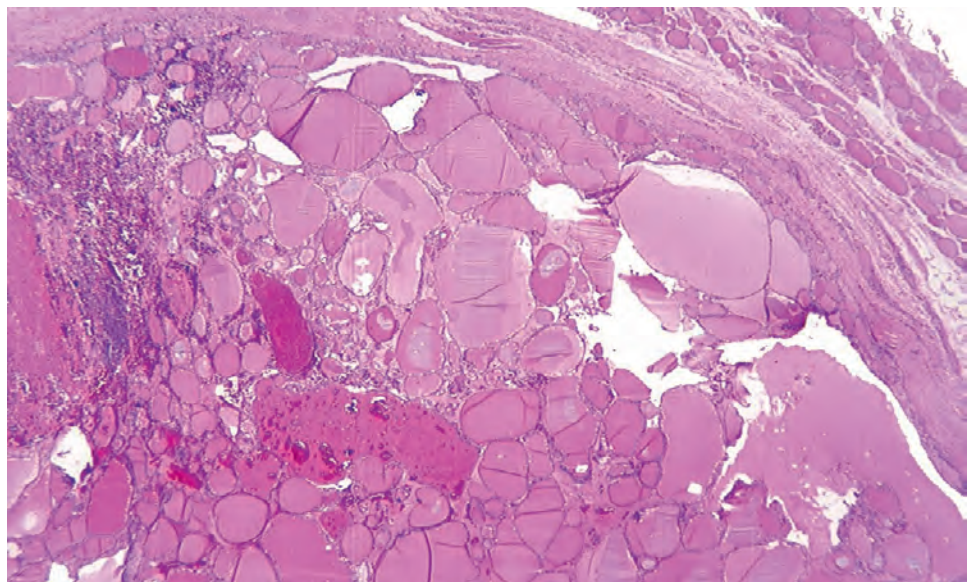
### FOLLICULAR VARIANT

Usually encapsulated, the tumor must be predominantly composed of small, tight follicles with scant, hyper eosinophilic colloid. Papillae are absent or less than 1 % of the tumor volume (Figs. 25.21 and 25.22). There are two types: *encapsulated with invasion* and *infiltrative*. By definition, invasion is present, otherwise the tumor would be considered as a NIFTP. The infiltrative form is sclerotic with easily identified invasion. The encapsulated with invasion type shows either capsular or lymphovascular invasion. The nuclear features determine the diagnosis in this variant. Specifically, the nuclei are large with pale to powdery to cleared nuclear chromatin and an increased



**FIGURE 25.22**

(A) Small, tight follicles with hyper eosinophilic colloid in this follicular variant of papillary carcinoma. (B) Nuclear chromatin clearing and overlap with small tight follicles and limited colloid production. (C) The nuclei are irregular in shape and size and misplaced around the follicle. Tumoral fibrosis separates the follicles. (D) Nuclear features of papillary carcinoma can be isolated to just a few follicles at a time. The whole tumor is still papillary carcinoma.

**FIGURE 25.23**

This macrofollicular variant of papillary carcinoma is surrounded by a capsule, compressing the peripheral parenchyma. The low power resemblance to adenomatoid nodule is deceiving.

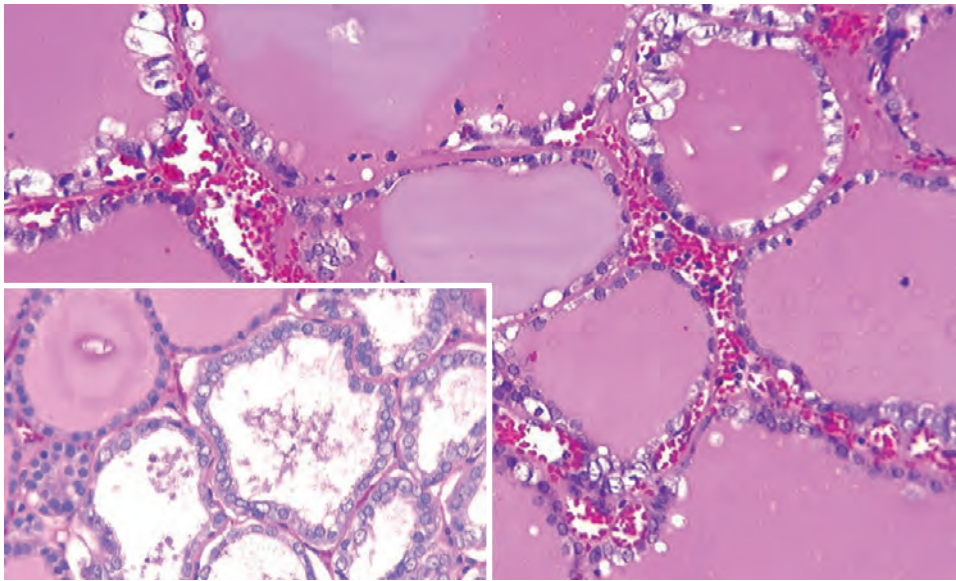
number of nuclear grooves and folds (Fig. 25.22). Internal sclerosis or fibrosis is seen (Fig. 25.49). This variant has a similar outcome to conventional PTC.

### MACROFOLLICULAR VARIANT

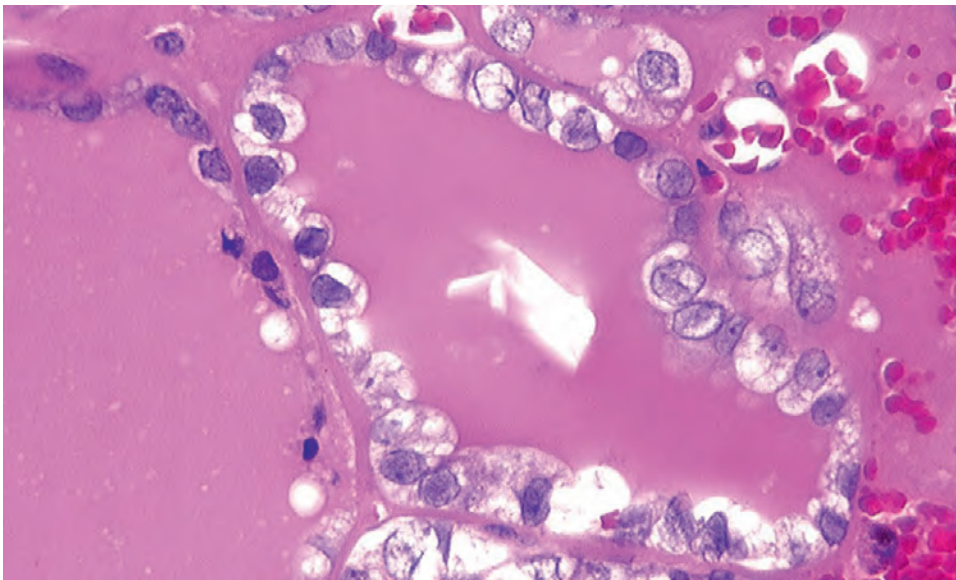
This is an uncommon variant that is difficult to recognize as it has an architectural resemblance to adenomatoid

nodules or hyperplastic nodules (Fig. 25.23). The tumor is composed of predominantly large/macrofollicles with a subtle increased cellularity, often accentuated at the periphery (Fig. 25.24). The colloid is often scalloped or vacuolated. The nuclei are often flattened and hyperchromatic, although classic papillary nuclei are scattered throughout the tumor (Fig. 25.25). Abortive, "rigid" or straight papillary structures will extend into the center of the colloid-filled follicle, usually lined by the atypical



**FIGURE 25.24**

Large follicles are lined by flattened to atypical follicular cells with scalloped colloid in this macrofollicular variant of papillary carcinoma. *Inset* demonstrates an area of increased cellularity and the cytologic features of papillary carcinoma.

**FIGURE 25.25**

The nuclear features are well demonstrated in this macrofollicular variant of papillary carcinoma. A crystalloid is seen in the center. Nuclear grooves, nuclear contour irregularities, and nuclear chromatin clearing is accentuated.

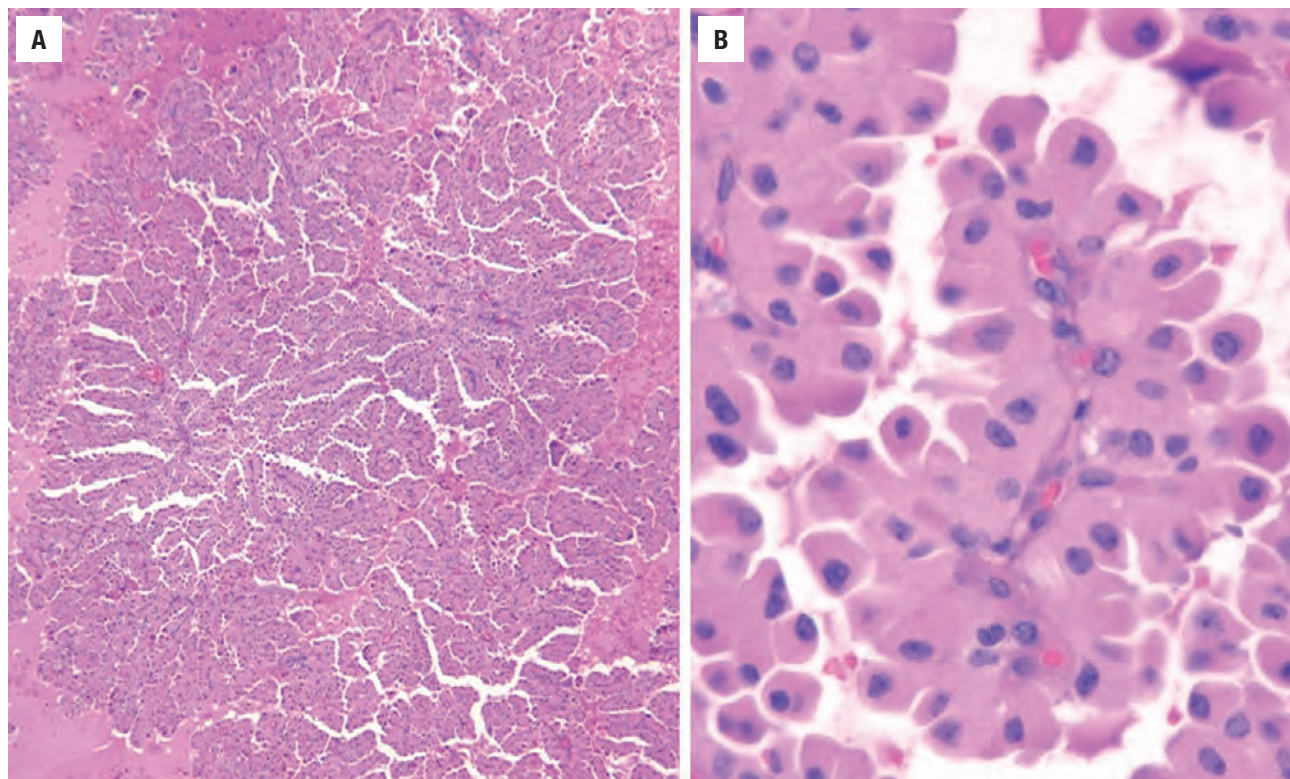
cells. This variant seems to metastasize less frequently than classic papillary carcinoma, but otherwise is similar in treatment and outcome.

#### ONCOCYTIC VARIANT

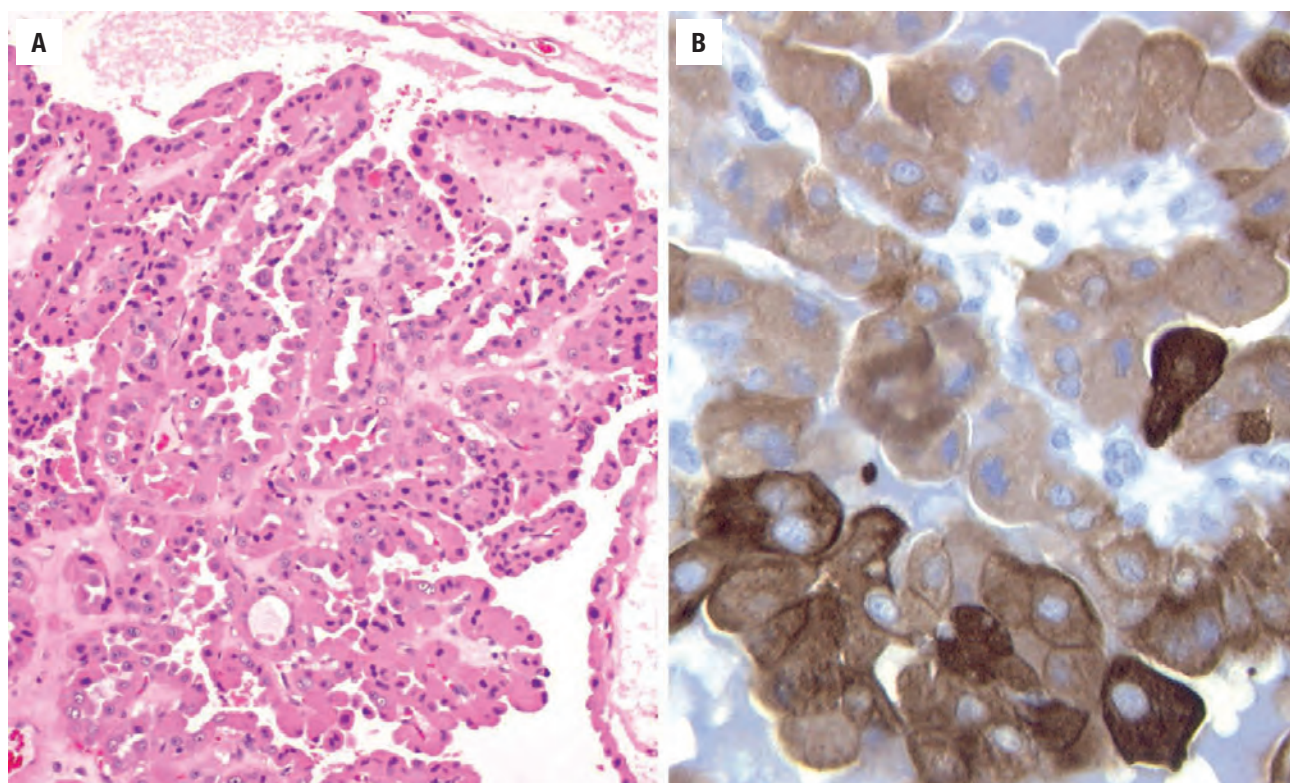
The macroscopic appearance is of a deep brown (“mahogany”) encapsulated neoplasm, which tends to be large and has cystic change. Lymphocytic infiltrate is common. More than 70 % of the tumor should have complex, arborizing papillary structures (Fig. 25.26), with fibrovascular stromal cores lined by enlarged cells with abundant oncocytic (oxyphilic, Askanazy, Hürthle) cytoplasm. Some authors use a lower cutoff, but this tends to dilute the category, with a few even suggesting

a follicular oncocytic variant. The oncocytic cytoplasm is compact and “glassy” with a fine granularity, representing an increased number of mitochondria. The enlarged nuclei tend to be apically oriented and slightly more hyperchromatic than classic papillary carcinoma (Fig. 25.27), with numerous intranuclear cytoplasmic inclusions (the latter a common finding in any tumor with abundant cytoplasm). Psammoma bodies are occasionally present. Degenerative changes are common. The cells are frequently immunoreactive with CK19, but this finding is nonspecific (Fig. 25.27). The diagnosis by FNA is very difficult, but clear nuclei with grooves and inclusions may help to separate it from a follicular neoplasm. Oncocytic cells can be seen in the tall cell variant of papillary carcinoma, from which it should be separated. The patient outcome and management for



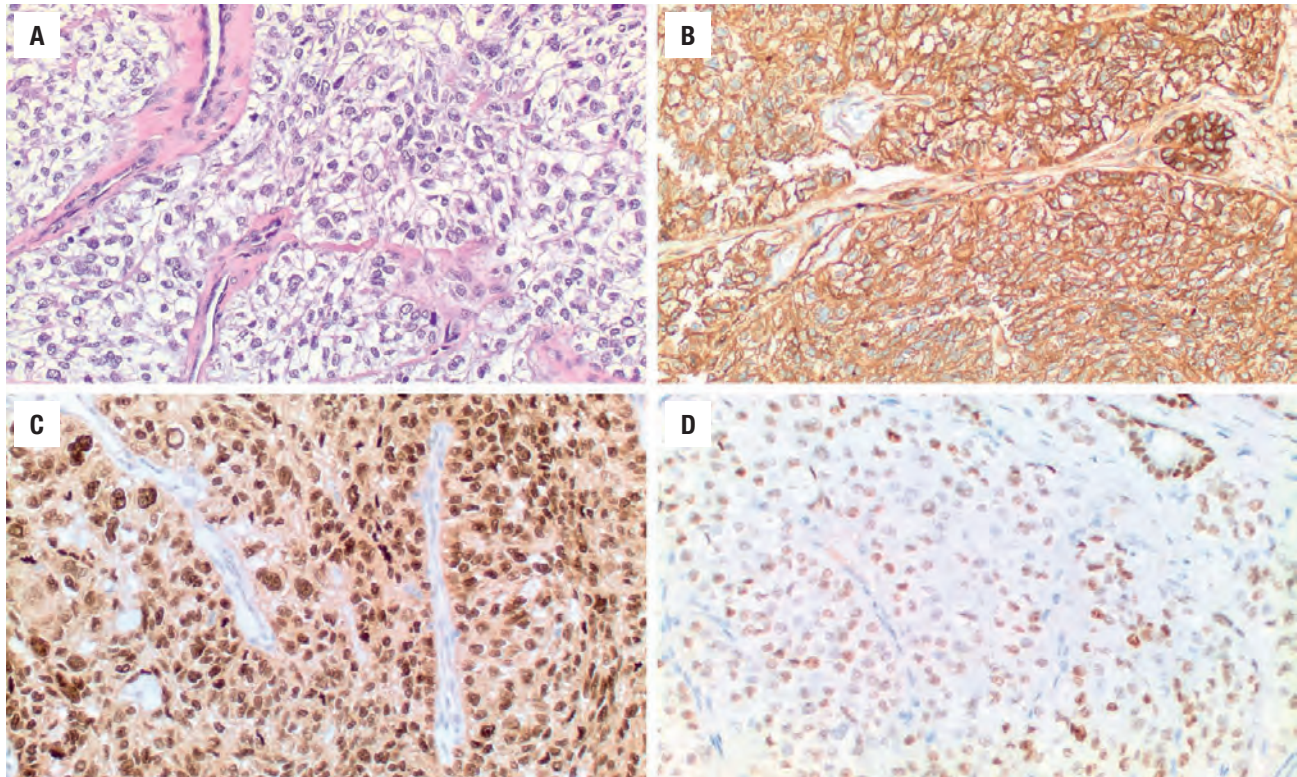
**FIGURE 25.26**

(A) Complex, arborizing papillary structures are composed of oncocytic cells in this oncocytic PTC variant. Hemorrhage and degeneration are noted. (B) Tumor nuclei show apical polarization on the papillary fronds with deeply eosinophilic cytoplasm in this oncocytic variant of PTC.

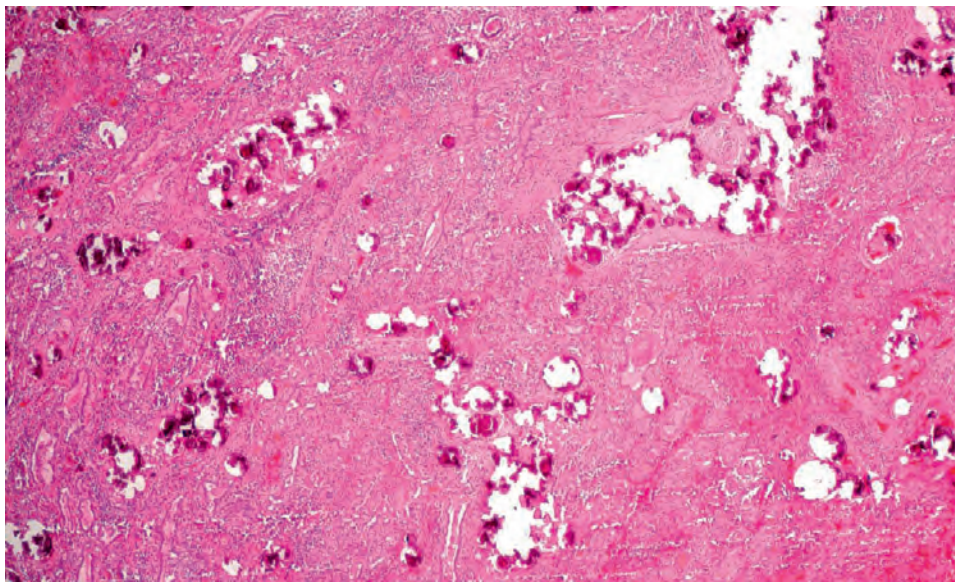
**FIGURE 25.27**

(A) Oncocytic cells within a papillary architecture. Note that the nuclei are luminal. (B) CK19 is known to be positive in the oncocytic variant of PTC but is not specific or sensitive.



**FIGURE 25.28**

Clear cell papillary thyroid carcinoma shows the nuclear features of PTC but in a tumor whose cytoplasm is cleared (**A**). The neoplastic cells are immunoreactive with thyroglobulin (**B**), PAX8 (**C**), and TTF1 (**D**).

**FIGURE 25.29**

A low magnification demonstrating innumerable psammoma bodies in clusters with lymphocytic thyroiditis. Many of the psammoma bodies are in lymphovascular spaces.

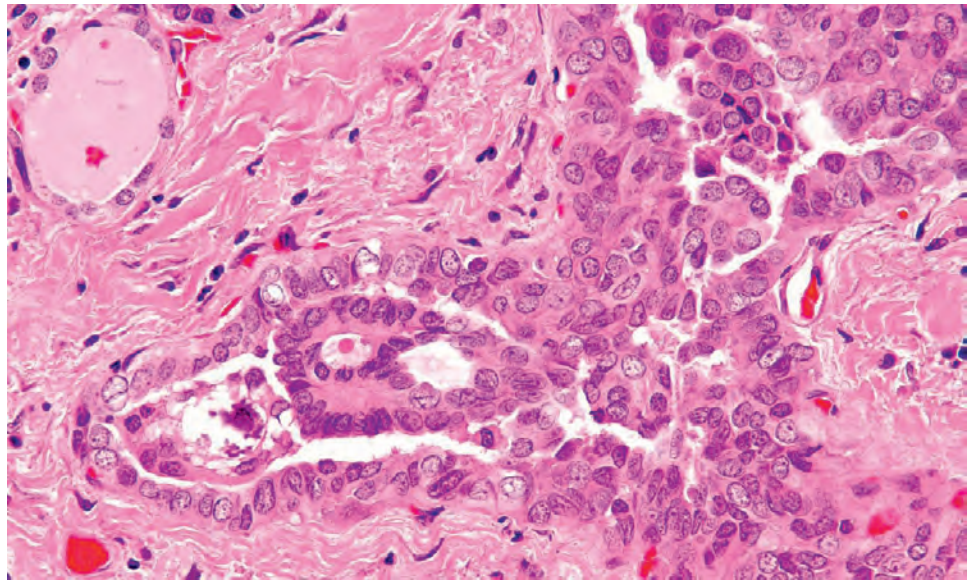
the oncocytic variant is identical to classical papillary carcinoma.

#### CLEAR CELL VARIANT

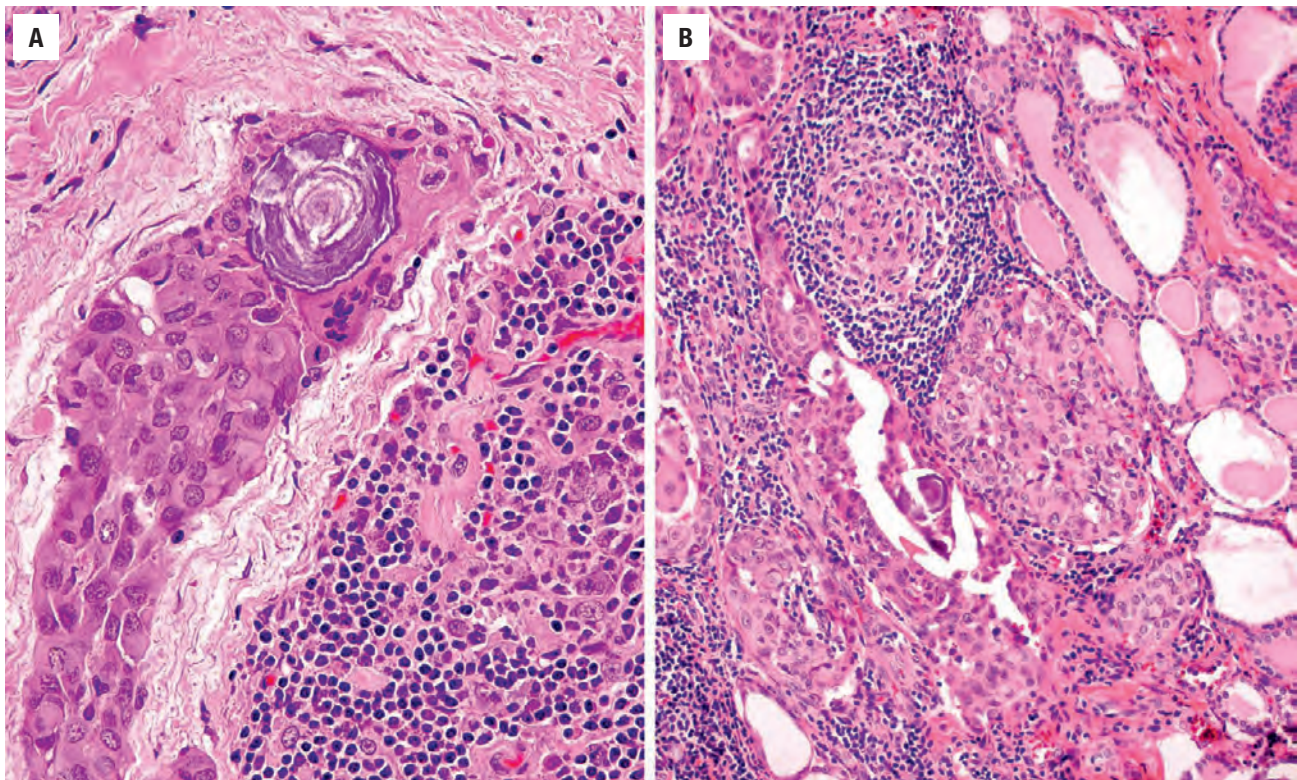
This is a very uncommon variant that is predominantly composed of cells with clear cytoplasm (**Fig. 25.28**).

Papillary or follicular patterns may predominate. Occasionally, a mixture of oncocytic and clear cells may be seen, as clearing results from degeneration of the oncocytic cells. Separation from metastatic renal cell carcinoma or medullary thyroid carcinoma can be made by the presence of colloid, but may require the use of TTF1, thyroglobulin (**Fig. 25.28**), calcitonin, and CAIX. The treatment and prognosis are identical to classic papillary carcinoma.



**FIGURE 25.30**

Dense fibrosis separates the tumor into nodules. Lymphovascular invasion is noted with tumor cells within a vascular space, associated with squamous metaplasia.

**FIGURE 25.31**

(A) Papillary carcinoma with squamous metaplasia associated with a psammoma body. There is lymphocytic thyroiditis. (B) Psammoma bodies and papillary carcinoma are noted within a lymph-vascular channel. There is well developed lymphocytic thyroiditis and fibrosis.

### SPINDLE CELL VARIANT

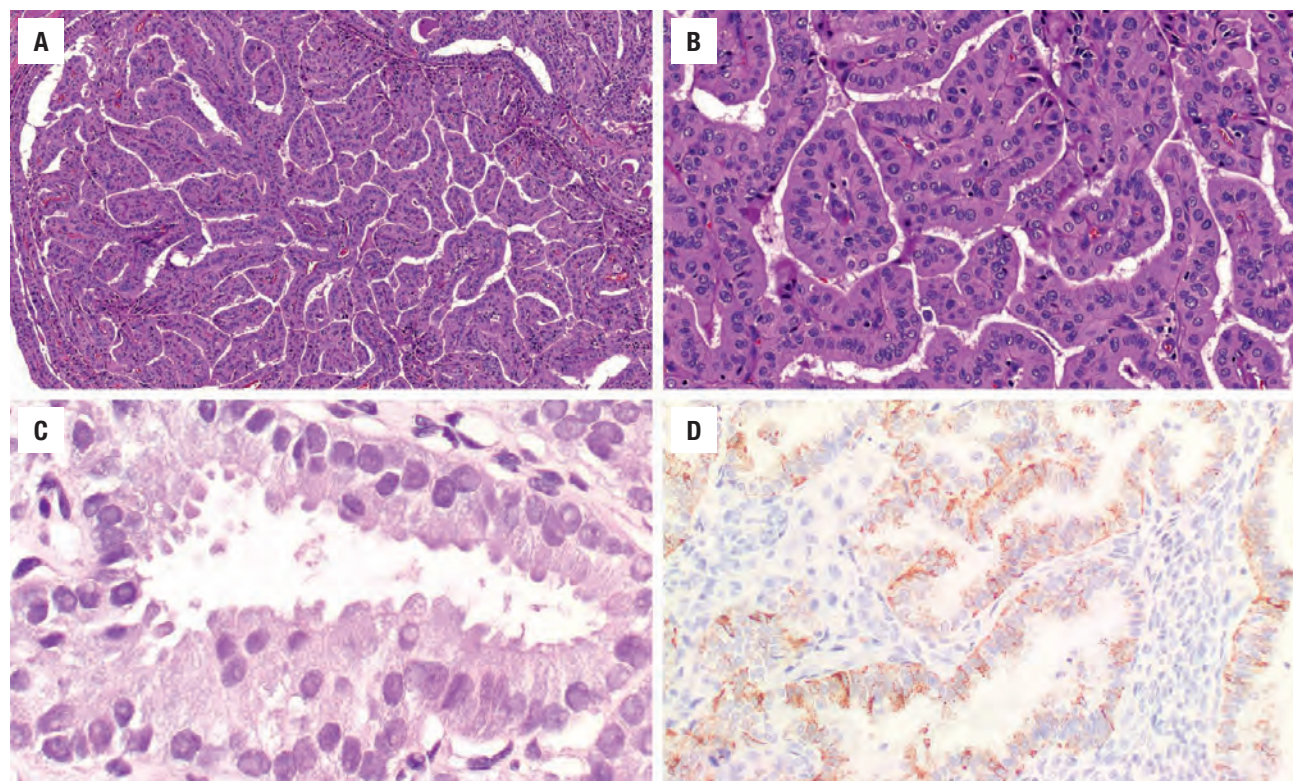
Exceedingly rare, this variant shows focal to diffuse spindle cell proliferation not adjacent to a previous FNA site. The cells must be proven to be epithelial by cytokeratin and TTF1. The cells are bland, lacking increased mitoses and necrosis (Fig. 25.14). This allows for separation from

an undifferentiated carcinoma where there is profound pleomorphism, necrosis, and increased mitoses.

### DIFFUSE SCLEROSING VARIANT

Usually developing in young patients (mean, 18 years), the tumor is characterized by diffuse involvement of one



**FIGURE 25.32**

Various patterns seen in tall cell variant of papillary thyroid carcinoma. (A) No colloid is seen with elongated follicles creating the papillary projections. (B) The cells are each at least three times taller than they are wide with prominent cellular borders. (C) The cytoplasm ranges from oncocytic, amphophilic, basophilic, and clear. Intranuclear cytoplasmic inclusions are common. (D) The neoplastic cells are highlighted with napsin.

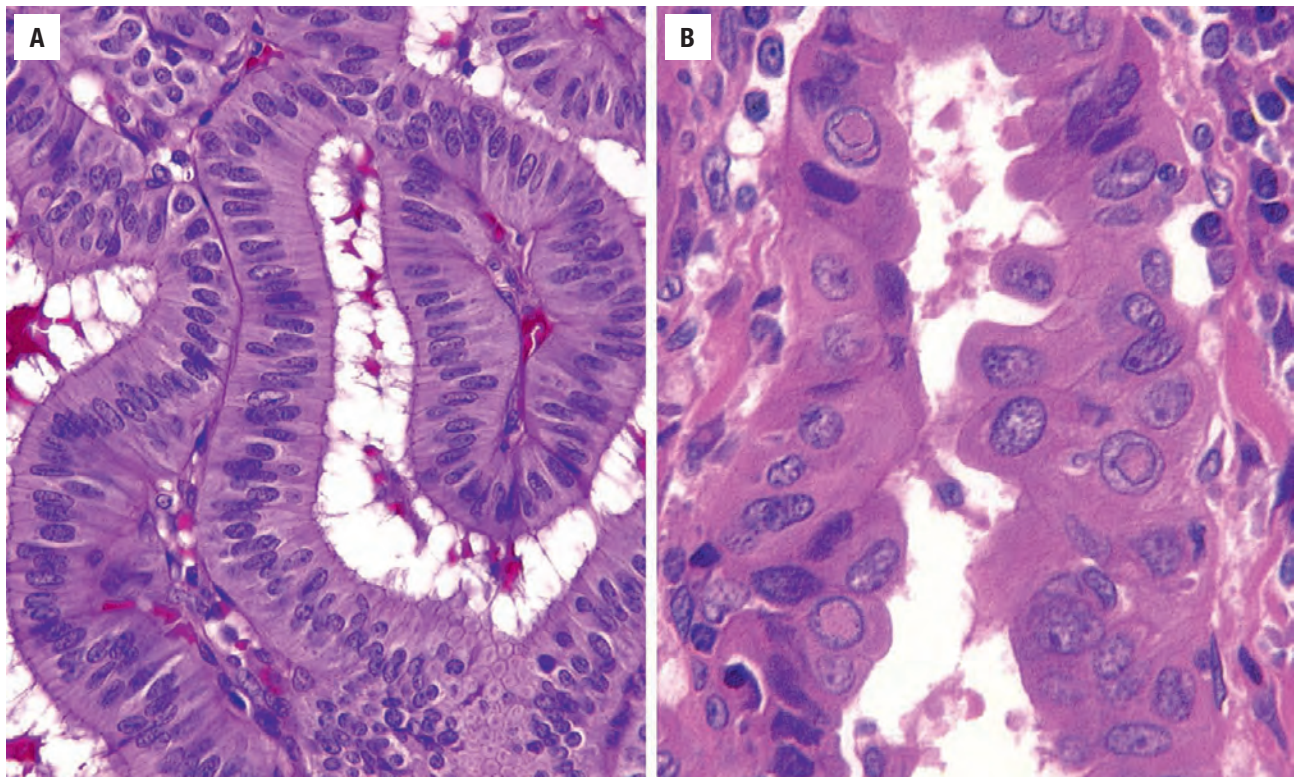
or both lobes with nearly 100 % of patients demonstrating cervical lymph node metastasis at the time of presentation, while up to 25 % develop distant metastases. The gland is firm, with white streaks and a gritty cut consistency, and an ill-defined border, if a dominant mass is noted. The histology shows an exaggeration of features of PTC, with extensive fibrosis, innumerable psammoma bodies, extensive intravascular and extrathyroidal extension, florid squamous metaplasia, and a background of dense lymphocytic thyroiditis (LT) (Figs. 25.29 and 25.30). Nuclear features of papillary carcinoma are present, often identified in papillary or solid groups of cells within vascular spaces (Fig. 25.31). Total thyroidectomy, lymph node dissection, and radioablative therapy will yield an excellent long-term prognosis despite the “biologically” aggressive clinical presentation. Lung metastases occur in up to 25 % of patients, necessitating close and careful patient follow-up.

### TALL CELL VARIANT

There is controversy as to whether the “tall cell” is a variant or just a pattern of growth within papillary carcinoma. When this cell type is the dominant finding in the neoplasm (range from 30 % to 70 %, but greater

than 30 % of the tumor area yields the most consistent correlation with outcome), the patients tend to be older (> 60 years), with an increased proportion of men, and the tumor tends to be large (> 5 cm), showing extrathyroidal extension. However, microscopic tumors may occur. Papillary structures and elongated parallel follicles with scant or no colloid are common (Fig. 25.32), along with intratumoral fibrosis. By definition, a tall cell is at least three times as tall as it is wide (plane of section must be taken into consideration). There is usually abundant, granular cytoplasm, resulting in an increased number of intranuclear cytoplasmic inclusions and nuclear grooves (Fig. 25.32). Inter cellular borders are sharply demarcated. The nuclei are enlarged with a central position of the nucleus rather than at the luminal aspect as seen in the oncocytic variant (Fig. 25.33). This variant stains positive with napsin, confounding when metastatic lung tumors are considered in the differential diagnosis (Fig. 25.32). There is a high association with *BRAF* and *TERT* mutations, and also a high de-differentiation rate to undifferentiated carcinoma. There is an increased incidence of lymph node metastasis and hematogenous spread to bone and lung, with a tendency for local recurrence and invasion into adjacent structures. Surgery and adjuvant therapy are necessary, with a worse prognosis than classic papillary carcinoma.



**FIGURE 25.33**

(A) Columnar variant with pseudostratification of nuclei with no colloid present. (B) Tall cell variant with oncocytic cells, intranuclear cytoplasmic inclusions, and cells three times as tall as they are wide.

### COLUMNAR CELL VARIANT

Men and women are equally affected by this rare variant. Tumors are usually large (> 5 cm) and encapsulated, but have intra- and extrathyroidal spread. There is prominent papillary growth with markedly elongated, parallel follicles (“railroad tracks”), which are separated by scant colloid (Fig. 25.34). The cells are tall with a syncytial arrangement. There is prominent nuclear stratification of elongated nuclei with coarse and heavy chromatin deposition, distinctly different from classic papillary carcinoma. Subnuclear or supranuclear vacuolization of the cytoplasm is common (Fig. 25.35). Squamous metaplasia is common (“endometrioid pattern”; Fig. 25.36). Mitotic figures may be present, along with necrosis in a few cases. There is often CDX2 immunoreactivity, but TTF1 is also seen. If the patient is older with a large tumor that has extrathyroidal extension, more aggressive surgery and radioablative therapy may be necessary. The prognosis is worse than for classic papillary carcinoma, although it may be more a feature of infiltration than cytologic variant. Some examples of columnar variant histologically overlap with the more indolent cribriform-morular variant (discussed below). In these very uncommon and unusual histologic variants, performing selected immunohistochemistry studies (such as  $\beta$ -catenin in cases with squamous metaplasia) may be of value.

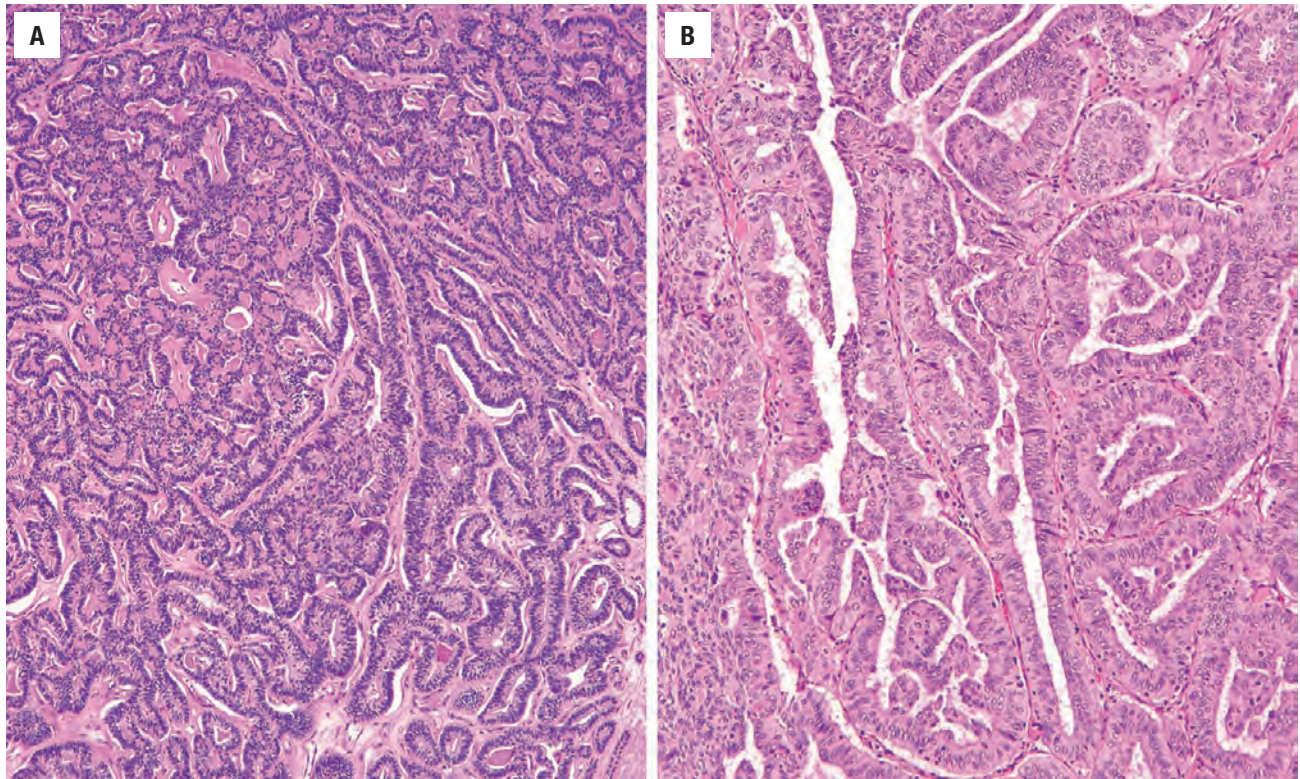
### SOLID VARIANT

Papillary carcinoma may have a solid or insular pattern, with oval nests or islands with scant colloid, and cells with a high nuclear-to-cytoplasmic ratio (Fig. 25.37). It is seen more often in children. This term is applied when the tumor is predominantly solid, trabecular, or nested, and does not show features of another variant. Sometimes the pattern is classified as poorly differentiated, but if the nuclear features of papillary carcinoma are present, then this pattern does not influence the management or the outcome. It is only when increased mitoses and necrosis are present that the tumor moves to the poorly differentiated category (Fig. 25.13).

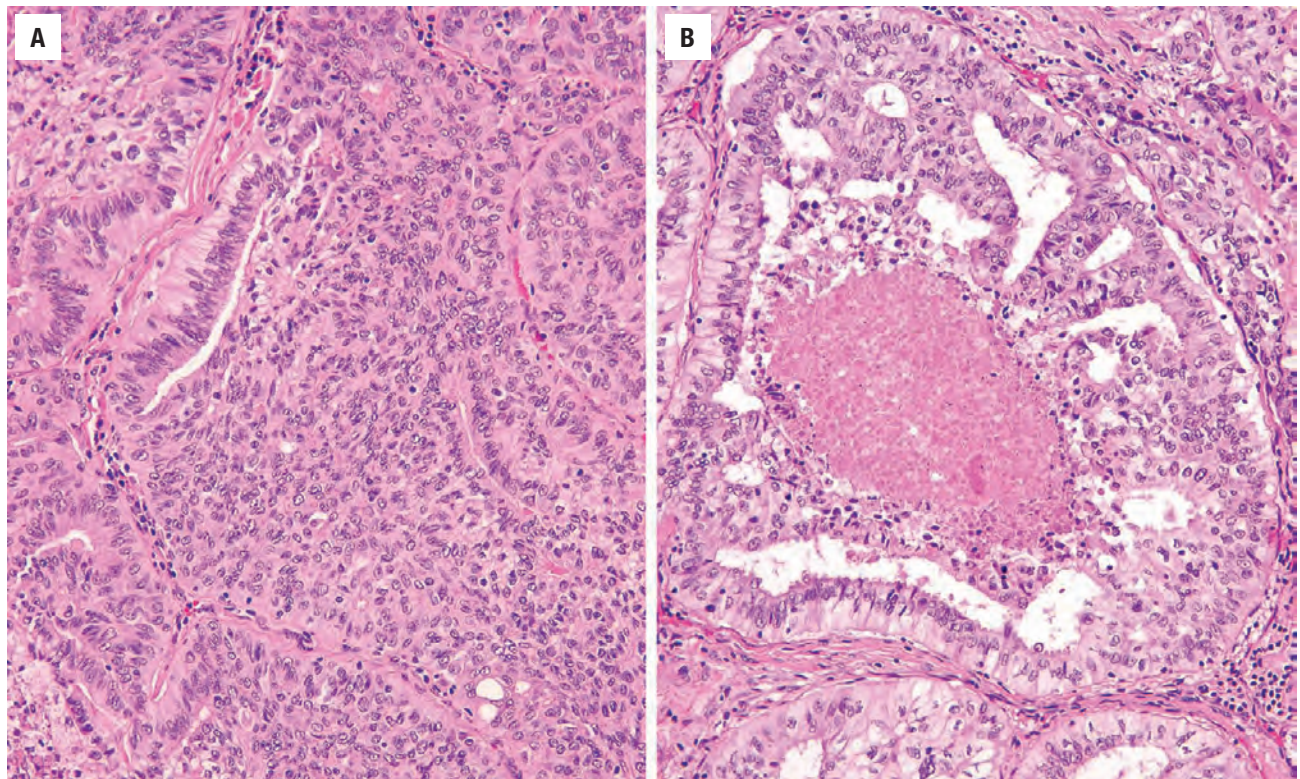
### CRIBRIFORM-MORULAR VARIANT

Seen almost exclusively in females, there is a high association with FAP, with a diagnosis of this variant prompting colonic examination and possibly genetic testing for germline *APC* mutation. In syndrome cases, there are often multiple encapsulated tumor nodules, showing a mixed pattern of growth: cribriform, trabecular, solid, papillary, and follicular (Fig. 25.38). Colloid is scant to absent. There are often whorls or morules composed of spindle cells without keratinization, showing an optically clear nucleus. The nuclear features of papillary carcinoma



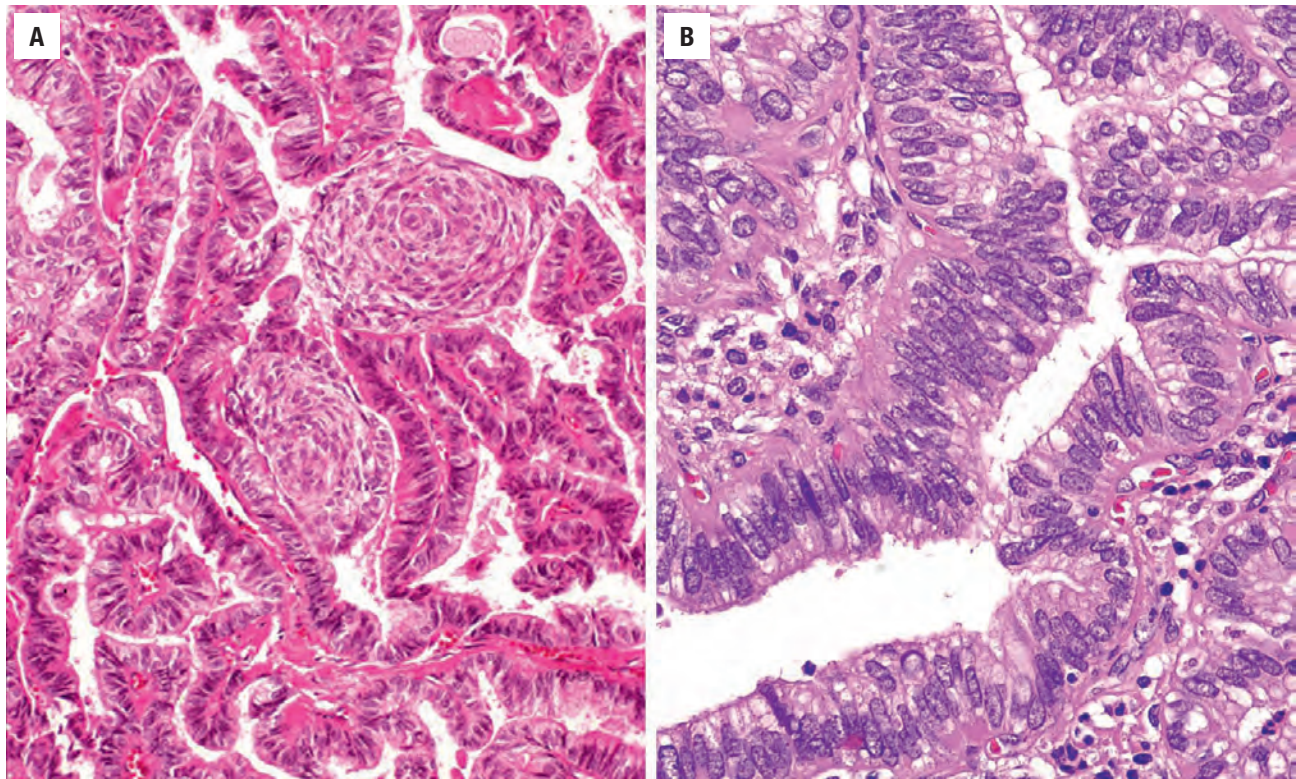
**FIGURE 25.34**

Columnar cell variant of PTC. (A) Papillary structures arranged in markedly elongated, parallel follicles (tram-tracks). There is scant colloid, with marked nuclear stratification (B).

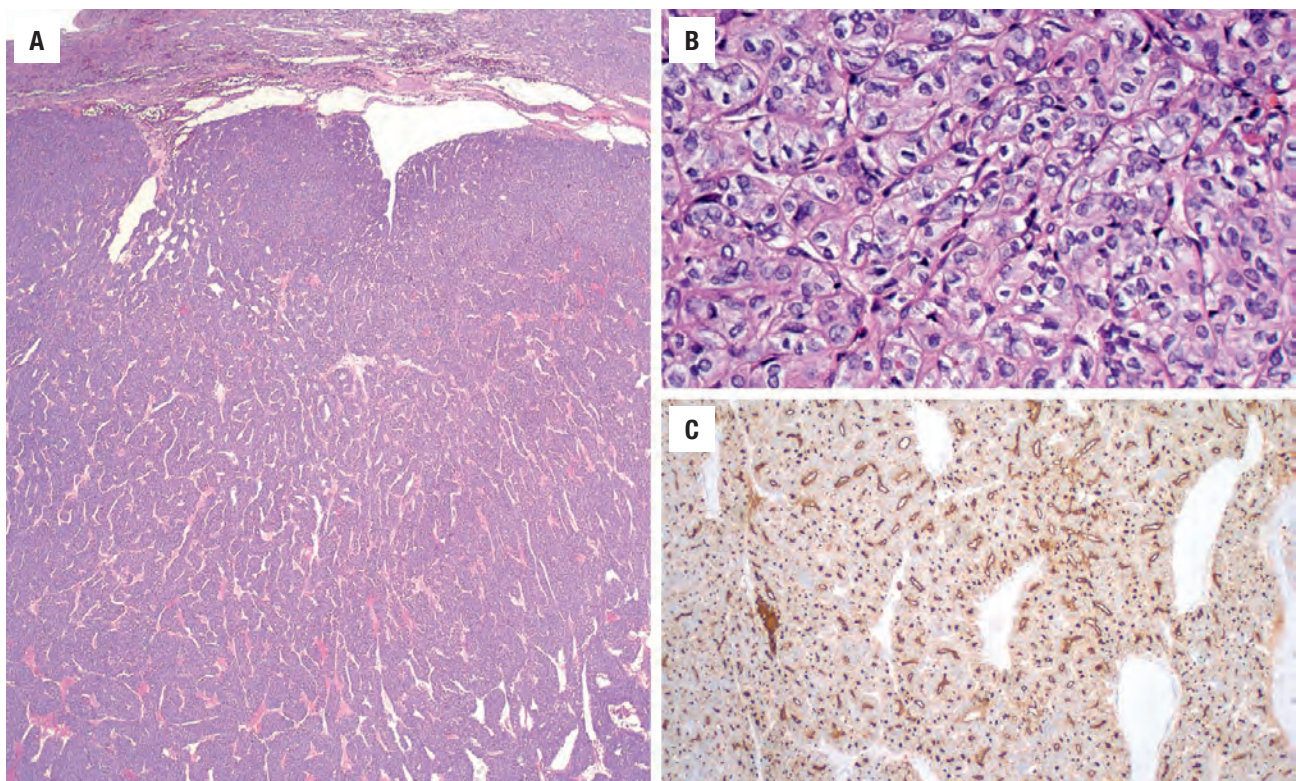
**FIGURE 25.35**

Columnar cell variant of PTC. (A) A syncytial architecture predominates in this tumor. Nuclear stratification with subnuclear vacuoles are noted. (B) The tumor cell nuclei have an elongate shape and demonstrate pronounced pseudostratification. Prominent subnuclear vacuoles are seen in cells arranged in a cribriform architecture. Central comedonecrosis is present.



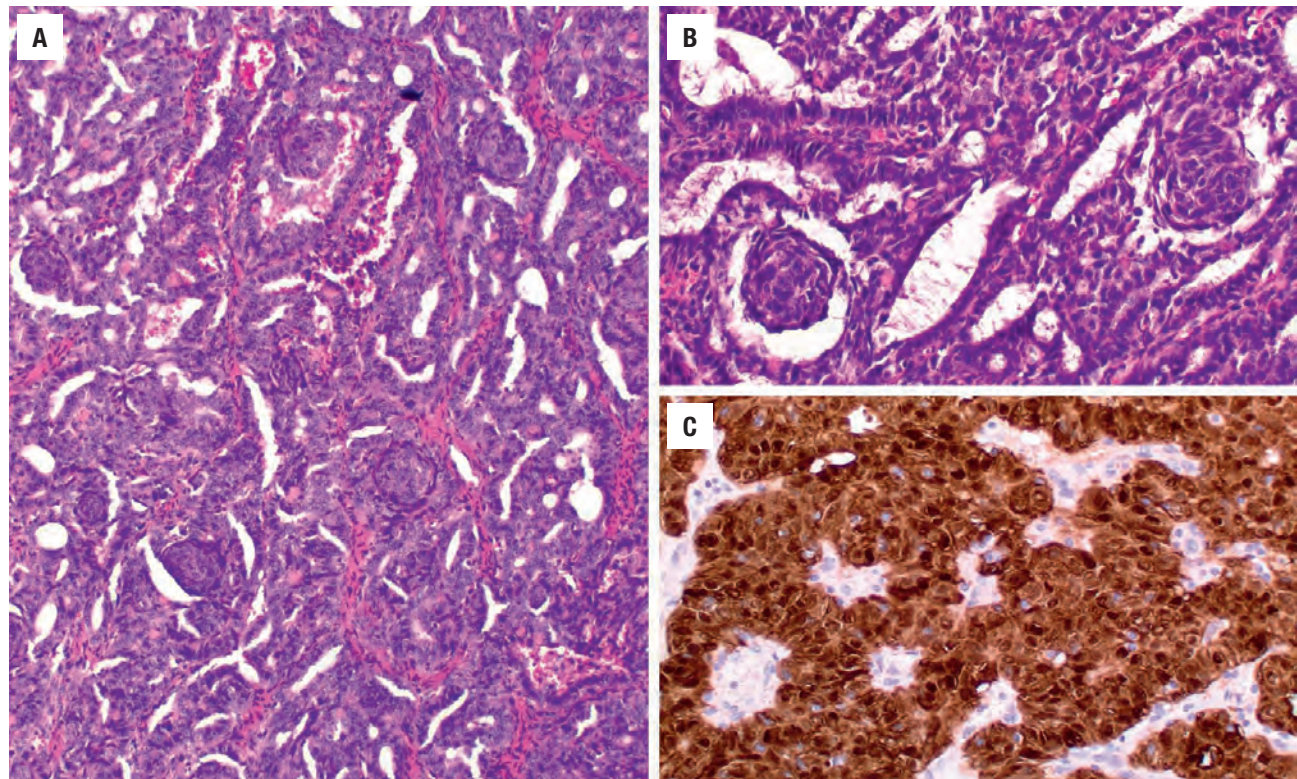
**FIGURE 25.36**

(A) Squamous metaplasia may be seen in the columnar cell variant of PTC. (B) The pseudostratified, elongated nuclei may have more coarse chromatin.

**FIGURE 25.37**

An insular architecture can be the predominant pattern in any thyroid tumor. (A) Classic papillary carcinoma with an insular architecture. (B) Small, tight trabeculae that create an insular appearance. (C) A strong and diffuse thyroglobulin reaction to confirm thyroid follicular cell origin.



**FIGURE 25.38**

(A) There is a cribriform to elongated pattern to this cribriform morular variant, with numerous squamous morules easily identified in a background that lacks colloid. (B) The squamous morules are whorls, juxtaposed to the elongated and partially stratified nuclei. (C) There is a strong nuclear expression of  $\beta$ -catenin.

are rare, taking more of a columnar shape, but still containing grooves and folds (Fig. 25.38). TTF1 and thyroglobulin staining is weak, patchy, and focal, while a strong nuclear  $\beta$ -catenin accumulation (Fig. 25.38) and immunoreactivity to ER and PR are characteristic.

### HOBNAIL VARIANT

This is an uncommon variant, requiring at least 30 % of the cells to have hobnail features although this percentage is a source of debate. The variant shows complex papillary and micropapillary structures. These structures are lined by follicular cells that have a hobnail appearance, with apically placed nuclei showing prominent nucleoli. The cells tend to be dyscohesive. This variant has necrosis, mitoses, and frequent extrathyroidal extension and lymphovascular invasion.

### PAPILLARY CARCINOMA-SIZE VARIATION

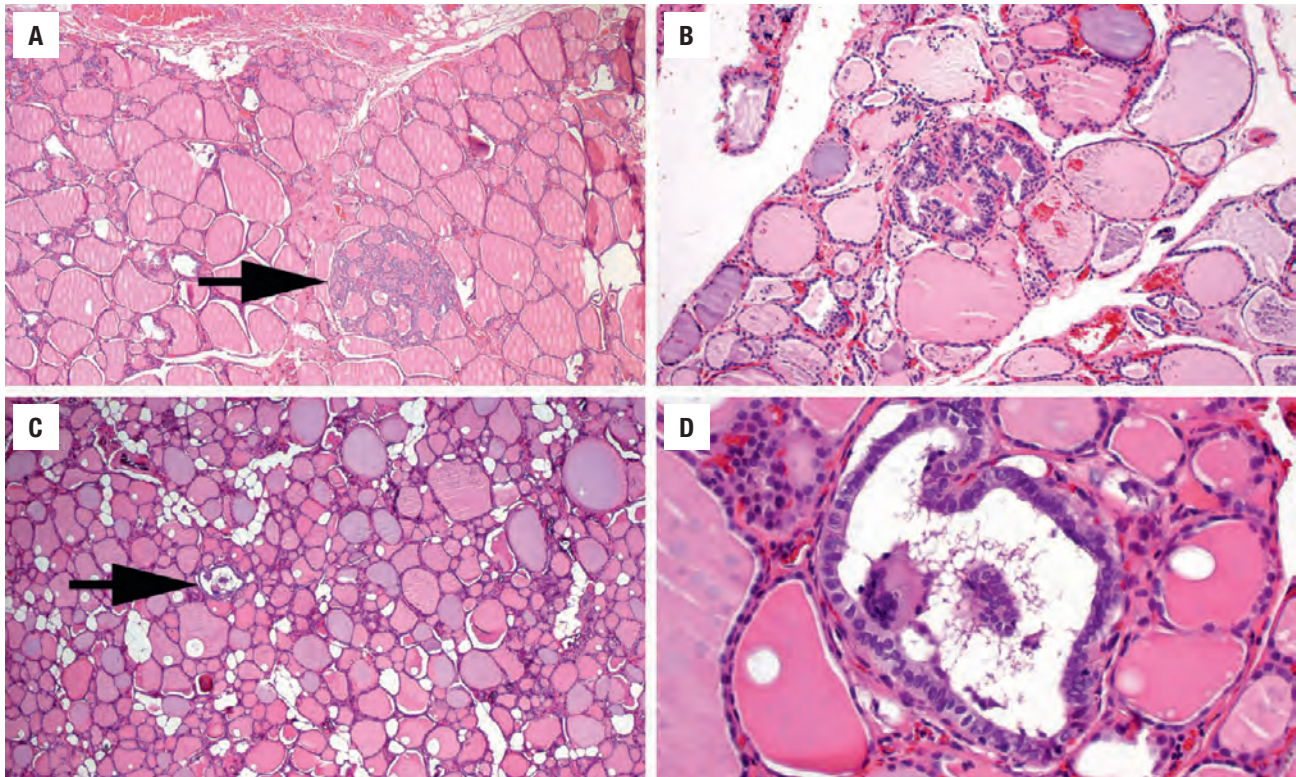
Any of the papillary carcinoma variants may be less than 1 cm in size, which is referred to as microscopic papillary carcinoma, or occult, incidental, or microcarcinoma (Fig. 25.39). This qualification should only be applied when the tumor is found incidentally in a thyroid gland removed for other reasons. The tumor has a proclivity to develop in the subcapsular region and is frequently sclerotic with

a radiating “scar-like” infiltration into the surrounding parenchyma. The term “microcarcinoma” should be used for adult patients, since children with small tumors may still have biologically aggressive neoplasms. Separation from intraglandular metastasis may be difficult, although the intravascular location, lack of capsule and sclerosis, and lack of “stellate” growth supports intraglandular metastasis. Most of these tumors are less than 2 mm in size and are of limited clinical consequence, with an outcome indistinguishable from the general population. Therefore, no additional therapy is necessary for tumors of this size. The noninvasive tumors may qualify as the newly recognized noninvasive follicular thyroid tumor with papillary-like nuclear features, but by definition, they are tumors > 1.0 cm.

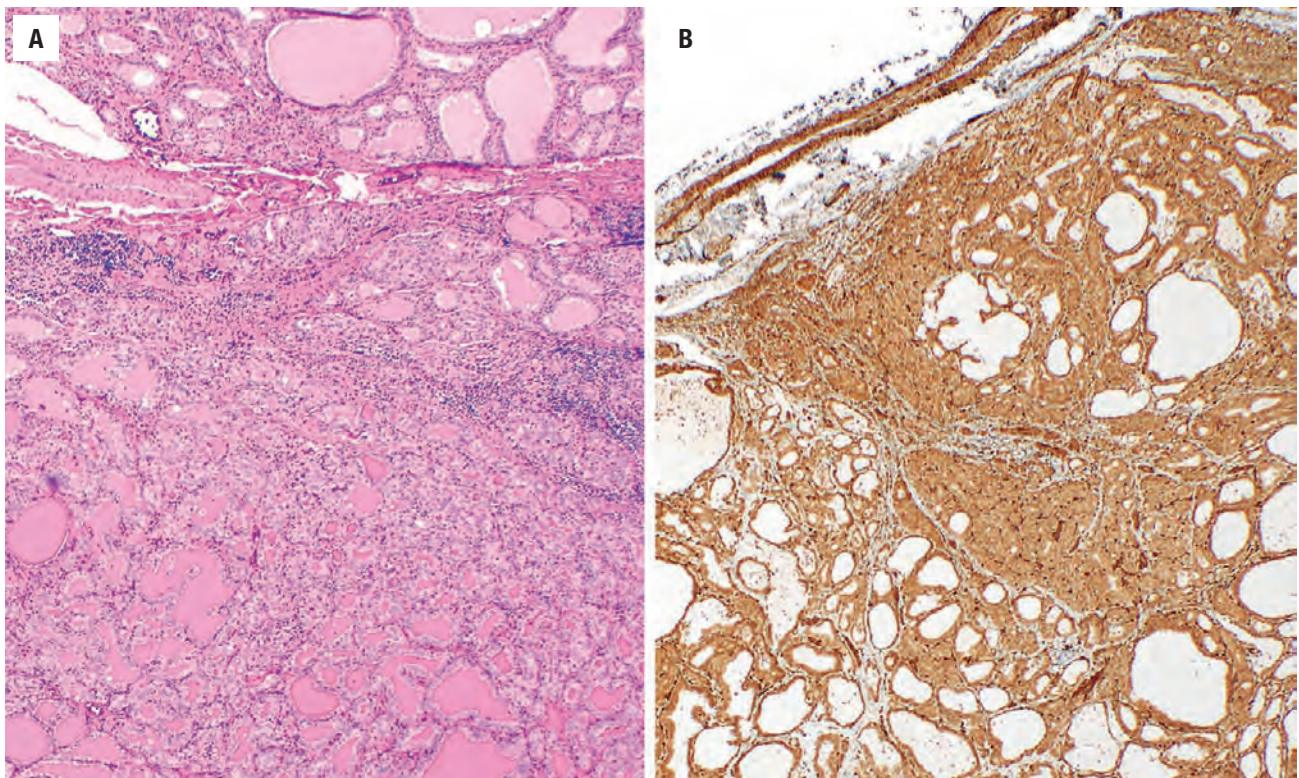
## FOLLICULAR CARCINOMA

Follicular carcinoma (FC) is the second most common malignant neoplasm of the thyroid gland, defined by invasive growth of an encapsulated follicular epithelial-derived cell that lacks the nuclear features of papillary carcinoma. There is a familial association in up to 4 % of FC in the U.S., with PTEN hamartoma tumor syndrome (Cowden disease, Werner syndrome) and Carney complex the most common (Fig. 25.40). Iodine deficiency, radiation exposure (5.2 times relative risk), and pre-existing thyroid



**FIGURE 25.39**

(A-D) Microscopic papillary carcinomas are distinct from the surrounding tissue and have both papillary architecture and show typical nuclear features. The tumors are frequently only a few follicles large. **C** is a low-power magnification, whereas **D** is a high power of the same tumor.

**FIGURE 25.40**

This thyroid gland neoplasm is surrounded by a very thin and delicate capsule (**A**), showing a strong PTEN immunohistochemistry reaction (**B**).



**FOLLICULAR THYROID CARCINOMA—DISEASE FACT SHEET****Definition**

- A malignant epithelial neoplasm with follicular cell differentiation, invasive growth, and lacking the nuclear features of papillary carcinoma

**Incidence and Location**

- Up to 10% of thyroid malignancies
- Increased in iodine-deficient areas and in patients with pre-existing thyroid disease or syndrome association (PTEN hamartoma tumor syndrome, Carney)

**Morbidity and Mortality**

- Recurrent laryngeal nerve damage and hypoparathyroidism
- Excellent long-term outcome (~90% 20-year survival depending on type)

**Sex and Age Distribution**

- Females > males (2:1)
- Usually in the 5th-6th decades
- Oncocytic tumors occur in patients about a decade older

**Clinical Features**

- Usually an asymptomatic, palpable mass
- Rarely dysphagia or hoarseness

**Radiographic Features**

- Ultrasound shows a solid or cystic mass, a capsule, and is used to guide fine needle aspiration
- Computed tomography is useful to determine extent of the mass and lymph node disease
- Nuclear scintigraphy rarely used

**Prognosis and Therapy**

- Excellent long-term prognosis (~90% 20-year survival)
- Surgery (lobectomy or thyroidectomy) with radioactive iodine

disease are known risk factors. Specifically, FA may be a direct precursor (similar genetic mutations may be seen, although lower frequency) since the histology is identical except for invasion, and patients with FC are about a decade older than patients with adenoma.

**CLINICAL FEATURES**

Up to 10% of thyroid carcinomas are FCs, reflecting a downward trend as the recognition of the follicular variant of papillary carcinoma has increased. FC is more common in women than men (about 2:1), with a peak incidence in the 5th and 6th decades, although recently the sex difference is not as distinct. The oncocytic type tends to occur in patients about a decade older. Patients usually present with an asymptomatic solitary, painless thyroid mass, which is usually solid on radiographic imaging. Hoarseness, dysphagia, dyspnea, and stridor are rare. FC tends to be larger than

**FOLLICULAR THYROID CARCINOMA—PATHOLOGIC FEATURES****Gross Findings**

- Solitary, encapsulated mass
- Invasion usually difficult to see on gross examination
- Usually < 5 cm

**Microscopic Findings**

- Capsule varies from thin to thick with smooth muscle-walled vessels in the capsule wall
- Capsular invasion: into and through the capsule
- Lymphovascular invasion: within or beyond capsule, showing direct extension, tumor thrombus, or endothelial lining
- Cellular tumors with follicular, solid, and trabecular growth
- Slightly enlarged cells with round to oval nuclei and coarse nuclear chromatin
- Oncocytic cells often have large, centrally placed macronucleoli within the nuclei
- Variant patterns and cytologic features

**Immunohistochemical Findings**

- Thyroglobulin, TTF1, PAX8, CK7 positive

**Molecular Findings**

- *PAX8-PPAR $\gamma$*  commonly identified
- *RAS* in up to 45% of tumors
- *TERT* seen in more biologically aggressive tumors

**Fine Needle Aspiration**

- Cellular aspirates with dispersed microfollicular arrangements of cells forming small “ring-like” structures; colloid is scant
- Cannot be reliably separated from follicular adenoma (FA) and adenomatoid nodules

**Pathologic Differential Diagnosis**

- FA, papillary thyroid carcinoma, medullary thyroid carcinoma, adenomatoid nodules

papillary carcinoma. Thyroid function tests are almost always normal. Lymph node metastasis is uncommon, although slightly more common in the oncocytic variant, as hematogenous spread is more common than lymphatic spread. Distant metastasis is seen in up to 20% of patients (lung and bone). Imaging cannot reliably distinguish between benign and malignant lesions. Iodinated contrast is to be avoided as it delays  $^{131}\text{I}$  therapy. Ultrasound may demonstrate a solid versus cystic lesion, and show a nonechogenic halo (capsule). Turbulent intratumoral blood flow is seen more often in carcinoma.

**PATHOLOGIC FEATURES****GROSS FINDINGS**

The tumors are usually solitary, well-circumscribed masses surrounded by a variably thick capsule separating

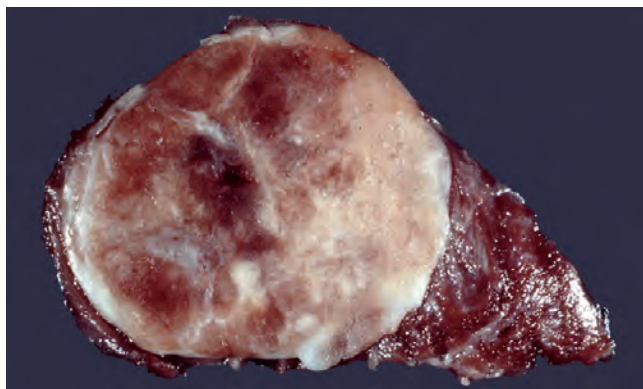


them from the uninvolved parenchyma. The capsule is usually thicker than an adenoma. The cut surface is often bulging and has a light tan to brown appearance (Fig. 25.41), although widely invasive tumors often have hemorrhage and necrosis (Fig. 25.42). Most tumors are less than 5 cm in size (generally 2 to 4 cm), although oncocytic tumors are slightly larger. The tumors are rarely multifocal. Oncocytic tumors may be mahogany-brown. In general, depending on size, a minimum of 10 blocks (2 to 3 sections per block) from the capsule-tumor interface are submitted for histologic evaluation.

#### MICROSCOPIC FINDINGS

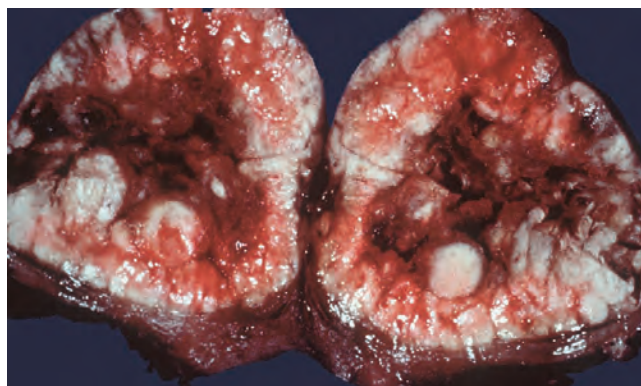
The tumors are surrounded by a variable fibrous connective tissue capsule, which ranges from thick (0.1 to 0.4 cm) and well-formed to thin, irregular, uneven, and poorly formed. The capsule has parallel layers of collagen containing smooth muscle-walled vessels. The

diagnostic feature of FC is invasion: capsular and/or lymphovascular penetration (either is sufficient for diagnosis). Capsular invasion is classified as single or multiple foci of tumor cells identified penetrating *into* (> 50 % partial capsule; Fig. 25.43) and *through* (entire thickness; Figs. 25.44 and 25.45) the capsule. In general, penetration beyond greater than 1/2 the capsular thickness, or beyond the tumor nodule in an area unassociated with a previous FNA site, qualify as capsular invasion. Parenchymal extension is defined by neoplastic cells surrounded by uninvolved thyroid parenchyma on either side of the protrusion. Deeper sections may be necessary to “connect” satellite nodules. Vascular invasion can involve single or multiple foci within small, medium, or large vessels (Fig. 25.46). Small vessels, usually within the capsule, have a limited caliber, while medium-sized vessels with or without smooth muscle walls, are noted within or immediately adjacent to the capsule. Vascular invasion is defined by direct extension of tumor cells into the vessel lumen, tumor thrombi adherent to the



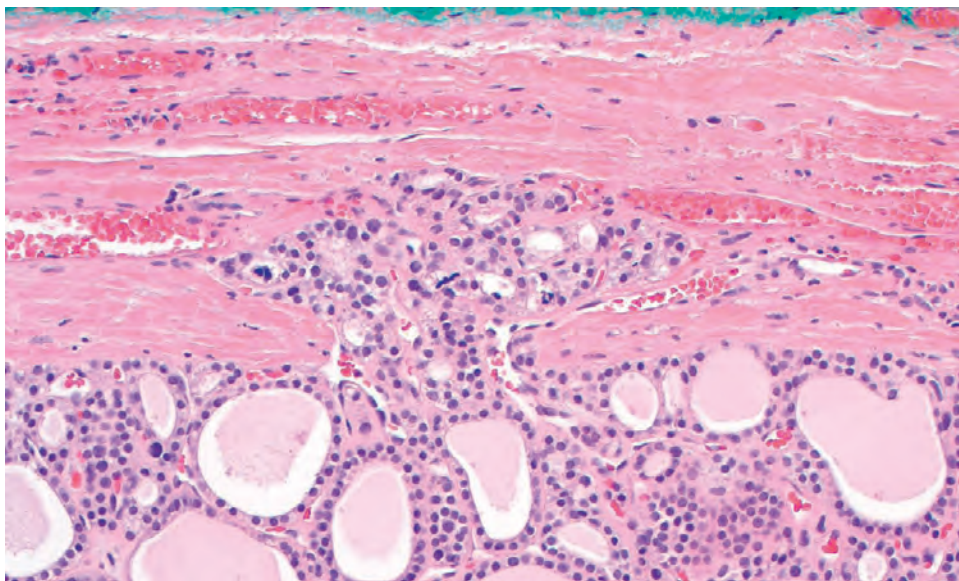
**FIGURE 25.41**

A solitary mass surrounded by a capsule has a distinctly different appearance from the surrounding uninvolved thyroid parenchyma.



**FIGURE 25.42**

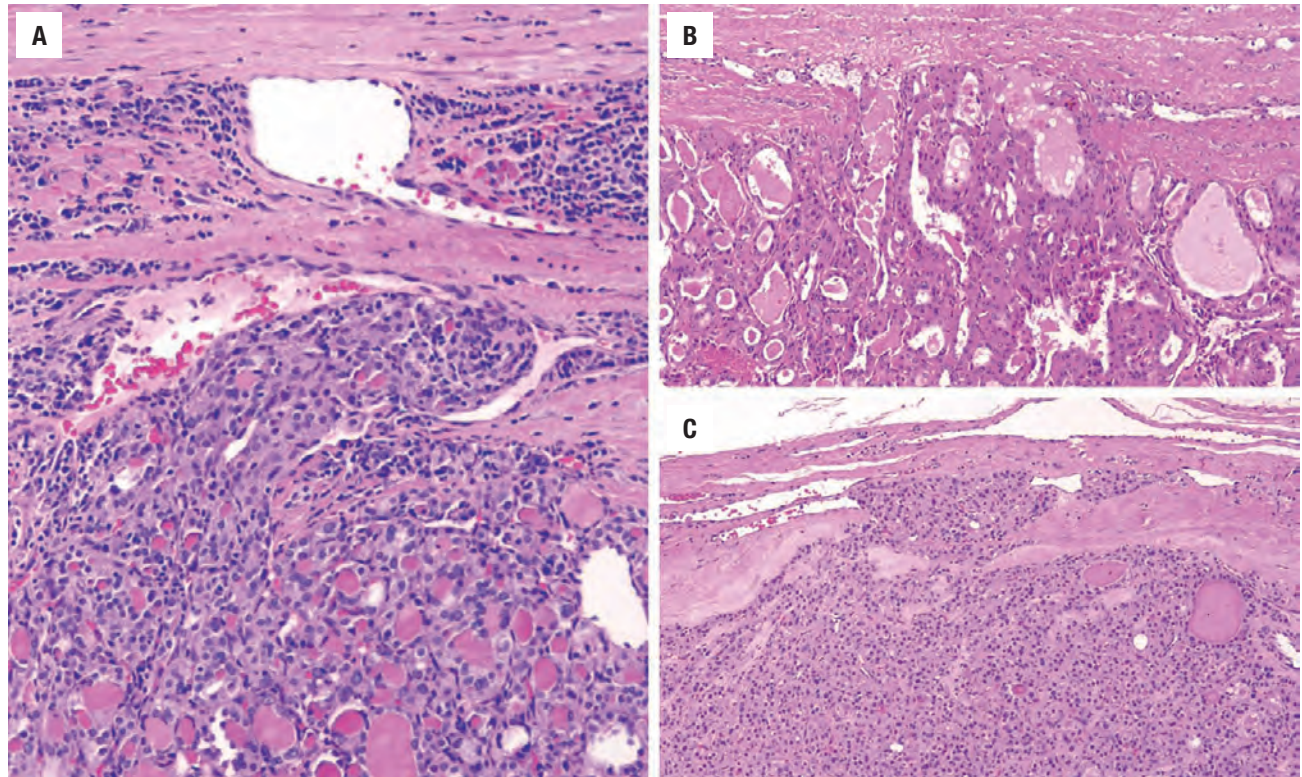
A widely invasive tumor with central hemorrhage, necrosis, and degeneration.



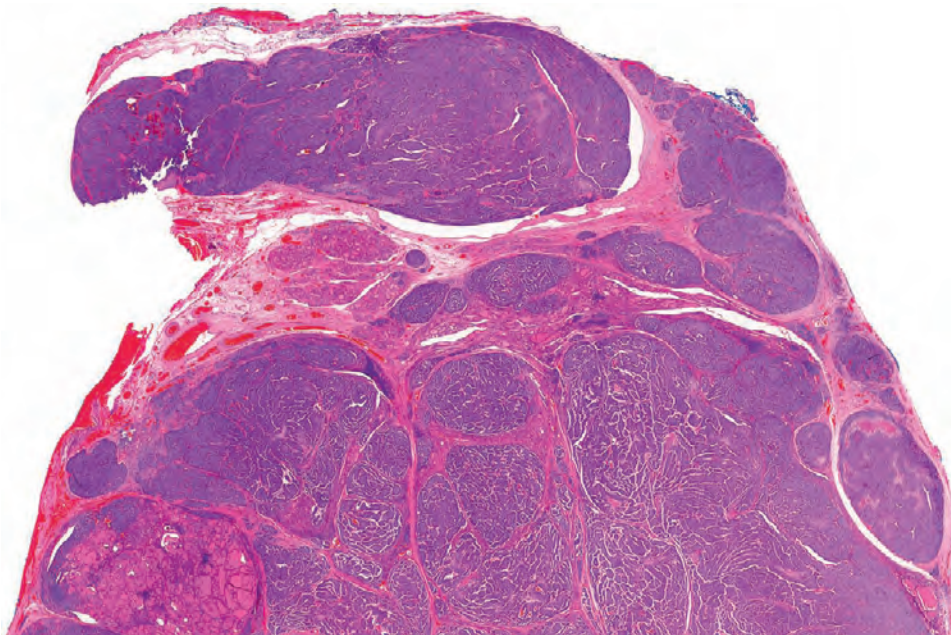
**FIGURE 25.43**

The tumor capsule is broken by the neoplastic cells penetrating through the capsule, showing a small “mushroom” shape.



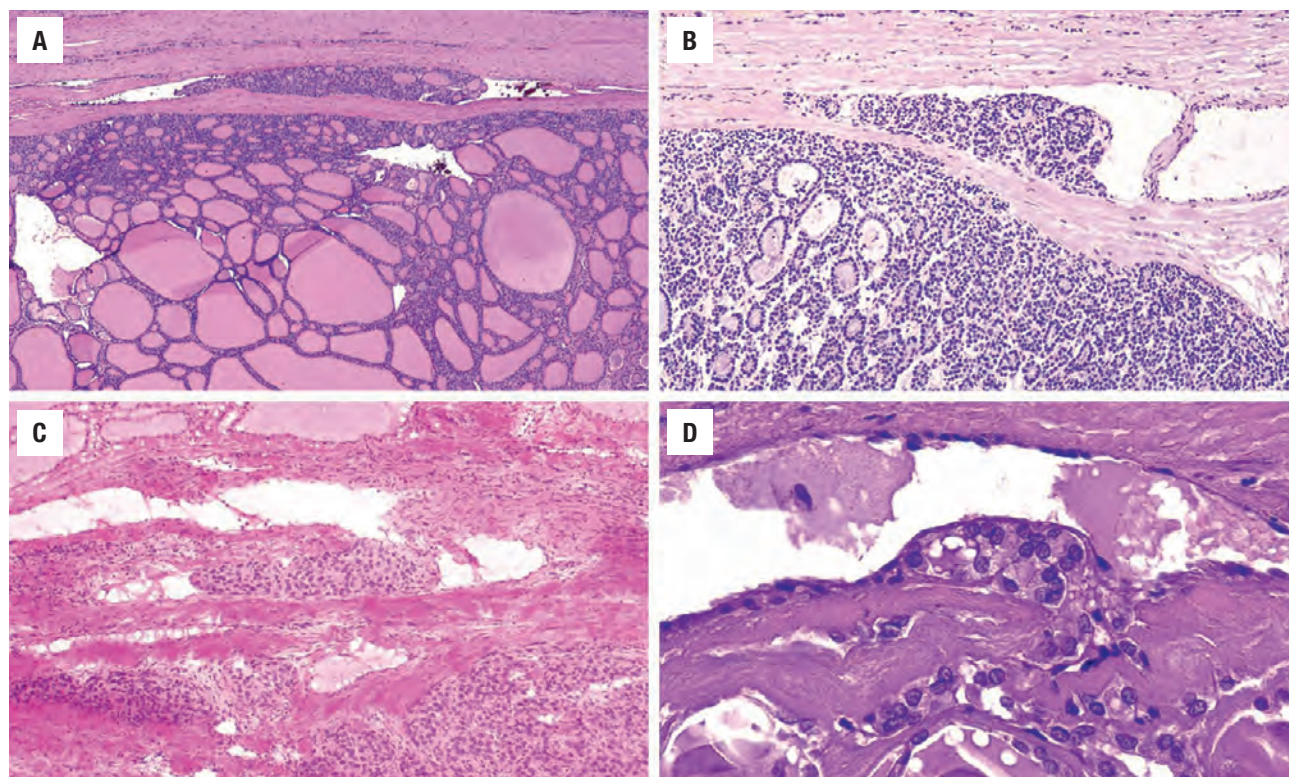
**FIGURE 25.44**

(A) Capsular penetration by the neoplastic cells in association with a vascular space. (B) Oncocytic tumor cells are invading into the capsule. (C) Capsular transgression noted on frozen section specimen.

**FIGURE 25.45**

There are numerous large, "mushroom-shaped" projections of neoplastic cells out into the surrounding parenchyma. Note that the capsule has "traveled" with the tumor in several areas, still present at the advancing edge. The tumor shows a more solid pattern.



**FIGURE 25.46**

Vascular invasion in follicular carcinoma. **(A)** Tumor thrombus filling a vascular space. **(B)** A tumor fragment attached to a vessel wall within the tumor capsule. **(C)** A frozen section showing tumor attached to the wall of an intermediate vessel. **(D)** There is no well-developed invasion yet, as there is an endothelial lining covering the tumor nest. Deeper or serial levels would be recommended in this setting.

vessel wall (often associated with blood clot), and/or tumor nests associated with endothelium (Fig. 25.47). Tumor plugs in vascular spaces *within* the tumor mass do not qualify as vascular invasion; nor do detached or artifactually dislodged tumor fragments free-floating in vascular spaces. An intravascular organizing thrombus (Masson disease) does not qualify as invasion. Also, “penetrating” vessels should not be misinterpreted to represent invasion, as these vessels frequently pull neoplastic cells with them, but do not represent true invasion. There is a movement toward quantifying the number of vessels involved, specifically listing if greater than 4 vessels are involved, which then qualifies the tumor as angioinvasive.

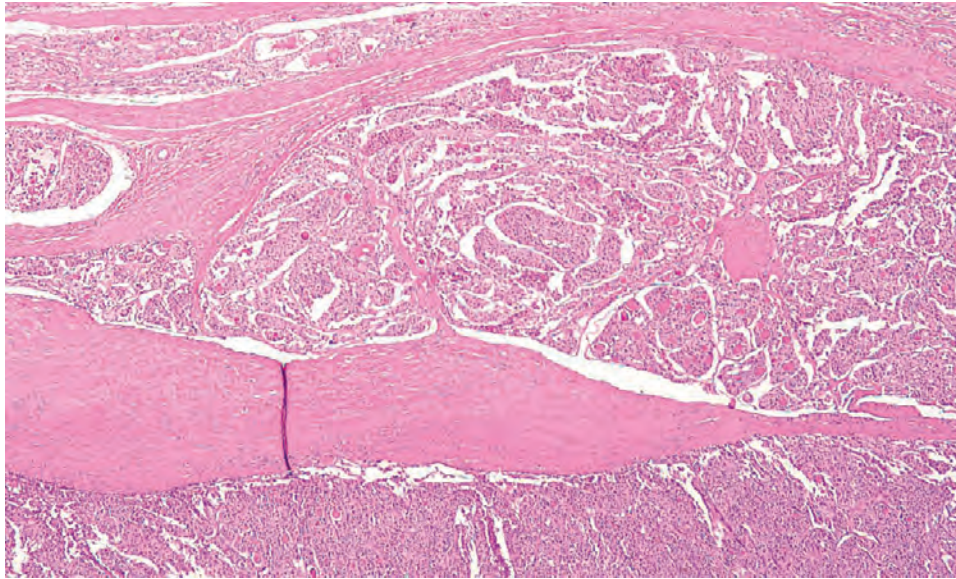
Many different patterns of growth can be seen in FC (microfollicular, trabecular, insular, solid, cystic; Fig. 25.48), but usually only one pattern predominates. The tumors are usually cellular with colloid easily identified. Oncocytic cells (oxyphilic, Askanazy, or Hürthle cell) have fine to slightly coarse, granular, abundant eosinophilic cytoplasm surrounding round to regular nuclei with coarse nuclear chromatin and eosinophilic, centrally placed nucleoli (Fig. 25.48). Colloid is usually less in oncocytic tumors, but identified as small droplets in the center of the follicle. While the majority of cases will have tumor cells that are round and regular, occasionally,

focal tumor cell spindling, tumor cell clearing, signet-ring formation, and even pleomorphism may be present (Fig. 25.49). Mitotic figures and necrosis may be seen, but degenerative changes are more common, especially in the central regions of the tumor or post FNA. Direct soft tissue and tracheal extension is rare. Extrathyroidal extension should be reported along with involvement of the surgical margin.

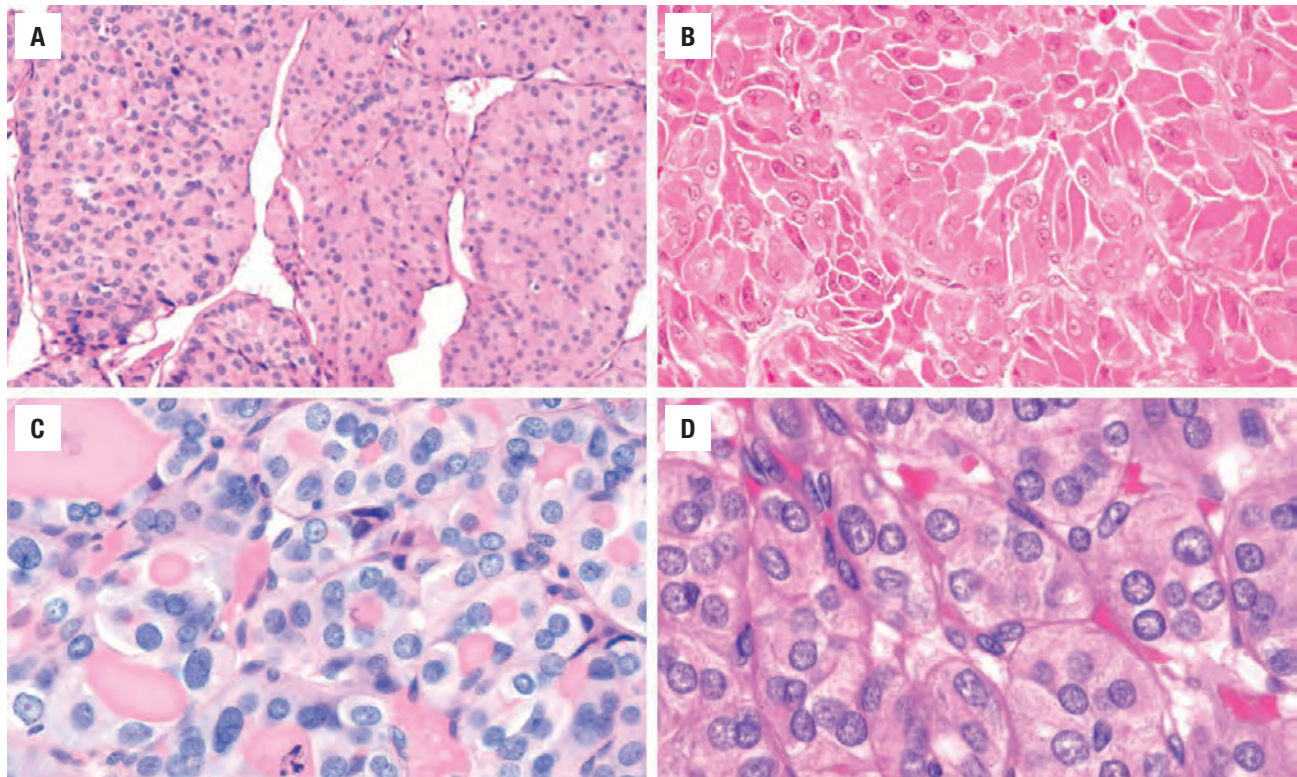
A number of variants or qualifiers are used in describing FCs, identified as follows:

- *Minimally invasive*: Limited capsular and/or lymphovascular invasion, although exact number of foci is undefined. Invasion is limited to small or medium capsular or pericapsular vascular spaces (generally <4 foci of either feature).
- *Widely invasive*: Uncommon type with extensive infiltration beyond the tumor capsule (“mushroom” invasion) into large vessels, and shows nodules of tumor within the parenchyma. Many times the capsule is attenuated or hard to identify. As the degree of invasion increases, the biologic behavior becomes more aggressive (Figs. 25.45 and 25.47).
- *Oncocytic variant (Hürthle, Askanazy, oxyphilic)*: Greater than 75% of the tumor is composed of large, polygonal, oncocytic cells (Figs. 25.44 and 25.48),



**FIGURE 25.47**

Large projections of tumor beyond the contour of the lesion with vascular invasion is diagnostic of a widely invasive follicular carcinoma.

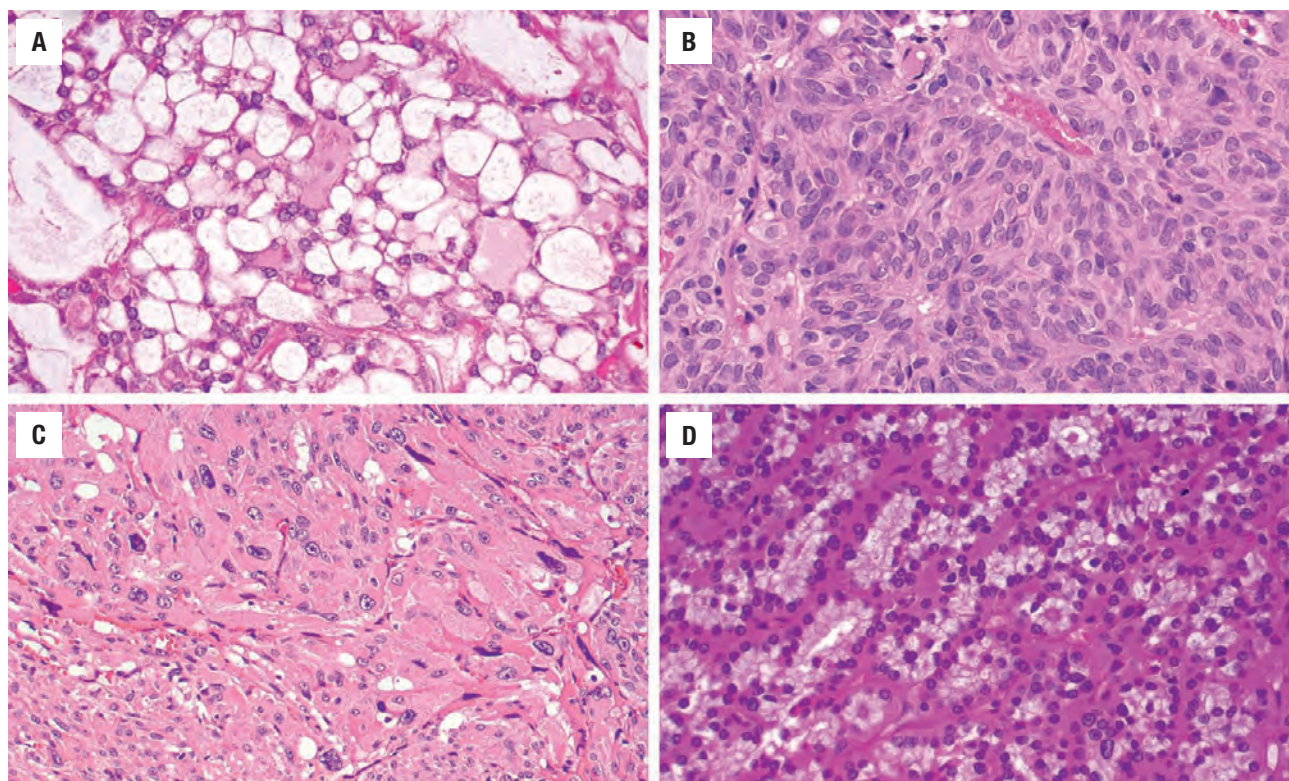
**FIGURE 25.48**

Patterns of growth and cytoplasmic appearance of follicular carcinoma. (A) Trabecular pattern with granular cytoplasm. (B) Solid pattern with oncocytic cytoplasm. (C) Slight nuclear variability in a follicular pattern. (D) Insular growth with focal colloid.

the cytoplasm of which is filled with abnormal mitochondria (abnormal dense bodies). The cytoplasm is coarse to deeply eosinophilic or “opacified.” Due to increased mitochondria, the tumors are more prone to infarction or degeneration. The tumors tend to be larger than conventional FC, and have scant to absent colloid. Thyroglobulin or TTF1 may be required to

confirm follicular derivation. There may occasionally be calcifications which can resemble psammoma bodies. The nuclei often contain large, centrally placed, brightly eosinophilic nucleoli. Pleomorphism tends to be more easily identified. There is no difference in outcome or management, although FCs with oncocytic cells tend to occur in older patients, have



**FIGURE 25.49**

Uncommon features in FTC include: (A) Signet-ring pattern. (B) Tumor cell spindling without colloid production. (C) Profound, focal nuclear pleomorphism. (D) Focal tumor cell cytoplasmic clearing in an oncocytic tumor (colloid is seen).

larger tumors, and more commonly have lymph node metastasis (up to 30 %). FNA will frequently result in infarction with associated hemorrhage, cyst formation, and eventual fibrosis.

- *Clear cell variant*: Any tumor may have clear cell change, especially prominent in oncocytic neoplasms (Fig. 25.49). It should be the dominant finding (> 75 %) for this variant to be diagnosed.
- *Spindle cell variant*: Tumor spindling should be the dominant finding (Fig. 25.49).
- *Signet-ring cell variant*: The nuclei are compressed and displaced by clear to amphophilic cytoplasm. The material is irregular thyroglobulin (Fig. 25.49).
- *Fatty metaplasia*: (fat cells within the follicular neoplasm) and *glomeruloid pattern* are very rare.

## ANCILLARY STUDIES

### IMMUNOHISTOCHEMICAL FINDINGS

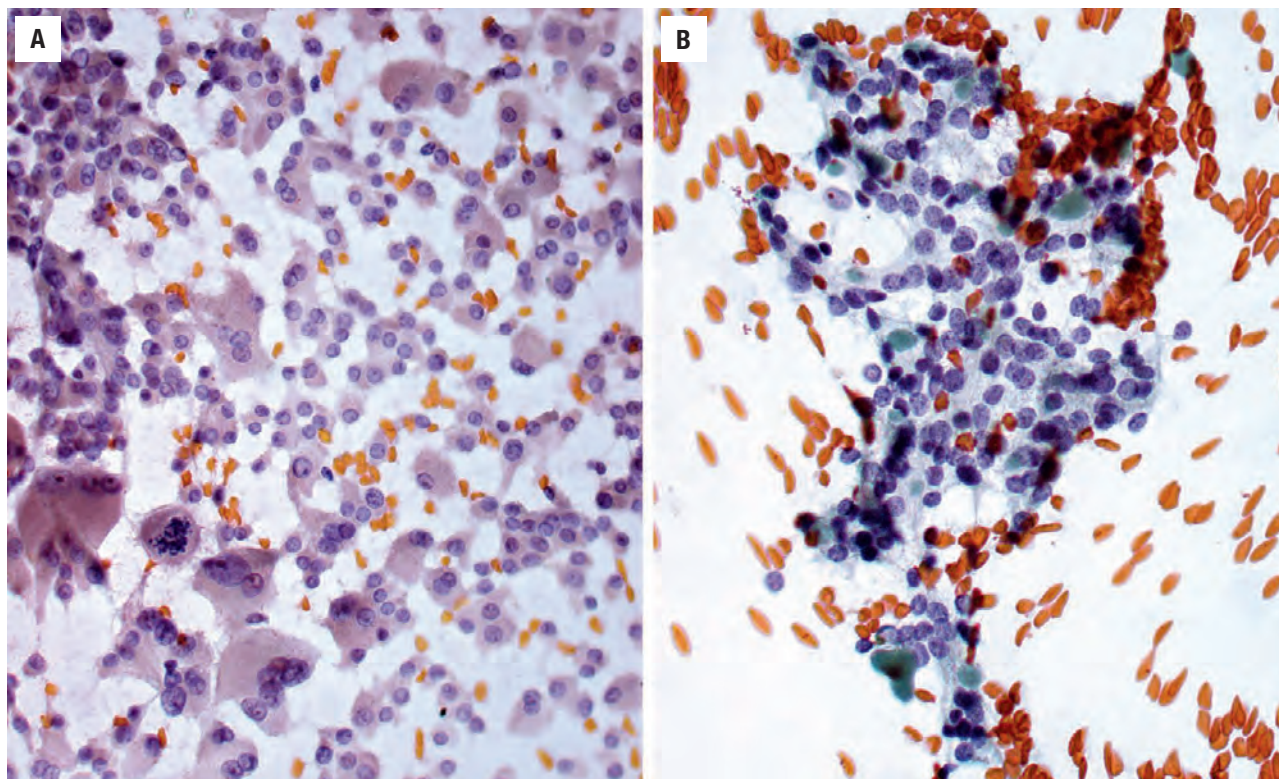
Immunohistochemistry may be of value in confirming that the neoplasm is of follicular derivation, but it is seldom necessary for diagnostic purposes. The cells would be thyroglobulin, TTF1, PAX8, and CK7 immunoreactive, while chromogranin, calcitonin, and pCEA are negative. Oncocytic tumors can show high background or

nonspecific staining, however, so interpreting results should be done with caution. Stains for endothelial markers (CD34, CD31, factor VIII-RAg) to accentuate vessels is of only limited value, as the endothelial cells are frequently discontinuous or lost in deeper sections, making interpretation difficult.

### FINE NEEDLE ASPIRATION

Separation between adenomatoid nodule, FA, and FC relies on the demonstration of capsular or lymphovascular invasion, making FNA of no value in making such a distinction. However, FNA is an excellent screening tool with a sensitivity of 78 %, specificity of 98 %, and positive predictive value of 99 % for these lesions. The aspirates are hypercellular with a dispersed microfollicular architecture or small, spherical three-dimensional clusters. There are often 6 to 12 nuclei forming a ring-like structure. The cytoplasmic borders are often indistinct. The cells are enlarged with uniform, round nuclei with coarse nuclear chromatin. Nuclear size and shape variability may be present (Fig. 25.50). Oncocytic cells may be the dominant finding (Fig. 25.50). The cells tend to be larger, with an eccentric nucleus, bi- or multinucleated, and often with a prominent nucleolus. There is usually scant or absent colloid. These findings are best reported as “thyroid follicular epithelial proliferation, favor neoplasm,” which translates into a tumor requiring surgical excision.



**FIGURE 25.50**

(A) Small follicles and sheets of oncocyctic cells showing mitoses and multinucleation in a “thyroid follicular neoplasm” fine needle aspiration (FNA; alcohol fixed, Papanicolaou stain). (B) An FNA smear showing a microfollicular pattern with nuclear size and shape variability and green droplets of colloid (alcohol fixed, Papanicolaou stain).

### FROZEN SECTION

If a FNA has been performed, then frozen section should be declined. It is nearly completely useless unless you “happen” upon an area of invasion. If a frozen section is demanded, two to three sections of the capsule should be sampled, and then “defer to permanent” should be invoked.

### MOLECULAR FINDINGS

Many FCs (up to 50%) will demonstrate rearrangements of the peroxisome proliferator-activated receptor gamma (*PPARγ*) gene, which produces a number of fusion proteins of which *PAX8-PPARγ* is the most common. This is a fusion between *PAX8* gene on 2q13 and *PPARγ* gene on 3p25 and can be detected with FISH. Almost never identified concurrently, *RAS* mutations are identified in about 45% of FCs. *GRIM-19* gene mutations can be seen in oncocyctic tumors. *PTEN* germline mutations are associated with FC and FV PTC. However, there is some overlap with FAs, papillary carcinoma, and undifferentiated carcinoma. *TERT* mutations are shown to be associated with a more aggressive clinical behavior.

### DIFFERENTIAL DIAGNOSIS

FA and *cellular adenomatoid nodules*, especially those with degenerative fibrosis, are sometimes difficult to separate from minimally invasive or low-grade FC. Neoplasms usually have muscle-walled vessels in the fibrous capsule, while an adenomatoid nodule usually does not. Tangential sectioning, irregular tumor contour, FNA, and frozen section artifacts all hamper interpretation. Adequate sampling of the *tumor-to-capsule-to-parenchymal* interface (at least one section per centimeter of tumor) is imperative before resorting to “atypical FA” or “follicular neoplasm of uncertain malignant potential.” Adenomatoid nodules are usually multiple, tend to be less cellular with more colloid than neoplasms, and do not have a true capsule.

*Follicular variant of papillary carcinoma* may occasionally be a problem, although the nuclear features should assist in the distinction. The newly recognized noninvasive follicular thyroid neoplasm with papillary-like nuclear features also shows nuclear findings of papillary carcinoma, even if only focally or in a patchy fashion. *Medullary thyroid carcinoma* can occasionally be oncocyctic, but



the nuclei tend to be finely stippled (neuroendocrine) and the cells are chromogranin, calcitonin, and pCEA immunoreactive. Tumor cells are frequently ovoid to spindled. Amyloid is often present. C-cell hyperplasia in the background may suggest the diagnosis, especially in inherited tumors. In the clear cell variant, *parathyroid tumors* and *metastatic renal cell carcinoma* may need to be separated from FC by using immunohistochemical studies along with the clinical history. A poorly differentiated carcinoma tends to have a more solid, trabecular, or insular growth pattern, shows necrosis and increased mitoses (> 3/10 high power fields), and shows limited to absent colloid production.

**PROGNOSIS AND THERAPY**

There has been a change in patient outcome over the past decades, especially with more neoplasms being found earlier in their development and with correct classification as minimally invasive. Overall, minimally invasive FC has an ~97% 20-year survival, with survival curves approaching those of normal age- and sex-matched controls. Hypoparathyroidism and recurrent laryngeal nerve damage is seen in up to 3% of patients. Widely invasive tumors, on the other hand, portend a more aggressive biologic behavior with ~50% 20-year survival. In any tumor type or grade, if metastasis develops, it occurs most commonly in lungs and bone, although the oncocytic type may have a higher frequency of lymph node metastases. When FCs are stratified by sex, age, size, and extent of invasion, there is no difference in recurrence or patient outcome when controlling for variant type, specifically the oncocytic variant. Therefore, “oncocytic” FCs should be managed in a fashion identical to FC. Adverse prognostic factors include age more than 55 years, extrathyroidal extension, tumor greater than 4 cm, distant metastases, and *TERT* mutations.

Conservative resection (lobectomy) versus radical surgery (total thyroidectomy) does not seem to yield statistically significant differences in patient outcome. Therefore, the most conservative treatment to completely remove the tumor is advocated. However, as radioablative iodine therapy is only effective after total thyroidectomy, there is a tendency toward this management. <sup>131</sup>I is not taken up by 25% of conventional FCs and up to 75% of oncocytic FCs, so it is ineffective. External beam radiation may be used in some patients.

**■ UNDIFFERENTIATED CARCINOMA**

Accounting for ~2% to 3% of all thyroid gland neoplasms, undifferentiated carcinoma (also known as *anaplastic carcinoma* and *pleomorphic carcinoma*), is a

**UNDIFFERENTIATED THYROID CARCINOMA—DISEASE FACT SHEET**

**Definition**

- Highly aggressive malignant neoplasm composed of undifferentiated cells that exhibit immunohistochemical or ultrastructural epithelial differentiation

**Incidence and Location**

- 2%-3% of all thyroid malignancies
- Higher in endemic goiter regions and in Europe
- Radiation exposure risk

**Morbidity and Mortality**

- Rapidly fatal in nearly all patients

**Sex and Age Distribution**

- Females > males (1.5:1)
- Most patients are older than 60 years

**Clinical Features**

- Rapidly expanding neck mass
- Usually have underlying long history of thyroid disease
- Hoarseness, dysphagia, and pain are common
- Frequent metastases identified at presentation

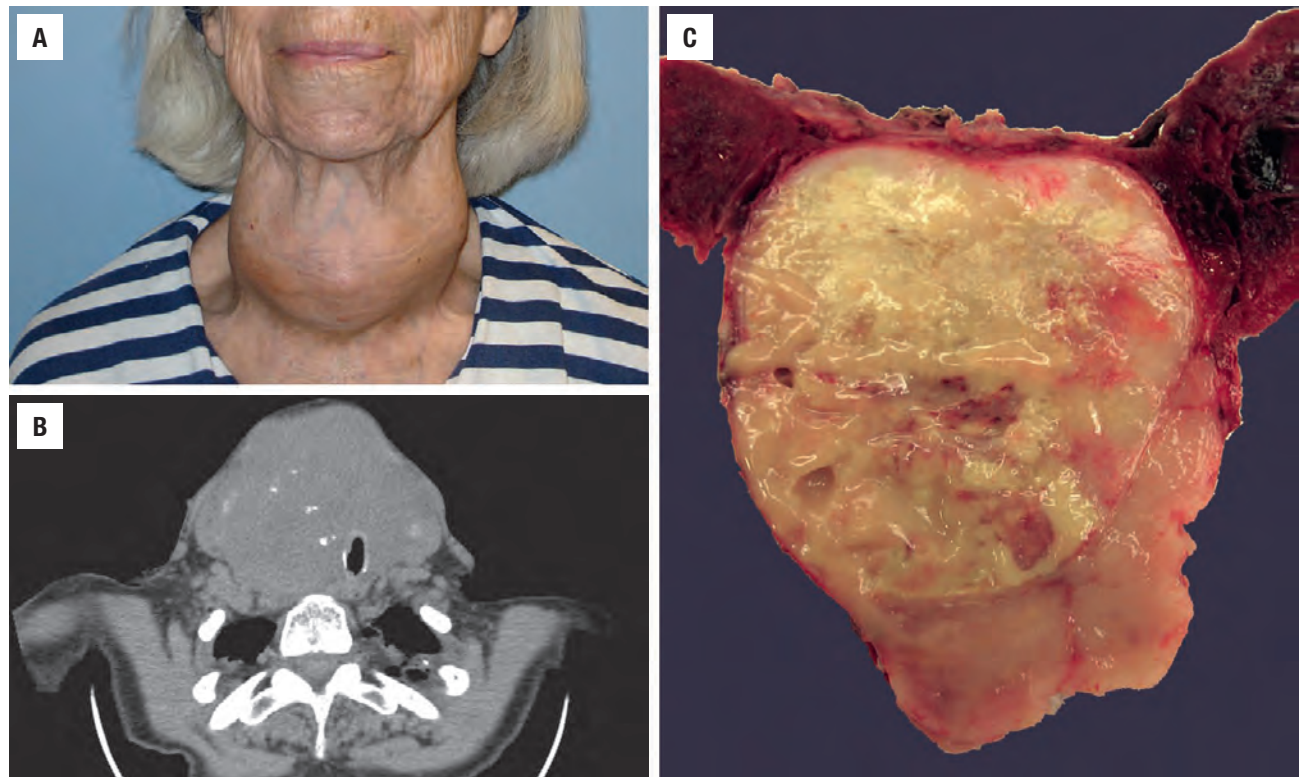
**Prognosis and Therapy**

- Poor prognosis, > 95% die of disease usually in less than 6 months (accounts for over 50% of all thyroid cancer deaths)
- Surgery and combination multimodality therapy

highly aggressive malignant neoplasm composed of undifferentiated thyroid follicular cells, requiring immunohistochemical or ultrastructural support to determine their epithelial origin. All are primary thyroid tumors by definition (not metastatic or direct extension). Risk factors include radiation exposure risk, low socioeconomic status, old age, along with iodine deficiency, and a long history of thyroid disease.

**CLINICAL FEATURES**

The vast majority of patients are over 60 years, but the sharp female predilection for other thyroid gland neoplasms is not sustained in this neoplasm: the female to male ratio is 1.5:1. Nearly all of the patients present with a rapidly (a few weeks) enlarging fixed and hard neck mass (Fig. 25.51), often associated with a long history of thyroid disease (goiter, FC, papillary carcinoma). Furthermore, the hoarseness, dysphagia, vocal cord paralysis, and pain often associated with the mass are indications of the widely invasive nature of the neoplasm. Extension into the soft tissues and surrounding organs (esophagus, trachea) is common. Hyperthyroidism may result due to rapid destruction of follicles and hormone

**FIGURE 25.51**

(A) A clinical photograph demonstrates a large thyroid mass with engorged veins. (B) A large mass entirely replacing the thyroid gland and expanding into the soft tissue with tracheal deviation is seen on computed tomography. (C) The cut surface shows the thyroid parenchyma invaded by a tumor that is fleshy, with a yellow to tan appearance, and demonstrating degeneration. (A, Courtesy Dr. G. Calzada.)

### UNDIFFERENTIATED THYROID CARCINOMA—PATHOLOGIC FEATURES

#### Gross Findings

- Large (mean: 6 cm), fleshy, bulky masses with necrosis and hemorrhage
- Infiltrating, often into adjacent soft tissues and organs

#### Microscopic Findings

- Widely invasive with extensive lymphovascular invasion
- Many different patterns of growth
- Poorly differentiated cells: polygonal, spindle, and epithelioid
- Profound pleomorphism
- Tumor giant cells, osteoclast-like giant cells, and squamous differentiation may be seen
- Increased mitotic figures, including atypical forms
- Bone and cartilage are sometimes present
- Necrosis, hemorrhage, and degeneration

#### Immunohistochemical Findings

- Keratin and epithelial membrane antigen, in up to 80% of cases (focal and limited)

- p63 may be positive, but thyroglobulin and TTF1 are rarely positive
- PAX8 is positive in about 75% of cases
- Vimentin and p53 positive in nearly all cases

#### Fine Needle Aspiration

- Biphasic population: tumor and uninvolved thyroid
- Highly cellular with single cells and focal clusters composed of remarkable atypical cells
- Mitotic figures are prominent
- Background necrosis and inflammatory cells may be seen

#### Pathologic Differential Diagnosis

- Exclude metastatic disease to thyroid; primary thyroid sarcomas and lymphoma



release. Metastases to cervical lymph nodes and/or lungs, bone, and brain are noted at clinical presentation in up to 50 % of patients. Leukocytosis can be seen due to the secretion of macrophage colony-stimulating factor. Radiographic studies show the extent of the disease and degree of infiltration (including vessels), along with necrosis and calcifications (Fig. 25.51).

## **PATHOLOGIC FEATURES**

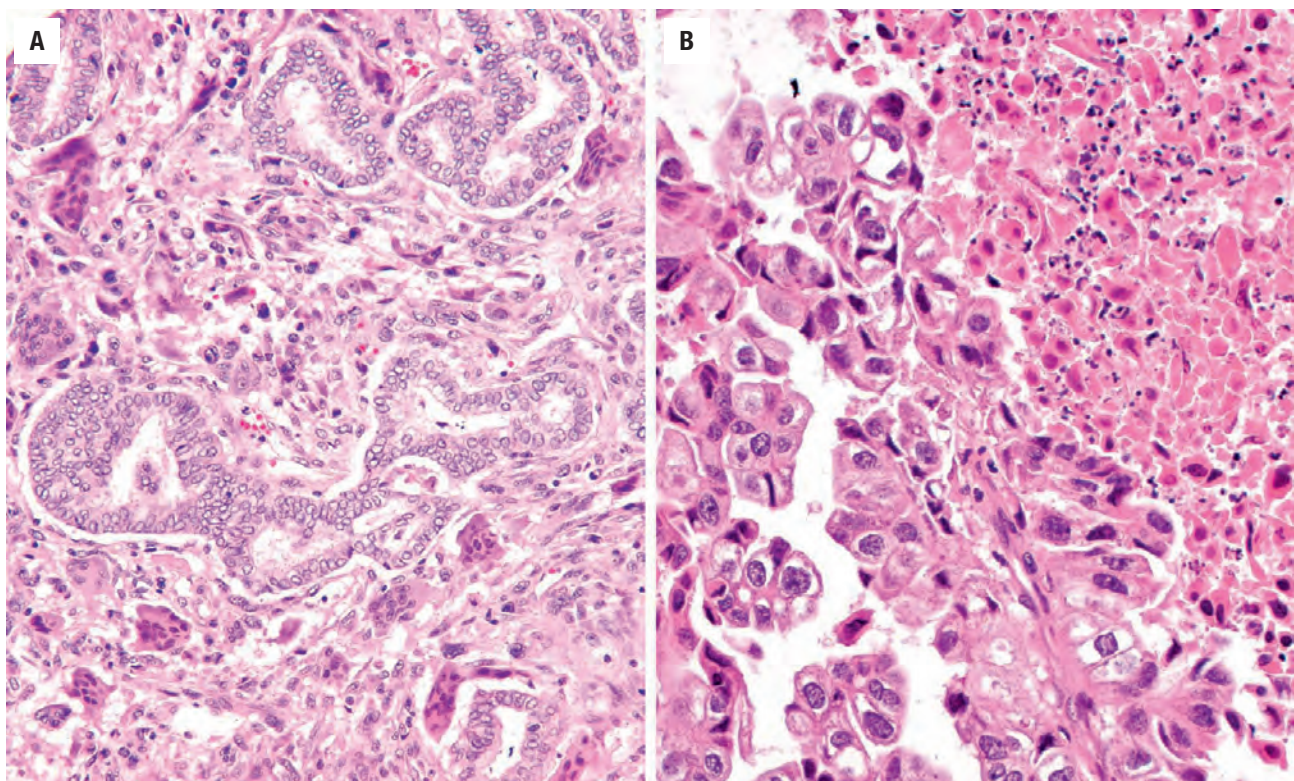
### **GROSS FINDINGS**

The tumors are usually a bulky (mean: 6 cm), fleshy, pale-tan solitary mass (60 %), often fixed and firm. Multifocal (40 %) or bilateral (25 %) tumors are not as common. Tumors typically completely replace the thyroid parenchyma and show extensive invasion beyond the thyroid gland into the perithyroidal tissues; thus all are stage pT4 by definition. Necrosis and hemorrhage are almost ubiquitous (Fig. 25.51). Adequate sampling to show preexisting or coexisting carcinoma is suggested.

### **MICROSCOPIC FINDINGS**

The remarkably infiltrative tumor is composed of a combination of pleomorphic, spindle, and epithelioid

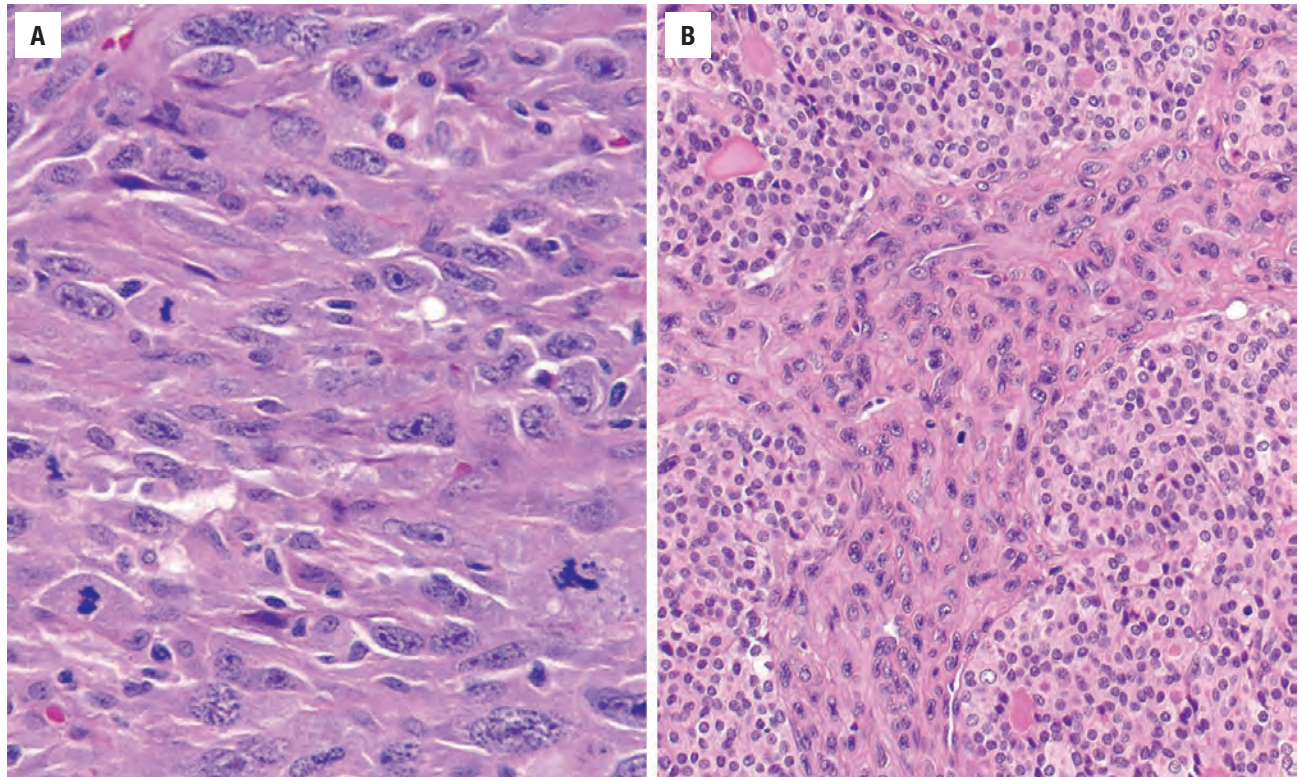
cells arranged in solid sheets to fascicular bundles which nearly completely efface the thyroid parenchyma (Figs. 25.52–25.54). Extrathyroidal extension, with soft tissue and local organ extension, is common. Extensive lymphovascular invasion is present, along with significant coagulative-type necrosis, hemorrhage, and degeneration. A desmoplastic stroma may be present. It is not uncommon to identify a concurrent neoplasm, with papillary carcinoma identified most commonly, while FC is next (Figs. 25.52 and 25.53). One cell type may predominate, but pleomorphism is usually profound. The spindle cell type often resembles various sarcomas (Fig. 25.53). Tumor giant cells filled with bizarre nuclei are common; nontumor osteoclast-like giant cells are described infrequently (Fig. 25.54). Squamous differentiation is also occasionally noted. Mitotic figures, including atypical forms, and necrosis are prominent features (Fig. 25.53). A rich acute inflammatory infiltrate and a vascular component may also be present, the latter a mimic of angiosarcoma (anastomosing) or hemangiopericytoma (staghorn; Fig. 25.54). Colloid is absent within the tumor, but entrapment of follicles may be seen. Thoroughly sampled tumors will often demonstrate foci of PTC (Fig. 25.52) or FC (Fig. 25.53), suggesting high-grade transformation of a pre-existing neoplasm in the development of undifferentiated carcinoma. A number of variants are recognized, although they do not alter outcome or management: osteoclastic, angiomatoid, lymphoepithelioma-like, rhabdoid, and paucicellular variants.



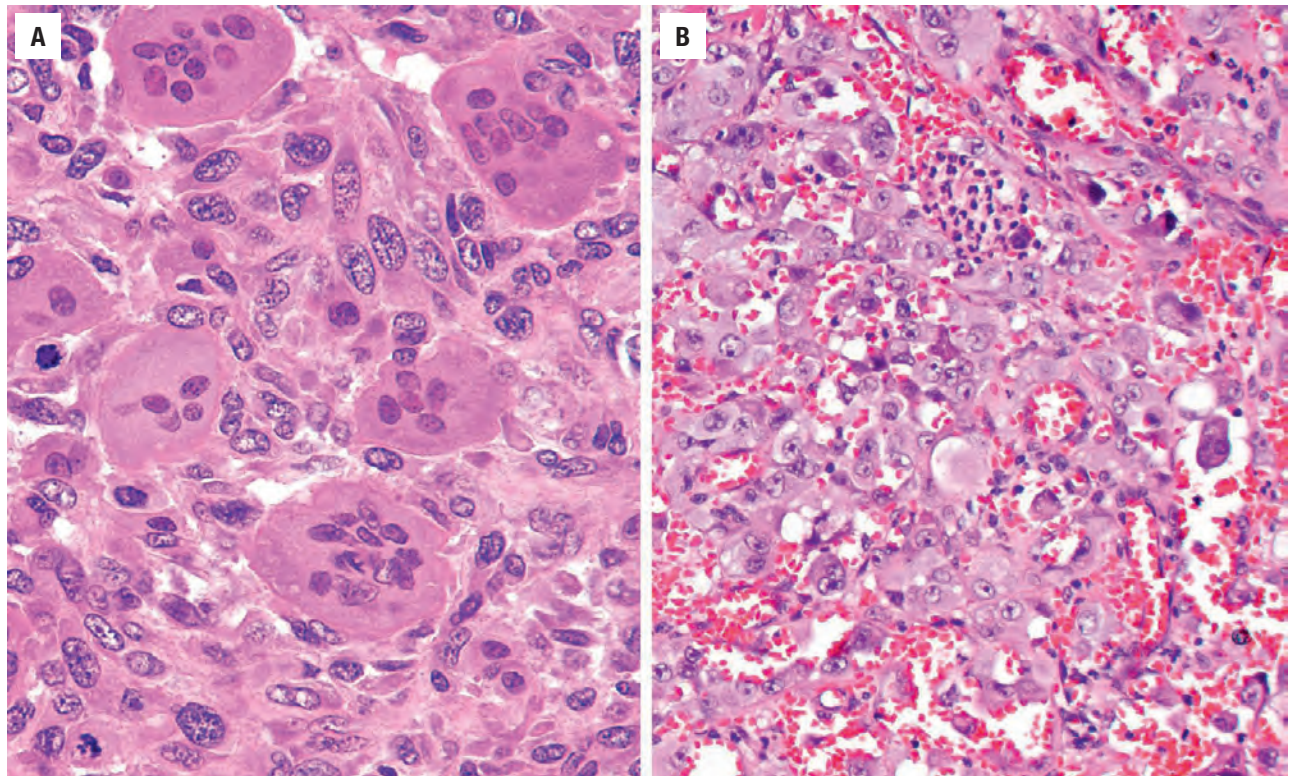
**FIGURE 25.52**

(A) Undifferentiated carcinoma arising in association with PTC. The undifferentiated component has spindle and giant cell features. (B) Dedifferentiation of a columnar variant of PTC with extensive necrosis and atypia.



**FIGURE 25.53**

(A) Spindle cells with numerous atypical mitoses comprise this undifferentiated carcinoma. (B) There is a follicular carcinoma that blends with a highly atypical spindled cell, pleomorphic population with increased mitoses in this undifferentiated carcinoma.

**FIGURE 25.54**

(A) Numerous osteoclast-like giant cells comprise this tumor. (B) This angiomatoid pattern shows extravasated erythrocytes and acute inflammatory cells.



## ANCILLARY STUDIES

### IMMUNOHISTOCHEMICAL FINDINGS

Cytokeratins (AE1/AE3 [Fig. 25.55], CAM5.2) and epithelial membrane antigen (EMA) are the most commonly identified “epithelial” markers, present in up to 80 % of cases, but often limited to focal areas and/or isolated cells (pleomorphic, spindle, and/or epithelioid cells). Vimentin is strongly positive. p63 is positive in many cases, while thyroglobulin and TTF1 are usually not identified (Fig. 25.55). Nuclear  $\beta$ -catenin is frequently expressed. PAX8 is seen in about 75 % of cases. *TP53* mutations are common, with strong reactivity for p53. When confronted with the differential diagnoses of sarcoma, melanoma, and lymphoma, specific phenotypic markers may help with the separation: desmin, myogenin, smooth muscle actin, CD31, CD34, S100 protein, HMB-45, SOX10, CD30, ALK, and CD45RB. Ki67 is frequently very high.

### FINE NEEDLE ASPIRATION

Aspirates are usually highly cellular, composed of single cells, small clusters, or sheets of large, highly pleomorphic cells (Fig. 25.56). Cytoplasm is often abundant, with bizarre, single or multiple nuclei containing prominent nucleoli. Mitotic figures, necrosis, and acute inflammatory cells are present. Colloid is usually absent. While a diagnosis of “poorly differentiated malignant neoplasm” can be rendered, the separation between a primary versus metastatic tumor, and determining whether it is a carcinoma, sarcoma, lymphoma, or melanoma would require ancillary techniques. Rarely, aspirates may be paucicellular or contain only necrotic debris and inflammatory cells. Core needle sampling may yield a more definitive diagnosis in these cases.

### MOLECULAR FINDINGS

The cytogenetics are often complex and show a progressive accumulation of chromosomal alterations (numerical and structural aberrations). The most common mutations are in *TP53* (nuclear expression), while *BRAF* V600E, *RAS*, *PIK3CA*, and *PTEN* are also seen in a range of 10 % to 20 % each.

## DIFFERENTIAL DIAGNOSIS

*Metastatic tumors* to the thyroid gland present the most common differential diagnostic difficulty, although primary sarcomas and lymphomas of the thyroid may also occur. A selection of pertinent and selected immunohistochemical markers will usually help make the

separation. However, PAX8 is present in thyroid and kidney tumors, while TTF1 can be seen in lung and isolated malignant cells of undifferentiated carcinoma. A pertinent caution: *melanoma* frequently has *BRAF* and *NRAS* mutations, so other markers may be required for this distinction. *Riedel thyroiditis* tends to have heavy fibrosis, inflammation, and vasculitis without cellular atypia. Further, this IgG<sub>4</sub> disease usually shows storiform fibrosis, obliterative phlebitis, and an increased number of plasma cells.

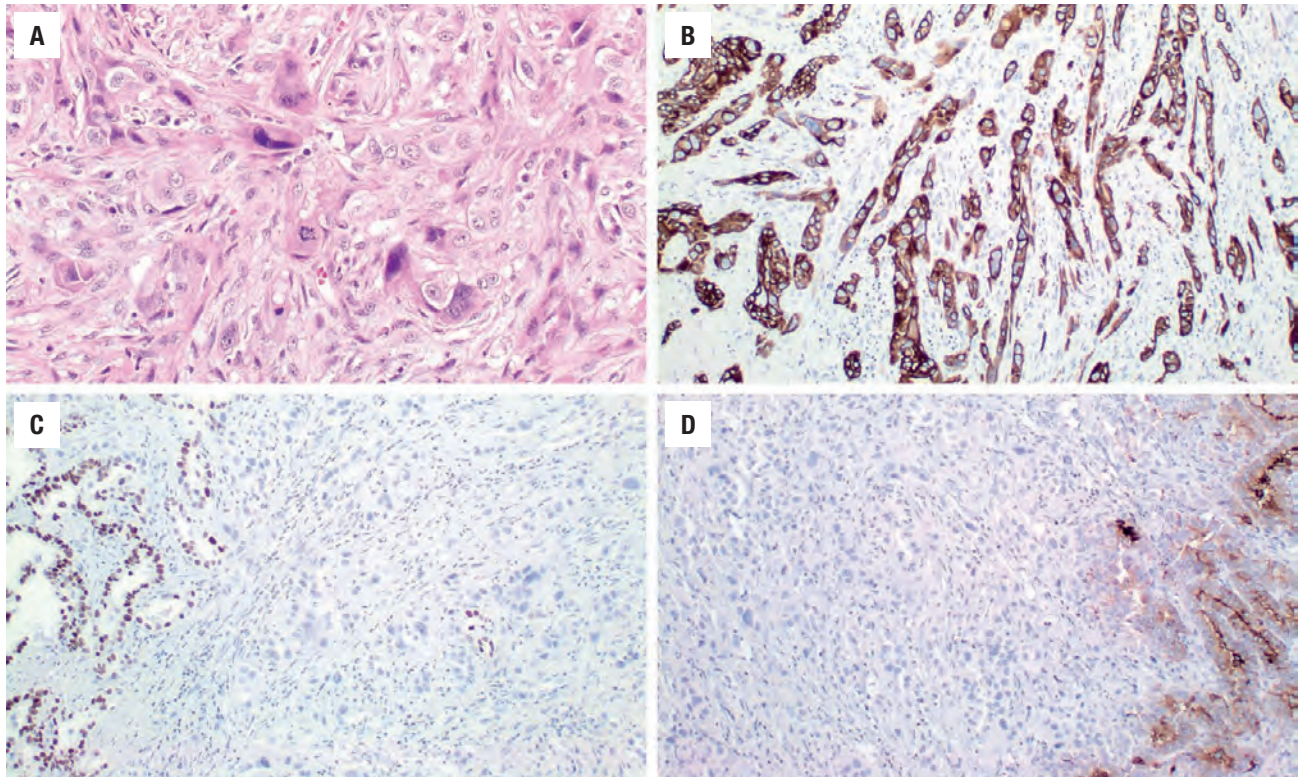
## PROGNOSIS AND THERAPY

The extremely grave clinical outcome of more than 95 % of patients dying from disease in less than 6 months accounts for over 50 % of *all* thyroid cancer deaths. All patients' tumors by definition are stage pT4, with a high proportion of patients showing lymph node metastases (50 %) and distant metastases (50 %: lung, bone, brain) at presentation. In spite of surgery and combination multimodality therapy, the adverse prognosis seems unaltered, although targeted therapies (gefitinib and bevacizumab) have shown promise. Chemosensitization may help. Hyperfractionation or accelerated dosing regimens of radiation improve efficacy. Only rarely will patients have a *better* prognosis, when the undifferentiated carcinoma is a *minor* component of a thyroid neoplasm that has been completely excised and aggressively managed with adjuvant chemotherapy and radiation.

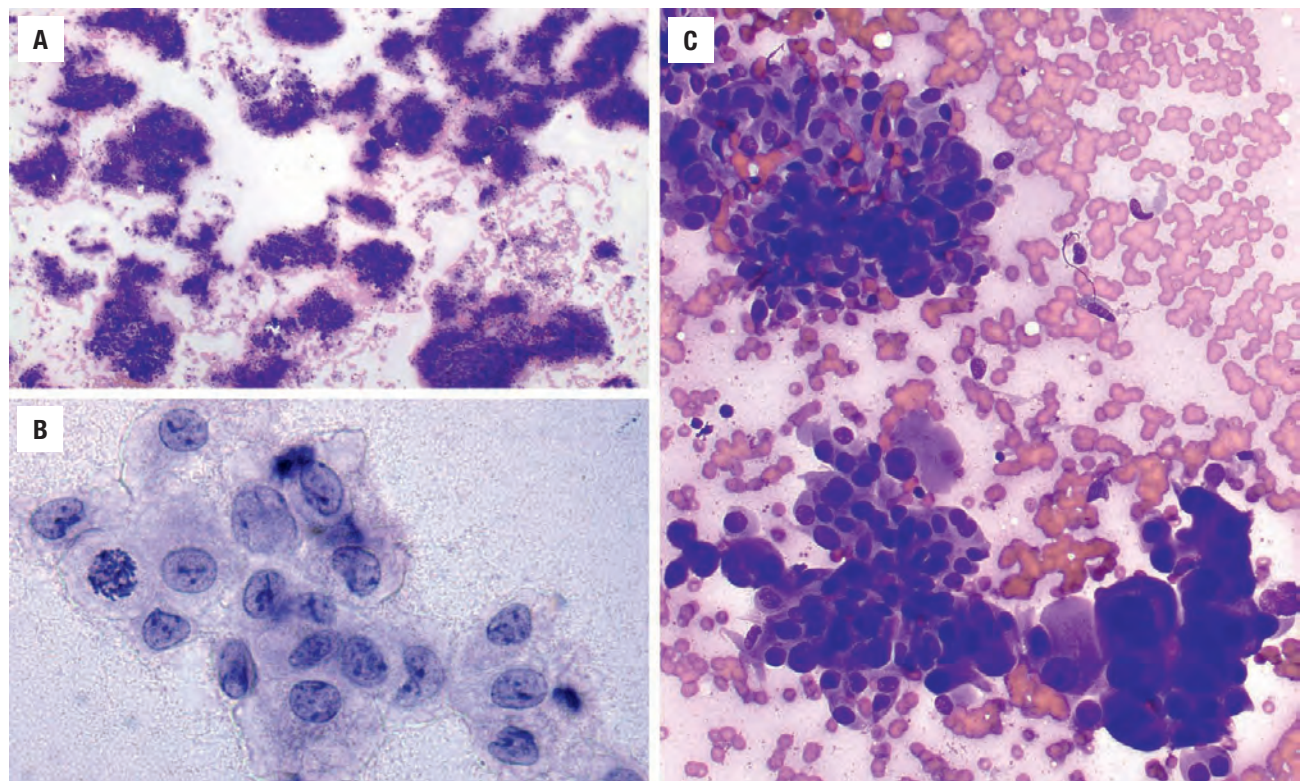
## MEDULLARY THYROID CARCINOMA

The ultimobranchial body (derived from the 4th branchial pouch) is believed to give rise to C-cells (parafollicular cells) which tend to be aggregated in the upper and middle lobes of the thyroid gland (not in the isthmus). The main peptide secreted by these cells is calcitonin, a hormone involved in calcium (and phosphorus) homeostasis. Calcitonin decreases serum calcium by: (1) inhibiting osteoclastic bone resorption; (2) inhibiting  $\text{Ca}^{+2}$  absorption by the intestines; and by (3) inhibiting renal resorption of  $\text{Ca}^{+2}$ , thus promoting its urinary secretion. Calcitonin gene-related peptide (CGRP) is also present. MTC is a malignant neuroendocrine neoplasm of the thyroid gland with evidence of C-cell differentiation. This tumor has a strong familial or inherited association with the multiple endocrine neoplasia (MEN) syndromes, as well as other inherited forms of medullary thyroid carcinoma when there is a germ-line mutation in the *RET* oncogene. These autosomal inherited syndromes include MEN2A (Sipple): parathyroid hyperplasia (hyperparathyroidism), medullary thyroid carcinoma, adrenal pheochromocytoma, and



**FIGURE 25.55**

(A) There is a pleomorphic spindle cell proliferation with increased mitoses that shows pancytokeratin (B), but lacks TTF1 (C), and thyroglobulin (D) immunoreactivity.

**FIGURE 25.56**

(A) Cellular smear of sheet of cells that have a high nuclear-to-cytoplasmic ratio and nuclear pleomorphism (Diff Quik). (B) There is marked nuclear pleomorphism and an atypical mitotic figure (alcohol fixed, Papanicolaou stain). (C) Fine needle aspiration demonstrates loosely cohesive cells with remarkable atypia and opacified cytoplasm in this undifferentiated carcinoma.



**MEDULLARY THYROID CARCINOMA—DISEASE FACT SHEET****Definition**

- A malignant neuroendocrine tumor of the thyroid gland showing C-cell differentiation

**Incidence and Location**

- About 2%–3% of thyroid malignancies
- 70% sporadic; 30% inherited (familial)
- Usually develops in upper to middle thyroid lobes (never isthmus)

**Morbidity and Mortality**

- Other disorders associated with familial disease (multiple endocrine neoplasia [MEN])
- 45%–85% at 10 years, stage and familial disease dependent

**Sex and Age Distribution**

- Females > males (1.1:1)
- 5th–6th decades for sporadic tumors
- 3rd decade for familial tumors

**Clinical Features**

- Sporadic cases usually have a unilateral, solitary thyroid mass
- Familial cases have multicentric and bilateral thyroid masses
- Frequently discovered as part of evaluation of parathyroid, adrenal, pituitary, pancreas, and gastrointestinal disease (MEN syndrome), in which thyroid symptoms may be subclinical
- Lymphadenopathy is common (up to 70% of patients at presentation)
- Hoarseness, stridor, obstruction
- Serum calcitonin levels elevated

**Radiographic Features**

- <sup>131</sup>I-meta-iodobenzylguanidine (MIBG) positive mass
- Positron emission tomography useful in identifying metastases

**Prognosis and Therapy**

- Clinical stage and inherited type dependent
- Excellent prognosis for small tumors confined to the thyroid, incidentally discovered and without lymph node metastases (100%)
- Low TNM stage, <50 years, calcitonin-rich, and abundant amyloid tumors have better prognosis
- Total thyroidectomy and central lymph node dissection
- Chemotherapy and/or targeted molecular therapies have variable effectiveness
- Screening identifies familial incidence

survival, differentiation, motility, and chemotaxis. Mutations of five extracellular cysteine codons (exon 10: 609, 611, 618, 620; exon 11: 634) collectively account for about 95 % of MEN2A and 85 % of familial medullary thyroid carcinoma (FMTC) kindred. Interestingly, codon 634 is involved in 80 % to 90 % of MEN2A cases (arginine for cysteine substitution most commonly) while 98 % of MEN2B are associated with point mutation in codon 918 of exon 16 (Met918Thr substitution), identified as germline mutations. Furthermore, up to two-thirds of sporadic medullary thyroid carcinomas have somatic *RET* mutations.

**CLINICAL FEATURES**

About 2 % to 3 % of all thyroid neoplasms are MTC. The sporadic (nonfamilial) and inherited (familial) forms of the tumor determine the clinical presentation. Although nearly 70 % of MTCs are sporadic, exclusion of an inherited form of the disease is necessary.

Sporadic medullary thyroid carcinoma is slightly more common in women than men (1.1:1) and tends to occur in the middle decades of life (5th and 6th decades). Patients usually present with a unilateral palpable thyroid gland mass, with up to 70 % having cervical lymphadenopathy at presentation, and about 10 % distant metastases. Hoarseness, stridor, and upper airway obstruction is only seen in about 15 % of patients. Serum calcitonin levels are almost invariably elevated, a finding not usually seen in other types of neuroendocrine carcinomas. Carcinoembryonic antigen (CEA) is also often elevated and calcium imbalances are not uncommon.

Familial medullary thyroid carcinoma (FMTC) may be discovered “incidentally” during work-up for MEN-associated disease in the parathyroid, adrenal, pituitary, pancreas, and gastrointestinal tract. These syndromes have an autosomal dominant mode of inheritance. MEN2A is most frequently associated with familial medullary thyroid carcinoma. The patients usually present at a young age (mean, 3rd decade) with multicentric and *bilateral* thyroid lobe nodules/enlargement. If there is an association with MEN2B, the patients are even younger (infancy to early childhood), with mucosal neuromas often bringing the patient to clinical attention. Neuromas of the oral cavity, lips, tongue, and gastrointestinal tract may present with clinical findings that are similar to Hirschsprung disease, but the distinction is made by rectal biopsy revealing loss of ganglion cells in the latter. It is important to note that the diverse nonthyroid signs and symptoms of the MEN syndrome may dominate the clinical presentation, with none of the findings referable to calcitonin increase. For example, patients may present primarily with paroxysmal hypertension, headache, and sweating secondary to a coexistent pheochromocytoma. Given the syndromic nature of the disease,

pancreatic endocrine tumors; and MEN2B (Wagenmann-Froboese syndrome): includes the above with the addition of soft tissue tumors (usually mucosal neuromas). Most of the mutations are a gain-of-function (activating) germline mutation of *RET* proto-oncogene involving 10q11.2, a member of the receptor tyrosine kinase superfamily (*RET*: REarranged during Transfection). The *RET* receptor activates signaling pathways responsible for cell proliferation,

hyperparathyroidism with calcium homeostasis derangements, pituitary hormone secretion, and pancreatic hormone secretion need to be carefully and completely evaluated. The very high plasma calcitonin level seen in MTC (for which there is no medical treatment) is responsible for the diarrhea and flushing seen in up to 30 % of patients. The other inherited, but non-MEN related forms of medullary thyroid carcinoma, are less common and often present at the same (older) age as the sporadic cases.

### RADIOGRAPHIC FEATURES

CT and ultrasound often show only a mass lesion (Fig. 25.57). However,  $^{131}\text{I}$ -meta-iodobenzylguanidine (MIBG) scintigraphy will greatly aid in the diagnosis. This radiopharmaceutical and guanethidine analog is a radio-compound that shows a remarkable affinity for neural crest-derived tissues and tumors that belong to the dispersed neuroendocrine system (DNES), where it is taken up by neurotransmitter vesicles. Therefore, medullary thyroid carcinoma will “light-up” with this technique, confirming the neuroendocrine nature of the neoplasm. Similarly, positron emission tomography (PET) can be used to identify distant metastases.

## PATHOLOGIC FEATURES

### GROSS FINDINGS

Sporadic tumors are usually unilateral, solitary masses, while familial tumors are multifocal and bilateral. Most tumors are usually located in the middle to upper third of each lobe. Depending upon the symptoms and whether familial or not, the tumor can range from a “microscopic” focus to completely replacing the thyroid lobe (up to 10 cm in greatest dimension), although usually 2 to 3 cm. Tumors are usually circumscribed, but infiltration can be seen (Fig. 25.57). The cut section is tan, yellow to pink, and is soft to rubbery or firm. A gritty cut surface represents the calcifications that may be seen. If the specimen is a prophylactic thyroidectomy in a familial syndrome patient, the lobes should be serially sectioned transversely and sections submitted sequentially from superior to inferior. A calcitonin immunohistochemical stain may be used to highlight C-cell hyperplasia or microscopic carcinoma.

### MICROSCOPIC FINDINGS

Normal C-cells are difficult to identify on routine light microscopy. They are small polygonal to spindle shaped

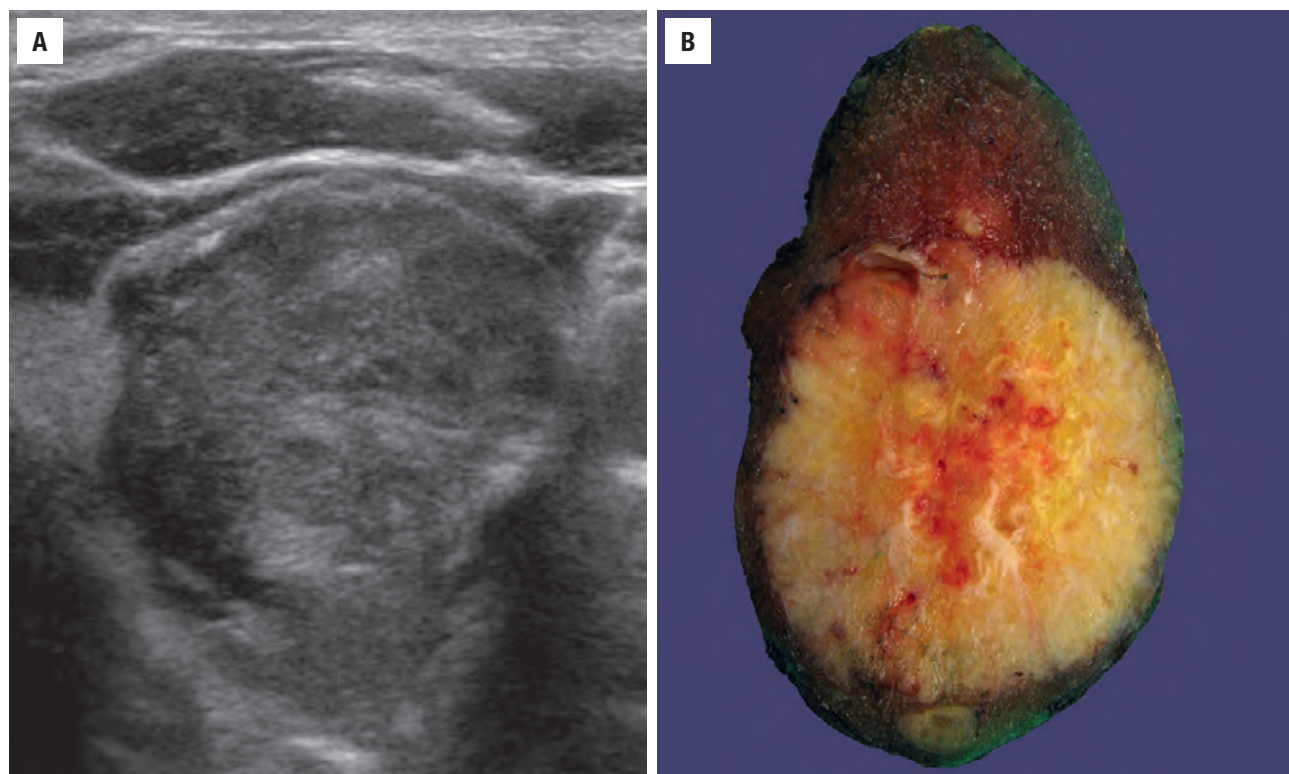


**FIGURE 25.57**

(A) Thyroid gland ultrasound shows a mass within the thyroid, focally with mixed echogenicity. (B) The gross tumor shows a bosselated periphery, with smaller nodules within the parenchyma. The tumor is yellow with areas of hemorrhage.



## MEDULLARY THYROID CARCINOMA—PATHOLOGIC FEATURES

### Gross Findings

- Sporadic tumors are unilateral and solitary
- Familial tumors are multifocal and bilateral
- Usually encapsulated or circumscribed with a tan-yellow soft to firm cut surface
- Usually 2-3 cm in dimension (smaller in familial cases)
- Calcifications can be seen

### Microscopic Findings

- Pre-neoplastic C-cell hyperplasia has bilateral nodules of > 50 cells per aggregate
- Invasive borders with lymphovascular invasion prominent
- Multiple patterns of growth
- Entrapment of benign follicular epithelial cells common
- Round to oval, spindled to plasmacytoid cells
- Round to oval nuclei with stippled, “salt-and-pepper” nuclear chromatin
- Intranuclear cytoplasmic inclusions common
- Mitotic figures and necrosis are uncommon
- Amyloid is present in up to 90% of tumors
- Many variants recognized

### Immunohistochemical Findings

- **Positive:** calcitonin, calcitonin gene related peptide, chromogranin, synaptophysin, PAX8, keratin, CD56, pCEA, TTF1

- **Negative:** thyroglobulin
- Amyloid positive (although Congo red apple-green birefringence is easier to interpret)

### Fine Needle Aspiration

- Cellular aspirates with single cells and small, loosely cohesive clusters
- Colloid absent but amyloid present
- Round to oval, spindle to polygonal cells
- Bi- and multinucleated cells with moderate pleomorphism
- Plasmacytoid appearance with eccentric nucleus placement
- Stippled to coarse nuclear chromatin
- Metachromatic red cytoplasmic granules on air dried preparations

### Molecular Findings

- Gain of function germline/somatic mutation of *RET* (A634C; M918T most common)

### Pathologic Differential Diagnosis

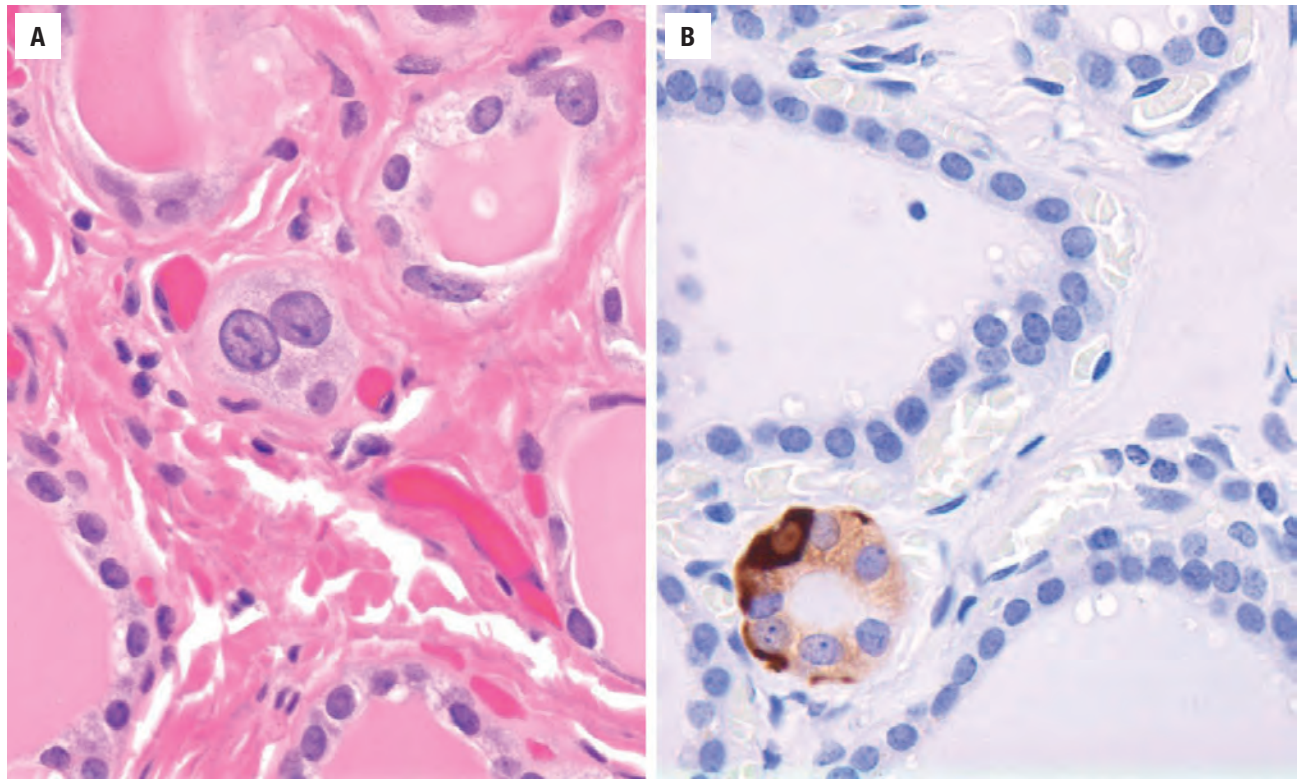
- C-cell hyperplasia can mimic intraglandular spread, solid cell nests and palpation thyroiditis
- Follicular adenoma, follicular carcinoma, papillary carcinoma, paraganglioma, hyalinizing trabecular tumor, amyloid goiter, undifferentiated carcinoma, metastatic tumor, lymphoma

cells identified immediately adjacent to or within thyroid follicles. The nuclei are pale and the cytoplasm is often clear or slightly granular (Fig. 25.58). Solid cell nests (SCNs), pavedment cell clusters without intercellular bridges, are thought to be remnants of the ultimobranchial body (Fig. 25.59), and are composed of C-cells and “main cells,” pluripotent cells with squamoid findings. They are found in the upper and outer lobes of the thyroid gland, frequently identified incidentally in thyroid glands removed for different reasons. They may be seen in and around areas of C-cell proliferation.

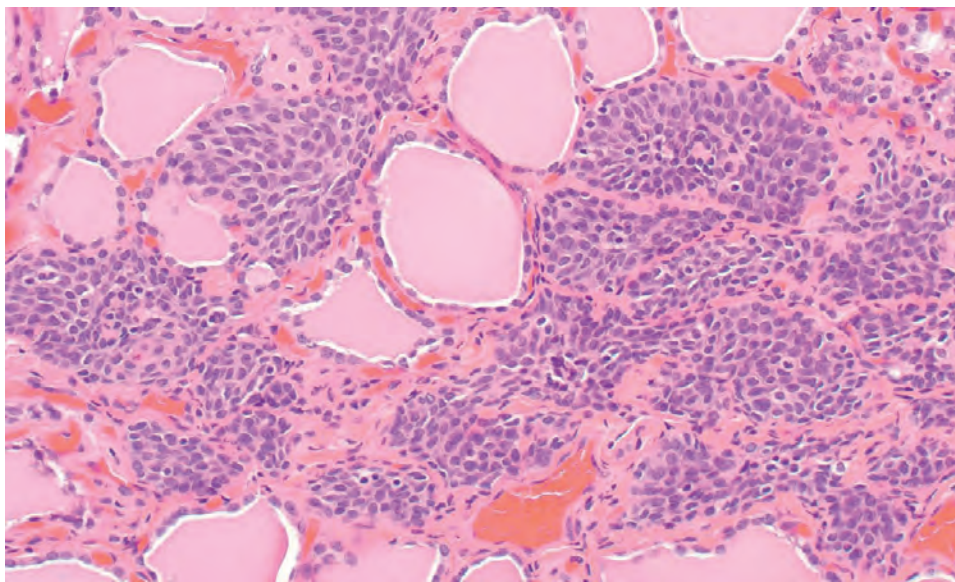
**Precursor lesion:** C-cell hyperplasia is thought to be either reactive (physiologic or secondary; Fig. 25.60) or pre-neoplastic, with the latter (also called medullary carcinoma in situ) considered the precursor of heritable MTC (Fig. 25.61). Many subjective points of separation exist. However, if there are aggregations of more than 50 C-cells, and especially if identified in nodules, bilaterally, or diffusely, pre-neoplastic C-cell hyperplasia is diagnosed. This form will have germline mutations in the *RET* gene. These small aggregates are often noted adjacent to MTC. These groups may be focal, diffuse, or nodular. These aggregates should not show dysplastic changes, amyloid deposition, or breach of the basement membrane (highlighted by type IV collagen stains). Furthermore, if the aggregate is less than 0.5 cm, the term “microcarcinoma” may be employed (Fig. 25.62). In contrast, physiologic C-cell hyperplasia, usually *not* identified by standard H&E, is composed of discrete,

small (<50 cells) aggregates of normal appearing C-cells without associated fibrosis or amyloid. With increased experience, physiologic C-cells can be recognized by H&E, with calcitonin immunohistochemistry used as confirmation. This type of response is seen widely in aging, chronic disease, renal disorders, hyperparathyroidism, and lymphocytic thyroiditis, among other disorders.

**Medullary thyroid carcinoma:** The borders are irregular, circumscribed to encapsulated, with tumor cells extending out into the thyroid parenchyma, entrapping benign, uninvolved follicular epithelium (Fig. 25.63). These entrapped areas can be seen quite deep within large tumors (Fig. 25.64). In very large tumors, extension into adjacent soft tissues and neck organs may be present. The term “microcarcinoma” should only be applied to tumors less than 0.5 cm rather than the usual 1.0 cm, since in general, this cutoff is associated with less metastatic potential. Lymphovascular invasion is usually prominent, often associated with a high incidence of lymph node metastases. A host of different patterns of growth and cell types are observed in MTC, including solid sheets, organoid, lobular, trabecular, insular, glandular, tubular, and papillary patterns, variably comprising spindle, oncocytic, clear, and amphicrine cell types (Figs. 25.65 and 25.66). The various patterns of growth are separated by a fibrovascular stroma. The cells are round to oval, spindled to plasmacytoid, with ill-defined eosinophilic or amphophilic granular cytoplasm. Pigmentation is

**FIGURE 25.58**

(A) Normal C-cells have a para-follicular distribution with slightly basophilic cytoplasm. (B) Individual C-cells are calcitonin immunoreactive (heavy, dark, granular cytoplasmic immunoreactivity).

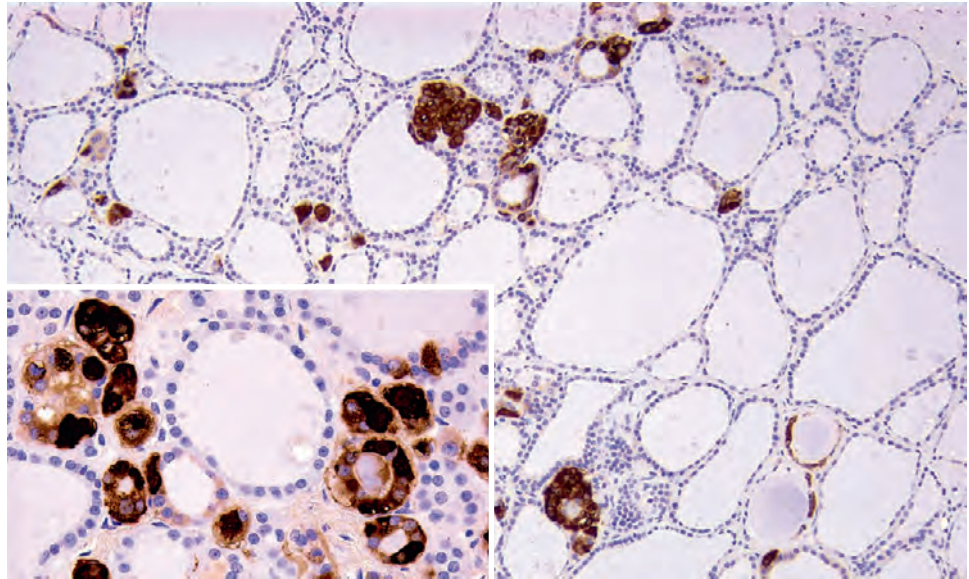
**FIGURE 25.59**

Ultimobranchial body remnants are called solid cell nests. These structures are seen around normal follicles with oval nuclei, coarse nuclear chromatin, and a lack of intercellular borders.

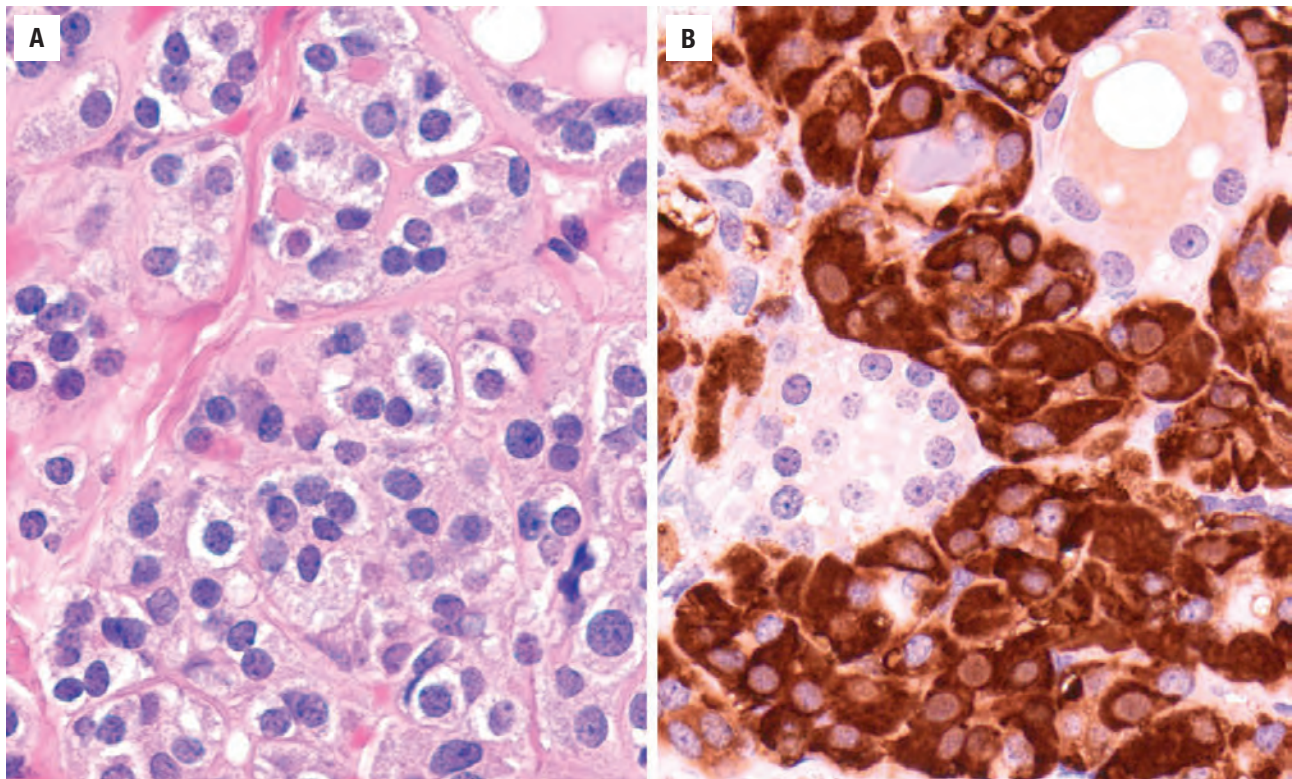
uncommon. The nuclei are usually round to oval and chromatin is coarse to stippled and “salt-and-pepper” in distribution (Fig. 25.67). Nucleoli are not prominent, except in the oncocyctic variant. Intranuclear cytoplasmic inclusions can be identified. Bi- and multinucleation is common, with moderate nuclear pleomorphism present.

An increased mitotic index and necrosis is usually identified only in large tumors. Amyloid, a homogeneous, acellular, eosinophilic, extracellular matrix material is seen in most cases (up to 90 %; Fig. 25.68). It has been demonstrated to be full-length calcitonin (pro-calcitonin) by spectrometric analysis, with katacalcin, a precursor



**FIGURE 25.60**

Small aggregates of C-cells are part of a physiologic response to chronic disease, aging, or other abnormalities. No nest contains more than 50 cells, the nodules do not coalesce, and there is no associated fibrosis or amyloid. *Inset* demonstrates small groups of cells, but usually still in a parafollicular distribution without destruction of the parenchyma (calcitonin immunohistochemistry).

**FIGURE 25.61**

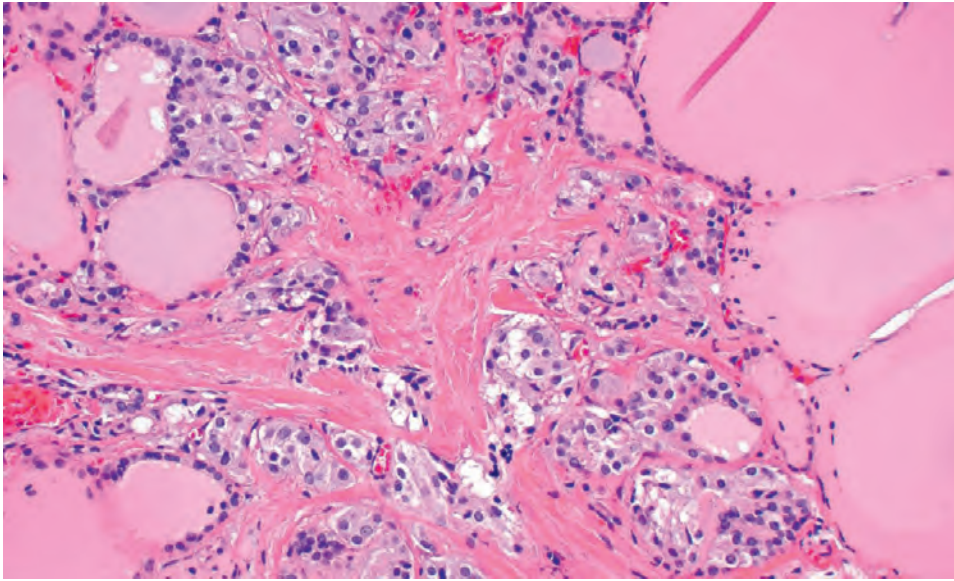
(A) Neoplastic C-cell hyperplasia shows aggregates of more than 50 C-cells with associated fibrosis. A small uninvolved thyroid follicle is present (*upper center*). (B) Calcitonin immunohistochemistry accentuates the cells around the thyroid follicles.

molecular, also present. Tumors without amyloid tend to have a worse prognosis. Mucin production is occasionally noted, but is of limited amount. Psammoma-like bodies may also be seen.

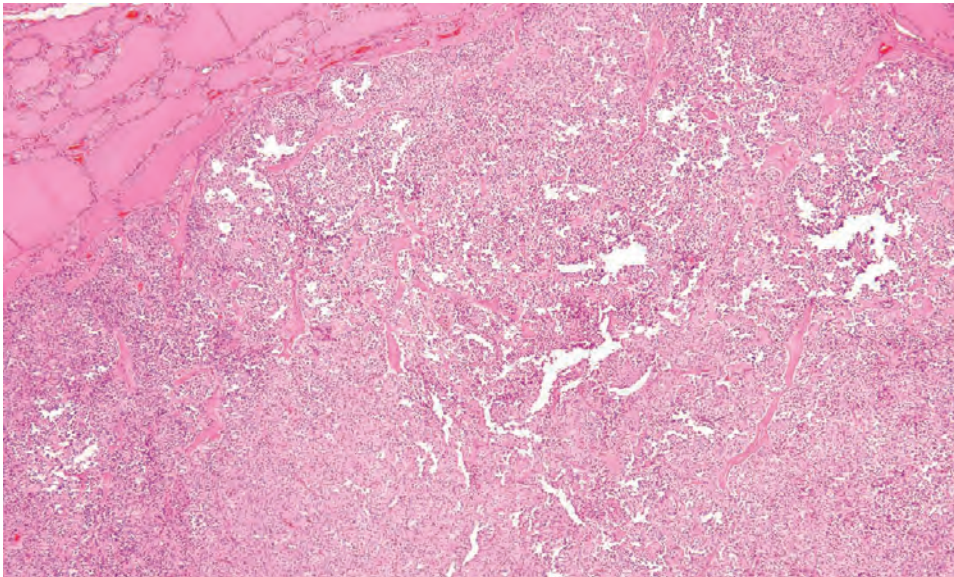
Numerous variants are recognized, but are of no specific clinical or management significance, but are often

confused with other tumor types: papillary/pseudopapillary, tubular/glandular, giant cell, small cell, spindle cell, oncocytic cell, clear cell, amphicrine, melanotic, squamous cell, paraganglioma-like, and angiosarcoma-like. Immunohistochemical confirmation is usually required.

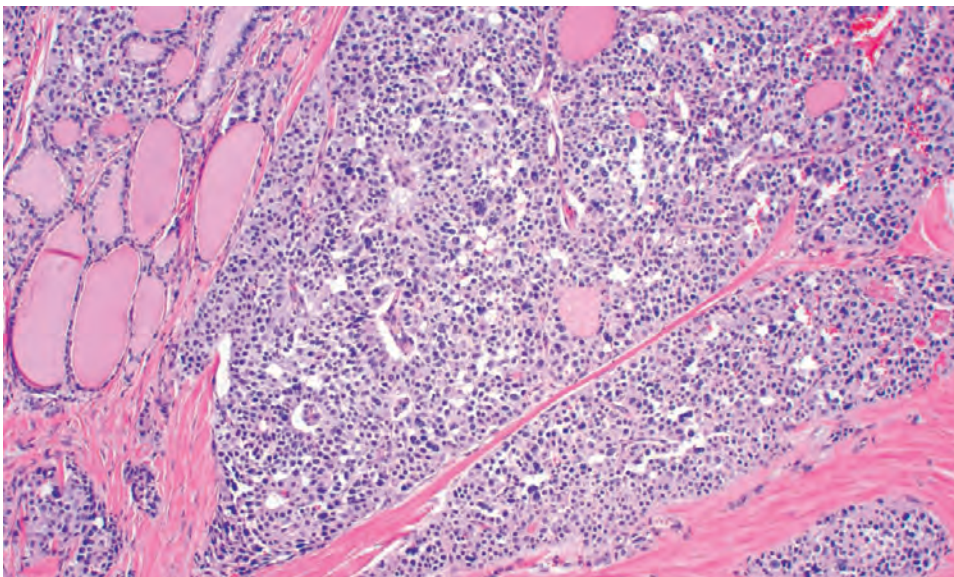


**FIGURE 25.62**

Microscopic medullary thyroid carcinoma shows destructive growth of more than 50 cells, fibrosis, and focal nuclear pleomorphism.

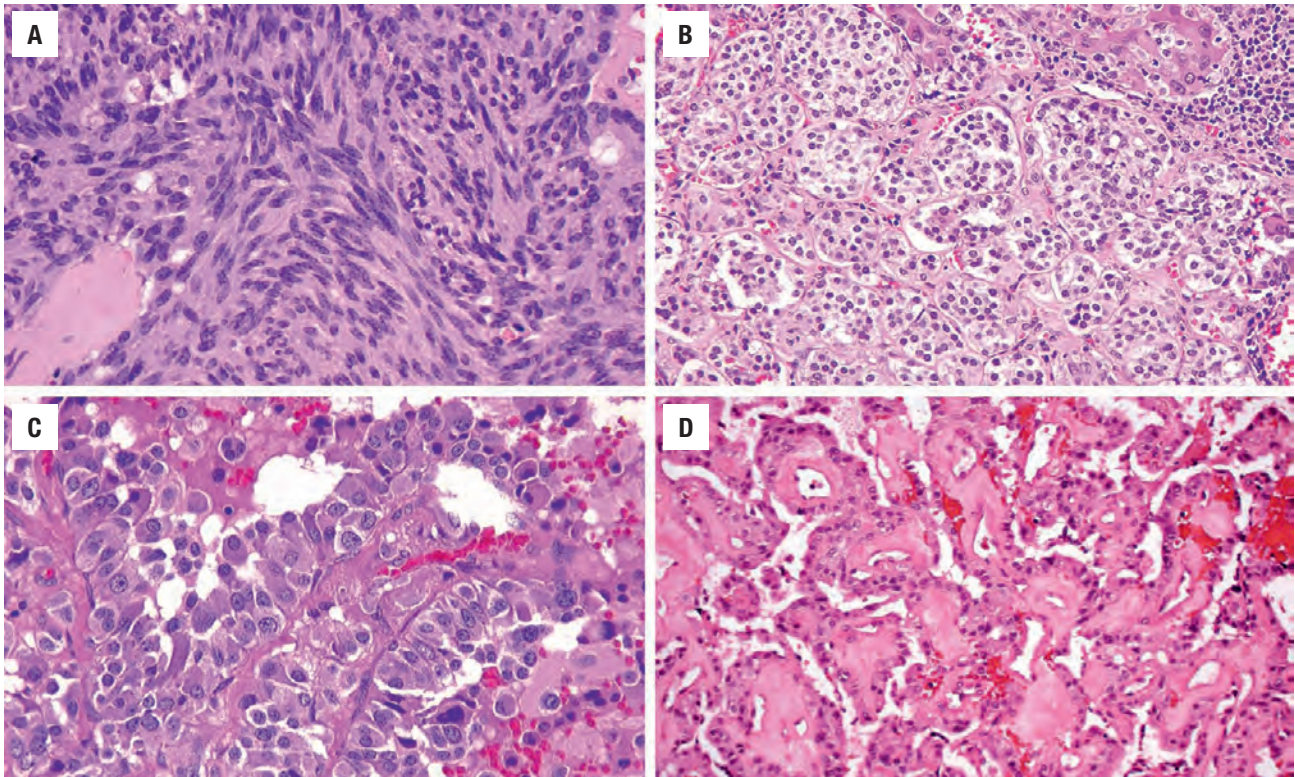
**FIGURE 25.63**

Predominantly solid growth pattern is noted in this medullary thyroid carcinoma. The interface between the tumor and the adjacent thyroid is irregular. Small wisps of pink amyloid are noted.

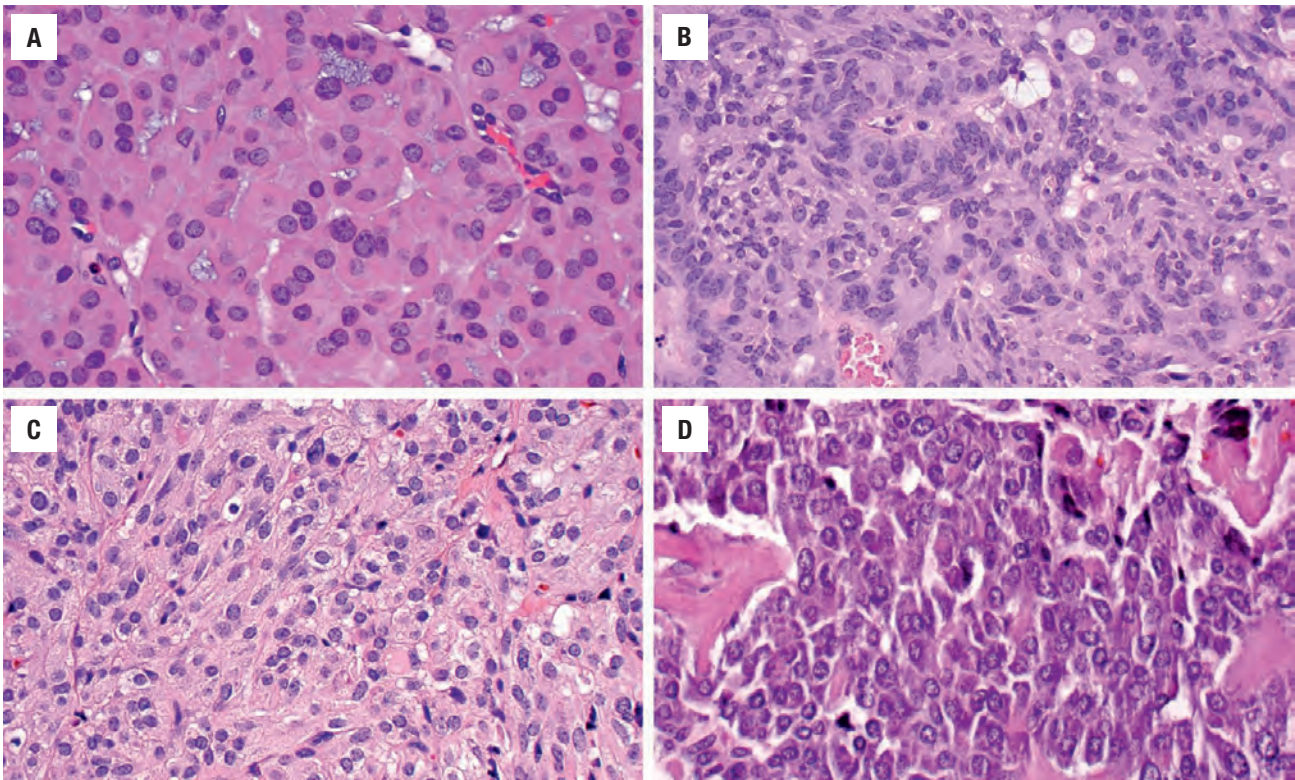
**FIGURE 25.64**

MTC has entrapped a number of benign thyroid follicular epithelial cells with associated colloid. There are more follicles on the left side of the image.



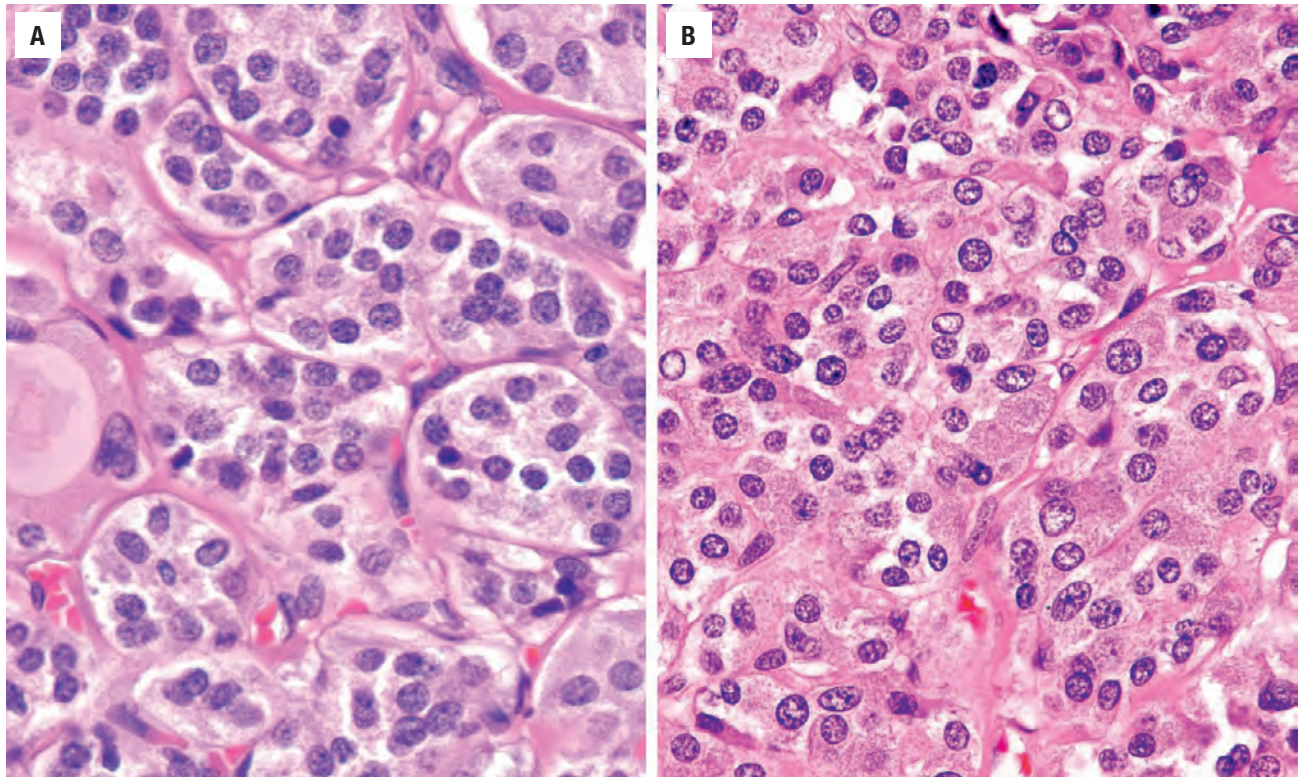


**FIGURE 25.65** Patterns of growth in MTC. (A) Spindled to fascicular. (B) Organoid. (C) Papillary architecture with basophilic granular cytoplasm. (D) Angiomatoid, simulating an angiosarcoma.

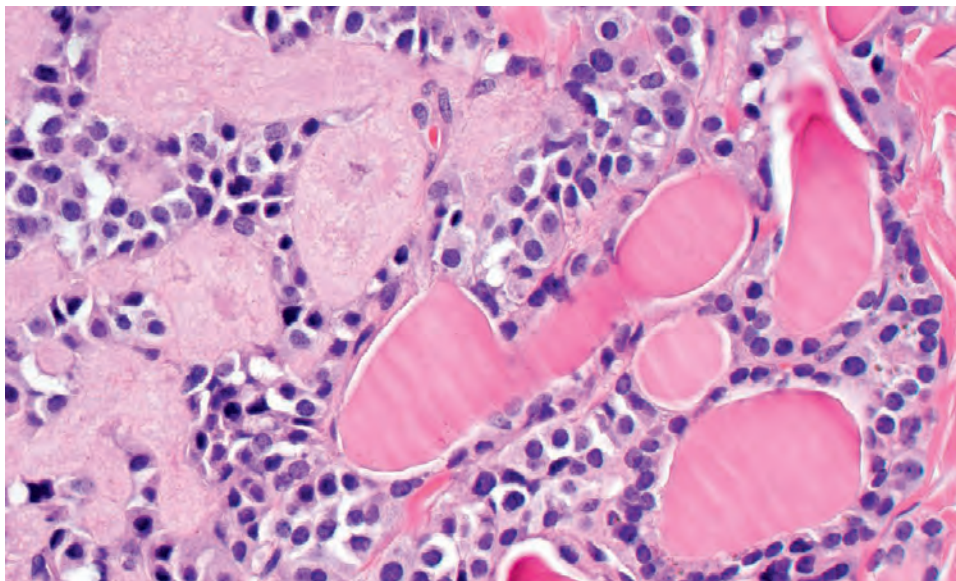


**FIGURE 25.66** Cell types in MTC. (A) Oncocytic. (B) Fusiform to columnar cells with basophilic, granular cytoplasm. (C) Spindled. (D) Plasmacytoid.



**FIGURE 25.67**

(A) Organoid pattern of growth with basophilic granular cytoplasm noted around nuclei with coarse, salt-and-pepper nuclear chromatin distribution. There is a single follicle on far left. (B) Follicular growth may mimic a follicular epithelial neoplasm. However, the nuclear chromatin is different.

**FIGURE 25.68**

Amyloid is common. *Left* side shows eosinophilic, amorphous, extracellular amyloid blending with surrounding tumor cells. Note the difference from the colloid (*right*), which is more brightly eosinophilic. These are entrapped thyroid follicles.



## ANCILLARY STUDIES

### HISTOCHEMICAL AND IMMUNOHISTOCHEMICAL FINDINGS

C-cells are easily accentuated by calcitonin (Fig. 25.69), CGRP, chromogranin, CD56, and synaptophysin, while keratin and polyclonal carcinoembryonic antigen (pCEA)

are also reactive. Rarely, CGRP is the only peptide positive. It is important to know that MTC is also TTF1 reactive although negative with thyroglobulin. Similarly, PAX8 is positive, but usually variable and weak.

Argyrophilic stains (Grimelius stain) can be employed, while the Fontana-Masson stain is negative. When amyloid is present, polarization of a Congo Red stain will give the characteristic apple-green birefringence. Alternatively,

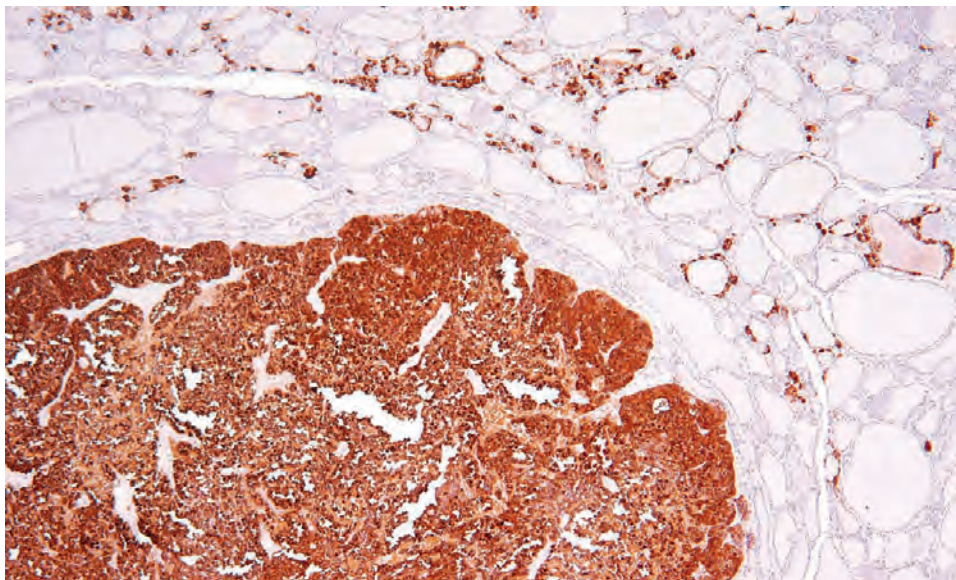


**FIGURE 25.69**

MTC is strongly and diffusely immunoreactive for calcitonin. Groups of C-cells in the background are highlighted around the MTC.

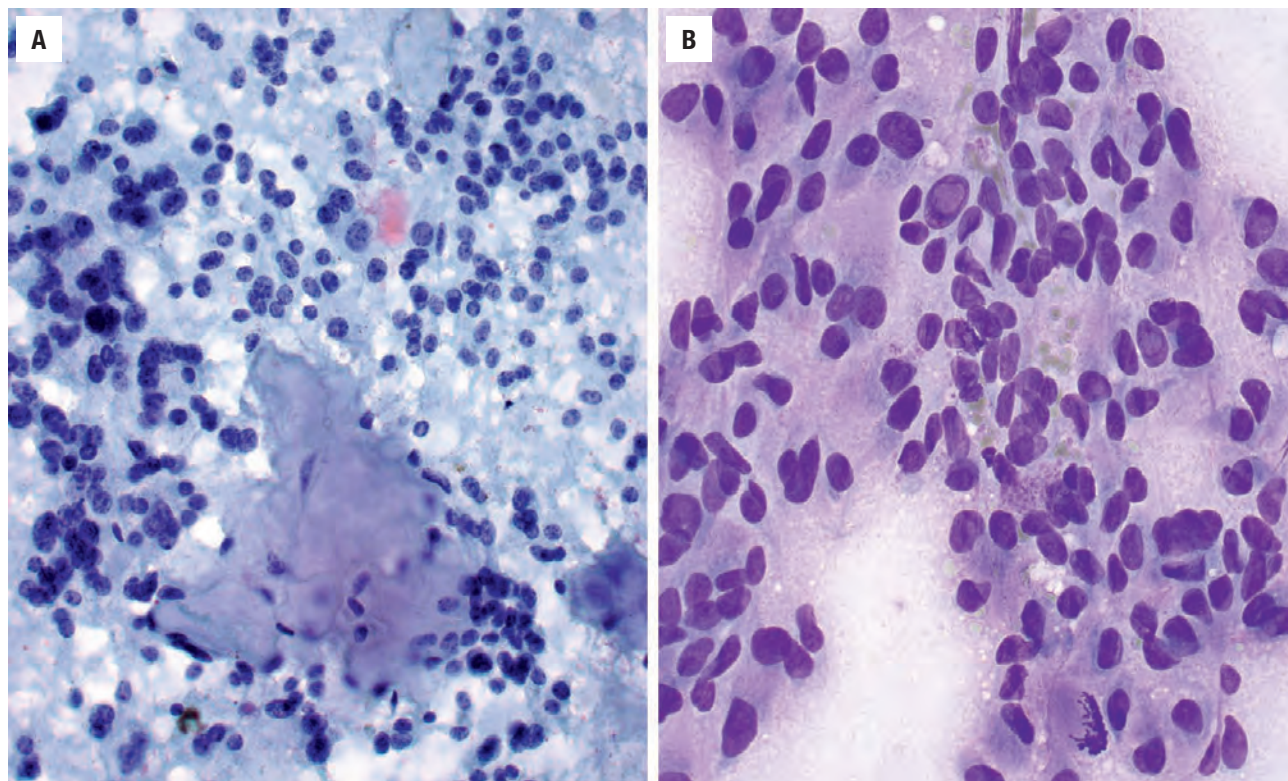


**FIGURE 25.70**

(A) Cellular aspirate with loosely cohesive tumor cells. Plasmacytoid architecture is prominent. There is nuclear pleomorphism as well as amorphous amyloid in the center (alcohol fixed, Papanicolaou stain). (B) There are clusters of cells with plasmacytoid and spindled cells. Note the intranuclear cytoplasmic inclusion and mitotic figure (air dried, Diff-Quik stain).

Crystal Violet yields purple metachromatic staining. Occasionally, amyloid immunohistochemistry may be performed, but it is a difficult stain to interpret due to significant diffusion artifacts.

#### FINE NEEDLE ASPIRATION

There is significant cytologic variability from case to case. Most aspirates are cellular with single cells or small, loosely cohesive clusters of cells (Fig. 25.70). Colloid is notably absent; however, the extracellular, homogeneous, amorphous eosinophilic clumps or spheres of amyloid (seen in about 60 % of aspirates) may sometimes be misinterpreted as colloid (Fig. 25.70). The tumor cells vary from round to oval, spindle-shaped, and polygonal. Bi- and multinucleation can be seen, along with moderate pleomorphism. The nuclear chromatin is stippled or coarsely granular (“salt-and-pepper”) with abundant, eosinophilic cytoplasm often eccentrically surrounding the nucleus. This plasmacytoid appearance is quite characteristic. Intranuclear cytoplasmic inclusions may be seen (Fig. 25.70). Air dried preparations often highlight the distinctive metachromatic red cytoplasmic granules.

#### MOLECULAR FINDINGS

Somatic *RET* mutations, most commonly the M918T mutation, have been shown to occur in 20 % to 80 % of sporadic MTC (the wide range is due to different detection techniques). Germline *RET* oncogene mutations are identified in all hereditary forms, although the mutations occur in different codons and with different degrees of penetrance. Germline mutations can be detected in peripheral blood samples rather than using tumor cells. *RAS* mutations are seen in some *RET* negative tumors, considered mutually exclusive.

#### DIFFERENTIAL DIAGNOSIS

Neoplastic C-cell hyperplasia (clusters of > 50 cells) may be mistaken for intraglandular spread of MTC, since fibrosis may be seen. However, the cells tend to have a more intense calcitonin immunoreactivity. SCNs and palpation thyroiditis can usually be separated by histology alone.

The differential diagnosis of MTC includes most of the primary tumors of the thyroid gland. Hyalinizing trabecular tumor, FC, papillary thyroid carcinoma, paraganglioma, amyloid goiter, undifferentiated carcinoma, and lymphoma may mimic MTC. Metastatic carcinomas are uncommon, although renal cell is the most frequent. Direct extension into the thyroid by laryngeal neuroendocrine carcinomas may occasionally cause diagnostic difficulty. Metastatic foci of MTC may be difficult to separate from other carcinomas, although immunohistochemical analysis for calcitonin, pCEA, and chromogranin aid in this distinction.

#### PROGNOSIS AND THERAPY

Clinical stage and inheritance pattern are most important in determining the patient's prognosis. If there is no metastatic disease, patients can enjoy nearly 100 % cure rates following surgery. This is especially true in tumors found incidentally (usually small and without metastasis) during screening for familial disease. Metastatic disease to cervical lymph nodes is common, while metastases to liver, lungs, and bone are less commonly identified. However, if there is metastatic disease or elevated calcitonin and/or CEA levels, the prognosis is more guarded and difficult to predict. Overall, there is between a 45 % and 85 % 10-year survival rate, dependent on stage. Survival is best for familial non-MEN related disease, followed by sporadic and MEN2A, which is better than MEN2B. Age (> 50 years) and TNM stage are the only independent prognostic factors. Extrathyroidal extension and postoperative persistent calcitonin elevation are also poor prognostic indicators. Patients with the M918T mutation tend to have a more aggressive clinical course.

Total thyroidectomy is the treatment of choice, with central lymph node dissection as clinically or radiographically indicated. Prophylactic thyroidectomy is used in patients with germline mutations. Specific *RET* mutations will dictate the specific age for the thyroidectomy: mutations in codon 611, 618, 620, and 634 mutations receive thyroidectomy before 5 years of age. Lymph node dissection is performed in tumors greater than 1 cm. Chemotherapy, somatostatin analogs, and targeted molecular therapy (tyrosine kinase inhibitors targeting *RET*) are being used with variable effectiveness. Parathyroid gland disease may also be present (50 % penetrance by age 82), especially if the MTC is familial, necessitating parathyroidectomy. Pheochromocytoma shows a 50 % penetrance by 68 years. <sup>131</sup>I radioablative therapy is useless since there is no thyroid hormone production. Follow-up of the patient's serum calcitonin and CEA levels, especially if elevated, is required to monitor for recurrence. Whenever MTC is found, the incidence of discovering a genetic form when evaluating relatives of the proband is elevated; thus, a valuable screening tool, irrespective of the specific technique employed (biochemical or molecular).

#### ■ PRIMARY THYROID GLAND LYMPHOMA

Thyroid gland lymphoma is defined as a primary lymphoma arising within the confines of the thyroid gland and usually associated with chronic LT. Acquired mucosa-associated lymphoid tissue (MALT) from autoimmune, immune deficiency, or inflammatory processes, results in a nodular or diffuse infiltrate of lymphoid cells, frequently with follicles and germinal centers, and associated



## PRIMARY THYROID GLAND LYMPHOMA—DISEASE FACT SHEET

### Definition

- Primary lymphoma arising within the thyroid gland and nearly always associated with chronic lymphocytic thyroiditis (LT)

### Incidence and Location

- About 2–5% of thyroid neoplasms
- About 2% of extranodal lymphomas

### Morbidity and Mortality

- Most arise within the setting of chronic LT and/or Hashimoto disease
- Mortality is grade and stage dependent

### Sex and Age Distribution

- Females > > males (4:1)
- Mean age: 7th decade

### Clinical Features

- Mass (often rapidly enlarging in high grade lymphoma) with associated pain, dysphagia, and hoarseness
- Hypothyroidism may be seen (usually a function of chronic LT)
- Associated cervical adenopathy in some cases

### Prognosis and Therapy

- Overall, 80% 5-year survival, but type, grade and stage dependent
- Poor prognosis: > 65 years, poor performance status, males, vocal cord paralysis, diffuse large B-cell lymphoma, high stage, extrathyroidal extension, vascular invasion
- Chemotherapy and radiation employed, dependent on grade and stage

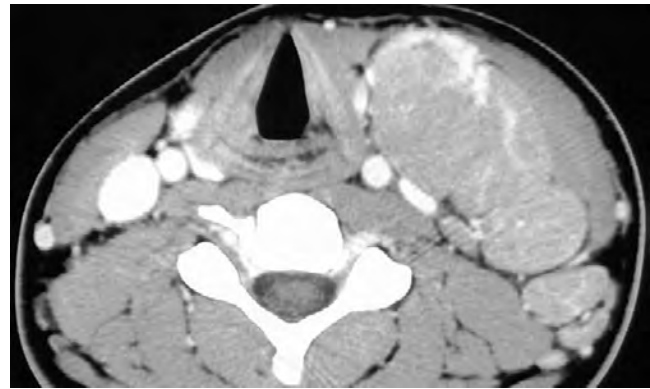


**FIGURE 25.71**

A computed tomography scan showing a large left thyroid gland mass, with associated lymphadenopathy. This is nonspecific, but was part of a thyroid diffuse large B-cell lymphoma.

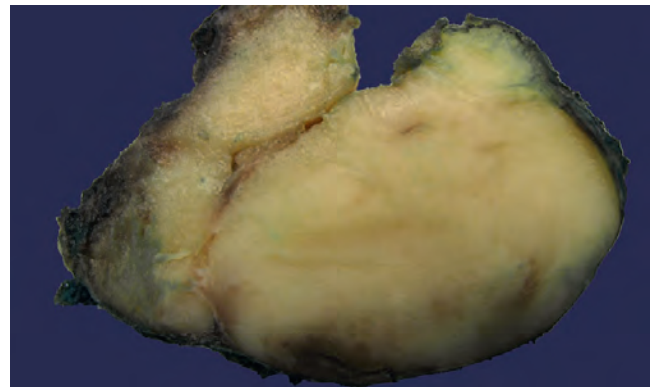


**FIGURE 25.72**

Malignant lymphoma with a characteristic “fish-flesh” appearance. Note the lack of any significant thyroid gland parenchyma.

oncocytic metaplasia of thyroid epithelium. There is a chronicity to the process. The MALT concept suggests a post-germinal center (activated) marginal zone B-cell forms the extranodal marginal zone B-cell lymphoma (EMZBCL). Although there is usually a lack of systemic involvement, regional lymph nodes may be affected. Follicular lymphoma (FL) and Hodgkin lymphoma (HL) are exceptional.

## CLINICAL FEATURES

Primary thyroid lymphomas account for about 2 to 5% of all thyroid gland neoplasms and about 2% of all extranodal lymphomas, and are essentially divided into two types: EMZBCL and diffuse large B-cell lymphoma (DLBCL). Primarily a disease of older individuals (mean, 65 years), there is a strong female to male predilection (4:1). Patients nearly always have a history of chronic LT (Hashimoto thyroiditis), the MALT setting considered

essential for the development of this lymphoma. In fact, there is an 80-fold increased risk of lymphoma in patients who have chronic LT. By definition, lymph node lymphomas directly extending into the thyroid are not considered primary thyroid lymphomas. Patients' symptoms are generally nonspecific, with the most common complaint a mass in the thyroid gland, with pain and obstructive symptoms, including dysphagia and/or hoarseness (seen in 30% of patients) related to compression. Hypothyroidism is usually due to underlying Hashimoto thyroiditis rather than the lymphoma. In DLBCL, the “end point” of many other types of B-cell lymphoma, patients often report a rapidly enlarging mass (Fig. 25.71). The duration of symptoms is usually short (mean, 4 months). Staging is the same as that used for lymphomas in general, with “E” added for extranodal. The perithyroidal lymph nodes may be involved, resulting in stage IE or IIE, followed by other lymph nodes or bone marrow. Patients usually lack constitutional or “B” symptoms (fever, profound night sweats, weight loss, anorexia).

**PRIMARY THYROID GLAND LYMPHOMA—PATHOLOGIC FEATURES****Gross Findings**

- Usually large (mean: 7 cm)
- Soft to firm, lobular and multinodular
- Effacement of the normal thyroid
- Cut surface is bulging, tan, and “fish-flesh”
- Usually homogeneous or mottled
- Extension into perithyroidal soft tissues

**Microscopic Findings**

- Extranodal marginal zone B-cell lymphoma and diffuse large B-cell lymphoma (DLBCL) with transitions between the two
- Constant background of chronic lymphocytic thyroiditis (LT)
- Extension into fat and skeletal muscle
- Atypical small lymphocytes, centrocytes, monocytoid B-cells, and plasma cells
- Dutcher bodies and Russell bodies
- Lymphoepithelial lesions (atypical lymphoid cells within the follicular epithelium) are diagnostic
- Diffuse architecture, large, atypical cells with increased mitotic figures suggests transformation into a DLBCL

**Immunohistochemical Findings**

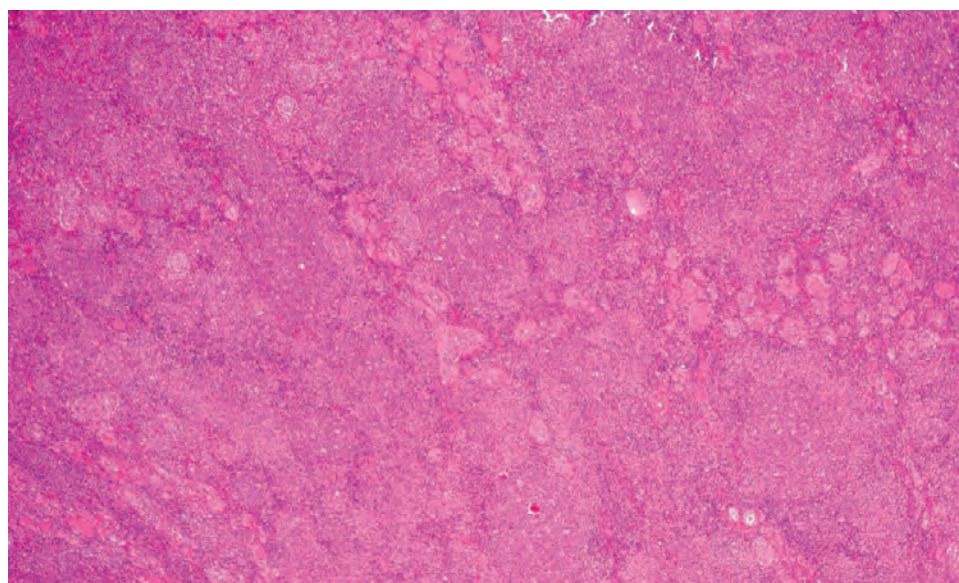
- CD20 (co-expressed with CD43 occasionally)
- CD79a, PAX5, and CD138
- BCL-2 in the colonizing B-cells within germinal centers
- Kappa or Lambda light chain restriction
- EMZBCL: Negative CD5, CD10, BCL6
- Keratin highlights the lymphoepithelial lesions

**Fine Needle Aspiration**

- Marginal zone B-cell lymphomas are a dispersed, noncohesive admixture of lymphocytes, centrocytes, monocytoid B-cells, immunoblasts, plasma cells, and histiocytes—perhaps indistinguishable from a LT
- DLBCL aspirates are hypercellular with dyscohesive, large, atypical neoplastic cells

**Pathologic Differential Diagnosis**

- Lymphocytic thyroiditis, undifferentiated carcinoma, myeloid sarcoma, melanoma, ectopic thymoma

**FIGURE 25.73**

Whereas lymphocytic thyroiditis can be seen in a few areas, there is a pseudofollicular to nodular effacement of the thyroid parenchyma by this MALT-like lymphoma.

**PATHOLOGIC FEATURES****GROSS FINDINGS**

The lymphomas are often large (mean, 7 cm), firm to soft, lobulated, and may be either a solid or cystic mass involving one or both thyroid lobes. The cut surface is often bulging, pale, with a “fish-flesh,” uniform, homogeneous to mottled appearance (Fig. 25.72). Foci of hemorrhage and necrosis are frequently noted. Extension into the surrounding soft tissues is common.

**MICROSCOPIC FINDINGS**

Lymphomas of the thyroid gland virtually always arise in the setting of chronic LT, whether part of clinical Hashimoto thyroiditis or not. There is a vaguely nodular to diffuse heterogeneous effacement of the thyroid gland (Fig. 25.73). Perithyroidal extension into fat and skeletal muscle (Fig. 25.74) is common, while lymphovascular invasion is more common in higher-grade tumors. Atrophy and fibrosis are frequently present in the adjacent thyroid gland parenchyma. Thyroid lymphoma is divided into two main groups: EMZBCL: 30% to 40% of cases and



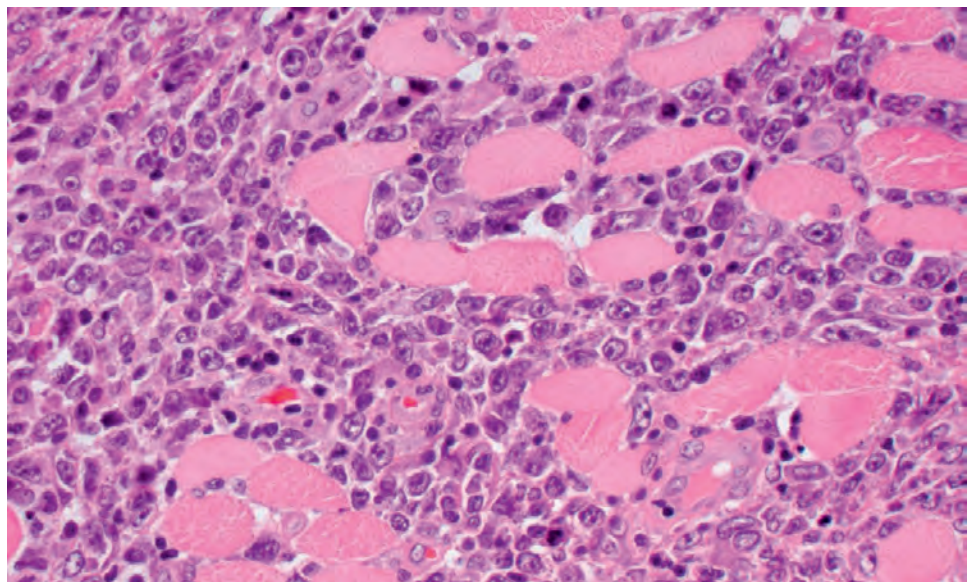
DLBCL: 60 % to 70 % of cases. In cases of EMZBCL, the B-cell infiltrate is composed of a heterogeneous population of atypical small lymphocytes, marginal zone (centrocyte-like) small cleaved cells, monocytoid B-cells, scattered large immunoblasts and centroblast-like cells, and plasma cells (Figs. 25.75 and 25.76). Monocytoid B-cells are monotonous populations of atypical lymphoid cells with abundant, pale cytoplasm with lobulated or kidney-shaped nuclei. Reactive germinal centers, which may often demonstrate colonization or follicle lysis by the neoplastic cells, are invariably present. These cells yield a darker zone within follicles on low-power examination. However, the follicular architecture may recapitulate a follicle center lymphoma, which is an uncommon tumor type in the thyroid gland. Lymphoepithelial lesions, which represent infiltration of epithelial follicular structures by atypical neoplastic B-cells, are a consistent feature and present in two forms: (1) rounded balls or masses, filling and distending the lumen

of the thyroid follicles (“MALT balls”; Fig. 25.77) or (2) single or aggregated lymphocytes within or between follicular epithelial cells (Fig. 25.78). Plasma cells (Fig. 25.79) and plasmacytoid cells with Dutcher bodies or cytoplasmic immunoglobulin (Mott cells; Fig. 25.80) are also seen, occasionally simulating a plasmacytoma. Concurrent disease within the gastrointestinal tract, salivary gland, lung, or breast may be present.

There may be single or multifocal areas of large cell transformation adjacent to the low-grade component, suggesting a transformation, transition, or “de-differentiation.” Alternatively, DLBCL may occur in the absence of any recognizable, pre-existent low-grade areas (Fig. 25.81). There are usually sheets of large cells that show a spectrum of cytologic features that resemble centroblasts, immunoblasts, monocytoid B-cells, and plasmacytoid cells (Fig. 25.82). Focal Reed-Sternberg-like (Fig. 25.83) or Burkitt-like cells may be noted that are

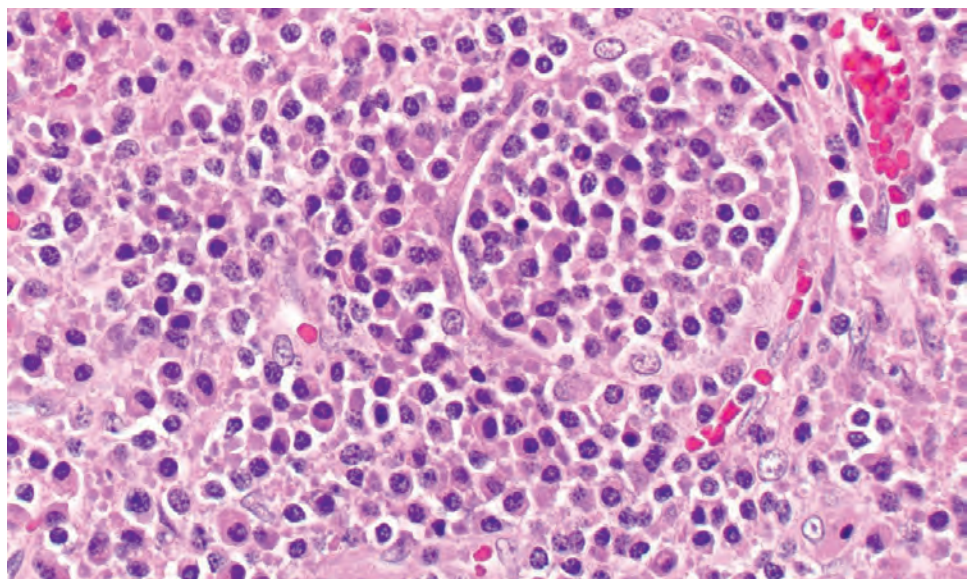
**FIGURE 25.74**

There are many plasmacytoid to centrocyte-like lymphoid cells infiltrating between skeletal muscle bundles in this lymphoma.

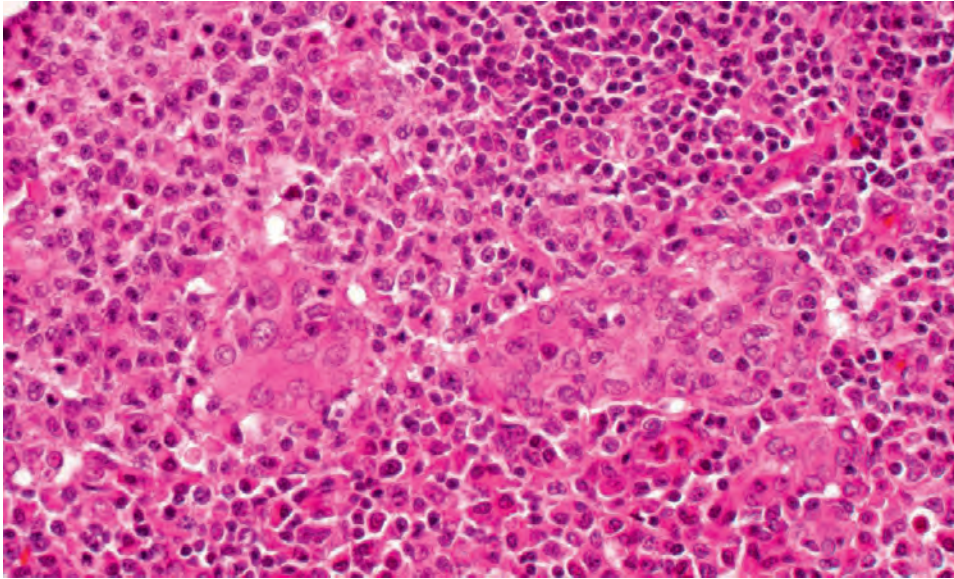


**FIGURE 25.75**

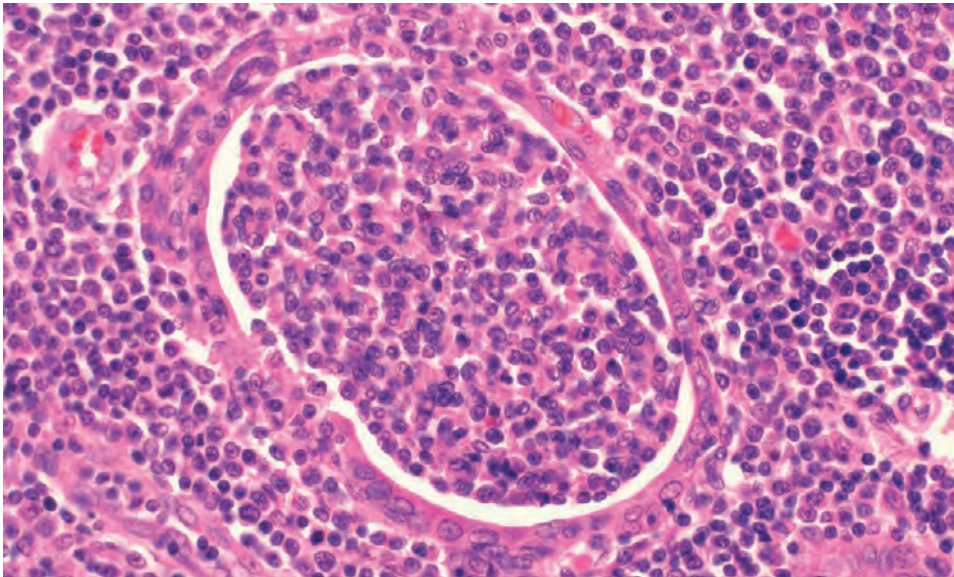
Atypical small lymphocytes, centrocyte-like cells, and monocytoid B-cells are arranged in sheets and small clusters, growing into the follicular epithelium of the thyroid gland (*upper*). Note the numerous plasmacytoid cells.



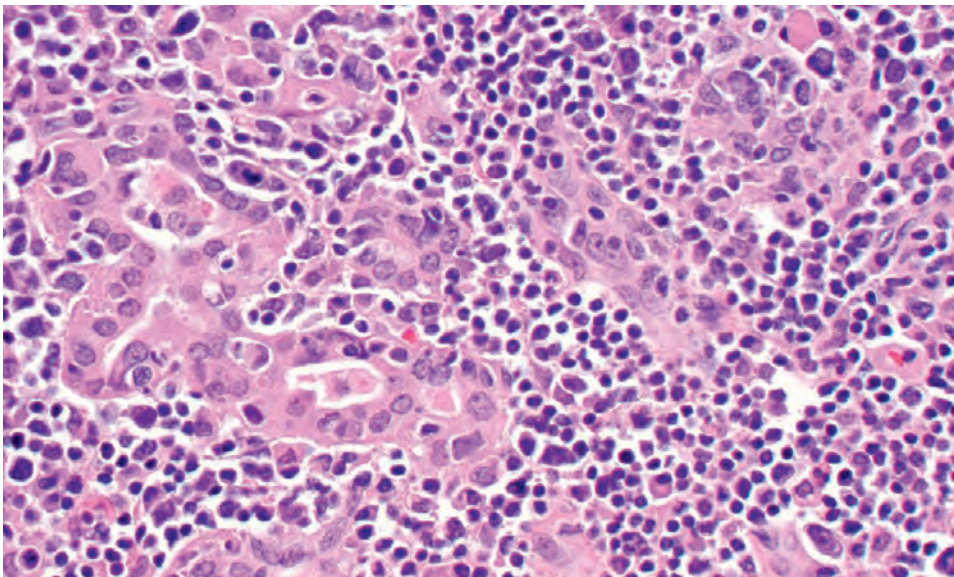


**FIGURE 25.76**

Monocytoid B-cells have an "epithelioid" appearance. Note the thyroid cells in the center, surrounded by plasmacytoid cells (*lower*) and monocytoid cells (*upper*).

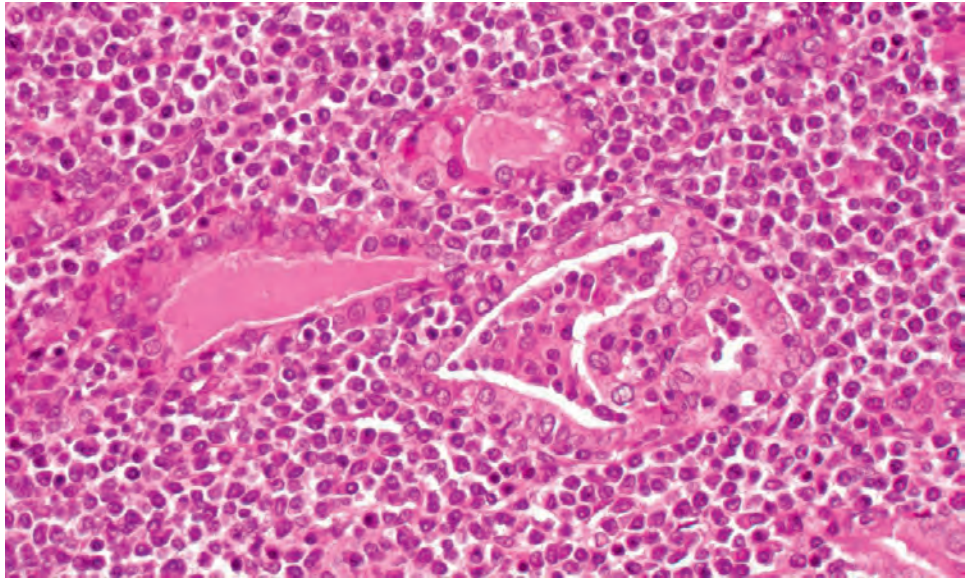
**FIGURE 25.77**

Masses of lymphoid cells are noted distending a thyroid follicle. This type of lymphoepithelial lesion is referred to as a "MALT ball."

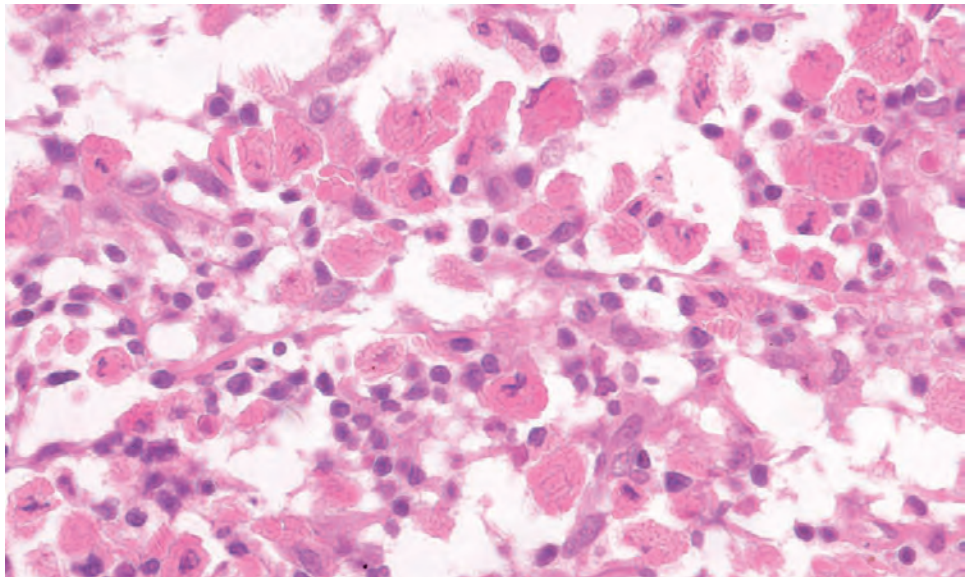
**FIGURE 25.78**

This lymphoepithelial lesion shows destruction of the follicular epithelium by the atypical lymphoid elements, which are seen effacing the background tissue.

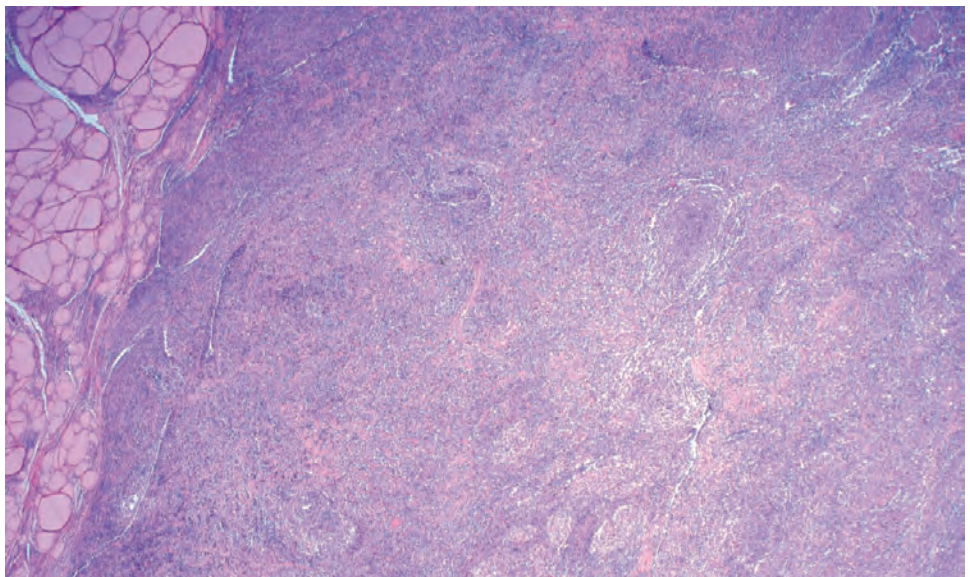


**FIGURE 25.79**

Prominent plasmacytoid differentiation is noted with Dutcher bodies (intranuclear cytoplasmic inclusions) in this MALT lymphoma. There is also a prominent lymphoepithelial lesion.

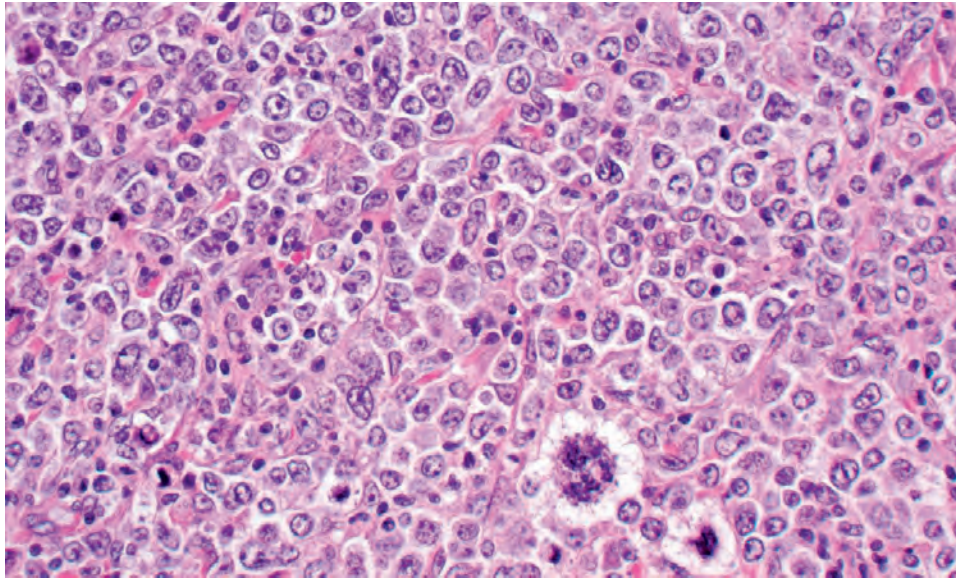
**FIGURE 25.80**

Crystalline type immunoglobulins are seen filling the cytoplasm of the neoplastic plasmacytoid cells of this EMZBCL.

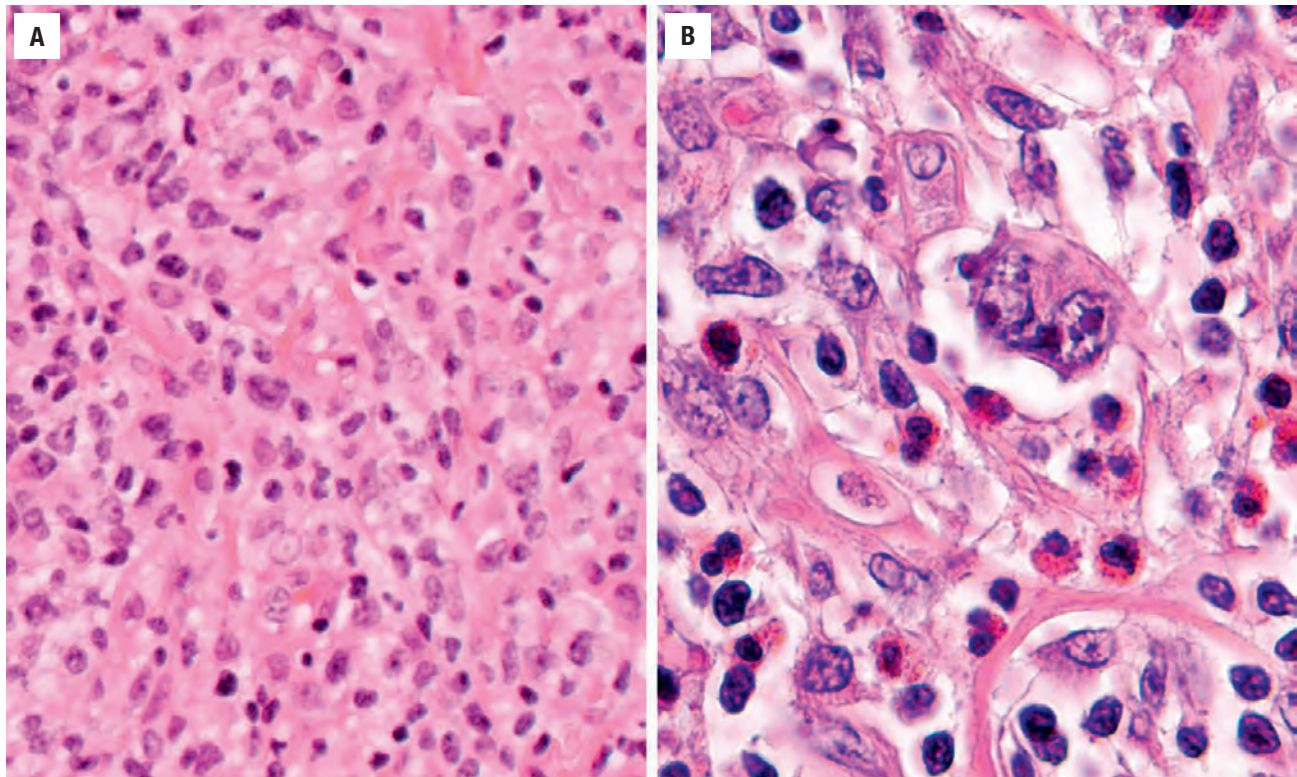
**FIGURE 25.81**

Thyroid tissue (*left*) has been replaced by a diffuse, large cell population of centroblastic-like B-cells in this diffuse large B-cell lymphoma.



**FIGURE 25.82**

Sheet-like growth of centroblast-like cells immunoblasts and monocytoid cells with significant atypia in this diffuse large B-cell lymphoma. Note the pleomorphism and mitoses.

**FIGURE 25.83**

(A) Large, cleaved cells are admixed with small cleaved lymphocytes in this diffuse large B-cell lymphoma (DLBCL). (B) Eosinophils and Reed-Sternberg-like cells are focally identified in this DLBCL.

associated with brisk mitotic activity, apoptosis, and a starry sky pattern (Fig. 25.84). Vascular invasion is seen more commonly in high-grade tumors. The uninvolved thyroid parenchyma may have adenomatoid nodules, adenomas, or carcinoma (papillary much more often than FC). T-cell lymphomas, extramedullary plasmacytoma, Burkitt lymphoma, and classical HL are rare in the thyroid gland.

## ANCILLARY STUDIES

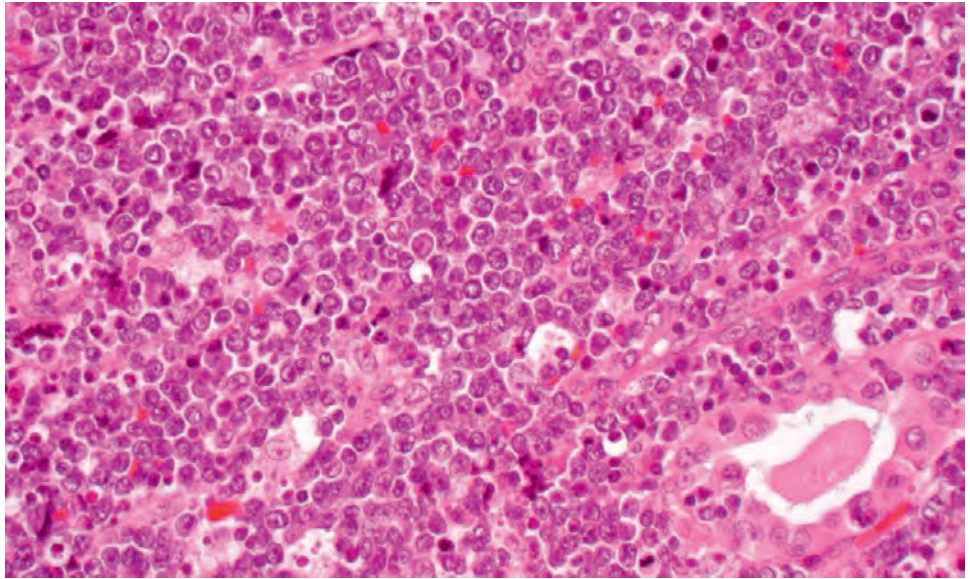
### IMMUNOHISTOCHEMICAL FINDINGS

The B-cell immunophenotype of EMZBCL and DLBCL is confirmed by immunoreactivity for CD20 (Fig. 25.85), CD79a (Fig. 25.86), PAX5, and/or CD138. BCL-2

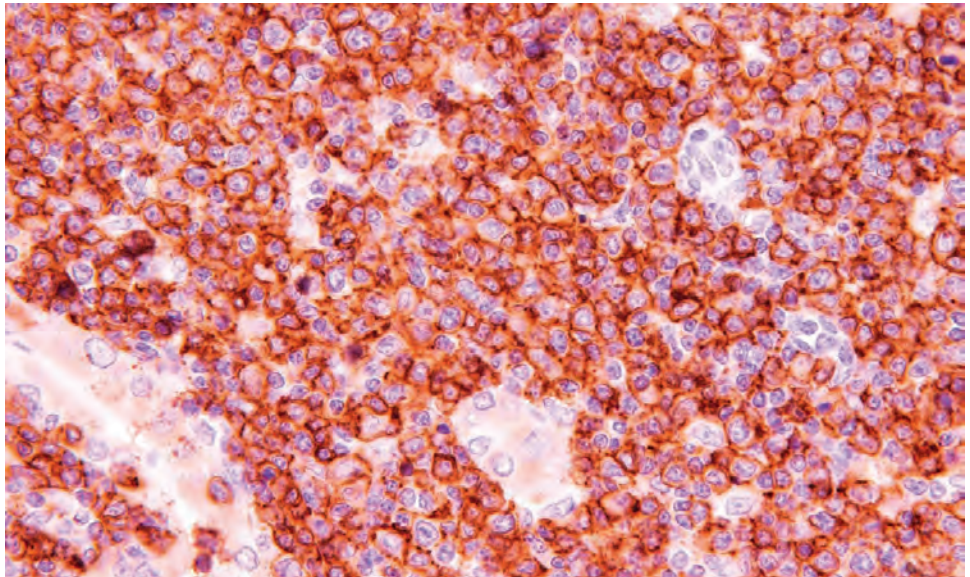


**FIGURE 25.84**

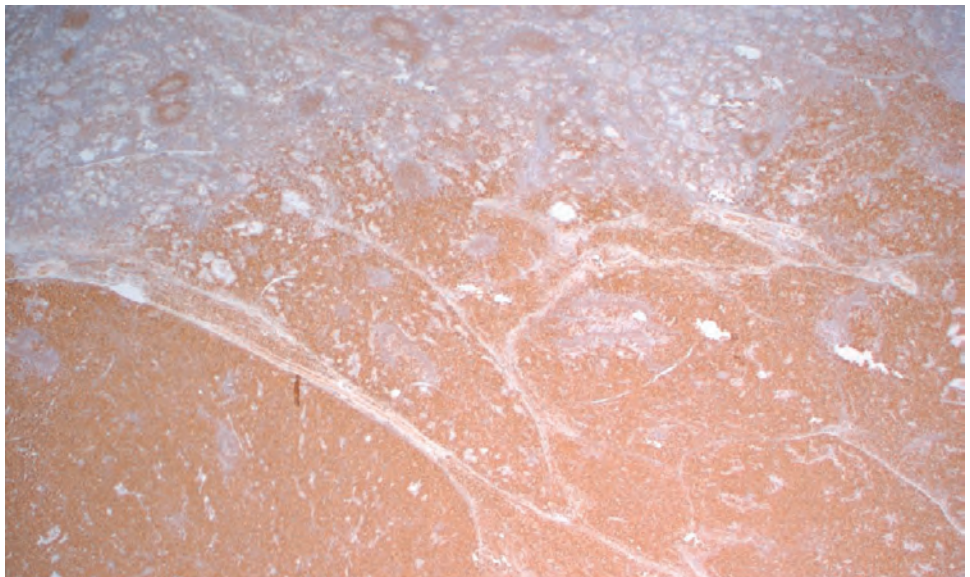
Burkitt-like pattern shows brisk mitotic activity, apoptosis, and a “starry-sky” pattern with numerous tingible body macrophages in this diffuse large B-cell lymphoma. There is a thyroid follicle (lower right).

**FIGURE 25.85**

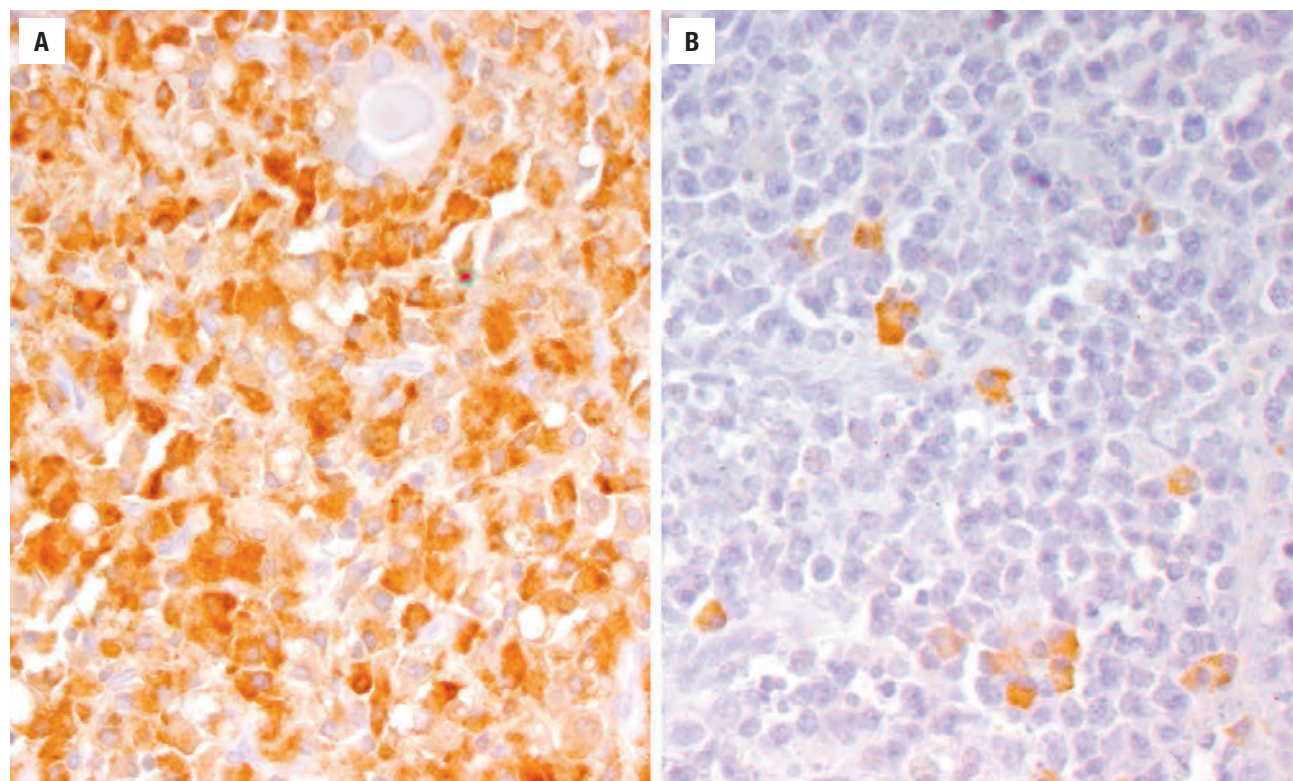
CD20 strongly and diffusely highlights the large, cleaved cells in this lymphoma. Note the unstained thyroid follicular epithelium.

**FIGURE 25.86**

Chronic lymphocytic thyroiditis (top) shows focal CD79a staining, while the EMZBCL shows strong and diffuse staining of most of the cells.





**FIGURE 25.87**

(A) Kappa-restricted population of atypical lymphoid cells. (B) Lambda highlights only rare plasma cells in this EMZBCL.

reactivity in the neoplastic, colonizing B-cells (but not in the residual, reactive germinal center cells) is also characteristic. Overall, the cells are negative for CD5, CD10, and BCL-6. Immunoglobulin light chain restriction for either  $\kappa$  or  $\lambda$  may be demonstrated (Fig. 25.87), especially in the plasma cell or plasmacytoid component. Coexpression of CD43 with CD20 may be seen in a small percentage of EMZBCL. An antibody to cytokeratin will highlight the epithelial remnants in the lymphoepithelial lesions (Fig. 25.88). FLs are divided by BCL2 rearrangement, separated by CD10 and BCL2 reactivity. Additional molecular (*FOXP1-IGH*; *BLC6*, *MYC*) and cytogenetic studies can be performed to confirm the nature of the tumor.

#### FINE NEEDLE ASPIRATION

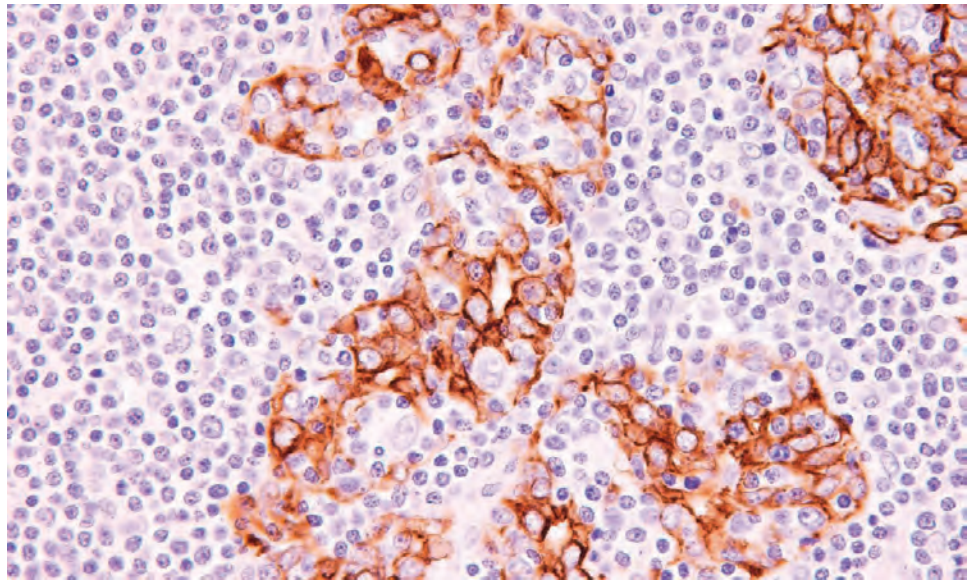
The full spectrum of dispersed, noncohesive admixture of lymphoid elements will often be present within the cellular aspirates from an EMZBCL (Fig. 25.89), making separation from LT nearly impossible. There may be a better yield if there is a single or dominant mass lesion rather than diffuse enlargement. However, there is usually an absence of tingible body macrophages in lymphoma. Similarly, thyroid follicular epithelium is usually absent. Moreover, the dyscohesive, monotonous population of large atypical cells (2 to 3 $\times$  the size of mature lymphocytes) with scant cytoplasm and large

nuclei with vesicular nuclear chromatin and background lymphoglandular bodies suggest a diagnosis of DLBCL. Immunohistochemistry, flow cytometry, and/or Ig heavy chain gene rearrangements can be performed on aspiration material.

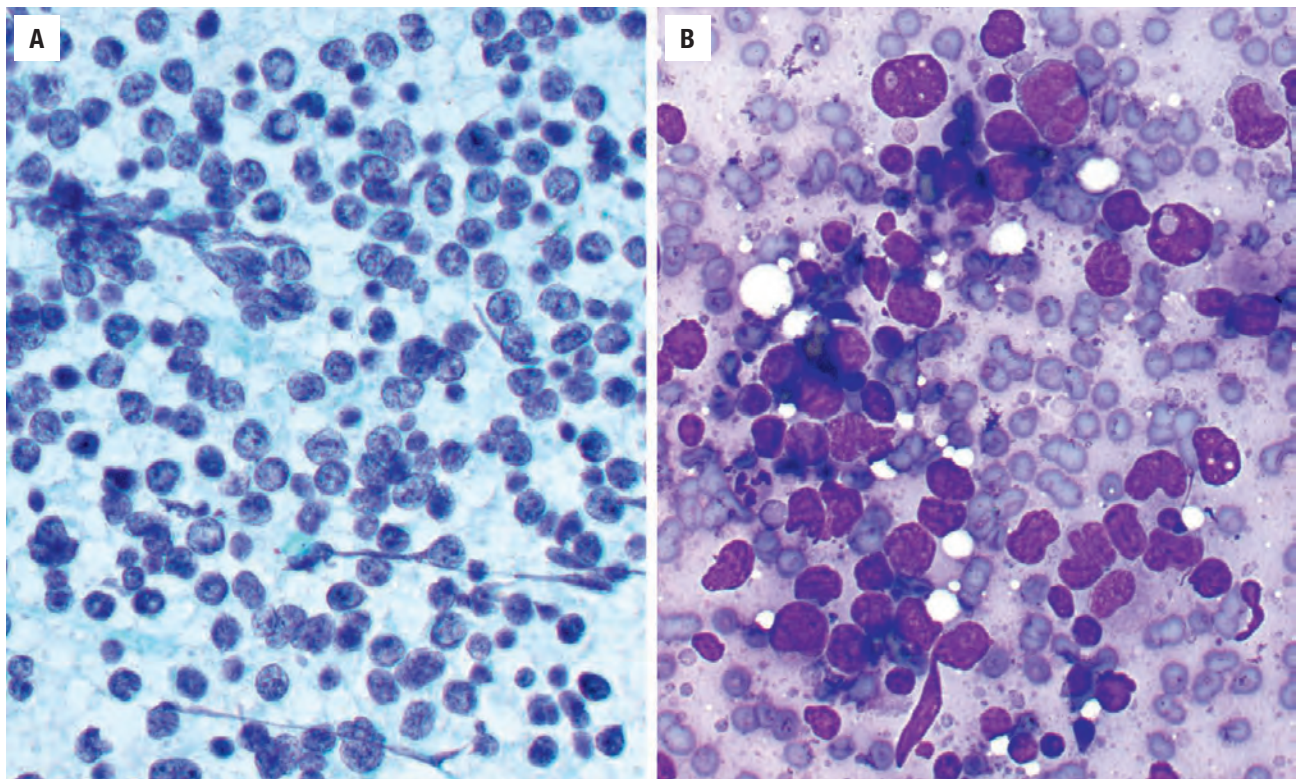
#### DIFFERENTIAL DIAGNOSIS

The distinction between EMZBCL and *chronic lymphocytic thyroiditis* may be difficult at times. In EMZBCL, the diffuse pattern, colonization of the benign germinal center, Dutcher bodies, and lymphoepithelial lesions should help with the separation. Usually there is no cytologic atypia and there may be oncocytic change in the thyroid follicular epithelial cells. In a few cases, however, immunohistochemical, flow cytometric, or molecular genetic analyses may be required. DLBCL may be indistinguishable from *undifferentiated carcinoma*, *melanoma*, or *myeloid sarcoma* by histology alone and may require a more thorough antibody panel, including CD45RB, CD20, cytokeratin, S100 protein, SOX10, Melan-A, and HMB45 and myelomonocytic markers (CD11b, CD14) to make the correct diagnosis. Rarely, an *ectopic thymoma* has both epithelial and lymphoid elements, but lacks lymphoepithelial lesions, a nondestructive pattern of growth, and would be positive with CD5.



**FIGURE 25.88**

A lymphoma immunostained for keratin highlights the residual thyroid follicles which are extensively infiltrated by neoplastic lymphoid cells, creating lympho-epithelial lesions.

**FIGURE 25.89**

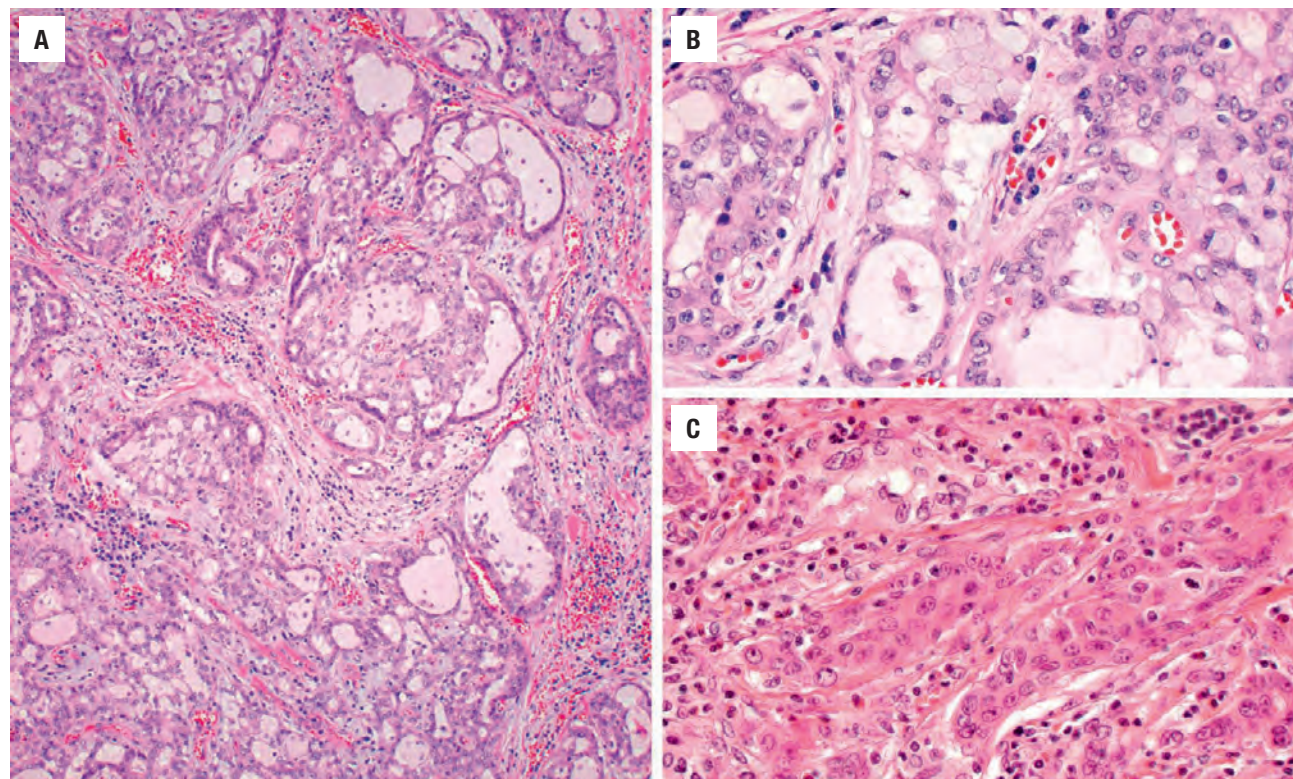
Fine needle aspiration is usually cellular without thyroid epithelial cells. (A) Enlarged lymphoid cells with lymphoglandular bodies in the background (alcohol fixed, Papanicolaou stain). (B) Greatly enlarged atypical lymphoid cells with background lymphoglandular bodies (air dried, Diff-Quik stain).

### PROGNOSIS AND THERAPY

The prognosis of thyroid MALT-type lymphomas is very favorable in general, although the prognosis is stage and histology dependent. In general, localized (stage IE or IIE) tumors with a low grade histology have an excellent prognosis (> 95 % disease specific 5-year survival),

whereas those with either a large cell component, or diffuse large B-cell type, have a worse overall survival (~30 % to 70 % disease specific 5-year survival for stage IVE versus IE, respectively) and are much more likely to die of disease. Poor prognostic features include age more than 65 years, poor performance status, males, vocal cord paralysis, DLBCL, high stage, extrathyroidal extension, and vascular invasion. Nearly all patients with



**FIGURE 25.90**

Mucoepidermoid carcinoma. (A) Cysts and small glands with intervening fibrosis. (B) Transitional, epidermoid, and mucocytes are easily identified. (C) There are a large number of eosinophils, along with areas of squamous and mucinous differentiation.

stage IVE die with disease. While surgery is used to “debulk” or decompress and obtain tissue for the diagnosis, chemotherapy and radiation (including hyperfractionation) are standard, with the regimen determined by the histologic grade and stage.

## ■ UNCOMMON THYROID NEOPLASMS

### MUCOEPIDERMOID CARCINOMA

Mucoepidermoid carcinoma is a rare, malignant thyroid tumor with a histologic appearance similar to its low-grade salivary gland counterpart. There are two histologic variants: mucoepidermoid carcinoma (MEC) and sclerosing mucoepidermoid carcinoma with eosinophilia (SMECE). While distinctive histologically, they have a similar indolent clinical behavior. Most cases develop in the setting of chronic LT, within which there is squamous metaplasia. Females are affected more often than males (7:1 for SMECE; 2:1 for MEC), with a mean age at presentation in the 5th to 7th decades of life. Patients present nonspecifically with a neck mass. Surgery is the treatment of choice, yielding a good long-term prognosis, although metastatic disease to lymph nodes can be seen

(in up to 35 % of patients) and extrathyroidal extension suggests a more aggressive behavior.

Tumors are ill-defined and unencapsulated, and predominantly composed of a solid mass. There is nearly always a background of chronic LT, specifically fibrosing Hashimoto thyroiditis in the SMECE type, often with an excess of eosinophils. However, prominent cystic foci may be seen. The tumor is composed of intertwined cords and nests of cells within a fibrous stroma (Fig. 25.90). As its name implies, the proliferation includes squamous cells admixed with mucocytes. The squamous cells have mild pleomorphism, increased nuclear to cytoplasmic ratio, round nuclei with prominent nucleoli, and eosinophilic cytoplasm. Horny pearl formation, individual cell keratinization, and intercellular bridges are present. Mucous cells have abundant clear to foamy appearing cytoplasm and peripherally located hyperchromatic nuclei (Fig. 25.90). Ciliated cells may be seen. Hyaline bodies resembling colloid may be seen in the cytoplasm of mucocytes. Intratumoral sclerosis composed of thick, acellular hyalinized bands of tissue can be seen. Psammoma bodies are occasionally present. Concurrent papillary thyroid carcinoma is seen in up to 50 % of cases, and may show areas of blending-transition, even though it is considered a distinct tumor type. Mucicarmine will highlight intracytoplasmic and intraluminal mucin. The epidermoid cells will be positive with keratins (high and low molecular weight), CK5/6, p63, PAX8, CD10, and galectin-3, while



**UNCOMMON THYROID GLAND NEOPLASMS—FACT SHEET****Mucoepidermoid Carcinoma**

- Low grade malignant thyroid tumor with histology identical to salivary gland tumors
- Painless neck mass usually in middle-aged females, managed by surgery, with an excellent prognosis
- Unencapsulated tumor with squamous/epidermoid cells and mucous cells
- Eosinophils often present, but lymphoplasmacytic infiltrate with sclerosis also seen
- Positive with CK5/6, p63, PAX8, CD10, and galectin-3

**Squamous Cell Carcinoma**

- Primary thyroid squamous cell carcinoma without mucocytes or direct extension from adjacent organs
- Older female patients (2:1 F:M) who present with a rapidly enlarging neck mass
- Radical surgery and radiotherapy still has a poor prognosis, with frequent metastases
- Widely invasive tumor with extrathyroidal extension, composed of cohesive sheets, ribbons, and nests of cells with polygonal to spindle shape
- Keratinization, keratin pearl formation, high mitotic index
- Positive with cytokeratin, CK5/6, CK19, p63, p40

**Spindle Cell Tumor With Thymus-Like Differentiation**

- A highly cellular biphasic tumor showing spindle-shaped epithelial cells that blend with glandular structures, showing primitive thymic differentiation
- Occurs in young female (2:1 F:M) patients with an asymptomatic thyroid mass
- Prolonged, indolent course after surgery
- Firm to hard, white-tan and fleshy, occasionally with cysts, up to 12 cm
- Spindle-shaped cells arranged in short, reticulated, intersecting, and streaming, tight to loose fascicles or bundles which merge with epithelial cells separated into lobules by dense fibrosis
- Epithelial cells are arranged in glands, tubules, papillae, or sheets
- Abrupt keratinization can be seen
- Delicate nuclear chromatin in both cell types
- Positive: CK-pan, CAM5.2, CK7, CD117, and INI1 (intact)

**Intrathyroid Epithelial Thymoma/Carcinoma Showing Thymus-Like Differentiation**

- Primary thyroid gland neoplasm that is architecturally and cytologically similar to thymic epithelial tumors
- Slightly more common in women, usually in the 5th decade
- Asymptomatic thyroid mass, often of the lower thyroid lobes
- Metastatic disease at presentation in up to 50% of patients
- Prolonged, indolent course after surgery and radiation
- Firm to hard, white-tan and fleshy, up to 12 cm, often infiltrative tumor
- Solid, nests and lobules, with an infiltrative growth
- Epithelioid, syncytial cells with large vesicular-appearing nuclei, pleomorphism, and prominent nucleoli
- Squamous differentiation is noted, often abrupt
- Dense fibrosis with prominent lymphoplasmacytic infiltrate
- Positive with HMWK, p63, CD5, CD117, PAX8, bcl-1, and GLUT-1

**Leiomyoma**

- Primary thyroid gland benign smooth muscle tumor
- Young patients, who present with small tumors

- Bundles or intersecting fascicles of bland smooth muscle cells, with blunt-cigar shaped nuclei and paranuclear vacuoles
- Positive: SMA, MSA, desmin, caldesmon, calponin

**Schwannoma**

- Primary thyroid gland benign peripheral nerve sheath tumor
- Densely packed spindle-cell areas adjacent to loosely arranged hypocellular areas
- Slender spindle cells with fibrillar cytoplasm and wavy-spindled nuclei
- Medium-sized vessels with hyalinized walls
- Positive: S100 protein, SOX10

**Solitary Fibrous Tumor**

- Collagen-producing spindle cells arranged in characteristic perivascular pattern
- Usually middle-aged female patients
- Large tumors with solid, white-gray-tan cut appearance
- Cellular mesenchymal tumor with syncytial arrangement of bland, spindled, and monotonous cells with elongated slender nuclei
- Separated by bundles of collagen and delicate open-patulous vascular spaces
- Positive: STAT6, CD34, BCL-2

**Angiosarcoma**

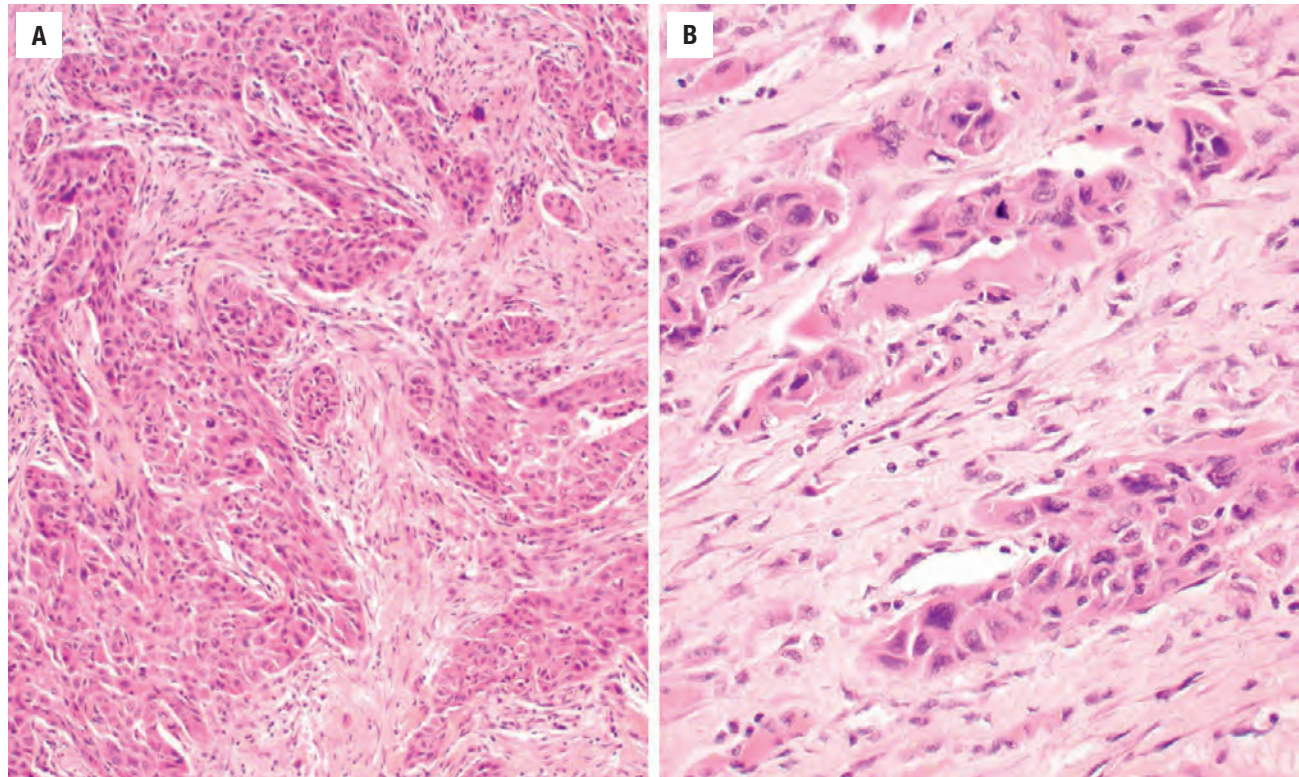
- Primary thyroid gland malignant neoplasm of endothelial cell differentiation
- Increased in areas with iodine deficiency and in occupational exposure to polymeric materials, usually in older patients, with women > men (5:1)
- Poor prognosis with high metastatic rate
- Variegated cut surface with extensive hemorrhage and necrosis, showing invasion
- Freely anastomosing vascular channels with irregular, cleft-like to patulous vascular spaces lined by large, epithelioid polygonal cells
- Neolumen formation with erythrocytes, vesicular nuclear chromatin, prominent macronucleoli
- High mitoses and hemosiderin laden macrophages
- Positive: CD34, CD31, ERG, FLI1, and pancytokeratin

**Leiomyosarcoma**

- Primary malignant thyroid gland neoplasm with smooth muscle differentiation
- Thought to arise from large vessel walls at the gland periphery
- Older patients who have a poor prognosis
- Large, nodular to bosselated tumor with significant invasion
- Entrapped follicles within the highly cellular bundles or fascicles of pleomorphic spindled cells, with blunt-ended, hyperchromatic nuclei, with perinuclear vacuoles
- Positive: vimentin, actin, and desmin, with a high Ki-67 index

**Malignant Peripheral Nerve Sheath Tumor**

- Primary malignant thyroid gland neoplasm showing peripheral nerve sheath differentiation
- Older patients, who usually have a poor outcome
- Arising from peripheral nerves, they invade, entrap and destroy the thyroid parenchyma, with significant vascular invasion and necrosis
- Highly cellular, tightly packed fascicles giving a herringbone appearance
- Highly pleomorphic spindled cells with fibrillary cytoplasmic extensions
- Positive: S100 protein, SOX10, p53

**FIGURE 25.91**

Squamous cell carcinoma arising primarily within the thyroid gland showing sheets and nests of invasive tumor cells (**A**). There are dyskeratosis, intercellular bridges, pleomorphism, and nuclear hyperchromasia (**B**).

the mucocytes are mCEA positive. Thyroglobulin and TTF1 may be focally positive, but calcitonin and S100 protein are negative. *BRAF* (V600E) mutation is not detected, and the *CRTC1-MAML2* fusion transcript may be rarely identified. The differential diagnosis includes squamous metaplasia, epithelial cysts in LT, medullary thyroid carcinoma, primary or secondary squamous cell carcinoma, undifferentiated carcinoma, and carcinoma showing thymus-like differentiation (CASTLE).

### SQUAMOUS CELL CARCINOMA

A thyroid gland primary squamous cell carcinoma is composed entirely of squamous cells without mucocytes and without direct invasion from adjacent organs (larynx, esophagus). A history of radiation exposure is occasionally present. This tumor is thought to be derived from thyroid follicular epithelium, via squamous metaplasia compounded by additional genetic alterations resulting in malignant transformation. A rare tumor, females are affected more often than males (2:1), with a mean age at presentation in the 6th and 7th decades. Patients usually present with a rapidly enlarging neck mass after a long history of pre-existing thyroid disease. Imaging studies are encouraged to exclude primaries in adjacent organs. Cervical lymph node enlargement is common. Early radical resection yields the best outcome by debulking the tumor.

Radical dose radiotherapy can be used, as radioiodine therapy does not work. Tumors follow a rapidly declining clinical course, with a very poor prognosis (mean survival: <1 year), essentially identical to undifferentiated thyroid carcinoma.

By definition, direct extension or metastasis must be excluded. The tumors are widely invasive and destructive, with extrathyroidal extension, soft tissue invasion, and both lymphovascular and perineural invasion. Tumors are arranged in cohesive sheets, ribbons, or nests, with variable pleomorphism (Fig. 25.91). The cells are polygonal, polyhedral, and spindled, with keratinization and keratin pearl formation. There is usually a high mitotic index, including atypical forms. Tumors are often high grade. An inflammatory infiltrate (Hashimoto thyroiditis) and stromal desmoplasia are common. Other tumors may be present (papillary carcinoma is most common), and in these cases, a diagnosis of “with squamous differentiation” is usually used. Tumor cells are usually positive with cytokeratin, CK5/6, CK19, p63, and p40 while negative with thyroglobulin, CEA, calcitonin, and CD5. *Metastatic squamous cell carcinoma* can usually be excluded on clinical or radiographic grounds. Extensive *squamous metaplasia* lacks atypia, does not form a mass, is not infiltrative, and lacks necrosis. *CASTLE* shows a greater degree of tumor spindling, has more keloid-like collagen deposition, and inflammatory cells, and is positive with CD5 and S100-A9.



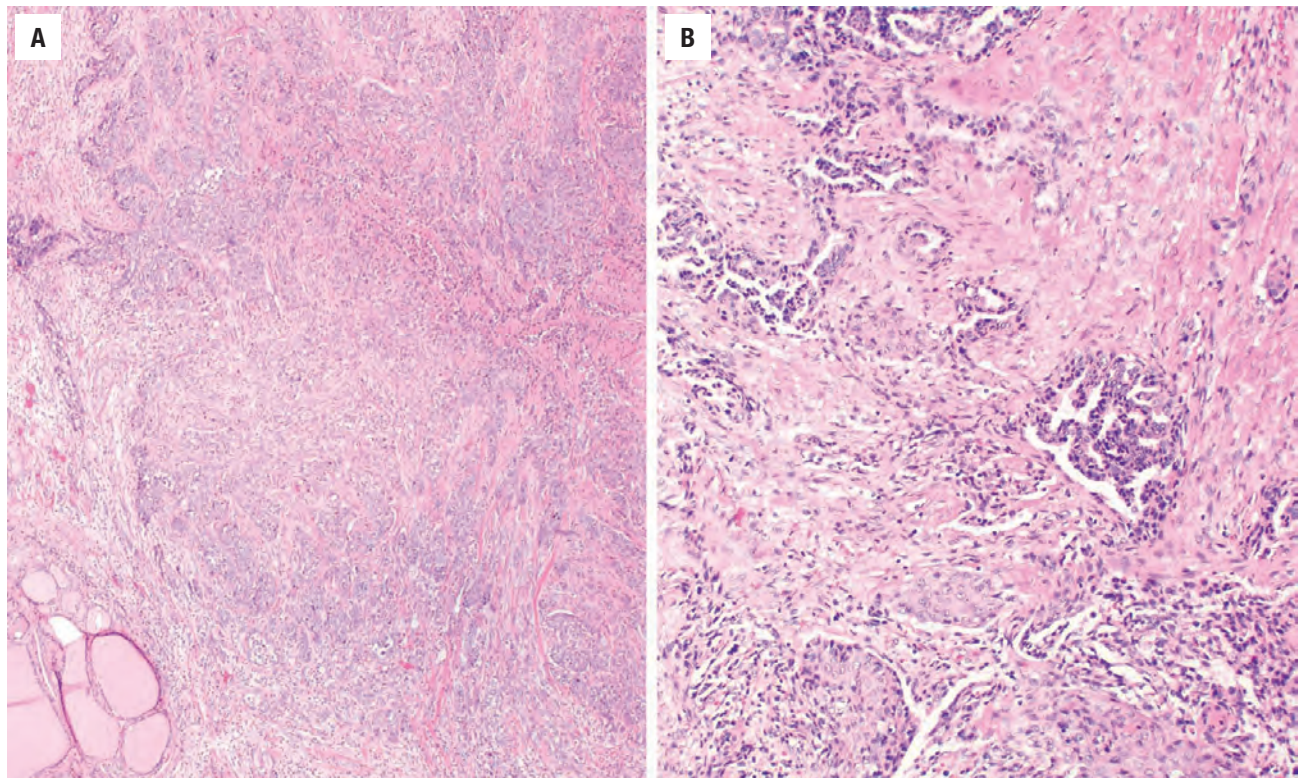
**THYMIC AND RELATED BRANCHIAL POUCH NEOPLASMS**

This is a rare group of tumors that have spindle cells and thymic-like areas of differentiation. They are thought to arise from thymic rests adjacent to or within the thyroid gland or from branchial pouch remnants. Spindle cell tumor with thymus-like differentiation (SETTLE) occurs in young patients (mean, 15 to 20 years), with males affected more often than females (2:1). Patients usually have an asymptomatic neck mass. Intrathyroid epithelial thymoma/CASTLE is slightly more common in women than men (1.3:1) and tends to develop in adults in the 5th decade. An asymptomatic neck or thyroid mass, which may or may not be invasive at the time of presentation, is the most common clinical presentation. Metastatic disease can be seen in up to 50% of patients.

The tumors are usually well demarcated and circumscribed, but tend to be only partially or incompletely encapsulated, but there is usually a sharp border with normal thyroid parenchyma. The tumors are up to 12 cm in greatest dimension, white-tan to yellow-gray, firm to hard, and may have small cysts present within a vaguely whorled to lobular mass. A gritty texture may be present.

Most are identified in the lower poles of the thyroid gland, related to ectopic thymic tissue or branchial pouch origin.

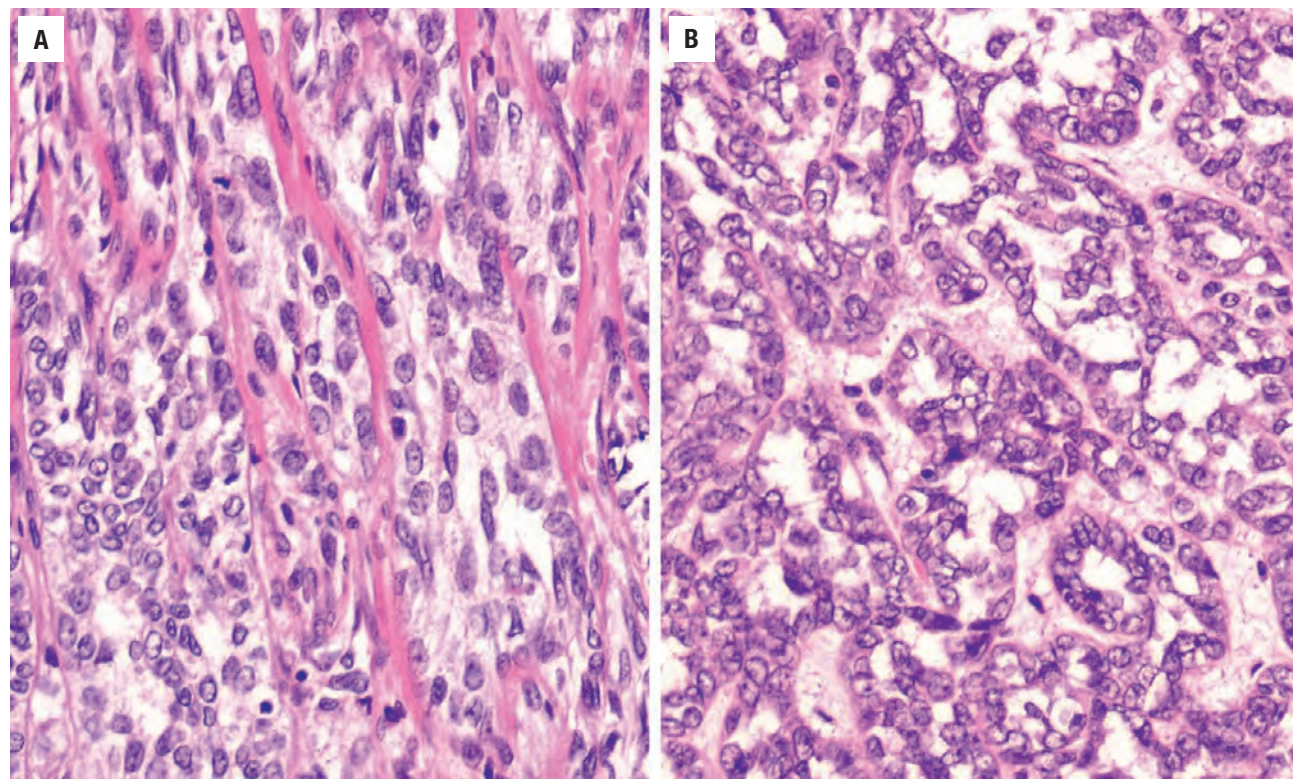
- *Spindle cell tumor with thymus-like differentiation (SETTLE)*: This is a highly cellular biphasic tumor showing primitive thymus histology, characterized by an admixture of spindle-shaped cells that merge with epithelial cells (Fig. 25.92). Sclerotic fibrosis abruptly separates the spindle cell component into a lobular pattern. Vascular invasion may be seen. The cells are arranged in short, reticulated, intersecting, and streaming fascicles or bundles. The elongated nuclei have a syncytial pattern with delicate nuclear chromatin and small nucleoli (Fig. 25.93). The epithelial cells are more polygonal and are arranged in glands, tubules, trabeculae, cords, papillae, glomeruloid structures, and sheets (Fig. 25.93). Sometimes abrupt keratinization may be seen. Branching cystic glands can occasionally be identified, lined by mucinous or ciliated respiratory cells. These pale staining cells are cuboidal to columnar. Calcifications can be seen in the stroma. Mitoses and necrosis are rare. It is important to note the



**FIGURE 25.92**

(A) There is a blending of spindled and epithelial cells in this spindle cell tumor with thymus-like differentiation (SETTLE). (B) Bands of fibrosis separate the tumor in the thyroid into lobules of spindle and epithelial cells in SETTLE.



**FIGURE 25.93**

(A) Spindled and epithelioid cells have delicate nuclei with small nucleoli. Note the wisps of fibrosis separating the tumor cells. (B) Epithelioid cells are arranged in tubules, glands, and papillary projections, with focal glomeruloid structures. Note the “optical” clearing of the nuclei.

often abrupt transition between the two components of this tumor.

- *Intrathyroid epithelial thymoma/CASTLE*: Similar to thymic carcinoma, the tumor is arranged in solid nests or lobules with an expansive or infiltrative growth of epithelioid cells into the surrounding thyroid parenchyma (Fig. 25.94) or adjacent soft tissue and organs (larynx, trachea). The tumor is conceptually a squamous cell carcinoma with a lymphocyte-rich stroma, lacking any follicular or papillary structures. The epithelioid cells have a resemblance to thymomas or thymic carcinomas with epithelioid to spindle-shaped cells arranged in sheets and nests (Fig. 25.95). The cells show mild to moderate nuclear pleomorphism, with large, round to oval nuclei with pale- to vesicular-appearing chromatin, distinct but small nucleoli, and abundant eosinophilic cytoplasm with indistinct cell borders (syncytial arrangement; Fig. 25.95). Mitotic figures are usually limited, far less than the high number seen in undifferentiated carcinoma. Squamous differentiation may be present including keratinization and intercellular bridges.

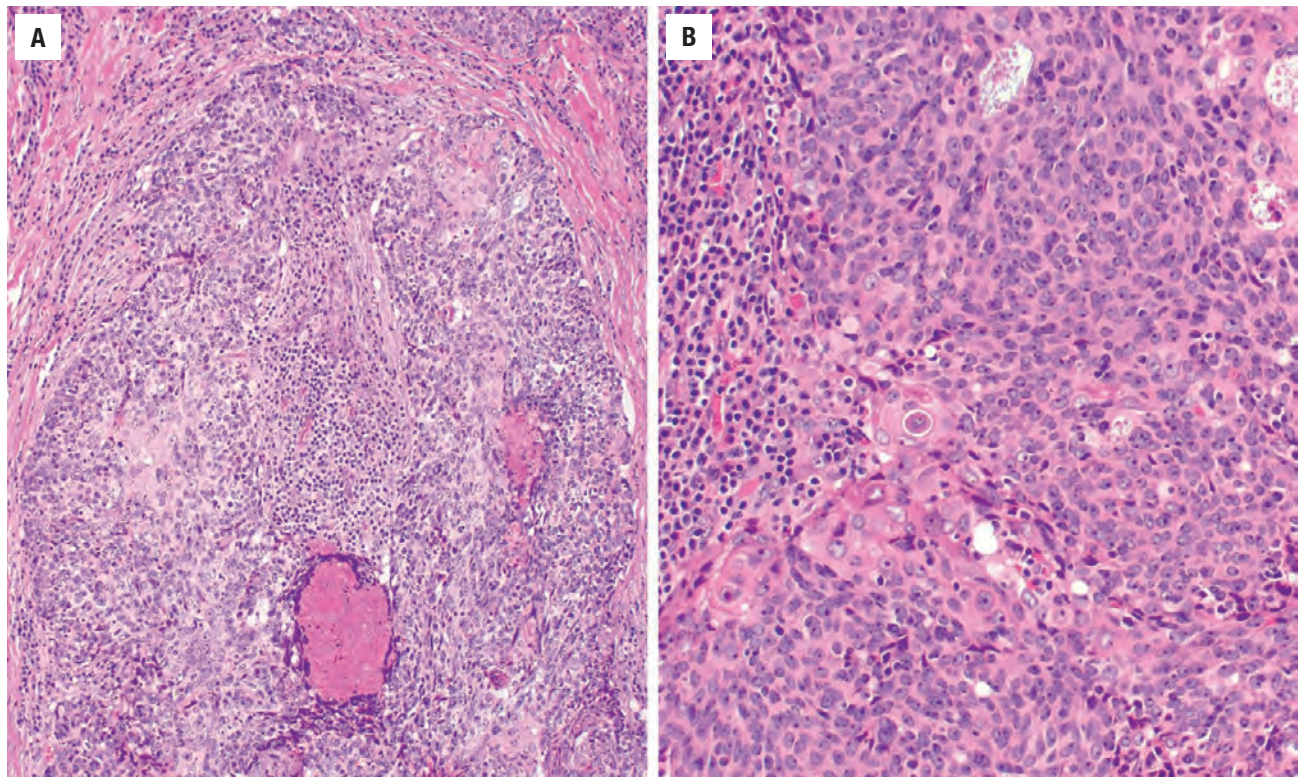
In SETTLE, both the spindle cells and epithelial cells are cytokeratin, CAM5.2, CK7, and CD117 positive, with an intact INI1 (Fig. 25.96), while negative with CD5. Rarely, myoepithelial markers are positive. By contrast, in CASTLE the tumor cells are HMWK, p63, CD5 (Fig. 25.97), CD117, PAX8, bcl-2, and GLUT-1 positive, with GLUT-1, CD5, and CD117 a unique combination.

In both tumors, the cells are negative for thyroglobulin, TTF1, calcitonin, CEA, EBER, S100 protein, synaptophysin, and CK20.

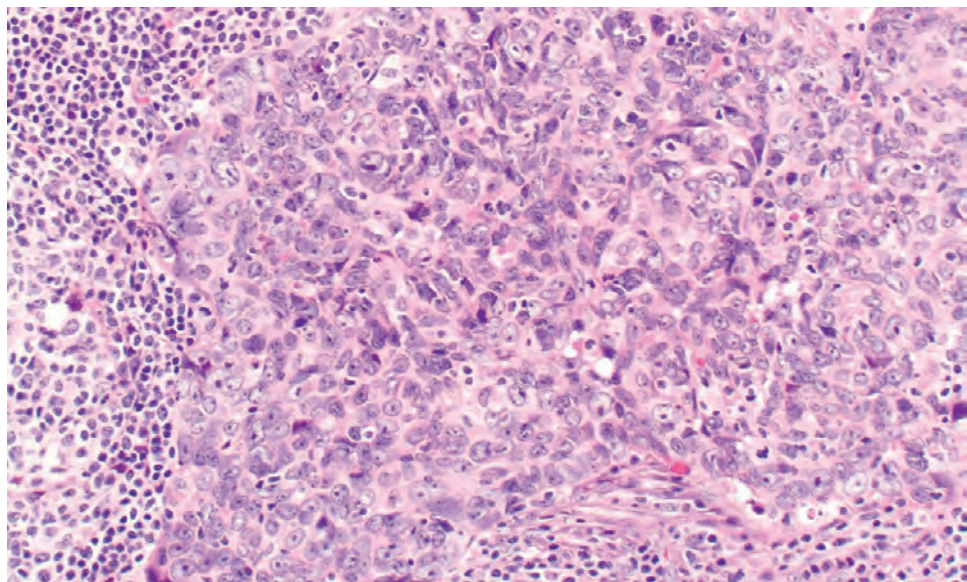
Thymic carcinoma, ectopic thymoma, synovial sarcoma, solitary fibrous tumor, teratoma, follicular dendritic cell sarcoma, spindle cell carcinoma, myoepithelial carcinoma of soft tissue, squamous cell carcinoma, medullary thyroid carcinoma, metastatic lymphoepithelial carcinoma, and undifferentiated carcinoma are all considered in the differential diagnosis of these thymic-like tumors. However, the distinct histologies of these tumors and their respective immunohistochemical profiles help with separation, especially employing CD5, Ki-67, and thyroid-specific markers.

Due to the rare nature of these tumors, a definitive prognosis is difficult to predict, although most pursue a



**FIGURE 25.94**

(A) There is a sheet-like to lobular architecture to the neoplastic cells, showing central comedonecrosis. Note the areas of squamous eddy formation. (B) There is an inflammatory infiltrate at the periphery of the broad sheet of atypical epithelium in this carcinoma showing thymus-like differentiation, composed of enlarged, polygonal, epithelioid cells.

**FIGURE 25.95**

This carcinoma showing thymus-like differentiation shows a syncytial arrangement of spindled to polygonal epithelioid cells. The nuclear chromatin is pale to vesicular, with small, but distinct nucleoli.

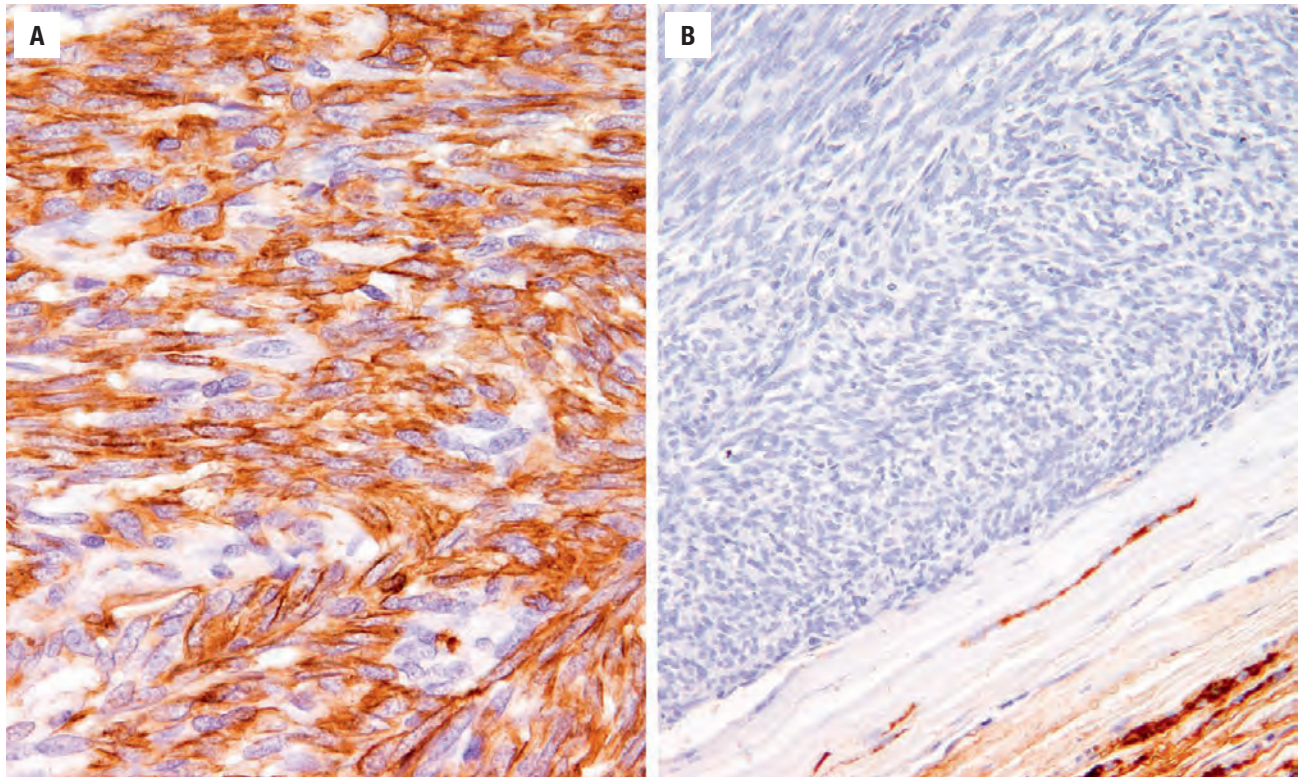
prolonged indolent course (~80% 10-year survival). Local recurrence and regional metastases have been reported more often in CASTLE (50%) than in SETTLE (26%), with delayed metastases seen more often in SETTLE (up to 70% of cases). Surgical excision is the treatment of choice (including selected lymph node dissection and resection of all delayed metastases), with neoadjuvant chemotherapy and radiation occasionally employed.

## MESENCHYMAL TUMORS

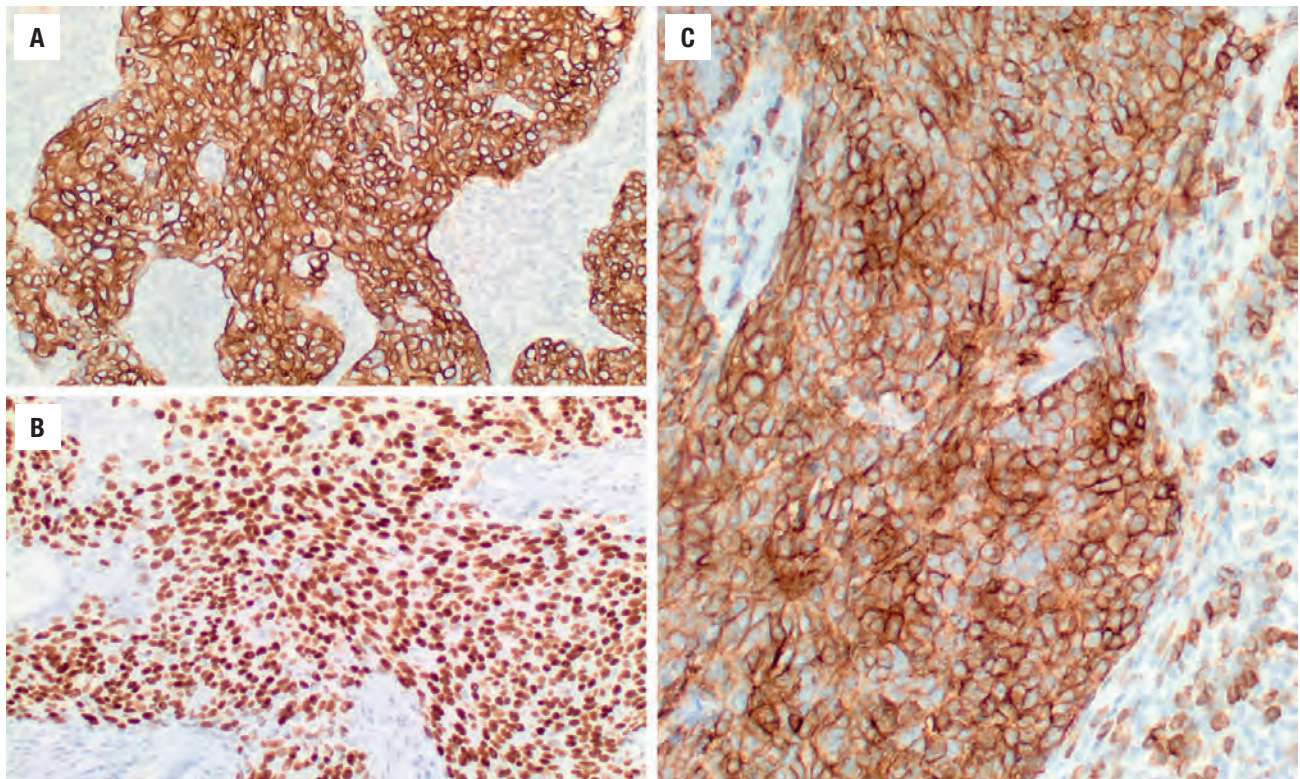
Many different benign and malignant mesenchymal tumors can be seen in the thyroid gland, although with limited frequency.

**Leiomyoma** is a benign primary thyroid neoplasm composed of cells with distinct smooth muscle differentiation histologically. They develop from smooth muscle-walled



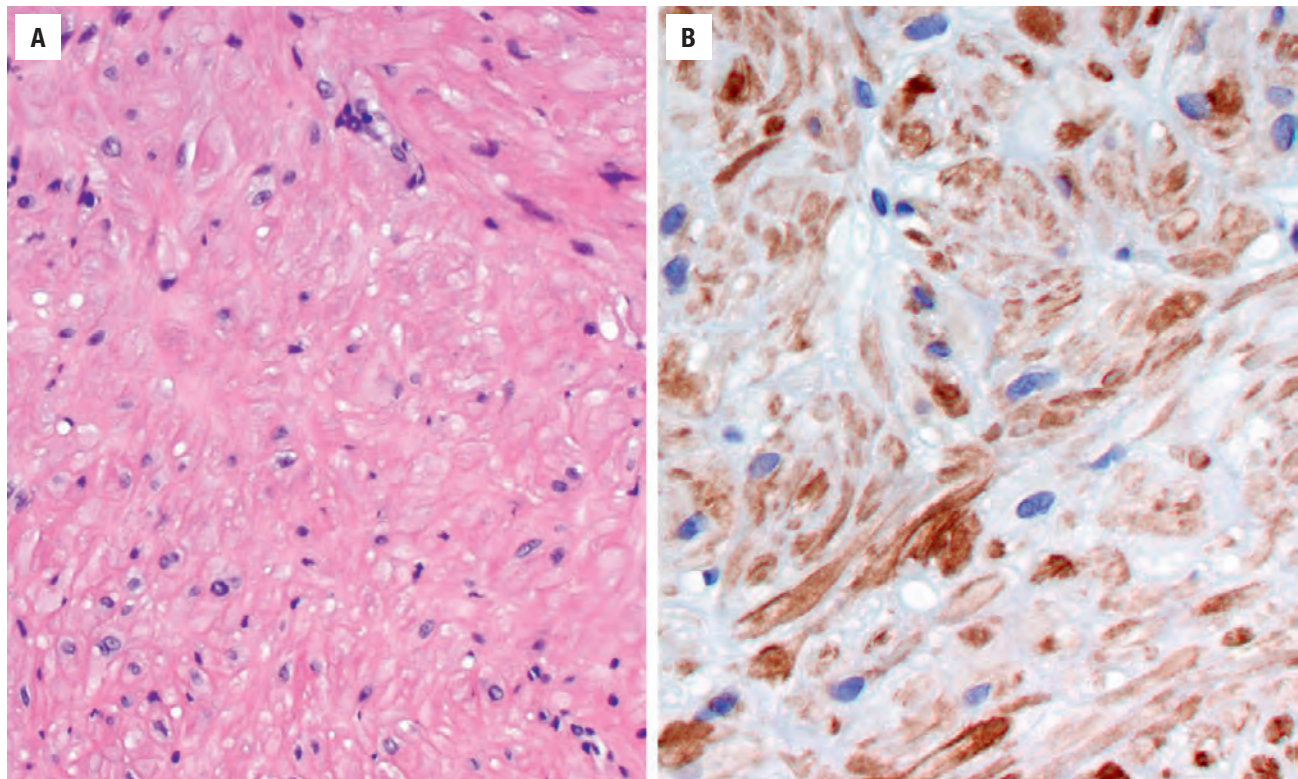
**FIGURE 25.96**

Keratin is strongly and diffusely immunoreactive in the neoplastic cells of a spindle cell tumor with thymus-like differentiation (**A**), whereas thyroglobulin is nonreactive (**B**).

**FIGURE 25.97**

Carcinoma showing thymus-like differentiation shows strong CK5/6 (**A**) and p63 (**B**) immunoreactivity, with a well-developed immunoreaction with CD5 (**C**; thymic T-cells are positive internal controls), the latter confirming the thymic-like differentiation.



**FIGURE 25.98**

(A) Leiomyoma composed of cytologically bland spindled tumor cells with vacuoles. (B) Strong and diffuse actin reaction.

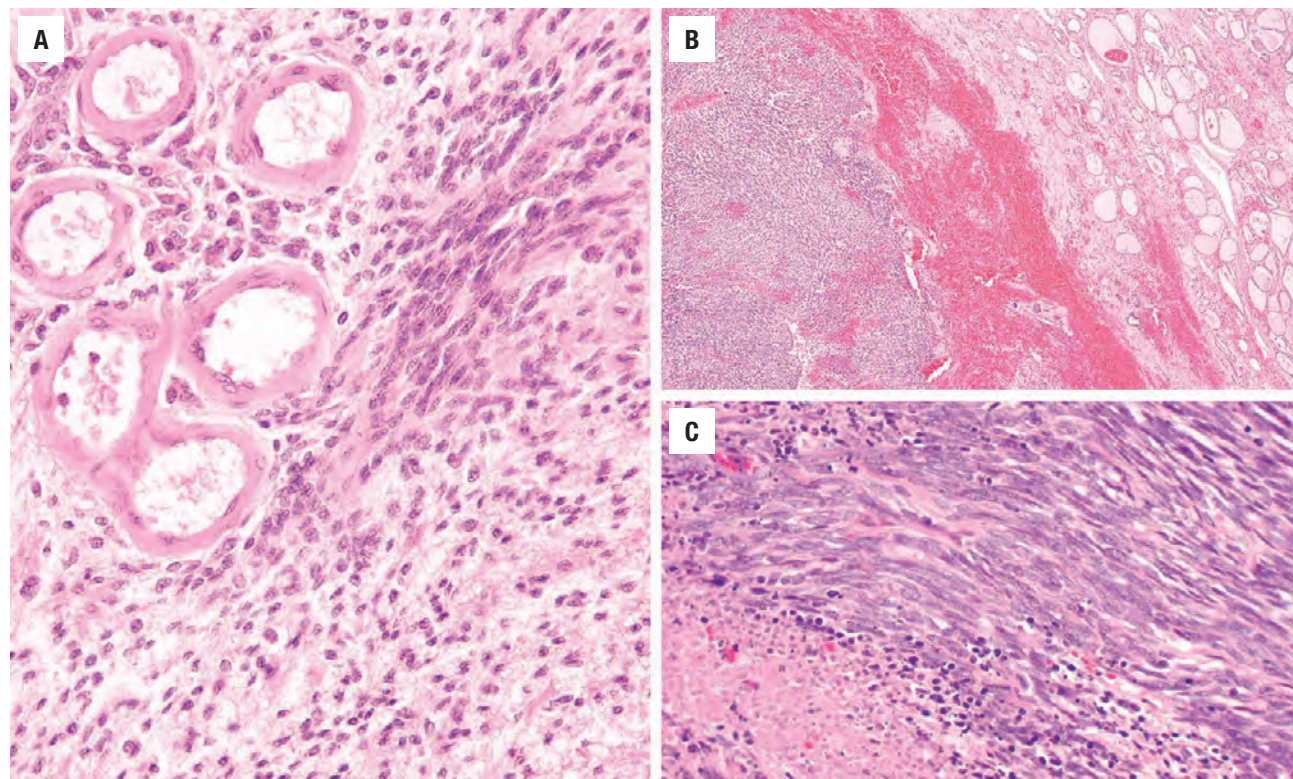
vessels at the thyroid gland periphery. Usually, patients are young with an equal sex distribution. Tumors are small (mean, 2 cm), well circumscribed, and unencapsulated with a smooth periphery. The cells are arranged in bundles or fascicles of bland smooth muscle fibers that intersect in an orderly fashion (Fig. 25.98). Cells are spindled and blunt-ended or cigar-shaped, with centrally placed nuclei. Paranuclear cytoplasmic vacuoles are sometimes prominent. The tumor cells are positive with vimentin, SMA, MSA, caldesmon, calponin, and desmin, but negative with S100 protein, SOX10, pancytokeratin, and calcitonin.

**Schwannoma** is a benign neoplasm composed of cells with evidence of distinct peripheral nerve-sheath differentiation histologically. They develop from the sympathetic and parasympathetic or possibly sensory nerves adjacent to the thyroid gland. All ages are affected with an equal sex distribution. Tumors are well circumscribed or encapsulated. The tumor cells show densely packed spindle-cell areas (Antoni A) adjacent to loosely arranged, hypocellular degenerated areas (Antoni B; Fig. 25.99). The slender fusiform cells are arranged in interlacing fascicles with fibrillar cytoplasmic extensions. Nuclear palisading (Verocay bodies) may be seen. The nuclei are wavy and spindled, lacking atypia. There are usually small to medium-sized blood vessels with heavily hyalinized walls. The tumor cells show strong and diffuse S100 protein, SOX10, and vimentin immunoreactivity.

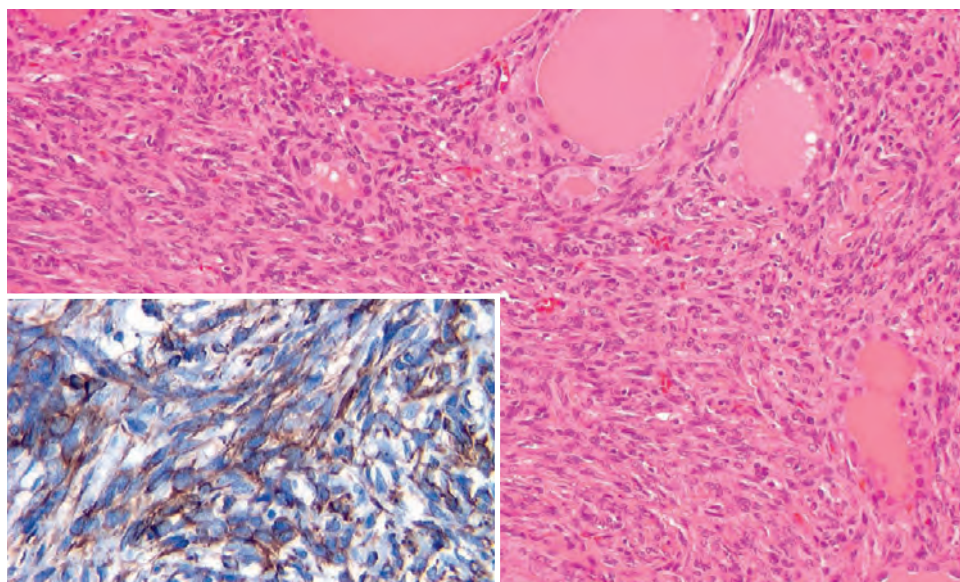
**Solitary fibrous tumor (SFT)** is a mesenchymal tumor composed of collagen-producing spindled cells arranged in a characteristic vascular pattern. Females are affected more often than males, usually as middle-aged patients. Tumors are relatively large (mean, 4.5 cm), well circumscribed, and frequently encapsulated, with a firm, solid, white-gray-tan cut appearance. Histologically, they are variegated, cellular, mesenchymal tumors, showing hypocellular areas alternating with hypercellular areas. The tumor cells are spindled, bland, and monotonous with elongated, slender nuclei arranged in a syncytial, nonspecific growth pattern (Fig. 25.100). The cells are separated by bundles of keloid-like collagen, and delicate, open to patulous vascular spaces. Extravasated erythrocytes, inflammatory cells, and mast cells are common. Myxoid change and inflammatory cells (mast cells usually) may be seen. The neoplastic cells are immunoreactive with STAT6, CD34, CD99, and bcl-2 (Fig. 25.100), with weak, variable reactions to actin. Pertinent negatives include S100 protein, thyroid markers, CD117, keratin, ALK1, desmin, and other muscle markers.

**Angiosarcoma** is a primary thyroid gland malignant tumor of endothelial cell differentiation. There is an increased incidence in regions with dietary iodine deficiency, especially in alpine areas of central Europe, and in patients with significant occupational exposure to industrial vinyl chloride and other polymeric materials. The tumors are thought to arise from endothelium and



**FIGURE 25.99**

(A) Schwannoma with spindled cells associated with loosely arranged hypocellular areas and heavily hyalinized vessels. (B) Highly cellular spindled cell malignant peripheral nerve sheath tumor (MPNST) within the thyroid gland. (C) The fascicles of this MPNST are associated with necrosis and mitoses.

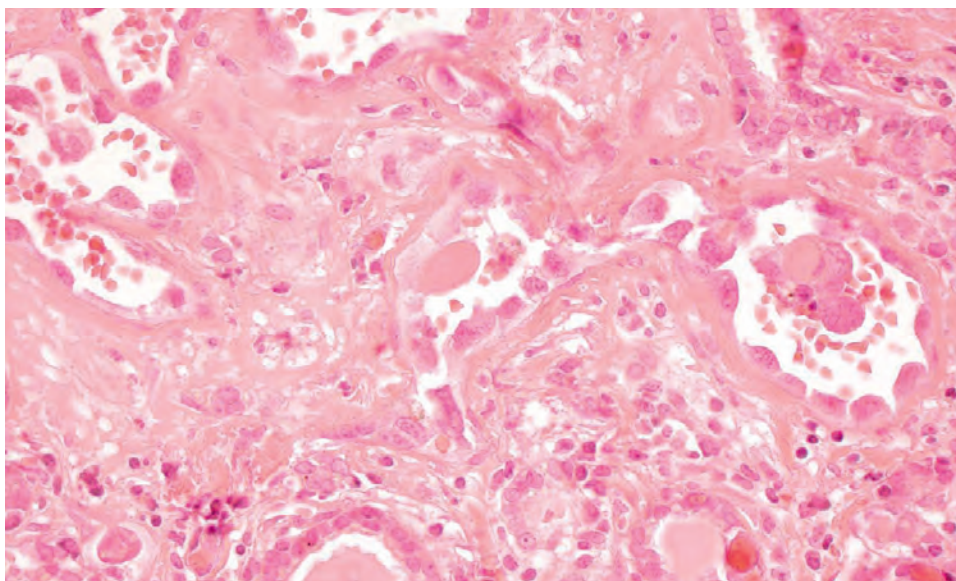
**FIGURE 25.100**

SFT infiltrates around the uninvolved thyroid follicles. Spindle cell population is separated by bands of collagen. *Inset* demonstrates positivity with bcl-2.

not follicular epithelial cells. Tumors usually present in the 7th decade of life, with women affected more often than men (5:1). Most patients have a long history of goiter, with a painless mass. Rarely, there may be a rapidly growing mass with pressure symptoms. It is important to realize that there may be severe bleeding at primary or metastatic sites which may complicate surgery. Total

thyroidectomy is the treatment of choice, with palliative chemotherapy. Adjuvant radiotherapy, frequently administered as brachytherapy with a radiation sensitizer may be employed. The overall prognosis is poor, with the majority of patients dying from disease in less than 6 months. Distant metastases develop to lung, gastrointestinal tract, and bone.



**FIGURE 25.101**

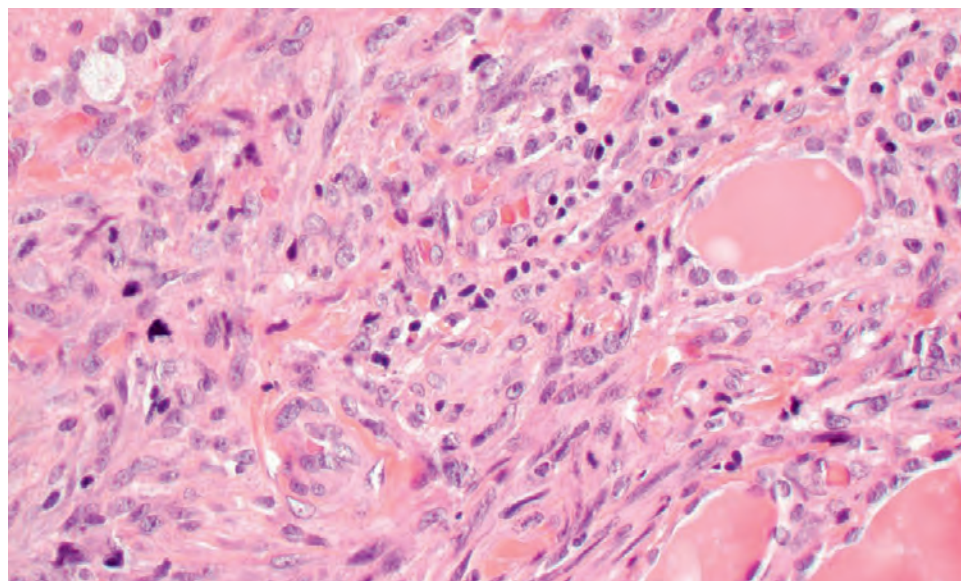
Pleomorphic endothelial cells lining irregular vascular spaces are the hallmark of angiosarcoma. Note the entrapped thyroid follicular epithelial cells (*bottom*).

The cut surface is variegated with extensive hemorrhage and necrosis within tumors that tend to be large (up to 12 cm). The periphery is irregular, with blending and invasion of the thyroid parenchyma. Freely anastomosing vascular channels are arranged in solid, spindled, papillary, and pseudoglandular patterns. Tumor necrosis and hemorrhage is usually seen throughout the tumor. There are increased mitoses, including atypical forms. Hemosiderin-laden macrophages are common. There are irregular, cleft-like to patulous vascular channels lined by large, epithelioid polygonal cells ([Fig. 25.101](#)). There is abundant eosinophilic to vacuolated cytoplasm surrounding round nuclei with vesicular chromatin and prominent macronucleoli. Neolumen formation with erythrocytes within the lumen may be seen. The lesional cells are positive with vascular endothelial markers, including CD31, FVIII-RAg, CD34, ERG, and FLI1. Keratin is also expressed in a majority of cases. It is important to not over interpret diffusion artifacts. The differential diagnosis includes undifferentiated carcinoma, degenerative adenomatoid nodules, post-FNA artifacts, medullary thyroid carcinoma, metastatic melanoma, and angiosarcoma.

**Leiomyosarcoma** (LMS) is a malignant primary thyroid neoplasm composed of cells with distinct smooth-muscle differentiation histologically. This is the malignant counterpart of leiomyoma. Patients tend to be older, presenting with a mass at the thyroid gland periphery. Patients usually have a poor prognosis. The tumors are large (up to 12 cm), showing a nodular to bosselated outer surface, and significant soft tissue invasion. There is often entrapment and destruction of thyroid follicles. Perineural and vascular invasion are frequently present, along with tumor necrosis. The tumors are highly cellular, arranged in bundles or disordered fascicles of spindled cells with centrally placed, hyperchromatic, blunt-ended,

cigar-shaped nuclei. Perinuclear cytoplasmic vacuoles are quite characteristic ([Fig. 25.102](#)). Nuclear pleomorphism is usually present, along with increased mitoses. The neoplastic cells are positive with vimentin, SMA, MSA, caldesmon, and desmin, showing a high Ki-67 index. The differential includes medullary thyroid carcinoma, undifferentiated carcinoma, and direct extension or metastatic LMS.

**Malignant peripheral nerve sheath tumor** (MPNST) of the thyroid gland is a malignant neoplasm composed of cells with evidence of distinct peripheral nerve sheath differentiation histologically. These are the malignant counterpart of schwannoma. Most patients have a poor outcome and die from disease. All ages are affected, although patients are usually older at initial presentation. Syndrome-associated tumors tend to develop in patients of younger age. There is an equal sex distribution. Tumors are tan to white and glistening with a “neural” appearance, sometimes showing thyroid gland effacement, cystic change, and necrosis. They may be seen arising from the perithyroidal nerves. The tumors arise within the thyroid gland, invading, entrapping, and destroying the parenchyma. Vascular invasion may be present. The tumors are highly cellular, arranged in tightly packed fascicles that are woven into a vague herringbone or marbled pattern, with only isolated Antoni B areas. The cells are spindled, with fibrillar cytoplasmic extensions arranged in a loose background. Pleomorphism, necrosis, increased mitoses ([Fig. 25.99](#)), and atypical mitoses are all easily identified. The cells are strongly positive with vimentin and p53, showing SOX10 and variable S100 protein reaction (often focal and weak). Other markers are negative, although a rare malignant triton tumor may show focal muscle markers where there is rhabdomyoblastic differentiation. The differential diagnosis includes Riedel thyroiditis, undifferentiated carcinoma,

**FIGURE 25.102**

Thyroid follicles are destroyed by this pleomorphic spindled cell population, showing numerous mitotic figures in this primary leiomyosarcoma.

medullary thyroid carcinoma, metastatic melanoma, and other sarcomas (both primary and metastatic). Other melanoma markers (HMB-45, Melan-A) should be positive in melanoma.

## **■ METASTATIC NEOPLASMS**

Tumors that occur in the thyroid as a result of lymphovascular spread from distant sites are considered as metastatic disease. While not covered in this section, it should be noted that direct extension into the thyroid from adjacent organs (larynx [squamous cell carcinoma], trachea, esophagus, lymph nodes [lymphoma], soft tissues) may sometimes need to be included in the differential diagnosis of thyroid masses. The thyroid gland is richly vascularized, predisposing to relatively high frequency of metastases.

### **CLINICAL FEATURES**

Seen in up to 7.5% of surgically removed glands, up to 25% of autopsied patients with disseminated malignancies will have thyroid gland metastases. This may be due to advances in radiographic techniques, increased use of FNA, or improved treatments resulting in longer survival. In clinical series, metastatic deposits are identified at a higher frequency in abnormal glands: those with adenomatoid nodules, thyroiditis, and follicular neoplasms. Furthermore, the metastatic deposits may be found within primary thyroid tumors (i.e., metastatic renal cell carcinoma to a papillary thyroid carcinoma). All ages are affected, but metastases are more common in older

### **METASTATIC NEOPLASMS—DISEASE FACT SHEET**

#### **Definition**

- Lymphovascular spread from distant sites to the thyroid gland, which is richly vascularized, predisposing to metastatic deposits

#### **Incidence and Location**

- Up to 25% in autopsied patients and 7.5% in clinical series
- Increased in peripheral vascular spaces or in other tumors

#### **Morbidity and Mortality**

- Usually poor clinical outcome, although exceptions occur

#### **Sex and Age Distribution**

- Females > males, although tumor type specific
- Usually older patients

#### **Clinical Features**

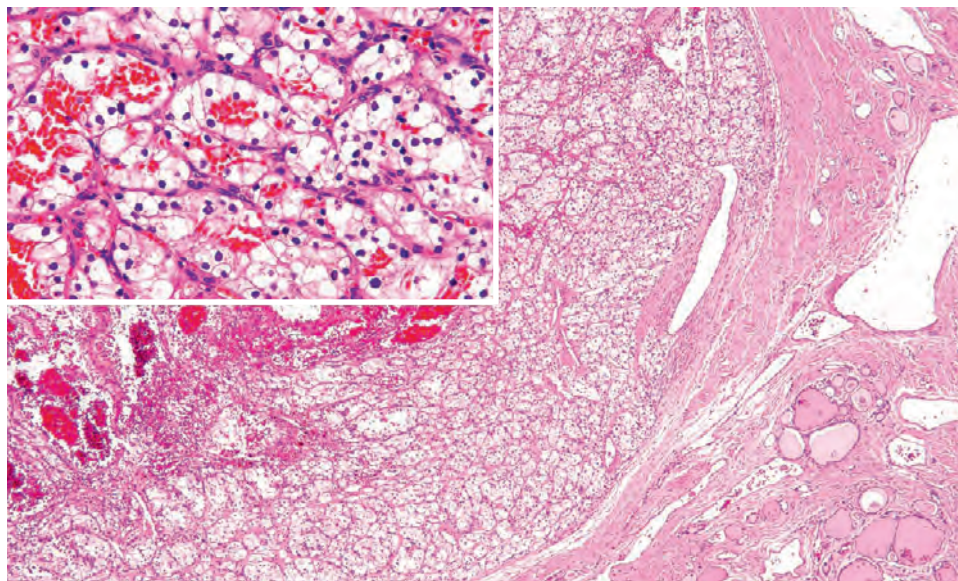
- Rapidly enlarging thyroid mass, although sometimes a thyroid disorder may be the clinical presentation
- In up to 40% of patients, the thyroid presentation is the initial manifestation of an occult primary

#### **Prognosis and Therapy**

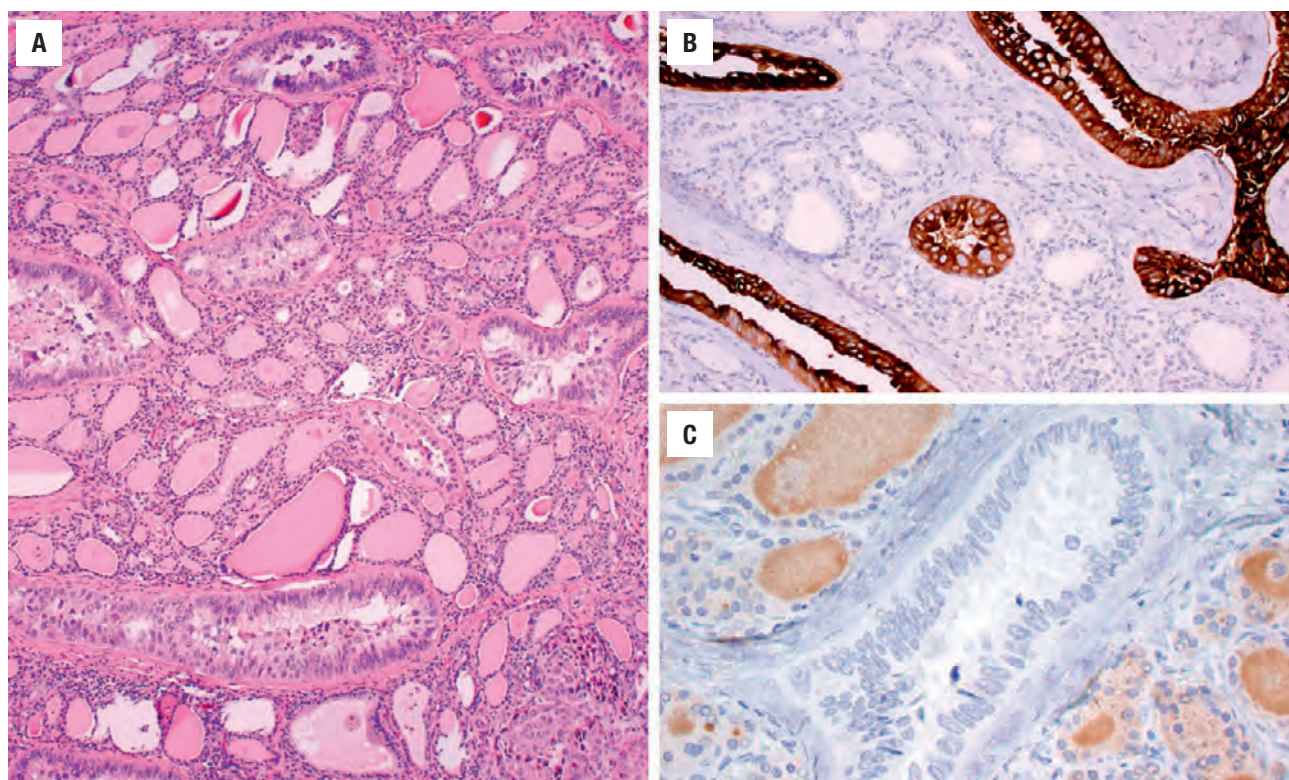
- Usually poor and determined by the underlying primary
- When limited to the thyroid gland, surgery may yield a prolonged survival

patients (mean, 62 years), and in females more often than males (1.2:1). A rapidly enlarging thyroid mass may be the presenting sign, although more often the underlying thyroid disease may result in the clinical presentation. In a number of patients (up to 40%), the thyroid gland metastatic deposit is the initial presentation



**FIGURE 25.103**

Encapsulated metastatic clear cell renal cell carcinoma to the thyroid gland may mimic a primary thyroid neoplasm with clear cells. *Inset* shows erythrocytes in the center of pseudo-glands. Prominent cell borders and small hyperchromatic nuclei are present.

**FIGURE 25.104**

(A) Metastatic lung adenocarcinoma to the thyroid gland within multiple vascular channels. (B) Strong and diffuse mCEA in the metastatic tumor. (C) Thyroglobulin is negative in the tumor, but positive in the adjacent follicles.

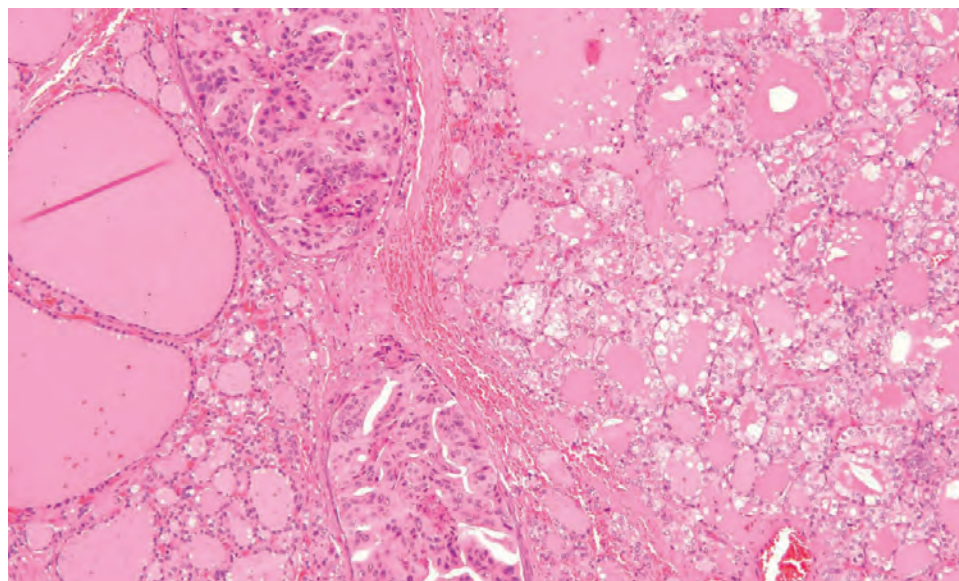
of the occult primary tumor. The most common primary sites in order of frequency are kidney (Fig. 25.103), lung (Fig. 25.104), breast (Fig. 25.105), stomach, prostate, and skin (melanoma). Kidney tumors are the most likely to present with an occult primary, while also having the longest latency period. Ultrasound can be used to show multifocal disease and bilateral metastases, and to guide biopsy.

## **PATHOLOGIC FEATURES**

### **GROSS FINDINGS**

Multifocal and bilateral disease is more common, but in clinically significant metastatic deposits, a unilateral solitary mass is more likely to result in clinical evaluation.



**FIGURE 25.105**

Vascular spaces are filled with neoplastic cells that have a different appearance from the adenomatoid nodules (*left*) and the papillary thyroid carcinoma (*right*). This is a metastatic breast carcinoma.

### METASTATIC NEOPLASMS—PATHOLOGIC FEATURES

#### Gross Findings

- Usually multifocal and bilateral
- Can metastasize to preexisting thyroid lesions

#### Microscopic Findings

- Usually resemble the primary tumor although de-differentiation may occur
- Kidney > lung > breast > stomach, prostate > skin
- Lymphovascular channels at thyroid gland periphery shows tumor most frequently
- Distinctly different architecture and histology from primary thyroid neoplasms (although clear cell metastatic renal cell carcinoma and metastatic neuroendocrine carcinomas may cause difficulty)

#### Immunohistochemical Findings

- Metastatic tumors have unique immunohistochemical profiles, distinctly different from thyroid primaries (caution with TTF1 and calcitonin results)

#### Pathologic Differential Diagnosis

- Clear cell adenoma/carcinoma, medullary thyroid carcinoma, lymphoma, direct extension

There is a predilection for larger vessels at the thyroid gland periphery. Metastatic deposits can be large, up to 15 cm in maximum dimension.

### MICROSCOPIC FINDINGS

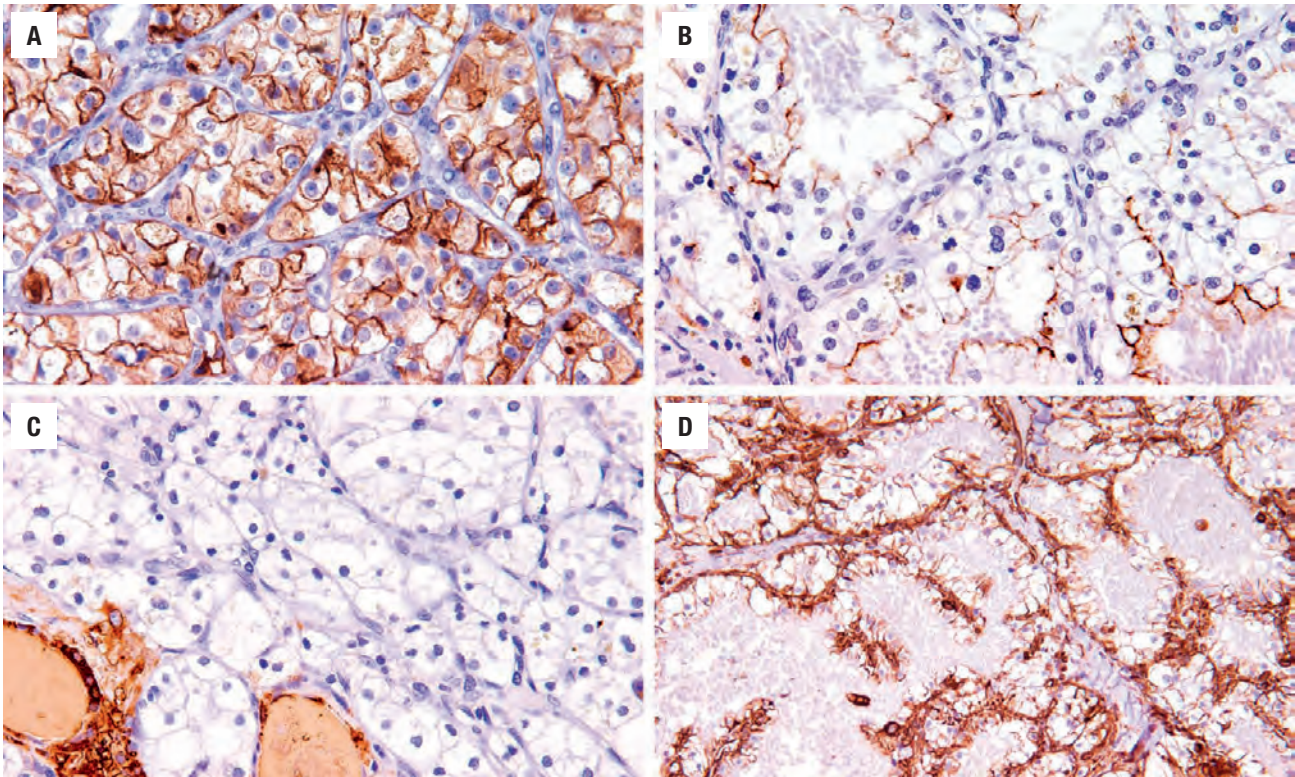
The thyroid gland is a richly vascularized endocrine organ, and hence, susceptible to metastatic deposits. For the most part, the metastatic deposits morphologically resemble the primary site, with rare examples of more

poorly differentiated tumor in the thyroid. Close examination of the periphery of the thyroid gland where the vasculature is the most dense, will help to identify intravascular metastatic deposits. Fibrous septa within the gland are widened by tumor within lymphatic channels (Figs. 25.104 and 25.105). When the tumor deposits form a mass lesion, they usually have an architecture and cytomorphology distinct from thyroid primaries. Metastatic clear cell renal cell carcinoma is an exception (Fig. 25.103). Carcinomas are most common (~80%), while LMS and melanoma are the most common noncarcinomas. Metastatic neuroendocrine (small cell) carcinomas may also pose some difficulty, as they may resemble a MTC; or they may also be TTF1 immunoreactive if they are from the lung, similar to lung adenocarcinoma and primary thyroid follicular neoplasms.

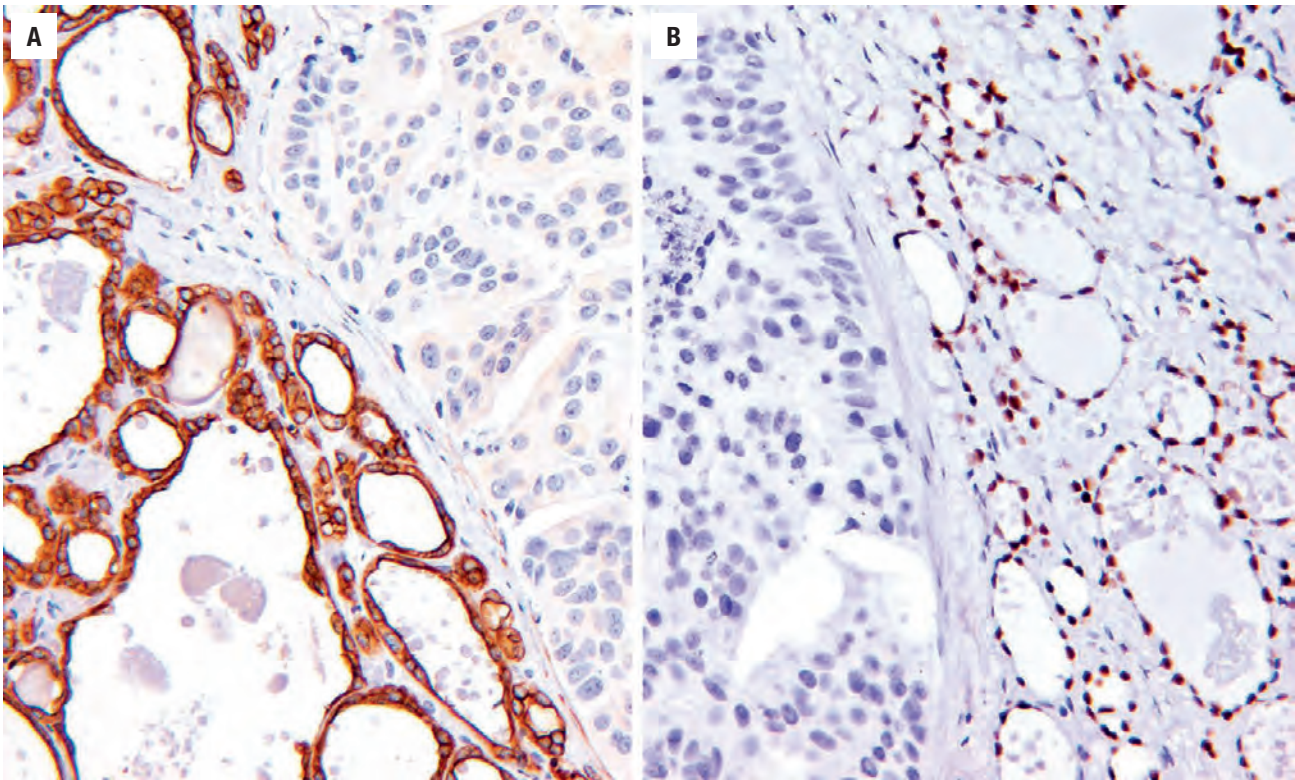
### ANCILLARY STUDIES

Primary thyroid follicular tumors will usually be thyroglobulin, TTF1, PAX8, and CK7 immunoreactive, while C-cell derived tumors will be calcitonin and chromogranin reactive. While there are exceptions, metastatic tumors will not be thyroglobulin reactive (Figs. 25.104, 25.106, and 25.107), and only rare examples of calcitonin immunoreactivity in metastatic neuroendocrine neoplasms are known. Diffusion artifact and/or entrapment of follicular epithelium within metastatic tumors must be excluded. FNA may help to confirm malignancy but it is frequently misinterpreted as to type. In general, the smears are cellular with two distinct cell populations (Fig. 25.108). Molecular studies can be helpful (PAX8-PPAR $\gamma$ , BRAF, RAS), although there are overlapping results with several tumors.



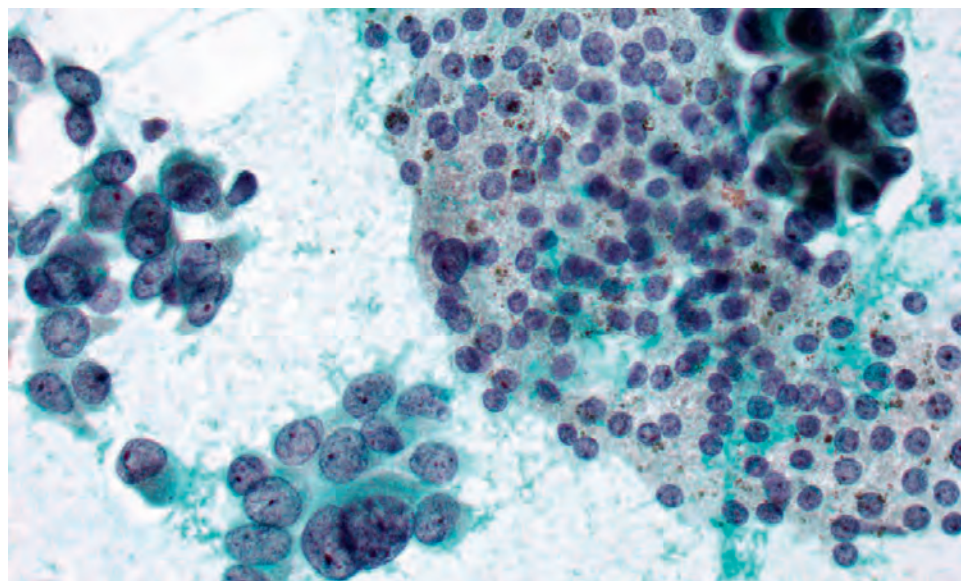


**FIGURE 25.106**  
Immunohistochemical panel can help to separate metastatic from primary neoplasms. This renal cell carcinoma is reactive with CD10 (A), negative for thyroglobulin (C), and positive with epithelial membrane antigen (B) and vimentin (D).

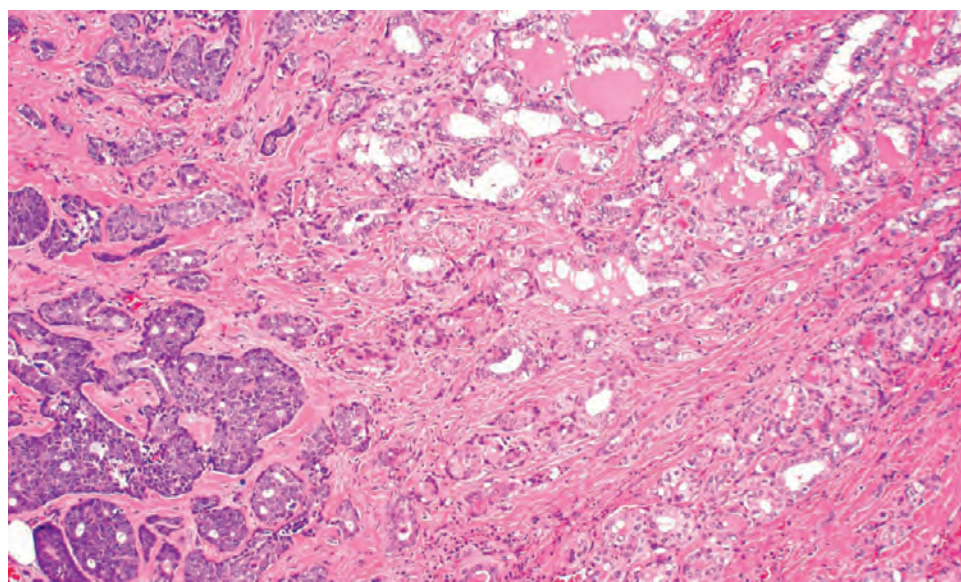


**FIGURE 25.107**  
Metastatic breast carcinoma is nonreactive with thyroglobulin (A) and TTF1 (B). Tumor cells are within a vascular space.



**FIGURE 25.108**

Two distinct populations are present: the thyroid follicular epithelium and the greatly enlarged, pleomorphic adenocarcinoma population (from a lung primary) (alcohol fixed, Papanicolaou stain).

**FIGURE 25.109**

Adenoid cystic carcinoma is directly invading from a larynx primary, colliding with a primary thyroid papillary carcinoma.

### DIFFERENTIAL DIAGNOSIS

A solitary metastatic renal cell carcinoma may be difficult to separate from the clear cell change seen in FAs or carcinomas, and more rarely in papillary and medullary thyroid carcinomas. The prominent vascularity, glandular lumina filled with erythrocytes, lack of colloid, sharp intercellular borders, and small, hyperchromatic nuclei favor a renal cell carcinoma. The neoplastic cells are RCC, CD10, CAIX, and EMA immunoreactive, while nonreactive for TTF1 or thyroglobulin; both are PAX8 positive. Direct extension from adjacent organs is usually radiographically and clinically distinctive (Fig. 25.109).

### PROGNOSIS AND THERAPY

For the most part, the prognosis is determined by the underlying primary and, almost by dint of metastases, correlates with a poor prognosis. However, if metastatic disease is limited to the thyroid, surgery can result in prolonged survival, especially for renal cell carcinoma, a primary tumor known for capricious behavior. Therefore, surgery is advocated if the tumor is slow growing or it is an isolated metastasis.

### SUGGESTED READINGS

The complete Suggested Readings list is available online at [ExpertConsult.com](http://ExpertConsult.com).



## SUGGESTED READINGS

## Papillary Carcinoma (Including Variants)

- Albores-Saavedra J, et al. The macrofollicular variant of papillary thyroid carcinoma: a study of 17 cases. *Am J Clin Pathol.* 1990;94:442–445.
- Albores-Saavedra J, et al. The many faces and mimics of papillary thyroid carcinoma. *Endocr Pathol.* 2006;17(1):1–18.
- Al-Brahim N, et al. Papillary thyroid carcinoma: an overview. *Arch Pathol Lab Med.* 2006;130(7):1057–1062.
- Asioli S, et al. Papillary thyroid carcinoma with prominent hobnail features: a new aggressive variant of moderately differentiated papillary carcinoma. A clinicopathologic, immunohistochemical, and molecular study of eight cases. *Am J Surg Pathol.* 2010;34(1):44–52.
- Baloch ZW, et al. Etiology and significance of the optically clear nucleus. *Endocr Pathol.* 2002;13:289–299.
- Baloch ZW, et al. Follicular-patterned lesions of the thyroid: the bane of the pathologist. *Am J Clin Pathol.* 2002;117:143–150.
- Baloch ZW, et al. Pathologic diagnosis of papillary thyroid carcinoma: today and tomorrow. *Expert Rev Mol Diagn.* 2005;5(4):573–584.
- Baloch ZW, et al. Microcarcinoma of the thyroid. *Adv Anat Pathol.* 2006;13(2):69–75.
- Baloch ZW, et al. Diagnostic terminology and morphologic criteria for cytologic diagnosis of thyroid lesions: a synopsis of the National Cancer Institute Thyroid Fine-Needle Aspiration State of the Science Conference. *Diagn Cytopathol.* 2008;36(6):425–437.
- Beckner M, et al. Oxyphilic papillary thyroid carcinomas. *Am J Clin Pathol.* 1995;103:180–187.
- Bejarano PA, et al. Thyroid transcription factor1, thyroglobulin, cytokeratin 7, and cytokeratin 20 in thyroid neoplasms. *Appl Immunol Mol Morphol.* 2000;8(3):189–194.
- Benndbaek FN, et al. Management of the solitary thyroid nodule: results of a North American survey. *J Clin Endocrinol Metab.* 2000;85:2493–2498.
- Berho M, et al. The oncocytic variant of papillary carcinoma of the thyroid: a clinicopathologic study of 15 cases. *Hum Pathol.* 1997;28:47–53.
- Bongiovanni M, et al. CDX2 expression in columnar variant of papillary thyroid carcinoma. *Thyroid.* 2013;23(11):1498–1499.
- Cameselle-Teijeiro J, et al. Cribriform-morular variant of papillary carcinoma: a distinctive variant representing the sporadic counterpart of familial adenomatous polyposis-associated thyroid carcinoma? *Mod Pathol.* 1999;12(4):400–411.
- Cancer Genome Atlas Research Network. Integrated genomic characterization of papillary thyroid carcinoma. *Cell.* 2014;159(3):676–690.
- Carcangiu ML, et al. Clear cell changes in primary thyroid tumors: a study of 38 cases. *Am J Surg Pathol.* 1985;9:705–722.
- Carcangiu ML, et al. Papillary carcinoma of the thyroid. A clinicopathologic study of 241 cases treated at the University of Florence, Italy. *Cancer.* 1985;55(4):805–828.
- Carcangiu ML, et al. Diffuse sclerosing variant of papillary thyroid carcinoma: clinicopathologic study of 15 cases. *Am J Surg Pathol.* 1989;13:1041–1049.
- Casey MB, et al. Distinction between papillary thyroid hyperplasia and papillary thyroid carcinoma by immunohistochemical staining for cytokeratin 19, galectin3, and HBME1. *Endocr Pathol.* 2003;14(1):55–60.
- Chan JK, et al. The grooved nucleus. A useful diagnostic criterion of papillary carcinoma of the thyroid. *Am J Surg Pathol.* 1986;10(10):672–679.
- Chan JK. Papillary carcinoma of thyroid: classical and variants. *Histol Histopathol.* 1990;5:241–257.
- Chisholm EJ, et al. Systematic review and meta-analysis of the adverse effects of thyroidectomy combined with central neck dissection as compared with thyroidectomy alone. *Laryngoscope.* 2009;119(6):1135–1139.
- Chow SM, et al. Diffuse sclerosing variant of papillary thyroid carcinoma—clinical features and outcome. *Eur J Surg Oncol.* 2003;29:446–449.
- Cohen Y, et al. BRAF mutation in papillary thyroid carcinoma. *J Natl Cancer Inst.* 2003;95(8):625–627.
- Corrado S, et al. Papillary thyroid carcinoma with predominant spindle cell component: report of two rare cases and discussion on the differential diagnosis with other spindled thyroid neoplasm. *Endocr Pathol.* 2014;25(3):307–314.
- Donnellan KA, et al. Papillary thyroid carcinoma and familial adenomatous polyposis of the colon. *Am J Otolaryngol.* 2009;30(1):58–60.
- Ferreiro JA, et al. Columnar cell carcinoma of the thyroid: report of three additional cases. *Hum Pathol.* 1996;27:1156–1160.
- Francis Z, et al. Serum thyroglobulin determination in thyroid cancer patients. *Best Pract Res Clin Endocrinol Metab.* 2008;22(6):1039–1046.
- Gamboa-Dominguez A, et al. Macro-follicular variant of papillary thyroid carcinoma: a case and control analysis. *Endocr Pathol.* 1996;7:303–308.
- Ganly I, et al. Prognostic implications of papillary thyroid carcinoma with tall cell features. *Thyroid.* 2014;24(4):662–670.
- Gharib H, et al. Fine-needle aspiration cytology of the thyroid. A 12-year experience with 11,000 biopsies. *Clin Lab Med.* 1993;13:699–709.
- Ghossein R, et al. Papillary thyroid carcinoma tall cell variant. *Thyroid.* 2008;18(11):1179–1181.
- Giordano TJ, et al. Molecular classification of papillary thyroid carcinoma: distinct BRAF, RAS, and RET/PTC mutations-specific gene expression profiles discovered by DNA microarray analysis. *Oncogene.* 2005;24(44):6646–6656.
- Grodski S, et al. An update on papillary microcarcinoma. *Curr Opin Oncol.* 2009;21(1):1–4.
- Gupta S, et al. Follicular variant of papillary thyroid cancer: encapsulated, nonencapsulated, and diffuse: distinct biologic and clinical entities. *Arch Otolaryngol Head Neck Surg.* 2012;138(3):227–233.
- Harach HR, et al. Familial adenomatous polyposis associated thyroid carcinoma: a distinct type of follicular cell neoplasm. *Histopathology.* 1994;25(6):549–561.
- Hay ID, et al. Predicting outcome in papillary thyroid carcinoma: development of a reliable prognostic scoring system in a cohort of 1779 patients surgically treated at one institution during 1940 through 1989. *Surgery.* 1993;114(6):1050–1057.
- Hay ID, et al. Papillary thyroid carcinoma managed at the Mayo Clinic during six decades (1940–1999): temporal trends in initial therapy and longterm outcome in 2444 consecutively treated patients. *World J Surg.* 2002;26(8):879–885.
- Hundahl SA, et al. A National Cancer Data Base report on 53,856 cases of thyroid carcinoma treated in the U.S., 1985–1995. *Cancer.* 1998;83(12):2638–2648.
- Ito Y, et al. Prognostic significance of extrathyroid extension of papillary thyroid carcinoma: massive but not minimal extension affects the relapse-free survival. *World J Surg.* 2006;30(5):780–786.
- Ivanova R, et al. Diffuse (or multinodular) follicular variant of papillary thyroid carcinoma: a clinicopathologic and immunohistochemical analysis of ten cases of an aggressive form of differentiated thyroid carcinoma. *Virchows Arch.* 2002;440(4):418–424.
- Joung JY, et al. Diffuse sclerosing variant of papillary thyroid carcinoma: Major genetic alterations and prognostic implications. *Histopathology.* 2016;69(1):45–53.
- Jun P, et al. The sonographic features of papillary thyroid carcinomas: pictorial essay. *Ultrasound Q.* 2005;21(1):39–45.
- Lang W, et al. Occult carcinomas of the thyroid: evaluation of 1020 sequential autopsies. *Am J Clin Pathol.* 1988;90:72–76.
- Lang BH, et al. Staging systems for papillary thyroid carcinoma: a review and comparison. *Ann Surg.* 2007;245(3):366–378.
- Lee JH, et al. Clinicopathologic significance of BRAF V600E mutation in papillary carcinomas of the thyroid: a meta-analysis. *Cancer.* 2007;110(1):38–46.
- Li C, et al. BRAF V600E mutation and its association with clinicopathological features of papillary thyroid cancer: a metaanalysis. *J Clin Endocrinol Metab.* 2012;97(12):4559–4570.
- Lino-Silva LS, et al. Thyroid gland papillary carcinomas with “micropapillary pattern,” a recently recognized poor prognostic finding: clinicopathologic and survival analysis of 7 cases. *Human Pathol.* 2012;43(10):1596–1600.
- Liu X, et al. Highly prevalent TERT promoter mutations in aggressive thyroid cancers. *Endocr Rel Cancer.* 2013;20(4):603–610.
- Lloyd RV, et al. Observer variation in the diagnosis of follicular variant of papillary thyroid carcinoma. *Am J Surg Pathol.* 2004;28:1336–1340.
- Ludvíková M, et al. Oncocytic papillary carcinoma with lymphoid stroma (Warthin-like tumour) of the thyroid: a distinct entity with favourable prognosis. *Histopathology.* 2001;39(1):17–24.

53. Melo M, et al. TERT promoter mutations are a major indicator of poor outcome in differentiated thyroid carcinomas. *J Clin Endocrinol Metab*. 2014;99(5):E754–E765.
54. Mizukami Y, et al. Papillary thyroid carcinoma in Kanazawa, Japan: prognostic significance of histological subtypes. *Histopathology*. 1992;20(3):243–250.
55. Mizukami Y, et al. Diffuse follicular variant of papillary carcinoma of the thyroid. *Histopathology*. 1995;27(6):575–577.
56. Motosugi U, et al. Thyroid papillary carcinoma with micropapillary and hobnail growth pattern: a histological variant with intermediate malignancy? *Thyroid*. 2009;19(5):535–537.
57. Nakamura T, et al. Macrofollicular variant of papillary thyroid carcinoma. *Pathol Int*. 1998;48(6):467–470.
58. Nakatani Y, et al. Biotin-rich, optically clear nuclei express estrogen receptor-beta: tumors with morules may develop under the influence of estrogen and aberrant beta-catenin expression. *Human Pathol*. 2004;35(7):869–874.
59. Nardone HC, et al. c-Met expression in tall cell variant papillary carcinoma of the thyroid. *Cancer*. 2003;98:1386–1393.
60. Nikiforov YE. RET/PTC rearrangement in thyroid tumors. *Endocr Pathol*. 2002;13:3–16.
61. Nikiforov Y, et al. Pediatric thyroid cancer after the Chernobyl disaster. Pathomorphologic study of 84 cases (1991–1992) from the Republic of Belarus. *Cancer*. 1994;74(2):748–766.
62. Nikiforov YE, et al. Solid variant of papillary thyroid carcinoma: incidence, clinicopathologic characteristics, molecular analysis, and biologic behavior. *Am J Surg Pathol*. 2001;25(12):1478–1484.
63. Nikiforov YE, et al. Nomenclature revision for encapsulated follicular variant of papillary thyroid carcinoma: a paradigm shift to reduce overtreatment of indolent tumors. *JAMA Oncol*. 2016;2(8):1023–1029.
64. Nikiforova MN, et al. Molecular genetics of thyroid cancer: implications for diagnosis, treatment and prognosis. *Expert Rev Mol Diagn*. 2008;8(1):83–95.
65. Osamura RY, et al. Current practices in performing frozen sections for thyroid and parathyroid pathology. *Virchows Arch*. 2008;453(5):433–440.
66. Park SY, et al. Analysis of differential BRAF(V600E) mutational status in multifocal papillary thyroid carcinoma: evidence of independent clonal origin in distinct tumor foci. *Cancer*. 2006;107(8):1831–1838.
67. Piersanti M, et al. Controversies in papillary microcarcinoma of the thyroid. *Endocr Pathol*. 2003;14:183–191.
68. Prendiville S, et al. Tall cell variant: an aggressive form of papillary thyroid carcinoma. *Otolaryngol Head Neck Surg*. 2000;122:352–357.
69. Rassael H, et al. Microscopic papillary carcinoma of the thyroid gland: a non-surgical entity. A clinicopathologic correlation of 90 cases. *Eur Arch Otorhinolaryngol*. 1998;225:462–467.
70. Rosai J, et al. Papillary carcinoma of the thyroid: a discussion of its several morphologic expressions, with particular emphasis on the follicular variant. *Am J Surg Pathol*. 1983;7:809–817.
71. Rosai J. Immunohistochemical markers of thyroid tumors: significance and diagnostic applications. *Tumori*. 2003;89(5):517–519.
72. Rosenbaum MA, et al. Contemporary management of papillary carcinoma of the thyroid gland. *Expert Rev Anticancer Ther*. 2009;9(3):317–329.
73. Schröder S, et al. The encapsulated papillary carcinoma of the thyroid. A morphologic subtype of the papillary thyroid carcinoma. *Cancer*. 1984;54(1):90–93.
74. Schröder S, et al. Clear-cell carcinomas of thyroid gland: a clinicopathological study of 13 cases. *Histopathology*. 1986;10:75–89.
75. Scognamiglio T, et al. Diagnostic usefulness of HBME1, galectin3, CK19, and CITED1 and evaluation of their expression in encapsulated lesions with questionable features of papillary thyroid carcinoma. *Am J Clin Pathol*. 2006;126(5):700–708.
76. Sujoy V, et al. Columnar cell variant of papillary thyroid carcinoma: a study of 10 cases with emphasis on CDX2 expression. *Thyroid*. 2013;23(6):714–719.
77. Taccaliti A, et al. Genetic mutations in thyroid carcinoma. *Minerva Endocrinol*. 2009;34(1):11–28.
78. Thompson LDR, et al. Diffuse sclerosing papillary thyroid carcinoma. A clinicopathologic and immunophenotypic analysis of 22 cases. *Endo Pathol*. 2006;16:331–348.
79. Veronese N, et al. Prognostic impact of extranodal extension in thyroid cancer: a metaanalysis. *J Surg Oncol*. 2015;112(8):828–833.
80. Volante M, et al. Poorly differentiated thyroid carcinoma: the Turin proposal for the use of uniform diagnostic criteria and an algorithmic diagnostic approach. *Am J Surg Pathol*. 2007;31(8):1256–1264.
81. Wenig BM, et al. Thyroid papillary carcinoma of columnar cell type: a clinicopathologic study of 16 cases. *Cancer*. 1998;82:740–753.
82. Woenckhaus C, et al. Spindle cell variant of papillary thyroid carcinoma. *Histopathology*. 2004;45(4):424–427.
83. Xing M, et al. Association between BRAFV600E mutation and mortality in patients with papillary thyroid cancer. *JAMA*. 2013;309(14):1493–1501.
84. Yamamoto Y, et al. Occult papillary carcinoma of the thyroid. A study of 408 autopsy cases. *Cancer*. 1990;65(5):1173–1179.
85. Zhu Z, et al. Molecular profile and clinicopathologic features of the follicular variant of papillary thyroid carcinoma. An unusually high prevalence of ras mutations. *Am J Clin Pathol*. 2003;120(1):71–77.

## Follicular Carcinoma

1. Armstrong MJ, et al. PAX8/PPAR $\gamma$  rearrangement in thyroid nodules predicts follicular pattern carcinomas, in particular the encapsulated follicular variant of papillary carcinoma. *Thyroid*. 2014;24(9):1369–1374.
2. Asa SL. My approach to oncocytic tumours of the thyroid. *J Clin Pathol*. 2004;57(3):225–232.
3. Baloch ZW, et al. Our approach to follicular-patterned lesions of the thyroid. *J Clin Pathol*. 2007;60(3):244–250.
4. Baloch ZW, et al. Fine-needle aspiration of the thyroid: today and tomorrow. *Best Pract Res Clin Endocrinol Metab*. 2008;22(6):929–939.
5. Brennan MD, et al. Follicular thyroid cancer treated at the Mayo Clinic, 1946 through 1970: initial manifestations, pathologic features, therapy, and outcome. *Mayo Clin Proc*. 1991;66:11–22.
6. Cameselle Teijeiro J, et al. Follicular thyroid carcinoma with an unusual glomeruloid pattern of growth. *Human Pathol*. 2008;39(10):1540–1547.
7. Carcangiu ML, et al. Icar cell change in primary thyroid tumors. A study of 38 cases. *Am J Surg Pathol*. 1985;9(10):705–722.
8. Carcangiu ML, et al. Hürthle cell neoplasms of the thyroid gland. A study of 153 cases. *Cancer*. 1991;68:1944–1953.
9. Evans HL, et al. Follicular and Hürthle cell carcinomas of the thyroid: a comparative study. *Am J Surg Pathol*. 1998;22:1512–1520.
10. Giusiano Courcambek S, et al. Pure spindle cell follicular carcinoma of the thyroid. *Thyroid*. 2008;18(9):1023–1025.
11. Hundahl SA, et al. A National Cancer Data Base report on 53,856 cases of thyroid carcinoma treated in the U.S., 1985–1995. *Cancer*. 1998;83:2638–2648.
12. Ito Y, et al. Prognostic factors of minimally invasive follicular thyroid carcinoma: extensive vascular invasion significantly affects patient prognosis. *Endocr J*. 2013;60(5):637–642.
13. Ko HM, et al. Clinicopathologic analysis of fine needle aspiration cytology of the thyroid. A review of 1,613 cases and correlation with histopathologic diagnoses. *Acta Cytol*. 2003;47(5):727–732.
14. LiVolsi VA, et al. Follicular neoplasms of the thyroid: view, biases, and experiences. *Adv Anat Pathol*. 2004;11(6):279–287.
15. LiVolsi VA, et al. Use and abuse of frozen section in the diagnosis of follicular thyroid lesions. *Endocr Pathol*. 2005;16(4):285–293.
16. Mazzaferri EL. An overview of the management of papillary and follicular thyroid carcinoma. *Thyroid*. 1999;9(5):421–427.
17. Mete O, et al. Pathological definition and clinical significance of vascular invasion in thyroid carcinomas of follicular epithelial derivation. *Mod Pathol*. 2011;24(12):1545–1552.
18. Ngeow J, et al. Utility of PTEN protein dosage in predicting for underlying germline PTEN mutations among patients presenting with thyroid cancer and Cowden-like phenotypes. *J Clin Endocrinol Metab*. 2012;97(12):E2320–E2327.
19. Nikiforov YE. Thyroid carcinoma: molecular pathways and therapeutic targets. *Mod Pathol*. 2008;21 Suppl 2:S37–S43.
20. Nikiforova MN, et al. PAX8-PPAR gamma rearrangement in thyroid tumors: RT-PCR and immunohistochemical analyses. *Am J Surg Pathol*. 2002;26:1016–1023.
21. Oertel YC, et al. Diagnosis of malignant epithelial thyroid lesions: fine needle aspiration and histopathologic correlation. *Ann Diagn Pathol*. 1998;2(6):377–400.



22. Schröder S, et al. Clear cell carcinomas of thyroid gland: a clinicopathological study of 13 cases. *Histopathology*. 1986;10(1):75–89.
23. Thompson LDR, et al. Minimally invasive follicular thyroid carcinoma. *Endocr Pathol*. 2001;12(4):417–422.
24. Thompson LD, et al. A clinicopathologic study of minimally invasive follicular carcinoma of the thyroid gland with a review of the English literature. *Cancer*. 2001;91(3):505–524.
25. van Heerden JA, et al. Follicular thyroid carcinoma with capsular invasion alone: a nonthreatening malignancy. *Surgery*. 1992;112(6):1130–1136.
26. Wartofsky L, et al. The use of radioactive iodine in patients with papillary and follicular thyroid cancer. *J Clin Endocrinol Metab*. 1998;83(12):4195–4203.
27. Wu S, et al. Follicular lesions of the thyroid: a retrospective study of 1,348 fine needle aspiration biopsies. *Diagn Cytopathol*. 2012;40 Suppl 1:E812.
28. Xu B, et al. Prognostic impact of extent of vascular invasion in lowgrade encapsulated follicular cell derived thyroid carcinomas: a clinicopathologic study of 276 cases. *Human Pathol*. 2015;46(12):1789–1798.
29. Quiros RM, et al. Evidence that one subset of anaplastic thyroid carcinomas are derived from papillary carcinomas due to BRAF and p53 mutations. *Cancer*. 2005;103(11):2261–2268.
30. Smallridge RC, et al. Anaplastic thyroid cancer: molecular pathogenesis and emerging therapies. *Endocr Relat Cancer*. 2009;16(1):17–44.
31. Sugitani I, et al. Prognostic factors and treatment outcomes for anaplastic thyroid carcinoma: ATC Research Consortium of Japan cohort study of 677 patients. *World J Surg*. 2012;36(6):1247–1254.
32. Venkatesh YS, et al. Anaplastic carcinoma of the thyroid. A clinicopathologic study of 121 cases. *Cancer*. 1990;66:321–330.
33. Wan SK, et al. Paucicellular variant of anaplastic thyroid carcinoma. A mimic of Reidel's thyroiditis. *Am J Clin Pathol*. 1996;105(4):388–393.
34. Wang Y, et al. Clinical outcome of anaplastic thyroid carcinoma treated with radiotherapy of once- and twice- daily fractionation regimens. *Cancer*. 2006;107(8):1786–1792.

### Medullary Thyroid Carcinoma

#### Undifferentiated (Anaplastic) Carcinoma

1. Albores-Saavedra J, et al. Changing patterns in the incidence and survival of thyroid cancer with follicular phenotype—papillary, follicular, and anaplastic: a morphological and epidemiological study. *Endocr Pathol*. 2007;18(1):1–7.
2. Bishop JA, et al. PAX8 immunostaining of anaplastic thyroid carcinoma: a reliable means of discerning thyroid origin for undifferentiated tumors of the head and neck. *Human Pathol*. 2011;42(12):1873–1877.
3. Carcangiu ML, et al. Anaplastic thyroid carcinoma. A study of 70 cases. *Am J Clin Pathol*. 1985;83:135–158.
4. Chiacchio S, et al. Anaplastic thyroid cancer: prevalence, diagnosis and treatment. *Minerva Endocrinol*. 2008;33(4):341–357.
5. Cornett WR, et al. Anaplastic thyroid carcinoma: an overview. *Curr Oncol Rep*. 2007;9(2):152–158.
6. Gaffey MJ, et al. Anaplastic thyroid carcinoma with osteoclast-like giant cells. A clinicopathologic, immunohistochemical, and ultrastructural study. *Am J Surg Pathol*. 1991;15(2):160–168.
7. Garcia Rostan G, et al. Frequent mutation and nuclear localization of beta catenin in anaplastic thyroid carcinoma. *Can Res*. 1999;59(8):1811–1815.
8. Goutsouliak V, et al. Anaplastic thyroid cancer in British Columbia 1985-1999: a population-based study. *Clin Oncol (R Coll Radiol)*. 2005;17(2):75–78.
9. Heron DE, et al. Anaplastic thyroid carcinoma: comparison of conventional radiotherapy and hyperfractionation chemoradiotherapy in two groups. *Am J Clin Oncol*. 2002;25(5):442–446.
10. Jiang JY, et al. Prognostic factors of anaplastic thyroid carcinoma. *J Endocrinol Invest*. 2006;29(1):11–17.
11. Kunstman JW, et al. Characterization of the mutational landscape of anaplastic thyroid cancer via whole exome sequencing. *Hum Mol Genet*. 2015;24(8):2318–2329.
12. Miettinen M, et al. Variable expression of keratins and nearly uniform lack of thyroid transcription factor 1 in thyroid anaplastic carcinoma. *Hum Pathol*. 2000;31:1139–1145.
13. Mills SE, et al. Angiomatoid carcinoma and 'angiosarcoma' of the thyroid gland. A spectrum of endothelial differentiation. *Am J Clin Pathol*. 1994;102(3):322–330.
14. Murugan AK, et al. Anaplastic thyroid cancers harbor novel oncogenic mutations of the ALK gene. *Cancer Res*. 2011;71(13):4403–4411.
15. Neff RL, et al. Anaplastic thyroid cancer. *Endocrinol Metab Clin North Am*. 2008;37(2):525–538.
16. Nikiforov YE. Genetic alterations involved in the transition from well-differentiated to poorly differentiated and anaplastic thyroid carcinomas. *Endocr Pathol*. 2004;15(4):319–327.
17. Nonaka D, et al. Diagnostic utility of thyroid transcription factors Pax8 and TTF2 (FoxE1) in thyroid epithelial neoplasms. *Mod Pathol*. 2008;21(2):192–200.
18. Papi G, et al. Primary spindle cell lesions of the thyroid gland; an overview. *Am J Clin Pathol*. 2006;125 Suppl:S95–S123.
19. Pudney D, et al. Clinical experience of the multimodality management of anaplastic thyroid cancer and literature review. *Thyroid*. 2007;17(12):1243–1250.
20. Albores-Saavedra JA, et al. C-cell hyperplasia and medullary thyroid microcarcinoma. *Endocr Pathol*. 2001;12:365–377.
21. Beerman H, et al. Melanin production in black medullary thyroid carcinoma (MTC). *Histopathology*. 1990;16(3):227–233.
22. Bose S, et al. Medullary carcinoma of the thyroid: a cytological, immunocytochemical, and ultrastructural study. *Diagn Cytopathol*. 1992;8:28–32.
23. DeLellis RA, et al. Calcitonin and carcinoembryonic antigen as tumor markers in medullary thyroid carcinoma. *Am J Clin Pathol*. 1978;70(4):587–594.
24. Eng C, et al. The relationship between specific RET protooncogene mutations and disease phenotype in multiple endocrine neoplasia type 2. International RET mutation consortium analysis. *JAMA*. 1996;276(19):1575–1579.
25. Erickson LA, et al. Analysis of Amyloid in Medullary Thyroid Carcinoma by Mass Spectrometry-Based Proteomic Analysis. *Endocr Pathol*. 2015;26(4):291–295.
26. Golouh R, et al. Amphicrine-composite calcitonin and mucin producing carcinoma of the thyroid. *Ultrastructural Pathol*. 1985;8(23):197–206.
27. Guyétant S, et al. Medullary thyroid microcarcinoma: a clinicopathologic retrospective study of 38 patients with no prior familial disease. *Human Pathol*. 1999;30(8):957–963.
28. Harach HR, et al. Glandular (tubular and follicular) variants of medullary carcinoma of the thyroid. *Histopathology*. 1983;7(1):83–97.
29. Harach HR, et al. Medullary (C cell) carcinoma of the thyroid with features of follicular oxyphilic cell tumours. *Histopathology*. 1988;13(6):645–656.
30. Kakudo K, et al. Medullary carcinoma of the thyroid. Giant cell type. *Arch Pathol Lab Med*. 1978;102(9):44–57.
31. Kaserer K, et al. Recommendations for reporting C cell pathology of the thyroid. *Wien Klin Wochenschr*. 2002;114(7):27–48.
32. Landon G, et al. Clear cell variant of medullary carcinoma of the thyroid. *Human Pathol*. 1985;16(8):844–847.
33. Moline J, et al. Multiple endocrine neoplasia type 2: an overview. *Gen in Med*. 2011;13(9):755–764.
34. Moura MM, et al. High prevalence of RAS mutations in RET-negative sporadic medullary thyroid carcinomas. *J Clin Endocrinol Metab*. 2011;96(5):E863–E868.
35. Nakazawa T, et al. cell-derived calcitonin-free neuroendocrine carcinoma of the thyroid: the diagnostic importance of CGRP immunoreactivity. *Int J Surg Pathol*. 2014;22(6):530–535.
36. Norton JA, et al. Multiple endocrine neoplasia type IIb: the most aggressive form of medullary thyroid carcinoma. *Surg Clin N Am*. 1979;59(1):109–118.
37. Papaparaskeva K, et al. Cytologic diagnosis of medullary carcinoma of the thyroid gland. *Diagn Cytopathol*. 2000;22(6):351–358.
38. Perry A, et al. Physiologic versus neoplastic C-cell hyperplasia of the thyroid: separation of distinct histologic and biologic entities. *Cancer*. 1996;77(4):750–756.
39. Pillarisetty VG, et al. Micromedullary thyroid cancer: How micro is truly micro? *Ann Surg Oncol*. 2009;16(10):2875–2881.
40. Rowland KJ, et al. Hereditary thyroid cancer syndromes and genetic testing. *J Surg Oncol*. 2015;111(1):51–60.

22. Sadow PM, et al. Mixed Medullary-follicular-derived carcinomas of the thyroid gland. *Adv Anat Pathol*. 2010;17(4):282–285.
23. Sambade C, et al. Follicular and papillary variants of medullary carcinoma of the thyroid. *Pathol Res Pract*. 1988;184(1):9810–9817.
24. Santoro M, et al. Activation of RET as a dominant transforming gene by germline mutations of MEN2A and MEN2B. *Science*. 1995;267(5196):381–383.
25. Wells SA, et al. Revised American Thyroid Association guidelines for the management of medullary thyroid carcinoma. *Thyroid*. 2015;25(6):567–610.
26. Ye L, et al. The evolving field of tyrosine kinase inhibitors in the treatment of endocrine tumors. *Endocr Rev*. 2010;31(4):578–599.

### Primary Thyroid Lymphoma

1. Anscombe AM, et al. Primary malignant lymphoma of the thyroid: a tumour of mucosa-associated lymphoid tissue: review of seventy-six cases. *Histopathology*. 1985;9:81–97.
2. Bacon CM, et al. Follicular lymphoma of the thyroid gland. *Am J Surg Pathol*. 2009;33(1):22–34.
3. Compagno J, et al. Malignant lymphoma and other lymphoproliferative disorders of the thyroid gland. A clinicopathologic study of 245 cases. *Am J Clin Pathol*. 1980;74:1–11.
4. Derringer GA, et al. Malignant lymphoma of the thyroid gland: a clinicopathologic study of 108 cases. *Am J Surg Pathol*. 2000;24:623–639.
5. Devine RM, et al. Primary lymphoma of the thyroid: a review of the Mayo Clinic experience through 1978. *World J Surg*. 1981;5(1):33–38.
6. Fonseca E, et al. Primary lymphomas of the thyroid gland: a review with emphasis on diagnostic features. *Arch Anat Cytol Pathol*. 1998;46(1–2):94–99.
7. Graff Baker A, et al. Prognosis of primary thyroid lymphoma: demographic, clinical, and pathologic predictors of survival in 1,408 cases. *Surgery*. 2009;146(6):1105–1115.
8. Green LD, et al. Anaplastic thyroid cancer and primary thyroid lymphoma: a review of these rare thyroid malignancies. *J Surg Oncol*. 2006;94(8):725–736.
9. Isaacson PG. Lymphoma of the thyroid gland. *Curr Top Pathol*. 1997;91:1–14.
10. Kato I, et al. Chronic thyroiditis as a risk factor of B-cell lymphoma in the thyroid gland. *Jap J Can Res Gann*. 1985;76(11):1085–1090.
11. Koida S, et al. Primary T-cell lymphoma of the thyroid gland with chemokine receptors of Th1 phenotype complicating autoimmune thyroiditis. *Haematologica*. 2007;92(3):e37–e40.
12. Mian M, et al. High response rate and improvement of longterm survival with combined treatment modalities in patients with poor risk primary thyroid diffuse large B-cell lymphoma: an International Extranodal Lymphoma Study Group and Intergruppo Italiano Linfomi study. *Leuk Lymph*. 2011;52(5):823–832.
13. Oertel JE, et al. Lymphoma of the thyroid and related disorders. *Semin Oncol*. 1987;14:333–342.
14. Pedersen RK, et al. Primary non-Hodgkin's lymphoma of the thyroid gland: a population based study. *Histopathology*. 1996;28:25–32.
15. Stone CW, et al. Thyroid lymphoma with gastrointestinal involvement: report of three cases. *Am J Hematol*. 1986;21(4):357–365.
16. Streubel B, et al. T(3;14)(p14.1;q32) involving IGH and FOXP1 is a novel recurrent chromosomal aberration in MALT lymphoma. *Leukemia*. 2005;19(4):652–658.
17. Thieblemont C, et al. Primary thyroid lymphoma is a heterogeneous disease. *J Clin Endocrinol Metab*. 2002;87(1):105–111.
18. Wang SA, et al. Hodgkin's lymphoma of the thyroid: a clinicopathologic study of five cases and review of the literature. *Mod Pathol*. 2005;18(12):1577–1584.
19. Watanabe N, et al. Clinicopathological features of 171 cases of primary thyroid lymphoma: a longterm study involving 24,553 patients with Hashimoto's disease. *Br J Haematol*. 2011;153(2):236–243.

### Mucoepidermoid Carcinoma and Sclerosing Mucoepidermoid Carcinoma With Eosinophilia

1. Albores-Saavedra J, et al. Clear cells and thyroid transcription factor I reactivity in sclerosing mucoepidermoid carcinoma of the thyroid gland. *Ann Diagn Pathol*. 2003;7(6):348–353.

2. Ando M, et al. Mucoepidermoid carcinoma of the thyroid gland showing marked ciliation suggestive of its pathogenesis. *Pathol Int*. 2008;58(11):741–744.
3. Baloch ZW, et al. Primary mucoepidermoid carcinoma and sclerosing mucoepidermoid carcinoma with eosinophilia of the thyroid gland: a report of nine cases. *Mod Pathol*. 2000;13(7):802–807.
4. Bondeson L, et al. Cytologic features in fine-needle aspirates from a sclerosing mucoepidermoid thyroid carcinoma with eosinophilia. *Diagn Cytopathol*. 1996;15(4):301–305.
5. Chan JK, et al. Sclerosing mucoepidermoid thyroid carcinoma with eosinophilia. A distinctive low-grade malignancy arising from the metaplastic follicles of Hashimoto's thyroiditis. *Am J Surg Pathol*. 1991;15(5):438–448.
6. Farhat NA, et al. Primary mucoepidermoid carcinoma of the thyroid gland: a report of three cases and review of the literature. *Endocr Pathol*. 2013;24(4):229–233.
7. Geisinger KR, et al. The cytomorphologic features of sclerosing mucoepidermoid carcinoma of the thyroid gland with eosinophilia. *Am J Clin Pathol*. 1998;109(3):294–301.
8. Hunt JL, et al. p63 expression in sclerosing mucoepidermoid carcinomas with eosinophilia arising in the thyroid. *Mod Pathol*. 2004;17(5):526–529.
9. Lai CY, et al. Sclerosing mucoepidermoid carcinoma with eosinophilia of thyroid gland in a male patient: a case report and literature review. *Int J Clin Exp Pathol*. 2015;8(5):5947–5951.
10. Minagawa A, et al. A case of primary mucoepidermoid carcinoma of the thyroid: molecular evidence of its origin. *Clin Endocrinol (Oxf)*. 2002;57(4):551–556.
11. Musso-Lassalle S, et al. A diagnostic pitfall: nodular tumor-like squamous metaplasia with Hashimoto's thyroiditis mimicking a sclerosing mucoepidermoid carcinoma with eosinophilia. *Pathol Res Pract*. 2006;202(5):379–383.
12. Nath V, et al. Mucoepidermoid carcinoma of the thyroid with concomitant papillary carcinoma: comparison of findings on fine needle aspiration biopsy and histology. *Endocr Pathol*. 2014;25(4):427–432.
13. Prichard RS, et al. Mucoepidermoid carcinoma of the thyroid: a report of three cases and postulated histogenesis. *Thyroid*. 2012;22(2):205–209.
14. Rocha AS, et al. Mucoepidermoid carcinoma of the thyroid: a tumour histotype characterised by P-cadherin neoexpression and marked abnormalities of E-cadherin/catenins complex. *Virchows Arch*. 2002;440(5):498–504.
15. Shah AA, et al. Thyroid sclerosing mucoepidermoid carcinoma with eosinophilia: a clinicopathologic and molecular analysis of a distinct entity. *Mod Pathol*. 2016 Dec 2.
16. Shehadeh NJ, et al. Sclerosing mucoepidermoid carcinoma with eosinophilia of the thyroid: a case report and review of the literature. *Am J Otolaryngol*. 2004;25(1):48–53.
17. Sim SJ, et al. Sclerosing mucoepidermoid carcinoma with eosinophilia of the thyroid: report of two patients, one with distant metastasis, and review of the literature. *Hum Pathol*. 1997;28(9):1091–1096.
18. Solomon AC, et al. Thyroid sclerosing mucoepidermoid carcinoma with eosinophilia: mimic of Hodgkin disease in nodal metastases. *Arch Pathol Lab Med*. 2000;124(3):446–449.
19. Tirado Y, et al. CRTC1/MAML2 fusion transcript in high grade mucoepidermoid carcinomas of salivary and thyroid glands and Warthin's tumors: implications for histogenesis and biologic behavior. *Genes Chromosomes Cancer*. 2007;46(7):708–715.
20. Wenig BM, et al. Primary mucoepidermoid carcinoma of the thyroid gland: a report of six cases and a review of the literature of a follicular epithelial-derived tumor. *Hum Pathol*. 1995;26(10):1099–1108.

### Squamous Cell Carcinoma

1. Burman KD, et al. Unusual types of thyroid neoplasms. *Endocrinol Metab Clin North Am*. 1996;25(1):49–68.
2. Cook AM, et al. Squamous cell carcinoma of the thyroid: outcome of treatment in 16 patients. *Eur J Surg Oncol*. 1999;25(6):606–609.
3. Fassan M, et al. Primary squamous cell carcinoma of the thyroid: immunohistochemical profile and literature review. *Tumori*. 2007;93(5):518–521.
4. Lam KY, et al. Primary squamous cell carcinoma of the thyroid gland: an entity with aggressive clinical behaviour and distinctive cytokeratin expression profiles. *Histopathology*. 2001;39(3):279–286.



5. Lee JR, et al. Squamous cell carcinoma of the thyroid gland. *J Med Assoc Ga.* 1980;69(9):755–758.
6. Nakhjavani M, et al. Direct extension of malignant lesions to the thyroid gland from adjacent organs: report of 17 cases. *Endocr Pract.* 1999;5(2):69–71.
7. Ryska A, et al. Massive squamous metaplasia of the thyroid gland—report of three cases. *Pathol Res Pract.* 2006;202(2):99–106.
8. Sahoo M, et al. Primary squamous-cell carcinoma of the thyroid gland: new evidence in support of follicular epithelial cell origin. *Diagn Cytopathol.* 2002;27(4):227–231.
9. Simpson WJ, et al. Squamous cell carcinoma of the thyroid gland. *Am J Surg.* 1988;156(1):44–46.
10. Sparano A, et al. Predictors of thyroid gland invasion in glottic squamous cell carcinoma. *Laryngoscope.* 2005;115(7):1247–1250.
11. Tsuchiya A, et al. Squamous cell carcinoma of the thyroid—a report of three cases. *Jpn J Surg.* 1990;20(3):341–345.
10. Papi G, et al. Primary spindle cell lesions of the thyroid gland; an overview. *Am J Clin Pathol.* 2006;125 Suppl:S95–S123.
11. Reimann JD, et al. Carcinoma showing thymus-like differentiation of the thyroid (CASTLE): a comparative study: evidence of thymic differentiation and solid cell nest origin. *Am J Surg Pathol.* 2006;30(8):994–1001.
12. Wang YF, et al. Thyroid carcinoma showing thymus-like elements: a clinicopathologic, immunohistochemical, ultrastructural, and molecular analysis. *Am J Clin Pathol.* 2015;143(2):223–233.

### Spindle Cell Tumor With Thymus-Like Differentiation

1. Chan JK, et al. Tumors of the neck showing thymic or related branchial pouch differentiation: a unifying concept. *Hum Pathol.* 1991;22(4):349–367.
2. Cheuk W, et al. Spindle epithelial tumor with thymus-like differentiation (SETTLE): a distinctive malignant thyroid neoplasm with significant metastatic potential. *Mod Pathol.* 2000;13:1150–1155.
3. Folpe AL, et al. Spindle epithelial tumor with thymus-like differentiation: a morphologic, immunohistochemical, and molecular genetic study of 11 cases. *Am J Surg Pathol.* 2009;33(8):1179–1186.
4. Grushka JR, et al. Spindle epithelial tumor with thymus-like elements of the thyroid: a multi-institutional case series and review of the literature. *J Pediatr Surg.* 2009;44(5):944–948.
5. Ippolito S, et al. Spindle epithelial tumor with thymus-like differentiation (SETTLE): clinicopathological features, differential pathological diagnosis and therapy. *Endocrine.* 2016;51(3):402–412.
6. Iwasa K, et al. Spindle epithelial tumor with thymus-like differentiation (SETTLE) of the thyroid. *Head Neck.* 2002;24:888–893.
7. Recondo G, et al. Spindle epithelial tumor with thymus-like differentiation: a case report and comprehensive review of the literature and treatment options. *Head Neck.* 2015;37(5):746–754.
8. Su L, et al. Spindle epithelial tumor with thymus-like differentiation: a case report with cytologic, histologic, immunohistologic, and ultrastructural findings. *Mod Pathol.* 1997;10(5):510–514.
9. Xu B, et al. Spindle epithelial tumor with thymus-like differentiation of the thyroid: a case report with pathological and molecular genetics study. *Human Pathol.* 2003;34(2):190–193.

### Carcinoma Showing Thymus-Like Differentiation

1. Asa SL, et al. Primary thyroid thymoma: a distinct clinicopathologic entity. *Hum Pathol.* 1988;19:1463–1467.
2. Berezowski K, et al. CD5 immunoreactivity of epithelial cells in thymic carcinoma and CASTLE using paraffin-embedded tissue. *Am J Clin Pathol.* 1996;106(4):483–486.
3. Chan JK, et al. Tumors of the neck showing thymic or related branchial pouch differentiation: a unifying concept. *Hum Pathol.* 1991;22:349–367.
4. Chan LP, et al. Carcinoma showing thymus-like differentiation (CASTLE) of thyroid: a case report and literature review. *Kaohsiung J Med Sci.* 2008;24(11):591–597.
5. Chow SM, et al. Carcinoma showing thymus-like element (CASTLE) of thyroid: combined modality treatment in 3 patients with locally advanced disease. *Eur J Surg Oncol.* 2007;33(1):83–85.
6. Ito Y, et al. Clinicopathologic significance of intrathyroidal epithelial thymoma/carcinoma showing thymus-like differentiation: a collaborative study with Member Institutes of The Japanese Society of Thyroid Surgery. *Am J Clin Pathol.* 2007;127(2):230–236.
7. Kakudo K, et al. Intrathyroid epithelial thymoma (ITET) and carcinoma showing thymus-like differentiation (CASTLE): CD5-positive neoplasms mimicking squamous cell carcinoma of the thyroid. *Histol Histopathol.* 2013;28(5):543–556.
8. Liu Z, et al. Clinical analysis of thyroid carcinoma showing thymus-like differentiation: report of 8 cases. *Int Surg.* 2013;98(2):95–100.
9. Ng WK, et al. Cytologic Diagnosis of “CASTLE” of thyroid gland: report of a case with histologic correlation. *Diagn Cytopathol.* 1996;15(3):224–227.
1. Al Ghamdi S, et al. Malignant schwannoma of the thyroid gland. *Otolaryngol Head Neck Surg.* 2000;122:143–144.
2. Anagnostouli M, et al. Thyroid gland neurofibroma in a NF1 patient. *Acta Neurol Scand.* 2002;106:58–61.
3. Andrian A, et al. Leiomyoma and neurilemoma: report of two unusual non-epithelial tumours of the thyroid gland. *Virchows Arch A Pathol Anat Histopathol.* 1988;413:367–372.
4. Andrian A, et al. FNA cytology of thyroid neurilemmoma (schwannoma). *Diagn Cytopathol.* 1992;8:311–312.
5. Aoki T, et al. Primary neurilemoma of the thyroid gland: report of a case. *Surg Today.* 1993;23:265–268.
6. Aron M, et al. Neural tumours of the neck presenting as thyroid nodules: a report of three cases. *Cytopathology.* 2005;16(4):206–209.
7. Biankin SA, et al. Leiomyoma of the thyroid gland. *Pathology.* 1999;31:64–66.
8. Bohórquez CL, et al. Solitary fibrous tumor of the thyroid with capsular invasion. *Pathol Res Pract.* 2003;199(10):687–690.
9. Cameselle-Teijeiro J, et al. Solitary fibrous tumor of the thyroid. *Am J Clin Pathol.* 1994;101(4):535–538.
10. Chetty R, et al. Leiomyosarcoma of the thyroid: immunohistochemical and ultrastructural study. *Pathology.* 1993;25(2):203–205.
11. Conzo G, et al. Leiomyosarcoma of the thyroid gland: a case report and literature review. *Oncol Lett.* 2014;7(4):1011–1014.
12. Cutlan RT, et al. Immunohistochemical characterization of thyroid gland angiomatoid tumors. *Exp Mol Pathol.* 2000;69(2):159–164.
13. Dickersin GR. The electron microscopic spectrum of nerve sheath tumors. *Ultrastruct Pathol.* 1987;11:103–146.
14. Eloy JA, et al. Metastasis of uterine leiomyosarcoma to the thyroid gland: case report and review of the literature. *Thyroid.* 2007;17(12):1295–1297.
15. Erkilic S, et al. Primary leiomyoma of the thyroid gland. *J Laryngol Otol.* 2003;117:832–834.
16. Eusebi V, et al. Keratin-positive epithelioid angiosarcoma of thyroid. A report of four cases. *Am J Surg Pathol.* 1990;14(8):737–747.
17. Farrag TY, et al. Solitary fibrous tumor of the thyroid gland. *Laryngoscope.* 2009;119(12):2306–2308.
18. Goldstein J, et al. Primary Schwannoma of the thyroid gland. *Int Surg.* 1982;67:433–434.
19. Gustafson LM, et al. Primary neurilemoma of the thyroid gland: a case report. *Am J Otolaryngol.* 2001;22:84–86.
20. Jayaram G. Neurilemmoma (schwannoma) of the thyroid diagnosed by fine needle aspiration cytology. *Acta Cytol.* 1999;43:743–744.
21. Just PA, et al. An unusual clinical presentation of a rare tumor of the thyroid gland: report on one case of leiomyosarcoma and review of literature. *Ann Diagn Pathol.* 2008;12(1):50–56.
22. Kandil E, et al. Primary peripheral nerve sheath tumors of the thyroid gland. *Thyroid.* 2010;20(6):583–586.
23. Kawahara E, et al. Leiomyosarcoma of the thyroid gland. A case report with a comparative study of five cases of anaplastic carcinoma. *Cancer.* 1988;62(12):2558–2563.
24. Leslie MD, et al. Malignant transformation of neurofibromas at multiple sites in a case of neurofibromatosis. *Postgrad Med J.* 1987;63:131–133.
25. Lucioni M, et al. Paediatric laryngeal malignant nerve sheath tumour. *Int J Pediatr Otorhinolaryngol.* 2007;71(12):1917–1920.
26. Maiorana A, et al. Epithelioid angiosarcoma of the thyroid. Clinicopathological analysis of seven cases from non-Alpine areas. *Virchows Arch.* 1996;429(2–3):131–137.
27. Miettinen M, et al. Sox10 A marker for not only schwannian and melanocytic neoplasms but also myoepithelial cell tumors of soft tissue: a systematic analysis of 5134 tumors. *Am J Surg Pathol.* 2015;39(6):826–835.

28. Mizuuchi Y, et al. Solitary fibrous tumor of the thyroid gland. *Med Mol Morphol*. 2014;47(2):117–122.
29. Pallares J, et al. Malignant peripheral nerve sheath tumor of the thyroid: a clinicopathological and ultrastructural study of one case. *Endocr Pathol*. 2004;15:167–174.
30. Papi G, et al. Primary spindle cell lesions of the thyroid gland; an overview. *Am J Clin Pathol*. 2006;125 Suppl:S95–S123.
31. Papi G, et al. Solitary fibrous tumor of the thyroid gland. *Thyroid*. 2007;17(2):119–126.
32. Papotti M, et al. Diagnostic controversies in vascular proliferations of the thyroid gland. *Endocr Pathol*. 2008;19(3):175–183.
33. Rodriguez I, et al. Solitary fibrous tumor of the thyroid gland: report of seven cases. *Am J Surg Pathol*. 2001;25(11):1424–1428.
34. Ryska A, et al. Epithelioid haemangiosarcoma of the thyroid gland. Report of six cases from a non-Alpine region. *Histopathology*. 2004;44(1):40–46.
35. Sugita R, et al. Primary schwannoma of the thyroid gland: CT findings. *AJR Am J Roentgenol*. 1998;171:528–529.
36. Surov A, et al. Primary Thyroid Sarcoma: A Systematic Review. *Anticancer Res*. 2015;35(10):5185–5191.
37. Tanahashi J, et al. Solitary fibrous tumor of the thyroid gland: report of two cases and review of the literature. *Pathol Int*. 2006;56(8):471–477.
38. Thompson LDR, et al. Peripheral nerve sheath tumors of the thyroid gland: a series of four cases and a review of the literature. *Endocr Pathol*. 1996;7:309–318.
39. Thompson LDR, et al. Primary smooth muscle tumors of the thyroid gland. *Cancer*. 1997;79:579–587.
40. Tullbah A, et al. Epstein-Barr virus-associated leiomyosarcoma of the thyroid in a child with congenital immunodeficiency: a case report. *Am J Surg Pathol*. 1999;23(4):473–476.
41. Vege DS, et al. Malignant peripheral nerve sheath tumors of the head and neck: a clinicopathological study. *J Surg Oncol*. 1994;55:100–103.
42. Wang TS, et al. Primary leiomyosarcoma of the thyroid gland. *Thyroid*. 2008;18(4):425–428.
43. Yildirim G, et al. Concurrent epithelioid malignant peripheral nerve sheath tumor and papillary thyroid carcinoma in the treated field of Hodgkin's disease. *Head Neck*. 2008;30(5):675–679.

## Metastatic Neoplasms

1. Chen H, et al. Clinically significant, isolated metastatic disease to the thyroid gland. *World J Surg*. 1999;23(2):177–180.
2. Cimino-Mathews A, et al. Diagnostic use of PAX8, CAIX, TTF-1, and TGB in metastatic renal cell carcinoma of the thyroid. *Am J Surg Pathol*. 2011;35(5):757–761.
3. Czech JM, et al. Neoplasms metastatic to the thyroid gland. *Surg Gynecol Obstet*. 1982;155:503–505.
4. Dušková J, et al. Secondary or second primary malignancy in the thyroid? metastatic tumors suggested clinically: a differential diagnostic task. *Acta Cytol*. 2014;58(3):262–268.
5. Heffess CS, et al. Metastatic renal cell carcinoma to the thyroid gland: a clinicopathologic study of 36 cases. *Cancer*. 2002;95:1869–1878.
6. Kim TY, et al. Metastasis to the thyroid diagnosed by fine-needle aspiration biopsy. *Clin Endocrinol*. 2005;62(2):236–241.
7. Lam KY, et al. Metastatic tumors of the thyroid gland: a study of 79 cases in Chinese patients. *Arch Pathol Lab Med*. 1998;122(1):37–41.
8. Liu YP, et al. Thyroid metastasis from breast cancer presenting with diffuse microcalcifications on sonography: a case report. *J Clin Ultrasound*. 2014;42(7):430–432.
9. Nabili V, et al. Collision tumor of thyroid: metastatic lung adenocarcinoma plus papillary thyroid carcinoma. *Am J Otolaryngol*. 2007;28(3):218–220.
10. Nakhjavani MK, et al. Metastasis to the thyroid gland. A report of 43 cases. *Cancer*. 1997;79:574–578.
11. Nakhjavani M, et al. Direct extension of malignant lesions to the thyroid gland from adjacent organs: report of 17 cases. *Endocr Pract*. 1999;5(2):69–71.
12. Papi G, et al. Metastases to the thyroid gland: prevalence, clinicopathological aspects and prognosis: a 10-year experience. *Clin Endocrinol*. 2007;66(4):565–571.
13. Pusztaszeri M, et al. Fine needle aspiration biopsy of secondary neoplasms of the thyroid gland: a multi-institutional study of 62 cases. *Cancer Cytopathol*. 2015;123(1):192–199.
14. Wood K, et al. Metastases to the thyroid gland: the Royal Marsden experience. *Eur J Surg Oncol*. 2004;30(6):583–588.



# Non-Neoplastic Lesions of the Parathyroid Glands

■ **Lester D.R. Thompson**

## ■ GENERAL CONSIDERATIONS

There are a variable number of glands (2 to 10), but usually four are present, symmetrically arranged within the upper and lower poles of the bilateral thyroid gland. Approximately 5% of people have more than four glands. The glands are usually soft, pliable, and measure < 0.5 cm (5 mm), with a combined weight of approximately 120 to 140 mg. It is agreed that no single gland should be more than 60 mg, although the lower glands are often slightly larger than the upper glands. Embryologically, the upper pair arise from the fourth branchial pouch, whereas the lower pair arise from the third branchial pouch. Notably, glands can be found anywhere along the normal route of migration, resulting in glands embedded within the thymus, pericardium, esophagus, and mediastinum.

The parathyroid gland is composed of four cell types:

- The chief cell (6 to 8  $\mu$ m), a small polygonal cell with central round nucleus and abundant cytoplasmic secretory granules, is the basic functional cell involved in parathyroid hormone (parathormone, PTH) secretion.
- The oxyphilic or oncocytic cell (12  $\mu$ m) is slightly larger than chief cells, with abundant granular cytoplasm, ultrastructurally shown to be packed with mitochondria. These cells increase in number as the patient ages and tend to occur in nodules.
- The water-clear cell (quite rare) has well-defined cell borders and abundant clear cytoplasm due to excessive glycogen.
- Adipocytes, which also increase with age, compose up to 60% of the cellular mass. A general rule of thumb: 50% parenchymal fat at 50 years of age. There also tends to be more stromal fat at the poles of the gland(s).

The cellular components are arranged in cords, sheets, and pseudoglandular or pseudoacinar patterns. Age, sex, body fat, and other factors affect normal parathyroid gland cellularity.

In short, the principal function of the parathyroid glands is calcium homeostasis, briefly discussed here (spatial constraints limit this discussion). Calcium homeostasis is maintained within narrow limits (approximately 8 to 10 mg/dL) by the balance between variables increasing serum calcium (dietary intake, intestinal absorption, and bone resorption) and those decreasing serum calcium (bone accretion and urinary/fluid excretion). Nearly 99% of calcium is stored in the skeletal system, and osteoclastic resorption is most important. The three most important hormones are PTH, calcitonin (secreted by thyroid C cells), and vitamin D.

PTH is a polypeptide hormone (84 amino acid residues; the n-terminal is active, whereas the c-terminal is assayed) that increases blood calcium levels by stimulating osteoclastic resorption of bone and decreasing urinary excretion of calcium, while increasing renal phosphate excretion. This results in hypophosphatemia and can cause metabolic acidosis due to inhibition of  $\text{HCO}_3^-$ . The half-life of PTH is 20 to 30 minutes. Abnormal or decreased function of the parathyroid glands results in disorders of calcium metabolism, characterized by too little (e.g., osteomalacia, pseudo hypoparathyroidism) or too much (e.g., milk-alkali syndrome, calcinosis) calcium. PTH also stimulates production of 1,25 dihydroxy-cholecalciferol (calcitriol), the hormonally active form of vitamin D, which increases the uptake of calcium from the gut, decreases urinary excretion of calcium, and increases the release of calcium from bone.

Parathyroid non-neoplastic disorders include aplasia, cysts, parathyroiditis, and hyperplasia. The discussion will be limited to hyperplasia.

Hyperparathyroidism is a state of elevated serum PTH as a result of excessive secretion. It is separated into primary, secondary, and tertiary, with primary hyperparathyroidism caused most commonly by adenoma (80%), hyperplasia (15%), and carcinoma (5%). The inappropriately increased PTH is due to an intrinsic abnormality in the gland(s) rather than a known stimulus for PTH secretion. Most hyperplasia results from secondary hyperparathyroidism, in which there is an increase

in parathyroid parenchymal cell mass within multiple glands in response to a known clinical stimulus for increased secretion of PTH, such as chronic renal failure, malabsorption, and abnormalities of vitamin D metabolism. It is usually characterized by hypocalcemia and hyperphosphatemia. Similarly, tertiary hyperparathyroidism is generally characterized by four-gland hyperplasia in a state of autonomous hypersecretion.

## ■ PRIMARY CHIEF CELL HYPERPLASIA

Primary chief cell hyperplasia is a non-neoplastic absolute increase in the parenchymal cell mass within multiple parathyroid glands without a known clinical stimulus for increased PTH secretion. There is an annual incidence of approximately 4 per 100,000 persons per year in the United States.

### CLINICAL FEATURES

Approximately 15% of all primary hyperparathyroidism is caused by primary chief cell hyperplasia. Women are

#### PRIMARY CHIEF CELL HYPERPLASIA—DISEASE FACT SHEET

##### Definition

- Non-neoplastic absolute increase in parathyroid parenchymal cell mass within all parathyroid tissue without a known stimulus

##### Incidence

- Approximately 40/million population

##### Morbidity and Mortality

- Calcium metabolism abnormality
- Cardiovascular disease may cause death

##### Sex and Age Distribution

- Females > males (2-3:1)
- Adults, 40-60 years (mean, 5th decade)
- Younger (25 years) in syndrome associated patients

##### Clinical Features

- 20% may be familial
- Asymptomatic, discovered during multichannel analyzer studies
- If symptomatic: fatigue, lethargy, anorexia, weakness, vomiting, depression, polyuria, polydipsia, hypertension
- “Bones, stones, abdominal moans” not seen often
- Nephrolithiasis, nephrocalcinosis
- Biochemical findings include elevated calcium, decreased inorganic phosphorus, and increased parathyroid hormone levels

##### Prognosis and Therapy

- Excellent, although recurrences occur (~15%)
- Surgery with autotransplantation

affected much more commonly than men (2 to 3:1), with the overall incidence increasing with age (especially in postmenopausal women). The mean age at presentation is the 5th decade. Most patients present with sporadic disease (80%), although approximately 20% of patients have familial disease (most commonly multiple endocrine neoplasia [MEN] syndromes). Patients tend to present much younger (mid-twenties) when syndrome associated, without a sex predilection. MEN1 (Wermer syndrome) is the most common syndrome, with nearly 90% of patients having parathyroid hyperplasia. The *MEN1* gene is localized on chromosome 11q13. Up to approximately 30% of patients with MEN2A (Sipple syndrome) have parathyroid proliferative disease but it is very rare in MEN2B. Patients may also present as part of autosomal dominant familial isolated hyperparathyroidism, calcium-sensing receptor (*CASR*) mutation, familial hypocalciuric hypercalcemia, neonatal severe primary hyperparathyroidism, and hyperparathyroidism–jaw tumor (HPT-JT) syndrome.

A fair number of patients are asymptomatic, the disorder discovered incidentally during routine multiphasic screening for other reasons. The presentation is often varied but vague, including fatigue, lethargy, anorexia, weakness, nausea, vomiting, constipation, polyuria, polydipsia, hypertension, arthralgias, and psychiatric symptoms. The classic triad of “bones, stones, and abdominal moans” is rarely seen in modern care but refers to osteitis fibrosa cystica (brown tumor of bone), kidney stones, and peptic ulcer disease, respectively. Work-up often reveals nephrocalcinosis, nephrolithiasis, and metastatic calcifications. Psychiatric or mental changes are frequent and include emotional instability, depression, psychosis, and confusion. Symptoms relate specifically to the degree (serum level) and duration of calcium elevation. Rarely, patients present with a neck mass.

Biochemical findings include an elevation of serum ionized calcium levels, with corresponding decrease in serum inorganic phosphorus concentrations and associated high serum alkaline phosphatase. Serum PTH levels, using the intact hormone assay, will usually be increased above the normal range of 10-65 pg/mL. In addition, there will be a high urine calcium, cAMP, hydroxyproline, and phosphate.

### RADIOGRAPHIC FEATURES

<sup>99m</sup>Tc sestamibi imaging is the preferred technique for detecting the topographic location of parathyroid tissue (Fig. 26.1), although limited in detecting hyperplasia, with greater clinical utility for detecting adenoma or carcinoma. In general, radiographic studies are primarily used in the setting of recurrent disease after failed surgery. Single-photon emission computed tomography (SPECT) with the use of <sup>99m</sup>Tc sestamibi as the radiotracer,



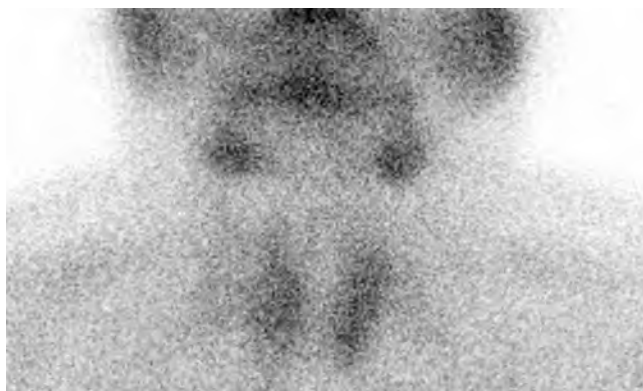


**FIGURE 26.1**

A delayed  $^{99m}\text{Tc}$  sestamibi image demonstrates uneven, increased uptake in all glands, consistent with hyperplasia. (Courtesy of Dr W. Chen.)

especially when combined with computed tomography, can help with preoperative localization. Unusual locations of (ectopic) parathyroid tissue may be identified with magnetic resonance imaging using gadolinium and fat-suppression techniques. However, hyperplasia does not enhance as much with gadolinium as does an adenoma. Ultrasound (US), when used by an experienced investigator, can be a good alternative if scintigraphic studies are inconclusive. Furthermore, US may be used to guide fine needle aspiration (FNA) or guide retrograde venous sampling to determine PTH levels.

## **PATHOLOGIC FEATURES**

### **GROSS FINDINGS**

In hyperplasia, all four glands will be affected, although sometimes not to the same degree, creating uneven or nodular hyperplasia or asymmetric enlargement, the latter more common in MEN1 associated disease. Traditionally, two glands should be sampled, including a “normal” gland to accurately separate adenoma and hyperplasia. However, with significant improvements in radiographic studies and intraoperative rapid PTH assessments, reliable and accurate separation may be achieved. Diffuse or nodular enlargement is noted, with cystic change occasionally identified. The glands are usually (approximately 50% of cases) less than 1 g in total weight, although approximately 30% are 1 to 5 g, and the remaining 20% are greater than 5 g. The glands are soft and tan-brown.

### **MICROSCOPIC FINDINGS**

#### **Primary Chief Cell Hyperplasia**

The histology of all the glands is similarly affected, although variation in cellularity is common. The parenchymal component shows increased cellularity with a

## **PRIMARY CHIEF CELL HYPERPLASIA—PATHOLOGIC FEATURES**

### **Gross Findings**

- All glands affected, although not equally (two glands sampled for accurate diagnosis)
- Diffuse or nodular enlargement
- Soft, tan-brown glands

### **Microscopic Findings**

- Variance between glands is common, but all are affected
- Parenchyma increased with decreased stromal fat content
- Cellularity increased
- Chief and oncocytic cells increased
- Solid, follicular, and cord-like patterns may be seen
- Secondary changes are common

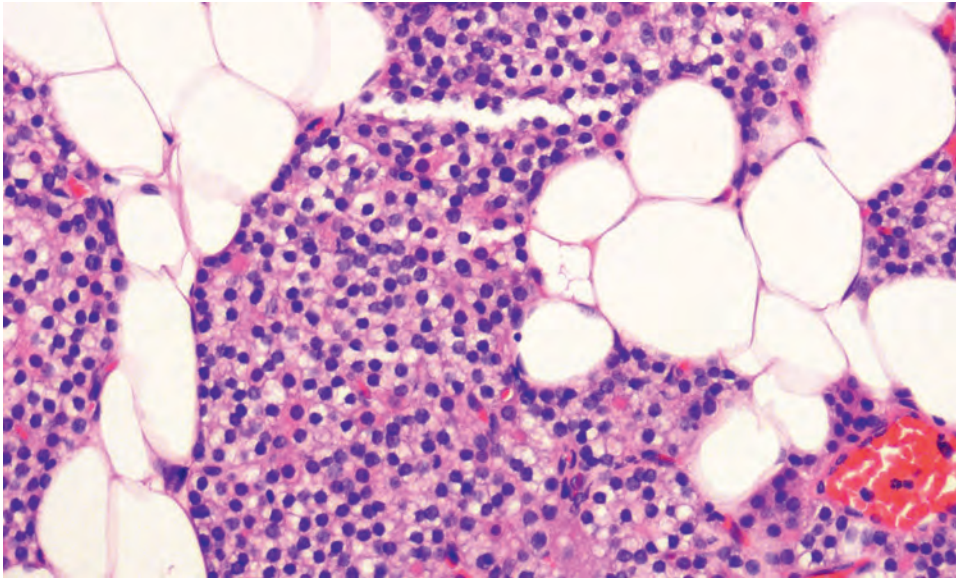
### **Pathologic Differential Diagnosis**

- Parathyroid adenoma, parathyroid carcinoma, thyroid gland tumors, metastatic renal cell carcinoma

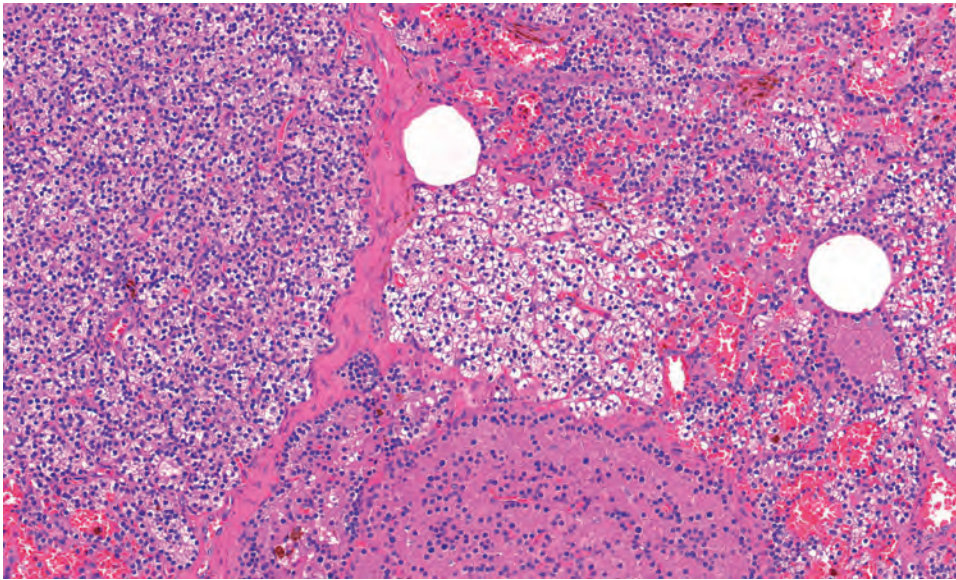
commensurate decrease in stromal fat (Figs. 26.2 and 26.3). The process can appear nodular, multinodular, or diffuse, depending on the increasing proportion of the gland involved (Fig. 26.4). Notably, the process may extend into the soft tissue surrounding the parathyroid gland and should not be overinterpreted as “invasive” (Fig. 26.5). Overall, the cellularity is increased, even if it varies between glands. In general, chief cells are preferentially increased, but oncocytes and clear cells may show variable degrees of increased cellularity (Fig. 26.6). A variety of different architectural patterns, including solid, follicular (Fig. 26.7), and cord-like patterns (Fig. 26.8), are noted, in addition to a vaguely nodular appearance (Fig. 26.9), the latter more common in elderly patients. Chief cells are polyhedral, with round, centrally located nuclei. The cytoplasm can be amphophilic, clear, or vacuolated. Oncocytic cells are much larger, with abundant eosinophilic, granular cytoplasm surrounding slightly larger nuclei (Fig. 26.10). Cellular atypia may be seen, but it is usually not widespread or profound. Mitoses are usually less than 5 per 10 high-power fields, without atypical forms. Secondary changes including fibrosis, hemorrhage, hemosiderin-laden macrophages, cholesterol clefts, and cyst formation are common findings (Fig. 26.11). Intracellular glycogen is often increased in hyperplastic glands above what is seen in atrophy or adenoma. Stromal adipose tissue is decreased.

#### **Water-Clear Cell Hyperplasia**

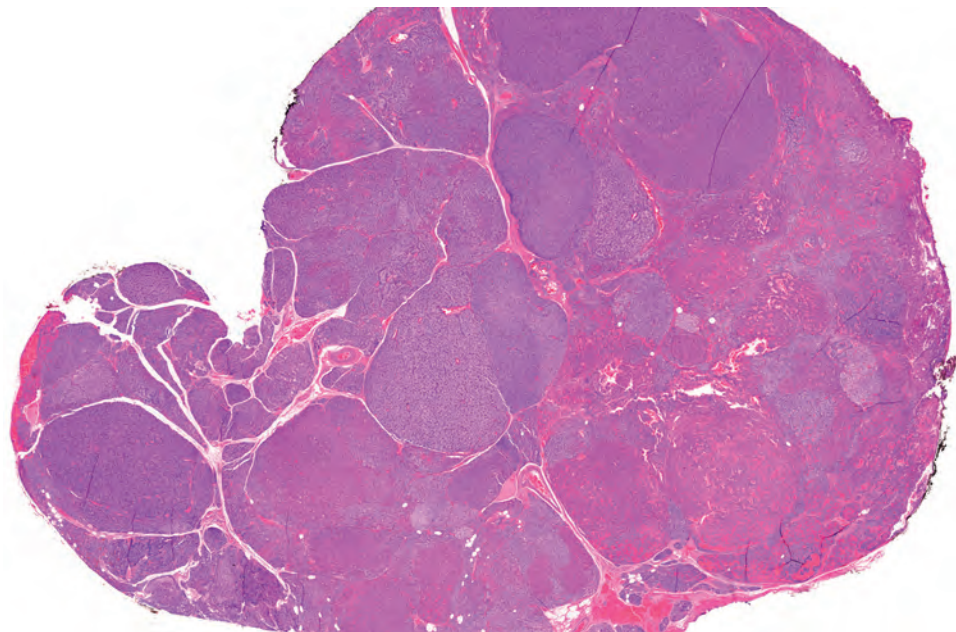
This very uncommon type of hyperplasia is seen slightly more often in men, most commonly in the 5th decade of life. The upper glands tend to be preferentially involved, and all reported cases have a combined gland weight of greater than 1 g. The large cells have cytoplasm

**FIGURE 26.2**

Normal parathyroid gland tissue showing an appropriate distribution of parathyroid parenchyma and stromal fat. There are chief cells and oncocytic cells within the parenchyma. The cellularity is ~50% and appropriate for a 50-year-old patient without health problems and a normal body habitus.

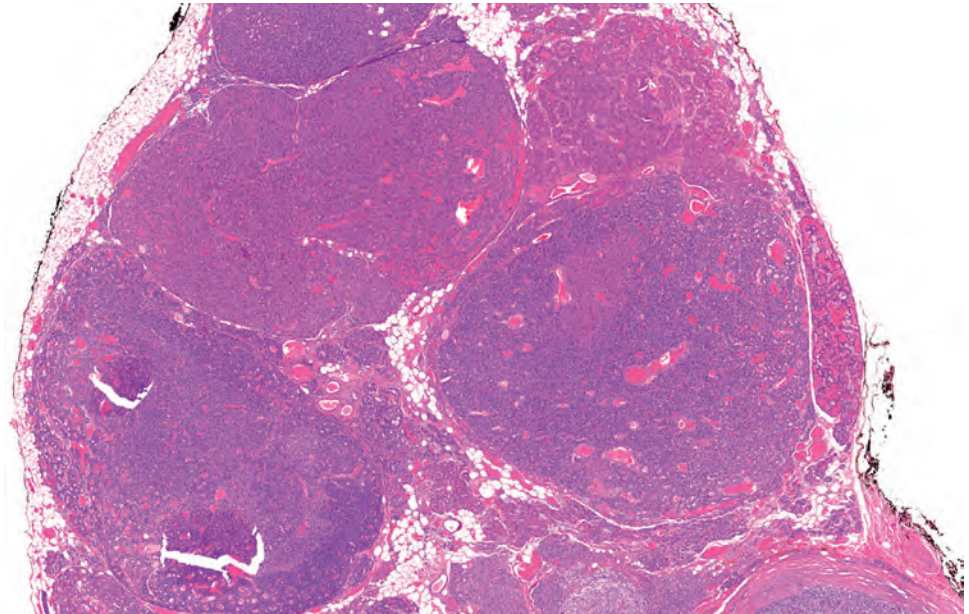
**FIGURE 26.3**

The entire gland reveals an increased parenchymal cellularity with a decrease in the amount of stromal adipose tissue in this hyperplastic parathyroid gland.

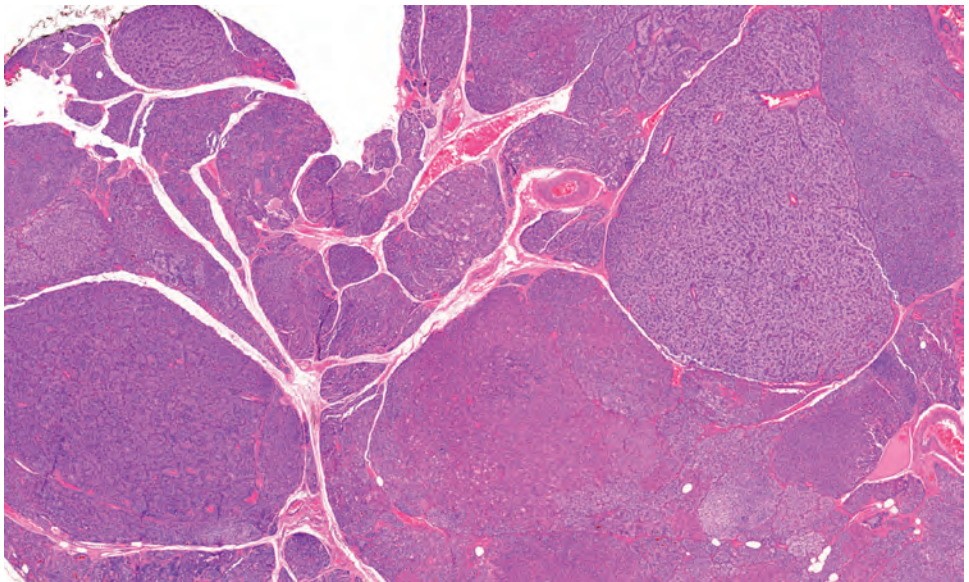
**FIGURE 26.4**

Multiple nodules are noted within this cellular parathyroid gland. There is fibrosis but not capsule formation. Note the presence of chief and oncocytic cells, arranged in variably sized nodules.

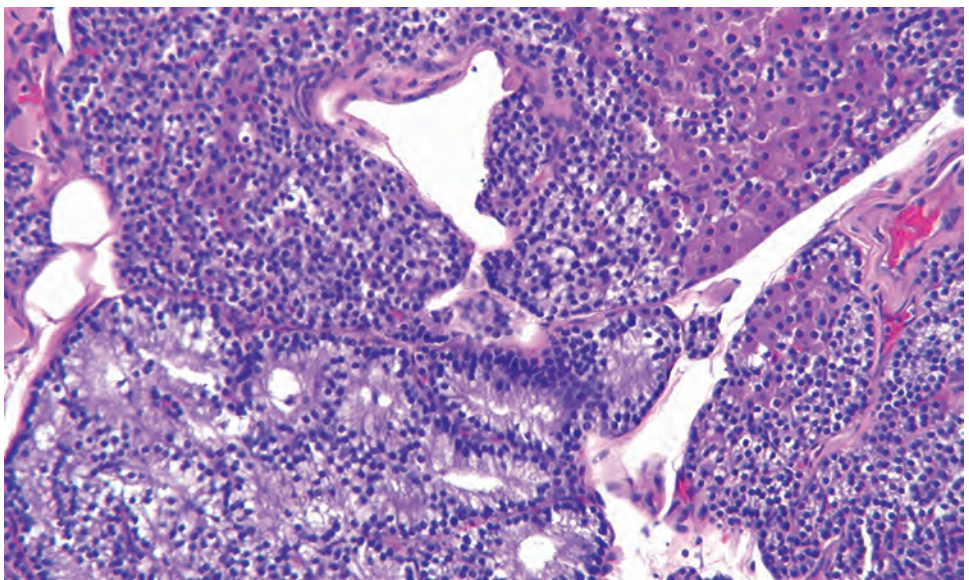


**FIGURE 26.5**

The hyperplastic parenchymal tissue has expanded into the adjacent adipose tissue, although separation from stromal adipose tissue can be challenging.

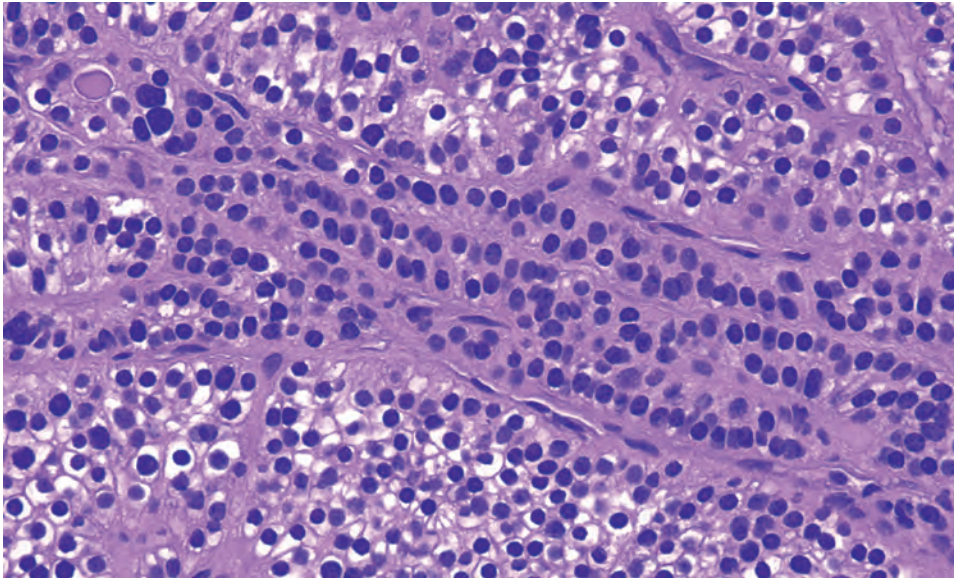
**FIGURE 26.6**

A hyperplastic gland shows a multinodular appearance, with variably sized nodules of both chief and oncocytic cells. There is virtually no stromal adipose tissue in this gland.

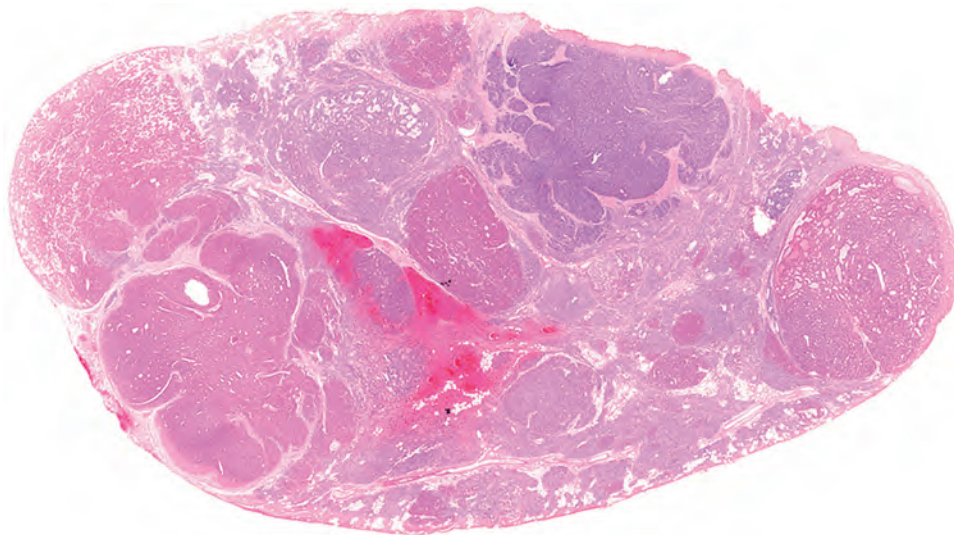
**FIGURE 26.7**

Solid and follicular patterns of growth are identified. A few oncocytic cells are also identified in the predominantly chief cell hyperplasia.

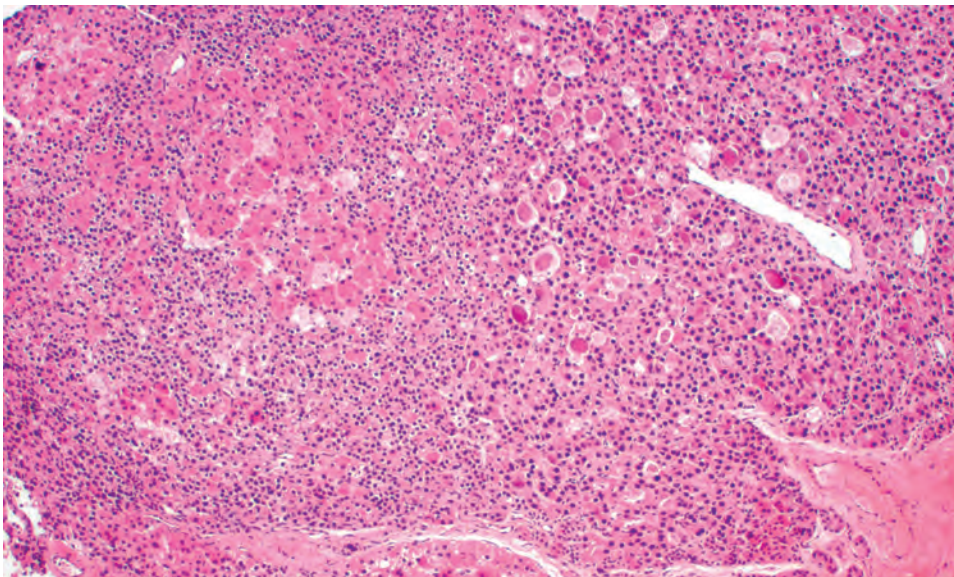


**FIGURE 26.8**

Cord-like growth is present in this example of parathyroid hyperplasia.

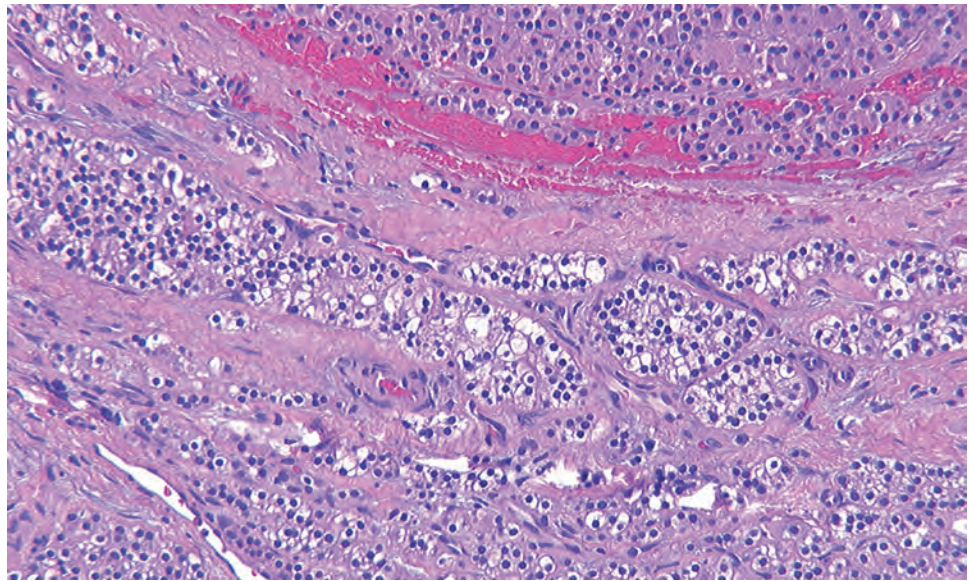
**FIGURE 26.9**

A number of nodules of oncocytic cells are noted in this sample of hyperplasia, associated with chief cell nodules in the immediately adjacent tissues. There is a remarkably decreased adipose tissue content.

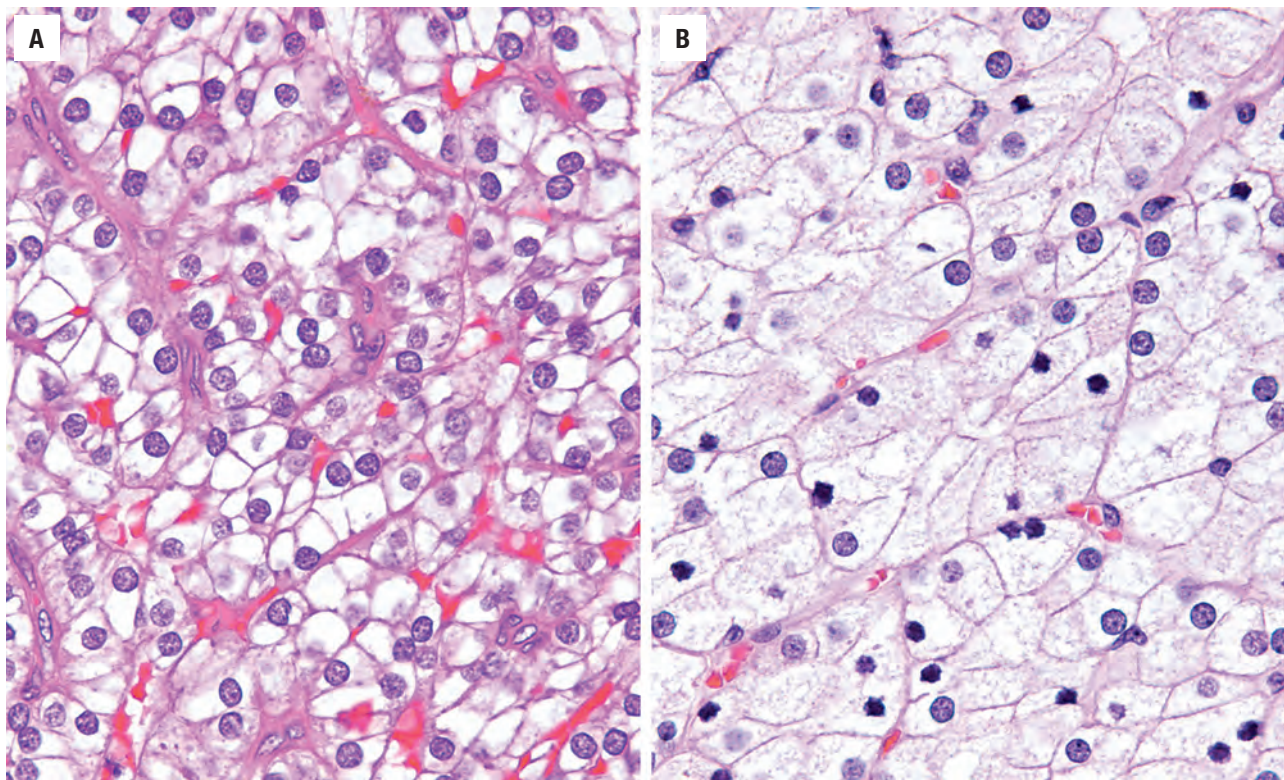
**FIGURE 26.10**

This nodule shows a predominantly oncocytic appearance, with large cells showing abundant granular eosinophilic cytoplasm but with a low nuclear to cytoplasmic ratio.



**FIGURE 26.11**

Fibrosis and hemorrhage are seen within this example of parathyroid hyperplasia.

**FIGURE 26.12**

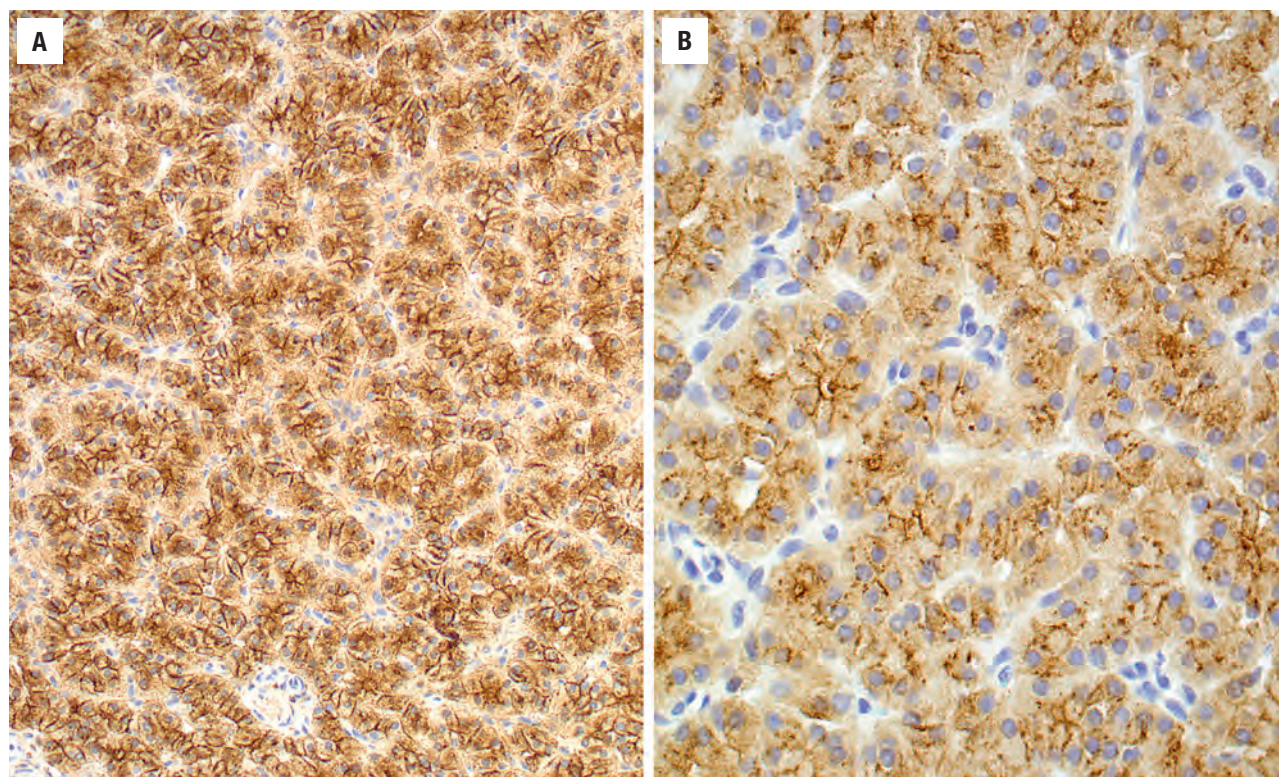
Water-clear cell hyperplasia presents with optically clear cytoplasm on frozen section material (**A**), but standard processing yields a finely reticulated cytoplasm on routine processing (**B**). The cell borders are prominent and the nuclei tend to be basally oriented.

that is completely clear on hematoxylin and eosin (Fig. 26.12). The feature is usually present on frozen section material, whereas usual processing may cause the artifact to be lost, resulting in a finely reticulated cytoplasm composed of numerous small vacuoles. Cell borders are prominent. The nuclei tend to be basally oriented. There is no stromal adipose tissue present. Neutral fat stains are negative, but glycogen is present in the cytoplasm.

#### ANCILLARY STUDIES

FNA does not reliably separate between adenoma and hyperplasia and therefore is not of value. The chief cells will be positive for keratins, chromogranin, synaptophysin, CD56, and PTH (Fig. 26.13), while negative for TTF1 and thyroglobulin, but immunohistochemical studies do not help with the principal differential diagnostic



**FIGURE 26.13**

This example of parathyroid hyperplasia shows the normal staining of the cells with chromogranin (**A**) and parathyroid hormone (**B**). Staining may be useful in separating between primary parathyroid diseases and metastases.

consideration: adenoma. CD4 may be positive on the cell surface (membranous pattern), usually of only chief cells. Fat staining of cryostat sections may help to discriminate between normal and slightly hyperplastic glands (less *intracytoplasmic* fat than normal cells) but is not always helpful. Cyclin D1 overexpression is seen in up to 30 % of hyperplastic glands.

The use of intraoperative PTH assays has profoundly altered the management of parathyroid disease. An intraoperative decline of PTH to normal levels at 10 minutes and greater than 50 % of the initial baseline value suggests surgical cure. Furthermore, the use of chemical evaluation is resulting in a decrease of intraoperative frozen section consultation in parathyroid surgery.

*MEN1* mutations are common in MEN1 patients, although most are a new sporadic mutation; *RET* mutations may be seen in MEN2A patients; *CASR* mutations are not usually present in sporadic parathyroid disease (although homozygous inactivating mutations seen in neonatal severe hyperparathyroidism); germline *HRPT2* mutations may be seen in HPT-JT syndrome associated hyperplasia.

### DIFFERENTIAL DIAGNOSIS

The principal differential is with parathyroid adenoma, although sometimes in recurrent disease, separation from

parathyroid carcinoma may be more difficult. Tiny glandular biopsies from normal associated glands are difficult to interpret because the distribution of parenchymal and fat cells is often irregular. Identification of a capsule, a single cell population, pseudoacinar growth, secretions, and cellular monotony are features seen more commonly in adenoma. Although not diagnostic, pleomorphism, when seen in multiple foci, suggests an adenoma. Reactive stromal fibrosis is seen in recurrent hyperplasia, whereas dense, acellular, perivascular fibrosis is seen in carcinoma. Carcinoma affects only a single gland and is usually found in a symptomatic patient with a very high serum calcium level. Other considerations include parathyromatosis or nests of hyperplastic epithelium usually within the soft tissues of the neck, lacking any fibroblastic reaction or an infiltrative pattern. These collections may be iatrogenic remnants from surgery for previous hyperparathyroidism or may be embryonic rests of parathyroid tissue that are stimulated by the underlying primary hyperparathyroidism. There is no pleomorphism, no intravascular location, and no other histologic features to suggest malignancy. Clear cell hyperplasia may be confused with metastatic renal cell carcinoma, especially if there is renal disease. Furthermore, bony metastasis generally may result in hypercalcemia due to the osteolytic effect, but these patients do not have hyperparathyroidism per se. Lipoadenoma results from an increase in both stromal fat and parenchymal cell volume, often with



stromal myxoid change. Lastly, lithium has been known to produce hyperparathyroidism, but it resolves with drug discontinuance.

### PROGNOSIS AND THERAPY

The serum calcium level may be lowered by hydration and by a variety of pharmacologic agents, including bisphosphonates (inhibition of bone resorption), hormone replacement (inhibition of PTH-related bone resorption), and calcimimetics (negative feedback inhibition). However, no long-term correction is achieved without surgery. Minimally invasive radio-guided parathyroidectomy is generally used for adenoma rather than hyperplasia (usually coupled with specialized radiographic studies, such as SPECT). Complete removal of three glands, while leaving a remnant of the fourth gland, is the most widely used surgery (subtotal parathyroidectomy). Autotransplantation into the forearm may also be performed to avoid neck dissection if recurrence develops. Recurrence may develop in approximately 15% of patients but may take years to develop. If there is asymmetric involvement and previous history is unknown, the diagnosis of an “adenoma” may be rendered. It is important to consider the presence of supernumerary glands, ectopic glands, or parathyromatosis whenever considering the recurrence or persistence of hyperplasia. Hypoparathyroidism may rarely result if all glands are removed. Subtotal parathyroidectomy is preferred for water-clear cell hyperplasia.

## ■ SECONDARY AND TERTIARY PARATHYROID HYPERPLASIA

Secondary hyperparathyroidism is a non-neoplastic increase in the parenchymal cell mass in all of the parathyroid gland tissue in response to a known clinical stimulus for increased PTH secretion. Tertiary hyperparathyroidism is characterized by increased parathyroid parenchymal cell mass associated with autonomous hyperfunction in patients with a history of chronic secondary hyperparathyroidism who are on dialysis or have undergone renal transplantation (the hypertrophied parathyroid glands fail to return to normal after therapy).

### CLINICAL FEATURES

The most common cause of secondary hyperparathyroidism is chronic renal failure, which results in abnormally low serum calcium levels—the clinical stimulus that results in the adaptive (compensatory) increase in production of PTH. Alternatively, other causes resulting in

## SECONDARY AND TERTIARY PARATHYROID HYPERPLASIA—DISEASE FACT SHEET

### Definition

- Non-neoplastic increase in parathyroid parenchymal cell mass within all parathyroid tissue with a known stimulus

### Incidence

- Especially common in patients with renal failure and/or on dialysis

### Morbidity and Mortality

- Control of calcium level may be difficult, leading to skeletal deformities and vessel calcification

### Sex and Age Distribution

- Females > males (3:1)
- Older patients in general but often after years of renal disease
- Renal disease occurs in all ages

### Clinical Features

- Chronic renal failure, malabsorption, vitamin D metabolism abnormalities, and pseudohypoparathyroidism may all cause disease
- Serum calcium level is decreased; serum parathyroid hormone is elevated
- Symptoms reflect underlying disease

### Prognosis and Therapy

- Depends on underlying renal disease
- Subtotal parathyroidectomy performed early to avoid skeletal deformities and vessel calcification

hyperparathyroidism include abnormalities of vitamin D metabolism, calcium deficiency, malabsorption, and low serum magnesium. Lithium therapy may result in reversible hyperparathyroidism. A broad age spectrum is affected, reflecting the underlying renal disease. Patients present with symptoms of increased PTH, which often results in osteomalacia and periarticular abnormal calcium deposition. The serum calcium level is usually decreased. In renal failure, parathyroid glands seem to expand diffusely and polyclonally, while later developing areas of nodular hyperplasia with diminished expression of both the vitamin D receptor and CASR. When more than one parathyroid gland progresses to nodular hyperplasia, the hyperparathyroidism is often refractory to medical treatment.

Tertiary hyperparathyroidism usually occurs after years of renal failure and is purported to be an autonomous parathyroid hyperfunction occurring in a setting of known secondary hyperparathyroidism. Most cases result from diffuse or nodular chief cell hyperplasia affecting multiple glands. The hypercalcemia that can result often threatens the kidney transplant graft function, requiring prompt treatment.

## PATHOLOGIC FEATURES

### GROSS FINDINGS

The findings are no different from primary hyperplasia, with all of the glands affected, whether it is uniform, nodular, or asymmetric. The glands are yellow to tan-brown. In tertiary disease, asymmetry can be quite startling, with glands often reaching up to 40 times the size of normal glands.

### MICROSCOPIC FINDINGS

There is an overall increase of parenchymal cells, including chief, oxyphilic, and transitional (intermediate

between chief and oxyphilic cells) types (Fig. 26.14), with a decrease in the amount of stromal adipocytes. The adipocyte decrease seems more pronounced if the disease has been present for a long duration (Fig. 26.15). Nodular or diffuse growth is present, along with sheets, cords, and acinar structures. The cells are quite enlarged in comparison to normal cells. Oxyphilic cells tend to be increased more than chief cells. However, in tertiary hyperparathyroidism, the chief cells are more frequently affected. Secondary changes, including fibrosis, calcification, cyst formation, hemorrhage, and hemosiderin-laden macrophages, are frequent.

## DIFFERENTIAL DIAGNOSIS

Primary chief cell hyperplasia is the main differential diagnostic consideration, although this is a clinical separation in most cases. Parathyroid adenoma and carcinoma are also considered in the differential diagnosis but are usually eliminated with clinical information. With recurrence of hyperparathyroidism, small islands of residual parenchyma within the fat may take on an atypical and “invasive” appearance, which should not be overinterpreted as carcinoma.

## PROGNOSIS AND THERAPY

Prevention and treatment of secondary hyperparathyroidism is a continual management predicament for the nephrologist and endocrinologist. Subtotal parathyroidectomy is the treatment of choice, with a small remnant

### SECONDARY AND TERTIARY PARATHYROID HYPERPLASIA—PATHOLOGIC FEATURES

#### Gross Findings

- Identical to primary hyperplasia although gland enlargement may be huge

#### Microscopic Findings

- Increased parenchyma with decreased adipocytes
- Nodular or diffuse growth
- Oncocytic cell increase may be more noticeable than chief cell
- Secondary changes are common

#### Pathologic Differential Diagnosis

- Primary chief cell hyperplasia, parathyroid adenoma, parathyroid carcinoma

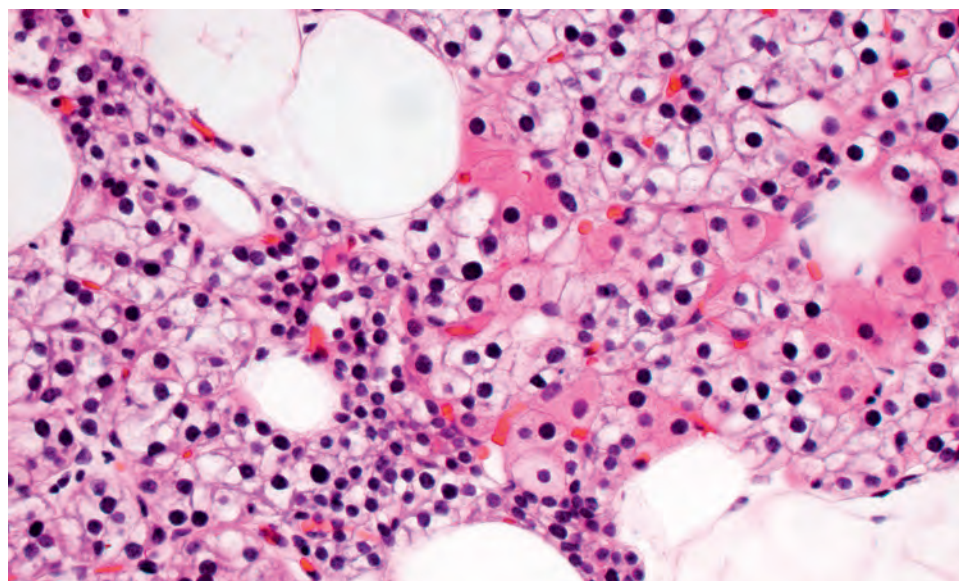


**FIGURE 26.14**

Hyperplasia shows chief cells, oncocytic cells, and transitional cells.



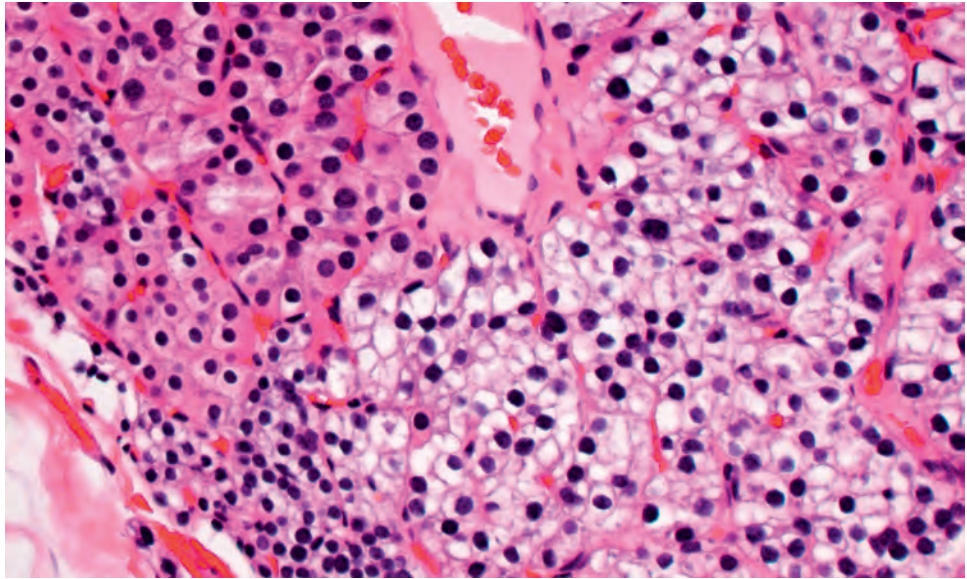


**FIGURE 26.15**

There are nodules of both oncocytic and chief cells, although no fat is present in this high-power view in a patient with long-standing disease.

of tissue left or autotransplanted. However, it is important to perform surgery early to avoid skeletal deformities and vessel calcifications because these changes will not regress post surgery. Recurrence of hyperparathyroidism is an ongoing management problem with renal failure patients. Likewise, the autonomous hyperfunction of the parathyroid glands results in an alteration of the “set-point” of serum calcium levels, which causes stimulation

of the parathyroid tissue in spite of “normal” calcium levels.

#### **SUGGESTED READINGS**

The complete list of Suggested Readings is available online at [ExpertConsult.com](http://ExpertConsult.com).

**SUGGESTED READINGS****Primary Chief Cell Hyperplasia**

1. Alevizaki M. Management of hyperparathyroidism (PHP) in MEN2 syndromes in Europe. *Thyroid Res*. 2013;6(suppl 1):S10.
2. Bell WC. Surgical pathology of the parathyroid glands. *Adv Exp Med Biol*. 2005;563:1–9.
3. Bombi JA, et al. Ultrastructural pathology of parathyroid glands in hyperparathyroidism: a report of 69 cases. *Ultrastruct Pathol*. 1993;17:567–582.
4. Bondeson AG, et al. Fat staining in parathyroid disease – diagnostic value and impact on surgical strategy: clinicopathologic analysis of 191 cases. *Hum Pathol*. 1985;16:1255–1263.
5. Bondeson L, et al. Cytopathological variables in parathyroid lesions: a study based on 1,600 cases of hyperparathyroidism. *Diagn Cytopathol*. 1997;16:476–482.
6. Carlson D. Parathyroid pathology: hyperparathyroidism and parathyroid tumors. *Arch Pathol Lab Med*. 2010;134(11):1639–1644.
7. Castleman B, et al. Parathyroid hyperplasia in primary hyperparathyroidism: a review of 85 cases. *Cancer*. 1976;38(4):1668–1675.
8. Dedeurwaerdere F, et al. Histopathology of the parathyroid glands. *Acta Otorhinolaryngol Belg*. 2001;55:95–101.
9. DeLellis RA, et al. Primary hyperparathyroidism: a current perspective. *Arch Pathol Lab Med*. 2008;132(8):1251–1262.
10. DeLellis RA. Parathyroid tumors and related disorders. *Mod Pathol*. 2011;24(suppl 2):S78–S93.
11. Duan K, et al. Clinicopathological correlates of hyperparathyroidism. *J Clin Pathol*. 2015;68(10):771–787.
12. Eslamy HK, et al. Parathyroid scintigraphy in patients with primary hyperparathyroidism: 99mTc sestamibi SPECT and SPECT/CT. *Radiographics*. 2008;28(5):1461–1476.
13. Fitko R, et al. Parathyromatosis in hyperparathyroidism. *Hum Pathol*. 1990;21:234–237.
14. Fraser WD. Hyperparathyroidism. *Lancet*. 2009;374(9684):145–158.
15. Grimelius L, et al. Histopathological diagnosis of parathyroid diseases. *Pathol Res Pract*. 1995;191:353–365.
16. Hsu YC, et al. Intramuscular and subcutaneous forearm parathyroid autograft hyperplasia in renal dialysis patients: A retrospective cohort study. *Surgery*. 2015;158(5):1331–1338.
17. Hunt JL. Molecular alterations in hereditary and sporadic thyroid and parathyroid diseases. *Adv Anat Pathol*. 2009;16(1):23–32.
18. Johnson SJ, et al. Best practice no 183. Examination of parathyroid gland specimens. *J Clin Pathol*. 2005;58(4):338–342.
19. Lew JL, et al. Surgical management of primary hyperparathyroidism: state of the art. *Surg Clin North Am*. 2009;89(5):1205–1225.
20. LiVolsi VA, et al. Parathyroid: The Pathology of hyperparathyroidism. *Surg Pathol Clin*. 2014;7(4):515–531.
21. Lloyd RV, et al. *Parathyroid gland. Endocrine Diseases. Atlas of Nontumor Pathology, First Series, Fascicle 1*. Washington, DC: Armed Forces Institute of Pathology; 2002:45–90.
22. Mihai R, et al. Imaging for primary hyperparathyroidism—an evidence-based analysis. *Langenbecks Arch Surg*. 2009;394(5):765–784.
23. Newey PJ, et al. Parafibromin—functional insights. *J Intern Med*. 2009;266(1):84–98.
24. Osamura RY, et al. Current practices in performing frozen sections for thyroid and parathyroid pathology. *Virchows Arch*. 2008;453(5):433–440.
25. Penner CR, et al. Primary parathyroid hyperplasia. *Ear Nose Throat J*. 2003;82(5):363.
26. Quiriny M, et al. Parathyroidectomy in primary hyperparathyroidism: retrospective study of 167 patients, experience in Jules Bordet Institute. *Acta Chir Belg*. 2014;114(2):118–124.
27. Rubello D, et al. Minimally invasive radio-guided surgery for primary hyperparathyroidism: From preoperative to intraoperative localization imaging. *Ann Endocrinol (Paris)*. 2010;71(6):511–518.
28. Seethala RR, et al. Parathyroid lipoadenomas and lipohyperplasias: clinicopathologic correlations. *Am J Surg Pathol*. 2008;32(12):1854–1867.
29. Szalat A, et al. Lithium-associated hyperparathyroidism: report of four cases and review of the literature. *Eur J Endocrinol*. 2009;160(2):317–323.
30. Týcová I, et al. Molecular patterns of diffuse and nodular parathyroid hyperplasia in long-term hemodialysis. *Am J Physiol Endocrinol Metab*. 2016;311(4):E720–E729.
31. Udelsman R. Primary hyperparathyroidism. *Curr Treat Options Oncol*. 2001;2:365–372.
32. Vulpio C, et al. Histology and immunohistochemistry of the parathyroid glands in renal secondary hyperparathyroidism refractory to vitamin D or cinacalcet therapy. *Eur J Endocrinol*. 2013;168(6):811–819.
33. Weber AL, et al. The thyroid and parathyroid glands. CT and MR imaging and correlation with pathology and clinical findings. *Radiol Clin North Am*. 2000;38:1105–1129.
34. Westin G, et al. Molecular genetics of parathyroid disease. *World J Surg*. 2009;33(11):2224–2233.
35. Yang QS, et al. Dual-phase <sup>99m</sup>Tc-MIBI imaging findings in sporadic primary hyperplasia of parathyroid glands. *Clin Nucl Med*. 2015;40(5):423–426.
36. Zhang Y, et al. Endocrine tumors as part of inherited tumor syndromes. *Adv Anat Pathol*. 2011;18(3):206–218.

**Secondary and Tertiary Parathyroid Hyperplasia**

1. Alkhalili E, et al. The utility of neck ultrasound and sestamibi scans in patients with secondary and tertiary hyperparathyroidism. *World J Surg*. 2015;39(3):701–705.
2. Fraser WD. Hyperparathyroidism. *Lancet*. 2009;374(9684):145–158.
3. Fukagawa M. Cell biology of parathyroid hyperplasia in uremia. *Am J Med Sci*. 1999;317:377–382.
4. Gioviale MC, et al. Post-transplantation tertiary hyperparathyroidism. *Ann Transplant*. 2012;17(3):111–119.
5. Jamal SA, et al. Secondary and tertiary hyperparathyroidism. *J Clin Densitom*. 2013;16(1):64–68.
6. Osamura RY, et al. Current practices in performing frozen sections for thyroid and parathyroid pathology. *Virchows Arch*. 2008;453(5):433–440.
7. Taieb D, et al. Parathyroid scintigraphy: when, how, and why? A concise systematic review. *Clin Nucl Med*. 2012;37(6):568–574.
8. Tominaga Y. Management of renal hyperparathyroidism. *Biomed Pharmacother*. 2000;54(suppl 1):25s–31s.
9. Vestergaard P, et al. Medical treatment of primary, secondary, and tertiary hyperparathyroidism. *Curr Drug Saf*. 2011;6(2):108–113.
10. Westin G, et al. Molecular genetics of parathyroid disease. *World J Surg*. 2009;33(11):2224–2233.



# Benign Neoplasms of the Parathyroid Gland

■ **Lester D.R. Thompson**

## ■ PARATHYROID ADENOMA

A parathyroid gland adenoma is an encapsulated benign neoplasm of the parathyroid parenchymal cells (either chief or oncocyctic cells). Parathyroid disease is separated into primary, secondary, or tertiary, based on whether the parathyroid gland is primarily the source of the disease or if the gland is reacting to exogenous stimulation, such as renal disease (Chapter 26). This distinction is sometimes quite difficult on histology alone and even more so if only a single gland is sampled. Intraoperative selective venous parathyroid hormone (PTH) assay is a clinical parameter which may assist with the distinction. Isolated cases of adenoma are associated with exposure to ionizing radiation (fourfold increase in Hiroshima-exposed patients), but the majority have no specific etiology. A small subset of cases present as part of the hyperparathyroidism–jaw tumor (HPT-JT) syndrome, an autosomal dominant disorder (*CDC73* gene at 1q25-q31) characterized by parathyroid adenoma or carcinoma, various fibro-osseous lesions of jaw (ossifying fibroma), and renal cysts or tumors. Up to 80 % of the patients will have HPT.

### CLINICAL FEATURES

Early detection of parathyroid disease has improved dramatically with increased use of multichannel auto-analyzers, with calcium levels determined as part of routine blood chemistries. Therefore, a true incidence is difficult to determine, although 2 to 3 per 1,000 patients per year is considered an approximate incidence. Parathyroid adenomas are the most common cause of primary HPT, accounting for approximately 80 %–85 % of HPT. Women are affected more frequently than men (approximately 2 to 3:1), with a peak incidence in the 4th to 5th decades, with an even more pronounced female incidence in patients older than 75 years (5:1). Blacks are affected more often than whites or Asians. There is a rare association with inherited syndromes (MEN1, MEN2, and

### PARATHYROID ADENOMA—DISEASE FACT SHEET

#### Definition

- An encapsulated benign neoplasm of either the chief or the oncocyctic cells

#### Incidence

- Approximately 2-3 per 1,000 persons per year

#### Morbidity and Mortality

- Associated with excess calcium, with cardiovascular abnormalities the most significant
- No mortality

#### Sex and Age Distribution

- Females > males (2-3:1)
- Mean age at presentation: 4th to 5th decades

#### Clinical Features

- Nonspecific findings of fatigue, weakness, and pain related to hypercalcemia
- Polydipsia, polyuria, and nephrolithiasis
- Pancreatitis and peptic ulcer disease are less common
- Mass lesion may be palpated
- Rarely associated with inherited syndromes

#### Radiographic Features

- <sup>99m</sup>Tc sestamibi scan helps to identify adenoma in up to 90% of cases
- Ultrasound and computed tomography can be used in addition

#### Prognosis and Therapy

- Excellent without recurrence (by definition)
- Surgery is treatment of choice

HPT-JT syndrome). The existence of two simultaneous adenomas is quite uncommon and difficult to prove by histology alone. Approximately 90 % of tumors develop in normally situated parathyroid glands, with the lower glands affected more commonly; however, mediastinum, esophagus, thymus, and other anatomic site tumors are recognized along with intrathyroidal neoplasms. Symptoms

of excess calcium and/or PTH may yield a nonspecific clinical presentation that includes fatigue, malaise, weakness, abdominal pain, depression, constipation, peptic ulcer disease, kidney stones, and/or pancreatitis. Nephrolithiasis is approximately twice as common in men than in women. However, calculi are not seen as frequently because biochemical screening results in early identification of the tumor before symptoms are well developed. A palpable mass is an uncommon finding.

By laboratory investigation, patients tend to have *higher* serum calcium levels than detected in patients with primary chief cell hyperplasia. Patients will also have elevated serum PTH levels, hypophosphatemia, and hyperphosphaturia.

### RADIOGRAPHIC FEATURES

A variety of techniques can be used to detect and localize abnormal parathyroid glands, including ultrasonography, computed tomography, magnetic resonance imaging, thallium subtraction scanning, and nuclear scintigraphy, specifically with  $^{99m}\text{Tc}$  sestamibi. Technetium seems to be the most useful in practical application, and it is concentrated by parathyroid tissue (Fig. 27.1), effectively identifying adenomas in up to 90% of cases. Still, this suggests it cannot be used in isolation. Specifically, with a greater

tendency to use minimally invasive parathyroid surgery, it is much more important to use scintigraphic studies, combined with ultrasound and intraoperative PTH measurement or gamma probe testing. Ultrasound-guided fine needle aspiration or retrograde venous sampling can also be of value in evaluating parathyroid disease.

### PATHOLOGIC FEATURES

#### GROSS FINDINGS

Almost always solitary, the gland is typically enlarged, and often ovoid, with a mean weight of approximately 1 g. The surface is smooth and surrounded by a thin capsule (Fig. 27.2), although multinodularity and multilobularity may develop. The cut surface is smooth, soft, and reddish-brown, often distinct from the yellowish-brown surrounding periphery of parathyroid parenchyma. If the adenoma is large (up to 10 cm), degenerative or cystic changes may be seen (Fig. 27.2), sometimes masking the true nature of the process, associated with prominent fibrosis and possible calcification.

#### MICROSCOPIC FINDINGS

A single gland is usually affected by a well-circumscribed and usually encapsulated mass with a fatless population

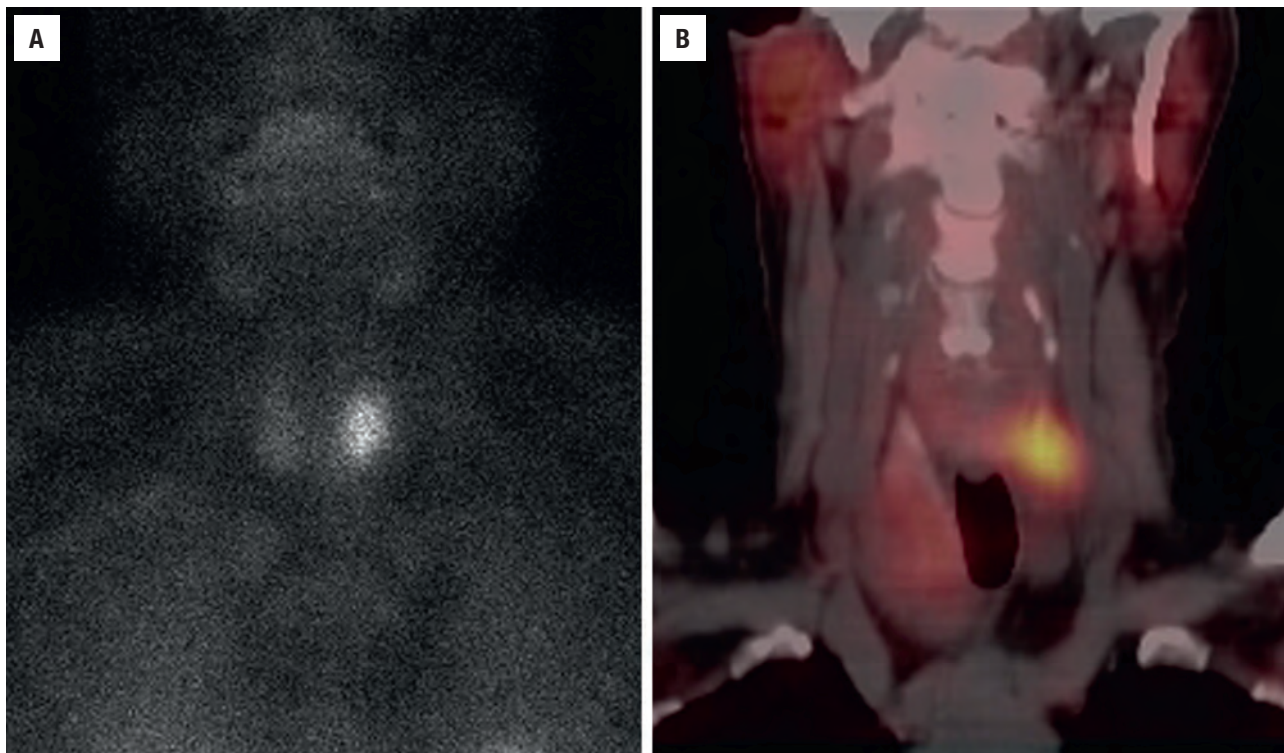


**FIGURE 27.1**

A  $^{99m}\text{Tc}$  sestamibi scan shows increased uptake disproportionate to the other parathyroid glands, a finding consistent with adenoma. (A) was obtained at 4-hour delay, whereas (B) was as a fused computed tomography and sestamibi image, helping establish a specific location.



**PARATHYROID ADENOMA—PATHOLOGIC FEATURES****Gross Findings**

- A single enlarged parathyroid gland (rarely, two adenomas may occur)
- Smooth, encapsulated mass
- Reddish brown, with rim of uninvolved parenchyma adjacent to proliferation
- Usually a mean weight of approximately 1 g

**Microscopic Findings**

- Single mass
- Encapsulated (although often a thin, irregular capsule)
- Fatless nodule
- Distinct histology within the neoplasm different from remaining gland
- Atrophy or compression of adjacent parathyroid parenchyma
- Usually a single histologic population of enlarged cells
- Glandular architecture with “secretions” more common in adenoma than hyperplasia
- Oncocytic adenoma: composed of oncocytes (>75% of cells)

**Immunohistochemical Findings**

- Pancytokeratin, parathyroid hormone, chromogranin, synaptophysin *positive*
- Parafibromin strong nuclear reaction (except in HPT-JT syndrome)
- PAX8, GATA3, and cyclin-D1 *positive* in most
- Ki-67: low proliferation index
- TTF1, thyroglobulin, galectin-3, and calcitonin *negative*

**Fine Needle Aspiration**

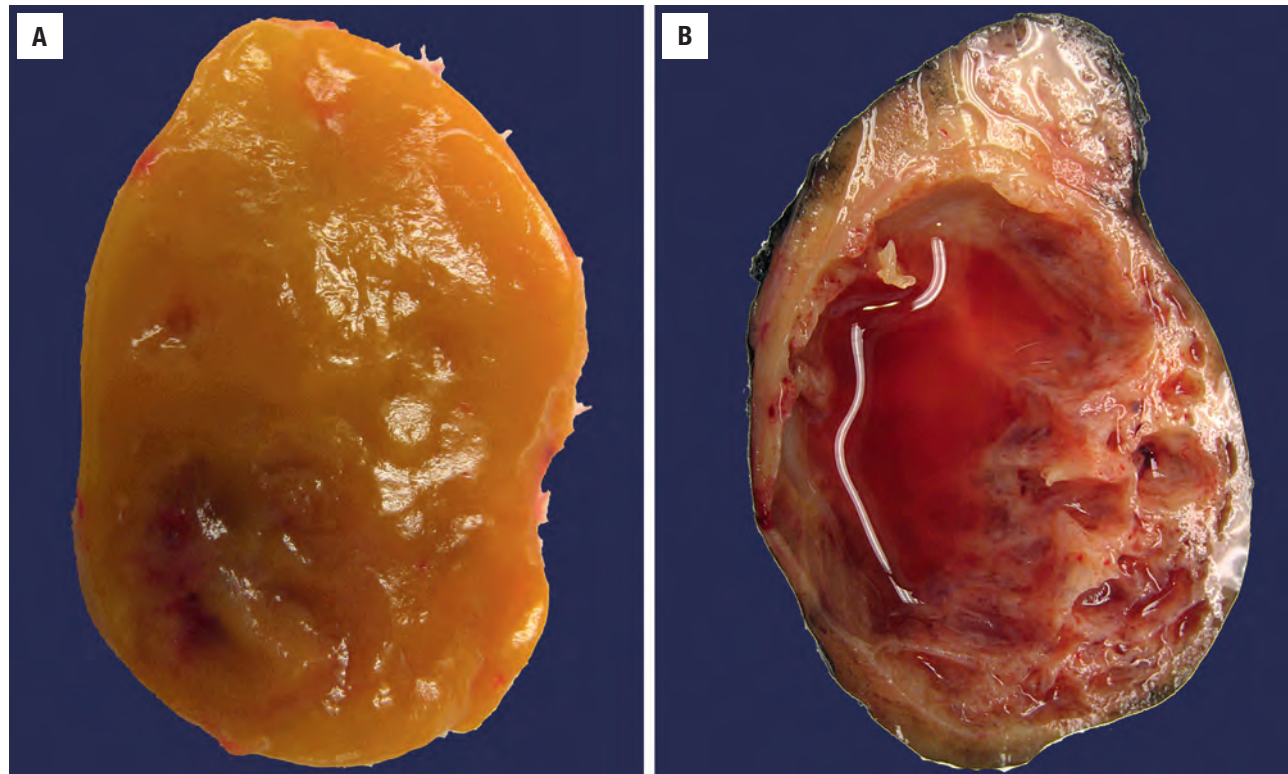
- Similar to thyroid follicular lesions
- Clear cytoplasm and distinct cell borders are helpful

**Molecular Findings**

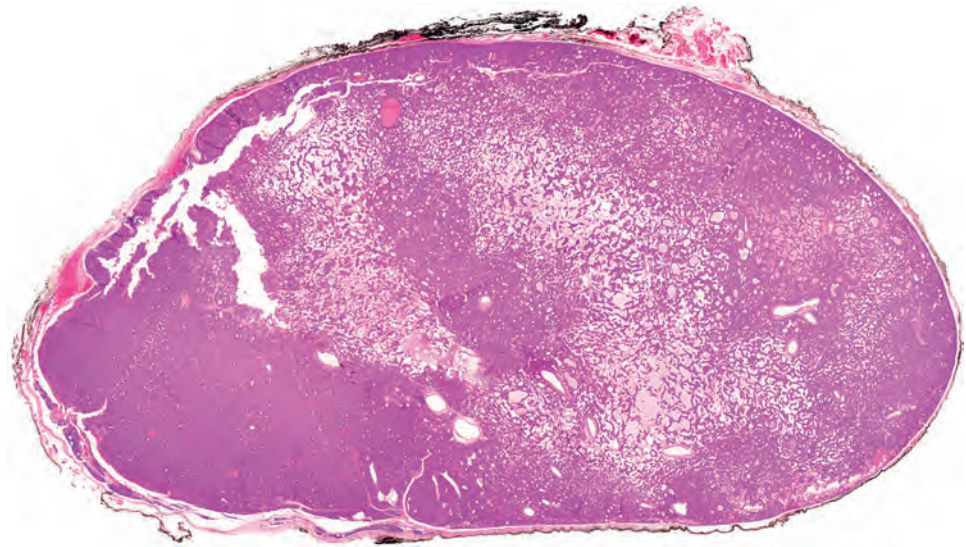
- *CCND1* overexpression (20%-40%) or translocation (~8%)
- Somatic mutations of *MEN1* in up to 40%
- *CDC73* somatic mutations in HPT-JT syndrome patients

**Pathologic Differential Diagnosis**

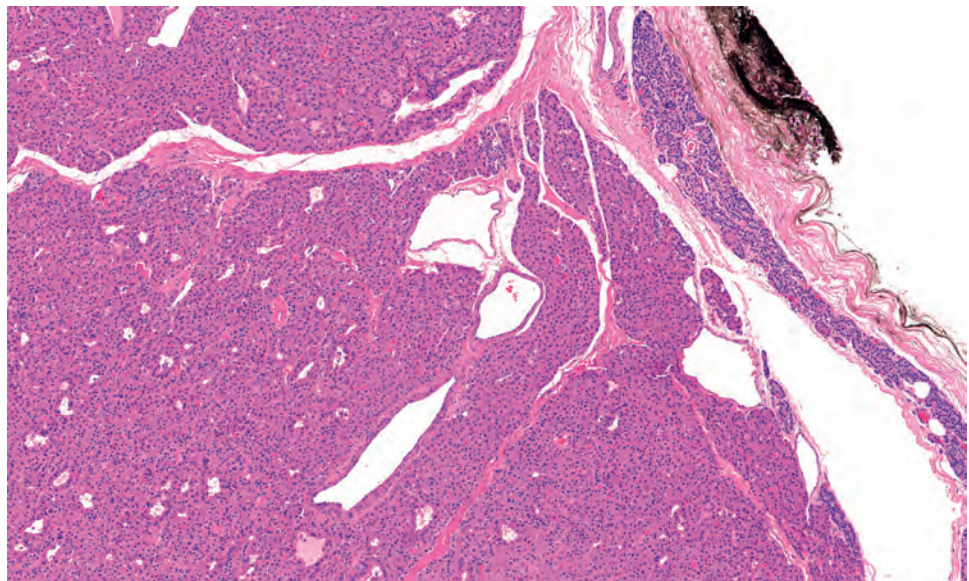
- Parathyroid hyperplasia, thyroid adenoma, parathyroid carcinoma, medullary thyroid carcinoma, metastatic renal cell carcinoma

**FIGURE 27.2**

(A) This parathyroid gland adenoma weighed 4.5 g, showing a homogeneous cut surface. No areas of atrophic or compressed parenchyma are seen. (B) This large adenoma (4.5 cm) has undergone cystic degeneration, showing multiple variable sized cysts.

**FIGURE 27.3**

A well-formed capsule separates the oncocyctic neoplasm from the surrounding, compressed uninvolved parathyroid parenchyma.

**FIGURE 27.4**

A thin, but well-formed fibrous capsule separates this adenoma from the surrounding nonatrophic parenchyma. Fat is focally present in the uninvolved parenchyma.

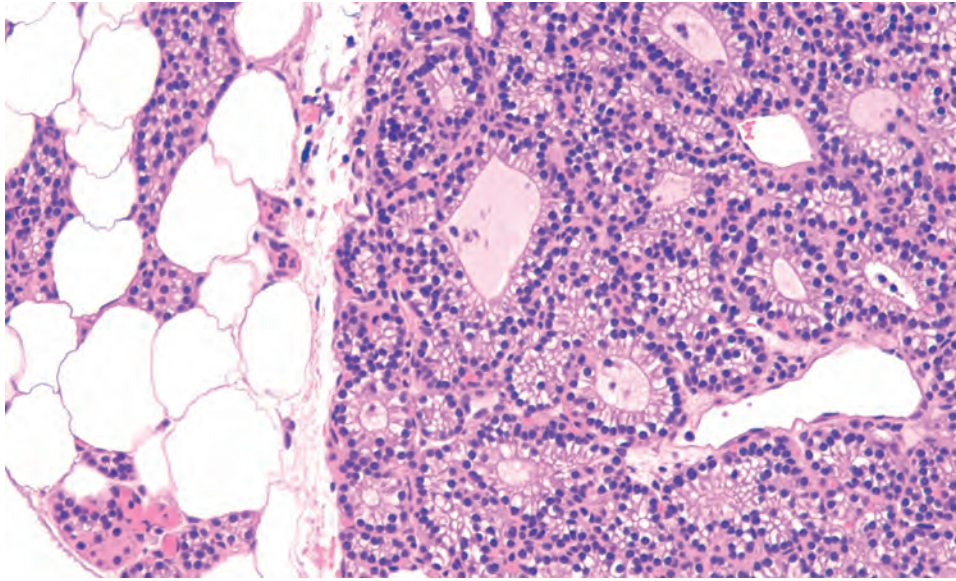
of cells within the tumor, distinct from the uninvolved, compressed, or atrophic parathyroid parenchyma (Figs. 27.3 and 27.4) immediately adjacent to the tumor. The capsule is sometimes extremely thin and attenuated (Fig. 27.5). The tumor is usually composed of a single cell proliferation of enlarged oncocyctic (Fig. 27.6) or chief cells (Fig. 27.7), with the latter the most common, although occasionally a mixture of both may be seen. The cells are often arranged in a solid or acinar-glandular (follicular) distribution, a finding uncommon in hyperplasia (Fig. 27.8). Peritheliomatous palisading (tumor growth centered around vessels) is occasionally identified. The neoplastic cells tend to be larger than the non-neoplastic cells in the adjacent parathyroid parenchyma. The chief cells have ample clear to slightly eosinophilic cytoplasm surrounding nuclei that are round to oval with heavy nuclear chromatin distribution (Fig. 27.9). Perinuclear halos may be seen. Nucleoli are small to

inconspicuous. Intracellular lipid (fat) within the cytoplasm is limited, if present at all. Tumor cell spindling is uncommon (Fig. 27.10).

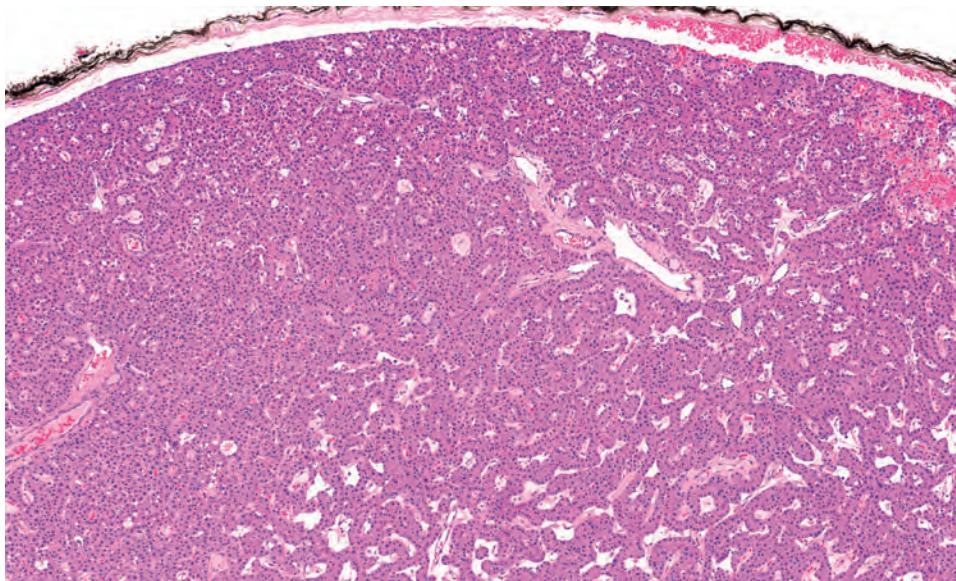
Nuclear pleomorphism may be seen, although it is usually focal or arranged in clusters (Fig. 27.10). Multinucleated giant cells may also be seen in isolation (Fig. 27.10). Mitoses are inconspicuous, with one or fewer mitoses per 10 high-power fields (HPFs). Eosinophilic “secretions” may sometimes be mistaken for colloid (Fig. 27.8) and may occasionally calcify, simulating a psammoma body. Amyloid may occasionally be identified between the neoplastic cells. Stroma is scant, but delicate fibrovascular bands separate the neoplastic cells. Hemosiderin-laden macrophages, inflammation, and fibrosis may be part of degenerative changes, especially in large tumors (Fig. 27.11).

Oncocyctic (oxyphilic) cell adenomas (approximately 5% of all adenomas) are arranged in sheets, cords, nests,

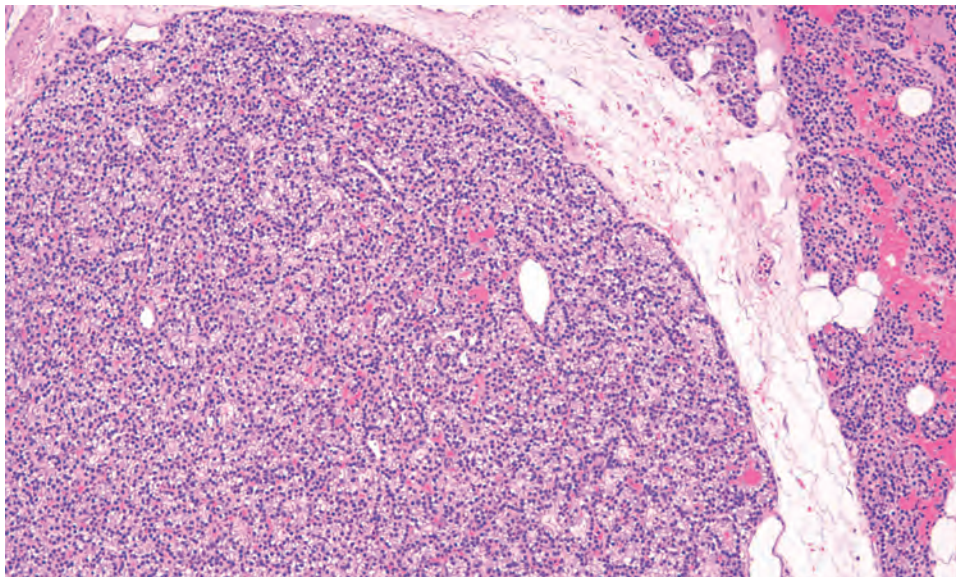


**FIGURE 27.5**

A nearly nonexistent capsule separates the adenoma from the surrounding parenchyma. The parenchyma contains cells that are smaller than the neoplasm and has fat. The neoplastic cells are arranged in a pseudoglandular distribution.

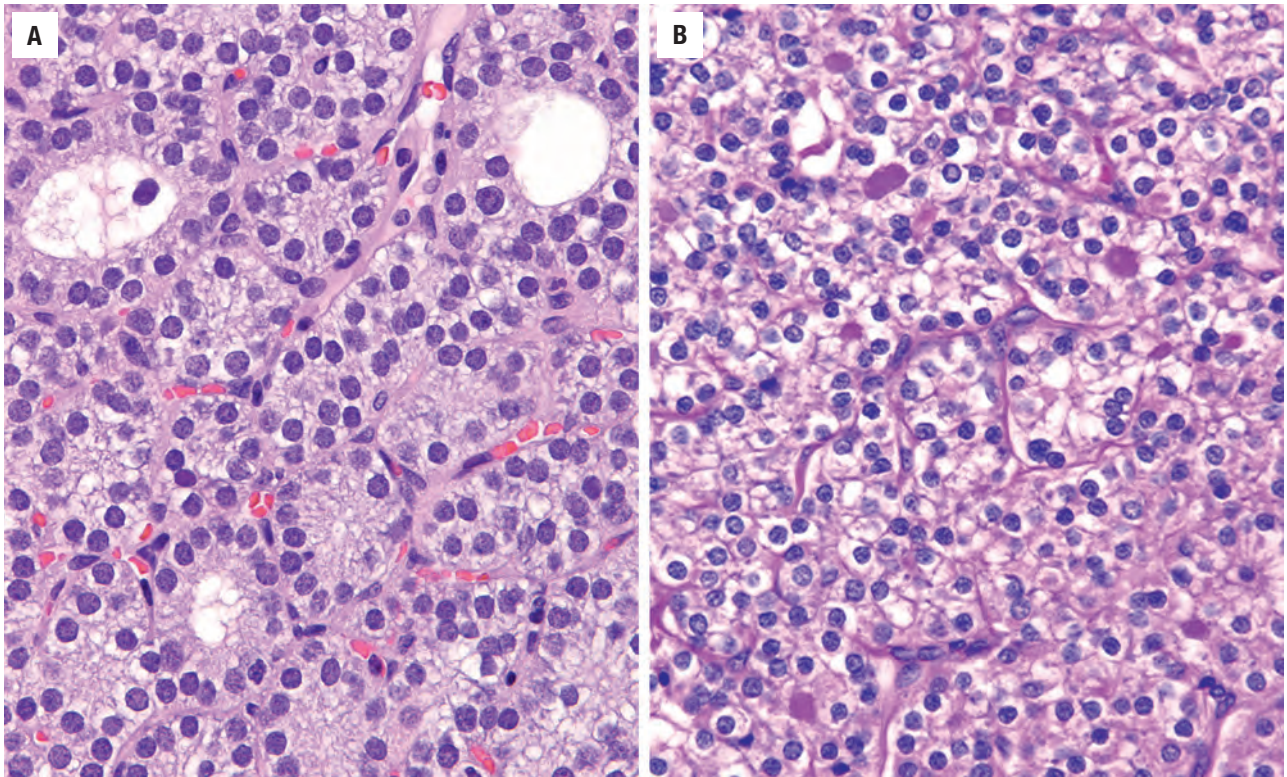
**FIGURE 27.6**

A thin capsule is seen at the top of the image but no uninvolved parenchyma is noted. This is an oncocytic adenoma.

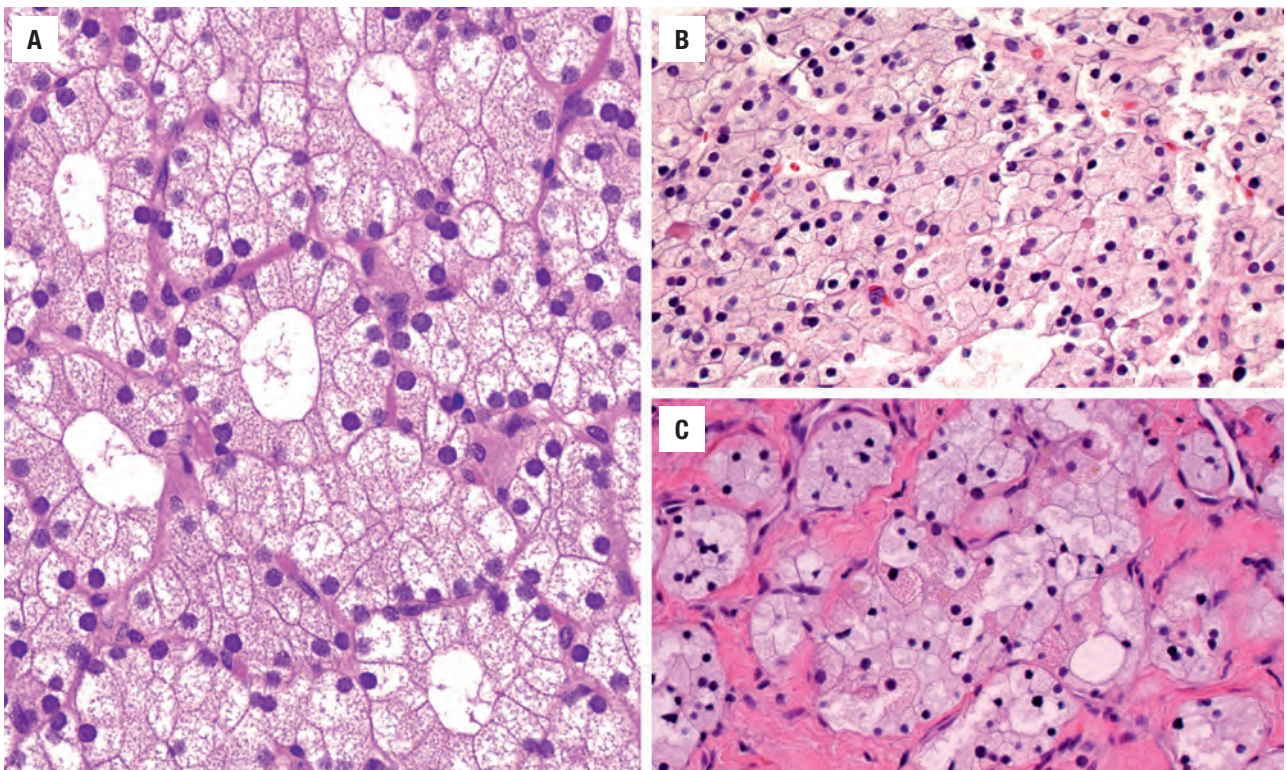
**FIGURE 27.7**

Chief cells compose this adenoma without any fat cells present. There is a thin, edematous capsule separating the tumor from uninvolved parenchyma which still contains adipocytes.



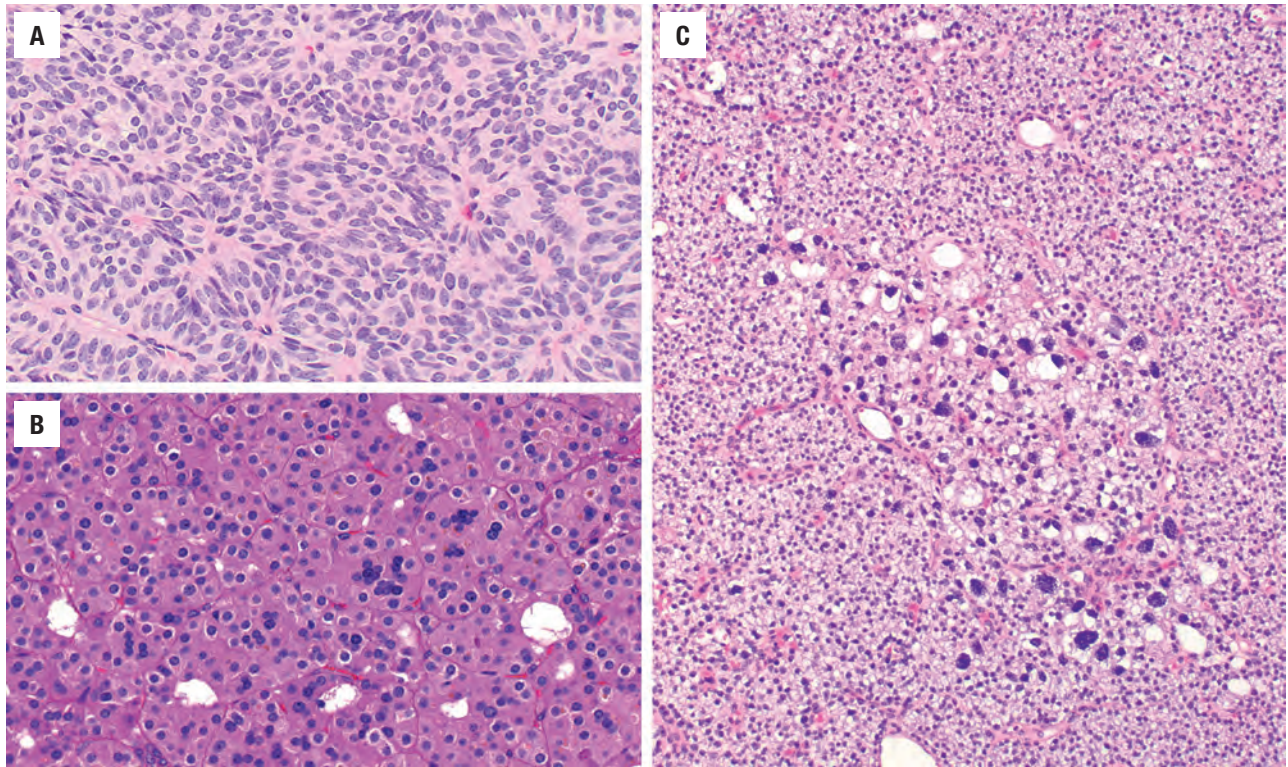
**FIGURE 27.8**

(A) A glandular pattern is commonly seen in adenomas, with cells arranged around a lumen. (B) Inspissated "colloid-like" material is noted. In a case such as this, immunohistochemistry may be of value.

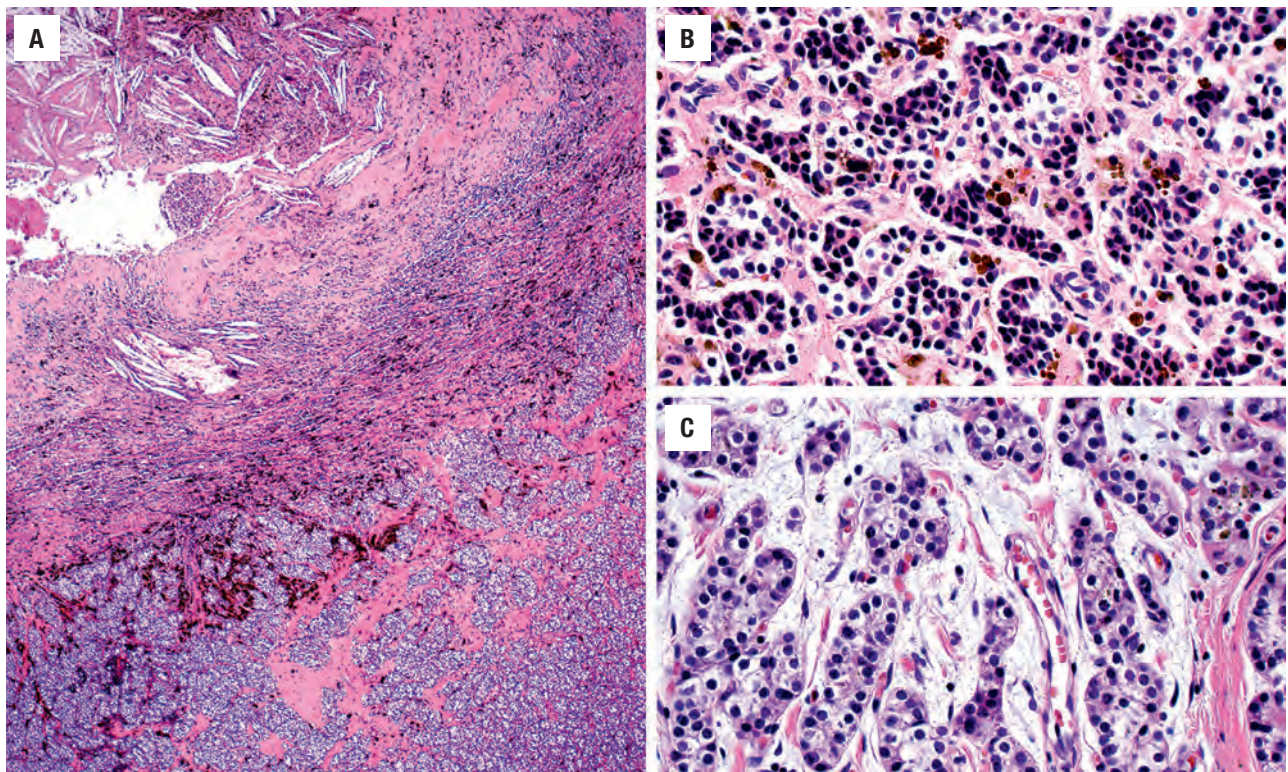
**FIGURE 27.9**

(A and B) Cytoplasmic clearing can be seen in parathyroid adenoma, although a slightly granular or vacuolated appearance may remain. Note the increased intralobular fibrosis (C).



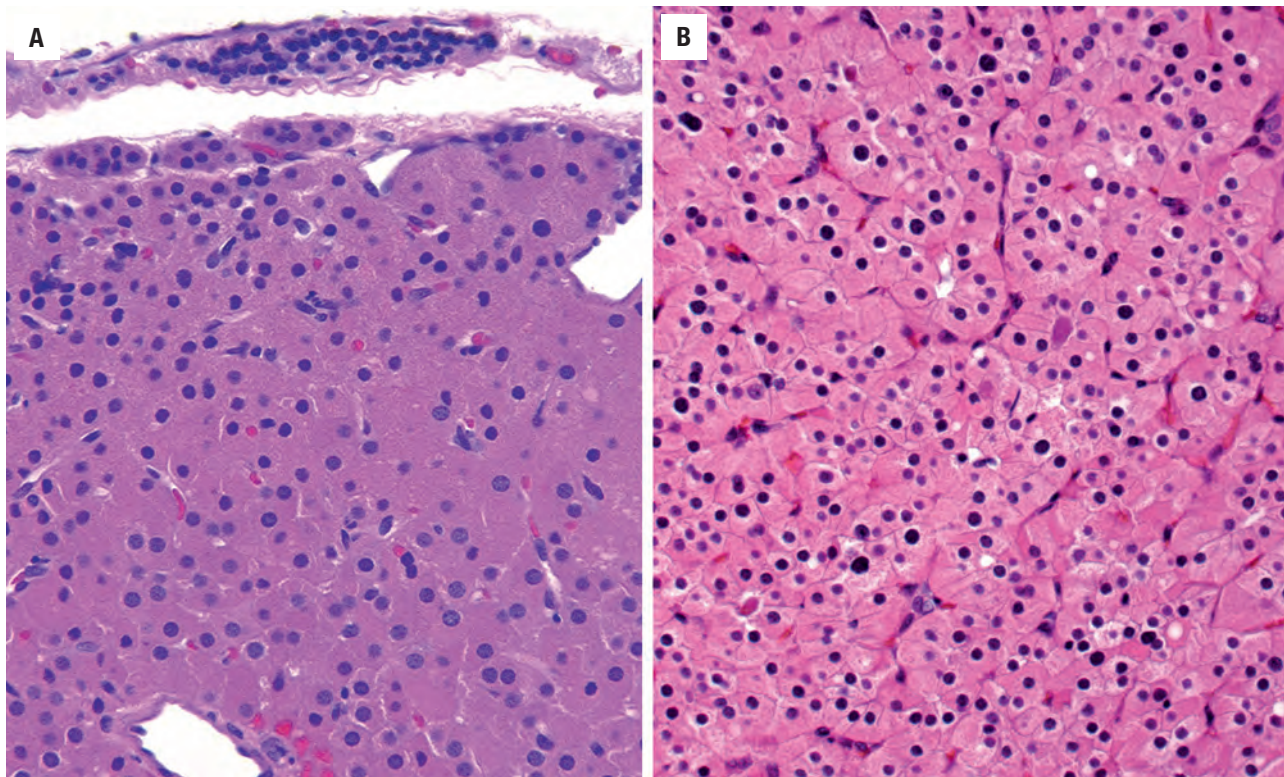
**FIGURE 27.10**

(A) Tumor cell spindling is focally present in this adenoma. (B) Multinucleated giant cells are seen. (C) Profound pleomorphism is focally present in this adenoma.

**FIGURE 27.11**

Degenerative changes are not uncommon in adenoma. (A) A large area of degeneration with fibrosis, hemosiderin-laden macrophages, and cholesterol clefts. (B) This "pseudoalveolar" pattern is associated with numerous hemosiderin-laden macrophages. (C) A myxoid-mucinous degeneration of the stroma is noted in this adenoma.



**FIGURE 27.12**

Granular, oncocytic, or oxyphilic cytoplasm may be seen in adenoma (compressed uninvoluted parathyroid is present at the upper region of [A]). Note the "inspissated" material in (B).

or glandular structures, composed predominantly (> 75 %) of cells with abundant eosinophilic, granular cytoplasm and may have prominent, centrally placed eosinophilic nucleoli (Fig. 27.12). There may be adenomas with a mixture of chief and oncocytic cells, but this is a feature much more frequently seen in hyperplasia. Water clear cell adenoma and lipoadenoma are recognized but are exceedingly rare. Lipoadenoma (hamartoma) is a proliferation of parenchymal and stromal adipose cells in an encapsulated tumor, separate from the rest of the gland. The diagnosis is exceedingly difficult in small biopsy samples because it may appear to be normal tissue. Sometimes the presence of myxoid stroma or degeneration may be helpful. Papillary architecture is very rare. Double adenomas are exceptional, requiring more than one hypercellular, enlarged gland, histologically confirmed normal glands, no familial history of MEN or HPT, and permanent cure with surgical removal of the enlarged glands (difficult to prove with years of follow-up required). If identified, the superior glands are more often affected.

## ANCILLARY STUDIES

### IMMUNOHISTOCHEMICAL FINDINGS

The parenchymal cells will be keratin, chromogranin, synaptophysin, and PTH immunoreactive, although the

interpretation of the PTH reaction is fraught with diffusion artifacts and serum reactions. Parafibromin will show a strong nuclear reaction in the vast majority of adenomas (notable exception for HPT-JT syndrome adenomas), with PAX8 (nuclear) reaction (approximately 40 % of adenoma), GATA3, and cyclin-D1 expression also seen. TTF1, thyroglobulin, galectin-3, and calcitonin are nonreactive. Ki-67 yields a low proliferation index (usually <5 %). If an adenoma is parafibromin positive (nuclear), it has not been reported to recur.

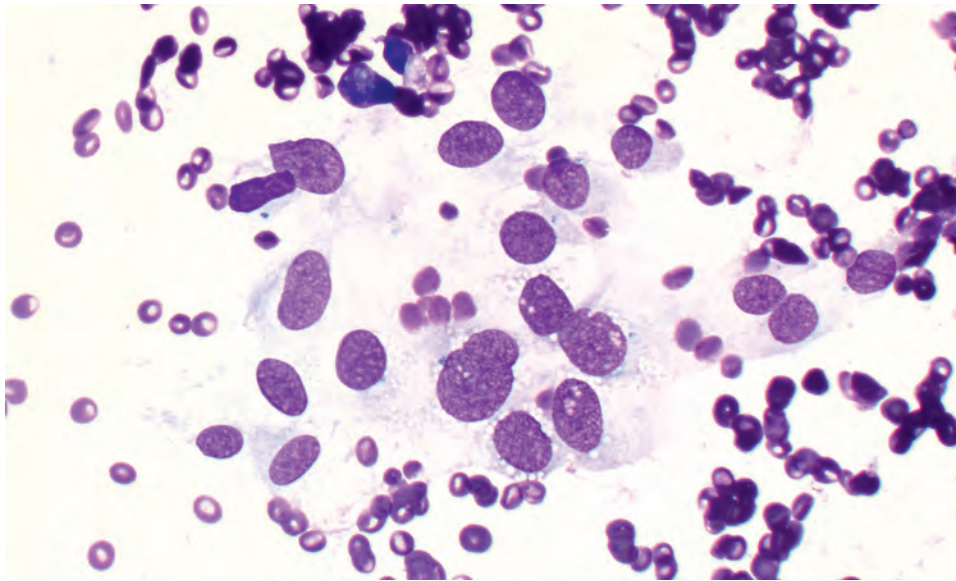
### HISTOCHEMISTRY

Fat stains (oil red O, Sudan black) have been used historically to show decreased intracellular fat in hyperfunctioning tumor cells but is of limited practical value.

### FINE NEEDLE ASPIRATION

Ultrasound-guided parathyroid sampling is used in some settings. Separation of a thyroid follicular neoplasm from a parathyroid proliferation is difficult. There are usually naked nuclei set within a few small sheets of cells, sometimes forming acinar or follicular structures. The nuclei are usually small and hyperchromatic, with isolated atypical cells (Fig. 27.13). Secretions and "colloid-like" substances may suggest a thyroid lesion. Clear to vacuolated cytoplasm may be noted, but separation



**FIGURE 27.13**

A loosely cohesive pattern is noted in this fine needle aspiration smear, showing delicate to vacuolated cytoplasm. Note there is slight nuclear pleomorphism (DiffQuik-stained smear).

from a metastatic renal cell tumor or a thyroid gland neoplasm may be difficult. Fluid PTH levels may help, but only if fluid is obtained from a cystic lesion. If cell block material is obtained, immunohistochemistry may be used. Molecular techniques may be used to confirm a parathyroid or thyroid neoplasm in certain settings.

#### MOLECULAR FINDINGS

A number of molecular findings are seen in the monoclonal proliferation of adenoma. There are alterations involving cyclin D1, with *CCND1-PRAD1* translocation resulting in cyclin-D1 overexpression. Adenomas tend to show adenomatous polyposis coli (*APC*) expression, whereas it is lost in carcinoma. Tumor suppressor gene *MEN1* (11q13) frequently shows somatic (rather than germline) mutations in the second wild-type allele in up to 40% of patients with adenoma, with an additional inactivating mutation of the remaining allele. *CDC73* somatic mutations are nearly exclusively identified in patients with the HPT-JT syndrome. Rarely, *CDKN1B* somatic mutations may be detected.

#### DIFFERENTIAL DIAGNOSIS

Parathyroid hyperplasia, parathyroid carcinoma, thyroid neoplasms, and metastatic renal cell carcinoma are the principal differential diagnostic considerations. Uneven, nodular hyperplasia will mimic an adenoma, especially if only a single gland is sampled. A “remnant” can be seen in both lesions. The easiest way to separate hyperplasia and adenoma is to sample more than one gland.

Hyperplasia should be considered (1) if more than one gland is enlarged or abnormal, (2) if there is an increase in the parenchyma to stromal fat ratio (age variability considered), and (3) if there is nodular distribution of both chief and oncocyctic cells. Clinical information about renal status, serum calcium, and/or PTH levels and condition of the remaining “in situ” glands will help to make the separation. Intraoperative changes in the serum PTH levels may also serve to confirm the diagnosis of adenoma (levels decrease dramatically after removal) versus hyperplasia (elevated level persists).

Carcinoma usually has a trabecular architecture; demonstrates thick, acellular bands of fibrosis; a thick capsule; capsular, lymphovascular, or perineural invasion; profound nuclear pleomorphism; increased mitotic figures, including atypical forms; and the presence of necrosis. Adherence to the thyroid gland, difficulty in removing the tumor, and extremely elevated serum calcium and/or PTH levels should raise suspicion of parathyroid carcinoma. In sites of previous surgery or FNA, the reactive changes in the stroma (hemosiderin-laden macrophages, cholesterol granuloma, foreign body giant cell reaction) may also simulate invasive growth or result in attachment to the surrounding tissues, factors which should be weighed carefully in determining the final diagnosis. Typically, there is a reduced to absent nuclear expression of parafibromin in parathyroid carcinoma. Occasionally, in cases which cannot be definitively separated, the term “atypical adenoma” can be used, while detailing the histologic features of concern (Fig. 27.14). It is interesting to note that when these tumors are followed, there is usually a benign clinical outcome.

Thyroid lesions do not have a rim of uninvolved parathyroid tissue, may have birefringent oxalate crystals, and will be TTF1 and/or thyroglobulin immunoreactive.

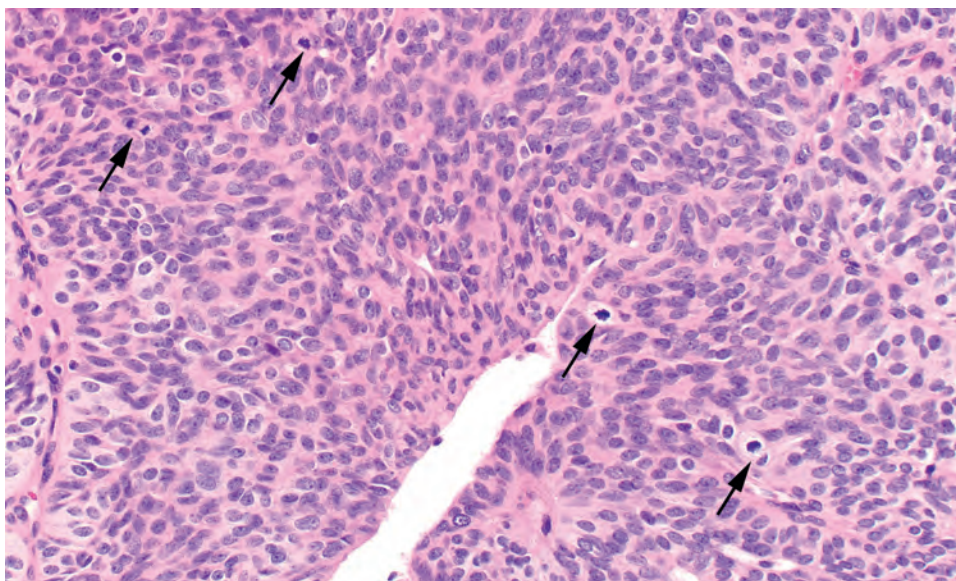


**FIGURE 27.14**

This parathyroid gland adenoma had no histologic features of note, other than six mitoses per 10 HPFs, with four captured in a single field (*arrows*). The qualifier “atypical adenoma” could be applied in this setting.

### PROGNOSIS AND THERAPY

Surgery is the treatment of choice if there is significant calcium elevation, other complications of HPT, or if the patient is older than 50 years. In the past, removal of the adenoma and sampling of a second gland was advocated. With the use of minimally invasive radio-guided parathyroidectomy, removal of a single gland can now be done with success. However, preoperative definitive anatomic and functional localization must be achieved, accompanied by intraoperative gamma probe readings

and rapid intact PTH determination. Surgery ameliorates the calcium effects of HPT, specifically those affecting the cardiovascular system. Recurrent HPT may be due to incomplete removal, parathyromatosis (ruptured, implanted, or remnant parathyroid adenoma tissue), or hyperfunction of the autografted parathyroid tissue.

### SUGGESTED READINGS

The complete list of Suggested Readings is available online at [ExpertConsult.com](http://ExpertConsult.com).



**SUGGESTED READINGS****Parathyroid Adenoma**

1. Akerstrom G, et al. Histologic parathyroid abnormalities in an autopsy series. *Hum Pathol.* 1986;17:520–527.
2. Arnold A, et al. Molecular pathogenesis of primary hyperparathyroidism. *J Bone Miner Res.* 2002;17(suppl 2):N30–N36.
3. Bai S, et al. Water-clear parathyroid adenoma: report of two cases and literature review. *Endocr Pathol.* 2012;23(3):196–200.
4. Bondeson AG, et al. Fat staining in parathyroid disease—diagnostic value and impact on surgical strategy: clinicopathologic analysis of 191 cases. *Hum Pathol.* 1985;16:1255–1263.
5. Bricaire L, et al. Frequent large germline HRPT2 deletions in a French National cohort of patients with primary hyperparathyroidism. *J Clin Endocrinol Metab.* 2013;98(2):E403–E408.
6. Carpten JD, et al. HRPT2, encoding parafibromin, is mutated in hyperparathyroidism-jaw tumor syndrome. *Nat Genet.* 2002;32(4):676–680.
7. Costa-Guda J, et al. Germline and somatic mutations in cyclin-dependent kinase inhibitor genes CDKN1A, CDKN2B, and CDKN2C in sporadic parathyroid adenomas. *Horm Cancer.* 2013;4(5):301–307.
8. DeLellis RA, et al. Primary hyperparathyroidism: a current perspective. *Arch Pathol Lab Med.* 2008;132(8):1251–1262.
9. DeLellis RA. Parathyroid carcinoma: an overview. *Adv Anat Pathol.* 2015;12(2):53–61.
10. DeLellis RA. Parathyroid tumors and related disorders. *Mod Pathol.* 2011;24(suppl 2):S78–S93.
11. Gill AJ, et al. Loss of nuclear expression of parafibromin distinguishes parathyroid carcinomas and hyperparathyroidism-jaw tumor (HPT-JT) syndrome-related adenomas from sporadic parathyroid adenomas and hyperplasias. *Am J Surg Pathol.* 2006;30(9):1140–1149.
12. Gotthardt M, et al. Clinical value of parathyroid scintigraphy with technetium-99m methoxyisobutylisonitrile: discrepancies in clinical data and a systematic metaanalysis of the literature. *World J Surg.* 2004;28:100–107.
13. Iacobone M, et al. Hyperparathyroidism-jaw tumor syndrome: a report of three large kindred. *Langenbecks Arch Surg.* 2009;394(5):817–825.
14. Juhlin CC, et al. Parafibromin and APC as screening markers for malignant potential in atypical parathyroid adenomas. *Endocr Pathol.* 2010;21(3):166–177.
15. Lieu D. Cytopathologist-performed ultrasound-guided fine-needle aspiration of parathyroid lesions. *Diagn Cytopathol.* 2010;38(5):327–332.
16. Mihai R, et al. Surgical strategy for sporadic primary hyperparathyroidism: an evidence-based approach to surgical strategy, patient selection, surgical access, and reoperations. *Langenbecks Arch Surg.* 2009;394(5):785–798.
17. Mihai R, et al. Imaging for primary hyperparathyroidism—an evidence-based analysis. *Langenbecks Arch Surg.* 2009;394(5):765–784.
18. Sharretts JM, et al. Clinical and molecular genetics of parathyroid neoplasms. *Best Pract Res Clin Endocrinol Metab.* 2010;24(3):491–502.
19. Shattuck TM, et al. Somatic and germ-line mutations of the HRPT2 gene in sporadic parathyroid carcinoma. *N Engl J Med.* 2003;349(18):1722–1729.
20. Simonds WF, et al. Familial isolated hyperparathyroidism is rarely caused by germline mutation in HRPT2, the gene for the hyperparathyroidism-jaw tumor syndrome. *J Clin Endocrinol Metab.* 2004;89(1):96–102.
21. Vasef MA, et al. Expression of cyclin D1 in parathyroid carcinomas, adenomas, and hyperplasias: a paraffin immunohistochemical study. *Mod Pathol.* 1999;12:412–416.
22. Weiland LH, et al. Lipoadenoma of the parathyroid gland. *Am J Surg Pathol.* 1978;2(1):3–7.
23. Westin G, et al. Molecular genetics of parathyroid disease. *World J Surg.* 2009;33(11):2224–2233.

# Malignant Neoplasms of the Parathyroid Gland

■ **Lester D.R. Thompson**

## ■ PARATHYROID CARCINOMA

Parathyroid carcinoma is a malignant neoplasm arising from the parathyroid parenchymal cells, comprising approximately 1% of all primary hyperparathyroidism (HPT) cases (no malignant adipose tumors are recognized in the parathyroid). Secondary parathyroid hyperplasia and neck irradiation are suggested as etiologic factors. There is also an increased incidence of carcinoma in patients with hereditary hyperparathyroidism–jaw tumor (HPT-JT) syndrome. There are no well-accepted histologic features that are used alone to diagnose carcinoma, but a constellation of features can help to confirm the diagnosis.

### CLINICAL FEATURES

Parathyroid carcinoma affects fewer than 1/1,000,000 population per year, develops in all ages, although more frequently in older adults (mean 6th decade) and up to a decade earlier than adenoma. There is no sex bias, distinctly different from the marked female predominance in patients with parathyroid adenoma. Japanese and Italian patients show a higher incidence of carcinoma than other races.

The clinical features are due primarily to the effects of excessive parathyroid hormone (PTH) secretion and hypercalcemia. Laboratory values of greater than 1,000 ng/L for PTH and greater than 16 mg/dL for serum calcium are very concerning for parathyroid carcinoma. The nonspecific symptoms (weakness, fatigue, anorexia, weight loss, nausea, polyuria, polydipsia) overlap with adenoma, but excessively high serum calcium levels (>16 mg/dL) are associated with nephrolithiasis, renal insufficiency, and bone “brown tumors.” Concurrent bone disease and kidney stones are more common in patients with carcinoma than adenoma. A palpable neck mass (in up to 75% of patients) suggests carcinoma and is often difficult to remove at surgery due to adherence to

### PARATHYROID CARCINOMA—DISEASE FACT SHEET

#### Definition

- A malignant neoplasm derived from parathyroid parenchymal cells

#### Incidence and Location

- Accounts for < 2% of primary hyperparathyroidism
- Slightly higher frequency in lower parathyroid glands

#### Morbidity and Mortality

- Adverse effects of hypercalcemia on the cardiovascular system
- Indolent tumor with recurrences and metastases, up to 15% mortality at 5 years

#### Sex, Race, and Age Distribution

- Equal sex distribution
- Japanese and Italian patients have a higher incidence
- Wide age range, although predominantly older patients; still ~10 years younger than patients with adenoma

#### Clinical Features

- Symptoms referable to excess calcium and parathyroid hormone
- Nephrolithiasis and bone “brown tumors”
- Palpable neck mass, often difficult to remove surgically
- Hoarseness is common with recurrent laryngeal nerve involvement
- May be part of hereditary hyperparathyroidism–jaw tumor syndrome
- High serum calcium and parathyroid hormone levels

#### Prognosis and Therapy

- Indolent with recurrences common (~50%)
- Approximately 50% 10-year survival
- Surgery

the soft tissues, nerves (recurrent laryngeal nerve involvement gives hoarseness), and/or thyroid gland. Carcinoma may develop in any parathyroid gland but is slightly more common in the *lower* parathyroid glands.

Most cases are sporadic, with only a small subset associated with familial disease forms. There are recurrent losses of chromosome 13q, the same region known to



contain the retinoblastoma (*RB1*) and *BRCA2* tumor suppressor genes. A genomic region frequently lost in parathyroid adenomas is 11q, the location of *MEN1*, but it is almost never identified in carcinoma, supporting the contention that parathyroid carcinomas arise de novo rather than from preexisting adenomas. Carcinoma is a component of HPT-JT syndrome, where it is identified in approximately 15% of patients. Carcinomas are rarely associated with prior irradiation, renal failure, and celiac disease. Radiographic studies are usually unreliable in separating adenoma from carcinoma but can aid in planning surgery.

## **PATHOLOGIC FEATURES**

### **GROSS FINDINGS**

Carcinomas are typically poorly circumscribed, large, and adherent to the surrounding soft tissues, nerves, and thyroid gland by thick fibrous bands. If there has been previous surgery, scarring and hemorrhage may simulate “invasion.” The cut surface is firm and white-tan and may have areas of necrosis. Tumors range from 1.5 to 6 cm (mean, 3 cm), developing in normally located or ectopic sites, and ranging up to 50 grams.

### **MICROSCOPIC FINDINGS**

No one histologic feature, other than metastatic disease, is considered diagnostic for parathyroid carcinoma. However, a constellation of features can usually be used to support the diagnosis. The most helpful features are those of invasive growth, including (1) definitive vascular invasion (endothelial lined space with attachment to

## **PARATHYROID CARCINOMA—PATHOLOGIC FEATURES**

### **Gross Findings**

- Large tumors (mean, 3 cm)
- Adherent to soft tissues and thyroid gland
- Firm, gray-white cut surface
- Central necrosis may be present

### **Microscopic Findings**

- Adherence to the thyroid gland
- Capsular, vascular, or perineural invasion
- Soft tissue extension
- Tumor cell necrosis (comedonecrosis)
- Trabecular growth with thick, acellular bands of fibrosis
- Tumor cell monotony, although profound pleomorphism can be seen
- High nuclear to cytoplasmic ratio
- Spindling of tumor cells
- Prominent, eosinophilic, irregular macronucleoli
- Increased mitotic figures, including atypical forms

### **Immunohistochemical Findings**

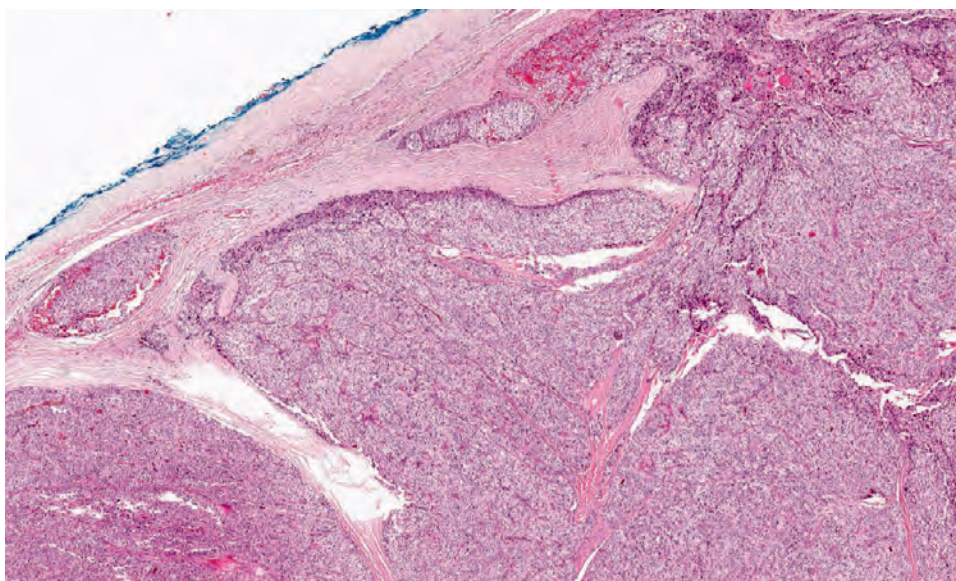
- Chromogranin and parathyroid hormone, along with keratins
- Loss of parafibromin
- Increased Ki-67 labeling index
- Cyclin D1 overexpression
- Negative TTF1 and thyroglobulin

### **Molecular Findings**

- Recurrent losses in chromosome 13q (region of *RB1* and *BRCA2*)
- *CDC73* shows germline inactivating mutations
- *CCND1* is overexpressed

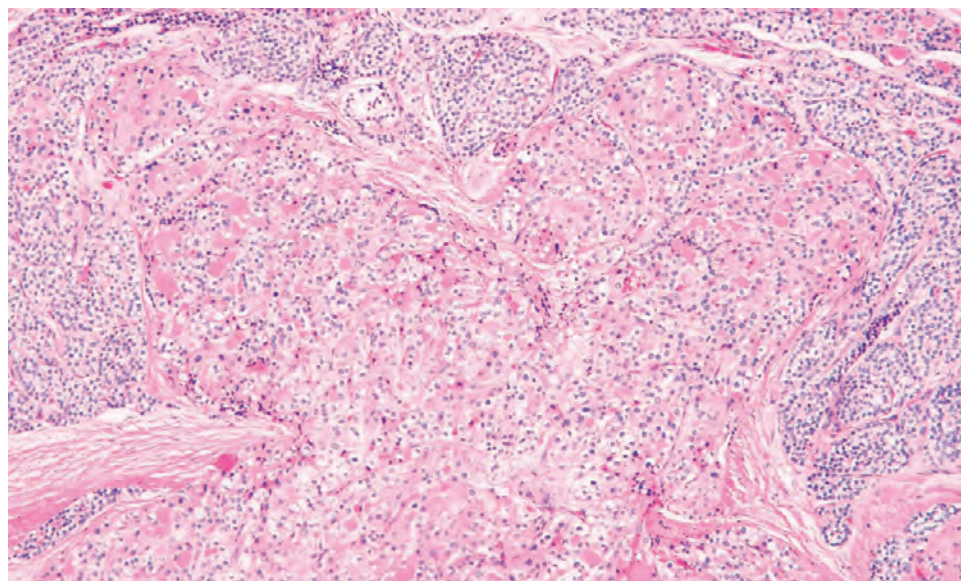
### **Pathologic Differential Diagnosis**

- Parathyroid adenoma, medullary carcinoma, thyroid follicular neoplasms, metastatic renal cell carcinoma

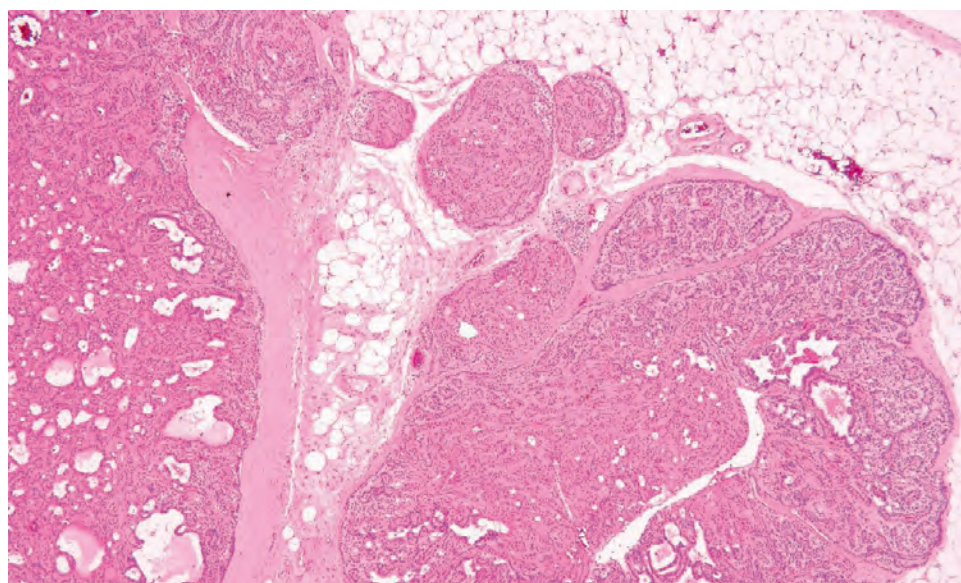


**FIGURE 28.1**

Neoplastic cells are identified within vascular spaces of the fibrous connective tissue capsule of this parathyroid carcinoma.

**FIGURE 28.2**

A "mushroom" projection of neoplastic cells through the capsule into the surrounding parathyroid parenchyma is seen in this parathyroid carcinoma.

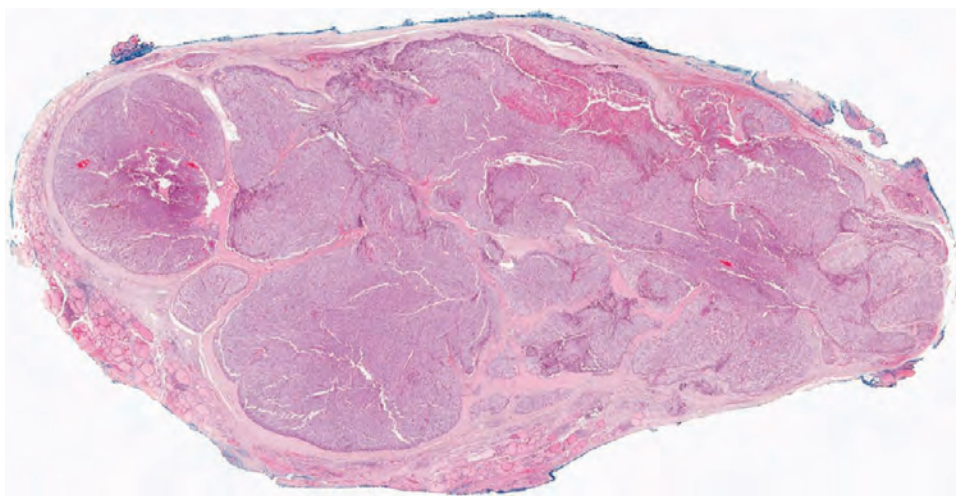
**FIGURE 28.3**

A thick capsule surrounding the neoplasm, with areas of invasion and direct extension into the surrounding periparathyroidal adipose tissue.

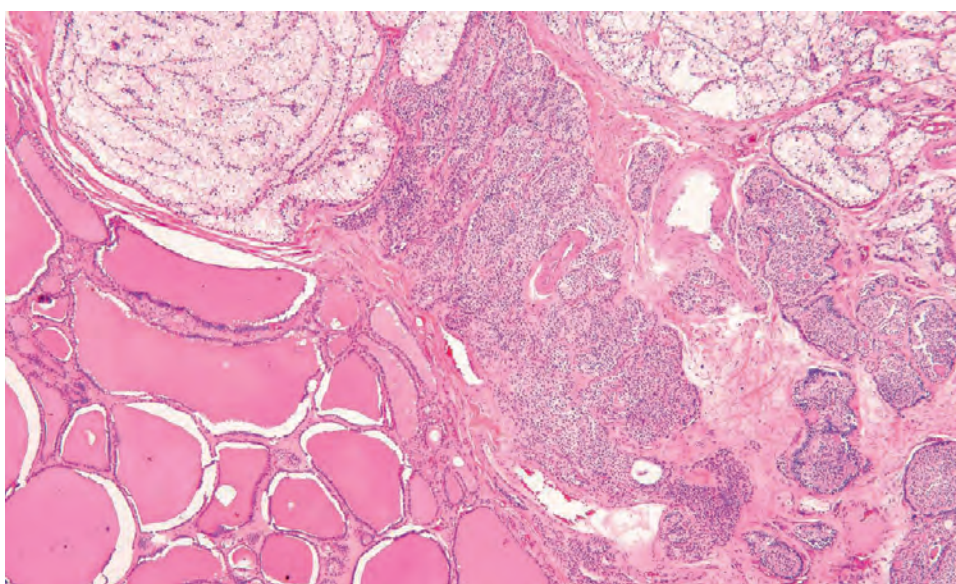
the wall by the neoplastic cells; [Fig. 28.1](#)), (2) capsular invasion ([Fig. 28.2](#)), (3) extension into the uninvolved periparathyroidal adipose tissue ([Fig. 28.3](#)), (4) invasion/attachment to the thyroid parenchyma ([Figs. 28.4](#) and [28.5](#)), and (5) perineural invasion, the latter almost diagnostic of carcinoma ([Fig. 28.6](#)), although this feature is not commonly identified (approximately 5%). Epithelial entrapment in fibrosis (usually secondary to degenerative changes) can mimic invasion and may be nigh unto impossible to separate from true invasion in some cases ([Fig. 28.7](#)). A thick capsule is frequently associated with band-like acellular, dense, broad areas of fibrosis, with occasional hemosiderin-laden macrophages or hemorrhage ([Fig. 28.8](#)). The fibrosis often shows a perivascular

distribution, with collagen expanding into the tumor. Small compartments are often formed by the fibrosis. True tumor necrosis, often in a central, comedonecrosis pattern, also suggests malignancy ([Fig. 28.9](#)). The tumor cells are arranged in solid, diffuse ([Fig. 28.10](#)), or organoid groups, with a trabecular pattern noted in a number of cases ([Fig. 28.11](#)). Many different patterns of growth can be seen in parathyroid carcinoma, including glandular, pseudoacinar, spindle cell, peritheliomatous (perivascular palisade), and papillary ([Fig. 28.12](#)). Cystic change tends to be seen more often in patients with HPT-JT syndrome. Chief cell neoplasms ([Fig. 28.13](#)) are more common than oncocytic neoplasms ([Fig. 28.14](#)), although the cytoplasmic quality does not influence patient outcome.

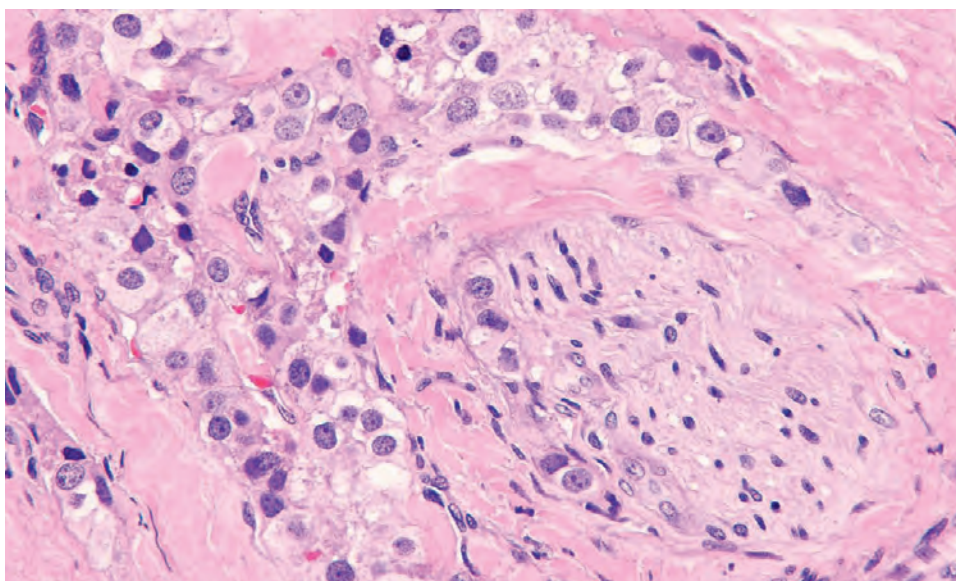


**FIGURE 28.4**

Solid nodules of tumor separated by large, thick bands of fibrosis are identified immediately adjacent to thyroid parenchyma (*lower and left*).

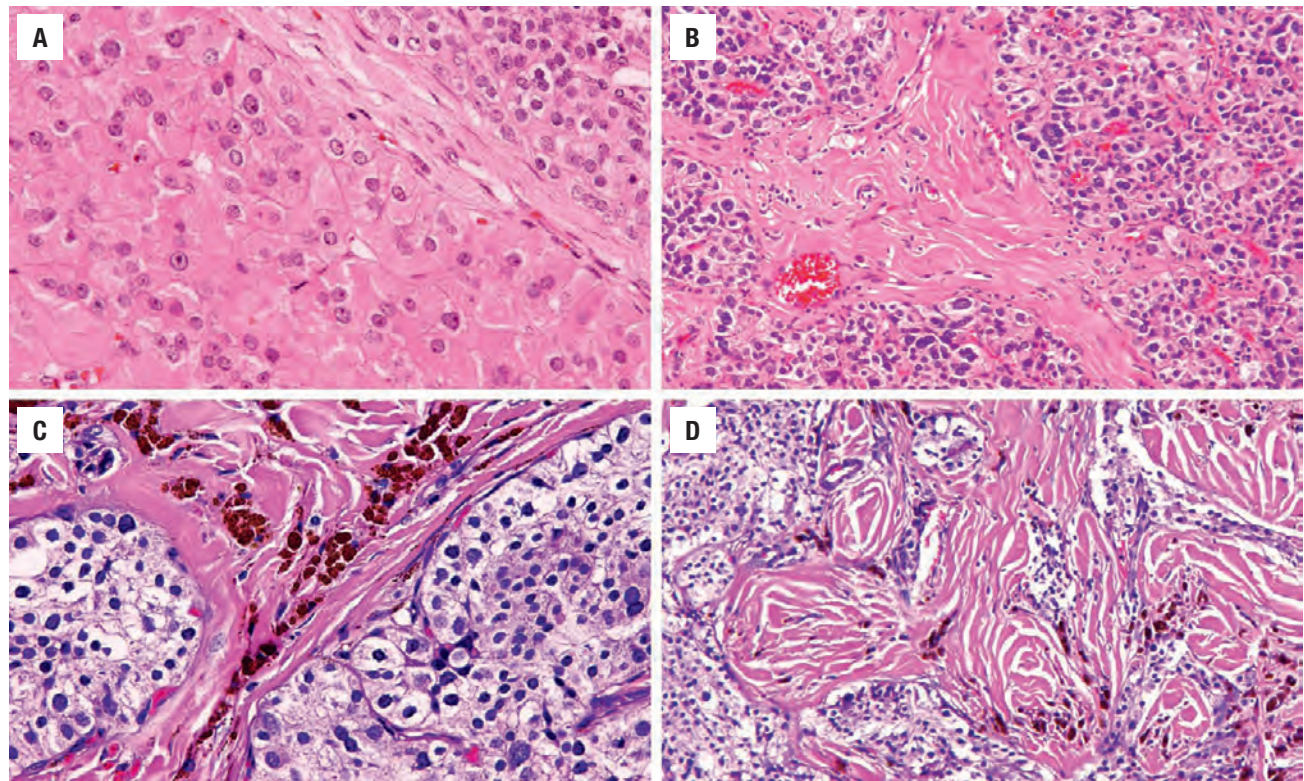
**FIGURE 28.5**

Neoplastic parathyroid cells are intimately associated with thyroid tissue (*lower left*).

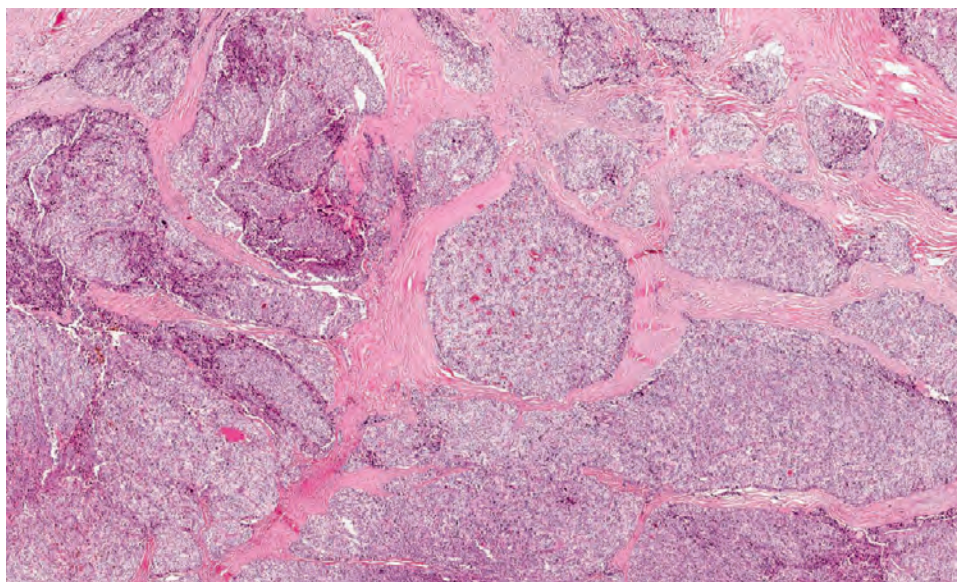
**FIGURE 28.6**

Perineural invasion, including intraneural invasion, is diagnostic of a parathyroid carcinoma in this example.



**FIGURE 28.7**

Fibrosis is common in parathyroid carcinoma. Scant fibrosis (A) to dense, acellular, eosinophilic perivascular fibrosis (B) is seen in parathyroid carcinoma. Hemosiderin may be deposited within the fibrosis to a variable degree (C and D).

**FIGURE 28.8**

Multiple nodules of monotonous cells are separated by dense fibrosis in this parathyroid carcinoma.



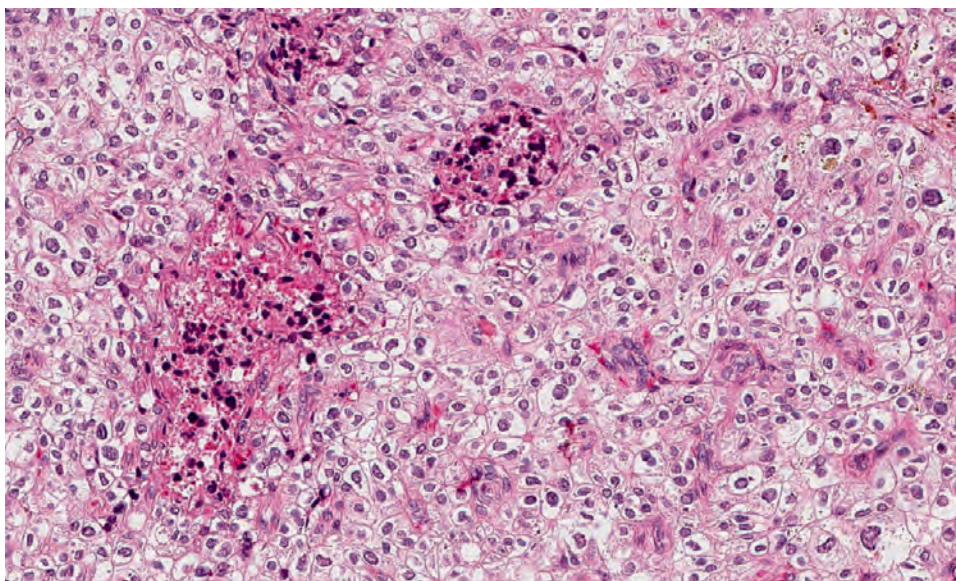


**FIGURE 28.9**

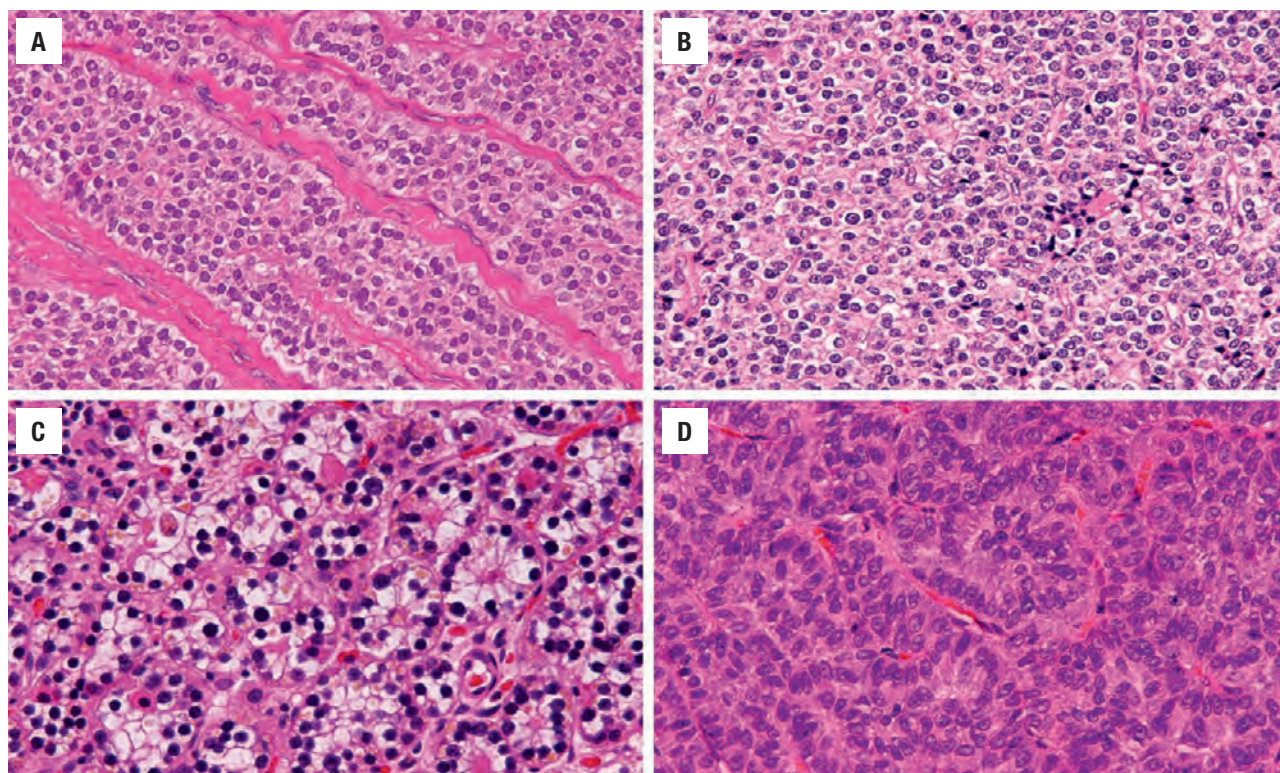
Comedonecrosis is a feature of carcinoma, not seen in benign conditions. However, it is an uncommon feature.



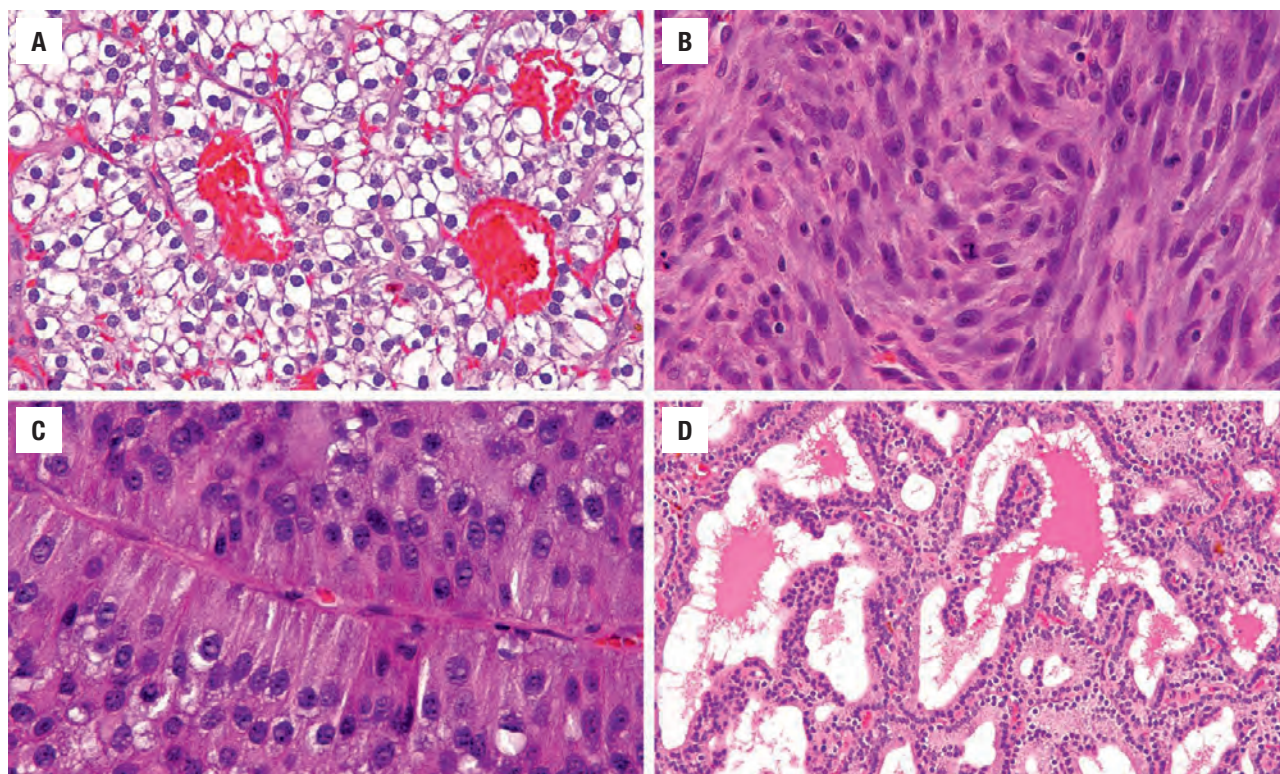
**FIGURE 28.10**

A monotonous, diffuse pattern suggests a neoplasm rather than hyperplasia, although more common in carcinoma than adenoma.



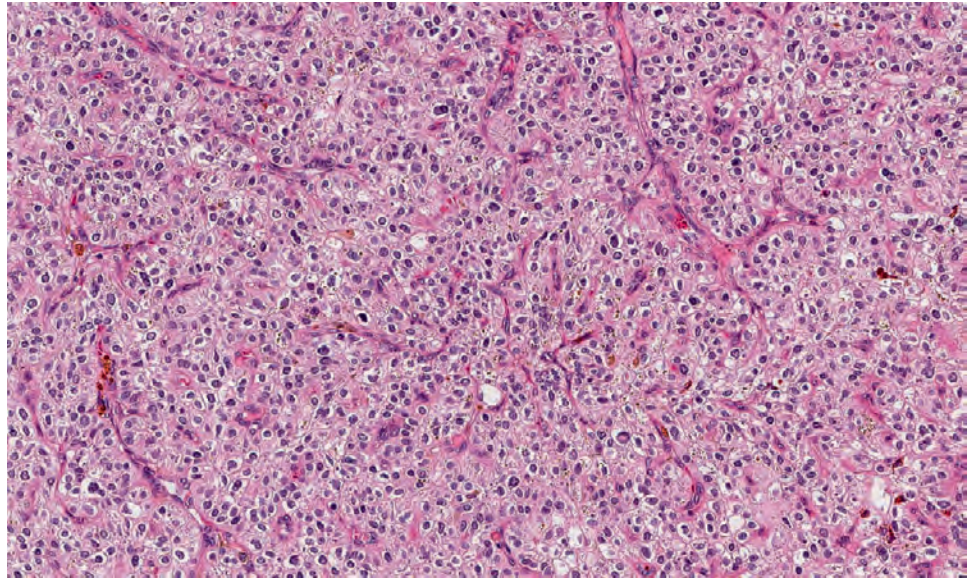
**FIGURE 28.11**

Many patterns can be seen in carcinoma, including trabecular (A), solid (B), follicular (C), and festoons (D).

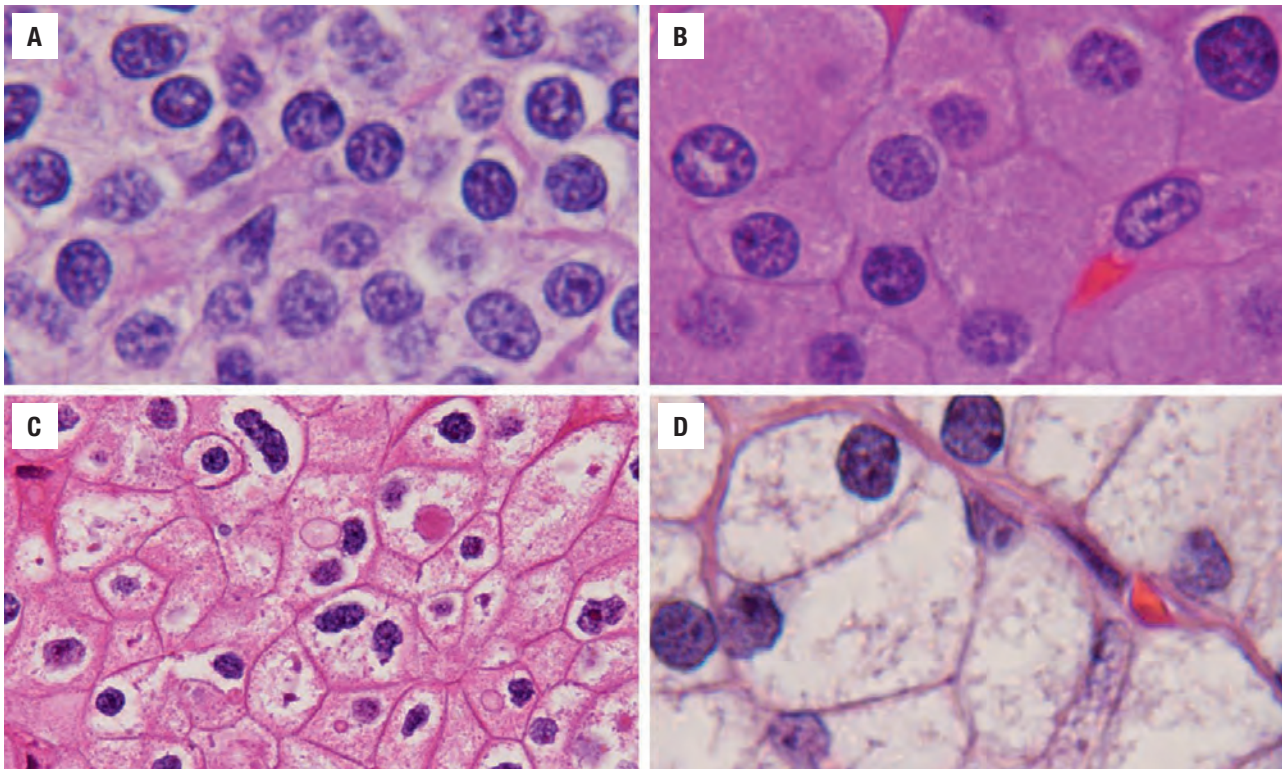
**FIGURE 28.12**

Many patterns can be seen in carcinoma, including pseudoglandular (A), spindled (B), peritheliomatous (C), and papillary (D).



**FIGURE 28.13**

This chief cell neoplasm shows enlarged cells with an increased nuclear to cytoplasmic ratio, along with dense, heavy nuclear chromatin distribution.

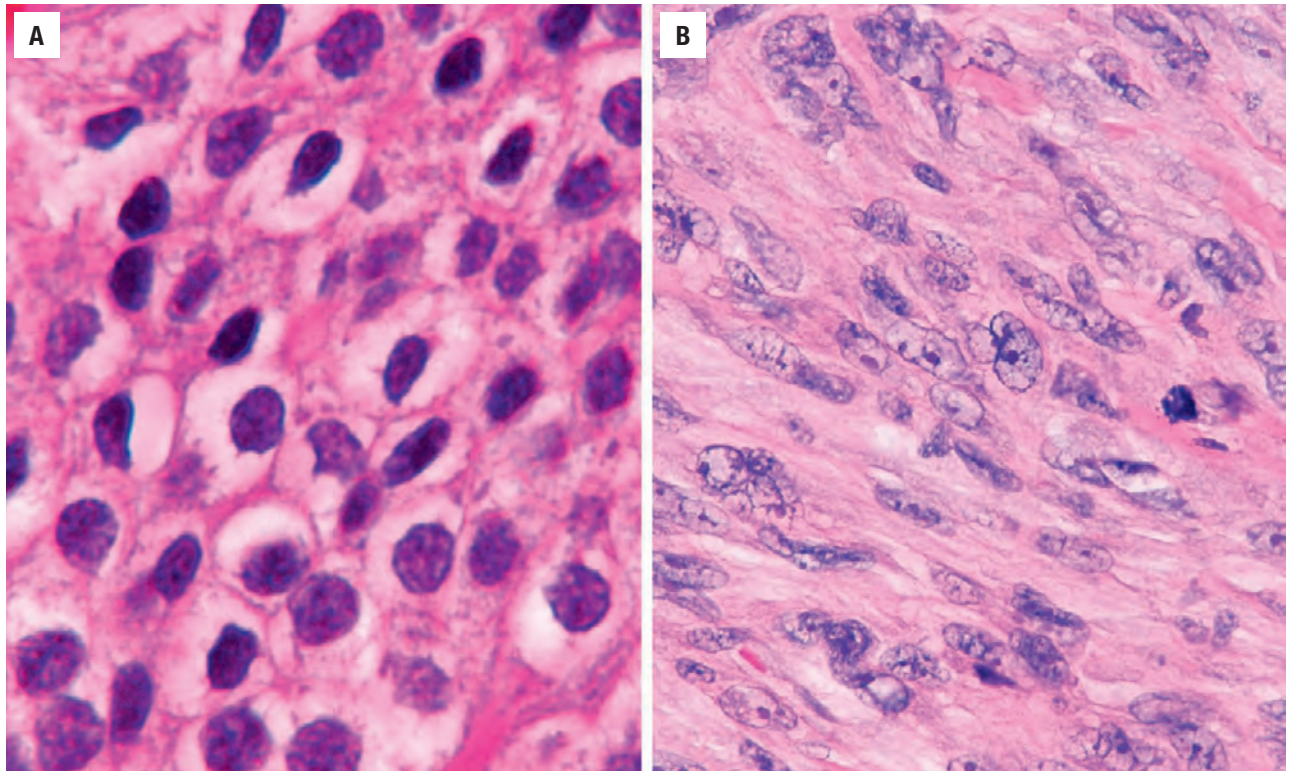
**FIGURE 28.14**

Cytoplasmic quality can range from amphophilic (A), oxyphilic (B), partially cleared (C), to completely clear (D). Note how the cell membranes are prominent in all types of cytoplasm.

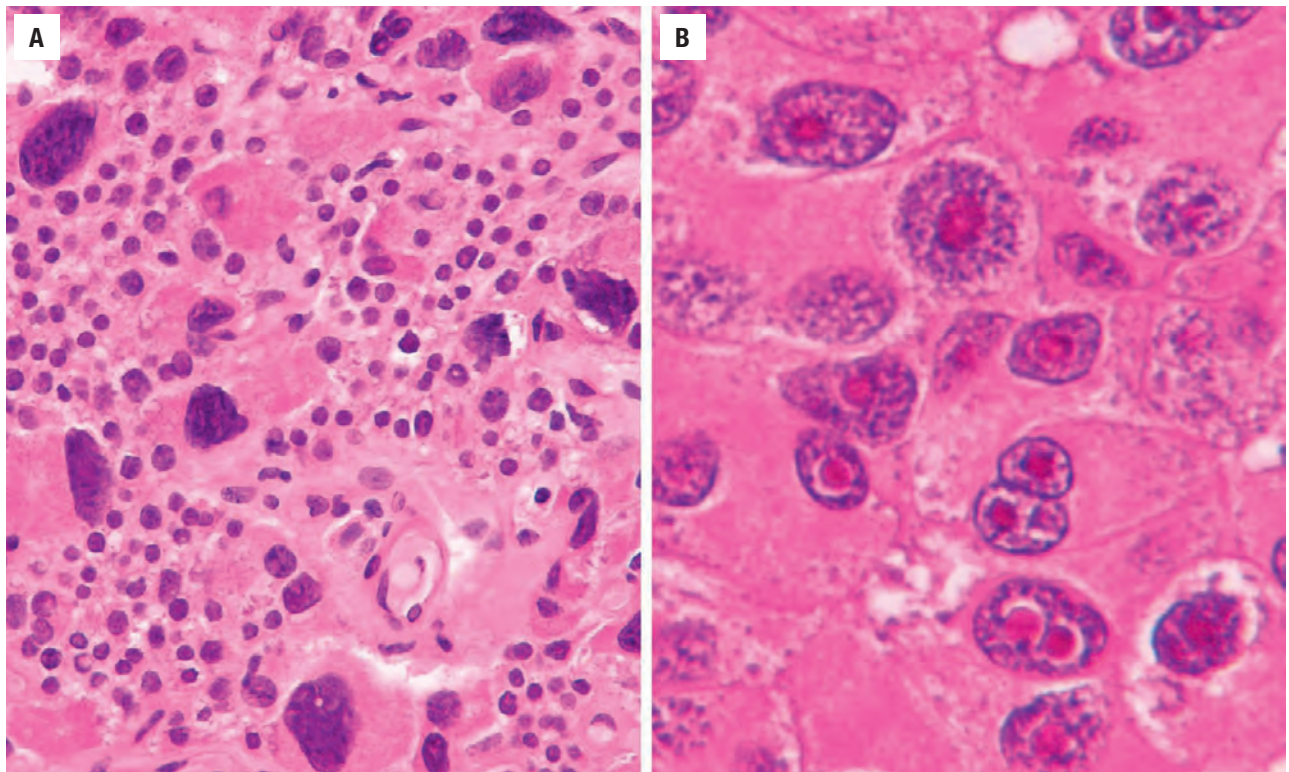
The nuclear chromatin tends to be dense to coarse. Tumor cell spindling, “watermelon seeds,” and pyknosis are seen more frequently in carcinoma, but not exclusively (Fig. 28.15). A monotonous cellular population (in which the cells may be atypical or not) suggests malignancy. Many tumors exhibit cells with an increased nuclear to cytoplasmic ratio, cellular enlargement, profound

pleomorphism, and prominent, irregular, eosinophilic macronucleoli (Fig. 28.16). Remarkably increased mitotic activity, including atypical forms, is more likely in carcinoma, but mitotic figures alone cannot separate between adenoma and carcinoma; however, atypical mitoses are only seen in carcinoma. Frozen section is discouraged, especially if it is an incisional biopsy, because it results



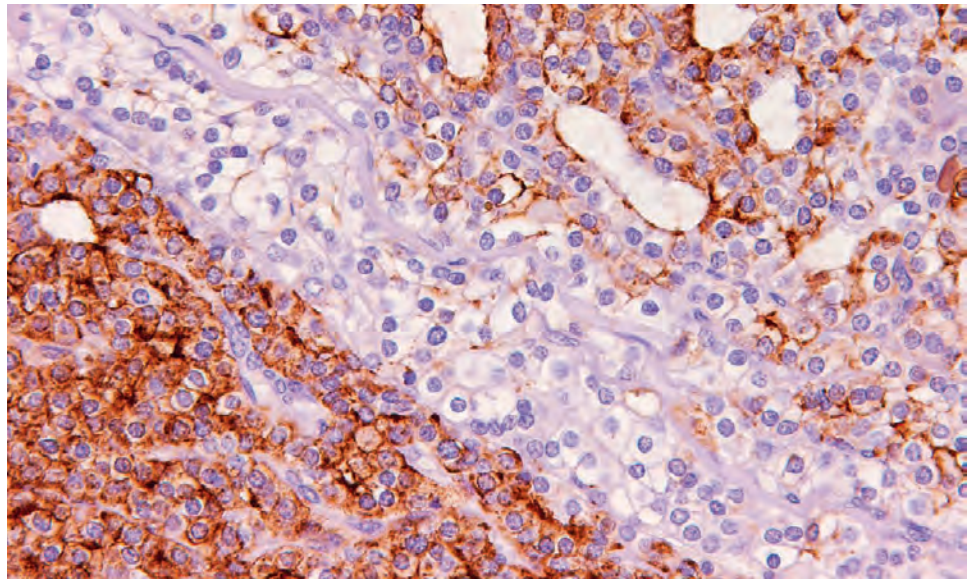
**FIGURE 28.15**

(A) Pyknotic, “watermelon seed” appearance to the nuclei is common in carcinoma. (B) Tumor cell spindling and remarkable anaplasia is seen in this parathyroid carcinoma.

**FIGURE 28.16**

(A) Profound nuclear pleomorphism. (B) Prominent, irregular, macro, eosinophilic nucleoli with a perinucleolar halo are almost diagnostic of carcinoma.



**FIGURE 28.17**

Variable expression of chromogranin is seen in this carcinoma, with heavy reaction in the lower left, focal reaction in the middle, and intermediate staining in the upper right.

in tumor cell seeding, with recurrent HPT, whether the original disease was benign or malignant. The triad of macronucleoli, greater than 5 mitoses/50 high-power fields, and coagulative necrosis seems to predict aggressive behavior.

## ANCILLARY STUDIES

### IMMUNOHISTOCHEMICAL FINDINGS

The neoplastic cells are immunoreactive with parathyroid hormone (PTH), chromogranin (Fig. 28.17), cytokeratins (such as CAM5.2), PGP9.5, GATA3, and galectin-3, with strong reactivity for transcription factor glial cells missing (Gcm)2, whereas nonreactive with TTF1 and thyroglobulin. There is a loss of parafibromin immunoreactivity in carcinoma (Fig. 28.18), although it is not universal, and may show decreased expression instead, especially when there is a background of chronic renal failure. Increased Ki-67 (Fig. 28.18) and cyclin D1 overexpression are seen more commonly in parathyroid carcinoma. Ki-67 proliferation is usually higher in carcinomas, but significant overlap with adenoma limits clinical utility. A variety of other markers may occasionally be expressed in parathyroid carcinoma (CK7, CK18, muc-1, epithelial membrane antigen [EMA], p16, and renal cell marker), (Fig. 28.19), whereas p27 is reduced and bcl2 and CK14 are lost (clinical application of these markers is limited).

### MOLECULAR FINDINGS

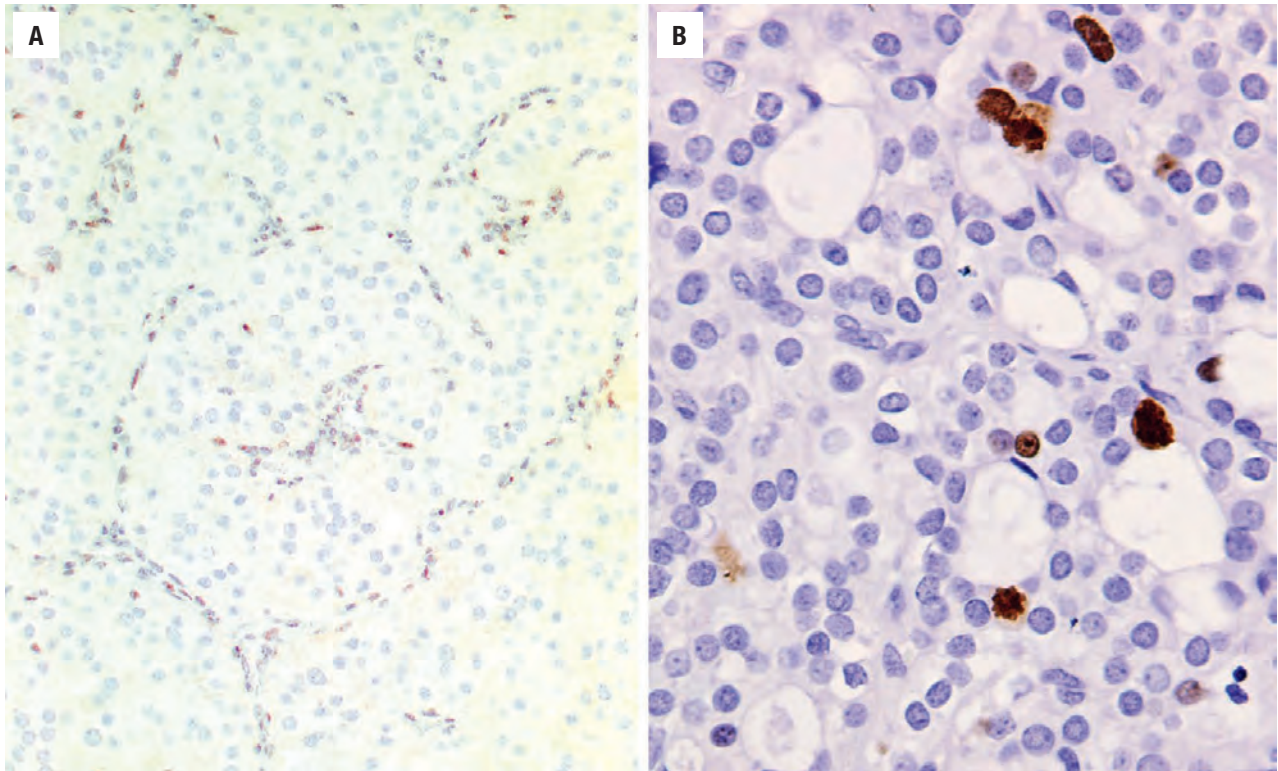
A variety of different genes are involved to a variable degree in parathyroid tumorigenesis (Table 28.1), along with related syndromes. Approximately 15 % of patients

with the HPT-JT syndrome develop parathyroid carcinoma. The tumor suppressor gene *CDC73* (1q25) shows a germline inactivating mutation in many cases of HPT-JT (approximately an 80 % penetrance), but approximately 20 % of patients with seemingly sporadic parathyroid carcinoma also have germline mutations in this tumor suppressor gene. Thought to be the major molecular driver in the pathogenesis of carcinoma, somatic mutations are also present in many cases. *CDC73* (cell division cycle 73; formerly *HRPT2*) encodes the protein parafibromin, a nuclear protein, that is lost with mutation. Therefore, nuclear parafibromin reaction is lost in many, but not all carcinomas, while remaining expressed in adenoma. Menin protein (encoded by *MEN1*) is required for the transforming growth factor (TGF)- $\beta$  to effectively inhibit parathyroid cell proliferation and PTH production. The high rate of somatic mutations in menin within tumors supports this contention, although not a major finding in carcinoma. Cyclin D1 (*CCND1*, formerly known as *PRAD1*: parathyroid adenomatosis 1) is overexpressed in both adenomas (20 % to 40 %) and carcinomas (up to 70 %), but somatic rearrangements or germline translocations or rearrangements have not been detected in carcinoma. Many other candidate genes (*PRUNE2*, *PIK3CA*, *MLL2*, *MTOR*, *ADCK1*) are being further evaluated.

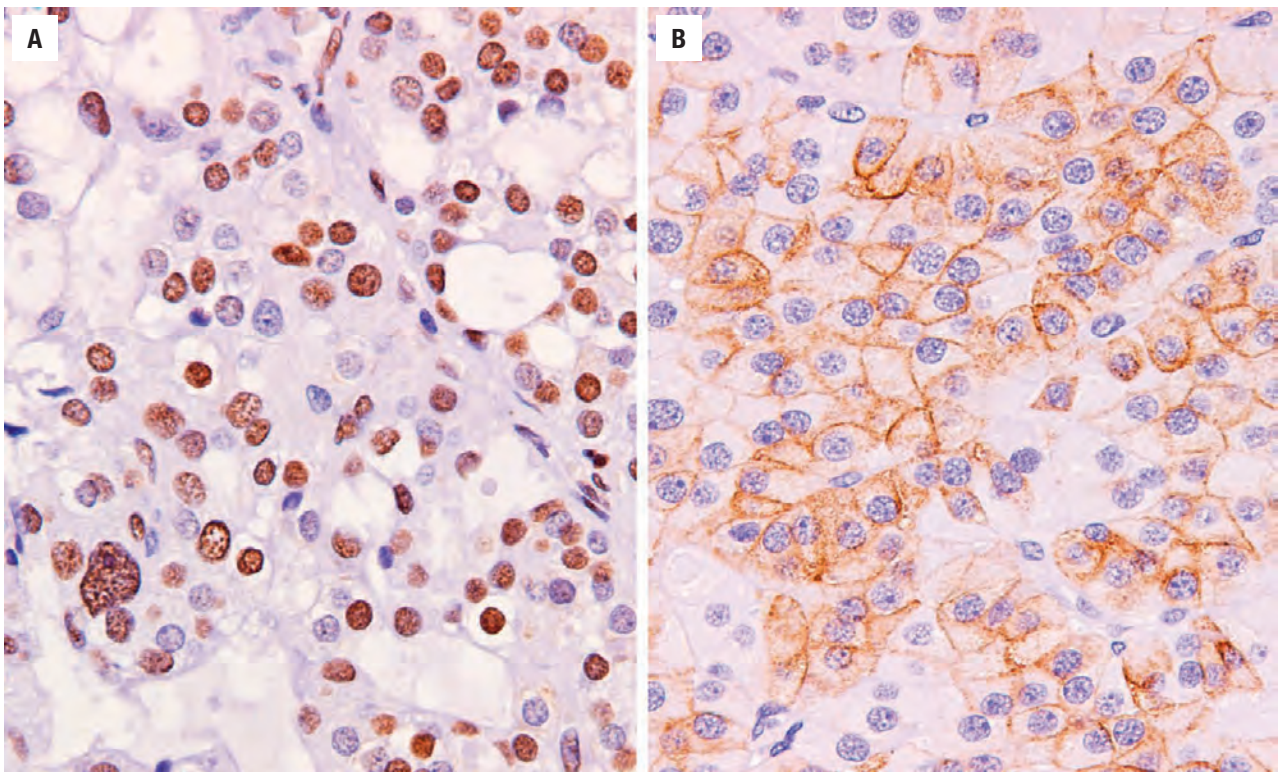
## DIFFERENTIAL DIAGNOSIS

Parathyroid carcinoma must be separated from parathyroid adenoma, thyroid conditions, and metastatic neoplasms. The most difficult separation is from parathyroid adenoma, especially in the setting of previous surgery or with “neck manipulation” (referred to as parathyromatosis). Vascular or perineural invasion predicts carcinoma, as do markedly increased serum calcium and PTH values. Adenomas



**FIGURE 28.18**

(A) Nuclei of the neoplastic cells are negative for parafibromin, whereas the endothelial cells show a strong reaction (internal control). (B) Ki-67 is strongly reactive within the nuclei of a number of cells.

**FIGURE 28.19**

(A) p16 is strongly and diffusely nuclear immunoreactive in nearly all of the neoplastic nuclei. (B) Renal cell marker reacts along the membranes of parathyroid carcinoma cells in some cases.



**TABLE 28.1****Genes associated with syndromic and sporadic parathyroid neoplasms**

| Gene         | Location | Protein Encoded | Syndrome Associated Parathyroid Disease   | Sporadic Parathyroid Disease                                      |
|--------------|----------|-----------------|---|---|
| <i>MEN1</i>  | 11q13    | Menin           | MEN1, typical adenomas  | Inactivating mutation in up to 35% of adenomas; rare in carcinoma |
| <i>CDC73</i> | 1q25     | Parafibromin    | Hyperparathyroidism–jaw tumor (HPT-JT) syndrome<br>Parathyroid carcinoma ~20% of patients | Inactivation in ~80% of carcinomas                                |
| <i>RET</i>   | 10q11.2  | c-Ret           | MEN2a<br>Parathyroid adenoma in > 99%   | Very rare   |
| <i>CCND1</i> | 11q13    | Cyclin D1       | n/a   | Overexpression in adenoma and carcinoma (but not usually mutated) |

are usually smaller, but with increased use of screening laboratory studies, this feature is not as useful in current practice. Unfortunately, large adenomas will frequently display fibrosis, hemosiderin deposits, and cystic degeneration, thereby mimicking carcinoma. Moreover, although a rim of uninvolved parathyroid parenchyma is rarely seen in parathyroid carcinoma, in large adenomas it may be more difficult to detect. When adenoma cells are arranged in acinar or glandular-type structures, eosinophilic material can be seen, a feature uncommon in carcinoma. The cells of an adenoma are enlarged but do not usually have the increased N:C ratio of a carcinoma; nucleoli are usually small and inconspicuous. Mitotic activity is usually low in adenomas, but mitotic figures alone cannot be used to separate benign from malignant tumors. Adenomas will be positive with parafibromin, p27, bcl-2, and MDM2.

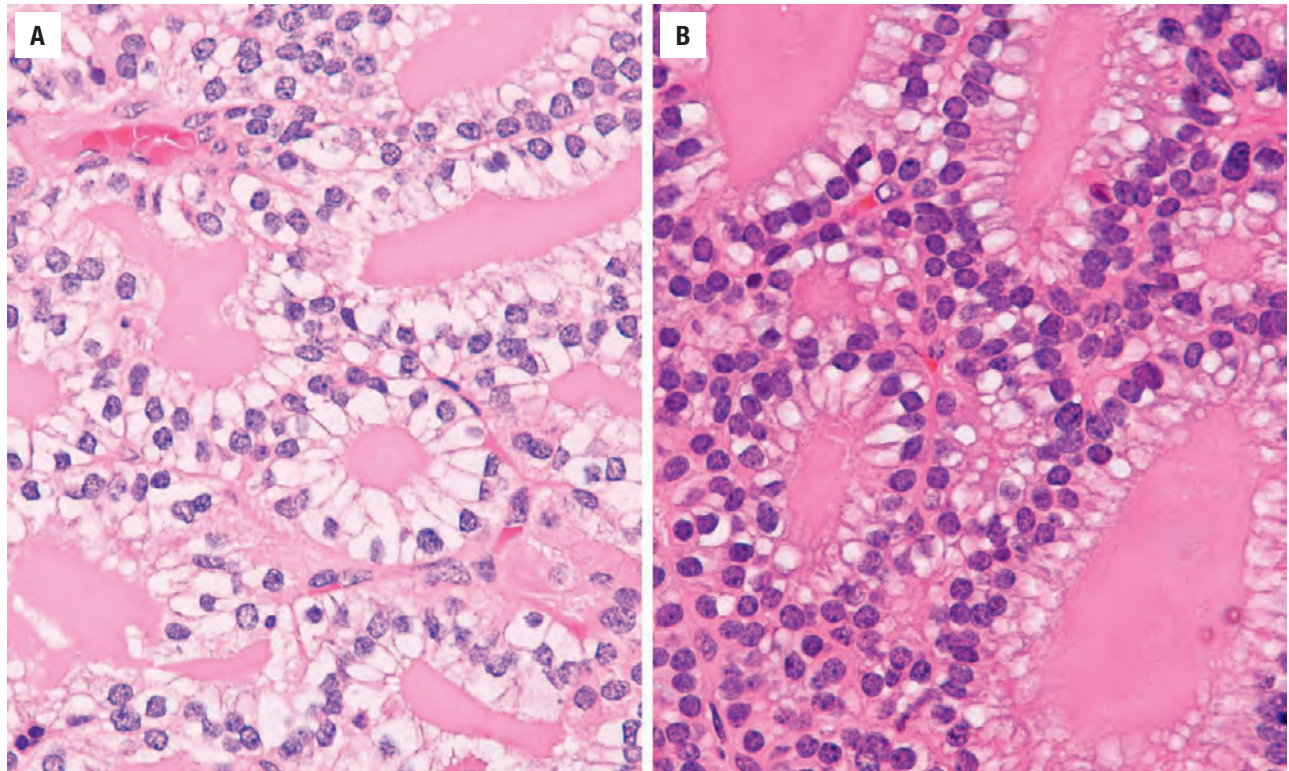
A thyroid follicular neoplasm may be simulated by the “follicular” pattern of growth and by inspissated material within the lumen in parathyroid carcinoma (Fig. 28.20). Parathyroid cells usually have clear cytoplasm and will display very prominent cell borders. Intrathyroidal parathyroid tissue often lacks a well-defined capsule and may show pseudoinvasive growth patterns. Immunohistochemistry will also help with separation (TTF1 and thyroglobulin). Medullary carcinoma may metastasize or directly invade into parathyroid tissue and will be chromogranin immunoreactive but will be calcitonin and CEA positive. Metastatic renal cell carcinoma may present as a “clear cell neoplasm” in the parathyroid gland (Fig. 28.21). However, the vascular pattern, sinusoidal growth and immunoreactivity with vimentin, CD10, PAX8, CAIX, and EMA without other markers will probably help to make this distinction in the correct clinical context.

As nice as it would be to have a definitive diagnosis in each case, the concept of an intermediate category must be addressed. The term “atypical adenoma” is suggested for a parathyroid neoplasm lacking unequivocal

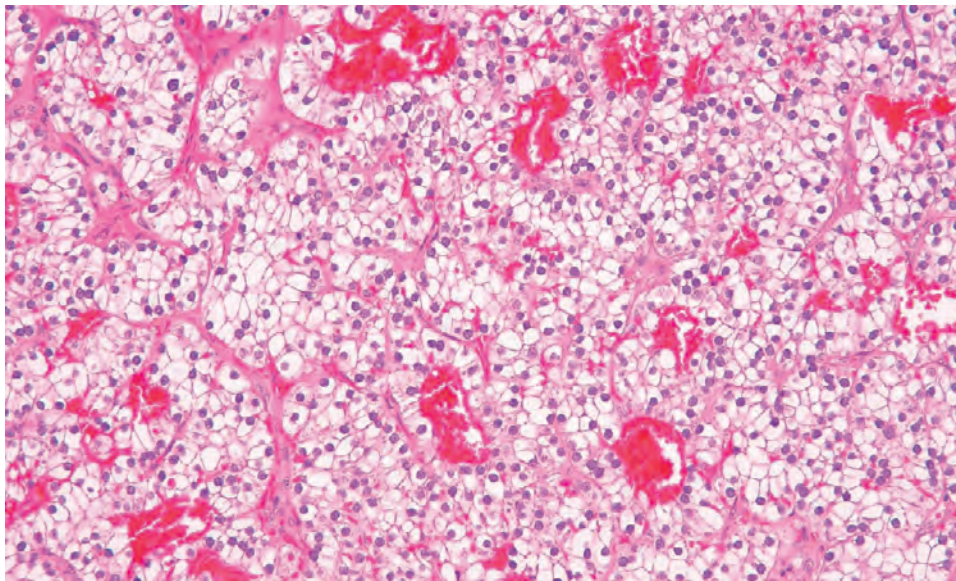
evidence of invasiveness, even though it may be adherent to surrounding tissues, but showing some other feature(s) suspicious for malignancy (such as increased mitoses; band-like fibrosis). These tumors are considered of uncertain malignant potential, requiring close clinical follow-up. The use of parafibromin for these difficult tumors may help to limit the use of this noncommittal term. Curiously, these cases, where follow-up is available, show a benign clinical outcome.

### PROGNOSIS AND THERAPY

Overall, there is a 5-year survival up to 85%, with a 10-year survival of approximately 60%. Local recurrence can occur in up to 60% of patients, usually within 3 years, by spread to contiguous neck structures. Recurrences should be documented by localization studies in a patient with recurrent hypercalcemia, but a prolonged survival can still be expected after palliative surgery. Disruption of the capsule during surgery may cause seeding of parathyroid tissue and give rise to persistent or recurrent HPT, referred to as parathyromatosis. Staging has been introduced with the 8th edition of the American Joint Committee on Cancer Staging (AJCC). There are possible factors associated with a worse prognosis, including male sex, old age at diagnosis, large tumor size, vascular invasion, and lymph node metastasis. The best outcome for parathyroid carcinoma occurs when there is complete resection at the first surgery. Adjuvant therapy does not play much of a role in management because it is the management of the metabolic effects of PTH and hypercalcemia that are important. When metastatic disease develops (usually late in the disease course), lymph nodes, lung, and mediastinum are affected more often than bone and liver. Although self-evident, benign “brown tumors” caused by profound HPT may mimic bone metastases.

**FIGURE 28.20**

Parathyroid carcinoma can have inspissated secretions that can mimic a thyroid neoplasm (**A**). The prominent cell borders and clear cytoplasm (**B**) will help with the separation from a thyroid neoplasm.

**FIGURE 28.21**

Parathyroid carcinoma may occasionally have a sinusoidal pattern of growth, including prominent cell borders, making separation from metastatic renal cell carcinoma a challenge. This metastatic renal cell carcinoma has prominent cell borders and a pseudoglandular pattern.

## ■ METASTATIC TUMORS

By definition, tumors that metastasize to or directly invade the parathyroid parenchyma or gland are considered metastatic tumors. Although the glands are vascular,

lymphatic spread is uncommon. Abnormal glands (hyperplasia, adenoma, carcinoma) are more likely to contain metastatic deposits than normal tissue, suggesting there is perhaps an alteration in vascularity or blood flow in the abnormal tissue. Lymphomas and leukemias are excluded by definition.



## CLINICAL FEATURES

Metastases are uncommon, present in less than 0.1 % of surgically removed parathyroids. The vast majority of patients are asymptomatic, although occasionally a mass in the neck, hoarseness, and pain may be the presenting finding. Multiple glands may be involved. Hypoparathyroidism is exceptionally rare. Women are affected slightly more frequently. Patients tend to be older (7th decade). The most common metastatic primary sites include breast (lobular > ductal carcinoma), melanoma, lung, kidney, and soft tissue primaries. Direct extension from a laryngeal or esophageal squamous cell carcinoma or lymphoma may also be identified.

### METASTATIC TUMORS—DISEASE FACT SHEET

#### Definition

- Tumors that metastasize to, or directly invade, the parathyroid gland

#### Incidence and Location

- Unknown due to asymptomatic presentation

#### Morbidity and Mortality

- Usually poor clinical outcome, although exceptions occur

#### Sex and Age Distribution

- Women slightly more commonly
- Tend to be older age at initial presentation

#### Clinical Features

- Vast majority of patients are asymptomatic

#### Prognosis and Therapy

- Usually poor and determined by the underlying primary

## PATHOLOGIC FEATURES

### GROSS FINDINGS

The gland may be slightly enlarged, but metastases are usually not identified at macroscopic examination. Direct extension may result in “attachment” to thyroid, larynx, or esophagus.

### MICROSCOPIC FINDINGS

The lymphatic or vascular location of tumor emboli will help to separate a primary lesion from metastatic disease. The histologic features of the primary site are usually maintained in the metastatic focus (Figs. 28.21 and 28.22). When there is direct extension (Fig. 28.23), the tumor is usually large, and the parathyroid gland involvement is incidental. Separation from thyroid gland (follicular or medullary) primary clear cell tumors and

### METASTATIC TUMORS—PATHOLOGIC FEATURES

#### Gross Findings

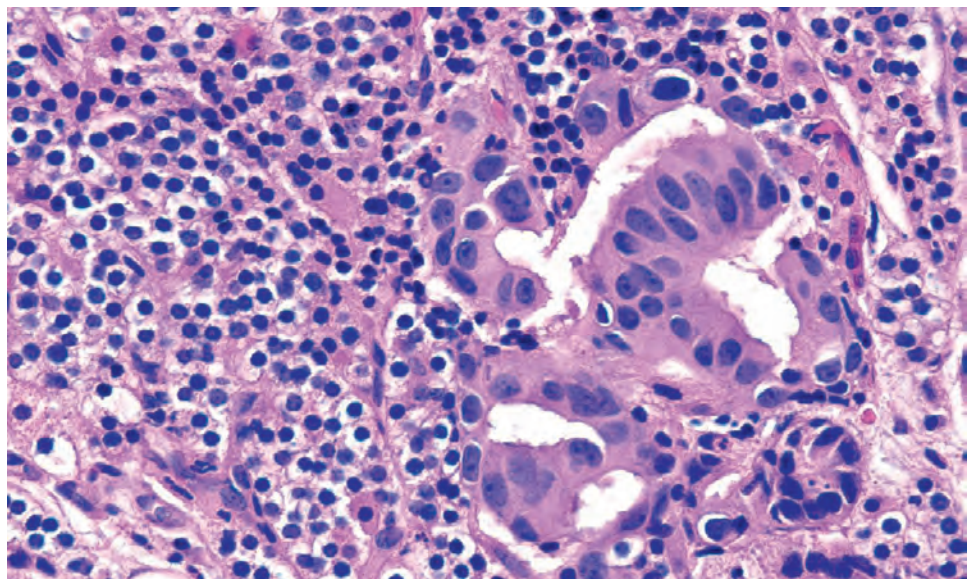
- Direct extension may have “attached” thyroid, larynx, or esophagus
- Metastases may be multinodular

#### Microscopic Findings

- Features of primary tumor are usually maintained
- Lymphomas and squamous cell carcinomas are easy to distinguish from primary lesions

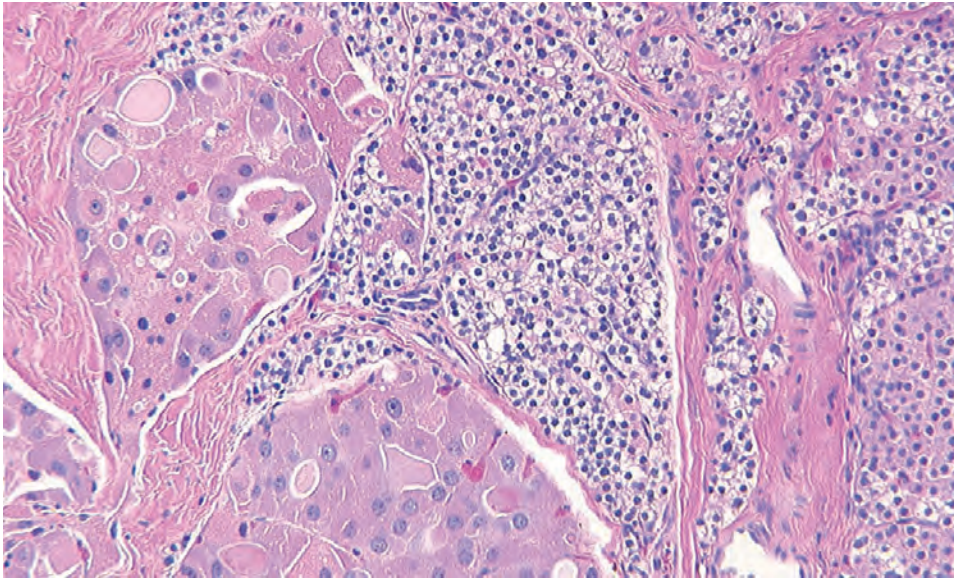
#### Pathologic Differential Diagnosis

- Clear cell neoplasms including follicular or medullary thyroid tumors and metastatic renal cell carcinoma



**FIGURE 28.22**

A neoplastic gland from a metastatic breast carcinoma is noted within the background parathyroid parenchyma.

**FIGURE 28.23**

Metastatic thyroid follicular carcinoma creates nodules of oncocytic epithelium within a cellular parathyroid gland. Immunohistochemistry may be required to confirm the diagnosis.

metastatic renal cell carcinoma may occasionally warrant the use of immunohistochemical studies to achieve the correct diagnosis.

#### PROGNOSIS AND THERAPY

The prognosis is usually guarded, with the nature of the underlying primary determining the overall outcome. In

light of the metastatic nature of the disorder at time of presentation, the management is symptomatic or palliative, with surgery usually used to remove the tumor and to get a histologic diagnosis.

#### SUGGESTED READINGS

The complete list of Suggested Readings is available online at [ExpertConsult.com](http://ExpertConsult.com).



## SUGGESTED READINGS

## Parathyroid Carcinoma

- Al-Kurd A, et al. Parathyroid carcinoma. *Surg Oncol*. 2014;23(2):107–114.
- Arvai K, et al. Molecular profiling of parathyroid hyperplasia, adenoma and carcinoma. *Pathol Oncol Res*. 2012;18(3):607–614.
- Asare EA, et al. Parathyroid carcinoma: an update on treatment outcomes and prognostic factors from the National Cancer Data Base (NCDB). *Ann Surg Oncol*. 2015;22(12):3990–3995.
- Bondeson L, et al. Cytopathological variables in parathyroid lesions: a study based on 1,600 cases of hyperparathyroidism. *Diagn Cytopathol*. 1997;16:476–482.
- Brown S, et al. Parathyroid carcinoma: increasing incidence and changing presentation. *ANZ J Surg*. 2011;81(7–8):528–532.
- Carlson D. Parathyroid pathology: hyperparathyroidism and parathyroid tumors. *Arch Pathol Lab Med*. 2010;134(11):1639–1644.
- Costa-Guda J, Arnold A. Genetic and epigenetic changes in sporadic endocrine tumors: parathyroid tumors. *Mol Cell Endocrinol*. 2014;386(12):46–54.
- DeLellis RA. Parathyroid carcinoma: an overview. *Adv Anat Pathol*. 2005;12(2):53–61.
- DeLellis RA. Challenging lesions in the differential diagnosis of endocrine tumors: parathyroid carcinoma. *Endocr Pathol*. 2008;19(4):221–225.
- Dudney WC, et al. Parathyroid carcinoma. *Otolaryngol Clin North Am*. 2010;43(2):441–453, xi.
- Erickson LA, et al. Oxyphil parathyroid carcinomas: a clinicopathologic and immunohistochemical study of 10 cases. *Am J Surg Pathol*. 2002;26:344–349.
- Erovic BM, et al. Biomarkers of parathyroid carcinoma. *Endocr Pathol*. 2012;23(4):221–231.
- Evans HL. Criteria for diagnosis of parathyroid carcinoma. *Surg Pathol*. 1991;4:244–265.
- Gill AJ. Understanding the genetic basis of parathyroid carcinoma. *Endocr Pathol*. 2014;25(1):30–34.
- Gill AJ, et al. Loss of nuclear expression of parafibromin distinguishes parathyroid carcinomas and hyperparathyroidism-jaw tumor (HPT-JT) syndrome-related adenomas from sporadic parathyroid adenomas and hyperplasias. *Am J Surg Pathol*. 2006;30(9):1140–1149.
- Hundahl SA, et al. Two hundred eighty-six cases of parathyroid carcinoma treated in the U.S. between 1985–1995: a National Cancer Data Base Report. *Cancer*. 1999;86:538–544.
- Iacobone M, et al. Hyperparathyroidism-jaw tumor syndrome: a report of three large kindred. *Langenbecks Arch Surg*. 2009;394(5):817–825.
- Isotalo PA, et al. Presence of birefringent crystals is useful in distinguishing thyroid from parathyroid gland tissues. *Am J Surg Pathol*. 2002;26(6):813–814.
- Kameyama K, et al. Parathyroid carcinomas: can clinical outcomes for parathyroid carcinomas be determined by histologic evaluation alone? *Endocr Pathol*. 2002;13(2):135–139.
- Kasaian K, et al. Complete genomic landscape of a recurring sporadic parathyroid carcinoma. *J Pathol*. 2013;230(3):249–260.
- Kruijff S, et al. Negative parafibromin staining predicts malignant behavior in atypical parathyroid adenomas. *Ann Surg Oncol*. 2014;21(2):426–433.
- Lee JY, et al. Upregulation of FGFR1 expression is associated with parathyroid carcinogenesis in HPT-JT syndrome due to an HRPT2 splicing mutation. *Int J Oncol*. 2014;45(2):641–650.
- Marcocci C, et al. Parathyroid carcinoma. *J Bone Miner Res*. 2008;23(12):1869–1880.
- Newey PJ, et al. Parafibromin—functional insights. *J Intern Med*. 2009;266(1):84–98.
- Sadler C, et al. Parathyroid carcinoma in more than 1,000 patients: A population-level analysis. *Surgery*. 2014;156(6):1622–1630.
- Schulte KM. Clinical presentation, staging and long-term evolution of parathyroid cancer. *Ann Surg Oncol*. 2010;17(8):2156–2174.
- Sharretts JM, Simonds WF. Clinical and molecular genetics of parathyroid neoplasms. *Best Pract Res Clin Endocrinol Metab*. 2010;24(3):491–502.
- Shifrin A, et al. Primary and metastatic parathyroid malignancies: a rare or underdiagnosed condition? *J Clin Endocrinol Metab*. 2015;100(3):E478–E481.
- Singh Ospina N, et al. Prevalence of parathyroid carcinoma in 348 patients with multiple endocrine neoplasia type 1 case report and review of the literature. *Clin Endocrinol (Oxf)*. 2016;84(2):244–249.
- Smith JF, Coombs RR. Histological diagnosis of carcinoma of the parathyroid gland. *J Clin Pathol*. 1984;37:1370–1378.
- Taggart JL, et al. Parathyroid carcinosarcoma: a rare form of parathyroid carcinoma with normal parathyroid hormone levels. *Int J Surg Pathol*. 2013;21(4):394–398.
- Thompson LD. Parathyroid carcinoma. *Ear Nose Throat J*. 2009;88(1):722–724.
- Villar-del-Moral J, et al. Prognostic factors and staging systems in parathyroid cancer: a multicenter cohort study. *Surgery*. 2014;156(5):1132–1144.
- Wei CH, Harari A. Parathyroid carcinoma: update and guidelines for management. *Curr Treat Options Oncol*. 2012;13(1):11–23.
- Westin G, et al. Molecular genetics of parathyroid disease. *World J Surg*. 2009;33(11):2224–2233.
- Woodard GE, et al. Parafibromin, product of the hyperparathyroidism-jaw tumor syndrome gene HRPT2, regulates cyclin D1/PRAD1 expression. *Oncogene*. 2005;24(7):1272–1276.
- Yu W, et al. Whole-exome sequencing studies of parathyroid carcinomas reveal novel PRUNE-2 mutations, distinctive mutational spectra related to APOBEC-catalyzed DNA mutagenesis and mutational enrichment in kinases associated with cell migration and invasion. *J Clin Endocrinol Metab*. 2015;100(2):E360–E364.

## Metastatic Tumors

- Barnes L. Metastases to the head and neck: an overview. *Head Neck Pathol*. 2009;3(3):217–224.
- Benisovich VI, et al. A case of adenocarcinoma of the lung associated with a neck mass and hypercalcemia. *Cancer*. 1991;68(5):1106–1108.
- Bogges MA, et al. Renal clear cell carcinoma appearing as a left neck mass. *Ear Nose Throat J*. 1996;75(9):620–622.
- Bumpers HL, et al. Endocrine organ metastases in subjects with lobular carcinoma of the breast. *Arch Surg*. 1993;128(12):1344–1347.
- de la Monte SM, et al. Endocrine organ metastases from breast carcinoma. *Am J Pathol*. 1984;114:131–136.
- Goddard CJ, et al. Symptomatic hypocalcaemia associated with metastatic invasion of the parathyroid glands. *Br J Hosp Med*. 1990;43(1):72.
- Horwitz CA, et al. Secondary malignant tumors of the parathyroid glands. Report of two cases with associated hypoparathyroidism. *Am J Med*. 1972;52(6):797–808.
- Ito Y, et al. Clinical significance of extrathyroid extension to the parathyroid gland of papillary thyroid carcinoma. *Endocr J*. 2009;56(2):251–255.
- Lee SH, et al. Concurrence of primary hyperparathyroidism and metastatic breast carcinoma affected a parathyroid gland. *J Clin Endocrinol Metab*. 2013;98(8):3127–3130.
- Lee HE, et al. Tumor-to-tumor metastasis: Hepatocellular carcinoma metastatic to parathyroid adenoma. *Pathol Int*. 2011;61(10):593–597.
- Levy MT, et al. Primary paraganglioma of the parathyroid: a case report and clinicopathologic review. *Head Neck Pathol*. 2010;4(1):37–43.
- Venkatraman L, et al. Primary hyperparathyroidism and metastatic carcinoma within parathyroid gland. *J Clin Pathol*. 2007;60(9):1058–1060.

# Diseases of the Paraganglia System

■ Vickie Y. Jo

## ■ PARAGANGLIOMA

Extra-adrenal paragangliomas arise from paraganglia distributed along the paravertebral sympathetic and parasympathetic chains and include tumors arising in the carotid body, jugulotympanic body, orbit, nasopharynx, larynx, vagal body, paraspinal chain (aorticosympathetic and visceral-autonomic), urinary bladder, and the organ of Zuckerkandl. Although the most common site of paraganglioma is within the adrenal gland (referred to as pheochromocytoma), this discussion will be limited to those arising in the head and neck, which is the most common site for extra-adrenal paragangliomas.

Paragangliomas are tumors of neural crest origin and may arise as sporadic lesions or in association with hereditary tumor syndromes (Table 29.1). It is now known up to half of all paragangliomas have *succinate dehydrogenase* (*SDH*) mutations; *SDH* mutations are present in at least 30 % of head and neck paragangliomas. The *SDH* enzyme complex localizes to the inner mitochondrial membrane and is a member of the tricarboxylic acid cycle and electron transport chain (in which it is known as complex II) and catalyzes the oxidation of succinate to fumarate. *SDH* is composed of four normally and ubiquitously expressed subunit proteins: *SDHA*, *SDHB*, *SDHC*, and *SDHD*. Inactivating mutations in any of the four nuclear-encoded genes result in dysfunction of the entire *SDH* complex (“*SDH* deficient”). *SDH* deficiency can be detected by immunohistochemistry (see section on “Ancillary Studies”). Germline *SDHD* mutations were first identified in 2000 in a subset of patients with hereditary paraganglioma-pheochromocytoma syndrome (HPGL/PCC); since that time, mutations have also been identified in *SDHA*, *SDHB*, *SDHC*, and the related *SDHAF2*. Most *SDH*-deficient head and neck paragangliomas are secondary to germline *SDH* mutations, and only rare somatic mutations have been reported. Mutations in *SDHD* are the most frequent in head and neck paragangliomas and are also associated with disease multifocality. HPGL/PCC is dominantly inherited, although transmittance of *SDHD* mutations appears to be paternal (unlike for *SDHA*, *SDHB*, and *SDHC*), which is suggestive of imprinting. Interestingly, the distribution of specific *SDH*

mutations differs for paragangliomas in other sites; for example, *SDH*-deficient thoracoabdominal paragangliomas are most commonly secondary to *SDHB* mutations. Carney-Stratakis syndrome is an autosomal dominant inherited syndrome due to germline mutations in one of the *SDH* genes, and patients develop paragangliomas and gastrointestinal stromal tumor (GIST). There are also known associations with *VHL*, *NF1*, and *RET* genes for paragangliomas. Paragangliomas, with GISTs and pulmonary chondromas, comprise Carney triad, which is not known to be inherited; affected patients are mostly women who may also develop adrenal cortical adenoma, esophageal leiomyoma, and pheochromocytoma. Due to the relatively high frequency of genetic susceptibilities associated with paragangliomas and pheochromocytomas, genetic counseling is recommended for affected patients even in the absence of family history.

## CLINICAL FEATURES

Because normal paraganglia are located throughout the body, paragangliomas have been described in nearly every anatomic location. The head and neck is the most common location for extra-adrenal paragangliomas, accounting for up to 70 % of tumors. The most common subsite is the carotid body (60 % of head and neck paragangliomas), followed by the middle ear (glomus tympanicum or glomus jugulare) and the vagus nerve (glomus vagale). The carotid body tumor is considered to be derived from the oxygen-sensing chemoreceptive organ at the bifurcation of the carotid artery and can become hyperplastic in people who live at high altitudes (presumably secondary to chronic hypoxia). In the head and neck, normal paraganglia are associated with the parasympathetic nervous system and are adjacent to cranial nerves or the arterial vasculature. It must be emphasized that cervical or thoracic sympathetic paragangliomas are distinct from parasympathetic paragangliomas arising in nearby locations. Cervical sympathetic paragangliomas are separate from the carotid body and other structures, and are vanishingly rare.



**TABLE 29.1****Genetic syndromes associated with paraganglioma and pheochromocytoma**

| Syndrome  | Gene Locus  | Gene                 | Paraganglia Tumor                         | Other Abnormalities   |
|---|---|----------------------|---|---|
| von Hippel-Lindau                                     | 3p26  | <i>VHL</i>           | Paraganglioma/pheochromocytoma in 10%-20% | Renal cysts and renal cell carcinoma<br>Visceral organ cysts<br>Hemangioblastomas |
| Hereditary paragangliomatosis                         |   |                      |   |   |
| PGL1  | 11q23   | <i>SDHD</i>          | Multiple paragangliomas (100%)            |   |
| PGL2  | 11q13   | <i>SDHAF2</i>        |   |   |
| PGL3  | 1q21  | <i>SDHC</i>          |   |   |
| PGL4  | 1p36.1-p35  | <i>SDHB</i>          |   |   |
| PGL5  | 5p15  | <i>SDHA</i>          |   |   |
| Carney-Stratakis Syndrome                             | Germline mutations in one of the <i>SDH</i> genes |                      | Paragangliomas (90%-100%)                 | Gastrointestinal stromal tumors   |
| Neurofibromatosis type I (von Recklinghausen disease) | 17q11.2   | <i>Neurofibromin</i> | Paraganglioma/pheochromocytoma in 1%-5%   | Neurofibromas<br>Schwannomas<br>Central nervous system gliomas                    |
| MEN2A   | 10q11.2   | <i>RET</i>           | Paraganglioma/pheochromocytoma in 50%-70% | Parathyroid hyperplasia<br>Medullary thyroid carcinoma                            |
| MEN2B   | 10q11.2   | <i>RET</i>           | Paraganglioma/pheochromocytoma in 50%-70% | Medullary thyroid carcinoma<br>Mucosal neuromas<br>Skeletal abnormalities         |

**PARAGANGLIOMA—DISEASE FACT SHEET****Definition**

- Neuroectodermal tumors arising from paraganglia along the parasympathetic or sympathetic nerves

**Incidence and Location**

- Rare (incidence estimate of 0.2-1/100,000 population)
- In the head and neck, the carotid body is the most common subsite (60%), followed by jugulotympanic and vagal

**Morbidity and Mortality**

- Infiltrative growth and local recurrence can lead to morbidity or death

**Sex and Age Distribution**

- Females > > males (especially at high altitude for carotid body tumors)
- 5th-6th decades

**Clinical Features**

- Slowly growing, painless mass, symptoms are mass related
- Occasionally may be a pulsatile lesion

- Middle ear lesions may produce tinnitus, hearing loss, and nerve dysfunction
- Tumors in the head and neck are rarely functional
- Approximately 10% are bilateral, multiple, pediatric, or malignant, with up to 50% familial/inherited
- At least 30% of head and neck paragangliomas are succinate dehydrogenase deficient
- Germline *SDHD* mutations are most common in head and neck paragangliomas

**Radiographic Features**

- Computed tomography shows enhancing mass in characteristic location
- Hyperintense T2-weighted magnetic resonance imaging
- Angiography shows splaying of the internal and external carotid arteries with a tumor blush
- <sup>123</sup>I-MIBG localizes tumor(s)

**Prognosis and Therapy**

- Good prognosis if completely resected, although may be indolent and recur/metastasize years later
- Surgery with preoperative adrenergic blockage and/or embolization

Most patients with head and neck paragangliomas are in the 5th to 6th decades; females are affected more often than males (5:1), although male patients more often present in the setting of inherited or familial tumors. Patients present with a slowly growing, painless mass and may have mass-related symptoms depending on the location of the tumor, such as tinnitus, hearing loss, and cranial nerve dysfunction in the middle ear. In superficial locations, paragangliomas are often described clinically as a pulsatile mass. Otic examination of middle ear tumors may demonstrate a pulsatile, reddish-purple mass behind the tympanic membrane. Approximately 10% of tumors are bilateral, multiple, pediatric, or malignant, with up to 50% familial/inherited. Tumors arising in patients with a genetic syndrome are more likely to be multiple and bilateral (Table 29.1).

Almost all head and neck paragangliomas are non-functioning; in this anatomic region only up to 4% are biochemically active. In contrast, extra-adrenal paragangliomas in the abdomen are most often associated with the sympathetic nervous system and are often functional, secreting catecholamines that produce clinical symptoms, such as headache, perspiration, palpitations, pallor, and hypertension.

### RADIOGRAPHIC FEATURES

The most common imaging modalities used to assess paragangliomas are computed tomography (CT), magnetic resonance imaging (MRI), angiography, and  $^{131}\text{I}$ -meta-iodobenzylguanidine (MIBG) scans. These studies usually accurately define location, size, and extent of the tumor. Contrast-enhanced CT scans will demonstrate an enhancing mass and are better for detailing adjacent fine osseous changes (Fig. 29.1). The Glasscock-Jackson classification

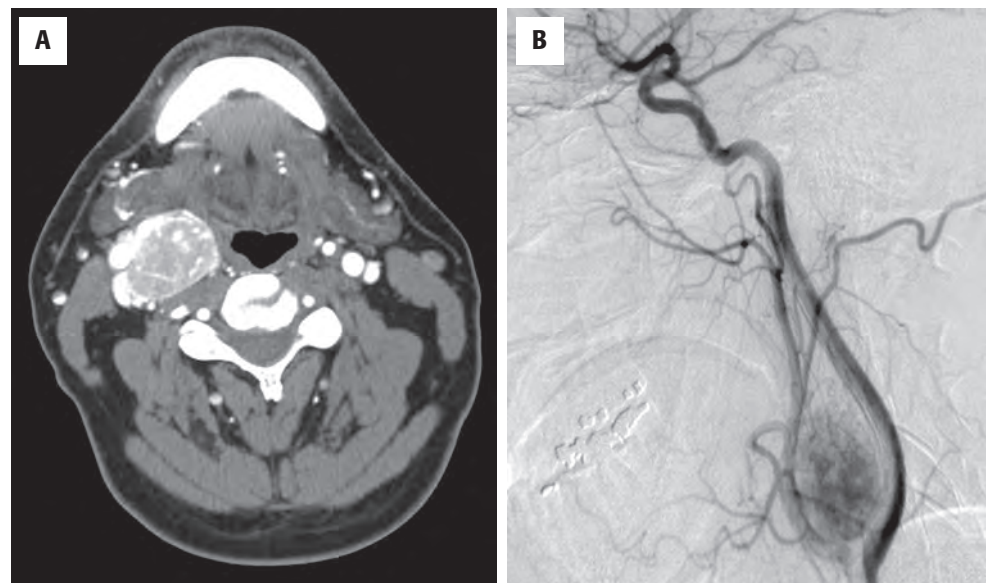
is used to document the extent of involvement of middle ear tumors based on CT studies: type I, limited to the cochlear promontory; type II tumors fill the middle ear space; whereas type III tumors extend farther into the mastoid air cells; type IV, extension is beyond the middle ear space into the mastoid bone and/or external auditory canal or anteriorly toward the carotid. Paragangliomas on contrast-enhanced MRI show a characteristic hyperintense T2-weighted image. Due to their vascularity, paragangliomas have a characteristic “salt and pepper” pattern on MRI caused by high-velocity flow voids (black dots) and foci of hemorrhage or slow flow (white dots).

Angiography is often used for patients who are undergoing operative resection and will demonstrate the characteristic pronounced tumor vascularity. In carotid body paragangliomas, the tumor will splay the internal and external carotid arteries, which is a diagnostic feature (Fig. 29.1).  $^{123}\text{I}$ -MIBG scans have been reported to aid in localization of paragangliomas, especially in occult or familial settings.  $^{111}\text{In}$  octreotide (Indium-111, a somatostatin analog) may also be sensitive for tumors greater than 1.5 cm. In some cases, ultrasound may be helpful in localizing superficial paragangliomas. Positron emission tomography (PET) using  $^{18}\text{F}$ fluorodeoxyglucose ( $^{18}\text{F}$ FDG-PET) will show avid uptake by the tumor cells.

### PATHOLOGIC FEATURES

#### GROSS FINDINGS

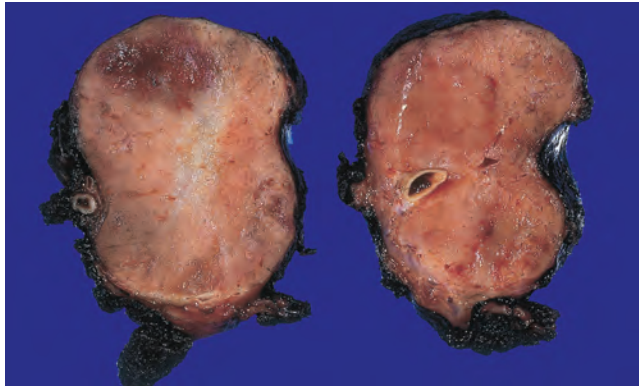
Most paragangliomas are resected en bloc. Because of the high vascularity, surgery can be bloody and difficult, and preoperative embolization may be performed. The resected specimen typically appears as a round to oval mass lesion with a smooth, encapsulated, or well-circumscribed



**FIGURE 29.1**

(A) Contrast-enhanced computed tomography scan demonstrates a large enhancing mass at the bifurcation of the carotid artery on the left. (B) Angiography demonstrates splaying of the internal and external carotid arteries by a well-vascularized tumor.



**FIGURE 29.2**

Gross image of a carotid body paraganglioma with a pseudocapsule and congested cut surface. (Courtesy of Dr. J. A. Ohara.)

### PARAGANGLIOMA—PATHOLOGIC FEATURES

#### Gross Findings

- Gray to hemorrhagic mass with fibrous pseudocapsule
- Average size of 3.8 cm but may grow large (up to 10 cm)

#### Microscopic Findings

- Organoid nests (“zellballen”) of various sizes
- Polygonal cells with granular, basophilic to eosinophilic cytoplasm
- May have hyperchromatic nuclei and bizarre pleomorphism
- Network of fibrovascular septae

#### Immunohistochemical Findings

- Chief cells positive with chromogranin, synaptophysin, NSE
- S100 protein and/or GFAP–positive sustentacular cells
- Loss of expression of SDHB immunohistochemistry (indicating succinate dehydrogenase deficiency) in ~30% of tumors

#### Pathologic Differential Diagnosis

- Depends on anatomic location: includes middle ear adenoma, ceruminous adenoma, meningioma, schwannoma, medullary thyroid carcinoma, hyalinizing trabecular adenoma of thyroid, parathyroid adenoma, typical/atypical carcinoid tumor (of larynx), metastatic renal cell carcinoma

periphery (Fig. 29.2). Carotid body tumors average 3.8 cm in size but can grow up to 10 cm in largest dimension. Resected tumors of the middle ear tend to be small and fragmented. Although most paragangliomas are firm in texture, the color may vary from light tan to dark reddish-brown, correlating with the amount of hemorrhage and congestion. The Shamblin staging system is applied to carotid body tumors, based on operative findings and gross examination. Stage 1 tumors are small and easily dissected from the adjacent vessels. Stage 2 tumors are larger and more adherent and partially surround the vessel. Stage 3 tumors are large and completely surround the carotid bifurcation.

### MICROSCOPIC FINDINGS

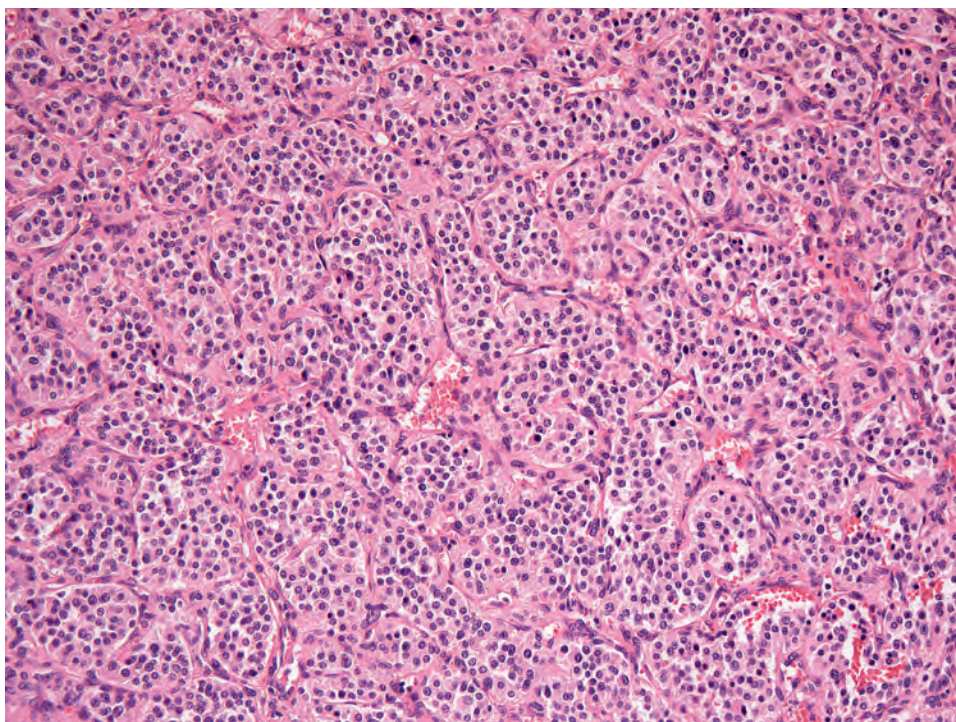
A fibrous pseudocapsule will usually surround a paraganglioma, but this can appear incomplete on microscopic sections. The periphery of the tumor should be examined for clear margins of resection because there are increased recurrence rates with incomplete excision. In some cases, capsular penetration and vascular invasion may be found, but these features are not indicative of malignancy. Paragangliomas have a characteristic architecture, with tumor cells arranged in round to oval nests that vary in size (the so-called zellballen pattern), with an extensively fibrovascular stroma (Fig. 29.3).

The cytomorphology of paraganglioma tumor cells is heterogeneous. The neoplastic chief cells (or type I cells) typically appear as round and epithelioid cells with variably sized, centrally to eccentrically placed round nuclei (Fig. 29.4). The cytoplasm may vary in appearance from finely granular eosinophilic to deeply basophilic (Fig. 29.4) and may also appear syncytial or show clear cell changes (Fig. 29.4). Tumor nuclei range in appearance from small and round to large and vesicular, sometimes hyperchromatic, with random bizarre pleomorphism (Fig. 29.5). Nucleoli may appear inconspicuous or extremely large. Nuclear pseudoinclusions are occasionally seen. Although nuclear hyperchromasia and pleomorphism may appear concerning for malignancy, these features alone are not predictive of malignancy. Mitoses are sparse and atypical forms should not be present. Rarely, other types of morphologic patterns can predominate, including sclerosing variants (see later), trabecular growth, angioma-like architecture, or spindled morphology (Fig. 29.6). Some tumors may have increased fibrosis that obscures the classic nested pattern, and infarct-type changes and foreign material may be seen in embolized tumors (Fig. 29.7). Hemorrhage may be present, but frank necrosis is not a common feature.

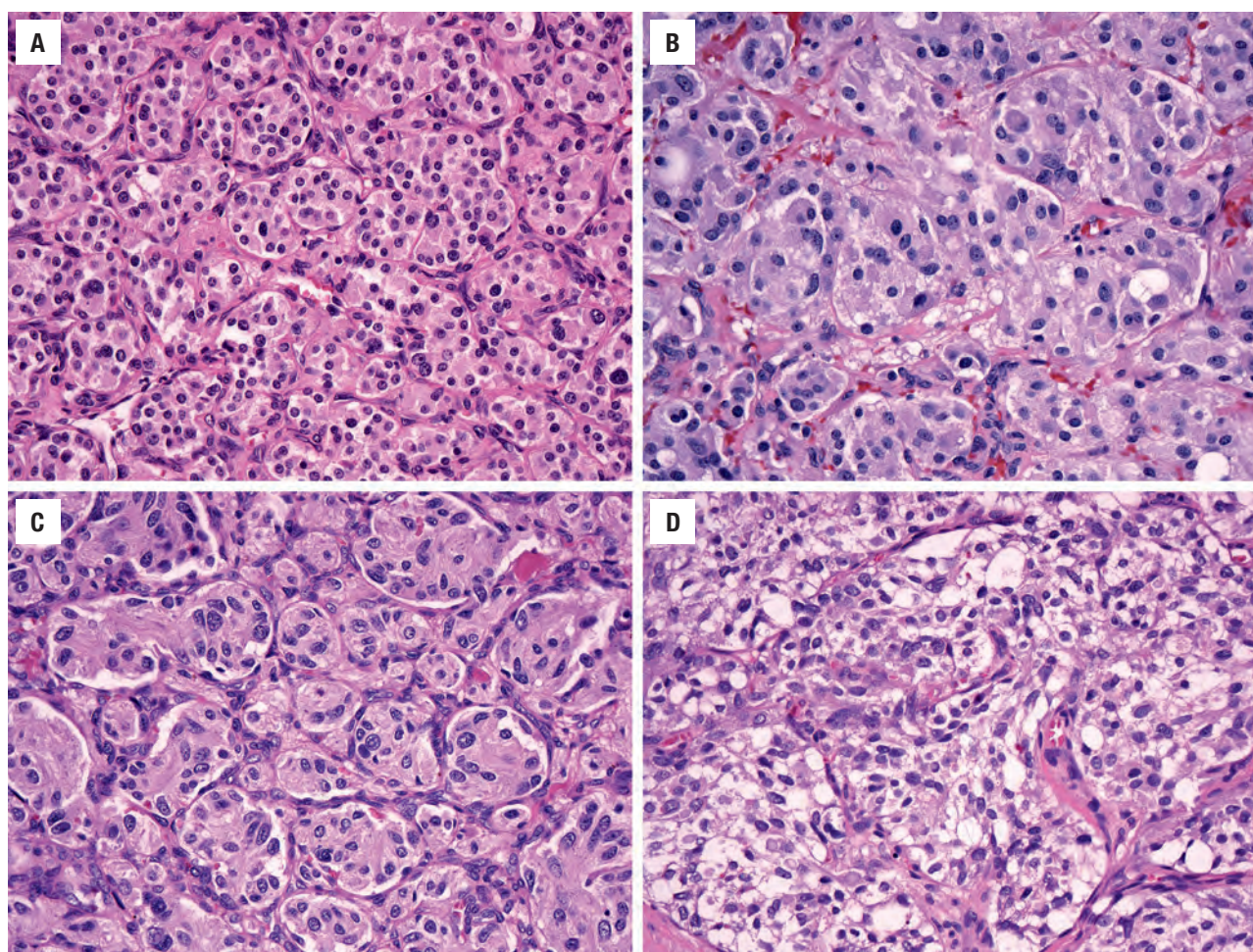
A characteristic feature in paragangliomas is the supporting network of stromal cells and vessels that surround the nests of neoplastic cells. These surrounding cells are called “sustentacular” (supporting) cells, also referred to as type II cells. They are histologically and ultrastructurally nondistinct but are highlighted with S100 protein and/or GFAP immunohistochemistry (see section on “[Ancillary Studies](#)”).

A subset of paraganglioma is characterized by extensively sclerotic stroma, in which tumor cells are arranged in irregular nests, cords, or strands and may impart an infiltrative growth pattern worrisome for malignancy (Fig. 29.8). These “sclerosing variants” can also show prominent spindled morphology and trabecular growth, as well as distortion and crush artifact, which can mimic small cell carcinoma (Fig. 29.8). Although paragangliomas with sclerosing features are thought to exhibit overall indolent behavior, higher recurrence rates may be observed secondary to difficulty in achieving complete resection.



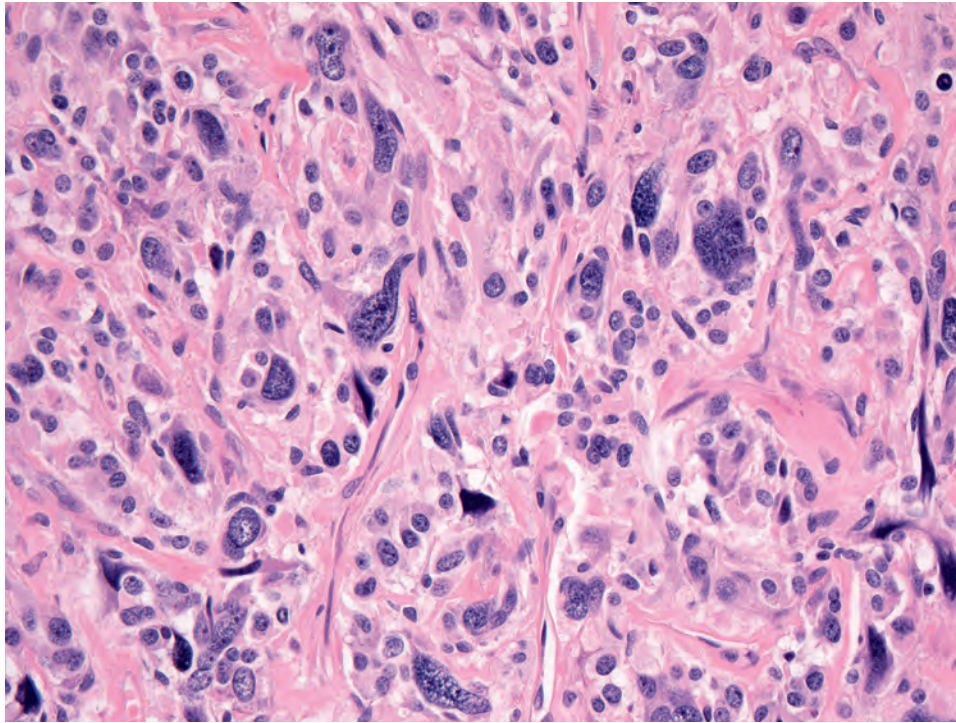
**FIGURE 29.3**

Paraganglioma is typically composed of tumor cells arranged in round to oval nests ("zellballen" pattern) with an extensively fibrovascular stroma.

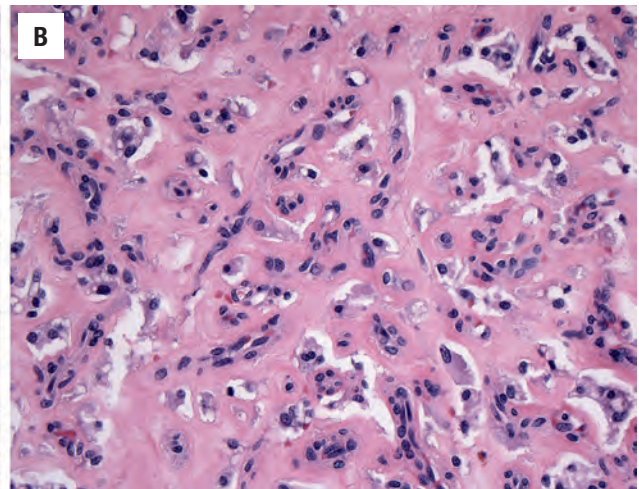
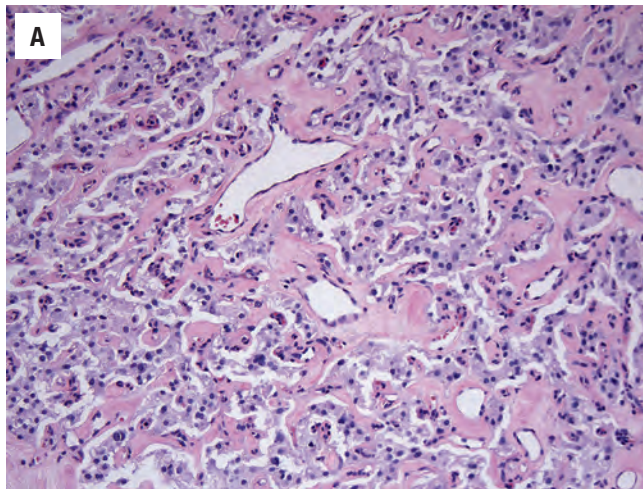
**FIGURE 29.4**

Paraganglioma may show heterogeneous cytomorphologic features. The round to epithelioid tumor cells have variably sized, centrally to eccentrically placed round nuclei, and cytoplasm may appear finely granular eosinophilic (A), deeply basophilic (B), or syncytial (C), or show clear cell changes (D).



**FIGURE 29.5**

Tumor nuclei may be large and vesicular, hyperchromatic, with significant and bizarre but isolated nuclei with pleomorphism.

**FIGURE 29.6**

Varying morphologic patterns may be seen in paragangliomas, such as trabecular growth (**A**) or angiomatous architecture (**B**).

Middle ear and laryngeal paragangliomas deserve special mention because the histologic features can be difficult to identify in these locations. Because of the fragmentation of middle ear paragangliomas and their tendency to have smaller nests and higher vascularity (Fig. 29.9), they can be mistaken for other middle ear tumors, such as middle ear adenoma. Laryngeal paragangliomas are extremely rare and must be differentiated from other neuroendocrine tumors in this region (such as typical/atypical carcinoid and medullary thyroid carcinoma).

Occasionally, paragangliomas can have pigmentation, which is thought to be neuromelanin, or they can contain

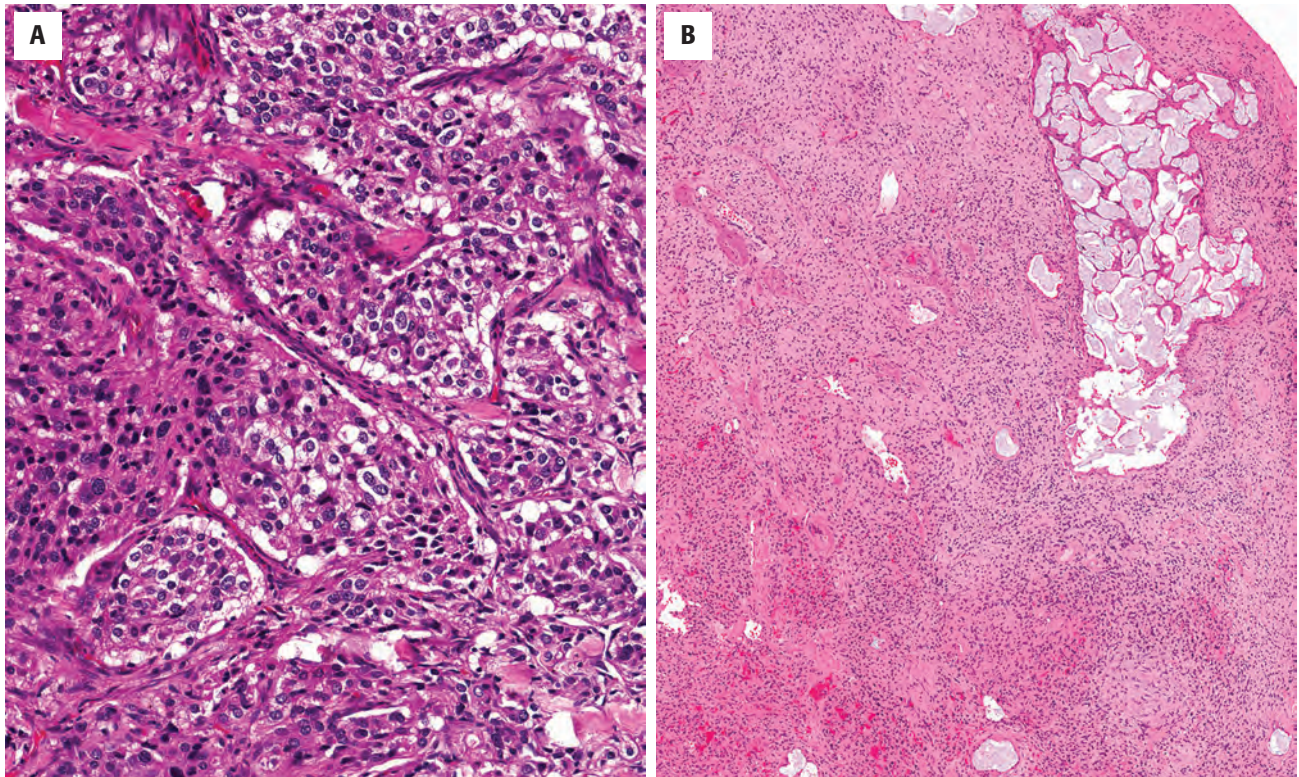
amyloid or show prominent eosinophilic cytoplasmic globules (Fig. 29.10). Although these features do not alter the prognosis, they may be a pitfall for correct diagnosis.

## ANCILLARY STUDIES

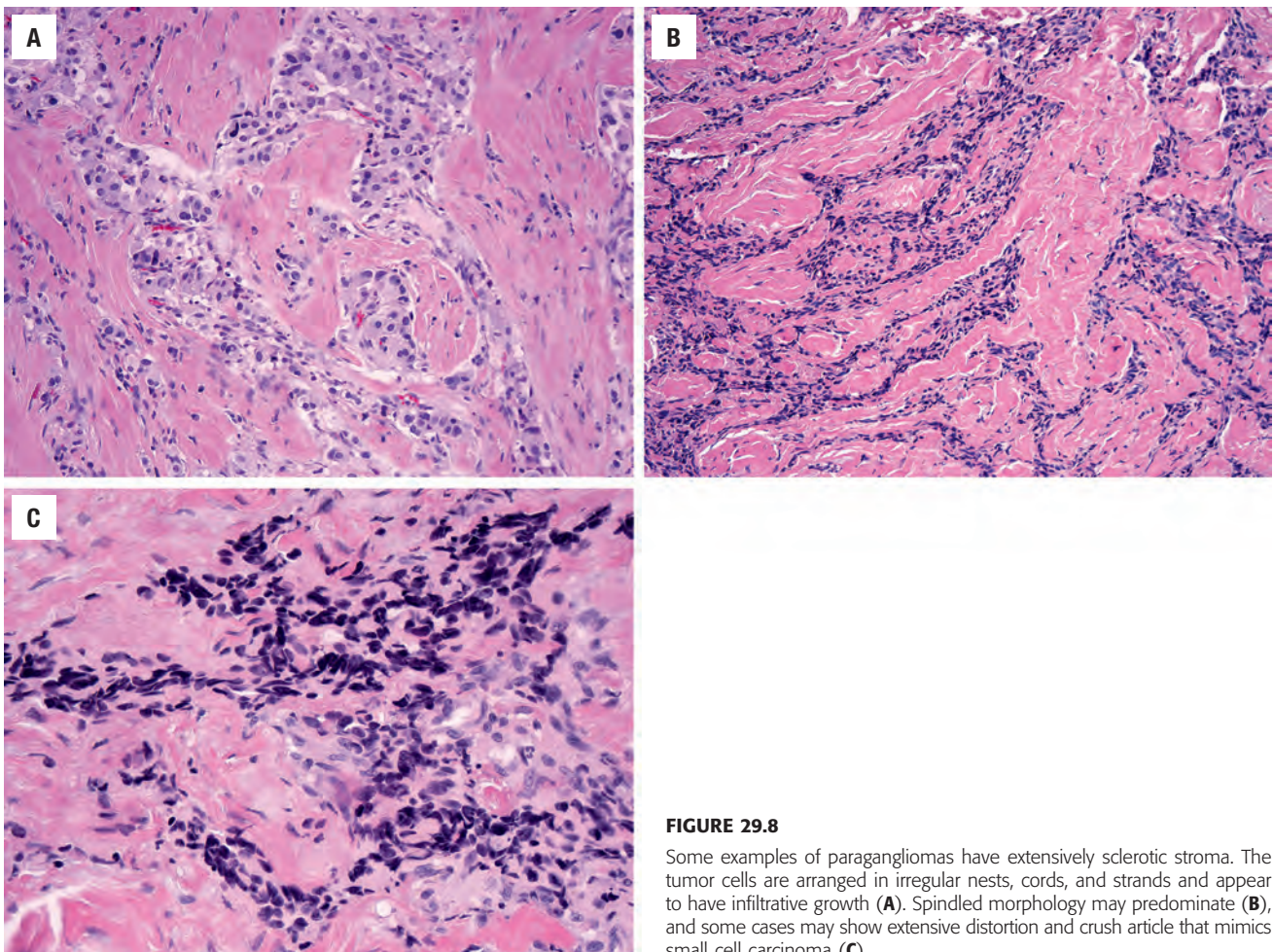
### ULTRASTRUCTURAL FINDINGS

Electron microscopy is not used often but shows the characteristic dense-core neurosecretory granules



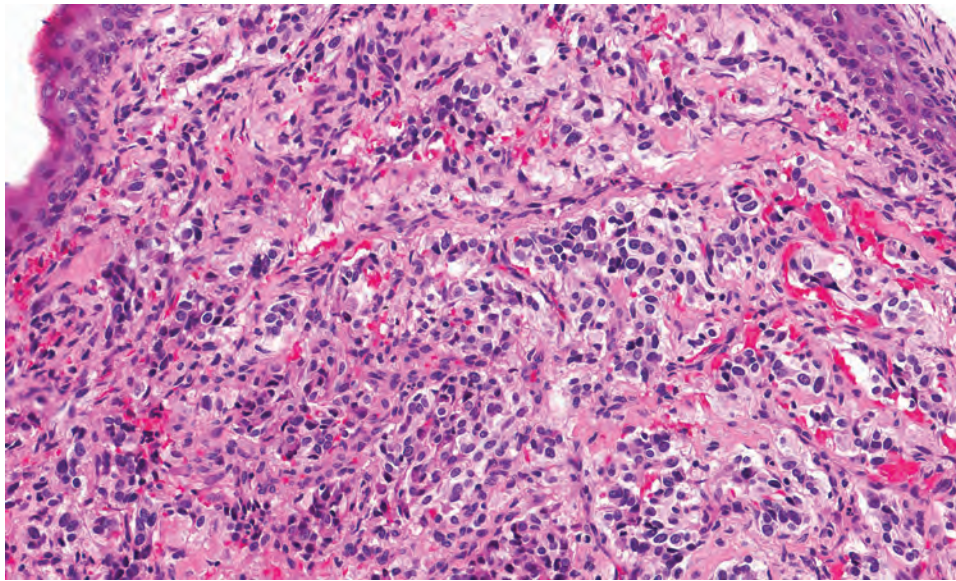
**FIGURE 29.7**

(A) In some examples, fibrosis separates the islands of tumor cells and obscures the nested pattern. (B) Note the foreign material used in presurgical embolization.

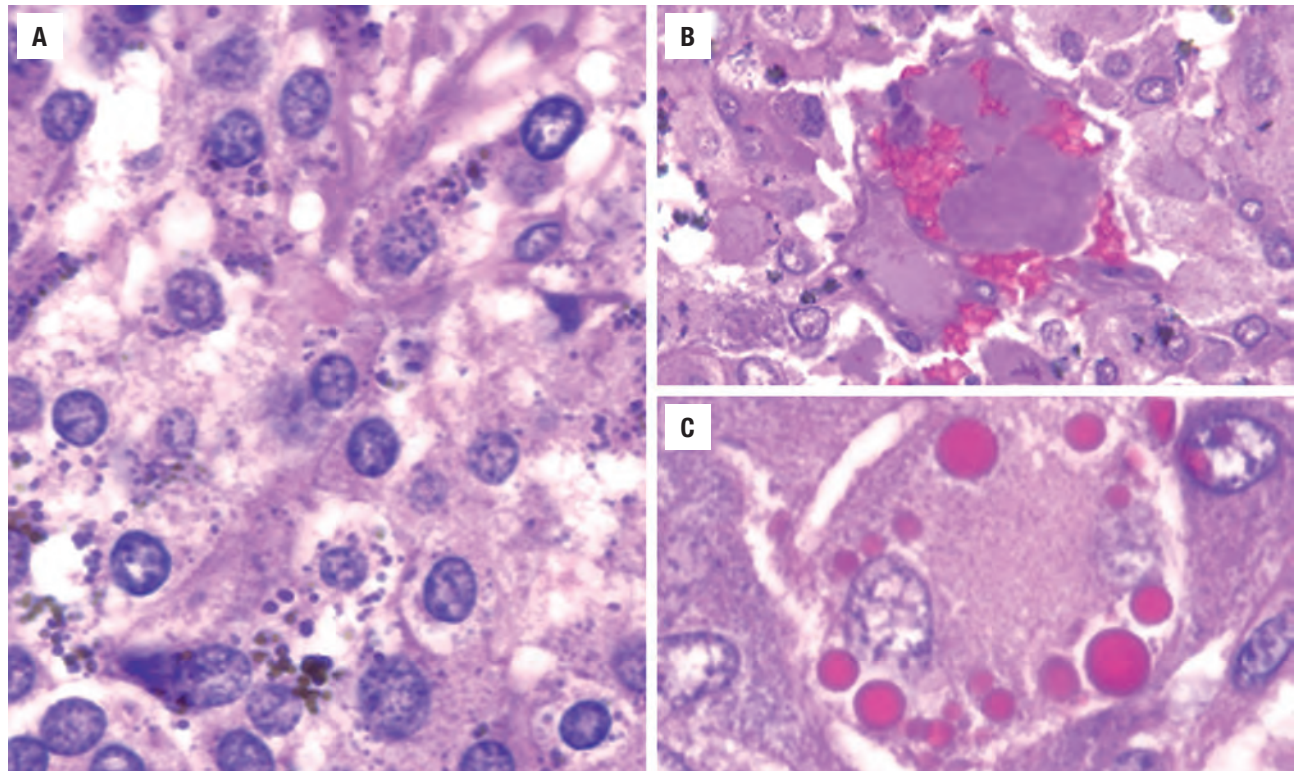
**FIGURE 29.8**

Some examples of paragangliomas have extensively sclerotic stroma. The tumor cells are arranged in irregular nests, cords, and strands and appear to have infiltrative growth (A). Spindled morphology may predominate (B), and some cases may show extensive distortion and crush artifact that mimics small cell carcinoma (C).



**FIGURE 29.9**

A jugulotympanic paraganglioma showing small nests and high vascularity.

**FIGURE 29.10**

(A) Neuromelanin pigment may be found in paraganglioma. (B) Amyloid deposition in a paraganglioma. (C) Eosinophilic cytoplasmic globules in a paraganglioma.

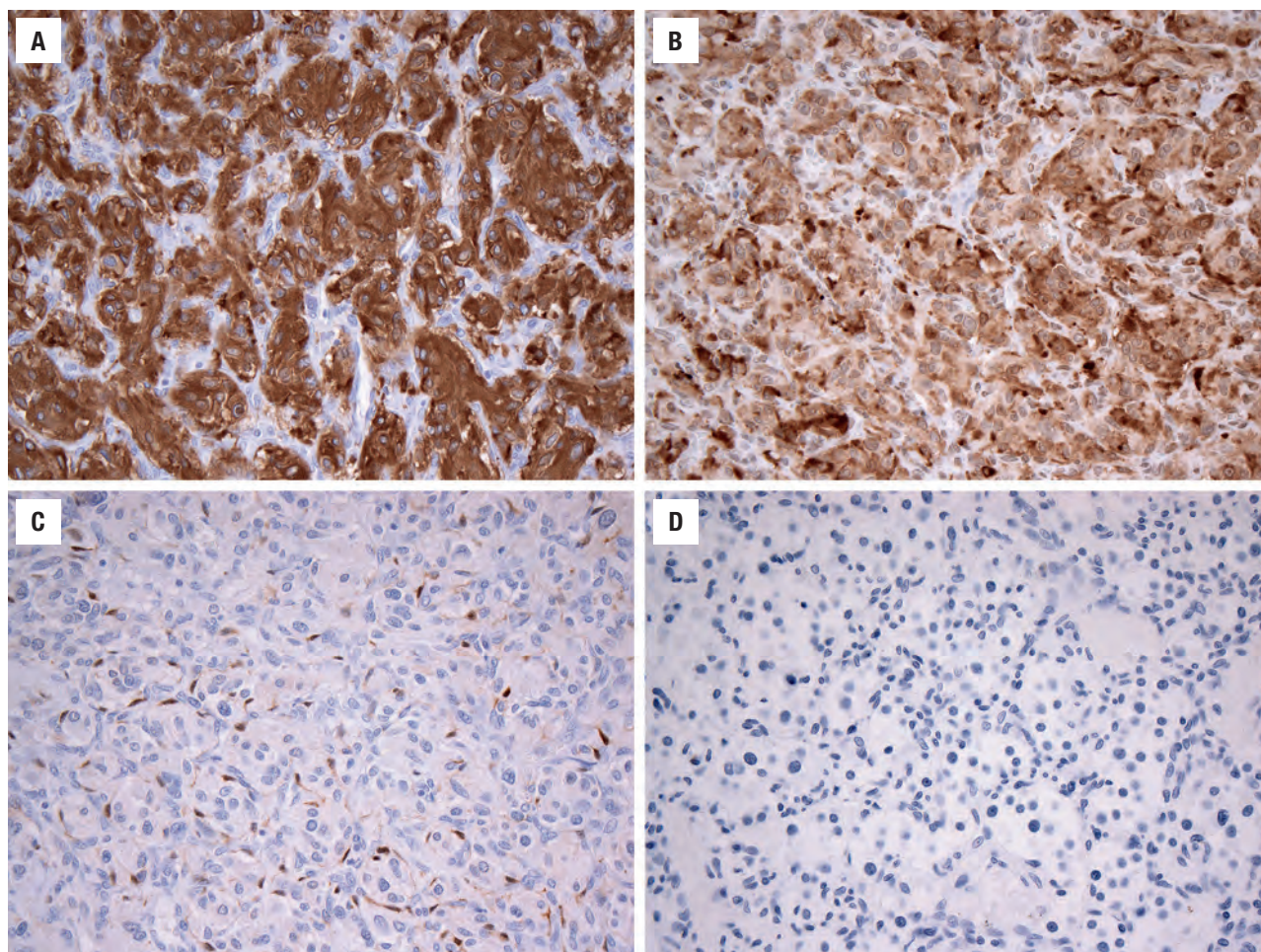
of neuroendocrine cells. The granules can vary in number and size, often correlating with the secretory characteristics.

#### IMMUNOHISTOCHEMICAL FINDINGS

The “nonchromaffin” cells of paragangliomas will invariably stain for neuroendocrine immunohistochemical

markers, including chromogranin, synaptophysin, neuron-specific enolase (NSE), and CD56 (Fig. 29.11). In a small subset of cases, positivity may be seen for a variety of specialized neuropeptides (i.e., somatostatin, substance P, adrenocorticotrophic hormone, and calcitonin). The supporting sustentacular cells have a unique staining pattern in that they are uniformly S100 protein positive, highlighting the periphery of the tumor (Fig. 29.11), and



**FIGURE 29.11**

Paraganglioma tumor cells are positive for synaptophysin (**A**) and chromogranin (**B**). S100 protein highlights the sustentacular cells (**C**). Keratin is consistently negative (**D**).

may occasionally be positive for glial fibrillary acidic protein (GFAP). Keratin is consistently negative in paragangliomas (Fig. 29.11).

SDH deficiency (which occurs in at least 30 % of head and neck paragangliomas) can be detected by immunohistochemistry, and antibodies are available for SDHB and SDHA. Loss of expression of SDHB reflects dysfunction of the entire SDH complex secondary to mutation in any of the *SDH* genes (or functional deficiencies due to other mechanisms, such as epigenetic events or hypermethylation) (Fig. 29.12). In contrast, loss of immunohistochemical expression of SDHA correlates only with mutation in *SDHA*. Retention of SDHB expression essentially excludes the possibility of an underlying *SDH* mutation.

#### FINE NEEDLE ASPIRATION

Fine needle aspiration (FNA) of paraganglioma is generally avoided because it may result in significant hemorrhage or potentially a vasovagal reaction. Furthermore, manipulation of a functional tumor can induce a

hypertensive crisis. Nonetheless, aspiration specimens in unsuspected cases show moderate cellularity, often with a hemorrhagic background. Smears show tumor cells singly dispersed or in groups, occasionally forming acini (or “pseudorosettes”) (Fig. 29.13). The polygonal tumor cells vary in size, with variably sized and shaped nuclei and wispy, pale cytoplasm. Binucleated, multinucleated, or giant cells may be seen.

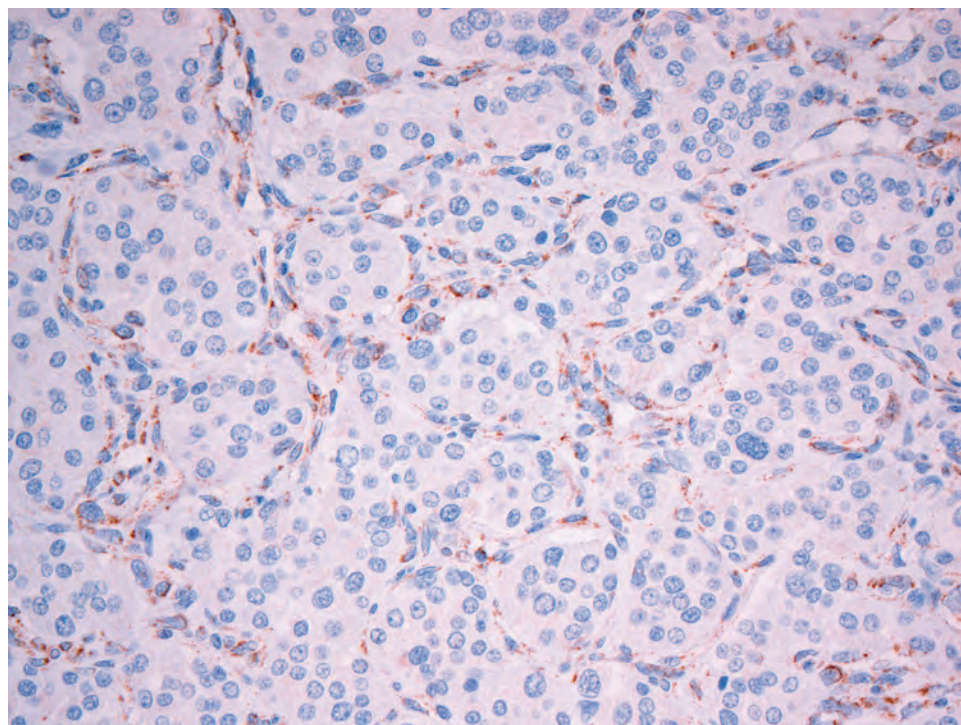
#### DIFFERENTIAL DIAGNOSIS

The differential diagnosis for paraganglioma depends on the location of the tumor.

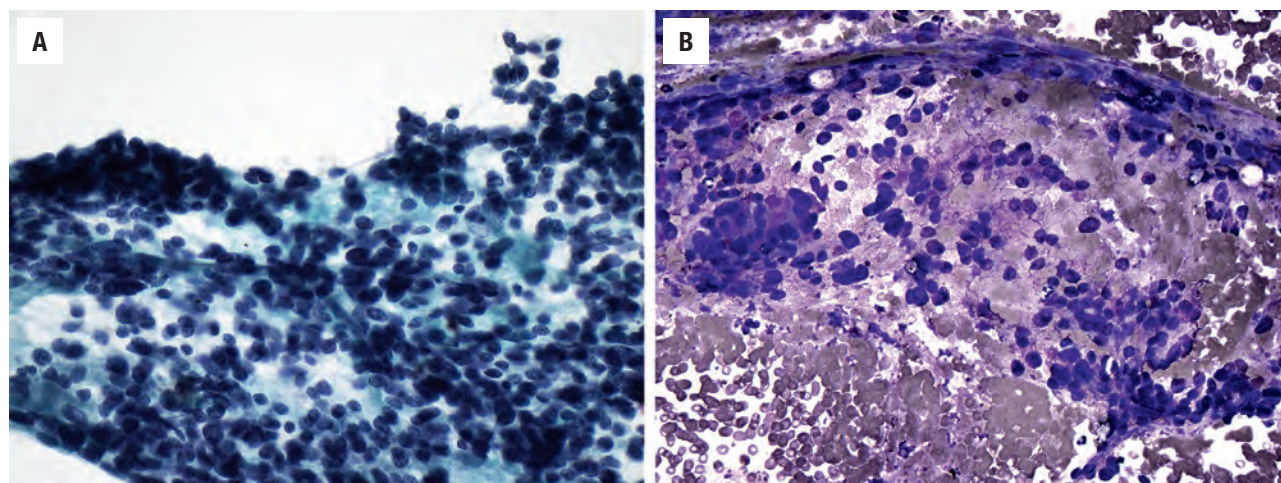
#### MIDDLE EAR/JUGULOTYMPANIC PARAGANGLIOMA

Paraganglioma may be difficult to separate from other tumors when biopsy samples from the middle ear are small and possibly crushed. The differential diagnosis includes middle ear adenoma, ceruminous adenoma,



**FIGURE 29.12**

Loss of SDHB expression indicates succinate dehydrogenase (SDH) deficiency secondary to dysfunction of the entire SDH complex, which may be caused by mutation in any of the *SDH* genes. Note the positive internal control of endothelial cells, which show the intact characteristic granular staining pattern.

**FIGURE 29.13**

(A) A Papanicolaou-stained, alcohol-fixed smear of a paraganglioma showing a population of round and polygonal tumor cells arranged in large groups and acini. (B) An air-dried, Romanowsky-stained smear shows tumor cells with moderate pleomorphism, wispy cytoplasm, and acinar formation.

meningioma, schwannoma, or rarely metastasis, such as metastatic renal cell carcinoma. Morphologic overlap can usually be resolved through use of a pertinent panel of immunohistochemistry studies (Table 29.2). Paraganglioma is negative for keratin and epithelial membrane antigen (EMA), which can help to separate most of these tumors. S100 protein can identify sustentacular cells in a paraganglioma, but this staining pattern should be distinguished from the diffuse nuclear positivity in schwannoma.

#### VAGAL AND CAROTID BODY TUMORS

In this location, paraganglioma must be differentiated from other neuroendocrine tumors, including medullary thyroid carcinoma, hyalinizing trabecular tumor of the thyroid, and parathyroid adenoma. Paragangliomas with predominant sclerosis may also mimic an infiltrative carcinoma. Medullary thyroid carcinoma will be positive for keratin, calcitonin, TTF1, PAX8, and carcinoembryonic antigen. Hyalinizing trabecular tumor of the thyroid

**TABLE 29.2**  
Immunohistochemical separation of middle ear tumors

| Stain         | Paraganglioma       | Middle Ear Adenoma | Meningioma | Schwannoma | Metastatic Renal Cell Carcinoma |
|---------------|---------------------|--------------------|------------|------------|---------------------------------|
| Chromogranin  | +                   | +                  | –          | –          | –                               |
| Synaptophysin | +                   | +                  | –          | –          | –                               |
| S100 protein  | +                   | –                  | ± (rare)   | +          | –                               |
| SDHB          | – (expression lost) | +                  | +          | +          | +                               |
| Cytokeratin   | –                   | +                  | ± (rare)   | ±          | +                               |
| EMA           | –                   | +                  | +          | +          | +                               |
| ISL1          | –                   | +                  | –          | –          | –                               |
| PAX8          | –                   | –                  | –          | –          | +                               |

EMA, Epithelial membrane antigen.

**TABLE 29.3**  
Immunohistochemical separation of neck tumors with neuroendocrine differentiation

| Stain         | Paraganglioma       | Medullary Thyroid Carcinoma | Typical and Atypical Carcinoid of Lung | Small Cell Carcinoma | Metastatic Neuroendocrine Neoplasms (GI/Pancreas) | Parathyroid Adenoma |
|---------------|---------------------|-----------------------------|--|----------------------|---|---------------------|
| Chromogranin  | +                   | +                           | +                                      | +                    | +   | +                   |
| Synaptophysin | +                   | +                           | +                                      | +                    | +   | +                   |
| S100 protein  | +                   | –                           | –                                      | –                    | –   | –                   |
| SDHB          | – (expression lost) | +                           | +                                      | +                    | +   | +                   |
| Cytokeratin   | –                   | +                           | +                                      | +                    | +   | +                   |
| Calcitonin    | –                   | +                           | –                                      | –                    | –   | –                   |
| TTF1          | –                   | +                           | ±                                      | +                    | –   | –                   |
| PTH           | –                   | –                           | –                                      | –                    | –   | +                   |
| PAX8          | –                   | +                           | –                                      | –                    | ±   | ±                   |
| CDX2          | –                   | –                           | –                                      | –                    | ±   | –                   |

shows a distinctive Ki-67 membranous staining pattern with the Dako MIB-1 antibody. Immunohistochemistry for parathyroid hormone (PTH) will identify parathyroid adenoma. Furthermore, these mimics are positive for keratin (Table 29.3), unlike paraganglioma. Clinical and radiographic correlation will also be of use in separating these tumors.

#### LARYNGEAL PARAGANGLIOMA

Laryngeal paraganglioma is very uncommon. The differential includes typical/atypical carcinoid and other neuroendocrine tumors that can secondarily involve the larynx, such as medullary thyroid carcinoma or metastases. Paragangliomas with sclerosing features may be

difficult to distinguish from small cell carcinoma. However, distinctive growth patterns, increased nuclear pleomorphism, necrosis, increased mitoses, and a carefully selected immunohistochemical panel will help in this differential. These mimics typically express keratin and EMA, which are negative in paragangliomas; furthermore, S100 protein can identify sustentacular cells in paraganglioma.

#### PROGNOSIS AND THERAPY

Paragangliomas are indolent tumors (estimated to have a 7-year doubling time) and generally have a good clinical



outcome, particularly in the sporadic setting. However, there are not very well-established histologic criteria for malignancy. Thus, even with histologically benign tumors, lifelong clinical follow-up (including biochemical and/or radiographic studies) is probably essential to monitor for potential recurrence or metastasis. The overall recurrence rate is approximately 5%. If recurrence or metastasis develops, the overall greater than 90% 5-year survival will decrease substantially to about 60% 5-year survival.

Surgery is the treatment of choice but must be individualized by taking into consideration the patient's age, medical status, tumor site and size, history of recurrences, and evidence of any cranial nerve deficits. There is a risk for patients to develop stroke or cranial nerve injury as a complication of the surgery (35%). In general, there is preoperative treatment (2 to 3 weeks prior) with  $\alpha$ - and  $\beta$ -blockers to suppress malignant hypertension and/or embolization to avoid excess bleeding. Gamma knife radiation has been used with mixed results, but radiation can be used effectively for poor surgical candidates and older adults.

## ■ MALIGNANT PARAGANGLIOMA

Malignant paragangliomas are uncommon, and reported rates in the head and neck range from 2% to 19%. The pathologist is rarely able to make the diagnosis of malignancy in the primary tumor based on histology alone because there are no reproducible, reliable, and well-accepted criteria for malignancy. Currently, the definition of malignancy for paraganglioma is the presence of metastatic disease. In some instances, the occurrence of multifocal, multiple, and bilateral tumors, in as many as 10% of cases, can make the determination of metastatic disease challenging. The most common sites of metastatic disease are regional lymph nodes, bone, liver, and lung. However, despite known metastatic disease, the clinical course is indolent and prolonged in many patients. Functional tumors allow for biochemical monitoring (urine or plasma levels) to identify recurrence.

### CLINICAL FEATURES

The clinical parameters of malignant tumors may be indistinguishable from benign tumors, although patients may be slightly younger (mean, 44 years) and without the same sex bias of benign tumors. However, patients are more likely to be symptomatic than patients with benign tumors. Interestingly, patients with inherited syndromes have malignancies *less often* than patients with sporadic disease.

### MALIGNANT PARAGANGLIOMA—DISEASE FACT SHEET

#### Definition

- Defined by the presence of metastasis

#### Incidence and Location

- Malignancy rates estimated between 2% and 19% in the head and neck
- Most malignant paragangliomas are abdominal

#### Morbidity and Mortality

- Protracted clinical course with late recurrences
- Functional tumors have symptomatic recurrences

#### Sex and Age Distribution

- Equal sex distribution
- 4th-5th decades

#### Clinical Features

- May be larger than benign tumors
- More likely to be functional (catecholamine secretion)

#### Prognosis and Therapy

- Less than 50% 10-year survival
- Regional lymph nodes are usual location of metastases
- Recurrences and metastases in up to 50%, often late
- Surgery (debulking), radiation, and radiolabeled analogs showing promise

### RADIOGRAPHIC FEATURES

The principal role of radiographic studies is to define the extent of disease and presence of multifocal or metastatic deposits preoperatively to allow for appropriate intervention (Fig. 29.14). Metastatic deposits can be FDG avid, suggesting PET scanning may be useful.  $^{123}\text{I}$ -MIBG studies or a labeled dopamine analog tracer may be useful for imaging as well as therapy.

### PATHOLOGIC FEATURES

#### GROSS FINDINGS

Malignant paragangliomas tend to be large and may demonstrate areas of confluent necrosis and hemorrhage. Extensive and significant gross capsular and/or vascular invasion may be noted.

#### MICROSCOPIC FINDINGS

Malignant paragangliomas generally appear histologically indistinct from their benign counterparts. The histologic findings of extensive capsular or vascular

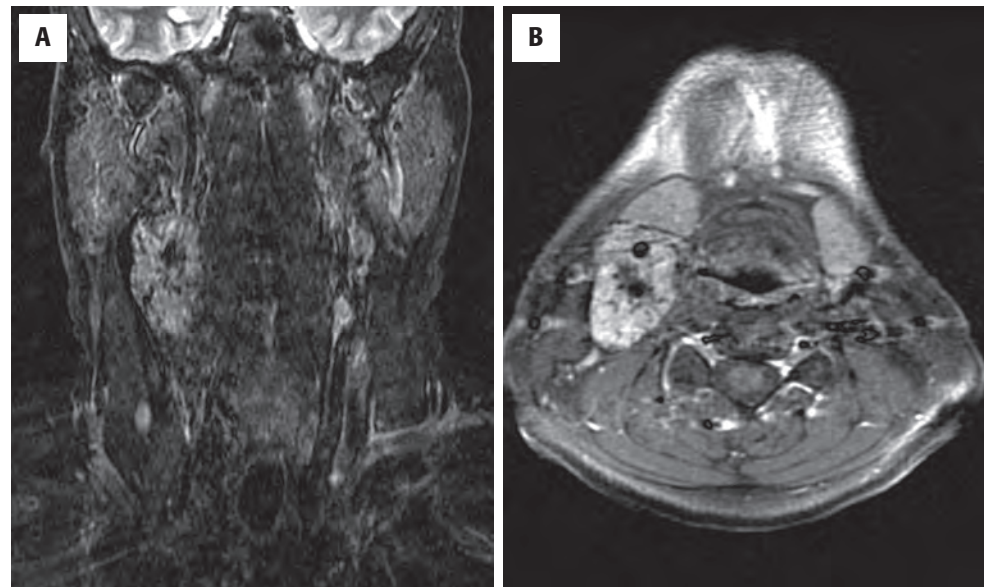


**FIGURE 29.14**

A malignant paraganglioma with known metastases to the lymph nodes. Note the bright signal on magnetic resonance imaging without contrast (**A**). The T1-WI postcontrast image shows a much brighter signal, with flow voids (**B**).

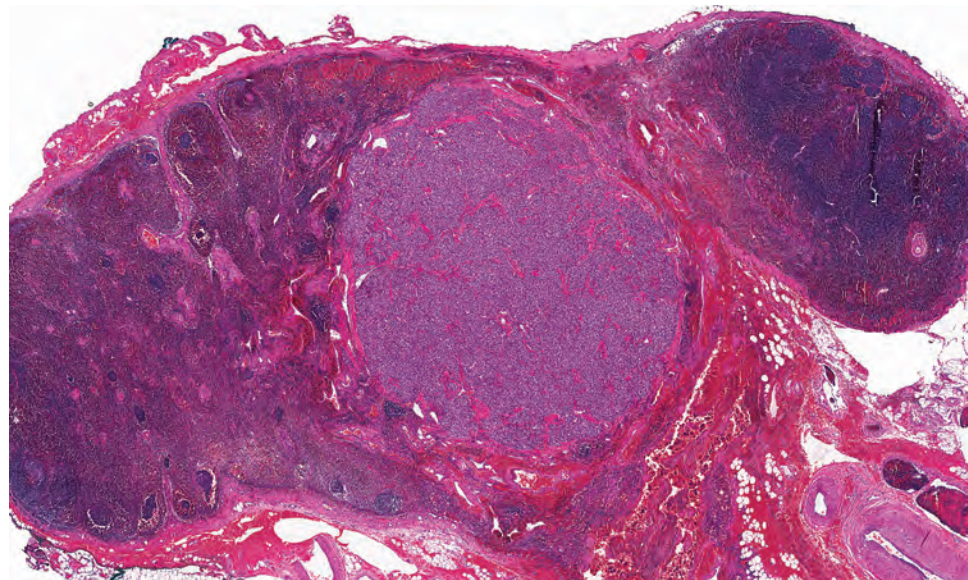


**FIGURE 29.15**

Metastatic paraganglioma in a cervical lymph node. Note the well-defined Zellballen architecture and relatively bland cytology, underscoring that definitive features of malignancy are usually absent in paragangliomas that show malignant behavior.

invasion, confluent necrosis, hypercellularity, large nests or diffuse growth, profound pleomorphism, increased mitoses ( $> 3/10$  high-power fields), and atypical mitotic figures have been analyzed for correlation with malignant behavior, but studies remain inconclusive. Metastases are most frequent to regional lymph nodes (70 %), a figure that is even higher in carotid body tumors ( $> 92$  %) (Fig. 29.15).

are positive for synaptophysin, chromogranin, and NSE immunohistochemistry. However, malignancy is suggested when there is a *loss* of S100 protein–positive sustentacular cells, correlating with a diffuse growth or large nest pattern, and if there is an increased proliferation index (Ki-67). Although the level is not absolute, a proliferative index of greater than 5 % to 8 % suggests malignancy. Loss of immunohistochemical expression of SDHB identifies tumors with germline *SDH* mutations.

#### ANCILLARY STUDIES

There are no currently available histochemical, immunohistochemical, ploidy, or molecular/genetic markers that accurately predict a malignant paraganglioma. Similar to their benign counterparts, malignant paragangliomas

#### DIFFERENTIAL DIAGNOSIS

Separation between benign and malignant paraganglioma causes the most difficulty and may be impossible to accurately diagnose. Paragangliomatosis (multifocal



**MALIGNANT PARAGANGLIOMA—PATHOLOGIC FEATURES****Gross Findings**

- Usually large tumors with hemorrhage and necrosis

**Microscopic Findings**

- Many are identical to benign paragangliomas
- No well-established histologic criteria for malignancy
- May be widely invasive lesions (capsule, vessels, into surrounding parenchyma/soft tissue)
- May show confluent necrosis
- Large nests or diffuse growth may be seen
- Profound pleomorphism can be observed
- Increased mitotic figures and atypical forms

**Immunohistochemical Findings**

- *Decreased* S100 protein—positive sustentacular cells suggests malignancy
- *Increased* Ki-67 labeling index suggests malignancy
- *Loss* of SDHB expression indicates succinate dehydrogenase deficiency

**Pathologic Differential Diagnosis**

- Benign paraganglioma, atypical carcinoid tumor (larynx or lung), neuroendocrine carcinoma, medullary thyroid carcinoma

**PROGNOSIS AND THERAPY**

Malignant paragangliomas are indolent but progressive, resulting in less than 50 % 10-year overall survival. When metastasis develops, the most common sites are lymph node, bone, liver, and lung. Surgery, especially debulking procedures, is the treatment of choice for metastatic disease, with symptomatic management of the excess catecholamines (alpha- and beta-blockade). Radiation may slow disease progression. Radiolabeled analogs (including tyrosine kinase inhibitors) may be used in functional tumors, but chemotherapy and radiation do not seem to impact survival. Ultimately, without accepted histologic criteria for malignancy in the primary tumors, all patients with paraganglioma need lifelong clinical follow-up to monitor for evidence of metastatic or recurrent disease.

**SUGGESTED READINGS**

The complete list of Suggested Readings is available online at [ExpertConsult.com](http://ExpertConsult.com).

disease) may sometimes be mistaken for metastatic tumor. Malignant paraganglioma may mimic other neuroendocrine tumors, such as medullary thyroid carcinoma, but the differential is easily resolved using immunohistochemistry, as previously discussed (Table 29.3).

## SUGGESTED READINGS

## Paraganglioma

- Ali-el-Dein B, et al. Abdominal and pelvic extra-adrenal paraganglioma: a review of literature and a report on 7 cases. *In Vivo*. 2002;16:249–254.
- Bauters C, et al. Hereditary pheochromocytomas and paragangliomas: a study of five susceptibility genes. *J Med Genet*. 2003;40:e75.
- Baysal BE, et al. Etiopathogenesis and clinical presentation of carotid body tumors. *Microsc Res Tech*. 2002;59:256–261.
- Bikhazi PH, et al. Molecular pathogenesis in sporadic head and neck paraganglioma. *Laryngoscope*. 2000;110:1346–1348.
- Boedeker CC, et al. Head and neck paragangliomas in von Hippel-Lindau disease and multiple endocrine neoplasia type 2. *J Clin Endocrinol Metab*. 2009;94(6):1938–1944.
- Chetty R. Familial paraganglioma syndromes. *J Clin Pathol*. 2010;63(6):488–491.
- Dalainas I, et al. Carotid body tumours. A 20-year single-institution experience. *Chir Ital*. 2006;58(5):631–635.
- Das DK, et al. Fine-needle aspiration diagnosis of carotid body tumor: report of a case and review of experience with cytologic features in four cases. *Diagn Cytopathol*. 1997;17(2):143–147.
- de Krijger RR, et al. New developments in the detection of the clinical behavior of pheochromocytomas and paragangliomas. *Endocr Pathol*. 2006;17(2):137–141.
- Edstrom Elder E, et al. The management of benign and malignant pheochromocytoma and abdominal paraganglioma. *Eur J Surg Oncol*. 2003;29:278–283.
- Erickson D, et al. Benign paragangliomas: clinical presentation and treatment outcomes in 236 patients. *J Clin Endo Metabol*. 2001;86:5210–5216.
- Ferlito A, et al. Identification, classification, treatment, and prognosis of laryngeal paraganglioma. Review of the literature and eight new cases. *Ann Otol Rhinol Laryngol*. 1994;103:525–536.
- Gardner P, et al. Carotid body tumors, inheritance, and a high incidence of associated cervical paragangliomas. *Am J Surg*. 1996;172(2):196–199.
- Jani P, et al. Familial carotid body tumours: is there a role for genetic screening? *J Laryngol Otol*. 2008;122(9):978–982.
- Kimura N, et al. Carotid body paraganglioma. In: El-Naggar AK, et al., eds. *Classification of Head and Neck Tumours*. 4th ed. World Health Organization Classification of Tumours. Lyon, France: IARC Press; 2017:277–280.
- Kimura N, et al. Vagal paraganglioma. In: El-Naggar AK, et al., eds. *Classification of Head and Neck Tumours*. 4th ed. World Health Organization Classification of Tumours. Lyon, France: IARC Press; 2017:283–284.
- Kimura N, et al. Extra-adrenal paragangliomas. In: Lloyd RV, et al., eds. *Classification of Endocrine Tumours*. 4th ed. World Health Organization Classification of Tumours. Lyon, France: IARC Press; 2017:190–192.
- Kimura N, et al. Sympathetic paragangliomas. In: Lloyd RV, et al., eds. *Classification of Endocrine Tumours*. 4th ed. World Health Organization Classification of Tumours. Lyon, France: IARC Press; 2017:192–195.
- Kimura N, et al. Middle ear paraganglioma. In: El-Naggar AK, et al., eds. *Classification of Head and Neck Tumours*. 4th ed. World Health Organization Classification of Tumours. Lyon, France: IARC Press; 2017:282.
- Koch CA, et al. New insights into the genetics of familial chromaffin cell tumors. *Ann N Y Acad Sci*. 2002;970:11–28.
- Kupferman ME, et al. Paragangliomas of the head and neck. *Curr Oncol Rep*. 2008;10(2):156–161.
- Lack EE, et al. Association of Directors of Anatomic and Surgical Pathology: recommendations for reporting of extra-adrenal paragangliomas. *Mod Pathol*. 2003;16:833–835.
- Maher ER, et al. The pressure rises: update on the genetics of pheochromocytoma. *Hum Mol Genet*. 2002;11:2347–2354.
- McCaffrey TV, et al. Familial paragangliomas of the head and neck. *Arch Otolaryngol Head Neck Surg*. 1994;120:1211–1216.
- McNichol AM. Differential diagnosis of pheochromocytomas and paragangliomas. *Endocr Pathol*. 2001;12:407–415.
- Milroy CM, et al. Immunohistochemical markers in the diagnosis of neuroendocrine neoplasms of the head and neck. *Ann Otol Rhinol Laryngol*. 1995;104:413–418.
- Moran CA, et al. Pigmented extraadrenal paragangliomas: a clinicopathology and immunohistochemical study of five cases. *Cancer*. 1997;79:398–402.
- Netterville JL, et al. Carotid body tumors: a review of 30 patients with 46 tumors. *Laryngoscope*. 1995;105(2):115–126.
- Papasprou K, et al. Management of head and neck paragangliomas: review of 120 patients. *Head Neck*. 2009;31(3):381–387.
- Pellitteri PK, et al. Paragangliomas of the head and neck. *Oral Oncol*. 2004;40:563–575.
- Plukker JT, et al. Outcome of surgical treatment for carotid body paraganglioma. *Br J Surg*. 2001;88:1382–1386.
- Rao AB, et al. From the archives of the AFIP. Paragangliomas of the head and neck: radiologic-pathologic correlation. *Radiographics*. 1999;19:1605–1632.
- Sajid MS, et al. A multicenter review of carotid body tumour management. *Eur J Vasc Endovasc Surg*. 2007;34(2):127–130.
- Shamblin WR, et al. Carotid body tumor (chemodectoma). Clinicopathologic analysis of ninety cases. *Am J Surg*. 1971;122:732–739.
- Tischler AS. Pheochromocytoma and extra-adrenal paraganglioma: updates. *Arch Pathol Lab Med*. 2008;132(8):1272–1284.
- Unlu Y, et al. Management of carotid body tumors and familial paragangliomas: review of 30 years' experience. *Ann Vasc Surg*. 2009;23(5):616–620.
- van der Mey AG, et al. Management of carotid body tumors. *Otolaryngol Clin North Am*. 2001;34:907–924.
- van Nederveen FH, et al. An immunohistochemical procedure to detect patients with paraganglioma and pheochromocytoma with germline SDHB, SDHC, or SDHD germline mutations: a retrospective and prospective analysis. *Lancet Oncol*. 2009;10:764–771.
- Wasserman PG, et al. Paragangliomas: classification, pathology, and differential diagnosis. *Otolaryngol Clin North Am*. 2001;34:845–862, v–vi.
- Weber PC, et al. Jugulotympanic paragangliomas. *Otolaryngol Clin North Am*. 2001;34:1231–1240.
- Whiteman ML, et al. <sup>111</sup>In octreotide scintigraphy in the evaluation of head and neck lesions. *AJNR Am J Neuroradiol*. 1973;18:1073–1080.
- Zeitler DM, et al. Preoperative embolization in carotid body tumor surgery: is it required? *Ann Otol Rhinol Laryngol*. 2010;119(5):279–283.

## Malignant Paraganglioma

- Andersen KF, et al. Malignant pheochromocytomas and paragangliomas—the importance of a multidisciplinary approach. *Cancer Treat Rev*. 2011;37(2):111–119.
- Argiris A, et al. PET scan assessment of chemotherapy response in metastatic paraganglioma. *Am J Clin Oncol*. 2003;26:563–566.
- Brown HM, et al. Predicting metastasis of pheochromocytomas using DNA flow cytometry and immunohistochemical markers of cell proliferation: a positive correlation between MIB-1 staining and malignant tumor behavior. *Cancer*. 1999;86:1583–1589.
- Chrisoulidou A, et al. The diagnosis and management of malignant pheochromocytoma and paraganglioma. *Endocr Relat Cancer*. 2007;14(3):569–585.
- de Krijger RR, et al. New developments in the detection of the clinical behavior of pheochromocytomas and paragangliomas. *Endocr Pathol*. 2006;17(2):137–141.
- Edstrom Elder E, et al. The management of benign and malignant pheochromocytoma and abdominal paraganglioma. *Eur J Surg Oncol*. 2003;29:278–283.
- Lee JH, et al. National Cancer Data Base report on malignant paragangliomas of the head and neck. *Cancer*. 2002;94(3):730–737.
- Shah MJ, et al. Flow cytometric DNA analysis for determination of malignant potential in adrenal pheochromocytoma or paraganglioma: an Indian experience. *Ann Surg Oncol*. 2003;10:426–431.
- Thompson LD. Pheochromocytoma of the Adrenal Gland Scaled Score (PASS) to separate benign from malignant neoplasms: a clinicopathologic and immunophenotypic study of 100 cases. *Am J Surg Pathol*. 2002;26:551–566.
- Zheng JW, et al. Recurrent malignant carotid body tumor: report of one case and review of the literature. *Chin Med J*. 2005;118(22):1929–1932.



Page numbers followed by “f” indicate figures, “t” indicate tables, and “b” indicate boxes.

## A

Abscesses, stellate, 492–494, 493f  
 Acanthosis, of squamous epithelium, 204, 204f  
 Accessory salivary glands, 241  
 Acinic cell adenocarcinoma, oncocytoma vs., 274  
 Acinic cell carcinoma (AcCC)  
   of parotid gland, 486f  
   of salivary glands, 293–300, 294b  
     ancillary studies of, 297, 298f–300f  
     clinical findings on, 293, 293f  
     multinodular oncocytic hyperplasia vs., 244  
     pathologic findings in, 294–297, 294b, 295f–297f  
 Ackerman tumor. *see* Verrucous squamous cell carcinoma (VSCC)  
 Acoustic neuroma. *see* Peripheral nerve sheath tumor  
 Acquired immunodeficiency syndrome (AIDS). *see* Human immunodeficiency virus (HIV)  
 Acquired mucosa-associated lymphoid tissue, 667–668  
 Actinic keratosis, 441  
*Actinomyces*, 182–183  
*Actinomyces israelii*, 182–183  
 Actinomycosis  
   cervical, 496–497, 496f, 497b  
   oral, 183–184, 185f  
 Active ossifying fibroma, of gnathic bones, 385–388, 386b  
   clinical features of, 386, 386f  
   differential diagnosis of, 387–388  
   pathologic features of, 386–387, 386b, 387f  
   prognosis and therapy for, 388  
   radiologic features of, 386  
 Acute rhinosinusitis, 1, 2f  
 Acute thyroiditis, 551–552, 551b  
   ancillary studies of, 551  
   clinical findings on, 551  
   differential diagnosis of, 552  
   pathologic findings in, 551, 552b, 552f  
   prognosis and therapy for, 552  
 Adenocarcinoma. *see also* Polymorphous low-grade adenocarcinoma (PLGA), of salivary glands; Sinonasal adenocarcinoma  
   basaloid. *see* Sialoblastoma, of salivary glands  
   of breast, 529f  
   ceruminous, 454–455, 481–484, 482b, 482f–484f

Adenocarcinoma (*Continued*)  
   metastatic  
     ceruminous adenocarcinoma vs., 483–484  
     in colon, 486f  
     to lymph nodes, 529, 529f  
     sinonasal adenocarcinoma vs., 60  
   neuroendocrine adenoma vs., 474  
   not otherwise specified  
     ceruminous, 482, 484  
     of salivary glands, 360–362, 360b, 361f  
   of salivary glands  
     basal cell, 346–348, 347f–348f, 351b  
     polymorphous, 309–317, 310b, 310f, 314b  
     with squamous metaplasia, 164  
     synovial sarcoma vs., 536  
 Adenoid cystic carcinoma (ACC)  
   basaloid squamous cell carcinoma vs., 160–161  
   ceruminous, 482, 483f, 484  
   epithelial-myoepithelial carcinoma vs., 322  
   polymorphous adenocarcinoma vs., 314–316  
   of salivary glands, 300–309, 301b  
     ancillary studies of, 305–308, 306f–309f  
     clinical findings on, 300, 301f  
     differential diagnosis of, 308–309  
     pathologic findings in, 58, 301–305, 302f–306f, 304b  
     prognosis and therapy of, 309  
   sialoblastoma vs., 346  
   small cell carcinoma vs., 356  
 Adenoma. *see also* Follicular adenoma, of thyroid gland; Neuroendocrine adenoma of middle ear; Parathyroid adenoma; Pleomorphic adenoma  
   atypical  
     follicular adenoma vs., 603, 604f  
     of parathyroid gland, 724  
   basal cell, salivary gland, 266–269, 266b, 267f–268f  
     congenital. *see* Sialoblastoma, of salivary glands  
     pleomorphic adenoma vs., 264  
     sialoblastoma vs., 346  
   canalicular, salivary gland, 269–272, 270b, 270f–271f  
   ceruminous, 453–457, 453b, 454f–456f  
     ceruminous adenocarcinoma vs., 483–484  
     neuroendocrine adenoma vs., 474

Adenoma (*Continued*)  
   follicular, 593–604, 593b  
     ancillary studies of, 599–603, 602f–603f  
     clinical findings on, 593  
     differential diagnosis of, 603–604  
     pathologic findings in, 594–599, 595b, 595f–601f  
     radiologic findings in, 593–594, 594f  
   paraganglioma-like. *see* Hyalinizing trabecular tumor  
   sebaceous, salivary gland, 279–281, 279b, 280f  
 Adenomatoid nodules  
   follicular adenoma vs., 603  
   follicular thyroid carcinoma vs., 651  
   macrofollicular variant of papillary carcinoma vs., 634–635, 634f  
   papillary carcinoma vs., 630, 630f–631f  
 Adenomatoid odontogenic tumor (AOT), of gnathic bones, 409–411, 409b  
   ancillary studies of, 411  
   clinical features of, 409  
   differential diagnosis of, 411  
   pathologic features of, 409–410, 410b  
   prognosis and therapy for, 411  
   radiologic features of, 409, 410f–411f  
 Adenosquamous carcinoma (ASC)  
   basaloid squamous cell carcinoma vs., 160–161  
   of larynx, hypopharynx, and trachea, 163–164, 163b, 163f  
   of oral cavity and oropharynx, 221, 235, 235f  
 Adipocytes, parathyroid, 701  
 Adrenal gland, paraganglioma of, 728  
 Adrenocorticotrophic hormone (ACTH), 47–50  
 Adult rhabdomyoma (AR), 129–131  
   ancillary studies of, 130, 130f  
   clinical features of, 129, 129b  
   differential diagnosis of, 131  
   granular cell tumor vs., 127–128  
   pathologic features of, 129, 129b, 130f  
   prognosis and therapy for, 131  
*Afipia felis*, 492  
 AFS. *see* Allergic fungal sinusitis  
 AIDS. *see* Human immunodeficiency virus (HIV)  
 Alcohol use/abuse  
   precursor squamous lesions and, 138  
   squamous cell carcinoma and, 143b, 219  
 ALHE. *see* Angiolymphoid hyperplasia with eosinophilia

- Allergic fungal sinusitis (AFS), 8–10, 8*b*, 9*f*–10*f*, 10*b*
- Allergic mucin, 9*f*
- Allergic rhinosinusitis, 1, 2*f*–3*f*
- Alveolar rhabdomyosarcoma, of sinonasal tract, 88, 89*f*–90*f*
- Alveolar soft part sarcoma, 213–214
- Amalgam tattoo, 176–177, 177*b*
- clinical findings on, 176, 176*f*
- differential diagnosis of, 177
- pathologic features of, 177, 177*b*, 177*f*
- prognosis and therapy for, 177
- radiologic findings in, 176
- Ameloblastic carcinoma, of gnathic bones, 423–425, 424*b*
- ameloblastoma and, 402, 403*f*
- ancillary studies of, 425
- clinical findings on, 423
- differential diagnosis of, 425
- pathologic findings in, 423–424, 424*b*, 424*f*
- prognosis and therapy for, 425
- radiologic findings in, 423
- Ameloblastic fibroma, 399–402
- odontogenic sarcoma *vs.*, 432, 432*f*
- Ameloblastic fibro-odontoma, 399–402
- Ameloblastic odontoma, 399–402
- Ameloblastoma, of gnathic bones, 395–402, 396*b*
- adenomatoid odontogenic tumor *vs.*, 411
- clinical features of, 395–396
- differential diagnosis of, 399–402
- odontogenic keratocyst *vs.*, 405–406
- pathologic features of, 396–399, 397*b*, 397*f*–402*f*
- prognosis and therapy for, 402, 403*f*
- radiologic features of, 396*f*–397*f*
- unicystic, dentigerous cyst *vs.*, 368
- Amiodarone-induced thyroid disease, 589–592, 590*b*
- clinical findings on, 590
- differential diagnosis of, 591–592, 592*f*
- laboratory studies on, 590
- pathologic findings in, 590, 590*b*, 591*f*
- prognosis and therapy for, 592
- Amyloid, 107–109, 108*f*–110*f*
- Amyloid goiter, 586–589, 587*b*
- ancillary studies of, 588–589, 589*f*
- clinical findings on, 587
- differential diagnosis of, 589
- pathologic findings in, 587, 588*f*, 589*b*
- prognosis and therapy for, 589
- Amyloidosis, 107–110, 108*b*
- ancillary studies of, 109, 110*f*
- clinical features of, 107
- differential diagnosis of, 109–110
- pathologic features of, 107–109, 108*b*, 108*f*–109*f*
- prognosis and therapy for, 110
- vocal cord polyps/nodules *vs.*, 102
- Anaplastic carcinoma. *see* Undifferentiated carcinoma
- Angiocentric NK/T-cell lymphoma. *see* Extranodal NK/T-cell lymphoma, nasal type
- Angiofibroma, nasopharyngeal. *see* Nasopharyngeal angiofibroma
- Angiolymphoid hyperplasia with eosinophilia (ALHE)
- of ear, 441–444, 442*b*
- clinical findings on, 441–442
- differential diagnosis of, 442
- pathologic findings in, 442, 442*b*, 443*f*
- prognosis and therapy for, 444
- lobular capillary hemangioma *vs.*, 207
- Angiomatosis, bacillary, 494–495, 494*b*–495*b*, 495*f*
- Angiosarcoma
- angiolymphoid hyperplasia with eosinophilia *vs.*, 442
- contact ulcer *vs.*, 105–106
- juvenile hemangioma *vs.*, 282
- Kaposi sarcoma *vs.*, 226
- lobular capillary hemangioma *vs.*, 33, 207
- of sinonasal tract, 94–95, 95*f*
- of thyroid gland, 678*b*, 684–685, 686*f*
- Angular cheilitis, 181
- Antibiotics
- for cat scratch disease, 494
- for rhinoscleroma, 14
- Antimicrobials, for rhinosinusitis, 2
- Antiretroviral therapy, 227
- Antrochoanal polyp, 2–3, 6*f*
- AOT. *see* Adenomatoid odontogenic tumor
- Aphthous stomatitis, recurrent, 192–194, 193*b*, 193*f*
- clinical findings on, 192
- differential diagnosis of, 193–194
- pathologic findings in, 193, 193*f*, 194*b*
- prognosis and therapy for, 194
- AR. *see* Adult rhabdomyoma
- Asboe-Hansen sign, 190
- ASC. *see* Adenosquamous carcinoma
- Atypia, cytologic
- in precursor squamous lesions, 138
- in reactive laryngeal epithelial changes, 115
- Atypical adenoma
- follicular adenoma *vs.*, 603, 604*f*
- of parathyroid gland, 724
- Atypical hyperplasia, 138
- Autoantibodies, for thyroiditis, 562
- Autoimmunity, for thyroiditis, 562
- B**
- Bacillary angiomatosis, 226, 494–495, 494*b*–495*b*, 495*f*
- Bartonella henselae*, 226, 492
- Bartonella quintana*, 492
- Basal cell adenocarcinoma, of salivary glands, 346–348, 347*f*–348*f*, 351*b*
- sialoblastoma *vs.*, 346
- Basal cell adenoma, of salivary glands, 266–269, 266*b*
- ancillary studies of, 267–269, 269*f*
- clinical findings on, 266
- congenital. *see* Sialoblastoma, of salivary glands
- differential diagnosis of, 269
- pathologic findings in, 266–267, 267*b*, 267*f*–268*f*
- pleomorphic adenoma *vs.*, 264
- prognosis and therapy of, 269
- sialoblastoma *vs.*, 346
- Basal zone hyperplasia, 116*f*, 138, 142
- Basaloid adenocarcinoma. *see* Sialoblastoma, of salivary glands
- Basaloid cells, 346–348, 347*f*
- Basaloid squamous cell carcinoma (BSCC)
- adenoid cystic carcinoma *vs.*, 308–309
- adenosquamous carcinoma *vs.*, 160–161
- of larynx, hypopharynx, and trachea, 160–161, 161*b*, 161*f*–162*f*
- of nasopharynx, 71
- of oropharynx, 232, 235*f*
- B-cell lymphoma
- diffuse large
- extranodal marginal zone lymphoma *vs.*, 343
- of thyroid gland, 668, 668*f*, 670–673, 672*f*–674*f*
- extranodal marginal zone
- of salivary glands, 340–343, 341*b*, 341*f*–344*f*, 343*b*
- of thyroid gland, 668–670, 670*f*–671*f*
- Benign immature teratoma, 513–514
- Benign lymphoepithelial lesion (BLEL), of salivary glands, 251, 252*b*, 253*f*–254*f*
- Benign mature teratoma, 513–514
- Benign mixed tumor. *see* Pleomorphic adenoma
- Biocollagenolytic (necrobiotic) necrosis, granulomatosis with polyangiitis and, 16, 17*f*
- Biphasic synovial sarcoma, 532–534, 533*f*, 535*f*
- Biphenotypic sinonasal sarcoma, 92, 93*f*
- respiratory epithelial adenomatoid hamartoma *vs.*, 21
- Birbeck granules, 504–507
- BLEL. *see* Benign lymphoepithelial lesion
- Bone cyst, simple gnathic, 375–376, 375*b*, 375*f*–376*f*
- BRAF* gene, 504–505, 628–630
- Branchial cleft anomalies
- of ear, 433–436, 433*b*
- clinical findings on, 433–434, 434*f*
- differential diagnosis of, 435–436
- pathologic findings in, 434–435, 434*b*, 435*f*–436*f*
- prognosis and therapy for, 436
- of neck, 488–492, 488*b*
- ancillary studies of, 489–490
- clinical findings on, 488
- differential diagnosis of, 490–492, 491*f*
- pathologic findings in, 488–489, 489*f*–490*f*, 490*b*
- prognosis and therapy for, 492
- radiologic findings in, 488
- Branchial cleft cysts, 488–489, 488*b*, 489*f*, 490*b*, 491*f*
- cat scratch disease *vs.*, 494
- laryngeal cysts *vs.*, 114
- metastatic squamous cell carcinoma *vs.*, 527
- Branchial pouch neoplasms, 680–682, 680*f*–683*f*
- Breast carcinoma/adenocarcinoma
- to ear and temporal bone, 484–485, 485*f*
- to lymph nodes, 529*f*
- to parathyroid gland, 726*f*



- Bronchial cysts, 490–492
- Brown tumor of hyperparathyroidism, 212  
central giant cell lesion *vs.*, 412–414
- BSCC. *see* Basaloid squamous cell carcinoma
- Burkitt-like cells, 670–673, 674f
- C**
- Ca ex PA. *see* Carcinoma ex pleomorphic adenoma
- Calcified odontogenic cyst, odontogenic keratocyst *vs.*, 405–406
- Calcifying epithelial odontogenic tumor (CEOT), of gnathic bones, 406–409, 406b  
ancillary studies of, 407  
clinical features of, 406  
differential diagnosis of, 408  
ghost cell odontogenic carcinoma *vs.*, 430  
pathologic features of, 407, 407f–408f, 409b  
prognosis and therapy for, 408–409  
radiologic features of, 407, 407f  
sclerosing odontogenic carcinoma *vs.*, 427–428
- Calcitonin, function of, 656–658, 692
- Calcitonin gene-related peptide (CGRP), 656–658
- Calcium, serum, parathyroid carcinoma and, 692, 711
- Canalicular adenoma, of salivary glands, 269–272, 270b, 270f–271f
- Candida*, 183, 184f
- Candida albicans*, 181
- Candidiasis, oral, 181, 182f
- Canker sores, 192
- Capillary lymphangioma, 509
- Capsular invasion  
in follicular thyroid carcinoma, 646–648, 646f–647f  
in parathyroid carcinoma, 714–722, 715f
- Carcinoid tumor  
of lung, typical and atypical, paraganglioma *vs.*, 738t  
of middle ear, 470
- Carcinoma. *see also* Acinic cell carcinoma; Adenoid cystic carcinoma; Ameloblastic carcinoma; Clear cell carcinoma; Mucoepidermoid carcinoma; Neuroendocrine carcinoma; Parathyroid carcinoma; Salivary duct carcinoma; Small cell carcinoma; Squamous cell carcinoma; Thyroid carcinoma  
chordoma *vs.*, 541  
ectopic pituitary adenoma *vs.*, 50  
epithelial-myoepithelial, in salivary glands, 291–293, 318b, 318f–321f, 322b  
lobular capillary hemangioma *vs.*, 207  
lymphoepithelial, 356b, 358–360, 359f  
metastatic  
benign lymphoepithelial lesion *vs.*, 252–254  
endolymphatic sac tumor *vs.*, 477  
nasopharyngeal, 69–72, 69b–70b, 70f–72f  
NUT, 66–68, 66b–67b, 67f–68f  
squamous cell, of sinonasal tract, 51–57, 52b, 53f–56f
- Carcinoma (*Continued*)  
uncommon, of salivary gland, 346–354, 351b  
basal cell adenocarcinoma, 346–348, 347f–348f, 351b  
clear cell carcinoma, 348–351, 350f, 351b, 352f  
oncocyctic carcinoma, 354, 354f–355f  
sebaceous carcinoma, 351, 351b, 352f–353f  
undifferentiated  
of salivary glands, 354–360, 355f, 356b, 357f–359f  
sinonasal, 61–66, 62b, 62f–63f, 64t–65t, 66f  
of thyroid gland, 652–656
- Carcinoma ex mixed tumor in situ, 262
- Carcinoma ex pleomorphic adenoma (Ca ex PA)  
chordoma *vs.*, 541  
of salivary glands, 335–340, 335b  
clinical findings on, 335, 335f  
differential diagnosis of, 340, 340f  
pathologic findings in, 335–336, 336b, 336f–339f  
prognosis and therapy for, 340
- Carcinoma in situ (CIS)  
of larynx, 138–141  
of oral cavity, 220–221, 222f
- Carcinoma showing thymus-like differentiation (CASTLE), 678b, 680–681, 682f–683f
- Carcinosarcoma, of salivary glands, 340f
- Carotid body tumors, 737–738, 738t
- CASTLE. *see* Carcinoma showing thymus-like differentiation
- Cat scratch disease (CSD), 492–494, 492b  
ancillary studies of, 493–494  
clinical findings on, 492  
differential diagnosis of, 494  
pathologic findings in, 492–493, 493b, 493f  
prognosis and therapy for, 494
- “Cauliflower ear” deformity, 444, 445f
- Cavernous hemangioma, 511
- Cavernous lymphangioma, 509
- C (calcitonin-producing)-cells, 656–660, 661f  
hyperplasia of, 660, 662f, 666–667, 666f  
ultimobranchial remnants *vs.*, 549
- CCND1* gene, 722, 724t
- CDNH. *see* Chondrodermatitis nodularis helices
- Cementoblastoma, of gnathic bones, 393–395, 393b  
clinical features of, 393  
differential diagnosis of, 395  
osteoblastoma *vs.*, 391–392  
osteoid osteoma *vs.*, 393  
pathologic features of, 393–395, 394b, 394f–395f  
prognosis and therapy for, 395  
radiologic features of, 393, 394f
- Cementoma, familial gigantiform, 381
- Cemento-osseous dysplasia. *see also* Osseous dysplasia  
ossifying fibroma *vs.*, 384–385
- Cemento-ossifying fibroma, 383. *see also* Ossifying fibroma
- Central giant cell granuloma, peripheral giant cell granuloma *vs.*, 212
- Central giant cell lesion  
cherubism *vs.*, 380  
of gnathic bones, 411–414, 413b  
clinical features of, 412  
differential diagnosis of, 412–414  
pathologic features of, 412, 413f, 414b  
prognosis and therapy for, 414  
radiologic features of, 412, 412f  
peripheral giant cell granuloma *vs.*, 212
- Central odontogenic fibroma, of gnathic bones, 388–390, 388b  
clinical features of, 388  
differential diagnosis of, 390  
pathologic features of, 388, 389f–390f, 390b  
prognosis and therapy for, 390  
radiologic features of, 388, 389f  
sclerosing odontogenic carcinoma *vs.*, 427–428
- Central ossifying fibroma, oral, 207
- Ceruminoma. *see* Ceruminous adenoma of ear
- Ceruminous adenocarcinoma, of ear and temporal bone, 481–484, 482b  
ancillary studies of, 483  
ceruminous adenoma *vs.*, 454–455  
clinical findings on, 481  
differential diagnosis of, 483–484  
pathologic findings in, 482, 482b, 483f–484f  
prognosis and therapy for, 484  
radiologic findings in, 481, 482f
- Ceruminous adenoma of ear, 453–457, 453b  
ancillary studies of, 454, 456f  
ceruminous adenocarcinoma *vs.*, 483–484  
clinical findings on, 453  
differential diagnosis of, 454–455  
neuroendocrine adenoma *vs.*, 474  
paraganglioma *vs.*, 736–737  
pathologic findings in, 453–454, 453b, 454f–456f  
prognosis and therapy for, 457
- Ceruminous papillary cystadenoma papilliferum, 454
- Ceruminous pleomorphic adenoma, 454
- Ceruminous syringocystadenoma papilliferum, 453–454
- Cervical actinomycosis, 496–497, 496f, 497b
- Charcot-Leyden crystals, 8–9, 9f
- Cheilitis, angular, 181
- Chemodectoma, of middle ear, 463
- Cherubism, 379–381, 379b–380b, 379f–380f  
central giant cell lesion *vs.*, 412–414  
peripheral giant cell granuloma *vs.*, 212
- Chief cell adenoma, of parathyroid gland, 704–706
- Chief cells  
of paraganglioma, 731  
of parathyroid gland, 693–700  
secondary and tertiary hyperplasia of, 700–702, 700b–701b, 701f–702f
- Cholesteatoma  
of ear and temporal bone, 446–450, 447b  
ancillary studies of, 450  
clinical findings on, 446–447, 448f  
differential diagnosis of, 450

- Cholesteatoma** (*Continued*)  
 first branchial cleft anomalies *vs.*, 435–436  
 pathologic findings in, 447–449, 447*b*, 449*f*  
 prognosis and therapy for, 450  
 radiologic findings in, 447, 448*f*  
 squamous cell carcinoma with, 478–480
- Cholesterol granuloma**, of ear and temporal bone, 450–452, 450*b*
- cholesteatoma** *vs.*, 450  
 clinical findings on, 450  
 differential diagnosis of, 451–452  
 pathologic findings in, 451, 451*b*, 451*f*  
 prognosis and therapy for, 452  
 radiologic findings in, 450–451
- Chondroblastic osteosarcoma**, of gnathic bones, chondrosarcoma *vs.*, 418*f*, 420
- Chondrodermatitis nodularis helices** (CDNH), 439–441, 439*b*  
 clinical findings on, 439, 440*f*  
 cystic chondromalacia *vs.*, 437  
 differential diagnosis of, 441  
 pathologic findings in, 439–441, 439*b*, 440*f*–441*f*  
 prognosis and therapy for, 441
- Chondroid syringoma**, 538, 539*f*
- Chondroid syringoma**, 453–454
- Chondroma**  
 chondromesenchymal hamartoma *vs.*, 21  
 chondrosarcoma *vs.*, 170–173  
 of larynx and trachea, 131–134, 131*b*  
 ancillary studies of, 132  
 clinical features of, 131, 132*f*  
 differential diagnosis of, 132–133, 133*f*  
 pathologic features of, 131–132, 131*b*, 132*f*–133*f*  
 prognosis and therapy for, 133–134
- Chondromalacia**, cystic, of ear, 436–438, 436*b*  
 clinical findings on, 436, 437*f*  
 differential diagnosis of, 437  
 pathologic findings in, 437, 437*b*, 437*f*–438*f*  
 prognosis and therapy for, 438
- Chondromesenchymal hamartoma** (CMH), 18, 20*f*
- Chondrometaplasia**, chondrosarcoma *vs.*, 170–173
- Chondromyxoid fibroma**,  
 chondromesenchymal hamartoma *vs.*, 21
- Chondrosarcoma**  
 of gnathic bones, 419–421, 420*b*  
 ancillary studies of, 420  
 clinical findings on, 419–420  
 differential diagnosis of, 420  
 myxoid, 420, 421*f*  
 osteosarcoma *vs.*, 419  
 pathologic findings in, 420, 420*b*, 421*f*  
 prognosis and therapy for, 421  
 radiologic findings in, 420
- of larynx and trachea, 168–173, 169*b*  
 chondroma *vs.*, 133–134  
 chordoma *vs.*, 541  
 clinical findings on, 169  
 differential diagnosis of, 170–173
- Chondrosarcoma** (*Continued*)  
 pathologic findings in, 170, 170*b*, 170*f*–172*f*  
 prognosis and therapy for, 173  
 radiologic findings in, 169, 169*f*  
 mesenchymal, 421–423, 422*b*  
 ancillary studies of, 422  
 clinical findings on, 422  
 differential diagnosis of, 423  
 pathologic findings in, 422, 422*b*, 423*f*  
 prognosis and therapy for, 423  
 radiologic findings in, 422
- Chordoma**, of neck, 537–541, 537*b*  
 ancillary studies of, 538–541, 540*f*  
 clinical findings on, 537  
 differential diagnosis of, 541  
 pathologic findings in, 538, 538*b*, 538*f*–540*f*  
 prognosis and therapy for, 541  
 radiologic findings in, 537–538
- Choristoma**, teratoma *vs.*, 616–618
- Choroid plexus papilloma**, 477
- Chronic lymphocytic thyroiditis**. *see* Lymphocytic thyroiditis, chronic
- Chronic rhinosinusitis**, 1, 3*f*
- “Church spire” keratosis**, 148, 151*f*
- Churg-Strauss disease**, granulomatosis with polyangiitis *vs.*, 18
- Cicatricial pemphigoid**, 188
- CIS**. *see* Carcinoma in situ
- Clear cell carcinoma**  
 calcifying epithelial odontogenic tumor *vs.*, 408  
 mucoepidermoid carcinoma *vs.*, 291–293  
 of salivary glands, 348–351, 350*f*, 351*b*, 352*f*
- Clear cell odontogenic carcinoma**, of gnathic bones, 428–429, 428*b*, 428*f*–429*f*
- Clear cell oncocytosis/oncocytoma**, 272–274
- Clear cell variant**  
 of follicular adenoma, 599, 600*f*  
 of follicular thyroid carcinoma, 650  
 of papillary thyroid carcinoma, 637, 637*f*
- Coccidioides immitis**, spherules of,  
 rhinosporidiosis cysts *vs.*, 16
- Collagen**, ropy, 518, 519*f*
- Colon adenocarcinoma**, metastatic, 486*f*
- Columnar papillomas**, 22
- Columnar variant**, of papillary thyroid carcinoma, 640, 641*f*–642*f*
- Comedonecrosis**  
 basaloid squamous cell carcinoma *vs.*, 160, 161*f*  
 in ceruminous adenocarcinoma, 482, 483*f*  
 in parathyroid carcinoma, 714–722, 718*f*  
 in salivary duct carcinoma, 328–333, 330*f*, 332*f*
- Complex odontoma**, 414, 414*b*, 416*f*
- Compound odontoma**, 414, 414*b*, 415*f*
- Computed tomography**, for squamous cell carcinoma of sinonasal tract, 52
- Condyloma acuminatum**  
 focal epithelial hyperplasia *vs.*, 205  
 oral, 200, 200*b*, 200*f*
- Congenital basal cell adenoma**. *see* Sialoblastoma, of salivary glands
- Congenital cyst of larynx**, 111–112
- Congenital granular cell epulis** (CGCE), 214–217, 215*b*, 215*f*–216*f*  
 ancillary studies of, 216  
 clinical features of, 215  
 differential diagnosis of, 216  
 granular cell tumor *vs.*, 213–214  
 pathologic features of, 215  
 prognosis and therapy for, 217
- Conjunctivitis**, ligneous, 102
- Contact ulcer**, 104–107, 105*b*  
 clinical features of, 104  
 differential diagnosis of, 105–106  
 pathologic findings in, 104–105, 105*b*, 105*f*–107*f*  
 prognosis and therapy for, 106–107  
 vocal cord polyps/nodules *vs.*, 102
- Contact ulcer**, spindle cell squamous cell carcinoma *vs.*, 158
- Conventional ameloblastomas**, 395–396
- Corticosteroids**  
 for granulomatosis with polyangiitis, 18  
 for mucous membrane pemphigoid, 190  
 for oral lichen planus, 188  
 for recurrent aphthous stomatitis, 194
- Cribriform adenocarcinoma** of minor salivary glands (CAMSG), 309, 316*f*
- Cribriform-morular variant**, of papillary thyroid carcinoma, 640–643, 643*f*
- Cribriform variant**, of adenoid cystic carcinoma, 301–302, 302*f*
- CSC73 gene**, associated with parathyroid neoplasms in, 724*t*
- CSD**. *see* Cat scratch disease
- Cutaneous CD30+ T-cell lymphoma**, 195
- Cyclophosphamide**, for granulomatosis with polyangiitis, 18
- Cylindrical cell carcinoma**. *see* Squamous cell carcinoma
- Cylindrical cell papillomas**, 22
- Cylindroma**. *see* Ceruminous adenoma of ear
- Cylindromatous variant**, of adenoid cystic carcinoma, 301–302, 303*f*
- Cystadenocarcinoma**  
 polymorphous adenocarcinoma *vs.*, 314–316  
 salivary duct carcinoma *vs.*, 333
- Cystadenomas**, papillary cystadenoma lymphomatosum *vs.*, 277
- Cystic chondromalacia**, of ear, 436–438, 436*b*  
 clinical findings on, 436, 437*f*  
 differential diagnosis of, 437  
 pathologic findings in, 437, 437*b*, 437*f*–438*f*  
 prognosis and therapy for, 438
- Cystic hygroma**, of neck, 509–511, 509*b*  
 ancillary studies of, 510–511  
 clinical findings on, 509, 510*f*  
 differential diagnosis of, 511  
 pathologic findings in, 509–510, 510*f*–511*f*, 511*b*  
 prognosis and therapy for, 511
- Cystic metastatic squamous cell carcinoma**. *see* Metastatic cystic squamous cell carcinoma



## Cysts

- branchial cleft, 488–489, 488*b*, 489*f*, 490*b*, 491*f*
- cat scratch disease *vs.*, 494
- laryngeal cysts *vs.*, 114
- metastatic squamous cell carcinoma *vs.*, 527
- bronchial, 490–492
- dentigerous, 366–368, 366*b*, 367*f*
- dermoid, 490–492
- eruption, 368
- laryngeal, 110–114, 111*b*
  - clinical features of, 110–111
  - differential diagnosis of, 114
  - pathologic features of, 111–114, 111*b*, 112*f*–113*f*
  - prognosis and therapy for, 114
- lymphoepithelial, 254–255, 255*b*, 255*f*–256*f*
- mucus retention, 244–248, 245*f*–246*f*, 247*b*
- nasopalatine duct, 376–377, 376*b*–377*b*, 377*f*
- periapical, 368–370, 369*f*, 370*b*
- simple bone, 375–376, 375*b*, 375*f*–376*f*
- thymic, 490–492, 491*f*
- thyroglossal duct, 114, 490–492, 542–546, 542*b*
  - clinical findings on, 542, 543*f*
  - differential diagnosis of, 544
  - pathologic findings in, 542–543, 543*f*–545*f*, 544*b*
  - prognosis and therapy for, 544–546
  - radiographic findings on, 542

**D**

- Dedifferentiated chordoma, of neck, 541
- Dental follicle, central odontogenic fibroma *vs.*, 390
- Dentigerous cyst, of gnathic bones, 366–368, 366*b*
  - clinical findings on, 366
  - differential diagnosis of, 368
  - odontogenic keratocyst *vs.*, 405–406
  - pathologic findings in, 366, 366*b*, 367*f*
  - prognosis and therapy for, 368
- de Quervain thyroiditis. *see* Granulomatous thyroiditis, subacute
- Dermal anlage tumor, 266
- Dermoid cysts
  - branchial cleft cyst *vs.*, 490–492
  - teratoma *vs.*, 616–618
- Desmoid-type fibromatosis, nasopharyngeal angiofibroma *vs.*, 45
- Desmoplasia, oral, 222–224
- Desmoplastic ameloblastoma, 396, 401*f*
  - sclerosing odontogenic carcinoma *vs.*, 427–428
- Desmoplastic fibroma, central odontogenic fibroma *vs.*, 390
- Developmental abnormalities, of salivary glands, 241–244, 241*b*, 242*t*
  - ancillary studies of, 243–244
  - clinical features of, 241–242, 243*f*
  - differential diagnosis of, 244
  - pathologic features of, 242–243, 242*b*, 243*f*–244*f*
  - prognosis and therapy for, 244

- Diffuse hyperplasia (Graves disease), 569*b*
  - ancillary studies of, 571–574, 574*f*
  - differential diagnosis of, 574
  - laboratory findings on, 584
  - papillary carcinoma *vs.*, 630
  - pathologic findings in, 569*f*–573*f*, 570*b*
  - prognosis and therapy for, 574–575
- Diffuse large B-cell lymphoma (DLBCL)
  - extranodal marginal zone lymphoma *vs.*, 343
  - of thyroid gland, 668, 668*f*, 670–673, 672*f*–674*f*
- Diffuse sclerosing variant, of papillary thyroid carcinoma, 637*f*–638*f*, 638–639
- DLBCL. *see* Diffuse large B-cell lymphoma
- Ductal cyst of larynx, 111–112
- Dutcher bodies, 669–670, 672*f*
- Dyshormonogenetic goiter, 583–586, 584*b*
  - ancillary studies of, 586
  - clinical findings on, 584
  - differential diagnosis of, 586
  - laboratory findings on, 584
  - papillary carcinoma *vs.*, 630
  - pathologic findings in, 584–586, 584*b*, 585*f*–587*f*
  - prognosis and therapy for, 586
- Dyskeratosis, laryngeal, 121, 121*f*
- Dysplasia
  - cemento-osseous, ossifying fibroma *vs.*, 384–385
  - fibrous
    - of gnathic bones, 371*b*–372*b*, 371*f*–372*f*
    - osseous dysplasia *vs.*, 381–382
    - ossifying fibroma *vs.*, 384–385
    - osteomyelitis *vs.*, 364
  - laryngeal reactive epithelial changes *vs.*, 121
  - of larynx, hypopharynx, and trachea, 138–139, 139*f*–142*f*, 140*t*
  - of oral cavity, 219–220
  - osseous
    - fibrous dysplasia *vs.*, 371
    - of gnathic bones, 381–382, 381*b*–382*b*, 382*f*
    - osteomyelitis *vs.*, 364

**E**

- Ear. *see also specific lesion or neoplasm*
  - benign neoplasms of, 453–477
    - ceruminous adenoma, 453–457, 453*b*, 454*f*–456*f*
    - endolymphatic sac tumor, 475–477, 475*b*, 476*f*–477*f*
    - Langerhans cell histiocytosis, 457–460, 457*b*–458*b*, 458*f*–460*f*
    - meningioma, 467–470, 468*b*, 469*f*–470*f*
    - middle ear adenoma (neuroendocrine adenoma of middle ear), 470–474, 471*b*–472*b*, 471*f*–474*f*
    - paraganglioma, 463–467, 464*b*, 465*f*–467*f*
    - peripheral nerve sheath tumor (schwannoma), 460–463, 461*b*, 462*f*–463*f*
- Ear (*Continued*)
  - malignant neoplasms of, 478–487
    - ceruminous adenocarcinoma, 481–484, 482*b*, 482*f*–484*f*
    - metastatic, 484–487, 485*b*, 485*f*–486*f*
    - squamous cell carcinoma, 478–481, 478*b*–479*b*, 479*f*–481*f*
  - non-neoplastic lesions of, 433–452
    - angiolymphoid hyperplasia with eosinophilia, 441–444, 442*b*, 443*f*
    - cholesteatoma, 446–450, 447*b*, 448*f*–449*f*
    - cholesterol granuloma, 450–452, 450*b*–451*b*, 451*f*
    - chondrodermatitis nodularis helices, 439–441, 439*b*, 440*f*–441*f*
    - cystic chondromalacia, 436–438, 436*b*–437*b*, 437*f*–438*f*
    - first branchial cleft anomalies, 433–436, 433*b*–434*b*, 434*f*–436*f*
    - relapsing polychondritis, 444–446, 444*b*–445*b*, 445*f*–446*f*
  - EBV. *see* Epstein-Barr virus
  - Ectomesenchymal chondromyxoid tumor, 217–218, 217*b*, 218*f*
  - Ectopic hamartomatous thymoma (EHT), 515–517, 515*b*
    - ancillary studies of, 517
    - clinical findings on, 515
    - differential diagnosis of, 517
    - pathologic findings in, 515–516, 515*f*–517*f*, 517*b*
    - prognosis and therapy for, 517
  - Ectopic pituitary adenoma, 46–50, 47*b*, 48*f*–49*f*
  - Ectopic thymoma, primary thyroid gland lymphoma *vs.*, 675
  - Ectopic thyroid, 178–179, 178*b*
    - clinical findings on, 178, 178*f*
    - differential diagnosis of, 179
    - pathologic findings in, 178, 178*b*, 179*f*
    - prognosis and therapy for, 179
    - radiologic findings in, 178
  - ELST. *see* Endolymphatic sac tumor
  - Embryoma. *see* Sialoblastoma, of salivary glands
  - Embryonal cyst of larynx, 111–112
  - Embryonal rhabdomyosarcoma
    - sinonasal inflammatory polyp *vs.*, 5–6
    - of sinonasal tract, 86–88, 88*f*–89*f*
  - EMC. *see* Epithelial-myoepithelial carcinoma
  - Emperipolesis, 14*f*
    - sinus histiocytosis with, 503, 504*f*
  - EMZBCL. *see* Extranodal marginal zone B-cell lymphoma
  - Encapsulated variant, of papillary thyroid carcinoma, 633, 633*f*
  - Encephalocele, nasal glial heterotopia *vs.*, 12
  - Endodermally derived tissues, of thyroid gland, 549–551
  - Endolymphatic sac tumor (ELST), 475–477, 475*b*
    - ancillary studies of, 476–477
    - clinical findings on, 475
    - differential diagnosis of, 477
    - pathologic findings in, 475–476, 475*b*, 476*f*–477*f*

- Endolymphatic sac tumor (ELST)  
(*Continued*)  
prognosis and therapy for, 477  
radiologic findings in, 475  
Epidermal inclusion cysts, 435–436  
Epidermoid carcinoma. *see* Squamous cell carcinoma  
Epidermoid cells, of mucoepidermoid carcinoma, 284–285, 286f  
Epidermoid cyst of thyroid gland, 544  
Epignathus, 616–618  
Epimyoeplithelial islands, 341–343, 342f  
Epiphora, squamous cell carcinoma and, 51–52  
Epistaxis, squamous cell carcinoma and, 51–52  
Epithelial lesions of larynx, reactive, 114–121, 114b  
ancillary studies of, 120–121  
clinical features of, 114–115  
differential diagnosis of, 121  
pathologic features of, 115–120, 115b, 116f–121f  
prognosis and therapy for, 121  
Epithelial-myoeplithelial carcinoma (EMC)  
adenoid cystic carcinoma *vs.*, 308–309  
mucoepidermoid carcinoma *vs.*, 291–293  
of salivary gland, 317–322, 318b  
ancillary studies of, 319–322, 321f  
clinical findings on, 317  
differential diagnosis of, 322  
pathologic findings in, 317–319, 318f–321f, 322b  
prognosis and therapy for, 322  
Epithelioid cells, of chordoma, 538–541, 538f, 541f  
Epithelioid hemangioma, 207  
Epstein-Barr virus (EBV)  
nasal type NK/T-cell lymphoma and, 82, 84  
nasopharyngeal carcinoma and, 69  
oral hairy leukoplakia and, 179, 181f  
Epulis, congenital granular cell, 214–217, 215b, 215f–216f  
Epulis gravidarum, 29  
Erdheim-Chester disease, 507–508  
Erosive lichen planus, 186f  
Eruption cyst, 368  
Erythema nodosum, 492  
Erythroplakia, 138, 219–220, 220f  
ES/PNET. *see* Ewing sarcoma  
ESCC. *see* Exophytic squamous cell carcinoma  
Esthesioneuroblastoma. *see* Olfactory neuroblastoma  
Everted papillomas, 22  
Ewing sarcoma, 95–97, 95b  
ancillary studies of, 96  
differential diagnosis of, 64t–65t, 96–97  
ectopic pituitary adenoma *vs.*, 50  
NUT carcinoma *vs.*, 68  
pathologic features of, 96, 96b, 97f–98f  
sinonasal undifferentiated carcinoma *vs.*, 63  
Exophytic papillomas, 22–23, 23t–24t, 24f–25f  
Exophytic squamous cell carcinoma (ESCC)  
of larynx, hypopharynx, and trachea, 150–152, 152b, 153f  
squamous papilloma *vs.*, 123  
External jugular phlebectasia, 114  
Extranodal marginal zone B-cell lymphoma (EMZBCL)  
of salivary glands, 340–343, 341b, 341f–344f, 343b  
of thyroid gland, 668–670, 670f–671f  
Extranodal NK/T-cell lymphoma  
Langerhans cell histiocytosis *vs.*, 507–508  
nasal type, 82–86, 82f–83f, 83b  
ancillary studies of, 85, 86f  
differential diagnosis of, 64t–65t, 85  
granulomatosis with polyangiitis *vs.*, 18  
pathologic features of, 83–84, 84b, 84f–85f  
relapsing polychondritis *vs.*, 445–446  
Extravasated mucocele, of salivary glands, 245f–246f
- F**  
FA. *see* Follicular adenoma  
Familial gigantiform cementoma, 381  
Fasciitis, nodular, of neck, 497–501, 498b  
ancillary studies of, 500–501  
clinical findings on, 497  
differential diagnosis of, 501, 502f  
pathologic findings in, 497–500, 498f–500f, 500b  
prognosis and therapy for, 501  
radiologic findings in, 497  
Fatty metaplasia, of follicular thyroid carcinoma, 650  
FC. *see* Follicular carcinoma  
Fetal rhabdomyoma, 501  
Fibroma. *see also* Ossifying fibroma  
ameloblastic, 399–402  
odontogenic sarcoma *vs.*, 432, 432f  
central odontogenic, sclerosing  
odontogenic carcinoma *vs.*, 427–428  
nuchal, lipoma *vs.*, 520  
oral, 197–198, 197b–198b, 198f–199f  
ossifying, of gnathic bones, 383–385, 383b  
clinical features of, 383  
differential diagnosis of, 384–385  
pathologic features of, 384b, 385f  
prognosis and therapy for, 384–385  
radiologic features of, 383, 384f  
Fibromatosis  
desmoid-type, nasopharyngeal  
angiofibroma *vs.*, 45  
nodular fasciitis *vs.*, 501  
Fibro-odontoma, ameloblastic, 399–402  
Fibrosarcoma  
nodular fasciitis *vs.*, 501  
of sinonasal tract, 91–92, 92f  
Fibrous dysplasia  
of gnathic bones, 370–373, 371b  
clinical findings on, 370  
differential diagnosis of, 371  
pathologic findings in, 370–371, 372b, 372f  
prognosis and therapy for, 373  
radiologic findings in, 370, 371f  
osseous dysplasia *vs.*, 381–382  
ossifying fibroma *vs.*, 384–385  
osteomyelitis *vs.*, 364  
Fibrous hamartoma of infancy, lipoma *vs.*, 520  
Fibrous histiocytoma, nodular fasciitis *vs.*, 501  
Fibrous variant of Hashimoto thyroiditis, 562  
invasive fibrous thyroiditis *vs.*, 561  
Fine-needle aspiration (FNA)  
for acute thyroiditis, 551  
for basal cell adenoma, of salivary glands, 269  
for branchial cleft anomalies, of neck, 489–490, 491f  
for cat scratch disease, 493  
for chordoma, 539–541, 541f  
for diffuse hyperplasia (Graves disease), 571–574  
for ectopic thyroid, 178  
for follicular thyroid adenoma, 602, 603f  
for follicular thyroid carcinoma, 650, 651f  
for granulomatous inflammation, 493  
for hyalinizing trabecular tumor, 611, 612f  
for invasive fibrous thyroiditis, 561  
for juvenile salivary gland hemangioma, 282, 283f  
for medullary thyroid carcinoma, 666f, 667  
for metastatic neoplasm of unknown primary, 530  
for metastatic squamous cell carcinoma of neck, 527, 527f  
for nodular fasciitis, 501, 501f  
for nodular hyperplasia, 582, 582f–583f  
for noninvasive follicular thyroid neoplasm, 607, 608f  
for oncocytoma, 274, 276f  
for papillary thyroid carcinoma, 628, 629f  
for paraganglioma, 736  
for parathyroid adenoma, 710–711  
for pleomorphic adenoma, 264  
for primary thyroid gland lymphoma, 675, 676f  
for salivary glands, developmental abnormalities of, 244  
for sebaceous adenoma, 281  
for spindle cell lipoma/pleomorphic lipoma, 520  
for squamous cell carcinoma  
of oral cavity, 222  
of oropharynx, 236  
for subacute granulomatous thyroiditis, 554, 556f  
for synovial sarcoma, 534, 536f  
for teratoma, 616  
for thyroglossal duct cyst, 544  
for thyroid ectopia and lingual thyroid, 547  
for thyroid lesions and nodules, 619



Fine-needle aspiration (FNA) (*Continued*)  
 for undifferentiated thyroid carcinoma, 656, 657f

First branchial cleft anomalies, 433–436, 433b  
 clinical findings on, 433–434, 434f  
 differential diagnosis of, 435–436  
 pathologic findings in, 434–435, 434b, 435f–436f  
 prognosis and therapy for, 436

Fistula, thyroglossal duct cyst, 542

Flexner-Wintersteiner rosettes, 78–80, 79f

“Floret cells”, 517–519, 519f

Florid osseous dysplasia, 381

Focal osseous dysplasia, 381

“Focus score,” for lymphocytes, 252

Follicular adenoma, of thyroid gland, 593–604, 593b  
 ancillary studies of, 599–603, 602f  
 clinical findings on, 593  
 differential diagnosis of, 603–604  
 follicular carcinoma *vs.*, 593, 651  
 papillary carcinoma *vs.*, 630  
 pathologic findings in, 594–599, 595b, 595f–601f  
 prognosis and therapy for, 604  
 radiologic findings in, 593–594, 594f

Follicular carcinoma (FC), of thyroid gland, 643–652, 644f, 645b  
 ancillary studies of, 650–651, 651f  
 clinical findings on, 645  
 differential diagnosis of, 651–652  
 follicular adenoma *vs.*, 593  
 hyalinizing trabecular tumor, 613  
 papillary carcinoma *vs.*, 630  
 pathologic findings in, 645–650, 645b, 646f–650f  
 prognosis and therapy for, 652  
 variants of, 648–650

Follicular lymphoma, extranodal marginal zone lymphoma *vs.*, 343

Follicular variant  
 of acinic cell carcinoma, 294–295, 296f  
 of papillary thyroid carcinoma, 633–634, 633f–634f  
 follicular carcinoma *vs.*, 651–652

Fordyce granules, 175–176, 175b  
 clinical findings on, 175, 175f  
 differential diagnosis of, 176  
 pathologic findings in, 175, 175b, 176f  
 prognosis and therapy for, 176

Frozen section, of follicular thyroid carcinoma, 651

Fungal thyroiditis, granulomatous thyroiditis *vs.*, 554–555, 557f

Fungiform papillomas, 22

Fungus ball, allergic fungal sinusitis *vs.*, 9–10, 10f

**G**

Gastroesophageal reflux disease (GERD), 104

GCT. *see* Granular cell tumor

Genes, associated with parathyroid neoplasms, 724t

Genetic studies  
 of chordoma, 541  
 of endolymphatic sac tumor (ELST), 477

Adenocarcinoma (*Continued*)  
 of follicular thyroid adenoma, 602–603  
 of neurofibromatosis type 2, 462  
 of paraganglioma, 466  
 of peripheral nerve sheath tumor (schwannoma), 462  
 of spindle cell lipoma/pleomorphic lipoma, 520  
 of synovial sarcoma, 536, 536f

Genetic syndromes, associated with  
 paraganglioma and pheochromocytoma, 729t

Ghost cell odontogenic carcinoma, of gnathic bones, 429–430, 430b  
 clinical findings on, 430  
 differential diagnosis of, 430  
 pathologic findings in, 430, 430b, 431f  
 prognosis and therapy for, 430  
 radiologic findings in, 430

Giant cell fibroma, 197–198, 199f

Giant cells. *see also* Central giant cell lesion; Peripheral giant cell granuloma  
 in papillary carcinoma, 623–627, 625f  
 in undifferentiated thyroid carcinoma, 654, 655f

Glandular pattern, of neuroendocrine adenoma, 472, 472f–473f

Glasscock-Jackson classification, of middle ear paraganglioma, 730

Glioma. *see* Nasal glial heterotopia (NGH)

Glomangiopericytoma (GPC), 35–40, 36b  
 ancillary studies of, 38, 40f  
 differential diagnosis of, 38–40, 41f  
 lobular capillary hemangioma *vs.*, 33  
 meningioma *vs.*, 35  
 pathologic features of, 36–38, 37f–39f

Glomus tumors  
 glomangiopericytoma *vs.*, 38–40  
 of middle ear, 463

Glossitis, median rhomboid, 183, 184f

Gnathic bones. *see also specific lesion or neoplasm*  
 benign neoplasms of, 383–416  
 active ossifying fibroma as, 385–388, 386b, 386f–387f  
 adenomatoid odontogenic tumor as, 409–411, 409b, 410f–411f  
 ameloblastoma as, 395–402, 396b–397b, 396f–403f, 410b  
 calcifying epithelial odontogenic tumor as, 406–409, 406b, 407f–408f, 409b  
 cementoblastoma as, 393–395, 393b–394b, 394f–395f  
 central giant cell lesion as, 411–414, 412f–413f, 413b–414b  
 central odontogenic fibroma as, 388–390, 388b, 389f–390f, 390b  
 odontogenic keratocyst as, 403–406, 404b–405b, 404f–406f  
 odontoma as, 414–416, 414b–415b, 415f–416f  
 ossifying fibroma as, 383–385, 383b–384b, 384f–385f  
 osteoblastoma as, 390–392, 391b–392b, 391f–392f  
 osteoid osteoma as, 391b–392b, 391f–392f, 392–393

Gnathic bones (*Continued*)  
 malignant neoplasms of, 417–432  
 ameloblastic carcinoma as, 423–425, 424b, 424f  
 chondrosarcoma as, 419–421, 420b, 421f  
 clear cell odontogenic carcinoma as, 428–429, 428b, 428f–429f  
 ghost cell odontogenic carcinoma as, 429–430, 430b, 431f  
 mesenchymal chondrosarcoma as, 421–423, 422b, 423f  
 odontogenic sarcoma as, 431–432, 431b–432b, 432f  
 osteosarcoma as, 417–419, 417b, 418f–419f, 418t, 419b  
 primary intraosseous carcinoma as, 425–426, 425b–426b  
 sclerosing odontogenic carcinoma as, 426–428, 426b–427b, 427f  
 non-neoplastic lesions of, 363–382  
 cherubism as, 379–381, 379b–380b, 379f–380f  
 dentigerous cyst as, 366–368, 366b, 367f  
 fibrous dysplasia as, 371b–372b, 371f–372f  
 nasopalatine duct cyst as, 376–377, 376b–377b, 377f  
 osseous dysplasia as, 381–382, 381b–382b, 382f  
 osteomyelitis as, 363–366, 363b–364b, 365f  
 osteonecrosis as, 373b–374b, 374f  
 periapical cysts as, 368–370, 369f, 370b  
 simple bone cyst as, 375–376, 375b, 375f–376f  
 tori as, 377–379, 378b, 378f

Goiter. *see also* Adenomatoid nodules  
 amyloid, 586–589, 588f–589f, 589b  
 dyshormonogenetic, 583–586, 584b, 585f–587f  
 multinodular. *see* Nodular hyperplasia

Gonadal teratoma, metastatic, 514–515

Gorlin syndrome, 403–404

GPC. *see* Glomangiopericytoma

Granular cell epulis, congenital, 214–217, 215b, 215f–216f

Granular cell tumor (GCT), 212–214, 213b–214b, 213f–214f  
 congenital granular cell epulis *vs.*, 216  
 of larynx, 125–129, 126b  
 adult rhabdomyoma *vs.*, 131  
 ancillary studies of, 127, 128f  
 clinical features of, 126, 126f  
 differential diagnosis of, 127–128, 127f–128f  
 pathologic features of, 126–127, 126b, 127f  
 prognosis and therapy for, 129  
 precursor squamous lesions *vs.*, 142  
 vocal cord polyps/nodules *vs.*, 102

Granuloma. *see also* Central giant cell lesion  
 eosinophilic, 504–505  
 peripheral giant cell, 208–212, 210b, 210f–212f, 212b  
 pyogenic, 29, 205–207, 205b–206b, 206f–207f. *see also* Contact ulcer; Lobular capillary hemangioma

Granuloma (*Continued*)

- Teflon, 115, 120
- traumatic ulcerative, 194–196, 195*b*
  - clinical findings on, 194*f*
  - differential diagnosis of, 195
  - pathologic findings in, 194, 195*b*, 195*f*–196*f*
  - prognosis and therapy for, 196
- Granulomatosis, lymphomatoid, nasal-type extranodal NK/T-cell lymphoma *vs.*, 85
- Granulomatosis with polyangiitis, 16–18, 17*f*, 18*b*. *see also* Wegener granulomatosis
  - contact ulcer *vs.*, 105–106
  - nasal-type extranodal NK/T-cell lymphoma *vs.*, 85
  - relapsing polychondritis *vs.*, 445–446
  - sinus histiocytosis *vs.*, 503–504
- Granulomatous inflammation, 492–494, 492*b*
  - ancillary studies of, 493–494
  - clinical findings on, 492
  - differential diagnosis of, 494
  - pathologic findings in, 492–493, 493*b*, 493*f*
  - prognosis and therapy for, 494
- Granulomatous rhinosinusitis, infectious, granulomatosis with polyangiitis *vs.*, 18
- Granulomatous thyroiditis, subacute, 552–557, 553*b*
  - acute thyroiditis *vs.*, 552
  - ancillary studies of, 554, 556*f*
  - clinical findings on, 553
  - differential diagnosis of, 554–555, 557*f*–558*f*
  - laboratory studies for, 553
  - pathologic findings in, 553, 554*b*, 554*f*–555*f*
  - prognosis and therapy for, 557
- Graves disease. *see* Diffuse hyperplasia
- GRIM-19 gene, 651

**H***Haemophilus influenzae*, 1

- Hairy leukoplakia (HL), oral, 179–181, 180*b*
  - clinical findings on, 179, 179*f*
  - differential diagnosis of, 181
  - histochemical studies in, 179
  - immunohistochemical findings in, 180, 181*f*
  - molecular studies in, 180–181
  - pathologic findings in, 179–181, 180*b*, 180*f*
  - prognosis and therapy for, 181
- Hamartoma
  - of parathyroid gland, 706–710
  - respiratory epithelial adenomatoid, 29
  - sinonasal adenocarcinoma *vs.*, 60
  - teratoma *vs.*, 514–515, 616–618
- Hand-Schüller-Christian syndrome, 504–505
- Hashimoto thyroiditis. *see* Lymphocytic thyroiditis, chronic
- Hashitoxicosis, 562
- Hassall corpuscles, 490–492, 491*f*

- Heck disease, 203, 203*b*–204*b*, 204*f*
- Hemangioma. *see also* Lobular capillary hemangioma
  - epithelioid, 207
  - glomangiopericytoma *vs.*, 38–40
  - juvenile salivary gland, 281–283, 281*b*
    - ancillary studies of, 282
    - clinical findings on, 281
    - differential diagnosis of, 282
    - pathologic findings in, 282, 282*b*, 282*f*–283*f*
    - prognosis and therapy for, 283
  - lobular capillary, angiolymphoid hyperplasia with eosinophilia *vs.*, 442
  - lymphangioma *vs.*, 511
- Hemangiopericytoma
  - lobular capillary hemangioma *vs.*, 207
  - sinonasal-type, 35–40, 36*b*, 37*f*–41*f*
- Hematoma, small, 248
- Herpes labialis, 182
- Herpes simplex virus (HSV)
  - recurrent aphthous stomatitis *vs.*, 193–194
    - type 1 oral, 183, 185*f*
    - type 8, Kaposi sarcoma and, 226
- Herpes zoster, 184
- Herpetiform aphthous ulcers, 192
- Heterotopia
  - nasal glial, 10–12, 11*f*, 12*b*
  - salivary gland, 241–244, 241*b*–242*b*, 242*t*, 243*f*–244*f*
  - teratoma *vs.*, 616–618
- Hibernoma, 131
- Highly active antiretroviral therapy (HAART), 203
- Histiocytoma, fibrous, nodular fasciitis *vs.*, 501
- Histiocytosis
  - Langerhans cell, of neck, 504–508, 505*b*, 506*f*–507*f*, 507*b*
  - sinus, with massive lymphadenopathy, 502–504, 503*b*, 504*f*
- Histiocytosis X, 504–505
- HL. *see* Hairy leukoplakia
- Hobnail variant, of papillary thyroid carcinoma, 643
- Hodgkin lymphoma
  - invasive fibrous thyroiditis *vs.*, 561
  - Langerhans cell histiocytosis *vs.*, 507–508
- Holmer-Miller sign, 42
- Homer Wright pseudorosettes, 78–80, 79*f*
- Hormones, ectopic pituitary adenoma and, 47–50
- HPV. *see* Human papillomavirus
- HPV-related carcinoma with adenoid cystic-like features, 53–54, 54*f*
  - adenoid cystic carcinoma (ACC) *vs.*, 60
- HSV. *see* Herpes simplex virus
- HTT. *see* Hyalinizing trabecular tumor
- Human immunodeficiency virus (HIV)
  - lymphoepithelial cyst and, 254, 255*f*
  - multifocal epithelial hyperplasia and, 203
  - oral hairy leukoplakia and, 179
- Human papillomavirus (HPV)
  - metastatic squamous cell carcinoma and, 521, 523*f*
  - oral lesions associated with, 200

Human papillomavirus (HPV) (*Continued*)

- oral squamous cell carcinoma and, 219
- precursor squamous lesions and, 138
- sinonasal papillomas, 122
  - ancillary studies of, 123
  - differential diagnosis of, 123–124, 125*f*
  - microscopic findings in, 123, 124*f*
  - prognosis and therapy for, 124–125
  - vaccine for, 125
- Hyalinizing clear cell carcinoma, 348
  - clear cell odontogenic carcinoma *vs.*, 429
- Hyalinizing trabecular tumor (HTT), 604, 608–613, 608*b*
  - ancillary studies of, 611, 612*f*
  - clinical findings on, 608
  - differential diagnosis of, 613
  - pathologic findings in, 609–611, 609*b*, 609*f*–611*f*
  - prognosis and therapy for, 613
- Hyams' grading system, for olfactory neuroblastoma, 80*t*
- Hygroma, cystic, of neck, 509–511, 509*b*
  - ancillary studies of, 510–511
  - clinical findings on, 509, 510*f*
  - differential diagnosis of, 511
  - pathologic findings in, 509–510, 510*f*–511*f*, 511*b*
  - prognosis and therapy for, 511
- Hypercalcemia, 724
- Hyperparathyroidism, 693
  - brown tumor of, 212
    - central giant cell lesion *vs.*, 412–414
  - parathyroid adenoma and, 701
  - primary, parathyroid carcinoma and, 713
  - secondary, 700
- Hyperparathyroidism-jaw tumor (HPT-JT) syndrome
  - parathyroid adenoma in, 703
  - parathyroid carcinoma in, 693, 713
- Hyperplasia. *see also* Diffuse hyperplasia (Graves disease); Parathyroid hyperplasia; Pseudoepitheliomatous hyperplasia
  - angiolymphoid, with eosinophilia, 441–444, 442*b*
    - clinical findings on, 441–442
    - differential diagnosis of, 442
    - lobular capillary hemangioma *vs.*, 207
    - pathologic findings in, 442, 442*b*, 443*f*
    - prognosis and therapy for, 444
  - basal zone, 116*f*, 142
  - intercalated duct, 258–260, 259*b*, 259*f*
  - keratinizing, verrucous squamous cell carcinoma *vs.*, 148
  - multifocal epithelial, 203–205, 203*b*–204*b*, 203*f*–204*f*
  - oncocytic, 241–242, 241*b*–242*b*, 242*t*, 243*f*–244*f*, 272
  - reactive papillary, 202
  - verrucous, 115–116, 117*f*
- Hyperplastic candidiasis, 181, 184*f*
- Hyperplastic squamous proliferations, 142
- Hyperthyroidism. *see* Diffuse hyperplasia (Graves disease)
- Hypoparathyroidism, 700



- Hypopharynx. *see also specific lesion or neoplasm*  
 benign neoplasms of, 122–137  
   adult rhabdomyoma, 129–131, 129b, 130f  
   chondroma, 131–134, 131b, 132f–133f  
   granular cell tumor, 125–129, 126b, 126f–128f  
   sinonasal papillomas, 122–125, 124f–125f  
 malignant neoplasms of, 138–174  
   chondrosarcoma, 170f–172f  
   metastatic/secondary tumors of, 173–174, 173b, 174f  
   neuroendocrine carcinoma, 164–168, 164b–165b, 165f–168f  
   precursor squamous lesions, 138–143, 138b–139b, 139f  
   squamous cell carcinoma, 143–148, 143b–144b, 144f–147f  
   squamous cell carcinoma variants, 148–164, 148b, 149t, 150f–163f, 152b, 155b, 161b, 163b  
 non-neoplastic lesions of, 101–121  
   amyloidosis, 107–110, 108b, 108f–110f  
   contact ulcer, 104–107, 105b, 105f–107f  
   reactive epithelial changes, 114–121, 114b–115b, 116f–121f  
 Hypothyroidism, in chronic lymphocytic thyroiditis, 562
- I**  
 Immunosuppressive agents, for  
   granulomatosis with polyangiitis, 18
- Infections  
   acute thyroiditis and, 552  
   of oral cavity and oropharynx, 181–185  
     clinical findings on, 181–183, 182f  
     differential diagnosis of, 184  
     pathologic finding of, 183–184  
     prognosis and therapy for, 185  
   rhinosinusitis and, 1  
   stellate abscesses in, 494  
 “Infiltrative” pattern, of neuroendocrine adenoma, 472, 473f
- Inflammatory myofibroblastic tumor, spindle cell squamous cell carcinoma *vs.*, 158, 159f
- Inflammatory myofibroblastic tumor (IMT), 134–137, 134b  
   ancillary studies of, 134–135, 136f  
   clinical features of, 134  
   differential diagnosis of, 135–137, 136f  
   pathologic features of, 134, 134b, 135f  
   prognosis and therapy for, 137
- In situ hybridization (ISH)  
   for Epstein-Barr virus, 180–181, 181f  
   for herpes simplex virus, 185f  
   for human papillomavirus, 123, 124f, 525, 526f  
   for sinonasal papillomas, 28–29
- Insular variant, of follicular adenoma, 596–599
- Intercalated duct hyperplasia, 258–260, 259b, 259f  
   ancillary studies of, 260  
   clinical features of, 259
- Intercalated duct hyperplasia (*Continued*)  
   differential diagnosis of, 260  
   pathologic features of, 259–260  
   prognosis and therapy for, 260
- Intercalated duct-type cells, 294
- Intermediate cells, of mucoepidermoid carcinoma, 284–285, 286f
- Intestinal-type adenocarcinoma, of sinonasal tract, 57–58, 59f, 60, 61f
- Intrathyroid epithelial thymoma/CASTLE, 678b, 680–681, 682f–683f
- Invasive fibrous thyroiditis, 557–561  
   ancillary studies of, 561  
   chronic lymphocytic thyroiditis *vs.*, 566–567  
   clinical findings on, 558  
   differential diagnosis of, 561  
   laboratory studies for, 558  
   pathologic findings in, 559–561, 559b, 559f–561f  
   prognosis and therapy for, 561  
   radiologic findings in, 558
- Invasive keratinizing-type squamous cell carcinoma, 233f
- Inverted papillomas, 23–26, 23t–24t, 26f–27f
- J**  
 Jugulotympanic paraganglioma, 735f, 736–737. *see also* Middle ear paragangliomas
- Juvenile (capillary) hemangioma (JH), 281–283, 281b–282b, 282f–283f
- Juvenile ossifying fibroma, of gnathic bones, 385–388, 386b  
   clinical features of, 386, 386f  
   differential diagnosis of, 387–388  
   pathologic features of, 386–387, 386b, 387f  
   prognosis and therapy for, 388  
   radiologic features of, 386
- Juvenile trabecular ossifying fibroma, 385–386
- K**  
 Kadish staging, for olfactory neuroblastoma, 80
- Kaposi sarcoma (KS), 224–227, 226b  
   ancillary studies of, 226  
   clinical features of, 225  
   differential diagnosis of, 226  
   lobular capillary hemangioma *vs.*, 207  
   pathologic features of, 225, 226b, 226f–227f  
   prognosis and therapy for, 227
- Keratinizing dysplasia of larynx, 138, 140f–141f
- Keratinizing hyperplasia of larynx, 148
- Keratinizing squamous cell carcinoma of nasopharynx, 71  
   of oral cavity and oropharynx, 223f  
   of sinonasal tract, 53, 53f
- Keratoses, 138  
   “church spire”, 148, 151f  
   laryngeal, 116–119, 116f, 118f
- Kikuchi-Fujimoto disease, 494
- Kimura disease, 442
- Kissing ulcer, 104–105, 105f
- Klebsiella rhinoscleromatis*, 12
- Koilocytes, 123, 200–201
- Koilocytosis, 116
- L**  
 Lane tumor. *see* Spindle cell “sarcomatoid” carcinoma
- Langerhans cell histiocytosis (LCH)  
   of ear and temporal bone, 457–460, 457b–458b, 458f–460f  
   of neck, 504–508, 505b, 506f–507f, 507b  
   sinus histiocytosis *vs.*, 503–504
- Langerhans cells, 505–507
- Langerin, 505–507, 507f
- Large cell carcinoma (LCC)  
   lymphoepithelial carcinoma *vs.*, 359  
   of salivary glands, 356–358, 356b
- Laryngeal intraepithelial neoplasia (LIN), 138
- Laryngeal paraganglioma, 738
- Laryngocoele, 110–114, 111b  
   clinical features of, 110–111  
   differential diagnosis of, 114  
   pathologic features of, 111–114, 111b, 112f–113f  
   prognosis and therapy for, 114
- Larynx. *see also specific lesion or neoplasm*  
   benign neoplasms of, 122–137  
     adult rhabdomyoma, 129–131, 129b, 130f  
     chondroma, 131–134, 131b, 132f–133f  
     granular cell tumor, 125–129, 126b, 126f–128f  
     sinonasal papillomas, 122–125, 124f–125f  
   malignant neoplasms of, 138–174  
     chondrosarcoma, 168–173, 169b–170b, 169f–172f  
     metastatic/secondary tumors of, 173–174, 173b, 174f  
     neuroendocrine carcinoma, 164–168, 164b–165b, 165f–168f  
     precursor squamous lesions, 138–143, 138b–139b, 139f  
     squamous cell carcinoma, 143–148, 143b–144b, 144f–147f  
     squamous cell carcinoma variants, 148–164, 148b, 149t, 150f–163f, 152b, 155b, 161b, 163b  
   non-neoplastic lesions of, 101–121  
     amyloidosis, 107–110, 108b, 108f–110f  
     contact ulcer, 104–107, 105b, 105f–107f  
     cysts, 110–114, 111b, 112f–113f  
     reactive epithelial changes, 114–121, 114b, 116f–121f  
     vocal cord polyps and nodules, 101–104, 101b–102b, 102f–104f
- LCC. *see* Large cell carcinoma
- LCH. *see* Langerhans cell histiocytosis;  
   Lobular capillary hemangioma
- LEC. *see* Lymphoepithelial carcinoma
- Leiomyomas  
   glomangiopericytoma *vs.*, 38–40  
   of thyroid gland, 678b, 682–684, 684f

- Leiomyosarcoma (LMS)  
 of sinonasal tract, 92–94, 94f  
 of thyroid gland, 678b, 686, 687f
- Lepromatous leprosy, 503–504
- LESA. *see* Lymphoepithelial sialadenitis
- Letterer-Siwe disease, 504–505
- Leukoplakia  
 of larynx, 114–115  
 malignant transformation of, 138  
 in oral cavity, 219–220, 220f  
 oral hairy, 179–181, 180b, 183b  
   clinical findings on, 179, 179f  
   differential diagnosis of, 181  
   pathologic findings in, 179–181, 180b, 180f–181f  
   prognosis and therapy for, 181  
 proliferative verrucous, 202
- Lichen planus, oral, 186–188, 186b  
 ancillary studies of, 186–188  
 clinical findings on, 186, 186f  
 differential diagnosis of, 188  
 pathologic findings in, 186, 187f, 188b  
 prognosis and therapy for, 188
- Ligneous conjunctivitis, 102
- Lingual thyroid, 178, 178f, 546–548, 547b, 547f
- Lipoadenoma, 706–710
- Lipoma, spindle cell/pleomorphic, 517–520, 518b  
 ancillary studies of, 520  
 clinical findings on, 518  
 differential diagnosis of, 520  
 pathologic findings in, 518–519, 518f–519f, 520b  
 prognosis and therapy for, 520
- Liposarcoma, 520
- Lithium, 700
- LMS. *see* Leiomyosarcoma
- Lobular capillary hemangioma (LCH), 205–207, 205b  
 ancillary studies of, 207  
 angiolymphoid hyperplasia with eosinophilia *vs.*, 442  
 clinical features of, 205  
 differential diagnosis of, 207  
 Kaposi sarcoma *vs.*, 226  
 pathologic features of, 206, 206b, 206f–207f  
 peripheral ossifying fibroma *vs.*, 208–210  
 prognosis and therapy for, 207  
 of sinonasal tract, 29–33, 29b–30b, 30f–32f
- Lung carcinoma, to ear and temporal bone, 484–485
- Lymph nodes. *see also* Neck  
 radiologic imaging of, 52
- Lymphadenoma, sebaceous, 279–281, 279b, 279f–280f
- Lymphadenopathy  
 in cat scratch disease, 492  
 sinus histiocytosis with massive, 502–504, 503b, 504f
- Lymphangioma, of neck, 509–511, 509b  
 ancillary studies of, 510–511  
 clinical findings on, 509, 510f  
 differential diagnosis of, 511  
 pathologic findings in, 509–510, 510f–511f, 511b  
 prognosis and therapy for, 511
- Lymphocytic infiltrate, 252, 253f
- Lymphocytic thyroiditis  
 chronic (Hashimoto thyroiditis), 562–567, 562b  
   ancillary studies of, 566, 567f  
   clinical findings on, 562  
   differential diagnosis of, 566–567, 568f  
   diffuse hyperplasia *vs.*, 574  
   laboratory studies for, 563  
   pathologic findings in, 563–566, 563b, 563f–566f  
   primary thyroid gland lymphoma *vs.*, 675  
   prognosis and therapy for, 567  
   radiologic findings in, 562–563  
 papillary carcinoma and, 637f–638f, 638–639
- Lymphoepithelial carcinoma (LEC), 254  
 of salivary glands, 356b, 358–360, 359f
- Lymphoepithelial cysts, of salivary glands, 254–255, 255b, 255f–256f
- Lymphoepithelial lesion, of salivary glands, benign, 251, 252b, 253f–254f
- Lymphoepithelial-like (undifferentiated) carcinoma  
 of oropharynx, 235–236, 236f
- Lymphoepithelial sialadenitis (LESA), 251–254  
 ancillary studies of, 252  
 clinical features of, 251–252  
 differential diagnosis of, 252–254  
 extranodal marginal zone B-cell lymphoma and, 340, 341f  
 lymphoepithelial carcinoma *vs.*, 359  
 pathologic features of, 252  
 prognosis and therapy for, 254
- Lymphoma. *see also* B-cell lymphoma;  
 Extranodal NK/T-cell lymphoma  
 benign lymphoepithelial lesion *vs.*, 252–254  
 cat scratch disease *vs.*, 494  
 cutaneous CD30+ T-cell, 195  
 ectopic pituitary adenoma *vs.*, 50  
 follicular, 343  
 histiocytic, 503–504  
 Hodgkin  
   invasive fibrous thyroiditis *vs.*, 561  
   Langerhans cell histiocytosis *vs.*, 507–508  
 lymphoepithelial carcinoma *vs.*, 359  
 mantle cell, 82  
 mucosa-associated lymphoid tissue  
   benign salivary lymphoepithelial lesion and, 251–252  
   laryngeal amyloidosis and, 107  
   of thyroid gland, 667–668  
 neuroendocrine carcinoma *vs.*, 167–168  
 primary thyroid gland, 667–677  
 small cell carcinoma *vs.*, 240, 356  
 squamous cell carcinoma *vs.*, 222–224
- Lymphomatoid granulomatosis, nasal-type  
 extranodal NK/T-cell lymphoma *vs.*, 85
- M**
- Macrofollicular variant  
 of follicular adenoma, 596–599  
 of papillary thyroid carcinoma, 634–635, 634f–635f
- Magnetic resonance imaging, for squamous cell carcinoma of sinonasal tract, 52
- Malignant paraganglioma, 739–741, 739b  
 ancillary studies of, 740  
 clinical findings on, 739  
 differential diagnosis of, 740–741  
 pathologic findings in, 739–740, 740f, 741b  
 prognosis and therapy for, 741  
 radiologic findings in, 739
- Malignant peripheral nerve sheath tumor (MPNST), of thyroid gland, 678b, 685f, 686–687
- Malignant teratoma, of neck, 513–514
- Malignant transformation  
 of sinonasal papilloma, 23–26, 27f  
 of squamous papilloma, 124–125
- “MALT balls”, 669–670, 671f
- Mammary analogue secretory carcinoma, of salivary glands, 322–326, 323b  
 ancillary studies of, 326  
 clinical findings on, 322  
 differential diagnosis of, 326, 328f  
 pathologic findings in, 322–323, 323b, 324f–327f  
 prognosis and therapy for, 326
- Mantle cell lymphoma, 82
- McCune-Albright syndrome, 370
- Median rhomboid glossitis, 183, 184f
- Medication-related osteonecrosis (MRON), 373
- Medullary carcinoma, of thyroid gland, 656–667, 658b  
 ancillary studies of, 666–667, 666f  
 clear cell variant of papillary carcinoma *vs.*, 637  
 clinical findings on, 658–659  
 differential diagnosis of, 667  
 follicular carcinoma *vs.*, 604, 651–652  
 hyalinizing trabecular tumor, 613  
 neuroendocrine carcinoma *vs.*, 167–168  
 papillary carcinoma *vs.*, 630  
 paraganglioma *vs.*, 738t  
 parathyroid carcinoma *vs.*, 724  
 pathologic findings in, 632b, 659–662, 660b, 663f–665f  
 prognosis and therapy for, 667  
 radiologic findings in, 659, 659f  
 thyroglossal duct cyst with, 543
- Melanoma. *see also* Oral mucosal melanoma  
 ectopic pituitary adenoma *vs.*, 50  
 lobular capillary hemangioma *vs.*, 207  
 metastatic, to lymph nodes, 529, 530f  
 primary thyroid gland lymphoma *vs.*, 675  
 small cell carcinoma *vs.*, 356  
 spindle cell squamous cell carcinoma *vs.*, 158  
 squamous cell carcinoma *vs.*, 222–224  
 undifferentiated thyroid carcinoma *vs.*, 656
- Melanotic neuroectodermal tumor of infancy, 74–77, 77f
- Membranous variant, of acinic cell carcinoma, 348, 348f
- MEN1* gene  
 genes associated with parathyroid neoplasms in, 724t  
 parathyroid adenoma and, 711  
 parathyroid carcinoma and, 713–714



- Meningioma  
 of ear and temporal bone, 467–470, 468*b*  
 ancillary studies of, 468–469, 470*f*  
 clinical findings on, 467–468  
 differential diagnosis of, 469–470  
 neuroendocrine adenoma *vs.*, 474  
 paraganglioma *vs.*, 466–467  
 pathologic findings in, 468, 468*b*, 469*f*  
 peripheral nerve sheath tumor (schwannoma) *vs.*, 462–463  
 prognosis and therapy for, 470  
 radiologic findings in, 468  
 extracranial, active ossifying fibroma *vs.*, 387–388  
 paraganglioma *vs.*, 738*t*  
 of sinonasal tract, 33–35, 33*b*–34*b*, 34*f*–35*f*
- Meningocele, 469–470  
 meningioma *vs.*, 35
- Merkel cell carcinoma, cutaneous, 356
- Merkel type, of small cell carcinoma, 357*f*
- Mesenchymal chondrosarcoma, of gnathic bones, 421–423, 422*b*  
 ancillary studies of, 422  
 clinical findings on, 422  
 differential diagnosis of, 423  
 pathologic findings in, 422, 422*b*, 423*f*  
 prognosis and therapy for, 423  
 radiologic findings in, 422
- Mesenchymal malignancies, of sinonasal tract and nasopharynx, 64*t*–65*t*, 86  
 angiosarcoma *as*, 94–95, 95*f*  
 biphenotypic sinonasal sarcoma *as*, 92, 93*f*  
 fibrosarcoma *as*, 91–92, 92*f*  
 leiomyosarcoma *as*, 92–94, 94*f*  
 rhabdomyosarcoma *as*, 64*t*–65*t*, 86–91, 88*f*–89*f*
- Mesenchymal tumors, of thyroid gland, 682–687
- Metaplasia  
 laryngeal, 116  
 oncocytic, 241–242, 241*b*–242*b*, 242*t*, 243*f*–244*f*, 272
- Metastasizing pleomorphic adenoma, 340, 340*f*
- Metastatic cystic squamous cell carcinoma  
 branchial cleft cyst *vs.*, 490–492  
 first branchial cleft anomalies *vs.*, 435–436  
 lymphoepithelial cyst *vs.*, 255
- Metastatic gonadal teratoma, 514–515
- Metastatic melanoma, to lymph nodes, 529, 530*f*
- Metastatic neoplasms. *see also*  
 Adenocarcinoma, metastatic; Breast carcinoma/adenocarcinoma;  
 Carcinoma, metastatic; Renal cell carcinoma, metastatic  
 cat scratch disease *vs.*, 494  
 of ear and temporal bone, 484–487, 485*b*  
 ancillary studies of, 487  
 clinical findings on, 484  
 differential diagnosis of, 487  
 pathologic findings in, 484–485, 485*b*, 485*f*–486*f*  
 prognosis and therapy for, 487
- Metastatic neoplasms (*Continued*)  
 epithelial-myoepithelial carcinoma *vs.*, 322  
 of larynx or hypopharynx, 173–174, 173*b*  
 clinical findings on, 173  
 differential diagnosis of, 173–174  
 pathologic findings in, 173, 173*b*, 174*f*  
 prognosis and treatment for, 174  
 medullary carcinoma *vs.*, 667  
 neuroendocrine carcinoma *vs.*, 167–168  
 papillary carcinoma *vs.*, 630  
 of parathyroid gland, 725–727, 726*b*  
 clinical features of, 726  
 pathologic findings in, 726–727, 726*b*, 726*f*–727*f*  
 prognosis and therapy for, 727  
 salivary gland, metastatic squamous cell carcinoma *vs.*, 527–528  
 small cell carcinoma *vs.*, 356  
 of thyroid gland, 687–691, 687*b*  
 ancillary studies of, 689, 690*f*–691*f*  
 clinical findings on, 687–688, 688*f*–689*f*  
 differential diagnosis of, 691, 691*f*  
 pathologic findings in, 688–689, 689*b*  
 prognosis and therapy for, 691  
 undifferentiated thyroid carcinoma *vs.*, 656  
 of unknown primary, 528–530, 528*b*  
 ancillary studies of, 529–530, 531*t*  
 clinical findings on, 528  
 differential diagnosis of, 530  
 pathologic findings in, 529, 529*f*–530*f*, 530*b*  
 prognosis and therapy for, 530
- Metastatic neuroendocrine neoplasms, paraganglioma *vs.*, 738*t*
- Metastatic papillary thyroid carcinoma  
 angiolymphoid hyperplasia with eosinophilia *vs.*, 442  
 endolymphatic sac tumor *vs.*, 477  
 lymphangioma *vs.*, 511
- Metastatic squamous cell carcinoma, of neck, 521–528, 521*b*  
 ancillary studies of, 524–527, 526*f*  
 differential diagnosis of, 527–528  
 pathologic findings in, 522–524, 522*b*, 523*f*–525*f*  
 prognosis and therapy for, 528  
 radiologic findings in, 522, 522*f*
- Microcystic type, of acinic cell carcinoma, 294–295, 296*f*, 297–300
- Microscopic medullary thyroid carcinoma, 660, 663*f*
- Middle ear adenoma. *see* Neuroendocrine adenoma of middle ear
- Middle ear corpuscles, 481
- Middle ear paragangliomas, 733, 736–737, 738*t*
- Mikulicz cells, 13, 14*f*
- Minimally invasive follicular carcinoma, 648
- Mitosoid cells, 201–202, 204*f*
- Mixed tumor. *see* Pleomorphic adenoma
- MMP. *see* Mucous membrane pemphigoid
- Molecular analysis  
 of follicular thyroid carcinoma, 651  
 of medullary thyroid carcinoma, 667  
 of papillary thyroid carcinoma, 628–630  
 of undifferentiated thyroid carcinoma, 656
- Molecular genetics  
 of Ewing sarcoma, 96  
 of extranodal NK/T-cell lymphoma, nasal type, 85  
 of Langerhans cell histiocytosis, 507
- Monocytoid B-cells, 669–670
- Monophasic synovial sarcoma, 532–533, 532*f*, 535*f*, 536
- Monostotic fibrous dysplasia, 370
- Mucin, allergic, 8–9, 9*f*
- Mucocele  
 Fordyce granules *vs.*, 176  
 paranasal sinus, 6–7, 6*b*–7*b*, 7*f*–8*f*  
 of salivary glands, 244–248, 245*f*–246*f*, 247*b*
- Mucocutaneous candidiasis, chronic, 181
- Mucocytes, of mucoepidermoid carcinoma, 285, 287*f*–289*f*, 292*f*
- Mucoepidermoid carcinoma (MEC)  
 ceruminous, 482, 484  
 epithelial-myoepithelial carcinoma *vs.*, 322  
 lymphoepithelial cysts *vs.*, 255  
 mucus retention cyst *vs.*, 248  
 necrotizing sialometaplasia *vs.*, 250  
 oncocytoma *vs.*, 244  
 rhinoscleroma *vs.*, 13–14  
 of salivary glands, 242, 284–293, 284*b*  
 ancillary studies of, 290–291, 291*f*–292*f*  
 clinical findings on, 284, 285*f*  
 differential diagnosis of, 291–293, 292*f*  
 pathologic findings in, 284–286, 285*f*–286*f*, 287*b*  
 prognosis and therapy for, 293  
 tumor grading, 287–288, 290*f*, 291*t*  
 of thyroid gland, 677–679, 677*f*, 678*b*
- Mucosa-associated lymphoid tissue (MALT) lymphoma  
 benign salivary lymphoepithelial lesion and, 251–252  
 laryngeal amyloidosis and, 107  
 of thyroid gland, 667–668
- Mucosal melanoma. *see also* Oral mucosal melanoma  
 malignant, differential diagnosis of, 64*t*–65*t*  
 neuroendocrine carcinoma *vs.*, 167–168  
 of sinonasal tract, 72–77, 73*b*  
 ancillary studies of, 74, 76*f*  
 clinical features of, 72–73, 73*f*  
 differential diagnosis of, 74–77, 77*f*  
 pathologic features of, 73–74, 73*b*, 74*f*–76*f*
- Mucous membrane pemphigoid (MMP), 188–190, 189*b*  
 ancillary studies of, 189, 190*f*  
 clinical findings on, 188, 188*f*  
 differential diagnosis of, 190  
 pathologic findings in, 188, 189*b*, 189*f*  
 prognosis and therapy for, 190
- Mucus retention cyst, of salivary glands, 244–248, 247*b*  
 clinical features of, 244–245, 245*f*–246*f*  
 differential diagnosis of, 248  
 pathologic features of, 247–248, 247*b*, 248*f*  
 prognosis and therapy for, 248  
 radiologic features of, 247

Multifocal epithelial hyperplasia, 203–205, 203b–204b, 203f–204f  
 Multiple endocrine neoplasia (MEN), medullary thyroid carcinoma in, 656–658  
 Mummification, cellular, 626f, 627  
 Mycetoma, allergic fungal sinusitis vs., 9–10, 10f  
 Myeloid sarcoma, primary thyroid gland lymphoma vs., 675  
 Myoepithelioma  
   epithelial-myoepithelial carcinoma vs., 322  
   pleomorphic adenoma vs., 264  
   rhinoscleroma vs., 13–14  
 Myofibroblastic tumor, inflammatory, 158, 159f  
 Myxoid chondrosarcoma, 420, 421f  
 Myxoma  
   lipoma vs., 520  
   odontogenic, 368  
   vocal cord polyps/nodules vs., 102

## N

NAME. *see* Neuroendocrine adenoma of middle ear  
 Nasal cavity. *see also specific lesion or neoplasm*  
   benign neoplasms of, 22–50  
     ectopic pituitary adenoma as, 46–50, 47b, 48f–49f  
     glomangiopericytoma (sinonasal-type hemangiopericytoma) as, 35–40, 36b, 37f–41f  
     lobular capillary hemangioma as, 29–33, 29b–30b, 30f–32f  
     meningioma as, 33–35, 33b–34b, 34f–35f  
     nasopharyngeal angiofibroma as, 40–45, 41b, 42f–46f, 43b  
     sinonasal papillomas as, 22–29, 23f–28f, 23t–24t  
   malignant neoplasms of, 51–100  
     differential diagnosis of, 64t–65t  
     Ewing sarcoma as, 95–97, 95b–96b, 97f–98f  
     extranodal NK/T-cell lymphoma as, 82–86, 82f–86f, 83b–84b  
     mesenchymal, 86  
     mucosal melanoma as, 72–77, 73b, 73f–77f  
     nasopharyngeal carcinoma as, 69–72, 69b–70b, 70f–72f  
     NUT carcinoma as, 66–68, 66b–67b, 67f–68f  
     olfactory neuroblastoma as, 77–82, 78b, 78f–79f, 80t, 81f  
     sinonasal adenocarcinoma as, 57–61, 57b–58b, 59f–60f  
     sinonasal undifferentiated carcinoma as, 61–66, 62b, 62f–63f, 64t–65t, 66f  
     squamous cell carcinoma as, 51–57, 52b, 53f–56f  
     teratocarcinosarcoma as, 97–100, 99b, 99f–100f  
   non-neoplastic lesions of, 1–21  
     allergic fungal sinusitis as, 8–10, 8b, 9f–10f, 10b

Nasal cavity (*Continued*)  
   granulomatosis with polyangiitis as, 16–18, 17f, 18b  
   nasal glial heterotopia as, 10–12, 11f, 12b  
   paranasal sinus mucocele as, 6–7, 6b–7b, 7f–8f  
   rhinoscleroma as, 12–14, 13b, 13f–14f  
   rhinosinusitis as, 1–2, 1b–2b, 2f–3f  
   rhinosporidiosis as, 15–16, 15b–16b, 15f  
   sinonasal hamartomas as, 18–21, 19b, 19f–21f, 21b  
   sinonasal inflammatory polyps as, 2–6, 4b, 4f–6f  
 Nasal glial heterotopia (NGH), 10–12, 11f  
 Nasopalatine duct cyst, 376–377, 376b–377b, 377f  
 Nasopharyngeal angiofibroma (NPA), 40–45, 41b, 43b  
   ancillary studies of, 45  
   differential diagnosis of, 45  
   lobular capillary hemangioma vs., 33  
   meningioma vs., 35  
   pathologic features of, 42–45, 42f–46f  
   radiologic features of, 42  
   sinonasal inflammatory polyp vs., 5–6  
   staging system for, 42t  
 Nasopharyngeal carcinoma (NPC), 69–72, 69b  
   ancillary studies of, 71, 72f  
   basaloid squamous cell, 71  
   differential diagnosis of, 71–72  
   keratinizing squamous cell, 71  
   lymphoepithelial carcinoma vs., 359  
   nonkeratinizing, 70–71, 70f–71f  
   pathologic features of, 70–71, 70b  
   radiologic features of, 69  
 Nasopharynx. *see also specific lesion or neoplasm*  
   benign neoplasms of, 22–50  
     ectopic pituitary adenoma as, 46–50, 47b, 48f–49f  
     glomangiopericytoma (sinonasal-type hemangiopericytoma) as, 35–40, 36b, 37f–41f  
     lobular capillary hemangioma as, 29–33, 29b–30b, 30f–32f  
     meningioma as, 33–35, 33b–34b, 34f–35f  
     nasopharyngeal angiofibroma as, 40–45, 41b, 42f–46f, 43b  
     sinonasal papillomas as, 22–29, 23f–28f, 23t–24t  
   malignant neoplasms of, 51–100  
     B-cell lymphoma as, 82  
     differential diagnosis of, 64t–65t  
     Ewing sarcoma as, 95–97, 95b–96b, 97f–98f  
     extranodal NK/T-cell lymphoma as, 82–86, 82f–86f, 83b–84b  
     mesenchymal, 86  
     mucosal melanoma as, 72–77, 73b, 73f–77f  
     nasopharyngeal carcinoma as, 69–72, 69b–70b, 70f–72f  
     NUT carcinoma as, 66–68, 66b–67b, 67f–68f

Nasopharynx (*Continued*)  
   olfactory neuroblastoma as, 77–82, 78b, 78f–79f, 80t, 81f  
   sinonasal adenocarcinoma as, 57–61, 57b–58b, 59f–60f  
   sinonasal undifferentiated carcinoma as, 61–66, 62b, 62f–63f, 64t–65t, 66f  
   squamous cell carcinoma as, 51–57, 52b, 53f–56f  
   teratocarcinosarcoma as, 97–100, 99b, 99f–100f  
   non-neoplastic lesions of, 1–21  
     allergic fungal sinusitis as, 8–10, 8b, 9f–10f, 10b  
     granulomatosis with polyangiitis as, 16–18, 17f, 18b  
     nasal glial heterotopia as, 10–12, 11f, 12b  
     paranasal sinus mucocele as, 6–7, 6b–7b, 7f–8f  
     rhinoscleroma as, 12–14, 13b, 13f–14f  
     rhinosinusitis as, 1–2, 1b–2b, 2f–3f  
     rhinosporidiosis as, 15–16, 15b–16b, 15f  
     sinonasal hamartomas as, 18–21, 19b, 19f–21f, 21b  
     sinonasal inflammatory polyps as, 2–6, 4b, 4f–6f  
 Neck. *see also specific lesion or neoplasm*  
   benign neoplasm of, 509–520  
     ectopic hamartomatous thymoma (EHT), 515–517, 515b, 515f–517f, 517b  
     lymphangioma, 509–511, 509b, 510f–511f, 511b  
     spindle cell lipoma/pleomorphic lipoma, 517–520, 518b, 518f–519f, 520b  
     teratoma, 512–515, 512b, 512f–514f, 514b  
   malignant neoplasms of, 521–541  
     chordoma, 537–541, 537b–538b, 538f–541f  
     metastatic neoplasm of unknown primary, 528–530, 528b, 529f–530f, 530b, 531t  
     metastatic squamous cell carcinoma, 521–528, 521b–522b, 522f–527f  
     synovial sarcoma, 531–537, 531b–532b, 532f–537f  
   non-neoplastic lesions of, 488–508  
     bacillary angiomatosis, 494–495, 494b–495b, 495f  
     branchial cleft anomalies, 488–492, 488b, 489f–491f, 490b  
     cat scratch disease, 492–494, 492b–493b, 493f  
     cervical actinomycosis, 496–497, 496f, 497b  
     Langerhans cell histiocytosis, 504–508, 505b, 506f–507f, 507b  
     nodular fasciitis, 497–501, 498b, 498f–502f, 500b  
     sinus histiocytosis with massive lymphadenopathy, 502–504, 503b, 504f  
 Necrotizing (malignant) external otitis, 445–446



- Necrotizing sialometaplasia (NS)  
adenosquamous carcinoma *vs.*, 164  
of larynx, 119–120, 120f  
mucoepidermoid carcinoma *vs.*, 291, 292f  
of salivary glands, 248–251, 249b  
clinical features of, 248–249, 249f  
differential diagnosis of, 250  
pathologic features of, 249–250, 249b,  
250f–251f  
prognosis and therapy for, 251  
squamous cell carcinoma *vs.*, 147,  
222–224
- Neurilemmoma. *see* Peripheral nerve sheath tumor
- Neuroblastoma, olfactory. *see* Olfactory neuroblastoma
- Neuroendocrine adenoma of middle ear (NAME), 470–474, 471b  
ancillary studies of, 472–474, 473f–474f  
ceruminous adenoma *vs.*, 454–455  
clinical findings on, 470–471, 471f  
differential diagnosis of, 474  
endolymphatic sac tumor *vs.*, 477  
histochemical findings in, 474  
meningioma *vs.*, 469–470  
paraganglioma *vs.*, 466–467  
pathologic findings in, 471–472, 472b,  
472f–473f  
prognosis and therapy for, 474
- Neuroendocrine carcinoma, 108b, 164–168, 164b  
ancillary studies of, 167, 168f  
basaloid squamous cell carcinoma *vs.*, 160–161  
clinical findings on, 164  
differential diagnosis of, 167–168  
large cell, 356  
pathologic findings in, 164–167, 165b,  
165f–167f  
prognosis and therapy for, 168  
sinonasal undifferentiated carcinoma *vs.*, 63  
squamous cell carcinoma *vs.*, 55–56
- Neuroendocrine differentiation, immunohistochemical separation of neck tumors with, 738t
- Neurofibroma  
lipoma *vs.*, 520  
peripheral nerve sheath tumor *vs.*, 462–463
- Neurofibromatosis  
type 1, 729t  
type 2, 460
- Neuroma  
acoustic. *see* Peripheral nerve sheath tumor  
medullary thyroid carcinoma *vs.*, 658–659
- Nevoid basal cell carcinoma syndrome (NBCCS), 403–404
- NF1 gene, 728
- NF2 gene, 462
- NGH. *see* Nasal glial heterotopia
- Nikolsky sign, 188, 190
- Nocardia, 184
- Nodular fasciitis, 497–501, 498b  
ancillary studies of, 500–501  
clinical findings on, 497  
differential diagnosis of, 501, 502f
- Nodular fasciitis (*Continued*)  
pathologic findings in, 497–500, 498f–500f, 500b  
prognosis and therapy for, 501  
radiologic findings in, 497
- Nodular hyperplasia (multinodular goiter), 575–583, 575b  
ancillary studies of, 582, 582f–583f  
clinical findings on, 575  
differential diagnosis of, 582–583  
laboratory studies for, 576  
pathologic findings in, 576–582, 576b,  
577f–581f  
prognosis and therapy for, 583  
radiologic findings in, 575, 576f
- Nodular oncocytic hyperplasia (NOH), 241–242, 241b–242b, 242t, 243f–244f
- Nodules, vocal cord, 101–104, 101b–102b, 102f
- Non-salivary gland-type adenocarcinoma, sinonasal, 57  
intestinal-type, 57–58, 59f, 60, 61f  
nonintestinal-type, 57–60, 60f
- Nonintestinal-type adenocarcinoma, sinonasal, 57–60, 60f
- Noninvasive follicular thyroid neoplasm, with papillary-like nuclear findings, 604–607, 605b, 605f  
ancillary studies of, 606–607  
clinical findings on, 604  
differential diagnosis of, 607  
pathologic findings in, 605–606, 606b,  
606f–607f  
prognosis and therapy for, 607  
radiographic findings on, 604
- Nonkeratinizing squamous cell carcinoma of nasopharynx, 70–71, 70f–71f  
of oral cavity and oropharynx, 233f–234f  
of sinonasal tract, 54, 54f
- Nonspecific glandular cells, 294
- Notochord  
benign tumors of, 541  
chordoma of, 537
- NPA. *see* Nasopharyngeal angiofibroma
- NPC. *see* Nasopharyngeal carcinoma
- Nuchal fibroma, 520
- Nuchal-type fibroma, lipoma *vs.*, 520
- Nuclear scintigraphy, of parathyroid adenoma, 704, 704f
- NUT carcinoma, 66–68, 66b  
ancillary studies of, 68, 68f  
differential diagnosis of, 68  
pathologic features of, 67–68, 67b, 67f  
sinonasal undifferentiated carcinoma *vs.*, 63  
squamous cell carcinoma *vs.*, 55–56
- O**
- Occult primary tumor, 528
- Odontogenic carcinoma, of gnathic bones  
ghost cell, 429–430, 430b  
clinical findings on, 430  
differential diagnosis of, 430  
pathologic findings in, 430, 430b, 431f  
prognosis and therapy for, 430  
radiologic findings in, 430  
sclerosing, 426–428, 426b  
ancillary studies of, 427  
clinical findings on, 426  
differential diagnosis of, 427–428
- Odontogenic carcinoma, of gnathic bones (*Continued*)  
pathologic findings in, 426–427, 427b, 427f  
prognosis and therapy for, 428  
radiologic findings in, 426
- Odontogenic cyst, inflammatory, 368
- Odontogenic fibroma, of gnathic bones, central, 388–390, 388b  
clinical features of, 388  
differential diagnosis of, 390  
pathologic features of, 388, 389f–390f, 390b  
prognosis and therapy for, 390  
radiologic features of, 388, 389f  
sclerosing odontogenic carcinoma *vs.*, 427–428
- Odontogenic keratocyst, of gnathic bones, 403–406, 404b  
clinical features of, 403–404  
differential diagnosis of, 405–406  
pathologic features of, 404–405, 405b, 405f–406f  
prognosis and therapy for, 406  
radiologic features of, 404f
- Odontogenic myxoma, dentigerous cyst *vs.*, 368
- Odontogenic sarcoma, of gnathic bones, 431–432, 431b–432b, 432f
- Odontogenic tumor, of gnathic bones  
adenomatoid, 409–411, 409b  
ancillary studies of, 411  
clinical features of, 409  
differential diagnosis of, 411  
pathologic features of, 409–410, 410b  
prognosis and therapy for, 411  
radiologic features of, 409, 410f–411f  
calcifying epithelial, 406–409, 406b  
ancillary studies of, 407  
clinical features of, 406  
differential diagnosis of, 408  
pathologic features of, 407, 407f–408f, 409b  
prognosis and therapy for, 408–409  
radiologic features of, 407, 407f  
squamous, sclerosing odontogenic carcinoma *vs.*, 427–428
- Odontoma  
ameloblastic, 399–402  
of gnathic bones, 414–416, 414b  
clinical features of, 414  
differential diagnosis of, 415–416  
pathologic features of, 414–415, 415b, 415f–416f  
prognosis and therapy for, 416  
radiologic features of, 414, 415f
- Olfactory neuroblastoma (ONB), 77–82, 78b  
ancillary studies of, 80–81, 81f  
differential diagnosis of, 64t–65t, 81  
ectopic pituitary adenoma *vs.*, 50  
Hyams' grading system for, 80t  
meningioma *vs.*, 35  
NUT carcinoma *vs.*, 68  
pathologic features of, 78–80, 78b, 79f–80f  
radiographic features of, 77, 78f  
sinonasal undifferentiated carcinoma *vs.*, 63

- OLP. *see* Oral lichen planus
- Oncocytes/oncocyctic cells
- of parathyroid adenoma, 706–710
  - of parathyroid gland
    - primary chief cell hyperplasia and, 693–700, 693b–694b, 694f–698f
    - secondary and tertiary hyperplasia and, 700–702, 700b–701b, 701f–702f
  - of salivary glands, 242, 243f
- Oncocyctic adenoma, 594, 599, 600f, 602f
- Oncocyctic carcinoma
- oncocyctoma *vs.*, 274
  - of salivary glands, 351b, 354, 354f–355f
- Oncocyctic cell papillomas, 22, 23t–24t, 26–28, 28f
- Oncocyctic hyperplasia, 241–242, 241b–242b, 242t, 243f–244f, 272
- Oncocyctic metaplasia, 241–242, 241b–242b, 242t, 243f–244f, 272
- Oncocyctic variant
- of follicular thyroid carcinoma, 646f, 648–650, 649f
  - of papillary thyroid carcinoma, 635–637, 636f
- Oncocyctoma
- adult rhabdomyoma *vs.*, 131
  - epithelial-myoepithelial carcinoma *vs.*, 322
  - of salivary glands, 272–275, 272b
  - ancillary studies of, 274
  - canalicular adenoma *vs.*, 272–274
  - clinical findings on, 272
  - differential diagnosis of, 274
  - electron microscopy for, 274, 275f
  - histochemical findings of, 274
  - oncocytosis in, 242
  - pathologic findings in, 272–274, 273f–275f, 274b
  - prognosis and therapy for, 275
- Oncocytosis, of salivary glands, 241–244, 241b–242b, 242t, 243f–244f
- oncocyctoma and, 272
- Oral cavity and oropharynx. *see also specific lesion or neoplasm*
- benign neoplasms of, 197–218
    - congenital granular cell epulis, 214–217, 215b, 215f–216f
    - fibroma, 197–198, 197b–198b, 198f–199f
    - lobular capillary hemangioma, 205–207, 205b–206b, 206f–207f
    - multifocal epithelial hyperplasia, 203–205, 203b–204b, 203f–204f
    - peripheral giant cell granuloma, 208–212, 210b, 210f–212f, 212b
    - peripheral ossifying fibroma, 207–210, 208b, 208f–209f
    - squamous papilloma, 200–203, 200b–201b, 200f–202f
  - malignant neoplasms of, 219–240
    - Kaposi sarcoma, 224–227, 226b, 226f–227f
    - oral mucosal melanoma, 227–229, 228f
    - small cell carcinoma, 237–240
    - squamous cell carcinoma, 219–224, 219b, 220f–225f, 221b, 230–237, 230b, 231f, 233f–235f, 238f
- Oral cavity and oropharynx (*Continued*)
- non-neoplastic lesions of, 175–196
    - amalgam tattoo, 176–177, 176f–177f, 177b
    - ectopic thyroid, 178–179, 178b, 178f–179f
    - Fordyce granules, 175–176, 175b, 175f–176f
    - hairy leukoplakia, 179–181, 179f–180f, 180b
    - infections, 181–185, 182f
    - mucous membrane pemphigoid, 188–190, 188f–190f, 189b
    - oral lichen planus, 186–188, 186b, 186f–187f, 188b
    - pemphigus vulgaris, 190–192, 190f–192f, 191b
    - recurrent aphthous stomatitis, 192–194, 193b–194b, 193f
    - traumatic ulcerative granuloma, 194–196, 194f–196f, 195b
- Oral hairy leukoplakia (OHL), 179–181, 180b
- clinical findings on, 179, 179f
  - differential diagnosis of, 181
  - pathologic findings in, 179–181, 180b, 180f–181f
  - prognosis and therapy for, 181
- Oral lichen planus (OLP), 186–188, 186b
- ancillary studies of, 186–188
  - clinical findings on, 186, 186f
  - differential diagnosis of, 188
  - pathologic findings in, 186, 187f, 188b
  - prognosis and therapy for, 188
- Oral mucosal melanoma (OMM), 227–229, 227b, 228f
- ancillary studies of, 228–229, 229f
  - clinical features of, 227–228
  - differential diagnosis of, 229
  - pathologic features of, 228, 228b
  - prognosis and therapy for, 229
- Organ of Zuckerkandl, 728
- Oropharyngeal carcinoma
- nasopharyngeal carcinoma *vs.*, 71–72
  - squamous cell carcinoma *vs.*, 55–56
- Oropharynx. *see* Oral cavity and oropharynx
- Orphan Annie nuclei, 623–627, 624f
- Orthokeratinized odontogenic cyst, odontogenic keratocyst *vs.*, 405–406
- Osseous dysplasia
- fibrous dysplasia *vs.*, 371
  - florid, 381
  - focal, 381
  - of gnathic bones, 381–382, 381b–382b, 382f
  - osteomyelitis *vs.*, 364
  - periapical, 381
- Ossifying fibroma
- of gnathic bones, 383–385, 383b
  - active, 385–388, 386b, 387f
  - clinical features of, 383, 386f
  - differential diagnosis of, 384–385
  - fibrous dysplasia *vs.*, 371
  - osseous dysplasia *vs.*, 381–382
  - pathologic features of, 384, 384b, 385f
- Ossifying fibroma (*Continued*)
- prognosis and therapy for, 384–385
  - radiologic features of, 383, 384f
  - of oral cavity
    - central, 207
    - peripheral, 207–210, 208b, 208f–209f
- Osteoblastoma, of gnathic bones, 390–392, 391b
- cementoblastoma *vs.*, 395
  - clinical features of, 390
  - differential diagnosis of, 391–392
  - pathologic features of, 391, 391f–392f, 392b
  - prognosis and therapy for, 392
  - radiologic features of, 390–391
- Osteoid osteoma, of gnathic bones, 391b, 392–393
- cementoblastoma *vs.*, 395
  - clinical features of, 392
  - differential diagnosis of, 393
  - pathologic features of, 391f–392f, 392–393, 392b
  - radiologic features of, 393
- Osteomyelitis, of gnathic bones, 363–366, 363b–364b, 365f
- fibrous dysplasia *vs.*, 371
  - osseous dysplasia *vs.*, 381–382
- Osteonecrosis, of gnathic bones, 373–375, 373b
- clinical findings on, 373
  - differential diagnosis of, 374
  - pathologic findings in, 373–374, 374b, 374f
  - prognosis and therapy for, 375
  - radiologic findings in, 373
- Osteoradionecrosis, 373
- Osteosarcoma, of gnathic bones, 417–419, 417b
- clinical findings on, 417, 418t
  - differential diagnosis of, 419
  - fibrous dysplasia *vs.*, 371
  - osteoblastoma *vs.*, 391–392
  - osteoid osteoma *vs.*, 393
  - pathologic findings in, 417–419, 418f–419f, 419b
  - prognosis and therapy for, 419
  - radiologic findings in, 417, 418f
- Otitis, external, necrotizing (malignant), 445–446
- P**
- PA. *see* Pleomorphic adenoma
- Paget disease, 364
- Palpation thyroiditis, granulomatous thyroiditis *vs.*, 554–555, 558f
- Papillary carcinoma, of thyroid gland, 619–632, 620b
- ancillary studies of, 627–630, 629f
  - clinical findings on, 619, 620f
  - differential diagnosis of, 630, 630f–631f
  - endolymphatic sac tumor *vs.*, 477
  - follicular carcinoma *vs.*, 630
  - histological variants of, 632–643
    - clear cell, 637, 637f
    - columnar, 640, 641f–642f
    - cribriform-morular, 640–643, 643f
    - diffuse sclerosing, 637f–638f, 638–639
    - encapsulated, 633, 633f



- Papillary carcinoma, of thyroid gland  
(*Continued*)  
  follicular, 633–634, 633f–634f  
  hobnail, 643  
  macrofollicular, 634–635, 634f–635f  
  oncocytic, 635–637, 636f  
  size variation, 643, 644f  
  solid, 640, 642f  
  spindle cell, 638  
  tall cell, 639, 639f–640f  
  metastatic, lymphangioma *vs.*, 511  
  pathologic findings in, 621–627, 621f–628f  
  prognosis and therapy for, 630–632, 631f  
  radiologic findings in, 620–621, 620f  
Papillary cystadenoma lymphomatosum, 275, 276b–277b, 277f–278f  
Papillary cystadenoma papilliferum, ceruminous, 454  
Papillary-cystic growth, of acinic cell carcinoma, 294–295  
Papillary-cystic variant, of acinic cell carcinoma, 297–300  
Papillary sinusitis, 2  
  sinonasal adenocarcinoma *vs.*, 60  
Papillary squamous cell carcinoma (PSCC)  
  of larynx, hypopharynx, and trachea, 150–152, 152b, 153f–154f  
  of oropharynx, 232, 234f  
  sinonasal papilloma *vs.*, 29  
  squamous papilloma *vs.*, 123–124, 202  
Papillary thyroid carcinoma  
  diffuse sclerosing variant of, invasive fibrous thyroiditis *vs.*, 561  
  metastatic, angiolymphoid hyperplasia with eosinophilia *vs.*, 442  
  thyroglossal duct cyst with, 543  
Papilloma. *see also* Squamous papilloma  
  choroid plexus, 477  
  koilocytosis in, 116  
  sinonasal, 22–29, 23f–28f, 23t–24t  
Parabasal hyperplasia, 138  
Paraganglia system diseases, 728–741. *see also specific disease*  
  malignant paraganglioma, 739–741, 739b, 740f, 741b  
  paraganglioma, 728–739, 729b, 729t, 730f–737f, 731b  
Paraganglioma, 463–467, 464b, 728–739, 729b  
  adult rhabdomyoma *vs.*, 131  
  ancillary studies of, 466, 467f, 733–736, 736f–737f  
  ceruminous adenoma *vs.*, 454–455  
  clinical findings on, 463–464, 728–730  
  differential diagnosis of, 466–467, 736–738, 738t  
  genetic syndromes associated with, 729t  
  granular cell tumor *vs.*, 127–128  
  hyalinizing trabecular tumor, 613  
  jugulotympanic, 735f  
  meningioma *vs.*, 35, 469–470  
  neuroendocrine adenoma *vs.*, 474  
  pathologic findings in, 464–466, 464b, 465f–466f, 730–733, 731b, 731f–735f  
  prognosis and therapy for, 467, 738–739  
  radiologic findings in, 464, 465f, 730, 730f  
Paraganglioma 1 (PGL1) genes, 466  
Paragangliomatosis, hereditary, 729t  
Parakeratosis, laryngeal, 116–119, 119f  
Paranasal sinus mucocele, 6–7, 6b–7b, 7f–8f  
Paranasal sinuses. *see also specific lesion or neoplasm*  
  benign neoplasms of, 22–50  
    ectopic pituitary adenoma *as*, 46–50, 47b, 48f–49f  
    glomangiopericytoma (sinonasal-type hemangiopericytoma) *as*, 35–40, 36b, 37f–41f  
    lobular capillary hemangioma *as*, 29–33, 29b–30b, 30f–32f  
    meningioma *as*, 33–35, 33b–34b, 34f–35f  
    nasopharyngeal angiofibroma *as*, 40–45, 41b, 42f–46f, 43b  
    sinonasal papillomas *as*, 22–29, 23f–28f, 23t–24t  
  malignant neoplasms of, 51–100  
    differential diagnosis of, 64t–65t  
    Ewing sarcoma *as*, 95–97, 95b–96b, 97f–98f  
    extranodal NK/T-cell lymphoma *as*, 82–86, 82f–86f, 83b–84b  
    mesenchymal, 86  
    mucosal melanoma *as*, 72–77, 73b, 73f–77f  
    nasopharyngeal carcinoma *as*, 69–72, 69b–70b, 70f–72f  
    NUT carcinoma *as*, 66–68, 66b–67b, 67f–68f  
    olfactory neuroblastoma *as*, 77–82, 78b, 78f–79f, 80t, 81f  
    sinonasal adenocarcinoma *as*, 57–61, 57b–58b, 59f–60f  
    sinonasal undifferentiated carcinoma *as*, 61–66, 62b, 62f–63f, 64t–65t, 66f  
    squamous cell carcinoma *as*, 51–57, 52b, 53f–56f  
    teratocarcinosarcoma *as*, 97–100, 99b, 99f–100f  
  non-neoplastic lesions of, 1–21  
    allergic fungal sinusitis *as*, 8–10, 8b, 9f–10f, 10b  
    granulomatosis with polyangiitis *as*, 16–18, 17f, 18b  
    nasal glial heterotopia *as*, 10–12, 11f, 12b  
    paranasal sinus mucocele *as*, 6–7, 6b–7b, 7f–8f  
    rhinoscleroma *as*, 12–14, 13b, 13f–14f  
    rhinosinusitis *as*, 1–2, 1b–2b, 2f–3f  
    rhinosporidiosis *as*, 15–16, 15b–16b, 15f  
    sinonasal hamartomas *as*, 18–21, 19b, 19f–21f, 21b  
    sinonasal inflammatory polyps *as*, 2–6, 4b, 4f–6f  
Paraneoplastic pemphigus (PNP), 190  
Parathyroid adenoma, 703–712, 703b  
  ancillary studies of, 710–711, 711f  
  carcinoma *vs.*, 722–724  
  clinical findings on, 703–704  
  differential diagnosis of, 711, 712f  
  genes associated with, 724t  
  paraganglioma *vs.*, 738t  
  pathologic findings in, 704–710, 705f–710f  
  prognosis and therapy for, 712  
Parathyroid adenoma (*Continued*)  
  radiographic findings of, 704, 704f  
  secondary or tertiary hyperplasia *vs.*, 701  
Parathyroid carcinoma, 713–724, 713b  
  adenoma *vs.*, 711  
  ancillary studies of, 722, 722f–723f  
  clinical findings on, 713–714  
  differential diagnosis of, 722–724, 725f  
  genes associated with, 724t  
  pathologic findings in, 714–722, 714b, 714f–721f  
  prognosis and therapy for, 724  
Parathyroid gland. *see also specific lesion or neoplasm*  
  benign neoplasms of, 703–712  
    adenoma, 703–712, 703b, 704f–712f, 705b  
  malignant neoplasms of, 713–727  
    carcinoma, 713–724, 713b–714b, 714f–720f  
    metastatic tumors, 725–727, 726b, 726f–727f  
  non-neoplastic lesions of, 692–702  
    primary chief cell hyperplasia, 693–700, 693b–694b, 694f–698f  
    secondary and tertiary hyperplasia, 700–702, 700b–701b, 701f–702f  
Parathyroid hormone (PTH), 692  
Parathyroid hyperplasia  
  adenoma *vs.*, 711  
  secondary and tertiary, 700–702, 700b–701b, 701f–702f  
  water-clear cell, 694–698  
Parathyroid tumors, follicular carcinoma *vs.*, 651–652  
Parathyromatosis, 722–724  
Parotid gland  
  anatomy of, 241  
  metastatic neoplasms from, 484–485, 486f  
PAX8 gene, 651  
PEH. *see* Pseudoepitheliomatous hyperplasia  
Pemphigoid, mucous membrane, 188–190, 189b  
  ancillary studies of, 189, 190f  
  clinical findings on, 188, 188f  
  differential diagnosis of, 190  
  pathologic findings in, 188, 189b, 189f  
  prognosis and therapy for, 190  
Pemphigus vulgaris (PV), 190–192, 191b  
  ancillary studies of, 191–192, 192f  
  clinical findings on, 190, 190f  
  differential diagnosis of, 192  
  pathologic findings in, 191, 191b, 191f  
  prognosis and therapy for, 192  
Periapical cyst, of gnathic bones, 368–370, 368b  
  clinical findings on, 368  
  differential diagnosis of, 370  
  pathologic findings in, 368–370, 369f, 370b  
  prognosis and therapy for, 370  
  radiologic findings in, 368  
Periapical osseous dysplasia, 381  
Perineural invasion, in parathyroid carcinoma, 714–722  
Periostitis, proliferative gnathic bone, 363–364, 365f  
Peripheral ameloblastomas, 395–396

- Peripheral giant cell granuloma (PGCG), 208–212, 210*b*, 210*f*–212*f*, 212*b*
- Peripheral nerve sheath tumor (PNST)  
of ear and temporal bone, 460–463, 461*b*  
ancillary studies of, 462  
clinical findings on, 461  
differential diagnosis of, 462–463  
meningioma *vs.*, 469–470  
paraganglioma *vs.*, 466–467  
pathologic findings in, 461–462, 461*b*, 462*f*–463*f*  
prognosis and therapy for, 463  
radiologic findings in, 461  
malignant, of thyroid gland, 678*b*, 685*f*, 686–687  
nasopharyngeal angiofibroma *vs.*, 45
- Peripheral ossifying fibroma (POF), 207–210, 208*b*, 208*f*–209*f*
- PGCG. *see* Peripheral giant cell granuloma
- Pheochromocytoma, 728, 729*t*
- Phlebectasia, external jugular, 114
- “Physaliphorous” cells, 538, 539*f*, 541, 541*f*
- Pilomatricomas, metastatic squamous cell carcinoma *vs.*, 527
- Pindborg tumor, 406. *see also* Calcifying epithelial odontogenic tumor
- Pituitary adenoma, ectopic, 46–50, 47*b*, 48*f*–49*f*
- Pleomorphic adenoma (PA)  
carcinoma *ex*, 335–340, 335*b*  
clinical findings on, 335, 335*f*  
differential diagnosis of, 340, 340*f*  
pathologic findings in, 335–336, 336*b*, 336*f*–339*f*  
prognosis and therapy for, 340  
ceruminous, 454  
chondroma *vs.*, 132–133, 133*f*  
chondrosarcoma *vs.*, 170–173  
chordoma *vs.*, 541  
epithelial-myoepithelial carcinoma *vs.*, 322  
metastasizing, 340, 340*f*  
oncocytoma *vs.*, 242  
polymorphous adenocarcinoma *vs.*, 314–316  
of salivary glands, 261–266, 261*b*  
ancillary studies of, 264, 265*f*  
clinical findings on, 261  
differential diagnosis of, 264, 265*f*–266*f*  
pathologic findings in, 261–262, 262*b*, 262*f*–264*f*  
prognosis and therapy for, 264–266  
of salivary glands, adenoid cystic carcinoma *vs.*, 308–309
- Pleomorphic carcinoma. *see* Undifferentiated carcinoma
- Pleomorphic lipoma, 517–520, 518*b*, 519*f*, 520*b*
- Pleomorphism, 115, 121
- Plexiform ameloblastoma, 400*f*–401*f*
- PLGA. *see* Polymorphous low-grade adenocarcinoma
- PNST. *see* Peripheral nerve sheath tumor
- POF. *see* Peripheral ossifying fibroma
- Polyangiitis, granulomatosis with, 16–18
- Polychondritis, relapsing, of ear, 444–446, 444*b*  
clinical findings on, 444, 445*f*  
cystic chondromalacia *vs.*, 437
- Polychondritis, relapsing, of ear (*Continued*)  
differential diagnosis of, 445–446  
pathologic findings in, 445, 445*b*, 445*f*–446*f*  
prognosis and therapy for, 446
- Polymerase chain reaction, for sinonasal papillomas, 28–29
- Polymorphous adenocarcinoma (PAC)  
adenoid cystic carcinoma *vs.*, 308–309  
of salivary glands, 309–317, 310*b*  
ancillary studies of, 314, 316*f*–317*f*  
clinical findings on, 309–310, 310*f*  
differential diagnosis of, 314–316  
pathologic findings in, 310–313, 311*f*–315*f*, 314*b*  
prognosis and therapy for, 317
- Polymorphous low-grade adenocarcinoma (PLGA), of salivary glands, 309, 310*b*  
adenoid cystic carcinoma *vs.*, 308–309
- Polyostotic fibrous dysplasia, 370
- Polypoid masses, 153
- Polyps. *see also* Sinonasal polyps  
nasopharyngeal angiofibroma *vs.*, 45  
vocal cords, 101–104, 101*b*  
clinical features of, 101  
differential diagnosis of, 102  
pathologic features of, 101–102, 102*b*, 102*f*–104*f*  
prognosis and therapy for, 102–104
- Positron emission tomography (PET), of cervical lymph nodes, 52
- PPAR $\gamma$  gene, 651
- Precursor lesion, of medullary thyroid carcinoma, 660, 662*f*–663*f*
- Precursor squamous lesions, of larynx, hypopharynx, and trachea, 138–143, 138*b*  
clinical findings on, 138–139, 139*f*  
differential diagnosis of, 142  
pathologic findings in, 139–141, 139*b*, 140*f*–142*f*, 140*t*  
prognosis and therapy for, 143
- Pregnancy tumor, gingival, 205
- “Pre-psammoma bodies”, 468–469, 470*f*
- Primary chief cell hyperplasia, of parathyroid gland, 693–700, 693*b*  
ancillary studies of, 698–699, 699*f*  
clinical findings on, 693  
differential diagnosis of, 699–700  
pathologic findings in, 694–698, 694*b*, 695*f*–698*f*  
prognosis and therapy for, 700  
radiologic findings in, 693–694, 694*f*
- Primary intraosseous carcinoma, of gnathic bones, 425–426, 425*b*–426*b*
- Primary thyroid gland lymphoma, 667–677, 668*b*  
ancillary studies of, 673–675, 674*f*–676*f*  
clinical findings on, 668, 668*f*  
differential diagnosis of, 675  
pathologic findings in, 668*f*–674*f*, 669–673, 669*b*  
prognosis and therapy for, 676–677
- Primitive neuroectodermal tumor (PNET). *see* Ewing sarcoma
- Prolactin, 47–50
- Prolapse of ventricle, laryngeal cyst *vs.*, 114
- Proliferative periostitis, of gnathic bones, 363–364, 365*f*
- Psammoma bodies  
in meningioma, 468–469, 470*f*  
in papillary thyroid carcinoma, 623–627, 625*f*–626*f*, 635–637, 637*f*–638*f*
- Psammomatoid ossifying fibroma, 385–386  
meningioma *vs.*, 35
- PSCC. *see* Papillary squamous cell carcinoma
- Pseudoepitheliomatous hyperplasia (PEH)  
granular cell tumor with, 127–128, 127*f*  
laryngeal, 116, 117*f*–118*f*  
squamous cell carcinoma *vs.*, 55–56
- Pseudomembranous candidiasis, 181, 182*f*
- Pseudorosettes  
in olfactory neuroblastoma, 78–80, 79*f*  
in paraganglioma, 736
- p16* gene, 220–221
- PTH. *see* Parathyroid hormone
- PV. *see* Pemphigus vulgaris
- Pyogenic granuloma, 29, 205–207, 205*b*–206*b*, 206*f*–207*f*. *see also* Contact ulcer; Lobular capillary hemangioma
- Pyostomatitis vegetans, 193–194
- R**
- Radiation changes  
to laryngeal epithelium, 115  
squamous cell carcinoma *vs.*, 147
- Ranula, 244–245
- RAS. *see* Recurrent aphthous stomatitis
- RAS gene, 602–603, 628–630
- RB1* gene, 713–714
- Reactive epithelial changes, of larynx, 114–121, 114*b*  
ancillary studies of, 120–121  
clinical features of, 114–115  
differential diagnosis of, 121  
pathologic features of, 115–120, 115*b*, 116*f*–121*f*  
prognosis and therapy for, 121
- Reactive papillary hyperplasia, 202
- Reactive squamous proliferations, 142
- Reactive vascular ectasia, 226
- REAH. *see* Respiratory epithelial adenomatoid hamartoma
- Recurrent aphthous stomatitis (RAS), 192–194, 193*b*, 193*f*  
clinical findings on, 192  
differential diagnosis of, 193–194  
pathologic findings in, 193, 193*f*, 194*b*  
prognosis and therapy for, 194
- Recurrent respiratory papillomatosis (RRP), 122
- Reed-Sternberg-like cells, 670–673, 673*f*
- Regenerative squamous proliferations, 142
- Relapsing polychondritis, of ear, 444–446, 444*b*  
clinical findings on, 444, 445*f*  
cystic chondromalacia *vs.*, 437  
differential diagnosis of, 445–446  
pathologic findings in, 445, 445*b*, 445*f*–446*f*  
prognosis and therapy for, 446



- Renal cell carcinoma, metastatic  
  calcifying epithelial odontogenic tumor  
  vs., 408  
  clear cell variant of papillary carcinoma  
  vs., 637  
  to ear and temporal bone, 486f  
  endolymphatic sac tumor vs., 477  
  follicular adenoma vs., 604  
  follicular thyroid carcinoma vs., 651–652  
  oncocytoma vs., 274  
  paraganglioma vs., 738t  
  parathyroid adenoma vs., 711  
  parathyroid carcinoma vs., 724  
  parathyroid chief cell hyperplasia vs.,  
  699–700
- Renal failure, parathyroid hyperplasia in,  
  700
- Reparative giant cell granuloma. *see* Central  
  giant cell lesion
- Reparative squamous proliferations, 142
- Respiratory epithelial adenomatoid  
  hamartoma (REAH), 18, 19f, 29
- RET* gene  
  associated with parathyroid neoplasms in,  
  724t  
  paraganglioma and, 728  
  thyroid carcinoma and, 628–630
- Rhabdomyoblasts, 86–88, 89f
- Rhabdomyoma  
  adult, 129–131  
  ancillary studies of, 130, 130f  
  clinical features of, 129, 129b  
  differential diagnosis of, 131  
  granular cell tumor vs., 127–128  
  pathologic features of, 129, 129b, 130f  
  prognosis and therapy for, 131  
  congenital granular cell epulis vs., 216  
  fetal, nodular fasciitis vs., 501  
  granular cell tumor vs., 213–214
- Rhabdomyosarcoma (RMS)  
  ectopic pituitary adenoma vs., 50  
  nodular fasciitis vs., 501  
  of sinonasal tract and nasopharynx,  
  86–91, 88f  
  alveolar, 88, 89f–90f  
  differential diagnosis of, 64t–65t  
  embryonal, 86–88, 88f–89f
- Rhinoscleroma, 12–14, 13b, 13f–14f  
  sinus histiocytosis vs., 503–504
- Rhinosinusitis, 1–2, 1b–2b, 2f–3f  
  allergic fungal sinusitis vs., 9–10  
  chronic, nasal-type extranodal NK/T-cell  
  lymphoma vs., 85  
  infectious granulomatous, granulomatosis  
  with polyangiitis vs., 18
- Rhinosporidiosis, 15–16, 15b–16b, 15f  
  sinonasal papilloma vs., 29
- Rhinosporidium seeberi*, 15
- Riedel thyroiditis, undifferentiated thyroid  
  carcinoma vs., 656
- Riga-Fede disease, 194
- RMS. *see* Rhabdomyosarcoma
- “Roman-bridging,” in salivary duct  
  carcinoma, 328–333, 330f, 332f
- Ropy collagen, 518, 519f
- Rosai-Dorfman disease, 502–504, 503b,  
  504f  
  rhinoscleroma vs., 13–14, 14f
- Rushton bodies, 368–370, 369f, 405, 405f
- Russell bodies, 13
- S**
- Saccular cyst of larynx, 111–112, 113f
- Salivary duct carcinoma (SDC), 328–335,  
  329b  
  ancillary studies of, 333, 334f  
  in carcinoma ex pleomorphic adenoma,  
  336, 339f  
  clinical findings on, 328, 328f  
  differential diagnosis of, 333  
  pathologic findings in, 328–333,  
  329f–333f, 330b  
  prognosis and therapy for, 333–335
- Salivary gland-type adenocarcinoma, 57, 59f
- Salivary glands. *see also specific lesion or  
  neoplasm*  
  anatomy of, 241  
  benign neoplasms of, 261–283  
  basal cell adenoma, 266–269, 266b,  
  267f–268f  
  canalicular adenoma, 269–272, 270b,  
  270f–271f  
  hemangioma, 281–283, 281b–282b,  
  282f–283f  
  oncocytoma, 272b, 273f–276f  
  papillary cystadenoma lymphomatosum,  
  275, 276b–277b, 277f–278f  
  pleomorphic adenoma, 261–266,  
  261b–262b, 262f–264f  
  sebaceous adenoma/lymphadenoma,  
  279–281, 279b, 280f  
  developmental abnormalities of, 241,  
  241b–242b, 242t, 243f–244f  
  malignant neoplasms of, 284–362  
  acinic cell carcinoma, 293f, 294b,  
  295f–300f  
  adenocarcinoma, not otherwise  
  specified, 360–362, 360b, 361f  
  adenoid cystic carcinoma, 301b,  
  301f–309f, 304b  
  carcinoma ex pleomorphic, 335b–336b,  
  335f–340f  
  epithelial-myoepithelial carcinoma,  
  318b, 318f–321f, 322b  
  extranodal marginal zone B-cell  
  lymphoma, 340–343, 341b, 341f–  
  344f, 343b  
  mucoepidermoid carcinoma, 284b,  
  285f–286f, 287b, 290f–292f,  
  291t  
  polymorphous adenocarcinoma, 310b,  
  310f–317f, 314b  
  salivary duct carcinoma, 328f–334f,  
  329b–330b  
  secretory carcinoma, 323b, 324f–328f  
  sialoblastoma, 344b, 344f–346f, 346,  
  346b  
  uncommon carcinomas, 346–354,  
  347f–350f, 351b, 352f–355f  
  undifferentiated carcinomas, 354–360,  
  355f, 356b, 357f–359f  
  non-neoplastic lesions in, 241–260  
  benign lymphoepithelial lesion, 251,  
  252b, 253f–254f  
  lymphoepithelial cysts, 254–255, 255b,  
  255f–256f
- Salivary glands (*Continued*)  
  mucus retention cyst, mucocele, and  
  sialolithiasis, 244–248, 245f–246f,  
  247b  
  necrotizing sialometaplasia, 248–251,  
  249b, 249f–251f
- Sarcoid granulomas, granulomatous  
  thyroiditis vs., 554–555, 557f
- Sarcoidosis, benign salivary  
  lymphoepithelial lesion vs., 252–254
- Sarcoma. *see also* Kaposi sarcoma  
  alveolar soft part, 216  
  Ewing, 64t–65t, 95–97, 95b–96b, 97f–98f  
  glomangiopericytoma vs., 38–40  
  of sinonasal tract, 87b  
  angiosarcoma as, 94–95, 95f  
  biphenotypic sinonasal sarcoma as, 92,  
  93f  
  fibrosarcoma as, 91–92, 92f  
  leiomyosarcoma as, 92–94, 94f  
  rhabdomyosarcoma as, 64t–65t, 86–91,  
  88f–90f  
  synovial, 158, 160f, 531–537, 531b–532b,  
  532f–537f
- “Sarcomatoid” carcinoma. *see* Spindle cell  
  “sarcomatoid” carcinoma (SCSC)
- Sarcomatoid squamous cell carcinoma,  
  inflammatory myofibroblastic tumor  
  vs., 135–137, 136f
- SCC. *see* Squamous cell carcinoma
- Schneiderian papillomas, squamous cell  
  carcinoma vs., 55–56
- Schwannoma. *see also* Peripheral nerve  
  sheath tumor  
  lipoma vs., 520  
  meningioma vs., 35  
  paraganglioma vs., 738t  
  of thyroid gland, 678b, 684, 685f
- Sclerosing mucoepidermoid carcinoma with  
  eosinophilia (SMECE), 677
- Sclerosing odontogenic carcinoma, of  
  gnathic bones, 426–428, 426b  
  ancillary studies of, 427  
  clinical findings on, 426  
  differential diagnosis of, 427–428  
  pathologic findings in, 426–427, 427b,  
  427f  
  prognosis and therapy for, 428  
  radiologic findings in, 426
- Sclerosing osteomyelitis  
  fibrous dysplasia vs., 371  
  of gnathic bones, 363–364, 365f  
  osseous dysplasia vs., 381–382
- Sclerosing polycystic adenosis, 257–258,  
  257b, 258f
- SDC. *see* Salivary duct carcinoma
- SDH* gene, 466, 728
- Sebaceous adenoma, of salivary glands,  
  279–281, 279b  
  ancillary studies of, 280–281  
  clinical findings on, 279  
  differential diagnosis of, 281  
  pathologic findings in, 279–280, 279b,  
  280f–281f  
  prognosis and therapy for, 281
- Sebaceous carcinoma, of salivary glands,  
  351, 351b, 352f–353f
- Sebaceous glands, benign ectopic, 175

- Sebaceous lymphadenoma, of salivary glands, 279–281, 279*b*, 279*f*–280*f*
- Secondary parathyroid hyperplasia, 700–702, 700*b*–701*b*, 701*f*–702*f*
- Secondary tumors, of larynx or hypopharynx, 173–174, 173*b*, 174*f*
- Secretory carcinoma, of salivary glands, 322–326, 323*b*
- ancillary studies of, 326
- clinical findings on, 322
- differential diagnosis of, 326, 328*f*
- pathologic findings in, 322–323, 323*b*, 324*f*–327*f*
- prognosis and therapy for, 326
- Seeding, parathyroid tumor cell, 724
- Seromucinous hamartoma (SH), 18, 20*f*
- Serous acinar cells, 294, 295*f*
- SETTLE. *see* Spindle cell tumor with thymus-like differentiation
- SFT. *see* Solitary fibrous tumor
- SHML. *see* Sinus histiocytosis with massive lymphadenopathy
- Sialadenitis
- acinic cell carcinoma *vs.*, 297–300
- benign salivary lymphoepithelial lesion *vs.*, 252–254
- lymphoepithelial, 251–254
- carcinoma *vs.*, 359
- extranodal marginal zone B-cell lymphoma and, 340, 341*f*
- Sialoblastoma, of salivary glands, 344–346, 344*b*
- ancillary studies of, 346
- clinical findings on, 344, 344*f*
- differential diagnosis of, 346
- pathologic findings in, 344, 345*f*–346*f*, 346*b*
- Sialolith, 245, 247*f*
- Sialolithiasis, of salivary glands, 244–248, 245*f*–247*f*, 247*b*
- Sialometaplasia, necrotizing. *see* Necrotizing sialometaplasia
- Signet-ring cell adenoma, follicular adenoma and, 599, 600*f*
- Signet-ring cell variant, of follicular thyroid carcinoma, 650, 650*f*
- Simple bone cyst, 375–376, 375*b*, 375*f*–376*f*
- Sinonasal adenocarcinoma, 57–61, 57*b*
- ancillary studies of, 60
- differential diagnosis of, 60
- non-salivary gland-type, 57
- pathologic features of, 58–60, 58*b*
- salivary gland-type, 57–58, 59*f*
- sinonasal hamartoma *vs.*, 21, 21*f*
- Sinonasal hamartomas, 18–21, 19*b*, 19*f*–21*f*, 21*b*
- Sinonasal papillomas, 22–29, 122*b*
- ancillary studies of, 123, 124*f*
- clinical features of, 122–123, 123*f*
- differential diagnosis of, 29, 123–124, 125*f*
- pathologic features of, 22–28, 23*f*–28*f*, 23*t*–24*t*, 123, 123*b*, 124*f*–125*f*
- prognosis and therapy for, 124–125
- rhinosporidiosis *vs.*, 16
- sinonasal adenocarcinoma *vs.*, 60
- squamous cell carcinoma *vs.*, 55–56
- Sinonasal polyps
- allergic fungal sinusitis *vs.*, 9–10
- inflammatory, 2–6, 4*b*, 4*f*–6*f*
- respiratory epithelial adenomatoid hamartoma *vs.*, 21
- lobular capillary hemangioma *vs.*, 33
- nasal glial heterotopia *vs.*, 12
- sinonasal papilloma *vs.*, 29
- with stromal atypia, 89–91, 91*f*
- Sinonasal sarcoma, biphenotypic, respiratory epithelial adenomatoid hamartoma *vs.*, 21
- Sinonasal tract. *see* Nasal cavity; Paranasal sinuses
- Sinonasal-type hemangiopericytoma, 35–40, 36*b*, 37*f*–41*f*
- Sinonasal undifferentiated carcinoma (SNUC), 61–66, 62*b*, 62*f*
- ancillary studies of, 63
- differential diagnosis of, 63, 64*t*–65*t*, 66*f*
- nasopharyngeal carcinoma *vs.*, 71–72
- NUT carcinoma *vs.*, 68
- pathologic features of, 62*b*, 63, 63*f*
- squamous cell carcinoma *vs.*, 55–56
- Sinus histiocytosis with massive lymphadenopathy (SHML), 502–504, 503*b*
- ancillary studies of, 503
- clinical findings on, 502
- differential diagnosis of, 503–504
- pathologic findings in, 502–503, 503*b*, 504*f*
- prognosis and therapy for, 504
- radiologic findings in, 502
- Sinuses. *see also* Paranasal sinuses
- thyroglossal duct cyst and, 542
- Sinusitis
- allergic fungal, 8–10, 8*b*, 9*f*–10*f*, 10*b*
- papillary, sinonasal adenocarcinoma *vs.*, 60
- Sistrunk procedure, for thyroglossal duct cyst, 543*f*
- Sjögren syndrome
- benign lymphoepithelial lesion and, 251–252
- extranodal marginal zone B-cell lymphoma and, 340
- Small cell carcinoma, 237–240, 237*b*
- ancillary studies of, 240
- clinical features of, 237
- differential diagnosis of, 240
- paraganglioma *vs.*, 738*t*
- pathologic features of, 237–240, 240*b*
- prognosis and therapy for, 240
- of salivary glands, 354–356, 355*f*, 356*b*, 357*f*–358*f*
- Small medullary carcinoma, ultimobranchial remnants *vs.*, 549
- “Small round blue cell” malignant neoplasms of sinonasal tract, 64*t*–65*t*
- SMARCB1-deficient sinonasal carcinoma, sinonasal undifferentiated carcinoma *vs.*, 63
- Smoking
- precursor squamous lesions and, 138*b*
- squamous cell carcinoma and, 219
- verrucous squamous cell carcinoma and, 148
- SNUC. *see* Sinonasal undifferentiated carcinoma
- Solid cell nests, medullary carcinoma *vs.*, 659–660, 661*f*
- Solid variant
- of acinic cell carcinoma, 294–295, 295*f*
- of adenoid cystic carcinoma, 301–302, 304*f*–305*f*
- of basal cell adenocarcinoma, 348
- of basal cell adenoma, 266, 267*f*
- of papillary thyroid carcinoma, 640, 642*f*
- Solitary fibrous tumor (SFT)
- glomangiopericytoma *vs.*, 38–40, 41*f*
- invasive fibrous thyroiditis *vs.*, 561
- of thyroid gland, 678*b*, 684, 685*f*
- SP. *see* Squamous papilloma
- Spindle cell lipoma/pleomorphic lipoma, 517–520, 518*b*
- ancillary studies of, 520
- clinical findings on, 518
- differential diagnosis of, 520
- pathologic findings in, 518–519, 518*f*–519*f*, 520*b*
- prognosis and therapy for, 520
- Spindle cell melanoma, 158
- Spindle cell sarcoma, 532–533, 532*f*–533*f*
- Spindle cell “sarcomatoid” carcinoma (SCSC)
- of larynx, hypopharynx, and trachea, 102, 153–158, 155*b*, 155*f*–160*f*
- of middle ear, 478–479, 481*f*
- of oropharynx, 232–235
- vocal cord polyps/nodules *vs.*, 102
- Spindle cell squamous cell carcinoma (SCSCC)
- chondrosarcoma *vs.*, 170–173
- of larynx, hypopharynx, and trachea, 153–158, 155*b*, 155*f*–160*f*
- of oral cavity, 221–222
- Spindle cell tumor with thymus-like differentiation (SETTLE), 678*b*, 680–681, 680*f*–681*f*, 683*f*
- Spindle cell variant
- of follicular thyroid carcinoma, 650, 650*f*
- of papillary thyroid carcinoma, 638
- Spindle cells, in undifferentiated thyroid carcinoma, 654, 655*f*
- Squamous cell carcinoma (SCC)
- basaloid
- adenoid cystic carcinoma *vs.*, 308–309
- of nasopharynx, 71
- calcifying epithelial odontogenic tumor *vs.*, 408
- of ear and temporal bone, 478–481, 478*b*
- ancillary studies of, 480–481
- cholesteatoma *vs.*, 450
- chondrodermatitis nodularis helices *vs.*, 441
- clinical findings on, 478, 479*f*
- cystic metastatic, first branchial cleft anomalies *vs.*, 435–436
- differential diagnosis of, 481
- pathologic findings in, 478–480, 479*b*, 480*f*–481*f*
- prognosis and therapy for, 481
- of gnathic bones, primary intraosseous carcinoma *vs.*, 426



- Squamous cell carcinoma (SCC) (*Continued*)  
 of larynx, hypopharynx, and trachea, 143–148, 143b  
 clinical findings on, 143  
 differential diagnosis of, 147, 147f  
 granular cell tumor *vs.*, 127–128  
 laryngeal cysts and, 114  
 neuroendocrine carcinoma *vs.*, 167–168  
 pathologic findings in, 143–147, 144b, 144f–147f  
 precursor lesions of, 138  
 prognosis and therapy for, 148  
 reactive epithelial changes and, 117f  
 metastatic  
 to lymph nodes, 529  
 of neck, 521–528, 521b–522b, 522f–527f  
 metastatic cystic  
 branchial cleft cyst *vs.*, 490–492  
 first branchial cleft anomalies *vs.*, 435–436  
 lymphoepithelial cyst *vs.*, 255  
 of oral cavity, 219–224, 219b  
 ancillary studies of, 222  
 clinical features of, 219–220, 220f  
 differential diagnosis of, 222–224  
 pathologic features of, 220–222, 221b, 222f–225f  
 prognosis and therapy for, 224  
 radiologic features of, 220, 221f  
 traumatic ulcerative granuloma *vs.*, 195  
 verrucous, 224f  
 of oropharynx, 230–237, 230b  
 ancillary studies of, 235f, 236, 238f–239f  
 clinical features of, 230–231, 231f  
 differential diagnosis of, 236–237  
 pathologic features of, 231–236, 232b, 233f–235f  
 prognosis and therapy for, 237  
 radiologic features of, 231, 231f  
 of salivary gland  
 mucoepidermoid carcinoma *vs.*, 291–293  
 necrotizing sialometaplasia *vs.*, 250  
 salivary duct carcinoma *vs.*, 333  
 of sinonasal tract, 51–57, 52b  
 ancillary studies of, 54, 55f–56f  
 differential diagnosis of, 55–56  
 NUT carcinoma *vs.*, 68  
 pathologic features of, 52–54, 52b, 53f–54f  
 of thyroid gland, 678b, 679, 679f  
 Squamous cell carcinoma (SCC) variants  
 adenosquamous  
 basaloid squamous cell carcinoma *vs.*, 160–161  
 of larynx, hypopharynx, and trachea, 163–164, 163b, 163f  
 of oral cavity and oropharynx, 221, 235, 235f  
 basaloid  
 adenoid cystic carcinoma *vs.*, 308–309  
 adenosquamous carcinoma *vs.*, 160–161  
 of larynx, hypopharynx, and trachea, 160–161, 161b, 161f–162f  
 of nasopharynx, 71  
 of oropharynx, 232, 235f  
 Squamous cell carcinoma (SCC) variants (*Continued*)  
 exophytic  
 of larynx, hypopharynx, and trachea, 150–152, 152b, 153f  
 squamous papilloma *vs.*, 123  
 of larynx, hypopharynx, and trachea, 148–164, 149f  
 papillary  
 of larynx, hypopharynx, and trachea, 150–152, 152b, 153f–154f  
 of oropharynx, 232, 234f  
 sinonasal papilloma *vs.*, 29  
 squamous papilloma *vs.*, 123–124, 202  
 spindle cell “sarcomatoid”  
 of larynx, hypopharynx, and trachea, 102, 153–158, 155b, 155f–160f  
 of middle ear, 478–479, 481f  
 of oropharynx, 232–235  
 squamous cell carcinoma *vs.*, 147  
 verrucous  
 of larynx, hypopharynx, and trachea, 148–150, 148b, 150f–152f  
 of oral cavity, 221, 224f  
 verrucous hyperplasia *vs.*, 115–116, 117f  
 Squamous intraepithelial lesion (SIL), 138  
 Squamous intraepithelial neoplasia (SIN), 138  
 Squamous morules, 643f  
 Squamous odontogenic tumor, sclerosing  
 odontogenic carcinoma *vs.*, 427–428  
 Squamous papilloma (SP)  
 of larynx, 122  
 ancillary studies of, 123  
 differential diagnosis of, 123–124, 125f  
 gross findings in, 123  
 microscopic findings in, 123, 124f  
 prognosis and therapy for, 124–125  
 of oral cavity, 200–203, 200b  
 ancillary studies of, 201  
 clinical features of, 200  
 differential diagnosis of, 201–202  
 pathologic features of, 200–201, 200f–202f, 201b  
 prognosis and therapy for, 203  
 squamous cell carcinoma *vs.*, 55–56, 147  
 SS. *see* Synovial sarcoma  
 Stellate abscesses, 492–494, 493f  
 Stomatitis, recurrent aphthous, 192–194, 193b, 193f  
 clinical findings on, 192  
 differential diagnosis of, 193–194  
 pathologic findings in, 193, 193f, 194b  
 prognosis and therapy for, 194  
*Streptococcus pneumoniae*, 1  
 Subacute thyroiditis. *see* Granulomatous thyroiditis  
 Sublingual gland, 241  
 Submandibular gland, 241  
 Sustentacular cells, of paraganglioma, 735–736  
 Sympathetic paragangliomas, thoracic, 728  
 Synovial sarcoma (SS), 531–537, 531b  
 ancillary studies of, 534–536, 535f  
 clinical findings on, 531  
 differential diagnosis of, 536  
 pathologic findings in, 532–533, 532b, 532f–534f  
 Synovial sarcoma (SS) (*Continued*)  
 prognosis and therapy for, 536–537  
 radiologic findings in, 531  
 spindle cell squamous cell carcinoma *vs.*, 158, 160f  
 Syringocystadenoma papilliferum, ceruminous, 453–454  
 Syringoma, chondroid, 453–454  
**T**  
 Tall cell variant, of papillary thyroid carcinoma, 639, 639f–640f  
 Tattoo, amalgam, 176–177, 177b  
 clinical findings on, 176, 176f  
 differential diagnosis of, 177  
 pathologic features of, 177, 177b, 177f  
 prognosis and therapy for, 177  
 radiologic findings in, 176  
 Teflon granuloma, of larynx, 115, 120  
 Temporal bone. *see also specific lesion or neoplasm*  
 benign neoplasms of, 453–477  
 endolymphatic sac tumor, 475–477, 475b, 476f–477f  
 Langerhans cell histiocytosis, 457–460, 457b–458b, 458f–460f  
 meningioma, 467–470, 468b, 469f–470f  
 peripheral nerve sheath tumor (schwannoma), 460–463, 461b, 462f–463f  
 malignant neoplasms of, 478–487  
 ceruminous adenocarcinoma, 481–484, 482b, 482f–484f  
 metastatic, 484–487, 485b, 485f–486f  
 squamous cell carcinoma, 478–481, 478b–479b, 479f–481f  
 Teratocarcinosarcoma, 97–100, 99b  
 ancillary studies of, 99  
 differential diagnosis of, 100  
 pathologic features of, 98–99, 99b, 99f–100f  
 Teratoma, 613–618, 613b  
 ancillary studies of, 615–616  
 cervical, 512  
 clinical findings on, 613  
 differential diagnosis of, 616–618  
 laryngeal cysts *vs.*, 114  
 metastatic gonadal, 514–515  
 of neck, 512b  
 ancillary studies of, 514  
 clinical findings on, 512, 512f  
 differential diagnosis of, 514–515  
 pathologic findings in, 513–514, 513f–514f, 514b  
 prognosis and therapy for, 515  
 pathologic findings in, 614–615, 614f–617f, 615b  
 prognosis and therapy for, 618  
 radiologic findings in, 614  
 Tertiary parathyroid hyperplasia, 700–702, 700b–701b, 701f–702f  
 Thrombus, mucocele *vs.*, 248  
 Thrush, 181  
 Thymic and related branchial pouch neoplasms, 680–682  
 Thymic cysts, 490–492, 491f  
 Thymoma, ectopic, primary thyroid gland lymphoma *vs.*, 675

- Thyroglossal duct cyst, 542–546, 542b  
 branchial cleft cyst *vs.*, 490–492  
 clinical findings on, 542, 543f  
 differential diagnosis of, 544  
 pathologic findings in, 542–543, 543f–545f, 544b  
 prognosis and therapy for, 544–546  
 radiographic findings on, 542
- Thyroid carcinoma. *see also* Follicular carcinoma (FC), of thyroid gland; Medullary carcinoma, of thyroid gland; Papillary carcinoma, of thyroid gland  
 metastatic  
   angiolympoid hyperplasia with eosinophilia *vs.*, 442  
   endolymphatic sac tumor *vs.*, 477  
   to lymph nodes, 529  
   lymphangioma *vs.*, 511  
 undifferentiated, 621b, 652–656, 652b–653b, 653f–655f, 657f  
   invasive fibrous thyroiditis *vs.*, 561  
   primary thyroid gland lymphoma *vs.*, 675
- Thyroid gland. *see also specific lesion or neoplasm*  
 benign neoplasm of, 593–618  
   follicular adenoma, 593–604, 593b, 594f–603f, 595b  
   hyalinizing trabecular tumor, 608–613, 608b, 609f–612f  
   noninvasive follicular thyroid neoplasm, 604–607, 605b–606b, 605f–607f  
   teratoma, 613–618, 613b, 614f–617f, 615b  
 ectopic, 546–548, 546f, 547b  
   ancillary studies of, 547  
   clinical findings on, 546  
   differential diagnosis of, 547–548  
   oral, 178–179, 178b, 178f–179f  
   pathologic findings in, 546–547, 547b, 547f  
   prognosis and therapy for, 548  
   radiologic findings in, 546  
 malignant neoplasms of, 619–691  
   follicular carcinoma, 643–652, 644f, 645b, 646f–651f  
   medullary carcinoma, 632b, 656–667, 658b, 659f, 660b, 663f–666f  
   metastatic, 687–691, 687b, 688f–691f, 689b  
   papillary carcinoma, 619–632, 620b, 620f–631f  
   primary lymphoma, 667–677, 668b–669b, 668f–676f  
   uncommon, 677–687, 678b  
   undifferentiated carcinoma, 621b, 652–656, 652b–653b, 654f–655f, 657f  
 non-neoplastic lesions of, 542–592  
   acute thyroiditis, 551–552, 551b–552b, 552f  
   amiodarone-induced thyroid disease, 589–592, 590b, 591f–592f  
   amyloid goiter, 586–589, 587b, 588f–589f, 589b  
   chronic lymphocytic thyroiditis, 562–567, 562b–563b, 563f–566f
- Thyroid gland (*Continued*)  
 diffuse hyperplasia (Graves disease), 567–575, 569b–570b, 569f–574f  
 dysmorphonogenetic goiter, 583–586, 584b, 585f–587f  
 invasive fibrous thyroiditis, 557–561, 559b, 559f–561f  
 nodular hyperplasia, 575–583, 575b–576b, 576f–583f  
 subacute granulomatous thyroiditis, 552–557, 553b–554b, 554f–557f  
 thyroglossal duct cyst, 542–546, 542b, 543f–545f, 544b  
 thyroid ectopia and lingual thyroid, 546–548, 546f–547f, 547b  
 ultimobranchial body remnants, 548–551, 548b, 549f–550f  
 parathyroid carcinoma adjacent to, 716f  
 uncommon malignant neoplasms of mesenchymal tumors, 682–687  
   mucoepidermoid carcinoma, 677–679, 677f  
   squamous cell carcinoma, 679, 679f  
   thymic and related branchial pouch neoplasms, 680–682
- Thyroid hormone replacement, for chronic lymphocytic thyroiditis, 567
- Thyroid neoplasms, parathyroid adenoma *vs.*, 711
- Thyroidectomy, for medullary thyroid carcinoma, 667
- Thyroiditis  
 acute, 551–552  
   ancillary studies of, 551  
   clinical findings on, 551  
   differential diagnosis of, 552  
   pathologic findings in, 551, 552b, 552f  
   prognosis and therapy for, 552  
 chronic lymphocytic (Hashimoto thyroiditis), 562–567, 562b  
   ancillary studies of, 566, 567f  
   clinical findings on, 562  
   differential diagnosis of, 566–567, 568f  
   laboratory studies for, 563  
   pathologic findings in, 563–566, 563b, 563f–566f  
   primary thyroid gland lymphoma *vs.*, 675  
   prognosis and therapy for, 567  
   radiologic findings in, 562–563  
 granulomatous, 553b  
   acute thyroiditis *vs.*, 552  
   ancillary studies of, 554, 556f  
   clinical findings on, 553  
   differential diagnosis of, 554–555, 557f–558f  
   laboratory studies for, 553  
   pathologic findings in, 553, 554b, 554f–555f  
   prognosis and therapy for, 557  
 invasive fibrous, 557–561  
   ancillary studies of, 561  
   clinical findings on, 558  
   differential diagnosis of, 561  
   laboratory studies for, 558  
   pathologic findings in, 559–561, 559b, 559f–561f
- Thyroiditis (*Continued*)  
 prognosis and therapy for, 561  
 radiologic findings in, 558  
 lymphocytic, 637f–638f, 638–639  
 Riedel, undifferentiated thyroid carcinoma *vs.*, 656
- Tobacco use  
 precursor squamous lesions and, 138  
 squamous cell carcinoma and, 143, 219
- Tonsillar cyst, 111–112, 113f
- Tori, of gnathic bones, 377–379, 378b, 378f
- Trabecular tumor, hyalinizing, 608–613, 608b  
 ancillary studies of, 611, 612f  
 clinical findings on, 608  
 differential diagnosis of, 613  
 follicular adenoma *vs.*, 604  
 paraganglioma *vs.*, 737–738  
 pathologic findings in, 609–611, 609b, 609f–611f  
 prognosis and therapy for, 613
- Trabecular variant, of basal cell adenoma, 266
- Trachea. *see also specific lesion or neoplasm*  
 benign neoplasms of, 122–137  
   adult rhabdomyoma, 129–131, 129b, 130f  
   chondroma, 131–134, 131b, 132f–133f  
   granular cell tumor, 125–129, 126b, 126f–128f  
   sinonasal papillomas, 122–125, 124f–125f  
 malignant neoplasms of, 138–174  
   chondrosarcoma, 168–173, 169b–170b, 169f–172f  
   neuroendocrine carcinoma, 164–168, 164b–165b, 165f–168f  
   precursor squamous lesions, 138–143, 138b–139b, 139f  
   squamous cell carcinoma, 143–148, 143b–144b, 144f–147f  
   squamous cell carcinoma variants, 148–164, 148b, 149t, 150f–163f, 152b, 155b, 161b, 163b  
 non-neoplastic lesions of, 101–121  
   amyloidosis, 107–110, 108b, 108f–110f  
   contact ulcer, 104–107, 105b, 105f–107f  
   reactive epithelial changes, 114–121, 114b, 116f–121f
- Transitional vocal cord epithelium, 142
- Transplant-associated Kaposi sarcoma, 225
- Traumatic cyst of larynx, 111–112
- Traumatic ulcerative granuloma, 194–196, 195b  
 clinical findings on, 194f  
 differential diagnosis of, 195  
 pathologic findings in, 194, 195b, 195f–196f  
 prognosis and therapy for, 196
- Tuberculosis thyroiditis, granulomatous thyroiditis *vs.*, 554–555
- Tubular variant  
 of adenoid cystic carcinoma, 301–302, 302f  
 of basal cell adenoma, 266
- Tubulotrabeular variant, of acinic cell carcinoma, 348, 349f



Tumor-to-capsule-to-parenchymal interface  
for follicular carcinoma, 651  
for papillary carcinoma, 621  
Turner syndrome, 509, 510f  
“Two-thirds rule”, 409  
Tzanck cells, 183, 185f

## U

Ulcer, contact, 104–107, 105b  
clinical features of, 104  
differential diagnosis of, 105–106  
pathologic features of, 104–105, 105b, 105f–107f  
prognosis and therapy for, 106–107  
spindle cell squamous cell carcinoma *vs.*, 158  
vocal cord polyps/nodules *vs.*, 102  
Ulcerative granuloma, traumatic, 194–196, 195b  
clinical findings on, 194f  
differential diagnosis of, 195  
pathologic findings in, 194, 195b, 195f–196f  
prognosis and therapy for, 196  
Ultimobranchial body, 656–658  
remnants, 548–551, 548b, 549f–550f, 659–660, 661f  
Ultrasound, for papillary carcinoma, 620–621, 620f  
Undifferentiated carcinoma  
of salivary glands, 354–360, 356b  
large cell carcinoma, 356–358, 356b  
lymphoepithelial carcinoma, 356b, 358–360, 359f  
small cell carcinoma, 354–356, 355f, 356b, 357f–358f  
sinonasal, 61–66, 62b, 62f–63f, 64t–65t, 66f  
of thyroid gland, 652–656, 652b  
ancillary studies of, 656, 657f  
clinical findings on, 652–654, 653f  
differential diagnosis of, 656

Undifferentiated carcinoma (*Continued*)  
invasive fibrous thyroiditis *vs.*, 561  
pathologic findings in, 621b, 653b, 654, 654f–655f  
primary thyroid gland lymphoma *vs.*, 675  
prognosis and therapy for, 656  
Unicystic ameloblastoma  
dentigerous cyst *vs.*, 368  
of gnathic bones, 395–396, 402f

## V

Vacuolated cells, 294  
Vagal paraganglioma, 737–738, 738t  
Vascular invasion  
in follicular thyroid carcinoma, 646–648, 648f–649f  
in parathyroid carcinoma, 714–722, 714f  
Venereal wart. *see* Condyloma acuminatum  
Verruca vulgaris  
oral, 200, 200b, 200f  
sinonasal papilloma *vs.*, 29  
Verrucous hyperplasia  
laryngeal, 115–116, 117f  
verrucous carcinoma *vs.*, 148  
Verrucous squamous cell carcinoma (VSCC)  
of larynx, hypopharynx, and trachea, 148–150, 148b, 150f–152f  
of oral cavity, 221, 224f  
verrucous hyperplasia *vs.*, 115–116, 117f  
VHL gene, 475, 477, 728  
Viral rhinosinusitis, 1  
Vitamin D, 692  
Vocal abuse or overuse, 101  
Vocal cord polyps and nodules, 101–104, 101b  
clinical features of, 101  
differential diagnosis of, 102  
pathologic features of, 101–102, 102b, 102f–104f  
prognosis and therapy for, 102–104

von Hippel-Lindau syndrome (VHL),  
endolymphatic sac tumor in, 475  
von Recklinghausen disease, 729t  
VSCC. *see* Verrucous squamous cell carcinoma

## W

Wagner-Meissner bodies, lipoma *vs.*, 520  
Waldeyer ring, metastatic squamous cell carcinoma in, 528  
Warthin tumor, 275–279, 276b–277b, 277f–278f  
“Warthin” variant, of papillary carcinoma, 628f  
Warts. *see* Condyloma acuminatum; Verruca vulgaris  
Water-clear cell hyperplasia, 694–698  
“Watermelon seed,” nuclei in carcinoma, 714–722, 721f  
Wegener granulomatosis (WG), 16. *see also* Granulomatosis with polyangiitis  
contact ulcer *vs.*, 105–106  
nasal-type extranodal NK/T-cell lymphoma *vs.*, 85  
relapsing polychondritis *vs.*, 445–446  
sinus histiocytosis *vs.*, 503–504  
Wickham striae, 186, 186f  
Widely invasive follicular carcinoma, 647f–648f, 648  
Work type I branchial cleft anomalies, 433  
Work type II branchial cleft anomalies, 433, 435f

## Z

Zellballen pattern, of paraganglioma, 464–466, 465f, 731, 732f  
Zymogen granules, 294, 295f, 298f